U.S. Department
of Commerce

Volume 90
Number 1
January 1992

Fishery Bulletin

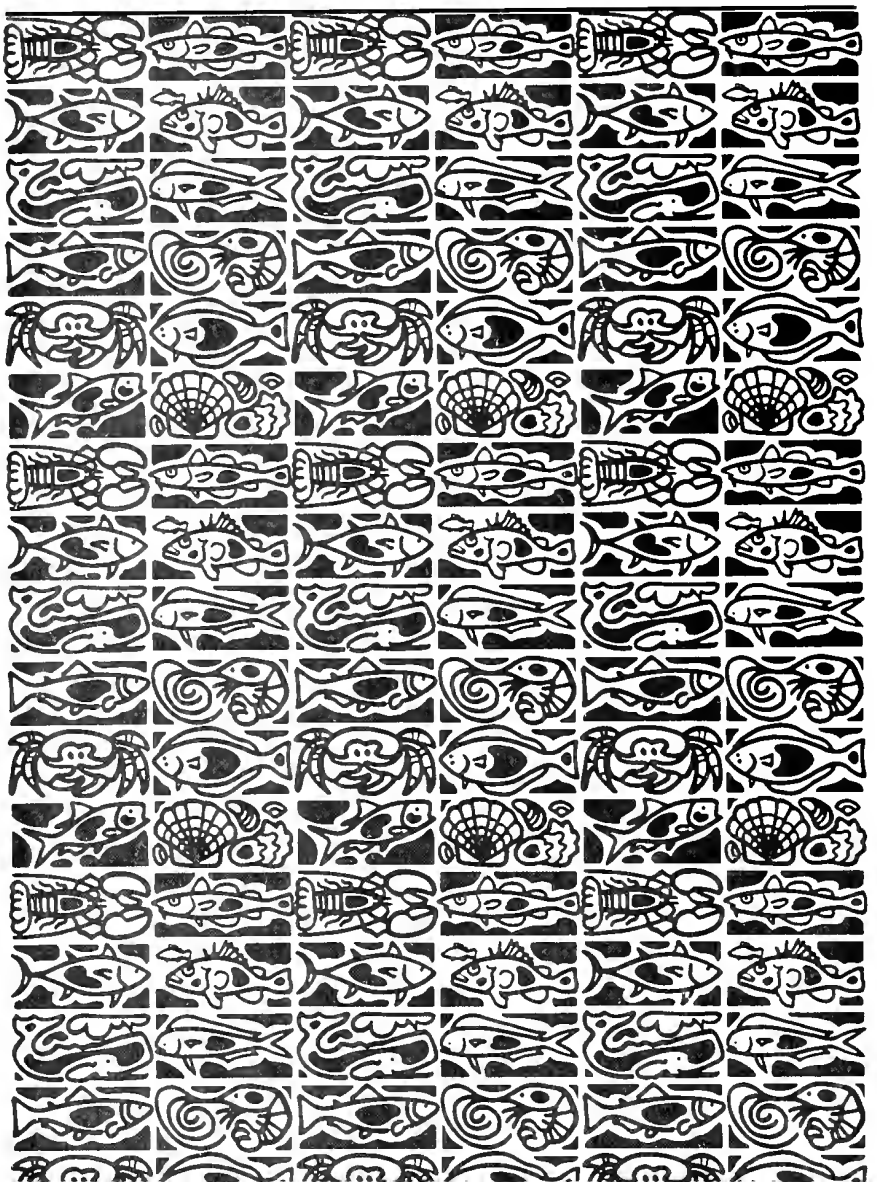

Fishery Bulletin

The *Fishery Bulletin* (ISSN 0090-0656) is published quarterly by the Scientific Publications Office, National Marine Fisheries Service, NOAA, 7600 Sand Point Way NE, BIN C15700, Seattle, WA 98115-0070. Second class postage is paid in Seattle, Wash., and additional offices. POSTMASTER send address changes for subscriptions to Fishery Bulletin, Superintendent of Documents, Attn: Chief, Mail List Branch, Mail Stop SSOM, Washington, DC 20402.

The Secretary of Commerce has determined that the publication of this periodical is necessary in the transaction of the public business required by law of this Department. Use of funds for printing of this periodical has been approved by the Director of the Office of Management and Budget.

For sale by the Superintendent of Documents, U.S. Government Printing Office, Washington, DC 20402. Subscription price per year: $16.00 domestic and $20.00 foreign. Cost per single issue: $9.00 domestic and $11.25 foreign. **See back page for order form.**

The *Fishery Bulletin* carries original research reports and technical notes on investigations in fishery science, engineering, and economics. The Bulletin of the United States Fish Commission was begun in 1881; it became the Bulletin of the Bureau of Fisheries in 1904 and the Fishery Bulletin of the Fish and Wildlife Service in 1941. Separates were issued as documents through volume 46; the last document was No. 1103. Beginning with volume 47 in 1931 and continuing through volume 62 in 1963, each separate appeared as a numbered bulletin. A new system began in 1963 with volume 63 in which papers are bound together in a single issue of the bulletin. Beginning with volume 70, number 1, January 1972, the *Fishery Bulletin* became a periodical, issued quarterly. In this form, it is available by subscription from the Superintendent of Documents, U.S. Government Printing Office, Washington, DC 20402. It is also available free in limited numbers to libraries, research institutions, State and Federal agencies, and in exchange for other scientific publications.

U.S. Department
of Commerce
Seattle, Washington

Volume 90
Number 1
January 1992

Fishery Bulletin

Contents

Notes

Abstract.—We summarize the methods for estimating relative abundance of seven dolphin stocks in the eastern tropical Pacific Ocean using sightings data collected on commercial tuna vessels by trained observers, developed by Buckland and Anganuzzi (1988a) and Anganuzzi and Buckland (1989). Their estimates of relative abundance, which may show large year-to-year fluctuations, are smoothed to provide estimates of the underlying trend in dolphin abundance between 1976 and 1988. The bootstrap method provides estimation of precision in a way that allows trend estimates to be used for management purposes, without the need to assume that trends in abundance are linear. Concerns about the validity of the estimates are addressed.

Estimating trends in abundance of dolphins associated with tuna in the eastern tropical Pacific Ocean, using sightings data collected on commercial tuna vessels

Stephen T. Buckland
Karen L. Cattanach
SASS Environmental Modelling Unit, MLURI
Craigiebuckler, Aberdeen AB9 2QJ, United Kingdom

Alejandro A. Anganuzzi
Inter-American Tropical Tuna Commission
8604 La Jolla Shores Drive, La Jolla, California 92093

Manuscript accepted 27 November 1991.
Fishery Bulletin, U.S. 90:1–12 (1992).

Incidental mortality of dolphins in the tuna fishery in the eastern tropical Pacific since 1959 has been sufficient to affect abundance of stocks of at least two species of dolphin: the spotted dolphin *Stenella attenuata* and the spinner dolphin *S. longirostris* (Smith 1983). Although there is less information available on stocks of the common dolphin *Delphinus delphis*, mortality estimates (e.g., Hall and Boyer 1988) suggest that abundance of stocks of this species may also have been reduced. To monitor possible effects of incidental mortality on the size of dolphin stocks, several attempts to estimate abundance have been made, usually applying line-transect methodology to data collected on either commercial tuna vessels ("tuna vessel data") or research vessels ("research vessel data") or both. Holt and Powers (1982) and Holt (1985, 1987) considered analyses of research vessel data alone, and of tuna vessel data combined with research vessel data. More recently, Holt and Sexton (1989, 1990a,b) analyzed data from research vessels alone. Tuna vessel data alone were analyzed by Hammond and Laake (1983), by Polacheck (1987), by Buckland and Anganuzzi (1988a), and by Anganuzzi and Buckland (1989).

The tuna vessel data are collected by scientific technicians placed by two organizations onboard commercial tuna purse seiners. The Inter-American Tropical Tuna Commission (IATTC) places technicians on vessels of the international fleet (including U.S.-registered vessels), and the National Marine Fisheries Service (NMFS) of the United States places technicians on U.S.-registered vessels only. Data were first collected by NMFS in 1974, and by IATTC in 1979.

Tuna vessel data provide a large database, with regular coverage of a substantial portion of the area occupied by the dolphin stocks. However, due to the nature of the fishery operations, the assumptions necessary for line-transect sampling to yield unbiased estimates of absolute abundance are often violated. Therefore, analytic procedures should as far as possible be insensitive to those violations. We summarize here the procedures of Buckland and Anganuzzi (1988a), as modified by Anganuzzi and Buckland (1989). Since these procedures are unlikely to remove all biases, the estimates should

be treated as indices of relative abundance, rather than estimates of absolute abundance of the stocks. The definition of a stock, and its boundaries, is problematic, but we follow the recommendations of Au et al. (1979), for reasons stated by Anganuzzi and Buckland (1989), except in two cases. A more southerly southern boundary was found to be necessary for the southern offshore stock of spotted dolphins (Anganuzzi et al. 1991), and we adopt the recommendation of Perrin et al. (1991) to combine the northern and southern whitebelly stocks of spinner dolphins. We also derive estimates for pooled offshore stocks of spotted dolphins and pooled stocks of common dolphins, since they are not differentiable in the field.

Buckland and Anganuzzi (1988a) provided three types of test for assessing whether abundance of a stock had changed over time. For several stocks, the tests failed to provide a clear indication of recent changes, since the occasional large fluctuation in annual estimates indicated that there were significant changes in abundance that were biologically implausible. We present here a method of smoothing the sequence of estimates of relative abundance. Used in conjunction with the bootstrap, it yields a simple method of assessing change over time which does not require that trends are assumed to be linear, and which does not yield biologically implausible rates of change.

Edwards and Kleiber (1989) have questioned the validity of estimating trends in abundance from sightings data collected on commercial tuna vessels. We carry out a simple simulation study to assess their assertions, and compare the relative abundance estimates calculated from tuna vessel data with those calculated from research vessel data for the years 1986–89, for which data from both sources are available.

Methods

The number of dolphins N in an area for a given stock and year is estimated by

$$\hat{N} = A \cdot \hat{s} \cdot \hat{D}$$

where A is the size of the area,
$\hat{s}$ is the estimated average school size for the stock in area A, and
$\hat{D}$ is the estimated density of schools in area A.

The line-transect method provides the estimate $\hat{D}$ (Burnham et al. 1980). Suppose schools farther than a distance w from the trackline are discarded from the analyses. Then

$$\hat{D} = \frac{n \cdot \hat{f}(0)}{2L} \quad (1)$$

where n is the number of schools detected in the area that are within the truncation distance w,
$\hat{f}(0)$ is the estimated probability density function of the n perpendicular distances, evaluated at perpendicular distance zero, and
L is the total length of transect in nautical miles within the area.

If we define the encounter rate E to be the expected number of sightings detected within w of the trackline per nautical mile of search, then its estimate is given by

$$\hat{E} = n/L.$$

Hence,
$$\hat{D} = \frac{\hat{E} \cdot \hat{f}(0)}{2} \quad (2)$$

and
$$\hat{N} = \frac{\hat{E} \cdot \hat{f}(0) \cdot \hat{s} \cdot A}{2}. \quad (3)$$

If $\hat{D}$ and $\hat{N}$ were estimates of absolute abundance, then the following assumptions would be required:

(i) Within each area or stratum, either the search effort of the tuna vessels is random or the dolphin schools are randomly distributed;
(ii) any movement of schools is slow relative to the speed of the vessel, at least before detection;
(iii) all schools on or close to the trackline are detected and identified;
(iv) sighting distances and angles are measured without error;
(v) sightings of schools are independent events;
(vi) school size is recorded without error, and for mixed schools percent of each species is recorded without error;
(vii) probability of detection of a school is independent of its size, at least out to perpendicular distance w.

If the estimates are used solely as indices of relative abundance, as here, then any or all of the above assumptions may fail without invalidating the estimates, provided that bias arising from the failure of an assumption is consistent across time. Even this proviso may be relaxed when trends in abundance over a long sequence of years are estimated; in this case it is merely necessary to assume that bias shows no trend with time. Catch-per-unit-effort methods for estimating relative abundance are known to show trends in bias over time in some instances, due to increased efficiency of vessels (Cooke 1985). We attempt to avoid such problems by incorporating a parameter that measures the

efficiency of search of the tuna vessels. This parameter, the effective search width, is estimated using line-transect theory. It may be interpreted as twice the distance at which the number of undetected dolphin schools closer to the vessel is equal to the number of detected schools further from the vessel, and is therefore the effective width of the strip of ocean searched by the vessel. As efficiency of the fleet to detect dolphin schools increases (e.g., through the use of helicopters, high-resolution radar, etc.), the effective search width increases, and bias in abundance estimates should remain unaffected.

We adopt a strategy of reducing bias as much as possible, so that the effect of any trend in bias over time on estimated trends in abundance is minimized. To estimate the different components of the estimator of Equation (3), separate stratification schemes are applied for encounter rate, effective search width, and school size. In stratifying for a given component, our aim is to define strata such that each stratum is relatively homogeneous with respect to that component, so that non-random search effort and non-random distribution of schools generate only small bias in any given stratum. Crude encounter rates, average school sizes, and average detection distances are estimated by 1° square. Where data are insufficient, the crude estimates are smoothed, and the same smoothing procedure interpolates for squares in which there was no tuna vessel effort. These estimates are used to allocate 1° squares to strata, yielding the separate stratifications for encounter rate, school size, and effective search width, respectively. Full details are given by Anganuzzi and Buckland (1989).

Thus the problem of abundance estimation has been reduced to three simpler problems: For a random point in the stock area, the expectations of encounter rate, school size, and effective search width are estimated, and the three estimates are multiplied together to obtain the final abundance estimate. Lack of independence between the three estimates does not bias the overall estimate, and independence is not assumed when estimating variance. A nonparametric bootstrap technique is used to obtain variances. The resampling unit in the bootstrap is the individual cruise, and for each bootstrap replicate the full estimation procedure is applied, thus generating bootstrap estimates of abundance. The sample variance of these estimates yields the required variance estimates, and confidence intervals are obtained by the percentile method. (See Buckland and Anganuzzi 1988a, for details.)

Bias arising from rounding errors in the recorded sighting distances r and angles θ is reduced by smearing the data, using the method favored by Buckland and Anganuzzi (1988b). The recorded location of each school relative to the tuna vessel at the time of detection is defined by r and θ, and that location is "smeared" over the sector defined by $r \cdot (1 \pm d)$ and $\theta \pm \phi/2$, to allow for inaccuracy in the recorded values. The smearing parameters d and ϕ are estimated from the data. When a small sighting angle is rounded to zero, the calculated perpendicular distance is zero, giving a spurious spike in the perpendicular distance distribution at zero distance. Smearing yields more robust estimation by removing or reducing this spike.

Here we take the estimates of Anganuzzi and Buckland (1989) and of Anganuzzi et al. (1991) and attempt to estimate the underlying trends in dolphin abundance by smoothing them. Various smoothing methods such as moving averages, running medians, and polynomial regression were investigated (Smith 1988). The chosen method was a compound running median known as "4253H, twice" (Velleman and Hoaglin 1981), which is constructed as follows.

Suppose that $\{X(t)\}$, $t = 1, \ldots, N$, is a time-series of length N, and let $\{S_i(t)\}$ be a smoothed version of it, found by calculating an i-period running median. We can construct compound smoothing methods such as $\{S_{ij}(t)\}$, which is simply $\{S_j(S_i(t))\}$. Thus, a 4253 running median method smooths a time-series using a 4-period running median, which is in turn smoothed by a 2-period running median, smoothed again by a 5-period running median, and then by a 3-period running median (i.e., $\{S_{4253}(t)\} = \{S_3(S_5(S_2(S_4(t))))\}$). Near the endpoints, where there are not enough values surrounding a point to be smoothed using the specified running median, a shorter-period running median may be used. The endpoints of the resultant time-series are calculated by estimating $X(0)$ and $X(N+1)$, the "observed" values at $t = 0$ and $t = N+1$, and then calculating

$$S_{4253}(1) = \text{median } \{\hat{X}(0), X(1), S_{4253}(2)\} \text{ and}$$

$$S_{4253}(N) = \text{median } \{S_{4253}(N-1), X(N), X(N+1)\}.$$

$\hat{X}(0)$ is found by extrapolating from the straight line which passes through the smoothed values at $t = 2$ and $t = 3$, i.e., $\hat{X}(0) = 3 \cdot S_{4253}(2) - 2 \cdot S_{4253}(3)$; similarly, $\hat{X}(N+1) = 3 \cdot S_{4253}(N-1) - 2 \cdot S_{4253}(N-2)$.

The H in "4253H, twice" denotes a linear smoothing method commonly used with running medians, which is known as Hanning. It is a 3-period weighted moving average for $t = 2, \ldots, N-1$, with weights {0.25, 0.5, 0.25}. The endpoints remain unchanged.

The pattern of the time-series may be recovered by calculating the residuals of the series (i.e., the differences between the smoothed and unsmoothed estimates), smoothing the residual series using the same method as for the time-series, and then adding the smoothed values of the residuals to the smoothed

values of the series. This is known as smoothing "twice." For example, if we define the residuals of the time-series smoothed by 4253H to be $\{E(t)\} = \{X(t) - S_{4253}(t)\}$, then the values of the times-series smoothed by "4253H, twice" can be defined by

$$\{S_{4253H,\,twice}(t)\} = \{S_{4253H}(t) + S_{4253H}(E(t))\}.$$

Thus the "4253H, twice" running median method uses a 4253 running median to smooth the time-series, estimates the endpoints of the smoothed series, and then smooths the resultant series by Hanning. The residuals of the series are calculated and are also smoothed, using the same method as above. The smoothed values of the residuals are then added to the smoothed values of the time-series to produce a time-series smoothed by "4253H, twice." The advantage of using running medians is that the magnitude of an extreme estimate does not affect the resultant smoothed time-series. The above method is sufficiently complex that its behavior cannot be readily understood. However, simpler methods were found to suffer from one or more of the following shortcomings: Estimated trends were not always smooth; implausible rates of change were sometimes indicated; trends near the start or end of the sequence of estimates were often poorly estimated.

Nonparametric bootstrap replicates are generated as described by Anganuzzi and Buckland (1989). We select here the bootstrap estimates that correspond to an 85% confidence interval for relative abundance in each year. The rationale for the choice of confidence level is that if two 85% confidence intervals do not overlap, the difference between the corresponding relative abundance estimates is significant at roughly the 5% level ($P \leqslant 0.05$); whereas if they do, the difference is not significant ($P > 0.05$). If the abundance estimates are assumed to be lognormally distributed, each with the same coefficient of variation, then the exact confidence level that gives this property is 83.4%. If one estimate has twice the coefficient of variation of the other, the confidence level increases slightly to 85.6%. Thus a choice of 85% makes some allowance for variability in the coefficient of variation.

For each abundance estimate, 79 bootstrap replicates are run, so that the 6th smallest and 6th largest bootstrap estimates provide an approximate 85% confidence interval (Buckland 1984). If this procedure is carried out independently for each year, confidence intervals are wide. Provided the assumed stock area spans the whole range of the stock, numbers of dolphins within it are unlikely to vary greatly in successive years, and a procedure that calculates confidence intervals for a given year incorporating information from years immediately preceding and following that year is more informative. For a given stock, we achieve this by carrying out one bootstrap replication for each year that a relative abundance estimate is available. These estimates are smoothed using the routine described above, and the process is repeated 79 times. For each year, the 6th smallest and 6th largest smoothed estimates provide approximate 85% confidence limits. We use the sequence of medians of the smoothed bootstrap estimates (i.e., the 40th estimate of each ordered set of 79) as the "best" indicator of trend, so that it is calculated in a comparable manner to the confidence limits. Larger numbers of bootstrap replicates are preferable, but available computer power was limited. Repeat runs for the northern offshore stock of spotted dolphins were carried out, to assess the Monte Carlo variability.

By using overlapping confidence intervals to test for a difference between years, independence between smoothed estimates for different years is assumed. Given the strong positive correlation in the smoothed estimates between successive years, the test is unlikely to detect a large change between one year and the next, but should be reliable for detecting trends over a period of perhaps five or more years, for which correlations between smoothed estimates are small.

Results

Figures 1–10 show the estimates of underlying trend for each of the main stocks associated with tuna in the eastern tropical Pacific Ocean. Since stock boundaries and stock identity are both uncertain, we also show trend estimates after pooling data from stocks that are not differentiable in the field. The broken horizontal lines in these plots correspond to the upper and lower 85% confidence limits for the 1988 relative abundance estimate. Years for which the entire confidence interval lies outside the region between the broken horizontal lines show a relative abundance significantly different from that for 1988. Because the smoothed estimate for the first or final year of a sequence can be poor, we show the unsmoothed estimate and corresponding 85% confidence limits for the first and last year on each plot.

Figures 1 and 2 show estimated trends for northern offshore spotted dolphins, with and without the abnormally low 1983 estimate, which corresponded with a very strong El Niño event. It is clear that the 1983 estimate affects the smoothed estimate of trend, but its effect is no greater than if it had been just smaller than the 1984 estimate. Thus abnormal estimates may be more safely retained when using this procedure, and subjective decisions of whether to treat an estimate as an outlier are avoided.

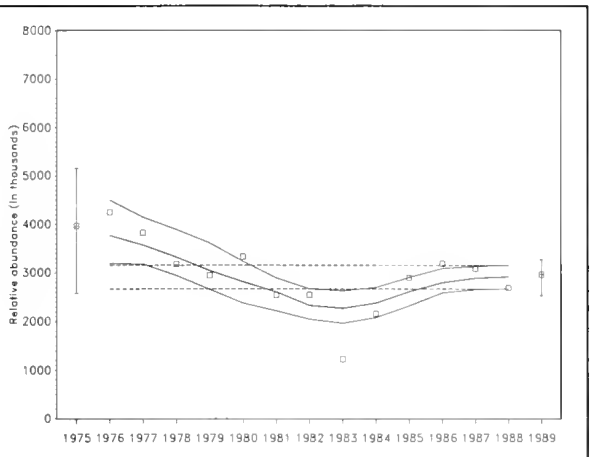

Figure 1

Smoothed abundance trends of northern offshore stock of spotted dolphin *Stenella attenuata* in the eastern tropical Pacific. Broken lines indicate approximate 85% confidence limits. Horizontal lines correspond to 85% confidence limits for the 1988 estimate. If lower limit lies above upper limit for an earlier year, abundance has increased significantly between that year and 1988 ($P<0.05$); if upper limit lies below lower limit for an earlier year, abundance has decreased significantly.

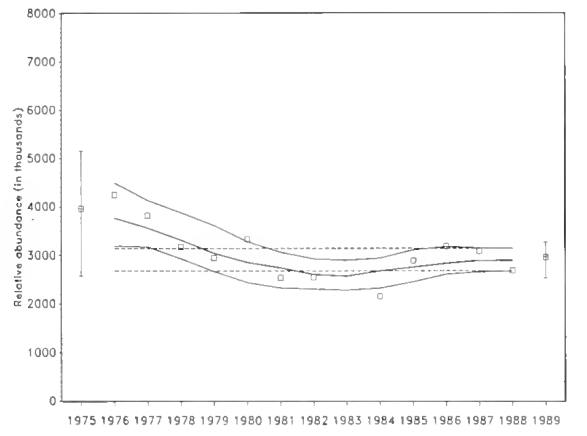

Figure 2

Smoothed abundance trends of northern offshore stock of spotted dolphin *Stenella attenuata* in the eastern tropical Pacific, excluding 1983 estimate. Broken lines indicate approximate 85% confidence limits. See Figure 1 for more details.

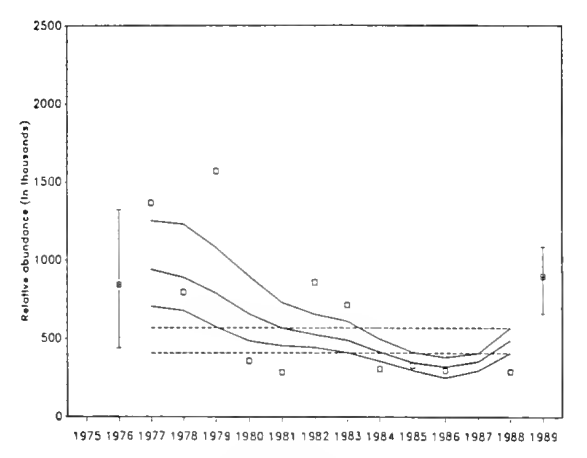

Figure 3

Smoothed abundance trends of southern offshore stock of spotted dolphin *Stenella attenuata* in the eastern tropical Pacific. Broken lines indicate approximate 85% confidence limits. See Figure 1 for more details.

The estimated trend from Figure 1 is downwards until around 1983. Estimated abundance in 1976 and 1977 was significantly higher than in 1988 ($P<0.05$), but there is some evidence of a recovery between 1983 and 1988 ($P<0.05$). Thus northern offshore spotted dolphins appeared to decrease through the 1970s and early 1980s, with numbers remaining stable or increasing since.

Figure 3 suggests there may have been a marked decline in numbers of southern offshore spotted dolphins since the late 1970s. The smoothed 1988 estimate is significantly lower than the smoothed estimates for 1977 and 1978, but there is evidence of an increase since 1986 ($P<0.05$), after a relatively high unsmoothed estimate for 1989. As shown by Anganuzzi et al. (1991), southern offshore spotted dolphins appear to occupy appreciably different regions from one year to another, and the extent of mixing with northern offshore spotted dolphins remains unclear. We therefore believe that trend estimates for this stock are unreliable. The estimated trends obtained by pooling data from the offshore stocks are shown in Figure 4. The estimates are dominated by the data from the larger northern offshore stock, and the plot is similar to Figure 1. The 1988 smoothed relative-abundance estimate is significantly higher than the 1983 and 1984 estimates, and significantly lower than all estimates preceding 1979.

Figure 5 suggests that the eastern spinner dolphin might have had a pattern of change similar to the northern offshore spotted dolphin, although estimated abundance in the late 1980s is roughly equal to that in the mid-1970s, so depletion between 1975 and 1983 may have been less than for northern offshore spotted dolphins. The 1988 smoothed estimate is just significantly higher than the smoothed estimates for 1981 and 1982 ($P<0.05$).

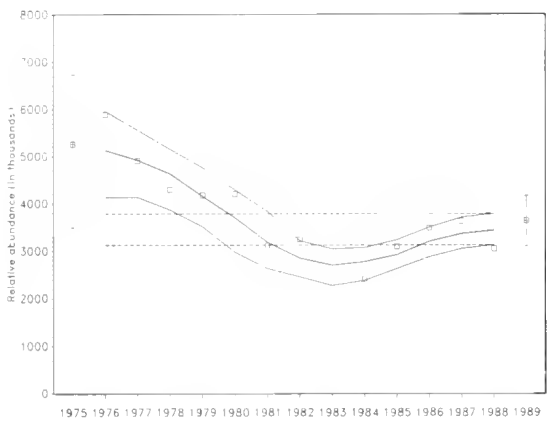

Figure 4
Smoothed abundance trends of pooled northern and southern offshore stocks of spotted dolphin *Stenella attenuata* in the eastern tropical Pacific. Broken lines indicate approximate 85% confidence limits. See Figure 1 for more details.

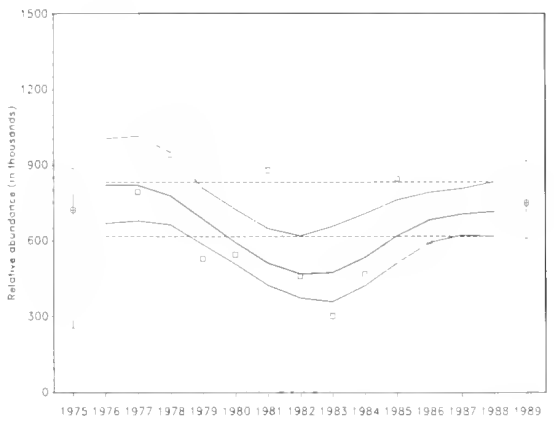

Figure 6
Smoothed abundance trends of whitebelly stock of spinner dolphin *Stenella longirostris* in the eastern tropical Pacific. Broken lines indicate approximate 85% confidence limits. See Figure 1 for more details.

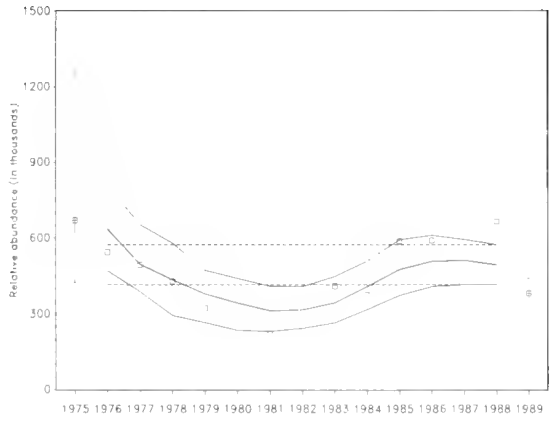

Figure 5
Smoothed abundance trends of eastern stock of spinner dolphin *Stenella longirostris* in the eastern tropical Pacific. Broken lines indicate approximate 85% confidence limits. See Figure 1 for more details.

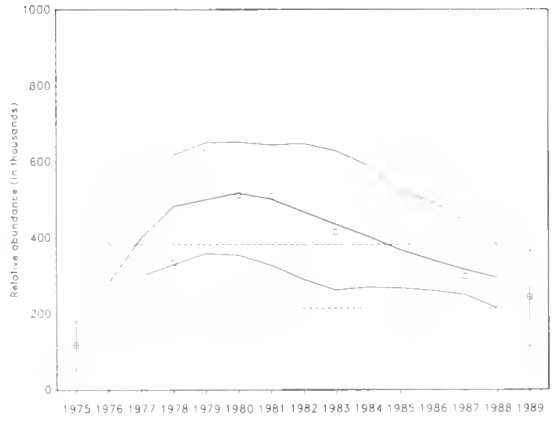

Figure 7
Smoothed abundance trends of northern stock of common dolphin *Delphinus delphis* in the eastern tropical Pacific. Broken lines indicate approximate 85% confidence limits. See Figure 1 for more details.

The estimated trend for whitebelly spinner dolphins (Fig. 6) is similar to that for eastern spinner dolphins and northern offshore spotted dolphins. There is some evidence that abundance in 1988 was higher than in 1982 ($P \cong 0.05$), but no other comparisons with 1988 are significant. The 1982 smoothed estimate is significantly lower than those for 1976–78.

End effects in Figure 7 give rise to an implausible trend in numbers of northern common dolphins during 1975–78. Since 1980, there may have been a decline in this stock, but no smoothed estimates differ significantly. The central stock of common dolphins (Fig. 8) shows evidence of a steep decline from 1977 to 1983, with stability since. The smoothed estimate for 1988 is significantly lower than for all years preceding 1980 ($P < 0.05$), but does not differ significantly from any later estimates. Data on the southern stock of common dolphins are sparse. There may have been a decreasing trend (Fig. 9), but unsmoothed estimates fluctuate widely and no smoothed estimates differ significantly.

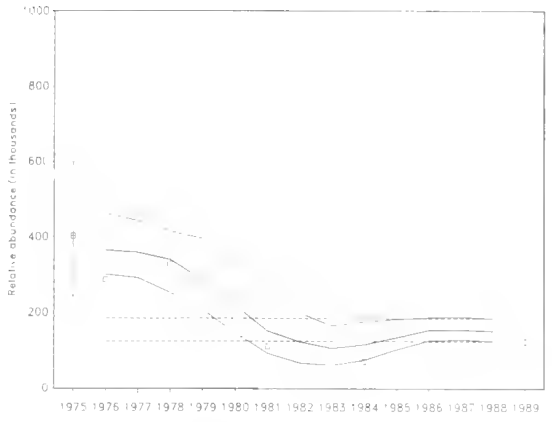

Figure 8
Smoothed abundance trends of central stock of common dolphin *Delphinus delphis* in the eastern tropical Pacific. Broken lines indicate approximate 85% confidence limits. See Figure 1 for more details.

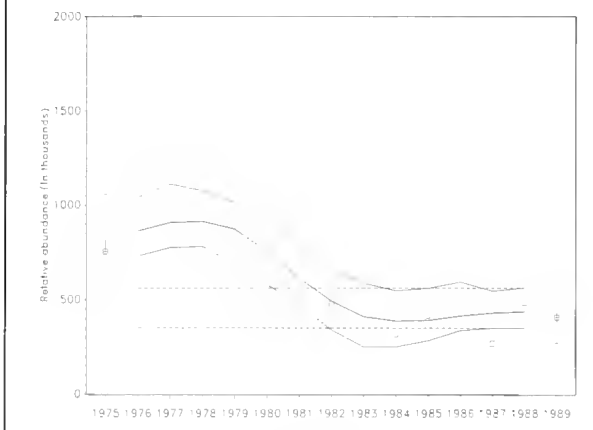

Figure 10
Smoothed abundance trends of pooled northern, central, and southern stocks of common dolphin *Delphinus delphis* in the eastern tropical Pacific. Broken lines indicate approximate 85% confidence limits. See Figure 1 for more details.

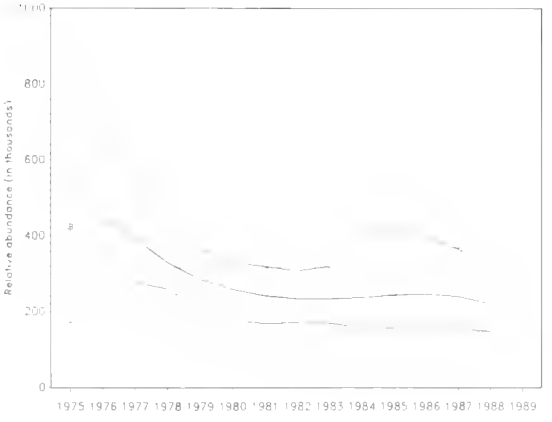

Figure 9
Smoothed abundance trends of southern stock of common dolphin *Delphinus delphis* in the eastern tropical Pacific. Broken lines indicate approximate 85% confidence limits. See Figure 1 for more details.

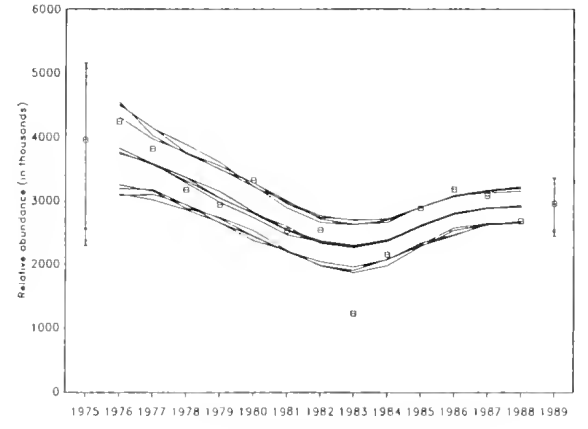

Figure 11
Smoothed abundance trends of northern offshore stock of spotted dolphin *Stenella attenuata* in the eastern tropical Pacific. Broken lines indicate approximate 85% confidence limits. Estimates and limits were determined from four independent sets of 79 bootstrap replicates, so that the plot indicates uncertainty in the estimates arising from Monte Carlo variation.

If data are pooled across stocks of common dolphins (Fig. 10), the 1988 smoothed estimate is significantly lower than all those preceding 1981.

Four independent sets of 79 bootstrap replicates were generated for the northern offshore stock of spotted dolphins. The resulting plots, one of which corresponds exactly to Figure 1, are superimposed in Figure 11. If an infinite number of replicates could be carried out for each set, the four plots would be identical. Thus Figure 11 indicates the uncertainty that can be expected in the median and interval estimates due to Monte Carlo variation.

Discussion

Unsmoothed estimates of relative abundance sometimes show larger year-to-year variation than is

plausible, even if full allowance is made for the precision of the estimates. An example is the 1983 estimate for the northern offshore stock of spotted dolphins, which is significantly lower than either the 1982 or the 1984 estimate. This has been attributed to the strong El Niño event of that year (Buckland and Anganuzzi 1988a). The change in environmental conditions appeared to cause spotted dolphins to split into smaller schools and to disperse more widely than is normal, so that tuna vessels were unable to locate areas of concentration. If, in normal years when concentrations occur in known areas, there is positive bias in the abundance index, then a relatively low estimate might be expected for 1983. This effect would be enhanced if many animals wandered beyond the normal range of the stock, so that the abundance index for 1983 corresponded to only that portion of the stock remaining within its normal bounds. Such effects may be regarded either as bias that fluctuates over time or as an additional source of variability that is unaccounted for in the variances of the abundance indices. Provided the effects are essentially random, and do not exhibit a consistent linear trend over time, the smoothing algorithm described above smooths out the large fluctuations and, in conjunction with the bootstrap, provides variance and interval estimates for the smoothed abundance indices that take full account of variability not allowed for in the variance estimates of the unsmoothed indices.

The validity of estimating trends in dolphin abundance from tuna-vessel sightings data has been questioned by Edwards and Kleiber (1989). They used a simple simulation model of non-random search vessel effort coupled with clustered distributions of dolphin schools to investigate bias. By allowing the clustering of schools to be slight in one year and extreme in the next, they showed that bias in the relative abundance estimates can be inconsistent between years. They define a change estimate as the ratio of relative abundance estimates for the two years. They state, "This two-sample change estimate is only a rough approximation to a trend estimate derived from a series of measurements. . .However, conclusions about the effects of inconsistent biases on this **change** estimate will be valid for **trend** estimates also, except for the unlikely case in which effects of various inconsistent biases cancel each other out, so that the trend estimate reflects the actual trend, but only fortuitously." (The emphasis on "change" and "trend" is theirs.) They also note that "It is obvious. . .that even relatively small changes of bias can lead to considerably inaccurate estimates of change and, by implication, estimates of trend." If this is so, there would be little value in estimating trends in abundance from tuna-vessel sightings data. We question whether the simulation model of Edwards and Kleiber (1989), which is a considerable simplification of reality, allows such strong conclusions. However, we use their results to assess the validity of their arguments. We take their worst-case scenario of a static environment, using the stratified and smoothed option, and average across their four replicates for the high-density case. The calculations indicate a downward bias of about 20% for the "simple, gentle" environmental topography of year 1 and an upward bias of about 100% for the "complex, steep" topography of year 2. Thus, if the population comprised 2500 schools (as in their simulations), the expected estimate would be around 2000 schools in the first year and 5000 in the second, a 2.5-fold estimated increase for a population that has constant size. Is this conclusion "valid for **trend** estimates also"? Suppose a population comprised 4 million animals in 1975, and decreased at a rate of 5% per annum until 1989. Suppose we again take an extreme scenario in which the "simple, gentle" environmental topography applied in El Niño years, and the "complex, steep" topography applied in all other years. The expectations of the estimates are shown in Table 1. Also shown are simulated estimates, for which errors were generated from a lognormal distribution which yields a coefficient of variation of 15%, close to that observed for estimates based on tuna vessel data. The errors were then added to the expected estimates. The estimated rate of decrease for the expected estimates is 5.0% per annum (SE 2.5%), and that for the simulated estimates is 4.7% per annum (SE 2.6%). Thus a scenario of extreme and inconsistent

Table 1

Actual abundance (millions), and expected and simulated relative-abundance estimate by year for a hypothetical stock, declining at an annual rate of 5%. Expected abundance is calculated assuming estimates are biased down by 20% in El Niño years (*) and up by 100% in other years.

Year	Actual abundance	Expected estimate	Simulated estimate
1975	4.00	8.00	8.04
1976*	3.80	3.04	3.37
1977	3.61	7.22	6.86
1978	3.43	6.86	5.86
1979	3.26	6.52	6.87
1980	3.10	6.19	8.66
1981	2.94	5.88	6.26
1982*	2.79	2.23	1.97
1983*	2.65	2.12	3.22
1984	2.52	5.04	4.98
1985	2.39	4.79	5.72
1986	2.28	4.55	4.02
1987*	2.16	1.73	1.65
1988	2.05	4.11	4.01
1989	1.95	3.90	4.75

bias does not invalidate the procedures when applied to a long sequence of estimates. In practice, a rate of change in abundance is unlikely to be roughly constant over such a long time-period, yet tests for trend over a short time-period have low power. Figures 1–10 provide a simple method to test for change over longer time-periods without the necessity of assuming the rate of change is constant.

The smoothing procedure used for generating trend estimates can perform poorly at the start (e.g., Fig. 7) or at the end of a sequence of estimates, so that sharp increases or declines during the first or last year or two should be treated with suspicion. The first and last smoothed estimate in a sequence are especially unreliable, and are omitted from Figures 1–10. Thus, changes in abundance are assessed relative to 1988 rather than 1989.

To assess the current status of dolphin stocks, and the effects of recent levels of mortality, it is necessary to determine whether trends in dolphin abundance are best estimated from tuna vessel data or research vessel data, or whether some combination of estimates from both sources is preferable. Given sufficient data and adequate coverage of the entire range of each stock, research-vessel estimates of trend would be preferred, since they are likely to be less biased. However, Holt and Sexton (1989, 1990ab), to exploit fully the small number of research vessel sightings, made assumptions that might be seriously violated. Firstly, data are pooled across all sightings of dolphin schools of at least 15 animals, irrespective of species, to improve precision of effective search-width estimates. This may introduce bias which is not consistent over time, especially if non-target species (those which are seldom associated with tuna, and are therefore seldom encircled by purse seines) have a different effective search width and a different rate of change in abundance than target species. Secondly, although abundance estimates are given by stock, encounter-rate estimates by stock area are ignored for stocks that are not separated in the field. Thus for offshore spotted dolphins, a single abundance estimate per year is generated and then prorated by stock area, to yield separate estimates for the northern and southern offshore stocks. If the southern offshore stock became extinct, and the northern offshore stock increased at a rate that ensured overall abundance remained constant, the expected trend in research vessel estimates would be zero for both stocks. The same applies to common dolphin stocks. The estimates of Holt and Sexton indicate that there are large numbers of common dolphins in the western sector of the eastern tropical Pacific, yet the species is seldom recorded there. Using the estimation methods of Holt and Sexton, valid trend estimates from research vessel data are not available separately for northern and southern offshore stocks of spotted dolphin or for the main stocks of common dolphin.

In Figures 12–15 we show the valid estimates of trend (i.e., those obtained after pooling data from stocks that are not differentiable in the field) from the research-vessel relative abundance estimates for 1986–89, taken from Sexton et al. (1991) and Gerrodette and Wade (1991). Also shown are the corresponding unsmoothed trend estimates from tuna vessel data. Vertical bars show ±2 standard errors. Plots are based on the relative abundance estimates and standard errors of Tables 2 and 3. The research vessel estimates indicate changes in abundance that are biologically implausible, even with full allowance for the estimated precision of the estimates. Thus either the precision of the surveys is appreciably worse than estimated or there is strong and inconsistent bias in the estimates from one year to the next. By contrast, despite the concerns over the validity of tuna vessel estimates, they yield biologically plausible rates of change during 1986–89 when the precision of the estimates is accounted for.

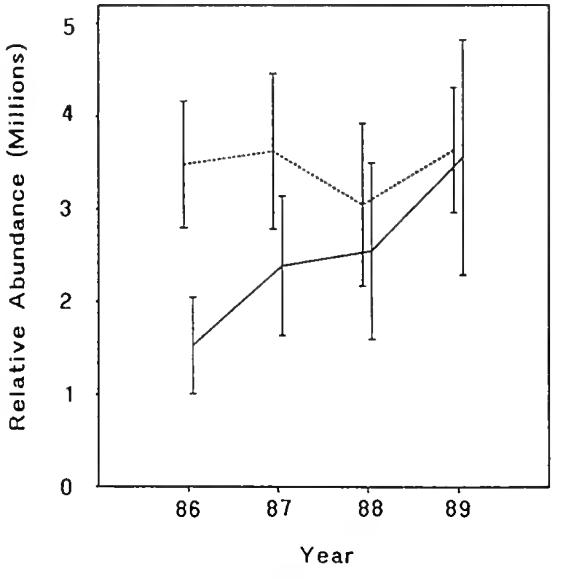

Figure 12

Unsmoothed abundance trends of northern and southern offshore stocks of spotted dolphin *Stenella attenuata* in the eastern tropical Pacific, estimated from research (solid line) and tuna vessel data. Vertical bars are ±2 standard errors.

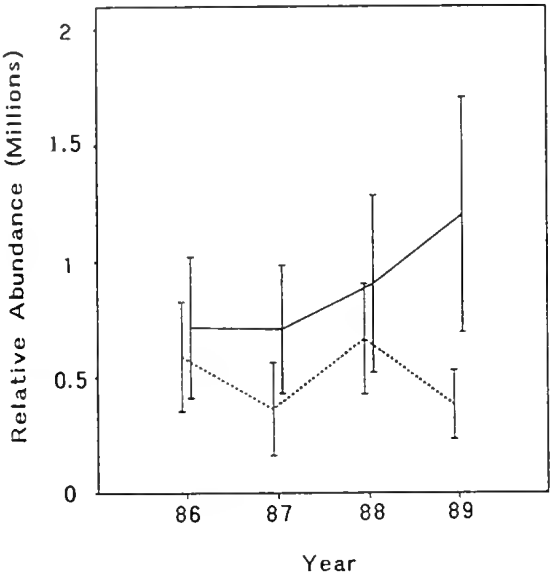

Figure 13

Unsmoothed abundance trends of eastern stock of spinner dolphin *Stenella longirostris* in the eastern tropical Pacific, estimated from research (solid line) and tuna vessel data. Vertical bars are ±2 standard errors.

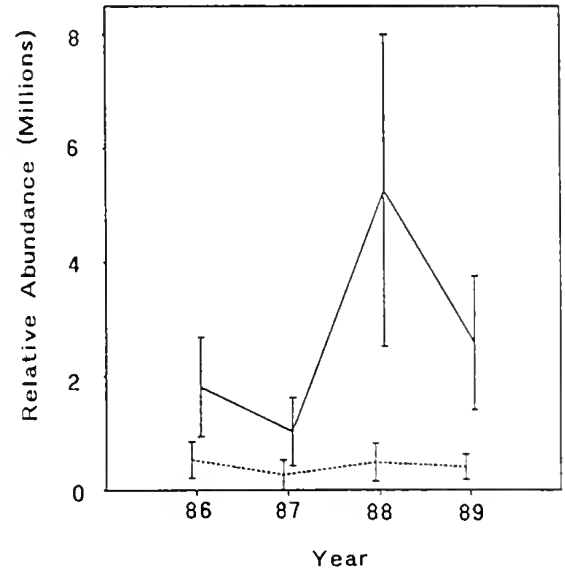

Figure 15

Unsmoothed abundance trends of northern, central, and southern stocks of common dolphin *Delphinus delphis* in the eastern tropical Pacific, estimated from research (solid line) and tuna vessel data. Vertical bars are ±2 standard errors.

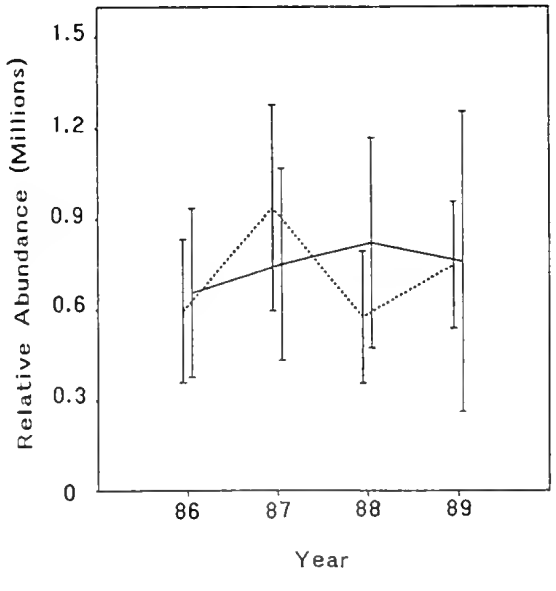

Figure 14

Unsmoothed abundance trends of whitebelly stock of spinner dolphin *Stenella longirostris* in the eastern tropical Pacific, estimated from research (solid line) and tuna vessel data. Vertical bars are ±2 standard errors.

Acknowledgments

We are grateful to Dr. J. Joseph, Dr. M. Hall, and Dr. M. Scott for comments on the methods outlined here, and to two reviewers and Dr. L. Jones for their constructive comments and criticisms. We also acknowledge the recent and continuing efforts of the Southwest Fisheries Science Center to evaluate methods for analyzing tuna vessel and research vessel sightings data; their program of work forced us to address more carefully the issue of how to estimate and test for trends in abundance.

Citations

Anganuzzi, A.A., and S.T. Buckland

1989 Reducing bias in estimated trends from dolphin abundance indices derived from tuna vessel data. Rep. Int. Whaling Comm. 39:323–334.

Anganuzzi, A.A., S.T. Buckland, and K.L. Cattanach

1991 Relative abundance of dolphins associated with tuna in the eastern tropical Pacific, estimated from tuna vessel sightings data for 1988 and 1989. Rep. Int. Whaling Comm. 41: 497–506.

Au, D., W.L. Perryman, and W. Perrin

1979 Dolphin distribution and the relationship to environmental features in the eastern tropical Pacific. Admin. Rep. LJ-79-43, Southwest Fish. Sci. Cent., NMFS, NOAA, La Jolla, CA 92038, 59 p.

Table 2

Unsmoothed relative-abundance estimates (standard errors in parentheses) of some stocks of dolphin in the eastern tropical Pacific, calculated from research vessel data collected 1986–89.

Year	Offshore spotted dolphin		Eastern spinner dolphin		Whitebelly spinner dolphin		Common dolphin	
1986	1527	(261)**	716	(152)	657	(140)	1810	(437)*
1987	2388	(377)	707	(138)	750	(159)	1026	(298)‡††
1988	2549	(476)	902	(191)	821	(174)	5263	(1368)*††
1989	3560	(634)**	1200	(254)	759	(248)	2586	(587)‡

*Estimates differ significantly ($P<0.05$)
‡Estimates differ significantly ($P<0.05$)
**Estimates differ significantly ($P<0.01$)
††Estimates differ significantly ($P<0.01$)

Table 3

Unsmoothed relative-abundance estimates (standard errors in parentheses) of some stocks of dolphin in the eastern tropical Pacific, calculated from tuna vessel data collected 1986–89.

Year	Offshore spotted dolphin		Eastern spinner dolphin		Whitebelly spinner dolphin		Common dolphin	
1986	3484	(342)	590	(118)	595	(119)	532	(159)
1987	3627	(420)	363	(100)	937	(170)	271	(132)
1988	3048	(439)	665*	(119)	575	(109)	487	(167)
1989	3640	(337)	381*	(74)	748	(105)	408	(111)

*Estimates differ significantly ($P<0.05$)

Buckland, S.T.
1984 Monte Carlo confidence intervals. Biometrics 40: 811–817.

Buckland, S.T., and A.A. Anganuzzi
1988a Trends in abundance of dolphins associated with tuna in the eastern tropical Pacific. Rep. Int. Whaling Comm. 38: 411–437.
1988b Comparison of smearing methods in the analysis of minke sightings data from IWC/IDCR Antarctic cruises. Rep. Int. Whaling Comm. 38:257–263.

Burnham, K.P., D.R. Anderson, and J.L. Laake
1980 Estimation of density from line transect sampling of biological populations. Wildl. Monogr. 72, 202 p.

Cooke, J.G.
1985 On the relationship between catch per unit effort and whale abundance. Rep. Int. Whaling Comm. 35:511–519.

Edwards, E.F., and P.M. Kleiber
1989 Effects of nonrandomness on line transect estimates of dolphin school abundance. Fish. Bull., U.S. 87:859–876.

Gerrodette, T., and P.R. Wade
1991 Monitoring trends in dolphin abundance in the eastern tropical Pacific using research vessels over a long sampling period: Analysis of 1989 data. Rep. Int. Whaling Comm. 41: 511–515.

Hall, M.A., and S.D. Boyer
1988 Incidental mortality of dolphins in the eastern tropical Pacific. Rep. Int. Whaling Comm. 38:439–441.

Hammond, P.S., and J.L. Laake
1983 Trends in estimates of abundance of dolphins (*Stenella* spp. and *Delphinus delphis*) involved in the purse-seine fishery for tunas in the eastern Pacific Ocean, 1977–81. Rep. Int. Whaling Comm. 33:565–588.

Holt, R.S.
1985 Estimates of abundance of dolphin stocks taken incidentally in the eastern tropical Pacific yellowfin tuna fishery. Admin. Rep. LJ-85-20, Southwest Fish. Sci. Cent., NMFS, NOAA, La Jolla, CA 92038, 32 p.
1987 Estimating density of dolphin schools in the eastern tropical Pacific Ocean by line transect methods. Fish. Bull., U.S. 85:419–434.

Holt, R.S., and J.E. Powers
1982 Abundance estimation of dolphin stocks involved in the eastern tropical Pacific yellowfin tuna fishery determined from aerial and ship surveys to 1979. Tech. Memo. 23, Southwest Fish. Sci. Cent., NMFS, NOAA, La Jolla, CA 92038, 95 p.

Holt, R.S., and S.N. Sexton
1989 Monitoring trends in dolphin abundance in the eastern tropical Pacific using research vessels over a long sampling period: Analyses of 1987 data. Rep. Int. Whaling Comm. 39:347–351.
1990a Monitoring trends in dolphin abundance in the eastern tropical Pacific using research vessels over a long sampling period: Analyses of 1986 data, the first year. Fish. Bull., U.S. 88:105–111.

1990b Monitoring trends in dolphin abundance in the eastern tropical Pacific using research vessels over a long sampling period: Analyses of 1988 data. Rep. Int. Whaling Comm. 40:471–476.

Perrin, W.F., P.A. Akin, and J.V. Kashiwada

1991 Geographic variation in external morphology of the spinner dolphin *Stenella longirostris* in the eastern Pacific and implications for conservation. Fish. Bull., U.S. 89:411–428.

Polacheck, T.

1987 Relative abundance, distribution and inter-specific relationship of cetacean schools in the eastern tropical Pacific. Mar. Mammal Sci. 3:54–77.

Sexton, S.N., R.S. Holt, and D. DeMaster

1991 Investigating parameters affecting relative estimates in dolphin abundance in the eastern tropical Pacific from research vessel surveys in 1986, 1987, and 1988. Rep. Int. Whaling Comm. 41:517–524.

Smith, K.L.

1988 Calibration and smoothing of relative dolphin abundance estimates. MSc. diss., University of Strathclyde.

Smith, T.D.

1983 Changes in sizes of three dolphin (*Stenella* spp.) populations in the eastern tropical Pacific. Fish. Bull., U.S. 81:1–14.

Velleman, P.F., and D.C. Hoaglin

1981 Applications, basics and computing of exploratory data analysis. Duxbury Press, Boston.

Abstract.– Osteological differences confirm the validity of two species of *Grammatorcynus*, *G. bicarinatus* (Quoy and Gaimard 1825) and the long-recognized *G. bilineatus* (Rüppell 1836). In addition to having fewer gill rakers (12–15 vs. 18–24), a smaller eye (3.1–4.6% vs. 4.0–6.0% FL), small black spots on the lower sides of the body, and reaching a larger size (110 cm FL vs. 60 cm), *G. bicarinatus* differs from *G. bilineatus* in having a shorter neurocranium, shorter parasphenoid flanges, lower posterior edge of maxillary shank, shorter quadrate process, narrower first postcleithrum, wider ethmoid, wider vomer, wider lachrymal, longer teeth, wider palatine tooth patch, wider opercle, and a thin posttemporal shelf between the anterior processes. All but one of the 16 osteological differences previously found between *Grammatorcynus bilineatus* and *Scomberomorus* and *Acanthocybium* are confirmed with the inclusion of *G. bicarinatus* in the genus. *Grammatorcynus bilineatus* is widespread in tropical and subtropical waters of the Indo-West Pacific from the Red Sea to Tokelau Islands in Oceania. The range of *G. bicarinatus* is restricted to the western and eastern coasts of Australia and southern Papua New Guinea.

Manuscript accepted 18 December 1991.
Fishery Bulletin, U.S. 90:13–53 (1992).

Morphology, systematics, and biology of the double-lined mackerels (*Grammatorcynus*, Scombridae)

Bruce B. Collette

Systematics Laboratory, National Marine Fisheries Service, NOAA
National Museum of Natural History, Washington, DC 20560

Gary B. Gillis

Observer Program, Alaska Fisheries Science Center, National Marine Fisheries Service
NOAA, 7600 Sand Point Way NE, Seattle, Washington 98115-0070
Current address: Department of Ecology and Evolutionary Biology
University of California, Irvine, California 92715

Until recently, most authors considered the genus *Grammatorcynus* to be monotypic (Fraser-Brunner 1950, Silas 1963, Zharov 1967, Collette 1979). Electrophoretic work (Lewis 1981, Shaklee 1983) indicated there were two species of double-lined mackerels in Australia. This was confirmed by Collette (1983) who showed there are two species: the double-lined mackerel or scad *G. bilineatus*, (Rüppell 1836), widespread in the Indo-West Pacific, with more gill rakers (18–24), a larger eye (4.0–6.0% FL), and a smaller maximum size (60 cm FL); and the shark mackerel *G. bicarinatus* (Quoy and Gaimard 1825), restricted to the waters of northern Australia and southern New Guinea, with fewer gill rakers (12–15), a smaller eye (3.1–4.6% FL), and a larger maximum size (110 cm FL). All morphological information concerning *Grammatorcynus* in Collette (1979) and Collette and Russo (1985b) was based solely on *G. bilineatus*.

The purposes of this paper are to describe osteological differences between the two species of *Grammatorcynus*, redefine the genus and both species, and summarize the literature on both species. The paper is divided into two parts. Part 1, Comparative Morphology, contains descriptions and illustrations of morphometry, meristic characters, soft anatomy, and osteology of the two species of *Grammatorcynus*; comparisons are made with *Scomberomorus* and *Acanthocybium* where appropriate. Part 2, Systematics and Biology, contains a generic description and accounts of both species, including synonymy, types of nominal species, diagnoses (based on characters from the first section), size, biology, interest to fisheries, geographic distribution, and material examined.

Methods and materials

Methods are those used by Collette and Russo (1985b) in a revision of *Scomberomorus*, and by Collette and Chao (1975) in a revision of the bonitos (Sardini).

Material of *Grammatorcynus* is listed at the end of each species account; 80 specimens of *G. bilineatus* and 11 *G. bicarinatus*. Abbreviations of institutions housing the material follow Leviton et al. (1985). Comparative material of *Scomberomorus* and *Acanthocybium* was listed in the species accounts in Collette and Russo (1985b).

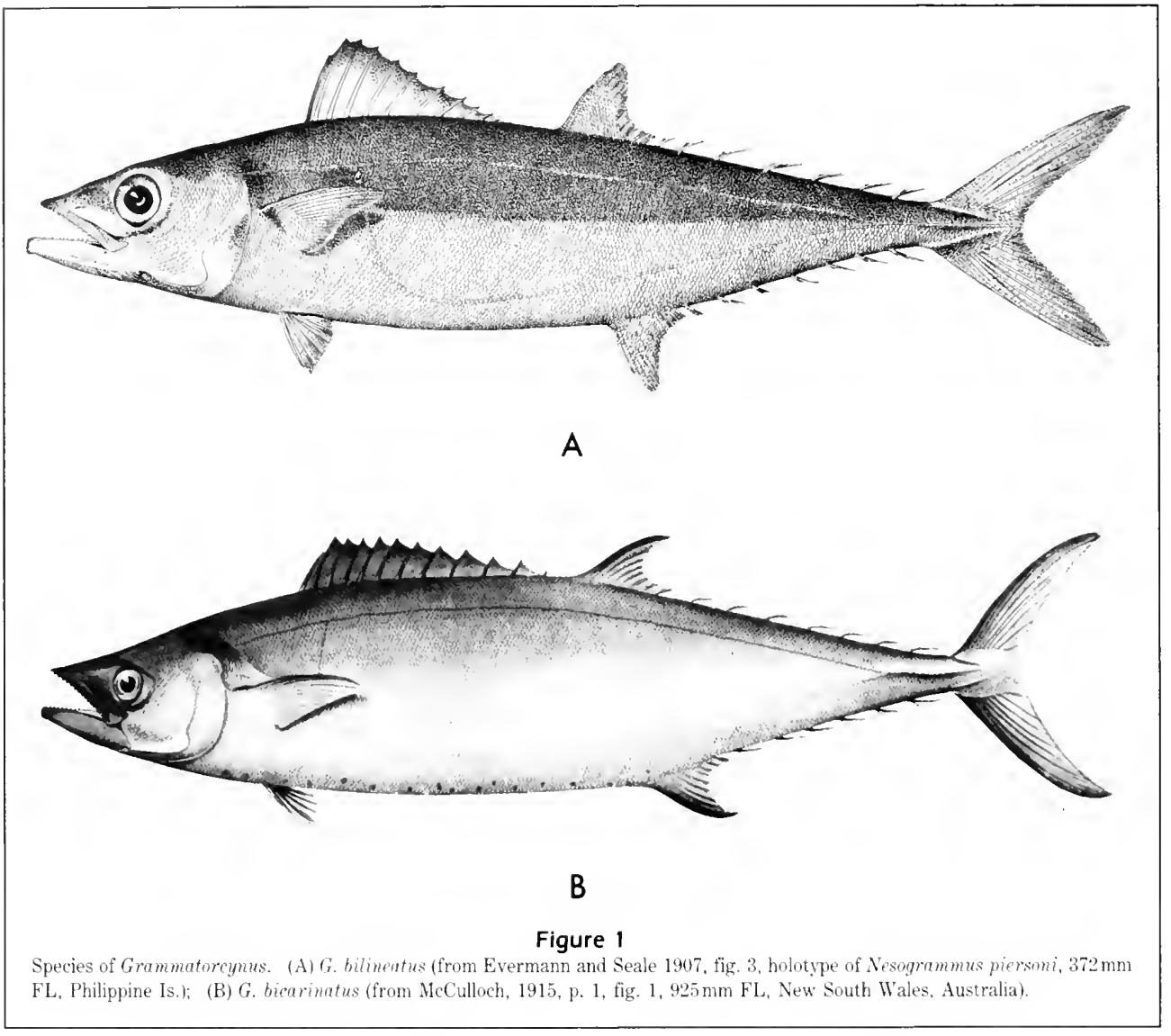

Figure 1

Species of *Grammatorcynus*. (A) *G. bilineatus* (from Evermann and Seale 1907, fig. 3, holotype of *Nesogrammus piersoni*, 372mm FL, Philippine Is.); (B) *G. bicarinatus* (from McCulloch, 1915, p. 1, fig. 1, 925mm FL, New South Wales, Australia).

Part 1: Comparative morphology

Morphological characters useful for distinguishing between species of *Grammatorcynus* and for evaluating phylogenetic relationships of the genus are divided into six categories: lateral line, color pattern, morphometry, meristic characters, soft anatomy, and osteology.

Lateral line

The genus *Grammatorcynus* differs from all other genera of Scombridae in having two lateral lines, hence their common name, double-lined mackerels. The dorsal-most lateral line is slightly convex, originates near the dorsal portion of the opercle, and continues posteriorly until it converges with the second lateral line, just anterior to the median caudal keel. The second lateral line originates from the first at a point below the first four spines of the dorsal fin. It starts ventrally, running under, or just posterior to, the pectoral fin, and abruptly turns into a concave line that continues posteriorly until meeting the dorsal lateral line (Fig. 1). The function of this additional lateral line is unknown. The characteristic two lateral lines are discernible in specimens as small as 56.9mm SL (Nishikawa 1979:133). Anomalies in the pattern of the lateral lines are occasionally found, but none appear to be species specific (Fig. 2; Silas 1963:fig. 3).

Color pattern

Dark spots are usually found on the ventral portion of *G. bicarinatus* (Fig. 1B). The spots are smaller than the pupil, originate near the ventral border of the oper-

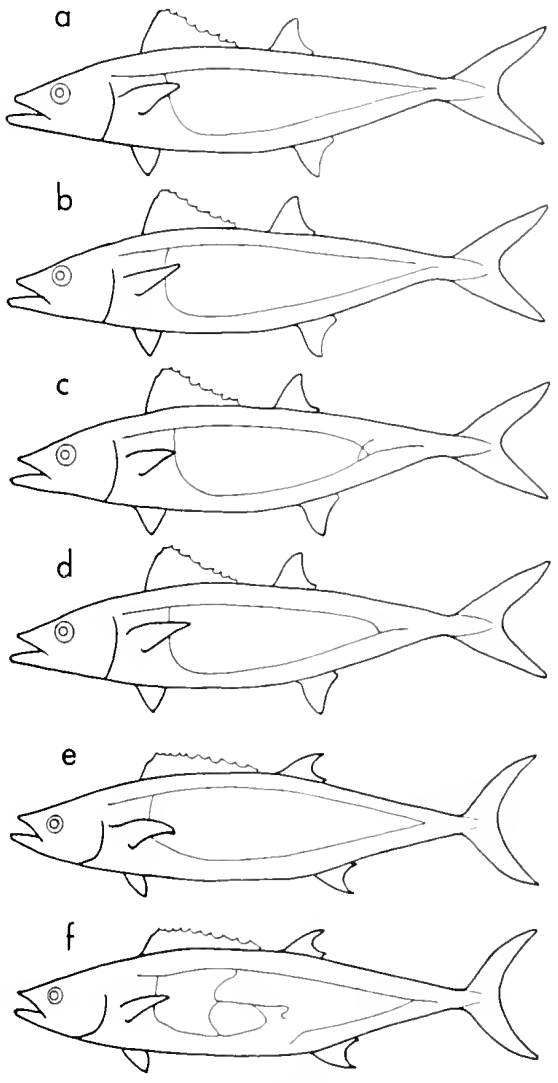

Figure 2
Variations in lateral line pattern in *Grammatorcynus*. (a) Usual pattern in *G. bilineatus*; (b–d) variations in pattern in *G. bilineatus*; (b) Australia, 410 mm FL; (c) Queensland, 416 mm FL; (d) Queensland, 400 mm FL; (e) usual pattern in *G. bicarinatus*; (f) variation in pattern in *G. bicarinatus*, Western Australia, 765 mm FL.

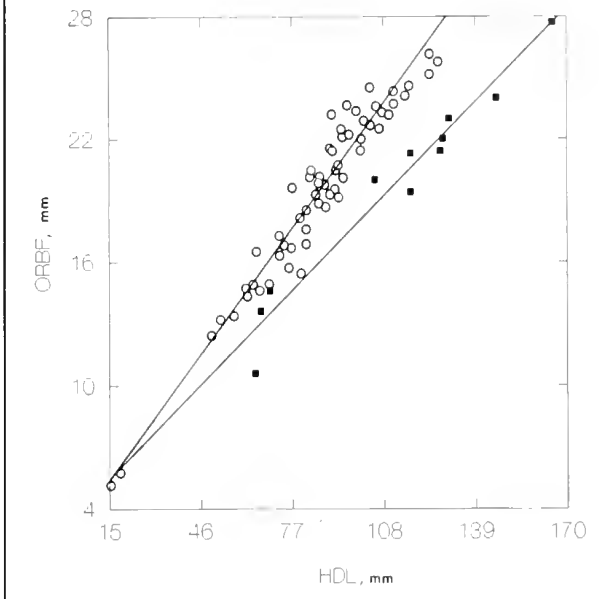

Figure 3
Orbit length (ORBF) compared with head length (HDL) in *Grammatorcynus*. Open circles = *G. bilineatus*, squares = *G. bicarinatus*.

culum, and continue posteriorly to the anal fin. They are found below the ventral lateral line on both sides of the fish. No spots were present in the two smallest specimens examined (AMS IB.5207-8, 306–315 mm FL). Spots are never present in *G. bilineatus* (Fig. 1A).

Morphometric characters

In addition to fork length, 26 measurements were routinely made on all specimens. Several morphometric characters separate the two species. A summary table shows the range and mean of all the characters as thousandths of fork length, and eight of the characters as thousandths of head length (Table 1). Scatter diagrams, with regression lines, show two of the best morphometric characters: *G. bicarinatus* has a smaller orbit (Fig. 3), and a longer first dorsal fin base (Fig. 4).

Meristic characters

Numbers of fin rays (first dorsal spines, second dorsal rays, dorsal finlets, anal rays, anal finlets, and pectoral rays), gill rakers, and teeth on the upper and lower jaws are systematically valuable in *Grammatorcynus*. They are discussed in the relevant osteological sections of the paper.

Soft anatomy

Viscera Emphasis was placed on the appearance of the viscera in ventral view, after removal of an oval segment of the belly wall. Previous descriptions of the viscera of *Grammatorcynus* include Kishinouye (1923), Silas (1963), and Collette and Russo (1985b).

The anterior end of the liver abuts the transverse septum anteriorly in the body cavity. The liver has three lobes. The right and left lobe are longer than the middle lobe, with the right lobe being longest (Fig. 5c–d). The liver is similar in shape in *Scomberomorus*,

Table 1

Morphometric comparison of *Grammatorcynus bilineatus* and *G. bicarinatus*.

	G. bicarinatus					*G. bilineatus*				
Character	*N*	Min	Max	Mean	SD	*N*	Min	Max	Mean	SD
Fork length (thousandths)	10	306	825	551	186	64	226	575	408	77
Snout-A	7	596	626	613	10	61	581	641	606	13
Snout-2D	7	536	558	549	8	61	528	619	547	14
Snout-1D	9	267	301	280	11	64	276	322	295	9
Snout-P2	9	234	272	253	13	63	236	306	258	12
Snout-P1	9	197	230	216	10	63	199	245	226	9
P1-P2	10	91	255	115	49	62	90	135	101	7
Head length	10	191	223	207	9	64	197	236	218	7
Max. body depth	8	177	210	192	13	57	164	234	196	14
Max. body width	8	105	129	115	8	56	91	136	114	9
P1 length	10	118	137	127	5	63	106	142	126	8
P2 length	10	65	81	74	5	63	70	87	77	3
P2 insertion-vent	7	313	345	332	12	62	262	354	328	14
P2 tip-vent	9	238	281	260	15	61	228	275	251	10
Base 1D	9	253	272	264	6	63	207	261	235	11
Height 2D	6	97	111	103	5	54	82	116	98	7
Base 2D	10	76	102	90	8	62	68	118	102	9
Height A	10	94	116	104	8	49	67	114	94	9
Base A	9	66	91	80	8	63	73	105	87	7
Snout (fleshy)	10	77	88	81	4	64	58	90	80	5
Snout (bony)	10	64	76	70	4	64	60	80	72	5
Maxilla length	10	91	110	102	6	63	89	108	98	5
Postorbital	10	87	98	92	3	62	78	98	91	3
Orbit (fleshy)	10	31	46	37	5	64	40	60	49	4
Orbit (bony)	10	48	69	59	8	64	53	88	68	6
Interorbital	9	59	71	64	4	62	56	74	62	3
2D-caudal	9	412	475	454	27	60	427	496	470	13
Head length (thousandths)	11	64	165	112	33	64	50	126	89	17
Snout (fleshy)	11	379	410	393	8	64	248	397	366	21
Snout (bony)	11	313	356	340	16	64	281	357	329	16
Maxilla length	11	475	510	495	12	63	420	480	448	15
Postorbital	11	412	471	446	17	62	350	450	419	15
Orbit (fleshy)	11	164	211	179	16	64	191	257	226	14
Orbit (bony)	11	238	319	282	25	64	252	381	313	24
Interorbit	10	274	322	308	13	62	253	327	283	13

but in *Acanthocybium* the right and left lobes are about the same size. Two efferent vessels lead directly from the anterior surface of the liver into the sinus venosus.

The stomach is sometimes visible in ventral view, partially covered by the liver and caecal mass, but often completely hidden. Stomach contents included crustaceans and small fishes.

The pyloric portion of the intestine arises from the anterior end of the stomach, where the main branches of the pyloric caeca join the intestine. The caeca branch and form a dense dendritic conglomeration, the caecal mass. The intestine continues posteriorly as a simple straight tube to the anus. A straight intestine is also found in *Acanthocybium* (Fig. 5b) and *S. niphonius*, but all other species of *Scomberomorus* have folds (2 or 4) in the intestine (Fig. 5a).

Osteology

The osteological description is divided into five sections: skull, axial skeleton, dorsal and anal fins, pectoral girdle, and pelvic girdle. Osteological terminology and organization generally follow that of Collette and Russo (1985b).

Skull Description of the skull is presented in two sections: neurocranium (Figs. 6–9) and branchiocranium.

Neurocranium Following a general description of the neurocranium, the four major regions are discussed: ethmoid, orbital, otic, and basicranial.

General characteristics In dorsal view (Fig. 6), the neurocranium of *Grammatorcynus* is more or less triangular in shape, narrow at its anterior margin,

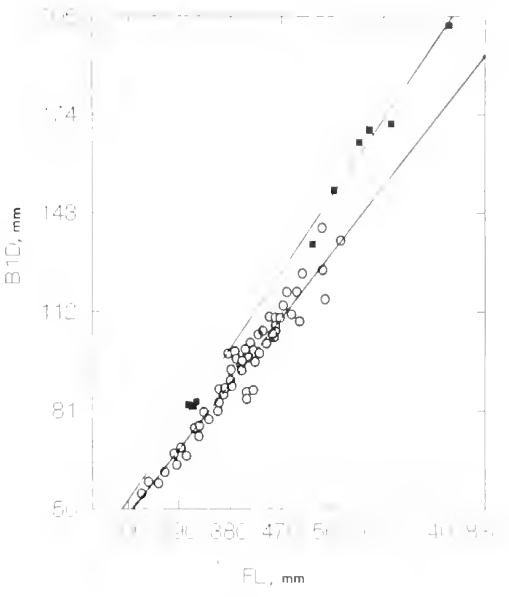

Figure 4
Length of first dorsal fin base (B1D) compared with fork length (FL) in *Grammatorcynus*. Open circles = *G. bilineatus*, squares = *G. bicarinatus*.

widening posteriorly. It is intermediate in shape between the elongate neurocranium of *Acanthocybium*, *Scomber*, and *Rastrelliger*, and the shorter, wider neurocranium of *Thunnus*. The posterodorsal surface is marked by a median ridge (supraoccipital crest), with two parallel ridges on either side. These five thin ridges of bone form six grooves, three on each side: dilator (very shallow), temporal (quite deep), and supratemporal (most easily seen in lateral view) (Allis 1903:49).

The median ridge originates just posterior to the thin, oval pineal foramen located between the posterior, median edges of the frontal bones. This ridge becomes larger posteriorly, and forms the supraoccipital crest. Internal or temporal ridges originate at the posterior portion of the frontals (midlevel of the orbit), continuing posteriorly to the epiotic. External or pterotic ridges also originate near the posterior margin of the frontals, continuing posteriorly to the pterotic.

Neurocrania of the two species of *Grammatorcynus* differ in size, relative to fork length. Length of the neurocranium, measured from the anterior tip of the vomer to the posterior margin of the basioccipital, is slightly longer in *G. bilineatus* (14–16% FL) than in *G. bicarinatus* (13% FL).

Ethmoid region This region is composed of the ethmoid, lateral ethmoid, and vomer. The nasal bone lies lateral to the ethmoid and lateral ethmoid, and, therefore, is included here.

Ethmoid The ethmoid (dermethmoid) has a smooth flat dorsal surface that is partially overlapped by the frontals. It connects ventrally to the vomer, posteriorly to the lateral ethmoids, and anterolaterally to the nasals. Its anterior border is nearly straight, with an anteromedian projection, unlike the relatively smooth, concave border in *Scomberomorus* and *Acanthocybium*. The ethmoid is clearly visible in dorsal view (Fig. 6), and is wider, relative to the length of the neurocranium, in *G. bicarinatus* (width 25–28% of length) than in *G. bilineatus* (19–21%).

Lateral ethmoid The lateral ethmoids (parethmoids) are massive, paired bones that extend downward from the middle region of the frontals and form the anterior margin of the orbit and the posterior and mesial walls of the nasal cavity. The ventral surface of the lateral ethmoid bears an articulating surface for the palatine, and the posterolateral process serves as an articulation surface for the lachrymal. The lateral expansion of the bone is greater in *G. bicarinatus* (45–50% of neurocranium length) than in *G. bilineatus* (39–42%) (Fig. 8).

Vomer The anterior process of the vomer bears a circular or oval patch of fine teeth on its ventral surface. Its pointed posterior end is firmly ankylosed dorsally with the parasphenoid. The anterior process is wider in *G. bicarinatus* (16–18% of neurocranium length) than in *G. bilineatus* (13–15%) (Fig. 8).

Nasal The nasal bones are flat, elongate bones that articulate with the lateral edge of the frontals. They project out beyond the ethmoid and, from a dorsal view, reach about as far anteriorly as the vomer. There is no such projection of the nasal bones in *Scomberomorus* or *Acanthocybium*. Length divided by width is 2.8–3.4 in *Grammatorcynus*, which is intermediate between the ranges of *Scomberomorus* (2.0–3.1) and *Acanthocybium* (3.1–4.2). The anterior end of the bone forms a short, slightly angled arm. No differences were found between the nasals of the two species of *Grammatorcynus*.

Orbital region The orbit (Fig. 7) is surrounded by the posterior wall of the lateral ethmoid, the ventral side of the frontal, the pterosphenoid, sphenotic, prootic, suborbital, and lachrymal bones. The left and right orbits are partially separated by the basisphenoid. The sclerotic bones enclose the eyeballs.

The orbit of *G. bilineatus* is larger than that of *G. bicarinatus* (Fig. 7), reflecting the difference in orbit length (Fig. 3). The maximum height of the orbit measured from the parasphenoid to the pterosphenoid is 24–25% of neurocranium length in *G. bilineatus* vs. 16–17% in *G. bicarinatus*. Orbit length in *G. bilineatus* is 51–54% of neurocranium length vs. 47–49% in *G. bicarinatus*.

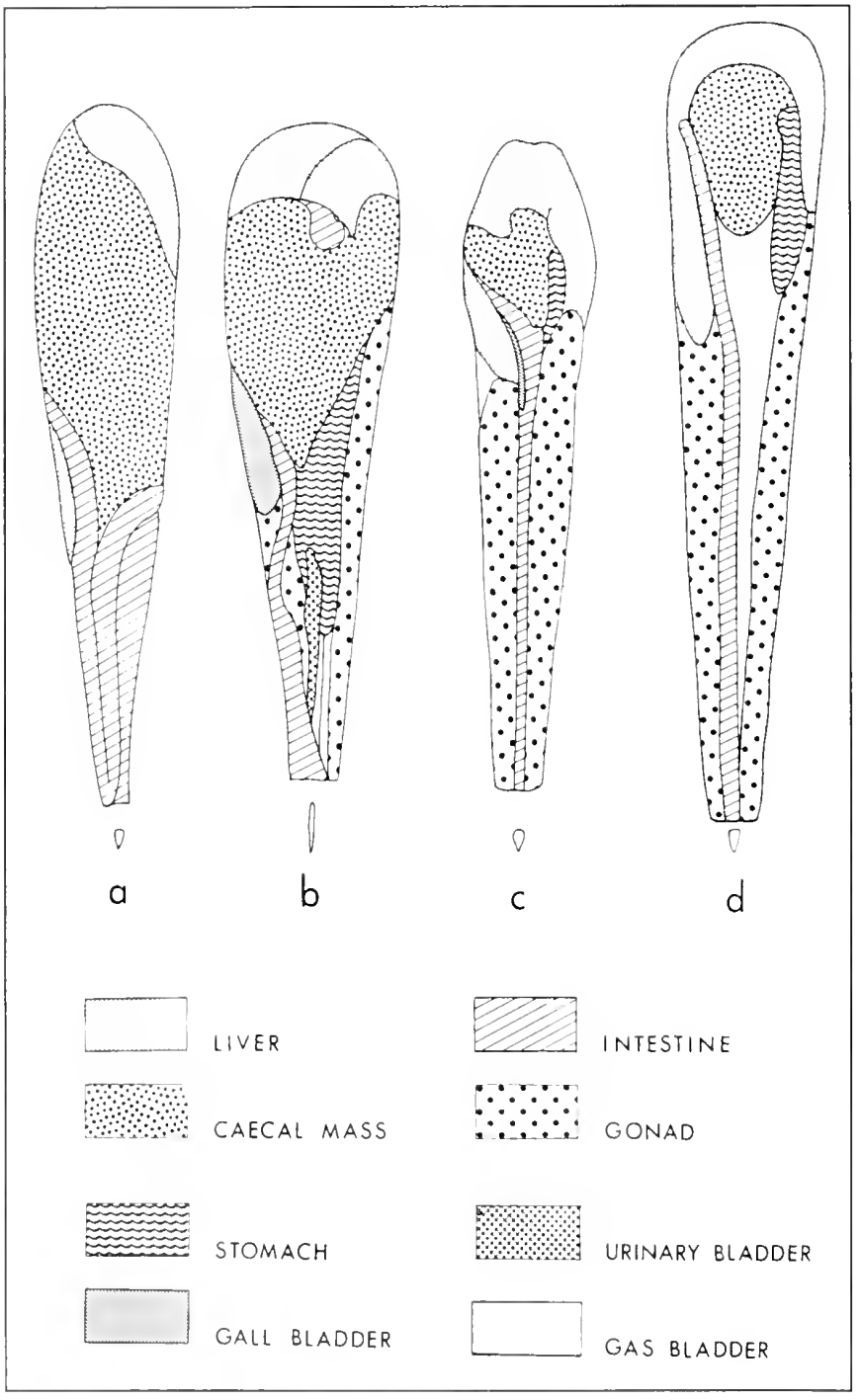

Figure 5
Ventral view of viscera. (a) *Scomberomorus maculatus*, Georgia, 290 mm FL; (b) *Acanthocybium solandri*, Campeche Banks, Mexico, 1280 mm FL; (c) *Grammatorcynus bilineatus*, Marshall Is., 424 mm FL; (d) *G. bicarinatus*, Australia.

Frontal The paired frontals form the largest portion of the dorsal surface of the neurocranium. A small, elongate oval pineal opening is present between the posterior ends of the frontals. A larger and more irregular foramen is present in *Acanthocybium*, but *Scomberomorus* lacks this opening (Collette and Russo 1985b: figs. 11–12).

In *Scomberomorus* and *Acanthocybium*, the frontals form a median ridge that increases in height posteriorly and joins the supraoccipital crest. *Grammatorcynus* lacks this ridge and the supraoccipital crest begins posterior to the pineal opening, giving the top of the skull a much flatter appearance than in the other two genera.

In ventral view (Fig. 8), the left and right frontals articulate with the pterosphenoids at the anterior end of a median opening into the brain cavity. The ridge around the anterior end of this space forms a point and

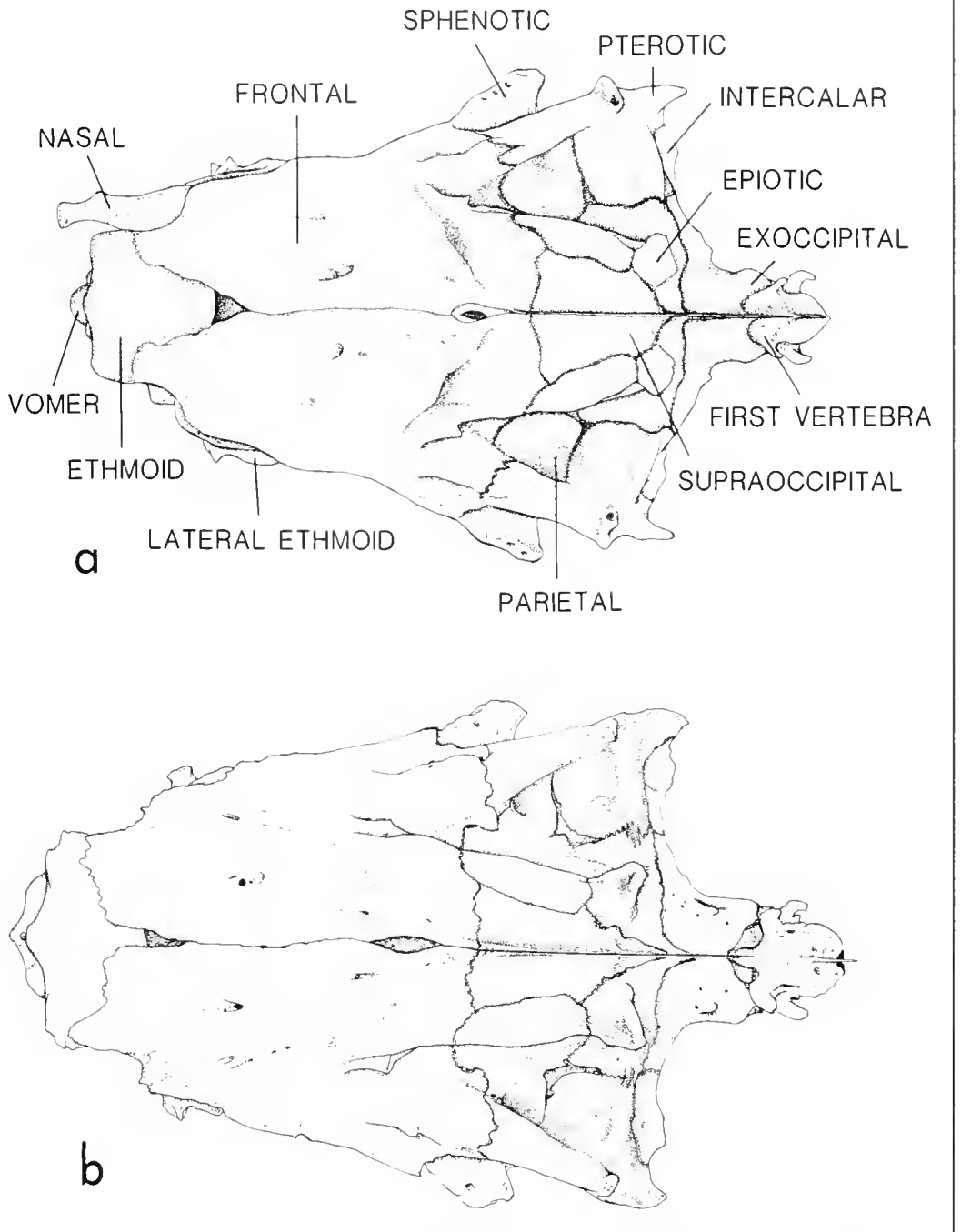

Figure 6

Dorsal view of skulls in *Grammatorcynus*. (a) *G. bilineatus*, Scott Reef, Timor Sea, 453 mm FL; (b) *G. bicarinatus*, Western Australia, Exmouth Gulf, 765 mm FL.

extends almost to the ethmoid in *G. bilineatus*. The ridge curves around the anterior end of the space and ends distinctly more posteriorly in *G. bicarinatus*. This difference cannot be seen in the ventral view of the skulls (Fig. 8) because the median part of the opening is obscured by the parasphenoid, so a separate outline figure has been made (Fig. 9).

Pterosphenoid The pterosphenoids (alisphenoids) form the posterodorsal margin of the orbit. They serve as the base for the median basisphenoid, and abut the prootics posteriorly and the frontals and sphenotics laterally.

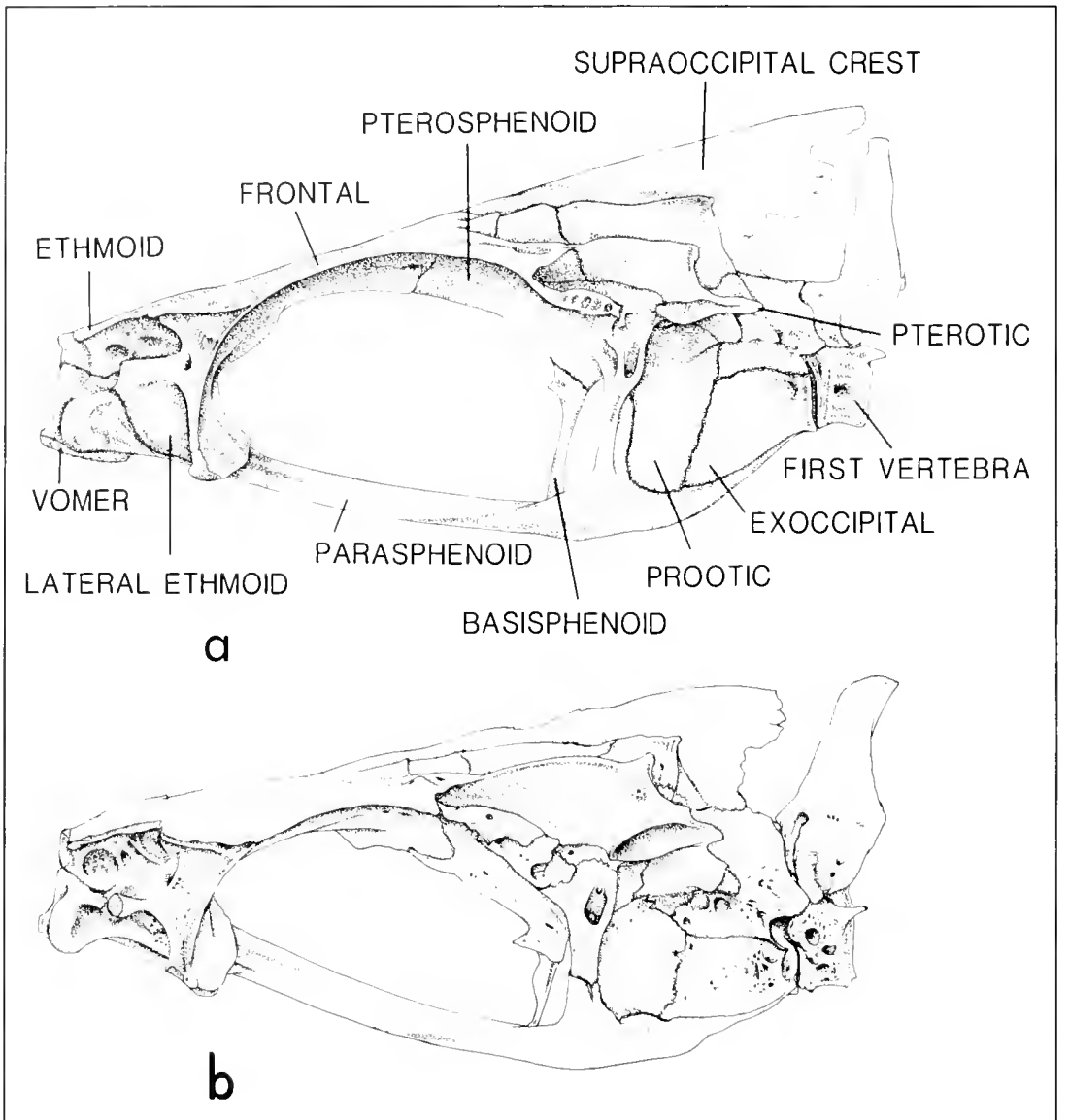

Figure 7

Lateral view of skulls in *Grammatorcynus*. (a) *G. bilineatus*, Scott Reef, Timor Sea, 453 mm FL; (b) *G. bicarinatus*, Western Australia, Exmouth Gulf, 765 mm FL.

Sclerotic The sclerotic bones consist of two thickened, semicircular segments connected by cartilage on the inner surface and by corneal membranes on the outside. The sclerotic bones of *Grammatorcynus* are relatively larger and thinner compared with *Scomberomorus* and *Acanthocybium*.

Basisphenoid The basisphenoid is a small, median, Y-shaped bone that connects the prootics and pterosphenoids dorsally with the parasphenoid ventrally (Fig. 7). The dorsal compressed vertical base bears a slight anterior process, but no posterior process. This is similar to the condition in *Scomberomorus*, but the anterior process is much shorter in *Grammatorcynus*. The basisphenoid is longer in *G. bilineatus* since the height of the orbit is greater in this species compared with *G. bicarinatus*.

Infraorbitals The bones of the infraorbital series (Fig. 10) enclose the infraorbital branch of the lateral sensory canal system. The canal enters the infraorbital series at what is usually considered the last element (dermosphenotic), and continues around the orbit, terminating on the first infraorbital (lachrymal).

The lachrymal, the first and largest element, is elongate with a mesially-directed articular process just anterior to the middle of the bone. It covers part of the maxilla, and articulates with the lateral ethmoid

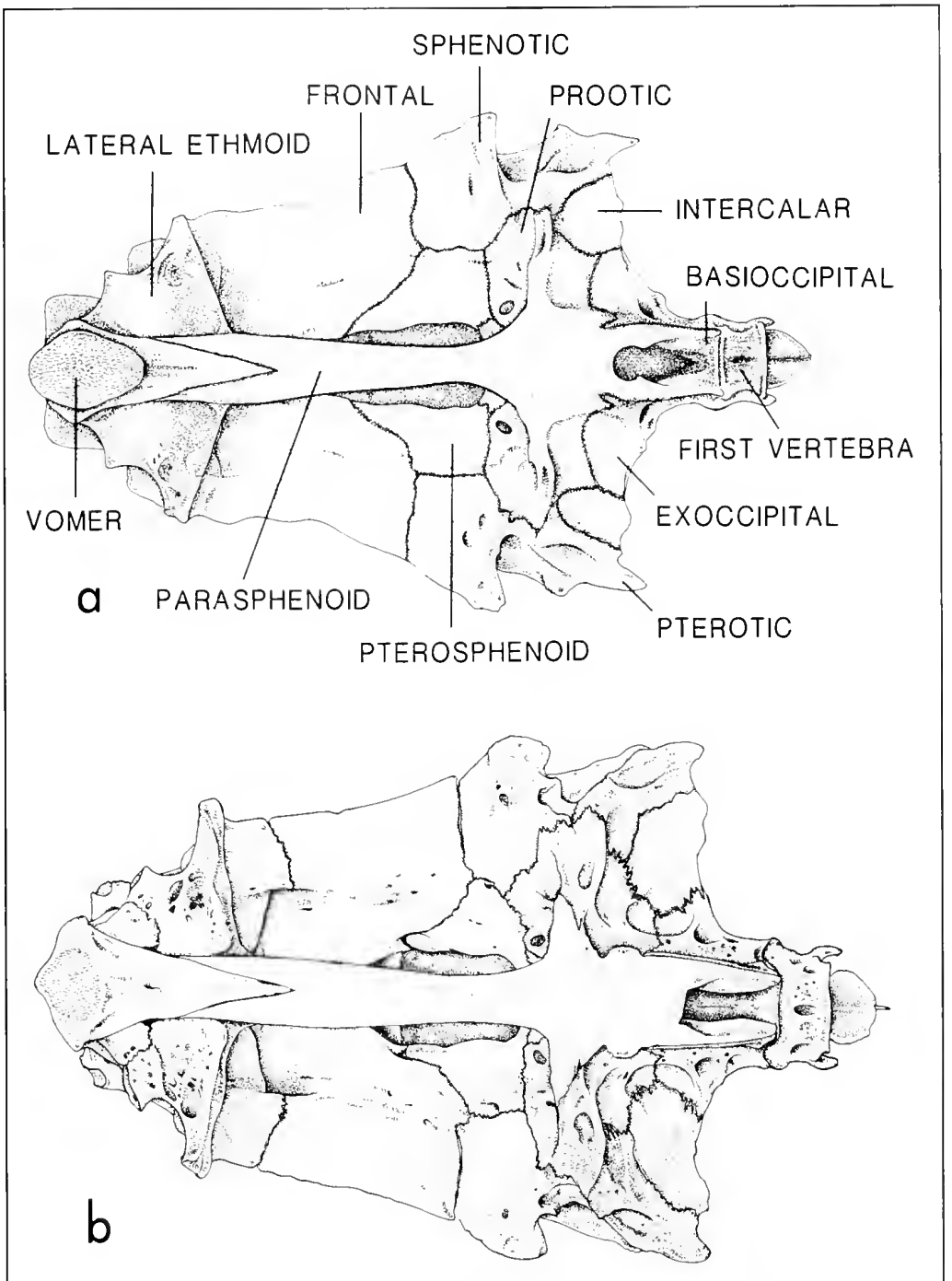

Figure 8

Ventral view of skulls in *Grammatorcynus*. (a) *G. bilineatus*, Scott Reef, Timor Sea, 453mm FL; (b) *G. bicarinatus*, Western Australia, Exmouth Gulf, 765mm FL.

dorsally by the articular process. The process is larger in *G. bicarinatus*, making the lachrymal wider (30–35% of total bone length) than in *G. bilineatus* (27–30%). The anterior portion has a small notch in it, much more indistinct than the forked anterior region in *Scomberomorus* (Fig. 10a). The posterior region is distinctly forked, with the ventral arm being wider and longer than the dorsal arm.

The second infraorbital connects to the forked posterior region of the lachrymal. It is a small, elongate bone. The third infraorbital is an elongate, tubular bone that connects to the posterior portion of the second

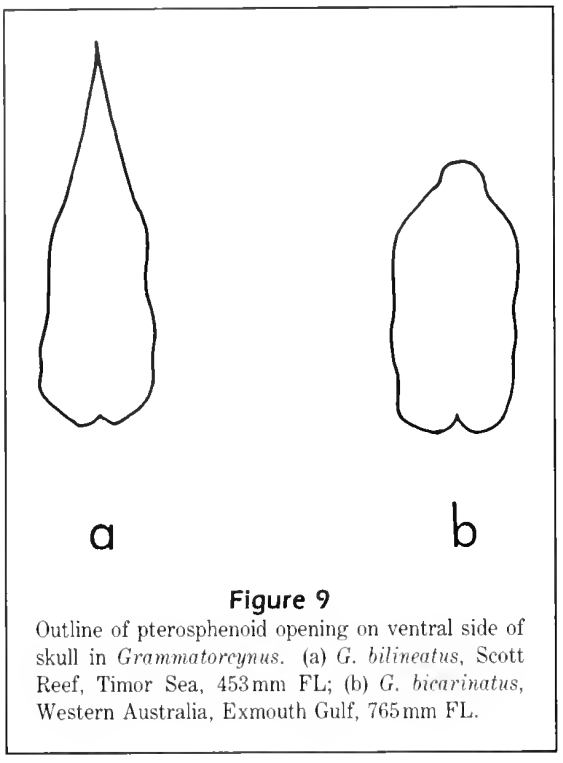

Figure 9
Outline of pterosphenoid opening on ventral side of skull in *Grammatorcynus*. (a) *G. bilineatus*, Scott Reef, Timor Sea, 453mm FL; (b) *G. bicarinatus*, Western Australia, Exmouth Gulf, 765mm FL.

infraorbital. It has a large, mesial, shelflike extension (subocular shelf of Smith and Bailey 1962). The fourth through penultimate elements total 13 in a specimen of *G. bilineatus* (Fig. 10c), are small, and are easily lost with cheek scales during dissection. No special effort was made to compare these bones in the two species.

Otic region This region encloses the otic chamber inside the skull, and is formed by the parietal, epiotic, supraoccipital, prootic, pterotic, sphenotic, and intercalar (opisthotic) bones.

Parietals The parietals articulate with the frontals anteriorly, the supraoccipital mesially, the pterotics laterally, sphenotics ventrally, and epiotics posteriorly. There is a short inner lateral crest on the parietals and epiotics, but this crest does not originate on the frontals as it does in *Scomberomorus* and *Acanthocybium*.

Epiotics The epiotics are irregular bones bounded by the parietals anteriorly, the supraoccipital mesially, the exoccipitals posteriorly, and the pterotics laterally. The medial process of the posttemporal bone attaches to a distinct roughened process on the posterior corner of the epiotic. *Scomberomorus* has a roughened area at the posterior end of the fronto-epiotic crest rather than a distinct process.

Supraoccipital The supraoccipital forms the dorsomedian portion of the posterior end of the neurocranium. It bears a well-developed crest that continues forward onto the parietals but stops at the pineal opening instead of extending all the way forward onto the frontals as in *Scomberomorus*. The supraoccipital consists of a thin crest on a roughly hexagonal base. The crest extends down over the exoccipitals along the median line where the dorsal walls of the exoccipitals suture with each other. It extends posteriorly over the first vertebral centrum (Fig. 7).

Prootics In ventral view (Fig. 8), the prootics connect with all the bones in the posterior part of the neurocranium. Each prootic is bordered ventrally by the parasphenoid; posteriorly by the basioccipital, exoccipital, and intercalar; laterally by the pterotic and sphenotic; and anteriorly by the parasphenoid and basisphenoid. The prootics are irregular in shape and meet each other along the ventromedian line of the brain case to form the posterior portion of the myodome.

Pterotics The pterotics form the lateral posterior corners of the neurocranium. Each pterotic is produced posteriorly to form a spine. A pterotic ridge continues anteriorly onto the parietal, but does not extend onto the posterior part of the frontal as it does in *Scomberomorus*. In ventral view (Fig. 8), the pterotics articulate with the sphenotics anteriorly and the prootics and intercalars medially.

Sphenotics The sphenotics form the most posterior dorsolateral part of the roof of the orbit. They continue the outer lateral shelf from the frontals, and articulate with the pterosphenoid medially and the prootic and pterotic posteriorly. A fossa at the juncture of the sphenotic and pterotic receives the anterior condyle of the hyomandibula. In dorsal or ventral view, the distance between the tips of the two sphenotics is the widest portion of the cranium, 60–67% the length of the neurocranium in *Grammatorcynus*.

Intercalars The intercalars (opisthotics) are flat bones that form part of the posterior border of the neurocranium interposed between the pterotics and exoccipitals. The anterior portion on the dorsal surface is concealed by the overlapping pterotic, thus exposing the bone on the dorsal surface less than on the ventral surface (compare in Figures 6 and 8). Each intercalar has a roughened area on its dorsal surface to receive the lateral arm of the posttemporal. There is no posterior projection from the intercalars in *Grammatorcynus* or *Acanthocybium* as there is in eight species of *Scomberomorus*, such as *S. commerson* and *S. concolor* (Collette and Russo 1985b:figs. 11a and 12b).

Basicranial region This region consists of the parasphenoid, basioccipital, and exoccipital bones, and forms the posteroventral base of the skull.

Parasphenoid The parasphenoid is a long, cross-shaped bone. It articulates with the vomer anteriorly and forms the ventral axis of the skull. It also

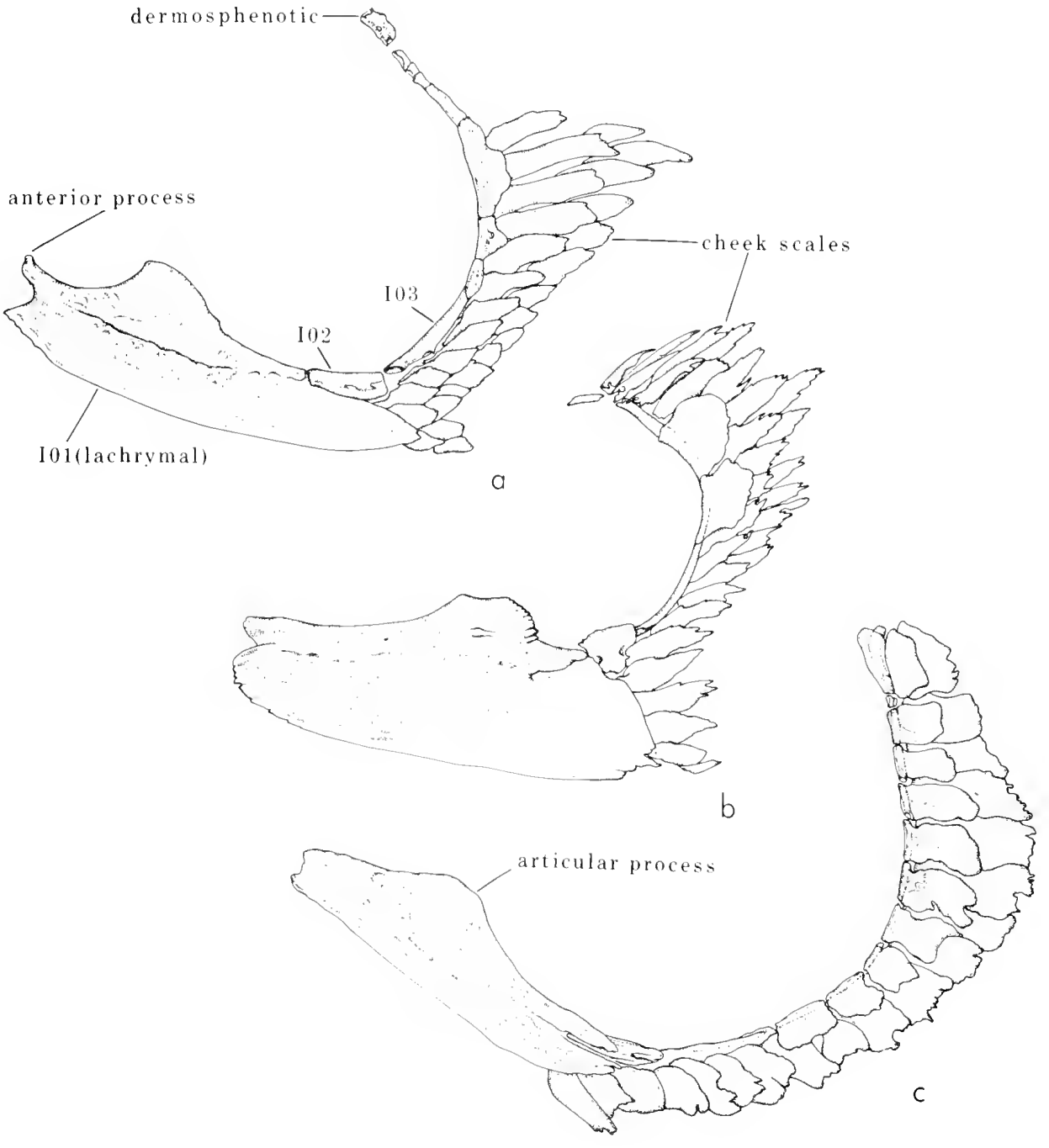

Figure 10

Left infraorbital bones in lateral view. (a) *Scomberomorus maculatus*, Cape Hatteras, NC, 534 mm FL; (b) *Acanthocybium solandri*, Revillagigedos Is., 1068 mm FL; (c) *Grammatocrynus bilineatus*, Timor Sea, 453 mm FL.

forms the ventral border of the orbits and connects with the lateral ethmoids, basisphenoid, prootics, and basioccipital bones dorsally. The lateral wings of the parasphenoid extend dorsolaterally along the ventral ridge of the prootic bones on either side, and have pointed ends which form part of the anteroventral wall of the posterior myodome. Posteriorly, the parasphenoid bifurcates into two lateral flanges that attach dorsally to the corresponding posteroventral flanges of the basioccipital bone, and surround the posterior

opening of the posterior myodome. These flanges are longer in *G. bilineatus* (18–21% of neurocranium length) than in *G. bicarinatus* (14%), making the posterior opening of the posterior myodome larger in *G. bilineatus* (Fig. 8). A ventrally projecting median keel is present in the area anterior to the origin of the lateral flanges. In ventral view, the parasphenoid narrows posteriorly until near the region of the median keel, where it widens slightly before the lateral wings. The anterior portion and the region just anterior to the lateral wings are about equal in width. In *Grammatorcynus*, the shaft of the parasphenoid is narrower than that of *Scomberomorus* and *Acanthocybium*. In *G. bilineatus*, the contour of the parasphenoid is concave, making the orbit larger than in *G. bicarinatus*, in which the parasphenoid is flat (Fig. 7).

Basioccipital The basioccipital has lateral flanges on either side of the skull and forms the roof and lateral walls of the posterior myodome. The lateral flanges expand ventrally to meet the flat posterior flanges of the parasphenoid. Anteriorly, the basioccipital is attached to the prootics and dorsally with the exoccipitals. The first vertebral centrum attaches to the posterior surface of the basioccipital.

Exoccipital The exoccipitals connect the skull with the first vertebra dorsally. The exoccipital articulates with the epiotic and supraoccipital bones anterodorsally, the intercalars laterally, and with the other exoccipital posterodorsally. In ventral view, the exoccipital articulates with the prootic anteriorly, basioccipital ventromedially, and intercalar laterally. In posterior view, the foramen magnum is framed by the exoccipitals.

Branchiocranium The branchiocranium is divided into five sections: mandibular arch, palatine arch, hyoid arch, opercular apparatus, and branchial apparatus.

Mandibular arch The mandibular arch is composed of the upper jaw (premaxilla, maxilla, and supramaxilla) and the lower jaw (dentary, angular, and retroarticular). Teeth are borne on the premaxilla and dentary, and the number of teeth on these bones differs between species.

Dentition Long, thin, slightly laterally compressed teeth are present in a single row in the upper and lower jaws of *Grammatorcynus*. *Scomberomorus* has large, triangular, laterally compressed teeth similar to those of *Acanthocybium*, which are blunter and more tightly compressed. The length of the jaw teeth differs between the species: *G. bicarinatus* has longer teeth than *G. bilineatus* (maximum length 6% vs. 4% dentary length). The number of jaw teeth in *Grammatorcynus* also varies. Teeth are often broken or lost, so the range in mean tooth count may not reflect accurately the actual number of teeth. However, the maximum number of teeth is useful. *Grammatorcynus bicarinatus* has a lower maximum tooth count on its upper jaw than *G. bilineatus* (25 vs. 37), and the same is true of the lower jaw, (23 vs. 32; Table 2). The maximum number of jaw teeth present in *Scomberomorus* is slightly higher than *G. bilineatus* (39, range 5–39 in the upper jaw; and 37, range 4–37 in the lower jaw). Collette and Russo (1985b) noted that in *Scomberomorus*, the species with the fewest teeth has the fewest gill rakers and the species with the most teeth has the most gill rakers. There is a similar correlation in *Grammatorcynus*: *G. bilineatus* also has more gill rakers (18–24 vs. 12–15 in *G. bicarinatus*).

Premaxilla The premaxilla (Fig. 11) is a long, curved bone with an arrowhead-shaped anterior end that extends dorsally and posteriorly as an ascending process. The posterior shank of the premaxilla is elongate and bears a row of 14–37 long, thin teeth on its ventral margin. There are two articular facets for the overlying maxilla at the junction of the posterior margin of the ascending process with the shank portion. Ascending processes of both premaxillae are closely approximated to each other mesially and fit into the median groove of the ethmoid bone. The ascending process forms an angle of 55–67° with the shank: *G. bilineatus* has a slightly larger angle (60–67°, Fig. 11c) than *G. bicarinatus* (55–58°, Fig. 11d). *Grammatorcynus* has a larger angle than any species of *Scomberomorus* except *S. guttatus* (60–61°). The ascending process is 33–40% of the total length of the premax-

Table 2
Number of teeth in upper and lower jaws of *Grammatorcynus*.

Species	Side	Min	Max	$\bar{x}$	Overall $\bar{x}$	N
Upper jaw						
G. bilineatus	L	14	37	23.5	24.0	39
	R	14	36	24.5		
G. bicarinatus	L	14	25	20.5	20.7	8
	R	17	24	20.9		
Lower jaw						
G. bilineatus	L	12	32	18.6	18.8	36
	R	14	30	19.1		
G. bicarinatus	L	16	20	17.5	17.5	7
	R	15	23	17.6		

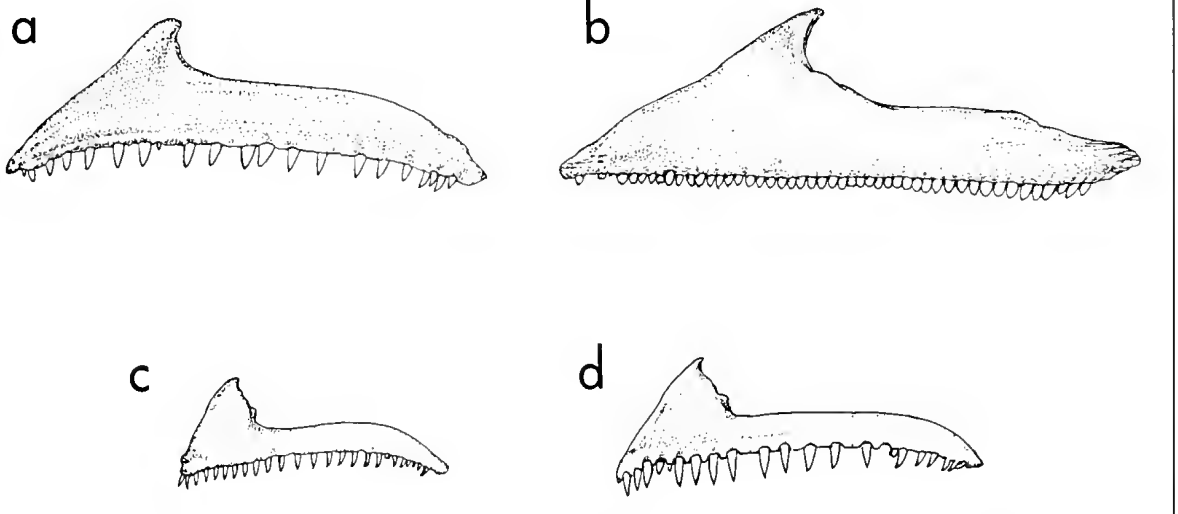

Figure 11

Left premaxillae in lateral view. (a) *Scomberomorus lineolatus*, Cochin, India, 786 mm FL, 2×; (b) *Acanthocybium solandri*, Miami, FL, 1403 mm FL, 1×; (c) *Grammatorcynus bilineatus*, Marshall Is., 424 mm FL, 2×; (d) *G. bicarinatus*, Great Barrier Reef, 563 mm FL.

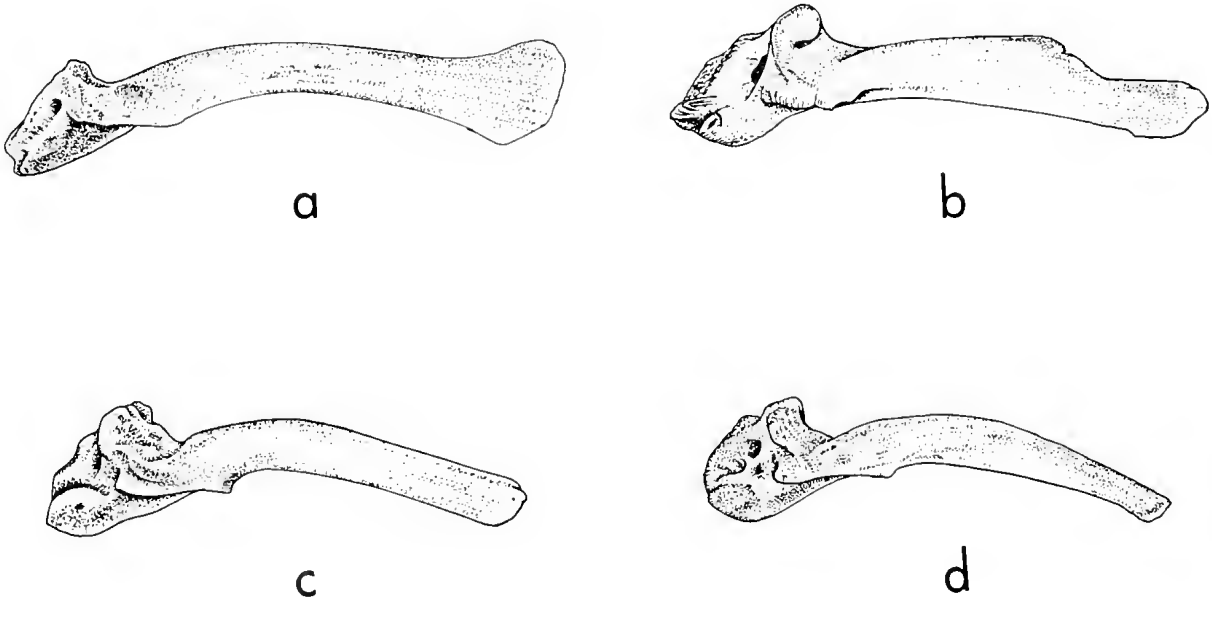

Figure 12

Left maxillae in lateral view. (a) *Scomberomorus munroi*, New Guinea, 512 mm FL, 2×; (b) *Acanthocybium solandri*, Miami, FL, 1403 mm FL, 1×; (c) *Grammatorcynus bilineatus*, Timor Sea, 453 mm FL, 2×; (d) *G. bicarinatus*, Great Barrier Reef, 563 mm FL.

illa. This is a small percentage relative to *Acanthocybium* (50%, Fig. 11b). *Scomberomorus* is intermediate (31–48%, Fig. 11a).

Maxilla The maxilla (Fig. 12) is a long, curved bone surmounting the premaxilla dorsolaterally by means of an anterior head and ventral sulcus. The head consists of a thick, massive inner condyle and a small lateral process. The inner condyle possesses a prominent knob at its dorsolateral aspect that fits into the articular surface of the vomer, and an anterior, deep

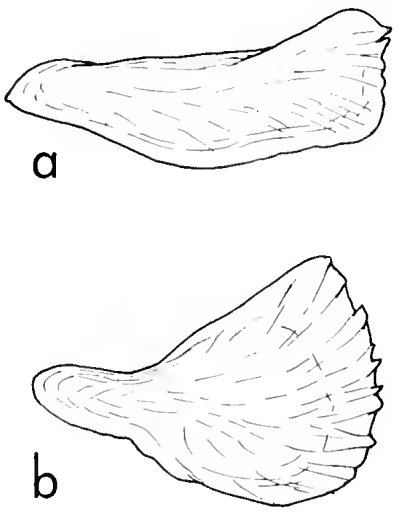

Figure 13
Supramaxillae in lateral view in *Grammatorcynus*. (a) *G. bilineatus*, Western Australia, 460mm FL; (b) *G. bicarinatus*, Australia, 625mm FL.

concavity facing the inner wall of the premaxilla. Immediately posterior to the head is a shallow depression that receives the anterior articulating process of the palatine. The shank of the maxilla is narrow and somewhat flattened. It remains at a relatively constant height along its entire length, unlike the shank of *Scomberomorus* (Fig. 12a) in which the posterior end of the shank expands into a flat plate. The posterior end is distinctly thinner than the middle of the shank in *Acanthocybium* (Fig. 12b).

The head of the maxilla is longer (25–29% of total maxilla length) in *Grammatorcynus* than in any species of *Scomberomorus* (18–25%) but shorter than in *Acanthocybium* (33%, Fig. 12b).

The height of the posterior end of the shank, relative to the total length of the maxilla, is less in *G. bicarinatus* (6–8%, Fig. 12d) than in *G. bilineatus* (8–11%, Fig. 12c). *Grammatorcynus bilineatus* is similar to those species of *Scomberomorus* that have the least well-developed (lowest) posterior expansions: *S. multiradiatus* (8–9%) and *S. sinensis* (9–11%). Other species of *Scomberomorus*, such as *S. munroi* (Fig. 12a), have larger posterior expansions (11–15%).

Supramaxilla The supramaxilla (Fig. 13) covers the posterior end of the maxilla. It is a small, flat bone that is expanded posterodorsally. The expansion is much more pronounced in *G. bicarinatus* (59–76% of bone length, Fig. 13b) than in *G. bilineatus* (35–42%, Fig. 13a).

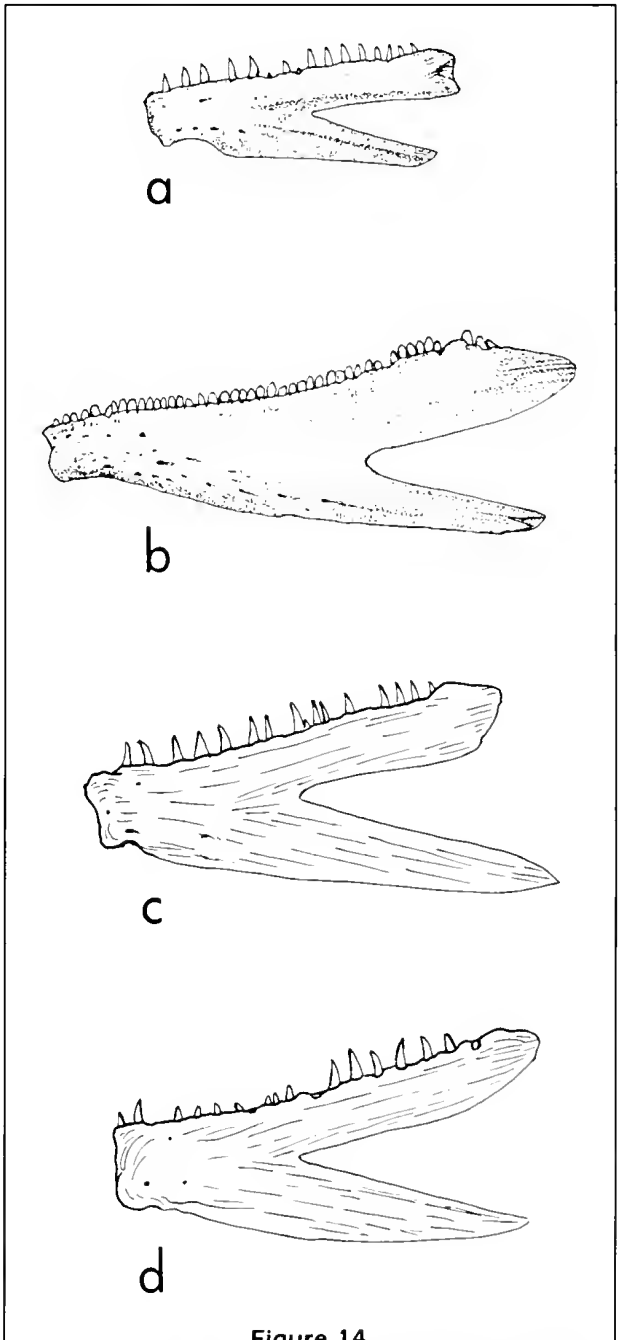

Figure 14
Left dentaries in lateral view. (a) *Scomberomorus semifasciatus*, Port Moresby, New Guinea, 510mm FL, 2×; (b) *Acanthocybium solandri*, Miami, FL, 1403mm FL, 1×; (c) *Grammatorcynus bilineatus*, Marshall Is., 424mm FL; (d) *G. bicarinatus*, Western Australia, 765mm FL, 1×.

Dentary The dentary (Fig. 14) is laterally flattened and bears a single row of 12–32 long, thin teeth on the dorsal margin. Posteriorly, the dentary has two arms of the same relative width (the ventral arm may be slightly narrower), unlike *Scomberomorus* (Fig. 14a) and *Acanthocybium* (Fig. 14b) where the ventral arm

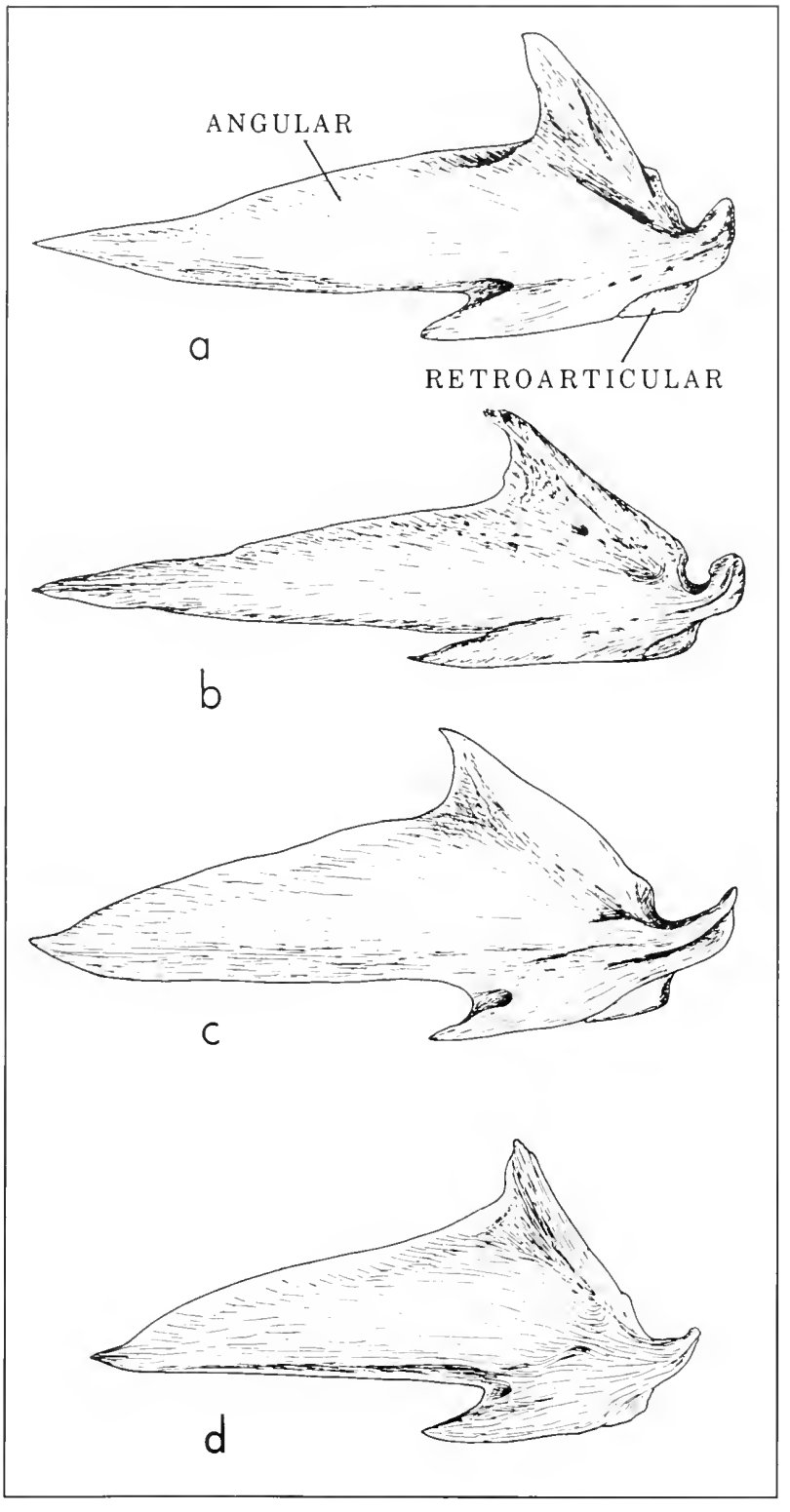

Figure 15
Left angulars and retroarticulars in lateral view. (a) *Scomberomorus semifasciatus*, Port Moresby, New Guinea, 510 mm FL, 3.5×; (b) *Acanthocybium solandri*, Miami, FL, 1403 mm FL, 1×; (c) *Grammatorcynus bilineatus*, Papua New Guinea, 382 mm FL, 4.5×; (d) *G. bicarinatus*, Western Australia, 765 mm FL, 2×.

is much narrower than the dorsal arm. The length of the dentary from its anterior margin to the tip of the ventral arm is 97–109% of the length of the dorsal arm. The ventral arm is longer in *G. bilineatus* (104–109% of dorsal arm length, Fig. 14c) than in *G. bicarinatus* (97–98%, Fig. 14d). The ventral arm is longer in *Grammatorcynus* than it is in *Scomberomorus* (86–97%) and *Acanthocybium* (91–96%). Species of *Grammatorcynus* and *Scomberomorus* have a notch on the anteroventral margin of the dentary that is absent in *Acanthocybium*. *Acanthocybium* has a prominent notch on the anterior margin of the dentary that is indistinct or absent in *Grammatorcynus* and *Scomberomorus*.

Angular (Fig. 15) The triangular anterior end of the angular (frequently called articular) fits into the dentary anteriorly. The posterior end of the angular bears three large processes: the dorsal process, directed forward and upward; the ventral process, directed forward; and the posterior process, directed backward and upward. The posterior process is hooked and carries a transverse articular facet for the quadrate. The length from the tip of the posterior process to the tip of the dorsal process is 40–47% of the total length of the bone. The length from the tip of the posterior process to the tip of the ventral process is slightly longer, 44–52% of bone length. The depth of the angular, measured from the tip of the dorsal process to the tip of the ventral process, is 36–48% of the total length, with the depth of *G. bicarinatus* being greater (44–48%, Fig. 15d) than that of *G. bilineatus* (36–41%, Fig. 15c). The ventral process is approximately as long or longer than the dorsal process in *Grammatorcynus*. In *G. bilineatus*, the ventral process is 84–105% of the length of the dorsal process, and in *G. bicarinatus* the ventral process is longer than the dorsal process (153–200%). Only *Acanthocybium* (99–148%, Fig. 15b), *S. commerson* (99–162%), and *S. queenslandicus* (115–136%) also have a

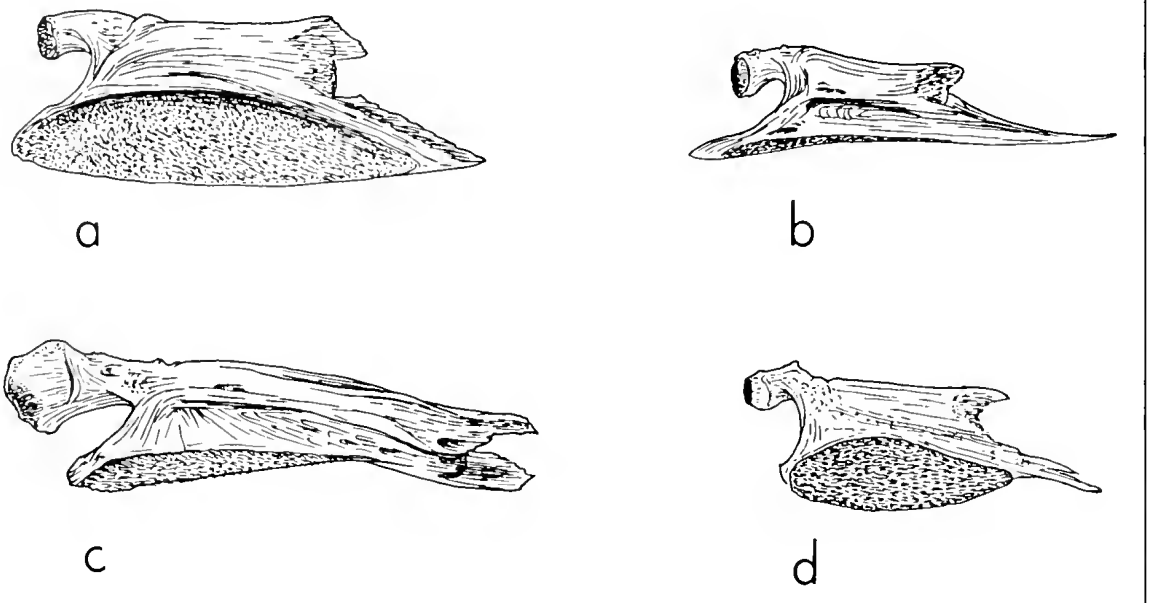

Figure 16

Left palatines in lateral view, slightly rotated to better show tooth patches. (a) *Scomberomorus semifasciatus*, New Guinea, 740 mm FL, 2×; (b) *Scomberomorus commerson*, New South Wales, 1155 mm FL, 1×; (c) *Acanthocybium solandri*, Miami, FL, 1403 mm FL, 1×; (d) *Grammatorcynus bilineatus*, Timor Sea, 453 mm FL, 2×.

ventral process as long or longer than the dorsal process. All other species of *Scomberomorus* (Fig. 15a) have ventral processes that are relatively shorter.

Retroarticular (Fig. 15) The retroarticular bone (frequently called the angular) is rhomboid and attached firmly, but not fused, to the posteroventral margin of the angular. No differences were found between the retroarticulars of the species of *Grammatorcynus*.

Palatine arch The palatine arch consists of four pairs of bones in the roof of the mouth: palatine, ectopterygoid, entopterygoid, and metapterygoid.

Palatine The palatine is forked both posteriorly and anterolaterally (Fig. 16). The dorsal branch of the anterolateral fork is hooked, and its anterior end articulates with a facet on the maxilla, immediately ventral to the nasal. The ventral branch appears almost indistinct in comparison with the longer ventral branch of *Acanthocybium* (Fig. 16c) and the even longer ventral branch of *Scomberomorus* (Fig. 16a–b). In *Scomberomorus*, the ventral branch is longer than the dorsal branch, which is not true of *Grammatorcynus* or *Acanthocybium*. The distance from the anterior end of the ventral branch to the end of the external branch divided by the distance from the tip of the dorsal hook to the end of the external branch is 118–125% in *Grammatorcynus*, 112–121% in *Acanthocybium*, and only 87–107% in *Scomberomorus*. The distance from the tip of the dorsal hook to the tip of the inner branch divided by the distance to the tip of the outer branch is 71–75% in *Grammatorcynus*, 54–84% in *Scomberomorus*, and 97–99% in *Acanthocybium*. Hence, *Acanthocybium* differs from both *Grammatorcynus* and *Scomberomorus* in that its posteriorly directed inner branch is almost as long as the outer branch. The tooth patch is short and wide in *Grammatorcynus* (Fig. 16d), more so in *G. bicarinatus* (width 38–42% of length, Fig. 17b) than in *G. bilineatus* (width 26–32% of length, Fig. 17a), long and narrow in *Acanthocybium*, and between the two extremes in *Scomberomorus*. The teeth are fine in all three genera, but are a little larger in *Grammatorcynus* and *Acanthocybium* than in most species of *Scomberomorus*.

Ectopterygoid The ectopterygoid is a T-shaped bone with the top of the T forming its posterior end. It joins with the entopterygoid dorsolaterally, the palatine laterally and anteriorly, and the quadrate and metapterygoid posteriorly (Fig. 18). Dividing the dorsal distance (from the anterior end of the bone to the tip of the dorsal arm) by the ventral distance (from the anterior end to the tip of the ventral process) results in a number that is greater than 100% in *Grammatorcynus* (107–116%, Fig. 18c) and *Acanthocybium* (103–109%, Fig. 18b), but only 85–100% in *Scombero-*

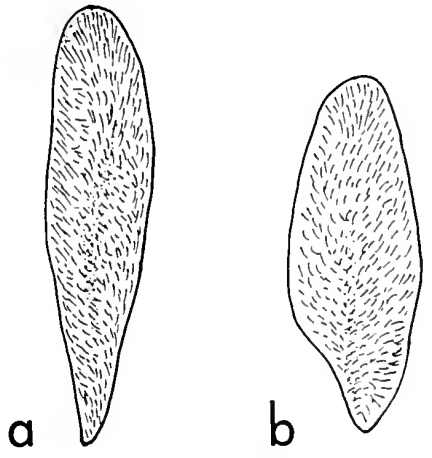

Figure 17
Palatine tooth patches in *Grammatorcynus*. (a) *G. bilineatus*, Queensland, 521 mm FL; (b) *G. bicarinatus*, Western Australia, 765 mm FL.

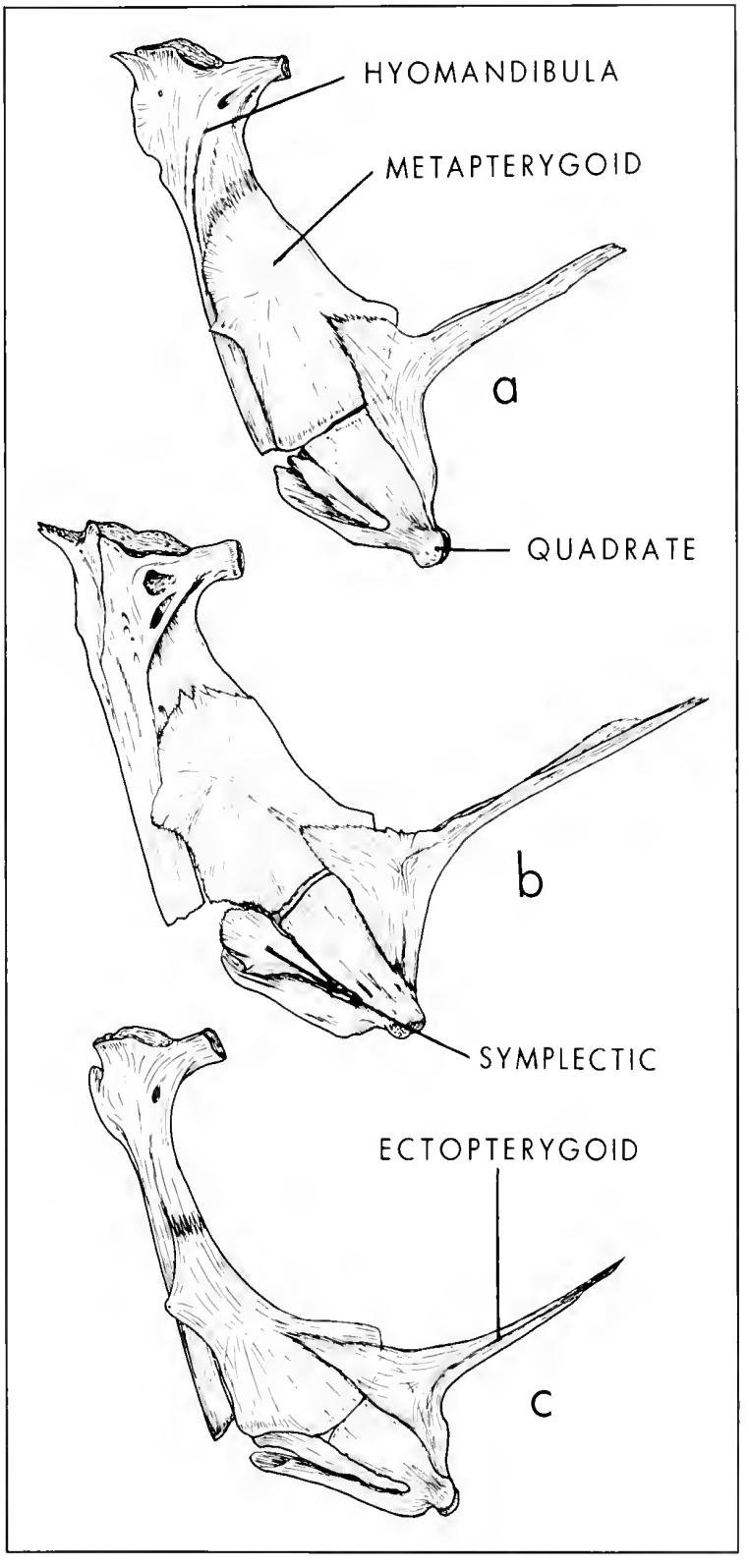

Figure 18 (right)
Left suspensoria in mesial view. (a) *Scomberomorus semifasciatus*, New Guinea, 510 mm FL, 2.5×; (b) *Acanthocybium solandri*, Revillagigedos Is., 1068 mm FL, 1.5×; (c) *Grammatorcynus bilineatus*, Marshall Is., 424 mm FL, 2×.

morus (Fig. 18a). The shank is longer in *Acanthocybium* than in the other two genera. The posterior edge of the ectopterygoid (from the tip of the dorsal process to the tip of the ventral process) relative to the ventral distance is long, 63–72% in *Grammatorcynus*, and relatively shorter in *Acanthocybium* (41–47%) and *Scomberomorus* (43–63%).

Entopterygoid The entopterygoid is elongate and oval in shape (width 35–41% of length, Collette and Russo 1985b: fig. 28). The outer margin of the entopterygoid is the thickest part of the bone and attaches to the inner margin of the ectopterygoid. The entopterygoid also connects with the palatine anteriorly and the metapterygoid posterolaterally. The mesial and posterior borders are free from contact with other bony elements. The dorsal surface is roughly convex. The dorsal surface is similarly convex in *Acanthocybium*, but the dorsal surface in *Scomberomorous* is concave. The ventral surface is convex in all three genera, and it forms the major part of the buccal roof. *Scomberomorus* contains species that have both narrower (*S. commerson*, width

23–28% of length) and wider (*S. maculatus* width 41–42% of length) entopterygoids. The entopterygoid of *Acanthocybium* (30–35%) is slightly narrower than that of *Grammatorcynus* (35–41%).

Metapterygoid The metapterygoid is a flat, quadrangular or somewhat triangular bone (Fig. 18). The posterodorsal margin of this bone is deeply grooved to receive the hyomandibula. The dorsal portion is strongly ankylosed to the lamellar region of the hyomandibula. The ventroposterior margin abuts the lowermost portion of the symplectic process of the hyomandibula, but does not touch the hyomandibula. There is a relatively long slit beween the two bones through which the hyoidean artery passes (Allis 1903). The ventral border is divided into two portions: the horizontal portion in contact with the quadrate and the anterior oblique portion ankylosed to the ectopterygoid. On the mesial surface, the metapterygoid has a triangular-shaped area that forms an interdigitating articulation with the upper arm of the ectopterygoid. The posteroventral margin of the metapterygoid articulates with the dorsal end of the symplectic in *Grammatorcynus* (Fig. 18c) and *Acanthocybium* (Fig. 18b), but does not do so in most species of *Scomberomorus* (Fig. 18a). The posterior, horizontal part of the ventral border is shorter than the anterior oblique part in *Grammatorcynus* (anterior part 132–181% of posterior part) and *Acanthocybium* (188–218%); however, in *Scomberomorus* the posterior part is longer than the anterior part (anterior part 39–86% of posterior part).

Hyoid arch The hyoid arch is composed of the hyomandibula, symplectic, quadrate, hyoid complex (hypohyals, ceratohyal, epihyal, interhyal, and the seven branchiostegal rays), and two median unpaired bones, the glossohyal and urohyal.

Hyomandibula The hyomandibula is an inverted L-shaped bone (Fig. 18) connecting the mandibular suspensorium and opercular bones to the neurocranium. Dorsally, there are three prominent condyles. The long dorsal condyle forms the base of the L and fits into the fossa at the junction of the pterotic and sphenotic bones. The anterior condyle articulates with the ventral fossa of the pterotic, and the lateral process is attached to the inside of the opercle. Anterolaterally, the hyomandibula is drawn out into a lamellar region that joins the metapterygoid. Posterolaterally, it has a long articulation with the preopercle. Ventrally, the hyomandibula has a long symplectic process; at the posterodorsal corner there is a small, sometimes almost indistinct spine. A strong vertical ridge extends from the ventral margin to just below the dorsal border, where it then curves anteriorly to confluence with the anterior condyle. The areas lying anterior and posterior to this ridge are grooved for articulation with the metapterygoid and preopercle, respectively; in situ, only the ridge and a portion of the upper broader surface are visible exteriorly. The upper surface of the symplectic is connected to the ventral border of the hyomandibula by way of a cartilage, best developed in *Acanthocybium*. There is one deep fossa on the inner surface of the hyomandibula in *Grammatorcynus* (Fig. 18c) and *Scomberomorus* (Fig. 18a); there are two such fossae in *Acanthocybium* (Fig. 18b).

The posterodorsal spine, which is quite small in *Grammatorcynus* and in most species of *Scomberomorus*, is best developed in *Acanthocybium*, *S. commerson* (Devaraj 1977), and *S. queenslandicus*. The maximum width (tip of anterior condyle to outer margin of posterior condyle) of the hyomandibula is least relative to the total length (ventral tip to dorsal margin of dorsal condyle) in *Grammatorcynus* (width 34–39% of length) and *S. multiradiatus* (36–39%). The hyomandibula is widest, relative to length in *S. sinensis* (45–52%). *Acanthocybium* and the other species of *Scomberomorus* fall between these two extremes (39–47%).

Symplectic The symplectic is a small bone that fits into a groove on the inner surface of the quadrate (Fig. 18). In *Grammatorcynus* the symplectic is slightly wider than it is in *Scomberomorus*; however, the groove into which the symplectic fits is narrower in *Grammatorcynus* than in *Scomberomorus*, so that the symplectic nearly fills the groove in *Grammatorcynus* and does not fill the groove in *Scomberomorus* (Fig. 18a). The symplectic is greatly expanded at its dorsal end in *Acanthocybium* (Fig. 18b). The symplectics in *Grammatorcynus* and *Acanthocybium* extend well beyond the dorsal margin and even beyond the dorsal end of the posterior process of the quadrate to make contact with the metapterygoids, making them much longer than the symplectics in most species of *Scomberomorus*. The symplectic of *G. bilineatus* (Fig. 19a) is longer than that of *G. bicarinatus* (Fig. 19b).

Quadrate The lower jaw is suspended from the cranium by means of the articulating facet of the ventral surface of the triangular quadrate (Fig. 18). The broad dorsal margin of the quadrate abuts the ventral border of the metapterygoid. There is a strong process on the posterior margin of the quadrate that is attached along the lower anterior arm of the preopercle. This process is quite long in *G. bilineatus* (its length measured from the ventral facet to the tip of the process is 134–145% of the distance from the ventral facet to the dorsal margin; Fig. 19a) and *Acanthocybium*, but shorter in *G. bicarinatus* (122–125%, Fig. 19b) and most species of *Scomberomorus*.

Hyoid complex This complex includes the two hypohyals (basihyal of Mago Leccia 1958), ceratohyal, epihyal, and interhyal bones, and the seven branchiostegal rays (Collette and Russo 1985b:fig. 29). The

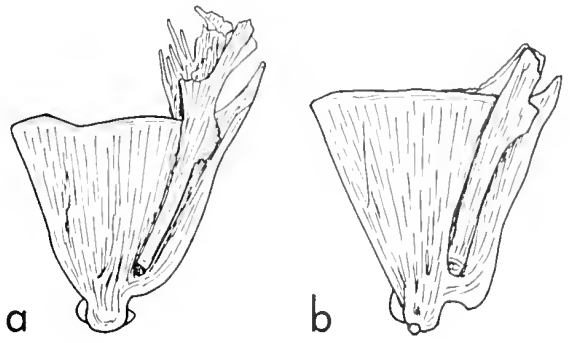

Figure 19
Quadrate and symplectic in *Grammatorcynus*. (a) *G. bilineatus*, Western Australia, 460 mm FL; (b) *G. bicarinatus*, Queensland, 563 mm FL.

hypohyals, ceratohyal, and epihyal are closely associated and form a functional unit.

Hypohyals The hypohyals comprise separate dorsal and ventral elements joined longitudinally. In lateral view, the ventral hypohyal is clearly larger than the dorsal hypohyal in *Grammatorcynus*, but in *Scomberomorus* not quite as large relative to *Grammatorcynus*. In *Acanthocybium* the ventral hypohyal is three times larger than the dorsal hypohyal. Laterally, the suture that runs between the dorsal and ventral hypohyals curves ventrally at various angles in *Grammatorcynus* and *Scomberomorus*, but runs almost horizontally in *Acanthocybium*. Mesially, a pointed lateral process at the anterodorsal end of the dorsal hypohyal forms a symphysis with the glossohyal, urohyal, basibranchial, and the process of the hypohyal from the opposite side in *Grammatorcynus* and *Scomberomorus*. *Acanthocybium* also has a pointed lateral process, but it appears to be further posterior due to also having an anterior pointed end to the hypohyals at the junction of the dorsal and ventral hypohyals. In addition, *Acanthocybium* has a prominent anterolateral process on the ventral hypohyal. The groove for the hyoidean artery runs along the outer surface of the epihyal, ceratohyal, and ventral portion of the dorsal hypohyal. In *Grammatorcynus* the groove in the dorsal hypohyal is relatively short, extending anteriorly 11–39% of the length of the dorsal hypohyal before becoming a covered tunnel leading to the inner side of the dorsal hypohyal. In *Scomberomorus* the groove extends 32–53% before becoming a tunnel to the inner side, and in *Acanthocybium* the groove extends 29–47% before becoming a foramen leading to the inner side. The opening on the inner side appears as a small to moderate pit, usually located in the ventral portion of the dorsal hypohyal in *Grammatorcynus* and *Scomberomorus*.

Ceratohyal The ceratohyal is a long flat bone, broadest at the posterior end, and with an anteroventral projection that articulates with the posteroventral notch of the ventral hypohyal. It is the largest bone of the hyoid complex. Posteriorly, the middle part of the ceratohyal interlocks with the epihyal by means of odontoid processes issuing from both elements (ceratohyal-epihyal suture of McAllister 1968), while the upper and lower portions are joined by cartilage. Four acinaciform branchiostegal rays are attached to the respective articular surfaces along the concave middle portion of the ventral margin in *Grammatorcynus* and *Acanthocybium*. In *Scomberomorus* the fifth branchiostegal ray is also usually attached to the ceratohyal (most posterior part) or on the space between the ceratohyal and epihyal, not on the anterior part of the epihyal. In *Grammatorcynus* and *Acanthocybium* the fifth branchiostegal ray is on the anterior part of the epihyal. The hyoidean groove runs the length of the ceratohyal on its lateral surface. The groove is so deep in 10 species of *Scomberomorus* (*brasiliensis*, *commerson*, *concolor*, *multiradiatus*, *munroi*, *niphonius*, *queenslandicus*, *semifasciatus*, *sierra*, and *tritor*) that it forms a thin slit through the bone, the ceratohyal window or "beryciform" foramen. This slit is rare in *Grammatorcynus* and *Acanthocybium*, and is either rare or occasional in the other eight species of *Scomberomorus*. The dorsal margin of the ceratohyal is usually concave, but sometimes flat in *Grammatorcynus*. It is deeply concave in *Acanthocybium*, and varies from concave to convex in *Scomberomorus*.

Epihyal The epihyal is a triangular bone that interlocks anteriorly with the ceratohyal and has a posterior process that articulates with the interhyal. Three branchiostegal rays articulate with the epihyal in *Grammatorcynus* and *Acanthocybium*. Only two branchiostegal rays are found on the ventral portion of the epihyal in *Scomberomorus*. In *Grammatorcynus* the depth of the epihyal is 66–80% of the length from the smooth anterior margin of the bone to the tip of the posterior process. Epihyal depth is narrowest in *Acanthocybium* (58–62%), and in *Scomberomorus* it varies from 68% in *S. commerson* and *S. cavalla* to 98% in *S. koreanus*, with intermediate values for the other species.

Interhyal The interhyal is a small flattened bone that is attached to the epihyal dorsal to the posterior process. It is directed obliquely upward and links the hyoid complex to the hyomandibula and symplectic. No differences in interhyals were noted.

Glossohyal The glossohyal (basihyal) is a median bone that supports the tongue and overlies the

first basibranchial bone at the anterior end of the branchial arch. In *Grammatorcynus* there is a quadrangular to oval tooth plate fused to and covering the dorsal surface of the glossohyal (Collette and Russo 1985b:fig. 30). No tooth plate is present in *Acanthocybium* or *Scomberomorus*. The glossohyal of *Grammatorcynus* is slightly wider (width 47–55% of length) than the roughly rod-shaped or conical-shaped glossohyal of *Scomberomorus* (35–54%) and the flattened spatulate glossohyal of *Acanthocybium* (42%).

Urohyal The urohyal is a compressed, median, unpaired bone (Fig. 20). The anterior end of this element lies between, and is connected with, the hypohyals of the left and right sides. The most prominent difference in the urohyal of *Grammatorcynus* is that in dorsal view, the posterior end of the dorsal margin is tripartite (Fig. 20c–d) instead of forked, as it is in *Scomberomorus* and *Acanthocybium* (Fig. 20a–b). The dorsal and anterior portions of the ventral margins are thickened in *Grammatorcynus*. The anterior end has an articulation head; the posterior end is deepest in *Scomberomorus*, and much less deep in *Grammatorcynus* due to the convex shape of the ventral margin. The maximum depth of the urohyal in *Grammatorcynus* is 15–20% of the length of the dorsal margin. The maximum depth in *Acanthocybium* is not as great as this (13–15%), and in *Scomberomorus* it is greater (16–24%). In *Grammatorcynus* the ventral margin of the urohyal is relatively short, only 68–71% of the length of the dorsal margin, compared with 80–91% in *Acanthocybium* and *Scomberomorus*.

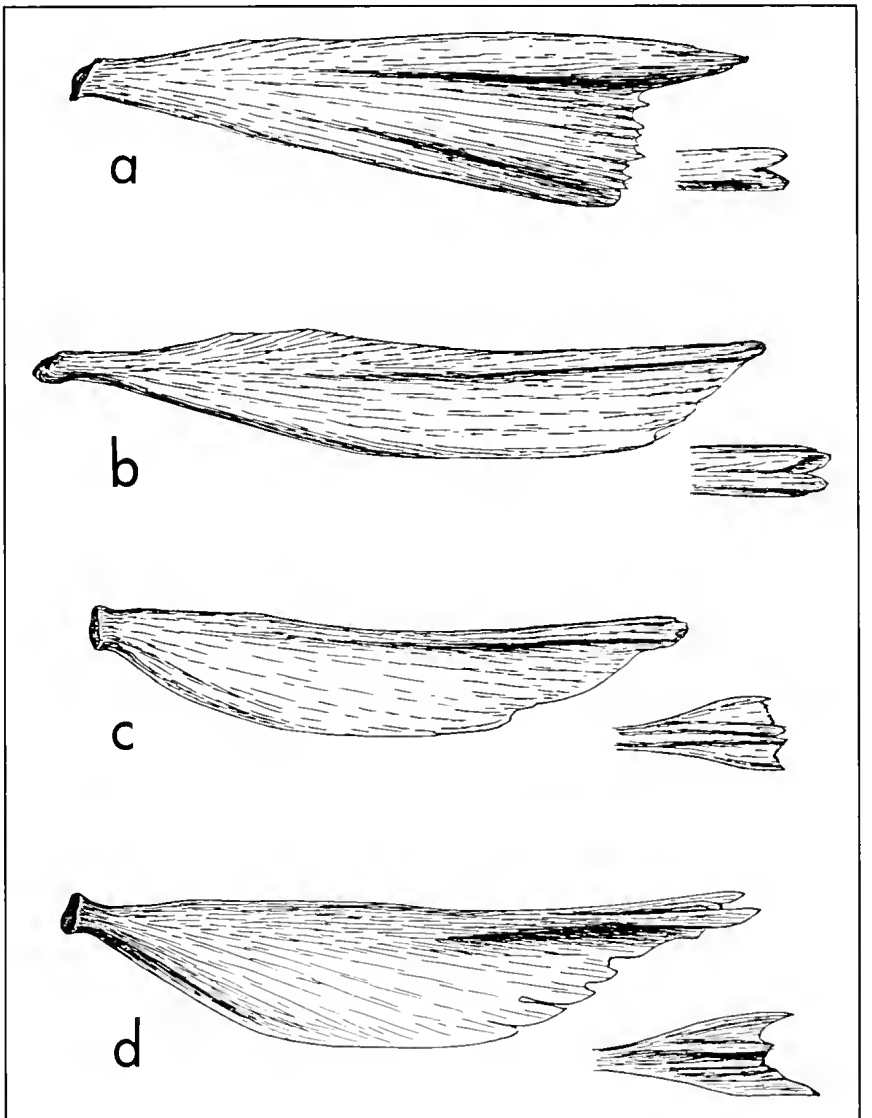

Figure 20

Urohyals in left lateral view. (a) *Scomberomorus queenslandicus*, Queensland, 641 mm FL; (b) *Acanthocybium solandri*, Indian O., 1088 mm FL; (c) *Grammatorcynus bilineatus*, New Guinea, 382 mm FL; (d) *G. bicarinatus*, Australia, 663 mm FL. Fig. (a) drawn twice as large as (b), (c) three times as large. Inset is the posterior end of the dorsal margin, in dorsal view.

Opercular apparatus Four wide, flat bones (opercle, preopercle, subopercle, and interopercle) fit together to form the gill cover.

Opercle The opercle (Fig. 21) is overlapped laterally on its anterior margin by the posterior half of the preopercle. The narrow, elongate, articular facet for the opercular process of the hyomandibula is located on the medial surface of the anterodorsal corner of the opercle. *Grammatorcynus* and most species of *Scomberomorus* have a weak process at the posterodorsal corner. This process is absent in *Acanthocybium*. In *Grammatorcynus* the width of the opercle is 63–79% of the total length of the bone; *G. bicarinatus* has a wider opercle (width 72–79% of length, Fig. 21d) than *G. bilineatus* (63–72%, Fig. 21c). Both species of *Grammatorcynus* have narrow opercles compared with the extremely wide opercles found in *Acanthocybium* (Fig. 21b).

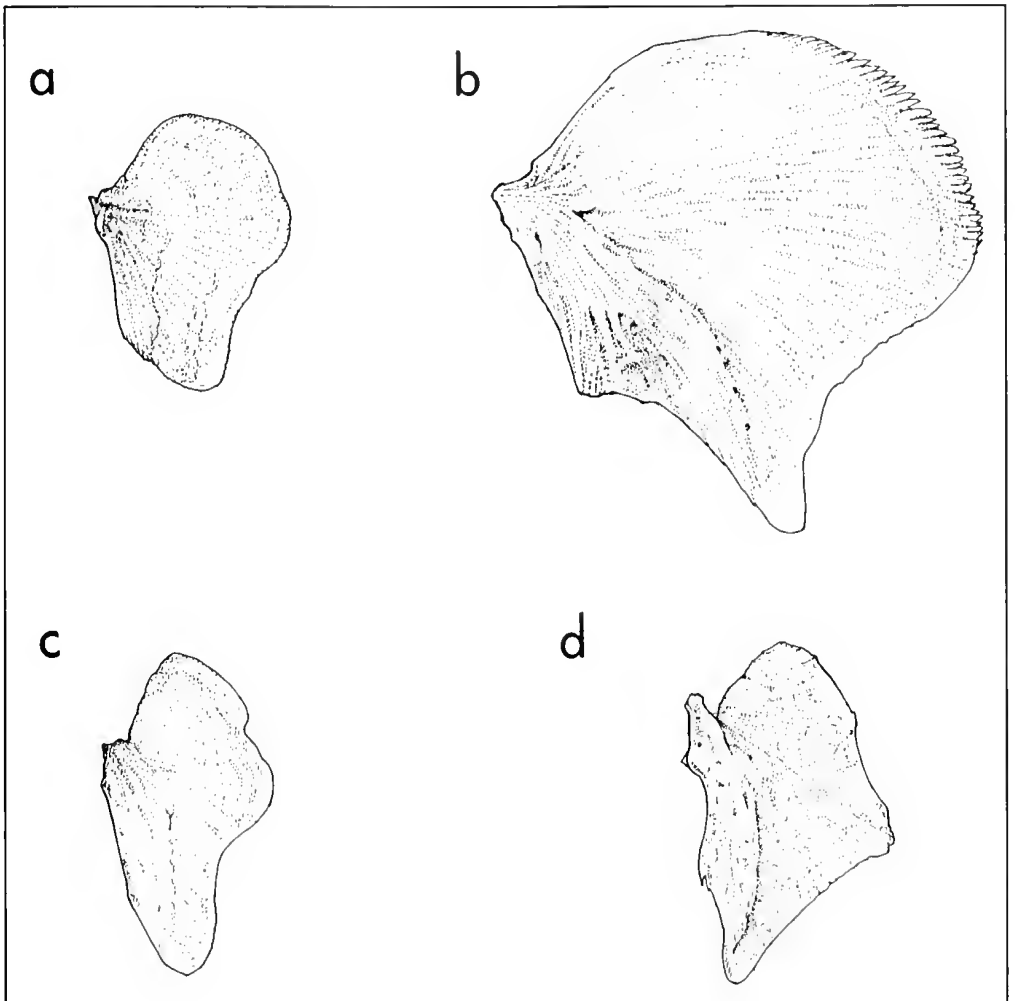

Figure 21

Left opercles in lateral view. (a) *Scomberomorus semifasciatus*, New Guinea, 510 mm FL; (b) *Acanthocybium solandri*, Revillagigedos Is., 1080 mm FL; (c) *Grammatorcynus bilineatus*, Marshall Is., 424 mm FL; (d) *G. bicarinatus*, Great Barrier Reef, 563 mm FL.

Preopercle The preopercle is a large, crescent-shaped flat bone, broadest at the lower posterior angle (Collette and Russo 1985b:fig. 33). The anterior portion of the bone is thickened into a bony ridge. A series of 5–7 pores along the lower margin of the ridge represents the preoperculomandibular canal of the lateral line system which continues onto the dentary. On the mesial side, the bony ridge possesses a groove for attachment to the hyomandibula and the quadrate. There is a shelf mesial to the anteroventral end of the preopercle in *Acanthocybium* that is absent in *Grammatorcynus* and *Scomberomorus*. The canals leading to the preopercular pores are visible through the bone in *G. bilineatus* and all species of *Scomberomorus*, but these canals could not be seen in the specimens of *G. bicarinatus* and *Acanthocybium* due to the thickness of the bone. The posterior margin of the preopercle is distinctly concave in *Grammatorcynus* and most species of *Scomberomorus*. However, it is only slightly concave or flat in *Acanthocybium* and *S. commerson*. In *Grammatorcynus* the distance from the anterior margin of the bony ridge to the posterior end of the lower lobe is 64–75% of the height of the preopercle measured from the ventral margin to the dorsal tip of the bone. In *Scomberomorus* the lower lobe is 69–80% of the height of the preopercle. The anterodorsal margin terminates in a pore similar to the preoperculomandibular lateral-line canal pore at the anteroventral margin of the bone.

Subopercle The subopercle is a flat, roughly triangular bone with a prominent anterior projection (Collette and Russo 1985b:fig. 34). Two ridges

converge posteriorly from the anterior projection on the lateral side of the bone. The upper ridge articulates with the lower posterior projection of the opercle, and the lower ridge connects to the posterodorsal margin of the interopercle. The dorsal ridge is much more prominent than the ventral ridge and extends over the main part of the subopercle as a discrete shelf. The weaker ventral ridge is more difficult to detect in most specimens of *Grammatorcynus*. The angle between the anterior projection and the anterior margin of the subopercle is acute in *Grammatorcynus* and *S. multiradiatus*; however, in *Acanthocybium* and the other species of *Scomberomorus* the angle is close to 90°. The length of the anterior projection in *Grammatorcynus* varies from 23 to 33% of the length of the anterior margin dorsal to the projection. The projection is slightly longer (28–33%) in *G. bicarinatus* than in *G. bilineatus* (23–28%). The projection is longest in *Acanthocybium* (36–45%) and shortest in *S. commerson* (20–25%), with the rest of the species of *Scomberomorus* having projections between 21 and 43%.

Interopercle The interopercle is roughly oval in shape, narrow at the anterior margin and widening posteriorly, with a crest on the superior margin (Collette and Russo 1985b:fig. 35). There is a well-developed facet on the mesial side to receive the articular process of the interhyal. The maximum depth of the interopercle relative to the length of the bone is 35–43% in *Grammatorcynus*. The maximum depth of the interopercle is a little greater in *Acanthocybium* (40–49%), and much greater in the species of *Scomberomorus* (45–61%). Often there is a well-formed notch anterior to the crest on the sloping anterior margin in *Grammatorcynus* and *Scomberomorus*, which is not as well developed in *Acanthocybium*. The posterior margin is rounded in *Grammatorcynus* and *Scomberomorus* but divided into two by a notch in *Acanthocybium*.

Branchial apparatus The branchial apparatus is composed of five pairs of gill arches, gill filaments, gill rakers, pharyngeal tooth patches, and supporting bones. The general arrangement in *Grammatorcynus* is similar to that found in other scombrids such as the Sardini (Collette and Chao 1975), *Thunnus* (Iwai and Nakamura 1964:22, fig. 1; de Sylva 1955:21, fig. 40), *Scomberomorus* (Mago Leccia 1958:327, pl. 12; Collette and Russo 1985b:fig. 36), and *Rastrelliger* (Gnanamuttu 1971:14, fig. 6). Most branchial bones bear patches of tiny teeth.

Basibranchials The three basibranchials form an anteroposterior chain. The first and second are about the same size, and considerably shorter than the third. The first is covered dorsally by the glossohyal.

In lateral view, the first basibranchial is narrowest in the middle. In *Grammatorcynus* and *Acanthocybium* it is elongate. In *Scomberomorus* it is short with a wide base where it joins with the second basibranchial. The second basibranchial has a prominent notch in the ventral margin and a distinct groove laterally that extends from the anteroventral margin to the middorsal region of the bone. This groove accepts the anterior end of the first hypobranchial. The third basibranchial has an expanded anterior end at its junction with the second basibranchial, and then tapers posteriorly. A prominent groove is present anteriorly that accepts the medial anterior end of the second hypobranchial. A section of cartilage extends posteriorly to articulate with the fourth and fifth ceratobranchials.

Hypobranchial Three hypobranchials are present. The first is interposed beween the second basibranchial and the first ceratobranchial. The second is about the same size as the first, fits into a groove on the third basibranchial, and extends to the second ceratobranchial. The third hypobranchial is smaller than the first or second, fits snugly against the posterolateral margin of the third basibranchial, and its posterior end articulates with the third ceratobranchial.

Ceratobranchials The five ceratobranchials are the longest bones in the branchial arches. They have a deep groove ventrally for the branchial arteries and veins. The ceratobranchials support most of the gill filaments and gill rakers. The first three are morphologically similar and articulate with the posterior ends of their respective hypobranchials. The fourth is more irregular and attaches to a cartilage posterior to the third basibranchial. The fifth ceratobranchial is also attached to the cartilage, has a dermal tooth plate fused to its dorsal surface, and the complex is termed the lower pharyngeal bone. It is covered with small conical teeth that are directed slightly posteriad.

Epibranchials The posterolateral end of each of the four epibranchials is attached to the ends of the first four ceratobranchials. Each epibranchial bears a groove posterodorsally for the branchial arteries and veins. The first epibranchial is the longest and bears two processes mesially. The anterior process articulates with the first pharyngobranchial, and the posterior process attaches with the interarcual cartilage. The second epibranchial is similar to the first, but slightly shorter. The anterior end has two processes, an anterior process that attaches to the second pharyngobranchial and a posterior process that is coupled with the third pharyngobranchial by way of an elongate cartilage. This process is relatively elongate in *Grammatorcynus*, but shorter in *Acanthocybium* and *Scomberomorus*. The third epibranchial is the shortest in the series. Laterally, it is attached with the third ceratobranchial; mesially, it is attached with the third pharyngobranchial. An elongate posterodorsal process

is present. This process joins with the fourth epibranchial, which is larger than the third and is interposed between the fourth ceratobranchial and pharyngobranchial. It is a curved bone with the angle formed by the lateral and medial arms being much more acute in *Grammatorcynus* than in *Acanthocybium* and *Scomberomorus*. A dorsal process arises from the middle of the bone and attaches to the third epibranchial.

Pharyngobranchials There are four pharyngobranchials attached basally to the epibranchial of their respective gill arch. The first is long and slender, articulates dorsally with the prootic, and is frequently called the suspensory pharyngeal (Iwai and Nakamura 1964). The elongate second pharyngobranchial bears a patch of teeth. The third is the largest element in the series; it has a broad patch of teeth on its ventral surface, a broad posterior end, and tapers to a narrow anterior end. In *Grammatorcynus* and *Acanthocybium* the third pharyngobranchial is shorter than in *Scomberomorus*. The fourth pharyngobranchial also bears a ventral tooth plate, has a rounded posterior end, and has an elongate strut (pharyngobranchial stay) mesially which overlaps the third pharyngobranchial. This stay is much shorter in *Grammatorcynus* and *Acanthocybium* than in *Scomberomorus*.

Gill rakers The hypobranchial, ceratobranchial, and epibranchial of the first gill arch support a series of slender, rigid gill rakers. The longest gill raker is at or near the junction of the upper and lower arches, between the ceratobranchial and epibranchial. Magnuson and Heitz (1971) have clearly shown that there is a correlation between numbers of gill rakers, gap between gill rakers, and size of food items in a number of species of Scombridae.

The number of gill rakers is easily countable and is an especially useful taxonomic character in differentiating between the two species of *Grammatorcynus*: *G. bilineatus* has more gill rakers (18–24) than *G. bicarinatus* (12–15) (Table 3). *Acanthocybium* differs from all other genera of Scombridae in completely lacking gill rakers. Three species of *Scomberomorus* have greatly reduced numbers of gill rakers: *S. multiradiatus* (1–4 gill rakers), *S. commerson* (1–8), and *S. queenslandicus* (3–9). *Scomberomorus concolor* stands out in having the most gill rakers (21–27). Other species of *Scomberomorus* fall between these extremes. There is a correlation between number of gill rakers and number of jaw teeth in *Grammatorcynus* and *Scomberomorus*. Species with the fewest gill rakers, *G. bicarinatus* and *S. multiradiatus*, also have the fewest jaw teeth, and species with the most gill rakers, *G. bilineatus* and *S. concolor*, have the most teeth.

Axial skeleton This section is divided into four parts: vertebral number, vertebral column, ribs and intermuscular bones, and caudal complex.

Vertebral number Vertebrae may be divided into precaudal (abdominal) and caudal. The first caudal vertebra is defined as the first vertebra that bears a notably elongate haemal spine and lacks pleural ribs. Vertebral counts include the urostyle which bears the hypural plate. *Grammatorcynus* has 31 vertebrae, which is less than *Scomberomorus* (41–56 vertebrae), which in turn is less than *Acanthocybium* (62–64). The same situation also applies to precaudal and caudal vertebrae. Both species of *Grammatorcynus* have 12 precaudal and 19 caudal (except for one specimen of *G. bicarinatus* with 11 plus 20 caudal). *Scomberomorus* has 16–23 precaudal and 20–36 caudal, and *Acanthocybium* has 31–33 precaudal and 31–33 caudal. The presence of only 31 vertebrae in *Grammatorcynus* is a primitive condition agreeing with *Scomber* and *Rastrelliger*, the most primitive members of the Scombrinae. The increased number of vertebrae in *Acanthocybium* is clearly a specialization.

Vertebral column The neural arches and spines are stout and compressed on the first to the fourth vertebra (especially the first 3) in *Grammatorcynus*. They extend farther back, to the fifth or sixth vertebrae, in most species of *Scomberomorus*, and extend farthest, to the seventh vertebra, in *Acanthocybium* and *S. commerson*. Posteriorly, toward the caudal peduncular vertebrae and caudal complex, the neural spines bend abruptly backward and cover most of the neural groove; caudally they merge into the caudal complex as in *Thunnus* (Kishinouye 1923, Gibbs and Collette 1967) and the bonitos (Collette and Chao 1975).

Table 3
Number of gill rakers on first arch in *Grammatorcynus*.

	12	13	14	15	16	17	18	19	20	21	22	23	24	N	$\bar{x}$
G. bilineatus							1	10	15	30	10	5	1	72	20.8
G. bicarinatus	1	—	7	3										11	14.1

The neural prezygapophyses on the first vertebra are modified to articulate with the exoccipital where the vertebral axis is firmly articulated with the skull. Neural postzygapophyses arise posterodorsally from the centrum and overlap prezygapophyses posteriorly. The postzygapophyses progressively merge into the neural spine in the peduncular region to disappear by the last 5–6 vertebrae. The basic structure and elements of the neural arches and neurapophyses are similar to those of other scombrids (Kishinouye 1923, Conrad 1938, Mago Leccia 1958, Nakamura 1965, Gibbs and Collette 1967, Collette and Chao 1975, Potthoff 1975, Collette and Russo 1985b).

Variable characters are found on the haemal arches and haemapophyses. Laterally directed parapophyses, arising from the middle of the centrum, appear on the 4th–6th vertebrae where the intermuscular bones and pleural ribs are encountered (see section on Ribs and Intermuscular Bones). The parapophyses become broader and longer posteriorly and gradually shift to the anteroventral portion of the centra. In lateral view, the first ventrally visible parapophyses are found on the 6th–7th vertebra in *Grammatorcynus*, the 7th–9th in *Scomberomorus* (usually the 8th), and on the 14th–15th in *Acanthocybium*.

Posteriorly, the distal ends of the paired parapophyses meet, forming the first closed haemal arch. The first closed haemal arch is on the 8th vertebra in *Grammatorcynus*, 10th–16th vertebra in *Scomberomorus*, and 25th–28th vertebra in *Acanthocybium*. This location is correlated with the total number of vertebrae. The haemal spines become elongate and point posteriorly until they abruptly become more elongate on the first caudal vertebra. The paired pleural ribs (see section on Ribs and Intermuscular Bones) attach to the distal ends of the parapophyses and arches and extend posteriorly to the last precaudal vertebra. The haemal arches and spines bend posteriorly at the caudal peduncle and then merge into the caudal complex symmetrically with the neural arches and spines on the caudal vertebrae.

Haemapophyses include pre- and postzygapophyses, but their relative positions are different from those of the neurapophyses, and they do not overlap. The first haemal postzygapophyses arise posteroventrally from the 6th–7th centrum in *Grammatorcynus*, the 6th–8th in *Scomberomorus*, and the 9th–10th in *Acanthocybium*. They reach their maximum length at about the junction of the precaudal and caudal vertebrae. The haemal postzygapophyses fuse with the haemal spine or disappear in the caudal peduncle region. The haemal prezygapophyses arise from the anterior base of the haemal arches on the 8th–11th vertebra in *Grammatorcynus*, the 10th–22nd in *Scomberomorus*, and the 23rd–25th in *Acanthocybium*.

Struts between the haemal arch and the centrum form the inferior foramina. Foramina are present from the 17th–19th to the 25th–28th vertebra in *Grammatorcynus*, the 21st–33rd to the 35th–52nd in *Scomberomorus*, and the 49th–51st to the 56th–57th in *Acanthocybium*.

Ribs and intermuscular bones Pleural ribs are present from the second or third vertebra posterior to the 12th–31st vertebra in the three genera. Intermuscular bones start on the back of the skull or the first vertebra and extend to the 10th–30th vertebra.

Correlated with its low number of vertebrae, *Grammatorcynus* has the fewest pleural ribs (10 pairs). *Acanthocybium* has the most pleural ribs (30 pairs) in agreement with its many vertebrae. Species of *Scomberomorus* are intermediate in number of vertebrae and also in number of pleural ribs (15–21). The first pleural rib articulates with the centrum of the third vertebra in *Grammatorcynus* and most species of *Scomberomorus*, and articulates with the centrum of the second vertebra in *Acanthocybium*, as noted by Devaraj (1977:44), and in at least one specimen each of *S. commerson*, *S. maculatus*, and *S. sinensis*. Pleural ribs usually extend posteriorly to about the last precaudal vertebra: 12 in *Grammatorcynus*, 17–23 in *Scomberomorus*, and 31 in *Acanthocybium*.

Intermuscular bones start on the first vertebra in *Grammatorcynus*, *Acanthocybium*, and some species of *Scomberomorus*. In some specimens of at least 13 species of *Scomberomorus*, the first intermuscular bone is attached to the exoccipital on the skull, and in *S. concolor*, *S. koreanus* (also noted by Devaraj 1977), and *S. sierra*, it appears to be the usual condition. *Grammatorcynus* has 19–21 pairs of intermuscular bones, many more than *Acanthocybium* (only 10 pairs, which seems odd given its high number of vertebrae and pleural ribs), but fewer than most species of *Scomberomorus* (20–30 pairs).

Caudal complex Three preural centra support the caudal fin in *Grammatorcynus*. In *Scomberomorus* four or five preural centra support the caudal fin, and in *Acanthocybium* there are five. The urostyle represents a fusion of preural centrum 1 and the ural centrum (Potthoff 1975). The urostyle is fused with the triangular hypural plate posteriorly and articulates with the uroneural dorsally. In *Grammatorcynus* there is very little compression of the preural centra. Preural centrum 4 is not shortened at all, preural centrum 3 is shortened slightly, and preural centrum 2 is shortened slightly more (Collette and Russo 1985b:fig. 39). In *Acanthocybium* and *Scomberomorus*, preural centra 2–4 are compressed more than any of the preural centra in *Grammatorcynus*, but still not as much as the centra in the bonitos and tunas (Collette and Chao

1975, Gibbs and Collette 1967). In *Grammatorcynus* the posterior-most neural and haemal spine bend away from the vertebral axis and parallel the dorsal and ventral edges of the hypural plate. In *Acanthocybium* and *Scomberomorus*, three posterior neural and haemal spines bend away from the vertebral axis more abruptly than in *Grammatorcynus*.

Table 4
Number of dorsal spines, second dorsal fin rays, and dorsal finlets in *Grammatorcynus*.

	Spines			Rays			Finlets		
	11	12	13	10	11	12	6	7	8
G. bilineatus	4	65	1	10	55	4	61	9	
G. bicarinatus		10		10			1	9	1

The triangular hypural plate is composed of 5 fused hypural bones (Potthoff 1975). In some specimens of *Grammatorcynus* (*G. bilineatus* 453 and 521 mm FL, and *G. bicarinatus* 563 mm FL) the dorsalmost (hypural 5) is partially fused with the dorsal part of the hypural plate (hypurals 3–4). However, in smaller specimens (382–424 mm FL) such fusion was absent, as is the case in *Scomberomorus* and *Acanthocybium*. There is a primitive hypural notch present on the middle of the posterior margin of the hypural plate. This notch is a remnant of the fusion of the dorsal part of the hypural plate with the ventral part (hypurals 1–2). The notch is absent in the more advanced bonitos and tunas (Collette and Chao 1975).

The parhypural is separate from the ventral hypural plate in *Grammatorcynus* and *Scomberomorus* but is fused with it in *Acanthocybium*. This fusion was also noted by Conrad (1938), Fierstine and Walters (1968), and Devaraj (1977). The two haemal arches preceding the parhypural are autogenous in the three genera, although Devaraj (1977) stated that they were fused with their centra in *Acanthocybium*.

The parhypural has a strongly-hooked process, the parhypurapophysis (or hypurapophysis), at its proximal end. The parhypurapophysis slopes slightly upwards similarly in *Grammatorcynus* and *Scomberomorus*. In *Acanthocybium* it has a right angle and then a level projection.

There are two epurals as in other scombrids (Potthoff 1975). In shape and size, the anterior epural (1) resembles the neural spine of adjacent preural centrum 3. The smaller, posterior epural (2) is a free splint located between the anterior epural and the uroneural and fifth hypural, which are joined together.

Dorsal and anal fins *Grammatorcynus* usually has 12 dorsal spines, rarely 11 or 13 (Table 4), fewer than either *Scomberomorus* (12–22) or *Acanthocybium* (23–27). Dorsal spine counts are roughly correlated with vertebral number: *Grammatorcynus* has the fewest precaudal, caudal, and total vertebrae, and the fewest dorsal spines, while *Acanthocybium* has the most precaudal and total vertebrae, and the most dorsal spines.

Table 5
Number of anal fin rays and finlets in *Grammatorcynus*.

	Rays			Finlets		
	11	12	13	5	6	7
G. bilineatus	12	42	17	1	61	8
G. bicarinatus	5	3	1		3	7

The range in number of second dorsal fin rays is 10–25 in the three genera. *Grammatorcynus* has 10–12 rays, 10 in *G. bicarinatus* and usually 11 in *G. bilineatus* (Table 4). There are usually more second dorsal rays in *Acanthocybium* (11–16) and *Scomberomorus* (15–25).

Dorsal finlets number 6–11 in the three genera. *Grammatorcynus* has 6–8, usually 7 in *G. bicarinatus*, and usually 6 in *G. bilineatus* (Table 4). *Acanthocybium* has 7–10, and *Scomberomorus* has 6–11. The total number of second dorsal elements is the same in both species of *Grammatorcynus*, 11+6=17 in *G. bilineatus*, 10+7=17 in *G. bicarinatus*.

Anal fin rays show a similar trend to that of dorsal fin rays. The range in the three genera is 11–29. *Grammatorcynus* has 11–13 (Table 5), similar to *Acanthocybium* (11–14), but much fewer than *Scomberomorus* (15–29).

Anal finlets range in number from 5 to 12 in the three genera. *Grammatorcynus* has 5–7, usually 6 in *G. bilineatus*, and usually 7 in *G. bicarinatus* (Table 5), generally fewer than *Acanthocybium* (7–10) or *Scomberomorus* (5–12). Again, the total number of anal elements is the same in both species, 12+6=18 in *G. bilineatus*, 11+7=18 in *G. bicarinatus*.

Pectoral girdle The pectoral girdle consists of the girdle itself (cleithrum, coracoid, and scapula), the radials to which the pectoral fin rays attach, and a chain of bones that connect the girdle to the rear of the skull (posttemporal, supracleithrum, supratemporal, and two postcleithra).

Posttemporal The posttemporal (Fig. 22) is a flat elliptical bone with two sturdy anterior processes that attach the pectoral girdle to the neurocranium. The median (dorsal) process articulates with the dorsal surface of the epiotic. The lateral (ventral) process is shorter, round in cross section, and its hollow anterior end articulates with the dorsal protuberance of the intercalar. There is a thin shelf visible between these two processes in *G. bicarinatus* (Fig. 22d) and *Scomberomorus* (Fig. 22a), but this shelf is hidden behind the flat, posterior portion of the bone in *G. bilineatus* (Fig. 22c) and *Acanthocybium* (Fig. 22b). A variably-sized notch is present at the middle of the posterior edge of the flat body of the bone. *Grammatorcynus* usually has a distinct, variably-sized anteriorly directed spine on the ventral margin of the median process about one-third of the distance from the body of the bone to the anterior tip of the process. In *Acanthocybium*, there is a separate process extending anteriorly from the ventral wall of the median process. This auxillary process (Kishinouye 1923) is as long or almost as long as the median process itself. It ends in a series of several pointed processes. (Both Conrad 1938 and Devaraj 1977 referred to the auxillary process as the median process.) The lengths of the median and lateral processes vary among the species under discussion. The lengths were measured from the midpoint of the shelf that connects the two processes, to the end of the processes. Both the median and lateral processes are longer, relative to the length of the entire bone, in *G. bilineatus* where the shelf is hidden posteriorly (median process is 53–60% length of entire bone, and lateral process is 35–40%) than in *G. bicarinatus* where the shelf is not hidden, and is found more near the midpoint of the bone (median process is 49% and lateral process is 30%). In *Acanthocybium* (shelf hidden) the median process is 56–65% the length of the entire bone, and the lateral process is 27–37%. In *Scomberomorus* (shelf evident) the median process is 36–51% and the lateral process is 15–36%.

Another useful taxonomic character is the presence (if present, shape is important) or absence of a spine or process at the base of the lateral process on the inner surface of the posttemporal. It is present as a wide flap in *Grammatorcynus* (Fig. 22c,d), a blunt process in *Acanthocybium* (Fig. 20b), and as a shelf with a point in *S. commerson*, *S. munroi*, *S. niphonius*, *S. plurilineatus* (Fig. 22a), and sometimes in *S. sinensis*. It is absent or small and inconspicuous in the other 13 species of *Scomberomorus*.

Supracleithrum The supracleithrum is an ovate bone, overlapped dorsolaterally by the posttemporal and overlapping the anterior part of the dorsal wing-like extension of the cleithrum. The anterior border of the bone on the mesial side is thickened into a ridge.

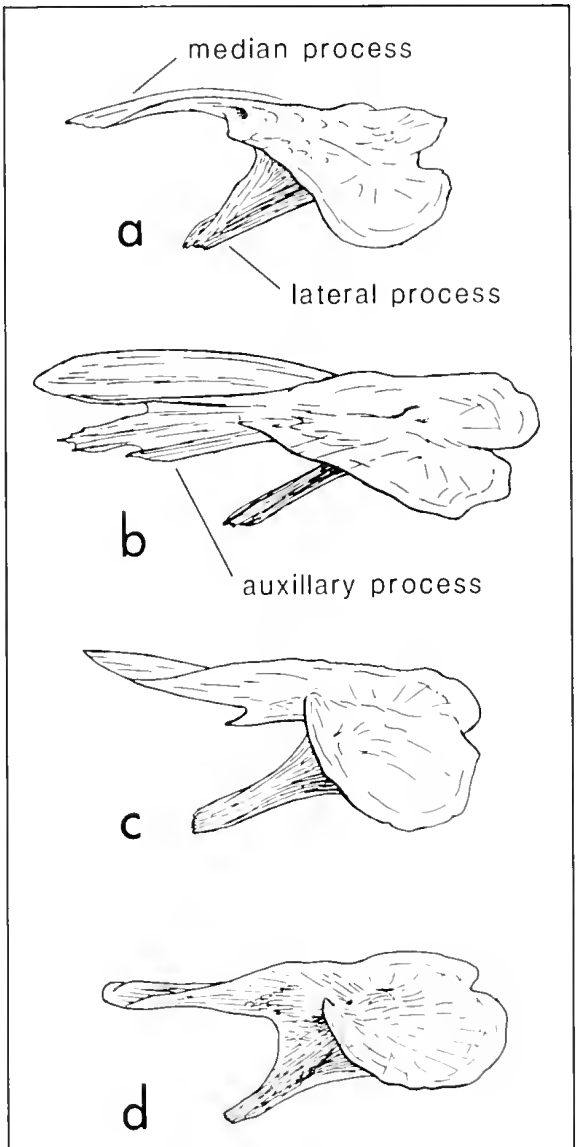

Figure 22
Lateral view of left posttemporals. (a) *Scomberomorus plurilineatus*, South Africa, 910 mm FL, 1×; (b) *Acanthocybium solandri*, Revillagigedos Is., 1068 mm FL, 1×; (c) *Grammatorcynus bilineatus*, Queensland, 521 mm FL, 1.5×; (d) *G. bicarinatus*, Western Australia, 565 mm FL.

Dorsally there is a small handle-shaped process that curves into the posterior margin to end in a notch at the posterodorsal aspect. Both the anterior and posterior borders are extended so that they form humps in *Grammatorcynus* (Collette and Russo 1985b: fig. 41). A branch of the lateralis system extends from the posterior notch of the posttemporal onto the supracleithrum. This short canal lies ventral to the dorsal process of the supracleithrum and extends to the posterior edge of the bone.

The maximum width of the supracleithrum varies from 43 to 75% of the total length of the bone in the three genera. It is widest in *Grammatorcynus*, width 72–82% (89% in one 475 mm FL specimen of *bilineatus*) of length (due to the extensions of anterior and posterior borders). *Scomberomorus* varies in width from 43% in *S. multiradiatus* to 62% in *S. niphonius*. There is no evidence that size is a factor in the size of the supracleithrum in *Grammatorcynus* as was noted by Collette and Russo (1985b) for *Scomberomorus*.

The dorsal process is prominent in *Grammatorcynus*, *S. cavalla*, *S. commerson*, *S. lineolatus*, and especially in *Acanthocybium*. In other species of *Scomberomorus*, it is either small or less sharply set off from the main body of the supracleithrum.

Supratemporal The supratemporal is a thin flat bone having three distinct arms and lying just underneath the skin where its lateral arm articulates with a dorsal articular surface on the pterotic. The anteriormost arm is the longest, while the ventrally directed arm is the shortest. The arm directed posteriorly is intermediate in length. The anterior margin is deeply concave, and the greatly convex posterior margin slightly overlaps the dorsal arm of the posttemporal.

The supratemporal bears a prominent lateral line canal that extends out almost to the tips of all three arms (Collette and Russo 1985b: fig. 42). In these three genera, the canal along the anterior margin of the bone is the longest, and the canal along the lateral side is next longest. In *Grammatorcynus*, the first canal is not branched like it is in most species of *Scomberomorus*, and the second canal is relatively longer.

Cleithrum The main body of the cleithrum is crescent-shaped with an anterodorsal spine and a posteriorly projecting plate at the upper end (Collette and Russo 1985b: fig. 43). The angle between the spine and the plate is much smaller in *Grammatorcynus* and *Scomberomorus* than in *Acanthocybium*. In *Grammatorcynus*, the spine does not extend as far dorsally as the plate. In *Acanthocybium* and most species of *Scomberomorus*, the spine extends about equally as far dorsally as the plate, and in *S. sinensis* the spine extends well beyond the dorsal margin of the plate. In *Grammatorcynus* and most species of *Scomberomorus*, the plate narrows posteriorly. The posterior plate is longer and of uniform width in *Acanthocybium*.

The lower part of the cleithrum is large and folded back upon itself as two walls: one lateral and the other mesial, which meet at their anterior margins and run parallel to each other. The mesial wall of the cleithrum forms a large triangular slit with the coracoid. In *Grammatorcynus* and *Scomberomorus*, the lateral wall of the cleithrum is narrow enough to allow part of the slit to be visible in a lateral view. This slit is hidden in lateral view in the species of *Scomberomorus* because of the great width of the lateral wall of the cleithrum (Devaraj 1977:46, Collette and Russo 1985b: figs. 43a–b).

Coracoid The coracoid is elongate and more or less triangular in shape. It connects with the scapula along its dorsal edge and with the mesial shelf of the cleithrum anterodorsally and anteroventrally. The coracoid is relatively wider in *Grammatorcynus* and *Scomberomorus* than in *Acanthocybium*.

Scapula The anterior margin of the scapula connects to the mesial shelf of the cleithrum. This attachment extends to the posterior projecting plate anterodorsally. The scapula is attached to the coracoid posteriorly and with the first two radials posterodorsally. The posterodorsal margin of the scapula is drawn out into a facet that accepts the most anterior ray of the pectoral fin. The scapula is pierced by a large, usually round, foramen near the lateral margin with the inner shelf of the cleithrum. A prominent suture leads to the dorsal and ventral margin of the scapula from the foramen. The suture is intermediate in size in *Grammatorcynus* relative to the large sutures present in *Acanthocybium*, *S. brasiliensis*, and *S. regalis*, and the small suture in *S. koreanus*.

Radials The four radials differ in size and shape and attach directly to the thickened posterior edges of the scapula and coracoid. The size of the radials increases posteroventrally. Small foramina are located beween the 2nd and 3rd and the 3rd and 4th radials counting posteriorly. In *Grammatorcynus* the first two radials, and sometimes a small portion of the third, attach to the scapula; the second two, sometimes only one and a large portion of the second, attach to the coracoid. In *Acanthocybium* and *Scomberomorus* the upper one-third of the third radial, along with the first two radials, always attaches to the scapula, and the ventral two-thirds of the third radial plus the fourth radial attach to the coracoid. A much larger foramen is present between the largest (fourth) radial and the coracoid. Posteriorly, this foramen is framed by a posterior process of the upper part of the fourth radial meeting an anterior process from the posterior margin of the coracoid. This process is only slightly developed in *Grammatorcynus*. The foramen is about equal in size to, or larger than the scapular foramen in *Grammatorcynus* and *Scomberomorus*, whereas in *Acanthocybium* the scapular foramen is much larger.

Pectoral fin rays The first (uppermost and largest) pectoral fin ray articulates directly with a posterior process of the scapula. The other rays attach to the radials. The number of pectoral rays varies from 19 to 26 in the three genera. *Grammatorcynus* has 21–26

pectoral fin rays, similar to *Acanthocybium* (22–26). *Scombermorus* shows greater variation (19–26) in this character and in most species averages less than either *Grammatorcynus* or *Acanthocybium*. There is a slight difference in number of pectoral fin rays between the species of *Grammatorcynus*: *G. bilineatus* has a range of 22–26, mode 25, $\bar{x}$ 24.4; *G. bicarinatus* 21–24, mode 24, $\bar{x}$ 23.2 (Table 6).

Table 6
Number of pectoral fin rays in *Grammatorcynus*.

	21	22	23	24	25	26	*N*	$\bar{x}$
G. bilineatus		1	11	19	27	4	62	24.4
G. bicarinatus	1	2	2	6			11	23.2

First postcleithrum The posterior projecting plate of the cleithrum has its posterior end attached to the first postcleithrum which connects ventrally to the second postcleithrum. The lamellar first postcleithrum has a narrower upper end and a wider, rounded lower margin (Fig. 23). The upper end is concave in *Grammatorcynus* (Fig. 23c–d) and pointed in both *Scomberomorus* (Fig. 23a) and *Acanthocybium* (Fig. 23b). The width of the postcleithrum varies from 46 to 62% of the length of the bone in *Grammatorcynus*. It is narrower in *G. bicarinatus* (width 46–52% of length, Fig. 23d) than in *G. bilineatus* (55–62%, Fig. 23c). In *Acanthocybium* (47–48%, Fig. 23b) the width is similar to that of *G. bicarinatus*. Species of *Scomberomorus* (Fig. 23a) have narrower postcleithra (24–41%) than the other two genera.

Second postcleithrum The second postcleithrum is broad and lamellar at the upper part with a short pointed ascending process and a long styliform descending process. *Grammatorcynus* (Fig. 24d) differs strikingly from *Acanthocybium* (Fig. 24c) and *Scomberomorus* (Fig. 24a–b) in having a distinct process extending anteriorly from the broad lamellar portion of the bone. The long descending process is so thin in most specimens that an accurate measurement of its length is nearly impossible because some portion of it usually breaks off. No differences were detected in this bone between the two species of *Grammatorcynus*.

Pelvic girdle The pelvic fin rays (I,5) attach directly to the paired basipterygia that make up the pelvic girdle. The bones are united along the midline and are imbedded in the ventral abdominal wall, free from contact with other bones. Each basipterygium is composed of three main parts: a wide anterodorsal plate, a thin, flat anterior process, and a strong posterior process.

To compare the pelvic girdles, the lengths of the three parts were measured from their bases to their tips. *Grammatorcynus* has the longest anterior process (46–51% of the length of the anterodorsal plate, Fig. 25d), *Acanthocybium* has the next longest (35–47%, Fig. 25c), and *Scomberomorus* the shortest (15–52%, Fig. 25a–b). *Grammatorcynus* (29–33%, Fig. 25d) and *Acanthocybium* (30–39%, Fig. 25c) have shorter posterior processes than the species of *Scomberomorus* (20–90%, Fig. 25a–b).

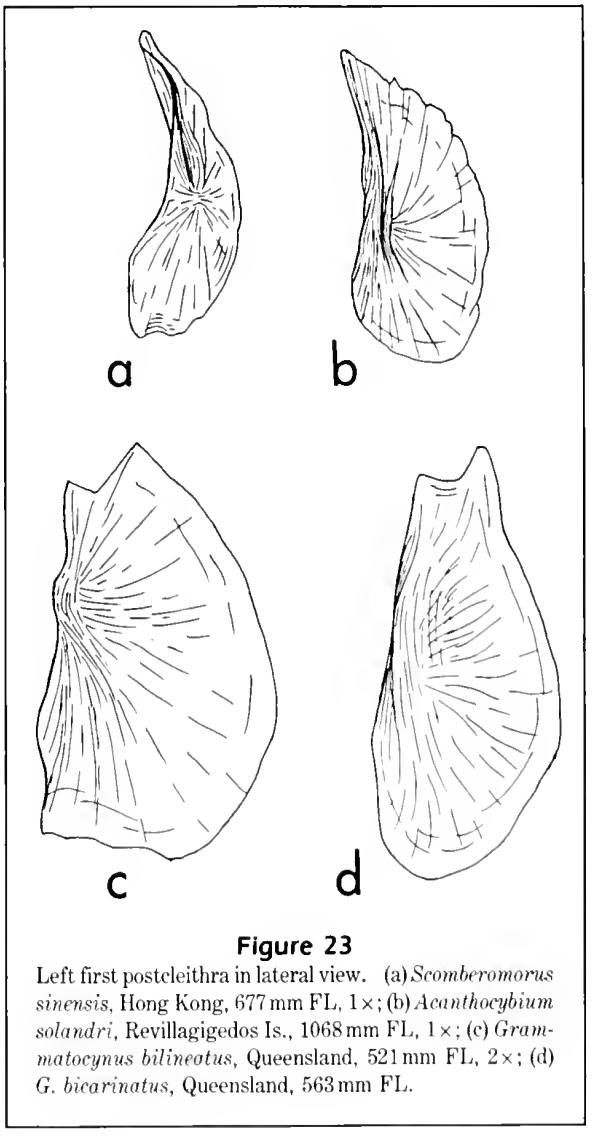

Figure 23
Left first postcleithra in lateral view. (a) *Scomberomorus sinensis*, Hong Kong, 677 mm FL, 1×; (b) *Acanthocybium solandri*, Revillagigedos Is., 1068 mm FL, 1×; (c) *Grammatocynus bilineatus*, Queensland, 521 mm FL, 2×; (d) *G. bicarinatus*, Queensland, 563 mm FL.

Grammatorcynus, some individuals of *Acanthocybium*, and several species of *Scomberomorus* have longer anterior than posterior processes. The lengths of the anterior process as a percentage of the posterior process are: *Grammatorcynus* (154–158%), *Acanthocybium* (91–156%), and *Scomberomorus* species (42–121%).

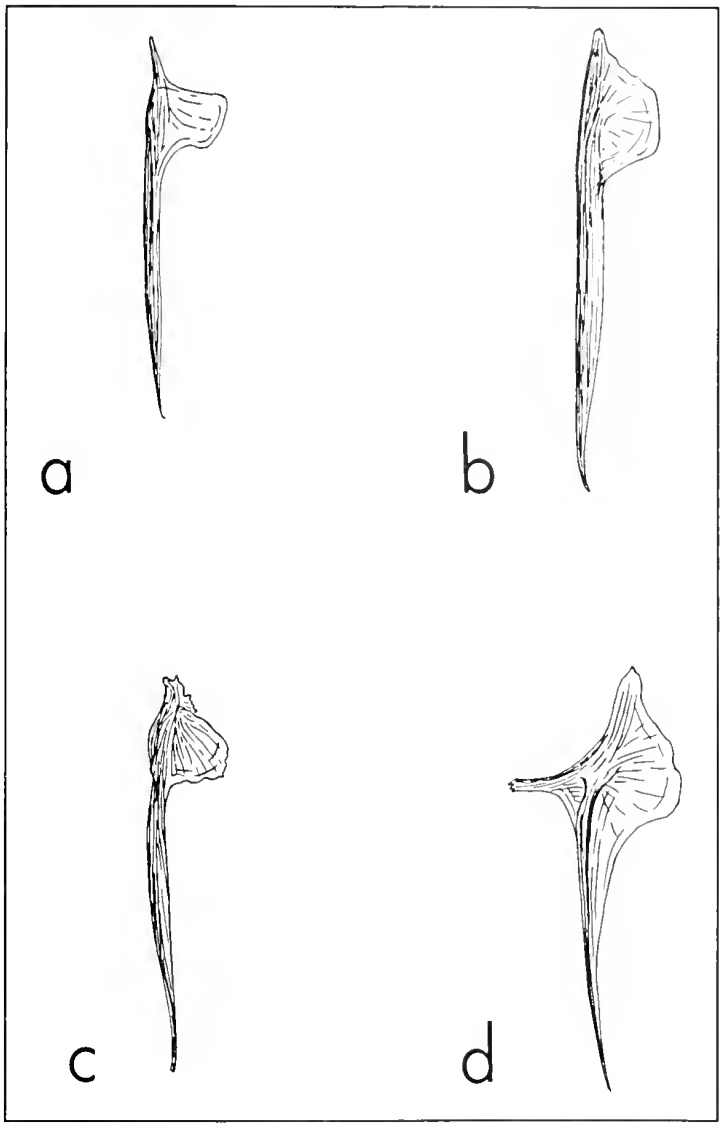

Figure 24
Left second postcleithra in lateral view. (a) *Scomberomorus queenslandicus*, Great Barrier Reef, 641 mm FL, 1×; (b) *S. koreanus*, Indonesia, 480 mm FL, 1.5×; (c) *Acanthocybium solandri*, Revillagigedos Is., 1068 mm FL, 1×; (d) *Grammatorcynus bilineatus*, Queensland, 382 mm FL, 2×.

Grammatorcynus differs from most other scombrids in having a single fleshy interpelvic process. *Auxis* and *Gymnosarda* also have a single interpelvic process; very large in the former, moderate-sized in the latter.

Part 2: Systematics and biology

Grammatorcynus Gill 1862

Grammatorcynus Gill 1862: 125 (original description; type-species *Thynnus bilineatus* Rüppell 1836 by original designation).
Nesogrammus Evermann and Seale 1907: 61 (original description; type-species *Nesogrammus piersoni* Evermann and Seale 1907 by original designation, = *Grammatorcynus bilineatus*).

Figure 25 (below)
Right basipterygia of the pelvic girdle in mesial view. (a) *Scomberomorus regalis*, Miami, FL, 469 mm FL, 1.5×; (b) *S. lineolatus*, Palk Strait, India, 428 mm FL, 2×; (c) *Acanthocybium solandri*, Miami, FL, 1403 mm FL, 1×; (d) *Grammatorcynus bilineatus*, Queensland, 521 mm FL, 1.5×.

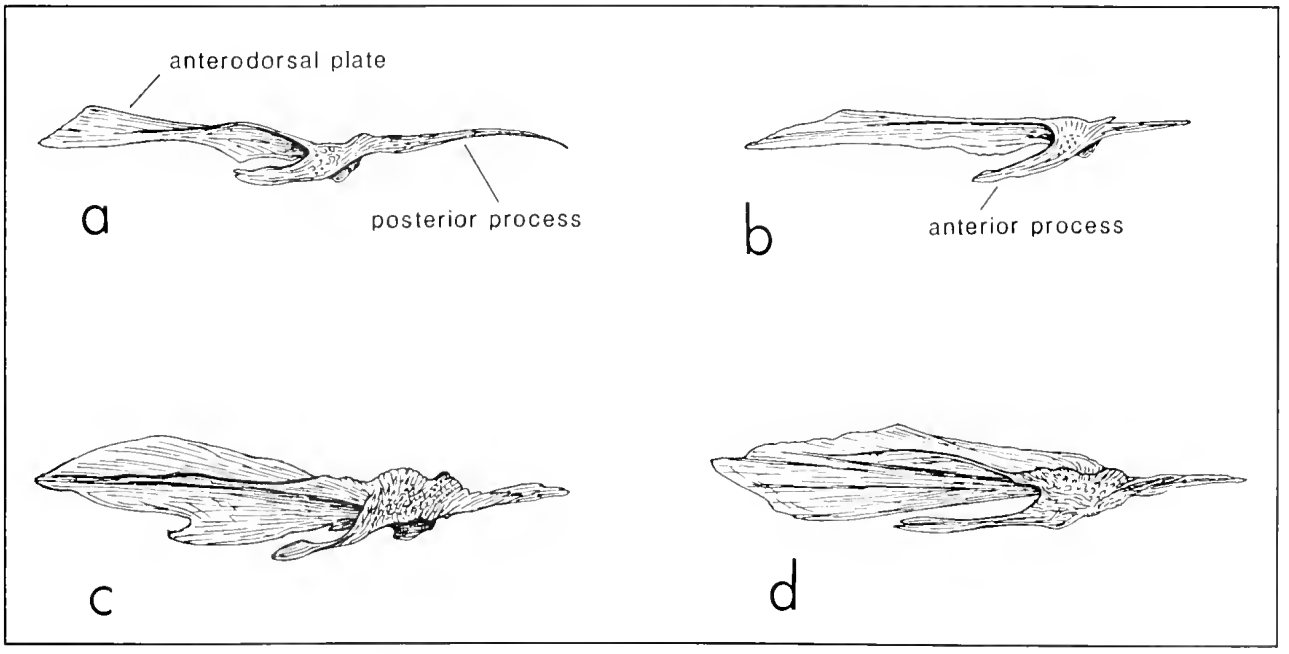

Diagnosis *Grammatorcynus* differs from all other scombrid genera in having a second ventral lateral line, and it differs from all other scombrids and billfishes in lacking a triangular bony stay on the fourth pharyngeal toothplate (Johnson 1986). Like the Scombrini, it has a low number of vertebrae (31) and the caudal fin rays are supported by only the last three vertebrae. Like the Scomberomorini, it has a well-developed median keel on the caudal peduncle, but it lacks the bony support for the keel that is present in bonitos and higher tunas. *Grammatorcynus* differs from *Scomberomorus* in having a pineal window, a single interpelvic process, and large scales.

Collette and Russo (1985b: 612) reported that *Grammatorcynus bilineatus* differed from *Scomberomorus* and *Acanthocybium* in 16 osteological characters. *Grammatorcynus bicarinatus* also differs in 15 of those 16 characters: **(1)** supracleithrum wide, 72–89% of length (narrow, 42–62% in *Scomberomorus* and *Acanthocybium*); **(2)** pores absent along dorsal branch of supratemporal (present); **(3)** nasal bones protrude far beyond ethmoid region (do not protrude far beyond); **(4)** posterior end of urohyal tripartite (forked); **(5)** glossohyal with large tooth patch fused to dorsal surface of bone (no fused tooth patch); **(6)** hyomandibula narrow, 34–39% of length (wide, 39–52%); **(7)** angle of lateral and medial arms of fourth epibranchial more acute (less acute); **(8)** anterior process of second epibranchial elongate (shorter); **(9)** three vertebrae support caudal fin rays (four or five vertebrae); **(10)** distinct anterior process on second postcleithrum (no such process); **(11)** anterior end of first postcleithrum notched (pointed); **(12)** first two pectoral radials attach to scapula (upper one-third of third radial also attaches to scapula); **(13)** jaw teeth conical (compressed and triangular); **(14)** shaft of parasphenoid narrow and concave or flat (wider and convex); and **(16)** posterior edge of ectopterygoid long, 63–72% of ventral distance (short, 41–63%). Unlike *G. bilineatus*, *G. bicarinatus* resembles *Scomberomorus* and *Acanthocybium* in having the upper margin of the dentary longer than the lower margin **(15)**.

Relationships Larval characters of *Grammatorcynus bilineatus* (as described by Wade 1951 from eight specimens 8.5–17.5 mm FL) were used by Okiyama and Ueyanagi (1977, 1978) and Ueyanagi and Okiyama (1979) to construct an "index of primitiveness" that divided the Scombrinae into four groups: mackerels, *Grammatorcynus*, tunas, and Spanish mackerels and bonitos. Nishikawa (1979) expanded the description of larvae based on 62 specimens, 4.75–56.9 mm SL, from Papua New Guinea. Nishikawa (1979) and Jenkins (1989) noted that *Grammatorcynus* larvae have preopercular spines characteristic of higher scombrids but absent in *Scomber* and *Rastrelliger*.

Lewis (1981) examined Australian scombrids electrophoretically and found that the two *Grammatorcynus* species showed fixed differences at 6 (23%) of 26 loci (GPD, ADA, ADH, GDA, PK_2, and PGM_1). Fixed differences were also observed at several other loci not used in his study, namely AD_2 and XO. He analyzed the electrophoretic data phenetically and cladistically. The two most parsimonious Wagner networks involved 308 steps. The species of *Grammatorcynus* were always paired and well-separated from

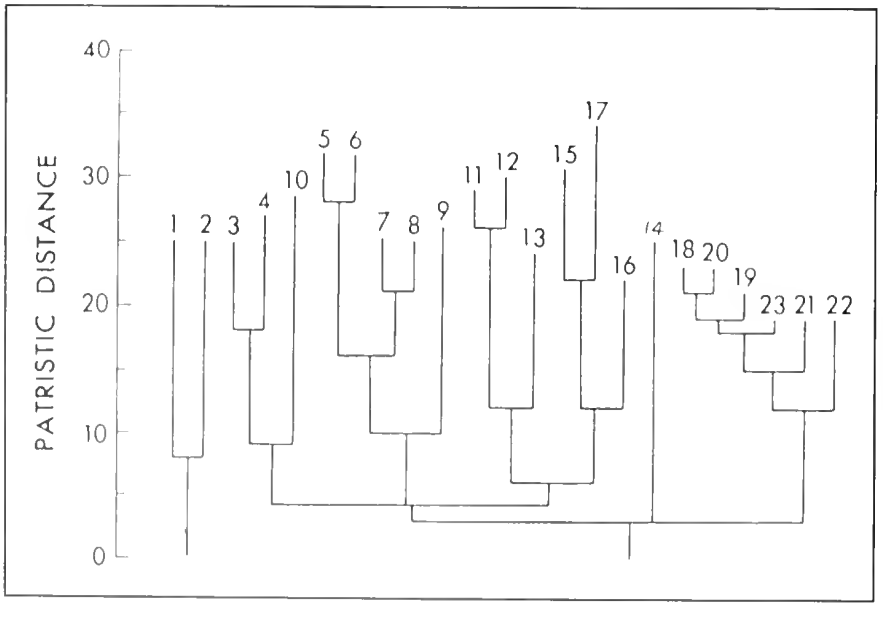

Figure 26
One of two equally parsimonious Wagner networks for 23 Australian species of Scombridae expressed in dendrogram form (from Lewis 1981: fig. 6.4). (1) *Scomber australasicus*, (2) *Rastrelliger kanagurta*, (3) *Grammatorcynus bicarinatus*, (4) *G. bilineatus*, (5) *Scomberomorus commerson*, (6) *S. queenslandicus*, (7) *S. multiradiatus*, (8) *S. semifasciatus*, (9) *S. munroi*, (10) *Acanthacybium solandri*, (11) *Sarda australis*, (12) *S. orientalis*, (13) *Cybiosarda elegans*, (14) *Gymnosarda unicolor*, (15) *Auxis* sp., (16) *Euthynnus affinis*, (17) *Katsuwonus pelamis*, (18) *Thunnus albacares*, (19) *T. tonggol*, (20) *T. obesus*, (21) *T. alalunga*, (22) *T. maccoyii*, (23) *T. thynnus orientalis*.

other Scomberomorini (Fig. 26). They were most often linked with *Acanthocybium* and then with species of *Scomberomorus*.

Based on both adult and larval morphological characters and Lewis' electrophoretic data, *Grammatorcynus* is clearly more advanced than the mackerels (Scombrini) and less advanced than the higher scombrids. Collette et al. (1984:fig. 312) placed it between *Gasterochisma* and the Scombrini on the one hand, and the more advanced Scomberomorini, Sardini, and Thunnini on the other hand. Collette and Russo (1985a,b) used *Grammatorcynus* as the primary outgroup in assessing relationships of the species of *Scomberomorus*. In his reappraisal of scombroid relationships, Johnson (1986: fig. 1 and p. 38–39) placed *Grammatorcynus* in its own tribe, Grammatorcynini, above the Scombrini, as the sister group of higher scombroids, which included the Sardini (including the Thunnini), Scomberomorini, Acanthocybiini, and billfishes.

Grammatorcynus bilineatus (Rüppell, 1836) Double-lined or scad mackerel

Thynnus bilineatus Rüppell 1836:39–40 (original description, Red Sea), pl. 12, fig. 2. Günther 1860: 366–367 (description). Klunzinger 1871:443 (Red Sea). Meyer 1885:270 (Celebes).

Grammatorcynus bilineatus. Gill 1862:125 (*T. bilineatus* type species of new genus). Kishinouye 1923: 413–415 (description, anatomy; Ryukyu and Marshall Is.), fig. 10 (skeleton); pl. 16, fig. 8 (transverse section of vertebrae; pl. 34, fig. 62 (drawing). Hardenberg 1935:137–138 (description; W Java Sea). Okada 1938:170 (E. Indies, Red Sea; nijiyō saba). Morice 1953:36–40 (anatomy; after Kishinouye 1923). Schultz 1960:411–412 (description; Bikini, Marshall Is.). Kuronuma 1961:16 (listed, Vietnam). Lewis 1968:51 (Eniwetok, Marshall Is., infested with parasitic copepod *Caligus asymmetricus*). Collette 1983: 715–716 (distinguished from *G. bicarinatus*), fig. 1A. Collette and Nauen 1983:39–40 (description, range, fig.). Collette et al. 1984:608 (fig. 326, larva after Nishikawa 1979), 618 (larvae). McPherson 1984 (color pattern in Queensland, fig.). Masuda et al. 1984: 224–225 (description); color pl. 220A. Collette and Russo 1985a:141–144 (outgroup for *Scomberomorus*). Collette and Russo 1985b (anatomy, osteology, figures, comparisons with *Scomberomorus*). Allen and Russell 1986:101 (Scott Reef, NW Australia). Grant 1987:362–363 (scad mackerel; Queensland; color photo 769). Allen and Swainston 1988: 144 (Dampier Archipelago northwards, NW Australia), 145 (color painting 966). Bauchot et al. 1989: 657 (large brain, encephalization index of 226). Zug et al. 1989:14 (Rotuma I.). Randall et al. 1990:443 (description, range), color plate VIII-14 (painting).

Nesogrammus piersoni Evermann and Seale 1907 (original description; Bulan, Sorsogon Province, Luzon, Philippine Is.); pl. 1, fig. 3.

Grammatorcynus bicarinatus not of Quoy and Gaimard 1825. Herre 1931:33 (Balabac and Jolo, Philippine Is.). Fraser-Brunner 1950:156 (synonymy), fig. 25. Umali 1950:9 (Zamboanga and Jolo, Philippine Is.). Warfel 1950:18 (Philippine Is.), fig. 13 (drawing of fish, gill arch, and liver). Wade 1951:456–458 (8 larvae, 8.5–17.5 mm; Philippine Is.), fig. 2 (8.5 mm specimen), fig. 3 (17.5 mm specimen). de Beaufort 1951:215–216 (description, synonymy), fig. 36. Herre 1953:248 (synonymy). Dung and Royce 1953: 168–169, table 97 (morphometric data on 17 specimens 408–580 mm FL, western Marshall Is.). Matsubara 1955:519 (2 lateral lines; range), fig. 222B. Munro 1958b:262–263 (New Guinea region records; CSIRO C492, New Hanover, examined). Jones et al. 1960:136 (Ross I., Port Blair, Andaman Is.). Collette and Gibbs 1963a:25 (monotypic genus). Collette and Gibbs 1963b:27 (description), pl. 7. Jones and Silas 1963:1781 (synonymy, Indian Ocean references, range). Silas 1963:811–833 (description, synonymy, synopsis of biological data). Kamohara 1964:34 (Miyako-jima, Ryukyu Is.). Jones and Kumaran 1964:364–365, figs. 70–71 (larvae, after Wade 1951). Jones and Silas 1964a:16,18 (description, synonymy, range), pl. 4, fig. (449 mm female from Port Blair, Andaman Is.). Jones and Silas 1964b:258 (in key; Andaman Is.). Gorbunova 1965: 55 (references to Wade 1951 and Silas 1963). Tongyai 1966:6 (in key), 17 (pl. 1, outline fig. of specimen from Phuket I.). Kamohara 1967:43 (description). Munro 1967:197–198 (description of *G. bicarinatus*; New Guinea specimens are *G. bilineatus*). Ben-Tuvia 1968:35 (Entedibir Is., Red Sea), fig. 3g. Ben-Yami 1968:40 (schools probably occur in region of Sahlak Archipelago, southern Red Sea). Jones 1968:998 (occur in catches in Andaman area). Jones 1969:26 (Laccadive Archipelago, India). Tongyai 1970:558 (Thai common names; Indian Ocean coast of Thailand). Tongyai 1971:3–5 (description, Thai common names, Thai distribution). Shiino 1972:70 (common names). Richards and Klawe 1972:72 (references to larvae). Gushiken 1973:49 (color photograph of 60 cm specimen from Okinawa). Helfman and Randall 1973:151 (Palau; common names mokorokor and biturturch). Magnuson 1973:350 (correlation of size, pectoral fin length, and presence of swim bladder). Lewis et al. 1974:83,87 (Bismarck Archipelago, Papua New Guinea). Springer et al. 1974:40 (Indonesia). Romimohtairo et al. 1974:35

(Gamber Bay, Gag I., Indonesia). Gorbunova 1974:26 (fig. 2, after Wade 1951). Orsi 1974:174 (listed, Vietnam). Masuda et al. 1975:256 (color photograph F), 79 (description; Okinawa southward). Cressey 1975: 216 (parasitic copepod *Shiinoa occlusa* from nasal cavity of a specimen from N. Celebes). Kailola 1975:235 (5 collections from Papua New Guinea). Uyeno and Fujii 1975:14 (table 1, comparison of caudal complex with other scombrids). Fourmanoir and Laboute 1976:183 (description; New Caledonia), color photograph. Shiino 1976:229 (common names). Anonymous 1977:15 (table 4, Bagaman I., Louisiade Archipelago, Papua New Guinea). Klawe 1977:2 (table 1, range). Collette 1979:29 (characters, range). Céng and Yāng 1979:472–473 (description; Sisha Is., South China Sea), fig. 335. Yamakawa 1979:43 (Miyako-jima, Ryukyu Is., after Kamohara 1964). Joseph et al. 1979:38 (range, figure). Nishikawa 1979:125–140 (early development; 62 postlarval and juvenile specimens, mostly from Papua New Guinea). Shirai 1980:64 (description, Ryukyu Is.), color photograph. Cressey and Cressey 1980:46 (parasitic copepod fauna: *Shiinoa occlusa* and *Caligus asymmetricus*). Rau and Rau 1980: 512–513 (description, Philippine Is.). Jones and Kumaran 1981:581–582 (description; Laccadive Archipelago), fig. 494. Wang 1981:161 (listed; S. China Sea). Johannes 1981:156–157 (biology, Palau). Lewis 1981:13 (species B, scad; maximum size 60cm FL, 3 kg), photograph. Kyushin et al. 1982:249 (description, common name nijō-saba), color photograph (specimen from Milne Bay, New Guinea). Cressey et al. 1983:238 (systematic position of genus), 264 (parasitic copepod fauna; 4 species of *Caligus* added). Lewis et al. 1983:7 (table 2, 203 specimens, 380–630mm FL; Fiji). Wass 1984:31 (Fiji; common name "namuauli"). Masuda et al. 1984:224–225 (description, Japan), pl. 220A. Gillett 1987:20 (caught by Satawal tuna fishermen, central Caroline Is.). Nishikawa and Rimmer 1987:5 (larval description; fig. 5, larva, postlarva, and juvenile from Nishikawa 1979). Dyer et al. 1989:65 (monogenean *Caballerocotyla* sp. from Okinawa specimen). Rivaton et al. 1989:67 (listed, New Caledonia).

Grammatorcynnus (sic) *bicarinatus* not of Quoy and Gaimard 1825. Roux-Estève and Fourmanoir 1955:201 (Abulat I., Red Sea).

Grommatorcynus (sic) *bicarinatus* not of Quoy and Gaimard 1825. Zhang 1981:302 (description of 3 larvae, Sisha Is., South China Sea; fig. 1, 6.4mm larva).

Grammatorcynos (sic) *bilineatus*. Myers 1988:168 (listed, Mariana Is.). Myers 1989:254 (description; range), underwater photo 134A, 280 (listed; Caroline, Mariana, and Marshall Is.).

Diagnosis *Grammatorcynus bilineatus* has more gill rakers (18–24 vs. 12–15), a larger eye (4.1–6.0% vs. 3.1–4.6% FL), lacks black spots on the lower sides of its body, and does not reach as large a size (max. 600mm FL) as *G. bicarinatus*.

Description Dorsal spines 11–13, usually 12; rays 10–12, usually 11; finlets 6, rarely 7 (Table 4). Anal fin with one spine, 11–13, usually 12 rays; 6 finlets, rarely 5 or 7 (Table 5). Pectoral fin rays 22–26, usually 24 or 25 (Table 6). Gill rakers on first arch 18–24, usually 21, $\bar{x}$ 20.8 (Table 3). Upper jaw teeth 14–37, $\bar{x}$ 23.5 (left), 24.5 (right) (Table 2); lower jaw teeth 12–32, $\bar{x}$ 18.6 (left), 19.1 (right) (Table 2). Morphometric data summarized in Table 1.

Grammatorcynus bilineatus has a longer neurocranium (14–16% FL vs. 13%), longer parasphenoid flanges (18–21% of neurocranium length vs. 14%), higher maximum number of teeth on the upper (37 vs. 25) and lower (32 vs. 23) jaws, higher posterior expansion of the maxilla (8–11% of maxilla length vs. 6–8%), longer quadrate process (134–145% of quadrate length vs. 122–125%), wider first postcleithrum (55–62% of length vs. 46–52%), narrower ethmoid (19–21% of length vs. 25–28%), narrower vomer (13–15% of length vs. 16–18%), narrower lachrymal (27–30% of length vs. 30–35%), shorter teeth (up to 4% of dentary length vs. up to 6%), narrower palatine tooth patch (26–32% of length vs. 38–42%), narrower opercle (63–72% of length vs. 72–79%), and the shelf between the posttemporal processes is hidden behind the flat posterior portion of the bone.

Color In life, the back is bright pale green, the upper sides and belly silvery, and there are no black spots on the belly as there are in *G. bicarinatus* (Grant 1987: 363). Underwater, it is reported to display a distinctive white patch on the caudal peduncle (McPherson 1984). There are color photographs of fresh specimens from Japan (Masuda et al. 1975:256, Shirai 1980:64), New Caledonia (Fourmanoir and Laboute 1976:183), South China Sea (Kyushin et al. 1982:249), and Australia (Grant 1987: fig. 769). An underwater photograph has been published from Micronesia (Myers 1989: photo 134A). There is a color painting in Randall et al. 1990 (pl. VIII-14).

Size Maximum size is about 63cm FL, 3.3kg weight (Lewis et al. 1983). Maturity seems to be attained at about 40–43cm FL (Silas 1963, Johannes 1981, Lewis et al. 1983).

Biology The best summary of biological information on *G. bilineatus* is Silas (1963). It is an epipelagic species found mostly in shallow reef waters where it

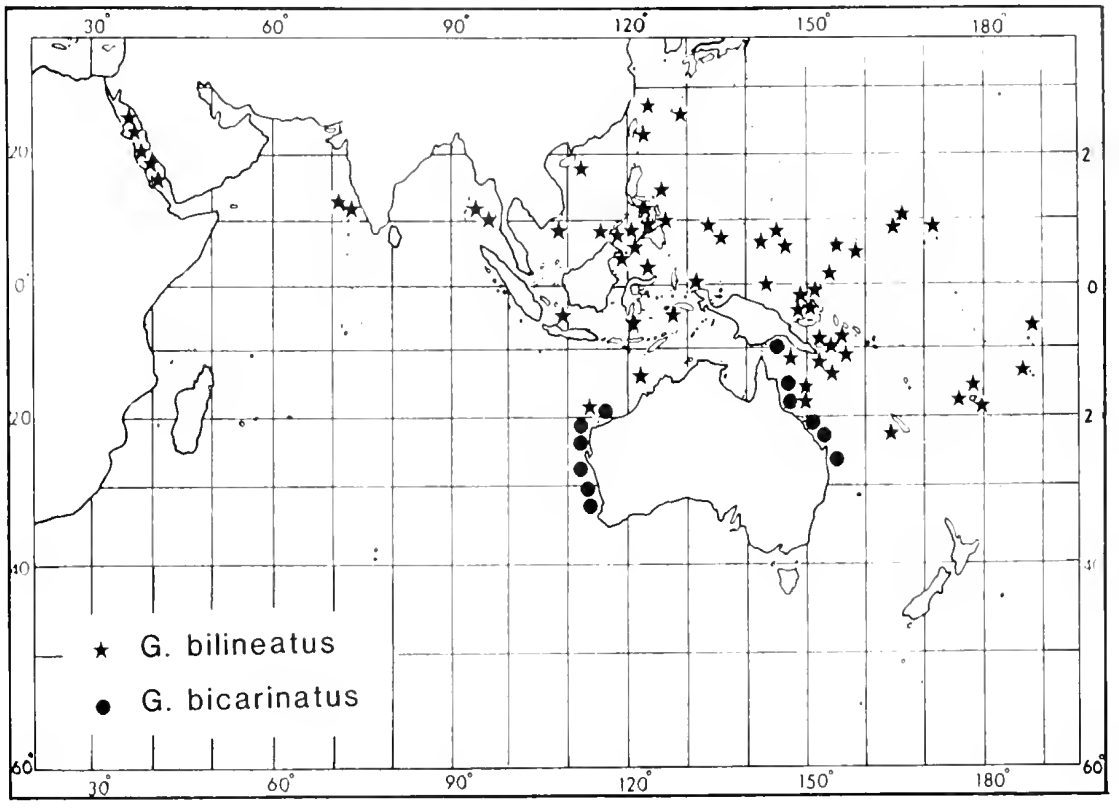

Figure 27
Distribution of *Grammatorcynus* based on specimens examined and literature records.

forms large schools. The spawning season in Fiji extends from October through March (Lewis et al. 1983). Larvae and juveniles have been illustrated from the Philippines (Wade 1951), Papua New Guinea (Nishikawa 1979), and the South China Sea (Zhang 1981). Food includes adult and juveniles of crustaceans and fishes, particularly clupeoids such as *Sardinella* and *Thrissocles*, but also includes other fishes such as *Sphyraena* and *Balistes* (Silas 1963:831).

Parasites Six species of parasitic copepods have been reported from *G. bilineatus* (Cressey and Cressey 1980, Cressey et al. 1983): Shiinoidae: *Shiinoa occlusa* Kabata; Caligidae: *Caligus asymmetricus* Kabata, *C. regalis* Leigh-Sharpe, *C. bonito* Wilson, *C. pelamydis* Krøyer, and *C. productus* Dana. The monogenean *Caballerocotyla* sp. was found on an Okinawan specimen (Dyer et al. 1989).

Interest to fisheries Double-lined mackerel are taken incidentally with hand lines off Port Blair, Andaman Islands (Silas 1963). It is common in the offshore zones of Fiji but is only occasionally seen in Fiji markets (Lewis et al. 1983). The flesh is reported to be mild and pleasantly flavored but it is necessary to remove the kidney tissue before cooking to avoid the ammonia smell. This characteristic has given rise to one of the Palauan names for the species, biturchturch, which means urine (Johannes 1981:187). It is valued for marlin bait in Queensland (McPherson 1984).

Range Widespread near coral reefs in the tropical and subtropical Indo-West Pacific (Fig. 27). Based on literature, specimens examined, and photographs, known from the Red Sea, Andaman Sea, East Indies, Philippines, South China Sea, Ryukyu Islands, New Guinea (New Britain, New Ireland, New Hanover, and the Louisiade Archipelago), Australia (northern Western Australia, from Dampier Archipelago north and Queensland), Solomon Islands, New Caledonia, Caroline Islands, Marshall Islands, Fiji, Tonga, and Tokelau Islands (photograph from Fakaofo Atoll received from Robert Gillett, Regional Fishery Support Programme, Suva, Fiji, Aug. 1985).

Table 7

Morphometric comparison of *Grammatorcynus bilineatus* from the Red Sea and the western Pacific Ocean.

	Red Sea					Western Pacific Ocean				
Character	*N*	Min	Max	Mean	SD	*N*	Min	Max	Mean	SD
Fork length (thousandths)	15	264	432	364	53	44	226	575	430	72
Snout-A	15	592	628	615	11	41	581	641	603	12
Snout-2D	15	534	557	547	7	41	528	619	548	16
Snout-1D	15	287	306	296	7	44	276	322	295	10
Snout-P2	15	249	271	261	7	43	236	306	257	12
Snout-P1	15	220	244	230	7	43	199	245	224	9
P1-P2	15	94	135	105	9	43	90	111	100	5
Head length	15	213	234	220	6	44	197	236	218	8
Max. body depth	13	182	213	201	8	40	164	234	193	15
Max. body width	12	97	122	111	8	40	91	136	115	9
P1 length	14	110	142	122	9	44	106	142	128	7
P2 length	14	74	81	77	2	44	70	87	76	4
P2 insertion-vent	14	312	352	333	12	43	262	354	326	15
P2 tip-vent	13	242	275	256	11	43	228	273	249	9
Base 1D	15	207	246	230	10	43	211	261	236	10
Height 2D	12	88	109	98	6	37	88	116	99	7
Base 2D	14	88	114	102	8	43	79	118	102	8
Height A	11	84	102	93	7	34	82	114	96	7
Base A	14	74	89	84	4	44	73	101	88	7
Snout (fleshy)	15	77	86	81	3	44	58	90	79	5
Snout (bony)	15	71	78	74	3	44	60	80	71	5
Maxilla length	15	95	108	101	4	43	89	107	97	5
Postorbital	15	89	98	93	2	43	78	98	91	4
Orbit (fleshy)	15	44	57	49	4	44	40	60	49	4
Orbit (bony)	15	60	75	68	5	44	53	88	68	7
Interorbital	15	58	67	62	3	43	56	74	62	3
2D-caudal	15	458	475	468	5	41	427	496	471	16
Head length (thousandths)	15	62	94	80	11	44	50	126	94	16
Snout (fleshy)	15	340	384	369	11	44	248	397	365	22
Snout (bony)	15	313	351	336	11	44	281	357	326	18
Maxilla length	15	443	469	459	8	43	420	480	443	14
Postorbital	15	397	433	420	12	43	350	450	419	16
Orbit (fleshy)	15	206	253	222	13	44	191	257	226	15
Orbit (bony)	15	283	336	307	15	44	252	381	313	27
Interorbit	15	268	298	283	9	43	253	327	284	14

Geographic variation The wide range of *G. bilineatus* plus the gaps in distribution due to its preference for coral reef habitats lead to the possibility that some populations differ morphologically from others. However, comparison of frequency distributions by geographic areas of meristic characters summarized in Tables 2–6 showed general uniformity in the range and modes of these characters. The Red Sea population is the most isolated from the rest, but it showed no meristic differentiation. Comparisons of ranges and means of morphometric data showed few differences between the Red Sea and Pacific populations (Table 7).

Dissections 11 (382–521 mm FL). USNM 270386 (410), Australia, diss. 1-28-69. USNM 270390 (453), Scott Reef, J. McCosker 73-8, diss. 4-1-76. USNM 270387 (424), Marshall Is., J. E. Randall, diss. 4-29-76. USNM 270384 (382), Kavieng, New Guinea, diss. 10-12-76. USNM 270385 (389), Cairns, Qld., G. McPherson, diss. 3-30-81. USNM 270389 (521), Port Douglas, Qld., diss. 3-31-81. USNM 270388 (416), Cairns, Qld., G. McPherson, diss. 1-5-83. USNM 270383 (475), Scott Reef, J. McCosker 72-18, diss. 1-10-83. USNM 270382 (399), Cairns, Qld., G. McPherson, diss. 1-11-83. USNM 270391 (400), Port Douglas, Qld., diss. 1-13-83. USNM 316130 (460), Scott Reef, J. McCosker 73-8, diss. 7-18-89.

Material examined 80 specimens (23.5–575 mm FL) from 58 collections.

Red Sea 16 (264–440) from 10 collections. SMF 2755 (1, 287); Massua; E. Rüppell; holotype of *Thynnus bilineatus*; stuffed. NMW uncat. (5, 362–432); Jambo; 1895–96; I.R.M. Exped. 62c. NMW uncat. (1, 424); Hassani; 1895–96; I.R.M.

Exped. 62b. NMW uncat. (1, 360); Djeddah; 1895–96; I.R.M. Exped. 62. NMW uncat. (2, 264–320); Rothes Meer; 1879–80; Klunzinger. NMW 16825 (2, 304–382); Rothes Meer; Klunzinger. MNHN 52–28 (1, 422); Mer Rouge; "Calypso". USNM 266928 (1, 327); near Entedebir; March 1962; ISRSE 4144. HUJ E62/4399 (1, 368); S Red Sea; March–April 1962; Israel; S Red Sea Exped. BPBM 28388 (1, 440); Saudi Arabia, Jeddah market; 11 May 1982; J.E. Randall.

Andaman Sea 4 (235–294) from 2 collections. MFLB uncat. (2, 282–294); Thailand, Phuket Province; 23 Feb. 1966. MFLB uncat. (2, 235–237); Thailand, Phuket Province; 27 Jan. 1970.

East Indies 4 (108–413) from 4 collections. BMNH 1872. 4.6.25(1, 413); N. Celebes; Meyer. AMNH 17583 (1, 108) Celebes. USNM 213564 (1, 395); Indonesia, Ambon fish market; V.G. Springer; 19 March 1974. USNM 213565 (1, 360); Indonesia, Buton I., Teluk Buton; V.G. Springer and M.F. Gomon; VGS 74-26; 28 March 1974.

Philippine Islands 5 (275–390) from 5 collections. USNM 55899 (1, 372); Luzon, Sorsogon Province, Bulan; C.J. Pierson; holotype of *Nesogrammus piersoni*. USNM 195044 (1, 343); Cebu market; 6 April 1908; Albatross. CAS SU 13575 (1, 275); Balabac I.; A.W.C.T. Herre; 1929. CAS SU 13687 (1, 342); Jolo; A.W.C.T. Herre; 1931. CAS SU 40469 (1, 390); Gulf of Leyte, Leyte; R.F. Annereaux; 12 Sept. 1945.

Okinawa ZUMT 16738 (1, 378); Okinawa. ZUMT 52381 (1, ca. 500); Okinawa, Ishigaki I.; 4 June 1966.

New Guinea 10 (23.5–410) from 6 collections. CSIRO C.492 (1, 226); New Hanover, Drei Inseln Harbor, Kulineva R. USNM 270384, 316162 (2, 363–382); New Ireland, Kavieng; 20 March 1976. DASF 4247 (1, 23.5); New Britain; Borgen Bay; 13 April 1972. DASF 4248 (1, 37.9); New Britain; Tavanatangir; 11 Oct. 1972. DASF 4250 (2, 54.3–65.5); New Britain; Dikarua I.; Cape Lambert; 28 Nov. 1972. USNM 320095 (3, 385–410); Hermit Is., E side Jalun I.; 2 Nov. 1978.

Australia 9 (389–521) from 4 collections. USNM 270383 (1, 475); Western Australia, Scott Reef; J.E. McCosker 72-18. USNM 270390, 316130 (2, 453–460); Western Australia, Scott Reef, 14°05′S, 121°50′E; J.E. McCosker 73-8. USNM 270382, 270385, 270388, 316161 (4, 389–416); Queensland, Cairns; G. McPherson and P. Cooper. USNM 270389, 270391 (2, 400–521); Queensland, off Port Douglas; Sept.–Oct. 1976.

Solomon Islands 2 (275–482) from 2 collections. USNM 205078 (1, 482); New Georgia, Gizo I.; W. Chapman; 30 May 1944. AMS I.19435-020 (1, 275); Solomon Is.; G. Smith.

Caroline Islands 15 (327–575) from 13 collections. CAS GVF 651 (1, 462); Palau Is., Rattakadakoru; Palau 145; 5 Sept. 1955. CAS GVF 933 (1, 439); Palau Is., Velasco Reef; Palau 147; 6 Oct. 1956. CAS GVF 934 (1, 432); Palau Is., Velasco Reef; Palau 148; 6 Oct. 1956. CAS GVF 946 (1, 454); Palau Is., Velasco Reef; Palau 149; 6 Oct. 1956. CAS GVF 1422 (1, 543); Palau Is., Ilruthapel I.; Palau 57–42; 20 Oct. 1957. CAS GVF 1867 (1, 461); Palau Is.; Palau 59–39; 15 April 1959. CAS GVF 1891 (1, 444); Palau Is., Angaur I.; Palau sta. 59-63; 16 June 1959. CAS GVF 1970 (2, 543–575); Palau Is., Kossol Passage, 7°56′18″N, 134°31′55″E; sta. 59-709; 30 July 1959. BPBM 10501 (2, 434–448); Palau; 23 April 1964. USNM 264910 (1, 510); between Ponape and Ant Atoll; R.A. Croft; 1983. CAS GVF (1, 408); Kapingamarangi, 1°6′N, 154°44′W; sta. 108; 4 Aug. 1958. CAS GVF 405 (1, 327); Kapingamarangi; sta. 102; 2 Aug. 1954. CAS GVF 33 (1, 462); Ifaluk; 2 Oct. 1953.

Marshall Islands 9 (254–549) from 7 collections. USNM 140986 (2, 419–468); Bikini Atoll lagoon, V. Brock and J. Marr; 2 April 1946. USNM 142054 (2, 503–549); Bikini Atoll lagoon off Bikini I.; V. Brock and J. Marr; 25 March 1946. USNM 142055 (1, 410) Bikini Atoll, W of Boro I., V. Brock; 6 April 1946. USNM 181932 (1, 382); Majuro Atoll; A.F. Bartsch; 1958. BPBM uncat. (1, 254); Majuro Atoll; P. Shiota; 30 Aug. 1972. USNM 270387 (1, 424); Enewetak Atoll; J.E. Randall; 2 April 1976. BPBM 12800 (1, 330); Enewetak; 4 April 1972; J.E. Randall.

Fiji Islands 2 (335–426) from 2 collections. USNM 176657 (1, 426); S of Suva; J.K. Howard; 4–15 Dec. 1952. USNM 243969 (1, 335); reef NNE Malamala I., V.G. Springer 82-24; 24 May 1982.

Rotuma Island USNM 285517 (396); Rotuma; G.D. Johnson; 14 May 1986.

Samoan Islands USNM 305080 (1, 465); American Samoa, East Bank, 12 mi. off E end of Tutuila; 1 July 1989.

Grammatorcynus bicarinatus (Quoy and Gaimard, 1825) Shark mackerel

Thynnus bicarinatus Quoy and Gaimard 1825:357 (original description; Baie des Chiens-Marins (= Shark Bay), W. Australia), pl. 61, fig. 1.

Grammatorcynus bicarinatus. McCulloch 1915:266–269 (description; off Cook I., near Tweed River Heads, New South Wales; 925 mm FL, 18.75 lbs.), pl. 1, fig. 1. Ogilby 1918:101 (reference to McCulloch 1915; caught off Moreton Bay, Queensland), 105 (30-lb. specimen in Queensland state fish market). McCulloch 1922:106 (New South Wales; rarely captured; to 3 ft.). McCulloch and Whitley 1925:142 (Moreton Bay, Queensland). McCulloch 1929:263–264 (synonymy). Anonymous 1945:7 (listed among marketable fish of Cairns, Queensland area). Whitley 1947:129 (W. Australia). Whitley 1948:24 (listed, W. Australia). Coates 1950:22 (Great Barrier Reef; 25 lbs. maximum; "shark mackerel"), fig. Serventy 1950:20 (common in W. Australia from Geraldton northwards but not extending in waters of the Kimberly Division of W. Australia). Munro 1958a:112 (description; Queensland, N New South Wales, and W. Australia), fig. 748 (after McCulloch). Whitley 1964a:232 (length to 48 in., weight 25 lb.), 239 (fig. 4f, range in Australia only), pl. 4 (fig. b, after McCulloch). Whitley 1964b:48 (listed). Marshall 1964:367 (description, Queensland), color plate 53, fig. 354. Grant 1965:176 (description after Munro 1958a; sought-after market fish in

Queensland), fig. Marshall 1966: 205 (description), color plate 53, fig. 354. Munro 1967:197–198 (text is based on Australian *G. bicarinatus*; New Guinea specimens are *G. bilineatus*), fig. 333. Grant 1972: 107 (same as 1965), fig. Coleman 1974:42 (color, habits), 43 (underwater color photograph, Heron I., Queensland). Grant 1975:165 (same as 1972), fig. Rohde 1976:50 (Lizard I., Queensland). Anonymous 1978:18 (listed among species being investigated by Queensland Fisheries Service). Grant 1978:195 (same as 1975), fig. Hutchins 1979:83 (may visit Rottnest I., W. Australia). Coleman 1981:268 (Australia, habits), color underwater photo (from Coleman 1974). Lewis 1981:12 (species A, shark mackerel; maximum size 110cm FL, 13.5kg) photograph. Grant 1982:632 (same as 1978 plus comments on ammonia smell of flesh). Collette 1983:716–718 (distinguished from *G. bilineatus*), fig. 1B. Collette and Nauen 1983:39–40 (description, range, fig.). Hutchins and Thompson 1983:62, 85 (W. Australia), p. 63 (fig. 290). Russell 1983:146 (Heron I., Barrier Reef based on Coleman 1974). McPherson 1984 (color pattern in Queensland, fig.). Collette and Russo 1985b:547 (in key). Hutchins and Swainston 1986: 102 (description, range), 103 (color painting 587), 141 (weight to 11.7kg). Grant 1987: 362 (shark mackerel; Queensland; color photo 768). Allen and Swainston 1988:144 (Geographe Bay north, Western Australia), 145 (color painting 965). Hutchins 1990:275 (sight record, Shark Bay, Western Australia). Randall et al. 1990:433 (description, range), color plate VII-13 (painting).

Diagnosis *Grammatorcynus bicarinatus* has fewer gill rakers (12–15 vs. 18–24), a smaller eye (3.1–4.6% vs. 4.1–6.0% FL), small black spots on the lower sides of its body, and reaches a larger maximum size (1100 mm FL) than *G. bilineatus*.

Description Dorsal spines 12; rays 10, finlets usually 7, rarely 6 or 8 (Table 4). Anal spines 1, rays 11–13, finlets 6 or 7, usually 7 (Table 5). Pectoral fin rays 21–24, $\bar{x}$ 23.2 (Table 6). Gill rakers on first arch 12–15, $\bar{x}$ 14.1 (Table 3). Upper jaw teeth 14–25, $\bar{x}$ 20.5 (left), 20.9 (right) (Table 2); lower jaw 15–23, $\bar{x}$ 17.5 (left), 17.6 (right) (Table 2). Morphometric data summarized in Table 1.

Grammatorcynus bicarinatus has a shorter neurocranium (13% vs. 14–16% FL), shorter parasphenoid flanges (14% vs. 18–21% neurocranium length), a lower maximum number of teeth on the upper (25 vs. 37) and lower (23 vs. 32) jaws, lower posterior edge of shank of maxilla (6–8% vs. 8–11% maxilla length), shorter quadrate process (122–125% vs. 134–145% quadrate length), narrower first postcleithrum (46–52% vs. 55–62% length), wider ethmoid (25–28% vs. 19–21% length), wider vomer (16–18% vs. 13–15% neurocranium length), wider lachrymal (30–35% vs. 27–30% length), longer teeth (maximum 6% vs. 4% dentary length), wider palatine tooth patch (38–42% vs. 26–32% length), wider opercle (72–79% vs. 63–72% length), and a thin posttemporal shelf between the anterior processes.

Color General color in life is bright, glowing green above, grading into the silver of the sides and belly, which is marked with scattered small black spots that are absent in *G. bilineatus* (Grant 1987:362). Underwater, it is reported to display a dark band along the lower lateral line (McPherson 1984). Color photographs have been published by Marshall (1964 and 1965: pl. 53, fig. 354) and Grant (1987: photo 768), and there are color paintings in Hutchins and Swainston (1986:103), Allen and Swainston (1988:965), and Randall et al. (1990: plate VIII-13). An underwater photograph was published by Coleman (1974:43 and 1981:268).

Size Maximum size is 110–130cm FL and 11.6–13.5 kg weight (Lewis 1981, Hutchins and Swainston 1986, Allen and Swainston 1988).

Biology Shark mackerel form dense concentrations near individual bays and reefs in Barrier Reef waters. With the rising tide, they move into shallow water over the reef flats, feeding on schools of clupeoid fishes (Grant 1982).

Interest to fisheries Shark mackerel are fished off Western Australia, the Northern Territory, Queensland, and northern New South Wales (Grant 1987). It is regarded as a light-tackle sportsfish with commercial value in Queensland (McPherson 1984). The name shark mackerel comes from the ammonia-like smell noticed when the fish is being filleted. This odor can be masked by brushing the fillets with lemon juice prior to cooking (Grant 1982, 1987).

Range Found over coastal reefs of all Australian warm waters (Grant 1987) with occasional stragglers south to 30° on both east (Cook I., New South Wales) and west (Shark Bay, Western Australia) coasts (Fig. 27) and in the Gulf of Papua (A.D. Lewis, South Pacific Comm., Noumea, pers. commun.). The apparent gap in distribution may be due to ecological reasons, the scarcity of reef habitats along the north coast of Australia, or to historical reasons, as outlined by Springer and Williams (1990).

Dissections 4 specimens (563–765mm FL). USNM 270392 (563), Cairns, Qld., diss. 1-3-83. USNM 316126 (765),

Exmouth Gulf, WA, B. Hutchins, diss. 1-18-83. USNM 316127-8 (2, 625–663), Australia, diss. 7-5-89.

Material examined 11 specimens (300–765 mm FL) from 8 collections. USNM 316129 (1, 563), Queensland, Fitzroy I. S of Cairns; Jan. 1984. USNM 176832 (1, 525), Great Barrier Reef; J.K. Howard; 8 April–29 May 1952. AMS IB.5207-8 (2, 306–315), Queensland, Gladstone District; P. Gibson. USNM 316126, uncat. (2, 607–765), Western Australia, Exmouth Gulf. WAM-P 27343 (1, 825), Western Australia, N. Muiron I., 21°39′S, 114°22′E. WAM-P 25821 (1, 320), Western Australia, S. Muiron I., 21°39′S, 114°20′E. WAM-P 22974 (head only, 105 mm), Western Australia, Kendrew I., 20°29′S, 116°22′E; 21 Feb. 1973; B. Hutchins. USNM 316127-8 (2, 625–663), Australia.

Acknowledgments

The original impetus for this study came from A.D. Lewis, now with the South Pacific Commission, Noumea, New Caledonia. In the course of his doctoral dissertation on population genetics of Australian scombroids (Lewis 1981), he discovered that there were two species in the genus *Grammatorcynus*, informed us of the problem, and provided us with frozen material needed to do a thorough anatomical study. We are deeply appreciative of his interest and efforts throughout the course of this study. Sally Rothwell spent the month of February 1983 working in the Systematics Laboratory on a Careers in Biology Program from Colgate University. Her efforts made completion of the 1983 preliminary paper possible. Frozen material, vital for this study, was provided through the efforts of A.D. Lewis, J.E. McCosker (CAS), B. Hutchins (WAM), and G. McPherson (Northern Fisheries Research Center, Queensland). Several assistants, students, and colleagues participated in dissections over the years: Linda Pushee Mercer, Frances Matthews Van Dolah, Sally Rothwell, and Joseph Russo. Preserved material was made available by A. Ben-Tuvia (HUJ), B.E. Bookheim (Department of Marine and Wildlife Resources, Pago Pago, American Samoa), W.E. Eschmeyer and P. Sonoda (CAS), R.A. Croft (Ponape State Government), B. Herzig (NMW), W. Klausewitz (SMF), A.D. Lewis (then in Papua New Guinea), G.J. Nelson (AMNH), J.R. Paxton (AMS), J.E. Randall and A.Y. Suzumoto (BPBM), J.B. Hutchins (WAM), and P.J.P. Whitehead (then at BMNH). Assistance with analyzing the morphometric data was provided by Ruth Gibbons. Osteological drawings were painstakingly rendered by Keiko Hiratsuka Moore. The map was produced by Martha S. Nizinski. Participation in this study by the second author was made possible by a Smithsonian Summer Internship in Vertebrate Zoology in the summer of 1989. Drafts of the manuscript were reviewed by G. David Johnson, Thomas A. Munroe, Yosuo Nishikawa, and William Smith-Vaniz.

Citations

Allen, G.R., and B.C. Russell
1986 Part VII. Fishes. *In* Faunal surveys of the Rowley Shoals, Scott Reef and Seringapatam Reef, North-western Australia. Rec. W. Aust. Mus. Suppl. 25:75–103.

Allen, G.R., and R. Swainston
1988 The marine fishes of north-western Australia. West. Aust. Mus., Perth, 201 p.

Allis, E.P. Jr.
1903 The skull, and the cranial and first spinal muscles and nerves in *Scomber scomber*. J. Morphol. 18(1-2):45–328.

Anonymous
1945 Marketable fish of the Cairns Area. N. Queensl. Nat. Club 2, 8 p.
1977 Report on Japan-Papua New Guinea joint skipjack tagging in the PNG area, October–December, 1975 on the R/V *Fuji Maru*. Res. Devel. Div., Fish. Agency Jpn., and Fish. Div., Dep. Primary Ind., Papua New Guinea, 30 p.
1978 Major Queensland bid to track Spanish mackerel. Aust. Fish. 37(3):18–19.

Bauchot, R., J.E. Randall, J.-M. Ridet, and M.-L. Bauchot
1989 Encephalization in tropical teleost fishes and comparison with their mode of life. J. Hirnforsch. 30(6):645–669.

Ben-Tuvia, A.
1968 Report on the fisheries investigations of the Israel South Red Sea Expedition, 1962. Bull. Sea Fish. Res. Stn. Haifa 52:21–25.

Ben-Yami, M.
1968 Observations on the distribution and behaviour of pelagic schooling fish in the southern Red Sea. Bull. Sea Fish. Res. Stn. Haifa 51:31–46.

Céng, B-g., and Y. Yāng
1979 Suborders Scombroidei, Thunnioidei. *In* Fishes of the islands in the South China Sea, p. 470–488. Science Press, Beijing.

Coates, G.
1950 Fishing on the Barrier Reef and inshore. T. Willmett & Sons, Townsville, 72 p.

Coleman, N.
1974 Australian marine fishes in colour. A.H. & A.W. Reed, Sydney, 108 p.
1981 Australian sea fishes north of 30°S. Doubleday, Sydney and Auckland, 297 p.

Collette, B.B.
1979 Adaptations and systematics of the mackerels and tunas. *In* Sharp, G.D., and A.E. Dizon (eds.), The physiological ecology of tunas, p. 7–39. Academic Press, NY.
1983 Recognition of two species of double-lined mackerels (*Grammatorcynus*: Scombridae). Proc. Biol. Soc. Wash. 96(4): 715–718.

Collette, B.B., and L.N. Chao
1975 Systematics and morphology of the bonitos (*Sarda*) and their relatives (Scombridae, Sardini). Fish. Bull., U.S. 73(3): 516–625.

Collette, B.B., and R.H. Gibbs Jr.
1963a A preliminary review of the fishes of the family Scombridae. FAO Fish. Rep. 6(1):23–32.

1963b Preliminary field guide to the mackerel- and tuna-like fishes of the Indian Ocean (Scombridae). Smithson. Inst., Wash. DC, 48 p.

Collette, B.B., and C.E. Nauen

1983 Scombrids of the world. FAO Species Catalogue. FAO Fish. Synop. 125, Vol. 2, 137 p.

Collette, B.B., and J.L. Russo

1985a Interrelationships of the Spanish mackerels (Pisces: Scombridae: *Scomberomorus*) and their copepod parasites. Cladistics 1(2):141–158.

1985b Morphology, systematics, and biology of the Spanish mackerels (*Scomberomorus*, Scombridae). Fish. Bull., U.S. 82(4):545–692.

Collette, B.B., T. Potthoff, W.J. Richards, S. Ueyanagi, J.L. Russo, and Y. Nishikawa

1984 Scombroidei: Development and relationships. *In* Moser, H.G., et al. (eds.), Ontogeny and systematics of fishes, p. 591–620. Spec. Publ. 1, Am. Soc. Ichthyol. Herpetol. Allen Press, Lawrence, KS.

Conrad, G.M.

1938 The osteology and relationships of the wahoo (*Acanthocybium solandri*), a scombrid fish. Am. Mus. Novit. 1000, 32 p.

Cressey, R.F.

1975 A new family of parasitic copepods (Cyclopoida, Shiinoidae). Crustaceana 28(2):211–219.

Cressey, R.F., and H.B. Cressey

1980 Parasitic copepods of mackerel- and tuna-like fishes (Scombridae) of the world. Smithson. Contrib. Zool. 311, 186 p.

Cressey, R.F., B.B. Collette, and J.L. Russo

1983 Copepods and scombrid fishes: A study in host-parasite relationships. Fish. Bull., U.S. 81(2):227–265.

de Beaufort, L.F.

1951 Percomorphi (concluded). *In* The fishes of the Indo-Australian Archipelago 9, p. 1–242. E.J. Brill, Leiden.

de Sylva, D.P.

1955 The osteology and phylogenetic relationships of the blackfin tuna, *Thunnus atlanticus* (Lesson). Bull. Mar. Sci. Gulf Caribb. 5(1):1–41.

Devaraj, M.

1977 Osteology and relationships of the Spanish mackerels and seerfishes of the tribe Scomberomorini. Indian J. Fish. 22(1-2):1–67.

Dung, D.I.Y., and W.F. Royce

1953 Morphometric measurements of Pacific scombrids. U.S. Fish Wildl. Serv. Spec. Sci. Rep. Fish. 95, 170 p.

Dyer, W.G., E.H. Williams Jr., and L.B. Williams

1989 Monogeneans from marine fishes of Okinawa, Japan. Proc. Helminthol. Soc. Wash. 56(1):64–68.

Evermann, B.W., and A. Seale

1907 Fishes of the Philippine Islands. Bull. U.S. Bur. Fish. 26:49–110.

Fierstine, H.L., and V. Walters

1968 Studies in locomotion and anatomy of scombroid fishes. Mem. South. Calif. Acad. Sci. 6:1–31.

Fourmanoir, P., and P. Laboute

1976 Poissons de Nouvelle Calédonie et des Nouvelles Hébrides. Editions Pacifique, Papeete, Tahiti, 376 p.

Fraser-Brunner, A.

1950 The fishes of the family Scombridae. Ann. Mag. Nat. Hist., Ser. 12, 3:131–163.

Gibbs, R.H. Jr., and B.B. Collette

1967 Comparative anatomy and systematics of the tunas, genus *Thunnus*. Fish. Bull., U.S. 66(1):65–130.

Gill, T.N.

1862 On the limits and arrangement of the family of scombroids. Proc. Acad. Nat. Sci. Phila. 14:124–127.

Gillett, R.

1987 Traditional tuna fishing: A study at Satawal, Central Caroline Islands. Bishop Mus. Bull. Anthropol. 1, 48 p.

Gnanamuttu, J.C.

1971 Osteology of the Indian mackerel, *Rastrelliger kanagurta* (Cuvier). Indian J. Fish. 13(1):1–26.

Gorbunova, N.N.

1965 Seasons and conditions of spawning of the scombroid fishes (Pisces, Scombroidei). Tr. Inst. Okeanol. Akad. Nauk SSSR 80:36–61 [in Russ., Engl. summ.].

1974 A review of larvae of scombrid fishes (Scombridae, Pisces). Tr. Inst. Okeanol. Akad. Nauk SSSR 96:23–76 [in Russ., Engl. summ.].

Grant, E.M.

1965 Guide to fishes. Queensl. Dep. Harbours and Marine, Brisbane, 280 p.

1972 Guide to fishes. Queensl. Dep. Primary Ind., Brisbane, 2d ed., 472 p.

1975 Guide to fishes. Coordinator-General's Dep., Brisbane, 3d ed., 640 p.

1978 Guide to fishes. Dep. Harbours and Marine, Brisbane, 4th ed., 768 p.

1982 Guide to fishes. Dep. Harbours and Marine, Brisbane, 5th ed., 896 p.

1987 Fishes of Australia. E.M. Grant Pty Ltd., Queensl., 480 p.

Günther, A.

1860 Catalogue of the acanthopterygian fishes in the collection of the British Museum, Vol. 2. London, 548 p.

Gushiken, S.

1973 Fishes of the Okinawa Islands. Ryukyu Fish. Assoc., Naha, 247 p.

Hardenberg, J.D.F.

1935 Some new or rare fishes of the Indo-Australian Archipelago IV. Treubia 15(2):131–140.

Helfman, G.S., and J.E. Randall

1973 Palauan fish names. Pac. Sci. 27(2):136–153.

Herre, A.W.C.T.

1931 The fishes of the Herre 1931 Philippine Expedition with descriptions of 17 new species. Newspaper Enterprise Ltd., Hong Kong, 106 p. [reprinted by N.K. Gregg, Kentfield, CA].

1953 Check list of Philippine fishes. U.S. Fish Wildl. Serv. Res. Rep. 20, 977 p.

Hutchins, B.

1979 A guide to the marine fishes of Rottnest Island. Creative Research, Perth, 103 p.

1990 Fish survey of South Passage, Shark Bay, Western Australia. *In* Berry, P.F., S.D. Bradshaw, and B.R. Wilson (eds.), Research in Shark Bay, p. 263–278. Rep. France-Aust. Bicent. Exped. Comm., West. Aust. Mus., Perth.

Hutchins, B., and R. Swainston

1986 Sea fishes of southern Australia. Swainston Publ., Perth, 180 p.

Hutchins, B., and M. Thompson

1983 The marine and estuarine fishes of southwestern Australia. A field guide for anglers and divers. West. Aust. Mus., Perth, 103 p.

Iwai, T., and I. Nakamura

1964 Branchial skeleton of the bluefin tuna, with special reference to the gill rays. Bull. Misaki Mar. Biol. Inst., Kyoto Univ. 6:21–25.

Jenkins, G.P.
1989 Scombridae—Mackerels, Spanish mackerels, bonitos, tunas. *In* Leis, J.M., and T. Trnski (eds.), The larvae of Indo-Pacific shorefishes, p. 291-297. New South Wales Univ. Press, Kensington.

Johannes, R.E.
1981 Words of the lagoon. Fishing and marine lore in the Palau District of Micronesia. Univ. Calif. Press, Berkeley, 245 p.

Johnson, G.D.
1986 Scombroid phylogeny: An alternate hypothesis. Bull. Mar. Sci. 39(1):1-41.

Jones, S.
1968 The scombroid fishery of India—present and future. *In* Proc., Symp. Scombroid Fishes, Mar. Biol. Assoc. India, Symp. Ser. 1(3):994-1000.
1969 Catalogue of fishes from the Laccadive Archipelago in the reference collections of the Central Marine Fisheries Research Institute. Bull. Cent. Mar. Fish. Res. Inst. 8, 32 p.

Jones, S., and M. Kumaran
1964 Eggs, larvae and juveniles of Indian scombroid fishes. *In* Proc., Symp. Scombroid Fishes, Mar. Biol. Assoc. India, Symp. Ser. 1(1):343-378.
1981 Fishes of the Laccadive Archipelago. Nature Conserv. and Aquat. Sci. Serv., Trivandrum, 760 p.

Jones, S., and E.G. Silas
1963 Tuna and tuna-like fishes from the Indian Seas. FAO Fish Rep. 3(6):1775-1796.
1964a A systematic review of the scombroid fishes of India. *In* Proc., Symp. Scombroid Fishes, Mar. Biol. Assoc. India, Symp. Ser. 1(1):1-105.
1964b Mackerel from the Andaman Sea. *In* Proc., Symp. Scombroid Fishes, Mar. Biol. Assoc. India, Symp. Ser. 1(1): 255-282.

Jones, S., E.G. Silas, and E. Dawson
1960 New records of scombroid fishes from the Andaman-Nicobar waters. J. Mar. Biol. Assoc. India 2(1):136-137.

Joseph, J., W. Klawe, and P. Murphy
1979 Tuna and billfish-Fish without a country. Inter-Am. Trop. Tuna Comm., La Jolla, 46 p.

Kailola, P.J.
1975 A catalogue of the fish reference collection at the Kanudi Fisheries Research Laboratory, Port Moresby. Dep. Agric., Stock, Fish., Port Moresby, Res. Bull. 16, 277 p.

Kamohara, T.
1964 Fishes obtained in the Okinawa and the Yaeyama Islands. Res. Rep. Kochi Univ. 13(5):31-43 [in Jpn.].
1967 Fishes of Japan in color. Hoikusha Publ. Co., Osaka, 135 p.

Kishinouye, K.
1923 Contributions to the comparative study of the so-called scombroid fishes. J. Coll. Agric. Imp. Univ., Tokyo 8(3): 293-475.

Klawe, W.L.
1977 What is a tuna? Mar. Fish. Rev. 39(11):1-5.

Klunzinger, C.B.
1871 Synopsis der Fische des Rothen Meeres. II. Theil. Verh. Zool. Bot. Ges. Wien 21:441-668.

Kuronuma, K.
1961 A check list of the fishes of Vietnam. Div. Agric., Nat. Res., U.S. Oper. Mission Vietnam, ICA Contract IV-153, 66 p.

Kyushin, K., K. Amaoka, K. Nakaya, H. Ida, Y. Tanino, and T. Senta
1982 Fishes of the South China Sea. Jpn. Mar. Fish. Res. Cent., Tokyo, 333 p.

Leviton, A.E., R.H. Gibbs Jr., E. Heal, and C.E. Dawson
1985 Standards in herpetology and ichthyology: Part I. Standard symbolic codes for institutional resource collections in herpetology and ichthyology. Copeia 1985:802-832.

Lewis, A.D.
1981 Population genetics, ecology and systematics of Indo-Australian scombrid fishes, with particular reference to skipjack tuna (*Katsuwonus pelamis*). Ph.D. thesis, Aust. Natl. Univ. 314 p.

Lewis, A.D., B.R. Smith, and R.E. Kearney
1974 Studies on tunas and baitfish in Papua New Guinea waters—II. Dep. Agric., Stock, Fish, Port Moresby, Res. Bull. 11, 113 p.

Lewis, A.D., L.B. Chapman, and A. Sesewa
1983 Biological notes on coastal pelagic fishes in Fiji. Fish. Div. (MAF) Fiji Tech. Rep. 4:1-68.

Lewis, A.G.
1968 Copepod crustaceans parasitic on fishes of Eniwetok Atoll. Proc. U.S. Natl. Mus. 125(3656):1-78.

Magnuson, J.J.
1973 Comparative study of adaptations for continuous swimming and hydrostatic equilibrium of scombroid and xiphoid fishes. Fish. Bull., U.S. 71(2):337-356.

Magnuson, J.J., and J.G. Heitz
1971 Gill raker apparatus and food selectivity among mackerels, tunas, and dolphins. Fish. Bull., U.S. 69(2):361-370.

Mago Leccia, F.
1958 The comparative osteology of the scombroid fishes of the genus *Scomberomorus* from Florida. Bull. Mar. Sci. Gulf Caribb. 8(4):299-341.

Marshall, T.C.
1964 Fishes of the Great Barrier Reef and coastal waters of Queensland. Angus & Robertson, Sydney, 566 p.
1965 Fishes of the Great Barrier Reef and coastal waters of Queensland. Livingston Publ. Co., Narberth, PA.
1966 Tropical fishes of the Great Barrier Reef. Angus & Robertson, Sydney, 239 p.

Masuda, H., C. Araga, and T. Yoshino
1975 Coastal fishes of southern Japan. Tokai Univ. Press, Tokyo, 379 p.

Masuda, H., K. Amaoka, C. Araga, T. Uyeno, and T. Yoshino (editors)
1984 The fishes of the Japanese Archipelago. Tokai Univ. Press, Tokyo, 437 p.

Matsubara, K.
1955 Fish morphology and hierarchy. Part 1. Ishizaki Shoten, Tokyo, 789 p. [in Jpn.].

McAllister, D.E.
1968 The evolution of branchiostegals and associated opercular, gular, and hyoid bones and the classification of teleostome fishes, living and fossil. Bull. Natl. Mus. Canada 221, 239 p.

McCulloch, A.R.
1915 Notes on, and descriptions of Australian fishes. Proc. Linn. Soc. NSW 40:259-277.
1922 Check list of the fish and fish-like animals of New South Wales. Part 3. Aust. Zool. 2(3):86-130.
1929 A check-list of the fishes recorded from Australia. Aust. Mus. Mem. 5(1):1-144.

McCulloch, A.R., and G.P. Whitley
1925 A list of the fishes recorded from Queensland waters. Mem. Queensl. Mus. 8(2):125-182.

McPherson, G.
1984 Two species of double-lined mackerel (family Scombridae) in Queensland waters. Queensl. Dep. Primary Ind. Leafl., 2 p.

Meyer, A.B.
1885 Catálogo de los peces recolectados en el Archipiélago de las Indias Orientales. Ann. Soc. Españ. Hist. Nat. 14:5-49.

Morice, J.
1953 Essai systématique sur les familles des Cybiidae, Thunnidae et Katsuwonidae, poissons scombroides. Rev. Trav. Inst. Pêches Marit. 18(1):35-63.

Munro, I.S.R.
1958a Families Polynemidae to Scomberomoridae. Handbook of Australian fishes 27:109-112. Aust. Fish. Newsl. 17(10): 17-20.
1958b The fishes of the New Guinea region. Papua New Guinea Agric. J. 10(4):97-369.
1967 The fishes of New Guinea. Dep. Agric., Stock, Fish., Port Moresby, New Guinea, 650 p.

Myers, R.F.
1988 An annotated checklist of the fishes of the Mariana Islands. Micronesica 21(1-2):115-180.
1989 Micronesian reef fishes. Coral Graphics, Guam, 298 p.

Nakamura, I.
1965 Relationships of fishes referable to the subfamily Thunninae on the basis of the axial skeleton. Bull. Misaki Mar. Biol. Inst., Kyoto Univ. 8:7-38.

Nishikawa, Y.
1979 Early development of the double-lined mackerel, *Grammatorcynus bicarinatus* (Quoy and Gaimard), from the western tropical Pacific. Far Seas Fish. Res. Lab., Bull. 17:125-140.

Nishikawa, Y., and D.W. Rimmer
1987 Identification of larval tunas, billfishes and other scombroid fishes (suborder Scombroidei): An illustrated guide. CSIRO Mar. Lab. Rep. 186, 20 p.

Ogilby, J.D.
1918 Ichthyological notes (no. 4). Mem. Queensl. Mus. 6: 97-05.

Okada, Y.
1938 A catalogue of vertebrates of Japan. Maruzen Co., Tokyo, 412 p.

Okiyama, M., and S. Ueyanagi
1977 Larvae and juvenile of the Indo-Pacific dogtooth tuna, *Gymnosarda unicolor* (Rüppell). Bull. Far Seas Fish. Res. Lab., Shimizu 15:35-49.
1978 Interrelationships of scombroid fishes: An aspect from larval morphology. Bull. Far Seas Fish. Res. Lab., Shimizu 16:103-113.

Orsi, J.J.
1974 A check list of the marine and freshwater fishes of Vietnam. Publ. Seto Mar. Biol. Lab. 21(3/4):153-177.

Potthoff, T.
1975 Development and structure of the caudal complex, the vertebral column, and the pterygiophores in the blackfin tuna (*Thunnus atlanticus*, Pisces, Scombridae). Bull. Mar. Sci. 25(2):205-231.

Quoy, J.R.C., and J.P. Gaimard
1824-1825 Voyage autour du Monde,... Exécuté sur les corvettes de S. M. l'Uranie et la Physicienne, pendant les années 1817, 1818, 1819 et 1820. 3, Zoologie, 712 p.

Randall, J.E., G.R. Allen, and R.C. Steene
1990 Fishes of the Great Barrier Reef and Coral Sea. Univ. Hawaii Press, Honolulu, 507 p.

Rau, N., and A. Rau
1980 Commercial marine fishes of the Central Philippines (bony fishes). German Agcy. for Tech. Coop. (GTZ), 629 p.

Richards, W.J., and W.L. Klawe
1972 Indexed bibliography of the eggs and young of tunas and other scombrids (Pisces, Scombridae) 1880-1970. NOAA Tech. Rep. NMFS SSRF-652, 107 p.

Rivaton, J., P. Fourmanoir, P. Bourret, and M. Kulbicki
1989 Catalogue des poissons de Nouvelle-Caledonie. ORSTOM Rapp. Prov., 170 p.

Rohde, K.
1976 Monogenean gill parasites of *Scomberomorus commersoni* Lacépède and other mackerel on the Australian east coast. Z. Parasitenkde. 51:49-69.

Romimohtairo, K., M. Hutomo, and Sumarna
1974 Results of the biological observations in Gamber Bay, Gag Island with a special note on the tuna and skipjack fishing ground in Irian Jaya waters. Oseanol. Indones. 3:29-45.

Roux-Estève, R., and P. Fourmanoir
1955 Poissons capturés par le mission de la *Calypso* en Mer Rouge. Ann. Inst. Oceanogr., Paris 30:195-203.

Rüppell, E.
1836 Neue Wirbelthiere zu der fauna von Abyssinien gehörig. Fische des rothen Meeres. Frankfurt am Main, 148 p. Lfg. 6:29-52.

Russell, B.C.
1983 Annotated checklist of the coral reef fishes in the Capricorn-Bunker Group, Great Barrier Reef Australia. Great Barrier Reef Marine Park Authority, Spec. Publ. Ser. 1, 184 p.

Schultz, L.P.
1960 Suborder Scombrina. Family Scombridae: Tunas. *In* Schultz, L.P., et al., Fishes of the Marshall and Marianas Islands. Bull. U.S. Nat. Mus. 202(2):410-417.

Serventy, D.L.
1950 Tuna survey of north Australia. Aust. Fish. Newsl. 9:18-20.

Shaklee, J.B.
1983 The utilization of isozymes as gene markers in fisheries management and conservation. *In* Isozymes: Current topics in biological and medical research, vol. 11:213-247. Liss, NY.

Shiino, S.M.
1972 List of English names of Japanese fishes with proposition of new names. Sci. Rep. Shima Marineland 1, 210 p. [in Jpn. and Engl.].
1976 List of common names of fishes of the world, those prevailing among English-speaking nations. Sci. Rep. Shima Marineland 4, 262 p.

Shirai, S.
1980 (rev. ed.) Ecological encyclopedia of the marine animals of the Ryukyu Islands in colour. Okinawa Kyoiku Shuppan, 636 p.

Silas, E.G.
1963 Synopsis of biological data on double-lined mackerel *Grammatorcynus bicarinatus* (Quoy and Gaimard) (Indo-Pacific). FAO Fish. Rep. 6, vol. 2:811-833.

Smith, C.L., and R.M. Bailey
1962 The subocular shelf of fishes. J. Morphol. 110(1):1-17.

Springer, V.G., and J.T. Williams
1990 Widely distributed Pacific Plate endemics and lowered sea-level. Bull. Mar. Sci. 46(3):631-640.

Springer, V.G., Burhanuddin, and M.F. Gomon
1974 List of fishes collected during Rumphius Expedition I. Oseanol. Indones. 1:39-45.

Tongyai, M.L.P.
1966 Background notes for Spanish mackerel, (*Scomberomorus* spp.) from Thai waters, studies, 1954-1965. Thai Mar. Fish. Lab., *Scomberomorus* Rep. Paper 1, 25 p.
1970 Plah in-see, *Scomberomorus* spp., of Thailand, 1967. *In* Marr, J.D. (ed.), The Kuroshio—A symposium on the Japan Current, p. 557-564. East-West Center Press, Honolulu.
1971 A taxonomic study of the pla in-si (Pisces: Scombroidei) of Thailand. Div. Mar. Fish. Tech., Dep. Fish., Ministry Agric., Bangkok, 36 p.

Ueyanagi, S., and M. Okiyama
1979 Larval fish characters and phylogeny of scombroid fishes. Kaiyo Kaguku 11(2):93–99 [in Jpn., transl. in NMFS Proc. Rep. 82–14, NMFS, NOAA, Seattle, 24 p.].

Umali, A.F.
1950 Key to the families of common commercial fishes in the Philippines. U.S. Fish Wildl. Serv. Res. Rep. 21, 47 p.

Uyeno, T., and S. Fujii
1975 A fish fossil of the family Scombridae from a Miocene bed in Toyama Prefecture, Japan. Bull. Nat. Sci. Mus. Tokyo, Ser. C (Geol.) 1(1):11–16.

Wade, C.B.
1951 Larvae of tuna and tuna-like fishes from Philippine waters. Fish. Bull., U.S. 51:445–485.

Wang, C.
1981 Studies on the fish fauna of the South China Sea Islands, Guangdong Province, China. Oceanol. Limnol. Sin. (Suppl.) p. 137–165. [in Chinese].

Warfel, H.E.
1950 Outlook for development of a tuna industry in the Philippines. U.S. Fish Wildl. Serv. Res. Rep. 28, 37 p.

Wass, R.C.
1984 An annotated checklist of the fishes of Samoa. NOAA Tech. Rep. NMFS SSRF-781, 43 p.

Whitley, G.P.
1947 New sharks and fishes from Western Australia. Part 3. Aust. Zool. 11(2):129–150.
1948 A list of the fishes of Western Australia. West. Aust. Fish. Dep., Fish. Bull. 2, 35 p.
1964a Scombroid fishes of Australia and New Zealand. *In* Proc., Symp. Scombroid Fishes, Mar. Biol. Assoc. India Symp. Ser. 1(1):221–253.
1964b A survey of Australian ichthyology. Proc. Linnean Soc. NSW 89(1):11–127.

Yamakawa, T.
1979 Studies of the fish fauna around the Nansei Islands, Japan. 1. Check list of fishes collected by Toshiji Kamohara and Takeshi Yamakawa from 1954 to 1971. Rep. Usa Mar. Biol. Stn., Suppl. 1:1–47.

Zhang, R.
1981 On the larvae of tuna-like fishes around waters of Xisha Qundao of the Nan Hai. J. Fish. China 5(4):301–315 [in Chinese, Engl. summ.].

Zharov, V.L.
1967 Classification of the scombroid fishes (suborder Scombroidei, order Perciformes). Vopr. Ikhtiol. 7(2):209–224 [in Russ.].

Zug, G.R., V.G. Springer, J.T. Williams, and G.D. Johnson
1989 The vertebrates of Rotuma and surrounding waters. Atoll Res. Bull. 316, 25 p.

Geographic variation in cranial morphology of spinner dolphins *Stenella longirostris* in the eastern tropical Pacific Ocean

Michael E. Douglas

Oklahoma Biological Survey and Department of Zoology
University of Oklahoma, Norman, Oklahoma 73019
Present address: Department of Zoology and Museum
Arizona State University, Tempe, Arizona 85287

Gary D. Schnell
Daniel J. Hough

Oklahoma Biological Survey and Department of Biology
University of Oklahoma, Norman, Oklahoma 73019

William F. Perrin

Southwest Fisheries Science Center, National Marine Fisheries Service, NOAA
P O. Box 271, La Jolla, California 92038

Abstract.– The spinner dolphin *Stenella longirostris* is widely distributed in the eastern tropical Pacific Ocean. Geographic patterns in 30 cranial features were determined from 246 museum specimens grouped into 25 5° latitude-longitude blocks. Statistically significant sexual dimorphism was demonstrated for one-half of the cranial characters, with males generally being larger. ANOVAs, as well as principal components, canonical variates, and cluster (UPGMA and function-point) analyses demonstrated geographic variation in all characters. Patterns of geographic variation in morphology were evaluated for all *S. longirostris* specimens using Mantel tests and matrix correlations; 20 of 30 characters showed significant "regional patterning," while most (25 of 30) exhibited "local" patterning. The latitude-longitude block with specimens of *S. l. centroamericana* was distinctive in a number of features. Also, eastern spinner dolphins (*S. l. orientalis*) were smaller than spinners found to the south, southwest, or west. Many of the cranial characters exhibited a concentric pattern of geographic variation similar to that found by previous investigators for several external characters. Hawaiian specimens are the largest incorporated into this study and, typically, are more like those from southern localities than animals from geographically closer blocks. The association between morphological characters and 13 environmental measures was assessed with Mantel tests and product-moment correlations, revealing statistical concordance of morphological patterns for a number of cranial characters with those for water depth, sea surface temperature in January and July, surface salinity, thermocline depth, and surface dissolved oxygen. Several of these environmental variables manifest the same distributional pattern found in many of the cranial features.

Manuscript accepted 9 December 1991.
Fishery Bulletin, U.S. 90:54–76 (1992).

Information on geographic variation of dolphins in the eastern tropical Pacific is of intrinsic scientific interest, but also has practical implications because fishermen in the region kill dolphins in the course of purse-seining for yellowfin tuna (Allen 1985). Tuna in the region associate with schools of dolphins, primarily *Stenella* spp. and *Delphinus delphis*, and the fishermen set their nets on the schools to capture the tuna below them. In the process, many dolphins die, as many as 80,000–125,000 annually in recent years (Hall and Boyer 1988, 1989, 1990). The U.S. Government has used a series of management units, or stocks, in regulating this exploitation of the dolphins by U.S. vessels. For the spinner dolphin, these have been the eastern spinner, Costa Rican spinner, northern whitebelly spinner, and southern whitebelly spinner stocks (Perrin et al. 1985). These divisions are based on morphology, including body length and shape, color pattern, shape of the dorsal fin, and cranial characters. The Costa Rican form occurs close to the coast of Central America and is relatively large, with relatively long beak, erect to forward-canted dorsal fin, and monotonic gray coloration. The eastern form is smaller, with shorter beak; it also has the erect or canted fin and is gray overall, but with light patches in the axillary and genital areas. The whitebelly forms have a tripartite color pattern of dark gray, light gray, and (ventrally) white, and the dorsal fin is highly variable, ranging in adults from falcate to erect. The northern and southern stocks were divided based on modal differences in cranial measurements; the boundary is at the Equator. The eastern spinner and northern whitebelly spinner stocks overlap broadly; overlap between the eastern spinner and southern whitebelly spinner is very slight (Perrin et al. 1985). Dolphins killed in the fishery are identified to stock based on the modal appearance of adults in the school and, in the case of the two whitebelly stocks, location.

Most recently, Perrin (1990) described three subspecies of *Stenella*

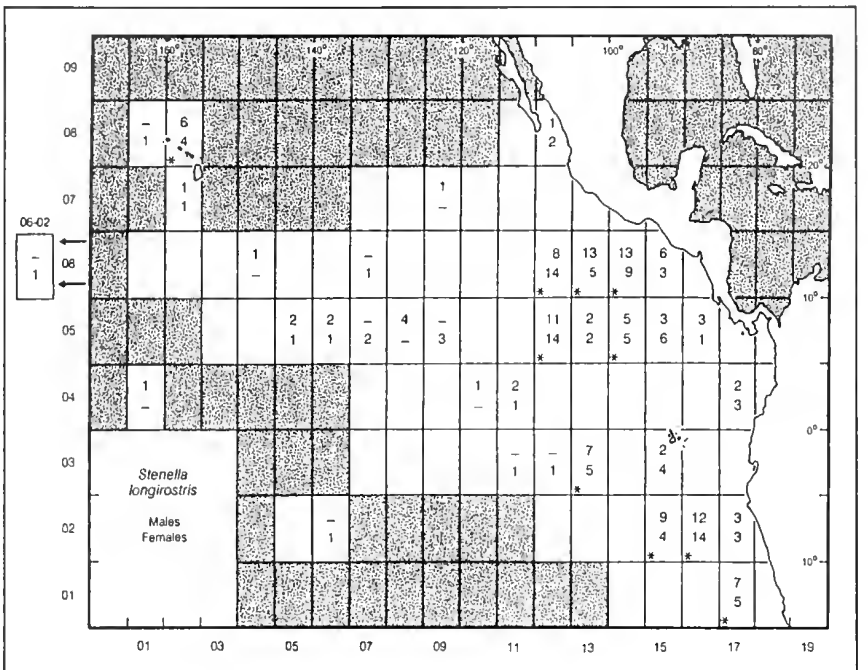

Figure 1

Known range of *Stenella longirostris* in eastern tropical Pacific Ocean (modified from Perrin 1990), with numbers of males (above) and females (below) available for each 5° latitude-longitude block (total of 246 specimens). Asterisks indicate 10 blocks included in analysis of sexual dimorphism. The 25 blocks with two or more specimens used as basis for analyses of geographic variation; for some aspects, the 10 blocks with single specimens projected onto axes based on the 25 blocks. Each block identified by numerical code (numbers on left and bottom margins are combined; e.g., block 0812 is just to east of southern tip of Baja California). One block (i.e., 06-02) is located off map to west (left).

longirostris: the pantropical spinner dolphin *S. l. longirostris* occurring in the Central, South, and Western Pacific, Indian, and Atlantic oceans; the Central American spinner *S. l. centroamericana* endemic to the coast of Central America and corresponding to the Costa Rican spinner management stock; and the eastern spinner *S. l. orientalis* endemic to the eastern tropical Pacific off Mexico, Central America, and northern South America and corresponding to the eastern spinner management stock. He concluded that the more offshore whitebelly forms constitute a broad zone of hybridization or intergradation between the eastern and pantropical forms. This view has support from results of a genetic study; Dizon et al. (1991) found no unique haplotypes in a restriction-enzyme examination of mitochondrial DNA of animals of the eastern and whitebelly morphological types.

Perrin et al. (1991) reexamined color pattern, body size and shape, and dorsal fin shape without *a priori* assignment of specimens to subspecies or management stock. They compared specimens from 5° geographic blocks. The results of their analyses support the taxonomic treatment by Perrin (1990); the whitebelly forms constitute a complex zone of highly variable animals intermediate between the eastern and pantropical types. Perrin et al. (1991) concluded that the pattern of geographic variation does not justify separation of northern and southern units on morphological grounds alone.

The purpose of the studies reported here was to carry out a parallel analysis of geographical cranial variation in the eastern Pacific, again making no *a priori* assignment of specimens to subspecies or management stock. We also examined relationships between cranial variation and environmental variables, in an effort to better understand the ecologies of the several forms of spinner dolphins.

Materials and methods

Data from 246 adult museum specimens (maturity judged by evaluating fusion of premaxilla with the maxilla at distal end of rostrum; Dailey and Perrin 1973) of spinner dolphins were used in this investigation (Fig. 1). We purposely included all appropriate specimens available, including those from the three named subspecies recognized from the region (Perrin 1990); furthermore, we did not differentiate between those with different color patterns ("eastern" and "whitebelly"; Perrin et al. 1985, 1991), in order to focus simply on cranial features. The animals used included 188 of 199 specimens used in the earlier study of sexual dimorphism (Douglas et al. 1986; the 11 remaining specimens not used had been incorrectly aged or had inadequate locality data) and 58 new specimens.

The first set of specimens was measured by M.E. Douglas and the new specimens by W.F. Perrin. In addition, Perrin remeasured 81 specimens of spinner dolphins and spotted dolphins *S. attenuata* measured by Douglas. This allowed a comparison to determine whether measurements were repeatable. Initially, 36 morphometric and meristic characters were evaluated (illustrations and character definitions given in Schnell et al. 1985a). Comparisons of measurements taken on the same specimens by the two investigators indicated

Table 1
Geographic variation and sexual dimorphism in *Stenella longrirostris* evaluated for 30 characters.

Character[a]	*F*-value[b]		Mean[c]		Correction factor[d]	Percentage difference[e]
	Block	Sex	Male	Female		
1 Condylobasal L.	22.19***	0.05	405.9	404.6	0.22	0.32
2 L. Rostrum (frm.Base)	15.93***	0.50	258.9	259.4	−0.61	−0.21
3 L. Rostrum (frm.Pterygoid)	20.71***	0.01	299.6	299.3	−0.08	−0.11
4 W. Rostrum (at Base)	15.19***	2.88	74.2	73.1	0.37	1.44
5 W. Rostrum (at 1/4 L.)	10.17***	11.82***	52.1	50.6	0.67	2.84
6 W. Rostrum (at 1/2 L.)	9.97***	10.20**	44.2	42.8	0.65	3.16
7 W. Premax. (at 1/2 L.)	5.65***	8.31**	21.4	20.8	0.31	3.02
8 W. Rostrum (at 3/4 L.)	2.92**	24.96***	32.5	30.5	1.01	6.34
9 Preorbital W.	38.05***	8.67**	139.9	137.5	1.00	1.76
10 Postorbital W.	49.34***	8.19**	155.7	153.3	0.93	1.57
11 Skull W. (at Zygomatic P.)	49.11***	14.89***	154.4	151.3	1.27	2.04
12 Skull W. (at Parietals)	6.27***	20.36***	130.1	127.2	0.10	0.52
13 Ht. Braincase	16.56***	15.52***	89.1	87.1	0.89	2.28
14 L. Braincase	18.71***	8.09**	101.7	100.3	0.67	1.47
15 Max. W. Premax.	6.55***	0.22	62.9	62.6	0.04	0.36
16 W. External Nares	3.88***	0.09	41.6	41.5	1.40	2.27
17 L. Temporal Fossa	4.32***	9.27**	50.4	48.7	0.82	3.52
18 W. Temporal Fossa	9.24***	17.82***	40.2	38.2	0.96	5.16
19 Orbital L.	6.56***	0.00	40.7	40.6	−0.01	−0.13
20 L. Antorbital P.	12.41***	11.46***	42.7	41.4	0.67	3.27
21 W. Internal Nares	22.50***	3.85	43.5	42.7	0.31	1.81
22 L. Up. Toothrow	16.23***	1.12	224.3	225.5	−0.82	−0.54
23 No. Teeth (Up.Lf.)	3.39***	3.88	53.2	52.5	0.42	1.30
24 No. Teeth (Up.Rt.)	5.19***	1.15	52.7	52.3	0.21	0.76
25 No. Teeth (Low.Lf.)	2.33*	0.80	51.3	51.1	0.17	0.39
26 No. Teeth (Low.Rt.)	2.61**	0.34	51.0	50.9	0.11	0.29
27 L. Low. Toothrow	13.99***	1.00	218.4	219.5	−0.76	−0.51
28 Ht. Ramus	21.64***	13.02***	55.4	54.1	0.60	2.51
29 Tooth W.	3.74***	13.84***	2.6	2.5	0.07	5.10
30 L. Ramus	18.06***	0.04	346.8	345.6	0.20	0.35

[a] Abbreviations: frm. = from; Ht. = height; L. = length; Lf. = left; Low. = lower; Max. = maximum; No. = number; P. = process; Premax. = premaxillary; Rt. = right; Up. = upper; W. = width.
[b] *F*-values from main effects two-way analysis of variance (5° block vs. sex) involving 10 blocks (*$P<0.05$; **$P<0.01$; ***$P<0.001$). Total of 170 individuals. Degrees of freedom 9 for among-block variation and 1 for between sexes.
[c] Unweighted mean for 10 blocks.
[d] Added to all individual female measurements and subtracted from all individual male measurements to correct for sexual differences.
[e] Difference between sexes (males minus females) multiplied by 100, with the resulting value divided by average of male and female means.

that 6 of the original 36 measurements (i.e., W. Lf. Premax. [at midline of Nares], W. Rt. Premax. [at midline of Nares], Separation of Pterygoids, L. Lf. Tympanic Cavity, L. Rt. Tympanic Cavity, and W. at Pterygobasioocipital Sutures; abbreviations used in these and other character names are listed in footnote a of Table 1) should be deleted, because we were not able consistently to repeat these measurements. For some other measurements, there were differences between investigators, but the differences were consistent (e.g., one obtained measurements that were smaller than those reported by the other). Therefore, we calculated regression equations for each of the remaining characters based on the 81 jointly-measured specimens. These regression equations were used to convert the measurements from the rest of the initial specimens to appropriate values for inclusion with the measurements taken by Perrin. Through these procedures, we developed a data set of 30 characters (listed in Table 1) for 246 specimens.

Only specimens that were largely complete were included in the analysis. Missing values (1.34% of total) were estimated by linear regression ("Missing Data Estimator" program developed by Dennis M. Power, Santa Barbara Mus. Nat. Hist., pers. commun.) onto the character that explained the greatest proportion of the variance for the variable under consideration.

Specimens then were assigned to 5° latitude-longi-

tude blocks, with each geographic block given a numerical code (see Fig. 1). We had specimens from 35 blocks, although 10 were represented by only a single specimen; the other 25 blocks were used as the basis for most analyses of geographic variation. While several of the remaining 25 blocks are represented by relatively small samples, tests for geographic patterning (described below) suggest that, in general, sample values are representative of what would be expected for these blocks based on their geographic positions. The 5° block size was selected, in part, because it was judged that available sample sizes would not permit detailed analysis of smaller geographic units. Furthermore, migratory movements and related factors were less likely to significantly influence results when these relatively large sampling areas were used.

Douglas et al. (1986) showed that *S. longirostris* in the eastern tropical Pacific was sexually dimorphic for 13 of 36 characters. Because some specimens used in that analysis were removed and new specimens added (see above), we reanalyzed the data with a two-way analysis of variance (ANOVA) for block and sex based on specimens in 10 blocks that had at least four of each sex (Fig. 1). We then produced a series of correction terms to adjust measurements of the larger sex downward and the smaller sex upward, thus producing sex-adjusted or "zwitter" measurements (for details on this adjustment, see Schnell et al. 1985a). These corrections enabled us to combine specimens for both sexes in an overall analysis of geographic variation.

Correlation, ordination and clustering

After conversion to zwitters, characters were then standardized so that means for blocks were zeros and standard deviations ones. Product-moment correlations were computed among characters, and the general associations among characters were summarized by clustering characters using the unweighted pair-group method with arithmetic averages (UPGMA).

This type of hierarchical cluster analysis also was performed to summarize average distance coefficients (Sneath and Sokal 1973) calculated for all pairs of blocks based on standardized data. Cophenetic correlation coefficients were computed to indicate the degree to which distances in the resulting dendrogram accurately represented original interblock morphologic distances.

In addition, we analyzed standardized data using a nonhierarchical K-group method called function-point cluster analysis (Katz and Rohlf 1973; described in Rohlf et al. 1979). Blocks are assigned to a series of subgroups at a specified level. The value for the w-parameter used by the function-point clustering method was varied. A hierarchical (but not necessarily non-overlapping) system of clusters can be obtained by conducting the analysis at more than one clustering level. Results are presented in the form of a modified skyline diagram (Wirth et al. 1966) where, for a given w-value, blocks joined in a common line are in the same cluster.

Based on standardized data, we constructed scatter diagrams of blocks projected onto the first two principal components (Sneath and Sokal 1973) extracted from a matrix of correlations among the 30 characters. Canonical variates analysis also was applied to determine the subset of variables that show the greatest degree of geographic variation—in this case, those that provide the greatest interblock separation relative to the degree of intrablock variation (Program P7M of BMDP; Dixon 1990). Plots of the first two canonical variables show the maximum separation of blocks in two-dimensional space. The original variables, which in combination exhibited maximum interblock variability, were then subjected to additional analyses.

Mantel test for geographic patterning

Using a test devised by Mantel (1967) and described by Sokal (1979), we analyzed interlocality variation in each character to determine whether values are geographically patterned, or vary spatially at random. This procedure enabled us to determine whether differences in character values between all pairs of samples are statistically associated in a linear manner with corresponding geographic distances. The observed association between sets of character differences and geographic distances was tested relative to its permutational variance, and the resulting statistic was compared against a Student's t-distribution with infinite degrees of freedom. Computations were performed using GEOVAR, a library of computer programs for geographic variation analysis written by David M. Mallis and furnished by Robert R. Sokal (State University of New York at Stony Brook).

Character differences were compared first with actual geographic distances (in nautical miles) between centers of blocks and then with reciprocals of distances. In evaluations of reciprocals, where distances are scaled in a nonlinear manner, longer distances are considered effectively to be equal, and the portion of the scale involving smaller distances is expanded. Thus, use of reciprocals of distances increases the power of analyses to reveal geographic patterns that are "local" in nature (i.e., involving closely placed blocks), whereas tests involving nautical-mile distances evaluate "regional" trends. Positive associations of character differences and nautical-mile distances are indicated by positive t-values, while negative t-values denote such associations when reciprocals of distances are used.

Table 2

Environmental measurements compiled for each 5° latitude-longitude block.*

1 Sea Current (N., Winter)—Average northern component (in knots) of the surface water current in winter (Innis et al. 1979; their fig. 2.2).
2 Sea Current (W., Winter)—Average western component (in knots) of the surface water current in winter (Innis et al. 1979; fig. 2.3).
3 Water Depth—Average sea depth (in m) (Bartholomew 1975; fig. 122).
4 Solar Insolation (Jan.)—Average incoming solar radiation for January (in gm. · cal/cm^2; Brunt 1934; table 2).
5 Solar Insolation (Annual)—Average annual incoming solar radiation in gm. · cal/cm^2; Brunt 1934; table 2).
6 Sea Surface Temp. (Jan.)—Average January sea surface temperature (in °C; Robinson 1976: fig. 2 north of 5°S; Wyrtki 1974: fig. 2 south of 5°S).
7 Sea Surface Temp. (July)—Average July sea surface temperature (in °C; Robinson 1976: fig. 74 north of 5°S; Wyrtki 1974: fig. 8 south of 5°S).
8 Sea Surface Temp. (Ann. Var.)—Average annual sea surface temperature variation (in °C; Robinson 1976: fig. 148 north of 5°S; Wyrtki 1974: fig. 26 south of 5°S).
9 Oxygen Min. Layer (Depth)—Annual mean depth (in m) of the absolute oxygen minimum surface with respect to the vertical (Levitus 1982: fig. 52).
10 Surface Salinity—Average salinity (‰) of surface sea water (Levitus 1982: microfiche F-02, frames 2–5).
11 Thermocline Depth (Winter)—Mean depths (in m) to the top of the thermocline for January, February, and March (Robinson 1976: figs. 12, 24, and 36 north of 5°S; Cromwell 1958: fig. 1a south of 5°S).
12 Thermocline Depth (Summer)—Mean depths (in m) to the top of the thermocline for July, August, and September (Robinson 1976: figs. 84, 96, and 108 north of 5°S; Cromwell 1958: fig. 1c south of 5°S).
13 Surface Dissolved Oxygen—Annual mean dissolved oxygen (mL/L) of surface sea water (Levitus 1982: microfiche F-03, frames 2–5).

* Abbreviations: Ann. Var. = Annual variation; Jan. = January; Min. = Minimum; N. = North; Temp. = Temperature; W. = West.

As an example of the Mantel procedure, consider the 25 blocks for which two or more specimens were available (Fig. 1). The geographic distances (in nautical miles) between each pair of the 25 blocks (300 pairs total) are computed. We then obtain the mean value for a given morphological character for each block; consider a character with large mean values in northern blocks, a gradual change as one proceeds south, and the smallest means in the most southerly blocks. We calculate the absolute character difference for each pair of blocks (300 difference values); in general, for this hypothetical case, close blocks geographically exhibit small differences in character means, while blocks far apart (e.g., a northern and a southern block) have the largest morphological differences. We and the Mantel test would identify this morphological character as having a strong regional pattern. We also compare reciprocals of geographic distance for each block pair with corresponding morphological differences; this approach indicates whether, in general, geographically close blocks also are similar morphologically (a case of local geographic patterning). The examplar morphological character, thus, would be identified as displaying a strong local pattern (in addition to the strong regional pattern). In general, a character showing a regional pattern (as we have defined it) also will exhibit a local pattern, but the reverse is not necessarily true. For instance, if the morphological character was large in both the north and south, was small for blocks in the middle, and had gradual changes between adjacent blocks, it would have a strong local pattern but no regional pattern (because many distant blocks are nearly identical morphologically). Detailed computational examples of the Mantel test can be found in Douglas and Endler (1982), Schnell et al. (1985b), and Manley (1985).

We also computed matrix correlations (Sneath and Sokal 1973) between character differences and the associated geographic distances or reciprocals of distances between localities. The significance of these coefficients cannot, however, be tested in the conventional way, because all pairs of localities were used and these are not statistically independent. However, the resulting values are useful as descriptive statistics indicating the degree of association of difference values.

Morphological-environmental covariation

Relatively little is known about the relationship (if any) of geographic variation in morphological characteristics of *S. longirostris* to differences in the environment. Therefore, as an initial exploratory analysis of covariation, we have calculated product-moment correlations of block means for morphological characters with environmental variables. Data were available for 13 environmental variables for the eastern tropical Pacific Ocean (Table 2). We also used UPGMA to summarize associations among these environmental variables for 51 blocks with specimens of *S. longirostris* or

S. attenuata or both; since these two dolphin species have broadly overlapping distributions in the eastern tropical Pacific, the blocks used are representative of areas inhabited by *S. longirostris*.

We conducted a principal components analysis of the 13 environmental variables for the 51 blocks in order to obtain summary variables that reflect overall environmental trends. Individual blocks were projected onto the resulting environmental principal components based on standardized data. These block variables were used as composite environmental variables for comparisons with morphological characteristics.

In addition to using matrix correlations and the Mantel procedure to test for local and regional patterning of variation in individual morphological characters, we compared difference patterns of selected morphological measures with those of environmental variables. In these tests, differences between each pair of blocks for a morphological variable were compared with those for an environmental variable.

Sources for environmental data are expanded over those used by Schnell et al. (1986: table 2) so as to accommodate the broader geographic representation resulting from increased numbers of specimens. Values for depth of the oxygen minimum layer were taken for all blocks from Levitus (1982). Data for sea surface temperatures and thermocline depths were not available in the previously used source for blocks west of 120°. Data for these and other blocks north of 5°S were taken from Robinson (1976). Overlapping blocks from the two sources for each environmental variable were used to produce regression equations. Previous data for blocks south of 5°S were converted using these regression equations. Overall, agreement of data for overlapping blocks from the two sources was relatively good. Correlations for sea surface temperatures were: January, 0.956; July, 0.951; annual variation, 0.929. Thermocline depth in winter had a correlation of 0.840, while that for summer values was lower (0.767). All correlations were statistically significant ($P<0.001$), and the associations of values from the two sources were basically linear.

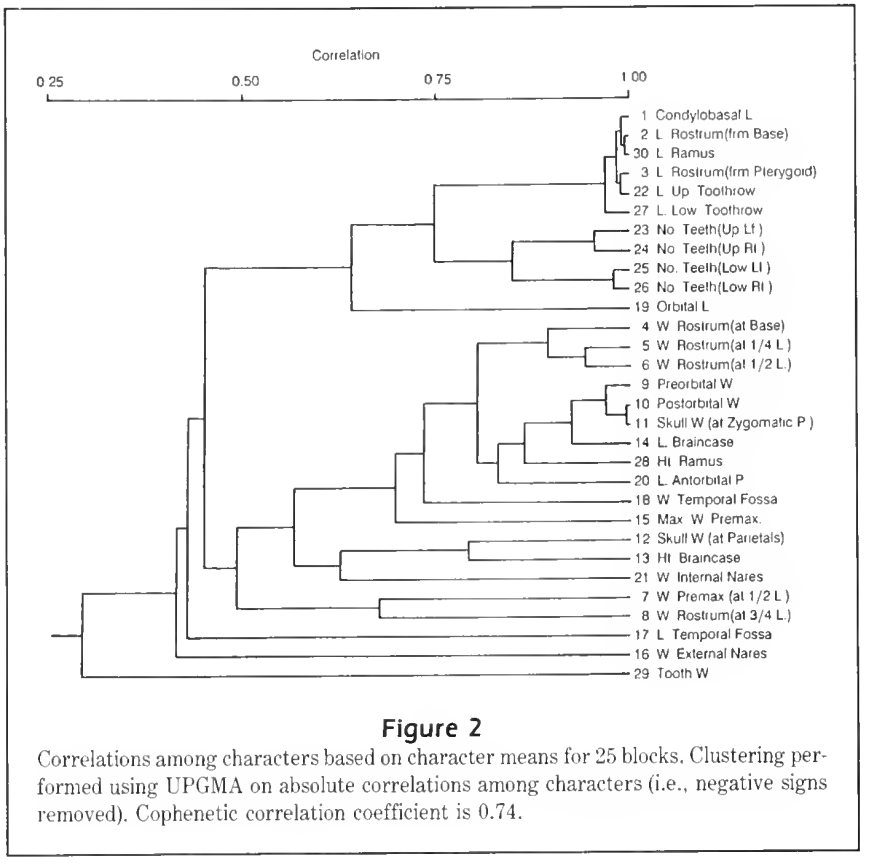

Figure 2

Correlations among characters based on character means for 25 blocks. Clustering performed using UPGMA on absolute correlations among characters (i.e., negative signs removed). Cophenetic correlation coefficient is 0.74.

Results

Sexual dimorphism

In the two-way ANOVA for block and sex, only three measurements showed a significant interaction for block and sex (W. Rostrum [at Base], L. Temporal Fossa and No. Teeth [Up.Lf.]). All characters exhibited significant variation by block (i.e., geographic variation), and 15 of the 30 characters displayed significant sexual dimorphism (Table 1). For most characters, males are larger than females. Character differences between sexes range up to 6.34% (see Table 1), with the most dimorphic character being W. Rostrum (at 3/4 L.).

Correlation, ordination and clustering

Figure 2 summarizes associations among characters based on means for the 25 blocks. Virtually all of the intercharacter correlations were positive in sign; a few indicated weakly negative associations. For the cluster analysis, absolute character correlations were analyzed (i.e., sign of correlation ignored), because we wanted to assess simply the degree of covariation. The character showing the most distinctive pattern relative to

Table 3

Principal component loadings for *Stenella longirostris* involving character means for 25 blocks.

Character	Component * I	Component * II	Character	Component * I	Component * II
1 Condylobasal L.	**0.914**	−0.325	16 W. External Nares	0.573	−0.045
2 L. Rostrum (frm.Base)	**0.872**	−0.397	17 L. Temporal Fossa	0.575	0.040
3 L. Rostrum (frm.Pterygoid)	**0.885**	−0.396	18 W. Temporal Fossa	0.647	0.599
4 W. Rostrum (at Base)	**0.856**	0.083	19 Orbital L.	0.782	−0.064
5 W. Rostrum (at 1/4 L.)	**0.838**	0.242	20 L. Antorbital P.	**0.849**	0.108
6 W. Rostrum (at 1/2 L.)	**0.880**	0.248	21 W. Internal Nares	0.631	0.427
7 W. Premax. (at 1/2 L.)	0.578	0.044	22 L. Up. Toothrow	**0.864**	−0.426
8 W. Rostrum (at 3/4 L.)	0.508	0.504	23 No. Teeth (Up.Lf.)	0.608	**−0.680**
9 Preorbital W.	**0.938**	0.255	24 No. Teeth (Up.Rt.)	0.688	−0.593
10 Postorbital W.	**0.917**	0.344	25 No. Teeth (Low.Lf.)	0.600	**−0.666**
11 Skull W. (at Zygomatic P.)	**0.916**	0.359	26 No. Teeth (Low.Rt.)	0.652	**−0.630**
12 Skull W. (at Parietals)	0.331	**0.659**	27 L. Low. Toothrow	**0.814**	−0.467
13 Ht. Braincase	0.625	**0.719**	28 Ht. Ramus	**0.872**	0.219
14 L. Braincase	**0.881**	0.326	29 Tooth W.	0.216	**0.752**
15 Max. W. Premax.	**0.811**	0.042	30 L. Ramus	**0.877**	−0.366

* Relatively high loadings highlighted in bold as follows: (component I)>|0.8|; (II)>|0.6|.

other morphological characters is Tooth W. In addition, correlations of L. Temporal Fossa and W. External Nares with other characters are relatively low. The rest of the characters are placed in two groups. The first cluster (characters listed between 1 and 19 at top of Fig. 2) includes lengths involving the anterior portion of the skull, tooth numbers, and Orbital L. The second group (characters 4 to 8 as listed in Fig. 2) includes a variety of skull widths, dimensions of the braincase, and Ht. Ramus.

Character loadings of a principal components analysis using 25 blocks are presented in Table 3. The first component explained 57.0% of the total character variance and the second 18.5% (cumulative total of 75.4%). Projections of all blocks onto these components are shown in Figure 3, while Figure 4 is a map summarizing geographically the projections onto the first component. This component, which reflects general skull size, has relatively

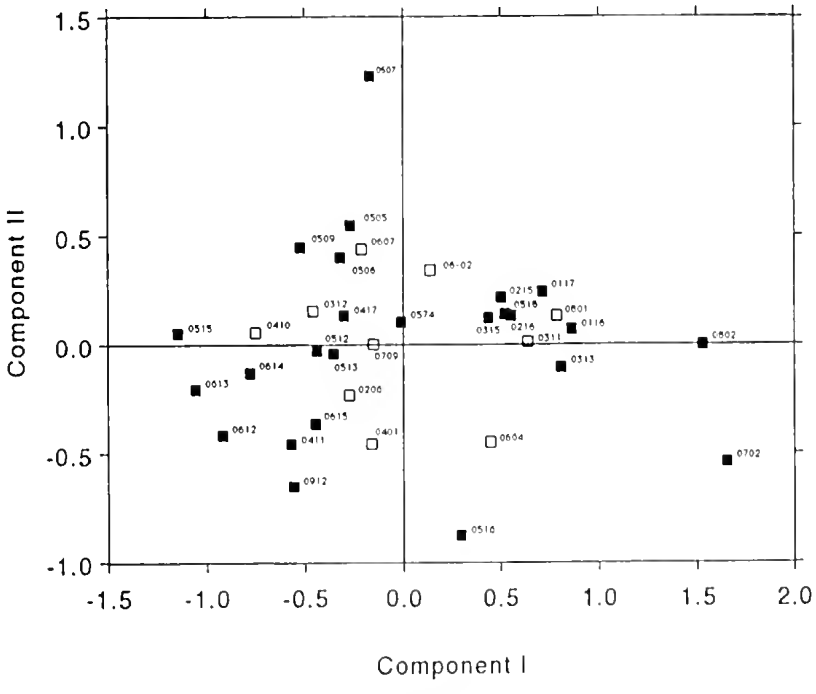

Figure 3

Projections of blocks onto first two principal components based on 30 characters. Solid symbols indicate 25 blocks on which analysis conducted. Open symbols represent blocks with only single specimens, which were projected onto axes generated from 25 blocks with two or more specimens.

high correlations (Table 3) with all characters except Tooth W. and Skull W. (at Parietals). Localities to the right in Figure 3 are from the Hawaiian Island area (0702 and 0802; see Fig. 4), where animals are larger. Specimens from southern blocks (e.g., 0116, 0117, 0313) also are larger than animals from other parts of the range. Blocks to the left in Figure 3, with negative loadings on component I, have smaller individuals. In general, *S. longirostris* from the northeastern blocks were the smallest (e.g., 0515, 0613, 0612).

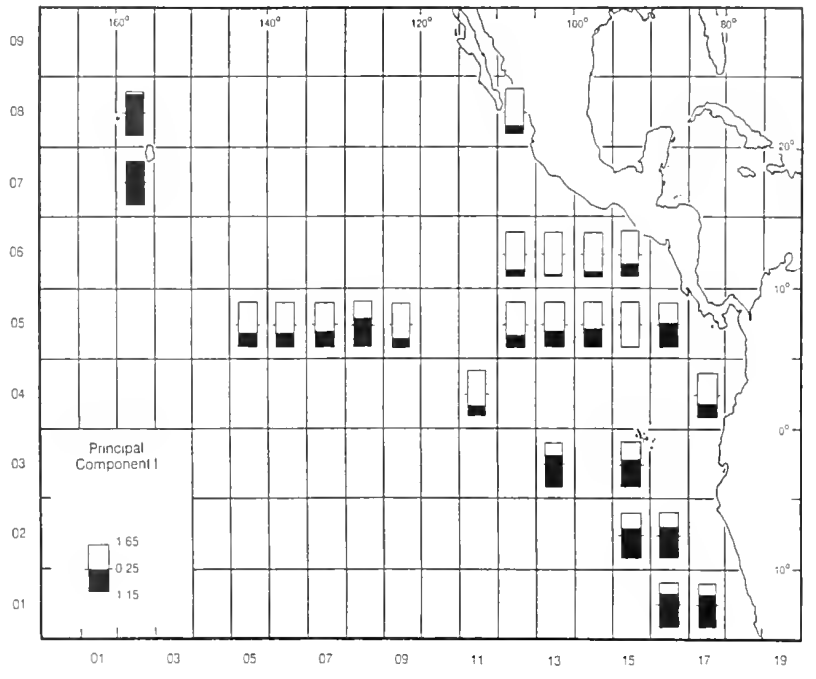

Figure 4
Geographic variation in principal component I. Bar represents range (low to high block values), and midpoint is marked. Darkened part of bar indicates value for particular block.

Component II has its highest positive correlations with Skull W. (at Parietals), Ht. Braincase, and Tooth W.; it has negative associations with characters 23–26, which involve numbers of teeth. Block 0507 is the most extreme, with a positive projection on this component (see Fig. 3); animals from this block have relatively wide skulls and reduced numbers of teeth. In contrast, block 0516 is at the other extreme, with relatively narrow skulls and greater numbers of teeth.

Figure 5 is a dendrogram depicting results from a UPGMA cluster analysis of the 25 geographic blocks. Four main clusters are evident, with block 0702 being the most divergent and in its own cluster. Block 0507 also is in a cluster by itself. The first group in the diagram (i.e., blocks 0116 through 0516 at top of Fig. 5) includes predominantly southern and western localities. Those in the largest cluster (listed from block 0411 to 0509 in Fig. 5) are situated to the north and/or east.

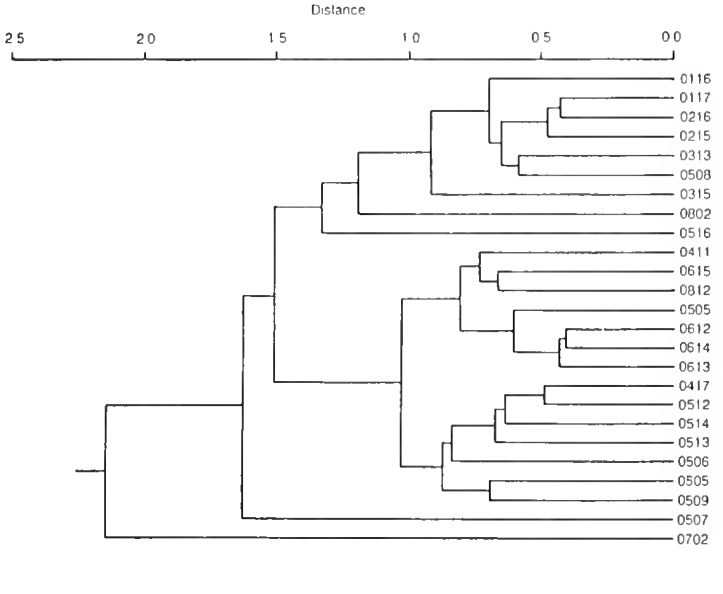

Figure 5
Distance phenogram summarizing UPGMA clustering of 25 blocks based on 30 characters. Cophenetic correlation is 0.80.

A modified skyline diagram (Fig. 6A) resulting from function-point clustering for 25 blocks based on 30 characters indicates an initial separation of block 0702 (which includes part of Hawaii) from the others. At a w-value of 3.50, there are three clusters: (1) block 0702; (2) the southern blocks in addition to blocks 0508 and 0802; and (3) the remaining northern and eastern blocks, including those just north of the Equator. Further subdivision results with smaller w-values (see Fig. 6A).

A similar analysis (Fig. 6B) was conducted using the five characters—Postorbital W., L. Rostrum (frm.

Pterygoid), W. Internal Nares, W. Premax. (at 1/2 L.), and W. Rostrum (at Base)—that, in combination, were best for discriminating among blocks (based on canonical variates analysis reported below). With a w-value of 1.79, block 0702 is separated from the remaining blocks. Note that four groups were formed when using a 1.47 w-value; there are two single-block groups (i.e., 0702 and 0802). When the w-value was lowered to 1.37, the same groups were formed, except that 0315 was in its own group and 0802 joined with a group of predominantly southern localities. With a 1.26 w-value, the clusters are the same except that block 0505 joins the northeastern blocks instead of those from the south. Three groups were formed with a 1.15 w-value: (1) block 0702; (2) a group of eight blocks, including southern blocks in addition to 0508, 0505, and 0802; and (3) the northern and eastern blocks, including 0411 and 0417, as well as 0506, 0507, and 0509. At smaller w-values, there is further subdivision.

A canonical variates analysis, using as initial data the information on all 30 measurements for 25 blocks, incorporated the five characters listed in Table 4. A two-dimensional plot of the 25 block centroids on canonical variables 1 and 2 is included as Figure 7; although not used to generate the axes, 10 blocks with only single specimens also are projected onto these variables. The geographic pattern of canonical variable 1 is depicted in Figure 8B. The eigenvalue for canonical variable 1 is 2.93 and that for the second is 0.55, with the two summarizing 82.0% of the variance for the five characters. These five characters in combination show the

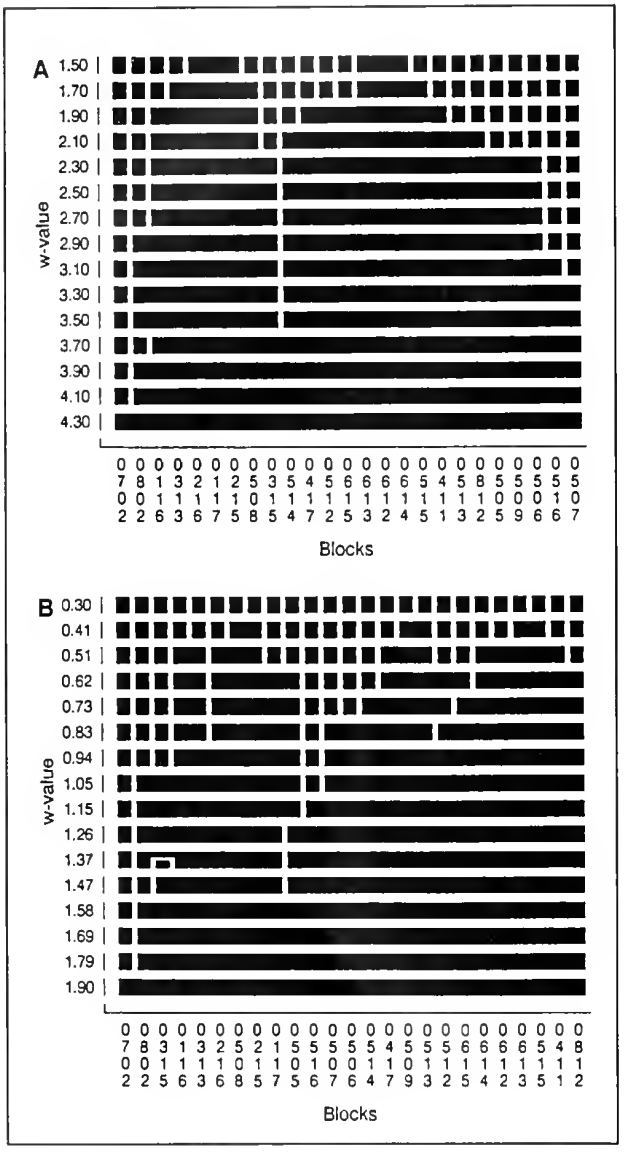

Figure 6

Modified skyline diagrams for 25 blocks, indicating groups formed using function-point clustering procedures and based on: (A) all 30 characters; (B) five characters that, in combination, best discriminate among blocks (Postorbital W., L. Rostrum [frm. Pterygoid], W. Internal Nares, W. Premax. [at 1/2 L.], and W. Rostrum [at Base]). For given w-value (i.e., row), blocks connected in common line are in same cluster.

Table 4

Canonical variates analysis of all specimens from 25 blocks.

Character		F-value to enter	Order of entry	Coefficients* 1	2
3	L. Rostrum (frm.Pterygoid)	4.53	2	0.0242 (0.2830)	−0.0662 (−0.7734)
4	W. Rostrum (at Base)	2.38	5	−0.0603 (−0.1622)	−0.1912 (−0.5145)
7	W. Premax. (at 1/2 L.)	2.30	4	−0.0291 (−0.0393)	0.2419 (0.3273)
10	Postorbital W.	23.21	1	0.2113 (0.8570)	0.0648 (0.2628)
21	W. Internal Nares	2.88	3	0.0958 (0.1870)	0.3324 (0.6489)
	Constant			38.9175	4.4931

*Unstandardized coefficients, with standardized values in parentheses, for canonical variates.

greatest among-group variability relative to that within groups and are used for more detailed comparisons with environmental variables (presented below).

As indicated in Table 4, the first canonical variable is most influenced by Postorbital W. (Fig. 8A). In Figure 7, blocks that are large for this character are to the right, while those that are small are to the left. When considering only those blocks with more than one specimen (i.e., those shown with solid symbols in Fig. 7), the two blocks from the vicinity of the the Hawaiian Islands (0802 and 0702) are to the right, as are blocks predominantly from the southern portion of the range. The blocks with single specimens (which tend to be more westerly) also are to the right. Specimens from blocks to the north and east are smaller; they are depicted to the left in Figure 7. Some west-central blocks group with the southern blocks, while others are intermediate or group with those to the northeast. The second canonical variable contrasts blocks from the Hawaiian Island area (0702, 0802) with the others (see Fig. 7); in the characters reflected by this variable, values of block 0812 (which is northern, but to the east) show some similarities to those for 0702 and 0802.

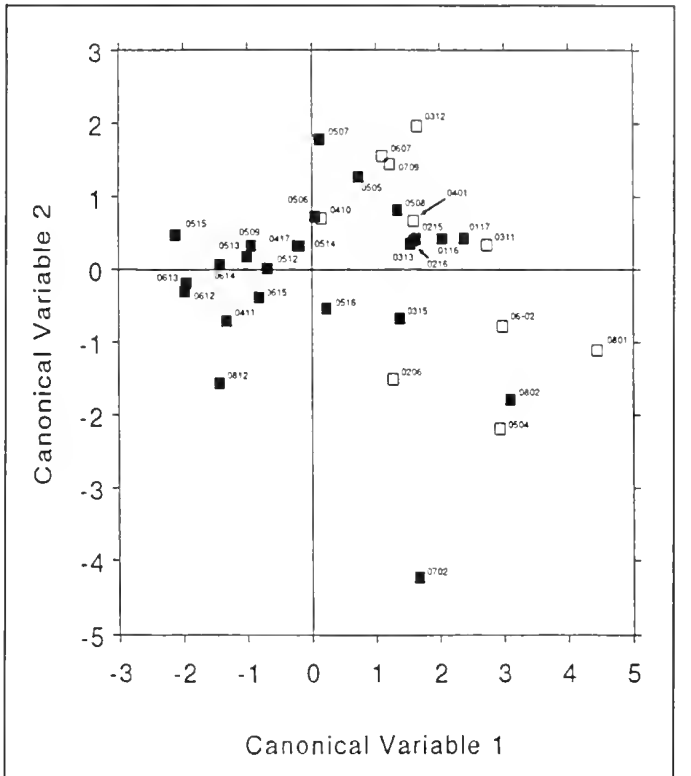

Figure 7

Projections of blocks onto first two canonical variables based on 30 characters. Solid symbols indicate 25 blocks on which analysis conducted. Open symbols represent blocks with only single specimens, which were projected onto axes generated from 25 blocks with two or more specimens.

Mantel test for geographic patterning

Individual characters were evaluated with respect to geographic patterning using Mantel tests, as well as matrix correlations that compare interblock geographic distances (or reciprocals of these distances) and character differences between localities. Of the 30 characters, 66.7% (20) show statistically significant regional patterning indicating that geographic distances (in nautical miles) and interblock character differences are interrelated (Table 5). For measures showing significant t-values the greatest character differences tend to be between blocks that are farthest away from each other, while nearer localities are more similar.

Local patterning, as indicated by a significant negative association of distance reciprocals and character differences, was found in 83.3% (25) of the characters (Table 5). All characters that showed regional patterning also exhibited local patterning.

Principal component projections also were assessed in terms of geographic patterning. As indicated at the bottom of Table 5, component I (Fig. 4) has strong regional and local patterning; component II has significant local patterning. Canonical variables 1 (Fig. 8B) and 2 both exhibit marked regional and local patterning (Table 5).

Morphological-environmental covariation

Figure 9 is a dendrogram indicating absolute correlations among the 13 environmental variables, subdividing them into five clusters. Sea Current (N., Winter) is in a group by itself and quite different from the others. Sea Current (W., Winter) and Oxygen Min. Layer (Depth) are in the second cluster, which joins with a group of five variables involving surface measures of temperature, oxygen, and salinity. The fourth cluster involves two measures of solar insolation, and the fifth reflects aspects of water depth.

The loadings of environmental variables on the first three environmental principal components are given in Table 6. The first component statistically explains 33.0% of the total character variance, the second 23.2%, and the third 15.8% (cumulatively 72.0%). Maps (Fig. 10) depict projections of the 25 blocks with two or more *S. longirostris* onto the first two environmental components. Environmental component I has relatively high values for blocks between 5° and 15°N, with intermediate values to the north and low values south of the Equator (Fig. 10A). Sea Surface Temp. (July)

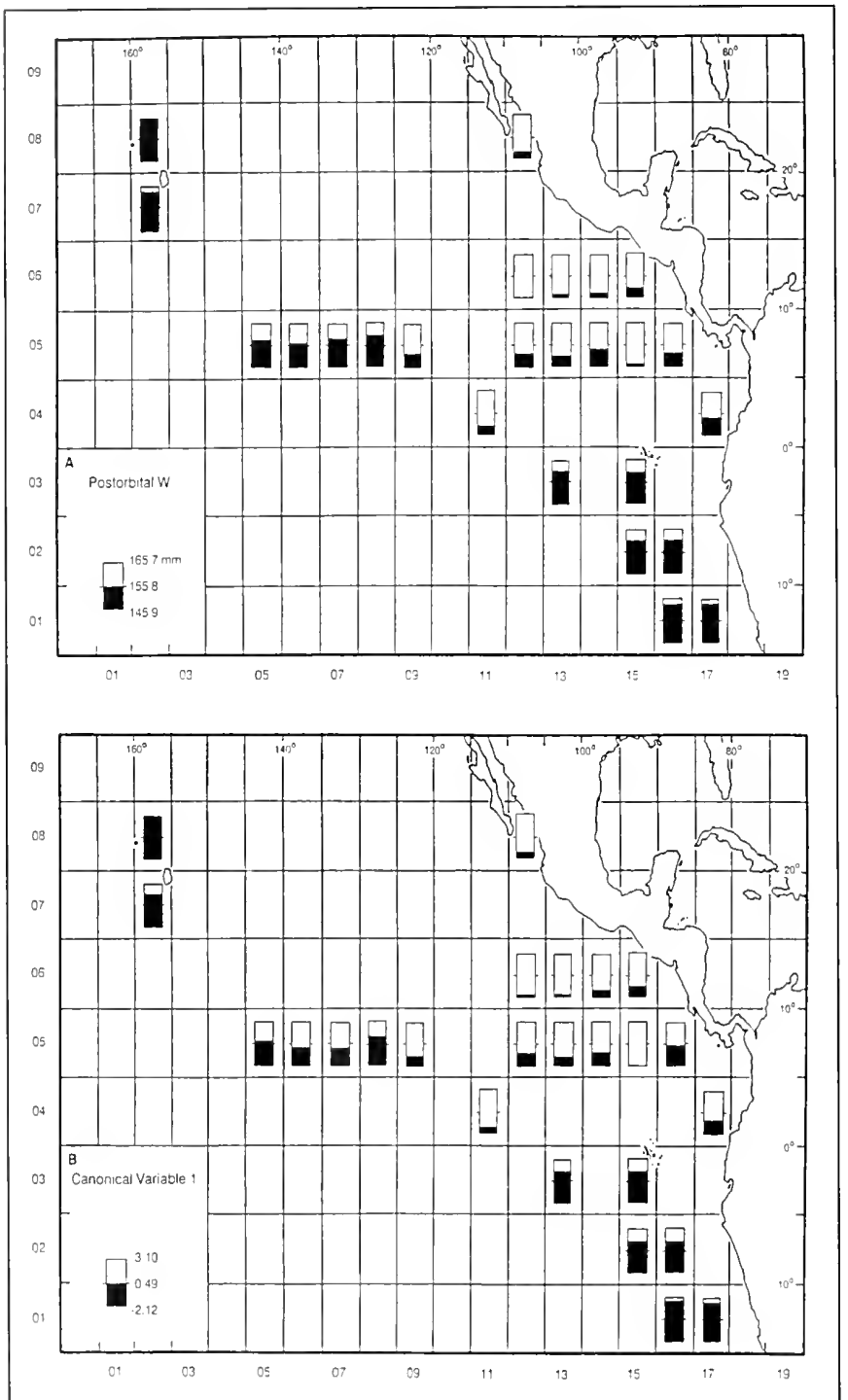

Figure 8

Geographic variation in (A) Postorbital W. and (B) canonical variable 1. Darkened part of bar indicates value for particular block.

has a high positive loading on component I, while that for Sea Surface Temp. (Ann. Var.) is negative. Five other variables have relatively high correlations with this component (Table 6). The second environmental component has high values for the two blocks adjacent to the Hawaiian Islands (Fig. 10B), with intermediate values in other western blocks. Strong negative projections on this component are found for blocks along the coast of South and Central America just north of the Equator. The most substantial loadings on this component are for the two thermocline variables (Table 6), while Water Depth and Surface Salinity also exhibit relatively high positive projections for component II. Environmental component III reflects mainly Solar Insolation (Annual), with Solar Insolation (Jan.) also having a relatively high positive loading (Table 6). The most extreme negative projection for component III is for the northern block near the coast (i.e., 0812), with the highest positive projects for blocks in the west-central portion of the study area (i.e., 0505 through 0509). In general, other blocks have relatively high projection values, except for 0802 (which is somewhat lower). Other components beyond the first three tended to represent only single environmental variables.

Several of the environmental measures showed few or no statistical associations with morphological characters (and resulting principal components or canonical variables), while others exhibited significant covariation (Table 7). The first environmental variable, Sea Current (N., Winter), is not significantly correlated with any of the 30 morphological measures. The other character summarizing sea-current information, Sea Current (W.,Winter), has a geographic pattern showing relatively weak statistical concordance with eight of the morphological characters. Toothrow lengths and three of the four tooth counts are among those with significant associations.

Table 5

Association of interlocality character differences with geographic distances (in nautical miles) and the reciprocals of these distances. Results from Mantel tests (t) and matrix correlations (r) for *Stenella longirostris*.

	Distance		Reciprocal of distance	
Character	t	r	t	r
1 Condylobasal L.	4.49***	0.445	−4.86***	−0.348
2 L. Rostrum (frm.Base)	3.89***	0.395	−4.35***	−0.315
3 L. Rostrum (frm.Pterygoid)	4.26***	0.437	−4.67***	−0.340
4 W. Rostrum (at Base)	3.49***	0.435	−3.86***	−0.316
5 W. Rostrum (at 1/4 L.)	3.16**	0.327	−3.48***	−0.255
6 W. Rostrum (at 1/2 L.)	3.12**	0.297	−3.68***	−0.258
7 W. Premax. (at 1/2 L.)	−0.48	−0.046	0.23	0.017
8 W. Rostrum (at 3/4 L.)	0.33	0.028	−1.98*	−0.132
9 Preorbital W.	4.59***	0.403	−6.36***	−0.429
10 Postorbital W.	3.57***	0.262	−5.97***	−0.373
11 Skull W. (at Zygomatic P.)	3.43***	0.255	−5.98***	−0.357
12 Skull W. (at Parietals)	1.83	0.199	−2.19*	−0.165
13 Ht. Braincase	1.51	0.146	−3.89***	−0.275
14 L. Braincase	3.62***	0.323	−4.85***	−0.329
15 Max. W. Premax.	2.05*	0.209	−3.58***	−0.260
16 W. External Nares	−0.48	−0.047	−0.38	−0.027
17 L. Temporal Fossa	1.87	0.193	−2.74**	−0.201
18 W. Temporal Fossa	3.84***	0.362	−4.69***	−0.327
19 Orbital L.	3.01**	0.325	−3.68***	−0.276
20 L. Antorbital P.	2.93**	0.229	−4.32***	−0.277
21 W. Internal Nares	0.56	0.047	−3.43***	−0.226
22 L. Up. Toothrow	3.96***	0.392	−4.47***	−0.319
23 No. Teeth (Up.Lf.)	3.46***	0.411	−3.61***	−0.286
24 No. Teeth (Up.Rt.)	3.46***	0.434	−3.30***	−0.271
25 No. Teeth (Low.Lf.)	1.62	0.178	−1.38	−0.105
26 No. Teeth (Low.Rt.)	1.52	0.158	−1.28	−0.093
27 L. Low. Toothrow	3.00**	0.285	−3.46***	−0.242
28 Ht. Ramus	3.03**	0.237	−4.77***	−0.306
29 Tooth W.	−0.55	−0.067	−0.13	−0.011
30 L. Ramus	3.91***	0.375	−4.47***	−0.314
Component I	3.77***	0.363	−4.64***	−0.327
Component II	1.13	0.134	−2.72**	−0.214
Canonical Variable 1	2.77**	0.220	−5.08***	−0.327
Canonical Variable 2	4.05***	0.520	−4.12***	−0.343

*$P<0.05$; **$P<0.01$; ***$P<0.001$.

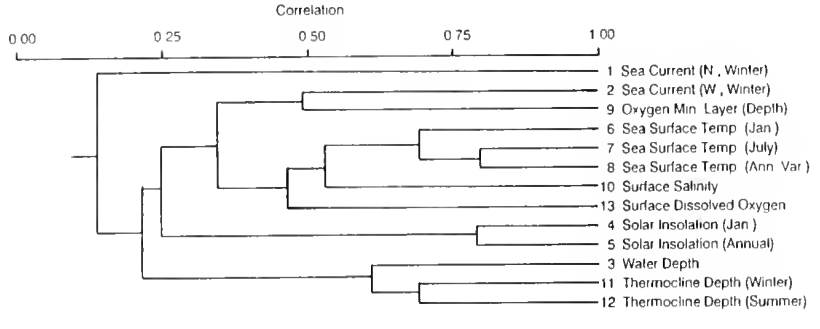

Figure 9

Clustering by UPGMA on absolute correlation values among environmental variables. Cophenetic correlation of 0.75.

Table 6

Principal component loadings for environmental variables.

Environmental variable	Component * I	II	III
1 Sea Current (N.,Winter)	−0.126	0.307	0.431
2 Sea Current (W.,Winter)	−0.495	−0.037	−0.091
3 Water Depth	−0.279	**0.783**	0.279
4 Solar Insolation (Jan.)	−0.683	−0.227	**0.627**
5 Solar Insolation (Ann.)	−0.274	−0.291	**0.872**
6 Sea Surface Temp. (Jan.)	0.768	−0.255	0.380
7 Sea Surface Temp. (July)	**0.942**	0.014	−0.101
8 Sea Surface Temp. (Ann.Var.)	**−0.848**	−0.224	−0.304
9 Oxygen Minimum Layer (Depth)	0.675	0.442	0.157
10 Surface Salinity	−0.608	**0.600**	−0.046
11 Thermocline Depth (Winter)	0.172	**0.888**	−0.269
12 Thermocline Depth (Summer)	−0.044	**0.836**	0.363
13 Surface Dissolved Oxygen	−0.596	0.089	−0.380

* Relatively high loadings highlighted in bold as follows: (component I) > |0.8|; (II and III) > |0.6|.

Table 7

Product-moment correlations of block means for morphological variables and components versus environmental variables and components based on 25 blocks of *Stenella longirostris*.[a]

Character	Environmental variable[b] 1	2	3	4	5	6	7	8	9	10	11	12	13	Environmental component I	II	III
1 Condylobasal L.						− −	− −						+ +	−		
2 L. Rostrum (frm.Base)						− −	−	+	+				+	−		
3 L. Rostrum (frm.Pterygoid)		+				− −	− −	+	−				+ +	−		−
4 W. Rostrum (at Base)			+ +			− −	−			+	+ + +	+ +			+ + +	
5 W. Rostrum (at 1/4 L.)			+ +			−	−			+	+ +	+ +			+ + +	
6 W. Rostrum (at 1/2 L.)			+ +				−			+	+	+ +			+ +	
7 W. Premax. (at 1/2 L.)													+		+ +	
8 W. Rostrum (at 3/4 L.)		−	+ +									+ +			+	
9 Preorbital W.			+ +			− − −	− − −			+ + +	+	+ +	+	− −	+ +	
10 Postorbital W.			+ +			− −	− − −			+ + +	+	+ +	+	− −	+ +	
11 Skull W. (at Zygomatic P.)			+ +			− −	− − −			+ + +	+	+ +	+	− −	+ +	
12 Skull W. (at Parietals)			+													
13 Ht. Braincase			+ +			−	− −			+ + +		+ +		−	+	
14 L. Braincase			+ + +			− − −	− − −			+ + +	+	+ +	+			
15 Max. W. Premax.					−	− −				+	+					
16 W. External Nares						−	−			+ +		+ + +	+	−		
17 L. Temporal Fossa						−	−						+	−		
18 W. Temporal Fossa			+ + +			−	−			+ +	+ +				+ + +	
19 Orbital L.		+				− −		−					+	−		
20 L. Antorbital P.			+			− −	− − −			+ +			+	− −		
21 W. Internal Nares			+	+ +			− − −							− −		
22 L. Up. Toothrow		+			−	− −	−	+	−				+ +	−		−
23 No. Teeth (Up.Lf.)		+				− −										−
24 No. Teeth (Up.Rt.)		+				− −										−
25 No. Teeth (Low.Lf.)																
26 No. Teeth (Low.Rt.)		+														
27 L. Low. Toothrow		+				− −	−	+	−				+	−	+	
28 Ht. Ramus			+ +			−	− −			+	+	+	+	−	+	
29 Tooth W.			+													
30 L. Ramus						− −	−	+	−				+ +	−		
Component I			+			− − −	− −			+ +	+	+	+	− −	+	
Component II		− −	+ +									+				+
Canonical Variable 1			+ +			− − −	− − −	+	−	+ +		+	+ +	− − −	+	
Canonical Variable 2		−		+ +	+ +						− −					+ +

Table 7 (continued)

[a] Blanks indicate nonsignificant correlations. Individual symbols refer to significant positive or negative correlations ($P<0.05$; >0.396); double symbols indicate highly significant correlations ($P<0.01$; >0.505); and triple symbols represent very highly significant correlations ($P<0.001$; >0.620).

[b] Environmental variables: (1) Sea Current (N., Winter); (2) Sea Current (W., Winter); (3) Water Depth; (4) Solar Insolation (Jan.); (5) Solar Insolation (Annual); (6) Sea Surface Temp. (Jan.); (7) Sea Surface Temp. (July); (8) Sea Surface Temp. (Ann. Var.); (9) Oxygen Min. Layer (Depth); (10) Surface Salinity; (11) Thermocline Depth (Winter); (12) Thermocline Depth (Summer); and (13) Surface Dissolved Oxygen.

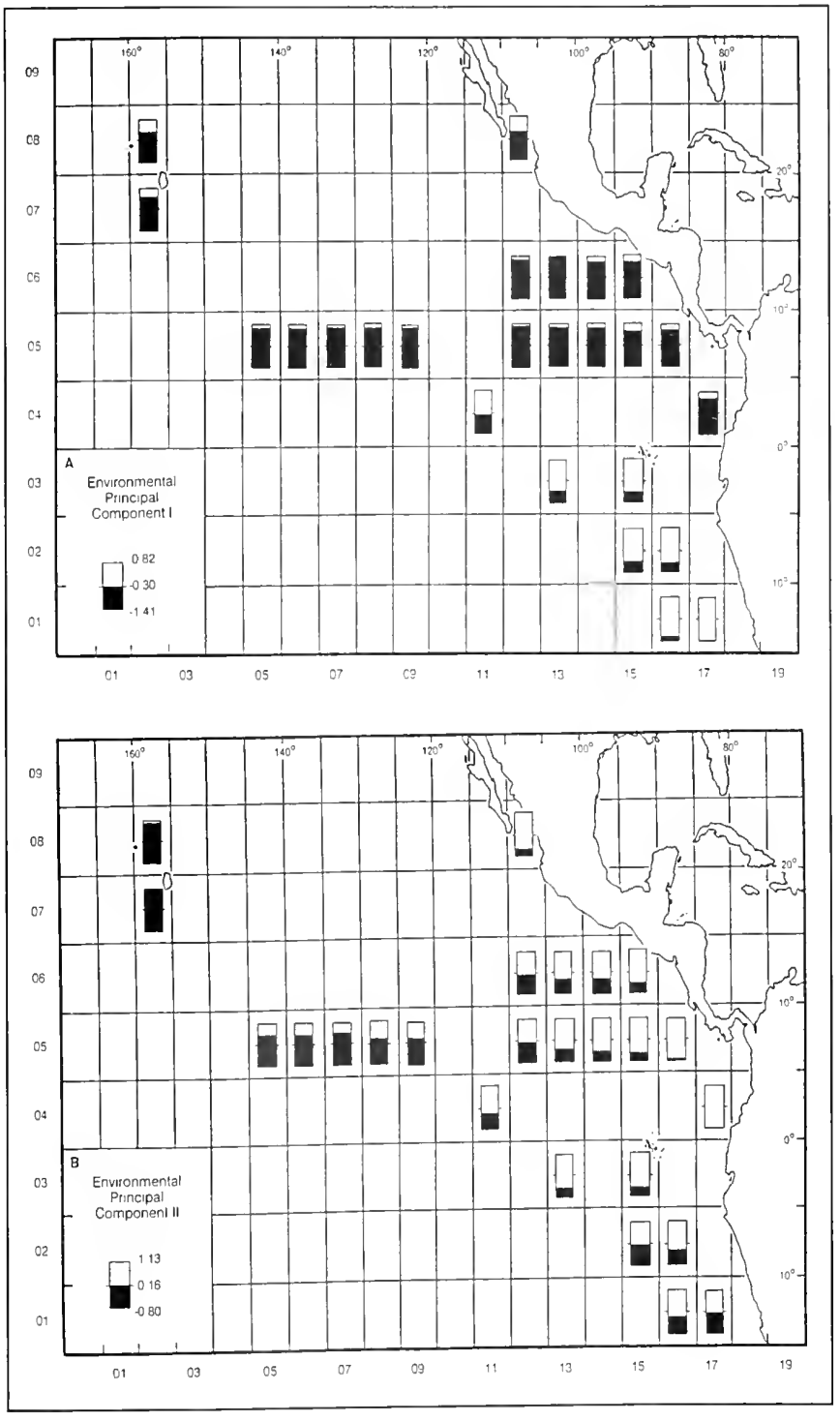

Figure 10
Geographic variation in environmental variables as summarized in (A) principal component I and (B) principal component II. Darkened part of bar indicates value for particular block.

Water Depth (variable 3; Fig. 11B) is positively correlated with 13 morphological measures, two of which (L. Braincase and W. Temporal Fossa) are very highly significant ($P<0.001$). The block values for W. Temporal Fossa (which have a 0.755 correlation with Water Depth values) are shown in Figure 11A. For the 13 variables, relatively large values typically were recorded in block 0117 and those in the vicinity of the Hawaiian Islands (0702 and 0802), all of which have relatively deep waters, while more shallow localities like 0516 and 0812 had individuals that were smaller for these characters.

The fourth environmental measure, Solar Insolation (Jan.), changes from high to low values uniformly from north to south. It is statistically associated with only one character, W. Internal Nares, which has small values for 0812; values tend to get higher as one proceeds south, but there are exceptions (such as 0802, which is relatively high). Canonical variable 2 has a pattern statistically similar to this environmental variable (bottom of Table 7).

Annual solar insolation (variable 5) has high values at the earth's Equator, with decreasing values as one proceeds toward either pole. Only two morphological variables have significant correlations with this environmental factor (Table 7), each of which are negative and relatively weak.

The sixth environmental variable, Sea Surface Temp. (Jan.), has significant negative correlations with 22 morphological characters, as well as principal component I (Fig. 4) and canonical variable 1 (Fig. 8B). Variable 7, which is Sea Surface Temp. (July) (Fig. 12), has a relatively high number (21) of significant negative associations with morphological measures, as well as with principal component I (Fig. 4) and canonical variable 1 (Fig. 8B). Postorbital W. (Fig. 8A) has the strongest correlation (−0.681) of any of the morphological characters with Sea Surface Temp. (July).

The eighth environmental variable, Sea Surface Temp. (Ann. Var.), exhibited relatively weak geographic concordance with six morphological characters, one of which was a negative association (Table 7). Also, only weak negative correlations of five morphological variables were found with depth of the oxygen minimum layer (variable 9).

Fourteen of the 30 morphological measures are significantly correlated with environmental variable 10, Surface Salinity (Fig. 13B). In addition to east-west changes from lower to higher values at a given latitude, salinity also exhibits a north-to-south trend of increasing values (below 15°N). The highest correlation (0.661) is with L. Braincase (Fig. 13A).

Thermocline Depth (Winter), variable 11, was positively associated with 13 morphological variables (Table 8), while Thermocline Depth (Summer), variable 12, has statistically significant positive correlations with 11 morphological traits. The final variable, Surface Dissolved Oxygen, covaries with 16 morphological variables. As suggested in the dendrogram in Figure 9, this environmental variable has a

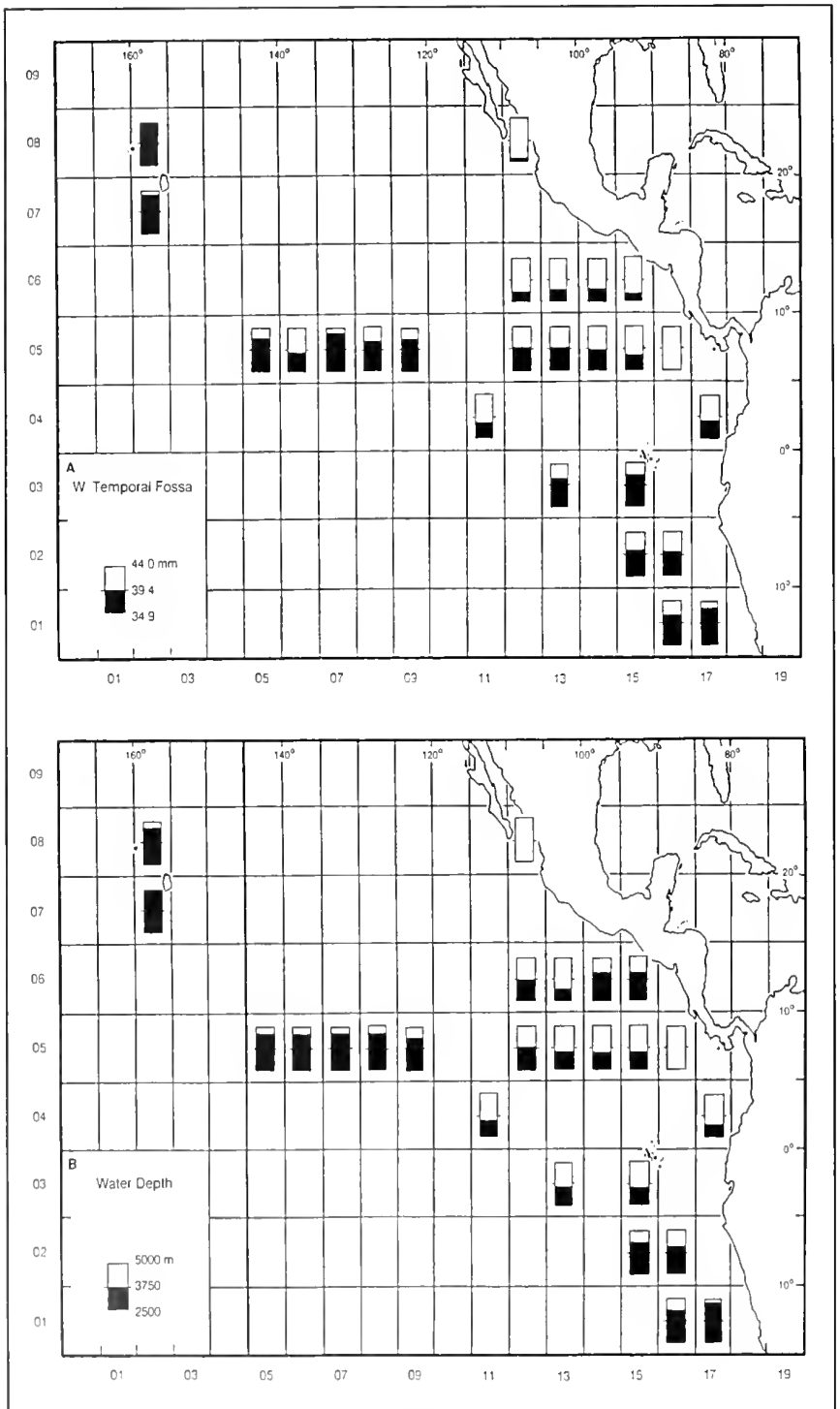

Figure 11

Geographic variation in (A) W. Temporal Fossa and (B) Water Depth. Darkened part of bar indicates value for particular block.

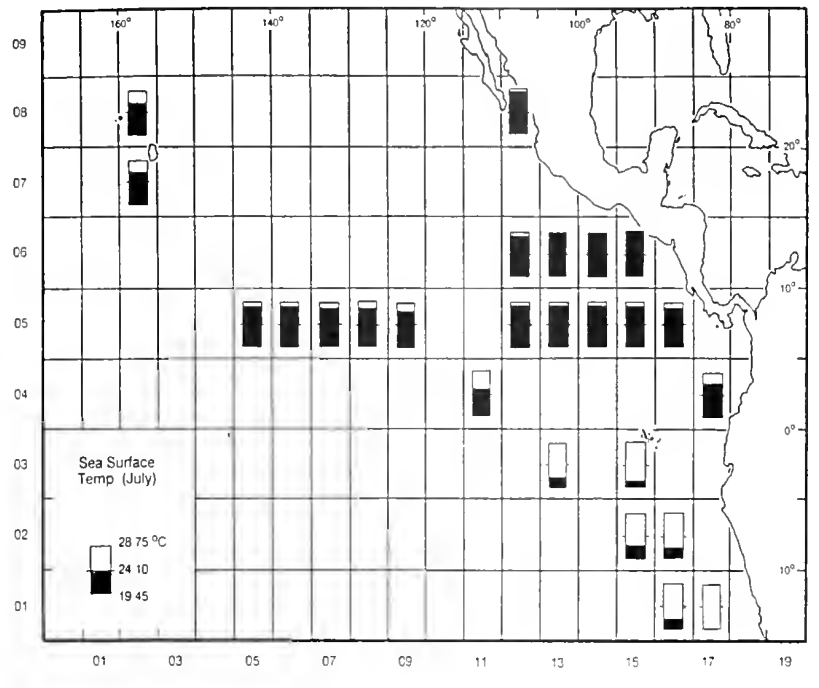

Figure 12
Geographic variation in Sea Surface Temp. (Jul.). Darkened part of bar indicates value for particular block.

pattern with similarities to those for sea surface temperatures.

Table 7 indicates that the pattern of correlations of environmental principal component I with cranial measures is similar to that of Sea Surface Temp. (July) (variable 7), which is expected given the strong loadings of this environmental variable on this component (see Table 6). Environmental principal component II has positive correlations with most skull-width measures (Table 7). The third environmental component has relatively few significant correlations with morphological characters; its strongest association is with one of the summary morphological variables, canonical variable 2.

In Table 8, we have summarized Mantel t-values and matrix correlations between selected

Table 8
Results of Mantel tests (t) and matrix correlations (r) for *Stenella longirostris*. Comparison of interlocality differences for 13 environmental variables and 3 environmental components against those for 5 morphological variables selected in canonical variates analysis.

	Postorbital W.		L. Rostrum (frm.Pterygoid)		W. Internal Nares		W. Premax. (at 1/2 L.)		W. Rostrum (at Base)	
Environmental variable	t	r	t	r	t	r	t	r	t	r
1 Sea Current (N.,Winter)	−0.56	−0.050	−0.59	−0.083	1.99*	0.215	−0.56	−0.073	−0.79	−0.141
2 Sea Current (W.,Winter)	−1.38	−0.092	0.12	0.010	−0.72	−0.053	0.59	0.048	−0.44	−0.044
3 Water Depth	3.23**	0.235	1.27	0.128	2.25*	0.186	−0.76	−0.073	2.22*	0.271
4 Solar Insolation (Jan.)	4.46***	0.339	2.60**	0.283	4.49***	0.393	0.77	0.079	1.81	0.241
5 Solar Insolation (Ann.)	2.14*	0.176	1.95	0.241	1.86	0.180	−0.54	−0.062	1.43	0.219
6 Sea Surface Temp. (Jan.)	5.47***	0.371	3.71***	0.327	3.63***	0.271	0.53	0.045	1.63	0.170
7 Sea Surface Temp. (July)	4.82***	0.353	1.73	0.176	4.65***	0.387	2.55*	0.244	0.64	0.079
8 Sea Surface Temp. (Ann.Var.)	1.64	0.114	1.22	0.113	3.80***	0.294	1.40	0.123	−0.40	−0.044
9 Oxygen Minimum Layer (Depth)	1.22	0.077	2.12*	0.158	3.54***	0.236	1.62	0.116	−0.61	−0.051
10 Surface Salinity	4.57***	0.323	0.37	0.035	1.03	0.082	0.06	0.005	0.62	0.072
11 Thermocline Depth (Winter)	2.92**	0.241	4.42***	0.548	−0.96	−0.093	−0.55	−0.063	3.87***	0.598
12 Thermocline Depth (Summer)	2.52*	0.172	1.63	0.146	−0.15	−0.001	−0.35	−0.030	3.41***	0.362
13 Surface Dissolved Oxygen	2.52*	0.204	1.43	0.172	1.88	0.179	0.93	0.105	−0.18	−0.027
Environmental Component I	3.63***	0.268	1.68	0.174	4.09***	0.345	2.02*	0.197	0.11	0.014
Environmental Component II	2.75**	0.212	3.85***	0.429	−1.11	−0.099	−0.75	−0.078	3.70***	0.508
Environmental Component III	1.39	0.120	1.19	0.160	1.99*	0.207	−0.97	−0.121	0.32	0.054

*$P<0.05$; **$P<0.01$; ***$P<0.001$.

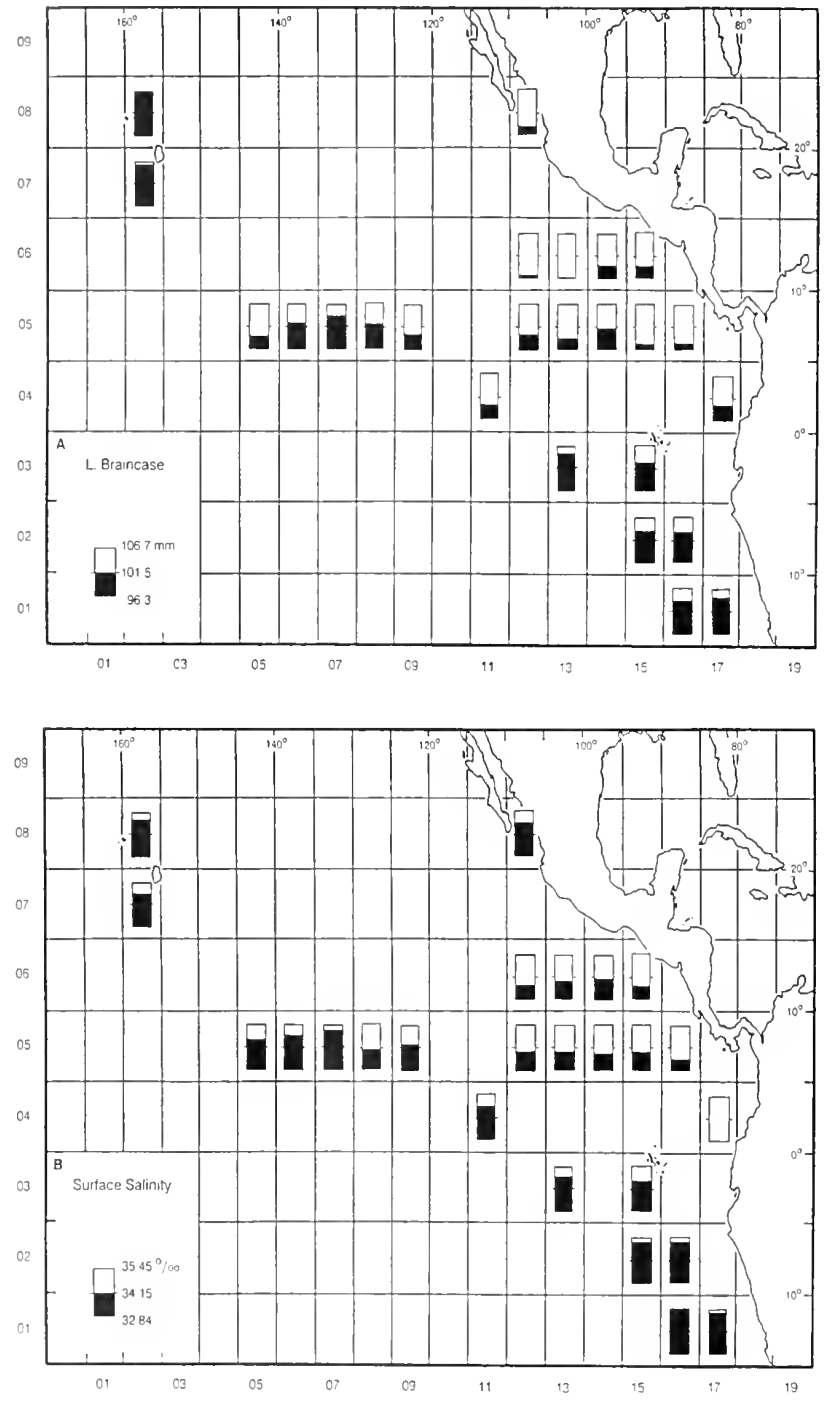

Figure 13

Geographic variation in (A) L. Braincase and (B) Surface Salinity. Darkened part of bar indicates value for particular block.

morphological and environmental variables. Assessing difference matrices using these techniques represents an alternate method with which to evaluate covariation of geographic patterns. For Postorbital W. (Fig. 8A), there are nine significant associations using the Mantel test (Table 8), with Sea Surface Temp. (Jan.) being the highest. The seven environmental variables displaying correlations in Table 7 with Postorbital W. also are judged concordant using the Mantel test. In addition, based on interblock difference values, there are statistically significant associations with the two measures of solar insolation (variables 4 and 5; see Table 8). The concordance with these two environmental variables is primarily on the strength of pattern similarities in the eastern portion of the range. Postorbital W. also shows significant associations with the first two environmental principal components.

Based on correlation tests for block means (Table 7), L. Rostrum (frm.Pterygoid) exhibited a geographic distribution of mean block values that was statistically associated with those for six environmental measures. Four significant associations were identified using the Mantel test (Table 8), only two of which were found by both tests (Sea Surface Temp. [Jan.] and Oxygen Minimum Layer [Depth]). It has a significant association with environmental component II.

In Table 8, a total of seven significant associations of difference values are recorded for W. Internal Nares with environmental variables, including the three listed in Table 7 as having statistically significant associations based on means. Difference values for environmental components I and III significantly covary with those of W. Internal Nares.

Using difference values, W. Premax. (at 1/2 L.) has only a weak correlation with a single environmental variable (Table 8); only a single significant association was found using correlations of mean values, and this was with another environmental variable (see Table 7). W. Premax. (at 1/2 L.) is weakly associated with environmental component I.

The W. Rostrum (at Base) exhibits covariation with three of the environmental variables based on the Mantel test (Table 8), two of which involve thermocline depth. The matrix correlation (Table 8) for W. Rostrum (at Base) with Thermocline Depth (Winter) is substantial (0.598), as it is with environmental component II (0.508). Mean values also showed an association of W. Rostrum (at Base) with the thermocline variables and Water Depth, as well as with three other environmental variables (Table 7).

Discussion

Sexual dimorphism

Our analysis of sexual dimorphism extends the studies of Douglas et al. (1986) in terms of additional specimens and minor adjustments in previously collected data. We found 15 of 30 variables were statistically dimorphic. Douglas et al. (1986) identified 13 of these as showing sexual differences, the increase of two characters (Postorbital W. and Tooth W.) being due primarily to increased numbers of specimens available. In five characters, including two rostral and two toothrow lengths, measurements for females were slightly larger than for males, although the differences were not statistically significant. For all other measures, males are larger than females, including all 15 where statistical significance was found.

Geographic variation

In 1889, when the existence of spinner dolphins in the eastern tropical Pacific was not yet known, True indicated that the absence of adequate samples made very difficult the task of taxonomically evaluating species in the genus *Stenella*. By the 1970s, Perrin (1975b) had available considerably more material for a monographic treatment of *S. attenuata* and *S. longirostris* from the eastern tropical Pacific and was able to make significant advances with respect to our understanding of morphological variation of *Stenella*. However, his work on *S. longirostris* also was hindered by the paucity of skeletal material from parts of the range. For our study, many additional specimens of *S. longirostris* were available. On the whole, our results are strongly supportive of those obtained by Perrin (1975b) for cranial characteristics, but we also have been able to substantially extend his analyses.

Perrin (1972) conducted an initial analysis of geographic variation in color patterns of *S. longirostris* in the eastern Pacific Ocean. He found geographic variation, particularly in the "dorsal field system" of coloration, which overlies a basic general pattern. These and other data suggested differentiation into eastern, whitebelly, and Hawaiian forms. The differences were analyzed further by Perrin (1975a,b), who indicated that the whitebelly form was in some ways similar to the Hawaiian form, but had a proportionately smaller beak. Perrin (1975b) described but did not name four races—the three mentioned above plus a Costa Rican form which occurs off the coast of Central America. Perrin et al. (1979b) evaluated possible differentiation in *S. longirostris* involving animals found south of the Equator in the eastern Pacific Ocean. They concluded that these *S. longirostris* are morphologically distinct from those to the northeast; characteristics showing such a trend include coloration, size, shape, and skeletal measures.

Recently, Perrin (1990) named and described three subspecies: *S. l. longirostris* (Gray's spinner dolphin), *S. l. orientalis* (eastern spinner dolphin), and *S. l. centroamericana* (Central American spinner dolphin). In our geographic variation assessment, we purposely included all adult specimens available, without an attempt *a priori* to differentiate previously described forms. However, the differences among the named forms are reflected in our results for cranial characteristics.

In our analyses, the Central American spinner dolphin of Perrin (1990) is shown to be different from other *S. longirostris* by the positioning of block 0516 on principal component II; it had the lowest value of any of the blocks (see Fig. 3). Three of the four specimens in block 0516 exhibit characteristics of Central American spinners (as does one of the nine from 0615). Character associations with the second principal component—summarized in Table 3—suggest that, after taking into account general size (summarized in and mathematically removed by component I), animals of this subspecies have relatively longer toothrows, greater numbers of teeth, a narrower skull at the parietals, and a shallower braincase than *S. longirostris* from other areas. Perrin (1990: table 2) provided comparative measurements and counts for *S. l. longirostris* and *S. l. centroamericana*, which show the Central American form to have longer toothrows and greater numbers of teeth. He did not include data on Ht. Braincase, but did characterize the Central American form as having a relatively long and narrow skull. While Skull W. (at Parietals) is slightly greater for *S. l. centroamericana* than *S. l. longirostris* (Perrin 1990: table 2), the former has a relatively narrow skull given its considerably greater length. Additional *S. l. centroamericana* specimens are needed, since the diagnosis and understanding of cranial variation in this subspecies still is based on very few animals.

Perrin (1990) suggested the existence of a zone of hybridization/intergradation between *S. l. longirostris*

and *S. l. orientalis* that may be about 2000km wide. *Stenella l. orientalis* is found primarily in the northeastern blocks we assessed. Our analyses confirm that, in general, adult spinner dolphins from this region are smaller than those from areas to the south, southwest, and west (for general trends, refer to block projections onto canonical variable 1 in Fig. 8B). The nominate subspecies, *S. l. longirostris*, of Perrin (1990) subsumes a series of broadly distributed populations. He indicated that *S. l. longirostris* likely includes areal entities (outside the eastern Pacific) worthy of formal taxonomic recognition, but to date these have not been evaluated properly because of a paucity of specimens from major portions of the range.

Extensive data on geographic variation in external morphology of *S. longirostris* in the eastern tropical Pacific were assessed by Perrin et al. (1991). They evaluated color patterns, dorsal-fin shapes, and total lengths for *S. longirostris* from throughout the geographic range covered in our study. Some external characters (e.g., ventral field coloration pattern) exhibited a "radial" or concentric pattern of variation, where spinners to the south, southwest and west were similar, but markedly different from those to the northeast. This pattern also was prevalent among cranial variables (e.g., see values for Postorbital W. [Fig. 8A], canonical variable 1 [Fig. 8B], and L. Braincase [Fig. 13A]).

We were able to incorporate specimens into our analyses from the general vicinity of the Hawaiian Islands. Perrin (1975b) evaluated Hawaiian specimens for cranial features and concluded that, in general, they were strikingly larger than other spinners. However, at the time, few specimens were available from southern localities. When these southern blocks are incorporated into the analysis, the Hawaiian specimens are not quite as extreme, although for most characters the Hawaiian specimens remain the largest (see Postorbital W. [Fig. 8A], W. Temporal Fossa [Fig. 11A] and L. Braincase [Fig. 13A], as well as principal component I [Figs. 3 and 4] and canonical variable 1 [Figs. 7 and 8B]). Also, for many of the characters the Hawaiian specimens are more similar to far-southern ones than to those from geographically closer western blocks located between 5° and 10°N. When evaluating other western single-specimen blocks that are situated closer to the Hawaiian Islands, some analyses (e.g., canonical variates analysis; see Fig. 7) indicate that spinners similar to Hawaiian specimens are present; however, additional specimens will be needed in order to clarify the trends in variation in this part of the Pacific.

In some descriptive analyses (e.g., see Figs. 6 and 7), block 0702 to the south of the Hawaiian Islands is depicted as quite distinct from other blocks, including the adjacent block to the north (0802). This incongruity is likely a statistical aberration related to the small sample size for 0702 (n 2), rather than to a biological difference. Checking the specimens from the two blocks indicated that they were taken in relatively close proximity, but were separated because of where the border between the blocks happened to be located. This apparent anomaly does not detract from the general conclusion that the spinners in the vicinity of the Hawaiian Islands are among the largest found in the overall study region.

Schnell et al. (1986) conducted an extensive analysis of geographic variation of offshore *S. attenuata*, a similar species that broadly overlaps in range with *S. longirostris*. The two species frequently are seen in mixed schools (Au and Perryman 1985, Reilly 1990). Reilly (1990) noted that 73% of the *S. longirostris* sightings from research vessels also included *S. attenuata*; 49% of the records of the more common *S. attenuata* involved schools that also had *S. longirostris*. While detailed comparisons evaluating interspecific geographic covariation in morphology are beyond the scope of this paper, our preliminary findings indicate that about one-half of the individual morphological characters show similar geographic patterns for blocks where both species are represented. However, two characters involving the temporal fossa (variables 17 and 18) exhibit negative correlations (the length correlation is statistically significant and the width nearly so)—localities where the fossa is larger in *S. attenuata*, it is smaller in *S. longirostris*. The temporal fossa reflects the size of muscles involved in the feeding apparatus. Also, the upper tooth counts show pronounced negative correlations interspecifically. Opposite trends in the two similar species for these characters may be an example of ecological character displacement related to differences in feeding and the types of food taken by the two species in given localities (Perrin 1984).

Genetic subdivision, management units, and implications of cranial variation

Considerable attention has been given to definition of stock units with a meaningful biological basis that can be employed to manage *S. longirostris* in the eastern Pacific (Perrin 1975a,b; Perrin et al. 1979b, 1985, 1991). One of the important questions with respect to the effectiveness or relevance of geographic management units is the degree to which the species is genetically subdivided. Perrin et al. (1991) noted a complex patchwork pattern of geographic variation in external and other characteristics in *S. longirostris* suggesting "that there is not a large amount of movement between the various regions." They pointed out that the complex geographic pattern of variation in the

zone of intergradation/hybridization of *S. l. orientalis* with *S. l. longirostris* is consistent with limited data on movements from tag returns (Perrin et al. 1979a), which indicate "a home range of a diameter of hundreds rather than thousands of kilometers."

Our findings strongly support these conclusions. All 30 characters studied showed geographic variation, with two-thirds having demonstrable regional patterning, and 25 of the 30 showing local patterning. These patterns emerge even though data are based on specimens pooled over season and for a number of years; consistent geographic patterns largely would be obscured if animals typically moved long distances within or between years. Clearly, as found by Schnell et al. (1986) for *S. attenuata*, in *S. longirostris* "there are notable patterns of geographic variation...indicating that geographic subdivision exists among populations."

We found concordance of geographic patterns in *S. longirostris* for a number of cranial characters as noted by Perrin et al. (1991) for external characters. Yet, some patterns are not concordant; in fact, there is a mosaic of patterns involving different characters and/or character suites. For example, many of the tooth counts, toothrow measurements, and rostrum and ramus lengths show very similar patterns of variation (as indicated in Fig. 2), while other characters like Tooth W. have a pattern among blocks that is not closely related to that of any other character. Not surprisingly, a number of skull widths covary. Overall, the findings for *S. longirostris* parallel the situation typically found in other mammals where geographic variation in morphological characters has been studied. Some observed patterns may be the consequence of action by selective forces, while others simply result from and are maintained because of isolation by distance. The findings are consistent with *S. longirostris* being genetically subdivided, stemming from individual animals or groups of animals having relatively limited home ranges.

For management stocks, Perrin et al. (1991) proposed an alternative management scheme where "an 'eastern spinner conservation zone' could be devised that would offer appropriate and unequivocal protection to the unique and coherent gene pool of the eastern subspecies." For instance, a zone bounded on the south by 10°N and and on the west by 125°W would encompass 84% of the schools that were identified in the field as being composed of "eastern" spinners, and would include very few "whitebelly" animals (Perrin et al. 1991). Based on the cranial measures we employed, spinners from the blocks in this portion of the range are very similar; the blocks typically were closely linked in cluster analyses and ordinations. Blocks from most other parts of the range did not show the same degree of consistency and concordance. Our data also provide additional biological justification for establishing a geographically defined management zone for *S. l. orientalis* that, operationally, would be easily understood and more effective for management purposes.

Perrin et al. (1991) also concluded that data on external characters do not support the division of whitebelly spinners into northern and southern stocks for management purposes. For cranial features, if one considers only eastern blocks, it is possible to achieve a considerable degree of separation between northern and southern whitebelly spinners. However, the situation becomes notably more complex when more westerly blocks are added. For virtually all cranial characters, the western blocks group with the more southerly blocks even though they are at the same latitude as blocks to the east containing northern whitebelly spinners; the only possible exception is W. Internal Nares, which shows a strong north to south gradient involving all blocks except for one in the vicinity of the Hawaiian Islands (i.e., 0802). The addition of cranial specimens from western locations has provided a more sophisticated picture of geographic variation of *S. longirostris* in the region under study.

Morphological-environmental covariation

Considerable heterogeneity exists in environmental parameters over the range of *S. longirostris* in the eastern tropical Pacific (see examples of environmental variation in Figs. 11–13). With two circulatory gyres adjacent to the region, one to the north and the other to the south, the eastern tropical Pacific has an easterly-flowing equatorial counter-current from 3° to 10°N latitude, and a number of fronts and convergences (Wyrtki 1966, 1967). These coupled with latitudinal and other gradients result in substantial spatial differences in environmental characteristics.

Spotted dolphin/environmental comparisons

Schnell et al. (1986) evaluated covariation in a similar suite of environmental and cranial morphological features for offshore *S. attenuata* in the eastern tropical Pacific. The *S. attenuata* investigation was focused in eastern areas (only 1 of 19 blocks was west of 115°W). Our analysis of *S. longirostris* covers considerably more of the ocean, and includes areas around the Hawaiian Islands, which potentially could have substantially different marine environments. The importance of particular environmental variables, of course, could be quite different when different geographic levels and different-sized areas are considered. Furthermore, environmental influence could well vary between species. Yet it can be instructive to compare results of environmental-morphologic patterns for

these two dolphin species with broadly overlapping geographic ranges in the tropical Pacific Ocean.

Sea surface temperatures (variables 6 and 7; July values depicted in Fig. 12) have negative correlations with a large number of morphological features in both studies (Table 7 and Schnell et al. 1986: table 6), indicating a general trend of larger animals in warmer waters. Surface Salinity (Fig. 13B) exhibits relatively strong morphologic correlations in both studies, reflecting a pattern that has both east-west and north-south components. Also, Thermocline Depth (Summer), which has relatively low values in northern localities and higher numbers in blocks as one proceeds to the west and south, is positively associated with a number of morphological measures in *S. longirostris* (Table 7), and covaries with *S. attenuata* cranial features as well.

Solar Insolation (Jan.) registers a north-south gradient. Our *S. longirostris* study produced virtually no significant correlations with this measure, while there were numerous positive correlations in the *S. attenuata* investigation. In the eastern portion of the *S. longirostris* range, a number of cranial features have north-south gradients, but the overall statistical association is negated with the addition of the western blocks, where animals often (irrespective of latitude) exhibit characteristics similar to those found in southern areas. The same findings were obtained for Solar Insolation (Ann.).

Three environmental variables—Water Depth (Fig. 11B), Thermocline Depth (Winter), and Surface Dissolved Oxygen—are positively correlated with cranial measures in *S. longirostris*, but show few of these associations in *S. attenuata*. Again, the differences in findings simply may reflect the inclusion of a wider geographic range of blocks in the *S. longirostris* study.

Schnell et al. (1986) indicated that for *S. attenuata* it would be helpful to have additional samples, particularly from western locations. They suggested that "Such a geographic broadening of representation may enable investigators to separate, at least in part, environmental-morphological correspondences that reflect causal relationships from trends [in morphology] maintained primarily as a result of isolation by distance." For *S. longirostris*, where additional western blocks are now represented (albeit in some cases with very limited samples), it is clear that the gradients in a relatively large number of cranial characteristics are not simply north-south trends, but rather what Perrin et al. (1991) described as a radial pattern. From northeastern blocks, these characters in *S. longirostris* change more-or-less gradually as one moves to the south, the southwest, or the west. There are several environmental variables exhibiting this type of pattern (e.g., Surface Salinity; Fig. 13B). At the same time, the January and July sea surface temperatures (for July values, see Fig. 12) have a predominantly north-south orientation (with the Hawaiian Island blocks being lower than expected, given their latitude) and are correlated with the largest number of cranial characters (see Table 7). When additional specimens of *S. attenuata* become available from westerly blocks not represented in samples available to Schnell et al. (1986), it will be of interest to determine whether patterns of cranial variation (and covariation with environmental measures) in this species will mirror those we have found for *S. longirostris*.

Significance of covariation with environmental measures While previous literature has little information on the relation of environmental and cranial variation in *S. longirostris*, other investigators (Au and Perryman 1985, Reilly 1990) have evaluated physical environmental parameters with respect to distributions of *S. longirostris* and several other species in the eastern tropical Pacific. They pointed out that the highest school densities for *S. longirostris* are in the area off the Mexican coast, which also is the most tropical and least seasonally variable portion of the range. We have demonstrated notable associations of cranial variation with physical environmental characteristics. Analyses involving environmental-cranial correlations, by their very nature, are descriptive and do not provide direct information on causal factors per se. Nevertheless, they clearly indicate that between areas where animals are different cranially, there often are marked habitat differences involving the physical environment.

The first two environmental principal components (Fig. 10) describe independent, orthogonal environmental patterns: component I has a general configuration of high values between 5° and 15°N, slightly lower values further to the north, and low values to the south (Fig. 10A), which is overlain by basically an east-to-west trend summarized in environmental principal component II. The important individual environmental covariates with morphological characters include surface temperatures, salinity, and measures of water depth. The physical environmental differences reflected by the principal components, as well as by individual environmental measures, describe basic habitat differences and likely reflect, indirectly, geographic differences in available prey species and their abundances. Given the marked environmental differences exhibited in the range of *S. longirostris*, the most surprising result would have been if this species had been relatively uniform geographically in cranial features—clearly, this is not the case. Our initial assessment of morphologic-environmental covariation further underscores the appropriateness of treating different parts of the range of *S. longirostris* in the eastern tropical Pacific

separately for management purposes. In particular, a growing base of information suggests giving special attention to the spinners from the relatively uniform area of the Pacific just to the west of the Mexican/Central American coast, and viewing the pattern of morphologic variation as being broadly concentric in nature.

Acknowledgments

S.B. Reilly and A.E. Dizon reviewed the manuscript and provided useful suggestions. We thank J. Gilpatrick and J.V. Kashiwada for preparing and curating some of the specimens, as well as assisting with preparation of data for analysis. Computer programs and assistance were provided by F.J. Rohlf, R.R. Sokal, and M.A. Schene. Support for aspects of this research was received by the University of Oklahoma through Contract 79-ABC-00167 from the U.S. Department of Commerce, National Oceanographic and Atmospheric Administration, and Purchase Orders 84-ABA-02177 and 40JGNF0532 from the National Marine Fisheries Service, Southwest Fisheries Science Center, La Jolla, CA. The following individuals provided access to museum specimens: S. Anderson, G.G. Musser, and D. Russell (American Museum of Natural History, New York, NY); M.C. Sheldrick (British Museum of Natural History, Tring, United Kingdom); S. Bailey, L.C. Binford, and J. Schoenwald (California Academy of Science, San Francisco, CA); P.J.H. van Bree (Instituut voor Taxonomische Zoologie, University of Amsterdam, Amsterdam, The Netherlands); D.R. Patten and J.E. Heyning (Los Angeles County Museum of Natural History, Los Angeles, CA); C.P. Lyman and M. Rutzmoser (Museum of Comparative Zoology, Harvard University, Cambridge, MA); W.Z. Lidicker Jr. (Museum of Vertebrate Zoology, University of California, Berkeley, CA); C.G. van Zyll de Jong (Museum of Natural Sciences, National Museum of Canada, Ottawa, Canada); J.G. Mead and C.W. Potter (National Museum of Natural History, Washington D.C.); D.W. Rice and A.A. Wolman (NOAA Northwest and Alaska Fisheries Science Center, Seattle, WA); L.J. Hansen (NOAA Southwest Fisheries Science Center, La Jolla, CA); G.F. Mees (Rijksmuseum van Natuurlijke Histoire, Leiden, The Netherlands); A. Rea (San Diego Museum of Natural History, San Diego, CA); M.L. Johnson and E. Kritzman (University of Puget Sound, Tacoma, WA); and G.L. Worthen (Utah State University, Logan, UT).

Citations

Allen, R.A.
1985 Dolphins and the purse-seine fishery for yellowfin tuna. *In* Beddington, J.R., R.J.H. Beverton, and D.M. Lavigne (eds.), Marine mammals and fisheries, p. 236–252. Allen and Unwin, London.

Au, D.W.K., and W.L. Perryman
1985 Dolphin habitats in the eastern tropical Pacific. Fish. Bull., U.S. 83:623–643.

Bartholomew, J., and Son
1975 The Times atlas of the world. Comprehensive Edition. Times Books, London, 223 p.

Brunt, D.
1934 Physical and dynamical meteorology. University Press, Cambridge, England, 411 p.

Cromwell, T.
1958 Thermocline topography, horizontal currents and "ridging" in the eastern tropical Pacific. Inter-Am. Trop. Tuna Comm. Bull. 3:135–152.

Dailey, M.D., and W.F. Perrin
1973 Helminth parasites of porpoises of the genus *Stenella* in the eastern tropical Pacific, with descriptions of two new species: *Mastigonema stenellae* gen. et sp. n. (Nematoda: Spiruroidea) and *Zalophotrema pacificum* sp. n. (Trematoda: Digenea). Fish. Bull., U.S. 71:455–471.

Dixon, W.D. (chief editor)
1990 BMDP statistical software, Vol. 1. Univ. Calif. Press, Berkeley.

Dizon, A.E., Ŝ.O. Southern, and W.F. Perrin
1991 Molecular analysis of mtDNA types in exploited populations of spinner dolphins (*Stenella longirostris*). Rep. Int. Whaling Comm. Spec. Issue 13:183–202.

Douglas, M.E., and J.A. Endler
1982 Quantitative matrix comparisons in ecological and evolutionary investigations. J. Theor. Biol. 99:777–795.

Douglas, M.E., G.D. Schnell, and D.J. Hough
1986 Variation in spinner dolphins (*Stenella longirostris*) from the eastern tropical Pacific Ocean: Sexual dimorphism in cranial morphology. J. Mammal. 67:537–544.

Hall, M.A., and S.D. Boyer
1988 Incidental mortality of dolphins in the eastern tropical Pacific tuna fishery in 1986. Rep. Int. Whaling Comm. 38: 439–441.
1989 Estimates of incidental mortality of dolphins in the eastern Pacific fishery for tropical tunas in 1987. Rep. Int. Whaling Comm. 39:321–322.
1990 Incidental mortality of dolphins in the tuna purse-seine fishery in the eastern Pacific Ocean during 1988. Rep. Int. Whaling Comm. 40:461–462.

Innis, G., J. Haefner, G. Worthen, and C. Fowler
1979 ETP ecosystem model documentation. Report for Southwest Fish. Cent., NMFS, NOAA, La Jolla, CA, 277 p.

Katz, J.O., and F.J. Rohlf
1973 Function-point cluster analysis. Syst. Zool. 22:295–301.

Levitus, S.
1982 Climatological atlas of the world ocean. NOAA Prof. Pap. 13, Rockville, MD.

Manley, B.J.F.
1985 The statistics of natural selection on animal populations. Chapman and Hall (Meuthen), NY.

Mantel, N.
1967 The detection of disease clustering and a generalized regression approach. Cancer Res. 27:209–220.

Perrin, W.F.
1972 Color patterns of spinner porpoises (*Stenella* cf. *S. longirostris*) of the eastern Pacific and Hawaii, with comments on delphinid pigmentation. Fish. Bull., U.S. 70:983–1003.
1975a Distribution and differentiation of populations of dolphins of the genus *Stenella* in the eastern tropical Pacific. J. Fish. Res. Board Can. 32:1059–1067.
1975b Variation of spotted and spinner porpoise (genus *Stenella*) in the eastern tropical Pacific and Hawaii. Bull. Scripps Inst. Oceanogr. 21:1-206.
1984 Patterns of geographical variation in small cetaceans. Acta Zool. Fenn. 172:137–140.
1990 Subspecies of *Stenella longirostris* (Mammalia: Cetacea: Delphinidae). Proc. Biol. Soc. Wash. 103:453–463.

Perrin, W.F., W.E. Evans, and D.B. Holt
1979a Movements of pelagic dolphins (*Stenella* spp.) in the eastern tropical Pacific as indicated by results of tagging, with summary of tagging operations, 1969–1976. NOAA Tech. Rep. NMFS SSRF-737, 14 p.

Perrin, W.F., P.A. Sloan, and J.R. Henderson
1979b Taxonomic status of the 'southwestern stocks' of spinner dolphin, *Stenella longirostris*, and spotted dolphin, *S. attenuata*. Rep. Int. Whaling Comm. 29:175–184.

Perrin, W.F., M.D. Scott, G.J. Walker, and V.L. Case
1985 Review of geographical stocks of tropical dolphins (*Stenella* spp. and *Delphinus delphis*) in the eastern Pacific. NOAA Tech. Rep. NMFS 28, 28 p.

Perrin, W.F., P.A. Akin, J.V. Kashiwada
1991 Geographic variation in external morphology of the spinner dolphin *Stenella longirostris* in the eastern Pacific and implications for conservation. Fish. Bull., U.S. 89:411–428.

Reilly, S.B.
1990 Seasonal changes in distribution and habitat differences among dolphins in the eastern tropical Pacific. Mar. Ecol. Prog. Ser. 66:1–11.

Robinson, M.K.
1976 Atlas of north Pacific Ocean monthly mean temperatures and mean salinities of the surface layer. Naval Oceanogr. Office Ref. Publ. 2, Wash. DC.

Rohlf, F.J., J. Kishpaugh, and D. Kirk
1979 NT-SYS. Numerical taxonomy system of multivariate statistical programs. State Univ. New York, Stony Brook.

Schnell, G.D., M.E. Douglas, and D.J. Hough
1985a Sexual dimorphism in spotted dolphins (*Stenella attenuata*) in the eastern tropical Pacific Ocean. Mar. Mammal Sci. 1:1–14.
1986 Geographic patterns of variation in offshore spotted dolphins (*Stenella attenuata*) of the eastern tropical Pacific Ocean. Mar. Mammal Sci. 2:186–213.

Schnell, G.D., D.J. Watt, and M.E. Douglas
1985b Statistical comparison of proximity matrices: Applications in animal behaviour. Anim. Behav. 33:239–253.

Sneath, P.H.A., and R.R. Sokal
1973 Numerical taxonomy. W.H. Freeman, San Francisco.

Sokal, R.R.
1979 Testing statistical significance of geographic variation patterns. Syst. Zool. 28:227–232.

True, F.W.
1889 Contributions to the natural history of the cetaceans, a review of the family Delphinidae. Bull. U.S. Natl. Mus. 36:1–191.

Wirth, M., G.F. Estabrook, and D.F. Rogers
1966 A graph theory model for systematic biology with an example for the Oncidiinae (Orchidaceae). Syst. Zool. 15:59–69.

Wyrtki, K.
1966 Oceanography of the eastern equatorial Pacific Ocean. Oceanogr. Mar. Biol. Annu. Rev. 4:36–68.
1967 Circulation and water masses in the eastern equatorial Pacific Ocean. Int. J. Oceanol. Limnol. 1:117–147.
1974 The dynamic topography of the Pacific Ocean and its fluctuations. Rep. H-16-74-S, Hawaii Inst. Geophysics, 19 p.

Geographic variation in population genetic structure of chinook salmon from California and Oregon

Graham A.E. Gall
Devin Bartley
Boyd Bentley
Department of Animal Science
University of California, Davis, California 95616

Jon Brodziak
Graduate Group in Applied Mathematics and Institute of Theoretical Dynamics
University of California, Davis, California 95616

Richard Gomulkiewicz
Graduate Group in Applied Mathematics and Institute of Theoretical Dynamics
University of California, Davis, California 95616
Present address: Department of Zoology, University of Texas, Austin, Texas 78712

Marc Mangel
Department of Zoology and Center for Population Biology
University of California, Davis, California 95616

Abstract.–We analyzed the protein products of 78 isozyme loci in 37 populations of chinook salmon *Oncorhynchus tshawytscha* from California and Oregon. Allele frequencies at 47 polymorphic loci revealed substantial genetic variability within the study area. The collections of chinook salmon studied could be differentiated into five major groups located in the following geographical areas: (1) Smith River–Southern Oregon area, (2) Middle Oregon Rivers, (3) Klamath–Trinity Basin, (4) Eel River–California Coastal area, and (5) Sacramento–San Joaquin Basin. Average heterozygosity estimates were lowest in collections from the Klamath–Trinity area and highest in the Oregon populations. Gene diversity analysis indicated that differences among fish within samples accounted for 89.4% of the total diversity, whereas intersample differences accounted for 10.6 %. Estimates of the average level of historical gene flow between populations ranged from 15.57 migrants per generation in the Sacramento–San Joaquin River system to 3.97 in the Klamath–Trinity Basin; an overall estimate of number of salmon exchanging genes between populations per generation was 2.11. Although these data appeared to reflect primarily population structures existing prior to the 20th century, evidence of some effects of hatchery management and transplantations was detected.

Manuscript accepted 13 August 1991.
Fishery Bulletin, U.S. 90:77–100 (1992).

Chinook salmon *Oncorhynchus tshawytscha* is the most abundant and commercially important species of Pacific salmon native to California and Oregon (Moyle 1976), but stocks have declined (Netboy 1974), in some cases to near extinction. Efforts to manage and preserve the chinook fishery have involved traditional methods such as tag and recapture estimations and restrictive fishing regulations. Recently, however, population genetic analysis of Pacific salmon has emerged as a major tool in fishery management to estimate population subdivision, migration, gene flow, and stock composition of ocean fisheries (Ryman and Utter 1987).

Genetic studies on chinook salmon have refined our understanding of these populations. Examination of large numbers of polymorphic loci revealed geographic associations among populations of chinook salmon (Gharrett et al. 1987, Utter et al. 1989, Bartley and Gall 1990, Shaklee et al. 1990b). Genetic differences among chinook salmon stocks from different geographic areas are being used to identify the stock composition of mixed ocean salmon fisheries (Pella and Milner 1987, Utter et al. 1987, Shaklee et al. 1990b, Brodziak et al. 1992). In addition, genetic studies have indicated the effects of climate and geological events on the population structure of chinook salmon (Gharrett et al. 1987, Bartley and Gall 1990).

Utter et al. (1989) and Bartley and Gall (1990) recently described California populations of chinook salmon using data sets with 53 isozyme loci for 35 populations, and 25 polymorphic loci for eight populations, respectively. The objectives of the study reported here were to further refine the description of chinook salmon populations in California and southern Oregon, expand the baseline genetic data available for genetic stock-identification studies (Shaklee et al. 1990b, Brodziak et al. 1992),

and provide estimates for heterozygosity, allele frequencies, and genetic identities as used for optimum estimation of stock composition of mixed fisheries.

Materials and methods

Samples

A total 37 samples of juvenile chinook salmon were collected from northern California and southern Oregon during 1987–88 (Fig. 1, Table 1). Fifteen of these samples were from fish hatcheries and pond rearing projects. All the samples represented fall-run fish with the exception of the upper Sacramento sample (#33) which represented winter run salmon. To collect outmigrant chinook salmon from the wild, two fyke nets (1.5×2.1×15m) were placed in a stream approximately 1.6km apart and allowed to set overnight. Juvenile salmon were removed from the nets the following morning and frozen on dry ice. Juvenile chinook from hatcheries were collected with dip nets. A small number of salmon was taken from each raceway that contained salmon until a total of 200 fish was collected. At the laboratory, liver, muscle, heart, and eye tissue were removed from 100 fish from each collection, placed in individual tubes, and stored at −80°C. The remaining 100 salmon were frozen at −80°C in an archival collection.

Electrophoresis

Tissue preparation and horizontal starch-gel electrophoresis followed standard procedures (Aebersold et al. 1987). Gels were made with 12% hydrolyzed potato starch (Connaught Labs.) and one of the following buffer solutions: CAM, an amine citrate buffer from Clayton and Tretiak (1972) adjusted to pH 6.8; TBCL, the discontinuous buffer system of Ridgway et al. (1970) at pH 8.0; TC-4, a Tris citrate buffer of 0.223 M Tris, 0.083 M citric acid pH 5.8 as electrode buffer, and a 3.7% mixture of buffer in distilled water for the gel (Schaal and Anderson 1974); and TG, a Tris glycine buffer of 0.025 Tris and 0.192 glycine pH 8.5 for both gel and electrode buffers (Holmes and Masters 1970). The protein systems analyzed, locus designations, tissue distribution of isozymes, and buffer systems used are presented in Table 2. Because of recent changes in genetic nomenclature (Shaklee et al. 1990a), other locus name synonyms are presented in Table 2 to facilitate comparisons with other studies. Allele designations followed Allendorf and Utter (1979).

Histochemical staining procedures followed Shaw and Prasad (1970) and Harris and Hopkinson (1976). The data set described herein constitutes baseline data

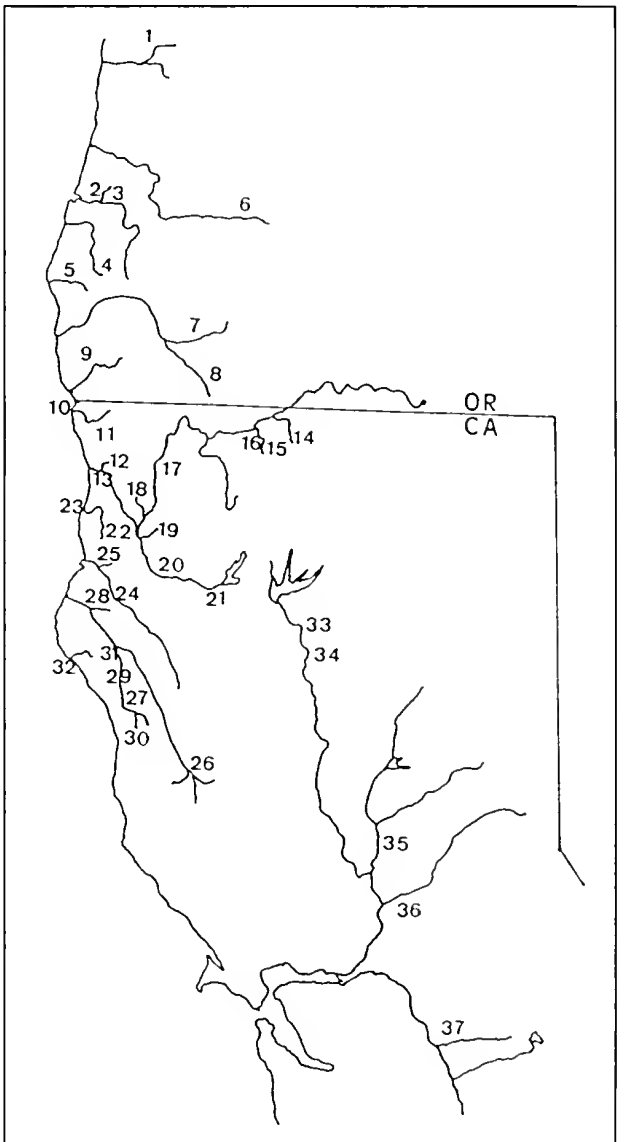

Figure 1
Collection sites of 37 samples of chinook salmon *Oncorhynchus tshawytscha*. Identification numbers are defined in Table 1.

reported in Gall et al. (1989) and used in maximum-likelihood estimates for the California mixed ocean salmon fishery (Brodziak et al. 1992). The duplicated isoloci AAT-1,2, IDH-3,4, MDH-1,2, MDH-3,4, and PGM-3,4 each were treated as two loci. Variant alleles were preferentially assigned to one locus, whereas common alleles were assigned to the other (Gharrett et al. 1987). Variation at the IDH-3,4 isoloci was ascribed to specific loci as described by Shaklee et al. (1990b). Our method of scoring isoloci is not the method of choice for studies of genetic mechanisms, as it may not reflect the true genetic distribution of alleles

Table 1

Thirty-seven collections of juvenile chinook salmon from five areas of California and Oregon. Locations of collections are designated on Figure 1 by identification number (ID#). N = number of fish analyzed.

Area	ID#	Collection site	N	No. of loci scored	Average heterozygosity (Nei 1973)
Middle Oregon	1	Fall Creek Hatchery	100	78	0.072
	2	Morgan Creek Hatchery	10	78	0.076
	3	Millacoma River	100	78	0.072
	4	Coquille River, South Fork	100	78	0.073
	5	Elk River Hatchery	100	78	0.076
	6	Rock Creek Hatchery	100	78	0.054
S. Oregon/N. California Coastal	7	Rogue River	100	78	0.052
	8	Applegate River	100	78	0.054
	9	Chetco River Hatchery	100	78	0.063
	10	Rowdy Creek Hatchery	62	77	0.067
	11	Smith River, Middle Fork	99	77	0.059
Klamath–Trinity Basin	12	Blue Creek	100	77	0.059
	13	Omagar Creek Pond-Rearing Facility	100	78	0.064
	14	Irongate Hatchery	99	78	0.031
	15	Bogus Creek	128	77	0.030
	16	Shasta River	100	77	0.028
	17	Salmon River	98	76	0.038
	18	Camp Creek Pond-Rearing Facility	100	77	0.044
	19	Horse Linto Creek	100	77	0.045
	20	Trinity River, South Fork	100	77	0.039
	21	Trinity River Hatchery	120	77	0.030
Eel River–California Coastal	22	Redwood Creek at Orick	95	77	0.050
	23	Redwood Creek Lagoon	100	77	0.054
	24	Mad River Hatchery	99	77	0.045
	25	Mad River, North Fork	61	77	0.054
	26	Eel River, Middle Fork	95	76	0.043
	27	Eel River, South Fork	99	78	0.048
	28	Van Duzen River	100	77	0.050
	29	Redwood Creek, South Fork Eel	93	77	0.046
	30	Hollow Tree Creek	100	78	0.045
	31	Salmon Creek, South Fork Eel	96	77	0.044
	32	Mattole River	100	77	0.049
Sacramento–San Joaquin	33	Upper Sacramento River	94	77	0.059
	34	Coleman Hatchery	100	77	0.063
	35	Feather River Hatchery	100	78	0.061
	36	Nimbus Hatchery	100	78	0.064
	37	Merced River Hatchery	100	78	0.057

(Allendorf and Thorgaard 1984, Waples 1988). However, our method of scoring increases the power of maximum-likelihood estimates of stock composition by equalizing the importance of variant alleles at isoloci and non-duplicated loci. Furthermore, our system was maintained for consistency with other research (Gall et al. 1989, Brodziak et al. 1992).

A missing heteromeric isozyme between GPI-1 and GPI-3 was observed in some fish. We scored this pattern, as described in Bartley and Gall (1990), by assigning variation to an artificial locus named GPI-H and labeling the common and variant alleles *Gpi-H(100)* and *Gpi-H(*)*, respectively. However, Utter et al. (1989) described breeding data that indicated the variation should be assigned to either GPI-1 or GPI-3.

Due to the difficulty of identifying heterozygote banding patterns from GPI-H, LDH-1, and MDHP-2, allele frequencies at these loci were calculated from the square root of the frequency of the alternate homozygote. The frequency of the *Tpi-3(106)* allele also was calculated from the square root of the frequency of the homozygous Tpi-3(106) pattern.

Table 2

Enzyme systems, IUBNC enzyme number, isozyme loci, buffer systems, and tissues used in electrophoretic analyses of chinook salmon. For loci, m = mitochondrial. M = muscle, H = heart, L = liver, E = eye. Buffers explained in the text. Locus designations (synonyms) are locus names used by (1) present study, (2) Bartley and Gall (1990), (3) American Fisheries Society (Shaklee et al. 1990a), and (4) Utter et al. (1989).

Enzyme name	Enzyme no.	Locus designations 1	2	3	4	Tissue	Buffer
Aspartate aminotransferase	2.6.1.1	AAT-1	AAT-1	*sAAT-1,2**	Aat-1,2	M,H	TC-4
		AAT-2	AAT-2			M,H	TC-4
		AAT-3		*sAAT-3**	Aat-3	E	TC-4
		AAT-4	AAT-3	*sAAT-4**		L	TC-4
		mAAT-1		*mAAT-1**		M,H	CAM
		mAAT-2		*mAAT-2**		M,H,L	CAM, TC-4
		mAAT-3		*mAAT-3**		M,H	CAM, TC-4
Acid phosphatase	3.1.3.2	ACP-1		*ACP-1**		M,L	CAM
		ACP-2		*ACP-2**		M	CAM
Adenosine deaminase	3.5.3.3	ADA-1		*ADA-1**		M	TG
		ADA-2		*ADA-2**		M	TG
Alcohol dehydrogenase	1.1.1.1	ADH	ADH	*ADH**		L	TC-4, TBCL
Aconitate hydratase	4.2.1.1	AH-1	AH	*sAH**		L,M,E	CAM, TC-4
		mAH-1		*mAH-1**		E,H	CAM
		mAH-2		*mAH-2**		E,H	CAM
		mAH-3		*mAH-3**		M,H	CAM
		mAH-4		*mAH-4**		M,H	CAM
Alanine aminotransferase	2.6.1.2	ALAT		*ALAT**		M	TG
Creatine kinase	2.7.3.2	CK-1	CK-1	*CK-A1**		M	TBCL, CAM
		CK-2	CK-2	*CK-A2**		M	TBCL, CAM
		CK-4	CK-3	*CK-A2**		E	CAM
Esterase	3.1.1.1	EST-3		*EST-D**		M,E	TG, TBCL
Fructose-biphosphate aldolase	4.1.2.13	FBALD-4	FBA	*FBALD-4**		E	CAM, TC-4
Fumarate hydratase	4.2.1.2	FH	FH	*FH**		M	CAM
Glycerol-3-phosphate dehydrogenase	1.1.1.8	G3PDH-1	GPDH-1	*G3PDH-1**		M	CAM, TC-4
		G3PDH-2	GPDH-2	*G3PDH-2**		M	CAM, TC-4
		G3PDH-3	GPDH-3	*G3PDH-3**		M	CAM, TC-4
		G3PDH-4	GPDH-4	*G3PDH-4**		M	CAM, TC-4
Glyceraldehyde-3-phosphate dehydrogenase	1.2.1.12	GAPDH-5	GAPDH-3	*GAPDH-5**		E	CAM, TC-4
		GAPDH-6	GAPDH-4	*GAPDH-6**		E	CAM, TC-4
Glucose-6-phosphate isomerase	5.3.1.9	GPI-1	GPI-1	*GPI-B1**	Gpi-1	M	TG, TBCL
		GPI-2	GPI-2	*GPI-B2**	Gpi-2	M	TG, TBCL
		GPI-3	GPI-3	*GPI-A**	Gpi-3	M,E	TG, TBCL
		GPI-H	GPI-H	*GPIr**	Gpi-1	M	TG, TBCL
Glutathione reductase	1.6.4.2	GR	GR	*GR**	Gr	M,E,L	TG TBCL
β-Glucuronidase	3.2.1.31	GUS		*GUS**		M	CAM, TC-4
Hydroacylglutathionine hydrolase	3.1.2.6	HAGH		*HAGH**		L,M,E	TG
L-Iditol dehydrogenase	1.1.1.14	IDDH-1	IDDH-1	*IDDH-1**		L	TBCL
		IDDH-2	IDDH-2	*IDDH-2**		L	TBCL
Isocitrate dehydrogenase	1.1.1.42	IDH-1	IDH-1	*mIDHP-1**		M	CAM
		IDH-2	IDH-2	*mIDHP-2**		M	CAM
		IDH-3	IDH-3	*sIDHP-1**	Idh-3,4	M,E,L	CAM, TC-4
		IDH-4	IDH-4	*sIDHP-2**		E,L	CAM, TC-4
L-Lactate dehydrogenase	1.1.1.27	LDH-1	LDH-1	*LDH-A1**		M	TBCL, TC-4
		LDH-2	LDH-2	*LDH-A2**		M	TBCL, TC-4
		LDH-3	LDH-3	*LDH-B1**		H,E	TBCL, TC-4
		LDH-4	LDH-4	*LDH-B2**	Ldh-4	L,E	TC-4
		LDH-5	LDH-5	*LDH-C**	Ldh-5	E	TC-4
α-Mannosidase	3.2.1.24	MAN	MAN	*αMAN**		L	TC-4

Table 2 (continued)

Enzyme name	Enzyme no.	Locus designations 1	2	3	4	Tissue	Buffer
Malate dehydrogenase (NADP)	1.1.1.40	MDHP-1		*sMEP-1**		M	TC-4
		MDHP-2		*sMEP-2**		M, E, L	TC-4
		mMDHP-1		*mMEP**		M	TC-4
Malate dehydrogenase (NAD)	1.1.1.37	MDH-1	MDH-1	*sMDH-A1,2**	Mdh-1, 2	E, M	TC-4
		MDH-2	MDH-2			E, M	TC-4
		MDH-3	MDH-3	*sMDH-B1,2**	Mdh-3, 4	M, E	CAM, TC-4
		MDH-4	MDH-4			M, E	CAM, TC-4
		mMDH-1		*mMDH-1**		M, E	CAM
		mMDH-2		*mMDH-2**		M, H	CAM
Mannose-6-phosphate isomerase	5.3.1.8	MPI	MPI	*MPI**	Mpi	E, M, L	CAM
Phosphogluconate dehydrogenase	1.1.1.44	PGDH	PGDH	*PGDH**		M, E, L	TC-4
Phosphoglucokinase	2.7.2.3	PGK-1		*PGK-1**		L	CAM
		PGK-2	PGK-2	*PGK-2**	Pgk-2	M, E, L	CAM
Phosphoglucosmutase	5.4.2.2	PGM-1	PGM-1	*PGM-1**	Pgm-1, 2	M, E	CAM
		PGM-2	PGM-2	*PGM-2**		M, E, L	TG, TC-4
		PGM-3		*PGM-3,4**		E, L, M	TG, TC-4
		PGM-4				E, L, M	TC-4
Pyruvate kinase	2.1.7.40	PK-1	PK-1	*PK-1**		M	TC-4
		PK-2	PK-2	*PK-2**		M	CAM
Superoxide dismutase	1.15.1.1	SOD-1	SOD-1	*SOD-1**	Sod	L, M	CAM
		mSOD		*mSOD**		H, M, E	TG
Triosphosphate isomerase	5.3. 1.1	TPI-3		*TPI-2.1**		E	TC-4
		TPI-4		*TPI-2.2**		M, E, L, H	TG, TBCl
β-N-Acetyl-D-glucosaminidase	3.2.1.30	a-GA		*βBGLUA**		L	TG, TBCL
Peptidases (substrates)	3.4.*.*						
Glycyl leucine		DPEP-1	PEPA-1	*PEP-A**	Dpep-1	M, E, H	CAM, TG
		DPEP-2	PEPA-2	*PEP-C**	Dpep-2	E	TG, TBCL
Phenylalanyl proline		PDPEP-2	PDPEP-2	*PEP-D2**		M, E	TC-4
Prolyl leucine		PEPLT		*PEP-LT**		M	TG
Leucylglycyl glycine		TAPEP	PEPB	*PEP-B1**	Tapep-1	M, E	TBCL, TG

Analyses

Genetic variability for each collection of salmon was assessed by calculating the frequencies of alleles at each locus and average heterozygosity assuming Hardy-Weinberg proportions (Nei 1973). A locus was considered variable if we observed polymorphism in at least one sample. Analyses were based on a maximum of 78 loci. If a sample was not scored for a particular locus, the locus was retained for analyses involving multiple samples. Deviations from expected Hardy-Weinberg genotypic proportions were tested by chi-square goodness-of-fit tests (Sokal and Rohlf 1981). Variant allele frequencies were pooled so the expected number of genotypes in a given class was always five or greater. Some loci could not be tested for goodness-of-fit because pooling allele frequencies to achieve a minimum class-size reduced the degrees of freedom to zero. In addition, the loci, PGM-3 and PGM-4, were excluded from goodness-of-fit tests due to the arbitrary nature of assigning variation to a specific locus. GPI-H, LDH-1, and MDHP-2 were excluded because of the method of calculating allele frequencies from the frequency of the alternate homozygotes.

Genetic identities (I) were calculated for each pair of samples (Nei 1972) and a dendrogram was constructed from estimates of I using the unweighted pair-group method (UPGMA) (Sneath and Sokal 1973). Total gene diversity (H_T) was partitioned to estimate within-sample (H_S) and between-sample (D_{ST}) components, and to estimate relative gene diversity ($G_{ST} = D_{ST}/H_T$) (Nei 1973, Chakraborty and Leimar 1987). Total gene diversity was partitioned into three hierarchical levels: panmixia (T), area or drainage (D), and sample (S) based on *a priori* geographic considerations (Table 1).

An estimate of average gene flow was calculated from Wright's (1943) fixation index

$$F_{ST} = 1/(4Nm + 1) \quad (1)$$

where Nm is the average number of migrants exchanging genes per generation. Equation (1) was solved for Nm by setting F_{ST} equal to the relative gene diversity appropriate for the hierarchical level of interest. This formulation provided an estimate of the number of migrant fish exchanging genes among samples per generation under the assumptions of selective neutrality of alleles and Wright's (1943) island model of migration. Slatkin and Barton (1989) discussed the sensitivity of equation (1) relative to various methods of estimating F_{ST} in the presence of selection and alternative population structures, and found it to be fairly robust.

Results

A total of 96 isozyme loci were examined. Thirty-one loci were monomorphic, 47 were categorized as polymorphic (Appendix A), whereas variability of an unknown and undefined nature was detected at 18 loci. Details of genetic polymorphisms not described elsewhere are outlined in Appendix B. The enzyme systems involving the 18 loci for which evidence of probable polymorphisms was detected (not listed in Table 2) and warrant further study included: two adenylate kinase loci, creatine kinase, four fructose biphosphate aldolase loci, four glyceraldehyde-3-phosphate dehydrogenase loci, two beta-galactosidase loci, alpha-glucoside, superoxide dismutase, two peptidase loci, and a highly anodal acromatic band. Because of difficulties defining a genetic model of inheritance, poor band resolution, or incomplete data, these 18 loci were not included in the analyses.

Tests of conformance to Hardy Weinberg genotypic proportions revealed 37 out of 462 cases (8%) of disequilibria. For wild samples of chinook salmon, 13 of 252 tests (5%) revealed disequilibrium, whereas in hatchery samples, 24 of 210 tests (11%) showed nonconformance to Hardy-Weinberg expectations. However, in the Klamath Basin, a higher percentage of disequilibrium was found (13 of 97 cases or 13%) in hatchery and wild samples. The proportion of disequilibrium observed in Klamath and non-Klamath samples was found to be significantly different ($P<0.05$) when tested for equality by the generalized likelihood-ratio test for binomial data (Larsen and Marx 1981) . The proportion of disequilibrium observed in hatchery (including pond rearing programs) and wild chinook salmon populations also was significantly different ($P<0.05$). The nature of the observed disequilibrium appeared to be random. That is, we did not observe consistent excesses or deficiencies of heterozygotes, nor did we observe specific loci that consistently deviated from Hardy-Weinberg expectations.

Estimates of average heterozygosity ranged from a low value of 0.028 in Shasta River (#16) to a high of 0.076 in the Morgan Creek (#2) and Elk River (#5) hatcheries. The Middle Oregon samples (#1–6) tended to have high estimates of average heterozygosity, whereas values for the Klamath-Trinity samples (#12–21) tended to be lower (Table 1).

Although genetic identity indices between all pairs of samples were greater than 0.982 (data not shown), the geographic distribution of alleles suggested population subdivision within the study area. For example, we found the *Aat-2(85)*, *Aat-3(90)*, *Aat-4(130)*, and *Iddh-1(0)* alleles predominantly in Oregon and north-coastal California (collections 1–11). The *mAh-4(112)*, *Gpi-H(*)*, and *Pgdh(90)* alleles were present mainly in the Sacramento/San Joaquin system (collections 33–37), whereas *Mdhp-1(92)* and *Gpi-2(60)* were less abundant in the Sacramento Basin compared with more northern areas. *Mdhp-2(78)* was a characteristic of the Klamath–Trinity system and a few coastal samples.

Cluster analysis of genetic identities revealed a strong geographic component to the grouping of chinook salmon samples. Five distinct clusters that reflected geographic areas were evident (Fig. 2): (1) Smith River–Southern Oregon rivers, (2) Klamath–Trinity Rivers, (3) Eel River system–California coastal rivers, (4) Middle Oregon rivers, and (5) Sacramento–San Joaquin system. The Smith River (#11) and the Rowdy Creek Hatchery (#10) samples were the most northern samples collected from California. Therefore, it is reasonable that they would be genetically similar to the southern Oregon samples. The sample from the Fall Creek Hatchery (#1) was the only sample from northern Oregon and therefore, appears as an independent cluster. Three samples, Rock Creek Hatchery (#6, middle Oregon), Blue Creek (#12, Klamath–Trinity Basin), and Omagar Creek (#13, Klamath–Trinity Basin), did not cluster in accordance with their geographic location.

Total gene diversity was 0.0620 (H_T) and average sample diversity was 0.0554 (H_S). Therefore, approximately 89.4% of the total genetic diversity was due to intrasample variability and 10.6% was due to intersample variation (Table 3). Further examination of the intersample diversity showed that genetic differences among samples within the five geographic groups identified from the dendrogram (see Table 1) accounted for about 3.2% of the total variation and 7.4% of the total diversity was due to differences between the major geographic areas. Gene diversity analysis for each geographic area treated separately revealed that although the Klamath–Trinity system possessed the lowest total gene diversity for a given area (H_D), relative gene diversity (G_{SD}) for this drainage was high

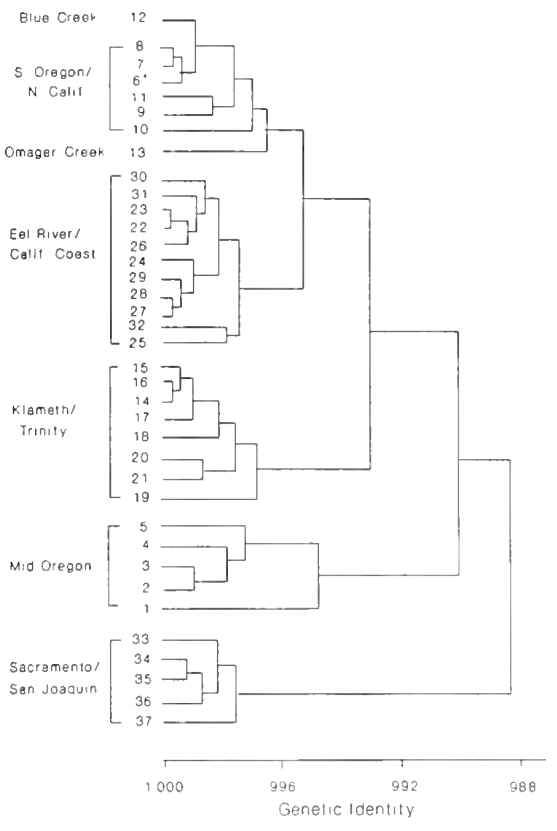

Figure 2

Dendrogram based on UPGMA clustering of genetic identity indices (Nei 1972). Identification numbers are defined in Table 1. Brackets on left side indicate geographic grouping, with Blue Creek and Omagar Creek as outliers (collection #6, indicated as 6*, was from mid-Oregon).

Table 3

Hierarchical gene diversity analyses of 37 samples of chinook salmon from Oregon and California.* H_{SD} = average gene diversity of samples within areas; H_D and G_{SD} = total gene diversity and relative gene diversity for a given area, respectively; Nm = average number of migrants exchanging genes per generation; H_S, H_T, and G_{ST} = within-sample, total, and relative gene diversity, respectively.

Area	H_{SD}	H_D	G_{SD}	Nm
Middle Oregon	0.0704	0.0741	0.0502	4.70
South Oregon/ N. California Coast	0.0586	0.0599	0.0223	10.96
Klamath–Trinity	0.0402	0.0428	0.0592	3.97
Eel River/California Coast	0.0473	0.0486	0.0271	8.98
Sacramento–San Joaquin	0.0607	0.0616	0.0158	15.57

*Total, ignoring subdivisions: H_S 0.0554, H_T 0.0620, G_{ST} 0.106, Nm 2.11

and comparable to the middle Oregon area which shared the highest total gene diversity (Table 3).

Based on an overall estimate of 0.106 for G_{ST} (Table 3), the number of immigrant individuals contributing genes to an average population, Nm, was estimated to be 2.11 individuals per generation. Estimates of gene flow within each geographic cluster were highest in the Sacramento–San Joaquin system (Nm 15.57) and lowest in the Klamath–Trinity drainage (Nm 3.97).

Discussion

The genetic structure of chinook salmon populations reported here appears similar to that reported previously. Distributions of variant alleles at Mdh-4, AH-1 Pgdh, Pgm-2, GPI-H, and Gpi-2 were similar to those reported by Bartley and Gall (1990). However, average heterozygosity estimates for the Klamath–Trinity drainage were somewhat higher than reported by Utter et al. (1989) and Bartley and Gall (1990). Bartley and Gall (1990) observed a range of 0.008–0.016 for this drainage, compared with the range of 0.028 for the Shasta River sample to 0.064 for the sample from Omagar Creek found in the present study. One reason for the higher estimates in the present study was the inclusion of the Mdhp-2 locus, which is highly polymorphic in the Klamath–Trinity drainage (Appendix A); Bartley and Gall (1990) and Utter et al. (1989) did not report data for this locus. Generally, comparisons of heterozygosity estimates between this study and earlier studies are difficult to interpret due to the improved laboratory procedures that have greatly increased the number of isozyme loci available for analysis.

Two samples from the Klamath–Trinity drainage, Blue and Omagar Creeks, were genetically differentiated from other samples from within the basin. For example, Mdhp-2(78) had an average frequency of 0.32 in eight other samples from the drainage, whereas the allele occurred at a frequency of 0.14 in Blue Creek and was not found in the Omagar Creek sample. Furthermore, Omagar and Blue Creeks had higher frequencies of the Tapep-1(130) and mMdh-1(-900) alleles than did other Klamath–Trinity samples. These frequencies indicated that fish from Omagar and Blue Creeks are genetically closer to southern Oregon populations than to Klamath–Trinity populations. This result was unexpected given the pattern of geographic clustering found by Utter et al. (1989) and Bartley and Gall (1990). However, earlier studies did not sample populations near or below the confluence of the Trinity and Klamath Rivers, as was done in the present study.

We do not know if the genetic structure of the Blue and Omagar Creek samples is characteristic of the lower Klamath–Trinity drainage. The Omagar Creek sample consisted of progeny of broodstock captured by instream gill nets at the mouth of Blue Creek and in the main section of the Klamath River; the Blue Creek sample was collected in the main stem of Blue Creek and was presumed to represent progeny of natural spawning. If accurate, our data suggest greater gene exchange between the lower Klamath and coastal populations of northern California–southern Oregon than between the lower and upper Klamath basin. Apparently northern California coastal populations of chinook salmon are genetically similar to southern Oregon populations because the two samples from the Smith River (samples 10 and 11) also clustered with the Oregon populations. This genetic similarity may have resulted from historical gene exchange in the form of transplants into the Klamath basin (Snyder 1931). Chinook salmon in the lower Klamath River are thought to be similar to Oregon populations in other characters, such as timing of spawning migration, fecundity, and size (Snyder 1931; Craig Tuss, U.S. Fish Wildl. Serv., Sacramento, CA 95616, pers. commun., Sept. 1990).

The relatively high incidence of Hardy-Weinberg disequilibria in hatchery and pond rearing programs may be the result of the limited number of broodstock used in production or non-random sampling of a hatchery's production, i.e., only sampling juveniles from a few raceways. For example, the Coleman National Fish Hatchery spawns approximately 10,000 fall-run chinook salmon. It is likely that our sample of 100 juveniles may not be an adequate representation of the hatchery output. The two samples with the highest number of deviations from Hardy-Weinberg expectations were both from pond rearing projects, Omagar and Camp Creeks. These pond rearing projects can serve a useful function by augmenting or establishing runs of chinook salmon in specific streams. However, care must be taken to maximize the effective population size of the broodstock and to prevent changes in the genetic variation.

The large number of significant departures from Hardy-Weinberg expectations for the Klamath samples compared with other samples was due primarily to the samples from Camp Creek and Omagar Creek. These two samples accounted for nine of the 13 significant tests within the Klamath system. Deleting data for these two Creeks from the comparison resulted in 6% (4 of 72) significant deviations for Klamath system samples versus 7% (24 of 349) for non-Klamath samples.

Our results indicate a geographic basis for genetic differentiation and subpopulation structure in chinook salmon populations from California and Oregon. Geographic affinities among chinook salmon populations have now been demonstrated along most of the western coastline of North America (Gharrett et al. 1987, Utter et al. 1989, Bartley and Gall 1990). Bartley and Gall (1990) identified three major clusters of chinook salmon populations in California that corresponded to the three major river drainages: the Sacramento–San Joaquin, the Eel, and the Klamath–Trinity. Utter et al. (1989) identified nine population units of chinook salmon over a large area from British Columbia to California. They found coastal populations from Oregon and Washington to be genetically similar to each other. Our data indicate that some coastal populations in California are differentiated from those in Oregon, but that northern California coastal populations of chinook salmon are similar to southern Oregon populations.

The level of intrasample gene diversity found in the present study, 89.4%, is similar to the values of 82.3 and 87.7% reported by Bartley and Gall (1990) and Utter et al. (1989), respectively. Overall estimates of gene flow of 1.16 (Bartley and Gall 1990) and 2.11 (this study) migrants per generation also are similar. The slightly lower level of population subdivision and therefore, higher level of gene flow found in the present study probably reflect a bias caused by the samples analyzed. Bartley and Gall (1990) analyzed a greater number of inland California populations than the present study. Most of their samples were from the three major drainages within California: the Klamath–Trinity, the Sacramento–San Joaquin, and the Eel. They suggested that straying and gene flow were higher among coastal streams than among separate drainages. Therefore, by including the large number of coastal samples in the present study, slightly higher overall estimates of gene flow and less apparent subdivision were expected. Separate gene diversity analyses of the groups from Oregon and northern California revealed that approximately 6% of the total diversity of the two Oregon groups was due to interpopulation differences compared with 12% for the three California groups. These results further support the expectation of lower levels of population subdivision when analyses involve many coastal samples.

The estimates of gene flow and population subdivision from hierarchical gene-diversity analyses varied among geographic areas. The Klamath–Trinity system would be expected to display lower levels of gene exchange if the lower and upper sections of the Klamath are separate subpopulations. However, deletion of the Blue Creek and Omagar Creek samples from the analysis changed the gene diversity estimates by less than 2%. The high level of estimated gene flow within the Sacramento–San Joaquin system most likely reflects the fact that four of the five samples were from

hatcheries. Although egg and fingerling transfers between areas have been reduced recently, a considerable amount of historical mixing of the hatchery stocks has occurred (Alan Baracco, Calif. Dep. Fish Game, Sacramento, CA 95616, pers. commun. Dec. 1986). Additionally, many salmon from the San Joaquin River stray into the Sacramento River on their spawning migration due to easier access and better water quality in the Sacramento River (Alan Baracco and Forrest Reynolds, Calif. Dep. Fish Game, Sacramento, CA 95616, pers. commun. Dec. 1986).

Independent estimates of straying based on coded-wire tagged fish indicate that chinook salmon in the Sacramento River do stray within the system. Rough estimates are that 2–5% of the Sacramento fall-run fish are from hatcheries in the San Joaquin River system. Approximately 1% of the fall-run chinook salmon returning to the Feather River Hatchery is composed of stray fish from the Nimbus (American River), Mokulumne, and Coleman Hatcheries. Straying also occurs in northern streams because chinook salmon marked on the Rogue River are recovered in the Klamath–Trinity drainage (Fred Meyer, Calif. Dep. Fish Game, Rancho Cordova, CA 95670, pers. commun. Feb. 1991). Therefore, it is not surprising that gene flow estimates for the Sacramento–San Joaquin drainage were high and that southern coastal populations from Oregon should resemble northern California coastal populations.

Stability of allele frequencies over time is often assumed in the methodology of genetic stock identification. Although the present study was not intended to uncover temporal variation of allele frequencies, some samples we examined also had been analyzed earlier. Eighteen locations from the present study were sampled in 1984–86 by Bartley and Gall (1990). For the interstudy comparison, loci chosen had to have a frequency of less than 0.95 for the common allele in at least two populations reported by Bartley and Gall (1990); isoloci were not used. Twelve loci fit the criterion: AH-1, DPEP-1, PDPEP-2, TAPEP, GPI-2, IDDH-2, IDH-2, MPI, PGDH, PGK-2, PGM-2, and SOD-1.

We found 18 instances of significant change in allele frequencies for seven hatchery samples (21.4%), 16 significant results for seven wild populations (19.0%), and five instances of significant change for a pond rearing project (41.7%) based on the G-statistic (Sokal and Rohlf 1981). Interstudy comparisons of the samples from Bogus Creek (= Bogas Creek in Bartley and Gall 1990), Shasta Creek, and the Feather River Fish Hatchery revealed no significant differences in allele frequencies.

Six hatcheries sampled in the present study also had been sampled by Utter et al. (1989). Loci selected to compare allele frequencies for these studies had to have a common allele frequency of less than 0.95 in one of the studies. Eight loci met the frequency criterion: AH, DPEP-1, TAPEP, GPI-2, GR, MPI, PGK-2, and SOD-1. Five of the six hatchery samples displayed significant changes in allele frequency between the two studies. Waples and Teel (1990) also reported significant changes in allele frequencies in hatcheries sampled in different years.

Although we observed differences in allele frequencies between this and earlier studies, we do not know if this represents temporal variation. It is tempting to make statements on the temporal stability or instability of allele frequencies in samples of chinook salmon from a given area, but without estimates of sampling variability for a given year, it is not possible to separate intrasample variation, random sampling error, and temporal variation. Nevertheless, given the presumed constancy of allele frequency data (Allendorf and Utter 1979), the number of significant G statistics uncovered in comparisons between samples in this study and those of Utter et al. (1989) and Bartley and Gall (1990) requires some explanation.

Waples and Teel (1990:149) stated, "tests of the equality of allele frequencies in temporally spaced samples must be interpreted with caution." In addition, Waples and Teel (1990) list inaccurate or artifactual genetic data, nonrandom sampling of fish for genetic analysis, selection, and migration as possible causes of significant change in allele frequencies. For example, large differences in allele frequencies at IDH-3 and IDH-4 between the present study and Bartley and Gall (1990) may be due to banding artifacts associated with tissue breakdown. One of us (Bentley) has observed the increased appearance of variant "alleles" at these loci in samples that were not properly frozen and stored. Therefore, the data for these two loci presented in Bartley and Gall (1990) may be artifactual. In addition, the analyses of Utter et al. (1989), Bartley and Gall (1990), and the present study were done by different personnel in different laboratories. Although standardization was attempted, scoring of gel banding patterns may have been inconsistent.

The level of temporal instability of allele frequencies is an important issue in the use of GSI to manage and conserve chinook salmon populations (Waples 1990, Waples and Teel 1990). However, sampling design should specifically address this question before one draws conclusions concerning wild or hatchery populations. Although we documented differences in allele frequencies between this and earlier studies, the overall association between genetic similarity and geographic location remains constant for populations of chinook salmon in California and Oregon.

Acknowledgments

This research was funded by the California Department of Fish and Game (Interagency Agreement No. C-1335, Genetic Analysis of Chinook and Coho Salmon Populations) and the Institute for Theoretical Dynamics at the University of California, Davis. We gratefully acknowledge the support and assistance of A. Baracco and L.B. Boydstun throughout the study. We thank personnel from the California Department of Fish and Game, the U.S. Fish and Wildlife Service, S. Downey, and W. Shoals for assistance with fish collections. The technical assistance from E. Childs, S. Fox, A. Marshall, C. Panattoni, and C. Qi is also appreciated. The valuable comments of F. Utter and two anonymous referees also are appreciated. We are especially grateful to the Northwest Fisheries Science Center of the National Marine Fisheries Service and the Washington Department of Fisheries Genetic Unit for their contribution to the development of a coastwide program of Genetic Stock Identification.

Citations

Aebersold, P.B., G.A. Winans, D.J. Teel, G.B. Milner, and F.M. Utter
1987 Manual for starch gel electrophoresis: A method for the detection of genetic variation. NOAA Tech. Rep. NMFS 61, 19 p.

Allendorf, F., and G.H. Thorgaard
1984 Tetraploidy and the evolution of salmonid fishes. *In* Turner, B. (ed.), Evolutionary genetics of fishes, p. 1–53. Plenum, NY.

Allendorf, F.W., and F.M. Utter
1979 Population genetics. *In* Hoar, W.J., and D.J. Randall (eds.), Fish physiology, vol. 8, p. 407–454. Academic Press, NY.

Bartley, D.M., and G.A.E. Gall
1990 Genetic structure and gene flow in chinook salmon populations of California. Trans. Am. Fish. Soc. 119:55–71.

Brodziak, J., B. Bentley, D. Bartley, G.A.E. Gall, R. Gomulkiewicz, and M. Mangel
1992 Tests of genetic stock identification using coded-wire tagged fish. Can. J. Fish. Aquat. Sci. (In press).

Chakraborty, R., and O. Leimar
1987 Genetic variation within a subdivided population. *In* Ryman, N., and F. Utter (eds.), Population genetics and fishery management, p. 89–120. Univ. Wash. Press, Seattle.

Clayton, J.W., and D.N. Tretiak
1972 Amine-citrate buffers for pH control in starch gel electrophoresis. J. Fish. Res. Board Can. 29:1169–1172.

Gall, G.A.E., B. Bentley, C. Panattoni, E. Childs, C. Qi, S. Fox, M. Mangel, J. Brodziak, and R. Gomulkiewicz
1989 Genetic stock identification: Chinook mixed fishery project 1986–1989. Rep. to Calif. Dep. Fish Game, Sacramento, by Univ. Calif., Davis, 420 p.

Gharrett, A.J., S.M. Shirley, and G.R. Tromble
1987 Genetic relationships among populations of Alaskan chinook salmon (*Oncorhynchus tshawytscha*). Can. J. Fish. Aquat. Sci. 44:765–774.

Harris, H., and D.A. Hopkinson
1976 Handbook of enzyme electrophoresis in human genetics. North Holland Publ. Co., Amsterdam, var. pag.

Holmes, R.S., and C.J. Masters
1970 Epigenetic interconversions of the multiple forms of mouse liver catalase. FEBS (Fed. Eur. Biochem. Soc.) Lett. 11:45–48.

Larsen, R.J., and M.L. Marx
1981 An introduction to mathematical statistics and its applications. Prentice Hall, Engelwood Cliffs, var. pag.

Moyle, P.B.
1976 Inland fishes of California. Univ. Calif. Press, Berkeley.

Nei, M.
1972 Genetic distance between populations. Am. Nat. 106: 283–292.
1973 Analysis of genediversity in subdivided populations. Proc. Natl. Acad. Sci. USA 70:3321–3323.

Netboy, A.
1974 The salmon: Their fight for survival. Houghton Mifflin, Boston, 613 p.

Pella, J.J., and G.B. Milner
1987 Use of genetic marks in stock composition analysis. *In* Ryman, N., and F. Utter (eds.), Population genetics and fishery management, p. 247–276. Univ. Wash. Press, Seattle.

Ridgway, G.J., S.W. Sherburne, and R.D. Lewis
1970 Polymorphisms in the esterase of Atlantic herring. Trans. Am. Fish. Soc. 99:147–151.

Ryman, N., and F. Utter (editors)
1987 Population genetics and fishery management. Univ. Wash. Press, Seattle, 420 p.

Schaal, B.A., and W.W. Anderson
1974 An outline of techniques for starch gel electrophoresis of enzymes from the America oyster *Crassostrea virginica* Gmelin. Tech. Rep. 74-3, Ga. Mar. Sci. Cent., 18 p.

Shaklee, J.B., R.W. Allendorf,D.C. Morizot, and G.S. Whitt
1990a Gene nomenclature for protein coding loci in fish. Trans. Am. Fish. Soc. 119:2–15.

Shaklee, J.B., C. Busack, A. Marshall, M. Miller, and S.R. Phelps
1990b The electrophoretic analysis of mixed-stock fisheries of Pacific salmon. *In* Ogita, Z-I., and C.L. Markert (eds), Isozymes: Structure, function, and use in biology and medicine, p. 235–265. Wiley-Liss, Inc., NY.

Shaw, C.R., and R. Prasad
1970 Starch gel electrophoresis of enzymes—a compilation of recipes. Biochem. Genet. 4:297–320.

Slatkin, M., and N.H. Baron
1989 A comparison of three indirect methods for estimating average levels of gene flow. Evolution 43:1349–1368.

Sneath, P.H.A., and R.R. Sokal
1973 Numerical taxonomy. W.H. Freeman, San Francisco, 573 p.

Snyder, J.O.
1931 Salmon of the Klamath River, California. Calif. Dep. Fish Game, Fish. Bull. 34:1–130.

Sokal, R.R., and F.J. Rohlf
1981 Biometry. W.H. Freeman, NY, 859 p.

Utter, F.M., D. Teel, G. Milner, and D. McIsaac
1987 Genetic estimates of stock comparisons of 1983 chinook salmon, *Oncorhynchus tshawytscha*, harvests off the Washington coasts and Columbia River. Fish. Bull., U.S. 85:12–23.

Utter, F.M., G. Milner, G. Stahl, and D. Teel
1989 Genetic population structure of chinook salmon, *Oncorhynchus tshawytscha*, in the Pacific Northwest. Fish. Bull., U.S. 87:239–264.
Waples, R.S.
1988 Estimation of allele frequencies at isoloci. Genetics 118: 371–384.
1990 Temporal changes of allele frequency in Pacific salmon: Implications for mixed-stock fishery analysis. Can. J. Fish. Aquat. Sci. 47:968–976.
Waples, R.S., and D.J. Teel
1990 Conservation genetics of Pacific salmon. 1. Temporal changes in allele frequency. Conserv. Biol. 4:144–156.
Wright, S.
1943 Isolation by distance. Genetics 28:114–138.

Appendix A

Allele frequencies at 47 variable isozyme loci. Identification numbers (ID#) defined in Table 1 and Figure 1; N = number of fish scored. Allele designations of Bartley and Gall (1990) are included in parentheses.

	AAT-2		Alleles			AAT-3		Alleles		AAT-4		Alleles	
	ID#	N	100 (100)	85 (90)	105	ID#	N	100	90	ID#	N	100	130
Middle Oregon	1	100	0.990	0.010		1	100	1.000		1	100	0.755	0.245
	2	100	0.930	0.070		2	100	0.995	0.005	2	100	0.785	0.215
	3	100	0.890	0.110		3	100	1.000		3	100	0.875	0.125
	4	100	0.920	0.080		4	100	0.995	0.005	4	100	0.835	0.165
	5	100	0.910	0.090		5	100	1.000		5	100	0.880	0.120
	6	100	1.000			6	100	0.975	0.025	6	100	1.000	
S. Oregon/	7	100	1.000			7	100	0.965	0.035	7	100	0.995	0.005
N. California Coastal	8	100	1.000			8	100	0.965	0.035	8	100	1.000	
	9	100	0.995	0.005		9	100	1.000		9	100	1.000	
	10	62	1.000			10	62	0.960	0.040	10	62	1.000	
	11	99	0.970	0.030		11	99	0.990	0.010	11	99	0.995	0.005
Klamath–Trinity Basin	12	100	1.000			12	100	0.990	0.010	12	100	0.975	0.025
	13	100	1.000			13	100	1.000		13	100	0.990	0.010
	14	98	1.000			14	99	1.000		14	98	0.995	0.005
	15	127	1.000			15	128	0.992	0.008	15	121	0.975	0.025
	16	100	1.000			16	100	1.000		16	100	0.970	0.030
	17	98	1.000			17	98	1.000		17	85	0.976	0.024
	18	106	1.000			18	106	1.000		18	106	0.877	0.123
	19	100	1.000			19	100	1.000		19	100	1.000	
	20	100	1.000			20	100	0.985	0.015	20	100	0.970	0.030
	21	120	1.000			21	120	1.000		21	120	0.996	0.004
Eel River–California Coastal	22	95	0.968	0.032		22	95	1.000		22	87	1.000	
	23	100	0.965	0.035		23	100	1.000		23	100	1.000	
	24	99	0.995	0.005		24	99	1.000		24	99	1.000	
	25	61	1.000			25	61	1.000		25	60	1.000	
	26	95	1.000			26	95	1.000		26	95	1.000	
	27	99	1.000			27	99	1.000		27	97	1.000	
	28	100	1.000			28	100	1.000		28	88	0.994	0.006
	29	93	1.000			29	93	1.000		29	93	1.000	
	30	100	0.995		0.005	30	100	1.000		30	94	1.000	
	31	96	1.000			31	96	1.000		31	93	0.984	0.016
	32	100	1.000			32	100	1.000		32	100	1.000	
Sacramento–San Joaquin	33	94	1.000			33	94	1.000		33	94	1.000	
	34	100	1.000			34	100	1.000		34	100	0.995	0.005
	35	100	1.000			35	100	1.000		35	100	1.000	
	36	100	1.000			36	100	1.000		36	100	1.000	
	37	100	1.000			37	100	1.000		37	100	1.000	

Appendix A (continued)

	mAAT-1		Alleles			mAAT-2		Alleles			mAAT-3		Alleles	
	ID#	*N*	−100	−77	−104	ID#	*N*	−100	−125	−90	ID#	*N*	−100	−450
Middle Oregon	1	100	1.000			1	100	0.985	0.015		1	100	1.000	
	2	100	0.970		0.030	2	100	0.960		0.040	2	100	0.965	0.035
	3	100	0.990		0.010	3	100	0.985		0.015	3	100	0.970	0.030
	4	100	1.000			4	100	0.975		0.025	4	100	0.955	0.045
	5	100	0.990		0.010	5	100	1.000			5	100	0.925	0.075
	6	100	0.985		0.015	6	100	0.945		0.055	6	100	1.000	
S. Oregon/	7	100	0.980		0.020	7	100	0.945	0.005	0.050	7	100	1.000	
N. California Coastal	8	100	0.980		0.020	8	100	0.945		0.055	8	100	1.000	
	9	100	0.985		0.015	9	100	0.975		0.025	9	100	0.995	0.005
	10	62	0.984		0.016	10	62	0.911		0.089	10	0		
	11	99	0.955	0.005	0.040	11	70	1.000			11	0		
Klamath–Trinity Basin	12	100	1.000			12	100	0.955		0.045	12	0		
	13	100	1.000			13	100	0.965		0.035	13	100	1.000	
	14	99	1.000			14	59	0.983		0.017	14	59	1.000	
	15	128	1.000			15	49	0.980		0.020	15	0		
	16	100	1.000			16	69	0.993		0.007	16	0		
	17	98	1.000			17	98	0.969		0.031	17	0		
	18	106	1.000			18	106	1.000			18	0		
	19	100	1.000			19	100	1.000			19	0		
	20	100	1.000			20	100	0.970		0.030	20	0		
	21	120	1.000			21	80	0.994		0.006	21	0		
Eel River–California Coastal	22	95	1.000			22	95	1.000			22	0		
	23	100	1.000			23	100	1.000			23	0		
	24	99	0.990	0.010		24	99	0.980	0.020		24	0		
	25	61	1.000			25	61	0.967	0.033		25	0		
	26	95	0.979	0.021		26	95	1.000			26	0		
	27	98	1.000			27	46	0.989		0.011	27	40	1.000	
	28	100	0.995	0.005		28	40	1.000			28	0		
	29	93	1.000			29	93	1.000			29	0		
	30	100	1.000			30	40	1.000			30	40	1.000	
	31	96	1.000			31	96	1.000			31	0		
	32	100	1.000			32	100	0.995		0.005	32	0		
Sacramento–San Joaquin	33	94	0.995		0.005	33	94	1.000			33	0		
	34	100	0.960		0.040	34	100	0.995	0.005		34	0		
	35	100	0.975		0.025	35	100	0.995		0.005	35	100	1.000	
	36	100	1.000			36	100	1.000			36	100	1.000	
	37	100	1.000			37	100	1.000			37	100	1.000	

	ADA-1		Alleles			ADH		Alleles		AH-1		Alleles		
	ID#	*N*	100	83	108	ID#	*N*	−100	−52	ID#	*N*	100 (100)	86 (90)	116 (110)
Middle Oregon	1	100	0.980	0.020		1	100	1.000		1	100	0.855	0.050	0.095
	2	100	0.990	0.010		2	100	0.975	0.025	2	100	0.890	0.095	0.015
	3	100	1.000			3	100	0.995	0.005	3	100	0.875	0.090	0.035
	4	100	0.990	0.010		4	100	1.000		4	100	0.855	0.135	0.010
	5	100	0.995	0.005		5	100	1.000		5	100	0.845	0.145	0.010
	6	100	1.000			6	100	0.990	0.010	6	100	0.890	0.100	0.010
S. Oregon/	7	100	1.000			7	100	1.000		7	100	0.935	0.065	
N. California Coastal	8	100	1.000			8	100	1.000		8	100	0.960	0.040	
	9	100	1.000			9	100	1.000		9	100	0.925	0.075	
	10	62	1.000			10	62	1.000		10	62	0.839	0.161	
	11	99	1.000			11	99	1.000		11	99	0.919	0.076	0.005
Klamath–Trinity Basin	12	100	0.995	0.005		12	100	1.000		12	100	0.940	0.060	
	13	100	1.000			13	100	1.000		13	100	1.000		
	14	99	1.000			14	99	1.000		14	99	0.990	0.005	0.005
	15	128	1.000			15	118	1.000		15	128	1.000		
	16	100	1.000			16	100	1.000		16	100	0.995		0.005
	17	0				17	97	1.000		17	98	1.000		
	18	106	1.000			18	106	1.000		18	106	0.953	0.047	
	19	100	1.000			19	100	1.000		19	100	1.000		

Appendix A (continued)

	ADA-1		Alleles			ADH		Alleles		AH-1		Alleles		
	ID#	*N*	100	83	108	ID#	*N*	−100	−52	ID#	*N*	100 (100)	86 (90)	116 (110)
Klamath–Trinity Basin (continued)	20	100	1.000			20	100	1.000		20	100	1.000		
	21	120	1.000			21	120	1.000		21	120	1.000		
Eel River–California Coastal	22	76	1.000			22	95	1.000		22	95	0.968	0.021	0.011
	23	100	1.000			23	100	1.000		23	100	0.945	0.040	0.015
	24	99	1.000			24	99	0.970	0.030	24	99	1.000		
	25	61	1.000			25	61	1.000		25	61	1.000		
	26	0				26	95	1.000		26	95	0.979	0.021	
	27	99	1.000			27	79	1.000		27	99	0.995	0.005	
	28	100	1.000			28	83	1.000		28	100	1.000		
	29	93	1.000			29	93	1.000		29	93	1.000		
	30	100	1.000			30	100	1.000		30	100	1.000		
	31	23	1.000			31	94	1.000		31	96	1.000		
	32	100	1.000			32	100	1.000		32	100	1.000		
Sacramento–San Joaquin	33	94	1.000			33	94	1.000		33	94	0.862	0.128	0.011
	34	100	1.000			34	100	1.000		34	100	0.775	0.200	0.025
	35	100	0.955		0.045	35	100	1.000		35	100	0.885	0.105	0.010
	36	100	0.960		0.040	36	100	1.000		36	100	0.835	0.130	0.035
	37	100	0.870		0.130	37	100	1.000		37	100	0.765	0.165	0.070

	mAH-1		Alleles		mAH-2		Alleles		mAH-3		Alleles	
	ID#	*N*	100	65	ID#	*N*	100	50	ID#	*N*	100	71
Middle Oregon	1	100	1.000		1	100	1.000		1	100	1.000	
	2	100	1.000		2	100	1.000		2	100	1.000	
	3	100	1.000		3	100	1.000		3	100	1.000	
	4	100	1.000		4	100	0.985	0.015	4	100	1.000	
	5	100	1.000		5	100	0.995	0.005	5	100	1.000	
	6	100	1.000		6	100	1.000		6	100	1.000	
S. Oregon/	7	100	1.000		7	100	1.000		7	100	0.995	0.005
N. California Coastal	8	100	0.980	0.020	8	100	1.000		8	100	0.995	0.005
	9	100	1.000		9	100	1.000		9	100	1.000	
	10	61	0.992	0.008	10	61	1.000		10	62	1.000	
	11	99	1.000		11	99	1.000		11	99	0.990	0.010
Klamath–Trinity Basin	12	100	0.995	0.005	12	100	1.000		12	100	0.995	0.005
	13	100	1.000		13	100	1.000		13	100	1.000	
	14	99	1.000		14	99	1.000		14	99	1.000	
	15	128	0.980	0.020	15	128	1.000		15	128	1.000	
	16	100	0.990	0.010	16	100	1.000		16	100	1.000	
	17	98	0.995	0.005	17	98	1.000		17	98	1.000	
	18	87	1.000		18	87	1.000		18	106	1.000	
	19	100	1.000		19	100	1.000		19	100	1.000	
	20	100	1.000		20	100	1.000		20	100	1.000	
	21	120	0.975	0.025	21	120	1.000		21	120	1.000	
Eel River–California Coastal	22	95	0.947	0.053	22	95	1.000		22	95	1.000	
	23	100	0.955	0.045	23	100	1.000		23	100	1.000	
	24	99	0.894	0.106	24	99	1.000		24	99	1.000	
	25	61	0.893	0.107	25	61	1.000		25	61	1.000	
	26	95	0.974	0.026	26	95	0.989	0.011	26	95	1.000	
	27	99	0.965	0.035	27	99	1.000		27	99	1.000	
	28	100	0.935	0.065	28	100	1.000		28	100	1.000	
	29	93	0.984	0.016	29	93	1.000		29	93	1.000	
	30	100	0.920	0.080	30	100	1.000		30	100	1.000	
	31	96	0.990	0.010	31	96	0.984	0.016	31	96	1.000	
	32	99	0.909	0.091	32	100	1.000		32	100	1.000	
Sacramento–San Joaquin	33	94	0.973	0.027	33	94	1.000		33	94	1.000	
	34	100	0.975	0.025	34	100	1.000		34	100	1.000	
	35	100	0.995	0.005	35	100	1.000		35	100	1.000	
	36	100	1.000		36	100	1.000		36	100	1.000	
	37	100	1.000		37	100	1.000		37	100	1.000	

Appendix A (continued)

	mAH-4		Alleles				CK-4		Alleles			
	ID#	*N*	100	119	112	123	ID#	*N*	100	105	95	98
Middle Oregon	1	100	1.000				1	100	1.000			
	2	100	1.000				2	100	1.000			
	3	100	0.950	0.050			3	100	1.000			
	4	100	0.975	0.020		0.005	4	100	0.955			0.045
	5	100	0.960	0.010		0.030	5	100	1.000			
	6	100	0.940	0.045		0.015	6	100	1.000			
S. Oregon/N. California Coastal	7	100	0.980	0.015		0.005	7	100	1.000			
	8	100	0.950	0.025		0.025	8	100	1.000			
	9	100	0.915	0.080		0.025	9	100	1.000			
	10	62	0.952	0.008		0.040	10	62	1.000			
	11	99	0.894	0.106			11	99	1.000			
Klamath–Trinity Basin	12	100	0.985			0.015	12	100	0.995	0.005		
	13	100	0.775	0.225			13	80	0.988			0.013
	14	99	0.899	0.101			14	99	1.000			
	15	128	0.938	0.051		0.012	15	118	1.000			
	16	100	0.955	0.030		0.015	16	100	1.000			
	17	98	0.929	0.046	0.005	0.020	17	98	1.000			
	18	106	0.943	0.028		0.028	18	106	1.000			
	19	100	0.905	0.095			19	100	1.000			
	20	100	0.980	0.015		0.005	20	100	1.000			
	21	120	0.942	0.054		0.004	21	120	1.000			
Eel River–California Coastal	22	95	0.874	0.121		0.005	22	95	1.000			
	23	100	0.900	0.100			23	100	1.000			
	24	99	0.924	0.076			24	99	0.985		0.015	
	25	61	0.828	0.172			25	61	1.000			
	26	95	0.868	0.132			26	95	1.000			
	27	99	0.874	0.126			27	99	1.000			
	28	100	0.835	0.165			28	100	1.000			
	29	93	0.871	0.129			29	93	1.000			
	30	99	0.778	0.222			30	100	1.000			
	31	96	0.786	0.214			31	96	1.000			
	32	100	0.900	0.100			32	100	1.000			
Sacramento–San Joaquin	33	94	0.957	0.011	0.032		33	94	1.000			
	34	100	0.925	0.020	0.055		34	100	1.000			
	35	100	0.860	0.035	0.105		35	100	1.000			
	36	100	0.925	0.020	0.055		36	100	1.000			
	37	100	0.905	0.065	0.030		37	100	1.000			

	EST-3		Alleles			GPI-2		Alleles			GPI-H		Alleles	
	ID#	*N*	100	97	107	ID#	*N*	100 (100)	60 (50)	135 (150)	ID#	*N*	100 (common)	* (*)
Middle Oregon	1	100	1.000			1	100	0.315	0.685		1	100	1.000	
	2	100	1.000			2	100	0.585	0.415		2	100	1.000	
	3	100	0.995	0.005		3	100	0.565	0.420	0.015	3	100	1.000	
	4	100	0.985	0.015		4	100	0.335	0.665		4	100	1.000	
	5	100	0.975	0.025		5	100	0.465	0.535		5	100	1.000	
	6	100	1.000			6	100	0.805	0.195		6	100	1.000	
S. Oregon/	7	100	1.000			7	100	0.720	0.280		7	100	1.000	
N. California Coastal	8	100	0.980	0.020		8	100	0.805	0.195		8	100	1.000	
	9	100	0.990	0.010		9	100	0.715	0.265	0.020	9	100	1.000	
	10	62	1.000			10	62	0.750	0.185	0.065	10	62	1.000	
	11	99	0.990	0.010		11	99	0.758	0.227	0.015	11	99	1.000	
Klamath–Trinity Basin	12	100	0.995	0.005		12	100	0.765	0.235		12	100	1.000	
	13	60	0.967	0.033		13	100	0.615	0.385		13	100	1.000	
	14	99	0.980	0.020		14	99	0.949	0.051		14	99	1.000	
	15	58	0.991	0.009		15	128	0.945	0.055		15	128	1.000	
	16	90	0.083	0.017		16	100	0.945	0.055		16	80	1.000	
	17	98	0.995	0.005		17	98	0.888	0.112		17	98	1.000	
	18	106	1.000			18	106	0.769	0.231		18	106	1.000	
	19	100	0.985	0.015		19	100	0.915	0.085		19	100	1.000	

Appendix A (continued)

	EST-3		Alleles			GPI-2		Alleles			GPI-H		Alleles	
	ID#	*N*	100	97	107	ID#	*N*	100 (100)	60 (50)	135 (150)	ID#	*N*	100 (common)	* (*)
Klamath-Trinity Basin	20	100	1.000			20	100	0.885	0.115		20	100	1.000	
(continued)	21	120	1.000			21	120	0.929	0.071		21	120	1.000	
Eel River-California Coastal	22	95	1.000			22	95	0.542	0.458		22	95	1.000	
	23	100	1.000			23	100	0.570	0.430		23	100	1.000	
	24	99	0.995	0.005		24	99	0.556	0.444		24	99	1.000	
	25	61	1.000			25	61	0.484	0.516		25	61	1.000	
	26	95	1.000			26	95	0.432	0.568		26	95	1.000	
	27	99	1.000			27	99	0.535	0.465		27	99	1.000	
	28	100	1.000			28	100	0.570	0.430		28	100	1.000	
	29	93	1.000			29	93	0.586	0.414		29	93	1.000	
	30	100	1.000			30	100	0.545	0.455		30	100	1.000	
	31	96	1.000			31	96	0.693	0.307		31	96	1.000	
	32	100	0.995		0.005	32	100	0.570	0.430		32	100	1.000	
Sacramento-San Joaquin	33	92	0.989	0.011		33	94	0.777	0.064	0.160	33	94	0.643	0.357
	34	100	0.995	0.005		34	100	0.940	0.040	0.020	34	100	0.717	0.283
	35	100	0.995	0.005		35	100	0.925	0.065	0.010	35	100	0.613	0.387
	36	100	1.000			36	100	0.930	0.070		36	100	0.654	0.346
	37	100	1.000			37	100	0.965	0.035		37	100	0.755	0.245

	GR		Alleles		HAGH		Alleles			IDDH-1		Alleles	
	ID#	*N*	100	85	ID#	*N*	100	143	78	ID#	*N*	100	0
Middle Oregon	1	96	1.000		1	100	1.000			1	100	0.950	0.050
	2	100	0.895	0.105	2	100	0.980	0.015	0.005	2	99	0.712	0.288
	3	97	0.943	0.057	3	100	0.985	0.015		3	99	0.864	0.136
	4	99	0.975	0.025	4	100	1.000			4	100	0.710	0.290
	5	80	1.000		5	100	1.000			5	99	0.934	0.066
	6	100	0.995	0.005	6	100	1.000			6	100	0.995	0.005
S Oregon/	7	100	0.995	0.005	7	100	1.000			7	100	1.000	
N. California Coastal	8	100	1.000		8	100	1.000			8	100	0.995	0.005
	9	100	1.000		9	100	1.000			9	99	0.919	0.081
	10	62	0.895	0.105	10	62	1.000			10	62	0.992	0.008
	11	99	0.975	0.025	11	99	1.000			11	99	0.990	0.010
Klamath-Trinity Basin	12	100	0.995	0.005	12	100	1.000			12	100	0.990	0.010
	13	100	1.000		13	100	1.000			13	100	0.995	0.005
	14	99	1.000		14	99	1.000			14	92	1.000	
	15	128	1.000		15	98	1.000			15	128	1.000	
	16	100	0.995	0.005	16	100	1.000			16	100	1.000	
	17	98	1.000		17	98	1.000			17	95	1.000	
	18	106	1.000		18	106	1.000			18	106	1.000	
	19	100	1.000		19	100	1.000			19	100	1.000	
	20	100	1.000		20	100	1.000			20	100	1.000	
	21	120	1.000		21	120	1.000			21	120	1.000	
Eel River-California Coastal	22	95	1.000		22	95	1.000			22	95	0.979	0.021
	23	100	1.000		23	100	1.000			23	100	0.990	0.010
	24	99	0.995	0.005	24	99	1.000			24	99	1.000	
	25	61	1.000		25	45	1.000			25	58	1.000	
	26	95	1.000		26	95	1.000			26	95	1.000	
	27	99	1.000		27	99	1.000			27	97	1.000	
	28	60	1.000		28	54	1.000			28	85	1.000	
	29	93	1.000		29	93	1.000			29	93	1.000	
	30	100	1.000		30	63	1.000			30	73	1.000	
	31	96	1.000		31	96	1.000			31	92	1.000	
	32	100	1.000		32	46	1.000			32	99	1.000	
Sacramento-San Joaquin	33	94	1.000		33	94	1.000			33	93	1.000	
	34	100	1.000		34	100	1.000			34	100	1.000	
	35	100	1.000		35	100	1.000			35	100	1.000	
	36	100	1.000		36	100	0.990		0.010	36	100	1.000	
	37	100	1.000		37	100	1.000			37	100	1.000	

Appendix A (continued)

	IDDH-2		Alleles			IDH-2		Alleles	
			100	61	20			100	154
	ID#	*N*	(100)	(50		ID#	*N*	(100)	(120)
Middle Oregon	1	100	1.000			1	100	1.000	
	2	99	0.995	0.005		2	100	1.000	
	3	99	0.990	0.010		3	100	1.000	
	4	100	0.990	0.010		4	100	1.000	
	5	99	0.990	0.010		5	100	1.000	
	6	100	0.940	0.060		6	100	1.000	
S Oregon/N. California Coastal	7	100	0.975	0.025		7	100	1.000	
	8	100	0.945	0.055		8	100	1.000	
	9	99	0.939	0.061		9	100	1.000	
	10	61	0.861	0.139		10	62	1.000	
	11	99	0.929	0.071		11	99	1.000	
Klamath–Trinity Basin	12	100	0.975	0.025		12	100	1.000	
	13	100	0.925	0.075		13	100	1.000	
	14	92	0.978	0.022		14	99	1.000	
	15	128	0.988	0.012		15	127	1.000	
	16	100	0.985	0.015		16	100	0.995	0.005
	17	95	0.937	0.063		17	98	0.995	0.005
	18	104	0.976	0.024		18	106	1.000	
	19	93	0.892	0.108		19	100	1.000	
	20	100	0.945	0.055		20	100	1.000	
	21	120	1.000			21	120	1.000	
Eel River–California Coastal	22	95	0.974	0.026		22	95	1.000	
	23	100	0.990	0.010		23	100	1.000	
	24	99	0.939	0.061		24	99	1.000	
	25	55	0.945	0.055		25	61	0.975	0.025
	26	95	0.995	0.005		26	95	0.974	0.026
	27	97	0.985	0.015		27	98	0.990	0.010
	28	83	0.982	0.018		28	100	0.990	0.010
	29	93	0.995	0.005		29	93	1.000	
	30	73	1.000			30	100	1.000	
	31	92	1.000			31	96	1.000	
	32	99	0.909	0.091		32	100	1.000	
Sacramento–San Joaquin	33	93	0.984		0.016	33	94	0.941	0.059
	34	100	0.990		0.010	34	100	0.905	0.095
	35	100	0.975		0.025	35	100	0.950	0.050
	36	100	0.990		0.010	36	100	0.830	0.170
	37	100	0.990		0.010	37	100	0.885	0.115

	IDH-3		Alleles						
			100	74	142	94	83	129	136
	ID#	*N*	(100)	(80)		(80)		(120)	
Middle Oregon	1	100	1.000						
	2	100	1.000						
	3	100	0.985					0.015	
	4	100	0.995					0.005	
	5	100	1.000						
	6	100	1.000						
S. Oregon/N. California Coastal	7	100	1.000						
	8	100	0.990					0.010	
	9	100	0.995						0.005
	10	62	1.000						
	11	99	1.000						
Klamath–Trinity Basin	12	100	1.000						
	13	100	1.000						
	14	99	1.000						
	15	124	1.000						
	16	99	1.000						
	17	98	1.000						
	18	106	1.000						
	19	100	1.000						

Appendix A (continued)

	IDH-3		Alleles						
	1D#	*N*	100 (100)	74 (80)	142	94 (80)	83	129 (120)	136
Klamath-Trinity Basin	20	100	1.000						
(continued)	21	120	0.992				0.008		
Eel River-California Coastal	22	95	0.995					0.005	
	23	100	1.000						
	24	99	1.000						
	25	61	1.000						
	26	95	1.000						
	27	99	1.000						
	28	100	1.000						
	29	93	1.000						
	30	100	1.000						
	31	96	1.000						
	32	100	1.000						
Sacramento-San Joaquin	33	94	0.949	0.005			0.048		
	34	100	0.995		0.005				
	35	100	1.000						
	36	100	0.990			0.010			
	37	100	1.000						

	IDH-4		Alleles			LDH-1		Alleles		LDH-4		Alleles			
	1D#	*N*	100 (100)	127 (120)	50	1D#	*N*	100	800	1D#	*N*	100 (100)	112 (115)	134	71 (75)
Middle Oregon	1	100	0.935	0.065		1	100	1.000		1	100	1.000			
	2	100	0.995	0.005		2	100	1.000		2	100	0.985		0.015	
	3	100	0.975	0.025		3	100	1.000		3	100	1.000			
	4	100	0.970	0.030		4	100	1.000		4	100	0.990		0.010	
	5	100	0.950	0.050		5	100	0.900	0.100	5	100	0.985			0.015
	6	100	0.930	0.070		6	100	1.000		6	100	1.000			
S. Oregon/	7	100	0.975	0.025		7	100	1.000		7	100	1.000			
N. California Coastal	8	100	0.945	0.055		8	100	1.000		8	100	0.980	0.010	0.010	
	9	100	0.975	0.025		9	100	1.000		9	100	1.000			
	10	62	0.879	0.121		10	62	1.000		10	62	1.000			
	11	99	0.985	0.015		11	99	1.000		11	99	1.000			
Klamath-Trinity Basin	12	100	0.980	0.020		12	100	0.859	0.141	12	100	1.000			
	13	100	0.900	0.100		13	100	1.000		13	100	1.000			
	14	99	1.000			14	99	1.000		14	99	1.000			
	15	128	0.996	0.004		15	127	1.000		15	128	1.000			
	16	99	1.000			16	100	1.000		16	100	1.000			
	17	98	0.980	0.020		17	98	1.000		17	98	1.000			
	18	102	1.000			18	106	1.000		18	106	1.000			
	19	100	0.990	0.010		19	100	1.000		19	100	1.000			
	20	100	0.980	0.020		20	100	1.000		20	100	1.000			
	21	120	1.000			21	120	1.000		21	120	1.000			
Eel River-California Coastal	22	95	0.868	0.132		22	95	0.897	0.103	22	95	1.000			
	23	100	0.845	0.155		23	100	0.900	0.100	23	100	1.000			
	24	99	0.899	0.101		24	99	1.000		24	99	1.000			
	25	61	0.885	0.115		25	61	1.000		25	61	1.000			
	26	95	0.900	0.100		26	95	1.000		26	95	1.000			
	27	99	0.859	0.141		27	99	1.000		27	99	1.000			
	28	100	0.865	0.135		28	100	1.000		28	100	1.000			
	29	93	0.785	0.215		29	93	1.000		29	93	1.000			
	30	100	0.810	0.190		30	100	1.000		30	100	1.000			
	31	96	0.859	0.141		31	96	1.000		31	96	1.000			
	32	100	0.765	0.235		32	100	1.000		32	100	1.000			
Sacramento-San Joaquin	33	94	0.915	0.085		33	94	1.000		33	94	1.000			
	34	100	0.905	0.090	0.005	34	100	1.000		34	100	1.000			
	35	100	0.895	0.105		35	100	1.000		35	100	1.000			
	36	100	0.875	0.125		36	100	1.000		36	100	1.000			
	37	100	0.995	0.005		37	100	1.000		37	100	1.000			

Appendix A (continued)

	LDH-5		Alleles			MDHP-1		Alleles		MDHP-2		Alleles	
	ID#	*N*	100	90	95	ID#	*N*	100	92	ID#	*N*	100	78
Middle Oregon	1	100	1.000			1	100	0.260	0.740	1	100	1.000	
	2	100	0.970	0.030		2	100	0.375	0.625	2	100	1.000	
	3	100	0.975	0.025		3	100	0.470	0.530	3	100	1.000	
	4	100	0.990	0.010		4	100	0.325	0.675	4	100	1.000	
	5	100	1.000			5	100	0.380	0.620	5	100	1.000	
	6	100	0.995	0.005		6	100	0.465	0.535	6	100	1.000	
S Oregon/	7	100	0.975	0.015	0.010	7	100	0.450	0.550	7	100	0.900	0.100
N. California Coastal	8	100	0.990	0.010		8	100	0.415	0.585	8	100	0.900	0.100
	9	100	1.000			9	100	0.325	0.675	9	100	0.900	0.100
	10	62	1.000			10	62	0.282	0.718	10	62	0.746	0.254
	11	99	1.000			11	98	0.362	0.638	11	98	1.000	
Klamath–Trinity Basin	12	100	0.985	0.015		12	100	0.315	0.685	12	100	0.859	0.141
	13	100	0.890	0.110		13	100	0.390	0.610	13	100	1.000	
	14	99	1.000			14	99	0.247	0.753	14	99	0.598	0.402
	15	127	1.000			15	123	0.228	0.772	15	123	0.558	0.442
	16	100	1.000			16	99	0.212	0.788	16	99	0.562	0.438
	17	98	1.000			17	98	0.245	0.755	17	98	0.622	0.378
	18	106	1.000			18	105	0.333	0.667	18	105	0.564	0.436
	19	100	1.000			19	100	0.465	0.535	19	100	0.827	0.173
	20	100	0.975	0.025		20	100	0.330	0.670	20	100	0.859	0.141
	21	120	1.000			21	120	0.150	0.850	21	120	0.726	0.274
Eel River–California Coastal	22	95	1.000			22	95	0.374	0.626	22	95	1.000	
	23	100	1.000			23	100	0.460	0.540	23	100	1.000	
	24	99	1.000			24	99	0.470	0.530	24	99	1.000	
	25	61	1.000			25	60	0.450	0.550	25	60	1.000	
	26	95	1.000			26	95	0.532	0.468	26	95	1.000	
	27	99	1.000			27	79	0.557	0.443	27	79	0.841	0.159
	28	100	1.000			28	100	0.480	0.520	28	100	0.900	0.100
	29	93	1.000			29	93	0.505	0.495	29	93	1.000	
	30	100	1.000			30	100	0.425	0.575	30	100	1.000	
	31	96	1.000			31	96	0.500	0.500	31	96	1.000	
	32	100	1.000			32	100	0.400	0.600	32	100	1.000	
Sacramento–San Joaquin	33	94	1.000			33	94	0.851	0.149	33	94	1.000	
	34	100	1.000			34	100	0.805	0.195	34	100	1.000	
	35	100	1.000			35	100	0.775	0.225	35	100	1.000	
	36	100	1.000			36	100	0.810	0.190	36	100	1.000	
	37	100	1.000			37	100	0.860	0.140	37	100	1.000	

	MDH-2		Alleles				MDH-4		Alleles			
	ID#	*N*	100	120	27	45	ID#	*N*	100 (100)	121 (120)	70 (70)	126
Middle Oregon	1	100	1.000				1	100	1.000			
	2	100	1.000				2	100	0.980	0.020		
	3	100	0.995			0.005	3	100	0.995	0.005		
	4	100	0.995		0.005		4	100	0.995	0.005		
	5	100	0.880		0.075	0.045	5	100	0.980	0.020		
	6	100	1.000				6	100	0.935	0.065		
S Oregon/N. California Coastal	7	100	1.000				7	100	1.000			
	8	100	1.000				8	100	0.975	0.025		
	9	100	0.990	0.005	0.005		9	100	0.950	0.045		0.005
	10	62	1.000				10	62	1.000			
	11	99	1.000				11	99	0.975	0.015	0.010	
Klamath–Trinity Basin	12	100	1.000				12	100	0.985	0.015		
	13	100	1.000				13	100	1.000			
	14	99	1.000				14	99	1.000			
	15	128	1.000				15	128	1.000			
	16	100	0.995			0.005	16	100	1.000			
	17	98	1.000				17	98	1.000			
	18	106	1.000				18	106	1.000			
	19	100	1.000				19	100	1.000			

Appendix A (continued)

	MDH-2		Alleles				MDH-4		Alleles			
	ID#	*N*	100	120	27	45	ID#	*N*	100 (100)	121 (120)	70 (70)	126
Klamath-Trinity Basin (continued)	20	100	1.000				20	100	0.995	0.005		
	21	120	1.000				21	120	1.000			
Eel River-California Coastal	22	95	1.000				22	95	0.995	0.005		
	23	100	0.995			0.005	23	100	0.985	0.015		
	24	99	1.000				24	99	1.000			
	25	61	1.000				25	61	1.000			
	26	95	1.000				26	95	1.000			
	27	99	1.000				27	99	1.000			
	28	100	1.000				28	100	1.000			
	29	93	1.000				29	93	1.000			
	30	100	1.000				30	100	1.000			
	31	96	1.000				31	96	1.000			
	32	100	1.000				32	100	1.000			
Sacramento-San Joaquin	33	94	1.000				33	94	0.979	0.021		
	34	100	1.000				34	100	0.920	0.070		0.010
	35	100	1.000				35	100	0.955	0.045		
	36	100	1.000				36	100	0.905	0.065		0.030
	37	100	1.000				37	100	0.935	0.040	0.025	

	mMDH-1		Alleles		mMDH-2		Alleles		MPI		Alleles	
	ID#	*N*	-100	-900	ID#	*N*	100	200	ID#	*N*	100 (100)	109 (110)
Middle Oregon	1	100	1.000		1	100	1.000		1	99	0.581	0.419
	2	100	0.980	0.020	2	100	0.995	0.005	2	100	0.695	0.305
	3	100	0.990	0.010	3	100	1.000		3	100	0.575	0.425
	4	100	0.995	0.005	4	100	1.000		4	100	0.505	0.495
	5	100	0.960	0.040	5	100	1.000		5	100	0.690	0.310
	6	100	0.915	0.085	6	100	0.995	0.005	6	100	0.900	0.100
S. Oregon/	7	100	0.940	0.060	7	100	1.000		7	100	0.890	0.110
N. California Coastal	8	100	0.940	0.060	8	100	0.995	0.005	8	99	0.828	0.172
	9	100	0.865	0.135	9	80	1.000		9	100	0.660	0.340
	10	62	0.960	0.040	10	62	1.000		10	62	0.815	0.185
	11	99	0.899	0.101	11	99	1.000		11	99	0.818	0.182
Klamath-Trinity Basin	12	100	0.910	0.090	12	100	0.995	0.005	12	100	0.860	0.140
	13	100	0.795	0.205	13	100	1.000		13	100	0.860	0.140
	14	99	1.000		14	99	1.000		14	99	0.970	0.030
	15	128	0.996	0.004	15	80	1.000		15	128	1.000	
	16	60	1.000		16	60	1.000		16	100	1.000	
	17	98	0.990	0.010	17	98	0.995	0.005	17	98	0.959	0.041
	18	70	1.000		18	106	1.000		18	106	0.953	0.047
	19	100	0.990	0.010	19	100	0.905	0.095	19	100	0.940	0.060
	20	100	0.970	0.030	20	100	1.000		20	100	0.975	0.025
	21	120	1.000		21	120	1.000		21	120	0.992	0.008
Eel River-California Coastal	22	95	0.995	0.005	22	95	0.995	0.005	22	95	0.805	0.195
	23	100	0.990	0.010	23	100	1.000		23	100	0.765	0.235
	24	99	0.995	0.005	24	99	1.000		24	99	0.904	0.096
	25	61	1.000		25	61	1.000		25	61	0.787	0.213
	26	95	0.989	0.011	26	95	1.000		26	95	0.853	0.147
	27	99	1.000		27	99	1.000		27	99	0.818	0.182
	28	100	1.000		28	73	1.000		28	99	0.808	0.192
	29	93	1.000		29	93	1.000		29	93	0.785	0.215
	30	100	1.000		30	100	1.000		30	100	0.800	0.200
	31	96	1.000		31	96	1.000		31	96	0.901	0.099
	32	100	1.000		32	100	1.000		32	100	0.610	0.390
Sacramento-San Joaquin	33	94	1.000		33	94	1.000		33	94	0.617	0.383
	34	100	1.000		34	100	1.000		34	100	0.585	0.415
	35	100	1.000		35	100	1.000		35	100	0.580	0.420
	36	100	1.000		36	100	1.000		36	100	0.545	0.455
	37	100	1.000		37	100	1.000		37	100	0.700	0.300

Appendix A (continued)

	PGDH		Alleles			PGK-2		Alleles		PGM-1		Alleles		
	ID#	N	100 (100)	90 (90)	85 (90)	ID#	N	100 (100)	90 (90)	ID#	N	100	210	50
Middle Oregon	1	100	1.000			1	100	0.660	0.340	1	100	0.855	0.065	0.080
	2	100	1.000			2	100	0.445	0.555	2	100	0.870	0.070	0.060
	3	100	1.000			3	100	0.435	0.565	3	100	0.910	0.070	0.020
	4	100	1.000			4	100	0.355	0.645	4	100	0.870	0.090	0.040
	5	100	1.000			5	100	0.465	0.535	5	100	0.880	0.090	0.030
	6	100	1.000			6	100	0.430	0.570	6	60	1.000		
S. Oregon/	7	100	1.000			7	100	0.395	0.605	7	100	1.000		
N. California Coastal	8	100	0.985		0.015	8	100	0.345	0.655	8	100	1.000		
	9	100	0.990		0.010	9	100	0.515	0.485	9	100	0.980	0.020	
	10	62	1.000			10	62	0.468	0.532	10	62	1.000		
	11	99	1.000			11	98	0.439	0.561	11	99	1.000		
Klamath-Trinity Basin	12	100	1.000			12	100	0.400	0.600	12	80	1.000		
	13	100	0.910		0.090	13	100	0.380	0.620	13	100	1.000		
	14	99	1.000			14	99	0.146	0.854	14	99	1.000		
	15	128	0.996	0.004		15	127	0.185	0.815	15	128	1.000		
	16	100	1.000			16	100	0.155	0.845	16	100	1.000		
	17	98	1.000			17	98	0.189	0.811	17	98	1.000		
	18	106	1.000			18	105	0.186	0.814	18	106	1.000		
	19	100	1.000			19	100	0.380	0.620	19	100	0.950		0.050
	20	100	1.000			20	100	0.320	0.680	20	100	1.000		
	21	120	1.000			21	120	0.292	0.708	21	120	1.000		
Eel River-California Coastal	22	95	1.000			22	95	0.379	0.621	22	95	1.000		
	23	100	1.000			23	100	0.345	0.655	23	80	0.994	0.006	
	24	99	1.000			24	99	0.525	0.475	24	99	1.000		
	25	61	1.000			25	61	0.459	0.541	25	61	1.000		
	26	95	1.000			26	95	0.242	0.758	26	95	1.000		
	27	99	1.000			27	99	0.480	0.520	27	99	1.000		
	28	100	1.000			28	99	0.439	0.561	28	100	1.000		
	29	93	1.000			29	93	0.392	0.608	29	93	1.000		
	30	100	1.000			30	100	0.245	0.755	30	100	1.000		
	31	96	1.000			31	96	0.365	0.635	31	96	1.000		
	32	100	1.000			32	100	0.315	0.685	32	100	1.000		
Sacramento-San Joaquin	33	94	0.979	0.021		33	94	0.590	0.410	33	94	1.000		
	34	100	0.975	0.025		34	100	0.495	0.505	34	100	1.000		
	35	100	0.960	0.040		35	100	0.490	0.510	35	100	1.000		
	36	100	0.920	0.080		36	100	0.605	0.395	36	100	1.000		
	37	100	0.900	0.100		37	100	0.670	0.330	37	100	1.000		

	PGM-2		Alleles				PGM-3		Alleles	
	ID#	N	100 (100)	166 (166)	144	120	ID#	N	100	94
Middle Oregon	1	100	1.000				1	100	0.710	0.290
	2	100	1.000				2	100	0.945	0.055
	3	100	0.970			0.030	3	100	0.885	0.115
	4	100	0.975			0.025	4	100	0.925	0.075
	5	100	1.000				5	100	0.900	0.100
	6	100	1.000				6	100	0.945	0.055
S. Oregon/N. California Coastal	7	100	0.995	0.005			7	100	0.970	0.030
	8	100	1.000				8	100	0.970	0.030
	9	100	0.965		0.030	0.005	9	100	0.950	0.050
	10	62	0.927		0.073		10	62	0.968	0.032
	11	99	0.995		0.005		11	99	0.934	0.066
Klamath-Trinity Basin	12	100	0.915	0.085			12	100	0.945	0.055
	13	100	0.975	0.025			13	100	0.930	0.070
	14	99	0.929	0.071			14	99	0.980	0.020
	15	128	0.902	0.098			15	114	0.987	0.013
	16	100	0.965	0.035			16	98	0.964	0.036
	17	98	0.964	0.036			17	98	0.923	0.077
	18	106	1.000				18	106	0.981	0.019
	19	100	0.860	0.135	0.005		19	100	0.970	0.030

Appendix A (continued)

	PGM-2 ID#	*N*	Alleles 100 (100)	166 (166)	144	120
Klamath–Trinity Basin (continued)	20	100	1.000			
	21	120	1.000			
Eel River–California Coastal	22	95	1.000			
	23	100	1.000			
	24	99	0.970	0.025	0.005	
	25	61	0.967		0.033	
	26	95	1.000			
	27	99	1.000			
	28	100	1.000			
	29	93	1.000			
	30	100	1.000			
	31	96	1.000			
	32	100	0.995	0.005		
Sacramento–San Joaquin	33	94	0.995	0.005		
	34	100	0.990	0.010		
	35	100	0.995	0.005		
	36	100	1.000			
	37	100	1.000			

	PGM-3 ID#	*N*	Alleles 100	94
	20	100	0.950	0.050
	21	120	0.900	0.100
	22	95	0.984	0.016
	23	100	0.965	0.035
	24	99	0.995	0.005
	25	61	1.000	
	26	95	1.000	
	27	99	1.000	
	28	100	1.000	
	29	93	1.000	
	30	100	1.000	
	31	96	1.000	
	32	100	1.000	
	33	94	0.995	0.005
	34	100	0.970	0.030
	35	100	0.970	0.030
	36	100	0.980	0.020
	37	100	0.975	0.025

	PGM-4 ID#	*N*	Alleles 100	94	108	88	90	97
Middle Oregon	1	100	0.100	0.520	0.015	0.285	0.080	
	2	100	0.325	0.565	0.050	0.010	0.035	0.015
	3	100	0.330	0.610	0.030	0.005	0.020	0.005
	4	100	0.385	0.540	0.055	0.005	0.015	
	5	100	0.265	0.675	0.030	0.030		
	6	100	0.505	0.430	0.055	0.010		
S. Oregon/ N. California Coastal	7	100	0.505	0.435	0.060			
	8	100	0.535	0.415	0.045	0.005		
	9	100	0.370	0.630				
	10	62	0.315	0.685				
	11	98	0.464	0.536				
Klamath–Trinity Basin	12	100	0.490	0.495		0.015		
	13	100	0.565	0.435				
	14	99	0.586	0.414				
	15	114	0.667	0.333				
	16	98	0.592	0.408				
	17	98	0.495	0.505				
	18	106	0.528	0.472				
	19	100	0.665	0.290	0.045			
	20	100	0.505	0.495				
	21	120	0.363	0.638				
Eel River–California Coastal	22	95	0.726	0.268	0.005			
	23	100	0.675	0.325				
	24	99	0.763	0.227		0.010		
	25	61	0.877	0.115		0.008		
	26	95	0.753	0.247				
	27	99	0.813	0.187				
	28	100	0.800	0.200				
	29	93	0.892	0.108				
	30	100	0.855	0.145				
	31	96	0.760	0.240				
	32	100	0.880	0.120				
Sacramento–San Joaquin	33	94	0.500	0.495		0.005		
	34	100	0.555	0.415	0.005	0.025		
	35	100	0.575	0.335		0.090		
	36	100	0.550	0.435		0.015		
	37	100	0.605	0.375		0.005		0.015

	SOD-1 ID#	*N*	Alleles −100 (−100)	−260 (−260)	580 (580)	1260
	1	99	0.788	0.202	0.010	
	2	100	0.770	0.230		
	3	100	0.765	0.230		0.005
	4	100	0.785	0.215		
	5	100	0.570	0.430		
	6	100	0.715	0.270	0.015	
	7	100	0.730	0.255	0.005	0.010
	8	100	0.780	0.210		0.010
	9	100	0.810	0.190		
	10	62	0.782	0.218		
	11	98	0.760	0.240		
	12	100	0.755	0.230		0.015
	13	100	0.815	0.185		
	14	99	0.990	0.010		
	15	128	1.000			
	16	100	1.000			
	17	94	0.968	0.027		0.005
	18	105	0.852	0.148		
	19	99	0.904	0.010		0.086
	20	100	0.845	0.090	0.060	0.005
	21	120	0.917	0.046	0.021	0.017
	22	92	0.750	0.250		
	23	100	0.635	0.365		
	24	99	0.798	0.202		
	25	59	0.636	0.364		
	26	95	0.700	0.300		
	27	99	0.778	0.222		
	28	87	0.793	0.207		
	29	92	0.837	0.163		
	30	99	0.798	0.202		
	31	91	0.714	0.286		
	32	100	0.715	0.270	0.015	
	33	93	0.661	0.339		
	34	100	0.790	0.210		
	35	100	0.755	0.240	0.005	
	36	100	0.690	0.300	0.010	
	37	100	0.715	0.270	0.015	

Appendix A (continued)

	TPI-3		Alleles			TPI-4		Alleles				DPEP-1		Alleles	
	ID#	*N*	100	106	104	ID#	*N*	100	104	102	101	ID#	*N*	100 (100)	90 (90)
Middle Oregon	1	99	0.783		0.217	1	100	1.000				1	100	0.715	0.285
	2	100	0.970		0.030	2	100	1.000				2	100	0.595	0.405
	3	100	0.960		0.040	3	100	1.000				3	100	0.660	0.340
	4	100	0.905		0.095	4	100	1.000				4	100	0.630	0.370
	5	100	0.890		0.110	5	100	1.000				5	100	0.715	0.285
	6	100	0.950		0.050	6	100	0.995	0.005			6	100	0.920	0.080
S. Oregon/	7	100	0.920		0.080	7	100	0.995		0.005		7	100	0.925	0.075
N. California Coastal	8	100	0.890		0.110	8	100	1.000				8	100	0.905	0.095
	9	100	0.840		0.160	9	100	0.975	0.025			9	100	0.810	0.190
	10	62	0.903		0.097	10	62	1.000				10	62	0.871	0.129
	11	99	0.753	0.101	0.146	11	99	0.970	0.030			11	99	0.848	0.152
Klamath–Trinity Basin	12	100	0.865		0.135	12	100	1.000				12	100	0.895	0.105
	13	100	0.965		0.035	13	100	1.000				13	100	0.770	0.230
	14	99	0.970		0.030	14	99	1.000				14	99	0.990	0.010
	15	128	1.000			15	128	1.000				15	128	1.000	
	16	100	1.000			16	100	1.000				16	100	1.000	
	17	98	0.964		0.036	17	98	0.995	0.005			17	98	0.964	0.036
	18	106	0.967		0.033	18	106	1.000				18	105	0.824	0.176
	19	100	0.940		0.060	19	100	1.000				19	100	0.940	0.060
	20	100	0.970		0.030	20	100	1.000				20	100	0.930	0.070
	21	120	0.979		0.021	21	120	1.000				21	120	1.000	
Eel River–California Coastal	22	95	0.984		0.016	22	95	0.989	0.005	0.005		22	95	0.942	0.058
	23	100	0.960		0.040	23	100	0.995	0.005			23	100	0.950	0.050
	24	99	1.000			24	99	0.995	0.005			24	99	0.965	0.035
	25	61	0.714	0.286		25	61	0.959	0.041			25	61	0.967	0.033
	26	95	1.000			26	95	0.968	0.032			26	95	0.963	0.037
	27	99	0.899	0.101		27	99	0.975	0.025			27	99	0.965	0.035
	28	100	0.859	0.141		28	100	0.975	0.025			28	100	0.955	0.045
	29	93	0.805	0.147	0.048	29	93	0.892	0.086	0.022		29	93	0.957	0.043
	30	100	1.000			30	100	0.875	0.125			30	95	0.937	0.063
	31	96	0.995		0.005	31	96	0.974	0.026			31	96	0.880	0.120
	32	100	0.895	0.100	0.005	32	100	0.955	0.045			32	100	1.000	
Sacramento–San Joaquin	33	94	0.936		0.064	33	94	1.000				33	94	0.894	0.106
	34	100	0.945		0.055	34	100	0.930		0.070		34	100	0.810	0.190
	35	100	0.915		0.085	35	100	0.960		0.040		35	100	0.850	0.150
	36	100	0.870		0.130	36	100	0.960		0.035	0.005	36	100	0.875	0.125
	37	100	0.830		0.170	37	100	0.965		0.035		37	100	0.950	0.050

	PDPEP-2		Alleles			PEPLT		Alleles		TAPEP-1		Alleles	
	ID#	*N*	100 (100)	107 (107)	83	ID#	*N*	100	110	ID#	*N*	100 (100)	130 (140)
Middle Oregon	1	100	0.995	0.005		1	100	1.000		1	100	0.725	0.275
	2	100	0.955	0.045		2	100	1.000		2	100	0.865	0.135
	3	100	0.980	0.020		3	100	1.000		3	100	0.880	0.120
	4	100	0.995	0.005		4	100	1.000		4	100	0.945	0.055
	5	100	1.000			5	100	1.000		5	100	0.895	0.105
	6	100	0.990	0.010		6	100	0.945	0.055	6	100	0.950	0.050
S. Oregon/	7	100	0.990	0.005	0.005	7	100	0.965	0.035	7	100	0.925	0.075
N. California Coastal	8	100	0.995	0.005		8	100	0.995	0.005	8	100	0.975	0.025
	9	100	1.000			9	100	1.000		9	100	0.940	0.060
	10	62	1.000			10	62	1.000		10	62	0.847	0.153
	11	99	1.000			11	99	1.000		11	99	0.955	0.045
Klamath–Trinity Basin	12	100	1.000			12	100	0.985	0.015	12	100	0.925	0.075
	13	100	1.000			13	100	1.000		13	100	0.860	0.140
	14	99	1.000			14	99	1.000		14	99	1.000	
	15	128	1.000			15	128	1.000		15	125	0.996	0.004
	16	100	1.000			16	100	1.000		16	100	1.000	
	17	98	1.000			17	98	1.000		17	98	1.000	
	18	106	1.000			18	106	1.000		18	106	1.000	

Appendix A (continued)

	PDPEP-2		Alleles			PEPLT		Alleles		TAPEP-1		Alleles	
	ID#	*N*	100 (100)	107 (107)	83	ID#	*N*	100	110	ID#	*N*	100 (100)	130 (140)
Klamath-Trinity Basin (continued)	19	100	1.000			19	100	1.000		19	100	1.000	
	20	100	1.000			20	60	1.000		20	100	0.980	0.020
	21	120	1.000			21	120	1.000		21	120	1.000	
Eel River-California Coastal	22	95	1.000			22	95	1.000		22	95	0.974	0.026
	23	100	1.000			23	100	1.000		23	100	0.960	0.040
	24	99	1.000			24	99	1.000		24	99	0.985	0.015
	25	61	1.000			25	61	1.000		25	61	0.992	0.008
	26	95	1.000			26	95	1.000		26	95	0.979	0.021
	27	98	1.000			27	60	1.000		27	99	0.965	0.035
	28	100	0.995	0.005		28	100	1.000		28	100	0.995	0.005
	29	93	1.000			29	93	1.000		29	93	1.000	
	30	100	1.000			30	100	1.000		30	100	0.990	0.010
	31	96	1.000			31	96	1.000		31	96	1.000	
	32	100	1.000			32	100	1.000		32	100	1.000	
Sacramento-San Joaquin	33	94	1.000			33	94	1.000		33	94	0.862	0.138
	34	100	0.995	0.005		34	100	1.000		34	100	0.890	0.110
	35	100	1.000			35	100	1.000		35	100	0.950	0.050
	36	100	0.990	0.010		36	100	1.000		36	100	0.940	0.060
	37	100	1.000			37	100	1.000		37	100	0.955	0.045

Appendix B
Recently discovered allozyme variability

Two monomeric mitochondrial loci of aconitate hydratase, mAH-1 and mAH-4, are polymorphic in chinook salmon. The *mAh-1(65)* allele was observed primarily in coastal California samples, although it is also present in the Sacramento system. Three alleles at mAH-4 were important in differentiating coastal and inland samples. Shaklee et al. (Wash. Dep. Fish., Olympia, WA 98504, pers. commun., Feb 1991) have recently performed breeding studies which confirmed the Mendelian model of inheritance for these loci.

Iditol dehydrogenase is coded by two loci in liver tissue. The enzyme is a tetramer for which both loci are assumed to be polymorphic. Variants were assigned to a particular locus based on relative staining intensities. The *Iddh-1(0)* allele was observed in Oregon and coastal northern California populations. The *Iddh-2(61)* allele was observed throughout the study area except in samples from the Sacramento system, whereas the *Iddh-2(20)* allele was only observed in the Sacramento samples.

Variation in NADP-dependent malate dehydrogenase was expressed at two cytosolic loci using chinook salmon muscle and heart tissue. MDHP-2 is also expressed in liver and eye tissue in juvenile fish. MDHP-1 variation has been described by Shaklee et al. (1990b). Due to the low levels of variability found in the Klamath-Trinity system, these MDHP loci wil be extremely important in the identification of fish from this area. The *Mdhp-2(78)* allele has nearly the same mobility as the *Mdhp-1(100)* allele, thus making identification of heterozygous samples difficult.

A duplicated and highly polymorphic monomeric PGM locus was designated by two loci, PGM-3 and PGM-4. These isoloci present particular difficulties when estimating allele and genotypic frequencies (Robin Waples and Paul Aebersold, NMFS Northwest Fish Sci. Cent., Seattle, WA 98115, pers. commun., June 1990). Six alleles have been identified in this system and several individuals with three and four different alleles were observed. Therefore, standards are required for correct analysis of banding patterns. Similar expressions of variants are seen in both liver and eye tissues. Conformance to Hardy-Weinberg proportions at these loci has been found using goodness-of-fit tests of expected and observed genotypes (Waples and Aebersold, pers. commun.) and a protocol for estimating allele frequencies from isoloci was presented by Waples (1988).

Triosphosphate isomerase is coded by four loci in chinook salmon. The products of TPI-1 and TPI-2 migrate cathodally, and those of TPI-3 and TPI-4 migrate anodally. Two variant alleles, *Tpi-3(104)* and *Tpi-3(106)*, were observed from eye tissue, and TPI-4 variation has been described by Shaklee (pers. commun.). Because *Tpi-3(106)* migrates close to *Tpi-4(100)*, only fish homozygous for the *Tpi-3(106)* allele can be

reliably scored. The *Tpi-3(106)* allele was observed in California coastal samples and samples from the Eel River.

The newly discovered alleles, *Ldh-1(800)*, *Mpdh-2(78)*, and *Tpi-3(106)*, could be visualized only in their homozygous form. If these alleles occur at low frequencies in samples of chinook salmon, they may not be detected because of the low probability of sampling the rare homozygote. This may account for the discontinuous distribution observed for some of these alleles (Appendix A). Consequently, *Ldh-1(800)* may be present at low frequency in more than just four samples.

Abstract.–The potential annual fecundity of Dover sole becomes fixed before the spawning season when the average diameter of the advanced stock of yolked oocytes exceeds 0.86 mm; hence potential annual fecundity is determinate. More central California females had atretic advanced oocytes than Oregon females, but rates of atresia were not sufficiently high to have an important effect on the potential annual fecundity of the population. A 1-kg female matured about 83,000 advanced yolked oocytes at the beginning of the season. Vitellogenesis continued for the advanced yolked oocytes during most of the spawning season while batches were repetitively matured and spawned. About nine batches were spawned over a six-month spawning season (December–May), and spawning ceased when the standing stock of advanced oocytes was exhausted. A 1-kg female released about 10,000 eggs per spawning, except for the first and last batches which were smaller than the rest. Near the end of the season, females may spawn more frequently than earlier in the year, increasing the daily production of eggs by the population even though fewer females are reproductively active. Annual reproductive effort of Dover sole was equivalent to about 14% of body wet weight per year. Fifty percent of the females had become sexually mature when they reached 332mm total length.

Various methodological issues were also treated in this paper, including validation of key assumptions underlying estimates of annual fecundity; fecundity sample-size requirements; evaluation of criteria and bias in estimating female sexual maturity; and comparisons of classification by histology and gross anatomy.

Manuscript accepted 15 January 1992.
Fishery Bulletin, U.S. 90:101–128 (1992).

Fecundity, spawning, and maturity of female Dover sole *Microstomus pacificus*, with an evaluation of assumptions and precision

J. Roe Hunter
Beverly J. Macewicz
N. Chyan-huei Lo
Carol A. Kimbrell

Southwest Fisheries Science Center, National Marine Fisheries Service, NOAA
P.O. Box 271, La Jolla, California 92038

Fecundity and sexual maturity estimates are staples of fishery science. Inevitably, they will be estimated for every species of economic consequence because of their importance in the dynamics of the population. A second reason for studying fecundity is that when fecundity estimates are combined with estimates of the abundance of eggs in the sea, they can be used to estimate the biomass of a stock. Our laboratory is currently evaluating such ichthyoplankton methods for estimating the biomass of Dover sole *Microstomus pacificus*, a large demersal resource occurring along the upper continental slope of the west coast of North America. The fecundity of Dover sole from Oregon has been estimated (Yoklavich and Pikitch 1989), but no estimate exists for the segment of the stock living in central California waters, nor have the assumptions underlying fecundity and sexual maturity assessments been studied with the thoroughness necessary for accurate estimates of adult biomass. Thorough analysis of these assumptions is usually lacking in the fecundity literature.

Our objectives were to describe the reproduction of Dover sole off central California and Oregon, and evaluate the assumptions underlying fecundity and sexual maturity estimates. We describe changes in the reproductive state of female Dover sole during the spawning season, estimate annual fecundity, batch fecundity, rates of atresia, annual rates of spawning, and length at 50% mature (ML_{50}).

Evaluation of the assumptions underlying annual fecundity estimates requires defining six fecundity terms, and those underlying maturity estimates require defining four terms for reproductive state.

Fecundity

Annual fecundity Total number of eggs spawned by a female per year.

Total fecundity Standing stock of advanced yolked oocytes.

Potential annual fecundity Total advanced yolked oocytes matured per year, uncorrected for atretic losses. In species with determinate fecundity, potential annual fecundity is considered to be equivalent to the total fecundity prior to the onset of spawning.

Determinate fecundity Annual fecundity is determinate when the potential annual fecundity becomes fixed prior to the onset of spawning. In fishes with determinate fecundity, total fecundity decreases with each

spawning because the standing stock of advanced yolked oocytes is not replaced during the spawning season.

Indeterminate annual fecundity Annual fecundity is indeterminate when the potential annual fecundity of a female is not fixed prior to the onset of spawning and unyolked oocytes continue to be matured and spawned during the spawning season.

Batch fecundity Number of hydrated oocytes released in one spawning; usually determined by counting the number of hydrated oocytes in the ovary.

Relative fecundity Fecundity divided by female weight.

Reproductive states

Active Females capable of spawning at the time of capture or in the near future (by the end of the survey or of a season, or other temporal end point). Ovaries of active females contain sufficient number of yolked oocytes for a spawning.

Inactive Females not capable of spawning at the time of capture nor in the near future, although some may have been mature in the past.

Mature Females that have spawned in the current reproductive season or can be expected to do so.

Immature Females that have not spawned in the current reproductive season nor can be expected to do so.

The central methodological issue in fishes with determinate fecundity (Hunter and Macewicz 1985a, Horwood and Greer Walker 1990) is to establish that potential annual fecundity is an unbiased estimate of annual fecundity. For this to be true in Dover sole requires four key assumptions. The first and most important assumption is that fecundity is determinate in Dover sole. This means that potential annual fecundity becomes fixed before spawning begins. Estimation of the standing stock of advanced oocytes (total fecundity) is meaningless if, during the spawning season, oocytes are added to that stock.

The second assumption is that the potential annual fecundity is equivalent to annual fecundity. Strictly speaking, this probably never happens because in any fish population some of the females resorb some of their advanced yolked oocytes rather than spawn them, a process known as atresia. If many females resorbed many of their advanced oocytes, potential annual fecundity would be a serious overestimate of annual fecundity in the population. In addition, not all ovulated oocytes are spawned; a few remain in the ovigerous folds of the ovary after spawning and are later resorbed. Retention of ovulated oocytes is probably seldom a serious bias.

The third assumption is that the females used to estimate potential annual fecundity have not spawned during the current reproductive season. Dover sole females that have spawned some of their stock of advanced oocytes cannot always be distinguished from those that have not begun spawning. Inclusion of partially spawned females in an estimate of potential annual fecundity of the population could be a significant bias.

The fourth assumption is that one is able to identify with certainty the oocytes that constitute the potential annual fecundity. An ovary may not be sufficiently developed to identify all of the oocytes destined to be spawned. On the other hand, if the ovary is highly advanced, spawning may have begun and some advanced oocytes lost. Clearly, an optimal range of ovarian development exists where these risks are minimized.

In addition to evaluating the above four assumptions (determinate fecundity, atresia, spawning, and immaturity) we consider several other methodological issues related to assessment of fecundity and female sexual maturity. These issues are (1) validation of our gross anatomical and histological classification of ovaries into active or inactive and mature or immature states; (2) four precision issues related to total fecundity estimates (number of tissue samples per ovary, number of females, location of ovarian tissue samples, and within-trawl and between-trawl variance); and (3) an evaluation of bias in the assessment of female sexual maturity.

Methods

Collections and shipboard measurements

Dover sole were collected along the central California coast (Point Conception to San Francisco Bay) during six research trawl cruises (Table 1). Dover sole were taken off the Oregon coast between Cape Lookout and Heceta Head during two cruises in 1988–89; miscellaneous collections provided by E. Pikitch off the Oregon coast in 1985 and 1986 were also used. Research trawls were one-half hour or one hour long, depending on depth. In central California waters, we used a 400-mesh Eastern trawl (mouth opening ~15 m wide and 1.5 m high; Wathne 1977). In Oregon waters, either an Alaska Fisheries Science Center (AFSC) modified 5-inch mesh, 90/120, high-rise "poly Nor'Eastern" trawl (fishing dimensions ~4.6 m high and 13.5 m wide at wing tips), a 5-inch mesh, 92/83, poly Nor'Eastern trawl, or a 5½-inch mesh, 75/90, high-rise Aberdeen trawl was used. Up to 100 Dover sole from

Table 1

Sources of reproductive data on female Dover sole *Microstomus pacificus*. Number of specimens in three levels of ovarian analysis and number of level-3 females with batch fecundity estimates.

Sampling protocol				Levels of ovarian analysis**				
Date (Begin/End)	State	No. positive trawl collections	Selection of females*	1	2	3	Total	Batch fecundity
				(no. females)				
3 Dec 85 – 12 Dec 85	CA	11	A	–	39	65	104	–
4 Nov 85 – 14 Dec 85	OR	4	Unknown	–	73	–	73	–
6 Feb 86 – 7 Feb 86	OR	3	Unknown	–	37	–	37	–
3 May 86	OR	2	Unknown	–	27	–	34	7
5 Mar 86 – 7 Mar 86	CA	8	A	1	135	3	139	–
2 May 86 – 4 May 86	CA	3	A	–	59	1	60	–
11 Jan 87 – 24 Jan 87	CA	27	B	45	387	103	535	–
5 Feb 87 – 15 Feb 87	CA	22	B	14	391	92	500	3
23 Feb 88 – 9 Apr 88	CA	51	C	1716	120	62	1941	43
28 Nov 88 – 14 Dec 88	OR	53	C	667	620	152	1439	–
21 Feb 89 – 31 Mar 89	OR	21	C	104	151	34	292	3
All Oregon		83		771	908	186	1875	10
All California		122		1776	1131	326	3279	46***
Oregon + California		205		2547	2039	512	5154	56***

*A = Random selection of both females and males until 25 females were collected.
B = Selection stratified by length (N 5) in <275 mm class, 10 in 275–424 mm class, and 10 in ≥425 mm.
C = Random selection of ≤100 fish (either females or males).
**Level 1 = gross anatomical; Level 2 = histological with anatomical; Level 3 = total fecundity with anatomical and histological.
***Five females with hydrated oocytes provided by W.W. Wakefield were included in estimate of batch fecundity.

each trawl haul were measured (total length) to the nearest millimeter, sexed, and their gonads classified; some females immediately after capture were also individually weighed to the nearest gram and their ovaries preserved in 10% neutral buffered formalin. Females selected for ovarian preservation were either taken randomly from the trawl catch or selected by length according to a quota for each of three length classes (<275 mm, 275–424 mm, and ≥425 mm) (see Table 1). The preserved ovaries were used to validate our shipboard classification of ovaries, to estimate fecundity, and to provide material for histological descriptions.

Gross anatomical classification of ovaries

Ovaries that were examined onboard the ship were assigned to one of three classes: no yolked oocytes present; yolked oocytes present; and translucent hydrated oocytes present. Ovaries with hydrated oocytes or other yolked oocytes were considered to be in the active state, while those ovaries in which observers saw no yolked oocytes were considered to be in the inactive state. This simple system based on gross anatomical examination of the ovary is more germane for biomass estimation work than are the more complicated systems which involve many more reproductive stages: for example, the seven-stage scale of Hjort (1910), or the five-stage scale of Hagerman

(1952). Eighty percent of the females that we classified using gross anatomical criteria were also classified as active or inactive using histological criteria. The results were compared to determine the accuracy of identifying active and inactive females by gross anatomical classification.

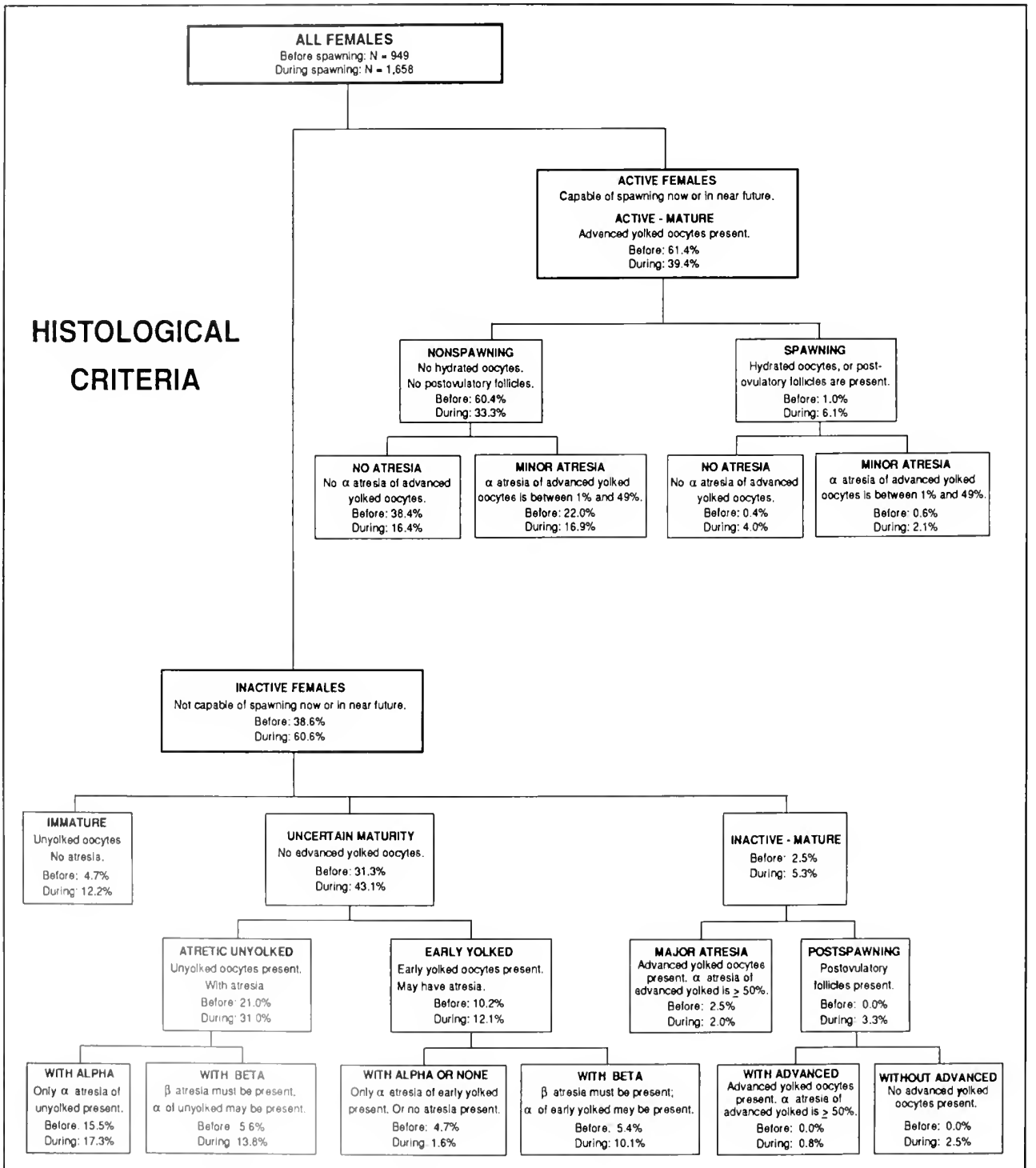

Figure 1

Dendrogram illustrating hierarchial classes of histological criteria of active and inactive ovaries of Dover sole *Microstomus pacificus*. Percentages of females (California and Oregon combined) in each class and subclass taken before (November–December) and during (January–May) the spawning season.

Histological methods

All of the preserved ovaries, regardless of development, had a piece removed for histological analysis. The pieces were dehydrated and then embedded in Paraplast. Subsequently histological sections were cut at 5–6μm and stained with Harris hematoxylin followed by eosin counterstain (H&E). Each ovary was classified histologically in the manner developed for northern anchovy *Engraulis mordax* by Hunter and Goldberg (1980) and Hunter and Macewicz (1980, 1985ab), with a few modifications appropriate for Dover sole ovarian structure. In the ovary we identified the presence or absence of the following: oocytes that have not begun vitellogenesis; oocytes in the first vitellogenic stages (0.15–0.55mm diameter); advanced yolked oocytes (0.47–1.4mm diameter) noting any stages of nucleus migration (precursor to hydration); hydrated oocytes; two stages of postovulatory follicles; and the different stages of atresia. The rate at which postovulatory follicles are resorbed in Dover sole is unknown. Hence no ages were assigned to postovulatory follicles.

Histological classification

We used histological analysis of the ovaries to assess the accuracy of our gross anatomical classification into active and inactive states, to define the optimal criteria for distinguishing mature from immature females, and to calculate various indices of spawning activity and postspawning states. The dendrogram (Fig. 1) indicates the histological characteristics used to classify ovaries into active and inactive states. The dendrogram also gives the frequency of the classes in each state for the prespawning period (November–December) and for the spawning season (January–May) using combined data from California and Oregon. The data are also given by cruise and region in Table 2.

Females were classed as active when histological analysis indicated that the ovary contained the sufficient number of advanced yolked oocytes for one spawning. Active females were then separated into spawning and nonspawning classes using additional histological criteria. Spawning females were those which showed histological evidence of past spawning

Table 2

Numbers of female Dover sole *Microstomus pacificus* in various histological subclasses. Listed by location, before or during the spawning season, and mean cruise date (year and month).

	Inactive										Active				
	Immature	Uncertain maturity						Mature			Mature				
		Atretic unyolked			Early yolked			Major atresia	Postspawning		Nonspawning		Spawning		
		Atresia present			No atresia	Atresia present			Advanced yolk		No atresia	Minor atresia	No atresia	Minor atresia	
Cruise		α only	β only	α and β		α only	β only	α and β		With	Without					All females
Oregon																
Before																
8512	1	4	0	9	0	0	2	9	5	0	0	20	23	0	0	73
8812	32	133	2	37	5	37	4	34	15	0	0	316	150	3	4	772
During																
8602	0	1	0	9	0	0	2	3	4	0	0	6	12	0	0	37
8903	23	70	2	16	1	3	7	18	2	1	3	24	14	3	1	188
8605	1	0	3	4	0	0	5	3	0	4	2	0	0	9	3	34
Total	57	208	7	75	6	40	20	67	26	5	5	366	199	15	8	1104
California																
Before																
8512	12	10	I	4	0	3	0	3	4	0	0	28	36	1	2	104
During																
8701	56	65	11	32	0	7	3	37	11	0	0	115	138	6	9	490
8702	43	99	8	70	2	11	7	36	10	0	1	91	86	12	10	486
8603	38	24	8	40	0	1	7	4	3	3	7	1	2	0	0	138
8803	30	18	4	11	0	4	14	17	3	4	15	31	28	35	11	225
8605	12	9	3	7	2	1	5	0	0	1	13	4	0	2	1	60
Total	191	225	35	164	4	27	36	97	31	8	36	270	290	56	33	1503

(postovulatory follicles present) or imminent spawning (hydrated oocytes or migratory nucleus-stage oocytes present), while the ovaries of nonspawning females showed no evidence of recent or imminent spawning but were capable of spawning in the near future. The fraction of active females classed as spawning was used as a spawning rate index. Spawning performance was also assessed by calculating the mean number of spawning states (postovulatory follicles, hydrated oocytes, migratory nucleus) per female in the spawning class.

Females with ovaries classified as active are considered mature. On the other hand, females with inactive ovaries could be either immature or mature because an ovary may have regressed to an inactive state after the female had attained sexual maturity. We designed our histological classification of inactive ovaries to distinguish as best as possible between mature and immature conditions. Inactive females were grouped into three classes (Fig. 1): immature, uncertain maturity, and inactive-mature. The inactive-mature class included ovaries showing clear histological evidence of past spawning (postspawning subclass) or past maturation of advanced yolked oocytes (major-atresia subclass). Postspawning ovaries contained either postovulatory follicles and no advanced yolked oocytes or postovulatory follicles and mostly atretic advanced yolked oocytes. The fraction of inactive females identified as postspawning was used as an index of the rate at which females passed from the active to the inactive state during the spawning season.

The five major histological classes of active and inactive females were subdivided into atretic subclasses using the first (α) and second (β) stages of resorption as defined by Bretschneider and Duyvene de Wit (1947) and Lambert (1970). One can identify the developmental stage of the oocyte only during the α stage of atresia because the oocyte is completely absorbed by the end of this stage. Subsequent stages (β, γ and δ) involve the resorption of the follicle. Thus, α atresia is of key importance to fecundity studies since the oocyte class can be identified. Subsequent stages may be useful for identifying past spawning activity.

For ovaries containing early yolked or only unyolked oocytes, classification was based solely on presence or absence of the following atresia: β, α of unyolked oocytes, and α of early yolked oocytes (classes immature and uncertain maturity of the inactive females) (Fig. 1).

Ovaries with advanced yolked oocytes were subdivided into two atretic subgroups using the extent of the α atresia of the advanced yolked oocytes: minor atresia, i.e., females with one oocyte to 49% of their advanced yolked oocytes in α; and major atresia, i.e., 50% or more of the advanced yolked oocytes in α. We showed in anchovy that the probability of spawning was very low when more than 50% of the advanced oocytes were atretic (Hunter and Macewicz 1985b). Therefore, ovaries with major atresia of advanced yolked oocytes were considered inactive (inactive-mature class) although the ovary contained some advanced yolked oocytes.

Estimation of total fecundity

We used the gravimetric method to estimate total fecundity of Dover sole. Total fecundity (Y_F) was the standing stock of advanced yolked oocytes in the ovary: $Y_F = Z \cdot C$, where Z is the ovary weight in grams, and C is oocyte density (number of advanced yolked oocytes per gram of ovarian tissue). We also measured diameters of 30 of the advanced yolked oocytes in at least one of the 2–5 tissue samples analyzed for each female for which fecundity was estimated. Advanced yolked oocytes were identified, counted, and measured using a digitizer linked by a video camera system to a dissection microscope.

We used the apparent density of yolk in whole oocytes after preservation, when viewed on the television monitor, to discriminate between developmental stages of yolked oocytes. We defined three stages of yolked oocytes: (1) only an initial layer of yolk along the periphery of the oocyte, appearing as a narrow band but not extending over 20% of the distance between the nucleus and the zona pellucida; (2) lightly-packed yolk possibly extending from the periphery to the nucleus with the nuclear area still evident; and (3) yolk dense enough to occlude the nucleus (Fig. 2) which is histologically equivalent to advanced yolked oocytes. Counts of stage-3 oocytes were used to estimate fecundity and measurements to estimate mean diameter of these advanced yolked oocytes.

Alpha atresia of stage-3 yolked oocytes were distinguished from other whole oocytes viewed on the television screen. The yolk within these α-atretic stage-3 oocytes appeared mottled and lighter due to yolk liquefaction and subsequent resorption, whereas in normal yolked oocytes it appeared dense, dark, and in compact globules (Fig. 2). In addition, the zona radiata (chorion, or membrane layers surrounding the oocyte) of the atretic oocytes was indistinct and irregular in appearance. It was not possible to accurately identify atretic oocytes in frozen, thawed, or poorly preserved ovaries. Atretic oocytes were not included in counts of advanced yolked oocytes used to estimate fecundity. To estimate rates of atresia, we recorded the number of α-atretic yolked oocytes in the random sample of 30 stage-3 oocytes measured. The number of α-atretic advanced yolked oocytes divided by 30 was used as an index of the intensity of atresia in all females used for fecundity estimation.

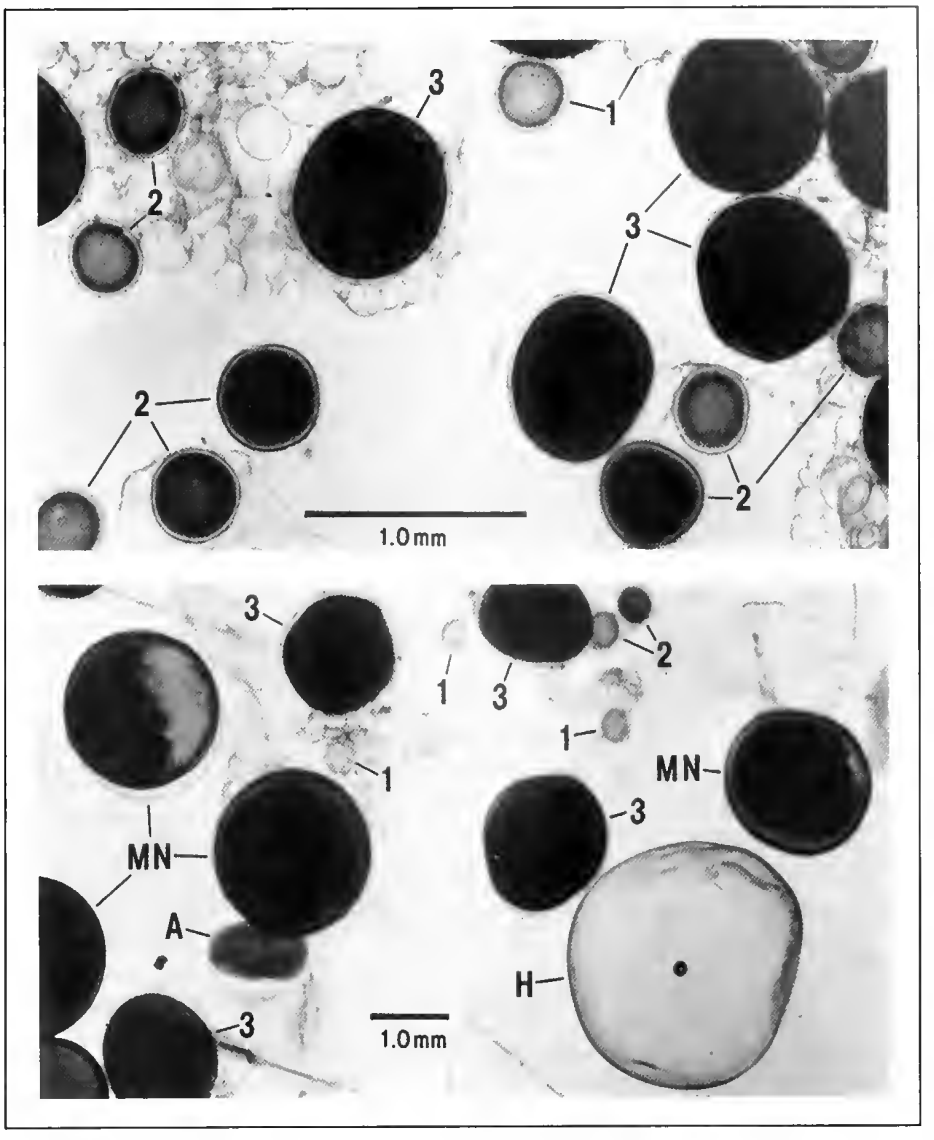

Figure 2
Three stages of preserved whole yolked oocytes of Dover sole *Microstomus pacificus* (stages defined in text). Lower panel also shows migratory nucleus (MN) oocytes, a hydrated (H) oocyte, and an α-atretic advanced yolked oocyte (A). The small air bubble on the hydrated oocyte is an artifact.

Batch fecundity

Batch fecundity was considered to be the number of migratory nucleus-stage oocytes or number of hydrated oocytes in the ovary. We used the gravimetric method to estimate numbers of these oocytes. Migratory nucleus-stage and hydrated oocytes stand out as discrete and easily identified oocyte maturity-classes (Fig. 2). Hydrated ovaries that contained new postovulatory follicles were not used to estimate batch fecundity.

We assigned each spawning batch to one of a possible five batch-order designations [1, 2, (2<B<U−1), (U−1), and U], where B is the batch-order number and U is the total number of spawning batches. The five batch-order designations were defined as follows: first batch (where B=1), nonhydrated, advanced yolked oocytes present and postovulatory follicles absent; second batch (where B=2), one class of postovulatory follicles and nonhydrated, advanced yolked oocytes present; intermediate batches (where B>2 but less than U−1), two classes of postovulatory follicles and nonhydrated, advanced yolked oocytes present; the penultimate batch (U−1), only two batches were present, one of hydrated and one of migratory nucleus oocytes, with no other advanced yolked oocytes present; and last batch (U), no advanced yolked oocytes present other than a single hydrated batch.

In this classification scheme, we assumed that (1) the presence of a single class of postovulatory follicles indicated one spawning had occurred; (2) the presence of two classes indicated at least two spawnings had occurred; and (3) the absence of postovulatory follicles indicated no spawning had occurred. The assumption of no spawning would not hold if the interval between spawnings was sufficiently long for postovulatory

follicles to be resorbed. We used this batch-order classification system to determine if batch fecundity varied with the order of the spawnings, as it does in some species (Alheit 1986, Hunter et al. 1989).

Estimation of length at 50% mature

We estimated the total length (mm) of female Dover sole when 50% had become mature using histological criteria. The fraction of females considered to be mature was estimated for 10 mm or for 50 mm length-classes, and the data were fit to a logistic curve (Dixon et al. 1988). We estimated the maturity threshold for females taken off central California and off Oregon, before and during the spawning season. In our analysis, we evaluated the extent to which changes in histological criteria affected the maturity estimate using six sets of histological criteria: (1) advanced yolked

Table 3

Conversion equations for Dover sole *Microstomus pacificus* by state, sex, or season.

Frozen to fresh for length and weight

Variable				Linear equation Y = a + bX					
Dependent Y	Independent X	State	Sex	a	b	r^2	F	N	Range of independent variable
Fresh length	Frozen length	Cal	All	9.47	1.01	0.99	25,550	251	196–512 mm
Fresh weight	Frozen weight	Cal	All	0*	1.22	—	10,229	111	54–1551 g
Fresh weight**	Frozen weight**	Cal	F	0*	1.29	—	19,575	147	76–1263 g

Length to weight

Variable				Exponential equation W = aL^b					
Dependent W	Independent L	State	Sex	a	SE	b	SE	N	Range of independent variable
Fresh weight (g)	Fresh length (cm)	Cal	F	0.00198	0.00011	3.45	0.016	1245	11.8–54.7 cm
		Cal	M	0.00173	0.00018	3.49	0.029	264	18.5–47.8 cm
		Cal	Unknown					4	12.8–23.5 cm
		Cal	F,M	0.00198	0.00009	3.45	0.013	1509	11.8–54.7 cm
		Ore	F	0.00141	0.00013	3.53	0.026	991	18.8–57.7 cm
		Ore	M	0.00156	0.00015	3.51	0.027	457	20.0–52.2 cm
		Ore	All	0.00159	0.00011	3.50	0.018	1448	18.8–57.7 cm
Fresh weight** (g)	Fresh length (cm)	Cal	F	0.0038	0.00048	3.27	0.033	1198	11.8–54.7 cm
		Ore	F	0.0012	0.00026	3.58	0.056	430	26.8–56.4 cm

Female weight and oocyte volume to ovary weight

Variable					Linear equation Y = a + bX_1 + cX_2						
Season	Dependent Y	Independent X_1	Independent X_2	State	a	b	c	r^2	F	N	Range of independent variable
Prespawning	Ovary weight (g)	Fish weight** (g)		Ore	9.07	0.013		0.09	38.9	388	122–2017 g
	Ovary weight (g)	Fish weight** (g)	Spher. vol.*** (mm^3)	Cal	−4.67	0.027	37.7	0.54	17.9	30	202–1124 g 0.33–0.70 mm^3
				Ore	−34.05	0.036	95.3	0.59	45.85	64	236–1816 g 0.33–0.59 mm^3
				Cal+ Ore	−26.06	0.036	76.3	0.59	68.2	94	202–1816 g 0.33–0.70 mm^3
Spawning	Ovary weight (g)	Fish weight** (g)		Cal	−7.05	0.032		0.41	826.7	1198	14–1736 g
				Ore	21.79	0.010		0.07	4.2	42	148–1597 g
				Cal+ Ore	−5.88	0.031		0.39	788.0	1240	14–1736 g

* Intercept not different from 0, line forced through origin.
** Without ovary.
*** Spherical volume = $4/3\pi r^3$; for mean oocyte diameters ≥0.86 mm.

oocytes or postovulatory follicles present; (2) early yolked oocytes with β atresia; (3) early yolked oocytes with only α atresia of the early yolked oocytes or no α or β atresia; (4) unyolked oocytes with β; (5) unyolked oocytes with only α of the unyolked oocytes; and (6) unyolked oocytes with no atresia. The sexual maturity for females identified by criterion 1 is certain, but some females may be excluded if only criterion 1 is used. Criteria 2–5, if added to criterion 1, broaden the maturity definition but increase the risk of misclassification. Criterion 6 is considered by definition to be immature. We evaluated these criteria to determine the optimal histological definition of maturity using a regression analysis of the lengths of females identified by each criterion.

Length, weight, and gonad weight relationships

To enable the reader to convert from one measurement to another, equations are provided to estimate fresh wet weight from frozen wet weight and from length for Dover sole taken in Oregon and central California waters (Table 3). Analysis of covariance indicated that the slope of the regression of the natural logarithms of weight on length did not differ between sexes for either state. The adjusted group mean for males differed from that for females in Oregon (N 1421, $F_{1,1418}$ 64.87, $P<0.005$ for length range 225–522 mm) but not in California. The slope of the regression of the natural logarithms of weight on length did not differ between central California and Oregon females but the adjusted group means were different (N 2215, $F_{1,2212}$ 79.18, $P<0.005$ for length range 188–547 mm). No difference existed between states in the equations for males. We do not attach too much biological importance to these differences; they could be related to differences in the timing of annual reproductive cycle or our sampling of it. Nonetheless, it seemed preferable to use the relationship for a specific sex or region, so all are listed.

An exponential model was fit to these data sets using a statistical program of weighted nonlinear regression (Dixon et al. 1988) where the weighting factor was the inverse of the variance of fish weight because the variance of fish weight increased with fish length. To compute the variance, fish lengths were divided into several segments, chosen so that within each segment the variance of fish weight was homogeneous. We preferred to obtain the estimates of coefficients directly from the nonlinear fitting so that fish weight could be directly estimated from the exponential model (Table 3).

Freezing of Dover sole caused a 9.47 mm shrinkage in total length, independent of fish length (Table 3). A sample of 251 Dover sole was measured just after capture and again, after thawing, four months later. The slope of the regression of fresh total length on frozen total length (after thawing) was not statistically different from 1, but the intercept, 9.47 mm, was significant. Freezing of females, with ovary removed, resulted in about a 22% loss in wet weight ($0.22 = 1 - \frac{1}{1.29}$; see Table 3).

We also provided equations to estimate ovary wet weight (g) from female wet weight (g, without ovary). This conversion is important if one wishes to express fecundity as a function of the total weight of the female, because all fecundity relations in this study are expressed as a function of female weight without an ovary. As ovary weight is a function of the developmental state of the ovary as well as the weight of the female, separate equations are provided for the prespawning period (November–December) when ovaries are less developed and for the spawning season when they are more fully developed. We also provided multiple regression equations to estimate ovary weight from female weight and the spherical volume of the average advanced yolked oocyte (computed from the mean diameter). These equations are used in the discussion to estimate ovary weight when an ovary contains an entire complement of fully matured advanced yolked oocytes.

Reproductive condition

Accuracy of gross anatomical classification

We rarely misclassified inactive ovaries using gross anatomical criteria. Of the 1272 females classified as inactive, only 14 (1.1%) were identified as active using histological criteria. This error rate is so low that differences could be attributable to clerical errors alone. A more common error in gross anatomical classification was to misclassify females as having active ovaries. One hundred and fifty-nine females (11.9%) were visually classified as having advanced yolked oocytes and were believed to be capable of spawning, while histological analysis indicated that their ovaries were inactive and future spawning was unlikely. The 159 females misclassified as active fell predominantly into two classes: females with ovaries in the early stages of vitellogenesis (40.8%), and females with advanced yolked oocytes with high levels of atresia (30.1%) (Table 4).

Misclassification of the early stages of vitellogenesis as active is expected because the gross anatomical criterion, "yolked oocytes visible," is not exact; observers are bound to differ on whether to include or exclude females that fall near the visible threshold

Table 4

Histological classification of female Dover sole *Microstomus pacificus* with inactive ovaries that were misclassified using gross anatomical criteria as having active ovaries. Data from central California and Oregon are combined.

Collection period	Percentage of females misclassified as active per inactive histological class: Immature	Unyolk atretic	Early yolked	Major atresia of adv. yolked	Post-spawning	Total no. misclassed females
Nov–Dec	0.0	2.0	48.9	48.9	0.0	49
Jan–May	4.5	23.6	37.2	21.8	12.7	110
Nov–May	3.1	17.0	40.8	30.1	8.8	159

for detection of yolked oocytes in the ovary. An exact criterion, such as oocyte diameter, would be more accurate but would be impractical for production work on the ship. Misclassification of highly atretic ovaries as active is also expected, since α-atretic advanced yolked oocytes are difficult if not impossible to see with the unaided eye. As highly-atretic advanced ovaries were rare in this study, our failure to detect them was a minor systematic error. Under environmental conditions unfavorable to reproduction, however, this could be an error of consequence.

Changes in ovarian condition during the spawning season

The fraction of females anatomically classed with active ovaries

Figure 3 (below)

Seasonal change in four indices of reproduction in Dover sole *Microstomus pacificus*. Indices are plotted as a function of elapsed time since 1 November; data are combined from different years; California (solid circles) and Oregon (open circles) data were combined to fit trend lines; numbers are the sample size of females. (upper left) Percentage of Dover sole with active ovaries; trend line is a weighted Weibull model (see text Eq. 1). (upper right) Percentage of females with active ovaries which had one or more spawning states; trend line is logistic model $P = \frac{e^{a+bL}}{1+e^{a+bL}}$, where a = −5.678 and b = 0.036. (lower left) Mean number of spawning states in active ovaries; bars are two standard errors of the mean. (lower right) Percentage of females with inactive ovaries identified as postspawning; trend line is logistic model where a = 8.495 and b = 0.042.

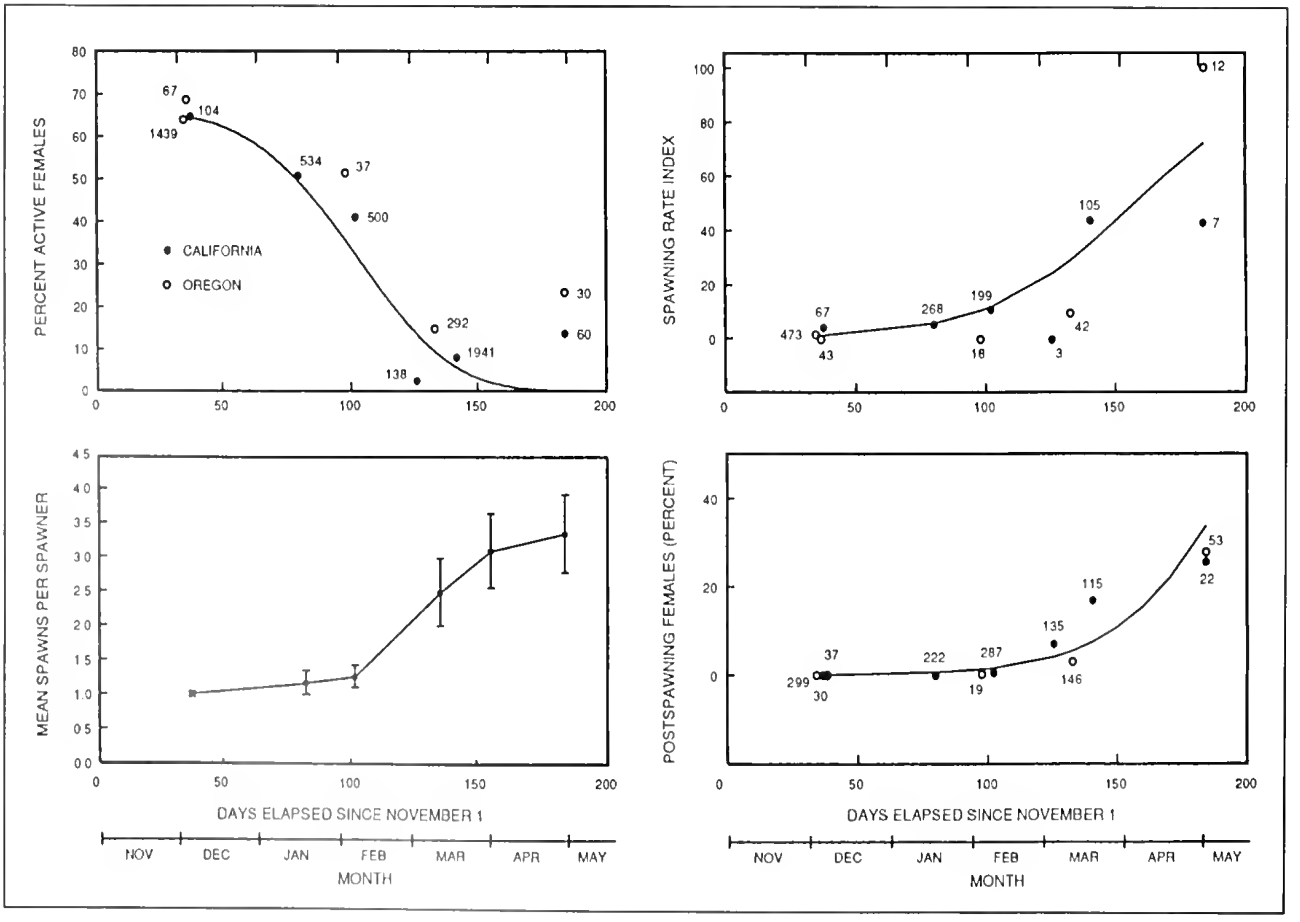

declined over the spawning season as females expended their stock of advanced yolked oocytes. We fitted a weighted Weibull function to the combined California and Oregon data, yielding the equation

$$P = 0.656\, e^{-\left(\frac{t}{111.5}\right)^{3.76}} \quad \text{(Eq. 1)}$$

where t is days elapsed since 1 November; P, the fraction active, is weighted by $\frac{N}{P(1-P)}$, and pseudo r^2 is 0.96. According to the equation, the percentage of females with active ovaries declined from 65% at the onset of the spawning season (about 6 December) to 40% by the end of January; by the end of February only 18% of the females had active ovaries (Fig. 3, upper left).

In California and Oregon, the mean diameter of the stock of advanced yolked oocytes increased steadily from December through April (Fig. 4). Thus reproductively active females continued vitellogenesis throughout most of the spawning season. By March or April the average advanced yolked oocyte is closer to the minimum size at which hydration begins (diameter 1.35 mm). Thus Dover sole may be able to spawn at a higher rate late in the spawning season, because less yolk would have to be added to the advanced oocytes for them to attain the size at hydration.

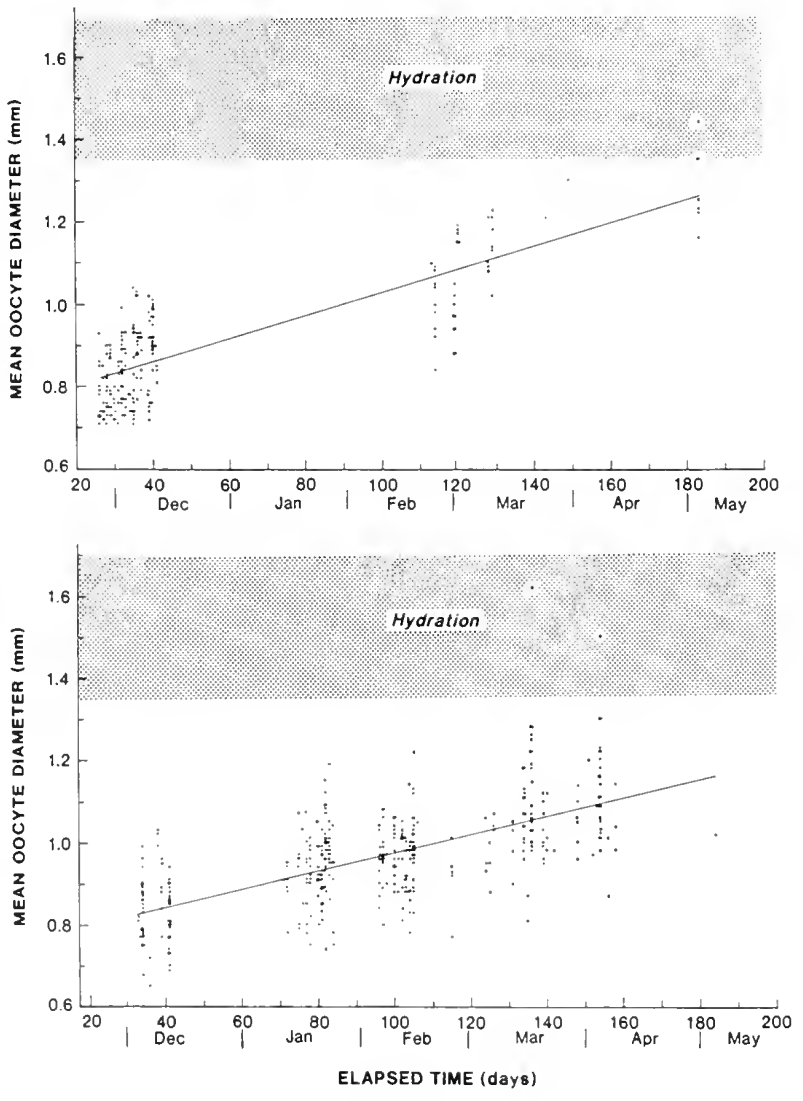

Figure 4

Increase in mean oocyte diameter (D) of the advanced yolked oocytes of Dover sole *Microstomus pacificus* from Oregon (top) and California (bottom) as a function of elapsed time (T) since 1 November. Data from different spawning seasons are combined; shaded area indicates size range of oocytes at the onset of hydration; trend lines are Oregon (D = 0.742 + 0.00282T, r^2 0.658, N 195) and California (D = 0.761 + 0.0022T, r^2 0.41, N 365).

Only 10 females taken in November–December were classed as spawning on the basis of their ovarian histology (Oregon and California data combined, N 949). They comprised only 1.0% of all females with preserved ovaries taken during this time and only 1.7% of those classed as active. Clearly, spawning is just beginning in November–December in California and Oregon waters. The spawning rate index increased from 1.3% in November–December to 12% by early February; it accelerated at the end of the season with spawning females comprising about 70% of all active females (percent calculated by the trend line in Fig. 3, upper right). Thus at the end of the season, most of the females with active ovaries had spawned recently. We believe this sharp increase in the index near the end of the season is evidence for a seasonal increase in spawning frequency.

A late seasonal increase also existed in the occurrence of multiple spawning stages within the same ovary. As many as five different past or potential spawning stages could be distinguished histologically in the same ovary: two stages of postovulatory folli-

cles, hydrated oocytes, migratory nucleus oocytes, and other advanced yolked oocytes. These data were expressed as the number of spawning states per spawner (spawns per spawner, Fig. 3, lower left). The average number of spawns per spawner increased from about one in mid-March to about three by early April. These data also indicated that spawning frequency may increase near the end of the spawning season.

The fraction of females with inactive ovaries that were classed as postspawning also increased late in the season (Fig. 3, lower right). This index can be considered a measure of the rate females in the population pass from the active to the inactive state. Although the duration of this stage was unknown, we were certain that it was ephemeral because there were always many fewer females classed as postspawning than the cumulative total of females that had passed from the active to inactive state. This index increased sharply in late-March through April, indicating that the rate females passed into the inactive stage accelerated during the last part of the season.

The sharp increases in the three indices described indicated that the daily production of eggs by the population may be higher in March than February even though fewer fish were spawning. For example, by mid-March (13 March), a half to a third as many females had reproductively active ovaries than in mid-February (10 Feb.). On the other hand, in mid-March as compared with mid-February, about twice as many females with active ovaries were classed as spawning, and the ovaries of the spawners contained evidence of about twice as many past or potential spawnings. Thus the reproductive output of the reproductively active females in the population in mid-March might be four times that of the active fish in mid-February. If this is true, half the number of active females could produce twice as many eggs per day. This is, of course, sheer speculation because the duration of these spawning stages is unknown. Nevertheless, the data presented in this section collectively suggest that the daily production of eggs by the population may increase near the end of the season even though fewer females are spawning.

Total fecundity

Location of tissue samples

A key assumption underlying the gravimetric method of fecundity estimation is that oocytes are randomly distributed in the ovary. To determine if advanced yolked oocytes are randomly distributed in the ovary, we compared the densities of advanced yolked oocytes in tissue samples taken from five different locations in the ovary of ten females. The location of a tissue sample within the ovary was defined in terms of three characteristics: longitudinal plane of the ovary (anterior end, middle, and posterior end); cross-sectional plane (interior near the lumen, exterior near the ovarian wall, or interior and exterior combined); and right and left lobes of the ovary. The characteristics of the five ovarian locations along with the mean oocyte density of each location are indicated in Table 5.

Initially we tested the overall effect of location of the tissue sample on oocyte density using two-way ANOVA; the effect of position was insignificant at the 5% level of significance (Table 5, lower). We also tested for possible differences between pairs of location characteristics: posterior end vs. middle; posterior vs. anterior ends of the ovary; right vs. left lobes of the ovary; and interior and exterior sections of the ovary. No significant differences were detectable between any of

Table 5

Effect of location of tissue samples within the ovary of Dover sole *Microstomus pacificus* on oocyte density (number of advanced yolked oocytes per unit sample weight) with mean and standard deviation (SD) and, below, two-way analysis of variance on results.

	Location in ovary of sample*			Oocyte density		
		Plane of section				
Position no.	Lobe	Long.	Cross.	*N*	Mean	SD
1	Rt	Post	Int & Ext	10	1803.7	468.1
2	Rt	Mid	Ext	10	1801.1	532.0
3	Rt	Mid	Int	10	1754.1	488.6
4	Rt	Ant	Ext	10	1886.1	440.2
5	Lt	Mid	Int	10	1839.3	537.6

Analysis of variance on five locations

Source	DF	SS	MS	*F*
Fish	9	10,379,034	1,153,226	
Position	4	96,638	24,160	1.373
Error	36	633,493	17,597	
Total	49	11,109,165		

*Long. = longitudinal, Rt = right lobe, Lt = left lobe, Post = posterior end, Mid = middle, Ant = anterior end, Int = internal, and Ext = external.

these four comparisons; F values ranged from 0.01 to 0.14, with the degrees of freedom being 1 and 45 for each comparison. Thus the advanced yolked oocytes in Dover sole are randomly distributed within the ovary, and tissue samples can be taken from any location or lobe without bias.

Optimal number of tissue samples

To develop a procedure for estimating the number of tissue samples needed for estimating total fecundity, we first considered the general fecundity model. The true total fecundity (Y_F) is the condition where all the advanced yolked oocytes in the ovary are counted, and the relation between female weight (W) and fecundity is defined as

$$Y_F = f(W) + A \qquad \text{(Eq. 2)}$$

where $f(W) = a+bW$, and A is the error term. The variance of A, σ^2_A, measures the deviation of the data set (Y_F, W) to the model f(W). As it was impractical to count all advanced yolked oocytes in the ovary, Y_F is estimated from counts of oocytes in weighed tissue samples, expressed as oocytes per gram of tissue or oocyte density. The precision of a fecundity estimate can be increased by increasing the number of tissue samples taken per female. On the other hand, if the amount of labor for fecundity work is fixed, then increasing the number of tissue samples per fish would reduce the number of fish that can be sampled. Thus we needed to know the minimum number of tissue samples necessary to guarantee a goodness-of-fit of the model to the data set.

We determined the optimum number of tissue samples by minimizing the variance of sample variance of A ($\sigma^2(s^2_A)$). This procedure led to using the ratio of the variance of oocyte counts between tissue samples within fish (σ^2_e) to the variance around the regression line (σ^2_A), i.e., $\theta = \sigma^2_e/\sigma^2_A$. The smaller the θ, the fewer tissue samples are needed.

Let's denote for the ith fish, $i = 1,..,n$,

W_i = fish weight,

Y_{Fi} = total number of advanced yolked oocytes in the ovary,

y_{ij} = advanced yolked oocyte count in the jth tissue sample, $j = 1,..,m$,

z_{ij} = weight of the jth tissue sample,

Z_i = formalin wet weight of ovary,

m = number of tissue samples from an ovary,

M_i = maximum number of tissue samples in an ovary,

$\hat{Y}_{Fij}$ = estimate of total number of advanced yolked oocytes in the ovary from the jth tissue sample $\left(\frac{y_{ij}}{z_{ij}}\right) Z_i$,

$\hat{Y}_{Fi}$ = estimated total number of advanced yolked oocytes in the ovary and is used for all analyses in fish fecundity in later sections

$$= \frac{\sum_{j=1}^{m} \hat{Y}_{Fij}}{m}, \text{ and}$$

$\hat{Y}_{Fi}$ = estimate of total fecundity from the regression model.

We write $\hat{Y}_{Fij}$ as

$$\hat{Y}_{Fij} = Y_{Fi} + (\hat{Y}_{Fij} - Y_{Fi})$$

$$= f(W_i) + A_i + e_{ij} \qquad \text{(Eq. 3)}$$

where $e_{ij} = \hat{Y}_{Fij} - Y_{Fi}$. The estimated total number of advanced yolked oocytes in the ovary is

$$\hat{Y}_{Fi} = \frac{\sum_{j=1}^{m} \hat{Y}_{Fij}}{m} = f(W) + A_i + e_i$$

$$= f(W) + \xi \qquad \text{(Eq. 4)}$$

and

$$\sigma^2_\xi = \sigma^2_A + \frac{\left(\frac{M-m}{M}\right)\sigma^2_e}{m}. \qquad \text{(Eq. 5)}$$

Thus the variance around the regression line σ^2_ξ based upon the data set $(\hat{Y}_{Fi}, W_i)$ is composed of two variance components: one is σ^2_A and the other is σ^2_e. The sample counterparts for σ^2_ξ and σ^2_e are s^2_ξ and s^2_e:

$$s^2_\xi = \frac{[\hat{Y}_F - f(W)]^2}{n-q} \qquad \text{(Eq. 6)}$$

is the mean square error from a regression analysis on $(\hat{Y}_{Fi}, W_i)$ where q is the number of regression coefficients and n is the number of fish, and

$$s^2_e = \frac{\sum_{i=1}^{n}\sum_{j=1}^{m} (\hat{Y}_{Fij} - \hat{Y}_{Fi})^2}{n(m-1)} \qquad \text{(Eq. 7)}$$

is the within-sample variance (Hunter et al. 1985). The estimate (s^2_A) of the variance around f(W) when Y_F is known (σ^2_A) can be estimated by subtraction:

$$s^2_A = s^2_\xi - \frac{\left(\frac{M-m}{M}\right) s^2_e}{m}. \qquad \text{(Eq. 8)}$$

According to Hunter et al. (1985), the optimum number of tissue samples can be determined for a given θ ($= s^2_e/s^2_A$), the cost of processing a tissue sample, and the cost of processing a fish. The ratio, $K = s^2_\xi/s^2_A$, measured the excess variance which is contributed by taking tissue samples rather than counting every advanced oocyte in the ovary.

We used Dover sole collected during January–February 1987 to determine the optimal number of tissue samples. Two tissue samples were taken from the ovaries of 99 Dover sole. The within-sample variance of oocyte density ($s^2_e = 1053 \times 10^4$) was obtained from an ANOVA, and the linear regression of $\hat{Y}_F$ on W ($\hat{Y}_F = 20{,}255 + 40.54W$) gave the MSE ($s^2_\xi = 18{,}469 \times 10^4$) (Table 6; Fig. 5, lower middle). Thus θ is 0.058 when calculated from equations (7 and 8) where $m = 2$. Because M was large (range 200–700), $\frac{M-m}{M}$ was assumed to equal 1, and s^2_A was computed as $s^2_\xi - (s^2_e/2) = 17{,}942 \times 10^4$. Hence when two tissue samples are used, the variance within tissue samples is only 5.8% of the variance around the fecundity-fish weight regression line. To quantify the excess variance due to subsampling, we computed $K = s^2_\xi/s^2_A = 1.03$. This means the variance around the regression line which was based on two tissue samples per fish (Eq. 4) is about 1.03 times that of an equation based on counts of all advanced yolked oocytes in the ovary (Eq. 2). Although the within-ovary variance was small, we recommend counting two tissue samples per female because the cost of processing the second sample was minimal.

Optimal number of females

In addition to the sample allocation based on cost of processing fish and cost of processing tissue samples, the number of females needed for a regression estimate of total fecundity was determined by modifying a procedure suggested by Thigpen (1987) to the 1987 fecundity data for Dover sole. The equation for determining the sample size (n) for a linear regression was

$$n - 1 = \frac{\left(\frac{1-r^2}{r^2}\right)}{CV(b)^2} \qquad \text{(Eq. 9)}$$

Table 6

Within-sample variance ($s^2_e \times 10^{-4}$) from ANOVA and the MSE ($s^2_\xi \times 10^{-4}$) from the regression analysis of fecundity ($Y \times 10^{-2}$) and weight of Dover sole *Microstomus pacificus*. California females taken January–February 1987.

Analysis of variance on total fecundity

Source	DF	SS	MS
Fish	98	8,559,008	87,337
Error	99	104,201	1,053
Total	197	8,663,209	

Analysis of variance on linear regression

Source	DF	SS	MS	F
Regression	1	2,488,019	2,488,019	134.72
Residual	97	1,791,468	18,469	

Predictor	Coeff.	SD	t
Constant	202.55	32.03	6.32
Fish wt.	40.54	3.49	11.61

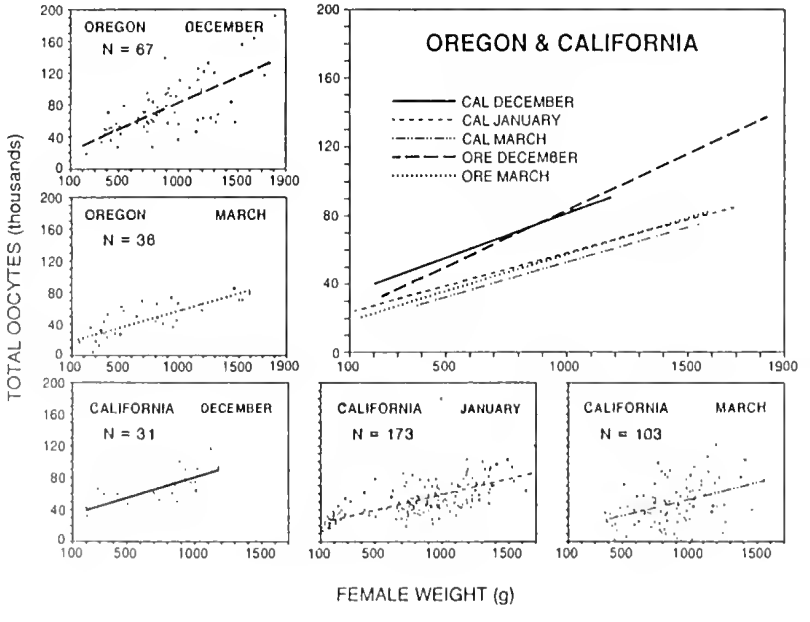

Figure 5

Total fecundity of Dover sole *Microstomus pacificus* as a function of female wet weight in grams (without ovary) for various months taken in central California and Oregon. Each point represents a single female; equations are given in Table 9.

where r^2 is the coefficient of determination, and CV(b) is the coefficient of variation for the regression coefficient (b). The coefficient of determination (r^2) for Dover sole total fecundity and fish weight was 0.58. Thus 73 females are required for a CV(b) = 0.10. In conclusion, two tissue samples from each of 70–80 Dover sole females were adequate for expressing the relation between weight and total fecundity, if a CV(b) of about 0.10 is desired.

Relation to ovarian development

The optimum time for estimating potential annual fecundity is early in the spawning season when the probability of spawning is low. Estimates taken in this period may be biased because all oocytes may not have been recruited into the advanced stock of yolked oocytes. In this section, we use Oregon Dover sole taken in November–December to examine the recruitment of oocytes into the advanced stock of yolked oocytes.

If substantial numbers of oocytes are maturing from early-yolked to more advanced stages, one would expect an overlap in the size distributions of oocytes in different development stages. When vitellogenesis of the early yolked oocytes does not continue, one would expect that a gap would develop between the less-advanced and the most-advanced oocytes as the yolked oocytes continued their maturation. In Dover sole, the diameter distributions of stage-1, -2, and -3 oocytes broadly overlap when the mean diameter of the advanced yolked oocytes (stage 3) is less than 0.7 mm (Fig. 6). The extent of overlap declines as the stage-3 oocytes grow from 0.7 mm to 0.8 mm. Separation of the advanced stock (stage 3) from the other vitellogenic stages (1 and 2) becomes complete as the advanced stock grows from 0.8 to 0.9 mm. It appears from this qualitative analysis that recruitment of stage-2 oocytes into the advanced stock probably ends when the mean diameter of stage 3 is between 0.8 and 0.9 mm.

We conducted a stepwise multiple regression analysis of total fecundity ($\hat{Y}_F$) on mean diameter of the advanced oocytes (D) and female weight (W) for females taken off Oregon in November–December. The coeffi-

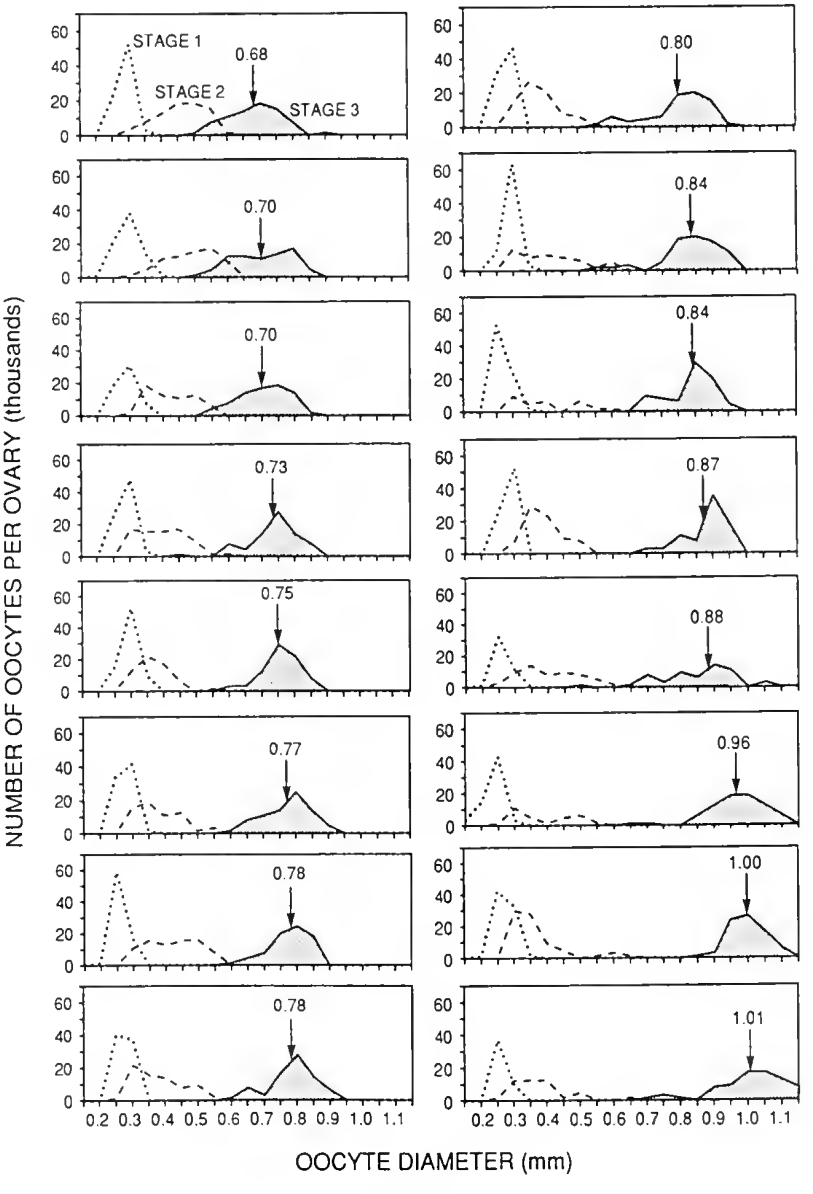

Figure 6

Frequency distribution of oocyte diameter of three vitellogenic oocyte stages in ovaries of Dover sole *Microstomus pacificus*. Each panel represents the ovary from one female. Fish arranged in order of the mean diameter of the advanced yolked oocytes, stage 3 (which is shaded); numbers and arrows indicate mean diameter of stage-3 oocytes. Mean total length was 420 mm and mean ovary-free weight of the females was 868 g. Fish were taken November–December 1988 along the Oregon coastline.

Table 7

Analysis of the relation between total fecundity ($\hat{Y}_F$) of Dover sole *Microstomus pacificus* and gonad-free body weight (W) and the average diameter of the advanced oocytes (D) using stepwise regression with analysis of variance. Specimens from Oregon in November–December 1988.

Stepwise regression

Step	1	2
Constant	22,398	−88,768
Weight (W)	45.4	47.8
t*	7.56	8.80
Diameter (D)		129,893
t*		6.01
S	25,654	23,096
R^2	27.58	41.69

Analysis of variance

Source	DF	SS	MS	F	P
Regression	2	5.68×10^{10}	2.84×10^{10}	53.27	<0.000
Error	149	7.95×10^{10}	5.33×10^{10}		
Total	151	1.36×10^{10}			

Source	DF	Sequential SS
Weight	1	3.76×10^{10}
Egg diameter	1	1.92×10^{10}

* For $P = 0.05$, $1.96 < t < 1.98$., df ≥ 120.

cient for diameter, as well as the one for weight, was positive and significant (Table 7). Thus the potential annual fecundity was not fully recruited as stage-3 oocytes in some of the Oregon Dover sole taken in November–December, since total fecundity increased with the mean diameter of the oocytes used to estimate total fecundity.

To determine the level of ovarian development (oocyte diameter) at which the full complement of oocytes was recruited into the advanced yolked oocyte class (stage 3), we conducted a series of stepwise multiple regression analyses by successively removing the data by 0.01 mm decrements from the lowermost oocyte diameter class starting at 0.71 mm. This analysis indicated that the threshold for a significant effect of oocyte diameter on total fecundity was between mean diameters of 0.85 and 0.86 mm (Table 8). The multiple regression coefficient for oocyte diameter was significant and positive when females with oocyte diameter

Table 8

Results of stepwise multiple regression of the total fecundity ($\hat{Y}_F$) of Dover sole *Microstomus pacificus* on gonad-free body weight (W) and mean oocyte diameter (D) for a succession of oocyte diameter-classes using the model $\hat{Y}_F = a + b_1 W + b_2 D$. Specimens taken along Oregon coast November–December 1988. Line separates oocyte diameter-classes where diameter is a significant variable, from those where it is not.

Oocyte diameter class (mm)	Constants		Multiple regression coefficients and their t-ratios for: Fish weight		Oocyte diameter		
	N	a	b_1	t	b_2	t*	r^2
0.71–1.04	152	−88,768	47.8	8.80	129,893	6.01	0.417
0.72–1.04	148	−90,147	48.3	8.90	130,860	5.87	0.424
0.74–1.04	133	−94,375	49.6	8.34	134,295	5.14	0.415
0.76–1.04	119	−90,710	51.3	7.98	128,688	4.17	0.407
0.78–1.04	105	−83,087	53.4	7.53	118,385	3.16	0.396
0.80–1.04	91	−90,344	55.9	7.29	123,891	2.60	0.400
0.82–1.04	85	−87,274	59.2	7.34	117,459	2.20	0.405
0.83–1.04	81	−111,317	56.9	7.44	145,193	2.77	0.440
0.84–1.04	77	−103,009	58.7	7.55	134,678	2.42	0.460
0.85–1.04	72	−90,464	60.1	7.33	120,166	1.95	0.457
0.86–1.04	67	−38,172	65.3	7.96	60,555	0.94	0.502
0.87–1.04	64	−33,982	63.5	7.30	57,891	0.87	0.482
0.88–1.04	60	−15,721	69.4	7.63	33,456	0.48	0.514
0.90–1.04	46	45,073	82.0	7.92	−40,601	−0.47	0.594
0.92–1.04	34	60,339	84.0	6.92	−58,185	−0.49	0.616

* For $P = 0.05$, t is 1.98 for df = 120, 2.00 for df = 60, and 2.06 for df = 25.

equal to or less than 0.86 mm were included, but was insignificant when only those having a diameter greater than 0.86 mm were considered. We concluded that ovaries in which the advanced stock of yolked oocytes has an average diameter of 0.85 mm or less are not sufficiently developed to be certain that the annual stock is fully recruited. Consequently, to estimate the potential annual fecundity, we used only females in which the average oocyte diameter of the advanced stock exceeded 0.85 mm.

No relationship between oocyte diameter and total fecundity was detected in the females taken off central California during November–December. Oocyte diameter may not have been a significant variable in central California because fewer females were examined and their ovaries were more advanced. In 48% of females from California, advanced yolked oocytes averaged more than 0.85 mm in diameter (N 65), whereas only 34% of the fish taken off Oregon had oocytes that did so (N 128).

Seasonal variation in total fecundity

Total fecundity of Dover sole decreased during the spawning season off both central California and Oregon (Fig. 5). Analysis of covariance indicated that equations expressing the relation between female weight and fecundity differed within the spawning season (Table 9). The total fecundity for a 1 kg female declined from about 80,000 advanced oocytes in December to about 50–60,000 during the spawning season (Table 9).

To further describe the decline in total fecundity over the season, we also regressed fecundity on female weight and elapsed time since 1 November. In both central California and Oregon the negative coefficients for elapsed time were significant, indicating that total fecundity declined with elapsed time (Table 9). Analysis of covariance indicated that multiple regression equations for California and Oregon were not different (analysis over a similar weight range of 174–1542 g; $F_{1,388}$ 1.59, P 0.208; adjusted mean fecundity for Oregon 57,849, SE 2092; adjusted mean fecundity for California 54,733, SE 1152). When we combined data for the two regions, we found that total fecundity declined on the average about 12% per month. This computation underestimated the actual rate of decline, since it did not take into account females that had spawned all of their advanced yolked oocytes.

Potential annual fecundity

Potential annual fecundity was considered to be equivalent to the standing stock of advanced yolked oocytes in fully developed, prespawning females. We consider

Table 9

Linear regression coefficients, confidence intervals, and estimates for the relationship between female weight (W, ovary-free, in g) and total fecundity ($\hat{Y}_F$) of Dover sole *Microstomus pacificus* from California and Oregon. Analysis of covariance for the effect of season on the relation between total fecundity and weight. Multiple regression coefficients are also given for the effect of elapsed time (T; days since 1 Nov.) and female weight on total fecundity.

Linear regression by month and state

State	Mean date of cruise	Linear equation $\hat{Y}_F = a + bW$ a	95% CI	b	95% CI	r^2	F	N	Regression estimate for 1 kg female	Analysis of covariance for effect of month with weight ranges similar Variables	df	F	P
Oregon	7 Dec 88	17,640	±15,460	65.5	±16.4	0.49	63.9	67	83,140	Weight	1	67.85	<0.005
	3 Mar 89	14,492	±8,530	42.9	±10.6	0.66	67.9	36	57,392	Month	1	20.06	<0.005
										Error	95		
										Total	97		
Central California	8 Dec 85	29,497	±6,121	51.6	±16.1	0.58	42.9	31	81,097	Weight	1	25.20	<0.005
	31 Jan 87	20,154	±6,344	38.9	±6.8	0.42	127.0	173	59,022	Month	2	18.91	<0.005
	23 Mar 88	12,072	±16,924	40.7	±18.6	0.15	18.9	103	52,772	Error	217		
										Total	220		

Multiple regression of total fecundity on weight and days elapsed since 1 November

Multiple regression equation $\hat{Y}_F = a + b_1W + b_2T$

State	a	95% CI	b_1	95% CI	b_2	95% CI	r^2	F	N	W_{min} (g)	W_{max} (g)	T_{min} (d)	T_{max} (d)
Oregon	35,162	±13,378	55.2	±11.2	−237	±104	0.59	74.9	103	147.7	1815.9	33	151
Central California	41,552	±8,142	40.3	±6.4	−224	±63	0.37	92.3	307	120.0	1690.3	34	160

Table 10

Relationship between total fecundity ($\hat{Y}_F$) and gonad-free body weight (g) or total length (mm) for California and Oregon Dover sole *Microstomus pacificus* females meeting specifications for potential annual fecundity estimation (females taken in November–December with average oocyte diameter >0.85 mm and no evidence of past or imminent spawning). Data are compared with Yoklavich and Pikitch (1989) estimates for Oregon.

Fecundity and weight

State	Linear equation $\hat{Y}_F = a + bW$ a	95% CI	b	95% CI	r^2	F	N	Estimate for 1 kg female	Gonad-free weight (g) Mean	Range
Oregon	17,640	±15,453	65.5	±16.4	0.488	63.86	67	83,140	870.5	236.0–1815.9
California	29,871	±12,996	50.9	±17.1	0.544	37.06	30	80,771	704.7	202.1–1124.2
Oregon + California	21,124	±9,248	62.0	±10.4	0.504	98.42	97	83,124	819.2	202.1–1815.9

Fecundity and length

State	Exponential equation $\hat{Y}_F = aL^b$ a	95% CI	b	95% CI	Pseudo r^2	F	N	Estimate for 453 mm female*	Total length (mm) Mean	Range
Oregon	$5.667 \cdot 10^{-6}$	$\pm 1.943 \cdot 10^{-5}$	3.806	±0.713	0.431	47.03	64	72,856	436	298–551
California	$6.101 \cdot 10^{-4}$	$\pm 5.042 \cdot 10^{-3}$	3.020	±1.380	0.084	2.57	30	64,094	423	296–526
Yoklavich & Pikitch**	$1.637 \cdot 10^{-6}$	$\pm 6.928 \cdot 10^{-6}$	4.021	±0.684	0.818	135.13	32	78,382	448	358–550

*Weight is about 1000 g using equation in Table 3.
**Estimated from Yoklavich and Pikitch (1989) original data.

Dover sole to be developed when the average diameter of the advanced oocytes (stage 3) exceeds 0.85 mm; prespawning females are those taken in November–December which show no histological evidence of recent past or of imminent spawning (no postovulatory follicles nor hydrated oocytes present).

Using only specimens that met these specifications, we regressed total fecundity on female weight (without ovary) for females taken in central California and Oregon. The two regression equations were quite similar; when the data are truncated so that the ranges of female weights were equal, no statistical difference existed between California and Oregon. Combining all data, we obtained the general equation

$$\hat{Y}_F = 21{,}124 + 62.0\,W \quad \text{(Eq. 10)}$$

where $\hat{Y}_F$ is estimated total fecundity from the regression line, and W is ovary-free female weight in grams. Therefore, the potential annual fecundity for a 1 kg Dover sole is about 83,000 oocytes (Table 10).

Fecundity of Dover sole was estimated recently by Yoklavich

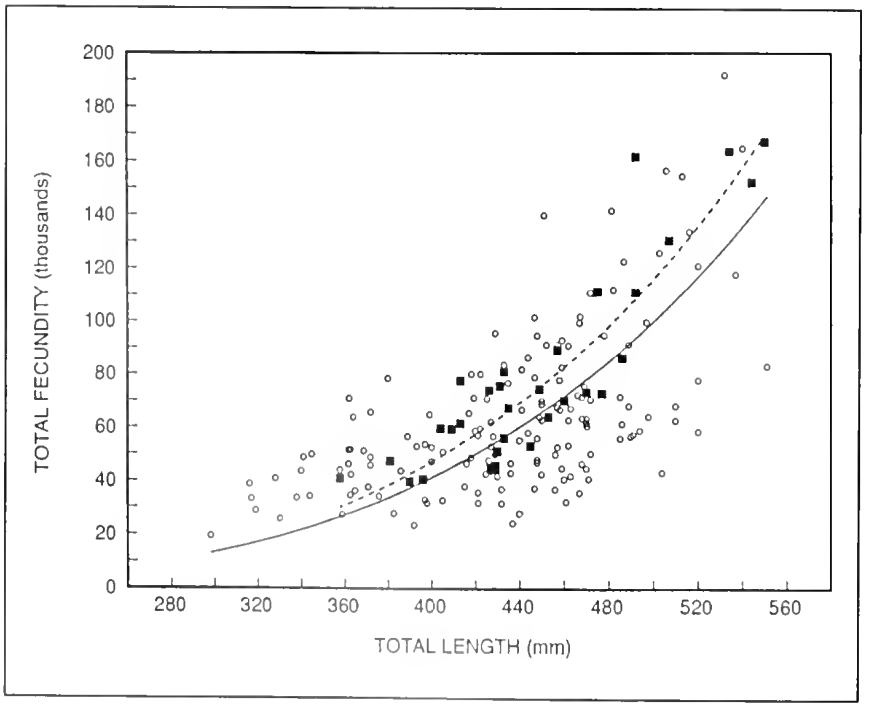

Figure 7

Total fecundity as a function of total length of Dover sole along the Oregon coast for our November–December 1988 data (open circles and solid line) and for data given by Yoklavich and Pikitch (1989) (filled squares and dashed line). Equations are given in Table 10.

Figure 8

Relative frequency distribution of the fraction of the random sample of advanced yolked oocytes measured that were atretic (α stage) from the Dover sole *Microstomus pacificus* females used in estimates of total fecundity shown by state: Oregon females, N 189; California females, N 361.

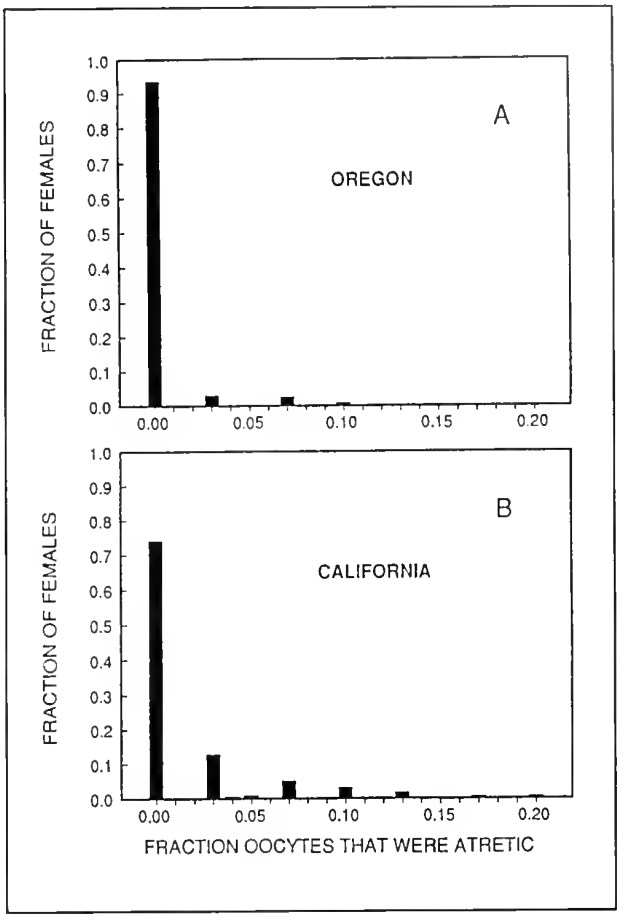

and Pikitch (1989) for females caught along the Oregon coast. Those authors used an exponential model and expressed annual fecundity as a function of length. The distribution of points in our data broadly overlapped the data of Yoklavich and Pikitch (1989) (Fig. 7). To compare our Oregon data with theirs, we truncated ours so that the length ranges of the two sets coincided and applied an analysis of covariance to log-transformed data. Analysis of covariance indicated that no significant difference existed between the two equations ($F_{1, 81}$ 2.03, P 0.158). In Table 10, the exponential equation for fecundity as a function of length is given for our data (not truncated) and for that of Yoklavich and Pikitch (1989). In summary, we found no statistical difference between California and Oregon, nor between our Oregon data and that of Yoklavich and Pikitch (1989).

Atretic losses

In fishes with determinate fecundity, a key question is whether atretic losses during a season constitute an important fraction of the potential annual fecundity. We identified whole atretic oocytes under a microscope while doing our fecundity work. To measure atretic losses, we counted the number of atretic oocytes (α advanced yolked oocytes) occurring in a random sample of 30 advanced yolked oocytes for each of the females used to estimate total fecundity (N 550).

In the fish used to estimate fecundity, the average fraction of advanced yolked oocytes that were atretic was low with the mean 0.015 (SD 0.032, N 361) in California, and even lower in Oregon females (mean 0.0033, SD 0.014, N 189). Atretic oocytes were observed in only 26% of California females and in only 6% of Oregon females (Fig. 8).

The total fecundity of California females was negatively correlated with the fraction of oocytes in the ovary that were atretic. A stepwise multiple regression of female weight, elapsed time, and fraction atretic on total fecundity (Table 11) indicated that the coefficient for the fraction

Table 11

Analysis of the relation between total fecundity ($\hat{Y}_F$) of Dover sole *Microstomus pacificus* ovary-free body weight, elapsed days since 1 November, and fraction of atretic oocytes using stepwise regression. Specimens from California.

	Stepwise regression		
Step	1	2	3
Constant	23,335	40,296	40,976
Weight	37.7	40.8	41.4
t*	2.11	14.03	14.23
Elapsed days		−205	−206
t		−7.85	−7.94
Fraction atretic			−63,278
t			−2.17
S	19,317	17,868	17,776
r^2	28.99	39.41	40.20

Analysis of variance					
Source	DF	SS	MS	F	P
Regression	3	7.58×10^{10}	2.53×10^{10}	79.99	<0.001
Error	357	1.13×10^{11}	3.16×10^{8}		
Total	360	1.89×10^{11}			

Source	DF	Sequential SS
Weight	1	6.28×10^{10}
Elapsed days	1	1.15×10^{10}
Fraction atretic	1	1.49×10^{9}

*For P = 0.05, t 1.97.

of oocytes that were atretic was significant and negative. According to the equation, when 10% of the advanced oocytes were atretic, total fecundity in a 1kg female was about 8% lower than when no advanced yolked oocytes were atretic. This analysis indicated that atretic losses of potential annual fecundity occurred, but on a population basis such losses were negligible. No relation between fecundity and atresia existed for Oregon females, probably because atresia was less prevalent in Oregon, with only 6% of females effected compared with 26% in central California.

The ovaries of many more females were examined histologically for atresia (N 2607) than were examined using the anatomical method, because we restricted the anatomical work to the fish used to measure total fecundity. Only 2% of all females examined histologically (Table 2) had ovaries in which 50% or more of the advanced yolked oocytes were in α atresia, but minor atresia was more common. Minor atresia occurred in 52% of the nonspawning California females and in 35% of the nonspawning Oregon females (Table 2).

The histological method was more sensitive than the anatomical one. Alpha atresia of advanced yolked oocytes was detected at least twice as frequently using histological techniques. The histological method was more sensitive because we could detect more subtle changes in oocyte structure and because we scanned about 150 oocytes per ovary, compared with 30 oocytes in the anatomical method. Despite the lack of sensitivity, the anatomical method was valuable because the standing stock of atretic oocytes could be easily estimated and directly related to total fecundity.

The histological evidence indicated that females with α-atretic advanced yolked oocytes were more common in central California waters than off Oregon. However, season and locality were confounded because most females from Oregon were taken prior to the spawning season while most females from California were taken during the season. To determine if either season or locality affected the relative frequency of atretic females, we combined the minor-atresia and major-atresia classes for California and Oregon and fit the stepwise logistic model

$$P = \frac{e^{\beta_0+\beta_1 X_1+\beta_2 X_2}}{1+e^{\beta_0+\beta_1 X_1+\beta_2 X_2}} \qquad \text{(Eq. 11)}$$

to the data (Table 12), where P is the fraction of females with atretic oocytes. The independent variables for location (X_1) are -1 for California and 1 for Oregon, and for season (X_2) are -1 for prespawning and 1 for during spawning. The estimates of coefficients for the equation are $\beta_0 = -0.183$ (SE 0.056) and $\beta_1 = -0.288$ (SE 0.056) (β_2 is not given because effect of season was not significant in an early regression analysis); the estimate of the atresia rate P for California is 0.525 (95% CI 0.479–0.572; Carter et al. 1986) and for Oregon is 0.384 (95% CI 0.338–0.433).

Table 12

Histological determination of number of Dover sole *Microstomus pacificus*, with α atresia of advanced yolked oocytes expressed as a percentage of all females with advanced yolked oocytes taken in central California and in Oregon, beginning (November–December) and during (January–May) the spawning season.

	Spawning season						
	Beginning		During		Beginning + During		
State	%	N	%	N	%	95% CI	N
Central California	59.2	71	51.9	617	52.5	47.9–57.2	688
Oregon	36.8	536	49.4	83	38.4	33.8–43.3	619

Table 13

Mean relative batch fecundity for five batch-order numbers (B), from the first batch to the last batch.

Batch-order no.[a] (B)	No. of females	Relative batch fecundity (oocytes/female wt(g))	
		Mean	SD
1	4	2.421	3.810
2	12	11.661	4.410
2<B<U-1	19	10.489	3.184
U-1	11	12.378	8.035
U	9	7.835	5.723

Analysis of variance on five batch orders

Source	DF	SS	MS	F	P
Batch order	4	371.2	92.8	3.44	0.015
Contrast[b]	1	352.6	352.6	13.08	0.001
Error	50	1347.6	27.0		
Total	54	1718.8			

[a]First batch spawned, B = 1; last batch spawned, B = U; penultimate batch, B = U-1.
[b]Comparison of relative fecundity of the first and last batch to the other batches.

Table 14

Comparison of fecundity between the penultimate batch and the last batch within the same Dover sole *Microstomus pacificus* female.

	Female weight (g)	Batch fecundity* (no. of oocytes)	
		Penultimate	Last
	270.00	4634	2121
	270.00	3716	323
	324.50	9374	1025
	539.00	11445	2903
	703.86	3906	411
	713.24	12213	6455
	752.11	2843	124
	793.54	6134	5856
	824.66	7022	3820
	1017.70	3621	29
	1247.82	11047	250
Mean	677.9	6905	2120
SD	309.8	3525	2355

*Paired t-test: t 4.99, df 10, P 0.0005.

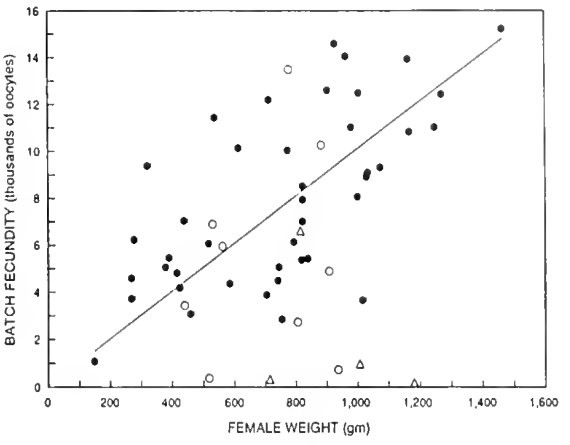

Figure 9

Batch fecundity of Dover sole *Microstomus pacificus* as a function of female weight (without ovary). Line is $\hat{Y}_B = 10.1W$ for the second through the penultimate spawning batches (filled circles); triangles = first spawning batch; open circles = last spawning batch.

This computation indicated that the occurrence of females with α atresia of advanced oocytes was significantly affected by locality of the samples but not by season. In short, more California females had one or more α-atretic advanced oocytes in their ovary than did Oregon females.

Batch fecundity

The first step in our analysis of batch fecundity ($\hat{Y}_B$) was to determine if the batch size varied with the order of spawning. Analysis of variance indicated that a significant batch-order effect existed (Table 13). The mean relative fecundity of the first (1) and last spawning batch (U) were significantly lower than the other batches (Table 13).

In eleven females, the only advanced oocytes left in the ovary were two "hydrated" spawning batches (Table 14). Each was in a different stage of development: one was fully hydrated (last batch), and the other was in the migratory nucleus stage (penultimate batch). In all of the eleven females, the last batch was always lower than the penultimate batch. The t-test for paired differences confirmed the effect of batch order on fecundity indicated by the ANOVA. The t-test also had less potential for bias because we used absolute rather than relative batch fecundity. The t-test indicated that the fecundity of the last batch differed from the penultimate batch (t 4.99, df 10, P 0.0005). We concluded that the batch size of a female Dover sole did change over the spawning season, with the last and the first batch being lower than the rest.

We determined the relation between batch fecundity and weight using regression analysis. We did not use the first and last batches since they were lower than the rest. The intercept for the regression of batch fecundity on female weight did not differ from zero (a 2142; t 1.87, df 40, P 0.07). Therefore we forced the regression line through 0, yielding the relationship $\hat{Y}_B = 10.1W$, where female weight ranged from 148 to 1464g (Fig. 9). This analysis indicated that the relative batch fecundity of Dover sole is about 10 oocytes per gram ovary-free female weight, except for the first and last batch. The relative fecundity for the first and last batches combined was also about 10 oocytes per gram (1 and U in Table 13). Thus the number of potential spawnings (S) per year can be calculated using $S = (\tilde{Y}_{FR}/10) + 1$, where $\tilde{Y}_{FR}$ is the relative potential annual fecundity ($\tilde{Y}_F/W$; $\tilde{Y}_F$ from Eq. 10). This means that the average 1kg female spawns its 83,000 advanced yolked oocytes in about nine batches.

Sexual maturity

To determine the optimal criteria for sexual maturity in female Dover sole, we established six sets of histological criteria for maturity (Table 15). The first set of criteria selects females with either advanced yolked

Table 15

Six sets of histological criteria for female sexual maturity in Dover sole *Microstomus pacificus*, with the mean length of the females in each set. (o) not present; (+) present; (–) not considered.

Criteria set no.	Certainty	Advanced yolked oocytes: with α atresia	Advanced yolked oocytes: no α atresia	Post-ovulatory follicles	Early yolked oocytes: with β atresia	Early yolked oocytes: only α atresia or none	Unyolked oocytes: with β atresia	Unyolked oocytes: only α atresia	Unyolked oocytes: no atresia	Mean length (mm): $\bar{x}$	Mean length (mm): ±2 SE	No. of females Calif. + Oregon (N 2595): No. in class	No. of females Calif. + Oregon (N 2595): Cumulative percent
1	Certain maturity	+	+	+	–	–	–	–	–	434	±3	1343	52
2	Uncertain	o	o	o	+	–	–	–	–	414	±7	218	60
3	Uncertain	o	o	o	o	+	–	–	–	397	±11	77	63
4	Uncertain	o	o	o	o	o	+	–	–	379	±6	279	74
5	Uncertain	o	o	o	o	o	o	+	–	350	±5	432	90
6	Certain immaturity*	o	o	o	o	o	o	o	+	297	±10	246	100

* Defined as certain immaturity because no histological evidence exists for maturity.

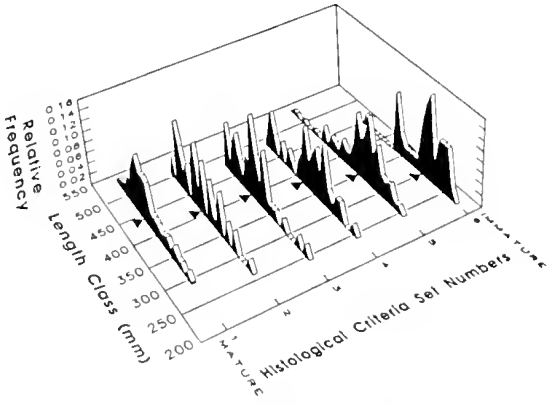

Figure 10

Length distribution of female Dover sole *Microstomus pacificus* identified by six sets of histological maturity criteria, ranging from criteria set 1 where maturity is certain, to set 6 where all females are considered to be immature (see Table 15). Females captured in November–December in California and Oregon; filled triangles indicate mean length of females.

oocytes or postovulatory follicles. The sexual maturity of these females is certain, but some mature females may be excluded if only the first set of criteria are used. Criteria sets 2 to 5, if added to the first set, broaden the maturity definition to include females having ovaries in the earliest stages of vitellogenesis and those showing possible signs of past reproductive activity (β- or α-stage atresia). Each additional criteria set that one might add to the first set increases the risk that immature fish will be classed as mature. Females in set 6 are considered to be immature because they have none of the characteristics mentioned in the other five sets.

Use of β atresia as a possible sign of past reproductive activity seems justified. Females with early yolked oocytes and β atresia (set 2) were larger on the average than those with no β atresia (set 3; t 2.45, P 0.015, df 293); and females with unyolked oocytes and β atresia (set 4) were larger than those with only α atresia of the unyolked (set 5; t 7.69, $P<0.001$, df 709). In addition, the ranking of criteria sets based on our intuitive appraisal of the risk of classification error is largely borne out by the length distributions of the females identified by the criteria set, since mean length decreased with criteria set number (Fig. 10).

To estimate the length at which 50% of the Dover sole are mature (ML_{50}) using all six histological criteria sets, we first used a maturity algorithm to estimate the fraction of fish that were mature in a given length-class. This algorithm is a regression method similar to those used to construct age-length keys (Bartoo and Parker 1983, Kimura and Chikuni 1987).

This analysis was based on two equations. The first equation was

$$q_{j|i} = q_{m|i}\, q_{j|m} + (1 - q_{m|i})\, q_{j|im} \qquad \text{(Eq. 12)}$$

where $q_{j|i}$ is the fraction of fish of length-class j in the ith criteria set; $q_{j|m} = q_{j|1}$ and $q_{j|im} = q_{j|6}$ because the criteria set 1 consists of all mature (m) fish and the criteria set 6 consists of all immature (im) fish; and $q_{m|i}$ the overall fraction of mature fish in the ith cri-

teria set. The second equation assumed that $q_{m|i}$ changed linearly with criteria set number i:

$$\hat{q}_{m|i} = b_1 + b_2 i. \quad \text{(Eq. 13)}$$

Combining equations (12) and (13) results in the final equation

$$y_{ij} = b_1 x_{1j} + b_2 x_{2j} \quad \text{(Eq. 14)}$$

where $y_{ij} = q_{j|i} - q_{j|im}$,
$x_{1j} = q_{j|m} - q_{j|im}$, and
$x_{2j} = i(q_{j|m} - q_{j|im})$.

For each criteria set i, we obtained the estimate of the fraction of mature fish ($q_{m|j|i}$) in each length-class j as

$$\hat{q}_{m|j|i} = \hat{q}_{m,j|i}/\hat{q}_{j|i} = [\hat{q}_{m|i}q_{j|m}]/\hat{q}_{j|i}.$$

We then obtained the estimated number of mature fish of length-class j in the criteria set i ($\hat{N}_{m|j|i}$) as the product of the total number of fish at length-class j ($N_{j|i}$) and the estimated fraction of mature fish at length-class j ($\hat{q}_{m|j|i}$):

$$\hat{N}_{m|j|i} = N_{j|i}\,\hat{q}_{m|j|i}.$$

The summation of $\hat{N}_{m|j|i}$ over all criteria (i) is the total number of mature fish at length-class j ($\hat{N}_{m|j} = \Sigma_i \hat{N}_{m|j|i}$). The total number of fish in length-class j ($N_j = \Sigma_i N_{j|i}$) and the number of mature fish ($\hat{N}_{m|j}$) were used to estimate ML_{50} for all females taken before the onset of spawning (California and Oregon data combined) using BMDPLR (Dixon et al. 1988).

We compared the above estimate with the ML_{50} for each of the five maturity definitions created by including progressively more criteria sets (Table 16). When the definition of sexual maturity is expanded by progressively adding criteria sets 2 to 5 to the definition, the ML_{50} decreased for each additional set of criteria added. Our estimate of ML_{50} from the model was 332mm and is most similar to maturity definition IV in Table 16. Thus, definition IV is the preferred histological definition of maturity because it is probably the least biased.

Inspection of Table 16 also indicated that the ML_{50} is always greater when measurements are made during the reproductive season than before it begins, regardless of the number of criteria sets used to define sexual maturity. This implied that during the spawning season the ovaries of some postspawning females are reabsorbed to the extent that they become indistinguishable from females defined as immature. Thus maturity should be estimated prior to the onset of spawning, and the definition of maturity should be broader than definition I.

We believe the preferable estimate of ML_{50} is one based on the maturity algorithm because it uses all the histological data, while those based on definitions use only a portion of it. The maturity algorithm should be applied only to data taken before the spawning season, since data collected later in the season will be biased. This method demands detailed histological classification which may be too costly for many purposes. Definition III could be used if tissue were examined microscopically or with a powerful hand lens, and it gives an ML_{50} value close to that provided by the model.

Table 16

Estimated length at which 50% of Dover sole females are sexually mature, using six histological definitions of ovarian maturity and a maturity algorithm that uses all data. California and Oregon data are combined; length at 50% mature estimated using logistic model (Dixon et al. 1988).

		Before spawning (*N* 854 females)			During spawning (*N* 1321 females)		
			No. of mature females			No. of mature females	
Definition no.	Histological criteria sets incl. in maturity definition[a]	Length at 50% mature (mm)	*N*	% of females	Length at 50% mature (mm)	*N*	% of females
I	1	373	541	63	419	568	43
II	1, 2	361	582	68	396	692	52
III	1, 2, 3	348	626	73	391	720	54
IV	1, 2, 3, 4	332	669	78	348	917	69
V	1, 2, 3, 4, 5	258	810	95	255	1184	90
Maturity algorithm	1, 2, 3, 4, 5, 6	332	691[b]	81[b]	389	742[b]	56[b]

[a] From Table 15.
[b] Estimated from maturity algorithm.

Table 17

Final maturity thresholds and logistic model parameters* for female Dover sole *Microstomus pacificus*, taken before the spawning season in California, Oregon, and the two states combined.

Region	Maturity definition	50% mature	95% CI	a	SE	b	SE	*N*
California	IV	298	215–391	−14.412	4.374	0.0483	0.0149	104
Oregon	IV	336	322–351	−9.268	0.806	0.0276	0.0022	750
California + Oregon	Maturity algorithm	332	305–367	−14.960	1.239	0.0450	0.0036	854

*$P = \frac{e^{a+bL}}{1+e^{a+bL}}$

We combined data from Oregon and California in this analysis because sample sizes (before spawning) were inadequate for application of the model separately. However, in Table 17 we provide estimates and fitting parameters based on definition IV for each region as well as those based on the model using the combined data. The ML_{50} estimated for definition IV was lower in California than in Oregon. However, analysis of covariance of the log transformation of fraction mature, $\mathrm{Ln}\left(\frac{q_m}{1-q_m}+1\right)$, on length and locality indicated that the difference between states was not significant (P 0.625, F 0.26). Thus our ML_{50} estimate for Dover sole along the California and Oregon coasts is 332 mm with 95% CI of 315–349 mm (Carter et al. 1986; Fig. 11). The ML_{50} we estimated from data in Hagerman (1952) for Dover sole from the Eureka California fishery is high (363 mm) compared with our final estimate for Oregon and California coasts (Fig. 11). However, Hagerman collected his specimens during the spawning season, and his estimate is similar to the ML_{50} for females taken during the spawning season (Definition IV, Table 16).

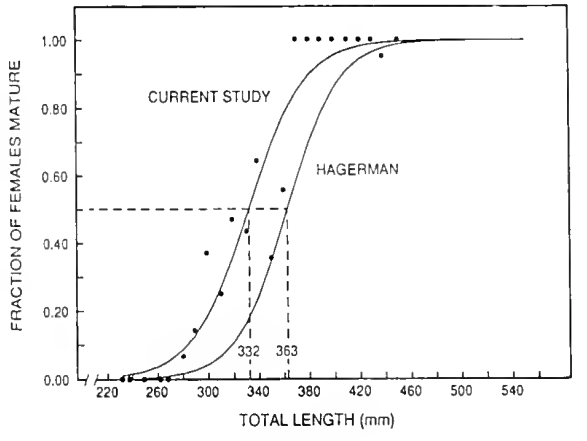

Figure 11

Fraction of female Dover sole *Microstomus pacificus* that were sexually mature as a function of total length. Points are for 10 mm length-class intervals; the fraction mature per length-class was assigned using maturity algorithm; data were from California and Oregon in November–December; logistic parameters are in Table 17. Present study is compared with Hagerman (1952), line only (logistic curve parameters, a −17.854, b 0.0450).

Discussion

Validation of fecundity assumptions

In the Introduction, we specified four assumptions required for an unbiased estimate of annual fecundity in Dover sole. These assumptions were that (1) fecundity was determinate; (2) potential annual fecundity was equivalent to actual fecundity; (3) females used to estimate annual fecundity had not spawned; and (4) recruitment of oocytes into the advanced stock of yolked oocytes had ceased for the season. The following is a review of the evidence for the four assumptions.

Five lines of evidence support the assumption of determinate fecundity for Dover sole: (1) in mature ovaries (mean diameter of advanced oocytes >0.85 mm), a hiatus existed between the advanced stock of mature oocytes and smaller, less mature oocytes; (2) total fecundity declined over the spawning season; (3) total fecundity was lower in females having postovulatory follicles; (4) the mean diameter of the advanced oocytes increased over the spawning season; and (5) our analysis of the order of spawning batches was consistent with the determinate fecundity assumption.

The second assumption, lack of significant atresia, also was supported by our analysis. Overall, atretic losses of advanced oocytes were negligible during the years of our study. Multiple regression analysis indicated that atresia had a small but significant effect on total fecundity of the California females that had

atretic oocytes. A few females suffered substantial losses in total fecundity, but such fish were rare and they had little effect on population means. Histological and anatomical evidence indicated that females with α-atretic advanced yolked oocytes were more common in central California than in Oregon waters. Atresia might be more common in central California Dover sole because bottom sediments are contaminated. Alternatively, females with atretic ovaries may be more common in central California waters because they are living near the southern end of their range where food supply and other habitat conditions may be less than optimal. Both explanations seem equally plausible at present.

The third assumption, that females used to estimate potential annual fecundity have not spawned in the current reproductive year, would be rejected for females taken in January through May. The assumption probably held for the females used to estimate annual fecundity in November–December because only 2.9% of the females from California and only 1% of the females in Oregon showed any histological signs of past or imminent spawning. The few females that showed histological signs of spawning were not used, of course, to estimate annual fecundity. Spawning may have gone undetected in some of the females used to estimate fecundity since postovulatory follicles are eventually resorbed. This does not seem likely for the November–December case because the spawning season had just begun and resorption is probably slow at the low temperatures of Dover sole spawning habitat.

Our fourth assumption, that all the oocytes that constitute the potential annual fecundity were included in our oocyte counts, is supported by two lines of evidence. The first is that no positive correlation existed between the mean diameter of the advanced oocytes and total fecundity. Such positive correlations were eliminated by excluding all ovaries in which the mean diameter of the advanced oocytes was less than 0.86 mm. A positive correlation between diameter and fecundity existed when all ovaries were considered (range in mean diameter of the advanced oocytes, 0.71–1.04 mm). This is evidence that recruitment of oocytes into the advanced class continued until the advanced stock was well separated from early vitellogenic oocytes (stages 1 and 2, Fig. 6). The second source of evidence is the form of the oocyte size-frequency distribution. A prominent gap between stage-2 and stage-3 oocytes existed when the mean diameter of stage-3 oocytes was between 0.84 and 0.96 mm (Fig. 6). The absence of significant numbers of oocytes in the intervening diameter classes (0.55–0.65 mm) indicates maturation of oocytes across this range either had ceased or was proceeding at a very slow pace. We conclude that recruitment of significant numbers of oocytes into the advanced stock probably ceases in Dover sole when the mean diameter of the advanced stock is between 0.86 and 0.96 mm.

Some authors working with other species (Hislop and Hall 1974 on *Melangius merlangus* (L.), Horwood and Greer Walker 1990 on *Solea solea*) consider all yolking oocytes to comprise the potential annual fecundity. In Dover sole this would mean that in addition to stage 3, the most advanced yolked oocytes, stages 1 and 2 would also be used to estimate annual fecundity. Such broad criteria are acceptable if all oocytes that began vitellogenesis ultimately become a part of the mature stock of oocytes that are spawned. This was not the case in Dover sole because oocytes in the early stages of vitellogenesis (stages 1 and 2) occurred in nearly all mature ovaries, including those in which some of the batches had already been spawned. The fate and dynamics of these small partially-yolked oocytes in advanced ovaries is uncertain; their numbers might either decrease due to resorption, increase and become part of next year's production, or remain in stable numbers until later in the year. It would seem impractical to adjust estimates of potential annual fecundity based on all vitellogenic oocytes for the fraction of those oocytes which do not continue vitellogenesis. Therefore, we believe use of the more mature yolked oocytes for estimating the potential annual fecundity is preferable.

An important implication of our discussions of the third and fourth assumptions is that timing the sampling of females is a critical element in estimating potential annual fecundity: Sample too early in the reproductive cycle and the ovaries are not sufficiently mature; sample too late and spawning is prevalent. The optimal time to sample Dover sole ovaries is when the average diameter of the advanced stock is between 0.86 and 1.1 mm (Fig. 12). When the diameter is less than 0.86 mm, the numbers of advanced oocytes are still increasing (indicated by the t value for the diameter coefficient in the fecundity equation, Fig. 12). When the diameter exceeds 1.1 mm, 20% or more of the females show histological signs of past or imminent spawning, and the assumption of no spawning cannot be safely made.

Spawning rates and reproductive energetics

The spawning season of Dover sole was protracted with postovulatory follicles occurring as early as December and hydrated oocytes as late as May, indicating a season of six months. This is a long season for a fish of determinate fecundity, since typically they are high-latitude species with short, 1–2 month spawning seasons. Batch fecundity was low, averaging about 10 oocytes per gram female weight, except for the first and last batch which average about 5 oocytes per gram. Dover sole spawn about nine times during their

protracted spawning season. Vitellogenesis does not cease when spawning begins, but rather it continues throughout most of the season as the advanced stocks of yolked oocytes are matured and spawned. Spawning frequency appears to increase near the end of the season. This may cause a higher daily production of eggs by the population in late-March or April than in February, even though fewer females have active ovaries in April.

To estimate reproductive effort of Dover sole, we calculated the hypothetical weight of the ovary when the entire advanced stock of oocytes had completed vitellogenesis and hydration had begun. The weight is hypothetical because a Dover sole ovary never contains a full complement of completely yolked oocytes, since vitellogenesis of the smaller advanced yolked oocytes continues after a female begins spawning. To compute the hypothetical weight, we assumed that all oocytes completed vitellogenesis when their average diameter was 1.5 mm. Hydration begins when the advanced yolked oocytes have a mean diameter of 1.3–1.7 mm. We estimated the gonad weight of a 1000 g female with oocytes having a mean diameter of 1.5 mm, using an equation in which gonad weight was expressed as a function of fish weight and volume of the average advanced oocyte (1.5 mm diameter has a volume of 1.77 mm^3; California plus Oregon data; Table 3). The ovary was estimated to weigh 144 g, or about 14% of the body weight. In other words, the annual reproductive effort of Dover sole was about 14% per year, and this effort was distributed over about nine spawnings averaging about 1.6% of their body weight per spawning. Gonad weight was considered to be a measure of reproductive effort by Gunderson and Dygert (1988); but they did not adjust the gonad weight for the full complement of yolk, and consequently their estimates are not comparable to these.

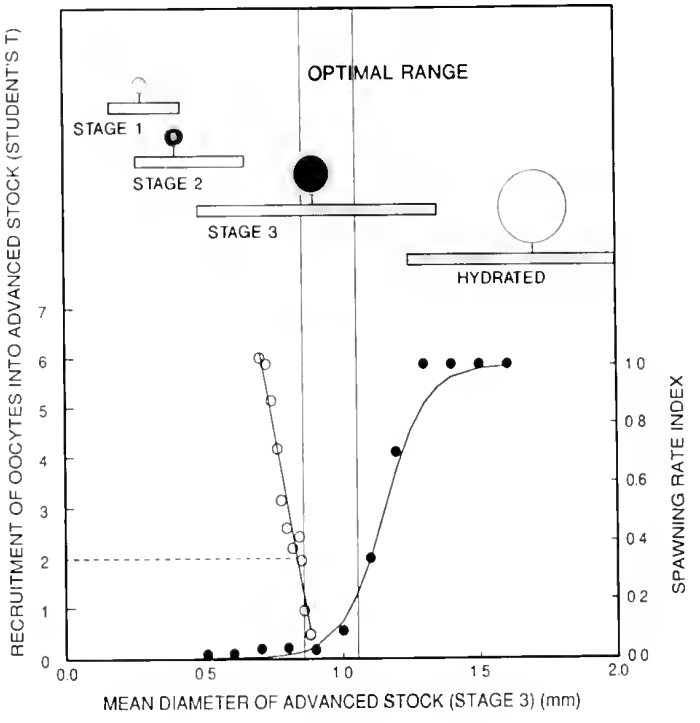

Figure 12

Optimal range of mean diameter of advanced yolked oocytes (stage 3) for determining potential annual fecundity of Dover sole (shaded area, 0.86–1.1 mm). Open circles, Student's t as a function of the minimum mean diameter of stage-3 oocytes included in the fecundity data set: when $t \geq 2$ (P 0.05), the mean oocyte diameter had a positive correlation with fecundity, indicating the stock of yolked oocytes for the season was not fully recruited into stage 3. Spawning rate index (filled circles) for females used in fecundity estimates; index = 0 when no females show signs of past or imminent spawning, and index = 1 when all females have postovulatory follicles or hydrated oocytes. Upper panel indicates diameter range of oocytes in three yolked oocyte stages and hydrated oocytes. Only stage-3 oocytes were used to estimate potential annual fecundity.

Assessment of sexual maturity

Our estimates of length at 50% mature (ML_{50}) were higher when females were taken during the spawning season than when they were sampled before spawning began, regardless of the histological criteria used. Thus, during the spawning season ovaries of some postspawning females had regressed far enough that they were histologically indistinguishable from immature females. This finding has two important implications: First, it indicates that even the broadest histological criteria, based on analysis of H&E sections, will not identify all postspawning females; second, it means that estimates of length or age at first maturity should always be conducted prior to the onset of spawning, when postspawning females with highly regressed ovaries are rare.

Another limit to our ability to assess sexual maturity is that we do not know how many of the females that begin vitellogenesis actually complete it during the current reproductive season. Dover sole ovaries with oocytes in the early vitellogenic stage occurred throughout the spawning season as well as before it began, indicating some females that begin vitellogenesis may not reach sexual maturity in the current

season. At this time, it is an arbitrary choice to consider as mature all females with vitellogenic ovaries or only those with advanced yolked oocytes. Our analysis showed that this arbitrary decision had a pronounced effect on ML_{50} estimates. Thus the criteria for maturity estimates should be precisely specified. It is particularly important to specify the minimum level of oocyte development necessary for a female to be considered as mature. Our preferred definition of maturity included females in the early stages of vitellogenesis with yolked oocytes as small as 0.18 mm diameter, and also included some females without vitellogenic oocytes (maturity IV, Table 16). Those females without vitellogenic oocytes had β atresia in the ovary. We believe that the presence of some β atresia is an inevitable consequence of the resorption of an active ovary or ovulation.

No discussion of sexual maturity would be complete without mentioning the gross anatomical systems used to classify ovaries, because they are the chief method used by fishery biologists to measure sexual maturity in marine fishes. Using gross anatomical criteria, we accurately separated active ovaries (advanced yolked oocytes present) from inactive ovaries (no advanced oocytes) with classification errors of 1–12%. Determining sexual maturity is a far more difficult task, however. Identification of mature females using gross anatomical methods has the same problems with postspawning and early vitellogenesis criteria as histological methods, but the potential for bias is greater. Anatomical criteria are less accurate and may be detectable for shorter periods than histological ones. For these reasons, differences between maturity studies should be interpreted with caution, especially when done by different observers, or with different methods, or when sampling at different times of the year. Many investigators have not been particularly careful to restrict sampling to early in the spawning season. The tendency will be to overestimate the ML_{50} using anatomical methods, especially when samples are taken midseason.

In an earlier paper on Dover sole, Hunter et al. (1990) concluded that size at 50% mature in Dover sole from central California in the 1980s differed from that of Dover sole in northern California in the late 1940s as determined by Hagerman (1952). Although a statistical difference existed between these two data sets, we are inclined to dismiss this difference, since it could be due to differences in criteria and sampling times. Similarly, Yoklavitch and Pikitch (1989) speculated that size at 50% maturity of Oregon Dover sole has changed because their estimate of maturity differed from Harry (1959). We believe that this difference also could easily be due to differences in criteria and timing of sampling. Our analysis of histological criteria for maturity clearly shows that differences in criteria or timing of sampling can produce differences in the ML_{50} as large as any of those seen in the Dover sole literature.

Acknowledgments

We appreciate and thank M. Yoklavich and E. Pikitch for providing original data and supplying some specimens, and W.W. Wakefield for providing some specimens. We thank all on shipboard who helped collect Dover sole ovaries: E. Lynn, W. Flerx, R. Dotson, R. Leong, E. Acuna, and D. Squires. We thank all others who served on the scientific crews and the crews of NOAA ships *David Starr Jordan* and *Miller Freeman*; they contributed greatly to the success of the cruises. Processing of laboratory specimens and estimation of fecundities were assisted by W. Kicklighter, M. Drawbridge, R. Leong, E. Lynn, D. Ramon, and S. Swailes. Computer programs were written by C. Vedovato, R. Young, and J. Butler. L. Jacobson provided suggestions on the modeling of sexual maturity. Illustrations were produced by R. Allen and H. Orr. K. Schaefer, J. Zeldis, and an anonymous reviewer reviewed the manuscript.

Citations

Alheit, J.
1986 Reproductive biology of sprat, *Sprattus sprattus*: Factors determining annual egg production. ICES CM 1986/H:58, 16 p.

Bartoo, N.W., and K.R. Parker
1983 Stochastic age-frequency estimation using the von Bertalanffy growth equation. Fish. Bull., U.S. 81:91–96.

Bretschneider, L.H., and J.J. Duyvene de Wit
1947 Sexual endocrinology of non-mammalian vertebrates. Monogr. Prog. Res., Vol. II. Elsevier, NY.

Carter, W.H. Jr., V.M. Chinchilli, J.D. Wilson, E.D. Campbell, F.K. Kessler, and R.A. Carchman
1986 An asymptotic confidence region for the ED_{100p} from the logistic response surface for a combination of agents. Am. Stat. 40:124–128.

Dixon, W.J., M.B. Brown, L. Engelman, M.A. Hill, and R.I. Jennrich
1988 BMDP statistical software manual, Vol 2. Univ. Calif. Press, Los Angeles, 1234 p.

Gunderson, D.R., and P.H. Dygert
1988 Reproductive effort as a predictor of natural mortality rate. J. Cons. Cons. Int. Explor. Mer 44:200–209.

Hagerman, F.B.
1952 The biology of the Dover sole, *Microstomus pacificus* (Lockington). Calif. Fish Game, Fish Bull. 85:1–48.

Harry, G.Y.
1959 Time of spawning, length at maturity, and fecundity of the English, petrale, and Dover soles (*Parophrys vetulaus*, *Eopsetta jordani*, and *Microstomus pacificus*, respectively). Fish Comm. Oreg. Res. Briefs 7:5–13.

Hislop, J.R.G., and W.B. Hall
1974 The fecundity of whiting, *Merlangius merlangus* (L.) in the North Sea, the Minch and at Iceland. J. Cons. Cons. Int. Explor. Mer 36:42–49.

Hjort, J.
1910 Report on herring investigations until January 1910. Publ. Circ. Cons. Explor. Mer 53.

Horwood, J.W., and M. Greer Walker
1990 Determinacy of fecundity in sole (*Solea solea*) from the Bristol Channel. J. Mar. Biol. Assoc. U.K. 70:803–813.

Hunter, J.R., and S.R. Goldberg
1980 Spawning incidence and batch fecundity in northern anchovy, *Engraulis mordax*. Fish. Bull., U.S. 77:641–652.

Hunter, J.R., and B.J. Macewicz
1980 Sexual maturity, batch fecundity, spawning frequency, and temporal pattern of spawning for the northern anchovy, *Engraulis mordax*, during the 1979 spawning season. Calif. Coop. Oceanic Fish. Invest. Rep. 21:139–149.
1985a Measurement of spawning frequency in multiple spawning fishes. *In* Lasker, R. (ed.), An egg production method for estimating spawning biomass of pelagic fish: Application to the northern anchovy, *Engraulis mordax*, p. 79–94. NOAA Tech. Rep. NMFS 36.
1985b Rates of atresia in the ovary of captive and wild northern anchovy, *Engraulis mordax*. Fish Bull., U.S. 83:119–136.

Hunter, J.R., N.C.H. Lo, and R.J. Leong
1985 Batch fecundity in multiple spawning fishes. *In* Lasker, R. (ed.), An egg production method for estimating spawning biomass of pelagic fish: Application to the northern anchovy, *Engraulis mordax*, p. 67–78. NOAA Tech. Rep. NMFS 36.

Hunter, J.R., B.J. Macewicz, and C.A. Kimbrell
1989 Fecundity and other aspects of the reproduction of sablefish, *Anoplopoma fimbria*, in Central California waters. Calif. Coop. Oceanic Fish. Invest. Rep. 30:61–72.

Hunter, J.R., J.L. Butler, C. Kimbrell, and E.A. Lynn
1990 Bathymetric patterns in size, age, sexual maturity, water content, and caloric density of Dover sole, *Microstomus pacificus*. Calif. Coop. Oceanic Fish. Invest. Rep. 31:132–144.

Kimura, D.K., and S. Chikuni
1987 Mixtures of empirical distributions: An iterative application of the age-length key. Biometrics 43:23–25.

Lambert, J.G.D.
1970 The ovary of the guppy *Poesilia reticulata*. The atretic follicle, a *Corpus atreticum* or a *Corpus luteum praeovulationis*. Z. Zellforsh. 107:54–67.

Thigpen, C.C.
1987 A sample size problem in simple linear regression. Am. Stat. 41:214–215.

Wathne, F.
1977 Performance of trawls used in resource assessment. Mar. Fish. Rev. 39(6):16–23.

Yoklavich, M.M., and E.K. Pikitch
1989 Reproductive status of Dover sole, *Microstomus pacificus*, off northern Oregon. Fish. Bull., U.S. 87:988–955.

Abstract.– Over the past several years researchers in Japan and the United States have independently been conducting extensive studies on the early life history of two discrete populations of walleye pollock *Theragra chalcogramma*, trying to understand recruitment variation. The population of interest to Japanese researchers spawns near Funka Bay, Hokkaido, Japan, while the population of interest to American researchers spawns in Shelikof Strait, Gulf of Alaska. This paper summarizes and compares characteristics of spawning and ecology of eggs, larvae, and early juveniles of the species in these two areas. Although the species has apparently adapted its early-life-history pattern to environmental differences in the two areas, some underlying similarities exist. The adults mainly spawn at a particular time of year following a spawning migration to a specific location so that the eggs and larvae can reach specific areas for subsequent development. In both areas oceanographic conditions are favorable for larval food production (copepod nauplii) when the walleye pollock larvae are present. Drift of the eggs into the bay, where copepod production is enhanced, seems important in Funka Bay, and drift of the larvae toward juvenile nursery grounds on the continental shelf as opposed to being swept offshore, seems important in Shelikof Strait. Interannual differences in larval drift and food production because of varying oceanographic conditions may contribute significantly to variations in year-class size.

Manuscript accepted 27 November 1991.
Fishery Bulletin, U.S. 90:129–138 (1992).

Comparisons of early-life-history characteristics of walleye pollock *Theragra chalcogramma* in Shelikof Strait, Gulf of Alaska, and Funka Bay, Hokkaido, Japan*

Arthur W. Kendall Jr.

Alaska Fisheries Science Center, National Marine Fisheries Service, NOAA
7600 Sand Point Way NE, Seattle, Washington 98115-0070

Toshikuni Nakatani

Laboratory of Principles of Fishing Grounds, Faculty of Fisheries
Hokkaido University, Hakodate, Japan 041

Walleye pollock *Theragra chalcogramma* is a dominant fish in the North Pacific Ocean and in the Bering Sea, both in terms of population size and importance to commercial fisheries. It is a major fishery resource in the Funka Bay area on the Pacific Ocean side of Hokkaido, Japan, and in Shelikof Strait, Gulf of Alaska. In both areas, most fishing is done just prior to and during the spawning season. In Funka Bay, walleye pollock are caught in bottom gillnets, while in Shelikof Strait midwater trawls are used. In Funka Bay the catch varied from about 4.3×10^4 metric tons (t) to about 10.7×10^4 t from 1976 to 1986. In Shelikof Strait, an intense fishery on the spawners existed from 1981 through 1988, although harvest has been severely restricted since 1986 because of reduced abundance of the population (Megrey 1989). The harvest in Shelikof Strait peaked in 1984 at about 31×10^4 t.

There is a growing interest in understanding recruitment in this species, and considerable work has been conducted independently by Japanese researchers in Funka Bay and by U.S. researchers in Shelikof Strait over the past several years. This paper compares the results of these studies (Table 1). While these studies reveal that the early-life-history strategy of walleye pollock allows this species to adapt to different environments, they also indicate that underlying similarities exist between populations. Although understanding causes of recruitment variation in either area is a distant goal, testable hypotheses have been developed in both areas. The comparisons presented in this paper may help researchers in both areas focus their studies toward an understanding of the recruitment process. They may also guide future studies of the species in other areas such as the Bering Sea.

Environmental comparisons

Physical setting

Funka Bay is located in the southern part of Hokkaido, Japan, at about 42°N (Fig. 1). Depths within the bay are generally less than 80 m, although there is a small area of water deeper than 100 m in the center of the bay. Immediately outside the bay the bottom slopes evenly to 500 m within 45 km. The area of the bay is 2270 km^2.

* Contribution FOCI-138 to Fisheries Oceanography Coordinated Investigations, NOAA.

Shelikof Strait is located in the northern Gulf of Alaska between the Alaska Peninsula and the Kodiak Archipelago at about 57°N (Fig. 1). Water depths within Shelikof Strait exceed 300m in some areas. At the northeast and southwest ends of the strait there are sill depths of about 200m. Depths of greater than 500m are reached on the continental slope immediately beyond the southwestern sill. The southern part of the strait and waters to the south comprising about 12,450km^2, are the areas occupied by eggs and larvae of walleye pollock originating in Shelikof Strait.

Table 1

Comparisons of early-life-history characteristics of walleye pollock *Theragra chalcogramma* and their spawning environments in Funka Bay, Japan, and Shelikof Strait, Gulf of Alaska.

	Funka Bay	Shelikof Strait
Latitude	45°50′–42°35′N	56°00′–59°00′N
Area	2270km^2	12,450km^2
Nominal annual catch	[a]70,000t	[b]100,000t
Spawning season	[c]Dec.–Mar.	[d]Early April
Spawning depth	[e]100–120m	[d]200–300m
Temperature at spawning depth	[e]2–6°C	[f]5.5°C
Depth of maximum egg concentrations	[e]0–40m	[f]150–200m
Egg specific gravity	[e]1.020–1.026g/cm^3	[f]1.024–1.031g/cm^3
Depth of maximum larval occurrence	[g]10–20m	[h]15–50m
Length of larvae when copepod nauplii are predominant components of diet	[e]<7–8mm	[h]<11mm
Larval growth rate	—	[h]0.21mm/day

[a]Nakayama et al. 1987, [b]Megrey 1989, [c]Maeda et al. 1976, [d]Kendall and Picquelle 1990, [e]Nakatani 1988, [f]Kendall and Kim 1989, [g]Kamba 1977, [h]Kendall et al. 1987.

Physical oceanography

The water of Funka Bay originates from the seasonal influx of two water masses: The Tsugaru Warm Water and the Oyashio Water. Tsugaru Warm Water enters the Bay in late-summer when surface waters exceed 15°C and there is a strong thermocline in the upper 20m (Nakatani 1988). Autumnal cooling produces isothermal conditions and cooling to about 4°C (Winter Funka Bay Water: Ohtani and Kido 1980). In late-winter or early-spring, the cold (<2°C), less saline (<33.0‰) Oyashio Water usually intrudes into the Bay above the Winter Funka Bay Water, producing a stratified condition with a temperature inversion. In late-spring and early-summer, seasonal warming of surface waters occurs and a thermocline develops. Throughout the year, bottom temperatures remain at 3–6°C.

Shelikof Strait has an estuarine type circulation, with less seasonal variation than Funka Bay. In its upper layers, the Alaska Coastal Current (ACC) flows to the southwest and is particularly pronounced on the Alaska Peninsula side of the Strait. During runoff seasons (late-spring to early-fall), substantial amounts of freshwater enter the strait, primarily from Cook Inlet, and flow along the Peninsula until thoroughly mixed with the ACC. From approximately 150m to the bottom, more saline water flows into the strait over the sill to the southwest (Kim 1987). During April and May (when walleye pollock eggs and larvae are present), near-surface water temperatures in the ACC are generally 0–4°C, warming to 7°C by late May, while the deeper waters are generally 4–5.5°C. Salinity varies from about 31 to 33.5‰.

In Funka Bay there is considerable interannual variation in the date when the Oyashio Water intrudes and in the length of time that surface temperatures remain cold (<3°C). In Shelikof Strait, interannual variation in the frequency, intensity, and track of storms affects water properties and transport.

Biological comparisons

Spawning

In Funka Bay, adult walleye pollock mature and spawn from November to March, with peak spawning activity occurring in January and February (Maeda et al. 1976 and 1981, Yoon 1981), whereas in Shelikof Strait most fish mature in February and March and spawning peaks in early April (Kim 1989, Kendall and Picquelle 1990). Pelagic eggs are present in Funka Bay from December until March, and in Shelikof Strait eggs are present mainly in April. There is some interannual variation in time of spawning in Funka Bay, and eggs have even been collected in November and April (Maeda et al. 1980). Thus the spawning season seems to occur earlier in the year and lasts longer in Funka Bay than in Shelikof Strait. Spawning occurs mainly at depths of 100–120m near the entrance of Funka Bay (Maeda et al. 1976, Nakatani 1988, Nakatani and Maeda 1989). In Shelikof Strait, spawning is concen-

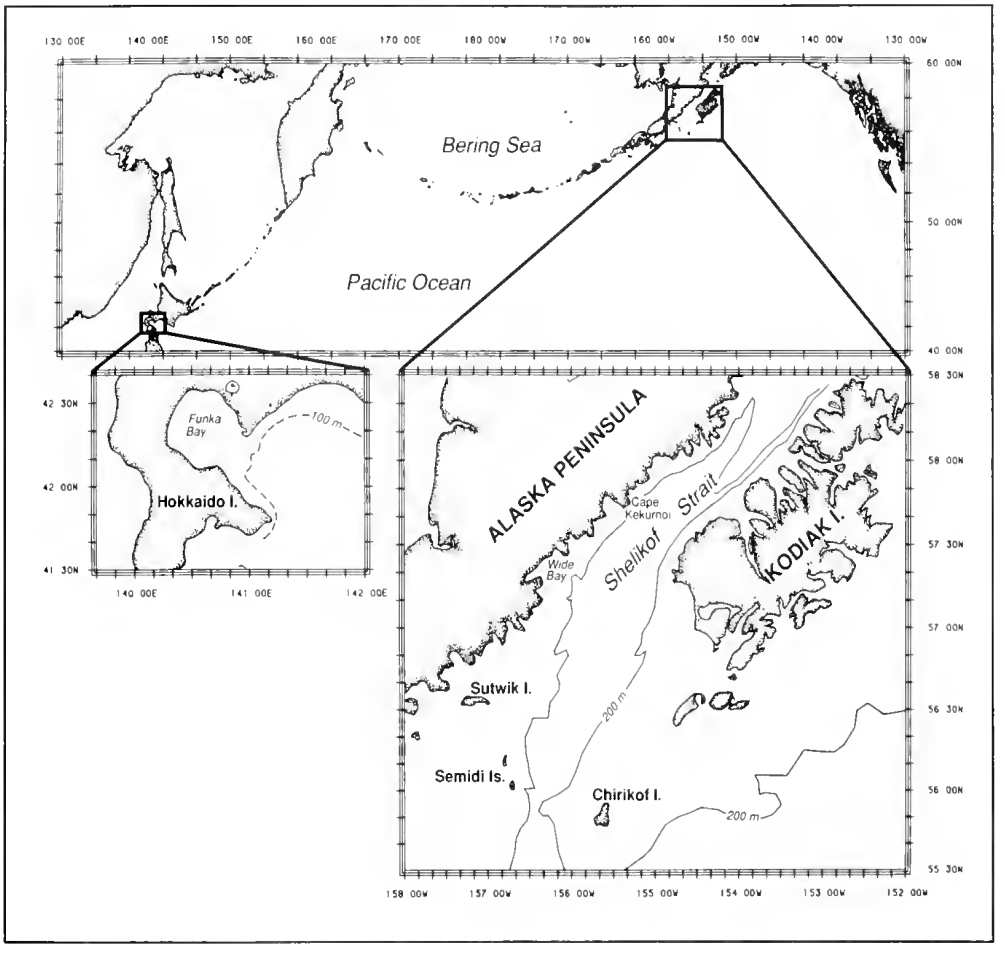

Figure 1
Location of Funka Bay, Japan, and Shelikof Strait, Gulf of Alaska. Insets are enlargements of the areas with pertinent bathymetry.

trated in a small area of deep water (>250 m) near Cape Kekurnoi (Fig. 1) (Kendall and Picquelle 1990).

Field surveys of adult walleye pollock in Funka Bay and Shelikof Strait show that fish congregate and migrate to a particular part of their range just prior to the spawning season. Final migration to a restricted spawning area takes place quickly. In Shelikof Strait, hydroacoustic surveys show that the fish separate into vertical strata, presumably by sex (females below males) and readiness to spawn (Muigwa 1989).

Although the fish move to the spawning area as a large group, spawning itself is by pairs. Behavior of spawning walleye pollock has been investigated using captive fish from Funka Bay (Sakurai 1982, 1989), as well as from Puget Sound, Washington (Baird and Olla 1991). The shallow tanks used by Sakurai (1989) may have prevented some of the vertical aspects of spawning behavior observed by Baird and Olla (1991). Although no such studies have been conducted on fish from Shelikof Strait, similarities between the behavior of fish from near the eastern (Puget Sound) and western (Funka Bay) extremes of the species distribution may indicate that spawning behavior varies little geographically. In experimental tanks, the fish form loose aggregations near the surface. Males frequently follow other males and females. Sakurai (1989) related male–male interaction to the agonistic behaviors associated with dominance; Baird and Olla (1991) considered the male's following behavior as a searching behavior for potential mates. Sakurai (1989) also observed courtship displays by males toward prospective mates. At the onset of a spawning, a female would swim down with a male following her. The male then made contact with her by rubbing his ventral surface first against her dorsum or side and then he swam beneath her, with their two vents in contact. Other males occasionally followed the pair closely and also made contact with the female. During vent-to-vent contact, the male rubbed his body rapidly against the female's abdomen, and presumably gametes were released at this time (they could not be seen in the water, but were found in the tank overflow within an hour). Most spawning took place in evening or morning twilight (Baird and Olla 1991).

Female walleye pollock characteristically spawn a number of batches of eggs over a fairly short period

each year. The interval between batches is a few days. The number of eggs per batch and size of eggs decrease with successive batches. These patterns have been observed both in Funka Bay (Sakurai 1982) and Shelikof Strait (Hinckley 1990).

Fecundity

Miller et al. (1986) related fecundity of walleye pollock from Shelikof Strait to gutted weight and fork length, while Sakurai (1982) related fecundity of walleye pollock from Funka Bay to whole weight and body length. Conversions were applied here to the Funka Bay length and weight data so fecundity could be compared with Shelikof Strait values based on

$$Y = 0.7634X + 23.4472 \ (r^2\ 0.96628,\ N\ 40)$$

where X = body weight and Y = gutted weight (Y. Sakurai, unpubl.); and

$$Y = 1.0659X + 4.050 \ (r^2\ 0.9959,\ N\ 53)$$

where X = body length and Y = fork length (T. Maeda, unpubl.).

The relative fecundity of Funka Bay fish is represented by the relationship $F = 8.73 \times 10^{-6} L^{3.98}$ and $F = 106.2 W^{1.21}$, where L = body length in mm and W = body weight in grams (N 94) (Sakurai 1982); therefore a 300g (gutted weight) fish produces 129,000 eggs and a 1000g fish yields 589,000 eggs. In Shelikof Strait, the relationship was found to be $F = 1.2604 L^{3.2169}$ and $F = 387.4551 W^{1.0160}$ (N 60), where L = fork length in cm and W = gutted weight in grams; this yields 127,000 eggs for a 300g fish and 433,000 eggs for a 1000g fish (Miller et al. 1986). Thus small fish from Funka Bay have about the same number of eggs, but larger fish have more eggs than those from Shelikof Strait (Fig. 2).

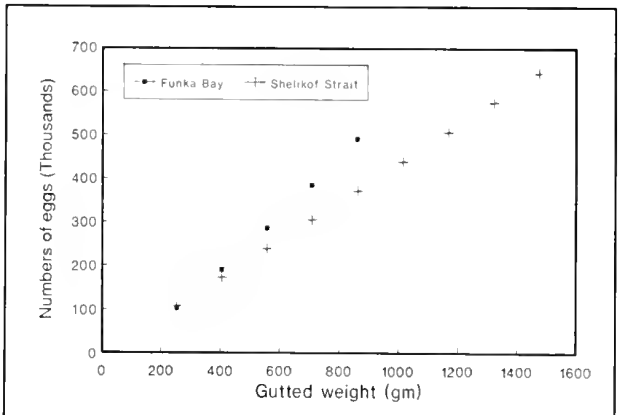

Figure 2
Fecundity-weight relationship for walleye pollock in Funka Bay, Japan (based on Sakurai 1982), and Shelikof Strait, Gulf of Alaska (based on Miller et al. 1986).

Eggs

Development Eggs from Funka Bay are more variable in size and slightly larger than those from Shelikof Strait. In Funka Bay, eggs are 1.15–1.68mm ($\bar{x}$ 1.46mm) in diameter (Nakatani and Maeda 1984, T. Nakatani, unpubl.). In Shelikof Strait, egg diameter ranges from 1.30 to 1.41mm, and egg size has been shown to vary interannually and decrease during the spawning season (Hinckley 1990).

Eggs from Funka Bay develop at a rate dependent on temperature according to the relationship

$$D = 31.70 \exp(-0.12T),$$

where D is days to 50% hatch and T is temperature (°C). Thus 50% hatch times are 22.1 days at 3°C, 17.4 days at 5°C, and 15.4 days at 6°C (Nakatani and Maeda 1984). No measurements of incubation time are available for eggs from Shelikof Strait; however, reared eggs from Auke Bay in southeast Alaska (58°20′N) required 19.2 days at 3°C, 14.1 days at 5°C, and 12.2 days at 6°C for 50% hatch (Haynes and Ignell 1983). Thus eggs from southeast Alaska developed to hatching more quickly, by about 2–3 days, than those from Funka Bay (Fig. 3).

Vertical distribution The vertical distribution and buoyancy of eggs have been investigated in both Funka Bay and Shelikof Strait. In Funka Bay, eggs rise in the water column as they develop. Stage-1 (fertilization to morula) eggs were found at a depth of roughly 30m (10–40m), whereas Stage-5 (embryo more than three-fourths yolk circumference) eggs were mainly at depths of 10–20m (Nakatani 1988). The specific gravity of Funka Bay eggs throughout development was within a range of 1.020–1.025g/cm^3 ($\bar{x}$ 1.0226g/cm^3). This resulted in an upward velocity of 4.9m/h in ambient water through the homogenized water column early in the spawning season (σ^t 26.41–27.17), and is consistent with field observations of shallower depths for older eggs compared with those recently spawned (Nakatani and Maeda 1984, Nakatani 1988).

In Shelikof Strait, the vertical distribution of eggs changes during development in response to their changing specific gravity. Newly spawned eggs are positively buoyant, and thus rise from the deep locations where they are spawned. In middle stages of development, the eggs become heavier and sink until just before hatching when they again rise toward the surface (Kendall and Kim 1989). The specific gravity

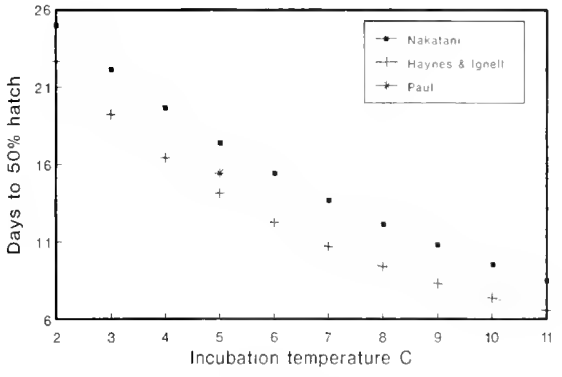

Figure 3
Incubation period of walleye pollock eggs from Funka Bay, Japan (based on Nakatani 1988); Resurrection Bay (based on A.J. Paul, Univ. Alaska, Seward, pers. commun.) and Auke Bay, Alaska (based on Haynes and Ignell 1983).

of eggs from Shelikof Strait varied from 1.0243 to 1.031 g/cm^3, whereas the water density varied from 1.0256 to 1.0259 g/cm^3 (in 1985). Less than 20% of eggs of all ages occurred above 162 m in Shelikof Strait. Over 80% of early- (fertilization to morula) and late-stage eggs (embryo more than one-half circumference of yolk to hatching) occurred between 216 and 277 m (near bottom), while over 60% of middle-stage eggs (gastrula) occurred between 162 and 216 m (Kendall and Kim 1989). Thus eggs in Shelikof Strait are heavier and occur deeper than those in Funka Bay.

Horizontal distribution The horizontal distribution pattern of eggs in Funka Bay was fairly consistent among the 3 years (1977, 1978, and 1987) for which data are presented (Nakatani 1988, Nakatani and Maeda 1981 and 1989). Younger eggs are mainly found just outside the entrance to the bay and older eggs are found inside the bay, indicating that spawning occurs outside the bay and the eggs drift into the bay as they develop. During the period 24 January to 11 February 1978, egg abundance reached 13,424 Stage-4 eggs/m^2 at a station just south of the entrance to the bay where large numbers of Stage 2–5 eggs were also present, producing a total of 23,817 eggs/m^2.

The egg distribution pattern in Shelikof Strait was most intensively examined in 1981; however, sampling in other years (1978–86) indicates similar patterns. The first appearance of low numbers of eggs occurs in March and early April, mainly in the southern part of the strait (Kendall and Picquelle 1990). The highest concentrations of eggs occur off Cape Kekurnoi in early April, where abundances of Stage-2 and -3 eggs exceeded 1000/m^2 in 1981. The combined abundance for all stages was 350,000 eggs/m^2 in the area of maximum concentration; about 15 times the maximum abundance observed in Funka Bay. By late April, egg abundance is reduced as eggs are spread more evenly throughout the southern two-thirds of the strait and the area immediately to the southwest of the strait. By late May, egg abundance is further reduced, but the area of occurrence is still similar to that seen in late April. As opposed to Funka Bay, there is little evidence of drift of eggs in Shelikof Strait. It appears that the adults spawn some eggs in the southwestern part of the strait as they move toward the main spawning area off Cape Kekurnoi. Later spawning in late April and May seems to be dispersed throughout the strait and occurs at a much reduced level. Measurements of currents in Shelikof Strait also indicate that little drift would be expected in the deep waters (>150 m) where most eggs occur (Kendall and Kim 1989).

Larvae*

Vertical distribution The ecology of walleye pollock larvae has been investigated in both Funka Bay and Shelikof Strait. In both areas most larvae occur above 50 m in the water column and exhibit limited diel vertical migration (Kamba 1977, Kendall et al. 1987). Few larvae are collected at the surface, but some larvae move up to 10–20 m depth in the evening. At night they are fairly evenly distributed throughout the upper 50 m, and in the early morning they are again concentrated above 20 m. During midday they are most abundant at 20 m and deeper to 50 m. The larvae sampled by Kendall et al. (1987) in Shelikof Strait averaged 11.0 mm (SD 1.7 mm), while those in Funka Bay sampled by Kamba (1977) had a wide range of lengths from 4.6 to 26.4 mm, although most were 4.6–12.8 mm. Kamba (1977) indicated that larger larvae (>13.7 mm) were more often collected in shallow tows at night and in deep tows during the day, suggesting that either the larger larvae migrated more than the smaller ones or that the larger larvae were more successful at avoiding the shallow nets during the day. No large larvae were collected by Kendall et al. (1987). Kamba (1977) concluded that the diel vertical movements of pollock larvae in Funka Bay corresponded to those of their zooplankton prey. Both Kamba (1977) and Kendall et al. (1987) found a diel pattern in gut fullness, with little food found in guts at night and most food found in guts during the day.

* Lengths of larvae and juveniles are reported here as standard length (SL, from the tip of the snout to the end of the notochord or base of the hypural plate), although in the Japanese literature they were given as total length (TL). Conversion from TL to SL is based on our paired measurements of 1048 fish (4.2–103 mm SL) which resulted in the relationship: SL(mm) = 0.108 + 0.907 TL(mm).

Horizontal distribution In the Funka Bay region, walleye pollock larvae are generally concentrated inside the bay from late January through early April (Nakatani 1988, Nakatani and Maeda 1989). Their abundance decreases during this time from >5000 larvae/m^2 in the area of maximum concentration in late January to 200–400 larvae/m^2 in early April. In many cases, surveys have disclosed more than one area of abundance within the bay. Their occurrence generally overlaps that of the Oyashio Water. For example, in 1980 the Tsugaru Warm Water remained in the bay longer than usual, and the Oyashio Water did not enter the bay until mid-March; before then, the larvae were concentrated at the mouth of the bay. It is possible that larvae entering the bay before the invasion of the Oyashio Water would experience low survival because of inadequate prey production.

In Shelikof Strait, most larvae are concentrated in one large patch that can be followed as it drifts to the southwest with the prevailing currents from April through May (Kendall et al. 1987). The velocity of drift may vary interannually and depend on weather patterns in the area as well as the strength of the ACC. In some years, it appears that most of the larvae drift out of the strait within 2–4 weeks after hatching, but in other years they remain for several more weeks because of the influence of nearshore eddies (Incze et al. 1989). There is considerable cross-strait shear in the current, so the drift of larvae is influenced by where they reach the surface layer from their deep incubation area (Kim and Kendall 1989). Larval abundances as high as 10,000/m^2 were observed in the patch in late April 1981, and by late May abundances of 2400/m^2 were present (Bates and Clark 1983).

Feeding Copepod nauplii, which were not identified to species, are the major prey item of first-feeding walleye pollock larvae (Kamba 1977, Kendall et al. 1987, Nakatani and Maeda 1983). Copepodids are the most important prey item in the diet of 11 mm larvae in Shelikof Strait and 8 mm larvae in Funka Bay. Copepod eggs were more prevalent in guts of larvae in Funka Bay than in Shelikof Strait (Nakatani and Maeda 1983, Kendall et al. 1987). Their digestibility and nutritional value for walleye pollock larvae are unknown. *Pseudocalanus* spp. was the most abundant copepod taxon in the water column in Shelikof Strait and Funka Bay when larvae were present (Kendall et al. 1987, Nakatani 1988). The nauplii in the guts of small larvae were probably mostly *Pseudocalanus* spp. and *Oithona* spp., and most of the copepodids in larger larvae were *Pseudocalanus* spp. Copepodids of *Pseudocalanus minutus* and *Oithona similis* were most abundant in larger larvae up to 30 mm in Funka Bay (Nakatani and Maeda 1983). The maximum prey size increases with growth of the larvae, but the minimum size remains fairly constant through fish up to about 73 mm (Kamba 1977).

Based on laboratory and field studies, naupliar abundances of about 10 per liter seem to be required to support growth of small (<8 mm) walleye pollock larvae (Paul 1983, Dagg et al. 1984). Prey densities above this threshold have been observed associated with the larval patch in Shelikof Strait before and during a storm (Incze et al. 1990). Naupliar abundances below this threshold were seen in Funka Bay throughout most of the larval period in 1987, but they were above 10 per liter in several other years (Nakatani and Maeda 1989). However, naupliar densities were probably underestimated, since they were collected on 100 μm sieves. Availability of smaller nauplii as larval food will require further observations.

Age and growth Daily growth increments on otoliths have been used to determine the age of larvae and early juveniles from both Shelikof Strait and Funka Bay. Based on a series of 109 larvae (6.0–14.6 mm SL) collected in Shelikof Strait in May 1983, the linear growth equation SL = 4.29 mm + 0.21 d (r^2 0.75), where d = age in days, was fit (Kendall et al. 1987). Growth based on 357 larvae and early juveniles 3.9–30.0 mm SL from the Shelikof spawning collected May through July 1987 fit a Laird-Gompertz function: SL at age t = 4.505 ($e^{7.854(1-e^{-0.004t})}$), where t = days after hatch (Yoklavich and Bailey 1989). The growth of larvae and juveniles from Funka Bay fit the function: TL = 121.5/(1 + $e^{-0.026(t-124.511)}$), with TL in mm (Nishimura and Yamada 1984). Thus larvae 50 days old from Funka Bay were about 14.0 mm SL (see footnote) while those from Shelikof Strait would range from 14.8 mm SL (Kendall et al. 1987) to 18.7 mm SL (Yoklavich and Bailey 1989) (Fig. 4).

Larval population length-frequency distributions depend on time of spawning, mortality of larvae, growth of larvae, and sampling bias. Except for sampling bias, these factors represent population processes occurring to the annual cohort of larvae. In Funka Bay, even though spawning takes place over a protracted period, larval survival appears low except during periods when adequate food is present. Mortality due to starvation is high for larvae that hatch before the spring increase of nauplii in Funka Bay (Nakatani and Maeda 1989, Nakatani 1991). Thus variations in size of larvae may depend more on differences in the birth dates of surviving larvae than on differences in growth rates.

In Shelikof Strait, spawning peaked during the first week of April in several years. By the end of April 1981, most larvae were about 4.8 mm. By the third week in May 1981, they were mostly 7–8 mm (Dunn et al. 1984), as they were in 1982 (Kendall et al. 1987).

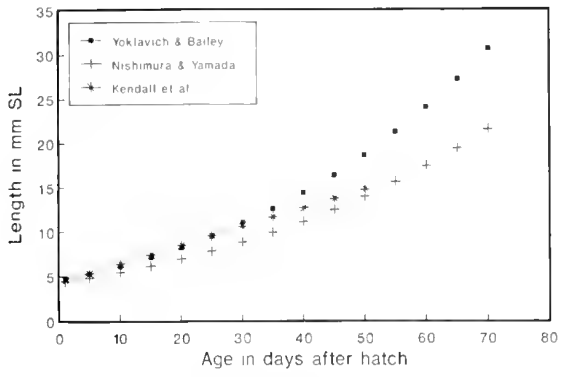

Figure 4

Growth of walleye pollock larvae and juveniles from Funka Bay, Japan (Nishimura and Yamada 1984), and larvae from Shelikof Strait, Gulf of Alaska (Kendall et al. 1987, Yoklavich and Bailey 1989).

However, in 1983 larvae averaged 11.23mm in late May (Kendall et al. 1987). No interannual differences in larval growth rates were discerned for larvae collected in Shelikof Strait in late May 1983, 1985, 1986, or 1987. Because larvae were larger in late May 1983 than in 1985, 1986, or 1987, they may have been survivors of an earlier spawning than those observed in the other years (Yoklavich and Bailey 1989).

Early juveniles

Young-of-the-year juvenile walleye pollock (18–73mm) have been sampled extensively in Funka Bay using midwater and bottom trawl nets (Nakatani and Maeda 1987). The juveniles are about 34mm in late May, 36mm in June, and 55–80mm in late July. In June, juveniles (22–66mm) are found mainly at 25–30m at night and at 10–15m during the day (Nakatani and Maeda 1987). The juveniles move deeper in the water column in May and June, and by late July most are on the bottom (Nakatani and Maeda 1987). In July, larger fish are caught in bottom trawls while smaller fish are still in the water column. As the juveniles grow and move toward deeper water and the bottom, they also move from inside the bay toward the entrance (in June) and to the shelf (100–300m) just outside the bay (by August) (Nakatani and Maeda 1987).

Some variation in size-at-date of juveniles among years has been observed (Fukuchi 1976, Nakatani and Maeda 1987), which may be due to interannual differences in growth rates, or differences in hatch dates of surviving juveniles.

Food organisms changed during juvenile growth with *Neocalanus plumchrus* being most important in fish >27mm long in midwater. Juveniles collected on the bottom fed on large-sized copepodids of *Neocalanus cristatus* and *Eucalanus bungii*, *Euphausia pacifica* (a euphausid), and *Parathemisto japonica* (an amphipod) (Nakatani and Maeda 1987).

Young-of-the-year juveniles from the Shelikof Strait spawning were sampled with a Methot midwater frame trawl (Methot 1986) in June and July 1987 (Hinckley et al. 1989), and by small-mesh midwater and bottom trawl surveys in late-summer of several years (Bailey and Spring, in review). Data from these studies have not yet been completely analyzed. However, in June and July the early juveniles (mainly 20–30mm) were found on the shelf along the Alaska Peninsula. As with the eggs and larvae, they formed a large discrete patch surrounded by a large area with lower abundances. From their pattern of distribution, it appears that at this size and time of year they still inhabit midwater depths and are not schooling (Hinckley et al. 1989). Fish were found to feed mainly on various life stages of *Pseudocalanus* spp., smaller fish ate primarily nauplii and copepodids, while adults became more important in larger fish. Differences in diet between fish sampled at different locations indicated that the food organisms were patchily distributed (Grover 1990).

Sampling in late-summer has concentrated mainly on the bays around Kodiak Island and along the Alaska Peninsula. Considerable interannual variation in sampling and pattern of distribution of juveniles characterized these surveys. In 1987, when the sampling area in late-summer included the shelf west of the Shumagin Islands, a concentrated patch of juveniles was found that was likely the product of the Shelikof Strait spawning, i.e., the eggs and larvae that had been followed through the spring during their drift to the southwest from Shelikof Strait (Bailey and Spring, in review).

Year-class determinants

Studies of walleye pollock early life history in both Funka Bay and Shelikof Strait have been designed to determine causes of year-class fluctuations. The basic premise is that these fluctuations result from events during early life history and have little relation to the abundance or other characteristics of the spawning population. The influence of hydrography and its effect on larval food supply has been the most intensively studied factor in both areas, but predation has also been considered in Shelikof Strait research.

In Funka Bay, walleye pollock early life history seems to be closely tied to the timing and extent of the influx of Oyashio Water (Nakatani 1984). This cold, low-salinity water carries *Pseudocalanus minutus* into the bay where they produce nauplii, the primary diet of small larvae in nearsurface waters. Walleye

pollock spawning seems to be timed and positioned to correspond to this influx. In years when this influx is delayed or absent, survival of larvae may be reduced (Nakatani and Maeda 1989). Years with an early invasion of the Oyashio Water have resulted in large year-classes of walleye pollock (Nakatani 1988). However, a strong year-class was also observed in 1980 when there was a late invasion (Nakatani and Maeda 1983, Nakayama et al. 1987). To predict population size fluctuations will require further studies on the causes of larval mortality.

Besides factors influencing larval food production in Shelikof Strait (Incze et al. 1990), the complex dynamics of the ACC as it exits the strait seem important in determining the rate of drift of the larval patch and its resultant position when the larvae are ready to settle (Reed et al. 1989). If the larvae are in the center of the ACC as it exits the strait, they may be carried quickly offshore through the sea valley between the Semidi Islands and Chirikof Island, as apparently happened in 1985 (Incze et al. 1989). Some of these larvae may remain offshore where larval feeding conditions are probably not ideal. The return of offshore larvae to the shelf for demersal settlement is also problematical. If the larvae are on the Alaska Peninsula side of the core of the ACC as it exits the strait, their drift will be slower, and they should remain in the coastal region where food production is probably enhanced. Their trajectory should carry them west along the Alaska Peninsula to shelf areas suitable for demersal settlement.

Storm winds blowing offshore from Wide Bay may displace the ACC as it exits the strait, and eddies have been observed in this area. The influence of such factors on the larval patch and larval food production may be important in determining the numbers of larvae reaching the juvenile stage.

Conclusions

It appears that within large areas of distribution, walleye pollock populations have evolved to spawn in very specific areas and during brief times of the year. Adults migrate to these areas annually for spawning. This spawning pattern produces concentrations of planktonic eggs and larvae that far exceed those reported for any other fish (>20,000 eggs/m^2; <5000 larvae/m^2). These spawnings are such that the eggs and larvae find themselves in areas where suitable food is abundant and where currents later carry larvae to suitable nursery areas. It appears that interannual variations in oceanographic conditions responsible for food production and larval drift impact larval survival, and hence year-class strength. Although there are marked differences in the geography and oceanography of Shelikof Strait and Funka Bay, walleye pollock have adapted to reproduce successfully in both areas. Adaptations in the early life history of walleye pollock to these differences in environment include timing and duration of the spawning season, specific gravity of the eggs, and differences in prey size in relation to larval size.

Time of spawning in both areas corresponds to seasonal transitions in hydrographic conditions (Nakatani 1988, Kim 1987). The spawning season is several months long in the lower-latitude Funka Bay area where there is considerable interannual variation in timing of the intrusion of the cold Oyashio Water, which increases copepod naupliar production. The Shelikof Strait area spawning is very peaked, taking place mainly over a few weeks and during the same time each year, early April. This is the time when currents are at an annual minimum due to reduced precipitation and weak winds. We do not know if low current strength is the seasonal signal that fish respond to, but presumably the signal is less variable than the intrusion of Oyashio Water.

Eggs are less dense in Funka Bay where water depths are only about one-third those of Shelikof Strait. In Funka Bay, the eggs rise in the water column after spawning and drift into the inner part of the bay. In Shelikof Strait, the eggs remain in the nearbottom water where they are spawned and show no appreciable drift. This difference in transport of eggs may relate to the desired location of hatching. Copepod production is enhanced when Oyashio Water enters Funka Bay and the egg drift pattern enables the eggs to hatch there. In Shelikof Strait, the upper layers of water during the spawning season are moving to the southwest at a rate that would flush eggs in surface waters out of the strait and into the offshore Alaska Stream in a few weeks. By remaining in the sluggish bottom waters, hatching is more likely to occur in southwest Shelikof Strait where larval prey may be more abundant. Interannual variations in storms in this area may effect copepod production and thereby larval condition.

In both areas, nauplii of species of small copepods, *Pseudocalanus* and *Oithona*, are dominant in the diet of first-feeding larvae. Eating small prey is energetically costly for larger larvae, so it may be critical for them to encounter more advanced stages of copepods (Incze et al. 1984). This may be more important in Shelikof Strait than in Funka Bay because larvae in Funka Bay start eating larger prey at a smaller size than do larvae in Shelikof Strait.

Drift of larvae to nursery grounds is more important in Shelikof Strait than it is in Funka Bay. It appears that most juveniles that result from spawning in Shelikof Strait inhabit shelf and nearshore areas 100–200km from the spawning location by the age of 4 months

(Hinckley et al. 1989). Juveniles from the Funka Bay spawning are mostly found in waters just outside the bay during their first summer (Nakatani 1988). In the following winter, some of them remain in the center of the bay (T. Maeda and T. Nakatani, unpubl. data).

Acknowledgments

Many investigators in Japan and the United States are studying the early life history of walleye pollock. Many have generously shared ideas and data with us and we thank them. In particular, Dr. Kevin Bailey, AFSC, and Dr. Jim Schumacher, PMEL, reviewed early drafts of this manuscript and gave numerous helpful suggestions, as well as Dr. Tatsuaki Maeda who conducted many of the Funka Bay studies that formed the basis for this paper with Dr. Toshikuni Nakatani. Dr. Lew Haldorson, University of Alaska, and Dr. Svein Sundby, Institute of Marine Research, Norway, provided valuable reviews of an earlier draft.

Citations

Bailey, K., and S. Spring
In review Comparison of larval, age-0 juvenile, and age-2 recruit abundance indices of walleye pollock *Theragra chalcogramma* in the western Gulf of Alaska. ICES J. Mar. Sci.

Baird, T.A., and B.L. Olla
1991 Social and reproductive behavior of walleye pollock *Theragra chalcogramma* of a captive group. Environ. Biol. Fish. 30:295–301.

Bates, R.D., and J. Clark
1983 Ichthyoplankton off Kodiak Island and the Alaskan Peninsula during spring 1981. NWAFC Proc. Rep. 83-89, Northwest & Alaska Fish. Cent., NMFS, NOAA, Seattle, WA 98115-0070, 105 p.

Dagg, M.J., M.E. Clarke, T. Nishiyama, and S.L. Smith
1984 Production and standing stock of copepod nauplii, food items for larvae of walleye pollock *Theragra chalcogramma* in the southeastern Bering Sea. Mar. Ecol. Prog. Ser. 19: 7–16.

Dunn, J.R., A.W. Kendall Jr., and R.D. Bates
1984 Distribution and abundance patterns of eggs and larvae of walleye pollock (*Theragra chalcogramma*) in the western Gulf of Alaska. NWAFC Proc. Rep. 84-10, Northwest & Alaska Fish. Cent., NMFS, NOAA, Seattle, WA 98115-0070, 66 p.

Fukuchi, M.
1976 Some aspects of bioenergetics of walleye pollock (*Theragra chalcogramma* Pallas) at early life stages. Ph.D. thesis, Univ. Hokkaido, Hokkaido, Japan.

Grover, J.J.
1990 Feeding ecology of late-larval and early-juvenile walleye pollock *Theragra chalcogramma* from the Gulf of Alaska in 1987. Fish. Bull., U.S. 88:463–470.

Haynes, E.B., and S.E. Ignell
1983 Effect of temperature on rate of embryonic development of walleye pollock, *Theragra chalcogramma*. Fish. Bull., U.S. 81:890–894.

Hinckley, S.
1990 Variation in egg size of walleye pollock (*Theragra chalcogramma*) with a preliminary examination of the effect of egg size on larval size. Fish. Bull., U.S. 88:471–483.

Hinckley, S., K. Bailey, J. Schumacher, S. Picquelle, and P. Stabeno
1989 Preliminary results of a survey for late stage larval walleye pollock and observations on larval drift in the western Gulf of Alaska, 1987. *In* Proc., Int. symp. on biology and management of walleye pollock, p. 297–306. Alaska Sea Grant Rep. 89-1, Univ. Alaska, Fairbanks.

Incze, L.S., M.E. Clarke, J.J. Goering, T. Nishiyama, and A.J. Paul
1984 Eggs and larvae of walleye pollock and relationships to the planktonic environment. *In* Ito, D.H. (ed.), Proceedings of the workshop on walleye pollock and its ecosystem in the eastern Bering Sea, p. 109–159. NOAA Tech. Memo. NMFS-F/NWC-62, Northwest & Alaska Fish. Cent., NMFS, Seattle, WA 98115-0070.

Incze, L.S., A.W. Kendall Jr., J.D. Schumacher, and R.K. Reed
1989 Interactions of a mesoscale patch of larval fish (*Theragra chalcogramma*) with the Alaska Coastal Current. Continental Shelf Res. 9:269–284.

Incze, L.S., P.B. Ortner, and J.D. Schumacher
1990 Microzooplankton, vertical mixing and advection in a larval fish patch. J. Plankton Res. 12:365–379.

Kamba, M.
1977 Feeding habits and vertical distribution of walleye pollock, *Theragra chalcogramma* (Pallas), in early life stage in Uchiura Bay, Hokkaido. Res. Inst. N. Pac. Fish., Hokkaido Univ., Spec. Vol., p. 175–197.

Kendall, A.W. Jr., and S. Kim
1989 Buoyancy of walleye pollock (*Theragra chalcogramma*) eggs in relation to water properties and movement in Shelikof Strait, Gulf of Alaska. *In* Beamish, R.J., and G.A. McFarlane (eds.), Effects of ocean variability on recruitment and evaluation of parameters used in stock assessment models, p. 169–180. Can. Spec. Publ. Fish Aquat. Sci. 108.

Kendall, A.W. Jr., and S.J. Picquelle
1990 Egg and larval distributions of walleye pollock, *Theragra chalcogramma*, in Shelikof Strait, Gulf of Alaska. Fish. Bull., U.S. 88:133–154.

Kendall, A.W. Jr., M.E. Clarke, M.M. Yoklavich, and G.W. Boehlert
1987 Distribution, feeding, and growth of larval walleye pollock, *Theragra chalcogramma*, from Shelikof Strait, Gulf of Alaska. Fish. Bull., U.S. 85:499–521.

Kim, S.
1987 Spawning behavior and early life history of walleye pollock, *Theragra chalcogramma*, in Shelikof Strait, Gulf of Alaska, in relation to oceanographic features. Ph.D. diss. Univ. Wash., Seattle, 221 p.
1989 Early life history of walleye pollock, *Theragra chalcogramma*, in the Gulf of Alaska. *In* Proc., Int. symp. on biology and management of walleye pollock, p. 117–139. Alaska Sea Grant Rep. 89-1, Univ. Alaska, Fairbanks.

Kim, S., and A.W. Kendall Jr.
1989 Distribution and transport of larval walleye pollock (*Theragra chalcogramma*) in Shelikof Strait, Gulf of Alaska, in relation to water movement. Rapp. P.-V. Reun. Cons. Int. Explor. Mer 191:127–136.

Maeda, T., T. Takahashi, M. Ijichi, H. Hirakawa, and M. Ueno
1976 Ecological studies on the Alaska pollock in the adjacent waters of the Funka Bay, Hokkaido-II spawning season. Bull. Jpn. Soc. Sci. Fish. 42:1213–1222 [in Jpn., Engl. abstr.].

Maeda, T., T. Nakatani, T. Takahashi, and M. Ueno
1980 On the population and developmental fluctuations of the Alaska pollock at the southern area off the Hokkaido in the Pacific Ocean. Bull. Jpn. Soc. Fish. Oceanogr. 37:29–33 [in Jpn.].

Maeda, T., T. Takahashi, and M. Ueno
1981 Annual life period of the adult Alaska pollock in the adjacent waters of the Funka Bay, Hokkaido. Bull. Jpn. Soc. Sci. Fish. 47:741–746 [in Jpn., Engl. abstr.].

Megrey, B.A.
1989 Exploitation of walleye pollock resources in the Gulf of Alaska, 1964–88: Portrait of a fishery in transition. *In* Proc., Int. symp. on biology and management of walleye pollock, p. 33–58. Alaska Sea Grant Rep. 89-1, Univ. Alaska, Fairbanks.

Methot, R.D.
1986 Frame trawl for sampling pelagic juvenile fish. Calif. Coop. Oceanic Fish. Invest. Rep. 27:267–278.

Miller, B.S., D.R. Gunderson, D. Glass, D.B. Powell, and B.A. Megrey
1986 Fecundity of walleye pollock (*Theragra chalcogramma*) from the Shelikof Strait, Gulf of Alaska. FRI-UW-8608, Coll. Fish., Univ. Wash., Seattle, 40 p.

Muigwa, N.M.
1989 Vertical distribution patterns of prespawning and spawning pollock (*Theragra chalcogramma*) in Shelikof Strait. *In* Proc., Int. symp. on biology and management of walleye pollock, p. 403–432. Alaska Sea Grant Rep. 89-1, Univ. Alaska, Fairbanks.

Nakatani, T.
1984 The early life history of walleye pollock *Theragra chalcogramma* (Pallas) in Funka Bay and the adjacent waters, Hokkaido. Aquabiology 34:341–347 [in Jpn., Engl. abstr.].
1988 Studies on the early life history of walleye pollock in Funka Bay and vicinity, Hokkaido. Mem. Fac. Fish., Hokkaido Univ. 35:1–46.
1991 Copepod nauplii as food of walleye pollock larvae (Pisces: Gadidae) in Funka Bay, Japan. Proc., Fourth int. conf. copepoda. Bull. Plankton Soc. Jpn., Spec. Vol., p. 515–525.

Nakatani, T., and T. Maeda
1981 Transport process of the Alaska pollack eggs in Funka Bay and the adjacent waters, Hokkaido. Bull. Jpn. Soc. Sci. Fish. 47:1115–1118.
1983 Distribution of walleye pollock larvae and their food supply in Funka Bay and the adjacent waters, Hokkaido. Bull. Jpn. Soc. Sci. Fish. 49:183–187 [in Jpn., Engl. abstr.].
1984 Thermal effect on the development of walleye pollock eggs and their upward speed to the surface. Bull. Jpn. Soc. Sci. Fish. 50:937–942 [in Jpn., Engl. abstr.].
1987 Distribution and movement of walleye pollock larvae *Theragra chalcogramma* in Funka Bay and the adjacent waters, Hokkaido. Bull. Jpn. Soc. Sci. Fish. 53:1585–1591 [in Jpn., Engl. abstr.; Engl. transl. avail. Alaska Fish. Sci. Cent., NMFS, NOAA, Seattle, WA 98115-0070].
1989 Distribution of copepod nauplii during the early life stages of walleye pollock in Funka Bay and vicinity, Hokkaido. *In* Proc., Int. symp. on biology and management of walleye pollock, p. 217–240. Alaska Sea Grant Rep. 89-1, Univ. Alaska, Fairbanks.

Nakayama, N., Y. Watanabe, H. Ida, and K. Nagasawa
1987 Observation report of walleye pollock fishery in the south region of Hokkaido, the Pacific Ocean, 1987, no. 1, p. 1–13 [in Jpn.].

Nishimura, A., and J. Yamada
1984 Age and growth of larval and juvenile walleye pollock, *Theragra chalcogramma* (Pallas), as determined by otolith daily growth increments. J. Exp. Mar. Biol. Ecol. 82:191–205.

Ohtani, K., and K. Kido
1980 Oceanographic structure in Funka Bay. Bull. Fac. Fish., Hokkaido Univ. 31:84–114 [in Jpn., Engl. abstr.].

Paul, A.J.
1983 Light, temperature, nauplii concentrations, and prey capture by first feeding pollock larvae, *Theragra chalcogramma*. Mar. Ecol. Prog. Ser. 13:175–179.

Reed, R.K., L.S. Ineze, and J.D. Schumacher
1989 Estimation of the effects of the flow on dispersion of larval pollock, *Theragra chalcogramma*, in Shelikof Strait, Alaska. *In* Beamish, R.J., and G.A. McFarlane (eds.), Effects of ocean variability on recruitment and evaluation of parameters used in stock assessment models, p. 239–246. Can. Publ. Fish. Aquat. Sci. 108.

Sakurai, T.
1982 Reproductive ecology of walleye pollock *Theragra chalcogramma* (Pallas). Ph.D. diss., Hokkaido Univ., 178 p. [Engl. transl. avail. Alaska Fish. Sci. Cent., NMFS, NOAA, Seattle, WA 98115-0070.
1989 Reproductive characteristics of walleye pollock with special reference to the ovarian development, fecundity and social behavior. *In* Proc., Int. symp. on biology and management of walleye pollock, p. 97–115. Alaska Sea Grant Rep. 89-1, Univ. Alaska, Fairbanks.

Yoklavich, M.M., and K. Bailey
1989 Growth of larval and juvenile walleye pollock from Shelikof Strait, Gulf of Alaska, as determined from daily increments in otoliths. *In* Proc., Int. symp. on biology and management of walleye pollock, p. 241–251. Alaska Sea Grant Rep. 89-1, Univ. Alaska, Fairbanks.

Yoon, T.
1981 Reproductive cycle of female walleye pollock *Theragra chalcogramma* (Pallas), in the adjacent waters of Funka Bay, Hokkaido. Bull. Fac. Fish. Hokkaido Univ. 32:22–38 [in Jpn., Engl. abstr.].

Abstract.—Catch and effort data for the abalone *Haliotis rubra* fishery off Victoria, Australia, revealed that catches were allied to incentive (price); annual catch was proportional to effort. The robustness of the fishery can be attributed to low fishing mortality (F around 0.1) and a relatively high minimum length of capture (120 mm). Exploitation models showed that egg production was at least 50% that of unfished stocks. The analyses also showed that egg production was sensitive to variation in the growth parameters; fast-growing populations were more vulnerable to recruitment overfishing than slow-growing populations. For slow-growing populations, yields could be considerably increased without endangering recruitment. It is suggested, from the available evidence, that overfishing has been overemphasized in the collapse of abalone fisheries.

Exploitation models and catch statistics of the Victorian fishery for abalone *Haliotis rubra*

Paul E. McShane

Marine Science Laboratories, Fisheries Division, Ministry for Conservation and Environment
P.O. Box 114, Queenscliff, Victoria 3225, Australia
Present address: Fisheries Research Division, Ministry of Agriculture and Fisheries
P.O. Box 297, Wellington, New Zealand

Recent and comprehensive descriptions of the state of the world's abalone (*Haliotis* spp.) fisheries include reviews of the abalone fisheries in California (Tegner 1989, Tegner et al. 1989 and 1992), British Columbia (Breen 1986, Sloan and Breen 1988), Australia (Prince and Shepherd 1992), Mexico (Guzman del Proo 1992) and Japan (Mottet 1978). A unifying theme of these reviews is that abalone fisheries are characterised by initial high productivity followed by irreversible decline. Australia has developed an abalone fishery only recently by world standards. In Victoria, the fishery for the abalone *Haliotis rubra* is productive, valuable, and apparently stable (McShane 1990). The government limits the number of operators in the fishery (71), the annual catch (1460 metric tons) since 1988, and minimum length of capture (120 mm).

A fundamental objective of fisheries science is to predict the production from a fishery under varying management strategies. A common approach is to consider the yield from an individual or year-class of individuals under different fishing conditions (Beverton and Holt 1957, Ricker 1975, Gulland 1988, Megrey and Wespestad 1988). Such exploitation models treat populations as the sum total of their individual members; yield is expressed as yield-per-recruit because the absolute level of recruitment is rarely known. Yield-per-recruit models have been applied to several abalone fisheries including those for *H. discus discus* (Ishibashi and Kojima 1979), *H. iris* (Sainsbury 1982a), *H. laevigata* (Sluczanowski 1984), *H. kamtschatkana* (Breen 1986, Sloan and Breen 1988), *H. rufescens* and *H. corrugata* (Tegner et al. 1989), and the Tasmanian fishery for *H. rubra* (Nash 1992).

Although yield-per-recruit models can provide information on appropriate harvest strategies to maximize yield, the results provide no indication of the sustainability of a particular harvest regime. Because of the historical tendency of abalone fisheries to collapse, increasing attention has been focused on management strategies which maintain egg production as well as yield (Sluczanowski 1984 and 1986, Breen 1986, Sloan and Breen 1988, Tegner et al. 1989, Nash 1992).

In the present paper, the productivity of the fishery for abalone *Haliotis rubra* off Victoria, Australia, is described. To investigate the effect of growth rate, the relative yields of weight and eggs for two hypothetical populations of *H. rubra*, fast- and slow-growing, are examined. Management implications of my results are discussed for *H. rubra* as well as for other abalone species generally.

Materials and methods

Fishery statistics

Data on annual catch, effort, and price (whole weight) for the Victorian abalone fishery were obtained from

Manuscript accepted 18 December 1991.
Fishery Bulletin, U.S. 90:139–146 (1992).

fishermen's returns and unpublished information supplied by the Victorian Fisheries Division. Information on the history of the Victorian abalone fishery was extracted from unpublished records supplied by the Victorian Fisheries Division (Dep. Conserv. Environ., 240 Victoria Pde, Melbourne 3002; see also McShane 1990).

Table 1
Estimates of rates of natural mortality (M) for *Haliotis rubra*.

Reference	Location	M(yr^{-1})
Beinssen and Powell (1979)	northeast Victoria	0.20
Nash (1992)	northern Tasmania	0.24–0.29
Shepherd et al. (1982)	South Australia	0.21–0.36
Prince et al. (1988)	southeast Tasmania	0.1–0.7

Yield-per-recruit

Generalised fisheries exploitation models such as yield-per-recruit rely heavily on several assumptions. For any "unit stock":

1 Growth rates do not vary with time or density of the exploitable stock. Thus growth can be modeled with one set of parameters, e.g., the von Bertalanffy growth equation (Ricker 1975). Departures from these assumptions are known for abalone (e.g., Newman 1968, Sloan and Breen 1988, Day and Fleming 1992). However, for stocks of *H. rubra* the assumptions are reasonable (McShane et al. 1988a).

2 The rate of natural mortality is known and does not vary with age, time or density of the stock. Natural mortality is an important parameter in yield-per-recruit models, yet it is often the most difficult to estimate accurately. Natural mortality of *H. rubra* is constant with age after the first year (Shepherd et al. 1982, McShane 1991, Shepherd and Breen 1992). Estimates of natural mortality are in Table 1.

3 Fishing (F) and natural (M) mortality are independent of each other. For abalone fisheries, fishing mortality cannot be considered applicable to the entire fishery. Individual exploitation rates are applied to substocks opportunistically according to weather and incentive (Sluczanowski 1984, McShane and Smith 1989a). Incidental mortality can be caused by fishing, for example, wounding of undersize individuals (Sloan and Breen 1988, Tegner 1989, Shepherd and Breen 1992).

4 Recruitment is constant. Recruitment measured as the density of post-settlement individuals is highly variable for *H. rubra* (McShane et al. 1988b, McShane and Smith 1991). However, variation in growth rates of prerecruit individuals within a population acts to smooth out year-to-year variation in those *H. rubra* reaching harvestable size (McShane 1991).

5 Individuals of the same age have the same weight and susceptibility to capture. Individual variation in the relationships of weight to length and length to age has been demonstrated for *H. rubra*, but reasonable generalizations of these relationships can be made for the stock (McShane et al. 1988a, McShane and Smith 1992).

To investigate the effects of various rates of fishing, the yield-per-recruit equation of Ricker (1975:237) was used. The increase in length with age of *H. rubra* was computed using the von Bertalanffy growth equation

$$L_t = L_\infty(1 - e^{-Kt-t_0})$$

where L_t is the shell length in mm of *H. rubra* at age t years, L_∞ is the hypothetical maximum length, K is the Brody growth constant, and t_0 is the hypothetical age when length is zero.

In calculating the yield-per-recruit of *H. rubra* at various ages, I assumed that individuals were recruited in the year corresponding to the minimum length at capture. The biomass of an individual of age t years, W_t (g), was assumed to be $0.00016L_t^3$, where L_t is in mm (McShane et al. 1988a).

Egg-per-recruit

A simple age-structured model was used in which the relative abundance of females of age t years (N_t) was computed as

$$N_t = N_0 e^{-Zt}$$

where Z is total mortality (F + M). The egg production of a female of age t years (E_t) has a linear relationship with length (L_t) for *H. rubra* (McShane et al. 1988b) such that

$$E_t = 0.03\ L_t - 2.4$$

where E is fecundity in millions of eggs, and L is shell length in mm; L_t is derived from the von Bertalanffy growth equation.

Total egg production (E_{tot}) is given by

$$E_{tot} = \sum_{t=0}^{t=25} N_t \cdot E_t$$

where t = 25 years is assumed to be the maximum age

Table 2

Parameters used in computations of yield and egg-per-recruit. Values for slow- and fast-growing populations of *Haliotis rubra* are derived from mark-recapture studies in Victoria, Australia (McShane 1990). Estimates provided are the von Bertalanffy growth parameters (see text for details).

Parameter	Fast	Slow
L_∞	152.1	139.7
K	0.37	0.20
t_0	−0.01	−0.12

(McShane et al. 1988a). Egg production under various combinations of F, M, and minimum length-at-capture was compared with egg production of an unfished population (F = 0).

Fast- and slow-growing populations of *H. rubra* were modeled. The generalised growth parameters (Table 2) were based on empirical estimates (McShane et al. 1988a, McShane 1990, McShane and Smith 1992). Both yield and egg-per-recruit were expressed graphically as a function of minimum length-at-capture (i.e., length-at-recruitment) and F, using two rates of natural mortality estimated for *H. rubra* (M = 0.1 and 0.2, Table 1). Length-at-recruitment was varied (in 10 mm increments) from 100 mm to 140 mm for fast-growing populations and from 70 mm to 130 mm for slow-growing populations. The value of F was varied from 0.1 to 1.5. A smooth surface was interpolated through points in 3-dimensional plots of yield and egg-per-recruit, following the method of McLain (1974) in which negative exponential weights are computed from distances between points in a regular grid and the irregularly spaced data points in the X–Y plane (Wilkinson 1990).

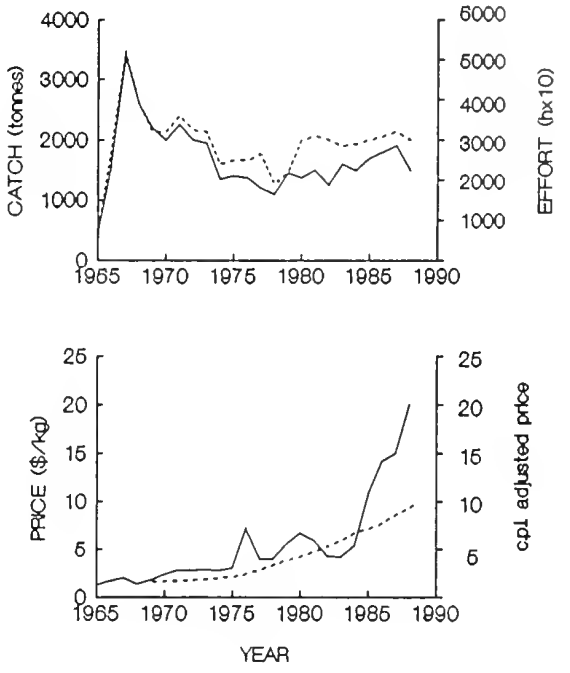

Figure 1

Comparison of (upper) annual catch and effort (dashed line), and (lower) actual price and CPI adjusted price (dashed line) of abalone *Haliotis rubra* in the fishery off Victoria, Australia, 1965–88.

Results

Fishery statistics

Annual variations in catch, effort, and value of the Victorian abalone fishery are described in Figure 1. Catch is highly correlated with effort (r 0.98, n 25, $P<0.001$). Although the catch rose in 1965–66 (accompanying development of export markets), the trend in both catch and effort is one of a slight but unalarming decrease followed by a slight increase during the 1980s. The introduction of catch quotas in 1988 is reflected in the decrease in catch in that year (Fig. 1). It is noteworthy that prior to 1988, price of abalone is a significant factor influencing the catch of the Victorian abalone fishery. Allowing for inflationary increases, the price of abalone doubled between 1967 and 1976–77 accompanying development of Japanese markets. Four exceptions to the steady rise in price have occurred. In 1967–68, a slight fall in price resulted from shipments of poor-quality abalone. Processing techniques were, at the time, in a developmental phase. Second, in 1976 an increase in price occurred concomitant with high demand by export markets and increased competition between processors for supply. The introduction of a competitive product, the Chilean "loco" *Concholepas concholepas*, on Asian markets coupled with buyer resistance to elevated prices of Australian abalone resulted in a decrease in price during 1977 (Stanistreet 1978). Note that there is a lag between price variation and catch and effort; the relative decrease in catch and effort in 1978 reflects the price drop in 1977 (Fig. 1). Buyer resistance also affected the price of abalone in 1981–82 and led to a decrease in effort and catch during this period.

More recently, the collapse of the large Mexican abalone fishery and the imposition of catch quotas on the Tasmanian and South Australian abalone fisheries (Prince and Shepherd 1992) decreased the world supply of abalone and increased the competitiveness of Victorian suppliers (McShane 1990). This and a decrease in the relative value of the Australian currency against

that of export markets resulted in a rapid increase in price of abalone during the 1980s.

Exploitation models

The yield and egg-production-per-recruit for individuals of various lengths under various levels of exploitation are shown for fast-growing (Fig. 2) and slow-growing (Fig. 3) populations of *H. rubra*. It can be seen that the relative yield-per-recruit is greater for fast-growing compared with slow-growing populations of *H. rubra*. The minimum lengths producing maximum yield-per-recruit are 130 mm for fast-growing populations and 120 mm for slow-growing populations. These maxima occurred at high exploitation rates (F~1) and were independent of the natural mortality rates applied to the model (0.1, 0.2). Natural mortality had an obvious effect on the decline of yield-per-recruit with minimum length. For M = 0.2, yield-per-recruit was less sensitive to variation in minimum length compared with M = 0.1. Note that at realistic levels of F (0.1, McShane and Smith 1989a), yield-per-recruit is comparatively low (Figs. 2 and 3). For such low rates of exploitation, the model shows that for fast-growing (in contrast to slow-growing) populations, yield-per-recruit is relatively insensitive to variation in the minimum length-at-capture. Similar results were obtained from yield-per-recruit analyses of other species of abalone, provided that rates of fishing mortality are relatively low (F < 0.3) (Ishibashi and Kojima 1979, Sainsbury 1982a, Sluczanowski 1984, Breen 1986, Sloan and Breen 1988, Tegner et al. 1989, Nash 1992).

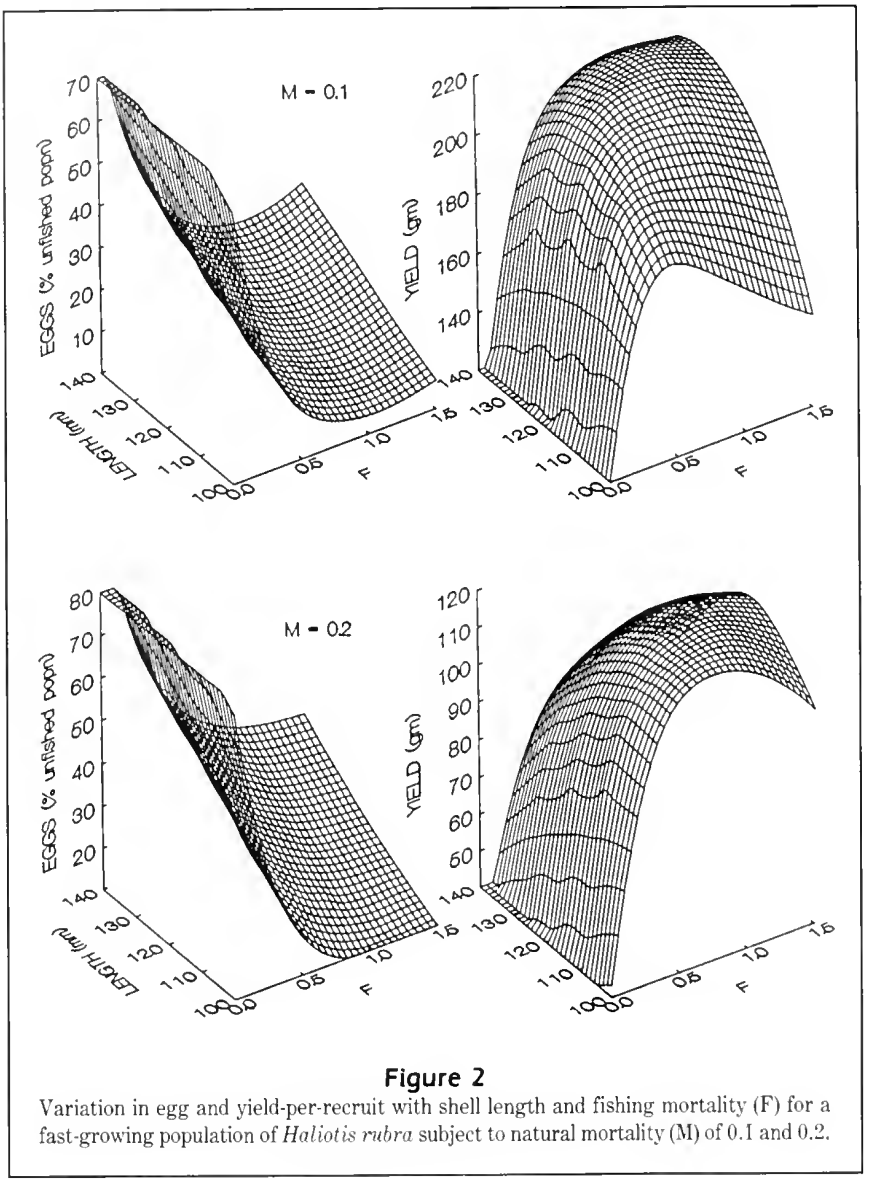

Figure 2
Variation in egg and yield-per-recruit with shell length and fishing mortality (F) for a fast-growing population of *Haliotis rubra* subject to natural mortality (M) of 0.1 and 0.2.

For fast-growing populations, exploitation rates producing maximum yield-per-recruit are associated with minimum egg production. Indeed, values of F > 0.3 are associated with egg production of less than 50% of an unfished population. Low egg production may cause recruitment failure in abalone stocks (Sloan and Breen 1988, Tegner et al. 1989). Egg production increases with minimum length; results of other studies show that fecundity of *H. rubra* is directly related to length (McShane et al. 1988b, Prince et al. 1988).

Egg production is less sensitive to variation in fishing mortality in slow-growing than in fast-growing populations of *H. rubra*. For minimum lengths over 120 mm, egg production rates are over 50% of an unfished population. At F = 0.1, egg production is over 60% of that of an unfished population for both M = 0.1 and 0.2.

Discussion

Catch levels for the Victorian abalone fishery suggest a robust fishery. But catch data are poor indicators of the stock abundance of abalone because fishermen can maintain catch rates by exploiting substocks (Breen

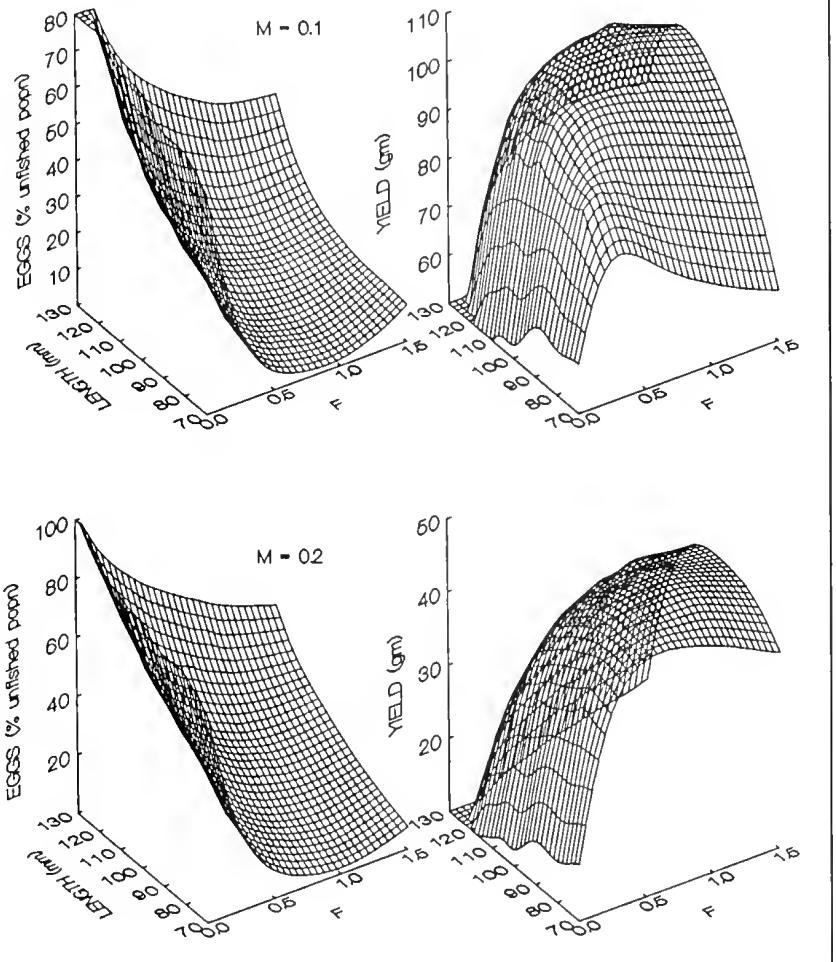

Figure 3

Variation in egg and yield-per-recruit with shell length and fishing mortality (F) for a slow-growing population of *Haliotis rubra* subject to natural mortality (M) of 0.1 and 0.2.

1980, Sloan and Breen 1988, McShane and Smith 1989a). Yet the available evidence is that the fishery is underexploited (McShane and Smith 1989ab; McShane 1990). Catches of *H. rubra* can be adjusted opportunistically by increasing effort when incentive (price) is high. Although Victorian abalone fishermen have the capacity to serially deplete substocks, rates of exploitation of *H. rubra* are generally low (see McShane and Smith 1989a). A surplus of harvestable individuals is maintained in substocks by the conservative fishing practices employed by Victorian abalone fishermen (McShane and Smith 1989a). With low exploitation rates ($F<0.3$), the egg-per-recruit model shows that there is adequate egg production by individuals above the present legal minimum length of 120 mm. However, as a consequence of reaching harvestable size in about 4 years, prerecruit individuals from fast-growing populations have fewer years of egg production than those *H. rubra* from slow-growing populations which reach harvestable size in about 10 years. Fast-growing populations of *H. rubra* are therefore vulnerable to recruitment overfishing should exploitation rates increase ($F>0.3$). This is unlikely in the Victorian abalone fishery because both the number of operators and the annual catch are controlled.

Most abalone fisheries are generally subject to pulse fishing. Substocks are fished, then left to recover (Sluczanowski 1984, McShane and Smith 1989a). Fast-growing populations are important in this regard because they can be fished at a higher frequency than slow-growing populations (Sluczanowski 1984). Thus fast-growing populations are subject to higher exploitation rates than slow-growing populations. Slow-growing populations are often characterised by large accumulations of prerecruit abalone which are food-limited (Sloan and Breen 1988, McShane 1990). Egg-per-recruit analysis shows that even at extraordinarily high rates of fishing mortality ($F>1$) egg production in slow-growing populations of *H. rubra* is above the assumed "safe" level of 50% of an unfished population (Sloan and Breen 1988, Tegner et al. 1989). The model shows that slow-growing populations could be "fished down" at a reduced size limit and high exploitation rate without endangering egg production. Such a harvesting strategy could reduce the abundance of the accumulated stock to a level where food is no longer a limiting factor (McShane and Smith 1989b). To date in Victoria, such slow-growing stocks are rarely fished because of a paucity of abalone of harvestable size (McShane and Smith 1989b).

Why is the Victorian fishery for *H. rubra* apparently robust in contrast to other abalone fisheries? The viability of the Victorian fishery can be attributed to a relatively low number of operators (limited entry has operated in Victoria since 1968) and an associated low exploitation rate (see McShane and Smith 1989a). A minimum length that maintains a safe level of egg production provides further safeguards against recruit-

ment overfishing, as does an annual catch quota. However, size limits introduced to the California abalone fishery were also conservative but failed to arrest the decline of the fishery (Tegner 1989, Tegner et al. 1992). The combination of high commercial effort and intense recreational and illegal harvest resulted in a removal of surplus stocks in the California (Tegner et al. 1992) and Mexican (Guzman del Proo 1992) abalone fisheries. Unrestrained recreational and illegal harvest remains a threat to the Victorian fishery, but with a comparatively low human population and a relatively inaccessible coastline the Victorian abalone fishery is less vulnerable to noncommercial overfishing than the California or Mexican abalone fisheries (McShane 1990).

While fishing can deplete stocks, there are a multitude of other factors that affect the abundance of abalone. For example, overfishing could not explain the recruitment failure which occurred in the abalone fishery of British Columbia (Breen 1986, Sloan and Breen 1988). Recruitment failure in various species of abalone has been attributed to sea temperature anomalies (Hayashi 1980, Forster et al. 1982, Shepherd et al. 1985) or natural variation (Sainsbury 1982b; see also McShane and Smith 1991). The collapse of the California abalone fishery for *H. rufescens* coincided with predator release (Lowry and Pearse 1973, Hines and Pearse 1982, Tegner 1989, Tegner et al. 1989, 1992). The importance of predation in controling abalone abundance is further exemplified by the recovery of stocks of *H. cracherodii* concomitant with a reduction in the abundance of major predators (Davis et al. 1992). The decrease in abundance of some California populations of abalone (*H. rufescens*, *H. cracherodii*) was attributed to low food availability caused by El Niño events (Tegner and Dayton 1987, Tegner et al. 1989), competition with other herbivores, and kelp harvest (Davis et al. 1992). Starvation in abalone causes a decrease in reproductive effort (Cox 1962) and an increased susceptibility to disease, both of which can cause a severe decline in stocks (Haaker et al. 1992, Tissot 1992). A major factor in the reduced abundance of abalone stocks in Japan is nearshore pollution (I. Hayashi, Igarashi-Jutaku 2-205, Niigata, Japan, pers. commun. 1990), a factor also implicated in the decline of California abalone stocks (see Tegner et al. 1992).

Variation in abiotic factors such as temperature have demonstrable effects on the survival and growth of exploited species (Cushing 1988). Such factors, apart from seasonal variation, vary stochastically and introduce uncertainty in fisheries management (Megrey and Wespestad 1988, Walters and Collie 1988). Faced with this uncertainty, fishery managers must proceed cautiously and gain a better understanding of the ecology of exploitable species, particularly of abalone which have a history of unexplained stock collapse.

Acknowledgments

I thank Dr. Paul Breen for helpful discussion and constructive comments on the manuscript. Drs. Linda Jones and Scoresby Shepherd offered helpful suggestions as did an anonymous reviewer.

Citations

Beinssen, K., and D. Powell
1979 Measurement of natural mortality in a population of blacklip abalone, *Notohaliotis ruber*. Rapp. P.-V. Reun. Cons. Int. Explor. Mer 175:23–26.

Beverton, R.J.H., and S.J. Holt
1957 On the dynamics of exploited fish populations. Fish. Invest. Ser. II Mar. Fish. G.B. Minist. Agric. Fish. Food 19, 533 p.

Breen, P.A.
1980 Measuring fishing intensity and annual production in the abalone fishery of British Columbia. Fish. Res. Board Can. Tech. Rep. 947, 49 p.
1986 Management of the British Columbia fishery for northern abalone (*Haliotis kamschatkana*). *In* Jameison, G.S., and N. Bourne (eds.), North Pacific workshop on stock assessment and management of invertebrates, p. 300–312. Can. Spec. Publ. Fish. Aquat. Sci. 92.

Cox, K.W.
1962 California abalones, family Haliotidae. Calif. Fish Game, Fish Bull. 118, 138 p.

Cushing, D.H.
1988 The study of stock and recruitment. *In* Gulland, J.A. (ed.), Fish population dynamics, 2d ed., p. 105–128. Wiley, NY.

Davis, G.E., D.V. Richards, P.L. Haaker, and D.O. Parker
1992 Mass mortality and fishery management of black abalone, *Haliotis cracherodii*, in Southern California. *In* Shepherd, S.A., M.J. Tegner, and S.A. Guzman del Proo (eds.), Abalone of the world: Biology, fisheries and culture. Blackwells, Oxford (in press).

Day, R.W., and A. Fleming
1992 The determinants and measurement of abalone growth. *In* Shepherd, S.A., M.J. Tegner, and S.A. Guzman del Proo (eds.), Abalone of the world: Biology, fisheries and culture. Blackwells, Oxford (in press).

Forster, G.R., G.W. Potts, and R. Swinfen
1982 Changes in the ormer populations of Guernsey and Jersey. J. Mar. Biol. Assoc. U.K. 62:717–727.

Gulland, J.A.
1988 Fish population dynamics, 2d ed. Wiley-Interscience, NY.

Guzman del Proo, S.A.
1992 Una revision sobre la biologia y pesqueria del abulon (*Haliotis* spp.) en Mexico. *In* Shepherd, S.A., M.J. Tegner, and S.A. Guzman del Proo (eds.), Abalone of the world: Biology, fisheries and culture. Blackwells, Oxford (in press).

Haaker, P.L., D.V. Richards, C. Friedman, G. Davis, D.O. Parker, and H. Togstad
1992 Abalone withering syndrome and mass mortality of black abalone, *Haliotis cracherodii*, in California. *In* Shepherd, S.A., M.J. Tegner, and S.A. Guzman del Proo (eds.), Abalone of the world: Biology, fisheries and culture. Blackwells, Oxford (in press).

Hayashi, I.
1980 Structure and growth of a shore population of the ormer, *Haliotis tuberculata*. J. Mar. Biol. Assoc. U.K. 60:431–437.

Hines, A.H., and J.S. Pearse
1982 Abalones, shells and sea otters: Dynamics of prey populations in central California. Ecology 63:1547–1560.

Ishibashi, K., and H. Kojima
1979 A study on the stock of Japanese black abalone, *Haliotis discus discus* in Tokushima Prefecture—III. Analysis on abalone fisheries management. Bull. Tokai Reg. Fish. Res. Lab. 98:65–75.

Lowry, L.F., and J.S. Pearse
1973 Abalone and sea urchins in an area inhabited by sea otters. Mar. Biol. (Berl.) 23:213–219.

McLain, D.H.
1974 Drawing contours from arbitrary data points. Computer J. 17:318–324.

McShane, P.E.
1990 The fisheries ecology of Victorian abalone. Ph.D. thesis, La Trobe Univ, Melbourne, 364 p.
1991 Density dependent mortality of the abalone *Haliotis rubra* (Mollusca:Gastropoda). Mar. Biol. (Berl.) 110:385–389.

McShane, P.E., and M.G. Smith
1989a Direct measurement of fishing mortality in abalone (*Haliotis rubra*) off southeastern Australia. Fish. Res. 8: 93–102.
1989b Victorian abalone fishery in good shape. Aust. Fish. 48:20–25.
1991 Recruitment variation in sympatric populations of the abalone *Haliotis rubra* (Mollusca:Gastropoda). Mar. Ecol. Prog. Ser. 73:203–210.
1992 Shell growth checks are unreliable indicators of age of the abalone *Haliotis rubra* (Mollusca:Gastropoda). Aust. J. Mar. Freshwater Res. (in press).

McShane, P.E., M.G. Smith, and K.H.H. Beinssen
1988a Growth and morphometry in abalone (*Haliotis rubra*) from Victoria. Aust. J. Mar. Freshwater Res. 39:161–6.

McShane, P.E., K.P. Black, and M.G. Smith
1988b Recruitment processes in *Haliotis rubra* (Mollusca: Gastropoda) and regional hydrodynamics in southeast Australia imply localised dispersal of larvae. J. Exp. Mar. Biol. Ecol. 124:175–203.

Megrey, B.A., and V.G. Wespestad
1988 A review of biological assumptions underlying fishery assessment models. *In* Wooster, W.S. (ed.), Fishery science and management—Objectives and limitations, p. 31–74. Lect. Notes Coastal Estuarine Stud. 28.

Mottett, M.G.
1978 A review of the fishery biology of abalones. Wash. Dep. Fish. Tech. Rep. 37, 78 p.

Nash, W.J.
1992 Determination of appropriate size limits by egg-per-recruit analysis, with an assessment of size limits as a management tool for blacklip abalone (*Haliotis rubra*) in Tasmania. *In* Shepherd, S.A., M.J. Tegner, and S.A. Guzman del Proo (eds.), Abalone of the world: Biology, fisheries and culture. Blackwells, Oxford (in press).

Newman, G.G.
1968 Growth of the South African abalone *Haliotis midae*. S. Afr. Div. Sea Fish. Invest. Rep. 67:1–24.

Prince, J.D., and S.A. Shepherd
1992 Australian fisheries for abalone and their management. *In* Shepherd, S.A., M.J. Tegner, and S.A. Guzman del Proo (eds.), Abalone of the world: Biology, fisheries and culture. Blackwells, Oxford (in press).

Prince, J.D., T.L. Sellers, W.B. Ford, and S.R. Talbot
1988 Recruitment, growth, mortality and population structure in a southern Australian population of *Haliotis rubra* (Mollusca: Gastropoda). Mar. Biol. (Berl.) 100:75–82.

Ricker, W.E.
1975 Computation and interpretation of biological statistics of fish populations. Bull. Fish. Res. Board Can. 191, 382 p.

Sainsbury, K.J.
1982a Population dynamics and fishery management of the paua, *Haliotis iris*. 2. Dynamics and management as examined using a size class population model. N.Z. J. Mar. Freshwater Res. 16:163–173.
1982b Population dynamics and fishery management of the paua, *Haliotis iris*. 1. Population structure, growth, reproduction and mortality. N.Z. J. Mar. Freshwater Res. 16:147–161.

Shepherd, S.A., and P.A. Breen
1992 Mortality in abalone: Its estimation, variability and causes. *In* Shepherd, S.A., M.J. Tegner, and S.A. Guzman del Proo (eds.), Abalone of the world: Biology, fisheries and culture. Blackwells, Oxford (in press).

Shepherd, S.A., G.P. Kirkwood, and R.L. Sandland
1982 Studies on southern Australian abalone (genus *Haliotis*). III. Mortality of *H. laevigata* and *H. ruber*. Aust. J. Mar. Freshwater Res. 33:265–272.

Shepherd, S.A., P.S. Clarkson, and J.A. Turner
1985 Studies on southern Australian abalone (genus *Haliotis*). V. Spawning, settlement and early growth of *H. scalaris*. Trans. R. Soc. S. Aust. 109:61–62.

Sloan, N.A., and P.A. Breen
1988 Northern abalone, *Haliotis kamtschatkana*, in British Columbia: Fisheries and synopsis of life history information. Can. Spec. Publ. Fish. Aquat. Sci. 103, 46 p.

Sluczanowski, P.R.
1984 A management oriented model of an abalone fishery whose substocks are subject to pulse fishing. Can. J. Fish. Aquat. Sci. 41:1008–1014.
1986 A disaggregate model for sedentary stocks: The case of South Australian abalone. *In* Jamieson, G.S., and N. Bourne (eds.), North Pacific workshop on stock assessment and management of invertebrates, p. 393–401. Can. Spec. Publ. Fish. Aquat. Sci. 92.

Stanistreet, K.
1978 Abalone sales prospects may be on the mend. Aust. Fish. 37:29–30.

Tegner, M.J.
1989 The California abalone fishery: Production, ecological interactions, and prospects for the future. *In* Caddy, J.F. (ed.), Scientific approaches to management of invertebrate stocks, p. 401–420. J. Wiley & Sons, NY.

Tegner, M.J., and P.K. Dayton
1987 El Niño effects on southern California kelp forest communities. Adv. Ecol. Res. 17:243–279.

Tegner M.J., P.A. Breen, and C.E. Lenner
1989 Population biology of red abalones, *Haliotis rufescens*, in southern California and management of the red and pink, *H. corrugata*, abalone fisheries. Fish. Bull., U.S. 87:313–339.

Tegner, M.J., J.D. DeMartini, and K.A. Karpov
1992 The California red abalone fishery: A case study in complexity. *In* Shepherd, S.A., M.J. Tegner, and S.A. Guzman del Proo (eds.), Abalone of the world: Biology, fisheries and culture. Blackwells, Oxford (in press).

Tissot, B.N.
1992 Mass mortality of the black abalone (*Haliotis cracherodii*) in the California Channel Islands. *In* Shepherd, S.A., M.J. Tegner, and S.A. Guzman del Proo (eds.), Abalone of the world: Biology, fisheries and culture. Blackwells, Oxford (in press).

Walters, C.J., and J.S. Collie
1988 Is research on environmental factors useful to fisheries management? Can. J. Fish. Aquat. Sci. 45:1848–1854.

Wilkinson, L.
1990 SYGRAPH: The system for graphics. SYSTAT, Inc., Evanston, IL.

Abstract.—On 1 October 1986, New Zealand introduced Individual Transferrable Quota (ITQ) management for most of its fisheries. ITQ management was implemented to address overfishing, overcapitalization, and excess government regulation. Quotas were based on catch histories, with a quota "buyback" (costing $42.4 million NZ) and prorated cuts to achieve total allowable catch (TAC) levels indicated by preliminary stock assessments. Fixed amounts of quota (defined by weight) were issued in perpetuity. Annual stock assessments are conducted. Government stated that it would buy or sell quota at market-determined prices in order to adjust TACs. On 1 April 1990, ITQs were redefined as proportions of annual TACs (known as "proportional ITQs"). Government extracts resource rent.

To date, there is little evidence of improvement in the condition of the fisheries resources. It is difficult to determine the economic effects of ITQ management; however, economic conditions have worsened due to factors which are unrelated to ITQ management. Revenues to government from the ITQ system have exceeded total costs, but there would have been a deficit if government had purchased quota to reduce TACs to the levels indicated by stock assessments. Government regulation has not been reduced.

Although there is general support for ITQ management in New Zealand, many problems have been encountered: quota overruns resulting from bycatch; inadequate stock assessment capability; disagreement over the level of resource rentals; and failure of government to enter the marketplace to reduce TACs when necessary.

Manuscript accepted 16 December 1991.
Fishery Bulletin, U.S. 90:147–160 (1992).

ITQs in New Zealand: The era of fixed quota in perpetuity

Michael P. Sissenwine
Headquarters, National Marine Fisheries Service, NOAA, Silver Spring, Maryland 20910

Pamela M. Mace
P O Box 7357, Silver Spring, Maryland 20907

The idea of managing fisheries by Individual Transferable Quotas (ITQs) is not new. Christy (1973) suggested the method, and Maloney and Pearce (1979) provided the economic rationale for it. Until recently, there were only a few applications of ITQ management (e.g., southern bluefin tuna, Geen and Nayar 1988; Lake Erie freshwater fisheries, Muse and Schelle 1989). One application that has received considerable attention is the ITQ management of fisheries in New Zealand. Two reasons for this attention are that (1) New Zealand is applying ITQ management on a more comprehensive national scale than ever before, and (2) New Zealand officials have done a good job of describing their ITQ system to the rest of the world (e.g., Clark et al. 1988, Crothers 1988). New Zealand's early experience with ITQ management is of interest to the United States because ITQ management is being planned or discussed for several fisheries (e.g., Pacific sablefish and halibut, South Atlantic wreckfish, and East Bering Sea groundfish). It has recently been implemented for Mid-Atlantic surf clams and ocean quahogs. This paper reviews the potential benefits and problems of New Zealand's ITQ management system based on firsthand observations of the authors.[1] The main body of the paper was completed in mid-1990. A postscript has been added to reflect more recent events through 1991.

Before describing the fisheries management situation in New Zealand, the authors want to caution that by pointing out problems, they are not condemning the ITQ system. Despite problems, there seems to be a general acceptance that ITQs are the way New Zealand fisheries will be managed. There is no widespread sentiment, either within government or the industry, to repeal ITQs. A regional poll conducted shortly after implementation of the ITQ system (Dewees 1989) found that the majority of the fishing industry favored it. It would be interesting to repeat the poll nationwide now. The authors are of the opinion that the industry would not want to return to the fisheries management situation (or lack thereof) that preceded ITQs.

New Zealand fisheries setting

Fisheries have always been important to New Zealand. Legend has it that a Maori (the native people of New Zealand) pulled up the North Island of New Zealand from the sea on a hook-and-line while fishing. Fishing was so important that the

[1] The authors of this paper were fortunate to have the opportunity to observe ITQ management in New Zealand firsthand. The first author made six trips to New Zealand during the first three and a half years of ITQ management, including approximately seven months employed by the New Zealand Fisheries Research Centre. The second author was employed by the New Zealand Fisheries Research Centre from August 1986 until May 1989. Both authors maintain contact with the fisheries management situation in New Zealand through their previous affiliations.

Treaty of Waitangi between the Maoris and the British, signed in 1840, deeds the Maoris' rights to their traditional fisheries.[2]

Although New Zealand is a small nation in terms of population and land area, its Exclusive Economic Zone (EEZ) of 1.3 million nm^2 (more than 15 times the land mass) is the fourth largest in the world. Most of the EEZ is deep; 72% of the zone has waters deeper than 1000 m, so it is difficult to judge the total potential yield.

Historically, New Zealand fisheries were restricted to coastal waters (<200 m in depth) and yielded less than 50,000 tons annually (Fig. 1). Deepwater fisheries (to 1500 m) developed during the 1970s, and the yield increased rapidly to a peak of about 500,000 tons in 1977. Most of the increase was due to foreign fishing. In 1978, New Zealand extended its jurisdiction to 200 miles. The yield decreased sharply for a few years, but it has since returned to about 500,000 tons. Since extended jurisdiction, domestic fishing has replaced almost all of the foreign fishing. However, it should be noted that much of the catch recorded as domestic is actually taken by foreign vessels and foreign crews under contract to New Zealand firms. In 1987, the first sale value of the catch was about $350 million NZ.[3] The export value of New Zealand fisheries products increased from $50 million NZ in 1977 to $676 million NZ in 1987. The 1987 figure represented about 6% of New Zealand's total exports (Bevin et al. 1989).

Fisheries management began with the Fisheries Act of 1908 which established authority for input controls, such as limited entry licensing, closed areas and seasons, controls on minimum fish sizes, and requirements for vessels to land at specific ports. The actual basis for the number of licenses allowed in the fisheries is unclear. Restrictive licensing was repealed in 1963.

New Zealand established authority for output controls (i.e., total allowable catches, or TACs) in 1978 when it extended jurisdiction. At the same time, a moratorium was placed on new fishing permits for rock lobsters and scallops. In 1980 the moratorium was extended to finfish permits. In 1983, a Deepwater Enterprise Allocation system was established. Deepwater Enterprise Allocations were a forerunner of ITQs. Quota for each of the species fished in deep water (below about 200 m) was allocated to nine companies which had already invested in deepwater harvesting and shoreside processing capability. The motivation for the Deepwater Enterprise Allocations was not over-

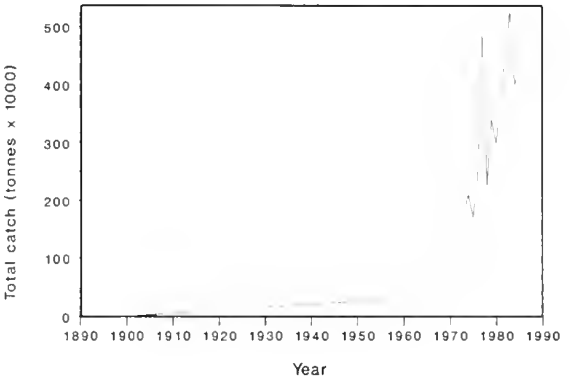

Figure 1
Annual yields from New Zealand EEZ, 1890–1990.

fishing or overcapitalization. It was intended to prevent these ills from occurring (Clark et. al. 1988) Presumably, it also encouraged investment in the deepwater fisheries and hastened the replacement of foreign fishing activity by domestic fishing. The quotas were initially awarded for a period of ten years, but were made permanent in 1985. Although the government had no authority to make quotas transferable, there was considerable de facto trading and leasing of shares among the nine companies.

New Zealand implemented ITQs for most of its fisheries in October 1986. The Government gave several reasons for introducing ITQs. According to Crothers (1988), "Fishery managers were faced with an open access inshore fishery under severe biological and economic pressure . . . many of the prime species were experiencing growth and probably recruitment overfishing . . . and the industry was overcapitalized, crippled by excessive government management intervention, and rapidly declining economic performance." A government publication titled "Inshore Finfish Fisheries: Proposed Policy for Future Management" (Anonymous 1984) stated that ". . . a broad description of the problem of the inshore fishery is that the major fish stocks are too low as a result of overfishing . . . there has been a moratorium on new entries to the inshore . . . part-time fisherman were removed administratively . . . this had a negligible effect on fishing effort or catch . . . the harvesting sector remains overcapitalized."[4] In summary, the government turned to

[2] The fishing heritage of the Maori people and the Treaty of Waitangi are more than a matter of passing interest. As will be discussed later in the paper, the Treaty of Waitangi has complicated implementation of ITQ management.

[3] Economic values are expressed in New Zealand dollars which equal about $0.58 U.S.

[4] While the removal of part-time fishermen may have had a negligible effect on fishing effort or catch, it did have social ramifications. Many of the part-time fishermen were Maoris. It could be argued that their removal was one of the factors that stimulated them to attempt to regain access to the fisheries through the courts under the Treaty of Waitangi.

ITQs because of perceived overfishing, overcapitalization, and crippling excess regulation.

Undoubtedly, the success of the Deepwater Enterprise Allocation system contributed to the decision to use ITQs to solve the perceived problems in the inshore fisheries. Clark et. al. (1988) labeled it as a model for inshore fisheries management. There was also a belief that problems could be solved only by applying some form of output controls (Sandrey and O'Donnell 1985), and that input controls had already been attempted and had failed (Crothers 1988). In fact, it is unclear how seriously input controls had been attempted, or how severely the fisheries were overfished or overcapitalized.[5] Of course, the failures of input controls or overfishing and overcapitalization are not prerequisites for ITQ management. It is better to put in place a property rights system, such as ITQs, before problems occur.

Implementation of ITQ management in New Zealand

The idea behind ITQ management of fisheries is quite simple. ITQs are intended to conserve the fisheries resource by setting a TAC. They increase economic efficiency by assigning ownership of portions of the TAC, thus eliminating competition between harvesters to obtain the largest possible share of the TAC. By making quota transferable, ownership should eventually rest with the most efficient harvesters, since they should be able to afford to pay the highest price to purchase quota. Excess capital is likely to be removed from the fishery as more efficient operators buy up enough quota to make optimal use of the capital that remains in the fishery.

In New Zealand, implementation of the ITQ management system began with stock assessments of all of the fisheries resources to be managed. Initially, this involved assessments of 153 management units, composed of 26 species-groups in up to 10 management areas per species-group. By April 1990, there were 169 management units, composed of 29 species-groups (45 species) and 10 major management areas. Forty-seven of these management units are of minor importance (in terms of amount of quota) with TACs established for administrative purposes only. There are insufficient data to conduct meaningful assessments for most management units. Initially, most of the TACs were based on one of two methods of estimation: (1) They were equated to landings in the most recent year(s) for which information was available, or (2) they were equated to the product of a trawl-survey biomass estimate and a stock productivity value in the range 0.05–0.15. The first method probably produced overly-optimistic estimates of sustainable yields since recent landings were often the highest on record. On the other hand, the second method may have resulted in overly-conservative estimates, since biomass estimates were conservative (due to conservative assumptions about the vulnerability of fish to trawl gear) and a maximum productivity level of 0.15 is low (although there are notable exceptions such as orange roughy). Other methods used to estimate a few of the initial TACs may have produced reasonable results. These included use of tagging data, yield-per-recruit analysis, and stock reduction analysis.

For the deepwater fisheries, TACs generally matched the sum of quota allocations under the Deepwater Enterprise Allocation system. These Deepwater Enterprise Allocations were converted directly to ITQs. In the inshore, a provisional maximum allocation was determined separately for each fishing permit holder as the average catch of that individual's best two out of the three fishing years of October–September 1981–82, 1982–83, and 1983–84. These catch histories were the basis for the initial allocation of quota defined in fixed amounts by weight. Since the allocations were based on the average of the best two-out-of-three years, it was likely that the "Sum of Catch Histories" (SCH) would exceed the maximum annual catch that had occurred during the base period. In addition, fishermen were given the right to appeal their allocations if they felt it did not represent their true share of the fisheries. Of the 1800 fishermen notified of their catch histories, about 1400 appealed, and many of these have subsequently increased their allocations. The appeals process is still ongoing even though the ITQ system has been fully implemented for more than three years.

If the SCH was equal to or less than the TAC, permit holders were allocated their catch histories as ITQ in perpetuity. TACs in excess of the SCHs were offered for sale. When the SCH exceeded the TAC, there was

[5] It is interesting that there were virtually no input controls on New Zealand fisheries during 1963–78 for rock lobsters and scallops and 1963–80 for finfish. Even after moratoria on new licenses were implemented in 1978 and 1980, there were no additional direct controls on fishing effort (e.g., limits on the number of days that could be fished), although there were some indirect controls (e.g., closed areas).

With regard to overcapitalization, the government estimated that the harvesting sector was overcapitalized by $28 million NZ in 1983, although details of how overcapitalization was defined and how it was estimated are lacking (Anonymous 1984). Investment (book value) in the harvesting sector in 1983 was estimated as $142 million NZ (Bevin et al. 1989). This indicates that the harvesting sector was overcapitalized by about 20%, which is almost certainly less than some North American fisheries (e.g., Mid-Atlantic surf clams, New England groundfish, Pacific halibut).

Clearly some inshore resources were overfished (e.g., snapper), but it is difficult to evaluate how serious the overfishing problem was in general. Stock assessment information is quite limited, as will be discussed later in this paper.

a Government buyback of quota. Crothers (1988) indicates that the buyback was to facilitate an orderly "rationalization" of the industry, and to help create a climate of support for ITQ management. Clark et al. (1988) indicates the buyback was to reduce the mismatch of fleet capacity to available catch. If the Government was not able to buy back as much quota as was necessary, prorated cuts in quota were made. This threat of proration probably encouraged permit holders to be more reasonable in determining the selling price of their provisional allocation of quota.

The buyback cost the Government $42.4 million NZ to purchase 15,700 tons of quota (the annual amount the owners would have been entitled to catch in perpetuity). Prorated cuts were made to reduce quota by an additional 9500 tons. Presumably, the Government felt that the potential increase in value of the fishery when overfished stocks recovered merited the cost of the buyback and the short-term losses that resulted from prorated cuts.

Relatively few stocks accounted for most of the cost of the buyback. Table 1 indicates that more than 85% of funds spent on the buyback were used to buy quota for four species (mostly in one management area where traditional inshore fisheries are prosecuted). Nearly 50% were used for the snapper fisheries. The total reduction from SCHs to TACs for the 1986–87 fishing year (which began 1 October 1986) was 6%. For the 21 species that were involved in the buyback and prorated cuts, the reduction was about 24%. For the four primary species involved, the reduction was 54%.

Table 2 gives detailed information for the four primary species affected by the buyback and prorated costs. It is noteworthy that, in all cases, the SCH greatly exceeded the actual catch in the year just prior to ITQs (1985–86). This means that a portion of the quota that was bought back probably would not have been caught. In fact, in all cases the actual catch in the first year of the ITQ system (1986–87) was lower than the TAC. This suggests there may have been a declining trend in the resource condition from the base period when SCHs were established to the point in time when ITQs were implemented. It also seems likely, in the authors opinion, that SCHs were inflated by the industry (i.e., a moral hazard phenomenon) in anticipation of ITQs. As a result, the government may have spent much of the $42.4 million NZ to buy back quota which would not have been caught; therefore, the buyback may have had relatively little effect on fishing mortality rates.

Since ITQ management was implemented in 1986, stock assessments have been conducted annually for each management unit, to the extent that the available data allow. These assessments are conducted in Fisheries Assessment Meetings (FAMs) during the middle

Table 1

Buybacks and prorated cuts for implementation of New Zealand ITQ management.

Species	Tons reduced (1000s)	Payments ($NZ millions)	% Total $
Snapper	5.7	19.4	45.7
Rig	3.0	7.7	18.1
School shark	3.7	4.3	10.0
Hapuku bass	1.7	5.1	12.0
17 other	11.0	5.9	14.2
Total	25.1	42.4	100.0

Table 2

Relevant information for the four main species included in the buyback and prorated cuts under New Zealand ITQ management. Values in thousands of tons or $millions NZ.

	Hapuku bass	Rig	School shark	Snapper
Tons reduced	1.7	3.0	3.7	5.7
Cost of buyback	5.1	7.7	4.3	19.4
SCH (sum of catch histories)	3.3	4.4	6.0	12.2
TAC 1986–87 (total allowable catch)	1.7	1.4	2.4	6.5
Catch 1985–86	1.7	2.9	3.7	8.6
Catch 1986–87	1.1*	1.1*	1.9*	5.4*

* Provisional

of the fishing year (April or May) in order to recommend TAC adjustments for the next fishing year (beginning in October). New Zealand law requires that the TAC be set to produce the maximum sustainable yield (MSY), as qualified by relevant factors including economic and environmental considerations and regional or global standards. Methods for estimating yields have been refined since 1985 when the initial TACs were calculated. New Zealand scientists now interpret MSY in two alternative ways: a static interpretation in which MSY is the maximum constant yield (MCY) that can be taken year after year from a fishery, and a dynamic interpretation in which MSY is the maximum average yield (MAY) that can be attained by varying the current annual yield (CAY) in response to fluctuations in stock size (Annala 1989 and 1990, Mace and Sissenwine 1989). MCY estimates are based on historic estimates of stock biomass from resource surveys, stock production models, or landings statistics. CAY estimates are generally based on recent estimates

of stock biomass and a target level of fishing mortality which is expected to produce MAY. Although the dynamic (CAY) strategy leads to higher average yields, the static (MCY) option has received the most attention for two reasons. First, the ITQ system was initially specified in terms of fixed weights of quota, valid in perpetuity. In practice, most TACs were constant. Second, the facilities for fisheries research are inadequate for providing frequent updates of stock status for all but a few of the more important fish stocks.

It should be recognized that FAMs are only part of the process of determining the level of TACs. The actual advice to the Minister of Fisheries on the setting of TACs is given by senior government officials who integrate stock assessment information with other considerations, including an evaluation of the risk to the resource of not adjusting a TAC. But the authors consider FAMs the best source of information on the condition of the fisheries resources, since they are open scientific meetings which formally document their deliberations and conclusions.

When ITQ management was implemented, the government stated that it would adjust the TAC by entering the market to buy or sell quota at market-determined prices. Government also reserved the option to make prorated cuts in quota. During the first three years of ITQ management, government either sold quota in perpetuity or leased annual quota for barracuda, hake, ling, orange roughy, hoki, and stargazer (Table 3). Most transactions were in the first year. A total of $84.2 million NZ was collected in quota sales and lease fees. But since the initial buyback when ITQs were implemented, government has not entered the marketplace to reduce any TACs,[6] despite the fact that the need for reductions has been indicated by several stock assessments (Annala 1989 and 1990; see next section).

Since ITQ management should increase resource rent, government charges an annual royalty (known as a resource rental) on quota holdings. In order to discourage speculation on quota (i.e., owning it without using it), resource rentals are charged on quota holdings rather than landings. This practice is an implied guarantee that fish are abundant enough for all quota to be caught without dissipating rent, which may not be the case due to assessment errors, failure to adjust TACs when assessments indicate TACs are too high, and because of varying economic conditions.

Gilbert (1988) estimated that the ITQ system could result in resource rents (referred to as surpluses in his paper) of 15–45% of the first sale value of the catch, depending on the species. His estimates reflect only the benefits of reducing effort relative to the open-access equilibrium (although the validity of an open-access equilibrium baseline is questionable for some of New Zealand's fisheries). They do not include the benefits of eliminating competition for shares of an overall TAC. If the average rent is 25% of the first sale value of the fishing, then there is the potential for government to extract at least $90 million NZ annually (i.e., 25% of the 1987 first sale) as resource rentals. Resource rentals averaged about $20 million NZ annually during the first three years of ITQ management.

Table 3
Revenues from sale/lease of quota under New Zealand ITQ management, 1986–89.

Species	Tons (1000s)	$NZ (millions)	% Total $
Barracuda	1.7	1.7	2.0
Hake	1.3	2.2	2.6
Ling	2.1	2.2	2.7
Orange roughy	7.8	23.4	27.8
Hoki	131.0	53.2	63.2
Stargazer	1.8	1.5	1.8
Total	145.7	84.2	100.1

On 1 April 1990, ITQs were redefined as portions of annual TACs. This eliminated the need for government to adjust TACs by entering the marketplace to buy and sell quota, and makes it more practical to vary TACs in response to the inherent variability in fisheries resources, and other factors (e.g., new scientific information). The change to proportional ITQs came at a time when government was facing a large liability (discussed further below) to buy quota to adjust TACs. Therefore, government agreed to freeze the rate of resource rentals for five years and redistribute the resource rentals to industry as compensation for TAC reductions.

What has happened under ITQ management

It is probably too early to conduct a formal evaluation of ITQ management in New Zealand. A transition period of 3–5 years, or longer, is to be expected. Many of the species in New Zealand are long-lived, and it is likely that adjustments in the condition of the resource, which ultimately affect the economic benefits, will be protracted. However, since some authors have already declared New Zealand's ITQ management a success

[6]The TAC for orange roughy on the Chatham Rise was reduced by exchanging quota in that area for quota on the Challenger Plateau. This was a temporary reduction for 1988–89, although stock assessments indicated that a permanent reduction was necessary.

(Clark et al. 1988), it is worth considering what has happened to date, to the extent this is possible given limitations in available information. As discussed earlier, government authors and government publications indicate that the ITQ system was put in place to address three problems: (1) conservation, (2) economic performance, and (3) government intervention. The initial effects of the ITQ system with respect to these problems are discussed below.

Conservation

There is little evidence of improvement in the condition of fisheries resources; but since stock assessment information is limited, it is difficult to know. The increase in TACs that lead to the revenues reported in Table 3 resulted from a reassessment of the stocks, and not an increase in abundance.[7] There is evidence that some stocks have declined, most notably orange roughy, which has been found to be much less productive than previously believed (Mace et al. 1990). The current TAC for the largest stock of orange roughy exceeds even the most optimistic estimates of long-term sustainable yield by a factor of three. ITQs are not responsible for the problem, but have done little to resolve it.

There are several species in addition to orange roughy in need of TAC reductions. There is accumulating evidence that TACs are too high in the long term for valuable species such as hoki, squid, paua, and rock lobster (Annala 1990). At the 1989 FAM (Annala 1989), MCY was estimated for 110 management units. Twenty-one of the estimates were within 10% of the TACs, 82 were less than 90% of the TAC, and only 7 were greater than 110% of the TAC. CAY was estimated for nine management units. One estimate was within 10% of the TAC, seven were less than 90% of the TAC, and one was greater than 110% of the TAC. In 36 cases, yield estimates were less than 50% of the TAC. Reductions in TACs, either immediate or gradually toward MCY or CAY estimates, were recommended for several species. In other cases, reductions were not recommended because of uncertainty in MCY or CAY estimates, because accumulated biomass was still being fished down (in new or developing fisheries), or because recent catches indicated it was unlikely the TAC would be reached. It should also be noted that "actual" TACs are now almost invariably higher than "official" TACs, mostly as a result of successful appeals to the Quota Appeals Authority. Some of the differences are trivial, but a comparison between actual and official TACs from Annala (1989) indicates that of the 122 scientifically-based TACs (i.e., excluding the 47 administrative TACs), 25% of the actual TACs exceeded the official TACs by more than 10%, and 6% were higher by more than 20%.

There are also many species for which the TAC greatly exceeds the catch. For example, in the 1987–88 fishing year, the TAC was undercaught by more than 10% in 122 (out of 169) management units (including 47 "administrative" management units that have TACs of only 10–30 tons), and by more than 20% in 104 management units (Annala et al. 1991). For the 1988–89 fishing year, the total catch for all management units was 66% of the sum of the actual TACs. In situations in which TACs are nonrestrictive, they have little conservation benefit. In these cases, the stocks are either being overfished (because TACs are too high), or they would not be overfished without the ITQ system. There are other cases in which TACs have been overrun (17 of the 169 management units exceeded the TAC by more than 10% in the 1987–88 fishing year; Annala et al. 1991). There are a number of mechanisms by which fishermen can legally exceed their quota. Most of these mechanisms were established in order to deal with bycatch in multispecies trawl fisheries.

The general conclusion is that TACs are not closely tied to the best available assessments of the fisheries resources, nor are catches strongly controled by the TACs. Some valuable stocks have probably declined in abundance. To date, the track record of ITQ management with respect to conservation is not good.

Economic effects

There is even less information on the economic effects of ITQ management. ITQ management could increase economic benefits through several mechanisms: (1) Conservation could lead to an increase in resource abundance and a decrease in harvesting costs; (2) the initial buyback of quota and prorated cuts might have caused some excess capital and labor to move to segments of the economy where they could add production; (3) transfer of quota might have led to consolidation of ownership by the most efficient operators, and resulted in some excess capital being removed from the fishery; and (4) elimination of competition for TACs might have resulted in a more efficient harvest and an increase in the value of product.

As discussed earlier, it is unlikely that ITQ management has resulted in an increase in population

[7] In the case of hoki, the increase in TAC from 100,000 tons in 1985–86 to 250,000 tons in 1986–87 was controversial. Some components of industry were skeptical of the assessment which was in part based on a single hydroacoustics survey. The hydroacoustics survey results were later found to be gross overestimates. So far, the hoki resource has sustained the increase in TAC, but stock assessment results (Annala 1990) suggest that a catch of 250,000 tons may not be sustainable over the longer term. Government is giving high priority to monitoring the stock.

abundance. On the other hand, the decline in the abundance of orange roughy probably has not increased harvesting costs so far. Although orange roughy abundance has decreased considerably, the catch has been stable. Since orange roughy are fished in dense, spatially and temporally predictable aggregations, the catch rate is probably relatively insensitive to overall population size (see Paloheimo and Dickie 1964, for a general discussion of the phenomenon).

It is difficult to determine whether the initial buyback of quota and prorated cuts reduced excess capital, but it seems unlikely. As noted earlier, it probably did not reduce fishing mortality in most cases because the quota that was bought back would probably not have been caught. Fishing mortality is a function of capital investment in the harvesting sector (e.g., number of vessels), labor inputs (e.g., number of days the vessels are operated), and technology. It seems unlikely that capital would have been removed from the fishery unless fishing mortality were reduced.

There is evidence that quota holdings have been consolidated, presumably to more efficient owners.[8] During the period October 1986–April 1988, there were 15,580 quota sales involving 453,000 tons, and 3417 leases of quota involving 253,000 tons, the sum of which exceeds the total amount of quotas (494,000 tons owned privately and 64,000 owned by government); therefore, some quota was involved in multiple transactions (Muse and Schelle 1988). According to Bevin et al. (1989), the total number of quota holders decreased by 5.7% during the first two years of ITQ management. The amount of quota held by the top ten quota owners increased from 57% to 80% of the total. The number of quota holders with more than 50 tons decreased by 37%. This consolidation in ownership of quota does not necessarily mean that vessel ownership has also been consolidated. Apparently, a number of vessel owners who have sold their ITQ allotments to fishing companies have also entered contracts to fish that quota for periods of several years.

Unfortunately, the authors have not been able to obtain reliable data on the number of vessels in the fishery prior to and since ITQ management. There are some data available (e.g., Anonymous 1987, Bevin et al. 1989), but the information is inconsistent. There are data that indicate a slight decrease in investment in the harvesting sector in 1987, after several years of steady growth (Bevin et al. 1989). On the other hand, the data indicate that employment and investment in the fisheries increased steadily through 1987 (Table 4).[9]

Table 4

Investment and employment (in harvesting sector and total; processing-sector values can be obtained by difference) in New Zealand fisheries, 1983–87 (from Bevin et al. 1989). Values are in $millions NZ (book-value) and numbers of employees.

	1983	1984	1985	1986	1987
Investment					
Harvesting	142	170	182	223	213
Total	353	405	437	510	550
Employment					
Harvesting	3700	4000	4450	3800	4240
Total	7500	8000	8650	9200	10240

It is also difficult to evaluate the effects of eliminating competition for TACs, but there are some positive signs. In informal discussions with members of the fishing industry, the authors have been told that harvesters have modified their fishing practices to reduce costs and/or increase the market value of their catches.

At this stage, it is unclear what economic effects ITQ management has had. But, all other things being equal, it seems reasonable that ITQ management should have increased economic benefits. Unfortunately, all other things are not equal.

Two events unrelated to ITQ management have adversely affected the economic condition of the New Zealand fishing industry. They are a weakening of the price of product in export markets (particularly orange roughy in the USA) and unfavorable exchange rates. As a result, the industry had only a 4.3% return on investment (before income taxes) during the one-year period beginning 1 April 1987 (Bevin et al. 1989).[10]

While the overall economic benefit of ITQ management to New Zealand is unclear so far, it was profitable for the government. As noted earlier, the government's revenues from sale or lease of quota was $84.2 million NZ. It also collected about $60 million dollars in

[8] There is a legal limit to how much consolidation can occur. It is illegal for a company to own more than 35% of the quota for a species in any management area, or more than 20% of the quota for a species overall. It is interesting that some segments of the fishing industry have viewed the potential of consolidation of ownership of quota negatively, while government fisheries managers have generally viewed it as part of the process of increasing economic efficiency (i.e., efficient harvesters can afford to buy quota from less efficient harvesters). New Zealand government officials also note that consolidation should reduce the cost of managing the ITQ system.

[9] Note that there was a high rate of inflation during this period (3.6, 9.4, 15.3, 18.2, and 9.6% in 1983–87, respectively, or 69% overall) which approximately offsets the increase in nominal value of capital investment.

[10] It should be recognized that the economic condition of the New Zealand industry is a controversial matter because of resource rentals and fuel excise taxes. Bevin et al. (1989) indicate that in 1987 the industry paid $55 million NZ in resource rentals and fuel excise taxes which reduced the rate of return on investment from 16.2% to 4.3% (before income taxes).

resource rentals during the first three years of ITQ management. This income exceeds the cost of the buyback ($42.4 million NZ) and the entire cost of the government's fisheries research, management, and enforcement programs (about $30 million NZ per year). And there is the potential for resource rentals to increase substantially (see previous discussion). On the other hand, the authors are of the opinion that government should increase fisheries research considerably if it is to produce adequate stock assessments to support ITQ management (i.e., to conserve without being too restrictive). Furthermore, if government had entered the marketplace and purchased quota to implement the reductions suggested by yield calculations performed at the 1989 Fisheries Assessment Meetings (Annala 1989), the cost would have far exceeded the revenue from the ITQ system (e.g., the reductions for orange roughy alone would have cost in the range of $60–150 million NZ).

Government intervention

The third problem that ITQ management was intended to solve was excess government intervention. To date, it has not reduced government intervention except by removing the moratorium on new licenses. The moratorium was replaced by the requirement to own quota. In addition, there are new recordkeeping/reporting requirements and complicated rules that are intended to cope with bycatch (Annala et al. 1991).

One form of government intervention that probably hampered the fishing industry was restrictions on the port at which harvesters were allowed to land their catch. However, this restriction was removed prior to ITQ management. Other forms of input controls, such as minimum fish size restrictions and closed areas or seasons, have usually not been removed. Some of these restrictions are necessary, in addition to a quota, in order to conserve the fisheries resources and to prevent potential yield from being wasted.[11] In other cases, regulations were put in place to aid one segment of the fishing industry relative to another. For example, large factory trawlers are restricted from fishing within 25 miles of the coast, which reduces direct competition with smaller vessels.

General reaction

It is not surprising that implementation of ITQs in New Zealand has been accompanied by controversy. The newspapers report numerous charges by the industry against the government. The industry is upset about the level of resource rentals. There are complaints about the fairness of the Quota Appeals Authority. There were complaints that government had overestimated the productivity of the hoki resource when it sold quota, and there are complaints that it has overestimated the severity of the problem with orange roughy now that it is attempting to reduce the quota. Although there is strong support from industry and government for ITQ management, many specific aspects of implementation are unpopular. This is probably unavoidable for a system that is relatively complex and so radically different from previous management.

Potential problems

From a theoretical perspective, ITQ management is an ideal method which generates maximum net economic returns, under some simplifying assumptions; but as Copes (1986) points out, there are many potential problems. Instead of reviewing Copes' list of potential problems that apply to ITQ management in general, this paper reviews actual and potential problems that apply specifically to New Zealand. They are (1) problems arising from redefinition of quota ownership, (2) implications of the Treaty of Waitangi, (3) inadequacy of the scientific basis of TACs, (4) bycatch, (5) high-grading, (6) enforcement, and (7) an adequate basis for setting resource rentals.

Redefinition of quota ownership

The need to redefine ITQs from fixed quantities in weight to proportions of the TAC resulted from government's failure to enter the marketplace to reduce TACs when necessary. Early versions of the proposed ITQ system included a "revolving fund" that would be administered by the New Zealand Treasury. Resource rentals and revenues from the sale of quota would have gone into the fund which could then be used to buy back quota as necessary. In fact, Crothers (1988) actually reported that the revolving fund existed. However, the fund never materialized and revenues paid to government by the fishing industry were used for other government functions. When faced with the overwhelming cost of buying back quota to reduce the TAC for orange roughy, the government announced its intention to change the ITQ system from fixed to proportional ITQ. The authors were surprised at how rapidly government was able to obtain the legal authority from Parliament to make such a fundamental, and economically significant, change in the system. It took approximately one year from the time that

[11] Fisheries management needs to consider two control variables: the fishing mortality rate which can be regulated by a quota, and the age- or size-at-first-capture which can be regulated by gear restrictions, area/season closures, or minimum fish size (Sissenwine and Shepherd 1987).

government announced its intentions to convert the system to proportional ITQs until the change became effective on 1 April 1990.

The actual details of how the conversion will be implemented had not been determined at the time this paper was written, but some difficulties are almost certain to be encountered. In order to gain industry acceptance of the change, government agreed to freeze resource rental rates for five years, and redistribute these funds to compensate industry for quota reductions. Industry may have misjudged the amount of compensation it will receive, since several of the species that are most likely to have large quota reductions are also the species that generate most of the resource rentals (e.g., orange roughy, hoki, squid). Therefore, the greater the reductions, the smaller the pool of funds available for compensation.

One implication of converting from ITQ in fixed amounts to proportional ITQ is that there will be pressure to change the method of yield estimation from an MCY strategy to a CAY strategy, with consequent increases in the amount and variety of assessment information required. With quota as a fixed amount, there was little change in TACs from year to year. With ITQs as a proportion of the TAC, there will be greater pressure from the industry to change TACs (particularly to increase them when stock size is perceived to be high).

Treaty of Waitangi

The Maori people have sued for rights to the fisheries under the terms of the Treaty of Waitangi. There are several related cases which had not been settled at the time this paper was written, but it appears that the Maori people are entitled to a significant amount of quota. Prior to the ITQ system, when there was no ownership of the fisheries, there was less incentive for the Maoris to exercise provisions of the Treaty of Waitangi. But when property rights were established, and many Maoris were excluded from the system because they were part-time fish harvesters who had already been removed from the fishery, it was inevitable that a controversy would follow. Bevin et al. (1989) reported that industry has delayed major investments in the fisheries because of uncertainty about Maori fishing rights. Industry is concerned that the eventual settlement with the Maoris will be at their expense (i.e., they will not be compensated for quota that is transferred to Maori ownership). The dispute over the Treaty of Waitangi has also caused government to delay adding important species into the ITQ system.

Stock assessments

The scientific basis for assessing fish stocks, setting TACs, and evaluating the overall performance of the ITQ system is generally inadequate. New Zealand had relatively little need for stock assessment capability prior to ITQs. For the most part, their fisheries management was laissez-faire. In the case of data for assessing deepwater species, New Zealand relied heavily on foreign research vessels. When ITQs were implemented, they were ill-prepared, in the opinion of the authors, to conduct stock assessments for all of the management units included in the system. The situation has improved since the implementation of ITQ management as New Zealand scientists have developed and refined the scientific basis for stock assessments, but they have had inadequate support (e.g., research vessels, data collection systems, and personnel). Inadequate assessment databases mean that the ITQ system is operating under high levels of uncertainty. The price of uncertainty is either conservative quotas or a high risk of stock collapses.

Bycatch

Some bycatch is inevitable in multispecies fisheries. This means harvesters will catch some fish for which they do not own quota. New Zealand planned to manage bycatch with a taxation scheme (referred to as surrendering catch to the government or "Crown"), which was intended to produce a neutral incentive for bycatch. The tax was supposed to be high enough so that harvesters would have no incentive to catch species for which they did not hold quota, but if they caught them as bycatch, it would be worth their while to land them for sale. The problem is knowing what the proper tax level is in order to result in a neutral incentive. In some cases, even taxing 100% of the ex-vessel value does not discourage fishing for species for which harvesters do not hold quota. This is because of vertical integration in the fishing industry and a very high value added during processing.

There are several other provisions for dealing with bycatch. Quota holders may overcatch by up to 10% in exchange for next year's quota. They may trade retrospectively for quota to cover catch they have already taken. They may trade quota of certain species to cover bycatch of certain other species (for specified combinations of species, often involving one-way trades only).

Another aspect of the bycatch problem is that it is difficult to distinguish between bycatch problems that are a conservation threat to the bycatch species and those that result from setting the wrong TAC, as a result of imprecise assessments. Regardless of whether

it is a conservation problem or not, bycatch constitutes a management problem. It also constitutes a problem for members of the fishing industry when they try to adjust their portfolios of quota holdings to match their landings. In theory, this can be done by buying and selling quota, assuming that the overall TACs match the relative catch rates experienced by the fishing industry in aggregate; but this may not be so.

Annala et al. (1991) reviewed the bycatch situation in detail. In the 1987–88 fishing year, the quota was overcaught for 33 (out of 169) management units, by up to 74%. Nine management units were overcaught by more than 20%. The frequency and magnitude of overcatching increased from 1986–87 to 1987–88.

Highgrading

Highgrading is the discarding or dumping of a lower valued size or species of fish, in favor of keeping more valuable fish. Although highgrading is illegal under the New Zealand ITQ system, it is known to occur (Annala et al. 1991). For example, it probably occurs in the snapper fishery where there is a premium paid for high quality fish for the Japanese "iki jime" (killed by spiking the brain) market, and in the oreo dory fishery where three species (spiky, and black and smooth oreo dory) with significantly different values are managed by a combined TAC. The amount of highgrading in New Zealand fisheries has not been quantified.

Clark and Duncan (1986) felt that highgrading would be "...a short term, transitional problem and should disappear once the fishery recovers and product value differential within the same stock diminish..." There is little evidence that the fishery has recovered. Nor should recovery of the fishery eliminate the incentive for highgrading, unless the ITQ system is administered such that TACs do not limit catch. If so, then other advantages of ITQ management would be undetermined. Nor are the authors aware of reasons why ITQ management should reduce value differences between species or levels of quality.

Enforcement

ITQ management is potentially difficult to enforce. New Zealand has some advantages over the United States when it comes to enforcement. First, the population is small, and therefore there is less scope for the development of a domestic black market, although black markets may be significant for some inshore species consumed domestically. Second, the country is remote, so that it is difficult to smuggle fish elsewhere. Third, most fish are exported, which involves record-keeping that helps to check the accuracy of quota reports. Finally, fisheries enforcement is carried out entirely by a single, coordinated agency.

New Zealand placed a high priority on establishing enforcement capability when it implemented ITQs. It reoriented enforcement from at-sea operations to shoreside investigations. The emphasis moved from conservation officers to accountants and investigators and "electronic surveillance" (computerized data recording). The industry is required to maintain and submit several different types of records that are necessary for monitoring catch and product flow. Penalties for quota violations are heavy. They may involve forfeiture of catch, vessel, and quota holdings, in addition to fines of up to $10,000 NZ. A second offense within seven years may result in prohibition from participation in any aspect of the fishing industry for up to three years. In addition, the fisheries enforcement agency passes information on to the tax department, which may then be used in income tax prosecutions. It is difficult to assess how well this enforcement approach is working.

Resource rentals

The New Zealand fishing industry is concerned about the basis of setting resource rentals, although it does not seem to dispute them in principle. The government planned to gradually increase resource rentals[12] until the fair market value of quota was reduced to approximately zero. In theory, government is extracting all of the resource rent from the fisheries at the point in time that there is no longer incentive to enter the fisheries. The industry argued that not all of the resource rent should be extracted, since investment in fishing is inherently risky.

It is arguable whether the market value of quota reflects resource rent in the fisheries. The price paid for quota should reflect the buyer's estimate of its net present value. However, the buyer's estimate may be incorrect (i.e., a bad investment). Even if the price paid for quota is correct, it may not reflect rent in a particular year. In practice, the price paid for quota has been extremely variable (e.g., from $13 per ton to $16,500 per ton for snapper; Bevin et al. 1989) for a variety of reasons (e.g., imperfect knowledge, inclusion of other assets in the price of quota, different discount rates, noncompetitive price setting). This makes it difficult to use the sales price of quota as a criterion for setting resource rentals.

[12]The law limits increases in resource rental rates to 20% per year.

Table 5
Problems and benefits of fisheries management by input controls, quotas (Q), and ITQs. The symbol "0" is used as the standard. The symbol "+" means a more difficult problem or greater benefit than "0." The symbol "++" means even greater problems or more benefit than "+."

	Type of management		
	Input	TACs	ITQs
Problems			
Stock assessments	0	+	+
Catch statistics	0	+	++
Enforcement	0	+	++
Bycatch	0	+	++
Benefits			
Conservation	0	0	0(+)
Economics	0	0	+

General issues

Many potential problems of ITQ management are problems associated with TAC management in general. In some cases they are exacerbated by individual quotas. Table 5 compares the problems and benefits associated with input controls (e.g., effort limits, closed areas or seasons), TACs, and ITQs. TAC management requires more frequent and timely stock assessments than management by most input controls (Sissenwine and Kirkley 1982). The problem is particularly severe for short-lived species (Copes 1986). The problem of providing stock assessments for ITQ management is about the same as that for TAC management. Catch statistics are one component of stock assessments. The need for catch statistics is generally greater for TAC management than for management by input controls. The need is even greater for ITQs because statistics on individual quota holders are the basis of management. Both TAC and ITQ management encourages "data fouling" or misreporting (Copes 1986), although the incentive is greater for ITQs. Similarly, enforcement is generally more of a problem for TAC management (although this is not universally true) because the catch has to be accurately enumerated. For ITQs, it must be accurately enumerated for individual quota owners, some of whom may have developed successful methods for circumventing the system. The bycatch problem is more difficult for TAC management than for input controls. For ITQs, the bycatch problem is even more difficult because individual quota owners must adjust their portfolios to match their multispecies catch rates.

In terms of the conservation benefits, input controls, TACs, and ITQs are all potentially effective (Sissenwine and Kirkley 1982). ITQs may have a potential advantage over TAC management because, with ownership, there should be greater incentive for the industry to cooperate. But limited-entry licensing (a form of input control) also conveys privileges that may encourage industry cooperation. In terms of economic benefits, ITQs are superior in theory. Both input controls and TAC management eventually allow dissipation of resource rent. For both forms of management, there is an incentive for fishermen to increase their cost of fishing, in order to gain a larger share of the resource, until the rent is dissipated. In practice, the actual economic benefits of input controls, TACs, and ITQs are probably fishery-specific.

Learning from New Zealand's experience

There is much to be learned from New Zealand's experience with ITQ management. New Zealand took a systems approach. Comprehensive new legislation was introduced. Enforcement needs, penalty schedules, reporting and recordkeeping requirements (including wholesalers and retailers), a quota trading system, a process for appealing initial allocations, a buyback scheme for "rationalization" of some fisheries, mechanisms for controling bycatch, the principle of resource rentals, and public and fishery industry education were all considered. New Zealand made some mistakes, but it would have probably made more if its approach had been piecemeal.

The authors are of the opinion that one mistake made by New Zealand fisheries managers was to establish ITQs in fixed amounts, valid in perpetuity. This method was used because it was thought that ITQs in fixed amounts would create a more certain environment for industry; they would provide a mechanism for government revenue-raising, since government believed TACs were conservative and future quota sales were likely; and the trading price for fixed amounts of quota would be the most effective method to obtain information to set resource rentals (Clark et. al. 1988).

Apparently, the government did not recognize how uncertain TACs might be (due, for example, to errors in stock assessments) or how often TACs might need to be adjusted (due, for example, to the inherent variability in the size of fish stocks) by entering the market to buy and sell quota, since the revolving fund (or some other method) was not established. It is also possible government did not expect the price of quota to be so high as to make it prohibitively expensive for the government to buy it to reduce quotas. In fact, the sales price of quota may not have been economically rational, in which case government would not want

to overpay to adjust TACs downward. But it should be noted that the Government did sell quota for similarly high prices. In any case, it seems more practical to define quota as a portion of the TAC, in an uncertain and dynamic environment.

In the authors' opinion, New Zealand fisheries managers underestimated the complexity of the bycatch problem. In a multispecies setting, the apparent independent fluctuations of each species complicate the bycatch problem. In general, insufficient information, variability between harvesters, and the complex organization of fisheries mean that it will be difficult to solve the bycatch problem by adjusting a tax on bycatch. Many fisheries are essentially single-species (e.g., surf clams, herring, scallops, lobsters). These are the best candidates for ITQ management with respect to bycatch. If ITQ management is to be applied to multispecies fisheries (e.g., New England groundfish), it might be better to exclude some of the minor species from the scheme, or to recognize that they may need to be "sacrificed" in order to optimize fishing on the more valuable species.

New Zealand lacked adequate stock assessment data for a quota-based management system such as ITQs. And, unfortunately, it will take time to develop appropriate time-series of data. In addition, there is much that needs to be learned about the basic biology of the deepwater species, many of which have only recently been discovered in commercially viable quantities. The basis for stock assessments is better in some other places (e.g., throughout North America and Europe), but the expectations for a high degree of precision may still make stock assessment capability problematic.

ITQ management requires adequate monitoring and enforcement capability to track individual catches. New Zealand's enforcement of ITQs is geared towards investigations by accountants and auditors, instead of traditional fisheries officers. In order for these investigators to be effective, the New Zealand fishing industry is required to maintain detailed "paper trails" for products. Penalties for violations are severe. It is too early to say whether this scheme is working, but it is obvious that it will be necessary to impose additional recordkeeping to enforce ITQs in most cases in the United States.

It is unclear how serious the overcapitalization problem was in New Zealand, but there are U.S. fisheries that are severely overcapitalized (e.g., New England groundfish). The buyback scheme in New Zealand probably did little to reduce overcapitalization. If a buyback scheme is intended to reduce overcapitalization, funds should be used to reduce capital, and not hypothetical catches that might not have been taken anyway.

A positive lesson that should be learned from New Zealand is the need to be clear about objectives when applying an ITQ system. Clearly, one of the intentions of New Zealand's fisheries managers was to increase resource rent in the fisheries and to extract the rent (through annual royalty payments[13]) for the general benefit of the country. What will be the objective for applying ITQ management elsewhere? If the objective is conservation, then quota management (or other forms of management) is sufficient in theory, although pressure from an overcapitalized fishing industry may prevent TACs from being set conservatively enough. If the objective is economic efficiency, then it is important to address distributional issues (resource rents, producer surplus, and consumer surplus).

There is a great potential for ITQ management, but it is not a panacea. When ITQ management is applied, it is important that it be approached with realism and based on adequate experience and data.

Postscript

Approximately 20 months have passed since New Zealand converted its ITQ program from one of fixed quota valid in perpetuity to one based on quota specified as a proportion of an annual TAC (also referred to as a percentage ITQ system in New Zealand or a percentage quota share system in the United States). As predicted in this paper, the transition has been controversial, in part because compensation available to the industry in the form of resource rentals has not been as large as anticipated. As a result, the fishing industry filed a $150 million NZ court action against the government. The lawsuit has since been settled out of court.

In spite of the change from fixed to variable quota, most TACs have remained unchanged from one year to the next. This is partly a result of inadequate information for stock assessments. However, there have been three notable reductions in TACs. The total hoki TAC has been reduced from 250,000 to 200,000 tons, Challenger orange roughy from 12,000 to 1900 tons, and Chatham Rise orange roughy from 32,800 to 23,800 tons. The reduction in hoki quota was a reflection of new stock assessment results suggesting that then-current TACs were unlikely to be sustainable; the reductions in orange roughy TACs resulted from assessment results suggesting that stock collapse was imminent.

The anticipated need for large reductions in the Chatham Rise orange roughy TAC was one of the

[13] At present, a legal basis for resource rentals in an ITQ system is lacking in the Unites States.

major factors that precipitated the change from fixed to variable ITQs, since it could have cost the government more than $100 million NZ to buy back sufficient quota to reduce the TAC to the estimated long-term sustainable level. After the change, it was agreed that the quota would be reduced at the rate of 5000 tons per year to the sustainable level, the latter being recalculated periodically as new data became available. Recent assessments (Francis and Robertson 1991) indicate a sustainable level of 7000–9000 tons and show that the risks of stock collapse under the proposed reduction schedule have increased due to the accumulation of new data which has resulted in a decrease in the point estimates of stock size and a decrease in uncertainty of the estimates. The results clearly indicate the need for a faster rate of reduction. However, the fishing industry continues to oppose quota reductions, and at this point in time the government has postponed the 5000-ton reduction schedule. The discovery of new orange roughy aggregations in the southern portion of the management area may alleviate the problem in the short term, but the low productivity of orange roughy stocks means that any accumulated biomass can be quickly fished down. Long-term sustainable yields from orange roughy stocks are estimated to be only about 1.5–2.5% of the recruited virgin biomass.

The problem of not reducing quotas when reductions are indicated by assessments is exacerbated by widespread rumors of quota busting, in spite of New Zealand's efforts to tailor enforcement to ITQ management. Some of these rumors have been confirmed by government sources.

New Zealand is now considering further evolution in its fisheries management system towards a form of comanagement. Topics being debated include the need to incorporate recreational fisheries into the management system, the need to include all remaining exploited species-stocks, and the pros and cons of eliminating the current limits on aggregation of quota (Pearse 1991). One objective is to transfer the costs of management and responsibility for the resource to the users of the resource, under the assumption that with ownership comes motivation for conservation. Stay tuned.

Citations

Annala, J.H.
1989 Report from the Fishery Assessment Plenary, May 1989: Stock Assessments and Yield Estimates. Fish. Res. Cent., N.Z. Minist. Agric. Fish., Wellington, 158 p.
1990 Report from the Fishery Assessment Plenary, April–May 1990: Stock Assessments and Yield Estimates. Fish. Res. Cent., N.Z. Minist. Agric. Fish., Wellington, 165 p.

Annala, J.H., K.J. Sullivan, and A. Hore
1991 Management of multispecies fisheries in New Zealand by individual transferable quotas. *In* Daan, N., and M.P. Sissenwine (eds.), Multispecies models for management of living resources. ICES Mar. Sci. Symp. 193:321–330.

Anonymous
1984 Inshore finfish fisheries: Proposed policy for future management. N.Z. Minist. Agric. Fish., Wellington, 31 p.
1987 Economic review of New Zealand fishing industry, 1986–1987. N.Z. Fish. Ind. Board, Wellington, 56 p.

Bevin, G., P. Maloney, and P. Roberts
1989 Economic review of the New Zealand fishing industry, 1987–1988. N.Z. Fish. Ind. Board, Wellington, 56 p.

Christy, F.T.
1973 Fishermen quotas: A tentative suggestion for domestic management. Occas. Pap. 19, Law of the Sea Inst., Univ. R.I., Narragansett.

Clark, I.N., and A.J. Duncan
1986 New Zealand's fisheries management policies—Past, present and future: The implementation of an ITQ based management system. *In* Fishery assess control programs worldwide, p. 107–141. Alaska Sea Grant Rep. 86-4, Univ. Alaska, Fairbanks.

Clark, I.N., P.J. Major, and N. Mollet
1988 Development and implementation of New Zealand's ITQ management system. Mar. Resour. Econ. 5:325–349.

Copes, P.
1986 A critical review of the individual quotas as a device in fisheries management. Land Econ. 62(3):278–291.

Crothers, S.
1988 Individual transferable quotas: The New Zealand experience. Fisheries (Bethesda) 13(1):10–12.

Dewees, C.M.
1989 Assessment of the implementation of individual transferable quotas in New Zealand's inshore fishery. N. Am. J. Fish. Manage. 9:131–139.

Francis, R.I.C.C., and D.A. Robertson
1991 Assessment of the Chatham Rise (ORH 3B) orange roughy fishery for the 1991/92 season. N.Z. Fish. Assess. Res. Doc. 91/3, N.Z. Minist. Agric. Fish., Wellington, 36 p.

Geen, G., and M. Nayar
1988 Individual transferable quotas in the southern bluefin tuna fishery: An economic appraisal. Mar. Resour. Econ. 5: 365–388.

Gilbert, D.J.
1988 Use of a simple age structured bioeconomic model to estimate optimal long run surpluses. Mar. Resour. Econ. 5:23–42.

Mace, P.M., and M.P. Sissenwine
1989 Biological reference points for New Zealand fisheries assessments. N.Z. Fish. Assess. Res. Doc. 89/11, N.Z. Minist. Agric. Fish., Wellington, 10 p.

Mace, P.M., J.M. Fenaughty, R.P. Coburn, and I.J. Doonan
1990 Growth and productivity of orange roughy (*Hoplostethus atlanticus*) on the north Chatham Rise. N.Z. J. Mar. Freshwater Res. 24:105–119.

Maloney, D.G., and P.H. Pearce
1979 Quantitative rights as an instrument for regulating commercial fisheries. J. Fish. Res. Board Can. 36:859–866.

Muse, B., and K. Schelle
1988 New Zealand's ITQ Program. Alaska Commer. Fish. Entry Comm. (CFEC 88-3), Juneau, 47 p.
1989 Individual fisherman's quotas: A preliminary review of some recent programs. Alaska Commer. Fish. Entry Comm. (CFEC 89-1), Juneau.

Paloheimo, J.E., and L.M. Dickie
1964 Abundance and fishing success. Rapp. P.-V Reun. Cons. Int. Explor. Mer 155:152-163.

Pearse, P.H.
1991 Building on progress: Fisheries policy development in New Zealand. Unpubl. rep. prepared for Minist. Agric. Fish., Wellington, NZ.

Sandrey, R.A., and D.K. O'Donnell
1985 New Zealand's inshore fishery: A perspective on the current debate. Agric. Econ. Res. Unit Res. Rep. 164, Lincoln College, Canterbury, NZ, 46 p.

Sissenwine, M.P., and J.E. Kirkley
1982 Fishery management techniques: Practical aspects and limitations. Mar. Policy 6:43-58.

Sissenwine, M.P., and J. Shepherd
1987 An alternative perspective on biological reference points and recruitment overfishing. Can. J. Fish. Aquat. Sci. 44: 913-918.

Seasonality in reproductive activity and larval abundance of queen conch *Strombus gigas*

Allan W. Stoner
Veronique J. Sandt
Isabelle F. Boidron-Metairon

Caribbean Marine Research Center
805 46th Place East, Vero Beach, Florida 32963

Abstract.–Reproductive behavior and larval abundance of queen conch *Strombus gigas* L. were investigated near Lee Stocking Island, Bahamas, with the primary purpose of determining relationships between physical variables, spawning frequency, and larval abundance. Monthly observations made by divers at the offshore spawning site showed that copulation increased as a linear function of bottom water temperature from April until the end of July, when maximum summer temperature was reached. Pairing, copulation, and egg-laying were all positively correlated with photoperiod throughout the study period. The last pairing and copulating conch were observed in the middle of the warmest period in August suggesting that stimuli other than temperature, such as declining photoperiod, induce the end of reproductive activity. The last egg mass was found in early October.

There was a significant correlation between spawning activity at the offshore reproductive site and larval abundance in the adjacent downcurrent inlet. The first conch veligers were found in plankton tows made in early June, five weeks after the first egg masses were observed at the end of April. High larval density was confined to July and August. Advanced-stage larvae, close to metamorphosis, were found only in the vicinity of a shallow, benthic nursery habitat. Comparison of reproductive season in queen conch populations of the Caribbean region showed no latitudinal trend. In all areas, reproduction was associated with long days and warm temperatures. Production of conch larvae at the time of high water temperature and steady trade wind conditions may promote rapid larval development and facilitate transport of the veligers to inshore nursery habitats.

Manuscript accepted 31 January 1992.
Fishery Bulletin, U.S. 90:161–170 (1992).

The queen conch *Strombus gigas* L. is the second most important fisheries species in the Caribbean region, after spiny lobster *Panulirus argus* (Brownell and Stevely 1981). Consequently, its general life history is well known (Randall 1964, Brownell and Stevely 1981, Berg and Olsen 1989). Sexes are separate and sexual maturity occurs at about 3½ years of age, a few months after the flared lip is formed (Egan 1985, Wilkins et al. 1987, Appeldoorn 1990). Fertilization is internal and copulation may precede spawning by several weeks (D'Asaro 1965). An individual female may spawn six to eight times during a single reproductive season (Davis and Hesse 1983). An egg mass, usually laid on clean, coral sand, takes 24–36 hours to produce and consists of a single continuous egg-filled tube folded upon itself to form a kidney-shaped aggregate of eggs and sand about 15 cm in length. Robertson (1959) estimated that between 385,000 and 430,000 eggs were laid in a single egg mass. Eggs hatch after 5–6 days; pelagic veligers remain in the water column for 18–40 days prior to metamorphosis (Randall 1964, D'Asaro 1965, Brownell 1977, Davis et al. 1987, Boidron-Metairon 1988, Mianmanus 1988).

Reproductive seasonality in queen conch has been reported for different sites within the Caribbean region (see Fig. 6), but the mechanisms which regulate reproductive behavior are poorly known. In this study, we provide the first report on abundance and seasonality of queen conch veligers in the field, and examine relationships between adult habitat, reproductive activity, temperature, photoperiod, and larval abundance.

Methods and materials

Study site

This study was conducted near Lee Stocking Island (southern Exuma Cays), Bahamas, an area known for high abundance of queen conch (Fig. 1). The islands and cays of the Exuma chain are bordered on the west by the shallow Great Bahama Bank (mean depth ~3 m) and on the east by the deep Exuma Sound. Waters from the Exuma Sound flow onto the Bank through numerous passes on the flood tide and are mixed with Bank water by wind-driven circulation. Surface drogue studies (N.P. Smith, Harbor Branch Oceanogr. Inst., Fort Pierce, FL 34946, unpubl. data) indicate that at the north end of Lee Stocking Island, water flows through Adderley Cay cut toward Shark Rock. At the south end of the Island, water flows through Rat Cay cut to the west between Barraterre Island and Children's Bay Cay. Most juvenile queen conch are located in shallow seagrass habitats on the Exuma Bank; largest populations are found near Shark Rock and southwest of Children's Bay Cay.

In Exuma Sound, approximately 1 km to the east of Lee Stocking

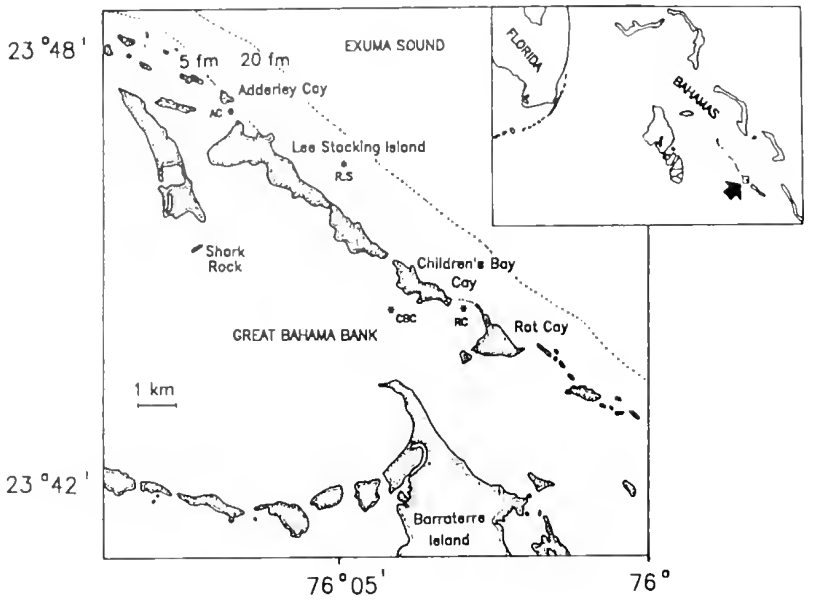

Figure 1

Map of the Lee Stocking Island, Bahamas, study site showing plankton sampling stations (*). RS = location of the Reproductive Site, where observations and plankton collections were made; RC = Rat Cay cut; AC = Adderley Cay cut; CBC = Children's Bay Cay nursery site.

Island, there is a coral ledge at which depths increase rapidly from 10 to 18m. Beyond the ledge is a 1km-wide platform with a gradual slope from 18 to 24m. Seaward from the platform, depth increases rapidly to the deep basin of Exuma Sound. This geomorphology is typical of the western side of the Exuma Sound. Highest number and density of adult *S. gigas* occur on the 18m-deep platform, which is beyond the normal free-diving range of conch fishermen. In this area, more than 99% of the conch are sexually mature (Stoner and Sandt 1992). In the colder months, the conch are found on algae-covered hardbottom; they move to sand for mating and egg-laying in the summer.

A study site of approximately 12 ha surface area on the 18m platform was chosen for the investigation of reproductive behavior and habitat association in adult conch (Fig. 2). The particular location, north of the 10m coral ledge, was selected because of an abundance of adult conch and close proximity of feeding and spawning habitats (Stoner and Sandt 1992). A scale map of the site was constructed from compass bearings and distances measured by scuba divers along the sides of primary habitat features or boundaries. Figure 2 shows all prominent features between the coral ledge and the 23m isobath.

Observations on reproductive behavior were made in three habitat types (1) Five hard-bottom domes (called "mounds"), each surrounded completely by bare sand, were examined. All of the mounds (designated with the letter "M" in Fig. 2) were located at depths of 18m at the base with tops between depths of 12 and 14m. (2) Sand habitats were divided into two major regions. S1 is the extensive sand flat between the 10m reef front and the mound zone. S2 is the sand area within the mound zone. (3) Rubble and boulder areas are found at the base of the 10m reef in a narrow band, with an extensive boulder field (B1) at the southeast end of the study site. The mounds and rubble, particularly in the B1 area, are covered with a turf of green algae (primarily *Cladophoropsis* spp.), plus abundant erect forms such as *Halimeda* spp. An area of mixed hardground, sand, and coral heads (H1) extends to the north and east of the study site.

Reproductive activity

Reproductive behavior was surveyed for 14 months, on a monthly basis during the period of highest activity (March–October 1988) and at 6–8 week intervals during January–February 1988 and November 1988–February 1989. Longer sampling intervals were used in the winter because preliminary observations near Lee Stocking Island in previous years indicated that no reproductive behavior occurs between November and March. During each survey, spanning 5–15 days, a scuba diver search for adult conch was made on mounds M1, M3, M4, and M5, in the boulder area (B1), in the rubble area (at the base of the coral ledge), and in both sand zones S1 and S2. During each survey period, all conch were counted on each of the mounds and at least one-half of the B1 area was examined. Very few conch were found on M2 and this mound was abandoned early in the study. After determining that most reproductive activity occurred on sand and not on hardground or rubble (Table 1), the sampling protocol was modified to locate at least 100 individuals on sand for each survey. During winter months, less than 100 conch were located on sand in several days searching; however, 100–300 animals were observed per month during most of the reproductive season.

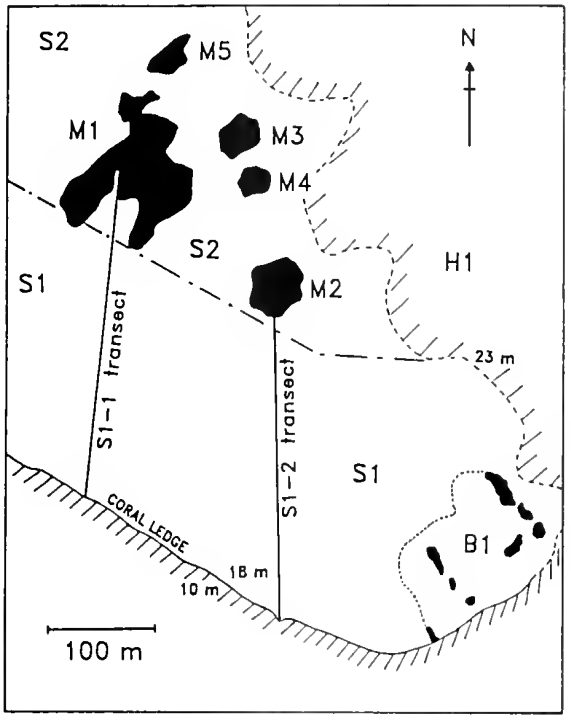

Figure 2
Map of the Reproductive Site (see Fig. 1) showing elevated Mounds (M), sand habitat (S1 and S2), boulder area (B1), and area of mixed hardground and sand (H1). S1-1 and S1-2 are transects over which density of conch were determined.

Table 1
Numbers and (percentages) of queen conch engaged in reproductive activity on three substratum types near Lee Stocking Island, Bahamas, 1988. Values for pairing and copulating represent number of male/female pairs.

	Behavioral type		
Substratum	Pairing	Copulating	Egg-laying
Sand	51 (94.4)	28 (84.4)	148 (99.3)
Rubble	0 (0.0)	2 (6.1)	0 (0.0)
Hardground	3 (5.6)	3 (9.1)	1 (0.7)

Each individual conch was classified in one of the following reproductive categories. (1) Pairing: Two conch were aligned, with the anterior part of the shell of one animal overlapping the posterior part of the shell of the other; but copulation was not observed. (2) Copulating: Animals were engaged in copulation, with the verge of the male beneath the mantle of the female. (3) Egg-laying: A female was actively laying an egg mass. (4) Non-reproductive: Conch was not engaged in reproductive behavior.

Seasonality in reproductive behavior was quantified by recording the percentage of total animals on sand in each behavioral category. Notes were made on the locations and substratum types (sand, rubble, hardground) where pairing, copulating, and egg-laying conch were found. Conch were measured for total shell length (spire to siphonal groove) and greatest shell lip thickness (approximately two-thirds of the distance posterior from the siphonal groove). Shell measurements were made to the nearest mm.

To estimate seasonal abundance of conch on sand, two quantitative transects across the S1 sand area (transects S1-1 and S1-2; Fig. 2) were examined each survey period. The transect surveys were made by a scuba diver who counted all adult conch within a known range while being towed 5 m above the sediment. High water transparency resulted in a mean transect width of 29 m (SD 6; range 20–40 m), which was measured with a tape on each survey date. The total survey area for each transect was calculated on the basis of horizontal visibility and the fixed distance of each transect line. For additional information on the abundance of queen conch on sand during the reproductive season, all adult conch were counted in circles of 20 m radii at locations of highest conch density in August 1987 (n 7 circles), and in June (n 2) and July 1988 (n 2).

Physical measurements

To provide information on sediment grain-size and organic content in the spawning habitat, sediment samples were taken from the surface adjacent to females laying eggs in August. Only eight samples were collected; however, the sediment in sand areas S1 and S2 appeared to be of uniform grain size. An effort was made to collect sediment samples from throughout the study site. Sediments were frozen until laboratory analysis. Organic content was determined by drying a subsample (~100 g wet wt) at 80°C to constant weight and incinerating at 500°C for 4 hours. Organic content was quantified as the percent difference between dry weight and ash-free dry weight. Another subsample (~50 g wet wt) was examined for granulometric properties. The sample was washed to remove salts and extract the silt-clay fraction (<62 μm). Silt-clay was analyzed with standard pipette procedures (Galehouse 1971), and the sand fraction with standard dry sieve procedures (Folk 1966).

Bottom-water temperature was recorded with a Ryan Instruments Temp Mentor placed at 17 m depth, near the base of the coral ledge. The thermograph recorded temperature with a precision of 0.2°C every

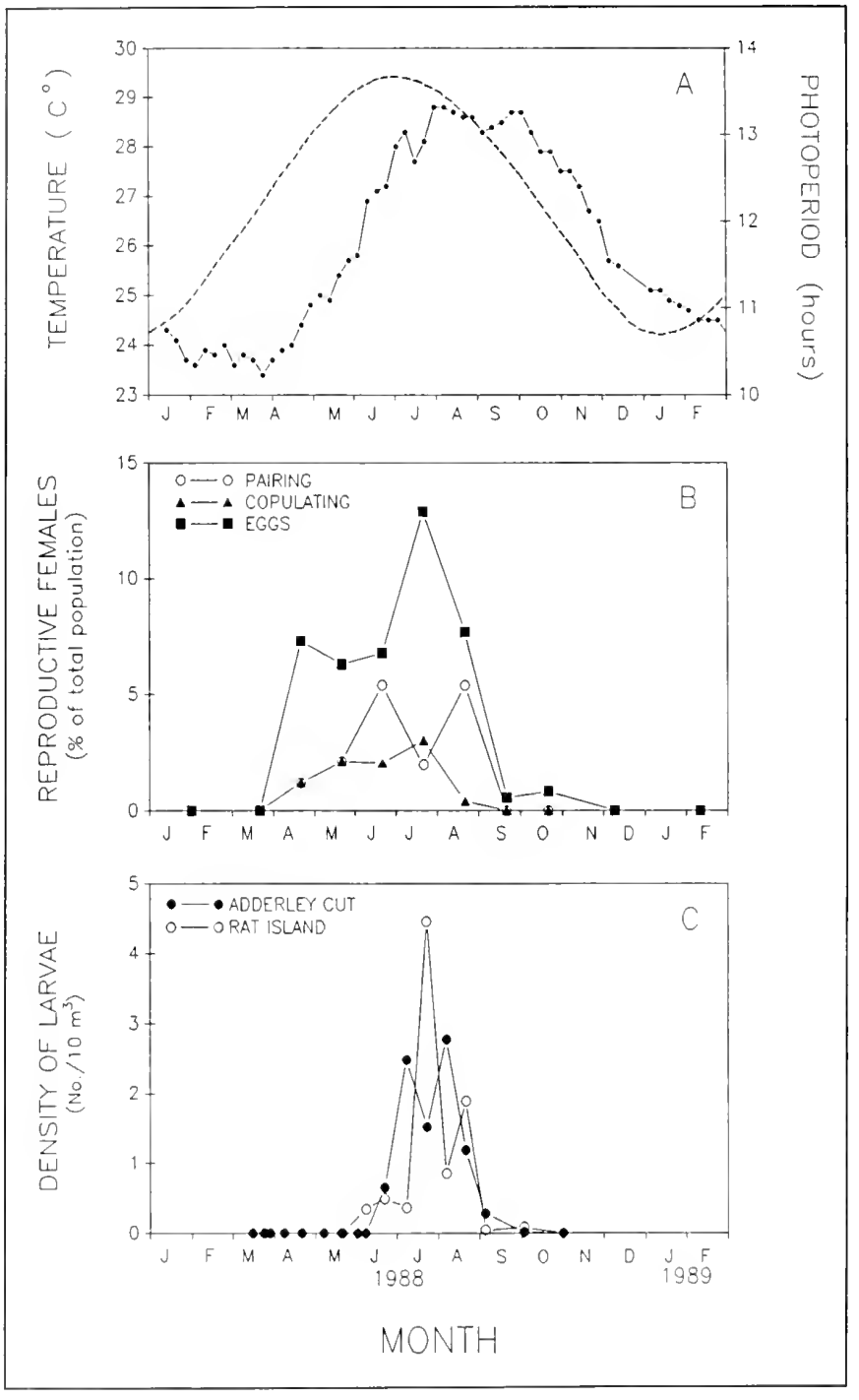

Figure 3

(A) Bottom-water temperature at 17 m depth with 7-day averages (solid line) and photoperiod in number of hours between sunrise and sunset (dashed line). (B) Number of queen conch *Strombus gigas* females on sand engaged in various reproductive activities. (C) Number of conch larvae in Rat Cay and Adderley Cay passes, January 1988–February 1989.

30 minutes; 7-day averages were generated and plotted (Fig. 3A). Surface-water temperature and weather conditions were recorded each time that plankton was collected.

To examine potential correlation between reproductive seasonality and photoperiod, a year-long photoperiod curve (Fig. 3A) was constructed for the study site. Numbers of hours and minutes between sunrise and sunset were calculated for local latitude at 9-day intervals using the Nautical Almanac.

Plankton collections

Daytime plankton collections were made for queen conch veligers from mid-March to October 1988. For seasonal analysis of larval abundance, collections were made every 2 to 3 weeks in the pass between Lee Stocking Island and Adderley Cay (Adderley Cay cut) and in the pass between Rat Cay and Children's Bay Cay (Rat Cay cut) (Fig. 1). Additionally, collections were made over the area surveyed for reproductive activity (Reproductive Site) with the primary purpose of detecting low densities of conch larvae at the onset and end of the reproductive season. Collections were not made at the Reproductive Site during peak reproduction, between July and mid-August. To examine densities and size-frequency of larvae on Exuma Bank, four collections were made over a known nursery for *S. gigas*, west of Children's Bay Cay (Fig. 1). This site is approximately 3.4 m deep and vegetated with the seagrass *Thalassia testudinum*.

In the passes, plankton were sampled during the first 2 hours of the flood tide; on the bank, tows were scheduled during the last 2 hours of flood tide. Plankton collections were made by towing a 0.5 m diameter conical net, 5 m long, with 202 μm mesh. Two tows were made at each site. Because the location of larvae in the water column was unknown, collections at the Reproductive Site were made by towing the net at 9 m depth (midwater column) for 10 minutes, then raised near

the surface at 1.5m depth for another 10 minutes. At the other three sites where there was considerable vertical mixing and shallow depth, the net was towed for 20 minutes in the upper 1.5m of the water column. Water volume sampled was calculated using a calibrated General Oceanics flowmeter, and larval abundance was expressed in numbers of veligers per $10\,m^3$.

To identify larvae, samples were refrigerated, sorted live (within 4 hours), and compared with laboratory-cultured larvae of the two most abundant *Strombus* spp. in the central Bahamas, *S. gigas* and *S. costatus*. Two other strombids occur in the Lee Stocking Island area (*S. gallus* and *S. raninus*); however, both are very rare relative to *S. gigas* and neither has been observed on the windward side of the island or in the inlets. Shell length, shell width, and shape of the shell tip were the principle criteria used to identify early-stage larvae. Number and shape of shell whorls and other shell characteristics were used to identify advanced larval stages. Measurement of shell length, from apex to siphonal edge, was made with an ocular micrometer and reported in microns for all intact shells.

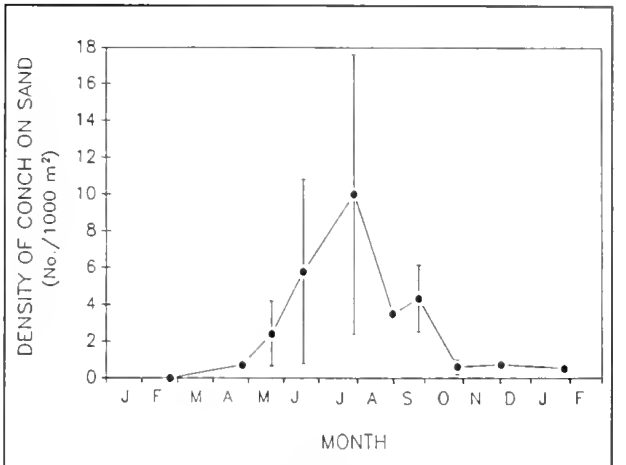

Figure 4

Density of queen conch *Strombus gigas* on sand at the Reproductive Site, off Lee Stocking Island, Bahamas, January 1988–February 1989. Values are mean ±SE for two transects.

Results

Conch reproduction

The reproductive season for *Strombus gigas* at Lee Stocking Island extended from mid-April to early October. The beginning of the season was marked by a massive migration of conch from hardground (mounds, rubble, and boulder areas) to sand habitats (Fig. 4) where first copulation, pairing, and spawning were observed on 14, 15, and 25 April 1988, respectively. In subsequent months, virtually all reproductive behavior occurred on sand (see later). The number of females engaged in reproductive activity increased gradually from April (9.7% of total sampled population) to July (18%) (Fig. 3B). In August, 13.8% of the population were reproductively active females; the percentage declined to less than 1.0% in September and October. Last copulation and pairing were seen in August, but egg-laying was observed through September. The last egg mass was discovered on 5 October 1988.

The number of reproductive conch increased with conch density on sand (Fig. 4) from January and February (0 conch/$1000\,m^2$) to July (10 conch/$1000\,m^2$). Density decreased after the beginning of August and was 0.61 conch/$1000\,m^2$ in October. Conch were aggregated on some dates and not distributed evenly along the transect lines. Large error bars in Figure 4 show that the two transect lines frequently had different densities of conch during the primary reproductive season. In August 1987, measurements in areas with high conch densities ranged from 11.1 to 20.7 conch/$1000\,m^2$. Values as high as 29.7 conch/$1000\,m^2$ (SE 2.0) were found in June 1988.

Low bottom-water temperatures were observed from early March to early April 1988 (near 23.6°C) (Fig. 3A). First pairing and copulating conch were seen at a temperature of 24°C in mid-April, and the first egg-laying female was found at 24.5°C. The number of copulating females increased as a linear function of bottom water temperature until the reproductive maximum (r 0.916, F 15.726, p 0.029; March through July 1988). There was no significant correlation between egg-laying and temperature (p 0.061) and pairing and temperature (p 0.285). Bottom temperature was relatively constant (28.3–28.8°C) from the end of July through September; the last pairing and copulating conch were observed during this period. Temperature decreased rapidly after September, and the last egg mass was found on 5 October. Water temperature was 26.5°C by late November 1988, decreasing to 25.1°C in late December.

All pairing and copulation were confined to the season with photoperiod greater than 12 hours, while egg-laying was observed until day length declined to 11 hours (Fig. 3A,B). Highest correlation occurred between length of day and copulation (r 0.870, F 24.838, p 0.001), but significant correlations were also found between photoperiod and both pairing (r 0.709, F 8.064, p 0.022) and egg-laying (r 0.838, F 18.896, p 0.002).

A few conch were buried partially in sand in mid-October 1987 and again in January and early February 1988. Burrowing was not seen again until mid-September 1988. In November, a few conch were buried

Table 2

Density of queen conch larvae at the Reproductive Site offshore from Lee Stocking Island, Bahamas, and at the nursery site near Children's Bay Cay on Exuma Bank, 1988. Values are numbers of conch larvae/10m^3 ± SD (n 2).

	Location	
Date	Reproductive Site	Children's Bay Cay
15 March	0±0	–
28 March	0±0	–
7 April	0±0	–
20 April	0±0	–
19 May	0±0	–
2 June	0.26±0.11	–
6 June	0.04±0.03	–
16 June	0.99±0.25	–
29 June	0.30±0.09	–
13 July	–	0.82±0.23
28 July	–	1.35±0.47
12 August	–	0.77±0.41
23 August	0.77±0.32	–
14 September	–	0.17±0.10
23 September	0±0	–
6 October	0±0	–

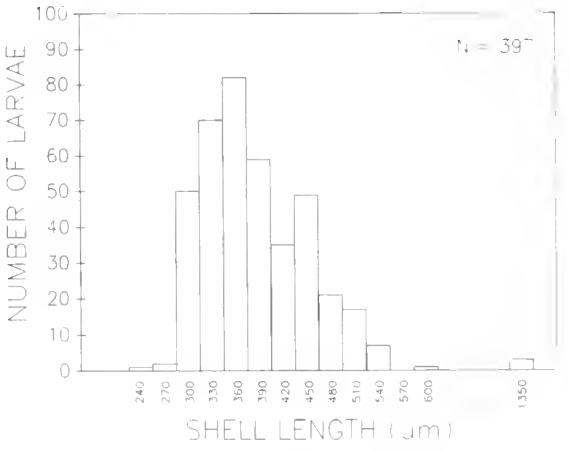

Figure 5

Length-frequency distribution for veligers collected near Lee Stocking Island, Bahamas, May–September 1988 (n 397).

in sand-filled depressions on the mounds. Some were almost entirely covered with sand and the shells were devoid of algae. It is possible that conch in the sand habitat were underestimated during winter months because of burial behavior; however, tag return data (Stoner and Sandt 1992) suggest that most adult conch move to hardground or rubble for the winter months.

The mean shell length of pairing, copulating, and egg-laying females ($\bar{x}$ 226mm, SD 23.6, n 180) was 2.3% larger than that for males in reproductive behavior ($\bar{x}$ 221mm, SD 17.4, n 180). However, pairwise ANOVA, using female-male pairs as statistical blocks, indicated no significant differences in shell length among pairs (F 1.155, p 0.358), or between females and males (F 0.847, p 0.366). Results were similar in the case of copulating conch (among pairs, F 1.105, p 0.430; between females and males, F 0.112, p 0.743).

Reproductive activity in *Strombus gigas* was rare on hardbottom substrata (i.e., mounds, rubble and boulder areas). Ninety-four percent of the pairing conch were observed on sand, none were observed on rubble, and only 5.6% were found on hardbottom (Table 1). Eighty-five percent of copulating conch were found on sand, with small percentages found on rubble and hardbottom.

A total of 149 egg-laying females were observed between April and October 1988; except for one female found laying eggs on hardbottom in area B1, all were found spawning on sand (Table 1). Nine observations of simultaneous pairing and egg-laying were made; only one simultaneous copulation and egg-laying was observed. All 148 females on sand were oriented perpendicular to sand waves, with the anterior end of the shell elevated near the crest of the wave and the egg mass near the trough. Mean grain size of sediments collected immediately adjacent to egg-laying females was 0.389 θ (774µm) (SD 0.248, n 8), which is in the coarse-sand classification. Sediments were poorly sorted as indicated by a mean sorting coefficient of 0.967 θ (SD 0.302, n 8). Organic content was 3.45% of dry weight (SD 0.69, n 8).

Larval abundance

Conch larvae were first collected at the Reproductive Site on 2 June 1988 at a density of 0.26 larvae/10m^3 (Table 2), 5 weeks after the first egg mass was discovered (Fig. 3B). Surface- and bottom-water temperatures were 27.5°C and 25.8°C, respectively. Veliger density at the Reproductive Site ranged from 0.04 larvae/10m^3 on 6 June to 0.99 larvae/10m^3 on 16 June. No plankton collections were made at this site between 29 June (0.30 larvae/10m^3) and 23 August (0.77/10m^3); during this interval, emphasis was shifted to the Children's Bay Cay site on Exuma Bank.

Larvae were not found until 6 June in Rat Cay cut and 20 June in Adderley Cay cut (Fig. 3C). By the end of June, surface-water temperature was near maximum (29.5°C and 29°C) in the two inlets. Highest density in the tidal passes was 4.46 larvae/10m^3 on 21 July at the Rat Cay cut, concurrent with maximum egg-laying frequency (13%) and surface and bottom temperatures

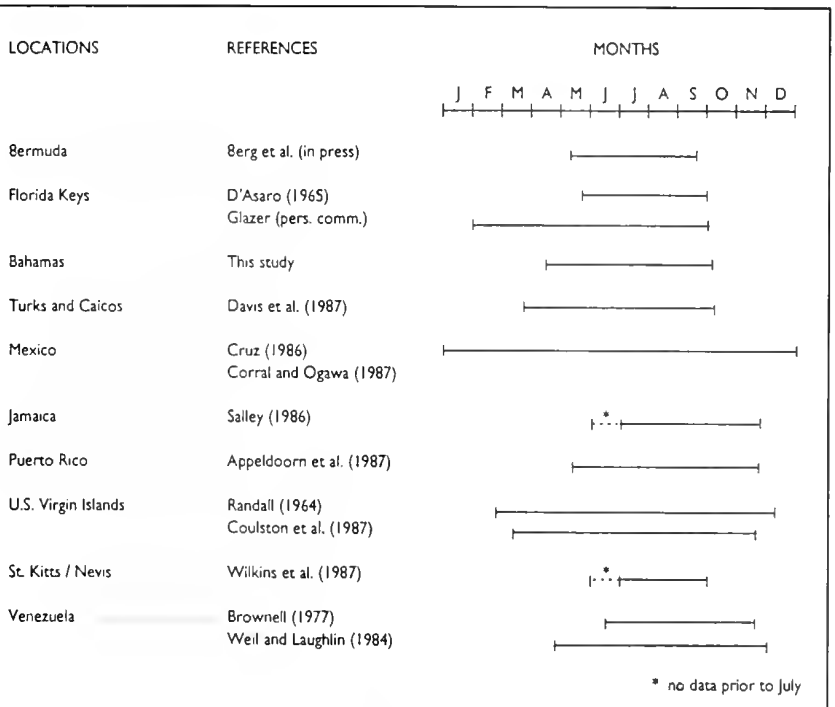

Figure 6

Reproductive seasons reported for *Strombus gigas* in the Caribbean region. Seasonality refers to any observations of reproductive behavior (copulating or egg-laying), and does not include histological results (see text). Locations are arranged in order of latitude from north (top) to south (bottom). Data for Mexico are for Banco Chinchorro on the Caribbean coast.

of 29.8°C and 28.1°C, respectively. Larvae continued to be found at the pass sites until the end of September, but were not present at the Reproductive Site after 23 August. No veligers were collected at any of the sites in October, concurrent with observation of the last egg mass. At this time, surface-water temperature had declined to 27.2°C and bottom temperature was 27.5°C.

Density of larvae at the Adderley Cay cut site showed a direct correlation with the percentage of females copulating (r 0.952, F 68.312, $p<0.0001$) and egg-laying (r 0.860, F 19.889, p 0.003). Densities of larvae at the Reproductive Site and the Rat Cay cut site were not correlated with copulation or egg-laying ($p>0.05$). Maxima in larval abundance occurred during months with highest water temperature, but there was no significant correlation between abundance of larvae and surface-water temperature at Adderley Cay cut (F 5.232, p 0.056) or Rat Cay cut (F 0.514, p 0.494) during the reproductive season (June–October). Log-transformation of the data did not improve the correlation coefficients.

Plankton collections over the nursery area, west of Children's Bay Cay, were begun on 13 July 1988; larval density was 0.82/10 m^3 (Table 2) and surface-water temperature was 31°C. Highest density at this site (1.35 larvae/10 m^3) occurred on 28 July, when numbers of copulating and spawning females were highest at the Reproductive Site. On 12 August, larval density declined to 0.77 larvae/10 m^3, concurrent with declines in reproductive activity. Larvae were last collected over the nursery area on 14 September at a density of 0.17 larvae/10 m^3; at this time, surface-water temperature on the Exuma Bank was 30°C and reproductive activity was near zero.

During the reproductive season, all but three of the conch veligers collected were between 340 and 600 μm in shell length ($\bar{x}$ 384 μm, SD 64, n 394) (Fig. 5). The largest three larvae (1350 μm) were removed alive from samples collected at the bank site in mid-July. Metamorphosis occurred within 24 hours in all three larvae.

Discussion

At Lee Stocking Island, the reproductive season for queen conch began in April and ended in early October. Although differences by a few months were found in the occurrence of reproductive behavior, there was no apparent trend related to latitude in beginning, end, or length of reproductive season in queen conch from Bermuda to Venezuela (Fig. 6).* The longest reproductive season was reported for the Caribbean coast of Mexico (Banco Chinchorro) (Cruz 1986, Corral and Ogawa 1987), where egg masses were found year-round. One of the shortest reproductive seasons was reported by D'Asaro (1965) for the Florida Keys, but more recent, intensive observations have shown that queen conch may spawn over at least a 9-month period in Florida (R. Glazer, Dep. Nat. Resour., Marathon, FL 33050, pers. commun., Sept. 1990).

* For geographic comparison, "reproductive seasonality" refers to any reported observation of pairing, copulation, or egg-laying in queen conch, except where noted in the text. Histological data are not included.

Geographic comparisons of seasonality in reproduction must be interpreted cautiously due to different methods, frequency and number of observations, annual variation, and different habitat types. For example, Brownell (1977) found that egg-laying in Los Roques, Venezuela, extended later into the season in deep water than in shallow water. Quantitative measures of reproductive activity provide a basis for examining mechanisms of seasonality, which is more useful than records of reproductive occurrence. In all studies that present seasonal curves for reproductive behavior or numbers of egg masses (e.g., Davis et al. 1984, Weil and Laughlin 1984, Corral and Ogawa 1987, and this study), maximum reproductive activity was reported during the warmest months of the year.

Control of gametogenesis and the physiology of egg production are still unknown for *S. gigas*, but histological studies of queen conch from Belize showed that mature eggs and sperm were in the gonads year-round (Egan 1985). External factors, therefore, are likely to mediate seasonality in the intensity of reproductive behavior and egg-laying.

Emphasis in the past has been placed on the potential role of water temperature in reproductive activity. Similar to observations in Los Roques, Venezuela (Brownell 1977, Weil and Laughlin 1984), reproductive activity at Lee Stocking Island began with rise in temperature. At both locations, reproductive activity intensified with increasing temperature to reach its maximum during the warmest period. Brownell (1977) suggested that a sharp temperature decline of 1.1°C from November to December was responsible for the termination of queen conch egg-laying in Los Roques. Similarly, egg-laying at Lee Stocking Island ended as bottom-water temperature began to decline steadily from 28.6°C in late September to 25.1°C in December. On the other hand, pairing, copulation, and egg-laying all decreased suddenly between August and September, during a period of high and relatively-stable water temperature, near 28.5°C.

Unlike the partial (early summer) correlation between reproductive behavior and temperature, pairing, copulation, and egg laying were all positively correlated with length of day throughout the year. Photoperiod, therefore, may be one of the important environmental variables which mediates the timing and length of reproductive season. Synergistic interaction between photoperiod and water temperature is possible.

In addition to decreasing length of day in late summer, increasing frequency and intensity of winds from the northeast produce a surge reaching the bottom at the Lee Stocking Island study site in the fall (Caribb. Mar. Res. Cent., Vero Beach, FL 32963, unpubl. data). The significance of wave disturbance is suggested by our own anecdotal observations of short-term decreases in reproductive activity concurrent with 1–2 day periods of reduced temperature and increased surge which occurred during the survey periods in early summer. Reductions in reproductive activity with increasing water turbulence have been noted for queen conch in the Caicos Islands (Davis et al. 1984) and for milk conch *Strombus costatus* in Puerto Rico (R.S. Appeldoorn, Dep. Mar. Sci., Univ. Puerto Rico, Mayaguez, PR 00709, pers. commun., May 1990).

As with temperature, photoperiod may influence the production of mature gametes or have a direct effect on the behavior of conch. It is likely that the combination of increasing water temperature, coupled with increasing length of day, triggers the mass migration of adult conch from hardground to sand habitats and to search for mates. Decreasing length of day and increasing wave surge appear to provide the best explanation for termination of the reproductive season, as pairing and copulation ended while bottom-water temperature was high. Experimental analysis will be required to determine the mechanisms involved in seasonal reproductive rates. Temperature, rates of temperature change, photoperiod, physical turbulence, and other seasonally variable environmental factors will need to be considered.

Similar to the findings of several others (D'Asaro 1965, Robertson 1959, Brownell 1977), egg-laying occurred primarily on clean coral sand with coarse grain size. Davis et al. (1984) noted that this type substrate may be critical for reproductive activity. Copulation and spawning stopped when they placed conch on a bottom type other than coral sand. At Lee Stocking Island, mating on hardbottom was observed, but was rare. Given that only one egg mass was found on substrate other than coral sand, it is clear that this is the preferred, if not critical, substrate for egg-laying.

This study provides the first report on abundance and distribution of queen conch veligers in the field. Veligers were present in the water column from 2 June to the end of September, in concordance with relatively constant rates of egg-laying from April through August. Despite a spawning season spanning 7 months, high numbers of larvae were present in the two inlets only during a 2-month period (July and August).

Although mechanisms involved in seasonality of larval production and survival are unknown as yet, it is clear that larvae were most abundant during the period of warmest water conditions. Summer spawning in Exuma Sound has adaptive significance. First, high temperatures are associated with higher developmental rates in pelagic larvae (Thorson 1950, McEdwards 1985, Boidron-Metairon 1987), decreasing the time larvae spend in the plankton and probably reducing larval mortality (Strathmann 1980). However, increase in temperature needs to be coupled with a food

supply sufficient to provide for higher feeding and metabolic rates (Scheltema and Williams 1982). Second, midsummer months are characterized by prevailing tradewind conditions (i.e., relatively constant winds and moderate seas from the southeast) in the Exuma Cays. General circulation over the reproductive site during this period was to the northwest, parallel to the Exuma island chain (N.P. Smith, Harbor Branch Oceanogr. Inst., Fort Pierce, FL 34946, unpubl. data). This would facilitate transport of pelagic larvae past the numerous inlets which veligers must enter to reach primary nursery habitats on Exuma Bank. As veligers are carried alongshore on the island shelf, they would readily be drawn through the inlets on flood tides. Northwest drift over the reproductive site may, in fact, explain the close correlation between larval abundance in Adderley Cay cut and reproductive activity occurring upcurrent. Winter weather patterns, with frequent passage of cold fronts and shifting winds and currents, would be less favorable for transport of conch larvae to the Exuma Bank nurseries.

On the basis of laboratory growth curves (Boidron-Metairon, unpubl. data), all but the three largest larvae collected in this study were less than approximately 2 weeks old in a larval life stage near 30 days. There are several possible explanations for the scarcity of advanced stage larvae: Late stages occupy habitats different from those of early-stage larvae (on or near the bottom), the abundance of older stages in the water column is reduced due to natural mortality, and/or the late stages are advected to different locations. Virtually nothing is known about transport or behavior of queen conch larvae in the field. Given the great significance of recruitment processes to management of this rapidly depleted fishery species, future research should include studies of larval transport and settlement.

In summary, highest reproductive activity occurred near Lee Stocking Island at a time of stable circulation patterns, high temperature (28–30°C), and long photoperiod. Maximum larval abundance in July and August placed high numbers of veligers in the water column at a time favorable for both high rates of development and transport to nursery habitats. Proximal mechanisms affecting short-term and seasonal variation in reproduction in queen conch may include temperature, rates of temperature change, photoperiod, wave-induced turbulence, and other variables associated primarily with season.

Acknowledgments

This research was supported by a grant from the Undersea Research Program of the National Oceanic and Atmospheric Administration (U.S. Department of Commerce) to the Caribbean Marine Research Center. We thank R.I. Wicklund, Director of the Caribbean Marine Research Center, for providing bottom-water temperature data for the reproductive site. Thanks to P. Bergman, N. Christie, K. McCarthy, O. Monterrosa and E. Wishinski for assistance in the field. R. Appeldoorn, P. Colin, L. Jones, J. Shenker, J.-P. Thonney, and anonymous reviewers provided helpful comments on the manuscript.

Citations

Appledoorn, R.S.
1990 Fishing pressure and reproductive potential in strombid conchs: Is there a critical stock density for reproduction? Mem. Soc. Cienc. Nat. La Salle (In press).

Appeldoorn, R.S., G.D. Dennis, and O. Monterrosa Lopez
1987 Review of shared demersal resources of Puerto Rico and the Lesser Antilles region. *In* Mahon, R. (ed.), Report and proceedings of the expert consultation on shared Fishery resources of the Lesser Antilles region. FAO Fish. Rep. 383: 36–57.

Berg, C.J. Jr., and D.A. Olsen
1989 Conservation and management of queen conch (*Strombus gigas*) fisheries in the Caribbean. *In* Caddy, J.F. (ed.), Marine invertebrate fisheries: Their assessment and management, p. 421–442. Wiley, NY.

Berg, C.J. Jr., J. Ward, B. Luckhurst, K. Nisbet, and F. Couper
In press Observations of breeding aggregations of the queen conch, *Strombus gigas*, in Bermuda. Proc. Gulf Caribb. Fish. Inst.

Boidron-Metairon, I.F.
1987 Effet de la temperature sur la duree des periodes larvaires de quatre especes d'Echinides des Caraibes. Bull. Soc. Sci. Nat. Ouest Fr. H.S:75–79.
1988 A new approach to comparative studies of *Strombus gigas* L. (Gastropoda: Strombidae) larvae at the developmental and nutritional levels. Proc. Gulf Caribb. Fish. Inst. (In press).

Brownell, W.N.
1977 Reproduction, laboratory culture and growth of *Strombus gigas*, *S. costatus*, and *S. pugilis* in Los Roques, Venezuela. Bull. Mar. Sci. 27:668–680.

Brownell, W.N., and J.M. Stevely
1981 The biology, fisheries, and management of the queen conch, *Strombus gigas*. Mar. Fish. Rev. 43(7):1–12.

Corral, J.L., and J. Ogawa
1987 Cultivo masivo de larva de caracol *Strombus gigas* en estanques de concreto. Proc. Gulf Caribb. Fish. Inst. 38: 345–352.

Coulston, M.L., R.W. Berey, A.C. Dempsey, and P. Odum
1987 Assessment of queen conch (*Strombus gigas*). Population and predation studies of hatchery reared juveniles in Salt River Canyon, St. Croix, U.S. Virgin Islands. Proc. Gulf Caribb. Fish. Inst. 38:294–306.

Cruz, R.S.
1986 Avances en la experimentacion de produccion massiva de caracol en Quintana Roo, Mexico. Proc. Gulf Caribb. Fish. Inst. 37:12–20.

D'Asaro, C.N.
1965 Organogenesis, development and metamorphosis in the queen conch, *Strombus gigas*, with notes on breeding habits. Bull. Mar. Sci. 15:359–416.

Davis, M., and C. Hesse
1983 Third world level conch mariculture in the Turks and Caicos Islands. Proc. Gulf Caribb. Fish. Inst. 35:73–82.

Davis, M., B.A. Mitchell, and J.L. Brown
1984 Breeding behavior of the queen conch *Strombus gigos* Linne, held in a natural enclosed habitat. J. Shellfish Res. 4:17–21.

Davis, M., C. Hesse, and G. Hodgkins
1987 Commercial hatchery produced queen conch, *Strombus gigas*, seed for research and grow-out market. Proc. Gulf Caribb. Fish. Inst. 38:326–335.

Egan, B.D.
1985 Aspects of the reproductive biology of *Strombus gigas*. M.S. thesis, Univ. British Columbia, Vancouver, 147 p.

Folk, R.L.
1966 A review of grain-size parameters. Sedimentology 6: 73–93.

Galehouse, J.S.
1971 Sediment analysis. *In* Carver, R.E. (ed.), Procedures in sedimentology petrology, p. 69–94. Wiley, NY.

McEdwards, L.R.
1985 Effects of temperature on the body form, growth, electron transport system activity, and development rate of an echinopluteus. J. Exp. Mar. Biol. Ecol. 93:169–181.

Mianmanus, R.T.
1988 Induction of settlement and metamorphosis in larvae of *Aplysia brasiliana* and *Strombus gigas* (Mollusca: Gastropoda). Ph.D. diss., Univ. Miami, Coral Gables, 171 p.

Randall, J.E.
1964 Contributions to the biology of the queen conch, *Strombus gigas*. Bull. Mar. Sci. 14:246–295.

Robertson, R.
1959 Observations on the spawn and veligers of conchs (*Strombus*) in the Bahamas. Proc. Malacol. Soc. 33:164–171.

Salley, S.
1986 Development of the statocyst of the queen conch larva, *Strombus gigas* L. (Gastropoda: Prosobranchia). M.S. thesis, McGill Univ., Montreal, 116 p.

Scheltema, R.S., and I.P. Williams
1982 Significance of temperature to larval survival and length of development in *Balanus eburneus* (Crustacea: Cirripedia). Mar. Ecol. Prog. Ser. 9:43–49.

Stoner, A.W., and V.J. Sandt
1992 Population structure and seasonal movements in deepwater queen conch, *Strombus gigas*. Bull. Mar. Sci. 51 (In press).

Strathmann, R.R.
1980 Why does a larva swim so long? Paleobiology 6:373–376.

Thorson, G.
1950 Reproductive and larval ecology of marine bottom invertebrates. Biol. Rev. 25:1–45.

Weil, E., and R. Laughlin
1984 Biology, population dynamics, and reproduction of the queen conch, *Strombus gigas* Linne, in the Archipielago de Los Roques National Park. J. Shellfish Res. 4:45–62.

Wilkins, R.M., M.H. Goodwin, and D.M. Reid
1987 Research applied to conch resource management in St. Kitts/Nevis. Proc. Gulf Caribb. Fish. Inst. 38:370–375.

Abstract.—The effect of benthic dredging on coastal fisheries has been of concern for several decades, but little work quantifying direct population impacts has been published. Modeling approaches have been used extensively to assess effects of power plant entrainment on fishery stocks. Several important differences between power plant and dredge operations prevent direct application of these models to dredge problems: Entrainment by dredges is short-term, has a moving intake, and affects all age-classes of the population. We present an equivalent adult loss model of impacts to the Washington coast Dungeness crab *Cancer magister* Dana fishery from dredging of a navigation channel in Grays Harbor, Washington. The model is driven by empirical population data to account for spatial and temporal variation in abundance and age-class structure. Results show that impacts are quite sensitive to the type of dredge used and the season in which dredging occurs. Contrary to initial expectations, the 0+ age-group loss was unimportant relative to losses from older age-classes. Despite many limitations, the model has proven useful for focusing impact assessment work, as a basis for scheduling construction to reduce impacts, and as a basis for scaling mitigation projects.

Manuscript accepted 17 January 1992.
Fishery Bulletin, U.S. 90:171–182 (1992).

Predicting effects of dredging on a crab population: An equivalent adult loss approach

Thomas C. Wainwright
David A. Armstrong
Paul A. Dinnel
José M. Orensanz
Katherine A. McGraw

School of Fisheries, WH-10
University of Washington, Seattle, Washington 98195

The effect of dredging on marine organisms has been an issue of environmental concern for several decades. Most studies on the impact of dredging and disposal of dredged material are concerned with changes in infaunal species assemblages and community characteristics, and generally measure effects by pre- and post-dredging comparisons. Very little work has been done on the direct effects of entrainment on populations of mobile epibenthic invertebrates or demersal fish, in part because such species are difficult to quantify. The reviews by Morton (1977) and Poiner and Kennedy (1984) indicate a strong research emphasis on habitat modification (by either dredging or disposal of sediments) and water column effects (turbidity, release of chemical pollutants) during dredging operations. Water column effects were also the focus of a workshop on anadromous fish and dredging (Simenstad 1990). Virtually no published works report on direct population losses due to entrainment or burial during dredging, except Stevens (1981) and Armstrong et al. (1982). There are few predictive models of dredging impacts other than that of Bella and Williamson (1980), who developed a model of dredging effects in Coos Bay, Oregon. Their model focused on water chemistry and sediments, but also gave some consideration to broad categories of animals.

In sharp contrast, power plant entrainment and impingement of fish has generated a large quantitative modeling literature (e.g. van Winkle 1977). Among the methods used in power plant assessments, the "equivalent adult loss" (Horst 1975, Goodyear 1977) and "production foregone" (Rago 1984) approaches are transferable to dredging operations, if sufficient biological and operational data are available. There are, however, several noteworthy differences between power plant and dredging operations which require different considerations in their analyses. Firstly, power plant water intakes operate continuously at a fixed location, while dredging operations are generally short-term, with a moving intake. This means that continuous, equilibrium approaches (e.g., MacCall et al. 1982) are not appropriate for dredging. Secondly, mobile benthic invertebrate populations are characterized by spatial aggregations and seasonal shifts in distribution which must be taken into account in estimating entrainment by a moving dredge. Finally, power plant entrainment is usually restricted to a single age-class (larvae or early juveniles), whereas dredging removes all age-classes present in the dredged habitat, but may kill age-classes at different rates.

The work we describe here applies an equivalent adult loss model (the "Dredge Impact Model" or "DIM") to assessing entrainment loss to the Dungeness crab *Cancer magister* Dana fishery in and around Grays Harbor, Washington. The Grays Harbor navigation channel (Fig. 1) extends from the harbor mouth to the city of Aberdeen, a distance of about 25 km. The U.S. Army Corps of Engineers currently removes an average of 1.2 million m^3 of sediment annually from the channel during maintenance dredging. To improve accessibility for deep draft vessels, the Corps planned to widen and deepen the channel by removing about 8.7 million m^3 of material over a two-year period (McGraw et al. 1988). Based on results and predictions of DIM, the Corps changed their original dredging program by modifying gear, volume dredged, and location/season combinations to minimize impact on crab within operational constraints (including weather and protection of other resources). Project construction took place throughout 1990, ending in January 1991. This paper extends an initial analysis (Armstrong et al. 1987), incorporating two additional years of biological data and providing a more thorough analysis of year-to-year variation. The study was undertaken in response to concerns of crab fishermen and resource managers that Grays Harbor is important as a juvenile crab nursery.

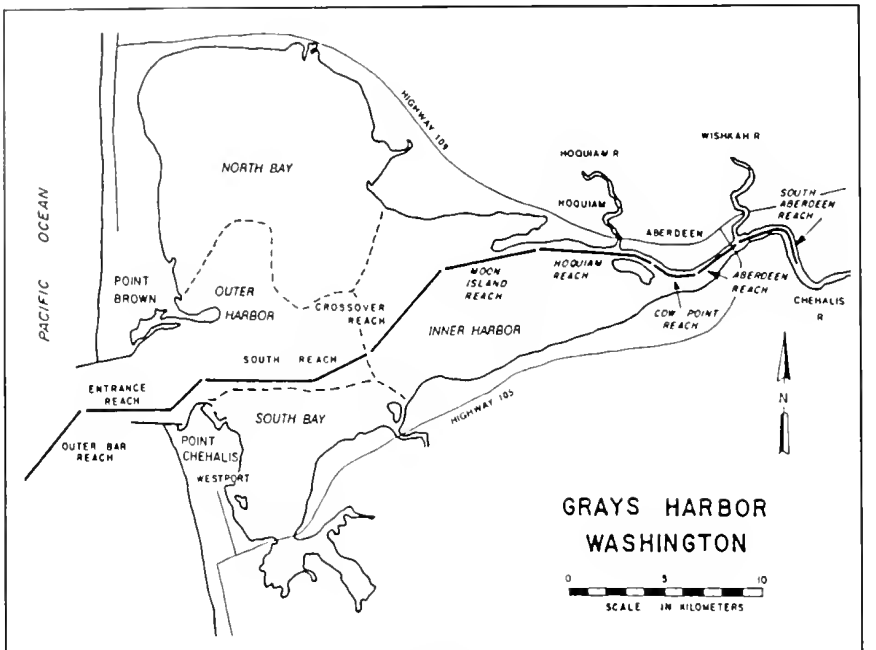

Figure 1

Map of Grays Harbor, Washington, showing existing navigation channel (heavy solid line) and sampling strata (separated by dashed lines).

Dungeness crab provide major fisheries along the west coast of North America, from central California to southern Alaska (Botsford et al. 1989). Since 1945, annual Washington coast crab landings have fluctuated between 1.2 and 9.5 thousand metric tons per year (Fig. 2). The general life-history pattern of Dungeness crab along the Washington coast is as follows (Gunderson et al. 1990, Jamieson and Armstrong 1991). Females molt to maturity along the open coast, generally in the spring. Mating occurs at this time, but eggs are not extruded until the following winter. Eggs generally hatch between December and March, and larvae remain in the water column for a few months. Late-stage larvae are found onshore in late-spring and summer, where they settle to the bottom and metamorphose. Settlement occurs both in nearshore coastal waters and in estuaries; within estuaries, crab settle in both subtidal and intertidal habitats. Crab settling in intertidal areas may remain there during their first summer, but move into the subtidal zone in fall. Few older crab are resident in the intertidal, but move on and off the tidal flats with the tides (Stevens et al. 1984). Crab settling in nearshore waters may remain there for life, but there is evidence of some migration into the estuary between their first and second summers. Crab remain in estuarine subtidal areas for up to two years, but late-juvenile and early-adult crab leave the estuary before reproduction, which occurs mainly along the open coast. Both female and male crab reach sexual maturity at about 2 years of age, but males may not breed until age-3 or older (Butler 1960 and 1961, Hankin et al. 1989).

Methods

Model structure

The calculation of crab loss is driven by two variables: crab abundance (uncontrolled) and volume dredged (controlled). Both of these vary in both space and time. The two types of data are related through an entrainment function that describes the number of crab entrained by each type of dredging gear as a function of local crab density and volume dredged. Not all crab entrained are killed, so a second relationship describes the number killed as a function of crab age and dredge type. To apply the model, crab abundance is measured

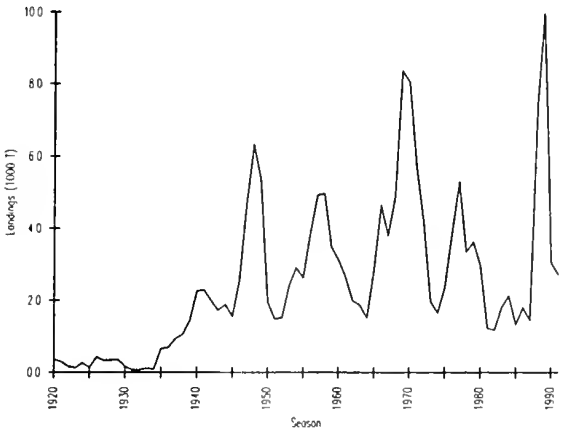

Figure 2

Historical landings in the Washington coastal Dungeness crab fishery. Sources: 1920–47, Cleaver (1949); 1948–50, Wash. Dep. Fish. (1951); 1951–87, Pac. Mar. Fish. Comm. (1989); 1988–91 are preliminary estimates (S. Barry, Wash. Dep. Fish., Olympia, pers. commun.).

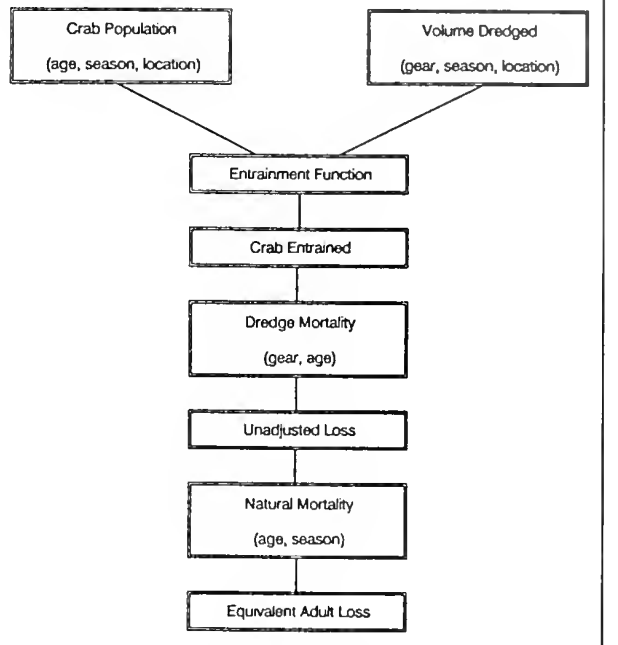

Figure 3

Flowchart of Dungeness crab adult loss model, showing main variables and structural categories (in parentheses).

as density stratified by age, season, and location. Dredging is described as the volume dredged by a particular gear in a location during a given season. Unadjusted loss figures are converted to equivalent adult loss by multiplying by the expected survival of crab from a certain age-class and season to adulthood. This approach is shown schematically in Figure 3, and described in detail below. Because we could not resolve older age-classes within our survey data, a crab was considered to reach adulthood in winter of its age 2+ year (i.e., approaching the end of its third year post-settlement).

Calculating losses in this manner requires an underlying concept of population dynamics and several simplifying assumptions. Creating a detailed model of local dynamics for a mobile benthic animal is difficult; there is continuous mortality and migration among habitats, the rates of which may vary with season, age, and locality. This may be summarized by the usual mass-balance equation for change in the population in a local area over a discrete time period:

$$N(t_1) = N(t_0) + R - M - E + I, \qquad (1)$$

where N is population abundance, t_0 and t_1 are two times, R is recruitment to the population (settlement), M is mortality, E is emigration, and I is immigration.

Mortality and migration rates are rarely known accurately (certainly not in our problem), so we have taken an empirical approach to defining population abundance. The approach is similar to, but simpler than, that taken by Boreman et al. (1981) for power plant entrainment in an estuary. The model is a discrete time, discrete age-population model with discrete habitat structure. To allow for seasonal changes in abundance or population structure, the year is subdivided into four seasons. Thus the population can be described as the numbers in various age-classes present in various habitat areas during particular seasons. In our model, abundance of any age-class in an area during a single time-step is taken to be the average abundance estimated from field surveys. We assume that all changes in abundance (i.e., mortality or migration) occur between time-steps, so that populations are constant throughout a step. This assumption introduces little error if the change during a step is small (less than about 10%), which will be true if time steps are relatively short and rates of change are relatively low. To meet this assumption in our application, we defined variable-length seasons of relatively constant population structure (see Data and Estimation section below).

The starting point for our calculations is estimated total crab density (D) for locations (l) and seasons (s), combined with age-class proportions (P). (Variables are fully defined in Table 1.) The second set of information needed for the calculation is the dredging schedule, expressed as volume dredged (V) by a specific gear type (g) in a specific location and season. For planning

Table 1
Model notation.

	Symbol	Description
Subscripts	a	age-class
	l	location
	s	season
	g	dredge gear
Population	D_{ls}	density
	P_{als}	age class proportions
	S_{as}	natural survival to adulthood
Dredging	V_{lsg}	volume dredged
Entrainment	e_g	entrainment rate
	m_{asg}	dredge-induced mortality proportion
Loss	E_{lsg}	total entrainment
	L_{alsg}	unadjusted loss
	EAL_{alsg}	equivalent adult loss

purposes, volume was measured as thousands of cubic yards (kcy) of dredged material (1 kcy = 765 m^3).

To obtain crab loss due to dredging from these two sets of information, we require crab entrainment rates (e), measured as numbers of crab entrained per unit volume dredged. Total entrainment (E) is

$$E_{lsg} = D_{ls} \cdot e_g \cdot V_{lsg}. \quad (2)$$

Postentrainment mortality (m), expressed as a proportion of those entrained, varies with gear type, age, and season. Age-specific loss (L) of crab in a single season, location, and gear combination will be

$$L_{alsg} = E_{lsg} \cdot P_{als} \cdot m_{asg}. \quad (3)$$

To compare the relative importance of losses from different age-classes, equivalent adult loss (EAL) for any season-location-gear combination is calculated as

$$EAL_{lsg} = \sum_{a} L_{alsg} \cdot S_{as}, \quad (4)$$

where S_{as} is the total natural survival to adulthood from age-class i in season k (assumed equal in all habitats). Total loss for the project is then

$$EAL_{tot} = \sum_{lsg} EAL_{lsg}. \quad (5)$$

Data and estimation

Population abundance Crab population surveys were conducted over a six-year period (1983–88) in Grays Harbor and along the adjacent coast. Stratified random sampling was done with a small beam trawl at biweekly or monthly intervals during spring and summer (May–September) with occasional sampling during fall and winter. From these surveys, crab densities were estimated for each stratum, and total population estimates were computed separately for Grays Harbor and the adjacent coast using the National Marine Fisheries Service BIOMASS program (Alaska Fish. Sci. Cent., 7600 Sand Point Way NE, Seattle, WA 98115), which uses standard stratified random survey statistical methods (Cochran 1962). Details of the survey design and population estimates can be found in Armstrong and Gunderson (1985) and Gunderson et al. (1990). In addition to the trawl surveys, intertidal crab were sampled in 0.25 m^2 quadrats at several locations within the harbor, and total intertidal population was estimated as described by Dumbauld and Armstrong (1987).

Growth and age-classes In general, age-class identification is difficult in crustaceans (Hartnoll 1982). The lack of retained hard parts prohibits direct aging techniques (such as scale analysis in fish), so age must be estimated from size. We relied on visual separations of age-classes in size-frequency plots from the population surveys, but molting and individual variability in growth obscure age-class modes except for young, rapidly growing crab. In all cases, young-of-the-year (age 0+) crab were easily identifiable as a separate size-group. Age 1+ size distributions sometimes overlapped older ages; in these cases, visual estimates of the separation point were supplemented by projecting growth from earlier observations. No reasonable separations could be made for older ages. For this reason, our analysis uses three age-classes: 0+, 1+, and >1+. Within Grays Harbor, we believe that most crab leave the estuary before their third year, so that almost all crab within the estuary identified as >1+ are actually age 2+, and this assumption is made in our analysis. Proportions in each age-class were then calculated from the total size-frequency distribution of each sampling stratum.

Definition of model seasons Seasons were defined to reflect important biological processes and major changes in crab abundance through the year. The spring season (April and May) reflects the start of settlement of the 0+ age-class and a period of migration into the estuary by age 1+ coastal crab; summer (June–September) is a period of continued settlement,

rapid growth, and steady mortality for 0+ crab and relative stability for older age-classes. Fall (October–December) and winter (January–March) are periods for which we have little sampling data, but both are periods of general population decline, migration from intertidal to subtidal areas within the estuary by 0+ crab, and emigration from the estuary by older age-classes. Where data were lacking during fall and winter, values were projected from late-summer populations according to the trends in numbers observed in years for which winter data were available.

Definition of geographic strata The population survey design had four strata within Grays Harbor: Outer Harbor, North Bay, South Bay, and Inner Harbor (Fig. 1). The navigation channel passes through two of these (Inner and Outer Harbor), and crab densities within various reaches of the channel were assumed to be the average densities for the corresponding sampling strata. In fact, crab densities estimated within the channel during entrainment studies are quite comparable with those estimated from the corresponding strata of the regular surveys (Dinnel et al. 1986, Dumbauld et al. 1988, Wainwright et al. 1990). Thus calculations for Bar, Entrance, and South Reaches used crab densities for the Outer Harbor, while Inner Harbor values were used from Crossover Reach to Aberdeen Reach. Crab densities decline upriver, and South Aberdeen Reach was assumed to have no crab.

Mortality Mortality estimates were calculated by regressing logarithm of population abundance on age. This method was applied separately for early juveniles (age 0+) and for older juveniles and adults (age 1+ and older). Because substantial migration of 0+ crab to or from the estuary does not occur, mortality rates specific to Grays Harbor could be calculated for this age-group. To estimate mortality, total estuarine 0+ and 1+ populations were calculated from the six years of trawl survey data. Estimates for 0+ subtidal populations were supplemented with intertidal estimates to provide a complete representation of the estuarine population. Direct calculation of mortality requires analysis of a population with no recruitment or migration. Settlement had essentially ended by July of each year, so we chose July of the 0+ year as the starting point for calculations. During the 1+ year, migration begins near the end of the summer as crab leave the estuary. Because of this, we chose June of the 1+ year as the endpoint for estimating first-year survival. First-year mortality estimates were calculated for each of five cohorts (1983–87 year-classes).

Estimation of mortality for older ages is more difficult for two reasons: age-class separation is difficult and inaccurate, and migration to and from the estuary occurs. Because of these problems, a different approach was used. To reduce problems of migration, population estimates for the estuary and adjacent coast were combined. Age-class separations were made using an instar analysis technique (Armstrong et al. 1987, Orensanz and Gallucci 1988) to identify instar composition of the population. Instar abundances were then assigned to year-classes. To reduce errors from sampling and age-class identification, monthly abundance estimates were averaged over all year-classes, then averaged over months within each survey season to give a single estimate for each age-class (a):

$$N_a = \text{mean}(N_{amy}), \tag{6}$$

where N_{amy} is the abundance estimate for age a in month m of sample year y. Then survival from age a to a+1 was calculated as

$$S_{a,a+1} = \frac{\bar{N}_{a+1}}{N_a}. \tag{7}$$

Because a single strong year-class biases estimates calculated in this way, the very strong 1984 year-class was excluded. The calculated age-specific natural mortality rates were then combined to produce the survival schedule (S_{as} in Eq. 4) used to calculate equivalent adult loss from unadjusted loss.

Estimating entrainment rate Numerous studies have been conducted to estimate the rate of entrainment of crab by various kinds of dredges, and the subsequent damage and mortality to entrained crab (McGraw et al. 1988). Entrainment and subsequent mortality are discussed separately below.

A regression relationship was used to predict the entrainment rate (crab entrained/kcy dredged; e in Eq. 2) from trawl-based density estimates (crab/ha). This approach was used by Armstrong et al. (1987) and McGraw et al. (1988) to estimate entrainment rates for a hopper dredge. More data have been collected since those studies, so a new relationship has been calculated. Sampling during the entrainment surveys consisted of two parts: sampling of the dredged material stream aboard a hopper dredge, and concurrent trawl surveys within the channel section being dredged. During each survey, sampling occurred over a two- to three-day period and covered several stations within the navigation channel. For each survey, mean entrainment (crab per kcy dredged) and mean density (crab per ha) were calculated over all samples within each station. This provided a total of 14 points which were used to calculate the regression. Details of survey methods are given in McGraw et al. (1988).

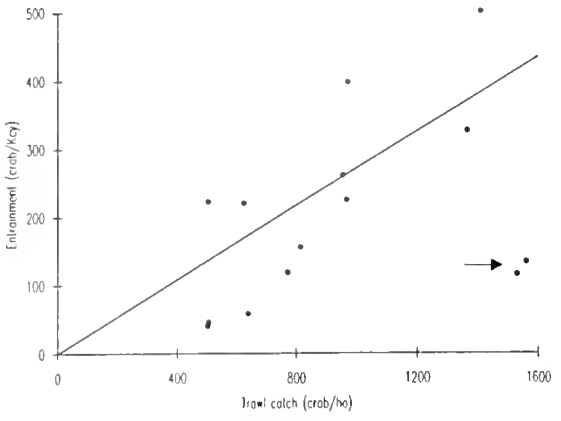

Figure 4

Relationship between trawl catch and entrainment of Dungeness crab by a hopper dredge. The line was fit by least-squares and non-parametric regression. Arrow indicates two outliers which were excluded from the least-squares regression.

To relate crab entrainment to crab density, several regression models were tried. The selection of a final model was based on both statistical measures of fit and biological reasonableness (i.e., an expectation that entrainment should increase with increasing crab density). First, a test for linearity ("XLOF" in the Minitab package; Minitab Inc., University Park, PA) was performed, and no significant nonlinearity was detected ($p>0.10$). Second, a linear least-squares regression was calculated; neither the slope nor the intercept were significantly different from zero for this model. However, this relationship was heavily influenced ("Cook's Distance Measure"; Weisberg 1985) by two points. When these two points were excluded, the best least-squares model was (Fig. 4)

$$Y = 0.27X, \quad (8)$$

where Y is entrainment by the dredge (crab/kcy), and X is trawl-estimated density (crab/ha). Finally, a non-parametric median-slope regression (Conover 1980) was calculated using all 14 data points. This method returned the same slope as the 12-point least-squares regression.

Entrainment for the other dredge types was calculated from this model based on relative entrainment factors given by Stevens (1981); entrainment by a pipeline dredge is assumed to be 100% of the hopper dredge value (this value is controversial, but is conservative), while a clamshell dredge entrains only about 5% of the hopper dredge value.

Table 2

Postentrainment mortality rates for Dungeness crab by age, season, and dredge type.

Dredge type	Age-class	Season	Size range (mm)	Mortality (%)
Hopper	0+	Apr–May	7–10	5
		Jun–Sep	11–30	10
		Oct–Dec	31–40	20
		Jan–Mar	41–50	40
	1+	Apr–Sep	51–75	60
		Oct–Mar	>75	86
	>1+	All	>75	86
Clamshell	All	All	All	10
Pipeline	All	All	All	100

Postentrainment mortality After entrainment, crab may be killed due to physical trauma during transport through pipes and pumps, burial under excessive sediment weight, or confined disposal in landfill by a pipeline dredge. Several estimates of postentrainment mortality (m in Eq. 3) have been made. For a hopper dredge, Stevens (1981) reported approximately 75% mortality, all sizes of crab combined. Armstrong et al. (1982) reported mortality rates by crab size for a hopper dredge, with 86% mortality for crab larger than 50mm carapace width (CW) and 46% mortality for those smaller than 50mm CW. Other studies indicate that hopper dredge mortality rates for small (<10mm) 0+ age-class crab range from 1% to 5% (K. Larson, Portland Dist., U.S. Army Corps of Eng., pers. commun., 1987). Gross mortality observations were also made during later entrainment studies (McGraw et al. 1988, Wainwright et al. 1990), but these recorded only obvious mutilations and so underestimate total mortality. We adopted a set of size-dependent mortality rates for a hopper dredge based on these studies (Table 2).

Little information is available concerning mortality of crab entrained by a clamshell dredge. Stevens (1981) reported an overall mortality rate of less than 10%, which seems reasonable considering the operation of the gear. We have used a 10% mortality rate for a clamshell dredge for all age-classes. Because its effluent goes to confined upland disposal, 100% mortality was assumed for all crab entrained by the pipeline dredge.

Simulations Scheduling of dredge operations was based on engineering constraints, weather limitations, avoidance of salmon migration periods, and avoidance of seasons and areas with high predicted crab loss. To help in this planning process, loss rates (expressed as crab per volume dredged) were calculated for each area and each season, based on average seasonal crab densities and age-class composition.

Table 3

Hypothetical project scenarios for Grays Harbor, WA, showing volume to be dredged by each dredge type in each area and season.

Harbor section	Season	Dredge	Volume (kcy)
Scenario 1: Full confined disposal			
Outer	Jan-Mar	Hopper	1698
Outer	Apr-May	Hopper	1132
Outer	Apr-May	Hopper	330
Outer	Jun-Sep	Hopper	2800
Inner	Jun-Sep	Hopper	1000
Inner	Jun-Sep	Pipeline	434
Inner	Oct-Dec	Hopper	2036
Inner	Oct-Dec	Pipeline	2224
Inner	Jan-Mar	Hopper	1714
Inner	Jan-Mar	Pipeline	670
		Total	14,038
Scenario 2: Limited confined disposal			
Outer	Apr-May	Hopper	1462
Outer	Jun-Sep	Hopper	2800
Outer	Jan-Mar	Hopper	1698
Inner	Apr-May	Clamshell	771
Inner	Jun-Sep	Hopper	1000
Inner	Jun-Sep	Clamshell	579
Inner	Oct-Dec	Hopper	2036
Inner	Oct-Dec	Clamshell	778
Inner	Oct-Dec	Pipeline	374
Inner	Jan-Mar	Hopper	1714
Inner	Jan-Mar	Clamshell	826
		Total	14,038

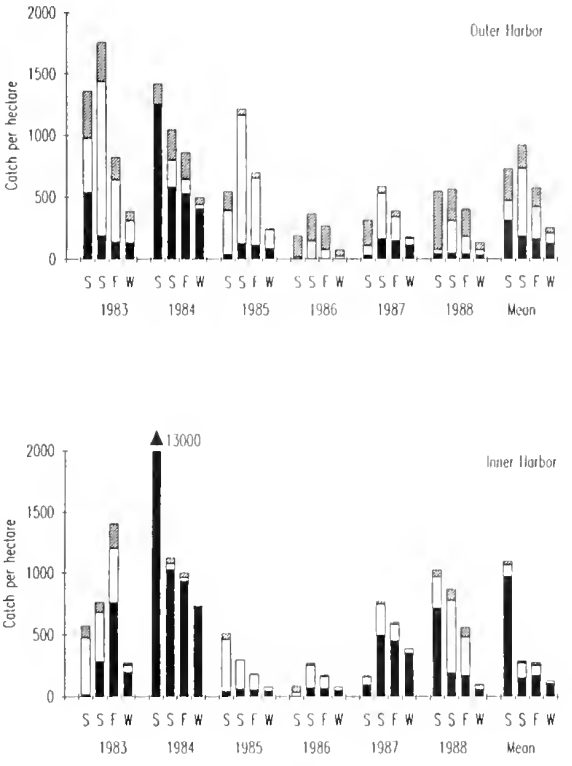

Figure 5

Seasonal abundance (catch per hectare) of Dungeness crab in the Outer and Inner Harbor strata of Grays Harbor, Washington, by age-class. Solid bars, age 0+; white, age 1+; hatching, age >1+.

Once project scheduling was determined, predictions of total crab loss were needed, which we calculated by simulating entrainment for planned construction scenarios. The scenarios we have used for calculating crab losses reflect the project as planned in 1987 (Table 3). There was some conflict between project costs and crab protection, particularly regarding the tradeoff between using gear that is economically efficient (hopper and pipeline) and that which minimizes loss (clamshell). Throughout most of the estuary, the efficiency of the hopper dredge makes alternatives uneconomic. In certain areas of the Inner Harbor, the pipeline dredge is economically most efficient but results in high post-entrainment mortality. The alternative dredge in those areas is a clamshell, which is generally more costly. To better evaluate this tradeoff, two scenarios are contrasted. Scenario 1 includes full use of a pipeline dredge where it is most effective; in Scenario 2, a clamshell dredge is substituted where feasible. Table 3 shows volumes dredged under each scenario by gear type, location, and season.

As initially planned, construction was to occur over two calendar years, extending through seven seasons. To simplify calculations, we compressed the project into a single model year (from spring of a given calendar year through winter of the next), and calculated entrainment and losses for each scenario separately based on each of the six years of survey-based crab abundance estimates. This produced a set of 12 (six years by two construction scenarios) model runs.

Because the project was revised in several ways since these calculations were made, results presented here do not reflect actual expected losses resulting from the project, and are presented only to illustrate the method.

Results

Population parameters

Age-class abundance Densities of crab in the Inner and Outer Harbor strata varied considerably among years and seasons (Fig. 5). Average seasonal total density ranged from 73 ha^{-1} to 13,000 ha^{-1}. Age 0+ crab were most abundant in 1984, and were usually more abundant in the Inner Harbor. Older crab were more

Table 4
Estimates of instantaneous mortality (Z) and annual survival (S) for age 0+ Dungeness crab, Grays Harbor, WA.

Year-class	Z (yr^{-1})	S (%)
83	3.4	3.4
84	2.2	11.5
85	3.5	3.0
86	1.6	19.8
87	1.9	15.2
Average	2.5	8.1

Table 5
Estimates of instantaneous mortality (Z) and annual survival (S) for older age-classes of Dungeness crab, Grays Harbor, WA, and adjacent coast combined. Estimates are for July–July, average for several years.

Age	Z (yr^{-1})	S (%)
1+ – 2+	1.6	19.5
2+ – 3+	0.8	45.0
3+ – 4+	1.0	38.0

Table 6
Survival schedule: percent of Dungeness crab surviving from each season to midwinter (15 Feb.) of the 2+ year.

		Age-class		
Season	Midpoint	0+	1+	2+
Apr–May	30 Apr	0.87	10.7	53.2
Jun–Sep	31 Jul	1.65	16.0	64.9
Oct–Dec	15 Nov	3.40	25.5	81.9
Jan–Mar	15 Feb	6.35	38.0	100.0

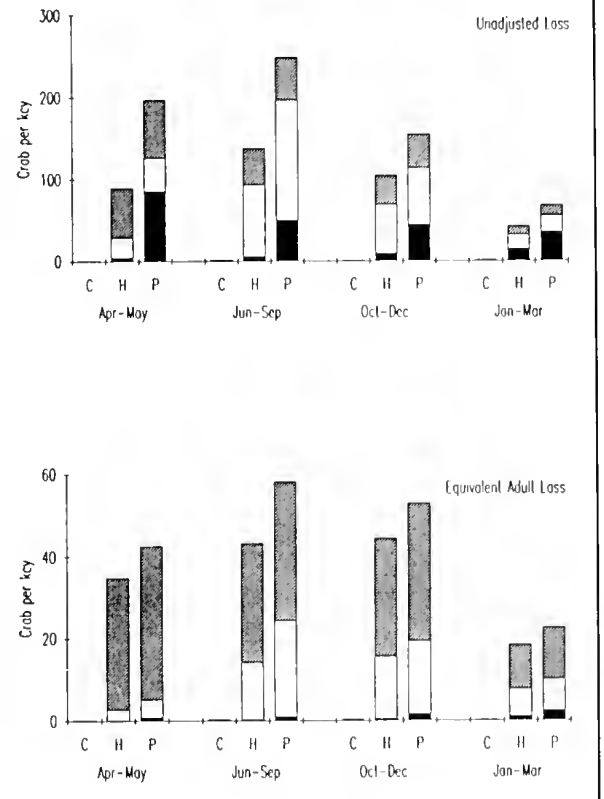

Figure 6
Entrainment rates of Dungeness crab by season and dredge type for the Outer Harbor, by age-class. (upper) Unadjusted losses; (lower) age 2+ equivalent losses. Dredge types: C = clamshell, H = hopper, P = pipeline. Age-classes as in Figure 5.

abundant in the Outer Harbor, where they reached peak densities in the summer season.

Mortality Estimated instantaneous mortality rates for age 0+ crab within Grays Harbor ranged from 1.6 to 3.5 yr^{-1}, with a mean of 2.5 yr^{-1}, corresponding to an annual survival of 8.1% (Table 4). For older crab, estimated mortality rates (Eq. 7) decreased to age 3+, then increased slightly between ages 3+ and 4+ (Table 5). These two results were combined to derive the seasonal survival schedule (Table 6) used in the model.

Gear and season comparisons

The results of gear/season comparison simulations are presented in Figures 6 and 7. These data show the strong contrast between the pipeline and clamshell dredges: the clamshell dredge has negligible impact. Comparing the unadjusted losses (Eq. 3) with age 2+ equivalent losses (Eq. 4) shows the relative unimportance of 0+ crab. Also notable are the high age 2+ equivalent losses in the Outer Harbor during summer and fall, when there are concentrations of age 1+ and older crab in this area (Fig. 5).

Impact estimates

Calculations of total age 2+ equivalent loss (Eq. 5) for the two project scenarios are shown in Figure 8. As expected, Scenario 1 (full use of the pipeline dredge with confined disposal) shows higher losses than Scenario 2. For both scenarios, a large part of the total loss occurs during the June–September season, due to large volumes being dredged in the Outer Harbor where older crab are concentrated at this time. The results indicate strong year-to-year variation in

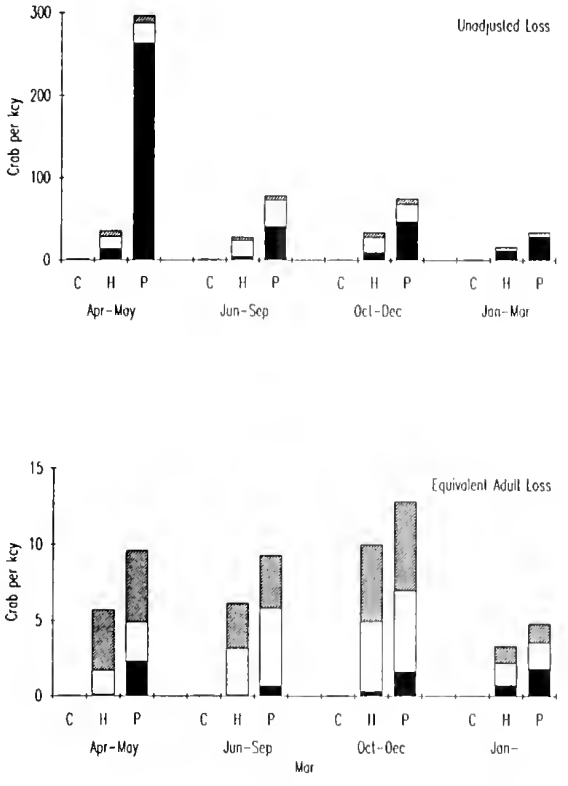

Figure 7
Entrainment rates of Dungeness crab by season and dredge type for the Inner Harbor, as in Figure 6.

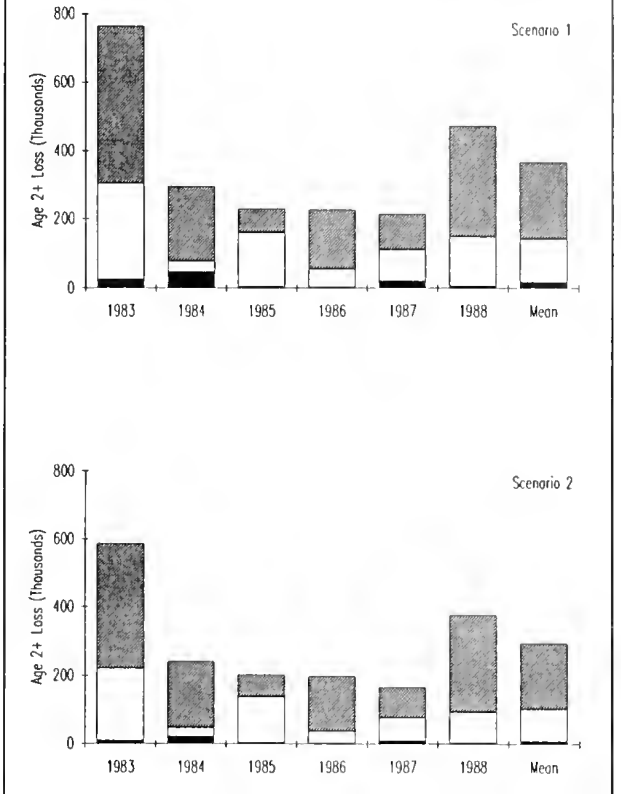

Figure 8
Total estimated age 2+ equivalent losses for hypothetical dredging in six years for two project scenarios. (upper) Full use of confined disposal; (lower) limited confined disposal. Age-classes as in Figure 5.

impacts, with 1983 construction resulting in impacts nearly three times the average for the other years. This is apparently because 1983 followed two years of strong settlement, as evidenced by the high abundance of both age 1+ and >1+ crab in that year (Fig. 5; see also Gunderson et al. 1990). This emphasizes the importance of population monitoring during construction to accurately assess impacts.

Discussion

Gear and season comparisons made with DIM provided several results which were subsequently used to schedule construction gear, season, and location combinations so as to reduce crab losses. As expected, the clamshell dredge (which moves slowly and does little mechanical damage to organisms) had insignificant impact in all seasons and areas. Comparing pipeline and hopper dredge effects, our initial impression was that, with confined disposal (resulting in 100% loss of all age-classes), the pipeline dredge would cause extremely high losses relative to the hopper dredge. This is true when one considers the unadjusted losses (Figs. 6A and 7A). However, when viewed on an equivalent adult loss basis (Figs. 6B and 7B), the pipeline dredge loss rate is only 10–50% higher than that of the hopper dredge. The equivalent adult loss viewpoint was also important in seasonal comparisons, especially in the Inner Harbor (Fig. 7) where unadjusted loss was highest in spring, but equivalent adult loss peaked in fall.

During any modeling endeavor in applied ecology, certain decisions must be made to limit the scope and applicability of the model. Many decisions are made simply on the basis of information or time available, while others reflect the biases and experiences of the authors. One of the major decisions in this project was the choice between predicting short-term losses via the equivalent adult loss approach, or accounting for potential longer-term losses due to reduction of the local reproductive stock via "production foregone" (Rago 1984) techniques. For local, short-term entrainment to have longer-term population effects requires a strong influence of current stock size on future recruitment.

For Dungeness crab, there is little evidence of stock-dependence. In fact, it is not clear whether a local stock, such as that in Grays Harbor, is self-reproducing or depends on larval drift from other areas. For this reason, we chose to use only short-term loss predictions.

The choice of slope for the regression of crab entrainment on trawl catch will strongly influence model results. We gave long consideration to the choice of regression models. Problems arise because there are few data points and large measurement errors associated with both variables. Costs of sampling (which involved simultaneous operations of a specially modified hopper dredge and a chartered trawler) prohibited any increase in data quantity or precision. Initially, we chose to use least-squares regression (LSR) with its underlying assumptions of normal errors with equal variances. There are two forms of LSR in common use: predictive LSR which assumes that all error is in measurement of the Y (dependent) variate, and functional LSR which incorporates errors in both X and Y variates. In the overall context of DIM, the entrainment regression serves the role of a calibration curve predicting entrainment from a set of observed trawl catches. For this reason, we used a predictive regression conditional on the observed trawl catches. (This implies that the result is not generalizable to any other method of crab density estimation, but such generalization is not needed here.) Two outliers were dropped from the LSR analysis; both points were from the same station in different years, and both were influenced by one or two extremely high trawl catches. Because we were not entirely satisfied with the assumptions of the LSR analysis, the data was reanalyzed using a nonparametric regression technique which is robust to non-normality, inequality of variances, and errors in measurement of the X variate. Because this analysis agreed with the final LSR model (Eq. 8), we accepted that model as the most reasonable.

Another limitation was our inability to reliably distinguish age-classes beyond 1+ and obtain mortality estimates for older age-groups. Because of this, we stopped our calculations at age 2+, but there is a strong desire to relate the results to fishery stocks with recruitment at 3–5 years of age. It is possible to perform some rough calculations of actual impact to fisheries, if we are willing to make some assumptions. Using Scenario 2 (limited confined disposal) as an example, estimated age 2+ equivalent losses ranged from 166 to 587 thousand crab (Fig. 8). The fishery harvests males only, so with a 50% sex ratio these numbers become 83–298 thousand age 2+ male crab lost. To relate these to the fishery, we need to know survival from age 2+ to recruitment. We have rough estimates of mortality from age 2+ to 3+ and from age 3+ to 4+ (Table 6) calculated from the trawl survey data set. These estimates are confounded with the decline in gear efficiency with crab size, and so are probably underestimates of true survival. They also depend on tenuous assumptions about size-at-age. Accepting these estimates and assuming the bulk of the fishery recruits at age 3+, our estimates of age 2+ loss correspond to losses to the fishery of 37–134 thousand age 3+ male crab. As exploitation rates are quite high (~70–90%; Methot and Botsford 1982), these numbers can be related directly to annual catch. The ten-year average catch for the Washington coast has been about 3000 metric tons, which corresponds to 3.3 million crab (average individual weight of 0.9kg). So, losses for this hypothetical scenario would be on the order of 1–4% of the average annual catch by the Washington coast fishery.

The model was limited by several other factors, particularly problems of data quality and parameter estimates. Primary among these was lack of data on beam trawl efficiency and size selectivity (Gunderson and Ellis 1986). We have implicitly assumed that the trawl sampling was 100% efficient for all sizes of crab, which is certainly not the case. The gear was designed for capturing juvenile crab, and we believe it to be relatively efficient for juvenile sizes, but crab approaching legal size are able to avoid or escape the small net. For estimating absolute numbers entrained, this is not a problem because the entrainment function is essentially a calibration of entrainment against trawl catch, regardless of trawl efficiency. However, to the extent that gear efficiency is below 100%, we underestimate total populations within the estuary. Calculations of entrainment as a proportion of the local population are thus biased upward. Trawl efficiency also affects natural mortality rate estimates, to which equivalent adult loss calculations are extremely sensitive.

Overall, DIM has proved useful even with its limitations. In project planning, the model allowed scheduling gear and work seasons to reduce impacts on the crab population, and provided some quantitative predictions of loss on which to base mitigation programs. DIM is now being used in conjunction with crab survey data gathered during construction to estimate actual crab losses and to fully define levels and type of mitigation. Beyond these intended uses, the model served to focus concerns about crab impacts, which tended to be somewhat ill-defined, onto specific questions of data quality and reliability of predictions, providing all sides a common basis for argument.

Acknowledgments

This work was done under a combination of support from the Seattle District, U.S. Army Corps of Engi-

neers (#DACW67-85-C-0033), Battelle Pacific Northwest Laboratories, Sequim, Washington, and Washington Sea Grant (#NA86AA-D-SG044 Project R/F-68). We appreciate the contributions of the Corps staff, notably Fred Weinmann, Gail Arnold, James Waller, and Ann Uhrich, and the valuable comments and discussion of the Grays Harbor Crab Study Panel convened by Walter Pearson. Louis Botsford provided invaluable suggestions for the initial model design. Loveday Conquest provided analysis of the entrainment regression and other statistical advice. The project could not have been completed without the cooperation of the crews of the COE dredge YAQUINA and the fishing vessel Karelia (Vern Heikkila at the helm). We also thank those (too numerous to name) who contributed greatly to field work, data analysis, and administrative support.

Citations

Armstrong, D.A., and D.R. Gunderson
1985 The role of estuaries in Dungeness crab early life history: A case study in Grays Harbor, Washington. *In* Melteff, B.R. (ed.), Proceedings, Symposium on Dungeness crab biology and management, p. 145–170. Alaska Sea Grant Rep. 85-3, Univ. Alaska, Fairbanks.

Armstrong, D.A., B.G. Stevens, and J.C. Hoeman
1982 Distribution and abundance of Dungeness crab and *Crangon* shrimp, and dredging-related mortality of invertebrates and fish in Grays Harbor, Washington. Tech. Rep. to Wash. Dep. Fish. and U.S. Army Corps of Eng., Seattle Dist. by School of Fisheries, Univ. Wash., Seattle, 349 p.

Armstrong, D.A., T.C. Wainwright, J. Orensanz, P.A. Dinnel, and B.R. Dumbauld
1987 Model of dredging impact on Dungeness crab in Grays Harbor, Washington. Fish. Res. Inst. Rep. FRI-UW-8702, School of Fisheries, Univ. Wash., Seattle, 167 p.

Bella, D.A., and K.J. Williamson
1980 Diagnosis of chronic impacts of estuarine dredging. J. Environ. Syst. 9:289–311.

Boreman, J., C.P. Goodyear, and S.W. Christensen
1981 An empirical methodology for estimating entrainment losses at power plants sited on estuaries. Trans. Am. Fish. Soc. 110:253–260.

Botsford, L.W., D.A. Armstrong, and J.M. Shenker
1989 Oceanographic influences on the dynamics of commercially fished populations. *In* Landry, M.R., and B.M. Hickey (eds.), Coastal oceanography of Washington and Oregon, p. 511–565. Elsevier, Amsterdam.

Butler, T.H.
1960 Maturity and breeding of the Pacific edible crab, *Cancer magister* Dana. J. Fish. Res. Board Can. 17:641–646.
1961 Growth and age determination of the Pacific edible crab *Cancer magister* Dana. J. Fish. Res. Board Can. 18:873–890.

Cleaver, F.C.
1949 Preliminary results of the coastal crab (*Cancer magister*) investigation. Wash. Dep. Fish. Biol. Rep. 49A:47–82.

Cochran, W.G.
1962 Sampling techniques, 2d ed. Wiley, NY, 413 p.

Conover, W.J.
1980 Practical nonparametric statistics, 2d ed. Wiley, NY, 462 p.

Dinnel, P.A., D.A. Armstrong, B.R. Dumbauld, and T.C. Wainwright
1986 Impact of dredging on Dungeness crab, *Cancer magister*, in Grays Harbor, Washington during August 1986. Fish. Res. Inst. Rep. FRI-UW-8611, School of Fisheries, Univ. Wash., Seattle, 34 p.

Dumbauld, B.R., and D.A. Armstrong
1987 Potential mitigation of juvenile Dungeness crab loss during dredging through enhancement of intertidal shell habitat in Grays Harbor, Washington. Fish. Res. Inst. Rep. FRI-UW-8714, School of Fisheries, Univ. Wash., Seattle, 64 p.

Dumbauld, B., D. Armstrong, P. Dinnel, and T. Wainwright
1988 Impact of dredging on Dungeness crab, *Cancer magister*, in Grays Harbor, Washington during August 1987. Fish. Res. Inst. Rep. FRI-UW-8820, School of Fisheries, Univ. Wash., Seattle, 25 p.

Goodyear, C.P.
1977 Mathematical methods to evaluate entrainment of aquatic organisms by power plants. Rep. FWS/OBS-76/20.3, U.S. Fish Wildl. Serv., Wash., DC.

Gunderson, D.R., and I.E. Ellis
1986 Development of a plumb staff beam trawl for sampling demersal fauna. Fish. Res. (Amst.) 4:35–41.

Gunderson, D.R., D.A. Armstrong, Y.-B. Shi, and R.A. McConnaughey
1990 Patterns of estuarine use by juvenile English sole (*Parophrys vetulus*) and Dungeness crab (*Cancer magister*). Estuaries 13:59–71.

Hankin, D.G., N. Diamond, M.S. Mohr, and J. Ianelli
1989 Growth and reproductive dynamics of adult female Dungeness crabs (*Cancer magister*) in northern California. J. Cons. Cons. Int. Explor. Mer 46:94–108.

Hartnoll, R.G.
1982 Growth. *In* Abele, L.G. (ed.), Embryology, morphology, and genetics (The Biology of Crustacea, vol. 2), p. 111–196. Academic Press, NY.

Horst, T.J.
1975 The assessment of impact due to entrainment of ichthyoplankton. *In* Saila, S.B. (ed.), Fisheries and energy production: A symposium, p. 107–118. Lexington Books, Lexington, MA.

Jamieson, G.S., and D.A. Armstrong
1991 Spatial and temporal recruitment patterns of Dungeness crab in the northeast Pacific. Mem. Queensl. Mus. 31:365–381.

MacCall, A.D., K.R. Parker, R. Leithiser, and B. Jessee
1982 Power plant impact assessment: A simple fishery production model approach. Fish. Bull., U.S. 81:613–619.

McGraw, K.A., L.L. Conquest, J.O. Waller, P.A. Dinnel, and D.A. Armstrong
1988 Entrainment of Dungeness crabs, *Cancer magister* Dana, by hopper dredge in Grays Harbor, Washington. J. Shellfish Res. 7(2):219–231.

Methot, R.D. Jr., and L.W. Botsford
1982 Estimated preseason abundance in the California Dungeness crab (*Cancer magister*) fisheries. Can. J. Fish. Aquat. Sci. 39:1077–1083.

Morton, J.W.
1977 Ecological effects of dredging and dredge spoil disposal: A literature review. Tech. Pap. U.S. Fish Wildl. Serv. 94, Wash., DC, 33 p.

Orensanz, J.M., and V.F. Gallucci
1988 A comparative study of postlarval life history schedules in four sympatric *Cancer* species. J. Crust. Biol. 8:187–220.

Pacific Marine Fisheries Commission
1989 Data series: Crab and shrimp section (Rev. 1989). Pac. Mar. Fish. Comm., Portland.

Poiner, I.R., and R. Kennedy
1984 Complex patterns of change in the macrobenthos of a large sandbank following dredging. Mar. Biol. 78:335–352.

Rago, P.J.
1984 Production forgone: An alternative method for assessing the consequences of fish entrainment and impingement losses at power plants and other water intakes. Ecol. Modell. 24:79–111.

Simenstad, C.A. (editor)
1990 Effects of dredging on anadromous Pacific Coast fishes: Workshop proceedings, Seattle, September 8–9, 1988. Wash. Sea Grant Prog., Univ. Wash., Seattle, 160 p.

Stevens, B.G.
1981 Dredging-related mortality of Dungeness crabs associated with four dredges operating in Grays Harbor, Washington. Seattle Dist., U.S. Army Corps of Eng. DA-79-45, Seattle, 148 p.

Stevens, B.G., D.A. Armstrong, and J.C. Hoeman
1984 Diel activity of an estuarine population of Dungeness crabs, *Cancer magister*, in relation to feeding and environmental factors. J. Crust. Biol. 4:390–403.

van Winkle, W. (editor)
1977 Proceedings of the conference on assessing the effects of power-plant-induced mortality in fish populations, Gatlinburg, Tennessee, May 3–6, 1977. Pergamon Press, NY, 380 p.

Wainwright, T.C., K.A. McGraw, D.A. Armstrong, B.R. Dumbauld, and L.L. Conquest
1990 Impact of dredging on Dungeness crab, *Cancer magister*, in Grays Harbor, Washington, during August 1989. Fish. Res. Inst. Rep. UW-FRI-9005, Univ. Wash., Seattle, 18 p.

Washington Department of Fisheries
1951 Washington commercial fisheries 1951 statistics. Wash. Dep. Fish., Seattle, 46 p.

Weisberg, S.
1985 Applied linear regression, 2d ed. Wiley, NY, 324 p.

Comparison of feeding and growth of larval round herring *Etrumeus teres* and gulf menhaden *Brevoortia patronus*

Weihzong Chen
East China Sea Fisheries Research Institute
300 Jun Gong Road, Shanghai, Peoples Republic of China

John J. Govoni
Stanley M. Warlen
Beaufort Laboratory, Southeast Fisheries Science Center
National Marine Fisheries Service, NOAA, Beaufort, North Carolina 28516

The round herring *Etrumeus teres* is one of several clupeid fishes, abundant in continental shelf waters of the Gulf of Mexico, that presently is not commercially exploited by the United States, although its sibling species *E. whiteheadi* is a fishery resource for South Africa (Roel and Melo 1990). The potential annual yield of this latent resource is estimated as 3.3×10^4 to 4.2×10^5 metric tons for the eastern Gulf (Houde 1977) and 1.1×10^5 to 1.1×10^6 metric tons for the entire Gulf (Reintjes 1980). Details relevant to the distribution and population dynamics of round herring, including elements of its early life history, are presently sketchy. Houde (1977) reported that round herring in the eastern Gulf of Mexico spawn from mid-October to the end of May between the 30 and 200 m isobaths. He surmised that there is a major spawning area about 150 km west-southwest of Tampa Bay, Florida, and a minor area just north of the Dry Tortugas. Off Texas and Louisiana, spawning occurs from 50 to 200 km offshore and may extend to the edge of the continental shelf (Fore 1971). Round herring and another clupeid, the gulf menhaden *Brevoortia patronus*, are sympatric; the latter spawns in inshore waters of the northern Gulf at least as far offshore as 130 km with a focus of spawning off Mississippi between mid-October and late March (Christmas and Waller 1975).

Differences between adult round herring and gulf menhaden are so obvious that systematists once referred these two species to separate families, Dussumieriidae and Clupeidae (Whitehead 1963), but their larvae are morphologically similar with one major exception, their jaw structure. (The misperception that, unlike other clupeids, round herring larvae do not possess a swimbladder (Fahay 1983) has been perpetuated in the literature.) At hatching larvae of both species are about 3.0 mm notochord length (NL) and are slender and elongate with a straight alimentary canal and a posterior anus (Houde and Fore 1973). Transformation to the juvenile form begins at about 18 mm standard length (SL) (Houde and Fore 1973). Round herring larvae develop teeth on their long, spatulate upper and lower jaws at about 6 mm SL (Houde and Fore 1973); but gulf menhaden do not develop teeth on their shorter, less compressed jaws until they are about 10 mm SL (Hettler 1984).

The diets of the larvae of these species might reflect differences in jaw structure and dentition. In addition, differences in diet quality and quantity may register different growth between these species. While feeding and growth of gulf menhaden larvae are documented (Govoni et al. 1983, Stoecker and Govoni 1984, Warlen 1988), similar information on the early life history of round herring is unavailable. In this paper, we compare the feeding and growth of larval round herring and gulf menhaden.

Materials and methods

Round herring and gulf menhaden larvae used in this study were removed from ichthyoplankton collections obtained during two cruises (December 1980 and February 1981) using MOCNESS gear (multiple opening/closing nets and environmental sensing system). Three stations were occupied, one each at the 18, 91, and 183 m isobaths, along three transects (off Cape San Blas, FL; off the Mississippi Delta, LA; and off Galveston Bay, TX (Sogard et al. 1987)). The objective of the sampling plan was to broadly canvass the continental shelf of the northern Gulf for larval gulf menhaden and two other species (Sogard et al. 1987); larval round herring were collected incidentally. Sampling at three discrete depths (surface, in the middle of the upper mixed layer, and within or below the thermocline) assured the collection of adequate numbers of specimens. In addition, larvae from a single collection taken at the Mississippi River plume front (Govoni et al. 1989) in December 1982 were examined to augment gut content data. Larvae were preserved in 5% formalin for food analysis and in 70% ethanol for growth studies (Table 1). To provide an indication of true dietary differences between species encountering the same food assortment, only those larvae from a single vertically and horizontally discrete collection (Govoni et al. 1986) that produced both species were used for diet comparisons

Manuscript accepted 25 November 1991.
Fishery Bulletin, U.S. 90:183–189 (1992).

Table 1

Time, location, and depth of collection in the northern Gulf of Mexico of round herring *Etrumeus teres* larvae examined for diet composition and growth determination.

Date	Time	Transect	Water column depth (m)	Sample depth (m)	No. of larvae collected	No. of larvae with food
6 Dec 80[1]	0645	Mississippi Delta	183	1	2	0
8 Dec 80[2]	0013	Cape San Blas	183	1	8	
8 Dec 80[2]	0013	Cape San Blas	183	51	2	
8 Dec 80[1]	0040	Cape San Blas	183	50	6	0
8 Dec 80[1]	0056	Cape San Blas	183	1	10	0
8 Dec 80[1]	0621	Cape San Blas	183	50	3	0
8 Dec 80[2]	1800	Cape San Blas	183	1	20	
8 Dec 80[2]	1800	Cape San Blas	183	102	1	
8 Dec 80[1]	1821	Cape San Blas	183	49	3	0
8 Dec 80[1]	1834	Cape San Blas	183	1	20	1
9 Dec 80[2]	0600	Cape San Blas	91	1	7	
9 Dec 80[2]	0600	Cape San Blas	91	35	1	
9 Dec 80[2]	0600	Cape San Blas	91	74	3	
9 Dec 80[1]	0617	Cape San Blas	91	35	13	0
9 Dec 80[1]	1237	Cape San Blas	91	37	2	0
9 Dec 80[2]	1800	Cape San Blas	91	1	19	0
9 Dec 80[1]	1806	Cape San Blas	91	75	3	0
9 Dec 80[1]	1817	Cape San Blas	91	35	3	0
9 Dec 80[1]	1827	Cape San Blas	91	1	20	4
10 Dec 80[2]	0005	Cape San Blas	91	1	19	
10 Dec 80[2]	0005	Cape San Blas	91	35	1	0
10 Dec 80[2]	0010	Cape San Blas	91	12	4	0
10 Dec 80[1]	0025	Cape San Blas	91	74	6	0
10 Dec 80[1]	0025	Cape San Blas	91	1	1	0
10 Dec 80[1]	0035	Cape San Blas	91	46	16	0
10 Dec 80[1]	0045	Cape San Blas	91	1	11	0
10 Dec 80[1]	1812	Cape San Blas	18	6	2	1
10 Dec 80[1]	1821	Cape San Blas	18	1	17	2
11 Dec 80[1]	0019	Cape San Blas	18	12	11	1
11 Dec 80[1]	0031	Cape San Blas	18	1	3	0
12 Feb 81[2]	1900	Galveston Bay	18	6	2	
13 Feb 81[2]	0600	Galveston Bay	91	35	5	
14 Feb 81[1]	0033	Galveston Bay	91	61	13	1
14 Feb 81[1]	0047	Galveston Bay	91	35	20	1
14 Feb 81[1]	0100	Galveston Bay	91	1	12	0
14 Feb 81[2]	0600	Galveston Bay	91	37	13	
14 Feb 81[1]	0620	Galveston Bay	91	77	8	0
14 Feb 81[1]	0635	Galveston Bay	91	27	20	0
14 Feb 81[1]	0644	Galveston Bay	91	1	20	0
14 Feb 81[1]	1823	Galveston Bay	91	74	20	1
14 Feb 81[1]	1846	Galveston Bay	91	1	20	7
18 Feb 81[1]	0014	Mississippi Delta	91	75	2	0
18 Feb 81[1]	0025	Mississippi Delta	91	1	20	8
18 Feb 81[2]	0600	Mississippi Delta	91	25	20	0
18 Feb 81[1]	0607	Mississippi Delta	91	25	20	2
18 Feb 81[1]	0625	Mississippi Delta	91	1	4	1
18 Feb 81[2]	1800	Mississippi Delta	91	40	8	
10 Dec 82[1]	0830	Mississippi Delta	18	1	88	26

[1]Collections for examination of diet.
[2]Collections for determination of growth.

(Table 1). Adequate numbers of larvae allowed growth comparisons of larvae collected on the Cape San Blas transect in December 1980 and larvae collected on the Mississippi Delta and Galveston Bay transects in February 1981.

Larvae were measured to the nearest 0.1 mm (NL before and SL after the formation of hypural plates). Guts were dissected and all gut contents were excised, identified, and measured. Percent similarity (Schoener 1970) was used to compare the diets of larval round herring and gulf menhaden from single collections.

Sagittal otoliths were removed from larvae, cleaned in distilled water, and mounted on glass microscope slides with clear acrylic resin; no griding or sectioning was necessary to resolve daily growth increments. Otoliths of round herring were semi-opaque and similar to those of gulf menhaden. Presumed daily increments were clearly discernable as bipartite structures consisting of adjoining incremental and discontinuous zones (Campana and Neilson 1985).

In describing the growth of larval round herring, we did not experimentally verify that their first otolith increment appeared 5 days after hatching or that subsequent increments were added daily as Warlen (1988) has done for gulf menhaden. We assumed that initial and subsequent increment deposition in round herring was similar to gulf menhaden. This assumption is justified, in part, by similarities in the period of some key developmental events. Incubation takes 36 hours at 20.5°C for round herring (O'Toole and King 1974), and 40–42 hours at 19–20°C for gulf menhaden (Hettler 1984). Complete adsorption of the yolk occurs in 4 days for round her-

ing reared in the laboratory at 24–26°C (Miller et al. 1979), as well as for gulf menhaden reared at 18–22°C (Hettler 1984). Further, we used alternative empirical methods to support our assumption that otolith growth increment formation occurs daily (Hales 1987). By comparing the width of marginal increments with the width of the proximal completely-formed increment, we determined the percentage of larvae with partially-formed or completely-formed marginal increments over a 24-hour period (8–10 December 1981; Table 1). The frequency of increment formation was inferred from these percentages and from the relationship of otolith radius and larval length.

The Laird version of the Gompertz growth model was used to describe growth from the logarithm of length and the estimated age of larvae (Zweifel and Lasker 1976). Growth curves of round herring and gulf menhaden larvae were compared by using the predictive, resampling method described by Kappenman (1981). Data for gulf menhaden growth were taken from Warlen (1988) for comparisons with the growth of round herring.

Results

Distribution and co-occurrence

In all, 419 round herring larvae were identified in the present collections, four fewer than gulf menhaden (Sogard et al. 1987). Collections of the larvae of both species indicate that they co-occur infrequently. Round herring and gulf menhaden larvae occurred together at 15 of 45 locations where collections produced either species. Larval round herring were collected most frequently throughout the water column at the offshore stations in water 91 m deep, although one of the largest single collections was made at 18 m (Table 1). Larval gulf menhaden were collected mostly inshore at the 18 m stations along each transect. The larvae of these species co-occurred mainly at the 91 m stations along each transect.

Diet comparisons

Only 56 round herring larvae had food in their guts. Larval round herring had eaten primarily copepod nauplii, copepodites, and adults, with pteropods (mainly *Limacina trochiformis*), tintinnids, invertebrate eggs, and *Eucalanus* spp. nauplii contributing lesser percentages (Table 2). *Eucalanus* nauplii were considered a discrete food organism separate from other copepod nauplii, because its form and size differed markedly; *Eucalanus* spp. nauplii have long, paddle-like appendages and are more than three times larger than the other copepod nauplii observed in the guts of larvae.

Table 2
The diet composition of 56 round herring *Etrumeus teres* larvae in the northern Gulf of Mexico.

	Percent frequency of occurrence	Percent total no.
Centric diatoms	1.8	1.3
Tintinnids	3.6	5.2
Pteropods	8.9	6.5
Pelecypods	1.8	1.3
Unidentified copepod nauplii	25.0	36.4
Unidentified *Eucalanus* nauplius	3.6	3.9
Copepodid and adult copepods	21.4	16.9
Calanoid copepodites and adults	5.4	3.9
Harpacticoid copepodites and adults	1.8	1.3
Cyclopoid copepodites and adults	16.1	11.7
Invertebrate eggs	10.7	11.7

Table 3
Comparison of the percent frequency of occurrence of food organisms in the diet of 26 larval round herring and gulf menhaden larvae collected simultaneously in the northern Gulf of Mexico.

	Percent frequency of occurrence	
Food organism	Round herring	Gulf menhaden
Tintinnid	3.8	4.2
Pteropods	19.2	2.1
Unidentified copepod nauplii	7.7	5.3
Unidentified *Eucalanus* nauplius	3.8	5.3
Unidentified copepodites and adult copepods	15.4	31.6
Calanoid copepodites and adults	3.8	33.7
Harpacticoid copepodites and adults	3.8	0
Cyclopoid copepodites and adults	30.8	11.6
Invertebrate eggs	11.5	6.3

The width of food organisms ranged from 40 to 280 μm, a width range comparable to that found for gulf menhaden (Govoni et al. 1983).

Of the 88 round herring larvae collected simultaneously with gulf menhaden, 26 had food in their guts. There were differences in the gut contents of these 26 round herring and 26 randomly selected gulf menhaden larvae collected simultaneously (Table 3). Larval round herring had eaten cylopoid copepods (*Oncaea* spp. and *Corycaeus* spp.) and pteropods more frequently, but calanoid copepodites and adult copepods less frequently, than had larval gulf menhaden. Percent similarity of the diets of these larvae was 52.2, a value that indicates marginal overlap in diet (Schoener 1970).

Growth comparisons

Marginal growth increments seemed to form from evening through early morning (Table 4). The allometric relationship ($\log_{10}$ radius = 0.126 $\log_{10}$SL+ 1.413; r^2 0.91) between otolith radius and standard length of 131 larvae also suggested a daily periodicity in otolith increment formation (Hales 1987).

Estimates of the length at hatching ($L_{(0)}$) for gulf menhaden provided by the Laird-Gompertz model 3.4mm SL (Fig. 1; Table 5), closely approximate the length-at-hatching of larvae incubated in the laboratory at a temperature of 20°C, 2.6–3.0mm SL (Hettler 1984). Estimates of $L_{(0)}$ for round herring, about 1.2 mm SL, however, are considerably lower than the lengths reported for larvae hatched in the laboratory: 3.8–4.0mm body length from eggs collected in the South Atlantic and incubated at 20.5°C (O'Toole and King 1974) and 6.0mm SL from eggs collected in the Pacific and incubated at 24–26°C (Miller et al. 1979). If the interval from hatching to deposition of the first growth increment is shorter in reality than the assumed 5 days, the Laird Gompertz growth curve would shift to the left, yielding a greater value for $L_{(0)}$, but the form of the growth curve, i.e., the growth rate, would remain the same.

Round herring grew faster than gulf menhaden through the first 20–40 days; gulf menhaden exhibited faster growth than round herring thereafter (Fig. 2). The fastest growth rate (≈0.85 mm/day) for round herring larvae occurred at about 15 days. Average growth rates through 27 days for December 1980 were 0.71 and 0.46mm/day for round herring and gulf menhaden; average rates through 50 days in February 1981 were 0.45 and 0.34mm/day. Annual differences in larval gulf menhaden growth are discussed in Warlen (1988).

Table 4

Percentage of round herring larvae with partially formed (narrow) or completed (wide) marginal otolith growth increments collected at three different times of day.

Time of capture (h)	No. of fish	Percentage	
		Partially formed	Completed
1800	9	22	78
2400	10	40	60
0600	6	100	0

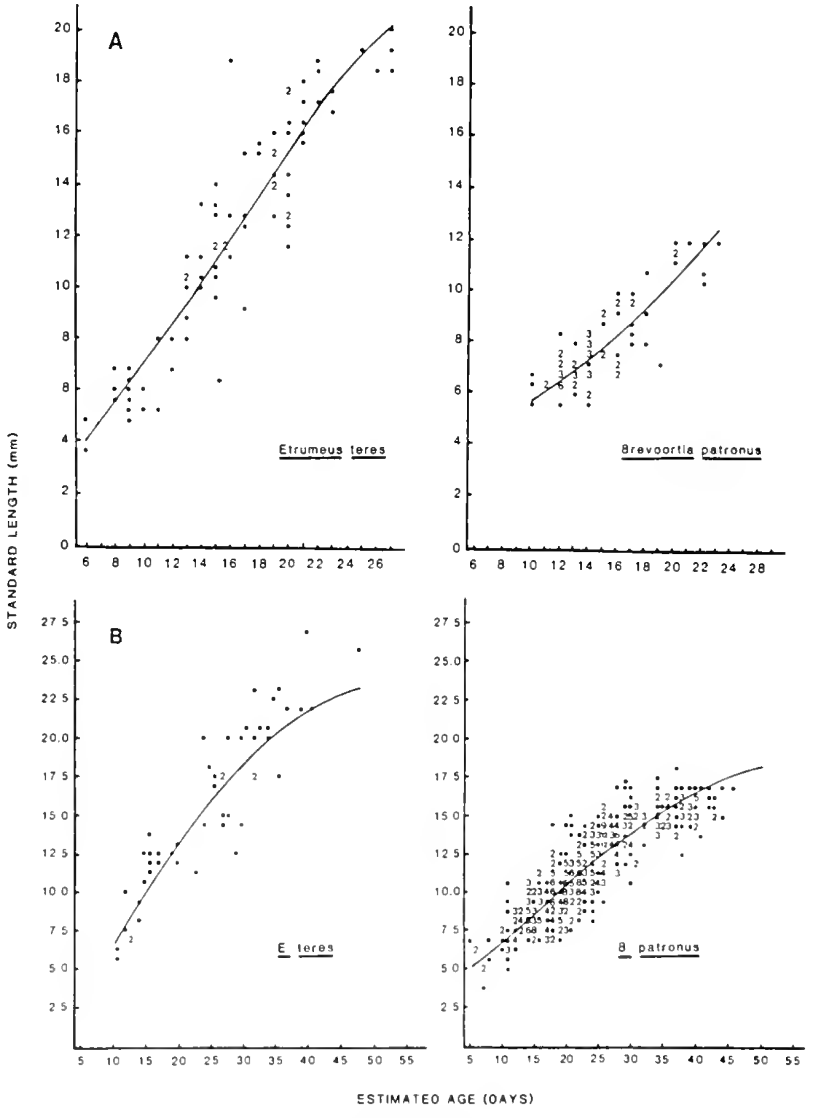

Figure 1

Growth of larval round herring *Etrumeus teres* and gulf menhaden *Brevoortia patronus* collected in December 1980 (A) and February 1981 (B) in the northern Gulf of Mexico. The log form of the Laird-Gompertz model was used to describe the growth of both species (numbers indicate location of coincident data points).

Table 5

Estimates of Laird-Gompertz growth model parameters* and mean age (d) and SL (mm) for larval round herring and gulf menhaden collected in the northern Gulf of Mexico during December 1980 and February 1981.

Date		Number of observations	Growth model parameters			Mean estimated age (d)	Mean SL (mm)
			$L_{(0)}$	$A_{(0)}$	α		
December 1980	Round herring	81	1.184 (0.310)	0.259 (0.055)	0.081 (0.015)	16.025 (0.590)	12.056 (0.501)
	Gulf menhaden	80	3.418 (0.995)	0.056 (0.037)	<0.001 (0.407)	14.862 (0.337)	8.034 (0.191)
February 1981	Round herring	50	1.240 (0.710)	0.232 (0.089)	0.077 (0.018)	25.200 (1.318)	15.620 (28.871)
	Gulf menhaden	561	3.401 (0.246)	0.087 (0.009)	0.045 (0.005)	23.401 (0.333)	11.493 (0.121)

* $L_{(0)}$ = length at hatching, $A_{(0)}$ = specific growth rate at hatching, α = exponential decay of the specific growth rate. Values in parentheses are asymptotic standard errors.

In two comparisons, the growth curves of these species differed, i.e., the sum of squares of the differences between observed and predicted lengths was greater when data for the two species were pooled than when the data were considered separately. In the comparison of larvae collected in December 1980, the sum of squares of deviations was 6.327 for pooled data and 2.736 for data considered separately (total observations = 161). In the comparison of larvae collected in February 1981, from two transects, the sum of squares of deviations was 13.255 for pooled data and 10.477 for data considered separately (total observations = 611).

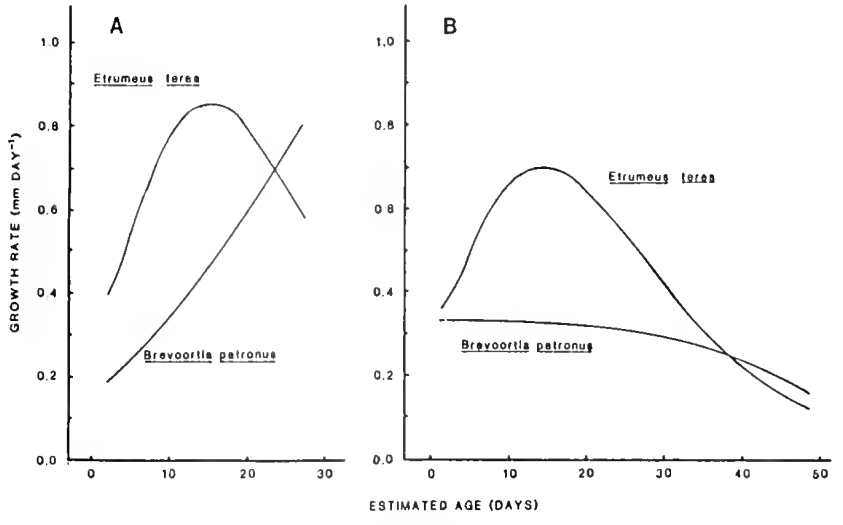

Figure 2

Age-specific growth rates of larval round herring *Etrumeus teres* and gulf menhaden *Brevoortia patronus* collected in December 1980 (A) and February 1981 (B) in the northern Gulf of Mexico. Specific growth rates-at-age were derived from the log form of the Laird-Gompertz growth model parameters.

Discussion

The large, spatulate, and toothed jaws of larval round herring might enable them to eat larger food organisms than gulf menhaden, but while the diets of larval round herring and gulf menhaden differed, the width of food organisms coincided. Diets, then, do not directly reflect differences in jaw structure and dentition. The pteropods eaten by both species were *Limacina trochiformis*, the cyclopoid copepods were primarily of the genera *Oncaea* and *Corycaeus*, and the calanoid copepods were primarily of the genera *Paracalanus* and *Acartia*. Round herring larvae ate more pteropods and cyclopoid copepods, but fewer calanoid copepods than did gulf menhaden larvae.

The more offshore distribution of larval round herring in the central and western northern Gulf of Mexico (Shaw and Drullinger 1990; present data) may explain differences in diet and growth. All of the food organisms eaten by larval round herring and gulf menhaden are broadly distributed in continental shelf waters, but some of the copepods have different patterns of distribution across the shelf in the northern

Gulf of Mexico (Ortner et al. 1989). *Acartia*, for example, occurs in greater abundance inshore, in less saline waters, whereas *Oncaea* and *Corycaeus* are more abundant in water of traditional salinities offshore (Ortner et al. 1989). Prior experience and learning can influence the capture efficiency, food selection, and ingestion rates of larval fishes (see review in Stoecker and Govoni 1984); and because larval round herring occupy more offshore waters, they may be conditioned to feed preferentially on the cyclopoids *Oncaea* and *Corycaeus*.

The difference in larval growth between these two species may reflect differences in the physical environment where these larvae grow. Offshore water in the northern Gulf of Mexico is typically warmer than inshore water during the winter. Inshore–offshore gradients in average water column temperature among the three stations along the three transects were 19.2 to 20.7 to 22.1°C for the Cape San Blas transect in December 1980; 16.1 to 15.0 to 18.1, 16.9 to 19.5 to 19.8, and 12.9 to 18.5 to 19.0°C for the Mississippi Delta, Cape San Blas, and Galveston Bay transects in February 1981. Temperature differences of this magnitude can account for intraspecific differences in growth rates among larval fish (Jones 1986, Warlen 1988) as seen here in the slower growth of round herring larvae in the cooler water of February 1981. The faster, early growth of round herring larvae, overall, probably results from the warmer waters of its offshore occurrence.

Acknowledgments

The collection of specimens examined in this paper was supported by a contract to the Beaufort Laboratory of the Southeast Fisheries Science Center, National Marine Fisheries Service, NOAA, from the Ocean Assessment Division, National Ocean Services, NOAA. This paper was developed while the senior author was a visiting scientist at the National Marine Fisheries Service, NOAA, Beaufort Laboratory.

Citations

Campana, S.E., and J.D. Neilson
1985 Microstructure of fish otoliths. Can. J. Fish. Aquat. Sci. 42:1014–1032.

Christmas, J.Y., and R.S. Waller
1975 Location and time of menhaden spawning in the Gulf of Mexico. Gulf Coast Res. Lab., Ocean Springs, MS, 20 p.

Fahay, M.P.
1983 Guide to the early stages of marine fishes occurring in the western North Atlantic Ocean, Cape Hatteras to the southern Scotian Shelf. J. Northwest Atl. Fish. Sci. 4:1–423.

Fore, P.L.
1971 The distribution of eggs and larvae of the round herring, *Etrumeus teres*, in the northern Gulf of Mexico. Am. Soc. Biol. Bull. 18, 34 p.

Govoni, J.J., D.E. Hoss, and A.J. Chester
1983 Comparative feeding of three species of larval fishes in the northern Gulf of Mexico: *Brevoortia patronus*, *Leiostomus xanthurus*, and *Micropogonias undulatus*. Mar. Ecol. Prog. Ser. 13:189–199.

Govoni, J.J., P.B. Ortner, F. Al-Yamani, and L.C. Hill
1986 Selective feeding of spot, *Leiostomus xanthurus*, and Atlantic croaker, *Micropogonias undulatus*, larvae in the northern Gulf of Mexico. Mar. Ecol. Prog. Ser. 28:175–183.

Govoni, J.J., D.E. Hoss, and D.R. Colby
1989 The spatial distribution of larval fishes about the Mississippi River plume. Limnol. Oceanogr. 34:178–187.

Hales, L.S.
1987 Distribution, abundance, reproduction, food habits, age, and growth of round scad, *Decapterus punctatus*, in the South Atlantic Bight. Fish. Bull., U.S. 85:251–268.

Hettler, W.F.
1984 Description of eggs, larvae, and early juveniles of gulf menhaden, *Brevoortia patronus*, and comparisons with Atlantic menhaden, *B. tyrannus*, and yellowfin menhaden, *B. smithi*. Fish. Bull., U.S. 82:85–95.

Houde, E.D.
1977 Abundance and potential yield of the round herring, *Etrumeus teres*, and aspects of its early history in the eastern Gulf of Mexico. Fish. Bull., U.S. 75:61–89.

Houde, E.D., and P.L. Fore
1973 Guide to identity of eggs and larvae of some Gulf of Mexico clupeid fishes. Fla. Dep. Nat. Resour., Mar. Res. Lab., Leafl. ser. IV, pt. 1, no. 23, 14 p.

Jones, C.
1986 Determining age of larval fish with the otolith increment technique. Fish. Bull., U.S. 84:91–103.

Kappenman, R.F.
1981 A method for growth curve comparisons. Fish. Bull., U.S. 79:95–101.

Miller, J.M., W. Watson, and J.M. Leis
1979 An atlas of common nearshore marine fish larvae of the Hawaiian Islands. Misc. Rep. PO-02, Univ. Hawaii Sea Grant Prog., Honolulu, 179 p.

Ortner, P.B., L.C. Hill, and S.R. Cummings
1989 Zooplankton community structure and copepod species composition in the northern Gulf of Mexico. Continental Shelf Res. 9:387–402.

O'Toole, M.J., and D.P.F. King
1974 Early development of the round herring, *Etumeus teres* (De Kay) from the south-east Atlantic. Vie Milieu 24:443–452.

Reintjes, J.W.
1980 Marine herring and sardine resources of the northern Gulf of Mexico. *In* Flandorfer, M., and L. Skuplen (eds.), Workshop for potential fishery resources of the northern Gulf of Mexico, New Orleans, 1980. Publ. MASGP-80-012, Miss.–Alabama Sea Grant Consort., 14 p.

Roel, B.A., and Y.C. Melo
1990 Reproductive biology of the round herring, *Etrumeus whiteheadi*. S. Afr. J. Mar. Sci. 9:177–187.

Schoener, T.W.
1970 Nonsynchronous spatial overlap of lizards in patchy habitats. Ecology 51:408–418.

Shaw, R.F., and D.L. Drullinger
1990 Early-life history profiles, seasonal abundance, and distribution of four species of clupeid larvae from the northern Gulf of Mexico, 1982 and 1983. NOAA Tech. Rep. NMFS 88, 60 p.

Sogard, S.M., D.E. Hoss, and J.J. Govoni
1987 Density and depth distribution of larval gulf menhaden, *Brevoortia patronus*, Atlantic croaker, *Micropogonias undulatus*, and spot, *Leiostomus xanthurus*, in the northern Gulf of Mexico. Fish. Bull., U.S. 85:601-609.

Stoecker, D.K., and J.J. Govoni
1984 Food selection by young gulf menhaden (*Brevoortia patronus*). Mar. Biol. (Berl.) 80:299-306.

Warlen, S.M.
1988 Age and growth of larval gulf menhaden, *Brevoortia patronus*, in the northern Gulf of Mexico. Fish. Bull., U.S. 86:77-90.

Whitehead, P.J.
1963 A revision of the recent round herrings (Pisces: Dussumieriidae). Bull. Br. Mus. (Nat. Hist.) Zool. 10:305-380.

Zweifel, J.R., and R. Lasker
1976 Prehatch and posthatch growth of fishes—a general model. Fish. Bull., U.S. 74:609-621.

Analytical correction for oversampled Atlantic mackerel *Scomber scombrus* eggs collected with oblique plankton tows

Denis D'Amours
Francois Grégoire

Division de la Recherche sur les Pêches
Ministère des Pêches et des Océans, Institut Maurice-Lamontagne
C.P. 1000, Mont-Joli, Québec G5H 3Z4, Canada

Atlantic mackerel *Scomber scombrus* is a pelagic species spawning on both sides of the North Atlantic ocean. In the east, mackerel spawn off the British Isles and in the North Sea (as reviewed by Lockwood 1988 and Daan et al. 1990). In the west, mackerel spawn in the Middle Atlantic Bight (Berrien 1978) and in the Gulf of St. Lawrence (Ware 1977). Atlantic mackerel is a moderately prolific species (Bigelow and Schroeder 1953); its fecundity has been estimated at 255,000 eggs for a medium-size female (30 cm FL) in the northeast Atlantic (Lockwood et al. 1981), and at 243,000 eggs for a similar-size female in the Middle Atlantic Bight (Morse 1980).

Mackerel eggs are concentrated near the surface when the water column is thermally stratified during spawning (Coombs et al. 1983, Ware and Lambert 1985). Sette's (1943) data from the Middle Atlantic Bight indicated that 80% of mackerel eggs were in the top 10 m. In the North Sea, Coombs et al. (1981) reported that 91% of mackerel eggs were above 26 m, and that more than 85% were between 0 and 16 m. In the Gulf of St. Lawrence, de Lafontaine and Gascon (1989) indicated that 89% of mackerel eggs were within 15 m of the surface. The distribution of mackerel eggs is thus characteristically non-homogeneous in the vertical plane.

In the Gulf of St. Lawrence and Middle Atlantic Bight, mackerel eggs are routinely surveyed for stock assessment purposes (e.g., Castonguay and Grégoire 1989, Berrien 1990). Surveys are carried out with oblique plankton tows, with bongo nets as described by Posgay and Marak (1980). However, accuracy of oblique plankton tows is known to be sensitive to nonhomogeneous vertical distribution of the sampled organisms (Smith and Richardson 1977). Ideally, there should be no hesitation at the surface when retrieving the net, as it would lead to a severe oversampling of the surface layer where the eggs are concentrated (Posgay and Marak 1980, Smith et al. 1985). In practice, it is difficult not to drag the plankton net at the surface for at least a few seconds; when the net is retrieved, it reaches the surface several meters behind the block, and is dragged at the surface until directly under the block, where it can be lifted out. During such dragging at the surface, the mouth of the net is typically nearly all submerged and samples the surface layer. It is usually assumed that such oversampling at the surface leads to a negligible bias in estimates of abundance.

In this paper, the bias caused by an oversampling of surface water on the calculated abundance of mackerel eggs is analyzed. An analytical correction for this bias is derived and applied to empirical data from a mackerel egg survey held in the Gulf of St. Lawrence in 1990 to reevaluate the annual production of eggs. Also, some potential effects of oversampling surface water are evaluated when computing total abundance and mortality rates of near surface organisms.

Manuscript accepted 9 December 1991.
Fishery Bulletin, U.S. 90:190–196 (1992).

Bias in computed egg abundance caused by oversampled surface water

Distribution of mackerel eggs

Concentrations of mackerel eggs are highest near the surface and decrease rapidly with depth. Sundby (1983) reported that under assumptions applicable in the present study, a negative exponential model (as Eq. 1, below) was appropriate to describe the vertical distribution of mackerel eggs. Ware and Lambert (1985) also concluded that the vertical distribution of mackerel eggs was best described by a negative exponential model. Data on the vertical distribution of mackerel eggs presented by Sette (1943) and by de Lafontaine and Gascon (1989) were fitted to negative exponential models; in both cases, over 90% of the variance in the egg distribution was explained. Therefore, a negative exponential model is appropriate to describe the distribution of mackerel eggs in the vertical plane.

Sampling mackerel eggs

Let the abundance of a population of eggs in a body of water decrease from the surface following an exponential model:

$$\frac{dN(z)}{dz} = -kN(z) \qquad (1)$$

where N(z) = concentration of eggs in number per volume at depth z, and k = rate constant. Upon integration of Eq. 1, the concentration of eggs at depth z is given by

$$N(z) = N_0 e^{-kz}, \quad (2)$$

where N_0 = concentration of eggs at the surface. When integrating Eq. 2, the total number of eggs (N_a) in number per surface area in this body of water is given by

$$N_a = \int_0^{\infty} N_0 e^{-kz} dz = \frac{N_0}{k}. \quad (3)$$

If an oblique plankton tow (Fig. 1A) is made through this distribution of eggs with a net of radius a, and a centered depth of α, the total number of eggs collected (N_H) will be equal to

$$N_H = \quad (4)$$

$$\int_0^{L_1} \int_{\alpha-a}^{\alpha+a} \int_{-\sqrt{a^2-(z-\alpha)^2}}^{+\sqrt{a^2-(z-\alpha)^2}} N(z)\, dydzdx_1$$

$$+ \int_0^{L_2} \int_{\alpha-a}^{\alpha+a} \int_{-\sqrt{a^2-(z-\alpha)^2}}^{+\sqrt{a^2-(z-\alpha)^2}} N(z)\, dydzdx_2,$$

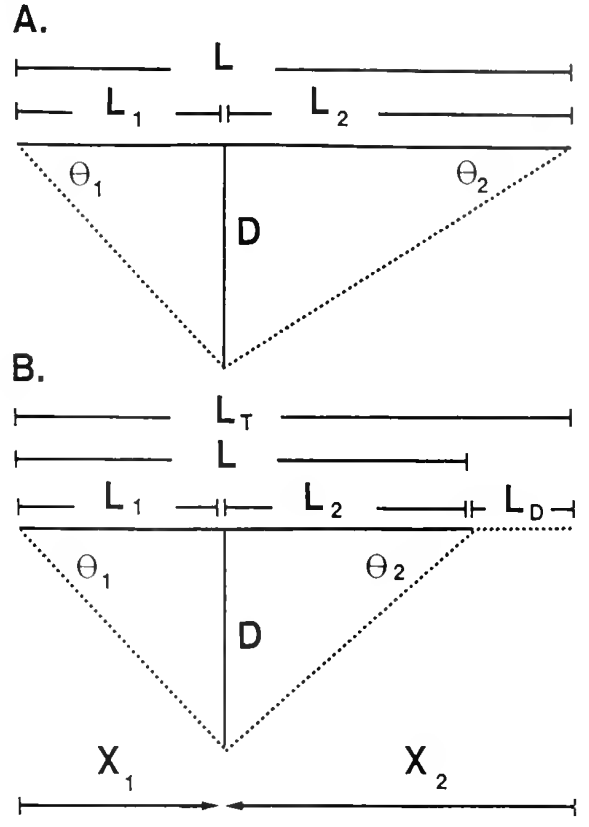

Figure 1

Path (broken line) of net during an oblique plankton tow: L's represent length components of the tow along horizontal references x_1 and x_2; D is the maximum depth of sampling, and θ's represent angles between path of net and horizon. In (A), the net is recovered upon reaching the surface; in (B), the net is dragged at the surface along L_D before recovery.

where x_1 is the horizontal distance from the start of the tow and x_2 is the horizontal distance from the end of the tow (Fig. 1A), and where z and y represent the vertical and horizontal openings of the net, respectively. Integrating Eq. 4 over the limits on z and y (as in D'Amours 1988),

$$N_H \approx \left[1 + \frac{(ka)^2}{8}\right] \left(\int_0^{L_1} N_0 e^{-kz} dx_1 + \int_0^{L_2} N_0 e^{-kz} dx_2 \right). \quad (5)$$

The term ka originates from the slight difference between the position of the geometric center of the net and the position of the center of abundance of the eggs within its opening (D'Amours 1988). Defining, $\tan \theta_i = \frac{D}{L_i}$, where D is the maximum depth of the tow, Eq. 5 can be rewritten as

$$N_H \approx \left[1 + \frac{(ka)^2}{8}\right] \left(\int_0^{L_1} N_0 e^{-k \tan \theta_1 x_1} dx_1 + \int_0^{L_2} N_0 e^{-k \tan \theta_2 x_2} dx_2 \right), \quad (6)$$

Evaluating Eq. 6 for kD≫0,

$$N_H \approx \frac{N_o}{k}\left(\frac{L}{D}\right)\left[1 + \frac{(ka)^2}{8}\right], \qquad (7)$$

where $L = L_1 + L_2$, and is the total horizontal length of the tow (Fig. 1A). It can now be seen that when the number of eggs collected in an oblique plankton tow (Eq. 7) is multiplied by the ratio D/L, and when the product ka is small, an approximation of Eq. 3 is obtained, which is a measure of the local abundance of eggs in number per surface area. The procedure of multiplying the total number of eggs collected in the oblique tow (equation 7) by the ratio of its maximum depth to its total horizontal length (D/L), is equivalent to the standardization procedure described by Smith and Richardson (1977). To obtain estimates of abundance in number per surface area, the standardization procedure consists of multiplying the number of eggs collected by the ratio of the maximun depth attained during the tow to the volume of water filtered. This standardization procedure is valid if all depth strata are sampled equally.

Now assume the same population of eggs, but where the net is dragged at the surface while being readied for recovery at the end of the tow. The length of drag at the surface is represented by L_D in Figure 1B. Along L_D, the mouth of the net is centered at depth α, which is equal to its radius a; i.e., oversampling occurs in the layer of water immediately below the surface, as deeply as the diameter of the net. Over L_D, the net will collect a number of eggs (N_S) equal to

$$N_S \approx L_D \int_{\alpha-a}^{\alpha+a} \int_{-\sqrt{a^2-(z-\alpha)^2}}^{+\sqrt{a^2-(z-\alpha)^2}} N(z)\, dy dz, \qquad (8)$$

which is approximated by (as in D'Amours 1988)

$$N_S \approx N_o\, e^{-k\alpha}\, L_D\left[1 + \frac{(ka)^2}{8}\right]. \qquad (9)$$

The total number of eggs (N_T) collected during an oblique tow, where the net is dragged at the surface at the end, will then be equal to the sum of N_H (Eq. 7) and N_S (Eq. 9):

$$N_T \approx \frac{N_o}{k}\left(\frac{L}{D}\right)\left[1 + \frac{(ka)^2}{8}\right] + N_o\, e^{-k\alpha}\, L_D\left[1 + \frac{(ka)^2}{8}\right]. \qquad (10)$$

The component N_S will add to the number of eggs collected, and its inclusion in the standardization procedure will result in a systematic overestimation of the abundance of eggs per surface area. When Eq. 10 is standardized with L_D included in the total length of the tow (L_T in Fig. 1B), and the result divided by the true theoretical abundance of eggs (Eq. 3), an expression is obtained which is the ratio (B) of the biased abundance to the true abundance of eggs:

$$B \approx L + D\left(k\, e^{-k\alpha}\, L_D\left[1 + \frac{(ka)^2}{8}\right]\right). \qquad (11)$$

Removal of bias from computed abundance of mackerel eggs

Assumption of constant filtration efficiency

In Eq. 11, L and L_D can be replaced by the proportion of the total duration of the tow they represent, under the assumption of constant filtration efficiency. This assumption is required to use tow time as a measure directly proportionnal to amount of water filtered, so as to separate L and L_D in Eq. 11. However, as pointed out by Smith and Richardson (1977), the filtration efficiency of a plankton tow declines typically with the duration of the tow, as the accumulated plankton reduces the porosity of the net. They warned that the diminishing efficiency of a net could result in an undersampling of surface water. To verify whether such undersampling of surface water occurred, which would offset oversampling at the end of the tow, the time-course of the efficiency of the plankton net must be assessed.

If filtration efficiency diminishes with time, the volume filtered per unit time will diminish with increasing tow duration. The residuals about a straight line fitted on the values of volume filtered against tow duration would then show a decreasing pattern of departure from linearity. The volumes filtered for the tows in the Gulf of St. Lawrence in 1990 were regressed against their respective total duration. The residuals of this regression did not indicate a decreasing de-

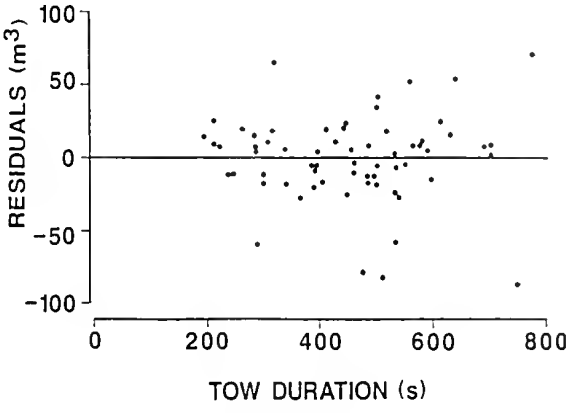

Figure 2
Residuals of a linear regression of volume filtered against tow duration of oblique plankton tows, from a mackerel egg survey held in the Gulf of St. Lawrence in 1990.

parture from linearity; somewhat unexpectedly, a tendency towards an increasing departure from linearity could be detected (Fig. 2). Therefore, it can be concluded that no surface undersampling occurred as a result of diminishing filtration efficiency. The apparent increasing departure from linearity can be explained by the fact that long tows (e.g., duration of 10 minutes) are deeper, i.e., well below the stratum where mackerel eggs are abundant. During short tows (e.g., duration of 6 minutes), the net is towed mainly in the stratum were eggs are present, and the filtration efficiency is less, though stationary, than in water devoid of eggs. During long, deep tows, more time is spent below the stratum containing mackerel eggs, and proportionally more free-flowing water is filtered there.

Correction of survey data

In Eq. 11, a rate constant k must be introduced to describe the distribution of the sampled organisms in the vertical plane. For the purpose of the demonstration, a rate constant $k = 0.15$/m was selected as representative of all mackerel egg stages at all stations; as discussed below, this rate constant is a representative value extracted from the literature on mackerel egg distribution. During the mackerel egg survey carried out in the Gulf of St. Lawrence in late-June and early-July 1990, the total duration of each oblique tow was measured, as well as the duration of the period during which the Bongo net was dragged at the surface before recovey (F. Grégoire, unpubl. data). The period of drag at the surface started when the net was visually spotted at the surface and ended when the net was lifted out of the water. From those measurements, values of L and L_D were calculated in percent of total tow time. With a rate constant $k = 0.15$/m, a net radius $a = 0.305$ m, a centered depth $\alpha = 0.305$ m along L_D, and a measured maximum depth D, a value of the degree of bias B was calculated for each tow as per Eq. 11. The corrected abundance of eggs was obtained by multiplying the computed biased abundance by [100%/B]. Using uncorrected and corrected abundances of eggs at each station, two total annual productions of mackerel eggs were computed for the Gulf of St. Lawrence in 1990 following the procedures of Ouellet (1987). The totals were 6.77×10^{14} eggs with uncorrected abundance, and 5.63×10^{14} eggs with corrected abundance. The difference of 1.14×10^{14} eggs, with a mean fecundity of 300,000 eggs and a sex ratio of 1:1, amounted to 7.6×10^8 mature mackerel.

The parameter D used in the above calculations was measured accurately with a bathymeter mounted on the plankton net. If triangulation had been used, where D is estimated by the amount of wire paid out and the angle subtended at the block, another source of bias would have been introduced owing to the approximative nature of the method. Assume a population of mackerel eggs in a body of water where $k = 0.15$ and $N_0 = 750$; if sampled to a depth D of 50 m with a net of radius $a = 0.305$ on a transect where $L = 1000$ m, a total of 100,000 eggs will be collected (Eq. 7). Standardization of this result by the ratio of D to L shows that the abundance of eggs is 5000 eggs/m^2. Had D been underestimated by 10% at 45 m, the abundance of eggs would have been underestimated also by 10% at 4500 eggs/m^2. If the same tow is repeated, but with $L_D = 75$ m and $\alpha = 0.305$ m, a total of 153,775 eggs will be collected. Standardization of this result with D correctly evaluated at 50 m indicates an abundance of 7152 eggs/m^2; with D underestimated by 10% at 45 m, standardization indicates an abundance of 6437 eggs/m^2. These examples show how an underestimation of 10% of D results in an abundance of eggs equal to 90% of the real value, and how a 7% (75 m/1075 m) oversampling at the surface results in an abundance of eggs equal to 143% of real value. Also, they show that when both an underestimation of D and an oversampling of the surface layer occur during a tow, the effects of both biases on the estimate of abundance are opposite, but not symmetrical, with the effect of the oversampling at the surface much more important than that from the underestimation in D.

A degree of bias (B in Eq. 11) was computed for various combinations of L_D (with $L = 100\% - L_D$) and rate constant k, with $a = \alpha = 0.305$ m, and $D = 50$ m (Fig. 3A). The degree of bias caused by an oversampling of surface water is a function of the time of sampling at the surface, and of the degree of contagion of the eggs near the surface, as described by the parameter k. For

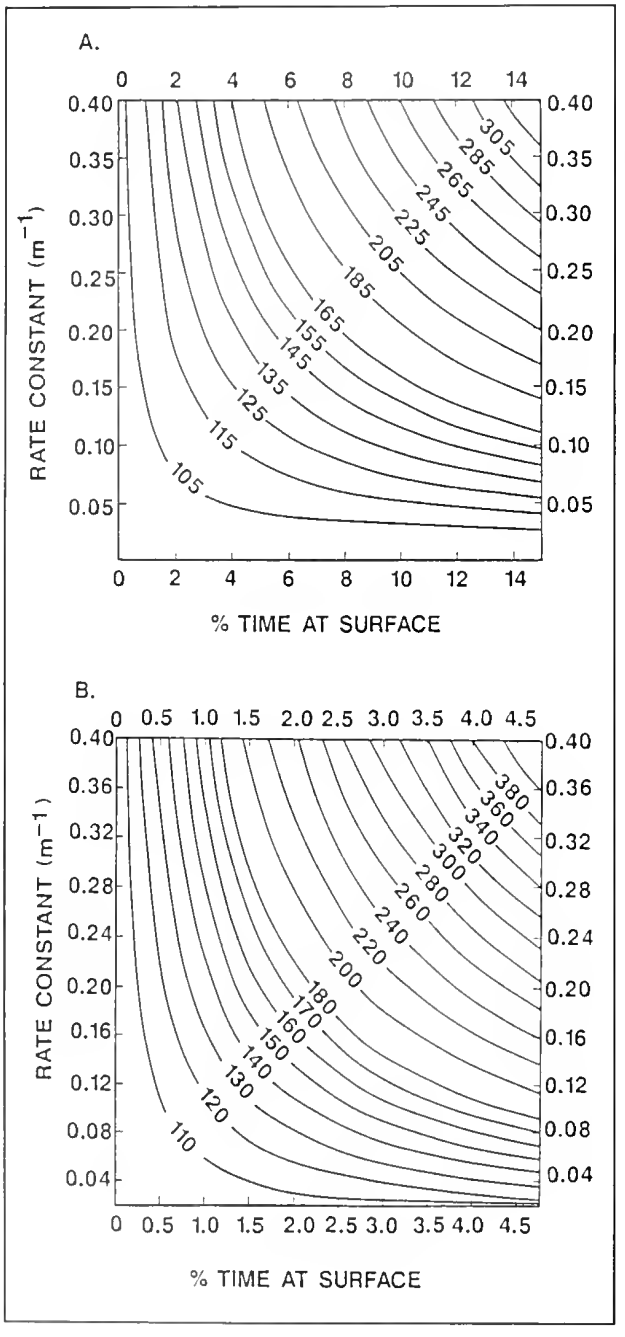

Figure 3

Isopleths (in %) of the ratio of biased abundance to true abundance per surface area of a theoretical population of fish eggs. The isopleths were computed for variable rate constants k of a negative exponential model describing the vertical distribution of the eggs, and for varying degree of oversampling surface water during an oblique plankton tow, L_D, expressed as percent of the total duration of the tow. In (A), the maximum sampling depth was set at 50 m; in (B), the maximum sampling depth was set at 200 m. All other parameters equal in (A) and (B).

example, with a sampling time at the surface representing 7% of the total duration of the tow, and with a rate constant of 0.15/m, the calculated abundance will be 140% of the real value. With eggs highly concentrated near the surface, that is with high values of k, even briefer towing times at the surface will still result in severe bias.

The degree of bias B was also computed for similarily varying k and L_D, again with $a = \alpha = 0.305$ m, but with maximum depth D increased to 200 m (Fig. 3B). For a rate constant of 0.15/m as in the previous example, but with towing time at the surface representing only 2% of the total duration (e.g., 12 seconds at the surface for a total tow time of 10 minutes), the calculated abundance of eggs will again be 140% of the real value. This somewhat counterintuitive result stems from the fact that by sampling deep strata, the fraction of the tow occurring in the stratum where eggs are present is proportionally smaller. As a result, brief times of oversampling at the surface have proportionally more effect on the calculated abundances of eggs than when the tow extends only to shallow strata.

Effects of oversampling surface water on variance of total abundance and on mortality rate

Effect on variance

Since the length of dragging at the surface is likely to vary (as a function of weather, crew handling of the net, etc.), a variance will be introduced in the computation of the total abundance of eggs over the studied body of water. It was assumed that the abundance of eggs (5000 eggs/m^2) was constant over the surface of a theoretical body of water where numerical experiments were carried out. Ten oblique tows were made in this theoretical body of water, with L = 1000 m, $a = \alpha = 0.564$ m, and k = 0.2/m, which are convenient values for illustrative purposes. A different length of drag at the surface (L_D) was assigned randomly to each tow; ten random numbers were multiplied by an arbitrary length of 6 m and the resulting L_D's were 6 (×2), 12, 24 (×3), 30, 36, 48, and 54 m. Ten estimates of abundance of eggs per unit surface area were calculated, and the mean was 5994 eggs/m^2, with 95% confidence intervals of 5646–6342 eggs/m^2. This illustrates that small and variable lengths of drag at the surface bias the estimated abundance over the whole body of water, and add a substantial margin of uncertainty to the estimate of local abundance.

In another numerical experiment, the abundance of eggs was again assumed constant throughout at 5000 eggs/m^2, except this time the degree of contagion

near the surface was made variable, i.e., the rate constant k varied randomly within bounds. Ten transects were carried out through these distributions of eggs, with L = 1000 m, $a = \alpha = 0.564$ m, and the length of drag at the surface (L_D) was held constant at 50 m. For each tow, a random value was assigned to the rate constant k: ten random numbers were multiplied by 0.1/m, and added to 0.15. The resulting values were 0.15, 0.16, 0.17 (×2), 0.20 (×2), 0.21 (×2), 0.22, 0.23 (×2), and the corresponding values of N_0 were adjusted so that $N_0/k = 5000$ eggs/m^2. Ten estimates of abundance of eggs per unit surface area were calculated, and the mean was 6876/m^2, with 95% confidence interval of 6713–7039 eggs/m^2. This indicates that even when maintaining a constant length of drag at the surface, similar problems of bias and variance still arise when the degree of contagion of the eggs varies.

Effect on mortality rates

Again for numerical experiments, the abundance of eggs at a theoretical station was assumed to be 5000 eggs/m^2, with $N_0 = 475$/m^3, and k = 0.095/m (i.e., 475/0.095 = 5000). An oblique tow with L = 1000 m, D = 50 m, $L_D = 50$ m, and $a = \alpha = 0.564$ m, was made through this concentration of eggs at time t_0, and the biased abundance was calculated to be 5873/m^2. For the purpose of the demonstration, it was assumed that the eggs suffered no mortality. Some time later at time t_1, the abundance of eggs was still the same, but they were closer to the surface, with $N_0 = 950$/m^3 and k = 0.19/m (i.e., 950/0.19 = 5000). The same oblique tow in this slightly rearranged concentration of eggs yielded a biased estimate of abundance of 6806/m^2, a relative increase of nearly 16% compared with the value at t_0, and an absolute bias of over 36%. In real situations, then, an increase in the degree of vertical contagion of the eggs over a sampling period could lead to an underestimation of the mortality rate if the surface water is oversampled, or to an overestimation if the degree of contagion decreases.

Conclusion

The oblique tow is a convenient method to obtain an estimate of abundance of eggs over a body of water. However, in actual operating conditions, it is rarely possible to carry out an oblique tow without dragging the net at the surface for some period of time, which may introduce a large bias in the estimate of abundance. The first practical recommendation to avoid such bias is to evaluate the assumption that a brief drag time at the surface will cause only a small bias in the estimation of abundance. If eggs are equally distributed over considerable depth, or concentrated in deeper water, this assumption is valid. If not, action should be taken to avoid dragging the net at the surface. If this is impossible, a measure of the amount of oversampling at the surface, and of the rate constant k, should be used to remove the bias from the data following Eq. 11.

In this study, the percent time of the tow spent at the surface was used as a measure of the amount of oversampling at the surface; this information is readily recorded in the field. However, the constant k describing the distribution of eggs had to be approximated from data available in the literature. Ware and Lambert (1985) reported values of k ranging from 0.1 to 1.1; they further indicated that variations in k were related to the steepness of the thermal gradient in the water column, the development stage of the eggs, and the degree of wind-induced mixing. Data on mackerel egg distribution by de Lafontaine and Gascon (1989) indicated a mean value k = 0.1, with the lowest values for the most recently spawned eggs. Data on mackerel egg distribution by Sette (1943) indicated a higher mean value k = 0.17, but with the highest values for the most recently spawned eggs. Differences in mean values of k as well as development-stage specific values may result from differences in local wind conditions as well as in differences in local water density. As discussed by Sundby (1983), the shape of a vertical distribution of mackerel eggs will be determined by the difference of density between the egg and the surrounding water, and by the degree of wind-induced mixing. The relationship reported by Sundby (1983) between wind velocity and vertical eddy diffusivity coefficient of mackerel eggs indicates that the rate constant k should diminish as the state of the sea increases. The definite application of the analytical correction proposed herein will require more site-specific studies on the factors affecting the vertical distribution of mackerel eggs and determining the value of k. Nonetheless, the value k = 0.15 used in this study is representative of realistic conditions in the field, and can be considered as a conservative estimate of the degree of vertical contagion of mackerel eggs. With more reliable values of k, the simple correction procedure suggested in this study could help increase the accuracy of biological parameters based on data from fish egg surveys where the technique of the oblique plankton tow has been used.

Acknowledgments

Dr. D. Booth and Mr. P. Gagnon reviewed an early version of the manuscript. This work followed a study by D'Amours (1988) during which help was provided by

Dr. Brian Petkau and Mr. Brian Leroux of the Statistical Consulting and Research Laboratory, Department of Statistics, University of British Columbia, Vancouver. I thank an anonymous reviewer and Dr. L.L. Jones for helpful reviews and comments.

Citations

Berrien, P.L.
1978 Eggs and larvae of *Scomber scombrus* and *Scomber japonicus* in continental shelf waters between Massachusetts and Florida. Fish. Bull., U.S. 76:95–115.

Berrien, P.
1990 Atlantic mackerel egg production and spawner biomass estimates for the Gulf of St. Lawrence and Northeastern United States waters in 1987. ICES CM 1990/H:18, 17 p.

Bigelow, H.B., and W.C. Schroeder
1953 Fishes of the Gulf of Maine. U.S. Fish. Wildl. Serv., Fish. Bull. 74, vol. 53, 577 p.

Castonguay, M., and F. Grégoire
1989 Le maquereau bleu (*Scomber scombrus* Linné) du nord-ouest de l'Atlantique, sous-régions 2 à 6 de l'OPANO en 1988. CAFSAC (Can. Atl. Fish. Sci. Advis. Comm.) Res. Doc. 89/39, 25 p.

Coombs, S.H., R.K. Pipe, and C.E. Mitchell
1981 The vertical distribution of eggs and larvae of blue whiting (*Micromesistius poutassou*) and mackerel (*Scomber scombrus*) in the eastern North Atlantic and North Sea. Rapp. P.-V. Réun. Cons. Int. Explor. Mer 178:188–195.

Coombs, S.H., J.A. Lindley, and C.A. Fosh
1983 Vertical distribution of larvae of mackerel *Scomber scombrus* and microplankton, with some conclusions on feeding conditions and survey methods. FAO Fish. Rep. 291(3):939–956.

Daan, N., P.J. Bromley, J.G.R. Hislop, and N.A. Nielsen
1990 Ecology of North Sea fish. Neth. J. Sea Res. 26: 343–386.

D'Amours, D.
1988 Vertical distribution and abundance of natant harpacticoids on a vegetated tidal flat. Neth. J. Sea Res. 22:161–170.

de Lafontaine, Y., and D. Gascon
1989 Ontogenetic variation in the vertical distribution of eggs and larvae of Atlantic mackerel (*Scomber scombrus*). Rapp. P.-V. Réun. Cons. Int. Explor. Mer 191:137–145.

Lockwood, S.J.
1988 The mackerel—Its biology, assessment and the management of a fishery. Fishing News Books Ltd., Farnham, Surrey, England, 181 p.

Lockwood, S.J., I.G. Baxter, J.C. Gueguen, G. Joakimsson, R. Grainger, A. Eltink, and S.H. Coombs
1981 The western mackerel spawning stock estimate for 1980. Cons. Int. Explor. Mer, CM 1981/H:13, 20 p.

Morse, W.W.
1980 Spawning and fecundity of Atlantic mackerel, *Scomber scombrus*, in the Middle Atlantic Bight. Fish. Bull., U.S. 78: 103–108.

Ouellet, P.
1987 Mackerel (*Scomber scombrus*) egg abundance in the southern gulf of St. Lawrence from 1979 to 1986, and the use of the estimate for stock assessment. CAFSAC (Can. Atl. Fish. Sci. Advis. Comm.) Res. Doc. 87/62, 40 p.

Posgay, J.A., and R.R. Marak
1980 The MARMAP Bongo zooplankton samplers. J. Northwest Atl. Fish. Sci. 1:91–99.

Sette, O.E.
1943 Biology of the Atlantic mackerel (*Scomber scombrus*) of North America. Part 1. Early life history. Fish. Bull., U.S. 50:149–237.

Smith, P.E., and S.L. Richardson
1977 Standard techniques for pelagic fish egg and larva surveys. FAO Fish. Tech. Pap. 175, 100 p.

Smith, P.E., W. Flerx, and R.P. Hewitt
1985 The CalCOFI vertical egg tow (CalVET) net. *In* Lasker, R. (ed.), An egg production method for estimating spawning biomass of pelagic fish: Application to the northern anchovy, *Engraulis mordax*. NOAA Tech. Rep. NMFS 36.

Sundby, S.
1983 A one-dimensional model for the vertical distribution of pelagic fish eggs in the mixed layer. Deep-Sea Res. 30: 645–661.

Ware, D.
1977 Spawning time and egg size of Atlantic mackerel, *Scomber scombrus*, in relation to the plankton. J. Fish. Res. Board Can. 34:2308–2315.

Ware, D., and T.C. Lambert
1985 Early life history of Atlantic mackerel (*Scomber scombrus*) in the southern Gulf of St. Lawrence. Can. J. Fish. Aquat. Sci. 42:577–592.

Association between the sessile barnacle *Xenobalanus globicipitis* (Coronulidae) and the bottlenose dolphin *Tursiops truncatus* (Delphinidae) from the Bay of Bengal, India, with a summary of previous records from cetaceans

Arjuna Rajaguru
Gopalsamy Shantha

Systematics Laboratory, National Marine Fisheries Service, NOAA
National Museum of Natural History, Washington, DC 20560

Several instances of association between cetaceans and cirripeds have been reported in the literature. Among the barnacles, *Coronula* spp., *Conchoderma* spp., and *Xenobalanus* sp. have been reported from various species of cetaceans of both temperate and tropical waters (Mackintosh and Wheeler 1929, Mackintosh 1942). Devaraj and Bennet (1974) reported a single specimen of *Xenobalanus globicipitis* found attached to the fluke of a finless black porpoise *Neophocaena phocaenoides* caught off Karwar, west coast of India. This type of phoretic partnership (i.e., transportation by one promotes well-being of the other) between 14 specimens of a sessile barnacle *Xenobalanus globicipitis* and a host, the bottlenose dolphin *Tursiops truncatus*, is recorded here from the Bay of Bengal on the east coast of India. This is the first record of the bottlenose dolphin as a host for *Xenobalanus globicipitis* from the central and northern Indian Ocean.

Five spinner dolphins *Stenella longirostris* (Gray 1828) (113.0–177.5 cm TL) and six bottlenose dolphins *Tursiops truncatus* (Montagu 1821) (95.3–367.5 cm TL), were collected from the Bay of Bengal, off Porto Novo (11°29′N; 79°46′E), southeast coast of India, between 15 March 1982 and 1 September 1987. These specimens were entangled accidentally in bottom-set gillnets (called *Motha Valai*, in Tamil vernacular) set mainly for sharks. The net is made of thick (no. 7-12) nylon thread (monofilament). The stretched mesh size is 10–12 cm, and there are about 120 meshes from the head to the foot rope; hence the net is about 12 m deep. Total length of the net is about 800 m (~ one-half mile). Fishing operations, which were carried out mostly at night, were confined to the upper continental shelf, up to 4 km from the coast, to depths of 18–22 m. The dolphins became entangled in the nets both day and night.

All entangled dolphins were examined for external and internal parasites (several dolphins had internal parasites). No barnacles were found on the spinner dolphins. One small bottlenose dolphin (148 cm male) caught on 28 January 1985 had numerous *Xenobalanus globicipitis* attached (Fig. 1A, B). None of the four larger (>150 cm) bottlenose dolphins had any barnacles. All barnacles were collected (four from the left fluke, eight from the right fluke, and one from each flipper) and preserved in formalin. The barnacles were still alive after more than 12 hours out of water. Measurements to the nearest millimeter (Fig. 2) are given in Table 1.

In the sessile barnacles, extreme reduction of plates is found in *Xenobalanus*. The shell is thin, small, white, irregularly star-shaped, and vestigial, containing only the basal parts of the animal. Connected to this thin, star-shaped shell is a cylindrical, smooth, flexible, peduncle-like body (Fig. 3). At the distal end of this greatly elongated pseudopeduncle is a reflexed hood, which bears two stumpy outpushings or 'horns,' but terga and scuta are absent. Cirri, mouth, a proboscoform penis, and associated organs project from the reflexed hood. The wall plates of this barnacle are embedded in the skin of the dolphin, with feeding appendages (cirri) and associated organs suspended by the long fleshy stalk. The body of *X. globicipitis* was dark-brown in live specimens, with a lighter colored hood; the penis was whitish.

Although belonging to the sessile group of the Cirripedia, this barnacle closely resembles stalked barnacles, especially *Conchoderma auritum* which is also found on cetaceans though never attached directly to the skin of its host. *Xenobalanus globicipitis* is always attached directly to the skin of its host (Pilsbry 1916, Barnard 1924). The resemblance is superficial, and is likely adaptive to being dragged through the water by the host. The closest affinities with *Xenobalanus* are the genera *Coronula*, *Platylepas*, and *Tubicinella* (Darwin 1854, Pope 1958).

The barnacles are found only around the rear margins of flippers and flukes. It is hypothesized that those that settle elsewhere are more easily swept off. A single immature barnacle (15 mm TL) was found attached to each flipper of the dolphin (Fig. 1A). All 12 mature barnacles (30–39 mm TL) (Table 1) were aggregated at the rear margin of the flukes (Fig. 1B). Pilsbry

Manuscript accepted 19 December 1991.
Fishery Bulletin, U.S. 90:197–202 (1992).

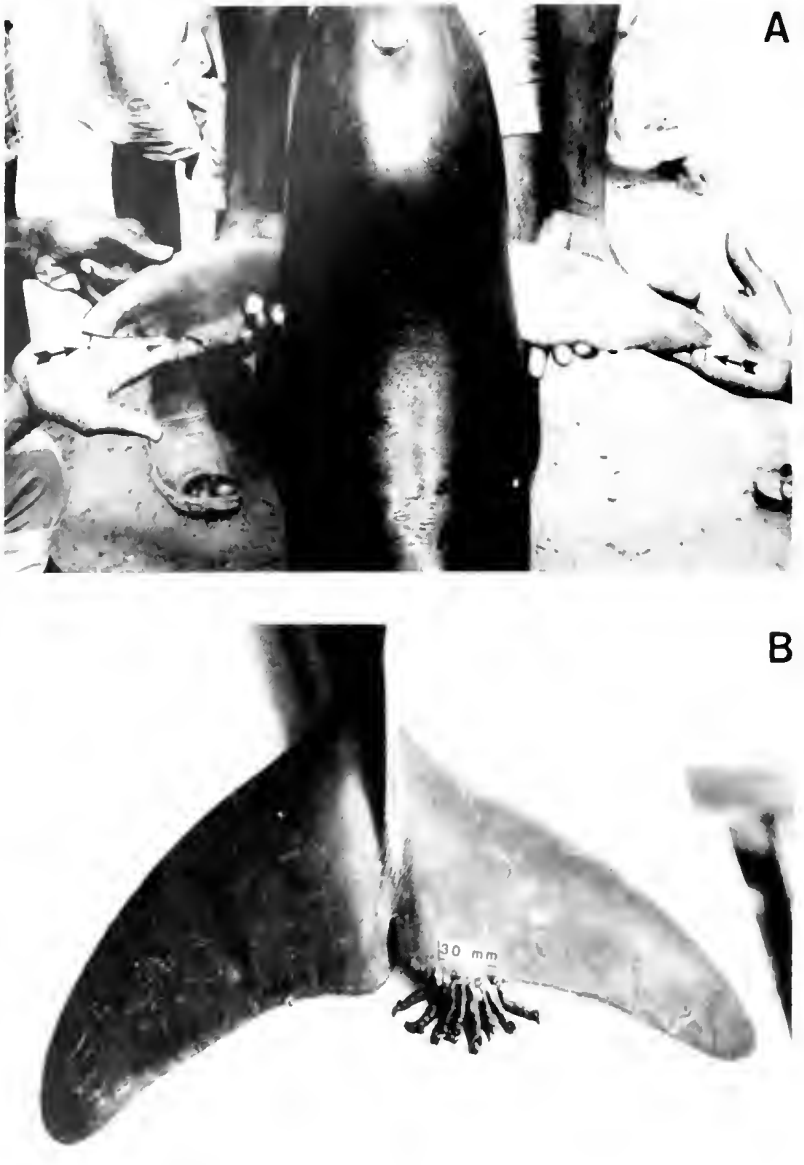

Figure 1
Sessile barnacles *Xenobalanus globicipitis* on a bottlenose dolphin *Tursiops truncatus*, caught in the Bay of Bengal, India. (A) Small barnacles on flippers. (B) Adult barnacles on tail flukes. Barnacles from the left fluke were removed prior to photographing; however, shell remnants are visible.

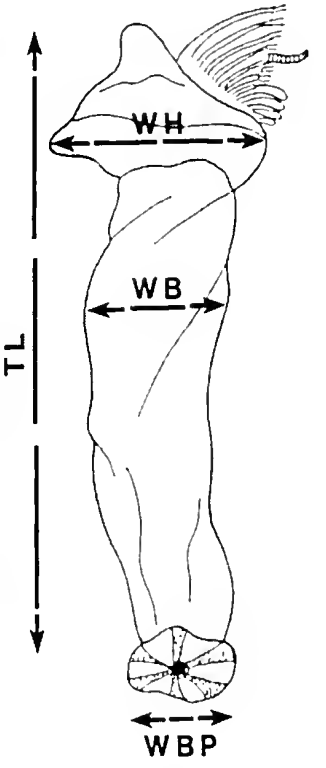

Figure 2
External measurements of the sessile barnacle *Xenobalanus globicipitis*. TL = total length, WB = width of body, WBP = width of basal plate, WH = width of hood.

(1916) reported that these barnacles grow in close groups. This aggregation permits cross-fertilization, which is common in hermaphroditic crustaceans (Barnes 1986).

Xenobalanus globicipitis occurs on about 19 species of cetaceans, from the small harbor porpoise *Phocoena phocoena* to the large blue whale *Balaenoptera musculus* (Table 2). The present record is the seventh report from a bottlenose dolphin. Six previous reports were from the central Atlantic coast of the United States (True 1891, Mead and Potter 1990), Gibraltar (Dollfus 1968, Pilleri 1970), and the east coast of South Africa (Barnard 1924, Ross 1984).

Based on a review of the literature, Rappé and Waerebeek (1988) suggested that *X. globicipitis* is an inhabitant of tropical and warm-temperate waters. They reported that occurrence of this species in the northeast Atlantic and Mediterranean is erratic, possibly related to sporadic incursions from adjacent tropical warm-temperate waters. Their information was based on only 23 reported localities. Our study shows 87 localities (Table 2) reported for *X. globicipitis*: 28 (32.2%) are located north of 40°N; 27 (31.0%) between 35° and 40°N; and 32 (36.8%) between 30°N and 30°S. From this it is clear that *X. globicipitis* is

Table 1

External measurements of the sessile barnacle *Xenobalanus globicipitis* collected from a bottlenose dolphin *Tursiops truncatus* (♂; 148 cm TL), entangled in a gillnet off Porto Novo, southeast coast of India, 28 January 1985

Attachment area	Specimen no.	TL	WH	WB	WBP
		(mm)			
Left fluke	1	37	11	7	5
	2	37	10	6	5
	3	37	11	6	5
	4	32	9	6	5
Right fluke	5	35	11	7	5
	6	30	11	7	5
	7	39	12	7	5
	8	35	12	7	5
	9	30	10	7	5
	10	34	11	8	8
	11	37	10	6	4
	12	30	9	6	5
Left flipper	13	15	5	3	3
Right flipper	14	15	4	3	3

Total length (TL): Basal plate to highest point of hood
Width of body (WB): Maximum width of elongated body
Width of basal plate (WBP): Maximum width of basal plate
Width of hood (WH): Maximum width of hood

a cosmopolitan species, occurring in temperate, warm-temperate, and tropical waters. In relation to the distribution of *X. globicipitis*, the bottlenose dolphin is distributed widely in temperate and tropical oceans. It is common from at least the north coast of Argentina to northern Norway (Kenney 1990).

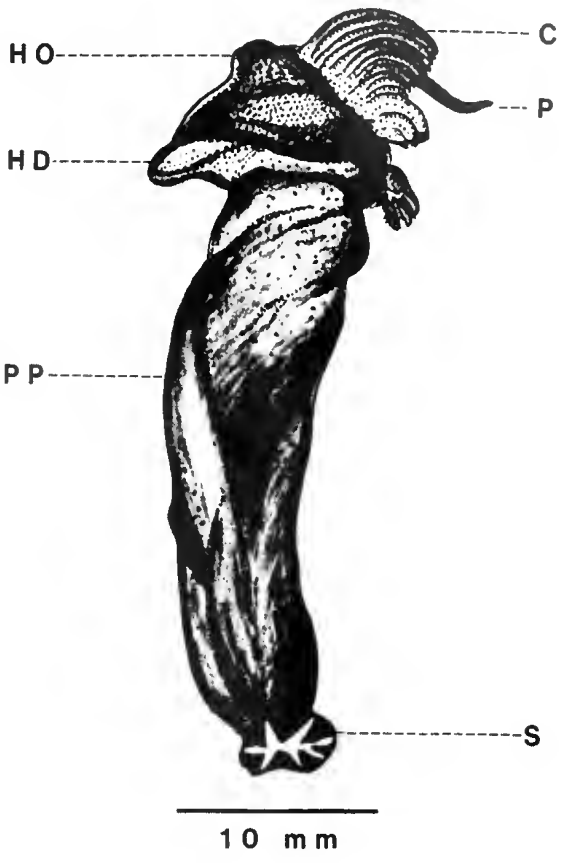

Figure 3

The sessile barnacle *Xenobalanus globicipitis*. C = cirri, HD = hood, HO = horn, P = penis, PP = pseudopeduncle, S = shell.

Table 2

Distribution and reported hosts of the sessile barnacle *Xenobalanus globicipitis*. Identification of host species names are updated.

Host	Reported by	Year	Locality
Order: Cetacea			
Suborder: Mysticeti			
Family: Balaenopteridae			
Balaenoptera borealis (Sei whale)	Broch	1924	Faröe Is., Greenland; Ingoy, Norway
	Cornwall	1927	Vancouver
	Nilsson-Cantell	1921	Faröe Is.
		1930	Saldanha Bay, S. Afr.
	Matthews	1938	Saldanha Bay
	Mackintosh	1942	Saldanha Bay
	Heldt	1950	Tunis
	Boxshall (in Rappé and Waerebeek)		Finnmark, Norway
Balaenoptera musculus (Blue whale)	Barnard	1924	Saldanha Bay
	Mackintosh and Wheeler	1929	South Africa
Balaenoptera musculus (Blue whale) (continued)	Nilsson-Cantell	1930	Saldanha Bay
	Mackintosh	1942	South Africa
	Cornwall	1955a	Pacific Canada
	Pike (in Cornwall)	1955b	No locality
	Boxshall (in Rappé and Waerebeek)		Shetland Is., Scotland
Balaenoptera physalus (Fin whale)	Calman	1920	Shetland Is.
	Barnard	1924	North Atlantic
	Barnard	1924	Antarctic
	Mackintosh and Wheeler	1929	South Africa
	Nilsson-Cantell	1930	S. Shetland Is.
	Nilsson-Cantell	1930	Saldanha Bay
	Mackintosh	1942	South Africa
	Raga and Sanpera	1986	Galicia, Spain

Table 2 (continued)

Host	Reported by	Year	Locality
Suborder: Odontoceti			
Family: Delphinidae			
Delphinus delphis (Common dolphin)	Hoek	1883	Atlantic
	Gruvel	1905	South Africa
	Gruvel	1920	South Africa
	Richard	1936	Oran, Algeria
	Stubbings	1965	Gorée, Senegal
	Pilleri	1970	W. Mediterranean
	Rappé	1988	Belgium
Grampus griseus (Risso's dolphin)	Gruvel	1920	Azores
	Richard	1936	Azores
	Richard	1936	Azores
	Pilleri and Gihr	1969	Barcelona, Spain
	Ross	1984	SE coast, S. Afr.
Sotalia sp. (Tucuxi)	Siciliano et al.	1988	Rio de Janeiro, Brazil
Stenella attenuata (Spotted dolphin)	Ross	1984	Mpelane, S. Afr.
Stenella coeruleoalba (Striped dolphin)	Raga et. al.	1982	Spanish coast, Medit. Sea
	Raga et. al.	1983	Spanish coast Medit. Sea
	Ross	1984	SE coast, S. Afr.
	Raga and Carbonell	1985	W. Mediterranean
	Boxshall (in Rappé and Waerebeek)		Mallorca
Stenella euphrosyne (Euphrosyne dolphin)	Pilleri	1970	Str. of Gilbraltar
Tursiops truncatus (Bottlenose dolphin)	True	1891	N. Carolina
	Dollfus	1968	Gibraltar
	Pilleri	1970	Gibraltar
	Present study	1985	Porto Novo, India
	Mead and Potter	1990	Central Atlantic coast, USA
	Ross	1984	Natal, S. Africa
	Barnard	1924	Natal, S. Africa
Unidentified delphinid	Pope	1958	Heron I., Queensl.
	Relini	1979	Ligurian Sea
Feresa attenuata (Pygmy killer whale)	Stubbings	1965	Yenn, Senegal
Globicephala macrorhynchus (Short-finned pilot whale)	Spivey	1977	Florida, Atlantic coast
Globicephala melas (Long-finned pilot whale)	Steenstrup	1852	Faröe Is.
	Hoek	1883	Faröe Is.
	Weltner	1897	Faröe Is.
	Gruvel	1912	Monaco
	Pilsbry	1916	Chesapeake Bay
	Gruvel	1920	Gibraltar
	Nilsson-Cantell	1921	Faröe Is.
	Richard	1936	Gibraltar
	Zullo	1963	Woods Hole
	Pilleri and Knuckey	1969	Spanish coast, Medit. Sea
	Kinze (in Rappé and Waerebeek)		Faröe Is.
	Raga et. al.	1983	Faröe Is.
	Pilsbry	1916	New England
Globicephalus sp.	Barnard	1924	North Atlantic
	Richard	1936	Mid-Atlantic
	Richard	1936	Baléares, Spain
Orcinus orca (Killer whale)	Gruvel	1920	Mediterranean
	Richard	1936	Monaco
	Richard	1936	Gibraltar
Pseudorca crassidens (False killer whale)	Gruvel	1912	Monaco
	Gruvel	1920	Miguel, Azores
	Richard	1936	Miguel, Azores
	Pilleri	1967	Spanish coast, Medit. Sea
Family: Phocoenidae			
Neophocaena phocaenoides (Finless black porpoise)	Devaraj and Bennet	1974	Karwar, India
Phocoena phocoena (Harbor porpoise)	Stubbings	1965	Hann, Senegal
Family: Ziphiidae			
Mesoplodon mirus (True's Beaked whale)	Ross	1984	SE coast, S. Afr.
Ziphius cavirostris (Goosebeaked whale [or] Cuvier's Beaked whale)	Bane and Zullo	1980	North Carolina
Unidentified whale	Broch	1924	Greenland
	Nilsson-Cantell	1930	W. Afr. (14°45′N; 18°34′W)
Unknown host	Nilsson-Cantell	1978	Bay of Biscay

Acknowledgments

Bruce B. Collette, Director, NMFS Systematics Laboratory, provided laboratory facilities and reviewed the manuscript, and the Fish Division, USNM, provided computer facilities. R. Natarajan and the authorities of Annamalai University, Tamil Nadu, India, provided facilities for this work. The senior author is grateful

to CSIR, New Delhi, for a Senior Research Fellowship for the Marine Mammal Project. William A. Newman verified the identification of *X. globicipitis*. Drafts of the manuscript were read by James G. Mead, William F. Perrin, and Austin B. Williams.

Citations

Bane, G.W., and V.A. Zullo
1980 (1981) Observations on a stranded goosebeaked whale (*Ziphius cavirostris*, Cuvier, 1823) and its ectocommensal barnacles (*Xenobalanus globicipitis*). J. Elisha Mitchell Sci. Soc. 96(1):1–3.

Barnard, K.H.
1924 Contributions to the crustacean fauna of South Africa. No. 7. Cirripedia. Ann. S. Afr. Mus. 20(1):1–103.

Barnes, R.D.
1986 Invertebrate zoology. W.B. Saunders, Philadelphia, 868 p.

Broch, Hj.
1924 Cirripedia Thoracica von Norwegen und dem norwegischen Nordmeere. Ein Systematik und biologischtiergeographische Studie. Skr. Vidensk. Selsk. Christiana, mat. naturv. KL, 17:1–121.

Calman, W.T.
1920 A whale-barnacle of the genus *Xenobalanus* from Antarctic seas. Ann. Mag. Nat. Hist., ser. 9, 6:165–166.

Cornwall, I.E.
1927 Some north Pacific whale barnacles. Contrib. Can. Biol. Fish., Toronto, new ser., 3(23):501–517.
1955a Cirripedia. Canada Pacific Fauna, Ottawa, fasc. 10C, 49 p.
1955b The barnacles of British Columbia. B.C. Prov. Mus., Handbk. 7:1–69.

Darwin, C.H.
1854 A monograph on the sub-class Cirripedia. II. The Balanidae, Verrucidae, etc. Ray Soc. Publ., 440 p.

Devaraj, M., and P.S. Bennet
1974 Occurrence of *Xenobalanus globicipitis* (Steenstrup) on the finless black porpoise, *Neomeris phocoenoides* in Indian seas. Indian J. Fish. 21(2):579–581.

Dollfus, R.Ph.
1968 *Xenobalanus globicipitis* Steenstrup (Cirripedia: Thoracica) recolté de la Côte Nord du Maroc. Bull. Inst. Pêches Marit. Maroc 16:55–60.

Gruvel, A.
1905 Monographie des Cirrhipèdes ou Thecostraces. Masson et Cie, Paris, 472 p.
1912 Sur le développement de la muraille chez le *Xenobalanus globicipitis* Steenstrup. C.R. Acad. Sci., Paris, 155: 1266–1268.
1920 Cirrhipèdes provenant des campagnes scientifiques de S.A.S. le Prince de Monaco (1885–1913). Rèsult. Campagnes Sci. accomp. sur son yacht par Albert I^{er}, Prince Souverain de Monaco, 53:1–88.

Heldt, J.H.
1950 Note au sujet de *Xenobalanus globicipitis* Steenstrup sur *Balaenoptera borealis* Lessou en Méditerranée. Bull. Soc. Hist. Nat. Tunis 3(1):25–28.

Hoek, P.P.C.
1883 Report on the Cirripedia collected by H.M.S. *Challenger* during years 1873–76. Rep. Sci. Res. Voyage H.M.S. *Challenger* 8(25):1–169.

Kenney, R.D.
1990 Bottlenose dolphins off the northeastern United States. *In* Leatherwood, S., and R.R. Reeves (eds.), The bottlenose dolphin, p. 369–386. Academic Press, San Diego.

Mackintosh, N.A.
1942 The southern stocks of whalebone whales. Discovery Rep. 22:199–298.

Mackintosh, N.A., and J.F.G. Wheeler
1929 Southern blue and fin whales. Discovery Rep. 1: 257–540.

Matthews, L.H.
1938 The sei whale, *Balaenoptera borealis*. Discovery Rep. 17:183–290.

Mead, J.G., and C.W. Potter
1990 Natural history of bottlenose dolphins along the central Atlantic coast of the United States. *In* Leatherwood, S., and R.R. Reeves (eds.), The bottlenose dolphin, p. 165–195. Academic Press, San Diego.

Nilsson-Cantell, C.A.
1921 Cirripeden-Studien. Zur Kenntnis der Biologie, Anatomie und Systematik dieser Gruppe. Zool. Bidr. Upps. 7:75–378.
1930 Thoracic cirripedes collected in 1925–27. Discovery Rep. 2:223–260.
1978 Cirripedia Thoracica and Acrothoracica. Marine Invertebrates of Scandinavia. Universistetes-forlaget, Oslo (5):1–135.

Pilleri, G.
1967 Behaviour of the *Pseudorca crassidens* (Owen) off the Spanish Mediterranean coasts. Rev. Suisse Zool. 74:679–683.
1970 *Xenobalanus globicipitis* Steenstrup on *Delphinus delphis*, *Stenella styx*, and *Tursiops truncatus* of the western Mediterranean. *In* Pilleri, G. (ed.), Investigations on cetacea, vol. II, p. 247–249. Hirnanatomisches Inst. der Univ., Berne, Switzerland.

Pilleri, G., and M. Gihr
1969 On the anatomy and behaviour of Risso's dolphin (*Grampus griseus* G. Cuvier). *In* Pilleri, G. (ed.), Investigations on cetacea, vol. I, p. 74–93. Hirnanatomisches Inst. der Univ., Berne, Switzerland.

Pilleri, G., and J. Knuckey
1969 Behaviour patterns of some Delphinidae observed in the western Mediterranean. Z. Tierpsychol. 26:48–72.

Pilsbry, H.A.
1916 The sessile barnacles (Cirripedia) contained in the collections of the U.S. National Museum, including a monograph of the American species. Bull. U.S. Nat. Mus. 93, 366 p.

Pope, E.C.
1958 The barnacle, *Xenobalanus globicipitis* Steenstrup in Australian Seas. Proc. R. Zool. Soc. N.S.W. 1956–57:159–161.

Raga, J.A., and E. Carbonell
1985 New dates about parasites on *Stenella coeruleoalba* (Meyen, 1833) (Cetacea: Delphinidae) in the western Mediterranean Sea. Invest. Cetacea 17:207–213.

Raga, J.A., and C. Sanpera
1986 Ectoparasitos y epizoitos de *Balaenoptera physalus* (L., 1758) en aguas atlanticas ibericas. Invest. Pesq. (Barcèlona) 50(4):489–498.

Raga, J.A., E. Carbonell, and M.A. Raduan
1982 Incidencias de parasitos en los cetaceos varados en las costas espanolas del Mediterraneo. Mem. Mus. Mar. Ser. Zool. 2(19):1–11.

Raga, J.A., M.A. Raduan, C. Blanco, and E. Carbonell
1983 Etude parasitologique du dauphin bleu et blanc *Stenella coeruleoalba* dans la Mediterranée occidentale. Rapp. P.-V. Reun. Comm. Int. Explor. Sci. Mer Medit. 28(5):211–212.

Rappé, G.
1988 Een vondst van *Xenobalanus globicipitis* in de Noordzee? Strandvlo 8(2):100–101.

Rappé, G., and K. van Waerebeek
1988 *Xenobalanus globicipitis* (Crustacea: Cirripedia) on cetaceans in the northeast Atlantic and the Mediterranean: A review. *In* Evans, P.G.H. (ed.), European research on cetaceans, p. 75–78. Proc., Second annual conf. European Cetacean Society, Troia, Portugal, 5–7 Feb. 1988. European Cetacean Society, Lisbon.

Relini, G.
1979 Remarks on cirripeds of Ligurian Sea. Rapp. Comm. Int. Mer. Médit. 25/26(4):131–132.

Richard, J.
1936 Notes sur les cétacés et les pinnipèdes. Result. Campagnes. Sci., Monaco 94:34–71.

Ross, G.J.B.
1984 The smaller cetaceans of the southeast coast of southern Africa. Ann. Cape Prov. Mus. Nat. Hist., 15(2):173–410.

Siciliano, S., L. Capistrano, and L. Lodi
1988 *Xenobalanus globicipitis* registrado em *Sotalia* sp. na bata de Guanabara - Rio de Janeiro - Brasil. Reunion Trabajo Especialistas Mamiferos Acuaticos, America del Sur, 25–30 de Julio. (Unpubl. Abstract #III-CL-36). Projeto Baleia, Jubarte, Rua José Higino 340, Ap. 102, Tijuca, Rio de Janiero, RJ 20520, Brazil.

Spivey, H.R.
1977 Those tenacious travelers of Florida's Atlantic coast. Fla. Nat. 50(6):6–10.

Steenstrup, J.
1852 Om *Xenobalanus globicipitis*, en ny Cirriped-Slaegt af Coronulafamilien. Vidensk. Medd. Naturhist. Foren. (1852): 62–64.

Stubbings, H.G.
1965 West African Cirripedia in the collections of the Institute Français d'Afrique Noire, Dakar, Senegal. Bull. Inst. Fr. Afr. Noire 27, ser. A (3):876–905.

True, F.W.
1891 Observations on the life history of the bottlenose porpoise. Proc. U.S. Nat. Mus. 13:197–203.

Weltner, W.
1897 Verzeichniss der bisher beschriebenen recenten Cirripeden Arten. Arch. Naturgesch. 63:227–280.

Zullo, V.A.
1963 A preliminary report on systematics and distribution of barnacles (Cirripedia) of the Cape Cod region. Publ. Mar. Biol. Lab., Woods Hole, 33 p.

Lack of biochemical genetic and morphometric evidence for discrete stocks of Northwest Atlantic herring *Clupea harengus harengus*

Susan E. Safford

U.S. Fish and Wildlife Service, P.O. Box 796 Turner's Falls, Massachusetts 01376
Present address: Graduate Center of Toxicology, 204 Funkhouser Building
University of Kentucky, Lexington, Kentucky 40506-0054

Henry Booke

U.S. Fish and Wildlife Service, P.O. Box 796, Turner's Falls, Massachusetts 01376

Historically, herring stock delineation has been based on spawning site because herring are presumed to return to their natal beds to spawn (Sindermann 1979). For example, Wheeler and Winters (1984) have estimated homing fidelity of spawning herring at 90%. Furthermore, some recognition of these historic stocks has been achieved through meristic studies (Anthony 1972, Parsons 1975, Cote et al. 1980), though these meristic differences disappear after several years, probably from environmental perturbations (Sindermann 1979). These means of defining a stock imply genetic differentiation, but do not measure it. A valid stock definition such as that in Booke (1981), "a species group, or population, of fish that maintains and sustains itself over time in a definable area," should include both genetic and geographic isolation. However, for managerial purposes it is often useful to divide large groups of a species into smaller groups, even if genetic or permanent geographic isolation cannot be demonstrated. Managerial units have sometimes been defined as stocks as in Anthony (1972), "a group of fish that remain sufficiently isolated so it can be managed as a unit separate from another one." A population can subdivide itself into discrete groups, which can be individually managed during the period of subdivision, such as a spawning season, even if these groups aren't genetically differentiated. Therefore, the goal of this study was to determine if the two spawning groups investigated constitute genetically differentiated stocks, and whether these groups could be identified either genotypically or phenotypically, regardless of stock status, outside the spawning grounds.

The first objective was to determine if herring which spawn in two geographically well-defined areas—Trinity Ledge, Nova Scotia, and Jeffries' Ledge, MA—constituted separate stocks through the demonstration of genetic differentiation by starch gel electrophoresis of enzymes. Electrophoretic studies on herring, including specimens from the two spawning grounds sampled in the present study, have been published (Kornfield et al. 1981 and 1982, Grant 1981 and 1984, King 1984). However, lack of standardization in technique, which has led to differences in the number and frequency of alleles at the same locus in different studies, makes it difficult to assess the true amount of electrophoretic differentiation among spawning groups. The second objective was to determine if these same groups of herring were separable phenotypically, whether or not genetic differences were detected. Included in this objective was the assessment of the temporal stability of a set of phenotypic characters measured over two years. This was important, as most morphometric and meristic studies which have indicated that significant phenotypic differences do exist between spawning groups of herring consist of only one year's data (Parsons 1975, Cote et al. 1980, Meng and Stocker 1984). The third and most important objective was to simultaneously measure the amount of electrophoretic and morphometric variation in the two spawning groups. Simultaneous performance of both kinds of analyses, previously done only by Ryman et al. (1984) on Northeast Atlantic herring, permits a better understanding of the level of variation between herring spawning groups.

Materials and methods

Sampling

Trinity Ledge (TL) fish were collected on 31 August 1983 and 5 September 1984, and Jeffries' Ledge (JL) fish on 1 November 1983 and 11 October 1984. All fish were taken on spawning grounds (Fig. 1) by commercial fishermen. The fish were transported frozen or packed in ice, and stored at −20°C for 1 week to 9 months until white muscle tissue samples were excised. The tissue samples were stored at −80°C until analyzed electrophoretically. A sample of 100 fish from each collection (400 total) was analyzed electrophoretically. These same fish were also analyzed morphometrically, except for 50 TL fish collected in 1983. Poor packing conditions made these 50 fish difficult

Manuscript accepted 23 September 1991.
Fishery Bulletin, U.S. 90:203–210 (1992).

to measure accurately, so an additional 50 herring were taken from the remaining TL 1983 sample for the morphometric analysis.

Morphometrics

Measurements Initially, 25 morphometric characters described by Meng and Stocker (1984) in their analysis of Pacific herring were measured on 100 Atlantic herring, 50 from each location, from the 1983 sample. The measurements followed Hubbs and Lagler (1958). Standard length (SL) was measured to the nearest 0.5 mm on a measuring board. The other measurements were taken with vernier calipers to the nearest thousandth of an inch and converted to millimeters. Multivariate analyses were used to determine if the groups were different from one another and which characters contributed to these differences. To address length bias, multiple analysis of covariance, performed under the MANOVA subroutine in the statistical package for the social sciences, was used to remove the effect of SL on the other variables (Sokal and Rohlf 1969, Steel and Torrie 1980). The results of multiple analysis of variance of the adjusted measurements versus spawning group, performed under the same subroutine, showed that the two groups were significantly different from each other and identified eight characters whose means were significantly different (Snedecor and Cochran 1967, Safford 1985) (Fig. 2). The binomial distribution predicted the probability of eight significant characters out of 25 as 1.77×10^{-5}, given a probability of 0.05 that a single character would be significantly different due to chance alone.

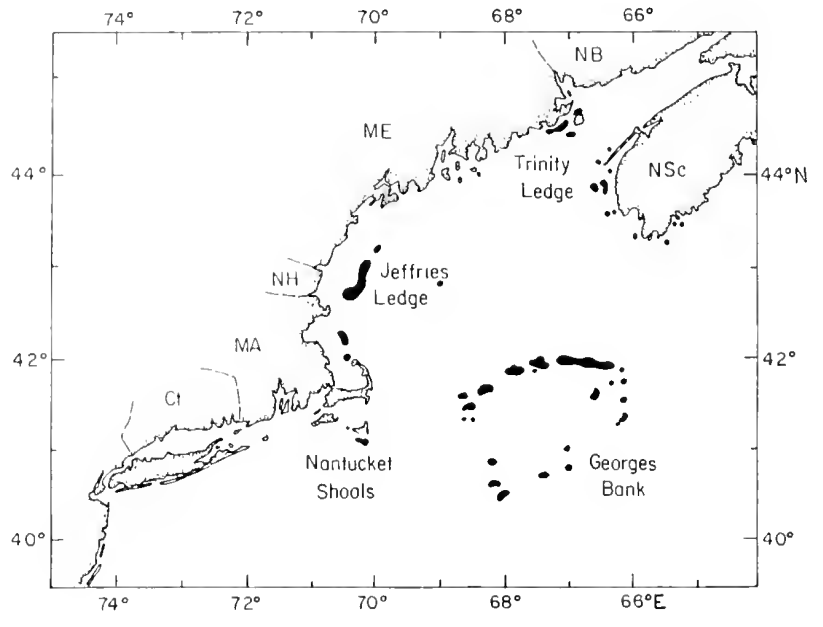

Figure 1
Atlantic herring spawning grounds in the Gulf of Maine region.

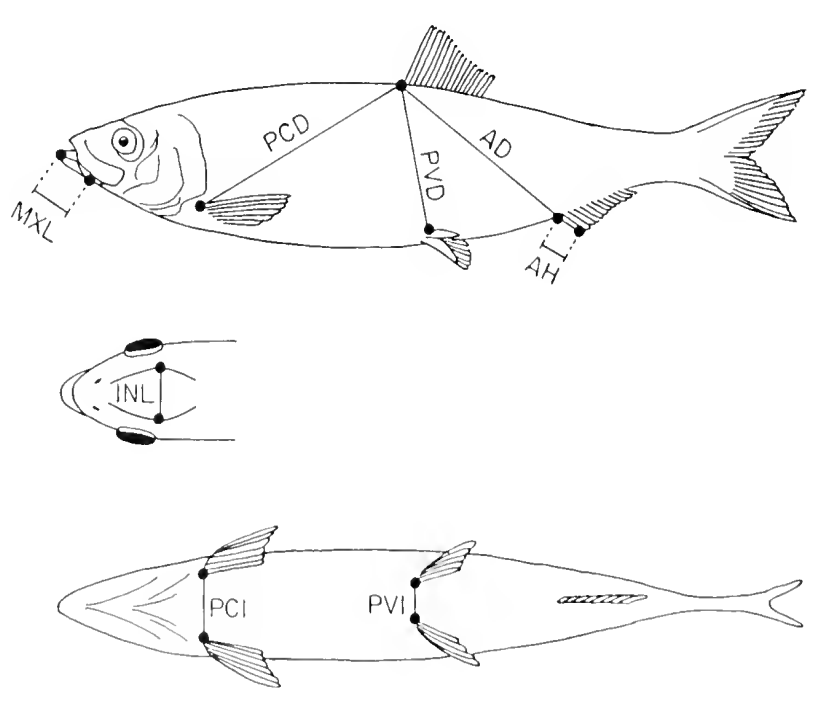

Figure 2
Eight morphometric measurements used to derive the discriminant function: MXL = maxillary length; PCD = pectoral to dorsal fin; PVD = pelvic to dorsal fin; AD = anal to dorsal fin; AH = anal fin height; INL = interorbital distance; PCI = distance between insertions of pelvic fins; PVI = distance between insertions of pectoral fins.

Discriminant function These eight characters were used to derive a discriminant function (Snedecor and Cochran 1967, Sokal and Rohlf 1969). Each measurement in subsequent samples was adjusted to the SL of the original sample to eliminate bias due to differences in the SL. Details of the construct of the discriminant function and the formulae used to adjust the subsequent measures can be found in Appendix A and Safford (1985).

The discriminant function was tested for spatial and temporal stability with additional samples from both 1983 and 1984. The additional sample data were treated as described in Appendix A to yield a z-score so the fish could be classified according to spawning group. The cut-off value for the z-score was set at zero, where fish with a z-score >0 were classified as Trinity Ledge fish and those with a z-score ≤ 0 were classified as Jeffries' Ledge fish (Norusis 1979, Safford 1985).

Table 1

Means (mm), unadjusted for standard length, and 95% confidence intervals of the eight morphometric characters used in the discriminant function derived from 100 Atlantic herring from the 1983 samples.

Character	Jeffries' Ledge (n 50)	Trinity Ledge (n 50)
Maxillary length (MXL)	27.90±0.57	31.06±0.51
Pectoral to dorsal fin (PCD)	81.46±1.98	93.44±1.82
Pelvic to dorsal fin (PVD)	48.41±1.53	59.43±1.63
Anal to dorsal fin (AD)	70.56±1.88	79.62±1.59
Height of anal fin (AH)	14.35±0.59	13.13±0.47
Interorbital distance (INL)	10.34±0.31	10.10±0.25
Distance between insertions of pectoral fins (PCI)	13.16±0.49	17.37±0.71
Distance between insertions of pelvic fins (PVI)	8.41±0.31	10.63±0.35
Standard length (SL)	233.50±18.03	251.50±14.19

Statistics A stepwise function employing the F-value of each character, ($p<0.05$), to accept or reject a character was derived to rank the variables. The distribution of phenotypic variation was measured by a nested analysis of variance (ANOVA), with years nested within groups, generated by nested procedures using PC-SAS packaged programs (SAS 1985). One-way ANOVA generated by the general linear models procedure in PC-SAS packaged programs (SAS 1985) was used to analyze differences in morphometric measurements, both between years within a spawning group and between spawning groups within a year.

Electrophoresis

Enzyme visualization Traditional starch gel electrophoresis of white muscle tissue samples as described by Utter et al. (1974), with some modifications, was used to resolve the enzymes. A detailed description of the gel composition and running conditions can be found in Safford (1985). Four polymorphic loci—phosphoglucomutase, *PGM-2** (5.4.2.2), glucose-6-phosphate isomerase, *GPI-2** (5.3.1.9), and two of lactate dehydrogenase, *LDH-1** and *LDH-2** (1.1.1.27)—were analyzed. The enzyme abbreviations and numbers follow the suggestions of Shaklee et al. (1989). Two buffer systems, Ridgway et al. (1970) and Markert and Faulhaber (1965), were used. The Ridgway gel buffer, used for LDH and GPI, was modified by doubling the amount of Tris (Sigma Chemical Co., St. Louis) in the recipe, which raised the pH to 8.5 and made the bands more distinct. The Markert-Faulhaber buffer was used for PGM because it improved band resolution. Stain recipes and techniques followed Shaw and Prasad (1970) with modifications which are detailed in Safford (1985). Photographs were taken immediately upon staining.

Statistics Allelic frequencies were compared between samples by chi-square contingency table analysis. Genotypic frequencies were tested for conformation to the Castle-Hardy-Weinberg (C-H-W) equilibrium with a chi-square goodness-of-fit test (Zar 1974). Gene diversity analyses were conducted according to Nei (1973), Chakraborty (1980), and Chakraborty et al. (1982).

Results

Morphometrics

Group means of eight morphometric characters were found to be significantly different ($p<0.01$) between samples taken from the two spawning areas in 1983. No overlap in range was found within the 95% confidence interval for seven of these variables, and overlap at the eighth variable was very small (Table 1). Therefore, it was concluded for this study that 50 fish from each sample were sufficient. The stepwise discriminant function accepted the first seven of these eight variables. Multiple analysis of variance of the eight characters versus locality for the 1984 samples revealed that only three of these characters—distance between insertions of the pelvic and dorsal fins (PVD), anal fin height (AH), and distance between the insertions of the pectoral fins (PCI)— were significantly different ($p<0.01$) between the two groups. Two of these characters, PVD and PCI, were among the three which

Table 2

Discriminant function analysis results of different Atlantic herring samples from known spawning grounds.

Sample	Number from each spawning ground classified as:		Percent from each spawning ground classified as:		Overall correct classification
	Jeffries' Ledge	Trinity Ledge	Jeffries' Ledge	Trinity Ledge	
1983 discriminant function construction sample ($N=N_1+N_2=100$)					
Jeffries' Ledge ($N_1=50$)	44	6	88%	12%	
Trinity Ledge ($N_2=50$)	7	43	14%	86%	87%
1983 Sample ($N=N_1+N_2=100$)					
Jeffries' Ledge ($N_1=50$)	38	12	76%	24%	
Trinity Ledge ($N_2=50$)	11	39	22%	78%	77%
1984 Sample ($N=N_1+N_2=198$)					
Jeffries' Ledge ($N_1=99$)	92	7	93%	7%	
Trinity Ledge ($N_2=99$)	84	15	85%	15%	54%

Table 3

Phenotypic variation of Atlantic herring in geographic and temporal hierarchies for each of eight morphometric characters. (*)$p \leq 0.01$; (+)$p \leq 0.001$. See Figure 2 for definitions of morphometric characters.

Source of variation:	Between spawning groups			Between years within a spawning group			Within samples		
Character	df	mean square	variance component (%)	df	mean square	variance component (%)	df	mean square	variance component (%)
MXL	1	120.3+	0.0	2	597.3+	59.0	390	4.2	41.0
AH	1	38.2*	0.7	2	29.0*	3.3	390	6.6	96.0
PCD	1	2136.1+	0.7	2	7778.3+	58.5	390	55.7	41.5
PVD	1	2655.8+	0.7	2	4483.7+	57.1	390	34.0	42.9
AD	1	1379.7	0.0	2	4475.3	53.4	390	41.9	46.6
INL	1	0.0	0.0	2	131.0+	63.6	390	0.6	36.4
PCI	1	282.3+	0.0	2	383.9+	46.5	390	4.4	53.5
PVI	1	45.8+	0.0	2	136.2+	46.3	390	1.6	53.7

accounted for most of the between-group variation in the 1983 sample. The percent correct classification by spawning group of three sets of samples (two from 1983, one from 1984) separated by the derived discriminant function is found in Table 2. Overall misclassification of fish collected in 1983 was 18%, while that of fish collected in 1984 was 46%.

The phenotypic variation of the unadjusted measurements was partitioned similarly within each morphometric character, except AH (Table 3). The partitioning of the phenotypic variation averaged across all characters is found in Table 4. None of the variation was explained by differences between spawning groups, while approximately one-half was partitioned within a spawning group between years. The remainder of the variation was within a sample. One-way ANOVA of between-year differences within a spawning group showed that within the TL group the means of all the characters, except AH ($p \leq 0.02$), were highly significantly different ($p \leq 0.0001$) between 1983 and 1984. In contrast, within the JL group three characters—distance between the insertions of the pelvic fins (PVI), AH, and PCI—were not significantly different between years. The remaining characters were significantly different ($p \leq .05$) between years.

Electrophoresis

Allelic frequencies within each sample for the four loci chosen for analysis are found in Table 5. Other enzyme systems were also investigated, but few specimens expressed enzyme activity at these loci (Safford 1985). We chose these loci because they had previously been shown to be polymorphic and to follow Mendelian in-

heritance in herring (Grant 1981, Kornfield et al. 1981 and 1982, King 1984). The designation of alleles is taken from Kornfield et al. (1982) and is based on direction of migration of the enzymes on the gel and their distance from the origin. *LDH** is encoded by three anodally migrating loci. The fastest locus, *LDH-3**, was present only in eye tissue and activity was found in only some of the fish, so this locus was not used in the present analysis. Each of the other two loci were represented by two alleles. *PGM** is encoded by two anodally migrating loci. The slower locus, *PGM-1**, was fixed for the same allele in all samples. The polymorphic locus, *PGM-2**, was represented by three alleles. However, the slowest allele was found in only one specimen. *GPI** is encoded by one anodally migrating locus, *GPI-2**, which was represented by five alleles in our samples.

Chi-square contingency table analysis revealed that *GPI-2** was significantly different ($p \leq 0.05$) between JL 1984 and both TL 1984 and JL 1983. This was probably due to a greater frequency of allele 150 in the JL 1984 sample. Its frequency was double (0.18) that found in the JL 1983 sample (0.09) and the TL 1984 sample (0.10). The chi-square goodness-of-fit test showed that the JL 1984 sample was not in C-H-W equilibrium at the *GPI-2** locus, which contained an excess of 150/−3 heterozygotes. The gene-diversity analysis results for the individual loci were similar within each locus, and revealed that more than 99% of the genetic diversity was found within a single sample. A comparison between the partitioning of the average gene diversity and the average phenotypic variation is shown in Table 4. The large between-year phenotypic variation is not reflected in the between-year genetic diversity index, as <1% of the gene diversity can be explained by between-year differences within a spawning group.

Discussion

In-depth discussions of the historical construct of herring stocks and the implications of recent electrophoretic findings can be found in Jorstad and Naevdal (1981), Smith and Jamieson (1986), and Kornfield and Bogdanowicz (1987). The traditional herring stock construct has not been supported by genetic stock structure analyses as none of the electrophoretic studies, including the present one, have found a large amount of genetic differentiation (Andersson et al. 1981, Grant 1981 and 1984, Jorstad and Naevdal 1981 and 1983,

Table 4

Distribution of relative gene diversity and phenotypic variation of Atlantic herring in geographic and temporal hierarchies. Gene diversity is based on four individual or pooled samples and four polymorphic loci. Phenotypic variation is averaged over 393 individuals, four individual or pooled samples, and eight morphometric characters.

	Gene diversity		Phenotypic variation		
Source of variation	Absolute	%	df	Mean square	Variance component (%)
Between spawning groups	0.00024	0.1	1	823.28	0.09
Between years within spawning groups	0.00074	0.4	2	2289.34	48.46
Within samples	0.20138	99.5	390	18.63	51.45

Table 5

Allelic frequencies of samples of Atlantic herring.

	Loci and alleles											
	LDH-1		*LDH-2*		*PGM-2*			*GPI-2*				
Location/Year	*100	0	100	72	112	100	95	150	100	40	−3	−75
Jeffries' Ledge (*N*)												
1983 (100)	0.980	0.020	0.955	0.045	0.025	0.975	0	0.090	0.630	0.140	0.120	0.020
1984 (100)	0.985	0.015	0.955	0.045	0.055	0.945	0	0.180	0.540	0.105	0.160	0.015
Trinity Ledge (*N*)												
1983 (100)	0.965	0.035	0.955	0.045	0.065	0.925	0.005	0.110	0.560	0.210	0.115	0.005
1984 (100)	1.000	0	0.945	0.055	0.025	0.975	0	0.100	0.630	0.120	0.130	0.020

* Allelic designations indicate direction of migration (+ anodal, − cathodal), and relative distance from origin (the farther away, the larger the number).

Kornfield et al. 1982, King 1984, Ryman et al. 1984). The conclusion that herring spawning groups are not discrete genetically-distinct stocks is further supported by the results of a recent study by Kornfield and Bogdanowicz (1987). They investigated the genetic relationships of ripe female herring from three locations, including Jeffries' Ledge and some of the 1983 Trinity Ledge samples analyzed in this study, by restriction endonuclease analysis of mitochondrial DNA (mtDNA). In other species, this technique has revealed genetic differentiation not uncovered by traditional enzyme electrophoresis (Avise et al. 1986). Kornfield and Bogdanowicz (1987) found that these spawning groups were not completely distinguished by the composite mtDNA digestion patterns generated, and no consistent geographic patterns were found for the unique composites. Therefore, they concluded that this approach also provided no evidence for the existence of genetically distinct stocks in the Gulf of Maine.

The significant departures from C-H-W equilibrium found in this and previous studies (Grant 1981, Ryman et al. 1984) may be considered contradictory to the hypothesis of the existence of a genetically homogenous herring population. However, these departures seem to be a feature of pelagic fish stocks (Smith et al. 1989). These disequilibria have been variously attributed to chance due to the low frequency of occurrence (Grant 1981, Ryman et al. 1984) and assortative mating (Smith et al. 1989). The significant departure in the present data has derived from an excess number of heterozygotes of one particular allelic combination in the JL 1984 data. One significant departure in 16 tests is slightly higher than would be expected by chance alone at the 5% probability level. An excess of heterozygotes can result from negative assortative mating; however, the data are not sufficient to support that hypothesis. Importantly, the C-H-W equilibrium applies to all generations in a population, thus significant departures may occur if sampling does not measure all generations in the same proportion in which they occur in the population. Based on SL, few immature and old fish were included, so this sample bias may have contributed to the significance level. Thus, the departure from C-H-W equilibrium is probably due to chance and perhaps some sampling bias. However, the distribution of alleles across generations within a population may warrant further investigation as disequilibrium, though explicable, is a feature of herring populations and some age-based selection may be occurring.

Although the genetic evidence argues for a single population of herring, significant phenotypic differences between spawning groups have been demonstrated (Parrish and Saville 1965, Burd 1969, Anthony 1972, Cote et al. 1980, Ryman et al. 1984). Morphometric and meristic characters, which have a complex underlying genetic structure, are believed to be greatly influenced by environmental parameters (Sindermann 1979, Ryman et al. 1984). Thus phenotypic differences may not reflect genetic differentiation, and small but detectable genetic differences may not significantly alter phenotypic characters. Differences in biochemical genetic and phenotypic variation can best be demonstrated when genetic and phenotypic analyses are performed on the same specimens. In their study, Ryman et al. (1984) screened 17 loci from herring caught in 17 locations ranging from the Gulf of Bothnia to the northeast Atlantic off Norway's western coast, and found significant allelic heterogeneity at only 4 loci. They concluded that the results resembled those of samples drawn from a single breeding population, as both the genetic diversity index and genetic distances were very small. They chose numbers of vertebrae and keeled scales as morphological characters. Morphological distances were used to construct a dendogram which differentiated herring in central Baltic fall spawning groups from a spring spawning Baltic group and the other fall spawning groups. Thus these meristic characters differed to some extent despite genetic similarities. Morphologic variation was partitioned by nested ANOVA with localities nested within larger geographic areas, and genetic variation was partitioned by genetic diversity analysis. They found over 99% of the gene diversity within a locality, compared with 50% of the phenotypic variation. Most important, $<1\%$ of the gene diversity was explained by between-geographic-group differences, while these differences explained 40% of the phenotypic variation.

The partitioning of variance in our samples was similar in many respects to that of Ryman et al. (1984). Over 99% of the genetic variance in our samples also occurred within a locality within a year, compared with approximately 50% of the morphometric variance component. However, the percent of the morphometric variance component explained by differences between spawning groups was similar for both the genetic and morphometric components (0.1%), in contrast to the large between-group morphometric variation found by Ryman et al. (1984). Results from both these studies demonstrate that most genetic diversity lies within a single locality at one point in time, further supporting the hypothesis that herring form a single panmictic population. Thus the current situation seems to be that despite the existence of discrete, defined spawning groups and apparent high homing fidelity, enough gene flow exists between spawning groups to prevent Northwest Atlantic herring from evolving into genetically distinct stocks. Alternatively, herring may have begun this process in recent geographic time, so that genetic differences have not had time to evolve. This lack of genetic differentiation also means that observed

phenotypic differences are most likely due primarily to differences in environmental conditions during development, and therefore will not be reliable indicators of stock identity. Further, if all measurable phenotypic characters are distributed similarly to those in the present study and Ryman et al. (1984), then the use of phenotypic characters to distinguish herring groups may be proscribed, as the large within-group variation would mask the subtler between-group differences.

These ideas need to be incorporated into current herring management policy. The results show that individuals from discrete spawning groups can not be reliably identified off the spawning grounds. Therefore, the contribution of each spawning group to various fisheries cannot be estimated. These results also suggest that the demise of a single spawning ground will not adversely affect the underlying genetic structure of the herring population, as few unique genes should be found exclusively within a spawning location. However, small discrete spawning grounds are apparently necessary to support a large population. Small spawning grounds may be necessary for appropriate spawning behavior or to ensure proper conditions for the larvae. Therefore, until the relationship between discrete spawning grounds and a healthy herring population is understood, management policy should include the maintenance of existing spawning grounds.

Acknowledgments

The authors thank Pamela Mace (Fisheries and Oceans, Canada) and the captain and crew of the FV *Barnegat* (Gloucester, MA) for field collection assistance, as well as three anonymous reviewers whose comments strengthened the paper. This work was supported by a two-year stipend to S. Safford from the Massachusetts Division of Marine Fisheries and additional funds from the Massachusetts Division of Fisheries and Wildlife and The Masssachusetts Co-operative Research Unit of Fisheries and Wildlife Biology.

Citations

Andersson, L., N. Ryman, R. Rosenberg, and G. Stahl
1981 Genetic variability in Atlantic herring (*Clupea harengus harengus*): Description of protein loci and population data. Hereditas 95:69–73.

Anthony, V.
1972 Population dynamics of the Atlantic herring in the Gulf of Maine. Ph.D. diss., Univ. Wash., Seattle, 266 p.

Avise, J.C., G.S. Helfman, N.C. Saunders, and L.S. Hales
1986 Mitochondrial DNA differentiation in North Atlantic eels: Population consequences of an unusual life history pattern. Proc. Natl. Acad. Sci. 83:4350–4354.

Booke, H.E.
1981 The conundrum of the stock concept—Are nature and nurture definable in fishery science? Can. J. Fish. Aquat. Sci. 38:1479–1480.

Burd, A.C.
1969 Trials with principal component analysis for herring racial studies. Int. Counc. Explor. Sea CM 1969/30, Pelagic Fish Comm., 11 p.

Chakraborty, R.
1980 Gene-diversity analysis in nested subdivided populations. Genetics 96:721–726.

Chakraborty, R., M. Haag, N. Ryman, and G. Stahl
1982 Hierarchical gene diversity analysis and its application to brown trout population data. Hereditas 97:17–21.

Cote, G., P. Lamoureux, J. Boulva, and G. Lacroix
1980 Separation des populations de hareng de l'Atlantique (*Clupea harengus harengus*) de l'estuaire du Saint-Laurent et de la peninsule gaspienne. Can. J. Fish. Aquat. Sci. 37:66–71.

Grant, W.S.
1981 Biochemical genetic variation, population structure, and evolution of Atlantic and Pacific herring. Ph.D. diss., Univ. Wash., Seattle, 135 p.
1984 Biochemical population genetics of Atlantic herring, *Clupea harengus*. Copeia 1984(2):357–364.

Hubbs, C., and K. Lagler
1958 Fishes of the Great Lakes region. Bull. 26, Cranbrook Inst. Sci., Bloomfield Hills, MI, 186 p.

Jorstad, K., and G. Naevdal
1981 Significance of population genetics on management of herring stocks. Int. Counc. Explor. Sea CM 1981/4:64.

Jorstad, K.E., and G. Naevdal
1983 Genetically distinct populations of herring. Contrib. XV Int. Cong. Genetics, New Delhi, India.

King, D.P.F.
1984 Genetic analysis of enzyme polymorphisms in herring. Heredity 52:121–131.

Kornfield, I., and S.M. Bogdanowicz
1987 Differentiation of mitochondrial DNA in Atlantic herring, *Clupea harengus*. Fish. Bull., U.S. 85(3):561–568.

Kornfield, I., P. Gagnon, and B. Sidell
1981 Inheritance of allozymes in Atlantic herring. Can. J. Genet. Cytol. 23:715–720.

Kornfield, I., B. Sidell, and P. Gagnon
1982 Stock definition in Atlantic herring: Genetic evidence for discrete fall and spring spawning populations. Can. J. Fish. Aquat. Sci. 39:1610–1621.

Markert, C.L., and I. Faulhaber
1965 Lactate dehydrogenase patterns in fish. J. Exp. Zool. 159:319–332.

Meng, H.J., and M. Stocker
1984 An evaluation of morphometrics and meristics for stock separation of Pacific herring (*Clupea harengus pallasi*). Can. J. Fish. Aquat. Sci. 41:414–422.

Nei, M.
1973 Analysis of gene diversity in subdivided populations. Proc. Natl. Acad. Sci. 70(12)Pt. 1:3321–3323.

Norusis, M.J.
1979 SPSS. Statistical algorithms. Release 8.0. SPSS, Inc., Chicago.

Parrish, B.B., and A. Saville
1965 The biology of the Northeast Atlantic herring populations. Oceanogr. Mar. Biol. Annu. Rev. 3:323–373.

Parsons, L.S.
1975 Morphometric variation in Atlantic herring from Newfoundland and adjacent waters. Int. Comm. Northwest Atl. Fish. Res. Doc. 11:73–92.

Ridgway, G.J., S.W. Sherburne, and R.P. Lewis
1970 Polymorphism in the esterases of Atlantic herring. Trans. Am. Fish. Soc. 99(1):147–151.

Ryman, N., U. Lagercrantz, I. Andersson, R. Chakraborty, and R. Rosenberg
1984 Lack of correspondence between genetic and morphological variability patterns in Atlantic herring (*Clupea harengus*). Heredity (53)3:687–704.

Safford, S.E.
1985 Stock identification through electrophoretic and morphometric analyses of two spawning populations of Northwest Atlantic herring (*Clupea harengus harengus*, Linnaeus). Master's thesis, Univ. Mass., Amherst, 111 p.

SAS
1985 SAS/STAT guide for personal computers, Version 6 Ed. SAS Inst., Inc., Cary, NC.

Shaklee, J.B., F.W. Allendorf, D.C. Morizot, and G.S. Whitt
1989 Genetic nomenclature for protein-coding loci in fish: Proposed guidelines. Trans. Am. Fish. Soc. 118:218–227.

Shaw, C.R., and R. Prasad
1970 Starch gel electrophoresis of enzymes: A compilation of recipes. Biochem. Genet. 4:297–320.

Sindermann, C.J.
1979 Status of Northwest Atlantic herring stocks of concern to the United States. Tech. Ser. Rep. 23, Sandy Hook Lab., NMFS, NOAA, Highlands, NJ, 449 p.

Smith, P.J., and A. Jamieson
1986 Stock discreteness in herrings: A conceptual revolution. Fish. Res. 4:223–234.

Smith, P.J., A.J. Birley, and A. Jamieson
1989 Electrophoretic studies and the stock concept in marine fishes. J. Fish. Biol. 35(Suppl. A):345–346.

Snedecor, G.W., and W.G. Cochran
1967 Statistical methods, 6th ed. Iowa State Univ. Press, Ames, 593 p.

Sokal, R.R., and F.J. Rohlf
1969 Biometry. W.H. Freeman, San Francisco, 776 p.

Steel, R.G.D., and J.H. Torrie
1980 Principles and procedures of statistics, biometrical approach, 2d ed. McGraw-Hill, NY.

Utter, F.M., H.O. Hodgins, and F.W. Allendorf
1974 Biochemical genetic studies of fishes: Potentialities and limitations. *In* Malins, D.C., and J.R. Sargent (eds.), Biochemical and biophysical perspectives in marine biology, Vol. 1, p. 213–238. Academic Press, NY.

Wheeler, J.P., and G.H. Winters
1984 Homing of Atlantic herring in Newfoundland waters as indicated by tagging data. Can. J. Fish. Aquat. Sci. 41: 108–117.

Zar, J.H.
1974 Biostatistical analysis. Prentice-Hall, Englewood Cliffs, NJ, 620 p.

Appendix A

The values of the eight morphometric characters were linearly combined to form a single value, a z-score, which was used to classify an individual into a group (Sokal and Rohlf 1969, Norusis 1979). The general formula for a z-score is

$$Z = C1X1 + C2X2 + \ldots + CnXn + e$$

where each C is the unstandardized canonical discriminant function coefficient for each character (Norusis 1979).

The general formula used to adjust each measurement was

$$R_v = Vn - b_o - b_i * SL$$

where R_v = adjusted measure,
V_n = original measure,
b_o = intercept,
b_i = slope of the univariate covariance equation, with
SL = 242.5 (mean SL of original sample).

Variability of monthly catches of anchovy *Engraulis encrasicolus* in the Aegean Sea

Konstantinos I. Stergiou
National Centre for Marine Research
Agios Kosmas, Hellinikon, Athens 16604, Hellas

In a recent paper, Stergiou (1990a) showed that the autoregressive terms of an ARIMA model describing the monthly fishery of the anchovy *Engraulis encrasicolus* in Hellenic waters indicated a 2- to 3-year periodicity in catches. A similar cycle has also been shown for anchovy in the Azov (Dement'eva 1987) and Adriatic Seas (S. Regner 1985). In comparison, long-term periodicities have been shown for *Engraulis mordax* off California (Soutar and Isaacs 1974). In this present study, I examined the variability of the Hellenic monthly catches of anchovy during the period 1964–87 using spectral analysis.

The purse-seine fishery landed 51,282 t of fish which comprised 49% of the total Hellenic catch in 1987 (Stergiou 1990b). Anchovy comprised 46.6% of the 1987 purse-seine catch; the remainder included sardine *Sardina pilchardus*, horse mackerel *Trachurus* sp., bogue *Boops boops*, chub mackerel *Scomber japonicus*, and bonito *Sarda sarda* (Stergiou 1990b). Ninety percent of the mean annual anchovy catch (1964–85) was caught in the northern, northwestern, and western Aegean Sea (Stergiou unpubl. data; no data are available for monthly catches per major fishing area). A recent study of genetic distances, based on electrophoretic variation, and of morphometric and meristic characters using multivariate analysis does not indicate separate stocks of anchovy (or sardine) in the Aegean Sea (Spanakis et al. 1989).

Monthly catches of anchovy (1964–87, 288 data points) and annual fishing effort (in horsepower, HP) of pelagic seiners were gathered from the Bulletins of the Hellenic National Statistical Service (1968–89). The monthly series was log-transformed and detrended to become stationary. The seasonal component was removed by differencing with lag = 12 (Chatfield 1984). To avoid a discontinuity at the end of the data, the resulting series was tapered by 20%. The Fast Fourier Transform was used to compute power spectral estimates, and smoothed (5 moving averages) squared amplitudes of the sinusoids were plotted.

Anchovy catches show a marked seasonal pattern (Fig. 1) and an increasing trend for the years following 1980. The increased trend in catch in recent years has raised concern about whether these high catches are sustainable. Due to higher prices of anchovy since the late 1970s, purse-seine fishing in Hellenic waters is anchovy-oriented rather than sardine-oriented (Stergiou 1986a, 1990a,b). Monthly fishing effort by pelagic seiners is not available. However, annual fishing effort of pelagic seiners increased considerably between 1964 and 1987 (from 363 boats, 20,316 HP, and 6152 tonnage of boats, to 502 boats, 112,310 HP, and 18,922 tonnage of boats; Hellenic Natl. Stat. Serv., 1968–89). Annual catches of anchovy are highly positively correlated with annual horsepower of the pelagic seiners [Ln(annual catch) = 8.25 + 0.000013HP; n 24, r + 0.89, $p<0.001$) (Fig. 2), indicating that the highly significant linear

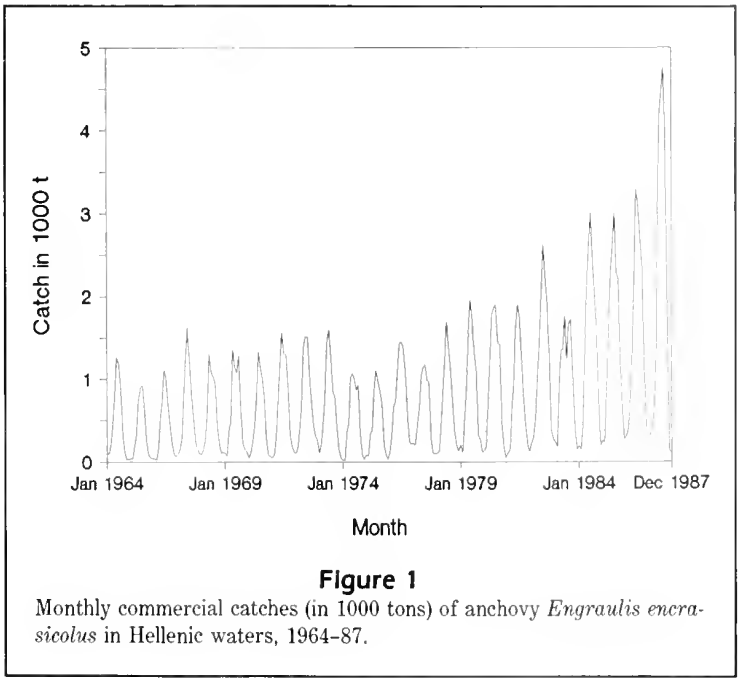

Figure 1
Monthly commercial catches (in 1000 tons) of anchovy *Engraulis encrasicolus* in Hellenic waters, 1964–87.

Manuscript accepted 26 July 1991.
Fishery Bulletin, U.S. 90:211–215 (1992).

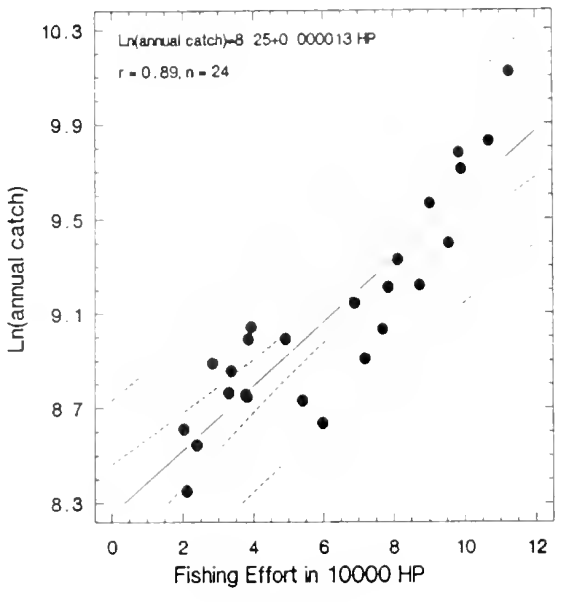

Figure 2

Regression line (solid) and 95% and 99% confidence limits (dotted) of the log annual commercial catch of anchovy and fishing effort in horsepower (HP), in Hellenic waters, 1964–87.

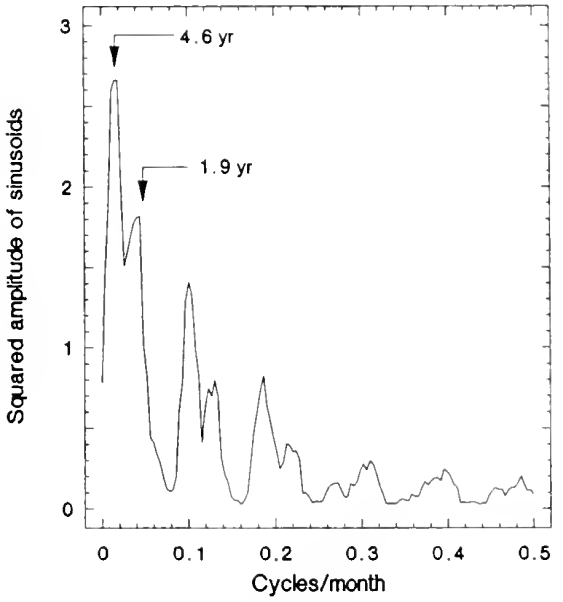

Figure 3

Spectrum of logged/detrended seasonally corrected monthly anchovy catches.

trend in monthly catches [Ln(monthly catch) = 5.38 + 0.0053T, n 288, r 0.38, $p<0.01$, where T = 1–288] is most likely attributed to increased fishing effort.

The spectrum of the resulting series (not shown here), which may be postulated to be free of any annual changes in effort, revealed a large major peak at 12 months (frequency 0.0833). This marked seasonal pattern is most likely related to the seasonal offshore-inshore migrations of anchovy and the nature of the purse-seine fishery (Stergiou 1990a). Purse-seine fishing in Hellenic waters does not occur in the open sea but is mainly restricted to coastal areas where schools of anchovy migrate seasonally. The anchovy starts its inshore migration in early spring, but peak abundance occurs in coastal waters in May–August. Offshore migration probably occurs in late summer–fall.

The smoothed spectrum of the seasonally corrected and detrended series (Fig. 3) reveals a prominent peak at 4.6 years (frequency 0.018) and a probable secondary peak at 1.9 years (frequency 0.043) (95% confidence intervals of the spectrum for 10 df: 0.4882–3.0798 squared amplitude of sinusoids). In contrast, non-sinusoidal periodic variability generates harmonics with periods of less than 1 year (Fig. 3).

Cycles of 2–3 and 4–5 years have also been identified in the air temperature in the northern (Thessaloniki) and western Aegean (Athens) (Table 1) and in different biotic (zooplankton, phytoplankton, fish eggs/larvae, fish) and abiotic variables (air temperature/pressure, sea temperature/salinity) in different areas of the Mediterranean, Black, and Azov Seas (Table 1). These cycles have also been suggested for annual anchovy catches and eggs/larvae, temperature, salinity, and zooplankton in the Adriatic Sea but the data set is limited (annual, 1962–76) and the cycles may not be statistically significant (D. Regner 1985). Correlations have been found between biotic/abiotic variables (primary production, zooplankton biomass, winds, river flow, air/sea temperature, salinity) and various abundance indices of the Mediterranean anchovy (Azov–Black Sea: Dement'eva 1987, Dekhnik and Rass 1988, Porumb and Marinescu 1979; Hellenic waters: Stergiou 1986b; Adriatic Sea: S. Regner 1985; western Mediterranean: Palomera and Lleonart 1989) and other species of *Engraulis* (see Bakun 1985).

Cycles with periods of 2–4 and 4–7 years have also been identified in the physical environment and marine populations in other areas of the world (e.g., Kort 1970, Shuntov et al. 1981, Colebrook and Taylor 1984, Mysak 1986). Such cycles have frequently been related to short-term ocean-atmosphere interactions (e.g., surface heat-exchange phenomena: Zupanovich 1968, Colebrook and Taylor 1984; advection: Kort 1970, Mysak 1986).

A comprehensive discussion of the mechanisms underlying such variability requires adequate biological

Table 1

Cycles identified in the variability of various climatic and biological parameters in the Mediterranean–Black Sea ecosystem. T = type of data (A = annual, M = monthly, D = daily); P = time period of available data; Me = method of analysis of data (sa = spectral analysis, acf = autocorrelation function, cgm = composite graphic method, i.e., comparison of graphs; see Dement'eva 1987).

Variable	Area	T	P	Me	Cycles, in years			Source
Sardine catch*	Adriatic	A	1853–1960	sa	2.3	3–3.5		Zupanovic 1968 Regner and Gacic 1974
Sardine catch	Hellas	M	1964–1982	sa		3.3		Stergiou 1988
Anchovy catch	Hellas	M	1964–1987	sa	1.9	3.3	4.6	This study
Anchovy catch*	Azov Sea	A	1955–1981	cgm	2–3			Dement'eva 1987
Carp catch*	Hellas[a]	A	1947–1983	sa		3–4		Economidis et al. 1988
Perch catch*	Hellas[a]	A	1947–1983	sa		3–4		Economidis et al. 1988
Copepods	Adriatic	M	1970–1974	acf	2–3			D. Regner 1985
Fish larvae	Adriatic	M	1971–1977	acf	3			S. Regner 1982
Fish eggs	Adriatic	M	1970–1974	acf	2–3			D. Regner 1985
Primary production	Adriatic	M	1970–1974	acf	2–3			D. Regner 1985
Diatoms*	Black Sea	A	1954–1987	sa	2.9		4.5	Petrova-Karadjova and Apostolov 1988
Air temp.*	Hellas[b]	A	1892–1981	sa	2.2–2.3		4	Flocas and Giles 1984
Air temp.*	Hellas[c]	A	1859–1981	sa	2.2–2.3		4	Flocas and Giles 1984
Air temp.*	Trieste	A	*	sa	2–2.9		4	Polli 1955
Air pressure*	Trieste	A	*	sa	2.3		4	Polli 1955
Air pressure*	Venice	A	*	sa	2.1–2.8		4	Polli 1955
Sea surface temp.	Adriatic	M	1970–1974	acf	2–3			D. Regner 1985
Sea surface temp.	Monaco	D	1946–1961	sa	1.8		4.4	Bethoux and Ibanez 1979
Sea surface salinity	Adriatic	M	1970–1974	acf	2–3			D. Regner 1985

* Together with cycles of 8–12 years (frequently related to the 11-year cycle in sunspot number, e.g., Gnevyshen and Ol' 1977).
[a] Lake Koronia, [b]Thessaloniki in summer, [c]Athens in summer.

and physical oceanographic information, probably on time scales of a few days and spatial scales of <1 km (*sensu* Leggett 1986). This information is not currently available. The distribution and biology of larval, juvenile, and adult anchovy and larval dispersal patterns have not been studied in Hellenic waters. However, some preliminary, conjectural discussion is presented here.

The anchovy spawning season in the eastern Mediterranean extends from April to September with a peak in the summer months (Demir 1965, S. Regner 1985). Anchovy larvae and postlarvae occur in the plankton between May and September with a peak in July–September (S. Regner 1985). This corresponds to the predictable period of the etesians winds. These dry northern, northeastern, and eastern winds blow each year over the Aegean Sea from the end of May until the end of October with a maximum frequency in July–August (Fig. 4; Carapiperis 1962, Mariopoulos 1961). Since anchovy spawning in the eastern Mediterranean does not seem to be affected by abiotic factors such as temperature or salinity (Demir 1965, S. Regner 1985), the summer spawning habit of anchovy may represent an important adaptation to the highly oligotrophic conditions of the stratified coastal Aegean waters in summer. By spawning in summer, anchovy larvae (1) do not compete with sardine larvae which occur in the plankton mainly in winter and spring (Yannopoulos 1977, Daoulas and Economou 1986, Regner et al. 1987), and (2) are released in a relatively food-rich environment due to the effect of the etesians winds. The increased frequency and intensity of the etesians winds

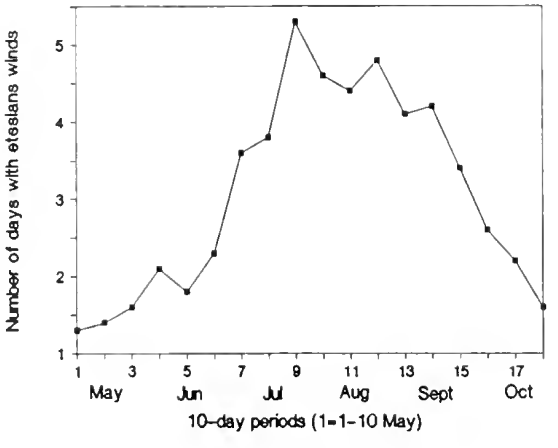

Figure 4

Mean number of days with etesians winds in Athens for May–October, 1893–1960 (data from Carapiperis 1962).

over the Aegean Sea in July–August when they frequently reach gale force (Carapiperis 1962) would probably deepen the mixed layer, and hence entrain nutrient-rich water from below the thermocline. Mullin et al. (1985) have shown that microzooplankton biomass and chlorophyll *a* levels can be doubled after wind-related events. In addition, an increase in the frequency and intensity of etesians winds may also result in an intensification of upwelling in the northern, northeastern, and eastern part of the Aegean Sea (Metaxas 1973, Theocharis et al. 1988). Hence, periods dominated by higher-than-average frequency of etesians in July–August may be associated with favorable feeding conditions for anchovy larvae which may be subject to lesser mortalities through starvation and predation, the main factors affecting larval mortality in Mediterranean anchovy (Azov–Black Sea: see Dekhnik and Rass 1988 for a review; Adriatic Sea: see S. Regner 1985 for a review; western Mediterranean: Palomera and Lleonart 1989).

Other factors may also affect variability in the anchovy abundance. For example, climatically-mediated long-term changes in production and plankton species composition in the eastern Mediterranean, changes in larval dispersion due to changing patterns of currents, as well as other factors, intrinsic or extrinsic, may affect the egg/larval/postlarval/juvenile phases. It has been maintained that in periods of increased air pressure gradient over the eastern Mediterranean, the water exchange between its basins intensifies (Pucher-Petkovic et al. 1971, Vucetic 1981). As a result, the salinity, nutrient content, temperature, and primary productivity of the Adriatic Sea and of the eastern Mediterranean basin rise, and the species composition of the phytoplankton community changes. These changes were accompanied by changes in the total biomass of small pelagic fish (sardine, anchovy, horse mackerel, etc). Such climate-plankton-small pelagic fish interactions in the eastern Mediterranean involve time lags of 2–3 years (Pucher-Petkovic et al. 1971). Lastly, cycles in anchovy catches may also be the result of social-economic factors (Stergiou 1991) and/or a change in the anchovy availability to purse seiners (changes in the distribution and/or density of schools as a response to changes in atmospheric and/or marine climatic patterns) rather than to changes in the abundance of anchovy itself.

Incorporation into management schemes of these cycles in abundance (e.g., Taylor and Prochaska 1984) is particularly important for anchovy and other small pelagic fish which are prone to collapse under intense fishing pressure and poor recruitment.

Acknowledgments

The author wishes to thank two anonymous reviewers for their constructive criticisms.

Citations

Bakun, A.
1985 Comparative studies and the recruitment problem: Searching for generalizations. Calif. Coop. Oceanic Fish. Invest. Rep. 26:30–40.

Bethoux, N., and F. Ibanez
1979 Analyse temporelle de la temperature de surface de la mer dans la baie de Monaco: Relation avec la temperature de l'air. Rapp. Comm. Int. Mer Medit. 25/26:47–49.

Carapiperis, L.N.
1962 The etesian winds II. On the frequency of the etesian winds. Notes, Natl. Observatory of Athens, Greece, Ser. II, Meteorologia 10:1–16 [Engl.].

Chatfield, C.
1984 The analysis of time series: An introduction. Chapman and Hall, NY.

Colebrook, J.M., and A.H. Taylor
1984 Significant time scales of long-term variability in the plankton and the environment. Rapp. P.-V. Reun. Cons. Int. Explor. Mer 183:20–26.

Daoulas, Ch., and A.N. Economou
1986 Seasonal variation of egg size in the sardine, *Sardina pilchardus* Walb., of the Saronikos Gulf: Causes and a probable explanation. J. Fish Biol. 28:449–457.

Dekhnik, T.V., and T.S. Rass
1988 Main aspects of the study on icthyoplankton. J. Ichthyol. 28:51–57.

Dement'eva, T.F.
1987 A method for correlation of environmental factors and year-class strength of fishes. J. Ichthyol. 27:55–59.

Demir, N.
1965 Synopsis of biological data on anchovy, *Engraulis encrasicolus*, (Linnaeus) 1758 (Mediterranean and adjacent seas). FAO Fish. Synop. 26, Rev. 1, 48 p.

Flocas, A.A., and B.D. Giles
1984 Air temperature variations in Greece. Pt. 2. Spectral analysis. J. Climatol. 4:541–546.

Economidis, P.S., A. Sinis, and G.P. Stamou
1988 Spectral analysis of exploited fish populations in lake Koronia (Macedonia, Greece) during the years 1947–1983. Cybium 12:151–159.

Gnevyshen, M.N., and A.I. Ol' (editors)
1977 Effects of solar activity on the earth's atmosphere and biosphere. Israel Prog. Sci. Transl., Jerusalem, 290 p.

Hellenic National Statistical Service
1968–1989 Results of the sea fishery survey by motor vessels. Sect. G, 20 issues (for years 1964–1987), Athens, Hellas.

Kort, V.G.
1970 Large-scale interaction between the ocean and the atmosphere using the North Pacific as an example. Oceanology 10:171–183.

Leggett, W.C.
1986 The dependence of fish larval survival on food and predator densities. *In* Skreslet, S. (ed.), The role of freshwater outflow in coastal marine ecosystems. NATO ASI Ser. G7: 117–137.

Mariopoulos, E.G.
1961 An outline of the climate of Greece. Publ. Meteor. Inst. Univ. Athens (Greece) 6:1-51 [Engl.].

Metaxas, D.A.
1973 Air-sea interaction in the Greek seas and resulted etesian wind characteristics. Tech. Rep. 5, Univ. Ioannina, Greece, School of Physics and Math., p. 1-32 [Engl.].

Mullin, M.M., E.R. Brooks, F.M.H. Reid, J. Napp, and E.F. Stewart
1985 Vertical structure of nearshore plankton off southern California: A storm and a larval fish food web. Fish. Bull., U.S. 83:151-167.

Mysak, L.A.
1986 El Niño, interannual variability and fisheries in the northwest Pacific Ocean. Can. J. Fish. Aquat. Sci. 43:464-497.

Palomera, I., and J. Lleonart
1989 Field mortality estimates of anchovy larvae, *Engraulis encrasicolus*, in the western Mediterranean. J. Fish. Biol. 35 (Suppl.):133-138.

Petrova-Karadjova, V.J., and E.M. Apostolov
1988 Influence of solar activity upon the diatoms of Black Sea plankton. Rapp. Comm. Int. Mer Medit. 31:224.

Polli, S.
1955 I cicli climatici di 5.6 e 8 anni e la loro realta' fisca. Riv. Meteor. Aueronaut. 2:1-12 [not seen, from Regner and Gacic 1974].

Porumb, I.I., and F. Marinescu
1979 Influence du facteur nourriture sur la formation des agglomerations d'anchois dans la zone neritique roumaine de la Mer Noire. Rapp. Comm. Int. Mer Medit. 25/26:47-48.

Pucher-Petkovic, T., M. Zore-Armanda, and I. Kacic
1971 Primary and secondary production of the Middle Adriatic in relation to climatic factors. Thallasia Jugosl. 7:301-311.

Regner, D.
1985 Seasonal and multiannual dynamics of copepods in the middle Adriatic Sea. Acta Adriat. 26:11-99.

Regner, S.
1982 Investigations of qualitative and quantitative composition of the larval fish stages in the plankton at the high sea of the central Adriatic. Stud. Mar. Fauna 11/12:45-60.
1985 Ecology of planktonic stages of anchovy, *Engraulis encrasicolus* (Linnaus, 1758), in the central Adriatic. Acta Adriat. 26:5-113.

Regner, S., and J. Gacic
1974 The fluctuation of sardine catch along the eastern Adriatic coast and solar activity. Acta Adriat. 15:1-15.

Regner, S., D. Regner, I. Marasovic, and F. Krsinic
1987 Spawning of sardine, *Sardina pilchardus* (Walbaum, 1792), in the Adriatic under upwelling conditions. Acta Adriat. 28:161-198.

Shuntov, B.P., N.A. Shurunov, and V.P. Vasil'kov
1981 Periodicity in the reproduction of fish from the New Zealand plateau based on data from commercial statistics. J. Ichthyol. 22:32-43.

Soutar, A., and J.D. Isaacs
1974 Abundance of pelagic fish during the 19th and 20th centuries as recorded in anaerobic sediments off California. Fish. Bull., U.S. 72:257-275.

Spanakis, E., N. Tsimenidis, and E. Zouros
1989 Genetic differences between populations of sardine, *Sardina pilchardus*, and anchovy, *Engraulis encrasicolus*, in the Aegean and Ionian seas. J. Fish. Biol. 35:417-437.

Stergiou, K.I.
1986a On the anchovy and sardine fishery in Greek waters, 1964-1982. Rapp. Comm. Int. Mer Medit. 30:241.
1986b Pre-war changes in the abundance of *Pagellus erythrinus*, *Merluccius merluccius*, and *Engraulis encrasicolus* in Greek waters and climatic change. FAO Fish. Rep. 361: 99-105.
1988 Spectral analysis of sardine fishery in Greek waters, 1964-1982. Rapp. Comm. Int. Explor. Mer Medit. 31:282.
1990a An autoregressive model of the anchovy *Engraulis encrasicolus* fishery in the eastern Mediterranean. Fish. Bull., U.S. 88:411-414.
1990b On the Greek fishery production. Greek Fish. News. 103:31-38 [in Greek].
1991 Describing and forecasting the sardine-anchovy complex in the eastern Mediterranean using vector autoregressions. Fish. Res. (Amst.) 11:127-141.

Taylor, G.T., and F.J. Prochaska
1984 Incorporating unobserved cyclical stock movements in fishery catch equations: An application to the Florida blue crab fishery. N. Am. J. Fish. Manage. 4:67-74.

Theocharis, A., D. Georgopoulos, Y. Krestenitis, and C. Koutitas
1988 Observations and modelling of upwelling in the Aegean Sea. Rapp. Comm. Int. Mer Medit. 31:212.

Vucetic, T.
1981 Biological production of the Adriatic plankton. FAO Fish. Rep. 253:65-71.

Yannopoulos, C.
1977 The reproduction and the egg size variations of *Sardina pilchardus* Walb. in the Thermaikos Gulf, Aegean Sea. Rapp. Comm. Int. Mer Medit. 24:73-75.

Zupanovic, S.
1968 Causes of fluctuations in sardine catches along the eastern coast of the Adriatic Sea. Anali Jandranskog Inst. 4:401-489.

Superintendent of Documents **Subscriptions** Order Form

Order Processing Code:
* 5178

☐ **YES,** enter my subscription as follows:

Charge your order. It's Easy! MasterCard VISA

To fax your orders (202) 512–2233

____ subscriptions to **FISHERY BULLETIN (FB)** for $24.00 per year ($30.00 foreign).

The total cost of my order is $_____. Price includes regular domestic postage and handling and is subject to change.

(Company or Personal Name) (Please type or print)

(Additional address/attention line)

(Street address)

(City, State, ZIP Code)

(Daytime phone including area code)

(Purchase Order No.)

May we make your name/address available to other mailers? YES ☐ NO ☐

Please Choose Method of Payment:

☐ Check Payable to the Superintendent of Documents

☐ GPO Deposit Account ☐☐☐☐☐☐☐ – ☐

☐ VISA or MasterCard Account

☐☐☐☐☐☐☐☐☐☐☐☐☐☐☐☐

☐☐☐☐ (Credit card expiration date)

Thank you for your order!

(Authorizing Signature) 11/91

Mail To: New Orders, Superintendent of Documents
P.O. Box 371954, Pittsburgh, PA 15250–7954

Fishery Bulletin

Guidelines for Contributors

Form of manuscript

The document should be in the following sequence: Title Page, Abstract (not required for Note), Text, Acknowledgments, Citations, Text footnotes, Appendices, Tables, Figure legends, and Figures.

Title page should include authors' full names and mailing addresses and the senior author's telephone and FAX numbers.

Abstract Not to exceed one double-spaced typed page. Should include a sentence or two explaining to the general reader why the research was undertaken and why the results should be viewed as important. Abstract should convey the main point of the paper and outline the results or conclusions. No footnotes or references.

Text A brief introduction should portray the broad significance of the paper. The entire text should be intelligible to readers from different disciplines. All technical terms should be defined, as well as all abbreviations, acronyms, and symbols in text, equations, or formulae. Abbreviate units of measure only when used with numerals or in tables and figures to conserve space. Measurements should be expressed in metric units, with other equivalent units given in parentheses. Follow the *U.S. Government Printing Office Style Manual*, 1984 ed., and the *CBE Style Manual*, 5th ed. Fishery and invertebrate nomenclature should follow the *American Fisheries Society Special Publication 12* (for fishes), *16* (for mollusks), and *17* (for decapod crustaceans).

Text footnotes should be numbered in Arabic numerals and typed on a separate sheet from the text. Footnotes are not used for reference material or personal communications, but rather to explain or define terms in the text and for contribution numbers on the title page.

Informal sources Personal communications, unpublished data, and untitled manuscripts in preparation are noted parenthetically in the text (full name, affiliation, brief address including zip code, and month and year when appropriate).

Acknowledgments Gather all acknowledgments into a brief statement at the end of the text. Give credit only for exceptional contributions and not to those whose contributions are part of their normal duties.

Citations All titled sources should be listed in the Citations section, including unpublished and processed material. In text, cite as Smith and Jones (1977) or (Smith and Jones 1977); if more than one citation, list chronologically (Smith 1936, Jones 1975, Doe In press). All sources cited in the text should be listed alphabetically by the senior authors' surnames under the heading CITATIONS. Abbreviations of periodicals and serials should conform to *Serial Sources for the BIOSIS Data Base*™. Indicate whether sources are in a language other than English. For informal literature, include address of author or publisher. Authors are responsible for the accuracy of all citations.

Tables should supplement, not duplicate, the text. Each table should be numbered and cited consecutively, with headings short but amply descriptive so that the reader need not refer to the text. For values less than one, zeros should precede all decimal points. Indicate units of measure in column headings; do not deviate from the unit of measure within a column. Table footnotes should be noted consecutively in Roman letters across the page from left to right and then down. Since all tables are typeset, they need not be submitted camera-ready.

Figures Photographs and line drawings should be of professional quality—clear and concise—and reducible to 42 picas for full-page width or to 20 picas for a single-column width, and to a maximum 55 picas high. All graphic elements in illustrations must be proportioned to insure legibility when reduced to fit the page format. Line weight and lettering should be sharp and even. Lettering should be upper and lower case, and vertical lettering should be avoided whenever possible (except for vertical, y, axis). Zeros should precede all decimal points for values less than one. Reproductions of line artwork are accepted in the form of high-quality photographic prints from negatives or photomechanical transfer (PMT). Halftones should be sharply focused with good contrast. Micron rules should be inserted on electron micrographs, even when magnification is included in the figure legend. There should be clear distinction between identifying letters (press-on or overlay) and background of photograph. Label each figure in pencil on the back. Send only xerox copies of figures to the Scientific Editor; originals or photographic prints will be requested later when the manuscript is accepted for publication.

Copyright Government publications are in the public domain, i.e., they are not protected by copyright.

Submission of manuscript

Disks Authors are encouraged to retain manuscripts on word-processing storage media (diskettes, floppy disks) and submit a double-spaced hardcopy run from the storage media. Submit disks as MS-DOS "print" or "nondocument" files (often called "ASCII files"). If a disk cannot be converted to an ASCII file, the author should indicate on the disk the source computer and software language along with the file name. Either 5¼-inch or 3½-inch disks from IBM-compatible or Apple/MacIntosh systems (non-graphics only) can be submitted, double-sided/double-density or high-density, limiting each file to 300 kilobytes. All 8-inch word-processing disks (e.g., Wang or NBI) must be converted onto 5¼- or 3½-inch MS-DOS print disks.

Send original hardcopy and two duplicated copies to:

Dr. Linda L. Jones, Scientific Editor
National Marine Mammal Laboratory
F/AKC3
National Marine Fisheries Service,
NOAA
7600 Sand Point Way NE
Seattle, WA 98115-0070

Copies of published articles and notes
The senior author and his/her organization each receive 50 separates free-of-charge. Additional copies may be purchased in lots of 100.

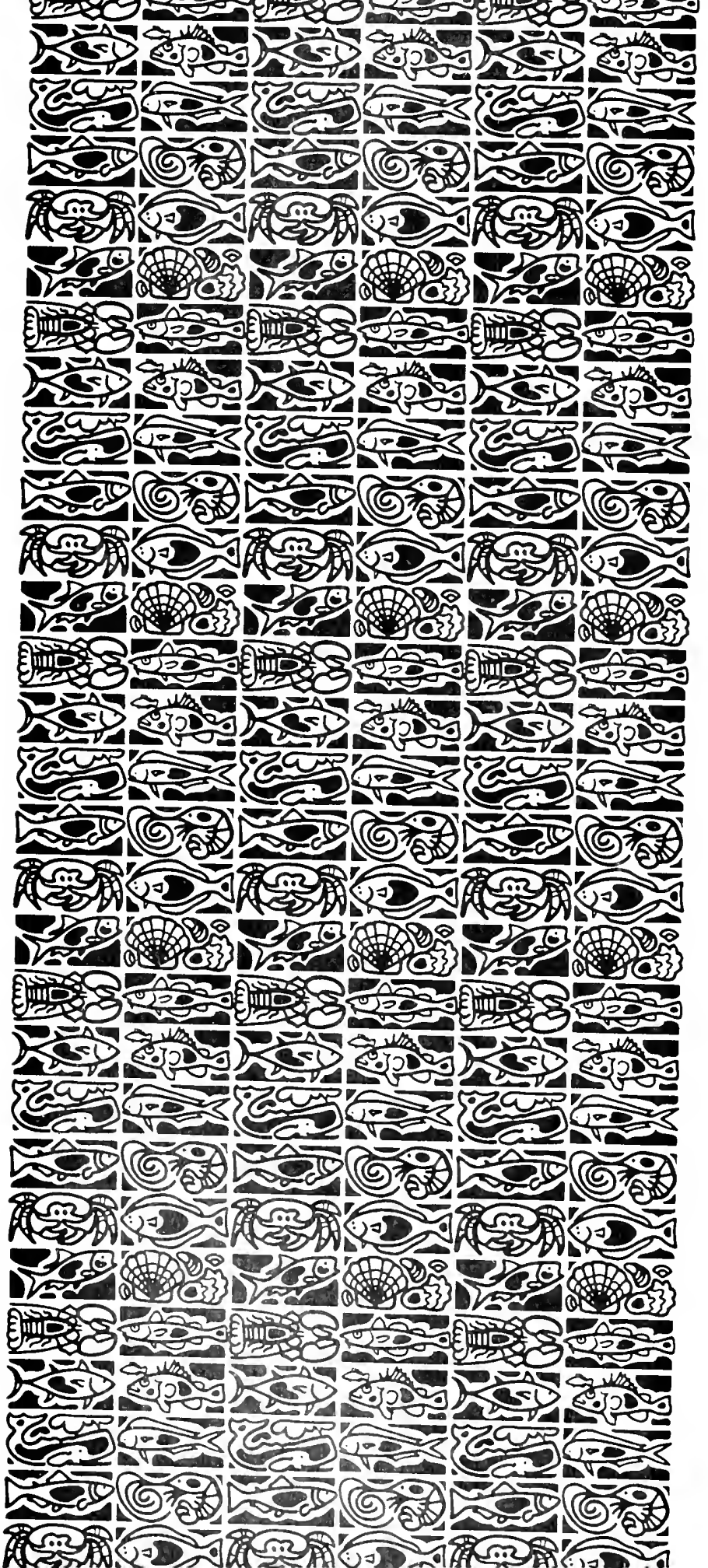

U.S. Department
of Commerce

Volume 90
Number 2
April 1992

Fishery Bulletin

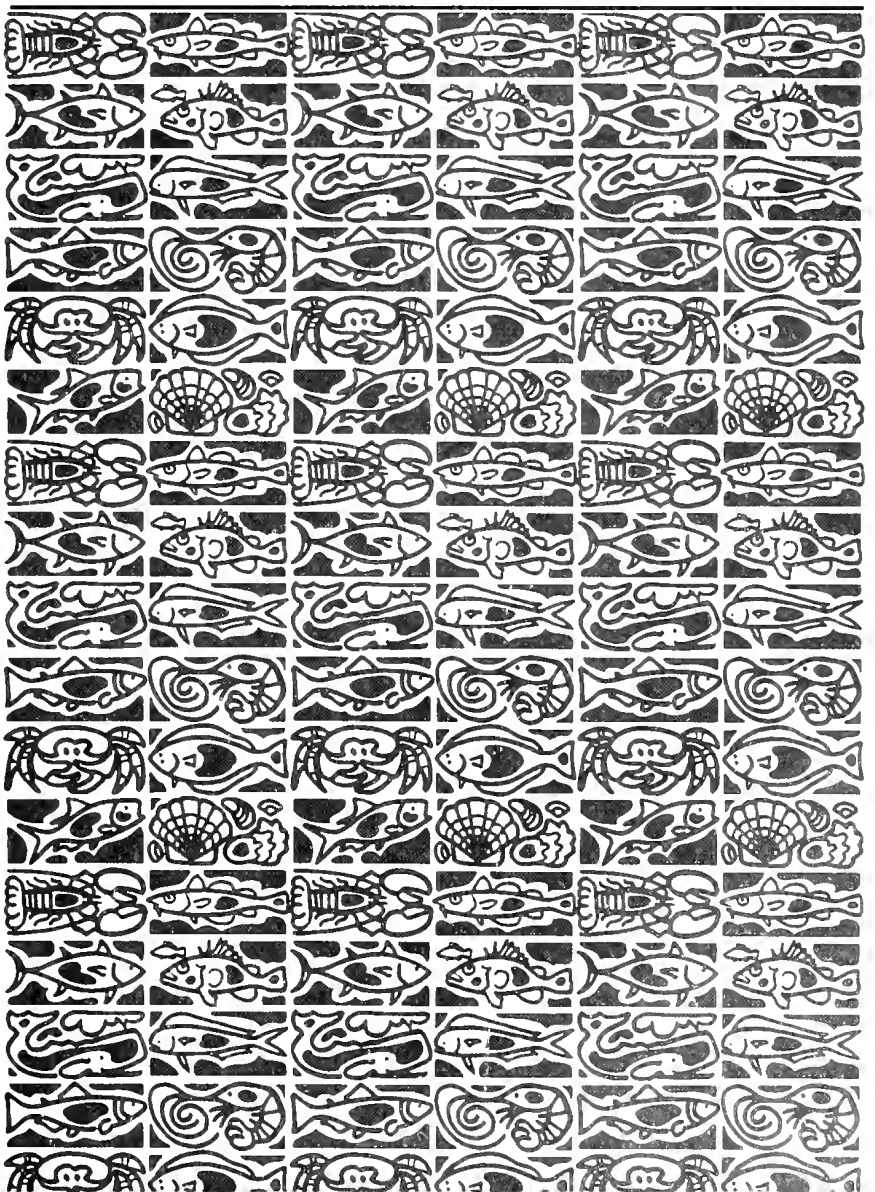

Fishery Bulletin

The *Fishery Bulletin* (ISSN 0090-0656) is published quarterly by the Scientific Publications Office, National Marine Fisheries Service, NOAA, 7600 Sand Point Way NE, BIN C15700, Seattle, WA 98115-0070. Second class postage is paid in Seattle, Wash., and additional offices. POSTMASTER send address changes for subscriptions to Fishery Bulletin, Superintendent of Documents, Attn: Chief, Mail List Branch, Mail Stop SSOM, Washington, DC 20402-9373.

The Secretary of Commerce has determined that the publication of this periodical is necessary in the transaction of the public business required by law of this Department. Use of funds for printing of this periodical has been approved by the Director of the Office of Management and Budget.

For sale by the Superintendent of Documents, U.S. Government Printing Office, Washington, DC 20402. Subscription price per year: $24.00 domestic and $30.00 foreign. Cost per single issue: $12.00 domestic and $15.00 foreign. **See back page for order form.**

The *Fishery Bulletin* carries original research reports and technical notes on investigations in fishery science, engineering, and economics. The Bulletin of the United States Fish Commission was begun in 1881; it became the Bulletin of the Bureau of Fisheries in 1904 and the Fishery Bulletin of the Fish and Wildlife Service in 1941. Separates were issued as documents through volume 46; the last document was No. 1103. Beginning with volume 47 in 1931 and continuing through volume 62 in 1963, each separate appeared as a numbered bulletin. A new system began in 1963 with volume 63 in which papers are bound together in a single issue of the bulletin. Beginning with volume 70, number 1, January 1972, the *Fishery Bulletin* became a periodical, issued quarterly. In this form, it is available by subscription from the Superintendent of Documents, U.S. Government Printing Office, Washington, DC 20402. It is also available free in limited numbers to libraries, research institutions, State and Federal agencies, and in exchange for other scientific publications.

U.S. Department of Commerce
Seattle, Washington

Volume 90
Number 2
April 1992

Fishery Bulletin

Contents

Notes

U.S. Department of Commerce
Seattle, Washington

Publications Awards 1989-90

National Marine Fisheries Service, NOAA

The Publications Advisory Committee of the National Marine Fisheries Service is pleased to announce the awards for best publications authored by NMFS scientists and published in the *Fishery Bulletin* volume 88 and *Marine Fisheries Review* volume 51. Eligible papers are nominated by the Fisheries Science Centers and Regional Offices and are judged by the NMFS Editorial Board. Only articles which significantly contribute to the understanding and knowledge of NMFS-related studies are eligible. We offer congratulations to the following authors for their outstanding efforts.

Fishery Bulletin 1990

Joseph E. Hightower

Multispecies harvesting policies for Washington-Oregon-California rockfish trawl fisheries. *Fishery Bulletin* 88:645-656. Dr. Hightower is retired from his position with the Southwest Fisheries Science Center, and is now with the North Carolina Cooperative Fish and Wildlife Center, North Carolina State University, Raleigh.

Marine Fisheries Review 1989

Joseph M. Terry and Lewis E. Queirolo

U.S. fisheries management and foreign trade linkages: Policy implications for groundfish fisheries in the North Pacific EEZ. *Marine Fisheries Review* 51(1):23-43. Drs. Terry and Queirolo are with the Alaska Fisheries Science Center, Seattle.

U.S. Department of Commerce
Seattle, Washington

Recent publications in the NOAA Technical Reports NMFS Series

102 Svrjcek, Ralph S. (editor)
Marine ranching: Proceedings of the seventeenth U.S.-Japan meeting on aquaculture, Ise, Mie Prefecture, Japan, October 16, 17, and 18, 1988. May 1991, 180 p.

103 Reid, Robert N., David J. Radosh, Ann B. Frame, Steven A. Fromm
Benthic macrofauna of the New York Bight, 1979-89. December 1991, 50 p.

104 Perez, Michael, and Thomas R. Loughlin
Incidental catch of marine mammals by foreign and joint venture trawl vessels in the U.S. EEZ of the North Pacific, 1973-88. December 1991, 57 p.

105 Wetherall, Jerry A. (editor)
Biology, oceanography, and fisheries of the North Pacific Transition Zone and Subarctic Frontal Zone. December 1991, 111 p.

106 Svrjcek, Ralph S. (editor)
Marine ranching: Proceedings of the eighteenth U.S.-Japan meeting on aquaculture, Port Ludlow, Washington, 18-19 September 1989. February 1992, 136 p.

107 Russell, Mike, Mark Grace, and Elmer J. Gutherz
Field guide to the searobins (*Prionotus* and *Bellator*) in the western North Atlantic. March 1992, 26 p.

Some NOAA publications are available by purchase from the Superintendent of Documents, U.S. Government Printing Office, Washington, DC 20402.

Age, growth, and reproduction of the goosefish *Lophius americanus* (Pisces:Lophiiformes)*

Michael P. Armstrong

School of Marine Science, Virginia Institute of Marine Science
College of William and Mary, Gloucester Point, Virginia 23062
Present address: Department of Zoology, University of New Hampshire
Durham, New Hampshire 03824

John A. Musick
James A. Colvocoresses

School of Marine Science, Virginia Institute of Marine Science
College of William and Mary, Gloucester Point, Virginia 23062

Abstract. – Age, growth, and reproduction were studied in goosefish *Lophius americanus* collected from National Marine Fisheries Service groundfish surveys and commercial fishing cruises between Georges Bank and Cape Hatteras in the western North Atlantic. Age and growth of *L. americanus* were determined from vertebral annuli, which became visible at the edge of the vertebral centra in May. Maximum ages of males and females were 9 and 11 years, respectively. Males appeared to experience higher mortality than females in the older age-classes. Von Bertalanffy growth curves calculated for males and females had excellent agreement with back-calculated lengths. The growth rate of *L. americanus* was intermediate to its eastern Atlantic congeners, *L. piscatorius* and *L. budegassa*. Male *L. americanus* matured at 3+ years (~370mm TL) and females at 4+ years (~485mm TL). Spawning took place primarily in May and June. Fecundity in 17 individuals of 610–1048mm TL ranged from 300,000 to 2,800,000 ova, and was linear with total length in that size range. Histological examination of the ovaries showed they are remarkably similar to ovaries of other lophiiform species. Females produced egg veils, which may function in dispersion, buoyancy, facilitating fertilization, and protection of the eggs and larvae.

The goosefish *Lophius americanus* (Valenciennes in Cuvier and Valenciennes 1837) is a benthic fish which occurs in the Northwest Atlantic Ocean from the northern Gulf of Saint Lawrence, southward to Cape Hatteras, North Carolina (Bigelow and Schroeder 1953, Scott and Scott 1988) and less commonly to Florida (Caruso 1983). It has a eurybathic depth distribution, having been collected from the tideline (Bigelow and Schroeder 1953) to approximately 840m (Markle and Musick 1974), although few large individuals occur deeper than 400m (Wenner 1978). Goosefish have been taken in temperatures of 0–24°C (Grosslein and Azarovitz 1982), but seem to be most abundant in temperatures of about 9°C in the Mid-Atlantic Bight (Edwards 1965), 3–9°C in Canadian waters (Jean 1965), and 7–11°C on the continental slope off Virginia (Wenner 1978). The goosefish is sympatric with the black-finned goosefish *L. gastrophysus* in deep water (>100–150m) from Cape Hatteras to the Florida coast, although strays of *L. gastrophysus* occur as far north as Washington Canyon, off Virginia (pers. observ., MPA).

Lophius americanus was confused with *L. piscatorius*, a European species, for many years. Thus all references to *L. piscatorius* in the western North Atlantic north of Cape Hatteras actually refer to *L. americanus* (Caruso 1977). There are several accounts of the species' life history (Gill 1905, Connolly 1920, Dahlgren 1928, Hildebrand and Schroeder 1928, Proctor et al. 1928, McKenzie 1936, Bigelow and Schroeder 1953, Grosslein and Azarovitz 1982, Scott and Scott 1988), but all are general in nature. Much of the information contained in these reports is anecdotal.

Goosefish are a bycatch of groundfishing and scalloping operations and are marketed under the name monkfish. They have traditionally been considered "trash" fish in the United States and discarded at sea or used in the production of fish meal, with a small amount being exported to Europe where *Lophius* has been highly esteemed as a food fish for centuries. Goosefish have become more popular with the American consumer due to dwindling catches and rising prices in recent years of the more traditional fishery products. Commercial landings have been increasing yearly since 1970 (Northeast Fisheries Science Center 1991). This

Manuscript accepted 20 March 1992.
Fishery Bulletin, U.S. 90:217–230 (1992).

* Contribution 1735, Virginia Institute of Marine Science.

study describes age, growth, and reproduction of this increasingly exploited fish.

Methods

Goosefish were collected during the spring and autumn groundfish surveys (1982–85) conducted by the National Marine Fisheries Service (NMFS) in the Mid-Atlantic Bight and southern New England (for survey methodology see Grosslein and Azarovitz 1982). Additional samples were obtained during the NMFS 1983 summer scallop survey off southern New England and during cruises aboard commercial groundfish trawlers and scallopers operating out of Hampton, Virginia. Sampling effort was concentrated in the area from southern New England to Virginia.

Goosefish greater than ~180mm were examined at sea. Smaller individuals were fixed in 10% formalin and saved for examination in the laboratory. Examination included measuring total and standard length and weight, excising a section of the vertebral column, removing both sagittal otoliths, recording stomach contents, macroscopic staging and weighing of the gonads, and preserving pieces of gonads for histological inspection and fecundity estimates.

Reproduction

Gonads were staged visually in the field and assigned to one of the following classes: immature, resting, developing, ripe, and spent. Both gonads were then removed from the body cavity and weighed to the nearest 0.1g. A small representative piece was excised from the midsection of selected gonads and preserved in Davidson's fixative for histological study.

Late-developing and ripe ovaries were selected for fecundity analyses. The extremely large size of goosefish ovaries precluded saving the entire organ. A subsample of about 100g was weighed to the nearest 0.1g and placed in modified Gilson's solution (Simpson 1951). After several months of storage, most of the ovarian connective tissue had dissolved. Ova were removed from the Gilson's solution, separated from any remaining ovarian tissue, rinsed in water, blotted on absorbent paper, and weighed. Three subsamples, each containing about 1000 ova, were removed and weighed to the nearest 0.001g. Ova in each sample were counted using a dissecting microscope. Fecundity was calculated as:

$$\text{Fecundity} = (W)(P)(N)$$

where W = total weight of both ovaries,

$$P = \frac{\text{weight of sample after Gilson's}}{\text{weight of sample before Gilson's}},$$

N = mean number of ova/g from 3 subsamples.

Gonad portions preserved in Davidson's fixative for histological preparations were dehydrated in a graded series of ethanol baths and Technicon reagents (S-29 dehydrant VC-670 solvent). They were then embedded in paraffin, sectioned at 7μm and stained using Harris' hematoxylin and counterstained with eosin Y. Gonad sections were viewed at 40×, 100×, and 400× to determine stages of oogenesis and spermatogenesis to verify accuracy of macroscopic field staging and to examine the histology of the goosefish ovary.

A gonasomatic index (GSI) was calculated for each sex as:

$$\text{GSI} = \frac{\text{gonad weight}}{\text{total weight of fish}} \times 100.$$

Age and growth

Weights were taken to the nearest gram in fish <1200g and to the nearest 25g increment in fish >1200g. Total length (TL) in millimeters was measured from the tip of the protruding lower jaw to the tip of the caudal fin rays. Because of the large size and loose suspension of the goosefish jaw apparatus, it was necessary to hold the head in a standard position while length was measured to reduce variation due to changes in head and jaw configuration. This position was achieved by applying light pressure to the top of the head, thereby causing a maximal amount of dorsal-ventral compression.

Vertebrae were chosen as the best method to age *L. americanus*, based on a preliminary examination which revealed that each vertebral centrum contained concentric rings which appeared to be annuli. Sagittal otoliths were also examined; however, otoliths from larger fish were opaque and had extremely irregular outer margins, which made it difficult or impossible to discern annuli.

A section of the vertebral column containing vertebrae numbers 3–11 was excised from each goosefish. These were stored in 50% isopropanol for 1–12 months. Vertebrae numbers 7–10 were similar in size and shape and also had the largest diameters. Vertebra number 8 was used in aging, but number 9 was used if number 8 was damaged in preparation.

Vertebra number 8 was disarticulated from the rest of the excised vertebral section. The neural and haemal arches and all excess fat, muscle, connective tissue and cartilage were removed by scalpel. The vertebra was then sliced along the midsagittal line producing two hourglass-shaped halves, similar to the method used by Lyczkowski (1971) and Lawler (1976) for preparing vertebrae from northern puffer *Sphaeroides maculatus*

and sandbar sharks *Carcharinus plumbeus*. These halves were then heated in an oven at 200°C for about 3 hours. Larger vertebra required one-half to 1 hour further heating. This heating made the alternating opaque and translucent bands of the vertebral centra more distinct.

Annuli were counted on the posterior face of the centrum. This was generally more concave than the anterior face, thus allowing greater separation of the rings. Each vertebra was read twice at an interval of at least one month to insure independence of readings. If they disagreed, a third reading was done. Agreement between any two readings was considered as the true count. If all three readings differed, the vertebra was considered unreadable and not used in the analysis. A random sample of fifty vertebrae was selected for verification by an independent reader.

Measurements of the vertebral rings and radius were made from the apex of the posterior and anterior faces of the centrum along an oblique line that followed the midline of the posterior centrum. All measurements and counts were made with a binocular dissecting microscope equipped with an ocular micrometer at 10× magnification using reflected light.

Regression analyses of vertebral radius on total length and weight on total length were calculated by the method of least squares. Length-at-age was back-calculated by the Lee method (Lagler 1956):

$$L' = C + S' (L - C)/S$$

where L' = total length of the fish at time of annulus formation,
L = total length of fish at time of capture,
S' = measurement to the annulus,
S = vertebral radius at time of capture,
C = correction factor; y-axis intercept of the regression of total length on vertebral radius.

Computation of the von Bertalanffy growth equations followed Ricker (1975).

Results

Reproduction

External sexual dimorphism was not apparent in *L. americanus*. Caruso (1975) noted sexual differences in nostril morphology, but this was not a useable field character. Sex was easily determined in mature individuals by examination of the gonads, which are markedly different in appearance. Gonads from small juveniles (<160–180 mm TL) were indistinguishable macroscopically. Both testes and ovaries from these juveniles were small, translucent, and string-like.

In females larger than ~180 mm TL the ovaries were long, wide, and ribbon-like. They were greatly coiled in the abdomen and supported by an extensive mesovarium. The two ovaries were fused at their posterior ends, forming a single, confluent organ. Dimensions of the ovary varied greatly depending on the stage of sexual development.

The testes were solid, sausage-like organs. A groove was present along the medial aspect of each testis. This groove contained blood vessels and served as the site of attachment for mesentary connective tissue.

A physical description of the gonads in the five developmental stages (immature, resting, developing, ripe, and spent) is presented in Table 1.

Table 1
Description of gonads at five maturity stages assigned to *Lophius americanus*, based on macroscopic examination.

Stage	Description
Ovaries	
Immature	Grayish-pink, relatively small, ribbon-like, appear almost empty, no vascularization.
Resting	Orangish-pink, contain material but no ova visible, larger than immature, little vascularization.
Developing	Pink, ova discernible by eye, abdominal cavity slightly bulging, highly vascular.
Ripe	Straw-colored to almost clear as ovary approaches spawning, distinct ova present, abdominal cavity greatly bulging, highly vascular.
Spent	Gray, extremely flaccid, appear almost empty, atretic ova appear as black or white dots, moderately vascular.
Testes	
Immature	White to tan, similar in shape as mature testes but very small, medial groove less distinct.
Resting	White to tan, much larger than immature, medial groove distinct, small amount of milt sometimes present when dissected.
Developing	Blotchy cream to tan, moderate to large amount of milt produced when dissected, very firm in texture.
Ripe	Blotchy cream to tan with areas of pink, extremely firm in texture, milt produced from genital pore when pressure is applied on abdomen, copious amounts present when dissected.
Spent	Grayish-tan, edges appear translucent, extremely flaccid, small amount of milt sometimes present when dissected.

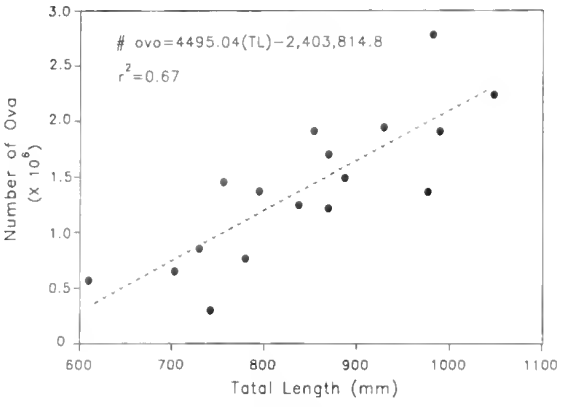

Figure 1

Relationship of fecundity with total length for *Lophius americanus*. Dashed line indicates least-squares regression. Regression equation and coefficient of determination are given. Each dot represents a single individual (n 17).

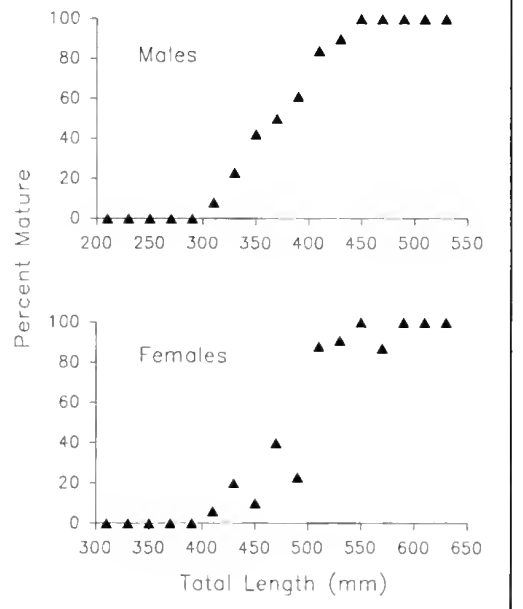

Figure 2

Percent of individuals sexually mature in relation to total length (mm) for *Lophius americanus*, based on macroscopic examination of the gonads. Lengths at 50% maturity are 368.9 mm for males and 485.3 mm for females.

Fecundity in 17 individuals of 610–1048 mm TL ranged from 301,150 to 2,780,632 ova. Fecundity increased linearly with TL in that size range (Fig. 1), the regression equation being

number of ova =

$$4495.04(\text{TL}) - 2{,}403{,}814.8 \quad (r^2\ 0.67).$$

Log transformations of one or both variables failed to provide a better fit.

Goosefish reached sexual maturity (by macroscopic staging) at 290–450 mm in males and 390–590 mm in females (Fig. 2). Linear regressions of proportion mature (arcsine-square root transformed) on TL for these size intervals were:

Proportion of males mature =

$$0.0089(\text{TL}) - 2.498 \quad (r^2\ 0.96)$$

Proportion of females mature =

$$0.0079(\text{TL}) - 3.056 \quad (r^2\ 0.86).$$

Values for length at 50% maturity were 368.9 mm in males and 485.3 mm in females.

Ovaries and testes followed similar patterns of development, with the exception that testes changed from a resting to developing state earlier in the year (Jan.–Feb.) (Fig. 3). No resting gonads were found for either sex in May or June. The percentage of spent gonads was highest in July–August, indicating that spawning had taken place in the previous time interval (May–June). Although the percentage of ripe gonads was highest in May–June, gonads in a near-spawning state were also found in March–April and July–August.

Gonasomatic values were calculated for 117 mature males and 98 mature females. The GSI peaked in May–June for females and March–April and May–June for males (Fig. 4). High index values in these months corresponded with the greatest incidence of ripe individuals (Fig. 3). Again, similar to observations based on gonad condition, males appeared to develop earlier in the season and remain ripe longer. No mature females were collected during the Jan.–Feb. interval.

GSI values for females were much greater than for males (Table 2). Females showed a large increase in GSI as the ovaries developed. The greatest value recorded was 50.9, from a ripe female. This value indicates that greater than half of the body weight was composed of ovarian mass. However, only a relatively small percentage of the ovarian weight from late-developing and ripe females was composed of ova. The actual percentage of the ovarian weight which was ova ranged from 12.9% to 33.5% for the seventeen females used for fecundity analysis. The remainder of the weight was ovarian tissue, and more importantly, the muco-gelatinous matrix surrounding the ova.

Slides were prepared from sections of 33 ovaries and 20 testes. Representatives from all the developmental

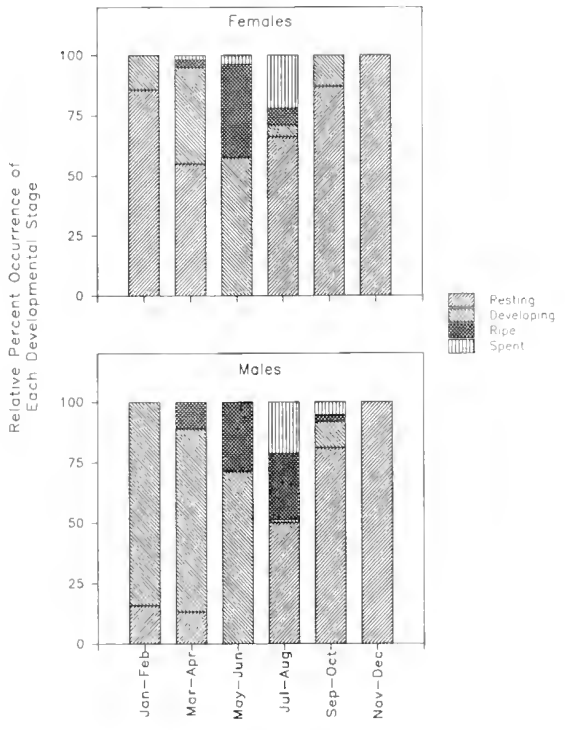

Figure 3

Seasonal progression of gonad condition in mature male and female *Lophius americanus*, based on macroscopic examination.

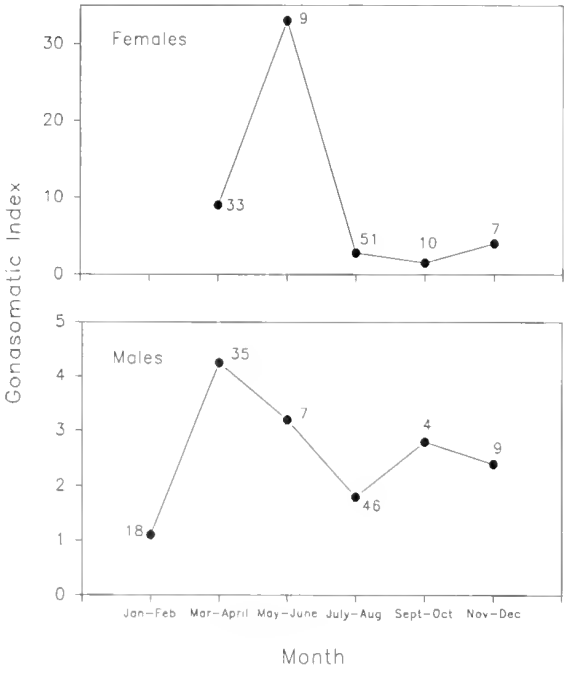

Figure 4

Seasonal progression of mean gonasomatic index values for male and female *Lophius americanus*. Numbers of mature individuals examined on each date are indicated.

Table 2

Gonasomatic index values at five gonad maturity stages for male and female *Lophius americanus*, based on macroscopic staging.

	Range	Mean(SE)	*n*
Females			
Immature	Trace-1.26	—	56
Resting	0.77-7.58	2.35(0.19)	53
Developing	3.82-22.12	12.26(1.18)	21
Ripe	18.23-50.90	33.96(2.73)	13
Spent	0.94-3.77	2.56(0.43)	12
Males			
Immature	Trace-0.83	—	37
Resting	0.31-3.42	1.46(0.17)	36
Developing	0.46-6.18	2.44(0.27)	43
Ripe	0.84-5.72	3.20(0.22)	23
Spent	0.18-4.19	1.16(0.20)	21

classes (immature, resting, developing, ripe and spent) were included.

Oogenesis proceeds through six distinguishable morphological stages similar to other fishes, such as black sea bass *Centropristis striata* (Mercer 1978):

Oogonia (4.5–11 μm) Densely packed, granular, deeply basophilic cells.

Stage 1 Small (15–50 μm) oocytes with a large nucleus, single nucleolus, and small amount of basophilic cytoplasm.

Stage 2 (30–200 μm) Previtellogenic oocytes with strongly basophilic cytoplasm and multiple nucleoli around the nucleus margin.

Stage 3 (110–390 μm) Vitellogenesis begins with the deposition of yolk vesicles in the less darkly-staining cytoplasm. A thin zona radiata can be seen in late stage-3.

Stage 4 (270–970 μm) Cytoplasm filled with yolk vesicles and globules, lightly staining. Zona radiata well developed and strongly acidophilic.

Stage 5 (>600 μm) Mature or nearly mature oocytes, uniform in appearance due to the coalescence of yolk globules. Often fractured or irregular in outline due to fixation and sectioning.

Based on the occurrence of these oocyte stages, the ovaries were placed in the following developmental classes:

Immature Stage 1 and 2 oocytes present, atretic bodies absent. The ovarian lamellae are pressed tightly together and lumen is small.

Resting Stage 1, 2, and 3 oocytes are present with stage 2 dominating.

Developing Oocyte stages 1, 2, 3, and small 4 are present with 3 dominating.

Ripe Oocyte stages 1, 2, 3, 4, and sometimes 5 are present with 4 dominating.

Spent Oocyte stages 1, 2, and 3 are present with 2 dominating. Atretic stage 4 and 5 oocytes and ruptured follicles are present.

Macroscopic and microscopic maturity classifications showed excellent agreement. Only two (6%) needed to be reclassified following histological examination. These included one reclassified from ripe to developing, and one from resting to immature.

Figures 5 and 6 show the histology of the ovary. The lumen is not centrally located but is at one side (Fig. 5). The ovigerous tissue extends into the lumen in the form of lamellae from one wall only. In late-developing and ripe ovaries, the mucogelatinous material that forms the egg veil can be seen surrounding the ovigerous lamellae and filling the lumen (Fig. 6). This material is produced by the epithelial cells (Fulton 1898), which can be seen lining the lumen and lamellae (Fig. 6).

Spermatogenesis proceeds through six distinct stages analogous to those described for *Tilapia* spp. (Hyder 1969) and *Caulolatilus microps* (Ross 1978). These stages are primary and secondary spermatogonia, primary and secondary spermatocytes, spermatids, and spermatozoa. Spermatogenesis in goosefish is not notably different from other teleosts, so the process is not described here.

The 20 testes examined histologically were placed in the following maturity classifications based on a modification of the system of Hyder (1969):

Immature Primary and/or secondary spermatogonia are present; primary and/or secondary spermatocytes may also be present.

Resting Primary and/or secondary spermatogonia and spermatocytes are present. Spermatids also

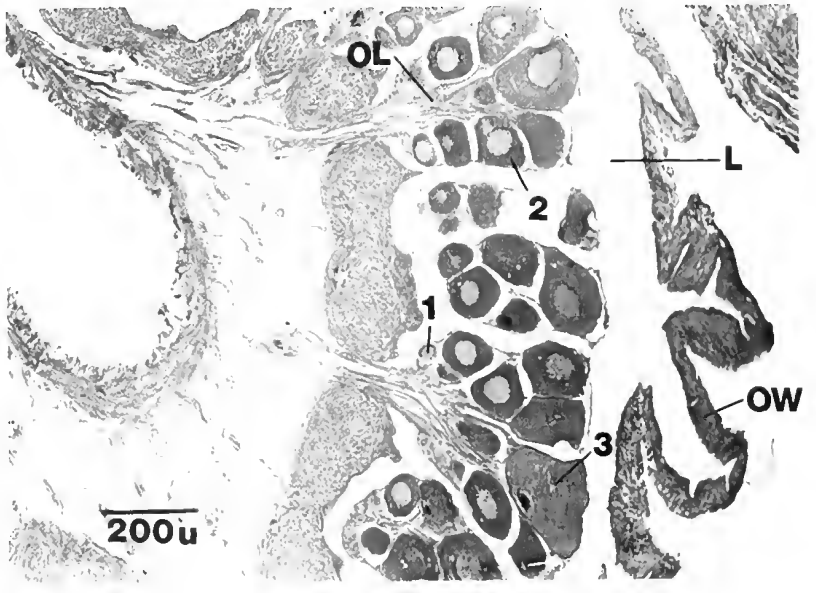

Figure 5

Photomicrograph of *Lophius americanus* ovary, classified as resting (40×): OL = ovigerous lamella; L = lumen of ovary; OW = nonovigerous ovarian wall; 1–3 = stages of oocyte development.

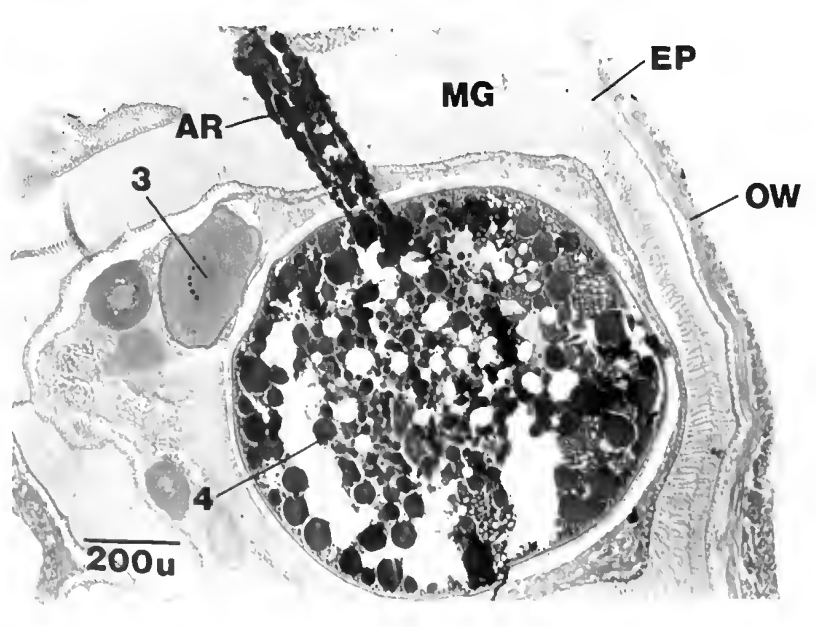

Figure 6

Photomicrograph of *Lophius americanus* ovary, classified as late developing (40×): MG = mucogelatinous matrix; EP = epithelial lining of lumen and lamellae; OW, = nonovigerous ovarian wall; AR = artifact; 3–4 = stages of oocyte development.

present. Small amount of spermatozoa may be present in lumen.

Developing Few primary and/or secondary spermatogonia visible; primary and/or secondary spermatocytes and spermatids present; spermatozoa present in lumen.

Ripe Few or no primary and/or secondary spermatogonia and spermatocytes visible; lumen densely packed with spermatozoa.

Spent No primary and/or secondary spermatogonia or spermatocytes visible; no spermatids present; few spermatozoa remaining in lumen.

In all cases, maturity classifications based on histological examination agreed with visual classifications applied in the field.

Age and growth

Growth marks on the vertebrae of *L. americanus* formed distinct steps on the centrum surface. Under magnification in reflected light, the surface texture of the step appeared coarser than the rest of the centrum. A narrow, dark, translucent band was on the outer side of each step. The step and the narrow band formed a continuous ring around the centrum and was considered to be the annulus. Broader, lighter opaque bands with relatively uniform surface texture were between the annuli. A broad, opaque band combined with a narrow, translucent band and step was interpreted as one year's growth. While these features were visible on fresh vertebrae, they became much more distinct when the vertebrae were heated. The step became deeper and the narrow, translucent band became opaque and dark relative to the rest of the centrum (Fig. 7).

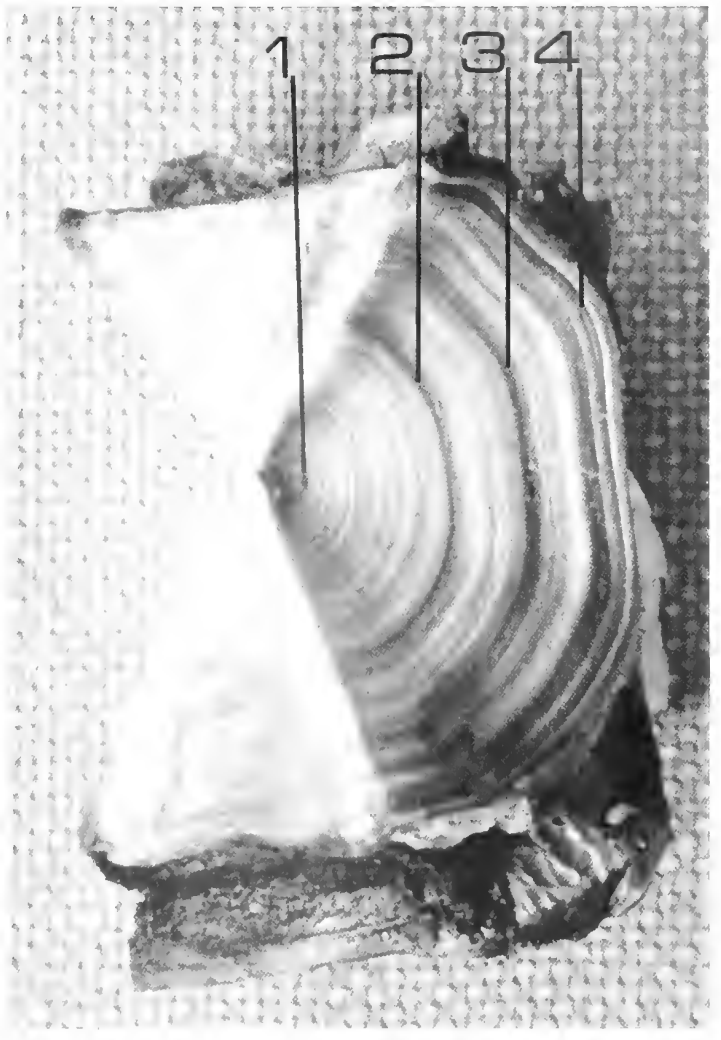

Figure 7
Vertebra from a 4-year-old *Lophius americanus*, after heating. Annuli are indicated.

Annuli were counted on vertebrae from 635 goosefish. In 200 (31.5%) cases, the first and second reading did not agree and a third reading was done. In most cases, the second reading differed by only one. In 25 (3.9%) cases, the third reading was different from both the first and second; these vertebrae were considered unreadable and discarded from the analysis.

Differences between readings were due to the presence of false annuli or because the true annuli were not distinct. False annuli appeared as dark bands but were not associated with a step. Another extraneous mark that sometimes occurred was a depression that formed a continuous ring on the centrum but was not a definitive step. This feature has also been found on black bullhead (Lewis 1949) and northern puffer (Lyczkowski 1971) vertebrae.

Annuli counts determined by the independent reader agreed with the original counts in 40 (80%) cases. In no case did the counts differ by more than one.

Van Oosten (1929) established the following criteria that must be met before checkmarks on scales or bones can be considered annuli: (1) Scales or bones must remain constant in number and identity throughout the life of the fish; (2) growth of the scale or bone must be proportional to the overall growth of the fish; (3) growth checkmarks must be formed at approximately the same time each year; and (4) back-calculated lengths should agree with empirical lengths. The first criterion is fulfilled by using vertebrae as the aging tool.

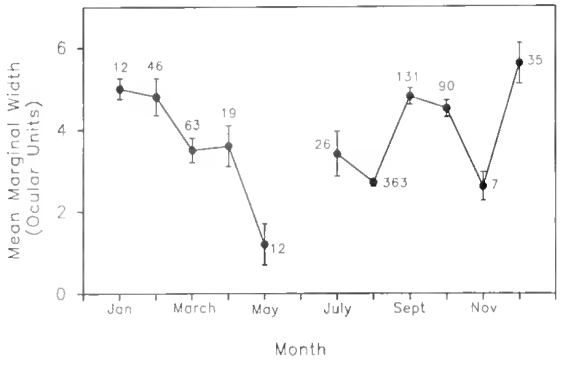

Figure 8

Monthly mean (± 1 SE of mean) marginal width for *Lophius americanus* vertebrae. Number of vertebrae examined each month is indicated. No vertebrae were collected during June.

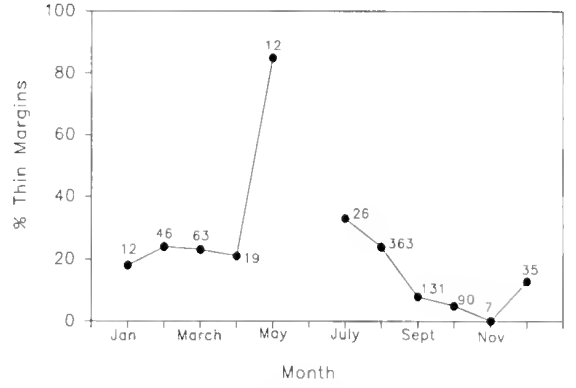

Figure 9

Percentage of *Lophius americanus* vertebrae having a marginal width less than one ocular unit by month. Number of vertebrae examined is indicated. No vertebrae were collected during June.

The regression of vertebral radius (VR) on TL revealed a strong linear relationship between the two variables. The regression equation based on 682 vertebrae from both sexes was as follows:

$$TL = 11.077(VR) + 40.018 \qquad (r^2\ 0.97).$$

This indicates that growth of vertebrae is proportional to growth of the fish, thereby satisfying the second criterion.

Monthly mean marginal increments were plotted for all age groups combined (Fig. 8). Sample size was not large enough to plot the age-groups separately. However, inspection of the data indicated that the seasonal progression of marginal increment was similar for all age-groups. Percentage of vertebrae showing a very small marginal increment (less than 1 ocular unit), indicating that little or no growth had occurred since the annulus was deposited, was also plotted (Fig. 9). The annuli were found to be closest to the edge of the vertebrae in May. Marginal increments were highest in December–February, following a period of growth during July–December. The percent of vertebrae with thin margins showed less variation than marginal increments. The percent was highest in May and decreased as the season progressed. These plots indicate that May is the time of annulus formation, and only one checkmark is formed per year. This appears to fulfill the third criterion that states that growth checks must be formed at approximately the same time each year; however, because data were pooled from several years, this cannot be stated with certainty. Although there was a decrease in the marginal increment from February to March, there was no corresponding rise in the percentage of very small margins (i.e., the mean

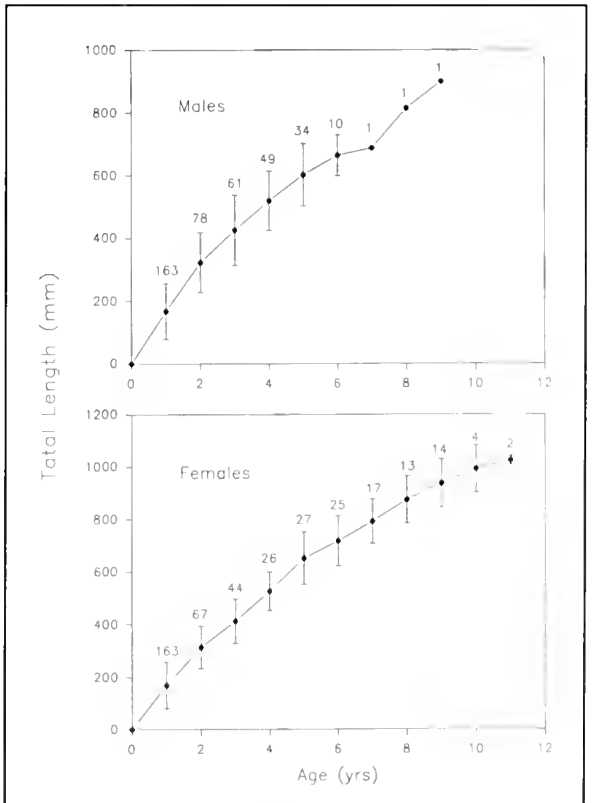

Figure 10

Mean observed lengths-at-age for *Lophius americanus*. Vertical bars indicate ranges of total length observed for each age. Sample sizes are indicated.

value of marginal width was not lowered by the presence of marginal widths <1). Although the relatively small sample sizes preclude making definitive conclusions, these data suggest that some process is causing

Table 3

Observed, von Bertalanffy, and back-calculated lengths-at-age (TL, mm) for male and female *Lophius americanus*, based on counts of vertebral annuli. The number examined for age 1 includes 142 unsexed individuals, which were used in the back-calculations for both sexes.

Age	Number examined	Mean observed length	von Bertalanffy length	Mean back-calculated lengths at successive annuli										
				I	II	III	IV	V	VI	VII	VIII	IX	X	XI
Males														
1	163	167	133	123										
2	78	322	256	127	267									
3	61	425	367	134	265	374								
4	49	519	469	127	263	377	472							
5	34	602	560	127	269	378	478	568						
6	10	664	644	109	241	352	465	549	634					
7	1	688	719	82	189	284	390	486	592	688				
8	1	815	788	109	255	367	473	602	675	731	793			
9	1	900	850	143	263	396	489	555	621	701	781	860		
			Mean	126	264	374	473	563	633	707	787	860		
		Annual growth increment		126	138	110	100	90	70	74	80	73		
Females														
1	163	169	121	124										
2	67	313	253	126	261									
3	44	412	373	124	257	361								
4	26	526	482	116	248	373	476							
5	27	652	581	130	278	405	507	600						
6	25	718	672	121	250	366	477	580	672					
7	17	792	754	124	265	386	485	573	662	757				
8	13	874	828	110	242	361	468	567	665	745	834			
9	14	937	896	119	250	373	475	567	652	740	821	901		
10	4	991	957	107	244	353	458	574	655	741	815	890	966	
11	2	1024	1014	117	254	380	488	591	677	757	826	894	962	1013
			Mean	123	258	374	483	581	664	748	826	898	965	1013
		Annual growth increment		123	135	116	109	98	83	84	78	72	67	48

the vertebrae to decrease slightly in diameter, possibly the resorbtion of the outer surfaces due to starvation in late winter.

Mean lengths were back-calculated for 256 males and 260 females. One hundred forty-two individuals, whose sex could not be determined because their gonads were undifferentiated (94–239 mm TL) but who were determined to have one annulus, were included in the back-calculations for each sex, bringing the total number used in the analysis to 398 males and 402 females.

The observed lengths were consistently higher than back-calculated or von Bertalanffy lengths for individual age-groups (Table 3). However, the differences are within the limits of seasonal growth, so the fourth criterion appears to have been fulfilled.

Males and females had very similar lengths-at-age until age 4. Above age 4, the mean lengths for females were slightly greater than males, with the difference becoming more pronounced with increasing age (Fig. 10).

The data suggest a difference in maximum age for the two sexes. The oldest male collected was 9 years old. Males older than 6 were exceptionally rare. Only one individual from each of the age groups 7, 8, and 9 was captured during the course of this study. The oldest female sampled was 11 years old. Fifty females greater than 6 years old were obtained. It appears that the number of older males is much fewer than females, indicating greater mortality of the males.

Mean back-calculated lengths-at-age were used to develop the vonBertalanffy growth equations. The resulting parameters and equation for females are:

$$K = 0.095$$
$$L_\infty = 1576 \text{ mm}$$
$$t_0 = 0.162$$
$$L_t = 1576.0\,(1 - e^{-0.095(t - 0.162)}).$$

The growth equation for males was calculated using three slightly different data sets. It was first calculated using all the mean back-calculated lengths available. The equation was then formulated after eliminating the two fish in age-groups 8 and 9 from the data set and finally it was calculated without age-groups 7, 8, or 9.

Because there was only one individual in each of these three oldest age-groups, these were possibly not good estimates of length for these ages. The parameters and equations are as follows.

All males:

$K = 0.097$
$L_\infty = 1460.0$
$t_0 = 0.015$
$L_t = 1460.0\ (1 - e^{-0.097(t-0.015)})$

Age-groups 8 and 9 eliminated:

$K = 0.166$
$L_\infty = 1018.0$
$t_0 = 0.211$
$L_t = 1018.0\ (1 - e^{-0.166(t-0.211)})$

Age-groups 7, 8, and 9 eliminated:

$K = 0.157$
$L_\infty = 1059.0$
$t_0 = 0.196$
$L_t = 1059.0\ (1 - e^{-0.157(t-0.196)})$

The length-weight relationships (Fig. 11) for 305 males and 311 females were:

Males

$\log_{10} W = 2.833\ (\log_{10} TL) - 4.347 \quad (r^2\ 0.95)$

Females

$\log_{10} W = 3.001\ (\log_{10} TL) - 4.770 \quad (r^2\ 0.98)$

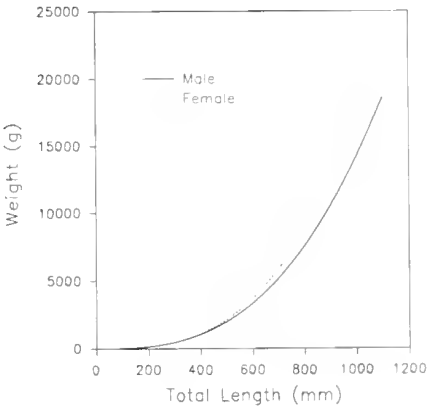

Figure 11
Length-weight relationship for male (n 305) and female (n 311) *Lophius americanus*.

Discussion

Reproduction

All female members of the Lophiiformes are thought to expel nonadhesive, mucoid egg rafts or veils with the possible exception of one species of antenariid angler fish (Pietsch and Grobecker 1980). These veils are buoyant and have a complex structure consisting of individual chambers, which each contain one to three eggs and an opening providing water circulation (Fulton 1898, Gill 1905, Rasquin 1958, Ray 1961). This method of egg production appears to be unique among the fishes.

The goosefishes, *Lophius* spp., have the most spectacular egg veils because of their large size. The egg veil of *L. americanus* can reach 6–12 m in length and 0.15–1.5 m in width (Martin and Drewry 1978). Several authors have provided detailed description of the egg veils of *L. americanus* (e.g., Agassiz and Whitman 1885, Connolly 1920, Dahlgren 1928) and *L. piscatorius* (Fulton 1898, Bowman 1919).

Estimates of fecundity presented by other authors are similar to those obtained in this study. Eaton et al. (1954) estimated 543,000 ova in the ovary of a 660 mm specimen. The regression of fecundity on TL presented here predicts 563,000 ova for a female of this size. Other estimates of fecundity range from 432,000 to 2,670,000 eggs, based on the examination of veils released from females of unknown size (Baird 1871, Nichols and Breder 1927, Berril 1929).

Female goosefish matured at a larger size and at a greater age (487 mm, age 4) than males (369 mm, age 3). This is a common trend among teleosts (Moyle and Cech 1982). In the case of goosefish, the female requires a larger body size to accommodate the large egg veil. Connolly (1920) was unable to determine size-at-maturity because of small sample size, but he stated that a goosefish 18 inches (457 mm) long (unstated sex) was immature, and all individuals over 31 inches (787 mm) were mature. McBride and Brown (1980), in a tabular summary of life-history parameters for several demersal fish species, present the age-at-maturity for *L. americanus* as 4 and 5 years for males and females, respectively. The source of their data is not stated. Martin and Drewry (1978) and several others also suggest that the age of maturity is 4 and 5 years for males and females. They state the source of this information as Connolly (1920). A review of Connolly's paper shows that he was quoting a publication by Fulton (1903), which deals with the growth of *L. piscatorius*, not *L. americanus*. At the time of Connolly's paper, the two species were considered synonymous. *L. piscatorius* is known to reach a larger maximum size and is larger at each age (based on data presented in the following age and growth discussion). The age-at-maturity cannot be considered the same

for the two species; in fact, it would be expected that the age- and length-at-maturity for *L. piscatorius* would probably be greater, as suggested here.

Data on gonad condition and the gonasomatic index indicate that spawning takes place in May–June in the area from Cape Hatteras to Southern New England. Because samples were collected and pooled from throughout this entire region, a seasonal progression of spawning from south to north as suggested in the literature cannot be demonstrated. Testes appear to develop earlier and remain ripe longer than ovaries. Fulton (1898) found the same to be true for *L. piscatorius*. This suggests that males may be multiple spawners. Multiple spawning in males would increase the chances of a ripe female encountering a ripe male, and thereby spawning successfully. It also serves to equalize the energetic investment of the sexes in reproduction. It appears that the investment of females is relatively high. The GSI was as high as 50%. Tsimenidis (1980) found values as high as 37% for the Mediterranean goosefish *L. budegassa*. A large part of the ovarian weight is composed of the mucogelatinous material that forms the veil. The caloric value of this material is unknown, but probably is rather low because of its low density and apparently high water content. However, the large amount of this material, combined with the great number of eggs produced, represents a sizeable energetic contribution by the female to reproduction.

Histological examination of the goosefish testes showed that spermatogenesis and the internal structure are not remarkably different from other teleosts. It also confirmed the validity of macroscopic staging of testes in the field. Examination of ovaries showed that oogenesis is similar to other teleosts but the structure of the ovary is somewhat different. The most significant differences were the presence of stalk-like lamellae containing the developing ova, and epithelium lining the lumen which is responsible for secreting the mucogelatinous matrix. Fulton (1898) was the first to suggest this mechanism of veil formation in the lophiids. His figures and descriptions of the histology of the ovaries of *L. piscatorius* indicate they are identical to those from *L. americanus* seen here. Rasquin (1958) provided detailed descriptions and photographs of the ovaries of two species of antennariid anglers (*Antennarius*, *Histrio*) and one species of ogcocephalid angler. These lophiiform species are known to produce egg veils. Although they are all only a fraction of the size of *L. americanus* and *L. piscatorius*, the histology of their ovaries was virtually identical to their larger relatives, including the presence of stalk-like ovigerous lamellae and secretory epithelium. It is reasonable to assume that all members of the order Lophiiformes known to produce egg veils have similar ovaries. This character may be useful in verifying veil production in some of the deepwater lophiiform families for which veil production has been assumed but not verified.

Pietsch and Grobecker (1980) suggest that the egg veil is an excellent device for broadcasting a large number of eggs over great geographical distances. In addition, the buoyancy of the veil causes the eggs to develop in relatively productive surface waters.

There seem to be additional selective advantages to the egg veil as well. It may function in facilitating fertilization of the eggs. When a veil is first extruded from the female, it absorbs a large quantity of water. As water is absorbed, sperm may be drawn into the egg chambers through the small circulation pores in the veil, thereby insuring fertilization. The veil likely functions by several methods in the protection of the eggs and embryos, since the embryos remain in the egg chamber for 2–3 days after hatching (Dahlgren 1928). Predators such as zooplankton are physically excluded from the egg chambers by the small size of the circulation pore. The veil may reduce or eliminate olfactory cues, thereby eliminating predators locating food items by this method. Wells (1977) suggests that the jelly coat of yellow perch *Perca flavescens* spawn may act in a similar manner. Finally, the mucogelatinous material of goosefish egg veils may be toxic or repugnant to potential predators. Newsome and Tompkins (1985) found that the egg mass of yellow perch contain some compound(s) that are not toxic but seem to deter predators. While such a protective device is rare among teleosts (Fuhrman et al. 1969, Orians and Janzen 1974), the presence of toxic or unpalatable compounds within the jelly coat of amphibian egg masses is well known (Licht 1969, Ward and Sexton 1981).

Age and growth

Females and males have about the same weight-at-length before maturity. After maturity the females are slightly heavier than males because of their large ovaries. As the ovaries ripen, weight differences between males and females become greater. The regression slopes for males and females approximate 3, implying isometric growth in the length-weight relationship. Tsimenidis and Ondrias (1980) calculated very similar length-weight regressions for *L. piscatorius* in the Mediterranean Sea.

Vertebrae appear to be valid aging tools for *L. americanus*. They satisfy all of Van Oosten's (1929) criteria. Vertebrae can readily be located and removed from goosefish and are relatively easy to prepare and read. The annuli are readily discernible since only 3% of the vertebrae were considered unreliable, and an inexperienced, independent reader agreed with the counts in 80% of the readings he performed.

These data indicate that the annuli become discernible in May. Because these rings are present on juveniles as well as adults, they appear to be related to seasonal patterns of growth rather than reproduction. The annuli are difficult to see when they are at the very edge of the vertebral centra. For this reason, they are probably not detected until some additional growth has occurred after they are laid down. Yasuda (1940) has shown that on vertebrae of *Scombrops* sp. annuli were formed 1.5 months later than on the otoliths. So it is likely that the annuli (composed of a step and a translucent band) found on goosefish vertebrae represent the end of fast growth (the step) in late-fall and a period of slow winter growth (the translucent band).

While several authors have studied growth in *L. piscatorius* and *L. budegassa* (Fulton 1903, Guillou and Njock 1978, Tsimenidis and Ondrias 1980), only Connolly (1920) has looked at growth in *L. americanus*. He based his growth estimates on vertebral annuli counts, but his sample size was only six individuals. His results were as follows: age 1, 114mm; age 4, 457mm; age 8, 737mm; age 9, 787mm; age 10, 940mm; age 12, 1016mm. These estimates are slightly lower than found in this study, but a slower growth rate would be expected in the colder Canadian waters in which Connolly conducted his study.

The growth rate of *L. americanus* is intermediate to *L. piscatorius* and *L. budegassa*. Figure 12 compares the mean back-calculated lengths for the two European species (from Tsimenidis and Ondrias 1980) with data presented here for *L. americanus*.

The differences in observed and back-calculated mean lengths between males and females past age 4 are small, but appear to be real. This is the most common form of sexual dimorphism among fishes (Moyle and Cech 1982). Tsimenidis and Ondrias (1980) found similar small differences between the sexes for *L. budegassa* and *L. piscatorius*.

More significant is the difference in mortality between the sexes implied by the data. The heavier mortality of males may be caused by increased predation due to their smaller size, but this does not seem likely. Perhaps the males exhibit behavioral or distributional differences which make them more susceptible to predation or fishing effort. A final possibility is that they simply reach senescence before females.

The von Bertalanffy growth equations fit the back-calculated lengths extremely well. The values for L_∞ for both sexes seem somewhat inflated. The maximum reported size for *L. americanus* is approximately 1220mm (Bigelow and Schroeder 1953). The largest female collected in this study was 1115mm and the calculated L_∞ was 1576mm. The largest male collected was 900mm compared with a calculated L of 1018–1460mm. The inflation of L_∞ is caused by a lack of representatives from the older age-classes. This is a common problem in age and growth studies. The asymptotic length is therefore not well defined for either sex in this study. The sampling effort was believed to be intense enough to sample these larger individuals if they were present in the population. It is concluded that these individuals are simply not present. This may be the result of commercial fishing pressure (groundfishing and scalloping), which tends to be selective towards larger individuals.

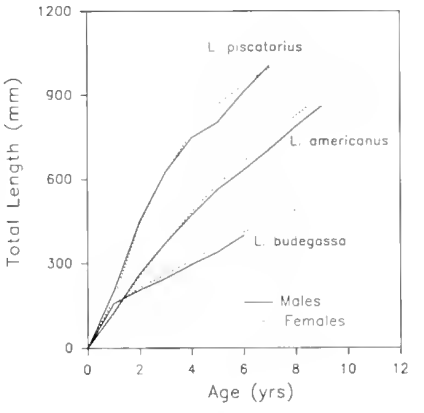

Figure 12
Back-calculated lengths-at-age for three species of *Lophius*. Data for *L. americanus* from present study; data for *L. piscatorius* and *L. budegassa* from Tsimenidis and Ondrias (1980).

Acknowledgments

We are indebted to all the graduate students and staff members at the Virginia Institute of Marine Science who assisted at various points in this study. D. Sved, M. Chittenden, and W. DuPaul provided helpful reviews of this manuscript. Ship time was provided by the Northeast Fisheries Science Center and the fishing vessels *Captain Wool*, *Virginia Queen*, *Virginia Cavalier*, and *Cara Lyn*. Funding was provided by Sea Grant, National Oceanic and Atmospheric Administration, U.S. Department of Commerce, under Grant NA86AA-D-SG042, through the Virginia Sea Grant Program, Project RC/F-10, J.A. Musick, Principal Investigator. This manuscript was based on a thesis submitted by the senior author in partial fulfillment of the M.A. degree, School of Marine Science, College of William and Mary.

Citations

Agassiz, A., and C.O. Whitman
1885 Studies from the Newport Marine Laboratory, XVI. The development of the osseus fishes. Part I. The pelagic stages of young fishes. Mem. Mus. Comp. Zool. 14(1):1-56.

Baird, S.F.
1871 Spawning of the goosefish *L. americanus*. Am. Nat. 5:785-786.

Berril, N.J.
1929 The validity of *L. americanus* as a species distinct from *L. piscatorius* with notes on rate of developement. Contrib. Can. Biol. Fish. 4(12):143-155.

Bigelow, H.B., and W.C. Schroeder
1953 Fishes of the Gulf of Maine. U.S. Fish. Wildl. Serv. Fish. Bull. 53(74), 577 p.

Bowman, A.
1919 The eggs and larvae of the angler (*Lophius piscatorius*) in Scottish waters. Rep. Fish. Board Scotl. Sci. Invest. for 1919, No. 1. 42 p.

Caruso, J.H.
1975 Sexual dimorphism of the olfactory organs of lophiids. Copeia 1975:380-381.
1977 The systematics of the fish family Lophiidae. Ph.D. diss., Tulane Univ., New Orleans, 220 p.
1983 The systematics and distribution of the lophiid angler fishes: II. Revision of the genera *Lophiomus* and *Lophius*. Copeia 1983:11-30.

Connolly, C.J.
1920 History of the new food fishes. III. The angler. Bull. Biol. Board Can. 3:1-17.

Cuvier, G., and A. Valenciennes
1837 Historie naturelle des poisons, vol. 12. F.G. Levrault, Paris, 507 p.

Dahlgren, U.
1928 The habits and life history of *Lophius*, the angler fish. Nat. Hist. 28(1):18-32.

Eaton, T.H. Jr., C.A. Edwards, M.A. McIntosh, and J.P. Rowland
1954 The structure and relationships of the anglerfish, *Lophius americanus*. J. Elisha Mitchell Sci. Soc. 70(2):205-218.

Edwards, R.L.
1965 Relation of temperature to fish abundance and distribution in the southern New England area. Int. Comm. Northwest Atl. Fish. Spec. Publ. 6:95-110.

Fuhrman, F.A., G.J. Fuhrman, D.L. Dull, and H.S. Moser
1969 Toxins from eggs of fishes and amphibia. J. Agric. Food Chem. 17:417-424.

Fulton, T.W.
1898 The ovaries and ovarian eggs of the angler or frog fish (*Lophius piscatorius*) and of the John Dory (*Zeus faber*). Sixteenth Annu. Rep. Fish. Board Scotl. 3:125-137.
1903 The distribution, growth, and food of the angler. Twenty-first Annu. Rep. Fish. Board Scotl. 3:186-199.

Gill, T.
1905 The life history of the angler. Smithson. Misc. Collect. 47(4):500-516.

Grosslein, M.D., and T.R. Azarovitz
1982 Goosefish, *Lophius americanus*. *In* Fish distribution. MESA N.Y. Bight Atlas Monogr. 15, New York Sea Grant Inst., Stony Brook.

Guillou, A., and J.C. Njock
1978 Analyse des structures de la peche dans les parts de la cote atlantique francaise de 1961 a 1975 et des incidences du chalutage sur les stocks des principales especes concernees par cette activite dans les mers adjacentes. Revue Trav. Inst. Peches Marit. 42(1,2):120-128 [in French].

Hildebrand, S.F., and W.C. Schroeder
1928 Fishes of Chesapeake Bay. Bull. U.S. Bur. Fish. 43, pt. 1, 388 p.

Hyder, M.
1969 Histological studies on the testes of *Tilapia leucesticta* and other species of the genus *Tilapia* (Pisces:Teleostei). Trans. Am. Microsc. Soc. 88(2):211-231.

Jean, Y.
1965 Seasonal distribution of monkfish along the Canadian Atlantic mainland. J. Fish. Res. Board Can. 22(2):621-624.

Lagler, K.F.
1956 Freshwater fishery biology, 2d ed. W.C. Brown, Dubuque, 248 p.

Lawler, E.F. Jr.
1976 The biology of the sandbar shark, *Carcharinus plumbeus*, in the lower Chesapeake Bay and adjacent waters. M.A. thesis, College of William and Mary, Williamsburg, 48 p.

Lewis, W.M.
1949 The use of vertebrae as indicators of the age of the northern black bullhead, *Ameriurus m. melas*. Iowa State Coll. J. Sci. 22(2):209-218.

Licht, L.E.
1969 Palatability of *Rana* and *Hyla* eggs. Am. Midl. Nat. 82:296-298.

Lyczkowski, J.M.
1971 Age and growth of the northern puffer, *Sphoeroides maculatus*. M.A. thesis, College of William and Mary, Williamsburg, 26 p.

Markle, D.F., and J.A. Musick
1974 Benthic-slope fishes found at 900 m depth along a transect in the western North Atlantic Ocean. Mar. Biol. (Berl.) 26: 225-233.

Martin, F.D., and G.E. Drewry
1978 Lophiidae. *In* Development of fishes of the mid-Atlantic Bight—An atlas of egg, larval and juvenile stages, vol. 6, Stromateidae through Ogocephalidae, p. 357-366. U.S. Fish Wildl. Serv. OBS 78/12, 416 p.

McBride, M.M., and B.E. Brown
1980 The status of the marine fishery resources of the northeastern United States. NOAA Tech. Memo. NMFS-F/NEC-5, Northeast Fish. Sci. Cent., Woods Hole, 13 p.

McKenzie, R.A.
1936 Some notes on the monkfish or angler (*Lophius piscatorius*). Can. Field Nat. 50:55-56.

Mercer, L.P.
1978 The reproductive biology and population dynamics of black sea bass, *Centropristis striata*. Ph.D. diss., College of William and Mary, Williamsburg, 196 p.

Moyle, P.B., and J.J. Cech Jr.
1982 Fishes, an introduction to ichthyology. Prentice-Hall, Englewood Cliffs, 593 p.

Newsome, G.E., and J. Tompkins
1985 Yellow perch egg masses deter predators. Can. J. Zool. 63:2882-2884.

Nichols, J.T., and C.M. Breder
1927 The marine fishes of New York and southern New England. Zoologica (NY) 9(1):1-192.

Northeast Fisheries Science Center
1991 Status of the fishery resources off the northeastern United States. NOAA Tech. Memo. NMFS-F/NEC-86, Northeast Fish. Sci. Cent., Woods Hole, 132 p.

Orians, G.H., and D.H. Janzen
1974 Why are embryos so tasty? Am. Nat. 108:581–592.

Pietsch, T.W., and D.B. Grobecker
1980 Parental care as an alternative reproductive mode in an antennariid angler fish. Copeia 1980:551–553.

Proctor, W., H.C. Tracy, E. Helwig, C.H. Blake, J.E. Morrison, and S. Cohen
1928 Fishes—A contribution to the life history of the angler (*Lophius piscatorius*). *In* Biological survey of the Mount Desert Region, Part 2, p. 1–29, Philadelphia.

Rasquin, P.
1958 Ovarian morphology and early embryology of the pediculate fishes *Antennarius* and *Histrio*. Bull. Am. Mus. Nat. Hist. 114(4):331–371.

Ray, C.
1961 Spawning behavior and egg raft morphology of the ocellated fringed frogfish, *Antennarius numifer* (Cuvier). Copeia 1961:230–231.

Ricker, W.E.
1975 Computation and interpretation of biological statistics of fish populations. Bull. Fish. Res. Board Can. 191, 382 p.

Ross, J.L.
1978 Life history aspects of the gray tilefish, *Caulolatilus microps* (Goode and Bean, 1878). M.A. thesis, College of William and Mary, Williamsburg, 120 p.

Scott, W.B., and M.G. Scott
1988 Atlantic fishes of Canada. Can. Bull. Fish. Aquat. Sci. 219, 731 p.

Simpson, A.C.
1951 The fecundity of the plaice. Fish. Invest. Ser. 2, Mar. Fish. G.B. Minist. Agric. Fish. Food 17(5), 27 p.

Tsimenidis, N.Ch.
1980 Contribution to the study of the angler-fishes *Lophius budegassa* Spinola, 1807 and *L. piscatorius* L., 1758 in Greek seas. Inst. Oceanogr. Fish. Res. (Athens) Spec. Publ. 4: 180–190.

Tsimenidis, N.Ch., and J.Ch. Ondrias
1980 Growth studies on the angler-fishes *L. piscatorius* and *L. budegassa* in Greek waters. Thalasographica 2(3):63–94.

Van Oosten, J.
1929 Life history of the lake herring (*Leucichthys artedi*, LeSeur) of Lake Huron as revealed by its scales, with a critique of the scale method. Bull. U.S. Bur. Fish. 44:265–428.

Ward, D., and O.J. Sexton
1981 Anti-predator role of salamander egg membranes. Copeia 1981:724–726.

Wells, L.
1977 Changes in yellow perch (*Perca flavescens*) populations of Lake Michigan, 1954–75. J. Fish. Res. Board Can. 34: 1821–1829.

Wenner, C.A.
1978 *Lophius americanus*. *In* Making a living on the continental slope and in the deep sea: Life history of some dominant fishes of the Norfolk Canyon area, p. 253–263, 267–268. Ph.D. diss., College of William and Mary, Williamsburg.

Yasuda, H.
1940 On the rings formed on scale, vertebral centrum, and otolith of the same individual fish. Jpn. Soc. Sci. Fish. Bull. 8:290–300.

Annual reproductive cycle of oocytes and embryos of yellowtail rockfish *Sebastes flavidus* (Family Scorpaenidae)

Michael J. Bowers

Tiburon Laboratory, Southwest Fisheries Science Center
National Marine Fisheries Service, NOAA
3150 Paradise Drive, Tiburon, California 94920

Abstract. – Female yellowtail rockfish *Sebastes flavidus*, a viviparous species employing intralumenal gestation following fertilization of ovulated eggs, were caught from Cordell Bank (seamount 20 miles west of Pt. Reyes, central California) on a monthly basis from May 1985 through April 1986 to determine their annual reproductive cycle. Since histological methods provide precise and detailed information, this method was employed to (1) examine oocytes and embryos to describe developmental stages, and (2) provide temporal assessment of the annual reproductive cycle. The description and staging scheme developed provide a basis to compare reproductive developmental patterns between cycles and populations.

Oogonia (Stage I) and early perinucleolus (Stage II) oocytes were present in samples from all months. Progressive growth of oocytes from early- to late perinucleolus (Stage III) was evident in spent and recovering ovaries, indicating the end of a reproductive year and the beginning of a new reproductive cycle. Initial yolk accumulation (Stage IV) occurred in July, and final yolk accumulation (Stage V) was predominant from September through January. In February, the majority of samples displayed fertilized ova in early-celled stages of embryonic development. Gestation continued for about 30 days with parturition occurring between January and March. Mature oocytes were also collected in March, suggesting the Cordell Bank yellowtail population has a prolonged reproductive season extending into April.

Manuscript accepted 9 March 1992.
Fishery Bulletin, U.S. 90:231–242 (1992).

Sixty species of rockfish (genus *Sebastes*) have been recorded in waters off the California coast; twenty species are utilized by commercial and recreational fisheries (Lenarz 1986). Rockfishes display a wide variety of life history patterns with respect to their habitat and seasonality of reproduction (Wyllie Echeverria 1987). The majority of investigations on rockfish reproduction have focused on the development, occurrence, and identification of larvae and juveniles. Evaluating annual reproductive success as a direct consequence of variations in oocyte viability has received less attention.

The *Sebastes* complex contributed approximately 37,806 mt to west coast fisheries in 1985 (PFMC 1990) and management of this resource is heavily dependent upon predictions of strong and weak year-classes. Since no single trait accurately represents reproductive capacities of fish populations (Eldridge et al. 1991), fisheries management is based on a variety of information. Year-class strength estimates may be enhanced by understanding factors influencing annual fluctuations in reproduction. Reproduction within this genus is characterized by intralumenal gestation, following fertilization of ovulated, mature eggs. This process is somewhat unique among teleosts occurring only in scorpaenids and zoarcids (Wourms et al. 1988). The investigation described here focuses on the development and temporal occurrence of oocytes and embryos within the ovary of yellowtail rockfish *Sebastes flavidus*. Characterization of oocyte growth and embryonic development provides a basis for assessing reproductive performance. This study is part of a larger effort to acquire information on the reproductive biology of yellowtail rockfish to ultimately determine factors that influence reproductive success.

Although characteristics of oocyte growth are generally similar among teleosts (Wallace and Selman 1981), numerous ovary maturity scales and oocyte classification schemes exist (Yamamoto 1956, Htun-Han 1978, Robb 1982, Howell 1983). These classification schemes are useful for determining reproductive strategies (synchronous, group-synchronous, or asynchronous) and evaluating aspects of reproductive trends. Each oocyte staging system is, however, less likely to be adapted for teleosts outside the genus of original study due to the variety of reproductive strategies. An oocyte classification scheme to assess the reproductive status of the marine, viviparous genus Sebastes in the Eastern Pacific has not been reported. Taking these factors under consideration, the objectives of the study reported here were two-fold: (1) to describe oocyte and embryonic development in *Sebastes flavidus* through one complete reproductive cycle, and (2) establish a staging

classification as a basis for the comparison of oocyte and embryonic development between populations, reproductive years, and other species of Sebastes. Such data may be used to monitor reproductive development during a particular year. In addition, descriptions of oocyte and embryonic development provide a basis to compare the impacts of environmental fluctuations and physiological responses with the production of viable offspring. An understanding of environmental and physiological interactions influencing reproductive success could provide valuable contributions to the understanding of recruitment dynamics and allow for more efficient resource management.

Materials and methods

Specimens were collected from Cordell Bank (38°00′N, 123°25′W), a seamount 20 miles west of Pt. Reyes, at monthly intervals. Adult female yellowtail rockfish were captured by hook-and-line at depths of 50–150 m, from May 1985 through April 1986. No samples were obtained in June 1985 due to inclement weather. Mean age and size of samples for each month are shown in Table 1.

Fish were held on ice and transported to the laboratory where pieces of ovaries (~4×4×6 mm) were dissected and fixed in 10% neutral buffered formalin. Routine paraffin embedding followed the guidelines of Humason (1967). Samples were sectioned at 6 μ thickness with a rotary microtome. Mounted sections were stained in hematoxylin and counterstained in eosin (H&E).

Cell measurements were made using a video coordinate digitizer (Model 582 AVCD, H.E. Inc., Las Vegas, NV) on cells sectioned through the nucleus. Oocytes were measured and staged randomly. Mean cell diameters were determined from a subsample of 10–20 cells for each stage. All cell diameters reported are from fixed tissues.

In each monthly sample, the first 200–400 cells encountered were counted and staged. Percent frequency distributions of the various oocyte stages were calculated by dividing the total number of a particular stage by the total number of oocytes observed, expressed as a percentage. Because the probability of an individual oocyte being sectioned is proportional to its size as well as its abundance, larger oocytes tend to be overestimated and smaller oocytes underestimated (Howell 1983). Nonetheless, frequency distributions do indicate seasonal changes within the ovary. Because of the wide range of cell diameters, overlapping sizes among oocyte stages, and shrinkage due to fixation, criteria for staging oocytes was based on histological appearances and cell structure.

Table 1

Monthly means and standard errors for age, standard length (SL), and weight (Wt) of *Sebastes flavidus* collected off central California, May 1985–April 1986, used for histological analysis.

Month	Age (yr)	SL (cm)	Wt (g)	*n*
May	14.7±2.0	37.4±1.0	1434±115	6
June	—	—	—	0
July	17.9±2.3	39.5±1.5	1600±146	9
Aug.	13.2±2.0	36.8±1.8	1387±181	4
Sept.	30.0±2.6	44.4±0.6	2349±111	6
Oct.	26.2±4.0	42.6±1.2	2017±157	7
Nov.	21.1±2.2	40.9±0.6	1780± 97	6
Dec.	18.7±2.1	39.3±1.1	1830±122	10
Jan.	15.4±1.8	36.1±1.1	1272±107	10
Feb.	14.6±1.8	36.1±1.1	1315± 83	10
Mar.	19.3±1.8	37.5±1.2	1489±102	10
Apr.	23.4±2.2	38.3±0.6	1387± 52	10

Although ovaries in varying stages of postfertilization development were observed, monthly collection of ovaries was inadequate for a detailed study of rapid embryonic development. Therefore, additional samples of embryonic stages were collected by catheterization from female yellowtail rockfish held in captivity. Ten adult female yellowtail rockfish captured after copulation were catheterized weekly for 6 weeks while being maintained in a flow-through, sand-filtered (to 10 μ) seawater system. Photoperiod was ambient. The mean temperature and salinity (10.4°C and 34.7‰) for the 2-month holding period (January and February) were well within the range of parameters at the sampling site.

Abbreviations used in figures

BC	blastodermal cap	MU	muscle
BR	brain	NC	notochord
C	capillary	NU	nucleoli
CH	chorion	N	nucleus
EB	embryonic body	OG	oil globule
EF	empty follicle	ON	oogonial nest
ER	erythrocyte	OP	optic vesicle
EY	eye	OV	oil vacuole
FOL	follicle	POF	postovulatory follicle
G	granulosa	RE	retina
GR	germ ring	SO	somite
HG	hind gut	T	theca
LC	lampbrush chromosome	VM	vitelline membrane
LN	lens	YG	yolk globule
LT	liver tissue	YM	yolk mass
MN	migratory nucleus		

Table 2

Classification and temporal occurrence of oocytes from *Sebastes flavidus* collected off central California, based on histological appearance. See text for additional histological descriptions.

Stage		Major histological characteristics	Temporal occurrence
I	Oogonia	Small cells (5–25 μ) found in clumps or "nests." Cytoplasm pale to clear. Basophilic nucleus occupying most of cell volume.	All year
II	Early perinucleolus	Wide range of cell diameters (20–100 μ). Intense basophilic cytoplasm. One or two large nucleoli in nucleus.	All year
III	Late perinucleolus	Diameters 50–140 μ. Small, clear vesicles present in cytoplasm. Cytoplasm pale-blue to light-gray. Several small nucleoli around inner margins of nuclear membrane.	Feb.–Oct.
IV	Initial yolk accumulation	Cell diameters 120–210 μ. Small spherical, eosinophilic yolk granules in a distinct cortical zone in cytoplasm. Cytoplasm vesicular and light-gray. Well-developed follicle surrounds a developing vitelline membrane. Several small nucleoli around the inner margins of nuclear membrane.	July–Oct.
V	Final yolk accumulation	Large cells (200–600 μ). Cell volume one-half to entirely full of yolk spheres. Lampbrush chromosomes visible in nucleoplasm. Lipid vacuoles appear larger as they coalesce.	Sept.–March
VI	Migratory nucleus	Cell diameters 600–750 μ. A single, large lipid vacuole present. Nuclear membrane indistinct or absent. Nuclear material irregularly shaped and no longer centrally located. Follicle may be distorted and irregularly shaped.	Dec.–March
VII	Ovulation & Fertilization	Mature oocyte free from follicle. The yolk mass is a single, large homogeneous mass, staining deep-purple. In fresh (unfixed) ovaries, ova appear clear or translucent.	Dec.–March

Results

Oocyte development

Major histological characteristics distinguishing stages for *S. flavidus* are listed in Table 2. All cells could be categorized into one of the seven stages. Terminology and nomenclature follow Moser (1967a) and Howell (1983).

Stage I: Oogonia These small cells were 5–25 μ in diameter and were found in clumps or "nests" along the lamellar branches (Figs. 1A, 4E). Larger oogonia in the 20 μ range possessed a deeply-stained chromatin network attached to a single, large basophilic nucleolus.

Stage II: Early perinucleolus These oocytes were 20–100 μ in cell diameter. While still closely associated with neighboring oogonia, there was noticeable movement away from oogonial nests. The most obvious feature of this cell was the intensely basophilic cytoplasm (Figs. 1B, 4E).

Stage III: Late perinucleolus Diameters were 50–140 μ. Clear vacuoles appeared in the cytoplasm of oocytes as small as 50 μ. Initially these vacuoles were distributed as a poorly organized ring surrounding the nucleus, but were seen randomly scattered throughout the cytoplasm of larger oocytes (Figs. 1B, 4E). As growth continued, they increased in size and number.

Stage IV: Initial yolk accumulation The earliest signs of yolk accumulation were seen in oocytes of 120–210 μ in diameter. Small, spherical globules of yolk were seen in a distinct cortical zone in the cytoplasm (Fig. 1C, D). The follicle enclosing the oocyte is more complex and composed of several identifiable structures (see below).

Stage V: Final yolk accumulation To simplify the staging of yolked oocytes, cells with approximately one-half their volume filled with yolk spheres, and cells whose volumes were entirely filled with yolk, were placed in Stage V. Yolk spheres increased in number and size. By the end of this stage, the cell diameter increased to about 650 μ. The cytoplasm was entirely filled with yolk spheres of various sizes (Fig. 2A). The vacuoles which were distributed throughout the cytoplasm began to coalesce, forming larger vacuoles.

An eosinophilic nucleoplasm with lampbrush chromosomes was visible (Fig. 2B). In the late Stage-V cell, the nucleus became irregularly shaped and the nuclear membrane was often indistinct (Fig. 2A).

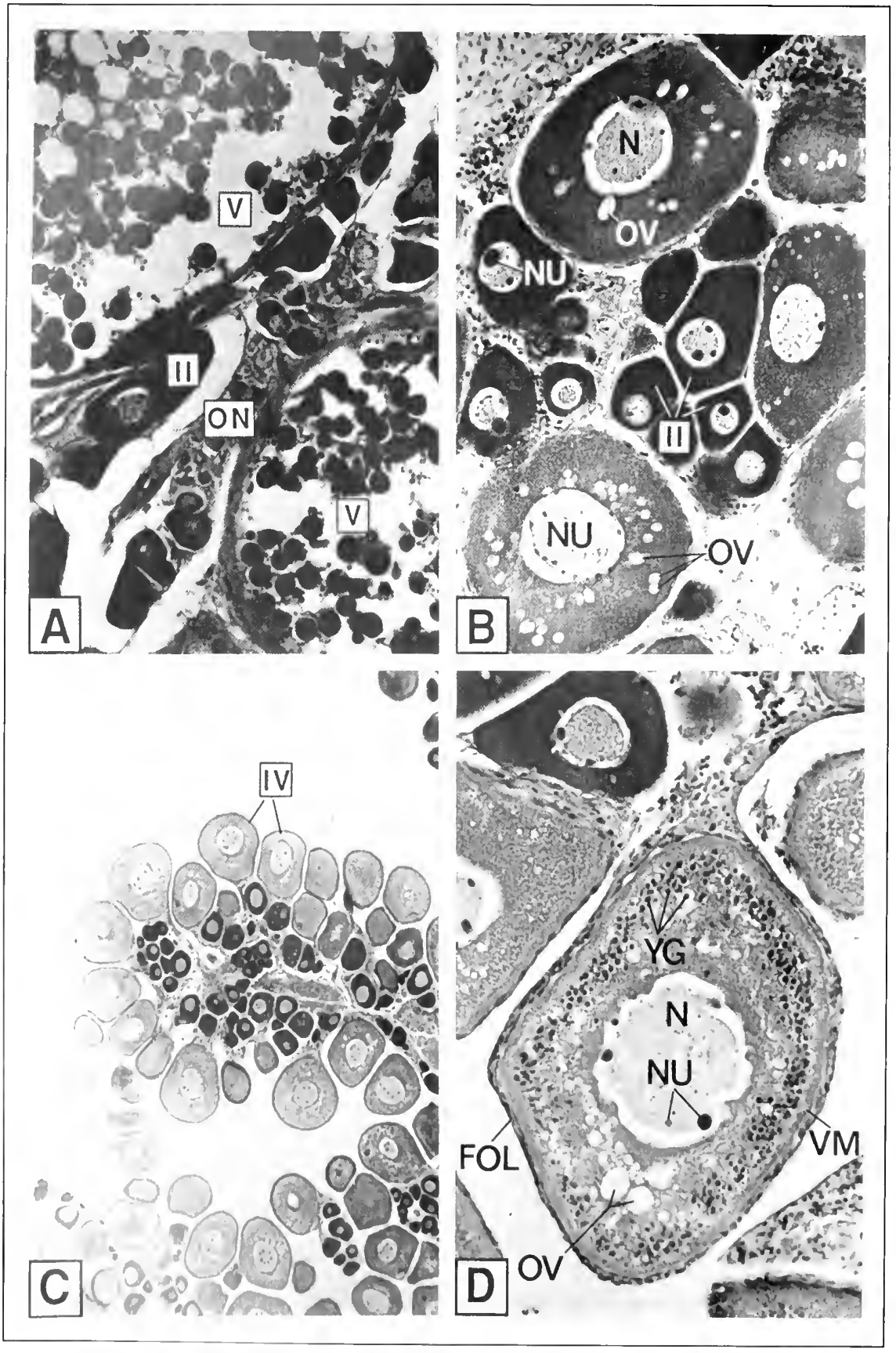
A
V
II
ON
V
B
N
OV
NU
II
NU
OV
C
IV
D
YG
N
NU
FOL
VM
OV

Figure 1 (left page)
(A) Oogonial nest (Stage-I oocyte) from *Sebastes flavidus*, containing several primary oocytes collected Dec. 1985, 400×. (B) Section of oocytes in ovary of *S. flavidus* collected May 1985, 250×. Basophilic properties of cytoplasm in Stage-II cells and their large nucleoli are shown. Distribution of vacuoles are seen in the larger Stage-III cells. (C) Cross-section of an ovary collected Aug. 1985 showing arrangement of Stage-IV oocytes in grape-like clusters on outer margins of a lamellar branch, 63×. (D) Typical Stage-IV (initial yolk accumulation) oocyte showing the first indications of yolk, 250×.

The cellular composition of the mature follicle was best observed in Stage-IV or Stage-V oocytes (Fig. 2D). A bilaminar vitelline membrane about 1 μ in thickness was next to the plasma membrane of the oocyte. Outside the vitelline membrane was a single inner epithelial layer, the granulosa. Encapsulating the granulosa was an intricate capillary network filled with erythrocytes. The theca, a single epithelial layer consisting of squamous cells with large nuclei, surrounded the profuse capillary system.

Stage VI: Migratory nucleus Cell diameters ranged from 600 to ~750 μ. Lipid material had coalesced to form a single, large vacuole, usually centrally located. Nuclear material was ameboid in appearance and no longer occupied a centralized position in the cell (Fig. 2C). Nucleoli were small, indistinct, or entirely absent.

Stage VII: Ovulation/Fertilization Histological evidence of ovulation was verified by observing the integrity of the surrounding follicle. Follicles appeared either as irregularly shaped and shrunken away from the oocyte or displayed a loss of continuity. Postovulatory follicles appeared throughout the sectioned ovary (Fig. 2C).

Because fertilization of the mature oocyte occurs rapidly after ovulation, distinction between ovulated oocytes and recently-fertilized oocytes was unnecessary. Therefore, fertilization was considered an event rather than a stage of histological distinction, and is included in Stage VII to maintain logical continuity of the developmental process. Following fertilization, however, the yolk material became a single homogeneous mass staining bright-purple in histological preparations, appearing clear or translucent in unfixed samples (Fig. 3A, B). This distinguishes fertilized from recently ovulated ova.

Embryonic development

A complete series of sequential embryonic developmental stages was not obtained from field collections due to the sampling interval and rapid development of embryos. Embryos from field collections were, however, satisfactorily placed into one of three broad categories: (1) early-celled, (2) embryonic body, or (3) eyed-larvae (where retinal pigmentation was visible).

Early-celled The early celled stage of embryonic development observed from field collections of yellowtail rockfish ovaries corresponded to stage 9 of Oppenheimer's classification for *Fundulus heteroclitus* (Oppenheimer 1937). The early-celled stage was seen as an undifferentiated mass of cells (blastodermal cap) on top of a large yolk mass (Fig. 3A). This stage was first collected in January, most frequently seen in February, and last occurred in March.

Embryos in a more advanced state (i.e., flattening or expansion of the blastula) occasionally occurred within an ovary primarily containing early-celled embryos. This suggests rapid cellular divisions and growth.

Embryonic body The appearance of an embryonic body was first seen in an ovary collected in February and last seen in March. This embryonic stage closely corresponds to Oppenheimer's stages 14 or 15 (Oppenheimer 1937). At the beginning of this stage, an undifferentiated mass of cells (taking on the appearance of tissue rather than individual cells) was located in a high ridge lying over the yolk mass. The oil globule was evident at the opposite pole (Fig. 3B). With further development, embryos displayed optic vesicles originating from lateral buds, distinguishing the cephalic region (Fig. 3C). By the end of this growth phase, somites along the trunk were visible along with lengthening of the tail. The head had further developed to include lens formation (Fig. 3D).

Figure 2 (overleaf, left page)
(A) Cross-section of ovary from *Sebastes flavidus* with clutch of oocytes in late Stage V, 63×. (B) Cross-section through nucleus of a Stage-V oocyte showing distribution of nucleoli and lampbrush chromosomes in the nucleoplasm, 400×. (C) Section through two nearly-mature oocytes in Stage VI (migratory nucleus), 63×. (D) Tangential section of Stage-V oocyte showing components of the follicle outside of vitelline membrane, 400×.

Figure 3 (overleaf, right page)
(A) Early-celled embryos from *Sebastes flavidus* ovary collected Feb. 1986, 63×. (B) First appearance of embryonic body, showing cellular differentiation. Whole embryo, formalin-fixed, 40×. (C) Section through developing embryo (embryonic body, late stage) showing optic vesicle formation originating from lateral expansions in cephalic region, 63×. (D) Embryonic body stage further developed than in Fig. 3C, with better definition of brain, retina, and lens formation, 63×.

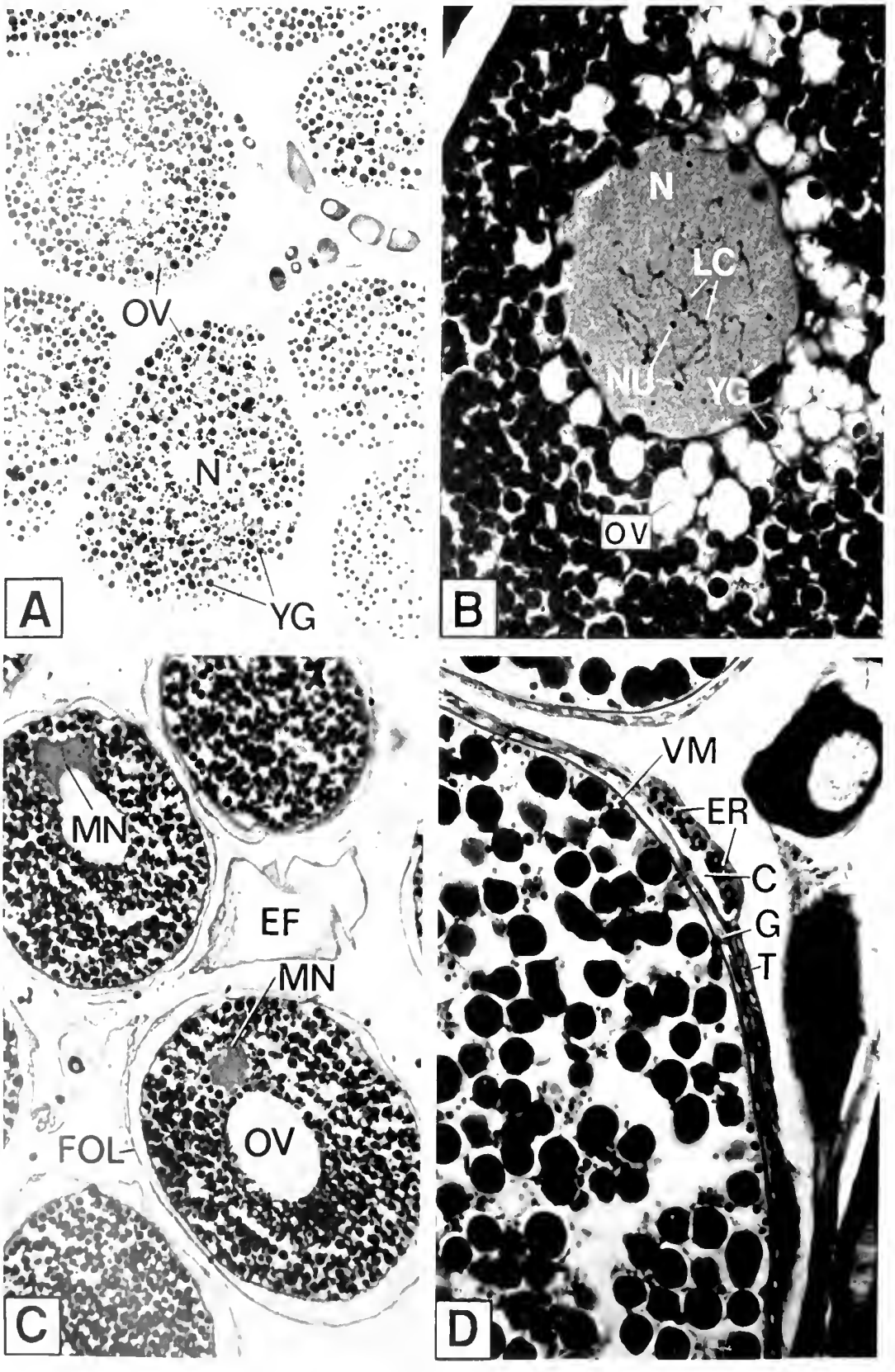

Figure 2

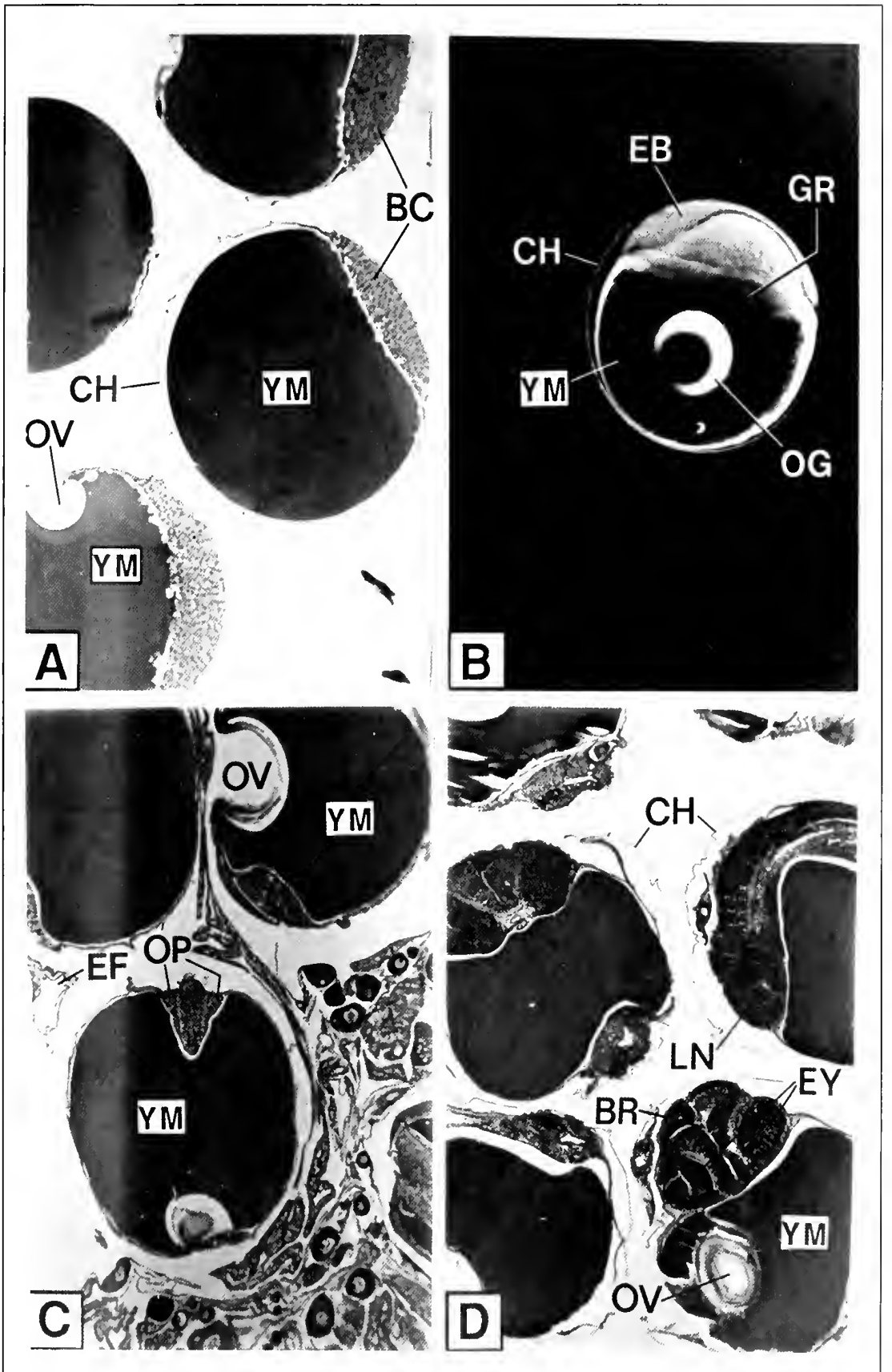

Figure 3

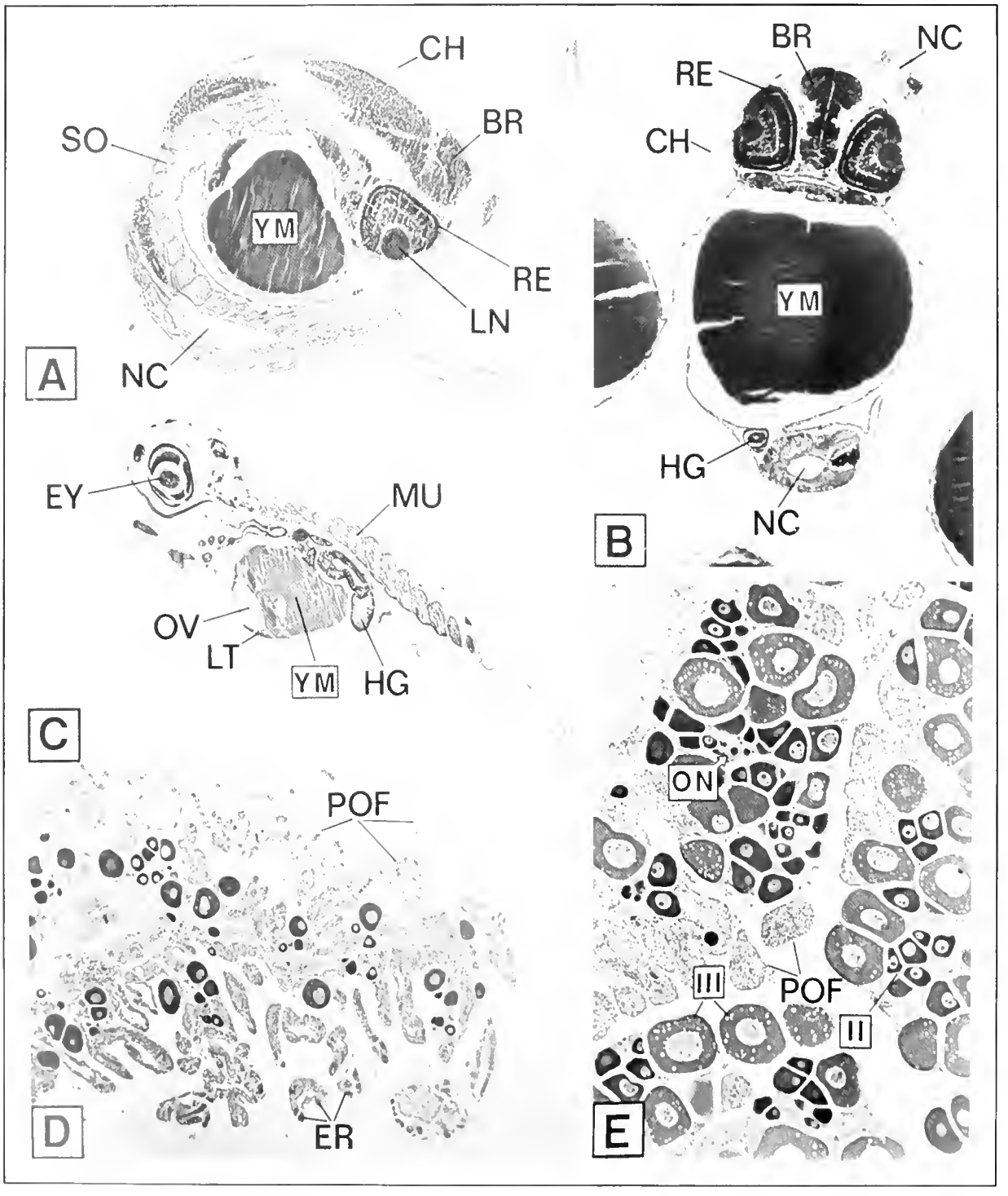

Figure 4 (above)

(A) Unhatched prolarvae of *Sebastes flavidus* collected Feb. 1986. Pigmentation of retina is apparent, as are well-formed somites, 63×. (B) Tangential section of unhatched prolarvae with completed pigmentation of the retina. Tail continues to lengthen and is seen to pass the head slightly, 63×. (C) Newly-hatched larva of *S. flavidus* showing close association of liver with oil vacuole, developing jaw and well-developed gut, 40×. (D) Cross-section of a recently-spent ovary of *S. flavidus* collected March 1986. Many empty and collapsed follicles are being resorbed, 40×. (E) Recovering and early developing ovary collected April 1986 showing reorganization of ovarian stroma as resorption nears completion, 63×.

Eyed-larvae Retinal pigmentation began as a black deposit outlining the periphery of the retina. Concurrently, somites were well formed in the thoracic and tail regions (Fig. 4A). Mature embryos (prehatching larvae) exhibited complete pigmentation of the eyes and a well-developed musculature system along the entire length of the tail (Fig. 4B). Embryos in this broad developmental category were in field samples collected in January and February. Had ovaries containing

hatched embryos (larvae) been collected in the field, they would have been included in this stage. Larvae were, however, taken from females held in the laboratory. These larvae were 4–6 mm in length and had open mouths with functional jaws. The yolk mass appeared to be reduced, and liver tissue was associated with a persistent oil globule (Fig. 4C).

Seasonal oocyte cycle Oogonial nests were observed in all samples, with about 25% frequency of occurrence throughout the entire reproductive cycle (Fig. 5). These Stage-I cells were most conspicuous early in the reproductive season and in ovaries of spent females.

Stage II or early-perinucleolus oocytes were also noted year-round and accounted for about one-third of all oocyte types observed (Fig. 5). The large nucleoli and dark cytoplasm were features that easily distinguish this stage. Mid- to late Stage-II cells were observed either singly or in groups around oocytes of later maturational stages (Stages III–VII) and were considered the 'resting' stage oocytes of other investigators (Bowers and Holliday 1961, Howell 1983).

In early spring, a broader range of Stage-II cell diameters was evident, indicating continued oocyte growth. Stage-III cells rapidly increased during March and April to a maximum frequency of 40% in April, and decreased in frequency by August as this clutch of oocytes developed (Fig. 5).

Copulation of yellowtail rockfish typically occurs over three months beginning in August and ending in October (Eldridge et al. 1991). The incidence and frequency of sperm in yellowtail rockfish ovaries were not evaluated in this study. However, small clumps or 'packages' of sperm were occasionally seen closely associated with the stroma or in spaces between developing (yolked) oocytes.

Initial yolk accumulation (Stage IV) was first documented in females collected in July, with all specimens collected in August showing this stage. In August, 34% of oocytes were Stage IV. Oocytes of Stage IV appeared as grape-like clusters on the outer margins of the lamellar branches, developing in a group-synchronous manner (Fig. 1C). The occurrence of Stage-IV oocytes sharply declined from August to November when no Stage-IV oocytes were observed (Fig. 5). As yolk accumulation continued, yolk spheres increased in size and number, filling the cytoplasm to about one-half its volume. At this point, oocytes were categorized as Stage V. Stage V was the most advanced oocyte observed from its first appearance in September until December when the frequency declined (Fig. 5). Oocytes in this developmental stage were most prevalent in November when they accounted for a mean of 48% of all oocytes. Stage-VI (Migratory nucleus) oocytes were first observed in December.

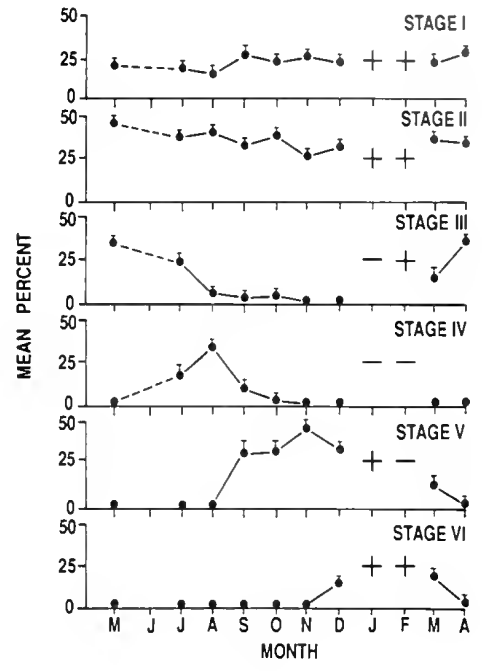

Figure 5
Mean monthly frequency distributions of oocyte Stages I–VI in ovaries of *Sebastes flavidus* during 1985–86. Error bars represent 1 SE. Plus signs = present, minus = not present. Monthly sample size same as in Table 1.

Ovaries with an advanced mode of Stage-VI oocytes continued to be collected over the next 3 months (January–March). This stage appeared to have a short duration, as ovaries containing Stage VII were also collected in some of the same months as Stage VI (December–February).

Ovary maturation was determined by using the most advanced oocyte or embryonic stage present in each monthly sample, and their frequency of occurrence was expressed as percent(s) (Fig. 6). Temporal ovarian development is illustrated and reflects a prolonged reproductive season.

While accurate frequency distributions on Stage-VII oocytes were not possible, the peak month of ovulation and fertilization appeared to be February. Sections of samples with Stage-VII oocytes showed eggs free from (e.g., outside) their follicular remnants. While continuity of follicular components (theca and granulosa) was disrupted, the integrity of the capillary network was maintained and there was a close association with the developing embryo.

Ovaries recently spawned (parturition) were seen as early as January and most frequently collected in March (Fig. 6). The ovary was greatly reduced in size,

reddish-blue in color, and very soft in texture. Histologically, the spent ovary displayed increased vascularization, a thickening of the tunica, and postovulatory follicles undergoing various stages of resorption (Fig. 4D). In addition, larvae remaining after parturition and yolked oocytes not reaching maturity are frequently seen in various stages of resorption.

Late-recovering and early-developing ovaries possessed reorganized lamellar branches containing Stages I, II, and early Stage-III oocytes as resorption nears completion (Fig. 4E). All samples collected in April were in this condition (Fig. 6), which marked the end of one reproductive season and the beginning of the next reproductive cycle.

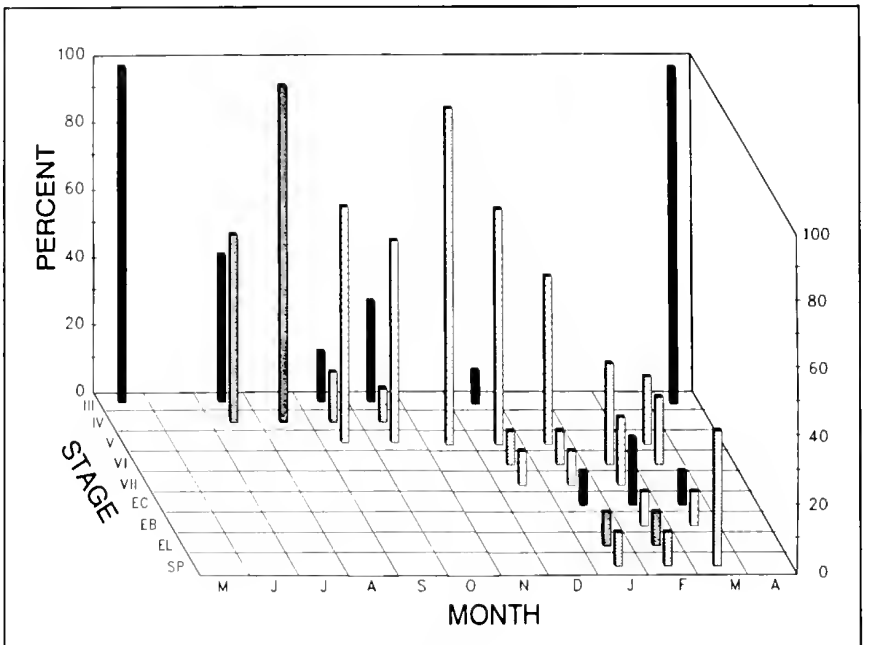

Figure 6

Percent distribution of ovarian maturation stages (derived from the most advanced oocyte or embryonic stage categorized histologically) from monthly collections of *Sebastes flavidus*; *n* is same as presented in Table 1. III = late perinucleolus, IV = early yolk, V = late yolk, VI = migratory nucleus, VII = ovulation/fertilization, EC = early-celled embryo, EB = embryonic body, EL = eyed-larvae, SP = spent.

Discussion

In the present study, I established an oocyte/embryonic classification that allows rapid determination of a rockfish population's status in the annual reproductive cycle. The use of this staging system allows one to establish oocyte frequency distributions and categorize ovaries as to their seasonal development, both temporally and spatially. This information, in turn, not only permits interannual and interpopulational comparisons, but may help reveal variations related to environmental factors.

Developmental events that occur in the oocytes of *Sebastes flavidus* are similar to those described for other teleosts with group-synchronous development (see review by Wallace and Selman 1981). Embryogenesis and the basic reproductive patterns follow observations reported for other members of the genus *Sebastes* (Moser 1967a, Wyllie Echeverria 1987). Temporal occurrence of reproductive events and seasonal variations of these events differ within the genus (Wyllie Echeverria 1987).

In the present work, oocyte development in *S. flavidus* has been categorized by separating oocyte growth into seven distinct stages. Oogonia and early-perinucleolus stages (Stages I and II, respectively) are found in the ovaries throughout the year. These stages appear to grow continuously, develop asynchronously, and, particularly in Stage-II cells, display a wide range of cell diameters. Development of unyolked oocytes in *S. flavidus* is similar to that described for *S. paucispinus* (Moser 1967a,b). However, seasonal occurrence of Stage-III oocytes differs between the two species. Stage-III oocytes in *S. flavidus* decline rapidly in number as yolk accumulation (Stage IV) is initiated. They are not observed again in the ovaries until after parturition and the beginning of the reorganization of the lamellar branches. While Moser (1967a) did not suggest a staging classification scheme, his descriptions for *S. paucispinus* included oocytes corresponding to Stage III (in the present study). In contrast to *S. flavidus*, these oocytes occurred in ovaries of *S. paucispinus* throughout the year (Moser 1967a). The temporal difference in occurrence of Stage-III oocytes between these two species is most likely a reflection of the number of broods produced annually. Viviparous species producing more than one brood annually require a reserve of Stage-III oocytes. In rockfish where two or more broods of young are produced in one reproductive season, a second clutch of yolked oocytes develops concurrently with the initial brood of gestating embryos. Moser (1967a) reported the second clutch of yolked oocytes to occur in *S. paucispinus* when the initial brood had reached eye-lens formation. A distinct seasonal absence of Stage-III oocytes, or a

clutch of yolked oocytes during embryonic gestation, distinguishes single from multiple spawners.

There were approximately 30–40 days between the appearance of fertilized ova and well-developed larvae or recently-spawned females. Therefore, gestation appears to be 30–40 days in *S. flavidus*. Moser (1967b) estimated 1–2 months gestation for the multiple-spawner *S. paucispinus*, and Boehlert and Yoklavich (1984) noted 37 days for *S. melanops*, a single-season spawner. Similarly, Mizue (1959) compared a multiple-spawner, *S. marmoratus* to a single-season spawner, *S. inermis*. His data suggest approximately 30–45 days for embryonic gestation in both species.

While the basic reproductive pattern among the various Sebastes species is similar, variations exist in reproductive strategy and life history (Boehlert and Yoklavich 1984). Temporal variations in reproductive seasonality of rockfishes are perhaps the most obvious and, therefore, well documented. Releasing larvae over an extended period of time increases the probability that a portion of the reproductive population would encounter favorable environmental conditions for the survival of the progeny. Wyllie Echeverria (1987) listed the peak parturition months for 34 species of *Sebastes* and reported that larval extrusion occurs for up to 9 months in some species. In her study, from samples collected over a 7-year period, the principal month of parturition for yellowtail rockfish was February. In the present study, and in more recent work (unpubl. data), March was the peak month of parturition; however, the samples were from a smaller geographical area. Phillips (1964), who sampled northern, central, and southern California rockfish populations, determined *S. flavidus* to be a "winter" spawner (November–March). Wyllie Echeverria (1987) reported parturition for yellowtail rockfish from north-central California to occur from January to July. In the present study, a shorter parturition time was observed for the Cordell Bank yellowtail population (January–March). This temporal variance may reflect a clinal reproductive variation in yellowtail rockfish populations. Care must be taken, however, when interpreting and comparing results where macroscopic characteristics are used. While field assessments by microscopic staging of whole oocytes or macroscopic examinations are less time-consuming, validation by histological methods is required for precise and detailed information (West 1990). Furthermore, studies on the impact of atresia and postovulatory follicles are relevant to understanding functional relationships between yellowtail rockfish reproduction and their environment. West (1990) suggests histology as the appropriate method of use for these types of studies.

A prolonged reproductive season is characteristic of the genus *Sebastes*, but the factors regulating such a mechanism are not clear. While temperature and photoperiod appear to effect later spawning in higher-latitude populations (Wooton 1984), inherent factors may also play a key role in the prolonged seasonality displayed by rockfishes. There is some evidence that age, at least in yellowtail rockfish, may account for some variation in parturition time within a season (M.J. Bowers, unpubl. data; Eldridge et al. 1991). In addition, Boehlert and Yoklavich (1984) estimated 5 days between hatching and birth in *S. melanops*, while parturition has been reported to occur immediately after hatching in the ovary in the subgenus *Sebasticus* (Tsukahara 1962). In this study, it could not be determined if hatched larvae remained in the ovaries of yellowtail rockfish. Further investigations are necessary to determine the occurrence, significance, and regulatory mechansims of larval retention.

Rockfish are an important economic resource to the Washington, Oregon, and California fisheries. Estimates of total commercial rockfish landings in 1985 were 37,806 mt (PFMC 1990). In the same year, recreational anglers landed approximately 4000 mt of rockfish in California alone. Yellowtail, blue, and black rockfishes represented 30% of the recreational landings (Lenarz 1986). Fluctuations in year-class strength cause the fishery to be somewhat unpredictable (Lenarz 1986), leaving it difficult for optimal management strategies to protect stock depletion and establish harvest guidelines. The earlier one can predict recruitment success, the more precise management decisions are likely to be. Leaman (1988) discussed the value of directing management models toward biological principles. Responses of yellowtail rockfish ovaries to environmental fluctuations are early indicators of reproductive performance. This study documents the process of oocyte development in yellowtail rockfish and provides a basis for interannual comparisons.

Acknowledgments

To Richard Powers, owner and operator of the *New Sea Angler*, my sincerest appreciation for his skill and assistance collecting samples. My greatest debt in connection with this work is to Dr. Bruce MacFarlane whose tireless enthusiasm, assistance, and patience are beyond mortal explanation.

Citations

Boehlert, G.W., and M. Yoklavich
1984 Reproduction, embryonic energetics, and the maternal-fetal relationships in the viviparous genus *Sebastes* (Pisces:Scorpaenidae). Biol. Bull. (Woods Hole) 167:354–370.

Bowers, A.B., and F. Holliday
1961 Histological changes in the gonad associated with the reproductive cycle of the herring (*Clupea harengus*). Dep. Agric. Fish. Scotl., Mar. Res. 5, p. 1-16.

Eldridge, M.B., J. Whipple, M. Bowers, B. Jarvis, and J. Gould
1991 Reproductive performances of yellowtail rockfish, *Sebastes flavidus*. Environ. Biol. Fishes 30:91-102.

Howell, W.H.
1983 Seasonal changes in the ovaries of adult yellowtail flounder, *Limanda ferruginea*. Fish. Bull., U.S. 81:341-355.

Htun-Han, M.
1978 The reproductive biology of the dab *Limanda limanda* (L.) in the North Sea: Seasonal changes in the ovary. J. Fish Biol. 13:351-359.

Humason, G.L.
1967 Animal tissue techniques, 3d ed. W.H. Freeman, San Francisco.

Leaman, B.M.
1988 Reproductive and population biology of Pacific ocean perch (*Sebastes alutus* (Gilbert)). Ph.D. thesis, Univ. Brit. Col., Vancouver, 200 p.

Lenarz, W.H.
1986 A history of California rockfish fisheries. *In* Proc., Int. Rockfish Symp., Oct. 1986, Anchorage, Alaska, p. 35-41. Alaska Sea Grant Rep. 87-2, Univ. Alaska, Fairbanks.

Mizue, K.
1959 Studies on a scorpaenous fish *Sebasticus marmoratus* Cuvier et Valenciennes. V. On the maturation and the seasonal cycle of the ovaries of the marine ovoviviparous teleost. Bull. Fac. Fish. Nagasaki Univ. 8:84-110 [in Jpn., Engl. summ.].

Moser, H.G.
1967a Seasonal histological changes in the gonads of *Sebastodes paucispinis* (Ayres), an ovoviviparous teleost (family Scorpaenidae). J. Morphol. 123:329-351.
1967b Reproduction and development of *Sebastodes paucispinis* and comparison with other rockfishes off southern California. Copeia 1967:773-797.

Oppenheimer, J.M.
1937 The normal stages of *Fundulus heteroclitus*. Anat. Rec. 68(1):1-15.

PFMC (Pacific Fishery Management Council)
1990 Status of the Pacific coast groundfish fishery through 1990 and recommended acceptable biological catches for 1991: Stock assessment and fishery evaluation. Document prepared for the Council and its advisory entities. Pac. Fish. Manage. Counc., Portland, OR 97201.

Phillips, J.B.
1964 Life history studies on ten species of rockfish (genus *Sebastodes*). Calif. Dep. Fish Game, Fish Bull. 126, 70 p.

Robb, A.P.
1982 Histological observations on the reproductive biology of the haddock, *Melanogrammus aeglefinus* (L.). J. Fish. Biol. 20:97-408.

Tsukahara, H.
1962 Studies on habits of coastal fishes in the Amakusa Islands. 2. Early life history of the rockfish, *Sebasticus marmoratus* (Cuvier et Valenciennes). Rec. Oceanogr. Works Jpn., Spec. 6:49-55.

Wallace, R.A., and K. Selman
1981 Cellular and dynamic aspects of oocyte growth in teleosts. Am. Zool. 21:325-343.

West, G.
1990 Methods of assessing ovarian development in fishes: A review. Aust. J. Mar. Freshwater Res. 41:199-222.

Wootton, R.J.
1984 Introduction: Strategies and tactics in fish reproduction. *In* Potts, G.W., and R.J. Wootton (eds.), Fish reproduction: Strategies and tactics, p. 1-12. Acad. Press, London.

Wourms, J.P., B.D. Grove, and J. Lombardi
1988 The maternal-embryonic relationship in viviparous fishes. *In* Hoar, W.S., and D.J. Randall (eds.), Fish physiology, Vol. XI, Part B, p. 1-34. Acad. Press, San Diego.

Wyllie Echeverria, T.
1987 Thirty-four species of California rockfishes: Maturity and seasonality of reproduction. Fish. Bull., U.S. 85:229-250.

Yamamoto, K.
1956 Studies on the formation of fish eggs. I. Annual cycle in the development of the ovarian eggs of the flounder, *Liopsetta obscura*. J. Fac. Sci. Hokkaido Univ., Ser. VI Zool. 12:362-373.

Abstract.– We sampled jewfish from recreational and commercial catches in the eastern Gulf of Mexico from November 1977 to January 1990 to obtain life history information. A single annual minimum in mean marginal increment ratios during May–August supported the hypothesis that jewfish up to at least age 10 can be aged by counting the opaque marks observed on otolith sections. Annual opaque mark formation was observed for a 3- and a 4-year-old jewfish using oxytetracycline (OTC) reference marks on otoliths (sagittae). Male jewfish (N 41) ranged 3–26 years old; females, 0–37 years (N 85). Growth was similar for males and females, averaging >100 mm/year through age 6, then slowing to about 30 mm/year by age 15, and finally declining to <10 mm/year after age 25. Observed total length and age data were described well by the following von Bertalanffy growth model: total length (mm) = $2006\ (1 - e^{(-0.126(\text{age (yrs)} + 0.49))})$. Jewfish spawned from June through December, with peak activity from July through September. Male jewfish matured at about 1100–1150 mm when 4–6 years old; females matured at 1200–1350 mm when 6 or 7 years old. The extensive overlap of length and age distributions of males and females, and the slight differences between their sizes and ages at maturity, prevent us from designating jewfish as a protogynous hermaphrodite. No transitional individuals were found. Their relatively slow growth, longevity, and behavioral characteristics, such as the tendency to form spawning aggregations, make jewfish populations highly susceptible to overfishing.

Manuscript accepted 11 March 1992.
Fishery Bulletin, U.S. 90:243–249 (1992).

Age, growth, and reproduction of jewfish *Epinephelus itajara* in the eastern Gulf of Mexico

Lewis H. Bullock
Michael D. Murphy
Florida Marine Research Institute, Florida Department of Natural Resources
100 Eighth Avenue SE, St. Petersburg, Florida 33701-5095

Mark F. Godcharles
Southeast Region, National Marine Fisheries Service, NOAA
9450 Koger Boulevard, St. Petersburg, Florida 33702

Michael E. Mitchell
Florida Marine Research Institute, Florida Department of Natural Resources
1481-A Market Circle, Port Charlotte, Florida 33953

The jewfish *Epinephelus itajara*, largest of the western North Atlantic groupers (possibly reaching 455 kg; Robins et al. 1986), ranges from the east coast of Florida throughout the Gulf of Mexico, Caribbean Sea, and south to Brazil (Smith 1971), and also in the Pacific Ocean from Costa Rica to Peru. Jewfish occur at depths ranging from several meters (shallow estuarine areas) to about 50 m. Juveniles can be found in holes and below undercut ledges in swift tidal creeks draining mangrove swamps. Large adults occur both inshore around structures such as piers and bridges, and offshore around ledges and wrecks (Bullock and Smith 1991).

Jewfish have recently been granted protected status, eliminating harvest in both the U.S. Exclusive Economic Zone (NMFS 1990a, b) and Florida's territorial waters (Florida Marine Fisheries Commission 1990). Prior to this designation, jewfish were captured by hook-and-line, speargun, shark and grouper/snapper longlines, and as a bycatch of shrimp trawling. Historically, the majority of the U.S. commercial catch has been landed along the Florida Gulf coast, where landings reached a high of approximately 61,700 kg in 1988 (Fla. Dep. Nat. Resour. Annual Landings Summ., Fla. Mar. Res. Inst., St. Petersburg, unpubl. data).

A comprehensive study of jewfish life history does not exist. Smith (1971) discussed their systematics, distribution, and ecology. Randall (1967) described food habits from nine individuals. Other researchers have contributed incidental observations on diet (Beebe and Tee-Van 1928, Tabb and Manning 1961, Odum 1971), habitat (Smith 1976, Odum et al. 1982), spawning (Schroeder 1924, Colin 1990), and parasites/pseudoparasites (Breder and Nigrelli 1934, Pearse 1934 and 1952, Manter 1947, Olsen 1952). Bullock and Smith (1991) provided basic life-history information on jewfish in the eastern Gulf of Mexico, but did not discuss age and growth or size/age-at-maturity. In this paper, we describe age and growth, spawning seasonality, and approximate size- and age-at-maturity for jewfish in the eastern Gulf of Mexico. We also briefly discuss the implications of these life-history characteristics as they relate to the jewfish's susceptibility to overfishing.

Methods and materials

Jewfish were sampled aperiodically from recreational and commercial catches from the eastern Gulf of Mexico, November 1977 through January 1990. Fifty-six percent (269/481) of the sampled jewfish were captured using spearguns, 27% by hook-and-line, 8% by bottom longline (either grouper/snapper or shark fisheries), and the remaining 9% by shrimp trawl, trap, or unrecorded methods. We attempted to determine sex, whole (WW) and/or gutted (GW) weight (kg), and total length (mm TL) for each specimen, although we could not determine whole weight and sex when fish had been eviscerated (N 271). Although eviscerated, unsexed fish could not be included in our study of reproduction, they were used in the age and growth analyses. If sagittae could be located, they were removed from the otic capsule (N 384) and stored dry. A portion of the gonad, if available (N 173), was preserved in 10% formalin and later transferred to 70% ethanol.

Otolith sections were examined for evidence of age marks. Transverse sections, approximately 0.5 mm thick, were cut from each sagitta with a Buehler Isomet low-speed saw. Sections were mounted on microscope slides with Histomount mounting media and examined for age marks under a dissecting microscope using reflected light. Age marks were counted independently by two readers. Later, a joint reading was conducted in an attempt to resolve differences between counts.

Monthly mean marginal increment ratios were calculated for fish with 1–10 annuli to determine the periodicity of mark formation. Marginal increment was standardized for differences in growth among age-classes by dividing the marginal increment for each fish by the distance between its penultimate and outermost annuli. We called this calculated value the 'marginal increment ratio' (*sensu* percentage of marginal increment; Hood et al. Unpubl. manuscr.). Fish were assigned ages based on the number of annuli and a biologically realistic hatching date of 1 September (time of peak spawning; see Results). All fish were assigned an age equal to their annulus count, except for fish collected prior to 1 September and that had already deposited an annulus during the most recent period of mark deposition (April–August; see Results). The assigned age for these fish was one less than their number of annuli.

Observations to determine the validity of age marks were made from two jewfish (290 mm TL, 509 g; and 375 mm TL, 934 g) that were injected intramuscularly with 50 mg oxytetracycline (OTC) per kg body weight on 3 November 1990 and 21 October 1989, respectively. These fish were maintained at ambient light and temperature in flow-through 1038-gallon seawater tanks located at the Keys Marine Laboratory in the Florida Keys. The smaller specimen survived 11 months after OTC treatment; the larger fish was sacrificed after 22 months.

Nonlinear regression of all available age and length data (using FSAS; Saila et al. 1988) was used to estimate parameters of the von Bertalanffy growth equation,

$$l_t = L_\infty(1 - e^{(-K(t-t_0))}),$$

where l_t is total length (mm), t is age (years), L_∞ is asymptotic length, K is the Brody growth coefficient, and t_0 is the age at zero length (von Bertalanffy 1957). Likelihood ratio tests were used to compare male and female von Bertalanffy parameter estimates (Kimura 1980, Cerrato 1990). Nonlinear regression was used to fit the exponential equation, WW or $GW = aTL^b$, to whole- or gutted-weight and total-length data.

Histological preparations of gonads were made to determine gonad developmental class, following the criteria presented by Moe (1969) for red grouper *Epinephelus morio*. Initially, gonad samples were embedded in paraffin, but beginning with fish sampled in 1988, gonads were embedded in plastic (glycol methacrylate) because of its superior tissue-infiltrating abilities. Gonad samples were sectioned to a thickness of 3.5 μm and stained with Weigert's hematoxylin and eosin Y for microscopic examination. Spawning was inferred from seasonal changes in the relative abundance of fish having ovaries containing vitellogenic oocytes or testes containing sperm in their efferent ducts. Sizes or ages at maturity were determined from changes in the proportion of mature fish over the entire age range or across 50 mm size-classes.

Results

Age and growth

Opaque bands can be recognized and counted on thin-sectioned jewfish sagittae. Initial counts of opaque bands by two independent readers agreed on 62% (237/384 fish) of sections analyzed, with 91% (348/384) of all counts either in agreement or differing by one. After a second, joint reading, agreement was reached on opaque-band counts for all but two sections, leaving 382 specimens for analysis of age and growth.

The annual pattern of monthly mean marginal increment ratios and observations from two OTC-marked jewfish support the hypothesis that annuli form once each year. Mean marginal increment ratios were greater than 70% during November–April and declined to a minimum of 20% in June. The mean marginal increment ratio remained less than 30% through August (Fig. 1). For a large number of specimens captured

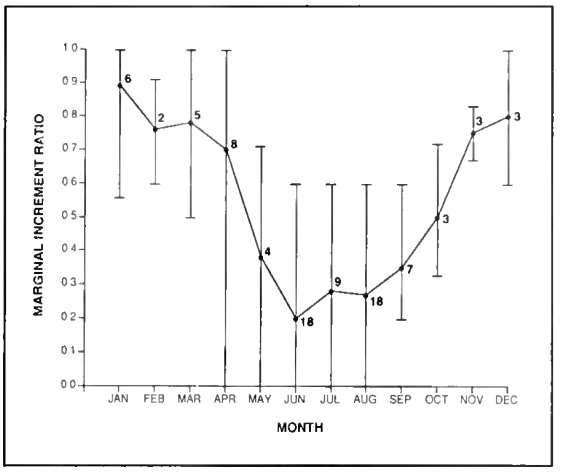

Figure 1

Monthly mean marginal increment ratios for jewfish with 1–10 opaque marks on otolith sections. Vertical lines indicate range of observations; sample size indicated by the number adjacent to the mean (*N* 86).

during April–August, we observed an opaque band at the outer edge of the otolith section and interpreted this as the deposition of a new annulus. After August, the mean marginal increment ratio increased until reaching a maximum during November–April. The observed annual minimum in monthly mean marginal increment ratios suggests that opaque bands form once each year in the otoliths of jewfish ≤10 years of age. The validity of age marks was confirmed for two OTC-marked jewfish. The OTC reference mark was clearly evident on otoliths of each of the two specimens. The otolith of the 3-year-old jewfish that had survived for 11 months in captivity contained a single annulus distal to the OTC mark. This fish, injected with OTC in November 1990, had apparently deposited an annulus prior to its death in October 1991. Its total length and weight were 505 mm TL and 2.7 kg. The 4-year-old specimen, injected with OTC in October 1989 and sacrificed in August 1991 after 22 months in captivity (total length and weight of ~735 mm TL and 9 kg), had deposited two annuli distal to the OTC reference mark.

A total of 481 jewfish were sampled for life-history data. Age data were determined for 382 individuals. Age range was 3–26 years for males (*N* 41), 0–37 for females (*N* 85), and 0–36 for fish of undetermined sex (*N* 256). Total lengths of jewfish sampled were 795–2057 mm for males (*N* 75), 338–2155 mm for females (*N* 131), and 75–2160 mm for fish of undetermined sex (*N* 275).

Jewfish grow slowly relative to their potential maximum size. Annual growth was most rapid (averaging >100 mm/year) through age 6, then declined to about 30 mm/year by age 15, and to less than 10 mm/year after age 25 (Table 1,

Table 1

Number of aged jewfish *Epinephelus itajara* from the eastern Gulf of Mexico, and average observed and predicted total lengths for age groups 0–37 years old. Predicted lengths are based on the von Bertalanffy growth equation mm TL = 2006 $(1 - e^{(-0.126(\text{age (yr)} + 0.49))})$.

	Average observed total length (mm)						Predicted total length (mm)		
Age	*N*	Male	*N*	Female	*N*	Unknown	Male	Female	Pooled*
0	0	—	1	338	4	170			—
1	0	—	3	517	0	—	434	382	344
2	0	—	5	717	1	711	605	563	541
3	2	863	4	708	4	751	759	725	714
4	1	1184	3	924	4	913	897	871	867
5	2	1080	1	1218	8	1067	1021	1002	1002
6	4	1078	0	—	5	1161	1132	1119	1121
7	5	1318	0	—	4	1423	1232	1225	1226
8	2	1476	2	1333	8	1437	1322	1319	1318
9	2	1400	2	1399	12	1368	1403	1404	1400
10	2	1398	6	1515	12	1516	1475	1481	1471
11	1	1660	6	1632	23	1544	1540	1549	1535
12	1	1690	7	1647	31	1612	1598	1611	1590
13	5	1620	10	1653	26	1644	1651	1666	1640
14	2	1849	7	1762	15	1723	1698	1715	1683
15	4	1828	4	1913	12	1737	1740	1760	1721
16	3	1909	4	1860	8	1735	1778	1800	1755
17	1	1770	2	1878	6	1879	1812	1836	1785
18	0	—	4	1820	8	1750	1843	1868	1811
19	0	—	0	—	6	1833	1870	1897	1834
20	0	—	2	1990	11	1842	1895	1923	1854
21	0	—	4	2023	8	1818	1917	1946	1872
22	0	—	2	2011	9	1820	1937	1967	1888
23	0	—	0	—	4	1938	1955	1986	1902
24	1	1905	1	1950	7	1936	1971	2003	1914
25	2	1955	0	—	4	1821	1985	2018	1925
26	1	1930	0	—	5	1891	1998	2032	1935
27	0	—	2	2065	3	1853	2010	2044	1943
28	0	—	1	1935	2	2006	2020	2055	1951
29	0	—	0	—	1	2090	2030	2065	1957
30	0	—	0	—	1	2040	2038	2073	1963
33	0	—	1	2015	2	1820	2058	2095	1977
34	0	—	0	—	1	2032	2064	2101	1980
36	0	—	0	—	1	1908	2073	2110	1986
37	0	—	1	1970	0	—	2077	2115	1988

* Including fish of unknown sex

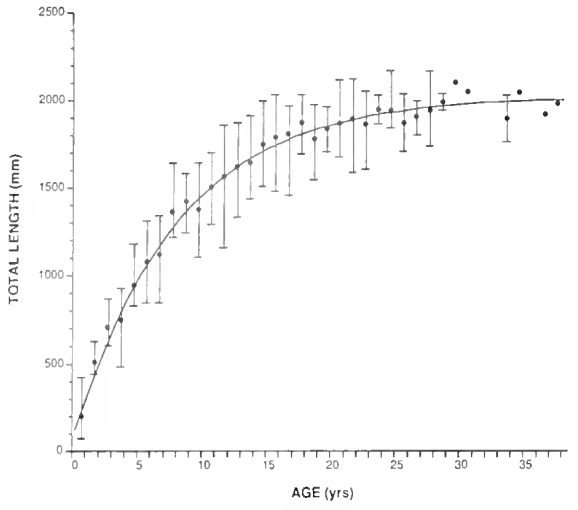

Figure 2

Observed ages (years) and total lengths (mm), and predicted growth modeled for jewfish collected from the eastern Gulf of Mexico. Parameters for the von Bertalanffy growth model are $L_\infty = 2006$ mm TL, K = 0.126/year, and $t_0 = -0.49$ year (N 382).

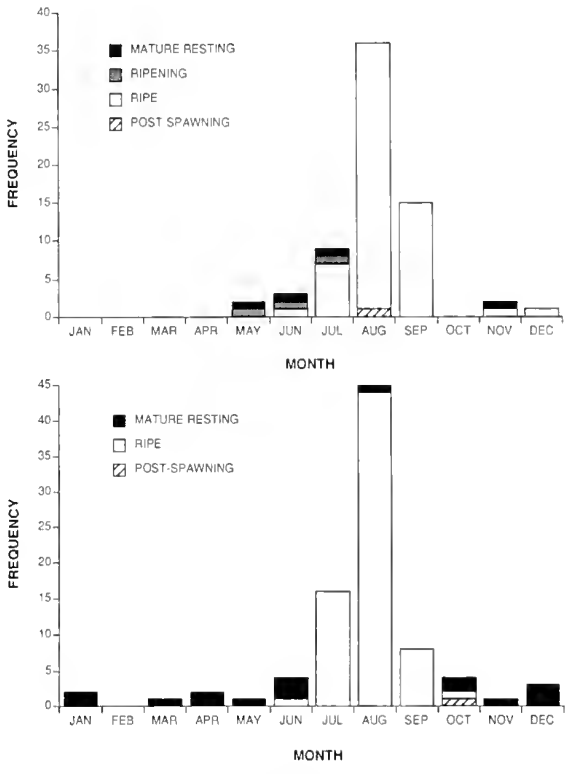

Figure 3

Monthly distribution of gonad classes for mature (upper) male (N 66) and (lower) female (N 86) jewfish collected from the eastern Gulf of Mexico. Histological criteria for gonad classes correspond to Moe's (1969) descriptions for red grouper.

Fig. 2). Average observed and predicted (von Bertalanffy equation) sizes-at-age were similar between sexes (Table 1). Results of likelihood ratio tests indicated no significant differences between sex-specific estimates of L_∞ (χ^2 0.136, df 1, $P>0.70$), K (χ^2 4.0×10^{-5}, df 1, $P>0.90$), or t_0 (χ^2 0.138, df 1, $P>0.70$). Estimates of the growth equation parameters (asymptotic standard error) for pooled length and age data were $L_\infty = 2006$ mm TL (23.3), K = 0.126/year (0.0057), and $t_0 = -0.49$ years (0.200).

The relationships of whole and gutted weight (kg) to total length (mm) were

$$WW = 1.31 \times 10^{-8} TL^{3.056} \quad (N\ 66,\ r^2\ 0.964)$$
$$GW = 2.94 \times 10^{-8} TL^{2.941} \quad (N\ 402,\ r^2\ 0.941).$$

Gutted and whole weights were linearly related (N 50, r^2 0.995) as follows:

$$WW = -0.717 + 1.1039\,GW$$
$$GW = 1.001 + 0.9018\,WW.$$

Reproduction

Jewfish spawn during June–December in the eastern Gulf of Mexico, with peak activity during July–September (Fig. 3). Ripe males and females first appeared in our collections during June. Nearly all gonads collected from mature fish in July, August, and September were classified as ripe. Most spawning appears to end by October, although a ripe male was collected in November and another in December. Spent fish were collected in August (one male) and October (one female). No transitional fish were found.

Male jewfish become sexually mature at a slightly smaller size and younger age than females. Male jewfish were first mature when about 1100–1150 mm TL at 4–6 years of age. All males <1150 mm TL (N 6, 795–1100 mm) were immature, whereas all larger males in our samples (N 55, 1155–2057 mm) were mature. Both 3-year-old males sampled were immature, whereas one large (1184 mm TL) 4-year-old male was mature. Fifty percent of males 5 or 6 years old (3 of 6 individuals) and all males age 7 or older (N 31) were mature. Female jewfish first mature when about 1200–1350 mm TL at age 6 or 7. All females <1225 mm (N 21, 338–1218 mm) and <6 years old (N 17, 0–5 yr) were immature. All larger (N 90, 1350–2155 mm) and older (N 68, 8–37 yr) females sampled were mature.

Discussion

Age and growth

The spring–summer period of annulus formation in jewfish seems somewhat protracted. However, there appears to be a considerable range for the duration of annulus deposition in grouper populations: 2 or 3 months for *Epinephelus morio*, *E. nigritis*, *E. drummondhayi*, and *E. niveatus* (Moe 1969, Matheson and Huntsman 1984, Moore and Labisky 1984, Manooch and Mason 1987) to 5–7 months for *Mycteroperca phenax* and *M. microlepis* (Matheson et al. 1986, Hood and Schlieder 1992). Moe (1969) discussed factors affecting annulus formation and concluded that spawning and its associated physiological processes probably caused annulus formation in red grouper. However, annulus formation does not always occur in phase with spawning in epinephelines. For example, Matheson et al. (1986) found *M. phenax* to spawn during April–August in the South Atlantic Bight, but annulus formation occurred during December–April.

The annual deposition of opaque bands, seen in 3- and 4-year old OTC-marked jewfish, needs to be validated for fish older than 10 years. Due to the difficulty in sampling large numbers of these older fish year-round, it is probably not feasible to utilize indirect validation techniques (i.e., marginal increment analysis). Validation will probably require direct observations of individuals that have been injected with OTC and recaptured after annulus deposition.

The growth rate of jewfish (i.e., K 0.13/year) falls within or near the range observed for some of its congeners in the South Atlantic Bight and Gulf of Mexico: speckled hind, 0.13/year (Matheson and Huntsman 1984) and red grouper, 0.11–0.18/year (Moe 1969, Muhlia-Melo 1975). However, jewfish growth is somewhat faster than that of the deepwater snowy grouper *E. niveatus* (K 0.07–0.09/year; Matheson and Huntsman 1984, Moore and Labisky 1984) and considerably greater than that of the second-largest grouper in the western North Atlantic Ocean, the warsaw grouper *E. nigritis* (K 0.05/year; Manooch and Mason 1987), which may reach weights >200 kg.

Reproduction

We found jewfish to be in peak spawning condition during July–September in the eastern Gulf of Mexico. This agrees with Schroeder's (1924) finding that jewfish spawned during July–August, when heavily exploited aggregations of jewfish appeared off the Florida Keys. Furthermore, Colin (1990) observed what he interpreted as courtship behavior in jewfish off southwest Florida during the full moons of August and September.

When compared with that of females, the slightly smaller size and younger age of males at first maturity is unexpected, given that jewfish are assumed to be protogynous hermaphrodites (Smith 1971). Furthermore, whereas the youngest fish in our sample was female, as would be expected for a protogynous fish, so was the oldest. However, Sadovy and Shapiro (1987) point out several factors that may obscure differences in length, age, and maturity between males and females of a protogynous fish: (1) Some females may never change sex for lack of genetic or environmental cues and therefore may attain sizes (ages) equal to or greater than males, (2) a fraction of the population may initiate female development but change to males prior to sexual maturation, and (3) size at sex-reversal may differ among subpopulations of the same species and thus may obscure differences in length or age distribution between the sexes. Conclusive evidence for protogynous hermaphroditism in jewfish (i.e., the presence of transitional individuals) was not found in this study. Transitional individuals in confirmed protogynous hermaphrodites, such as *E. morio* (Moe 1969) and *M. microlepis* (Collins et al. 1987, Hood and Schlieder 1992), never represent a large percentage of the population; therefore, more extensive collections than ours may be needed to detect the presence of these individuals.

Fisheries implications

The life-history characteristics that we describe imply that jewfish are highly vulnerable to overfishing. Their slow growth, longevity, and presumed low natural mortality specify a population composed of cohorts that reach their maximum biomass at relatively old ages (Alverson and Carney 1975). Thus the greatest yield from a cohort of jewfish would be attained at either low rates of fishing or when only large fish are harvested. If jewfish are indeed protogynous hermaphrodites, fishing may also disrupt their spawning and recruitment by limiting the number of older males available for spawning (Smith 1982, Bannerot et al. 1987, Huntsman and Waters 1987). In addition, behavioral traits exhibited by large jewfish, such as their general unwariness of spearfishermen and apparent site-specific spawning aggregations (Shroeder 1924, Colin 1990), make them readily available for capture. Fisheries managers of Florida territorial and U.S. Exclusive Economic Zone waters have recognized the jewfish's susceptibility to overfishing and have recently banned all harvest of jewfish from waters under their jurisdictions.

Acknowledgments

We would like to thank the following fishermen for providing juvenile specimens: D. Bellamy, I. Bellamy, J. Rhodes, and R. Woodring. This study would not have been possible without the fine cooperation from the following: T. Nachman, G. Brown, G. Migliano, M. Nahon, W. Tappan, F. Devens, D. Harger, E. McManus, R. Ruiz-Carus, J. Swanson, W. Gibbs, W. Bell, and Capt. T. Reynolds. Special thanks go to Capt. D. DeMaria, who not only permitted us to thoroughly sample his catches but was also the major impetus for bringing about protection for the jewfish in Florida.

This manuscript benefited from review by R. Taylor, R. Crabtree, and P. Hood of the Florida Marine Research Institute, Department of Natural Resources. This study was partially supported by funds provided to the State of Florida under PL 99-659 of the Department of Commerce.

Citations

Alverson, D.L., and M.J. Carney
1975 A graphic review of the growth and decay of population cohorts. J. Cons. Cons. Int. Explor. Mer 36:133–143.

Bannerot, S., W.W. Fox Jr., and J.E. Powers
1987 Reproductive strategies and the management of snappers and groupers in the Gulf of Mexico and Caribbean. *In* Polovina, J.J., and S. Ralston (eds.), Tropical snappers and groupers: Biology and fisheries management, p. 561–603. Westview Press, Boulder.

Beebe, W., and J. Tee-Van
1928 The fishes of Port-au-Prince Bay, Haiti, with a summary of the known species of marine fish of the Island of Haiti and Santo Domingo. Zoologica (NY) 10:1–279.

Breder, C.M. Jr., and R.F. Nigrelli
1934 The penetration of a grouper's digestive tract by a sharp-tailed eel. Copeia 1934(4):162–164.

Bullock, L.H., and G.B. Smith
1991 Seabasses (Pisces: Serranidae). Mem. Hourglass Cruises VIII (II), 243 p.

Cerrato, R.M.
1990 Interpretable statistical tests for growth comparisons using parameters in the von Bertalanffy equation. Can. J. Fish. Aquat. Sci. 47:1416–1426.

Colin, P.L.
1990 Preliminary investigations of reproductive activity of the jewfish, *Epinephelus itajara*. *In* Abstr. Gulf Caribb. Fish. Inst., 43rd Annu. Sess., Miami, 4–9 Nov. 1990, p. 9, 10.

Collins, M.R., C.W. Waltz, W.A. Roumillat, and D.L. Stubbs
1987 Contribution to the life history and reproductive biology of gag, *Mycteroperca microlepis* (Serranidae), in the South Atlantic Bight. Fish. Bull., U.S. 85:648–653.

Florida Marine Fisheries Commission
1990 Jewfish: Designation as protected species; prohibition of harvest in state waters; possession, landing, and sale prohibited. Florida Administrative Code 46-14.008, Tallahassee.

Hood, P.B., and R.C. Schlieder
1992 Age, growth and reproduction of gag, *Mycteroperca microlepis*, in the eastern Gulf of Mexico. Bull. Mar. Sci. 51(3).

Hood, P.B., M.F. Godcharles, and R. Barco
Unpubl. Age, growth, reproduction, and the feeding ecology of black sea bass, *Centropristis striata* (Pisces: Serranidae). Fla. Mar. Res. Inst., Fla. Dep. Nat. Resour., St. Petersburg, 38 p.

Huntsman, G.R., and J.R. Waters
1987 Development of management plans for reef fishes—Gulf of Mexico and U.S. South Atlantic. *In* Polovina, J.J., and S. Ralston (eds.), Tropical snappers and groupers: Biology and fisheries management, p. 533–560. Westview Press, Boulder.

Kimura, D.K.
1980 Likelihood methods for the von Bertalanffy growth curve. Fish. Bull., U.S. 77:765–776.

Manooch, C.S. III, and D.L. Mason
1987 Age and growth of the warsaw grouper and black grouper from the southeast region of the United States. Northeast Gulf Sci. 9:65–75.

Manter, H.W.
1947 The digenetic trematodes of marine fishes of Tortugas, Florida. Am. Midl. Nat. 38:257–416.

Matheson, R.H. III, and G.R. Huntsman
1984 Growth, mortality, and yield-per-recruit models for speckled hind and snowy grouper from the United States South Atlantic Bight. Trans. Am. Fish. Soc. 113:607–616.

Matheson, R.H. III, G.R. Huntsman, and C.S. Manooch III
1986 Age, growth, mortality, food, and reproduction of the scamp, *Mycteroperca phenax*, collected off North Carolina and South Carolina. Bull. Mar. Sci. 38:300–312.

Moe, M.A. Jr.
1969 Biology of the red grouper *Epinephelus morio* (Valenciennes) from the eastern Gulf of Mexico. Fla. Dep. Nat. Resour. Mar. Res. Lab. Prof. Pap. Ser. 10, 95 p.

Moore, C.M., and R.F. Labisky
1984 Population parameters of a relatively unexploited stock of snowy grouper in the lower Florida Keys. Trans. Am. Fish. Soc. 113:322–329.

Muhlia-Melo, A.
1975 Aspectos biológicos pesqueros de *Epinephelus morio* (Val.). M.S. thesis, Univ. Nac. Autónoma México, Mexico City, D.F., 68 p.

NMFS (National Marine Fisheries Service)
1990a Fishery management plan for the reef fish of the Gulf of Mexico, Amendment 2. Gulf of Mexico Fish. Manage. Counc., Tampa, 20 p.
1990b Fishery management plan for the snapper-grouper fishery of the South Atlantic Region, Amendment 2. South Atl. Fish. Manage. Counc., Charleston, 28 p.

Odum, W.E.
1971 Pathways of energy flow in a south Florida estuary. Univ. Miami Sea Grant Prog. Sea Grant Tech. Bull. 7, 162 p.

Odum, W.E., C.C. McIvor, and T.J. Smith III
1982 The ecology of the mangroves of south Florida: A community profile. U.S. Fish Wildl. Serv. Biol. Serv. FWS-OBS-81/24, 144 p.

Olsen, L.S.
1952 Some nematodes parasitic in marine fishes. Publ. Inst. Mar. Sci. Univ. Tex. 2:173–215.

Pearse, A.S.
1931 Observations on the parasites and commensals found associated with crustaceans and fishes at Dry Tortugas, Florida. Carnegie Inst. Washington Publ. Pap. Tortugas Lab. 28(435):104–115.

1952 Parasitic crustacea from the Texas coast. Publ. Inst. Mar. Sci. Univ. Tex. 2(2):5–42.

Randall, J.E.

1967 Food habits of reef fishes of the West Indies. Stud. Trop. Oceanogr. Inst. Mar. Sci. Univ. Miami 5:665–847.

Robins, C.R., G.C. Ray, J. Douglass, and R. Freund

1986 A field guide to Atlantic coast fishes of North America. Peterson Field Guide Ser. 32, Houghton Mifflin, Boston, 354 p.

Sadovy, Y., and D.Y. Shapiro

1987 Criteria for the diagnosis of hermaphroditism in fishes. Copeia 1987:136–156.

Saila, S.B., C.W. Recksiek, and M.H. Prager

1988 Basic fishery science programs, a compendium of microcomputer programs and manual of operation. Elsevier Sci. Publ., NY, 230 p.

Schroeder, W.C.

1924 Fisheries of Key West and the clam industry of southern Florida. Appendix XII to the Report of the U.S. Commissioner of Fisheries for 1923. Bur. Fish. Doc. 962, 74 p.

Smith, C.L.

1971 A revision of the American groupers: *Epinephelus* and allied genera. Bull. Am. Mus. Nat. Hist. 146:67–242.

1982 Patterns of reproduction in coral reef fishes. *In* Huntsman, G.R., W.R. Nicholson, and W.W. Fox Jr. (eds.), The biological bases for reef fishery management, p. 49–66. NOAA Tech. Memo. NOAA-TM-NMFS-SEFC-80, Beaufort Lab., Southeast Fish. Sci. Cent., Beaufort, NC.

Smith, G.B.

1976 Ecology and distribution of eastern Gulf of Mexico reef fishes. Fla. Mar. Res. Publ. 19, 78 p.

Tabb, D.C., and R.B. Manning

1961 A checklist of the flora and fauna of northern Florida Bay and adjacent brackish waters of the Florida mainland collected during the period July 1957 through September 1960. Bull. Mar. Sci. Gulf Caribb. 11:552–649.

von Bertalanffy, L.

1957 Quantitative laws in metabolism and growth. Q. Rev. Biol. 32:217–231.

Abstract.– Allozymes were used to examine spatial and temporal components of genetic variation among populations of queen conch in the Florida Keys and Bimini over a 4-year period. Spatial and temporal genetic variation were both significant ($P<0.001$) despite high levels of genetic similarity among samples (mean Nei's I, 0.994). However, no consistent pattern of variation was observed. The gene diversity among localities (G_{LT} 0.50%) did not differ significantly ($P>0.05$) from the diversity among years or samples within localities (G_{SL} 0.60%). In addition, Florida Keys and Bimini populations were very similar genetically to those studied previously in the Caribbean Sea and Bermuda (mean Nei's I, 0.988). In general, populations of queen conch appear to be structured as a mosaic of spatial and temporal genetic patchiness within a continuum of high genetic similarity. This genetic similarity is presumably maintained by larval drift and gene flow. However, the observed patterns of genetic variation suggest a dynamic population structure. This structure may reflect presettlement stochastic events and processes in the marine environment.

Genetic patchiness among populations of queen conch *Strombus gigas* in the Florida Keys and Bimini*

Donald E. Campton
Department of Fisheries and Aquaculture, University of Florida
7922 NW 71st Street, Gainesville, Florida 32606-0300

Carl J. Berg Jr.
Florida Marine Research Institute, Florida Department of Natural Resources
13365 Overseas Highway, Marathon, Florida 33050
Current address: P.O. Box 769, Kilauea, Hawaii 90754

Lynn M. Robison
Department of Fisheries and Aquaculture, University of Florida
7922 NW 71st Street, Gainesville, Florida 32606-0300
Current address: Department of Fisheries and Allied Aquacultures
Auburn University, Auburn, Alabama 36849

Robert A. Glazer
Florida Marine Research Institute, Florida Department of Natural Resources
13365 Overseas Highway, Marathon, Florida 33050

The queen conch *Strombus gigas* is a large marine gastropod of significant economic importance to the Caribbean Sea area (reviewed by Berg and Olsen 1989). The native range of the species extends from south Florida to Venezuela and eastward from Central America to the Bahama and West Indies Islands. An isolated population also inhabits the coastal waters of Bermuda. The species has been heavily exploited in commercial, recreational, and subsistance fisheries throughout its geographic range. Many populations are considered depleted or overfished.

The life history of queen conch suggests the potential for extensive gene flow through larval dispersal (Scheltema 1971, 1986). Laboratory studies indicate that larvae maintain the planktonic stage for 12–35 days ($\bar{x}$ 21 days) before settling and metamorphosis (Ballantine and Appledoorn 1983, Davis and Hesse 1983). Larvae entrained in swift, Caribbean currents (1–3 km/h) could thus be transported significant distances (Kinder et al. 1985). However, dispersal and recruitment patterns of *S. gigas* during the planktonic stage are largely unknown. Effective management and rehabilitation of the species throughout its geographic range necessitate an understanding of population structure, patterns of gene flow, and genetic relationships.

In a recent allozyme study, Mitton et al. (1989) found a high level of genetic similarity among populations of queen conch from eight localities throughout the Caribbean Sea. However, significant spatial heterogeneity in allele frequencies indicated that the sampled populations were not totally panmictic. In addition, allele frequencies for the geographically disjunct population of Bermuda were distinctive at one locus.

Manuscript accepted 4 March 1992.
Fishery Bulletin, U.S. 90:250–259 (1992).

* Journal Series R-01534, Florida Agricultural Experiment Station.

In the study described here, allozymes were used to examine the genetic structure of queen conch populations in the Florida Keys and Bimini. We collected conch from the same localities in multiple years to compare spatial and temporal components of genetic variation. Testing the relative significance of those two components was a major objective of our study.

Materials and methods

Sampled populations

Queen conch were collected between 1987 and 1990 from four localities in the Florida Keys and from Bimini, a linear distance of approximately 350 km (Table 1, Fig. 1). Samples of conch were obtained in multiple years from Ballast Key, Coffins Patch, and Craig Key. Single samples were obtained from Key Biscayne and Bimini. All animals were collected by scuba diving or snorkeling.

The shell length, or major axis, of each conch was measured with calipers to the nearest mm. Based on size distributions, the Coffins Patch population (or aggregation) appeared to be a single year-class or cohort that we sampled in three consecutive years (Table 1). All other populations represented mixtures of year-classes with new recruits added each year.

Tissues

Conch collected in 1987 (three samples) were processed according to the methods of Mitton et al. (1989): Only the distal tip of the digestive gland, including gonad and associated connective tissue, was retained for enzyme extraction. We were not able to resolve some of the enzymes or presumptive loci reported by Mitton et al. (1989) but were able to resolve some enzymes and loci not examined previously. Consequently, from each of 12 conch collected from Ballast Key in February, 1988 (Table 1), we dissected six tissues for further screening of enzymes and loci: (1) foot muscle, (2) proboscis with radula, (3) eyes and eyestalks, (4) crystalline style, (5) mantle tissue, and (6) distal tip of the digestive gland (Little 1965). Thirty-eight enzymes

Table 1

Means ± standard errors (SE) and ranges of shell length for samples of queen conch *Strombus gigas* collected from four localities in the Florida Keys and Bimini, 1987–90.

			Length (mm)	
Locality	Year	*N*	Mean ± SE	Range
Ballast Key	1987	56	167 ± 6.2	96–241
	1988[a]	12	125 ± 5.6	91–157
	1988[b]	30	135 ± 4.2	69–167
Coffins Patch	1988	100	58 ± 0.4	46–71
	1989	102	98 ± 0.6	87–112
	1990	100	142 ± 0.9	117–170
Craig Key	1987	105	177 ± 2.5	127–267
	1989	71	225 ± 3.5	137–257
	1990	92	187 ± 3.5	125–252
Key Biscayne	1987	79	155 ± 3.5	99–216
Bimini	1989	96	194 ± 2.0	127–236

[a] February collection.
[b] April collection.

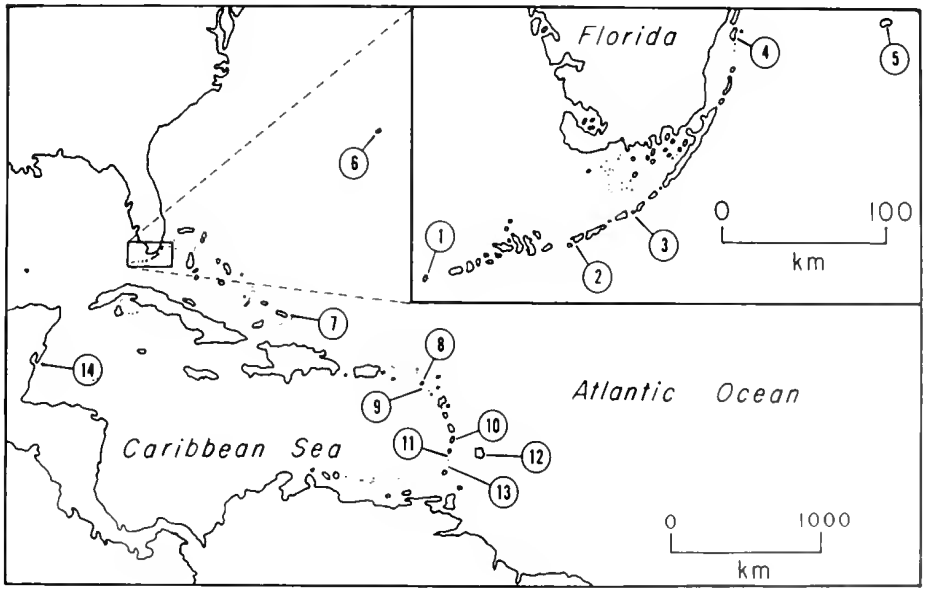

Figure 1

Localities from which queen conch *Strombus gigas* were collected. For the study described here, conch were collected from (1) Ballast Key, (2) Coffins Patch, (3) Craig Key, (4) Key Biscayne, and (5) Bimini. Localities 6–14 are from Mitton et al. (1989): (6) Bermuda, 1 site; (7) Turks and Caicos Islands, 4 sites; (8) St. Kitts, 2 sites; (9) Nevis, 1 site; (10) St. Lucia, 2 sites; (11) Bequia, 1 site; (12) Barbados, 1 site; (13) Grenadines, 3 sites; and (14) Belize, 2 samples, 1 each of the normal and melanic forms.

were assayed in each tissue using a variety of electrophoresis buffers.

On the basis of the aforementioned analyses, three tissues were retained from all conch collected subsequently in 1988–90: (1) foot muscle, (2) proboscis with radula, and (3) digestive gland with gonad. The three tissues were dissected from each individual, placed in separate cryotubes or plastic bags, and frozen in the field with liquid nitrogen or dry ice. All tissues were stored at −80°C until prepared for enzyme extraction.

Table 2

Enzymes and loci resolved in queen conch *Strombus gigas*. Tissues are digestive gland (D), foot muscle (F), and proboscis (P).

Enzyme	Enzyme number	Locus	Tissue	Optimum buffer[a]
Aspartate aminotransferase	2.6.1.1	*AAT-1**	D,P	TC
		*AAT-2**	F,P	TC
Argenine kinase	2.7.3.3	*ARGK**	F	TC
Dipeptidase[b] (substrates: Leu-Ala, Leu-Tyr)	3.4.13.11	[b]*DPEP-1**	D,F,P	TLBC-2,TC
		*DPEP-2**	D,F,P	TLBC-1
		*DPEP-3**	D,F,P	TLBC-1
Glucose-6-phosphate dehydrogenase	1.1.1.49	*G6PDH**	D	TLBC-2
Glucose-6-phosphate isomerase	5.3.1.9	*GPI**	D,F,P	TC
Isocitrate dehydrogenase ($NADP^+$)	1.1.1.42	*IDHP-1**	D,F,P	AC
		*IDHP-2**	D,F,P	AC
Malate dehydrogenase[b]	1.1.1.37	*MDH-1**	F,P	AC
		[b]*MDH-2**	D,P	AC
Octopine dehydrogenase	1.5.1.11	*ODH**	F,P	TLBC-1
Phosphoglucomutase[b]	5.4.2.2	[b]*PGM-1**	D,F,P	TC
		[b]*PGM-2**	D,F,P	TC
		*PGM-3**	F	TC
Phosphogluconate dehydrogenase[b]	1.1.1.44	[b]*PGDH**	F,P	AC
Tripeptide aminopeptidase (substrate: Leu-Gly-Gly)	3.4.11.4	*TPEP-1**	D,F,P	TLBC-1
		*TPEP-2**	D,F,P	TLBC-1

[a] AC: 0.04 M citric acid adjusted to pH 7.5 with N-(3-aminopropyl) morpholine (Clayton and Tretiak 1972); TBE: Tris-borate-EDTA, pH 8.6 (Boyer et al. 1963); TC: TC buffer of Siciliano and Shaw 1976; TLBC-1: LiOH buffer of Ridgway et al. (1970); TLBC-2: LiOH buffer of Selander et al. (1971).
[b] Enzymes and loci assayed also by Mitton et al. (1989).

Electrophoresis

Allozymes were detected by horizontal starch-gel electrophoresis following the procedures of Aebersold et al. (1987). Enzymes were extracted by homogenizing each tissue separately in 0.5–1.0 volumes of 0.05M PIPES, 0.05% Triton X-100, and 0.2mM pyridoxal-5′-phosphate (adjusted to pH 6.8 with 1.0M NaOH). Gels were prepared with a 12.5% mixture (wt:vol) of Connaught starch (Fisher Sci. Co.) and one of five buffer solutions (Table 2). Histochemical staining of gels followed standard procedures (Morizot and Schmidt 1990). Gels were stained by agar overlay for all enzymes except AAT.

Presumptive loci and alleles were designated by the nomenclature system outlined by Shaklee et al. (1990), except peptidase loci were identified by their di- or tripeptide acronyms (DPEP, TPEP). Multiple loci of a particular enzyme were designated numerically (1, 2, etc.) from fastest to slowest anodic mobility. Alleles of a particular locus were designated by their relative, anodic mobilities (most frequent allele = **100*).

Statistics

Genotypic proportions at each locus were tested for goodness-of-fit to Hardy-Weinberg expectations using the likelihood-ratio test or G-statistic (Sokal and Rohlf 1981). Allele frequencies at each locus were tested for homogeneity among samples by contingency table (samples × alleles) G-tests (Sokal and Rohlf 1981). This total G-statistic, or likelihood ratio, was then partitioned into hierarchical components representing temporal and spatial components of genetic variation within and among localities, respectively (e.g., Smouse and Ward 1978). An approximate F-ratio was then constructed as (G among localities/df)/(G among years within localities/df) to test whether the genetic heterogeneity among localities was significantly greater than the heterogeneity among years within localities. The total gene diversity (Nei 1973) was similarly partitioned into within- and among-locality components following the algorithm of Chakraborty et al. (1982). In all tests of statistical significance, significance probabilities were adjusted for the number of tests (loci) evaluated simultaneously (Rice 1989).

Nei's (1972) index of gene identity was calculated between all population samples. The genetic similarities among all populations, including those sampled by Mitton et al. (1989), were represented graphically in a UPGMA dendrogram (Sneath and Sokal 1973). The 1987 sample from Ballast Key was excluded from these latter analyses because of small sample size (n 12).

Table 3

Allele frequencies for samples of queen conch *Strombus gigas* from the Florida Keys (4 sites) and Bimini. "ND" indicates no data for that locus.

		Ballast Key			Coffins Patch			Craig Key			Key Biscayne	Bimini
Locus	Alleles	1987	1988[a]	1988[b]	1988	1989	1990	1987	1989	1990	1987	1990
*AAT-1**	*100*	0.713	1.00	0.62	0.723	0.755	0.696	0.663	0.671	0.678	0.648	0.591
	120	0.287	—	0.38	0.277	0.245	0.304	0.338	0.329	0.322	0.352	0.403
	130	—	—	—	—	—	—	—	—	—	—	0.005
*AAT-2**	*100*	ND	1.00	1.00	0.975	0.980	0.955	ND	0.993	0.973	ND	0.973
	150		—	—	0.025	0.020	0.045		0.007	0.022		0.016
	31		—	—	—	—	—		—	—		0.011
	180		—	—	—	—	—		—	0.005		—
*DPEP-1**	*100*	0.472	0.42	0.57	0.536	0.536	0.460	0.567	0.521	0.522	0.513	0.565
	108	0.528	0.58	0.43	0.464	0.464	0.540	0.433	0.479	0.478	0.487	0.435
*GPI**	*100*	0.929	1.00	0.98	1.000	0.990	1.000	0.985	1.000	0.995	0.994	0.995
	117	0.071	—	0.02	—	—	—	0.015	—	0.005	0.006	0.005
	78	—	—	—	—	0.010	—	—	—	—	—	—
*IDH-2**	*100*	ND	1.00	1.00	1.000	0.975	0.976	1.000	0.979	0.956	1.000	0.978
	82		—	—	—	0.025	0.024	—	0.021	0.044	—	0.022
*MDH-1**	*100*	ND	1.00	1.00	1.000	0.951	0.960	ND	0.944	0.944	ND	0.982
	120		—	—	—	0.049	0.040		0.056	0.056		0.018
*MDH-2**	*100*	0.794	1.00	1.00	1.000	1.000	1.000	0.955	1.000	1.000	1.000	1.000
	138	0.206	—	—	—	—	—	0.005	—	—	—	—
*ODH**	*100*	ND	1.00	1.00	0.990	0.990	1.000	ND	0.993	0.995	ND	0.995
	68		—	—	0.005	0.010	—		0.007	0.005		0.005
	134		—	—	0.005	—	—		—	—		—
*PGM-1**	*100*	0.723	0.83	0.62	0.665	0.706	0.645	0.737	0.697	0.658	0.709	0.660
	111	0.250	0.17	0.38	0.335	0.279	0.350	0.263	0.275	0.342	0.291	0.340
	89	0.027	—	—	—	0.015	0.005	—	0.028	—	—	—
*PGDH**	*100*	ND	0.59	0.63	0.686	0.721	0.695	ND	0.641	0.696	ND	0.681
	150		0.41	0.37	0.314	0.279	0.305		0.359	0.293		0.319
	200		—	—	—	—	—		—	0.011		—

[a] Data for these conch (February collection) were excluded from the statistical analyses because of small sample size.
[b] April collection.

Results

Nineteen presumptive loci encoding 11 enzymes were resolved electrophoretically (Table 2). Ten loci were polymorphic and were used exclusively in the population analyses (Table 3).

Florida Keys and Bimini populations

Allele frequencies for samples of queen conch from the Florida Keys and Bimini were very similar (Table 3). The gene identity between samples, averaged over the ten polymorphic loci, ranged from 0.978 to 0.999 and averaged 0.994 for all pairwise comparisons. Most alleles were present in all samples, but some rare ($P<0.01$) alleles were detected as only one or two heterozygotes (e.g., *AAT-1*130*). An exception to this latter generalization was the presence of the *MDH-2*138* allele at a frequency of 0.206 (35 **100/100*, 11 **100/138*, and 5 **138/138*) among 51 scored individuals collected from Ballast Key in 1987. Only one heterozygote for this allele was observed elsewhere during the study.

Genotypes conformed ($P>0.05$) to Hardy-Weinberg proportions at all loci except *DPEP-1**. At this latter locus, significant ($P<0.01$) deficits of heterozygotes were detected in 7 of 10 samples. Overall, 285, 279, and 244 individuals had the **100/100*, **100/108*, and **108/108* genotypes, respectively, at *DPEP-1**. This overall deficit of heterozygotes occurred despite similar ($P>0.05$) allele frequencies among samples (Table 3).

Spatial and temporal variation in allele frequencies accounted for minor but approximately equal amounts of gene diversity. The total gene diversity (H_T) averaged 0.202 for the ten polymorphic loci. Of this total, 0.60% and 0.50% were due to temporal and spatial variation within and among localities, respectively

Table 4

Hierarchical likelihood-ratio tests (G-statistics) for homogeneity of allele frequencies among samples of queen conch *Strombus gigas* from the Florida Keys and Bimini. Degrees of freedom are in parentheses.

Source of variation	*AAT-1**	*AAT-2**	*DPEP-1**	*GPI**	*IDH-2**	*MDH-1**
Total	19.68(18)	20.03(18)	7.84(9)	43.22(18)**	21.09(8)*	24.51(6)**
Among localities	16.26(8)	15.21(9)	2.42(4)	32.66(8)*	9.48(4)	9.57(3)
Within localities	3.42(5)	4.82(4)	5.42(5)	10.57(5)	11.61(4)	14.95(3)*
Ballast Key	1.62(1)	—	1.38(1)	2.81(1)	—	—
Coffins Patch	1.71(2)	2.37(2)	3.04(2)	4.36(2)	4.41(2)	14.94(2)**
Craig Key	0.09(2)	2.45(2)	1.00(2)	3.40(2)	7.20(2)	0.01(1)
(Approx. F-ratio[a])	2.97(8,5)	1.40(9,4)	0.56(4,5)	1.93(8,5)	0.82(4,4)	0.64(3,3)

Source of variation	*MDH-2**	*ODH**	*PGM-1**	*PGDH**	Total
Total	116.83(9)***	7.03(12)	34.13(18)	10.97(12)	305.33(128)***
Among localities	95.42(4)***	2.02(6)	8.79(8)	6.65(6)	198.48(60)***
Within localities	21.41(3)***	5.00(5)	25.34(10)*	4.32(4)	106.86(48)***
Ballast Key	19.54(1)***	—	5.49(2)	—	30.84(6)***
Coffins Patch	—	4.97(4)	6.58(4)	0.61(2)	42.99(22)**
Craig Key	1.87(2)	0.03(1)	13.27(4)	3.71(2)	33.03(20)*
(Approx. F-ratio[a])	3.34(4,3)	0.37(6,5)	0.43(8,10)	1.03(6,4)	1.49(60,48)

[a] Approximate F-ratio = (G among localities/df)/(G within localities/df).
*$P<0.05$; **$P<0.01$; ***$P<0.001$; after adjustment for number of tests (Rice 1989).

(G_{SL} 0.0060, G_{LT} 0.0050). The remaining 98.9% (H_S/H_T) was due to within-sample heterozygosity.

Allele-frequency heterogeneity among samples was significant ($P<0.05$) at several loci and was due to both spatial and temporal components of variation (Table 4). Temporal variation at Ballast Key ($P<0.001$) and Coffins Patch ($P<0.01$) was due primarily to variation at *MDH-2** and *MDH-1**, respectively. On the other hand, the heterogeneity among years at Craig Key ($P<0.05$) was due primarily to the cumulative effects of variation at *IDH-2** and *PGM-1**. Significant allele-frequency variation also existed among localities, but this latter variation did not exceed the temporal variation within localities as measured by F-ratio comparisons ($P>0.05$) at each locus.

Comparisons with Caribbean Sea and Bermuda populations

Allele frequencies at *DPEP-1**, *MDH-2**, *PGM-1**, and *PGDH** for the Florida Keys and Bimini populations of *S. gigas* can be compared directly with those for populations sampled by Mitton et al. (1989). In that previous study, queen conch were collected from 16 sampling sites representing eight major localities throughout the Caribbean Sea area (Fig. 1). In addition, conch were collected from one site in Bermuda.

Patterns of genetic variation among populations in the Caribbean Sea and Bermuda were similar to those for populations in the Florida Keys and Bimini (Table 5). Total gene diversities (H_T) for the two groups of populations were essentially equal (0.355 and 0.354, respectively). However, the diversity within and among localities was somewhat greater for Caribbean Sea and Bermuda populations (G_{LT} 1.69%, G_{SL} 1.14%) than for populations from the Florida Keys and Bimini (G_{LT} 0.39%, G_{SL} 0.68%). This latter result might be expected considering the relative geographic scales over which populations were sampled in the two studies (Fig. 1). In this context, summing G_{LT} and G_{SL} for Florida Keys and Bimini populations yields a percentage of gene diversity (1.07%) that is approximately equal to G_{SL} (sites within localities) for the Caribbean Sea and Bermuda populations (1.14%).

A dendrogram based on Nei's index of gene identity clearly reflected the high genetic similarity among populations of *S. gigas* (Fig. 2). The average gene identity (based on the four aforementioned loci) among populations sampled by Mitton et al. (1989) was 0.984, among those sampled here was 0.993, and between populations (samples) of the two studies was 0.988. Twenty-three of these populations clustered together at the 0.99 level or above. The Bermuda population and the 1987 Ballast Key population (sample) formed a separate subcluster, due primarily to divergent allele frequencies at *MDH-2**. The Vieux Fort (St. Lucia) and Six Hill Cay (Turks and Caicos Islands) populations also clustered separately, due primarily to slightly divergent

Table 5

Percentages of total gene diversity (H_T) among localities (G_{LT}), among samples and sites within localities (G_{SL}), and within samples and sites (H_S/H_T) for populations of queen conch *Strombus gigas* from the Florida Keys and Bimini (this study) and from the Caribbean Sea and Bermuda (Mitton et al. 1989). Data represent the means for *DPEP-1**, *MDH-2**, *PGM-1**, *PGDH**.

		Gene diversity (%)		
Populations	H_T	G_{LT}	G_{SL}	H_S/H_T
Florida Keys and Bimini	0.354	0.39	0.68	98.94
Caribbean Sea and Bermuda	0.355	1.69	1.14	97.17
All populations	0.354	1.24	1.01	97.75

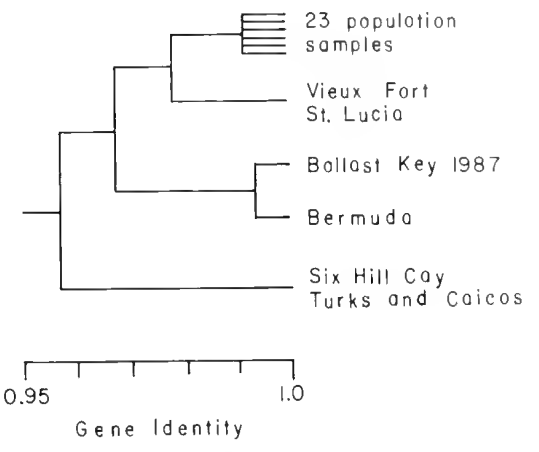

Figure 2

UPGMA dendrogram of genetic similarities among population samples of queen conch *Strombus gigas* based on allele frequencies at *DPEP-1**, *MDH-2**, *PGDH**, and *PGM-1**, and Nei's (1972) index of genetic identity.

allele frequencies at *PGDH** and *DPEP-1**, respectively (Mitton et al. 1989).

In summary, populations of *S. gigas* are very similar genetically and do not appear to be structured geographically. However, those populations cannot be considered totally panmictic.

Discussion

Population structure

Benthic marine invertebrates with planktonic larvae often exhibit spatial and temporal genetic variation similar to that described here for *S. gigas*. For example, Watts et al. (1990) found significant allele-frequency variation among three populations of sea urchin *Echinometra mathaei* separated by only 4km. Moreover, that heterogeneity over a 4km distance was approximately equal to the genetic heterogeneity among populations separated by over 1300km. Those investigators also detected significant allele-frequency variation among year-classes within each of the three microspatial sample sites. Similar patterns of heterogeneity were reported for the limpet *Siphonaria jeanae* (Johnson and Black 1982, 1984ab) and seastar *Acanthaster planei* (Nash et al. 1988, Nishida and Lucas 1988).

Significant microspatial genetic heterogeneity, despite high macrospatial genetic similarity, has been termed "genetic patchiness" (e.g., Johnson and Black 1984b). Such genetic patchiness could be due to either postsettlement natural selection or genetic heterogeneity among groups of recruits that are spatially or temporally separated (Watts et al. 1990). Under both hypotheses, planktonic dispersal is believed to maintain high genetic similarity among populations over broad geographic areas. However, under postsettlement natural selection, one would expect genetic variation among localities to be greater than the temporal variation within localities because of local adaptation. Conversely, under the model of presettlement genetic heterogeneity, spatial and temporal components of genetic variation are expected to be equal because the population structure would result from presettlement events that were independent of the specific localities at which settlement occurred. Under this latter model, spatial heterogeneity among localities would simply reflect the temporal heterogeneity within localities.

Results obtained here for *S. gigas* are most consistent with the presettlement hypothesis of genetic patchiness. Populations of queen conch throughout their geographic range are very similar genetically, yet spatial and temporal components of genetic variation appear significant and approximately equal. Mitton et al. (1989) obtained similar results for macrospatial (among-locality) and microspatial (within-locality) components of genetic variation. These results suggest a dynamic population structure in which allele-frequency heterogeneity may exist among groups of recruits that settle in different years at the same locality or at different localities in the same year. Johnson and Black (1982, 1984ab) and Watts et al. (1990) reached similar conclusions regarding genetic patchiness among populations of limpet and sea urchin, respectively.

Several mechanisms can be invoked to explain genetic patchiness due to presettlement events. Johnson and Black (1984ab) and Watts et al. (1990) suggest that

selective mortality prior to settlement, possibly reflecting stochastic variation in the marine environment (e.g., water temperature, salinity), may be responsible for the "chaotic genetic patchiness" that they observed. Alternatively, temporal variation in the source of recruits for each locality and/or genetic drift resulting from a finite number of breeders could also generate random genetic patchiness on both temporal and spatial scales (e.g., Waples 1989). None of these aforementioned hypotheses can be excluded with the available data.

The effective number of breeders (N_e) contributing to a cohort of larvae that settle together at a particular location is unknown for *S. gigas*. Males and females breed in aggregations at characteristic locations over a 6–9 month period, and each female may produce several egg masses of approximately 310,000–750,000 eggs each during the breeding season (Robertson 1959, Randall 1964, Weil and Laughlin 1984, Berg and Olson 1989). Several females within an aggregation may lay their egg masses simultaneously, and because the rate of embryonic development is temperature-related, hordes of larvae are released synchronously. These larvae can thus be entrained together into the water column and affected simultaneously by marine and oceanic processes. Consequently, hordes of larvae from a finite number of parents could potentially be presented simultaneously to a substrate that would induce settlement and metamorphosis.

Recently, Bucklin et al. (1989) and Bucklin (1991) obtained evidence that ocean currents and related processes (e.g., upwellings, eddies, offshore jets) can spatially and temporally maintain genetically discrete cohorts of zooplankton in the marine environment. For example, Bucklin et al. (1989) concluded that such processes "prevented homogenization of the plankton assemblages during transport" and that "plankton populations in complex flow fields may show patchiness in biological, biochemical, and/or genetic character at small time/space scales." Their results suggest that similar processes could affect significantly the distribution of pelagic larvae following their release into the water column.

The source of *S. gigas* recruits for the Florida Keys is unknown. The Florida Current, which sweeps eastward past the Florida Keys and subsequently forms the Gulf Stream, is created by the massive flow of warm water northward from the Caribbean Sea through the Yucatan Channel. This current could entrain large numbers of larvae from numerous locations prior to flowing eastward past the Florida Keys (Mitton et al. 1989). Stochastic variations in water currents, surface winds, and meteorological events (e.g., tropical storms) could thus affect significantly the source of *S. gigas* recruits for any particular locality. During the course of our study, we attempted to gain permission to collect conch from Cuba and Yucatan, Mexico—two possible sources of recruits for the Florida Keys—but were unable to do so.

One potential shortcoming of our study was that the temporal effects of recruitment were confounded with other population processes; that is, temporal genetic variation was measured among mixed aggregations of conch sampled in different years at the same locality and not among separate year-classes or cohorts. With the exception of the Coffins Patch population or aggregation (see below), all samples consisted of mixed age- and size-classes with new recruits added each year. In addition, some of the temporal genetic variation may have been due to migration of juveniles and adults into and out of the study areas (Hesse 1979, Weil and Laughlin 1984, Stoner et al. 1988, Stoner 1989). Consequently, we cannot separate the temporal effects of recruitment from other population processes. However, our goal was not to estimate temporal genetic variation among cohorts or year-classes *per se*, but rather to provide a measure of within-population (i.e., within-locality) variation by which the significance of genetic variation among localities could be evaluated. Population processes causing temporal genetic variation within localities would similarly affect the genetic variation among localities. Some measure of temporal variation was thus needed before the microevolutionary significance of genetic variation among localities could be ascertained. Alternatively, some form of stratified sampling of year- and/or size-classes would be required to separate recruitment or year-class effects from other potential sources of temporal genetic variation.

Possible evidence that recruitment, migration, or similar population processes may significantly affect the population structure of *S. gigas* was the presence of the *MDH-2*(138)* allele at a frequency of 0.206 in the 1987 sample from Ballast Key but the near absence of this allele in the 1988 sample and elsewhere during our study. Mitton et al. (1989) similarly reported, for the Bermuda population, a frequency of 0.30 for a "fast" *MDH-2** allele that was also rare elsewhere. However, the Bermuda population is believed to be self-sustaining with little planktonic recruitment from the Gulf Stream or elsewhere (Mitton et al. 1989). Conversely, Ballast Key is situated within the Florida Current and is the most upstream locality from which we collected conch for the present study. Two distinct aggregations of *S. gigas* may have been sampled at Ballast Key in 1987 and 1988, respectively.

Anomalous results

Coffins Patch Size distributions suggest that the Coffins Patch population was most likely a single year-class

or cohort that we sampled in three consecutive years (1988–90). This population or cohort presumably resulted from a large recruitment event during the summer and fall of 1987. We estimated that the 1987 aggregation at Coffins Patch consisted of at least 250,000 animals covering an area of approximately 30 hectares (Berg and Glazer, unpubl.).

Although the Coffins Patch aggregation appeared to be a single cohort, we detected a significant allele-frequency variation among years (1988–90) at *MDH-1**. This difference was due to the absence of the *MDH-1* (120)* allele in the 1988 sample (n 100) versus the presence of eight **100/120* heterozygotes in both the 1989 (n 102) and 1990 (n 100) samples. The 1989 sample also had one **120/120* homozygote. Sampling error does not adequately explain those results because the probability of obtaining all **100/100* homozygotes in the 1988 sample was only $(0.955^2)^{100} = 0.0001$ (assuming the true frequency of the **120* allele was 0.045 [mean of 1989 and 1990 samples] and random mating). Similarly, differential mortality among genotypes does not adequately explain those results unless heterozygotes were initially very rare and the subsequent mortality of **100/100* homozygotes was extremely high.

Alternatively, recruitment to the Coffins Patch area in 1987 may have been from more than one source population. This could have resulted in an aggregation that was not distributed randomly. Subsequent mixing and/or possible immigration of juveniles (e.g., Stoner 1989) could thus explain changes in allele frequencies between 1988 and 1989. None of these hypotheses can be excluded with the available data.

Regardless of actual mechanism, the presence of only one highly abundant year-class at Coffins Patch over a 3-year period indicates that recruitment to specific localities in the Florida Keys can be highly variable and unpredictable. This observation thus supports the interpretation that genetic patchiness may simply reflect stochastic events prior to settlement.

DPEP-1* We observed a consistent deficit of heterozygotes (with respect to Hardy-Weinberg expectations) at *DPEP-1** but not at other loci. Similar deficits of heterozygotes have been reported often for marine mollusks (reviewed by Gaffney et al. 1990). Such deficits are frequently associated with positive correlations between body size and individual heterozygosity. We also observed a positive correlation between body size and heterozygosity, but genotypic variation at *DPEP-1** did not contribute to that correlation. These results will be described in detail elsewhere (Campton et al. In press).

PGM-2* One possible point of inconsistency between the study described here and that of Mitton et al. (1989) concerns data for *PGM-2**. Mitton et al. (1989) presented only limited data for this latter locus (9 of 17 populations), but those investigators consistently observed a high frequency (0.57–0.69) polymorphism for a "slow" allele. In contrast, we found *PGM-2** to be fixed for a single allele. Only *PGM-1** and *PGM-2** are expressed in digestive gland tissue, which was the only tissue assayed by Mitton et al (1989). However, we also scored PGM in foot muscle which clearly revealed a third, more cathodal locus (*PGM-3**). We also observed three distinct loci in foot tissue of a second conch species, *S. costatus*.

At least three possibilities could thus account for the apparent difference between our results and those of Mitton et al. (1989) at *PGM-2**: (1) our inability to resolve the variant electromorph at *PGM-2**, (2) the partial expression of the *PGM-3** locus in digestive gland tissue (e.g., Allendorf et al. 1983) of individuals sampled by Mitton et al. (1989), thus giving false readings of heterozygotes at *PGM-2**, or (3) the reported allele-frequency difference between the two groups of populations are indeed real. Of the three possibilities, we believe explanations (1) and (2) are the most likely because of the high consistency of our allele frequencies with those of Mitton et al. (1989) at all other loci. Consequently, we believe that this apparent discrepancy at *PGM-2** most likely reflects laboratory-specific adaptations of basic electrophoretic procedures. In this context, we were able to resolve several loci not resolved by Mitton et al. (1989) and vice-versa.

Conclusions

The major finding of our study was the existence of spatial and temporal genetic patchiness among populations of queen conch in the Florida Keys and Bimini. We suggest that such genetic patchiness most likely results from presettlement stochastic events and processes in the marine environment. Nevertheless, these populations are all very similar genetically, presumably reflecting high levels of gene flow due to larval drift. These interpretations are consistent with the results of Mitton et al. (1989) and also explain similar patterns of "chaotic genetic patchiness" in other taxa of marine invertebrates.

Acknowledgments

We thank R. Estling, A. Kirkley, and W. Schumacher for their assistance in the laboratory.

Citations

Aebersold, P.B., G.A. Winans, D.J. Teel, G.B. Milner, and F.M. Utter
1987 Manual for starch gel electrophoresis: A method for the detection of genetic variation. NOAA Tech. Rep. NMFS 61, 19 p.

Allendorf, F.W., R.F. Leary, and K.L. Knudsen
1983 Structural and regulatory variation of phosphoglucomutase in rainbow trout. Isozymes Curr. Top. Biol. Med. Res. 9:123-142.

Ballantine, D.L., and R.S. Appeldoorn
1983 Queen conch culture and future prospects in Puerto Rico. Proc. Gulf Caribb. Fish. Inst. 35:57-63.

Berg, C.J. Jr., and D.A. Olsen
1989 Conservation and management of queen conch (*Strombus gigas*) fisheries in the Caribbean. *In* Caddy, J.F. (ed.), Marine invertebrate fisheries: Their assessment and management, p. 421-442. John Wiley, NY.

Boyer, S.H., D.C. Fainer, and E.J. Watson-Williams
1963 Lactate dehydrogenase variant from human blood: Evidence for molecular subunits. Science (Wash. DC) 141: 642-643.

Bucklin, A., M.M. Rienecker, and C.N.K. Mooers
1989 Genetic tracers of zooplankton transport in coastal filaments off northern California. J. Geophys. Res. 94(C6: 8277-8288.

Bucklin, A.
1991 Population genetic responses of the planktonic copepod *Metridia pacifica* to a coastal eddy in the California Current. J. Geophys. Res. 96(C8):14,799-14,808.

Campton, D.E., C.J. Berg Jr., L.M. Robison, and R.A. Glazer
In press Deficits of heterozygotes and correlation between size and heterozygosity in the marine mollusk, *Strombus gigas* (Gastropoda: Strombidae). Evolution.

Chakraborty, R., M. Haag, N. Ryman, and G. Stahl
1982 Hierarchical gene diversity analysis and its application to brown trout populations. Hereditas 97:17-21.

Clayton, J.W., and D.N. Tretiak
1972 Amine-citrate buffers for pH control in starch gel electrophoresis. J. Fish. Res. Board Can. 29:1169-1172.

Davis, M., and C. Hesse
1983 Third world level conch mariculture in the Turks and Caicos Islands. Proc. Gulf Caribb. Fish Inst. 35:73-82.

Gaffney, P.M., T.M. Scott, R.K. Koehn, and W.J. Diehl
1990 Interrelationships of heterozygosity, growth rate and heterozygote deficiencies in the coot clam, *Mulinia lateralis*. Genetics 124:687-699.

Hesse, K.O.
1979 Movement and migration of the queen conch, *Strombus gigas*, in the Turks and Caicos Islands. Bull. Mar. Sci. 29: 303-311.

Johnson, M.S., and R. Black
1982 Chaotic genetic patchiness in an intertidal limpet, *Siphonaria* sp. Mar. Biol. (Berl.) 70:157-164.
1984a The Wahlund effect and the geographical scale of variation in the intertidal limpet *Siphonaria* sp. Mar. Biol. (Berl.) 79:295-302.
1984b Pattern beneath the chaos: The effect of recruitment on genetic patchiness in an intertidal limpet. Evolution 38: 1371-1383.

Kinder, T.H., G.W. Hebrun, and A.W. Green
1985 Some aspects of the Caribbean circulation. Mar. Geol. 68:25-52.

Little, C.
1965 Notes on the anatomy of the queen conch, *Strombus gigas*. Bull Mar. Sci. 15:338-358.

Mitton, J.B., C.J. Berg Jr., and K.S. Orr
1989 Population structure, larval dispersal, and gene flow in the queen conch, *Strombus gigas*, of the Caribbean. Biol. Bull. (Woods Hole) 177:356-362.

Morizot, D.C., and M.E. Schmidt
1990 Starch gel electrophoresis and histochemical visualization of proteins. *In* Whitmore, D.H. (ed.), Electrophoretic and isoelectric focusing techniques in fisheries management, p. 23-80. CRC Press, Boca Raton.

Nash, W.J., M. Goddard, and J.S. Lucas
1988 Population genetic studies of the crown-of-thorns starfish, *Acanthaster planci* (L.), in the Great Barrier reef region. Coral Reefs 7:11-18.

Nei, M.
1972 Genetic distance between populations. Am. Nat. 106: 283-292.
1973 Analysis of gene diversity in subdivided populations. Proc. Natl. Acad. Sci. USA 70:3321-3323.

Nishida, M., and J.S. Lucas
1988 Genetic differences between geographic populations of the crown-of-thorns starfish throughout the Pacific region. Mar. Biol. (Berl.) 98:359-368.

Randall, J.E.
1964 Contributions to the biology of the queen conch, *Strombus gigas*. Bull. Mar. Sci. 14:246-295.

Rice, W.R.
1989 Analyzing tables of statistical tests. Evolution 43: 223-225.

Ridgway, G.J., S.W. Sherburne, and R.D. Lewis
1970 Polymorphisms in the esterases of Atlantic herring. Trans. Am. Fish. Soc. 99:147-151.

Robertson, R.
1959 Observations on the spawn and veligers of conchs (*Strombus*) in the Bahamas. Proc. Malacol. Soc. Lond. 33:164-171.

Scheltema, R.S.
1971 Larval dispersal as a means of genetic exchange between geographically separated populations of shallow-water benthic marine gastropods. Biol Bull. (Woods Hole) 140:284-322.
1986 On dispersal and planktonic larvae of benthic invertebrates: An eclectic overview and summary of problems. Bull. Mar. Sci. 39:241-256.

Selander, R.K., M.H. Smith, S.H. Yang, W.E. Johnson, and J.B. Gentry
1971 Biochemical polymorphism and systematics in the genus *Peromyscus*. I. Variation in the old field mouse (*Peromyscus polionotus*). Studies in Genetics VI. Univ. Texas Publ. 7103: 49-90.

Shaklee, J.B., F.W. Allendorf, D.C. Morizot, and G.S. Whitt
1990 Gene nomenclature for protein-coding loci in fish. Trans. Am. Fish. Soc. 119:2-15.

Siciliano, M.J., and C.R. Shaw
1976 Separation and visualization of enzymes on gels. *In* Smith, I. (ed.), Chromatographic and electrophoretic techniques. Vol. II, Zone electrophoresis (4th ed.), p. 185-209. Year Book Med. Publ., Chicago.

Smouse, P.E., and R.H. Ward
1978 A comparison of the genetic infrastructure of the Ye'cuana and the Yanomama: A likelihood analysis of genotypic variation among populations. Genetics 88:611-631.

Sneath, P.H.A., and R.R. Sokal
1973 Numerical taxonomy. W.H. Freeman, San Francisco.

Sokal, R.R., and F.J. Rohlf
1981 Biometry. W.H. Freeman, San Francisco.
Stoner, A.W.
1989 Winter mass migration of juvenile queen conch *Strombus gigas* and their influence on the benthic environment. Mar. Ecol. Prog. Ser. 56:99–104.
Stoner, A.W., R.N. Lipcius, L.S. Marshall Jr., and A.T. Bardales
1988 Synchronous emergence and mass migration in juvenile queen conch. Mar. Ecol. Prog. Ser. 49:51–55.
Waples, R.S.
1989 Temporal variation in allele frequencies: Testing the right hypothesis. Evolution 43:1236–1251.
Watts, R.J., M.S. Johnson, and R. Black
1990 Effects of recruitment on genetic patchiness in the urchin *Echinometra mathaei* in western Australia. Mar. Biol. (Berl.) 195:145–151.
Weil, E.M., and R.G. Laughlin
1984 Biology, population dynamics, and reproduction of the queen conch *Strombus gigas* Linnaeus in the Archipielago de Los Roques National Park. J. Shellfish Res. 4:45–62.

Detecting environmental covariates of Pacific whiting *Merluccius productus* growth using a growth-increment regression model

Martin W. Dorn

Alaska Fisheries Science Center, National Marine Fisheries Service, NOAA
7600 Sand Point Way NE, BIN C15700, Seattle, Washington 98115-0070

Abstract.—The growth patterns of Pacific whiting *Merluccius productus*, also known as Pacific hake, were examined for the period 1978–88 using fishery-based estimates of length-at-age. Mean length-at-age and a delta method variance estimate of mean length-at-age were computed for geographic and temporal strata in the U.S. fishery. These calculations took into account the two-phase sampling design used to sample the catch. A factorial analysis of variance of length found significant differences due to age, year, region, sex, and time-period during the fishery. Length increases with age and season. Pacific whiting found in the north are larger, and females are larger than males. The mean length-at-age began declining in 1978, and reached a minimum in 1984. From 1984 to 1986, there was a slight rebound in length-at-age, but after 1986 length-at-age again declined. To investigate the influence of population density and environmental covariates on annual growth, a generalized form of the von Bertalanffy growth model was developed. Deviations from a baseline model for sex-specific asymptotic growth were significantly correlated with changes in sea-surface temperature and adult biomass. Regression results indicate that a 0.5°C increase in mean summer sea-surface temperature would reduce annual growth by 24% at age 1 and 12% at age 4. In contrast, the effect of adult biomass on annual growth becomes greater with age. An increase of 200,000 metric tons (approximately 10% of the mean population biomass) would reduce annual growth by 5% at age 4 and by 10% at age 7. It is proposed that the effect of population density is greater for the older Pacific whiting because their diet has shifted from euphausiids, whose abundance is closely coupled with environmental processes, towards fish species with multiyear life cycles that can be affected by intense Pacific whiting predation.

Manuscript accepted 18 February 1992.
Fishery Bulletin, U.S. 90:260–275 (1992).

This paper describes research on the growth of Pacific whiting, also known as Pacific hake, a gadoid species that is an important component of the California Current ecosystem (Francis 1983). The coastal population of Pacific whiting is currently the target of a major fishery with an average (1977–88) annual harvest of 147,000 metric tons (t) (Dorn and Methot 1990). Adult Pacific whiting migrate north in spring and summer, feeding in the productive waters along the continental shelf and slope from northern California to Vancouver Island, British Columbia. In late autumn, Pacific whiting migrate south to spawning areas from Point Conception, California, to Baja California (Bailey et al. 1982). The U.S. fishery operates from April to November and in recent years has been conducted primarily under joint-venture arrangements, with U.S. fishing boats delivering fish to processing vessels from the Soviet Union, Poland, Japan, and other nations. The Canadian fishery for Pacific whiting is conducted in similar fashion, except that independent fishing by the foreign fleet still accounts for a significant portion of the catch.

Hollowed et al. (1988) observed that the mean length-at-age of Pacific whiting had declined in recent years, and hypothesized that the disruption of normal circulation and temperature patterns associated with the 1983 El Niño may have been the causative factor. The recruitment of strong 1980 and 1984 year-classes increased the population biomass of Pacific whiting to a maximum in 1986. The decline in the length-at-age could also have been a density-dependent growth response to this increase in population abundance. Since the Pacific whiting resource is managed by setting an annual quota in tons based on a conversion using weight-at-age from a projected yield in numbers (Dorn and Methot 1990), changes in growth must be taken into account when making management recommendations about the resource.

The objective of this paper is to examine the pattern of growth variability displayed by the coastal Pacific whiting population, and, in particular, to determine whether environmental covariates or fluctuations in population density could account for the recent changes in length-at-age. Analysis of variance, while useful as an exploratory technique to identify the sources of variability in length-at-age, is inadequate to describe changes in asymptotic growth. The nonlinear regression model presented in this paper is a simple, biologically realistic model for exploring the environmental determinants of asymptotic growth. Its potential utility is not limited to the application described in this paper, i.e., growth of Pacific whiting.

Methods

The U.S. Foreign Fisheries Observer Program at the Alaska Fisheries Science Center (AFSC) uses a two-phase sampling design to sample the catch of Pacific whiting (French et al. 1981). The first phase consists of obtaining a large initial sample of fish and recording the length and sex. For the second phase of sampling, a subsample of fixed size is selected for each combination of length category and sex. All fish in these subsamples are aged using otoliths.

Typically, each observer samples 2–3 hauls or joint-venture deliveries per day for length and sex, and 150 otoliths (5 per centimeter-length category per sex) are collected over a two-month cruise. The numbers of aged and measured fish from 1978–88 are given in Table 1. This information resides in a data base maintained by the Resource Ecology and Fisheries Management Division (REFM) at the Alaska Fisheries Science Center.

Kimura and Chikuni (1987) point out that, with a two-phase sampling design, estimates of mean length-at-age are biased when obtained simply by averaging the lengths of the aged fish. To avoid this bias, stratified length-at-age estimates were compiled from fishery data for the years 1978–88 using separate age-length keys for each stratum (see Appendix for details). Three spatial strata were defined as: (1) the area from lat. 39°00′N to lat. 43°00N, including part of the International North Pacific Fishery Commission (INPFC) Monterey region and the Eureka INPFC region (EUR); (2) the area from lat. 43°00N north to Cape Falcon (lat. 46°45N) in the southern part of the Columbia INPFC region (SCOL); and (3) the area north of Cape Falcon to the U.S.–Canada border including the northern part of the Columbia INPFC region and the U.S. portion of the Vancouver INPFC region (VNC) (Fig. 1).

Table 1

Number of Pacific whiting *Merluccius productus* sampled from the midwater trawl fishery during the years 1978–88 off Washington, Oregon, and northern California.

	Early period April–June		Middle period July–August		Late period Sept.–Nov.		Annual total	
Year	Aged	Measured	Aged	Measured	Aged	Measured	Aged	Measured
1978	2060	31,819	2801	66,153	978	26,799	5839	124,771
1979	1072	37,678	1552	83,584	500	52,094	3124	173,356
1980	844	15,674	2927	43,038	1565	43,536	5336	102,248
1981	1287	26,961	1928	55,174	1053	53,605	4268	135,740
1982	1913	77,529	1463	66,683	882	27,604	4258	171,816
1983	1480	82,186	1277	70,499	475	14,173	3232	166,858
1984	1344	70,888	1304	108,272	662	64,524	3310	243,684
1985	200	23,329	1690	142,592	550	101,089	2440	267,010
1986	1203	125,542	1393	238,779	474	109,786	3070	474,107
1987	1021	102,191	1414	188,361	740	140,902	3175	431,454
1988	1192	125,714	1349	194,246	502	100,184	3043	420,144
Total	13,616	719,511	19,098	1,257,381	8381	734,296	41,095	2,711,188

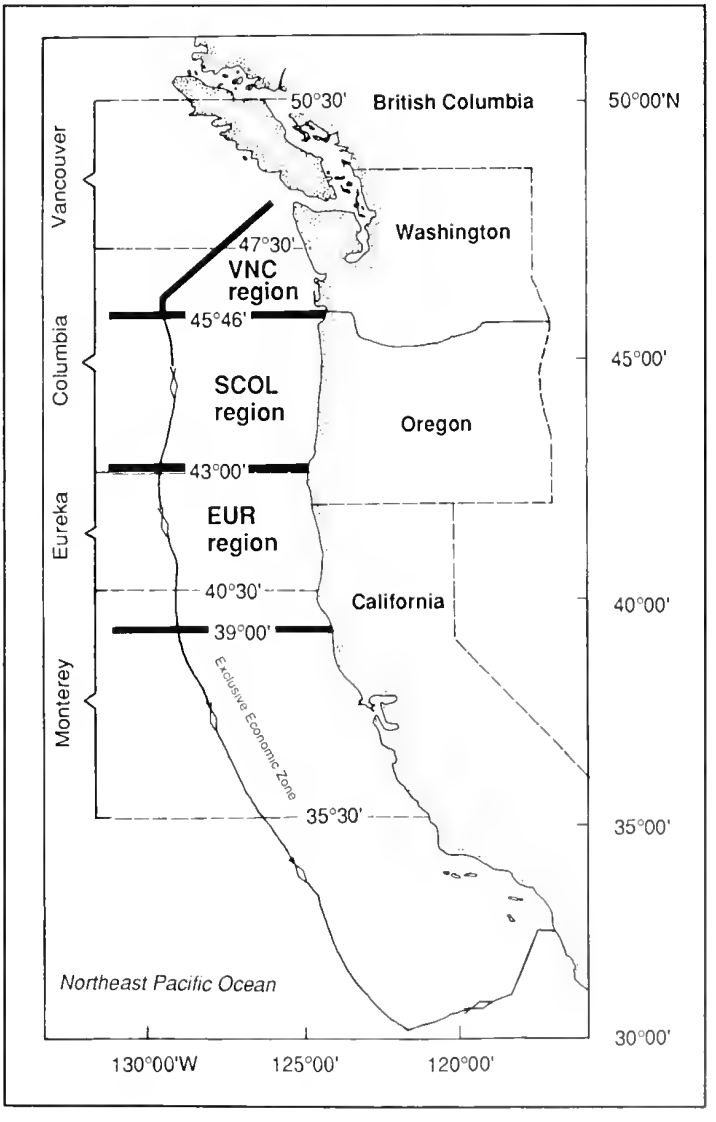

Figure 1

Spatial strata used to compile length-at-age for midwater trawl fishery samples of Pacific whiting *Merluccius productus*.

Each of these geographic regions encloses a center of Pacific whiting abundance and a concentration of fishing activity (Dorn and Methot 1990). Three time-periods were also defined as strata: (1) early (April–June), (2) middle (July–August), and (3) late (September–November). These time-periods divide the fishing season into three roughly equal parts. Over the years 1978–88, 27.9% of the catch came from the early time-period, 47.4% came from the middle time-period, and 24.7% came from the late time-period. In compiling the length-at-age estimates for the spatial and temporal strata, all data collected within that strata were aggregated and assumed to originate from random sampling of the catch within that strata.

Some of the detrimental effects of ageing error bias and low sampling intensity of uncommon age groups—common problems in analyzing fishery length-at-age data—can be reduced if the precision of the length-at-age estimates is known. A delta-method variance estimator of length-at-age for a two-phase sampling plan was derived and implemented for the U.S. fishery samples. Details of this estimator and a procedure for combining the length-at-age from different strata are described in the Appendix.

Two general methods of analyzing the growth in length of fish have been used widely in fishery research. The first method interprets individual observations of length-at-age or mean length-at-age in the population by fitting asymptotic growth curves, most typically the von Bertalanffy (or monomolecular) growth curve (Boehlert and Kappenman 1980, Kimura 1980, Shepherd and Grimes 1983). Using this technique to study environmental effects on growth on an annual scale is difficult because growth curves summarize the growth history of a year-class or a population over the lifespan of the organism. One approach to generalizing growth curves is to include seasonal environmental effects on growth. An example of this is the work of Pauly and Gaschütz (1979); they incorporated a sine wave in the von Bertalanffy growth curve to model the seasonal growth cycle.

The second common approach to analyzing growth data is analysis of variance (ANOVA). Factorial designs have been used to investigate regional growth variability (Francis 1983, Reish et al. 1985). Multiple linear regression is often used to examine the effect of the environment or population density on growth (Kreuz et al. 1982, Ross and Almeida 1986, Peterman and Bradford 1987). A factorial ANOVA of length using age, year, region, sex, and time-period as factors is reported in the Results. It should be recognized, however, that analysis of variance does not account for changes in asymptotic growth, except by fitting interaction terms that tend to obscure the analysis. It is used in this paper only as an exploratory technique to identify the sources of variability in length.

Because asymptotic growth is a universal feature of fish growth, a model to examine the effect of the environment on growth should account for this characteristic. At the same time, such a model must be general enough to allow for covariates to influence annual growth. To meet this objective, a simple extension of the asymptotic von Bertalanffy growth model was developed. The model has a framework similar to analysis of covariance, in that it allows for the possibility of differences in growth between constituent subgroups of the population and differences in growth due to the influence of population density or environmental covariates.

The von Bertalanffy growth model for the mean length l_a of a year-class at age a is given by

$$l_a = l_\infty (1 - e^{-k(a-a_0)}),$$

where l_∞ is the asymptotic maximum length, k is a growth coefficient, and a_0 is the hypothetical age at length zero. Subtracting the length at age a+1 from the length at age a gives the first difference of this equation, the annual growth increment from age a to age a+1,

$$l_{a+1} - l_a = l_\infty (1 - e^{-k})\, e^{-k(a-a_0)}.$$

Defining $g_0 = \ln[l_\infty(1 - e^{-k})]$, and $g_1 = -k$, a simple expression for annual growth is obtained:

$$l_{a+1} - l_a = \exp(g_0 + g_1(a - a_0)).$$

As might be expected, the parameter a_0 becomes redundant in this model for annual growth, since it is confounded with the parameter g_0. One possibility is simply to drop it from the equation. Another alternative, and the one used in this analysis, is to use a_0 to scale chronological age to some initial age for which the growth model is intended to apply. In the Pacific whiting data, there are growth increments from age 1 to age 2, so a_0 is set to 1. In this parameterization, structural growth coefficients, g_0 and g_1, describe simple elements of asymptotic growth: $\exp(g_0)$ is the annual growth increment at age a_0, and g_1 is the exponential decline in the annual growth increment (Fig. 2).

To assess the effect of an environmental covariate, x, this model is augmented with an additional coefficient for that environmental variable,

$$l_{a+1\,t+1\,s} - l_{ats} = \exp[g_0 + \sum_i g_{0i}\, x_i + (g_1 + \sum_j g_{1j}\, x_j)(a - a_0)] + e_{ats},$$

where $e_{ats} \sim N(0, w_{ats}\sigma^2)$. The additional subscripts in this equation are: t for year, s for sex, and i and j to index different environmental variables (e.g., x_i and x_j). The case weights, w_{ats}, are determined by the sum of the estimation variance for the two length-at-age estimates used to calculate the growth increment.

In this regression model, environmental variables can enter as either intercept or slope terms. An intercept coefficient affects g_0 and indicates a constant percent change in the growth increment regardless of age. Slope coefficients affect g_1 and provide flexibility for a varying percent change in the growth increment with age. Together these two types of coefficients, intercept and slope, cover a wide range of different ways that environmental conditions can effect growth at different ages. Note also that in this formulation, it is possible to use indicator variables to parameterize growth differences between different constituent groups of the population; for example, sex differences or geographic differences in growth. This model resembles a linear ANOVA model proposed by Weisberg (1986) to analyze back-calculated fish lengths, though he does not use von Bertalanffy growth to scale the annual growth increments.

The general procedure for fitting a nonlinear regression model in Ratkowsky (1983) was followed using the PAR algorithm in the BMDP statistical package for estimating a nonlinear regression model using weighted least-squares (Dixon 1983). Mean-square error was estimated by fitting a full model consisting of the coefficients g_0 and g_1, and separate intercept and slope coefficients for all environmental covariates (temperature, upwelling, biomass, recruitment strength) assessed in the analysis. Mean-square error was estimated by dividing the residual sum of squares for this model by the degrees of freedom. A full model should account for all the explainable variability, so that the residual error gives an estimate of mean-square error. A P-value of <0.05 was established as the criteria for statistical significance. Because of the presence of negatively-valued growth increments due to measurement error, it was not possible to take the logarithm of the growth increment and analyze the model using linear regression.

The analysis with this model uses the change in mean length of an age-group from the early period of the fishery (April–June) of one year to the early period of the following year. Geographic strata are not used in the analysis because the migratory nature of the coastal population of Pacific whiting would make any conclusions regarding regional growth patterns impossible to defend. It is assumed that the annual increment in growth from one spring to the next is due to conditions prevalent during the summer season of active growth. Although growth increments could be studied for shorter time-periods, this was considered inappropriate for our study because of possible lags between environmental conditions and the growth response of the fish. In addition, the fishery estimates of length-at-

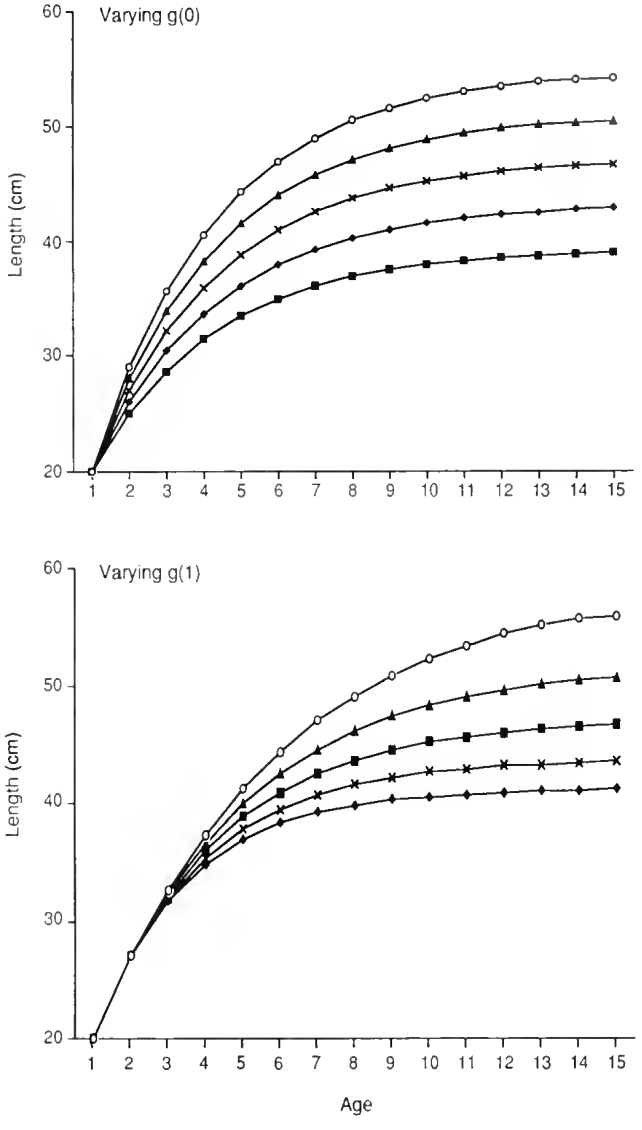

Figure 2

Families of asymptotic von Bertalanffy growth curves parameterized by g_0, the initial growth increment, and g_1, the exponential decline in the annual growth increment with age. All curves were constrained to pass through 20 cm at age 1.

Table 2

Environmental and stock biomass covariates of Pacific whiting *Merluccius productus* growth, assessed using the growth-increment regression model. Mean summer (April–August) sea-surface temperature (°C) is an average over lat. 40–50°N, and from the coast, west to long. 125°W. The Bakun upwelling indices are mean summer coastal upwelling (April–August) from lat. 42–48°N. Stock biomass is measured in millions of tons of age-2 and older fish in the coastal whiting population. Anomalies of temperature, upwelling index, and biomass are calculated as the annual value minus the mean over 1978–87.

Year	Temperature[a] (°C)	Temperature anomaly	Upwelling[b] index	Upwelling anomaly	Biomass[c]	Biomass anomaly
1978	13.1	0.6	49.5	0.3	1.503	−0.268
1979	12.5	0.0	49.2	0.1	1.709	−0.062
1980	12.2	−0.3	67.1	18.0	1.640	−0.131
1981	12.5	0.0	50.0	0.9	1.384	−0.387
1982	12.1	−0.3	55.9	6.7	2.000	0.230
1983	13.4	0.9	31.5	−17.6	1.805	0.035
1984	11.9	−0.5	45.7	−3.4	1.742	−0.029
1985	12.1	−0.4	45.3	−3.8	1.685	−0.086
1986	12.6	0.1	49.6	0.5	2.225	0.455
1987	12.3	−0.2	47.6	−1.5	2.012	0.242
Average 1978–87	12.47		49.15		1.771	

[a] J.G. Norton, Pac. Fish. Environ. Group, P.O. Box 831, Monterey, CA 93942, pers. commun., Aug. 1989.
[b] Mason and Bakun (1986).
[c] Dorn and Methot (1990).

Table 3

Recruitment in billions of age-2 fish to the Pacific whiting *Merluccius productus* population for year-classes 1965–84 (modified from Dorn and Methot 1990). The recruitment anomaly is calculated as the annual number of recruits minus the average over 1965–84.

Year	Recruits	Recruit anomaly
1965	0.692	−0.331
1966	0.786	−0.237
1967	1.110	0.087
1968	0.636	−0.387
1969	0.315	−0.708
1970	3.597	2.574
1971	0.169	−0.854
1972	0.306	−0.717
1973	1.432	0.409
1974	0.139	−0.884
1975	0.220	−0.803
1976	0.094	−0.929
1977	1.716	0.693
1978	0.035	−0.988
1979	0.145	−0.878
1980	4.604	3.581
1981	0.022	−1.001
1982	0.042	−0.981
1983	0.183	−0.840
1984	4.221	3.198
Average 1965-84	1.023	

age are not point estimates in time, but averages over 2 or 3 months. As a result, relating the growth increment to the environment over a short time-period would tend to blur environmentally-determined growth differences.

The environmental variables and stock abundance measures examined in the analysis were intentionally limited to a few variables which would characterize the environment of the population on the largest scale possible. The environmental variables are summer averages over the geographic range of the mature stock. Mean summer (April–August) sea-surface temperature (°C), provided by J.G. Norton (Pac. Fish. Environ. Group, Monterey, CA 93942, pers. commun., Aug. 1989), represents the mean value obtained from ships of opportunity between lat. 40°N and 50°N, and from the North American coast west to long. 125°W (Table 2). The Bakun upwelling indices are a mean of the monthly coastal upwelling indices during April–August from lat. 42–48°N and are in units of metric tons of water transported through the Ekman layer per second per 100 m of coastline (Mason and Bakun 1986). Stock biomass is measured in millions of tons of age-2 and older fish in the coastal whiting population, and is estimated using the stock synthesis model (Dorn and Methot 1990). The estimates of year-class strength in Table 3 come from the same source.

Results

Length analysis of variance

Annual length-at-age estimates by sex for 1978–88 were obtained using the procedures described in the

Appendix for calculating strata estimates of length-at-age, and for combining the strata estimates to produce an annual estimate (Fig. 3). The decline in length-at-age is evident in graphs of both male and female length-at-age.

The factorial analysis of mean length variance is given in Table 4. Weighted analysis of variance was used with the sampling variances as weights. The F-tests for age, year, region, sex, and time-period were all highly significant ($P<0.0001$). Because of the large number of observations (2072), this result is not surprising. The parameter estimates in Table 4 are defined such that the intercept term represents the mean length of a 1-year-old male in the early part of the season in 1978 in the EUR region. Parameter estimates for the other factor levels can be interpreted as the difference between mean length of Pacific whiting identified by that factor level and those identified by the intercept characteristic with all other factors being held constant.

The results of the ANOVA can be summarized as follows. Length increases with age to age 10, then varies irregularly to age 15 (Table 4). Length increases 0.55 cm from the early period (April–June) to the middle period (July–August), and increases an additional 0.46 cm from the middle period to the late period (September–November). There is an increase of 1.36 cm from the EUR region in the south to the VNC region in the north, indicating that the larger Pacific whiting of an age-group migrate farther north. On average, female Pacific whiting are larger than males by 0.55 cm. Since the ANOVA model does not contain a sex-age interaction, this difference in mean length would apply to all ages. In general, these results are consistent with the previously reported findings on the growth of Pacific whiting (Dark 1975, Francis 1983). The ANOVA year coefficients show the decline in length since 1978. Mean length-at-age reached a minimum in 1984. There was a slight rebound in length-at-age from 1984 to 1986, but after 1986 length-at-age began to decline again.

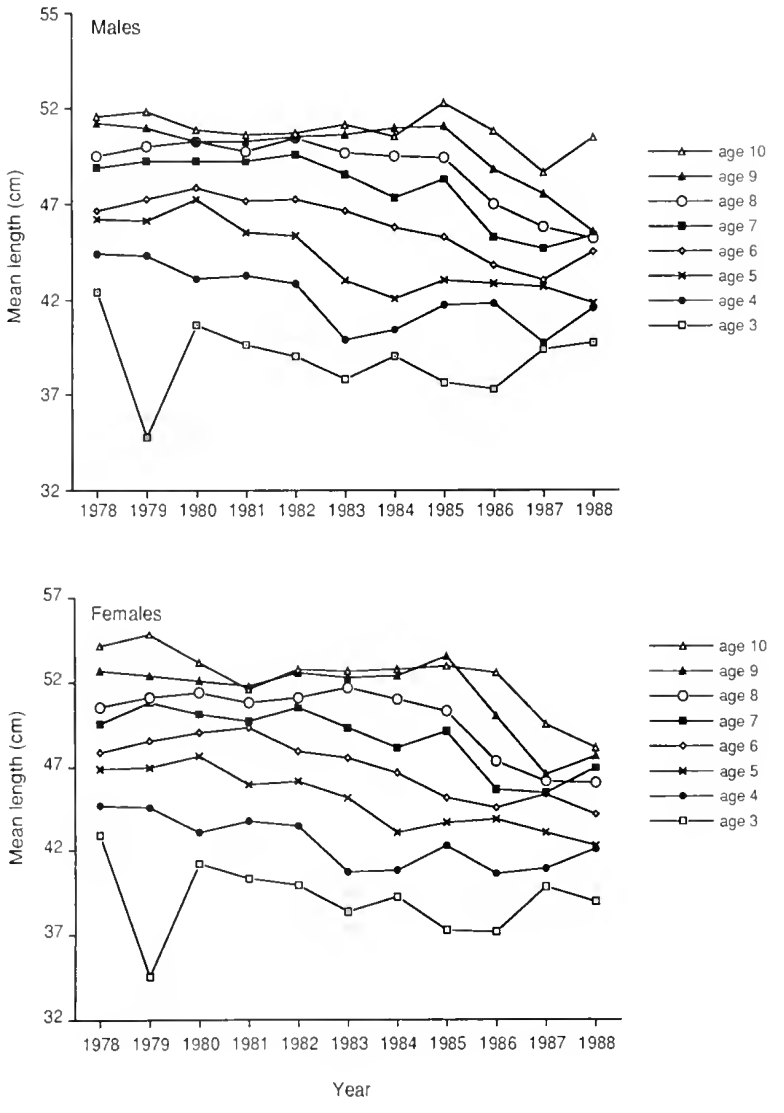

Figure 3

Mean U.S. fishery length-at-age estimates by sex for Pacific whiting *Merluccius productus*, 1978–89. The extremely low estimates of mean length for male and female age-3 fish in 1979 were due to asymmetric error in the ageing of the strong 1977 year-class.

Models containing interaction terms between factors were also analyzed. All the two-way interaction terms were statistically significant, but much less so than the main effects. The addition of more than 200 parameters to describe the two-way interactions would make interpretation difficult. Yet a model with only main effects is clearly inadequate, since it implies, for example, that both the 2-year-old and 12-year-old whiting declined in mean length by the same amount from 1983 to 1984.

Growth increment regression

Before considering the effects of environmental co-

variates, the growth increment model was used to investigate sex differences in growth. This was done by fitting a model with only g_0, g_1, and indicator variables for sex. The P-value for the intercept coefficient for sex was 0.059, but the P-value for the slope term was 0.998. By the criteria established earlier, neither coefficient would be considered statistically significant, although the P-value for the intercept coefficient is close to the critical value. The estimate of the intercept coefficient for sex (0.058) indicates that the females grow approximately 6% ($e^{0.058}$) more than males on an annual basis, regardless of age. A difference of this magnitude is sufficient to account for the greater asymptotic size of the females. Figure 4 shows the fitted sex-specific curves for the annual growth increment. Despite the lack of statistical significance of the intercept term for sex, it was retained in the model while evaluating the significance of environmental covariates on growth. The larger size attained by the female Pacific whiting is compelling evidence that there are sex-specific differences in Pacific whiting growth. Including this term in the baseline model is important because it accounts for this sex-specific variability in growth.

Table 4

Factorial analysis of variance of Pacific whiting *Merluccius productus* length-at-age using midwater trawl fishery samples over 1978–88. The model contains the factors age, year, geographic region, sex, and season. The intercept term estimates the mean length of a 1-year-old male in the early part of the season in 1978 in the EUR region; the other terms estimate the difference in the mean length of fish with that factor level and those with intercept characteristic.

Source	df	SS	Mean square	F-value	$P>F$
Age	14	1,112,327.5	79,452.0	3611.5	<0.001
Year	10	33,126.7	3,312.7	150.6	<0.001
Region	2	5,810.9	2,905.4	132.1	<0.001
Sex	1	2,239.2	2,239.2	101.8	<0.001
Season	2	3,531.0	1,765.5	80.3	<0.001
Error	2042	44,841.1	22.0		

Parameter		Estimate (cm)	SE of estimate
Intercept		26.88	0.211
Age:	2	7.90	0.201
	3	13.22	0.189
	4	17.02	0.147
	5	18.44	0.182
	6	19.39	0.200
	7	20.76	0.205
	8	22.29	0.190
	9	24.04	0.262
	10	29.92	0.308
	11	26.51	0.361
	12	26.07	0.290
	13	27.56	0.528
	14	27.69	0.555
	15	29.94	0.453
Year:	1979	−0.82	0.198
	1980	−0.50	0.174
	1981	−1.54	0.170
	1982	−2.33	0.169
	1983	−3.31	0.187
	1984	−4.64	0.169
	1985	−3.00	0.157
	1986	−2.64	0.175
	1987	−3.03	0.176
	1988	−4.00	0.174
Region:	SCOL	0.57	0.071
	VNC	1.36	0.089
Sex:	Females	0.55	0.052
Season:	Middle	0.53	0.065
	Late	0.99	0.079

Table 5 shows the analysis of variance using the annual growth-increment regression model. The model was built in a forward stepwise fashion, adding the environmental term to the baseline model that resulted in the largest reduction in the residual sum of squares. Temperature and population biomass were significant covariates in the model. Temperature had significant intercept ($P<$ 0.001) and slope terms (P 0.026). For biomass, only the slope term was significant (P 0.002).

The parameter estimates in Table 5 indicate that a 0.5°C increase in mean summer sea-surface temperature will bring about a 24% reduction in the annual growth increment at age 1. At age 4, the same increase in temperature would be expected to produce a 12% reduction in annual growth, and by age 7, the percent reduction would be close to zero. The model predicts an increase in growth due to increasing temperature above age 7, but as annual growth is very slight by this age, the consequences of this prediction are not important. One concern about the reliability of these results is that they may be overdependent on growth during the 1983 El Niño, when sea-surface temperature was the highest during the study. To investigate this possibility, a model was fit to the data excluding the

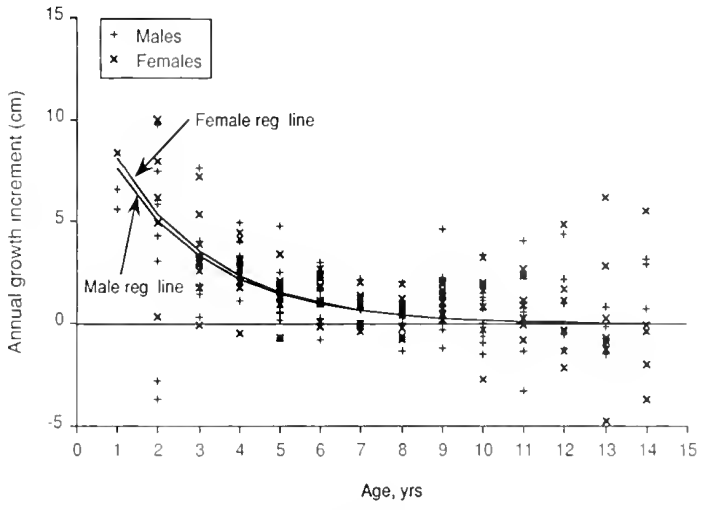

Figure 4

Growth-increment regression curves with different initial growth-increment coefficients (g_0) for male and female Pacific whiting *Merluccius productus*. The distribution of actual growth increments for the years 1978–89 illustrates the saddle-shaped variability of length-at-age statistics based on fishery sampling (N 211). Points represent observed annual growth increments per age-group per year.

Table 5

Analysis of variance of annual length increments using the nonlinear regression model. The coefficient g_0 is an intercept term: $\exp(g_0)$ estimates the growth increment from age 1 to age 2. The coefficient g_1 determines the slope of the exponential decline of the annual growth increment with age under average environmental conditions. Terms relating to covariates are identified as either intercept terms (g_0) or as slope terms (g_1).

Source	df	SS	Mean square	F-value	$P>F$
g_1	1	4067.8	4067.8	1166.5	<0.001
g_0 (sex)	1	12.6	12.6	3.6	0.059
g_0 (temp.)	1	93.5	93.5	26.8	<0.001
g_1 (biomass)	1	36.3	36.3	10.4	0.002
g_1 (temp.)	1	17.4	17.4	5.0	0.026
Error	204	711.4	3.5		

Parameter	Estimate	SE of estimate
g_0	1.995	0.038
g_1	−0.383	0.015
g_0 (sex)	0.058	0.029
g_0 (temp.)	−0.544	0.098
g_1 (biomass)	−0.086	0.027
g_1 (temp.)	0.099	0.043

growth increments from 1983. The parameter estimates followed the same trend as the results in Table 5, with increases in sea-surface temperature associated with large reductions in growth of younger fish, and a decreasing percent reduction with age.

For population biomass, an increase of 200,000t (~10% of the mean population biomass) would cause a 5% reduction in annual growth at age 4, and the percent reduction would increase with age, reaching a 10% reduction at age 7. Because the intercept term for biomass was not significant, growth of the age-1 fish would not be affected by changes in population biomass. During the 10 years studied, range in adult biomass was from 26% above to 22% below the mean of 1.771 million t (1978–87). This lack of contrast in adult biomass makes any interpretation very tentative, but the results do suggest that the effect of population density on growth is relatively small in comparison with the effect of temperature.

None of the other environmental covariates or measures of population density tested in the model were significant. The coefficient for upwelling was highly significant in a model without temperature, but when temperature was included in the regression, upwelling was no longer significant. Because water temperature and the upwelling index are statistically correlated off the coast of Oregon (Kruse and Huyer 1983), the parallel effects of temperature and upwelling index are not unexpected. The same parallel effect was found between year-class abundance and adult biomass. However, adult biomass accounted for more of the variability in annual growth than did year-class abundance. This suggests that the crowding that occurs when a strong year-class recruits to the population is experienced by all the adults, and not just the individuals which make up the strong year-class.

Figure 5 shows the standardized residuals from the final model, plotted against age and year. No trends are evident with respect to age. This plot also shows that the use of the estimation variances as weighting terms in the least-squares fit was successful in stabilizing the error variance with respect to age. However, there still is a noticeable trend in the standardized residuals by year, with positive residuals associated with the earlier years in the time-series (1979 and 1980), and negative residuals with the later years (1985 and 1987). This indicates that the environmental covariates examined thus far are not completely successful in accounting for the decline in mean length-at-age over the past decade.

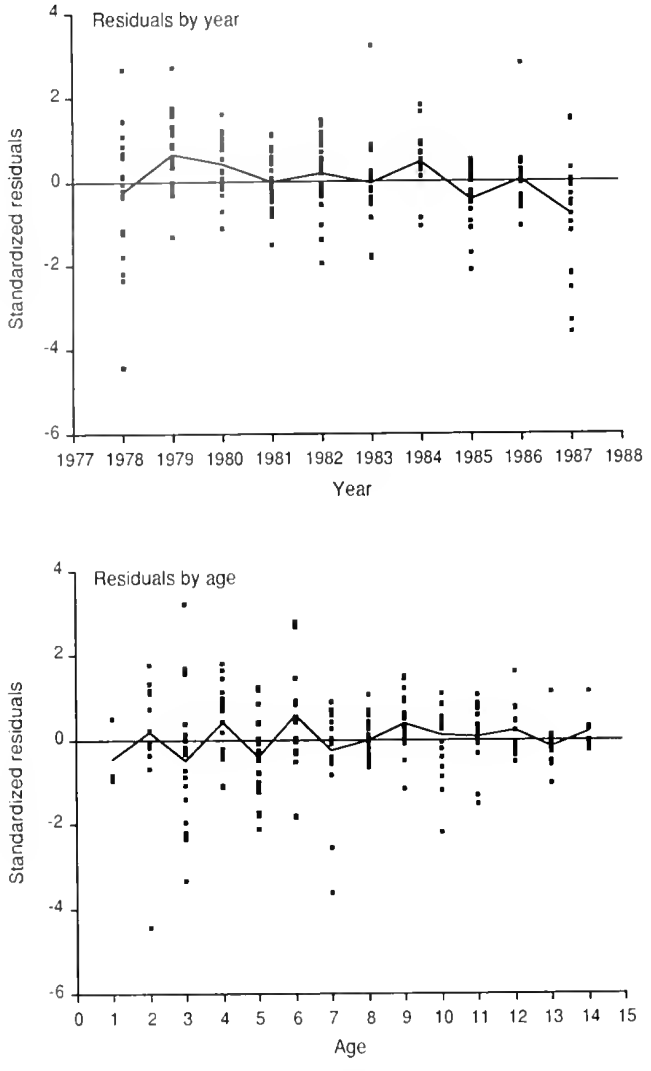

Figure 5

Standardized residuals by age and by year for the final model, which included g_0 and g_1 (coefficients modeling asymptotic growth), and coefficients for sex, sea-surface temperature, and population density. Lines connect averages of the residuals at each cluster of points.

Discussion

Although density-dependent growth has been demonstrated for many fishes (Shepherd and Grimes 1983, Reish et al. 1985, Ware 1985, Ross and Almeida 1986, Peterman and Bradford 1987, Overholtz 1989), few researchers would argue that density-dependent growth is an important characteristic of all fish populations. The age-structured yield models first developed by Beverton and Holt (1957)—currently used to manage many temperate marine fish stocks—use a fixed schedule of weight-at-age to calculate the yield, regardless of the level of population abundance. For a stock of Atlantic mackerel, however, the historically observed variation in weight-at-age attributable to density-dependent growth had a significant effect on the projected yields from the fishery (Overholtz et al. 1991). For Pacific whiting, this potential for changes in weight-at-age to influence yield is taken into account by using the weight-at-age observed in recent years to project the yield for the upcoming year (Dorn and Methot 1990). To obtain a fishing mortality rate that gives the long-term sustainable yield, the average weight-at-age over the history of the fishery is used. This strategy tacitly assumes that the current decline in weight-at-age is not a permanent change in the population.

Parrish et al. (1981) state that the principal resident species of the California Current system do not exhibit density-dependent growth. They contend that the population size of these species is controlled by environmental variability during the larval stages. As a result, the adults are seldom plentiful enough to reach a food-limited carrying capacity.

A contrasting viewpoint is found in Boehlert et al. (1989) who present evidence that the large biomass removals of *Sebastes* spp. in the years 1966–70 off the west coast of the United States resulted in increases in the annual growth of two members of this genus: canary rockfish *S. pinniger* and splitnose rockfish *S. diploproa*. They maintain that the decline in the total abundance of *Sebastes* spp. has had an effect on food availability for individual rockfish species. Although euphausiids are shared by most *Sebastes* species as the principal prey (Brodeur and Percy 1984), they are also a major link in the food chain of the California Current ecosystem, supporting numerous fish and invertebrate populations. For this reason, it is unlikely that changes in the abundance of *Sebastes* spp. alone could have had a substantial impact on the overall abundance of euphausiids in the California Current ecosystem. However, since rockfish are spatially restricted to habitats with limited area, the density-dependent growth displayed by *S. pinniger* and *S. diploproa* may be due to density-dependent changes in the food availability within these habitats. The possibility that cropping by Pacific whiting and other species significantly affects the abundance of euphausiids in the California Current ecosystem at large has not yet been adequately tested, though Mullin and Conversi (1989) were unable to detect any change in the abundance of euphausiids in the California current system after the start of the

large-scale fishery for Pacific whiting *Merluccius productus* in 1966.

Environmental influence on growth has been observed for many marine fish species (Kreuz et al. 1982, Anthony and Fogarty 1985). Because it can be easily measured and is associated with widespread changes in the aquatic environment, water temperature is the covariate most often studied. Water temperature may have a direct physiological effect on the growth of fish, or it may be indirectly linked to growth. For example, decreases in water temperature occur with the onset of upwelling in many coastal marine environments. On the west coast of North America, the availability of coastal upwelling indices on monthly, weekly, and daily time scales (Mason and Bakun 1986) has made it possible to investigate the direct effect of upwelling on growth, although convincing evidence of a link has not yet been found (Kreuz et al. 1982, Francis 1983, Boehlert et al. 1989).

Results from the Pacific whiting growth-increment regression show that an environmental covariate, sea-surface temperature, and population density could explain the deviations from a simple baseline model for asymptotic growth. The effect of temperature was greatest on the youngest ages present in the fishery samples and declined as age increased. In contrast, the effect of population biomass on annual growth increased with age. Temperature was the most important covariate, both in terms of its statistical significance and its effect on growth. This association of enhanced growth and reduced sea temperature is consistent with what is known about the California Current, a major eastern boundary current system. Kreuz et al. (1982) found an identical inverse effect on the growth of English sole *Parophrys vetulus* and Dover sole *Microstomus pacificus* at two locations off the Oregon coast.

Two mechanisms are believed to contribute to the high productivity of the California Current system. Coastal upwelling, generated by wind-driven offshore transport in the surface Ekman layer, brings low temperature, low salinity, and nutrient-rich water to the surface (Bakun and Nelson 1977). A second mechanism is the southward advection of water from the Alaskan Subarctic Gyre. This water is characterized by low temperatures, high nutrient content, and a large standing stock of zooplankton (Roesler and Chelton 1987). Regardless of which mechanism is dominant during a particular year, low mean sea-surface temperature during the summer can be expected to be associated with high productivity.

The diet of Pacific whiting provides the link between primary productivity and growth. The major prey of Pacific whiting are euphausiids, primarily *Thysanoessa spinifera* and *Euphausia pacifica* (Livingston 1983, Rexstad and Pikitch 1986). In summer, the abundance and pattern of distribution of these short-lived species (1–2 yr) are closely tied to upwelling and primary productivity (Simard and Mackas 1989). Rexstad and Pikitch (1986) found that euphausiids comprised 90% by weight of the diet of Pacific whiting 30–44 cm in length collected during a trawl survey in 1983 off the coasts of Oregon and Washington. Above 45 cm, a length which corresponds approximately to ages 5–7, this percentage drops to 20%. In the diet of the older Pacific whiting, euphausiids are largely replaced by small schooling fish and shrimp. These include northern anchovy *Engraulis mordax*, Pacific herring *Clupea harengus pallasi*, eulachon *Thaleichthys pacificus*, pink shrimp *Pandalus jordani*, and rockfish *Sebastes* spp. (Livingston 1983).

This shift in dietary preferences by Pacific whiting may help explain the effect of population biomass on growth. When the biomass of Pacific whiting is high, predation on fish species with multiyear life cycles may become intense enough to reduce their availability to the whiting population. In contrast, euphausiid abundance is closely coupled to annual variations in productivity, so whiting predation would likely have little effect on their abundance.

Some supporting evidence for density-dependent growth of Pacific whiting is found in Dark (1975), who also documented a decline in length-at-age using fishery samples from an earlier period in the fishery, 1964–69. At the time of Dark's research, estimates of population abundance were not available for Pacific whiting. It is now believed that the 1961 year-class was exceptionally strong, nearly the same size as the record 1980 year-class (Dorn and Methot 1990). Consequently, this earlier decline in length-at-age may also be partly attributable to increases in population density as the 1961 year-class moved into the population.

Although weight-at-age is the measure of size typically used in stock assessment models, the analysis in this paper focuses on length rather than weight. A practical reason for this strategy is that most at-sea sampling platforms are not sufficiently stable to obtain accurate individual weights of fish. Indeed, the weights-at-age used in stock assessment models for Pacific whiting are obtained by first estimating length-at-age, then converting to weight using a length-weight relationship (Dorn and Methot 1990). In addition, growth in length has several characteristics that make it amenable for analytical modeling. Except in very rare instances, changes in fish length are always positive or zero. The annual growth increment in length summarizes the growth response of the organism to environmental conditions that are prevalent throughout the year, or are short-term. In contrast, weight-at-age has a seasonal pattern of increase and decline, associated

with spawning, migration, and feeding, which would have to be accounted for in a model before analyzing environmental influences on growth.

Underlying this seasonal pattern of variation in weight is the length-weight relationship characteristic to a species, determined by the overall shape of the fish. Extreme departures from the typical length-weight relationship are unlikely to persist. Fish that are heavy in relation to their length in one year would tend to grow faster in length than average, while underweight fish would tend to experience slower growth in length. Adjustments to an individual's annual reproductive effort can also dampen departures from the typical length-weight relationship (Tyler and Dunn 1976).

During the period covered by this analysis, the length-weight relationship of Pacific whiting has varied from year to year, most noticeably in 1983, when mean weight was extremely low at a given length (Dorn and Methot 1990). The link between anomalies in the length-weight relationship and annual growth increments is best demonstrated by the results of a trial model that used the anomaly in the estimated weight at 45cm from the annual length-weight regression (Dorn and Methot 1990) as the only predictor variable for the annual growth increment. This variable was highly significant in the model ($P<0.001$), indicating that the annual growth increment is low during years where the length-weight relationship is below average. This result also supports the hypothesis that variation in Pacific whiting length-at-age is caused by environmental processes that affect the availability of food.

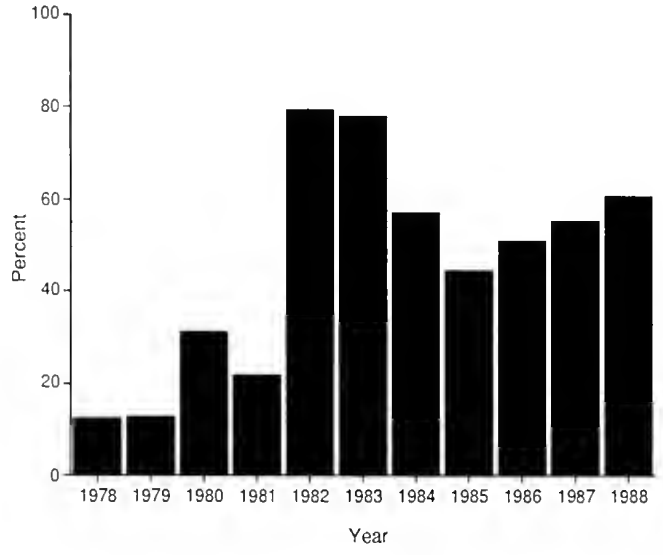

Figure 6

Percent of the Pacific whiting *Merluccius productus* catch biomass taken north of Cape Falcon (lat. 46°45'N) near the mouth of the Columbia River, during 1978–88. Catch of Pacific whiting from the Canadian zone is included in the calculations.

The analysis presented in this paper is based exclusively on fishery data. It should be acknowledged that there are numerous problems associated with the use of fishery statistics to infer growth patterns of fish within a population. Incomplete, size-dependent recruitment to a fishery can make fishery data on length-at-age a biased estimate of population length-at-age. Ageing error can distort the estimates of length-at-age when the year-classes have large differences in abundance. Shifts in the geographic and temporal pattern of the fishery, or shifts in the geographic distribution of the population itself, can cause spurious changes in estimates of length-at-age. The lengths for less abundant age-groups are not estimated as precisely as those for abundant age-groups. This is particularly true of extremely young and old fish, as these age-groups may be represented in fishery samples by only one or two individuals which determine the mean length for that age-group.

The severity of some of these problems can be reduced by using the procedures described in the Appendix for compiling strata estimates of length-at-age and calculating variance estimates. Length-at-age for temporal and geographic strata can be examined separately before being combined to produce annual summary statistics. Length-at-age estimates based on only a few individuals can be discounted in the analysis by using the estimated variances of length-at-age as weights. Nevertheless, some factors affecting growth can only be addressed by modeling fisheries as both a source of information on the stock and a major influence on its dynamics. The growth-increment regression model used in this paper assumes that the fishery samples the population without bias, so it is not the appropriate framework for studying these processes. Models with size-selective fishing mortality and stochastic growth have been developed for exploited fish populations (Deriso and Parma 1988, Parma and Deriso 1990). The practical application of these models is limited by the difficulty of distinguishing between different sources of growth variability using only catch data.

Size-selective mortality may have played a role in causing variation in length-at-age of Pacific whiting over the years covered by this analysis. Since the length ANOVA found a significant increase in length from south to north, a northward shift in the fishery would tend to increase length-at-age in the catch. At the same time, however, the length-at-age of the survivors of the

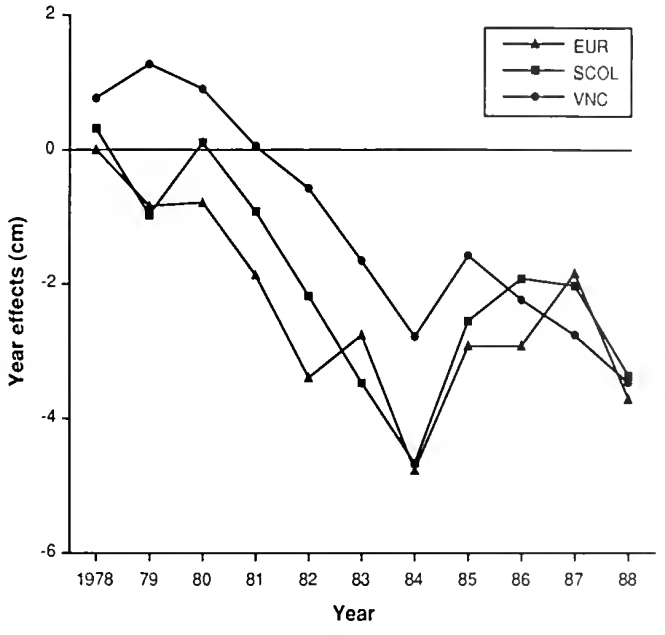

Figure 7

Estimated coefficients for a region-year interaction in a factorial analysis of variance, with the terms age, year, region, sex, season, and region-year interaction, for U.S. fishery length-at-age estimates of Pacific whiting *Merluccius productus* over 1978–88.

fishery would decrease, and this would tend to decrease the length-at-age in the catch in the following year from what it would have been otherwise. From 1978 to 1982, the fraction of the Pacific whiting catch taken north of Cape Falcon (near the mouth of the Columbia River at lat. 46°45′N) increased from 10% to 80%, and was 60% in 1988 (Fig. 6). The lack of fit of the growth-increment regression model with respect to year in Figure 5 may have been a result of this northward shift in fishing mortality.

However, it is difficult to predict the long-term effects of a shift in the geographic pattern of exploitation on length-at-age, because little is known about the extent of mixing from one year to the next of fish migrating from different regions. Without mixing between regions, an increase in fishing in the northern part of the range would reduce the abundance of larger individuals of an age-group, reducing the overall population length-at-age, while length-at-age of the southern fish would be unaffected. A more likely hypothesis is that some inter-regional mixing occurs from year to year. In this case, the length-at-age in all regions would decrease, though the magnitude of the decrease should be greatest in the north where the higher fishing occurred. Ultimately, this would tend to reduce latitudinal variation in length-at-age.

To support this hypothesis, there is some evidence of a change in the degree of latitudinal segregation by size of Pacific whiting. Figure 7 shows the coefficients for a region-year interaction for a length ANOVA with main effects being age, year, region, sex, and season. The absence of interaction between year and region would be identified by parallel year effect lines for each region, and would indicate that size-specific migratory pattern has remained constant. From 1978 to 1985, the region-year interaction does not appear prominent. After 1985, however, the lengths-at-age in the three regions become much closer together; in particular, the lengths of the fish in the VNC region, instead of being 1–2 cm larger than the fish in the other regions, are the same size or smaller.

Recently, Smith et al. (1990) examined the length-at-age data from the fishery for Pacific whiting in the Canadian waters over the same years examined by this paper. They used a generalized form of the von Bertalanffy growth model that makes length-at-age a function of length-at-age in the previous year, plus environmental covariates modeled in different ways according to a hypothesized mechanism by which the environmental covariate affects growth or apparent growth. Significant covariates in their model were population biomass, a suite of oceanographic variables measuring the strength of southward advection of water from the Alaskan Subarctic Gyre, and several variables that model size-selective mortality. Since fish younger than age 5 are not common in the Canadian samples, their analysis could not examine the sources of growth variability of the younger fish. Consequently, the analysis presented here on the environmental covariates of Pacific whiting growth in U.S. waters is a necessary complement to the paper by Smith et al. (1990). For example, an inverse relationship between temperature and growth, which is most pronounced for the younger fish, was not detected by Smith et al. (1990), and can partly account for the fact that the fish currently recruiting to Canadian waters at age 5 are much smaller than those recruiting in the late 1970's.

A major contention of Smith et al. (1990) is that expansion of the Canadian fishery is largely responsible for the decline in length-at-age observed since 1976. They used the ratio of the Canadian catch (in biomass) to the total population biomass during the current year as a covariate in their nonlinear regression model, a phenomenological approach that sidesteps the need to model the population dynamics. Although the monotonically increasing Canadian catch of Pacific whiting

since 1976 (except for 1985) and the declining length-at-age over the same period guarantees a statistically significant result, the real role of the Canadian fishery in determining length-at-age can be established only in a wider context that considers the magnitude and the geographic pattern of the fishery for Pacific whiting in U.S. waters. The region-year interaction coefficients in Figure 7 show that, up until 1984, the severity of the decline in length-at-age was similar in all three geographic regions in U.S. waters, extending from California north to the U.S.–Canada border. This is difficult to reconcile with the contention that the Canadian fishery is primarily responsible for the decline in length-at-age.

Both Smith et al. (1990) and this study used growth models that do not take into account the dynamics of the population, and as a consequence both have shortcomings which limit the growth- related phenomena to which they can be applied. An important direction for further research is the development of models for Pacific whiting that simultaneously model the growth and the population dynamics of the stock, including size-specific migratory behavior.

Acknowledgments

I thank Anne Hollowed, Daniel Kimura, Patricia Livingston, and Richard Methot for their comments on a preliminary version of this paper. In addition, suggestions by two anonymous reviewers significantly improved this paper.

Citations

Anthony, V.C., and M.J. Fogarty
1985 Environmental effects on recruitment, growth, and vulnerability of Atlantic herring (*Clupea harengus*) in the Gulf of Maine region. Can. J. Fish. Aquat. Sci. 42(Suppl. 1):158–173.

Bailey, K.M., R.C. Francis, and P.R. Stevens
1982 The life history and fishery of Pacific whiting, *Merluccius productus*. Calif. Coop. Oceanic Fish. Invest. Rep. 23: 81–98.

Bakun, A., and C.S. Nelson
1977 Climatology of upwelling related processes off Baja California. Calif. Coop. Oceanic Fish. Invest. Rep. 19:107–127.

Beverton, R.J.H., and S.J. Holt
1957 On the dynamics of exploited fish populations. Fish. Invest. Minist. Agric. Fish. Food (G.B.) Ser. II(19), 533 p.

Boehlert, G.W., and R.F. Kappenman
1980 Variation of growth with latitude in two species of rockfish (*Sebastes pinniger* and *S. diploproa*) from the northeast Pacific Ocean. Mar. Ecol. Prog. Ser. 3:1–10.

Boehlert, G.W., M.M. Yoklavich, and D.B. Chelton
1989 Time series of growth in the genus *Sebastes* from the northeast Pacific Ocean. Fish. Bull., U.S. 87:791–806.

Brodeur, R.D., and W.G. Pearcy
1984 Food habits and dietary overlap of some shelf rockfishes (genus *Sebastes*) from the northeastern Pacific Ocean. Fish. Bull., U.S. 82:269–294.

Dark, T.A.
1975 Age and growth of Pacific hake, *Merluccius productus*. Fish. Bull., U.S. 73:336–355.

Deriso, R.B., and A.M. Parma
1988 Dynamics of age and size for a stochastic population model. Can. J. Fish. Aquat. Sci. 45:1054–1068.

Dixon, W.J. (editor)
1983 BMDP statistical software. Univ. Calif. Press, Berkeley, 734 p.

Dorn, M.W., and R.D. Methot
1990 Status of the Pacific whiting resource in 1989 and recommendations for management in 1990. NOAA Tech. Memo. NMFS F/NWC-182, Alaska Fish. Sci. Cent., Seattle, 84 p.

Francis, R.C.
1983 Population and trophic dynamics of Pacific hake (*Merluccius productus*). Can. J. Fish. Aquat. Sci. 40:1925–1943.

French, R., R. Nelson Jr., and J. Wall
1981 Results of U.S. observer sampling on Japanese, U.S.S.R., Korean, and Polish fishing vessels, 1979. Int. North Pac. Fish. Comm., Annu. Rep. 1980:96–122.

Hollowed, A.B., S.A. Adlerstein, R.C. Francis, M. Saunders, N.J. Williamson, and T.A. Dark
1988 Status of the Pacific whiting resource in 1987 and recommendations to management in 1988. NOAA Tech. Memo. NMFS F/NWC-138, Alaska Fish. Sci. Cent., Seattle, 54 p.

Kimura, D.K.
1980 Likelihood methods for the von Bertalanffy growth curve. Fish. Bull., U.S. 77:765–776.
1989 Variability in estimating catch in numbers-at-age and its impact on cohort analysis. *In* Beamish, R.J., and G.A. McFarlane (eds.), Effects of ocean variability on recruitment and an evaluation of parameters used in stock assessment models, p. 56–66. Can. Spec. Publ. Fish. Aquat. Sci. 108.

Kimura D.K., and S. Chikuni
1987 Mixtures of empirical distributions: An iterative application of the age-length key. Biometrics 43:23–34.

Kreuz, K.F., A.V. Tyler, G.H. Kruse, and R.L. Demory
1982 Variation in growth of Dover soles and English soles as related to upwelling. Trans. Am. Fish. Soc. 111:180–192.

Kruse, G.H., and A. Huyer
1983 Relationships among shelf temperatures, coastal sea level, and the coastal upwelling index off Newport, Oregon. Can. J. Fish. Aquat. Sci. 40:238–242.

Livingston, P.A.
1983 Food habits of Pacific whiting, *Merluccius productus*, off the west coast of North America, 1967 and 1980. Fish. Bull., U.S. 81:629–636.

Mason, J.E., and A. Bakun
1986 Upwelling index update, U.S. West Coast, 33N–48N latitude. NOAA Tech. Memo. NMFS-SWFC-67, Southwest Fish. Sci. Cent., La Jolla, 81 p.

Muflin, M.M., and A. Conversi
1989 Biomasses of euphausiids and smaller zooplankton in the California current—Geographic and interannual comparisons relative to the Pacific whiting, *Merluccius productus*, fishery. Fish. Bull., U.S. 87:633–644.

Overholtz, W.J.
1989 Density-dependent growth in the northwest Atlantic stock of Atlantic mackerel (*Scomber scombrus*). J. Northwest Atl. Fish. Sci. 9:115–121.

Overholtz, W.J., S.A. Murawski, and W.L. Michaels
1991 Impact of compensatory responses on assessment advice for the Northwest Atlantic mackerel stock. Fish. Bull., U.S. 89:117–128.

Parma, A.M., and R.B. Deriso
1990 Dynamics of age and size composition in a population subject to size-selective mortality: Effects of phenotypic variability in growth. Can. J. Fish. Aquat. Sci. 47:274–289.

Parrish, R.H., C.S. Nelson, and A. Bakun
1981 Transport mechanisms and reproductive success of fishes in the California Current. Biol. Oceanogr. 1(2):175–203.

Pauly, D., and G. Gaschütz
1979 A simple method for fitting oscillating length growth data with a program for pocket calculators. Int. Counc. Explor. Sea CM 1979/G:24.

Peterman, R.M., and M.J. Bradford
1987 Density-dependent growth of age 1 English sole (*Parophrys vetulus*) in Oregon and Washington coastal waters. Can. J. Fish. Aquat. Sci. 44:48–53.

Ratkowsky, D.A.
1983 Nonlinear regression modeling. Marcel Dekker, NY, 276 p.

Reish, R.L., R.B. Deriso, D. Ruppert, and R.J. Carroll
1985 An investigation of the population dynamics of Atlantic menhaden (*Brevoortia tyrannus*). Can. J. Fish. Aquat. Sci. 42(Suppl. 1):147–157.

Rexstad, E.A., and E.K. Pikitch
1986 Stomach contents and food consumption estimates of Pacific hake, *Merluccius productus*. Fish. Bull., U.S. 84: 947–956.

Roesler, C.S., and D.B. Chelton
1987 Zooplankton variability in the California Current, 1951–1982. Calif. Coop. Oceanic Fish. Invest. Rep. 28:107–127.

Ross, M.R., and F.P. Almeida
1986 Density-dependent growth of silver hakes. Trans. Am. Fish. Soc. 115:548–554.

Shepherd, G., and C.B. Grimes
1983 Geographic and historic variations in growth of weakfish, *Cynoscion regalis*, in the Middle Atlantic Bight. Fish. Bull., U.S. 81:803–813.

Simard, Y., and D.L. Mackas
1989 Mesoscale aggregations of euphausiid sound scattering layers on the continental shelf of Vancouver Island. Can. J. Fish. Aquat. Sci. 46:1238–1249.

Singh, B.D., and D. Singh
1965 Some remarks on double sampling for stratification. Biometrika 52:587–590.

Smith, B.D., G.A. McFarlane, and M.W. Saunders
1990 Variation in Pacific hake (*Merluccius productus*) summer length-at-age near southern Vancouver Island and its relationship to fishing and oceanography. Can. J. Fish. Aquat. Sci. 47:2195–2211.

Tyler, A.V., and R.S. Dunn
1976 Ration, growth, and measures of somatic and organ condition in relation to meal frequency in winter flounder, *Pseudopleuronectes americanus*, with hypotheses regarding population homeostasis. J. Fish. Res. Board Can. 33:63–75.

Ware, D.M.
1985 Life history characteristics, reproductive value, and resilience of Pacific herring (*Clupea harengus pallasi*). Can J. Fish. Aquat. Sci. 42(Suppl. 1):127–137.

Weisberg, S.
1986 A linear model approach to backcalculation of fish length. J. Am. Stat. Assoc. 81:922–929.

Appendix: Variance estimates of mean length-at-age using a two-phase sampling procedure

The length and age samples collected by observers in the Pacific whiting fishery are recorded by haul or joint-venture delivery. The position and date of each sampled haul and joint-venture delivery are also recorded. In compiling the length-at-age estimates for spatial and temporal strata, all the data collected within that strata are aggregated and assumed to originate from random sampling from the catch within that strata.

Sampling design

A large initial random sample is obtained from the catch, and the length and sex of each fish is recorded. For the second phase of sampling, a subsample of fixed size is selected for each combination of length category and sex. All fish in these subsamples are aged using otoliths or other ageing structures.

Notation

i = 1,...,I length categories
j = 1,...,J age categories
n' = first-phase sample size
n'_i = number of fish of n' in length category i
q_i = probability that a fish is in length category i
n_i = subsample sizes
n_{ij} = number of the subsample taken from length category i of age j
q'_{ij} = pr(j|i), probability of age j given length i
q_{ij} = pr(i|j), probability of length category i given age j
p_j = pr(j), probability of age j
l_i = midpoint of *ith* length category
$\bar{l}_j$ = mean length of age j fish

To simplify notation, subscripts for males and females are not defined. The variance estimator obtained here is conditional on the first- and second-phase sample sizes. Separate estimates for males and females can be obtained by separating the samples by sex and conditioning on the number of each sex in the first- and second-phase samples. The same variance estimator is appropriate for separate sex estimates.

Sampling distributions

Assuming that the first-phase sample size n' is much smaller than the size of the population being sampled, the distribution of n'_i can be modeled by the multinomial distribution,

$$f(\{n'_i\} \mid n', \{q_i\}) = \left(\frac{n'!}{\prod_i n'_i!} \right) \prod_i q_i^{n'_i},$$

where $\sum_i q_i = 1$. Estimators for $\{q_i\}$ and the elements of the variance-covariance matrix of $\{q_i\}$ are

$$\hat{q}_i = \frac{n'_i}{n'},$$

$$\hat{\mathrm{Var}}(\hat{q}_i) = \frac{\hat{q}_i(1-\hat{q}_i)}{n'},$$

$$\hat{\mathrm{Cov}}(\hat{q}_i, \hat{q}_h) = -\frac{\hat{q}_i \hat{q}_h}{n'}.$$

To obtain a distribution for $\{n_{ij}\}$, it is convenient to condition on the fixed subsamples n_i. As in the case of the first phase of sampling, it is assumed that n_i is much less than the number in the population of that length category, so that a product of multinomial distributions is obtained for the second phase of sampling,

$$f(\{n_{ij}\} \mid \{n_i\}, \{q'_{ij}\}) = \prod_i \left[\left(\frac{n_i!}{\prod_j n_{ij}!} \right) \prod_j q'^{n_{ij}}_{ij} \right],$$

where $\sum_j q'_{ij} = 1$ for all i. Estimators for $\{q'_{ij}\}$ and the elements of the variance-covariance matrix of $\{q'_{ij}\}$ are

$$\hat{q}'_{ij} = \frac{n_{ij}}{n_i},$$

$$\hat{\mathrm{Var}}(\hat{q}'_{ij}) = \frac{\hat{q}'_{ij}(1-\hat{q}'_{ij})}{n_i},$$

$$\hat{\mathrm{Cov}}(\hat{q}'_{ij}, \hat{q}'_{hk}) = -\frac{\hat{q}'_{ij} \hat{q}'_{hk}}{n_i},$$

for $i = h$ and zero otherwise.

A troublesome inconsistency with this approach is that the n_i are assumed to be predetermined quantities. In fact, n_i is necessarily less than or equal to n'_i, the number in the *i*th length category from the first-phase sampling, and n'_i is a random variable that can take values between zero and the $\min(n', N_i)$ where N_i is the number of fish of length category i in the total catch. Singh and Singh (1965) address this issue while developing variance estimators for what in this fisheries application would correspond to mean age. While they were able to obtain estimators which correctly modeled the sampling procedures, they also found that their exercise in theoretical rigor did not result in any appreciable difference in practice.

Estimation of mean length-at-age

An unbiased estimate of $\bar{l}_j$ is given by

$$\bar{l}_j = \sum_i l_i q_{ij},$$

where q_{ij} is the probability of length i given age j. An expression for q_{ij} is obtained using Bayes theorem,

$$q_{ij} = \frac{q_i q'_{ij}}{\sum_i q_i q'_{ij}}.$$

A variance approximation for mean length-at-age

Because the above expression for mean length-at-age is nonlinear in the observations $\{n'_i\}$ and $\{n_{ij}\}$, a delta-method approximation is derived. Delta-method estimators can be algebraically complex but all have the same simple structure. For mean length-at-age, a delta-method approximation is given by

$$\mathrm{Var}(\bar{l}_j) \approx \mathbf{d}_j^{\mathrm{T}} \mathbf{V} \mathbf{d}_j,$$

where $\mathbf{d}_j$ is the vector of partial derivatives of $\bar{l}_j$ with respect to $\{q_i\}$ and $\{q'_{ij}\}$, and $\mathbf{V}$ is the variance-covariance matrix of $\{q_i\}$ and $\{q'_{ij}\}$. Defining

$$A_j = \sum_i l_i \hat{q}_i \hat{q}'_{ij},$$

and

$$\hat{p}_j = \sum_i \hat{q}_i \hat{q}'_{ij},$$

the elements of the vector of partial derivatives are given by

$$\frac{\partial \bar{l}_j}{\partial q_i} = \frac{\hat{q}'_{ij}(l_i \hat{p}_j - A_j)}{\hat{p}_j^2}$$

and

$$\frac{\partial \bar{l}_j}{\partial q'_{ij}} = \frac{\hat{q}_i(l_i \hat{p}_j - A_j)}{\hat{p}_j^2}.$$

Combining these expressions with the estimators for the variance-covariance matrix of q_i and q'_{ij} given earlier,

$$\hat{\mathrm{Var}}(\bar{l}_j) = \left[\frac{1}{\hat{p}_j}\right]^4 \left\{\sum_i (l_i\hat{p}_j - A_j)^2 \left(\frac{\hat{q}_i(1-\hat{q}_i)\hat{q}'^2_{ij}}{n'} + \frac{\hat{q}'_{ij}(1-\hat{q}'_{ij})\hat{q}_i^2}{n_i}\right) - \sum_{i\neq h}\sum \hat{q}_i\hat{q}_h\hat{q}'_{ij}\hat{q}'_{hj}(l_i\hat{p}_j - A_j)\frac{(l_h\hat{p}_j - A_j)}{n'}\right\}.$$

Combining length-at-age from different strata

An estimate of combined mean length-at-age is

$$\bar{l}_j = \sum_h \left(\frac{c_{jh}}{c_j}\right)\bar{l}_{jh},$$

where l_{jh} is the length-at-age in the h*th* stratum, and c_{jh} is the catch-at-age for the same stratum.

Again using a delta-method approximation,

$$\mathrm{Var}(\bar{l}_j) = \sum_h \mathrm{Var}(c_{jh})\left[\frac{(\bar{l}_{jh}\,c_j - \sum_h c_{jh}\,\bar{l}_{jh})}{c_j^2}\right]^2 + \sum_h \mathrm{Var}(\bar{l}_{jh})\left[\frac{c_{jh}}{c_j}\right]^2.$$

The complete expression should include a term involving $\mathrm{Cov}(c_{jh}, \bar{l}_{jh})$. This term was always negligible compared with the other two terms, and depended on the method used to calculate the catch-at-age. Consequently, it is not included here. The variance estimator for combined length-at-age for several strata requires an estimate of the variance of catch-at-age. A method for obtaining this is given in Kimura (1989).

Influence of sectioning otoliths on marginal increment trends and age and growth estimates for the flathead *Platycephalus speculator*

Glenn A. Hyndes
School of Biological and Environmental Sciences, Murdoch University
Murdoch, Western Australia 6150, Australia

Neil R. Loneragan
School of Biological and Environmental Sciences, Murdoch University
Murdoch, Western Australia 6150, Australia
Present address: CSIRO Division of Fisheries
P.O Box 120, Cleveland, Queensland 4163, Australia

Ian C. Potter
School of Biological and Environmental Sciences, Murdoch University
Murdoch, Western Australia 6150, Australia

Abstract. – Comparisons are made between estimates of ages and growth of the flathead *Platycephalus speculator* Klunzinger, from a temperate Western Australian estuary, using data obtained from whole and sectioned otoliths. The consistent annual trends shown by the width of the opaque zone on the periphery (marginal increment) of sectioned otoliths, irrespective of the number of translucent zones, demonstrate that the translucent zones in these otoliths correspond to annuli. While the marginal increments on whole otoliths also showed a similar marked and consistent annual trend when a single translucent zone was present, they were far less conspicuous when two or more translucent zones were observed. The large sample size and strong trends shown by marginal increments on otoliths exhibiting one translucent zone accounts for the fact that, when data for all whole otoliths are pooled, the marginal increment still shows a consistent annual trend. Sectioning of otoliths enhances the ability to differentiate between the outer opaque and translucent zones, and also often reveals one or more additional inner translucent zones in older fish. The use of whole otoliths frequently underestimated age by one year in 2+ to 4+ fish and two years in 5+ to 10+ fish, and by as much as five or six years in the oldest fish (11+ and 12+). The respective 95% confidence limits for the parameters L_∞, K, and t_0 in the von Bertalanffy growth equations for males, calculated using data from sectioned otoliths, overlapped those calculated from data for whole otoliths, and the same was true for K with females. This similarity in growth curves in particularly the first four years of life can be attributed to the fact that approximately 74 and 65% of the growth of males and females, respectively, occurred in the first three years, when underestimates of age were limited.

Manuscript accepted 18 February 1992.
Fishery Bulletin, U.S. 90:276–284 (1992).

Since assessments of fish stocks often rely on information on age composition, it is crucial that any age estimates used for such assessments are validated (Beamish and McFarlane 1983, Casselman 1987). Validation that growth zones on hard structures, such as otoliths, scales, and spines, are formed annually is often implied by establishing that the pattern of growth on the periphery of these structures follows a consistent annual trend (e.g., Johnson 1983, Maceina et al. 1987, Potter et al. 1988, Beckman et al. 1989). In otoliths of fish in temperate waters, an opaque zone generally starts to form in the spring immediately outside the translucent zone laid down during the preceding winter. The width of this opaque zone usually increases between spring and autumn. Although a subsequent retardation of growth during winter results in formation of the translucent zone at the edge of the otolith, this translucent zone frequently cannot be readily detected until the following spring, when it becomes delineated by the formation of a new opaque zone. The distance outside the outer translucent zone constitutes the marginal increment. Therefore, if the outer opaque and translucent zones are formed annually, the marginal increment should decline only once during the year. Verification that trends shown by the marginal increments follow a pattern consistent with annual growth is an important method for establishing that the alternating translucent and opaque zones each correspond to annuli and are thus appropriate for use in ageing (Brothers 1983).

Many workers have presented data which showed that an annual trend was followed either by the marginal increment, when data for all otoliths in each sample were pooled, or by the overall incidence of otoliths possessing either translucent or opaque zones on their outer edge. When these have shown a consistent annual trend, it has often been concluded that all translucent zones correspond to annuli (e.g., Nel et al. 1985, Reis 1986, Rincon and Lobon-Cervia 1989, Crozier 1990, Hayse 1990). However, trends shown in such pooled data will be strongly influenced by those of the dominant groups, *vis a vis* the number of translucent zones, and may

not be representative of all groups. Furthermore, trends shown by the marginal increment in some long-lived fish become clear only after the otoliths have either been sectioned or broken and burnt (Campana 1984, Collins et al. 1988). This accounts for estimates of age sometimes being lower when whole otoliths have been used than when either sectioned or broken and burnt otoliths were employed (Beamish 1979a, Campana 1984, Collins et al. 1988).

Although the Platycephalidae occurs along the coasts and within estuaries throughout the Indo-west Pacific region, the majority of the 41 species of flathead found in Australia are restricted to its southern waters (Sriramachandra-Murty 1975, Paxton and Hanley 1989). Despite wide distribution and, in some cases, the commercial and recreational importance of the Platycephalidae, estimates of the age and growth of representatives of this family are limited to those obtained for *Platycephalus bassensis*, *P. castelnaui*, and *P. speculator* by Brown (1977) and for *P. richardsoni* by Colefax (1934), Fairbridge (1951), and Montgomery (1985), the populations of which were all located in southeastern Australia. The most abundant species of flathead on the temperate southern coast of Western Australia is *P. speculator*, a species which has been shown to breed within Wilson Inlet, the largest estuary of this region (Hyndes et al. In press).

Previous attempts to age platycephalids have used whole sagittal otoliths (Colefax 1934, Fairbridge 1951, Brown 1977, Montgomery 1985). However, a preliminary investigation of the translucent zones in the sagittal otoliths of *P. speculator* from southwestern Australia showed that the outer opaque and translucent zones on the otoliths of larger fish often became clear only when the otoliths had been sectioned.

The present study was undertaken to determine the age structure and growth of *P. speculator* in Wilson Inlet, where this species is abundant and contributes to the local commercial and recreational estuarine fisheries (Lenanton and Potter 1987). Emphasis has been placed on elucidating the degree to which sectioning the otoliths influences marginal increment trends, age estimates, and growth equations. In addition, marginal increment data were pooled for both whole and sectioned otoliths to examine whether the resultant overall annual marginal increment trends were strongly influenced by that of a group(s) of otoliths with a particular number(s) of translucent zones.

Materials and methods

Sampling locality and regime

Wilson Inlet (117°25′E and 34°50′S) has a narrow entrance channel which opens into a wide basin (48 km^2) supplied by two main tributary rivers. Water depth in the basin is generally less than 2 m. *Platycephalus speculator* was collected monthly from within the basin of Wilson Inlet between September 1987 and April 1989 using beach seines (mesh size in pocket 9.5 mm) during the day and gillnets (six stretched-mesh sizes, 38–102 mm), otter trawls (mesh size in pocket 25 mm) and plankton trawls at night (mesh size 1 mm).

Bottom water temperatures near the entrance channel of Wilson Inlet and 12 km further up the estuary near the top end of the basin were recorded at the time of sampling.

Age determination

Each fish was measured (total length) and weighed to the nearest 1 mm and 0.1 g, respectively. Sex was recorded when the gonad could be identified as either ovary or testis, which was usually possible in fish >100 mm in length. Both of the sagittal otoliths of 1305 juvenile and adult fish were cleaned, dried, and stored in gelatin capsules.

Whole otoliths were placed in methyl salicylate solution and examined microscopically under reflected light against a black background. The marginal increment, i.e., the distance between the outer edge of the outermost translucent zone and the periphery, was measured on one of the otoliths of each fish and expressed either as (1) a proportion of the distance between the focus and the outer edge of the translucent zone when only one translucent zone was present, or (2) as a proportion of the distance between the outer edges of the two outermost translucent zones when two or more translucent zones were present. Measurements were always made along the same axis, to the nearest 0.05 mm (Fig. 1). The number of translucent zones on each otolith was recorded.

These otoliths were later mounted and embedded in black epoxy resin (Bedford 1983, Augustine and Kenchington 1987) and cut into 1.5–2 mm transverse sections using the diamond saw described by Augustine and Kenchington (1987). Sections were mounted on glass slides and their surfaces ground on sequentially finer grades (400–1200) of carborundum paper. Sections were then coated with clear nail polish and examined microscopically under reflected light. Measurements of the marginal increment and counts of the number of translucent zones in these sectioned otoliths were carried out in precisely the same manner as described above for whole otoliths.

Mean marginal increment values were plotted separately for both whole and sectioned otoliths with 1–4 and ≥5 translucent zones to ascertain if they follow a consistent annual trend and thus permit the translucent zones to be considered as annuli. Width and

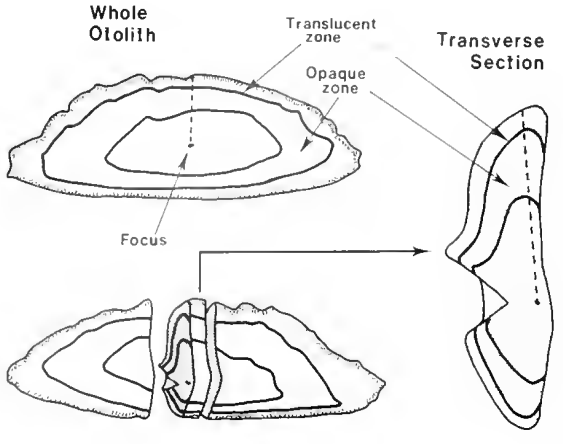

Figure 1

Schematic diagram showing the translucent and opaque zones in a whole and sectioned sagittal otolith of *Platycephalus speculator*. Broken line represents the axis along which measurements were taken.

thickness of the whole otoliths of 123 fish, covering the full range of sizes, were measured to the nearest 0.01 mm to examine the relationship between otolith width and thickness. The number of translucent zones in 140 otoliths, of which up to 20 otoliths came from each age-class (estimated from sectioned otoliths), were counted in whole and sectioned otoliths by a second 'reader' who had no previous experience in examining otoliths of this species. The reproducibility of age estimates for each method was determined by using the coefficient of variation (Sokal and Rohlf 1981, Chang 1982).

Von Bertalanffy growth curves were fitted to individual lengths of males and females at the estimated age-at-capture by a nonlinear technique (Gallucci and Quinn 1979) using a nonlinear subroutine in SPSS (SPSS 1988) and assuming a 'birth date' of 1 January. This date corresponds approximately to the midpoint of the period when, on the basis of gonadosomatic indices and trends shown by oocyte development, *P. speculator* exhibited peak spawning activity in Wilson Inlet (Hyndes et al. In press). The von Bertalanffy equation is $L_t = L_\infty\ [1 - e^{-K(t-t_0)}]$, where L_t is the length at age t (yr), L_∞ is the mean asymptotic length predicted by the equation, K is the growth coefficient, and t_0 is the hypothetical age at which fish would have zero length if growth followed that predicted by the equation. Comparisons have been made between the age estimates and von Bertalanffy growth curves, calculated from data obtained using whole and sectioned otoliths and assuming that, in both cases, the translucent zones correspond to annuli.

Results

Marginal increments

Annual trends in the mean marginal increments for whole and sectioned otoliths with one translucent zone were similar (Fig. 2). However, the sharp decline which occurred in the marginal increment after the winter (June–August) of 1988 was detected earlier in sectioned otoliths (October) than in whole otoliths (December). Although the data for 1987 were not as extensive, they still exhibited a similar marked decrease at the same time of year. In both years, the marginal increment on both whole and sectioned otoliths subsequently rose consistently through the summer, before leveling off in the late autumn and winter (Fig. 2).

Annual trends in mean marginal increments of sectioned otoliths with two, three, and four translucent zones parallel those in sectioned otoliths with one translucent zone, with marginal increments falling sharply in the spring (October) of both 1987 and 1988 (Fig. 2). Although the marginal increment on whole otoliths with two, three, and four translucent zones also declined in spring, the decrease was far less pronounced and the trends less consistent.

Since the number of otoliths with five or more translucent zones was small, values for the marginal increments on all such otoliths were pooled. Although seasonal trends shown by the marginal increment in sectioned otoliths with ≥ 5 translucent zones were slightly less consistent than in those with 1–4 such zones, they still followed a similar annual trend (Fig. 2). Furthermore, the translucent zones were still clearly visible and had the same appearance as those in otoliths with 1–4 translucent zones. No clear annual trend could be seen in the marginal increments of whole otoliths displaying ≥ 5 translucent zones (Fig. 2).

The above trends in marginal increments of sectioned otoliths (with a sharp decline only occurring at one time of the year, i.e., in the spring) show that the first four translucent zones on otoliths of *P. speculator* are laid down annually. Since the same trends were exhibited in pooled data for the fifth and subsequent translucent zones, these zones were presumably also, at least in most of these cases, laid down annually. We thus consider the translucent zone on sectioned otoliths as an annulus which can be used for ageing *P. speculator* from Wilson Inlet. The data also show that the outer opaque zone starts to form when water temperatures are rising from their winter (July) minima of about 11°C towards their summer (December–February) maxima of ~22°C (c.f. Figs. 2,3).

The annual trend shown by the mean marginal increment based on all sectioned otoliths, irrespective of the number of translucent zones, was essentially

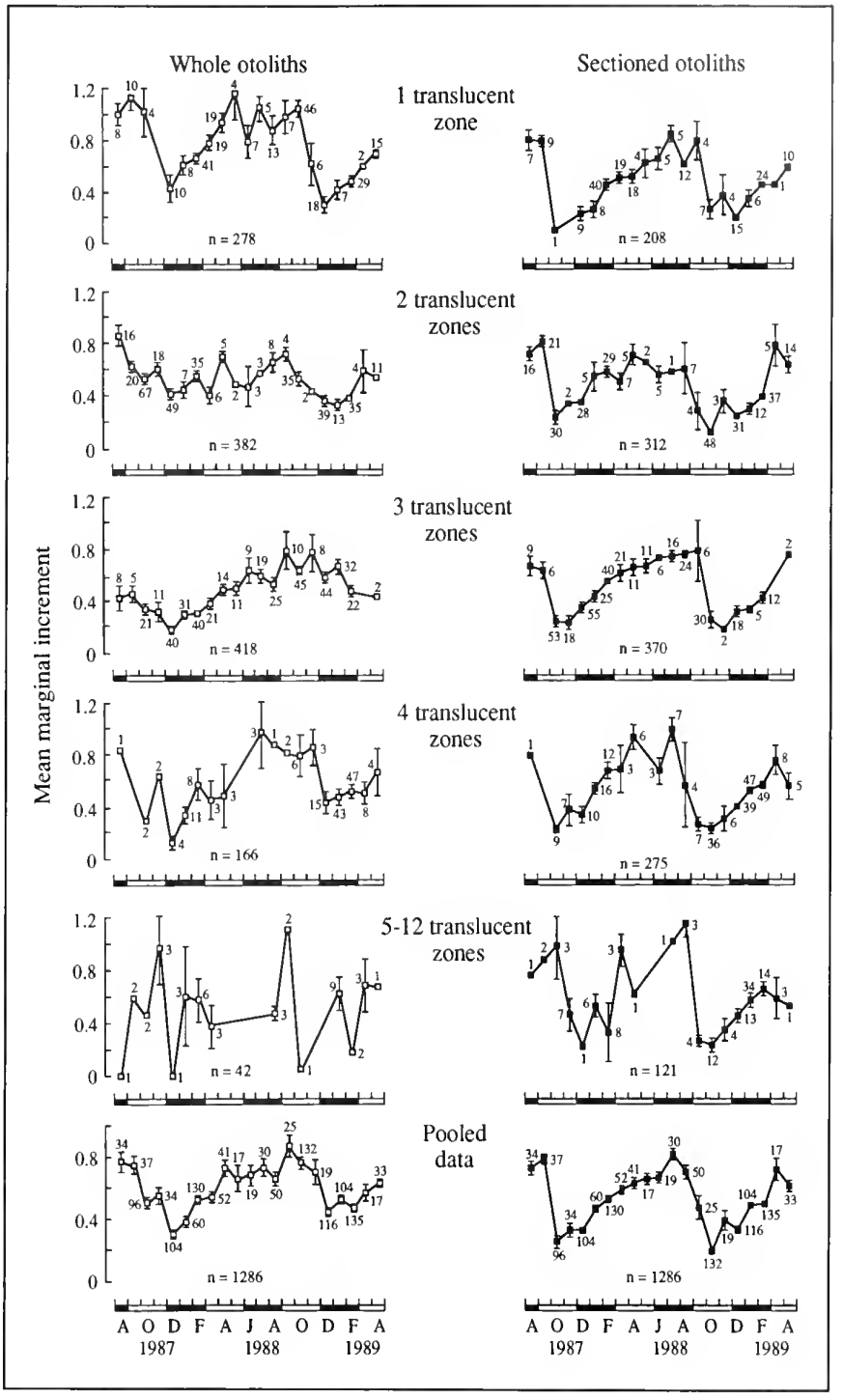

Figure 2
Mean marginal increments ± SE for whole and sectioned sagittal otoliths of *Platycephalus speculator*. Note that the marginal increment is given as a relative value, i.e., as a percentage of the distance between the focus and the outer translucent zone when only one zone was present, or as a percentage of the distance between the outer edges of the two outermost translucent zones when two or more such zones were present. In this Figure and in Figs. 3 and 6, the black bars on the x-axis refer to winter (June–Aug.) and summer (Dec.–Feb.) and the open bars to spring (Sept.–Nov.) and autumn (March–May).

the same as that of otoliths with 1–4 translucent zones (Fig. 2). Mean marginal increments based on all whole otoliths followed similar annual trends, but they were not as pronounced or consistent, and the variation about the means was greater (Fig. 2).

Length-frequency data

Few fish < 180 mm in length were caught (Fig. 4), reflecting the fact that smaller individuals of this benthic species did not tend to be collected by seine and gill-nets.

The three fish caught in the middle of spring (October) of 1987, which had otoliths with a single translucent zone bounded by a very narrow opaque zone, measured 91–106 mm in length (Fig. 4). This group is assumed to represent the 0+ age-class, i.e., the result of spawning which peaked in early January 1987 and can therefore be referred to as the 1987 year-class. The larger fish, which produced modal length-classes at 325–349 mm and 400–424 mm in October 1987 (Fig. 4), had otoliths with a narrow opaque zone bounding two and three translucent zones, respectively. The groups with two and three translucent zones therefore represent the 1+ and 2+ age-classes, or the 1986 and 1985 year-classes, respectively. Fish with otoliths exhibiting one, two, and three translucent zones in December 1987 and February 1988 are designated as representing the 1987, 1986, and 1985 year-classes, which is consistent with their length distributions (Fig. 4). The marked difference between the lengths of the 1987 year-class in October and December 1987 suggests that this year-class underwent remarkable growth between these months. However, the three fish caught in October were taken by beach seine in the shallows and are thus presumed to represent the lower end of the length range of this year-class, whereas those fish of the

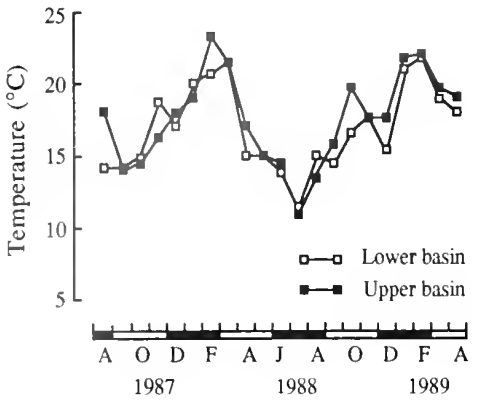

Figure 3
Bottom-water temperatures recorded at sites at lower and upper ends of the basin of Wilson Inlet, Western Australia, August 1987–April 1989.

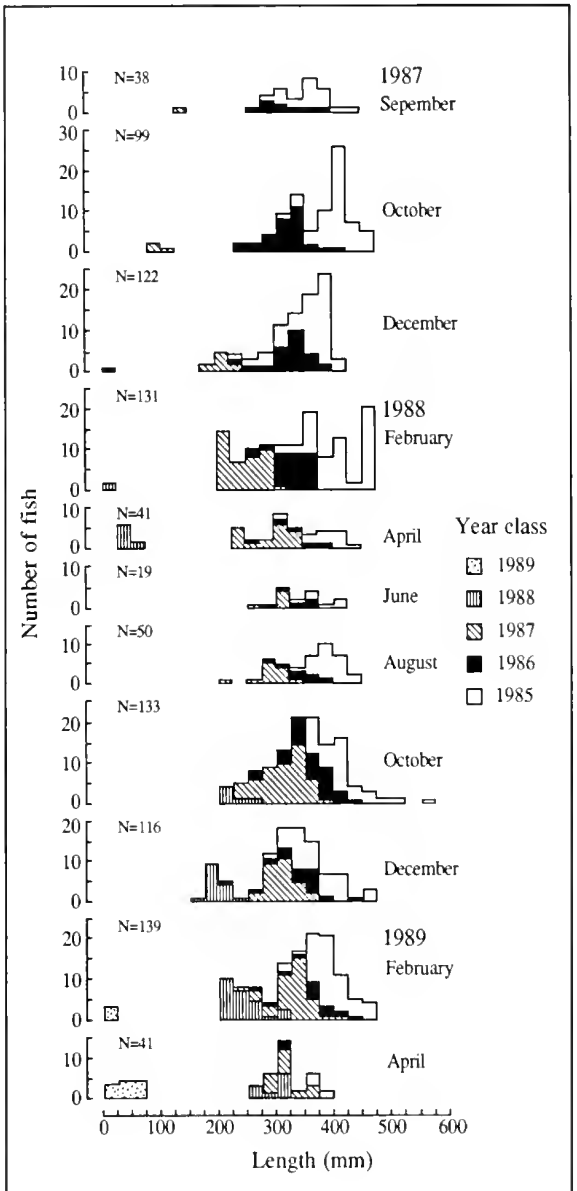

Figure 4
Length-frequency histograms for the 1985–89 year-classes of *Platycephalus speculator*.

corresponding cohort caught in December were taken in gillnets which, because of the mesh sizes of these nets, would have taken only the larger members of that year-class.

Larval *P. speculator*, ranging up to a length of 13 mm, were collected in plankton trawls in December 1987, February 1988, and February and April 1989 (Fig. 4). Otoliths of juveniles caught in April 1988 and 1989, and which from their lengths (23–89 mm) clearly corresponded to the 0+ age-class, did not have a translucent zone. The group of fish representing the 1988 year-class had reached 198–231 mm by December 1988, and 258–323 mm by April 1989. These length ranges are similar to those attained by the previous (1987) year-class in December 1987 and April 1988 (Fig. 4). The modal length of the 1+ age-class in October 1988 (= 1987 year-class) was identical to that of the 1+ age-class in October 1987 (= 1986 year-class). Six year-classes were usually found in samples from each month, and as many as eleven year-classes were present in February 1988 (older year-classes are not shown in Fig. 4). Maximum lengths for each sex were 696 mm for a 10+ female and 545 mm for a 12+ male.

Estimated ages and growth curves using whole and sectioned otoliths

All of the 197 otoliths which showed one translucent zone (= annulus) in sectioned otoliths also displayed a single zone prior to sectioning (Fig. 5). However, 44% of otoliths with two or more translucent zones after sectioning produced underestimates using whole otoliths. Between 23% and 57% of the otoliths with 2–4 annuli each showed one less translucent zone prior to sectioning and thus underestimated ages by 1 year. Discrepancies between the number of translucent zones in sectioned and whole otoliths were even more marked in otoliths with 5 or more translucent zones. Indeed, the numbers of annuli were as many as 5 or 6 less in whole otoliths than the 11 or 12 annuli observed in sectioned otoliths (Fig. 5). The proportion of underestimates using whole otoliths was greatest in spring for those otoliths which showed 2 or 3 translucent zones after sectioning (Fig. 6).

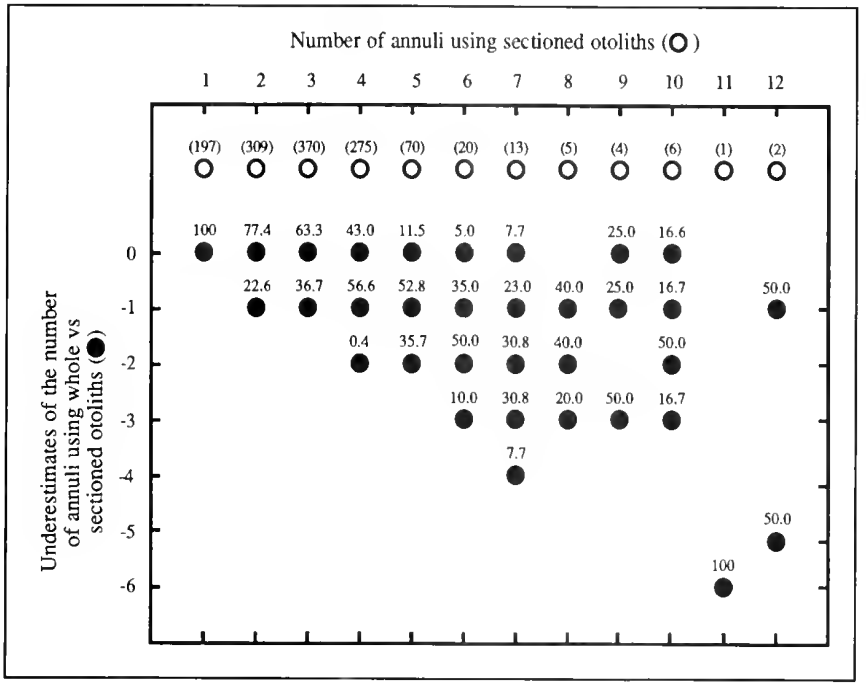

Figure 5
Number of otoliths with 1–12 annuli based on sectioned sagittal otoliths of *Platycephalus speculator*, and underestimates of the number of annuli observed on the same whole sagittal otoliths. Numbers in parentheses indicate the number of fish of different ages based on sectioned otoliths, while numbers above the closed circles indicate the percentage of underestimates using whole otoliths.

The coefficient of variation for replicate age estimates between readers was far less for sectioned otoliths (1.2%) than for the same otoliths prior to sectioning (8.7%). While the estimated age varied by only 1 year for each of the six sectioned otoliths for which there was disagreement, the estimated ages varied by as much as 3 years for the 53 whole otoliths for which there were discrepancies.

The relationship between width and thickness of sagittal otoliths of *P. speculator* is curvilinear, demonstrating that width does not increase proportionately with thickness (Fig. 7). The relationship between otolith width (W) and otolith thickness (T) is described by the following polynomial equation:

$$W = -0.283 + 4.635T - 1.175T^2 \quad (r^2\ 0.82,\ n\ 123).$$

The von Bertalanffy growth parameters for both male and female flathead were initially determined using individual lengths at estimated age (Table 1). Examination of the length-at-age plots showed that the curve for both sexes fell below the majority of the points for fish >5 years old, i.e., the asymptote was too pronounced to accommodate lengths of the older fish. Individual lengths of the fish were grouped into intervals of 0.1 years and the curves determined again by weighting the data by the inverse of the sample size for each age interval (Beckman et al. 1990). This procedure resulted in a better fit of the curve (Fig. 8). Although the values for t_0 for males and females were shifted slightly away from zero (namely from −0.134 to −0.332 and from −0.056 to −0.423, respectively), differences in the lengths of males and females at

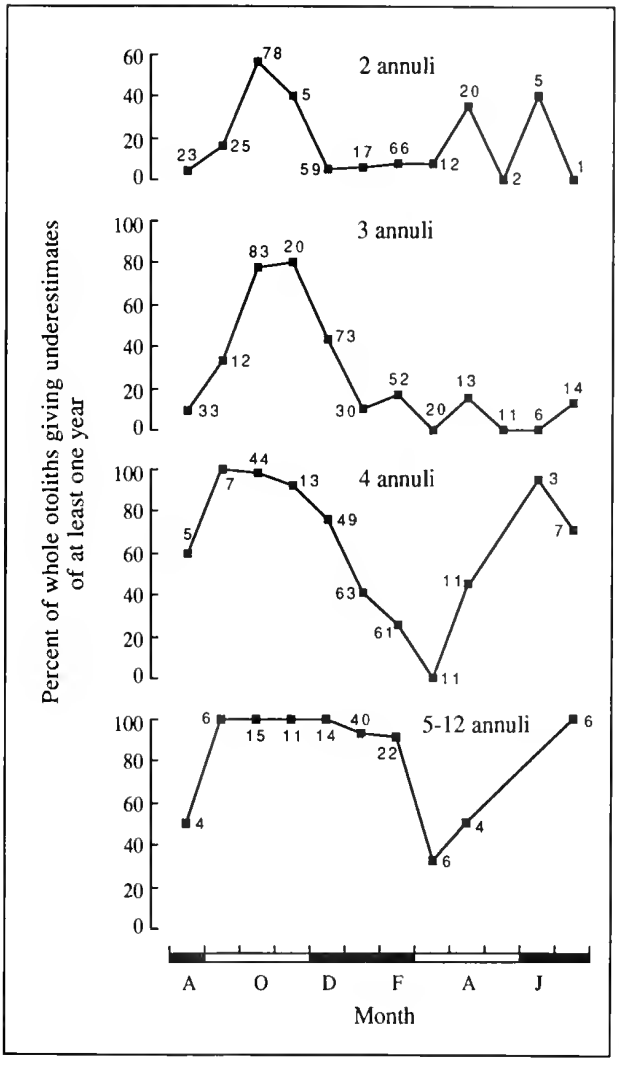

Figure 6
Seasonal incidence of underestimates by one or more annuli when using whole vs. sectioned sagittal otoliths of *Platycephalus speculator*.

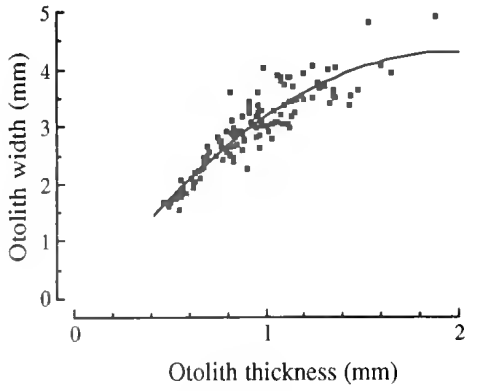

Figure 7
Relationship between width and thickness of the sagittal otoliths of *Platycephalus speculator*.

Table 1
Parameter estimates (95% confidence limits) for the von Bertalanffy growth model fitted to 630 male and 711 female *Platycephalus speculator*, determined from whole and sectioned otoliths using individual lengths-at-age and weighted lengths of each age-group in each month.

		Individual lengths			Weighted lengths		
Sex	Parameter	Est.	Lower	Upper	Est.	Lower	Upper
Sectioned otoliths							
Male	L_∞	429.2	419.9	438.5	477.4	468.6	486.2
	K	0.573	0.525	0.621	0.408	0.380	0.437
	t_0	−0.134	−0.201	−0.067	−0.332	−0.411	−0.253
Female	L_∞	481.8	469.4	494.2	601.0	588.2	619.8
	K	0.593	0.547	0.639	0.309	0.283	0.335
	t_0	−0.056	−0.109	−0.003	−0.423	−0.515	−0.331
Whole otoliths							
Male	L_∞	426.9	417.3	436.4	484.9	473.5	496.3
	K	0.700	0.641	0.760	0.466	0.429	0.502
	t_0	−0.068	−0.125	−0.012	−0.244	−0.292	−0.156
Female	L_∞	457.8	445.6	470.0	659.6	626.1	693.2
	K	0.767	0.694	0.840	0.264	0.231	0.296
	t_0	−0.088	−0.148	−0.028	−0.698	−0.837	−0.560

ages 1, 2, 3, and 4 were never altered by more than 22mm and the change was generally less than 12mm. The coefficient of determination (r^2) for the von Bertalanffy curve was 0.85 for both sexes using individual lengths-at-age, and 0.93 for males and 0.89 for females using the weighted procedure.

The respective parameters L_∞, K, and t_0 in the von Bertalanffy growth equations for males determined using weighted data obtained from sectioned otoliths overlapped those when the same approach was employed for whole otoliths, and the same was true for K with females (Table 1, Fig. 8). The von Bertalanffy growth-equation parameters using weighted data from sectioned otoliths show that female *P. speculator* grow towards a larger asymptotic size (L_∞) than males (Table 1, Fig. 8). Individual lengths of *P. speculator* in December–February at the end of their first and second years of life were 190–310mm and 210–370mm, respectively, for males, and 210–300mm and 250–400 mm, respectively, for females (Fig. 8).

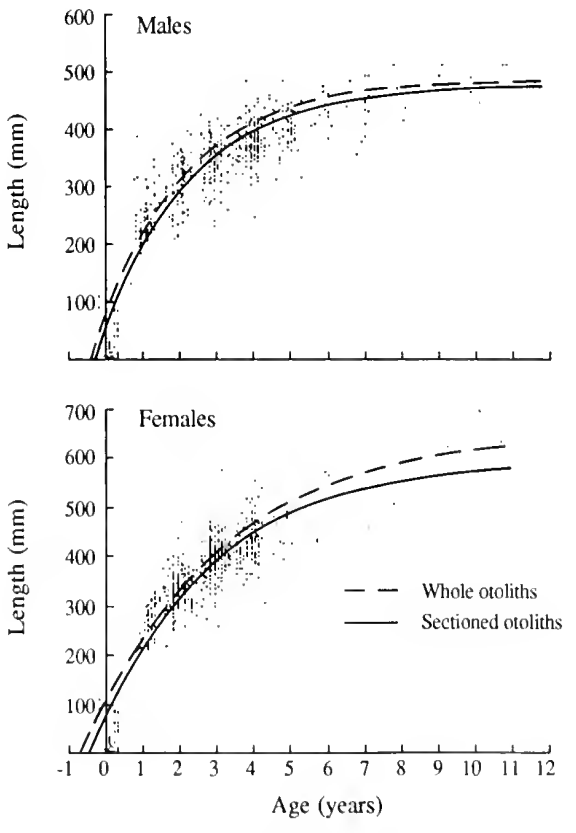

Figure 8
Von Bertalanffy growth curves fitted to length-at-age data, weighted by the inverse of the sample size of each 0.1 year age-group, using whole and sectioned otoliths of male and female *Platycephalus speculator*.

Discussion

Marginal increments

Marginal increments of the otoliths of *P. speculator* with two or more translucent zones exhibited conspicuous trends only after the otoliths were sectioned. This is largely due to the fact that sectioning of otoliths results in more accurate measurement of their peripheral and/or penultimate opaque zones, because one or both of the two outermost translucent zones have become more clearly delineated. This is similar to the situation with starry flounder *Platychthys stellatus*, in which annual trends in the marginal increments of

otoliths with four or more annuli were observed only after otoliths had been broken and burnt (Campana 1984). Likewise, in the case of king mackerel *Scomberomorus cavalla*, the percentage of otoliths with an opaque zone on their edge exhibited an annual trend only after the otoliths were sectioned (Collins et al. 1988).

The consistency in annual trends of marginal increments among sectioned otoliths of *P. speculator*, despite differing numbers of translucent zones, accounts for the clear annual trend in marginal increments when data for all otoliths in each of the monthly samples were pooled. The contrast between the conspicuous trend shown in pooled data for whole otoliths, and the relatively poor trend exhibited in whole otoliths with two or more translucent zones, shows how trends can be unduly influenced by those of a relatively large sample size of otoliths exhibiting a particularly strong annual trend, such as was present with those otoliths having one translucent zone. For validation of the use of translucent zones as annuli, it is thus important to establish that the trends shown by the marginal increments on otoliths with differing numbers of translucent zones each follow a consistent annual trend (Johnson 1983, Maceina et al. 1987, Potter et al. 1988, Beckman et al. 1989).

Age and growth estimates

Our results demonstrate that, while age estimates between sectioned and whole otoliths corresponded when one translucent zone was present, ages of older fish were underestimated by 2–4 years or as much as 5 or 6 years using whole otoliths. Increased resolution of the growth zones after sectioning is reflected in the far lower variability between age estimates made by two independent readers using sectioned otoliths.

Although otoliths with two or three translucent zones frequently yielded counts of one less zone prior to sectioning, many underestimates occurred with the otoliths taken from fish between mid-spring and early summer (October–December). In other words, they were collected during the period when sectioning enabled the new opaque zone to be detected approximately 2 months earlier than was possible with whole otoliths.

Our inability to detect all of the translucent zones in whole otoliths can in part be attributed to the growth pattern of the otolith. Whereas the first translucent zone can be easily detected in whole otoliths, the disproportionate increase in otolith thickness relative to its width results in the translucent zones becoming increasingly more closely apposed and therefore difficult to distinguish from one another. This parallels the situation recorded by Beamish (1979a, b) for Pacific hake *Merluccius productus*, and for several species of rockfish (*Sebastes*), and also by Campana (1984) for starry flounder *Platychthys stellatus*.

Despite the fact that a large proportion of ages were underestimated using whole otoliths, the von Bertalanffy growth curves derived from data using whole otoliths, particularly of males, did not differ markedly from those obtained using sectioned otoliths. This can be attributed to the fact that approximately 74 and 65% of growth for males and females, respectively, occurred in the first 3 years of life when underestimates of age were limited.

Implications for management

The vast majority of male *P. speculator* reach sexual maturity at the end of their first year of life (Hyndes et al. In press).Since males have attained only 190–310 mm by this time (Fig. 8), they will only occasionally have reached 300mm, the minimum legal length for capture of this species. However, the majority of females do not first attain sexual maturity until they are 2 years old (Hyndes et al. In press), by which time they have reached 250–400mm. Thus, the females of *P. speculator* can be exploited before they have had the opportunity to spawn.

In summary, this study has demonstrated that, in the case of the flathead *P. speculator*, it is crucial to section its otoliths in order to obtain an accurate estimate of age. Sectioning reduces the problems of distinguishing between peripheral translucent zones which, due to the growth pattern of the otolith, become increasingly more closely apposed with increasing size. While the results presented in this paper refer only to *P. speculator*, they parallel in some respects those obtained for *Platychthys stellatus* and *Scomberomorus cavalla* (Campana 1984, Collins et al. 1988). Such age underestimates have obvious implications in estimating mortalities for use in fisheries management. Our results also demonstrate the importance of plotting marginal increments for otoliths with different numbers of translucent zones, to establish that such zones are laid down annually on the otoliths of fish representing each presumed age-group. Since the females of *P. speculator* are being caught before they have spawned for the first time, there is a case for increasing the minimum legal size for capture.

Acknowledgments

We thank F. Baronie, D. Gaughan, P. Geijsel, P. Humphries, L. Laurenson, and F. Neira for their assistance with sampling. The sectioning saw was kindly provided by S. Blaber of the CSIRO Marine Labora-

tories at Cleveland, Queensland. Helpful discussions were provided by N. Hall, L. Laurenson and L. Pen. L. Pen also estimated the number of translucent zones in otoliths for the precision estimates. Gratitude is expressed to J. Casselman, R. Fletcher, M. Moran, N. Hall, two anonymous referees, and the scientific editor for constructive criticism of our work and this paper. Financial support was provided by the Western Australian Department of Fisheries.

Citations

Augustine, O., and T.J. Kenchington
1987 A low cost saw for sectioning otoliths. J. Cons. Cons. Int. Explor. Mer 43:296–298.

Beamish, R.J.
1979a Differences in the age of Pacific hake (*Merluccius productus*) using whole and sections of otoliths. J. Fish. Res. Board Can. 36:141–151.
1979b New information on the longevity of the Pacific hake (*Sebastes alutus*). J. Fish. Res. Board Can. 36:1395–1400.

Beamish, R.J., and G.A. McFarlane
1983 The forgotten requirement for age validation in fisheries biology. Trans. Am. Fish. Soc. 112:735–743.

Beckman, D.W., C.A. Wilson, and A.L. Stanley
1989 Age and growth of red drum, *Sciaenops ocellatus*, from offshore waters of the northern Gulf of Mexico. Fish. Bull., U.S. 87:17–27.

Beckman, D.W., A.L. Stanley, J.H. Render, and C.A. Wilson
1990 Age and growth of black drum in Louisiana waters of the Gulf of Mexico. Trans. Am. Fish. Soc. 119:537–544.

Bedford, B.C.
1983 A method for preparing sections of large numbers of otoliths embedded in black polyester resin. J. Cons. Cons. Int. Explor. Mer 41:4–12.

Brothers, E.B.
1983 Summary of round table discussions on age validation. *In* Prince, E.D., and L.M. Pulos (eds.), Proceedings, International workshop on age determination of oceanic pelagic fishes: Tunas, billfishes, and sharks, p. 35–44. NOAA Tech. Rep. NMFS 8.

Brown, I.W.
1977 Ecology of three sympatric flatheads (Platycephalidae) in Port Phillip Bay, Victoria. Ph.D. thesis, Monash Univ., Victoria, 304 p.

Campana, S.E.
1984 Comparison of age-determination methods for the starry flounder. Trans. Am. Fish. Soc. 113:365–369.

Casselman, J.M.
1987 Determination of age and growth. *In* Weatherly, A.H., and H.S. Gill (eds.), The biology of fish growth, p. 209–242. Academic Press, London.

Chang, W.Y.B.
1982 A statistical method for evaluating the reproducibilty of age determination. Can. J. Fish. Aquat. Sci. 39:1208–1210.

Colefax, A.N.
1934 A preliminary investigation of the natural history of the tiger flathead (*Neoplatycephalus macrodon*) on the south-eastern Australian coast. I. Distribution and supply; length statistics. Proc. Linn. Soc. N.S.W. 49:71–91.

Collins, M.R., D.J. Schmidt, C.W. Waltz, and J.L. Pickney
1988 Age and growth of the king mackerel, *Scomberomorus cavalla*, from the Atlantic coast of the United States. Fish. Bull., U.S. 87:49–61.

Crozier, W.W.
1990 Age and growth of the angler-fish (*Lophius piscatorius* L.) in the North Irish Sea. Fish. Res. (Amst.) 7:267–278.

Fairbridge, W.S.
1951 The New South Wales tiger flathead, *Neoplatycephalus macrodon* (Ogilby). Aust.J. Mar. Freshwater Res. 2:117–118.

Gallucci, V.F., and T.J. Quinn
1979 Reparameterizing, fitting and testing a simple growth model. Trans. Am. Fish. Soc. 10:14–25.

Hayse, J.W.
1990 Feeding habits, age, growth and reproduction of Atlantic spadefish *Chaetodipterus faber* (Pisces: Ephippidae) in South Carolina. Fish. Bull., U.S. 88:76–83.

Hyndes, G.A., F.J. Neira, and I.C. Potter
In press Reproductive biology and early life history of the marine teleost *Platycephalus speculator* Klunzinger (Platycephalidae) in a temperate Australian estuary. J. Fish Biol.

Johnson, A.G.
1983 Age and growth of yellowtail snapper from South Florida. Trans. Am. Fish. Soc. 112:173–177.

Lenanton, R.C.J., and I.C. Potter
1987 Contribution of estuaries to commercial fisheries in temperate Western Australia and the concept of estuarine dependence. Estuaries 10:28–35.

Maceina, M.J., D.N. Hata, T.L. Linton, and A.M. Landry
1987 Age and growth analysis of spotted seatrout from Galveston Bay, Texas. Trans. Am. Fish. Soc. 116:54–59.

Montgomery, S.S.
1985 Aspects of the biology of the tiger flathead *P. richardsoni* and the associated fishery. Masters thesis, Univ. New South Wales, Sydney, 228 p.

Nel, S.A., I.C. Potter, and N.R. Loneragan
1985 The biology of the catfish *Cnidoglanis macrocephalus* (Plotosidae) in an Australian Estuary. Estuarine Coastal Shelf Sci. 21:895–909.

Paxton, J.R., and J.E. Hanley
1989 Platycephalidae. *In* Walton, D.W., and R. Longmore (eds.), Zoological catalogue of Australia, 7, Pisces, Petromyzontidae to Carangidae, p. 465–472. Brown Prior Anderson, Burwood, Victoria.

Potter, I.C., A.J. Cheal, and N.R. Loneragan
1988 Protracted estuarine phase in the life cycle of the marine pufferfish *Torquigener pleurogramma*. Mar. Biol. (Berl.) 98: 317–329.

Reis, E.G.
1986 Age and growth of the estuarine catfish, *Netuma barba* (Siluriformes, Ariidae), in the estuary of the Patos Lagoon (Brasil). Fish. Bull., U.S. 84:679–686.

Rincon, P.A., and J. Lobon-Cervia
1989 Reproductive and growth strategies of the red roach, *Rutilus arcasii* (Steindachner, 1866), in two contrasting tributaries of the River Duero, Spain. J. Fish Biol. 34:687–705.

Sokal, R.R., and F.J. Rohlf
1981 Biometry, 2d ed. W.H. Freeman, NY, 859 p.

SPSS Inc.
1988 SPSS-X™ user's guide. SPSS Inc, Chicago, 1072 p.

Sriramachandra-Murty, V.
1975 On the fishes of the family Platycephalidae of the seas around India. J. Mar. Biol. Assoc. India 17:679–694.

Abstract.– Morphological changes during metamorphosis of Dover sole *Microstomus pacificus* are described from 2220 larvae and juveniles. Unlike most flounders, initiation of eye migration is uncoupled from metamorphosis and from the habitat change from planktonic to benthic. Dover sole larvae are optically asymmetrical during most of their planktonic life. Major features associated with metamorphosis are reduction in body depth with associated reductions in lengths of neural and hemal spines, increase in relative eye diameter, loss of canine-like teeth coincidental with acquisition of incisor-like teeth, resorption of posterior process of coracoid, development of body scales, change in body pigmentation, and development of the gut loop in the secondary body cavity. From initiation to completion, metamorphosis appears to take about 9 months, during which time there is little increase in body length.

Available evidence indicates that most spawning off Oregon occurs in spring, with April and May as peak hatching months. Settlement from the plankton occurs in winter, with January to March as peak settlement months. Duration of planktonic life appears to be about 2 years, with a minimum duration of about 18 months. Metamorphosing larvae settle over a broad "landing" zone (55–377 m), quantitatively distinct from, but overlapping, the narrower spring nursery zone (40–170 m). As yet, there is no evidence of delayed metamorphosis. Metamorphosis is protracted, seems to be seasonally-triggered, and may involve a significant period during which larvae switch between midwater and bottom habitats.

Manuscript accepted 18 March 1992.
Fishery Bulletin, U.S. 90:285–301 (1992).

Metamorphosis and an overview of early-life-history stages in Dover sole *Microstomus pacificus**

Douglas F. Markle
Phillip M. Harris
Christopher L. Toole

Department of Fisheries and Wildlife, 104 Nash Hall
Oregon State University, Corvallis, Oregon 97331-3803

There is uncertainty about the length of the pelagic life of Dover sole *Microstomus pacificus*. Hagerman (1952) noted that the "pelagic life is prolonged for several months and metamorphosis is delayed." Allen and Mearns (1977) thought a 9-month planktonic stage was "probably not unusual." Pearcy et al. (1977a) examined the early life history in greater detail and concluded that "Dover sole larvae are pelagic for at least a year." Hayman and Tyler (1980), although citing Pearcy et al. (1977a), constructed a time-line indicating a 9-month pelagic larval stage.

There is also little agreement on estimated body length at the end of the first year of life. Pearcy et al. (1977a) estimated growth to be 20–30 mm standard length (SL) during the first year, but also concluded that metamorphosis took place after about 1 year at 30–50 mm SL (the extra 10–30 mm of growth was not explained). Hagerman (1952) and Demory (1972), both limited by small sample sizes, mention lengths of 66–75 mm total length (TL) for nominal 1-year-old specimens.

Uncertainty about duration and growth in the pelagic phase has important implications for age estimates. Whether based on scales or otolith sections, no researcher has documented the age or size at which the first nominal annulus forms (Demory 1972, Chilton and Beamish 1982, Pikitch and Demory 1988, Hunter et al. 1990).

From the large midwater trawl collections made by W.G. Pearcy and colleagues (OSU) from 1961 to 1982, and juvenile bottom-trawl surveys conducted off Oregon from 1988 to 1990, we describe metamorphosis and other stages in the early life history of Dover sole and address questions relating to the duration and timing of these stages.

Materials and methods

Midwater trawl collections

A total of 796 Dover sole larvae were obtained from 425 midwater trawl stations off Oregon. Details of sampling methods are given in Pearcy (1976, 1980) and Pearcy et al. (1977 a,b). Because the midwater trawls were made for a variety of reasons, there are constraints on interpretation of these data. The most important constraints are seasonal, diel, depth, and gear. Seasonal coverage was best from June to September, and poorest in May and October (Table 1). There was a pronounced diel bias. Relatively few samples were collected between 0600 and 2000 hours (Table 2). Most samples were collected at night between 2200 and 0500 hours. The range of collec-

* Technical paper 9837, Oregon State University Agricultural Experiment Station.

Table 1
Distribution of midwater trawl stations by month, 1961–82.

Month	No. of stations	Percent of total
January	94	3.8
February	127	5.1
March	157	6.4
April	174	7.0
May	85	3.4
June	306	12.4
July	397	16.1
August	237	9.6
September	479	19.4
October	74	3.0
November	165	6.7
December	173	7.0
Total	2468	99.9

Table 2
Distribution of midwater trawl stations by time of day, 1961–82.

Hour of set	No. of stations	Percent	Hour of set	No. of stations	Percent
0100	192	7.8	1300	51	2.1
0200	158	6.4	1400	60	2.4
0300	177	7.2	1500	60	2.4
0400	184	7.4	1600	65	2.6
0500	154	6.2	1700	52	2.1
0600	82	3.3	1800	60	2.4
0700	68	2.8	1900	65	2.6
0800	61	2.5	2000	78	3.2
0900	61	2.5	2100	95	3.8
1000	69	2.8	2200	119	4.8
1100	45	1.8	2300	133	5.4
1200	55	2.2	2400	167	6.8

tion depths was 0–6000 m, but 81.8% of the samples were from depths <500 m. Eleven different gear types were used: Tucker trawl, Cobb trawl, 0.9 m Isaacs-Kidd midwater trawl (IKMT), 1.8 m IKMT, 2.4 m IKMT, 3.0 m IKMT, 2.4 m rectangular midwater trawl (RMT), 2.7 m RMT, 1 m^2 multiple plankton sampler, 65 m^2 midwater trawl, and 100 m^2 midwater trawl. Some gears were operated with and without opening-closing devices (Pearcy 1980). Eighty-eight percent of the collections were made with either a 1.8 m or 2.4 m Isaacs-Kidd midwater trawl (IKMT). All specimens were preserved in 10% formalin and transferred to 50% isopropanol.

Juvenile bottom-trawl collections

A bottom-trawl survey of juvenile Dover sole was conducted bimonthly, January to November 1989, in three areas off Oregon (Fig. 1). In March 1988 and 1990, a more limited survey was conducted in the central (Foulweather) area. Each area was 10 miles wide and oriented to the coast such that the depth range of 50–400 m could be covered in the shortest distance. Each area was subdivided into six strata bounded by isobaths at 50, 80, 100, 120, 160, 220 and 400 m. Trawl stations were randomly chosen such that a minimum of three 5-minute trawls were attempted in each stratum. When time permitted, additional stations were added in strata with highest concentrations of Dover sole (100–119 and 120–159 m). All trawling was conducted from the FV *Olympic* during daylight hours. The gear was a commercial, 34.9 mm mesh, two-seam shrimp trawl with a 27.4 m headrope, rigged with a 28.5 m footrope and tickler chain. The posterior 3/4 of the codend had a 6.4 mm liner. The catch was sorted on board, all fish species were counted and measured, and all Dover sole <200 mm SL were frozen or fixed in 10% formalin and returned to the laboratory for morphological analysis. All formalin-fixed specimens were preserved in 50% isopropanol before measurement.

Morphological analysis

All measurements reported herein were made in the laboratory on defrosted or formalin-fixed, isopropanol-preserved specimens. We found no significant differences (P 0.93) between measurements of 39 defrosted juvenile Dover sole (46.9–71.0 mm SL) when remeasured over a year after fixation and preservation.

Measurements were taken on 2220 larvae, juveniles, and adults. Using the staging system developed herein, the numbers examined in each stage were: Stage 1, 811; Stage 2, 29; Stage 3, pelagic captures, 12; Stage 3, benthic captures, 409; Stage 4, pelagic captures, 1; Stage 4, benthic captures, 461; and Stage 5, 497. On all specimens returned to the laboratory, we measured TL, SL, body depth at anus (BD1A), maximum body depth, snout to posterior extent of intestine length (SINT), and body weight. Length measurements were taken to the nearest 0.1 mm using an ocular micrometer on specimens <20 mm SL and dial calipers on larger specimens. Body weight was determined to the nearest 0.001 g for Stages 1 and 2 and to the nearest 0.1 g for Stages 3, 4, and 5 (see staging description below). Weights were taken from undamaged, pat-dried individuals. Weight loss in isopropanol-preserved larvae was as great as 10% after 2 minutes of air exposure due to alcohol evaporation. Although specimens were exposed for less time before weighing, a 10% weighing error was

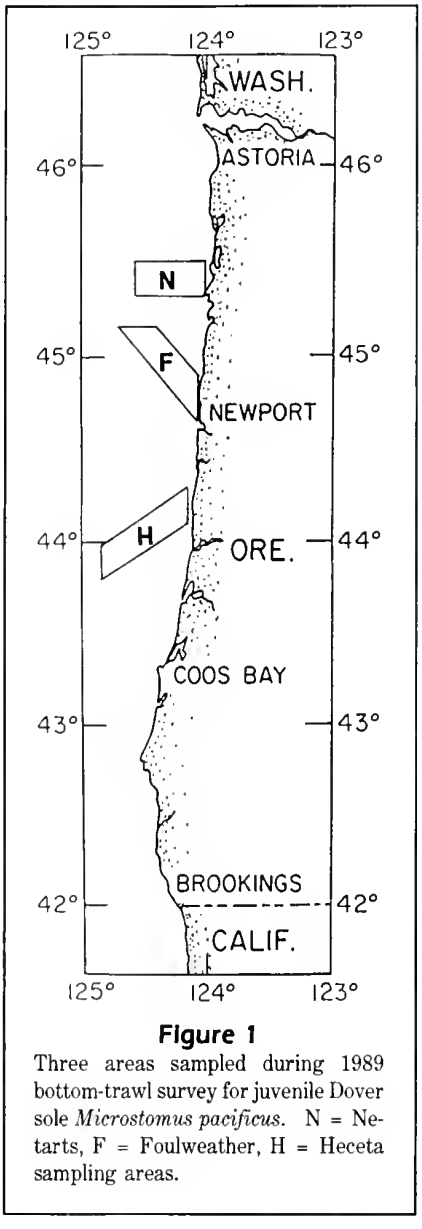

Figure 1
Three areas sampled during 1989 bottom-trawl survey for juvenile Dover sole *Microstomus pacificus*. N = Netarts, F = Foulweather, H = Heceta sampling areas.

assumed for this study. Considering the change in weight of three orders of magnitude between 10 and 50 mm SL, the weighing error was considered acceptable for this study.

A smaller subset of 201 specimens was examined to describe metamorphosis in greater detail, and all were deposited in the Oregon State University Fish Collection (OS). These specimens were either cleared and differentially stained with alizarin red S and alcian blue (Potthoff 1984), radiographed, or both. This subset included only postflexion Stage-1, most Stage-2, and representatives of Stages 3–5 larvae. In addition to routine measurements listed above, we measured right eye diameter, interorbital width, right upper jaw length, length of gastrointestinal tract as measured from anus to most posterior part of intestinal loop, length of first caudal neural spine, length of dorsal fin pterygiophore anterior to first caudal neural spine, length of dorsal fin pterygiophore posterior to first caudal neural spine, length of first hemal spine, length of anal fin pterygiophore anterior to first caudal hemal spine, and length of anal fin pterygiophore posterior to caudal hemal spine. Counts of vertebrae and rays of dorsal, anal, caudal, pectoral, and pelvic fins also were made.

A staging system describing Dover sole ontogeny was developed following the suggestions of Youson (1988). Our terminology deviates from Balon (1979, 1984) and Youson (1988) in our use of five numbered stages for early development, rather than numbered stages for metamorphosis only. Dover sole have a protracted metamorphosis, and our stages can be related, generally, to flatfish metamorphosis. We suggest terminology for each stage that incorporates traditional concepts of larval and juvenile periods as well as the metamorphic phase of the larval period. Metamorphosis occurs in Stages 2–4.

We were especially concerned with describing the beginning of metamorphosis, the initiation event, and the completion of metamorphosis, the climax event (Youson 1988). The initiation event was described based on six characters that reach the adult state during the plankton-to-benthos transition (see Results below). Another character, body scale formation, could be documented only in cleared and stained specimens and was concordant with completion of the six initiation-event characters. Development of the intestinal loop in the secondary body cavity, quantified by SINT, is the last character to change in Dover sole metamorphosis. The climax event was described based on the rate of change of the ratio of natural logarithms of two measurements (SINT and SL). Both initiation and climax events are further corroborated by body shape changes.

We use the concept of competency, as developed in the marine invertebrate developmental literature, as part of our definition of stages. The term regrettably has become a synonym for metamorphosis, as in the phrase "competent to metamorphose" (Pechenik 1986). Doyle (1975), using the term "delay" stage, noted that the onset of competency included both developmental criteria (strict metamorphosis as used herein) and a behavioral criterion, the ability to settle. In some invertebrates, attachment to a substrate is a prerequisite to metamorphosis; thus settlement must occur prior to metamorphosis. In fishes there is not necessarily a connection between metamorphosis (Youson 1988) and competence. However, Cowen (1991) applied the terms to fish and kept the marine invertebrate connection intact. Competency has been defined more narrowly

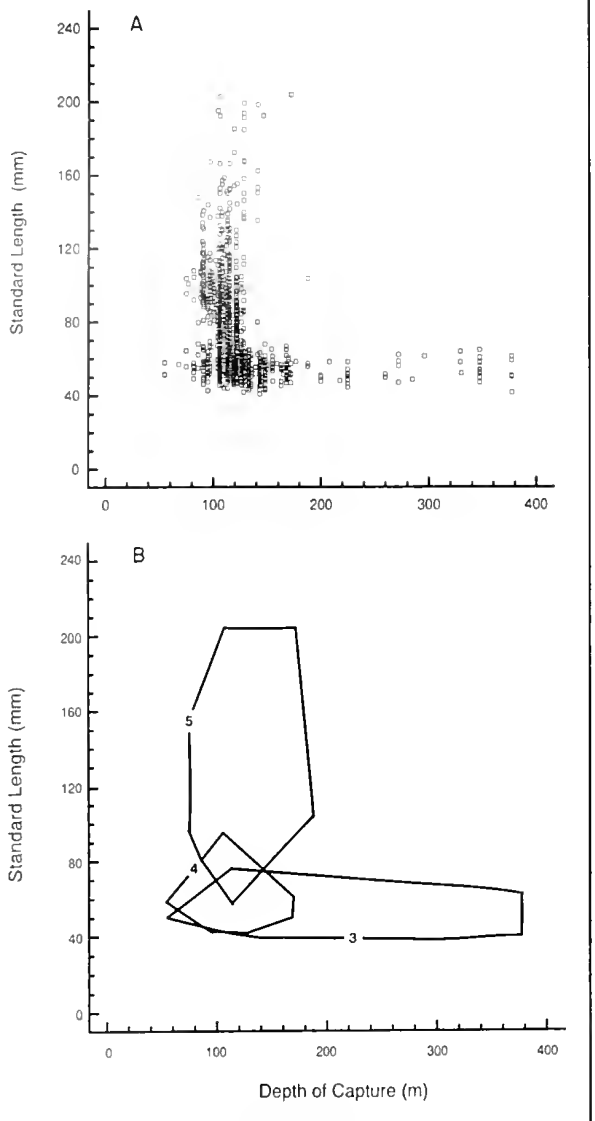

Figure 2
Relationship between body depth at anus and standard length in Dover sole *Microstomus pacificus*: (A) scatterplot of data points, Stages 1–5; (B) polygons circumscribing areas bounded by specimens in Stages 1–5.

Table 3
Characters used to quantify metamorphosis in Dover sole *Microstomus pacificus*.

Character	Character state
Teeth	0 Canines 1 Canines, incisors developing 2 Incisors
Eye position	0 Left side of head or dorsal ridge 1 Right side of head, adult position
Position of dorsal fin	0 First ray posterior to left eye 1 First ray equal with posterior margin or anterior to left eye
Posterior process of coracoid	0 Straight, angled posteriorly 1 Resorption beginning, tip curled into hook 2 Resorption complete, process absent
Pectoral fin shape	0 Round, paddlelike shape, < adult shape complement of rays, no radials formed 1 Intermediate shape, adult complement of rays, cartilaginous radials 2 Adult morphology
Pigmentation	0 Planktonic coloration 1 Benthic coloration

as the ability to settle (Jackson and Strathmann 1981), a conceptual improvement that removes predefined connections to metamorphosis. We identify precompetent, competent, and postcompetent stages during metamorphosis of Dover sole.

Time-series analysis

Two approaches were used to construct a time-line of early development: modal progression analysis (MPA, Bhattacharya 1967) and an analysis of seasonality of stages. MPA was facilitated using the computer program ELEFAN (Pauly 1987), but its utility was limited by sample sizes. Analysis of seasonality of stages was corroborated partly by monitoring growth of a single metamorphosing individual held in the laboratory at 13°C. The Stage-3 specimen was 57.7 mm SL when captured on 20 March 1989. It was measured regularly and progressed completely through Stage 4 to an early Stage 5, when it was sacrificed on 15 June 1989.

Results

Morphology and development

Stage 1 (premetamorphic larvae), 6.1–58.5 mm SL

For convenience and because of our emphasis on metamorphosis, all premetamorphic planktonic specimens are referred to as Stage 1. However, the premetamorphic phase of the larval period could be usefully divided into two intervals, the first approximating Stage I of Pearcy et al. (1977a). A transition from the first interval to the second occurs around 10–15 mm SL, during which eye migration begins, body depth increases (Fig. 2), the first dorsal and anal fin rays form, and caudal fin flexion begins. During the second interval, specimens acquire the adult numbers of vertebrae, and dorsal, anal, caudal, and pelvic fin rays; the stomach and intestine coil; 3–4 pyloric cecae develop; and a pigmentation pattern of dashes develops into a solid

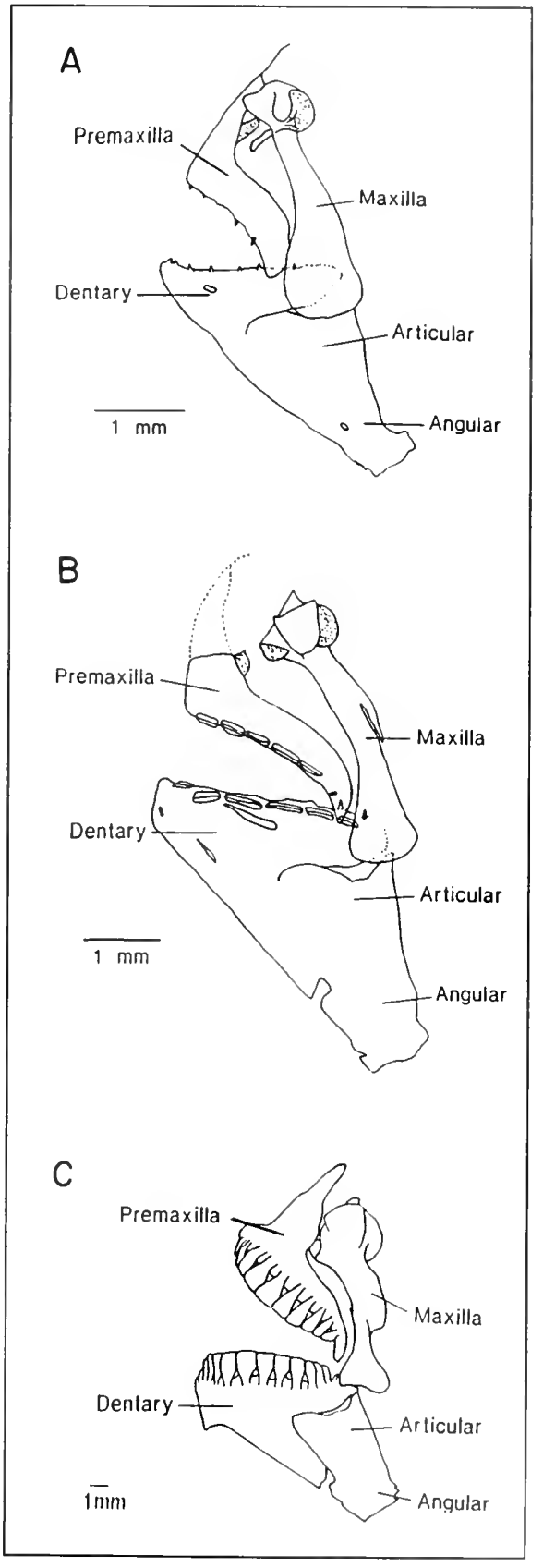

Figure 3
Jaw dentition during metamorphosis in Dover sole *Microstomus pacificus*, left lateral views: (A) OS12578, Stage 1 with canine teeth; (B) OS11377, Stage 2 with canine and developing incisor teeth; and (C) OS11288, Stage 5 with developed incisor teeth.

outline at the base of the dorsal and anal fins around 35–40 mm SL (Pearcy et al. 1977a).

Stage 2 (metamorphic precompetent larvae), 42.3–60.4 mm SL Six morphological characters that define the initiation event of metamorphosis are, in their approximate order of development: jaw dentition, completion of eye migration, position of anterior margin of dorsal fin, position or presence of posterior process of the coracoid, pectoral fin morphology, and beginning of asymmetrical coloration. Numerical scores given to the two or three states of each character are shown in Table 3. A metamorphosing presettlement individual can have a metamorphic score of 1 to 8. A score of 9 defines Stage 3, metamorphic competent larvae.

Dover sole larvae have canine-like teeth on left and right jaws (Fig. 3A). During Stage 2, incisor-like teeth develop on the left premaxilla and dentary (Fig. 3B). The canine-like teeth are lost from both jaws coincident with eruption of incisors in the left jaw (Fig. 3C).

In Stage 1 larvae, anterior dorsal-fin pterygiophores and fin rays are posterior to the orbit of the left eye which is located on the dorsal ridge of the cranium (Fig. 4A). During Stage 2, these pterygiophores move anterior to the orbit of the left eye (Fig. 4B).

The posterior process of the coracoid in larvae is a long, slender element that projects posteriorly above the visceral cavity, underneath the skin (Fig. 5A). During metamorphosis the process is resorbed. At the beginning of resorption, during Stage 2, the distal end of the process curls anteriorly into a hook (Fig. 5B). In our samples there is some indication that the process deteriorates (poor staining with alcian blue), but there is no gradual reduction in length or thickness of the process. Specimens either have the process or have lost it (Fig. 5C).

The pectoral fin in Stage-1 larvae is a paddle-shaped membrane with a thin, fleshy base and without radials. During Stage 2, a fleshy rectangular base, cartilaginous radials, and the adult complement of fin rays form (Fig. 5).

The Stage-1 larval color pattern consists of little or no pigment on the midlateral areas. A transitional pattern, in which melanophores aggregate along myosepta, is followed by the first indication of melanophores aggregating in two approximately circular groups anteriorly and posteriorly along the lateral line (Fig. 6). We score larval

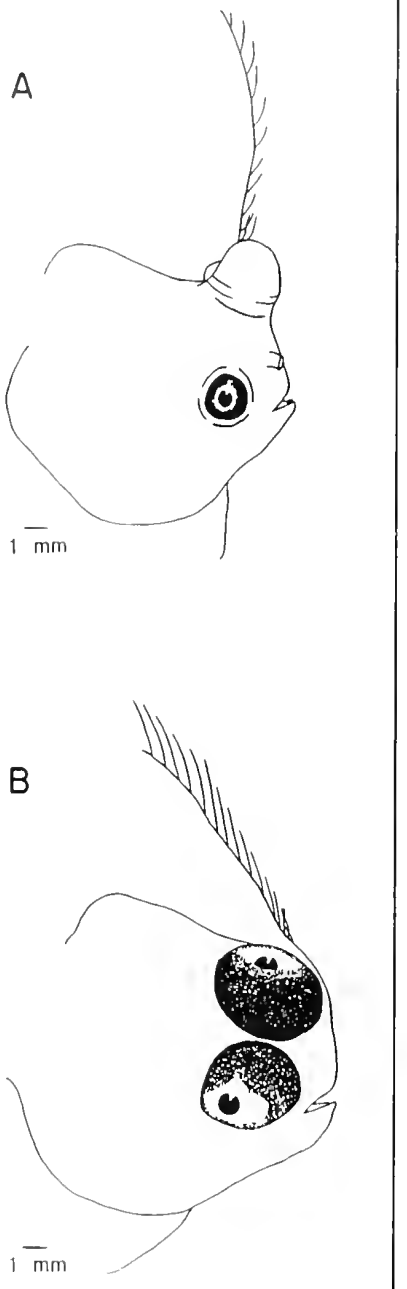

Figure 4
Position of dorsal fin rays and size of eyes in developing Dover sole *Microstomus pacificus*: (A) OS12558, Stage 1; and (B) OS12563, Stage 2.

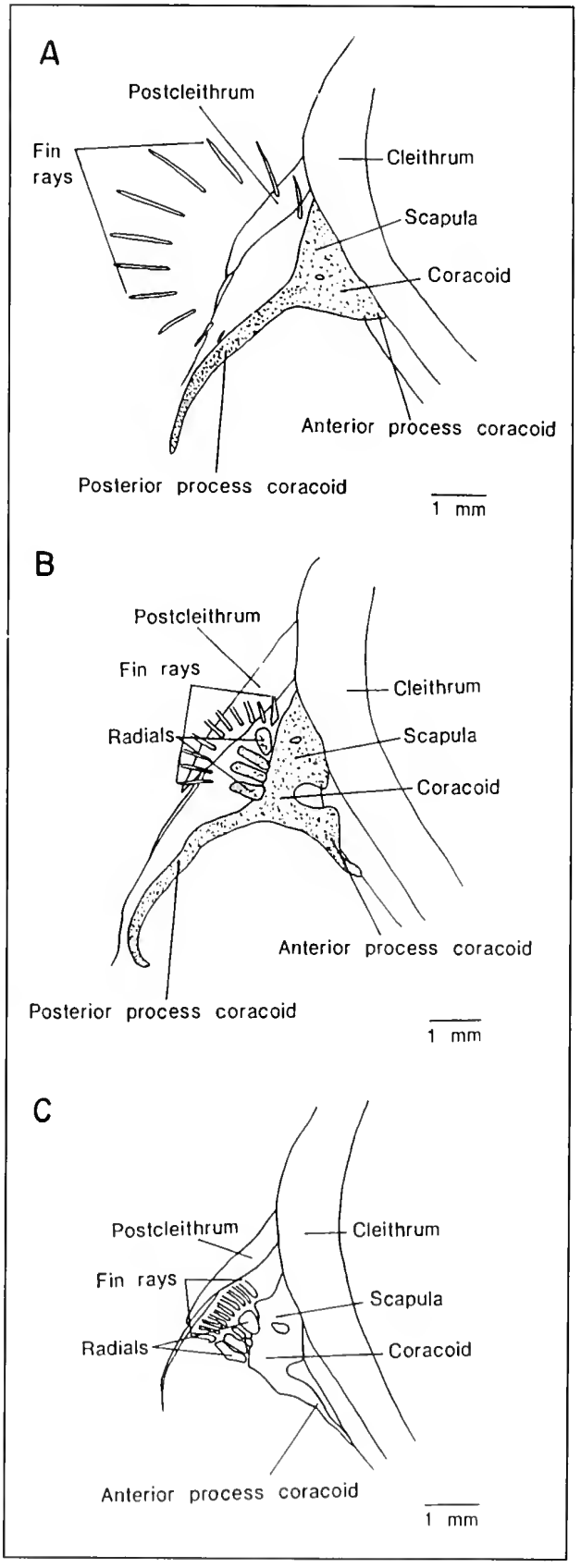

Figure 5
Pectoral fin development in Dover sole *Microstomus pacificus*: (A) OS12558, Stage 1 with straight ventral process of coracoid; (B) OS11377, Stage 2 with hooked tip on ventral process of coracoid; and (C) OS12563, Stage 3 after resorption of ventral process of coracoid.

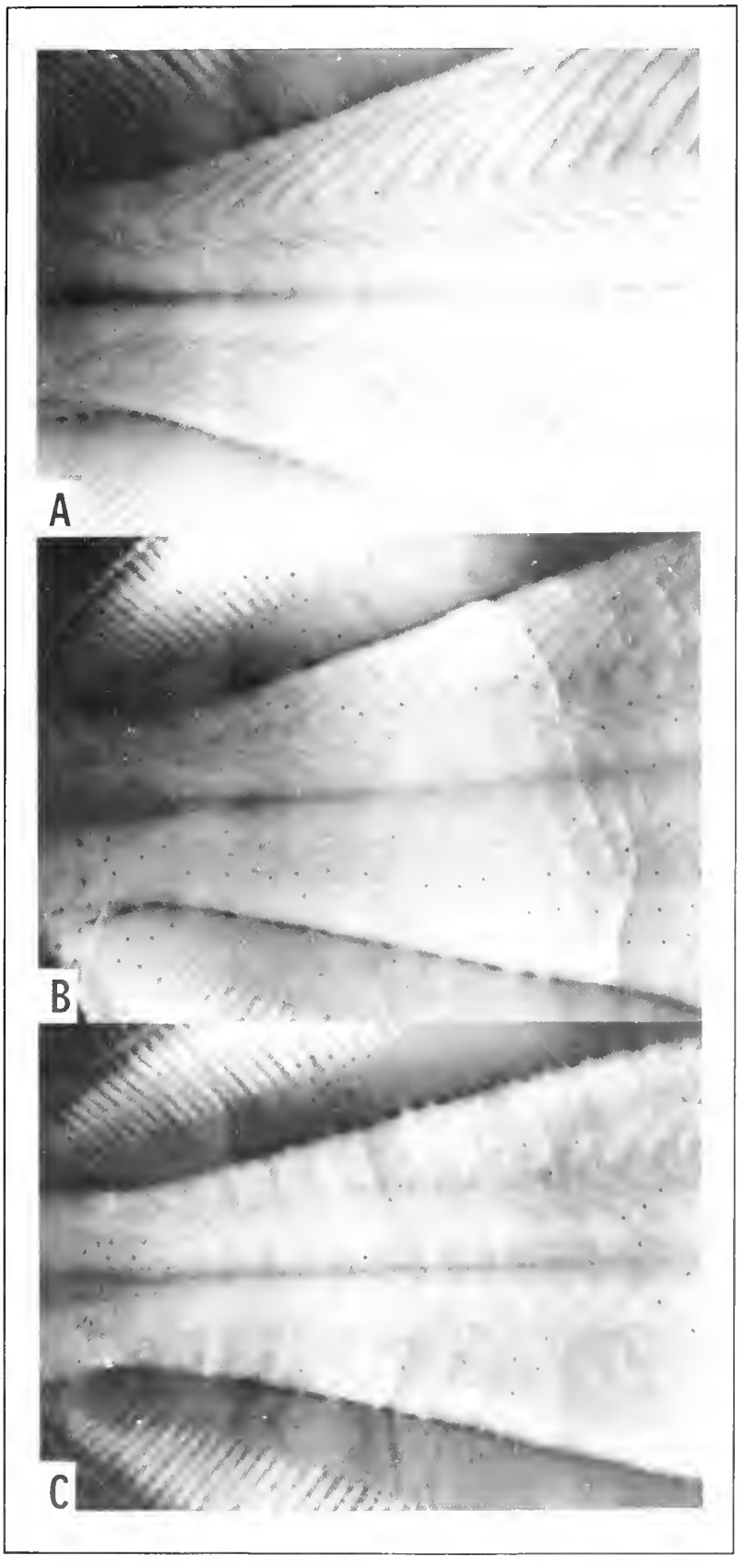

Figure 6

Right-side midlateral pigmentation patterns during development in Dover sole *Microstomus pacificus*: (A) OS13115, Stage 2, developmental score 5, larval pattern of no melanophores on myomeres; (B) OS13118, Stage 2, developmental score 8, transitional pattern of melanophores on myosepta; and (C) OS13117, Stage 3, aggregated pattern of melanophores in circular area on caudal peduncle and anterior trunk.

and transitional patterns equally and consider the circular aggregations as the first indication of asymmetrical coloration.

Coincident with changes in these six features are changes in features that are not easily coded: gradual loss of otic spines, reduction in body depth (Figs. 3 and 8), reduction in interorbital width (Fig. 7), increase in right eye diameter (Fig. 7), and increase in right upper jaw length (Fig. 3). Development of body scales also begins in Stage-2 specimens with metamorphic scores of 7 or 8. Body scales first form above and below the lateral line, anteriorly near the pectoral fin base, and on the caudal peduncle.

Stage 3 (metamorphic competent larvae), 40.7–74.9 mm SL Stage-3 specimens have a metamorphic score of 9, indicating that all six initiation-event features have either begun or reached the adult state. These specimens have a translucent appearance, intermediate between the earlier transparent stages and later opaque stages. Stage-3 specimens have asymmetrical coloration, retain the coiled, larval gut configuration, and have resorbed the posterior process of the coracoid. Some morphometric features initiated in Stage 2, such as increasing right eye diameter and shrinkage in body depth, continue in Stage 3 (Fig. 2). Ossification of pelvic-fin rays and radials is initiated in Stage 3, apparently after settlement (1 of 10 pelagic specimens and 4 of 4 benthic Stage-3 specimens have ossified pelvic fin rays and radials).

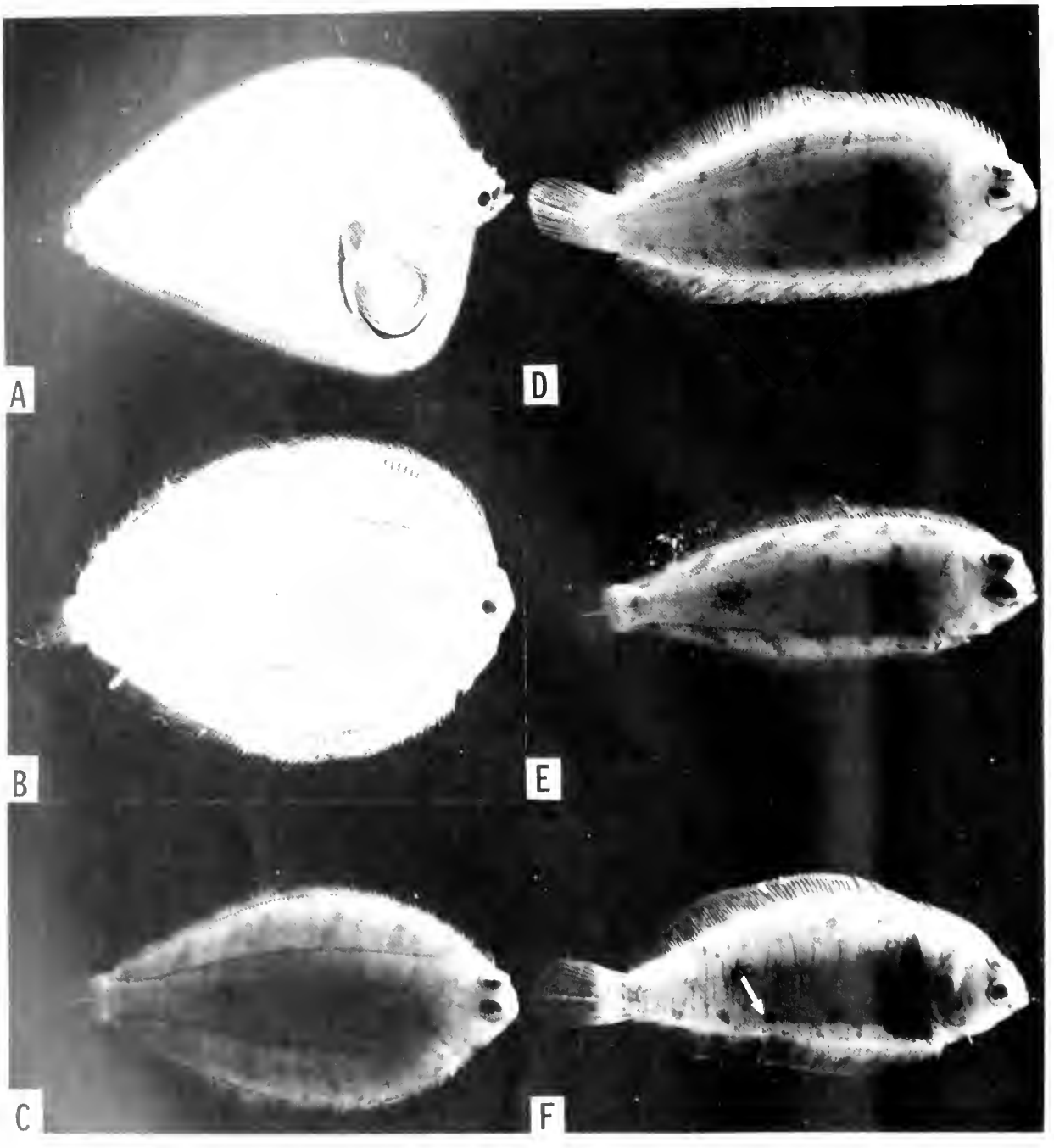

Figure 7

Dover sole *Microstomus pacificus* right lateral view: (A) OS13214, Stage 1, 20.4 mm SL; (B) OS11377, Stage 2, 54.5 mm SL; (C) OS13202, Stage 3 benthic capture, 52.4 mm SL; (D) OS13202, early Stage 4, 61.5 mm SL (intestinal loop is dark area above anal fin); (E) OS13203, late Stage 4, 58.4 mm SL; (F) OS13204, early Stage 5, 78.4 mm SL, arrow points to posterior end of intestinal loop.

Stage 4 (metamorphic postcompetent larvae), 41.7–79.3 mm SL Adult Dover sole have a long intestinal loop in the secondary body cavity above anal fin pterygiophores (Hagerman 1952). This intestinal loop (Fig. 7) forms after settlement, and its initiation is the defining feature of Stage 4. Continuous metamorphic changes in morphology, such as shrinkage in body depth, are completed during Stage 4 (Fig. 2).

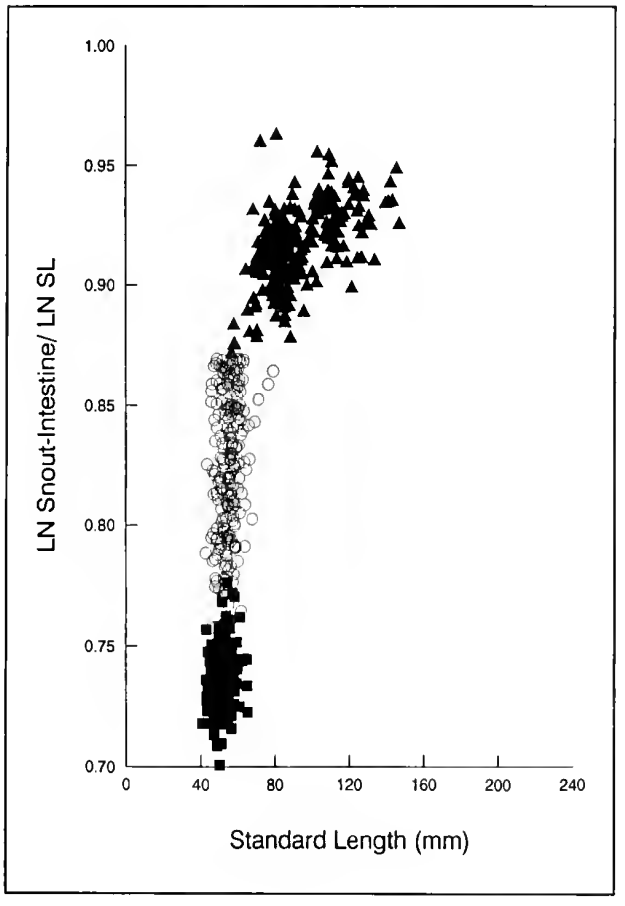

Figure 8
Relationship between the ln SINT/ln SL ratio and standard length during development of Dover sole *Microstomus pacificus*. Symbols represent Stage 3 (■), Stage 4 (○), and Stage 5 (▲).

Stage 5 (juvenile), 48.9 mm SL to sexual maturity
We define the climax event, and Stage 5, as the point at which length of the intestinal loop attains adult proportions. The continuous nature of this process is illustrated in the logarithm ratios of SINT/SL (Fig. 8). We chose a cut-off ratio by calculating the ratio for 2 mm SL increments and examining the rate at which the ratio changes over length. The greatest rate of change occurs between 67 and 69 mm SL, during which the mean ratio changes from 0.85 to 0.89. We chose the midpoint of these ratios and therefore define Stage 5 as those individuals with a ratio of ln (SINT)/ln (SL) > 0.87. Coincident with this change is an overall darkening of body color such that Stage 5 specimens look like small adults.

General features of early development and metamorphosis

Unlike most flounders, initiation of eye migration in Dover sole is uncoupled from the change in habitat from planktonic to benthic, as well as from the process of metamorphosis (as defined herein). Eyes are symmetrical up to a maximum size of only 13.4 mm SL, and the left eye can be on the midline in specimens as small as 9.5 mm SL (Pearcy et al. 1977a). Eye migration in Dover sole is arrested during planktonic growth, with the left eye stopping at the dorsal margin of the cranium at 15–20 mm SL (Fig. 4A). It remains in this position until metamorphosis. Thus, during most of their planktonic life, the eyes of Dover sole are asymmetrical.

There is a complex relationship between body depth and SL (Fig. 2), including (1) an interval of rapid increase from about 10 mm to at least 60.4 mm SL in some individuals, (2) a compensatory shrinkage phase over the size range 40.7–74.9 mm SL, and (3) a more typical linear growth phase that may begin in specimens as small as 41.7 mm SL. Body depth reduction is a regressive process (Youson 1988) in which lengths of neural and hemal spines and pterygiophores are reduced (Fig. 9). Two- and three-fold reductions occur in lengths of first caudal neural and hemal spines and their immediate anterior and posterior pterygiophores. Consequently, metamorphosing Stage-3 specimens 40–50 mm SL have neural and hemal elements comparable in length to those of 20–30 mm SL Stage-1 larvae. Neural and hemal elements and dorsal and anal pterygiophores in Stage-1 larvae are cartilaginous or weakly ossified, and vertebral centra lack zygopophyses. Complete ossification of neural and hemal elements and formation of zygopophyses occurs in Stages 2 and 3.

During most of metamorphosis, especially in Stages 2 and 3, body length appears to be arrested (Fig. 10). Although the sample size of Stage-2 larvae limits our confidence in further analysis, the data show little indication of growth between Stages 2 and 3 (Fig. 10). Because metamorphosis occurs over a broad range of sizes, similarity in size minima and maxima between stages also suggests little or no growth in body length. For example, the minimum sizes for Stages 2, 3, and 4 are almost identical (42.3, 40.7 and 41.7 mm SL, respectively). During Stage 4 there is finally some indication of growth because the smallest Stage-5 juvenile is 48.9 mm SL, more than 7 mm larger than the smallest Stage-4 larva. Yet, even this juvenile is 26 mm smaller than the largest metamorphosing Stage-3 larva.

There is an apparent loss in body weight during metamorphosis because of a decrease in mean weight from 2.6 to 2.4 g from Stage 2 to Stage 4 (Fig. 11). However, the small sample size of Stage 2 and our measuring error preclude attaching significance to the

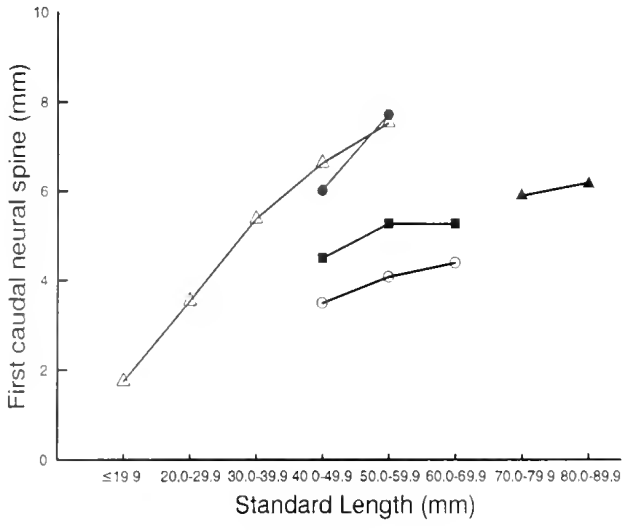

Figure 9

Change in length of first caudal neural spine during development of Dover sole *Microstomus pacificus*. Symbols represent Stage 1 (△), Stage 2 (●), Stage 3 (■), Stage 4 (○), and Stage 5 (▲).

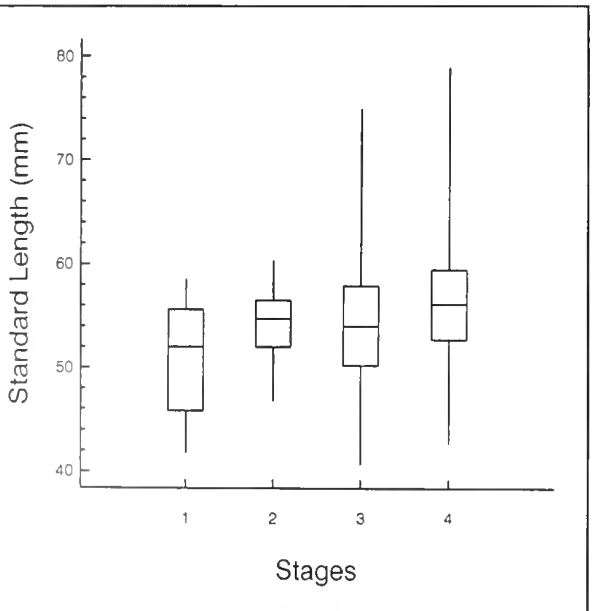

Figure 10

Mean standard length (horizontal line), size interval for 50% of observations (box), and size range for Stage-1 specimens >40 mm, all Stage-2 specimens, and all January and March Stage-3 and Stage-4 specimens of Dover sole *Microstomus pacificus*.

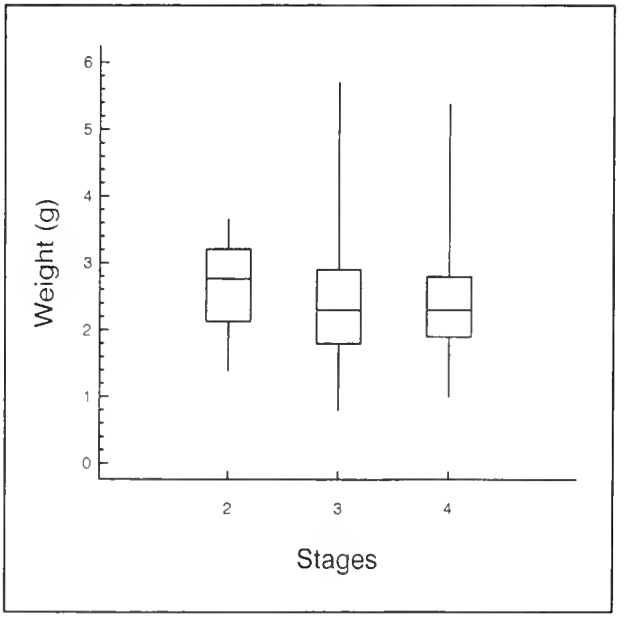

Figure 11

Mean weight (horizontal line), weight interval for 50% of observations (box), and weight range for Stages 2–4 in Dover sole *Microstomus pacificus*.

apparent loss. During the second year of life in the plankton (see next section), body weight increases an order of magnitude from a mean of about 0.30 g for Stage 1 in February to 2.0–4.0 g for Stage 2. All individuals that reach a size of 40 mm SL are at least 0.74 g; Stage-2 specimens are at least 1.39 g; Stage 3, at least 0.80 g; and Stage 4, at least 1.0 g. Because our sample size for Stage 3 is relatively large, our best estimate of a weight threshold for metamorphosis is ~0.8 g. However, if the suggestion of weight loss during metamorphosis is not an artifact (Fig. 11), the weight threshold may be closer to the minimum weight of Stage 2. Further complicating an estimate of that threshold is the observation that our lightest Stage-2 specimen (42.6 mm SL and 1.39 g) was caught in January with a developmental score of 7, and presumably may already have lost weight.

Because SINT increases during metamorphosis and BD1A decreases, the SINT/BD1A ratio provides an additional means of visualizing the relationship between the metamorphic process and developmental stages (Fig. 12).

Timing and duration of stages

Temporal change in size of Stage-1 larvae <40 mm SL was analyzed using MPA (Fig. 13). Small larvae, about 6–8 mm, were found from February to June. The smallest identifiable mode was in April, and from November to March modes were level around 22–25 mm. Two notable features of these data are apparent accelerated growth in June and reduced availability of larger

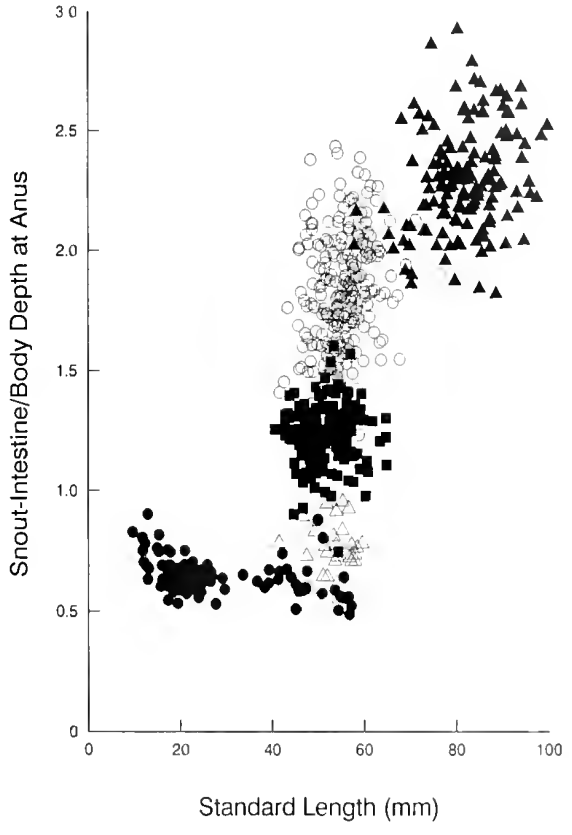

Figure 12

Relationship between the SINT/BD1A ratio and standard length during development of Dover sole *Microstomus pacificus*. Symbols represent Stage 1 (●), Stage 2 (△), Stage 3 (■), Stage 4 (○), and Stage 5 (▲).

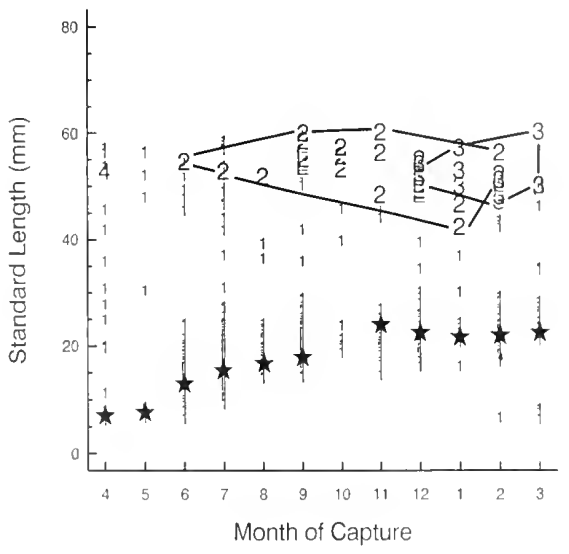

Figure 13

Relationship between standard length and month of capture for Dover sole *Microstomus pacificus*, Stages 1–4 collected in midwater trawls. Stars indicate modes determined by modal progression analysis in larvae <40 mm SL. Stage-2 and -3 specimens are circumscribed by lines.

Table 4

Seasonal catch-per-effort for planktonic Stage-2 and Stage-3 Dover sole *Microstomus pacificus* larvae off Oregon. *N* = number of trawls.

Month of collection	*N*	No. of Stage 2 based on metamorphic score								No. of Stage 3
		1	2	3	4	5	6	7	8	
January	128	–	–	–	–	–	–	2	–	2
February	167	–	–	–	–	–	–	–	2	4
March	147	–	–	–	–	–	–	–	–	2
April	201	–	–	–	–	–	–	–	–	0
May	106	–	–	–	–	–	–	–	–	0
June	278	1	–	–	–	–	–	–	–	0
July	291	–	–	–	–	–	1	–	–	0
August	303	1	1	–	–	–	–	–	–	0
September	217	–	1	–	4	2	1	–	–	0
October	129	–	–	–	–	1	1	–	1	0
November	217	–	–	–	–	–	–	2	1	0
December	126	–	–	–	–	–	–	2	6	2

specimens after March (Fig. 13). All small larvae (<10 mm SL) were collected on one day, 12 June 1971, between 50 and 67 km offshore, whereas larger larvae from June were collected considerably further offshore, 108–275 km on various dates. There appears to be little or no coherent size progression after the 24.5 mm mode in March. Specimens >30 mm are found in every month, and weakly-defined modes can be visualized around 50 mm in June, July, and September. Accelerated growth in April and May would seem to be required if the modal size were to double from about 25 mm in March to 50 mm in the second summer of life. Paradoxically, April is a time when micronekton biomass is normally low (Pearcy 1976).

Stage-2 specimens were caught from June to February (Table 4). The coherent progression of metamorphic scores for Stage-2 larvae indicates that metamorphosis begins as early as June; Stage-3 larvae are present as early as December and as late as March. About 6 months seems to be required to progress through Stage 2.

The seasonal distribution of Stage-3 larvae in benthic samples was consistent with their planktonic distribution (Table 5). During bimonthly sampling in 1989, 98.5% of Stage-3 specimens were caught in January or March. Five Stage-3 specimens were caught in May, and most new settlers appear to be in Stage 5 by July

Table 5
Seasonal distribution of Dover sole *Microstomus pacificus* stages in bottom-trawl samples off Oregon, 1989.

Month of collection	*N*	Number (%) Stage 3	Stage 4	Stage 5
January	371	177 (48)	12 (3)	182 (49)
March	655	155 (24)	347 (53)	153 (23)
May	222	5 (2)	113 (51)	104 (47)
July	60	0	11 (18)	49 (82)
September	154	0	5 (3)	149 (97)
November	267	0	3 (1)	264 (99)

(Table 5). Individuals appear to require about 45 days to progress through Stage 3. Our laboratory-held specimen progressed through Stage 4 in 43 days. Overall, the progression through Stages 2–4 appears to require about 1 year for the population as a whole and about 9 months for an individual.

The length and weight of benthic Stage 3 larvae were compared between January and March 1989. Mean length in March (51.5 mm SL) was significantly smaller than the mean length in January (56.3 mm SL, $P < 0.00001$). March specimens were also significantly lighter (2.0 g) than January specimens (2.7 g, $P < 0.0001$). A similar pattern (earliest individuals in a stage being largest) was seen in Stage-2 larvae. The mean length of Stage-2 larvae captured between January and March (late in the season, Table 4) was smaller (53.0 mm vs. 54.3 mm SL) and lighter (2.4 vs. 2.8 g) than Stage-2 larvae captured between June and December (early in the season, Table 4), but the differences were not significant (length $P < 0.4642$; weight $P < 0.1227$).

Habitat of stages

On average, Stage-1 specimens were caught in nets fished to a maximum depth of 338 m, Stage-2 specimens in nets fished to 538 m, and planktonic Stage-3 specimens in nets fished to 293 m. All planktonic Stage-3 larvae were caught at night, between 1835 and 0544 hours, and 93% of Stage-2 larvae were caught at night, between 1802 and 0748 hours. Sampling effort was also greatest at night (Table 1; opening-closing nets collected 516 Dover sole but most (509) were Stage 1). The minimum depth of capture in the discrete depth samples was < 100 m for 82%, and < 300 m for 95%, of Stage-1 specimens. Only six Stage-2 specimens were caught in discrete depth samples, and only two of these in nets not fishing the surface. One Stage-2 larva was caught at 100–150 m and the other at 400–500 m. The single Stage-3 larva collected in a discrete depth sample was collected at 0–330 m.

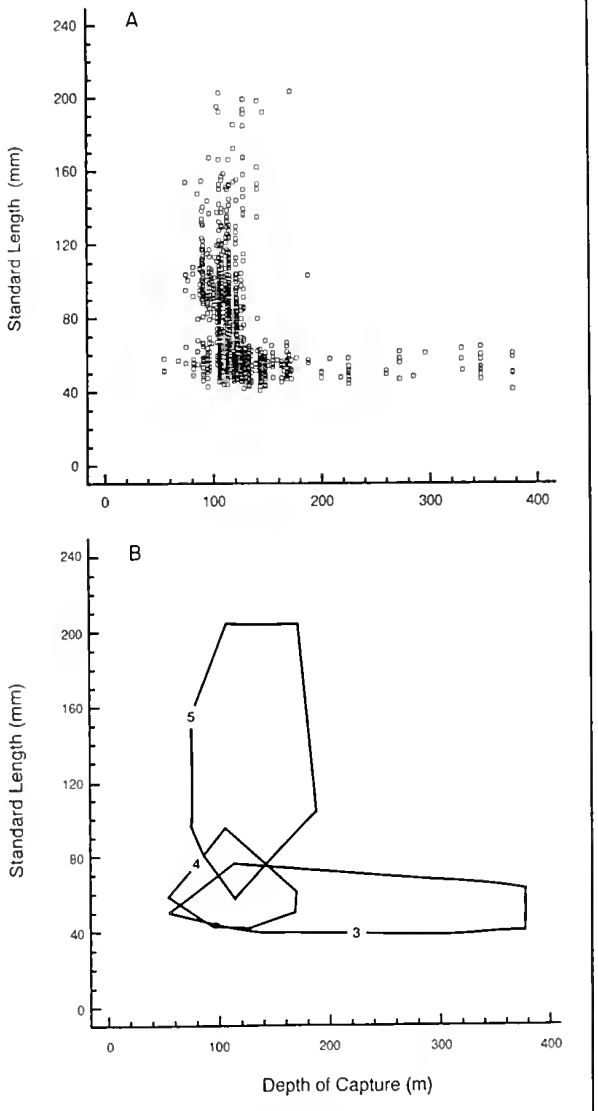

Figure 14
Relationship between standard length and depth of capture of developing Dover sole *Microstomus pacificus*, caught in bottom trawls off Oregon, January and March 1989: (A) scatterplot of data points, Stages 3–5; (B) polygons circumscribing areas bounded by specimens in Stages 3–5.

Benthic specimens were caught at depths shallower than the maximum depth fished by non-closing midwater nets. Based on our stratified sampling, a comparison of depth of capture of stages shows that Stage-3 specimens were caught at an average depth of 146 m (SE 2.65, range 55–377 m), Stage-4 specimens in January and March at an average depth of 118 m (SE 0.68, range 40–170 m), and Stage-5 specimens in January and March at an average depth of 110 m (SE

0.48, range 75–188 m). Compared with Stages 4 and 5, the greater average depth and variance of benthic Stage-3 larvae indicate a much broader depth distribution (Fig. 14).

Stage-3 larvae occupy a transitional "landing" zone quantitatively distinct from, but overlapping, the late-larval and juvenile nurserygrounds. Although Stage-3 larvae caught in bottom trawls quickly take to the bottom when placed in aquaria (pers. observ.), their nighttime capture in midwater trawls and daytime capture in bottom trawls suggest they may be engybenthic (nearbottom) or benthopelagic, rather than exclusively benthic.

Behavior associated with metamorphosis presumably includes some short-term (hours to days) switching between midwater and bottom habitats. In one individual in our data set, the behavior continued into Stage 4. A 53.0 mm Stage-4 specimen was caught 19 April 1963 off the mouth of the Columbia River at 0411 hours in a midwater trawl fished to 73 m over a bottom depth of about 125 m. Its gut loop was well developed and contained sand grains. Additional evidence is provided by midwater Cobb trawl samples collected by W. Lenarz and colleagues (NMFS Southwest Fish. Sci. Cent., Tiburon, CA 94920) between Monterey and San Francisco, California, from 28 March to 2 April 1990. In eight nighttime (2235–0447 hour) samples, fished at 0–110 m (most 0–30 m) over bottom depths of 33–1462 m, they collected 14 Stage-3 larvae (40.4–51.2 mm SL) and 16 Stage-4 larvae (42.4–53.4 mm SL). Stage-3 larvae were collected over bottom depths of 73–1462 m, and Stage-4 larvae were collected over bottom depths of 33–91 m. Thus, settling Stage-3 larvae were found in a "landing" zone at 55–377 m and in a wedge of the water column above and seaward of that zone.

Discussion

Time-line

Dover sole spawn in deep water in winter, December to February, according to Hagerman (1952), and November to April according to the circumstantial evidence of Harry (1959). Yoklavich and Pikitch (1989) provide evidence that smaller Dover sole have an earlier, shorter spawning season than larger fish, and that Dover sole now mature at significantly smaller sizes than reported by Hagerman (1952) or Harry (1959). These observations suggest the possibility that size-selective exploitation might have shifted the spawning season to earlier dates.

However, other observations suggest that peak hatching of Dover sole off Oregon is later, not earlier, than indicated by Hagerman (1952) or Harry (1959). Results of sampling the commercial Dover sole catch off southern Oregon (43°N) from March 1990 to September 1991 indicate running ripe females were caught from February through July with a peak in April (Mike Hosie, Oreg. Dep. Fish Wildl., Charleston, OR 97420, pers. commun.). Spent females increased from less than 10% of all females in April to 100% by early August. However, these observations may be biased towards later-spawning fish because the commercial catch is culled of small fish (Yoklavich and Pikitch 1989). Experiments performed in 1972 by S. Williams at Newport, Oregon, showed that hatching took 18 days at 12.5°C, 27 days at 10.0°C, and 38 days at 7.5°C (Mike Hosie, pers. commun.). In agreement with these observations, small larvae (<10 mm SL) in this study were collected from February to July, with most caught in April and May (Fig. 13, Pearcy et al. 1977a). In ten NMFS ichthyoplankton cruises conducted at 40–48°N from 1980 to 1987, high densities of Dover sole eggs were found in each of six cruises conducted in March, April, or May; none or trace amounts were found in four cruises conducted in August, November, or January (Urena 1989; M. Doyle, NMFS Alaska Fish. Sci. Cent., Seattle, WA 98115, pers. commun.). Finally, "spawning" adults off Alaska have been collected primarily in May and June (Hirschberger and Smith 1983), and eggs are collected in June (Kendall and Dunn 1985). Thus, the weight of evidence seems to indicate that most Dover sole off Oregon hatch from February (Fig. 13) to August (Urena 1989), with a peak in April and May (see also the time-line in Hayman and Tyler 1980).

Settlement is restricted to the period from January to March or April (Table 5), whereas metamorphosis requires a protracted period of up to one year, occurs at sizes >40 mm SL (Fig. 3), includes little growth in body length, and may include loss of weight. Cessation in growth of body length before and during metamorphosis has been documented in other flounders (Fukuhara 1986, 1988). If the modal size of Stage-1 larvae is ~25 mm in March, then the average duration of the planktonic period of Dover sole is about 21 months (Fig. 15). However, the timing of settlement has a size component; larger larvae tend to settle before smaller larvae. It seems reasonable that larger larvae are those that grow faster, but it is also possible that they are slow growers or have otherwise delayed metamorphosis and, therefore, are more than 2 years old (see Discussion below).

Distribution and relative abundance of metamorphic planktonic stages provide additional insight. Larger planktonic specimens were generally rare in midwater trawl collections (Fig. 13). However, Stage-2 larvae, with developmental scores of 7 and 8, and Stage-3 larvae were the most abundant of all metamorphic stages found in midwater (Table 4), even though they

were collected in months with few samples (Table 1). Planktonic Stage-2 larvae were caught in nets fished deeper than either Stage-1 or planktonic Stage-3 larvae. The rarity of larger planktonic and early metamorphic stages may reflect movement deeper into the mesopelagic zone and lower relative sampling effort in deeper water. Late in Stage 2 (developmental scores 7 and 8) and in Stage 3 this trend appears to be reversed, as these stages were caught more frequently. If metamorphosis is a time of increased vulnerability, deeper water may provide a predation refuge. Alternatively, the behavior may place metamorphosing specimens in a water mass that facilitates late larval transport.

Settlement seems remarkably gradual, coincides with the downwelling season, ends with the spring transition in the oceanographic regime (Huyer et al. 1979), and occurs over a very broad "landing" zone (Fig. 14). Stage-3 larvae settling outside the nursery zone may experience differential mortality, or their broad depth distribution may reflect a process of testing the habitat in search of the preferred nurseryground. Capture of Stage-3 and -4 specimens in both nighttime midwater and daytime bottom trawls suggests a diel vertical search pattern.

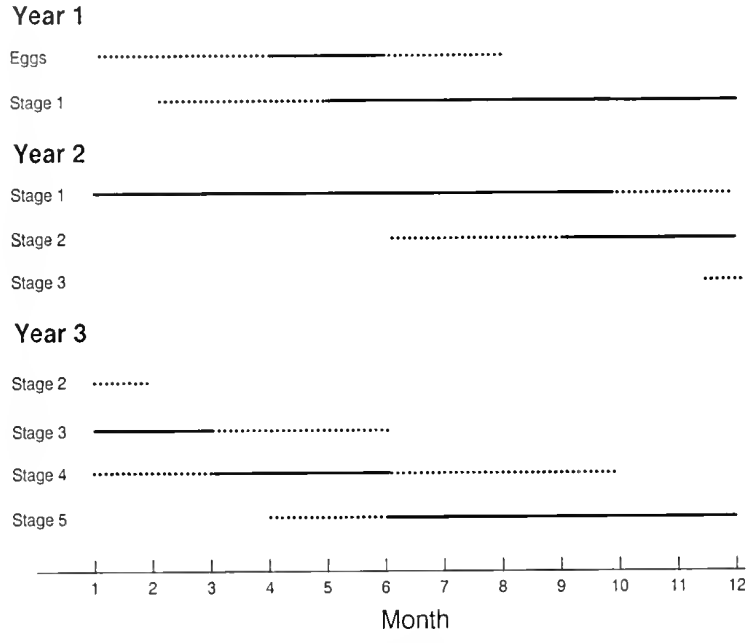

Figure 15

Hypothetical time-line of development for a cohort of Dover sole *Microstomus pacificus*, off Oregon. Solid lines represent presumed peak times for the different stages, and dotted lines represent the ranges.

Egg and larval drift

A proposed recruitment mechanism for Dover sole (Hayman and Tyler 1980, Parrish et al. 1981) focuses on inshore-offshore transport. The long planktonic period of Dover sole implies that alongshore transport also may be important. Our data allow some first-order generalizations about the distribution of early-life-history stages and may give further insight into the recruitment mechanism.

Urena (1989) found that greatest abundances of Dover sole eggs were in neuston samples collected beyond the 200 m isobath. In April and May in the upper 50 m, the current flows southward at about 10–15 cm/second at the 200 m isobath (Huyer 1977, fig. 9; Huyer et al. 1979) and is even weaker further offshore (Huyer and Smith 1978). At 10 cm/second, eggs could be transported 260 km southward in 30 days, assuming that their transport was not interrupted by offshore jets or gyres. Onshore-offshore transport of eggs should be variable. During upwelling, the upper 20 m may experience an average offshore velocity of 2–5 cm/second (Huyer 1983), and the upper 5 m may experience an average offshore velocity of 15 cm/second (Peterson et al. 1979). The short duration of the egg stage, restricted area of high offshore velocity, and the return inshore of water masses during relaxation after upwelling (Peterson et al. 1979) suggest that average offshore transport of eggs should be slow, but nontrivial. Deepwater spawning may help reduce both alongshore and onshore-offshore transport.

Stage-1 larvae also are found beyond the 200 m isobath (Pearcy et al. 1977a) and, like eggs, would be vulnerable to the southward flow of the California Current. In fact, the large surface area of the body of Dover sole larvae might facilitate such transport. Although there are important seasonal changes in direction (Huyer et al. 1979), on an annual basis the average surface current around 100 km offshore is ~0.5–1.0 cm/second to the south (Hickey 1979, fig. 8b). If Stage 1 lasts an average of 15 months, and assuming a mean flow of 0.75 cm/second, these larvae would travel an additional 295 km southward.

We suggest that early Stage-2 larvae move into deeper water. The California Undercurrent is a northward-flowing countercurrent located below 200 m and

influencing an area up to 500km off the shelf (McLain and Thomas 1983). Its velocity is <10cm/second over the continental slope north of Cape Mendocino (Hickey 1979) and weaker seaward of the slope. Somewhat further south, between Pt. Arena and Pt. Reyes, the current is 3–10cm/second from July to October and <1 cm/second from October to January (Huyer et al. 1989). If eggs and Stage-1 larvae are displaced, on average, 555km (260+295) southward of their spawning site, a northward-flowing undercurrent of 3.25cm/second would be sufficient to return Stage-2 larvae to the vicinity of their spawning site in 6 months. This does not seem to be an unreasonable average velocity for the undercurrent from July to January.

The depth range of the Stage 3 "landing" zone (55–377m) corresponds with the northward undercurrent located at 200–300m (Huyer and Smith 1985). However, these larvae appear to need a mechanism to bring them shoreward. The surface Ekman layer, 0–20m, within which wind-driven transport occurs (Huyer 1983), could be reached if larvae moved up in the water column during storms. Diel offbottom migrations could be part of this mechanism. Alternatively, as the body surface area is reduced during this stage, larvae may become less passive and move actively inshore.

Delayed metamorphosis and settlement

The protracted process of metamorphosis in Dover sole is contrary to expectations based on the ideas of saltatory ontogeny (Balon 1981). In general, ontogenetic transformations are expected to occur rapidly because intermediate forms are presumed to be maladapted. For example, loss of teeth from the right side of the jaw and development of incisors on the left side seem to hold no advantage for a planktonic larva, yet this is the situation in Dover sole for several months during the precompetent Stage 2. Delayed metamorphosis is also related to the concept of saltatory ontogeny; because the transition is assumed to be quick, an organism without the proper cues simply delays metamorphosis and settlement. In other words, it keeps the morphology appropriate for the habitat. Typically, field researchers identify a minimum threshold size or developmental stage for metamorphosis and assume that planktonic specimens greater than the threshold size or in the threshold stage have delayed metamorphosis (Pechenik 1986). Others have used a minimum age as a threshold (Cowen 1991).

Pearcy et al. (1977a) suggested that larger "holdover" Dover sole larvae (>50mm SL) delayed metamorphosis and few successfully recruited to the benthic juvenile stage. Delayed metamorphosis is predicted for coastal organisms subjected to offshore transport (Jackson and Strathmann 1981) and there is some evidence for delayed metamorphosis in fishes (Victor 1986, Cowen 1991). An advantage of delayed metamorphosis is extension of the settlement season beyond what would be expected based on the spawning season (Victor 1986). Contrary to this expectation, the duration of Dover sole settlement is seasonally restricted and, off Oregon, no greater than the duration of the spawning season. Because precompetent larvae are probably a great distance from their settlement site, cues for metamorphosis are likely to be seasonal rather than site-related.

Experimental studies focusing on flounders have shown (1) fast-growing individuals metamorphose at smaller sizes, (2) fast-growing individuals retain their faster growth rate for at least several weeks after metamorphosis, (3) age at metamorphosis (defined by eye migration) is more variable than size at metamorphosis, and (4) a target size or threshold must be reached prior to metamorphosis (Policansky 1982, Chambers and Leggett 1987, Chambers et al. 1988). Other fishes and organisms may have age-triggered, size-triggered, or age- and size-triggered metamorphosis (Policansky 1983). Policansky (1983) points out that a size threshold would be expected when there is a size difference in available food between different habitats or a minimum energy requirement to successfully function at a certain stage.

We suggest two contrasting interpretations of the early life history of Dover sole. If size and age at metamorphosis are positively correlated, as is the case in winter flounder (Chambers et al. 1988), then larger, earlier settlers are older and slower-growing than smaller, later settlers. The difference in age could be the difference between early and late spawners or between different years of spawning. Alternatively, variation in size at metamorphosis may simply reflect differential growth rates operating for a long time, probably at least 2 years. As a consequence, larger, earlier settlers would be the faster growers rather than slower growers. One could distinguish between these alternatives and demonstrate delayed metamorphosis by documenting different year-classes among settlers.

In terms of life-history strategies, delayed metamorphosis and protracted metamorphosis may confer similar advantages. Extension of settlement through delayed metamorphosis allows for adaptive responses to short-term oceanographic variability and avoidance of settling during unfavorable conditions. If metamorphosis and settlement are cued to favorable seasons, protracted metamorphosis and the ability of competent metamorphosing individuals (Stage-3 larvae) to spend several months moving between midwater and bottom habitats should also compensate for any short-term unfavorable oceanographic conditions.

Acknowledgments

This study was funded, in part, by Oregon Sea Grant with funds from NOAA, Office of Sea Grant, Department of Commerce, under grant NA85AA-D-SG095 (project R/OPF-29) and from appropriations made by the Oregon State Legislature; by the Pacific Outer Continental Shelf Region of the Minerals Management Service, U.S. Department of the Interior, Washington, D.C., under Contract 14-12-0001-30429; and by National Marine Fisheries Service contract NA-87-ABH-00014. Some ship time was generously donated by T.N. Thompson. C. Ridgley, D. Nelson, S. Banks, and R. Melendez helped collect data. Shipboard work was made as pleasant as circumstances permitted by T.N. Thompson and the crew of FV *Olympic*. A. Kendall (NMFS, Seattle, WA), W. Lenarz (NMFS, Tiburon, CA), and G. Moser and J. Butler (NMFS, La Jolla, CA) shared results of ongoing research. W. Pearcy, D. Stein, and collaborators saved, documented, and made available 20 years of planktonic and midwater trawl collections that were invaluable for this study.

Citations

Allen, M.J., and A.J. Mearns
1977 Life history of the Dover sole. Annu. Rep. South Calif. Coastal Water Res. Proj. 77-1, El Segundo, p. 223–228.

Balon, E.K.
1979 The theory of saltation and its application to the ontogeny of fishes: Steps and thresholds. Environ. Biol. Fishes 4: 97–101.
1981 Saltatory processes and altricial to precocial forms in the ontogeny of fishes. Am. Zool. 21:573–596.
1984 Reflections on some decisive events in the early life of fishes. Trans. Am. Fish. Soc. 113:178–185.

Bhattacharya, C.G.
1967 A simple method for resolution of a distribution into Gaussian components. Biometrics 23:115–135.

Chambers, R.C., and W.C. Leggett
1987 Size and age at metamorphosis in marine fishes: An analysis of laboratory-reared winter flounder (*Pseudopleuronectes americanus*) with a review of variation in other species. Can. J. Fish. Aquat. Sci. 44:1936–1947.

Chambers, R.C., W.C. Leggett, and J.A. Brown
1988 Variation in and among early life history traits of laboratory-reared winter flounder *Pseudopleuronectes americanus*. Mar. Ecol. Prog. Ser. 47:1–15.

Chilton, D.E., and R.J. Beamish
1982 Age determination methods for fishes studied by the groundfish program at the Pacific Biological Station. Can. Spec. Publ. Fish. Aquat. Sci. 60, 102 p.

Cowen, R.K.
1991 Variation in the planktonic larval duration of the temperate wrasse *Semicossyphus pulcher*. Mar. Ecol. Prog. Ser. 69:9–15.

Demory, R.L.
1972 Scales as a means of aging Dover sole (*Microstomus pacificus*). J. Fish. Res. Board Can. 29:1647–1650.

Doyle, R.W.
1975 Settlement of planktonic larvae: A theory of habitat selection in varying environments. Am. Nat. 109:113–126.

Fukuhara, O.
1986 Morphological and functional development of Japanese flounder in early life stage. Bull. Jpn. Soc. Sci. Fish. 52:81–91.
1988 Morphological and functional development of larval and juvenile *Limanda yokohamae* (Pisces: Pleuronectidae) reared in the laboratory. Mar. Biol. (Berl.) 99:271–281.

Hagerman, F.B.
1952 The biology of the Dover sole. Calif. Dep. Fish Game, Fish. Bull. 85:1–48.

Harry, G.Y. Jr.
1959 Time of spawning, length at maturity, and fecundity of the English, Petrale, and Dover soles (*Parophrys vetulus*, *Eopsetta jordani*, and *Microstomus pacificus*, respectively). Oreg. Fish Comm. Res. Briefs 7:5–13.

Hayman, R.A., and A.V. Tyler
1980 Environment and cohort strength of Dover sole and English sole. Trans. Am. Fish. Soc. 109:54–70.

Hickey, B.M.
1979 The California Current System—Hypotheses and facts. Prog. Oceanogr. 8:191–279.

Hirschberger, W.A., and G.B. Smith
1983 Spawning of twelve groundfish species in the Alaska and Pacific Coast regions, 1975–81. NOAA Tech. Memo. NMFS F/NWC-44, Northwest Fish. Sci. Cent., Seattle, WA 98112, 50 p.

Hunter, J.R., J.L. Butler, C. Kimbrell, and E.A. Lynn
1990 Bathymetric patterns in size, age, sexual maturity, water content, and caloric density of Dover sole, *Microstomus pacificus*. Calif. Coop. Oceanic Fish. Invest. Rep. 31:132–144.

Huyer, A.
1977 Seasonal variation in temperature, salinity and density over the continental shelf off Oregon. Limnol. Oceanogr. 22:442–453.
1983 Coastal upwelling in the California Current system. Prog. Oceanogr. 12:259–284.

Huyer, A., and R.L. Smith
1978 Physical characteristics of Pacific northwestern coastal waters. *In* Krauss, R. (ed.), The marine plant biomass of the Pacific Northwest coast, p. 37–55. Oregon State Univ. Press, Corvallis.
1985 The signature of El Niño off Oregon, 1982–1983. J. Geophys. Res. 90:7133–7142.

Huyer, A., E.J.C. Sobey, and R.L. Smith
1979 The spring transition in currents over the Oregon continental shelf. J. Geophys. Res. 84:6995–7011.

Huyer, A., P.M. Kosro, S.J. Lentz, and R.C. Beardsley
1989 Poleward flow in the California Current system. *In* Neshyba, S.J., Ch.N.K. Mooers, R.L. Smith, and R.T. Barber (eds.), Poleward flows along eastern ocean boundaries, p. 144–159. Springer-Verlag, NY.

Jackson, G.A., and R.R. Strathmann
1981 Larval mortality from offshore mixing as a link between precompetent and competent periods of development. Am. Nat. 118:16–26.

Kendall, A.W. Jr., and J.R. Dunn
1985 Ichthyoplankton of the continental shelf near Kodiak Island, Alaska. NOAA Tech. Rep. NMFS 20, 89 p.

McLain, D.R., and D.H. Thomas
1983 Year-to-year fluctuations of the California Countercurrent and effects on marine organisms. Calif. Coop. Oceanic Fish. Invest. Rep. 24:165–181.

Parrish, R.H., C.S. Nelson, and A. Bakun
1981 Transport mechanisms and reproductive success of fishes in the California Current. Biol. Oceanogr. 1(2):175–203.

Pauly, D.
1987 A review of the ELEFAN system for analysis of length-frequency data in fish and aquatic invertebrates. *In* Pauly, D., and G. Moran (eds.), Length-based methods in fisheries research, p. 7–34. Int. Cent. Living Aquat. Res. Manage., Manila.

Pearcy, W.G.
1976 Seasonal and inshore-offshore variations in the standing stocks of micronekton and macrozooplankton off Oregon. Fish. Bull., U.S. 74:70–80.
1980 A large, opening-closing midwater trawl for sampling oceanic nekton, and comparison of catches with an Isaacs-Kidd midwater trawl. Fish. Bull., U.S. 78:529–534.

Pearcy, W.G., M.J. Hosie, and S.L. Richardson
1977a Distribution and duration of pelagic life of larvae of Dover sole, *Microstomus pacificus*; Rex sole, *Glyptocephalus zachirus*; and Petrale sole, *Eopsetta jordani*, in waters off Oregon. Fish. Bull., U.S. 75:173–183.

Pearcy, W.G., E.E. Krygier, R. Mesecar, and F. Ramsey
1977b Vertical distribution and migration of oceanic micronekton off Oregon. Deep-Sea Res. 24:223–245.

Pechenik, J.A.
1986 Field evidence for delayed metamorphosis of larval gastropods: *Crepidula plana* Say, *C. fornicata* (L.), and *Bittium alternatum* (Say). J. Exp. Mar. Biol. Ecol. 97:313–319.

Peterson, W.T., C.B. Miller, and A. Hutchinson
1979 Zonation and maintenance of copepod populations in the Oregon upwelling zone. Deep-Sea Res. 26A:467–494.

Pikitch, E.K., and R.L. Demory
1988 An assessment of scales as a means of aging Dover sole. Trans. Am. Fish. Soc. 117:345–349.

Policansky, D.
1982 Influence of age, size, and temperature on metamorphosis in the starry flounder, *Platichthys stellatus*. Can J. Fish. Aquat. Sci. 39:514–517.
1983 Size, age and demography of metamorphosis and sexual matuartion in fishes. Am. Zool. 23:57–63.

Potthoff, T.
1984 Clearing and staining techniques. *In* Moser, G., et al. (eds.), Ontogeny and systematics of fishes, p. 35–37. Spec. Publ. 1, Am. Soc. Ichthyol. Herpeteol. Allen Press, Lawrence, KS.

Urena, H.M.
1989 Distribution of the eggs and larvae of some flatfishes (Pleuronectiformes) off Washington, Oregon and Northern California, 1980–1983. Unpubl. M.S. thesis, Oregon State Univ., Corvallis, 192 p.

Victor, B.C.
1986 Delayed metamorphosis with reduced larval growth in a coral reef fish (*Thalassoma bifasciatum*). Can. J. Fish. Aquat. Sci. 43:1208–1213.

Yoklavich, M.M., and E.K. Pikitch
1989 Reproductive status of Dover sole, *Microstomus pacificus*, off northern Oregon. Fish. Bull., U.S. 87:988–995.

Youson, J.H.
1988 *First metamorphosis. In Hoar*, W.S., and D.J. Randall (eds.), Fish physiology, vol. XI. The physiology of developing fish, Part B. Viviparity and posthatching juveniles, p. 135–196. Academic Press, San Diego.

Estimating stock abundance from size data

Michael L. Parrack

Miami Laboratory, Southeast Fisheries Science Center
National Marine Fisheries Service, NOAA
75 Virginia Beach Drive, Miami, Florida 33149-1099

Abstract.—The projection of resource production and the effect of removals on fisheries populations are based on abundance estimates, particularly estimates of the most current abundance. Monte Carlo methods were used to investigate a size-based method of estimating abundance for instances where the age of caught fish cannot be established, but where size samples and a growth schedule exist. Neither process variability (recruitment dates, growth rates, and unobserved change rates) nor sampling error (catch estimation, growth rate estimation, and relative abundance sampling) adversely affected estimation, although low sampling intensities often decreased precision. Abundances of recently recruited fish too small to occur in relative abundance samples more than once were estimated with large uncertainty. Inappropriately wide size-class widths caused uncertain abundance estimates of larger size-classes. However, if size-classes were of suitable width, the abundance of fish large enough to occur in abundance samples more than once were accurately and precisely estimated even in cases of high process variability and small sample sizes. Sampling gear efficiency (catchability) coefficients were often estimated without large bias but imprecisely. The exponent of the unobserved change rate (including natural mortality) was estimated precisely, but estimates were often biased. High correlations between estimates of the unobserved change rate and sampling gear efficiencies were not often observed. Estimation characteristics were unlike those based on virtual population analysis calculations. Maximum-likelihood estimates of the most recent abundances were accurate and precise, yet calculations of historical abundances were biased and extremely imprecise.

Manuscript accepted 9 March 1992.
Fishery Bulletin, U.S. 90:302–325 (1992).

Most often, the objective of fisheries regulations is to insure that stock abundance does not decrease or, if abundance is low, to increase it. The welfare of the entire stock may be of concern, or only a part of it such as the adult portion (spawning stock). These objectives are obtained by limiting yields (weight caught) to stock growth or, in instances were abundance is low, to less than stock growth. Abundance estimates are the bases for this regulation strategy. An opinion as to whether stock abundance is currently depressed or not is based on a comparison of an estimate of current abundance with estimates of previous abundances. Stock production (growth) in the immediate future is projected from the estimate of current abundance. Since the production projection is the basis for the yield limit, the estimate of current abundance determines the yield limit. Because it is a critical element of regulatory responsibility, abundance estimation methodology is of major interest.

Most estimation methods are based on age data. These methods specify that the population is entirely composed of unique groups of fish of equal age (cohorts) and that all members of a cohort grow into the first exploitable size (recruit) instantaneously before fishing begins once each year. These two requirements rarely, if ever, occur. Most populations spawn during several months, or sometimes throughout the entire year, so that annual or even monthly cohorts do not really exist. The growth of the young fish to sizes large enough to be caught is a continuous process so that recruitment is typically an ongoing phenomena. These biological realities are often ignored, and age-based analysis methods are used anyway.

Since the primary data element of age-based methods is the number of caught fish of each age, the ages of caught fish must be determined. Sometimes this requirement is difficult to satisfy. Major circuli from differing bone densities or the chemical composition of skeletal structures (scales, fin spines, or otoliths) have been validated as age marks in only 3.4% of age determination studies (Beamish and McFarlane 1983). Even in cases where indirect evidence of validation seems ample (Kreuz et al. 1982), direct measurement of growth from mark and recapture data can document a very different reality (Pikitch and Demory 1988). Collecting and processing samples can be so difficult and time consuming that large data voids occur. Frequent molting and the absence of bony tissue preclude the possibility of using hardpart ageing methods for many invertebrates, and the technology to determine age from somatic tissue does not currently exist.

These problems can be avoided by methods that model populations in terms of size and time rather than age and years (or months). Size-based methods need not require that the population be composed of age-specific cohorts nor that recruitment be an instantaneous, one-time event. The first size-based methods, however, are not so constructed.

The original technique to assess fish stocks from size instead of age data is a stepwise double-estimation procedure (see Pauly et al. 1987 for an example). Size-specific catches are first transformed to age-specific catches by using an inverted growth equation (Ricker 1975:221) or statistical estimators based on growth data (Clark 1981, Bartoo and Parker 1982, Shepherd 1985, Hoenig and Heisey 1987, Kimura and Chikuni 1987) so that the stock is assumed to be composed of age-specific cohorts. Size-to-age transformation methods that require size-frequencies only (i.e., growth data are not required) are available (Macdonald and Pitcher 1979, Pauly 1982, Fournier et al. 1990), but Monte Carlo tests have shown pronounced weaknesses in these methods (Hampton and Majkowski 1987, Rosenberg and Beddington 1987, Basson et al. 1988). Virtual population analysis (Ricker 1948, Fry 1949, Jones 1961, Gulland 1965, Murphy 1965) is then applied to the transformed catch, but the system of cohort-specific catch equations is underdetermined (Agger et al. 1971, Doubleday 1975, Ulltang 1977, Pope and Shepherd 1982). The inclusion of auxiliary data (total fishing effort, catch effort, or other relative abundance samples) using any of several statistical procedures (Laurec and Bard 1980; Paloheimo 1980; Anon. 1981b, 1983, 1984, 1986; Parrack 1981, 1986; Collie and Sissenwine 1983; Deriso 1985; Pope and Shepherd 1985; Mendelssohn 1988) eliminates that problem, so abundances can be estimated. If based on actual age data, virtual population analysis using auxiliary information does estimate stock abundances and fishing mortality rates reasonably well if the natural mortality rate is known (Deriso 1985, Pope and Shepherd 1985), but if the method is used without actual age data, its statistical characteristics are unknown. If the population is not composed of true age-specific cohorts or if the ageing of caught fish is problematic, the method is not appropriate. Spawning often is too protracted to establish cohorts and fish cannot be aged with reasonable certainty; yet because it is simple and tractable, this method is used anyway.

Several size-based abundance estimation methods do not employ data auxiliary to catches (Jones 1974 and 1981, Brethes and Desrosiers 1981, Lai and Gallucci 1988). Instead of using fishing effort or relative abundance samples to overcome the determination problem, they assume that the size-frequency of the catch, and thus of the stock (and recruitment magnitudes), is constant (in steady state). That assumption greatly restricts the usefulness of these methods.

Three items seem important when considering stock-abundance estimators. First, the data an estimator requires often may preclude its use if such data is not usually available. Next, since the likelihood procedure requires one, often a sampling distribution for an observed statistic is assumed even though support for the assumption cannot be offered. The resulting estimator thus might be entirely based on an inappropriate probability expression. Last, the statistical properties of an estimator are of concern. An estimator may be too imprecise to be useful unless sample sizes are unrealistically large, or its bias may be too large to ignore during estimation.

Since the method of least squares is not based on probability theory, statistical characteristics of such estimators are very uncertain. The likelihood procedure tends to generate estimators with superior statistical characteristics, but success is not guaranteed. Commonly, estimators of parameters of nonlinear models are problematic. They cannot be written in closed form so their expectations, which lead to bias and variance expressions, cannot be derived analytically. Since the estimator's performance characteristics cannot be predicted, they must be established from Monte Carlo studies. If such studies do not exist, the estimator's usefulness is unknown.

The first size-based procedure, a least-squares estimator, was developed (Beddington and Cooke 1981) and applied to sperm whales (Anon. 1981a, Cooke and Beddington 1982, Cooke et al. 1983b, Shirakihara and Tanaka 1983, de la Mare and Cooke 1984) to assess the northwestern Pacific stock (Beddington et al. 1983, Cooke and de la Mare 1983b, Shirakihara and Tanaka 1983). It is based entirely on size-specific catches and assumes a known adult-progeny ratio instead of using fishing effort or other auxiliary data. The statistical characteristics of the estimator were established with extensive Monte Carlo studies (Cooke et al. 1983a, Cooke and de la Mare 1983a, Shirakihara and Tanaka 1984, de la Mare and Cooke 1985 and 1987, Shirakihara et al. 1985, de la Mare 1988).

The method of Fournier and Doonan (1987) was derived by the likelihood method by assuming that catch and effort are each lognormal random variables and that the first four moments of length-frequencies are normal random variables. Monte Carlo tests established the estimator's ability to predict optimal long-term fishing effort, but the errors of the stock-abundance estimates are not described. The maximum-likelihood method of Schnute et al. (1989) assumes that the annual ratio of total yield to total effort is a normal random variable. The statistical characteristics of the estimator are not described.

The method of Sullivan et al. (1990) is a least-squares estimator based on catches, but Kalman filter methodology also may be used to obtain estimates (Sullivan 1989). The method does not require data other than catches even though it is well known that, in the case of age-based (VPA) methods, the system of catch equations without auxiliary data is not determined (Agger

et al. 1971, Doubleday 1975, Ulltang 1977, Pope and Shepherd 1982). Sullivan et al. (1990) suggest expanding the number of terms in the sum of squares to include effort and abundance indices if meaningful weights for these auxiliary data can be found (guidance for finding such weights is not provided). The statistical characteristics of the estimator are not yet described.

The lack of Monte Carlo tests of the performance of these estimators is a particular concern because, without knowledge of their statistical behavior, little certainty can be placed on the resulting estimates. Some of the estimators were developed by the likelihood method, but the justification for assuming the chosen sampling distributions often seems weak or lacking. The usefulness of those estimators that require total fishing effort seem limited, since that statistic is often estimated from catch and effort samples rather than enumerated. Most of the methods estimate the parameters of individual growth as part of the solution vector. This seems questionable in view of findings in a study of the separation of central moments of individual distributions from distribution mixtures (Hasselbald 1966), studies of the magnitude of correlation between estimates of growth-equation parameters (Gallucci and Quinn 1979), and of the performance of methods that estimate growth parameters from size distributions (Hampton and Majkowski 1987, Rosenberg and Beddington 1987, Basson et al. 1988). Also, most of the methods are based on elaborate population models, a characteristic that leads to two problems. First, such models often include deterministic stock-recruitment functions, and such functions are regarded as unrealistic representations of the dynamics of fish stocks. Second, since the population model is extensive, it includes a large number of parameters that must be estimated. It is well known that an exact representation of a real-world system is not possible; hence, a suitably parsimonious model that is a useful approximation with an informative structure is superior (Box 1979). The most germane variables are the current size-specific abundances since they will determine stock production in the immediate future.

The object of this study was to develop an abundance estimator that would be appropriate in almost all cases, whether or not the population is composed of cohorts, or whether or not age data is available. Effort was taken to write the estimation model as parsimonious as possible, to base estimation on data commonly collected from most fisheries, and to insure that the correct sampling distribution was used in the likelihood procedure. The bulk of the study was directed at describing the statistical characteristics of the estimator over a broad range of conditions from Monte Carlo simulations.

Methods

Abundance estimator

An abundance estimator was developed that uses a model of individual growth, size-specific catches and catch dates, and size-specific abundance observations (sighting data, research cruise catch-per-tow, etc.). The estimator makes three assumptions:

(1) Unobserved phenomena that change stock abundance (immigration, emigration, unrecorded catch, predation, and disease) are a (continuous) Poisson process with combined rate z,
(2) the size of an individual on a date is a known deterministic function of size on another date, and
(3) the sample average of relative abundance observations is a normally-distributed random variable with an expectation equal to a portion of absolute abundance.

The estimator uses a growth model to relate sizes and dates and an abundance model to project abundance from observed catches scaled to relative abundance observations.

Consider T time-periods, not necessarily of equal duration, so that $0 \leqslant t \leqslant T$. Within period t, relative abundance was observed on date y_t, then a catch occurred on date c_t. The number of fish caught on date c_t was C_t. Abundance on the date of the relative abundance observation (date y_t) is of interest; let this abundance (numbers of fish) be N_t. From assumption (1),

$$N_{t+1} = [N_t\, e^{-z_t(c_t - y_t)} - C_t]\, e^{-z_t(y_{t+1} - c_t)}.$$

Abundance on the date of the final abundance sample (i.e., N_T) is of most interest because stock production in the immediate future depends on it. Writing the above equation in terms of N_T as a time-series gives a simple forward projection of abundance on each relative abundance sampling date:

$$N_t = N_T\, e^{\sum_{k=t}^{T-1} z_k(y_{k+1} - y_k)} + \sum_{k=t}^{T-1} C_k\, e^{z_k(c_k - y_k) + \sum_{i=t}^{k-1} z_i(y_{i+1} - y_i)}.$$

If the unobserved change rate is assumed temporally invariant, this simplifies to

$$N_t = N_T\, e^{z(y_T - y_t)} + \sum_{k=t}^{T-1} C_k\, e^{z(c_k - y_t)}.$$

Each catch is subtracted separately; catching is not assumed to occur continuously at a constant rate. Abundance changes due to unobserved events are, however, assumed to occur continuously at a constant rate.

The model suggested by Chapman (1961) and Richards (1959) may be used to include growth. Letting A, m, b, and k be parameters, s the size, and t the time from birth, the general model

$$s_t = (A^{1-m} - b\, e^{-k \cdot t})^{\frac{1}{1-m}}$$

is the "logistic" function of Verhulst if m = 2, the Brody (monomolecular, von Bertalanffy) model if m = 0, and it approaches the Gompertz function as m approaches unity. Using the rationale of Fabens (1965) where s_1 is the size at time t_1 and s_2 is the size at time t_2, the above growth model leads to

$$s_2 = (A^{1-m} - (A^{1-m} - s_1^{1-m})\, e^{-k(t_2-t_1)})^{\frac{1}{1-m}}. \qquad (1)$$

This satisfies assumption (3), without reference to the actual age of individuals, by expressing size as a continuous function of time, but if growth is intermittent or has changed, a specialized model is most appropriate. From (1), or a more suitable model, let

l' = the size of a fish on date y_T that was size s on date y_t,
u' = the size of a fish on date y_T that was size s+1 on date y_t,
a' = the size of a fish on date c_k that was size s on date y_t, and
b' = the size of a fish on date c_k that was size s+1 on date y_t,

where l', u', a', and b' fall in size-classes l, u, a, and b. Including size in the abundance equation gives

$$N_{t,s} = \qquad (2)$$

$$\int_{l'}^{u'} N_{T,w}\, dw\, e^{z(y_T - y_t)} + \sum_{k=t}^{T-1} \int_{a'}^{b'} C_{k,w}\, dw\, e^{z(c_k - y_t)}.$$

If size-classes are suitably narrow, the frequency of size within size-classes tends to be proportional to size. The frequency of size within a class is therefore approximated by a trapezoid (i.e., trapezoidal integral approximation). The number of fish within the size class is

$$F_s = \int_s^{s+1} f_w\, dw = \tfrac{1}{2}(s+1-s)\,(f_s + f_{s+1})$$

$$= \tfrac{1}{2}(f_s - f_{s+1}),$$

where s is a size class, f_s is the frequency at size s, and F_s is the number within size-class s. Let the largest fish fall in class S:

$$f_S = \tfrac{1}{2}F_S \text{ because } f_{S+1} = 0.$$

Rewriting gives $f_S = 2\,F_S$.

Proceeding to smaller sizes,

$$F_{S-1} = \tfrac{1}{2}(f_{S-1} + f_S) = \tfrac{1}{2}(f_{S-1} + 2F_S)$$

$$\text{so } f_{S-1} = 2(F_{S-1} - F_S).$$

$$F_{S-2} = \tfrac{1}{2}(f_{S-2} + f_{S-1}) = \tfrac{1}{2}(f_{S-2} + 2F_{S-1} + 2F_S)$$

$$\text{so } f_{S-2} = 2(F_{S-2} - F_{S-1} + F_S).$$

$$\vdots \qquad \vdots$$

$$F_s = \tfrac{1}{2}(f_s + f_{s+1})$$

$$= \tfrac{1}{2}(f_s + 2F_{s+1} - 2F_{s+2} + \ldots \pm 2F_S).$$

Rearrangement gives the general expression for the frequency at size-class bounds:

$$f_s = 2(F_s - F_{s+1} + F_{s+2} - F_{s+3} + \ldots \pm F_S).$$

The frequency of any size, s, within class s is also required:

$$f_{s'} = f_s + \frac{f_{s+1} - f_s}{s+1-s}(s'-s) = f_s + (s'-s)(f_{s+1} - f_s).$$

The approximate integrals for equation (2) are thus:

If $u = l$: $\int_{l'}^{u'} N_{t,w}\, dw =$

$$\tfrac{1}{2}(u'-l)(\eta_l + (l'-l)(\eta_{l+1} - \eta_l) + (u'-l)(\eta_{l+1} - \eta_l),$$

or

if $u > l$: $\int_{l}^{u'} N_{t,w}\, dw =$

$$\tfrac{1}{2}(l+1-l')(\eta_l + (l'-l)(\eta_{l+1} - \eta_l) + \eta_{l+1}) + \ldots$$

$$\ldots \tfrac{1}{2}(u'-u)(2\eta_u + (u'-u)(\eta_{u+1} - \eta_u))$$

$$+ \sum_{i=l+1}^{u-1} N_{T,i},$$

and

$$\text{if } b = a: \int_{a'}^{b'} C_{k,w}\, dw =$$

$$\tfrac{1}{2}(b'-a')(\varsigma_a+(a'-a)(\varsigma_{a+1}-\varsigma_a)+\varsigma_b$$

$$+(b'-b)(\varsigma_{b+1}-\varsigma_b)),$$

or

$$\text{if } b < a: \int_{a'}^{b'} C_{k,w}\, dw =$$

$$\tfrac{1}{2}(a+1-a')(\varsigma_a+(a'-a)(\varsigma_{a+1}-\varsigma_a)+\varsigma_{a+1})+\ldots$$

$$\ldots\tfrac{1}{2}(b'-b)(2\varsigma_b+(b'-b)(\varsigma_{b+1}-\varsigma_b)),$$

where $\eta_s = 2(N_{T,s}-N_{T,s+1}+N_{T,s+2}-N_{T,s+3}+\ldots\pm N_{T,S}$,

and $\varsigma_s = 2(C_{k,s}-C_{k,s+1}+C_{k,s+2}-C_{k,s+3}+\ldots\pm C_{k,S}$.

On a sampling date, r measures are recorded and sample mean calculated for each size class:

$$Y_{t,s} = \sum_{k=1}^{r} \frac{Y_{t,s,k}}{r}.$$

According to assumption (3), the expectation of relative abundance is

$$E[Y_{t,s}] = f[\beta|Y,C] = q_s N_{t,s},$$

where β contains the sampling-gear efficiency coefficients (the q_s), the unobserved change rate (z), and the abundance of each size-class on date y_T (the $N_{T,s}$). $N_{t,s}$ is as defined by (2), Y indicates a matrix of relative abundance observations and C catches. Since it is a mean, clearly

$$Y_{t,s} \sim N\left(f[\beta|Y,C], \frac{\sigma^2[Y_{t,s}]}{r}\right)$$

(assumption 3). This implies the likelihood,

$$L(\beta) = \prod_{t,s}^{n} (2\pi)^{-1/2}\, \sigma[Y_{t,s}]^{-1}\, e^{-\frac{1}{2}(Y_{t,s}-f[\beta|Y,C])^2+\sigma^2[Y_{t,s}]},$$

where n is the product of the number of size-classes and sampling dates. Maximizing its logarithm (constant terms ignored),

$$-\sum_{t}^{T}\sum_{s}^{S}(Y_{t,s}-f[\beta|Y,C])^2 \div \sigma^{II}[Y_{t,s}] \qquad (4)$$

with respect to β yields maximum-likelihood estimates of the q_s, the $N_{T,s}$, and z. Maximization was achieved by minimizing the negative of (4) by the "Marquardt" method (Morrison 1960, Marquardt 1963, Conway et al. 1970, Gallant 1975, Press et al. 1986).

This estimator is equivalent to common least-squares if size and date variances are equal, but that restriction seems unlikely. Since

$$\sigma^2[Y_{t,s}] = N_{t,s}^2\, \mathrm{Var}[q_s], \qquad (5)$$

abundance is the dominant term. Abundance is dependent on reproductive success and a mortality history. Both are time-variant, so an assumption of equal variances is inappropriate.

This abundance estimator possesses few restrictions. Relative-abundance measures and catches can occur on any date. Any number of catches, or none at all, can occur between relative abundance samples or visa versa. The period of data collection may be short; the time-series may be brief. Individual growth can follow any form. Most important, recruitment to the exploited stock can occur continuously so that breeding (spawning) and birth (hatching) need not happen just once during each period. Reproduction may be continuous so age-specific cohorts need not exist. This estimator is not a cohort analysis, but it uses similar data.

Monte Carlo tests

Each test was designed to collect a history of estimator performance over many applications of the method in similar circumstances. Each test was composed of several trials. On each trial, a new exploited population was simulated, followed by relative abundance sampling, growth rate estimation, and catch estimation. Next, β was estimated by (4) from the data collected in the second step. Last, estimation error for each element of $\hat{\beta}$ was calculated. The familiar measure of error, $e = (\hat{\beta}-\beta)$, where β is the vector of population parameters estimated by $\hat{\beta}$, was not appropriate because β changed from one simulation to the next. Error was measured by the sufficient statistic $\in = \hat{\beta} \div \beta$. The bias of each element of β was estimated as the average $\in$ over the n trials (Monte Carlo samples). If a particular estimate was unbiased, then $\mu[\in] = 1$ for that parameter. The estimated error variance of each parameter, $s^2[\in]$, was also calculated.

A significance level for bias larger than 10% was found by computing the probability of the standard normal random variable as follows:

$$\text{significance level } \begin{pmatrix} \text{HO: } \mu[\in] \geqslant 0.9 \\ \text{HA: } \mu[\in] < 0.9 \end{pmatrix} =$$

$$\int_{-\infty}^{Z} f_p \, dp, \; Z = (\bar{\in} - 0.9) \div [s(\in)/\sqrt{n}].$$

$$\text{significance level } \begin{pmatrix} \text{HO: } \mu[\in] \leqslant 1.1 \\ \text{HA: } \mu[\in] > 1.1 \end{pmatrix} =$$

$$\int_{Z}^{\infty} f_p \, dp = 1.0 - \int_{-\infty}^{Z} f_p \, dp, =$$

$$(\bar{\in} - 1.1) \div [S(\in)/\sqrt{n}].$$

The results between tests were statistically compared by placing confidence intervals on the difference between the biases (Law and Kelton 1982:319) and using the variance ratio test (F test) to compare error variances.

In each Monte Carlo test, the intent was to complete trials until the estimate of bias was within a given bound with a prescribed probability (Law and Kelton 1982). Several parameters were estimated, so several biases were involved. It was too costly to confirm that all bias estimates were trustworthy and many parameters were not of primary interest, so the error of last-period total stock size ($\in[N(T.)]$) was used as the reference statistic. Trials were completed until

$$1.96^2 \cdot s^2(\in[N(T.)]) \div n \leqslant \Phi^2,$$

where Φ was usually small. The 95% confidence bound half-lengths for all parameters were computed to indicate how well bias was estimated for each parameter.

The method of Schrage (1979) was used to generate uniform random variables because it is portable and known to perform well (Law and Kelton 1982:227–228). Normal random variables were generated by the polar method (Law and Kelton 1982:259). The method of Scheuer and Stoller (1962) was used to generate correlated bivariate normal random numbers.

In most trials, the lives of 20,000 fish were individually simulated over 20 time-periods. A history of abundance and catch was created, then abundance sampling, catch estimation, and growth parameter estimation was simulated. Each fish possessed a unique growth pattern and recruitment date and independently encountered unobserved events and fishing death. The result of these encounters, growth rates, and recruitment dates were tabulated into size-class and date-specific matrices of numerical abundance and catch. The sequence of events of the population simulation is diagrammed in Appendix 1. A detailed description of the simulation and justification of control variable levels is given by Parrack (1990).

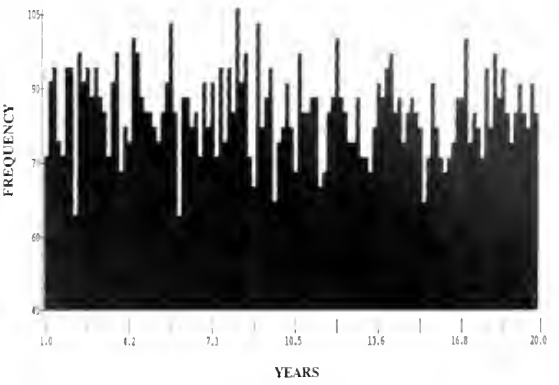

Figure 1

Frequency of recruitment dates from one trial of uniform recruitment simulations.

Von Bertalanffy growth was simulated by fixing m of equation (1) null. For each fish, A and k of (1) were drawn as normal random variables. The expectations were set near those estimated for many stocks, including Pacific cod (N.J.C. Parrack 1986), and their coefficients of variation (cv) were set as high or higher than common in other studies ($\leqslant 0.4$).

Two kinds of recruitment were considered, uniform and seasonal. The uniform pattern (Fig. 1) simulated continuous recruitment of constant magnitude. The date each fish recruited to the minimum size category was drawn as a U(1,20) random variable. Seasonal recruitment dates were drawn from normal distributions so that recruitment magnitudes varied U(1,20) between periods and so that a typical "pulse" of young fish recruited once each period, with some recruitment occurring continuously. The recruitment peak was simulated to occur randomly during April, May, and June by drawing the expected recruitment date for each period U(0.25,0.50). Protracted and contracted seasonal recruitment patterns were considered. Seasonal protracted recruitment was simulated by drawing the standard deviation of recruitment dates U(0.20,0.33) so that 80% of recruitment occurred randomly within ±3–5 months of the peak (Fig. 2). Seasonal contracted recruitment was simulated by drawing the standard deviation U(0.13,0.26) so that 80%

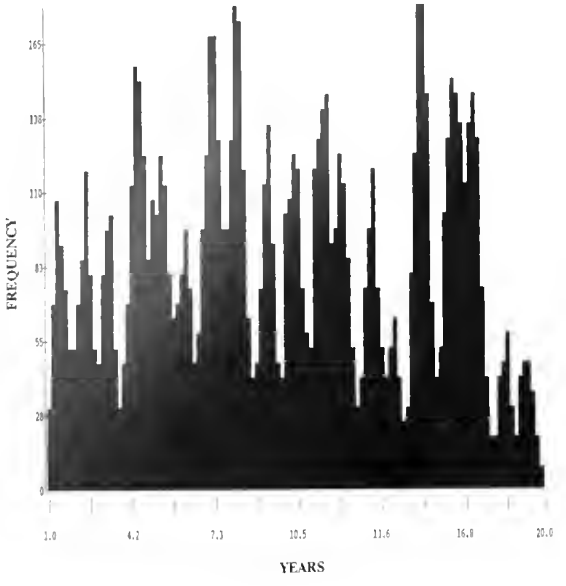

Figure 2
Frequency of seasonal, protracted recruitment dates from one trial. Peak recruitment occurs 1 April–1 June, 80% occurs within 3–5 months of the peak, and recruitment levels vary.

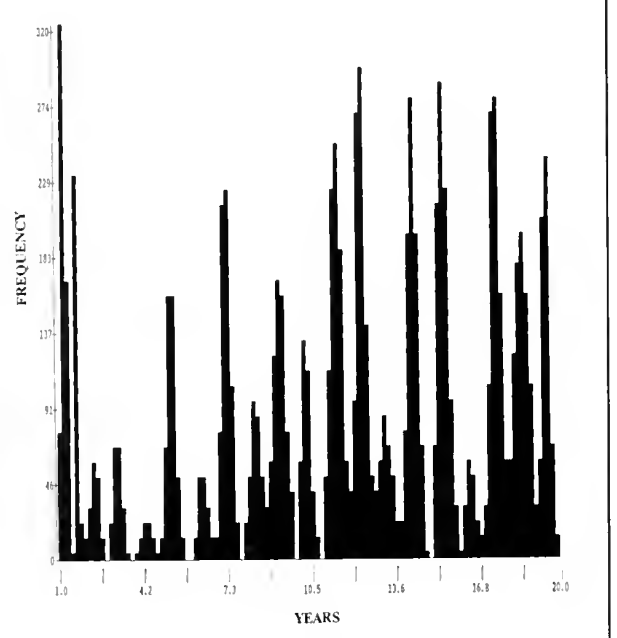

Figure 3
Frequency of seasonal, contracted recruitment dates from one trial. Peak recruitment occurs 1 April–1 July, 80% occurs within 2–4 months of the peak, and recruitment levels vary 20-fold between time periods.

of recruitment occurred randomly within ±2–4 months of the peak (Fig. 3).

The unobserved change rate was simulated both temporally invariant and variant. If variant, then $z_t \sim U(z_1, z_2)$ on each new trial; z_1 and z_2 were simulation control variables. Catching was simulated either as a single event that occurred once each midperiod or as a continuous event in each period. Fishing mortality was not imposed until period 6 so that the stock would accumulate as soon as possible after simulation initialization. In most tests the fishing mortality rate was drawn $U(F_1, F_2)$ on each new trial; F_1 and F_2 were control variables. Period-specific rates were set constant over all trials in two tests to guarantee a stock depletion caused by a rapid increase in fishing levels.

Sampling simulation included the generation of catch estimates, growth parameter estimates, and relative abundance measures. Populations and catches were generated over 20 time-periods. Relative abundance samples and catch estimates were simulated in the last four periods only, but catches were considered to be removed after the date of abundance samples so catch in the last period was irrelevant to estimation (and thus was not computed).

Size-class and date-specific catch estimates were drawn from a Gaussian distribution with catches from the simulator as the expectations and with variances specified by a cv. The estimator of catches was thus unbiased, and estimation errors (estimator variances) were proportional to catches.

A complete simulation of growth sampling and estimation was deemed too costly, so a reasonable proxy of unbiased estimation was used. Let A_i be a growth parameter of fish i such that $A_i \sim N(A, \sigma^2[A])$. Defining the uniqueness in growth of fish i as $\tau_i = A_i - A$, $\sigma^2[A] = \Sigma\tau_i^2/N$. Let A_i be unbiasedly measured by a_i with normal error so that $a_i = A_i + e_i$, $e_i \sim N(0, \sigma^2[e])$. Since $e_i = a_i - A_i$, $\sigma^2[e] = \Sigma e_i^2/N$, $\sigma^2[a_i] = E\{a_i - E[a_i]\}^2 = \sigma^2[A] + \sigma^2[e] + 2\sigma[\tau,e]$ where the last term is null because τ and e are independent. Using the sample mean of g fish to estimate A, $\sigma^2[A] = (\sigma^2[A] + \sigma^2[e])/g$, so that growth-parameter estimation variance is separated into two parts, that of inherent variability from fish to fish and that of growth measurement error. CV's were used as simulation control input instead of variances, so growth parameter estimates were $N(A, A^2(cv[A]^2 + cv[e]^2)/g)$ random variables. In reality, all growth parameters are estimated simultaneously. As a rule, growth parameter estimates are highly negatively correlated (Gallucci and Quinn 1979, Knight 1968, Burr 1988) with correlation coefficients often −0.90 or less. Estimates of k and A of (1) were drawn as normal random correlated variables (Rubinstein 1981:86) with a correlation coefficient of −0.95. The

number of fish sampled for growth (g) was specified in the simulation indirectly as a probability level and limit of a confidence bound. For a $1-\alpha$ level confidence interval on A of bound length $2\Phi A$,

$$\Phi A = Z(1-\alpha/2)\,\sigma[\hat{A}]$$

$$= Z(1-\alpha/2)\sqrt{A^2(cv[\hat{A}]^2+cv[e]^2)/g},$$

so

$$g = Z^2\left(1-\frac{\alpha}{2}\right)(cv[\hat{A}]^2 + cv[e]^2) \div \Phi^2.$$

On each sampling date r, relative abundance samples, $1 \leqslant k \leqslant r$, were simulated as

$$Y_{t,s} = \sum_{k=1}^{r} Y_{t,s,k} \div r = \sum_{k=1}^{r} q_{s,k}\, N_{t,s} \div r,$$

$$q_{s,k} \sim N\,(q_s,\ cv[q]^2\, q_s^2),$$

where cv[q] and the q_s were simulation constants. The q_s were 0.025, 0.05, 0.175, 0.225, 0.2425, and 0.25 (smallest to largest size-class) in most simulations. Several other variations were tried, and it was found that these constants did not affect results at all. Cv's of q were 0.4 or less. The observation and its variance were calculated as the maximum likelihood estimates,

$$Y_{t,s} = \sum_{k}^{r} Y_{t,s,k}/r$$

$$s^2[Y_{t,s}] = \sum_{k}^{r} (Y_{t,s,k} - Y_{t,s})^2/(r^2-r).$$

The sample size (r) was fixed indirectly by two control variables, the probability level and confidence-bound width for $Y_{t,s}$ where $\sigma^2[Y_{t,s}]$ is as (5). If a $1-\alpha$ level confidence interval on $Y_{t,s}$ was to be of bound length $2 \bullet \Phi \bullet N_{t,s} \bullet q_s$ then:

$$\Phi\, N_{t,s}\, q_s = \left(1-\frac{\alpha}{2}\right)\sigma[Y_{t,s}],$$

$$r = Z^2(1-\alpha/2)\, cv[q]^2 \div \Phi^2.$$

Sampling error entered the simulation as variation in q_s, not as variation in the $Y_{t,s}$; the variance of the abundance index was not an input.

These simulations encompassed many possibilities, but not all. Random variation was simulated in all process variables (z, growth parameters and recruitment magnitude, duration, and timing), but time trends were not. A different unobserved change rate was drawn for each time-period ($z_t \sim N(\mu_z,\ \sigma^2[z])$), but the expectation and variance were constant over time and size. Different growth parameters were drawn for each fish, but the expectations and variances were the same for all fish. Recruitment magnitudes for each time-period were drawn from a uniform distribution so time trends were not simulated. A different recruitment peak (i.e., the expectation of recruitment date) was drawn for each time-period from a common expectation and variance. A duration of recruitment (i.e., variance of recruitment date) was drawn for each time-period, but with the same expectation and variance. Random variation was simulated in sampling variables (catch estimates, growth parameter estimates, and the q_s), but biased estimates were not simulated. Although a different vector of sampling efficiencies (the q_s) were drawn for each sampling date, the expectation and variance for each size was temporally constant.

Results

The Monte Carlo tests fall into two categories: those that investigate the influence of population process variability on estimation errors, and those that test the effects of sampling and data estimation. Process variability includes recruitment phenomena, growth rates, and unobserved change due to emigration, immigration, natural death, and unrecorded catch. Sampling variation and data estimation includes four topics: catch estimation error, unrecorded dates of catch, growth parameter estimation error, and variability in sampling-gear efficiency coefficients, and thus in the abundance indices. Each of these items were studied separately in 14 tests.

Population process variability

For these tests, catches, dates of catch, and population growth parameters were considered to be known, and sampling gear efficiencies (the q's) invariant so that all sampling variation was absent. Catches were taken at midperiod. The probability of death due to catching in each period was an U(0.05, 0.2) random variable, and asymptotic size was 11.95 units (i.e., 119.5 cm, with 10 cm intervals).

Recruitment patterns Uniform recruitment test results (Table 1) show little bias and high precision in estimates of abundance and q's. Significance levels for the hypothesis of bias = 1.0 (unbiased) versus bias ≠ 1.0 (biased) were <0.00005 in almost every case, but bias

Table 1

Monte Carlo tests of populations processes. Catches, dates of catch, and population growth parameters were assumed known. Sampling gear efficiencies (q) were invariant. The probability of death due to catching in each period was a U(0.05, 0.2) random variable. Catches occurred at midperiod. Asymptotic size (i.e., $\mu[A]$) was 11.95.

	Recruitment patterns				Variable growth	Variable, rapid	Variable, slow
	Uniform	Protracted	Contracted	z variable	Test 1	growth - Test 2	growth - Test 3
$\mu[k]$	0.17	0.17	0.17	0.17	0.17	0.34	0.085
cv[A & k]	0.00	0.00	0.00	0.00	0.40	0.40	0.40
Loss rate z	0.10	0.10	0.10	U(0.1,0.4)	0.10	0.10	0.10
Recruit levels	constant	U(1, 20)	U(1, 20)	U(1, 20)	U(1, 20)	U(1, 20)	U(1, 20)
Recruit dates	U(1, 20)	$N(\mu, \sigma^2)$	$N(\mu, \sigma^2)$	$N(\mu, \sigma^2)$	$N(\mu, \sigma^2)$	$N(\mu, \sigma^2)$	$N(\mu, \sigma^2)$
$\mu(t)$		U(0.25, 0.5)	U(0.25, 0.5)	U(0.25,0.5)	U(0.247, 0.5)	U(0.247, 0.5)	U(0.247, 0.5)
$\sigma(t)$		U(0.2, 0.33)	U(.13, 0.26)	U(0.2, 0.33)	U(0.2, 0.33)	U(0.2, 0.33)	U(0.2, 0.33)
95% CI of bias of N(T.)							
½ width achieved	0.0024	0.0114	0.0160	0.0139	0.0434	0.0457	0.0498
Number of trials	1010	210	775	105	109	327	32

Variable	Bias	$s^2[\epsilon]$	Bias	$s^2[\epsilon]$	Bias	$s^2[\epsilon]$	Bias	$s^2[\epsilon]$	Bias	$s^2[\epsilon]$	Bias	$s^2[\epsilon]$	Bias	$s^2[\epsilon]$
N(T, 3)	0.9711	0.0032	1.1319	0.0333	1.3138	0.2460	1.1569	1.0508	0.7575	0.0204	0.8594	0.0319	0.8542	0.0456
N(T, 4)	0.9923	0.0152	0.9140	0.2824	0.9780	1.5205	0.9833	0.0955	1.0697	0.0588	0.7410	0.0152	0.8815	0.0379
N(T, 5)	0.9986	0.0055	0.9710	0.0527	0.9802	0.1454	1.0191	0.0364	0.9596	0.0134	0.9087	0.0168	0.9745	0.0044
N(T, 6)	0.9941	0.0010	1.0271	0.0078	1.0632	0.0165	1.0511	0.0341	0.9964	0.0010	1.0168	0.0101	1.0051	0.0036
N(T, 7)	0.9989	0.0016	0.9651	0.0072	0.9383	0.0133	0.9742	0.0046	0.9850	0.0010	0.9892	0.0041	0.9989	0.0036
N(T, 8)	1.0049	0.0005	1.0044	0.0012	1.0018	0.0041	0.9925	0.0017	1.0041	0.0003	0.9899	0.0013	1.0364	0.0043
N(T, 9)	0.9912	0.0008	0.9933	0.0024	0.9940	0.0036	1.0003	0.0024	0.9924	0.0004	0.9911	0.0004	1.0219	0.0100
N(T,10)	1.0084	0.0009	0.9916	0.0036	0.9905	0.0087	0.9735	0.0122	1.0200	0.0007	0.9991	0.0004	1.0836	0.0241
N(T,11)	0.9752	0.2291	0.6789	1.5190	0.4585	2.1818	0.2999	5.7229	1.0590	0.4399	1.2595	0.1852	1.9661	1.5290
N(T,12)									2.3825	2.7796	3.2020	1.3185	3.7363	5.9230
N(T,13)									2.9063	5.4646	3.8776	2.0041	5.5877	13.3879
N(T,14)									3.3177	8.3135	4.8876	1.9756	9.0415	77.7329
N(T,15)									3.9400	19.2576	6.3783	2.9742	11.3780	166.9735
N(T,16)									4.4074	45.0368	8.3752	6.7119	14.2365	403.7108
N(T,17)									5.5771	120.2284	11.3020	27.2042	14.9405	905.7713
N(T,18)									5.1845	203.8775	15.4323	50.7470	18.1915	903.7181
N(T,19)									9.6012	870.1467	23.3307	358.9141	26.6017	1253.4483
N(T,20)									1.3244	222.7073	26.9926	486.5381	11.0799	640.3803
N(T,21)									4.1712	169.5628	38.8813	2180.3053	24.4425	2117.6233
N(T,22)									-1.5598	53.1271	40.2471	3481.6977	2.3077	9.6225
N(T,23)									1.9878	41.6990	48.5059	4438.4966		
N(T,24)									-8.5990	2.7742	33.4447	6841.2892		
N(T,25)											32.0736	4537.5995		
N(T,26)											1.6141	5790.4488		
N(T.)	0.9908	0.0015	1.0064	0.0071	1.0491	0.0516	1.0245	0.0053	1.0988	0.0535	1.8714	0.1781	1.1147	0.0206
q(3)	1.0331	0.0039	0.9010	0.0209	0.8103	0.0410	0.8891	0.0268	1.3544	0.0543	1.2201	0.0676	1.4094	0.1195
q(4)	1.0178	0.0036	0.8844	0.0085	0.7299	0.0185	0.8728	0.0091	1.1304	0.0161	1.3772	0.0487	1.1669	0.0297
q(5)	0.9977	0.0030	0.9787	0.0067	0.9292	0.0181	0.9581	0.0058	1.0987	0.0118	1.2252	0.0325	1.0611	0.0064
q(6)	1.0090	0.0012	1.0212	0.0033	1.0177	0.0091	1.0161	0.0043	1.0478	0.0031	1.1014	0.0104	1.0094	0.0043
q(7)	0.9870	0.0011	1.0758	0.0062	1.1436	0.0137	1.0855	0.0073	1.0110	0.0023	1.0738	0.0063	0.9641	0.0025
q(8)	1.0133	0.0015	0.9290	0.0046	0.8422	0.0100	0.8780	0.0157	0.9706	0.0056	1.0444	0.0033	0.9198	0.0114
q(9)	1.0311	0.0039	1.0462	0.0199	1.0381	0.0275	0.9848	0.0437	0.9363	0.0100	1.0057	0.0044	0.9531	0.0258
q(10)	0.9717	0.0190	0.9655	0.1925	0.9282	0.2356	0.7786	0.3357	0.8790	0.0230	0.9282	0.0058	0.8257	0.0304
q(11)	0.7365	0.1902	0.6016	1.5307	0.8387	1.7031	0.1939	2.5069	0.5449	0.3805	0.4157	0.0087	0.4976	0.0643
q(12)									0.4371	0.0403	0.3132	0.0056	0.3373	0.0272
q(13)									0.3349	0.0263	0.2554	0.0047	0.2187	0.0129
q(14)									0.2587	0.0174	0.1940	0.0588	0.1427	0.0084
q(15)									0.1777	0.0124	0.1510	0.0221	0.0983	0.0038
q(16)									0.1242	0.0051	0.1171	0.0049	0.0654	0.0019
q(17)									0.0887	0.0036	0.0822	0.0029	0.0437	0.0015
q(18)									0.0589	0.0020	0.0580	0.0012	-0.2827	2.9493
q(19)									0.0394	0.0022	0.0365	0.0009	0.7259	13.8313
q(20)									-0.0925	1.0754	0.0247	0.0003	-0.1340	0.1934
q(21)									0.2614	2.9476	0.0165	0.0001	-0.0174	0.0165
q(22)									-0.1324	0.5450	0.0200	0.0473	-9.6131	278.5656
q(23)									-0.3803	3.0233	0.5313	53.3122		
q(24)									0.0163	0.0000	0.0122	0.2028		
q(25)									0.0177	0.0001	-0.0096	0.0421		
q(26)											-2.1688	167.9745		
z	1.5847	0.0715	1.6436	0.1442	1.8264	0.2772			1.9012	0.3023	2.7344	0.5514	0.9394	0.1280
exp(z)	1.0608	0.0008	1.0676	0.0017	1.0877	0.0034			1.0959	0.0036	1.1926	0.0075	0.9946	0.0013

was not large; the significance levels for the hypotheses of bias $\leq 10\%$ were >0.99995 for all estimates. Precision was not a problem, although error variances were not zero.

Since sampling variation was zero and the estimation model encompassed all of the population characteristics simulated, the estimation bias and imprecision were unexpected. The only possible source of that error are the integral approximations required in estimation.

The estimate of the unobserved change rate (z) was biased high by about 60% and its error variance was large. It entered estimation in an exponent, so the term in the model was the exponent of z (the reciprocal of "survival" from unobserved change), not z. The error term was again computed on the exponent of the estimate of z instead of z. The estimated bias was ten times lower and the error variance was several orders of magnitude less. This result proved consistent in all tests of population processes.

Partial correlation coefficients between parameter estimates did not exhibit meaningful trends. Although some adjoining abundance estimates were correlated (probably because the abundances were), evidence of other correlations were absent. Estimates of z were not correlated with the estimates of the q's or abundances; estimates of the q's were not correlated with abundance estimates. This result proved consistent. The correlation matrices for this and following tests are not shown for the sake of brevity but are presented in Parrack (1990).

The two seasonal recruitment tests (protracted and contracted patterns) show increased bias and imprecision. As the recruitment frequency contracted, bias and error variance-of-abundance estimates of the smallest and largest size-classes increased. This problem was worst for the largest size-class. Estimates of the q's also degraded.

Unobserved change rate The estimator assumes that the rate of change due to phenomena that cannot be observed (natural death, migration, unrecorded catch) is constant over periods. Since the assumption is undoubtedly false, estimation errors resulting from assigning a U(0.1,0.4) random variable to z for each period were investigated. Other simulation characteristics were as in the seasonal protracted recruitment test. The 95% confidence intervals on the difference of abundance estimation bias between this test and the protracted recruitment test included zero for size-classes 3 and 4, most others, and total abundance. Error variances were likely equal for size-classes 3, 4, and total abundance (SL 0.005, SL<0.000, SL<0.000). Correlations between estimates were low. A fourfold random variability in z did not affect estimation at all.

Growth Three tests consider highly variable growth. The cv's of asymptotic size and k were 0.4. Test 1 simulated the same growth parameters as the protracted recruitment test (k 0.17), test 2 considered growth twice as rapid (k 0.34), and test 3 growth twice as slow (k 0.085). All other simulation control variables are the same as the protracted recruitment test, so the results are comparable.

The results of all three tests were very similar. All reflected the high variation of asymptotic size: the parameter vector included size-classes larger than the asymptote. Abundance and q estimates of these classes (12 and larger) were worthless; huge bias and imprecision occurred. Abundances of smaller size-classes in all three tests were more precise than in the protracted recruitment test where growth was not variable. Biases and error variances of abundance and q estimates for size-class 11 and smaller were very similar in the three tests; performance seemed unaffected by growth rates. The exponent of z was again estimated much better than z in all three tests; estimates were precise although significant bias was present in the case of rapid, variable growth. Evidence of correlated estimates was absent. The introduction of an extremely high level of variation on individual growth parameters did not negatively affect estimates.

Data estimation and sampling

Errors attributable to sampling and the compilation of various input statistics were studied in seven tests. Catches are rarely censused as assumed by the estimator; estimates are usually the available statistics. The estimator models the dates of each catch, yet catch statistics are usually summed over an interval of dates. Growth rates are assumed to be known, but that is never possible; growth parameters must be estimated. Last, the variability in sampling-gear efficiency coefficients, and thus in the abundance indices, is also a source of uncertainty.

Most of the simulation control variables in these seven tests were the same as in the protracted recruitment test. Asymptotic size was 11.95, growth k was 0.17, the unobserved loss rate (z) was fixed at 0.1, and the seasonal, protracted recruitment pattern was employed; thus recruitment levels varied 20-fold between periods. Catching was simulated differently than in the protracted recruitment test. Catching was continuous (see Appendix 1, step 4) instead of a single subtraction at midperiod, and the fishing mortality rate (F) was a U(0.1,0.4) random variable.

Catch dates A single scenario was used to investigate the importance of recording each catch date and modeling each catch separately. The summed catch over each period was assumed to be known, but not

Table 2

Monte Carlo tests for the effects of sampling variation. $\mu[A]=11.95$, $\mu[k]=0.17$, $z=0.1$, and seasonal, protracted recruitment was simulated. Catching was simulated as a continuously occurring event. The instantaneous rate of fishing mortality was a U(0.1,0.4) random variable.

			Growth parameter measurement error			Relative abundance	
	Unknown catch date	Catch estimation error	40% Error	15% Error	with process variance	cv[q] 0.4, *r* 3	cv[q] 0.2, *r* 16
cv[A & k]	0.00	0.00	0.00	0.00	0.20	0.00	0.00
Catch estimation							
catch dates	absent	absent	absent	absent	absent	absent	absent
cv[C(t,s)]	0.00	0.40	0.00	0.00	0.00	0.00	0.00
Growth estimation							
cv[error]	0.00	0.00	0.40	0.15	0.15	0.00	0.00
precision level	–	–	–	–	0.02	–	–
probability level	–	–	–	–	0.95	–	–
fish sampled, g	1	1	1	1	601	1	1
Sampling efficiency							
cv[q(s)]	0.00	0.00	0.00	0.00	0.00	0.40	0.10
precision level	–	–	–	–	–	0.50	0.05
probability level	–	–	–	–	–	0.95	0.95
sample size, r	1	1	1	1	1	3	16
95% CI of bias of N(T.)							
½width achieved	0.0155	0.0197	0.4789	0.0210	0.0198	0.0354	0.0198
Number of trials	101	84	192	198	79	200	52

Variable	$\bar{\epsilon}$	$s^2[\epsilon]$	$\bar{\epsilon}$	$s^2[\epsilon]$	$\bar{\epsilon}$	$s^2[\epsilon]$	$\bar{\epsilon}$	$s^2[\epsilon]$	$\bar{\epsilon}$	$s^2[\epsilon]$	$\bar{\epsilon}$	$s^2[\epsilon]$	$\bar{\epsilon}$	$s^2[\epsilon]$
N(T, 3)	1.1081	0.0295	1.1817	0.0646	1.8710	217.1297	1.1439	0.1424	0.9947	0.0355	1.3381	5.2758	1.0972	0.0768
N(T, 4)	0.9710	0.3532	1.0314	0.2057	1.0034	3.4342	0.9228	1.0249	1.0184	0.0767	0.9247	3.0564	0.9288	0.0823
N(T, 5)	1.0009	0.0253	0.9350	0.0398	1.1353	3.4290	1.0028	0.1066	1.0026	0.0108	0.8733	0.2110	0.9128	0.0471
N(T, 6)	1.0162	0.0052	1.0197	0.0034	1.3096	6.9835	1.0375	0.0511	0.9902	0.0011	1.0156	0.0289	1.0092	0.0056
N(T, 7)	0.9740	0.0051	0.9660	0.0055	1.3544	12.7702	0.9675	0.0170	0.9953	0.0009	0.9530	0.0430	0.9191	0.0119
N(T, 8)	1.0000	0.0010	0.9956	0.0079	1.6209	17.9277	1.0437	0.0598	1.0019	0.0010	1.0243	0.0194	1.0239	0.0045
N(T, 9)	1.0003	0.0007	0.9939	0.0061	1.5861	11.9433	1.0458	0.0952	0.9959	0.0008	0.9703	0.0079	0.9688	0.0024
N(T,10)	0.9914	0.0045	0.9973	0.0012	2.6909	26.6738	1.3480	1.1729	1.0096	0.0019	1.0077	0.0112	1.0021	0.0004
N(T,11)	0.8191	3.9963	0.7914	1.2824	3.4334	111.2210	1.2774	5.3882	1.1619	0.3091	1.1734	1.1168	0.9568	0.1516
N(T,12)									2.3955	1.6866				
N(T,13)									3.4498	5.9767				
N(T,14)									3.2299	16.5785				
N(T,15)									3.6964	41.8706				
N(T,16)									0.4291	92.2468				
N(T,17)									6.5117	174.0005				
N(T,18)									1.5430	10.9191				
N(T,19)									18.1902	768.6451				
N(T.)	1.0242	0.0063	1.0259	0.0086	1.4105	11.4628	1.0416	0.0226	1.0542	0.0081	1.0345	0.0653	0.9799	0.0053
q(3)	0.9180	0.0200	0.8754	0.0291	1.3725	9.3538	0.9143	0.0715	1.0346	0.0290	0.9655	0.1063	0.9661	0.0460
q(4)	0.8578	0.0062	0.8729	0.0126	1.5114	25.7585	0.8825	0.0451	1.0391	0.0157	0.8933	0.0776	0.9397	0.0124
q(5)	0.9715	0.0051	0.9725	0.0103	2.0644	87.9064	1.0305	0.3386	1.0472	0.0098	1.0162	0.0709	1.0402	0.0091
q(6)	1.0046	0.0043	1.0141	0.0065	1.9815	47.7841	1.0593	0.1689	1.0315	0.0021	1.0467	0.0553	1.0629	0.0045
q(7)	1.0783	0.0059	1.0679	0.0065	2.0977	54.6183	1.0887	0.0294	1.0112	0.0022	1.1524	0.0767	1.1242	0.0159
q(8)	0.9093	0.0058	0.9342	0.0061	1.5326	20.5395	0.9387	0.0249	0.9900	0.0058	0.9596	0.0590	0.9590	0.0075
q(9)	1.0159	0.0190	1.0447	0.0239	1.7836	46.8489	1.0023	0.0620	0.9735	0.0082	1.1949	0.1016	1.1582	0.0194
q(10)	1.0151	0.1572	1.0147	0.0816	1.4402	25.2990	0.8819	0.1195	0.9388	0.0293	1.0083	0.1004	0.9874	0.0182
q(11)	0.5695	0.8583	0.8320	1.4223	1.4677	34.9181	0.9667	0.5829	0.6416	0.0701	0.9200	0.6084	0.8700	0.1365
q(12)									0.3774	0.0303				
q(13)									0.2138	0.0091				
q(14)									0.1017	0.0042				
q(15)									0.0488	0.0012				
q(16)									-3.1478	425.1308				
q(17)									0.0866	0.0670				
q(18)									-0.0707	0.0967				
q(19)									1.2251	4.4242				
z	0.8137	0.1022	1.6881	0.2587	0.2301	25.5499	1.0396	0.0219	0.1835	0.0000	0.8525	1.0626	0.8542	0.2896
exp(z)	0.9820	0.0010	1.0736	0.0031	0.9828	0.0416	1.0527	0.0067	1.0898	0.0022	0.9913	0.0104	0.9869	0.0029

the dates of the catches. The accumulated catch each period was assigned to the midpoint of each period for estimation. The results (Table 2) were almost identical with those of the protracted recruitment test (Table 1). The 95% confidence interval (Welch 1938) on the difference between total-abundance estimation bias of the protracted recruitment test and this test included zero (−0.0014 to 0.0372). The error variances were very similar (0.0072 and 0.0063). Estimates were not correlated. The absence of exact catch dates did not affect estimation.

Catch estimation error The effects of estimating catches rather than enumerating them were investigated by drawing size-class-specific catch estimates as normal random variables with expectation $C(t,s)$ and variance $(cv[C] \cdot C(t,s))^2$. This simulated unbiased catch estimation and estimation error proportional to catches. A large degree of catch estimation uncertainty was imposed ($cv[C] = 0.40$). Simulation control variables were the same as in the catch date test and the protracted recruitment test. Results were also similar. The bias of total abundance estimates was about the same for all three tests and the error variances were nearly so. Correlated estimates were not evident. Confidence intervals (95%) on the difference in bias between this test and the protracted recruitment test included zero for all size-classes and total abundance. The error variance for size-class 3 was different ($SL < 0.0005$) and might have been different for size-class 4 (SL 0.052), but probably not for total abundance (SL 0.142) and all others. Imprecise catch estimates did not impact bias or error variance.

Growth parameter estimation error The effect of imprecise growth parameter estimates was also considered. Estimates of growth parameters were simulated as normal correlated random variables with expectations equal to those of the population. As explained in the Monte Carlo methods section, the variance of a growth parameter estimate is composed of two parts: process variation due to variant individual growth, and growth measurement error. Simulation control constants were therefore the cv of A and of k, the growth measurement error cv, the two constants required to compute the sample size used to estimate the growth parameters, and the correlation coefficient between estimates (−0.95). Simulation constants were as in the catch date test except those related to growth parameter estimation.

Three tests were carried out, two without process variation. First, the effect of two measurement error cv's was studied in the absence of growth variability. The sample size was set at one fish in these two tests so affects due to measurement error would be magnified. Then, the combined effect of process variation and estimation error was considered.

In the first test with extremely imprecise growth parameter estimates (cv 0.4), Monte Carlo trials were carried out until it became obvious that little more information would be gained with further computations. Error variances were huge (Table 2). Only the exponent of z was reasonably estimated. Many estimates were correlated, particularly those of z with those of sampling-gear efficiency coefficients. Even without individually variant growth rates (an unlikely prospect), large growth-parameter measurement error created significant uncertainty.

The second test simulated 15% measurement error. A 95% confidence interval on the difference between the bias of total abundance estimates between this and the protracted recruitment test included zero, but the error variances were probably different ($SL < 0.0001$); most error variances were higher. Bias was unaffected although error variance approximately doubled. The estimates did not seem correlated. The introduction of a 15% growth measurement error increased error variances but did not affect bias.

The third test simulated both process error (cv 0.2) and 15% growth measurement error, but with a sample size such that 95% confidence intervals on the estimate of the expectation of growth parameters were with precision ±2% ($g = 601$ fish). The 95% confidence interval on the difference in bias of total abundance estimates between this test and the protracted recruitment test included zero (−0.0220 to 0.0238) although error variances perhaps differed ($SL \approx 0.05$). Estimates were not correlated. Apparently 15% (or less) measurement error, even with natural growth variation, minimally affects estimation.

Gear efficiency variability The estimator is derived from the density function of relative abundance observations (Y), but the effect of Y variability on estimation error was not of large interest. The variance of Y is $\sigma^2[Y_{t,s}] = N_{t,s}{}^2 cv[q]^2$. The dominant term is the square of abundance, so as abundance increases, $\sigma^2[Y_{t,s}]$ increases. This may be dampened a bit by an increase in q with size, but the dominant factor in the variance expression for the observations is abundance. Abundance levels cannot be controlled or anticipated beforehand, so knowledge of the effect of Y variability is of little value. Knowledge of the effect of q variability is useful, however, since care may be taken in the selection and design of sampling gear.

Studies that document the statistics necessary to calculate the variability of relative abundance sampling-gear efficiencies are not common. Studies of commerical fishery statistics offer different but useful information. Yield is a portion of biomass; the pro-

portion is the product of fishing effort and q for the fishing method. Since yield is the product of q, effort, and biomass, then yield-per-effort equals the product of q and biomass and q is yield-per-effort divided by biomass. It then follows that the cv's of q and yield-per-effort are equal. The cv of yield-per-effort of the Pacific halibut longline fishery is estimated to be 0.02 (Quinn et al. 1982), and that of Newfoundland flounder trawlers on the Grand Bank (Smith 1980) is estimated to be about the same. The levels used in these simulations (0.4 and 0.2) are about an order of magnitude higher than those.

Effects of the variability in q on estimation errors were investigated in three tests. All simulation constants were as in the protracted recruitment test except those related to abundance sampling. Simulation control constants were cv[q] and the two constants required to compute the sample size. Although they were probably unrealistically large, a cv[q] of 0.4 was used in the first test and 0.2 was used in the second.

First, the impact of extreme variability (cv 0.4) and extremely light sampling was tested. The sample size (r 3) was such that a 95% confidence interval on relative abundance was within ±50% of the expectation. The extremely high cv[q] and low relative-abundance sample size were not reflected in error variances as much as expected (Table 2), but error variances were higher than those of the protracted recruitment test. Most abundance estimates were biased by less than 10%. Estimates were not correlated.

Next, the cv[q] was reduced to 0.1 and the sample size was increased so that a 95% confidence interval on relative abundance was within ±5% of the expectation (r 16). The result was very similar to those of the first test except error variances were much lower. Biases of abundance estimates were ±10% or less and estimates were not correlated.

There was no evidence that high variation in the q_s biased abundance estimates even if sample sizes were insufficient, but error variances were affected. Error variance was considerably reduced with reasonable sample sizes.

Bias

The results of these experiments (Tables 1 and 2) show that abundances and gear efficiencies (q's) of the smallest and largest size-classes were often biased. Bias did not occur with uniform, constant recruitment and no sampling variation, but as process and sampling variation increased, bias in estimates of the smallest and largest sizes became pronounced.

Each expected value is a proportion of calculated abundance. The abundance calculation sums future catches (data), last-period abundance (estimates), and an amount for unobserved changes (estimate). Future catches and terminal abundance are thus the major components of each projection. Both catch and final abundance must be integrated over size. The integration of catch over size at each catch date following the date of the expected value is required. The integration of abundance over size on the date of the final relative abundance sample is also necessary. All integrals are approximated, so these calculations are the source of the bias. The amount of error incurred at each integration depends on how well the trapezoidal rule approximates the size distribution. Since the size frequency within a size-class is never smooth, the approximation will be in error with the amount depending on the degree of smoothness within the size-class. If growth is variable or the number of fish is small, clumps in size frequencies can result from chance alone, but the major factor is the growth and recruitment pattern combination.

Narrowing the size-classes eliminates this problem. If they are narrowed enough to eliminate clumping caused by the particular recruitment frequency contraction, the size frequency within size-classes will be smooth and the trapezoidal approximation will be accurate. The seasonal contracted pattern of recruitment test 3 was again used to demonstrate this. An asymptotic size of 120 cm was simulated with recruitment occurring at 20 cm. First, it was assumed that the data were collected in 20 cm intervals so that the asymptotic size was 6 and the recruitment size was class 1. In the second case, it was assumed that data were collected in 2 cm groups so that the asymptotic size was 60 and the recruitment size was class 10. The unobserved change rate was set at 0.2 in both tests, and all other simulation control variables were as in the contracted recruitment test.

Ninety-two trials were required to obtain a 95% confidence interval half-length of 0.05 on the bias of total abundance in bias test 1 with 20 cm interval data. Estimates of the smallest and largest size-class abundances were biased and the error variances were very large (Table 3), particularly for the largest size-class. The estimate of the survival from unobserved change (z) was, however, reasonably accurate and precise.

Only 16 trials were required to obtain a 95% confidence interval half-length of 0.03 on the bias of total abundance in bias test 2 with two-unit size-interval data because the error variances were very low. Estimates of the first three size groups were probably biased by 10% or more, but the rest were not. Only six of the 47 estimates were probably biased at all (0.95 level). The estimate of the exponent of z was also not biased. Although the matrix was too large to be included (194 rows and columns), there was no evidence that estimates were correlated.

Table 3

Biases for 20 cm size-class width data (bias test 1, 92 trials) versus biases for 2 cm size-class width data (bias test 2, 16 trials).

Bias test	Variable	Estimates: Bias	Estimates: $s^2[\in]$	Bias 95% CI ½-width	Significance levels: HO:Bias≥0.9 HA:Bias<0.9	Significance levels: HO:Bias≤1.1 HA:Bias>1.1
1	N(20–39)	1.2941	0.1332	0.0746	1.0000	0.0000
2	N(20–21)	1.8093	0.5273	0.3558	1.0000	0.0000
2	N(22–23)	1.5883	0.2529	0.2464	1.0000	0.0001
2	N(24–25)	1.5190	0.3576	0.2930	1.0000	0.0025
2	N(26–27)	1.1204	0.0790	0.1377	0.9991	0.3856
2	N(28–29)	0.9746	0.0578	0.1178	0.8927	0.9815
2	N(30–31)	0.8908	0.0124	0.0545	0.3699	1.0000
2	N(32–33)	1.0826	0.0440	0.1028	0.9997	0.6303
2	N(34–35)	0.9963	0.0002	0.0073	1.0000	1.0000
2	N(36–37)	1.0142	0.0032	0.0276	1.0000	1.0000
2	N(38–39)	0.9924	0.0005	0.0109	1.0000	1.0000
1	N(40–59)	1.0071	0.0234	0.0313	1.0000	1.0000
2	N(40–41)	1.0052	0.0003	0.0089	1.0000	1.0000
2	N(42–43)	1.0009	0.0000	0.0032	1.0000	1.0000
2	N(44–45)	1.0013	0.0001	0.0041	1.0000	1.0000
2	N(46–47)	0.9977	0.0001	0.0042	1.0000	1.0000
2	N(48–49)	1.0060	0.0008	0.0136	1.0000	1.0000
2	N(50–51)	0.9966	0.0004	0.0097	1.0000	1.0000
2	N(52–53)	1.0022	0.0000	0.0030	1.0000	1.0000
2	N(54–55)	0.9985	0.0001	0.0046	1.0000	1.0000
2	N(56–57)	0.9998	0.0000	0.0013	1.0000	1.0000
2	N(58–59)	0.9969	0.0001	0.0047	1.0000	1.0000
1	N(60–79)	0.9741	0.0288	0.0347	1.0000	1.0000
2	N(60–61)	1.0046	0.0001	0.0045	1.0000	1.0000
2	N(62–63)	0.9975	0.0002	0.0077	1.0000	1.0000
2	N(64–65)	0.9998	0.0000	0.0018	1.0000	1.0000
2	N(66–67)	0.9998	0.0001	0.0059	1.0000	1.0000
2	N(68–69)	1.0026	0.0002	0.0062	1.0000	1.0000
2	N(70–71)	0.9959	0.0002	0.0071	1.0000	1.0000
2	N(72–73)	1.0034	0.0001	0.0060	1.0000	1.0000
2	N(74–75)	1.0025	0.0001	0.0050	1.0000	1.0000
2	N(76–77)	1.0039	0.0003	0.0081	1.0000	1.0000
2	N(78–79)	1.0004	0.0001	0.0049	1.0000	1.0000
1	N(80–99)	1.0517	0.0745	0.0558	1.0000	0.9553
2	N(80–81)	0.9982	0.0003	0.0080	1.0000	1.0000
2	N(82–83)	1.0009	0.0001	0.0045	1.0000	1.0000
2	N(84–85)	1.0037	0.0002	0.0067	1.0000	1.0000
2	N(86–87)	1.0013	0.0000	0.0010	1.0000	1.0000
2	N(88–89)	0.9995	0.0000	0.0016	1.0000	1.0000
2	N(90–91)	0.9992	0.0001	0.0054	1.0000	1.0000
2	N(92–93)	0.9994	0.0000	0.0009	1.0000	1.0000
2	N(94–95)	0.9963	0.0001	0.0041	1.0000	1.0000
2	N(96–97)	0.9989	0.0000	0.0017	1.0000	1.0000
2	N(98–99)	0.9974	0.0000	0.0022	1.0000	1.0000
1	N(100–119)	6.4942	254.5641	3.2603	0.9996	0.0006
2	N(100–101)	1.0003	0.0000	0.0007	1.0000	1.0000
2	N(102–103)	0.9997	0.0003	0.0091	1.0000	1.0000
2	N(104–105)	0.9979	0.0003	0.0105	1.0000	1.0000
2	N(106–107)	0.9997	0.0000	0.0005	1.0000	1.0000
2	N(108–109)	1.0009	0.0000	0.0005	1.0000	1.0000
2	N(110–111)	0.9981	0.0000	0.0035	1.0000	1.0000
2	N(112–113)	1.0000	0.0000	0.0005	1.0000	1.0000
1	N(T.)	1.1808	0.0592	0.0497	1.0000	0.0007
2	N(T.)	1.0388	0.0049	0.0342	1.0000	0.9998

Bias test	Variable	Estimates: Bias	Estimates: $s^2[\in]$	Bias 95% CI ½-width	Significance levels: HO:Bias≥0.9 HA:Bias<0.9	Significance levels: HO:Bias≤1.1 HA:Bias>1.1
1	q(20–39)	0.8296	0.0207	0.0294	0.0000	1.0000
2	q(20–21)	0.6373	0.0560	0.1160	0.0000	1.0000
2	q(22–23)	0.6924	0.0504	0.1101	0.0001	1.0000
2	q(24–25)	0.7464	0.0621	0.1221	0.0068	1.0000
2	q(26–27)	0.9410	0.0465	0.1057	0.7766	0.9984
2	q(28–29)	1.0818	0.0616	0.1216	0.9983	0.6151
2	q(30–31)	1.1408	0.0234	0.0749	1.0000	0.1431
2	q(32–33)	0.9545	0.0300	0.0849	0.8959	0.9996
2	q(34–35)	0.7751	0.0463	0.1055	0.0101	1.0000
2	q(36–37)	0.6608	0.0531	0.1129	0.0000	1.0000
2	q(38–39)	0.7494	0.0379	0.0954	0.0010	1.0000
1	q(40–59)	1.0050	0.0125	0.0228	1.0000	1.0000
2	q(40–41)	0.9352	0.0099	0.0487	0.9216	1.0000
2	q(42–43)	1.0218	0.0205	0.0701	0.9997	0.9856
2	q(44–45)	1.0357	0.0093	0.0473	1.0000	0.9961
2	q(46–47)	0.8792	0.0154	0.0608	0.2513	1.0000
2	q(48–49)	0.7148	0.0542	0.1141	0.0007	1.0000
2	q(50–51)	0.7373	0.0333	0.0894	0.0002	1.0000
2	q(52–53)	0.8691	0.0090	0.0464	0.0960	1.0000
2	q(54–55)	1.0389	0.0438	0.1025	0.9961	0.8786
2	q(56–57)	1.0358	0.0056	0.0365	1.0000	0.9997
2	q(58–59)	0.8082	0.0187	0.0670	0.0036	1.0000
1	q(60–79)	0.9049	0.0193	0.0284	0.6333	1.0000
2	q(60–61)	0.6377	0.0760	0.1351	0.0001	1.0000
2	q(62–63)	0.8143	0.0401	0.0982	0.0434	1.0000
2	q(64–65)	0.9890	0.0204	0.0700	0.9936	0.9991
2	q(66–67)	1.0381	0.0257	0.0785	0.9997	0.9388
2	q(68–69)	0.8908	0.0447	0.1036	0.4306	1.0000
2	q(70–71)	0.7287	0.0583	0.1183	0.0023	1.0000
2	q(72–73)	1.0168	0.0152	0.0604	0.9999	0.9965
2	q(74–75)	1.0449	0.0163	0.0626	1.0000	0.9577
2	q(76–77)	0.8313	0.0415	0.0998	0.0886	1.0000
2	q(78–79)	0.7050	0.0727	0.1321	0.0019	1.0000
1	q(80–99)	0.7632	0.2257	0.0971	0.0029	1.0000
2	q(80–81)	0.9684	0.0392	0.0970	0.9167	0.9961
2	q(82–83)	1.0334	0.0214	0.0717	0.9999	0.9657
2	q(84–85)	0.6644	0.0478	0.1071	0.0000	1.0000
2	q(86–87)	0.9742	0.0679	0.1277	0.8727	0.9732
2	q(88–89)	0.7991	0.0914	0.1481	0.0909	1.0000
2	q(90–91)	0.7715	0.0667	0.1266	0.0233	1.0000
2	q(92–93)	0.9841	0.0515	0.1148	0.9244	0.9761
2	q(94–95)	0.7314	0.1194	0.1749	0.0294	1.0000
2	q(96–97)	0.8420	0.0390	0.1000	0.1279	1.0000
2	q(98–99)	0.9202	0.1227	0.1835	0.5856	0.9726
1	q(100–119)	0.1117	0.5453	0.1509	0.0000	1.0000
2	q(100–101)	0.7954	0.1388	0.1952	0.1467	0.9989
2	q(102–103)	0.9848	1.5099	0.6680	0.5983	0.6323
2	q(104–105)	1.0579	0.0507	0.1224	0.9943	0.7497
2	q(106–107)	0.8840	0.0867	0.1923	0.4350	0.9862
2	q(108–109)	0.8992	0.0936	0.2682	0.4976	0.9289
2	q(110–111)	1.0052	0.1531	0.3835	0.7047	0.6860
2	q(112–113)	1.0121	0.0004	0.0238	1.0000	1.0000
1	exp(z)	0.9716	0.0135	0.0237	1.0000	1.0000
2	exp(z)	0.9783	0.0169	0.0637	0.9920	0.9999

Estimates of the first three size-classes were both biased and imprecise. Poor estimates of the smallest few size-classes were expected. These classes lacked a catch history at the time of the last sample, so these estimates of abundance (at the time of the last relative abundance sample) were a function of the last-period relative abundance sample only.

Examples

Two tests were used to discover what might be expected when assessing populations with no periodicity in recruitment at all; recruitment dates were completely protracted uniformly through time (Fig. 1). Most control variables were the same in the two tests. Data were assumed to be available in two-unit size intervals. A 120-unit asymptotic size fell in size-class 60, and a 30-unit recruitment size in class 15. The growth parameter k was left at 0.17. Continuous fishing was simulated; the fishing mortality rate (F) for each period was drawn from a U(0.3,0.8) distribution. The expectations of sampling efficiencies (q_s) were arbitrarily chosen so that their regression on size was sigmoid, reaching an asymptote at size-class 30 (0.028, 0.031, 0.033, 0.038, 0.044, 0.053, 0.069, 0.101, 0.153, 0.190, 0.218, 0.234, 0.242, 0.247, 0.249, and 0.250). Catch estimates were simulated to be imprecise (cv 0.4). A 10% growth measurement error was simulated. Sampling intensities were the same in both tests; sample sizes for growth parameter estimates and for relative abundance observations were such that a 95% CI was of width ±5%.

Although the levels of population processes were the same in both tests, the amount of process variability was much higher in test 2. Normal growth variability was simulated in test 1 and extreme variability in test 2. The rate of unobserved change in test 1 was constant, but varied three-fold in test 2. The variance of sampling efficiencies was set one order of magnitude larger than that observed for commercial fishing gear in test 1 and twice that in test 2.

Error variances-of-abundance estimates were very low in the case of normal process variability (Table 4). Estimates of all but the smallest six size-classes were biased by 10% or less, if at all, and were precise. Bias (more than 10%) and imprecision of the smallest six size-class estimates was expected because the smaller fish were barely represented in the catch and appeared in the relative abundance samples just once. Estimates of the sampling efficiencies (the q_s) tended to be imprecise. Some were biased from 20% to 30% and a few even more. The estimate of survival from unobserved change was biased low (about 15%), yet precise. Estimates did not tend to be correlated. The correlations between the estimate of the unobserved change rate (z) and other estimates (Table 5), particularly of the q_s, were of interest because other studies found corre-

Table 4

Monte Carlo test results for two examples of constant, uniform recruitment.

	Example 1, Normal process variability					Example 2, High process variability				
Loss rate z	0.20					U(0.2, 0.6)				
Growth cv[A & k]	0.20					0.40				
Growth estimation										
cv[error]	0.10					0.10				
precision level	0.05					0.05				
probability level	0.95					0.95				
fish sampled, g	77					262				
Sampling efficiency										
cv[q(s)]	0.20					0.40				
precision level	0.05					0.05				
probability level	0.95					0.95				
sample size, r	62					246				
95% CI of bias of N(T.)										
½ width achieved	0.0149					0.024				
Number of trials	97					64				
	Estimates		Bias 95% CI	Significance levels		Estimates		Bias 95% CI	Significance levels	
	Bias	Variance	½ width	HO:Bias≥0.9 HA:Bias<0.9	HO:Bias≤1.1 HA:Bias>1.1	Bias	Variance	½ width	HO:Bias≥0.9 HA:Bias<0.9	HO:Bias≤1.1 HA:Bias>1.1
N(T,15)	0.7669	0.0368	0.0382	0.0000	1.0000	0.5605	0.0273	0.0405	0.0000	1.0000
N(T,16)	0.7556	0.0520	0.0454	0.0000	1.0000	0.6660	0.0633	0.0616	0.0000	1.0000
N(T,17)	0.8022	0.0718	0.0533	0.0002	1.0000	0.7294	0.0567	0.0583	0.0000	1.0000
N(T,18)	0.9012	0.0960	0.0617	0.5157	1.0000	0.7382	0.0765	0.0678	0.0000	1.0000
N(T,19)	0.8423	0.0689	0.0522	0.0152	1.0000	0.7538	0.0754	0.0673	0.0000	1.0000

Table 4 (continued)

	Estimates		Bias 95% CI ½ width	Significance levels HO:Bias≥0.9 HA:Bias<0.9	Significance levels HO:Bias≤1.1 HA:Bias>1.1	Estimates		Bias 95% CI ½ width	Significance levels HO:Bias≥0.9 HA:Bias<0.9	Significance levels HO:Bias≤1.1 HA:Bias>1.1
	Bias	Variance				Bias	Variance			
N(T,20)	0.8227	0.0662	0.0512	0.0015	1.0000	0.7826	0.0722	0.0658	0.0002	1.0000
N(T,21)	0.9475	0.0440	0.0418	0.9871	1.0000	0.8975	0.0738	0.0666	0.4702	1.0000
N(T,22)	1.0006	0.0001	0.0019	1.0000	1.0000	0.9982	0.0003	0.0042	1.0000	1.0000
N(T,23)	1.0007	0.0001	0.0020	1.0000	1.0000	1.0012	0.0004	0.0051	1.0000	1.0000
N(T,24)	0.9973	0.0001	0.0024	1.0000	1.0000	0.9993	0.0005	0.0053	1.0000	1.0000
N(T,25)	0.9992	0.0001	0.0019	1.0000	1.0000	0.9979	0.0002	0.0037	1.0000	1.0000
N(T,26)	0.9995	0.0001	0.0020	1.0000	1.0000	0.9946	0.0003	0.0040	1.0000	1.0000
N(T,27)	0.9979	0.0000	0.0012	1.0000	1.0000	0.9938	0.0002	0.0038	1.0000	1.0000
N(T,28)	0.9984	0.0000	0.0013	1.0000	1.0000	0.9970	0.0001	0.0022	1.0000	1.0000
N(T,29)	0.9992	0.0000	0.0012	1.0000	1.0000	0.9944	0.0004	0.0050	1.0000	1.0000
N(T,30)	0.9973	0.0000	0.0013	1.0000	1.0000	0.9944	0.0002	0.0032	1.0000	1.0000
N(T,31)	1.0008	0.0001	0.0016	1.0000	1.0000	0.9948	0.0002	0.0038	1.0000	1.0000
N(T,32)	0.9965	0.0001	0.0016	1.0000	1.0000	0.9956	0.0001	0.0028	1.0000	1.0000
N(T,33)	0.9984	0.0000	0.0010	1.0000	1.0000	0.9954	0.0001	0.0030	1.0000	1.0000
N(T,34)	0.9973	0.0000	0.0014	1.0000	1.0000	0.9951	0.0005	0.0055	1.0000	1.0000
N(T,35)	0.9987	0.0001	0.0015	1.0000	1.0000	0.9948	0.0002	0.0034	1.0000	1.0000
N(T,36)	0.9950	0.0002	0.0026	1.0000	1.0000	0.9944	0.0004	0.0051	1.0000	1.0000
N(T,37)	0.9974	0.0001	0.0017	1.0000	1.0000	0.9960	0.0001	0.0029	1.0000	1.0000
N(T,38)	0.9977	0.0001	0.0020	1.0000	1.0000	0.9980	0.0002	0.0034	1.0000	1.0000
N(T,39)	0.9984	0.0000	0.0011	1.0000	1.0000	0.9989	0.0001	0.0029	1.0000	1.0000
N(T,40)	0.9984	0.0001	0.0014	1.0000	1.0000	0.9946	0.0002	0.0035	1.0000	1.0000
N(T,41)	0.9980	0.0001	0.0016	1.0000	1.0000	0.9964	0.0001	0.0029	1.0000	1.0000
N(T,42)	0.9975	0.0001	0.0016	1.0000	1.0000	0.9983	0.0001	0.0019	1.0000	1.0000
N(T,43)	0.9988	0.0001	0.0015	1.0000	1.0000	0.9991	0.0000	0.0017	1.0000	1.0000
N(T,44)	0.9985	0.0001	0.0016	1.0000	1.0000	0.9971	0.0001	0.0026	1.0000	1.0000
N(T,45)	0.9996	0.0000	0.0006	1.0000	1.0000	0.9977	0.0001	0.0026	1.0000	1.0000
N(T,46)	0.9997	0.0000	0.0006	1.0000	1.0000	0.9995	0.0000	0.0009	1.0000	1.0000
N(T,47)	0.9997	0.0000	0.0014	1.0000	1.0000	1.0041	0.0016	0.0113	1.0000	1.0000
N(T,48)	1.0000	0.0000	0.0000	1.0000	1.0000	1.0475	0.0902	0.0931	0.9990	0.8655
N(T,49)	0.9984	0.0001	0.0022	1.0000	1.0000	0.9992	0.0000	0.0016	1.0000	1.0000
N(T,50)	1.0245	0.0480	0.0579	1.0000	0.9947	1.2121	1.1789	0.3952	0.9392	0.2892
N(T,51)	0.9994	0.0000	0.0011	1.0000	1.0000	1.0000	0.0000	0.0000	1.0000	1.0000
N(T,52)	0.9744	0.0256	0.0503	0.9981	1.0000	1.0000	0.0000	0.0000	1.0000	1.0000
N(T,53)	0.9152	0.2376	0.1663	0.5709	0.9853	1.2839	0.9669	0.5151	0.9280	0.2420
N(T,54)	1.0519	0.0840	0.1093	0.9968	0.8060	0.9500	0.0250	0.0980	0.8413	0.9987
N(T,55)	1.0000	0.0000	0.0000	1.0000	1.0000	0.8944	0.1003	0.2069	0.4790	0.9743
N(T,56)	1.0000	0.0000	0.0000	1.0000	1.0000	0.8500	0.1350	0.2940	0.3694	0.9522
N(T,57)	1.0000	0.0000	0.0000	1.0000	1.0000	1.2500	0.2500	0.4900	0.9192	0.2743
N(T,58)	0.9000	0.0400	0.1960	0.5000	0.9772	2.0500	2.2050	2.0580	0.8633	0.1828
N(T,59)	0.6500	0.3675	0.6860	0.2375	0.9007	1.4500	0.0050	0.0980	1.0000	0.0000
N(T,60)	0.1000	0.6050	1.0780	0.0729	0.9655					
N(T.)	0.9023	0.0056	0.0149	0.6165	1.0000	0.7959	0.0096	0.0240	0.0000	1.000
q(15)	1.3860	0.1273	0.0710	1.0000	0.0000	1.9296	0.3080	0.1360	1.0000	0.0000
q(16)	1.4553	0.2337	0.0962	1.0000	0.0000	1.7558	0.6789	0.2019	1.0000	0.0000
q(17)	1.4210	0.3804	0.1227	1.0000	0.0000	1.4925	0.1753	0.1026	1.0000	0.0000
q(18)	1.2625	0.2663	0.1027	1.0000	0.0010	1.6064	0.6341	0.1951	1.0000	0.0000
q(19)	1.3163	0.2459	0.0987	1.0000	0.0000	1.5429	0.4501	0.1644	1.0000	0.0000
q(20)	1.3521	0.2433	0.0982	1.0000	0.0000	1.4564	0.4088	0.1566	1.0000	0.0000
q(21)	1.1274	0.0701	0.0527	1.0000	0.1544	1.2697	0.1354	0.0901	1.0000	0.0001
q(22)	1.0136	0.0295	0.0342	1.0000	1.0000	1.0701	0.0400	0.0490	1.0000	0.8842
q(23)	1.0494	0.0236	0.0306	1.0000	0.9994	1.0805	0.0313	0.0434	1.0000	0.8113
q(24)	1.0770	0.0349	0.0372	1.0000	0.8875	1.0460	0.0401	0.0491	1.0000	0.9846
q(25)	1.0515	0.0266	0.0324	1.0000	0.9983	1.0328	0.0437	0.0512	1.0000	0.9949
q(26)	1.0264	0.0288	0.0338	1.0000	1.0000	0.9658	0.0560	0.0580	0.9870	1.0000
q(27)	0.9990	0.0386	0.0391	1.0000	1.0000	1.0400	0.0476	0.0534	1.0000	0.9861
q(28)	1.0209	0.0333	0.0363	1.0000	1.0000	0.9478	0.0739	0.0666	0.9202	1.0000
q(29)	0.9869	0.0450	0.0422	1.0000	1.0000	0.9101	0.0623	0.0611	0.6264	1.0000
q(30)	0.9408	0.0390	0.0393	0.9790	1.0000	0.9330	0.0487	0.0540	0.8843	1.0000
q(31)	0.9596	0.0434	0.0415	0.9976	1.0000	0.8261	0.0839	0.0710	0.0206	1.0000
q(32)	0.9150	0.0425	0.0410	0.7631	1.0000	0.9050	0.0622	0.0611	0.5634	1.0000
q(33)	0.9620	0.0444	0.0419	0.9981	1.0000	0.8922	0.0814	0.0699	0.4138	1.0000
q(34)	0.9051	0.0598	0.0486	0.5808	1.0000	0.8964	0.0935	0.0749	0.4623	1.0000
q(35)	0.9179	0.0619	0.0495	0.7603	1.0000	0.8245	0.0933	0.0748	0.0240	1.0000
q(36)	0.8685	0.0924	0.0605	0.1537	1.0000	0.7950	0.1000	0.0775	0.0039	1.0000
q(37)	0.8611	0.0802	0.0563	0.0883	1.0000	0.7620	0.0863	0.0720	0.0001	1.0000
q(38)	0.8240	0.0971	0.0620	0.0082	1.0000	0.7804	0.1357	0.0903	0.0047	1.0000
q(39)	0.7925	0.0791	0.0560	0.0001	1.0000	0.7502	0.1244	0.0871	0.0004	1.0000

Table 4 (continued)

	Estimates		Bias 95% CI ½ width	Significance levels HO:Bias≥0.9 HA:Bias<0.9	Significance levels HO:Bias≤1.1 HA:Bias>1.1	Estimates		Bias 95% CI ½ width	Significance levels HO:Bias≥0.9 HA:Bias<0.9	Significance levels HO:Bias≤1.1 HA:Bias>1.1
	Bias	Variance				Bias	Variance			
q(40)	0.8476	0.1304	0.0722	0.0775	1.0000	0.7426	0.0887	0.0747	0.0000	1.0000
q(41)	0.7956	0.0730	0.0546	0.0001	1.0000	0.7352	0.4793	0.1737	0.0315	1.0000
q(42)	0.6863	1.5698	0.2546	0.0500	0.9993	0.7424	0.1202	0.0885	0.0002	1.0000
q(43)	0.8525	0.1842	0.0882	0.1455	1.0000	0.8617	0.1037	0.0829	0.1827	1.0000
q(44)	0.8133	0.0973	0.0648	0.0044	1.0000	0.8777	0.1561	0.1044	0.3375	1.0000
q(45)	1.0254	2.2033	0.3119	0.7846	0.6804	0.8420	0.0913	0.0799	0.0774	1.0000
q(46)	0.8358	0.1309	0.0774	0.0519	1.0000	1.0564	0.9370	0.2606	0.8803	0.6284
q(47)	0.3470	25.6967	1.1397	0.1708	0.9023	63.2003	<99999.99	121.9043	0.8417	0.1590
q(48)	0.8576	0.6898	0.1974	0.3370	0.9919	1.0744	0.3067	0.1716	0.9768	0.6152
q(49)	0.7220	0.4331	0.1638	0.0166	1.0000	0.0008	75.0753	3.0502	0.2817	0.7600
q(50)	0.9710	3.3934	0.4868	0.6124	0.6983	2.7969	115.6154	3.9135	0.8290	0.1977
q(51)	−0.3572	73.2005	2.4998	0.1621	0.8734	0.7113	2.1593	0.6141	0.2735	0.8926
q(52)	−3.7106	632.0744	12.6793	0.2380	0.7715	0.8225	0.6106	0.3610	0.3370	0.9340
q(53)	1.0422	0.3956	0.2146	0.9031	0.7011	1.7977	6.0280	1.2861	0.9144	0.1438
q(54)	1.0498	0.3516	0.2237	0.9054	0.6700	2.2403	8.9080	1.8499	0.9222	0.1135
q(55)	0.0243	7.1499	1.2023	0.0767	0.9602	3.6459	67.4526	5.3658	0.8421	0.1762
q(56)	4.1165	89.6428	6.1858	0.8459	0.1696	3.2914	12.9452	2.8790	0.9482	0.0679
q(57)	0.8978	0.0700	0.2116	0.4919	0.9694	0.9321	0.0669	0.2536	0.5980	0.9028
q(58)	−3.1313	74.4663	8.4568	0.1751	0.8366	0.6640	0.2346	0.6713	0.2454	0.8985
q(59)	−5.6513	172.1638	14.8479	0.1936	0.8136	0.7438	0.0005	0.0294	0.0000	1.0000
q(60)	−0.3459	7.3840	3.7661	0.2584	0.7741					
exp(z)	0.6422	0.0084	0.0182	0.0000	1.0000					

lations (Paloheimo 1980, Collie and Sissenwine 1983). These estimates do not seem highly correlated.

The unobserved change rate was a random variable in the second test, so its estimation error was not computed. Error characteristics-of-abundance estimates were extremely similar to those of example one; apparently high process variability does not adversely affect estimation even in the presence of sampling variance.

The contracted seasonal recruitment pattern (Fig. 3), conventionally interpreted as age-specific cohorts, was used in the last two examples. Growth parameters were the same as the two previous examples and growth variation was moderate (cv 0.1). Sampling efficiencies were also unchanged and their variability set at that of example 1 (cv[q]=0.2). The unobserved change rate randomly varied five-fold ($z_t \sim U(0.05, 0.25)$). Catching was continuous so each period's catch was assigned to midperiod for estimation. Overfishing was simulated by rapidly increasing exploitation enough to decrease stock abundance 36% during the four periods of sampling (last four). The fishing mortality rates for periods 6–19 were: 0.05, 0.1, 0.15, 0.2, 0.25, 0.3, 0.6, 0.4, 0.5, 0.8, 0.6, 0.8, 1.0, and 1.2. Example 3 simulated very low sampling levels and example 4, high levels. It was of interest to find if abundance would be correctly estimated during overfishing under either sampling condition.

Table 5

Correlation coefficients between estimates of the unobserved change rate (z) and all other estimates.

Estimate	Rho	Estimate	Rho	Estimate	Rho	Estimate	Rho
N(T,15)	0.46	N(T,38)	0.08	q(15)	−0.53	q(38)	−0.18
N(T,16)	0.34	N(T,39)	0.11	q(16)	−0.30	q(39)	0.09
N(T,17)	0.45	N(T,40)	0.21	q(17)	−0.36	q(40)	−0.03
N(T,18)	0.20	N(T,41)	0.22	q(18)	−0.24	q(41)	0.02
N(T,19)	0.27	N(T,42)	0.22	q(19)	−0.18	q(42)	−0.09
N(T,20)	0.23	N(T,43)	0.15	q(20)	−0.18	q(43)	−0.14
N(T,21)	0.23	N(T,44)	0.08	q(21)	−0.22	q(44)	−0.01
N(T,22)	0.11	N(T,45)	0.31	q(22)	−0.22	q(45)	−0.07
N(T,23)	0.27	N(T,46)	0.20	q(23)	−0.16	q(46)	0.03
N(T,24)	0.22	N(T,47)	0.04	q(24)	−0.15	q(47)	0.11
N(T,25)	0.21	N(T,48)	0.19	q(25)	−0.27	q(48)	0.11
N(T,26)	0.10	N(T,49)	0.13	q(26)	−0.31	q(49)	0.08
N(T,27)	0.19	N(T,50)	0.26	q(27)	−0.26	q(50)	0.12
N(T,28)	0.22	N(T,51)	0.22	q(28)	−0.10	q(51)	0.02
N(T,29)	0.29	N(T,52)	0.11	q(29)	−0.35	q(52)	−0.11
N(T,30)	0.09	N(T,53)	0.16	q(30)	−0.10	q(53)	0.15
N(T,31)	0.17	N(T,54)	0.12	q(31)	−0.43	q(54)	0.15
N(T,32)	0.19	N(T,55)	0.21	q(32)	0.09	q(55)	0.02
N(T,33)	0.21	N(T,56)	0.16	q(33)	−0.17	q(56)	−0.05
N(T,34)	0.25	N(T,57)	0.06	q(34)	−0.19	q(57)	0.15
N(T,35)	0.18	N(T,58)	0.03	q(35)	−0.02	q(58)	−0.11
N(T,36)	0.08	N(T,59)	0.06	q(36)	0.04	q(59)	−0.11
N(T,37)	0.23	N(T,60)	−0.03	q(37)	−0.01	q(60)	−0.06

Example 3 was the limited-data case. The growth measurement error was large (cv 0.20) and the sample size for growth parameter estimation was moderate (95% CI of width ±5%, 77 fish). The precision of catch estimates was low (cv[C] = 0.4) and relative abundance sampling was meager (95% CI of width ±30%, two samples each period).

Error variances of the smallest seven size class abundance estimates were very large (Table 6), but error variances were low for size-classes 25 and larger. Usefully narrow confidence intervals on the bias of these estimates were obtained with few trials. Significance levels suggested that abundance estimates of size-classes 17–21 might not have been biased and unbiased estimation seemed likely for size-classes 22 and larger. Estimates of sampling gear efficiencies (q(s)) also seemed accurate although error variances were high.

Example four simulated sufficient sampling. A growth parameter measurement error (cv 0.05) and sample size (99% CI of width ±1%, 829 fish) more characteristic of databases for heavily sampled fisheries were used. Catches were precisely estimated (cv[C] = 0.2) and relative abundance sampling was at a very sufficient level (99% CI of width ±3%, 295 samples each period).

Biases (Table 6) were very similar to those of example 3. Abundance estimates for the smaller size-classes that appeared in relative abundance samples just once were probably biased by more than 10%, but the rest were not. Estimates of q for the smallest 10 size-classes were biased by more than 10% and the rest were probably not. Most error variances for stocksize estimates were several times smaller than those of example 3, and some were an order of magnitude smaller. Likewise, the error variance of q estimates was also smaller. As may be expected, sufficient sampling levels increased precision but did not affect bias. Abundance estimates of sizes that appeared in abundance samples more than once were estimated accurately when overfishing occurred, whether or not sampling levels were sufficient or not.

Estimates of historical stock sizes are usually used to find out if stock abundance is increasing or decreasing. Errors of virtual population analysis back-calculations of cohort-specific abundances converge as dates decrease (Agger et al. 1971, Pope 1972, Jones 1981). Conventional wisdom is thus that abundance estimates for the last period are extremely uncertain, but due to the convergence, estimated abundance trends are reliable. For this size-based estimator, (2) provides abundance calculations before date y(T) from the estimates available at the solution of (4).

Error characteristics of historical abundance estimates (Table 7) were unexpected. Bias and error variance increased as dates decreased. Last-period

Table 6

Examples for seasonal, contracted recruitment and overfishing.

	Example 3, Limited sampling					Example 4, Sufficient sampling				
Catch estimation										
catch dates	absent					absent				
cv[C(t,s)]	0.40					0.20				
Growth estimation										
cv[error]	0.20					0.05				
precision level	0.05					0.01				
probability level	0.95					0.99				
fish sampled, g	77					829				
Sampling efficiency										
cv[q(s)]	0.20					0.20				
precision level	0.30					0.03				
probability level	0.95					0.99				
sample size, r	2					295				
Number of trials	83					128				
	Estimates		Bias 95% CI	Significance levels HO:Bias≥0.9	HO:Bias≤1.1	Estimates		Bias 95% CI	Significance levels HO:Bias≥0.9	HO:Bias≤1.1
	Bias	Variance	½ width	HA:Bias<0.9	HA:Bias>1.1	Bias	Variance	½ width	HA:Bias<0.9	HA:Bias>1.1
N(T,15)	9.3261	759.7793	5.9301	0.9973	0.0033	12.8103	1297.3179	6.2399	0.9999	0.0001
N(T,16)	8.3623	546.7384	5.0304	0.9982	0.0023	8.3910	128.6375	1.9649	1.0000	0.0000
N(T,17)	2.0437	320.3240	3.8505	0.7198	0.3155	3.4678	49.7123	1.2215	1.0000	0.0001
N(T,18)	1.8321	42.6741	1.4054	0.9032	0.1536	1.2202	1.3293	0.1997	0.9992	0.1191
N(T,19)	0.9011	1.3723	0.2520	0.5033	0.9391	0.7992	0.3075	0.0961	0.0199	1.0000
N(T,20)	1.1948	1.6789	0.2788	0.9809	0.2525	0.8677	0.3403	0.1011	0.2657	1.0000

Table 6 (continued)

	Estimates		Bias 95% CI	Significance levels		Estimates		Bias 95% CI	Significance levels	
	Bias	Variance	½ width	HO:Bias≥0.9 HA:Bias<0.9	HO:Bias≤1.1 HA:Bias>1.1	Bias	Variance	½ width	HO:Bias≥0.9 HA:Bias<0.9	HO:Bias≤1.1 HA:Bias>1.1
N(T,21)	1.3401	5.0248	0.4823	0.9632	0.1646	1.7942	1.3107	0.1983	1.0000	0.0000
N(T,22)	0.9265	0.1610	0.0863	0.7262	1.0000	0.8043	1.2599	0.1945	0.1673	0.9986
N(T,23)	0.9335	0.4053	0.1370	0.6840	0.9914	0.8082	0.7830	0.1533	0.1203	0.9999
N(T,24)	0.9017	0.7664	0.1895	0.5072	0.9799	0.9673	0.1843	0.0744	0.9619	0.9998
N(T,25)	0.9988	0.0606	0.0533	0.9999	0.9999	1.0007	0.0106	0.0179	1.0000	1.0000
N(T,26)	0.9540	0.0476	0.0472	0.9875	1.0000	1.0021	0.0032	0.0098	1.0000	1.0000
N(T,27)	0.9890	0.0186	0.0295	1.0000	1.0000	0.9898	0.0055	0.0129	1.0000	1.0000
N(T,28)	0.9865	0.0129	0.0246	1.0000	1.0000	0.9855	0.0109	0.0181	1.0000	1.0000
N(T,29)	0.9596	0.0341	0.0400	0.9983	1.0000	0.9795	0.0174	0.0230	1.0000	1.0000
N(T,30)	1.0184	0.0600	0.0530	1.0000	0.9987	0.9979	0.0235	0.0269	1.0000	1.0000
N(T,31)	0.9606	0.0254	0.0349	0.9997	1.0000	0.9916	0.0084	0.0161	1.0000	1.0000
N(T,32)	0.9922	0.0073	0.0188	1.0000	1.0000	0.9945	0.0029	0.0094	1.0000	1.0000
N(T,33)	1.0158	0.0266	0.0359	1.0000	1.0000	0.9861	0.0022	0.0082	1.0000	1.0000
N(T,34)	0.9851	0.0117	0.0240	1.0000	1.0000	0.9824	0.0040	0.0112	1.0000	1.0000
N(T,35)	0.9700	0.0138	0.0260	1.0000	1.0000	0.9846	0.0025	0.0090	1.0000	1.0000
N(T,36)	0.9908	0.0339	0.0411	1.0000	1.0000	0.9921	0.0008	0.0052	1.0000	1.0000
N(T,37)	0.9852	0.0071	0.0195	1.0000	1.0000	0.9988	0.0004	0.0038	1.0000	1.0000
N(T,38)	0.9807	0.0027	0.0126	1.0000	1.0000	0.9992	0.0006	0.0048	1.0000	1.0000
N(T,39)	0.9874	0.0116	0.0278	1.0000	1.0000	0.9957	0.0003	0.0037	1.0000	1.0000
N(T,40)	0.9841	0.0024	0.0132	1.0000	1.0000	0.9986	0.0004	0.0042	1.0000	1.0000
N(T,41)	0.9992	0.0010	0.0090	1.0000	1.0000	1.0001	0.0001	0.0028	1.0000	1.0000
N(T,42)	1.0102	0.0314	0.0549	1.0000	0.9993	1.0002	0.0000	0.0013	1.0000	1.0000
N(T,43)	0.9924	0.0012	0.0115	1.0000	1.0000	0.9987	0.0001	0.0025	1.0000	1.0000
N(T,44)	0.9798	0.0101	0.0452	0.9997	1.0000	0.9986	0.0001	0.0027	1.0000	1.0000
N(T,45)	0.9833	0.0012	0.0158	1.0000	1.0000	1.0000	0.0000	0.0000	1.0000	1.0000
N(T,46)	0.9854	0.0006	0.0141	1.0000	1.0000	1.0000	0.0000	0.0000	1.0000	1.0000
N(T,47)	1.0000	0.0010	0.0253	1.0000	1.0000	1.0000	0.0000	0.0000	1.0000	1.0000
N(T,48)	0.8000	0.0200	0.1960	0.1587	0.9987	1.0000	0.0000	0.0000	1.0000	1.0000
N(T,49)						1.0000	0.0000	0.0000	1.0000	1.0000
N(T.)	1.1369	32.0777	1.2185	0.6484	0.4763	1.1493	29.8091	0.9459	0.6973	0.4593
q(15)	0.3282	0.1186	0.0741	0.0000	1.0000	0.2474	0.0501	0.0388	0.0000	1.0000
q(16)	0.3998	0.2084	0.0982	0.0000	1.0000	0.2984	0.0519	0.0395	0.0000	1.0000
q(17)	0.7850	0.7019	0.1802	0.1055	0.9997	0.6889	0.2424	0.0853	0.0000	1.0000
q(18)	1.3854	0.9594	0.2107	1.0000	0.0040	1.2926	0.6908	0.1440	1.0000	0.0044
q(19)	1.9397	2.7953	0.3597	1.0000	0.0000	1.6785	0.6126	0.1356	1.0000	0.0000
q(20)	1.3499	0.6184	0.1692	1.0000	0.0019	1.4341	0.3226	0.0984	1.0000	0.0000
q(21)	0.9199	0.4187	0.1392	0.6104	0.9944	0.6845	0.0844	0.0503	0.0000	1.0000
q(22)	0.6958	0.2367	0.1047	0.0001	1.0000	0.5667	0.0730	0.0468	0.0000	1.0000
q(23)	0.7353	0.2491	0.1074	0.0013	1.0000	0.6515	0.0753	0.0475	0.0000	1.0000
q(24)	0.9467	0.5200	0.1561	0.7213	0.9729	0.7885	0.0992	0.0546	0.0000	1.0000
q(25)	1.0306	0.3424	0.1266	0.9784	0.8584	0.9317	0.0882	0.0515	0.8861	1.0000
q(26)	1.0431	0.2997	0.1185	0.9910	0.8266	1.0073	0.0575	0.0415	1.0000	1.0000
q(27)	1.0743	0.3260	0.1236	0.9971	0.6583	0.9851	0.0475	0.0377	1.0000	1.0000
q(28)	1.0729	0.4116	0.1389	0.9927	0.6489	0.9155	0.0586	0.0419	0.7658	1.0000
q(29)	1.0112	0.3553	0.1290	0.9545	0.9113	0.9105	0.0767	0.0482	0.6652	1.0000
q(30)	0.9345	0.4927	0.1519	0.6719	0.9836	0.9002	0.0721	0.0471	0.5027	1.0000
q(31)	1.0777	0.5119	0.1568	0.9869	0.6096	0.8955	0.0796	0.0495	0.4297	1.0000
q(32)	1.0668	0.3685	0.1339	0.9927	0.6864	0.9643	0.1123	0.0587	0.9841	1.0000
q(33)	1.0548	0.2669	0.1139	0.9961	0.7818	1.0293	0.1086	0.0578	1.0000	0.9918
q(34)	1.0891	0.4220	0.1442	0.9949	0.5588	0.9230	0.1037	0.0569	0.7862	1.0000
q(35)	1.2517	1.4470	0.2670	0.9951	0.1327	0.9907	0.1106	0.0597	0.9985	0.9998
q(36)	1.0885	0.5550	0.1664	0.9868	0.5537	1.0126	0.1046	0.0591	0.9999	0.9981
q(37)	1.0643	0.3099	0.1286	0.9939	0.7066	1.0658	0.1899	0.0814	1.0000	0.7950
q(38)	1.2725	1.2458	0.2713	0.9964	0.1064	0.9944	0.0895	0.0589	0.9992	0.9998
q(39)	0.9949	0.7569	0.2239	0.7970	0.8211	1.0445	0.2018	0.0923	0.9989	0.8806
q(40)	1.1630	0.5160	0.1934	0.9962	0.2617	0.9748	0.1302	0.0806	0.9656	0.9988
q(41)	1.3898	1.4057	0.3320	0.9981	0.0435	0.9666	0.2227	0.1130	0.8761	0.9896
q(42)	1.4005	2.9713	0.5342	0.9668	0.1351	1.0596	0.2525	0.1316	0.9913	0.7265
q(43)	1.0215	0.2530	0.1643	0.9263	0.8256	−0.7903	123.8881	3.4933	0.1715	0.8556
q(44)	0.9185	0.2248	0.2132	0.5674	0.9524	1.1289	0.8725	0.3051	0.9293	0.4263
q(45)	4.0163	137.2726	5.4127	0.8704	0.1455	1.4194	2.0954	0.5674	0.9636	0.1350
q(46)	1.2540	0.3985	0.3572	0.9740	0.1990	1.0488	0.0964	0.1396	0.9816	0.7639
q(47)	1.2032	0.2502	0.4002	0.9312	0.3067	1.9698	5.6933	1.4101	0.9315	0.1133
q(48)	1.1792	0.2007	0.6210	0.8109	0.4013	1.0484	0.0029	0.0473	1.0000	0.9839
q(49)						0.9818	0.0718	0.2626	0.7291	0.8113

Table 7
Error statistics of historical abundance estimates from example 4.

Variable	n	Error variance	Bias estimate	Variable	n	Error variance	Bias estimate	Variable	n	Error variance	Bias estimate
N(1,15)	128	115.5114	5.9596	N(1,27)	128	0.1871	0.9173	N(1,39)	91	0.4743	0.7745
N(2,15)	128	86.8395	6.0680	N(2,27)	128	0.1899	0.8982	N(2,39)	91	0.5662	0.9049
N(3,15)	128	119.8275	5.3517	N(3,27)	128	0.4459	1.0290	N(3,39)	91	0.4302	1.0320
N(4,15)	128	1296.6914	12.8388	N(4,27)	128	0.0056	0.9896	N(4,39)	91	0.0003	0.9957
N(1,16)	128	30.4340	4.2588	N(1,28)	128	0.4354	0.9534	N(1,40)	77	1.1408	0.9088
N(2,16)	128	184.7422	7.4660	N(2,28)	128	0.2830	1.0502	N(2,40)	77	0.7205	1.0607
N(3,16)	128	68.0011	6.3408	N(3,28)	128	0.4060	1.1279	N(3,40)	77	0.4176	0.9065
N(4,16)	128	128.6176	8.3893	N(4,28)	128	0.0109	0.9854	N(4,40)	77	0.0004	0.9986
N(1,17)	128	10.8289	1.7620	N(1,29)	127	0.3800	0.9685	N(1,41)	67	0.8746	1.0508
N(2,17)	128	50.7792	2.9860	N(2,29)	127	0.6222	1.2014	N(2,41)	67	0.7359	0.9693
N(3,17)	128	6.3308	2.2878	N(3,29)	127	0.6897	1.1322	N(3,41)	67	0.6803	1.1584
N(4,17)	128	49.7113	3.4675	N(4,29)	127	0.0174	0.9794	N(4,41)	67	0.0001	1.0001
N(1,18)	128	0.5225	0.8387	N(1,30)	125	1.3161	1.1217	N(1,42)	56	0.2236	0.5534
N(2,18)	128	1.8065	1.0217	N(2,30)	125	0.6497	1.1361	N(2,42)	56	0.9773	0.8919
N(3,18)	128	1.3119	1.1786	N(3,30)	125	0.6635	1.1661	N(3,42)	56	0.8370	1.0048
N(4,18)	128	1.3292	1.2202	N(4,30)	125	0.0234	0.9971	N(4,42)	56	0.0000	1.0002
N(1,19)	128	0.2076	0.5674	N(1,31)	125	0.4402	0.9570	N(1,43)	39	0.3770	0.7205
N(2,19)	128	0.6367	0.7745	N(2,31)	125	0.7042	1.1035	N(2,43)	39	0.7222	1.0594
N(3,19)	128	0.2891	0.8107	N(3,31)	125	1.2571	1.1914	N(3,43)	39	0.5246	0.9171
N(4,19)	128	0.3074	0.7989	N(4,31)	125	0.0084	0.9916	N(4,43)	39	0.0001	0.9987
N(1,20)	128	0.3131	0.6707	N(1,32)	125	0.4139	0.8962	N(1,44)	36	0.3870	0.8145
N(2,20)	128	0.7200	0.8515	N(2,32)	125	0.4712	1.0943	N(2,44)	36	0.3686	0.8018
N(3,20)	128	0.4237	0.9559	N(3,32)	125	0.6876	1.1207	N(3,44)	36	0.2355	0.8025
N(4,20)	128	0.3411	0.8679	N(4,32)	125	0.0029	0.9944	N(4,44)	36	0.0001	0.9986
N(1,21)	128	1.3938	1.2717	N(1,33)	125	0.2451	0.7301	N(1,45)	25	0.4571	0.8148
N(2,21)	128	0.9207	1.3560	N(2,33)	125	0.4089	1.0021	N(2,45)	25	0.3210	0.8143
N(3,21)	128	1.5664	1.6328	N(3,33)	125	0.6057	1.1316	N(3,45)	25	0.1735	0.7110
N(4,21)	128	1.3111	1.7941	N(4,33)	125	0.0022	0.9864	N(4,45)	25	0.0000	1.0000
N(1,22)	128	3.4192	1.7054	N(1,34)	123	0.7671	0.8896	N(1,46)	19	0.3338	0.6204
N(2,22)	128	6.9873	2.0668	N(2,34)	123	0.5906	0.9968	N(2,46)	19	0.3380	0.5746
N(3,22)	128	7.5242	2.6186	N(3,34)	123	0.9354	1.1637	N(3,46)	19	0.1914	0.8296
N(4,22)	128	1.2599	0.8042	N(4,34)	123	0.0040	0.9824	N(4,46)	19	0.0000	1.0000
N(1,23)	128	1.1626	1.6450	N(1,35)	119	0.2867	0.8088	N(1,47)	11	0.1290	0.4227
N(2,23)	128	1.6512	1.5052	N(2,35)	119	0.6020	1.0950	N(2,47)	11	0.2434	0.4377
N(3,23)	128	8.1272	2.3806	N(3,35)	119	0.7955	1.1538	N(3,47)	11	0.0694	0.9398
N(4,23)	128	0.7830	0.8082	N(4,35)	119	0.0025	0.9846	N(4,47)	11	0.0000	1.0000
N(1,24)	128	1.2296	1.3307	N(1,36)	115	0.2635	0.6926	N(1,48)	5	0.1338	0.4633
N(2,24)	128	2.6137	1.3469	N(2,36)	115	0.4223	0.9411	N(2,48)	5	0.0132	1.0800
N(3,24)	128	23.1672	1.9363	N(3,36)	115	0.7491	1.0997	N(3,48)	5	0.1087	0.7000
N(4,24)	128	0.1842	0.9673	N(4,36)	115	0.0008	0.9921	N(4,48)	5	0.0000	1.0000
N(1,25)	128	0.5672	0.9923	N(1,37)	110	0.2637	0.6720	N(1,49)	4	0.1558	0.3750
N(2,25)	128	0.7867	0.9758	N(2,37)	110	0.5350	0.8555	N(2,49)	4	0.4950	1.1000
N(3,25)	128	5.6842	1.4490	N(3,37)	110	0.6735	1.0410	N(3,49)	4	0.0050	0.9500
N(4,25)	128	0.0106	1.0005	N(4,37)	110	0.0004	0.9986	N(4,49)	4	0.0000	1.0000
N(1,26)	128	0.2515	0.8747	N(1,38)	99	0.8277	0.8260				
N(2,26)	128	0.8233	0.9564	N(2,38)	99	0.2681	0.7480				
N(3,26)	128	3.1000	1.2203	N(3,38)	99	0.8225	1.2851				
N(4,26)	128	0.0032	1.0024	N(4,38)	99	0.0006	0.9989				

abundance estimates were accurate, but those of preceding periods were not. Error variances of estimates before the last period tended to be one to two orders of magnitude higher than those of the last period. This implies that abundance trends estimated in this manner probably will be wrong. In this example, the problem is large enough to mask much of the 36% decrease in abundance; the downward abundance trend would not be clear in calculations of historical stock sizes.

Discussion

These Monte Carlo tests show that size-based methods can be accurate and precise estimators of stock abundance. Population characteristics need not conform to the restrictive assumptions of traditional VPA methods. Any sort of fish stock can be successfully addressed with size-based techniques, an important aspect when assessing populations where ageing is impossible or where recruitment is not periodic.

These results imply that little will be gained from the extensive age sampling programs that are the foundation of VPA-based methods. They are not needed if size-based methods are used; only size samples and the rate of growth are required. Light, periodic growth sampling is sufficient to monitor possible growth rate changes through time. Also, since growth rates are required instead of ages, mark-recapture methods can be used to obtain growth measures if hardpart interpretations (age is not observed on hardparts; instead, characteristic marks are interpreted as annular occurrences) are difficult or expensive to obtain.

The method of abundance estimation developed in this study, a meticulous bookkeeper of size data as is the method of Beddingto.. and Cook (1981), is primitive compared with other size-based methods (Fournier and Doonan 1987, Schnute et al. 1989, Sullivan 1989, Sullivan et al. 1990). Its degree of success in estimating abundance suggests that complete population-model structures are unnecessary. Estimates were usefully accurate and precise even with very high process variability. Very pronounced individual growth variation did not cause estimation problems. These results show that precise, accurate abundance estimates are possible with any recruitment pattern imaginable. It was a particular surprise to find that temporally variant (fourfold) unobserved change rates ("natural mortality" of Ricker (1948) but including migration and unrecorded catch) did not affect estimation at all. That result is reassuring, since the rate is probably extremely variable in nature.

Sampling problems did not seem to degrade estimation either. The level of catch estimation error proved unimportant and there was no indication that exact catch dates need to be recorded. Highly variable sampling efficiencies (q_s) did not cause estimation problems, particularly when sample sizes were adequate. Highly variable individual growth rates (20%) and significant growth measurement error (15%) did not adversely affect abundance estimation when sampling was sufficient. Very large growth-parameter measurement error (40%) and small sample size destroyed performance; although bias was not a problem, extreme error variances and correlated estimates were.

It is of particular interest that this was the only test where estimates of the unobserved change rate (z) and sampling efficiencies (q) were highly correlated. The lack of a pronounced correlation between sampling gear efficiencies and the unobserved change rate in all other tests except this one was unexpected; similar studies of VPA-based methods (Paloheimo 1980, Collie and Sissenwine 1983) found such correlation a major characteristic. It thus seems possible that ageing errors, or the violation of a connected VPA assumption, contributed to correlation in those studies.

Abundances of most size-classes were estimated precisely with little or no bias, but biased and imprecise abundance estimates occurred in three circumstances. First, abundances of very small fish that were recruited between the next-to-last and last relative abundance sample were estimated poorly. A recruitment group had to be present in the relative abundance samples twice to be estimated with a useful degree of certainty. In practice, this problem is easily fixed if obtaining certain estimates of recent recruitment of small fish is important enough to justify the cost of additional samples during the last period. Since the estimator is not based on equal time units, only dates, additional sample(s) will monitor the size-classes of interest several times instead of just once. Second, wide size-classes caused bias and imprecision, particularly for larger sizes. This bias was easily eliminated by narrowing size-classes. Last, calculations of historical abundances were in large error. It is well known that VPA calculations are poor for the most recent period of data and improve as dates decrease. Though they are not germane to current production levels, estimates of the oldest stock sizes are the most certain ones in VPA. The exact opposite is true for this size-based method. Estimates of historical abundances obtained in the solution calculation should not be used; error variances of these computations are very large. Since the estimates of the final-period abundances are accurate and precise, this is probably not a problem even if historical stock-size estimates are needed. Although the procedure was not tested, these estimates might be obtained by starting with the initial four periods of data, estimating the fourth period abundance vector, and then progressing forward one period at a time. Abundance in the first three periods cannot be estimated but subsequent abundances can. The relation between the number of periods in the data and estimation errors was not investigated, but the authors- experience with VPA-based methods indicates little, if any, would be gained with a longer time-series.

This study shows that *a priori* knowledge of the unobserved change rate (z) is not required to accurately and precisely estimate abundance with this size-based method, yet it is well known (Paloheimo 1980, Collie and Sissenwine 1983, Deriso 1985, Pope and Shepherd 1985) that such knowledge is necessary when applying VPA-based procedures.

This study suggests that the unobserved change rate (z) will often be estimated with bias, yet z should be included in the vector of estimates anyway. Monte Carlo tests of the Beddington and Cook model established that simultaneous estimation of a natural mortality schedule (analogous to the unobserved change rate in this study) is necessary to avoid biased abundance estimates (de la Mare 1988). If z is fixed instead

of estimated, abundance estimation bias is assured because stock size is a function of that rate. It thus seems prudent to include the rate in the vector of estimates to avoid abundance estimation bias even if it is not useful. When necessary, Monte Carlo methods can be used to establish interval estimates on e^{-z}. This study indicates that estimates of e^{-z} are often biased, yet precise. The estimate of error variance over the 97 trials of example 1 was 0.0084, so the 95% CI width is $\pm 1.96\sqrt{(0.0084 \div 97)}$ or ± 0.0182, and the bias adjustment is 0.6422.

Acknowledgments

I express very sincere appreciation to Douglas G. Chapman for his knowledgeable and diligent guidance of this research and William G. Clark whose critical suggestions and encouragement significantly broadened the scope of this study. I am indebted to Bradford E. Brown, of the Southeast Fisheries Center of the National Marine Fisheries Service, who provided computer resources and other critical support. I especially thank Nancie J. Parrack for many helpful suggestions as the study progressed and Stephen B. Mathews for technical recommendations as well as a critical review of the original manuscript.

Citations

Agger, P., I. Boetius, and H. Lassen
1971 On errors in virtual population analysis. Int. Counc. Explor. Sea Doc. CM 1971/H:16, 10 p.

Anonymous
1981a Report of the sub-committee on sperm whales (Appendix 11). Rep. Int. Whaling Comm. 31:100–101.
1981b Report of the ad hoc working group on the use of effort data in assessments. Int. Counc. Explor. Sea Doc. CM 1981/G:5, 65 p.
1983 Report of the working group on methods of fish stock assessment. Int. Counc. Explor. Sea Doc. CM 1983/Assess:17, 73 p.
1984 Report of the working group on methods of fish stock assessments. Int. Counc. Explor. Sea Doc. CM 1984/Assess: 19, 56 p.
1986 Report of the ad hoc multispecies assessment working group. Int. Counc. Explor. Sea Doc. CM 1986, 10 p.

Bartoo, N.W., and K.R. Parker
1982 Stochastic age-frequency estimation using the von Bertalanffy growth equation. Fish. Bull., U.S. 81:91–96.

Basson, M., A.A. Rosenberg, and J.R. Beddington
1988 The accuracy and reliability of two new methods for estimating growth parameters from length-frequency data. J. Cons. Cons. Int. Explor. Mer 44:277–285.

Beamish, R.J., and G.A. McFarlane
1983 The forgotten requirement for age validation in fisheries biology. Trans. Am. Fish. Soc. 112:735–743.

Beddington, J.R., and J.G. Cooke
1981 Development of an assessment technique for male sperm whales based on the use of length data from the catches, with special reference to the North-west Pacific stock. Rep. Int. Whaling Comm. 31:747–760.

Beddington, J.R., J.G. Cooke, and W.K. de la Mare
1983 Estimations of the western North Pacific sperm whale population using the length distribution of catches. Rep. Int. Whaling Comm. 33:747–749.

Box, G.E.P.
1979 Robustness in the strategy of scientific model building. *In* Launer, R.L., and G.N. Wilkinson (eds.), Robustness in statistics, p. 201–236. Academic Press, NY.

Brethes, J.F., and G. Desrosiers
1981 Estimation of potential catches of an unexploited stock of soft-shell clam (*Mya arenaria*) from length composition data. Can. J. Fish. Aquat. Sci. 38:371–374.

Burr, R.L.
1988 Inferring the distribution of the parameters of the von Bertalanffy growth model from length moments. Can. J. Fish. Aquat. Sci. 45:1779–1788.

Chapman, D.G.
1961 Statistical problems in dynamics of exploited fisheries populations. *In* Proc., 4th Berkeley symp. math. stat. and probability. Contrib. Biol. and Probl. Med. 4:153–168. Univ. Calif. Press.

Clark, W.G.
1981 Restricted least-squares estimates of age composition from length composition. Can J. Fish. Aquat. Sci. 38:297–307.

Collie, J.S., and M.P. Sissenwine
1983 Estimating population size from relative abundance data measured with error. Can. J. Fish. Aquat. Sci. 40:1871–1879.

Conway, G.R., N.R. Glass, and J. C. Wilcox
1970 Fitting nonlinear models to biological data by Marquardt's algorithm. Ecology 51(3):503–507.

Cooke, J.G., and J.R. Beddington
1982 Further development of an assessment technique for male sperm whales based on length data from the catches. Rep. Int. Whaling Comm. 32:239–241.

Cooke, J.G., and W.K. de la Mare
1983a Description of and simulation studies on the length-specific sperm whale assessment technique. Rep. Int. Whaling Comm. 33:741–745.
1983b Further analyses for the location of the possible stock boundary for the North-West Pacific sperm whale based on length distributions of males. Rep. Int. Whaling Comm. 33: 275–277.

Cooke, J.G., W.K. de la Mare, and J.R. Beddington
1983a Some aspects of the reliability of the length data for the western North Pacific stock of sperm whales. Rep. Int. Whaling Comm. 33:265–267.
1983b An extension of the sperm whale model for the simulation of the male population by length and age. Rep. Int. Whaling Comm. 33:731–733.

de la Mare, W.K.
1988 Extended sensitivity trials on the length-specific method for estimating the size of exploited sperm whale populations. Rep. Int. Whaling Comm. 38:243–248.

de la Mare, W.K., and J.G. Cooke
1984 A new model for the female sperm whale incorporating aspects of the reproductive cycle. Rep. Int. Whaling Comm. 34:251–254.
1985 Analyses of the sensitivity of the length-specific estimation procedure to some departures from underlying assumptions. Rep. Int. Whaling Comm. 35:193–197.

1987 Further sensitivity trials in the length specific method for estimating the size of exploited sperm whale populations. Rep. Int. Whaling Comm. 37:219-222.

Deriso, R.B.
1985 Catch-age analysis with auxiliary information. Can. J. Fish. Aquat. Sci. 42:815-824.

Doubleday, W.G.
1975 A least squares approach to analyzing catch at age data. Int. Comm. Northwest Atl. Fish. Res. Doc. 75/35, 22 p.

Fabens, A.J.
1965 Properties and fitting the von Bertalanffy growth curve. Growth 29:265-289.

Fournier, D.A., and J.J. Doonan
1987 A length-based assessment method utilizing a generalized delay-difference model. Can. J. Fish. Aquat. Sci. 44:422-437.

Fournier, D.A., J.R. Sibert, J. Majkowski, and J. Hampton
1990 MULTIFAN: A likelihood-based method for estimating growth parameters and age composition from multiple length-frequency data sets illustrated using data for southern bluefin tuna. Can. J. Fish. Aquat. Sci. 47:301-317.

Fry, F.E.J.
1949 Statistics of a lake trout fishery. Biometrics 5:27-67.

Gallant, A.R.
1975 Nonlinear regression. Am. Stat. 29(2):73-81.

Gallucci, V.F., and T.J. Quinn II
1979 Reparameterization, fitting, and testing a simple growth model. Trans. Am. Fish. Soc. 108:14-25.

Gulland, J.A.
1965 Estimation of mortality rates. Annex to Rep. Arctic Fish. Working Group, Int. Counc. Explor. Sea Doc. CM 1965(3), 9 p.

Hampton, J., and J. Majkowski
1987 An examination of the accuracy of the Elefan computer programs for length based stock assessment. *In* Pauly, D., and G.P. Morgan (eds.), Length-based methods in fisheries research, p. 203-216. ICLARM (Int. Cent. Living Aquat. Resour. Manage.) Conf. Proc. 13, Manila.

Hasselblad, V.
1966 Estimation of parameters for a mixture of normal distributions. Technometrics 8:431-444.

Hoenig, J.M., and D.M. Heisey
1987 Use of a log-linear model with the EM algorithm to correct estimates of stock composition and to convert length to age. Trans. Am. Fish. Soc. 116:232-243.

Jones, R.
1961 The assessment of long-term effects of changes in gear selectivity and fishing effort. Mar. Res. (Scotl.) 1961(2):1-19.
1974 Assessing the long term effects of changes in fishing effort and mesh size from length composition data. Int. Counc. Explor. Sea Doc. CM 1974/F:33, 13 p.
1981 The use of length composition data in fish stock assessments (with notes on VPA and cohort analysis). FAO Fish. Circ. 734, 60 p.

Kimura, K.K., and S. Chikuni
1987 Mixtures of empirical distributions: An iterative application of the age-length key. Biometrics 43:23-35.

Knight, W.
1968 Asymptotic growth: An example of nonsense disguised as mathematics. J. Fish. Res. Board Can. 25:1303-1307.

Kreuz, K.F., A.V. Tyler, and G.H. Kruse
1982 Variation in growth of Dover soles and English soles as related to upwelling. Trans. Am. Fish. Soc. 111:180-192.

Lai, H.L., and V.F. Gallucci
1988 Effects of parameter variability on length-cohort analysis. J. Cons. Cons. Int. Explor. Mer 45:82-92.

Laurec, A., and F.X. Bard
1980 Analyse multicohorte sur deux classes d'age. Int. Com. Cons. Atl. Tunas Collect. Vol. Sci. Pap XV (SCRS-1979):1-20.

Law, A.M., and W.D. Kelton
1982 Simulation modeling and nalysis. McGraw-Hill, NY, 400 p.

Macdonald, P.D.M., and T.J. Pitcher
1979 Age groups from size frequency data: A versatile and efficient method of analyzing distributing mixtures. J. Fish. Res. Board Can. 36:987-1001.

Marquardt, D.W.
1963 An algorithm for least-squares estimation of non-linear parameters. J. Soc. Ind. Appl. Math 11(2):431-441.

Mendelssohn, R.
1988 Some problems in estimating population sizes from catch-at-age data. Fish. Bull., U.S. 86:617-630.

Morrison, D.D.
1960 Methods for nonlinear least squares problems and convergence proofs, tracking programs, and orbit determination. Proc. Jet Propul. Lab. Sem. (1960):1-9.

Murphy, G.I.
1965 A solution of the catch equation. J. Fish. Res. Board Can. 9:450-491.

Paloheimo, J.E.
1980 Estimation of mortality rates in fish populations. Trans. Am. Fish. Soc. 109:378-386.

Parrack, M.L.
1981 An assessment of the Atlantic bluefin tuna resource. Int. Com. Cons. Atl. Tunas Collect. Vol. Sci. Pap. XV:259-272.
1986 A method of analyzing catches and abundance indices from a fishery. Int. Com. Cons. Atl. Tunas Collect. Vol. Sci. Pap. XXIV:209-221.
1990 Estimating stock abundance from size data. Ph.D. diss., School Fish., Univ. Wash., Seattle, 116 p.

Parrack, N.J.C.
1986 Aspects of Pacific cod biology and population dynamics in the North Pacific. M.S. thesis, Univ. Wash., Seattle, 157 p.

Pauly, D.
1982 Studying single species dynamics in a tropical multispecies context. *In* Pauly, D., and G.I. Murphy (eds.), Theory and management of tropical fisheries, p. 33-70. ICLARM (Int. Cent. Living Aquat. Resour. Manage.) Conf. Proc. 9, Manila.

Pauly, D., M.L. Palomares, and F.C. Gayanilo
1987 VPA estimates of monthly population length composition, recruitment, mortality, biomass and related statistics of Peruvian anchoveta, 1953 to 1981. *In* Pauly, D., and I. Tsukayama (eds.), The Peruvian anchoveta and its upwelling ecosystem: Three decades of change, p. 142-166. ICLARM (Int. Cent. Living Aquat. Resour. Manage.) Stud. Rev. 15, Manila.

Pikitch, E.K., and R.L. Demory
1988 Assessment of scales as a means of aging Dover sole. Trans. Am. Fish. Soc. 117:345-349.

Pope, J.G.
1972 An investigation of the accuracy of virtual population analysis using cohort analysis. Int. Comm. Northwest Atl. Fish. Res. Bull. 9:65-74.

Pope, J.G., and J.G. Shepherd
1982 A simple method for the consistent interpretation of catch-at-age data. J. Cons. Cons. Int. Explor. Mer 40:176-184.
1985 A comparison of the performance of various methods for tuning VPAs using effort data. J. Cons. Cons. Int. Explor. Mer 42:129-151.

Press, W.H., B.P. Flannery, S.A. Teukolsky, and W.T. Vetterling
1986 Numerical recipes, the art of scientific computing. Cambridge Univ. Press, Cambridge, 818 p.

Quinn, T.J., S.H. Hoag, and G.M. Southward
1982 Comparison of two methods of combining catch-per-unit-effort data from geographic regions. Can. J. Fish. Aquat. Sci. 39:837–846.

Richards, F.J.
1959 A flexible growth function for empirical use. J. Exp. Botany 10(29) 290–300.

Ricker, W.E.
1948 Methods of estimating vital statistics of fish populations. Indiana Univ. Publ. Sci. Ser. 15, 101 p.
1975 Computation and interpretation of biological statistics of fish populations. Bull. Fish. Res. Board Can. 191, 382 p.

Rosenberg, A.A., and J.R. Beddington
1987 Monte Carlo testing of two methods for estimating growth from length frequency data, with general conditions for their applicability. *In* Pauly, D., and G.P. Morgan (eds.), Length-based methods in fisheries research, p. 283–289. ICLARM (Int. Cent. Living Aquat. Resour. Manage.) Conf. Proc. 13, Manila.

Rubinstein, R.Y.
1981 Simulation and the Monte Carlo method. John Wiley, NY, 278 p.

Scheuer, E.M., and D.S. Stoller
1962 On the generation of normal random vectors. Technometrics 4:278–281.

Schnute, J.T., L.J. Richards, and A.J. Cass
1989 Fish survival and recruitment: Investigations based on a size-structured model. Can. J. Fish. Aquat. Sci. 46:743–769.

Schrage, L.
1979 A more portable Fortran random number generator. ACM (Assoc. Comput. Machines) Trans. Math. Software 5: 132–138.

Shepherd, J.G.
1985 Deconvolution of length compositions. Int. Counc. Explor. Sea Methods Working Group, Working paper, 7 p.

Shirakihara, K., and S. Tanaka
1983 An alternative length-specific model and population assessment for the western North Pacific sperm whales. Rep. Int. Whaling Comm. 33:287–294.
1984 Simulation studies on length-specific population assessment techniques for western North Pacific sperm whales. Rep. Int. Whaling Comm. 34:259–264.

Shirakihara, K., S. Tanaka, and T. Nakano
1985 Further simulation studies on length-specific population assessment techniques for western North Pacific sperm whales. Rep. Int. Whaling Comm. 35:199–203.

Smith, S.J.
1980 Comparison of two methods of estimating the variance of the estimate of catch per unit effort. Can. Fish. Aquat. Sci. 37:2346–2351.

Sullivan, P.J.
1989 Kalman filter approach to catch at length analysis. Ph.D. diss., Univ. Wash., Seattle, 160 p.

Sullivan, P.J., H.L. Lai, and V.F. Gallucci
1990 A catch-at-length analysis that incorporates a stochastic model of growth. Can. J. Fish. Aquat. Sci. 47:184–198.

Ulltang, O.
1977 Sources of errors in and limitations of virtual population analysis (cohort analysis). J. Cons. Cons. Int. Explor. Mer 37:249–260.

Welch, B.L.
1938 The significance of the difference between two means when the population variances are unequal. Biometrika 25:350–362.

Appendix: Simulation steps of Monte Carlo tests

Control variables are F_1, F_2, z_1, p_t, μ_1, μ_2, σ_1, σ_2, μ_k, cv[k], μ_A, cv[A], cv[q], cv[C]

Compute the following once each trial for $1 \leqslant t \leqslant\leqslant T$:

1 If the F_t are variable, $F_t \sim U(F_1, F_2)$

2 If the z_t are variable, $z_t \sim U(z_1, z_2)$

3 If a single catch occurs once each period, then

- A probability of unobserved events (z) during y_t to c_t is $Pr[z']_t = 1 - e^{-z_t(c_t - y_t)}$,
- B probability of being caught (on date c_t) is $Pr[C]_t = F_t$,
- C probability of unobserved events (z) during c_t to y_{t+1} is $Pr[z']_t = 1 - e^{-z_t(y_{t+1} - c_t)}$, or

4 If catching is continuous, then

- A probability of death during y_t to y_{t+1} is $Pr[D]_t = 1 - e^{-(z_t + F_t)(y_{t+1} - y_t)}$, and
- B $Pr[z]_t = Pr[D]_t \; z_t \div (z_t + F_t)$.

5 If recruitment is seasonal, then

- A $p_t \sim U(1,20)$ where p_t is the proportion recruited during period t,
- B $\delta_t = \sum_{i=1}^{t} p_i \sum_{j=1}^{T-1} p_j$ = the accumulative frequency,
- C $\mu_t \sim U(\mu_1, \mu_2)$, and
- D $\sigma_t \sim U(\sigma_1, \sigma_2)$.

Compute the following once for each fish:

6 Draw growth parameters k and A such that

- A $k \sim N(\mu_k, (\mu_k \; cv[k]^2)$,
- B $A \sim N(\mu_A, (\mu_A \; cv[A]^2)$.

7 Draw a recruitment data, t_1, such that

- A if recruitment is uniform, then $t_1 \sim U(1,20)$, or
- B if recruitment is seasonal,
  - (1) draw t with probability specified by δ,
  - (2) draw $t_1 \sim N(\mu_t, \sigma^2_t)$.

8 If fishing is continuous, then

- A for the time period of recruitment draw u where $u \sim U(0,1)$.
  - (1) If $u \leqslant z_{t1}(1 - e^{-(z_{t1} + F_{t1})(y_{t1+1} - t_1)} \div (z_{t1} + F_{t1})$, the fish exited of unobserved causes; STOP.
  - (2) If not, but if $u \leqslant 1 - e^{-(z_{t1} + F_{t1})(y_{t1+1} - t_1)}$, the fish was caught; go to step 8C(2)(a).
  - (3) If neither occurred, the fish lived through the time period of recruitment; continue.
- B Add a fish to the abundance matrix.
  - (1) $t = t + 1$.
  - (2) $t_1 = y_t$.
  - (3) s_1 = the lower bound of the minimum size-class.
  - (4) Compute the size-class from equation (1).
  - (5) $N_{t,s2} = N_{t,s2} + 1$.
  - (6) If $t = T$, STOP.
- C Draw u where $u \sim U(0,1)$.
  - (1) If $u \leqslant Pr[z]_t$, the fish exited dur to unobserved events; STOP.
  - (2) If not, but if $u \leqslant Pr[D]_t$, the fish was caught.
    - (a) Draw u where $u \sim U(0,1)$.
    - (b) $t_2 = t + u$.
    - (c) Compute the size-class equation (1).
    - (d) Add to the catch matrix: $C_{t,s} = C_{t,s} + 1$; STOP.

(3) If neither occurred, the fish survived; go to step 8B.

9 If fishing occurs just once each period, then

A If $t_1 < c_{t1}$, the fish recruited before the catch.
(1) Draw u where $u \sim U(0,1)$.
(2) If $u \leqslant 1 - e^{-z_{t1}(c_{t1} - t_1)}$, the fish exited unobserved events before date c_t; STOP.
(3) If not, the fish survived to the catch date; go to step 9F.

B If $t_1 = c_{t1}$, the fish recruited on the catch date; go to step 9F.

C If $t_1 > c_{t1}$, the fish recruited after the catch.
(1) Draw u where $u \sim U(0,1)$.
(2) If $u \leqslant 1 - e^{-z_{t1}(y_{t1+1} - t_1)}$, the fish exited due to unobserved events before the next abundance sample (date y_{t+1}); STOP.
(3) If not, the fish survived fishing and so was alive on the next sampling date: $t = t + 1$.

D Add a fish to the abundance matrix.
(1) $t_2 = y_t$.
(2) s_1 = lower bound of the minimum size-class.
(3) Compute the size-class from equation (1).
(4) $N_{t,s2} = N_{t,s2} + 1$.
(5) If $t = T$, STOP.

E Draw u where $u \sim U(0,1)$. If $u \leqslant Pr[z']_t$, the fish exited due to unobserved events before the date of catch; STOP.

F Draw u where $u \sim U(0,1)$. If $u \leqslant Pr[C]_t$, the fish was caught on date c_t.
(1) $t_2 = c_t$.
(2) s_1 = lower bound of the minimum size-class.
(3) Compute the size-class when caught from equation (1).
(4) $C_{t,s2} = C_{t,s2} + 1$.
(5) STOP.

G Draw u where $u \sim U(0,1)$.
(1) If $u \leqslant Pr[z']_t$, the fish exited due to unobserved events before the next abundance sampling date; STOP.
(2) If not, the fish survived to the next relative abundance sample date.
(a) $t = t + 1$.
(b) Go to step 9D.

Collect samples once each trial:

10 Draw an extimate of the growth parameters such that
$\rho[\hat{A}, \hat{k}] = -0.95$,
$\hat{k} \sim N(\mu_k, \mu_k^2(cv[k]^2 + cv[e_k]^2)\text{divg}$, and
$\hat{A} \sim N(\mu_A, \mu_A^2(cv[A]^2 + cv[e_A]^2) \pm g$.

11 Draw an extimate of catch for all t and s where $\hat{C}_{t,s} \sim N(C_{t,s}, C_{t,s}\, cv[C]^2)$.

12 For each t and s draw $q_{t,s,k} \sim N(q_s, (q_s\, cv[q]^2)$ for $1 \leqslant k \leqslant r$.

13 Calculate $Y_{t,s}$ and $s^2[Y_{t,s}]$.

14 Determine the largest sampled size-class.

Biology of two co-occurring tonguefishes, *Cynoglossus arel* and *C. lida* (Pleuronectiformes: Cynoglossidae), from Indian waters

Arjuna Rajaguru

Systematics Laboratory, National Marine Fisheries Service, NOAA
National Museum of Natural History, Washington, DC 20560

Abstract.—Feeding ecology, age and growth, length-weight relationships, and reproductive biology of two species of tonguefishes, *Cynoglossus arel* and *C. lida*, from Porto Novo, southeast coast of India, were studied during October 1981–September 1982. These tonguefishes are benthophagus; adults feed primarily on polychaetes, while juveniles more often consume smaller prey such as hyperiid amphipods and copepods. A negative correlation between spawning activity and gastrosomatic index/hepatosomatic index was noted for *C. arel*. In *C. lida*, a higher percentage of empty stomachs was observed in males than in females.

Age and growth of these tonguefishes were determined by three methods, viz, (1) Petersen method, (2) probability plot, and (3) von Bertalanffy's equation. Rate of growth from the time of hatching through the first year is higher than that of older year-classes. Both species reach commercial size during their 2d and 3d year, and have a life-span of 3–4 years. Value of L_∞ (theoretical maximum attainable length) is 570 mm for male and 615 mm for female *C. arel*, and 335 mm for male and 340 mm for female *C. lida*.

Analyses of the length-weight relationship showed a significant difference in length-weight slopes of male and female *C. arel*. Due to gonad development, mature female *C. lida* deviated significantly from the 'cube law.'

Cynoglossus arel and *C. lida* have prolonged spawning periods of 10 months, with a spawning peak in January and September, respectively. Individuals spawn only once during each season. Both sexes of both species attain first sexual maturity during the 2d year. In male *C. lida*, higher values of the gonadosomatic index (GSI) in September indicate the occurrence of fully-mature specimens during this period. A rise in Kn values (relative condition factor) corresponds with a rise in gonadal activity in female *C. arel*. The correlation coefficient shows that fecundity in *C. arel* is correlated with total length, total weight, ovary length, and ovary weight, whereas in *C. lida* it is correlated only with ovary length and ovary weight.

Manuscript accepted 4 March 1992.
Fishery Bulletin, U.S. 90:328–367 (1992).

Out of 77 species of flatfishes occurring along the east and west coasts of India (Rajaguru 1987), only one species, viz, the Malabar sole *Cynoglossus macrostomus*, constitutes an important fishery along the Malabar coast (west coast of India) (Bal and Rao 1984). The Indian halibut *Psettodes erumei*, because of its larger size and delicious flesh, fetches a high value in fish markets (Pradhan 1969); however, it does not comprise a high value fishery. Other species of flatfishes which contribute to fisheries along the Indian coasts are: *Cynoglossus macrolepidotus*, *C. arel*, *C. dubius*, *C. lida*, *C. puncticeps*, *C. bilineatus*, *C. lingua*, *Paraplagusia* spp., *Solea* spp., and *Pseudorhombus* spp. (Seshappa 1973, Ramanathan 1977, Rajaguru 1987). However, none of these species comprises a single-species fishery. Separate statistics are not reported for these species; all flatfish species are jointly reported as 'soles' (CMFRI 1969, Fischer and Bianchi 1984). Average landings of flatfishes along the Indian coast is about 2% of the total marine fish catches (Ramanathan 1977, Rajaguru 1987). Most of these flatfish species became prominent in the landings only after the introduction of trawlers (Devadoss and Pillai 1973). These species, except the malabar sole *Cynoglossus macrostomus*, are generally not the target species, but are taken incidentally in the penaeid shrimp fishery. Along the Porto Novo Coast, of the 47 flatfish species (Rajaguru 1987), only *Psettodes erumei*, *Pseudorhombus arsius*, *Cynoglossus arel*, and *C. lida* occur throughout the year. The latter two species are taken in a fishery throughout the year, even during the northeast monsoon period, when other marine fish are generally absent.

The biology of these two tonguefishes is poorly known, except for work on age and growth of 138 *C. lida* from the west coast of India (Seshappa 1978). The present study examines various aspects of biology, including feeding ecology, age, growth, length-weight relationships, and reproductive biology of *C. arel* and *C. lida* in Porto Novo coastal waters.

Objectives of the study on the feeding ecology of these two species of tonguefishes are to determine (a) the diet of juveniles and adults, (b) differences in diet between seasons, and (c) relationships between feeding morphology, digestive morphology, and diet. An age and growth study was also undertaken to (a) evaluate differences in growth patterns between males and females, (b) determine age of recruitment to the Porto Novo fishery, and (c) determine longevity of these two tonguefishes. The objective of the studies on length-weight relationships is to determine if there is a significant deviation from the cube law of length-weight relationship related to ontogeny and gonadal development. The final aspect

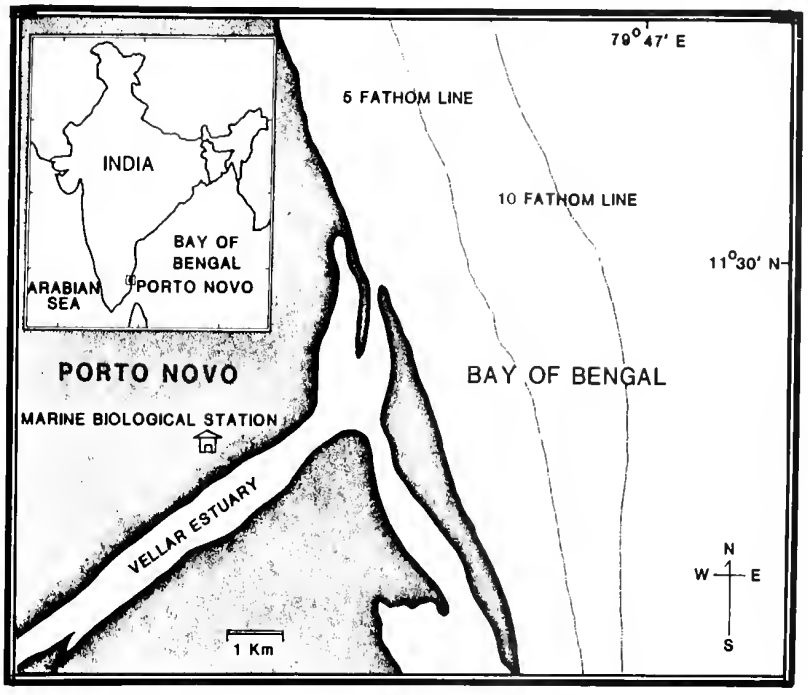

Figure 1
Map showing 5- and 10-fathom lines off Porto Novo coast, India.

of the study is reproductive biology. The objectives are to (1) determine the spawning season, spawning periodicity, age and size at first maturity, and (2) examine relationships between fecundity and total length, total weight, ovary length and ovary weight.

Materials and methods

Samples of large-scaled tonguefish *Cynoglossus arel* (Bloch and Schneider 1801) and shoulder-spot tonguefish *C. lida* (Bleeker 1851) were collected twice weekly (a total of 96 collections) from commercial fish catches landed in Porto Novo, southeast coast of India (11°29'N, 79°46'E; Fig. 1), from October 1981 to September 1982. Fishing operations were confined to the upper continental shelf, to a depth of 18–22 m, up to 4 km from the coast.

A total of 1220 specimens of *C. arel* (627 males, 569 females, 24 juveniles) and 1382 specimens of *C. lida* (718 males, 640 females, 24 juveniles) were collected for stomach analyses. For the age and growth study, a total of 1203 specimens of *C. arel* (634 males and 569 females), and 1374 specimens of *C. lida* (724 males and 650 females) were utilized; since juveniles were available only for 4 months, they were not included in the age and growth study. Length-weight equations were computed using data of 1281 specimens of *C. arel* (655 males, 599 females, and 27 juveniles) and 1519 specimens of *C. lida* (768 males, 723 females, and 28 juveniles). A total of 1196 specimens of *C. arel* (627 males and 569 females) and 1358 specimens of *C. lida* (718 males and 640 females) were examined for the reproductive biology studies. Some specimens were used for all four studies. Size range of the specimens was as follows: *C. arel* (males 95–360 mm TL, females 99–435 mm TL, juveniles 83–128 mm TL) and *C. lida* (males 97–248 mm TL, females 98–242 mm TL, juveniles 81–125 mm TL). Total length (TL) of each fish was measured to the nearest 1 mm; total weight (TW) was recorded to the nearest 0.1 g. Sex, maturity stages, TL, and TW were noted in fresh-caught fish. Size of monthly samples utilized for various analyses is given in Appendix.

Feeding ecology

Stomachs were removed and preserved in 5% formalin. Some empty stomachs were shrunken and contained mucus, while others were expanded but completely empty; the latter type is believed to occur in fish which have recently regurgitated (Daan 1973). Regurgitated stomachs, as well as fish with food remains in their mouths, were discarded.

Gastrosomatic index (GI) and hepatosomatic index (HI) were calculated to examine monthly variations in feeding intensity and to correlate these variations with breeding cycles, using the following formulae:

$$\text{Gastrosomatic index} = \frac{\text{Weight of gut (including contents)} \times 100}{\text{Weight of fish}}$$

$$\text{Hepatosomatic index} = \frac{\text{Weight of liver} \times 100}{\text{Weight of fish}}$$

For stomach analysis, the Index of Relative Importance (IRI) (Pinkas et al. 1971) was used. It incorporates percentage by number (N), volume (V), and frequency of occurrence (F) in the formula

$$IRI = (\%N + \%V) \times \%F.$$

The percentage IRI was calculated for the entire data set of juveniles, males, and females, and by length intervals (45 mm interval for *C. arel*, and 21 mm for *C. lida*).

Stomach contents were sorted, identified to the lowest possible taxa, and enumerated. Appendages and remains of the unidentified crustaceans are classified as "crustacean fragments." Volume of each taxonomic group of prey was measured by water displacement. To determine ontogenetic variations in feeding habits, stomach contents of juveniles were analyzed separately from those of adults.

Age and growth

Length measurement data were grouped into size-classes at intervals of 15 mm for *C. arel* and 7 mm for *C. lida*. Percentage frequencies were calculated by month. Sexes were treated separately, to determine whether there were differences in growth patterns between males and females. The Petersen method, probability plot method, and von Bertalanffy's equation were used to determine age and growth. Attempts to detect growth layers in hard parts (scales, otoliths, opercular bones, and supraoccipital crests) were not successful.

Petersen method This method of growth analysis is based on the assumption that the lengths of individuals of the same age in a population are distributed normally. When there are distinct intra-annual spawning periods, the length-frequency distribution may be multimodal, representing successive age-groups. The rate of growth slows with age (Ford 1933), and as a result the modes overlap, making interpretation difficult. In the case of fishes, such as tonguefishes, which have a prolonged spawning period, various broods entering the fishery overlap. In this case, it is necessary to trace a size-group for as many months as possible after it enters the commercial fishery and to find the average monthly growth rate for different size-classes. Approximate values of average size at different ages may then be calculated.

Probability plot method Plots of cumulative percentages of length distribution on probability paper provide estimates of the length ranges of fish in each age-group (Harding 1949, Cassie 1954). Hence fish lengths were used to obtain an approximation of the length-at-age structure. One difficulty in this method is the uncertainty surrounding whether the deviations represent virtual inflexion points of the lines. Another difficulty is locating each inflexion point, since any bend in the line is considered an inflexion point. Following this procedure, the line was divided into separate parts and for each (Cassie 1954), partial straight lines were drawn from which, a mean length was calculated for each age-group.

von Bertalanffy's equation The most widely accepted growth model is that of von Bertalanffy (1938),

$$L_t = L_\infty (1 - e^{-k(t-t_0)})$$

where L_t = length at age t,
L_∞ = theoretical maximum attainable (asymptotic) length,
k = a constant, expressing the rate of change in length increments with respect to t,
t_0 = hypothetical age at zero length, and
e = base of Naparian or natural logarithm.

The value of t_0 was calculated as follows:

$$-t_0 = 1/k\,[\log_e (L_\infty) - \log_e (L_\infty - L_t)] - t.$$

Walford's (1946) procedure was used to substitute $L_t + 1$ for L_t. The equation now can be written as

$$L_t + 1 = L_\infty (1 - e^{-k}) + L_t\, e^{-k}.$$

Length-weight relationship

Length-weight curves were obtained by using the equation $W = aL^b$. The least-squares regression of the logarithmic transformation,

$$\log_{10} W = \log_{10} a + b \log_{10} L,$$

where $\log_{10} W = Y$, $\log_{10} a = a$, $\log_{10} L = X$, $b = n$, was used for estimating the values of a and b (Snedecor 1956). This linear equation was fitted separately for males, females, and unsexed juveniles of *C. arel* and *C. lida* from monthly data.

To determine whether increased weight at a given length was caused by increased gonad weight in mature fish, the length-weight relationship was compared between different stages of maturity. Adults of both sexes of *C. arel* and *C. lida* were classified into three stages (Rajaguru 1987):

Immature (Stage I for both sexes): n 56 male and 47 female *C. arel*; 105 male and 54 female *C. lida*;
Maturing (Stage II for males, Stages II–III pooled for females): n 221 male and 224 female *C. arel*; 259 male and 342 female *C. lida*; and
Mature (Stage III for males, Stages IV–VI pooled for females): n 359 male and 292 female *C. arel*; 363

male and 254 female *C. lida*. (Refer to section on Reproductive biology, for Stages I–VI.)

The significance of variation in the estimate of b, from the expected value B (=3) for an ideal fish was tested by the *t*-test in both sexes of *C. arel* and *C. lida* (James 1967):

$$t = \frac{b - B}{Sb}$$

where B = hypothetical b (=3), and Sb = standard error of b.

Analysis of covariance (Snedecor 1956) was used for all comparisons.

Reproductive biology

Tonguefishes have no secondary sexual characters to distinguish the sexes. In females with gonads in advanced stages of maturity, ovaries can be seen easily through the body wall when the fish is held against light. In earlier stages of maturity, sexes are distinguishable only after dissection. Extension of gonads into body cavity, and their color, shape, and size, were noted after dissection. Ovary length was measured to the nearest mm, while weight of testis/ovary was recorded to the nearest mg. Ovaries were fixed in modified Gilson's fluid (Simpson 1951) for ova diameter studies.

To investigate the distribution pattern of ova in different regions of the ovary, ova were taken from anterior, middle, and posterior regions of eyed-side and blind-side lobes of ovaries in different stages of maturity (Clark 1934, Hickling and Rutenberg 1936, de Jong 1940). Ova diameter measurements in each part were noted separately. Results showed a uniform distribution of ovum size in different parts of both ovarion lobes. Hence to study development of ova, random samples of ~500 ova per ovary were measured from ovaries representing Stages I–VI (a total of 108 ovaries, at 18 ovaries/stage in *C. arel*, and a total of 168 ovaries, at 28 ovaries/stage in *C. lida*), using an ocular micrometer at a magnification which gave a value of 12.5 μ (0.0125 mm) to each micrometer division (m.d.). Ova diameter-frequency polygons were drawn after grouping the ova into 3 m.d. (0.04 mm) class-intervals.

Spawning seasons in both species were determined from percentage occurrence of different maturity stages during various months of the year.

Generally, gonad weight depends on size and stage of gonadal development. To account for effects of differential body size on gonad size, gonad weight was expressed as a percentage of body weight (Nikolsky 1963). This ratio,

$$\frac{\text{Weight of gonad} \times 100}{\text{Weight of fish}},$$

is termed gonadosomatic index (GSI). To determine the spawning season, GSIs for various months were calculated.

Relative condition factor (Kn) was calculated for individual fish of both sexes from the formula (Le Cren 1951),

$$Kn = W/\bar{W}$$

where, W = observed weight, and $\bar{W}$ = calculated weight ($\bar{W} = a + bx$). Monthly mean values of Kn were also calculated to confirm the spawning season.

To determine minimum length-at-first-maturity (i.e., Lm or L_{50} = length at which 50% of fish are mature), specimens of *C. arel* and *C. lida* were grouped into 15 mm and 7 mm class-intervals, respectively. Sexes were treated separately. Percentage occurrence of immature and mature fish of various length-groups was determined, and then percentage occurrence of mature fish was plotted for both sexes.

Fecundity was determined by the gravimetric method. For this study, 26 ovaries of *C. arel* (from specimens 200–439 mm TL) and 19 of *C. lida* (161–201 mm TL) were used. Since some ova might already have been shed, ovaries with oozing ova were not used. Ovaries were removed, measured to the nearest mm, and weighed to the nearest mg. From each ovary, three subsamples (each ~50 mg) were taken and weighed after removing excess moisture, and fixed in modified Gilson's fluid. From each of these subsamples, yolked ova were separated and counted. Mean number of ova from three subsamples was multiplied by the ratio of subsample weight: ovary weight to obtain an estimation of the total number of mature ova in the ovary. Numbers of ova per mm body length, per g body weight, per mm ovary length, and per mg ovary weight were also calculated. Fecundity of *C. arel* and *C. lida* was related to total length (TL), total weight (TW), ovary length (OL), and ovary weight (OW) using linear regression. Statistical comparisons (Snedecor 1956) of fecundity to TL, TW, OL, and OW were made.

To determine the differential distribution of sexes during the spawning migration, as well as during aggregation, the sex ratio was calculated for each month. To test the homogeneity in distribution of males and females, the chi-square formula was used.

Classification of maturity stages

Maturity stages were indexed for both sexes of *C. arel* and *C. lida*, following the ICES scale (Lovern and Wood 1937), with the following modifications. Color, shape, and extension of the ovary into the body cavity,

Figure 2
Percentage contribution of food items to the diet of juvenile, male, and female *Cynoglossus arel* and *C. lida* caught commercially off Porto Novo, India, October 1981–September 1982. Only values >5% IRI are individually shown; values <5% IRI are clumped together into a single category, the unshaded wedge of the pie chart. PO = polychaetes, PR = prawns; CF = crustacean fragments, FS = fish scales, AM = amphipods, CO = copepods, TN = tintinnids, FI = fishes, MI = miscellaneous.

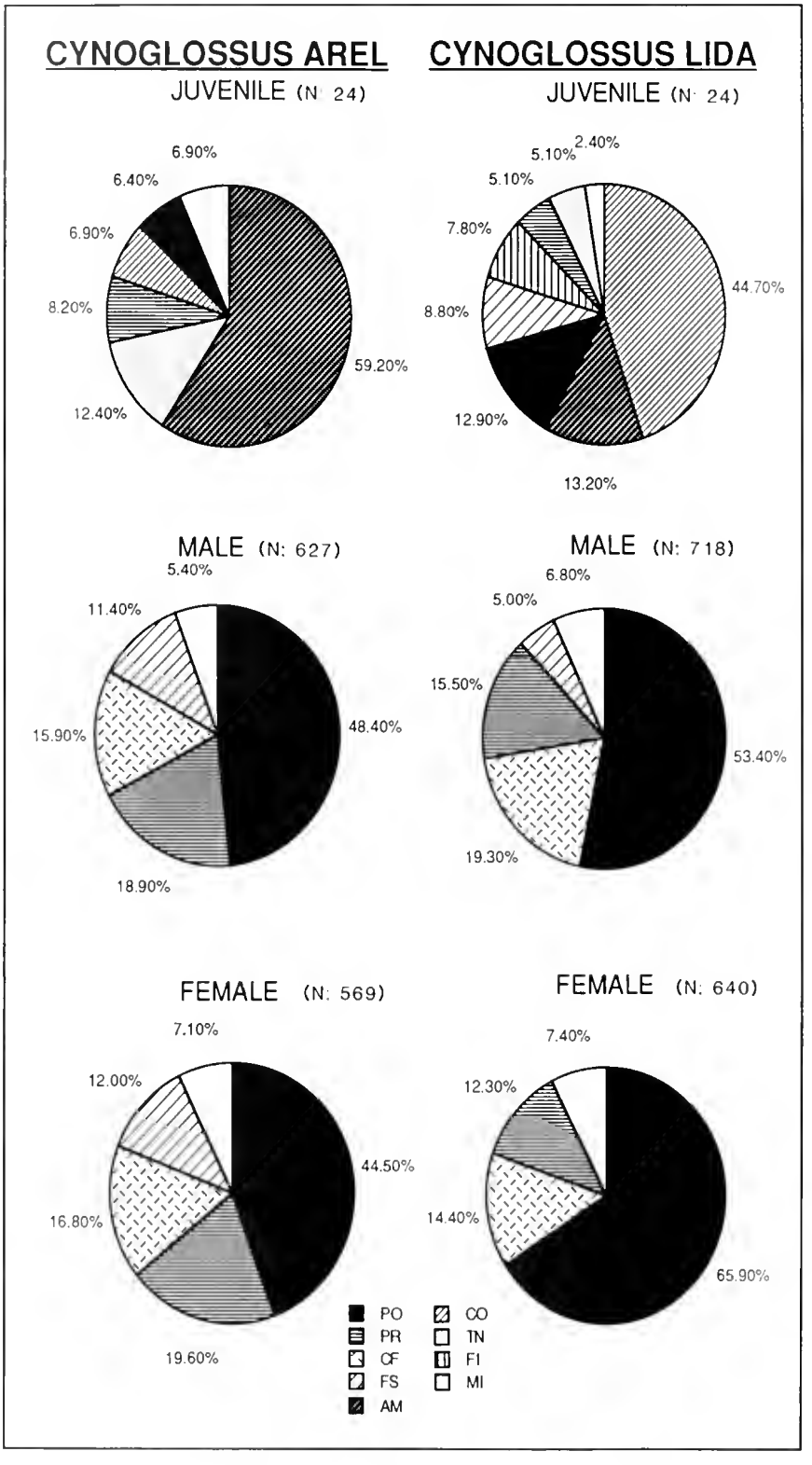

as well as color and shape of ova, were considered to define stage of maturity in females. Degree of transparency of the ovary was also used as a criterion, since it is one of its characteristic features during early as well as fully-mature phases. Color and size of testis were used to determine the stage of maturity in males. In both species, testes were divided into four stages, and ovaries into seven stages as follows:

Males:

Stage I (Immature) Testis minute, pale white.

Stage II (Maturing) Testis slightly enlarged, sac-like, creamy white; no milt oozes out on pressure.

Stage III (Mature) Testis enlarged, sac-like, creamy white; whitish milt running from vent on slight pressure.

Stage IV (Spent) Not found during the present study.

Females:

Stage I (Immature) Ovary very small, thread-like and transparent; under microscope, yolkless and transparent ova seen with prominent nuclei in the center; ova invisible to naked eye.

Stage II (Virgin maturing) Ovary slightly thicker, translucent and yellowish; occupying 1/3 to 1/2 of body cavity; ova invisible to naked eye; under a microscope, translucent ova seen with yolk granules around nucleus.

Stage III (Maturing) Ovary yellowish, granular, extending to more than 1/2 the length of body cavity, with vascularization; ova small; under microscope, opaque; nucleus hidden by yolk.

Stage IV (Mature) Ovary creamy yellow, with

Table 1

Percent IRI of various food items of male *Cynoglossus arel* caught commercially off Porto Novo, India, October 1981–September 1982. *N* = number of stomachs analyzed; Crustacean fr. = crustacean fragments; UI = unidentified. (Data presented to one decimal point; 0.0 denotes value of <0.05, and dash denotes absence of food item.)

	Jan.	Feb.	Mar.	Apr.	May	June	July	Aug.	Sep.	Oct.	Nov.	Dec.	Total	
Food items *N*	53	24	54	46	56	35	69	44	56	75	86	29	627	%
Polychaetes	28.0	0.3	62.2	52.4	25.2	60.4	57.9	75.6	70.1	73.2	56.1	19.1	580.5	(48.4)
Prawns	19.1	21.0	12.5	12.5	58.7	25.4	23.9	13.4	22.0	11.2	5.2	1.8	226.7	(18.9)
Crustacean fr.	23.5	15.6	14.0	25.2	10.9	9.6	8.1	3.6	0.6	4.3	4.2	70.9	190.5	(15.9)
Fish scales	26.6	53.1	10.4	2.8	1.4	2.7	2.3	1.8	4.9	3.7	26.7	0.3	136.7	(11.4)
Amphipods	0.4	0.2	0.7	1.0	3.3	0.6	7.5	5.1	0.0	2.4	2.2	3.4	26.9	(2.2)
Fish bone	1.3	—	—	—	—	—	—	—	—	—	5.2	0.6	7.1	(0.6)
Fish spine	—	5.8	—	—	0.0	—	0.0	—	—	—	—	—	5.8	(0.5)
Bivalves	0.1	0.3	0.1	0.1	0.0	0.3	0.1	0.1	0.0	4.2	0.3	—	5.7	(0.5)
Lingula sp.	—	—	—	5.4	0.0	—	—	—	—	—	—	0.0	5.4	(0.5)
Fishes	—	3.1	0.1	—	0.4	—	0.1	—	0.1	—	0.0	0.3	4.1	(0.3)
Crabs	0.9	0.4	0.0	0.4	0.1	0.8	0.1	0.1	0.4	0.2	0.1	—	3.6	(0.3)
Isopods	—	0.1	0.0	—	—	—	—	0.0	1.7	0.4	0.0	0.0	2.3	(0.2)
Algae	—	—	—	—	—	—	—	—	0.0	0.0	0.0	2.2	2.2	(0.2)
Fish eggs	—	—	0.0	—	—	—	—	—	0.0	0.1	—	1.3	1.4	(0.1)
Copepods	0.1	—	0.0	—	0.0	0.0	0.0	0.3	—	0.0	—	—	0.4	(0.0)
Gastropods	—	—	0.0	—	—	—	—	0.0	0.0	0.2	0.0	0.1	0.3	(0.0)
Squilla sp.	—	0.1	—	—	0.0	0.1	—	—	—	—	0.0	—	0.2	(0.0)
Coscinodiscus	—	—	—	—	—	—	—	—	0.2	—	—	—	0.2	(0.0)
Brittle star	—	—	—	0.1	—	—	0.0	—	—	—	—	—	0.1	(0.0)
Medusae	—	—	—	—	—	—	—	—	0.0	0.0	0.0	—	0.0	(0.0)
Egg mass (UI)	—	—	—	—	—	—	—	—	—	—	—	0.0	0.0	(0.0)
Nematode	0.0	—	0.0	—	—	—	0.0	0.0	—	—	—	—	0.0	(0.0)
Sand dollar	—	—	—	—	—	—	—	—	—	—	0.0	—	0.0	(0.0)
Echinoderm (UI)	—	—	—	—	—	—	—	—	0.0	—	—	—	0.0	(0.0)

prominent blood vessels; occupying 2/3 of body cavity; ova visible to naked eye and rich with yolk.

Stage V (Ripe) Ovary resembling Stage IV, but occupying more than 2/3 of the body cavity; under a microscope, ova slightly translucent with yolk granules; ova not running out of genital aperture on application of gentle pressure.

Stage VI (Oozing) Ovary yellowish and transparent, occupying entire length of body cavity; ripe ova running out through genital aperture on application of gentle external pressure on ovary; under a microscope, ova transparent.

Stage VII (Spent) Not found during the study.

Results

Feeding ecology

Food composition In *Cynoglossus arel*, polychaetes made up the bulk (44.5–48.4% IRI) of the diet of adults (Tables 1–2, Fig. 2). At least 11 species of polychaetes, viz, *Nephtys polybranchia*, *N. oligobranchia*, *Clymene annandalei*, *Phyllodoce* sp., *Ancistrosyllis constricta*, *Nereis chilkaensis*, *Diopatra* sp., *Onuphis* sp., *Eunice* sp., *Terebellides stroemi*, and *Sternaspis* sp., were consumed. The next most important prey items were prawns (18.9–19.6% IRI), crustacean fragments (15.9–16.8% IRI), and fish scales (11.4–12.0% IRI). The prey species which were consumed in smaller quantities included bivalves (represented by *Amussium* sp., *Placenta* sp., *Arca* sp., and *Pinna* sp.), gastropods (by *Umbonium* sp., *Turritella* sp., and *Dentalium* sp.), and fishes (by gobiids and *Cynoglossus monopus*) (Tables 1–2).

In adult *C. lida*, polychaetes (same species as in *C. arel*) dominated (53.4–65.9% IRI) (Tables 3–4, Fig. 2), while crustacean fragments (14.4–19.3% IRI) and prawns (12.3–15.5% IRI) ranked next in importance. The prey species which were consumed in smaller quantities included bivalves (represented by *Placenta* sp.), gastropods (by *Umbonium* sp. and *Turritella* sp.), and fishes (by gobiids and *Cynoglossus monopus*) (Tables 3–4).

Food of juveniles and adults Differences can be seen in stomach contents between juveniles and adults of both species (Tables 1–5, Fig. 2). Larger tonguefishes ate larger individuals of food species than did

Table 2

Percent IRI of various food items of female *Cynoglossus arel* caught commercially off Porto Novo, India, October 1981–September 1982. See Table 1 for abbreviations.

	Jan.	Feb.	Mar.	Apr.	May	June	July	Aug.	Sep.	Oct.	Nov.	Dec.	Total	
Food items *N*	39	45	49	55	54	40	56	54	35	54	54	34	569	%
Polychaetes	4.6	10.7	25.2	74.4	19.6	36.4	60.7	71.9	71.6	72.9	37.4	48.3	533.7	(44.5)
Prawns	30.8	17.9	26.4	9.5	41.0	41.1	19.0	3.3	10.8	14.3	12.7	8.7	235.5	(19.6)
Crustacean fr.	28.0	35.1	25.4	11.8	33.6	17.6	5.1	2.1	4.6	2.4	7.6	28.7	202.0	(16.8)
Fish scales	21.6	23.2	14.3	2.0	0.7	1.5	8.0	20.9	1.1	9.0	40.5	0.7	143.5	(12.0)
Amphipods	0.2	0.7	1.3	1.4	2.1	1.8	5.4	0.9	–	0.3	0.8	3.2	18.1	(1.5)
Fish bone	13.9	–	–	–	–	–	–	–	–	0.2	0.0	–	14.1	(1.2)
Fish spine	–	7.9	2.6	–	–	–	0.0	0.0	–	–	–	–	10.5	(0.9)
Crabs	0.7	0.0	1.6	0.2	2.6	1.4	0.1	0.0	0.7	0.1	0.4	2.6	10.4	(0.9)
Isopods	0.1	–	0.0	–	–	0.0	0.0	0.0	7.3	0.0	–	0.0	7.4	(0.6)
Fish eggs	–	0.0	–	–	–	–	–	–	–	0.0	0.0	6.1	6.1	(0.5)
Bivalves	0.1	1.6	1.0	0.1	0.0	0.0	0.0	0.0	1.7	0.1	0.2	0.5	5.3	(0.4)
Fishes	–	2.3	0.4	–	–	0.1	0.4	0.9	0.7	0.1	0.2	–	5.1	(0.4)
Lingula sp.	–	–	1.8	0.6	–	–	–	0.0	–	–	–	–	2.4	(0.2)
Gastropods	0.0	–	0.0	0.0	0.0	–	–	–	1.2	0.0	0.1	0.7	2.0	(0.2)
Lucifer	–	–	–	–	–	–	1.2	–	0.0	–	–	0.1	1.3	(0.1)
Copepods	–	0.6	–	–	0.4	–	0.0	0.0	–	0.0	–	0.0	1.0	(0.1)
Ciliates (UI)	–	–	–	–	–	–	–	–	–	0.5	–	–	0.5	(0.0)
Algae	–	–	–	–	–	–	–	–	0.0	0.0	0.0	0.4	0.4	(0.0)
Coscinodiscus	–	–	–	–	–	–	–	–	0.3	–	–	–	0.3	(0.0)
Squilla sp.	–	–	–	0.0	0.0	–	0.0	–	–	–	0.1	0.0	0.1	(0.0)
Brittle star	–	–	–	–	–	–	–	0.0	–	0.1	–	–	0.1	(0.0)
Medusae	–	–	–	–	–	–	0.1	–	0.0	–	–	–	0.1	(0.0)
Sand dollar	–	–	–	–	–	0.1	–	–	–	–	–	–	0.1	(0.0)
Nematode	0.0	0.0	0.0	–	0.0	–	–	0.0	–	–	–	0.0	0.0	(0.0)
Egg mass (UI)	–	–	–	0.0	–	–	–	0.0	–	–	0.0	0.0	0.0	(0.0)
Tube-like worm	–	–	–	–	–	–	–	–	0.0	–	–	–	0.0	(0.0)
Jelly fish	–	–	–	–	–	–	0.0	–	–	–	–	–	0.0	(0.0)
Sepia	–	–	–	–	–	0.0	–	–	–	–	–	–	0.0	(0.0)

smaller tonguefishes. In *C. arel*, amphipods (59.2% IRI) dominated diets of juveniles, followed by tintinnids (12.4% IRI). Smaller-sized prawns (8.2% IRI), copepods (6.9% IRI), and polychaetes (6.4% IRI) were next in importance. Fish remains, isopods, smaller crabs, and nematodes were found in decreasing order of importance and never composed more than 5% of the IRI. Breadth of the diet is much smaller in juveniles than adults (compare Tables 1–4 and 5). Only 10 types of food items occurred in stomachs of relatively few juveniles examined, whereas 29 different types of prey were noted in stomachs of adult *C. arel* (Tables 1–2, 5). In adult stomachs, fewer amphipods and more polychaetes were found than in juvenile stomachs. Prawns were the third most important prey in the diet of the juveniles, whereas in adults they were the second most important. Algal filaments were found only in stomachs of adults, while tintinnids were found only in stomachs of juveniles.

Juvenile *C. lida* fed on only 10 types of prey items and usually smaller sizes, whereas adults consumed 24 types of relatively large-sized prey items (Tables 3–5). Copepods (44.7% IRI) were preyed upon predominantly by juveniles of *C. lida* (Fig. 2), while polychaetes were dominant in the diet of adults. Hyperiid amphipods (13.2% IRI), which were of secondary importance and abundant in the diet of juveniles, occurred in smaller quantities in adult stomachs. Crustacean fragments were the second most important food item for adults. Other food items of juveniles are listed in Table 5.

However, the sample sizes for the juveniles of both tonguefishes are quite smaller than those of the adults. Therefore, the differences in number of prey in adults and juveniles may reflect differences in sample sizes.

Food of males and females A total of 76% of males and females of *C. arel*, and 65% of males and 73% of females of *C. lida*, had identifiable prey in their stomachs. In *C. lida*, females consumed 19 types of food items and males consumed 24 types (Tables 3–4). Polychaetes were relatively more abundant (Fig. 2) in the diet of females than males (65.9% vs. 53.4% IRI).

Table 3

Percent IRI of various food items of male *Cynoglossus lida* caught commercially off Porto Novo, India, October 1981–September 1982. See Table 1 for abbreviations.

	Jan.	Feb.	Mar.	Apr.	May	June	July	Aug.	Sep.	Oct.	Nov.	Dec.	Total	
Food items *N*	32	59	64	84	38	56	25	43	46	83	160	28	718	%
Polychaetes	5.4	42.3	31.2	89.4	21.4	67.6	27.8	93.8	87.4	83.0	89.2	2.8	641.3	(53.4)
Crustacean fr.	64.5	12.6	26.4	1.0	16.5	4.9	18.2	0.1	2.5	0.7	1.6	83.1	232.1	(19.3)
Prawns	17.5	9.6	26.6	3.8	57.3	21.5	23.3	3.6	8.0	6.2	5.1	3.8	186.3	(15.5)
Fish scales	6.4	20.4	12.7	0.8	2.7	0.2	3.8	0.2	0.5	6.5	0.6	5.2	60.0	(5.0)
Amphipods	0.6	2.4	0.2	3.2	1.9	5.7	24.7	2.0	–	3.4	3.3	0.2	47.6	(4.0)
Algae	5.2	4.3	–	–	–	–	–	0.0	0.0	–	–	4.4	13.9	(1.2)
Medusae	–	8.3	–	–	–	–	–	–	–	–	0.0	–	8.3	(0.7)
Lucifer	0.0	–	–	–	0.1	–	2.1	–	0.1	–	–	–	2.3	(0.2)
Copepods	0.0	–	2.0	0.0	–	–	–	0.0	0.0	–	–	0.1	2.1	(0.2)
Lingula sp.	–	0.0	0.2	1.6	–	–	–	–	–	–	0.0	–	1.8	(0.2)
Crabs	–	0.1	0.4	0.1	0.1	0.1	–	0.1	0.0	–	0.0	0.1	1.0	(0.1)
Isopods	0.3	0.0	0.3	–	–	–	–	–	0.3	–	–	0.0	0.9	(0.1)
Fishes	–	–	–	0.1	–	–	–	–	0.7	–	–	–	0.8	(0.1)
Fish eggs	0.1	0.1	–	–	–	–	–	–	–	–	–	0.3	0.5	(0.0)
Gastropods	–	0.0	–	–	–	–	–	0.1	0.2	–	0.1	–	0.4	(0.0)
Coscinodiscus	–	–	–	–	–	–	–	–	0.3	–	–	–	0.3	(0.0)
Bivalves	–	0.0	–	–	–	–	–	0.1	0.0	0.2	0.1	–	0.4	(0.0)
Nematode	0.0	0.0	–	–	–	–	–	–	0.0	–	–	0.0	0.0	(0.0)
Brittle star	–	–	–	0.0	–	–	–	–	–	–	–	–	0.0	(0.0)
Squilla sp.	–	0.0	–	–	–	–	–	–	–	–	0.0	–	0.0	(0.0)
Fish spine	–	–	–	0.0	–	–	–	–	–	–	0.0	–	0.0	(0.0)
Octopus sp.	–	0.0	–	–	–	–	–	–	–	–	–	–	0.0	(0.0)
Tape worm	–	–	–	0.0	–	–	–	–	–	–	–	–	0.0	(0.0)
Egg mass (U1)	–	0.0	–	–	–	–	–	–	–	–	–	–	0.0	(0.0)

Table 4

Percent IRI of various food items of female *Cynoglossus lida* caught commercially off Porto Novo, India, October 1981–September 1982. See Table 1 for abbreviations.

	Jan.	Feb.	Mar.	Apr.	May	June	July	Aug.	Sep.	Oct.	Nov.	Dec.	Total	
Food items *N*	42	16	18	51	31	59	25	62	25	76	207	28	640	%
Polychaetes	17.7	58.8	58.1	84.5	60.8	73.4	63.3	95.0	93.4	87.9	94.2	4.0	791.1	(65.9)
Crustacean fr.	48.5	12.5	7.7	2.0	5.2	5.0	10.3	0.6	1.2	0.8	0.3	78.7	172.8	(14.4)
Prawns	26.5	13.6	17.3	7.6	31.3	20.3	16.7	1.8	2.9	4.2	2.5	2.5	147.2	(12.3)
Amphipods	0.3	12.0	8.2	4.1	2.4	0.9	7.9	2.6	–	0.9	2.8	0.0	42.1	(3.5)
Fish scales	4.4	–	1.2	0.0	0.2	0.4	1.4	0.0	–	6.0	0.0	2.6	16.2	(1.4)
Fish eggs	0.4	0.1	0.3	–	–	–	–	–	0.9	–	–	7.5	9.2	(0.8)
Lingula sp.	–	–	6.7	1.8	–	–	–	0.0	–	–	–	–	8.5	(0.7)
Algae	1.3	1.2	–	–	–	–	–	–	–	–	–	4.6	7.1	(0.6)
Crabs	0.1	1.0	–	–	0.1	–	–	0.0	–	–	0.0	0.1	1.3	(0.1)
Isopods	0.0	0.1	0.2	0.0	0.0	0.0	–	–	0.9	0.1	0.0	–	1.3	(0.1)
Bivalves	0.3	–	–	–	–	0.0	0.3	–	0.3	0.1	0.2	–	1.2	(0.1)
Squilla sp.	0.1	0.5	–	–	–	0.0	–	–	–	–	–	–	0.6	(0.1)
Nematode	0.3	0.1	–	–	–	–	–	–	0.0	0.0	0.0	0.0	0.4	(0.0)
Copepods	0.0	–	0.2	–	–	0.0	0.1	–	–	0.0	0.0	–	0.3	(0.0)
Gastropods	0.0	0.1	–	–	–	–	–	–	0.3	–	0.0	–	0.4	(0.0)
Coscinodiscus	–	–	0.1	–	–	–	–	–	0.1	–	–	–	0.2	(0.0)
Medusae	0.1	–	–	–	–	–	–	–	–	–	–	–	0.1	(0.0)
Egg mass (U1)	0.0	–	–	–	–	–	–	–	–	–	–	–	0.0	(0.0)
Fish spine	–	–	–	–	–	–	–	0.0	–	–	–	–	0.0	(0.0)

Table 5

Percent IRI of various food items of juvenile *Cynoglossus arel* and *C. lida* caught commercially off Porto Novo, India, October 1981–September 1982. See Table 1 for abbreviations. (Data presented to one decimal point; dash denotes absence of food item.)

	C. arel						*C. lida*				
	Mar.	June	Oct.	Nov.	Total		Apr.	Nov.	Dec.	Total	
Food items *N*	6	5	7	6	24	%	8	9	7	24	%
Amphipods	50.0	83.0	60.4	43.5	236.9	(59.2)	3.0	32.8	3.9	39.7	(13.2)
Copepods	7.6	—	0.1	19.9	27.6	(06.9)	75.9	1.7	56.4	134.0	(44.7)
Tintinnids	11.1	—	16.4	21.9	49.4	(12.4)	—	12.0	3.3	15.3	(5.1)
Polychaetes	17.1	8.5	—	—	25.6	(6.4)	13.3	18.7	6.7	38.7	(12.9)
Prawns	—	1.3	20.4	10.9	32.6	(8.2)	2.5	12.7	—	15.2	(5.1)
Fish scales	1.0	1.6	1.2	3.0	6.8	(1.7)	1.7	18.4	6.3	26.4	(8.8)
Fishes	—	—	—	—	—	—	—	—	23.4	23.4	(7.8)
Crustacean fr.	11.1	5.1	—	—	16.2	(4.1)	—	0.8	—	0.8	(0.3)
Isopods	2.2	—	0.8	0.8	3.8	(1.0)	—	—	—	—	—
Ciliates (UI)	—	—	—	—	—	—	3.6	—	—	3.6	(1.2)
Nematode	—	0.3	0.1	0.1	0.5	(0.1)	—	3.0	—	3.0	(1.0)
Crabs	—	—	0.6	—	0.6	(0.2)	—	—	—	—	—

In *C. arel*, males consumed 24 types of food and females had 28 types of prey (Tables 1–2). Polychaetes were slightly more important in diets of males (48.4% IRI) than in females (44.5% IRI) (Tables 1–2, Fig. 2). The difference in numbers of identified prey in males and females is due to rare species occurring in some individuals.

Table 6

Percent frequency of occurrence (%F), percent of total number (%N), percent of total volume (%V), and index of relative importance (IRI) for food items of male and female *Cynoglossus arel* caught off Porto Novo, India, October 1981–September 1982. Size groups: 95–139 mm TL (*n* 10 ♂, *n* 15 ♀), and 140–184 mm TL (*n* 122 ♂, *n* 96 ♀) combined. *n* = number of stomachs analyzed; Crustacean fr. = crustacean fragments; UI = unidentified. (Data presented to one decimal point; 0.0 denotes value of <0.05, and dash denotes absence of food item.)

	Male (*n* 132)					Female (*n* 111)				
Food items	%F	%V	%N	IRI	%IRI	%F	%V	%N	IRI	%IRI
Polychaetes	27.7	62.8	30.7	2590.0	66.3	24.8	52.7	27.8	1996.4	62.7
Crustacean fr.	15.8	12.5	24.4	583.0	15.0	16.1	15.0	31.5	748.7	23.5
Prawns	14.9	15.9	10.4	391.9	10.0	11.2	10.7	7.5	203.8	6.4
Fish scales	10.9	1.7	17.0	203.8	5.2	9.9	0.4	3.8	41.6	1.3
Amphipods	12.4	0.9	8.6	117.8	3.1	11.8	0.7	7.5	96.8	3.0
Bivalves	2.0	1.5	1.4	5.8	0.2	3.8	2.2	2.3	17.1	0.5
Gastropods	2.0	0.1	0.6	1.4	0.0	2.5	0.2	1.5	4.3	0.1
Isopods	1.5	0.5	0.5	1.5	0.0	1.2	0.4	0.4	1.0	0.0
Copepods	1.5	0.0	0.6	0.9	0.0	2.5	0.0	1.3	3.3	0.1
Crabs	1.5	0.6	0.5	1.7	0.0	3.2	2.1	1.5	11.5	0.4
Fish	0.5	2.0	0.2	1.1	0.0	1.2	11.9	1.0	15.5	0.5
Fish bone	0.5	0.0	0.2	0.1	0.0	—	—	—	—	—
Fish spine	1.0	0.0	0.5	0.5	0.0	—	—	—	—	—
Fish egg	1.9	0.1	1.1	2.3	0.1	3.8	0.4	7.7	30.8	1.0
Squilla	—	—	—	—	—	0.6	0.0	0.2	0.1	0.0
Lingula sp.	1.0	0.5	1.1	1.6	0.0	1.2	1.5	2.9	5.3	0.2
Nematode	0.5	0.0	0.2	0.1	0.0	1.2	0.1	0.8	1.1	0.0
Algae	2.4	0.1	1.1	2.9	0.1	3.1	0.1	1.3	4.3	0.1
Brittle star	1.0	0.4	0.5	0.9	0.0	—	—	—	—	—
Echinoderm (UI)	0.5	0.2	0.2	0.2	0.0	—	—	—	—	—
Egg mass (UI)	0.5	0.2	0.2	0.2	0.0	—	—	—	—	—
Lucifer	—	—	—	—	—	1.9	1.6	1.0	4.9	0.2

Table 7

Percent frequency of occurrence (%F), percent of total number (%N), percent of total volume (%V), and index of relative importance (IRI) for food items of male and female *Cynoglossus arel* caught off Porto Novo, India, October 1981–September 1982. Size group: 185–229 mm TL (*n* 338 ♂, *n* 229 ♀). See Table 6 for abbreviations.

	Male (*n* 338)					Female (*n* 229)				
Food items	%F	%V	%N	IRI	%IRI	%F	%V	%N	IRI	%IRI
Polychaetes	28.2	57.5	30.5	2481.6	60.5	22.2	58.8	33.6	2051.3	58.8
Prawns	19.3	25.6	18.1	843.4	20.5	20.7	22.1	16.8	805.2	23.1
Crustacean fr.	14.7	8.6	18.2	394.0	9.6	14.2	7.9	18.0	367.8	10.5
Fish scales	13.6	1.7	18.1	269.3	6.6	12.4	0.6	7.1	95.5	2.8
Amphipods	11.6	0.7	7.3	92.8	2.3	12.4	0.8	9.3	125.2	3.6
Bivalves	3.3	1.4	1.5	9.6	0.2	2.3	3.5	4.0	17.3	0.5
Gastropods	0.4	0.0	0.1	0.0	0.0	1.2	0.3	2.6	3.5	0.1
Isopods	1.5	0.5	0.4	1.4	0.0	1.6	0.5	0.6	1.8	0.1
Copepods	1.3	0.0	0.4	0.5	0.0	1.2	0.0	0.3	0.4	0.0
Crabs	3.1	1.5	1.0	7.8	0.2	3.5	1.8	1.3	10.9	0.3
Fish	0.2	0.6	0.1	0.1	0.0	0.4	1.2	0.1	0.5	0.0
Fish egg	0.7	0.0	0.4	0.3	0.0	1.4	0.1	3.3	4.8	0.1
Squilla	–	–	–	–	–	0.4	0.2	0.1	0.1	0.0
Lingula sp.	0.6	1.6	3.4	3.0	0.1	0.8	0.2	0.5	0.5	0.0
Nematode	0.2	0.0	0.1	0.0	0.0	0.4	0.0	0.1	0.0	0.0
Algae	0.7	0.0	0.2	0.1	0.0	1.0	0.0	0.6	0.5	0.0
Egg mass (UI)	–	–	–	–	–	0.4	0.1	0.1	0.1	0.0
Lucifer	–	–	–	–	–	1.9	0.9	0.7	3.0	0.1
Sepia	–	–	–	–	–	0.2	0.1	0.1	0.0	0.0
Sand dollar	–	–	–	–	–	0.2	0.5	0.1	0.1	0.0
Tube-like worm	0.6	0.3	0.2	0.3	0.0	0.8	0.2	0.3	0.4	0.0
Jelly fish	–	–	–	–	–	0.2	0.1	0.1	0.0	0.0
Coscinodiscus	–	–	–	–	–	0.2	0.0	0.3	0.1	0.0

Food vs. fish size In *C. arel*, the dominant size-group in both sexes is 185–229 mm TL (54% of males, and 40% of females). Females in this size-group had eaten 23 types of prey, while males consumed only 16 types (Table 7). In the remaining size-groups of both sexes, there is no obvious difference in the number of prey types consumed (Tables 6, 8–9). In both sexes of *C. arel*, fish <275 mm TL preyed predominantly on polychaetes (55.1–66.3% IRI in males, 53.4–62.7% IRI in females), whereas in fish >275 mm TL the polychaetes were of lesser importance (10.5% IRI in females, <5.0% IRI in males), with fish remains being the most abundant (54.5% IRI in males, and 48.9% IRI in females) (Tables 6–9, and Fig. 3).

In both sexes of *C. lida*, fewer prey types were consumed by fish >200 mm TL (8–9 prey types) and by fish <136 mm TL (10–13 types), compared with fish 137–199 mm TL (16–19 types). Among fish <200 mm TL, polychaetes were the most abundant prey in both sexes (67.2–89.0% IRI in females, 61.0–81.5% IRI in males) (Tables 10–13, Fig. 4). Among the fish >200 mm TL, polychaetes were the most abundant prey only in females (90.2% IRI), whereas polychaetes were the second-most important prey in males (28.2% IRI) and prawns the most abundant prey (52.6% IRI) (Table 14, Fig. 4).

Seasonal variations in diet composition In male *C. arel*, polychaetes were dominant, except in February, May, and December (Table 1). During these 3 months, other prey items, viz, prawns (in May), crustacean fragments (in December), and fish remains (in February) were more important in the diet. In females, polychaetes also formed the primary food during 6 months (April, July, August, September, October, and December). In other months, prawns (January, March, May, and June), crustacean fragments (February), and fish remains (November) were the primary food consumed (Table 2).

In male *C. arel*, prawns were the secondary prey item for 6 months (February, June, July, August, September, and October), with polychaetes in May and December, crustacean fragments in March and April, and fish remains in January and November. In females, crustacean fragments were the secondary prey item for 5 months (January, March, April, May, and December), prawns for 3 months (July, September, and October), polychaetes for 2 months (June and November), and fish remains for 2 months (February and August). The tertiary food group in the diet of

Table 8

Percent frequency of occurrence (%F), percent of total number (%N), percent of total volume (%V), and index of relative importance (IRI) for food items of male and female *Cynoglossus arel* caught off Porto Novo, India, October 1981–September 1982. Size group: 230–274 mm TL (*n* 136 ♂, *n* 182 ♀). See Table 6 for abbreviations.

	Male (*n* 136)					Female (*n* 182)				
Food items	%F	%V	%N	IRI	%IRI	%F	%V	%N	IRI	%IRI
Polychaetes	23.2	46.8	21.7	1589.2	55.1	23.7	50.1	25.8	1798.8	53.4
Prawns	18.8	20.0	12.4	609.1	21.1	18.0	24.9	17.0	756.0	22.4
Crustacean fr.	14.8	10.0	18.6	423.3	14.7	17.3	11.9	24.5	629.7	18.7
Fish scales	10.3	0.5	3.6	42.2	1.5	10.7	0.5	4.9	57.8	1.7
Amphipods	11.8	1.1	6.3	87.3	3.0	10.5	0.4	3.8	44.1	1.3
Bivalves	3.3	3.0	2.8	19.1	0.7	2.7	1.0	1.0	5.4	0.2
Gastropods	2.6	0.1	0.6	1.8	0.1	1.6	0.0	0.3	0.5	0.0
Isopods	1.8	1.3	1.2	4.5	0.2	1.8	0.8	0.8	2.9	0.1
Copepods	1.5	0.0	0.3	0.5	0.0	–	–	–	–	–
Crabs	3.7	2.2	1.3	13.0	0.4	5.9	5.5	3.8	54.9	1.6
Fish	1.5	3.9	0.3	6.3	0.2	0.9	2.0	0.2	2.0	0.1
Fish bone	2.2	9.6	29.7	86.5	3.0	0.2	0.0	0.1	0.0	0.0
Fish spine	–	–	–	–	–	0.9	0.1	0.5	0.5	0.0
Fish egg	0.7	0.0	0.2	0.1	0.0	0.9	0.1	1.4	1.4	0.0
Squilla	1.1	0.6	0.2	0.9	0.0	0.9	0.5	0.3	0.7	0.0
Lingula sp.	0.4	0.0	0.1	0.0	0.0	0.9	1.3	3.0	3.9	0.1
Nematode	0.4	0.0	0.1	0.0	0.0	0.5	0.0	0.1	0.1	0.0
Algae	1.1	0.0	0.4	0.0	0.0	0.5	0.1	0.2	0.2	0.0
Egg mass (UI)	–	–	–	–	–	0.9	0.1	11.8	10.7	0.4
Lucifer	–	–	–	–	–	0.5	0.1	0.1	0.1	0.0
Sand dollar	0.4	0.8	0.1	0.4	0.0	–	–	–	–	–
Tube-like worm	0.4	0.1	0.1	0.1	0.0	–	–	–	–	–
Coscinodiscus	–	–	–	–	–	0.2	0.0	0.1	0.0	0.0
Brittle star	–	–	–	–	–	0.5	0.6	0.3	0.5	0.0

Table 9

Percent frequency of occurrence (%F), percent of total number (%N), percent of total volume (%V), and index of relative importance (IRI) for food items of male and female *Cynoglossus arel* caught off Porto Novo, India, October 1981–September 1982. Size groups: 275–319 mm TL (*n* 12 ♂, *n* 24 ♀); 320–364 mm TL (*n* 9 ♂, *n* 8 ♀); 365–409 mm TL (*n* 0 ♂, *n* 9 ♀), and 410–454 mm TL (*n* 0 ♂, *n* 6 ♀) combined. See Table 6 for abbreviations.

	Male (*n* 21)					Female (*n* 47)				
Food items	%F	%V	%N	IRI	%IRI	%F	%V	%N	IRI	%IRI
Fish scales	13.9	31.2	66.3	1355.3	54.5	15.3	23.4	60.8	1288.3	48.9
Prawns	20.8	19.2	2.7	455.5	18.3	18.5	16.9	2.9	366.3	13.9
Crustacean fr.	25.0	11.6	4.9	412.5	16.6	16.1	19.6	10.2	479.8	18.2
Polychaetes	11.1	8.4	0.9	103.2	4.2	14.5	16.9	2.2	277.0	10.5
Amphipods	5.6	4.5	0.2	26.3	1.1	4.0	0.1	0.2	1.2	0.0
Bivalves	–	–	–	–	–	3.3	0.5	0.1	2.0	0.1
Gastropods	–	–	–	–	–	1.6	0.0	0.0	0.0	0.0
Isopods	4.2	0.7	0.2	3.8	0.2	0.8	0.1	0.0	0.1	0.0
Copepods	–	–	–	–	–	1.6	0.1	3.0	5.0	0.2
Crabs	5.5	1.5	0.2	9.4	0.0	6.5	2.0	0.3	15.0	0.6
Fish	4.2	10.1	0.2	43.3	1.8	7.3	10.8	0.3	81.0	3.1
Fish bone	1.4	5.0	10.8	22.1	1.0	2.4	0.1	0.1	0.5	0.0
Fish spine	2.7	7.5	12.7	54.5	2.2	4.0	9.5	19.8	117.2	4.5
Fish egg	–	–	–	–	–	0.8	0.0	0.0	0.0	0.0
Squilla	1.4	0.3	0.0	0.4	0.0	–	–	–	–	–
Nematode	1.4	0.0	0.0	0.0	0.0	3.3	0.0	0.1	0.3	0.0
Algae	1.4	0.0	0.0	0.0	0.0	–	–	–	–	–
Coscinodiscus	1.4	0.0	0.9	1.3	0.1	–	–	–	–	–

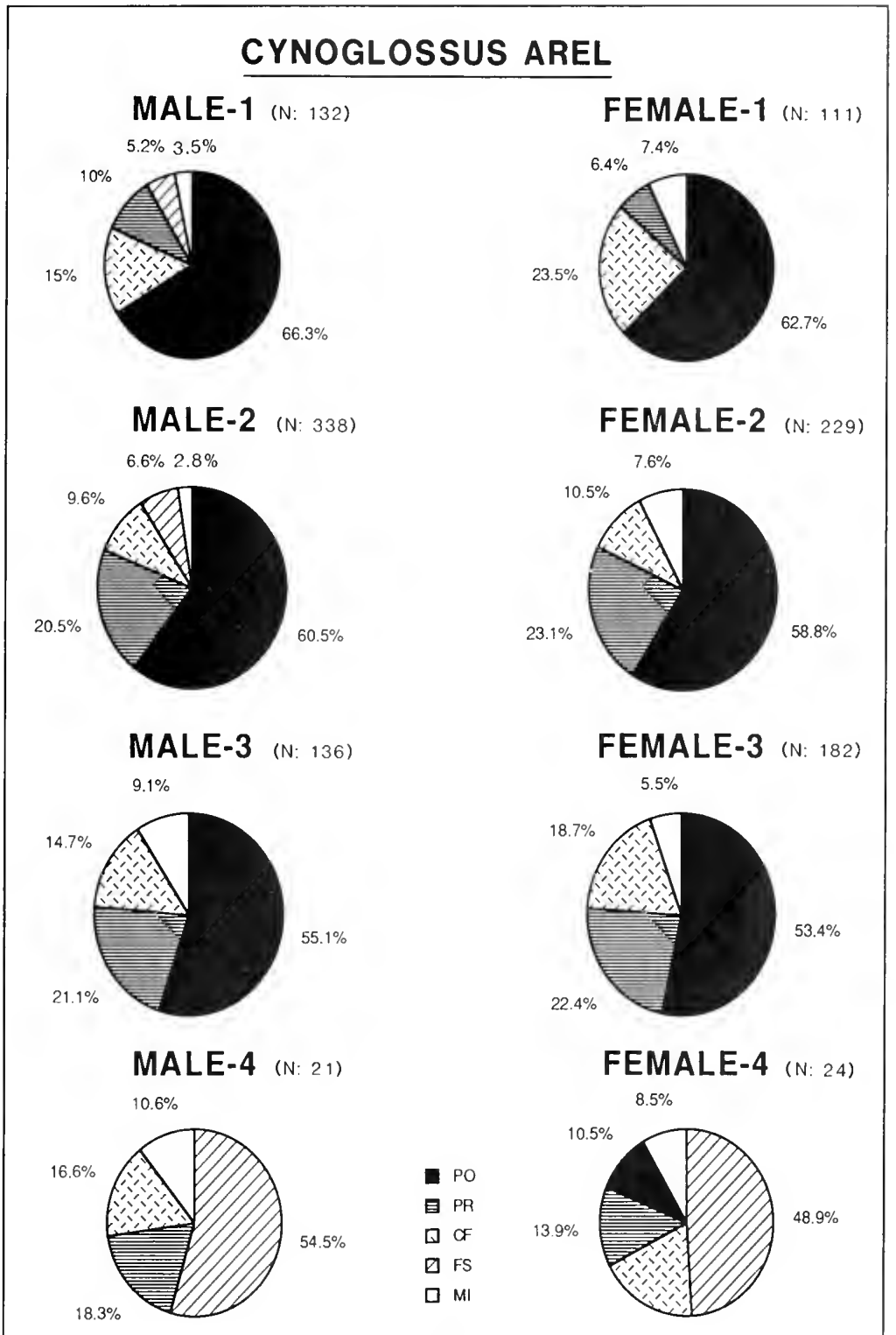

Figure 3

Percentage contribution of food items to the diet of various size groups of male and female *Cynoglossus arel* caught commercially off Porto Novo, India, October 1981–September 1982. Male-1 (*n* 132) and Female-1 (*n* 111) = size group 95–184 mm TL; Male-2 (*n* 338) and Female-2 (*n* 229) = 185–229 mm TL; Male-3 (*n* 136) and Female-3 (*n* 182) = 230–274 mm TL; Male-4 (*n* 21) = 275–364 mm TL; and Female-4 (*n* 47) = 275–454 mm TL. Only values >5% IRI are individually shown; values <5% IRI are clumped together into a single category, the unshaded wedge of the pie chart. PO = polychaetes, PR = prawns, CF = crustacean fragments, FS = fish scales, MI = miscellaneous.

Table 10

Percent frequency of occurrence (%F), percent of total number (%N), percent of total volume (%V), and index of relative importance (IRI) for food items of male and female *Cynoglossus lida* caught off Porto Novo, India, October 1981–September 1982. Size groups: 95–115 mm TL (*n* 6 ♂, *n* 13 ♀), and 116–136 mm TL (*n* 85 ♂, *n* 56 ♀) combined. *n* = number of stomachs analyzed; Crustacean fr. = crustacean fragments. (Data presented to one decimal point; 0.0 denotes value of <0.05, and dash denotes absence of food item.)

	Male (*n* 91)					Female (*n* 69)				
Food items	%F	%V	%N	IRI	%IRI	%F	%V	%N	IRI	%IRI
Polychaetes	29.0	73.4	42.6	3364.0	81.5	30.4	66.2	35.4	3088.6	70.2
Prawns	16.9	10.9	8.5	327.9	8.0	17.4	13.8	9.9	412.4	9.4
Crustacean fr.	8.9	8.4	19.6	249.2	6.1	13.0	16.2	34.5	659.1	15.0
Fish scales	13.0	0.8	9.0	22.1	0.5	10.9	0.4	4.3	51.2	1.2
Amphipods	13.0	0.6	6.7	94.9	2.3	17.4	0.8	8.1	154.9	3.5
Bivalves	–	–	–	–	–	1.1	0.3	0.3	0.7	0.0
Isopods	1.6	0.5	0.5	1.6	0.0	1.1	0.3	0.3	0.7	0.0
Copepods	1.6	0.0	0.5	0.8	0.0	–	–	–	–	–
Crabs	2.4	1.7	1.3	7.2	0.2	–	–	–	–	–
Fish egg	2.4	0.1	1.3	3.4	0.1	1.1	0.0	0.9	1.0	0.0
Lingula sp.	4.0	2.2	5.0	28.8	0.7	3.3	1.9	4.1	19.8	0.5
Algae	5.6	0.2	4.2	24.6	0.6	4.3	0.1	2.2	9.9	0.2
Lucifer	0.8	0.3	0.3	0.5	0.0	–	–	–	–	–
Brittle star	0.8	0.9	0.5	1.1	0.0	–	–	–	–	–

Table 11

Percent frequency of occurrence (%F), percent of total number (%N), percent of total volume (%V), and index of relative importance (IRI) for food items of male and female *Cynoglossus lida* caught off Porto Novo, India, October 1981–September 1982. Size group: 137–157 mm TL (*n* 211 ♂, *n* 136 ♀). See Table 10 for abbreviations.

	Male (*n* 211)					Female (*n* 136)				
Food items	%F	%V	%N	IRI	%IRI	%F	%V	%N	IRI	%IRI
Polychaetes	25.5	61.7	28.4	2297.6	61.0	30.0	62.0	29.9	2757.0	67.2
Crustacean fr.	15.3	16.7	30.7	725.2	19.2	15.5	16.5	31.8	748.7	18.3
Prawns	15.6	13.6	8.3	341.6	9.1	14.5	17.0	10.9	404.6	9.9
Fish scales	16.3	1.4	12.8	231.5	6.1	11.4	0.5	5.2	65.0	1.6
Amphipods	12.3	1.1	10.5	142.7	3.9	13.6	0.6	5.5	83.0	2.0
Bivalves	1.8	0.8	0.7	2.7	0.1	1.8	0.7	0.7	2.5	0.1
Gastropods	0.3	0.0	0.1	0.0	0.0	0.9	0.0	0.2	0.2	0.0
Isopods	0.9	0.4	0.4	0.7	0.0	1.4	0.4	0.4	1.1	0.0
Copepods	0.9	0.0	0.6	0.5	0.0	0.9	0.0	0.3	0.3	0.0
Crabs	1.3	0.7	0.4	1.4	0.0	0.9	0.7	0.5	1.1	0.0
Fish	0.3	1.1	0.1	0.4	0.0	–	–	–	–	–
Fish spine	0.3	0.0	0.2	0.1	0.0	–	–	–	–	–
Fish egg	0.6	0.0	0.2	0.1	0.0	2.3	0.5	9.7	23.5	0.6
Squilla	–	–	–	–	–	0.4	0.2	0.1	0.1	0.0
Lingula sp.	0.9	1.0	2.0	2.7	0.1	1.4	0.7	1.3	2.8	0.1
Nematode	0.3	0.0	0.1	0.0	0.0	1.4	0.0	0.5	0.7	0.0
Algae	5.3	0.2	3.3	18.6	0.5	3.2	0.2	2.9	9.9	0.2
Lucifer	0.9	0.4	0.2	0.5	0.0	–	–	–	–	–
Coelenterate	0.9	0.7	0.9	1.4	0.0	–	–	–	–	–
Coscinodiscus	–	–	–	–	–	0.4	0.0	0.1	0.0	0.0
Tape worm	0.3	0.2	0.1	0.1	0.0	–	–	–	–	–

Table 12

Percent frequency of occurrence (%F), percent of total number (%N), percent of total volume (%V), and index of relative importance (IRI) for food items of male and female *Cynoglossus lida* caught off Porto Novo, India, October 1981–September 1982. Size group: 158–178 mm TL (*n* 284 ♂, *n* 260 ♀). See Table 10 for abbreviations.

	Male (*n* 284)					Female (*n* 260)				
Food items	%F	%V	%N	IRI	%IRI	%F	%V	%N	IRI	%IRI
Polychaetes	29.0	61.2	28.4	2598.4	67.4	32.2	75.9	47.4	3970.3	81.3
Crustacean fr.	11.2	16.2	30.1	518.6	13.5	10.7	8.2	20.4	306.0	6.3
Prawns	16.2	14.9	9.2	390.4	10.1	18.3	12.5	10.4	419.1	8.6
Fish scales	14.9	1.4	12.7	210.1	5.6	8.9	0.4	4.4	42.7	0.8
Amphipods	9.7	0.8	7.1	76.6	2.0	14.7	0.6	8.1	127.9	2.6
Bivalves	0.5	0.4	0.4	0.4	0.0	2.5	0.7	0.9	4.0	0.1
Gastropods	2.6	0.2	1.2	3.6	0.1	1.4	0.1	0.5	0.8	0.0
Isopods	–	–	–	–	–	0.5	0.1	0.1	0.1	0.0
Copepods	0.8	0.0	0.2	0.2	0.0	0.8	0.0	0.3	0.2	0.0
Crabs	1.3	0.6	0.4	1.3	0.0	1.3	0.3	0.3	0.8	0.0
Fish spine	0.3	0.0	0.2	0.1	0.0	–	–	–	–	–
Fish egg	1.3	0.0	0.5	0.7	0.0	1.4	0.1	3.1	4.5	0.1
Squilla	0.5	0.5	0.2	0.4	0.0	1.0	0.4	0.3	0.7	0.0
Lingula sp.	0.5	0.1	0.2	0.2	0.0	0.8	0.4	1.0	1.1	0.0
Nematode	0.8	0.0	0.2	0.2	0.0	1.0	0.0	0.5	0.5	0.0
Algae	7.2	0.3	4.7	36.0	0.9	3.6	0.1	2.0	7.6	0.2
Egg mass (UI)	0.3	0.1	0.1	0.1	0.0	0.3	0.1	0.1	0.1	0.0
Coelenterate	2.1	3.2	3.9	14.9	0.4	0.3	0.1	0.1	0.1	0.0
Coscinodiscus	0.5	0.0	0.2	0.1	0.0	0.3	0.0	0.1	0.0	0.0
Octopus sp.	0.3	0.1	0.1	0.1	0.0	–	–	–	–	–

Table 13

Percent frequency of occurrence (%F), percent of total number (%N), percent of total volume (%V), and index of relative importance (IRI) for food items of male and female *Cynoglossus lida* caught off Porto Novo, India, October 1981–September 1982. Size group: 179–199 mm TL (*n* 111 ♂, *n* 144 ♀). See Table 10 for abbreviations.

	Male (*n* 111)					Female (*n* 144)				
Food items	%F	%V	%N	IRI	%IRI	%F	%V	%N	IRI	%IRI
Polychaetes	31.8	60.0	33.7	2979.7	70.8	35.7	82.4	56.5	4958.7	89.0
Prawns	20.6	16.9	12.6	607.7	14.4	14.9	9.1	8.3	259.3	4.7
Crustacean fr.	11.2	12.8	28.8	465.9	11.1	10.0	5.4	14.9	203.0	3.6
Fish scales	10.6	0.5	6.0	68.9	1.6	10.0	0.3	3.5	38.0	0.7
Amphipods	10.0	0.4	4.7	51.0	1.2	13.1	0.5	6.6	93.0	1.7
Bivalves	1.2	0.4	0.5	1.1	0.2	2.3	0.5	0.6	2.5	0.0
Gastropods	0.6	0.0	0.2	0.1	0.0	1.4	0.2	1.5	2.4	0.0
Isopods	1.2	0.3	0.3	0.7	0.0	3.2	0.5	0.7	3.8	0.1
Copepods	1.2	0.0	0.3	0.4	0.0	0.4	0.0	0.1	0.0	0.0
Crabs	1.2	0.4	0.3	0.8	0.0	1.4	0.3	0.3	0.8	0.0
Fish	0.5	1.8	0.2	1.0	0.0	–	–	–	–	–
Fish spine	–	–	–	–	–	0.4	0.0	0.2	0.1	0.0
Fish egg	1.8	0.0	0.5	0.9	0.0	2.3	0.1	2.8	6.7	0.1
Lingula sp.	–	–	–	–	–	0.4	0.6	1.8	1.0	0.0
Nematode	1.2	0.0	0.3	0.4	0.0	0.9	0.0	0.2	0.2	0.0
Algae	4.7	0.1	2.8	13.6	0.3	2.7	0.1	1.6	4.6	0.1
Lucifer	0.5	0.4	0.3	0.4	0.0	–	–	–	–	–
Coelenterate	1.2	6.0	8.3	17.2	0.4	–	–	–	–	–
Coscinodiscus	0.5	0.0	0.2	0.1	0.0	0.9	0.0	0.4	0.4	0.0

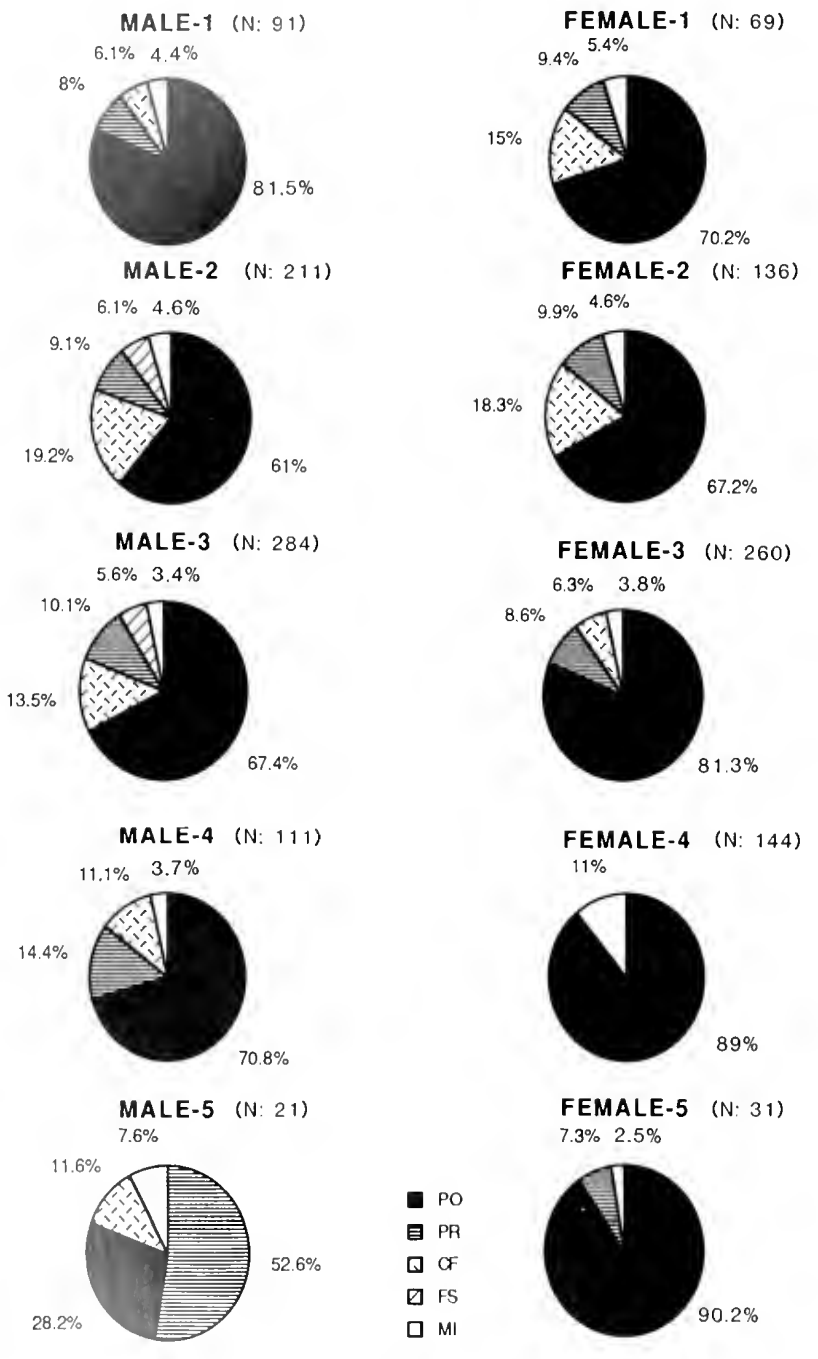

Figure 4

Percentage contribution of food items to the diet of various size groups of male and female *Cynoglossus lida* caught commercially off Porto Novo, India, October 1981–September 1982. Male-1 (n 91) and Female-1 (n 69) = size group 95–136 mm TL; Male-2 (n 211) and Female-2 (n 136) = 137–157 mm TL; Male-3 (n 284) and Female-3 (n 260) = 158–178 mm TL; Male-4 (n 111) and Female-4 (n 144) = 179–199 mm TL; and Male-5 (n 21) and Female-5 (n 31) = 200–262 mm TL. Only values >5% IRI are individually shown; values <5% IRI are clumped together into a single category, the unshaded wedge of the pie chart. PO = polychaetes, PR = prawns, CF = crustacean fragments, FS = fish scales, MI = miscellaneous.

male and female *C. arel* is shown in Figure 5. All other food items occurred sporadically (Tables 1–2).

In male *C. lida*, polychaetes were the dominant prey for 9 months (Table 3). In the remaining months, crustacean fragments (January and December) and prawns (May) dominated. In females, polychaetes were the primary food item for every month, except in January and December when crustacean fragments were the most important prey item (Table 4).

Prawns were next in importance in both sexes of *C. lida*. In males, prawns formed the secondary prey item except in February, May, July, October, and December. During these 5 months, fish remains (February, October, and December), polychaetes (May), and amphipods (July) were the secondary prey. In females, prawns were the secondary food, except in August and October–December. During these 4 months, amphipods (August and November), fish remains (October), and fish eggs (December) were consumed by females. The tertiary food group in the diet of male and female *C. lida* is shown in Figure 5. Organisms of lesser importance are listed in Tables 3–4.

Gastro- (GI) and hepatosomatic (HI) indices and occurrence of empty stomachs in relation to spawning In male *C. arel*, a peak occurrence of empty stomachs (Fig. 6) occurred in January, which is the peak spawning period. Lowest gastro- and hepatosomatic indices were also observed in January (Fig. 6). However, over the rest of the year, these factors did not appear to be related. The gastro- and hepatosomatic indices did not track the percentage occurrence of empty stomachs throughout the year.

Table 14

Percent frequency of occurrence (%F), percent of total number (%N), percent of total volume (%V), and index of relative importance (IRI) for food items of male and female *Cynoglossus lida* caught off Porto Novo, India, October 1981–September 1982. Size groups: 200–220 mm TL (*n* 19 ♂, *n* 27 ♀); 221–241 mm TL (*n* 1 ♂, *n* 3 ♀), and 242–262 mm TL (*n* 1 ♂, *n* 1 ♀) combined. See Table 10 for abbrevations.

	Male (*n* 21)					Female (*n* 31)				
Food items	%F	%V	%N	IRI	%IRI	%F	%V	%N	IRI	%IRI
Polychaetes	25.0	25.7	16.4	1052.5	28.2	39.1	84.8	70.8	6084.0	90.2
Prawns	25.0	42.5	36.1	1965.0	52.6	21.7	10.7	11.9	490.4	7.3
Crustacean fr.	10.0	12.2	31.1	433.0	11.6	10.9	1.8	6.2	87.2	1.3
Fish scales	10.0	0.3	3.4	37.0	1.0	8.7	0.1	2.3	20.9	0.3
Amphipods	15.0	0.6	8.2	132.0	3.4	8.7	0.3	4.2	39.2	0.5
Bivalves	—	—	—	—	—	4.3	2.1	3.4	23.7	0.4
Isopods	5.0	1.3	1.6	14.5	0.4	—	—	—	—	—
Copepods	—	—	—	—	—	2.2	0.0	0.4	0.9	0.0
Crabs	5.0	2.0	1.6	18.0	0.5	—	—	—	—	—
Fish	5.0	15.4	1.6	85.0	2.3	—	—	—	—	—
Lingula sp.	—	—	—	—	—	2.2	0.2	0.4	1.3	0.0
Nematode	—	—	—	—	—	2.2	0.0	0.4	0.9	0.0

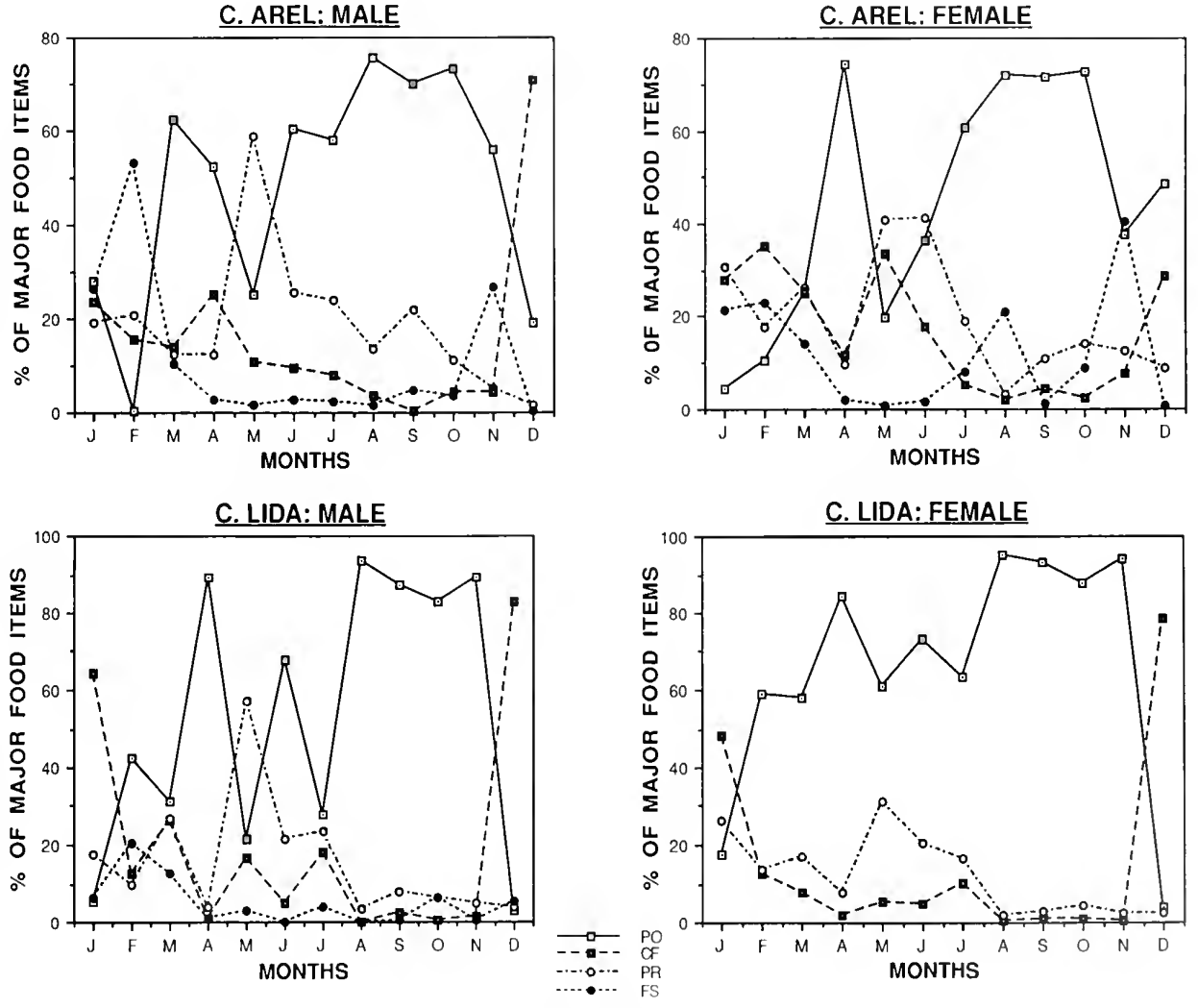

Figure 5

Seasonal variations in percentage contribution of major food items to the diet of male and female *Cynoglossus arel* and *C. lida* caught commercially off Porto Novo, India, October 1981–September 1982. Only values >5% IRI value are graphed. (Refer to Appendix for monthly sample size). PO = polychaetes, CF = crustacean fragments, PR = prawns, FS = fish scales.

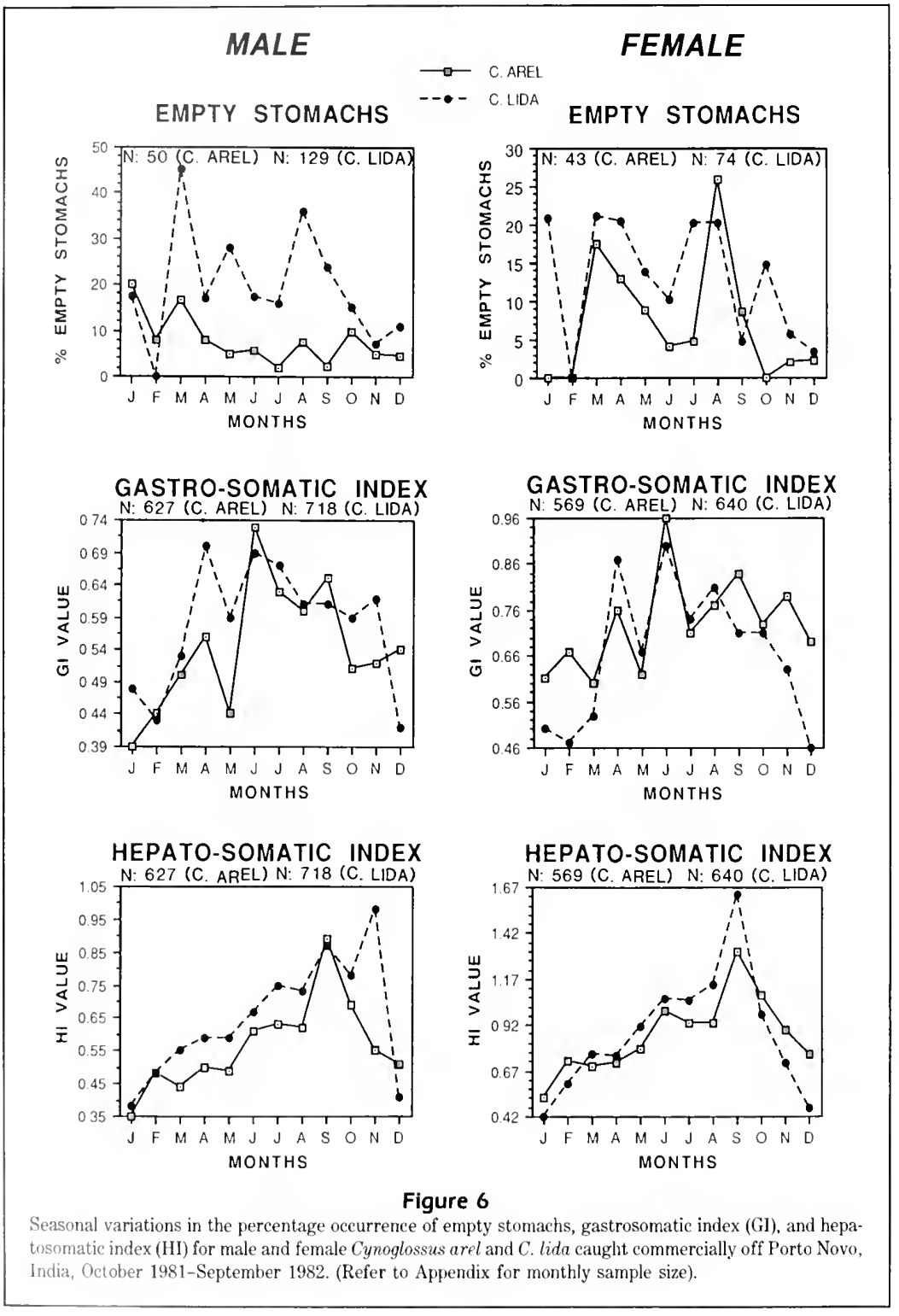

Figure 6

Seasonal variations in the percentage occurrence of empty stomachs, gastrosomatic index (GI), and hepatosomatic index (HI) for male and female *Cynoglossus arel* and *C. lida* caught commercially off Porto Novo, India, October 1981–September 1982. (Refer to Appendix for monthly sample size).

In female *C. arel*, occurrence of empty stomachs did not correspond with spawning. However, the lowest values of gastro- and hepatosomatic indices were recorded (Fig. 6) only during the peak spawning period (in January).

In both sexes of *C. lida*, gastro-/hepatosomatic indices and the occurrence of empty stomachs did not reveal any relationship (Fig. 6) with peak spawning activities (in September) of this species.

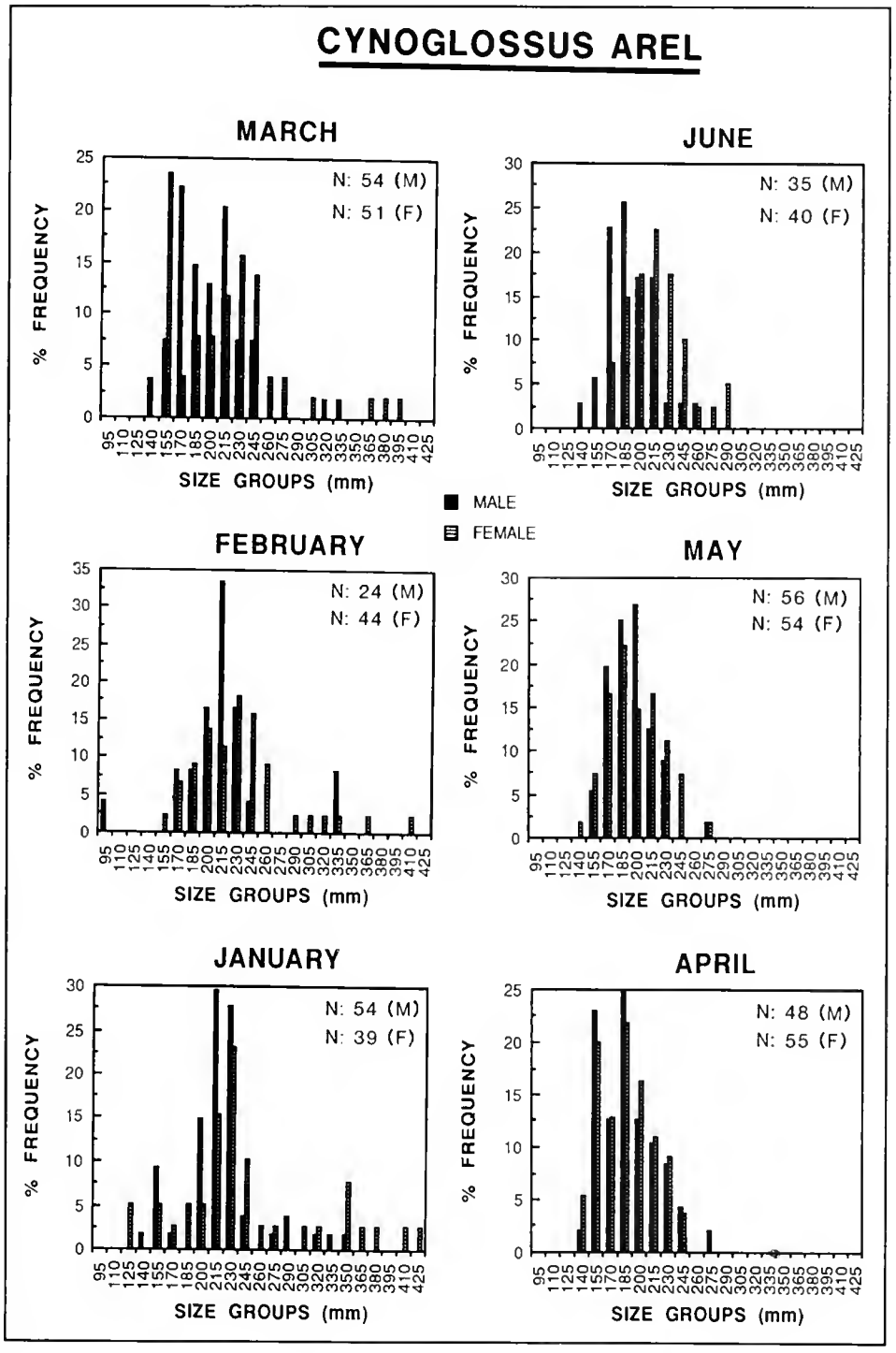

Figure 7A
Size-frequency histograms for male (M) and female (F) *Cynoglossus arel* (January–June) caught commercially off Porto Novo, India, October 1981–September 1982.

Age and growth

Petersen method Progression of modes in the length-frequency data could be traced for both sexes of *C. arel* and *C. lida* (Figs. 7,8).

In male *C. arel* (Fig. 7), the first mode was the 155–169 mm length-group in January. A progressive shift during subsequent months until October, to the 290–304 mm length-group, indicated a growth of 135 mm in 9 months. Assuming the same rate of growth, a fish would attain a length of 180 mm in the first year. Beyond November, it was not possible to trace length-groups.

In female *C. arel* (Fig. 7), the first mode was the 125–139 mm length-group in September. A progressive shift during subsequent months until March, to the 230–240 mm length-group, indicated a growth of 105 mm in 6 months. Groups could not be traced beyond April. At the same rate of growth, a fish would have

Figure 7B
Size-frequency histograms for male (M) and female (F) *Cynoglossus arel* (July–December) caught commercially off Porto Novo, India, October 1981–September 1982.

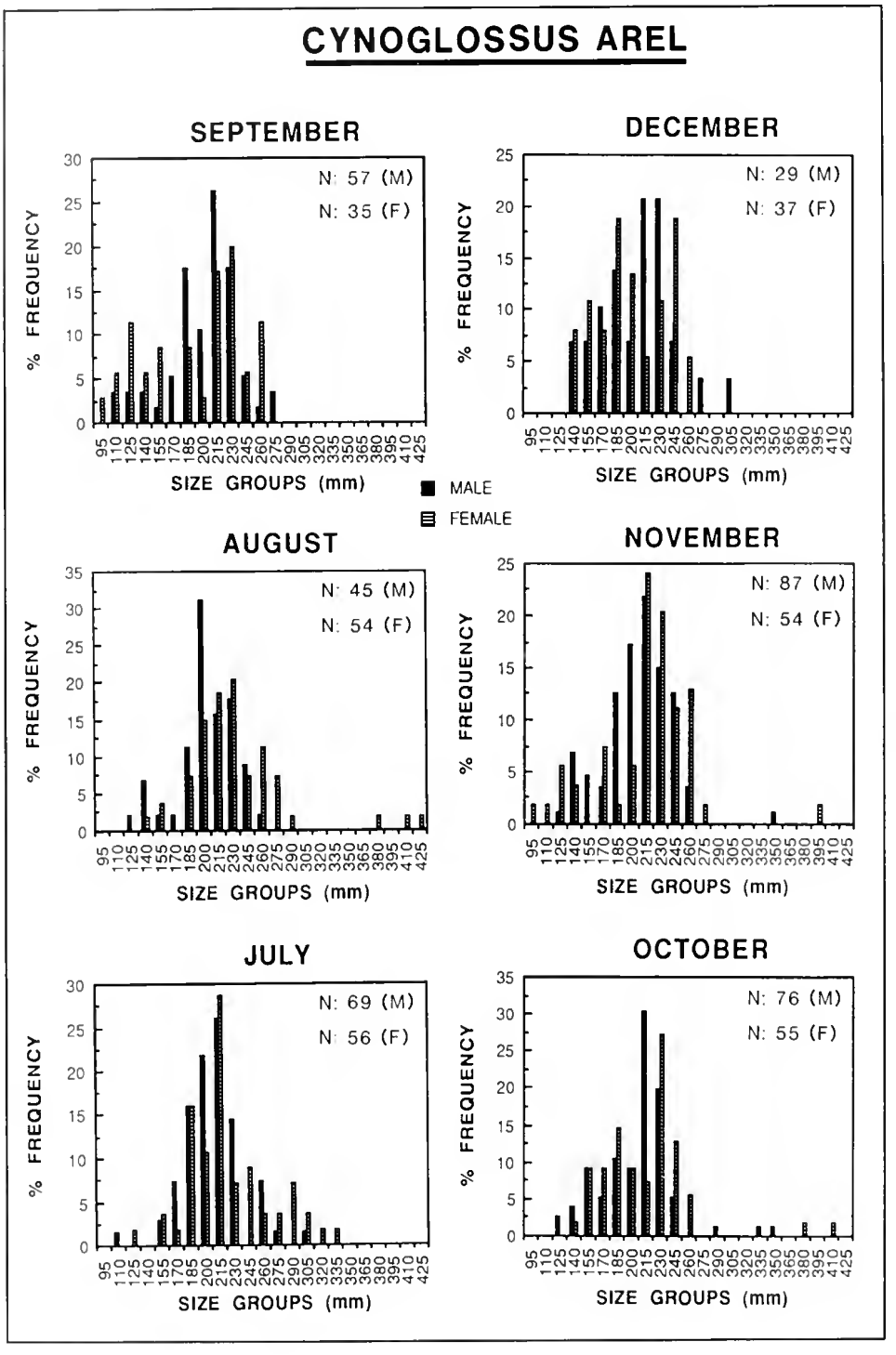

attained a length of 210 mm in the first year. There was another mode at the 200–214 mm length-group during February. A progressive shift of this mode during subsequent months until November, to the 260–274 mm length-group, indicated a growth of 60 mm in 9 months. Groups could not be traced beyond December. Based on this rate of growth, a fish would reach 290 mm at the end of the second year. Because of poorer representation in older size-groups, later modes were not traced.

In male *C. lida* (Fig. 8), the first mode was the 102–108 mm size-group in November. This was traced to the 179–185 mm size-group in May, 77 mm of growth in 6 months. Length-groups could not be traced beyond June. At this rate, a fish would be 154 mm at the end of the first year. The mode at the 151–157 mm size-group in March was traced to the 179–185 mm size-group in November, 28 mm growth in 8 months. At this rate of growth, a fish at the end of the second

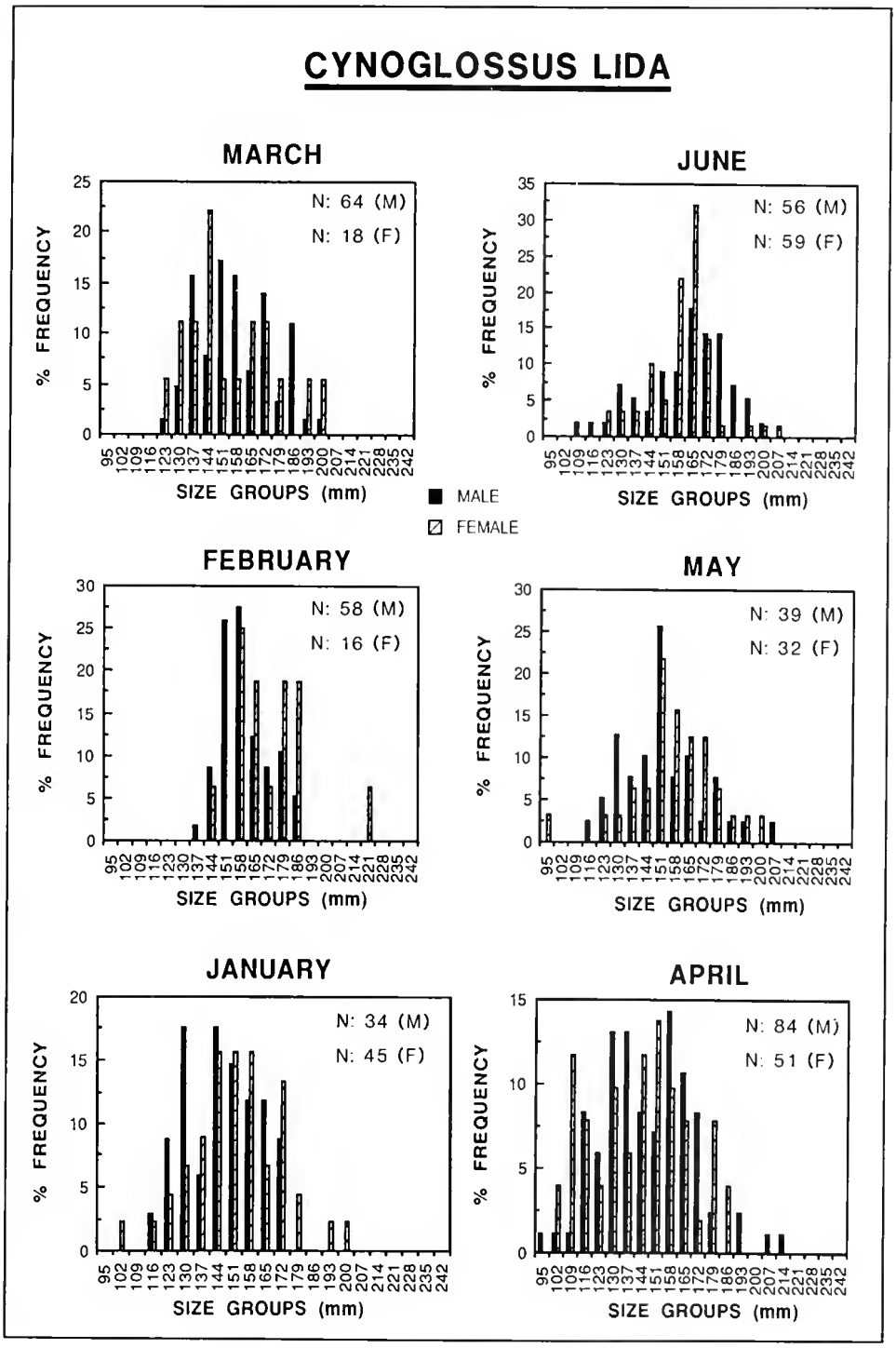

Figure 8A
Size-frequency histograms for male (M) and female (F) *Cynoglossus lida* (January–June) caught commercially off Porto Novo, India, October 1981–September 1982.

year would be 196mm. Further modes could not be traced.

In female *C. lida* (Fig. 8), the first mode was the 102–108mm size-group in November. This was traced to the 193–199mm size-group in June, 91mm growth in 7 months. At this rate, a fish would be 156mm in the first year. The mode at the 151–157mm size-group in January was traced back to the 193–199mm size-group in January, 42mm growth in 12 months. A fish would be 198mm at the end of the second year. The mode at the 193–199mm size-group in May was traced to the 207–213mm size-group in December, 14mm growth in 7 months. At this rate, a fish at the end of the third year would be 222mm.

The rate of growth from the time of hatching and throughout the first year would be more rapid than that of the older year-classes.

Figure 8B
Size-frequency histograms for male (M) and female (F) *Cynoglossus lida* (July–December) caught commercially off Porto Novo, India, October 1981–September 1982.

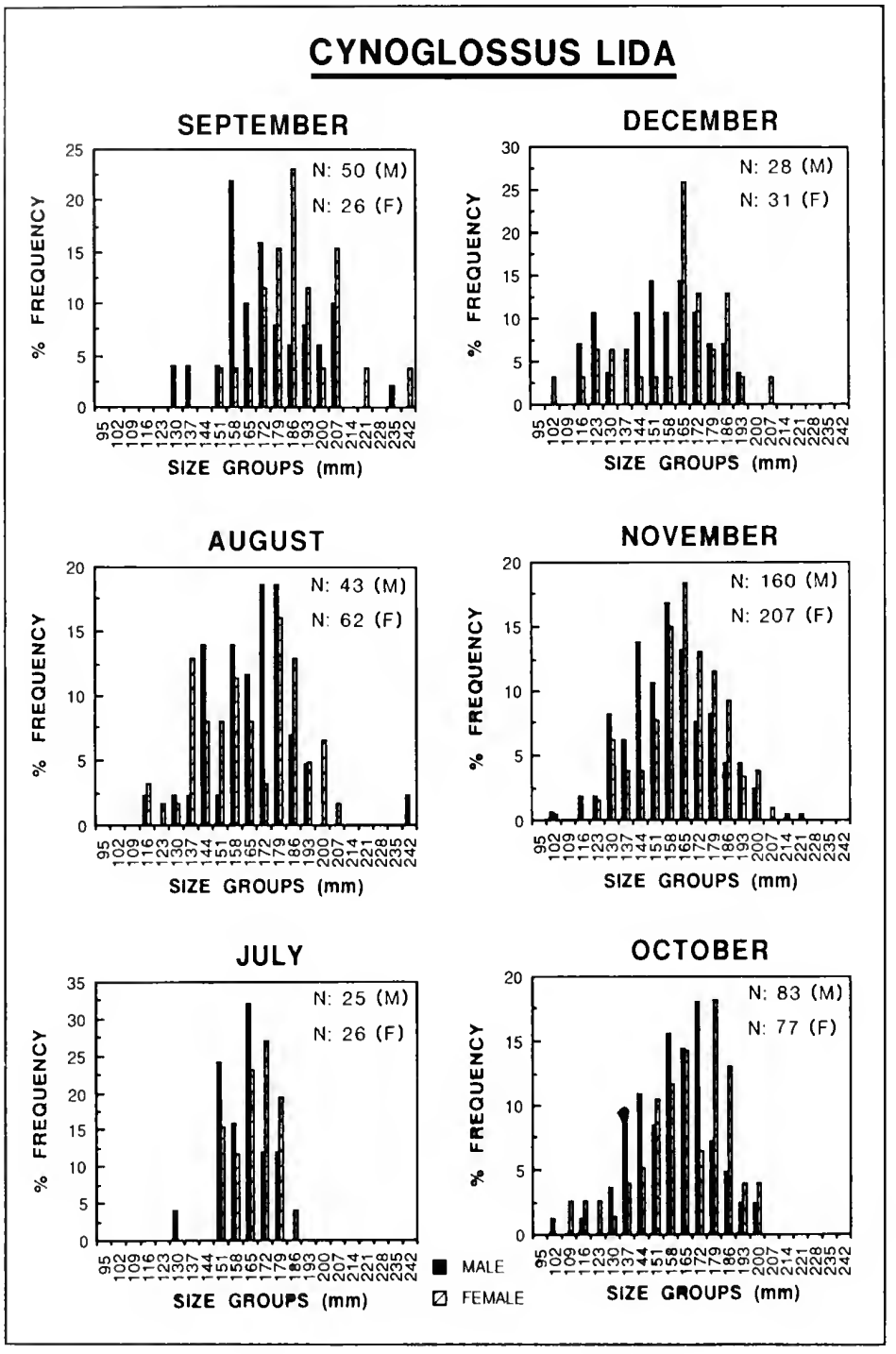

Probability plot method Cumulative percentage distribution of lengths was calculated for *C. arel* and *C. lida*, and plotted against the midpoints of length-groups on probability paper (Fig. 9I, J). These points formed approximately straight lines, but slight deviations could be recognized. Based on the probability plots, male *C. arel* attained 194 mm, 272 mm, and 333 mm in the 1st, 2d, and 3d years, respectively, while females reached 201, 312, and 393 mm for these years. In *C. lida*, males attained 151, 188, and 218 mm, while females reached 153, 188, and 216 mm, in the 1st, 2d, and 3d years, respectively.

von Bertalanffy's equation Plots of $L_t + 1$ against L_t, showing a straight-line relationship for *C. arel* and *C. lida*, were drawn. A least-square line was then fitted and an estimate of L_∞ was obtained (Fig. 9A, C, E, G). By this Ford-Walford graph, L_∞ was 570 mm for male

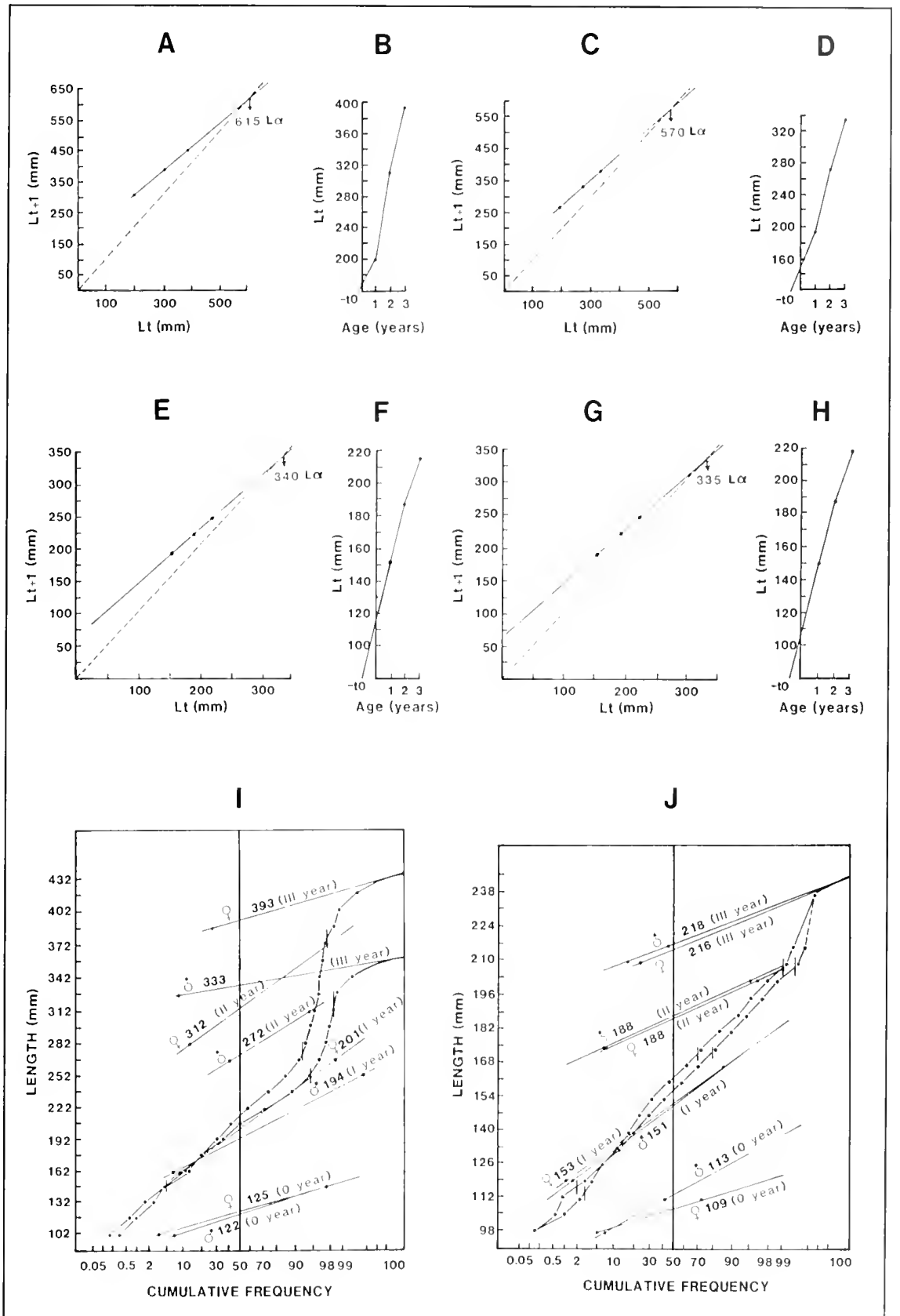

Figure 9

Age and growth of *Cynoglossus arel* and *C. lida* caught commercially off Porto Novo, India, October 1981–September 1982. Ford-Walford plot for female (A) and male (C) *C. arel*, and for female (E) and male (G) *C. lida*; theoretical growth curve for female (B) and male (D) *C. arel*, and female (F) and male (H) *C. lida*; probability plot for male and female *C. arel* (I) and *C. lida (J).*

and 615 mm for female *C. arel*; 335 mm for male and 340 mm for female *C. lida*.

Based on values obtained, the von Bertalanffy's equations are:

C. arel

Male $L_t = 570(1-e^{-0.2376(t+0.7753)})$

Female $L_t = 615(1-e^{-0.3151(t+0.2645)})$

C. lida

Male $L_t = 335(1-e^{-0.2326(t+1.6348)})$

Female $L_t = 340(1-e^{-0.2231(t+1.8029)})$

Male *C. arel* reached 194, 272, and 333 mm in the 1st, 2d, and 3d years, respectively (Fig. 9D), while females attained a length of 201, 312, and 393 mm for the 1st, 2d, and 3d years, respectively (Fig. 9B). Male *C. lida* reached 151, 188, and 218 mm (Fig. 9H), while females attained lengths of 153, 188, and 216 mm in the 1st, 2d, and 3d years, respectively (Fig. 9F).

Estimates of age and growth, based on the three different methods, are presented in Table 15.

Length-weight relationships

The linear relationships in logarithmic values of length and weight for males, females, and juveniles are shown in Figure 10A. These were typical length-weight relationships in which length increase is rapid initially, but later slows down with a corresponding increase in weight. Correlation coefficient values (r) are highly significant as follows:

Table 15

Mean length (mm) attained in different years of life (per 3 methods) by *Cynoglossus arel* and *C. lida* caught commercially off Porto Novo, India, October 1981–September 1982.

Species		Year	Method: Petersen	Method: Probability plot	Method: von Bertalanffy
Cynoglossus arel	Male	I	180	194	194
		II	—	272	272
		III	—	333	333
	Female	I	210	201	201
		II	290	312	312
		III	—	393	393
Cynoglossus lida	Male	I	154	151	151
		II	196	188	188
		III	—	218	218
	Female	I	156	153	153
		II	198	188	188
		III	222	216	216

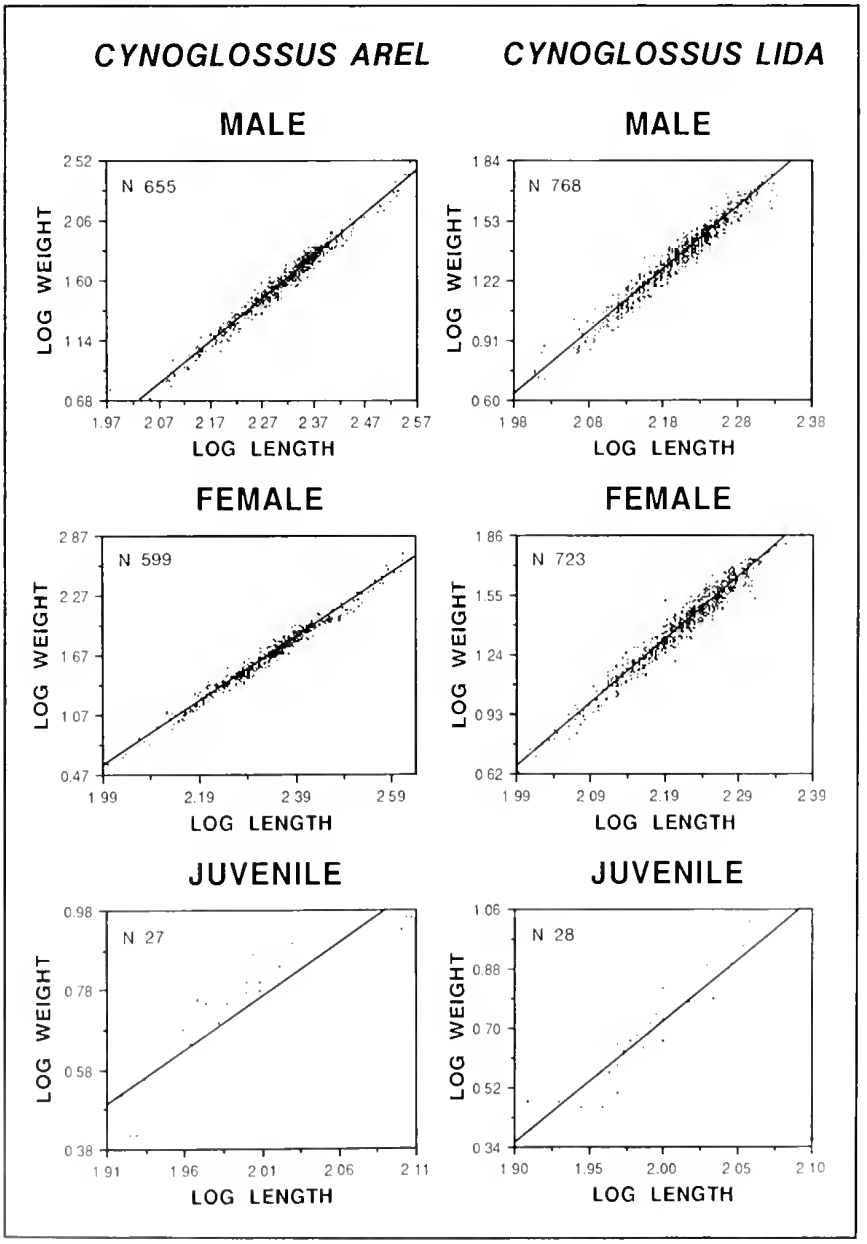

Figure 10A

Length-weight relationships for male, female, and juvenile *Cynoglossus arel* and *C. lida* caught commercially off Porto Novo, India, October 1981–September 1982.

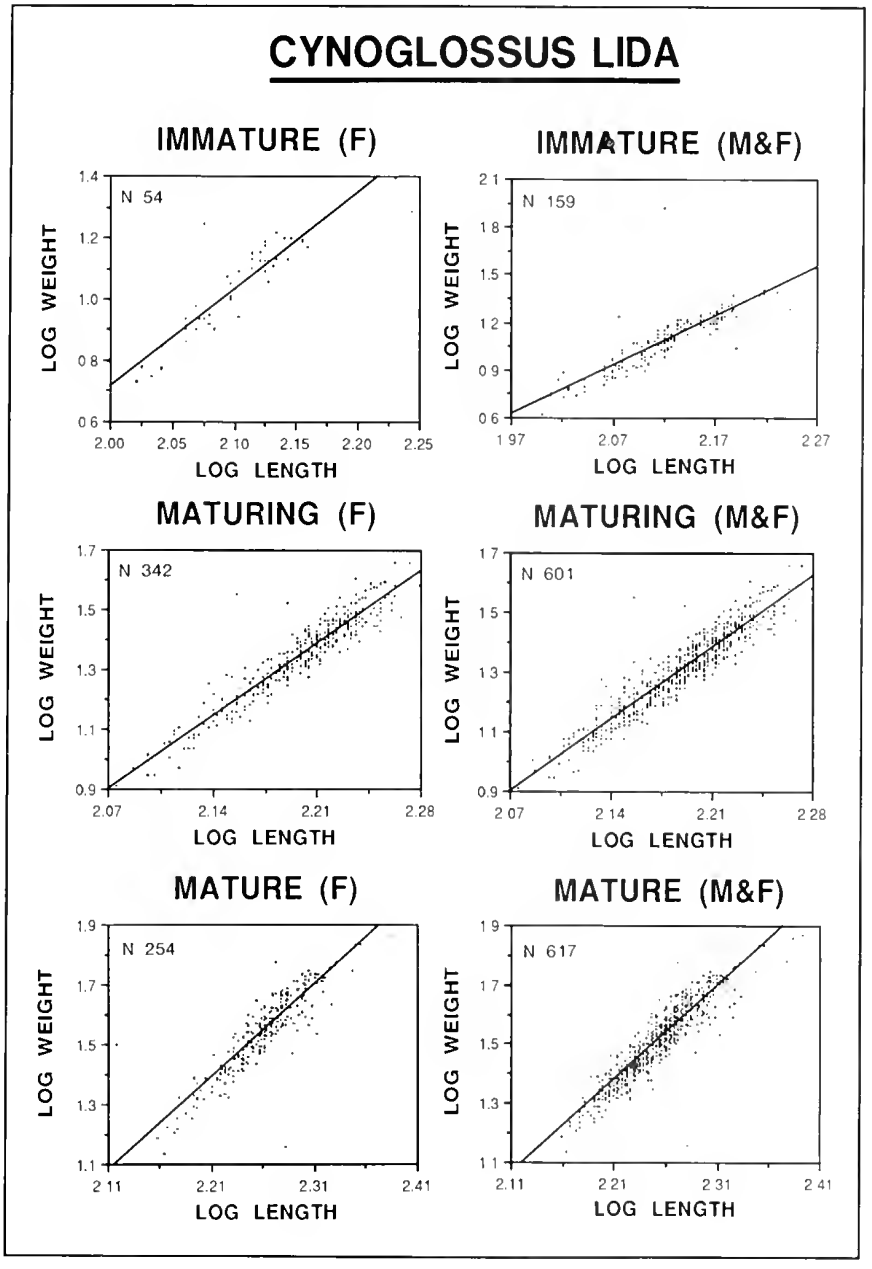

Figure 10B
Length-weight relationships for immature, maturing, and mature females (F), and pooled sexes (M&F) of *Cynoglossus lida* caught commercially off Porto Novo, India, October 1981–September 1982.

differences noted for the remaining 8 months (Table 17). In *C. lida*, no significant differences were observed in regression coefficients of length and weight between males and females.

Analysis of covariance was employed to determine whether growth patterns differed significantly between stages of maturity (immature, maturing, and mature) in males and females. No significant differences were noted for *C. arel* ($P>0.05$). Hence immature, maturing, and mature male and female *C. arel* were combined irrespective of sexes. As there was no significant difference in the regression of Y and X between maturity stages irrespective of sexes, the data for male, female, and juvenile *C. arel* were pooled for the entire year, irrespective of months and maturity stages, and the linear equation was fitted for males, females, and juveniles. Analysis of covariance was again employed for the pooled data to test whether growth patterns differed significantly between sexes of *C. arel*. Significant differences were obtained in the b value between male, female, and juvenile *C. arel*. On comparing males and females, males and juveniles, and females and juveniles, significant values were obtained. Since the growth rates of males, females, and juveniles differed significantly from one another, three separate equations, relating logW to logL, are presented for *C. arel* as follows,

C. arel Male logW = −5.9551 + 3.2665 logL
Female logW = −5.8231 + 3.2100 logL
Juvenile logW = −4.8615 + 2.7901 logL,

and the parabolic equations are

Male $W = 0.0000011\ L^{3.2665}$
Female $W = 0.0000015\ L^{3.2100}$
Juvenile $W = 0.0000138\ L^{2.7901}$.

C. arel Male 0.9870 ($P<0.001$)
Female 0.9905 ($P<0.001$)
Juvenile 0.8747 ($P<0.001$)

C. lida Male 0.9782 ($P<0.001$)
Female 0.9756 ($P<0.001$)
Juvenile 0.9409 ($P<0.001$).

Calculated b, a, r values, and observed F values are presented in Tables 16 and 17.

Linear equations were computed separately for males and females of each month to examine variations in growth patterns. In *C. arel*, significant differences were observed in regression coefficients during January, February, May, and July, with no significant

Table 16

Results of linear regressions of length-weight relations in *Cynoglossus arel* and *C. lida* caught off Porto Novo, India, October 1981–September 1982. r* = all r values were significant at 0.1% level.

	Cynoglossus arel				*Cynoglossus lida*			
Sample	*N*	r*	a	b	*N*	r*	a	b
				By months				
Male								
January	52	0.9920	−5.6785	3.1411	24	0.9900	−6.4285	3.5199
February	34	0.9902	−4.9278	2.8233	48	0.9872	−5.8703	3.2715
March	51	0.9785	−5.7827	3.1860	85	0.9822	−6.4397	3.5300
April	46	0.9834	−5.5809	3.0970	86	0.9878	−5.4470	3.0715
May	57	0.9813	−6.3448	3.4326	62	0.9823	−5.6679	3.1747
June	44	0.9887	−6.3781	3.4432	54	0.9705	−5.6760	3.1793
July	70	0.9868	−5.8109	3.1991	37	0.9677	−6.0573	3.3573
August	54	0.9951	−6.0999	3.3202	45	0.9860	−5.6693	3.1758
September	59	0.9913	−5.9119	3.2575	62	0.9809	−5.2038	2.9803
October	81	0.9907	−6.1854	3.3770	83	0.9678	−5.5118	3.1283
November	70	0.9922	−6.1151	3.3468	135	0.9823	−5.4126	3.0827
December	37	0.9930	−6.0433	3.3060	47	0.9879	−5.7740	3.2354
Total	655	0.9870	−5.9551	3.2665	768	0.9782	−5.7717	3.2315
Female								
January	49	0.9959	−5.9501	3.2687	31	0.9899	−6.1744	3.4089
February	52	0.9913	−5.6840	3.1432	45	0.9935	−5.8431	3.2598
March	47	0.9926	−5.7543	3.1782	38	0.9866	−6.1015	3.3718
April	58	0.9825	−5.3251	2.9920	54	0.9893	−5.6817	3.1849
May	52	0.9812	−5.6617	3.1412	43	0.9703	−5.7400	3.2157
June	41	0.9831	−6.0536	3.3047	54	0.9624	−5.1232	2.9342
July	55	0.9807	−5.0773	2.8787	44	0.9601	−5.9178	3.2983
August	66	0.9969	−6.2004	3.3643	64	0.9886	−5.6065	3.1489
September	39	0.9955	−5.8507	3.2361	37	0.9533	−5.2175	2.9923
October	57	0.9928	−5.9232	3.2654	80	0.9739	−5.7639	3.2454
November	45	0.9870	−5.8994	3.2511	168	0.9680	−5.7278	3.2335
December	38	0.9921	−6.0110	3.2960	65	0.9898	−5.9707	3.3277
Total	599	0.9905	−5.8231	3.2100	723	0.9756	−5.9084	3.2987
Juvenile								
All months	27	0.8747	−4.8615	2.7901	28	0.9409	−6.5983	3.6579
				By maturity stages				
Male								
Immature	56	0.9524	−4.7589	2.7205	105	0.8264	−5.5077	3.1101
Maturing	221	0.8111	−5.4998	3.0714	259	0.9260	−5.8584	3.2713
Mature	359	0.8909	−5.4090	3.0404	363	0.9328	−5.5189	3.1182
Female								
Immature	47	0.9266	−4.5468	2.6221	54	0.8867	−5.0851	2.9124
Maturing	224	0.9463	−4.8001	2.7575	342	0.9392	−6.2651	3.4629
Mature	292	0.9104	−4.9627	2.8516	254	0.8054	−5.5588	3.1443
Male and female								
Immature	103	0.9391	−4.6496	2.6699	159	0.8542	−5.3162	3.0209
Maturing	445	0.8725	−5.0463	2.8687	601	0.9399	−6.2280	3.4439
Mature	651	0.9089	−5.1071	2.9122	617	0.8726	−5.6599	3.1843

In *C. lida*, the tests made to check the relationship between length and weight during various stages of maturity (immature, maturing, and mature) in males and females showed significant differences between the three maturity stages in females alone and in pooled sexes, whereas males showed no significant differences. Hence logarithmic equations for immature, maturing, and mature females, as well as pooled sexes of *C. lida*, are presented as follows,

C. lida

Female alone

Immature logW = −5.0851 + 2.9124 logL

Maturing logW = −6.2651 + 3.4629 logL

Mature logW = −5.5588 + 3.1443 logL

Pooled sexes

Immature logW = −5.3162 + 3.0209 logL

Maturing logW = −6.2280 + 3.4439 logL

Mature logW = −5.6599 + 3.1843 logL.

The linear relationships in logarithmic values of length and weight for immature, maturing, and mature female, as well as pooled sexes of *C. lida*, are shown in Figure 10B.

Although female maturity exhibited a significant effect on the length-weight relationship, all data for male, female, and juvenile *C. lida* were treated separately, irrespective of month and maturity stage. Analysis of covariance was used to find variations in the growth patterns of males, females, and juveniles. Significant differences were observed in regression coefficients of males, females, and juveniles. While comparing males and juveniles, a significant difference was noted; however, no significant differences were observed in comparing males and females, and females and juveniles. Hence two logarithmic equations, one common equation for adults (male and female) and another for juveniles, are presented for *C. lida* as follows,

C. lida

Male & female logW = −5.8643 + 3.2761 logL

Juveniles logW = −6.5983 + 3.6579 logL,

and the parabolic equations are

Table 17

Observed F values and their significance in length-weight relationships of *Cynoglossus arel* and *C. lida* caught commercially off Porto Novo, India, October 1981–September 1982. *$P<0.05$.

Samples		*C. arel*	*C. lida*
Comparison between male, female, and juvenile			
January	Male × Female	8.0000*	1.8571
February	Male × Female	12.2941*	0.0000
March	Male × Female	0.0000	1.6923
April	Male × Female	1.1667	1.8182
May	Male × Female	5.5000*	12.0000
June	Male × Female	1.1429	2.1765
July	Male × Female	10.1667*	0.0000
August	Male × Female	1.8333	9.0000
September	Male × Female	8.0000	0.0000
October	Male × Female	2.3125	1.1875
November	Male × Female	1.0625	3.1333
December	Male × Female	0.0000	1.1250
All months			
Male × Female × Juvenile		4.8571*	3.7368*
Male × Female		4.2500*	3.3889
Male × Juvenile		6.8000*	5.5882*
Female × Juvenile		4.6522*	3.1905
Comparison between maturity stages			
Male			
Immature × Maturing × Mature		1.5915	1.2727
Immature × Maturing		2.1798	1.3333
Immature × Mature		3.5556	0.0000
Maturing × Mature		24.6667	2.1176
Female			
Immature × Maturing × Mature		1.0303	4.3913*
Immature × Maturing		1.0625	11.6296*
Immature × Mature		1.2826	1.4038
Maturing × Mature		1.6098	4.6000
Male and female combined			
Immature × Maturing × Mature		1.7971	7.2162*
Immature × Maturing		2.2131	13.6765*
Immature × Mature		3.4789	1.4000
Maturing × Mature		5.0714	8.6452*

Male and female $W = 0.0000014\ L^{3.2761}$
Juvenile $W = 0.0000003\ L^{3.6579}$

The *t*-test was employed, and the calculated b value was found to differ significantly from the hypothetical B value (=3), at 5% level, in male and female *C. arel* and in adult and juvenile *C. lida*, whereas juvenile *C. arel* showed no significant difference:

C. arel Male $t = 12.8125$
Female $t = 11.5385$
Juvenile $t = -0.6788$

C. lida Male & female $t = 14.8441$
Juvenile $t = 2.5470$

Hence it is clear that the cubic formula is not a proper representation of length-weight relationship in male and female *C. arel* and in adult and juvenile *C. lida*.

Reproductive biology

Seasonal occurrence of maturity stages Female *C. arel* with Stage-I ovaries occurred throughout the year, with a peak in September (Fig. 11). Stage-II ovaries were also present during all months, with higher percentages in April and October. Individuals with Stage-III ovaries occurred throughout the year, with higher proportions during March–May and July. Specimens with Stage-IV (mature ovaries) were present throughout the year, with a peak in November. Stage-V (ripe ovaries) were also noted during all months of the year, but maximum abundance was observed in November and December. Specimens with Stage-VI (oozing ovaries) were collected in all months except April and May. High incidence of oozing ovaries was observed in January and February. This indicates that the spawning occurs for up to 10 months (June–March). Occurrence of Stage-VI specimens, with a peak in January, indicates that the maximum number of individuals may spawn during January, which is the post-(northeast) monsoon period in Porto Novo.

In male *C. arel* (Fig. 12), immature (Stage-I), maturing (Stage-II), and mature (Stage-III) individuals occurred throughout the year. High percentages of individuals with Stage-I testes occurred in March and October–December. Maturing specimens (Stage II) were abundant from February to September. Occurrence of mature males (Stage III) showed a peak in January. Occurrence of a higher percentage of fully-mature specimens in January indicated that even though the spawning probably occurred year-round, the majority of individuals might spawn during the post-(northeast) monsoon period (January) in Porto Novo.

Female *C. lida* (Fig. 11) with Stage-I (immature) ovaries occurred for 9 months (absent in February, March, and July), with a peak in April. Stage-II (virgin maturing) individuals were present during all months except February and March, with a peak in December. Stage-III (maturing) ovaries were present throughout the year, with abundance in January, March, June, November, and December. Stage-IV (mature) specimens were present during all months of the year, with higher proportions during February, March, May, and July. Stage-V (ripe) individuals occurred throughout the year, except in December, with maximum abundance in February and September–October. Specimens with Stage-VI (oozing) ovaries were noted for 10 months (absent in January and December), with a peak in September. This indicates that the spawning period lasts for 10 months (February–November), while a

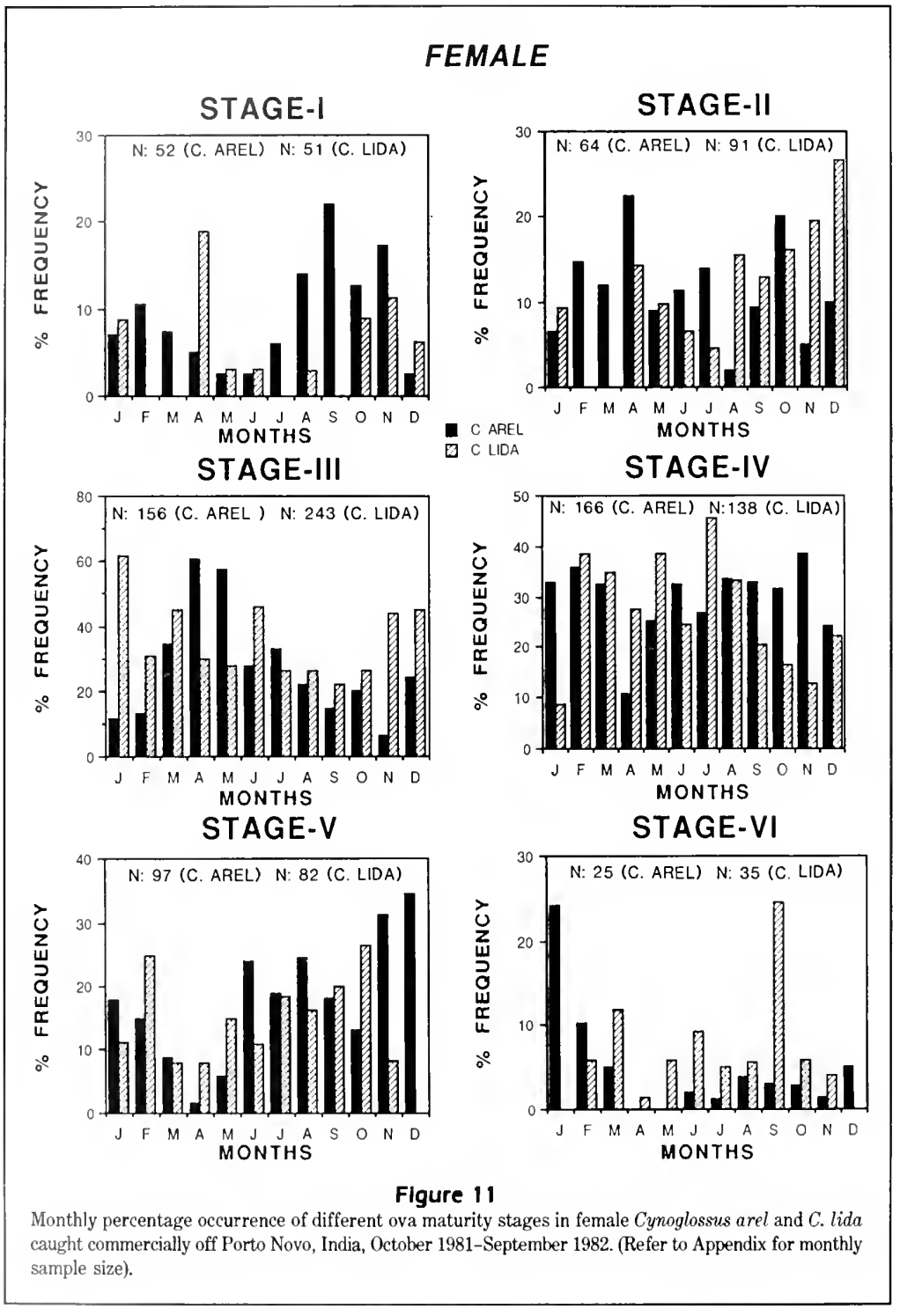

Figure 11

Monthly percentage occurrence of different ova maturity stages in female *Cynoglossus arel* and *C. lida* caught commercially off Porto Novo, India, October 1981–September 1982. (Refer to Appendix for monthly sample size).

maximum number of individuals spawn in September, which is the pre- (northeast) monsoon period in Porto Novo.

In male *C. lida* (Fig. 12), immature (Stage-I) specimens occurred throughout the year, except July and September, with a peak in January. Specimens at Stage II (maturing) were observed throughout the year, with high percentages at all months, except August and September. Stage-III (mature) males were available throughout the year, with a peak in September. This indicates that spawning occurs throughout the year, but a maximum number of males also seemed to spawn during September. Maximum occurrence of mature males in September corresponds with maximum occurrence of oozing females in the same period, and supports this view.

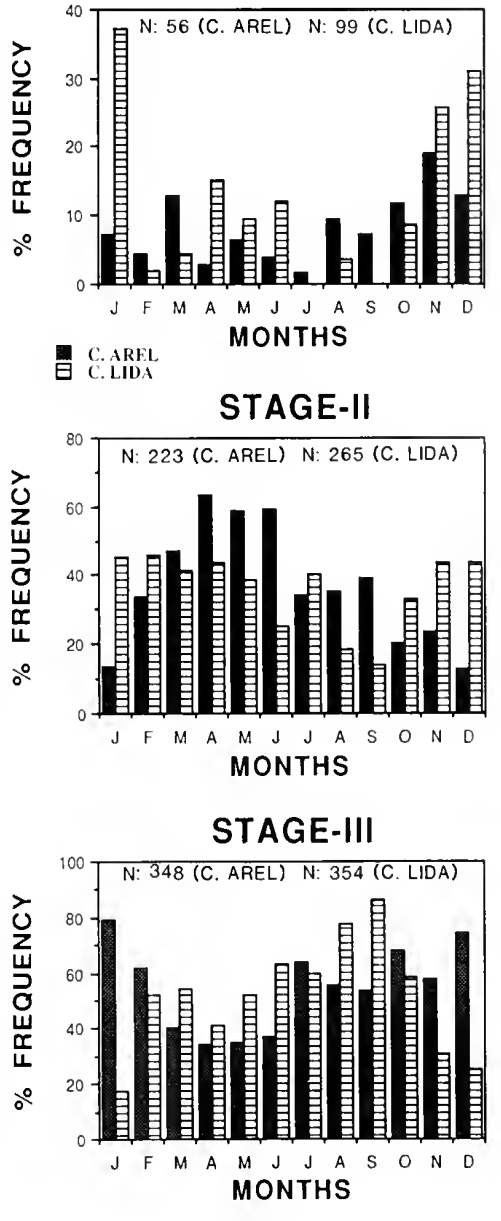

Figure 12
Monthly percentage occurrence of different testis maturity stages in male *Cynoglossus arel* and *C. lida* caught commercially off Porto Novo, India, October 1981–September 1982. (Refer to Appendix for monthly sample size).

Ova diameter Ova diameter frequencies, from ovaries of Stage I–VI, are shown in Figure 13 for *C. arel* and *C. lida*. Since immature, transparent, and microscopic ova (≤0.11 mm) outnumbered the maturing ova during all stages of maturity, only ova >0.11 mm were taken into consideration, from Stage II onwards. Progressive maturation to spawning condition was evident from increasing ova diameters of the most advanced mode at each stage.

For *C. arel* (Fig. 13) in Stage I, maximum number of ova measured 0.01–0.04 mm; however, a few relatively larger ova (0.09–0.11 mm) were also recorded. In Stage II, a mode was discernible with a stock of ova (0.16–0.19 mm) separated from immature stock. In Stage III, the previous mode (at 0.16–0.19 mm) shifted to 0.24–0.26 mm. In Stage IV, a mode made by opaque ova was observed at 0.36–0.38 mm. In Stage V, two modes were found, one with a peak at 0.43–0.45 mm, and another at 0.50–0.53 mm. In Stage VI, the preceding two modes formed jointly a single mode, with fully mature, transparent, and large-sized ova of 0.54–0.56 mm.

For *C. lida* (Fig. 13) in Stage I, immature ova measured 0.01–0.04 mm. In addition, a few relatively larger ova (0.09–0.11 mm) were also seen. In Stage II, a mode was discernible with a stock of ova at 0.09–0.11 mm, which was separated clearly from immature ova. In Stage III, the previous mode was shifted to 0.20–0.23 mm. In Stage IV, a mode of opaque ova was located at 0.31–0.34 mm. In Stage V, a mode of ripe ova was noted at 0.35–0.38 mm. In Stage VI, fully mature, transparent, and large-sized ova formed a mode at 0.39–0.41 mm.

Results indicate that individuals of *C. arel* and *C. lida* spawn only once during each season. Further, mature modes were wide-based (0.49–0.83 mm in *C. arel*, and 0.34–0.64 mm in *C. lida*); therefore, the spawning period of these species must be extended.

Gonadosomatic Index In male *C. arel* (Fig. 14), the highest GSI peak was in March, and the lowest GSI value was observed in January. In female *C. arel* (Fig. 14), the highest GSI peak was observed in November, and the lowest value was in January. In both sexes of *C. arel*, the peak values of GSI did not correspond with the observed spawning period in that year.

In male *C. lida* (Fig. 14), the highest GSI peak occurred in September, and the lowest value was in January, November, and December. In female *C. lida* (Fig. 14), the highest GSI peak was observed in May, while the lowest value was in December. Only in male *C. lida* did the high GSI peak coincide with the observed peak spawning period in September.

Relative condition factor (Kn) In male *C. arel* (Fig. 14), the highest Kn value peak was observed in February, and the lowest value was in October. In female *C. arel* (Fig. 14), the highest Kn peak was observed in January, and the lowest value was in November. Only

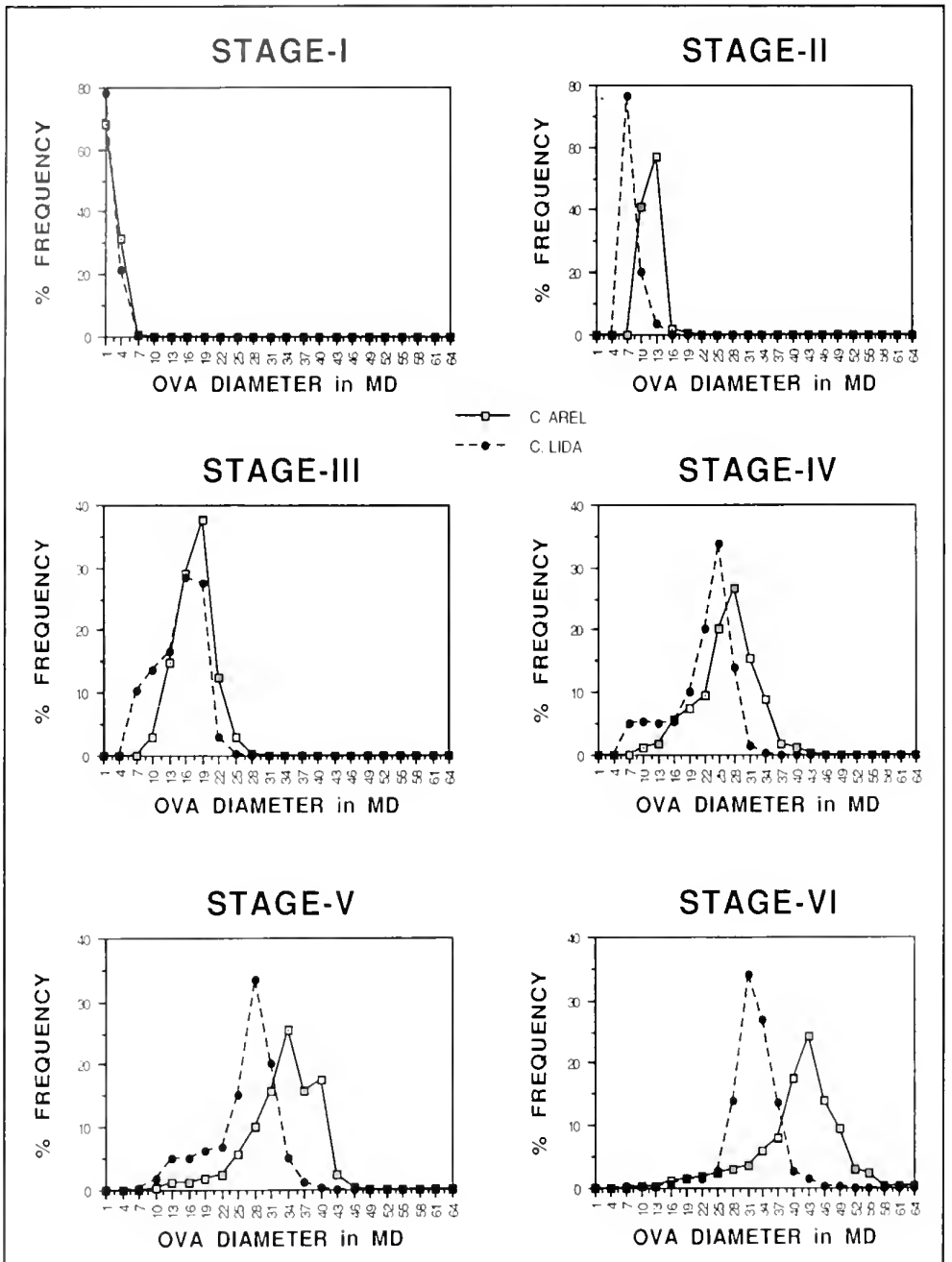

Figure 13

Percentage frequency of ova diameter in various maturity stages in *Cynoglossus arel* and *C. lida* caught commercially off Porto Novo, India, October 1981–September 1982. MD = micrometer division. (Number of fish examined for each stage: 18 *C. arel*, 28 *C. lida*).

in female *C. arel* did a rise in Kn value correspond with a rise in gonadal activity, indicating the spawning period (in January).

In male *C. lida* (Fig. 14), the highest Kn peak was seen in January and the lowest value was in February. In females of *C. lida* (Fig. 14), the highest Kn peaks were seen in January, July, and December, and the lowest value in May. In both sexes of *C. lida*, a rise in Kn value did not indicate the spawning period.

Size-at-first-maturity Both sexes of *C. arel* began to mature after the 140–154 mm size-group (Fig. 15). From the 155–169 mm size-group onwards, percentage occurrence of mature males and females increased steadily. Maturity reached 100% in the 245–259 mm size-group in males, and in the 275–289 mm size-group

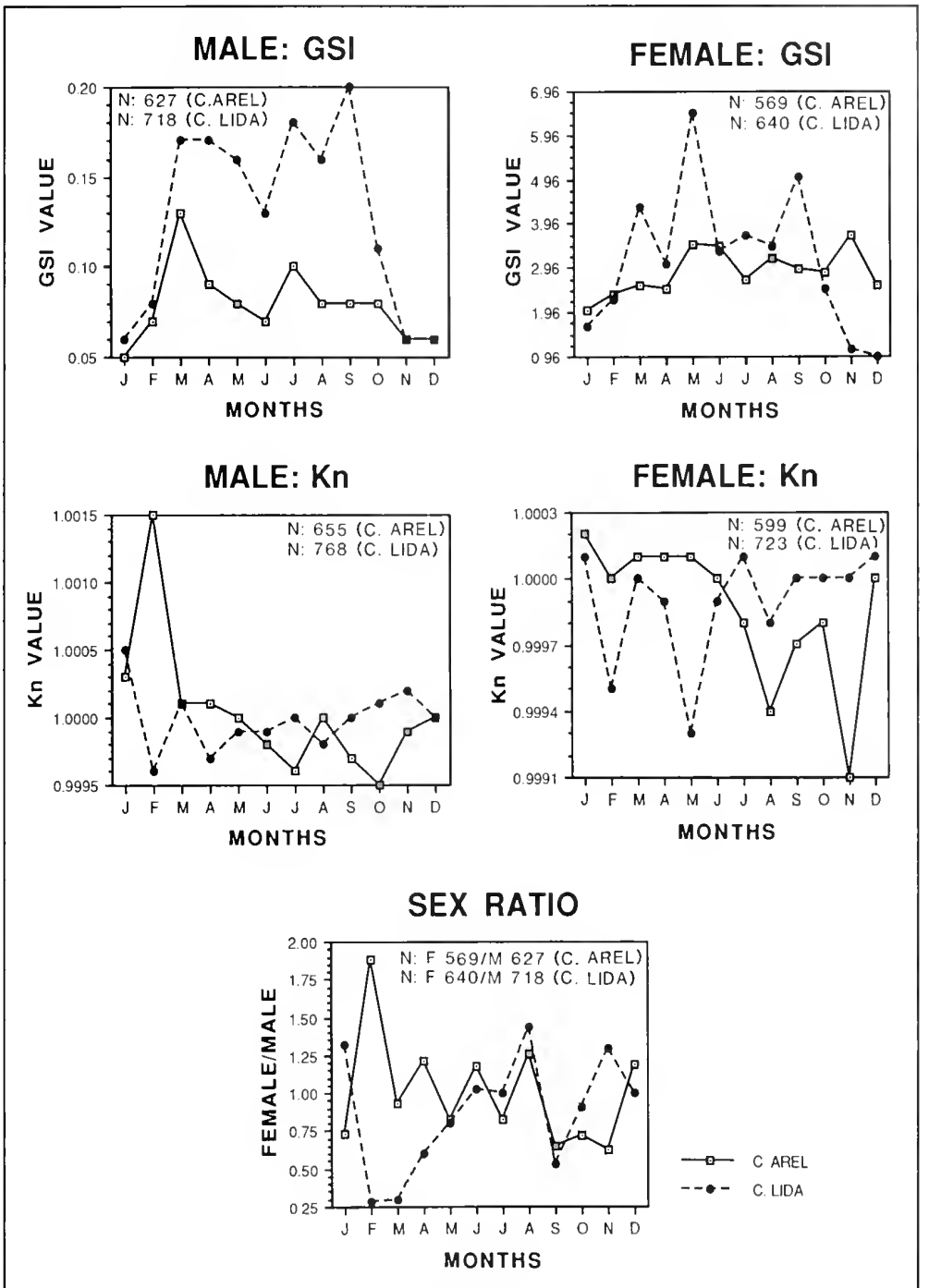

Figure 14

Relative condition factor (Kn), gonadosomatic index (GSI), and sex ratio (female/male) in *Cynoglossus arel* and *C. lida* caught commercially off Porto Novo, India, October 1981–September 1982. (Refer to Appendix for monthly sample size).

in females. The calculated Lm for *C. arel* was 217 mm for males and 225 mm for females.

In *C. lida*, no specimen of either sex was mature until the 137–143 mm size-group, and the percentage occurrence of mature specimens increased gradually from then on (Fig. 15). All male fish were mature at the 186–192 mm size-group, and females at the 193–199 mm size-group. In *C. lida*, Lm ($= L_{50}$) was calculated as 167 mm for males and 179 mm for females. In both species, males mature at a smaller size than females.

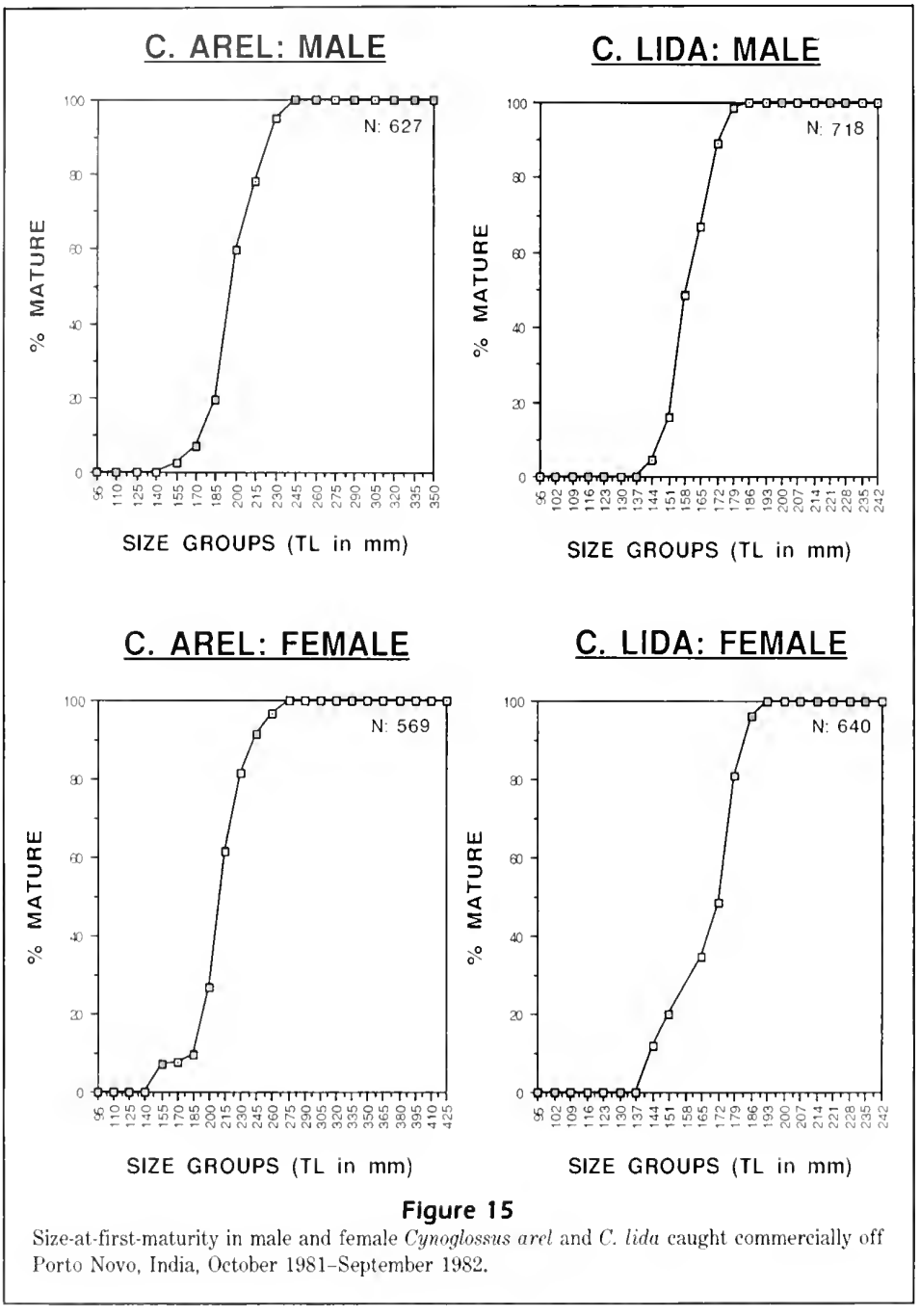

Figure 15

Size-at-first-maturity in male and female *Cynoglossus arel* and *C. lida* caught commercially off Porto Novo, India, October 1981–September 1982.

Age-at-first-maturity In their first year, males of *C. arel* grow to 180 mm according to the Petersen method, and to 194 mm according to the probability plot method and von Bertalanffy's equation (Rajaguru 1987). Female *C. arel* reached 201 mm as per the probability plot method and von Bertalanffy's equation, and 210 mm according to the Petersen method, at the end of their first year of life (Rajaguru 1987). Hence it appears that 50% of male and female *C. arel* attain first maturity at the beginning of their second year of life.

Male *C. lida*, at the end of their first year of life, would grow to 151–154 mm based on all three methods (Rajaguru 1987). Females of *C. lida* reach 153 mm according to von Bertalanffy's equation and the probability plot method, and 156 mm according to the Petersen method, at the end of the first year of their life (Rajaguru 1987). Therefore, 50% of male and female *C. lida* attain first sexual maturity during the second year of their life.

Fecundity Fecundity varied from 14,972 to 127,001 eggs/ovary in *C. arel*, and 11,267 to 81,004 eggs/ovary

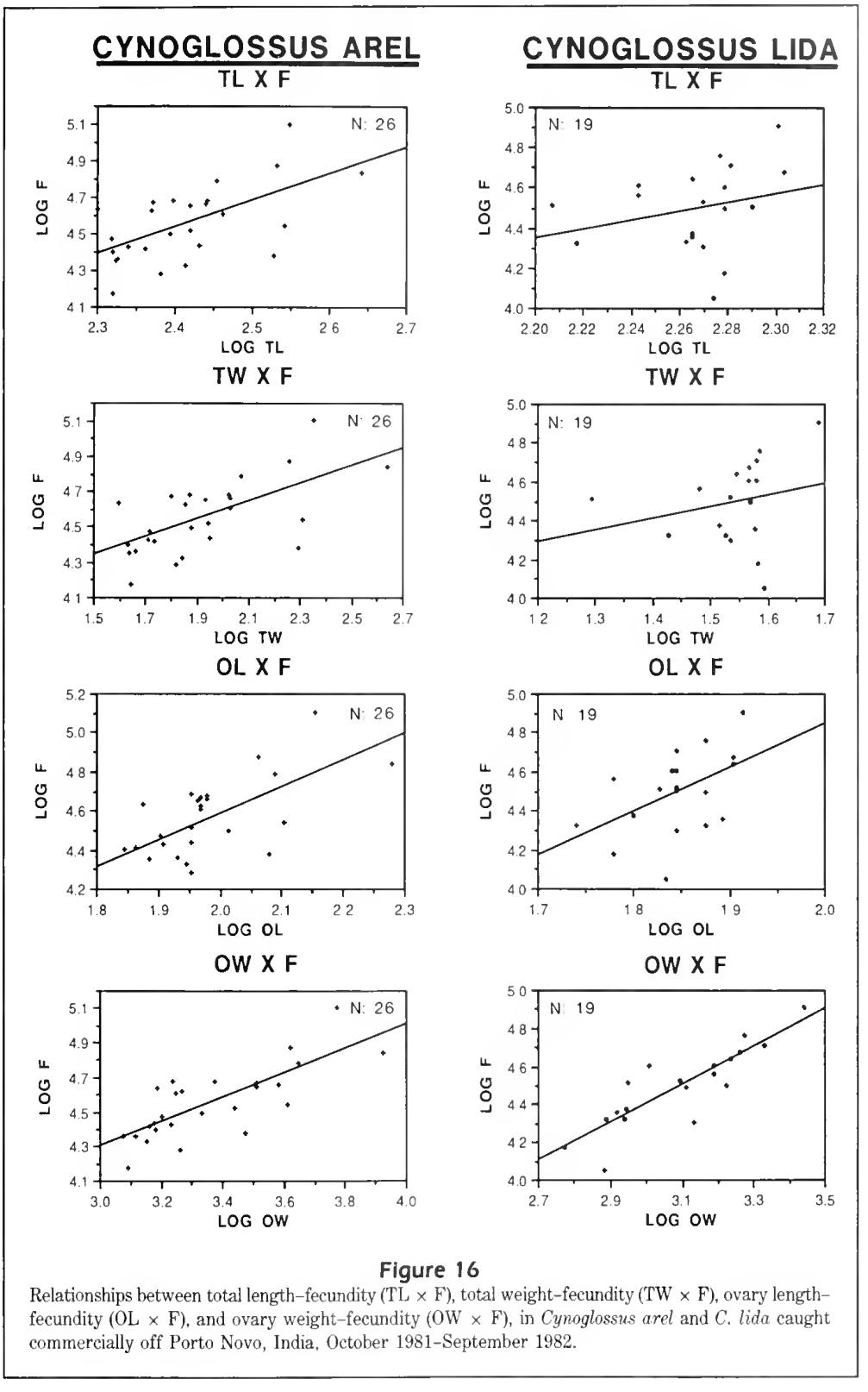

Figure 16

Relationships between total length–fecundity (TL × F), total weight–fecundity (TW × F), ovary length–fecundity (OL × F), and ovary weight–fecundity (OW × F), in *Cynoglossus arel* and *C. lida* caught commercially off Porto Novo, India, October 1981–September 1982.

in *C. lida*. Number of ova/g body weight was 124–1096 ($\bar{x}$ 464) in *C. arel*, and 287–1664 ($\bar{x}$ 988) in *C. lida*. Scatter diagrams of fecundity (F) against TL, TW, OL, and OW are shown in Figure 16.

Fecundity was found to increase with TL (Fig. 16). The calculated equation for F against TL is,

C. arel $\log F = 1.0629 + 1.4459 \log TL$

C. lida $\log F = -0.4923 + 2.2006 \log TL$.

The correlation coefficient (r) for this relationship in *C. arel* is 0.6043 ($P<0.001$) and is statistically significant; in *C. lida*, it is 0.2579 ($P>0.05$) and is not statistically significant.

Fecundity against TW showed a linear relationship (Fig. 16), and equations for the transformed data are,

$$\textit{C. arel} \quad \log F = 3.5907 + 0.4995 \log TW$$
$$\textit{C. lida} \quad \log F = 3.5536 + 0.6108 \log TW.$$

The correlation coefficient (r) for this relationship in *C. arel* is 0.6345 and is highly significant ($P<0.001$); in *C. lida*, the correlation coefficient of 0.2302 ($P>0.05$) did not indicate a significant correlation between these two variables.

Ovary length showed a straight-line relationship with fecundity (Fig. 16). In logarithmic form, the relationships between F and OL can be expressed as follows;

$$\textit{C. arel} \quad \log F = 1.8472 + 1.3693 \log OL$$
$$\textit{C. lida} \quad \log F = 0.3206 + 2.2630 \log OL.$$

The correlation coefficient in *C. arel* is 0.6632 ($P<0.001$) and is statistically significant; in *C. lida*, it is 0.4990 ($P< 0.05$), showing a high degree of correlation.

Fecundity plotted against OW showed a linear relationship (Fig. 16) and equations for these two variables are,

$$\textit{C. arel} \quad \log F = 2.1858 + 0.7050 \log OW$$
$$\textit{C. lida} \quad \log F = 1.3909 + 1.0038 \log OW.$$

The correlation coefficient in *C. arel* is 0.7729 ($P<0.001$), indicating a high degree of correlation between these two variables. In *C. lida*, the correlation coefficient of 0.8606 ($P<0.001$) is highly significant.

In the present study, the exponential value (b) for total length-fecundity was higher than for total weight-fecundity. Similarly, the b value for ovary length-fecundity was higher than for ovary weight-fecundity.

Sex ratio The sex ratio was about 1:1 for both species (Table 18, Fig. 14). However, the ratio varied in monthly samples, and chi-square values showed a significant deviation from the expected 1:1 ratio for 3 months (February, September, and November) in *C. arel*, and during February–April, September, and November in *C. lida*. Since data were pooled for one year, the chi-square value conformed to the expected 1:1 ratio in *C. arel*; whereas in *C. lida*, it deviated significantly from the expected 1:1 ratio. The deviation may be due to multiple testing.

Discussion

Feeding ecology

Cynoglossus arel and *C. lida* feed predominantly on polychaetes and crustaceans, followed by other phyla such as molluscs, echinoderms, and coelenterates. These similarities in diets indicate common feeding strategies within the tonguefishes and soles (Seshappa and Bhimachar 1955, Kuthalingam 1957, de Groot 1971, Braber and de Groot 1973ab, Stickney 1976, Pearcy and Hancock 1978, Langton and Bowman 1981, Wakabara et al. 1982, Langton 1983, Honda 1984).

Table 18

Sex ratio of *Cynoglossus arel* and *C. lida* caught commercially off Porto Novo, India, October 1981–September 1982. F = Probability.

	Cynoglossus arel							*Cynoglossus lida*						
Months	♂ N	♀ N	♂ %	♀ %	♂:♀	χ^2	F	♂ N	♀ N	♂ %	♀ %	♂:♀	χ^2	F
Jan.	53	39	57.6	42.4	1.4:1.0	2.1304	>0.05	32	42	43.2	56.8	0.8:1.0	1.3514	>0.050
Feb.	24	45	34.8	65.2	0.5:1.0	6.3913	<0.05	59	16	78.7	21.3	3.7:1.0	24.6533	<0.001
Mar.	54	49	52.4	47.6	1.1:1.0	0.2427	>0.05	64	18	78.0	22.0	3.6:1.0	25.8049	<0.001
Apr.	46	55	45.5	54.5	0.8:1.0	0.8020	>0.05	84	51	62.2	37.8	1.7:1.0	8.0667	<0.010
May	56	45	55.4	44.6	1.2:1.0	1.1980	>0.05	38	31	55.1	44.9	1.2:1.0	0.7101	>0.050
June	35	40	46.7	53.3	0.9:1.0	0.3333	>0.05	56	59	48.7	51.3	0.9:1.0	0.0783	>0.050
July	69	56	55.2	44.8	1.2:1.0	1.3520	>0.05	25	25	50.0	50.0	1.0:1.0	0.0000	—
Aug.	44	54	44.9	55.1	0.8:1.0	1.0204	>0.05	43	62	41.0	59.0	0.7:1.0	3.4381	>0.050
Sep.	56	35	61.5	38.5	1.6:1.0	4.8462	<0.05	46	25	64.8	35.2	1.8:1.0	6.2113	<0.050
Oct.	75	54	58.1	41.9	1.4:1.0	3.4186	>0.05	83	76	52.2	47.8	1.1:1.0	0.3082	>0.050
Nov.	86	54	61.4	38.6	1.6:1.0	7.3143	<0.01	160	207	43.6	56.4	0.8:1.0	6.0191	<0.050
Dec.	29	34	46.0	54.0	0.9:1.0	0.3968	>0.05	28	28	50.0	50.0	1.0:1.0	0.0000	—
Total	627	560	52.8	47.2	1.1:1.0	3.7818	>0.05	718	640	52.9	47.1	1.1:1.0	4.4801	<0.050

Diet of fishes is related not only to their feeding behavior, but also to their digestive morphology and mouth structure (Stickney et al. 1974). In *C. arel* and *C. lida*, jaws are asymmetrical so that the mouth points to the bottom when opened, aiding feeding upon benthic prey. Flatfishes that feed on benthose usually have asymmetrical jaws (Pearcy and Hancock 1978). *Cynoglossus arel*, *C. lida*, and other tonguefishes are, in general, polychaete feeders. These fishes have small stomachs (not highly demarcated) and long intestines, and lack gillrakers and pyloric caecae.

Although there were similarities in food items, importance of prey species differed between adults and juveniles. Juveniles of *C. arel* and *C. lida*, probably owing to their very small mouths, fed predominantly on smaller prey such as amphipods and copepods, and ingested fewer types (only 10) of food items. Adults of both species, in contrast, had eaten 24 and 29 types, respectively, of relatively large-sized prey, primarily polychaetes, prawns, crustacean fragments, and fish remains. Mouth size severely limits the size of prey which can be ingested (Stickney 1976). According to Honda (1984), the extent of food demand and ability for food acquisition increase with growth and development of fish. Lande's (1976) findings on the dab *Limanda limanda* revealed that larger fish consumed large-sized prey compared with smaller fish. Pearcy and Hancock (1978) studied feeding habits of Dover sole *Microstomus pacificus*, rex sole *Glyptocephalus zachirus*, slender sole *Lyopsetta exilis*, and Pacific sanddab *Citharichthys sordidus* off Oregon, and concluded that the number and size of prey taxa generally increased with size in these flatfishes, due to the ability of larger fish to consume a larger range of prey sizes than smaller fish.

During the present investigation, fewer empty stomachs were noted in female than male (11.6% vs. 18.0%) *C. lida*. A similar trend was observed by Langton (1983) for yellow-tail flounder *Limanda ferruginea* off the northeastern United States. In female and male *C. arel*, the percentage occurrence of empty stomachs was similar (7.7% vs. 8.0%).

Sexual differences in food and feeding habits of flatfishes have not been reported. In this study, there was some indication of differences in prey between males and females. The primary food group (polychaetes) was the same in both sexes of *C. lida*; however, polychaetes were somewhat more important in females (IRI 65.9%) than males (IRI 53.4%). Moreover, the breadth of the diet was somewhat less in females which fed upon only 19 food types, in contrast to males in which 24 prey types were consumed.

The present analysis on feeding intensity reveals that in males of *C. arel*, the peak occurrence of empty stomachs had a positive correlation with peak spawning activity (in January). Spawning fish contained the least amounts of prey, or had empty stomachs. This result is consistent with the findings of Ramanathan and Natarajan (1980) on Indian halibut *Psettodes erumei* and flounder *Pseudorhombus arsius*, and with those of Langton (1983) on yellowtail flounder *Limanda ferruginea*. However, in female *C. arel* and both sexes of *C. lida*, the occurrence of empty stomachs had no obvious relationship with spawning activities. Seshappa and Bhimachar (1955) also reported that in Malabar sole *C. semifasciatus*, feeding intensity was not interrupted by increased reproductive activity.

Male and female *C. arel* showed an inverse relationship between gastrosomatic/hepatosomatic indices and breeding cycle, with the lowest values observed during peak spawning (in January). This indicates that gut/liver energy reserves may be used for gonadal recrudescence. Such a correlation was observed by Ramanathan (1977) for the Indian halibut *Psettodes erumei* and flounder *Pseudorhombus arsius*. Wingfield and Grimm (1977) found HI to be highest in the prespawning season and lowest in the postspawning period of the Irish Sea plaice *Pleuronectes platessa*. However, *C. lida* did not show a relationship between gastrosomatic/hepatosomatic indices and breeding cycle.

Although the primary diet of these two demersal flatfishes consisted of benthic prey such as polychaetes, prawns, echinoderms, and molluscs, it was surprising to find that pelagic amphipods ($\leqslant$59.2% IRI) and copepods ($\leqslant$44.7% IRI) were also relatively important in their diets, especially in juveniles. *Cynoglossus arel* and *C. lida* are demersal flatfishes that have never been caught in the pelagic waters off Porto Novo, either during day or night. These tonguefishes are not known to undergo vertical feeding migrations. Based on the present study, it is speculated that these tonguefishes ingested pelagic prey such as hyperiid amphipods and copepods when these prey organisms approached or contacted the bottom during vertical migrations through the water column. Hyperiid amphipods have been reported to undertake extensive vertical migrations (Bowman et al. 1982, Roe et al. 1984, Clark et al. 1989). Isaacs and Schwartzlose (1965) and Pereyra et al. (1969) have reported that in the eastern North Pacific Ocean, demersal fishes feed on pelagic prey, when such prey approach the bottom along the edge of the continental shelf.

Polychaetes, prawns, amphipods, copepods, crustaceans, and fishes were important prey for both *Cynoglossus arel* and *C. lida*. These tonguefishes shared 25 different food items as prey (out of 30 food types in *C. arel*, and out of 26 in *C. lida*). High overlap in diet may reflect abundant prey resources, reducing competition. Lande (1976) observed such a high prey

abundance for Norwegian flatfishes. However, during the present study, some individuals had full and gorged stomachs, filled only with either polychaetes or prawns. This might indicate either greater availability or patchy distribution of the major food items. Seshappa and Bhimachar (1955) reported for Malabar sole *Cynoglossus semifasciatus*, from the west coast of India, that during certain months the guts were gorged with only one prey, mostly polychaetes.

During the present investigation, most stomachs of *C. arel* and *C. lida* were found to contain considerable quantities of sediment (sand and mud). In some specimens, the entire stomach was filled with sediment. Algal filaments were also found in some stomachs. Sediment and algal filaments were probably ingested accidentally with bottom-living polychaetes and other infauna. Since demersal fishes browse near the sea bottom, some amount of sediment may frequently be in their gut. This has been reported for other flatfishes, such as Malabar sole *Cynoglossus semifasciatus* (Seshappa and Bhimachar 1955) and *C. lingua* (Kuthalingam 1957), and for other demersal fishes (Sedberry and Musick 1978). Stickney (1976) stated that the high percentage occurrence of sand in the stomachs of blackcheek tonguefish *Symphurus plagiusa* might be due to ingestion of a significant quantity of detrital material in its feeding activities. It is unknown if sediment ingestion in *C. arel* and *C. lida* is accidental or represents a deliberate feeding action. *In situ* or aquarium studies on feeding habits would be required to answer this question.

Nematodes, present in stomachs of several specimens of *C. arel* and *C. lida*, were not attached to the stomach wall but, rather, appeared to be free-living species.

Age and growth

In the present study, distinct annual markings were not seen in scales, otoliths, opercular bones, and supraoccipital crests of *C. arel* and *C. lida*. Struhsaker and Uchiyama (1976) have stated that tropical and subtropical fishes are difficult to age, because they generally experience little seasonal and environmental changes and so do not develop annual rings clearly.

It was observed in *C. arel* and *C. lida* that after very rapid growth during the first year, there is a considerable reduction in the growth rate during the years when sexual maturity sets in; afterwards, the growth rate decreases slightly with age. This observation is consistent with the findings of Ford (1933) and Devold (1942).

Females of *C. arel* show faster growth, compared with males, and also live longer. According to Pitt (1966, 1967), since males mature earlier than females, it seems likely that energy is diverted at an earlier age from growth to reproduction, so that the rate of growth in males is reduced at an earlier age than in females. Results of age and growth studies on yellowtail flounder *Limanda ferruginea* from New England (Lux and Nichy 1969), *Limanda herzensteini* from Japan (Wada 1970a), Agulhas sole *Austroglossus pectoralis* from South Africa (Zoutendyk 1974a), and *Solea solea* from Spain (Ramos 1982) are also consistent with Pitt's view. In contrast to the above view, no significant difference was observed between the growth patterns in males and females of *C. lida*.

It is important to know at what age fishes are recruited to the fishery. The present study reveals that *C. arel* and *C. lida* reach commercial size during their 2d and 3d year. Botha et al. (1971) stated that Agulhas sole *Austroglossus pectoralis* off South Africa reached commercial size during their 3d–5th years, and at certain times their 2d–4th years. Lux and Nichy (1969) observed that yellowtail flounder *Limanda ferruginea* of the New England fishing grounds recruited to the commercial fishery during their 3d and 4th years. According to Seshappa and Bhimachar (1955), the bulk of commercial catches of Malabar sole *Cynoglossus semifasciatus* consisted of 2d-year individuals.

Cynoglossus arel and *C. lida* have a life-span of a little over 3 years in the southeast coast of India. The longevity for *C. lida* from the west coast of India has also been reported to be 3–4 years (Seshappa 1978). Longevity in most tropical fish species is relatively shorter and seldom exceeds 2–3 years (Qasim 1973b). However, temperate flatfishes were reported to have a longevity of 6–30 years (Devold 1942, Arora 1951, Pitt 1967, Lux and Nichy 1969, Lux 1970, Wada 1970a, Zoutendyk 1974a, Smith and Daiber 1977).

Length-weight relationships

During the present analyses, *C. arel* showed differences in characteristic length-weight slopes for males and females. Similar observations were made by Ketchen and Forrester (1966) and Powles (1967), while analyzing the length-weight relationships of Petrale sole *Eopsetta jordani* and American plaice *Hippoglossoides platessoides*, respectively. However, *C. lida* showed no significant differences in characteristic length-weight slopes for males and females. Zoutendyk (1974b) on Agulhas sole *Austroglossus pectoralis*, and Smith and Daiber (1977) on summer flounder *Paralichthys dentatus*, did not report significant differences in length-weight characteristics of males and females.

Cynoglossus arel and *C. lida* showed significant regression coefficients (b-values), which differed significantly from the hypothetical B value (= 3). Webb (1972) made similar observations for yellow-bellied flounder *Rhombosolea leporina*.

Significant deviation from the 'cube law' was observed in mature females of *C. lida* due to gonad development. Similar findings were observed by Dawson (1962) in hogchokers *Trinectes maculatus*, and by Lux (1969) in yellowtail flounder *Limanda ferruginea*.

In male and female *C. arel*, and male, female, and juvenile *C. lida*, the exponent values are >3, indicating that the weight increase is more in relation to length. But the exponent value for juveniles of *C. arel* is <3, indicating that an increase in weight is less compared with length.

During the present investigation, specimens <83 mmTL in *C. arel* and <81 mmTL in *C. lida* were not available from the continental shelf off Porto Novo. Arora (1951) reported such an absence of juveniles in the commercial catches for California sand dab *Citharichthys sordidus*. Non-availability of juveniles in commercial catches might be due to the gears operated or due to their occurrence in deeper waters, since spawning of cynoglossines in inshore waters has not been reported (Seshappa and Bhimachar 1955).

Reproductive biology

Spawning periods of *C. arel* and *C. lida* were prolonged, lasting for 10 months. The present study agrees with Qasim's (1973a) view that in Indian waters many fish species may be prolonged breeders. Seshappa and Bhimachar (1955) reported that the spawning season in the Malabar sole *Cynoglossus semifasciatus* off the west coast of India was prolonged (8 months).

In *C. arel* and *C. lida*, ova in different maturity stages taken from anterior, middle, and posterior regions of both lobes of ovaries showed no variation in their mean diameter. It is therefore concluded that the development of ovarian eggs proceeds uniformly throughout the ovary. Such a distribution of ova has been reported for Indian halibut *Psettodes erumei* and flounder *Pseudorhombus arsius* (Ramanathan and Natarajan 1979).

Male *C. arel* and *C. lida* attained maturity earlier than females. Pitt (1966) observed that males of American plaice *Hippoglossoides platessoides* were obviously smaller than females at first maturity. Results obtained by Lux and Nichy (1969) for yellowtail flounder *Limanda ferruginea* (New England), by Wada (1970b) for *Limanda herzensteini* (Japan), by Zoutendyk (1974a) for Agulhas sole *Austroglossus pectoralis* (South Africa), and by Ramos (1982) for *Solea solea* (Spain) were similar to the present findings.

The GSI is used widely as an index of gonadal activity and as an index for spawning preparedness. In male and female *C. arel* and in female *C. lida*, GSI did not accurately reflect gonadal activity; the relation of gonadal weight to body weight did not change with stage of gonadal development. de Vlaming et al. (1982) stated that the GSI is widely and consistently used for gonadal size and activity without verification of its validity. According to de Vlaming et al. (1982), the GSI is not always the best way of expressing gonadal activity, and so this index should not be applied without validation. Chrzan (1951) concluded that the ratio of gonad weight to body weight, which normally characterizes sexual maturity, could not be determined exactly. According to Delahunty and de Vlaming (1980), the exponential relationship between ovarian weight and body weight did not change with the phase of oocyte development. However, in male *C. lida*, higher values of GSI indicated the occurrence of fully-mature specimens during this period, and a sudden fall in GSI value after September appeared to be due to spawning. Such a relationship between GSI and gonadal activity was reported for Indian halibut *Psettodes erumei* and flounder *Pseudorhombus arsius* (Ramanathan and Natarajan 1979).

In male *C. arel* and male and female *C. lida*, a rise in Kn value did not correspond with a rise in gonadal activity. Webb (1973) observed no significant variation in body condition, with onset of spawning, in sand flounder *Rhombosolea plebeia* and yellow-bellied flounder *R. leporina* off New Zealand. However, in female *C. arel*, a rise in Kn value corresponded with a rise in gonadal activity, and thus showed a positive correlation.

A linear relationship between fecundity and other variables (total length, total weight, ovary length, and ovary weight) was observed in *C. arel* and *C. lida*. The result agrees with those of Hoda (1976). The correlation coefficient between fecundity and total length, total weight, ovary length, and ovary weight showed a high positive degree of correlation in *C. arel*. In *C. lida*, the correlation coefficient between fecundity and ovary length and ovary weight showed a high positive degree of correlation; whereas the correlation coefficient between fecundity and total length and total weight did not show significant correlations. Hence in *C. lida*, fecundity was dependent only on ovary length and ovary weight.

In *C. arel* and *C. lida*, fecundity was better correlated with total length and ovary length than with total weight and ovary weight. According to Colman (1973), in sand flounder *Rhombosolea plebeia* and yellow-bellied flounder *R. leporina* off New Zealand, fecundity increased at a rate greater than the cube of length, and more than proportionately to weight; fecundity was probably slightly less proportional to ovary weight. Colman (1973) suggested that this might be due to large ovaries containing either great quantities of ovarian fluid or connective tissue or a high proportion of nondeveloping eggs.

In *C. arel* and *C. lida*, age of fish had no effect on the number of eggs. Among fish of the same length, older ones did not contain more eggs than younger ones. This result is consistent with the findings of Simpson (1951) and Bagenal (1957).

More fecund *C. lida* (relative fecundity 287–1664, $\bar{x}$ 988) laid smaller eggs (⩽0.6250 mm d.m.), while less fecund *C. arel* (relative fecundity 124–1096, $\bar{x}$ 464) laid larger eggs (⩽0.8125 mm d.m.). Dahl (1918) and Svärdson (1949) also found that more fecund species lay smaller eggs.

In *C. arel* and *C. lida*, males outnumbered females and were relatively smaller in size than females. The present finding is inconsistent with Qasim's (1966) view that the sex which outnumbers the other attains a much bigger size.

Chi-square values showed a significant deviation from the expected 1:1 ratio for 3 months in *C. arel* and for 5 months in *C. lida*. Such a deviation could be due to a partial segregation of mature forms through habitat preference (Reynolds 1974), due to migration (Collignon 1960) or behavioral differences between sexes (Polonsky and Tormosova 1969), thus rendering one sex to be more easily caught than another.

During the present investigation, spent individuals of *C. arel* and *C. lida* were not found throughout the study period, since spawning of tonguefishes appears to take place mainly in deeper waters, as observed by Seshappa and Bhimachar (1955) for Malabar sole *Cynoglossus semifasciatus*. This is a gap in the reproductive biology of these tonguefishes. Deep-sea fishing is needed to confirm this type of spawning behavior by the tonguefishes.

For *C. arel*, the spawning peak was in January which is the post-(northeast) monsoon period along the southeast coast of India. Monsoonal floods end by this time, and food resources (like copepods and amphipods, which are essential food items of juveniles) are abundant; this season would appear to be a favorable time for spawning. The spawning peak of *C. lida* was in September, which is the pre-(northeast) monsoon period along the southeast coast of India; this period coincides with the most active southwest monsoon period along the west coast of India. Most of the rivers originating in the west receive floodwaters through the southwest monsoon and empty them into the Bay of Bengal, which thus gets rich primary food resources at this time. This period would also appear to be a favorable time for spawning, because of food abundance.

Thus *C. arel* and *C. lida*, though co-occurring sympatrically in the continental shelf waters off Porto Novo, share available food resources and appear to avoid competition for food and space for their juveniles by exhibiting spawning peaks during different periods (pre-/post-northeast monsoon).

Acknowledgments

I am indebted to Dr. Bruce B. Collette, Systematics Laboratory, for his many helpful suggestions in the modification of this manuscript for publication, and for providing the facilities of the Systematics Laboratory. My sincere thanks to Dr. Thomas Munroe for critically reviewing part (food and feeding) of the manuscript. Comments made by the editor, and two anonymous reviewers helped in modifying this manuscript. Special thanks go to Ms. Ruth E. Gibbons, for her suggestions regarding computer graphics. Grateful acknowledgement is extended to the University Grants Commission, New Delhi, to Dr. R. Natarajan, and to the authorities of Annamalai University, India, for offering financial support and necessary facilities to carry out this study as a part of my Ph.D. program. I thank Dr. K. Sriraman, Tamil Nadu Fisheries, Porto Novo, for his help in the statistics. My sister, Miss G. Shantha, helped me in processing the data. Computer help extended by Mr. H.A. Kurt Luginbyhl, Dr. Jeffrey Williams, Mr. Tom Orrell, and Mr. Jeffrey Howe is greatly appreciated.

Citations

Arora, H.L.
1951 An investigation of the California sand dab, *Citharichthys sordidus* (Girard). Calif. Fish Game 37(1):3–42.

Bagenal, T.B.
1957 The breeding and fecundity of the long rough dab *Hippoglossoides platessoides* (Fabr.) and the associated cycle in condition. J. Mar. Biol. Assoc. U.K. 36(2):339–375.

Bal, D.V., and V. Rao
1984 Marine fisheries. Tata McGraw-Hill, New Delhi, 470 p.

Botha, L., D.K. Lucks, and D.S. Chalmers
1971 Mesh selectivity experiments on the east coast sole. S. Afr. Ship. News & Fishing Ind. Rev. 26(10):50–57.

Bowman, T.E., A.C. Cohen, and M.M. McGuiness
1982 Vertical distribution of *Themisto gaudichaudii* (Amphipoda:Hyperiidea) in deep-water dumpsite 106 off the mouth of Delaware Bay. Smithson. Contrib. Zool. 351, 24 p.

Braber, L., and S.J. deGroot
1973a On the morphology of the alimentary tract of flatfishes (Pleuronectiformes). J. Fish. Biol. 5(2):147–153.
1973b The food of five flatfish species (Pleuronectiformes) in the southern North Sea. Neth. J. Sea Res. 6(1–2):163–172.

Cassie, R.M.
1954 Some uses of probability paper in the analysis of size frequency distributions. Aust. J. Mar. Freshwater Res. 5(3): 513–522.

Chrzan, F.
1951 Studies on the biology of the cod in the Gulf of Gdansk. Rep. Sea Fish. Inst. (Gdynia, Poland) 6:1–28.

Clark, F.N.
1934 Maturity of the California sardine (*Sardina caerulea*) determined by ova diameter measurements. Calif. Dep. Fish. Game Fish Bull. 42, 49 p.

Clark, M.R., K.J. King, and P.J. McMillan
1989 The food and feeding relationships of black oreo, *Allocyttus niger*, smooth oreo, *Pseudocyttus maculatus*, and eight other fish species from the continental slope of the south-west Chatham Rise, New Zealand. J. Fish. Biol. 35(4):465–484.

CMFRI
1969 Marine fish production in India, 1950–1968. Bull. Cent. Mar. Fish. Res. Inst. 13, Cochin, India, 144 p.

Collignon, J.
1960 Contribution à la connaissance des *Otolithus* des côtes d'Afrique Equatoriàle. Bull. Inst. Études Centrafracaines Brazzaville, N.S. 19–20:55–84.

Colman, J.A.
1973 Spawning and fecundity of two flounder species in the Hauraki Gulf, New Zealand. N.Z. J. Mar. Freshwater Res. 7(1&2):21–43.

Daan, N.
1973 A quantitative analysis of the food intake of North Sea cod, *Gadus morhua*. Neth. J. Sea Res. 6(4):479–517.

Dahl, K.
1918 Studies of trout and trout waters in Norway. Salmon Trout Mag. 17:58–79.

Dawson, C.E.
1962 Length-weight and standard length-total length relationships of South Carolina hogchokers, *Trinectes maculatus*. Trans. Am. Fish. Soc. 91(1):89–90.

deGroot, S.J.
1971 On the interrelationships between morphology of the alimentary tract, food and feeding behaviour in flatfishes (Pisces:Pleuronectiformes). Neth. J. Sea Res. 5(2):121–196.

de Jong, J.K.
1940 A preliminary investigation of the spawning habits of some fishes of Java Sea. Treubia Buitenzorg 17(4):307–330.

Delahunty, G., and V.L. deVlaming
1980 Seasonal relationships of ovary weight, liver weight and fat stores with body weight in the gold fish, *Carassius auratus* (L.). J. Fish. Biol. 16(1):5–13.

Devadoss, P., and P.K.M. Pillai
1973 Observations on the food of juveniles of *Psettodes erumei* (Bloch). Indian J. Fish. 20(2):664–667.

deVlaming, V., G. Grossman, and F. Chapman
1982 On the use of the Gonadosomatic Index. Comp. Biochem. Physiol. 73A(1):31–39.

Devold, F.
1942 Plaice investigations in Norwegian waters. Rep. Norw. Fish. Mar. Invest. VII(3), 83 p.

Fischer, W., and G. Bianchi
1984 FAO species identification sheets for fishery purposes. II. W. Indian Ocean-Fishing area 51. FAO, Rome.

Ford, E.
1933 An account of the herring investigations conducted at Plymouth during the years from 1924–'33. J. Mar. Biol. Assoc. U.K. 19(1):305–384.

Harding, J.P.
1949 The use of probability paper for the graphical analysis of polymodal frequency distributions. J. Mar. Biol. Assoc. U.K. 28(1):141–153.

Hickling, C.F., and E. Rutenberg
1936 The ovary as an indicator of the spawning period in fishes. J. Mar. Biol. Assoc. U.K. 21(1):311–317.

Hoda, S.M.S.
1976 Reproductive biology and length-weight relationship of *Thryssa dussumieri* (Val.) of the Pakistan coast. J. Mar. Biol. Assoc. India 18(2):272–287.

Honda, H.
1984 Food acquisition patterns in some demersal teleosts. Tohoku J. Agric. Res. 35(1):33–54.

Isaacs, J.D., and R.A. Schwartzlose
1965 Migrant sound scatterers: Interaction with the sea floor. Science (Wash. DC) 150(3705):1810–1813.

James, P.S.B.R.
1967 The ribbonfishes of the family Trichiuridae of India. Mem. Mar. Biol. Assoc. India 1, 226 p.

Ketchen, K.S., and C.R. Forrester
1966 Population dynamics of the Petrale sole, *Eopsetta jordani*, in waters off western Canada. Bull. Fish. Res. Board Can. 153, 195 p.

Kuthalingam, M.D.K.
1957 Life history and feeding habits of *Cynoglossus lingua* (Ham. Buch.). J. Zool. Soc. India 9(2):208–215.

Lande, R.
1976 Food and feeding habits of the dab (*Limanda limanda* [L.]) in Borgenfjorden, north Trondelag, Norway. Norw. J. Zool. 24(3):225–230.

Langton, R.W.
1983 Food habits of yellow-tail flounder, *Limanda ferruginea* (Storer), from off the northeastern United States. Fish. Bull., U.S. 81(1):15–22.

Langton, R.W., and R.E. Bowman
1981 Food of eight northwest Atlantic pleuronectiform fishes. NOAA Tech. Rep. NMFS-SSRF 749,16 p.

Le Cren, E.D.
1951 The length-weight relationship and seasonal cycle in gonad weight and condition in the perch (*Perca fluviatilis*). J. Anim. Ecol. 20(2):201–219.

Lovern, J.A., and H. Wood
1937 Variations in the chemical composition of herring. J. Mar. Biol. Assoc. U.K. 22(1):281–293.

Lux, F.E.
1969 Length-weight relationships of six New England flatfishes. Trans. Am. Fish. Soc. 98(4):617–621.
1970 Note on growth of American plaice, *Hippoglossoides platessoides* (Fabr.) in ICNAF Subarea 5. Int. Comm. Northwest Atl. Fish. Spec. Publ. 7:5–7.

Lux, F.E., and F.E. Nichy
1969 Growth of yellowtail flounder, *Limanda ferruginea* (Storer), on three New England fishing grounds. Int. Comm. Northwest Atl. Fish. Res. Bull. 6:5–25.

Nikolsky, G.V.
1963 The ecology of fishes. Academic Press, NY, 352 p.

Pearcy, W.G., and D. Hancock
1978 Feeding habits of dover sole, *Microstomus pacificus*; rex sole, *Glyptocephalus zachirus*; slender sole, *Lyopsetta exilis*; and Pacific sand dab, *Citharichthys sordidus*, in a region of diverse sediments and bathymetry off Oregon. Fish. Bull., U.S. 76(3):641–651.

Pereyra, W.T., W.G. Pearcy, and F.E. Carvey Jr.
1969 *Sebastes flavidus*, a shelf rockfish feeding on mesopelagic fauna, with consideration of the ecological implications. J. Fish. Res. Board Can. 26:2211–2215.

Pinkas, L., M.S. Oliphant, and I.L.K. Iverson
1971 Food habits of albacore, bluefin tuna and bonito in Californian waters. Calif. Fish Game 152, 105 p.

Pitt, T.K.
1966 Sexual maturity and spawning of American plaice, *Hippoglossoides platessoides* (Fabricius), from Newfoundland and Grand Bank areas. J. Fish. Res. Board Can. 23(5):651–672.
1967 Age and growth of American plaice, *(Hippoglossoides platessoides)* in the Newfoundland area of the Northwest Atlantic. J. Fish. Res. Board Can. 24(5):1077–1099.

Polonsky, A.S., and I.D. Tormosova
1969 The spawning of the jack-mackerel of the northeast Atlantic and the distribution of its eggs and larvae. Trudy Atl. Nauchno-Issled. Inst. Rybn. Khoz. Okeanogr. 23:27-48 [in Russian].

Powles, P.M.
1967 Length-weight relationships for American plaice, witch, and yellowtail, in ICNAF Subarea 4. Int. Comm. Northwest Atl. Fish. Res. Bull. 4:121-123.

Pradhan, M.J.
1969 Fishery and biology of *Psettodes erumei* (Schneider) an Indian Ocean flatfish. Bull. Natl. Inst. Sci. India 38, Part II. Proc., Symp. Indian Ocean, Sect. IV, Fisheries, p. 885-894.

Qasim, S.Z.
1966 Sex ratio in fish population as a function of sexual differences in growth rate. Curr. Sci. (Bangalore) 35(6):140-142.
1973a An appraisal of the studies on maturation and spawning in marine teleosts from Indian waters. Indian J. Fish. 20(1):166-181.
1973b Some implications of the problem of age and growth in marine fishes from the Indian waters. Indian J. Fish. 20(2):351-371.

Rajaguru, A.
1987 Studies on taxonomy of Indian flatfishes (Teleostei: Pleuronectiformes) and biology of two species of *Cynoglossus* Ham. Buch., 1822 (Cynoglossidae) from Porto Novo. Unpubl. Ph.D. diss., Annamalai Univ., Tamil Nadu, India, 301 p.

Ramanathan, N.
1977 Studies in flatfishes of Porto Novo waters (Teleostei: Pleuronectiformes). Unpubl. Ph.D. diss., Annamalai Univ., Tamil Nadu, India, 250 p.

Ramanathan, N., and R. Natarajan
1979 Breeding biology of *Psettodes erumei* (Bloch. and Schn.) and *Pseudorhombus arsius* (Ham. Buch.) (Pisces:Pleuronectiformes), along Porto Novo coast (S. India). Aquaculture 18(3):269-282.
1980 Food and feeding habits of *Psettodes erumei* (Bloch and Schn.) and *Pseudorhombus arsius* (Ham. Buch.). Matsya (Bull. Indian Soc. Ichthyol.) 6:39-42.

Ramos, J.
1982 Estudio de la edad y crecimiento del lenguado, *Solea solea* (Linneo, 1758) (Pisces:Soleidae). Invest. Pesq. 46 (1):15-28.

Reynolds, J.D.
1974 Biology of small pelagic fishes in the new Volta Lake in Ghana. Part III: Sex and reproduction. Hydrobiologia 45(4): 489-508.

Roe, H.S.J., P.T. James, and M.H. Thurston
1984 The diel migrations and distributions within a mesopelagic community in the north east Atlantic. 6. Medusae, ctenophores, amphipods and euphausiids. Prog. Oceanogr. 13: 425-460.

Sedberry, G.R., and J.A. Musick
1978 Feeding strategies of some demersal fishes of the continental slope and rise off the mid-Atlantic coast of the USA. Mar. Biol. (Berl.) 44:357-375.

Seshappa, G.
1973 The flatfish resources of the west coast of India. Proc., Symp. Living Resour. Seas around India, CMFRI (Cochin, India), p. 470-482.
1978 Some observations on the size distribution and the occurrence of growth rings in the scales of three species of *Cynoglossus* at Calicut. Indian J. Fish. 25 (1&2):188-196.

Seshappa, G., and B.S. Bhimachar
1955 Studies on the fishery and biology of the Malabar sole, *Cynoglossus semifasciatus* Day. Indian J. Fish. 2(1):180-230.

Simpson, A.C.
1951 The fecundity of the plaice. Fish. Invest. Minist. Agrl. Fish. U.K. Ser. II, 17(5), 27 p.

Smith, R.W., and F.C. Daiber
1977 Biology of the summer flounder, *Paralichthys dentatus*, in Delaware Bay. Fish. Bull., U.S. 75(4):823-830.

Snedecor, G.W.
1956 Statistical methods, 5th ed. Iowa State Coll. Press, Ames, 534 p.

Stickney, R.R.
1976 Food habits of Georgia estuarine fishes. II. *Symphurus plagiusa* (Pleuronectiformes:Cynoglossidae). Trans. Am. Fish. Soc. 105(2):202-207.

Stickney, R.R., G.L. Taylor, and R.W. Heard III
1974 Food habits of Georgia estuarine fishes. 1. Four species of flounders (Pleuronectiformes:Bothidae). Fish. Bull., U.S. 72:515-525.

Struhsaker, P., and J.H. Uchiyama
1976 Age and growth of the nehu, *Stolephorus purpureus* (Pisces: Engraulidae), from the Hawaiian islands as indicated by daily growth increments of sagittae. Fish. Bull., U.S. 74:9-17.

Svärdson, G.
1949 Natural selection and egg number in fish. Rep. Inst. Freshwater Res., Drottningholm 29:115-122.

von Bertalanffy, L.
1938 A quantitative theory of organic growth. Hum. Biol. 10(2):181-213.

Wada, K.
1970a Studies on the population biology of the flatfish, *Limanda herzensteini* Jordan et Snyder in Niigata Region. Bull. Jpn. Sea Reg. Fish. Res. Lab. 22:31-43.
1970b Studies on the population biology of the flatfish, *Limanda herzensteini* Jordan et Snyder in Niigata Region. II. Maturity and spawning. Bull. Jpn. Sea Reg. Fish. Res. Lab. 22: 45-57.

Wakabara, Y., E.K. deRezende, and A.S. Tararam
1982 Amphipods as one of the main food components of three pleuronectiforms from the continental shelf of South Brazil and North Uruguay. Mar. Biol. (Berl.) 68:67-70.

Walford, L.A.
1946 A new graphic method of describing growth of animals. Biol. Bull. (Woods Hole) 90(2):141-147.

Webb, B.F.
1972 Fish populations of the Avon-Heathcote estuary. 1. General ecology, distribution, and length-frequency. N.Z. J. Mar. Freshwater Res. 6(4):570-601.
1973 Fish populations of the Avon-Heathcote estuary. 2. Breeding and gonad maturity. N.Z. J. Mar. Freshwater Res. 7(1&2):45-66.

Wingfield, J.C., and N.S. Grimm
1977 Seasonal changes in plasma cortisol, testosterone and oestradiol-17β in the plaice, *Pleuronectes platessa* L. Gen. Comp. Endocrinol. 31:1-11.

Zoutendyk, P.
1974a The biology of the Agulhas sole, *Austroglossus pectoralis*, Part-2. Age and growth. Trans. R. Soc. S. Afr. 41(1):33-41.
1974b The biology of the Agulhas sole, *Austroglossus pectoralis*, Part-3. Length-weight relationships. Trans. R. Soc. S. Afr. 41(2):99-108.

Appendix

Monthly sample sizes (n) for various studies on biology of *Cynoglossus arel* and *C. lida* caught commercially off Porto Novo, India, October 1981–September 1982. GI = gastrosomatic index; HI = hepatosomatic index; GSI = gonadosomatic index; L-W = length-weight relationships; Kn = relative condition factor.

	GI/HI/GSI/Sex ratio				L-W/Kn				Age and growth			
	C. arel		*C. lida*		*C. arel*		*C. lida*		*C. arel*		*C. lida*	
Months	♂	♀	♂	♀	♂	♀	♂	♀	♂	♀	♂	♀
January	53	39	32	42	52	49	24	31	54	39	34	45
February	24	45	59	16	34	52	48	45	24	44	58	16
March	54	49	64	18	51	47	85	38	54	51	64	18
April	46	55	84	51	46	58	86	54	48	55	84	51
May	56	54	38	31	57	52	62	43	56	54	39	32
June	35	40	56	59	44	41	54	54	35	40	56	59
July	69	56	25	25	70	55	37	44	69	56	25	26
August	44	54	43	62	54	66	45	64	45	54	43	62
September	56	35	46	25	59	39	62	37	57	35	50	26
October	75	54	83	76	81	57	83	80	76	55	83	77
November	86	54	160	207	70	45	135	168	87	54	160	207
December	29	34	28	28	37	38	47	65	29	37	28	31
Total	627	569	718	640	655	599	768	723	634	569	724	650

Abstract.—The inverse method for mortality and growth estimation (IMMAGE) is a new approach to obtain unbiased estimates of mortality and growth parameters for larval fishes from length-frequency data biased by the size selectivity of plankton nets. The performance of IMMAGE is compared with methods which attempt to eliminate selection bias from sampled length-frequencies. Using Monte Carlo simulations, IMMAGE estimates growth and mortality parameters that are more accurate and precise than those produced by other methods.

Inverse method for mortality and growth estimation: A new method for larval fishes

David A. Somerton

Honolulu Laboratory, Southwest Fisheries Science Center
National Marine Fisheries Service, NOAA
2570 Dole Street, Honolulu, Hawaii 96822-2396
Present address: Alaska Fisheries Science Center
National Marine Fisheries Service, NOAA
7600 Sand Point Way NE, Seattle, Washington 98115-0070

Donald R. Kobayashi

Honolulu Laboratory, Southwest Fisheries Science Center
National Marine Fisheries Service, NOAA
2570 Dole Street, Honolulu, Hawaii 96822-2396

Estimation of the growth and mortality rates of larval fishes is complicated by the sampling biases that can result from the size selectivity of plankton nets. Size selectivity due to net avoidance by larvae, for example, results in an underestimation of larval abundance that progressively increases with increasing larval length. This bias leads to an underestimation of mean length-at-age and therefore growth rate, because larger larvae in each age-class are underrepresented relative to smaller larvae. Such bias also leads to an overestimation of mortality rate, because older larvae are underrepresented relative to younger larvae. Size selectivity due to extrusion of larvae results in an underestimation of larval abundance that progressively decreases with increasing larval length and likewise leads to bias in estimates of growth and mortality rates.

Growth studies rarely address such size selection, and when they do, the approach taken is usually to devise a sampling procedure that provides unbiased length-frequencies (Methot and Kramer 1979, Yoklavich and Bailey 1990). Mortality studies, by comparison, almost always address size selection and do so after the fact by taking one of several approaches to eliminate the selection bias from the sampled length-frequencies. One approach taken by mortality studies is to divide the sampled length-frequencies by length-specific estimates of capture probability. Such capture probabilities have been obtained from field studies and estimated as (1) catch ratios of large to small mesh nets (Lenarz 1972, Leak and Houde 1987), (2) catch ratios of day to night sampling (Houde 1977, Zweifel and Smith 1981, Morse 1989, Somerton and Kobayashi 1989), or (3) catch ratios of plankton nets to purse seines (Murphy and Clutter 1972, Leak and Houde 1987). Capture probabilities have also been based on theoretical escapement models (Ware and Lambert 1985). A second approach taken by mortality studies is to simply eliminate the biased portions of the length distribution. Such elimination may exclude only small (Morse 1989) or large larvae (Houde 1977, Methot and Kramer 1979) or both (Essig and Cole 1986). Elimination of biased length-frequencies also has been combined with the use of capture probabilities (Houde 1977, Morse 1989).

Manuscript accepted 9 March 1992.
Fishery Bulletin, U.S. 90:368–375 (1992).

Although the various approaches may differ in the specifics of their application, all are based on the premise that length-frequency data must first be corrected for selection bias before they can be utilized to estimate growth and mortality. Here we introduce a new approach which reorders and joins the processes of data correction and parameter estimation. This approach, which is based on a stock assessment technique known as synthesis modeling (Methot 1989, 1990), will herein be referred to as the inverse method for mortality and growth estimation (IMMAGE). The use of IMMAGE is examined to estimate growth and mortality rates from biased length-frequency data. Additionally, the performance of IMMAGE, using Monte Carlo simulation, is compared with approaches used to correct selection bias in length-frequency data prior to parameter estimation.

Materials and methods

IMMAGE vs. bias correction

To understand how IMMAGE works and why it is an inverse method for obtaining estimates of growth and mortality parameters, the bias-correction approach should first be examined (Fig. 1a–d). One variant of the bias-correction approach might include (1) estimating the unbiased length-frequency distribution (Fig. 1b) by dividing the observed length-frequency distribution (Fig. 1a) by length-specific estimates of capture probability; (2) converting the unbiased length-frequency distribution to an age-frequency distribution (Fig. 1c) using age and length information; and (3) estimating the instantaneous mortality rate (M) as the slope of a straight line fit to the logarithms of numbers at age (Fig. 1d).

The IMMAGE approach, if applied to the same data, would include (1) choosing initial values for M and the number of day-0 larvae (N_0); (2) estimating an unbiased age-frequency distribution (Fig. 1e) based on the values of M and N_0; (3) estimating the unbiased length-frequency distribution (Fig. 1f) from the age-frequency distribution using age and length information; (4) estimating the observed (i.e., biased) length-frequency distribution (Fig. 1g) by multiplying the unbiased length-frequency distribution by estimates of capture probability; and (5) iteratively varying M and N_0, and repeating steps 2–4, until the best fit is achieved between the estimated and observed length-frequency distributions.

Thus both approaches estimate M by fitting a mortality model. However, in the bias correction approach, the model is fit to numbers-at-age derived from the observed length-frequencies; while in the IMMAGE approach, the model is fit to the observed length-frequencies themselves. Growth parameters are estimated by IMMAGE in a similar manner, except a growth model rather than a mortality model is fit to the length-frequencies.

To estimate the observed length distribution, IMMAGE requires specification of a process model and ancillary data. The process model contains parameters that are iteratively varied to achieve the best fit to the observed length-frequency distribution; the ancillary data are parameters assumed to be known. For growth estimation, the process model consists of a growth function describing the mean length-at-age and a variance function describing the variance in length-at-age. Ancillary data include estimates of the capture probability at each length. For mortality estimation, the process model consists of a mortality function describing the instantaneous mortality rate at age or length. Ancillary data include the mean and variance in length-at-age, and the capture probability at each length. Growth and mortality process models are not restricted to any particular form and may include linear or nonlinear functions.

The performance of IMMAGE and several of the bias correction approaches to parameter estimation was examined by using a Monte Carlo simulation model. For growth parameter estimation, bias correction approaches were not examined because no application to larval fishes could be found in the literature. For mortality parameter estimation, three bias correction approaches were examined: (1) elimination of the biased portions of the observed length-frequency distribution, (2) division of the observed length-frequency distribution by estimates of capture probability (correction), and (3) elimination of the biased ages from a corrected age distribution.

Monte Carlo model

The Monte Carlo simulation model is designed to mimic the sequence of steps typically used in growth and mortality studies. A central feature of this model is the simulated collection of three types of data: length-frequency samples, selection samples, and ageing samples.

Length-frequency samples are either unbiased, representing random samples drawn from a larval fish population, or biased, representing samples collected with a plankton net. Selection samples are two independent length-frequency samples, one biased and the other unbiased, used to estimate length-specific capture probabilities. Such samples represent those that might be produced by an experiment to estimate the length-selection characteristics of a plankton net (i.e., day to night catch comparisons). Ageing samples are length-frequency samples in which each length mea-

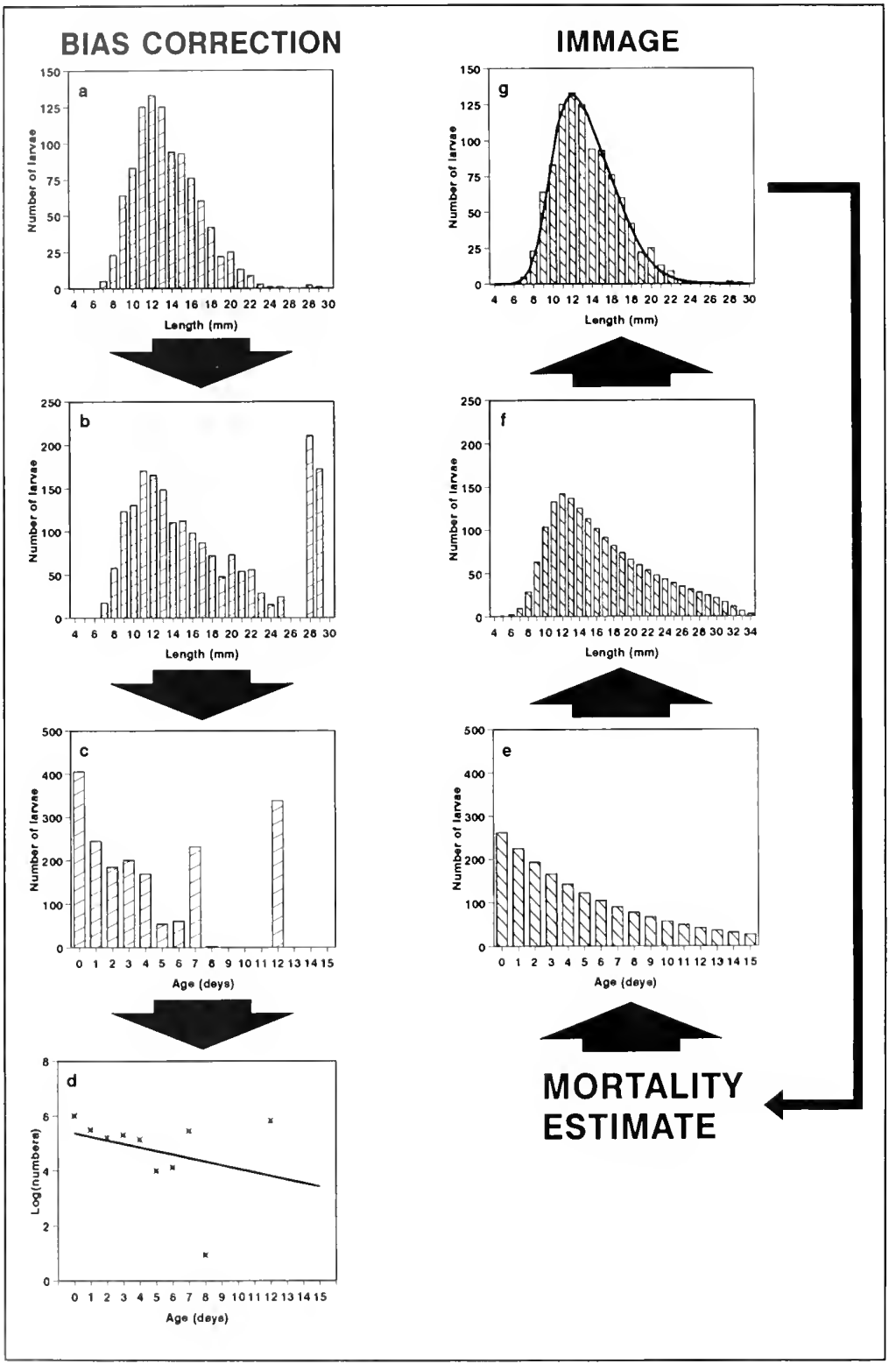

Figure 1
Comparison of the bias-correction and IMMAGE approaches to estimating instantaneous mortality rate (M) from selection-biased length-frequency data. Bias correction (left column) begins by dividing (a) the observed length-frequency distribution by estimates of capture probability to estimate (b) the unbiased length distribution. The unbiased length distribution is then converted to (c) an age distribution, and M is estimated with (d) linear regression. IMMAGE (right column) begins by creating (e) an unbiased age distribution using initial estimates of M and the number of day-0 larvae, N_0. The unbiased age distribution is converted to (f) an unbiased length distribution using the ageing sample. (g) The unbiased length distribution is multiplied by the capture probabilities to estimate the sampled length distribution (solid line), then mortality estimates are varied iteratively to minimize the residual sum of squares between the observed (histogram) and the estimated length distributions.

surement is associated with an age. Ageing samples are considered biased when used in growth parameter estimation but are considered unbiased when used in mortality parameter estimation. This distinction is made because mortality parameters can be influenced by selection bias in ageing samples as well as by selection bias in the length-frequency samples. To simplify interpretation of the results and avoid compounding the effects of the two sources of bias, bias in the ageing samples has been ignored in the mortality estimation.

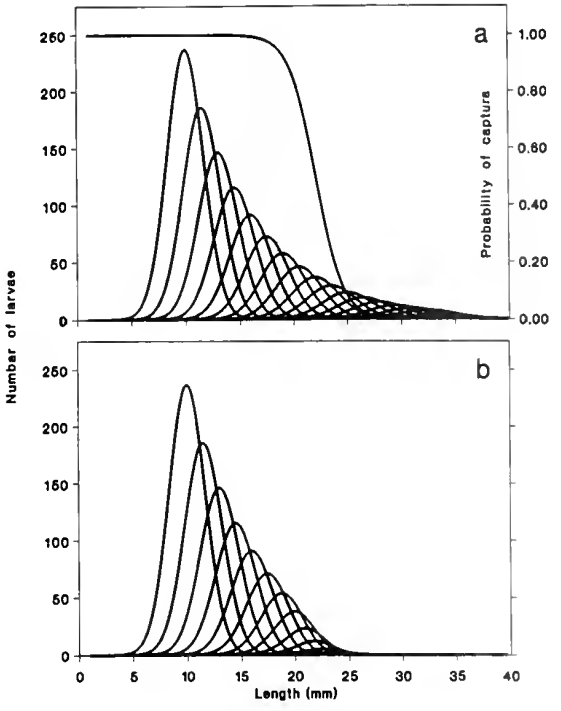

Figure 2

(a) Unbiased length distribution and relative abundance of each age-class in the simulated population of larvae, and the assumed values of capture probability (solid line) and the length of 95% selection (dotted line). With the length elimination method of bias corrector, all lengths to the right of the 95% selector line are eliminated. (b) Length distribution and relative abundance of each age-class within a sample collected with a size-selective plankton net. This distribution is created by multiplying the length distribution shown in (a) by the capture probabilities.

Unbiased length-frequency samples for these three types of data were generated by simulating the random sampling of a larval fish population (Fig. 2a) with a constant daily recruitment, a constant instantaneous daily mortality rate (M) of 0.20, and a length distribution at each age conforming to a normal probability distribution. Mean (l_t) and variance ($Var(l_t)$) of length-at-age were chosen, for simplicity, to be linear functions of age:

$$l_t = 10.00 + 1.50t, \text{ and} \quad (1)$$

$$Var(l_t) = 2.50 + 0.25t, \quad (2)$$

where t is age (in days) and l_t is length (in millimeters). Samples were drawn from the cumulative length probability distribution of this population that was constructed by dividing each of the population length-frequencies by the total sample size, then cumulatively summing across all lengths. Individual lengths within a sample were chosen by determining which category in the cumulative length probability distribution just exceeded the value of a generated uniform random number.

Biased length-frequency samples were generated by simulating the sampling of the model population by using a plankton net, which allowed zero extrusion and produced capture probabilities ($P_{c,l}$) described by an inverse logistic function:

$$P_{c,l} = 1 - \frac{1}{1 + 9.00 \times 10^7 \, e^{-2.61\,l}}, \quad (3)$$

where l is length (in mm) [Fig. 2a; parameters in Eq. (1–3) were chosen arbitrarily and were not intended to represent any particular species or sampling gear]. Samples were drawn by using the same procedure as used for unbiased samples except the population length distribution was multiplied by the capture probabilities (Fig. 2b).

Ageing samples were generated similar to length-frequency samples, but after each length was drawn, an associated age was also drawn by using the cumulative age probability distribution at each length and an additional uniform random number. The sample sizes used in the simulations [1000 length-frequency samples, 300 ageing samples, 600 selection samples, with the biased sample size set equal to the unbiased sample size × the average probability of capture determined from Equation (3)] were arbitrarily chosen but were similar to those used in Somerton and Kobayashi (1989, unpubl. data).

Growth simulations

Growth simulations examining the performance of IMMAGE consisted of 1000 repetitions of the following sequence. First, a biased ageing sample and a selection sample were generated. Second, capture probabilities were estimated from the selection sample by fitting an inverse logistic function of length, using nonlinear regression, to the ratios of the biased to the unbiased length-frequencies. Third, initial parameter estimates for the growth process model [Eq. (1) and (2)] were obtained from the ageing sample by fitting straight lines to length-at-age and variance of length-at-age. Fourth, the unbiased length distribution of each age-class was estimated as a normal distribution with mean and variance predicted from Eq. (1) and (2) evaluated at the current parameter estimates. Fifth, the biased length-frequency distribution of each age-class was estimated by multiplying the unbiased length-frequency distribution by the estimated capture probabilities. Sixth, parameter estimates for Eq. (1) and (2)

were iteratively varied, and steps 4 and 5 were repeated, until the minimum residual sum of squares (RSS) was achieved. The RSS was defined as

$$\sum_j \sum_i (F_{ij} - \hat{F}_{ij})^2, \quad (4)$$

where F_{ij} and $\hat{F}_{ij}$ are the observed and estimated frequency within the ith length interval and the jth age-class.

Mortality simulations

Mortality simulations examined the performance of IMMAGE and three bias-correction approaches: length elimination, division by capture probabilities, and age elimination. Each of the 1000 repetitions of a simulation began by generating a biased length-frequency sample, an unbiased ageing sample, and a selection sample. For all simulations, except those examining IMMAGE, mortality estimation began with an attempt to derive an unbiased age distribution. If length elimination was used, this was accomplished in two stages. First, an unbiased length-frequency distribution was estimated by eliminating all length categories with a capture probability of <0.95 [based on capture probabilities defined by Equation (3), length-classes 3–18 were retained; Fig. 2a]; a probability of 0.95 was used instead of 1.00 because it is better defined. Second, the age-frequency distribution was estimated from the unbiased length-frequency distribution by using the ageing sample and a procedure known as age-slicing (Mesnil and Shepherd 1990). To do this, lengths from the ageing sample were regressed on the ages, and the fitted linear regression equation was evaluated to determine the length corresponding to each age boundary (i.e., 0.5, 1.5, 2.5 days, and so on). Age-frequencies were then estimated by summing length-frequencies between age boundaries.

If division by capture probabilities was used, the age-frequency distribution was estimated by first dividing the observed length-frequency distribution by estimates of capture probability, then converting the length-frequencies to age-frequencies using age-slicing. If age elimination was used, age-classes with a capture probability of <0.95 at the mean length also were eliminated from the age-frequency distribution (age-classes 0–5 days were retained; Fig. 2a). For all three cases, instantaneous mortality rate was then estimated as the slope of an unweighted linear regression to the natural logarithm of numbers-at-age (Ricker 1975).

For simulations examining IMMAGE, mortality estimation proceeded as follows. First, initial values of M and N_0 were obtained from the ageing sample by fitting a straight line to the logarithm of numbers-at-age. Second, values of l_t and $\mathrm{Var}(l_t)$ were estimated from the ageing sample by fitting straight lines to length-at-age and $\mathrm{Var}(l_t)$-at-age, using linear regression, and then evaluating the fitted regression equations at each t. Third, capture probabilities were estimated from the selection sample. Fourth, the unbiased age distribution was estimated as $N_t = N_0 e^{-Mt}$. Fifth, the unbiased length distribution of each age-class was estimated as N_t times a normal probability distribution with a mean equal to l_t and a standard deviation equal to the square root of $\mathrm{Var}(l_t)$. The unbiased length distribution for the population was then estimated by summing the age-specific length distributions over all age-classes. Sixth, the biased (observed) length distribution was estimated by multiplying the unbiased population length distribution by the estimated capture probabilities. Seventh, N_0 and M were iteratively varied, and steps 4–6 repeated, until the minimum RSS was achieved. The RSS was defined as

$$\sum_j (F_j - \hat{F}_j)^2, \quad (5)$$

where F_j and $\hat{F}_j$ are the observed and estimated frequencies within the jth length interval.

The IMMAGE application used in the simulations (i.e., one that assumes linear growth and constant mortality) is available from the authors as a stand-alone program (IMMAGE, written in Microsoft QuickBasic) designed to run on IBM-compatible microcomputers.

Results and discussion

Growth

The type of size selection examined in the simulations (i.e., a decrease in the probability of capture with increasing larval length) complicates the estimation of growth and mortality in slightly different ways. For growth estimation, the primary effect is that the largest larvae in each age-class are undersampled relative to the smallest larvae, and the mean lengths-at-age are therefore underestimated (Fig. 2b). Since the bias progressively increases with age, plots of mean length against age are curvilinear and falsely indicate a declining growth rate (Fig. 3). Such curvilinear or even asymptotic growth patterns are often reported in studies of wild-caught larvae (Bailey 1982, Laroche et al. 1982, Lough et al. 1982, Thorrold 1988, Warlen 1988). Although there may be biological reasons to expect such a pattern, especially for species with pronounced ontogenetic changes in body form, length-selective sampling may be a contributing factor.

IMMAGE estimates of the slope (1.499 ± 0.005; $\bar{x}$ 1000 replicates ± 2 SE) and intercept (10.002 ± 0.012)

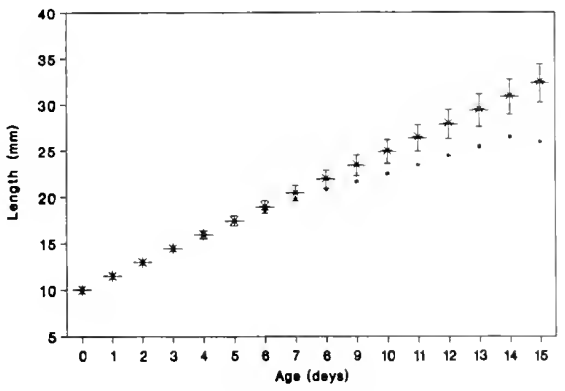

Figure 3

Mean length-at-age in the simulated population (*), mean length-at-age estimated without correction for size selection (■), and mean length-at-age (±2 SE) estimated with IMMAGE (vertical bars).

of the linear growth function [cf. Eq. (1)] were both unbiased, as were all of the estimates of mean length-at-age over the entire age range (Fig. 3). This indicates that, at least for linear growth, IMMAGE provides unbiased estimates of growth parameters from biased length and age samples.

Mortality

For mortality estimation, the primary effect of the decrease in capture probability with increasing larval length is that relative abundance is progressively underestimated with increasing age (Fig. 2b). If ignored, such a progressive underestimation would result in positively biased mortality estimates. In the simulated population, for example, mortality estimates obtained from the observed length-frequency samples ($M = 0.450 \pm 0.004$) had a highly significant positive bias of 125% (Fig. 4a).

Elimination of the biased length-frequencies was only partially effective in reducing the bias in estimated mortality rates, because the mortality estimates ($M = 0.364 \pm 0.007$) still had a highly significant positive bias of 80% (Fig. 4b). In practice, length elimination is likely to be even less effective than it appears here, because it is usually applied to cases where the capture probabilities are crudely known, whereas exact knowledge is assumed in the simulations.

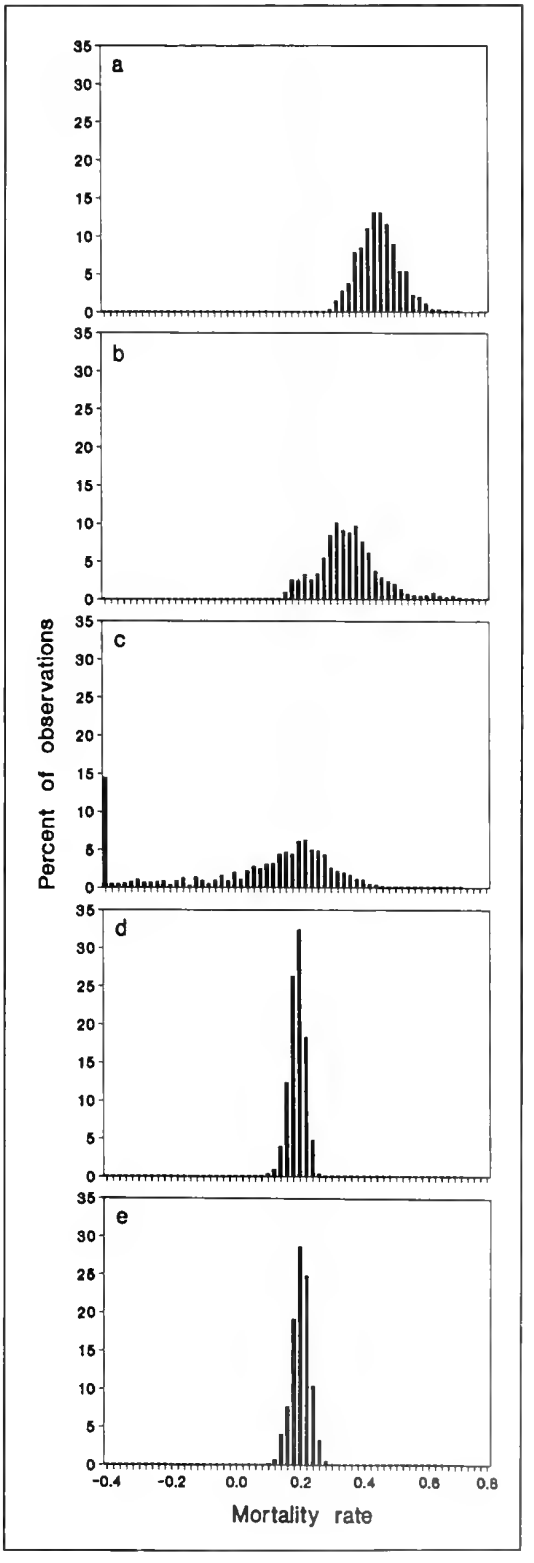

Figure 4 (right)

Frequency distribution of 1000 simulated estimates of instantaneous mortality rate computed from (a) observed length-frequency data, (b) observed length-frequency data after eliminating all length-frequencies with a capture probability of < 0.95, (c) observed length-frequency data divided by estimates of capture probability, (d) corrected age-frequency data after eliminating all age-frequencies with a capture probability of < 0.95, and (e) observed length-frequency data using IMMAGE.

Dividing the observed length-frequency distribution by estimates of capture probability was as ineffective because the mortality estimates (-0.035 ± 0.030) had a highly significant negative bias of 83% (Fig. 4c). The negative bias and the strong negative skew in the frequency distribution are due to the infrequent generation of large larvae. When such larvae occur in a sample, their relative abundance is greatly magnified by their extremely small capture probabilities. The overestimation of large length-classes results in a corresponding overestimation of old age-classes. Because the overestimated age-frequencies are at the extreme of the age range, they exert considerable influence on the slope of the mortality regression and thereby result in the underestimation of M.

Elimination of the biased age-frequencies nearly eliminates this problem and results in mortality estimates (0.192 ± 0.002) with a significant but small negative bias of 4% and a considerable reduction in variance (Fig. 4d). The apparently greater effectiveness of age elimination compared with length elimination is a function of the variance in length-at-age within the larval fish population. For example, when length elimination is applied to the simulated population, essentially all of the undersampled lengths are removed. However, this creates a new bias in the age distribution, because some age-classes experience greater elimination than others (Fig. 2a). Clearly, if no variation exists in length-at-age, length elimination will be identical to age elimination. To our knowledge, the use of age elimination has not been reported in the literature.

Mortality estimates produced by IMMAGE (0.201 ± 0.002) are unbiased and, along with age elimination, have the smallest variance (Fig. 4e). This superior performance is achieved because, unlike length or age elimination, IMMAGE uses all of the sampled length-frequency data and, unlike correction, uses capture probability multiplicatively and therefore avoids magnifying the sampling error.

Practical application of IMMAGE

The application of IMMAGE using the Monte Carlo simulation has been chosen because of its simplicity. Although linear growth, constant mortality, and monotonically increasing size selection may not always be suitable for a particular application, the IMMAGE procedure is extremely adaptable in the way growth, mortality, and size selection can be specified. For example, growth could be specified as an exponential or a Laird-Gompertz function, and size selection could be specified as a double logistic function (Somerton and Kobayashi 1989) describing extrusion and avoidance simultaneously. Mortality could be specified as either a stage-specific function, where the mortality rates of yolksac and feeding larvae differ, or an inverse function of age (Lo 1986). More importantly perhaps, mortality could also be specified as a function of length.

Although mortality rates of larvae likely decline with length for many species (Pepin 1991), length-dependent mortality rates are difficult to estimate because such mortality induces a progressive bias in mean length-at-age (if the largest larvae in an age-class survive better than the smallest, the apparent growth rate is positively biased; Methot and Kramer 1979). This problem can be circumvented with IMMAGE by estimating the size-selected length-frequency distribution using a length-based population model (Somerton and Kobayashi 1990) which mimics the growth and survival of individual members of an age-class over time. Using such an approach, the likelihood of size-dependent mortality could be tested against constant or age-dependent mortality based on goodness-of-fit to the observed length-frequencies.

Several variations on the application of IMMAGE described herein may be more appropriate in other cases. First, the estimation of growth and mortality parameters could be accomplished simultaneously rather than separately by allowing the mortality process model to include growth parameters as variables rather than as known quantities. Second, the objective function used for parameter estimation could be specified as a likelihood function rather than a sum-of-squares function. This would be especially appropriate in cases where the errors about the observed length-frequencies are not normally distributed. Third, prior estimates of some parameters could be included in the growth and mortality process models rather than estimating all parameters directly from the three samples (i.e., ageing, length-frequency, and selection samples).

We believe the best way of estimating parameter variances for an IMMAGE application is to use a sample reuse technique known as boot-strapping (Efron and Tibshirani 1991), because all sources of sampling variability can be included. Boot-strapping IMMAGE, however, is computationally intensive and potentially time-consuming. To facilitate variance estimation on slow computers, we have therefore included in the IMMAGE program an approximate technique that is based on the inverse of the information matrix (Ratkowsky 1983).

When obtaining larval fish samples free of selection bias is difficult, IMMAGE can still obtain unbiased estimates of growth and mortality parameters. Not only does IMMAGE provide estimates that are more accurate and precise than other approaches, its greater flexibility in form allows estimation of length-dependent mortality rates that are perhaps biologically more realistic than the constant rates now estimated.

Acknowledgments

We thank George Boehlert, Ed DeMartini, Chyan Huei Lo, Sue Picquelle, and Tim Ragen for reviewing the manuscript and offering helpful suggestions. In addition, we thank Rick Methot who gave us the original idea of the inverse estimation procedure.

Citations

Bailey, K.M.
1982 The early life history of Pacific hake *Merluccius productus*. Fish Bull., U.S. 80:589–598.

Efron, B., and R. Tibshirani
1991 Statistical analysis in the computer age. Science (Wash. DC) 253:390–395.

Essig, R.J., and C.F. Cole
1986 Methods of estimating larval fish mortality from daily increments in otoliths. Trans. Am. Fish. Soc. 115:34–40.

Houde, E.D.
1977 Abundance and potential yield of the round herring, *Etrumeus teres*, and aspects of its early life history in the eastern Gulf of Mexico. Fish. Bull., U.S. 75:61–89.

Laroche, J.L., S.L. Richardson, and A.A. Rosenberg
1982 Age and growth of a pleuronectid, *Parophrys vetulus*, during the pelagic larval period in Oregon coastal waters. Fish. Bull., U.S. 80:93–104.

Leak, J.C., and E.D. Houde
1987 Cohort growth and survival of bay anchovy *Anchoa mitchilli* larvae in Biscayne Bay, Florida. Mar. Ecol. Prog. Ser. 37:109–122.

Lenarz, W.
1972 Mesh retention of larvae of *Sardinops caerulea* and *Engraulis mordax* by plankton nets. Fish. Bull., U.S. 70: 789–798.

Lo, N.
1986 Modeling life-stage-specific instantaneous mortality rates, an application to northern anchovy *Engraulis mordax* eggs and larvae. Fish. Bull., U.S. 84:395–407.

Lough, R.G., M. Pennington, G.R. Bolz, and A.A. Rosenberg
1982 Age and growth of larval Atlantic herring, *Clupea harengus*, in the Gulf of Maine–Georges Bank region based on otolith growth increments. Fish. Bull., U.S. 80:187–199.

Mesnil, B., and J.G. Shepherd
1990 A hybrid age- and length-structured model for assessing regulatory measures in multiple-species, multiple-fleet fisheries. J. Cons. Cons. Int. Explor. Mer 47:115–132.

Methot, R.D.
1989 Synthetic estimates of historical abundance and mortality for northern anchovy. *In* Edwards, E.F., and B. Megrey (eds.), Mathematical analysis of fish stock dynamics, p. 66–82. Am. Fish. Soc. Symp. 6, Bethesda.
1990 Synthesis model: An adaptable framework for analysis of diverse stock assessment data. *In* Low, L.L. (ed.), Proceedings, Symposium on application of stock assessment techniques to gadids, p. 259–277. Int. North Pac. Fish. Comm. Bull. 50.

Methot, R.D., and D. Kramer
1979 Growth of northern anchovy larvae, *Engraulis mordax*, in the sea. Fish. Bull., U.S. 77:413–423.

Morse, W.W.
1989 Catchability, growth and mortality of larval fish. Fish. Bull., U.S. 87:417–446.

Murphy, G.I., and R.I. Clutter
1972 Sampling anchovy larvae with a plankton purse seine. Fish. Bull., U.S. 70(3S):789–798.

Pepin, P.
1991 Effect of temperature and size on development mortality and survival of marine fish. Can. J. Fish. Aquat. Sci. 48: 503–518.

Ratkowsky, D.A.
1983 Nonlinear regression modeling. Marcel Dekker, NY, 276 p.

Ricker, W.E.
1975 Computation and interpretation of biological statistics of fish populations. Bull. Fish. Res. Board Can. 191, 382 p.

Somerton, D.A., and D.R. Kobayashi
1989 A method for correcting catches of fish larvae for the size selection of plankton nets. Fish. Bull., U.S. 87:447–455.
1990 Robustness of the Wetherall length-based method to population disequilibrium. Fish. Bull., U.S. 89:307–314.

Thorrold, S.
1988 Estimating some early life history parameters in a tropical clupeid, *Herklotsichthys castelnaui*, from daily growth increments in otoliths. Fish. Bull., U.S. 87:73–83.

Ware, D.M., and T.C. Lambert
1985 Early life history of Atlantic mackerel (*Scomber scombrus*) in the southern Gulf of St. Lawrence. Can. J. Fish. Aquat. Sci. 42:577–592.

Warlen, S.M.
1988 Age and growth of larval gulf menhaden, *Brevoortia patronsis*, in the northern Gulf of Mexico. Fish. Bull., U.S. 86:77–90.

Yoklavich, M.M., and K.M. Bailey
1990 Hatching period, growth and survival of young walleye pollock *Theragra chalcogramma* as determined from otolith analysis. Mar. Ecol. Prog. Ser. 64:12–23.

Zweifel, J., and P. Smith
1981 Estimates of abundance and mortality of larval anchovies (1951–75): Application of a new method. Rapp. P.-V. Réun. Cons. Int. Explor. Mer 178:248–259.

Abstract.–The seasonal distribution and relative abundance of river herring *Alosa pseudoharengus* and *A. aestivalis* off Nova Scotia is examined using Canadian Department of Fisheries and Oceans data from bottom-trawl surveys (1970–89) and the International Observer Program (1980–89). River herring occurred throughout the year in regions characterized by strong tidal mixing and upwelling in the Bay of Fundy and off southwestern Nova Scotia. During spring, river herring were most abundant in the warmer, deeper waters of the central Scotian Shelf, particularly between Emerald and Western Banks, and in areas of warm slope water intrusion along the Scotian Slope, the western and southern edges of Georges Bank, and in the eastern Gulf of Maine–Bay of Fundy. Most catches occurred at bottom temperatures of 7–11°C offshore at mid-depths in spring (101–183 m), in shallower nearshore waters in summer (46–82 m) and in deeper offshore waters in fall (119–192 m). Diel variation in catch occurred during summer and fall but not during spring, with largest catches during daylight. Seasonal distribution patterns of small (<19 cm FL) and large (>19 cm FL) river herring overlapped geographically. Small fish preferred shallow regions (<93 m) during spring and fall, while large fish occurred in deeper areas (>93 m) during all seasons. The temporal and spatial distribution of river herring off the coast of Nova Scotia is likely influenced by zooplankton concentrations and occurrence of bottom temperatures >5°C. The pattern of seasonal movement is generally inshore and northward during spring, and offshore and southward in the fall.

Manuscript accepted 6 March 1992.
Fishery Bulletin, U.S. 90:376–389 (1992).

Seasonal distribution of river herring *Alosa pseudoharengus* and *A. aestivalis* off the Atlantic coast of Nova Scotia

Heath H. Stone
Brian M. Jessop
Department of Fisheries and Oceans, Biological Science Branch
P O Box 550, Halifax, Nova Scotia B3J 2S7, Canada

River herring (a collective term for the alewife *Alosa pseudoharengus* and the blueback herring *A. aestivalis*) are anadromous clupeids native to the Atlantic coast of North America. These closely-related species are remarkably similar in morphology and life history and differ only slightly in terms of meristics, morphometrics, growth parameters and time of spawning (Bigelow and Schroeder 1953, Leim and Scott 1966, Messieh 1977, Loesch 1987). Alewives and blueback herring are sympatric; alewife range from Newfoundland to North Carolina, and blueback herring from the Gulf of St. Lawrence to Florida (Bigelow and Schroeder 1953). They are fished commercially in the Maritime provinces of Canada and Atlantic coastal United States during their spring spawning migrations and are often marketed together as alewife, gaspereau, or river herring, depending on local convention.

Both species often co-occur in freshwater (Loesch et al. 1982, Jessop and Anderson 1989), estuarine (Stone and Daborn 1987), and marine (Neves 1981) habitats. While the freshwater life histories of alewives and blueback herring have been well documented (reviewed by Loesch 1987), less information is available on their distribution and movements at sea, particularly in Canadian coastal areas. Off the Atlantic coast of Nova Scotia, bottom trawls have caught river herring on the western Scotian Shelf, with alewives collected during spring and fall (Vladykov 1936, Neves 1981, Vinogradov 1984) and blueback herring in spring and summer (Netzel and Stanek 1966, Neves 1981). In the inner Bay of Fundy, river herring aggregate during summer in the turbid estuarine waters of Minas Basin (Rulifson 1984, Stone and Daborn 1987) and Cumberland Basin (Dadswell et al. 1984). In the outer Bay of Fundy, alewives and blueback herring have been captured during summer and autumn in herring weirs, purse seines (Jessop 1986), and during bottom-trawl surveys (Neves 1981). Neves (1981) examined the marine distribution and seasonal movements of river herring along the continental shelf from Cape Hatteras, North Carolina, to southwestern Nova Scotia. In this paper, we describe the seasonal marine distribution and relative abundance of river herring off Nova Scotia based on 20 years of combined alewife and blueback herring catch data from Canadian research vessel surveys, thereby extending northward the analysis by Neves (1981) of their distribution off the Atlantic coast of the United States. Offshore distributions are interpreted in relation to water depth and temperature within the survey area.

Although marine exploitation of alewives and blueback herring in the Maritime provinces by incidental

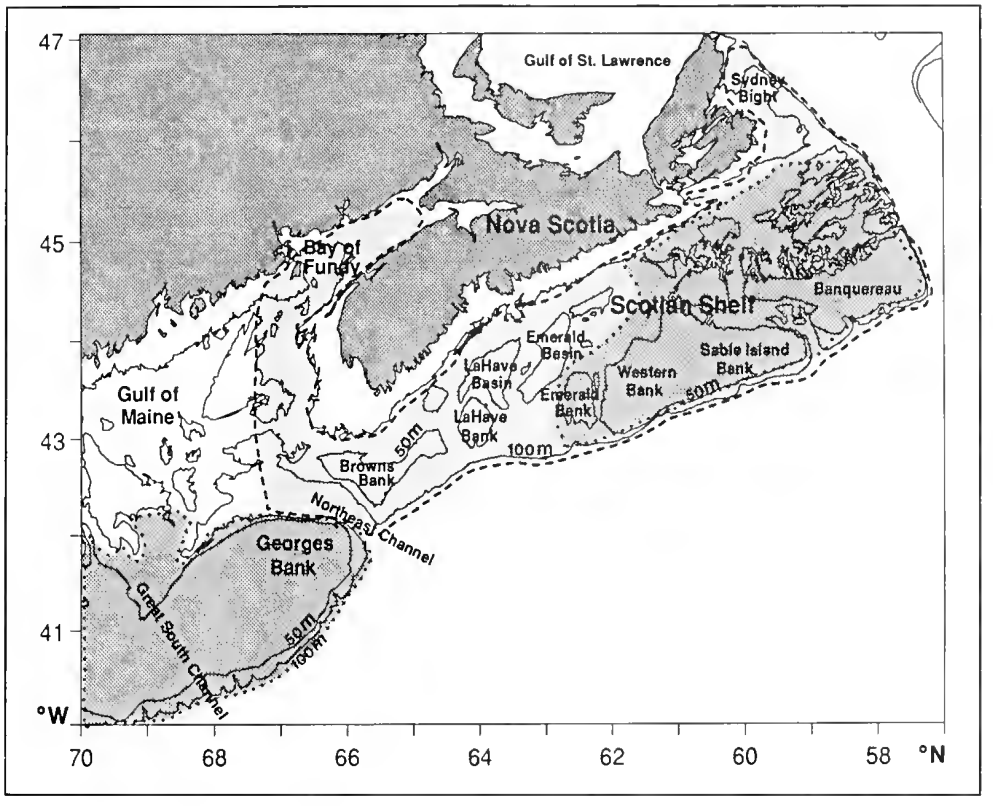

Figure 1
Topographical map of Canadian groundfish survey areas (1970–89) and geographic features mentioned in text. Spring (1979–85), summer (1970–89), and fall (1978–84) survey coverage of the Scotian Shelf and Bay of Fundy (- - -) is shaded light-gray. Spring (1986–89) survey coverage of the eastern shelf and Georges Bank (. . .) is shaded dark-gray. Offshore banks are delineated by the 100 m depth contour; basins and the outer edge of the continental shelf are delineated by the 200 m depth contour.

catches in offshore bottom-trawl fisheries from 1984 to 1989 has averaged 1,400 t, which is <17% of the freshwater exploitation (Statistics Branch, Dep. Fish. Oceans, P.O. Box 550, Halifax, Nova Scotia B3J 2S7), only a limited amount of information on marine distribution is available from commercial fishing operations. More comprehensive information comes from the bycatch of the annual bottom trawl surveys of the Scotian Shelf–Bay of Fundy region conducted by the Canadian Department of Fisheries and Oceans (DFO) to monitor temporal changes in the abundance of commercially exploited groundfish species and associated environmental conditions (Halliday and Koeller 1981). Additional information on river herring distribution was obtained from 10 years of bycatch data from foreign and domestic fishing operations compiled by the DFO International Observer Program.

Description of survey area

The survey area, which includes the Scotian Shelf, eastern Gulf of Maine, Bay of Fundy, and, recently, Georges Bank, is topographically and hydrographically complex (Fig. 1). The oceanographic and biological characteristics of this area influence the distribution of other species (Sinclair 1988) and are assumed to do so for river herring.

The Scotian Shelf is characterized by deep central basins (>200 m) and shallow offshore banks (<50 m). Over the deeper parts of the shelf, three distinct vertical layers occur: a surface mixed layer with seasonal temperature changes, an intermediate layer with temperatures <5°C regardless of season, and a warm bottom layer derived from cross-shelf intrusions of slope water (Hatchey 1942, Smith et al. 1978). The coldest water at any depth occurs in the northeastern Shelf and the warmest in the bottom waters of the central Shelf (also termed the Scotian Gulf) where intrusion of warm slope water to adjacent Emerald and LaHave Basins is a persistent feature (McLellan 1954). Nutrient-rich upwellings along the shelf-slope interface sustain high levels of biological productivity (Fournier et al. 1977). Consequently, pelagic fish production on the shelf-slope is much higher than on the shelf (Mills and Fournier 1979).

The Bay of Fundy and eastern Gulf of Maine regions are vertically well mixed due to the action of strong tidal currents (Greenburg 1984). Strong, persistent summertime fronts in sea-surface temperature occur near the mouth of the Bay and off southwestern Nova Scotia (Loder and Greenburg 1985). The upwelling of nutrient-rich deep water from the Gulf of Maine and Scotian Shelf supports high biological productivity during spring and summer (Fournier et al. 1984). Secondary production in the outer Bay of Fundy occurs

Table 1

Summary of river herring (*Alosa* spp.) catch (in numbers) and effort for spring, summer, and fall groundfish surveys conducted off Nova Scotia by the Canadian Department of Fisheries and Oceans, 1970–89. Parentheses enclose percentages of total numbers of sets containing catch. SD = sample standard deviation.

Season	Year	No. of surveys	No. of sets	Catch-per-set $\bar{x}$	Catch-per-set SD	Total no. of fish	Sets with catch
Spring (Feb–Apr)	1979–89	11	1231	6.6	73.85	8117	268 (21.8)
Summer (June–July)	1970–89	20	1892	2.0	18.05	3703	214 (11.3)
Fall (Sept–Dec)	1978–84	7	982	1.6	9.47	1537	120 (12.3)
Total	1970–89	38	4105	3.3	42.53	13357	602 (14.7)

predominantly within the water column and provides forage to pelagic fish species (Emerson et al. 1986).

On Georges Bank, frontal regions generated by tidal mixing along the northern and southern edges are highly productive due to advection of nutrients from deeper waters on both sides of the bank (Cohen et al. 1982). Intrusions of warm, saline slope water occur into the southern Gulf of Maine through the Great South Channel (Mountain et al. 1989) and the Northeast Channel (Ramp and Wright 1979).

Materials and methods

Survey design and sampling

River herring catch and length-frequency data were obtained from 38 bottom-trawl surveys conducted between 1970 and 1989 (Table 1). The main study area (Scotian Shelf, eastern Gulf of Maine, and Bay of Fundy; Fig. 1) was surveyed at least once annually during this period. A single summer (June–July) survey was conducted annually between 1970 and 1977; spring (February–April), summer, and fall (September–December) surveys were made from 1978 to 1984; and spring and summer surveys from 1985 to 1989. Changing research requirements shifted spring survey effort to Georges Bank and the eastern Scotian Shelf in 1986, thereby excluding the western shelf region and the Bay of Fundy (Fig. 1). Recent (1987–89) summer surveys also included some coverage of northeastern Georges Bank.

All surveys used a stratified random design with trawl stations allocated to depth strata in proportion to stratum area and randomly positioned within strata. Stratum depth ranges were 0–92 m (0–50 fm), 93–183 m (51–100 fm), and 184–366 m (101–200 fm). Before 1981, summer cruises used a No. 36 Yankee bottom trawl with a 10 mm stretched-mesh liner in the cod end; all other cruises used a Western IIA trawl with a 10- or 20 mm stretched-mesh liner. Tows at each sampling station were for 30 minutes. Halliday and Koeller (1981) and Smith (1988) give further details of Canadian groundfish survey methods.

Total number and weight (kg) of river herring in the catch were recorded for each tow as was bottom-water temperature (°C), tow deployment time (Atlantic Standard Time), latitude, longitude, and bottom depth (m). Fork lengths (FL) were measured (to nearest cm) for all fish in catches of <250 fish; otherwise, catches were subsampled (no fixed procedure) for length. Alewife and blueback herring were not differentiated and sex was not determined.

Catches of river herring in Canadian surveys probably consist mainly of alewives since both species tend to be vertically separated by depth. Blueback herring frequent upper levels; alewives frequent mid-depths (Neves 1981) where they are more available to capture in bottom-trawl gear. All of the river herring catch from 1990 spring and summer groundfish surveys (n 1048) were confirmed by examination to be alewives. However, because river herring were not identified to species during the 1970–89 surveys, upon which our analysis is based, we cannot exclude the possibility that the catch included a small proportion of blueback herring captured incidentally when setting or hauling the gear.

Data analysis

Catch-per-set was standardized to a tow length of 1.75 nm with no adjustment for differences between gear types. Only cruises with catches of one or more fish were analyzed; 17 cruises on the eastern Scotian Shelf with no catches were omitted. River herring >33 cm FL were excluded from the data set (<0.5% of all fish measured), since they exceed the maximum fork lengths recorded for alewife and blueback herring (Loesch 1987) and are believed to be incorrectly identified American shad *Alosa sapidissima*.

Seasonal distributions of relative abundance were obtained from plots of average catch-per-set data (including zero catches) aggregated by 20-minute rectangles of latitude and longitude. Seasonal, rather than monthly, distributions gave a more complete picture of offshore distribution patterns. The locations of 2, 5, and 10°C isotherms, generated from plots of the mean bottom-water temperature in 20-minute rectangles, were superimposed on seasonal distribution plots. Differences in the seasonal distribution of two size-groups of river herring (i.e., ≤19 cm and >19 cm FL) were examined by plotting the capture locations of each group. The size-at-first-spawning of Saint John River blueback herring (Jessop et al. 1982), which mature at a smaller size than alewife, was used as the separation criterion.

Approximate randomization tests, with 1000 permutations (Edgington 1987) were used to examine the following relationships: (a) effects of season (spring, summer, fall) and depth (<93 m, 93–183 m, >183 m) on mean catch-per-set (including sets with no catches), (b) diel variability in seasonal catch-per-set (day and night, based on gear deployment times in relation to monthly morning and evening civil twilight times for the appropriate geographic location), and (c) mean fork length by season and depth. All comparisons used catch or fork-length data from a 6-year time-series (1979–84) in which annual sampling occurred during spring, summer, and fall. Each dependent comparison (i.e., depth effect within season, season effect within depth), used a Bonferroni significance level (α 0.05, divided by the number of dependent comparisons) (Day and Quinn 1989).

Randomization procedures were used for the analysis because statistically significant heteroscedasticity in the variances of (a) transformed (ln X + 1) catch per set data by season and depth (Cochran's C = 0.372, $P<$ 0.0001, df 239, 9), (b) transformed (ln X + 1) diel catch-per-set by season (Cochran's C = 0.365, $P<0.0001$, df 359, 6), and (c) fork length by season and depth (Cochran's C = 0.293, $P<0.0001$, df 637, 9) violates an assumption of parametric statistics. This violation is compounded by unequal sample sizes.

Bycatch data

Set locations and fork lengths of river herring bycatch in foreign and domestic commercial groundfish operations (1980–89) obtained from the DFO International Observer Program database were compared with research survey data. Catch locations were plotted for spring (February–May) and summer (June–August), when fishing effort and bycatch were highest. Fork length distributions were truncated at 33 cm due to assumed misclassification (4% of fish measured exceeded this length). Annual landings of alewife in metric tons (t) for the Scotian Shelf–Bay of Fundy region (4VWX) from 1970 to 1989 were obtained from Northwest Atlantic Fisheries Organization (NAFO) Statistical Bulletins and correlated (Spearman rank) with catch indices from research vessel surveys. The analysis was conducted to determine if survey indices (i.e., mean number and mean weight per set · season^{-1} · year^{-1}) were consistent with bycatch landings as an indicator of relative abundance.

Results

Seasonal distribution and abundance

A total of 13,357 river herring were captured in 602 (15%) of 4105 bottom-trawl sets conducted between 1970 and 1989 (Table 1). Spring survey catches were the highest and most variable, followed by summer. The proportion of sets with river herring from spring surveys was nearly double that from the other two seasons. A maximum catch of 2292 river herring occurred on 17 March 1980 in the Scotian Gulf region, south of Emerald Basin.

During spring surveys, river herring dominated in three regions: the Scotian Gulf, southern Gulf of Maine, and off southwestern Nova Scotia from the Northeast Channel north to the central Bay of Fundy (Fig. 2). Catches also occurred along the southern edge of Georges Bank and in the canyon between Banquereau and Sable Island Banks. Relative abundance was highest in the Scotian Gulf between Emerald and Western Banks, and on the southern slope of Georges Bank. Most catches of river herring occurred where bottom temperatures exceeded 5°C (Fig. 2), although in the Bay of Fundy, captures occurred at lower temperatures.

Summer distributions of river herring were less extensive than in spring and were limited mainly to the eastern Gulf of Maine (off southwestern Nova Scotia) and the Bay of Fundy, with a few occurrences nearshore in the central Shelf region (Fig. 2). Catches were highest along the northern shore of the Bay of Fundy, with very few fish captured in the Scotian Gulf and on the eastern Scotian Shelf. Bottom temperatures exceeded 5°C at all capture locations.

Fall distributions of river herring were more extensive than in summer (Fig. 2). Moderate to large catches were obtained from southwestern Nova Scotia to the Bay of Fundy, the central Scotian Shelf, and Sydney Bight. As in the case of spring and summer surveys, very few fish were captured on the eastern half of the Scotian Shelf. All catches occurred at bottom temperatures exceeding 5°C.

Bycatch of river herring from foreign fishing fleets (1980–89) occurred mainly during spring in a narrow

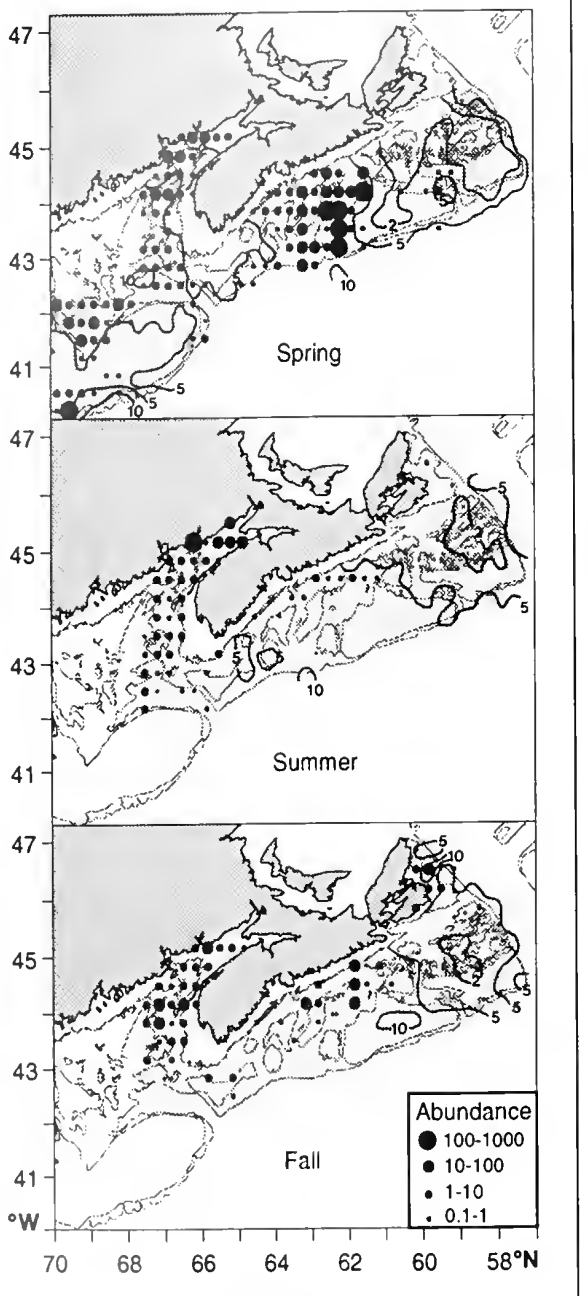

Figure 2

Distribution and relative abundance ($\bar{x}$ catch per 20-min square) of river herring from spring (1979–89), summer (1970–89), and fall (1978–84) groundfish surveys conducted off the Atlantic coast of Nova Scotia. Area sampled is indicated by shading, and mean catch (n/tow) for each 20-min square is represented by a solid circle, scaled to catch level. Isotherms for 2, 5, and 10°C of bottom temperature are also indicated.

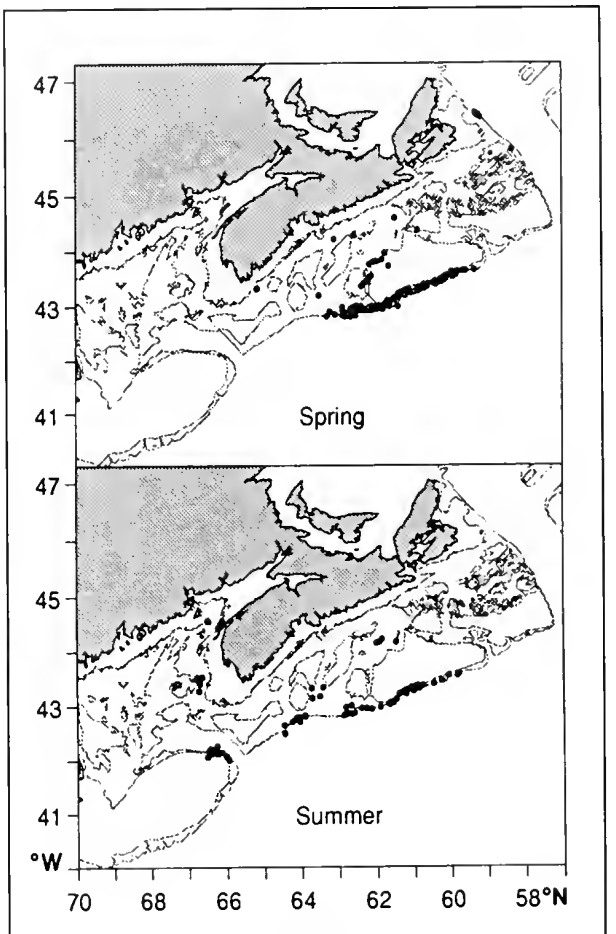

Figure 3

Spring and summer set locations of river herring bycatch from foreign and domestic fishing operations on the Scotian Shelf recorded by Canadian International Observers, 1980–89.

band along the edge of the Scotian Shelf from Emerald Bank east to Sable Island Bank (Fig. 3). This distribution reflects the location of the Soviet and Cuban silver hake fishery (M. Showell, Bedford Inst. Oceanogr., Dartmouth, N.S. B2Y 4A2, pers. commun., Jan. 1991) and indicates a more widespread occurrence of river herring along the shelf break than was apparent from bottom-trawl surveys. Bycatch from domestic fishing operations during spring occurred on the edge of Western and Emerald Banks and corresponds with catch locations from spring groundfish surveys.

Summer bycatch locations were similar to spring but extended further south and west along the shelf edge, with clusters of catches on the northern edge of Georges Bank, off southwestern Nova Scotia, and in the mouth of the Bay of Fundy (Fig. 3). River herring distribution along the shelf break, as indicated from spring and summer bycatches in the silver hake fishery, reflects the spatial distribution of that fishery. The number of summer observations from a reduced foreign fishing effort (n 86) was much less than spring (n 460). In both seasons, most bycatches occurred in

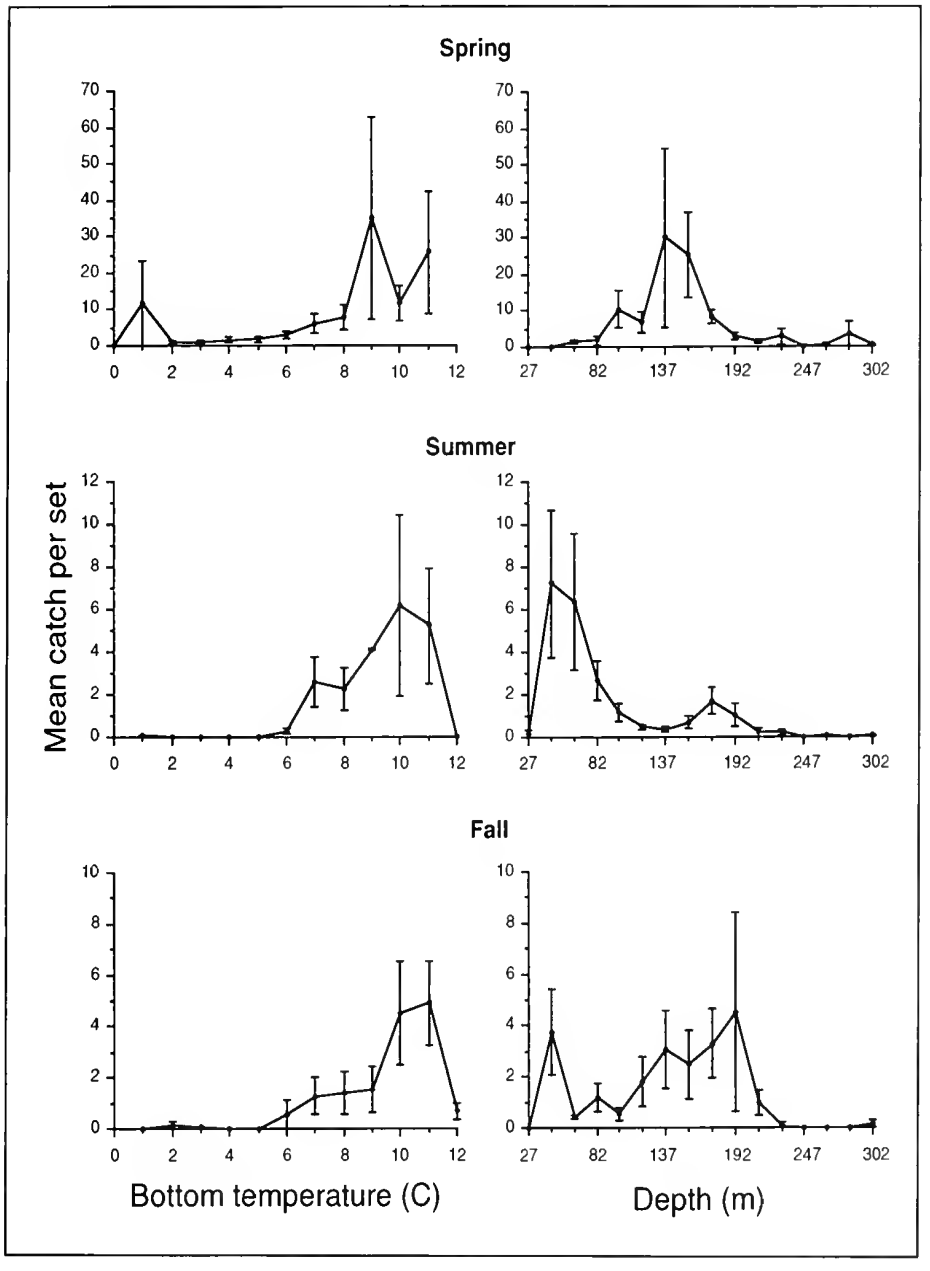

Figure 4
Mean catch-per-set of river herring within 1°C intervals of bottom temperature and 18.2 m (10 fm) depth intervals from spring, summer, and fall groundfish surveys, 1979–84, conducted off the Atlantic coast of Nova Scotia. Vertical bars represent ±1 SE. Sample sizes are ≥10 sets for each temperature and depth interval.

regions where bottom temperatures from groundfish surveys exceeded 5°C.

Temperature, depth, and diel effects on catch

The relationship between catch, bottom temperature, and depth was examined by plotting mean catch-per-set by season for intervals of 1°C and 18.3 m (10 fm) (Fig. 4). Despite much variability in the data, most catches occurred within the 7–11°C range regardless of season, with maximum catches within 9–11°C from spring through fall. An exception is the moderate catches at bottom temperatures <2°C during spring surveys in the Bay of Fundy (Figs. 2 and 4). The depth distribution of catches was more variable; spring catches occurred mainly at intermediate depths of 101–174 m, summer catches in shallow areas (46–82 m), and fall catches at mixed depths (i.e., 46 m, 119–192 m).

Mean catch-per-set of river herring for annual (1979–84) spring, summer, and fall surveys varied significantly by season and depth (Table 2, Fig. 5). Season effects within depth strata were significant for depths of <93 m and 93–183 m, but not for depths >183 m where all catches were low. Catches were highest within the <93 m strata during summer and within the 93–183 m depth strata during spring. Depth-within-season interaction was significant only during

Table 2

Summary of results from approximate randomization tests used to examine the following relationships: (a) effects of season and depth on mean catch-per-set, (b) diel variability in seasonal catch-per-set, and (c), mean fork length (FL) by season and depth. All comparisons used catch and fork-length data from Canadian groundfish surveys conducted 1979–84. Interaction effects with an asterisk are significant at the adjusted Bonferroni significance level of $P \leq 0.017$.

	Catch by season and depth		Catch by season and time		FL by season and depth	
Source	n	P	n	P	n	P
Main effects						
Season	2157	0.002	2157	0.006	5739	0.001
Depth	2157	0.010	–	–	5739	0.001
Time	–	–	2157	0.80	–	–
Interactions						
Season effect within depth						
<93 m	800	0.008*	–	–	1564	0.001*
93–183 m	836	0.001*	–	–	3769	0.001*
>183 m	521	0.027	–	–	406	0.001*
Depth effect within season						
spring	788	0.002*	–	–	3807	0.001*
summer	565	0.028	–	–	1114	0.001*
fall	804	0.060	–	–	818	0.001*
Season effect within time						
day	–	–	1231	0.228	–	–
night	–	–	926	0.033	–	–
Time effect within season						
spring	–	–	788	0.043	–	–
summer	–	–	565	0.001*	–	–
fall	–	–	804	0.017*	–	–

spring when the range in catches was greatest; summer and fall catches were similar at all depths (Table 2).

Mean catch-per-set of river herring varied significantly by season but not by time-period (Table 2, Fig. 6). Interactions of season effect within time-period were nonsignificant for day and night; interactions of time effect within season were significant for summer and fall but not for spring. For summer and fall surveys, catches from sets conducted during daylight were significantly higher than those conducted at night. While night catches from spring surveys tended to be higher than day catches (but not significantly so), they were extremely variable ($\bar{x}$ 13.4, sample SD 131.32). The proportion of sets with catch during day and night showed a seasonal pattern similar to that for mean catch, i.e., similar in spring (20% vs. 24%) and higher during the day in summer (15% vs. 5%) and fall (16% vs. 9%).

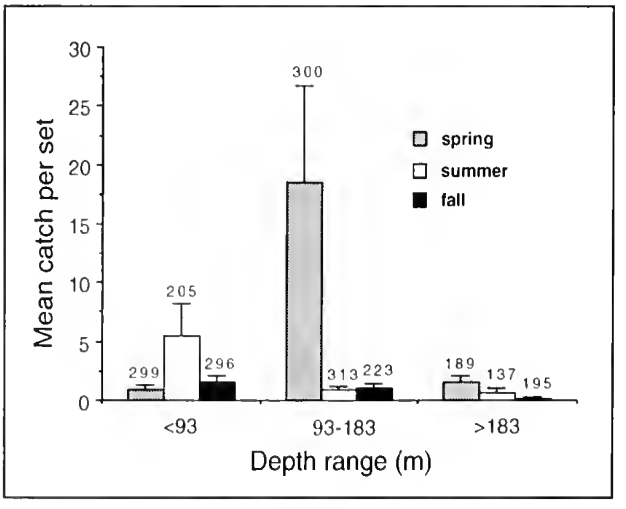

Figure 5

Mean catch-per-set of river herring by depth strata from spring, summer, and fall groundfish surveys, 1979–84, conducted off the Atlantic coast of Nova Scotia. Vertical bars represent +1 SE. Number of tows is indicated above error bars.

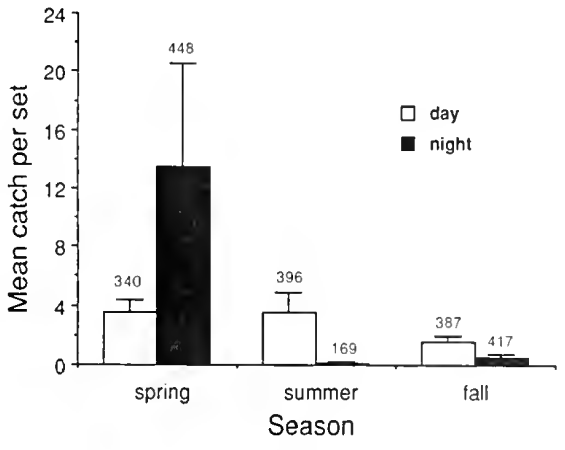

Figure 6

Mean catch-per-set of river herring in day and night collections from spring, summer, and fall groundfish surveys, 1979–84, conducted off the Atlantic coast of Nova Scotia. Vertical bars represent +1 SE. Number of tows is indicated above error bars.

Survey catch indices and NAFO landings

Seasonal catch indices (annual mean number and weight of river herring per set) from research vessel surveys were uncorrelated with NAFO bycatch data for the Scotian Shelf–Bay of Fundy area (4VWX) (Table 3). However, landings from the central and eastern shelf (4VW) were significantly correlated with spring (1979–89) survey indices. The relationship between mean weight index and 4VW NAFO landings (Fig. 7) gave the highest Spearman rank correlation coefficient (r_s 0.74).

Table 3

Spearman rank correlation coefficients for river herring (*Alosa* spp.) catch indices from spring (1979–89), summer (1970–89), and fall (1978–84) groundfish surveys vs. NAFO landings from the Scotian Shelf–Bay of Fundy (4VWX) and the central and eastern Scotian Shelf (4VW). (n = number of years; * significant at $P<0.05$; ** significant at $P<0.01$).

NAFO areas	Spring (n 11)	Summer (n 20)	Fall (n 7)
Mean catch/set · yr^{-1}			
4VWX	−0.23	−0.15	−0.07
4VW	0.60*	−0.01	−0.18
Mean weight/set · yr^{-1}			
4VWX	−0.19	−0.17	−0.29
4VW	0.74**	−0.05	−0.09

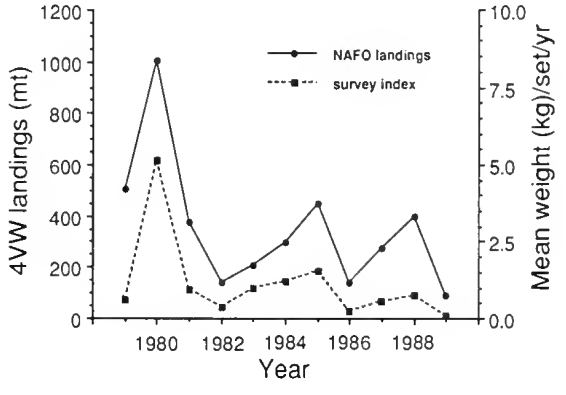

Figure 7

Annual landings in metric tons (t) reported to the Northwest Atlantic Fisheries Organization for the central and eastern Scotian Shelf (4VW), and spring survey catch index (kg/set·yr^{-1}) for 1979–89.

Seasonal length-composition and distribution

River herring from bottom-trawl collections measured 5–33 cm FL ($\bar{x}$ 23.7 cm; Table 4). Mean fork length in spring catches was less than in summer or fall. Fork lengths of river herring from foreign and domestic fisheries were 22–33 cm ($\bar{x}$ 29.6 cm) and were of comparable size in spring and summer sample collections. The larger size of bycatch fish compared with those from bottom-trawl surveys is probably due to the larger cod end mesh size (6 cm stretched) of commercial gear permitting escapement of smaller fish.

In all seasons, large river herring (>19 cm FL) were more abundant than small (≤19 cm) fish (Fig. 8). Polymodal length-frequency distributions indicated the

Table 4

River herring (*Alosa* spp.) fork-length statistics by season from groundfish surveys conducted by the Canadian Department of Fisheries and Oceans and from foreign and domestic bycatches recorded by Canadian International Observers. All fork lengths were truncated at 33 cm (see 'Materials and methods' for explanation). SD = sample standard deviation.

Season	Years	Fork length (cm) n	$\bar{x}$	SD	range
Groundfish survey data					
Spring (Feb–Apr)	1979–89	7543	22.7	5.08	5.0–33.0
Summer (June–July)	1970–89	3167	25.4	3.77	9.0–33.0
Fall (Sept–Dec)	1978–84	1512	24.8	4.92	5.0–33.0
Combined	1970–89	12213	23.7	4.91	5.0–33.0
Bycatch data					
Spring (Feb–May)	1980–89	1754	29.4	2.14	20.0–33.0
Summer (June–Aug)	1980–89	249	30.4	1.45	26.0–33.0
Combined	1980–89	2032	29.6	2.13	20.0–33.0

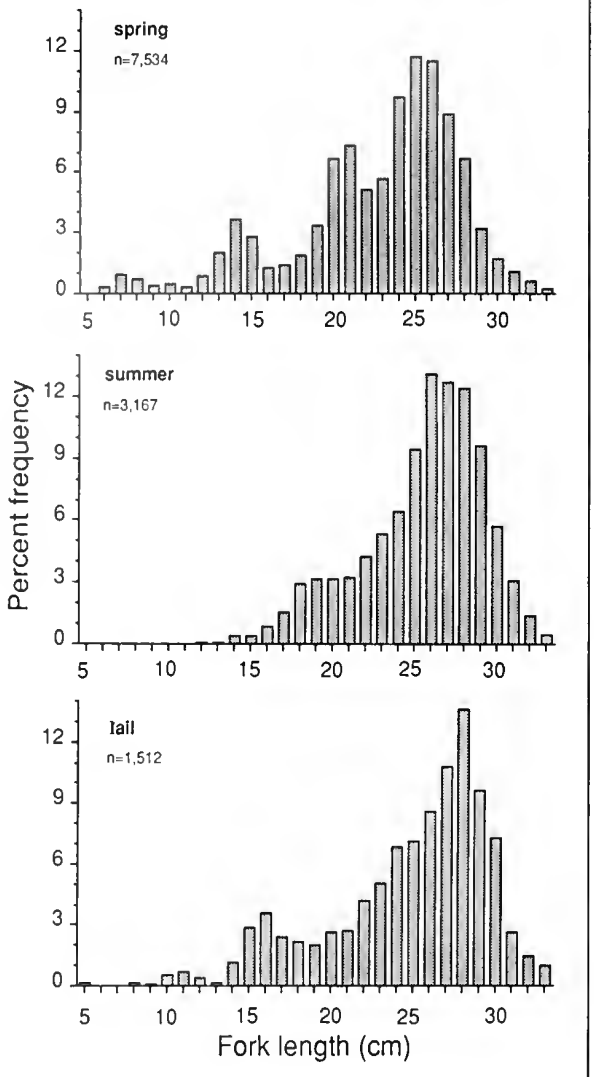

Figure 8
Length-frequency distributions of river herring from spring (1979–89), summer (1970–89), and fall (1978–84) groundfish surveys conducted off the Atlantic coast of Nova Scotia.

presence of at least three year-classes in the fall and four in the spring. Smaller individuals (≤19 cm FL) represented a larger proportion of the overall length composition in spring and fall than in summer.

River herring >19 cm FL were more densely and extensively distributed in all seasons than smaller fish. During summer and fall, most river herring ≤19 cm long were captured within the Bay of Fundy, although a few occurred in the central Shelf region and in Sydney Bight (fall only) (Fig. 9). The greatest overlap in the spatial distribution of both size-groups was during spring, especially in offshore regions (i.e., central Scotian Shelf, southern Gulf of Maine).

The mean fork length of trawl-caught (1979–84) river herring varied significantly by season of capture and depth (Table 2, Fig. 10). Interactions of season effect within depth strata and depth effect within season were all significant. Smaller fish were caught more frequently at depths <93 m during spring and fall. Larger fish occurred at all depths during summer (more numerously at <93 m depth) and at depths ≥93 m during spring and fall. In all three depth strata, river herring from spring surveys averaged smaller in length than those captured in summer and fall because of the greater occurrence of fish ≤19 cm throughout the survey area during spring (Fig. 9).

Discussion

Canadian groundfish survey data indicate persistent patterns in the temporal and spatial distribution of river herring off the Atlantic coast of Nova Scotia which appear to be greatly influenced by oceanographic features. In spring, river herring were most abundant in the warmer, deeper waters of the Scotian Gulf, particularly along the edges of Emerald and Western Banks and within the channel separating them, and in regions of warm slope-water intrusion along the Scotian Slope, the western and southern edges of Georges Bank, and the eastern Gulf of Maine. In all seasons, river herring occurred in the Bay of Fundy and off southwestern Nova Scotia, regions characterized by strong tidal mixing and upwelling, but were rarely present on the eastern Scotian Shelf.

Water temperature evidently influences temporal and spatial patterns in river herring depth distribution. In all seasons, most catches occurred within the 7–11°C range but shifted from mid-depths offshore in spring (101–183 m) to shallower, nearshore waters in summer (46–82 m), and to deeper offshore waters in fall (119–192 m). River herring were not present in colder regions on the eastern and western Scotian Shelf. Catches of river herring along the U.S. continental shelf were most frequent at bottom temperatures of 4–7°C and depths <92 m (Neves 1981). Spring catches of river herring at bottom temperatures <5°C in the Bay of Fundy indicate some flexibility in thermal selection, as might be expected of a migratory anadromous fish. American shad, which are closely related to alewives and blueback herring, can remain for extended periods in temperatures outside their usual range (7–13°C) and migrate rapidly between areas with different temperature regimes (Dadswell et al. 1987).

Seasonal shifts in zooplankton abundance, which are influenced by local oceanographic features, may also influence river herring distribution patterns off Nova Scotia. Both alewives and blueback herring are zoo-

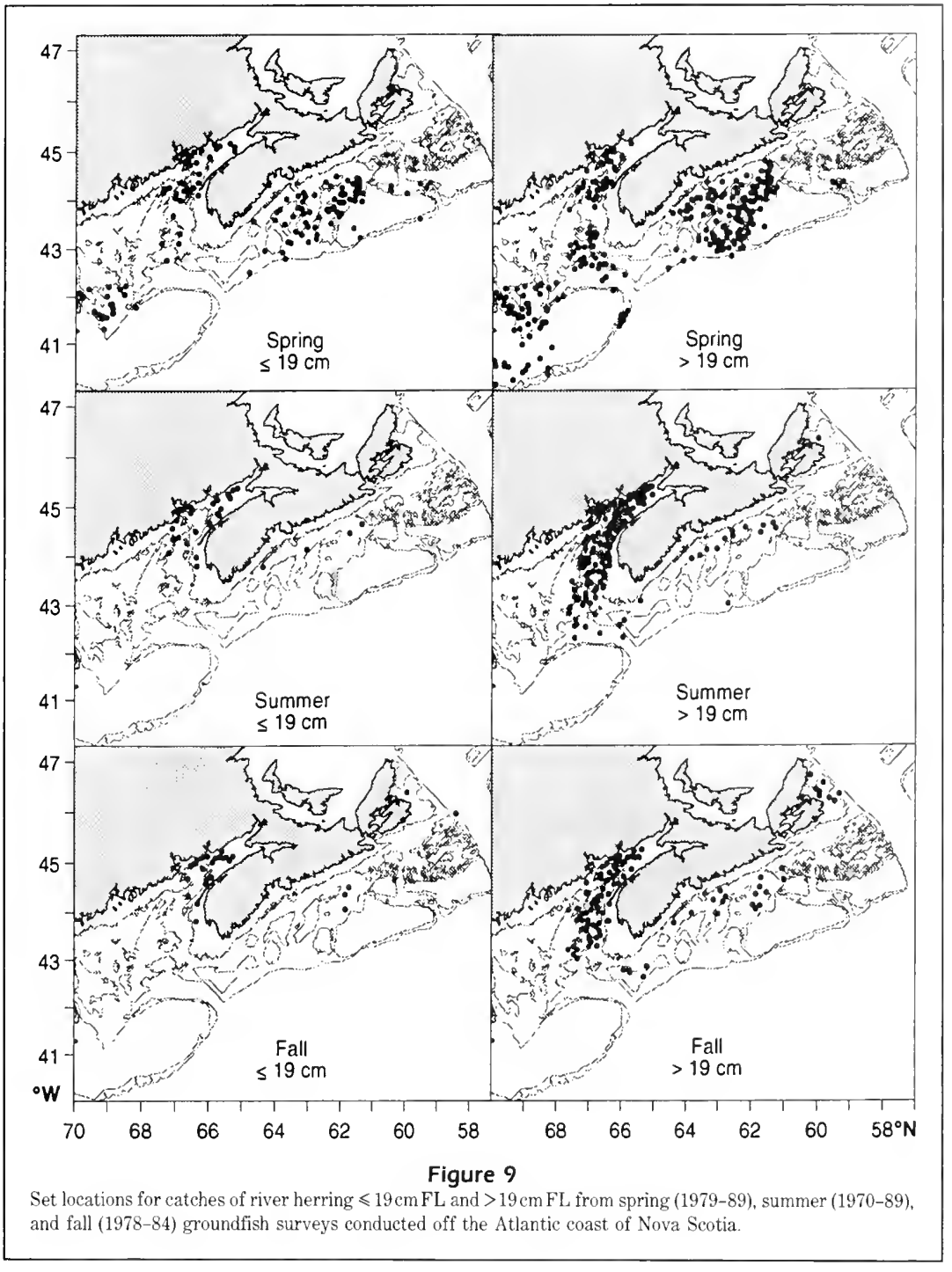

Figure 9

Set locations for catches of river herring ≤ 19 cm FL and > 19 cm FL from spring (1979–89), summer (1970–89), and fall (1978–84) groundfish surveys conducted off the Atlantic coast of Nova Scotia.

planktivores. Stomach contents of river herring collected on Georges Bank and the Scotian Shelf consisted mainly of euphausiids and calanoid copepods (Vinogradov 1984). These prey items are concentrated during winter and spring in deep basins of the Scotian Shelf (Sameoto and Herman 1989, Herman et al. 1991) as well as the outer Shelf and Shelf Slope (Sameoto 1982). Calanoid copepods dominate zooplankton production on Georges Bank during spring (Sherman et al. 1987) and are abundant during summer and fall in the eastern Gulf of Maine–outer Bay of Fundy region (Emerson et al. 1986) along with large populations of euphausiids (Kulka et al. 1982). Aggregations of river herring during spring on the central Shelf, Shelf Slope, and Georges Bank, during summer in the Bay of Fundy–eastern Gulf of Maine, and during fall in the

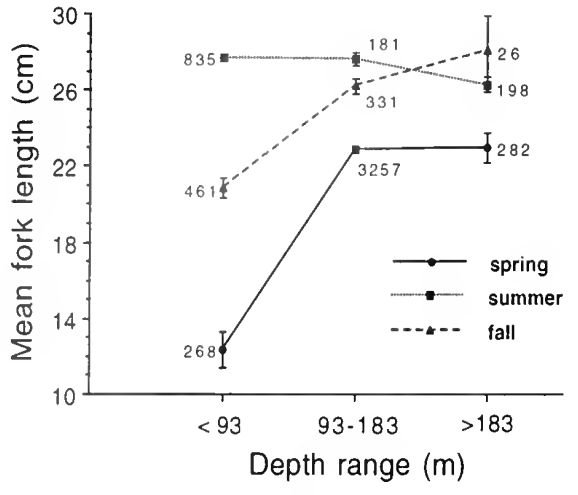

Figure 10

Mean fork length (cm) of river herring by depth strata from spring, summer, and fall groundfish surveys, 1979–84, conducted off the Atlantic coast of Nova Scotia. Vertical bars represent 95% CI. The number of fish in each category is adjacent to symbols.

outer Bay of Fundy and central Scotian Shelf coincide with high secondary productivity and an abundance of prey. River herring may move inshore in summer and offshore in winter in order to exploit seasonally available food resources.

The diurnal pattern of vertical migration by river herring accounts for the higher catches and proportion of sets with catches during daylight hours in summer and fall. Alewives and blueback herring that are closer to the bottom during the day are more susceptible to capture in bottom-trawling gear (Neves 1981, Loesch et al. 1982). Diel migrations, involving an upward movement at dusk followed by a downward movement at dawn, occur in landlocked adult alewives (Janssen and Brandt 1980), as well as anadromous juvenile (Jessop 1990) and adult river herring (Neves 1981). While spring catches did not follow this pattern, the presence of a cold (<5°C) intermediate water mass over warmer, deeper waters on the Scotian Shelf (Hatchey 1942), where the largest catches occurred, may have restricted the extent of vertical migration resulting in more captures at night. Our study indicates that few river herring are captured in areas where bottom temperatures are <5°C during spring; therefore, vertical migrations may be confined by a water temperature inversion.

Catch indices by number and weight from spring groundfish surveys (when relative abundance is greatest) both appear to be useful indicators of river herring bycatch in foreign and domestic trawl fisheries on the eastern and central shelf regions (4VW). Poor correlations, obtained when the Bay of Fundy–eastern Gulf of Maine bycatch landings (NAFO area 4X) were included in the analysis, were puzzling. Survey data indicate the presence of river herring in this area from spring through fall. Underreporting of river herring bycatches in domestic fishing operations (i.e., bottom trawl, gillnet, purse seine) may explain the poor correlations when landings from 4X and 4VW were combined. Catches from the central and eastern shelf region (4VW) are largely bycatches from the silver hake fishery. The frequent presence of DFO observers aboard these vessels may reduce the incidence of misreporting. Another possibility is the seasonal immigration of American-origin river herring into the Bay of Fundy–eastern Gulf of Maine region (Rulifson et al. 1987) which would increase the variability in the NAFO landings for area 4X.

The small proportion of fish ≤19 cm in summer collections, relative to spring and fall collections, may reflect their movement outside the survey area into coastal embayments and estuarine habitats in Maine and the inner Bay of Fundy. These areas serve as important summer feeding areas for river herring (Stone and Daborn 1987) and other anadromous fish species (Haedrich and Hall 1976). Summer resident river herring generally leave the inner Bay of Fundy in autumn when secondary production declines (Stone 1985).

Both large (>19 cm FL) and small (≤19 cm FL) river herring occurred nearshore from spring through fall, but were widely distributed offshore during spring (i.e., southern Gulf of Maine, Scotian Gulf). Most river herring ≤19 cm FL are sexually immature while those >19 cm FL are generally mature fish which have spawned previously or are maturing to spawn for the first time. Smaller, immature river herring evidently migrate offshore seasonally as do larger, mature fish. Size-related differences in depth distribution were such that small river herring occurred in shallow regions (<93 m) during spring and fall, while larger fish occurred in deeper areas (≥93 m) in all seasons. Janssen and Brandt (1980) reported that the nocturnal depth distribution of adult landlocked alewife differed by size-class, with the smaller fish at shallower depths.

Both Canadian and American marine survey data provide evidence of distinct seasonally and geographically separate aggregations of river herring. Off the Atlantic coast of the United States, the Middle Atlantic Bight is an important overwintering area for river herring, while in summer they concentrate further north in the Nantucket Shoals and on Georges Bank (Neves 1981). Aggregations of river herring in spring and fall on the central Scotian Shelf and in the eastern Gulf of Maine–Bay of Fundy suggest that these areas are important overwintering sites off Nova Scotia,

although the Scotian Shelf has not been surveyed during winter months (i.e., November–February). The main summer concentration extends northward from southwestern Nova Scotia into the Bay of Fundy.

Other members of the clupeid family also exhibit spatial and temporal discontinuity in marine distribution patterns. American shad winter off Florida, the mid-Atlantic Bight, and in the Scotian Shelf–Bay of Fundy region (Neves and Depres 1979, Dadswell et al. 1987), while summer concentrations occur off Newfoundland and Labrador (Hare and Murphy 1974), the inner Gulf of St. Lawrence (Dadswell et al. 1987), the Gulf of Maine (Neves and Depres 1979), and in the inner Bay of Fundy (Dadswell et al. 1983). Atlantic herring populations in the Gulf of Maine–Scotian Shelf region have several geographically separate areas for summer feeding (southwest Nova Scotia, Georges Bank, Bay of Fundy) and overwintering (Long Island Sound, Chedabucto Bay) (Sinclair and Isles 1985).

Seasonal movement patterns of river herring inferred from American and Canadian survey data involve a north-south progression and an inshore-offshore movement similar to that described for American shad populations along the Atlantic coast of North America (Neves and Depres 1979, Dadswell et al. 1987). During spring, river herring from the Middle Atlantic Bight move north as far as the Nantucket Shoals, Georges Bank, coastal Gulf of Maine and even the inner Bay of Fundy for the summer, then return south to the mid-Atlantic coast in winter and early spring (Neves 1981, Rulifson et al. 1987). The spring aggregation of mature river herring observed in Canadian survey catches from the southern Gulf of Maine likely consists of fish which will move inshore to spawn in rivers along the eastern seaboard of the United States, although some may enter Canadian rivers. A large component of the overwintering population on the Scotian Shelf moves inshore during spring to spawn in rivers along the Atlantic coast of Nova Scotia, the Bay of Fundy, and perhaps the Gulf of Maine. American shad tagged in rivers in Nova Scotia (Melvin et al. 1986) and in Quebec (Vladykov 1956) were recaptured on the Scotian Shelf in winter. The large aggregation of river herring in the eastern Gulf of Maine, apparent during spring surveys, may include fish in transit from overwintering areas on the Shelf to spawning rivers along the Bay of Fundy–Gulf of Maine coast. Considering their preference for water temperatures above 5°C, the migration route would occur along the Shelf Slope and into the eastern Gulf of Maine through the Northeast Channel. Postspawning river herring probably feed during summer in the Bay of Fundy–eastern Gulf of Maine before returning offshore to the central Shelf in the fall to overwinter. Some may move offshore soon after spawning, as indicated by the presence of large fish ($\bar{x}$ FL 30.4 cm) in the summer bycatch from the silver hake fishery along the shelf slope. Another component of the Shelf overwintering population may move north around Cape Breton to the Gulf of St. Lawrence in spring to spawn in natal rivers, returning in autumn to the Scotian Shelf to overwinter. This hypothesis is supported by the fall concentration of river herring in the Sydney Bight area and movement of an alewife accidently tagged in the Sydney Bight fall fishery for Atlantic herring, to the Margaree River (southern Gulf of St. Lawrence) where it was recaptured the following spring (Jessop, unpubl. data).

Most river herring overwintering on the Scotian Shelf probably originate in the Canadian Maritime Provinces and U.S. Gulf of Maine region. Some river herring of Canadian Maritime origin evidently migrate south to overwinter off the Middle Atlantic Bight as do American shad (Melvin et al. 1986, Dadswell et al. 1987). The tagging of over 50,000 river herring in the Saint John River, New Brunswick, produced two recaptures off North Carolina the following spring and other recoveries along the intervening coast (Jessop, unpubl. data). In another study, most recaptures from over 19,000 river herring tagged during summer and fall in the upper Bay of Fundy occurred in spring fisheries in Nova Scotia rivers, but one occurred off Massachusetts and several came from North Carolina (Rulifson et al. 1987). Summer aggregations of river herring in the Bay of Fundy–eastern Gulf of Maine may therefore consist of a mixture of stocks from the entire Atlantic coast, as do similar aggregations of American shad (Dadswell et al. 1987).

An understanding of the seasonal movements, stock composition, and exploitation of river herring populations which overwinter on the Scotian Shelf may help fishery managers to explain high variability in the returns of spawning fish regionally and to particular river systems. Stock composition and migratory routes remain to be examined.

Acknowledgments

We thank M. Dadswell and K. Frank for critically reviewing earlier drafts of the manuscript. We also wish to thank J. McMillan and C. Harvie for their assistance in data analysis and G. Black for helping with the offshore distribution plots. The constructive comments of the anonymous reviewers are also appreciated.

Citations

Bigelow, H.B., and W.C. Schroeder
1953 Fishes of the Gulf of Maine. Bull. U.S. Fish. Wildl. Serv. 74, 577 p.

Cohen, E.B., M.D. Grosslein, and M.P. Sissenwine
1982 Energy budget of Georges Bank. *In* Mercer, M.C. (ed.), Multispecies approaches to fisheries management advice, p. 95–107. Can. Spec. Publ. Fish. Aquat. Sci. 59.

Dadswell, M.J., G.D. Melvin, and P.J. Williams
1983 Effect of turbidity on the temporal and spatial utilization of the inner Bay of Fundy by American shad (*Alosa sapidissima*) (Pisces: Clupeidae) and its relationship to local fisheries. Can. J. Fish. Aquat. Sci. 40(Suppl. 1):322–330.

Dadswell, M.J., R. Bradford, A.H. Leim, D.J. Scarratt, G.D. Melvin, and R.G. Appy
1984 A review of research on fishes and fisheries in the Bay of Fundy between 1976 and 1983 with particular reference to its upper reaches. *In* Gordon, D.C., and M.J. Dadswell (eds.), Update on the marine environmental consequences of tidal power development in the upper reaches of the Bay of Fundy, p. 163–294. Can. Tech. Rep. Fish. Aquat. Sci. 1256, 686 p.

Dadswell, M.J., G.D. Melvin, P.J. Williams, and D.E. Themelis
1987 Influences of origin, life history and chance on the Atlantic coast migration of American shad. *In* Dadswell, M.J., et al. (eds.), Common strategies of anadromous and catadromous fishes, p. 313–330. Am. Fish. Soc., Bethesda.

Day, R.W., and G.P. Quinn
1989 Comparisons of treatments after an analysis of variance in ecology. Ecol. Monogr. 59:433–463.

Edgington, E.S.
1987 Randomization tests. Marcel Dekker, NY.

Emerson, C.W., J.C. Roff, and D.J. Wildish
1986 Pelagic-benthic energy coupling at the mouth of the Bay of Fundy. Ophelia 26:165–180.

Fournier, R.O., J. Marra, R. Bohrer, and M. Van Det
1977 Plankton dynamics and nutrient enrichment of the Scotian Shelf. J. Fish. Res. Board. Can. 34:1001–1018.

Fournier, R.O., M. Van Det, N.B. Hargraves, J.S. Wilson
1984 Physical factors controlling summer distribution of chlorophyll *a* off southwestern Nova Scotia. Limnol. Oceanogr. 29:517–526.

Greenburg, D.A.
1984 A review of the physical oceanography of the Bay of Fundy. *In* Gordon, D.C., and M.J. Dadswell (eds.), Update on the marine environmental consequences of tidal power development in the upper reaches of the Bay of Fundy, p. 9–30. Can. Tech. Rep. Fish. Aquat. Sci. 1256, 686 p.

Haedrich, R.L., and C.A.S. Hall
1976 Fishes and estuaries. Oceanus 19:55–63.

Halliday, R.G., and P.A. Koeller
1981 A history of Canadian groundfish trawling surveys and data usage in ICNAF divisions 4TVWX. *In* Doubleday, W.G., and D. Rivard (eds.), Bottom trawl surveys. Can. Spec. Publ. Fish. Aquat. Sci. 58:27–41.

Hare, G.M., and H.P. Murphy
1974 First record of American shad (*Alosa sappidissima*) from Labrador waters. J. Fish. Res. Board Can. 31:1536–1537.

Hatchey, H.B.
1942 The waters of the Scotian Shelf. J. Fish. Res. Board Can. 5:377–397.

Herman, A.W., D.D. Sameoto, C. Shunnian, M.R. Mitchell, B. Petrie, and N. Cochrane
1991 Sources of zooplankton on the Nova Scotia Shelf and their aggregations within deep shelf basins. Continental Shelf Res. 11:211–238.

Janssen, J., and S.W. Brandt
1980 Feeding ecology and vertical migration of adult alewives (*Alosa pseudoharengus*) in Lake Michigan. Can. J. Fish. Aquat. Sci. 37:177–184.

Jessop, B.M.
1986 Alewife and blueback herring in the Gulf of Maine area. Can. Atl. Fish. Sci. Adv. Comm. Res. Doc. 67, 7 p.
1990 Diel variation in density, length composition, and feeding activity of juvenile alewife, *Alosa pseudoharengus* Wilson, and blueback herring, *A. aestivalis* Mitchill, at near-surface depths in a hydroelectric dam impoundment. J. Fish. Biol. 37: 813–822.

Jessop, B.M., and W.E. Anderson
1989 Effects of heterogeneity in the spatial and temporal pattern of juvenile alewife (*Alosa pseudoharengus*) and blueback herring (*A. aestivalis*) density on estimation of an index of abundance. Can. J. Fish. Aquat. Sci. 46:1564–1574.

Jessop, B.M, A.H. Vromans, and W.E. Anderson
1982 Life-history data on alewife and blueback herring, Mactaquac Dam, 1975–81. Can. Data Rep. Fish. Aquat. Sci. 367, 43 p.

Kulka, D.W., S. Corey, and T.D. Isles
1982 Community structure and biomass of euphausiids in the Bay of Fundy. Can. J. Fish. Aquat. Sci. 39:326–334.

Leim, A.H., and W.B. Scott
1966 Fishes of the Atlantic Coast of Canada. Bull. Fish. Res. Board Can. 155, 485 p.

Loder, J.W., and D.A. Greenburg
1985 Predicted positions of tidal fronts in the Gulf of Maine. Continental Shelf Res. 4:397–414.

Loesch, J.G.
1987 Overview of life history aspects of anadromous alewife and blueback herring in freshwater habitats. *In* Dadswell, M.J., et al. (eds.), Common strategies of anadromous and catadromous fishes, p. 89–103. Am. Fish. Soc., Bethesda.

Loesch, J.G., W.H. Kriete, and E.J. Foell
1982 Effects of light intensity on the catchability of juvenile anadromous *Alosa* species. Trans. Am. Fish. Soc. 111:41–44.

McLellan, H.J.
1954 Bottom temperatures on the Scotian Shelf. J. Fish. Res. Board Can. 11:404–418.

Melvin, G.D., M.J. Dadswell, and J.D. Martin
1986 Fidelity of American shad, *Alosa sapidissima* (Clupeidae), to its river of previous spawning. Can. J. Fish. Aquat. Sci. 43:640–646.

Messieh, S.N.
1977 Population structure and biology of alewives (*Alosa pseudoharengus*) and blueback herring (*A. aestivalis*) in the Saint John River, New Brunswick. Environ. Biol. Fishes 2:195–210.

Mills, E.L., and R.O. Fournier
1979 Fish production and the marine ecosystems of the Scotian Shelf, eastern Canada. Mar. Biol. 54:101–108.

Mountain, D.G., M. Pastuszak, and D. A. Busch
1989 Slope water intrusion to the Great South Channel during autumn, 1977–85. J. Northwest Atl. Fish. Sci. 9:97–102.

Netzel J., and E. Stanek
1966 Some biological characteristics of blueback, *Pomolbus aestivalis* (Mitchell) and alewife, *Pomolbus pseudoharengus* (Wilson), from Georges Bank, July and October, 1964. Int. Comm. North Atl. Fish. Bull. 3:106–110.

Neves, R.J.
1981 Offshore distribution of alewife, *Alosa pseudoharengus* and blueback herring, *A. aestivalis*, along the Atlantic coast. Fish. Bull., U.S. 79:473–485.

Neves, R.J., and L. Depres
1979 The oceanic migration of American shad, *Alosa sapidissima*, along the Atlantic coast. Fish. Bull., U.S. 77: 199–212.

Ramp., S.R., and W.R. Wright
1979 Northeast Channel flow: The view after one year's measurements. Int. Counc. Explor. Sea CM 1979/C:54.

Rulifson, R.A.
1984 Tagging studies of river herring (*Alosa pseudoharengus* and *A. aestivalis*) in Bay of Fundy, Nova Scotia. N.C. Dep. Nat. Resour. Comm. Develop., Div. Mar. Fish., Completion Rep. AFC-22, E. Carolina Univ., Greenville, 26 p.

Rulifson, R.A., S.A. McKenna, and M.L. Gallagher
1987 Tagging studies of striped bass and river herring in upper Bay of Fundy, Nova Scotia. N.C. Dep. Nat. Resour. Comm. Develop., Div. Mar. Fish., Completion Rep. AFC-28-1, E. Carolina Univ., Greenville, 175 p.

Sameoto, D.D.
1982 Zooplankton and micronekton abundance in acoustic scattering layers on the Nova Scotian slope. Can. J. Fish. Aquat. Sci. 39:760–777.

Sameoto, D.D., and A.W. Herman
1989 Life cycle and distribution of *Calanus finmarchicus* in deep basins on the Nova Scotia shelf and seasonal changes in *Calanus* spp. Mar. Ecol. Prog. Ser. 66:225–237.

Sherman, K., W.G. Smith, J.R. Green, E.B. Cohen, M.S. Berman, K.A. Marti, and J.R. Goulet
1987 Zooplankton production and the fisheries of the northeastern shelf. *In* Backus, R.H., and D.W. Bourne (eds.), Georges Bank, p. 268–282. MIT Press, Cambridge.

Sinclair, M.
1988 Marine populations: An essay on population regulation and speciation. Univ. Wash. Press, Seattle, 252 p.

Sinclair, M., and T.D. Isles
1985 Atlantic herring (*Clupea harengus*) distributions in the Gulf of Maine–Scotian Shelf area in relation to oceanographic features. Can. J. Fish. Aquat. Sci. 42:880–887.

Smith, P.C., B. Petrie, and C.R. Mann
1978 Circulation, variability, and dynamics of the Scotian Shelf and Slope. J. Fish. Res. Board Can. 35:1067–1083.

Smith, S.J.
1988 Abundance indices from research survey data. *In* Rivard, D. (ed.), Collected papers on stock assessment methods, p. 16–43. Can. Atl. Fish. Sci. Adv. Comm. Res. Doc. 61.

Stone, H.H.
1985 Composition, morphometric characteristics and feeding ecology of alewives (*Alosa pseudoharengus*) and blueback herring (*A. aestivalis*) (Pisces: Clupeidae) in Minas Basin. MSc. thesis, Acadia Univ., Wolfville, N.S., 191 p.

Stone, H.H., and G.R. Daborn
1987 Diet of alewives, *Alosa pseudoharengus* and blueback herring, *A. aestivalis* (Pisces: Clupeidae) in Minas Basin, Nova Scotia, a turbid, macrotidal estuary. Environ. Biol. Fishes 19:55–67.

Vinogradov, V.I.
1984 Food of silver hake, red hake and other fishes on Georges Bank and adjacent waters, 1968–1974. NAFO (Northwest Atl. Fish. Organ.) Sci. Counc. Stud. 7:87–94.

Vladykov, V.D.
1936 Occurrence of three species of anadromous fishes on the Nova Scotian banks during 1935 and 1936. Copeia 1936:168.
1956 Distant recaptures of shad tagged in Quebec. Naturaliste Canadien (Quebec) 83:235–248.

Long-term coded wire tag retention in juvenile *Sciaenops ocellatus*

Britt W. Bumguardner
Robert L. Colura

Texas Parks and Wildlife Department, Perry R. Bass Marine Fisheries Research Station
HC 2, Box 385, Palacios, Texas 77465

Gary C. Matlock

Texas Parks and Wildlife Department, Fisheries and Wildlife Division
4200 Smith School Road, Austin, Texas 78744

Red drum *Sciaenops ocellatus*, a popular sport fish in the Gulf of Mexico and associated estuarine systems, have been subjected to increasing fishing pressure in recent years which has led to declining population size in Texas (Matlock 1982) and poor annual survival in Texas bays (Green et al. 1985). Commercial harvest of both inshore stocks of red drum in Texas prior to 1981 (Matlock 1982) and offshore stocks in the Gulf of Mexico prior to 1987 (Goodyear 1987) contributed to the apparent population decline in red drum. Documented commercial landings in the Gulf of Mexico were less than 50% of estimated recreational harvest prior to 1984. However, documented commercial landings increased to more than double the estimated recreational harvest from 1984 to 1986, primarily due to expansion of an oceanic purse seine fishery which began in 1978 (Goodyear 1987).

In Texas, reported commercial landings of red drum were more than double estimated recreational landings for 1976–77, then declined to slightly more than recreational landings for 1978–80. Estimated recreational landings were relatively stable, with a general downward trend, during 1976–80 (Matlock 1982). The sale of red drum harvested from Texas public waters was prohibited by legislative action as of 1 September 1981 (Maddux et al. 1989), while the purse seine fishery for offshore stocks of adult red drum was closed by the Gulf of Mexico Fisheries Management Council in 1986. Increasing sportfishing pressure and catastrophic freezes, which caused extensive fish kills in bays along the northern Gulf of Mexico (Maddux et al. 1989), have also contributed to imposition of increasingly restrictive sport bag and size limits for red drum in Texas.

Development of controlled spawning and pond culture techniques for red drum has allowed large-scale production and stocking of red drum fingerlings to enhance declining populations (Colura et al. 1976, Arnold et al. 1977, McCarty et al. 1986). Over 68 million red drum fingerlings have been stocked for population enhancement in Texas coastal waters since 1975, with the majority of fingerlings stocked since 1983 (Dailey 1990). Development of a reliable method for identifying stocked fish would allow evaluation of this stocking program. The fish, which are typically <50 mm total length (TL) when stocked (Dailey 1990), are frequently released in spring and summer when no small red drum ($\leq$100 mm TL) occur naturally in bays (McEachron and Green 1986), as red drum spawn in the fall (Comyns et al. 1991). Survival of fish stocked in spring and summer can be monitored by analysis of length-frequencies for about 9 months, at which time variation in growth masks the initial length differences. Fish stocked in fall cannot be monitored by length-frequency methods due to onset of the spawning season and resultant confusion of stocked and wild fish of similar size (Dailey and McEachron 1986, Matlock et al. 1986).

For stocking to be considered successful, hatchery fish must survive long enough to be recruited to the fishery and then to offshore schools of mature red drum. When evaluation of stocking success is based on recapture of tagged fish which must grow large enough to enter the fishery, determination of long-term tag retention and detection rates is necessary for accurate evaluation of fingerling stocking success. Appreciable tag loss or nondetection would result in underestimation of the proportion of hatchery fish in the population (Heimbach et al. 1990).

Tagging of hatchery fish has had little success (Matlock et al. 1984 and 1986, Gibbard and Colura 1980, Bumguardner et al. 1990). Only 10 of 5942 hatchery-reared red drum ($\bar{x}$ 452 mm TL) tagged with monel jaw tags on the opercula were recaptured within 8 months of release (Matlock et al. 1984). Three fish from over 38,000 fingerlings (40–120 mm TL) tagged in the snout with coded wire microtags and released in St. Charles Bay, Texas, were recaptured (Matlock et al. 1986). The low recapture rate of microtagged fish was probably due to tag loss. Gibbard and Colura (1980) reported 27% retention of coded wire tags placed in the nose of red drum fingerlings (50 mm mean TL) after 1 year. Bumguardner et al. (1990) conducted a short-term study (114 days) of red drum fingerlings ($\bar{x}$ 52 mm TL) tagged in the adductor mandibularis (cheek

Manuscript accepted 9 March 1992.
Fishery Bulletin, U.S. 90:390–394 (1992).

muscle) with coded wire microtags. Loss of coded wire tags was initially high (32.7% after 24 hours), but the rate of tag loss declined substantially 23 days post-tagging.

Tag retention by the same group of fish initially tagged by Bumguardner et al. (1990) was monitored 115–464 days post-tagging to determine if additional tag loss occurred. Tag detection rates using two methods of tag detection—a Northwest Marine Technology Field Sampling Device, and examination of X-ray negatives—were also determined and contrasted with tag detection rates reported for the two methods by Bumguardner et al. (1990). Our primary objective was to determine if tag retention rates declined between 114 and 464 days post-tagging, and to what extent tag loss and nondetection affected estimates of tag retention rates. While Bumguardner et al. (1990) considered mortality a component of tag loss and reported differential mortality between tagged and untagged fish, we limited the scope of this project to investigation of tag loss and nondetection rates. We did not consider mortality a component of tag loss because the facilities to maintain a group of control fish were not available.

Table 1

Coded wire microtag retention for red drum *Sciaenops ocellatus* through 464 days post-tagging, determined with the NMT Field Sampling Device.

Activity	No. fish	Interval (days)	No. fish examined	No. fish retaining tags	Tag retention (%)	Cumulative tag retention (%)
Tagged	2124	0–1	220[a]	148	67.3	67.3
Stocked in 0.1-ha ponds	1500	2–23	844[b]	397	69.8[c] ±31.2	47.0[c] ±20.2
Restocked in 0.2-ha ponds	599	24–114	238[b]	108	96.6[c] ±25.8	45.4[c] ±12.1
Held in tank[d]	52	115–285	33[b]	31	93.9	42.6 (93.9)[e]
Stocked in 0.4-ha pond	32	286–464	31[b]	26	89.3	38.0 (83.9)[f]

[a] Fish selected randomly from the total number of fish tagged.
[b] Number of fish surviving at the end of the interval.
[c] Reported as weighted average for three ponds with standard error.
[d] First 52 fish encountered while monitoring tag retention were overwintered in indoor tanks.
[e] Cumulative percent tag retention for days 115–285 used to calculate percent tag retention for 286–464 day interval.
[f] Cumulative percent tag retention for days 115–464 used to calculate percent tag retention for 286–464 day interval.

Materials and methods

Coded-wire microtag retention for red drum was monitored from tagging to 464 days post-tagging. About 2100 red drum fingerlings ($\bar{x}$ 52 mm TL) were tagged with coded wire microtags on 13 July 1987. Tags (1.07 × 0.25 mm) were inserted horizontally in the cheek muscle using a Northwest Marine Technology (NMT) Model MK2A tagging unit (Northwest Mar. Technol., Shaw I., WA) equipped with a plastic side mold to orient fish for consistent tag placement. An NMT Quality Control Device was used to magnetize tags and separate tagged from untagged fish.

Tagged fish were held in a 3.0 × 0.6 × 0.6 m tank for 24 hours, stocked in three 0.1-ha ponds at 500 fish/pond for 23 days, then transferred to three 0.2-ha ponds for 91 days (Table 1). Surviving fish harvested from each 0.1-ha pond were restocked as a group in separate 0.2-ha ponds. Fish were fed a commercially-prepared trout feed daily while in ponds. Tag retention was determined at 24 hours (prestocking), 23 days (harvest from 0.1-ha ponds), and 114 days (harvest from 0.2-ha ponds) post-tagging with an NMT Field Sampling Device (FSD) (Bumguardner et al. 1990). Fish were harvested from 0.2-ha ponds 114 days post-tagging, and 52 fish ($\bar{x}$ 220 mm TL) confirmed by the FSD as retaining tags were placed in a 4200 L circular fiberglass tank on 11 October 1987 for overwintering. As available tank space was limited, overwintering was restricted to 52 fish confirmed as retaining tags. Experience has shown indoor overwintering is required to insure survival of red drum in hatcheries during episodic freezing conditions on the Texas coast. Fish were fed 300 g chopped fish and shrimp daily. Fish were treated with a 0.25 mg/L Cu^{++} bath on four occasions for a protozoan parasite infestation tentatively identified as *Amyloodinium* sp. Fish were immersed in a 20 mg/L oxytetracycline HCl bath, and about 10 mL of injectable oxytetracycline solution (50 mg oxytetracycline HCl/mL solution) was placed in chopped shrimp and fish offered as feed to combat a bacterial infection. Surviving fish (n 33) were removed from the tank on 22 April 1988 (285 days after tagging), measured and checked for tag presence with the FSD.

The 33 surviving fish ($\bar{x}$ 352 mm TL) were placed in a 0.4-ha pond, with the exception of one fish that had lost the caudal fin, presumably as the result of a bacterial infection. These fish were fed a a 35% protein

floating fish ration (Texas Farm Products, Nacogdoches, TX), 0.45kg/day, 5 days/week, as a supplement to natural forage available in the pond. Fish were harvested on 11 October 1988, 464 days post-tagging. Microtag retention was determined with the FSD, fish were measured ($\bar{x}$ 473mmTL), and 10 of 31 surviving fish were selected at random and preserved in 50% formalin for X-ray analysis of tag retention. X-ray negatives of the preserved fish were visually inspected to confirm the presence or absence of tags as determined by the FSD.

Tag retention was determined for each interval, and overall or cumulative tag retention was determined at the end of each interval. As mortality was not considered tag loss in this study, cumulative tag retention reflects only the percentage of tag losses from shedding and nondetection of tags. A problem encountered in the course of this program was the calculation of tag retention rates when fish which had shed tags were not removed from the group at the end of the interval (2–23 days, 24–114 days, and 286–464 days). The percent decrease in cumulative tag retention was selected as an estimate of the percentage of fish losing tags in these intervals. Conversely, when fish that had lost tags were removed from the group, determination of tag retention for that interval (days 115–285) was simple (no. fish with tags/total no. fish examined), but cumulative tag retention had to be calculated. Tag retention for the interval in question was multiplied by cumulative tag retention from the previous interval to determine cumulative tag retention for the interval. The relationship used in these calculations was

$$TR_i = \frac{CTR_i}{CTR_{i-1}} \times 100,$$

where TR_i is percent tag retention for interval i, CTR_i is percent cumulative tag retention for interval i, and CTR_{i-1} is percent cumulative tag retention for the interval prior to interval i. Percent tag retention and percent cumulative tag retention for 1–23 and 24–114 day intervals for fish from individual ponds were used to calculate weighted means reported in Table 1. The weighting factor used was the number of fish harvested from each pond.

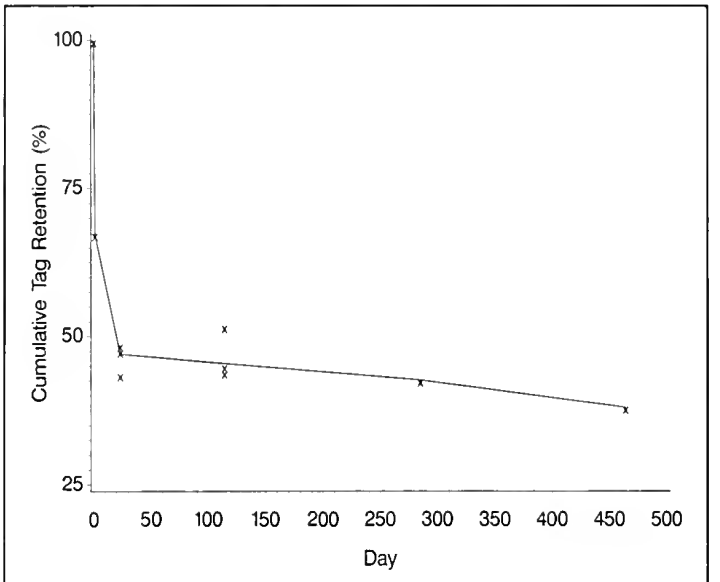

Figure 1
Observed values (X) of cumulative tag retention for microtagged red drum *Sciaenops ocellatus* fingerlings through 464 days post-tagging.

Results and discussion

Tag retention for surviving fish at 115–464 days post-tagging was 83.9%. Tag retention was 93.9% at 115–285 days post-tagging, and 89.3% at 286–464 days post-tagging (Table 1). Cumulative retention of coded wire microtags for red drum was 38.0% at 464 days post-tagging (Table 1, Fig. 1). Lack of replication at all intervals prevented statistical comparison of tag retention for different intervals. However, tag retention values of 96.6% for 24–114 days, 93.9% for 115–285 days, and 89.3% for 286–464 days post-tagging indicate cumulative tag retention decreased in the interval 24–464 days post-tagging, although at a slower rate than for the period 0–23 days (Table 1). Numerous authors (Gibbard and Colura 1980, Klar and Parker 1986, Fletcher et al. 1987, Williamson 1987, Bumguardner et al. 1990, and Dunning et al. 1990) have reported that the majority of coded-wire tag losses occur within a relatively short period (14–90 days) post-tagging. Our results agree with this generalization, but indicate tag losses may continue at a much reduced rate for extended periods after tagging. While our results are based on a small unreplicated sample (n 31 fish at study end), we believe they indicate long-term tag loss may be important when estimating the contribution of hatchery fish to a population. Accounting for this continued tag loss would prevent underestimation of the proportion of tagged fish occurring in the population (Heimbach et al. 1990).

Although Bumguardner et al. (1990) reported the FSD failed to detect tags present in 9% of live fish 114 days after tagging as determined by examination of X-ray negatives (n 186), no difference in tag detection between the FSD and X-ray negatives was found in this

study. Both X-ray negatives and the FSD indicated that 3 of 10 preserved fish lost tags. The criteria used to select fish for this study, i.e., confirmation of tag presence by the FSD, may have biased the comparison by eliminating fish with weakly magnetized tags.

Inserting coded wire tags horizontally in the cheek musculature of red drum fingerlings resulted in low tag retention. The site of tag insertion and tag orientation may affect tag retention. Tags implanted in striped bass *Morone saxatilis* and largemouth bass *Micropterus salmoides* cheek musculature resulted in higher retention rates than tags placed in snouts of striped bass and largemouth bass (Klar and Parker 1986, Fletcher et al. 1987, Williamson 1987). Changing the plane of tag insertion in the cheek muscle may increase tag retention. Dunning et al. (1990) reported coded-wire microtag retention in striped bass (65–100 mm TL) was greater when tags were inserted vertically rather than horizontally in the cheek muscle. A possible explanation of poor retention and high initial loss of wire microtags implanted horizontally in the cheek muscle of small fish may be the small margin of error in depth placement of the tag, due to size and thickness of the target area. Tags may be implanted too deeply, penetrate the muscle, and lodge in the buccal cavity. Anesthetized fish could retain the tag in the buccal cavity while passing through the Quality Control Device which magnetizes the tag and confirms tag presence, but then eject the tag after regaining equilibrium in the recovery tank. Changing tag orientation in the cheek muscle from horizontal to vertical would provide a thicker target for tag insertion and may be responsible for higher reported retention of microtags inserted vertically rather than horizontally in the cheek muscle of small fish.

Stocked red drum fingerlings are typically harvested at about 25 mm TL. Attempts to tag red drum of that size with wire microtags have resulted in high mortality (Gene McCarty, Texas Parks Wildl. Dep., Austin, unpubl. data). Tagging larger fish might improve retention rates and would reduce tagging mortality, but the fish would not be representative of the size of fish normally stocked. These factors would complicate any attempt to evaluate the effectiveness of stocking hatchery-reared red drum fingerlings using fish tagged with coded wire microtags.

Acknowledgments

We would like to acknowledge the assistance of Maxine Kubecka, D.V.M., Linda Kocurek, and the staff of the Palacios Veterinary Clinic in obtaining X-ray negatives. We also thank Paul Hammerschmidt for reviewing the manuscript. This study was conducted with partial funding from the U.S. Department of the Interior, Fish and Wildlife Service, under DJ 15.605 (Project F-36-R).

Citations

Arnold, C.R., T.D. Williams, W.H. Bailey, and J.L. Lasswell
1977 Laboratory spawning and rearing of red drum and southern flounder. Proc., Annu. Conf., Southeast. Assoc. Fish Wildl. Agencies 31:437–440.

Bumguardner, B.W., R.L. Colura, A.F. Maciorowski, and G.C. Matlock
1990 Tag retention, survival and growth of red drum fingerlings marked with coded wire tags. Am. Fish. Soc. Symp. 7:286–292.

Colura, R.L., B.T. Hysmith, and R.E. Stevens
1976 Fingerling production of striped bass (*Morone saxatilis*), spotted seatrout (*Cynoscion nebulosus*), and red drum (*Sciaenops ocellatus*) in saltwater ponds. Proc. World Maricult. Soc. 7:79–92.

Comyns, B.H., J. Lyczkowski-Schultz, D.L. Nieland, and C.A. Wilson
1991 Reproduction of red drum, *Sciaenops ocellatus*, in the north central Gulf of Mexico: Seasonality and spawner biomass. *In* Hoyt, R. (ed.), Larval fish recruitment and research in the Americas, p. 17–26. NOAA Tech. Rep. NMFS 95.

Dailey, J.A.
1990 Fish stocking in Texas Bays: 1975–1989. Manage. Data Ser. 49, Texas Parks Wildl. Dep., Fish. Div., Coastal Fish. Br., Austin, 32 p.

Dailey, J.A., and L.W. McEachron
1986 Survival of unmarked red drum stocked into two Texas bays. Manage. Data Ser. 116, Texas Parks Wildl. Dep., Coastal Fish. Br., Austin, 8 p.

Dunning, D.J., Q.E. Ross, B.R. Friedman, and K.L. Marcellus
1990 Coded wire tag retention by, and tagging mortality of, striped bass reared at the Hudson River hatchery. Am. Fish. Soc. Symp. 7:262–266.

Fletcher, D.H., F. Haw, and P.K. Bergman
1987 Retention of coded wire tags implanted into cheek musculature of largemouth bass. N. Am. J. Fish. Manage. 7: 436–439.

Gibbard, G.L., and R.L. Colura
1980 Retention and movement of magnetic nose tags in juvenile red drum. Proc., Texas Chap. Am. Fish. Soc. 3:22–29.

Goodyear, C.P.
1987 Status of the red drum stocks of the Gulf of Mexico. Contr. CRD 86/87-34, NMFS Southeast Fish. Sci. Cent., Miami, 121 p.

Green, A.W., H.R. Osburn, G.C. Matlock, and H.E. Hegen
1985 Estimated survival rates for immature red drum in northwest Gulf of Mexico bays. Fish. Res. (Amst.) 3:263–277.

Heimbach, D.G., D.J. Dunning, H. Wilson, and Q.E. Ross
1990 Sample-size determination for mark-recapture experiments: Hudson River case study. Am. Fish. Soc. Symp. 7: 684–690.

Klar, G.T., and N.C. Parker
1986 Marking fingerling striped bass and blue tilapia with coded wire tags and microtaggants. N. Am. J. Fish. Manage. 6:439–444.

Maddux, H.R., H.R. Osburn, D.L. Trimm, and K.W. Spiller
1989 Trends in finfish landings by sport-boat fishermen in Texas marine waters, May 1974–May 1988. Manage. Data Ser. 8, Texas Parks Wildl. Dep., Fish Div., Coastal Fish. Br., Austin, 496 p.

Matlock, G.C.
1982 The conflict between user groups of red drum and spotted seatrout in Texas. *In* Stroud, R. (ed.), Proc., 7th Annu. Mar. Rec. Fish. Symp. p. 101–109. Sport Fish. Inst., Wash., DC.

Matlock, G.C., B.T. Hysmith, and R.L. Colura
1984 Returns of tagged red drum stocked into Matagorda Bay, Texas. Manage. Data Ser. 63, Texas Parks Wildl. Dep., Coastal Fish. Br., Austin, 6 p.

Matlock, G.C., R.J. Kemp Jr., and T.J. Heffernan
1986 Stocking as a management tool for a red drum fishery, a preliminary evaluation. Manage. Data Ser. 75, Texas Parks Wildl. Dep., Coastal Fish. Br., Austin, 27 p.

McCarty, C.E., J.E. Geiger, L.N. Sturmer, B.A. Gregg, and W.P. Rutledge
1986 Marine finfish culture in Texas: A model for the future. *In* Stroud, R. (ed.), Fish culture in fishery management, p. 249–262. Am. Fish. Soc., Fish Cult. Fish. Manage. Sec., Bethesda.

McEachron, L.W., and A.W. Green
1986 Trends in relative abundance and size of selected finfish in Texas bays: November 1975–June 1984. Manage. Data Ser. 91, Texas Parks Wildl. Dep., Coastal Fish. Br., Austin, 271 p.

Williamson, J.H.
1987 Evaluation of wire nosetags for marking largemouth bass. Prog. Fish-Cult. 49:156–158.

Growth and mortality of *Lutjanus vittus* (Quoy and Gaimard) from the North West Shelf of Australia

Tim L.O. Davis
Grant J. West
CSIRO Division of Fisheries, Marine Laboratories
GPO Box 1538, Hobart, Tasmania 7001, Australia

The tropical waters of the North West Shelf of Australia are highly productive (Tranter 1962) and support a diverse fish fauna (Sainsbury et al. 1985). A significant multispecies trawl fishery has developed in the region, its total catch peaking in 1973 at 37,000 t, although this had decreased to 2700 t in 1989 (Jernakoff and Sainsbury 1990). *Lutjanus vittus* is an important and highly valued fish in this trawl fishery, comprising about 4% of the total catch (Jernakoff and Sainsbury 1990).

Assessment of fish yields of the North West demersal trawl fishery is based mainly on a Beverton and Holt dynamic pool model (Sainsbury 1987), which requires estimates of mortality and growth parameters for each species. In this paper we investigate the age, growth, population structure, and mortality of *L. vittus* collected from random trawl surveys of the North West Shelf during 1982–83.

Materials and methods

Field collection

Material was obtained from the CSIRO North West Shelf program (Young and Sainsbury 1985), which surveyed the shelf waters within latitudes 116–119°E about every two months between August 1982 and October 1983 (Fig. 1). Fish were caught with a Frank and Bryce trawl (30.5 m foot rope and a 20 mm cod-end liner) towed at 3.5–4.5 knots for 30 minutes during the day. Demersal tows were made at computer-generated random positions in 13 strata defined by water depth (10–50 m, 50–120 m, and 120–210 m), sediment type (nominally shelly sand, sand, sandy silt, and silt), and two geographical zones in which different fishing regimes were planned in the future (Table 1). Sixty-two trawl positions were produced for each sampling survey, with effort being allocated according to the mean and variance of catches determined by preliminary surveys and the area of each stratum. On average, 58 trawls were completed each survey.

At each random station the total weight of *L. vittus* and the fork length by 10 mm classes of each *L. vittus* was recorded. A subsample of 20–40 fish, approximately representing the size/frequency composition of the total catch (Kimura 1977) was then selected from each station for further analysis. Fork length was measured to the nearest mm and total weight to the nearest g, and sex were recorded. Sagittal otoliths and urohyals were collected for age determination.

Manuscript accepted 18 February 1992.
Fishery Bulletin, U.S. 90:395–404 (1992).

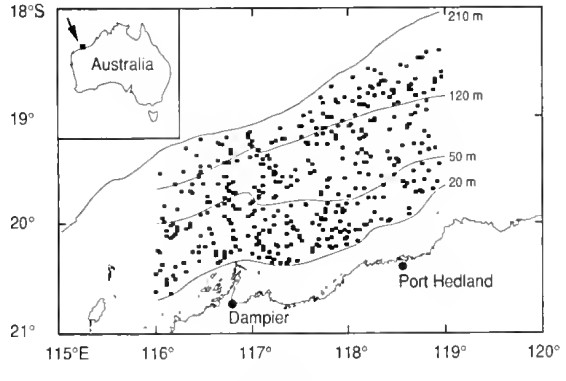

Figure 1
Distribution of 407 random stations sampled during seven cruises on the North West Shelf, September 1982–October 1983. The 20, 50, 120, and 200 m depth contours used to stratify sampling are shown.

Table 1
Stratified random trawl survey on the North West Shelf. The 13 strata sampled during each survey based on depth, geographical zones, and sediment type. Area (km^2) of each stratum and number of random trawls made in each stratum (in parenthesis) on each survey are shown.

	Sand	Shelly-sand	Silt	Sandy-silt
20–49 m				
116°E–117°30′E	3278(6)	3123(4)		
117°30′E–119°E	6309(6)	1732(4)		
50–119 m				
116°E–117°30′E	6123(7)	2381(4)		5505(5)
117°30′E–119°E	9679(7)	2381(4)		1423(5)
120–200 m				
116°E–117°30′E			4577(4)	
117°30′E–119°E		4886(4)	2412(2)	

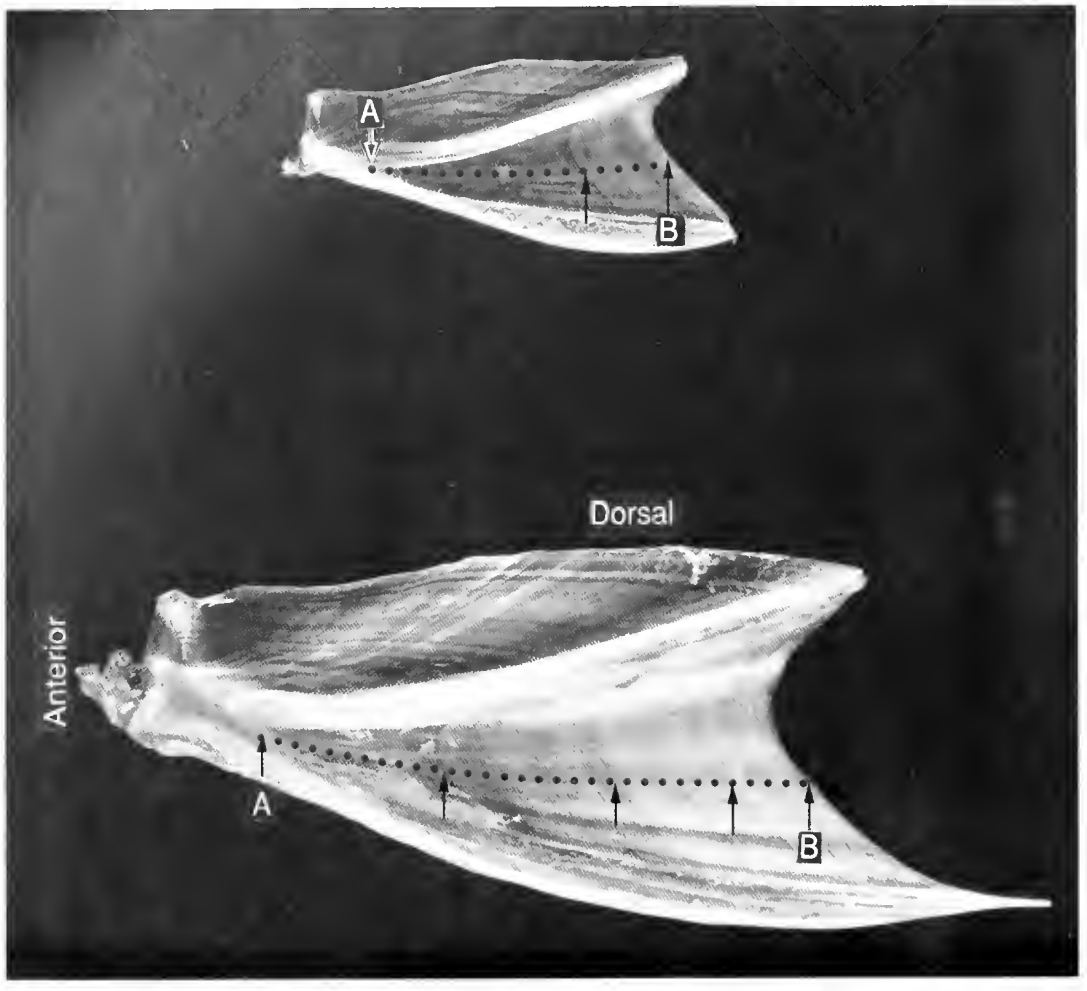

Figure 2
Urohyal bone of *Lutjanus vittus* with one check (129 mm FL) and three checks (242 mm FL). A–B taken as line of measurement.

Age determination

A preliminary examination of the sagittal otoliths, urohyals, scales, and vertebrae from 60 *L. vittus* indicated that checks were more clearly defined in otoliths and urohyals than in other hard parts. Due to their thickness and opacity, otoliths in older fish required sectioning because inner checks were obscured. As urohyals required little preparation before reading, they were chosen as the primary ageing structure; their only disadvantage being that checks in older fish were represented by a cluster of bands, so that determining the point at which the check was formed was somewhat subjective. Otoliths were referred to only when interpretation of urohyals was difficult. Urohyals were frozen and the flesh later removed by dipping in boiling water for 5 minutes, scrubbing, rinsing, and air drying before long-term storage.

Urohyals were examined dry on a black surface under incident light using a dissecting microscope. Checks under this lighting appeared as dark (hyaline) bands (Fig. 2). The distance from the origin to each check and the outer margin of the urohyal was measured along the axis indicated in Figure 2. The periodicity of check formation was determined from analysis of the temporal pattern of marginal increment development (distance from the outermost check to the outer margin of the urohyal) calculated as the index of completion (C) using the formula of Tanaka et al. (1981):

$$C = W_n/W_{n-1}, \quad (1)$$

where W_n = marginal increment, and W_{n-1} = previous complete increment. Analysis of variance was

used to test for significant differences in this index with time of year after arcsine square-root transformation.

Growth analysis

Two forms of length-at-age data were available: lengths were back-calculated to the last annulus (Whitney and Carlander 1956, Carlander 1981) to provide length-at-age data unconfounded by differences in the time of year of sampling. Absolute age-at-observed-length was also assigned, using an artificial January 1 birthdate.

The von Bertalanffy growth curve parameters were fitted to both sets of length-at-age data by direct non-linear least-squares estimation. The null hypothesis that there was no difference between males and females in the three growth-curve parameters was tested using the extra sum-of-squares principle (Draper and Smith 1981, Ratkowsky 1983). The mean lengths at the last annulus of fish aged 1–6 years were also compared between sexes using analysis of variance.

Population structure and mortality

Sex-specific length-frequency distributions and sex-specific age-length keys were obtained from the subsamples from each random station, pooled for each sampling period. It was assumed that neither the sex ratio nor the sex-specific growth rate varied in some systematic way between the different strata. The log-likelihood ratio χ^2 was used to test for departures from a 1:1 sex ratio.

For each sampling period in 1983, the length frequency of the total population was determined using the following equation (K.J. Sainsbury, CSIRO Div. Fish., pers. commun. 1991):

$$F_i = \sum_{j=1}^{j=13} f_{ij} A_j / n_j, \qquad (2)$$

where F_i is the relative frequency of size-class i in the population, f_{ij} is the frequency of size-class i in stratum j, A_j is the area of stratum j, and n_j is the number of trawls in stratum j. These length frequencies were then broken down by sex, using sex-specific length-frequency distribution determined for each sampling period in 1983. The sex-specific age structure at each sampling period was then calculated using the sex-specific age-length keys determined for each sampling period (Ricker 1975, Kimura 1977). A catch curve for each sex was then constructed (Gulland 1969) and total instantaneous mortality estimated by least-squares linear regression of the descending right-hand of the catch curve. Equality of mortality rates between the sexes was determined by analysis of covariance.

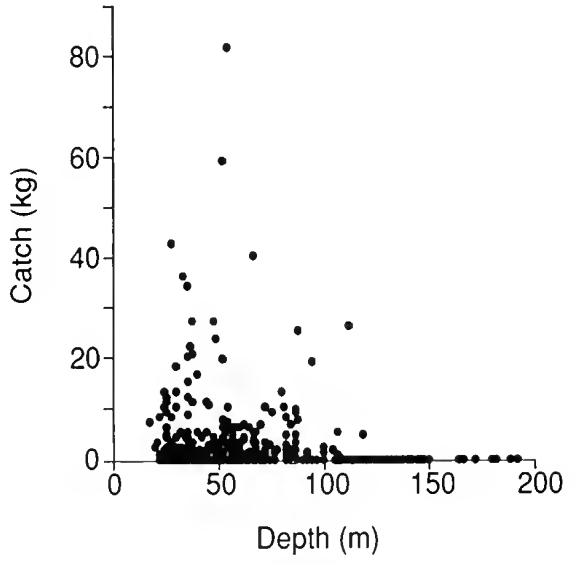

Figure 3
Catch per trawl of *Lutjanus vittus* by water depth on the North West Shelf of Australia, 1982–83.

Results

Depth distribution

Lutjanus vittus were caught in depths from 20 m (the shallowest depth sampled) to 120 m, with the largest catches being at 30–70 m (Fig. 3). There was a positive correlation between individual fish lengths and depth (r 0.337, t 24.7, df 4754, $P<0.001$). While almost the full size-range was encountered at most depths, there was a marked absence of fish <200 mm at depths >90 m (Fig. 4).

Length/weight relationship

In the regression of log weight/log length, the test for homogeneity of slopes between sexes was found to be not significant (ANCOVA, F 0.318, df 1, 2604, P 0.57) and, assuming a common slope, there was no significant difference in the intercepts for the two sexes (ANCOVA, F 1.76, df 1, 2605, P 0.19). Both sexes and juveniles whose sex could not be determined were then combined and a general relation between length (L in mm) and weight (W in g) for *L. vittus* was determined:

$$W = 9.99 \times 10^{-6} L^{3.086}$$

(F 367248, df 1, 2797, $P<0.001$).

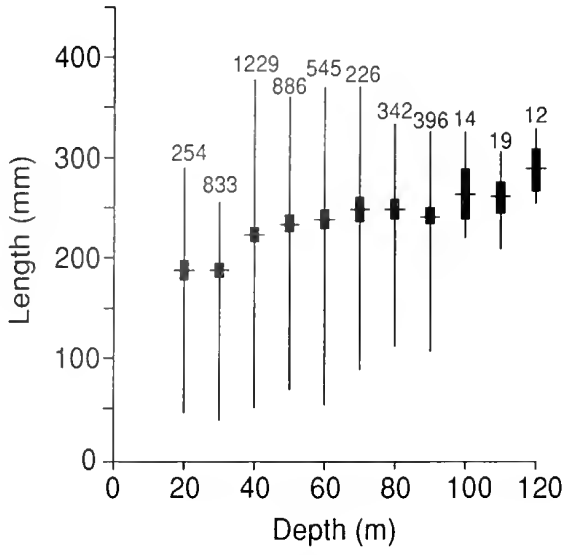

Figure 4

Mean length, 95% confidence limits (vertical bars), length range, and sample size of *Lutjanus vittus* by 10 m depth intervals.

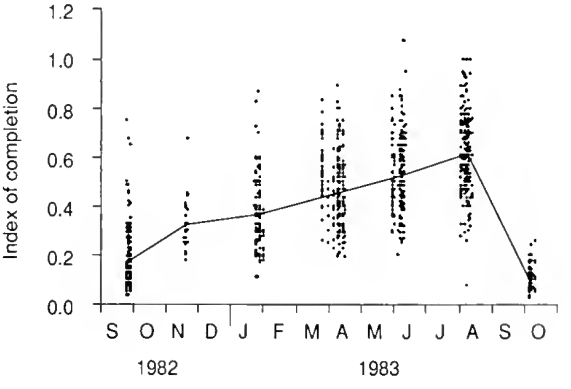

Figure 5

Seasonal change in the index of completion (amount of bone growth since the last check was formed) in *Lutjanus vittus* urohyals with 1–6 checks. Individual indices are plotted against day of sampling, and the line links the mean index for each sampling period.

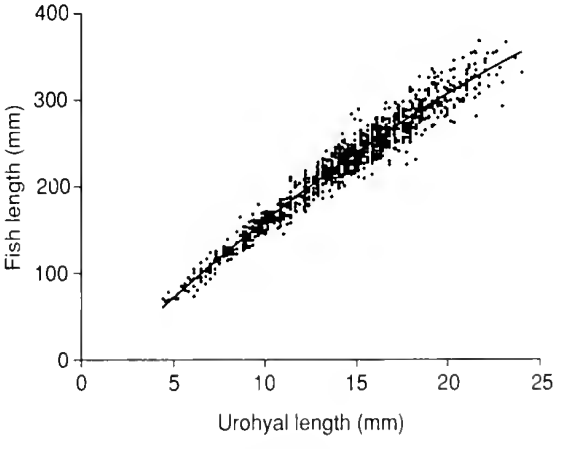

Figure 6

Curvilinear relationship between urohyal length and fish length in *Lutjanus vittus*.

Annulus formation

Evidence that checks are formed annually was obtained by examining the index of completion at about 2-month intervals throughout one season. The index of completion is a measure of the amount of bone growth since the last check was formed, expressed as a proportion of the previous growth increment. The indices of completion for fish aged 1–6 years were combined after each age-group was observed to follow the same seasonal changes in the index (Fig. 5). There were significant ($P<0.001$) differences in this index with time of year for urohyals having one, two, three, four, five and six checks (ANOVA, F 31.4, df 4, 172; F 80.1, df 6, 246; F 100.7, df 6, 263; F 40.0, df 6, 141; F 15.5, df 6, 69; F 88.8, df 5, 233, respectively). While there was considerable variation in this index at any one sampling period, there was a steady increase in the mean index from October to August, followed by a marked drop between August and October. It appears that checks are laid down some time between August and October.

Back-calculation

Lengths were back-calculated to the last annulus, using a proportional method based on the regression of fish length on urohyal length—the body proportional hypothesis (BPH) of Francis (1990). A quadratic equation best described the relationship between body length (L in mm) and urohyal length (U in mm) (Fig. 6):

$$L = -25.48 + 20.485U - 0.193U^2 \quad (r^2\ 0.95,\ \text{df}\ 1102).$$

The mean absolute difference between using BPH and SPH (regression of fish length on urohyal length) was 1.6 mm; BPH back-calculated smaller lengths in fish <150 mm and larger lengths in fish >200 mm.

Growth

Von Bertalanffy growth curves were fitted to length-at-age data for each sex separately. Fish whose sex

Table 2

Mean lengths back-calculated to the last annulus, 95% confidence limits, and sample number (n) at each age (years) for male and female *Lutjanus vittus*.

Age (yr)	Mean length (mm)	95% CL	n
Males			
1	90	87–93	92
2	164	160–167	104
3	214	210–217	122
4	261	256–266	66
5	295	288–302	52
6	313	304–322	22
7	338	330–347	14
Females			
1	89	87–92	92
2	167	163–170	148
3	216	214–219	159
4	251	247–253	115
5	276	271–282	45
6	291	284–298	17

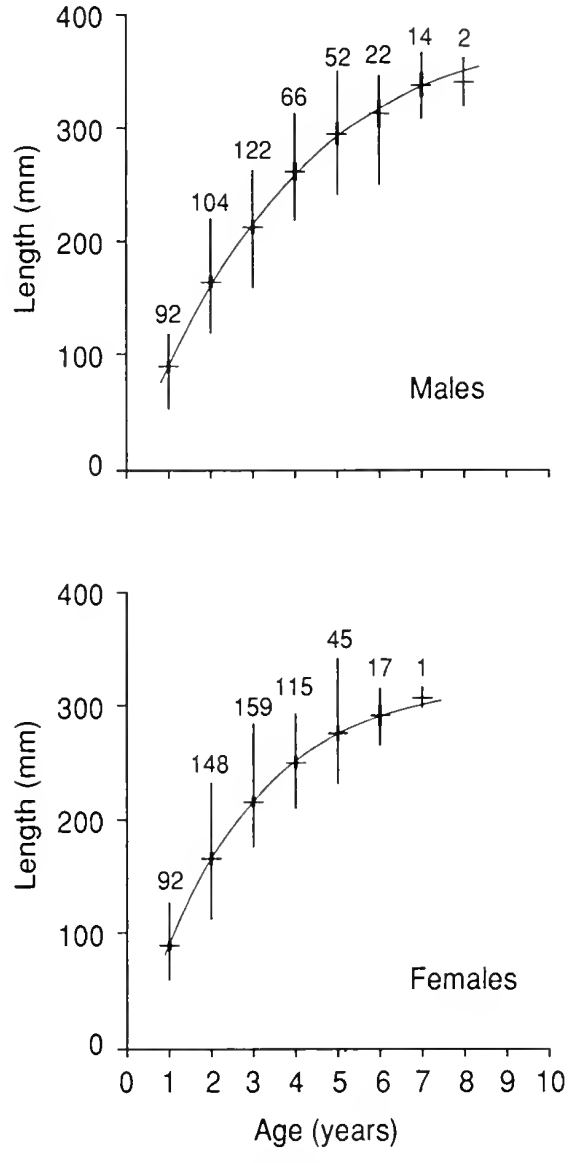

Figure 7

Growth of male and female *Lutjanus vittus*. Mean back-calculated lengths to the last annulus, 95% confidence limits (vertical bars), range, and sample size have been plotted. Von Bertalanffy growth curves were fitted to individual observations.

could not be identified (104 juveniles) presented a problem, because excluding them created a bias since fish that could be sexed in age-class 1 (40 males and 40 females) were larger animals. There were significant differences ($P<0.001$) in back-calculated and observed lengths between age-class 1 males, females, and juveniles (one-way ANOVA, F 50.7, df 2, 181; F 89.0, df 2, 181, respectively). Multiple comparison by the Tukey test indicated that age-class 1 fish that could be sexed were significantly larger than juveniles by about 17 mm for back-calculated lengths and 33 mm for observed lengths. To eliminate this bias, juveniles were ranked by size. The smallest was randomly assigned a sex, and then each juvenile in order was assigned to alternate sexes. The mean lengths back-calculated to the last annulus at each age for male and female (including assigned sexes in age-class 1) are presented in Table 2 and Figure 7.

Back-calculated length-at-age data minimize the effects of seasonal growth but do not completely eliminate it, because the time of check formation ranges over several months (Fig. 5). Assigning an absolute age using an arbitrary birthdate will only compensate for growth differences between fishes caught at different times of the year when there is little seasonal variation in growth rate. However, assigning absolute ages does enable age-class 0 data to be used in determining growth curves (Fig. 8). While back-calculated lengths cannot use age-class 0 data, they do enable a more realistic time-scale parameter (t_0) to be estimated.

The least-squares estimates of the von Bertalanffy growth curve parameters are quite different between the sexes for both forms of length-at-age data (Table 3). Independent of any assumed growth curve, there were significant differences in mean back-calculated lengths between sexes for age-classes 4–6 years (ANOVA, F 42.1, df 1, 311, $P<0.001$) but age-classes 1–3 were not significantly different (F 0.32, df 1, 605, P 0.569). Only fish whose sex was determined

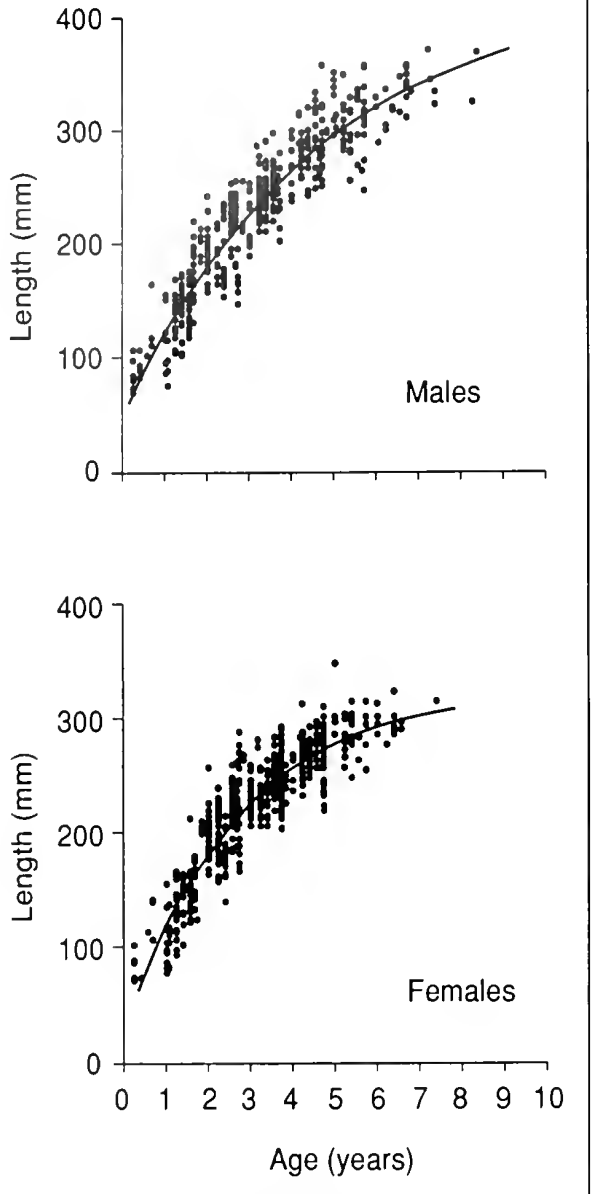

Figure 8
Growth of male and female *Lutjanus vittus* assigned an absolute age assuming a 1 January birthdate.

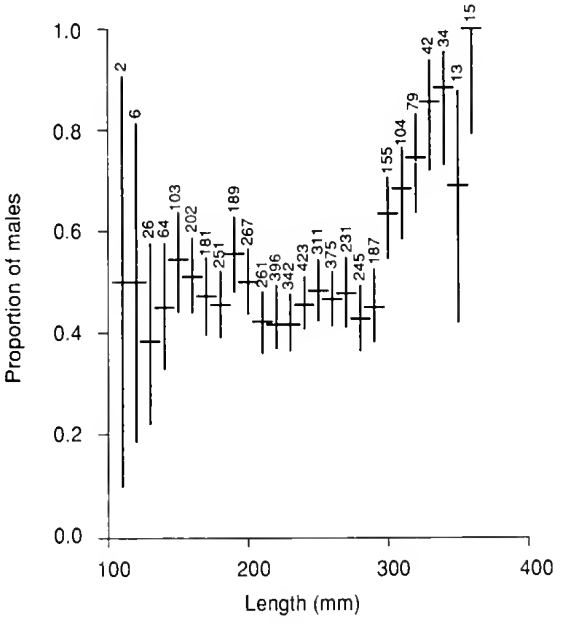

Figure 9
Proportion of males by 10 mm length-class. Means, 95% binomial confidence limits (vertical lines), and sample size are plotted.

were used in this analysis. Both males and females grow at the same rate for the first three years, after which females grow at a markedly slower rate than males.

Sex ratio

There was a marked departure from a 1:1 sex ratio (Fig. 9; likelihood ratio χ^2 152.1, df 29, $P<0.001$) which can be attributed to different growth rates between the sexes. Below 300 mm, sex ratios did not differ from 1:1 (likelihood ratio χ^2 23.3, df 18, P 0.18) but in all larger size groups there was a predominance of males.

Table 3
Estimated parameters (± SE) of the von Bertalanffy growth curve for *Lutjanus vittus*.

		Growth curve parameters			*F* test of parameter estimates		
	df	L_∞ (mm)	K	t_0 (yr)	*F*	df	*P*
Back-calculated length-at-age							
Males	473	403(10.4)	0.26(0.01)	0.02(0.05)	21.7	3, 1045	<0.001
Females	578	323(6.6)	0.39(0.02)	0.17(0.04)			
Length at absolute age							
Males	486	422(15.9)	0.22(0.02)	−0.56(0.09)	19.9	3, 1066	<0.001
Females	586	325(7.7)	0.37(0.03)	−0.23(0.08)			

Length-frequency distributions

Length-frequency distributions of the population were determined separately for males and females (Fig. 10). Each length-class was separated into age-classes based on the urohyal data. There was a jump in age-class between samples taken in August and October because a new check was formed in the intervening period. While

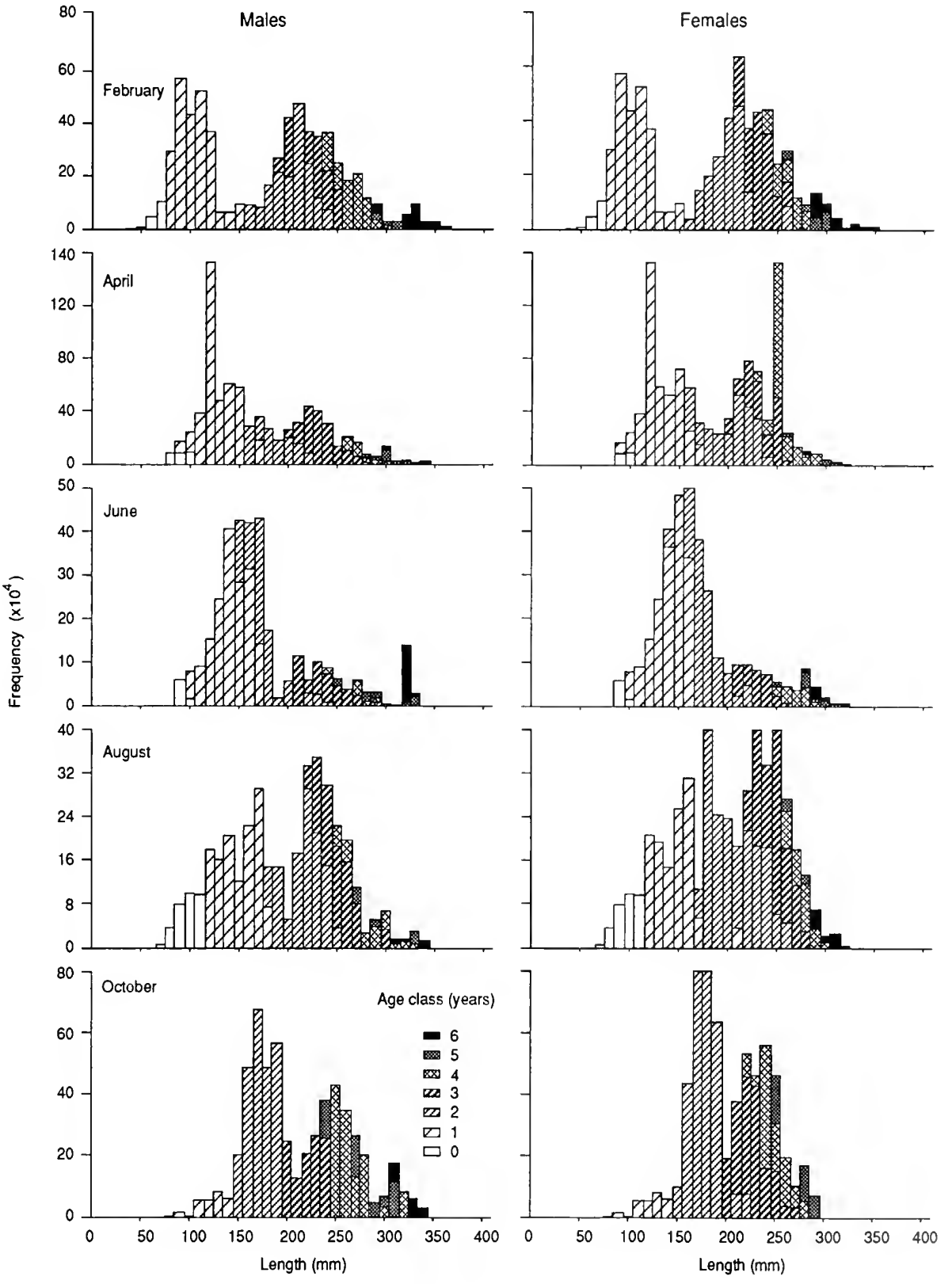

Figure 10

Total population length-frequency distribution of male and female *Lutjanus vittus* at each sampling period in 1983. Hatching within each distribution indicates the age-class structure determined from urohyal ageing. All age-groups increment by 1 year, August–September, due to check formation.

separation of sexes would have reduced variance in the length-frequency distribution of the older age-classes due to growth differences between sexes, there was still considerable size overlap of age-classes and difficulty in identifying modes after age 2 (Fig. 10). There was a clear progression in the length of age-classes 1 and 2 through the year, although age-class-2 fish of both sexes were somewhat larger than expected in February based on the progression in length of this age-class in subsequent months.

Mortality

The relative abundance of each age-class by sex was determined for the five periods sampled in 1983 (Fig. 11). A line was fitted by least squares to the descending limb of the catch curve. Fish not considered to be fully recruited to the sampling gear (circled points) were excluded. There was no significant difference in the slopes of the lines for males and females (ANCOVA, F 0.85, df 1, 47, P 0.36) and no significant sex effect (ANCOVA, F 1.23, df 1, 47, P 0.27) so a catch curve was fitted to the combined data. The instantaneous rate of annual mortality (Z) for males and females was estimated to be 0.98 (SE 0.076).

Discussion

Lutjanus vittus was caught at depths of 20m (the shallowest depth sampled) to 120m, with larger fish tending to inhabit deeper waters. This tendency has also been observed in other shallow-water lutjanids such as *L. aya* (Moseley 1966), *L. griseus* (Starck 1971), and *L. bohar* (Wright et al. 1986).

Most ageing studies on lutjanids have relied on otoliths as the principal structure (see review by Manooch 1987).However, a few authors (i.e., Reshetnikov and Claro 1976, Pozo and Espinosa 1982, Claro 1983, Palazón and González 1986) have used urohyals. Reshetnikov and Claro (1976) had difficulty determining the boundaries of the annual increment after the second or third annulus in urohyals because the annuli were made up of multiple bands. It was our experience that, despite this problem, increments were still easier to measure on urohyals than on whole otoliths, and preparation was far less time-consuming.

Our preliminary investigation indicated that the same number of checks were formed on a variety of hard structures, including urohyals. Data on marginal increments in urohyals showed a seasonal pattern with one check being formed each year, consistent with most other studies on lutjanids in tropical waters. However, studies on two lutjanid species from Cuban shelf waters have suggested that checks are formed twice a year

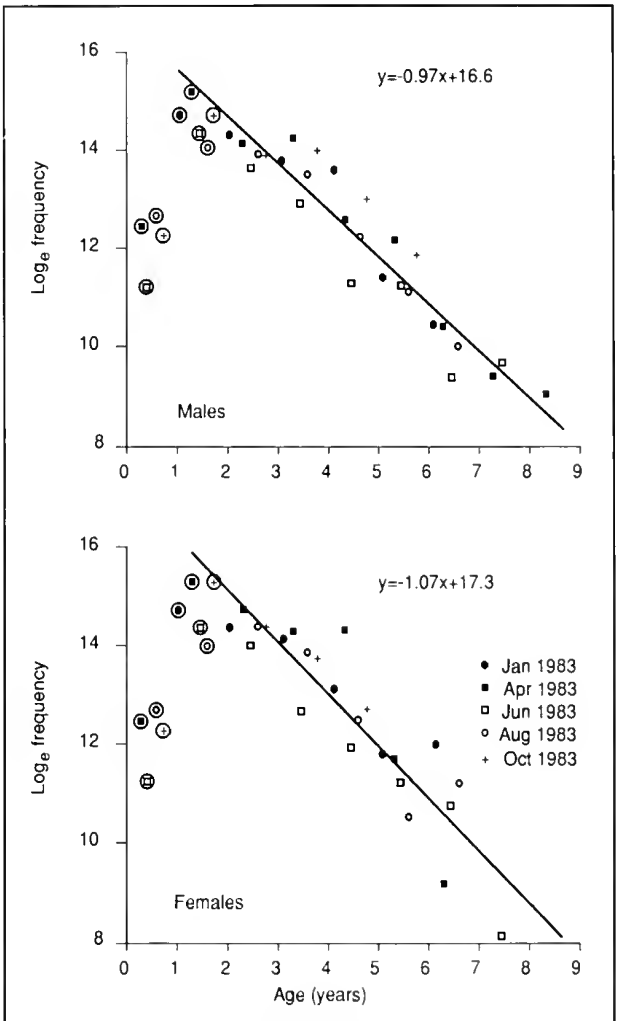

Figure 11

Log$_e$ frequency against absolute age for male and female *Lutjanus vittus*. Data for fish <2 years old (circled) were excluded from the regressions, as they were incompletely recruited age-classes.

(Espinosa and Pozo 1982, Pozo and Espinosa 1982).

The growth of male and female *L. vittus* was significantly different after 3 years of age, with females growing markedly slower than males. There are few documented cases of growth rates differing between sexes in lutjanids. However, female *L. vittus* in New Caledonia were found to grow at a slower rate, and slight growth differences were found in *L. amabilis* in New Caledonia (Loubens 1980) and *L. synagris* in Trinidad (Manickchand-Dass 1987). All mature females observed were 3 years of age or older (unpubl. data), and it seems likely that females grow more slowly than males at this stage because they expend proportionally more energy on gamete production than do males. Stunting in females from a sexually precocious population of *Lates calcarifer* was also attributed

to channeling energy into gonadal growth at the expense of somatic growth at a relatively early age (Davis 1984).

Length-frequency distributions did not show the modal structure one would expect knowing the age structure of the population. The length-frequencies showed three modes, whereas direct ageing suggested there should be at least six. Length-based methods of ageing work best with fish that spawn over a short period of time, have short life spans, and are fast growing; characteristics not typical of lutjanids (Manooch 1987).

A preponderance of females at larger sizes has been reported in studies of other lutjanids, e.g., *L. synagris* (Rodriguez Pino 1962, Erhardt 1977), *Etelis carbunculus* (Everson 1984), *E. coruscans*, *Aprion viriscens* (Everson et al. 1989), and *Rhomboplites aurorubens* (Grimes and Huntsman 1980). The latter authors attributed the preponderance to differential mortality and longevity. *L. vittus* goes against this trend: males predominate the larger size-classes, as is the case for *Lutjanus amabilis* (Loubens 1980) and *Lutjanus buccanella* (Thompson and Munro 1983). The preponderance of males at larger sizes appears to be due largely to a reduction in growth rates of mature females.

No significant differences were found in the instantaneous rate of annual mortality (Z) between male and female *L. vittus*. One of the assumptions of estimating mortality using the catch curve method of Gulland (1969) is that the mortality rate is constant for all years used in the estimation. This may not be the case for female *L. vittus* after 6 years of age. However, the data points in the oldest age-groups are based on smaller sample sizes, so the mortality curve at this stage should be interpreted with caution. Using the relationship between natural mortality (M) and the growth coefficient (K) for snappers and groupers determined by Ralston (1987) from published data provides us with estimates for M of 0.59 for males and 0.92 for females. The value for males seems reasonable, but that for females is unlikely if total mortality is about 0.98. Clearly, regression methods to produce estimates of M such as those used by Pauly (1980) and Ralston (1987) should be applied with caution.

Acknowledgments

This paper is dedicated to the memory of Mr. Otto Augustine, a technician with the CSIRO Division of Fisheries. He was responsible for the ageing of many fish species in the Division's programs from the late sixties up until his death in 1990. He determined the age and marginal increment data used in this paper. We wish to thank W. Thomas for laboratory assistance and all people who assisted in the fieldwork on the Northwest Shelf Program. We are grateful to K.J. Sainsbury for providing length-frequency and catch data from his research program, and K. Haskard for statistical advice. S. Blaber and J.S. Gunn reviewed the manuscript.

Citations

Carlander, K.D.
1981 Caution on the use of the regression method of back-calculating lengths from scale measurements. Fisheries (Bethesda) 6:2–4.

Claro, R.
1983 Ecologia y ciclo de vida del caballerote, *Lutjanus griseus* (Linnaeus), en la plataforma Cubana: 2. Edad y crecimiento, estructura de las poblaciones, pesquerias. Rep. Invest. Inst. Oceanol. Acad. Cienc. Cuba 8, 26 p.

Davis, T.L.O.
1984 A population of sexually precocious barramundi, *Lates calcarifer*, in the Gulf of Carpentaria, Australia. Copeia 1984: 144–149.

Draper, N.R., and H. Smith
1981 Applied regression analysis, 2d ed. Wiley, NY, 407 p.

Erhardt, H.
1977 Beitrage zur biologie von *Lutjanus synagris* (Linnaeus 1758) an der Kolumbianischen Atlantikkuste. Int. Rev. Gesamten Hydrobiol. 62:161–171.

Espinosa, L., and E. Pozo
1982 Edad y crecimento del sesí (*Lutjanus buccanella* Cuvier, 1828) en la plataforma suroriental de Cuba. Rev. Cubana Invest. Pesq. 7(1):80–100.

Everson, A.R.
1984 Spawning and gonadal maturation of the ehu, *Etelis carbunculus*, in the Northwestern Hawaiian Islands. *In* Grigg, R.W., and K.Y. Tanoue (eds.), Proc., Second symposium on resource investigations in the northwestern Hawaiian Islands, vol. 2, p. 128–148. UNIHI-SEAGRANT-MR-84-01, Univ. Hawaii, Honolulu.

Everson, A.R., H.A. Williams, and B.M. Ito
1989 Maturation and reproduction in two Hawaiian eteline snappers, uku, *Aprion virescens*, and onaga, *Etelis coruscans*. Fish. Bull., U.S. 87:877–888.

Francis, R.I.C.C.
1990 Backcalculation of fish length: A critical review. J. Fish Biol. 36:883–902.

Grimes, C.B., and G.R. Huntsman
1980 Reproductive biology of the vermilion snapper, *Rhomboplites aurorubens*, (Cuvier) from North and South Carolina waters. Fish. Bull., U.S. 78:137–146.

Gulland, J.A.
1969 Manual of methods for fish stock assessment. Part 1. Fish population analysis. FAO Man. Fish. Sci. 4:1–154.

Jernakoff, P., and K.J. Sainsbury
1990 CSIRO's northern demersal finfish stock assessments: 1980 to 1990. Bur. Rural Resour., Dep. Primary Ind. Energy Aust. Inf. Pap. IP/6/90, Canberra, A.C.T., Aust., 169 p.

Kimura, D.K.
1977 Statistical assessment of the age-length key. J. Fish. Res. Board Can. 34:317–324.

Loubens, G.
1980 Biologie de quelques espèces de poissons du lagon néo-caldonien. II. Sexualité et reproduction. Cah. Indo-Pac. II(1):41-72.

Manickchand-Dass, S.
1987 Reproduction, age and growth of the lane snapper, *Lutjanus synagris* (Linnaeus), in Trinidad, West Indies. Bull. Mar. Sci. 40 (1):22-28.

Manooch, C.S. III
1987 Mortality rates of snappers and groupers. *In* Polovina, J.J., and S. Ralston (eds.), Tropical snappers and groupers: Biology and fisheries management, p. 329-373. Westview Press, Boulder.

Mori, K.
1984 Early life history of *Lutjanus vitta* (Lutjanidae) in Yuya Bay, the Sea of Japan. Jpn. J. Ichthyol. 30(4):374-392.

Moseley, F.N.
1966 Biology of the red snapper, *Lutjanus aya* Bloch, of the Northwestern Gulf of Mexico. Publ. Inst. Mar.Sci. Univ. Tex. 11:90-101.

Pauly, D.
1980 On the interrelationships between natural mortality, growth parameters, and mean environmental temperature in 175 fish stocks. J. Cons. Perm. Int. Explor. Mer 39:175-192.

Palazón, J.L., and L.W. González
1986 Edad y crecimiento del pargo cebal, *Lutjanus analis* (Cuvier, 1828) (Teleostei: Lutjanidae) en la isla de Margarita y alrededores, Venezuela. Invest. Pesq. 50(2):151-165.

Pozo, E., and L. Espinosa
1982 Estudio de la edad y el crecimento del pargo del alto (*Lutjanus vivanus* Cuvier, 1828) en la plataforma suroriental de Cuba. Rev. Cubana Invest. Pesq. 7(2):1-23.

Ralston, S.V.D.
1987 Mortality rates of snappers and groupers. *In* Polovina, J.J., and S. Ralston (eds.), Tropical snappers and groupers: Biology and fisheries management, p. 375-404. Westview Press, Boulder.

Ratkowsky, D.A.
1983 Nonlinear regression modeling: A unified practical approach. Marcel Dekker, NY, 276 p.

Reshetnikov, Y.S., and R.M. Claro
1976 Cycles of biological processes in tropical fishes with reference to *Lutjanus synagris*. J. Ichthyol. 16:711-723.

Ricker, W.E.
1975 Computation and interpretation of biological statistics of fish populations. Bull. Fish. Res. Board Can. 191, 382 p.

Rodriguez Pino, Z.
1962 Estudios estadísticos y biológicos sobre la biajaiba (*Lutjanus synagris*). Cent. Invest. Pesq., Notas Sobre Invest. 4:1-91.

Sainsbury, K.J.
1987 Assessment and management of the demersal fishery on the continental shelf of northwestern Australia. *In* Polovina, J.J., and S. Ralston (eds.), Tropical snappers and groupers: Biology and fisheries management, p. 465-503. Westview Press, Boulder.

Sainsbury, K.J., P.J. Kailola, and G.G. Leyland
1985 Continental shelf fishes of northern and northwestern Australia. Clouston & Hall and Peter Pownall Fish. Inf. Serv., Canberra, Aust., 375 p.

Starck, W.A. II
1971 Biology of the gray snapper, *Lutjanus griseus*. *In* Starck, W.A. II, and R.E. Schroeder (eds.), Investigations on the gray snapper, *Lutjanus griseus*, p. 1-150. Stud. Trop. Oceanogr. (Miami) 10, Univ. Miami Press.

Tanaka, K., Y. Mugiya, and J. Yamada
1981 Effects of photoperiod and feeding on the daily growth patterns in otoliths of juvenile *Tilapia nilotica*. Fish. Bull., U.S. 79:459-465.

Thompson, R., and J.L. Munro
1983 The biology, ecology and bionomics of the snappers, Lutjanidae. *In* Munro, J.L. (ed.), Caribbean coral reef fishery resources, p. 94-109. ICLARM Stud. Rev. 7, Int. Cent. Living Aquat. Resour. Manage., Manila.

Tranter, D.J.
1962 Zooplankton abundance in Australian waters. Aust. J. Mar. Freshwater Res. 13:106-129.

Whitney, R.R., and K.D. Carlander
1956 Interpretation of body-scale regression for computing body length of fish. J. Wildl. Manage. 20:21-27.

Wright, A., P.J. Dalzell, and A.H. Richards
1986 Some aspects of the biology of the red bass, *Lutjanus bohar* (Forsskal), from the Tigak Islands, Papua New Guinea. J. Fish Biol. 28:533-544.

Young, P.C., and K.J. Sainsbury
1985 CSIRO's North West Shelf program indicates changes in fish populations. Aust. Fish. 44(3):16-20.

Correlation of winter temperature and landings of pink shrimp *Penaeus duorarum* in North Carolina

William F. Hettler

Beaufort Laboratory, Southeast Fisheries Science Center
National Marine Fisheries Service, NOAA, Beaufort, North Carolina 28516-9722

In habitats where low water temperature is not a limiting factor, pink shrimp *Penaeus duorarum* production has been related to rainfall and surface-water inflow (Browder 1985, Sheridan 1991). In contrast, North Carolina landings of pink shrimp were correlated with water temperature during the previous winter, but not to rainfall (Hettler and Chester 1982). In that study, the average water temperature of the two coldest consecutive weeks of each year recorded at a single temperature station located at the Beaufort Laboratory was a predictor of spring landings (through July) for the entire North Carolina fishery. Fifteen years of temperature records and landings were used to determine this relationship. Since the last year reported (1981), 10 additional years of temperature and landings data have become available. This note presents these new data and uses the resulting 25-year time-series to report that average minimum winter water temperature remains a reliable basis for forecasting landings of this species.

The temperature/landings relationship previously published (Hettler and Chester 1982) was recalculated after adding the 1982–91 temperature and landings data (Table 1, Fig. 1). No evidence of curvilinearity in the relationship could be found by fitting higher-order polynomial models. A time-series model was not appropriate because pink shrimp are 'annuals' and their annual population levels generally show low autocorrelation as suggested by the 1962–91 North Carolina pink shrimp heads-off landings data (Fig. 1). Thus the simple linear model was retained. The new regression to determine spring pink shrimp landings in North Carolina was

$$\text{Landings (kg)} = 83747(T) - 245208,$$

where T was the average temperature of the two coldest consecutive weeks (°C). The relationship was significant ($P<0.001$, r^2 0.803). The more general relationships of average winter water temperature (Dec–Mar) or average midwinter water temperature (Jan–Feb) did not correlate with landings over the 25-year time-series.

Predicted landings of pink shrimp were calculated and averaged within 25% of the actual landings for the recent 10-year period. Landings in 1991 were within >0.1% of the prediction. Possible causes of the relatively large deviations in some years' landings from the predicted are discussed in Hettler and Chester (1982) and include errors in the process of estimating landings, year-to-year changes in fishing effort, and, in addition, possible local thermal anomalies.

These new data continue to support the hypothesis that reduced pink shrimp landings in North Carolina are probably a result of cold kill of overwintering shrimp caused by cold water temperatures. In the coldest years (1963, 1977, 1978, and 1990) when spring landings were less than 100,000kg, lethal cold water probably penetrated all but the most highly protected overwintering estuarine habitat. North Carolina is the northern limit in the range of pink shrimp, thus this species is more likely to encounter low temperature stress in this location than in more southerly locations. The linearity of the model is perhaps a consequence of these shrimp's inherent vulnerability to cold water temperatures interact-

Table 1

Actual and predicted landings (heads-off) of pink shrimp *Penaeus duorarum* in the North Carolina spring fishery, February–July, based on average water temperature of the two coldest consecutive weeks of the preceding winter.

Year	Temp. °C	Landings (kg)		Percent over (+) or under (−)
		Actual	Predicted	
1982	5.0	197,630	173,527	+13.9
1983	8.8	451,163	491,765	−8.3
1984	5.9	184,380	248,899	−25.9
1985	5.4	126,797	207,025	−38.7
1986	6.9	307,514	332,646	−7.6
1987	8.3	551,521	449,892	+22.6
1988	6.1	433,125	265,648	+63.0
1989	8.1	639,166	433,142	+47.5
1990	3.7	66,853	64,656	+3.4
1991	10.0	592,381	592,262	<+0.1

Manuscript accepted 20 March 1992.
Fishery Bulletin, U.S. 90:405–406 (1992).

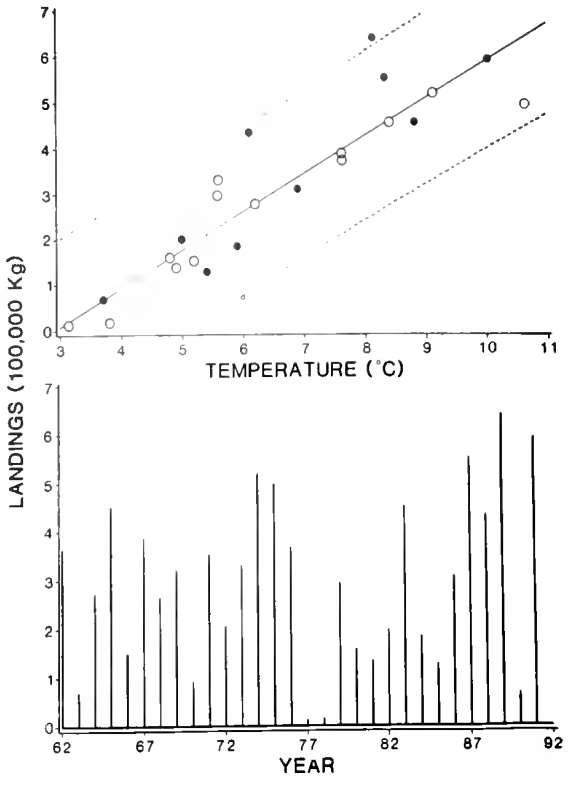

Figure 1

(Upper) Regression and 95% confidence limits for 25 years of temperatures and landings (heads-off) of pink shrimp *Penaeus duorarum*. Open circles represent years before 1982 reported by Hettler and Chester (1982); closed circles represent the years 1982–91. (Bottom) Spring landings (heads-off) of pink shrimp in North Carolina since 1962.

ing with the geographical/spatial distribution and availability of habitats that respond differently to dropping temperatures. The safest habitats would include favorable sediments for deep burrowing, deep water, and physiologically isosmotic salinity.

Acknowledgment

Landings data for 1982–91 were provided by the North Carolina Division of Marine Fisheries, NC/NMFS Cooperative Regional Statistics Program.

Citations

Browder, J.A.
1985 Relationship between pink shrimp production on the Tortugas grounds and water flow patterns in the Florida Everglades. Bull. Mar. Sci. 37:839–856.

Hettler, W.F., and A.J. Chester
1982 The relationship of winter temperature and spring landings of pink shrimp, *Penaeus duorarum*, in North Carolina. Fish. Bull., U.S. 80:761–768.

Sheridan, P.F.
1991 Tortugas pink shrimp forecast. *In* Baxter, K.N. (ed.), Shrimp resource review, briefing book, p. 39. NMFS Southeast Fish. Sci. Cent., Galveston, TX.

Growth of five fishes in Texas bays in the 1960s

Gary C. Matlock
Texas Parks and Wildlife Department
4200 Smith School Road, Austin, Texas 78744

The estuarine sport and commercial fish fisheries in Texas have historically relied upon five species: black drum *Pogonias cromis*, red drum *Sciaenops ocellatus*, sheepshead *Archosargus probatocephalus*, southern flounder *Paralichthys lethostigma*, and spotted seatrout *Cynoscion nebulosus*. Regulation of these fisheries dramatically increased as human demand for fish generally increased through the 1980s. For example, the sale of red drum and spotted seatrout caught in Texas was prohibited in 1981, use of nets in coastal waters was prohibited in 1988, and size, bag, and possession limits were imposed for each species by 1988. Growth information was used in selecting appropriate regulations for optimizing yield and sustaining recruitment. However, comprehensive, coastwide growth rates were available only for red drum, black drum, and spotted seatrout caught in the late 1970s and 1980s when exploitation was extremely high (Doerzbacher et al. 1988, Green et al. 1990). Potential yields may be underestimated when based on growth rates obtained when fishing mortality is high. Tagging data from which growth parameters could be estimated for those species had been collected sporadically from the late 1950s through the early 1970s (Green 1986) when fishing effort was presumably lower than in the 1980s, but these data have not been examined. The objective of this study was to describe quantitatively the growth of black drum, red drum, sheepshead, southern flounder, and spotted seatrout tagged in the 1960s.

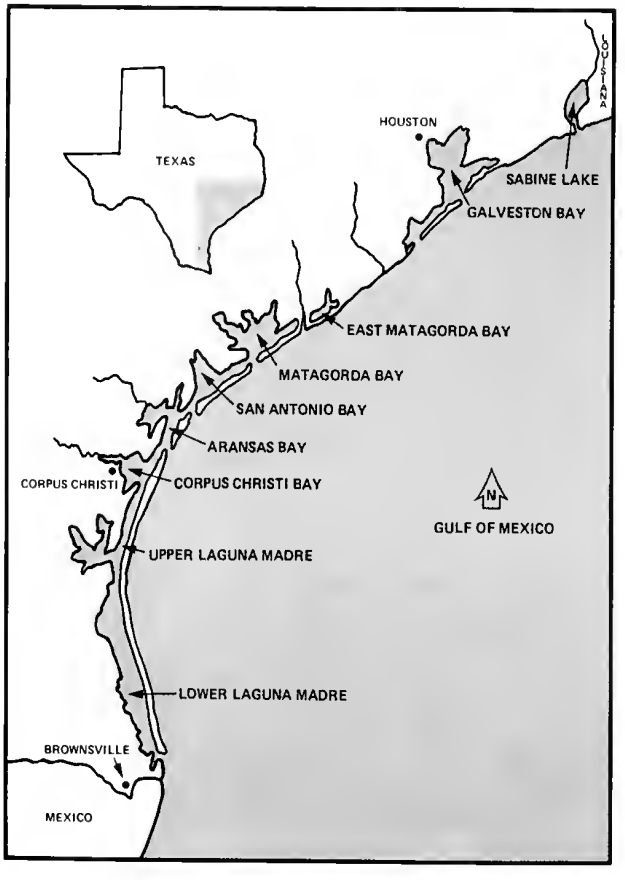

Figure 1
Location of Texas bay systems.

Methods

Data on total length (TL, mm) at tagging and recapture, and the number of days free until recapture for five fishes—black drum, red drum, sheepshead, southern flounder, and spotted seatrout—tagged by the Texas Parks and Wildlife Department (TPWD) in Texas bays (Fig. 1) and recaptured during the period 1950–75 were obtained from Green (1986). No length data were available for fish tagged in the Matagorda Bay system, however. Data resulted from a variety of projects designed to obtain life history information on fishes, mainly red drum and spotted seatrout. Fish for tagging were obtained using rod and reel, trotlines, and trammel and gill nets. Monel strap tags and internal abdominal tags were primarily used. The release of tagged fish and requests for information concerning recaptured fish were advertised through the news media and posters placed in areas frequented by fishermen. Non-monetary rewards of various types were usually offered for returned tags. Additional details are contained in Green (1986). The mean daily growth rate (G) was used to examine the suitability of the von Bertalanffy model for describing growth of each species. The growth rate was calculated as follows:

Manuscript accepted 9 March 1992.
Fishery Bulletin, U.S. 90:407–411 (1992).

$$G = (l_r - l_m)/d,$$

where l_r = TL at recapture,
l_m = TL at tagging, and
d = time in days between tagging and recapture.

A plot of mean daily growth rate versus TL at tagging for each species suggested asymptotic growth, since growth rate generally declined as size-at-tagging increased. Therefore, the von Bertalanffy growth model was chosen as an empirically-based description of growth (Moreau 1987) to which these tagging data were fit. Of the currently available estimating procedures for using tag data to describe growth following the von Bertalanffy growth equation, Fabens' (1965) method provides the most accurate estimates (Sundberg 1984). Data were analyzed using the Fishery Science Application System (Saila et al. 1988) and Fabens' (1965) iterated least-squares method for estimating K and L_∞ in the von Bertalanffy growth equation,

$$l_r = l_m + (L_\infty - l_m)[1 - \exp(-Kd)]$$

where l_r, l_m, and d are defined as above, and
L_∞ = the average TL in a population of fish allowed to grow indefinitely following the von Bertalanffy growth function, and
K = Brody's growth coefficient (per day).

Before analysis, data were screened following procedures of Doerzbacher et al. (1988) to eliminate outliers. Fish with growth rates >3mm/day or <−3 mm/day were eliminated from the data set. The mean ±3SD for the remaining data were then calculated, and fish with growth rates outside this range were also eliminated from the data set. Sufficient data were available to analyze tagged red drum separately by bay system (except for Sabine Lake and Matagorda Bay). Data for each of the other species were analyzed for all tagging locations combined.

The measure of effectiveness (P) used by Phares (1980) which is similar to the multiple correlation coefficient of linear regression (R^2) was used to determine how well the von Bertalanffy model fit the data:

$$P = (SSL - SSE)/SSL,$$

where SSL is the sum of squares of $(l_r - l_m)$, and SSE is the residual sum of squares of the model,

$$SSE = (l_r' - l_r)^2,$$

where l_r' is the model's predicted length-at-recapture, and n is the number of recaptured tagged fish (after data screening). The value of l_r' for each tagged fish was calculated following Parrack (1979):

$$l_r' = L_\infty - (L_\infty - l_m)\, e^{-K(d)}.$$

Standard errors of each estimated K and L_∞ were estimated using 10-fold cross-validation technique (a form of jackknife resampling) described by Verbyla and Litvaitis (1989). For each data set, the original data were randomly partitioned into ten subsamples, nine of which each contained 10% of the data, and one which contained the remainder. The first subsample was excluded from the data set, and K and L_∞ were reestimated. The first subsample was recombined with the data set, and the second subsample was excluded, and so on, until all 10 subsamples had been excluded. The standard error of each parameter of the original data set is approximated by the standard deviation of the mean of the 10 separate estimates made after removing each subsample.

Results and discussion

Most of the data reported for recaptured tagged fish during the 1960s were included in the analyzed data set (i.e., few outliers were found). Of 1630 recaptured fish, only 72 (4.4%) fish were excluded from the analyses (Table 1). Red drum from the lower Laguna Madre had the greatest proportion of outliers (13 of 69 fish). However, the size range at tagging of the remaining 56 fish was comparable to the range of red drum tagged in other bays. These results are similar to those of Doerzbacher et al. (1988) for red drum and black drum, and are supported by Ferguson et al. (1984) who demonstrated that red drum lengths reported by sport-fishermen were accurate.

Mean daily growth rates of tagged fish during the time between release and recapture were about 0.2 mm/day for all species, except red drum which averaged about 0.4–0.7 mm/day (Table 1). These means mainly represent the growth of smaller fish within each range because the size data were skewed toward small fish. For example, of 254 recaptured black drum, over 250 were <300mmTL at tagging and recapture. However, the estimates of daily growth for black drum, red drum, sheepshead, and spotted seatrout in this study were within the ranges of those reported by Colura et al. (1984), Cornelius (1984), Beckman et al. (1988, 1990, 1991), Doerzbacher et al. (1988), Murphy and Taylor (1989), Matlock (1990), and Green et al. (1990).

The estimated L_∞ for black drum, red drum, southern flounder, and spotted seatrout tagged in Texas

Table 1

Size, time free, and growth rate of five fishes tagged and released in Texas bays and recaptured by sport and commercial fishermen during the period 1950–75. Outliers were removed (screened) before anaylsis following the procedures described by Doerzbacher et al. (1988).

					TL (mm) at release		TL (mm) at recapture		Time free (days)		Growth rate (mm/day)	
Species	Bay system	No. tagged	No. in analysis	No. screened	Range	Mean (SD)	Range	Mean (SD)	Range	Mean (SD)	Range	Mean (SD)
Black drum	All bays	28,423	254	6	160–750	317 (101)	175–965	373 (116)	4–4143	273 (467)	−1.167–1.438	0.187 (0.125)
Red drum	Galveston	1370	73	2	155–620	342 (104)	241–762	453 (123)	2–1079	204 (200)	−0.500–1.667	0.624 (0.395)
	San Antonio	1272	101	4	220–720	397 (96)	220–915	506 (120)	11–2432	204 (259)	−0.679–1.847	0.569 (0.343)
	Aransas	3061	435	7	175–615	360 (85)	230–838	473 (107)	2–784	206 (169)	−0.378–1.729	0.565 (0.365)
	Corpus Christi	835	58	4	185–520	322 (93)	280–762	462 (123)	3–692	199 (142)	0–1.686	0.733 (0.396)
	Upper Laguna Madre	2857	147	5	133–693	426 (121)	203–774	544 (110)	6–831	250 (177)	0.600–1.526	0.416 (0.316)
	Lower Laguna Madre	2202	56	13	151–685	326 (122)	171–1016	440 (146)	11–5078	412 (824)	−0.274–0.938	0.395 (0.267)
Sheepshead	All bays	6530	56	6	200–555	313 (74)	210–555	336 (75)	1–630	148 (119)	−0.085–0.779	0.167 (0.209)
Southern flounder	All bays	3176	21	0	255–505	337 (78)	250–560	394 (84)	1–546	197 (169)	0–0.647	0.223 (0.192)
Spotted seatrout	All bays	20,517	357	25	192–762	373 (90)	192–762	406 (98)	1–1315	173 (196)	−0.786–1.220	0.171 (0.276)

bays was about 840–950 mm TL, whereas the sheepshead estimate was about 470 mm (Table 2). Daily growth coefficients (K) were about 0.0005 (0.183 annualized) for black drum, southern flounder, and spotted seatrout, and about 0.001 (0.365 annualized) for red drum and sheepshead (Table 1). The 1960s estimates of L_∞ for black drum, red drum, sheepshead, and spotted seatrout in Texas were generally higher than comparable estimates made in the 1980s. Red drum L_∞ in the 1960s ranged from 879 mm in the upper Laguna Madre to 1177 mm in the Aransas Bay system; L_∞ was 918 mm in the 1980s (Doerzbacher et al. 1988). Values for black drum, sheepshead, and spotted seatrout were as follows (1960s vs. 1980s): 844 mm vs. 798 mm (Doerzbacher et al. 1988); fork length (FL) 478 mm vs. 419 mm (males) and 447 mm (females) (Beckman et al. 1991); and 836 mm vs. 691 mm (Green et al. 1990), respectively. No estimates were available for southern flounder in the 1980s.

Red drum growth varied among bays. Estimates of L_∞ for red drum in each bay system approximated 930 mm, except in Aransas Bay where L_∞ was 1177 mm, and K (annualized) varied between 0.3 and 0.5. Reasons for the interbay variation in L_∞ and K for red drum in the 1960s are unknown. However, factors affecting growth (e.g., fishing mortality, food supply, red drum density, and environmental conditions like salinity and temperature) varied among bays (Matlock 1984).

The estimated values of L_∞ for black drum and red drum from fish tagged in the 1960s and 1980s appear to be underestimates because the data include few adult fish which reside mostly in the Gulf of Mexico (Matlock 1987, 1991). The addition of older adults would probably increase L_∞ and reduce K for both species, but the change in parameter estimates would depend on the average maximum age and size actually reached relative to the largest fish included in the analysis. Parameter estimates (standard error) for the von Bertalanffy model for black drum (0–58 years old) growth in Florida were 1172 mm (±9 mm) and 0.124 mm (±0.0003 mm), respectively. When the von Bertalanffy growth equation was fit to length and age (from otoliths) data for adults off Louisiana, the estimate for L_∞ was 1000 mm FL (Beckman et al. 1991); recall, L_∞ for Texas black drum was 844 mm TL. However, Beckman et al. (1991) questioned the biological significance of their L_∞ estimates because an asymptotic

Table 2

Estimates of parameters (daily K and L_∞) in the von Bertalanffy growth equation for five fishes tagged in Texas bays during the period 1950–75 (N = number of fish used in analysis). Approximate standard errors (SE) were estimated using ten-fold validation (Verbyla and Litvaitis 1989). Annualized K and associated SE were estimated by multiplying daily K and daily SE by 365 days. Measure of effectiveness (P) reflects how well the von Bertalanffy model fit the data (Phares 1980).

Species	Bay system	N	K (±1 SE) Daily	K (±1 SE) Annual	L_∞ (mm) (±1 SE)	P (%)
Black drum	All bays	254	0.00048 (0.000039)	0.175 (0.014)	844 (40)	77.7
Red drum	Galveston	73	0.00116 (0.000118)	0.423 (0.043)	900 (61)	91.7
	San Antonio	101	0.00112 (0.000119)	0.409 (0.043)	978 (77)	88.3
	Aransas	435	0.00075 (0.000036)	0.274 (0.013)	1177 (33)	90.2
	Corpus Christi	58	0.00138 (0.000210)	0.504 (0.077)	940 (82)	90.0
	Upper Laguna Madre	147	0.00127 (0.000085)	0.464 (0.031)	879 (27)	90.0
	Lower Laguna Madre	56	0.00075 (0.000221)	0.274 (0.810)	957 (88)	87.0
Sheepshead	All bays	56	0.00098 (0.000289)	0.358 (0.105)	478 (36)	43.9
Southern flounder	All bays*	21	0.00063 (0.000066)	0.230 (0.024)	848 (32)	80.4
Spotted seatrout	All bays	357	0.00045 (0.000040)	0.164 (0.015)	836 (36)	63.0

*Convergence criteria (successive estimates differ by $<2\times10^{-6}$) was not met after 25 iterations.

size was not attained within the size range sampled and growth was practically linear beyond age 5. Further, neither the von Bertalanffy nor power model accurately described the growth of black drums younger than age 5. A similar result was found for red drum when the von Bertalanffy model was fit to data from fish from the Gulf of Mexico (Beckman et al. 1989). The estimates for L_∞ were 909 mm FL for males and 1013 mm FL for females, but estimates for K (0.137 for males and 0.088 for females) were smaller than published estimates based primarily on young fish (Beckman et al. 1989). They suggested that separate models may be necessary to describe growth of young red drum from estuarine areas or old fish from offshore.

The estimates for spotted seatrout growth are probably more accurate than those for the other four species. The sample size is large, and fish of all sizes are well represented in the data set, including adult spotted seatrout which generally reside in the bays (Perret et al. 1980). Estimates for L_∞ and K using published length-at-age data collected from spotted seatrout in the Gulf of Mexico sporadically during 1929–84 were 655 mm and 0.2 mm, respecitvely (Condrey et al. 1985).

The L_∞ estimate for southern flounder (848 mm TL) may be an overestimate, whereas L_∞ for sheepshead (478 mm TL) may be an underestimate. State records for southern flounder and sheepshead caught in Texas salt waters are 711 mm and 641 mm, respectively (Anonymous 1989). Reasons for the apparent bias are unknown but may be related to the few recaptures of tagged southern flounder (21 fish) and the few large sheepshead recaptured. Only one sheepshead was >500 mm TL.

Citations

Anonymous
1989 Texas state fish records. Tex. Parks Wildl. Dep. PWD-L-9000-5-3/89, Austin, 1 p.

Beckman, D.W., A.L. Stanley, J.H. Render, and C.A. Wilson
1990 Age and growth of black drum in Louisiana waters of the Gulf of Mexico. Trans. Am. Fish. Soc. 119:537–544.
1991 Age and growth-rate estimation of sheepshead *Archosargus probatocephalus* in Louisiana waters using otoliths. Fish. Bull., U.S. 89:1–8.

Beckman, D.W., G.R. Fitzhugh, and C.A. Wilson
1988 Growth rates and validation of age estimates of red drum, *Sciaenops ocellatus*, in a Louisiana salt marsh impoundment. Contrib. Mar. Sci. (Suppl.) 30:93–98.

Beckman, D.W., C.A. Wilson, and A.L. Stanley
1989 Age and growth of red drum, *Sciaenops ocellatus*, from offshore waters of the northern Gulf of Mexico. Fish. Bull., U.S. 87:17–28.

Colura, R.L., C.W. Porter, and A.F. Maciorowski
1984 Preliminary evaluation of the scale method for describing age and growth of spotted seatrout (*Cynoscion nebulosus*) in the Matagorda Bay system, Texas. Manage. Data Ser. 57, Tex. Parks Wildl. Dep., Coastal Fish. Br., Austin, 17 p.

Condrey, R.E., G. Adkins, and M.W. Wascom
1985 Yield-per-recruit of spotted seatrout. Gulf Res. Rep. 8(1):63–67.

Cornelius, S.E.
1984 Contribution to the life history of black drum and analysis of the commercial fishery of Baffin Bay, Vol. II. Tech. Rep. 6, Caesar Kleberg Wildl. Res. Inst., Kingsville, TX, 241 p.

Doerzbacher, J.F., A.W. Green, and G.C. Matlock
1988 A temperture compensated von Bertalanffy growth model for tagged red drum and black drum in Texas bays. Fish. Res. (Amst.) 6:135–152.

Fabens, A.J.
1965 Properties and fitting of the von Bertalanffy growth curve. Growth 25:265–289.

Ferguson, M.O., A.W. Green, and G.C. Matlock
1984 Evaluation of the accuracy and precision of volunteered size data from tagged red drum returns. N. Am. J. Fish. Manage. 4:181–185.

Green, A.W., L.W. McEachron, G.C. Matlock, and H.E. Hegen
1990 Use of abdominal streamer tags and maximum-likelihood techniques to estimate spotted seatrout survival and growth. Am. Fish. Soc. Symp. 7:286–292.

Green, L.
1986 Fish tagging on the Texas coast, 1950–1975. Manage. Data Ser. 99, Tex. Parks Wildl. Dep., Coastal Fish. Br., Austin, 206 p.

Matlock, G.C.
1984 A basis for the development of a management plan for red drum in Texas. Ph.D. diss., Texas A&M Univ., College Station, 287 p.
1987 Maximum total length and age of red drum off Texas. Northeast Gulf Sci. 9:49–52.
1990 The life history of red drum. *In* Chamberlain, G.W., R.J. Miget, and M.G. Haby (compilers), Red drum aquaculture, p. 1–22. TAMU-SG-90-603, Texas A&M Univ. Sea Grant Coll. Prog., College Station.
1991 Maximum total length and age of black drum off Texas. Northeast Gulf Sci. 11:171–174.

Moreau, J.
1987 Mathematical and biological expression of growth in fishes: Recent trends and further developments. *In* Summerfelt, R.C., and G.E. Hall (eds.), The age and growth of fish, p. 81–113. Iowa State Univ. Press, Ames.

Murphy, M.D., and R.G. Taylor
1989 Reporduction and growth of black drum, *Pogonias cromis*, in northeast Florida. Northeast Gulf Sci. 10:127–137.

Parrack, M.L.
1979 Aspects of brown shrimp, *Penaeus aztecus*, growth in the northern Gulf of Mexico. Fish. Bull., U.S. 76:827–836.

Perret, W.S., J.E. Weaver, R.O. Williams, P.L. Johansen, T.D. McIlwain, R.C. Raulerson, and W.M. Tatum
1980 Fishery profiles of red drum and spotted seatrout. Gulf States Mar. Fish. Comm. 6, Ocean Springs, MS, 60 p.

Phares, P.L.
1980 Temperature associated growth of white shrimp in Louisiana. NOAA Tech. Memo. NMFS-SEFC-56, Southeast Fish. Sci. Cent., Galveston, TX, 19 p.

Saila, S.B., C.W. Recksiek, and M.H. Prager
1988 Basic fishery science programs, a compendium of microcomputer programs and maual of operation. Dev. Aquacult. Fish. Sci. 18, Elsevier Sci. Publ. Co., NY, 178 p.

Sundberg, P.
1984 A Monte Carlo study of three methods for estimating the parameters in the von Bertalanffy growth equation. J. Cons. Cons. Int. Explor. Mer 41:248–258.

Verbyla, D.L. and J.A. Litvaitis
1989 Resampling methods for evaluating classfication accuracy of wildlife habitat models. Environ. Manage. 13:783–787.

A mortality model for a population in which harvested individuals do not necessarily die: The stone crab

Victor R. Restrepo

University of Miami, Rosenstiel School of Marine and Atmospheric Science
Cooperative Institute for Marine and Atmospheric Studies
4600 Rickenbacker Causeway, Miami, Florida 33149

Stone crabs *Menippe mercenaria* support a valuable commercial fishery in the Gulf of Mexico, with most of the catch occurring near southwest Florida. Florida landings increased from about 400,000 lbs per fishing season (15 October–15 May) in the early 1960s to an average 2.7 million lbs since 1988. The 1990 landings were valued at over $15 million.

The stone crab fishery is unique in that only the crabs' claws can be harvested, provided that the claws are of legal size (70 mm in propodus length); declawed crabs must be returned to the ocean. Stone crabs can regenerate their massive claws which contain much of the crabs' edible meat (a large claw can weigh 250 g). In a sense, stone crabs are a "reusable resource" because claw regeneration by previously declawed crabs accounts for 1–10% of the annual landings (Savage et al. 1975, Ehrhardt and Restrepo 1989).

The main difficulty associated with estimating mortality rates in this unique fishery is that existing models are not applicable to the crabs' population dynamics. Traditional fisheries models are usually based on the equation (see Beverton and Holt 1957),

$$\frac{dN}{dt} = -(F+M)\,N_t,$$

where N is the population size, t is time, and F and M are the instantaneous fishing and natural mortality rates. An implication of this model is that all harvested animals die. Up to 50% of harvested stone crabs may survive, depending on fishing practices such as the amount of time animals are exposed to air and on the extent of the injury caused by declawing (Davis et al. 1979). Therefore, the above model is not appropriate for this fishery or others like it. In this paper I develop a mortality model that accounts for the possibility that harvested individuals may survive. The model can be used to estimate fishing mortality rates for stone crabs.

The model

Consider a closed population of large-sized individuals (large enough to lose both claws to fishing upon capture), in which catches are monitored for a short period of time. This time-period should be sufficiently short to ensure that declawed crabs will not have time to regenerate their claws. Claw regeneration in large stone crabs takes one year or more (Restrepo 1990), so this should not be a major constraint. The population dynamics during this time-period can be modeled by subdividing the population into harvestable and unharvestable crabs (those with and without legal-sized claws, respectively). Harvestable crabs may become unharvestable if they survive fishing; unharvestable crabs may not become harvestable within the time-interval, since it is assumed that claw regeneration does not occur.

Let

^{h}N, ^{n}N = population sizes (in numbers) of harvestable and unharvestable crabs,

F = rate of capture (assumed to be the same for both types of crabs),

^{h}M, ^{n}M = natural mortality rates for harvestable and unharvestable crabs, and,

S = fraction of harvestable crabs that survive claw removal and release ($0 \leqslant S \leqslant 1$).

For simplicity, assume that harvest and natural mortality rates remain fixed during the time-period. Note also that unharvestable crabs are immediately returned to the water upon capture so that their mortality due to capture is negligible. The differential equations describing the two-compartment model are

$$\frac{d^{h}N_t}{dt} = -(^{h}M + FS + F(1-S))^{h}N_t$$

$$= -(^{h}M + F)^{h}N_t, \text{ and} \qquad (1a)$$

$$d^{n}N_t = -\,^{n}M\,^{n}N_t + FS\,^{h}N_t. \qquad (1b)$$

Equation (1a) is the standard mortality model and simply shows that crabs disappear from the population due to fishing and natural mortality. Losses due to fishing are $F\,^{h}N_t$. Of these, a fraction $(1-S)$ actually die, and a fraction (S) become part of the unharvestable population (Eq. 1b). Thus, F is a true fishing mortality only when $S=0$.

Equation (1a) has the general solution

$$^{h}N_t = {}^{h}N_0\, e^{-(F+{}^{h}M)t}, \qquad (2)$$

Manuscript accepted 11 March 1992.
Fishery Bulletin, U.S. 90:412–416 (1992).

where ${}^{h}N_0$ is the population size at the beginning of the time-period (t = 0). This solution can be substituted into Equation (1b) to solve it since, without claw regeneration, ${}^{h}N_t$ is independent of ${}^{n}N_t$ (i.e., by assumption, there is no transfer from the nonharvestable into the harvestable population):

$$\frac{d{}^{n}N_t}{dt} = - {}^{n}M\,{}^{n}N_t + FS\,{}^{h}N_0\, e^{-(F+{}^{h}M)t}. \qquad (3)$$

This is a first-order linear differential equation that can be solved with the integrating factor

$$e^{\int {}^{n}M\,dt} = e^{{}^{n}Mt}.$$

Multiplying (3) throughout by this factor gives

$$\frac{d[e^{{}^{n}Mt}\,{}^{n}N_t]}{dt} = FS\,{}^{h}N_0\, e^{-(F+{}^{h}M-{}^{n}M)t}.$$

Integrating and letting ${}^{n}N_t = {}^{n}N_0$ at t = 0 gives the solution to Equation (3):

$${}^{n}N_t = \qquad (4)$$

$$\frac{FS\,{}^{h}N_0\,(1-e^{-(F+{}^{h}M-{}^{n}M)t})\,e^{-{}^{n}Mt}}{F+{}^{h}M-{}^{n}M} + {}^{n}N_0\, e^{-{}^{n}Mt}.$$

The dynamics explained by Equations (2) and (4) depend on six parameters (${}^{h}N_0$, ${}^{n}N_0$, ${}^{h}M$, ${}^{n}M$, S, and F). The main usefulness of these two equations lies in simulation modeling (e.g., for yield-per-recruit analyses) in which parameters are given as inputs rather than estimated from fitting the equations to data. However, as shown below, the number of parameters can be reduced to three by taking the ratio $R = {}^{n}N_t/{}^{h}N_t$. Note that the ratio of the two population types is largely independent of the level of sampling intensity, provided that the availabilities of harvestable and unharvestable crabs to the sampling gear do not change. Obtaining estimates of either ${}^{n}N_t$ or ${}^{h}N_t$ alone would be a more difficult task which could involve tagging or detailed survey statistics (see Seber 1982 for a discussion on the estimation of abundance). Dividing Equation (4) by Equation (2) gives

$$R_t = a\, e^{bt} - c, \qquad (5)$$

where $R_t = \dfrac{{}^{n}N_t}{{}^{h}N_t}$,

$$a = \frac{FS}{F+{}^{h}M-{}^{n}M} + \frac{{}^{n}N_0}{{}^{h}N_0},$$

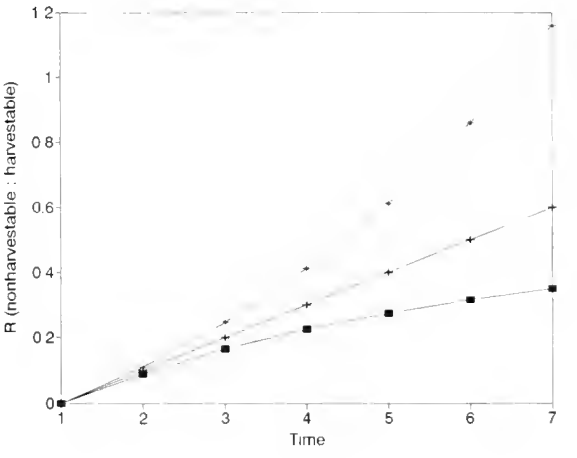

Figure 1

Expected trends in the ratio R (number of nonharvestable: harvestable stone crabs *Menippe mercenaria*) for three values of b in Eq. (5). Lower curve: b is negative and the trend exhibits convex curvature. Middle curve: b approaches zero and the trend is a straight line. Upper curve: b is positive and the trend is concave-upwards.

$$b = F+{}^{h}M-{}^{n}M, \text{ and}$$

$$c = \frac{FS}{F+{}^{h}M-{}^{n}M}.$$

Equation (5) shows that in a closed population and in the absence of claw regeneration, the ratio of nonharvestable to harvestable crabs should change exponentially with a concave, convex, or straight trend depending on the value of b. Consider a hypothetical population in which ${}^{h}N_0 = 1000$, ${}^{n}N_0 = 0.0$, S = 0.5, F = 0.2 per month, and ${}^{h}M = 0.2$ per month. When ${}^{n}M = 0.6$, $b = -0.2$, and R increases with convex curvature (Fig. 1, filled squares). When ${}^{n}M$ approaches 0.4, b approaches zero, and R increases linearly (Fig. 1, crosses). When ${}^{n}M = 0.2$ (${}^{n}M = {}^{h}M$), b is positive and the trend in R is a concave-upwards curve (Fig. 1, asterisks). In practice, some of the model's assumptions may not be always met. For instance, if ${}^{n}M = 0.2$ per month and 250 crabs recruit to the harvestable stock at the beginning of months 5, 6, and 7, then the trend in R decreases starting in month 5, while fishing is still ongoing (Fig. 2).

Application of the model to a data set

No studies have been carried out in which the data necessary for the model have been collected. For this reason the estimates presented below are meant to

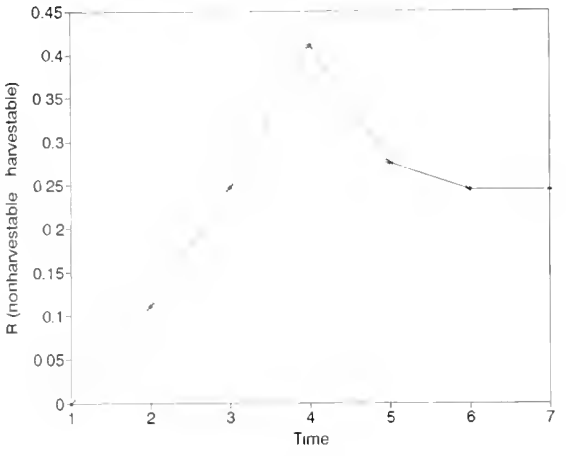

Figure 2

Trend in the ratio R (number of nonharvestable:harvestable stone crabs *Menippe mercenaris*) when the assumption of a closed population is not met. The value of b is positive, as in the upper curve in Fig. 1, but recruitment of harvestable crabs occurs in months 5, 6, and 7.

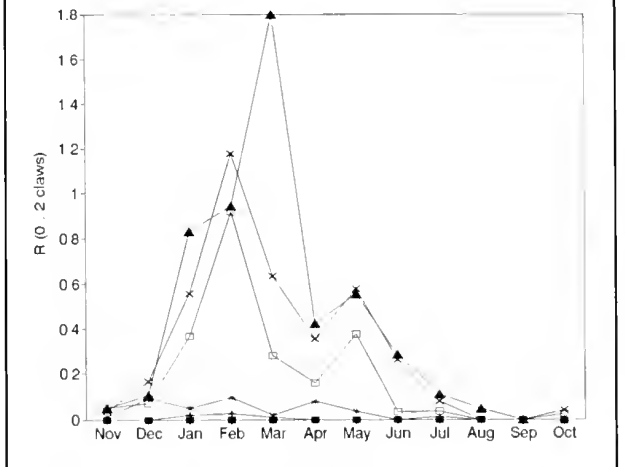

Figure 3

Observed values of the ratio of male stone crabs *Menippe mercenaria* without claws to those with two normal (not regenerated) claws, by size-group. Data from Sullivan (1979).

illustrate how the model can be applied. The data set I used (Sullivan 1979) was collected during 1975 and 1976 in an area where the fishery has been traditionally most intense. This data set contains detailed information on every individual captured, including carapace size, claw sizes, and claw status (presence/absence, regeneration stage, etc.).

The first step in analyzing the data is to define exactly how to categorize crabs in order to meet the assumption that unharvestable crabs do not become harvestable due to claw regeneration during the study period. One way to do so is as follows (Restrepo 1990): "Harvestable" crabs are those with two normal, legal-sized claws (normal claws are defined as those that have no signs of regeneration); "nonharvestable" are those without claws.

With this definition, all harvestable crabs that are caught will likely lose both claws and hence become part of the nonharvestable population if they survive. Conversely, crabs without any claws will not quickly become part of the harvestable population because it would take several regenerative molts (years) before their claws looked normal. Note that the definition above excludes from the analysis all crabs that have either one or two sublegal claws which could, through molting, become part of the harvestable population. In terms of meeting the model's assumptions, the above definition still poses a problem in that crabs with only one claw of legal size (which are relatively uncommon), whether normal or not, may become part of the nonharvestable stock upon declawing.

Figure 3 shows the observed trend in the ratio R [0 claws:2 normal claws] of male stone crabs from Sullivan's (1979) data, for several size-groups. (Female crabs are also harvested, but they are excluded from this analysis because few of them reach sizes at which both claws are of legal size.) Note that R is relatively constant and near zero for crabs <90 mm in carapace width (CW) (Fig. 3). Based on claw size—carapace width relationships (Restrepo 1990), the smaller of the crabs' claws (the "pincer") becomes harvestable only when the carapace reaches 90 mm in width. Thus males with two normal claws are not expected to lose both claws to fishing at sizes <90 mm CW, a fact which is corroborated by Figure 3. Otherwise, R values for the smaller crabs would show larger deviations from the zero line in Figure 3. For this reason, the analyses were conducted with crabs >90 mm CW (Fig. 4).

The trend in the observed R values (Fig. 4, filled squares) is reminiscent of that in Figure 2: it appears to increase concavely upwards from November to February, suggesting that ${}^{n}M < {}^{h}M + F$, and it then decreases starting in March. This decline is possibly a consequence of recruitment of large crabs with normal claws into the fishing grounds, suggesting a failure of the closed-population assumption. Empirical evidence for a similar recruitment peak of large males in the spring was found by Ehrhardt et al. (1990) in Everglades National Park. In addition to recruitment, the decline in R after February could also be attributed to declawed crabs being removed from the study site in greater numbers after this month (some vessels may remove the claws at the end of the day as they travel from the fishing grounds to port). Because of these

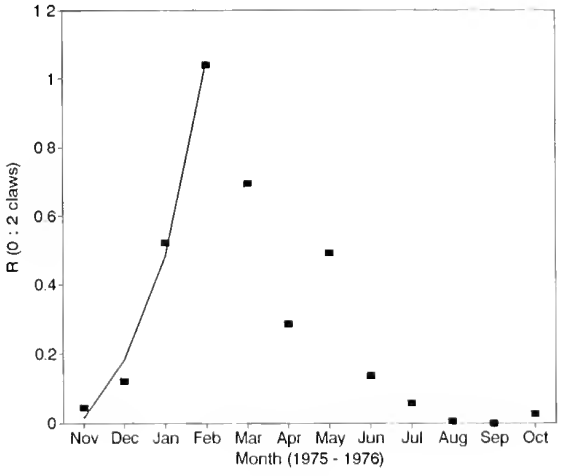

Figure 4

Grouped values from Fig. 3 for crabs ≥ 90 mm CW (symbols). Solid line: fit of Eq. (5) to the first four observations (estimates of fitted parameters are given in Table 1).

Table 1

Parameter estimates and correlation matrix obtained by fitting Equation (5) to Sullivan's (1979) data on stone crab *Menippe mercenaria*.

			Correlation with		
Parameter	Estimate	SE	â	b̂	ĉ
a	0.191	0.175	1.000		
b	0.618	0.252	−0.994	1.000	
c	0.175	0.229	0.972	−0.949	1.000

problems, only the first four data points in the series were used to estimate the parameters in Equation (5).

The least-squares parameter estimates, standard errors and correlation matrix are given in Table 1 (fit shown in Fig. 4). Note that the errors and correlations are extremely high, owing to the small amount of data used (4 data points to estimate 3 parameters). From these estimates, the following are obtained:

$$\frac{{}^{n}N_0}{{}^{h}N_0} = \hat{a} - \hat{c} = 0.016$$

$$FS = \hat{c}\,\hat{b} = 0.109$$

$$F + {}^{h}M - {}^{n}M = \hat{b} = 0.618.$$

Thus by fitting Equation (5) to the data, the relevant parameters that are estimated are the initial ratio (which could be measured directly, anyway) and the product FS. Due to the indeterminacy in the estimates of FS and $F + {}^{h}M - {}^{n}M$, auxiliary information is required before the harvest rate (F) can be deduced. One possibility is to assume that the natural mortalities of clawed and clawless crabs are identical. If so, then $F = \hat{b}$ and $S = \hat{c}$. This would result in $F = 0.618$/month and $S = 17.6\%$; instantaneous mortality due to fishing would be $F(1-S) = 0.51$/month. If ${}^{n}M > {}^{h}M$ as suggested by Bert et al. (1978), then the value of F will be less than that estimated by $\hat{b}$. Note that $F = \hat{b} = 0.618$/month translates into about 4.3/year (during a 7-month fishing season), which appears to be unreasonably high, giving indirect support to Bert et al.'s (1978) contention.

Conclusions

An application of the model to estimate current exploitation rates has not been carried out. As shown in the previous section, the data required to do so are relatively simple (crab size, number of claws, and type of claws) but cannot be obtained from the fishery landing statistics. Therefore, a research sampling program would have to be set up to monitor the population and obtain an estimate using the model. Such a sampling program should give consideration to the following requirements:

1 The areal coverage should be large enough to ensure that declawed crabs are not removed from the study site by the fishing vessels.

2 Time-periods when recruitment, immigration, or emigration take place should not be included in the analyses.

3 Counts of both harvestable and nonharvestable individuals should be made periodically (e.g., weekly) so the counts represent the number of individuals at a particular time, rather than the average number of individuals during a long time-period as was done in the preceding section.

4 To avoid imprecision and parameter correlations such as those in Table 1, a large number of R values should be available for parameter estimation.

Acknowledgments

I am grateful to Nelson Ehrhardt, David Die, and Clay Porch for their discussions and to an anonymous reviewer for helpful comments. Special thanks are due to the Marine Research Lab of the Florida Department of Natural Resources for allowing me the use of their data. Financial support for this study was provided by

the Florida Sea Grant College Program under project No. R/LR-b-24, and through the Cooperative Institute for Marine and Atmospheric Studies by the National Oceanic and Atmospheric Administration Cooperative Agreement No. NA90-RAH-0075.

Citations

Bert, T.M., R.E. Warner, and L.D. Kessler
1978 The biology and Florida fishery of the stone crab *Menippe mercenaria* (Say) with emphasis on southwest Florida. Fla. Sea Grant Tech. Rep. 9, Univ. Fla. Sea Grant Prog., Gainesville, 82 p.

Beverton, R.J.H., and S. Holt
1957 On the dynamics of exploited fish populations. Fish. Invest. Minist. Agric. Fish. Food U.K. (Ser. 2), 19, 533 p.

Davis, G.E., D.S. Baughman, J.D. Chapman, D. MacArthur, and A.C. Pierce
1979 Mortality associated with declawing stone crabs, *Menippe mercenaria*. Rep. SFRC T-552, Natl. Park Serv., South Fla. Res. Cent., Homestead, 23 p.

Ehrhardt, N.M., and V.R. Restrepo
1989 The Florida stone crab fishery: A reusable resource? *In* Caddy, J.F. (ed.), Marine invertebrate fisheries: Their assessment and management, p. 225–240. Wiley, NY.

Ehrhardt, N.M., D.J. Die, and V.R. Restrepo
1990 Abundance and impact of fishing on a stone crab (*Menippe mercenaria*) population in Everglades National Park, Florida. Bull. Mar. Sci. 46:311–323.

Restrepo, V.R.
1990 Population dynamics and yield-per-recruit assessment of southwest Florida stone crabs, *Menippe mercenaria*. Ph.D. thesis, Univ. Miami, Coral Gables, 225 p.

Savage, T., J.R. Sullivan, and C.E. Kalman
1975 An analysis of stone crab (*Menippe mercenaria*) landings on Florida's west coast, with a brief synopsis of the fishery. Fla. Dep. Nat. Resour. Mar. Res. Lab. Publ. 13, St. Petersburg, 37 p.

Seber, G.A.F.
1982 The estimation of animal abundance, 2d ed. Charles Griffin, London.

Sullivan, J.R.
1979 The stone crab, *Menippe mercenaria*, in the southwest Florida fishery. Fla. Dep. Nat. Resour. Mar. Res. Publ. 36, St. Petersburg, 37 p.

Optimal course by dolphins for detection avoidance

Carlos A.M. Salvadó
Pierre Kleiber
Andrew E. Dizon

Southwest Fisheries Science Center, National Marine Fisheries Service, NOAA
P.O. Box 271, La Jolla, California 92038-0271

One of the assumptions of line transect sampling is that movement of animals being counted is not in response to the approaching vessel before the animals are detected (Burnham et al. 1980). By observing from a helicopter the reaction of dolphins to an approaching survey vessel, Au and Perryman (1982) and Hewitt (1985) demonstrated that dolphin schools can detect the approach and maneuver to attempt to avoid detection. Because it may be that dolphin exhibit forms of optimal behavior (Au and Weihs 1980), it is of interest to determine whether there is a direction the dolphin should take that maximizes their distance to the vessel at the point of closest approach and, if there is such a direction, to determine whether dolphin use it. If this is so, this may be the way of determining through aerial means when dolphin first react to an approaching vessel and whether it is after they are detected by a shipboard observer.

Since the advent of purse-seine fishing in the eastern tropical Pacific in 1959, dolphin that associate with yellowfin tuna (i.e., primarily *Stenella attenuata*, *S. longirostris*, and *Delphinus delphis*) are chased, caught in nets, and sometimes drowned (Perrin 1968, 1969). Stuntz and Perrin (1979) reported that these species of dolphin are more difficult to capture in areas where purse-seine-vessel fishing effort has been greatest, implying that evasive behavior may be learned. It has also been reported by Au and Perryman (1982) that evasive maneuvers by dolphin upon approach of a vessel sometimes begin at a distance that is approximately the shipboard observer's horizon. Because the visual horizon of even a leaping dolphin is shorter than that of a shipboard observer, it is likely that they are reacting to the vessel sound. It is therefore plausible that by experiencing repeatedly the approach of such vessels, dolphin not only have learned to evade but do so optimally by choosing through trial and error the direction of escape, if it exists, in which the noise amplitude increases the least. Because the attenuation of sound is proportional to the distance transversed by it, escaping from a sound source in the direction where the amplitude increases the least is the same direction that maximizes the distance between a uniformly-moving source and receiver at the point of closest approach.

Here, we formulate the following problem: Upon detecting the approach of a vessel, a dolphin attempts to avoid detection by retreating. If the velocity of the vessel is V_B and that of the dolphin is V_D, is there a direction in which a dolphin can escape to maximize its distance from the vessel at the point of closest approach (Fig. 1)? And if so, what direction is it? We will show that there is such a direction: If α is the angle between V_B and V_D, the angle $\alpha = \arccos(V_D/V_B)$, where V_B and V_D are, respectively, the speeds of the vessel and the dolphin, will maximize the distance

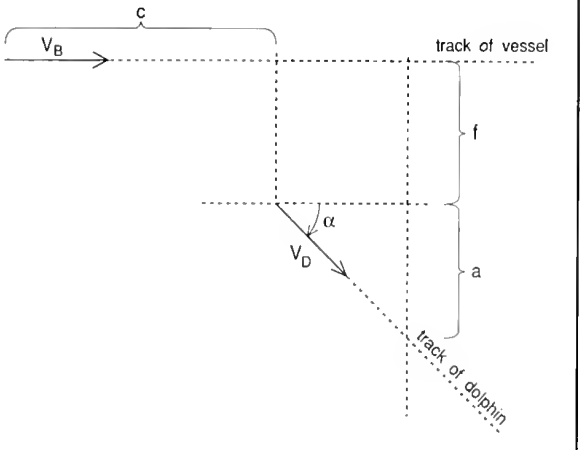

Figure 1
The vessel traveling at speed V_B and the dolphin traveling at V_D as seen in the stationary frame of reference. The direction α is the one chosen by the dolphin. Distance f is the perpendicular distance between the initial position of the dolphin and the projected path of the vessel, while a + f is the distance between vessel and dolphin when the dolphin is abeam.

Manuscript accepted 5 February 1992.
Fishery Bulletin, U.S. 90:417–420 (1992).

between vessel and dolphin at the point of closest approach.

Finally, to ease the task of data analysis by whoever makes the necessary observations, we have derived the expressions that relate dolphin speed and direction to their range and bearing from the vessel. In a cartesian coordinate system let V_x and V_y be, respectively, the x and y components of the dolphin velocity minus, respectively, the x and y components of the vessel velocity. Both V_x and V_y are constructed using range and bearing measurements of the dolphin from the vessel. Then $V_D=[(V_x+V_B)^2+V_y^2]^{1/2}$ and $\alpha=\arctan[V_y/(V_x+V_B)]$.

Problem solution

As stated in the formulation above, the problem makes sense only for the case $V_D \leqslant V_B$. With reference to Figure 2, to maximize the distance between vessel and dolphin at the point of closest approach, we must find the maximum value of r_{min} with respect to angle $0 \leqslant \alpha \leqslant \pi$.

For the purpose of the following exposition, we define initial position to be that position of the vessel (or the dolphin) at the time when the dolphin detects the approaching vessel and begins evasion. Initial time is the time corresponding to the initial position.

In Figure 2, at the point of closest approach the distance between vessel and dolphin is given by

$$r_{min} = (a+f)\cos\beta, \tag{1}$$

where $0 \leqslant \beta \leqslant \pi/2$, f is the perpendicular distance between the initial position of the dolphin and the projected path of the vessel, and (a+f) is the distance between vessel and dolphin when the dolphin is abeam. The vector diagram of Figure 2 shows that the apparent track of the dolphin as seen from the vessel is a function of α, the direction of escape of the dolphin. Therefore, to solve the problem as posed, we must find the extreme value of Eq. (1) with respect to angle α.

By computing the derivative with respect to α of Eq. (1), we find that r_{min} is rendered an extreme value when

$$\frac{dr_{min}}{d\alpha} = \cos\beta\,\frac{da}{d\alpha} - (a+f)\sin\beta\,\frac{d\beta}{d\alpha} \tag{2}$$

vanishes. Depending on the functional dependence of a and β on α, an equation of the form of Eq. (2), could vanish either term by term or by cancellation of the terms. For the former case, each term could vanish trivially (i.e., a and β are independent of α), or non-trivially (i.e., both a and β are rendered extreme values

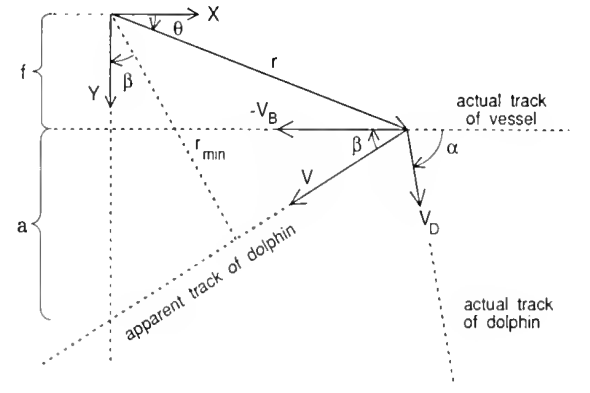

Figure 2

The apparent motion of the dolphin as seen in the moving frame of reference of the vessel. The apparent velocity **V** of the dolphin is the resultant of the vector addition of $-\mathbf{V}_B$ and $\mathbf{V}_D$. Distance f is the perpendicular distance between the initial position of the dolphin and the projected path of the vessel, while a+f is the distance between vessel and dolphin when the dolphin is abeam.

with respect to α simultaneously).

In Figure 1, c is the distance along the projected path of the vessel between the vessel's initial position and the point that is abeam of the dolphin's initial position. Let t_c be the time it takes the vessel to transverse distance c, and t that time from the initial time until the vessel has the dolphin abeam. From the application of the Pythagorean Theorem we can deduce

$$(V_D t)^2 = a^2 + [V_B(t-t_c)]^2. \tag{3}$$

Because

$$a = V_D t \sin\alpha, \tag{4}$$

it can then be shown by substitution of Eq. (4) into Eq. (3) that

$$t = \frac{t_c}{1-(V_D/V_B)\cos\alpha}. \tag{5}$$

By substituting Eq. (5) into Eq. (4), we find that as a function of α, a is given by

$$a = \frac{V_D t_c \sin\alpha}{1-(V_D/V_B)\cos\alpha}. \tag{6}$$

Because at least a is a function of α, we can conclude that in general Eq. (2) does not vanish trivially. However, β is also a function of α as can be deduced by the application of the Law of Sines to Figure 2:

$$\beta = \arctan\left[\left(\frac{V_D}{V_B}\right)\frac{\sin\alpha}{1-(V_D/V_B)\cos\alpha}\right]. \quad (7)$$

Next we investigate whether Eq. (2) vanishes nontrivially. Computing the derivative with respect to α of Eq. (6), we get

$$\frac{da}{d\alpha} = \frac{V_D t_c[\cos\alpha-(V_D/V_B)]}{[1-(V_D/V_B)\cos\alpha]^2}. \quad (8)$$

which vanishes only if

$$\alpha = \arccos\left(\frac{V_D}{V_B}\right) = \alpha_0. \quad (9)$$

Noting the similarity between a and β given respectively in Eq. (6) and (7), we can easily and simply express one in terms of the other. Writing

$$\beta = \arctan\left[\frac{a}{V_B t_c}\right], \quad (10$$

the derivative of β with respect to α is given by

$$\frac{d\beta}{d\alpha} = \frac{\cos^2\beta}{V_B t_c}\frac{da}{d\alpha}. \quad (11)$$

Substituting into Eq. (2) the equivalence of Eq. (11), we find that

$$\frac{dr_{min}}{d\alpha} = \cos\beta\left[1-\frac{(a+f)\sin\beta\cos\beta}{V_B t_c}\right]\frac{da}{d\alpha}, \quad (12)$$

which allows us to conclude that r_{min} is extreme at the point $\alpha=\alpha_0$ because, as we found in Eq. (8), a is extreme at that point. However, as can be appreciated in Eq. (12), there may be other points where r_{min} is extreme. We now investigate whether r_{min} is extreme for values of α other than α_0.

Other extreme values of r_{min} may be attained if

$$\cos\beta = 0 \quad (13)$$

or

$$(a+f)\sin\beta\cos\beta = V_B t_c \quad (14)$$

are physically realizable. Eq. (13) is satisfied for $\beta = n\pi/2$ ($n=1,3,5,...$), and of these only $\beta=\pi/2$ concerns us. It corresponds to the upper limit of the physically realizable range of $0\leqslant\beta\leqslant\pi/2$, and represents the uninteresting case $V_D=V_B$ (i.e., $\alpha_0=0$) which is the trivial special case of this problem: r_{min} is rendered constant when $V_D=V_B$ (i.e., the dolphin swims with the same velocity as the vessel), so the vanishing of Eq. (2) is trivially satisfied.

In Eq. (14) let $f=0$. This limit will not diminish the generality of the solution. The direction a dolphin should take to maximize its distance to the vessel at the point of closest approach will not depend on how close the dolphin is initially to the projected path of the vessel. So without loss of generality we investigate if there is a physically realizable angle β such that

$$a\sin\beta\cos\beta = V_B t_c \quad (15)$$

is satisfied. With the result from Eq. (10) and the identity $\tan\beta = \sin\beta\cos^{-1}\beta$, Eq. (15) can be expressed as the condition $\sin\beta=\pm1$ which is satisfied by the same uninteresting case that satisfies Eq. (13). Therefore, we can conclude that the nontrivial extreme value attained by r_{min} at $\alpha=\alpha_0$ is unique in the interval $0\leqslant\alpha\leqslant\pi$.

We only have left to show that the extreme value attained by r_{min} at $\alpha=\alpha_0$ is a maximum. Let a_0 and β_0 be the respective values of a and β at $\alpha=\alpha_0$. The second derivative of r_{min} with respect to α evaluated at $\alpha=\alpha_0$ is given by

$$\frac{d^2 r_{min}}{d\alpha^2}\Big|_{\alpha_0} = \cos\beta_0\left[1-\frac{a_0\sin\beta_0\cos\beta_0}{V_B t}\right]\frac{d^2 a}{d\alpha^2}\Big|_{\alpha_0}. \quad (16)$$

Because the second derivative of a with respect to α evaluated at $\alpha=\alpha_0$ is

$$\frac{d^2 a}{d\alpha^2}\Big|_{\alpha_0} = \frac{-V_D t_c}{[1-(V_D/V_B)^2]^{3/2}} < 0, \quad (17)$$

to determine whether Eq. (16) is negative we must show that

$$a_0\sin\beta\cos\beta_0 < V_B t_c. \quad (18)$$

We have shown already that Eq. (15) can only be satisfied for an angle $\beta=\pi/2$. Then Eq. (18) is satisfied for $0\leqslant\beta<\pi/2$. We have seen already that $\beta=\pi/2$ when $\alpha=0$, so $da/d\alpha=0$ at that point also. Therefore, we can also conclude that the nontrivial extreme value achieved by r_{min} at $\alpha=\alpha_0$, unique in the interval $0\leqslant\alpha\leqslant\pi$, is a maximum. Because Eq. (2) vanishes term by term, the same result is achieved by finding the extreme value with respect to α of either β or a.

In conclusion, a dolphin escaping at speed V_D at an angle α relative to the velocity V_B of an approaching vessel will maximize its distance to the vessel at the point of closest approach if $\alpha=\arccos(V_D/V_B)$.

Determination of dolphin velocity from range and bearing measurements

In this section we relate the dolphin velocity to practical *in situ* measurements. We will derive a relationship between dolphin speed and direction to its range $0 \leq r < \infty$ and bearing $0 \leq \theta \leq 2\pi$ from the vessel that triggers the dolphin to flight.

For the times $\{t_i: i = 1,2,...,n\}$ we perform the corresponding measurements $\{r_i, \theta_i: i = 1,2,...,n\}$. It is not necessary that the measurements be made from the vessel, but with reference to it (e.g., aerial measurements). However, it is necessary that there be no other vessel in the vicinity that perturbs the measurements by reaction of the dolphin to its presence.

The measurements of range and bearing of the dolphin from the vessel are equivalent to the cylindrical coordinates of the dolphin with respect to the moving frame of reference of the vessel. The cartesian coordinates $-\infty < x < \infty$ and $-\infty < y < \infty$ with respect to the same frame of reference are determined from

$$x = r \cos \theta \text{ and } y = r \sin \theta. \quad (19)$$

Let Δx, Δy, and Δt be, respectively, the increments of the variables x, y, and t. For each of the $(n-1)$ consecutive intervals, we can compute the average speeds in the x and y directions by

$$V_x = \frac{\Delta x}{\Delta t} \text{ and } V_y = \frac{\Delta y}{\Delta t}. \quad (20)$$

These are the components of the dolphins' apparent velocity V in the frame of the moving vessel (Fig. 2). We can express the dolphin velocity in the moving frame as a function of its speed and direction in the stationary frame by

$$V_x = V_D \cos \alpha - V_B \text{ and } V_y = V_D \sin \alpha, \quad (21)$$

which are a system of two coupled, nonlinear equations with V_D and α as unknowns. The solution to this set of equations is given by

$$V_D = \sqrt{V_x + V_B + V_y^2}, \quad (22)$$

where we have chosen the positive root, and

$$\alpha = \arctan\left(\frac{V_y}{V_x + V_B}\right). \quad (23)$$

With these results we can compare the $(n-1)$ time-intervals the direction α taken by the dolphin given Eq. (23), with the optimal direction given in Eq. (9) computed from the result given Eq. (22).

Acknowledgments

We gratefully acknowledge the valuable suggestions by Dave Au and Bill Perrin, and a correction of an erroneous definition by Tim Gerrodette.

Citations

Au, D., and W. Perryman
1982 Movement and speed of dolphin schools responding to an approaching ship. Fish. Bull., U.S. 80:371-379.

Au, D., and D. Weihs
1980 At high speeds dolphins save energy by leaping. Nature 284(5756):548-560.

Burnham, K.P., D.R. Anderson, and J.L. Laake
1980 Estimation of density from line transect sampling of biological populations. Wildl. Monogr. 72, 202 p.

Hewitt, R.P.
1985 Reaction of dolphins to a survey vessel: Effects on census data. Fish. Bull., U.S. 83:187-193.

Perrin, W.F.
1968 The porpoise and the tuna. Sea Frontiers 14:166-174.
1969 Using porpoise to catch tuna. World Fishing 18(6): 42-45.

Stuntz, W.E., and W.F Perrin
1979 Learned evasive behavior by dolphins involved in the eastern tropical Pacific tuna purse seine fishery. *In* Abstracts from presentations at the Third Biennial Conference of the Biology of Marine Mammals, Seattle, Oct. 7-11, 1979, p. 58. [Avail. Library, Natl. Mar. Mammal Lab., Seattle 98115.]

Effects of microprobe precision on hypotheses related to otolith Sr:Ca ratios

Christopher L. Toole

Department of Fisheries and Wildlife, Oregon State University
104 Nash Hall, Corvallis, Oregon 97331-3803
Present address: Environmental and Technical Services Division
National Marine Fisheries Service, NOAA
911 NE 11th Street, Suite 620, Portland, Oregon 97232

Roger L. Nielsen

College of Oceanography, Oregon State University
Ocean Administration 104, Corvallis, Oregon 97331-5503

Several recent studies have used the electron microprobe to infer environmental temperature at the time of otolith formation from the concentration ratio of strontium and calcium. Sr/Ca ratios of otoliths from fish held at constant temperature or collected at known temperature were examined using atomic absorption spectrophotometry (Radtke 1984, 1989) or wavelength dispersive electron microprobe analysis (Townsend et al. 1989, Kalish 1989, Radtke et al. 1990). These studies, with the exception of Kalish (1989), concluded that there is a negative linear relation between environmental temperature and otolith Sr/Ca ratio. This relationship, coupled with assignment of age to each microprobe sample site, has been used to infer the relative temperature histories of wild-caught fish (Radtke 1984,1987,1989; Radtke and Targett 1984; Radtke and Morales-Nin 1989; Townsend et al. 1989; Radtke et al. 1990). The most ambitious application of the method used otolith Sr/Ca ratios to contrast the calculated temperature histories of different subpopulations of larval herring in the Gulf of Maine (Townsend et al. 1989).

Using the electron microprobe to calculate individual fish temperature histories from otolith Sr/Ca ratios is potentially a useful technique for fisheries biologists. However, precision of back-calculated temperature estimates should be examined in greater detail. Previous studies do not explicitly state confidence limits for mean responses or prediction limits for new observations. The scatter of points in Radtke (1989), Townsend et al. (1989), and Radtke et al. (1990) suggest that widths of 95% prediction limits may be on the order of one to several °C for most levels of Sr/Ca examined. While this might be acceptable for studies of fish which are exposed to wide variations in environmental temperature, it is of less use for species which experience more subtle temperature changes.

Future validation experiments may improve the predictive capabilities of the Sr/Ca vs. temperature relationship by examining effects of other variables. For instance, the regression model might be expanded to include growth rate (Kalish 1989) and some measure of physiological stress (Townsend et al. 1989), since these also appear to influence the Sr/Ca ratio.

However, one component of the variation not likely to change in future experiments employing the electron microprobe is the model error term associated with measurement. Usually measurement error is considered insignificant in relation to other sources of variation and is incorporated into the total error term:

$$Y = a + b*X + \in_{Total}$$

where $\in_{Total} = \in_{Measurement} + \in_{Other}$. Measurement error can be thought of as a lower bound to the variation associated with the regression model when other sources of error are minimized.

We suspect that measurement error may be nontrivial when deriving Sr/Ca vs. temperature relationships. Sr/Ca ratios associated with a 1°C change in environmental temperature were approximately 0.00013–0.00036 in previous studies (Table 1). It is difficult to evaluate the significance of these small values without more information on the analytical precision of Ca and Sr detection in fish otoliths using the electron microprobe. Of the studies cited above, only Kalish (1989) reported analytical precision for representative values of Sr and Ca. In that study, measurement error associated with Sr was 3.5% and that associated with Ca was 0.5% for an Sr/Ca ratio of 0.002.

One purpose of the present study was to examine the precision associated with measuring Sr/Ca ratios in fish otoliths, and to demonstrate how this error affects temperature estimates derived from published regressions. Our approach was to intensively sample one otolith from one fish at three beam-power densities and four counting times. By using one otolith, between-fish effects could be ignored. Within-fish Sr/Ca effects were minimized by referencing samples to the same growth zones, leaving the different analytical techniques as the primary source of variation.

Manuscript accepted 15 January 1992.
Fishery Bulletin, U.S. 90:421–427 (1992).

Table 1
Published Sr/Ca vs. temperature relationships.

Source and species examined	Equation
Radtke et al. (1990)	T = 19.172 − 2.955 * (Sr/Ca * 1000)
Clupea harengus	1°C = 0.000338 (Sr/Ca)
Atlantic herring	Sr/Ca range 0.002–0.0045
Townsend et al. (1989)	T = 12.6 − 2.81 (Sr/Ca * 1000)
Clupea harengus	1°C = 0.000356 (Sr/Ca)
Atlantic herring	Sr/Ca range 0.001–0.0045
Radtke (1989)	(Sr/Ca * 1000) = 16.371 − 0.219 * T
Fundulus heteroclitus	1°C = 0.000219 (Sr/Ca)[a]
Mummichog	Sr/Ca range 0.009–0.013
Radtke (1984)	(Sr/Ca * 1000) = 4.19 − 0.13 * T[b]
Gadus morhua	1°C = 0.000130 (Sr/Ca)[a]
Atlantic cod	Sr/Ca range 0.0028–0.0038

[a] Assumes that slope of Sr/Ca on temperature (T) will also predict T on Sr/Ca.
[b] Not stated explicitly in Radtke (1984), but later reported in Kalish (1989).

A second purpose was to determine the effect of beam exposure on the constancy of Sr/Ca ratios. This was necessary because analytical techniques, such as increasing the counting time, will improve the precision of an analysis but may reduce its accuracy through beam damage to the specimen (e.g., Smith 1986, Potts 1987). This problem is encountered in the analysis of other carbonates, but is particularly severe for otoliths, which contain organic material in addition to $CaCO_3$ (Degens et al. 1969). CO_2 is lost during electron beam exposure and, because it is not actually measured by the microprobe but assumed to occur on a 1:1 basis with cations such as Sr and Ca, concentrations of those elements will increase with increasing beam damage. However, if Sr and Ca are not fractionated from one another by beam damage, their ratio should remain unchanged. Absence of change would indicate that methods which improve precision can be implemented without affecting the accuracy of Sr/Ca ratio determinations.

Methods

Dover sole *Microstomus pacificus* is a common Pacific coast flatfish. Juvenile Dover sole 54–104 mm SL were captured by trawling off the Oregon coast on 17 March 1990 and immediately injected with oxytetracycline (OTC). Within 12 hours, fish were transferred to aquaria in Corvallis, Oregon, where they were held for up to 48 days. The OTC produced a fluorescent band which delineated growth prior to capture from subsequent growth under laboratory conditions. Only portions of the otolith formed under natural conditions (inside the OTC band) were analyzed.

An otolith from a randomly selected fish was mounted on a slide with a toluene-based medium. It was ground using 600-grit paper along the saggital plane to a level near the central primordium. The mounting medium was then melted, the otolith was removed, washed, and remounted on its opposite side with heat-setting epoxy. The second side was then ground to the central primordium and polished with a series of diamond and alumina grits, ending with 0.05 μm alumina. The specimen was cleaned ultrasonically in detergent and water between grit changes and given final rinses in water and methanol. Prior to microprobe analysis, the specimen was carbon coated.

Beam power density and precision

Wavelength-dispersive electron microprobe analysis was performed with a Cameca SX-50 microprobe with a 40° beam angle. Three levels of beam-power density were obtained by varying the beam diameter while holding accelerating voltage and beam current constant at 15 KV and 20 nA, respectively. These voltage and current settings are common to most of the previous studies (R. Radtke, Hawaii Inst. Geophys., Univ. Hawaii, Honolulu 96822, pers. commun. 1990), although Kalish (1989) used a 10 nA current. Defocused beam diameters of 5, 7, and 10 μm resulted in beam-power densities of 1.019, 0.520, and 0.255 nA/μm. The most common beam diameter used in previous studies was 5 μm (R. Radtke, pers. commun. 1990), although Kalish (1989) rastered a 12.5 μm × 12.5 μm square.

Sr and Ca concentrations were calculated as normalized mole fractions (equivalent to the atomic ratios of Kalish 1989). Mole fractions are more informative than weight percentages for examination of Sr/Ca ratios, since the substitution of Sr for Ca in otolith aragonite theoretically occurs on a per-atom basis (e.g., Radtke 1989). Normalization also reduces effects of beam damage on concentrations.

Precision of elemental measurements was determined as the coefficient of variation (CV) (Williams 1987),

$$CV = \sigma_{\text{k-ratio}}/\text{k-ratio}$$

where the k-ratio is the ratio of x-ray counts from the otolith to those of the standard (i.e., the calibrated fraction of that element in the otolith) and $\sigma_{\text{k-ratio}}$ is the

standard deviation of that measurement. For a single microprobe analysis, this is calculated as

$$CV = \left[\left[\left[\frac{\sum_{i=1}^{n} N_i^2 - \frac{\left(\sum_{i=1}^{n} N_i\right)^2}{n}}{\left(\frac{\sum_{i=1}^{n} N_i}{n}\right)}\right]^{0.5}\right]^2_{\text{Standard}} + \left[\frac{N_p + \left(\frac{t_p}{t_b}\right) * N_i}{(N_p - N_b)}\right]^2_{\text{Otolith}}\right]^{0.5}$$

where n = number of samples taken on the standard,
N_i = x-ray count (corrected for background count) from ith sample on the standard,
N_p = x-ray count for peak wavelength of element in sample,
N_b = x-ray counts from background wavelengths of element in sample,
t_p = peak wavelength counting time, and
t_b = background wavelength counting time.

Approximate 95% confidence limits for each element measured in each sample were considered ±2*CV, since the Poisson distribution underlying these calculations approximates a normal distribution when sample size (the number of x-rays detected by the spectrometer during an analysis) is high (Williams 1987). X-ray counts in this experiment were on the order of 10^2–10^3 for Sr and 10^4–10^5 for Ca. Confidence limits for the Sr/Ca ratio were also calculated as ±2*CV, but in this case the standard deviation of the k-ratio was calculated as

$$\sigma_{Sr/Ca} = \left[\left(\frac{\sigma_{Sr}}{\text{k-ratio}_{Sr}}\right)^2 + \left(\frac{\sigma_{Ca}}{\text{k-ratio}_{Ca}}\right)^2\right]^{0.5}.$$

Sr and Ca were analysed using the TAP (Sr L-α) and PET (Ca K-α) crystals. Background counts were taken at ±(0.005*sin θ) (where θ is the angle of the spectrometer crystal when it is detecting peak counts) for the same length of time as the peak count. Due to interference with a second-order Ca K-α peak, only one background count was made for Sr. Strontianite (NMNH R10065) and calcite (USNM 136321) were used as standards.

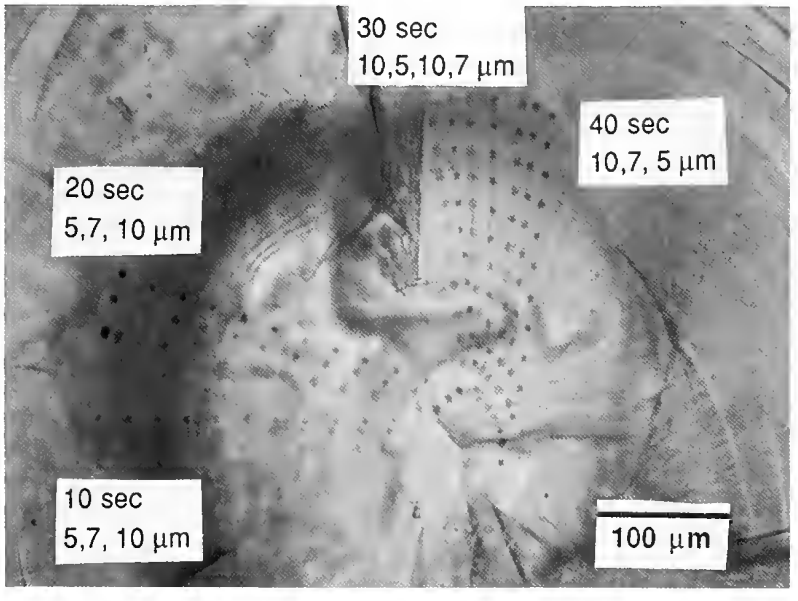

Figure 1
Photomicrograph of otolith from 65.7 mm SL juvenile Dover sole *Microstomus pacificus*, showing location of 12 microprobe transects used for analysis. Each circular area represents one analysis. Note hyaline area near central primordium at inner end of transects and more opaque area towards outer end. The 13th transect was an accidental repetition of the 10 µm, 30-sec transect. Bar indicates 100 µm.

Counting time and precision

Counting time refers to the length of time a spectrometer is collecting counts of characteristic x-rays for an element during one analysis. Counting times of 10, 20, 30, and 40 sec were compared for each beam-power density. The most commonly used counting time for both elements in previous studies was 20 sec (R. Radtke, pers. commun. 1990), although Kalish (1989) analyzed Sr at 100 sec and Ca at 20 sec. Precision was determined as with beam-power density.

Transects of twelve analyses each were made for the 12 combinations of beam power density (4) and counting time (3) (combined $N = [12*3*4] = 144$). These transects passed from an area near the central primordium to an area just inside the discontinuity created by accessory primordia (Fig. 1). This discontinuity

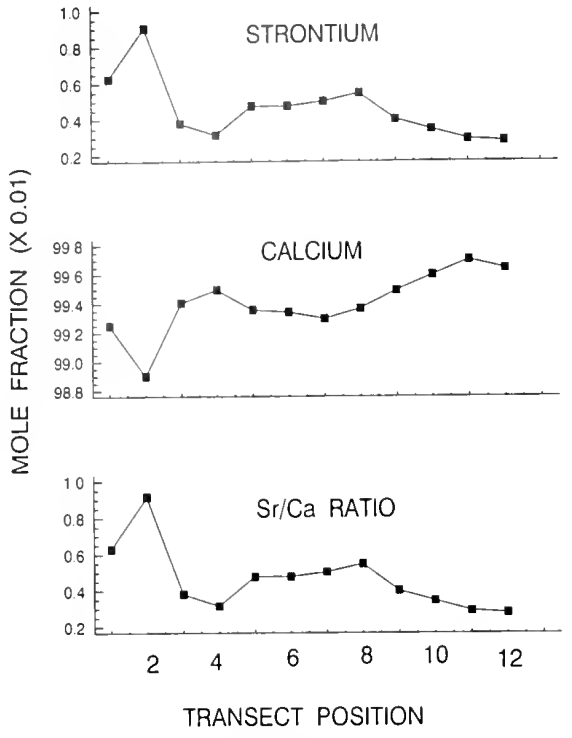

Figure 2

Example of changes in Sr and Ca concentration and the Sr/Ca ratio along one of 12 transects made on a Dover sole otolith. A 7 μm beam and 20-sec counting time were used. Position 1 is the point closest to the central primordium, and position 12 is closest to the otolith edge.

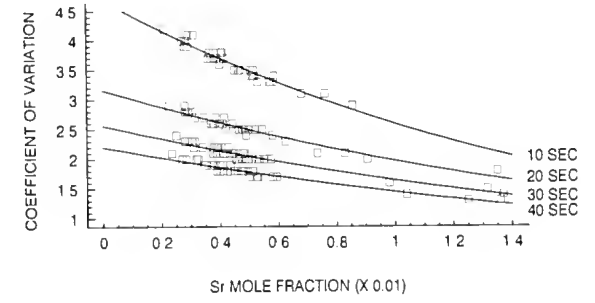

Figure 3

Relation of coefficient of variation (measurement error) to elemental concentration for transects from one Dover sole otolith. Each regression represents three transects with 12 points each (N 36). Regression equations are presented in Table 2.

Table 2

Relationship between Sr concentration and coefficient of variation (CV) for different counting times, based on microprobe transects along the saggital plane of a Dover sole *Microstomus pacificus* otolith. Each equation was derived from three transects of twelve points each (N 36). Equations are in the form: CV = exp(A + (B * Sr mole fraction)). Standard errors in parentheses.

Seconds	A	B	R^2
10	1.546 (0.012)	−59.261 (2.558)	0.940
20	1.150 (0.011)	−47.156 (2.076)	0.938
30	0.941 (0.010)	−44.454 (1.806)	0.947
40	0.789 (0.010)	−42.135 (1.863)	0.938

was >100 μm inside the OTC mark. Starting and ending points for all transects were referenced to specific growth areas identified by dark continuous bands, and the remaining points were evenly spaced between these two points. Locations at the start of the transects were in a translucent area of the otolith assumed to have little organic material (Dannevig 1955), while the end points were in a more opaque area, which probably contained more organic material.

Exposure time and accuracy

Counting time and exposure time were distinguished in this experiment. Counting time is the minimum time the specimen is exposed to the electron beam, while exposure time also includes the time necessary to collect background counts and counts of other elements.

Six sequential analyses were made at each of six locations (combined N 36) to determine changes in elemental concentration. The locations were the start and endpoints of each 20-sec transect used for the precision analysis. Sequential analyses at each location were made in increments of 20-sec counting times, which corresponded to exposure times of 65, 130, 195, 260, 325, and 390 sec. These exposure times were approximately twice as long as those which would result from an analysis of Sr and Ca alone, because S was also analyzed (results not reported).

Statistical analyses

The effect of elemental concentration on Sr precision (CV's) was examined with linear and nonlinear regressions. To determine if beam-power density affected Sr precision, multiple regressions containing normalized concentration and "dummy variables" corresponding to beam size were analyzed with partial-F tests (Neter et al. 1989:364–370). Each of the four counting times was analyzed separately.

Widths of 95% confidence intervals associated with Sr/Ca ratios were determined with linear and nonlinear regressions for each counting time. The ratios and widths of confidence intervals were then converted to temperatures using the four previously published Sr/Ca vs. temperature regressions in Table 1.

The effect of exposure time on Sr/Ca constancy was analyzed with a multiple regression containing exposure time and each location (coded as 0's and 1's) as independent variables. Locations were included to remove possible effects of initial Sr/Ca concentrations, which varied between sites. After determining that interactions and nonlinear terms did not improve a model with parallel straight lines, the common slope was compared with a slope of 0 using a t-test.

Whenever the null hypothesis could not be rejected at $\alpha = 0.05$, statistical power $(1-\beta)$ of the test was calculated as in (Neter et al. 1989:74–75). The power of a test was considered acceptable if $(1-\beta) > 0.80$ (Peterman 1990).

Results

The twelve transects made under different beam conditions on the otolith of a 65.7 mm SL juvenile Dover sole exhibited consistent patterns of strontium and calcium concentrations. Sr concentrations were highest at the two innermost positions and lowest at the two outermost positions in all transects. Sr/Ca ratios mirrored the pattern of Sr. Ca concentrations were approximately 100–500 times higher than Sr concentrations. An example of one of the 12 transects (7 μm beam at 20-sec counting time) is presented in Figure 2.

Relative error of Sr measurements decreased as counting time and elemental concentrations increased, and this was best described by an exponential regression model (Fig. 3, Table 2). The coefficient of variation was 1.4–4.2% for Sr concentrations of 0.2–1.2%. When the effect of elemental concentration was removed, Sr CV's increased with decreasing beam-power density (Table 3); however, this effect was small compared with those of elemental concentration and counting time. Differences in Sr CV's attributable to beam-power density was 0.012–0.076%.

The coefficient of variation associated with Ca measurements was 0.5% for 10- and 20-sec counts and 0.4% for 30- and 40-sec counts, regardless of Ca concentration and beam-power density.

Regressions of the widths of 95% confidence intervals for Sr/Ca determinations against measured Sr/Ca ratios are presented in Figure 4 and Table 4. These regressions include only the effects of elemental concentration and counting time; the effect of beam-power density is omitted. Although relative error decreases

Table 3

Relationship between Sr coefficient of variation (CV) and beam power density, holding Sr concentration as a nonlinear covariate, based upon microprobe transects along the saggital plane of a Dover sole otolith. Each regression represents three transects with 12 points each (N 36). Equations are in the form: $CV = A_1 + A_2Z_1 + A_3Z_2 + B_1*(\text{Sr mole fraction}) + B_2*(\text{Sr mole fraction})^2$ where A is the intercept for the 10 μm beam (0.255 nA/μm density), $A + A_2Z_1$ is the intercept for the 7 μm beam (0.520 nA/μm density), and $A + A_3Z_2$ is the intercept for the 5 μm beam (1.019 nA/μm density); Z_1 and Z_2 are dummy variables for the 7 and 5 μm beams; and B_1 and B_2 are fitted slope parameters. Partial-F tests indicate the significance of beam power density effects in the model. Standard errors in parentheses.

	Counts			
Parameter	10-sec	20-sec	30-sec	40-sec
A_1	4.990	3.394	2.767	2.420
	(0.101)	(0.043)	(0.051)	(0.041)
A_2	−0.013	−0.019	−0.027	−0.039
	(0.027)	(0.018)	(0.017)	(0.014)
A_3	−0.076	−0.055	−0.052	−0.053
	(0.027)	(0.018)	(0.017)	(0.014)
B_1	−389.80	−219.41	−169.07	−151.79
	(40.88)	(13.49)	(15.73)	(12.81)
B_2	17940.3	7746.5	5386.3	5229.6
	(3996.70)	(921.47)	(959.47)	(796.05)
R^2 (adj.)	0.954	0.969	0.959	0.962
$F^*_{(0.05, 2, 31)}$	4.479	4.833	4.531	8.443
P	0.020	0.015	0.019	0.001

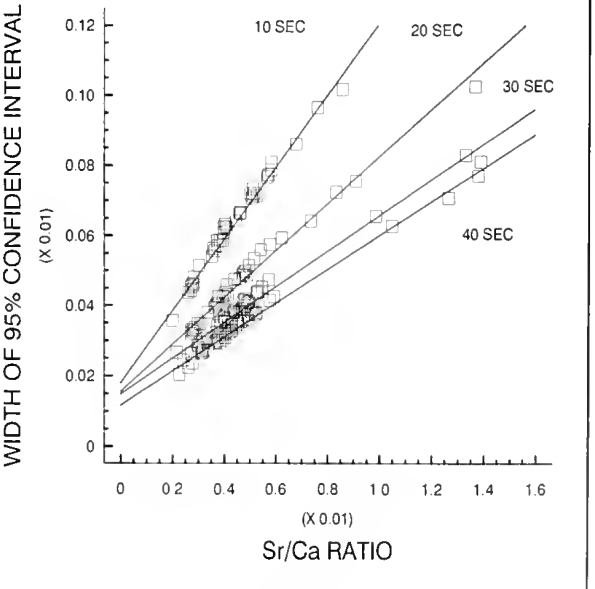

Figure 4

Relationship between Sr/Ca ratios and 95% confidence intervals of measurements at different counting times, based upon microprobe transects along the saggital plane of one Dover sole otolith. Each regression represents three transects of 12 points each (N 36). Regression equations are presented in Table 4.

Table 4

Relationship between Sr/Ca ratios and 95% confidence interval of measurements at different counting times, based upon microprobe transects along the saggital plane of a Dover sole otolith. Each equation was derived from three transects of 12 points each (N 36). Form of the relationship is: 95% CI = A + (B*Sr/Ca ratio). Standard errors in parentheses.

Seconds	A	B	R^2
10	1.791E-4	0.1024	0.9861
	(9.829E-6)	(0.0021)	
20	1.551E-4	0.0669	0.9823
	(7.990E-6)	(0.0015)	
30	1.477E-4	0.0508	0.9817
	(6.579E-6)	(0.0012)	
40	1.166E-4	0.0482	0.9888
	(4.843E-6)	(0.0009)	

with increasing Sr/Ca, the actual width of the confidence interval increases. Conversion of Sr/Ca ratios and 95% confidence limits to temperatures, using the 20-sec regression and previously published temperature vs. Sr/Ca ratios, is presented in Figure 5. Confidence limits associated with calculated temperatures were 0.6–4.7°C, depending upon species, study, and temperature level.

The model which best fit the six multiple exposures is presented in Figure 6. The common slope of $-1.3*10^{-7}$ was not different from a slope of 0 ($t_{0.05,29} = 0.176$, $P = 0.86$). This experiment could have detected a change as small as $1.86*10^{-6}$ Sr/Ca per sec increased exposure (or $1.21*10^{-4}$ for each 65-sec treatment) at $\alpha = 0.05$ and $(1-\beta) = 0.90$, had such an effect existed.

Discussion

Our results confirm that measurement error associated with Sr/Ca determinations is nontrivial. At the standard counting time of 20 sec, measurement error associated with Sr/Ca determinations (expressed as 95% confidence intervals) was equal to or greater than the Sr/Ca increment representative of a 1°C temperature change in three of the four previously-published studies. Even in Townsend et al. (1989), at temperatures <4°C, measurement error was >1°C. The highest measurement error in the studies was representative of a 4.7°C temperature change. Inferred temperature differences between otolith regions or between fish should be considered in light of these values. Statistical error in the Sr/Ca vs. temperature regressions will add to the measurement error associated with temperature calculations.

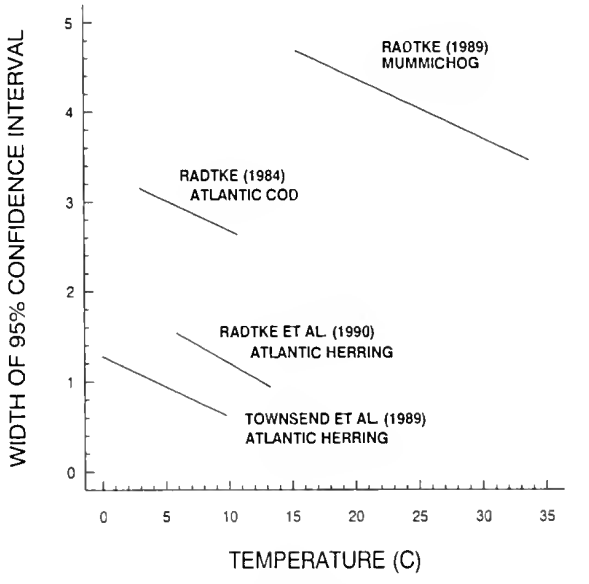

Figure 5

Relationship between back-calculated temperature estimates and 95% confidence intervals (for measurement error only) surrounding those estimates. Temperature vs. Sr/Ca conversions are from Table 1. Confidence intervals are converted from Sr/Ca confidence intervals for 20-sec counts in Table 4 and Figure 4.

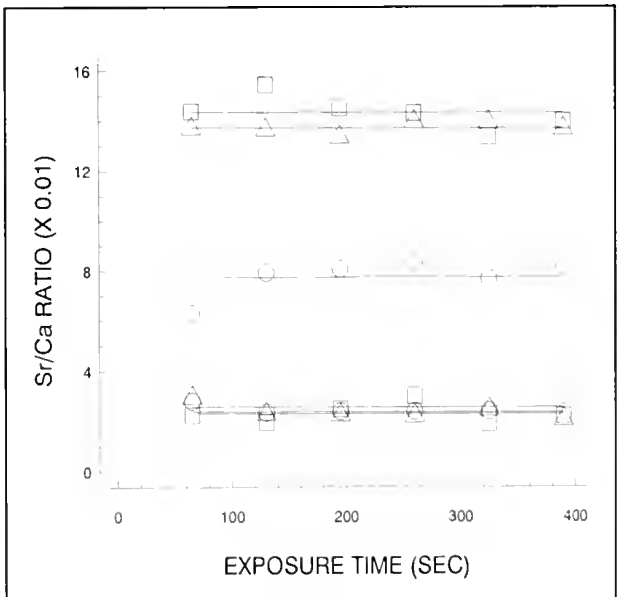

Figure 6

Relationship between Sr/Ca level and exposure time, based upon microprobe samples at six sites on one Dover sole otolith. Six sequential analyses were made at each site (N 36). The six exposure times corresponded to counting times of 20, 40, 60, 80, 100, and 120 sec. The equation describing the relationship is: Sr/Ca level = $0.0023 + (0.0054*Z_1) + (0.00026*Z_2) + (0.0114*Z_3) + (6.6\times10^{-5}*Z_4) + (0.012*Z_5) - (1.30\times10^{-7}*$ exposure time), where Z_1–Z_5 are dummy variables for locations. Adjusted $R^2 = 0.991$, $P < 0.0001$.

At least 40-sec counts would be necessary to detect a 1°C change in temperature experienced by herring (Townsend et al. 1989, Radtke et al. 1990) at all temperature levels examined in those studies. Detection of a 1°C temperature change in cod (Radtke 1984) and *Fundulus* (Radtke 1989) would require much longer counting times, beyond the range examined in this experiment.

This experiment documents the improvement in precision which is possible when otoliths are analyzed at longer counting times and higher beam power densities. Neither treatment appeared to affect the level of Sr/Ca accuracy under the range of conditions examined. Obvious burns on the otolith (Fig. 1) indicate that beam damage did occur in all of our experimental treatments, and we suspect that it also occurred in other studies using similar analytical conditions. However, whatever effect this may have had on the accuracy of the molecular weight percent concentrations for Ca and Sr, the ratio of the two elements remained constant, indicating no observable fractionation.

One implication of these results is that Sr/Ca precision can be increased, with no apparent loss of accuracy, when analyses are conducted for 40-sec rather than 20-sec counting times, and at 5 μm rather than 10 μm beam sizes, at an accelerating voltage of 20 nA. The 5 μm beam allows greater temporal resolution, which is helpful when matching the sample location to structures such as daily growth increments. These may be as small as 0.1–0.2 μm, depending upon species, growth rate, and age (Campagna and Neilson 1985).

Because the level of precision may affect conclusions of studies relating otolith Sr/Ca levels to environmental temperature, it is important to know the analytical conditions under which each study is conducted. Minimal information required includes beam current and voltage, beam size, counting time for each element, standards used, and precision of measurements. This information has not been reported in sufficient detail in some of the previous studies, making interpretation difficult. The methods described in this experiment are proposed as a means of defining measurement precision in future studies of Sr/Ca ratios in fish otoliths.

Acknowledgments

We are grateful to Douglas Markle for his advice and support. Comments by John Kalish on an earlier draft greatly improved the final version. This work was funded in part by the Oregon Sea Grant Program, Project No. NA85AA-D-SG095; Pacific Outer Continental Shelf Region of the Minerals Management Service, Department of Interior Contract No. 14-12-0001-30429; and the Oregon State University Research Office. We also thank Capt. Terry Thompson of the FV *Olympic* for donation of a portion of the ship time.

Citations

Campagna, S.E., and J. Neilson
1985 Microstructure of fish otoliths. Can. J. Fish. Aquat. Sci. 42:1014–1032.

Dannevig, E.H.
1955 Chemical composition of the zones in cod otoliths. J. Cons. Cons. Int. Explor. Mer 21:156–159.

Degens, E.T., W. Deuser, and R. Haedrich
1969 Molecular structure and composition of fish otoliths. Mar. Biol. (Berl.) 2:105–113.

Kalish, J.M.
1989 Otolith microchemistry: Validation of the effects of physiology, age, and environment on otolith composition. J. Exp. Mar. Biol. Ecol. 132:151–178.

Neter, J., W. Wasserman, and M. Kutner
1989 Applied linear regression models. Irwin, Boston, 667 p.

Peterman, R.M.
1990 Statistical power analysis can improve fisheries research and management. Can. J. Fish. Aquat. Sci. 47:2–15.

Potts, P.J.
1987 A handbook of silicate rock analysis. Chapman & Hall, NY, 622 p.

Radtke, R.L.
1984 Cod fish otoliths: Information storage structures. *In* The propagation of cod *Gadus morhua* L. Flodevigen Rapp. 1:273–298.
1987 Age and growth information available from the otoliths of the Hawaiian snapper, *Pristipomoides filamentosus*. Coral Reefs 6:19–25.
1989 Strontium-calcium concentration ratios in fish otoliths as environmental indicators. Comp. Biochem. Physiol. 92A: 189–193.

Radtke, R.L., and B. Morales-Nin
1989 Mediterranean juvenile bluefin tuna: Life history patterns. J. Fish Biol. 35:485–496.

Radtke, R.L., and T. Targett
1984 Rythmic structural and chemical patterns in otoliths of the Antarctic fish *Notothenia larsoni*: Their application to age determination. Polar Biol. 3:203–210.

Radtke, R.L., D. Townsend, S. Folsom, and M. Morrison
1990 Strontium:calcium concentration ratios in otoliths of herring larvae as indicators of environmental histories. Environ. Biol. Fish. 27:51–61.

Smith, M.P.
1986 Silver coating inhibits electron microprobe beam damage of carbonates. J. Sedimentary Petrol. 56:107–108.

Townsend, D.W., R. Radtke, M. Morrison, and S. Folsom
1989 Recruitment implications of larval herring overwintering distributions in the Gulf of Maine, inferred using a new otolith technique. Mar. Ecol. Prog. Ser. 55:1–13.

Williams, K.L.
1987 An introduction to X-ray spectrometry: X-ray fluorescence and electron microprobe analysis. Allen & Unwin, London, 370 p.

Superintendent of Documents **Subscriptions** Order Form

Order Processing Code:
* 5178

☐ **YES,** enter my subscription as follows:

Charge your order. It's Easy! MasterCard VISA

To fax your orders (202) 512–2233

____ subscriptions to **FISHERY BULLETIN (FB)** for $24.00 per year ($30.00 foreign).

The total cost of my order is $_____. Price includes regular domestic postage and handling and is subject to change.

(Company or Personal Name) (Please type or print)

(Additional address/attention line)

(Street address)

(City, State, ZIP Code)

(Daytime phone including area code)

(Purchase Order No.)

May we make your name/address available to other mailers? YES ☐ NO ☐

Please Choose Method of Payment:

☐ Check Payable to the Superintendent of Documents

☐ GPO Deposit Account ☐☐☐☐☐☐☐ – ☐

☐ VISA or MasterCard Account

☐☐☐☐☐☐☐☐☐☐☐☐☐☐☐☐

☐☐☐☐ (Credit card expiration date)

Thank you for your order!

(Authorizing Signature) 11/91

Mail To: New Orders, Superintendent of Documents
P.O. Box 371954, Pittsburgh, PA 15250–7954

Fishery Bulletin

Guidelines for Contributors

Form of manuscript

The document should be in the following sequence: Title Page, Abstract (not required for Note), Text, Acknowledgments, Citations, Text footnotes, Appendices, Tables, Figure legends, and Figures.

Title page should include authors' full names and mailing addresses and the senior author's telephone and FAX numbers.

Abstract Not to exceed one double-spaced typed page. Should include a sentence or two explaining to the general reader why the research was undertaken and why the results should be viewed as important. Abstract should convey the main point of the paper and outline the results or conclusions. No footnotes or references.

Text A brief introduction should portray the broad significance of the paper. The entire text should be intelligible to readers from different disciplines. All technical terms should be defined, as well as all abbreviations, acronyms, and symbols in text, equations, or formulae. Abbreviate units of measure only when used with numerals or in tables and figures to conserve space. Measurements should be expressed in metric units, with other equivalent units given in parentheses. Follow the *U.S. Government Printing Office Style Manual*, 1984 ed., and the *CBE Style Manual*, 5th ed. Fishery and invertebrate nomenclature should follow the *American Fisheries Society Special Publication 12* (for fishes), *16* (for mollusks), and *17* (for decapod crustaceans).

Text footnotes should be numbered in Arabic numerals and typed on a separate sheet from the text. Footnotes are not used for reference material or personal communications, but rather to explain or define terms in the text and for contribution numbers on the title page.

Informal sources Personal communications, unpublished data, and untitled manuscripts in preparation are noted parenthetically in the text (full name, affiliation, brief address including zip code, and month and year when appropriate).

Acknowledgments Gather all acknowledgments into a brief statement at the end of the text. Give credit only for exceptional contributions and not to those whose contributions are part of their normal duties.

Citations All titled sources should be listed in the Citations section, including unpublished and processed material. In text, cite as Smith and Jones (1977) or (Smith and Jones 1977); if more than one citation, list chronologically (Smith 1936, Jones 1975, Doe In press). All sources cited in the text should be listed alphabetically by the senior authors' surnames under the heading CITATIONS. Abbreviations of periodicals and serials should conform to *Serial Sources for the BIOSIS Data Base*™. Indicate whether sources are in a language other than English. For informal literature, include address of author or publisher. Authors are responsible for the accuracy of all citations.

Tables should supplement, not duplicate, the text. Each table should be numbered and cited consecutively, with headings short but amply descriptive so that the reader need not refer to the text. For values less than one, zeros should precede all decimal points. Indicate units of measure in column headings; do not deviate from the unit of measure within a column. Table footnotes should be noted consecutively in Roman letters across the page from left to right and then down. Since all tables are typeset, they need not be submitted camera-ready.

Figures Photographs and line drawings should be of professional quality—clear and concise—and reducible to 42 picas for full-page width or to 20 picas for a single-column width, and to a maximum 55 picas high. All graphic elements in illustrations must be proportioned to insure legibility when reduced to fit the page format. Line weight and lettering should be sharp and even. Lettering should be upper and lower case, and vertical lettering should be avoided whenever possible (except for vertical, y, axis). Zeros should precede all decimal points for values less than one. Reproductions of line artwork are accepted in the form of high-quality photographic prints from negatives or photomechanical transfer (PMT). Halftones should be sharply focused with good contrast. Micron rules should be inserted on electron micrographs, even when magnification is included in the figure legend. There should be clear distinction between identifying letters (press-on or overlay) and background of photograph. Label each figure in pencil on the back. Send only xerox copies of figures to the Scientific Editor; originals or photographic prints will be requested later when the manuscript is accepted for publication.

Copyright Government publications are in the public domain, i.e., they are not protected by copyright.

Submission of manuscript

Disks Authors are encouraged to retain manuscripts on word-processing storage media (diskettes, floppy disks) and submit a double-spaced hardcopy run from the storage media. Submit disks as MS-DOS "print" or "non-document" files (often called "ASCII files"). If a disk cannot be converted to an ASCII file, the author should indicate on the disk the source computer and software language along with the file name. Either 5¼-inch or 3½-inch disks from IBM-compatible or Apple/MacIntosh systems (non-graphics only) can be submitted, double-sided/double-density or high-density, limiting each file to 300 kilobytes. All 8-inch word-processing disks (e.g., Wang or NBI) must be converted onto 5¼- or 3½-inch MS-DOS print disks.

Send original hardcopy and two duplicated copies to:

Dr. Linda L. Jones, Scientific Editor
National Marine Mammal Laboratory
F/AKC3
National Marine Fisheries Service,
NOAA
7600 Sand Point Way NE
Seattle, WA 98115-0070

Copies of published articles and notes
The senior author and his/her organization each receive 50 separates free-of-charge. Additional copies may be purchased in lots of 100.

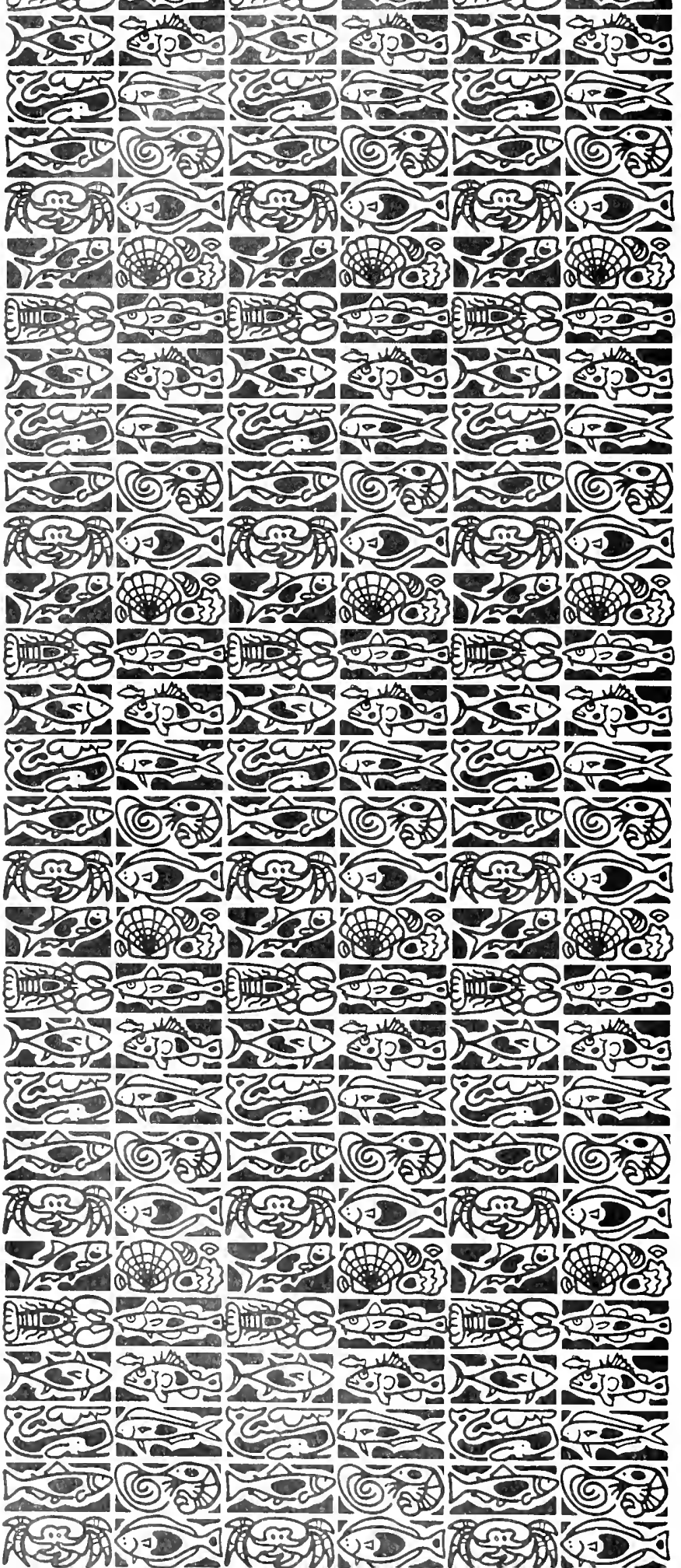

U.S. Department
of Commerce

Volume 90
Number 3
July 1992

Fishery Bulletin

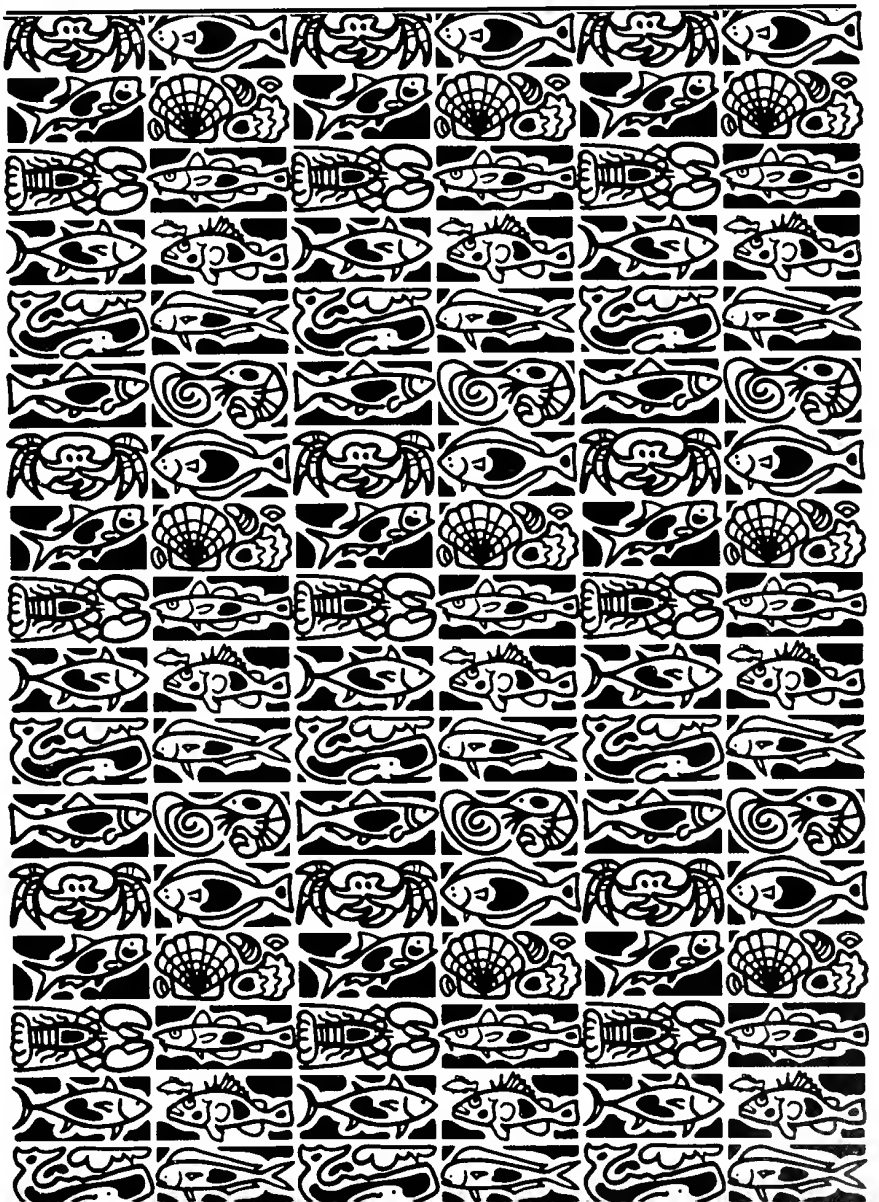

Fishery Bulletin

The *Fishery Bulletin* (ISSN 0090-0656) is published quarterly by the Scientific Publications Office, National Marine Fisheries Service, NOAA, 7600 Sand Point Way NE, BIN C15700, Seattle, WA 98115-0070. Second class postage is paid in Seattle, Wash., and additional offices. POSTMASTER send address changes for subscriptions to Fishery Bulletin, Superintendent of Documents, Attn: Chief, Mail List Branch, Mail Stop SSOM, Washington, DC 20402-9373.

The Secretary of Commerce has determined that the publication of this periodical is necessary in the transaction of the public business required by law of this Department. Use of funds for printing of this periodical has been approved by the Director of the Office of Management and Budget.

For sale by the Superintendent of Documents, U.S. Government Printing Office, Washington, DC 20402. Subscription price per year: $24.00 domestic and $30.00 foreign. Cost per single issue: $12.00 domestic and $15.00 foreign. See **back page for order form.**

The *Fishery Bulletin* carries original research reports and technical notes on investigations in fishery science, engineering, and economics. The Bulletin of the United States Fish Commission was begun in 1881; it became the Bulletin of the Bureau of Fisheries in 1904 and the Fishery Bulletin of the Fish and Wildlife Service in 1941. Separates were issued as documents through volume 46; the last document was No. 1103. Beginning with volume 47 in 1931 and continuing through volume 62 in 1963, each separate appeared as a numbered bulletin. A new system began in 1963 with volume 63 in which papers are bound together in a single issue of the bulletin. Beginning with volume 70, number 1, January 1972, the *Fishery Bulletin* became a periodical, issued quarterly. In this form, it is available by subscription from the Superintendent of Documents, U.S. Government Printing Office, Washington, DC 20402. It is also available free in limited numbers to libraries, research institutions, State and Federal agencies, and in exchange for other scientific publications.

U.S. Department of Commerce
Seattle, Washington

Volume 90
Number 3
July 1992

Fishery Bulletin

Contents

Notes

Errata

(1)

Markle, Douglas F., Phillip M. Harris, and Christopher L. Toole

Metamorphosis and an overview of early-life-history stages in Dover sole *Microstomus pacificus*.
Fish. Bull., U.S. 90(2):285–301.

Table 4 (p. 295) should have reference to *N* (no. of trawls) deleted; the text on p. 297–298 correctly refers to Table 1 for the correct number of trawls each month.

The line art which appears in Figure 2 (p. 288) should be replaced by the following (right column):

(2)

Stone, Heath H., and Brian M. Jessop

Seasonal distribution of river herring *Alosa pseudoharengus* and *A. aestivalis* off the Atlantic coast of Nova Scotia.
Fish. Bull., U.S. 90(2):376–389.

Figure 1 (p. 377) should be corrected as follows: Depths should read 100 and 200 m, as the caption states, rather than 50 and 100 m.

(3)

Authorship of the following article should be corrected to read as follows:

Bartley, Devin, Boyd Bentley, Jon Brodziak, Richard Gomulkiewicz, Marc Mangel, and Graham A.E. Gall

Geographic variation in population genetic structure of chinook salmon from California and Oregon.
Fish. Bull., U.S. 90(1):77–100.

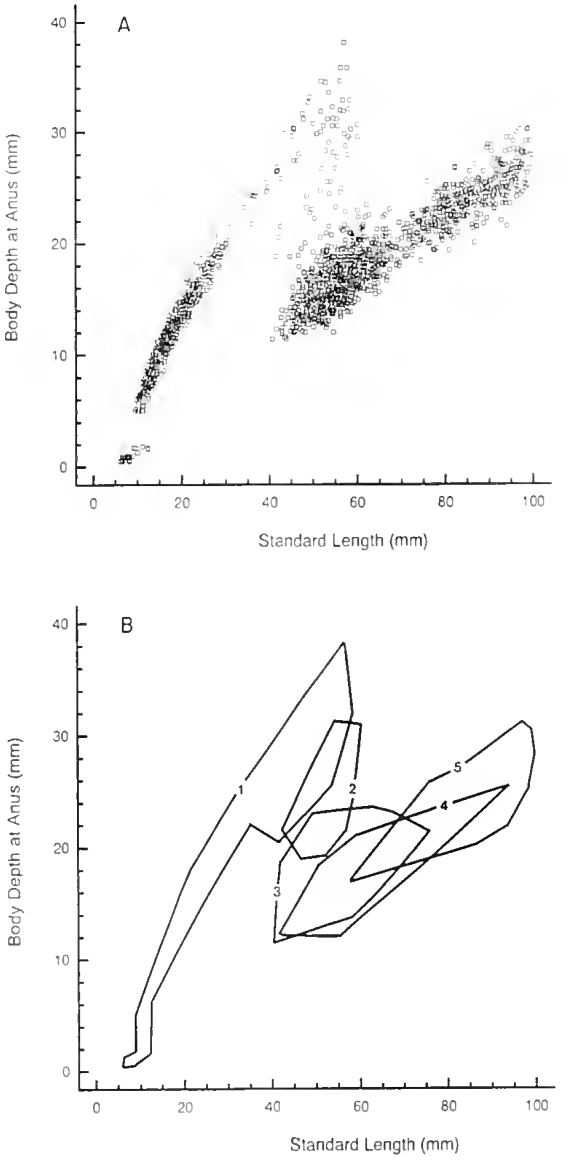

Figure 2

Relationship between body depth at anus and standard length in Dover sole *Microstomus pacificus*: (A) scatterplot of data points, Stages 1–5; (B) polygons circumscribing areas bounded by specimens in Stages 1–5.

Population characteristics of individually identified humpback whales in southeastern Alaska: Summer and fall 1986

C. Scott Baker
University of Hawaii, Pacific Biomedical Research Center
Kewalo Marine Laboratory, 41 Ahui Street, Honolulu, Hawaii 96813

Janice M. Straley
Institute of Marine Sciences, University of Alaska, Fairbanks, Alaska 99775

Anjanette Perry
University of Hawaii, Pacific Biomedical Research Center
Kewalo Marine Laboratory, 41 Ahui Street, Honolulu, Hawaii 96813

Abstract.–In the summer and fall of 1986 a total of 257 humpback whales *Megaptera novaeangliae* were individually identified during nonsystematic vessel surveys of southeastern Alaska. The majority of adult animals (n 130, 54.6%) identified in 1986 had been identified previously in southeastern Alaska during the years 1979–85. Capture-recapture estimates suggested that this regional subpopulation increased in abundance from 1979 to 1986, and included 547 individual whales (95% CL: 504–590) at the time of the 1986 surveys. An average reproduction rate of 0.36 calves/mature female·year^{-1} (95% CL: 0.28–0.43) was estimated for this regional subpopulation using individual identification records collected during 1980–86. In the Frederick Sound–Stephens Passage area, the largest number of whales was found during August and their predominant prey appeared to be euphausiids. In the Glacier Bay–Icy Strait area, the relative abundance of whales was greatest in June and July and their predominant prey appeared to be schooling fish. Low levels of interchange between surveyed areas for much of the summer season indicated strong preferences for local habitats among individual whales. The documented presence of some individual whales for at least 6 months is evidence that southeastern Alaska is the primary feeding ground for many of the whales identified in these surveys.

Manuscript accepted 18 May 1992.
Fishery Bulletin, U.S. 90:429–437 (1992).

Humpback whales *Megaptera novaeangliae* in the central and eastern North Pacific, like those in the western North Atlantic (Katona and Beard 1990), appear to form several geographically-isolated subpopulations during the summer and fall feeding season (Baker et al. 1986, Perry et al. 1990). Following their yearly migration south, individuals from these feeding herds intermingle in the waters of either Hawaii or Mexico during the winter breeding season (Darling and Jurasz 1983, Baker et al. 1985, Darling and McSweeney 1985, Baker et al. 1986).

The coastal waters of southeastern Alaska (56–59°N lat.) seem to encompass the primary feeding ground of a single 'herd' or regional subpopulation estimated to number between 327 and 421 individual whales as of 1983 (Baker et al. 1986). Although the exact geographic boundaries of each herd are unknown, whales from southeastern Alaska appear to remain segregated from those that summer to the west in the Gulf of Alaska, including Prince William Sound, and those which summer to the south along the coast of central California (Baker et al. 1986, Perry et al. 1990). Fidelity to a particular feeding ground appears to be maternally directed (Martin et al. 1984, Baker et al. 1987, Clapham and Mayo 1987) and may persist across many generations, as suggested by geographic segregation of mitochondrial DNA haplotypes (Baker et al. 1990).

Within southeastern Alaska, however, the distribution of whales is not homogeneous and intermingling of individuals is not random (Baker 1985a, Baker et al. 1985). Some whales return with considerable fidelity to specific areas or 'neighborhoods' such as Glacier Bay, Sitka Sound or Frederick Sound and, at least during part of the feeding season, may establish restricted local ranges (Jurasz and Palmer 1981, Perry et al. 1985, Baker et al. 1988, Straley 1990). Changes in distribution and local movement within a season appear to reflect changes in prey availability. The relatively early arrival of whales into the Glacier Bay area indicates that this may be an important area for early-summer feeding on schooling fish, including capelin *Mallotus villosus*, sand lance *Ammodytes hexapterus*, and Pacific herring *Clupea harengus* (Wing and Krieger 1983, Krieger and Wing 1984 and 1986, Perry et al. 1985).

By late summer, whales typically congregate in Frederick Sound and Stephens Passage where large swarms of euphausiids, primarily *Thysonoessa raschii* and *Euphausii pacifica*, are common (Krieger and Wing 1984, 1986). Some whales feed throughout fall and early winter in areas such as Seymour Canal and Sitka Sound where euphausiids and schooling herring appear to remain available (Baker et al. 1985, Straley 1990).

Here we summarize the results of nonsystematic surveys of individually identified humpback whales in southeastern Alaska during the summer and through late fall of 1986. The 1986 surveys were designed to overlap in geographic range and seasonal timing with previous coverage during the years 1979–85 (Baker et al. 1985, Baker 1985b). In keeping with recommended management plans (Anonymous 1984), our surveys documented regional abundance and distribution of humpback whales in areas that may be impacted directly or indirectly by vessel activity in Glacier Bay National Park. More specifically, we sought to evaluate trends in the abundance, reproductive rates, and primary prey of humpback whales in southeastern Alaska across the years 1979–86. Documentation of long-term trends in these population characteristics are valuable for assessing the influences of human activity, such as mining, logging, or petroleum exploration and development, or natural environmental fluctuations such as El Niño events, on the habitat use and recovery of this endangered species (National Marine Fisheries Service 1991).

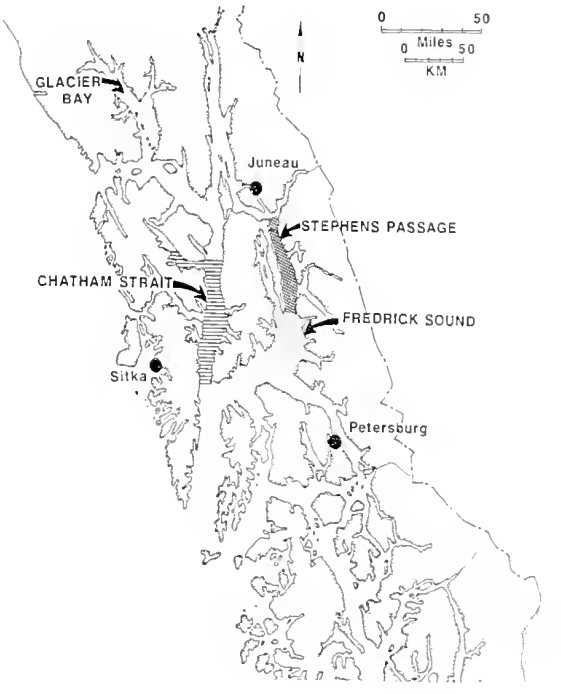

Figure 1
Southeastern Alaska region and primary survey areas (shaded).

Methods

Vessel surveys

Humpback whales were observed and individually identified primarily in two areas or subregions of southeastern Alaska (Fig. 1): Glacier Bay and the adjacent waters of Icy Strait (referred to collectively as Glacier Bay); and the contiguous waters of Stephens Passage and Frederick Sound, including Seymour Canal (referred to collectively as Frederick Sound). Photographs of whales were also collected in Chatham Strait and Sitka Sound on an opportunistic basis throughout the summer and fall.

Whales in Glacier Bay were censused by one of us (CSB) from 22 May to 10 September under the auspices of the National Park Service. A total of 42 one-day surveys were conducted aboard a 17-foot fiberglass boat powered by a 50-hp outboard motor. The lower and middle bay (i.e., from Bartlett Cove to the mouths of Muir Inlet and the West Arm) were surveyed not less than twice and not more than three times a week. The mouth of Glacier Bay and the adjacent waters of Icy Strait were surveyed at least once and not more than twice a week. Study period and survey coverage were designed to overlap and extend previous coverage during the summers of 1982–85 (Baker et al. 1985, Baker 1985b).

Whales in Frederick Sound were censused during three summer surveys: 31 July–3 August; 29 August–1 September; and 12 September–15 September. These survey cruises were conducted aboard the RV *Sashin*, a 22-foot stern-drive vessel provided by the Auke Bay Laboratory, National Marine Fisheries Service. Each cruise originated and ended in Juneau and surveyed the length of Stephens Passage and Frederick Sound south to Cape Fanshaw and west to Pybus Bay (see shaded area, Fig. 1). A fourth survey of Frederick Sound was conducted from 29 November to 9 December aboard the MV *Fairweather*, a 43-foot, diesel-powered cabin cruiser. This cruise originated and ended in Sitka, Alaska, and surveyed the southern half of Chatham Strait and Frederick Sound, north to Seymour Canal. The dates and geographic coverage of Frederick Sound surveys were chosen to coincide with those of similar previous surveys during the summers of 1984–85 (Krieger and Wing 1986, CSB unpubl. data), the fall or winters of 1979–85 (Straley 1990),

and with field efforts during the summers of 1981–82 (Baker et al. 1985).

Prey assessment

Humpback whale prey species were assessed in Glacier Bay with a Ross Fineline 250C recording fathometer equipped with a 22° beam, 105-kHz transducer. In Frederick Sound, prey were assessed with a Lowrance recording fathometer equipped with a 250-kHz transducer. Putative identification of primary prey species type (e.g., euphausiids vs. schooling fish) was based on qualitative differences in target strength, as judged from the relative intensity of fathometer recordings, and the size, shape, and depth of prey schools. These interpretations were based on reference to previous documentation of humpback whale prey using quantitative hydroacoustics and net sampling (Wing and Krieger 1983, Krieger and Wing 1984 and 1986). On occasion, observations of feces from feeding whales or the presence of prey species at the surface provided direct confirmation of primary prey species type.

Individual identification

We attempted to individually identify all humpback whales encountered by collecting photographs of the ventral surface of the whales' flukes. The uniqueness of the coloration, shape, and scarring pattern of the flukes' ventral side allowed for the reliable identification of individual whales (Katona et al. 1979). Because our primary objective was to collect individual identification photographs for use in capture-recapture analyses and the estimation of long-term reproductive rates, we did not attempt to count unidentified whales along the survey tracks. Consequently, all references to 'sightings' or 'observations' of whales are based only on photographs of unique individuals.

Methods for processing and comparison of fluke photographs followed that described by Perry et al. (1988). Photographs of whales were taken with a 35 mm single-lens reflex camera equipped with a motor drive and a 300 mm telephoto or 70–210 mm zoom lens. High-speed (ASA 400–1600) black-and-white film was used. From each observation of a whale or group of whales, the best photograph of each individual's flukes was printed and assigned a "fluke observation" or identification number. Information on the location, date, and social affiliation of each fluke identification was stored in a data retrieval file at the University of Hawaii Computing Center. During the matching of fluke photographs, a whale that was identified on more than one occasion was also assigned an "animal" number. This number allowed us to reference all fluke observations, or identifications, of that individual. All fluke photographs were judged to be of either good, fair, or poor quality. Good- and fair-quality photographs showed at least 50% of both flukes at an angle sufficiently vertical to distinguish the shape of the flukes' trailing edges. For this study, poor-quality photographs were deleted from the data set.

Table 1

Between-years reidentification and the Petersen population estimate using Bailey's correction (in parentheses) of humpback whales *Megaptera novaeangliae* in southeastern Alaska.

Year	Identified: no. [newly]	Reidentification year						
		1980	1981	1982	1983	1984	1985	1986
1979	83	32	41	48	11	36	33	40
	[83]	(307)	(294)	(310)	(353)	(435)	(498)	(484)
1980	121	–	58	53	11	48	53	51
	[89]		(306)	(410)	(514)	(479)	(457)	(556)
1981	148	–	–	85	26	73	66	63
	[71]			(315)	(280)	(388)	(451)	(553)
1982	182	–	–	–	31	80	81	79
	[66]				(290)	(436)	(453)	(544)
1983	50	–	–	–	–	35	29	23
	[12]					(269)	(340)	(498)
1984	193	–	–	–	–	–	80	76
	[76]						(486)	(599)
1985	203	–	–	–	–	–	–	79
	[74]							(606)
1986	238	–	–	–	–	–	–	–
	[108]							
Sum	579							

Results

Abundance and regional fidelity

A total of 257 humpback whales, including 19 calves, were individually identified in southeastern Alaska during 1986. This total includes 29 adults identified only in Glacier Bay, 183 identified only in Frederick Sound, 16 identified only in Sitka Sound or Chatham Strait, and 10 adults common to more than one subregion. The majority (n 130, 54.6%) of the 238 adults identified in 1986 had been identified in southeastern Alaska previously, based on comparison with photographs collected by University of Hawaii researchers and associates during the years 1979–85 (Perry et al. 1988). The addition of the 108 newly identified individuals to the existing catalogue of photographs resulted in a cumulative total of 579 adult whales identified in southeastern Alaska across the 8 study years (Table 1).

To determine the fidelity of humpback whales to regional feeding grounds, photographs collected from southeastern Alaska during 1986 were compared with

photographs of 95 individuals from the western Gulf of Alaska (von Ziegesar and Matkin 1989), 18 from central California collected during 1977–85 (Perry et al. 1988), and 225 individuals from central California identified during 1987–88 (Calambokidis et al. 1990). This comparison provided no evidence of movement by individual whales between these three feeding regions. Two whales previously identified in both southeastern Alaska and Prince William Sound (Baker et al. 1986) were not reidentified in southeastern Alaska in 1986, suggesting that their immigration to southeastern Alaska may have been temporary.

The identification and reidentification of individual animals across years lends itself to the estimation of abundance using capture-recapture formulae (e.g., Hammond 1986). Table 1 summarizes abundance estimates of the southeastern Alaska feeding herd from a pair-wise comparison of all yearly samples using the Petersen estimate with Bailey's correction (Caughley 1977). The yearly estimates range from a low of 269 (1983–84) to a high of 606 (1985–86). The weighted mean of the Petersen estimate (i.e., the Schnabel estimate; Seber 1982) across the 8-year study indicated that this regional subpopulation has included 547 animals (95% CL: 504–590).

Possible inequalities of individual reidentification probabilities were examined by calculating the identification frequencies for individual whales across the 8 study years (Table 2). The observed frequency distribution showed fewer 2- or 3-year reidentification records and more single identifications and reidentification records of extreme frequencies than expected when compared with a zero-truncated Poisson distribution calculated according to Caughley (1977). The significant departure of the observed from the expected distribution (χ^2 [4] 291, $p<0.001$) suggests that all individual whales were not equally available for reidentification during the study period. Possible causes of this unequal 'catchability' include births, deaths, and permanent emigration across the 8-year study, as well as heterogeneity of reidentification probabilities due to local habitat preferences and the limited range of surveys.

Table 2

Observed and expected frequency of yearly identifications for 579 adult humpback whales *Megaptera novaeangliae* in southeastern Alaska during the years 1979–86.

	Identification frequency (years)						
	1	2	3	4	5	6	7+
Observed	330	81	56	46	32	24	10
Expected	216	186	108	47	16	6	—

Note: Expected frequencies were calculated from the zero-truncated Poisson distribution according to the methods described by Caughley (1977).

Reproductive rates

Among the 238 adults individually identified in 1986, there were 32 cows accompanied by calves assumed to be less than a year old. Using this census information we estimated the crude birth rate in 1986 to be 0.125, calculated as the total number of identified cows (n 32) divided by the total number of identified whales of all classes (n 257, including only identified calves). This estimate, however, may have been biased by the greater visibility of cow/calf pairs and by additional effort directed towards individually identifying members of this age/sex class.

An alternate estimate of annual reproductive rates was calculated using the identification histories of individual females known to be reproductively mature prior to the 1986 surveys (Baker et al. 1987). Of the 41 mature females previously identified by Baker et al. (1987), 24 were reidentified during the 1986 surveys and 9 were accompanied by a calf, yielding an estimate of 0.375 calves/mature female·year^{-1}. The addition of the 1986 identifications provides an updated estimate of the long-term calving rates for 41 females previously discussed by Baker et al. (1987) (Table 3). Between 1980 and 1986, these 41 females were observed with 58 individual calves across 162 seasonal identifications. Although annual calving rates appeared to alternate

Table 3

Calving rates of mature female humpback whales *Megaptera novaeangliae* in southeastern Alaska, based on reproductive histories of 41 individuals identified in two or more summer seasons (see Baker et al. 1987).

	Identification year							
	1980	1981	1982	1983	1984	1985	1986	Sum
Females identified	8	33	33	12	31	21	24	162
Total calves	2	9	15	3	15	5	9*	58
Calves/female	0.25	0.27	0.45	0.25	0.48	0.24	0.38	0.36

*Includes one calf thought to have died during the summer. See text for details.

Table 4

Within-year (between-survey) reidentification and the Petersen population estimates with Bailey's correction (in parentheses) of adult humpback whales *Megaptera novaeangliae* in Glacier Bay, 1986.

Survey month	Identified: no. [newly]	No. reidentified June	July	Aug	Sept
June	27	–	17	12	7
	[27]		(42)	(39)	(37)
July	27	–	–	12	9
	[10]			(39)	(30)
August	18	–	–	–	10
	[3]				(18)
September	10	–	–	–	–
	[0]				
Sum	40				

Table 5

Within-year (between-survey) reidentification and the Petersen population estimates with Bailey's correction (in parentheses) of adult humpback whales *Megaptera novaeangliae* in Frederick Sound, 1986.

Survey dates	Identified: no. [newly]	No. reidentified 1	2	3	4
31 July–3 Aug	72	–	22	19	13
	[72]		(247)	(234)	(283)
29 Aug–1 Sept	78	–	–	23	9
	[56]			(211)	(429)
12–15 Sept	64	–	–	–	4
	[30]				(704)
29 Nov–7 Dec	54	–	–	–	–
	[36]				
Sum	194				

between high and low years from 1981 to 1986, a Test of Independence indicated that these year-to-year differences were not significant (χ^2 [6] 6.88, p 0.332). Average calving rate across the 7-year study was 0.36 calves/year (95% binomial CL: 0.284–0.432), similar to the previously reported rate of 0.37 for the years 1980–85 (Baker et al. 1987).

Local abundance and interchange

Capture-recapture estimates of seasonal abundance for the Glacier Bay and Frederick Sound subregions were calculated using the Petersen formula with Bailey's correction and treating each survey or survey period as a sample (Tables 4 and 5). In Glacier Bay, the number of individual whales identified was greatest during June and July and declined through August and September

Table 6

Local movement of humpback whales *Megaptera novaeangliae* between Glacier Bay (GB) and Frederick Sound (FS) during the summer and fall of 1986.

Animal no.	From Last ident. date	To First ident. date	Interval (days)
#117	GB, 25 July	FS, 30 Aug	36
#161	GB, 22 July	FS, 2 Aug	8
#155	GB, 22 July	FS, 30 Aug	39
#196	FS, 31 July	GB, 8 Aug	8
#221	GB, 29 July	FS, 31 Aug	33
#350	GB, 21 July	FS, 30 Aug	40
#564	GB, 22 July	FS, 26 Aug	35
#566	GB, 11 July	FS, 30 Aug	50
#587	GB, 14 Aug	FS, 4 Dec	112
#616	GB, 16 July	FS, 31 July	15
#616	FS, 31 July	GB, 14 Aug	14
#616	GB, 14 Aug	FS, 30 Aug	16

(Table 4). The percentage of newly-identified whales declined rapidly through the summer, suggesting that the census of identified individuals approached a complete count of the whales in this subregion. Capture-recapture estimates based on monthly censuses ranged from 18 to 42 and agreed closely with the total number of 40 adults identified in this subregion.

In Frederick Sound, the number of individual whales identified during each survey remained constant from late July to mid-September and declined by late fall (Table 5). The percentage of newly-identified whales decreased through the three summer surveys but increased in the late-fall survey. The Frederick Sound capture-recapture estimates from the three summer surveys ranged from 211 to 247, exceeding the total of 158 individuals identified during this period but not approaching the between-year estimates of regional abundance (see Table 1). Capture-recapture estimates increased considerably when summer surveys were compared with the fall surveys. Ranging from 283 to 704, the fall estimates agreed more closely with across-year estimates for the entire southeastern Alaska region. The larger capture-recapture estimates from the fall survey and the increase in percentage of newly identified whales suggested the dissolution of population stratification observed during the summer months or the arrival of individuals from unsurveyed areas of southeastern Alaska.

Documented interchange between the southeastern Alaska subregions was limited to 12 transits by 10 individual whales (Table 6). Eight one-way transits were from Glacier Bay to Frederick Sound, and a single one-way transit was from Frederick Sound to Glacier Bay. One individual, animal #616, traveled from Glacier

Bay to Frederick Sound and back between 16 July and 14 August. Animal #616 was last identified in Frederick Sound on 30 August.

Regional occupancy

The interval between the first and last identification of an individual whale provided a minimum estimate of its occupancy in southeastern Alaska (Baker et al. 1985). Although it was not possible to document continuous residency of individual whales in either of the primary study areas (i.e., Glacier Bay or Frederick Sound), there was no evidence that individuals migrated to other known feeding regions between surveys (see 'Abundance and regional fidelity'). The longest documented regional occupancy was 192 days for animal #587. This individual was first identified on 1 June in Glacier Bay and last identified on 9 December in Frederick Sound. Animal #587's identification record, discussed by Baker et al. (1987), showed that she lost a calf sometime during the summer of 1986. Three other adults and one calf had documented occupancies of nearly equivalent length: 191 days for #616, an animal of unknown age-sex class (see also Table 6); 183 days for #350, an animal of unknown age-sex class; and 186 days for #161 and her calf.

Foraging behavior

During summer surveys, whales in Frederick Sound tended to occur in aggregations of 20 to 80 animals often clustered along submerged ridges and mounts, as determined by reference to fathometer recordings and navigational charts. Observations of whale feces and fathometer recordings of dense scattering layers below feeding whales indicated that euphausiids were the primary prey for these aggregations. During the late-fall survey, we were unable to collect fathometer recordings or to observe whale feces in order to confirm the primary prey species. However, the surface-movement and diving patterns of whales and the location of feeding aggregations were similar to that observed during summer surveys, suggesting that euphausiids were again the primary prey.

The predominant prey of humpback whales in Glacier Bay was schooling fish, as evidenced by fathometer recordings and observations of schooling fish at the surface. Within the Bay, whales fed singly or in pairs on dense schools of capelin and sandlance. Outside the Bay, in the adjacent waters of Icy Strait, the predominant prey of humpback whales appeared to be herring as demonstrated in previous years using hydroacoustic techniques and net tows (Wing and Krieger 1983, Krieger and Wing 1984 and 1986). As in previous years (Baker 1985a), whales near Icy Strait formed a socially cohesive pod of 7 to 9 individuals that appeared to cooperate in foraging on schools of herring.

Discussion

Population characteristics

The number of individual whales photographically identified during the 1986 surveys, 238 adults and 19 calves, can be considered a minimum estimate of abundance for the southeastern Alaska feeding herd. Capture-recapture analyses of across-year identification records, however, provide estimates of this regional population that are two or three times larger than that based on the 1986 census alone. Although these analyses are more likely than simple counts to provide realistic estimates of regional abundance, they should be interpreted with caution since the behavior of whales seldom conforms strictly to the theoretical assumptions underlying these models (e.g., Hammond 1986, Perry et al. 1990). Violation of the assumption of equal catchability among southeastern Alaska whales, for example, is indicated by the analysis of reidentification frequencies across the 8-year study period. Births, deaths and permanent emigration obviously contribute to this unequal catchability (i.e., reidentification inequality). Another probable source of unequal catchability is heterogeneity due to local habitat preference by individual whales and the variable and limited geographic coverage of the surveys. While births and deaths cause a positive bias in the Petersen estimate of abundance, reidentification heterogeneity causes a negative bias (Hammond 1986 and 1990).

Assuming, however, that adult mortality among humpback whales is low (e.g., Buckland 1990) and that permanent emigration to other feeding regions is infrequent (e.g., Perry et al. 1990), the weighted Petersen estimate of 547 whales (95% CL: 503–590) may be our most robust for the southeastern Alaska subpopulation in 1986. By using the cumulative reidentification records of individuals across years and weighting the final estimate by the largest sample year, the weighted Petersen should be less biased than the between-year Petersen estimates by heterogeneity due to local habitat preferences or variation in survey effort. Births during the study period are included in the cumulative population estimate when the calves mature sufficiently to become available for individual identification. The weighted Petersen is also consistent with other estimates derived from the individual identification records. The upper confidence interval of this estimate overlaps with the total count of 579 whales identified during the 8-year study and agrees closely with the unbiased Petersen estimates from the pair-

wise comparisons of years with the largest sample of identified whales, 1984–86 and 1985–86 (see Table 1).

Regardless of the exact number of individuals inhabiting this region, the individual identification surveys and mark-recapture estimates suggest that the southeastern Alaska herd increased from 1979 to 1986. In Frederick Sound, overall survey effort decreased since 1981–82 but, with the exception of 1983 when only a single 4-day survey was conducted, the number of identified whales increased. As confirmed by photographic documentation, a general increase in the number of whales in the Glacier Bay area during the last few years was the result of the continued return of past residents and the recruitment of their offspring (Baker et al. 1988). In terms of overall regional abundance, the mark-recapture estimates from pair-wise comparisons of 1986 to previous years suggest an increase from 484 to 606 across 1979–86, while estimates from contiguous years suggest an increase from 307 to 606 (Table 1). Requiring an annual rate of increase from 3.4 to 10.4%, these trends in estimated abundance are within the range reported for population growth of other unexploited baleen whales based on individual identification data (e.g., Hammond 1990, Best and Underhill 1990, Bannister 1990). More accurate estimates of the current abundance and the true rate of increase in the southeastern Alaska subpopulation will require further detailed analyses of survival rates and the biases introduced by heterogeneity of identification records.

Although apparently sufficient to sustain some degree of population growth, the observed reproduction rate of humpback whales in southeastern Alaska seemed low in comparison with other studied populations and to the maximum reproductive potential of 0.50, or even 1.00 (calves/mature female·year^{-1}) as observed in some individually identified females (Darling 1983, Glockner-Ferrari and Ferrari 1984 and 1990, Baker et al. 1987, Clapham and Mayo 1987 and 1990, Straley 1989). The estimated calving rate of 0.36 (calves/mature female·year^{-1}) across the 1980–86 study suggests that females from this region give birth to a calf that survives its first migration from the wintering grounds about once every 2.8 years. In the Gulf of Maine, Clapham and Mayo (1990) report an average reproduction rate of 0.41 (calves/mature female·year^{-1}) and an average calving interval of 2.35 years for the period 1979–87, using individual identification methods similar to those used here. Pregnancy rates from exploited populations, as summarized by Baker et al. (1987), all exceed the estimated calving rate for southeastern Alaska, although this historical comparison is confounded by differences in methodology.

Seasonal trends and foraging strategies

The number of whales identified in Glacier Bay and Icy Strait was greatest during late June and early July, and declined through August and September. Since survey effort in Glacier Bay was high relative to total number of whales identified, and constant throughout the study period, we believe that trends in the monthly censuses or counts of individuals reflected changes in seasonal abundance for this subregion. Although surveys of Frederick Sound were not frequent enough to track the seasonal increase in whales during early summer, the greatest numbers of whales were found during late July and August, approximately 1 month after the local peak in Glacier Bay.

We could not determine if these seasonal trends reflect primarily changes in the timing of migratory arrival on the feeding grounds or the pattern of local movement among subregions of southeastern Alaska. Within the geographic limits of our surveys, seasonal changes in influx were accompanied by some local movement between subregions; the decline in numbers of whales in Glacier Bay was, in part, the result of their relocation to Frederick Sound. Studies in previous years also demonstrated that local movement between these subregions tends to be one-directional, resulting in the whales congregating in Frederick Sound during late summer and fall (Baker 1984, Perry et al. 1985, Krieger and Wing 1986). Large areas of available habitat in southeastern Alaska remain entirely unsurveyed (see Fig. 1), including the outer coast of Baranof Island and the inside passage to the south of Frederick Sound. The increase in percentage of newly-identified whales during the late-fall survey of 1986 suggests local movement from these unsurveyed areas.

Local movement may be an attempt to take advantage of seasonal changes in prey availability. Humpback whales in Frederick Sound fed almost entirely on euphausiids while those in Glacier Bay fed almost entirely on schooling fish. Movement from Glacier Bay to Frederick Sound was presumably accompanied by a shift in primary prey species. Similar contrasts in the primary prey species of whales in these two subregions have been documented in previous years (Krieger and Wing 1984 and 1986). Some whales, however, showed a strong preference for particular prey species or local habitat throughout the summer. This was indicated by the persistence of certain individual whales feeding on herring in Icy Strait late through the summer, when other whales had moved to feed on euphausiids in Frederick Sound.

Stock identity and management

The summer and late-season surveys of 1986 and previous years (Baker et al. 1985) demonstrated that many whales remained to feed in southeastern Alaska for much of the summer and into late fall. Intervals between first identification and last reidentification of some individual whales indicated seasonal occupancies of at least 6 months. Since no surveys were conducted from 15 September to 29 November, it was not possible to document continuous residency of individual whales in either of the primary study areas (i.e., Glacier Bay or Frederick Sound). However, comparisons of individual identification photographs collected in the central and western Gulf of Alaska, including Prince William Sound, and along the coast of central California indicate that whales which summer in southeastern Alaska seldom migrate to alternate feeding grounds within seasons or across years (Baker et al. 1986, Perry et al. 1990). These observations are strong evidence that southeastern Alaska is the migratory terminus and primary feeding ground for a distinct herd or seasonal subpopulation of humpback whales.

Comparisons of individual identification photographs and analysis of mitochondrial DNA haplotypes demonstrate that many members of the southeastern Alaska feeding herd migrate to wintering grounds near the islands of Hawaii (Darling and Jurasz 1983, Baker et al. 1986, Perry et al. 1990, Baker et al. 1990). The migratory connection between these primary seasonal habitats provides a unique opportunity to study and protect a population of humpback whales that spends the majority of its time within U.S. coastal waters (National Marine Fisheries Service 1991).

Acknowledgments

Surveys of humpback whales in southeastern Alaska during 1986 were made possible by funding from the U.S. Marine Mammal Commission (contract number MM3309822-5) and the cooperation of personnel from Glacier Bay National Park and the Auke Bay Laboratory, National Marine Fisheries Service. C.S. Baker was supported by employment to Glacier Bay National Park and Preserve during these surveys and by a postdoctoral fellowship from the Smithsonian Institution during the preparation of this manuscript. The views and opinions expressed in this paper do not necessarily reflect those of these agencies. Photographs collected during 1979 and 1980 were made available by the National Marine Mammal Laboratory, Seattle, courtesy of W.S. Lawton. Photographs collected during 1981, 1982, and 1984 were made available courtesy of L.M. Herman, University of Hawaii. We thank the following people for their assistance in the field: Gary Vequist, Glacier Bay National Park; Ken Krieger, George Snyder, and Bruce Wing, Auke Bay Laboratory, NMFS; Carol and Jim Greenough, and Chuck Johnstone, Sitka, Alaska. The manuscript benefited from a thorough review by S. Swartz, Marine Mammal Commission, L. Jones and H. Braham, National Marine Mammal Laboratory, and the comments of two anonymous reviewers.

Citations

Anonymous
1984 Glacier Bay National Park and Preserve, Alaska; Protection of humpback whales; Proposed rules. Federal Register 49:15482–15494.

Baker, C.S.
1984 Population characteristics and feeding behavior of humpback whales in southeastern Alaska during 1984. Unpubl. rep. to NMFS Auke Bay Lab., Auke Bay, AK, 44 p.
1985a The population structure and social organization of the humpback whale (*Megaptera novaeangliae*) in the central and eastern North Pacific. Ph.D. diss., Univ. Hawaii, Honolulu, 307 p.
1985b The humpback whales of Glacier Bay and adjacent waters: Summer 1985. Unpubl. rep. to Glacier Bay Natl. Park, Gustavus, AK, 33 p.

Baker, C.S., L.M. Herman, A. Perry, W.S. Lawton, J.M. Straley, and J.H. Straley
1985 Population characteristics and migration of humpback whales in southeastern Alaska. Mar. Mammal Sci. 1:304–323.

Baker, C.S., L.M. Herman, A. Perry, W.S. Lawton, J.M. Straley, A.A. Wolman, G.D. Kaufman, H.E. Winn, J.D. Hall, J.M. Reinke, and J. Ostman
1986 Migratory movement and population structure of humpback whales (*Megaptera novaeangliae*) in the central and eastern North Pacific. Mar. Ecol. Prog. Ser. 31:105–119.

Baker, C.S., A. Perry, and L.M. Herman
1987 Reproductive histories of female humpback whales (*Megaptera novaeangliae*) in the North Pacific. Mar. Ecol. Prog. Ser. 41:103–114.

Baker, C.S., A. Perry, and G. Vequist
1988 Humpback whales of Glacier Bay, Alaska. Whalewatcher 22(3):13–17.

Baker, C.S., S.R. Palumbi, R.H. Lambertsen, M.T. Weinrich, J. Calambokidis, and S.J. O'Brien
1990 The influence of seasonal migration on the geographic distribution of mitochondrial DNA haplotypes in humpback whales. Nature (Lond.) 344:238–240.

Bannister, J.
1990 Southern right whales off western Australia. *In* Hammond, P.S., et al. (eds.), Individual recognition of cetaceans: Use of photo-identification and other techniques to estimate population parameters, p. 279–288. Rep. Int. Whaling Comm. Spec. Issue 12.

Best, P.B., and L.G. Underhill
1990 Estimating population size in southern right whales (*Eubalaena australis*) using naturally marked animals. *In* Hammond, P.S., et al. (eds.), Individual recognition of cetaceans: Use of photo-identification and other techniques to estimate population parameters, p. 183–190. Rep. Int. Whaling Comm. Spec. Issue 12.

Buckland, S.T.
1990 Estimation of survival rates from sightings of individually identified whales. *In* Hammond, P.S., et al. (eds.), Individual recognition of cetaceans: Use of photo-identification and other techniques to estimate population parameters, p. 149–154. Rep. Int. Whaling Comm. Spec. Issue 12.

Calambokidis, J., J.C. Cubbage, G.H. Steiger, K.C. Balcomb, and P. Bloedel
1990 Population estimates of humpback whales in the Gulf of the Farallones. *In* Hammond, P.S., et al. (eds.), Individual recognition of cetaceans: Use of photo-identification and other techniques to estimate population parameters, p. 325–334. Rep. Int. Whaling Comm. Spec. Issue 12.

Caughley, G.
1977 Analysis of vertebrate populations. Wiley, NY, 288 p.

Clapham, P.J., and C.A. Mayo
1987 Reproduction and recruitment of individually-identified humpback whales, *Megaptera novaeangliae*, in Massachusetts Bay: 1979–1985. Can. J. Zool. 65:2853–2863.
1990 Reproduction of humpback whales (*Megaptera novaeangliae*) observed in the Gulf of Maine. *In* Hammond, P.S., et al. (eds.), Individual recognition of cetaceans: Use of photo-identification and other techniques to estimate population parameters, p. 171–176. Rep. Int. Whaling Comm. Spec. Issue 12.

Darling, J.D.
1983 Migration, abundance and behavior of Hawaiian humpback whales, *Megaptera novaeangliae* (Borowski). Ph.D. diss., Univ. Calif., Santa Cruz, 147 p.

Darling, J.D., and C.M. Jurasz
1983 Migratory destinations of North Pacific humpback whales (*Megaptera novaeangliae*). *In* Payne,R. (ed.), Communication and behavior of whales, p. 359–368. Westview Press, Boulder.

Darling, J.D., and D.J. McSweeney
1985 Observations on the migrations of North Pacific humpback whales (*Megaptera novaeangliae*). Can. J. Zool. 63: 308–314.

Glockner-Ferrari, D., and M. Ferrari
1984 Reproduction in humpback whales, *Megaptera novaeangliae*, in Hawaiian waters. *In* Perrin, W.P., et al. (eds.), Reproduction in whales, dolphins, and porpoises, p. 237–242. Rep. Int. Whaling Comm. Spec. Issue 6.
1990 Reproduction in the humpback whales (*Megaptera novaeangliae*) in Hawaiian waters, 1975–1988: The life history, reproductive rates, and behavior of known individuals identified through surface and underwater photography. *In* Hammond, P.S., et al. (eds.), Individual recognition of cetaceans: Use of photo-identification and other techniques to estimate population parameters, p. 161–169. Rep. Int. Whaling Comm. Rep. Spec. Issue 12.

Hammond, P.S.
1986 Estimating the size of naturally marked whale populations using capture-recapture techniques. *In* Donovan, G.P., (ed.), Behavior of whales in relation to management, p. 253–282. Rep. Int. Whaling Comm. Spec. Issue 8.
1990 Heterogeneity in the Gulf of Maine? Estimating humpback whale population size when capture probabilities are not equal. *In* Hammond, P.S., et al. (eds.), Individual recognition of cetaceans: Use of photo-identification and other techniques to estimate population parameters, p. 135–140. Rep. Int. Whaling Comm. Spec. Issue 12.

Jurasz, C.M., and V.P. Palmer
1981 Censusing and establishing age composition of humpback whales (*Megaptera novaeangliae*) employing photodocumentation in Glacier Bay National Monument, Alaska. Unpubl. rep. to Natl. Park Serv., Alaska Reg. Office, Anchorage, 44 p.

Katona, S.K., and J.A. Beard
1990 Population size, migrations and feeding aggregations of the humpback whale (*Megaptera novaeangliae*) in the western North Atlantic Ocean. *In* Hammond, P.S., et al. (eds.), Individual recognition of cetaceans: Use of photo-identification and other techniques to estimate population parameters, p. 295–307. Rep. Int. Whaling Comm. Spec. Issue 12.

Katona, S., B. Baxter, O. Brazier, S. Kraus, J. Perkins, and H. Whitehead
1979 Identification of humpback whales by fluke photographs. *In* Winn, H.E., and B.L. Olla (eds.), Behavior of marine animals, vol. 3, p. 33–44. Plenum Press, NY.

Krieger, K., and B.L. Wing
1984 Hydroacoustic surveys and identification of humpback whale forage in Glacier Bay, Stephens Passage and Frederick Sound, southeastern Alaska, Summer 1983. NMFS Auke Bay Lab., Juneau, 60 p.
1986 Hydroacoustic monitoring of prey to determine humpback whale movements. NOAA Tech. Memo. NMFS F/NWC-66, NMFS Auke Bay Lab., Juneau, 62 p.

Martin, A.R., S.K. Katona, D. Matilla, D. Hembree, and T.D. Waters
1984 Migration of humpback whales between the Caribbean and Iceland. J. Mammal. 65:330–333.

National Marine Fisheries Service
1991 Recovery plan for the humpback whale (*Megaptera novaeangliae*). Prepared by the Humpback Whale Recovery Team for the Natl. Mar. Fish. Serv., Silver Spring, MD, 105 p.

Perry, A., C.S. Baker, and L.M. Herman
1985 The natural history of humpback whales in Glacier Bay, Alaska. Final rep. to Natl. Park Serv., Alaska Reg. Office, Anchorage, 22 p.
1990 Population characteristics of individually identified humpback whales in the central and eastern North Pacific: A summary and critique. *In* Hammond, P.S., et al. (eds.), Individual recognition of cetaceans: Use of photo-identification and other techniques to estimate population parameters, p. 307–318. Rep. Int. Whaling Comm. Spec. Issue 12.

Perry, A., J.R. Mobley, C.S. Baker, and L.M. Herman
1988 Humpback whales of the central and eastern North Pacific: A catalog of individual identification photographs. Sea Grant Misc. Rep. UNIHI-SEAGRANT-MR-88-02, Univ. Hawaii, Honolulu, 37 p.

Seber, G.A.F.
1982 The estimation of animal abundance and related parameters. Macmillan, NY, 654 p.

Straley, J.M.
1989 Population characteristics of humpback whales (*Megaptera novaeangliae*) in Glacier Bay and adjacent waters: 1989. Unpubl. rep. to Glacier Bay Natl. Park, Gustavus, AK, 33 p.
1990 Fall and winter occurrences of humpback whales (*Megaptera novaeangliae*) in southeastern Alaska. *In* Hammond, P.S., et al. (eds.), Individual recognition of cetaceans: Use of photo-identification and other techniques to estimate population parameters, p. 319–324. Rep. Int. Whaling Comm. Spec. Issue 12.

Von Ziegesar, O., and C.O. Matkin
1989 A catalogue of Prince Williams Sound humpback whales identified by fluke photographs between the years 1977 and 1988. North Gulf Oceanic Soc., P.O. Box 15244, Homer, AK, 28 p.

Wing, B.L., and K. Krieger
1983 Humpback whale prey studies in southeastern Alaska, summer 1982. Unpubl. rep. to NMFS Auke Bay Lab., Juneau, 60 p.

Abstract. – To test the hypothesis that year-class strength in marine fishes is determined in the early-larval stages, and that these stages can be used to predict recruitment, I modeled the recruitment process using a modified form of key-factor analysis. Using data compiled from the fish literature, I found a significant relationship (R^2 0.90, $P \ll 0.001$, n 97) between the mean and interannual variance of stage-specific mortality rates that provided variance estimates for the model. The R^2 values for the true correlation between abundances of small larvae and subsequent recruitment for four example species of marine fish were predicted to lie between 0.10 and 0.57, depending on the assumptions of the model. I therefore suggest that recruitment levels are fixed after the early-larval period. However, the precision of sample correlations are too low (10-yr data series) to empirically test whether abundances or mortality rates of early larvae are in reality strongly or poorly correlated with recruitment. After metamorphosis, the strength of the true relationship and the precision of sample correlations increase sufficiently to permit precise forecasting of recruitment. Recruitment is a complex process in which variation in all life stages contributes substantially to the variability in final abundance; therefore, researchers should recognize the importance of the later prerecruit stages and the interactions among all stages.

Manuscript accepted 6 May 1992.
Fishery Bulletin, U.S. 90:439–453 (1992).

Precision of recruitment predictions from early life stages of marine fishes

Michael J. Bradford

Department of Biology, McGill University
1205 Ave Dr Penfield, Montreal, Quebec H3A-1B1, Canada
Present address: Department of Fisheries and Oceans, West Vancouver Laboratory
4160 Marine Drive, West Vancouver, BC V7V 1N6, Canada

A major problem in the management of marine fisheries is the unpredictable fluctuations in stock size resulting from variable recruitment. Hjort (1913) first recognized this recruitment variability and proposed a number of hypotheses that linked the survival of small first-feeding larvae and subsequent year-class strength (reviewed by Wooster and Bailey 1989). These hypotheses have formed the basis of much research on the early life history of fishes, research which has been largely focused on the 'critical period' during the transition from endogenous to exogenous modes of feeding. While much has been learned about the biology of larval fish, the evidence for a critical period of increased mortality and a link between the larval stage and recruitment remains equivocal (May 1974, Ware and Lambert 1985, Peterman et al. 1988, Campana et al. 1989). Explanations for this failure have ranged from sampling and technical difficulties, such as inappropriate scales of sampling (Leggett 1986, Taggart and Leggett 1987, McGurk 1989), to the suggestion that no such critical period exists, and that all prerecruit stages contribute to some degree to variability in year-class strength (Sissenwine 1984, Anderson 1988, Peterman et al. 1988).

There have been few attempts to model the recruitment process to assess the likelihood that early-larval mortality is a dominant feature of year-class variability. Manipulations of life tables have shown that small changes in larval mortality have the potential to cause great variation in recruitment (Smith 1985, Houde 1987 and 1989, Pepin and Myers 1991); however, the influence of the larval stages in a fully dynamic model incorporating variability in all stages has not been investigated. In particular, the role of postlarval mortality in causing recruitment variability is unclear and has been the cause of some controversy (Sissenwine 1984, Peterman et al. 1988, Taggart and Frank 1990, Wooster and Bailey 1989).

An often-stated justification for research on the early life history of fish is to provide short-term forecasts of recruitment, thereby allowing managers to adjust fishing regulations in response to changes in stock size (Gulland 1989). While it is obvious that the stages very close to recruitment will give the most accurate predictions, sampling these stages is often difficult and expensive (Smith 1985), unless they are caught incidentally in other fisheries. Rather, efforts have usually been concentrated on finding a predictive relationship between recruitment and the abundance or some measure of survival of larvae and recruits, on the working assumption that Hjort's hypothesis of year-class determination at this early stage is valid (Peterman et al. 1988, Cushing 1990).

The utility of short-term (i.e., annual) predictors of recruitment in the

management of fish stocks has recently been challenged by Walters and Collie (1988) and Walters (1989). In simulated management examples, Walters (1989) finds that only extremely accurate forecasts of recruitment can offer significant improvements over using the long-term mean recruitment in stock assessment models. Thus, while studies of the early stages of marine fish may reveal insights into their ecology, it is unclear whether sufficiently accurate forecasts of recruitment will ever be possible from these early stages.

In this paper I first pose the question, "How strong are the correlations between abundances or mortality rates of the early life stages and recruitment likely to be?" I develop a simple analytical model based on key-factor analysis (Varley and Gradwell 1960, Manly 1977). I use parameter estimates compiled from a literature survey to calculate the expected correlations between life stages for the prediction of fish recruitment. I suggest that the assertion that year-class strength is fixed in the early-larval stages is not general, and, furthermore, under likely field conditions it will be difficult to quantitatively test this hypothesis.

The model

I developed a simple model to simulate the variability in population numbers and the strength of correlations between life stages. In brief, the model generated annual abundances and mortality rates over a specified number of years from which correlations between early-life-history stages and recruitment were calculated. This process was repeated in a Monte Carlo fashion to estimate the sampling distribution of the correlation coefficients.

I divided the egg-recruit period into four intervals: (1) egg-yolksac larvae, (2) early-feeding larvae, (3) late-feeding larvae, and (4) juveniles from metamorphosis to age 1, which I assumed to be the age of recruitment. I assumed that populations would be sampled at five distinct times that divide the egg-recruit period into four intervals. Sampling points were: eggs spawned (N_e), first-feeding larvae (N_f), young larvae (N_l),metamorphs (N_m), and recruits (N_r). First-feeding larvae were operationally defined as larvae that have just begun to feed, while young larvae were defined as having an age of 10 days after the onset of feeding.

In any year, the number of recruits is the product of the number of eggs spawned and the survival rates of the prerecruit stages:

$$\text{Recruitment} = \text{Eggs} \cdot S_{ys} \cdot S_{el} \cdot S_{ll} \cdot S_j,$$

where the subscripts refer to the egg-yolksac, early-larval, late-larval, and juvenile periods outlined above. Expressing survival rates as instantaneous mortalities, $M = -\ln(S)$, and taking logs of the abundances give the usual equation of key-factor analysis (Varley and Gradwell 1960):

$$N_r = N_e - M_{ys} - M_{el} - M_{ll} - M_j, \quad (1)$$

where N_r and N_e are log abundances of recruits and eggs of a particular cohort, and the M_i values are interval-specific instantaneous mortalities for four intervals defined above. I assume, following Hennemuth et al. (1980) and Peterman (1981), that log abundances and instantaneous mortality rates are normally distributed with stage-specific variances described below. This multiplicative process results in lognormally distributed recruitment, consistent with empirical results (Hennemuth et al. 1980). All subsequent references to abundance made in this paper are to log-transformed values.

Since I am interested in short-term forecasting, I assumed that stock size and, therefore, mean egg production are stationary in time and that variation in egg production is independent of recruitment. Thus, in the absence of density-dependent processes, recruitment is linearly related to egg production.

To introduce stochastic variation in the model, the abundance of eggs, N_e, and the interval-specific mortality rates were simulated as normal random variables. As the time-series of egg production was stationary and my interest is in correlations rather than abundances, the abundance of eggs and the mortality rates all had a mean of 0.

To start the sequence of calculations in a given model year, the initial abundance of eggs was randomly chosen. In the simplest version of the model, which assumes mortality in each interval is independent of the others and is density-independent, the following equation was then used to calculate the numbers of each subsequent stage:

$$N_{k+1} = N_k - m_k, \quad (1)$$

where N_k is the abundance of stage k, and m is a normal random deviate that simulates random interannual variability in mortality of interval k.

The complete independence of mortality of one stage with that of a subsequent stage is probably an unrealistic assumption because, for example, years which are good for yolksac larval survival may also be good for the survival of older larvae. This can be modeled by introducing covariances between the interval-specific mortality rates (Gerrodette et al. 1984). Covariation between interval-specific mortality rates was modeled by assuming that there was a positive corre-

lation between the mortality rate of adjacent intervals across years. The mortality of a given interval in any model year then depends partially on the mortality of the previous period in that same year. With ρ equal to the correlation between adjacent interval-specific mortality rates, I used the following equation to calculate the mortality rate of successive intervals:

$$M_{k+1} = \rho \left\{ \frac{SD(M_{k+1})}{SD(M_k)} \right\} M_k + (1 - \rho^2)^{1/2} M_{k+1}.$$

In this equation, the actual mortality for stage $k+1$ is a linear combination of the random variables simulating the variability in stages k and $k+1$. The correlation coefficient determines how much mortality in stage $k+1$ is similar to that of stage k. The ratio of standard deviations in the first term scales the contribution of the mortality of the previous interval to the appropriate variance. To simplify, I assumed throughout this paper that there was no covariance between the number of eggs spawned and mortality in subsequent intervals.

Finally, density-dependent mortality was incorporated in some versions of the model. Density-dependent mortality was added to the juvenile period, following suggestions of Houde (1987) and Smith (1985) that this is the most likely interval for density effects. While a number of formulations are possible, I chose a power function (Peterman 1982):

$$Y = aX^b,$$

where in this case X and Y are the abundances of juveniles and recruits, respectively. For density-independent mortality, $b = 1$; b is <1 for density-dependent cases. The parameter a is thus the density-independent survival rate. After taking logs, the log of the abundance of recruits is now a function of the log of the number of metamorphs, N_m, and the density-independent mortality, M_j:

$$N_r = bN_m - M_j. \quad (2)$$

In the stochastic simulations, this equation was used to calculate recruitment with a random normal deviate substituted for M_j.

The full model was run for 1000 10-yr trials in SAS (1987), and a matrix of abundances and mortality rates for each stage was built up. For each 10-yr trial, correlation coefficients were calculated between the various predictors of recruitment (i.e., abundances and mortality rates of each of the prerecruit stages), and the numbers of recruits and summary statistics of the distributions of correlation coefficients were derived.

Table 1

Daily mortality rates (M) and interval durations (t, in days) for four species used as examples in the analysis. Egg mortality includes the yolksac period up to first feeding; larval periods explained in text. Values were adapted from Houde (1987; cod *Gadus morhua*, and herring *Clupea harengus*), Smith (1985; anchovy *Engraulis mordax*), and Zijlstra and Witte (1985; plaice *Pleuronectes platessa*).

	Egg		Early larvae		Late larvae		Juveniles	
Species	M	t	M	t	M	t	M	t
Cod	0.061	18	0.160	10	0.063	46	0.010	291
Herring	0.050	21	0.080	10	0.034	70	0.015	264
Anchovy	0.250	7	0.160	10	0.050	79	0.012	269
Plaice	0.068	38	0.104	10	0.045	77	0.008	245

Model parameters

To generalize the results, I used four fish species as examples (Table 1). These were not chosen to be representative of a specific stock or situation, but rather to indicate the effect of different life histories on our ability to forecast recruitment. To parameterize the model for a specific species, the interannual variance of the number of eggs laid and the mortality of each prerecruit stage was required.

I obtained estimates of the variance in the number of eggs spawned from published reconstructions of stock abundances (Table 2). Except for cod, I used the residuals of linear regressions of log(eggs) on time to estimate the variance, since time trends existed for some stocks.

Estimates of the variability in mortality rates for all prerecruit stages are unavailable; I therefore sought a predictive relationship between interannual variance and the mean of daily mortality rates. This allowed estimation of the variances of mortality rates of the early life stages from mean daily rates. I surveyed the literature for papers containing 2 or more years of estimates of age- or stage-specific mortality for the same population or stock. All stages from egg to adult were used, for marine, freshwater, and anadramous fish species. No screening of the data was done except for estimates from adult fish, where only estimates using methods independent of catch-data analysis were used (i.e., tagging). Most adult estimates were from lightly or unfished stocks. In some cases I estimated mortality from annual estimates of abundance or from regressions of log abundance on time. All estimates were converted to daily values using annual estimates of stage duration if available, or the long-term average stage duration. Daily mortalities were then averaged

over the number of years of data available, and the variance calculated. Both variates were log-transformed, and a least-squares regression was fitted to the data.

I used the variance-mean relationship to calculate the interannual variance in mortality from mean daily mortality rates extracted from published life tables (Table 1). I split the larval period and defined the first 10 days of feeding as the early stage. This period corresponds to the usual definition of the 'critical period' for first-feeding larvae (Leggett 1986): few marine larvae can survive more than 10 days without feeding (Miller et al. 1988). Except for anchovy, where values were taken directly from Smith (1985), the daily mortality rate for the early period was set at twice the average rate for the whole larval period. Mortality rates for the late period were adjusted so that the mortality for the total larval period matched the published life tables. The result of these calculations was that the daily mortality rates of the early-larval interval were about 2.5 times those for the late-larval period. It is difficult to assess whether this decline is realistic, because there is considerable variability in the decline in mortality over time in empirical studies; in many cases mortality has been found to be nearly constant over much of the larval period (Dahlberg 1979), while there are other cases where significant declines have been observed (i.e., Savoy and Crecco 1988). Declines in mortality with larval age may be accentuated by a possible bias due to sampling interval (Taggart and Frank 1990). The variance in mortality over the duration of a particular interval was then calculated as the product of the square of the interval's duration (in days), and the variance of the daily mortality rate predicted from the variance-mean relationship.

Table 2

Interannual variability in log-transformed egg production and recruitment, compiled from literature values. All egg estimates are residuals from linear regressions of log abundance on time, except for cod where an intermediate value between herring and plaice was used.

Species	$Var(N_e)$	$Var(N_r)$
Cod	0.075	0.40
Herring	0.081	1.92
Anchovy	0.282	1.91
Plaice	0.055	0.14

Data sources
Cod: mean of 5 northwest Atlantic stocks in Koslow et al. (1987).
Herring: mean of 7 northwest Atlantic stocks in Winters and Wheeler (1987).
Anchovy: eggs—Peterman et al. (1988), recruitment—Methot (1989).
Plaice: Bannister (1978).

Covariation in mortality rates

Two scenarios were developed concerning the effects of covariation between mortality rates. In the independent case, all mortality rates were varied independently of one another, while for the 'covariance' version, mortality rates of adjacent stages were assumed to be correlated across years. Few data are available to estimate the strength of these correlations, so I assumed ρ values for the correlations between adjacent M_k based on the likelihood of common agents of mortality. I assigned a relatively low ρ value of 0.25 for the correlation between the egg/yolksac period and the early-larval mortality because early-larval mortality is thought to be strongly affected by feeding success, which does not affect egg survival. Nonetheless, predation pressures are probably similar for both stages, causing some covariation in mortality rates. A ρ value of 0.5 was used between the early- and late-larval intervals because of the similarity of habitat between these two periods. For the pelagic species, anchovy and herring, $\rho = 0.25$ was used for the correlation between the late-larval and juvenile intervals, while for the demersal species, cod and plaice, I set $\rho = 0$, reflecting the major habitat shifts associated with metamorphosis.

Density-dependence

To explore the effects of density-dependence on correlations, I ran the model with $b = 1.0$, the density-independent case, or $b = 0.7$, simulating moderately strong density-dependent mortality. The variance of juvenile mortality predicted from Figure 1 is in fact the sum of both the density-independent and density-dependent sources of mortality. To estimate the density-independent component of mortality (M_j) required for Eq. (2), I had to remove the density-dependent mortality from the total juvenile mortality predicted by Figure 1. Rearranging Eq. (2) and solving for the total juvenile mortality (M_{jtot}) yields

$$M_{jtot} = N_m - N_r = (1 - b)N_m + M_j.$$

In the models without covariances between mortality rates, and in the covariance model for cod and plaice where there is no covariation in mortality across metamorphosis, taking variances yields

$$Var(M_j) = Var(M_{jtot}) - (1 - b)^2 Var(N_m).$$

In these cases, to find $Var(M_j)$ I ran the stochastic

model up to the metamorph stage and calculated the median $Var(N_m)$. $Var(M_j)$ was then found by subtraction using $Var(M_{jtot})$ predicted from Figure 1 (Table 3). For herring and anchovy in the covariance model, the equation above should include a term for the covariance between M_{jtot} and N_m. In these cases, $Var(M_j)$ was found by trial by running the model with different values of $Var(M_j)$ and matching the median M_{jtot} with the value predicted from the regression equation of Figure 1.

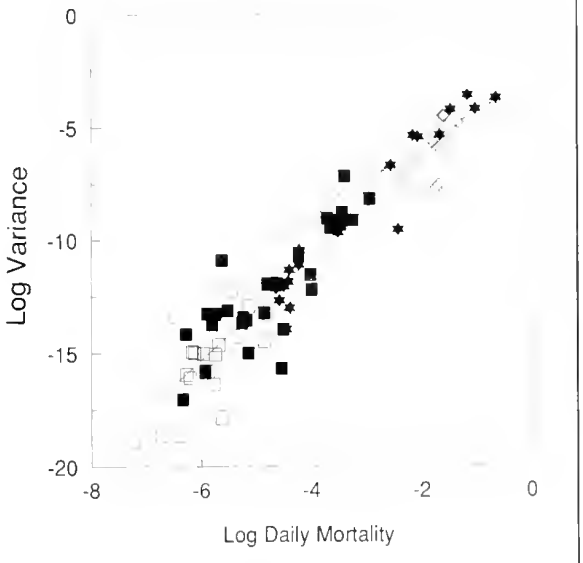

Figure 1

Relationship between interannual variance in daily mortality rates and mean daily mortality from published values. Symbols indicate eggs (*), larvae (◊), juveniles (■), and adults (□). Equation of the line: $\ln\{Var(M)\} = 2.231 \ln(M) - 1.893$ (R^2 0.90, $P<0.0001$). Regression uses the square root of number of years comprising each data point as weights.

Table 3

Variances of juvenile mortality rates $V(M_j)$ used in the four versions of the model and the variance of log recruitment, $V(N_r)$, generated by the model. Model versions include density-dependent (DD) or independent (DI) juvenile mortality and, in some cases, covariance between stage-specific mortality rates (COV). Variances for M_j in the DD models are for the density-independent component only, and were found by simulation.

	DI		DI-COV		DD		DD-COV	
Species	$V(M_j)$	$V(N_r)$	$V(M_j)$	$V(N_r)$	$V(M_j)$	$V(N_r)$	$V(M_j)$	$V(N_r)$
Cod	0.45	1.49	0.45	2.04	0.35	0.87	0.34	1.15
Herring	0.91	1.49	0.91	2.08	0.85	1.14	0.92	1.59
Anchovy	0.58	2.54	0.58	3.91	0.40	1.36	0.45	2.16
Plaice	0.22	1.64	0.22	2.46	0.09	0.79	0.09	1.04

To provide objective criteria for evaluating recruitment hypotheses, I defined two performance criteria for the correlations with recruitment. Recruitment research is commonly cast as a search for the stage when "year-class strength is determined" or "recruitment is fixed." I define such a stage as having an $R^2>0.50$ with recruitment, i.e., being able to account for at least half of the variability in year-class strength. A more rigorous standard of $R^2>0.80$ was set for correlations to be used for management purposes (Walters 1989).

Results

Variance-mean relationship

There was a highly significant relationship (R^2 0.90, $P<0.0001$, n 97) between the log of mean daily stage-specific mortality and the log of the interannual variance in the daily mortality rate (Fig. 1). The variance in mortality rate was independent of the number of years of data comprising each point (multiple regression with mean mortality, P 0.81 for sample size). The square root of sample size was used as a weight in all analyses. There was no significant effect of life history (freshwater, marine, or anadramous) on the variance-mean relationship (ANCOVAR; for slopes and adjusted means, all $P>0.20$). There was no difference in the relationship between the variance and mean of mortality among the egg, juvenile, and adult stages ($P>0.5$), but the slope for the larval stage was significantly different from the other three stages (intercept P 0.10, slope P 0.010). Because there were a number of studies on the same species, I also averaged the data across both species and stage to decrease the non-independence of the data due to common phylogeny. The variance-mean regression for this averaged dataset was almost identical to the full set (R^2 0.92, $P<0.0001$, n 53); the regression parameters differed by <2%. In this case, the regression for the larvae was not different than for the other three stages (intercept P 0.28, slope P 0.11), suggesting the significant effect found for the full dataset may have been due to the overrepresentation of some species. I therefore used the overall regression (Fig. 1) to predict the variance of mortality of all stages, rather than using a separate regression for larvae. This is a conservative procedure for rejecting Hjort's hypothesis, because the single regression predicts a more variable mortality for the early-larval stage than does the separate larval regression; the single regression produces stronger correlations between abundance of

early larvae and recruitment than the separate larval regression.

Correlations between early life history and recruitment

Correlations between abundances at early life stages and recruitment increased in strength as the interval between the two stages decreased (Figs. 2, 3). Overall, covariances in mortality rates across stages increased R^2 values between early abundances and recruitment by 0.01–0.25, while density-dependent juvenile mortality had only a small and usually negative effect on R^2 values.

Correlations between egg or first-feeding larvae and recruitment were weak; the average R^2 over all species and models was 0.05 for eggs and 0.20 for first-feeding larvae. None of the values exceeded 0.50, indicating that these early stages have little predictive capability. At the end of the early-larval stage, R^2 values increased; and in 4 of 16 cases in Figures 2 and 3 the R^2 values exceeded 0.50. However, no values exceeded 0.80, the suggested requirement for recruitment forecasting to be beneficial for management (Walters 1989).

In nearly all cases, the majority (R^2>0.50) of recruitment variation was predictable at the age of metamorphosis. The exception was the herring example, which gave low correlations because of high variability in the juvenile mortality rate. Half the correlations met the forecasting requirement of R^2>0.80 by the age of metamorphosis; these cases occurred in species with the lowest juvenile mortality rates.

The success of larval mortality rates in predicting recruitment was lower than for larval abundance estimates. The correlation between the mortality rate of the early-larval period and recruitment was strongly affected by the presence of covariation between stage-specific mortality rates; without these covariances the average R^2 was 0.12; the largest value was 0.18. When the covariances were incorporated, these correlations are increased, although none exceed 0.5 (Fig. 4). Ten of 16 R^2 values exceeded 0.50 for the much

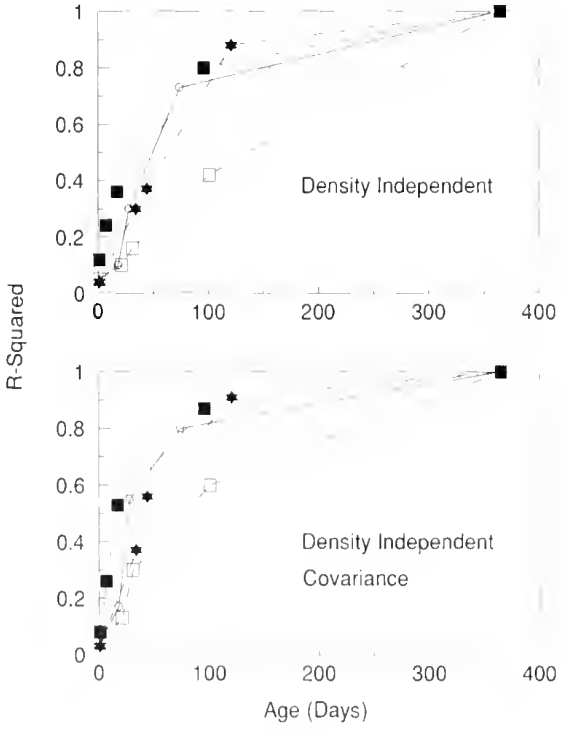

Figure 2

Predicted R^2 values for correlations between recruitment and early life stages for cod (O), anchovy (■), plaice (*), and herring (□). For each species, symbols represent, from left to right: abundance of eggs (at t = 0), first-feeding larvae, 10-d larvae, and metamorphs. Dotted line indicates the strength of correlations required for recruitment prediction (Walters 1989). Both examples include density-independent juvenile mortality; lower panel also incorporates covariance between interval-specific mortality rates.

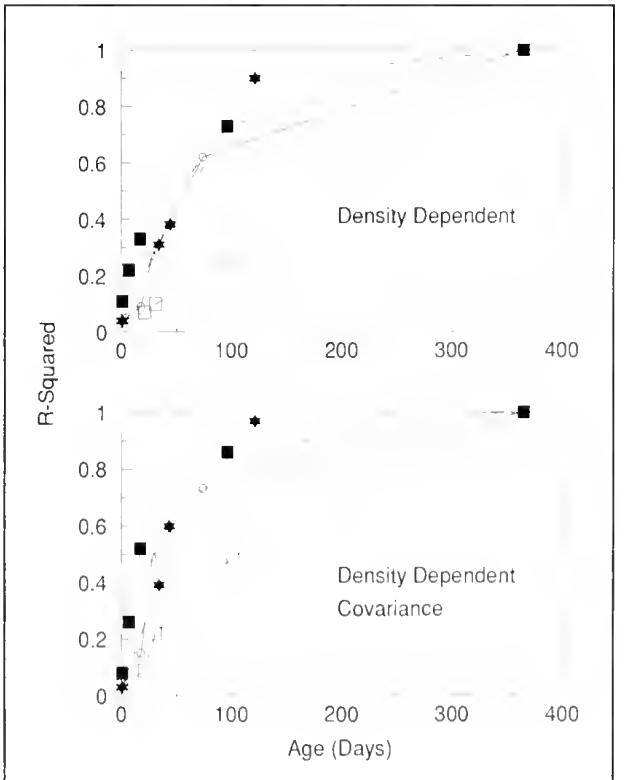

Figure 3

As in Figure 2, except both versions include density-dependent juvenile mortality; lower panel also incorporates mortality covariances.

longer late-larval period. The recruitment-forecasting threshold of 0.8 was never reached for correlations between recruitment and any larval mortality rate.

A wide range of R^2 values can result from a short time-series. For example, the 95% range of R^2 values for the correlation of early cod larvae with recruitment (10-yr time-series) in the density-independent model that includes covariance in mortality rates extended from 0.07 to 0.86 (Fig. 5). The 95% range decreases if the true relationship between the variables is stronger; for cod metamorphs the conclusion that this stage can be used to describe the majority of recruitment variation will nearly always be reached (Fig. 5).

Sensitivity analysis

Two sensitivity analyses were conducted to assess dependence of the results on input parameters. First, stage-specific variances in mortality were recalculated with the slope of the variance-mean regression set at its 95% confidence limits; the intercept was derived by constraining the line through the mean of both variables. For the cod-DI model, increasing the slope to the upper confidence limit increased the R^2 for the correlations between the abundance of recruits and early larvae or metamorphs by about 0.05; decreasing the slope lowered R^2 values by similar amounts. There was little effect on correlations involving the egg or first-feeding stages. I also recalculated the correlations with the intercept of the variance-mean regression at its 95% confidence limits. With the intercept at its lower limit, R^2 values increased by 0.01–0.04, and at the upper limit the correlations decreased by a similar amount. Thus, the overall results are not particularly sensitive to the sampling error associated with the data in Figure 1.

I also varied the length of the early-larval period. In the life tables (Table 2), I fixed the early-larval period at 10 days and set the daily mortality rate at twice the average for the whole larval period. In sensitivity runs I varied this period from 5 to 15 days; duration and mortality rate of the late-larval period were recalculated to keep the total mortality for the larval period constant. The duration of this period of high larval mortality had a strong effect on the strength of the correlation between abundance of larvae sampled at the end of the early period and recruitment. When the early-larval period was increased by 5 days, the R^2 in the cod-DI model increased by 0.21 (Fig. 6).

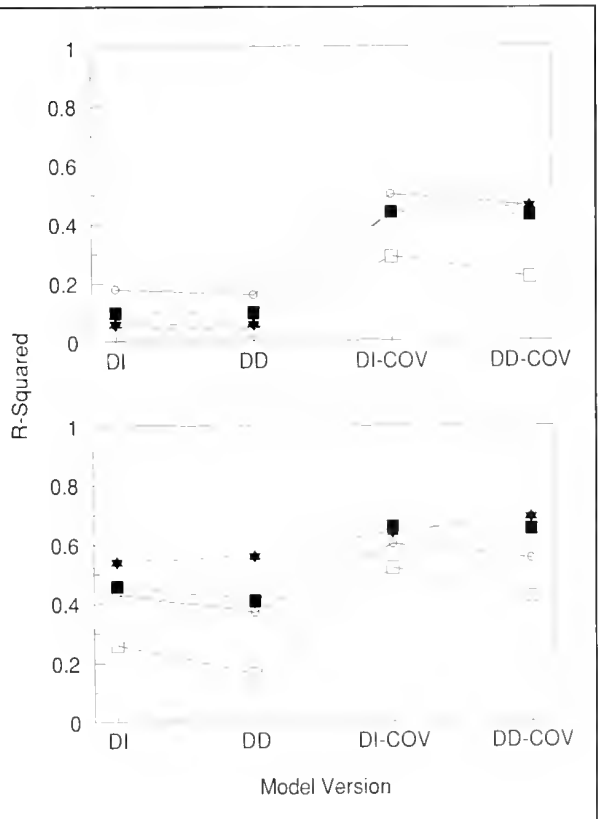

Figure 4

Predicted R^2 values for correlations between recruitment and early- and late-larval mortality rates for cod (O), anchovy (■), plaice (*), and herring (□). Axis labels refer to four versions of the model, incorporating density-independent (DI) or -dependent (DD) juvenile mortality and covariances between mortalities (COV).

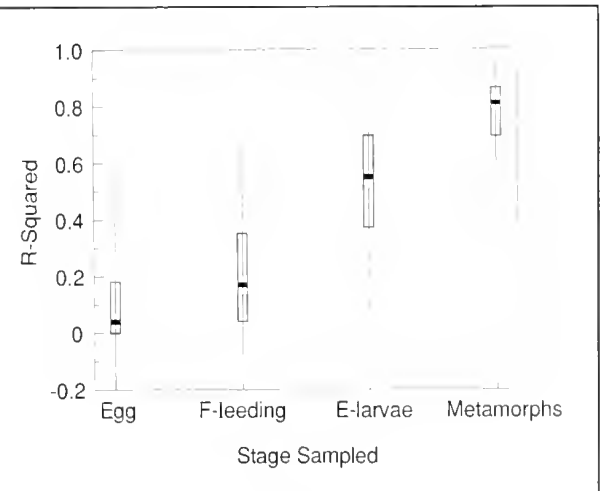

Figure 5

Variability in sample R^2 values (10-yr series) for the correlation between recruitment and abundances of early stages for cod in the model, with density-independent juvenile mortality and mortality covariances. Shown are the median (bar), interquartile (rectangle), and 95% ranges (line). Data are from 1000 runs; note that the criterion for significance ($R^2>0$, α 0.05) is 0.40.

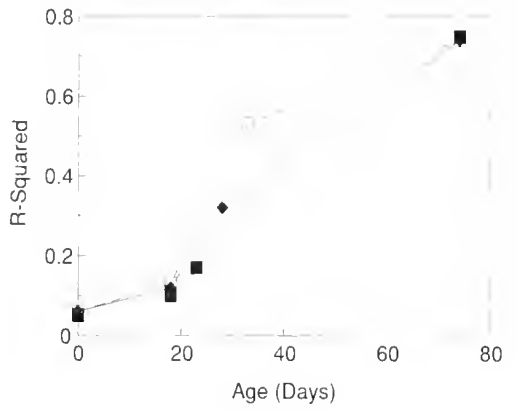

Figure 6

Effects of altering length of the early-larval stage on recruitment correlation for the cod DI-COV model. Early stage is defined as having twice the daily mortality rate of the total larval period. Shown are results with the early stage set at 5 (■), 10 (◆), and 15 (□) days. Symbols represent, from left to right: egg, yolk-sac larvae, early larvae, and metamorph stages.

Discussion

My results indicate that only predictions of recruitment based on abundances of postmetamorphic fish are likely to be useful for the management of marine fishes. The contribution to recruitment variation made by egg number (and, therefore, stock biomass) is very small, a prediction confirmed by most stock-recruit data (Parrish 1973). Correlations involving the abundance of early larvae are stronger, but are still too weak for forecasting. The model R^2 values for correlations involving early larvae are similar to the range, extending from 0.01 to 0.66, for published values compiled by Peterman et al. (1988). Accurate recruitment forecasting may be possible by sampling during the late-larval period (Graham and Sherman 1987). However, this is highly dependent on parameters and the dynamics of the particular species; only for cases with low variability in juvenile mortality or with mortality rates correlated across stages are the abundances of late larvae likely to be useful for recruitment forecasting.

Research on recruitment variability has been oriented to the early-larval stages largely as the result of Hjort's (1913) hypotheses and the observation that most of the individuals of a year-class die during the first few weeks of life (Wooster and Bailey 1989). In my four example species, the average cumulative mortality on the cohort to the 10-d larval stage is 93% (Table 1), yet the variation in abundance of these larvae explains more than 50% of recruitment variability in less than half of the cases. Variability in the late-larval and juvenile stages is still large enough to influence the strength of correlations of recruitment with larval abundances. My results suggest that the stage 'when year-class strength is determined' (defined here as $R^2>0.5$) occurs after this early critical period. However, the sensitivity analysis indicates that the strength of the correlation between the abundance of larvae and recruitment will depend strongly on the rate at which mortality declines during the larval period, and at what age the larvae are being sampled.

Strong linkages in mortality rates across intervals also render the definition of a 'critical period' less concise. Correlations between early life stages and recruitment were stronger when there were linkages, because survival to the age of sampling will be correlated to survival in the future. An estimate of mortality or abundance in one stage will be an index of mortality in all early life stages. This may be especially true for the early-larval stages (the classical 'critical period') because small larvae are probably subjected to a similar source of mortality as older larvae, especially if spawning occurs over a protracted period, mixing larvae of different ages together in the same body of water. In addition, environmental conditions during an early stage may affect survival of the cohort in the future. Poor feeding conditions of early larvae, for example, may have a long-term effect on growth and survival (Frank and McRuer 1989). In these cases, recruitment will be somewhat predictable from the early-larval stages, but this is not support for a strict interpretation of Hjort's hypothesis that an early critical period determines recruitment because mortality is correlated across all prerecruit stages.

The difficulty and expense of obtaining accurate estimates of abundances of eggs and larval fish have led to increased interest in finding indirect estimates of mortality rates that may be simpler to collect and could provide an index of year-class strength. Such measures include estimates of growth (Houde 1987), condition, lipid content (Theilacker 1986), and RNA/DNA ratios (Buckley and Lough 1987) as well as oceanographic variables such as upwelling and wind events (Peterman and Bradford 1987). My results show that such mortality estimates made on small larvae are not likely to be strongly correlated with recruitment (Fig. 4). Mortality estimates on older larvae will have stronger correlations, potentially closer to a value of 0.50. Note that the correlations in Figure 4 are for direct estimates of mortality, indirect indices will be more poorly related to recruitment. A combination of larval abundances and mortality rate estimates may allow more precise prediction of recruitment (Graham and Sherman 1987, Frank and McRuer 1989); if estimates are accurate and are based on older larvae,

correlations nearly as strong as those predicted for metamorphs might be possible.

The correlations will be weaker if sampling errors are included in the estimates of abundance. Preliminary simulations with random sampling errors with a coefficient of variation of 50% (untransformed abundances) decreased R^2 values in Figures 2 and 3 by 0.10–0.15 (Bradford unpubl.). Biased estimates, e.g., due to gear avoidance (Lo et al. 1989), will not affect correlations between an early stage and recruitment, unless the magnitude of the bias is correlated with the estimate. Precision, through the use of consistent technique across years, is more important for the purposes of forecasting. Large-scale surveys of abundance of late larvae or juveniles may be sufficiently accurate for the forecasting of recruitment (Lo et al. 1989) if the stage sampled is likely to be strongly correlated with recruitment (Fig. 5).

An implicit, though infrequently stated, assumption of research on early-life-history influences on recruitment is that the mean and the interannual variance of mortality rates are correlated. High mortality alone will not cause recruitment variation; it must also be coupled with high interannual variability. The data compiled in Figure 1 provide evidence that this is generally true, and that the interannual variability in the larval period is proportionately no greater than that found for other stages. In addition, my sensitivity analysis suggests that the general conclusions of this paper are robust to the sampling variability of this relationship. However, detailed investigation of the recruitment dynamics of an individual species will require estimation of the variance of stage-specific mortality rates, because the predictive power of Figure 1 is still relatively low for any particular case, and the biology of an individual species may not result in rates that follow the overall average pattern. Examples are provided by species which spawn during periods of extreme climatic events such as wind storms (e.g., capelin *Mallotus villosus* or red drum *Sciaenops ocellatus*, reviewed by Taggart and Frank 1990). In these cases, interannual variability in the mortality of the earliest stages is probably larger than predicted by the regression of Figure 1, and the correlation between the early stages and recruitment is likely to be stronger than I have predicted. In contrast, for the North Sea plaice a relationship (R^2 0.7) was found between egg abundance and recruitment (Zijlstra and Witte 1985), which is higher than my model predicts for this species (although just within the 95% range). This species has relatively low recruitment variation, suggesting that larval and juvenile survival rates are not as variable as predicted by Figure 1, or that density-dependent mortality might be important in regulating recruitment (Zijlstra and Witte 1985).

The recruitment variances generated by various versions of the model tend to be higher than published values (Tables 2, 3). These literature estimates will likely be underestimates of the true variability in recruitment, because errors in catch sampling and ageing can greatly reduce recruitment variability estimated from sequential population analysis (Rivard 1989, Bradford 1991). Alternatively, my recruitment variances could be too high because I have either overestimated the variances of mortality rates or underestimated the severity of density-dependent mortality. Since the data in Figure 1 include sampling error, all of the variances in Tables 2 and 3 will be somewhat inflated. If sampling error is proportional to the rate of mortality, the sensitivity analysis suggests that removing sampling error (i.e., lowering the intercept of Fig. 1) will have only a slight effect on recruitment correlations.

One additional source of variability not explicitly considered in my analysis is the effect of varying stage duration, due to interannual variability in growth rates. Houde (1987, 1989) has demonstrated through life-table manipulation that small variations in larval growth may have large effects on the number of metamorphs produced. The effect on recruitment will be buffered somewhat as shortening the larval period will increase the length and, therefore, the total mortality of the juvenile stage. However, if the variation in growth rates is due to temperature, Pepin (1991) suggests that the offsetting effects of temperature on development and mortality will result in no net effect of temperature variation on cumulative mortality over the egg and larval stages. In this case, by not including variation in growth rates I will have overestimated the variability in larval mortality. However, to some extent the effects of growth-rate variation are already included in my model because many of the estimates in Figure 1 are based on total stage length and will, therefore, include the effects of varying stage duration caused by variation in growth rates in the calculation of the average daily mortality rate.

The sampling variability of correlations from short datasets makes it difficult to draw inferences about the causes of recruitment variability. This low precision suggests that confidence limits around the sample estimates, r or R^2, should always be supplied, much in the same way that standard errors are given for sample means. A population correlation from Figures 2 and 3 is a value that would be obtained from a very long time-series of data, and is a true measure (in the context of the model) of the contribution of an early life stage to recruitment variation. However, there is a good chance (e.g., >30% for early larvae in Fig. 5) that a sample correlation between the abundance of an early stage and recruitment may not be significantly different from 0. Even if the correlation is significant,

statements about whether the relationship is, in reality, weak or strong cannot be made because the 95% confidence limits around the sample correlation are wide (Fig. 5). Published correlations between early life stages and recruitment vary greatly in strength (e.g., Peterman et al. 1988, Stevenson et al. 1989, Cushing 1990); unfortunately with short data series, true differences in the biology of these species cannot be distinguished from sampling error. The correlations between early larval abundances and recruitment compiled by Peterman et al. (1988) also illustrate this point: in only 1 of 7 cases do the 95% confidence limits around R^2 not include both 0.2 and 0.8. This problem of low precision is less serious when the true correlation is likely to be fairly high (Fig. 5, metamorphs).

The precision of correlations is also relevant to analyses involving oceanographic or climatic variables and recruitment. These studies usually invoke hypotheses that the environmental variables are agents of larval mortality, either through transport or their effects on the production or concentration of larval food (Shepherd et al. 1984, Hollowed and Bailey 1989); therefore, their true correlations with recruitment can be no stronger than the correlations for mortality rates directly (Fig. 4). Yet the sampling variability of R^2 for a short series of data suggests that there will be a good chance of finding at least one strong sample correlation among a group of 4–5 predictors that may be, in reality, only weakly related to recruitment. Adding more data will result in the sample correlation declining towards ρ; this frequently results in the sample correlation becoming nonsignificant (Koslow et al. 1987, Walters and Collie 1988, Prager and Hoenig 1989). My model results suggest environmental variables will be strongly correlated with recruitment only if the environmental factor is related to mortality across all prerecruit stages (e.g., Fig. 4; covariance models).

In summary, my analysis indicates that it is unlikely that estimates of abundance of survival rates of the egg and early-larval stages of marine fish will lead to useful predictions of recruitment. Although mortality in the earliest life stages is a major source of recruitment variability, the late-larval and juvenile periods are also important. Peterman et al. (1988), Fritz et al. (1990), and Pepin and Myers (1991) argue for the need for coordinated research on all prerecruit stages, rather than focusing only on the early stages, and my results support this view. The modeling approach I have developed here can be easily modified for any particular species to estimate *a priori* the likelihood of success of proposed recruitment research and to suggest particularly fruitful avenues of investigation.

Acknowledgments

This analysis would not have been possible without the efforts of many scientists in estimating the vital rates of fish populations in multiyear studies. I thank G. Cabana for discussions of variability and correlations and for help collecting data. This paper has been improved through the comments of G. Cabana, M. LaPointe, B. McKenzie, R.M. Peterman and D. Roff, and two reviewers. Partial support was provided by postgraduate fellowships from the National Science and Engineering Research Council of Canada (NSERC) and the Max Bell Foundation, and NSERC operating grants to D. Roff.

Citations

Ahlstrom, E.H.
1954 Distribution and abundance of egg and larval populations of the Pacific sardine. Fish. Bull., U.S. 56:83–140.

Alexander, G.R., and D.S. Shetter
1969 Trout production and angling success from matched plantings of brook trout and rainbow trout in East Fish Lake, Michigan. J. Wildl. Manage. 33:682–692.

Al-Hossaini, M., Q. Lui, and T.J. Pitcher
1989 Otolith microstructure indicating growth and mortality among plaice, *Pleuronectes platessa*, post-larval sub-cohorts. J. Fish. Biol. 35(Suppl. A):81–90.

Allen, R.L.
1977 Status of the upper Columbia river salmon and steelhead runs. *In* Schwiebert, E. (ed.), Columbia river salmon and steelhead, p. 23–30. Am. Fish. Soc. Spec. Publ. 10, Bethesda.

Anderson, J.T.
1984 Early life history of redfish (*Sebastes* spp.) on Flemish Cap. Can. J. Fish. Aquat. Sci. 41:1106–1116.
1988 A review of size dependent survival during pre-recruit stages of fishes in relation to recruitment. J. Northwest Atl. Fish. Sci. 8:55–66.

Bannister, R.C.A.
1978 Changes in plaice stocks and plaice fisheries in the North Sea. Rapp. P.-V. Reun. Cons. Int. Explor. Mer 172:86–101.

Bannister, R.C.A., D. Harding, and S.J. Lockwood
1974 Larval mortality and subsequent year-class strength in the plaice (*Pleuronectes platessa*). *In* Blaxter, J.H.S. (ed.), The early life history of fish, p. 21–37. Springer-Verlag, NY.

Barnaby, J.T.
1944 Fluctuations in abundance of red salmon, *Oncorhynchus nerka*, of the Karluk River, Alaska. Fish. Bull., U.S. 50: 237–295.

Bradford, M.J.
1991 Effects of ageing errors on recruitment time series estimated from sequential population analysis. Can. J. Fish. Aquat. Sci. 48:555–558.

Buckley, L.J., and R.G. Lough
1987 Recent growth, biochemical composition, and prey field on larval haddock (*Melanogrammus aeglefinus*) and Atlantic cod (*Gadus morhua*) of Georges Bank. Can. J. Fish. Aquat. Sci. 44:14–25.

Campana, S.E., K.T. Frank, P.C.F. Hurley, P.A. Koeller, F.H. Page, and P.C. Smith
1989 Survival and abundance of young Atlantic cod (*Gadus morhua*) and haddock (*Melanogrammus aeglefinus*) as indicators of year-class strength. Can. J. Fish. Aquat. Sci. 46 (Suppl. 1):171–182.

Chadwick, E.M.P.
1982 Stock-recruitment relationship for Atlantic salmon (*Salmo salar*) in Newfoundland rivers. Can. J. Fish. Aquat. Sci. 39: 1496–1501.
1987 Causes of variable recruitment in a small Atlantic salmon stock. *In* Dadswell, M.J., et al. (eds.), Common strategies of anadromous and catadromous fishes, p. 390–401. Am. Fish. Soc. Symp. 1, Bethesda.

Clady, M.D.
1975 Early survival and recruitment of smallmouth bass in northern Michigan. J. Wildl. Manage. 39:194–200.

Cushing, D.H.
1990 Plankton production and year-class strength in fish populations: An update of the match/mismatch hypothesis. Adv. Mar. Biol. 26:250–294.

Dahlberg, M.D.
1979 A review of survival rates of fish eggs and larvae in relation to impact assessments. Mar. Fish. Rev. 41(3):1–12.

Dey, W.P.
1981 Mortality and growth of young-of-year striped bass in the Hudson river estuary. Trans. Am. Fish. Soc. 110:151–157.

Dragesund, O., and O. Nakken
1973 Relationship between parent stock size and year class strength in Norwegian spring spawning herring. Rapp. P.-V. Reun. Cons. Int. Explor. Mer 164:15–29.

Farris, D.A.
1960 Abundance and distribution of eggs and larvae and survival of larvae of jack mackerel (*Trachurus symmetricus*). Fish. Bull., U.S. 61:247–279.

Foerster, R.E.
1968 The sockeye salmon (*Oncorhynchus nerka*). Fish. Res. Board Can. Bull. 162, 422 p.

Forney, J.L.
1971 Development of dominant year classes in a yellow perch population. Trans. Am. Fish. Soc. 100:739–749.

Frank, K.T., and J.K. McRuer
1989 Nutritional status of field-collected haddock (*Melanogrammus aeglefinus*) larvae from southwestern Nova Scotia: An assessment based on morphometric and vertical distribution data. Can. J. Fish. Aquat. Sci. 46(Suppl. 1):125–133.

Franklin, D.R., and L.L. Smith
1963 Early life history of the northern pike with special reference to the factors influencing the numerical strength of year classes. Trans. Am. Fish. Soc. 92:91–110.

Freeburg, M.H., W.W. Taylor, and R.W. Brown
1990 Effect of egg and larval survival on year-class strength of lake whitefish in Grand Traverse Bay, Lake Michigan. Trans. Am. Fish. Soc. 119:92–100.

Fritz, E.S., L.B. Crowder, and R.C. Francis
1990 The National Oceanic and Atmospheric Administration plan for recruitment fisheries oceanography research. Fisheries (Bethesda) 15:25–31.

Gerrodette, T., D. Goodman, and J. Barlow
1984 Confidence limits for population projections when vital rates vary randomly. Fish. Bull, U.S. 83:207–215.

Graham, J.J., and K.M. Sherman
1987 Recruitment mechanisms of 2-year-old atlantic herring to the Maine fishery: The larval stage. *In* Hoyt, R.D. (ed.), 10th annual larval fish conference, p. 61–68. Am. Fish. Soc. Symp. 2, Bethesda.

Gulland, J.A.
1989 Fish populations and their management. J. Fish. Biol. 35A:1–9.

Harding, D., J.H. Nichols, and D.S. Tungate
1978 The spawning of plaice (*Pleuronectes platessa*) in the southern North Sea and English Channel. Rapp. P.-V. Reun. Cons. Int. Explor. Mer 172:102–113.

Hatch, J.T., and J.C. Underhill
1988 Abundance, distribution, and mortality of larval lake herring in western Lake Superior. *In* Hoyt, R.D. (ed.), 11th annual larval fish conference, p. 95–103. Am. Fish. Soc. Symp. 5, Bethesda.

Heessen, H.J.L., and A.D. Rijnsdorp
1989 Investigations on egg production and mortality of cod (*Gadus morhua*) and plaice (*Pleuronectes platessa*) in the southern and eastern North Sea in 1987 and 1988. Rapp. P.-V. Reun. Cons. Int. Explor. Mer 191:15–20.

Hennemuth, R.C., J.E. Palmer, and B.E. Brown
1980 A statistical description of recruitment in eighteen selected fish stocks. J. Northwest Atl. Fish. Sci. 1:101–111.

Hjort, J.
1913 Fluctuations in the great fisheries of northern Europe viewed in the light of biological research. Rapp. P.-V. Reun. Cons. Int. Explor. Mer 19:1–228.

Hollowed, A.B., and K.M. Bailey
1989 New perspective on the relationship between recruitment of Pacific hake (*Merlucius productus*) and the ocean environment. *In* Beamish, R.J., and G.A. McFarlane (eds.), Effects of ocean variability on recruitment and an evaluation of parameters used in stock assessment models, p. 207–220. Can. Spec. Publ. Fish. Aquat. Sci. 108.

Houde, E.D.
1987 Fish early life dynamics and recruitment variability. *In* Hoyt, R.D. (ed.), 10th annual larval fish conference, p. 17–29. Am. Fish. Soc. Symp. 2, Bethesda.
1989 Subtleties and episodes in the early life of fishes. J. Fish. Biol. 35A:29–38.

Howe, A.B., P.G. Coates, and D.E. Pierce
1976 Winter flounder estuarine year-class abundance, mortality, and recruitment. Trans. Am. Fish. Soc. 105:647–657.

Johannessen, A.
1986 Recruitment studies of herring in Lindaaspollene, western Norway, 1–3. Fiskeridir. Skr. Ser. Havunders. 18: 139–240.

Jonsson, B., S. Skulason, S.S. Snorrason, O.T. Sandlund, H.J. Malmquist, P.M. Jonasson, R. Gydemo, and T. Lindem
1988 Life history variation of polymorphic Arctic charr (*Salvelinus alpinus*) in Thingvallavatn, Iceland. Can. J. Fish. Aquat. Sci. 45:1537–1547.

Kawanabe, H.
1969 The significance of social structure in production of the ayu, *Plectoglossus altivelis*. *In* Northcote, T.G. (ed.), Symposium on salmon and trout in streams, p. 243–265. H.R. MacMillan Lect. Fish., Univ. Brit. Col., Vancouver.

Koslow, J.A., K.R. Thompson, and W. Silvert
1987 Recruitment to northwest Atlantic cod (*Gadus mordua*) and haddock (*Melanogrammus aeglefinus*) stocks: The influence of stock size and climate. Can. J. Fish. Aquat. Sci. 44:22–39.

Kramer, R.H., and L.L. Smith
1962 Formation of year classes in largemouth bass. Trans. Am. Fish. Soc. 91:29–41.

Leggett, W.C.
1986 The dependence of fish larval survival on food and predator densities. *In* Skreslet, S. (ed.), The role of freshwater outflows in coastal marine systems, p. 117–137. Springer-Verlag, Berlin.

Lo, N.C.H., J.R. Hunter, and R.P. Hewitt
1989 Precision and bias in estimates of larval mortality. Fish. Bull., U.S. 87:399–416.

Lockwood, S.J.
1980 Density-dependent mortality in 0-group plaice (*Pleuronectes platessa*) populations. J. Cons. Cons. Int. Explor. Mer 39:148–153.

Manly, B.J.F.
1977 The determination of key factors from life table data. Oecologia 31:111–117.

Manooch, C.S., and G.R. Huntsman
1977 Age, growth, and mortality of the reg porgy, *Pagrus pargrus*. Trans. Am. Fish. Soc. 106:26–35.

Mansfield, P.J., and J.D. Jude
1986 Alewife (*Alosa pseudoharengus*) survival during the first growth season in southeastern Lake Michigan. Can. J. Fish. Aquat. Sci. 43:1318–1326.

Mathews, S.B.
1984 Variability of marine survival of Pacific salmonids: A review. *In* Pearcy, W.G. (ed.), The influence of ocean conditions on the production of salmonids in the north Pacific, p. 161–182. Oreg. State Univ., Corvallis.

Mathews, S.B., and F.W. Olson
1980 Factors affecting Puget Sound coho salmon (*Oncorhynchus kisutch*) runs. Can. J. Fish. Aquat. Sci. 37:1373–1378.

May, R.C.
1974 Larval mortality in marine fishes and the critical period concept. *In* Blaxter, J.H.S. (ed.), The early life history of fish, p. 3–19. Springer-Verlag, Berlin.

McDonald, J., and J.M. Hume
1984 Babine Lake sockeye salmon (*Oncorhynchus nerka*) enhancement program: Testing some of the major assumptions. Can. J. Fish. Aquat. Sci. 41:70–92.

McGurk, M.D.
1989 Advection, diffusion and mortality of Pacific herring larvae *Clupea harengus pallasi* in Bamfield Inlet, British Columbia. Mar. Ecol. Prog. Ser. 51:1–18.

McNeil, W.J.
1969 Survival of pink and chum salmon eggs and alevins. *In* Northcote, T.G. (ed.), Symposium on salmon and trout in streams, p. 101–117. H.R. MacMillan Lect. Fish., Univ. Brit. Col., Vancouver.

Methot, R.D.
1989 Synthetic estimates of historical abundance and mortality for the northern anchovy. *In* Edwards, E.F., and B.A. Megrey (eds.), Mathematical analysis of fish stock dynamics, p. 66-82. Am. Fish. Soc. Symp. 6, Bethesda.

Miller, T.J., L.B. Crowder, J.A. Rice, and E.A. Marshall
1988 Larval size and recruitment mechanisms in fishes: Towards a conceptual framework. Can. J. Fish. Aquat. Sci. 45:1657–1670.

Nickelson, T.E.
1986 Influences of upwelling, ocean temperature, and smolt abundance on marine survival of coho salmon (*Oncorhynchus kisutch*) in the Oregon production area. Can. J. Fish. Aquat. Sci. 43:527–535.

Nielson, L.A.
1980 Effect of walleye (*Stizostedion vitreum vitreum*) predation on juvenile mortality and recruitment of yellow perch (*Perca flavescens*) in Oneida Lake, New York. Can. J. Fish. Aquat. Sci. 37:11–19.

Palomera, I., and J. Lleonart
1989 Field mortality estimates of anchovy larvae, *Engraulis encrasicolus*, in the western Mediterranean. J. Fish. Biol. 35(Suppl. A):133–138.

Parker, R.R.
1968 Marine mortality schedules of pink salmon of the Bella Coola River, central British Columbia. J. Fish. Res. Board Can. 25:757–794.

Parrish, B.B. (editor)
1973 Fish stocks and recruitment. Rapp. P.-V. Reun. Cons. Int. Explor. Mer 164.

Pearcy, W.G.
1962 Ecology of an estuarine population of winter flounder, *Pseudopleuronectes americanus*. III. Distribution, abundance, growth, and production of juveniles; survival of larvae and juveniles. Bull. Bingham Oceanogr. Collect. Yale Univ. 18: 39–64.

Pepin, P.
1991 Effect of temperature and size on development, mortality and survival rates of the pelagic early life stages of marine fish. Can. J. Fish. Aquat. Sci. 48:503–518.

Pepin, P., and R.A. Myers
1991 Significance of egg and larval size to recruitment variability of temperate marine fish. Can. J. Fish. Aquat. Sci. 48:1820–1828.

Peterman, R.M.
1981 Form of random variation in salmon smolt-adult relations and its influence on production estimates. Can. J. Fish. Aquat. Sci. 38:1113–1119.
1982 Nonlinear relation between smolts and adults in Babine Lake sockeye salmon (*Oncorhynchus nerka*) and implications for other salmon populations. Can. J. Fish. Aquat. Sci. 39: 904–913.

Peterman, R.M., and M.J. Bradford
1987 Wind speed and mortality rate of a marine fish, the northern anchovy, *Engraulis mordax*. Science (Wash. DC) 235:354–356.

Peterman, R.M., M.J. Bradford, N.C.H. Lo, and R.D. Methot
1988 Contribution of early life stages to interannual variability in recruitment of northern anchovy (*Engraulis mordax*). Can. J. Fish. Aquat. Sci. 45:8–16.

Poole, J.C.
1969 A study of winter flounder mortality rates in Great South Bay, New York. Trans. Am. Fish. Soc. 98:611–616.

Prager, M.H., and J.H. Hoenig
1989 Superposed epoch analysis: A randomization test of environmental effects on recruitment with application to chub mackerel. Trans. Am. Fish. Soc. 118:608–618.

Pritchard, A.L.
1948 Efficiency of natural propagation of the pink salmon (*Oncorhynchus gorbuscha*) in McClinton Creek, B.C. J. Fish. Res. Board Can. 7:224–236.

Rivard, D.
1989 Overview of the systematic, structural, and sampling errors in cohort analysis. *In* Edwards, E.F., and B.A. Megrey (eds.), Mathematical analysis of fish stock dynamics, p. 49–65. Am. Fish. Soc. Symp. 6, Bethesda.

Roberson, K., and R.H. Holder
1987 Development and evaluation of a streamside sockeye salmon (*Oncorhynchus nerka*) incubation facility, Gulkana River, Alaska. *In* Smith, H.D., L. Margolis, and C.C. Wood (eds.), Sockeye salmon (*Oncorhynchus nerka*) population biology and future management, p. 191–197. Can. Spec. Publ. Aquat. Sci. 96.

SAS
1987 SAS/STAT guide for personal computers, version 6. SAS Inst. Inc., Cary, NC.

Savoy, T.F., and V.A. Crecco
1988 The timing and significance of density-dependent and density-independent mortality of American shad, *Alosa sapidissima*. Fish. Bull., U.S. 86:467–488.

Seelbach, P.W.
1987 Effect of winter severity on steelhead smolt yield in Michigan: An example of the importance of environmental factors in determining smolt yield. *In* Dadswell, M.J., et al. (eds.), Common strategies of anadromous and catadromous fishes, p. 441–450. Am. Fish. Soc. Symp. 1, Bethesda.

Shepherd, J.G., J.G. Pope, and R.D. Cousens
1984 Variations in fish stocks and hypotheses concerning their links with climate. Rapp. P.-V. Reun. Cons. Int. Explor. Mer 185:255–267.

Shetter, D.S.
1961 Survival of brook trout from egg to fingerling stage in two Michigan trout streams. Trans. Am. Fish. Soc. 90: 252–258.

Sissenwine, M.P.
1984 Why do fish populations vary? *In* May, R.M., (ed.), Exploitation of marine communities, p. 59–94. Springer-Verlag, Berlin.

Smith, P.E.
1985 Year-class strength and survival of 0-group clupeoids. Can. J. Fish. Aquat. Sci. 42(Suppl. 1):69–82.

Stevenson, D.K., K.M. Sherman, and J.J. Graham
1989 Abundance and population dynamics of the 1986 year class of herring along the Maine coast. Rapp. P.-V. Reun. Cons. Int. Explor. Mer 191:345–350.

Sunby, S., H. Bjorke, A.V. Soldal, and S. Olsen
1989 Mortality rates during the early life stages and year-class strength of northeast Arctic cod (*Gadus morhua*). Rapp. P.-V. Reun. Cons. Int. Explor. Mer 191:351–358.

Taggart, C.T., and K.T. Frank
1990 Perspectives on larval fish ecology and recruitment processes: Probing the scales of relationships. *In* Sherman, K., C.M. Alexander, and B.D. Gold (eds.), Large ecosystems: Patterns, processes and yields, p. 151–164. Am. Assoc. Adv. Sci., Wash. DC.

Taggart, C.T., and W.C. Leggett
1987 Short-term mortality in post-emergent larval capelin *Mallotus villosus*. I. Analysis of multiple *in situ* estimates. Mar. Ecol. Prog. Ser. 41:205–217.

Taylor, W.W., M.A. Smale, and M.H. Freeberg
1987 Biotic and abiotic determinants of lake whitefish (*Coregonus clupeaformis*) recruitment in northeastern Lake Michigan. Can. J. Fish. Aquat. Sci. 44(Suppl. 2):313–323.

Theilacker, G.H.
1986 Starvation-induced mortality of young sea-caught jack mackerel, *Trachurus symmetricus*, determined with histological and morphological methods. Fish. Bull., U.S. 84:1–17.

Thorne, R.E., and J.J. Ames
1987 A note on variability of marine survival of sockeye salmon (*Oncorhynchus nerka*) and effects of flooding on spawning success. Can. J. Fish. Aquat. Sci. 44:1791–1795.

Turner, J.L., and H.K. Chadwick
1972 Distribution and abundance of young-of-year striped bass, *Morone saxatilis*, in relation to river flow in the Sacramento-San Joaquin estuary. Trans. Am. Fish. Soc. 101:442–452.

Uphoff, J.H.
1989 Environmental effects on survival of eggs, larvae, and juveniles of striped bass in the Choptank River, Maryland. Trans. Am. Fish. Soc. 118:251–263.

Van Woert, W.F.
1980 Exploitation, natural mortality, and survival of smallmouth bass and largemouth bass in Shasta Lake, California. Calif. Fish Game 66:163–171.

Varley, G.C., and G.R. Gradwell
1960 Key factors in population studies. J. Anim. Ecol. 29: 399–401.

Walters, C.J.
1989 Value of short-term forecasts of recruitment variation for harvest management. Can. J. Fish. Aquat. Sci. 46: 1969–1976.

Walters, C.J., and J.S. Collie
1988 Is research on environmental factors useful to fisheries management? Can. J. Fish. Aquat. Sci. 45:1848–1854.

Walton, C.J.
1987 Parent–progeny relationships for an established population of anadramous alewives in a Maine lake. *In* Dadswell, M.J., et al. (eds.), Common strategies of anadromous and catadromous fishes, p. 451–454. Am. Fish. Soc. Symp. 1, Bethesda.

Ward, B.R., and P.A. Slaney
1988 Life history and smolt-to-adult survival of Keogh River steelhead trout (*Salmo gairdneri*) and the relationship to smolt size. Can. J. Fish. Aquat. Sci. 45:1110–1122.

Ware, D.M., and T.C. Lambert
1985 Early life history of Atlantic mackerel (*Scomber scombrus*) in the southern Gulf of St. Lawrence. Can. J. Fish. Aquat. Sci. 42:577–592.

Watanabe, Y., and N.C.H. Lo
1989 Larval production and mortality of Pacific saury, *Cololabis saira*, in the northwestern Pacific Ocean. Fish. Bull., U.S. 78:601–613.

Winters, G.H., and J.P. Wheeler
1987 Recruitment dynamics of spring-spawning herring in the Northwest Atlantic. Can. J. Fish. Aquat. Sci. 44:882–900.

Wooster, W.W., and K.M. Bailey
1989 Recruitment of marine fishes revisited. *In* Beamish, R.J., and G.A. McFarlane (eds.), Effects of ocean variability on recruitment and an evaluation of parameters used in stock assessment models, p. 153–159. Can. Spec. Publ. Fish. Aquat. Sci. 108.

Zijlstra, J.J., and J. IJ. Witte
1985 On the recruitment of 0-group plaice in the North Sea. Neth. J. Zool. 35:360–376.

Zijlstra, J.J., R. Dapper, and J. IJ. Witte
1982 Settlement, growth and mortality of post-larval plaice (*Pleuronectes platessa*) in the western Wadden Sea. Neth. J. Sea. Res. 15:250–272.

Appendix

Daily mortality rates and interannual variances plotted in Figure 1. Stage refers to egg (E), larval (L), juvenile (J), or adult (A) periods. For anadromous salmon, fry-smolt and smolt-adult mortality were classified as juvenile and adult mortality, respectively. N is the number of years of data in each study.

Species	Stage	M	var(M)	N	Study
Alosa pseudoharengus	L	0.0490	4.31E-04	9	Mansfield and Jude 1986
	L	0.1980	1.07E-04	8	Walton 1987
A. sapidissima	L	0.0524	2.96E-04	8	Savoy and Crecco 1988
	L	0.0978	1.28E-03	8	
	L	0.2290	3.50E-03	8	
	J	0.0027	1.30E-07	8	
	J	0.0185	5.08E-06	8	
Clupea harengus	E	0.3135	2.80E-02	2	Dragesund and Nakken 1973
	L	0.2060	1.10E-02	2	
	L	0.0275	3.38E-04	11	Graham and Sherman 1987
	L	0.1168	1.83E-03	4	Johannessen 1986
	L	0.0900	8.98E-03	2	McGurk 1989
Cololabis saira	L	0.0726	9.19E-04	14	Watanabe and Lo 1989
Coregonus artedii	L	0.5000	1.63E-02	2	Hatch and Underhill 1988
C. clupeaformis	E	0.0299	6.40E-05	2	Taylor et al. 1987
	L	0.0143	9.30E-05	2	
	L	0.0216	2.10E-04	2	Freeberg et al. 1990
Engraulis encrasicolis	L	0.2000	1.11E-02	3	Palomera and Lleonart 1989
E. mordax	E	0.3600	1.53E-02	13	Peterman et al. 1988
	L	0.1860	5.52E-04	13	
	J	0.0180	9.77E-06	13	
Esox lucius	L	0.1650	3.60E-03	3	Franklin and Smith 1963
Gadus morhua	E	0.1890	4.84E-03	3	Campana et al. 1989
	L	0.1940	2.37E-03	3	
	E	0.2304	1.48E-02	7	Heessen and Rijnsdorp 1989
	L	0.1010	5.63E-04	8	Sunby et al. 1989
	J	0.0312	8.90E-05	7	
Melanogrammus aeglefinus	E	0.1270	4.43E-03	3	Campana et al. 1989
	L	0.2630	8.56E-03	3	
Micropterous dolomieui	E	0.0890	7.12E-05	3	Clady 1975
	L	0.0310	7.74E-05	3	
	A	0.0007	6.00E-09	2	Van Woert 1980
M. salmoides	L	0.0224	9.90E-05	3	Kramer and Smith 1962
	J	0.0078	1.80E-06	4	
Morone saxatilis	L	0.1770	4.50E-04	2	Dey 1981
	J	0.0040	2.00E-06	2	
	L	0.1550	4.30E-03	6	Uphoff 1989
	J	0.0530	2.80E-04	10	Turner and Chadwick 1972
Oncorhynchus gorbuscha	E	0.0097	5.32E-06	6	Pritchard 1948
	J	0.0260	7.80E-05	3	Parker 1968
	A	0.0080	1.65E-06	3	
O. kisutch	A	0.0028	1.37E-07	8	Mathews 1984
	A	0.0078	5.15E-07	17	Mathews and Olson 1980
	A	0.0049	3.51E-07	22	Nickelson 1986
O. mykiss	J	0.0036	1.85E-05	3	Seelbach 1987
	A	0.0020	1.02E-07	4	Allen 1977
	A	0.0022	3.08E-07	7	Ward and Slaney 1988

Appendix (continued)

Species	Stage	M	var(M)	*N*	Study
Oncorhynchus nerka					
Sixmile Creek	E	0.0103	3.15E-06	2	Foerster 1968
Scully Creek	E	0.0116	8.82E-07	6	
Williams Creek	E	0.0111	5.91E-06	3	
Chilko Creek	E	0.0123	2.24E-06	7	
Tally Creek	E	0.0146	1.53E-05	11	
Port John Lake	E	0.0123	1.20E-05	9	
Karymai Spring	E	0.0120	7.23E-06	8	
Chilko Lake	J	0.0018	3.96E-08	7	
Karymai Spring	J	0.0056	1.31E-06	8	
Cultus Lake	J	0.0053	1.47E-06	10	
Port John Lake	J	0.0028	1.77E-06	8	
Babine Lake	J	0.0052	1.17E-06	10	
	J	0.0032	1.72E-06	14	McDonald and Hume 1984
	A	0.0026	2.98E-07	7	Foerster 1968
	A	0.0021	3.26E-07	24	Peterman 1982
Karluk River	A	0.0017	7.86E-09	6	Barnaby 1944
Summit Lake	A	0.0036	1.73E-08	3	Roberson and Holder 1987
Ten Mile Lake	A	0.0032	2.88E-07	6	
Gulkana Hatchery	A	0.0031	7.65E-08	9	
Lake Washington	A	0.0034	4.42E-07	11	Thorne and Ames 1987
Oncorhynchus spp.	E	0.0147	2.90E-05	23	McNeil 1969
Pagrus pagrus	A	0.0012	7.76E-09	3	Manooch and Huntsman 1977
Perca flavescans	J	0.0146	2.36E-05	6	Forney 1971
	J	0.0320	1.53E-04	8	
	A	0.0079	8.90E-06	12	Nielson 1980
Plecoglossus altivelis	J	0.0097	6.70E-06	3	Kawanabe 1969
Pleuronectes platessa	E	0.0783	1.24E-03	11	Harding et al. 1978
	E	0.1165	4.70E-03	2	Heessen and Rijnsdorp 1989
	L	0.0525	7.24E-04	4	Bannister et al. 1974
	L	0.0112	6.46E-05	7	Zijlstra et al. 1982
	J	0.0336	7.69E-04	2	Al-Hossaini et al. 1989
Firemore	J	0.0303	1.07E-04	4	Lockwood 1980
Filey Bay	J	0.0245	1.18E-04	4	
	J	0.0030	1.08E-06	5	Zijlstra et al. 1982
Pseudopleuronectes americanus	J	0.0389	1.09E-04	3	Howe et al. 1976
	J	0.0058	3.04E-07	2	Pearcy 1962
	A	0.0019	1.18E-07	5	Poole 1969
Salmo salar	J	0.0019	7.07E-07	7	Chadwick 1982
	J	0.0027	1.38E-07	10	Chadwick 1987
	A	0.0058	2.36E-06	9	
Salvelinus alpinus	A	0.0015	1.53E-06	2	Jonsson et al. 1988
S. frontinalis	J	0.0082	6.47E-05	6	Shetter 1961
	J	0.0110	8.76E-07	9	
	J	0.0106	1.55E-07	3	
S. salvelinus	A	0.0042	4.59E-06	5	Alexander and Shetter 1969
Sardinops caerulea	L	0.0831	3.32E-04	2	Ahlstrom 1954
Scomber scomber	E	0.5260	2.50E-02	4	Ware and Lambert 1985
	L	0.5110	2.12E-02	3	
Sebastes spp.	L	0.0680	1.25E-03	2	Anderson 1984
Trachurus symmetrichus	L	0.1387	4.62E-04	3	Farris 1960

Abstract. – Complete series of field-collected larvae were used to describe the post-yolksac development of two common southern California marine sculpins, *Clinocottus analis* and *Orthonopias triacis*. Characters diagnostic of *C. analis* include nape pigment, dorsal head pigment, heavy rows of dorsal gut melanophores, 18–33 postanal ventral melanophores (PAVM). Postflexion larvae develop multiple preopercular spines (9–12) and several post-temporal/supracleithral spines, and later stages also acquire a W-shaped patch of pigment on the body under the second dorsal fin. Characters diagnostic of *Orthonopias triacis* include a heavy cap of dorsoposterior gut pigment, 26–55 PAVM, occasionally one or two dorsocranial melanophores, and, rarely, one melanophore at the nape; postflexion *O. triacis* develop four preopercular spines. Comparison with other cottid species is included.

Field collection data (1978–85) indicate *C. analis* and *O. triacis* larvae both occur in greatest densities off rocky habitats along the 15 m isobath. A key is provided for known preflexion marine sculpin larvae found in southern California.

Post-yolksac larval development of two southern California sculpins, *Clinocottus analis* and *Orthonopias triacis* (Pisces: Cottidae)

Richard F. Feeney

Section of Fishes, Natural History Museum of Los Angeles County
900 Exposition Boulevard, Los Angeles, California 90007

Clinocottus analis and *Orthonopias triacis* are two common marine sculpins (Pisces: Cottidae) of the rocky intertidal and subtidal areas of southern California (Miller and Lea 1972, Eschmeyer et al. 1983). The range of *C. analis* extends from Cape Mendocino, northern California, to Asuncion Pt., Baja California Sur; *O. triacis* extends from Monterey, central California, to San Geronimo I., central Baja California (Fig. 1).

A description of the embryology and larval development of *Clinocottus analis* was first attempted by Eigenmann (1892) who gave a preliminary description of the eggs and yolksac larvae of *C. analis* from reared eggs obtained in San Diego Bay CA, and subsequently by Budd (1940) from eggs obtained in Monterey Bay CA. In both studies the larvae died at the end of the yolksac stage. Bolin (1941) described the embryology and yolksac development of reared *Orthonopias triacis*.

Hubbs (1966) described many characteristics of *C. analis* embryology, especially in response to temperature, but gave no description of the larvae. Washington (1986) presented a description of a limited series of postflexion *C. analis* larvae and juveniles identified on the basis of meristic and morphological characters. A 7.0 mm *O. triacis* was previously illustrated (Washington et al. 1984). No description, however, of a complete larval series of either species exists, despite the common occurrence of adults in California coastal waters and the existence of several partial descriptions of their larval development in the literature.

The following is a description of larval series for both *C. analis* and *O. triacis* based on field-collected specimens from southern California and Baja California, Mexico. Comparison with other cottid species and occurrence is discussed. A key to known southern California preflexion cottid larvae is included to summarize early-life-history information from many sources including Richardson and Washington (1980), Richardson (1981), Washington et al. (1984), Washington (1986), Feeney (1987), and Matarese et al. (1989). This work is intended to aid in identification and hopefully stimulate further research on the development of related species.

Materials and methods

A total of 145 larvae and 9 juveniles of *Clinocottus analis* and 322 larvae and 4 juveniles of *Orthonopias triacis* were studied. Specimens were examined from the Scripps Vertebrate Collection (SIO), the Southwest Fisheries Science Center (SWFSC), the California Academy of Sciences (CAS), and the Natural History Museum of Los Angeles County, Section of Fishes (LACM).

The SIO specimens (21) are preserved in 50% isopropanol and were collected in Baja California at Bahia Todos Santos (SIO H51-19B); the lot

Manuscript accepted 6 May 1992.
Fishery Bulletin, U.S. 90:454–468 (1992).

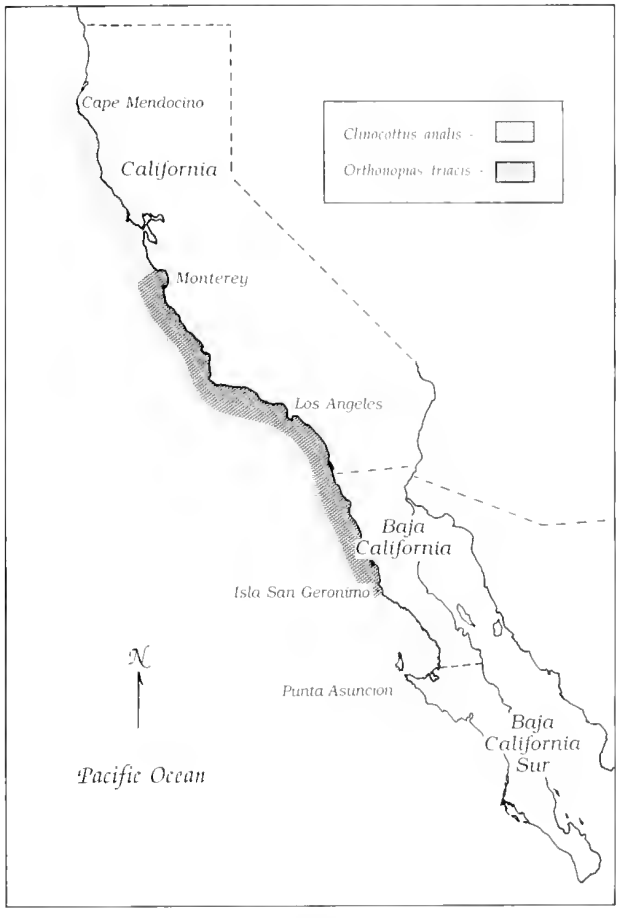

Figure 1
Geographic range of *Clinocottus analis* and *Orthonopias triacis*.

contained an excellent series of both *C. analis* and *O. triacis* postflexion larvae, the discovery of which became the impetus for the present study.

The SWFSC material (10 specimens) is preserved in 5% formalin; some specimens (6) were collected in Baja (6607-AX-110.32; 6806-JD-110.32; SWFSC/SIO H51-106), the remainder were collected in California. Two *C. analis* specimens (SWFSC/SIO H46-63) and two *O. triacis* (SWFSC 6607-AX-110.32) were cleared and stained.

CAS material included one lot of postflexion *C. analis* (SU 68789, 70% ethanol), collected in Monterey Bay, California.

LACM specimens (fixed in 5% formalin and preserved in either 5% formalin or 70% ethanol) were collected in coastal waters (<75 m depth) of the Southern California Bight between Pt. Conception and the Mexican border. Most specimens were collected during the Coastal Resources and 316b phases of the Ichthyoplankton Coastal and Harbor Studies (ICHS) Program and during the Bightwide Program; methods and station locations can be found in Brewer et al. (1981), Brewer and Smith (1982), and Lavenberg et al. (1986). Also, five postflexion *C. analis* specimens (LACM 45404-1, 45414-1–45417-1; in ethanol) were collected at the Catalina Island Marine Science Center (Ninos 1984). Six additional *C. analis* juveniles from the general LACM collection were used: four collected at Santa Barbara Island (LACM 31546-4), one at Catalina Island (LACM 35695-1), and one at Palos Verdes Peninsula (LACM 1993).

Morphometric data, including preanal length, body depth, pectoral length, head length, and eye diameter were measured from 50 *C. analis* and 54 *O. triacis* specimens. Data were entered into an "Excel" spreadsheet program on a Macintosh IIci. Means and standard deviation of morphometric measurements were computed using "SYSTAT." Frequency plots of melanophores vs. length were made using "SYGRAPH" and the "LOWESS" (locally-weighted least squares) scatterplot smoothing method (Wilkinson 1989).

Specimens were illustrated using a camera lucida attached to a Wild M3 stereomicroscope.

Occurrence data are based on specimens taken during 1978–85 on ICHS and Bightwide cruises using a variety of sampling gears. During Coastal Resources collections (ICHS cruises, 1978–79) oblique bongo samples and discrete depth samples were taken monthly along a grid of 10 transects, each with 4 stations. The transects were evenly spaced along the coast from Point Conception to San Diego. The stations corresponded to bottom depths of 8, 15, 22, and 36 m. Additionally, 8 stations (4 sites each) were located in Los Angeles–Long Beach Harbor and San Diego Bay. Integrated water-column samples were collected by fishing a 70 cm bongo sampler from the bottom to the surface. Discrete depth samples were collected at the surface (manta sampler), at the mid-depth of the water column (70 cm bongo sampler) and at the bottom (70 cm bongo sampler equipped with wheels). All samplers had nets of 335 μ mesh Nitex, and attached flowmeters gave estimates of the volume of water filtered. During the 316b phase (ICHS cruises, 1979–80) the number of transects was increased to 20 and the number of stations was reduced to 2 (8 and 22 m) except for 4 "expanded" transects (Ormond Beach, Playa del Rey, Seal Beach, San Onofre), which retained 4 stations (8, 15, 22, and 36 m). For epibenthic sampling, the benthic bongo sampler was replaced by a larger "Auriga" sampler. Collections were taken monthly during the 316b phase. Samples were sporadically taken in 1981, but no data from them are used here.

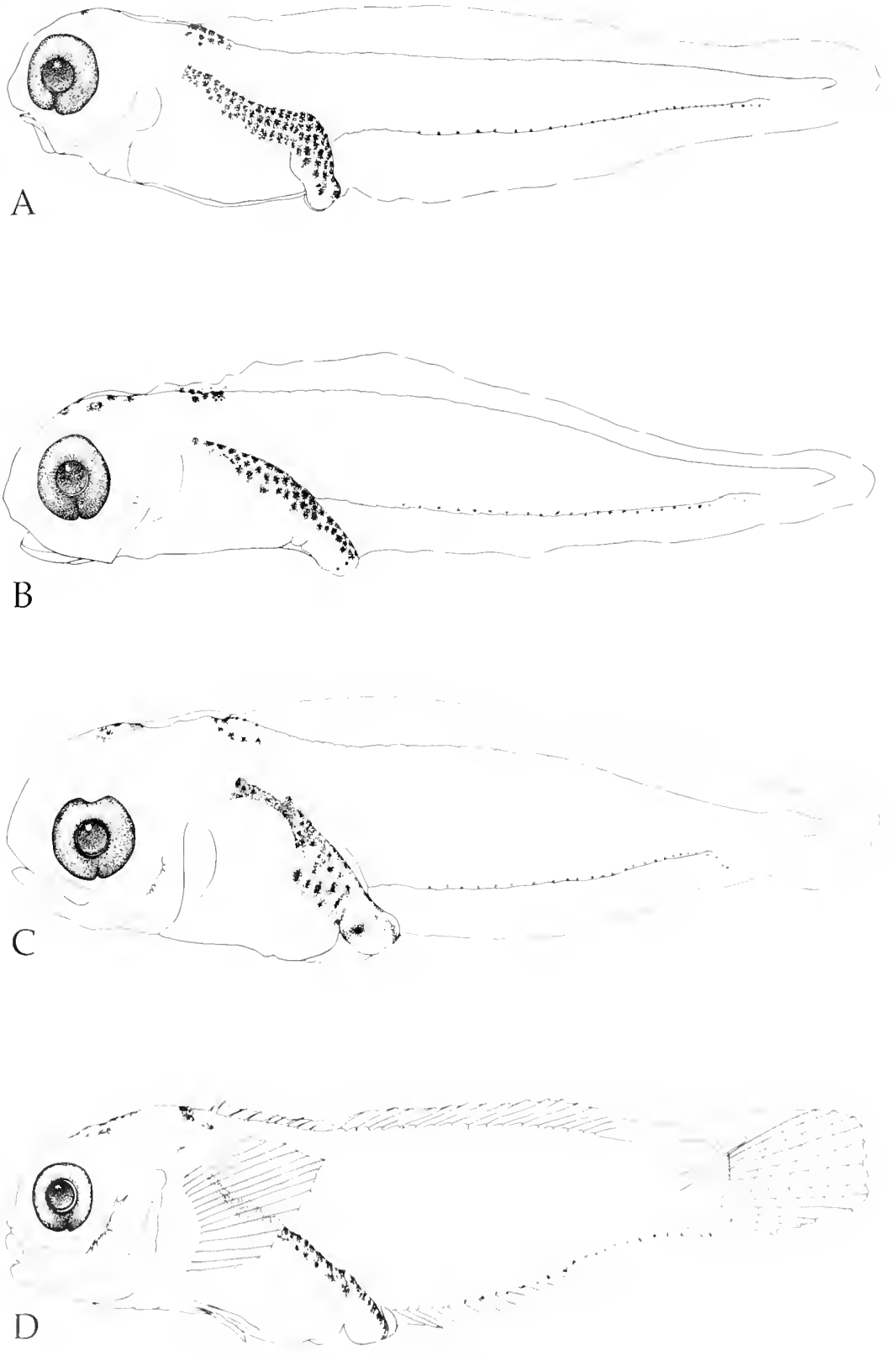

Figure 2

Field-collected *Clinocottus analis* larvae: (A) 3.9 mm (LACM KH #22), (B) 5.6 mm (LACM KH #22), (C) 5.6 mm (LACM 018-SO-36-AU-01), (D) 8.6 mm (SIO H51-19B).

The Bightwide program began in 1982 and samples were taken bimonthly at the four "expanded" 316b transects. During the Bightwide program, a fifth station (75m) was added to each transect. Only oblique bongo samples were taken during the Bightwide phase. Additional details are provided in Lavenberg et al. (1986).

Estimates of larval abundance ($n/10\,m^2$ of sea surface) for each taxon were estimated (for methods, see Smith and Richardson 1977). These abundances were plotted against variables, such as transect, station depth, gear type and date, to determine patterns of local occurrence.

Identification

Yolksac and small post-yolksac larvae of *Clinocottus analis* and *Orthonopias triacis* were identified by comparison with descriptions of reared larvae (Eigenmann 1892, Budd 1940, Bolin 1941). Larger preflexion and flexion larvae were associated to postflexion larvae and juveniles using pigment characters, number of preopercular spines, length of gut, and location of the anus. Washington (1986) was helpful in linking postflexion *C. analis* individuals to juveniles using melanophore patterns and meristics. For definition of terms, see Feeney (1987).

Table 1

Morphometrics of larvae and juveniles of *Clinocottus analis* and *Orthonopias triacis*, represented as a mean percentage of standard length ± the standard deviation, with range in parentheses.

Measurement stage	*Clinocottus analis*	*Orthonopias triacis*
Preanal length		
Preflexion	46.0±3.4(40.0–52.2)	38.8±3.0(31.5–44.8)
Flexion	47.1±2.2(44.6–48.5)	41.7±2.8(37.8–47.2)
Postflexion	50.5±2.1(46.9–54.5)	43.5±3.0(39.1–48.3)
Juvenile	47.3±1.1(46.0–48.4)	43.5±2.7(39.9–46.3)
Body depth		
Preflexion	24.8±2.2(19.7–29.7)	24.3±3.1(19.8–33.2)
Flexion	23.8±2.2(21.3–25.3)	24.3±2.9(19.8–28.5)
Postflexion	28.7±2.0(25.6–32.7)	25.9±2.4(22.1–29.5)
Juvenile	26.4±2.7(24.5–30.4)	23.6±1.6(21.7–25.3)
Pectoral length		
Preflexion	8.5±1.3 (6.6–11.3)	8.1±1.2 (6.1–11.3)
Flexion	8.9±2.0 (7.3–11.2)	10.2±2.6 (6.3–16.0)
Postflexion	27.8±4.3(16.9–32.5)	18.2±5.0(10.8–25.4)
Juvenile	35.4±1.8(33.0–36.8)	34.9±2.0(32.4–37.1)
Head length		
Preflexion	21.8±2.1(18.6–26.1)	21.2±1.7(18.0–24.4)
Flexion	23.3±0.7(22.5–23.8)	24.1±2.7(19.3–29.1)
Postflexion	30.2±1.8(25.6–32.8)	28.0±2.3(25.0–31.4)
Juvenile	36.6±4.4(33.8–43.2)	34.5±1.3(33.1–35.7)
Eye diameter		
Preflexion	10.7±1.1 (8.3–12.5)	10.0±0.8 (8.5–12.2)
Flexion	10.1±0.2 (9.9–10.2)	9.2±0.9 (7.8–10.7)
Postflexion	8.9±0.6 (8.0–10.5)	9.1±1.1 (8.1–10.8)
Juvenile	10.0±0.6 (9.4–10.7)	10.9±1.1 (9.9–12.4)

Results

Description of *Clinocottus analis* larvae

Distinguishing characters Distinguishing characters of *Clinocottus analis* preflexion larvae include heavy dorsoposterior gut pigment, nape pigment (usually with a nape bubble), 18–25 postanal ventral melanophores (PAVM), and melanophores on the head over the midbrain. Late preflexion larvae may develop up to 33 PAVM. Larger flexion and postflexion larvae develop multiple preopercular spines (9–12) similar to other *Clinocottus* and *Oligocottus* species (Washington 1986). Transforming larvae develop a W-shaped patch of pigment under the 2d dorsal and have an advanced anus. In juveniles, the preopercular spines coalesce to one bifurcate spine; small, prickly scales begin to develop under the 2d dorsal fin. The anus advances about halfway to pelvic fin origin.

Morphology *Clinocottus analis* yolksac larvae hatch at lengths of 3.7–4.5mm (Eigenmann 1892, Budd 1940); preserved field-collected larvae are found as small as 3.1mm (due to shrinkage during preservation). Larvae are robust with fully pigmented eyes at hatching. Dorsal gut diverticulae (wings) as seen in some *Artedius* (Washington 1986) are absent; however, sometimes a bump can be seen in that area.

The preanal length averages 46% of notochordal length (NL), which is closer to Eigenmann's illustration (est. 44%) than to Budd's illustration (est. 33%); the minimum preanal length from field-collected specimens was 40% NL (Table 1). During flexion the preanal length increases slightly to an average of 47%. In postflexion larvae, preanal length increases to an average 51.5% standard length (SL). In juveniles, the pectoral fin and head lengthen to an average 35 and 37% SL, respectively (Table 1).

In postflexion larvae, the anus is slightly advanced of the anal fin origin. In transforming postflexion larvae, the anus advances from the anal fin to about one-third the distance to the pelvic fin origin. In juveniles, the anus advances almost halfway to the pelvic fins.

At 9.8mm a cirrus appears on each dorsal orbit (Fig. 3B).

Fin development In postflexion larvae, fin elements start to form; the caudal rays become segmented. Pelvic fins appear as buds (Table 2). At 9.8mm, fin rays, including the pelvics, are well-formed.

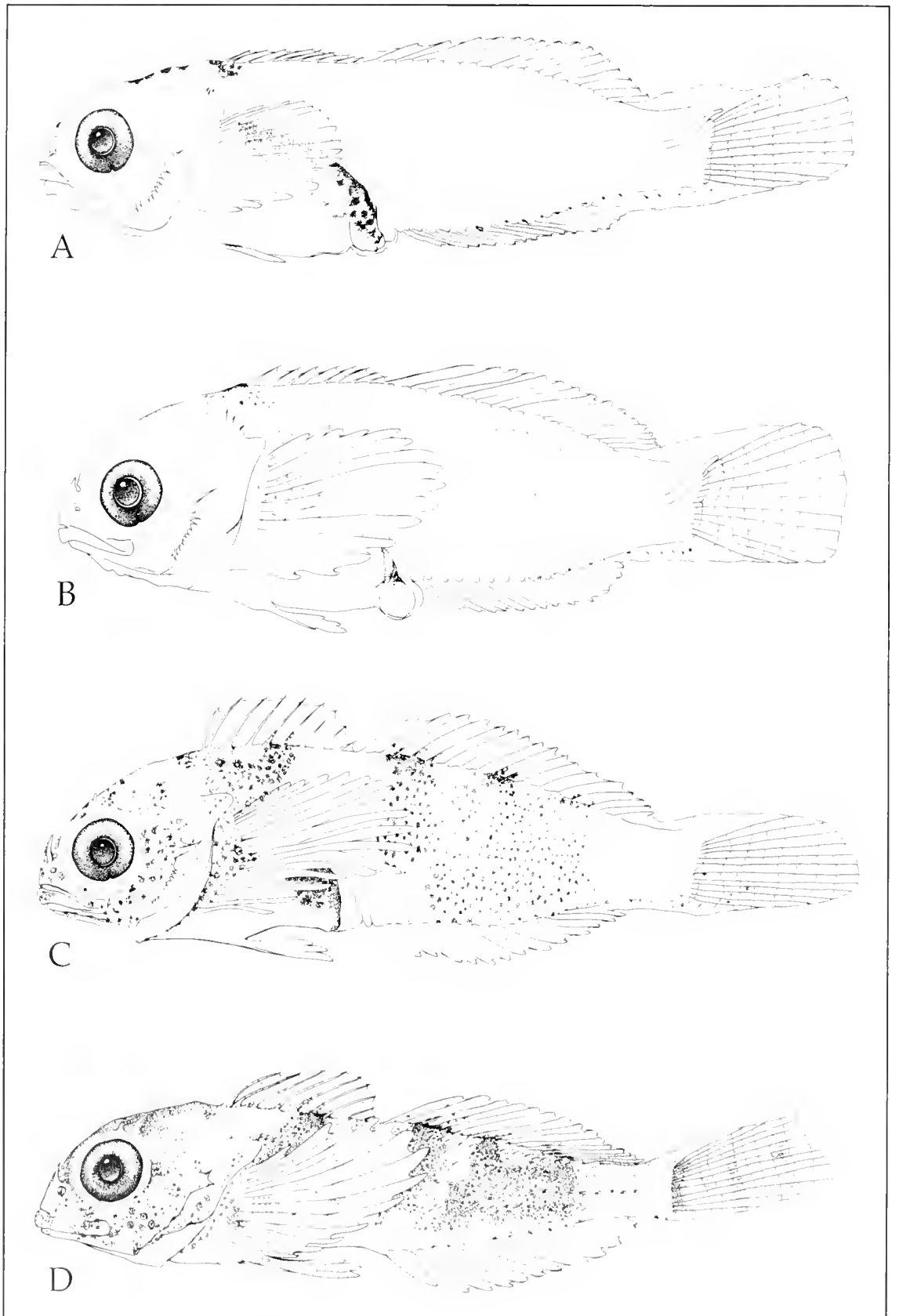

Figure 3

Field-collected *Clinocottus analis* larvae and juveniles: (A) 9.7 mm (SIO H51-19B), (B) 9.8 mm (SIO H51-19B), (C) 10.6 mm (LACM 008-88-22-MA-01), (D) 13.3 mm (LACM 45404-1).

Spination Preopercular spines begin to develop in the late preflexion stage at ~5.5 mm NL; the 5.6 mm specimen (in Fig. 2B) has developed 2 spines. During flexion, the number of preopercular spines increases to 5 (Table 2, Fig. 2C).

In postflexion larvae, the preopercular spines number 6–12 (Table 2); the upper spine is elongated. A post-temporal/supracleithral spine appears at 8 mm (Fig. 2D).

By 9.7 mm, a pair of nasal spines appear (Fig. 3A). The dorsalmost preopercular spine elongates to about twice the length of other spines. The number of post-temporal/supracleithral spines increases to 3. At 9.8 mm, a small spine (not illustrated) may be present where the sensory canal forms over the parietal, anterior to the nape; the spine persists in specimens up to 11 mm SL (CAS SU 68789).

In juveniles, multiple preopercle spines (about 10) coalesce to 1 elongate, bifurcated uppermost spine and 2 convex undulations ventrally where the other spines had been. Larval post-temporal spines form the anteriormost part of the lateral line which later becomes decorated with a series of multispined scales. Smaller spines (prickles) form laterally below the 2d dorsal and lateral line.

Pigmentation In yolksac *Clinocottus analis*, about 140 dense melanophores in 6–7 rows line the dorsoposterior gut (peritoneal) membrane (Eigenmann 1892, Budd 1940). Nape melanophores number 11–15 with several extending onto a bubble of skin that is usually present at the anterior nape. A stellate melanophore can usually be found on the head over one or both sides of the midbrain. A row of 18–25 PAVM is present from about the 6th postanal myomere to the caudal area; the last 2–3 melanophores usually extend down into the finfold.

Post-yolksac larvae retain much of the appearance of the yolksac larvae (Fig. 2A). The number of PAVM may increase to 33, but usually ranges in the mid-20s, generally decreasing in larger larvae (Fig. 4).

Late preflexion larvae develop numerous head melanophores over the midbrain (Fig. 2B). One 4.6 mm specimen had 19 midbrain melanophores and one forebrain melanophore; however, the melanophores over the midbrain usually number 10–15 with no forebrain pigment. Melanophores sometimes form at the anus in this stage; however, these usually form in the postflexion stage. One 5.2 mm specimen had 5–6 melanophores in a circle around the anus.

By 9.7 mm, the number of PAVM has decreased to less than 23 (Fig. 4). In a 9.8 mm specimen (Fig. 3B), melanophores begin to form below the nape and laterally below the second dorsal fin.

Table 2

Meristics of larvae and juveniles of *Clinocottus analis* (specimens inside the two dashed lines are undergoing flexion of the notochord).

Size (mm)	D_1	D_2	A	P	V	PS	PCV	CV	TV	M	PAVM
3.1	–	–	–	–	–	0	–	–	–	35	29
4.2	–	–	–	–	–	0	–	–	–	33	28
5.6	–	–	–	–	–	2	–	–	–	34	24
5.2	–	–	–	–	–	?	–	–	–	34	25
5.6	–	–	–	–	–	5?	–	–	–	34	26
8.4	IX?	17?	13	15?	buds	6–8	–	–	–	32	21
9.7	IX	16	14	15	I,3	10	–	–	–	33	14
10.5	IX	17	14	15	I,3	10	–	–	–	31?	17?
10.9*	IX	17	13	15	I,3	11?	11	22	33	–	–
11.1	IX	17	13	15	I,3	9	–	–	–	32	9
11.4*	IX	17	14	15	I,3	11	11	22	33	–	–
13.3**	IX	16	13	15	I,3	1	11	21	32	–	11
15.1	IX	16	13	15	I,3	1†	–	–	–	–	14
15.8**	IX	16	13	15	I,3	1	11	21	32	–	8
21.0	IX	16	13	15	I,3	1†	–	–	–	–	8

D_1 dorsal fin spines
D_2 dorsal rays
A anal fin rays
P pectoral fin rays
V pelvic rays
PS preopercle spines
PCV precaudal vertebrae
CV caudal vertebrae
TV total vertebrae
M myomeres
PAVM postanal ventral melanophores

* cleared and stained larvae
** x-rayed
† The one preopercle spine has a double point.

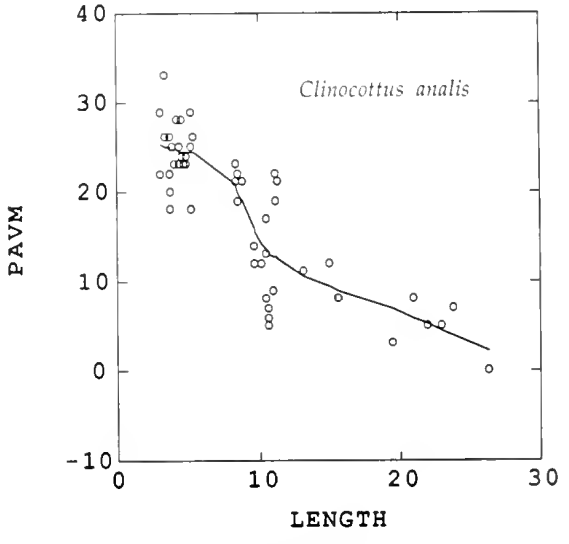

Figure 4

Frequency of postanal ventral melanophores (PAVM) vs. length (mm) with a LOWESS regression line at F = 0.5 (half the points included in a running window) for *Clinocottus analis* larvae and juveniles.

Transforming postflexion larvae develop a wide band of pigment under the second dorsal that is typically W-shaped and extends ventrally almost to the anal fin (Fig. 3C). Another band of dense pigment forms under the first dorsal fin and extends down across and onto the pectoral fin base. The head becomes heavily pigmented; about 15 large stellate melanophores (along with numerous small ones) extend across the preopercle and below the eye. Two or three melanophores appear on the posterior maxillary. Melanophores surround the nasal openings and spine. A band of pigment runs across the anterior upper lip (premaxillary). The lower jaw and chin also have pigment. The ventral gut is not pigmented. Several of the caudal rays are pigmented.

Juvenile *C. analis* continue to add pigment dorsolaterally while still retaining some of the larval pigmentation (Fig. 3D). The W-shaped patch is still present under the second dorsal, as well as a band of pigment under the first dorsal and across the pectoral fin base. The number of PAVM continue to decrease (Fig. 4). Two new patches of melanophores appear on the caudal peduncle and over the hypural plates. Melanophores appear in the dorsal, pectoral and caudal fins.

Meristics *Clinocottus analis* postflexion larvae have 6 branchiostegal rays and twelve (6+6) principal caudal rays which are consistent with adult counts. Other meristics are given in Table 2. Numbers of fin and vertebral elements match well with modes given by Howe and Richardson (1978).

Comparison with other species

Clinocottus analis larvae have no anterior gut pigment like *C. recalvus* larvae (Morris, 1951). *Clinocottus acuticeps* also has forebrain pigment and a longer trailing gut than *C. analis*, no early head pigment, fewer PAVM, and hindgut diverticulae (Washington 1986). *Clinocottus embryum* has fewer nape and PAVM. *Clinocottus globiceps* has anterior gut pigment and only four or five PAVM.

Preflexion *Oligocottus maculosus* have shorter guts (preanal averages 39.1% SL) than *C. analis* (Washington 1986). *Oligocottus snyderi* has no head pigment and few PAVM (~6). Larvae of *O. rubellio* (rosy sculpin) and *O. rimensis* (saddleback sculpin) have not been described. A 15.6mm juvenile *O. rubellio* (LACM 42918-1) differs from *C. analis* juveniles by having more cirri on the head, no W-shaped pigment patch laterally, and no banding anywhere, just a fine covering of light melanophores. *Oligocottus rimensis* differs by having an elongate body and a high number of dorsal soft rays (16–19). A 17.1mm *O. rimensis* (LACM 943) is developing saddles of pigment typical of adults but lacks the W-shaped patch of *C. analis*. *Oligocottus rimensis* has a single large preopercular spine (single pointed) and 3 smaller spines, similar to the "*Myoxocephalus*" group (Washington et al. 1984), i.e., 4 preopercle spines throughout their early development; the dorsal spine elongates in juveniles. *Oliocottus rimensis* juveniles also have no head cirri and the first pelvic ray appears double (split in two).

Clinocottus analis differs from some *Artedius* (*A. fenestralis*, *A. lateralis*, *A.* spp.) by having no large gut diverticulae (wings). Species of *Artedius* without wings (*A. creaseri*) differ by having anterior gut pigment and fewer PAVM (~10) (See Appendix 1).

Occurrence

Oblique bongo samples from coastal waters (8, 15, 22, 36, and 75m depths) of the Southern California Bight taken during the period 1978–84 (see Lavenberg et al. (1986) for methods) indicate *C. analis* larvae (mostly preflexion) were captured at the greatest densities along the 15m isobath off rocky tidepool areas in southern California, especially off Palos Verdes Peninsula and Gaviota in 1979–80. Larvae occurred during all months of the year, with peak abundance in July. Wells (1986) found that *C. analis* spawn throughout the year, with a peak in September–November in 1971–72, based on gonosomatic index values and the appearance of juveniles in the tidepools.

In discrete depth (neuston, middepth, epibenthic) samples taken in the Southern California Bight in October 1978 and June 1979–July 1980, 100% of the *C. analis* larvae (almost exclusively notochordal and flexion sizes) were caught in epibenthic samplers (benthic bongo or auriga nets) indicating the smaller larvae are near the bottom. Large postflexion individuals were common in neuston tows (manta nets) taken during the Coastal Resources Program (1978–79 except October; not fully sorted to date) at Coho Bay (Pt. Conception), and Playa del Rey and Seal Beach (stations on each side of Palos Verdes; no station at Palos Verdes) indicating larger postflexion, metamorphosing larvae are located near the surface. Ninos (1984) collected many larger postflexion larvae (~10mm) during surface night-lighting at Catalina Island. At Palos Verdes, juveniles (<25mm) are found back in the intertidal in small pools, separated from the larger adults (Wells 1986).

Description of *Orthonopias triacis* larvae

Distinguishing characters Distinguishing characters for *Orthonopias triacis* larvae include a heavy cap of pigment on the dorsoposterior gut, 26–55 PAVM, nape melanophores usually absent, no wings, short gut

(preanal length 31.5–44.8%SL in preflexion larvae), and 4 preopercular spines in late-flexion and postflexion larvae. Postflexion larvae and juveniles have an anus advanced from the anal fin. Juveniles develop rows of spiny scales between the dorsal fin and lateral line.

Morphology *Orthonopias triacis* larvae hatch at 2.9–3.8mm (Bolin 1941); field-collected larvae are as small as 2.6mm (after preservation). At 4.3mm, the caudal fin anlage is forming (Fig. 5B). Flexion occurs in larvae between 4.2 and 7.2mm (Table 3).

In preflexion larvae, the preanal length averages 39%SL (Table 1). During flexion the preanal length increases to an average of 42%SL. Postflexion preanal length averages 43.5%SL. Small juveniles (13.2mm, LACM W67-153, not illustrated) also have an average preanal distance of 43.5%SL.

In postflexion larvae, the anus starts to advance anteriorly from the developing anal fin. In larger postflexion larvae (Fig. 6C), a cirrus forms on the orbit. Small juveniles (13.2mm, LACM W67-153, not illustrated) have a cirrus on the orbit and one in the interorbital space; they also have lateral line scales and scale bands under the dorsal fin.

Larger juveniles (Fig. 6D) have numerous cirri and spines on the head; a smaller cirrus forms on the maxillary and cirri develop between the preopercular spines. The anus is located about halfway to pelvic origin.

Fin development In postflexion larvae, complete rays are formed by 7.2mm in all fins except the pelvics, which are present as buds (Table 3).

Spination Preopercular spines start to form in *Orthonopias triacis* during flexion at 4.2–5.8mm (Fig. 5C, Table 3). Postflexion larvae typically have 4 preopercular spines of about equal size and equally spaced (Fig. 6B). Sometimes an accessory preopercular spine is present; a 7.3mm larva possesses a smaller spine adjacent to the 2 large spine from the top.

Small juveniles (13.2mm, LACM W67-153, not illustrated) still retain the 4 preopercular spines (Table 3). In larger juveniles (Fig. 6D, Table 3), preopercular spines are reduced to 3 and a bump where the ventralmost one used to be; the dorsalmost spine becomes bifurcate.

In large postflexion larvae (Fig. 6C), nasal spines are present. Three post-temporal/supracleithral spines appear above the opercular flap near the point where the lateral line will start to form. A small foramen is present on the parietals where a sensory canal forms.

Table 3

Meristics of larvae and juveniles of *Orthonopias triacis* (specimens inside the two dashed lines are undergoing flexion of the notochord).

Size (mm)	D_1	D_2	A	P	V	PS	PCV	CV	TV	M	PAVM
2.6	–	–	–	–	–	0	–	–	–	34	40
3.4	–	–	–	–	–	0	–	–	–	36	51
4.3	–	–	–	–	–	0	–	–	–	36	30
4.2	–	–	–	–	–	1	–	–	–	37?	43
4.9	–	–	–	–	–	2	–	–	–	34	35
5.5	–	–	–	–	–	2	–	–	–	35	35
6.5	–	–	–	–	–	4	–	–	–	35	27
7.2	–	–	–	–	–	4	–	–	–	34	28
6.8	IX?	16?	11?	14?	buds	5*	–	–	–	34	25
7.3	IX?	16?	12?	14?	buds	4	–	–	–	35	33
8.2**	IX	16	12	14	I,3	4	11	24	35	–	–
9.2	IX	16	12	14	I,3	4	–	–	–	35	7?
13.2	IX	17	12	15	I,3	4	–	–	–	–	1
17.2	IX	17	12	14	I,3	4	–	–	–	–	0
23.0†	IX	17	12	14	I,3	3††	11	24	35	–	8

* Second (from dorsum) preopercle spine has smaller spine next to it.
** cleared and stained larvae
† x-rayed
†† Dorsal preopercle spine has a double point.

Pigmentation Yolksac *Orthonopias triacis* have pigmented eyes at hatching, a cap of dense pigment on the dorsoposterior gut, and about 35 PAVM that start on the 3d or 4th postanal myomere. One or a pair of head melanophores is sometimes present (Bolin 1941).

The dorsoposterior gut pigment in field-collected larvae is composed of ~80–90 melanophores in a circular pattern (Fig. 5A). Small larvae (<4mm) have 32–55 PAVM (Fig. 7); preflexion larvae >4mm have 26–43 PAVM. One or two head melanophores over the midbrain occur in about 33% of preflexion larvae. Nape pigment is usually absent; one punctate melanophore occurs at the nape in about 25% of preflexion larvae.

Flexion larvae have similar pigment as above (Fig. 5D, 6A). The first few PAVM are formed as dashes of pigment at the start of the anal fin base (Fig. 6A). A 7.0mm specimen (Washington et al. 1984) has at least 3 head melanophores and 1 nape melanophore, and seems to be just completing flexion. A 5.8mm specimen (that may have shrunk to a greater extent because it was ETOH-preserved) completing flexion has 12 head melanophores and 2 nape melanophores (LACM 009-80-36-BB-01).

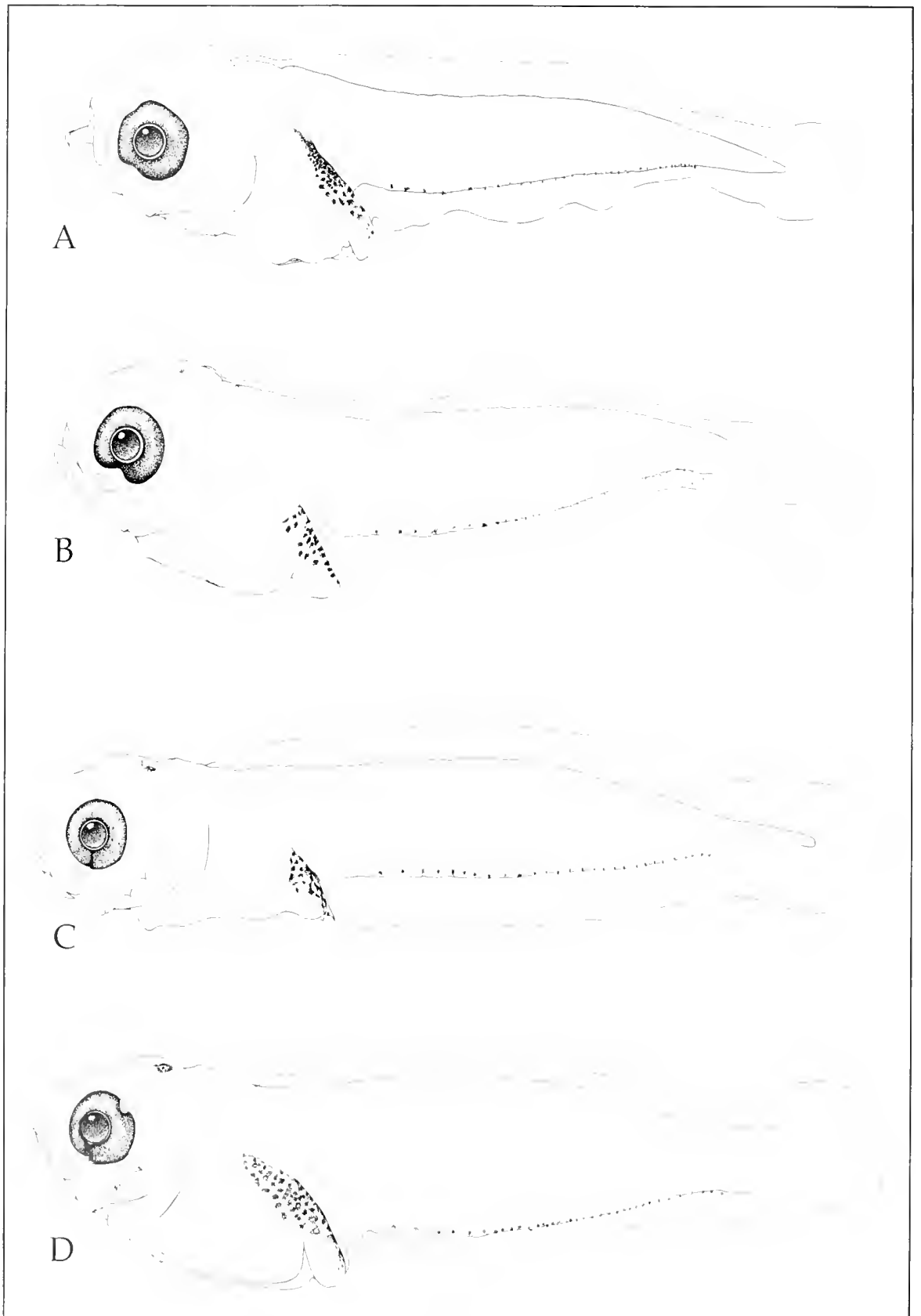

Figure 5

Field-collected *Orthonopias triacis* larvae: (A) 3.3 mm (LACM 026-PV-22-OB-02p), (B) 4.3 mm (LACM 026-PV-15-OB-01p), (C) 5.8 mm (SIO H51-19B), (D) 5.5 mm (LACM 012-80-08-BB-01).

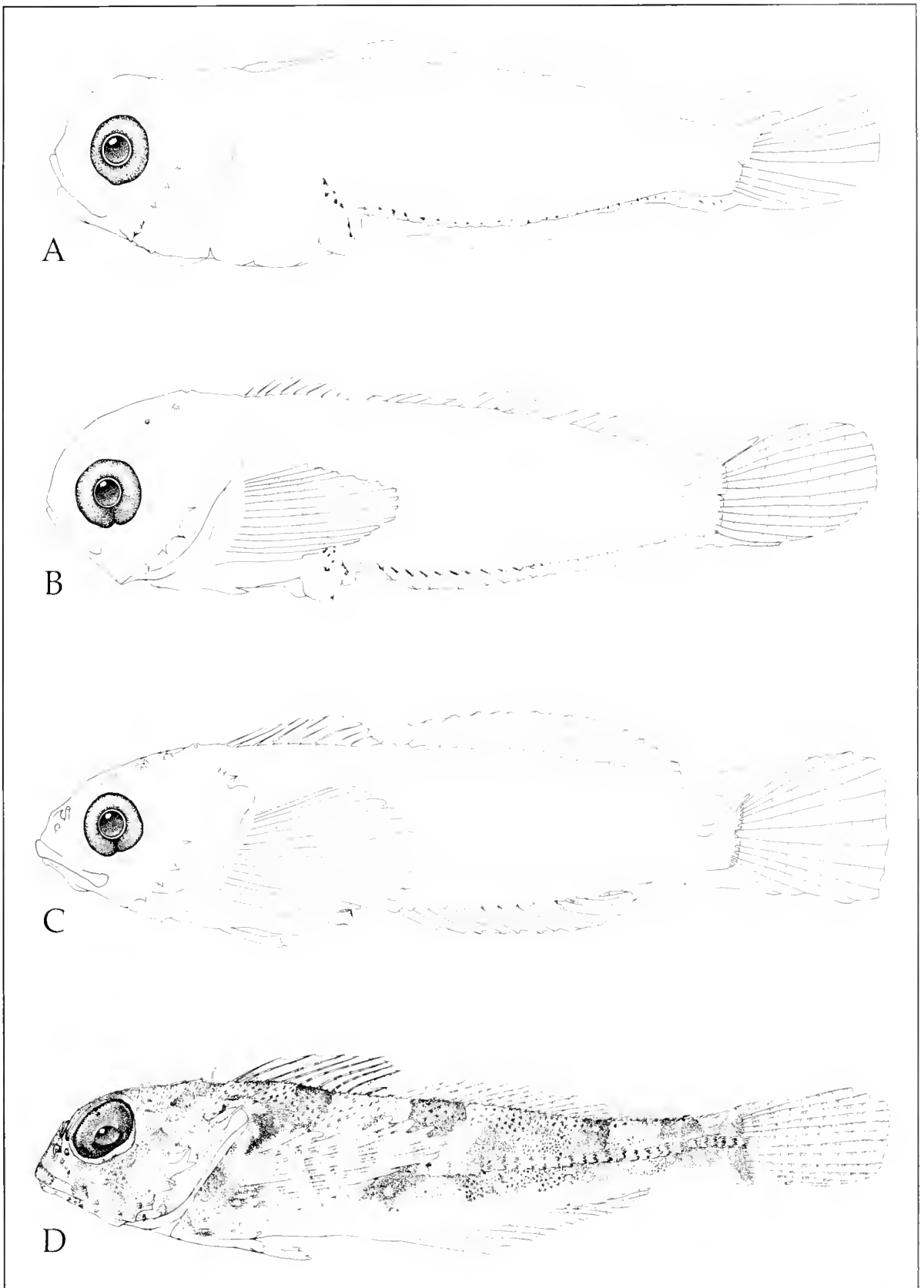

Figure 6

Field-collected *Orthonopias triacis* larvae and juveniles: (A) 5.9mm (LACM 026-PV-15-OB-01p), (B) 7.2mm (LACM 012-88-36-BB-01), (C) 9.2mm (SIO H51-19B), (D) 23.0mm (LACM 9423-8).

Postflexion PAVM pigment takes the form of dashes at the base of each anal ray. At least 3 melanophores can be found on the head over the midbrain. In larger postflexion larvae, the number of PAVM is greatly reduced (Fig. 7).

Small juveniles (13.2mm, LACM W67-153, not illustrated) have numerous melanophores over the midbrain. Few or no PAVM may be present (Fig. 7). In the 13.2mm juvenile, a dark patch of melanophores on the pectoral fin base extends to and around the pelvic girdle and meets at the ventral midline. Bands of pigment extend down from the dorsum and stop just ventral to lateral line.

In larger juveniles (Fig. 6D) a patch of melanophores is present on the pectoral fin base, but may not be continuous across the pelvic girdle as it is in the 13.2mm juvenile. Light circles appear in the dense pigment below the lateral line.

Meristics Meristics for *O. triacis* (Table 3) are comparable to published accounts. Modes for the fin elements matched those given in Howe and Richardson (1978). Vertebrae (35) were 1 greater than the mode (34) in Howe and Richardson. Branchiostegal rays (BR) form during flexion; a 5.6mmFL larva had 5 visible BR. In postlarvae and juveniles, branchiostegal rays = 6, PCR = 6+6.

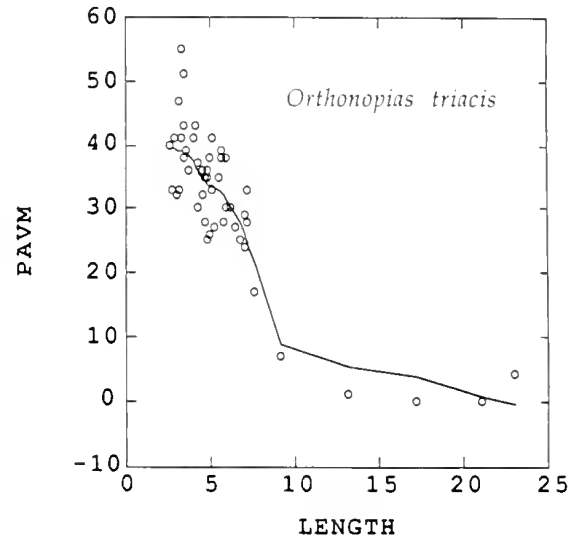

Figure 7
Frequency of postanal ventral melanophores (PAVM) vs. length (mm) with a LOWESS regression line at F = 0.5 (half the points included in a running window) for *Orthonopias triacis* larvae and juveniles.

Comparison with other species

Orthonopias triacis are similar to *Artedius meanyi* larvae (Washington 1986) by possession of 4 preopercular spines, a short compact gut, and an eye cirrus; *A. meanyi* postflexion larvae and juveniles also develop small, prickly scales on the head and below the dorsal fin. *Artedius meanyi* differ in having far fewer PAVM (<13), pigment in the dorsal finfold, anterior gut melanophores, and in undergoing flexion at a larger size (6.2–9.4mm). *Artedius meanyi* and *O. triacis* were put in the "*Myoxocephalus*" group by Washington et al. (1984) due to the presence of 4 preopercular spines.

Orthonopias triacis larvae are similar to others within the "*Myoxocephalus*" group, including *Icelinus* and *Chitonotus*, in having no heavy nape pigment and a high number of PAVM; *Icelinus quadriseriatus* has 25–63 PAVM (Feeney 1987) and *Chitonotus* has 24–45 PAVM (Richardson and Washington 1980). *Orthonopias triacis* lacks ventral gut pigment (see Appendix 1).

Orthonopias triacis can not be assigned to the "*Artedius/Clinocottus/Oligocottus*" group, as tentatively suggested by Richardson (1981), because it lacks the multiple preopercular spine pattern, gut diverticulae, and trailing gut. *Clinocottus analis* postflexion larvae (this paper) are similar to *O. triacis* because of the advanced anus and presence of head pigment, nasal spines, post-temporal/supracleithral spines, cirri over the eye, and similar meristics. *Clinocottus analis* differs in having multiple (>5) preopercular spines, a 'W' shaped pigment patch on the side of the body, and a longer gut (preanal = 46.0–54.5% SL vs. 39.1–48.3% SL in *O. triacis*).

Orthonopias triacis larvae initially have more PAVM than *C. analis*; however, the number of PAVM decreases with length more quickly than *C. analis* (Figs. 6, 7); linear regressions (not shown) of *O. triacis* PAVM have a greater negative slope (−2.413 vs. −1.161) than *C. analis*. Linear regression lines were not used, however, in the final plots (Figs. 6, 7) because LOWESS smoothing (Wilkinson 1989) indicates that the relationship between PAVM and length may be nonlinear, especially in *O. triacis*. Additional large postflexion and juvenile specimens need to be examined to verify this relationship.

Occurrence

During 1978–84, *O. triacis* larvae (like *C. analis*) were collected in highest densities off Palos Verdes and other rocky areas, at the 15m isobath during the entire year, peaking in spring and summer. Approximately 72% of the larvae in discrete depth tows were collected in epibenthic tows and none in neuston tows. Flexion larvae were rarely collected. Postflexion individuals have not been found in the 1978–79 neuston tows as were

C. analis. Postflexion/metamorphosing individuals apparently do not exhibit neustonic behavior like *C. analis*. Juvenile *O. triacis* have been collected subtidally on reefs and off rocky areas (LACM collection data).

Conclusions

Clinocottus analis larvae can be grouped with the "*Artedius*" group of cottid larvae based on the high number of preopercular spines (9–12) (Washington et al. 1984). The advanced anus of postflexion larvae is typical of *Clinocottus*. Swank (1988) showed that *Clinocottus analis* is more closely related to other species within the genus rather than to *Oligocottus maculosus*; *C. analis* was found to be the most divergent in the genus. Larval characters presented here lend support to her conclusions. *Clinocottus analis* larvae share many characters with other *Clinocottus*, but still have some significant differences, i.e., a high PAVM count and development of prickly spines on the body.

Orthonopias triacis larvae can be grouped, along with *A. creaseri*, *A. meanyi*, *Chitonotus*, and *Icelinus*, in the "*Myoxocephalus*" group (Washington et al. 1984) because of the presence of four preopercular spines. Body morphology of *O. triacis* is most similar to *A. meanyi*.

Orthonopias triacis and *C. analis* preflexion larvae co-occur in the same areas (15 m isobath near rocky habitats), but can be easily distinguished using pigment and morphological characters. Larger postflexion larvae can be distinguished by the number of preopercular spines.

Acknowledgments

I thank the following for their help: David Ambrose, Daniel Cohen, Pamela and Lissette Feeney, Javier Gago, Robert Lavenberg, Gerald E. McGowen, Geoffrey Moser, Margaret Neighbors, Debra Oda, Brenda and Jim Rounds, Jeremyn Schmitz, Helga Schwarz, Jeffrey Seigel, Camm C. Swift, H.J. Walker, Brian White, William Watson, and the Natural History Museum of Los Angeles County.

Citations

Bolin, R.L.
1941 Embryonic and early larval stages of the cottid fish *Orthonopias triacis* Starks and Mann. Stanford Ichthyol. Bull. 2:73–82.

Brewer, G.D., and P.E. Smith
1982 Northern anchovy and Pacific sardine spawning off southern California during 1978–80: Preliminary observations of the importance of the nearshore coastal region. Calif. Coop. Oceanic Fish. Invest. Rep. 23:160–171.

Brewer, G.D., R.J. Lavenberg, and G.E. McGowen
1981 Abundance and vertical distribution of fish eggs and larvae in the Southern California Bight: June and October 1978. Rapp. P.-V. Reun. Cons. Int. Explor. Mer 178:165–167.

Budd, P.L.
1940 Development of the eggs and early larvae of six California fishes. Calif. Div. Fish Game, Fish Bull. 56, 50 p.

Eigenmann, C.H.
1892 The fishes of San Diego, California. Proc. U.S. Natl. Mus. 15:123–178.

Eschmeyer, W.N., E. Herald, and H. Hammann
1983 A field guide to Pacific Coast fishes of North America. Peterson Field Guide Ser. 28, Houghton Miffin, Boston, 336 p.

Feeney, R.F.
1987 Development of the eggs and larvae of the yellowchin sculpin, *Icelinus quadriseriatus* (Pisces: Cottidae). Fish. Bull., U.S. 85:201–212.

Howe, K.M., and S.L. Richardson
1978 Taxonomic review and meristic variation in marine sculpins (Osteichthyes: Cottidae) of the northeast Pacific Ocean. Final rep. NOAA-NMFS Contract 03-78-M02-120, School Oceanogr., Oreg. State Univ., Corvallis, 142 p.

Hubbs, C.
1966 Fertilization, initiation of cleavage, and developmental temperature tolerance of the cottid fish, *Clinocottus analis*. Copeia 1966:29–42.

Lavenberg, R.J., G.E. McGowen, A.E. Jahn, and J.H. Petersen
1986 Abundance of Southern California nearshore ichthyoplankton: 1978–1984. Calif. Coop. Oceanic Fish. Invest. Rep. 27:53–64.

Matarese, A.C., A.W. Kendall Jr., D.M. Blood, and B.M. Vinter
1989 Laboratory guide to early life history stages of northeast Pacific fishes. NOAA Tech. Rep. NMFS 80, 652 p.

Miller, D.J., and R.N. Lea
1972 Guide to coastal marine fishes of California. Calif. Dep. Fish Game, Fish Bull. 157, 249 p.

Morris, R.W.
1951 Early development of the cottid fish, *Clinocottus recalvus* (Greeley). Calif. Fish Game 37:281–300.

Ninos, M.
1984 Settlement and metamorphosis in *Hypsoblennius* (Pisces, Blenniidae). Ph.D. diss., Univ. South. Calif., Los Angeles, 181 p.

Richardson, S.L.
1981 Current knowledge of larvae of sculpins (Pisces: Cottidae and allies) in northeast Pacific genera with notes on relationships within the family. Fish. Bull., U.S. 79:103–121.

Richardson, S.L., and B.B. Washington
1980 Guide to the identification of some sculpin (Cottidae) larvae from marine and brackish waters off Oregon and adjacent areas of the northeast Pacific. NOAA Tech. Rep. NMFS Circ-430, 56 p.

Smith, P.E., and S.L. Richardson
1977 Standard techniques for pelagic fish egg and larva surveys. FAO Fish. Tech. Pap. 175, 100 p.

Swank, E.S.
1988 Biochemical systematics of the genus *Clinocottus* (Cottidae). Bull. South. Calif. Acad. Sci. 87(2):57–66.

Washington, B.B.
1986 Systematic relationships and ontogeny of the sculpins *Artedius, Clinocottus,* and *Oligocottus* (Cottidae: Scorpaeniformes). Proc. Calif. Acad. Sci. 44:157-223.

Washington, B.B., W.N. Eschmeyer, and K.M. Howe
1984 Scorpaeniformes: Relationships. *In* Moser, H.G., et al. (eds.), Ontogeny and systematics of fishes, p. 438-447. Spec. Publ. 1, Am. Soc. Ichthyol. Herpetol. Allen Press, Lawrence, KS.

Wells, A.W.
1986 Aspects of ecology and life history of the woolly sculpin, *Clinocottus analis,* from Southern California. Calif. Fish Game 72:213-226.

Wilkinson, L.
1989 Sygraph: The system for graphics. Systat, Inc., Evanston, 600 p.

Appendix 1: Key to known southern California sculpin larvae (preflexion stage)

Comments: The following key is provided as a guide to identifying known Southern California sculpin larvae. Some larvae may not key out exactly due to variation in pigment or because they are a species that is not described yet (see table at end of key). Types (e.g., *Artedius* type 16) are named as they are labeled in the LACM collection. Equivalent types in literature are noted.

1 Wings (gut diverticulae) present 2

Wings absent (or as bumps only) 4

2(1) Postanal ventral melanophores 3-12 3

Postanal ventral melanophores 22-32 ..... ***Artedius lateralis***

3(2) Nape pigment present; myomeres 32-35 ..... ***Artedius* type 16**
(= *Artedius* type 3 (Washington 1986); may be either *A. corallinus* or *A. notospilosus*)

Nape pigment absent; myomeres 36-37 ..... ***Artedius* type A**
(= undescribed; has wings like other *Artedius*, no nape pigment, and only 3-8 PAVM)

4(1) Body covered with melanophores 5

Body melanophores restricted to ventral midline, gut, nape or head region 9

5(4) ~26-28 myomeres; stubby body (hatches at 6-7mm) ..... ***Rhamphocottus richardsonii****

36-41 myomeres; elongate body 6

6(5) Elongate pectoral fin (>20% of the body); pigment extending into dorsal and anal finfold (hatches at ~7-9mm) ..... ***Nautichthys oculofasciatus****

Pectoral fins not elongate (<15% of body); no pigment extending into fins 7

7(6) Lateral body relatively unpigmented; preanal length 36-42% of notochordal length ..... ***Hemilepidotus spinosus***

Lateral body covered with melanophores; preanal length ~44-46% of notochordal length 8

8(7) Series of elongate melanophores present along the lateral midline; pointed snout ..... ***Radulinus* sp.**

No distinct series of elongate melanophores along the lateral midline; blunt snout ..... ***Scorpaenichthys marmoratus***

9(4) Otic capsule pigment present (may be present in *Paricelinus hopliticus*) 10

Otic capsule pigment absent 11

10(9) Nape pigment present (several melanophores); dorsal gut pigment not in bands ..... ***Oligocottus/Clinocottus* type D**
(= *C. recalvus* (Morris 1951) or *C. globiceps* or *O. maculosus* (Washington 1986). These specimens are most similar to larger *C. recalvus* from same locality; however, they share characters with all three species (e.g., otic capsule pigment) or with one species (e.g., nape bubble like *O. maculosus*).

Nape pigment absent (or 1 melanophore occipitally); dorsal gut pigment in bands ..... ***Leptocottus armatus***

11(9) Nape pigment present **12**

Nape pigment absent (rarely present in *Orthonopias* triacis and flexon *Chitonotus pugetensis*) ... **19**

12(11) Anterior gut pigment present; ventral gut pigment present **13**

Anterior gut pigment absent; ventral gut pigment absent **14**

13(12) Myomeres 40–42; postanal ventral melanophores ~37–38; pigment on snout ..... ***Paricelinus hopliticus****

Myomeres 27–30; postanal ventral melanophores <15; pigment on snout absent ..... ***Enophrys taurina*?**
(= undescribed; only one specimen collected, similar to *E. bison* description (Richardson and Washington 1980) except for scattered ventral gut pigment)

14(12) Postanal ventral melanophores 5–14 ..... **15**

Postanal ventral melanophores 15–33 ..... **16**

15(14) Preanal myomeres 7–9; head pigment usually absent; gut pigment light and scattered ..... ***Oligocottus synderi***

Preanal myomeres 10–12; head pigment present; gut pigment heavy ..... ***Oligocottus/Clinocottus* type B**
(= undescribed; looks much like *C. analis* but has only 10–14 PAVM)

16(14) Nape melanophores <6 ..... **17**

Nape melanophores >6 ..... **18**

17(16) Postanal ventral melanophores 15–21; dorsal gut pigment light to moderate ..... ***Clinocottus embryum****

Postanal ventral melanophores 21–33; dorsal gut pigment heavy ..... ***Artedius harringtoni***

18(16) Head pigment absent; dorsal gut pigment moderate; nape melanophores ~18 ..... ***Oligocottus/Clinocottus* type C**
(= undescribed; no head pigment, 17–31 PAVM; lighter pigment than *C. analis*, may be *O. maculosus*)

Head pigment present (except in smallest larvae (<3.0mm)); dorsal gut pigment heavy; nape melanophores <17 ..... ***Clinocottus analis***

19(11) Postanal ventral melanophores 7–18 ..... **20**

Postanal ventral melanophores ≥24 ..... **21**

20(19) Ventral gut pigment absent; preanal myomeres 8–10 ..... ***Artedius creaseri***

Ventral gut pigment present; preanal myomeres 11–12 ..... ***Cottus asper***

21(19) Ventral gut pigment present 22

Ventral gut pigment absent ..... ***Orthonopias triacis***

22(21) ~5 parallel lines (striations) of pigment oriented horizontally on posterior gut .... ***Synchirus gilli****

No parallel lines of pigment on posterior gut 23

23(22) Two or more prominent anterior gut melanophores present 24

Anterior gut melanophores absent (or one only) 26

24(23) Dorsal head pigment absent; jaw angle pigment present 25

Dorsal head pigment present (except in larvae ~3.5 mm or smaller); jaw angle pigment usually absent ..... ***Chitonotus pugetensis***

25(24) Anterior gut melanophores ~2; myomeres 33–37 ..... ***Icelinus/Chitonotus*** (= not a type, but a category for ambiguous or damaged specimens that may be either *Icelinus* or *Chitonotus*)

Anterior gut melanophores ~10; myomeres 38–40 ..... ***Icelinus*** **type A** (= undescribed; probably *I. tenuis* based on high myomere counts (38–40))

26(23) Jaw angle (quadrate) pigment present ..... ***Icelinus quadriseriatus***

Jaw angle pigment absent ..... ***Icelinus/Chitonotus***

*I have not examined larvae of this type; characters were taken from the literature.

Appendix table

The following larvae have not been described and are probably unknown, which should be taken into consideration when using the key, especially if the larva(e) do not key out exactly.

Taxa	Comments
Artedius corallinus	15–16 dorsal rays; *A.* type 3?; intertidal (see Washington 1986).
Artedius notospilotus	*A.* type 3? (Washington 1986).
Icelinus burchami fuscescens	Rare; found in deep water (126–549 m); 16–18 dorsal rays.
Icelinus cavifrons	X–XI dorsal spines (>98%); IX dorsal spines (<2%).
Icelinus filamentosus	15–18 dorsal rays.
Icelinus fimbriatus	Rare; found at moderate depths (60–265 m); X–XI dorsal spines.
Icelinus oculatus	Rare; found in deep water (109–274 m); X–XI dorsal spines; 37 vertebrae.
Icelinus sp. nov.	X dorsal spines; rare?
Leiocottus hirundo	16–17 dorsal rays; recent occurrence on reefs in Santa Barbara area and Santa Cruz I., California.
Oligocottus rimensis	16–19 dorsal rays; juveniles lack 'W'-shaped pigment on side; intertidal.
Oligocottus rubellio	Juveniles lack 'W'-shaped pigment on side; intertidal.
Psychrolutes phrictus	Rare, found in deep water (839–2800 m), 22–26 pectoral rays; may = "cottoid A" (Richardson and Washington 1980).
Radulinus vinculus	Rare; southern range limit is Anacapa I.
Zesticelus profundorum	Rare; 25–26 vertebrae; deep water (88–2580 m).

Abstract. – To investigate the genetic basis of stock structure of the weakfish *Cynoscion regalis*, a total of 370 individuals was collected from four geographic sites along the mid-Atlantic coast of the United States over a period of 4 years. Restriction fragment length polymorphism (RFLP) analysis of weakfish mitochondrial DNA, employing either 6 or 13 restriction endonucleases, demonstrated a low level of intraspecific mtDNA variation, with a mean nucleotide sequence divergence of 0.13% for the pooled samples. The common mtDNA genotype occurred at a frequency of 0.91–0.96 in all samples, and no significant heterogeneity was found among samples in the occurrence of the common mtDNA genotype or rare variants. The lack of spatial partitioning of rare mtDNA genotypes among collection sites suggests considerable gene flow along the mid-Atlantic coast. Together these data are consistent with the hypothesis that weakfish comprise a single gene pool, and indicate that the fishery should be managed as a single, interdependent unit.

A genetic analysis of weakfish *Cynoscion regalis* stock structure along the mid-Atlantic Coast*

John E. Graves
Jan R. McDowell
Virginia Institute of Marine Science, School of Marine Science
College of William and Mary, Gloucester Point, Virginia 23062

M. Lisa Jones
Department of Biology, College of William and Mary, Williamsburg, Virginia 23185

The weakfish *Cynoscion regalis* is broadly distributed along the Atlantic coast of the United States. It is common from Long Island NY to Cape Canaveral FL, and has occasionally been reported from as far north as Nova Scotia and as far south as the Gulf of Mexico (Bigelow and Schroeder 1953, Weinstein and Yerger 1976). Weakfish abundance varies considerably on both a spatial and temporal basis, especially in the northern part of the species' range (Bigelow and Schroeder 1953).

The life history of the weakfish has been well studied (reviewed in Wilk 1979). Spawning occurs in estuarine and coastal waters from late spring through early fall, with a peak of activity in late May and early June. There appears to be little offshore transport of the early-life-history stages, and young-of-the-year remain in shallow estuarine and coastal waters during their first summer. Like many fishes along the mid-Atlantic coast, weakfish move offshore to overwinter as coastal waters cool during the fall, returning in the spring when inshore temperatures increase.

The seasonal inshore and offshore movements of weakfish could lead to significant mixing of fish from different coastal areas. Tagging studies by Nesbit (1954) showed that a large proportion of weakfish tend to return to the same coastal region in which they were tagged, although many fish were recaptured in areas distant from the original tagging location. The differential size distribution of weakfish along the mid-Atlantic coast is consistent with the hypothesis that mixing of weakfish from different coastal areas occurs. Larger (older) weakfish are more predominant in northern waters during the summer, and the mean size of weakfish tends to decrease as one moves down the Atlantic coast (Wilk and Silverman 1976). Whether this represents an ontogenetic change in seasonal movements or differential survival or growth of fish from different coastal areas is not known.

Weakfish support an important commercial and recreational fishery. Commercial landings over the past 110 years have undergone dramatic fluctuations. Combined commercial and recreational landings were at a recent peak during 1980 at 36,400 metric tons (t) and subsequently dropped to about 19.1 t over a period of 2 years (Vaughan et al. 1991). The total catch has remained fairly constant for the last 8 years, although a significant decline in landings from northern waters has been noted over the period (Vaughan et al. 1991). For example, the combined commercial

Manuscript accepted 4 June 1992.
Fishery Bulletin, U.S. 90:469–475 (1992).

* Contribution 1749 of the Virginia Institute of Marine Science and School of Marine Science, College of William and Mary.

and recreational catch in New York dropped from 840t in 1982, to 224t in 1986, to 10t in 1990 (NMFS Current Fishery Statistics Series). The recreational catch typically represents a sizable fraction of the total landings, and at times surpasses the commercial catch (Wilk 1979).

Many weakfish are lost from the fishery as incidental bycatch in shrimp trawling operations. The incidental weakfish bycatch, which is greatest in the southern part of the species' range, consists mostly of young-of-the-year fish. It is difficult to determine the magnitude of the weakfish bycatch, but it is estimated that it exceeds the combined recreational and commercial catch in the southern states (South Carolina, Georgia and Florida) and may approach 30% of the total coastal fishery for adults (Keiser 1976, Mercer 1983, Vaughan et al. 1991).

The Fishery Management Plan for Weakfish was adopted in 1985 by the Atlantic States Marine Fisheries Commission (Mercer 1985). At that time, the genetic basis of weakfish stock structure was not well understood, and most states have independently managed their weakfish fisheries. As a result, different gear restrictions and minimum sizes are enforced along the mid-Atlantic coast. For example, Florida, Georgia, South Carolina, North Carolina, New Jersey, and Connecticut have no recreational minimum size limit, but a 9-inch size limit is enforced in Virginia, 10 inches in Maryland and Delaware, and 12 inches in New York and Rhode Island.

A thorough understanding of weakfish stock structure is essential for effective management of the fishery. Several management decisions require knowledge of the interdependence of fishery resources from different coastal areas. The recent decline in landings from northern waters has coincided with increased catches of large weakfish in the North Carolina winter offshore (sinknet) fishery (Vaughan et al. 1991), but it is not known if the two fisheries operate on the same stock of fish. On a larger geographic scale, the relationship between bycatch mortality of young weakfish in southern waters and landings of older weakfish in northern waters in subsequent years has not been determined. A detailed genetic analysis of weakfish stock structure would provide information required to test hypotheses of the independence of weakfish from different coastal areas.

Several studies have investigated weakfish stock structure employing a variety of ecological and morphological techniques including mark and recapture data (Nesbit 1954), scale circuli patterns (Perlmutter et al. 1956), morphological characters (Seguin 1960, Scoles 1990), and relative growth rates and reproductive characters (Shepherd and Grimes 1983, 1984). Most of these studies concluded that weakfish comprise two or more stocks; however, the inability to distinguish between ecophenotypic and genetic character variation in these studies has confounded interpretation of the results.

There are few studies on the biochemical genetics of the weakfish. Crawford et al. (1989) analyzed water-soluble protein variation using starch gel electrophoresis. They found no significant genetic differentiation between weakfish collected from Buzzards Bay MA to Cape Hatteras NC, and so were unable to disprove the null hypothesis that weakfish along the mid-Atlantic coast share a common gene pool. Of the 25 protein-encoding loci surveyed in the Crawford et al. (1989) study, only two were polymorphic within the pooled sample, and the mean heterozygosity was low relative to other marine fishes.

Studies of protein variation have been extremely useful in demonstrating the intraspecific genetic structure of many marine fishes (reviewed in Ryman and Utter 1987). For those species which display little intraspecific variation, like the weakfish, sample sizes must be very large to detect significant differentiation between putative stocks, if it exists. In such cases, analysis of a more rapidly evolving set of molecular characters may provide a better estimate of population structure with a more manageable number of samples. Restriction fragment length polymorphism (RFLP) analysis of mitochondrial DNA (mtDNA) has provided such a tool, and the technique has been useful in resolving stock structure within species which exhibit little protein variation (reviewed by Ovenden 1990).

This paper reports the results of an RFLP analysis of weakfish mtDNA to determine if fish along the mid-Atlantic coast share a common gene pool. The study began as a spatial and temporal investigation of a large number of individuals from a few collection sites along the central mid-Atlantic coast with 6 restriction endonucleases. Because there was a high degree of genetic homogeneity among these samples, we expanded the investigation to include an intensive analysis of weakfish from the northern and southern ends of the species' range with 13 restriction endonucleases.

Materials and methods

For our sampling protocol we assumed that if separate genetic stocks of weakfish exist, they should be separated at the time of spawning. We therefore restricted our collections to female weakfish that were ready to spawn as evidenced by high gonadosomatic indices (GSI). For example, the mean GSI of the New York 1988 sample was 7.7% ± 3.1SD.

Ripe, female weakfish were obtained from commercial fishermen, sportfishing tournaments, and the

National Marine Fisheries Service Inshore Trawl Survey. Dates and locations of capture, and the size composition of the collections are presented in Table 1. Freshly-caught weakfish were measured for standard length and then dissected. Ovaries were removed and quickly frozen at −20°C.

Mitochondrial DNA was obtained by the rapid isolation procedure of Chapman and Powers (1984) for the initial survey of mtDNA genetic heterogeneity. After ethanol precipitation, the mtDNA-enriched DNA pellet was rehydrated in 75 μL of distilled water, and the yield from ~7 g of ovarian tissue was usually sufficient for at least 7 restriction digestions visualized with ethidium bromide.

The 1988 and 1989 samples were surveyed with the following six restriction endonucleases: *Ava*I, *Bam*HI, *Bgl*I, *Hind*III, *Nci*I, and *Pvu*II. Restriction fragments were separated by horizontal gel electrophoresis on 0.8–1.5% agarose gels run at 2 v/cm for 16 h. Gels of restriction digestions of isolations containing high yields of mtDNA were visualized after ethidium bromide staining with ultraviolet light illumination (Maniatis et al. 1982) and photographed with a Polaroid CU-5 camera using a Wratten #5 filter. For those samples in which there was not sufficient mtDNA for direct visualization, restriction digestions were endlabeled before electrophoresis with the appropriate ^{35}S nucleotide triphosphate using the Klenow fragment (Maniatis et al. 1982). After electrophoresis, the gels were rinsed with a scintillation enhancer, dried, and autoradiographed at −70°C for 5 d.

To compare the genetic relationship of weakfish from the northern and southern ends of their range in greater detail, mtDNA was purified from ovarian tissues using the CsCl density-gradient centrifugation protocol of Lansman et al. (1981). The mtDNA from these samples was surveyed with the 6 restriction endonucleases listed above and the following 7 enzymes: *Apa*I, *Ava*II, *Ban*I, *Bcl*I, *Eco*RV, *Hinc*II, and *Hha*I. The restriction digestions were endlabeled, separated on agarose gels, and autoradiographed as described above.

The different fragment patterns produced by each restriction endonuclease were each assigned a letter. A composite mtDNA genotype, consisting of the letters representing the fragment patterns generated by each restriction endonuclease, was then constructed for each individual. The nucleon diversity (Nei 1987) was calculated for each sample and for the pooled samples. The percent nucleotide sequence divergence between mtDNA genotypes was estimated by the site approach of Nei and Li (1979) and the percent mean nucleotide sequence divergences within and among weakfish samples were calculated following the method of Nei (1987), with the latter value being corrected for within-group heterogeneity. The distribution of genotypic frequencies was evaluated for homogeneity between collections using the G-test (Sokal and Rohlf 1981).

Table 1
Weakfish *Cynoscion regalis* collection data.

Sample	Location	Date	*N*	Standard length Mean, range (mm)
NY88	Long Island NY	6/88	58	560, 254–750
NY89	Long Island NY	5/89	65	619, 216–750
DE88	Lewes DE	5/88	74	597, 256–761
DE89	Lewes DE	5/89	51	521, 290–744
DE91	Lewes DE	6/91	25	522, 390–670
NC88	Hatteras NC	6/88	72	278, 221–342
SO91	SC, GA, FL	5/91	25	201, 174–273

Table 2
Distribution of weakfish *Cynoscion regalis* mtDNA genotypes based on 6 restriction endonucleases among the different collections. The order of restriction enzyme morphs, represented from left to right, is *Hind*III, *Pvu*II, *Bgl*I, *Bam*HI, *Nci*I, and *Ava*I. Fragment sizes for each restriction pattern are available from the senior author upon request.

	Sample							
Genotype	NY88	NY89	DE88	DE89	DE91	NC88	SO91	Total
AAAAAA	55	60	67	48	22	69	24	345
AAAAAC	0	2	2	0	1	1	0	6
AAAAAB	0	0	2	0	1	0	1	4
AAAAFA	1	0	0	1	0	1	0	3
AAAADA	0	2	0	1	0	0	0	3
ABAAAA	1	1	0	0	0	0	0	2
AAAABA	1	0	1	0	0	0	0	2
AAAACA	0	0	2	0	0	0	0	2
DAAAAB	0	1	0	0	0	0	0	1
AAAAEA	0	0	0	0	0	1	0	1
CAAAAA	0	0	0	0	0	1	0	1
Total	58	66	74	50	24	73	25	370

Results

Weakfish mtDNA demonstrated very little variation. Of the 370 weakfish surveyed with 6 restriction endonucleases, 345 shared a common mtDNA genotype (Table 2). Ten variant genotypes were encountered in

the analysis, distributed among the remaining 25 individuals. In each case, variant genotypes were closely related to the common genotype, differing by no more than two restriction site changes. Restriction site gains or losses were inferred from completely additive changes in fragment patterns. No length polymorphisms or heteroplasmy were observed. A total of 43 restriction sites were detected in the 6-enzyme survey, and the average individual was scored for 29 sites, representing about 1.0% of the weakfish mtDNA genome.

The common mtDNA genotype, AAAAAA, occurred in the great majority of fish in all samples, ranging in frequency from 0.905 (DE88) to 0.960 (DE89, SO91), with a value of 0.932 for the pooled sample (Table 2). The next most-common genotype, AAAAAC, occurred in the pooled sample at a frequency of 0.017, and was present in 4 of the 7 samples. Because of the predominance of a single genotype in all samples, nucleon diversities were relatively low (Table 3), ranging from 0.079 (DE89) to 0.180 (DE88), with a value of 0.130 for the pooled samples. As all variant mtDNA genotypes were related to the common genotype by no more than 2 restriction site changes, the percent mean nucleotide diversity within each sample was also quite low (Table 3), ranging from 0.06 (DE89) to 0.18 (NY89).

Little genetic differentiation was detected among weakfish samples collected at the same location over 2 or more years (Table 4). Among samples collected in Delaware during 1988, 1989, and 1991, and in New York during 1988 and 1989, the percent mean nucleotide sequence divergences, corrected for within-sample variation (Nei 1987), ranged from 0.00 (DE88/DE91, NY88/NY89) to 0.01 (DE89/DE91).

Little genetic differentiation was encountered among samples of weakfish collected along the mid-Atlantic coast. The nucleotide sequence divergences among samples collected at geographically distant sites during the same spawning season ranged from 0.00 (NY88/NC88) to 0.03 (NY89/DE89). These values are of the same magnitude as those found among samples of weakfish collected at the same site over 2 or more years, indicating a lack of spatial genetic structuring.

An analysis of the distribution of mtDNA genotypes also revealed no significant heterogeneity among temporal or spatial collections. To avoid a bias caused by including expected values <1, we initially pooled all alternate genotypes for an analysis of heterogeneity. The results of a G-test (Sokal and Rohlf 1981) revealed no significant spatial or temporal differences in the distribution of the common and pooled rare genotypes among the 7 samples (G_H 2.88, $0.75>p>0.50$). Expanding the analysis to include the common genotype and all 10 rare genotypes separately (each with expected values <1 in one or more collections) did not significantly change the outcome. Once again, the null hypothesis of homogeneity could not be disproved (G_H 51.62, $0.50>p>0.25$).

The low level of variation detected in our analysis of weakfish mtDNA could be the result of many factors. After reviewing the 1988 and 1989 results, we felt that we might have biased our estimates of mean nucleotide sequence divergence by using 6 restriction endonucleases that, by chance, were not variable within weakfish. To test this hypothesis, we analyzed the DE91 and SO91 weakfish collections with an additional 7 restriction endonucleases. The average individual in the 13-enzyme analysis was scored for 65 restriction sites, or approximately 2.4% of the weakfish mtDNA molecule. Of the 49 fish in the two samples surveyed, only one variant mtDNA genotype was found (one fish from the SO91 sample with the common 6-enzyme mtDNA genotype exhibited a site gain relative to the common pattern for the enzyme *Bcl*I). As a result,

Table 3

Genotypic diversity and percent mean nucleotide sequence diversities for 7 weakfish *Cynoscion regalis* collections. Values for both 6 and 13 restriction enzyme surveys are listed for the Delaware (DE) 1991 and southern (SO) 1991 samples.

Sample		Nucleon diversity	Percent mean nucleotide sequence diversity
NY88		0.102	0.09
NY89		0.171	0.18
DE88		0.180	0.15
DE89		0.079	0.06
DE91	(6)	0.163	0.19
	(13)	0.239	0.10
NC88		0.107	0.11
SO91	(6)	0.080	0.09
	(13)	0.080	0.04
Total		0.130	0.13

Table 4

Percent mean nucleotide sequence divergences between weakfish *Cynoscion regalis* collections. Values are based on results from 6 restriction endonucleases and have been corrected for within-group sequence diversity (Nei 1987).

	NY89	DE88	DE89	DE91	NC88	SO91
NY88	0.00	0.00	0.00	0.01	0.00	0.00
NY89	—	0.00	0.03	0.00	0.00	0.00
DE88	—	—	0.00	0.00	0.00	0.00
DE89	—	—	—	0.01	0.02	0.00
DE91	—	—	—	—	0.00	0.00
NC88	—	—	—	—	—	0.00

the nucleon diversity, which is sensitive to the number of enzymes employed, increased for only one of the two samples. The within-sample percent mean nucleotide sequence diversity, which is not as sensitive to the number of restriction sites surveyed, was slightly lower for both samples (Table 4), and the corrected values of percent mean nucleotide sequence divergence between the DE91 and SO91 samples was essentially the same whether based on 6 or 13 informative restriction enzymes.

Discussion

The presence of alleles unique to samples from particular geographic locations has been used to infer intraspecific genetic structuring and to determine levels of gene flow among collection sites (Slatkin 1989). This model assumes that increased frequencies of "private" alleles are a direct result of limited gene flow. An inspection of the above data reveals several genotypes that are present at very low frequencies (Table 2); however, it is interesting to note that most genotypes represented by more than a single individual occur in two or more geographic samples. For example, the genotype AAAAFA was encountered three times in the analysis of 370 weakfish, occurring in the NY88, NC88, and DE89 samples. The lack of spatial partitioning of rare alleles is strongly suggestive of a high rate of gene flow among collection locations.

The level of mtDNA variation found within the weakfish is among the lowest reported for any species of fish. While it is difficult to compare nucleon diversities from different studies because the value is dependent upon the number of restriction sites surveyed, relative levels of variability can be determined from comparisons of studies involving about the same numbers and types of restriction endonucleases. The nucleon diversity of the 1991 weakfish samples surveyed with 13 enzymes was 0.157, a value that falls well below the range of 0.473–0.998 reported by Avise et al. (1989) for other fishes analyzed with about the same number of enzymes. The nucleon diversity of the weakfish was also substantially below the mean value of 0.943 reported for the red drum *Sciaenops ocellatus* (Gold and Richardson 1991). Relatively low values of nucleon diversity have been found for the black drum *Pogonias cromis* (0.584) and the spotted seatrout *Cynoscion nebulosus* (0.531), a congener of the weakfish (C. Furman and J.R. Gold, Texas A&M Univ., College Station, pers. commun., Aug. 1991). However, these values are still substantially larger than those we found for the weakfish. Comparisons of nucleotide sequence diversities among these species also indicate that the weakfish is relatively depauperate in terms of mtDNA variation. The mean percent nucleotide sequence diversities within 7 black drum samples (0.142) and 5 spotted seatrout samples (0.222) are substantially higher than that within the 7 weakfish samples (0.10) surveyed in this study.

The finding of relatively low levels of mtDNA variation within the weakfish is consistent with the lack of allozyme variation reported by Crawford et al. (1989). Low levels of mtDNA variation have generally been attributed to small effective population sizes of females, resulting in relatively rapid sorting of gene trees (Nei 1987, Avise et al. 1988, Chapman 1990, Bowen and Avise 1990). Variations in weakfish abundance over the last 110 years have been reflected in commercial catches, which have fluctuated from a high of 44.5 million pounds in 1908 to a low of 3.1 million pounds in 1967 (Vaughan et al. 1991), but it is unlikely that such variations over recent history have drastically reduced the effective population size of female weakfish. Population bottlenecks on a larger time-scale (e.g., glaciation events) or cyclical fluctuations in population size may have resulted in the reduced genetic diversity within the weakfish, but such explanations are merely speculative and do not necessarily agree with the observation that other sciaenids with similar distributions and life histories do not exhibit such low levels of mtDNA diversity.

Reductions in effective population size can also occur due to differential reproductive contribution, resulting from skewed sex ratios, limited mating opportunities, or varying of survival among progeny. While little is known of weakfish spawning behavior or differential recruitment success, the sex ratio tends to be very close to 1.0 (Wilk 1979). Thus, the cause or causes contributing to the low genetic variation observed among weakfish relative to other fishes is problematic.

In addition to low levels of within-sample variation, we detected little temporal or spatial genetic differentiation among weakfish samples. Because there were few variant mtDNA genotypes, and almost all of the rare variant genotypes occurred in more than one population, the uncorrected mean nucleotide sequence divergences among weakfish samples were of the same magnitude as mean nucleotide diversities found within samples. Thus, the mean difference among mtDNA genotypes randomly drawn from within a single sample was equivalent to the mean difference among mtDNA genotypes drawn from different samples.

Low levels of within-group mtDNA variation do not preclude the occurrence of significant between-group differentiation. Bowen and Avise (1990) recently reported low values of mtDNA diversity within samples of Atlantic and Gulf of Mexico black sea bass *Centropristis striata* (within-sample percent nucleotide sequence diversity of 0.03), yet their study revealed

significant differentiation between the two populations (an uncorrected percent mean sequence divergence of 0.75). The lack of significant population structuring within the weakfish relative to the black sea bass is evidenced in a comparison of the ratio of between-group to within-group sequence divergences: For the black sea bass the ratio is 24, while for the weakfish it is ~1.

The results of our investigation suggest that weakfish comprise a single genetic stock throughout the species' range. No significant genetic differentiation was found among geographic samples or among samples taken at the same site over several years. Consequently, at the level of genetic resolution we employed, we cannot disprove the null hypothesis that weakfish share a common gene pool. The inference that gene flow occurs throughout the species' range is supported by the homogeneous distribution of rare mtDNA genotypes.

The genetic homogeneity found within the weakfish in this study and in the allozyme analysis of Crawford et al. (1989) contrast with the geographical variation of morphological and life-history characters reported in other studies (Perlmutter et al. 1956, Seguin 1960, Shepherd and Grimes 1983 and 1984, Scoles 1990). The degree of plasticity of weakfish morphological and life-history characters to different environmental conditions has not been determined, but in light of research on other fishes (Barlow 1961), it would not be surprising if much of the geographic variation previously described among weakfish is ecophenotypic.

Our inference that there is sufficient gene flow among weakfish along the mid-Atlantic coast to prevent even minor genetic differentiation from occurring has several management implications. There is clearly some interdependence among areas, a conclusion also supported by the tagging data of Nesbit (1954). To obtain a meaningful estimate of the magnitude of the interdependence between these areas would require a tagging study much more extensive than that of Nesbit (1954), which would involve considerable time and expense. Until such information is available, it would be best to manage the weakfish resource conservatively, as a single interdependent stock.

Acknowledgments

This study would not have been completed without the assistance of several individuals along the mid-Atlantic coast. The perseverance and efforts of all those who collected weakfish samples are gratefully acknowledged, especially Alice Webber, New York Department of Environmental Conservation; Rich Seagraves, Delaware Division of Fish and Wildlife; and Charlie Wenner, South Carolina Wildlife and Marine Resources. A portion of this project was initiated by Herb Austin and Brian Meehan, Virginia Institute of Marine Science. Ana Beardsley provided technical assistance. Carol Furman and John Gold kindly shared unpublished data. Dan Scoles, Herb Austin, and Mark Chittenden critically read the manuscript. Funding for this study was provided by the Atlantic States Marine Fisheries Commission (88-1WSID), the U.S. Fish and Wildlife Service (F-60-R), and the Commonwealth of Virginia. M. Lisa Jones was supported by a Howard Hughes Summer Fellowship in Molecular Biology.

Citations

Avise, J.C., R.M. Ball, and J. Arnold
1988 Current versus historical population sizes in vertebrate species with high gene flow: A comparison based on mitochondrial DNA lineages and inbreeding theory for neutral mutations. Mol. Biol. Evol. 5:331–344.

Avise, J.C., B.W. Bowen, and T. Lamb
1989 DNA fingerprints from hypervariable mitochondrial genotypes. Mol. Biol. Evol. 6:258–269.

Barlow, G.W.
1961 Causes and significance of morphological variation in fishes. Syst. Zool. 10:105–117.

Bigelow, H., and W. Schroeder
1953 Fishes of the Gulf of Maine. U.S. Fish Wildl. Serv., Fish. Bull. 53, 577 p.

Bowen, B.W., and J.C. Avise
1990 Genetic structure of Atlantic and Gulf of Mexico populations of sea bass, menhaden, and sturgeon: Influence of zoogeographic factors and life-history patterns. Mar. Biol. (Berl.) 107:371–381.

Chapman, R.W.
1990 Mitochondrial DNA analysis of striped bass populations in Chesapeake Bay. Copeia 1990:355–366.

Chapman, R.W., and D.A. Powers
1984 A method for the rapid isolation of mitochondrial DNA from fishes. Tech. Rep. UM-SG-TS-84-01, Maryland Sea Grant Prog., Univ. Md., College Park, 11 p.

Crawford, M.K., C.B. Grimes, and N.W. Buroker
1989 Stock identification of weakfish, *Cynoscion regalis*, in the middle Atlantic region. Fish. Bull., U.S. 87:205–211.

Gold, J.R., and L.R. Richardson
1991 Genetic studies in marine fishes. IV. An analysis of population structure in the red drum (*Sciaenops ocellatus*) using mitochondrial DNA. Fish. Res. (Amst.) 12:213–241.

Keiser, R.K. Jr.
1976 Species composition, magnitude and utilization of the incidental catch of the South Carolina shrimp fishery. Tech. Rep. 16, S.C. Mar. Resour. Cent., Charleston, 94 p.

Lansman, R.A., R.O. Shade, C.F. Shapira, and J.C. Avise
1981 The use of restriction endonucleases to measure mitochondrial DNA sequence relatedness in natural populations. III. Techniques and potential applications. J. Mol. Evol. 17:214–226.

Maniatis, T., I.F. Fritsch, and J. Sambrook
1982 Molecular cloning: A laboratory manual. Cold Spring Harbor Lab., Cold Spring Harbor NY, 545 p.

Mercer, L.P.
1983 A biological and fisheries profile of weakfish, *Cynoscion regalis*. Spec. Sci. Rep. 39, N.C. Dep. Nat. Resour. & Community Dev., Div. Mar. Fish., 107 p.
1985 Fishery management plan for the weakfish (*Cynoscion regalis*) fishery. Spec. Sci. Rep. 46, N.C. Dep. Nat. Resour. & Community Dev., Div. Mar. Fish. Fish. Manage. Rep. 7, Atl. States Mar. Fish. Comm., 129 p.

Nei, M.
1987 Molecular evolutionary genetics. Columbia Univ. Press, NY, 512 p.

Nei, M., and W-H. Li
1979 Mathematical model for studying genetic variation in terms of restriction endonucleases. Proc. Natl. Acad. Sci. 76:5269–5273.

Nesbit, R.A.
1954 Weakfish migration in relation to its conservation. U.S. Fish Wildl. Serv., Spec. Sci. Rep. Fish. 115, 81 p.

Ovenden, J.R.
1990 Mitochondrial DNA and marine stock assessment: A review. Aust. J. Mar. Freshwater Res. 41:835–53.

Perlmutter, A., S.W. Miller, and J.C. Poole
1956 The weakfish (*Cynoscion regalis*) in New York waters. N.Y. Fish Game 3:1–43.

Ryman, N., and F. Utter (editors)
1987 Population genetics and fishery management. Univ. Wash. Press, Seattle, 420 p.

Scoles, D.
1990 Stock identification of weakfish, *Cynoscion regalis*, by discriminant function analysis of morphometric characteristics. Masters thesis, College of William & Mary, Williamsburg, 51 p.

Seguin, R.
1960 Variation in the Middle Atlantic coast population of the grey squeteague, *Cynoscion regalis* (Bloch and Schneider), 1801. Ph.D. diss., Univ. Delaware, Newark, 70 p.

Shepherd, G.R., and C.B. Grimes
1983 Geographic and historic variations in growth of weakfish, *Cynoscion regalis*, in the middle Atlantic Bight. Fish. Bull., U.S. 81:803–813.
1984 Reproduction of weakfish, *Cynoscion regalis*, in the New York Bight and evidence for geographically specific life history characteristics. Fish. Bull., U.S. 82:501–511.

Slatkin, M.
1989 Gene flow and the geographic structure of natural populations. Science (Wash. DC) 236:787–792.

Sokal, R.R., and F.J. Rohlf
1981 Biometry. W.H. Freeman, NY.

Vaughan, D.S., R.J. Seagraves, and K. West
1991 An assessment of the Atlantic weakfish stock, 1982–1988. Atl. States Mar. Fish. Comm. Spec. Rep. 21, Wash. DC, 29 p. + tables.

Weinstein, M.P., and R.W. Yerger
1976 Protein taxonomy of the Gulf of Mexico and Atlantic Ocean seatrouts, genus *Cynoscion*. Fish. Bull., U.S. 74: 599–607.

Wilk, S.J.
1979 Biological and fisheries data of weakfish, *Cynoscion regalis* (Bloch and Schneider). NOAA Tech. Ser. Rep. 21, NMFS Sandy Hook Lab., Highlands NJ, 49 p.

Wilk, S.J., and M.J. Silverman
1976 Fish and hydrographic collections made by the research vessels *Dolphin* and *Delaware II* during 1968–1972 from New York to Florida. NOAA Tech. Rep. NMFS SSRF-697, 159 p.

Abstract. – Five submersible dives were conducted to evaluate the behavior of deepwater shrimp and the relationship of their density to bottom type and trap yield. Differences in behavior of two species of *Heterocarpus* were observed: *H. ensifer* tended to group around large anemones and other benthic relief over otherwise flat, sandy bottom and were very active in the presence of a baited container; whereas *H. laevigatus* were solitary and showed little activity around a baited container. Greater densities of *H. laevigatus* were observed on volcanic than on coralline substrate, indicating a possible association with this bottom type. Trap catches were regressed against observed *H. laevigatus* densities yielding an estimate of the catchability coefficient. This coefficient differed from that obtained from a previously conducted Leslie model depletion study. Factors contributing to this difference may include comparing estimates of catchability based on data from different areas, bias in the estimate of catchability based on observed density, and bias in the estimate of catchability from the depletion study. A combined fishing and visual census study is suggested as the best assessment technique.

An assessment of the exploitable biomass of *Heterocarpus laevigatus* in the main Hawaiian Islands. Part 2: Observations from a submersible

Robert B. Moffitt
Frank A. Parrish

Honolulu Laboratory, Southwest Fisheries Science Center
National Marine Fisheries Service, NOAA
2570 Dole Street, Honolulu, Hawaii 96822-2396

Tropical deepwater pandalid shrimp have potential for commercial harvesting in many areas of the Pacific (Struhsaker and Aasted 1974, Wilder 1977, Moffitt 1983, King 1984, Tagami and Barrows 1988). These shrimp are readily trapped but not easily trawled (Struhsaker and Aasted 1974). The largest and most commercially desirable species in Hawaii is *Heterocarpus laevigatus* (Tagami and Barrows 1988); the smaller *H. ensifer* has less commercial appeal but is also abundant (Struhsaker and Aasted 1974). In the early 1980s, several boats initiated a trap fishery targeting *H. laevigatus*, and landings rose to a high of 159 metric tons (t) in 1984 (HDLNR 1986). By 1985, most vessels left the fishery, and the annual landings dropped to <6 t/yr (West. Pac. Fish. Inf. Network, NMFS Honolulu Lab., unpubl. data).

Early predictions of maximum sustainable yield for Hawaiian shrimp, based on little or no direct data, were as much as 1000–2000 t/yr (Struhsaker and Aasted 1974, HDLNR 1979). Recent research on population dynamics combined with systematic trapping surveys has resulted in more refined estimates of exploitable biomass and maximum sustainable yield for *H. laevigatus* in various island locations (Dailey and Ralston 1986, Ralston 1986, Moffitt and Polovina 1987, Ralston and Tagami 1992). The most recent estimate of exploitable biomass for the main Hawaiian Islands, 271–1050 t, is based on an estimate of the catchability coefficient (q) obtained through a Leslie model depletion study, coupled with catch-per-unit-effort (CPUE) values and habitat area estimates obtained through systematic trapping (Ralston and Tagami 1992).

The relationship of observed target-species density to fishing-gear CPUE has been used to estimate stock biomass and catchability (Ralston et al. 1986, Kulbicki 1988). Estimates of abundance obtained through visual census techniques are generally higher than those based on catches of fishing gear, and the relative reliability of the various assessment methods must be analyzed on a case-by-case basis (Uzmann et al. 1977, Powles and Barans 1980, Kulbicki and Wantiez 1990, Matlock et al. 1991).

In the present study, we conducted submersible dives at several sites in the Hawaiian Islands to observe shrimp behavior both away from and in the vicinity of a baited container and to record density and substrate associations of *H. laevigatus*. Observations of shrimp behavior and substrate associations have applications to commercial fishermen in terms of

Manuscript accepted 26 May 1992.
Fishery Bulletin, U.S. 90:476–482 (1992).

trapping technique and site selection. The mean of observed densities recorded during submersible dives is regressed against yields of a trap set at the dive sites to obtain an estimate of q, and this value is compared with that reported by Ralston and Tagami (1992). An accurate estimate of catchability is important in order to better estimate exploitable biomass for management purposes.

Methods

A total of five submersible dives were conducted in the main Hawaiian Islands, at two sites off leeward Oahu in February 1988 and three sites off the Kona coast of the Island of Hawaii in August 1988 (Table 1). The Oahu sites were selected for their proximity to port and because of previously-observed concentrations in the area of unidentified red shrimp at appropriate depths (400–900 m) for *Heterocarpus*. The three Kona sites were selected as extremes in *H. laevigatus* yield for the area during a trapping survey using pyramid traps conducted in March 1988 (see Tagami and Barrows (1988) and Ralston and Tagami (1992) for trap description and trapping methods). Catches of *H. laevigatus* were lowest for the Kona area (<1 kg/trap-night) at one of the sites and highest (>10 kg/trap-night) at the remaining two sites.

Table 1
Locations of five study sites off the islands of Oahu and Hawaii and 1988 sampling dates.

Site no.	Location	Dive date	Trap date
Oahu			
1	21°19.3′N, 158°10.1′W	8 Feb.	13 Mar.
2	21°31.0′N, 158°16.8′W	9 Feb.	13 Mar.
Kona			
1	19°14.0′N, 155°54.9′W	23 Aug.	18 Mar.
2	19°20.7′N, 155°54.2′W	24 Aug.	18 Mar.
3	19°47.5′N, 156°07.8′W	25 Aug.	15 Mar.

Visual censuses

All dives used the *Pisces V*, a three-man submersible that allowed simultaneous observations by two researchers through separate view ports with non-overlapping fields of view directed diagonally forward and down. A video camera continuously recorded the bottom throughout each dive as well. The same two researchers estimated shrimp abundance on all dives and independently reviewed the dive video tapes as a check on observer bias. On each survey, the submersible descended to depths of 480–920 m, then traveled to an arbitrary starting location at ~600–750 m depth. At this point, a baited container was placed on the bottom and observations of shrimp behavior in the presence of bait were recorded. After observing shrimp behavior for ~15 min, the submersible traveled a haphazard, rectangular track at a speed of ~2 knots along the contours within the zone of maximum shrimp abundance (defined below), returning to the baited container for retrieval at the end of the dive. At preselected time-intervals (5 or 10 min), the submersible settled to the bottom and counts of shrimp were taken by each observer in an independent quadrant filling the field of view. The estimated area of each quadrant was 10 m^2, which was calibrated by underwater observation of known dimensions with the submersible attached to its launch-and-retrieval vehicle. The minimum distance between observation sites was ~100 m. The number of observations of shrimp density varied between dives, for bottom time was dependent on battery power.

Bottom depth, temperature, and substrate type were recorded with each shrimp count. The substrate within each quadrant was categorized by composition and particle size of the major component. Substrate composition included coralline, volcanic, and mixed; particle size included sand, rock both small (~<15 cm diameter) and large (>15 cm diameter), and pavement.

A χ^2 goodness-of-fit test using a Poisson distribution for the expected frequencies was conducted to determine whether *H. laevigatus* were concentrated or evenly distributed over the bottom at each dive site. Mean *H. laevigatus* density and 95% CI was calculated for each dive site based on a Poisson distribution,

$$CL = D_{(i)} \pm (1.96)\left(\frac{(D_{(i)})}{n_{(i)}}\right)^{1/2},$$

where $D_{(i)}$ and $n_{(i)}$ are the mean density and number of observations for each dive site. Expected density values (De) for each site were calculated using trap landings for the site and the normalized catchability coefficient (q) reported by Ralston and Tagami (1992), using the following formula:

$$De_{(i)} = \frac{CPUE_{(i)}}{q}.$$

Confidence limits for the expected density values for each site could not be calculated, since variance cannot be computed for CPUE, based as it is on the catch of a single trap.

An analysis of variance (ANOVA) was performed to determine whether higher mean densities of *H. laevi-*

gatus could be attributed to different dive sites or bottom types and to determine whether there was observer bias. Independent variables for the ANOVA were dive site, substrate material, substrate particle size, and observer.

Comparisons of trap landings and density estimates

Trap catch rates were obtained in March 1988 from one pyramid shrimp trap set at each of the five dive sites and allowed to soak overnight (see Ralston and Tagami (1992) for details). Trap catches of *H. laevigatus* were regressed against mean densities obtained from visual counts for the five study sites, fitting a linear model with a zero intercept. The slope of this regression is an estimate of q, which was compared with that reported by Ralston and Tagami (1992).

Results

A total of 923 shrimp were captured in the 5 pyramid traps set at the study sites. Of these, 705 (76%) were *H. laevigatus* (Table 2), 217 were *H. ensifer*, and 1 was *Acanthephyra eximia*. During the scheduled observation periods on the submersible dives, a total of 494 shrimp were observed (194 total quadrant observations). Of these, only 95 (19%) were *H. laevigatus*, and the remainder consisted primarily of *Plesionika* sp., tentatively identified as *P. ensis*, and a few individuals of *P. alcocki*, *H. ensifer*, *A. eximia*, and *Gnathophausia longispina*. All *H. laevigatus* observed from the submersible appeared well within the size range of those captured in the traps, indicating that both stock assessment methods sample the same population.

Visual censuses

During our dives, the shrimp showed little reaction to the presence of the submersible or its lights. When the submersible came within a few inches of the shrimp, they swam a short distance avoiding collision. When the photoflash was used, the shrimp within a few feet of the submersible started, darting a distance of 1–4 cm. No other reactions to the submersible or its lights were observed. Several behavioral differences were noted between the various species observed.

A total of 94% (89 of 95) of the *H. laevigatus* observed during census periods were seen between 550 and 675 m, the depth range herein defined as the zone of maximum abundance. Individuals of *H. laevigatus* were observed at each dive site, but not necessarily during the scheduled census periods conducted within the zone of maximum abundance. Only counts taken within this depth range were used in the analysis.

Table 2

Trap catches, predicted densities, and mean observed densities with 95% CL of *Heterocarpus laevigatus* at five study sites off the islands of Oahu and Hawaii in 1988. N = the number of observations.

Dive site	Trap catch (*n*/trap)	Density (*n*/ha)		CL	N
		Predicted	Observed		
Oahu					
1	5	0.53	0	–	34
2	26	2.7	0	–	8
Kona					
1	0	0	200	(−680)–1080	10
2	376	40	1360	(−570)–3290	14
3	298	31	890	220–1560	76

Heterocarpus laevigatus were observed as solitary individuals on the bottom, usually stationary but occasionally walking, and rarely swimming near the bottom. They showed little activity in the presence of a baited container and were not observed crawling over or entering it. Conversely, *H. ensifer* were found in groups near relief features (e.g., large sea anemones) at shallower (450–550 m) depths, either stationary on the bottom or swimming about 1 m above the bottom. They were very active in the presence of a baited container, aggregating quickly and crawling over and entering the container through the mesh and other holes. *Plesionika alcocki* usually were seen on the bottom, whereas *P. ensis* generally were seen hanging motionless in the water column ~1–2 m off the bottom. Each showed some activity around the baited container. *Acanthephyra eximia* and *G. longispina* were observed swimming 1–2 m off the bottom, but were not seen at the baited container.

Bottom temperature varied during the dives from a low of 3.9°C at 920 m to a high of 6.0°C at 480 m. The temperature range within the zone of maximum *H. laevigatus* abundance was 4.8–5.9°C.

Bottom type varied considerably among the sites. The bottom at the two Oahu sites was classified as coralline sand making up an even, featureless plain with a gradual (<20°) slope. The bottom at the three Kona coast sites was much steeper, generally about a 35–45° slope, but with some sections near vertical or even slightly undercut at the Kona site 3. At Kona site 1, the bottom was nearly uniformly composed of small (5–10 cm diameter), sharp-edged volcanic rocks and very little coralline material. Kona site 2 differed from site 1 in that the small volcanic rocks were more weathered and the substrate had a greater coralline component. Kona site 3 had many sandy areas, at

Table 3

Analysis of variance for *Heterocarpus laevigatus* density by dive, bottom type, and observer.

Source	df	SS	MS	F	*P*
Dive	4	31.25	7.81	6.87	0.0001
Substrate material	2	24.53	12.26	10.79	0.0001
particle size	3	5.96	2.98	2.62	0.0765
Observer	1	3.40	3.40	2.99	0.0859
Error	132	150.08	1.14	—	—
Corrected total	141	215.22	—	—	—

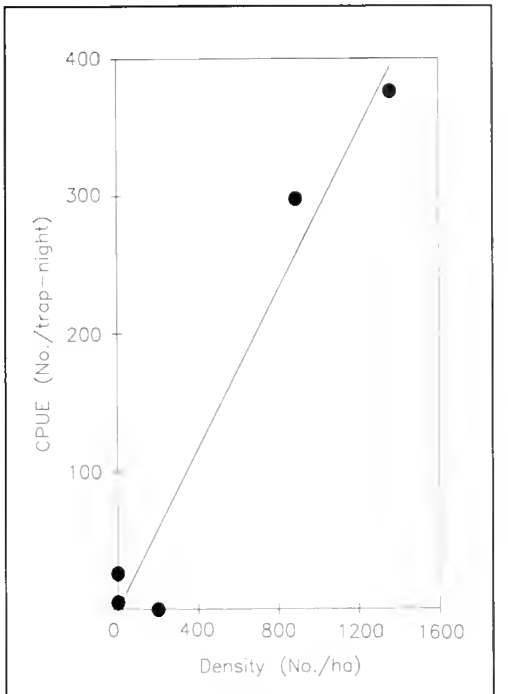

Figure 1

Regression of trap catch per unit effort (CPUE; number per trap-night) and observed density of *Heterocarpus laevigatus* (number/hectare) at five sites in the Hawaiian Islands.

times covering the entire $10\,m^2$ quadrant, as well as areas of exposed limestone often forming undercut cliffs, and areas of small weathered volcanic rocks.

The distribution of *H. laevigatus* over the bottom was evaluated in several ways. No significant values were found for the χ^2 goodness-of-fit tests ($P>0.10$) of the density observations recorded at each dive site, suggesting that the shrimp were randomly distributed (in a Poisson manner) instead of clumped at each dive site. The mean and confidence intervals of *H. laevigatus* density observed at each dive site are presented in Table 2. Pooling data from all dive sites for the independent variables (dive site, substrate material, substrate particle size, and observer), only dive site and substrate material were significantly correlated with shrimp density (ANOVA, $P<0.05$; Table 3). The distribution of residuals did not differ significantly from a normal distribution. Independent review of the dive video by each observer yielded complete agreement on *H. laevigatus* counts and substrate classification, indicating a lack of observer bias in shrimp density estimation and substrate associations.

Comparisons of trap landings and density estimates

Mean observed densities were regressed on trap catches for each dive site (Fig. 1) (r^2 0.97, P 0.0003). The least-squares regression equation is

$$CPUE_i = 0.2896\ (D_i), \qquad (SE\ 0.02364).$$

An estimate of catchability is obtained directly from the value of the slope (0.2896ha/trap-night) with a confidence interval calculated as 0.2144–0.3648/trap-night. This estimate of catchability is <1/30th that reported by Ralston and Tagami (1992) and is reflected in the differences between observed and expected *H. laevigatus* densities for Kona sites 2 and 3 (Table 2).

Discussion

Differences in behavior between *H. laevigatus* and *H. ensifer*, the two species with greatest commercial potential, may lead to some practical applications for fishermen. The high activity level noted for *H. ensifer* in the presence of a baited container has also been reported by Gooding et al. (1988) and Saunders and Hastie (1989). The rapid attraction and entry of this species into traps, even during daylight hours, indicate that a short soak time may be adequate for commercial harvesting. The lower activity level of *H. laevigatus* observed in our study and reported by Saunders and Hastie (1989) may indicate that a longer soak time is more appropriate for this species. If so, a small vessel with a limited number of traps could maximize total catch by making two short sets during daylight hours on *H. ensifer* grounds, followed by an overnight set on *H. laevigatus* grounds, assuming that suitable concentrations of both species are present within a reasonable proximity.

Previous observations of *H. ensifer* from a submersible found higher densities on flat, silty, sandy areas than over low-relief, rocky outcroppings (Gooding et al. 1988). Although statistical analysis of substrate associations were not conducted for *H. ensifer* in this study, we did observe a similar substrate association. *Heterocarpus ensifer* were abundant at the Oahu dive sites at depths (500–800 m), although this is deeper than their reported optimum range of 300–600 m (Gooding 1984). The substrate on these two dives was flat, coralline sand with few isolated, low-profile features (e.g., sea anemones, small rocks) around which the shrimp appeared to concentrate. No rocky outcroppings were observed on these dives. Very few *H. ensifer* were observed at the three Kona dive sites, where the bottom was steep and composed largely of rocky rubble with few sandy patches, though the dive depths again were deeper than the optimum range for this species.

The substrate associations of *H. laevigatus* appeared to differ from those of *H. ensifer*. Although the differences in substrate particle size were not significant, the ANOVA test revealed significantly higher densities on volcanic compared with coralline substrates (Table 3) with data from all dive sites pooled. The significant results for substrate type, however, must be viewed with caution because of the significance of dive site to *H. laevigatus* density and the unbalanced sample design. Not only were all substrate types not present on a single dive, but those types present were not found in equal proportions on any dive. Therefore, differences in density attributed to substrate type may actually be a reflection of differences related by some other factor to dive site. In particular, the Kona dive sites were largely volcanic, and the majority of the *H. laevigatus* observed were from Kona sites 2 and 3. Although Kona site 1 also was largely volcanic, the volcanic rocks differed from those observed at sites 2 and 3, in that the appearance was of a more recent rock slide (sharper edges vs. weathered). This apparent instability may be responsible for the low shrimp density observed at site 1. Other aspects of the bottom, such as slope, substrate complexity, stability, and current patterns may be of considerable importance and should be investigated in future work on the substrate associations of *H. laevigatus*.

With visual censusing techniques, there is always a concern regarding the reliability of abundance estimates. Various factors, including sampling techniques, species behavior, and physical conditions, can bias results (Colton and Alevizon 1981, Sale and Douglas 1981, Brock 1982, Ralston et al. 1986, Matlock et al. 1991). Some authors believe that density estimates based on direct visual surveys, though often much higher, are more reliable than those estimated from fishing gear catches (Uzmann et al. 1977, Powles and Barans 1980, Kulbicki and Wantiez 1990). Individuals of the target species, *H. laevigatus*, were easily counted because they were in the open and reacted almost with indifference to the presence of the submersible, and because the low, uncomplicated relief at the study sites offered little opportunity for their concealment. Avoidance of the submersible by the shrimp seems unlikely. Observed densities were much greater than expected, yet these would be underestimates if avoidance occurred. We cannot discount the possibility of bias in our density estimates caused by attraction of shrimp to the baited container placed at the beginning of our dives. However, we observed no increased density gradient in the vicinity of the container, and density observations were taken well away from the container site (>100 m), presumably outside the drawing range of the bait, leading us to believe that bias due to this source was small.

Recalculation of exploitable biomass for the main Hawaiian Islands using Ralston and Tagami (1992) data and methods, but substituting the q value obtained in this study, would lead to a 33-fold increase in the estimate of exploitable biomass (~9000 t instead of 271 t). Just as Ralston and Tagami (1992) suggest that their estimate may be too low, we suggest that 9000 t may be unreasonably high, considering the preliminary nature of this estimate and the failure of the Hawaiian fishery that was at least partly due to drops in catch rates at annual yields of <200 t (Tagami and Barrows 1988). The acceptance of either of these estimates would drastically affect management decisions, and careful evaluation of these two values must be made. Contributions to the difference between the two estimates may be from three sources: actual differences in catchability for the two studies related to differences in time and study locations, error in our estimate of q, and error in the Ralston and Tagami (1992) estimate.

The estimation of q can be influenced by a variety of factors including currents, water turbidity and temperature, type of bait, soak time of fishing gear, and density of the target species (Morgan 1974, Richards and Schnute 1986, Miller 1990). For the two studies involved in this discussion, many of the potential sources of error were standardized. Both studies used the same traps, same bait, and same soak times. They did not, however, conduct studies at the same location or time, and the range of catch rates encountered differed for the two studies. In both studies it is assumed that catchability is constant for all catch rates and densities involved, but this may not be true, particularly between studies. Unfortunately, we are unable to evaluate the extent of the error involved from these sources.

The estimate of q presented in this study could also be biased. Sources of potential bias include lack of

representative catch rates for study sites, error in density estimation, incompatibility of CPUE and density estimates collected at different points in time, and the few data pairs involved. Not only were shrimp catches for each dive site based on a single trap-night of effort, but also traps generally were set at depths greater than the observed range of maximum abundance determined from our submersible observations (~750 m vs. 550–675 m). This results in no estimate of error for CPUE estimates at each site and no way to determine whether the traps were set within the range of maximum shrimp abundance at the time of trapping. If the traps were not set within this zone, yields at our sites may underrepresent relative shrimp abundance, leading to a lower-than-actual estimate of q. Another potential source of error in our q estimate is the accuracy of our density estimate. Confidence limits on our density estimates are quite broad, allowing for a fair degree of error. At many dive sites this problem is related to the few observations of density taken within the zone of maximum abundance. Additional problems in density estimation associated with the presence of bait in the water during the dives have already been addressed. The question of compatibility between data pairs of density estimates and CPUE values obtained at different points in time stems from possible changes in density or in q over time. Although trap catch rates in the Mariana Archipelago did not vary significantly on a seasonal basis (Polovina et al. 1985), suggesting that q does not vary seasonally, *H. laevigatus* may undergo temporal changes in depth range on either a diurnal or seasonal basis (King 1984, Dailey and Ralston 1986). If such movements do occur (the evidence is not strong) and depth range expands or contracts during these changes, densities observed during midday periods in February and August may differ from those occurring during trapping in March. Finally, although the fit is quite good, our estimate of q is based on only five data pairs covering limited values of CPUE and density.

The potential error in the Ralston and Tagami (1992) q estimate depends on the appropriateness of using their habitat area estimate in normalizing q and the validity of the assumption of constant catchability for all members of the population. These error sources are not necessarily greater than those discussed above, but are much easier to quantify. Even when an accurate estimate of biomass is obtained for a study site, calculation of a normalized q is dependent on the estimated habitat area of the study site. Estimated habitat area is apt to be larger when depth range is estimated from trap catches, as opposed to visual surveys, because of the ability of the traps to draw shrimp outside of their normal depth range. Recalculating the habitat area of the Ralston and Tagami study site using the observed depth range (550–675 m) instead of the reported range (420–640 m) results in a reduction in area to 63% of the original value (748 ha instead of 1187 ha). Normalizing q with this reduced study-site area estimate gives an adjusted q value of 5.999 ha/trap-night (CI 2.6709–9.3271 ha/trap-night. The ratio of this adjusted value to the q obtained in the present study is 20.7 instead of the original 32.7. Ralston and Tagami (1992) discuss the effect on their q value of a large portion of the population not being susceptible to trap capture for the duration of the study period. They supply evidence that their original estimate of catchability may have been four times too high, resulting in a four-fold underestimation of exploitable biomass. Other authors have reported similar overestimates of catchability resulting from depletion studies (Morgan 1974, Morrissy 1975, Miller 1990). A further four-fold reduction of the Ralston and Tagami q value results in a ratio of 5.9 relative to our q value and only 1.8 for the extremes of the 95% CL (the minimum value for the Ralston and Tagami confidence interval compared with our maximum value). Coupling these quantifiable factors with the non-quantifiable factors discussed above could bring the two estimates of catchability into agreement.

Because of the importance of accurate estimates of exploitable biomass to the management process, it would be desirable to conduct a combined technique survey of the *H. laevigatus* resource. This should include direct visual density estimation with a trapping study conducted at the same time and place to obtain a reliable estimate of catchability and thereby exploitable biomass. Until that time, the expanded exploitable biomass estimate (1050 t) for the main Hawaiian Islands as presented by Ralston and Tagami (1992) should be accepted for management purposes as a reasonable, conservative approximation.

Acknowledgments

We would like to thank the staff of the Hawaii Undersea Research Laboratory for their support during the field portion of this study. We have also appreciated the comments and suggestions made by various reviewers, including M.G. King, S. Ralston, W.B. Saunders, M.P. Seki, and D.T. Tagami, which have helped to form this paper.

Citations

Brock, R.E.
1982 A critique of the visual census method for assessing coral reef fish populations. Bull. Mar. Sci. 32:269–276.

Colton, D.E., and W.S. Alevizon
1981 Diurnal variability in a fish assemblage of a Bahamian coral reef. Environ. Biol. Fishes 6:341–345.

Dailey, M.D., and S. Ralston
1986 Aspects of the reproductive biology, spatial distribution, growth, and mortality of the deepwater caridean shrimp, *Heterocarpus laevigatus* in Hawaii. Fish. Bull., U.S. 84: 915–925.

Gooding, R.M.
1984 Trapping surveys for the deepwater caridean shrimps, *Heterocarpus laevigatus* and *H. ensifer*, in the Northwestern Hawaiian Islands. Mar. Fish. Rev. 46(2):18–26.

Gooding, R.M., J.J. Polovina, and M.D. Dailey
1988 Observations of deepwater shrimp, *Heterocarpus ensifer*, from a submersible off the island of Hawaii. Mar. Fish. Rev. 50(1):32–39.

HDLNR (Hawaii Department of Land and Natural Resources)
1979 Hawaii fisheries development plan. Dep Land Nat. Resour., State of Hawaii, Honolulu, 297 p.
1986 Hawaii fisheries plan, 1985. Div. Aquat. Resour., Dep. Land Nat. Resour., State of Hawaii, Honolulu, 163 p.

King, M.G.
1984 The species and depth distribution of deepwater caridean shrimps (Decapoda, Caridea) near some Southwest Pacific islands. Crustaceana 47:174–191.

Kulbicki, M.
1988 Correlation between catch data from bottom longlines and fish censures in the SW lagoon of New Caledonia. *In* Choat, J.H., et al. (eds.), Proc. 6th Int. Coral Reef Symp., Townsville, Aust., 2:305–312.

Kulbicki, M., and L. Wantiez
1990 Comparison between fish bycatch from shrimp trawlnet and visual censuses in St. Vincent Bay, New Caledonia. Fish. Bull., U.S. 88:667–675.

Matlock, G.C., W.R. Nelson, R.S. Jones, A.W. Green, T.J. Cody, E. Gutherz, and J. Doerzbacher
1991 Comparison of two techniques for estimating tilefish, yellowedge grouper, and other deepwater fish populations. Fish. Bull., U.S. 89:91–99.

Miller, R.J.
1990 Effectiveness of crab and lobster traps. Can. J. Fish. Aquat. Sci. 47:1228–1251.

Moffitt, R.B.
1983 *Heterocarpus longirostris* MacGilchrist from the Northern Mariana Islands. Fish. Bull., U.S. 81:434–436.

Moffitt, R.B., and J.J. Polovina
1987 Distribution and yield of the deepwater shrimp *Heterocarpus* resource in the Marianas. Fish. Bull., U.S. 85:339–349.

Morgan, G.R.
1974 Aspects of the population dynamics of the western rock lobster, *Panulirus cygnus* George. II Seasonal changes in the catchability coefficient. Aust. J. Mar. Freshwater Res. 25:249–259.

Morrissy, N.M.
1975 The influence of sampling intensity on the 'catchability' of marron, *Cherax tenuimanus* (Smith) (Decapoda: Parastacidae). Aust. J. Mar. Freshwater Res. 26:47–73.

Polovina, J.J., R.B. Moffitt, S. Ralston, P.M. Shiota, and H.A. Williams
1985 Fisheries resource assessment of the Mariana Archipelago, 1982–85. Mar. Fish. Rev. 47(4):19–25.

Powles, H., and C.A. Barans
1980 Groundfish monitoring in sponge-coral areas off the southeastern United States. Mar. Fish. Rev. 42(5):21–35.

Ralston, S.
1986 An intensive fishing experiment for the caridean shrimp, *Heterocarpus laevigatus*, at Alamagan Island in the Mariana Archipelago. Fish. Bull., U.S. 84:927–934.

Ralston, S., and D.T. Tagami
1992 An assessment of the exploitable biomass of *Heterocarpus laevigatus* in the main Hawaiian Islands. Part 1: Trapping surveys, depletion experiment, and length structure. Fish. Bull., U.S. 90:494–504.

Ralston, S., R.M. Gooding, and G.M. Ludwig
1986 An ecological survey and comparison of bottom fish resource assessments (submersible versus handline fishing) at Johnston Atoll. Fish. Bull., U.S. 84:141–155.

Richards, L.J., and J.T. Schnute
1986 An experimental and statistical approach to the question: Is CPUE and index of abundance? Can. J. Fish. Aquat. Sci. 43:1214–1227.

Sale, P.F., and W.A. Douglas
1981 Precision and accuracy of visual census technique for fish assemblages on coral patch reefs. Environ. Biol. Fish. 6: 333–339.

Saunders, W.B., and L.C. Hastie
1989 Deep-water shrimp survey and feasibility study, Republic of Palau, Western Caroline Islands. Pac. Fish. Dev. Found., Final Rep., Proj. 63A, Honolulu.

Struhsaker, P., and D.C. Aasted
1974 Deepwater shrimp trapping in the Hawaiian Islands. Mar. Fish. Rev. 36(10):24–30.

Tagami, D.T., and S. Barrows
1988 Deep-sea shrimp trapping for *Heterocarpus laevigatus* in the Hawaiian Archipelago by a commercial fishing vessel. NOAA Tech. Memo. NMFS-SWFC-103, NMFS Honolulu Lab., 14 p.

Uzmann, J.R., R.A. Cooper, R.B. Theroux, and R.L. Wigley
1977 Synoptic comparison of three sampling techniques for estimating abundance and distribution of selected megafauna: Submersible vs camera sled vs otter trawl. Mar. Fish. Rev. 39(12):11–19.

Wilder, M.J.
1977 Biological aspects and fisheries potential of two deepwater shrimps *Heterocarpus ensifer* and *Heterocarpus laevigatus* in waters surrounding Guam. M.S. thesis, Univ. Guam, Agana, 79 p.

Abstract.– Research and commercial trapping data show variation in recruitment to the fishery for spiny lobster *Panulirus marginatus* at Maro Reef, relative to Necker Island which is 670 km to the southeast. Recruitment to the fishery at Maro Reef is shown to be highly correlated with the difference in sea level 4 years earlier between French Frigate Shoals and Midway Islands. Geosat altimeter data indicate that the relative sea level between French Frigate Shoals and Midway is an indicator of the strength of the Subtropical Counter Current. Mechanisms linking the Subtropical Counter Current with larval advection and survival are discussed. The sea level index provides a forecast of recruitment 4 years later to the fishery at Maro Reef.

Variability in spiny lobster *Panulirus marginatus* recruitment and sea level in the Northwestern Hawaiian Islands*

Jeffrey J. Polovina

Honolulu Laboratory, Southwest Fisheries Science Center
National Marine Fisheries Service, NOAA
2570 Dole Street, Honolulu, Hawaii 96822-2396
Joint Institute of Marine and Atmospheric Research (JIMAR)
University of Hawaii, Honolulu, Hawaii 96822
Department of Oceanography, School of Ocean and Earth Science and Technology
University of Hawaii, Honolulu, Hawaii 96822

Gary T. Mitchum

Joint Institute of Marine and Atmospheric Research (JIMAR)
University of Hawaii, Honolulu, Hawaii 96822
Department of Oceanography, School of Ocean and Earth Science and Technology
University of Hawaii, Honolulu, Hawaii 96822

Significant correlations between commercial landings or recruitment estimates and one or more environmental indices are commonly reported in the fisheries literature, but few have served as accurate predictors of future population levels (Drinkwater and Myers 1987). However, such correlations can lead to the formulation or support of hypotheses regarding the factors responsible for population changes. For example, an inverse correlation between the survival of Pacific mackerel *Scomber japonicus* to age 1 and the strength of the California Current, and the lack of correlation between survival and plankton biomass, have been offered as evidence that advection, rather than starvation, controlled survival of the planktonic stages of this species (Sinclair et al. 1985).

Correlative studies on lobsters suggest that population size results from changes in survival and advection at the larval stage, but in at least one instance, density-dependent mechanisms after postsettlement may dampen this variation (Pollock 1986). Fluctuations in sea-surface temperature appear to result in changes in larval survival and catches 6 years later for the clawed lobster *Homarus americanus* in Maine (Fogarty 1988). Variation in the strength of the Leeuwin Current, which may be linked to El Niño Southern Oscillation (ENSO) events, is suggested as a cause of variation in the number of larvae returned to the coast and subsequent recruitment to the fishery for the western rock lobster *Panulirus argus* (Pearce and Phillips 1988). Changes in recruitment levels of the California spiny lobster *P. interruptus* to the northern portion of its habitat may be episodic, influenced by large-scale, interannual El Niño events (Pringle 1986). Variation in postlarval recruitment in the South African rock lobster *Jasus lalandii* is thought to arise from changes in the paths and velocities of extensive offshore currents, which eventually return larvae to the coast. However, density-dependent phenomena influ-

* Contribution 2820 of the School of Ocean and Earth Science and Technology, University of Hawaii; JIMAR Contribution 91-0243.

Manuscript accepted 20 May 1992.
Fishery Bulletin, U.S. 90:483–493 (1992).

encing juvenile and adult stages may substantially dampen this variation and produce fairly stable recruitment to the fishery (Pollock 1986).

In the Northwestern Hawaiian Islands (NWHI), a substantial drop in catches and catch-per-unit-effort (CPUE) of spiny lobster *P. marginatus* Quoy and Gaimard 1825 was recently documented (Polovina 1991). This study examines whether these declines in catches and CPUE are due to overfishing or to oceanographic factors which impact spiny lobster population dynamics.

NWHI lobster fishery

The NWHI region is an isolated range of islands, islets, banks, and reefs that extend 2775 km northwest from Nihoa Island to Kure Atoll (Fig. 1). In 1977 after research cruises documented a substantial lobster population in the NWHI, a commercial trap fishery was initiated. The fishery targeted two species: the endemic spiny lobster *P. marginatus* and the slipper lobster *Scyllarides squammosus* Mike-Edwards 1837. A fishery management plan implemented in 1983 mandated that vessels submit logbooks recording daily catch and number of traps set (effort); the plan also established a minimum harvest size for spiny lobster and prohibited the harvest of egg-bearing females. Subsequent amendments to this plan added a minimum legal size for slipper lobster and required that traps have escape vents. In 1990, low catches and CPUE prompted a 6-month closure of the fishery (May–November 1991).

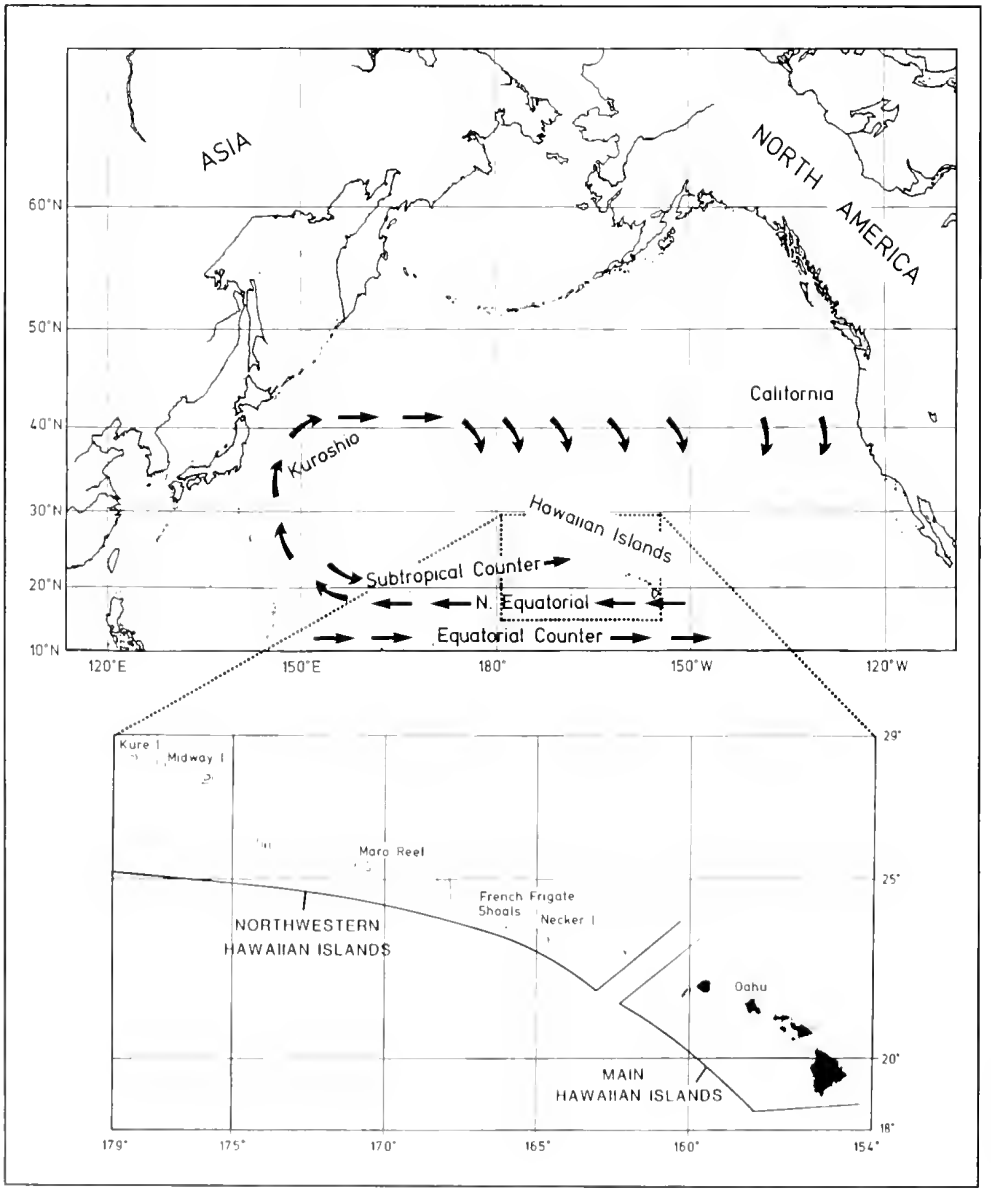

Figure 1
Pacific Ocean and major currents with an inset of the Hawaiian Archipelago, including the Northwestern Hawaiian Is.

Since 1983, the lobster fleet has been composed of 9–14 vessels (20–30 m long), each averaging 3 trips per year. The vessels set about 800 traps per day and remain at sea almost 2 months per trip. Landings in recent years have averaged almost 1 million lobsters, valued at about US$6 million ex-vessel. Because of heavy fishing since 1986, the population has been fished down to the point that 3-year-old recruits comprised most of the fishery catches (Polovina 1991). Since 1988, about 80% of landings have been spiny lobster (Table 1). Two banks—Necker I. at the southeast end of the NWHI, and Maro Reef which is 670 km northwest of Necker I.—account for over 60% of the fishery's catches. There is no recreational lobster fishery in the NWHI.

Table 1

Annual landings of spiny (*Panulirus marginatus*) and slipper (*Scyllarides squammosus*) lobsters, trapping effort, and percentage of spiny lobster in the landings, 1983–90.[1]

Year	Lobster landings (10^3) Spiny	Slipper	Total	Trap hauls (10^3)	CPUE	% spiny lobster
1983[2]	158	18	176	64	2.75	90
1984	677	207	884	371	2.38	78
1985	1022	900	1922	1041	1.83	53
1986	843	851	1694	1293	1.31	50
1987	393	352	745	806	0.92	53
1988	888	174	1062	840	1.26	84
1989	944	222	1166	1069	1.09	81
1990	591	187	778	1182	0.66	76

[1] Data were provided to the NMFS Honolulu Lab., as required by the Crustacean Fishery Management Plan of the W. Pac. Reg. Fish. Manage. Counc., Honolulu.
[2] April–December 1983.

Spiny lobster spawn over a broad spring, summer, and fall period. After hatching, the eggs are planktonic; the planktonic period for the larvae is estimated at 12 months based on spawning season and larval tow data (NMFS Honolulu Lab., unpubl. data). Further, the larval tow data suggest that mid- to late-stage spiny lobster larvae are close to the surface at night and move down to ~100 m during the day (Polovina, pers. observ.). Based on growth curves estimated from both tagging (MacDonald 1984) and length-based methods (Polovina and Moffitt 1989), spiny lobster reach the minimum legal size (which is slightly larger than the size at onset of sexual maturity) approximately 3 years after they settle onto benthic habitat. After settlement, the lobster probably do not move between banks since interbank depths exceed 1000 m.

Regional oceanography

The Hawaiian Archipelago lies within the subtropical gyre formed by the Kuroshio Current to the west and the north, the California Current to the east, and the North Equatorial Current to the south (Fig. 1). The speed of the gyre in the vicinity of the archipelago is slow (<5 cm/s; Roden 1991). An eastward-flowing current within the subtropical gyre, named the Subtropical Counter Current (SCC), was predicted by Yoshida and Kidokoro (1967) and subsequently confirmed by Robinson (1969) and Uda and Hasunuma (1969) (Fig. 1). More recent work has shown that, in at least the western portion, the interior of the subtropical gyre is composed of a quasi-stationary banded structure of easterly- and westerly-flowing currents (White and Hasunuma 1982). The SCC consists of two bands of eastward flow at 23° and 28°N, with mean annual speeds of 8 and 6 cm/s, respectively (White and Hasunuma 1982).

In addition to these large-scale features, the mesoscale oceanography around the Hawaiian Archipelago is a complex system of fronts and eddies resulting from both interactions between alternating east and west currents and interactions between current and the topography of the archipelago.

Data and analysis

Research data

Standardized trapping surveys, using the same traps set at the same sites, were conducted at Necker I. and Maro Reef during June and July of 1986–88 and 1990. The size-frequency data were converted to age-frequency data with a von Bertalanffy growth curve (MacDonald 1984). The age-frequency distribution was standardized for the number of traps deployed to estimate the relative age-frequency distribution of the population.

Fishery data

Although detailed catch and effort data were not available until after the logbook regulations were established in 1988, catch and effort were generally light and were concentrated around Necker I. from the inception of the fishery until 1984 (Fig. 2). The combined CPUE for slipper and spiny lobsters in 1983–90 generally declined from 2.8 to ~0.7 lobster per trap-

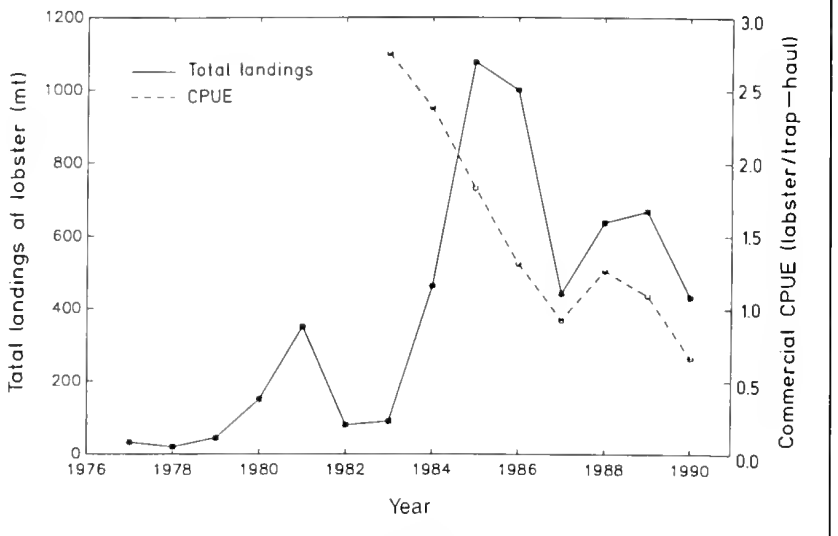

Figure 2

Total slipper (*Scyllarides squammosus*) and spiny (*Panulirus marginatus*) lobster landings and CPUE from the Northwestern Hawaiian Is., 1977-90.

haul (Fig. 2), based on catch and effort data reported in the logbooks. Catch data in the logbooks are checked against landings by enforcement agents, so misreporting is not a problem. Common assessment approaches, such as length-based cohort analysis, are not applicable to this fishery, given the relatively short time-series of catch and effort data, the difficulty in routinely ageing lobsters, and the lack of information on the size-frequency from the landings and the nature of a stock-recruitment relationship. While a dynamic surplus production model has been applied to the data, an implicit assumption about the form of the stock recruitment relationship is required (Polovina 1991).

A more general approach is to begin with a model which expresses N_t as the number of exploitable lobsters at time t as a function of N_{t-1}, Z as the total instantaneous mortality from time t-1 to t, and r as the number which recruit and survive from t-1 to t as

$$N_t = r + N_{t-1}\, e^{-z}.$$

Using the relationship that the product of catchability (q) and $N_{(t)}$ is $CPUE_{(t)}$, this model becomes

$$CPUE_t = q*r + CPUE_{t-1}\, e^{-M-qf},$$

where M and f are annual instantaneous natural mortality and fishing effort, respectively, during the period t-1 to t. This CPUE model, a simple version of a size-structured model developed by Schnute et al. (1989), was used to estimate population parameters and to evaluate the extent that fishing effort explains the observed variation in CPUE. This model assumes constant catchability and recruitment; hence, the differences between predicted and observed CPUE are interpreted as variation in recruitment, catchability, or both.

The commercial data do not indicate whether effort was directed at slipper or spiny lobster. However, the catches can be grouped into two periods based on the proportion of spiny to slipper lobsters. In period 1 (1983–84 and 1988–90), ~80% of the landings were spiny lobster; in period 2 (1985–87), ~56% of the landings were spiny lobster (Table 1). The change in proportion of spiny lobster catches is likely due to changes in targeting and abundance. The CPUE model is modified so that a catchability coefficient can be estimated for each period. Our modified CPUE model regresses the CPUE of spiny lobster above the minimum size in month t ($CPUE_t$) on the CPUE of the same month in the previous year:

$$CPUE_t = R*Q_t\, e^{-\frac{(M+Q_t f_t)}{2}} + (CPUE_{t-12})\,(e^{-M-Q_t f_t})\left(\frac{Q_t}{Q_{t-12}}\right)$$

with

$$Q_t = q_1 I_{1,t} + q_2 I_{2,t}$$

where q_1 is the catchability of spiny lobster during period 1, q_2 is the catchability during period 2, M is the annual instantaneous natural mortality, R is the annual recruitment, f is the cumulative fishing effort during the period (t-12, t-1), and $I_{i,t}$ (i=1,2) is the indicator or set function which takes the value 1 if t is within period i or otherwise takes the value 0. Estimates of R, q_1, q_2, and M were obtained by minimizing the sum of squares of the difference between the square root of the observed and predicted CPUE with a simplex algorithm.

Sea level data

To examine the relationship between lobster recruitment variation at Maro Reef and physical factors such

as variation in the SCC, we focused on the analysis of sea level data from the NWHI. Our choice of sea level was primarily a practical one. In comparison to current or upper-layer temperature records, the sea level records are of long duration, and the data are measured continuously and are available in nearly real-time. An additional advantage is that sea-surface height data from the Geosat satellite altimeter are available to provide a spatial description that complements the temporal description available from the sea level stations.

Data on the difference in sea level between the gauges at French Frigate Shoals (FFS) and at Midway Is. have been available since 1976 (Figs. 1,3). This sea level difference (denoted as FFS–Midway sea level) serves as an index of the geostrophic current anomalies across the NWHI in the region of Maro Reef. For example, an increase in the sea level height at FFS relative to Midway Is., measured from tide gauges, indicates the strengthening of a current that is across the gradient between the two locations and is flowing from the southwest to the northeast.

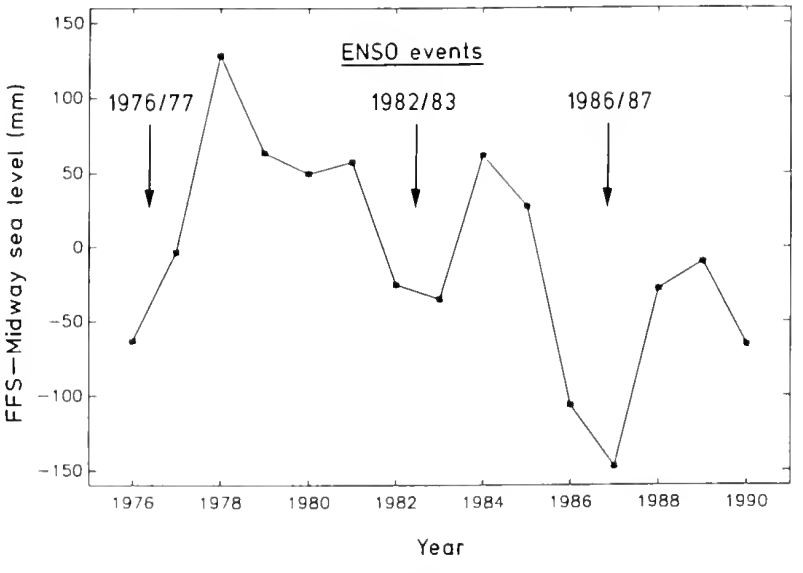

Figure 3
Annual French Frigate Shoals (FFS)–Midway sea level differences from tide gauges, 1976–90 (ENSO = El Niño Southern Oscillation).

To interpret these flow anomalies as a manifestation of the variations in SCC strength, the spatial structure of the sea-surface height variation was examined by mapping the variability observed by the Geosat altimeter during November 1986–November 1988. These 2 years were selected because more accurate orbit estimates were available during this time-period and would result in more accurate sea-surface height fields. The Geosat geophysical data records were obtained from NOAA (Cheney et al. 1987) and were processed with software developed at the University of Hawaii.

Averages of the Geosat data over November 1986–November 1987 were subtracted from the averages over November 1987–November 1988. Before using the Geosat data, we checked that the resulting sea level differences from the altimeter were consistent with the corresponding sea level differences from tide gauges at FFS and Midway (not shown). Choosing these time-periods also allowed us to contrast conditions during the ENSO period of 1986–87, when the FFS–Midway sea level was low (~520 mm), with conditions during the normal period of 1987–88, when the FFS–Midway sea level was higher (~600 mm).

Puerulus settlement

During the last planktonic stage (i.e., postlarval or puerulus stage), spiny lobster acquire the benthic morphological features of adults and become active swimmers seeking benthic habitat. MacDonald (1986) studied puerulus settlement in the Hawaiian Archipelago with traps known as Witham Collectors at Kure Atoll (north of Midway Is.) in 1979–83 and at FFS in 1981–85. He computed mean catch per collector over 12-month periods (June–May) at Kure Atoll and FFS. These data will be compared with the FFS–Midway sea level data.

Results

The fit of the model to the commercial CPUE data and the resulting residuals indicate the model fits the trend in CPUE, but considerable unexplained variation exists in CPUE within and between years (Fig. 4). For example, given the fishing effort, CPUE was greater than expected in 1988 but declined more than expected in 1990. Since the model assumes both constant recruitment and constant catchability, the residuals may reflect variation in these factors. From the fit of the model, $R = 1.2 \times 10^6$ adult lobsters/yr, $M = 0.71$/yr, $q_1 = 1.2 \times 10^{-6}$, and $q_2 = 0.6 \times 10^{-6}$. Thus 1.2 million lobsters recruit to the fishery annually; with an M of 0.71/yr, only 50% of the 3-year-olds survive 1 year (in

the absence of fishing). Further, a CPUE of 1.2 spiny lobster/trap-haul means the exploitable population is 1 million spiny lobster. An independent estimate of M from tagging at FFS is 0.5/yr (MacDonald 1984).

Commercial trapping effort since 1985 has averaged about 1 million trap-hauls (Table 1); using the q_1 estimate as catchability, annual fishing mortality (F) is estimated as 1.2/yr or 1.7×M. With these figures and the estimates of growth and age at onset of sexual maturity, the Beverton-Holt yield equation estimates the spawning-stock biomass per recruit, when effort is 1 million trap-hauls, is 40% of what it would be in the absence of fishing (Polovina 1991). Thus, the ratio of F to M and the relative spawning-stock biomass calculations suggest that the spawning biomass in 1985–86 was not fished down to a level that would cause the poor recruitment to the fishery 4 years later (1989–90).

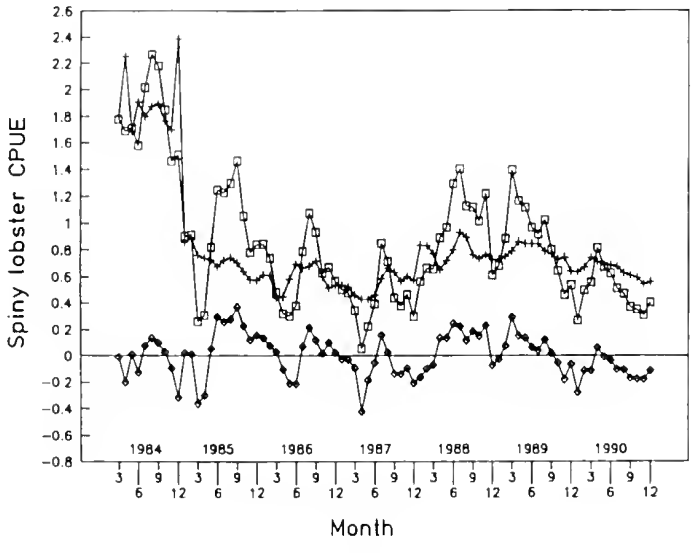

Figure 4

Fit of the CPUE model (+) to monthly CPUE (□) for spiny lobster *Panulirus marginatus* in the Northwestern Hawaiian Is., and residuals from the fit (◆).

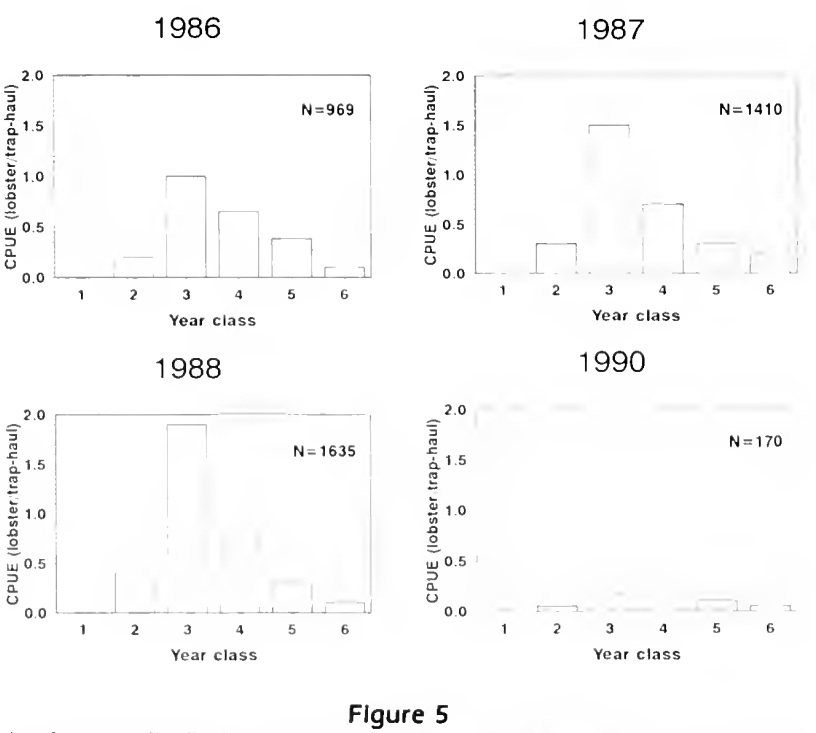

Figure 5

Age-frequency distributions of spiny lobster *Panulirus marginatus*, based on research sampling in 1986–88 and 1990 at Maro Reef (N = no. of spiny lobster in the sample).

Much of the variation in residuals from the CPUE model is due to variation in recruitment at Maro Reef. For example, for the entire NWHI in 1990, trapping effort increased 11% from the previous year while the catch declined 33%, resulting in a 39% decline in CPUE. However, the decline in CPUE was most striking at Maro Reef, where CPUE declined 42% even though effort decreased by 37%. At Necker I., CPUE also declined (40%) but effort increased 35%.

The estimated age-frequency distributions based on research cruises at Maro Reef show a strong 3-year-old class in 1988 and a striking absence of all age-classes in 1990 (Fig. 5). This is consistent with the hypothesis that recruitment of the 3-year-olds to the fishery was weak in 1990 and subsequent fishing reduced all older age-classes. Necker I. had many more 2-year-olds in the samples since some trapping sites include nursery habitat; but between years, the abundance of 2-year-olds was relatively constant, whereas older lobsters declined in 1990, likely because of the increase in fishing effort (Fig. 6).

The NWHI lobster fleet is very mobile and shifts its trapping locations according to abundance of lobsters. By 1985, both Maro

Reef and Necker I. had gone through a period of fishing down the pre-exploitation population; the relative change in catches between the two banks may reflect changes in their relative recruitment. Since both banks are not always fished each month, we pooled the catches by quarter. A 3-quarter moving average of the ratio of quarterly catches at Maro Reef to the combined quarterly catches at Necker I. and Maro Reef shows considerable variation (Fig. 7). For example, catches from Maro in 1985 and 1988 represented almost 80% of the catches from the two banks, but in 1990 they represented less than 20%. A 3-quarter moving average of the residuals from the CPUE model shows the same trend as the ratio of catches from Maro Reef relative to Necker I. and Maro Reef combined (Fig. 7). This suggests that the variation in recruitment, catchability, or both at Maro Reef is responsible for most of the variation not explained by fishing effort observed for the entire NWHI.

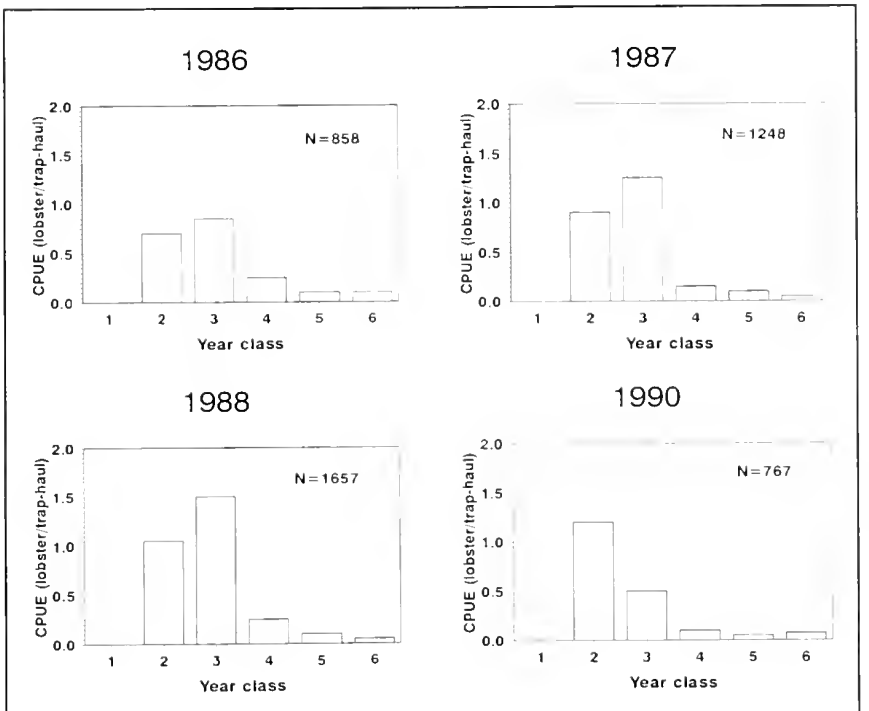

Figure 6
Age-frequency distributions of spiny lobster *Panulirus marginatus*, based on research sampling in 1986–88 and 1990 at Necker I. (N = no. of spiny lobster in the sample).

Variation between sea level and the SCC

Differences in sea level over the Pacific, between a year when the FFS–Midway sea level was high and a year when it was low, appear as a ridge of positive values, extending from southwest to northeast, that parallels a trough of negative values to the northwest (Fig. 8). Midway lies in the trough, Honolulu is on the ridge, and FFS lies on the gradient, which corresponds to the region of the most energetic geostrophic flow anomalies. This ridge and trough indicate that the change in the FFS–Midway sea level from low to high reflects the increase in a ridge extending across the western Pacific. The increase in the ridge and trough pattern represents an increase in the current flow along the gradient of this ridge. The path of this gradient or flow across the Pacific is consistent with the general path of the SCC. Thus FFS–Midway sea level measures a large-scale oceanographic feature which is represented by the height of the sea level ridge stretching across the Pacific. The height and location of this sea level ridge

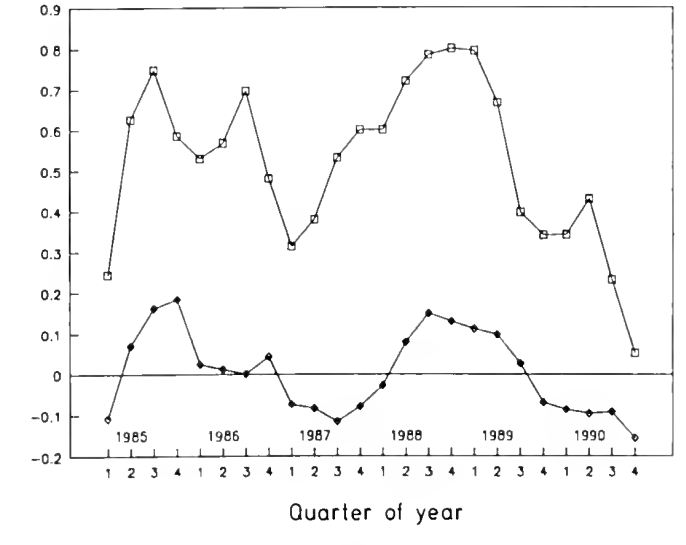

Figure 7
Three-quarter moving average of the ratio of quarterly landings of spiny lobster *Panulirus marginatus* at Maro Reef to quarterly landings at Maro Reef and Necker I. (□), and 3-quarter moving average of the residuals from the fit of the CPUE model to monthly spiny lobster CPUE (◆).

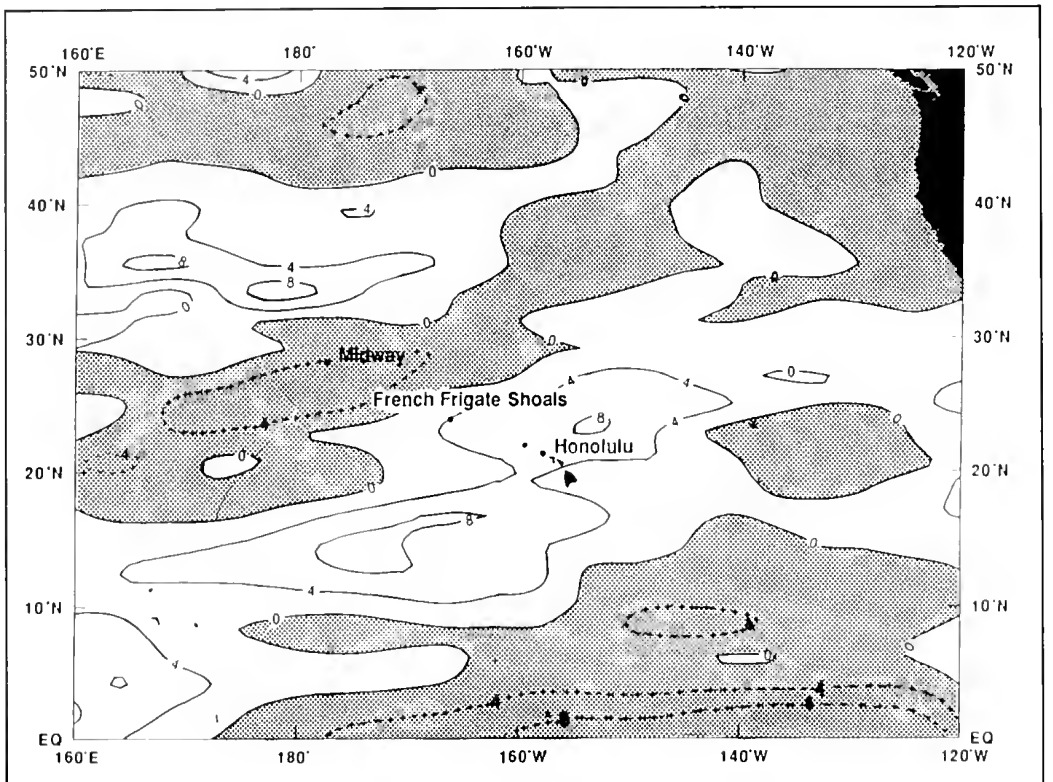

Figure 8

Differences between mean sea level during a non-ENSO (El Niño Southern Oscillation) period (Nov. 1987–Sept. 1988) and an ENSO period (Nov. 1986–Sept. 1987) from Geosat data. Negative values denoted by shaded areas.

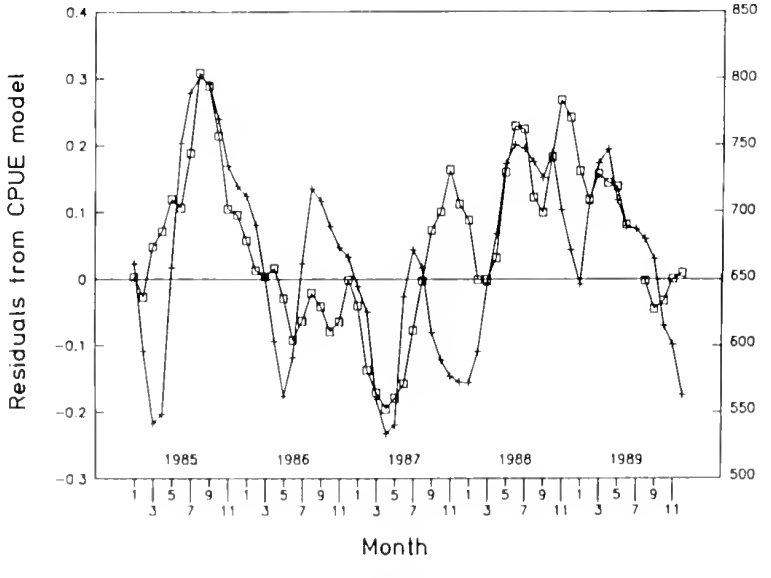

Figure 9

Overlay of 3-month moving average of French Frigate Shoals (FFS)–Midway sea level advanced by 4 years (□) with a 3-month moving average of residuals from the fit of the CPUE model (+).

correspond to the SCC strength and position, respectively.

Relationship between sea level and lobster abundance

Lagged cross-correlations between FFS–Midway sea level and the variables (i.e., the ratio of catches at Maro Reef to the combined catches at Maro Reef and Necker I., and the residuals from the CPUE model) have their strongest correlations (r 0.82 and 0.68, respectively) with sea level lagged by exactly 4 years. When sea level is lagged by 4 years and overlayed with these time-series, there is good agreement (Figs. 9,10). Based on research samples pooled over 1986–88, the mean estimated age of lobsters caught by the fishery is 3.8 years (after settlement).

Based on the comparison of FFS–Midway sea level with the available puerulus settlement data from MacDonald (1986) in the same year, the FFS–Midway sea level correlates positively with mean puerulus catches at Kure Atoll (r 0.78, P 0.11) and shows no significant correlation with mean puerulus catches at FFS (r −0.37, P>0.25) (Fig. 11).

Discussion

The research and commercial catch and effort data presented here show that the recruitment of 3-year-old spiny lobster to the fishery has varied considerably at Maro Reef but has remained stable at Necker I., 670 km to the southeast. Fishing effort is not considered sufficiently heavy to explain a decline in recruitment, especially a decline at one bank and not the other. The relationship between recruitment to the fishery at Maro Reef and the FFS–Midway sea level advanced by 4 years suggests that environmental factors impacting the larval stage are responsible for the recruitment variation. The Geosat data suggest that the FFS–Midway sea level measures the SCC. Hence the SCC strength or location dictates recruitment strength to the fishery 4 years later. Consistent with this hypothesis is the mean age of lobsters in the commercial catches as well as the correlation between puerulus settlement at Kure Atoll and FFS–Midway sea level. The lack of correlation between puerulus settlement at FFS and sea level is consistent with the observation that recruitment at the lower end of the NWHI is not linked to the same pattern of variation as Maro Reef. Annual variation in both SCC strength and position has been observed in the western Pacific (White and Hasunuma 1982). In summary, the temporal pattern of spiny lobster recruitment differs between Necker I. and Maro Reef. At Maro Reef, large-scale oceanographic features appear to control the abundance of late-stage larvae, which in turn results in interannual variation in recruitment to the fishery.

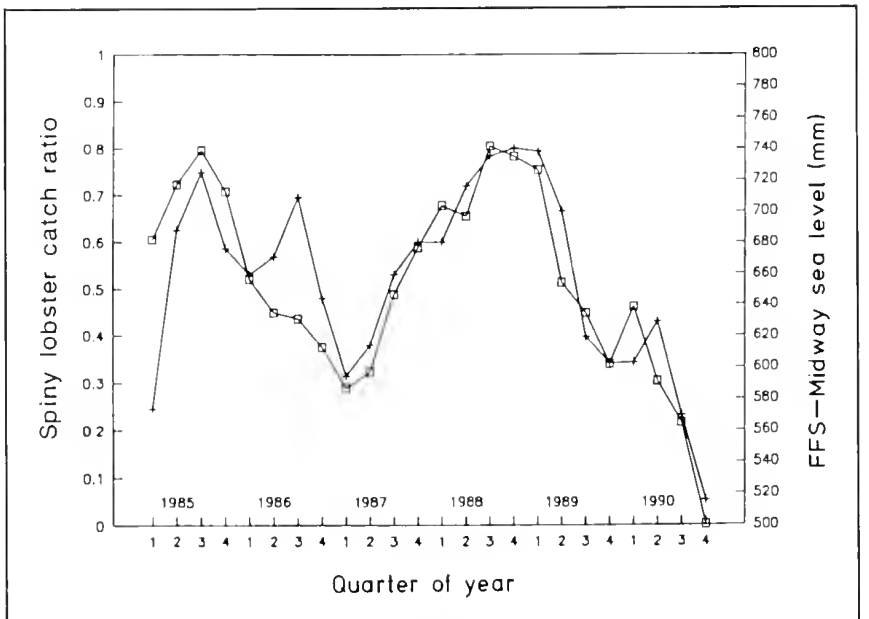

Figure 10

Overlay of 3-quarter moving average of French Frigate Shoals (FFS)–Midway sea level advanced by 4 years (□), with a 3-quarter moving average of the ratio of Maro Reef to Maro Reef plus Necker I., spiny lobster landings (+).

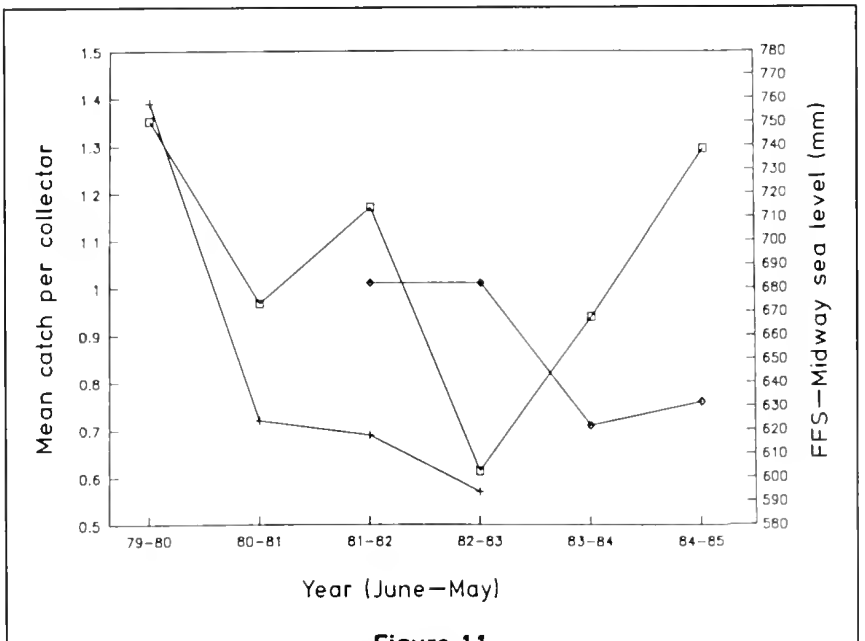

Figure 11

Mean annual puerulus settlement from traps at Kure Atoll (+) and French Frigate Shoals (FFS) (◊) and FFS–Midway sea level (□), all computed on a June–May year.

The underlying mechanism linking the correlation between the SCC and subsequent recruitment at Maro Reef is not known. It is possible that the SCC returns larvae, which have been advected west of the archipelago, back to Maro Reef. The SCC has been hypothesized to transport *Acropora* coral from Johnston Atoll (lat. 16°45′N., long. 169°31′W) to FFS (Grigg 1982). In addition, larvae of a spiny lobster species not recorded as an adult in Hawaii have been transported from the Marshall Is. to the Hawaiian Archipelago (Phillips and McWilliam 1989).

However, it may be that the SCC impacts not advection but larval survival. Laboratory studies have shown that spiny lobster larvae suffer a high level of mortality when water temperatures drop below 20°C (T. Kazama, NMFS Honolulu Lab., pers. commun., Sept. 1991). In the years we estimated that the SCC was weak, water temperatures <20°C in the winter have been observed at Maro Reef but not Necker I. If little larval mixing occurs between Maro Reef and Necker I., larval mortality at Maro Reef resulting from low winter temperatures could account for the observed recruitment variation.

A third hypothesis is that when the SCC has a particular speed and location, it produces fronts which retain larvae near Maro Reef. When the SCC is weak or shifts, these fronts are not formed near Maro Reef. Preliminary evidence from the drifter buoys and larval sampling in our study suggests fronts north of Maro Reef and south of Necker I. may be important for lobster larvae (Polovina, pers. observ.)

One potential management application of the lagged relationship between FFS–Midway sea level and recruitment is that it provides up to a 4-year forecast of recruitment to the fishery at Maro Reef. A 3-quarter moving average of the FFS–Midway sea level shifted forward by 4 years forecasts poor recruitment in 1991, followed by an improvement beginning in late 1992 (Fig. 12). During January–May 1991 before the fishery was closed for 6 months, recruitment at Maro Reef clearly had not recovered, as only 1052 spiny lobster were harvested from Maro Reef while 34,746 spiny lobster were harvested from Necker I. Recall that the relative catches between banks provide an index of relative abundance, since the fleet moves to maximize the CPUE. The FFS–Midway sea level data forecast that catches at Maro Reef will improve beginning in late 1992 (Fig. 12). Data from larval tows are consistent with this forecast. Standardized larval tows, taken in June and November 1989 over a grid of stations from the 200 m isobath out to 56 km around both Necker I. and Maro Reef, caught 3802 and 3342 late-stage phyllosomes, respectively (J. Polovina, unpubl. data). A t-test, based on a lognormal distribution, finds no significant difference in the mean abundance of larvae between Maro Reef and Necker I. If we assume that larval abundance was high around Necker I. in 1989, then good larval recruitment apparently has returned to Maro Reef. This is consistent with the observed higher sea-level values in 1989 (shown as 1993 values in Fig. 12, since the sea level has been advanced by 4 years) and suggests that catches will be high at Maro Reef in 1993.

The FFS–Midway sea level time-series from 1976 to 1990 (Fig. 3) shows that ENSO events may result in poor recruitment to the fishery 4 years later, but the series also shows a long-term decline. Reasons for the low FFS–Midway sea level during ENSO events are not known, but may be related to a decrease in surface water supplied to the SCC in the western Pacific. Such a change could be associated with the circulation disruptions observed in the tropical Pacific during ENSO events (Meyers and Donguy 1984). The long-term decline in sea level from 1976 to 1990 suggests there is a low-frequency component in the variation in SCC strength and, hence, lobster recruitment. Thus, it may be some time before recruitment to the fishery is at the early 1980s' level.

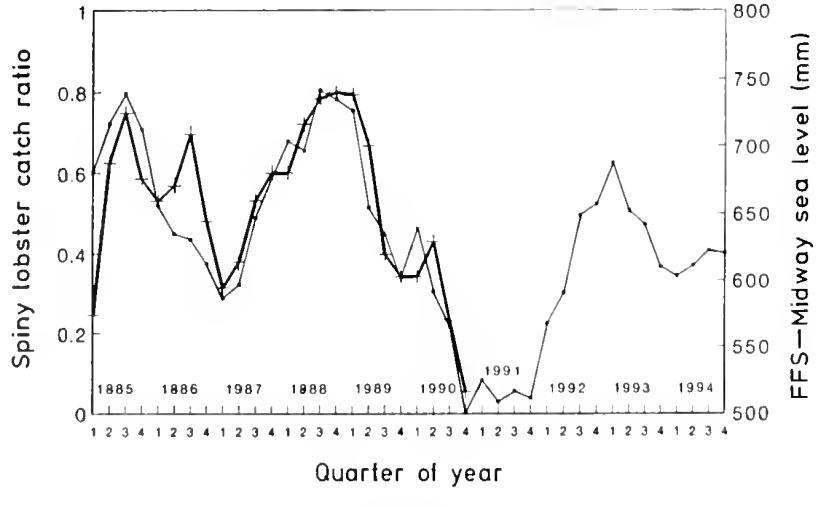

Figure 12

Three-quarter moving average of the ratio of quarterly landings of spiny lobster *Panulirus marginatus* at Maro Reef to quarterly landings at Maro Reef and Necker I. (bold line) overlayed with the 3-quarter moving average of French Frigate Shoals (FFS)–Midway sea level deviation advanced by 4 years (thin line).

Acknowledgments

Partial support for this study was provided by the National Science Foundation under grant OCE8911163 by the TOGA Sea Level Center through NOAA Cooperative Agreement NA90RAH00074 to the Joint Institute for Marine and Atmospheric Research (JIMAR), University of Hawaii; and by NASA through the Jet Propulsion Laboratory as part of the TOPEX Altimetry Research in Ocean Circulation Mission.

Citations

Cheney, R.E., B.C. Douglas, R.W. Agree, L.L. Miller, and D.L. Porter
1987 Geosat altimeter geophysical data record (GDR) user handbook. NOAA Tech. Memo. NOS NGS-46, Natl. Geod. Surv., Rockville, MD, 29 p.

Drinkwater, K.F., and R.A. Myers
1987 Testing predictions of marine fish and shellfish landings from environmental variables. Can. J. Fish. Aquat. Sci. 44: 1568–1573.

Fogarty, M.J.
1988 Time series models of the Maine lobster fishery: The effect of temperature. Can. J. Fish. Aquat. Sci. 45:1145–1153.

Grigg, R.W.
1981 *Acropora* in Hawaii. Part 2. Zoogeography. Pac. Sci. 35(1):15–24.

MacDonald, C.D.
1984 Studies on recruitment in the Hawaiian spiny lobster, *Panulirus marginatus*. *In* Proc. Res. Invest. NWHI, p. 199–220. UNIHI-SEAGRANT-MR-84-01, Univ. Hawaii Sea Grant Coll. Prog., Honolulu.
1986 Recruitment of the puerulus of the spiny lobster, *Panulirus marginatus*, in Hawaii. Can. J. Fish. Aquat. Sci. 43: 211–2125.

Meyers, G., and J.R. Donguy
1984 The North Equatorial Counter Current and heat storage in the western Pacific Ocean during 1982–83. Nature (Lond.) 5991 (312)258–260.

Pearce, A.F., and B.F. Phillips
1988 ENSO events, the Leeuwin Current, and larval recruitment of the western rock lobster. J. Cons. Cons. Int. Explor. Mer 45:13–21.

Phillips, B.F., and P.S. McWilliam
1989 Phyllosoma larvae and the ocean currents off the Hawaiian Islands. Pac. Sci. 43(4):352–361.

Pollock, D.E.
1986 Review of the fishery for and biology of the Cape rock lobster, *Jasus lalandii*, with notes on larval recruitment. Can. J. Fish. Aquat. Sci. 43:2107–2117.

Polovina, J.J.
1991 Status of lobster stocks in the Northwestern Hawaiian Islands, 1990. Admin. Rep. H-91-04, Honolulu Lab., NMFS Southwest Fish. Sci. Cent., Honolulu, 15 p.

Polovina, J.J., and R.B. Moffitt
1989 Status of lobster stocks in the NWHI, 1988. Admin. Rep. H-89-3, Honolulu Lab., NMFS Southwest Fish. Sci. Cent., Honolulu, 10 p.

Pringle, J.D.
1986 California spiny lobster (*Panulirus interruptus*) larval retention and recruitment: A review and synthesis. Can. J. Fish. Aquat. Sci. 43:2142–2152.

Robinson, M.K.
1969 Theoretical predictions of Subtropical Countercurrent confirmed by bathythermograph (BT) data. Bull. Jpn. Soc. Fish. Oceanogr. Spec. (Prof. Uda's Commem. Pap.):115–121.

Roden, G.I.
1991 Effects of the Hawaiian Ridge upon oceanic flow and thermohaline structure. Deep-Sea Res. (Suppl. 1) 38:S623–S654.

Schnute, J.T., J. Richards, and A.J. Cass
1989 Fish survival and recruitment: Investigations based on a size-structured model. Can. J. Fish. Aquat. Sci. 46:743–767.

Sinclair, M., M.J. Tremblay, and P. Bernal
1985 El Niño events and variability in a Pacific mackerel (*Scomber japonicus*) survival index: Support for Hjort's second hypothesis. Can. J. Fish. Aquat. Sci. 43:602–608.

Uda, M., and K. Hasunuma
1969 The eastward Subtropical Countercurrent in the Western North Pacific Ocean. J. Oceanogr. Soc. Jpn. 25:201–210.

White, W.B., and K. Hasunuma
1982 Quasi-stationary banded structure in the mean zonal geostrophic current regimes of the western North Pacific. J. Mar. Res. 40(4):1035–1046.

Yoshida, K., and T. Kidokoro
1967 Subtropical countercurrent in the North Pacific—An eastward flow near the Subtropical Convergence. J. Oceanogr. Soc. Jpn. 23:88–91.

Abstract. – A deepwater trapping survey for *Heterocarpus laevigatus* was conducted around the main islands of the Hawaiian Archipelago to estimate exploitable biomass and potential yield. Stratified sampling by depth zone and island was conducted over a 3-year period to evaluate shrimp catch rates. Catchability of the traps was estimated from a 12-day intensive fishing experiment performed at a small, isolated site in the Kaulakahi Channel; habitat areas were determined by digitizing nautical charts.

Results from a Leslie analysis of the depletion experiment showed that *H. laevigatus* is very susceptible to capture by traps (i.e., catchability $\hat{q}$ = 9.48 ha/trap-night). There was no evidence of a change in size structure through the course of the experiment.

Shrimp catch rates varied greatly by island and depth of capture. Exploitable biomass was greatest in the 460–640 m depth range; negligible amounts of shrimp occurred shallower than 350 m and deeper than 830 m. Catch rates were highest at Niihau and lowest at Oahu. The total exploitable biomass of shrimp in the main Hawaiian Is. was estimated to be 271 MT, a figure substantially less than previously believed.

Analysis of multiple size-frequency distributions for each sex showed no evidence of modal size progression. Assuming equilibrium conditions, application of the Wetherall et al. (1987) method to these data resulted in estimates of M/K = 1.01 for female shrimp and 0.74 for males. From these results and estimates of L_∞ we calculate that $F_{0.1}/M = 0.75$ for females and 0.86 for males.

An assessment of the exploitable biomass of *Heterocarpus laevigatus* in the main Hawaiian Islands. Part 1: Trapping surveys, depletion experiment, and length structure

Stephen Ralston

Tiburon Laboratory, Southwest Fisheries Science Center
National Marine Fisheries Service, NOAA
3150 Paradise Drive, Tiburon, California 94920

Darryl T. Tagami

Honolulu Laboratory, Southwest Fisheries Science Center
National Marine Fisheries Service, NOAA
2570 Dole Street, Honolulu, Hawaii 96822-2396

The caridean shrimp, *Heterocarpus laevigatus* Bate 1888, is an abundant deepwater inhabitant of the Hawaiian Is., where it has been fished sporadically since 1970 (Anon. 1979). Two early research surveys (Clarke 1972, Struhsaker and Aasted 1974) showed that large catches of this species, and its smaller congener *H. ensifer*, could readily be taken in baited traps in water depths of 365–825 m (200–450 fm).* Based on catch rates from around the island of Oahu, the deepwater shrimp resource seemed sufficiently abundant to support a commercial fishery (2.6 kg/trap-night for *H. laevigatus* and 6.6 kg/trap-night for *H. ensifer*; Struhsaker and Aasted 1974).

To date, however, attempts to harvest the resource have met with limited success, even though 75 MT of *H. laevigatus* were landed by one vessel during a 14-month period (Tagami and Barrows 1988). At its peak in 1983–84, a short-lived fishery developed, involving as many as 7 medium-sized (23–40 m) boats. At that time over 190 MT of *H. laevigatus* were landed, with an ex-vessel value of $1.5 million ($7.85/kg; Hawaii Dep. Land & Nat. Resour., Div. Aquat. Resour.). The fishery soon failed, however, primarily due to problems with gear loss, product processing, and localized stock depletions. Even so, the product was well received by the public, and rejuvenating the shrimp fishery remains a fishery development goal of the State of Hawaii (Anon. 1984).

With this interest in developing the Hawaiian fishery, major gaps in our knowledge of local *H. laevigatus* shrimp stocks have become apparent (see Gooding 1984, Dailey and Ralston 1986), although elsewhere in the Pacific more extensive data are available (e.g., Wilder 1977, King 1984 and 1986, Ralston 1986, Moffitt and Polovina 1987). Particularly lacking are estimates of the absolute abundance of the *H. laevigatus* stock in Hawaii and its ability to withstand sustained fishing pressure.

The primary objective of the work presented here was to estimate the exploitable biomass of *H. laevigatus* in the main Hawaiian Is. A secondary objective was to estimate growth and mortality rates through analysis of length-frequency data. Together

* Depths are given in meters with fathom equivalents (1.0 fm = 1.83 m), although contouring and stratification were based on nautical charts in fathoms.

Manuscript accepted 27 May 1992.
Fishery Bulletin, U.S. 90:494–504 (1992).

these findings could form a basis for estimating the potential yield of the shrimp resource.

To determine the exploitable biomass of shrimp at spatially discrete locations in Hawaii, the formula (Ricker 1975) was used:

$$\text{CPUE} = q\left[\frac{B}{A}\right]$$

where CPUE is the catch-per-unit-effort, q is the catchability coefficient of the fishing gear, B is exploitable biomass, and A is the area occupied by the population. This relationship is based on the explicit assumption that catch rate is strictly proportional to shrimp density (B/A), and that q is the proportionality constant equating these quantities. By rearrangement we have,

$$B = \frac{\text{CPUE} \cdot A}{q}.$$

Thus, to estimate the exploitable shrimp biomass at a locality we need (1) an unbiased estimate of catch rate, (2) a measure of the habitat area over which the catch rate prevails, and (3) knowledge of the sampling gear's efficiency (i.e., an estimate of q).

To accomplish these three objectives, the study was divided into two phases. First, a depletion experiment was conducted to estimate the catchability coefficient (q). This was followed by a depth-stratified sampling program for *H. laevigatus* around each of the main islands of the Hawaiian archipelago (i.e., Hawaii, Maui, Kahoolawe, Lanai, Molokai, Oahu, Kauai, and Niihau).

Methods

Shrimp trapping was conducted during a series of nine cruises of the NOAA ship *Townsend Cromwell* (Table 1). During each cruise, standard fishing gear was utilized to gather CPUE statistics at specific geographical locations. The gear employed was a top-loading pyramidal shrimp trap, identical in construction to those used commercially in Hawaii from 1983 to 1984. Each trap was made of welded steel reinforcement bars, had a 1.83 m^2 base, an overall volume of 1.84 m^3, and was covered by 1.27×2.54 cm mesh hardware cloth. A full description and illustration of the gear is given in Tagami and Barrows (1988).

Typically, 6–10 solitary traps were set daily and allowed to soak overnight. Traps were generally deployed in the afternoon and hauled the following morning, being in the water for a period of 16–20 hours. All traps were baited with approximately 3 kg of chopped mackerel *Scomber japonicus*. After hauling to the surface, each trap was emptied and the contents were sorted to species, counted, and weighed to the nearest 0.01 kg. Random subsamples of ~200 *H. laevigatus* were routinely collected, from which carapace length (CL) was measured to the nearest 0.1 mm using dial calipers. For all measured shrimp, sex was determined by examining the endopodite of the first pleopod (spatulate in males, pinnate in females; see King and Moffitt 1984). In addition, the ovigerous condition of females was recorded.

Table 1
Summary of shrimp-trapping cruise dates and locations.

Date	Location	No. of traps hauled
April 1985	Molokai	3
	Lanai	1
May 1986	Kaulakahi Channel	105
July 1986	Kaulakahi Channel	10
Sept. 1986	Kaulakahi Channel	10
Nov. 1986	Kaulakahi Channel	12
Sept./Oct. 1987	Niihau	68
	Kauai	128
	Kaulakahi Channel	11
Feb./March 1988	Kaulakahi Channel	10
	Oahu	8
	Hawaii	31
Oct. 1988	Kaulakahi Channel	17
	Molokai	20
	Lanai	18
	Maui	38
	Kahoolawe	8
March 1989	Oahu	67
	Molokai	32

Depletion experiment

To estimate q, an intensive fishing experiment was conducted (see also Ralston 1986). Depletion experiments, including the Leslie method used here (Ricker 1975), have three restrictive assumptions. First, all individuals in the exploitable portion of the population are equally likely to be captured with the fishing gear. Second, the fished population is closed, or else additions exactly balance removals other than those due to fishing. Third, fishing removals account for all changes in stock biomass, such that natural mortality, growth, and recruitment have negligible effects during the period of fishing. Thus, the best site for a depletion experiment is a naturally isolated, small area so that removals can be carried out over as short a time-interval as possible.

A small rise midway in the Kaulakahi Channel (21° 54.5′N, 159°56.5′W) separating Kauai and Niihau was

chosen for the work. This nearly circular rise (Fig. 1) with a crest at 421 m (230 fm), has an area of 1187 ha (horizontal planar area <640 m or 350 fm) and is isolated from the Islands of Kauai and Niihau by depths >730 m (400 fm; Fig. 2). The site lies in the required depth range for *H. laevigatus* and has relatively high densities of the target species.

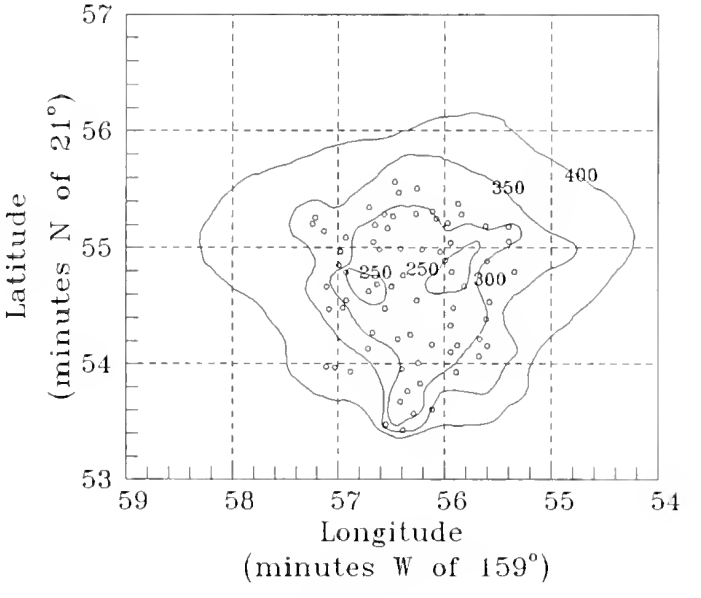

Figure 1
Contour map of the Kaulakahi Channel study site. Depths are in fathoms, and circles represent trap-set locations.

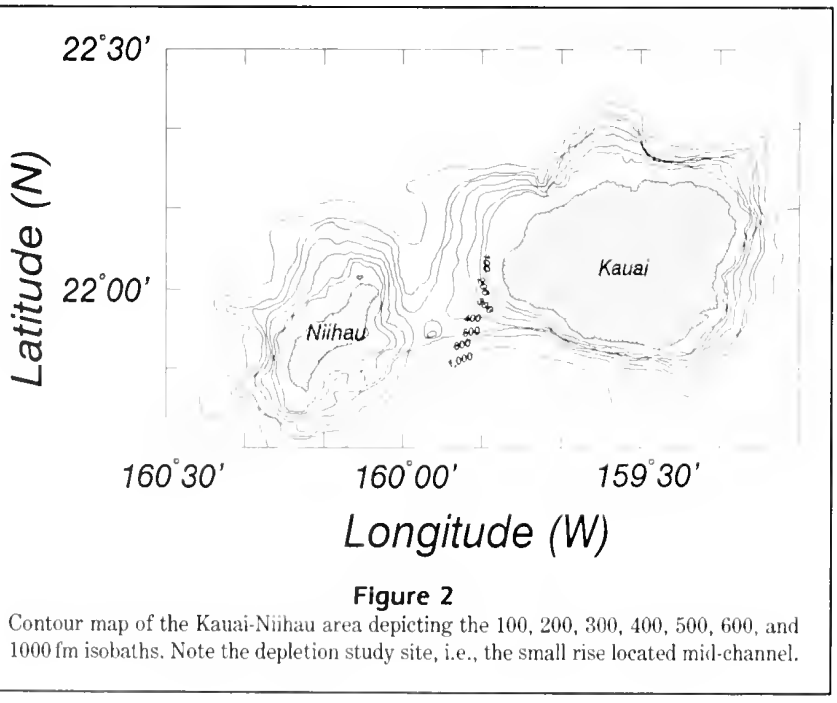

Figure 2
Contour map of the Kauai-Niihau area depicting the 100, 200, 300, 400, 500, 600, and 1000 fm isobaths. Note the depletion study site, i.e., the small rise located mid-channel.

The intensive fishing experiment was conducted 13–24 May 1986. During each of the 12 days of the experiment, 6–14 pyramidal shrimp traps were set between depths of 421 and 695 m (230 and 380 fm). Following the Leslie method (Ricker 1975, Seber 1982), catchability was estimated directly from the slope of the linear regression of CPUE on corrected cumulative catch. That is,

$$\begin{aligned} CPUE_i &= q \cdot B_i \\ &= q(B_0 - K_i) \\ &= qB_0 - qK_i, \end{aligned}$$

where $CPUE_i$ is the catch-per-unit-effort on day i (kg/trap-night), q is the catchability coefficient/trap-night of the pyramid traps, B_i is the average biomass (kg) present on day i, B_0 is the biomass (kg) of shrimp present at the start of the experiment, and K_i is the corrected cumulative removals for day i, defined as

$$K_i = \frac{1}{2} C_i + \sum_{n=1}^{i-1} C_n,$$

where $C_n (n = 1, 2, \ldots, i)$ is the catch (kg) taken on each day of the experiment. Note that the estimate of catchability ($\hat{q}$) pertains strictly to the interaction between the traps we used and the stock resident in the study area, which is normalized to unit area after multiplying by 1187 ha (i.e., the area of the study site).

Determination of habitat areas

The distribution of *H. laevigatus* is strongly dependent on bottom depth. Little or no shrimp occur in waters outside the 366–915 m (200–500 fm) range (Struhsaker and Aasted 1974, Gooding 1984, Dailey and Ralston 1986). In the main portion of the Hawaiian Archipelago (Hawaii, Maui, Lanai, Kahoolawe, Molokai, Oahu, Kauai, and Niihau) a number of islands share a common 915 m (500 fm) depth contour (e.g, Kauai and Niihau; Fig. 2). Even so, in our study each island was treated as a separate stock for

purposes of geographically stratifying the analysis. An exception was made for the islands of Maui, Lanai, Kahoolawe, and Molokai (MLKM), which share, in addition to the 915 m (500 fm) contour, a common 366 m (200 fm) isobath. These four islands were, therefore, treated as a single geographic locality.

Estimates of the amount of suitable shrimp habitat, in hectares (1 ha = 0.01 km^2), were obtained by determining the horizontal planar area lying between charted depth contours. A large digitizing tablet was used to calculate all area estimates directly from nautical charts (NOAA charts 19016, 19019, and 19022, and Defense Mapping Agency bottom contour charts). These charts included 915 m (500 fm) isobaths, but we manually contoured all of the 366 m (200 fm) isobaths using the sounding data provided on each chart. In addition, good detailed bathymetry was available for the islands of Kauai and Niihau, and at these sites the 458 m (250 fm), 549 m (300 fm), 640 m (350 fm), 732 m (400 fm), and 824 m (450 fm) isobaths were contoured and digitized as well.

Each contour was digitized three times by each author, providing a minimum estimate of measurement error in our calculation of habitat areas. These errors were typically small (median CV 0.5%, range 0.1–1.9%). A potentially more serious type of error concerns discrepancies between the actual locations of contours and their representations on charts. However, we had no information concerning the magnitude of this type of error and, given that measurement errors were negligible, we assumed that our estimates of habitat area were accurate and precise.

These data were then used to calculate habitat areas for each 92 m (50 fm) depth interval between 366 and 915 m (200–500 fm). First, the relative distribution of habitat was calculated from the Kauai and Niihau data. To estimate depth-specific habitat areas for the three remaining sites (Oahu, MLKM, and Hawaii), the combined relative proportions of habitat for each depth interval obtained at Kauai–Niihau were applied to the estimates of total habitat area between 366 and 915 m (200–500 fm). In support of this procedure, results in Mark and Moore (1987) indicate that slope-depth relationships among the main islands of the archipelago are, in general, similar.

Depth-stratified sampling

For the second phase of the assessment, each of the island areas was targeted for comprehensive trapping surveys to determine abundance patterns (i.e., catch rate) with depth and to estimate standing stocks (Table 1). A depth-stratified sampling approach was used. From preliminary data gathered at Kauai and Niihau during the September 1987 cruise, the mean and variance in CPUE were calculated for each of the six 92 m (50 fm) depth intervals lying in the 366–915 m (200–500 fm) range. Based on the results of this vertical distribution survey, sampling effort was optimally partitioned into depth strata by Neyman allocation (Cochran 1977), i.e., trap allocations to each depth interval were based on the product of abundance (CPUE · habitat area) and the standard deviation of CPUE at that depth. As each cruise progressed, CPUE means and variances were recalculated daily and the trap allocation schedule was updated.

From the results of the surveys, exploitable biomass was estimated (Eq. 1) for each depth interval at each site visited. This calculation assumes that the catchability estimate, which was determined at the depletion experiment study site, can be extended to all other localities sampled. An estimate of the variance of the biomass for each stratum was obtained from Eq. 1 using the delta method (Seber 1982), resulting in

$$\mathrm{VAR[B]} \approx \frac{\mathrm{A}^2}{\hat{\mathrm{q}}^2}\,\mathrm{VAR[CPUE]} + \frac{\mathrm{A}^2 \cdot \mathrm{CPUE}^2}{\hat{\mathrm{q}}^4}\,\mathrm{VAR}[\hat{\mathrm{q}}]$$

if all covariance terms are zero (a reasonable first assumption) and VAR[A] is negligible (see above). Confidence intervals were then calculated using the distribution of standard normal scores ($\alpha = 0.05$, $Z = 1.96$).

Length-frequency analysis

The Kaulakahi Channel experimental depletion site was visited on seven separate occasions during May 1986–March 1988 (Table 1). During each visit a length-frequency sample of *H. laevigatus* was obtained, with the ultimate goal of analyzing the progression of size modes over time (egg bearing is strongly seasonal; Dailey and Ralston 1986, Moffitt and Polovina 1987). Additional length-frequency samples were obtained during the course of the depth-stratified sampling at each of the island sites.

Mortality and growth parameters were estimated from length-frequency distributions using the regression method of Wetherall et al. (1987). This technique requires an equilibrium population size-structure, an undesirable and restrictive assumption. Even so, data are available to support its use. Dailey and Ralston (1986) present length-frequency data for male and female shrimp sampled during the earliest stages of the fishery (1983–84). The data are very similar to those presented here, suggesting that exploitation has yet to seriously affect size composition. Additionally, the time-invariance of the size-frequency data we collected at the Kaulakahi study site (see below) indicates equilibrium conditions.

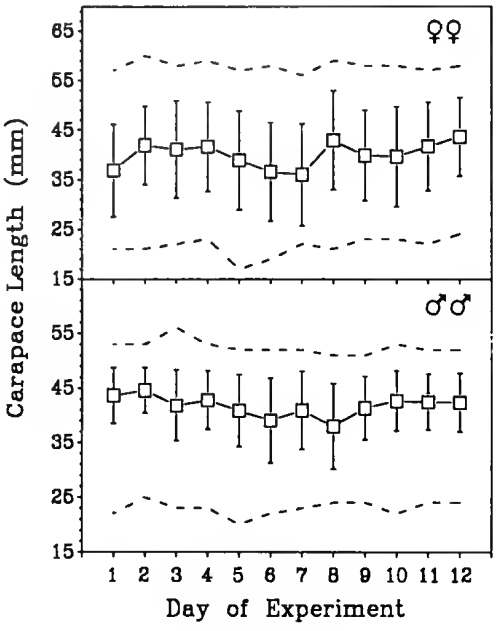

Figure 3

Distributions of carapace length for male and female *Heterocarpus laevigatus* during the depletion experiment. Open squares are means bracketed by ±1 SD; dashed lines represent maximum and minimum observed sizes.

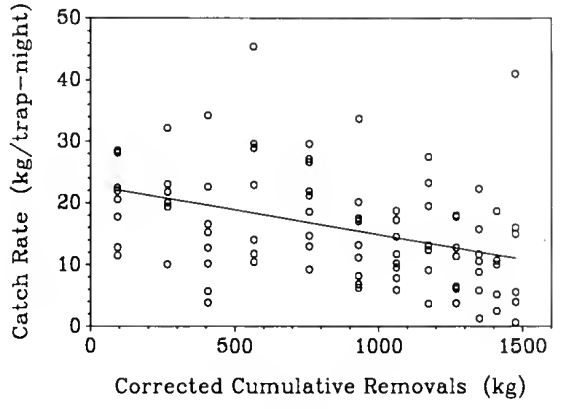

Figure 4

Leslie model applied to the experimental depletion of *Heterocarpus laevigatus* at the Kaulakahi Channel study site. Each point represents one valid trap-night of fishing.

For each sex, the von Bertalanffy asymptotic length (CL_∞) and the ratio (Θ) of the total mortality rate (Z/yr) to the von Bertalanffy growth coefficient (K/yr) were estimated from a weighted regression of mean lengths ($CL_{\mu i}$) on full vulnerability cutoff lengths (CL_{ci}). In the analysis, the CL_{ci} were incremented in 1.0 mm steps above CL_{co}, the minimum size of full vulnerability to the gear, and the $CL_{\mu i}$ were recalculated at each step. Using the morphometric functional regressions presented in Dailey and Ralston (1986), CL_{co} was set equal to 30 mm (the length of *H. laevigatus* with carapace width = 12.7 mm), corresponding to the least dimension of the wire mesh covering the traps. This approach to estimating CL_{co} deviates from that used in previous applications of the regression method to *H. laevigatus* stocks. Dailey and Ralston (1986) and Moffitt and Polovina (1987) both assumed that shrimp were not fully selected by baited traps until reaching a CL greater than the modal size of length-frequency distributions from trap catches.

Because the size-structure we observed was similar to the unexploited stock (see above), it follows that $\Theta = M/K$, where M is natural mortality/yr. Likewise, using the length-weight regressions of Dailey and Ralston (1986), we estimated the asymptotic weights (W_∞) for each sex as the predicted weight at $CL = CL_\infty$. The average size at entry to the fishery (CL_ρ, *sensu* Beverton and Holt 1957) was obtained by averaging the minimum size caught and CL_{co}. Given estimates of M/K, W_∞, and CL_ρ, we used the tables presented in Beverton and Holt (1966) to determine sex-specific values of yield-per-recruit (Y/R) at various levels of exploitation (F/M). From these data we computed values of $F_{0.1}/M$, the exploitation level at which the marginal increase in Y/R declines to 10% of its value at the origin (Gulland and Boerema 1973, Gulland 1983).

Results

Depletion experiment

During the depletion experiment, 123 pyramid shrimp traps were set at the Kaulakahi Channel study site. Of these, 19 were lost, resulting in 104 effective trap-nights of standard fishing effort and a gear loss rate of 15%. A total of 45,482 *H. laevigatus* were caught, which collectively weighed 1499 kg. The average size of each shrimp was therefore 33.0 g. During the 12-day course of the experiment, no change occurred in the daily mean size of shrimp caught (Fig. 3; $r_{♀} = 0.32$, df 10; $r_{♂} = -0.28$, df 10).

Individual trap catches were regressed on values of corrected cumulative removals to date (Fig. 4). Traps that did not fish properly (e.g., the funnel entrance was ajar upon retrieval) were not included, although cumulative removals (K_i) included all shrimp caught in the study area (<695 m or 380 fm). Therefore, each point represents an observation of CPUE from one valid

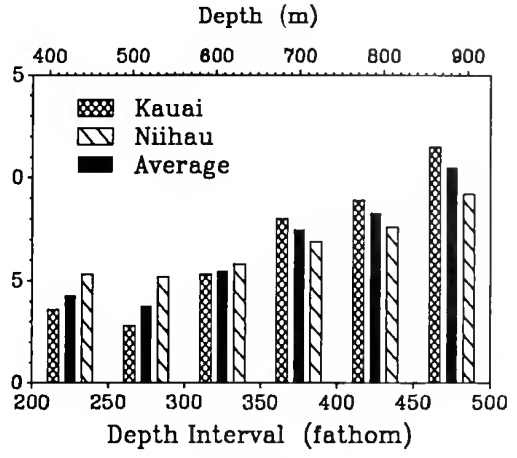

Figure 5

Distribution of habitat by depth at Kauai and Niihau. The composite average distribution is based on pooling habitat at these two sites.

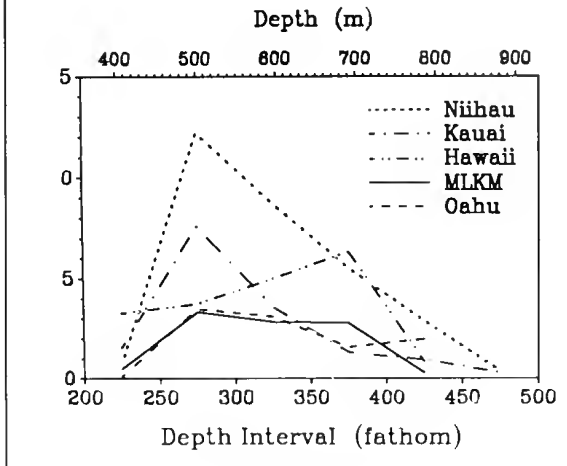

Figure 6

Average CPUE of *Heterocarpus laevigatus* relative to depth at each site sampled.

trap-night of fishing. Also presented is the ordinary least-squares regression equation relating these variables. The equation of the line is

$$CPUE_i = 22.84 - 0.007988[K_i],$$

with standard errors of the slope and intercept equal to 0.001997 and 1.9368, respectively. The regression is highly significant ($F_{1,89} = 16.00$, P 0.0001). The residuals show no obvious departure from linearity, an indication of constant catchability.

Under the Leslie model, the exploitable biomass at the start of the experiment is defined by the x-intercept, i.e., 2859 kg. Because the study site covered 1187 ha, this amounts to an initial density of 2.4087 kg/ha, which produced an initial catch rate ($CPUE_0$) equal to 22.84 kg/trap-night (i.e., the y-intercept). Then, $\hat{q}$ expressed on a hectare basis, rather than defined in terms of the study site, is estimated to be 9.4798 ha/trap-night. In real terms, one overnight soak of a single, large pyramidal shrimp trap is estimated to have captured ~0.8% of the shrimp in the entire study area, which is equivalent to all the shrimp in ~9.5 ha, were they randomly dispersed. The standard error of $\hat{q}$/ha is the product of A (1187 ha) and the standard error of $\hat{q}$ measured over the study site (0.001997) (Seber 1982).

It is instructive to note that an initial density of 2.4087 kg/ha is equivalent to an average of 73 shrimp/ha (see statistics for mean shrimp weight above). Based on this density, the average utilization of habitat by each shrimp was 137 m^2, a remarkable figure given the relatively high catch rate encountered at the beginning of the depletion experiment (22.83 kg/trap-night).

Depth-stratified sampling

Habitat areas by 92 m (50 fm) depth intervals were estimated for the Oahu, Hawaii, and MLKM sites by assuming that the proportionate distribution of habitat between 366 and 915 m (200–500 fm) at these sites was the same as the composite distribution obtained at Kauai and Niihau. While there were some differences in the distribution of habitat with depth between Kauai and Niihau (Fig. 5, Table 2), they were relatively minor. At both sites the amount of habitat in the 458–549 m (250–300 fm) depth interval was slightly less than in the 366–458 m (200–250 fm) interval; but with increasing depth below that, the amount of habitat per 92 m (50 fm) depth interval increased steadily.

There were, however, marked differences in CPUE with depth among the five localities sampled (Fig. 6, Table 2). Catch rates at Niihau were particularly high relative to the other areas, especially at 458–549 m (250–300 fm). Catch rates at Oahu and MLKM were much lower. The modes of the distributions at Kauai and Niihau were shifted to the shallow end of the depth range, whereas at Hawaii it was shifted deeper.

Results presented in Table 2 provide estimates of the exploitable biomass (B), as well as variance estimates, for the depth intervals sampled at each site. Although catch rates at Niihau are quite high, the reduced amount of habitat at this island (69,530 ha) is sufficient to support only a small stock of shrimp (35.7 MT). Oahu, with its much lower catch rates, has a larger exploit-

Table 2
Depth-stratified sampling results for *Heterocarpus laevigatus* in the main Hawaiian Is.

Depth range (m)	Depth range (fm)	No. traps set	Mean CPUE kg/trap	VAR[CPUE]	Habitat area (ha)	B (kg)	VAR[B]
Kauai							
366–458	200–250	29	1.566	0.894	12,760	2,108	1,897,271
458–549	250–300	37	7.587	1.093	12,070	9,663	7,608,356
549–640	300–350	25	3.607	0.322	14,410	5,481	2,621,353
640–732	350–400	18	1.324	0.436	16,940	2,367	1,742,930
732–824	400–450	6	0.953	0.203	17,770	1,786	912,472
824–915	450–500	7	0.299	0.038	20,200	637	197,960
Totals		122			94,150	22,042	14,980,342
Niihau							
366–458	200–250	9	0.788	0.586	10,670	887	791,140
458–549	250–300	18	12.214	7.253	10,570	13,611	20,586,349
549–640	300–350	19	8.719	3.335	11,010	10,127	10,907,759
640–732	350–400	10	5.533	2.737	11,730	6,847	7,120,644
732–824	400–450	4	2.903	0.906	12,210	3,739	2,377,052
824–915	450–500	4	0.380	0.094	13,340	535	204,092
Totals		64			69,530	35,746	41,987,037
Oahu							
366–458	200–250	6	0.122	0.017	41,570	535	342,588
458–549	250–300	20	3.482	3.239	40,100	14,726	71,490,061
549–640	300–350	33	3.115	0.480	45,070	14,810	24,568,526
640–732	350–400	13	1.594	0.698	50,800	8,542	24,613,230
732–824	400–450	2	1.990	0.303	53,300	11,187	17,379,858
824–915	450–500	0	0.000	0.000	59,510	0	0
Totals		74			290,350	49,800	138,394,264
Hawaii							
366–458	200–250	1	3.270	2.152	38,720	13,357	47,049,206
458–549	250–300	4	3.750	2.223	37,320	14,767	48,097,991
549–640	300–350	11	5.008	3.882	41,980	22,171	106,796,660
640–732	350–400	11	6.325	3.036	47,300	31,560	137,841,468
732–824	400–450	4	0.858	0.889	49,630	4,491	25,603,225
824–915	450–500	0	0.000	0.000	55,430	0	0
Totals		31			270,350	86,345	365,388,550
Maui-Lanai-Kahoolawe-Molokai							
366–458	200–250	15	0.500	0.110	69,420	3,662	6,716,452
458–549	250–300	43	3.338	0.399	66,920	23,567	54,580,681
549–640	300–350	42	2.823	0.168	75,250	22,409	41,983,921
640–732	350–400	19	2.795	0.653	84,790	25,004	91,353,003
732–824	400–450	1	0.300	0.079	88,970	2,815	7,443,949
824–915	450–500	0	0.000	0.000	99,370	0	0
Totals		120			484,730	77,457	202,078,006

able biomass of *H. laevigatus* than does Niihau. In aggregate, we estimate the exploitable stock at all islands to be $B_{\Sigma tot} = 271.4$ MT ($p[217.3 \leq B_{\Sigma tot} \leq 325.5] = 0.95$, SE 27.6MT, CV 10.18%).

Analysis of length-frequency data

Although the Kaulakahi Channel study site was sampled on seven different occasions over a 29-month period (May 1986–October 1988), during which over 6800 female and 11,800 male shrimp were sexed and measured, there was little evidence of progression in size modes (Fig. 7). The CL frequency distributions of male shrimp were particularly stagnant, and those of females showed no coherent pattern that could be attributed to the influx of year-classes into the exploitable population.

Due to the apparent stationary behavior of these

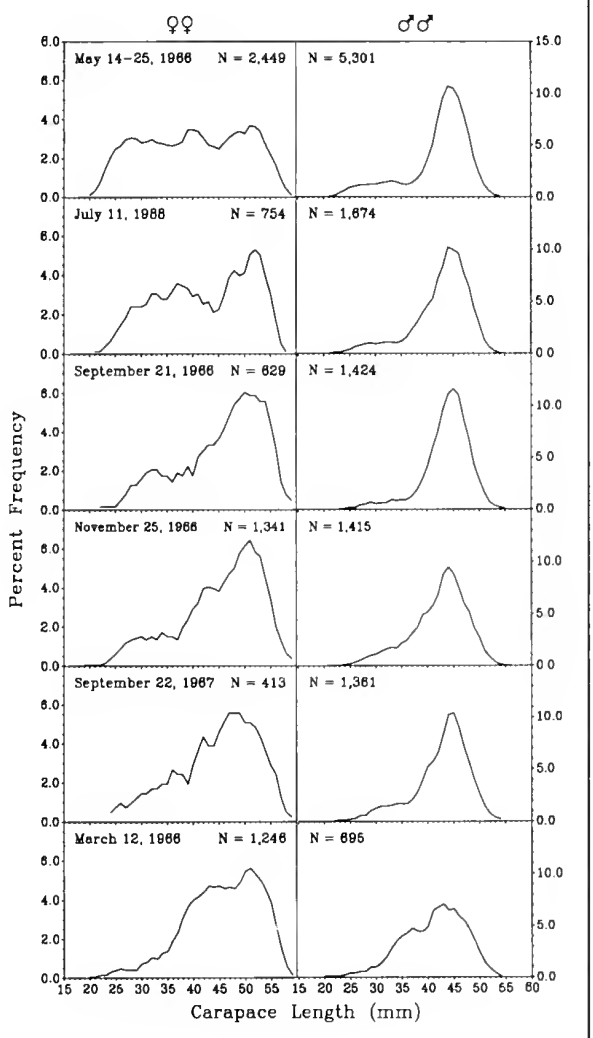

Figure 7

Length-frequency distributions of female and male *Heterocarpus laevigatus* at the Kaulakahi Channel study site.

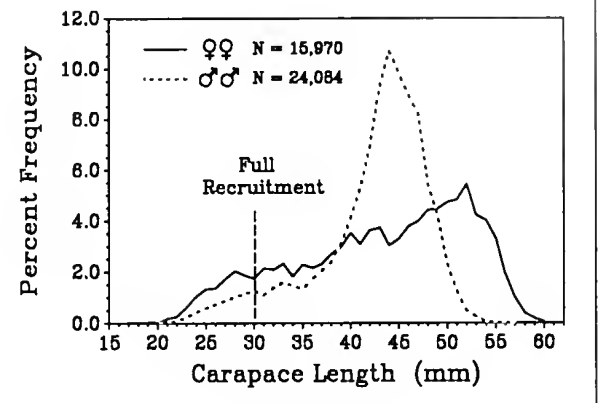

Figure 8

Composite length-frequency distributions for all female and male *Heterocarpus laevigatus* sampled.

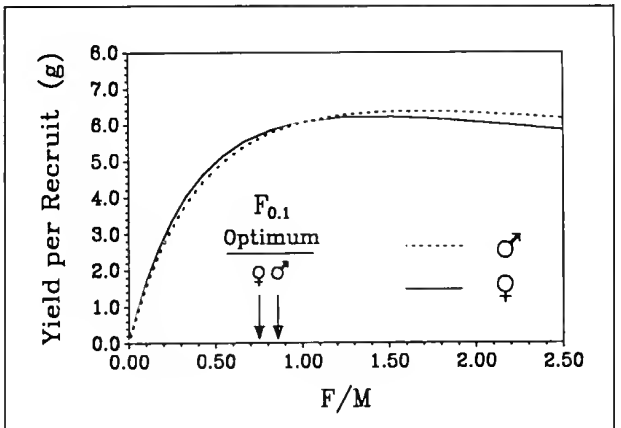

Figure 9

Yield-per-recruit of *Heterocarpus laevigatus* and estimates of optimum exploitation level ($F_{0.1}/M$).

distributions, all the length data were pooled (Fig. 8). It is evident from the figure that female shrimp reach substantially larger sizes than do males, in agreement with previously published work (Dailey and Ralston 1986, Moffitt and Polovina 1987). Superimposed on the combined length-frequency distributions of males and females is the estimated size of *H. laevigatus* when fully vulnerable to the traps (i.e., $CL_{co} = 30$ mm CL). The carapace width of shrimp this size is equal to 1.27 cm (0.5″), the minimum mesh size of the traps.

We applied the Wetherall et al. (1987) regression method to these length-frequency data and estimated that $\Theta_{♀} = 1.01 \pm 0.052$ and $\Theta_{♂} = 0.74 \pm 0.075$. For females we estimated that $CL_{\infty} = 58$ mm (SE 0.37) and for males $CL_{\infty} = 50$ mm (SE 0.44), corresponding to $W_{\infty} = 80$ g for females and 55 g for males.

The smallest shrimp we captured in the pyramid traps was 16 mm CL. Below this size, selectivity of the gear was zero. By equating carapace width and mesh size, we determined that $CL_{co} = 30$ mm. Thus, our estimate of the size at 50% recruitment to the fishery (CL_{ρ}) is 23 mm. Given this result, and sex-specific estimates of Θ and W_{∞}, we calculate that for females $F_{0.1}/M = 0.75$ and for males $F_{0.1}/M = 0.86$ (Fig. 9).

Discussion

In this assessment, projections of exploitable biomass depend greatly on the estimate of catchability obtained from the Leslie depletion experiment. Due to its major role in the calculations, sources of bias in its estimation must be considered carefully.

There is evidence to show that estimates of crustacean population size obtained through survey removal methods like the Leslie and DeLury methods (Ricker 1975) may severely misrepresent the actual size of the population. In his study, Morrissy (1975) found that DeLury estimates of population number of *Cherax tenuimanus* were anywhere from 39 to 53% of those based on a complete count of the population. Similarly, DeLury estimates of the population density of *Panulirus cygnus* were 25% of those estimated from diver counts (Morgan 1974a).

The most likely origin of bias in these situations is that not all individuals in the exploitable portion of the population are equally vulnerable (*sensu* Morrissy 1973) to the gear. For example, when sampling with baited drop nets, the catch of *C. tenuimanus* in intermolt, expressed as a known fraction of the actual population, was much higher than the catch in a premolt condition; individuals in molt stages immediately preceding and following ecdysis were not caught at all (Morrissy 1975).

It is possible that a similar bias was operating during the depletion study at the Kaulakahi Channel study site. The presence of shrimp in the exploitable portion of the population, which were less susceptible to trapping, would result in overestimation of catchability and underestimation of biomass. Factors such as molt stage (Morgan 1974b, Morrissy 1975), sex (Morrissy 1973), and feeding history (Sainte-Marie 1987) are known to cause variation in vulnerability to trapping. Although social dominance, mediated through differences in size, can affect catchability (Morrissy 1973, Chittleborough 1974), it is unlikely to have substantially biased our results because the catch size-structure remained unchanged during the experiment (Fig. 3). Also, Gooding et al. (1988) did not see "any overt aggressive behavior" among *H. ensifer* that were active around baits. Lastly, seasonal and interannual alterations in catchability due to temperature (Chittleborough 1970, Morgan 1974b), salinity (Morgan 1974b), and food availability (Chittleborough 1970) operate over longer time-scales than the depletion experiment.

Two other lines of evidence support the premise that shrimp biomass was underestimated. Although results presented in Figure 4 indicate that 12 days of trapping dropped the catch rate to 48% of its starting value (10.87 kg/trap-night), it had risen to 19.73 kg/trap-night when resampled 47 days later (data from 9–11 July 1986 cruise; see Table 1). If catchability is estimated from the decline in catch rate that occurred between the beginning of the depletion study (22.84 kg/trap-night) to the time the site was resampled 2 months later, and we assume the decline was due only to trap removals (1499.00 kg), we obtain $\hat{q} = 2.4624$ ha/trap-night. This represents a 74% reduction in the estimate, which in turn would inflate biomass estimates by a factor of 3.85 (i.e., $B_{\Sigma_{tot}} = 1050$ MT). This relative bias is similar to that reported by Morgan (1974a) for *Panulirus cygnus* (see above).

From submersible observations of *H. laevigatus* density, Moffitt and Parrish (1992) obtained $\hat{q} = 0.2895$ ha/trap-night for the same traps we used, amounting to a 33-fold difference relative to our Leslie analysis. They, too, expressed concerns about bias in catchability estimates derived from depletion experiments due to variable susceptibility to the gear. Conversely, their estimate of catchability was based on comparing site-specific March 1988 trap catches with submersible observations made during August, even though *H. laevigatus* undergoes seasonal vertical migrations (King 1983, Dailey and Ralston 1986). In addition, at the start of each dive, they deployed a baited trap in the area of the submersible. Both factors could lead to underestimation of catchability.

It is clear that biased estimates of q will result if the probability of capture is not uniform among shrimp. In an attempt to solve this problem, Quinn (1987) developed a depletion model that explicitly incorporated a term for non-constant catchability. Application of his model to Pacific halibut effectively accounted for short-term trends in q, but auxiliary estimates of fishing and natural mortality were required, data that are unavailable here.

The primary objective of this study was to determine the exploitable biomass of *H. laevigatus* in the main Hawaiian Is. (MHI). Even if shrimp biomass were as high 1050 MT, rather than 271 MT (see above), our results indicate that the MHI stock is much smaller than previously believed, and that prior estimates of maximum sustainable yield (MSY) are much too high. For example, Struhsaker and Aasted (1974), using figures from a fishery for *H. reedi* off the coast of Chile, speculated that *H. ensifer* in Hawaii could sustain a level of production equal to 10–20 kg/ha · yr^{-1}. If *H. laevigatus* were assumed to be equally productive (e.g., Anon. 1979), then, given there are ~350,000 ha of prime habitat at 458–640 m (250–350 fm) in the MHI alone (Table 2), the resulting estimate of MSY exceeds stock biomass many times over. Moreover, catch rates of *H. laevigatus* in the distant Northwestern Hawaiian Is. (Nihoa to Kure), which represent a similar amount of shrimp habitat as the MHI, are no more than half those observed in the MHI (Gooding 1984, Tagami and Barrows 1988, Tagami and Ralston 1988).

Our estimates of $\Theta_{\varphi} = 1.01$ and $\Theta_{\sigma} = 0.74$ are much lower than those given in Dailey and Ralston (1986), who reported $\Theta_{\varphi} = 2.9$ and $\Theta_{\sigma} = 4.3$. By requiring CL_{co} to be greater than the modal size, they effectively constrained Θ to values much greater than unity. A similar requirement was imposed by Moffitt and Polovina

(1987), who estimated $\Theta_{\varphi} = 1.9$ and $\Theta_{\sigma} = 2.1$ for *H. laevigatus* in the Mariana Is. Additionally, use of the "mode" criterion to establish the minimum size at full vulnerability results in substantially greater sensitivity of Θ to input estimates of CL_{co}. For example, if CL_{co} is 30 mm as we suggest (Fig. 8), ±2 mm perturbations in CL_{co} result in −9% and +12% changes in estimates of Θ_{σ}. However, if the mode of the size-frequency distribution is used instead ($CL_{co} = 44$ mm), the same perturbations alter estimates of Θ_{σ} by −16% and +46%. Similar sensitivity was observed in estimates of Θ_{φ}. In summary, it is our belief that independent estimates of CL_{co} are superior to those obtained from the size data analyzed, particularly when there is no reason to suspect that agonistic interactions affect the catch size-structure.

Lower values of Θ indicate a reduction in the instantaneous mortality rate (Z), an increase in the von Bertalanffy growth coefficient (K), or both. We favor the first hypothesis, largely because of the cold (4–6°C), trophically-impoverished habitat in which *H. laevigatus* reside. In many respects these shrimp represent a crustacean analog to Pacific ocean perch *Sebastes alutus*, which grow very slowly, exhibit extreme longevity, and display low rates of natural mortality (Leaman and Beamish 1984). Consequences of this life-history pattern are that (1) under pristine conditions, individuals accumulate in the largest size-categories (Fig. 8), (2) the ratio of production to biomass is low, and (3) stocks are very susceptible to overfishing.

Acknowledgments

We would like to thank the scientists and crew of the NOAA RV *Townsend Cromwell* for their assistance in helping us complete this study. This paper benefited from reviews by G.W. Boehlert, A.D. MacCall, R.B. Moffitt, and J.J. Polovina.

Citations

Anonymous
1979 Hawaii fisheries development plan. Hawaii Dep. Land and Nat. Resour., Honolulu, 297 p.
1984 Status of fisheries assessment of development and management needs for selected crustacean species in the western Pacific region. West. Pac. Reg. Fish. Manage. Counc., Honolulu, 60 p.

Beverton, R.J.H., and S.J. Holt
1957 On the dynamics of exploited fish populations. U.K. Minist. Agric. Fish., Fish. Invest. (Ser. 2) 19, 533 p.
1966 Manual of methods for fish stock assessment. Part. 2. Tables of yield functions. FAO Fish. Tech. Pap. 38, Rev. 1, 67 p.

Chittleborough, R.G.
1970 Studies on recruitment in the western Australian rock lobster *Panulirus longipes cygnus* George: Density and natural mortality of juveniles. Aust. J. Mar. Freshwater Res. 21: 131–148.
1974 Home range, homing and dominance in juvenile western rock lobsters. Aust. J. Mar. Freshwater Res. 25:227–234.

Clarke, T.A.
1972 Collections and submarine observations of deep benthic fishes and decapod crustacea in Hawaii. Pac. Sci. 26:310–317.

Cochran, W.G.
1977 Sampling techniques. Wiley, NY, 428 p.

Dailey, M.D., and S. Ralston
1986 Aspects of the reproductive biology, spatial distribution, growth, and mortality of the deepwater caridean shrimp, *Heterocarpus laevigatus*, in Hawaii. Fish. Bull., U.S. 84: 915–925.

Gooding, R.M.
1984 Trapping surveys for the deepwater caridean shrimps, *Heterocarpus laevigatus* and *H. ensifer* in the Northwestern Hawaiian Islands. Mar. Fish. Rev. 46(2):18–26.

Gooding, R.M., J.J. Polovina, and M.D. Dailey
1988 Observations of deepwater shrimp, *Heterocarpus ensifer*, from a submersible off the island of Hawaii. Mar. Fish. Rev. 50(1):32–39.

Gulland, J.A.
1983 Fish stock assessment. A manual of basic methods. Wiley, NY, 223 p.

Gulland, J.A., and L.K. Boerema
1973 Scientific advice on catch levels. Fish. Bull., U.S. 71: 325–335.

King, M.G.
1983 The ecology of deepwater caridean shrimps (Crustacea: Decapoda: Caridea) near tropical Pacific Islands with particular emphasis on the relationship of life history patterns to depth. Ph.D. thesis, Univ. South Pacific, Suva, Fiji, 258 p.
1984 The species and depth distributions of deepwater caridean shrimps (Decapoda, Caridea) near some southwest Pacific Islands. Crustaceana 47:174–191.
1986 The fishery resources of Pacific island countries. Part 1. Deep-water shrimps. FAO Fish. Tech. Pap. (272.1), 45 p.

King, M.G., and R.B. Moffitt
1984 The sexuality of tropical deepwater shrimps (Decapoda: Pandalidae). J. Crustacean Biol. 4:567–571.

Leaman, B.M., and R.J. Beamish
1984 Ecological and management implications of longevity in some northeast Pacific groundfishes. Int. N. Pac. Fish. Comm. Bull. 42:85–97.

Mark, R.K., and J.G. Moore
1987 Slopes of the Hawaiian ridge. *In* Decker, R.W. (ed.), Volcanism in Hawaii, p. 101–107. U.S. Geol. Surv. Prof. Pap. 1350.

Moffitt, R.B., and F.A. Parrish
1992 An assessment of the exploitable biomass of *Heterocarpus laevigatus* in the main Hawaiian Islands. Part 2: Observations from a submersible. Fish. Bull., U.S. 90:476–482.

Moffitt, R.B., and J.J. Polovina
1987 Distribution and yield of the deepwater shrimp *Heterocarpus* resource in the Marianas. Fish. Bull., U.S. 85:339–349.

Morgan, G.R.
1974a Aspects of the population dynamics of the western rock lobster, *Panulirus cygnus* George. 1. Estimation of population density. Aust. J. Mar. Freshwater Res. 25:235–248.

1974b Aspects of the population dynamics of the western rock lobster, *Panulirus cygnus* George. II. Seasonal changes in the catchability coefficient. Aust. J. Mar. Freshwater Res. 25: 249–259.

Morrissy, N.M.

1973 Normal (Gaussian) response of juvenile marron, *Cherax tenuimanus* (Smith) (Decapoda: Parastacidae), to capture by baited sampling units. Aust. J. Mar. Freshwater Res. 24: 183–195.

1975 The influence of sampling intensity on the 'catchability' of marron, *Cherax tenuimanus* (Smith) (Decapoda: Parastacidae). Aust. J. Mar. Freshwater Res. 26:47–73.

Quinn, T.J. III

1987 Standardization of catch-per-unit-effort for short-term trends in catchability. Nat. Resour. Model. 1(2):279–296.

Ralston, S.

1986 An intensive fishing experiment for the caridean shrimp, *Heterocarpus laevigatus*, at Alamagan Island in the Mariana Archipelago. Fish. Bull., U.S. 84:927–934.

Ricker, W.E.

1975 Computation and interpretation of biological statistics of fish populations. Fish. Res. Board Can. Bull. 191, 382 p.

Saint-Marie, B.

1987 Meal size and feeding rate of the shallow-water lysianassid *Anonyx sarsi* (Crustacea: Amphipoda). Mar. Ecol. Prog. Ser. 40:209–219.

Seber, G.A.F.

1982 The estimation of animal abundance, 2d ed. Griffin, London, 506 p.

Struhsaker, P., and D.C. Aasted

1974 Deepwater shrimp trapping in the Hawaiian Islands. Mar. Fish. Rev. 36(10):24–30.

Tagami, D.T., and S. Barrows

1988 Deep-sea shrimp trapping *Heterocarpus laevigatus* in the Hawaiian Archipelago by a commercial fishing vessel. NOAA Tech. Memo. NOAA-TM-NMFS-SWFC-103, NMFS Honolulu Lab., 14 p.

Tagami, D.T., and S. Ralston

1988 An assessment of exploitable biomass and projection of maximum sustainable yield for *Heterocarpus laevigatus* in the Hawaiian Islands. Admin. Rep. H-88-14, Honolulu Lab., Southwest Fish. Sci. Cent., 22 p.

Wetherall, J.A., J.J. Polovina, and S. Ralston

1987 Estimating growth and mortality in steady-state fish stocks from length-frequency data. *In* Pauly, D., and G.R. Morgan (eds.), Length-based methods in fisheries research, p. 53–74. ICLARM Conf. Proc. 13., Int. Cent. Living Aquat. Resour. Manage., Manila, and Kuwait Inst. Sci. Res., Safat, Kuwait.

Wilder, M.J.

1977 Biological aspects and fisheries potential of two deepwater shrimps *Heterocarpus ensifer* and *Heterocarpus laevigatus* in waters surrounding Guam. M.S. thesis, Univ. Guam, Agana, 79 p.

Interannual variation and overlap in the diets of pelagic juvenile rockfish (Genus: *Sebastes*) off central California

Carol A. Reilly
Tiburon Laboratory, Southwest Fisheries Science Center
National Marine Fisheries Service, NOAA, 3150 Paradise Drive, Tiburon, California 94920

Tina Wyllie Echeverria
Tiburon Laboratory, Southwest Fisheries Science Center
National Marine Fisheries Service, NOAA, 3150 Paradise Drive, Tiburon, California 94920
Present address: School of Fisheries and Ocean Sciences
University of Alaska, Fairbanks, Alaska 99775-1080

Stephen Ralston
Tiburon Laboratory, Southwest Fisheries Science Center
National Marine Fisheries Service, NOAA, 3150 Paradise Drive, Tiburon, California 94920

Abstract.– The diets of pelagic juveniles of widow rockfish *Sebastes entomelas*, yellowtail rockfish *S. flavidus*, chilipepper *S. goodei*, shortbelly rockfish *S. jordani*, and bocaccio *S. paucispinis* were compared using samples collected during 1984–87. All five species co-occur as pelagic juveniles off central California. Frequency of occurrence, percent by number, and a ranking index of prey items were determined from 1088 stomachs. Major prey of pelagic juvenile rockfish were the various life stages of calanoid copepods and subadult euphausiids (including eggs).

For each year, dietary overlap was quantified between interspecific pairs using the Colwell and Futuyma (1971) index. Amount of overlap varied from year to year. Long-term intraspecific dietary overlap, based on the 4 years of data, was generally less than interspecific overlap within years. Year-to-year variation in the diets of these species was generally greater than within-year variation among them, suggesting that, as a group, pelagic juvenile rockfishes are opportunistic feeders. Also, if interannual variation in the distribution and abundance of foods has a major impact on recruitment, the high dietary overlaps of these co-occurring species would suggest parallel survival and year-class success.

Multivariate analysis of variance was used to examine the effects of latitude, depth, and fish size on food consumption. Alterations in diet were related to latitude, depth, and a latitude-depth interaction for three species in 1987 and, also, for shortbelly rockfish in 1984–86. Diet was apparently unrelated to fish size.

Manuscript accepted 20 May 1992.
Fishery Bulletin, U.S. 90:505–515 (1992).

Rockfishes of the genus *Sebastes* are a major component of the west coast groundfish fishery (Gunderson and Sample 1980), yet little is known of their early life history. Kendall and Lenarz (1987) noted a particular lack of information on the biology of the pelagic juvenile life-stage. To date most work on pelagic juveniles has addressed problems in identification (e.g., Moser et al. 1977, Laroche and Richardson 1980 and 1981, Matarese et al. 1989), growth (Boehlert 1981a, Boehlert and Yoklavich 1983, Penney and Evans 1985, Laidig et al. 1991, Woodbury and Ralston 1991), and vertical distribution (Boehlert 1977 and 1981b, Moser and Alhstrom 1978, Moser and Boehlert 1991, Lenarz et al. 1991).

Female rockfishes undergo internal fertilization and the eggs develop within the ovary for a 40–50 day period (Kendall and Lenarz 1987). Larvae hatch internally, are extruded approximately 1 week later, and begin feeding. Larvae grow and transform into juveniles, a developmental stage characterized by the attainment of full meristic characters. Many rockfishes have a pelagic juvenile stage. Pelagic juveniles ranging in size from 15–100 mm SL are abundant off central California from April to June, although distributional patterns vary markedly among species and years (Wyllie Echeverria et al. 1990). The pelagic juvenile stage ends with settlement into demersal or nearshore habitats.

Evidence strongly indicates that the recruitment of marine fishes is heavily influenced by events that occur early in the life history (Blaxter 1974). A frequently proposed explanation is that the availability and abundance of foods appropriate for first-feeding larval and later juvenile stages are critical to adequate survival and growth. A reduction in the fine-scale density of suitable prey items, whether due to an absolute decrease in prey abundance (Hjort 1914) or to a randomized dispersion of what formerly was a patchy prey resource (Lasker 1975), can have a negative impact on survival. Reduced prey densities can affect survivorship directly through starvation, or indirectly by reducing growth rates and thereby prolonging exposure to other size-specific mortality factors

(e.g., predation, advection, etc.). Regardless of the mechanism, variation in the availability of food can have a major effect on year-class strength (Lasker 1981). The study of food utilization patterns and diet overlap is, therefore, useful in understanding survival mechanisms during the pelagic juvenile life stage. Moreover, annual variation in the extent of interspecific dietary overlap may indicate changes in the distribution and abundance of prey (e.g., Zaret and Rand 1971). Since this may well be critical in determining the success of a year-class, similarity in food habits among pelagic juvenile rockfish may result in similar recruitment dynamics.

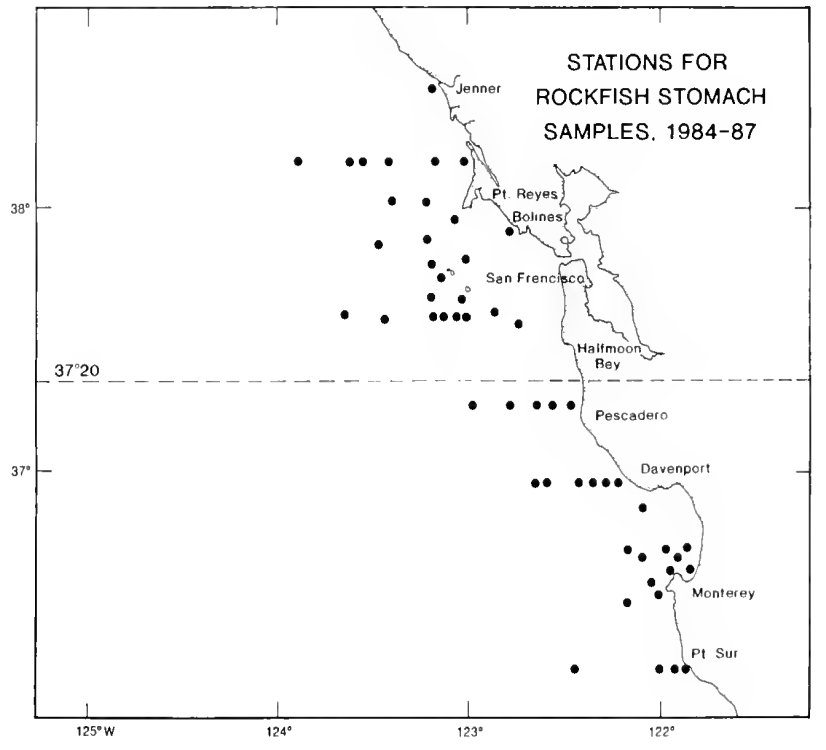

Figure 1
Map of the central California coast showing locations of midwater trawl stations where *Sebastes* stomach samples were obtained, 1984–87.

Previous published dietary studies of juvenile rockfish have been limited to (1) experimental work on food ration and growth in black rockfish (*S. melanops*, Boehlert and Yoklavich 1983); (2) a description of the diet of newly settled Pacific ocean perch (*S. alutus*, Carlson and Haight 1976); (3) a comparison of the food habits of seven *Sebastes* spp. in a nearshore kelp-forest habitat (Singer 1985); and (4) predation on barnacle larvae by a mixed assemblage of settled kelp resident juvenile rockfishes (Gaines and Roughgarden 1987). The purpose of this study was to examine the feeding ecology of several co-occurring young-of-the-year pelagic juvenile rockfishes, including widow rockfish *S. entomelas*, yellowtail rockfish *S. flavidus*, chilipepper *S. goodei*, shortbelly rockfish *S. jordani*, and bocaccio *S. paucispinis*. Specific goals of this study were to (1) identify the food habits of these five species during the pelagic juvenile stage, (2) determine the extent of dietary overlap among the five species, and (3) determine the degree of interannual variation in patterns of prey utilization.

Materials and methods

Juvenile rockfish used in this study were obtained from midwater trawl samples made during a series of annual pelagic juvenile rockfish surveys conducted off central California during 1984–87. Details of these surveys are described in Wyllie Echeverria et al. (1990). The primary purpose of the surveys was to estimate the distribution and abundance of the pelagic-stage juveniles of age-0 rockfishes. Survey areas and dates differed somewhat from year to year (Fig. 1, Table 1). The surveys were conducted during June, except in 1987 when the survey extended from late-May to June. In 1984 and 1985, the survey area extended from Point Sur (lat. 36°18′N) to Point Cabrillo (lat. 39°20′N). Bottom depths at each trawl station ranged from <50 m at nearshore localities to >3700 m beyond the continental shelf. The sampling plan was revised in 1986; seven transects composed of 36 stations were selected based on previous records of rockfish abundance and the availability of ship time. These stations were sampled repetitively during three consecutive sweeps of the area. After 1985, the survey area extended from Cypress Point (lat. 36°35′N) to Point Reyes (lat. 38° 00′N), with station depths ranging from <50 to 1000 m.

Collections were made from the RV *David Starr Jordan* with a modified Cobb midwater trawl net having a 24.4 m head rope and 0.76 cm mesh liner in the codend. The standard depth sampled was 30 m. However, at shallow stations (bottom depth <100 m) the net was set at 5–10 m. At some deep stations samples were

Table 1

Number of juvenile *Sebastes* stomachs examined from juvenile rockfish surveys, 1984–87.

Year	Survey dates	Species	No. of stomachs	Range (mm SL)
1984	8–24 June	Widow rockfish	15	40–63
		Yellowtail rockfish	40	36–56
		Chilipepper	20	38–55
		Shortbelly rockfish	120	30–65
		Bocaccio	50	21–77
1985	5–30 June	Widow rockfish	75	43–63
		Yellowtail rockfish	30	39–48
		Shortbelly rockfish	85	49–75
1986	3–25 June	Yellowtail rockfish	10	35–47
		Shortbelly rockfish	168	15–47
		Bocaccio	25	18–40
1987	23 May–21 June	Widow rockfish	105	48–80
		Yellowtail rockfish	17	39–52
		Chilipepper	125	41–76
		Shortbelly rockfish	150	17–78
		Bocaccio	53	22–86
Total stomachs examined			1088	

also collected at 100 m. Nets were fished for 15 min at depth during the night, ~30 min after sunset, or before sunrise.

Five specimens of each species were randomly subsampled from each haul for dietary analysis. Generally, no samples were taken if fewer than five individuals were taken in a haul. Specimens were tentatively identified to species and preserved whole in 10% buffered formalin, usually within 1 hour of collection. Identifications were later verified ashore with meristics keys (Matarese et al. 1989, Moreland and Reilly 1991); samples were transferred to 70% isopropyl alcohol within 1 month of collection. Standard length (SL) was later measured to the nearest 0.1 mm. Stomachs were removed and stored in 70% isopropyl alcohol until examined.

Stomach contents were examined with a dissecting microscope. Empty stomachs were noted and the digestive state of each prey item was coded on a scale of 1–3, with 3 representing digestion too advanced for identification. All prey types were identified to the lowest possible taxonomic level and counted. When possible, a subsample of all prey types was measured along the longest axis with an ocular micrometer. Heads or eyes were used to obtain total counts when food items were fragmented. For each rockfish species, the proportion of prey types in the diet was calculated as the percentage of total prey numbers consumed in a year, summed over all the individuals examined for stomach contents.

A ranking index, modified from Hobson (1974), was calculated for the major food items. The index (I_r) is the product of proportional frequency of occurrence and percent by number, calculated for all specimens of a species in a year. To quantify dietary overlap among species, the index of Colwell and Futuyma (1971) was used, that is,

$$C_{ih} = 1.0 - 0.5 \left(\sum_{j=1}^{n} p_{ij} - p_{hj} \right),$$

where p_{ij} and p_{hi} are the numerical proportions of prey $j = 1 \ldots N$ found in the diets of species i and h, respectively. The index has a minimum value of zero, when no overlap occurs, and a maximum value of one, when all prey are shared in equal proportions by the two species.

Multivariate analysis of variance (MANOVA) was used to examine relationships among latitude, bottom depth, and the diets of chilipepper, shortbelly, and widow rockfish (Green 1978, SAS 1985). Although only in 1987 were there sufficient data to analyze the diets of all three species, adequate samples of shortbelly rockfish were obtained during all years (1984–87). Thus, examination of overall variation in diet through time, vis-à-vis latitude and depth, was limited to shortbelly rockfish. Analyses were confined to the three prey types of highest frequency of occurrence during the year examined, which varied among the different species and years. The numerical proportions of the three prey types (the dependent variables) were arcsine-transformed (Sokal and Rohlf 1981) prior to MANOVA testing. Latitude, depth, and a latitude-depth interaction term were the independent variables. Station latitude was classified as either north or south of lat. 37°20'N. Similarly, station depth was divided into deep (>100 m) or shallow (<100 m) categories. Data for chilipepper, shortbelly, and widow rockfish sampled in 1987 were also divided into large (>1987 median SL) and small (<1987 median SL) size-classes to examine diet variation as a function of fish size. Shortbelly rockfish were sufficiently numerous during all years to analyze diet variation as a function of predator size. Prey types for this analysis were again limited to the three prey categories with the highest overall frequencies of occurrence in a year, and the dependent variables were the arcsine-transformed numerical proportions in the diet.

Table 2

Summary of stomach contents for five species of pelagic juvenile *Sebastes*, 1984. FO = frequency of occurrence; % = percent by number.

	Widow rockfish (*n* 15)		Yellowtail rockfish (*n* 40)		Chilipepper (*n* 20)		Shortbelly rockfish (*n* 120)		Bocaccio (*n* 50)	
Prey category	FO	%	FO	%	FO	%	FO	%	FO	%
EUPHAUSIACEA										
Furcilia	33.3	10.1	50.0	12.3	30.0	6.8	54.2	35.1	36.0	24.1
Calyptopis			2.5	0.3			1.0	0.1	2.0	0.2
Juveniles	20.0	3.2	15.0	3.4	15.0	2.6	14.1	10.2	38.0	25.3
AMPHIPODA										
Hyperiid juveniles							1.0	0.1	4.0	0.3
CUMACEA							1.7	0.1		
DECAPODA										
Natantia juveniles	6.7	0.5					1.0	0.2		
COPEPODA										
Calanus spp.	46.7	41.0	52.5	28.7	40.0	27.2	40.8	15.1	34.0	31.6
Candacia sp.			5.0	0.4			6.7	0.5	2.0	0.2
Copepods (unidentified)	26.7	17.6	47.5	14.7	15.0	10.5	36.7	12.0	30.0	15.8
Juveniles	20.0	27.7	17.5	40.2	40.0	52.9	10.8	26.8	2.0	0.9
OSTEICHTHYES										
Fish larvae (unidentified)									20.0	1.7

Results

Frequency of occurrence and percent number

Stomachs from 1088 pelagic juvenile rockfish collected from midwater trawls during the four survey years (Table 1) were examined. Frequency of occurrence and percent number for specific prey types of each rockfish species varied considerably from year to year (Tables 2–5). In 1984, bocaccio differed from all other rockfish species in the frequency of occurrence of fish larvae as a prey type (Table 2). Euphausiid eggs occurred in the stomachs of all three species in 1985, although there is a disparity in the percent number (Table 3). Euphausiid eggs were much less frequent in the diets of the three rockfish species in 1986 (Table 4), whereas juvenile euphausiids occurred more frequently. Overall, data from 1984–87 show that prey items having a high frequency of occurrence generally had a high percentage by number. Euphausiid eggs and juveniles and unidentified copepods often had high percentages by number relative to their frequencies of

Table 3

Summary of stomach contents for three species of pelagic juvenile *Sebastes*, 1985. FO = frequency of occurrence; % = percent by number.

	Widow rockfish (*n* 75)		Yellowtail rockfish (*n* 30)		Shortbelly rockfish (*n* 85)	
Prey category	FO	%	FO	%	FO	%
EUPHAUSIACEA						
Furcilia	22.7	1.7	30.0	1.2	14.1	0.4
Calyptopis	2.7	0.1	6.7	1.5	1.2	0.1
Juveniles	5.3	0.7	10.0	0.2	16.5	0.4
Euphausiid eggs	18.7	8.2	36.7	59.1	48.2	59.3
AMPHIPODA						
Hyperiid juveniles	6.7	0.1	3.3	0.1	7.1	0.1
LARVACEA	6.7	4.1			7.1	2.4
CHAETOGNATHA	1.3	0.1				
DECAPODA						
Natantia juveniles			3.3	0.1	1.2	0.1
COPEPODA						
Calanus spp.	22.7	1.7	16.7	1.2	25.9	1.2
Candacia sp.	2.7	0.1	3.3	0.1	1.2	0.1
Copepods (unidentified)	13.3	3.7			17.6	2.9
Eucalanus sp.	8.0	1.8			3.5	0.1
Euchirella sp.	2.7	0.2			3.5	0.1
Juveniles	44.0	77.6	56.7	36.5	57.6	33.3
Metridia sp.			3.3	0.1	1.2	0.1
OSTEICHTHYES						
Fish larvae (unidentified)	1.3	0.1				

Table 4

Summary of stomach contents for three species of pelagic juvenile *Sebastes*, 1986. FO = frequency of occurrence; % = percent by number.

	Yellowtail rockfish (*n* 10)		Shortbelly rockfish (*n* 168)		Bocaccio (*n* 25)	
Prey category	FO	%	FO	%	FO	%
EUPHAUSIACEA						
Furcilia	10.0	1.6	13.2	0.9	4.0	0.2
Calyptopis	10.0	0.6	3.6	0.1		
Juveniles	70.0	7.1	59.9	10.0	52.0	22.0
Euphausiid eggs			4.8	1.1		
CUMACEA	10.0	1.0	1.2	0.1		
DECAPODA						
Natantia juveniles	20.0	1.0	0.6	0.1		
COPEPODA						
Calanus spp.			38.3	6.6	64.0	30.5
Copepods (unidentified)			34.1	3.9	28.0	5.9
Epilabidocera sp.	40.0	8.7				
Juveniles	50.0	80.1	71.9	77.3	44.0	41.4

occurrence. Euphausiid eggs and juvenile copepods were the smallest significant prey of pelagic juvenile rockfish. It is therefore not surprising that these categories often display high percentages by number. Likewise, the category 'unidentified copepods' typically was based on counts of small items (e.g., head fragments).

Ranking index

Prey having both a high frequency of occurrence and percentage by number are the most important items in the diet (Tables 2–5). *Calanus* spp. copepods were particularly important in 1984 when all rockfish species consumed substantial numbers of this

Table 5

Summary of stomach contents for five species of pelagic juvenile *Sebastes*, 1987. FO = frequency of occurrence; % = percent by number.

	Widow rockfish (*n* 105)		Yellowtail rockfish (*n* 17)		Chilipepper (*n* 125)		Shortbelly rockfish (*n* 150)		Bocaccio (*n* 53)	
Prey category	FO	%	FO	%	FO	%	FO	%	FO	%
EUPHAUSIACEA										
Furcilia	6.6	0.20	11.8	1.1	8.0	1.30	40.7	4.00	1.9	0.1
Calyptopis	8.5	0.30	5.9	0.4	2.4	0.40	6.7	1.60	1.9	0.1
Juveniles	39.6	9.00	76.5	31.1	19.8	10.30	6.7	0.60	30.2	10.7
Euphausiid eggs	27.4	52.00	5.9	7.7	10.4	35.80	28.7	65.80	1.9	10.5
Euphausiids (unidentified)	8.5	0.30	5.9	0.2	8.0	0.60	8.0	0.20		
Euphausia sp.									3.8	0.2
Thysanoessa sp.	1.0	0.01								
AMPHIPODA										
Hyperiids	1.0	0.01			1.6	0.10	1.0	0.01	1.9	0.1
CUMACEA					1.0	0.04				
DECAPODA										
Natantia juveniles	1.0	0.04			1.0	0.04				
Crab megalopa					3.2	0.20				
Crab zoea					1.6	0.10	1.0	0.01		
CIRRIPEDIA										
Cypris larva							1.0	0.10		
COPEPODA										
Calanus spp.	33.0	19.80	47.1	13.9	28.0	22.80	44.0	20.30	32.1	11.5
Candacia sp.					1.0	0.10			1.9	0.2
Copepods (unidentified)	22.6	7.30	5.9	1.1	8.0	4.10	4.0	1.00	13.2	45.8
Eucalanus sp.	1.9	0.10							1.9	0.1
Euchaeta sp.									1.9	0.8
Rhincalanus sp.	1.0	0.01					1.0	0.01		
Juveniles	24.5	10.00	17.7	44.5	14.4	24.30	16.0	6.30	5.7	19.3
TEUTHOIDEA										
Squid larva									1.9	0.1
OSTEICHTHYES										
Fish larvae									15.1	0.6
Eggs	3.8	1.00					2.0	0.40		

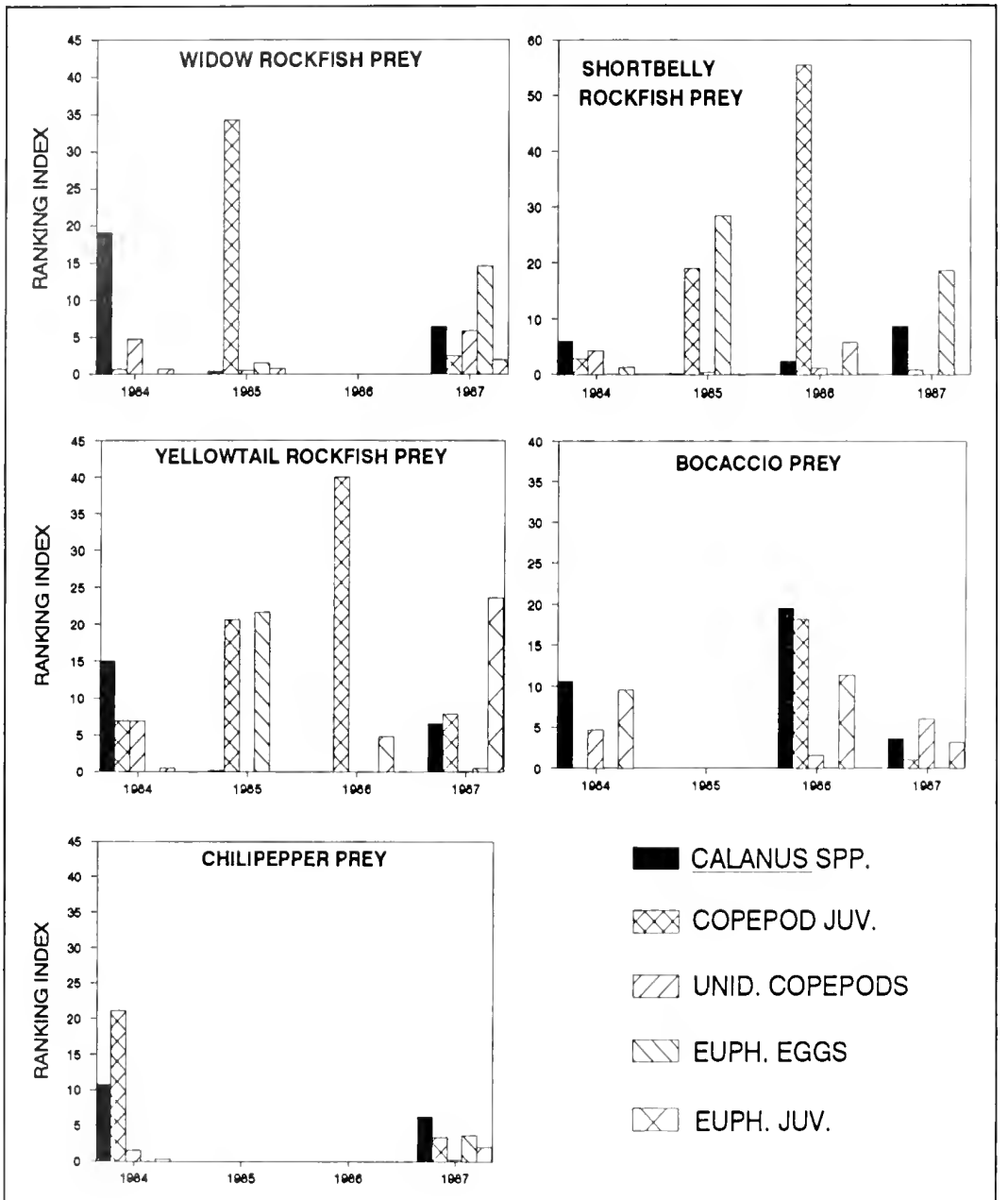

Figure 2

Histograms of the prey ranking index across years for five species of pelagic juvenile *Sebastes*. *Calanus* spp. = *Calanus* spp. copopods; copepod juv. = copopod juveniles; unid. copepods = unidentified copepods; euph. eggs = euphausiid eggs; euph. juv. = euphausiid juveniles.

prey. Likewise, 1985 was a year in which copepod juveniles and euphausiid eggs dominated the diets of the three species examined (widow, yellowtail, and shortbelly rockfish) and copepod juveniles were again important to all species in 1986.

Interspecific prey utilization patterns were less obvious. There is some indication that widow and chilipepper rockfish consumed more copepod juveniles and *Calanus* spp. copepods than did the other species. Similarly, shortbelly rockfish appeared to consume more euphausiid eggs, while bocaccio consumed more euphausiid juveniles. Likewise, there was some suggestion that bocaccio fed on larger prey than the other species (e.g., euphausiid adults and fish larvae). Nonetheless, no distinctive separation in primary prey species was evident among the five species examined.

Based on the I_r ranking index, it is apparent that the diet of pelagic juveniles is typically dominated by

a single prey type each year, followed by several prey types with indices at much lower values (Fig. 2). There were few instances in which the two most important prey types were similar in ranking index, e.g., yellowtail rockfish consuming euphausiid eggs (21.7) and juvenile copepods (20.7) in 1985. This result suggests that each year these species, to a large extent, specialize on foods that are intermittently abundant. Also, the ranking index data, together with information on frequency of occurrence and percent by number, indicate the major prey items of pelagic juvenile rockfish were various life stages of copepods and subadult euphausiids.

Dietary overlap

The extent of interspecific dietary similarity was quantified by comparing dietary overlaps among all possible pairs of species within each year (1984–87). Ten species pairs were possible, but not all pairs were observed each year since all five species were not always collected (Table 6). Overlap indices are sensitive to the taxonomic level to which prey items are categorized; thus, statistical tests of significance concerning the data are arbitrary. Therefore, the convention established by Langton (1982) and Brodeur and Pearcy (1984) was invoked. Overlap index values of 0.00–0.29 were considered low, values of 0.30–0.60 were considered medium, and values >0.60 were considered high.

Using these criteria, annual comparisons of the distribution of overlap indices for 1984 indicate that 60% of all comparisons were classified as medium and 40% were classified as high. Results from 1985 and 1986 indicate that 67% of the scores were medium and 33% were high. In contrast, index values during 1987 generally had the lowest amount of overlap: 10% low, 70% medium, and 20% high. Based on these findings we conclude that, although overall patterns of dietary overlap do vary from one year to the next, variations are relatively modest (only in 1987 was any low overlap observed). Moreover, in this study most within-year species pairings showed >30% overlap. The principal exception to this generalization was for yellowtail and shortbelly rockfish sampled in 1987. Their diets were quite dissimilar.

Overlap indices were also calculated for all possible interannual intraspecific combinations. These calculations allow an assessment of the temporal stability of the diet relative to the amount of interspecific dietary overlap displayed during a given year. The frequency distribution of dietary overlap values derived from self-pairing of rockfish species from different years is shifted well to the left (toward zero) of the distribution of interspecific scores obtained within a year (Fig. 3). These findings show that in any particular year the different species of rockfish are opportunistic feeders that utilize relatively similar prey items, but substantial dietary change can occur from year to year.

Table 6

Diet overlap indices for individual pairings of pelagic juvenile *Sebastes* (1984–87). Wid = widow rockfish; Yel = yellowtail rockfish; Chi = chilipepper; Sho = shortbelly rockfish; Boc = bocaccio.

	Year			
Species pair	1984	1985	1986	1987
Wid–Yel	0.84	0.53	–	0.39
Wid–Chi	0.58	–	–	0.69
Wid–Sho	0.52	0.46	–	0.77
Wid–Boc	0.57	–	–	0.50
Yel–Chi	0.61	–	–	0.52
Yel–Sho	0.58	0.90	0.91	0.22
Yel–Boc	0.64	–	0.46	0.48
Chi–Sho	0.38	–	–	0.56
Chi–Boc	0.41	–	–	0.49
Sho–Boc	0.61	–	0.51	0.30

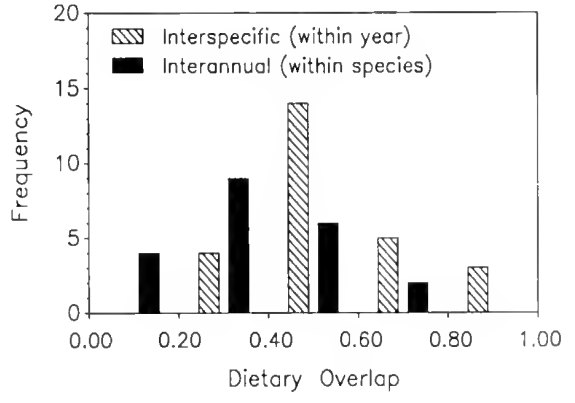

Figure 3

Frequency of dietary overlap indices among all interspecific *Sebastes* pairs within years, compared with frequency of overlap indices calculated for each *Sebastes* species self-paired across years.

Latitude and depth effects

Dietary variation with respect to station latitude (north or south of lat. 37°20′N), station depth (deeper or shallower than 100 m), and the interaction of these variables were analyzed using MANOVA (Table 7). The statistical significance of each analysis depended on the particular combination of species and year examined. In 1987, highly significant ($P<0.001$) diet variations occurred with depth for shortbelly and widow rockfish.

Table 7

Results of MANOVA of depth, latitude, and depth by latitude effects on three principal prey types of pelagic juvenile *Sebastes*. Cal = *Calanus* spp.; CoJv = copepod juveniles; EJv = euphausiid juveniles; EuEg = euphausiid eggs; ELv = euphausiid larvae; UnCo = unidentified copepods; Fur = furcilia.

					MANOVA model effects					
		Prey type			Depth		Latitude		Depth * latitude	
Species	Year	I	II	III	Wilks' λ	*P*	Wilks' λ	*P*	Wilks' λ	*P*
Chilipepper	87	Cal	CoJv	EJv	0.9019	0.0580[b]	0.9186	0.1044	0.9715	0.5525
Widow	87	Cal	EuEg	EJv	0.6638	0.0001**	0.9536	0.2813	0.9805	0.6632
Shortbelly	87	Cal	EuEg	ELv	0.7649	0.0001**	0.9805	0.5059	0.9243	0.0252*
Shortbelly	86	Cal	CoJv	EJv	0.8917	0.0005**	0.7522	0.0001**	0.9404	0.0234*
Shortbelly	85	Cal	EuEg	CoJv	0.8934	0.0472*	0.9293	0.1600	0.9185	0.1121
Shortbelly	84	Cal	UnCo	Fur	0.9647	0.3110	0.9213	0.0429*	0.9095	0.0240*

Significance levels:
[b]borderline
*$P<0.05$
**$P<0.01$

In that year, latitude had no discernible influence on the diet of these two species, although for shortbelly rockfish a significant interaction between depth and latitude was evident. These findings strongly suggest that spatial variability in the environment (i.e., latitude and depth of the water column) can influence, to some extent, the diets of pelagic juvenile rockfish in a species-specific manner.

Results for the full time-series of shortbelly rockfish data (1984–87) also show that spatial patterns change over time. Although depth had a highly significant effect on diet in 1986 and 1987, it was not significant in 1984 or 1985. Similarly, latitude had no appreciable relationship to the diet of shortbelly rockfish in 1985 and 1987, but it had a highly significant effect in 1986. Importantly, whenever a latitude correlation with diet was present, the interaction term (depth * latitude) was significant as well. We believe that the erratic influence of spatial structure on the shortbelly diet is likely due to the dynamic nature of the nearshore pelagic/neritic physical environment.

Using the 1987 data, we examined the least-squares means (Searle et al. 1980) of the transformed numerical proportions of the individual prey types to learn exactly how dietary composition varied when statistically-significant model effects occurred. In that year, the diet of chilipepper showed borderline significance with depth ($P = 0.058$); the least-squares means revealed that chilipepper consumed more *Calanus* spp. copepods in shallow water, and more juvenile copepods and juvenile euphausiids at bottom depths >100 m. Likewise, all three prey types (*Calanus* spp., euphausiid eggs, and juvenile euphausiids) of widow rockfish were consumed in greater proportion in deep water, especially euphausiid eggs. For shortbelly rockfish, which displayed a significant interaction term, consumption of *Calanus* spp. copepods was noticeably depressed at shallow southern stations. Euphausiid eggs were consumed in much greater quantities at deep stations, both north and south, while fewer larval euphausiids (furcilia and calyptopis) were found in fish from northern deep stations.

Predator size

Results were inconsistent when these same data (i.e., numerical proportions in the diet of the three most frequently occurring prey items for 1984–87 shortbelly rockfish, 1987 chilipepper, and 1987 widow rockfish) were also explored with MANOVA to assess the effect of fish size on composition of the diet. In each instance, fish were assigned to either small or large size-classes, based on whether standard lengths were smaller or larger than the annual median of that species.

Of the six cases examined (Table 8) two yielded significant ($P<0.05$) results. Large shortbelly rockfish sampled in 1986 tended to eat a higher proportion of *Calanus* spp. copepods, whereas small fish had a higher fraction of juvenile euphausiids and juvenile copepods in their diet. Results from that year, therefore, support the view that large fish tend to consume large prey. Even so, a significant size effect was demonstrated for 1985 shortbelly rockfish, which was exactly the opposite of 1986; large fish consumed fewer *Calanus* spp. copepods and a greater percentage of euphausiid eggs than did small fish. Sample size was not adequate to statistically analyze fish length jointly with distributional patterns. However, in 1985, 34 of

Table 8

Results of MANOVA of fish size on three principal prey types of pelagic juvenile *Sebastes*. Cal = *Calanus* spp.; CoJv = copepod juveniles; EJv = euphausiid juveniles; EuEg = euphausiid eggs; ELv = euphausiid larvae; UnCo = unidentified copepods; Fur = furcilia.

		Prey type			Fish size	
Species	Year	I	II	III	Wilks' λ	P
Chilipepper	87	Cal	CoJv	EJv	0.9927	0.9088
Widow	87	Cal	EuEg	EJv	0.9678	0.4407
Shortbelly	87	Cal	EuEg	ELv	0.9634	0.2132
Shortbelly	86	Cal	CoJv	EJv	0.9362	0.0161*
Shortbelly	85	Cal	EuEg	CoJv	0.8801	0.0261*
Shortbelly	84	Cal	UnCo	Fur	0.9928	0.8654

*$P<0.05$

the 42 shortbelly rockfish that were classified as small came from deep stations. Results presented earlier (Table 7) showed that the diet of shortbelly rockfish varied significantly with depth in 1985 (i.e., fewer euphausiid eggs and copepod juveniles at deep stations). Thus, the conclusion that small fish consumed large prey in 1985 is, to some degree, confounded with this spatial effect.

Discussion

The five species of pelagic juvenile rockfish examined in this study consumed pelagic zooplankton almost exclusively. Relatively few prey types made up the major portion of the diet each year. Various life history stages of calanoid copepods and euphausiids dominated. Carlson and Haight (1976) reported that copepods and euphausiids were important in the diet of pelagic juvenile Pacific ocean perch *S. alutus*. Singer (1985) recently reported that settled juveniles of several rockfish species consumed copepods and zoea larvae in a central California kelp forest. Other studies (Robb and Hislop 1980, Bowman 1981, Conway 1980) have also demonstrated that calanoid copepods and euphausiids are extremely important foods to pelagic juvenile fishes in the northeastern Pacific Ocean. These studies demonstrate that the diets of pelagic juvenile rockfishes are similar to those of other species possessing pelagic juvenile life stages.

A significant finding of this study is that *Sebastes* spp. juveniles periodically forage heavily on euphausiid eggs. Euphausiid eggs have not been previously reported as a prey item of pelagic juvenile rockfish and yet they were a very important dietary component both in 1985 and 1987. During those years, euphausiid eggs averaged over 37% of the prey items consumed by the five species studied. However, euphausiid eggs were absent from samples collected in 1984 and were a minor component in 1986.

Some species of euphausiids brood their eggs prior to hatching (e.g., *Nyctiphanes* spp.), whereas other species release eggs upon fertilization (e.g., *Euphausia pacifica* and *Thysanoessa spinifera*). Since adult euphausiids were not found in any stomachs in 1985 (Table 3), and since only the latter genera were encountered in large swarms in the study area in 1987 (Smith and Adams 1988), rockfish must have consumed eggs after release. It was not expected that a nonmotile prey would constitute such an important food resource to pelagic juvenile rockfish. The appearance of eggs in clumped masses in guts suggests that eggs were not individually picked from the plankton.

Another interesting finding was the consumption of fish larvae by bocaccio juveniles. A total 15–20% of all bocaccio sampled in 1984 and 1987 contained larval fish. In our surveys, bocaccio grow faster and reach larger sizes as pelagic juveniles ($\geq$ 100 mm SL) than do other species (Woodbury and Ralston 1991). They are also distributed at shallower depths (Lenarz et al. 1991).

We used the I_r statistic to rank the importance of individual prey items in the diet. This statistic differs from a similar statistic used by Hobson (1974) in that it is the product of proportional frequency of occurrence and percent by number, rather than percent by volume. Use of this statistic allowed us to characterize the prey types consumed by *Sebastes* in each of the 4 years studied. No obvious species-specific patterns emerged in the absence of a temporal component.

Our results indicate that pelagic juvenile *Sebastes* tend to respond similarly to environmental fluctuations in their food base, suggesting an opportunistic feeding strategy. Intraspecific dietary overlap between interannual pairings was much lower than were interspecific interannual pairings. On a relative basis, interannual differences in diet were tracked similarly among the five species we examined. Annual changes in diet are likely to reflect annual differences in the composition, availability, and abundance of prey.

It was not possible to infer from our results whether or not food is limiting to pelagic juvenile rockfishes, given the relatively large interannual variation in the diet among these species and the likelihood that variation in the availability of prey is likely responsible.

Even so, high dietary overlap observed among co-occurring pelagic juvenile rockfishes suggests that similar recruitment dynamics must exist if the distribution and abundance of foods has a major impact on recruitment.

Intraspecific spatial variation was observed (Table 7), even though substantial interspecific overlap exists in patterns of food utilization. In some instances, parallel spatial differences were observed for different species. For example, in 1987 both widow and shortbelly rockfish fed on euphausiid eggs to a much greater extent in deep water (>100 m) than in shallow water. In other cases, however, species-specific differences in diet due to depth were reversed. In 1987, for example, the consumption of *Calanus* spp. copepods by chilipepper was higher in shallow water, while consumption by widow rockfish was higher in deep water.

With the exception of the predator-size MANOVA discussed previously (i.e., shortbelly rockfish in 1985), sample sizes for each treatment combination in all MANOVA tests were reasonably well balanced. Therefore, it is unlikely that our conclusions were compromised by our choice of statistical tests.

The spatial incongruity of within-year dietary patterns among species also extended to interannual within-species comparisons. For example, shortbelly rockfish sampled in 1984 and 1987 consumed substantially fewer *Calanus* spp. copepods in the shallow southern quadrant than anywhere else. However, in 1986 consumption of this prey was greatest in fish taken in this region.

These interspecific (within-year) and interannual (within-species) comparisons demonstrate a lack of stability in the specifics of how spatial dietary effects are expressed. It is likely that the complex nearshore pattern of circulation that characterizes the study area (frontal structures, mesoscale eddies, turbulent jets, and upwelling plumes are common recurrent features; Mooers and Robinson 1984, Flament et al. 1985, Njoku et al. 1985, Schwing et al. 1990) defines the spatial distribution of the zooplanktonic animals upon which these rockfish feed. Thus, the dynamic nature of the physical environment off central California generates spatial instabilities in the distribution and abundance of prey.

Acknowledgments

We are grateful to all personnel of the Tiburon Laboratory, Southwest Fisheries Science Center, National Marine Fisheries Service, particularly the staff of the Groundfish Analysis Investigation, who participated in the juvenile rockfish recruitment surveys in 1984–87. We thank Master Milt Roll and the officers and crew of the RV *David Starr Jordan* for their valuable help in collecting juvenile rockfish during these research cruises. Sharon Moreland (currently of the Army Corps of Engineers) taught us identification techniques for young-of-the-year pelagic juvenile rockfish. Tony Chess (Tiburon Laboratory) assisted with identification of copepods, and Margaret Knight (Scripps Institute of Oceanography) confirmed identification of the euphausiid eggs. Jim Bence (Tiburon Laboratory) generously assisted us with statistical analyses. This paper was greatly improved by thoughtful, constructive reviews by Pete Adams, Jim Bence, George Boehlert, Ted Hobson, Ralph Larson, Bill Lenarz, Jeannette Whipple, and three anonymous reviewers.

Citations

Blaxter, J.H.S. (editor)
1974 The early life history of fish. Springer-Verlag, NY, 765 p.

Boehlert, G.W.
1977 Timing of the surface-to-benthic migration in juvenile rockfish, *Sebastes diploproa*, off southern California. Fish. Bull., U.S. 75:887–890.
1981a The effects of photoperiod and temperature on laboratory growth of juvenile *Sebastes diploproa* and a comparison with growth in the field. Fish. Bull., U.S. 79:789–794.
1981b The role of temperature and photoperiod in the ontogenetic migration of prejuvenile *Sebastes diploproa* (Pisces: Scorpaenidae). Calif. Fish. Game 67:164–175.

Boehlert, G.W., and M.M. Yoklavich
1983 Effects of temperature, ration, and fish size on growth of juvenile black rockfish, *Sebastes melanops*. Environ. Biol. Fish. 8:17–28.

Bowman, R.E.
1981 Food of 10 species of northwest Atlantic juvenile groundfish. Fish. Bull., U.S. 79:200–206.

Brodeur, R.D., and W.G. Pearcy
1984 Food habits and dietary overlap of some shelf rockfishes (Genus *Sebastes*) from the northeastern Pacific Ocean. Fish. Bull., U.S. 82:269–293.

Carlson, H.R., and R.E. Haight
1976 Juvenile life of Pacific Ocean perch, *Sebastes alutus*, in coastal fiords of southeastern Alaska: Their environment, growth, food habits, and schooling behavior. Trans. Am. Fish. Soc. 105:191–201.

Colwell, R.K., and D.J. Futuyma
1971 On the measurement of niche breadth and overlap. Ecology 52:567–576.

Conway, D.V.P.
1980 The food of larval blue whiting, *Micromesistius poutassou* (Risso), in the Rockall area. J. Fish Biol. 16:709–723.

Flament, P., L. Armi, and L. Washburn
1985 The evolving structure of an upwelling filament. J. Geophys. Res. 90(C6):11,765–11,778.

Gaines, S.D., and J. Roughgarden
1987 Fish in offshore kelp forests affect recruitment to intertidal barnacle populations. Science (Wash. DC) 235:479–481.

Green, P.E.
1978 Analyzing multivariate data. Dryden Press, Hinsdale, IL, 519 p.

Gunderson, D.R., and T.M. Sample
1980 Distribution and abundance of rockfish off Washington, Oregon, and California during 1977. Mar. Fish. Rev. 42(3–4): 2–16.

Hjort, J.
1914 Fluctuations in the great fisheries of northern Europe viewed in the light of biological research. Rapp. P.-V. Reun. Cons. Perm. Int. Explor. Mer 20:1–228.

Hobson, E.S.
1974 Feeding relationships of teleostean fishes on coral reefs in Kona, Hawaii. Fish. Bull., U.S. 72:915–1031.

Kendall, A.W. Jr., and W.H. Lenarz
1987 Status of early life history studies of northeast Pacific rockfishes. *In* Proc. Int. Rockfish Symp., Oct. 1986, Anchorage, Alaska, p. 99–128. Alaska Sea Grant Rep. 87-2, Univ Alaska, Fairbanks.

Laidig, T.E., S. Ralston, and J.R. Bence
1991 Dynamics of growth in the early life history of shortbelly rockfish, *Sebastes jordani*. Fish. Bull., U.S. 89:611–621.

Langton, R.W.
1982 Diet overlap between Atlantic cod, *Gadus morhua*, silver hake, *Merluccius bilinearis*, and fifteen other northwest Atlantic finfish. Fish. Bull., U.S. 80:745–759.

Laroche, W.A., and S.L. Richardson
1980 Development and occurrence of larvae and juveniles of the rockfishes *Sebastes flavidus* and *Sebastes melanops* (Scorpaenidae) off Oregon. Fish. Bull., U.S. 77:901–924.
1981 Development of larvae and juveniles of the rockfishes *Sebastes entomelas* and *S. zacentrus* (Family Scorpaenidae) and occurrence off Oregon, with notes on head spines of *S. mystinus*, *S. flavidus*, and *S. melanops*. Fish. Bull., U.S. 79: 231–258.

Lasker, R.
1975 Field criteria for survival of anchovy larvae: The relation between inshore chlorophyll maximum layers and successful first feeding. Fish. Bull., U.S. 73:453–462.
1981 The role of a stable ocean in larval fish survival and subsequent recruitment. *In* Lasker, R. (ed.), Marine fish larvae — morphology, ecology, and relation to fisheries, p. 80–87. Univ. Wash. Press, Seattle.

Lenarz, W.H., R.J. Larson, and S. Ralston
1991 Depth distributions of late larvae and pelagic juveniles of some fishes of the California current. Calif. Coop. Oceanic Fish. Inst. Rep. 32:41–46.

Matarese, A.C., A.W. Kendall Jr., D.M. Blood, and B.M. Vinter
1989 Laboratory guide to early life history stages of northeast Pacific fishes. NOAA Tech. Rep. NMFS 80, 652 p.

Mooers, C.N.K., and A.R. Robinson
1984 Turbulent jets and eddies in the California current and inferred cross-shore transports. Science (Wash. DC) 223: 51–53.

Moreland, S.L., and C.A. Reilly
1991 Key to the juvenile rockfishes of central California. *In* Laidig, T.E., and P.B. Adams (eds.), Methods used to identify pelagic juvenile and larval rockfish (genus *Sebastes*) occurring along the coast of central California, p. 59–180. NOAA Tech. Memo. NOAA-TM-NMFS-SWFC-166, NMFS Tiburon Lab.

Moser, H.G., and E.H. Ahlstrom
1978 Larvae and pelagic juveniles of blackgill rockfish, *Sebastes melanostomus*, taken in mid-water trawls off southern California and Baja California. J. Fish. Res. Board Can. 35:981–996.

Moser, H.G., E.H. Ahlstrom, and E.M. Sandknop
1977 Guide to the identification of scorpionfish larvae (Family Scorpaenidae) in the eastern Pacific with comparative notes on species of *Sebastes* and *Heliocolenus* from other oceans. NOAA Tech. Rep. NMFS Circ. 402, 71 p.

Moser, H.G., and G.W. Boehlert
1991 Ecology of pelagic larvae and juveniles of the Genus *Sebastes*. Environ. Biol. Fish. 30:203–224.

Njoku, E.G., T.P. Barnett, R.M. Laurs, and A.C. Vastano
1985 Advances in satellite sea surface temperature measurement and oceanographic applications. J. Geophys. Res. 90(C6):11,573–11,586.

Penney, R.W., and G.T. Evans
1985 Growth histories of larval redfish (*Sebastes* spp.) on an offshore Atlantic fishing bank determined by otolith increment analysis. Can. J. Fish. Aquat. Sci. 42:1452–1464.

Robb, A.P., and J.R.G. Hislop
1980 The food of five gadoid species during the pelagic 0-group phase in the northern North Sea. J. Fish Biol. 16:199–217.

SAS Institute Inc.
1985 SAS User's guide: Statistics, version 5 edition. SAS Institute Inc., Cary, NC, 956 p.

Schwing, F.B., S. Ralston, D.M. Husby, and W.H. Lenarz
1990 The nearshore physical oceanography off the central California coast during May–June, 1989: A summary of CTD data from juvenile rockfish surveys. NOAA Tech. Memo. NOAA-TM-NMFS-SWFSC-153, NMFS Tiburon Lab., 142 p.

Searle, S.R., F.M. Speed, and G.A. Milliken
1980 Population marginal means in the linear model: An alternative to least squares means. Am. Stat. 34(4):216–221.

Singer, M.M.
1985 Food habits of juvenile rockfishes (*Sebastes*) in a central California kelp forest. Fish. Bull., U.S. 83:531–541.

Smith, S.E., and P.B. Adams
1988 Daytime surface swarms of *Thysanoessa spinifera* (Euphausiacea) in the Gulf of the Farallones, California. Bull. Mar. Sci. 42(1):76–84.

Sokal, R.R., and F.J. Rohlf
1981 Biometry. W.H. Freeman, San Francisco, 859 p.

Woodbury, D., and S. Ralston
1991 Interannual variation in growth rates and back-calculated birthdate distributions of pelagic juvenile rockfishes (*Sebastes* spp.) off the central California coast. Fish. Bull., U.S. 89: 523–533.

Wyllie Echeverria, T., W.H. Lenarz, and C. Reilly
1990 Survey of the abundance and distribution of pelagic young-of-the-year rockfishes off central California. NOAA Tech. Memo. NOAA-TM-NMFS-SWFC-147, NMFS Tiburon Lab., 125 p.

Zaret, T.M., and A.S. Rand
1971 Competition in tropical stream fishes: Support for the competitive exclusion principle. Ecology 52:336–342.

Abstract.—The red hind *Epinephelus guttatus*, a grouper of commercial importance in the central western Atlantic, is believed to be overexploited in a number of areas. Red hind taken by fish trap and hook-and-line in western Puerto Rico and the U.S. Virgin Island of St. Thomas were aged using sectioned otoliths (sagittae). Ages were validated by marginal increment analysis for fish ages 1–10 yr, and by a field study involving oxytetracycline injection for fish ages 1–4; a single opaque and translucent zone (viewed under transmitted light) is deposited annually. For Puerto Rico, the von Bertalanffy growth function (VBGF) was $L_t = 514.5\ (1 - e^{-0.101(t+2.94)})$. Back-calculated mean fork lengths ranged from 163 mm at age-1 yr, to 448 mm at maximum age-17. For St. Thomas, the VBGF was $L_t = 601.0\ (1 - e^{-0.071(t+4.69)})$. Back-calculated mean fork lengths ranged from 194 mm at age-1, to 470 mm at maximum age-18. Sex and stage of sexual maturation were determined for a subsample of aged fish from Puerto Rico. Fifty percent of females had attained sexual maturity by age 3 yr. Ages of females were 1–9 yr; males, 2–17 yr, and individuals undergoing sexual transition from female to male, 3–7 yr. The male to female sex ratio was 1:2.6. The occurrence of sexually-transitional individuals, as well as significant differences between the sexes in both size and age, confirm protogynous hermaphroditism for fish from Puerto Rico.

Age and growth of red hind *Epinephelus guttatus* in Puerto Rico and St. Thomas

Yvonne Sadovy
Miguel Figuerola*
Ana Román

Fisheries Research Laboratory, Department of Natural Resources
P.O. Box 3665, Mayagüez, Puerto Rico

The red hind *Epinephelus guttatus* is a serranid of considerable commercial importance throughout the Caribbean, the Bahamas, and Bermuda (Burnett-Herkes 1975, Mahon 1987). In Puerto Rico and the U.S. Virgin Islands, this species is one of the most-frequently reported groupers in commercial landings. It is taken by hook-and-line, fish trap, and speargun, over the insular shelf to a depth of about 80 m.

Grouper are relatively long-lived and slow-growing fishes. These characteristics, combined with the protogynous sexual pattern (female to male sex change) reported for many grouper, and intensive fishing over short-term traditional spawning aggregations, render grouper species especially vulnerable to overexploitation (Bannerot et al. 1987, Manooch 1987, Ralston 1987, Shapiro 1987, Bohnsack 1989).

There are indications that red hind resources of Puerto Rico and the U.S. Virgin Islands are being overexploited. Commercial grouper landings reported in Puerto Rico have declined consistently and substantially over the last decade, from 386 mt in 1978 to 47 mt (of which 38% were red hind) in 1990 (Matos and Sadovy 1989, Sadovy In press, Sadovy and Figuerola 1992). Yield-per-recruit analyses indicate growth overfishing (harvesting at too small a size to maximize potential yield) in western Puerto Rico (Stevenson 1978, Sadovy and Figuerola 1992). All known annual spawning aggregations in both Puerto Rico and St. Thomas are heavily exploited. In addition, recent length-frequency data from commercial catches in St. Thomas indicate that mean length declined substantially between 1984 and 1988 (Beets and Friedlander 1992), although it is not clear to what extent this decline is attributable to overfishing, or is related to annual variation in recruitment (Appeldoorn et al. 1992), or a combination of the two.

Little is known of the life history of the red hind. Previous studies on age and growth in this species have been conducted in Bermuda using whole otoliths (Burnett-Herkes 1975), and in Jamaica using length-frequency analysis (Thompson and Munro 1974). However, neither study is recent and neither validated the ageing techniques. The sexual pattern is reported to be protogyny in Bermuda (Smith 1959, Burnett-Herkes 1975), and protogyny is also indicated for Puerto Rico stocks (Shapiro et al. unpubl. data). The objectives of this study were to determine age and growth of the red hind in two heavily-exploited areas—western Puerto Rico and St. Thomas, U.S. Virgin Islands—and to confirm sexual pattern. This information is necessary to allow stock assessments to be made for this species, and to permit the development of a management policy for the red hind in the region.

Manuscript accepted 27 May 1992.
Fishery Bulletin, U.S. 90:516–528 (1992).

* Reprint requests should be addressed to this author.

Methods

Samples of *Epinephelus guttatus* were obtained from local fishermen and from Fisheries Research Laboratory (FRL) research programs using hook-and-line and arrowhead fish traps (3.2 cm (1.25 in.) galvanized mesh). Monthly collections were made between September 1987 and January 1989 with a minimum of 80 fish for most months from Puerto Rico. Smaller monthly samples from February 1988–January 1989 were received from St. Thomas, which lies on the same geological platform. Fish from St. Thomas were taken by hook-and-line and by fish trap (3.81 cm (1.5 in.) galvanized mesh).

For each fish, the weight (whole weight to nearest gm) and length (fork length (FL) and standard length (SL) to nearest mm) were measured. Otoliths (sagittae) were extracted, washed, and stored dry prior to processing. Preliminary work determined these calcareous structures to be more suitable than other calcareous structures for ageing purposes: dorsal spines exhibited growth lines but the central portion was often eroded resulting in an incomplete growth history, and scale markings were irregular and thus considered unreliable for ageing. Gonads in good condition were removed whenever possible, fixed in Davidson's fixative (Yevich and Barszcz 1981), embedded in paraffin, sectioned at 8 μm, and stained with hematoxylin and eosin.

Examination of whole otoliths under transmitted light revealed alternating opaque and translucent zones (terminology follows that of Wilson et al. 1983). To count the zones, however, otoliths had to be sectioned. Preliminary sectioning in two planes (frontal and transverse; $N = 20$ otoliths in each plane) established that transverse sections most clearly revealed growth zones. For sectioning, otoliths were mounted with glue, using a hot glue gun, on small cards, and sectioned through the focus with a single 7.2 cm (3 in.) diameter, low-concentration diamond blade on a Buehler Isomet low-speed saw. From each otolith, three sections of 0.36–0.43 mm were mounted on glass slides using Flo-Texx mounting medium.

Otolith width (OW) of a sample of unsectioned otoliths from a wide size-range of fish was measured to describe the OW/FL relationship. Measurements of otolith sections were made from the point where the sulcus meets the focus to the dorsal margin of the otolith (the region of most rapid growth) and to the proximal edge of each opaque zone. Measurements were also made from the distal edge of the outermost (opaque) zone to the dorsal margin for marginal increment analysis. Total number of opaque zones was noted. Measurements were made with an ocular micrometer, to the nearest micrometer unit (where 1 mm = 32 micrometer units). Each otolith was read twice. When readings disagreed by more than one opaque zone, the otolith was eliminated. Readings of a subsample of otoliths from Puerto Rico, of a wide range of ages and size-groups, were also made by an independent researcher.

To validate the temporal significance of opaque zones, a field study was undertaken. Individuals were captured by hook-and-line baited with squid from a 30 × 30 m area on a shallow (7 m) relatively-unfished reef known as "El Negro," 6 km off western Puerto Rico. The study site was visited over a 15-month period between April 1988 and June 1989. Individuals were tagged with a numbered FLOY anchor tag inserted into the dorsal musculature, and/or with FLOY abdominal tags for identification. Each fish was measured (FL) and injected with a dosage of 100 mg/kg body weight of Terramycin 100 (Pfizer) (1 mL contains 100 mg oxytetracycline-OTC-hydrochloride), and released. The dosage necessary to produce a visible mark under longwave ultraviolet light was established by preliminary tests (50 and 100 mg/kg body weight were tested; 50 mg/kg body weight did not consistently leave OTC marks) and the correct dosage determined on-site from a weight/FL relationship. Fish recaptured were measured and the otoliths examined for opaque zone formation following deposition of the OTC time marker.

Data were analyzed separately for Puerto Rico and St. Thomas using Lotus 1-2-3 and Basic Fishery Science Programs (Saila et al. 1988). The Kolmogorov-Smirnov two-sample test and the t-test were used to compare size-frequency distributions and mean size, respectively (Sokal and Rohlf 1981). Weight (W) on FL regressions were calculated using the relationship $W = aFL^b$. The SL:FL and OW:FL regressions were determined. The Lee method (Carlander 1981) of back-calculating body length from prior annuli was used:

$$L_i = a + [(L_c - a)(O_i/OR)],$$

where: L_i = length at time of ith annulus formation
a = intercept
L_c = length at time of capture (FL)
O_i = otolith radius at time of ith annulus formation
OR = otolith radius at time of capture.

This method requires knowledge of the relationship between OR along the line of measurement and FL. The constant a is obtained from this relationship and used in Lee's formula.

Growth was assumed to conform to the von Bertalanffy growth function (VBGF) (Ricker 1975). This

was calculated from the Saila et al. (1988) statistical package (FISHPARM program using Marquadt's non-linear least-squares method) and fitted to mean back-calculated lengths-at-age. The VBGF is

$$L_t = L_\infty (1 - e^{-K(t-t_0)}),$$

where L_t = length at age t
L_∞ = asymptote of the growth-in-length curve
K = Brody growth coefficient
t = age of the fish
t_0 = the theoretical origin of the growth curve, i.e., age at which fish would have zero length if it had always grown in a manner described by the equation.

To establish chronological age at the time of first opaque zone formation, data on the early growth of juvenile red hind were assembled from field collections and observations taken over 9-month periods following spawning in January of 1985 and 1987 (Sadovy, unpubl. data). Since spawning occurs over a limited period, during, at most, 2 months each year (Erdman 1976, Beets and Friedlander 1992, Shapiro et al. In press), and settlement may be assumed to occur between 3 weeks to 2 months after spawning (Colin et al. 1987), growth rates of individuals in the months following settlement could be estimated.

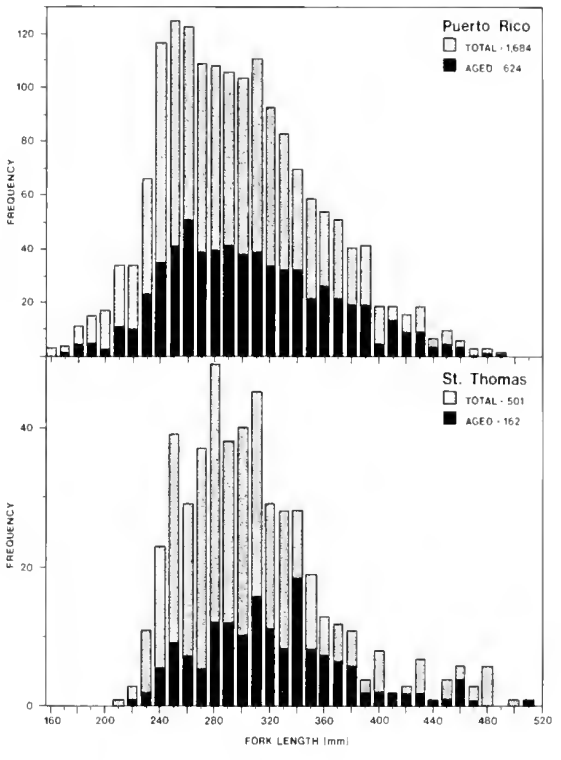

Figure 1
Size-frequency distributions of all *Epinephelus guttatus* collected (stippled) from Puerto Rico and St. Thomas, and subsamples from which otoliths were analyzed (solid).

Results

Samples

Of 1684 *Epinephelus guttatus* collected from Puerto Rico, otoliths were sectioned from 1098. Opaque and translucent zones were detectable in almost all otolith sections. When zones lacked sufficient definition for focus-to-ring measurements, the otoliths were discarded as unsuitable for use in calculating growth parameters, although some were used to assign ages to sexed fish by counts of opaque zones. A total of 624 (63%) otoliths were used to count growth zones and for focus-to-ring measurements. Of these, a subsample of 73 otoliths was read by an independent researcher; only one was rejected because of a discrepancy of more than one zone compared with our readings. Of the 501 St. Thomas samples, otoliths were sectioned from 490, and 162 (33%) were judged to be sufficiently clear for analysis; it is not known why otolith legibility was so low for St. Thomas samples.

Size-frequency distributions of all fish collected in Puerto Rico and in St. Thomas, and the subsamples used for analysis of otoliths from each location, are shown in Figure 1. For Puerto Rico, size-frequency distributions of individuals and subsamples used for age determination did not differ significantly (Kolmogorov-Smirnov: D = 0.043, NS). This confirmed our impression that illegible otoliths occurred at all fish sizes and ages, and affirmed that their elimination introduced no bias to the calculation of growth parameters. For St. Thomas, however, the distributions differed significantly (D = 0.150, $p<0.05$). Therefore, growth parameters derived for St. Thomas should be treated with caution.

Frequency distributions of the distance from the focus to each opaque zone in Puerto Rico collections are shown in Figure 2. Relationships of SL:FL and W:FL were established for each location.

Puerto Rico:

FL = 3.86 + 1.2044 SL (r^2 0.99; N 227)
Log W = −5.21 + 3.1422 Log FL (r^2 0.97; N 1619)

St. Thomas:

FL = 24.49 + 1.1101 SL (r^2 0.98; N 494)
Log W = −4.68 + 2.9402 Log FL (r^2 0.92; N 493)

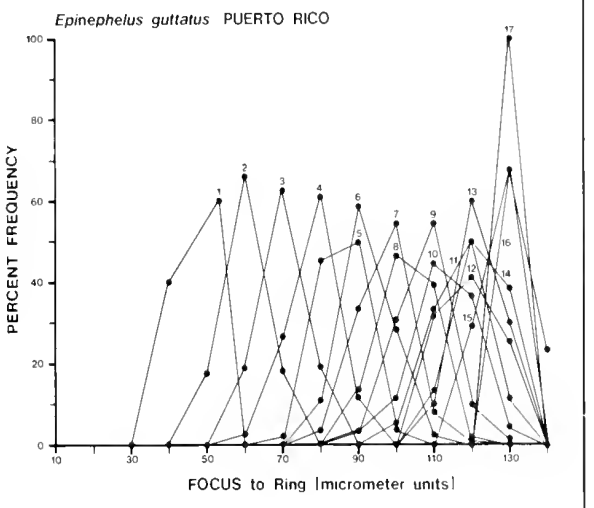

Figure 2
Frequency distributions of the distance from focus to proximal edge of each opaque zone (1–17) in sectioned sagittae of *Epinephelus guttatus* from Puerto Rico.

Validation

Marginal increment analysis Mean marginal increments for Puerto Rico fish were plotted on a monthly basis for annuli I–VI individually, and combined for annuli VII–X because of low monthly sample sizes for these older age-groups (Fig. 3). These data indicate that, at least for annuli II–V, the opaque zone begins to form between about April and May and is a true annulus. For annulus VI, the zone is laid down later, between May and July. For annuli VII–X combined, opaque zones are apparently deposited annually between May and July.

Since sample sizes from St. Thomas were too low for marginal increment analysis by individual age-group, otoliths from all age-groups were combined and plotted on a monthly basis by the percent of sections that lacked a marginal increment. These data indicate that the time of opaque zone formation (i.e., spring/summer) is similar for both Puerto Rico and St. Thomas (Fig. 4). A possible 'pseudoannulus' was detected in 74 (12%) of sectioned otoliths. This was a wide, weakly-discernible band always located between the focus and the first annulus. It occurred sporadically in fish of all sizes.

Field validation study Of a total of 139 fish tagged, injected, and released, 8 females from age-classes 1–4 were recaptured 5–16 months following tagging. Mean monthly growth rates for recaptured individuals from Puerto Rico measured 1–8 mm (Table 1). One individual (#00038) was recaptured in February 1991, 18 km from the tagging site on an offshore bank, a known spawn-

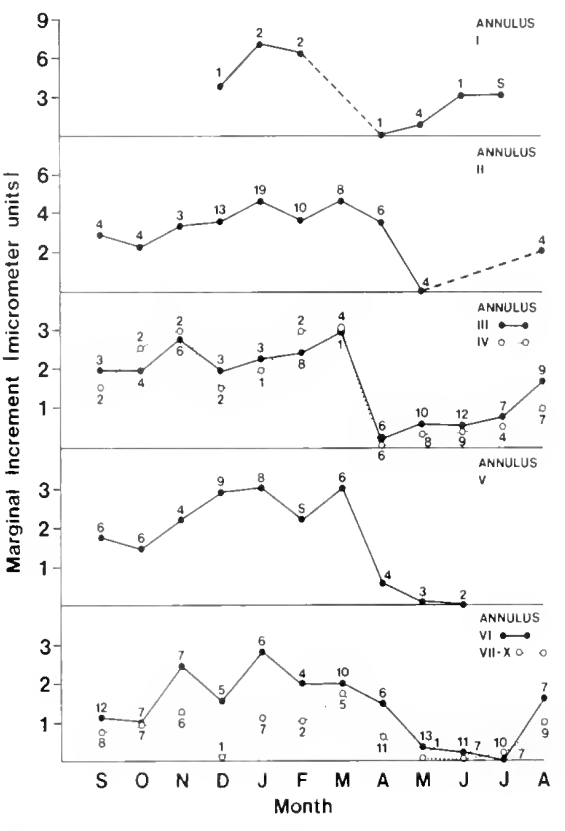

Figure 3
Marginal increment analyses for annuli I–X for *Epinephelus guttatus* from Puerto Rico (1 micrometer unit = 0.031 mm). Numbers above plots are sample sizes. Dashed lines connect samples separated by more than one month.

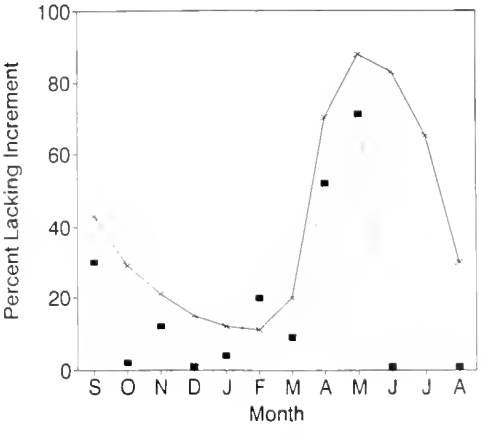

Figure 4
Percentage of otolith sections lacking a marginal increment for *Epinephelus guttatus* from Puerto Rico (solid line) and St. Thomas (dashed line) for age groups 1–10.

Table 1

Temporal significance of opaque growth zones in otoliths of *Epinephelus guttatus* from Puerto Rico, based on OTC-marked/recaptured fish. OR = otolith radius; MI = marginal increment; OTC = oxytetracycline mark.

Tag no.	Date (D/M/Y) Capture Recapture	FL (mm) Capture Recapture	Days in field	Measurements (32 micrometer units = 1 mm) Focus to ring 1	2	3	4	OTC	OR	MI	No. of opaque zones
00094	01/06/88 31/10/88	163 203	152	37*	—	—	—	[1]46	55	4	1
00078	25/05/88 04/05/89	127 151	344	45*	59	—	—	[1]52	63	0	2
00076	01/06/88 14/02/89	202 231	258	40	52	61	—	[2]65	72	4	3
00468	13/05/88 20/03/89	210 220	311	38	54	60	—	[2]68	73	5	3
00418	02/06/88 31/10/88	214 220	151	34	51	62*	—	[1]64	71	0	3
00385	19/08/88 10/02/89	218 248	175	39	50	69	—	[3]60	70	0	3
[4]00038	11/10/89 14/02/91	261 289	491	43	61	75	—	[3]72	85	3	3
00426	08/06/88 07/02/89	287 317	244	45	60	73	87	[2]90	95	4	4

[1]OTC mark lies within opaque zone indicated by asterisk.
[2]OTC mark lies at junction of opaque and translucent zones.
[3]OTC mark lies within translucent zone.
[4]Fish originally tagged June–December 1988; inner OTC mark 52[(3)]. Retagged 11/10/89 (only retag data presented).

Table 2

Mean back-calculated and observed fork lengths (mm) at time of opaque zone formation (yr) for age-groups 1–17 of 624 *Epinephelus guttatus* from Puerto Rico.

Age-group	*N*	Mean length at capture	SD	1	2	3	4	5	6	7	8	9	10	11	12	13	14	15	16	17
1	19	184	47	161																
2	97	247	21	168	213															
3	90	256	23	162	203	234														
4	52	272	26	159	195	226	253													
5	87	306	30	163	205	237	263	286												
6	126	321	33	165	207	237	262	283	303											
7	52	342	42	163	205	236	262	284	305	325										
8	29	353	34	169	209	236	260	283	304	320	336									
9	26	374	36	160	209	241	269	290	310	327	340	357								
10	27	393	32	170	213	244	271	293	312	329	346	361	374							
11	5	413	41	163	211	247	270	298	315	333	349	366	382	399						
12	4	416	30	160	194	226	257	283	302	321	335	352	366	382	394					
13	2	422	17	168	219	250	275	296	313	334	347	360	372	384	399	410				
14	5	448	31	172	212	247	278	304	323	340	354	368	383	409	417	432				
15	0	—	—																	
16	1	448	—	155	213	238	262	277	289	308	332	353	372	387	393	405	414	424	436	
17	2	458	46	159	216	247	271	293	312	323	336	348	362	380	395	406	416	431	440	448
Back-calculated mean lengths (weighted)				164	206	236	262	286	306	326	342	359	375	390	401	412	426	429	439	448
Growth increments					42	30	26	24	20	20	16	16	16	15	11	11	14	3	10	9

ing aggregation area. To reach the bank, this fish must have crossed water of at least 194 m depth, a substantial depth for similar-sized individuals of this species (Sadovy et al., unpubl. data).

During the tagging study, significant data loss occurred; in approximately 60% of tagged fish resighted, the identifying number of the dorsal tag had detached, leaving behind a monofilament anchor partially embedded in dorsal musculature. On the other hand, resightings of fish marked with abdominal tags indicated that all had retained both the numbered tag anchor and the attached color streamer.

Data for age-groups of recaptured fish indicated that no more than one opaque zone is deposited annually, although sample size was limited. Opaque zone formation had begun in or after February, had terminated prior to August, and occurred somewhat later in the year in older age-groups.

Recaptures were initiated as early as 5 months after tagging because individuals typically disappeared from the immediate study site within a few months of capture. Results covering less than a 12-month field period should be treated with caution, although all results were consistent with the marginal increment analysis in terms of both the temporal nature of opaque zones and the time of their annual deposition.

Age and growth

For Puerto Rico, the FL/OR relationship is

$$FL = 33.2180 + 3.0743\ OR \quad (r^2\ 0.76;\ N\ 624).$$

Table 2 shows the mean back-calculated lengths for ages 1–17 years from 624 fish. The following growth parameter estimates were obtained from the von Bertalanffy growth function (with asymptotic SE in parentheses):

$$L_\infty = 514.5\,\text{mm FL} \quad (6.29)$$
$$K = 0.1013 \quad (0.003765)$$
$$t_0 = -2.944 \quad (0.1357).$$

Figure 5 shows empirical mean lengths and their standard deviations, as well as back-calculated and theoretical (VBGF) growth curves, for Puerto Rico.

For St. Thomas the FL/OR relationship is

$$FL = 94.7206 + 2.4757\ OR \quad (r^2\ 0.68;\ N\ 162).$$

Table 3 shows the mean back-calculated lengths for age-groups 1–18 from 162 fish. The following growth parameter estimates were obtained from the von Bertalanffy growth function (with asymptotic SE in parentheses):

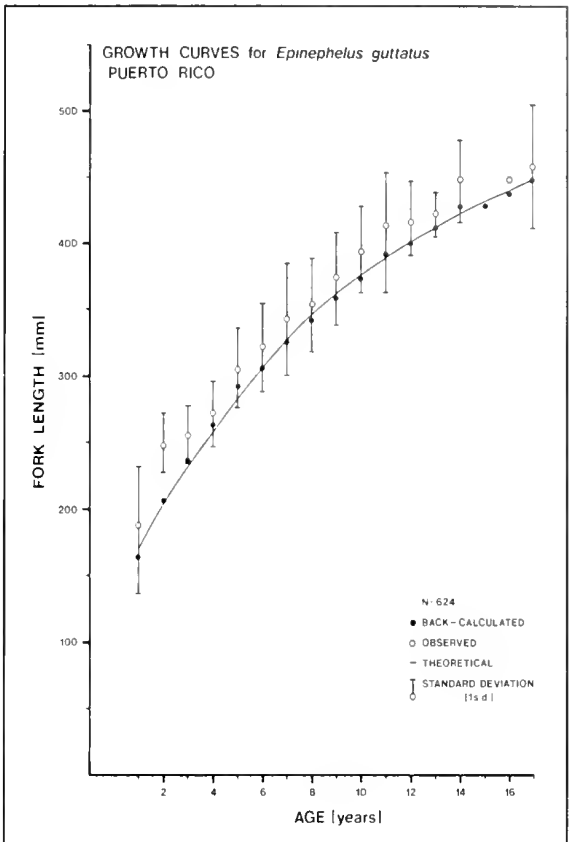

Figure 5
Empirical, back-calculated, and theoretical (von Bertalanffy) growth curves for *Epinephelus guttatus* from Puerto Rico.

$$L_\infty = 601.0\,\text{mm FL} \quad (32.82)$$
$$K = 0.0705 \quad (0.009954)$$
$$t_0 = -4.690 \quad (0.5920).$$

Figure 6 shows the empirical mean lengths and their standard deviations, as well as back-calculated and theoretical growth curves, for St. Thomas.

For Puerto Rico, the OW/FL relationship is

$$OW = 1.4205 + 0.0108\ FL \quad (r^2\ 0.93;\ N\ 315;\ \text{Fig. 7}).$$

For St. Thomas, the OW/FL relationship is

$$OW = 0.5591 + 0.0049\ FL \quad (r^2\ 0.93;\ N\ 101).$$

When mean back-calculated fork lengths for annuli I–V for age-groups 1–14 from Puerto Rico and St. Thomas are plotted (Fig. 8), two points are worthy of note. If regressions for each annulus are calculated for all available ages up to age-group 14, all are statistically

Table 3

Mean back-calculated and observed fork lengths (mm) at time of opaque zone formation (yr) for age-groups 1–18 of 162 *Epinephelus guttatus* from St. Thomas.

Age-group	N	Mean length at capture	SD	1	2	3	4	5	6	7	8	9	10	11	12	13	14	15	16	17	18
1	7	249	12	204																	
2	10	260	17	195	232																
3	39	280	25	190	229	259															
4	10	284	28	185	213	243	265														
5	16	319	28	195	229	260	286	308													
6	27	335	27	195	228	255	278	298	316												
7	11	348	29	194	227	255	278	297	317	333											
8	13	362	29	195	230	258	282	303	320	333	349										
9	9	370	55	195	226	252	275	296	315	331	343	358									
10	5	356	28	184	212	238	261	279	296	312	324	333	345								
11	5	391	45	195	228	253	279	300	317	332	345	355	367	378							
12	3	424	51	203	242	273	294	311	329	346	358	375	388	401	411						
13	1	460	—	206	234	270	290	332	348	365	382	396	410	424	438	452					
14	3	442	22	222	246	269	291	318	339	355	368	378	391	399	412	420	430				
15	2	492	12	215	263	290	316	343	362	378	389	405	421	434	450	460	469	478			
16	0	—	—																		
17	0	—	—																		
18	1	475	—	192	217	248	273	299	324	350	368	386	401	414	427	432	439	452	460	465	470
Back-calculated mean lengths (weighted)				194	228	256	279	301	318	335	349	362	377	400	423	438	445	469	460	465	470
Growth increments					34	28	23	22	17	17	14	13	15	23	23	38	7	24	−9	5	5

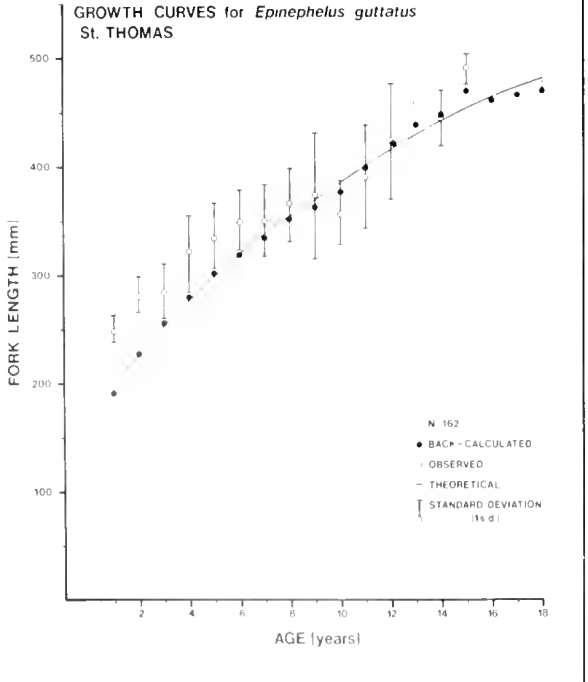

Figure 6

Empirical, back-calculated, and theoretical (von Bertalanffy) growth curves for *Epinephelus guttatus* from St. Thomas.

significant ($p<0.05$), with the exception of annuli I and II for Puerto Rico. Also of note are two distinct depressions in back-calculated mean lengths for each geographic location. For Puerto Rico these are indicated at age-groups 4 and 12, and for St. Thomas at age-groups 4 and 10. These points will be addressed in the discussion.

Data on growth during the months following spawning indicate rapid growth from the time of settlement in February or March at ~40 mm FL (N 29), to 60 mm FL in April/May (N 3), 108 mm (N 2) in August, and 115 mm (N 4) in October.

Age, sex, and size

A total of 186 individuals from Puerto Rico were sexed, by histological examination of gonads, and aged. Of these, 131 were female and 50 were male; 5 were considered to be in sexual transition between female and male, with gonads consisting of degenerating sexually-mature (i.e., vitellogenic) ovarian tissue and scattered areas of spermatogenic tissue exhibiting various stages of spermatogenesis (Sadovy and Shapiro 1987). All males exhibited testes with an ovarian-like configuration and lumen (Sadovy and Shapiro 1987).

Mean observed FL, standard deviation, and sample size by sex and age-class from Puerto Rico are shown

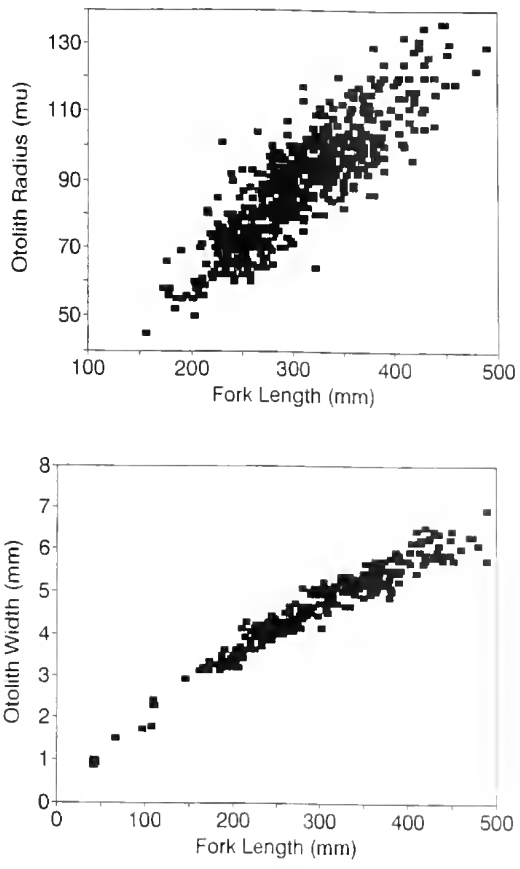

Figure 7

(upper) Relationship between otolith radius and fork length for *Epinephelus guttatus* from Puerto Rico (1 micrometer unit = 0.0312 mm). (lower) Relationship between unsectioned otolith width and fork length for *Epinephelus guttatus* from Puerto Rico.

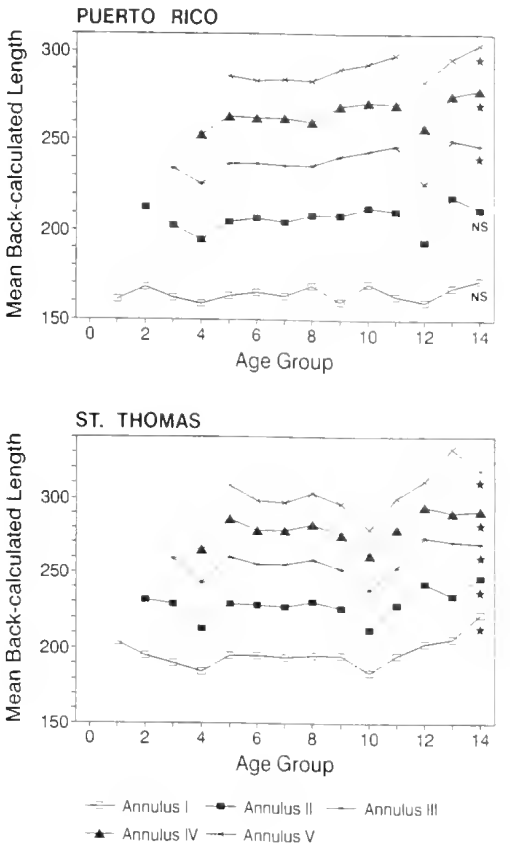

Figure 8

(upper) Mean back-calculated fork length of annuli I–V for *Epinephelus guttatus* from Puerto Rico. Asterisks denote significance at $p<0.05$; NS = nonsignificant. (lower) Mean back-calculated fork length of annuli I–V for *Epinephelus guttatus* from St. Thomas. Asterisks denote significance at $p<0.05$.

in Table 4. Fork length at time of capture (i.e., observed FL) did not differ significantly between the sexes for age-groups 2–8 (Table 4). However, both age- and size-frequency distributions from both Puerto Rico and St. Thomas differed significantly by sex (age: $D=0.593$, $p<0.01$; size: $D=0.576$, $p<0.01$) (Fig. 9).

Females were found at ages 1–9, males at ages 2–17, and individuals undergoing sexual transition at ages 3–7 (Table 4). No sexually-mature individuals were detected below age 2 years. Fifty percent of females had attained sexual maturity by age 3.

Discussion

Validation and formation of opaque zones

Opaque zones incrementally deposited in the sagittae of the red hind *Epinephelus guttatus* were validated as annual in this study, both by marginal increment analysis and by a field study involving the marking of otoliths by OTC. Although the possibility of bi- or multi-annual growth lines (Deelder 1981, Lee et al. 1983) for fish aged 11 years and over could not be discarded, these age-groups constituted a small percentage of sampled individuals; hence, the validation may be applied confidently to the exploited segment of red hind stocks in the region.

It is not known what causes the formation of opaque and translucent zones in this species. However, since zones are found in both adults and juveniles, they are clearly not caused exclusively by spawning activity (Nekrasov 1980). Opaque zone formation has been proposed to be associated with low somatic growth rates, and translucent zones with high growth rates, in the white grunt *Haemulon plumieri* (Sadovy and Severin 1992). A similar relationship is proposed for the red

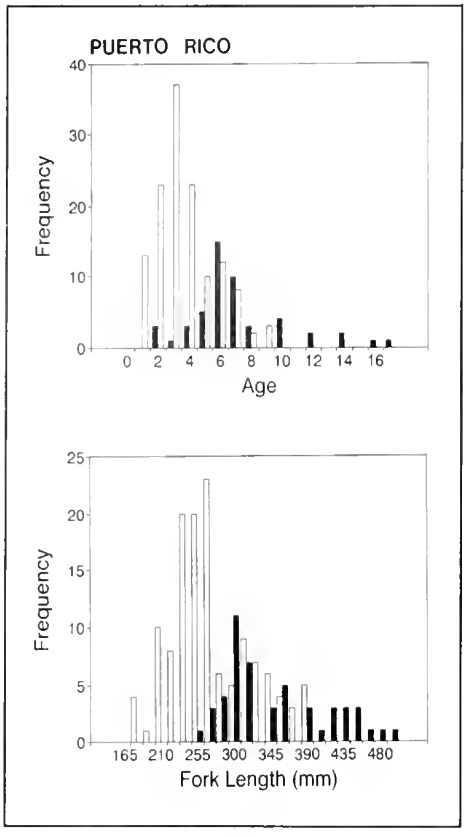

Figure 9
(upper) Age-frequency distributions of female (stippled) and male (solid) *Epinephelus guttatus* from Puerto Rico. (lower) Size-frequency distributions of female (dotted) and male (solid) *Epinephelus guttatus* from Puerto Rico.

hind (Sadovy and Severin, unpubl. data). Since time of opaque zone formation was earlier in the year in younger than in older fish, zone formation is unlikely to be caused by a simple environmental factor acting directly and equally on all individuals. Time of opaque zone formation is February–July, which is similar to that reported for four other groupers of the genus *Epinephelus* from the western Atlantic (Table 5). The pattern of earlier annual opaque zone formation in younger individuals noted in our study was also reported in otoliths from *E. morio* (Moe 1969) and *Mycteroperca microlepis* (Collins et al. 1987), and in pike *Esox lucius* (aged using cleithra; Casselman 1983).

Data on growth of red hind in the months following settlement indicate rapid growth from the time of settlement at ~40mmFL (*N* 29), to 115mmFL the following October. These data indicate that the first opaque zone, which is laid down between March and April at a back-calculated 164mmFL (SD 18mm) in Puerto Rico and 194mmFL (SD 17mm) in St. Thomas, represents an age 1+ year fish (13–15 months old, depending on month of spawning).

Growth parameters and longevity

Red hind in Puerto Rico and St. Thomas are long-lived and attain their maximum size slowly, following fast growth during the first year. Thompson and Munro (1974), using length-frequency analysis, calculated $L_\infty = 520$mmFL for Jamaica–Pedro Bank fish, and $L_\infty = 500$mmFL for Jamaica-Port Royal fish. Burnett-Herkes (1975),

Table 4
Mean observed fork length (mm) and standard deviation for male and female red hind, *Epinephelus guttatus*, by age-group. Fish from Puerto Rico collected September 1987–September 1988 (*$p<0.05$). NS = nonsignificant.

	Observed fork length (mm)								
	Female			Male				Transitional fish	
Age	$\bar{x}$	SD	*N*	$\bar{x}$	SD	*N*	Student's *t*	FL	*N*
1	196.3	16.3	13	–	–	–	–		0
2	238.7	20.6	23	253.7	34.2	3	1.1076 NS		0
3	251.5	18.6	37	301.0	–	1	0.1410 NS	275	1
4	267.2	28.0	23	280.7	10.5	3	0.8150 NS	278	1
5	307.2	28.4	10	288.0	7.3	5	1.4621 NS		0
6	344.9	35.8	12	322.2	30.4	15	1.7823 NS	315	1
7	340.6	25.9	8	336.6	49.4	10	0.2066 NS	258; 380	2
8	362.5	17.5	2	368.7	50.4	3	0.2536 NS		0
9	326.7	12.5	3	–	–	0	–		0
10	–	–	–	418.0	14.9	4	–		0
11	–	–	–	–	–	0	–		0
12	–	–	–	440.0	10.0	2	–		0
13	–	–	–	–	–	0	–		0
14	–	–	–	470.0	10.0	2	–		0
15	–	–	–	–	–	0	–		0
16	–	–	–	448.0	–	1	–		0
17	–	–	–	490.0	–	1	–		0
Total	268.0	50.0	131	342.0	65.0	50	8.1597*	301	5

Table 5
Caribbean and western Atlantic *Epinephelus* spp. aged by whole or sectioned otoliths.

Species	Growth parameters* L_∞ (mm FL)	K	t_0 (yr)	Time of opaque zone formation	Max. age (yr)	Source
E. nigritus	2394	0.054	−3.616	April–May	41	Manooch and Mason 1987
E. niveatus	1320	0.087	−1.012	May–July	17	Moore and Labisky 1984
E. niveatus	1255	0.074	−1.920	May–July	17	Matheson and Huntsman 1984
E. drummondhayi	967	0.130	−1.010	April–June	15	Matheson and Huntsman 1984
E. morio	928	0.113	0.091	—	14+	Melo 1975 (cited in Manooch 1987)
E. morio	792	0.179	−0.449	March–July	25+	Moe 1969
E. guttatus	601	0.071	−4.690	March–June?	18+	This study; St. Thomas
E. guttatus	515	0.101	−2.944	February–July	17+	This study; Puerto Rico
E. guttatus	507	0.180	−0.440	—	17+	Burnett-Herkes 1975; also used length-frequency data

*L_∞ = asymptote of the growth-in-length curve; K = Brody growth coefficient; t_0 = theoretical origin of von Bertalanffy growth curve (Ricker 1975).

using whole otoliths and length-frequency analyses for ageing, reported $L_\infty = 507$ mm FL in Bermuda. The largest fish sampled in the present study were 490 mm FL in Puerto Rico and 504 mm FL in St. Thomas. In several years of intensive sampling of thousands of red hind from local commercial landings, Fisheries Research Laboratory (FRL) data recorded <2% of individuals >500 mm FL (FRL, unpubl. data). These data reflect asymptotic lengths established in the present study. Randall (1983) reported the largest West Indian specimen collected to be 673 mm FL, and Smith (1971) reported the largest fish he examined to be 510 mm SL (618 mm FL using the above FL/SL relationship).

Growth parameters obtained using otoliths as the ageing structure for western Atlantic species of the genus *Epinephelus* are shown in Table 5. The data for *E. guttatus* in Puerto Rico and St. Thomas fall within the range of values of L_∞, K, and maximum age reported for western Atlantic grouper. A maximum of 17 growth zones in Puerto Rico and 18 growth zones in St. Thomas were recorded. We consider the estimated longevity of 17+ and 18+ to be reasonable for commercially-taken red hind in Puerto Rico and St. Thomas, respectively. Luckhurst et al. (1992) recorded 22 (±1) opaque zones in an unusually-large 720 mm FL individual from Bermuda.

Lengths-at-capture were consistently higher than back-calculated lengths for each age-group (Figs. 5, 6). The higher observed mean fork lengths generally reflect additional growth between previous ring formation and time of capture. However, the notably high observed mean FL of ages-1 and -2 fish for both Puerto Rico and St. Thomas may be due, in part, to selection by the fishery of the largest fish in these younger age-groups. Similar selection was also reported for the first two age-classes in *E. morio* (Moe 1969) and may be especially common in longer-lived, slower-growing species, such as grouper (Bannerot 1984). When sampling is biased towards larger individuals of young year-classes, there may be artificial depression of K in the VBGF (Ricker 1975). A downward bias would generally produce conservative management advice in terms of justifying imposition of minimum size regulations based on future returns to the fishery (Bannerot 1984).

The relationship between FL and OR for both locations is somewhat weaker than in other studies of fish age and growth. Since the OW/FL relationships for otoliths from both locations are strong, this indicates that variability is introduced by the position on the sectioned otolith selected for measurement and counting of opaque zones, rather than by a poor relationship between body length and otolith size (Fig. 7).

The regressions for mean back-calculated fork lengths of annuli I–V of age-groups 1–14 for Puerto Rico and St. Thomas are statistically significant, with two exceptions (Fig. 8). Such a trend could suggest a reverse "Rosa-Lee" phenomenon, indicating enhanced survivorship of fast-growing fish (Ricker 1975). If this were true, it would result in an upward bias of the parameter K in the VBGF. However, sample sizes for individuals above age-group 10 are very low, and regressions for age-groups 5–10 are not significant, with the exception of annulus II for Puerto Rico. Since these age-groups comprise the bulk of commercial landings, we believe that bias to estimates of growth parameters derived in the present study is negligible. Furthermore, since a similar increase is apparent in most age-groups

below age-group 4, there is clearly no consistent relationship between growth rate and mortality.

The depressions in back-calculated mean lengths (Fig. 8) apply to years 1983–84 (age-group 4) and 1975–76 (age-group 12) for Puerto Rico, and 1984 (age-group 4) and 1978 (age-group 10) for St. Thomas. In the case of older age-classes, small sample sizes could have produced sampling errors. However, we believe that in the case of 1984, this pattern is unlikely to be the result of sampling artifacts. Possible explanations for lower mean back-calculated lengths in both locations include environmental factors, such as unusually low temperatures or reduced food availability, or alterations in fishing effort and associated demographic changes. We know of no changes in fishing effort or gear during the early 1980s at either location. Reduced environmental temperatures or food availability may have caused age-1 and -2 fish to experience a decrease in growth rate that carried over into later years. Interestingly, catch curves developed from the same data set indicate a particularly low recruitment into the fishery of age-4 fish in 1984 (Sadovy and Figuerola 1992). This trend in the catch curves is strikingly similar for both locations, strongly suggesting a region-wide phenomenon. Poor recruitment into the fishery of a young age-class could result from slow growth early in life of individuals of that cohort.

Examination of temperature records for the region indicates that the winter of 1984 was the first since that of 1975 in which the mean minimum temperature dropped below 26°C (lat. 14.7°–18.2°) (Atwood and Hendee In press). In summary, we suggest that lower temperatures may have retarded growth in young individuals and that this reduction in size-at-age early in life was carried through the growth history of the animal.

Age and sex

Among sexed individuals, the majority (80%) of females were ages 1–5, and the males ages 2–10. Empirical mean lengths for age-groups 2–8 did not differ by sex. Moe (1969) also found the empirical growth curves of the sexes of *E. morio* to be similar, indicating that there are no marked differences in growth between the sexes or sexual phases of an individual. The combination of histological data, especially the presence of transitionals, size/age frequency distributions, and a female-biased sex ratio, confirm protogyny for this species in Puerto Rico. However, the presence of males as young as the youngest mature female indicates that at least some males may develop directly from a juvenile phase without passing through an initial functional female phase.

The red hind and fishery management

The condition of growth overfishing in the red hind (Sadovy and Figuerola 1992), and the general vulnerability of grouper species to fishing pressure, indicate the urgent need for management, stock monitoring, and assessment throughout its geographic range. In particular, given the apparent importance of spawning aggregations for annual reproductive output in the red hind (Bohnsack 1989; Shapiro 1987), and the intensity with which these are exploited locally (Sadovy, unpubl.), the possibility of recruitment overfishing needs to be addressed.

Acknowledgments

We thank the Caribbean Fishery Management Council, NMFS/NOAA, which is largely responsible for funding this research, and Omar Muñoz-Roure and Miguel Rolón for support in the early phases of developing this study. We are particularly grateful to Richard Appeldoorn, Jim Burnett-Herkes, Mark Collins, George Dennis III, Doug DeVries, Allyn Johnson, Angie McGehee, Charles Manooch III, and George Mitcheson for information, help, and advice. Charles Manooch kindly evaluated a subsample of otoliths. Stephen Ralston drew our attention to implications in the data we have discussed and represented as Figure 8. Thanks are due to Jim Beets who provided the otolith samples from St. Thomas. The cooperation and support of the Exploration Team of the Fisheries Research Laboratory and of local fishermen, especially Santiago Vélez Ocasio and Wilfredo Vélez Ocasio, were much appreciated. We thank Bonny Bower-Dennis who prepared some of the figures.

Citations

Appeldoorn, R., J. Beets, J. Bohnsack, S. Bolden, D. Matos, S. Meyers, A. Rosario, Y. Sadovy, and W. Tobias
1992 Shallow water reef fish stock assessment for the U.S. Caribbean. NOAA Tech. Memo. NMFS-SEFSC-304, NMFS Southeast Fish. Sci. Cent., Miami, 70 p.

Atwood, D.K., and J.C. Hendee
In press An assessment of global warming stress on Caribbean coral reef ecosystems. Proc. Gulf Caribb. Fish. Inst. 44.

Bannerot, S.P.
1984 The dynamics of exploited groupers (Serranidae): An investigation of the protogynous hermaphroditic reproductive strategy. Ph.D. diss., Univ. Miami, Coral Gables, 393 p.

Bannerot, S.P., W.W. Fox Jr., and J.E. Powers
1987 Reproductive strategies and the management of snappers and groupers in the Gulf of Mexico and Caribbean. *In* Polovina, J.J., and S. Ralston (eds.), Tropical snappers and groupers: Biology and fisheries management, p. 561–603. Westview Press, Boulder.

Beets, J., and A. Friedlander
1992 Stock analysis and management strategies for red hind, *Epinephelus guttatus*, in the U.S. Virgin Islands. Proc. Gulf Caribb. Fish. Inst. 42:66–80.

Bohnsack, J.A.
1989 Protection of grouper spawning aggregations. Coastal Resour. Div. Contrib. CRD 88-89-06, NMFS Southeast Fish. Sci. Cent., Miami, 8 p.

Burnett-Herkes, J.
1975 Contribution to the biology of the red hind, *Epinephelus guttatus*, a commercially important serranid fish from the tropical western Atlantic. Ph.D. diss., Univ. Miami, Coral Gables, 154 p.

Carlander, K.D.
1981 Caution on the use of the regression method of back-calculating lengths from scale measurements. Fisheries (Bethesda) 6(1):2–4.

Casselman, J.M.
1983 Age and growth assessment of fish from their calcified structures—techniques and tools. *In* Prince, E.D., and L.M. Pulos (eds.), Proc., Int. workshop on age determination of oceanic pelagic fishes, p. 1–17. NOAA Tech. Rep. NMFS 8.

Colin, P.L., D.Y. Shapiro, and D. Weiler
1987 Aspects of the reproduction of two groupers, *Epinephelus guttatus* and *E. striatus* in the West Indies. Bull. Mar. Sci. 40(2):220–230.

Collins, M.R., C.W. Waltz, W.A. Rourvillat, and D.L. Stubbs
1987 Contribution to the life history and reproductive biology of gag, *Mycteroperca microlepis* (Serranidae), in the south Atlantic Bight. Fish. Bull., U.S. 85:648–653

Deelder, C.L.
1981 On the age and growth of cultured eels, *Anguilla anguilla* (Linnaeus, 1758). Aquaculture 26:13–22.

Erdman, D.S.
1976 Spawning patterns of fishes from the northeastern Caribbean. Contrib. Agric. Pesq., Dep. Agric. Commonwealth of Puerto Rico 8(2):1–37.

Lee, D.W., E.D. Prince, and M.E. Crow
1983 Interpretation of growth bands on vertebrae and otoliths of Atlantic bluefin tuna, *Thunnus thunnus*. *In* Prince, E.D., and L.M. Pulos (eds.), Proc., Int. workshop on age determination of oceanic pelagic fishes, p. 61–69. NOAA Tech. Rep. NMFS 8.

Luckhurst, B., J. Barnes, and Y. Sadovy
1992 Record of an unusually large red hind, *Epinephelus guttatus* (Serranidae), from Bermuda with comments on its age. Bull. Mar. Sci. 51(2):267–270.

Mahon, R. (editor)
1987 Report and proceedings of the expert consultation on shared fishery resources of the Lesser Antilles region, Mayagüez, Puerto Rico, 8–12 Sept. 1986. FAO Fish. Rep. 383, 278 p.

Manooch, C.S. III
1987 Age and growth in snappers and groupers. *In* Polovina, J.J., and S. Ralston (eds.), Biology and management of snappers and groupers, p. 329–373. Westview Press, Boulder.

Manooch, C.S. III, and D.L. Mason
1987 Age and growth of the Warsaw grouper and black grouper from the southeast region of the United States. Northeast Gulf Sci. 9(2):65–75.

Matheson, R.H. III, and G.R. Huntsman
1984 Growth, mortality, and yield-per-recruit models for speckled hind and snowy grouper from the United States South Atlantic Bight. Trans. Am. Fish. Soc. 113:607–616.

Matos, D., and Y. Sadovy
1989 CODREMAR/NMFS cooperative statistics program for 1988–1989, Annual report July 1989. Coop. Stat. Prog., NMFS, St. Petersburg FL, and Puerto Rico Dep. Nat. Resour., 56 p.

Melo, A.M.
1975 Aspectos biológicos pesqueros de *Epinephelus morio* (Val.). Unpubl. thesis, Univ. Nac. Autón. México, México D.F, 68 p.

Moe, M.A.
1969 Biology of the red grouper *Epinephelus morio* (Valenciennes), from the eastern Gulf of Mexico. Fla. Dep. Nat. Resour. Mar. Res. Lab. Prof. Pap. Ser. 10, 95 p.

Moore, C.M., and R.L. Labisky
1984 Population parameters of a relatively unexploited stock of snowy grouper in the lower Florida Keys. Trans. Am. Fish. Soc. 113:322–329.

Nekrasov, V.V.
1980 The causes of annulus formation in tropical fishes. Hydrobiol. J. (Engl. transl. Gidrobiol. Zh.) 2:35–39.

Ralston, S.
1987 Mortality rates of snappers and groupers. *In* Polovina, J.J., and S. Ralston (eds.), Tropical snappers and groupers: Biology and fisheries management, p. 375–404. Westview Press, Boulder.

Randall, J.E.
1983 Caribbean reef fishes, 2d ed., rev. T.F.H. Publ., Neptune, NJ, 350 p.

Ricker, W.E.
1975 Computation and interpretation of biological statistics of fish populations. Bull. Fish. Res. Board Can. 191, 382 p.

Sadovy, Y.
In press Grouper stocks of the western central Atlantic: The need for management and management needs. Proc. Gulf. Caribb. Fish. Inst. 43.

Sadovy, Y., and M. Figuerola
1992 The status of the red hind fishery in Puerto Rico and St. Thomas, as determined by yield-per-recruit analysis. Proc. Gulf. Caribb. Fish. Inst. 42:23–38.

Sadovy, Y., and K.P. Severin
1992 Trace elements in biogenic aragonite: Correlation of body growth rate and strontium levels in the otoliths of the white grunt, *Haemulon plumieri* (Pisces: Haemulidae). Bull. Mar. Sci. 50(2):237–257.

Sadovy, Y., and D.Y. Shapiro
1987 Criteria for the diagnosis of hermaphroditism in fishes. Copeia 1987 (1):136–156.

Saila, S.B., C.W. Recksiek, and M.H. Prager
1988 Basic fishery science programs: A compendium of microcomputer programs and manual of operation. Dev. Aquacult. Fish. Sci. 18, Elsevier Press, Amsterdam, 230 p.

Shapiro, D.Y.
1987 Reproduction in groupers. *In* Polovina, J.J., and S. Ralston (eds.), Tropical snappers and groupers: Biology and fisheries management, p. 295–327. Westview Press, Boulder.

Shapiro, D.Y., Y. Sadovy, and M.A. McGehee
In press Size, composition, and spatial structure of the annual spawning aggregation of the red hind, *Epinephelus guttatus* (Pisces: Serranidae). Copeia.

Smith, C.L.
1959 Hermaphroditism in some serranid fishes from Bermuda. Pap. Mich. Acad. Sci. Arts Lett. 44:111–119.
1971 A revision of the American groupers: *Epinephelus* and allied genera. Bull. Am. Mus. Nat. Hist. 146:69–241.

Sokal, R.R., and F.J. Rohlf
1981 Biometry, 2d ed. W.H. Freeman, San Francisco, 859 p.

Stevenson, D.K.
1978 Management of a tropical fish pot fishery for maximum sustainable yield. Proc. Gulf. Caribb. Fish. Inst. 30:95–115.

Thompson, R., and J.L. Munro
1974 The biology, ecology and bionomics of Caribbean reef fishes: Serranidae (hinds and groupers). Res. Rep. Zool. Dep., Univ. West Indies, Jamaica, 3(5b), 82 p.

Wilson, C.A., E.B. Brothers, J.M. Casselman, C.L. Smith, and A. Wild
1983 Glossary. *In* Prince, E.D., and L.M. Pulos (eds.), Proc., Int. workshop on age determination of oceanic pelagic fishes, p. 207–208. NOAA Tech. Rep. NMFS 8.

Yevich, P.R., and C.A. Barszcz
1981 Preparation of aquatic animals for histopathological examination. Aquat. Biol. Sect., Biol. Methods Br., Environ. Monit. & Support Lab., U.S. Environ. Protect. Agcy, Cincinnati, 81 p.

Abstract.–Spawning patterns, larval distribution, and juvenile growth characteristics were examined for tautog *Tautoga onitis* in New Jersey and the Mid-Atlantic Bight. We analyzed data from plankton surveys (1972–1990) over the continental shelf and in the Great Bay–Mullica River estuarine system. Data on size and abundance of juveniles were derived from throw trap and trawl collections in New Jersey estuaries (1988–89). In addition, we validated the daily deposition of otolith increments and used increment counts to estimate juvenile age and growth patterns. Extensive egg and larval collections indicated that spawning occurs from April through September, with a peak in June and July. Spawning over the continental shelf is concentrated off Long Island and Rhode Island. Based on validated daily increments in sagittal otoliths and the formation of a well-defined settlement mark, tautog larvae spend about 3 weeks in the plankton. Both spawning and settlement occur over a prolonged period, based on otolith back-calculations. Three methods of estimating young-of-the-year growth rates, including length-frequency progressions, otolith age/fish-size comparisons, and direct measurement of growth in caging experiments, indicated an average growth rate of about 0.5 mm/day during the peak midsummer growing season. Length-frequency distributions suggested tautog reach a modal size of about 75 mm SL after their first summer, and 155 mm by the end of their second summer.

Manuscript accepted 20 May 1992.
Fishery Bulletin, U.S. 90:529–539 (1992).

Early life history of the tautog *Tautoga onitis* in the Mid-Atlantic Bight*

Susan M. Sogard
Marine Field Station, Institute of Marine and Coastal Sciences
Rutgers University, Great Bay Boulevard, Tuckerton, New Jersey 08087
Present address: Hatfield Marine Science Center
Oregon State University, Newport, Oregon 97365

Kenneth W. Able
Marine Field Station, Institute of Marine and Coastal Sciences
Rutgers University, Great Bay Boulevard, Tuckerton, New Jersey 08087

Michael P. Fahay
Sandy Hook Laboratory, Northeast Fisheries Science Center
National Marine Fisheries Service, NOAA, Highlands, New Jersey 07732

The tautog *Tautoga onitis* is one of two labrid wrasses common along the northeast coast of the United States (the other is the cunner *Tautogolabrus adspersus*). Tautog occur in coastal areas from Nova Scotia to South Carolina, but are abundant only from Cape Cod to the Delaware Capes (Bigelow and Schroeder 1953). Adult tautog form a minor component of local commercial fisheries and a major component of the recreational catch. They reach a maximum size of about 90 cm and 10 kg (Bigelow and Schroeder 1953), and an age of 34 years (Cooper 1967). Large juveniles and adults depend on young mussels *Mytilus edulis* for food (Olla et al. 1974), and the diet of recently-settled juveniles consists primarily of copepods and amphipods (Grover 1982). Spawning takes place from May to August, with a peak in June (Kuntz and Radcliffe 1918, Colton et al. 1979, Eklund and Targett 1990). Egg and larval development are described in detail by Kuntz and Radcliffe (1918) and Williams (1967); additional information on life history is presented in Auster (1989).

Both juvenile and adult tautog are dependent on habitats with structure or cover, which presumably aids in protection from predators (Olla et al. 1974 and 1979, Olla and Studholme 1975). Tautogs typically become quiescent at night, resting in association with some type of shelter (Olla et al. 1974). Smaller fish (subadults <25 cm) may range only a few meters from that shelter during daytime activity, while larger individuals (adults >30 cm) cover a broader area for foraging, returning to the same general shelter area at night (Olla et al. 1974).

Declining water temperatures in the fall trigger an offshore migration of adults (age 4+). An increase in schooling behavior and night activity also occurs (Olla et al. 1980), perhaps related to migratory activity. Laboratory studies indicate that adults attain a dormant state at temperatures <5°C. Juveniles (age 2–3) also become torpid in winter, but they remain inshore, either partially buried or in close proximity to structure (Olla et al. 1974). In spring and summer adults return to inshore habitats. On hard-bottom reefs off Maryland

* Contribution 92-07 of the Rutgers University Institute of Marine and Coastal Sciences.

Table 1
Collection sources for *Tautoga onitis* eggs, larvae, and juveniles used in analyses of seasonal distribution and growth comparisons.

Stage	Sampling location	Years sampled	Sampling frequency	No. of tows or samples	Data source
Eggs	Mullica River, Great Bay, Little Egg Inlet	1972–75	monthly or bimonthly	462	Milstein and Thomas 1977
Larvae	Nova Scotia to North Carolina	1977–87	monthly or bimonthly	11,438	MARMAP
	Great Bay, Little Sheepshead Creek	1989–90	weekly	913	Rutgers Marine Field Station Plankton Survey
Early juveniles	Great Bay, Little Egg Harbor	1988–89	biweekly, May–September	436	Sogard and Able 1991
	Great Bay; artificial seagrass	1988	weekly, June–September	54	Sogard 1990
Late juveniles	Great Bay, Little Egg Harbor	1988–89	monthly	808	Rutgers Marine Field Station Trawl Survey

and Virginia (25–35m in depth) fish-trap catches of tautog are lowest in summer (Eklund and Targett 1991), perhaps due to inshore migrations of winter residents. Tagging studies conducted by Cooper (1966) suggest relatively discrete populations of tautog, with adults returning to the same spawning location following their winter residence offshore.

These prior studies of habitat requirements, behavior, and growth have focused primarily on fishes older than 1 year. In this paper we concentrate on life-history aspects for young-of-the-year individuals, particularly larvae and juveniles that have just recently metamorphosed and settled from the plankton. We present information on spatial and temporal distribution of eggs and larvae, larval stage duration, juvenile habitat, daily growth, and otolith-size/fish-size relationships.

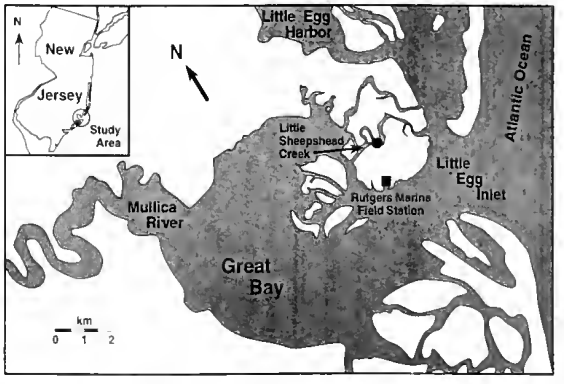

Figure 1
Map of Mullica River–Great Bay estuary system in New Jersey, and location of plankton sampling site in Little Sheepshead Creek.

Materials and methods

Reproductive seasonality and larval distribution

Information on timing of spawning and spatial distribution of tautog larvae was obtained from three sources (Table 1). Egg abundances were assessed in plankton collections during December 1972–December 1975 in the Mullica River–Great Bay estuary and adjacent ocean off Little Egg Inlet, New Jersey (Fig. 1). Sampling was conducted with 0.5m and 1.0m diameter plankton nets and 20cm and 36cm diameter bongo samplers with 0.5mm mesh. Surface, midwater, and bottom tows were made with the plankton nets; the bongos were fished obliquely. Data used in this study were reanalyzed from a report by Milstein and Thomas (1977).

Larval occurrences over the continental shelf were determined from collections made on Marine Resources Monitoring, Assessment and Prediction (MARMAP) surveys (Sherman 1988) by the National Marine Fisheries Service (NMFS). Surveys were conducted from Cape Hatteras, North Carolina, to Cape Sable, Nova Scotia. Sampling stations are shown in Figure 2; sampling methods are described in Sibunka and Silverman (1989).

Our third source of plankton data was obtained from a sampling program at the Rutgers University Marine Field Station. A 1m diameter, 1mm mesh net was fished at the surface and just above the bottom on night flood tides in Little Sheepshead Creek, adjacent to Great Bay (Fig. 1).

Juvenile length-frequency comparisons

Monthly patterns in length-frequency distributions were assessed from collections across several sites in the Little Egg Harbor and Great Bay estuaries (Fig. 1) using throw-trap and otter trawl sampling (Table 1). A throw trap is a $1\,m^2$ open box that is thrown onto

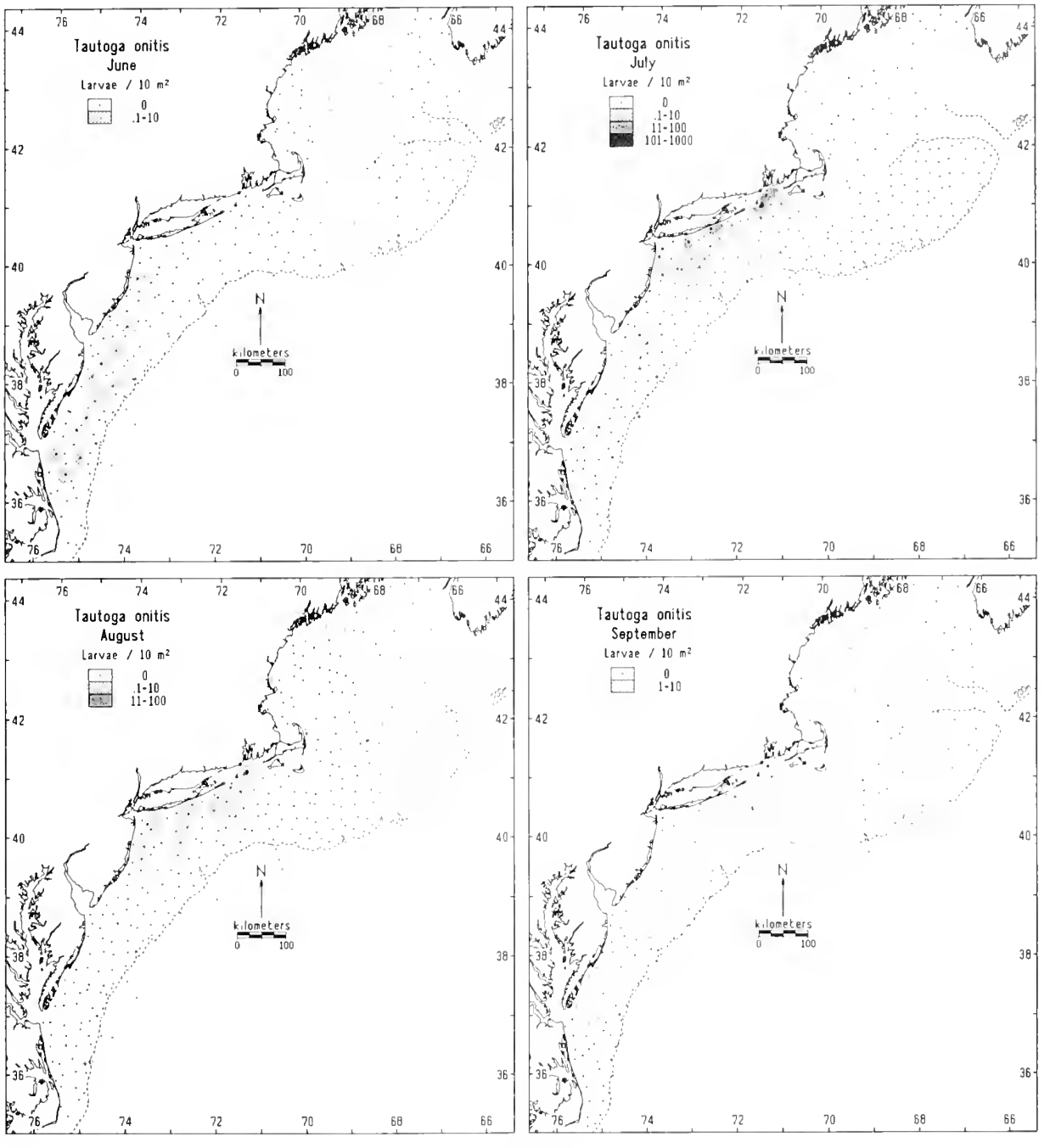

Figure 2

Average monthly distributions of *Tautoga onitis* larvae based on 11 years (1977–87) of sampling in the Mid-Atlantic Bight. Density calculations are based on collections within 1 km^2 blocks.

the desired substrate, with all animals subsequently removed with a 1 m wide net scraped across the bottom substrate. All throw-trap sampling was conducted at low tide in shallow (<0.5 m at low tide) vegetated and unvegetated habitats. Further details on the throw-trap method and sampling schedule are presented in Sogard and Able (1991). Additional length data were obtained from tautog collected with throw traps from artificial seagrass habitats on a shallow sandflat in Great Bay (Sogard 1990).

Tautog in deeper waters (1–8 m) of the Great Bay–Little Egg Harbor estuarine system were collected

during the Rutgers Marine Field Station trawl survey. A 4.9m otter trawl (6.3mm mesh cod end, 19mm mesh wings) was towed for 2 minutes at a total of 14 stations, which were representative of a variety of habitat types. Four replicate trawls were taken at each station.

Otolith increment analysis

More detailed information on planktonic stage duration, settlement patterns, and growth of young-of-the-year tautog was derived from analysis of otolith increments. To validate a daily rate of increment formation, the number of increments following a tetracycline-induced fluorescent mark on the sagitta was compared with the actual number of days elapsed. Juvenile tautog (19–63mm SL) were immersed for 24h in a 500mg/L solution of oxytetracycline dihydrate in natural seawater (20–25 ppt) diluted with distilled water to about 17 ppt. They were then held in laboratory aquaria, fed daily with *Artemia*, and preserved in 95% ethanol after 6–30 days. The sagittae of these individuals were removed, embedded in Spurr resin, and polished in the sagittal plane to the central primordium on both sides, using a series of 400–1500 grit sandpaper and alumina powder (0.3 μm), following the methods of Secor et al. (1991). The number of increments following the tetracycline mark was counted with UV microscopy at 400–1000× magnification.

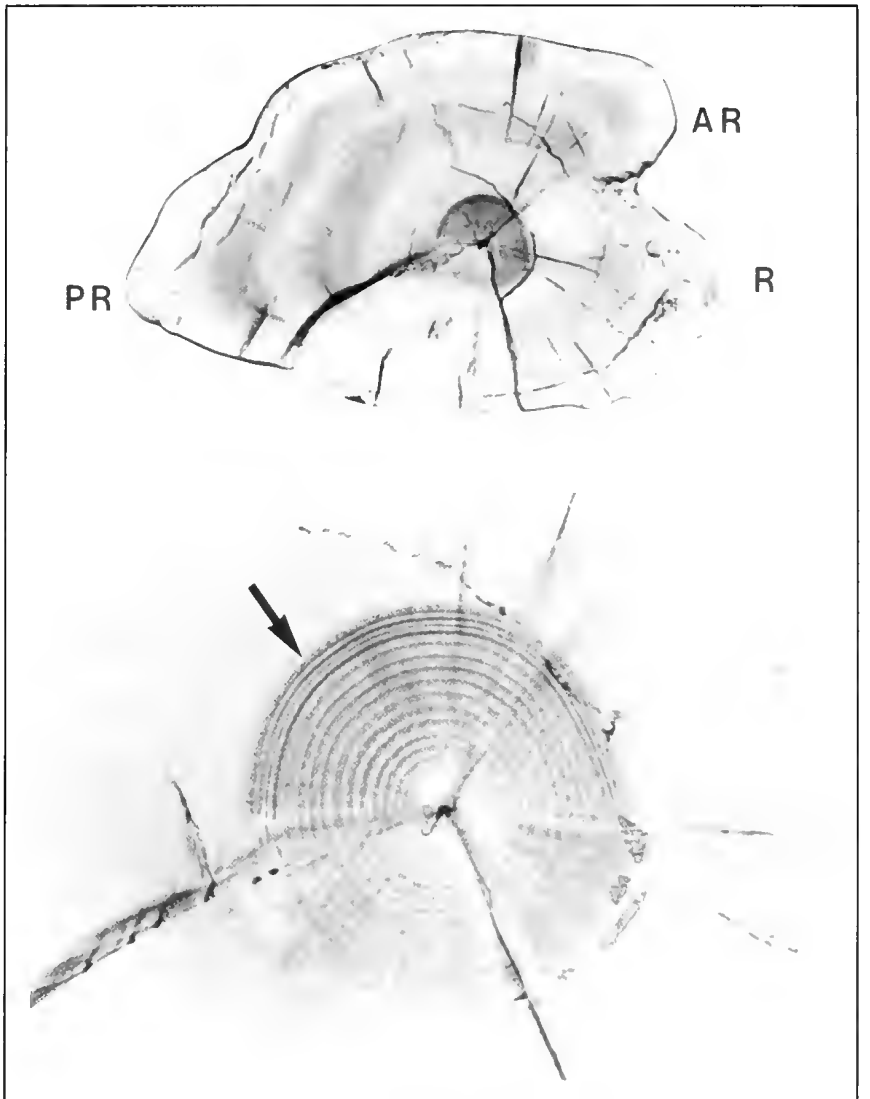

Figure 3

Ground and polished left sagitta of a 38.7mm SL juvenile *Tautoga onitis*. (upper) Photographed at 100× magnification; scale bar = 200μm. R = rostrum, PR = postrostrum, AR = antirostrum. Tip of the rostrum was partially destroyed during polishing. (lower) Closeup view of central region (400×). Arrow points to transition between pelagic and demersal stage increments. Scale bar = 50μm.

The degree of correspondence between otolith size and fish size was determined for 55 juvenile tautog by comparing radial measurements of the rostrum, postrostrum, and antirostrum (Fig. 3) with standard lengths. Radial measurements were made with an image analysis system attached to an Olympus BH-2 microscope, using a magnification on the monitor of 160× or 410×, depending on the size of the otolith. The relationship between otolith radial measurements and length (SL) of the fish was determined by regression analysis. Because preliminary analysis of a matched set of sagittae found no significant differences between left and right radius measurements (paired comparisons t-tests: n 8, $P>0.10$ for all three radii), either sagitta was used in subsequent analyses.

Increments were counted for a series of tautog (n 37, 7.6–62.8mm SL) collected from early-July through late-September in 1988. Larval and juvenile increments were distinguished on the basis of an apparent settlement mark in the sagittae (see below). Increments were counted independently on three different dates by the same reader, and the results were averaged. Preliminary counts of matched sagittae found no difference

between left and right (paired comparisons t-test: $P>0.10$), with the two sides differing by <2%. Thus, either sagitta could be used for increment counts.

The mean duration of the planktonic stage was estimated by the mean number of increments preceding the settlement mark. Birth and settlement dates were estimated by subtracting the number of total increments and juvenile increments, respectively, from the date of capture. Assuming that initial increment formation occurred at about the time of hatching, as in other wrasses (Victor 1982), our estimates of birthdates should correspond within a few days to the date of hatching.

Juvenile growth rates

We used three independent methods to estimate growth rates of young-of-the-year juveniles during the summer. The relationship between otolith age (total increments) and standard length was fit to a linear equation, using the slope as an estimate of daily growth. We also examined the progression of mean lengths for tautog collected on a weekly basis in 1988 (primarily from artificial seagrass experiments). Weekly mean lengths were determined and regressed on time, with the slope of the resulting equation used as a second estimate of daily growth. Growth rates based on these two indirect estimates were compared with a third, direct measurement of individual tautog growth in field caging experiments by Sogard (In press).

Results

Reproductive seasonality and larval distribution

In the Great Bay–Mullica River estuarine system, tautog eggs occurred in plankton collections from April through August, with peak abundances in June and July (Table 2). Initial occurrence and peak abundance of eggs were earlier in the Mullica River than in the bay and adjacent inlet, suggesting that spawning began earlier in the season in the upper part of the estuary, and continued later in the summer in the lower estuary and offshore waters. Tautog larvae in weekly plankton collections in Great Bay (Table 1) occurred in July and August of 1989 (n 12) and July of 1990 (n 9). Larvae were collected in the offshore MARMAP surveys from May through October, with a peak in July (Table 3, Fig. 2).

Based on geographic distribution of larvae, spawning was concentrated in southern New England waters (Fig. 2). Spawning activity in continental shelf waters appeared to follow a northward progression through the summer, beginning as early as May in the southern part of the region (Table 3).

Daily increment validation

Results of the validation tests indicated that increments on sagittae of juvenile tautog were deposited on a daily basis. The slope of the regression comparing the actual number of days elapsed with the number of increments following tetracycline marks did not differ from 1 ($P>0.05$, r^2 0.86, Fig. 4). Comparison of sagittal

Table 2

Monthly mean densities (no./1000 m^3) of *Tautoga onitis* eggs in Mullica River, Great Bay, and adjacent Atlantic Ocean off Little Egg Inlet, New Jersey, December 1972–December 1975. Plankton sampling was conducted throughout the year, but eggs were not collected in months not appearing in the table.

	Mullica River	Great Bay	Atlantic Ocean
April	66	3	0
May	116	726	853
June	169	165	1259
July	22	2221	1984
August	0	13	20

Table 3

Abundance of *Tautoga onitis* larvae ($\bar{x}$ no./100 m^3) collected during MARMAP survey cruises, 1977–87, by subarea and month. Mean abundance is followed by number of occurrences (2d line) and total number of stations sampled (3d line).

Subarea	May	June	July	Aug	Sept	Oct
Georges Bank	—	0.01	—	—	—	—
	0	1	0	0	0	0
	332	152	213	312	144	396
Southern New England	—	—	1.75	0.19	0.08	0.01
	0	0	26	18	4	1
	225	131	231	191	103	224
New Jersey	—	0.07	0.06	0.03	—	—
	0	4	9	4	0	0
	209	139	176	174	120	143
Delmarva Peninsula	—	0.16	0.02	0.01	—	—
	0	6	3	1	0	0
	163	82	104	140	126	45
Virginia and North Carolina	0.08	0.09	0.01	0.01	—	—
	7	3	1	1	0	0
	135	66	76	122	103	37

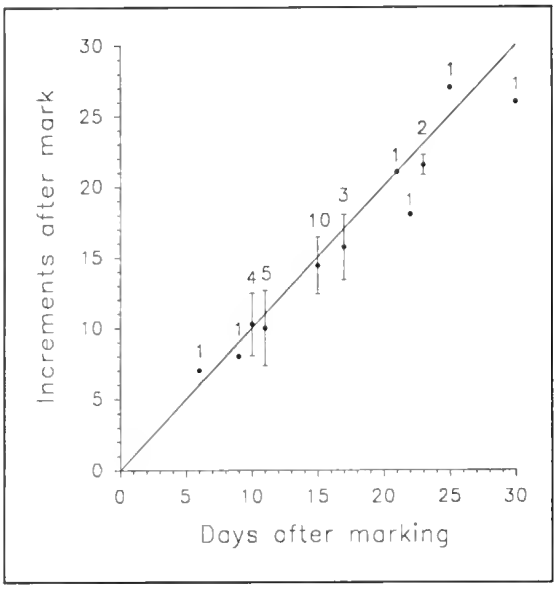

Figure 4

Validation of daily deposition of otolith increments in *Tautoga onitis*, comparing the number of increments outside a tetracycline-induced mark with the number of days since marking. Numbers above data points are numbers of fish tested; error bars are SD's. Resulting regression line does not deviate significantly ($P>0.05$) from a line of one-to-one correspondence.

radius measurements with standard length demonstrated a strong correspondence for all three radii (Fig. 5). For all three cases, a square-root equation provided the best fit.

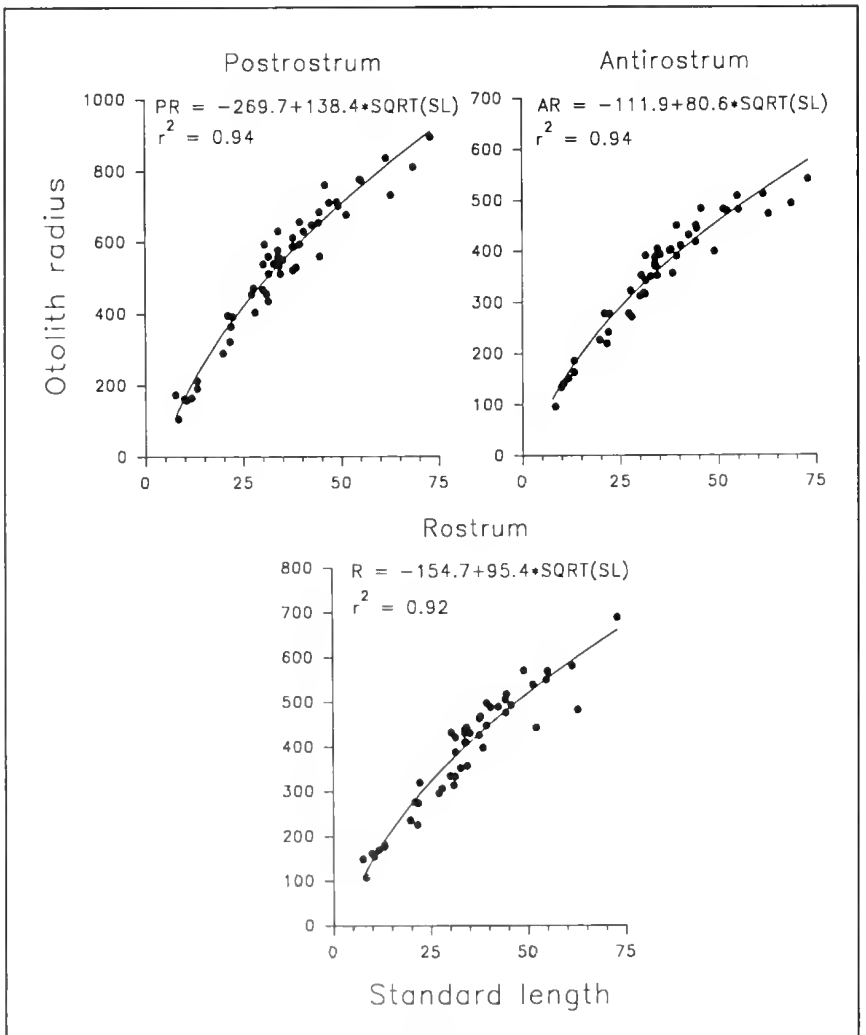

Figure 5

Regressions comparing otolith radial measurements (see Fig. 3) with standard length of juvenile *Tautoga onitis*. Displayed curves fit the square-root equations derived in regression analysis.

Settlement marks and larval stage duration

An obvious transition in the appearance of increments occurred in the sagittae (Fig. 3). Inner increments were generally more distinct because they were higher in contrast, darker in appearance, and more circular than increments outside the transitional area. In the sagittal plane, outer increments diverged in morphology, with increased deposition along the eventual axes of rostrum, postrostrum, and antirostrum. Sagittae of larval tautog (n 5) were comprised of only the darker, inner increments. Thus, we believe this transition in increment contrast and shape takes place at or near the time of settlement, when the individual has completed transformation and moved from a planktonic to epibenthic lifestyle. Settlement marks are a common feature of labrid otoliths, allowing ready distinction of larval and juvenile increments (Victor 1986).

The total number of increments (separated into larval and juvenile stages) was counted for 37 individuals collected in the Great Bay and Little Egg Harbor sampling. The number of increments deposited during the

pelagic larval stage was remarkably similar, with a mean of 20.4 (SD 2.7). Assuming that the first increment is deposited at about the time of hatching, tautog spend 3 weeks in the plankton before settling to the benthos. Subtraction of total increments from the date of collection resulted in a wide spread of estimated birth (hatch) dates, with a mean of 4 June and a range of 17 April–22 July. These dates are consistent with the general timing of the collection of eggs and larvae (Tables 2, 3). Settlement dates, estimated by subtracting only the juvenile-stage increments from the date of capture, were correspondingly widespread, with a mean of 25 June and a range of 6 May–13 August.

Juvenile habitat, size composition, and growth

In throw-trap samples collected in the shallow waters of Great Bay and Little Egg Harbor, juvenile tautog were collected only on vegetated substrates, and were more abundant in sea lettuce (*Ulva lactuca*, *n* 19) than in eelgrass (*Zostera marina*, *n* 2) (Sogard and Able 1991). Juveniles <40 mm in length were rare in the deeper waters sampled by trawls, but the larger young-of-the-year and 1-year-old tautog collected by trawling were most abundant in eelgrass beds. Of 14 sampling stations throughout Great Bay and Little Egg Harbor, two were in eelgrass habitats. These two stations accounted for 69% of the 235 tautog collected by trawling in 1988 and 1989.

Combined length-frequency data from throw-trap sampling and trawling efforts suggested that most tautog in the Great Bay–Little Egg Harbor system, based on these sampling techniques, belonged to one of two year-classes (Fig. 6). Young-of-the-year first appeared in July, primarily in the shallower (<1 m) habitats sampled by throw trapping. In the deeper areas (>1 m) sampled by otter trawl, larger young-of-the-year fishes increased in number in August collections. By September, the young-of-the-year dominated the trawl samples while decreasing in throw-trap sampling.

Modal progression of length-frequency distributions demonstrated relatively rapid growth for both young-of-the-year and 1-year-old tautog during the summer months. In contrast, comparison of young-of-the-year sizes in October with 1-year-old lengths in June indicated only minor growth during the fall, winter, and spring. Juvenile tautog attained a size of 40–100 mm

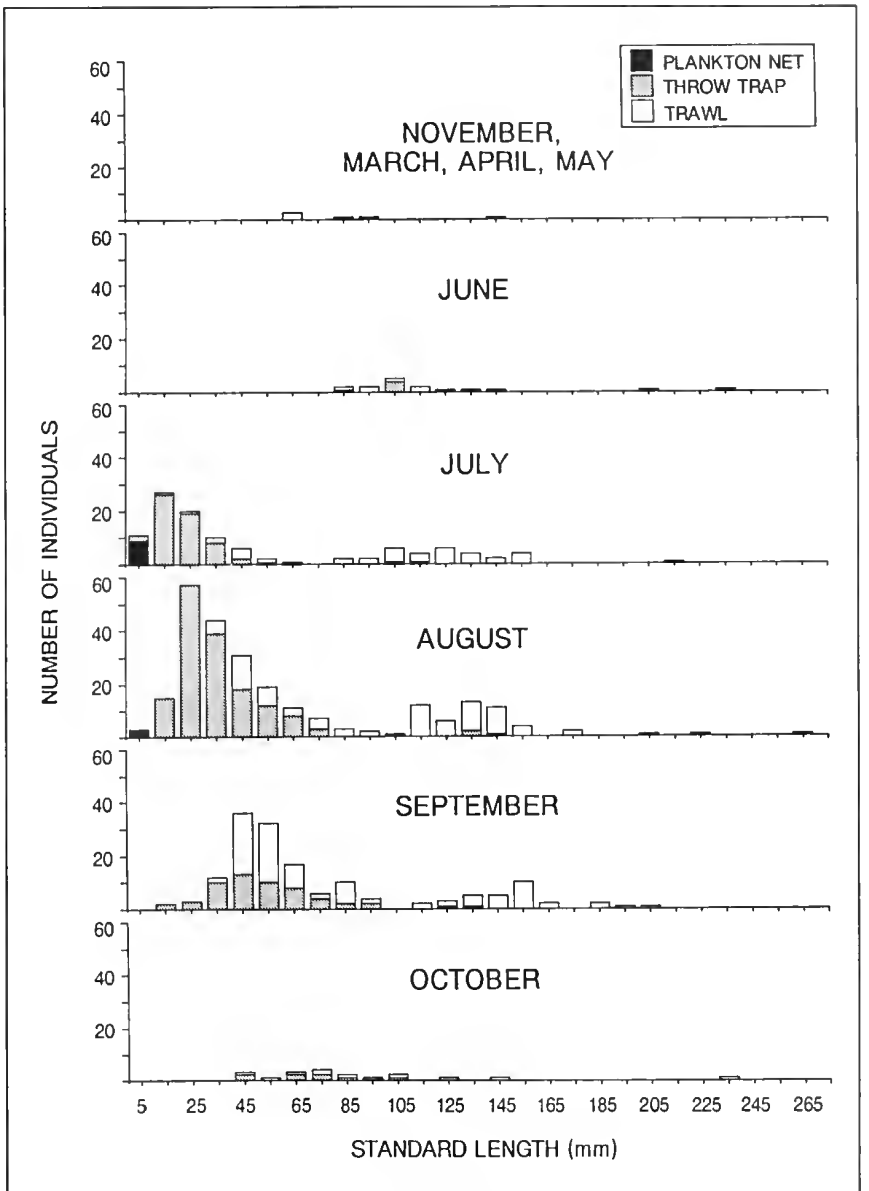

Figure 6

Length-frequency distributions of *Tautoga onitis* collected in the Little Egg Harbor–Great Bay estuarine system. Plankton samples were collected on a weekly basis throughout the year. Throw-trap samples were collected from shallow habitats (<1 m at low tide), May–October; trawl samples were collected from deeper habitats (1–8 m) monthly, with no tautog collected during December–February.

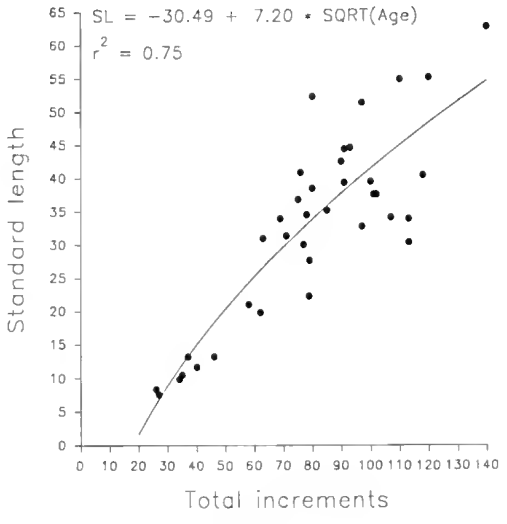

Figure 7
Total number of increments vs. standard length for 37 juvenile *Tautoga onitis*. The plotted square-root equation provided the best fit in regression analyses.

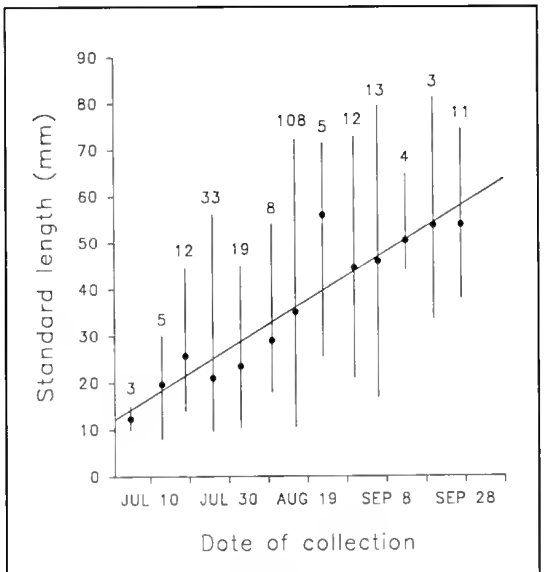

Figure 8
Mean and range in standard length of juvenile *Tautoga onitis* collected on a weekly basis in 1988. All fish were collected with throw traps, primarily from artificial seagrass substrates. The regression line was fit to means for each sampling date (n 13). Numbers above ranges are the number of tautog collected each week.

SL in their first growing season, with a modal size of 75 mm in October (Fig. 6). One-year-old fish reached a size of 110–170 mm SL by the end of their second summer, with a modal size in September of 155 mm.

Comparison of otolith ages (total increment counts) with standard lengths provided a general estimate of juvenile growth. The resulting relationship was best described by a square-root equation (Fig. 7), indicating a slight decline in absolute growth rate with age. If the data are fit to a linear equation, a slope of 0.47 results, thus estimating an average rate of 0.47 mm/day during the early juvenile stage. Substantial variability was evident, especially among older individuals (Fig. 7).

To obtain an estimate of growth based on length-frequency distributions, we compared length with the date of capture for 236 juveniles collected only by throw traps in 1988. When the mean length each week was regressed on time (Julian date), the resulting slope provided an estimated growth rate of 0.52 mm/day (Fig. 8).

Discussion

Spawning patterns

Based on the seasonal occurrence of eggs and larvae, the peak spawning period for tautog in the Mid-Atlantic Bight and inshore New Jersey waters is during the summer. Spawning appears to follow a geographical progression, beginning earlier in the southern part of the region. Consistent with this pattern, Eklund and Targett (1990) report that gonosomatic indices of adult tautog off Maryland and northern Virginia are highest in May.

The egg collections in New Jersey and high egg and larval abundances in areas such as Narragansett Bay (Bourne and Govoni 1988) demonstrate that tautog spawn primarily inside estuaries or nearshore waters. The MARMAP collections indicate that spawning activity involves offshore continental shelf waters as well, since all of the tautog larvae obtained during MARMAP surveys were preflexion stage.

Otolith deposition patterns

Otolith increments of juvenile tautog can be reliably used to obtain valuable age and growth information. The strong correspondence of otolith size (based on radial measurements) with fish size suggests that accurate back-calculation of size-at-age is possible. Increments on the sagittae are deposited on a daily basis and can be readily separated into planktonic and demersal stages, due to the distinct contrast in microstructure at the time of settlement. We did not, however, test increment deposition rates under conditions of poor or negative growth. These conditions have resulted in less than daily increments in other species (Geffen 1982, Lough et al. 1982, McGurk 1984, Alhossaini and Pitcher 1988, Siegfried and Weinstein 1989,

Sogard 1991, Szedlmayer and Able In press), and we caution that this may also be the case for tautog otoliths.

Settlement

Increment counts preceding the settlement mark averaged 20.4, suggesting larvae spend approximately 3 weeks in the plankton before settling to the benthos. This estimate of larval stage duration is similar to that derived by Victor (1986) for a sample of five tautog ($\bar{x}$ 25.4). The planktonic stage for tautog is relatively short compared with other labrids; Victor (1986) estimated average larval durations of 17–104 days for other wrasse species.

The earliest estimated date of settlement, based on otolith increments, was earlier than the first collections of juveniles with throw traps, suggesting that tautog were not available to the collecting gear during and immediately after settlement. The smallest juveniles for which we have otolith information were 7.6–13.2 mm SL and had 11–23 increments ($\bar{x}$ 16.3) deposited after the settlement mark. Victor (1983) reported that newly settled wrasses of the species *Halichoeres bivittatus* bury in sediments immediately following settlement from the plankton and remain buried for an average of 5 days. We do not know if a similar behavior occurs in *Tautoga onitis*.

Juvenile habitat utilization

Our collection of juvenile tautog primarily in vegetation is in accord with prior studies, which demonstrated an association with structured habitats (Olla et al. 1974, Olla et al. 1979). Several studies comparing eelgrass vs. unvegetated substrates noted significantly higher densities of tautog in grassbeds, with few or no tautogs collected on bare substrates (Briggs and O'Connor 1971, Orth and Heck 1980, Weinstein and Brooks 1983, Heck et al. 1989). The importance of sea lettuce as a nursery habitat has received only limited attention, although Nichols and Breder (1926) mentioned its attraction to small juvenile tautog. In a separate study that also quantitatively compared sea lettuce and eelgrass habitats in New Jersey, using suction sampling, Able et al. (1989) also noted higher abundances of early juvenile tautog in sea lettuce patches than in eelgrass, although the total catch was relatively small. Larger juveniles make extensive use of rocky reef habitats (Olla et al. 1979). The importance of hard substrates for newly settled tautog has not been examined.

All of the smaller juvenile tautog (<35 mm SL) that we collected were from sea lettuce patches or artificial seagrass plots. These individuals were a brilliant green in color. As noted by Nichols and Breder (1926), this color closely matches that of *Ulva lactuca*, but presumably would be conspicuous on a bare sand substrate. In our sampling, these early juveniles were absent from eelgrass beds. The larger juveniles collected during trawl sampling (in eelgrass and other habitats) had a dark, mottled coloration similar to that of the adults as depicted by Bigelow and Schroeder (1953).

Over the course of our summer sampling, we observed a shift in concentration of young-of-the-year from the shallow areas sampled by throw traps to deeper waters sampled by otter trawl (Fig. 6). This shift suggests that newly-settled juveniles concentrate in shallow waters, moving to deeper sections of the estuary with growth.

Although trawling was conducted year round, individuals of age 1 or older were common only from June through September. This pattern could result from inaccessibility to the gear. Some individuals may move out of shallow habitats in the fall to deeper areas of the estuary with more stable sheltering refuges. Behavioral responses displayed by tautog in cold temperatures, i.e., dormancy and remaining in close contact with sheltering structure (Olla et al. 1974) or burying in sediments (Olla et al. 1979), would also reduce capture rates in winter. In addition, some individuals may leave the estuary to winter offshore, although Olla et al. (1974) suggest that most tautogs less than 4 years old remain inshore.

Tautogs older than 1 year may be more abundant in the estuary than trawl catches would indicate. Larger individuals inhabit holes and crevices of eroding salt marsh banks, and other physical structures such as pilings and rock jetties, where they would not be available to trawling gear.

Juvenile growth

Our estimates of sizes attained by juvenile tautog at the end of the first and second summers are larger than the mean lengths (TL) at ages 1 and 2 calculated for Rhode Island tautog from opercular bone annuli (Cooper 1967). Warmer temperatures in New Jersey may support faster mean growth rates than in Rhode Island. In addition, more southern estuaries in the tautog's range have an extended summer season, allowing both earlier spawning in the spring and continued rapid growth prior to declining water temperatures in the fall.

Analysis of length progressions and otolith ages resulted in two similar estimates of natural growth rates for juvenile tautog (0.52 mm/day and 0.47 mm/day). Individual growth rates of juvenile tautog were also measured in the field in caging experiments (Sogard In press). To summarize results of Sogard

(In press), growth rates varied significantly, depending on location in the estuary and habitat type (vegetated or unvegetated). Across four experiments and a total of 141 tautog, growth averaged 0.18 mm/day, with a range of −0.47 to +0.84 mm. At the site (Great Bay 1) and habitat (sea lettuce) supporting the fastest growth, the mean rate was 0.45 mm/day. Thus, length-frequency patterns and otolith ages reported in this study provided growth estimates that were higher than the overall average in caging experiments but comparable to rates for tautog caged in the best habitats. Based on throw-trapping results, juvenile tautog were rare at those sites and habitats where growth in cages was poor (Sogard In press). Thus, for the areas where tautog were likely to be common, the directly measured growth rate in cages was comparable to rates indirectly calculated for unrestrained fishes. The three methods together estimated a rapid growth rate of about 0.5 mm/day for southern New Jersey estuaries during the first summer.

Acknowledgments

We thank Dan Roelke and additional Rutgers Marine Field Station personnel for their assistance in field sampling. Dave Witting and Steve Szedlmayer coordinated the plankton sampling and trawling collections, respectively, in Great Bay. Susan Kaiser provided valuable help in data compilation and analysis. We are especially grateful to Rich McBride for his assistance with the otolith validation studies. Financial support was provided through New Jersey Sea Grant NA89AA-D-SG057 (NJSG-92-258).

Citations

Able, K.W, K.A. Wilson, and K.L. Heck Jr.
1989 Fishes of vegetated habitats in New Jersey estuaries: Composition, distribution, and abundance based on quantitative sampling. Publ. 1041, Cent. Coastal & Environ. Stud., Rutgers Univ., New Brunswick, 38 p.

Alhossaini, M., and T.J. Pitcher
1988 The relation between daily rings, body growth and environmental factors in plaice, *Pleuronectes platessa* L., juvenile otoliths. J. Fish Biol. 33:409–418.

Auster, P.J.
1989 Species profiles: Life histories and environmental requirements of coastal fishes and invertebrates (North Atlantic and Mid-Atlantic)—tautog and cunner. U.S. Fish Wildl. Serv. Biol. Rep. 82, 13 p.

Bigelow, H.B., and W.C. Schroeder
1953 Fishes of the Gulf of Maine. Fish. Bull., U.S. 53, 577 p.

Bourne, D.W., and J.J. Govoni
1988 Distribution of fish eggs and larvae and patterns of water circulation in Narragansett Bay, 1972–1973. *In* Weinstein, M.P. (ed.), Larval fish and shellfish transport through inlets, p. 132–148. Am. Fish. Soc. Symp. 3, Bethesda.

Briggs, P.T., and J.S. O'Connor
1971 Comparison of shore-zone fishes over naturally vegetated and sand-filled bottoms in Great South Bay. N.Y. Fish Game J. 18:25–41.

Colton, J.B., W.G. Smith, A.W. Kendall Jr., P.L. Berrien, and M.P. Fahay
1979 Principle spawning areas and times of marine fishes, Cape Sable to Cape Hatteras. Fish. Bull., U.S. 76:911–915.

Cooper, R.A.
1966 Migration and population estimation of the tautog, *Tautoga onitis* (Linnaeus), from Rhode Island. Trans. Am. Fish. Soc. 95:239–247.
1967 Age and growth of tautog, *Tautoga onitis* (Linnaeus), from Rhode Island. Trans. Am. Fish. Soc. 96:134–142.

Eklund, A.M., and T.E. Targett
1990 Reproductive seasonality of fishes inhabiting hard bottom areas in the Middle Atlantic Bight. Copeia 1990: 1180–1184.
1991 Seasonality of fish catch rates and species composition from the hard bottom trap fishery in the Middle Atlantic Bight (U.S. east coast). Fish. Res. (Amst.) 12:1–22.

Geffen, A.J.
1982 Otolith ring deposition in relation to growth rate in herring (*Clupea harengus*) and turbot (*Scophthalmus maximus*) larvae. Mar. Biol. (Berl.) 71:317–326.

Grover, J.J.
1982 The comparative feeding ecology of five inshore, marine fishes off Long Island, New York. Ph.D. diss., Rutgers Univ., New Brunswick, 197 p.

Heck, K.L. Jr., K.W. Able, M.P. Fahay, and C.T. Roman
1989 Fishes and decapod crustaceans of Cape Cod eelgrass meadows: Species composition and seasonal abundance patterns. Estuaries 12:59–65.

Kuntz, A., and L. Radcliffe
1918 Notes on the embryology and larval development of twelve teleostean fishes. Bull. U.S. Bur. Fish. 35:87–134.

Lough, R.G., M. Pennington, G.E. Bolz, and A.A. Rosenberg
1982 Age and growth of larval Atlantic herring, *Clupea harengus* L., in the Gulf of Maine—Georges Bank region based on otolith growth increments. Fish. Bull., U.S. 80:187–199.

McGurk, M.D.
1984 Ring deposition in the otoliths of larval Pacific herring *Clupea harengus pallasi*. Fish. Bull., U.S. 82:113–120.

Milstein, C.B., and D.L. Thomas
1977 Summary of ecological studies for 1972–1975 in the bays and other waterways near Little Egg Inlet and in the ocean in the vicinity of the proposed site for the Atlantic Generating Station, New Jersey. Bull. 18, Ichthyol. Assoc., Ithaca, NY, 757 p.

Nichols, J.T., and C.M. Breder Jr.
1926 The marine fishes of New York and southern New England. Zoologica (NY) 9:1–192.

Olla, B.L., and A.L. Studholme
1975 The effect of temperature on the behavior of young tautog, *Tautoga onitis* (L.). *In* Barnes, H. (ed.), Proc., Ninth Euro. Mar. Biol. Symp., p. 75–93. Aberdeen Univ. Press, Aberdeen.

Olla, B.L., A.J. Bejda, and A.D. Martin
1974 Daily activity, movements, feeding, and seasonal occurrence in the tautog, *Tautoga onitis*. Fish. Bull., U.S. 72:27–35.
1979 Seasonal dispersal and habitat selection of cunner, *Tautogolabrus adspersus*, and young tautog, *Tautoga onitis*, in Fire Island inlet, Long Island, New York. Fish. Bull., U.S. 77:255–261.

Olla, B.L., A.L. Studholme, A.J. Bejda, and C. Samet
1980 Role of temperature in triggering migratory behavior of the adult tautog *Tautoga onitis* under laboratory conditions. Mar. Biol. (Berl.) 59:23–30.

Orth, R.J., and K.L. Heck Jr.
1980 Structural components of eelgrass (*Zostera marina*) meadows in the lower Chesapeake Bay—Fishes. Estuaries 3:278–288.

Secor, D.H., J.M. Dean, and E.H. Laban
1991 Manual for otolith removal and preparation for microstructural examination. Tech. Rep. BI1191-1, Belle Baruch Inst., Columbia, SC, 85 p.

Sherman, K.
1988 Ichthyoplankton surveys: A strategy for monitoring fisheries change in a large marine ecosystem. *In* Smith, W.G. (ed.), An analysis and evaluation of ichthyoplankton survey data from the northeast continental shelf ecosystem, p. 3–9. NOAA Tech. Memo. NMFS-F/NEC-57, NMFS Northeast Fish. Sci. Cent., Woods Hole.

Sibunka, J., and M. Silverman
1989 MARMAP surveys of the continental shelf from Cape Hatteras, North Carolina to Cape Sable, Nova Scotia (1984–1987). Atlas No. 3. Summary of operations. NOAA Tech. Memo. NMFS-F/NEC-68, NMFS Northeast Fish. Sci. Cent., Woods Hole, 197 p.

Siegfried, R.C. III, and M.P. Weinstein
1989 Validation of increment deposition in the otoliths of spot (*Leiostomus xanthurus*). Estuaries 12:180–185.

Sogard, S.M.
1990 Parameters of habitat quality for epibenthic fishes and decapod crustaceans in New Jersey estuaries. Ph.D. diss., Rutgers Univ., New Brunswick, 195 p.
1991 Interpretation of otolith microstructure in juvenile winter flounder (*Pseudopleuronectes americanus*): Ontogenetic development, daily increment validation, and somatic growth relationships. Can. J. Fish. Aquat. Sci. 48:1862–1871.
In press Variability in growth rates of juvenile fishes in different estuarine habitats. Mar. Ecol. Prog. Ser.

Sogard, S.M., and K.W. Able
1991 A comparison of eelgrass, sea lettuce macroalgae, and marsh creeks as habitat for epibenthic fishes and decapods. Estuarine Coastal Shelf Sci. 33:501–519.

Szedlmayer, S.T., and K.W. Able
In press Daily increment formation in larval and juvenile summer flounder, *Paralichthys dentatus*. Can. J. Fish. Aquat. Sci.

Victor, B.C.
1982 Daily otolith increments and recruitment in two coral-reef wrasses, *Thalassoma bifasciatum* and *Halichoeres bivittatus*. Mar. Biol. (Berl.) 71:203–208.
1983 Settlement and larval metamorphosis produce distinct marks on the otoliths of the slippery dick, *Halichoeres bivittatus*. *In* Reaka, M.L. (ed.), Results of workshop on coral reef ecology, Philadelphia, 1983, sponsored by Am. Soc. Zool. Symp. Ser. Undersea Res., NOAA Undersea Res. Prog. 1(1):47–52.
1986 Duration of the planktonic larval stage of one hundred species of Pacific and Atlantic wrasses (family Labridae). Mar. Biol. (Berl.) 90:317–326.

Weinstein, M.P., and H.A. Brooks
1983 Comparative ecology of nekton residing in a tidal creek and adjacent seagrass meadow: Community composition and structure. Mar. Ecol. Prog. Ser. 12:15–27.

Williams, G.C.
1967 Identification and seasonal size changes of eggs of the labrid fishes, *Tautogolabrus adspersus* and *Tautoga onitis*, of Long Island Sound. Copeia 1967:452–453.

Fish-habitat associations on a deep reef at the edge of the Oregon continental shelf

David L. Stein
Department of Oceanography, Oregon State University, Corvallis, Oregon 97331-2914

Brian N. Tissot
Department of Zoology, Oregon State University, Corvallis, Oregon 97331-2914
Present address: Department of Biology, College of Arts and Sciences
University of Hawaii, Hilo, Hawaii 96720

Mark A. Hixon
Departments of Oceanography and Zoology, Oregon State University
Corvallis, Oregon 97331-2914

William Barss
Oregon Department of Fish and Wildlife, Newport, Oregon 97365

Abstract. – Heceta Bank is a large reef on the edge of the central Oregon continental shelf that supports a wide variety of commercial fisheries. Using the research submersible *Delta*, we studied fish abundances on Heceta Bank and the relationship between species composition of fish assemblages and bottom types. Cluster analysis indicated that fish assemblages were most unique on mud, boulder, rock ridge, mud and cobble, and mud and boulder substrates. Rockfishes, particularly pygmy *Sebastes wilsoni*, sharpchin *S. zacentrus*, rosethorn *S. helvomaculatus*, and yellowtail *S. flavidus*, were the most abundant fishes and dominated all substrates except mud, where Dover sole *Microstomus pacificus* and zoarcids *Lycodes pacificus* were most abundant.

Principal component analysis (PCA) and canonical correlation analysis (CCA) were used to determine the sources of variation within the data. PCA demonstrated that habitat variability was a fundamental cause of heterogeneity among fish assemblages. In contrast, CCA showed how species occurrences were related to specific substrates.

Ontogenetic shifts in behavior and substrate preference occurred in pygmy rockfish. Small juveniles often formed dense schools above the bank's shallower rocky ridges. Larger individuals occurred in nonpolarized assemblages on the bottom in cobble and boulder fields.

Manuscript accepted 11 May 1992.
Fishery Bulletin, U.S. 90:540–551 (1992).

Heceta Bank is a major commercial fishery zone off central Oregon. It supports a wide variety of fisheries: a demersal trawl fishery for many species of flatfishes; a longline fishery for halibut *Hippoglossus stenolepis*; midwater trawl and vertical longline fisheries for rockfishes (*Sebastes* spp.); a midwater trawl fishery for hake *Merluccius productus*; and during upwelling, a troll fishery for salmon (*Oncorhynchus* spp). Despite its importance to commercial fisheries, little was known about Heceta Bank prior to our 1987 submersible studies (Pearcy et al. 1989). From those exploratory dives we learned that (1) the bank is composed of diverse substrates, each supporting fish assemblages differing in species composition and relative abundances; (2) shallow areas of the bank act as a nursery for juvenile rockfishes; and (3) commercially valuable species of rockfish are associated with the shallow bank top in untrawlable areas, which thus serve as refugia from most commercial fishing.

Our 1987 studies focused on initial exploration and description of the Bank. Here we report results from our 1988 submersible-based surveys in which we again studied the fishes occurring on the Bank, concentrating specifically on their associations with various bottom types. We selected sampling stations that represented the range of habitats described by Pearcy et al. (1989) (Fig. 1). Our objectives were to (1) further develop methods of collecting and analyzing data that could be gathered from a submersible to study rocky banks; (2) identify the species occurring on Heceta Bank and estimate their relative and absolute abundances; (3) obtain detailed information about the variability of bottom types occurring within each station; and (4) assess the composition of fish assemblages in relation to different bottom types.

Methods

Data collection

We used the submersible *Delta* to make 18 dives at six stations on Heceta Bank in September 1988 (Fig. 1). These stations represented all substrates and depths within range of the submersible (to 366 m).

At each station we made three daylight dives, each by a different observer (DS, MH, WB). Dives began and ended at least an hour after dawn and an hour before sunset, respectively, minimizing the possible effects of diurnal migration by fishes. Almost all dives at each station were made on the same day.

Our methods basically follow those developed for use by scuba divers working on shallow reefs (Brock 1954, Ebeling 1982). Each observer made two 30-minute visual belt transects during each dive, yielding 6 transects per station (i.e., a total of 36 transects, 12 by each observer). To determine if there were any discernible effects from lights or motor noise of the submersible on the fishes, a 10-minute rest was taken with all lights and machinery off between each pair of transects. To minimize variability caused by within-transect substrate changes, all transects within a station started as closely as possible at the same position, as determined by Loran C. However, due to limits in the accuracy of Loran C and variability in current speed and direction, transects within stations were usually 100–300 m apart.

The observer in the submersible viewed the bottom through a single bow port which limited observation to about a 90° view. Submersible altitude above bottom (at height of observers' eyes from the bottom) was held as closely as possible to 2 m, as measured by an altimeter on the vehicle and by a chain suspended from the submersible (see below). Widths of the viewing path at altitudes of 0.5–2.0 m were determined empirically by "flying" the vehicle at right angles across a decimeter-striped 3 m pole placed on the bottom and noting the length of the pole visible to the observer between two fixed points on the submersible. At 2 m altitude, the transect width was 2.3 m. Thus, the density of fishes (no./m^2) was calculated as the number of fishes seen along a transect divided by 2.3 times the transect length in meters. To aid in estimating fish length and maintaining vehicle altitude, an ~0.4 m long fiberglass rod, striped in alternating black and white decimeters, was hung by chain from the vehicle within the observer's view. Chain length was adjusted so that when the rod was just above the bottom, the observer's altitude was 2 m.

The goal of the observer during a dive was to identify, count, and estimate the lengths (to the nearest decimeter) of all fishes seen along the transect. Fishes were categorized into "schooling" when five or more individuals formed a polarized group (i.e., all fish

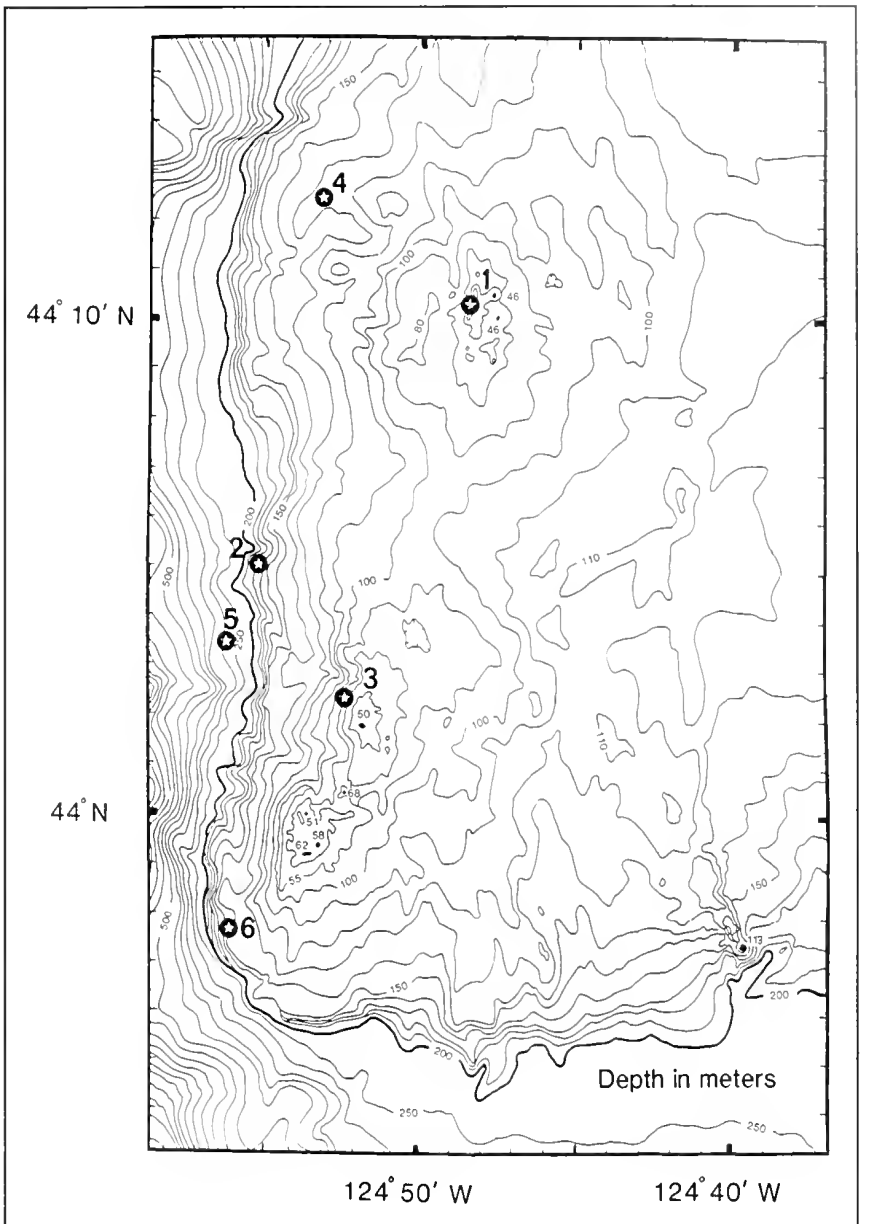

Figure 1
Bathymetric chart of Heceta Bank, Oregon, indicating locations of the six stations sampled.

moving syncronously in the same direction). Non-polarized aggregations or solitary individuals were considered "non-schooling." Data were collected by continuous audio tape recordings of the observer during transects, continuous video records (also including audio, time, and date), and 35mm still photographs automatically triggered every 30 seconds. We used a PhotoSea 1000 35mm still camera and a PhotoSea 2000 video camera, both on fixed mounts outside the vehicle. The video camera was mounted on the starboard bow of the submersible and recorded a field of view that partially overlapped that of the observer within the submersible. The audio track of the videotape recorded the observers comments which allowed real-time integration of fish observations and bottom-type descriptions (see below). Visibility always extended at least to the limits illuminated by the lights (i.e., ~3m or more except where limited by topography). Immediately following each dive, data were entered by computer into a relational database system and verified against the audio tapes.

We tried to minimize inherent biases of submersible studies as suggested by Ralston et al. (1986), such as fishes not seen or unidentified, diurnal variability, and effects of vehicle on fishes. Through a detailed analysis of fish and bottom-type observations recorded in the continuous video coverage of each transect, several observer-related factors affecting data collection were discovered. First, the diving observer usually noted fishes first, then bottom type. When fishes were present coincidentally with a substrate change, fish records were frequently correlated with the wrong bottom type. Second, observers tended to record substrate types based upon larger (high-relief) features rather than small (low-relief) ones, even when the smaller ones were preponderant. Apparently, boulders impressed observers more than cobble or mud, even when the latter were most abundant. Neither of these sources of error was intuitively obvious or suspected. If left uncorrected, these errors would have changed the apparent fish-substrate associations.

Due to these inherent biases, we extracted data on bottom types from the videotape record of each transect. In order to standardize any bias in the evaluation of bottom types, a single observer (BT) reviewed all videotapes. Dominant substrates were categorized using a two-code combination of seven possible categories: mud (code M), sand (S), pebble (P, diameter <6.5cm), cobble (C, >6.5 and <25.5cm), boulders (B, >25.5cm), flat rock (F, low vertical relief), or rock ridges (R, high vertical relief). Substrate was noted as either "primary" if it covered at least 50% of the area viewed (the first code), or "secondary" if it covered more than 20% of the area viewed (the second code). For example, a mud-boulder bottom type (code MB) consisted of at least 50% cover by mud with at least 20% cover by boulders. In contrast, a mud bottom (MM) consisted of >80% cover by mud.

We defined each transect segment of uniform bottom type as a "habitat patch." Transects within stations were therefore represented by a series of habitat patches defined by the frequency of substratum change along a transect. As a result, the size of habitat patches varied both within and among transects in conjunction with the area of uniform bottom types. The average habitat patch measured 150.8m^2 (SE 15.4m^2, n 524).

Data analysis

Although data were collected on all observed fish, data analysis focused on the distribution and abundance of non-schooling fishes rather than schooling fishes, because data for the former were more reliable. First, due to the lack of a manipulator on the submersible, we were unable to collect schooling fishes, which were typically small and unidentifiable, to obtain voucher specimens for positive identification. Second, schooling species were generally more abundant above the bottom in midwater and were not common in the transect path.

We tested for statistical differences among stations and observers in non-schooling fish abundance using a nested two-factor analysis of variance (ANOVA). Thirty-minute transect segments served as nested replicates. Sample variances were examined for homogeneity using Bartlett's test (Sokal and Rohlf 1981) prior to using the ANOVA. Because the raw data were heteroscedastic, the analysis examined the log-transformed total abundance of non-schooling fish per m^2.

To examine the variation in fish assemblages among transects, data were analyzed using principal component analysis (PCA). The PCA was an R-mode analysis of the variance-covariance matrix based on the log-transformed abundance of non-schooling fish per m^2. By definition, the axes examined in PCA are statistically independent of on another (Pimentel 1979). Rare species were eliminated from analysis by selecting only species present on at least 10 of the possible 36 transects. A total of 30 taxa met this criterion and were used in the analysis.

To examine the overall similarity of fish assemblages occurring on different substrates, data were analyzed using hierarchical cluster analysis. The analysis was limited to 21 species which were present on at least 12 of the possible 36 transects. The data in this analysis were the log-transformed total number of individuals per m^2 of each species that occurred on each substrate combination. A dendrogram was constructed using

Euclidean distance as a measure of similarity and the group-average clustering method (Pimentel 1979).

To examine specific associations between fish abundance and bottom-type characteristics, data were examined using canonical correlation analysis (CCA). CCA maximizes correlations among two sets of variables while it minimizes correlations within sets (Pimentel 1979). We used CCA to quantify associations between abundances of non-schooling fish species (data set 1) and bottom types (data set 2). Our primary goal was to extract meaningful, natural associations between fishes and habitat factors potentially influencing their distribution and abundance. CCA estimates these associations using four metrics (Pimentel 1979). First, the *canonical correlation* measures the overall association between the two data sets. Second, the *redundancy coefficient* measures the amount of overall variation in one data set as predicted by the other. While the canonical correlation coefficient describes the goodness-of-fit of the two data sets, which can be influenced by a single high correlation between one variable in each data set, the redundancy coefficient measures the extent of overlap in the variation of the two data sets. Third, the *variable loadings* indicate which variables are correlated on a particular axis. The fourth metric, *canonical variate scores*, measures the contribution of each sampling unit (in this analysis, the habitat patch) to the fish-habitat pattern depicted on each axis. Canonical variate scores are derived for each data set: scores for the habitat data indicate the relative cover of specific bottom types on each axis, while scores for the fish data indicate the relative abundance of specific fish on each axis. Canonical variate scores derived from CCA represent a powerful way to measure the abundance of fish in reference to habitat type. In essence, the method controls for the effects of sampling across a range of different habitats, and thus increased our power to detect meaningful spatial variation in fish abundance.

Data for CCA were derived using observations of habitat patches, which were discrete segments of uniform bottom type within each transect (n 524 segments for all transects). For each habitat patch, the abundances of 21 fish species were tabulated relative to the summed total area (in m^2) comprised by the habitat. For mixed bottom types, the total patch area was apportioned 80% to the primary substrate and 20% to the secondary substrate.

Results

The six stations represented a wide variety of substrates, ranging from shallow rocky ridges separated by sand, to intermediate-depth cobble and boulder fields, to deep mud and pebble bottoms (Figs. 1,2). Stations 1 and 3 (shallow bank tops) were rocky ridges at 60–80 m depth separated by sand and boulder-filled valleys; station 2 (bank saddle) was primarily mud with interspersed cobble at 150–200 m; station 4 was mud, ridge, and cobble at 145–175 m; station 5 was mud at 250–340 m; and station 6 was boulder and cobble grading into mud at 200–270 m. Because transects were always run into the current to insure controllability of the vehicle, distance traveled along the transects was not standardized, but was in the range 467–2367 m ($\bar{x}$ length 1357 m, SE 460 m).

Nested two-way ANOVA of transects and observers, based on the relative abundances of all non-schooling fish species summed, indicated significant differences among stations (F 6.22, df 5,18, $P<0.01$), but not among observers (F 1.39, df 2,18, $P>0.05$), or in interactions among observer transects and stations (F 0.48, df 10,18, $P>0.05$). A Student-Newman-Keuls multiple-range test separated the mean number of non-schooling fish at stations into two subgroups: station 4, where fish were most abundant at 2.09 fish/m^2, and all other stations, which ranged between 1.84 fish/m^2 (station 6) and 0.31 fish/m^2 (station 1).

Species identified: Number and size

We identified 38 taxa to species in our 1988 dives. This represents a 23% increase over the 31 species identified in 1987 (Pearcy et al. 1989). The increase was due primarily to species that were uncommon, suggesting that we identified most or all of the numerically important species on Heceta Bank. There were distinct differences in taxonomic composition and abundances between non-schooling and schooling fishes. About 89% of the non-schooling fishes seen were identified to species; fewer than 2% were not identified to family or genus. All schooling fishes seen were *Sebastes*. Of these, only 49% were identified to species; the remainder were identified to genus only (Table 1). Most of the schooling fish were small or juvenile fish that we could not identify without voucher specimens.

We counted 10,102 non-schooling fish, ranging from 3829 individuals of pygmy rockfish *Sebastes wilsoni* to one individual in each of ten species (Table 1). Schooling fishes comprised 22,470 individuals, over 50% of which (12,820) were unidentified small *Sebastes*. The most abundant identifiable schooling species was again the pygmy rockfish, with 8390 individuals. The least-abundant schooling species was widow rockfish *Sebastes entomelas* with 20 counted. The total number of fish schools seen (all species) was 145, ranging from 70 pygmy rockfish schools to one school of widow rockfish. The number of individuals per school ranged from about 10 to 330.

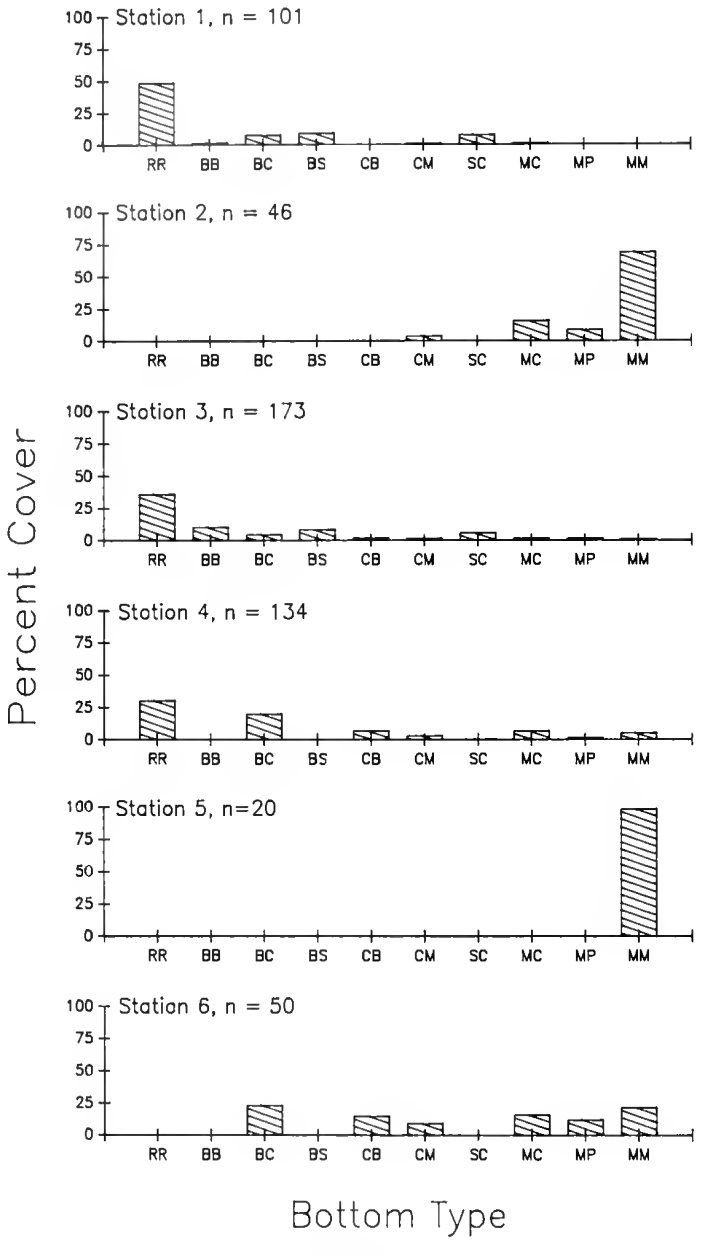

Figure 2

Percent cover of the ten most abundant bottom-type combinations at Heceta Bank, Oregon. RR = rock ridge; BB = boulder; BC = boulder–cobble; BS = boulder–sand; CB = cobble–boulder; CM = cobble–mud; SC = sand–cobble; MC = mud–cobble; MP = mud–pebble; MM = mud (see text for a description of bottom-type codes). n = number of habitat patches sampled per station.

Among non-schooling species, the estimated total length ranged from 105 cm (dogfish shark *Squalus acanthias*) to a mean of 12 cm (unidentified small *Sebastes*) (Table 1). Many smaller fishes were seen, but could be identified only to genus (*Sebastes* juveniles) or family (Gobiidae). Among schooling species, average length varied from 42 cm (yellowtail rockfish *Sebastes flavidus*) to 11 cm (*Sebastes* juveniles).

Ontogenetic habitat changes

Several rockfish species occurred both in schools and singly, including pygmy, yellowtail, sharpchin *S. zacentrus*, redstripe *S. proringer*, and canary *S. pinniger*. Pygmies were the single-most abundant species identified in either category. Schools of pygmy rockfish consisted of significantly smaller individuals, averaging 16.1 cm, whereas non-schooling aggregations and solitary individuals averaged 19.4 cm TL (ANOVA, F 18.0, df 1,699, $P<0.01$). Furthermore, schools were usually associated with ridge tops shallower than 100 m, while non-schooling fish were on cobble and boulder bottoms at depths of 100–150 m. A similar analysis of the data for yellowtail, sharpchin, redstripe, and canary rockfish showed no significant difference between sizes of individuals in and out of schools (ANOVA, all $P>0.05$).

Differences among stations: Fish assemblages

Results of the PCA indicated striking differences among stations in both the composition of fish assemblages and the similarity of individual transects within stations (Table 2, Fig. 3). Bartlett's sphericity test indicated that the first two axes described significant non-random patterns of variation among species, and accounted for 70% of the total variation. The first axis, which accounted for 49% of the variation, primarily contrasted transects at station 4 (intermixed mud and rocky ridges) vs. transects at station 5 (mud) (Fig. 3). Transects from stations 1 and 3 (shallow rocky bank tops) formed intermediate homogeneous groups, while transects from stations 2 and 6 (medium-depth boulder and cobble fields) formed intermediate heterogenous groups. Variable loadings indicated that this axis primarily contrasted variation in the relative abundance of rosethorn, pygmy, canary, sharpchin, yellowtail, and greenstriped rockfish, which were abundant at stations 1, 3, and 4 with the relative abundance of thornyhead rockfish, rex sole, sablefish, poachers, and zoarcids, which were abundant at station 5 (Table 2).

Table 1

Numbers of individuals, average total lengths, and standard errors of lengths for schooling and non-schooling fish species identified on Heceta Bank, Oregon, September 1988.

Species	No. seen	Mean length (cm)	SE
Schooling			
Unident. small rockfish (*Sebastes* spp.)	12820	11.1	1.02
Pygmy rockfish (*S. wilsoni*)	8390	16.1	0.72
Yellowtail rockfish (*S. flavidus*)	590	42.3	1.94
Sharpchin rockfish (*S. zacentrus*)	320	24.1	2.38
Redstripe rockfish (*S. proriger*)	220	25.0	4.73
Canary rockfish (*S. pinniger*)	110	41.7	4.70
Widow rockfish (*Sebastes entomelas*)	20	35.0	*
Non-schooling			
Pygmy rockfish (*S. wilsoni*)	3829	19.4	0.23
Sharpchin rockfish (*S. zacentrus*)	2030	23.7	0.28
Rosethorn rockfish (*S. helvomaculatus*)	931	21.6	0.10
Dover sole (*Microstomus pacificus*)	436	30.3	0.37
Unident. sculpins (Cottidae)	319	15.8	0.09
Shortspine thornyhead (*Sebastolobus alascanus*)	310	21.7	0.32
Blackbelly eelpout (*Lycodes pacificus*)	307	25.4	0.29
Greenstriped rockfish (*Sebastes elongatus*)	288	26.5	0.33
Unident. poachers (Agonidae)	248	22.5	0.15
Slender sole (*Lyopsetta exilis*)	240	22.5	0.16
Unident. small rockfish (*Sebastes* spp.)	130	11.6	1.35
Yellowtail rockfish (*S. flavidus*)	126	43.6	0.62
Rex sole (*Glyptocephalus zachirus*)	120	27.3	0.49
Unident. flatfish (Pleuronectidae)	93	21.3	1.21
Canary rockfish (*S. pinniger*)	78	46.9	0.98
Thornback sculpin (*Paricelinus hopliticus*)	57	14.8	0.05
Spotted ratfish (*Hydrolagus colliei*)	54	44.1	0.53
Unident. fish	47	18.2	1.30
Unident. large rockfish (*Sebastes* spp.)	47	23.1	0.94
Redstripe rockfish (*S. proriger*)	38	29.0	1.14
Ronquils (Bathymasteridae)	33	14.7	0.16
Sablefish (*Anoplopoma fimbria*)	33	54.7	3.53
Kelp greenling (*Hexagrammos decagrammus*)	29	32.2	0.64
Non-schooling (continued)			
Yelloweye rockfish (*S. ruberrimus*)	27	45.4	1.78
Petrale sole (*Eopsetta jordani*)	26	27.3	0.55
Threadfin sculpin (*Icelinus filamentosus*)	26	23.5	0.52
Longnose skate (*Raja rhina*)	23	72.8	40.6
Sandpaper skate (*R. kincaidii*)	22	30.0	2.77
Lingcod (*Ophiodon elongatus*)	20	46.5	9.96
Blacktail snailfish (*Careproctus melanurus*)	15	30.3	0.69
English sole (*Parophrys vetulus*)	15	32.3	1.65
Splitnose rockfish (*S. diploproa*)	13	31.9	2.03
Black eelpout (*Lycodes diapterus*	13	28.1	1.10
Redbanded rockfish (*S. babcocki*)	11	28.6	3.78
Eared blacksmelt (*Bathylagus ochotensis*)	11	15.0	*
Big skate (*R. binoculata*)	10	68.0	32.4
Hagfish (*Eptatretus* sp.)	10	34.0	3.83
Unident. blennies (Blenniidae)	6	15.0	*
Bocaccio (*S. paucispinis*)	5	53.0	3.13
Sculpin (*Icelinus* sp.)	4	27.5	1.25
Tiger rockfish (*S.nigrocinctus*)	4	40.0	1.67
Sanddab (*Citharichthys* sp.)	3	15.0	*
Unident. blotched rockfish (*Sebastes* spp.)	3	25.0	*
Eelpout (*Lycodapus* spp.)	2	15.0	*
Arrowtooth flounder (*Atheresthes stomias*)	1	45.0	—
Darkblotched rockfish (*S. crameri*)	1	35.0	—
Spiny dogfish (*Squalus acanthias*)	1	105.0	—
Unident. smelt (Osmeridae)	1	15.0	—
Pacific Ocean perch (*S. alutus*)	1	25.0	—
Pacific cod (*Gadus macrocephalus*)	1	55.0	—
Sand sole (*Psettichthys melanostictus*)	1	35.0	—
Silvergray rockfish (*S. brevispinis*)	1	55.0	—
Unident. eelpout (Zoarcidae)	1	35.0	—
Unident. skate (Rajidae)	1	15.0	—

* No observed variation; all fish estimated to be same length.

The second axis, which described 20% of the variation of relative fish abundance, presented an additional independent pattern of variation among stations (Table 2, Fig. 3). This axis primarily contrasted transects at stations 1 and 3 (shallow rock ridge) with transects from all other stations. As in the first axis, transects within stations along the second axis were heterogeneous; that is, the relative abundances of the fishes seen varied among transects. Station 1 transects were relatively homogeneous compared with transects at stations 2, 3, and 6, which varied considerably. Variable loadings indicated that this axis represented variation in the relative abundance of kelp greenlings and lingcod, which were abundant on bank tops, versus thornyhead and sharpchin rockfish, zoarcids, threadfin sculpin, and dover, rex, and slender sole, which were abundant at other stations.

Fish-habitat associations

Of the 49 possible combinations of bottom type (7×7 types), 27 were encountered. Cluster analysis indicated that habitat types had varying degrees of similarity in fish assemblages (Fig. 4). Mud had the most distinct

Table 2

Results of principal component analysis. Underlined bold characters indicate high variable loadings, with positive and negative loadings being inversely correlated along each axis. Thus, PC1 depicts a gradient from soft-bottom species (negative loadings) to hard-bottom species (positive loadings). PC2 depicts a secondary gradient from hard-bottom species (negative loadings) to soft-bottom species (positive loadings).

	PC1	PC2
Eigenvalue	3.056	1.266
Percent of total variation	49.3	20.4
Chi-square	1778	1557
Degrees of freedom	434	405
Variable loadings		
Canary rockfish (*Sebastes pinniger*)	**0.826**	0.135
Yelloweye rockfish (*S. ruberrimus*)	0.477	−0.230
Yellowtail rockfish (*S. flavidus*)	**0.657**	−0.092
Redbanded rockfish (*S. babcocki*)	−0.552	0.338
Redstripe rockfish (*S. proriger*)	0.411	0.180
Sculpins (Cottidae)	**0.748**	0.036
Threadfin sculpin (*Icelinus filamentosus*)	0.339	**0.447**
Kelp greenling (*Hexogrammos decagrammus*)	0.189	**−0.621**
Lingcod (*Ophiodon elongatus*)	0.203	**−0.525**
Rosethorn rockfish (*S. helvomaculatus*)	**0.888**	−0.296
Pygmy rockfish (*S. wilsoni*)	**0.892**	0.372
Sharpchin rockfish (*S. zacentrus*)	**0.714**	**0.602**
Splitnose rockfish (*S. diploproa*)	−0.595	0.266
Greenstriped rockfish (*S. elongatus*)	**0.670**	0.286
Shortspine thornyhead (*Sebastolobus alascanus*)	**−0.690**	**0.446**
Eelpouts (Zoarcidae)	**−0.701**	**0.606**
Hagfish (*Eptatretus* sp.)	−0.222	0.385
Spotted ratfish (*Hydrolagus colliei*)	−0.326	**0.461**
Poachers (Agonidae)	**−0.751**	**0.519**
Sablefish (*Anoplopoma fimbria*)	−0.668	0.400
Searchers (Bathymasteridae)	0.441	−0.141
Blacktail snailfish (*Careproctus melanurus*)	−0.641	0.198
Dover sole (*Microstomus pacificus*)	−0.503	**0.761**
English sole (*Parophrys vetulus*)	−0.066	0.140
Petrale sole (*Eopsetta jordani*)	−0.005	0.192
Rex sole (*Glyptocephalus zachirus*)	−0.644	**0.448**
Slender sole (*Lyopsetta exilis*)	−0.180	**0.582**
Big skate (*Raja binoculata*)	−0.179	0.115
Longnose skate (*R. rhina*)	0.311	0.021
Sandpaper skate (*R. kincaidii*)	−0.429	0.238

fish assemblage, followed by boulder, rocky ridge, mud and cobble, and mud and boulder habitats. In contrast, habitats involving combinations of boulder, mud, sand, and cobble had comparatively similar fish assemblages.

The results of the cluster analysis provide information relevant to the interpretation of the PCA results (Figs. 3, 4). Stations that displayed little among-transect variability in fish assemblages were composed primarily of rocky ridge (stations 1 and 3), and mud (station 5): habitats that had relatively distinct fish assemblages. In contrast, stations with high among-transect variability (primarily stations 2 and 6) were composed of mixtures of mud, cobble, and boulders: habitats sharing relatively similar fish assemblages.

There were additional habitat patterns evident in the distribution of the most abundant rockfish species (Table 3). Comparing abundances of the four most abundant species *within subhabitats*, pygmy rockfish dominated all except mud, mud and cobble, and flat rock. Sharpchin dominated mud and cobble; rosethorn, the flat rock (Table 3). Comparing abundances for each subhabitat *within species*, it is clear that each species, even though it might not be numerically dominant overall, was most abundant in a particular habitat. Thus, pygmy rockfish were most abundant on mud and boulder; sharp chin and greenstriped rockfish on mud and cobble; rosethorn rockfish on boulder; and yellowtail rockfish on rock ridges.

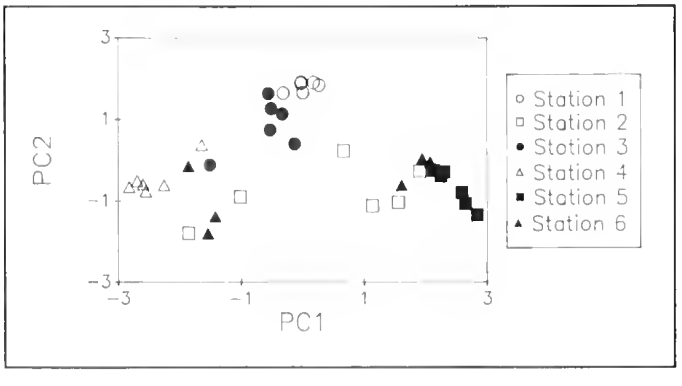

Figure 3

Ordination of first and second principal component scores for 36 transects sampled at six stations on Heceta Bank. The analysis is based on the relative abundances of 30 fish taxa observed (see Table 2 for species list).

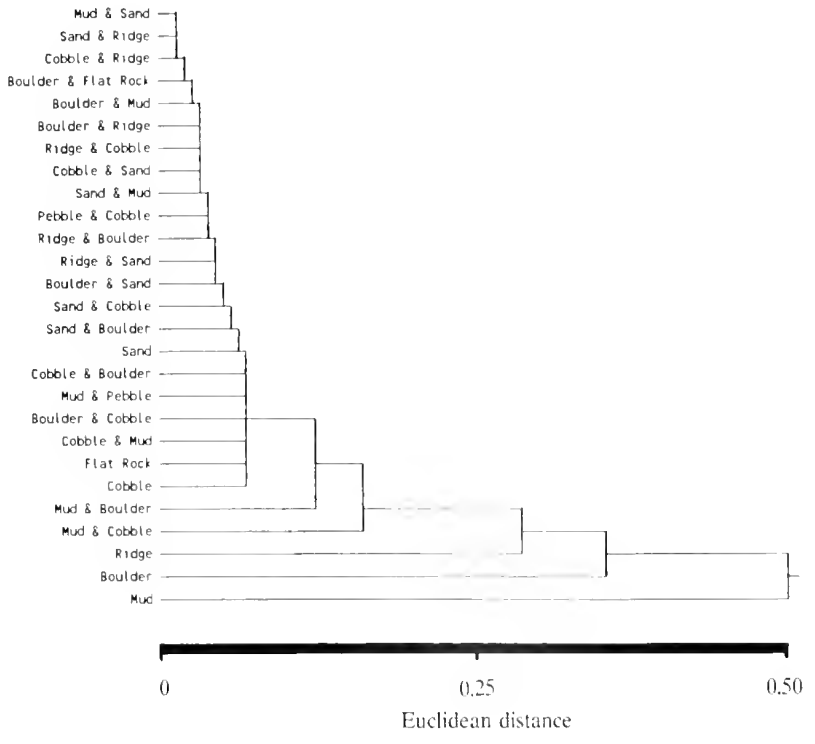

Figure 4

Cluster analysis of all observed bottom types based on the relative abundances of 21 fish taxa (see Table 4 for species list).

In general, the degree of bottom-type relief varied inversely with depth (Fig. 5). High relief substrates such as rock ridges, boulder, and cobble occurred at relatively shallow 80–100 m depths, while low-relief muddy substrates, such as mud and boulder, mud and cobble, and pure mud, occurred relatively deeper, at 160–240 m depths (Fig. 5).

CCA described associations between species abundance and the distribution of specific habitat types (Table 4, Fig. 6). Bartlett's test indicated that the first three axes represented significant canonical correlations. The low values of the redundancy coefficient for these axes (0.10–0.03, measuring variability in fish abundance explained by habitat variation) demonstrated strong correlations between several species and habitats rather than general associations among all species and all habitats.

Table 3

Average number of fish per hectare ($10^4 m^2$) on the seven most distinct habitat types, as determined by cluster analysis (see Fig. 4). Only the 21 most abundant taxa are listed, these taxa used in the canonical correlation analysis. Most-abundant taxon in each category underlined in bold characters. Species absent from a specific habitat are indicated with dashes.

Species	Mud	Mud & cobble	Mud & boulder	Cobble	Boulder	Flat rock	Rock ridge
Agonidae	186	464	1122	–	25	–	18
Bathymasteridae	7	7	–	–	–	–	15
Big skate	7	–	51	–	–	–	–
Canary rockfish	–	14	102	–	–	158	82
Cottidae	24	79	51	67	–	158	73
Dover sole	**499**	343	2295	–	–	–	15
Greenstriped rockfish	64	364	204	266	25	–	79
Kelp greenling	–	–	–	67	76	316	27
Lingcod	–	–	–	67	–	–	30
Longnose skate	7	14	51	–	–	–	6
Pygmy rockfish	21	2129	**8926**	**999**	**2772**	–	**1785**
Redstripe rockfish	–	7	–	–	–	–	43
Rex sole	107	57	1887	–	–	–	–
Rosethorn rockfish	26	343	408	933	161	**474**	675
Sharpchin rockfish	60	**2930**	2754	133	–	–	277
Shortspine thornyhead	239	443	2193	–	–	–	–
Slender sole	76	107	408	–	–	–	–
Spotted ratfish	26	14	510	–	–	–	–
Yelloweye rockfish	–	7	–	–	25	–	27
Yellowtail rockfish	–	29	–	67	176	–	191
Zoarcidae	282	279	1887	–	50	–	18

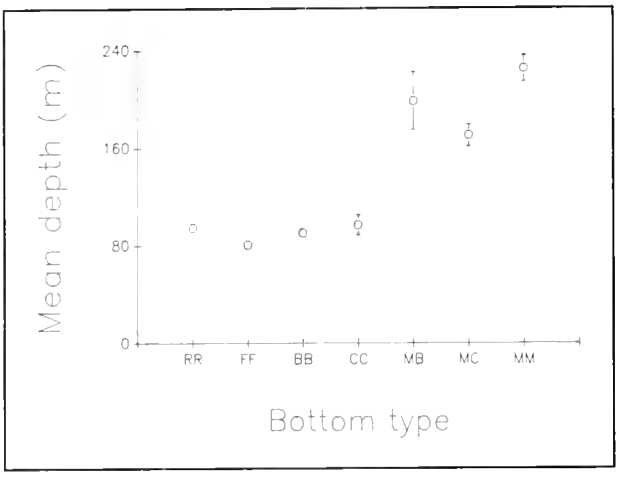

Figure 5

Average depth (±1 SE) of the eight most distinct bottom type combinations on Heceta Bank, Oregon. Bottom codes and sample sizes are as follows: RR = rock ridge (n 109); FF = flat rock (n 4); BB = boulder (n 29); CC = cobble (n 8); MB = mud-boulder (n 11); MC = mud-cobble (n 45); MP = mud-pebble (n 26); MM = mud (n 55) (see text for a description of bottom type codes). n = number of habitat patches sampled per station.

Because bottom-type changes were highly correlated with changes in depth (Fig. 5), the CCA did not confound species associations with bottom types from different depths. Each axis measured associations occurring within the depth range of the habitat indicated by the variable loadings on each axis.

The first axis described variation in fish abundance associated with mud habitats (160–240 m). Variable loadings indicate that thornyheads, zoarcids, poachers, and rex and Dover sole commonly occur on mud (Table 4). Canonical variate scores on this axis were significantly different among stations in both the habitat and fish scores: station 5, the only pure mud station (Fig. 2), was significantly different from all others (Kruskal-Wallis, $p<0.01$) (Fig. 6A).

The second axis contrasted an additional independent fish-habitat association. Variables loadings indicated that ratfish, and rosethorn, sharpchin, yelloweye, canary, and pygmy rockfish were associated with boulder and cobble fields at 75–100 m depths. Canonical scores for the second axis also differed significantly among stations on both habitat and fish scores: station 6, the station with the highest cover of boulder-cobble (Fig. 2), was significantly different from all other stations (Kruskal-Wallis, $p<0.01$) (Fig. 6B).

The third axis indicated an additional association between fish and habitat. Variables loadings indicated that greenstriped and yellowtail rockfish, lingcod, and cottids were associated with sand

Table 4

Results of canonical correlation analysis. Variables with high loadings are indicated in underlined boldface characters. High negative loadings on the first canonical axis, CC1, indicate fish that were abundant in mud habitats. Similarily, high loadings on CC2 and CC3 indicate fish that were abundant on cobble–boulder bottoms and rock ridge–sand valley bottoms, respectively.

	CC1	CC2	CC3
Canonical correlation	0.849	0.786	0.489
Chi-square	1197	656	249
Degrees of freedom	147	120	95
	Canonical variate loadings		
Fish			
Canary rockfish (*S. pinniger*)	0.032	**−0.278**	0.090
Yelloweye rockfish (*S. ruberrimus*)	0.035	**−0.382**	−0.139
Yellowtail rockfish (*S. flavidus*)	0.048	−0.021	**0.434**
Redstripe rockfish (*S. proriger*)	0.015	−0.218	−0.098
Cottidae	0.029	−0.200	**0.360**
Kelp greenling (*Hexagrammos decagrammus*)	0.048	−0.140	0.102
Lingcod (*Ophiodon elongatus*)	0.017	−0.134	**0.367**
Rosethorn rockfish (*S. helvomaculatus*)	0.026	**−0.842**	0.295
Pygmy rockfish (*S. wilsoni*)	−0.007	**−0.571**	0.012
Sharpchin rockfish (*S. zacentrus*)	−0.075	**−0.837**	−0.052
Greenstriped rockfish (*S. elongatus*)	−0.155	−0.037	**0.618**
Shortspine thornyhead (*Sebastolobus alascanus*)	**−0.461**	0.066	−0.104
Zoarcidae	**−0.696**	0.077	−0.080
Spotted ratfish (*Hydrolagus colliei*)	−0.337	**−0.504**	−0.172
Agonidae	**−0.678**	0.079	−0.020
Bathymasteridae	0.027	0.043	0.080
Dover sole (*Microstomus pacificus*)	**−0.951**	0.028	−0.005
Rex sole (*Glyptocephalus zachirus*)	**−0.665**	0.065	−0.086
Slender sole (*Lyopsetta exilis*)	−0.088	0.047	−0.081
Big skate (*Raja binoculata*)	−0.324	0.037	−0.059
Longnose skate (*Raja rhina*)	−0.048	0.069	−0.129
Variance extracted	0.132	0.113	0.051
Redundancy	0.095	0.070	0.012
Habitat			
Mud	**−0.998**	0.052	−0.017
Sand	0.037	0.041	**0.665**
Pebble	−0.013	0.070	−0.023
Cobble	−0.041	**−0.514**	0.269
Boulders	0.026	**−0.925**	−0.159
Flat Rock	0.020	0.026	−0.060
Rocky Ridge	0.095	−0.007	**0.529**
Variance extracted	0.144	0.161	0.118
Redundancy	0.104	0.100	0.028

and ridge habitats at 75–100m depths. Canonical variate scores among stations differed on the third axis with respect to habitat scores, but not on fish scores. With respect to habitat, stations 1 and 3, which had the highest amount of sand and ridge cover (Fig. 2), were significantly different from stations 2, 4, and 6 (Kruskal-Wallis, $p<0.01$) (Fig. 6C). In contrast, with respect to fish abundance, stations were highly variable, and not significantly different among stations (Kruskal-Wallis, $p>0.05$) (Fig. 6C).

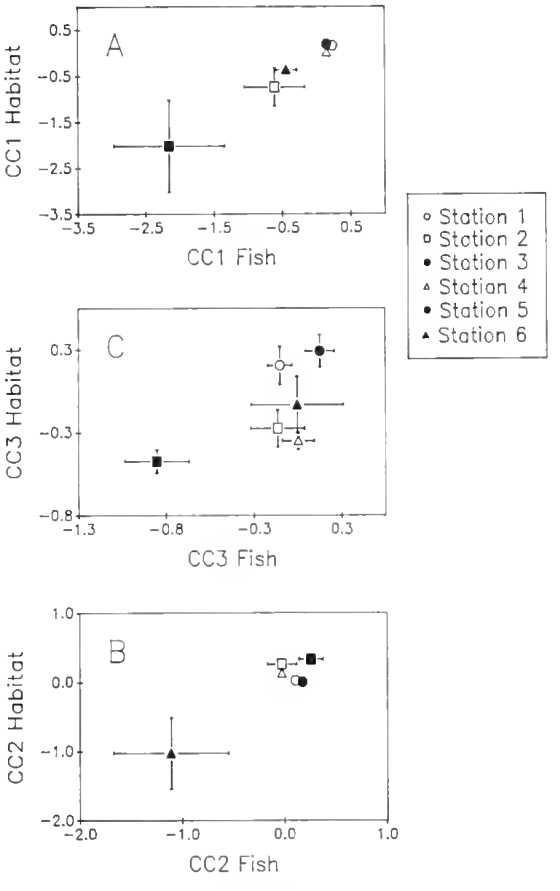

Figure 6

Average canonical variate scores for each station (±1 SE) on three canonical correlation axes (see Table 4). Canonical scores for habitat indicate the relative cover of specific bottom types on each axis, while scores for the fish data indicate the relative abundance of specific fish on each axis.

Discussion

The principal objective of our study was to develop methods to estimate spatial variation in fish abundance on Heceta Bank. However, the high variability of bottom types encountered required that we understand the effects of bottom-type variation on fish abundance and distribution.

Fish-habitat associations

The principal components analysis showed that stations with the least variability in fish abundance among replicate transects were those at stations composed of rock ridge, such as the bank tops (stations 1 and 3), and of mud (station 5). In contrast, high variability in fish abundance among replicate transects occurred at stations having combinations of mud, cobble, and boulders (stations 2, 4 and 6). Moreover, canonical correlation analysis indicated that fish assemblages associated with these habitats were unique. Mud, cobble–boulder, and ridge–sand habitats displayed different species composition and relative abundance.

In most sampling situations, such as use of a bottom trawl or bottom-set gillnet, analysis would be limited to a fish-only PCA-type appproach. Within-station variability, such as that documented here, would be largely unaccounted for without detailed information about bottom type. In the present study, canonical correlation analysis of fish abundance relative to bottom type provided key information on a major source of within-station variability.

The ability to estimate bottom-type composition and determine the relationships of species with each substrate is a critical advantage of submersible studies. In shallow water, this has been done using scuba (e.g., Hixon 1980, Larson 1980, Hallacher and Roberts 1985). However, there are few such studies below scuba depths. In the northeastern Pacific, Carlson and Straty (1981) and Straty (1987) used a submersible to study habitat and nursery areas for rockfishes in southeastern Alaska. Straty (1987) concentrated on species of juvenile rockfishes and their occurrence in relation to substrate type and relief; he did not attempt to quantify abundances. Richards (1986) similarly investigated distributions of deep rockfishes at 21–140m and related their occurrence to bottom type. Although she was able to show substrate associations for three species (*Sebastes elongatus*, *S. maliger*, and *S. ruberrimus*), only three substrate categories were used, and abundances of fishes were determined on the basis of distance of maximum visibility. Nevertheless, she recognized the importance of such studies and developed initial methods for obtaining data on this subject.

Abundances of species

We know of no comparable data to that presented here for fish abundances on Heceta Bank. However, similar studies have been done on inshore reefs in central California. Miller and Geibel (1973), using scuba tech-

niques similar to our submersible methods, estimated abundances of juvenile and adult rockfishes along transects on an inshore reef supporting an extensive kelp forest. Their estimates of juvenile abundances are much higher than ours: more than 46,000 fish/ha compared with our maximum of 15,039 fish/ha (station 3). Comparing abundances of adults at the same stations, they estimated 3133–5046 fish/ha vs. 558–1724 fish/ha at our station 3. The maximum estimated number of adult fishes at any of our stations was 9635 fish/ha (station 4). However, our estimates at the shallow bank top stations (1 and 3) are low because they did not include most of the schooling fishes, which were above the submersible. We have no accurate estimates of the abundances of these fishes, primarily yellowtail and widow rockfish. They occurred in schools of thousands.

Availability of comparative data

There are few data sets comparable with ours that were obtained by other methods. Rough bottoms are untrawlable, reducing usable gear to longlines or set nets. Even where these are used, if substrate varies over the length of the longline or net, they "integrate" the fishes over those different bottom types, preventing association of species with specific substrate types. Using otter trawls with foot rope rollers, Barss et al. (1982) studied fish assemblages associated with "rough" (rocky bottom fishable with nets using rollers) and "smooth" bottom on the west (offshore) side of Heceta Bank. The areas with most relief were unfishable (including our stations 1 and 3). They found distinct differences in catches between the two types of areas, but admitted that their results were biased by the type of gear they were forced to use in order to trawl on rough bottom.

Recently, Matthews and Richards (In press) used gillnets to compare fish assemblages on trawlable and untrawlable bottoms west of Vancouver Island. Their goal was to determine whether, as commercial fishermen believe, untrawlable bottom west of Vancouver Island provides refuges for commercially exploited fishes (primarily Pacific Ocean perch) caught nearby. They concluded there were no reservoir populations. However, given the mesh size of their bottom-set gillnets, they were unlikely to sample either juveniles or semipelagic species such as yellowtail and widow rockfish. Thus, given our current and previous observations of juvenile and yellowtail rockfish associated with shallow, high-relief rocky ridges (Pearcy et al. 1989), we suggest that these unfished areas could still provide refuges for fishes in either of those categories.

Habitat shifts

Ontogenetic habitat shifts, such as those desribed here for pygmy rockfish, are common among rockfish species. Westrheim (1970), Carlson and Haight (1976), and Straty (1987) found that juvenile Pacific Ocean perch *Sebastes alutus* were usually shallower than adults. Carr (1983) described the growth-related migration of juvenile *S. atrovirens*, *S. carnatus*, *S. chrysomelas*, and *S. caurinus* to the bottom in a central California kelp forest. However, Hallacher (1977), studying adults and juveniles of *S. mystinus* and *S. serranoides* in Monterey Bay at depths of ~25 m or less, found that abundances of both increased with depth, maxima occurring at the greatest depths sampled. This difference could be related to degree of association with the bottom as adults. The species Carr (1983) studied were benthic as adults, whereas the latter two species occur in the water column.

Conclusions

The results presented here show the utility of using a submersible rather than bottom set nets, traps, or longlines to study fish-substrate associations in deep water areas where substrate is heterogeneous. Other methods, such as Remote Operated Vehicles, rely on video and still camera images, which are not as adequate for accurate identification as the human eye. Moreover, other types of gear do not allow detailed characterization of the substrate sampled, but rather integrate the catch from a variety of habitats. We believe that the methods presented here, in addition to describing basic fish-habitat associations, allowed us to control the effects of sampling across a range of different habitats, and increased our ability to detect meaningful spatial variation in fish abundance.

Acknowledgments

We thank the crews of the RV *William A. McGaw* and RS *Delta* for help in obtaining the data; their cooperation and expertise are appreciated and gratefully acknowledged. Comments by L. E. Hallacher and L. Richards greatly improved the manuscript. The research was supported by the Minerals Management Service, Department of the Interior, under MMS Agreement No. 14-12-0001-30445, and the National Undersea Research Program of NOAA.

Citations

Barss, W.H., S.L. Johnson, and R.L. Demory
1982 Biological studies on rockfish and associated species from Heceta Bank off Oregon, 1980–81. Oreg. Dep. Fish Wildl. Completion Rep. Proj. 1-151-R2, Comm. Fish. Res. Dev. Act., Newport, 28 p.

Brock, V.E.
1954 A preliminary report on a method of estimating reef fish populations. J. Wildl. Manage. 18:297–308.

Carlson, H.R., and R.E. Haight
1976 Juvenile life of Pacific Ocean perch, *Sebastes alutus*, in coastal fiords of southeastern Alaska: Their environment, growth, food habits, and schooling behavior. Trans. Am. Fish. Soc. 105(2):191–201.

Carlson, H.R., and R.R. Straty
1981 Habitat and nursery grounds of Pacific rockfish, *Sebastes* spp., in rocky coastal areas of southeastern Alaska. Mar. Fish. Rev. 43(7):13–19.

Carr, M.
1983 Spatial and temporal patterns of recruitment of young-of-the-year rockfishes (genus *Sebastes*) into a central California kelp forest. M.S. thesis, San Francisco State Univ., 104 p.

Ebeling, A.W.
1982 Scuba diver observations and statistical analysis. *In* DeWees, C.M. (ed.), Guidelines for marine ecological surveys, nekton, p. 6–9. Calif. Sea Grant Coll. Mar. Adv. Prog., Univ. Calif., Davis.

Hallacher, L.
1977 Patterns of space and food use by inshore rockfishes (Scorpaenidae: *Sebastes*) of Carmel Bay, California. Ph.D. thesis, Univ. Calif., Berkeley, 115 p.

Hallacher, L.E., and D.A. Roberts
1985 Differential utilization of space and food by the inshore rockfishes (Scorpaenidae: *Sebastes*) of Carmel Bay, California. Environ. Biol. Fish. 12:91–110.

Hixon, M.A.
1980 Competitive interactions between California reef fishes of the genus *Embiotoca*. Ecology 61:918–931.

Larson, R.J.
1980 Competition, habitat selection, and the bathymetric segregation of two rockfish (*Sebastes*) species. Ecol. Monogr. 50:221–239.

Matthews, K.R., and L.J. Richards
In press Rockfish (Scorpaeidae) assemblages of trawlable and untrawlable habitats of Vancouver Island, British Columbia. N. Am. J. Fish. Manage.

Miller, D.J., and J.J. Geibel
1973 Summary of blue rockfish and lingcod life histories; a reef ecology study; and giant kelp, *Macrocystis pyrifera*, experiments in Monterey Bay, California. Calif. Dep. Fish Game Fish Bull. 158:1–137.

Pearcy, W.G., D.L. Stein, M.A. Hixon, E. Pikitch, W. Barss, and R. Starr
1989 Submersible observations of deep-reef fishes of Heceta Bank, Oregon. Fish. Bull., U.S. 87:955–965.

Pimentel, R.A.
1979 Morphometrics, the multivariate analysis of biological data. Kendall-Hunt, Dubuque, 276 p.

Ralston, S., R.M. Gooding, and G.M. Ludwig
1986 An ecological survey and comparison of bottom fish resource assessments (submersible versus handline fishing) at Johnston Atoll. Fish. Bull., U.S. 84(1):141–155.

Richards, L.J.
1986 Depth and habitat distributions of three species of rockfish (*Sebastes*) in British Columbia: Observations from the submersible PISCES IV. Environ. Biol. Fishes 17(1):13–21.

Sokal, R.R. and F.J. Rohlf
1981 Biometry: The principals and practice of statistics in biological research, 2d ed. W.H. Freeman, NY, 859 p.

Straty, R.R.
1987 Habitat and behavior of juvenile Pacific rockfish (*Sebastes* spp. and *Sebastolobus alascanus*) off southeastern Alaska. *In* Cooper, R.A., and A.N. Shepard (eds.), Scientific applications of current diving techniques on the U.S. continental shelf, p. 109–123. Symp. Ser. Undersea Res., NOAA Undersea Res. Prog. 2(2), Wash. DC.

Westrheim, S.J.
1970 Survey of rockfishes, especially Pacific Ocean perch, in the northeast Pacific Ocean, 1963–66. J. Fish. Res. Board Can. 27:1781–1809.

Management advice from a simple dynamic pool model

Grant G. Thompson

Resource Ecology and Fisheries Management Division
Alaska Fisheries Science Center, National Marine Fisheries Service, NOAA
7600 Sand Point Way NE, Seattle, Washington 98115-0070

Abstract.—This paper is devoted to a theoretical examination of two rules of thumb commonly used in fishery management: (I) the fishing mortality rate associated with maximum sustainable yield (F_{MSY}) equals the natural mortality rate, and (II) the equilibrium stock biomass at maximum sustainable yield equals one-half the pristine stock biomass. Taken together, these rules of thumb are shown to be inconsistent with any simple dynamic pool model in which three conditions hold: (1) the first derivative of the stock-recruitment relationship is uniformly nonnegative, (2) the second derivative of the stock-recruitment relationship is uniformly nonpositive, and (3) the first derivative of the weight-at-age relationship is uniformly positive. An example of such a model is presented and the equilibrium solution derived analytically. In this model, F_{MSY} can be either greater than or less than the natural mortality rate, while the equilibrium stock biomass at maximum sustainable yield is consistently less than one-half the pristine stock biomass. To illustrate the utility of the theoretical framework developed, the model is applied to the eastern Bering Sea stock of rock sole *Pleuronectes bilineatus*.

Manuscript accepted 4 June 1992.
Fishery Bulletin, U.S. 90:552–560 (1992).

Two rules of thumb

Despite its acknowledged shortcomings (e.g., Larkin 1977), management for maximum sustainable yield (MSY) remains a common strategy among fisheries professionals. Under a constant harvest rate policy, this strategy is implemented by exploiting the stock at the fishing mortality rate corresponding to MSY (F_{MSY}). Alternatively, this strategy could be implemented by exploiting the stock so as to maintain its biomass at the level corresponding to MSY, $B(F_{MSY})$. To estimate F_{MSY} and $B(F_{MSY})$, fishery scientists and managers employ a variety of approaches, ranging from highly sophisticated simulation models to simple "rules of thumb." Frequently used examples of the latter can be found in the form of two hypotheses employed by Alverson and Pereyra (1969) in their analysis of the potential yield of certain fish stocks. These hypotheses (hereafter referred to as Rules I and II) are

$$\frac{F_{MSY}}{M} = 1 \qquad \text{(I)}$$

and

$$\frac{B(F_{MSY})}{B(0)} = 0.5, \qquad \text{(II)}$$

where F is the instantaneous rate of fishing mortality per year, F_{MSY} is the value of F that produces MSY in equilibrium, M is the instantaneous rate of natural mortality per year, B(F) is the equilibrium stock biomass corresponding to a fishing mortality rate of F, $B(F_{MSY})$ is the equilibrium stock biomass when $F = F_{MSY}$, and B(0) is the pristine stock biomass (i.e., equilibrium stock biomass when F = 0).

Alverson and Pereyra (1969) presented a sketchy derivation of Rules I and II, leaving open the question of which models might be capable of leading to the hypothesized relationships. A number of authors have subsequently examined specific models in this context and shown them to be inconsistent with Rules I and II. Gulland (1971) and Beddington and Cooke (1983) cast doubt on the robustness of Rules I and II in terms of their applicability to the "simple" model of Beverton and Holt (1957), but did not generalize their conclusions beyond that particular model. Likewise, Francis (1974) demonstrated inconsistencies between Rules I and II and a set of assumptions derived from the Schaefer (1954) model, although his argument was weakened somewhat by computing MSY in terms of numbers, not biomass. Deriso (1982) showed that the discrete fishing mortality rate generated by his delay-difference model at MSY was consistently higher than the discrete natural mortality rate when recruitment was constant, while under several other stock-recruitment assumptions the relationship was reversed. Shepherd (1982) also demonstrated that Rules I and II did not adequately describe the behavior of a particular surplus production model.

Since none of these authors addressed the possibility that other

models might support Rules I and II, it remains to be seen whether these rules are inconsistent only for isolated special cases, or are actually incompatible with a major class of models.

Review of simple dynamic pool models

One place to start in the search for models that might be compatible with Rules I and II is within the family of simple dynamic pool models. As distinguished from surplus production models such as those of Schaefer (1954) and Pella and Tomlinson (1969), dynamic pool models describe stock dynamics in terms of the individual processes of recruitment, growth, and mortality, and incorporate age structure at least implicitly (e.g., Pitcher and Hart 1982). Within the broad class of dynamic pool models, a model will be referred to here as "simple" if it reflects the following assumptions: (A) Cohort dynamics are of continuous-time form, (B) vital rates are constant with respect to time and age, (C) fish mature and recruit to the fishery continuously and at the same invariant ("knife-edge") age, (D) mean body weight-at-age is determined by age alone, (E) the stock (or population) consists of the pool of recruited individuals, (F) maximum age is infinite, (G) the stock is in an equilibrium state determined by the fishing mortality rate, and (H) recruitment is determined by stock biomass alone. Within the framework provided by these assumptions, particular models are distinguished by the forms assigned to the weight-at-age and stock-recruitment functions.

Assumptions (A–C) imply that simple dynamic pool models conform to the following pair of equations:

$$\frac{\delta n(F, a)}{\delta a} = -n(F, a)Z, \tag{1}$$

and

$$n(F, a) = n(F, a_r)\, e^{-Z(a-a_r)}, \tag{2}$$

where a = age, n(F, a) is the stationary population distribution (in numbers) by ages a when the stock is exploited at a fishing mortality rate of F, Z is the instantaneous rate of total mortality (F + M), and a_r is the age of recruitment.

Equation (1) gives the instantaneous rate of change, by age, of the distribution n. When integrated with Z constant (Assumption B), Equation (1) gives Equation (2), numbers as a function of age. Assumption (D) implies that Equation (2) can be cast in terms of biomass by multiplying both sides of the equation by the weight-at-age function w(a):

$$b(F, a) = W(a)\, n(F, a_r)\, e^{-Z(a-a_r)}, \tag{3}$$

where b(F, a) is the stationary population distribution (in biomass) by ages a when the stock is exploited at a fishing mortality rate of F.

Assumptions (B), (C), (E), and (F) imply that total equilibrium stock numbers can be obtained by integrating Equation (2) from $a = a_r$ to $a = \infty$, giving

$$N(F) = \frac{n(F, a_r)}{Z}, \tag{4}$$

where N(F) represents total equilibrium numbers when the stock is exploited at a fishing mortality rate of F.

Likewise, equilibrium stock biomass is obtained by integrating Equation (3) from $a = a_r$ to $a = \infty$:

$$B(F) = n(F, a_r) \int_{a_r}^{\infty} w(a)\, e^{-Z(a-a_r)}\, da. \tag{5}$$

In the case where $a = a_r$, Assumptions (G) and (H) imply that the left-hand side of Equation (3), recruitment biomass, is a deterministic function of equilibrium stock biomass r(B(F)):

$$b(F, a_r) = r(B(F)). \tag{6}$$

Average weight of individuals in the stock W(F) can be written

$$W(F) = \frac{\int_{a_r}^{\infty} w(a)\, e^{-Z(a-a_r)}\, da}{\int_{a_r}^{\infty} e^{-Z(a-a_r)}\, da}$$

$$= Z \int_{a_r}^{\infty} w(a)\, e^{-Z(a-a_r)}\, da. \tag{7}$$

Equation (5) can then be rewritten

$$B(F) = \frac{W(F)\, n(F, a_r)}{Z}. \tag{8}$$

For the case of a pristine stock (F = 0), Equations (4) and (8) imply that equilibrium stock size (in terms of

numbers and biomass, respectively) is given by

$$N(0) = \frac{n(0, a_r)}{M}, \quad (9)$$

and

$$B(0) = \frac{W(0)\, n(0, a_r)}{M}. \quad (10)$$

Inconsistency of Rules I and II

The argument of Francis (1974) can be generalized to address more fully the compatibility of Rules I and II. The method to be used is as follows: First, it will be shown that if Rules I and II were to hold simultaneously with the properties of simple dynamic pool models, these rules would imply a particular result. It will then be shown that this result is incompatible with a major subset of the family of simple dynamic pool models, thus proving that Rules I and II are also incompatible with this subset.

Rule II and Equation (10) imply

$$B(F_{MSY}) = \frac{W(0)\, n(0, a_r)}{2M}. \quad (11)$$

Equation (8) implies that $B(F_{MSY})$ must also conform to

$$B(F_{MSY}) = \frac{W(F_{MSY})\, n(F_{MSY}, a_r)}{F_{MSY} + M}. \quad (12)$$

Solving Equations (11) and (12) for F_{MSY} gives

$$F_{MSY} = \left(\frac{2W(F_{MSY})\, n(F_{MSY}, a_r)}{W(0)\, n(0, a_r)} - 1 \right) M. \quad (13)$$

Next, Rule I and Equation (13) imply

$$\frac{n(F_{MSY}, a_r)}{n(0, a_r)} = \frac{W(0)}{W(F_{MSY})}. \quad (14)$$

The left-hand side of Equation (14) can be rewritten

$$\frac{n(F_{MSY}, a_r)}{n(0, a_r)} = \frac{w(a_r)\, n(F_{MSY}, a_r)}{w(a_r)\, n(0, a_r)} = \frac{b(F_{MSY}, a_r)}{b(0, a_r)} = \frac{r(B(F_{MSY}))}{r(B(0))}. \quad (15)$$

Now let the discussion be restricted to models in which the first derivative of the stock-recruitment relationship is uniformly nonnegative. In such cases, Equation (15) indicates that the left-hand side of Equation (14) is less than or equal to 1 if equilibrium stock biomass decreases as a function of F [i.e., if $B(F_{MSY}) < B(0)$, then $r(B(F_{MSY})) < r(B(0))$]. To examine the conditions under which this occurs, let Equation (8) be rewritten

$$B(F) = \frac{W(F)\, r(B(F))}{w(a_r)\, Z}. \quad (16)$$

Equation (16) can be differentiated as follows:

$$\frac{dB(F)}{dF} = \frac{r(B(F)) \left[Z \left(\frac{dW(F)}{dF} \right) - W(F) \right]}{Z \left[w(a_r)\, Z - W(F) \left(\frac{dr(F(F))}{dB(F)} \right) \right]}. \quad (17)$$

The numerator in Equation (17) is negative whenever $dW(F)/dF < 0$, which is easily shown to be true whenever w(a) is monotone increasing, a characteristic typical of all commonly used growth functions (Schnute 1981).

Thus, it follows that dB(F)/dF will likewise be negative whenever the denominator in Equation (17) is positive; that is, whenever

$$\frac{w(a_r)\, Z}{W(F)} > \frac{dr(F(F))}{dB(F)}. \quad (18)$$

By Equation (16), the left-hand side of (18) can be rewritten as the ratio of r(B(F)) to B(F), giving

$$\frac{r(B(F))}{B(F)} > \frac{dr(B(F))}{dB(F)}. \quad (19)$$

Given that the discussion has been restricted to models with stock-recruitment relationships that are nondecreasing (nonnegative first derivative), a sufficient condition for Equation (19) to hold is for dr(B(F))/dB(F) to be nonincreasing (nonpositive second

derivative). Therefore, for all simple dynamic pool models in which r(B(F)) is nondecreasing and dr(B(F))/dB(F) is nonincreasing, the left-hand side of Equation (14) is less than or equal to 1.0.

Turning to the right-hand side of Equation (14), note that this expression is necessarily greater than 1.0 whenever $dW(F)/dF<0$, a condition which has already been noted to hold whenever w(a) is monotone increasing.

Summarizing the argument, then, it has been shown that Rules I and II cannot hold simultaneously for any simple dynamic pool model in which the first derivative of the stock-recruitment relationship is uniformly nonnegative, the second derivative of the stock-recruitment relationship is uniformly nonpositive, and the first derivative of the weight-at-age relationship is uniformly positive.

Example of a simple dynamic pool model

Growth, biomass, recruitment, and yield

As an alternative to Rules I and II, it is possible to examine the behavior of F_{MSY}/M and $B(F_{MSY})/B(0)$ explicitly for a particular model. The model to be examined here incorporates a linear weight-at-age function (Schnute 1981). Let

$$w(a) = w(a_r)\left(\frac{a-a_0}{a_r-a_0}\right), \tag{20}$$

where a_0 represents the age intercept.

Biomass at age is then

$$b(F,a) = \frac{b(F, a_r)\,(a-a_0)\,e^{-Z(a-a_r)}}{a_r-a_0}. \tag{21}$$

For a given value of $b(F, a_r)$, biomass at age can be integrated from $a=a_r$ to $a=\infty$ to obtain the corresponding equilibrium stock size. Equation (21) can be integrated by parts, giving the following expression for equilibrium stock biomass (Hulme et al. 1947):

$$B(F) = \left(\frac{b(F, a_r)}{a_r-a_0}\right)\int_{a_r}^{\infty}(a-a_0)\,e^{-Z(a-a_r)}\,da$$

$$= \left(\frac{b(F, a_r)}{Z}\right)\left(1+\frac{1}{Z(a_r-a_0)}\right). \tag{22}$$

The stock-recruitment relationship of Cushing (1971) will be used to complete the model, giving recruitment as a power function of stock size:

$$b(F, a_r) = pB(F)^q, \tag{23}$$

where p and q are constants, and $0\leqslant q\leqslant 1$. In the limiting case of $q=0$, recruitment is constant, while in the other limiting case of $q=1$, recruitment is proportional to biomass.

The Cushing stock-recruitment relationship has the advantage of rendering Equation (22) explicitly solvable. Substituting Equation (23) into Equation (22) and rearranging terms gives the following equation for equilibrium stock biomass:

$$B(F) = \left[\frac{p}{Z}\left(1+\frac{1}{Z(a_r-a_0)}\right)\right]^{\frac{1}{1-q}}. \tag{24}$$

Multiplying both sides of Equation (24) by F then gives the equation for yield Y(F) shown below:

$$Y(F) = F\left[\frac{p}{Z}\left(1+\frac{1}{Z(a_r-a_0)}\right)\right]^{\frac{1}{1-q}}. \tag{25}$$

A partitioning of stock production

From this point on, it will prove helpful to make use of a new parameter K″, defined as follows:

$$K'' = \frac{1}{M(a_r-a_0)}. \tag{26}$$

The parameter K″ has a special biological interpretation in the context of the present model. To develop this interpretation, first multiply Equation (22) through by Z, yielding:

$$Z\,B(F) = b(F, a_r)\left(1+\frac{1}{Z(a_r-a_0)}\right). \tag{27}$$

Assuming no immigration or emigration, stock losses due to mortality must equal stock gains due to recruitment and growth at equilibrium (Russell 1931). Since the left-hand side of Equation (27) represents losses due to mortality, the right-hand side must equal the sum of equilibrium recruitment and growth. Therefore, Equation (27) can be rearranged to define equilibrium stock growth G(F) as follows:

$$G(F) = Z\,B(F) - b(F,a_r) = \frac{b(F, a_r)}{Z(a_r-a_0)}. \tag{28}$$

Dividing Equation (28) through by $b(F, a_r)$ gives the ratio between the two components of stock production, i.e., growth and recruitment:

$$\frac{G(F)}{b(F, a_r)} = \frac{1}{Z(a_r - a_0)}. \quad (29)$$

In the case of a pristine stock, Equation (29) reduces to

$$\frac{G(0)}{b(0, a_r)} = \frac{1}{M(a_r - a_0)} = K''. \quad (30)$$

In other words, K'' is simply the pristine ratio of growth to recruitment. At values of $K''>1$ pristine production is dominated by growth, while at $K''=1$ the two components of pristine production are equal, and at values of $K''<1$ pristine production is dominated by recruitment.

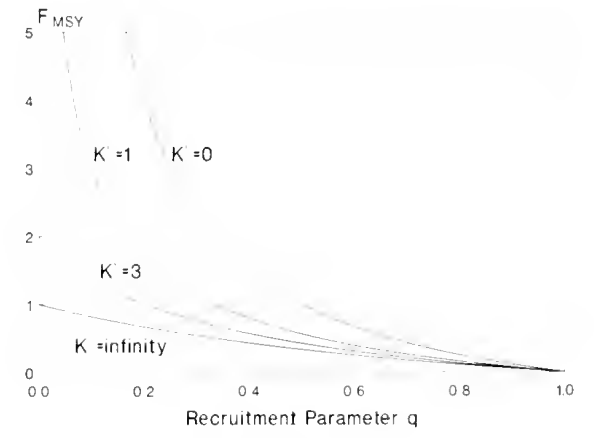

Figure 1

Ratio of F_{MSY} to M. For a given K'' value, the ratio decreases toward zero as q approaches 1.0. Higher K'' values result in lower values of the ratio, reaching a lower limit as K'' approaches infinity.

Fishing mortality at maximum sustainable yield

Differentiating Equation (25) with respect to F and setting the resulting expression equal to zero gives the following equation for F_{MSY}:

$$F_{MSY} = \frac{-\left(\frac{q+1}{a_r - a_0}\right) + M + \sqrt{\left(\frac{q+1}{a_r - a_0}\right)^2 + \left(\frac{(6q-2)M}{a_r - a_0}\right) + M^2}}{2q} - M. \quad (31)$$

Using F' to denote the ratio F/M, Equation (31) can be simplified via Equation (26) to

$$F'_{MSY} = \frac{-(q+1)K'' + 1 + \sqrt{(q+1)^2 K''^2 + (6q-2)K'' + 1}}{2q} - 1. \quad (32)$$

Figure 1 illustrates the behavior of F'_{MSY} as a function of q for four values of K'' (0, 1, 3, and ∞). Note that F'_{MSY} can deviate substantially from the value of 1.0 suggested by Rule I. The locus of parameter values for which Rule I holds under Equation (32) is

$$q = \frac{1}{K''+2}, \quad (33)$$

implying that q must be less than 0.5 in order for Rule I to hold.

When $q=1$, Equation (32) falls to zero. As q approaches zero, Equation (32) approaches an upper limit F'_{max} defined by

$$F'_{max} = \frac{K''+1}{K''-1}. \quad (34)$$

The limits of Equation (32) as K'' approaches zero and infinity are, respectively,

$$\lim_{K''\to 0} F'_{MSY} = \frac{1-q}{q} \quad (35)$$

and

$$\lim_{K''\to \infty} F'_{MSY} = \frac{1-q}{1+q}. \quad (36)$$

When pristine growth and recruitment are exactly balanced ($K'' = 1$), Equation (32) reduces to

$$F'_{MSY} = \sqrt{\frac{1}{4} + \frac{2}{q}} - \frac{3}{2}. \quad (37)$$

In the case of Equation (34), Rule I is always an underestimate (i.e., F'_{MSY} is always greater than 1.0). In the case of Equation (35), Rule I is an underestimate whenever $q<0.5$ and an overestimate whenever $q>0.5$. In the case of Equation (36), Rule I is always an overestimate, except in the limiting case where $q=0$. In the case of Equation (37), Rule I is an underestimate whenever $q<1/3$ and an overestimate whenever $q>1/3$.

Biomass at MSY relative to pristine biomass

Substituting $M+F_{MSY}$ for Z in Equation (24) gives $B(F_{MSY})$. Likewise, substituting M for Z in Equation (24) gives B(0). Forming a ratio from these two biomasses gives

$$\frac{B(F_{MSY})}{B(0)} = \left(\frac{K'' + F'_{MSY} + 1}{(K''+1)(F'_{MSY}+1)^2} \right)^{\frac{1}{1-q}}, \quad (38)$$

where F'_{MSY} is given by Equation (32).

Equation (38) is illustrated in Figure 2. Note that all of the curves in Figure 2 exhibit the same upper bound (1/e, about 0.37), which is reached in the limit as q approaches 1.0. Thus, Rule II always overestimates Equation (38) by a minimum of about 36%. At values of $q>0.5$, the biomass ratio is always greater than 0.25, but at lower values of q the ratio can be much smaller.

Multiplying Equations (32) and (38) gives the ratio MSY/MB(0), which is plotted in Figure 3. This ratio describes a stock's maximum sustainable fishery-induced losses as a proportion of its pristine losses. Alverson and Pereyra (1969) suggested that the MSY/MB(0) ratio should equal 0.5, a figure obtained by multiplying Rules I and II together. Note that this suggestion errs on the high side whenever K'' exceeds 1.0, as well as whenever q exceeds ~0.23.

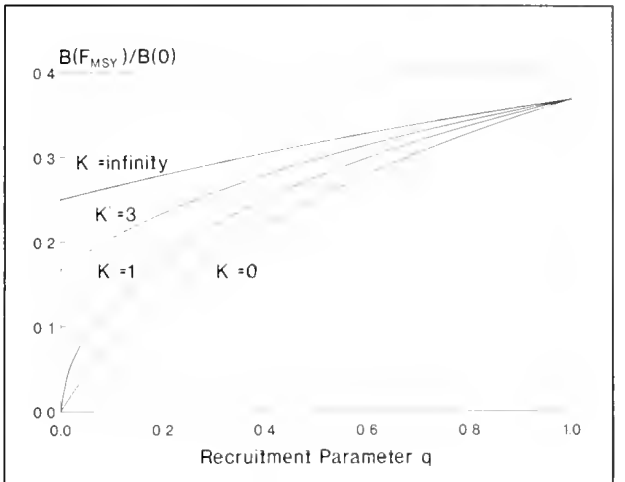

Figure 2

Ratio of $B(F_{MSY})$ to B(0). For any given K'' value, the ratio increases toward a value of 1/e as q approaches 1.0. Higher K'' values result in higher values of the ratio, reaching an upper limit as K'' approaches infinity.

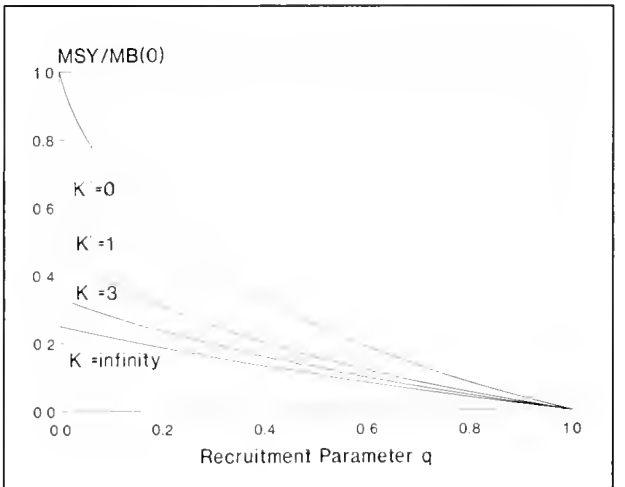

Figure 3

Ratio of MSY to the product of M and B(0). For a given K'' value, the ratio decreases toward a value of zero as q approaches 1.0. Higher K'' values result in lower values of the ratio, reaching a lower limit as K'' approaches infinity.

Applying the model to rock sole

As an illustration of the approach suggested above, the model can be applied to the eastern Bering Sea stock of rock sole *Pleuronectes bilineatus*. This stock is exploited by a multispecies flatfish fishery, and is also the target of an important roe fishery (Walters and Wilderbuer 1988).

The parameters to be estimated are q and K''. The parameter q can be determined from data on stock biomass and recruitment. Trawl survey estimates of rock sole stock biomass are available for the years 1979–88 (Walters and Wilderbuer 1988). In addition, age composition of the stock has been determined for the years 1979–87. In order to obtain an estimate of age composition for 1988, the "iterated age-length key" approach of Kimura and Chikuni (1987) was applied to the 1986 age-length key and the 1988 length-

frequency distribution. Assuming that rock sole recruit at age 3 (Walters and Wilderbuer 1988), these data provide seven years of information on the stock-recruitment relationship. Fitting Eq. (23) to these seven points (assuming lognormal error, Fig. 4) gives $q = 0.235$.

The composite parameter K'' can be estimated from its constituent parameters a_r, a_0, and M (Eq. 26). Walters and Wilderbuer (1988) set $a_r = 3$ and $M = 0.2$. The parameter a_0 can be derived by regressing a line through the mean weights-at-age, as shown in Figure 5 ($R^2 = 0.904$). This gives an a_0 value of 1.475 years, implying a K'' value of 3.279.

With these parameter values, Equation (32) gives $F'_{MSY} = 0.880$, or $F_{MSY} = 0.176$. This estimate of F_{MSY} compares favorably with the value of 0.155 that Walters and Wilderbuer (1988) derived from a surplus production model. It is relatively close to (within 12% of) the value indicated by Rule I.

However, Rule II does not fare so well in this example. Equation (38) estimates the ratio between $B(F_{MSY})$ and $B(0)$ at a value of 0.245, 51% below the value predicted by Rule II.

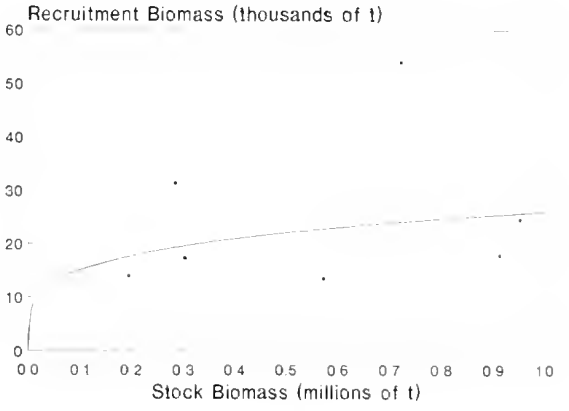

Figure 4

Stock-recruitment data and curve for eastern Bering Sea rock sole *Pleuronectes bilineatus*. Age-3 biomass (lagged 3 yr) is plotted against stock biomass for the years 1979–88.

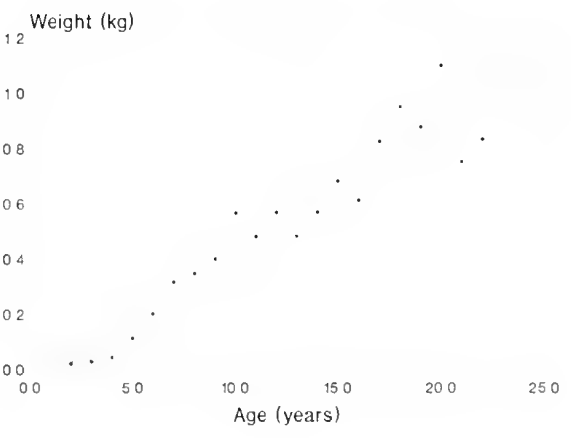

Figure 5

Weight-at-age data and relationship for eastern Bering Sea rock sole *Pleuronectes bilineatus*. Data are from the 1986 trawl survey conducted by the Alaska Fisheries Science Center.

Discussion

The topic of this paper, management advice from a simple dynamic pool model, has been considered from the perspective of how two commonly used rules of thumb compare with simple dynamic pool models in general, and how they compare with one such model in particular.

Choice of functional forms

Within the family of simple dynamic pool models, a particular model is defined by its stock-recruitment and growth functions. As Paulik (1973) and Ricker (1979) state, the choice of functional form for these two processes is largely a matter of convenience. The linear growth and Cushing stock-recruitment functions have been chosen for the proposed model, in part because of the tractability they confer. For example, their use permits explicit specification of F_{MSY} (impossible in other known examples of simple dynamic pool models, except in the special case where $F_{MSY} = F_{max}$). Another advantage is economy of parametrization: only two parameters (K'' and q) are required. The main disadvantage is the possibility that the simplicity of these functional forms might ignore critical behaviors.

The linear growth assumption is probably the more controversial of the two choices. The primary criticism of the linear growth equation is that it implies a constant growth rate, whereas other commonly used functions exhibit decreasing growth rates at upper ages (Beverton and Holt 1957), usually manifested in the form of an upper asymptote. In practice, however, the absence of an asymptote may be inconsequential or even preferable (Knight 1968, Ricker 1979) for two reasons: (1) In exploited populations, individuals may only rarely survive to reach the portion of the growth curve where a marked decrease in growth rate would be most discernible; and (2) in functional forms that incorporate an asymptote, this parameter is often poorly estimated, being highly correlated with at least one other parameter in the equation.

Robustness of the rules of thumb

Neither Rule I nor Rule II is particularly robust when applied to simple dynamic pool models in general or to the model developed here in particular. Rule I can drastically over- or underestimate the true relationship between F_{MSY} and M. When q exceeds 0.5, Rule I consistently overestimates the ratio between F_{MSY} and M, whereas when q is less than 0.5, the ratio can range both well above and well below the value suggested by Rule I.

Although these results do not provide much theoretical support for Rule I, it is still possible that Rule I holds as an empirical generalization (it turned out to be fairly close in the case of eastern Bering Sea rock sole, for example). If Rule I does hold as an empirical generalization, Equation (33) indicates that this implies an inverse relationship between the relative importance of growth in pristine production (K″) and the degree of density-dependence in the stock-recruitment relationship (q). Further work is necessary to see if such an inverse relationship is supported on the basis of life history or other theory.

Rule II consistently overestimates the ratio between $B(F_{MSY})$ and B(0) in the model presented here (Eq. 38, Fig. 2). In the case of eastern Bering Sea rock sole, Rule II was off by 51%. The problem with Rule II stems from the "diminishing returns" nature of the relationship between F and B(F), wherein successive increases in F result in less and less of an impact on biomass. Rule II, on the other hand, was inspired by the Schaefer (1954) model, in which the relationship between F and B(F) is linear (i.e., it exhibits constant returns to scale).

Interestingly, the upper asymptote displayed in Figure 2 corresponds exactly to the asymptote observed in a pair of surplus production models proposed by Pella and Tomlinson (1969, reparametrized by Fletcher 1978) and Fowler (1981), models that are conceptually very different from the one presented here. Mathematically, the isomorphism stems from the fact that all three models involve functions that raise a parameter x to an exponent of the form $1/(1-x)$. The fact that this result can be obtained from both surplus production and dynamic pool models indicates that it may be worthy of further investigation.

Since the rule of thumb setting MSY/MB(0) equal to 0.5 was derived by multiplying Rules I and II, it is affected by the upward bias inherent in Rule II. This is reflected in the eastern Bering Sea rock sole example, where the estimated value for the MSY/MB(0) ratio was only 0.216. It appears that the "MSY/MB(0) rule" can be a good approximation only when Rule I results in a major underestimate, which in the context of the model developed here requires two things: (1) Recruitment must be relatively independent of stock size, and (2) pristine production must be relatively dependent on recruitment (Fig. 3). Another consequence of this relationship is that Rule I can never hold when MSY/MB(0) = 0.5, and vice-versa. This conclusion stands in stark contrast to the traditional view which holds that the MSY/MB(0) rule derives from Rule I. Instead, it seems more likely that the two are mutually exclusive, at least in the context of simple dynamic pool models.

Acknowledgments

I would like to thank James Balsiger, Nicholas Bax, Roderick Hobbs, Daniel Kimura, Richard Methot, and Thomas Wilderbuer of the Alaska Fisheries Science Center for reviewing all or portions of this paper in various stages of development. Comments provided by Ian Fletcher of the Great Salt Bay Experimental Station were especially helpful. Three anonymous reviewers also supplied constructive suggestions.

Citations

Alverson, D.L., and W.T. Pereyra
1969 Demersal fish explorations in the northeastern Pacific Ocean—an evaluation of exploratory fishing methods and analytical approaches to stock size and yield forecasts. J. Fish. Res. Board Can. 26:1985-2001.

Beddington, J.R., and J.G. Cooke
1983 The potential yield of fish stocks. FAO Fish. Tech. Pap. 242, 47 p.

Beverton, R.J.H., and S.J. Holt
1957 On the dynamics of exploited fish populations. Fish Invest. Minist. Agric., Fish. Food (G.B.) Ser. 2, 19, 533 p.

Cushing, D.H.
1971 The dependence of recruitment on parent stock in different groups of fishes. J. Cons. Cons. Int. Explor. Mer 33: 340-362.

Deriso, R.B.
1982 Relationship of fishing mortality to natural mortality and growth at the level of maximum sustainable yield. Can. J. Fish. Aquat. Sci. 39:1054-1058.

Fletcher, R.I.
1978 Time-dependent solutions and efficient parameters for stock-production models. Fish. Bull., U.S. 76:377-388.

Fowler, C.W.
1981 Density dependence as related to life history strategy. Ecology 62:602-610.

Francis, R.C.
1974 Relationships of fishing mortality to natural mortality at the level of maximum sustainable yield under the logistic stock production model. J. Fish. Res. Board Can. 31: 1539-1542.

Gulland, J.A.
1971 The fish resources of the ocean. Fishing News (Books) Ltd., Surrey, England, 255 p.

Hulme, H.R., R.J.H. Beverton, and S.J. Holt
1947 Population studies in fisheries biology. Nature (Lond.) 159:714-715.

Kimura, D.K., and S. Chikuni
1987 Mixtures of empirical distributions: An iterative application of the age-length key. Biometrics 43:23–35.

Knight, W.
1968 Asymptotic growth: An example of nonsense disguised as mathematics. J. Fish. Res. Board Can. 25:1303–1307.

Larkin, P.A.
1977 An epitaph for the concept of maximum sustainable yield. Trans. Am. Fish. Soc. 106:1–11.

Paulik, G.J.
1973 Studies of the possible form of the stock-recruitment curve. Rapp. P.-V. Reun. Cons. Perm. Int. Explor. Mer 164: 302–315.

Pella, J.J., and P.K. Tomlinson
1969 A generalized stock production model. Bull. Inter-Am. Trop. Tuna Comm. 13:419–496.

Pitcher, T.J., and P.J.B. Hart
1982 Fisheries ecology. AVI Publ. Co., Westport, CT, 414 p.

Ricker, W.E.
1979 Growth rates and models. *In* Hoar, W.S., D.J. Randall, and J.R. Brett (eds.), Fish physiology, vol. 8, p. 677–743. Academic Press, NY.

Russell, E.S.
1931 Some theoretical considerations on the 'overfishing' problem. J. Cons. Cons. Int. Explor. Mer 6:3–20.

Schaefer, M.B.
1954 Some aspects of the dynamics of populations important to the management of the commercial marine fisheries. Bull. Inter-Am. Trop. Tuna Comm. 1:27–56.

Schnute, J.
1981 A versatile growth model with statistically stable parameters. Can. J. Fish. Aquat. Sci. 38:1128–1140.

Shepherd, J.G.
1982 A family of general production curves for exploited populations. Math. Biosci. 59:77–93.

Walters, G.E., and T.K. Wilderbuer
1988 Rock sole. *In* Condition of groundfish resources of the eastern Bering Sea and Aleutian Islands region in 1988, p. 106–117. Unpubl. manuscr. submitted to Int. N. Pac. Fish. Comm., Sept. 1988. NMFS Alaska Fish. Sci. Cent., Seattle, 219 p.

Abstract. – A simple dynamic pool model is used to examine the problem of stock-recruitment parameter uncertainty from a Bayesian perspective. Probabilities associated with different parameter values are used to weight the losses (i.e., opportunity costs to society) associated with any given fishing mortality rate. By choosing appropriate forms for the loss and probability density functions, the model is shown to result in an analytic solution. Because this solution gives the fishing mortality rate that maximizes the expected value of the logarithm of sustainable yield, it is denoted F_{MELSY}. The solution is a monotone-decreasing function of parameter uncertainty, converging on the fishing mortality rate corresponding to maximum sustainable yield as the degree of uncertainty approaches zero. As an empirical illustration, the model is applied to the eastern Bering Sea stock of rock sole *Pleuronectes bilineatus*.

A Bayesian approach to management advice when stock-recruitment parameters are uncertain

Grant G. Thompson

Resource Ecology and Fisheries Management Division
Alaska Fisheries Science Center, National Marine Fisheries Service, NOAA
7600 Sand Point Way NE, Seattle, Washington 98115-0070

Manuscript accepted 4 June 1992.
Fishery Bulletin, U.S. 90:561–573 (1992).

Exploiting a stock at the fishing mortality rate (F) associated with maximum sustainable yield (MSY) is a common fishery management strategy. For the most part, three simple propositions are sufficient to justify this strategy: (1) The stock exhibits a sustainable yield determined by the fishing mortality rate, (2) more sustainable yield is always preferable to less, and (3) the parameters underlying the stock's dynamics are known with certainty. However, parameters governing stock dynamics are typically not known with certainty, and in such cases it is possible to demonstrate that the appropriate F value may be less than the value corresponding to MSY (F_{MSY}).

The approach to be used in this demonstration is taken from Bayesian decision theory (e.g., Raiffa 1968, DeGroot 1970). Early applications of Bayesian theory to fisheries problems were presented by Rothschild (1972), Lord (1973, 1976), Walters (1975), and Walters and Hilborn (1976). Of the many more recent applications, those presented by Ludwig and Walters (1982), Clark et al. (1985), and Walters and Ludwig (1987) bear most closely on the present study.

For simplicity, it will be assumed here that stock dynamics are deterministic but governed by parameters which may be imprecisely estimated. This approach is distinct from the more common one of assuming that stock dynamics are the product of a deterministic system (with parameter values given and fixed) modified by a random error term. Important early examples of the latter approach include Ricker (1958), Larkin and Ricker (1964), and Tautz et al. (1969). Ludwig and Walters (1982) and Mangel and Clark (1983) incorporate both approaches in a systematic fashion which makes the distinction especially clear.

The basic model

Thompson (1992) developed a simple dynamic pool model which can be solved explicitly for F_{MSY}. In terms of biomass per recruit, the model is basically that of Hulme et al. (1947); thus, body weight is taken to be a linear function of age, with intercept a_0. The main departure from Hulme et al. is that biomass at recruitment age a_r is taken to be proportional to stock biomass raised to a power q (Cushing 1971). With these specifications, sustainable yield Y(F) can be written

$$Y(F) = F\left[\left(\frac{p}{M}\right)\left(\frac{1+K''+F'}{(1+F')^2}\right)\right]^{\frac{1}{1-q}}, \quad (1)$$

where M is the instantaneous rate of natural mortality, $F' = F/M$, p is the proportionality term in the Cushing stock-recruitment relationship, and $K'' = 1/[M(a_r - a_0)]$ (which can be interpreted in this model as the pristine ratio of growth to recruitment). The

Cushing exponent q is constrained to fall between 0 and 1. In the limiting case of $q=0$, recruitment is constant, while in the other limiting case of $q=1$, recruitment is proportional to biomass.

Differentiating Equation (1) with respect to F and setting the resulting expression equal to zero gives the following equation for F_{MSY}:

$$F'_{MSY} = \frac{-(q+1)K'' + 1 + \sqrt{(q+1)^2K''^2 + (6q-2)K'' + 1}}{2q} - 1, \quad (2)$$

where $F'_{MSY} = F_{MSY}/M$.

A common rule of thumb is that F'_{MSY} should equal 1. The locus of parameter values for which this rule holds precisely is given by

$$K'' = \frac{1}{q} - 2. \quad (3)$$

Analyzing the model in a Bayesian framework

Parameter estimates in any model are by definition associated with some degree of uncertainty. For example, parameters governing the stock-recruitment relationship are particularly difficult to estimate precisely (Larkin 1973, Paulik 1973, Ludwig and Walters 1981, Walters and Ludwig 1981 and 1987, Shepherd 1982, Clark 1985, Clark et al. 1985, Rothschild and Mullen 1985, Shepherd and Cushing 1990). In the presence of such uncertainty, a Bayesian approach would use the probabilities associated with different parameter values to weight the losses (i.e., opportunity costs to society) associated with choosing a particular fishing mortality rate. Following similar studies by Ludwig and Walters (1982), Clark et al. (1985), and Walters and Ludwig (1987), the present analysis will focus on the uncertainty surrounding a single parameter, in this case the stock-recruitment exponent q. This uncertainty takes the form of a probability density function (pdf) P(q) which describes the relative credibility of alternative q values.

To simplify notation, define z(F, q) as the ratio of Y(F) to MSY for an arbitrary value of q drawn from P(q). Then, the "Bayes decision" (DeGroot 1970) is the value of F that minimizes

$$E\{L[z(F, q)]\} = \int_0^1 L[z(F, q)]\, P(q)\, dq, \quad (4)$$

where L[z(F, q)] represents the losses resulting from selection of a particular value of F given a particular value of q, and $E\{L[z(F, q)]\}$ is the expected value of L[z(F, q)] (the "risk," DeGroot 1970). The minimum value of $E\{L[z(F, q)]\}$ is referred to as the "Bayes risk" (DeGroot 1970). The integral is taken over the interval 0 to 1 because the Cushing stock-recruitment relationship constrains q to that range.

The Bayes decision can be derived by differentiating $E\{L[z(F, q)]\}$ with respect to F and solving for the value that sets the derivative equal to zero. The validity of this procedure requires that all parameter values, including those describing P(q), remain constant into the future. The solution corresponding to such an assumption is sometimes known as a "myopic Bayes" solution (Ludwig and Walters 1982, Mangel and Clark 1983, Mangel and Plant 1985, Parma 1990). A more general alternative is to allow for the possibility that parameter estimates will be updated in the future, but this approach is vastly more difficult (Clark et al. 1985, Mangel and Plant 1985, Walters and Ludwig 1987).

Minimizing risk under a logarithmic loss function

Of course, specification of the functions L and P is crucial to this problem. Following Lord (1976) and Ludwig and Walters (1982), one possible choice is to assume that L is a linear function of $z(L(z) = 1 - z)$. Another common form is the quadratic $L(z) = (1-z)^2$, which has been used in the fisheries literature by Walters (1975), Hightower and Grossman (1987), and Charles (1988). One of the oldest alternatives is the logarithmic loss function, $L(z) = -\ln(z)$, dating back to the work of Bernoulli in 1738 (transl. 1954). Logarithmic loss (or, conversely, utility) seems first to have been used in the fisheries literature by Gleit (1978), followed by Lewis (1981, 1982), Mendelssohn (1982), Opaluch and Bockstael (1984), Ruppert et al. (1984, 1985), Deriso (1985), Walters (1987), Walters and Ludwig (1987), Getz and Haight (1989), Hightower and Lenarz (1989), Hightower (1990), Parma (1990), and Parma and Deriso (1990).

Linear, quadratic, and logarithmic loss functions are compared in Figure 1. As Figure 1 indicates, the logarithmic loss function corresponds to a "preservationist" viewpoint, in which extinction of the stock is absolutely unacceptable (i.e., the loss corresponding to extinction is infinite). Because the logarithmic loss function is clearly identifiable as a risk-averse alternative function (see Discussion), it is a good candidate for illustrating how a Bayesian approach can differ from more traditional approaches which do not incorporate uncertainty in an explicit fashion.

To incorporate the logarithmic loss concept into the model, first note that Equation (1) allows z(F, q) to be written

$$z(F, q) = \frac{Y(F)}{MSY} = \frac{F\left[\left(\frac{p}{M}\right)\left(\frac{1+K''+F'}{(1-F')^2}\right)\right]^{\frac{1}{1-q}}}{F_{MSY}\left[\left(\frac{p}{M}\right)\left(\frac{1+K''+F'_{MSY}}{(1+F'_{MSY})^2}\right)\right]^{\frac{1}{1-q}}} = \frac{F'}{F'_{MSY}}\left[\left(\frac{1+F'_{MSY}}{1+F'}\right)^2\left(\frac{1+K''+F'}{1+K''+F'_{MSY}}\right)\right]^{\frac{1}{1-q}}. \quad (5)$$

For an arbitrary value of q, the (logarithmic) loss associated with a given choice of F is thus

$$L[z(F, q)] = \ln(F'_{MSY}) - \frac{2\ln(1+F'_{MSY}) - \ln(1+K''+F'_{MSY})}{1-q} - \ln(F') + \frac{2\ln(1+F') - \ln(1+K''+F')}{1-q}. \quad (6)$$

Substituting Equation (6) into Equation (4), the risk can be written

$$E\{L[z(F, q)]\} = \int_0^1 P(q)\left(\ln(F'_{MSY}) - \frac{2\ln(1+F'_{MSY}) - \ln(1+K''+F'_{MSY})}{1-q}\right) dq$$

$$- \int_0^1 P(q)\left(\ln(F') - \frac{2\ln(1+F') - \ln(1+K''+F')}{1-q}\right) dq. \quad (7)$$

From Equation (2), it is clear that F'_{MSY} involves only K'' and q. Thus, regardless of the form of P(q), the first integral on the right-hand side of Equation (7) is independent of F. Therefore, the problem of finding the Bayes decision is equivalent to minimizing the second integral on the right-hand side of Equation (7). Remembering that the integral (taken over the interval 0 to 1) of a constant multiplied by P(q) is equal to the constant itself, the following proxy objective function is obtained:

$$E_1\{L[z(F, q)]\} = -\ln(F') + [2\ln(1+F') - \ln(1+K''+F')]\int_0^1 \frac{P(q)}{1-q} dq. \quad (8)$$

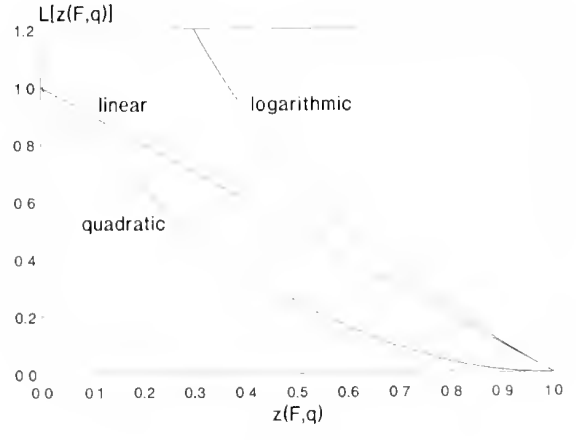

Figure 1

Three possible loss functions. Loss, or relative utility foregone, is plotted against the ratio of Y(F)/MSY for quadratic, linear, and logarithmic loss functions.

Incorporating a beta probability density function

The next step in determining the Bayes decision is to select a form for the pdf P(q). Bayesian decision theory frequently makes use of the beta family of pdfs (e.g., DeGroot 1970, Holloway 1979). The beta distribution would seem to be a natural candidate for P(q), since it constrains q to the necessary (0,1) range. In its standard form, the beta distribution can be written

$$P(q) = \left(\frac{\Gamma(\alpha+\beta)}{\Gamma(\alpha)\,\Gamma(\beta)}\right) q^{\alpha-1}\,(1-q)^{\beta-1}, \tag{9}$$

where α and β are positive constants and $\Gamma(\cdot)$ is the gamma function, which, except for $\Gamma(1)=1$, can be described in terms of the recursion formula

$$\Gamma(\alpha) = (\alpha-1)\,\Gamma(\alpha-1). \tag{10}$$

By Equations (9) and (10), then, the integral in Equation (8) can be evaluated as follows:

$$\int_0^1 \frac{P(q)}{1-q}\,dq = \left(\frac{\Gamma(\alpha+\beta)}{\Gamma(\alpha)\,\Gamma(\beta)}\right)\int_0^1 q^{\alpha-1}\,(1-q)^{\beta-2}\,dq = \left(\frac{\Gamma(\alpha+\beta)}{\Gamma(\alpha)\,\Gamma(\beta)}\right)\left(\frac{\Gamma(\alpha)\,\Gamma(\beta-1)}{\Gamma(\alpha+\beta-1)}\right)$$

$$= \left(\frac{\Gamma(\beta-1)}{\Gamma(\beta)}\right)\left(\frac{\Gamma(\alpha+\beta)}{\Gamma(\alpha+\beta-1)}\right) = \frac{\alpha+\beta-1}{\beta-1}. \tag{11}$$

Substituting Equation (11) into Equation (8) then gives

$$E_1\{L[z(F,\,q)]\} = -\ln(F') + \frac{[2\ln(1+F') - \ln(1+K''+F')]\,(\alpha+\beta-1)}{\beta-1}. \tag{12}$$

Differentiating Equation (12) with respect to F' and setting the resulting expression equal to zero yields the quadratic expression

$$\alpha F'^2 + [K''(2\alpha+\beta-1) + \alpha - \beta + 1]\,F' - (\beta-1)\,(K''+1) = 0. \tag{13}$$

Before solving Equation (13), it would be helpful to cast the solution in terms of parameters which are more intuitive than α and β, for example the mean and variance of P(q). The beta distribution has mean m and variance v as follows:

$$m = \frac{\alpha}{\alpha+\beta} \qquad \text{and} \qquad v = \frac{\alpha\beta}{(\alpha+\beta)^2\,(\alpha+\beta+1)}. \tag{14 and 15}$$

Conversely, Equations (14) and (15) can be solved simultaneously to describe α and β in terms of m and v:

$$\alpha = \left(\frac{m(1-m)}{v} - 1\right) m \qquad \text{and} \qquad \beta = \left(\frac{m(1-m)}{v} - 1\right)(1-m). \tag{16 and 17}$$

Unlike the normal distribution, the variance of the beta distribution exhibits a maximum possible value for a given mean. Remembering that α and β are constrained to be positive, the maximum possible value of v can be derived from either Equation (16) or Equation (17) by setting the left-hand side equal to 0 and solving for v. This exercise results in a maximum v equal to $m(1-m)$. Thus, α and β can be written in terms of the mean and a scaled variance $v'\left(=\dfrac{v}{m(1-m)}\right)$ as follows:

$$\alpha = \left(\frac{1}{v'} - 1\right) m \qquad \text{and} \qquad \beta = \left(\frac{1}{v'} - 1\right)(1-m). \qquad (18) \text{ and } (19)$$

For a given set of K″, m, and v′ values, Figure 2 shows the risk (depicted by the area under a particular curve) associated with three possible F′ values.

Fishing mortality at maximum expected log-sustainable yield

Substituting Equations (18) and (19) into Equation (13) and solving for F′ gives the value that minimizes risk. Because of the form used for the loss function, this process is equivalent to finding the level of F′ that maximizes the expected value of the logarithm of sustainable yield. It is thus convenient to refer to this value as F'_{MELSY} (for "maximum expected log sustainable yield"), which for this particular model can be written

$$F'_{MELSY} = \frac{[(m+2)\,K''-2]\,v' - (m+1)\,K'' + 1 + \sqrt{k_2\,v'^2 - k_1\,v' + k_0}}{2\,m(1-v')} - 1, \qquad (20)$$

where $k_2 = (m+2)^2\,K''^2 + (12m-8)\,K'' + 4$,
$k_1 = (2m^2+6m+4)\,K''^2 + (18m-8)\,K'' + 4$, and
$k_0 = (m+1)^2\,K''^2 + (6m-2)\,K'' + 1$.

Figure 3 illustrates how F'_{MELSY} varies with K″, m, and v′. A few special cases are of particular interest. For example, when q is known with certainty, i.e., m = q and v′ = 0, Equation (20) reduces to Equation (2). Equation (2) is thus the "certainty equivalent" solution (Ludwig and Walters 1982). The ratio between F_{MELSY} and F_{MSY} is illustrated in Figure 4. Differences in K″ tend to have less influence on this ratio than differences in either m or v′.

Other important special cases of Equation (20) include the limits as K″ approaches zero and infinity, which are shown respectively below:

$$\lim_{K''\to 0} F'_{MELSY} = \frac{1-m(1-v') - 2v'}{m(1-v')} \qquad \text{and} \qquad \lim_{K''\to\infty} F'_{MELSY} = \frac{1-m(1-v') - 2v'}{1+m(1-v') - 2v'}. \qquad (21) \text{ and } (22)$$

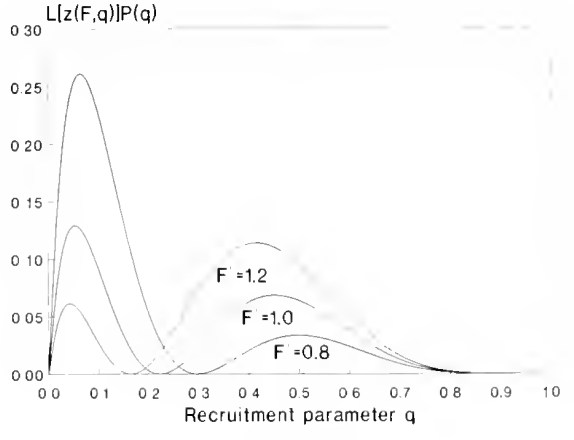

Figure 2
Risk under different F levels. The area under a curve is the risk associated with the F level that defines the particular curve. Parameter values used to generate these curves were K″ = 2.5, m = 0.2, and v′ = 1/11.

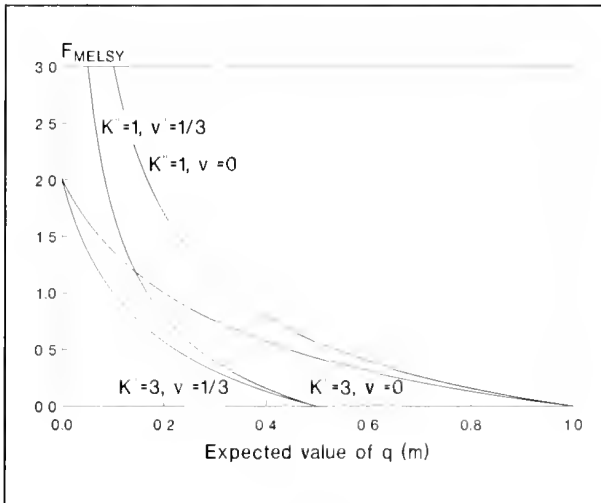

Figure 3
Values of F'_{MELSY} resulting from different combinations of parameter levels. F'_{MELSY} tends to decrease as K″, m, or v′ increases.

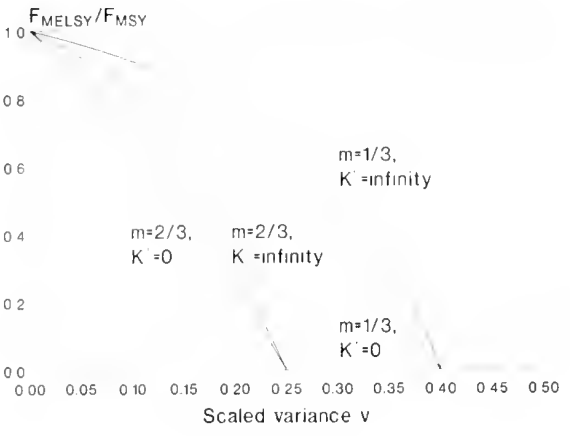

Figure 4

Ratio of F'_{MELSY} to F'_{MSY} under different combinations of parameter levels. The ratio tends to decrease as K″ decreases or as m or v′ increases.

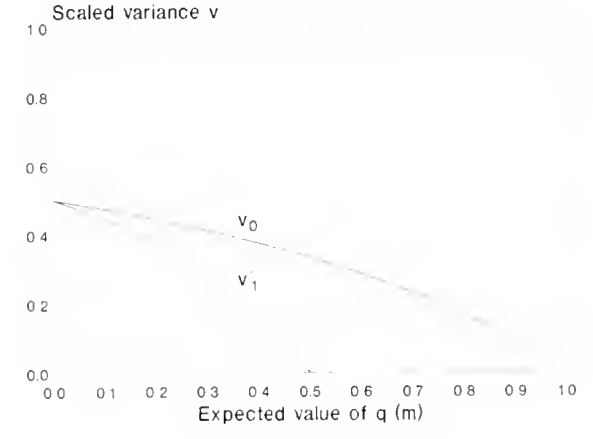

Figure 5

Limiting values of v′. The solid curve shows v'_0, the locus at which $F'_{MELSY}=0$. The dashed curve shows v'_1, the locus limiting the parameter subspace for which F'_{MELSY} can exceed 1. For (m, v′) combinations below the v'_1 curve, F'_{MELSY} can take any value, depending on K″. For (m, v′) combinations between the two curves, F'_{MELSY} can range between 0 and 1, again depending on K″. For (m, v′) combinations on or above the v'_0 curve, $F'_{MELSY}=0$.

Equation (20) also implies that F'_{MELSY} falls to zero whenever v′ reaches a critical value v'_0 defined as

$$v'_0 = \frac{1-m}{2-m}. \tag{23}$$

By Equation (19), v'_0 corresponds to a β value of 1. Whenever $\beta \leq 1$, the right-hand tail of the beta distribution fails to reach zero, implying a non-zero probability that q = 1. When q = 1, any positive F value causes the stock to go extinct. Given the preservationist attitude implicit in the logarithmic loss function, any possibility of extinction is unacceptable, so F'_{MELSY} drops to zero in this case. Note that F'_{MELSY} is never positive for values of v′ greater than 0.5.

Just as Equation (2) could be solved to determine the locus of parameter values under which F'_{MSY} takes on the special value of 1 (Eq. 3), Equation (20) can be solved to determine the following locus of parameter values under which $F'_{MELSY}=1$:

$$K'' = \frac{1-2v'}{m(1-v')} - 2. \tag{24}$$

In the certainty equivalent case, Equation (24) reduces to Equation (3). As K″ approaches zero, Equation (24) defines an upper limit on v′ (v'_1) for the special case where $F'_{MELSY}=1$:

$$v'_1 = \frac{1-2m}{2-2m}. \tag{25}$$

Under Equation (3), F'_{MSY} could exceed 1 only if q were less than 0.5. While Equation (25) implies essentially the same property (replacing F'_{MSY} with F'_{MELSY} and q with m), it adds a similar restriction on v′, namely that F'_{MELSY} can exceed 1 only if v′ is less than 0.5. [Note that this is a weaker version of the restriction implied by Equation (23). Equations (23) and (25) are compared in Figure 5.]

Biomass at MSY compared with biomass at MELSY

Dividing Equation (1) through by F gives equilibrium stock biomass. By substituting Equations (20) and (2) into this expression and setting q = m, the ratio of stock biomass at MSY to stock biomass at MELSY is given by

$$\frac{B(F_{MSY})}{B(F_{MELSY})} = \left[\left(\frac{F'_{MELSY}+1}{F'_{MSY}+1}\right)^2\left(\frac{K''+F'_{MSY}+1}{K''+F'_{MELSY}+1}\right)\right]^{\frac{1}{1-m}}, \tag{26}$$

with limits

$$\lim_{K'\to 0}\left(\frac{B(F_{MSY})}{B(F_{MELSY})}\right) = \left(\frac{1-2v'}{1-v'}\right)^{\frac{1}{1-m}} \quad \text{and} \quad \lim_{K'\to\infty}\left(\frac{B(F_{MSY})}{B(F_{MELSY})}\right) = \left(\frac{(1+m)(1-2v')}{(1+m)(1-v') - v'}\right)^{\frac{1}{1-m}}. \qquad (27) \text{ and } (28)$$

Equations (26–28) decline from a value of 1 at $v' = 0$ to a minimum at $v' = v'_0$. The minimum value depends on K″ and m, but is never greater than 1/e.

Estimating the parameters of the beta distribution

To fit the Cushing stock-recruitment curve to a set of n stock-recruitment data points, it seems reasonable to assume the following model:

$$y_i = \rho + qx_i + \varepsilon_i, \qquad (29)$$

where x_i represents the natural logarithm of the ith stock biomass datum, y_i represents the natural logarithm of the ith recruitment datum (lagged according to the age of recruitment), $\rho = \ln(p)$, and ε_i is an independent error term distributed as $N(0,\sigma^2)$.

Press (1989) presented a Bayesian approach to estimating the parameters of the pdf of q using Equation (29) as the underlying model. The following paragraphs summarize this presentation, which begins by rephrasing the problem in the form of Bayes' theorem:

$$h(q,\rho,\sigma \mid \mathbf{x}, \mathbf{y}) \propto \left(\prod_{i=1}^{n} f(y_i \mid x_i,q,\rho,\sigma)\right) g_1(q)\, g_2(\rho)\, g_3(\sigma), \qquad (30)$$

where $\mathbf{x}$ is the vector $(x_1, \ldots, x_n)'$; $\mathbf{y}$ is the vector $(y_1, \ldots, y_n)'$; $h(q,\rho,\sigma \mid \mathbf{x}, \mathbf{y})$ represents the posterior pdf of the parameters q, ρ, and σ; $f(y_i \mid x_i,q,\rho,\sigma)$ represents the conditional pdf of y_i given the observed value of x_i and any particular values of q, ρ, and σ; and $g_j(\cdot)$ represents the prior pdf of the jth parameter.

Given the assumptions implicit in Equation (29), $f(y_i \mid x_i,q,\rho,\sigma)$ can be written

$$f(y_i \mid x_i,q,\rho,\sigma) = \frac{\exp\left(\dfrac{-(y_i-\rho-qx_i)^2}{2\sigma^2}\right)}{\sqrt{2\pi\sigma^2}}. \qquad (31)$$

A special case of interest is the one in which the $g_j(\cdot)$ are all "vague" (also called noninformative or indifference) priors. These are pdfs which reflect indifference regarding the probability of alternative parameter values. Press (1989) treated $g_1(q)$ and $g_2(\rho)$ as constants, implying that all values on the real line are equally likely in the prior distribution. Since σ is constrained to be positive, however, Press set $g_3(\sigma) = 1/\sigma$, reflecting a uniform prior distribution for $\ln(\sigma)$.

Using Equation (31) and the priors specified by Press (1989), Eq. (30) gives a straightforward solution. The classical least-squares estimates of q and ρ ($\hat{q}$ and $\hat{\rho}$, respectively) obtain as the maximum-likelihood estimates. In their posterior pdf, q and ρ jointly follow a bivariate Student's t distribution, so that marginally the posterior pdf of q, $h_1(q \mid \mathbf{x}, \mathbf{y})$, follows a univariate 3-parameter t distribution with $n-2$ degrees of freedom:

$$h_1(q \mid \mathbf{x},\mathbf{y}) = \frac{\Gamma\left(\dfrac{n-1}{2}\right)}{\Gamma\left(\dfrac{n-2}{2}\right)\sqrt{\pi(n-2)\, s_q^2}\left(1 + \dfrac{(q-\hat{q})^2}{(n-2)\, s_q^2}\right)^{n-1}}, \qquad (32)$$

where s_q^2 is the estimated variance of $\hat{q}$ given by

$$s_q^2 = \frac{\sum_{i=1}^{n} (y_i - \hat{\rho} - \hat{q}x_i)^2}{(n-2)\sum_{i=1}^{n} (x_i - \bar{x})^2}. \quad (33)$$

For the present application, the solution given by Press (1989) needs to be modified in only one respect. His suggested form for $g_1(q)$ implies a uniform distribution over the entire real line, whereas here P(q) has been specified *a priori* to be zero for all values less than 0 or greater than 1. Given Equations (30) and (31), this implies that the suggested uniform shape for $g_1(q)$ should be truncated outside the range 0 to 1. This in turn implies that $h_1(q \mid \mathbf{x},\mathbf{y})$ should also be truncated outside the range 0 to 1 (and rescaled appropriately).

Strictly speaking, then, P(q) follows a truncated t distribution in this approach, rather than the hypothesized beta. However, a beta distribution can be made to approximate the truncated t by solving for m and v as follows:

$$m = \frac{\int_0^1 q\, h_1(q \mid \mathbf{x},\mathbf{y})\, dq}{\int_0^1 h_1(q \mid \mathbf{x},\mathbf{y})\, dq} \quad (34)$$

and

$$v = \frac{\int_0^1 (q-m)^2\, h_1(q \mid \mathbf{x},\mathbf{y})\, dq}{\int_0^1 h_1(q \mid \mathbf{x},\mathbf{y})\, dq}. \quad (35)$$

Applying the model to rock sole

As an illustration of the approach suggested above, the model can be applied to the eastern Bering Sea stock of rock sole *Pleuronectes bilineatus*. This stock is exploited by a multispecies flatfish fishery, and is also the target of an important roe fishery (Walters and Wilderbuer 1988).

The parameters to be estimated are K″, m, and v′. Thompson (1992) estimated K″ for this stock at a value of 3.279, and described a set of stock and recruitment data ($n = 7$) which can be used to estimate m and v′. Fitting Equation (29) to these data gives $\hat{q} = 0.235$ and $s_q^2 = 0.114$ (Fig. 6). Substituting these parameters into Equations (34) and (35) gives $m = 0.369$ and $v = 0.057$, with $v' = 0.243$. The relationship between the truncated t distribution defined by these values and the beta approximation is shown in Figure 7 ($R^2 = 0.97$).

With parameter values $K'' = 3.279$, $m = 0.369$, and $v' = 0.243$, Equation (20) gives $F'_{MELSY} = 0.365$. Multiplying through by M (set at 0.2 by Walters and Wilderbuer 1988) gives $F'_{MELSY} = 0.073$. Substituting m for q in Equation (2) yields $F'_{MSY} = 0.607$, or $F_{MSY} = 0.121$. This value of F_{MSY} differs somewhat from the value of 0.176 given by Thompson (1992), which was based on the least-squares estimate of q ($\hat{q}$) instead of the

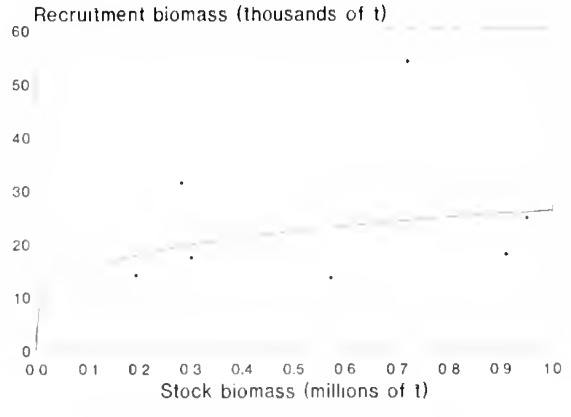

Figure 6

Stock-recruitment data and curve for eastern Bering Sea rock sole *Pleuronectes bilineatus*. Age-3 biomass (lagged 3 yr) is plotted against stock biomass for the years 1979–88. The curve is the least-squares fit.

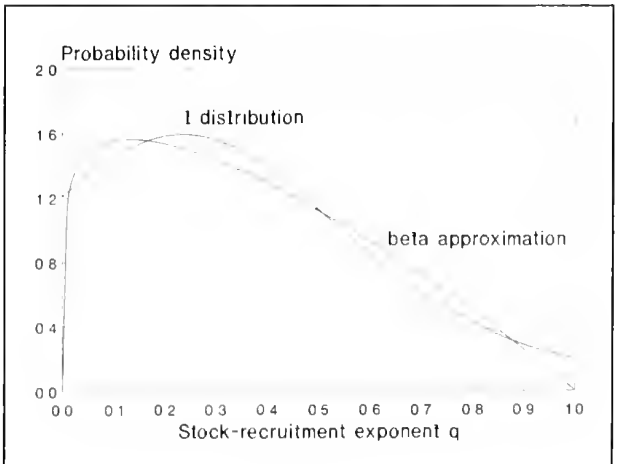

Figure 7

Comparison of truncated t and beta pdfs for the stock-recruitment exponent q in the eastern Bering Sea rock sole *Pleuronectes bilineatus* example.

Bayesian estimate (m). These two F_{MSY} values bracket the value of 0.155 which Walters and Wilderbuer (1988) derived from a surplus production model. Regardless of which F_{MSY} value is chosen, however, it exceeds F_{MELSY} by a significant amount.

Discussion

Evaluation of assumptions

The approach described here consists of three main components: the basic model represented by Equation (1), the logarithmic loss function, and the beta form for P(q). These components were chosen in part because they are tractable, making possible the analytic solution for F'_{MELSY} given by Equation (20). In addition, each has some degree of theoretical support, as described below.

The basic model The basic model was evaluated by Thompson (1992). In brief, the model includes terms for all of the requisite features of dynamic pool models (recruitment, growth, natural mortality, fishing mortality). The distinguishing features of the model (linear growth and a Cushing stock-recruitment relationship) satisfy the principal theoretical requirements for growth and stock-recruitment functions given by Schnute (1981) and Ricker (1975), respectively. Although the basic model is a simple one, it approximates more complicated models fairly well under a wide range of parameter values.

Logarithmic loss function The logarithmic loss function may require a bit more discussion. As mentioned earlier, this loss function is only one of several possibilities, two of the other most-common being the linear and quadratic forms. The principal argument against the linear loss function is that it implies strict risk neutrality, whereas most individuals tend to be at least somewhat risk-averse. Thus, if fishery managers tend to be risk-averse, a linear loss function would be inappropriate, except over a narrow range of yield values.

In contrast, the quadratic loss function implies a degree of risk aversion. In addition, the quadratic form has properties which prove convenient for a number of statistical applications. However, it has also been the subject of substantial criticism (Pratt 1964, Samuelson 1967, Box and Tiao 1973). Although the quadratic loss function does fall into the "risk-averse" category, this functional form manifests its risk aversion somewhat perversely by exhibiting increasing absolute risk aversion (Pratt 1964). In other words, a fishery manager using a quadratic loss function would be less willing to take risks as yields became higher.

The logarithmic loss function is another risk-averse alternative. It can be described as a special case of the isoelastic marginal loss function defined by $L(z) = (1 - z^{\phi})/\phi$, where $\phi > 0$ (the logarithmic case being obtained in the limit as ϕ approaches zero). Unlike the quadratic loss function, isoelastic marginal loss functions exhibit decreasing absolute risk aversion (Pratt 1964). Isoelastic marginal loss functions also display the convenient property of constant *relative* risk aversion R(z), defined as $-zL''(z)/L'(z)$ (Pratt 1964). Specifically, $R(z) = 1 - \phi$ for the isoelastic marginal loss family. The logarithmic case, where $R(z) = 1$, thus represents a clear risk-averse alternative to the risk-neutral linear loss function, where $\phi = 1$ and $R(z) = 0$.

The fact that the logarithmic loss function tends toward negative infinity as the resource approaches extinction may be viewed as problematic by some. On the other hand, Smith (1985) views this behavior as a requisite characteristic for any loss function to be used in the context of renewable resources, arguing that it "introduces a useful conservation motive into the decision making process." Opaluch and Bockstael (1984) go even further, stating, "It is well known that the log function exhibits the best properties of the simple functional forms. . . ."

Beta probability density function The principal justification for using the beta pdf to describe P(q) is that the beta is a natural choice for the pdf of any continuous variable which is constrained to fall within the 0 to 1 range. The fact that it allows for an explicit solution to Equation (7) is another argument in its favor.

Unfortunately, the method presented here for estimating the parameters of P(q) is based on a model (Press 1989) which yields a truncated t distribution, not a beta distribution. If this model is accepted as a true description of reality, then the beta form for P(q) is only an approximation. Of course, most functional forms used in modeling are only approximations, so the question is whether the advantages of increased tractability provided by the beta distribution outweigh any attendant losses of accuracy. Holloway (1979) argues in the affirmative after noting the difficulty of identifying natural processes which yield the beta distribution as a formal result.

In general, the effectiveness of Bayes decisions is relatively insensitive to small changes in the assumed pdf (DeGroot 1970). This being the case, the question really is whether the difference between the truncated t distribution and the beta approximation is typically small. To assess the magnitude of this difference, the goodness-of-fit between the truncated t and beta distributions was examined for a wide range of n, $\hat{q}$, and s_q^2 values (Fig. 8). Note that $R^2 > 0.95$ for a wide range of parameter values, indicating that the loss of

accuracy resulting from the beta approximation is often small.

Another fact to keep in mind is that the model presented by Press (1989) is only one possibility. Despite the pessimism conveyed by Holloway (1979), it is conceivable that other models could yield the beta distribution as an exact result.

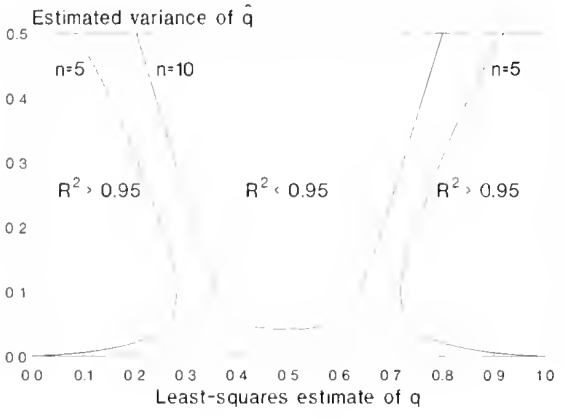

Figure 8

Loci of parameter values under which a beta approximation to the truncated t distribution gives an R^2 value of 0.95. R^2 was calculated by comparing the two distributions at q values of 0.01, 0.02, . . ., 0.99. For $n = 5$, parameter combinations lying to the interior of the two curves correspond to R^2 values <0.95. For $n = 10$, R^2 values <0.95 correspond to parameter combinations lying above the curve.

Comparison with previous studies

Of the many previous applications of Bayesian decision theory to fisheries, the studies by Ludwig and Walters (1982), Clark et al. (1985), and Walters and Ludwig (1987) are most closely related to the present work. The various features of the four approaches are outlined in Table 1. The three previous studies exhibit certain common features which distinguish them from the present study, namely: (1) use of a discrete time scale; (2) inclusion of an explicit adaptive management strategy; (3) inclusion of environmental stochasticity as well as parameter uncertainty; (4) inclusion of a positive discount rate in the objective function; (5) assumption of a normal form for the pdf of the uncertain parameter; and (6) inability to derive an exact analytic solution, even in the myopic case (except for one special instance considered by Clark et al.). The present study is also the only one of the group which includes both a biomass-based model and a risk-averse loss function.

Ludwig and Walters (1982) found that the deterministic optimum escapement level can be less than half the value of the Bayesian solution. Although the continuous form of the model used in the present study makes it difficult to talk about escapement per se, equilibrium stock size might serve as a suitable proxy

Table 1

Comparison of four studies describing Bayesian approaches to fishery management.

Feature	Ludwig and Walters (1982)	Clark et al. (1985)	Walters and Ludwig (1987)	This study
Time scale	discrete	discrete	discrete	continuous
Yield metric	numbers	biomass	numbers	biomass
Adaptive strategy included	yes	yes	yes	no
Age structure included	no (discrete generations)	yes	no (discrete generations)	yes
Discounting included	yes	yes	yes	no
Harvesting costs included	no	yes	no	no
Stochasticity included	yes	yes	yes	no
Loss function	linear	linear	logarithmic	logarithmic
Growth function	none	isometric von Bertalanffy	none	linear
Stock-recruitment function	Ricker (1954)	a) Cushing b) stock-independent c) linear-threshold	Cushing	Cushing
Uncertain parameter	Ricker exponent	a) ln(Cushing multiplier) b) mean ln(recruitment) c) mean ln(recruitment)[1]	Cushing exponent (q)	q
Pdf	normal	normal	normal	beta
Analytic solution obtained	no	case (b) (myopic only)	approximate[2] (myopic only)	yes

[1] Only recruitment data from stock sizes above the threshold were used to calculate the mean.
[2] Approximate solution valid only for pdfs with variance <0.01.

for comparison with the results of Ludwig and Walters. As Equations (26–28) indicate, a variety of parameter combinations allow for $B(F_{MSY})$ to be less than half of $B(F_{MELSY})$. Since the results presented by Ludwig and Walters (1982) were derived from a numbers-based model, Equation (27) is particularly relevant. Under this equation, a v′ value greater than 1/3 is sufficient to guarantee that the stock size at MSY will be less than half the stock size at MELSY, regardless of the value of m. At values of m>0.5, a v′ value of 0.227 is sufficient.

Clark et al. (1985) found that the relationship between the myopic Bayes and certainty-equivalent solutions depended on the model used. In the special case where recruitment is independent of stock size, for example, they found that the myopic Bayes solution always exceeded the certainty equivalent solution. For the same model, the authors also found that the myopic Bayes solution always increased with the level of uncertainty. These results are precisely the opposite of those obtained in the present study, where F_{MELSY} is always less than F_{MSY} and decreases monotonically with v′. In their "full cohort model" with a stock-recruitment relationship, however, Clark et al. (1985) obtained results similar to those of the present study. In one example, the myopic Bayes solution prescribed a 30–50% reduction in F relative to the certainty-equivalent solution. Using yet another model, Walters and Ludwig (1987) also found that the myopic Bayes solution was a monotone-decreasing function of uncertainty.

Conclusion

This paper describes an approach for treating the problem of parameter uncertainty in a systematic fashion. Although fisheries are often managed as though stock parameters are known with certainty, it would be preferable to develop a management approach more consistent with the fact that such certainty is the exception rather than the rule. Such an approach was developed here in the context of Bayesian decision theory. When applied to the particular model presented, this approach indicates that the optimal fishing mortality rate F_{MELSY} (Eq. 20) is always less than F_{MSY} (Eq. 2) except in the limiting case where q is known with certainty (Fig. 4).

This result provides formal support for the intuitive conclusion (e.g., Kimura 1988) that fishing mortality should be strongly constrained when the stock-recruitment relationship is uncertain. Similarly, Equation (25) indicates that if recruitment is highly dependent on stock size (specifically, if m exceeds 0.5), F_{MELSY} will always be less than the natural mortality rate.

The rock sole example illustrates the basic conservatism of the F_{MELSY} approach. In this example, F_{MELSY} was less than F_{MSY} by about 40%. Given that neither the F_{MSY} value (0.121) nor the fit from the stock-recruitment regression (Fig. 6) was atypical of groundfish stocks, the ratio between F_{MELSY} and F_{MSY} in this example provides a practical illustration of the extent to which an explicit accounting for uncertainty can influence management strategy. The magnitude of the effort reduction prescribed in this example is similar to results described by Ludwig and Walters (1982) and Clark et al. (1985). The confirmatory nature of these studies may suggest that the conventional wisdom regarding optimal exploitation rates should be reexamined. At the very least, the F_{MELSY} approach provides a low-end estimate of the maximum acceptable harvest rate and a warning against taking F_{MSY} estimates too seriously.

A great deal of the conservatism resulting from the F_{MELSY} approach as developed here stems from the assumption that all values of q are logically possible, despite the fact that a q value of 1 results in extinction under any level of fishing. One alternative might be to examine q in the context of life-history theory, to determine if it is possible to justify some other upper limit on the logically permissible range. A related alternative would be to use a nonuniform prior in estimating P(q). The assumption of a uniform prior may be overly pessimistic, since fishery biologists often have an intuitive feel for stock-recruitment parameters, even in the absence of data for a particular stock. Such information could be used to define an alternate prior pdf. Another possibility would be to establish an empirical prior based on the results of other stock-recruitment studies, but this would likely require a fairly elaborate weighting scheme so that stock-recruitment parameters from the most dissimilar stocks or environments would have the least influence on the form of the resulting pdf.

An additional factor which may add to the conservatism of the F_{MELSY} strategy as developed here is the use of the myopic Bayes solution rather than an actively adaptive solution. An actively adaptive solution would attempt to anticipate and make use of changes in available information resulting from alternative management actions (e.g., Walters and Hilborn 1976, Smith and Walters 1981, Ludwig and Walters 1982, Ludwig and Hilborn 1983, Clark et al. 1985, Walters 1986, Milliman et al. 1987, Walters and Ludwig 1987, Parma 1990, Parma and Deriso 1990). However, myopic Bayes (or similar) solutions often perform nearly as well as their actively adaptive counterparts (Mendelssohn 1980, Walters and Ludwig 1987, Parma 1990, Parma and Deriso 1990), and if the myopic Bayes solution is reestimated each year, the result is a

passively adaptive strategy which is asymptotically optimal over time (Walters 1987). Most important for the purposes of the present study, though, is the fact that the myopic Bayes solution is computationally much simpler than the actively adaptive solution.

In conclusion, it should be stressed that while the approach suggested here was developed in the context of a particular model and particular loss and probability density functions, this development was meant primarily to illustrate the approach, not to limit it. More sophisticated applications—utilizing alternative assumptions, functional forms, and solution techniques—are certainly to be encouraged. In particular, future research might incorporate recruitment stochasticity, positive discount and cost rates, additional objective function components (e.g., yield variability), and uncertainty in other parameters and variables (e.g., the natural mortality rate, growth rate, and stock size).

Acknowledgments

I would like to thank James Balsiger, Nicholas Bax, Russell Kappenman, Daniel Kimura, Richard Methot, and Thomas Wilderbuer of the Alaska Fisheries Science Center for reviewing all or portions of this paper in various stages of development. Three anonymous reviewers also provided helpful suggestions. In addition, I would like to thank Robert Burr and Loveday Conquest of the University of Washington's Center for Quantitative Science for their assistance.

Citations

Bernoulli, D.
1954 Exposition of a new theory on the measurement of risk. Econometrica 22:23-36.

Box, G.E.P., and G.C. Tiao
1973 Bayesian inference in statistical analysis. Addison-Wesley, Reading, MA, 588 p.

Charles, A.T.
1988 In-season fishery management: A Bayesian model. Nat. Resour. Model. 2:599-629.

Clark, C.W.
1985 Bioeconomic modelling and fisheries management. John Wiley, NY, 291 p.

Clark, C.W., A.T. Charles, J.R. Beddington, and M. Mangel
1985 Optimal capacity decisions in a developing fishery. Mar. Resour. Econ. 2:25-53.

Cushing, D.H.
1971 The dependence of recruitment on parent stock in different groups of fishes. J. Cons. Cons. Int. Explor. Mer 33: 340-362.

DeGroot, M.H.
1970 Optimal statistical decisions. McGraw-Hill, NY, 489 p.

Deriso, R.B.
1985 Risk adverse harvesting strategies. Lect. Notes Biomath. 61:65-73.

Getz, W.M., and R.G. Haight
1989 Population harvesting: Demographic models of fish, forest, and animal resources. Princeton Univ. Press, Princeton, 391 p.

Gleit, A.
1978 Optimal harvesting in continuous time with stochastic growth. Math. Biosci. 41:111-123.

Hightower, J.E.
1990 Multispecies harvesting policies for Washington-Oregon-California rockfish trawl fisheries. Fish. Bull., U.S. 88:645-656.

Hightower, J.E., and G.D. Grossman
1987 Optimal policies for rehabilitation of overexploited fish stocks using a deterministic model. Can. J. Fish. Aquat. Sci. 44:803-810.

Hightower, J.E., and W.H. Lenarz
1989 Optimal harvesting policies for the widow rockfish fishery. *In* Edwards, E.F., and B.A. Megrey (eds.), Catch-at-age, bioenergetics, system, and sampling models for microcomputer analyses for fishery dynamics, p. 83-91. Am. Fish. Soc. Symp. 6, Bethesda.

Holloway, C.A.
1979 Decision making under uncertainty: Models and choices. Prentice-Hall, Englewood Cliffs, NJ, 522 p.

Hulme, H.R., R.J.H. Beverton, and S.J. Holt
1947 Population studies in fisheries biology. Nature (Lond.) 159:714-715.

Kimura, D.K.
1988 Stock-recruitment curves as used in the stock-reduction analysis model. J. Cons. Cons. Int. Explor. Mer 44:253-258.

Larkin, P.A.
1973 Some observations on models of stock and recruitment relationships for fishes. Rapp. P.-V. Reun. Cons. Int. Explor. Mer 164:316-324.

Larkin, P.A., and W.E. Ricker
1964 Further information on sustained yields from fluctuating environments. J. Fish. Res. Board Can. 21:1-7.

Lewis, T.R.
1981 Exploitation of a renewable resource under uncertainty. Can. J. Econ. 14:422-439.
1982 Stochastic modeling of ocean fisheries resource management. Univ. Wash. Press, Seattle, 109 p.

Lord, G.E.
1973 Characterization of the optimum data acquisition and management of a salmon fishery as a stochastic dynamic program. Fish. Bull., U.S. 71:1029-1037.
1976 Decision theory applied to the simulated data acquisition and management of a salmon fishery. Fish. Bull., U.S. 74: 837-846.

Ludwig, D., and R. Hilborn
1983 Adaptive probing strategies for age-structured fish stocks. Can. J. Fish. Aquat. Sci. 40:559-569.

Ludwig, D., and C.J. Walters
1981 Measurement errors and uncertainty in parameter estimates for stock and recruitment. Can. J. Fish. Aquat. Sci. 38:711-720.
1982 Optimal harvesting with imprecise parameter estimates. Ecol. Model. 14:273-292.

Mangel, M., and C.W. Clark
1983 Uncertainty, search, and information in fisheries. J. Cons. Cons. Int. Explor. Mer 41:93-103.

Mangel, M., and R.E. Plant
1985 Regulatory mechanisms and information processing in uncertain fisheries. Mar. Resour. Econ. 1:389-418.

Mendelssohn, R.
1980 Using Markov decision models and related techniques for purposes other than simple optimization: Analyzing the consequences of policy alternatives on the management of salmon runs. Fish. Bull., U.S. 78:35–50.
1982 Discount factors and risk aversion in managing random fish populations. Can. J. Fish. Aquat. Sci. 39:1252–1257.

Milliman, S.R., A.P. Grima, and C.J. Walters
1987 Policy making within an adaptive management framework, with an application to lake trout (*Salvelinus namaycush*) management. Can. J. Fish. Aquat. Sci. 44(Suppl. 2):425–430.

Opaluch, J.J., and N.E. Bockstael
1984 Behavioral modeling and fisheries management. Mar. Resour. Econ. 1:105–115.

Parma, A.M.
1990 Optimal harvesting of fish populations with non-stationary stock-recruitment relationships. Nat. Resour. Model. 4:39–76.

Parma, A.M., and R.B. Deriso
1990 Experimental harvesting of cyclic stocks in the face of alternative recruitment hypotheses. Can. J. Fish. Aquat. Sci. 47:595–610.

Paulik, G.J.
1973 Studies of the possible form of the stock-recruitment curve. Rapp. P.-V. Reun. Cons. Int. Explor. Mer 164:316–324.

Pratt, J.W.
1964 Risk aversion in the small and in the large. Econometrica 32:122–136.

Press, S.J.
1989 Bayesian statistics: Principles, models, and applications. John Wiley, NY, 237 p.

Raiffa, H.
1968 Decision analysis: Introductory lectures on choices under uncertainty. Addison-Wesley, Reading, MA, 309 p.

Ricker, W.E.
1954 Stock and recruitment. J. Fish. Res. Board Can. 11: 559–623.
1958 Maximum sustained yields from fluctuating environments and mixed stocks. J. Fish. Res. Board Can. 15:991–1006.
1975 Computation and interpretation of biological statistics for fish populations. Fish. Res. Board Can. Bull. 191, 382 p.

Rothschild, B.J.
1972 An exposition on the definition of fishing effort. Fish. Bull., U.S. 70:671–679.

Rothschild, B.J., and A.J. Mullen
1985 The information content of stock-and-recruitment data and its non-parametric classification. J. Cons. Cons. Int. Explor. Mer 42:116–124.

Ruppert, D., R.L. Reish, R.B. Deriso, and R.J. Carroll
1984 Optimization using stochastic approximation and Monte Carlo simulation (with application to harvesting of Atlantic menhaden). Biometrics 40:535–545.
1985 A stochastic population model for managing the Atlantic menhaden (*Brevoortia tyrannus*) fishery and assessing managerial risks. Can. J. Fish. Aquat. Sci. 42:1371–1379.

Samuelson, P.A.
1967 General proof that diversification pays. J. Financial & Quant. Analysis 2:1–13.

Schnute, J.
1981 A versatile growth model with statistically stable parameters. Can. J. Fish. Aquat. Sci. 38:1128–1140.

Shepherd, J.G.
1982 A versatile new stock-recruitment relationship for fisheries, and the construction of sustainable yield curves. J. Cons. Cons. Int. Explor. Mer 40:67–75.

Shepherd, J.G., and D.H. Cushing
1990 Regulation in fish populations: Myth or mirage? Philos. Trans. R. Soc. Lond. B 330:151–164.

Smith, A.D.M., and C.J. Walters
1981 Adaptive management of stock-recruitment systems. Can. J. Fish. Aquat. Sci. 38:690–703.

Smith, J.B.
1985 A discrete model of replenishable resource management under uncertainty. Mar. Resour. Econ. 1:283–308.

Tautz, A., P.A. Larkin, and W.E. Ricker
1969 Some effects of simulated long-term environmental fluctuations on maximum sustained yield. J. Fish. Res. Board Can. 26:2715–2726.

Thompson, G.G.
1992 Management advice from a simple dynamic pool model incorporating constant marginal cost and discount rates. Fish. Bull., U.S. 90:552–560.

Walters, C.J.
1975 Optimal harvest strategies for salmon in relation to environmental variability and uncertainty in production parameters. J. Fish. Res. Board Can. 32:1777–1784.
1986 Adaptive management of renewable resources. MacMillan, NY, 374 p.
1987 Approaches to adaptive policy design for harvest management. Lect. Notes Biomath. 72:114–122.

Walters, C.J., and R. Hilborn
1976 Adaptive control of fishing systems. J. Fish. Res. Board Can. 33:145–159.

Walters, C.J., and D. Ludwig
1981 Effects of measurement errors on the assessment of stock-recruitment relationships. Can. J. Fish. Aquat. Sci. 38:704–710.
1987 Adaptive management of harvest rates in the presence of a risk averse utility function. Nat. Resour. Model. 1:321–337.

Walters, G.E., T.K. Wilderbuer
1988 Rock sole. *In* Condition of groundfish resources of the eastern Bering Sea and Aleutian Islands region in 1988, p. 106–117. Unpubl. manuscr. submitted to Int. N. Pac. Fish. Comm., Sept. 1988. NMFS Alaska Fish. Sci. Cent., Seattle, 219 p.

Eastern Pacific species of the genus *Umbrina* (Pisces: Sciaenidae) with a description of a new species

H.J. Walker Jr.
Scripps Institution of Oceanography
University of California at San Diego, La Jolla, California 92093-0208

Keith W. Radford
Department of Biology, Mesa College
7250 Mesa College Drive, San Diego, California 92111

Abstract.—The only cosmopolitan sciaenid genus, *Umbrina*, is represented in the eastern Pacific Ocean by eight species: *U. analis*, *U. bussingi*, *U. dorsalis*, *U. galapagorum*, *U. reedi*, *U. roncador*, *U. wintersteeni* n. sp., and *U. xanti*. *Umbrina analis* is removed from the synonymy of *U. xanti*. Lectotypes are designated for *U. dorsalis*, *U. galapagorum* and *U. xanti*. *Umbrina wintersteeni*, which usually occurs in shallow, protected waters of the southern Gulf of California and the west coast of southern Baja California Sur, apparently is morphologically intermediate between two major groups of eastern Pacific species. Distinguishing characters of *U. wintersteeni* include peritoneum and inside gill cover with little or no pigment; barbel relatively short and stout; anal fin with six soft rays; anal fin darkly pigmented to dusky; pelvic fins usually dusky; second anal spine of moderate length.

Manuscript accepted 6 August 1992.
Fishery Bulletin, U.S. 90:574-587 (1992).

Of the more than 70 genera in the percoid family Sciaenidae, only *Umbrina* has a worldwide distribution (Chao 1986a). The approximately 15 species that constitute *Umbrina* occur in tropical to temperate waters over the continental shelf to the upper slope. In the New World, *Umbrina* comprises four species in the Atlantic (Gilbert 1966, Miller 1971) and eight in the Pacific (this study). Most eastern Pacific species are collected with beach seines over sand or sand-mud bottoms, along open coasts or in bays, and probably support artisanal or sportfisheries wherever they are found. In southern California the yellowfin croaker *U. roncador* and spotfin croaker *Roncador stearnsii*) together make up about 10 percent of the surf fisherman's catch (Frey 1971).

No review of the eastern Pacific species of *Umbrina* has been published, although McPhail (1958) wrote extensive keys to all known eastern Pacific sciaenids, and Lopez S. (1980) described a new species of *Umbrina* from this area. The purposes of this paper are to review the eastern Pacific species of *Umbrina*, provide a key and characters useful in their identification, and describe a new species.

Materials and methods

Counts and measurements generally follow those of Hubbs and Lagler (1958). Gill raker counts include rudiments. Unless otherwise stated, standard length (SL) is used throughout. Vertebral and procurrent caudal ray counts were made from radiographs. A short, stout barbel is defined as one whose length roughly equals its width at midlength (seen in side view); an elongate barbel is at least twice as long as wide. Mean percentages of certain morphometrics used in species diagnoses were calculated usually from 30 specimens, occasionally ~20 (when available), selected from the entire size range of the species. Standard errors associated with these means were calculated strictly to show relative variation for a particular proportion and were always 0.6% (once) or less. All pigmentation notes were made from alcohol-preserved specimens. Institutional abbreviations follow Leviton et al. (1985). There have been many instances where eastern Pacific species have been ascribed to *Umbrina* (e.g., *U. panamensis* = *Menticirrhus panamensis*; *U. imberbis* = *Sciaena*, probably *callaensis*), and these are beyond the scope of this paper. Type material

of all synonyms listed in the species accounts was examined by the authors and/or C.L. Hubbs (deceased).

Systematics

Genus *Umbrina* Cuvier

Synonymy

Umbrina Cuvier 1816:297 (type species *Sciaena cirrosa* Linnaeus, by monotypy, see Opinion 988, Bull. Zool. Nom. (1972):123).

Attilus Gistel 1848:109 (type species *Sciaena cirrosa* Linnaeus, by monotypy).

Asperina Ostroumoff 1896:30 (type species *A. improviso* (=*U. cirrosa*) Ostroumoff, by monotypy).

Diagnosis Deep-bodied to moderately elongate, compressed sciaenid fishes with a single mental barbel, usually with an apical pore; swim bladder single-chambered, usually carrot-shaped, with no diverticula, located entirely abdominally; preopercular margin with bony serrations; two anal spines, the second long and thick.

Description As in Gilbert (1966), Trewavas (1977), and Chao (1978, 1986a,b), with some additions: back slightly arched; ventral profile nearly straight; head oblong; snout thick and protuberant with 5–7 rostral and 5 marginal pores; chin with two pairs of lateral pores surrounding the short barbel; mouth small, inferior, horizontal or nearly so; teeth small, villiform, set in bands in both jaws, outer row of teeth in upper jaw may be slightly enlarged; sagitta (largest otolith) thick, oval, with smooth inner surface and crested or nodular outer surface; cauda of sulcus bent sharply and not reaching ventral edge of sagitta, ostium reaching anterior edge; gill rakers short; caudal fin truncate to slightly emarginate or pointed; scales ctenoid; vertebrae 10–11 + 14–16 = 25–26; dorsal fin rays IX–X + I,21–33; anal rays II,5–10; pectoral rays 14–20; overall background coloration white to silver or yellow to brown; usually with dark-brown stripes: oblique dorsolaterally, more longitudinal midlaterally and on peduncle area, becoming faint or absent ventrally, usually faint or absent on head.

Relationships The genera *Sciaena* and *Umbrina* are the only representatives of the tribe Sciaenini (Chao 1986a). Characters of the swim bladder are the most important factors in assessing the phylogenetic relationships among suprageneric groups of sciaenids and the single-chambered swim bladder, lacking appendages, characteristic of the sciaenines, is the most primitive (plesiomorphic) form (Chao 1986a). The genus *Sciaena* (species have no barbels) is a polyphyletic assemblage containing numerous species and is in need of revision (Chao and Miller 1975, Chao 1986a). Although apparently monophyletic, we presently can only define *Umbrina* with synplesiomorphies or homoplastic apomorphies (e.g., pored mental barbel) (L.N. Chao, Bio-Amazonica Conserv. Int., Brazil, pers. commun., Sept. 1991).

Key to the eastern Pacific species of *Umbrina*

1A Inside gill cover dark to black, particularly in area of pseudobranch 2
1B Inside gill cover pale or lightly punctate 4

2A Dorsal fin with 21–23 soft rays; no stripes on body ..... ***U. bussingi***
2B Dorsal fin usually with 26–30 soft rays; dark to dusky horizontal or oblique stripes on body 3

3A Anal fin normally with 7 soft rays; peritoneum dark ..... ***U. roncador***
3B Anal fin normally with 6 soft rays; peritoneum light ventrally (may be dark dorsally) ..... ***U. xanti***

4A Anal fin with 9(8) soft rays; dorsal fin with IX + I spines ..... ***U. reedi***
4B Anal fin with 6–7(8) soft rays; dorsal fin with X + I spines 5

5A Dorsal fin usually with 30–33 soft rays; snout length less than eye diameter ..... ***U. dorsalis***
5B Dorsal fin usually with 24–29 soft rays; snout length greater than eye diameter (adults) 6

6A Body stripes distinct; pectoral fin rays 17 or fewer; dorsal fin soft rays 27 or fewer 7
6B Body stripes indistinct or lacking; pectoral fin rays usually 18 or more; dorsal fin rays 27 or more ..... ***U. galapagorum***

7A Second anal spine ~1.5 in head; pelvic fins with little or no pigment ..... ***U. analis***
7B Second anal spine ~2.0 in head; pelvic fins usually dusky to dark ..... ***U. wintersteeni***

Umbrina bussingi Lopez S.

Figure 1

Synonymy

Umbrina bussingi Lopez S. 1980:203–208 (original description: holotype LACM 38715-1; Costa Rica).

Diagnosis A small species of *Umbrina* (max. length 252 mm) characterized by the following combination of characters: inside gill cover dark to black; no dark-brown stripes; caudal fin pointed; barbel compressed,

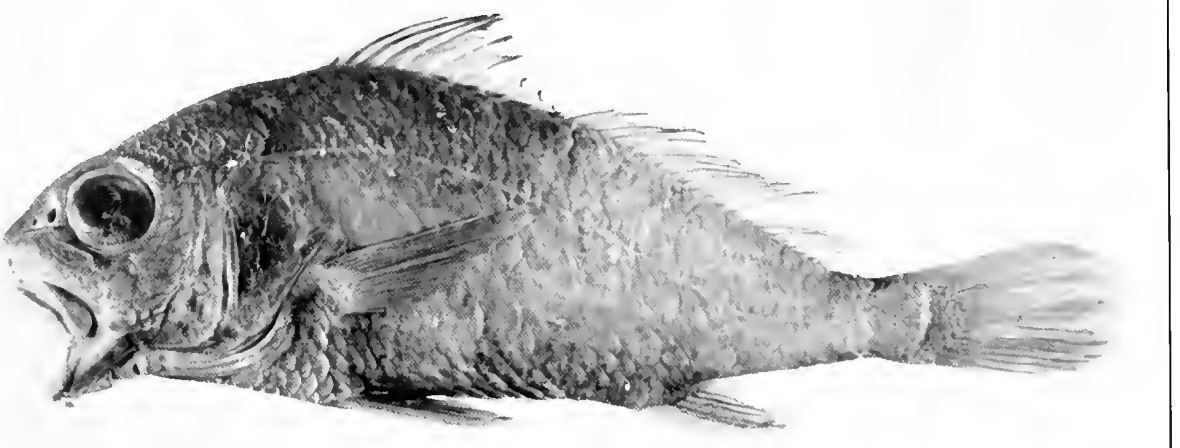

Figure 1
Umbrina bussingi, 230 mm SL, LACM 9099-28.

with anterior, slit-like (vertical) pore (large adults); peritoneum dark to dusky ventrally and laterally, lighter dorsally; soft dorsal fin rays 21–23; soft anal rays 7; pectoral rays usually 18–19; procurrent caudal rays 7–8 + 7–8(9); dorsal spines X + I; gill rakers usually 19–20; vertebrae 10 + 15; length of second anal spine, $\bar{x}$ 17% SL; body depth, $\bar{x}$ 32% SL; eye length, $\bar{x}$ 9% SL; upper-jaw length, $\bar{x}$ 13% SL; pectoral fin length, $\bar{x}$ 26% SL.

Description Counts and measurements are given in Tables 1–6. Soft dorsal and anal fin rays as in Diagnosis. Pectoral rays 17–19; gill rakers 17–22; barbel not fully developed (usually bulbous) on specimens ≥154 mm; pigment inside operculum appears externally as large, dark spot; no dark-brown stripes at any size; background color uniformly light- (in young, to ~155 mm) to medium-brown; second anal spine relatively long and thick; body fairly deep; eye large, relatively smaller in larger specimens, but length always greater than snout length; head and upper jaw relatively long; pectoral fins extremely long, proportionately shorter at larger sizes; lateral line scales 47–49, $\bar{x}$ 47.95, SE 0.18; spinous dorsal fin dark to dusky, lighter in smaller specimens; soft dorsal, pelvic, and caudal fins light to dusky, becoming darker with increasing size, most pigment on pelvic and caudal fins appearing on distal two-thirds; pectoral fins essentially unpigmented; anterior, proximal portion of anal fin darkly pigmented at most sizes, dark pigment on most of fin at larger sizes.

Distribution Southern Gulf of California, south of Los Frailes to Golfo de Chiriqui, Panama (Fig. 2). A relatively deep-living species, taken in depths of 32 m to >183 m (Lopez S. 1980).

Umbrina roncador Jordan and Gilbert
Figure 3

Synonymy

Umbrina roncador Jordan and Gilbert 1882:277–278 (original description: holotype USNM 29371, Bahia Pequeña, Baja California Sur).

Sciaena thompsoni Hubbs 1921:1–3 + pl. (original description: holotype UMMZ 55053, Santa Catalina I., CA).

Diagnosis An intermediate-sized species of *Umbrina* (reported to ~381 mm) characterized by the following: inside gill cover dark to black, particularly in area of pseudobranch; peritoneum usually dark; soft dorsal fin rays usually 26–29; soft anal rays usually 7; pectoral rays usually 17–18; procurrent caudal rays usually 9–10 + 8–9; dorsal spines X + I; gill rakers usually 18–20; vertebrae 10 + 15; barbel relatively elongate, slender, more robust at sizes greater than ~200 mm; length of second anal spine, $\bar{x}$ 12% SL; body depth, $\bar{x}$ 29%; eye length, $\bar{x}$ 6%; upper jaw length, $\bar{x}$ 11%; pectoral fin length, $\bar{x}$ 17%.

Description Counts and measurements are given in Tables 1–6. Soft rays of second dorsal fin 24–31; soft anal rays 6–7; pectoral rays 15–20; gill rakers 15–22; snout length greater than eye diameter (adults); pigment inside operculum usually appears externally as large, dark spot, dark pigment around pseudobranch

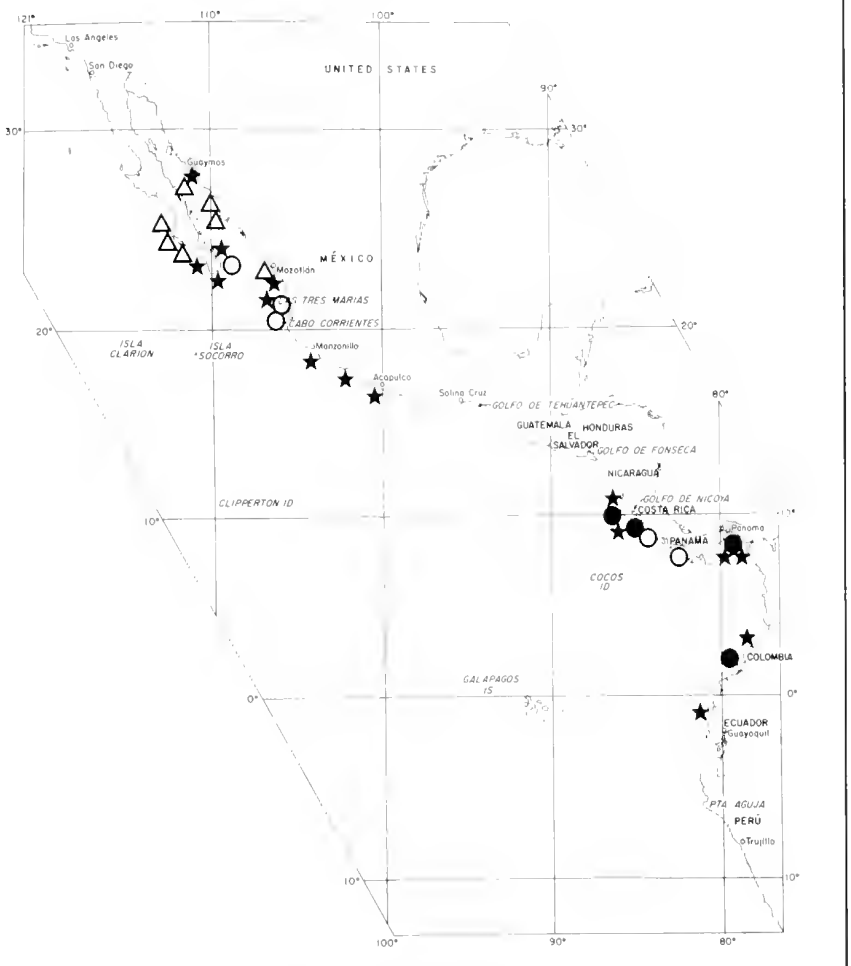

Figure 2
Geographic distribution of *Umbrina bussingi* (○), *U. dorsalis* (★), *U. analis* (●), and *U. wintersteeni* n. sp. (△).

usually present by 50–65 mm; barbel fully developed by ~70 mm, indistinguishable or flat at sizes <30 mm, bulbous between ~30 and 70 mm; lateral line scales 49–54, $\bar{x}$ 50.85, SE 0.04; virtually all brown stripes present by 70 mm; 5–8 dark, vertical bars occasionally on specimens 25–180 mm, usually faint when >80 mm; dorsal fin dusky at most sizes; pectoral, pelvic, anal, and caudal fins usually with little or no pigment, caudal occasionally dusky.

Distribution Point Conception to Bahia Magdalena and disjunctly in the northern Gulf of California, north of 27°N (Fig. 4). Taken in bays and the surf zone to ~45 m (Miller and Lea 1972).

Umbrina xanti Gill
Figure 5

Synonymy

Umbrina xanti Gill 1862:257–258 (original description: syntypes USNM 7156, USNM 2996, USNM 3693, USNM 3694, Cabo San Lucas, Baja California Sur; lectotype USNM 7156 (79

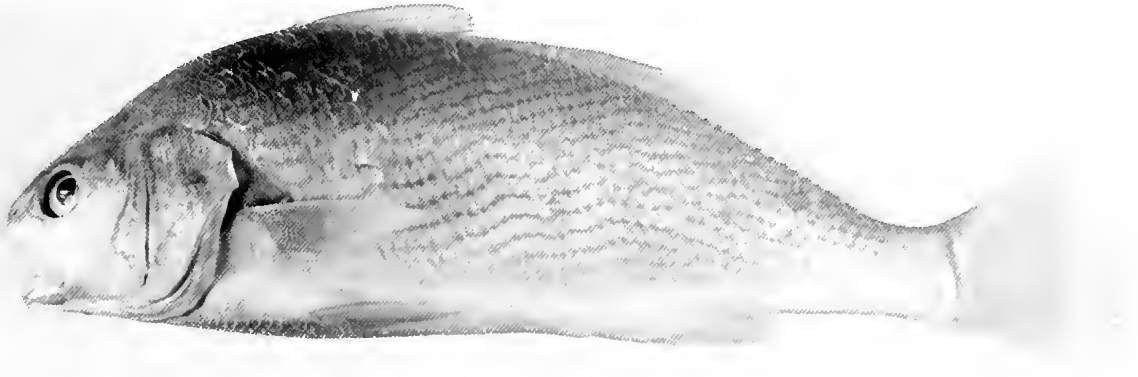

Figure 3
Umbrina roncador, 217 mm SL, SIO 64-65.

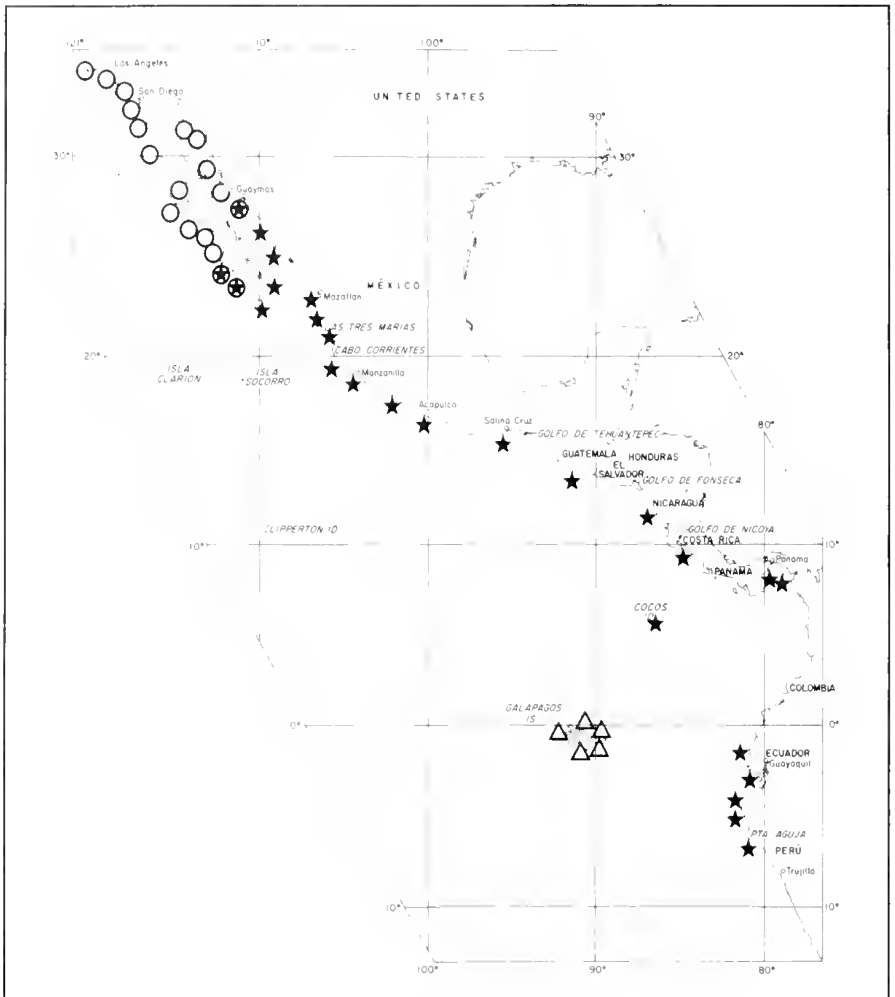

Figure 4
Geographic distribution of *Umbrina roncador* (○), *U. xanti* (★) plus one specimen from Chile at 19°36′S, 70°13′W), and *U. galapagorum* (△).

mm), herein designated; paralectotypes USNM 316653, [removed from USNM 7156] USNM 2996, USNM 3693, USNM 3694, MCZ 35976 [removed from USNM 3693]).

Umbrina sinaloae Scofield 1896:220–221 (original description: syntypes CASSU 1632, Mazatlan, Sinaloa, Mexico).

Diagnosis A small species of *Umbrina* (max. length 295 mm) characterized by the following: gill cover dark to black, particularly in area of pseudobranch; peritoneum usually light ventrally, punctate or occasionally dark dorsally; soft dorsal fin rays usually 27–29; soft anal rays usually 6; pectoral rays usually 17–18; procurrent caudal rays usually 8–9 + 8–9; dorsal spines X + I; gill rakers usually 17–19; vertebrae 10 + 15; barbel relatively elongate, slender; length of second anal spine, $\bar{x}$ 12% SL; body depth $\bar{x}$ 29%; eye length, $\bar{x}$ 7%; upper jaw length, $\bar{x}$ 10%; pectoral fin length, $\bar{x}$ 16%.

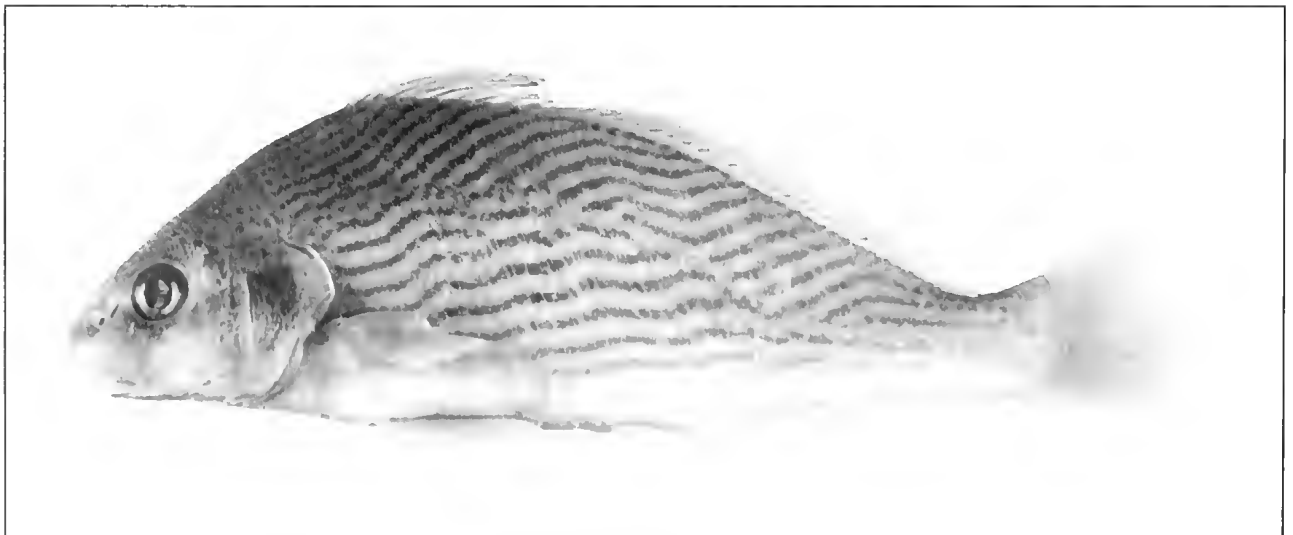

Figure 5
Umbrina xanti, 188 mm SL, SIO 63-522.

Description Counts and measurements are given in Tables 1–6. Soft rays of second dorsal fin 26–30; soft anal rays 6–7; pectoral rays 14–19; gill rakers 16–21; snout length greater than eye diameter (adults); pigment inside operculum generally appears externally as large, dark spot; dark pigment around pseudobranch evident by 35–40 mm; barbel fully developed by 45 mm, usually knobby between 30 and 45 mm; lateral line scales 48–52, $\bar{x}$ 50.02, SE 0.05; nearly all brown stripes present by 75–80 mm; dark, vertical bars 6–9, occasionally and only on specimens <100 mm; dorsal fin dusky; pectoral, pelvic, anal and caudal fins usually with little or no pigment, caudal occasionally dusky.

Distribution Bahia Magdalena and the southern Gulf of California (south of 27°N) to northern Peru (incl. Isla del Coco, Fig. 4), one specimen from Pisagua, Chile, 19°36′S, 70°13′W. Found in tide pools (juveniles) and along beaches, to 36 m.

Umbrina reedi Günther
Figure 6

Synonymy
Umbrina reedi Günther 1880:25 (original description: holotype BMNH 1919.5.14.283; I. Juan Fernandez, Chile).

Diagnosis A large species of *Umbrina* (max. length 650 mm) characterized by the following: inside gill cover pale to lightly punctate; peritoneum dark ventrally and laterally, lighter dorsally; large, dark spot in axil of pectoral fin; soft dorsal fin rays usually 24–25; soft anal rays usually 9; pectoral rays usually 18; procurrent caudal rays usually 9–10 + 8–9; dorsal spines IX + I; gill rakers usually 19–20; vertebrae 10 + 15; barbel relatively short, stout; length of second anal spine, $\bar{x}$ 14% SL; body depth, $\bar{x}$ 35%; eye length, $\bar{x}$ 7%; upper jaw length, $\bar{x}$ 13%; pectoral fin length, $\bar{x}$ 23%.

Description Counts and measurements are given in Tables 1–6. Soft rays of second dorsal fin 21–26; soft anal rays 8–10; pectoral rays 17–19; gill rakers 18–22; body and caudal peduncle deep; snout length greater than eye diameter at sizes greater than ~150 mm; pectoral fins relatively long; upper jaw long; barbel bulbous at 28 mm, not fully developed until ~120 mm; lateral line scales 49–52, $\bar{x}$ 49.90, SE 0.17; caudal peduncle and midlateral brown stripes evident by 120 mm; dorsolateral stripes undifferentiated on most specimens, appearing as irregular dashes of pigment; dorsal and caudal fins dusky; pectoral, pelvic and anal fins dark (pectorals frequently dusky), lighter on specimens less than ~130 mm.

Distribution Islands off Chile: Islas Juan Fernandez (~33°40′S, 78°55′W) and San Felix (~26°17′S, 80°06′W). From the surf zone to 30 m.

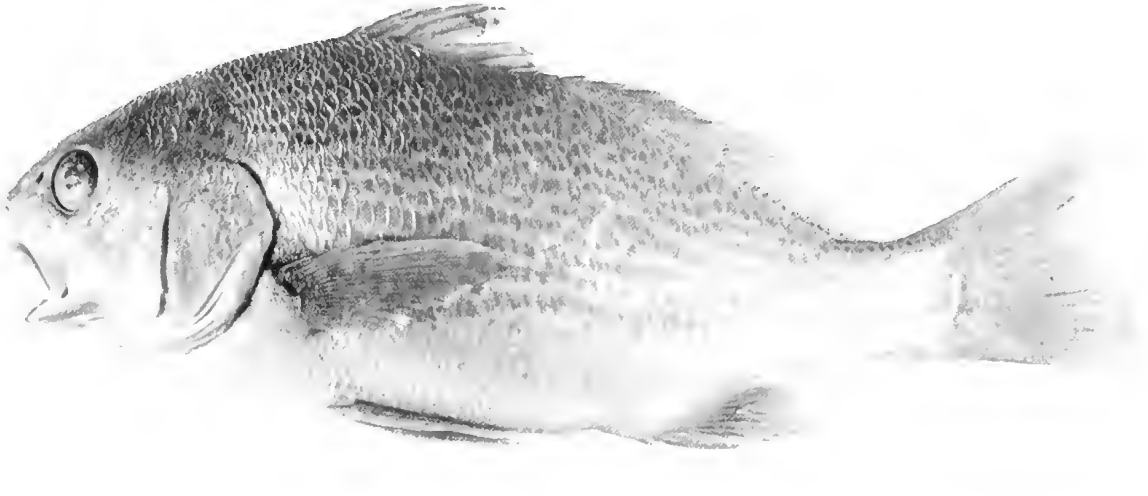

Figure 6
Umbrina reedi, 268 mm SL, SIO 65-657.

Figure 7
Umbrina dorsalis, 236mm SL, SIO 62-705.

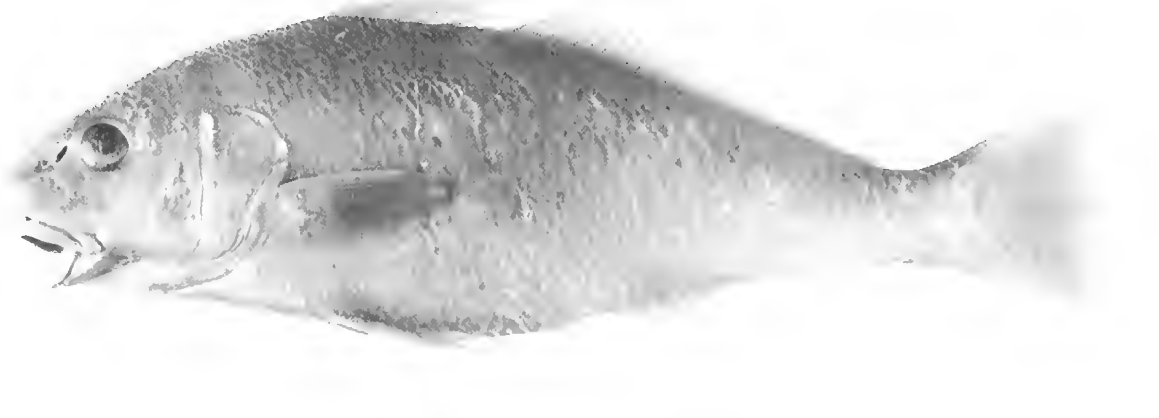

Figure 8
Umbrina galapagorum, 273mm SL, SIO 79-51.

Umbrina dorsalis Gill
Figure 7

Synonymy
Umbrina dorsalis Gill 1862:257 (original description: syntypes USNM 3696, Cabo San Lucas, Baja California Sur; lectotype USNM 3696 (77mm), herein designated; paralectotypes USNM 316654 [removed from USNM 3696]).

Diagnosis An intermediate-sized species of *Umbrina* (max. length 332mm) characterized by the following: inside gill cover and peritoneum pale to lightly punctate; soft dorsal fin rays usually 30–32; soft anal rays usually 7; pectoral rays usually 16–17; procurrent caudal rays usually 7–8 + 6–7; dorsal spines X + I; gill rakers usually 19–21; vertebrae 10 + 16; barbel relatively long and thick; length of second anal spine, $\bar{x}$ 15% SL; body depth, $\bar{x}$ 38%; eye length, $\bar{x}$ 8%; upper jaw length, $\bar{x}$ 13%; pectoral fin length, $\bar{x}$ 21%.

Description Counts and measurements are given in Tables 1–6. Soft rays of second dorsal fin 28–33; soft anal rays 7–8; pectoral rays 15–17; gill rakers 18–25; eye relatively large, proportionately smaller in larger specimens, generally greater than snout length; upper jaw long; body and caudal peduncle deep; barbel fully developed by 75mm, bulbous between 30 and 65mm; lateral line scales 49–54, $\bar{x}$ 51.73, SE 0.15; virtually all brown stripes present by 75mm, no stripes on speci-

mens <65 mm; 5–8 wide, dark bars (saddles) on specimens 30–65 mm; dorsal and pelvic (posterior) fins dusky to dark; pectoral and caudal fins light to dusky (posterior pectoral fin dark on specimens <45 mm); anal fin dark to dusky.

Distribution South of Bahia Magdalena and in the southern Gulf of California to Equador (Fig. 2). Found in tidepools (juveniles) to ~5 m.

Umbrina galapagorum Steindachner
Figure 8

Synonymy
Umbrina galapagorum Steindachner 1878:20–21 (original description: syntypes MCZ 8601, USNM 120437, James I., Galapagos Is.; lectotype MCZ 8601 (94 mm), herein designated; paralectotype USNM 120437).

Diagnosis An intermediate-sized species of *Umbrina* (max. length 413 mm) characterized by the following: inside gill cover lightly punctate or dusky, usually little or no pigment in area of pseudobranch; brown stripes indistinct or absent; peritoneum pale or lightly punctate; soft dorsal fin rays usually 27–29; soft anal rays usually 6–7; pectoral rays usually 17–19; procurrent caudal rays usually 9–10 + 8–9; dorsal spines X + I; gill rakers usually 18–19; vertebrae 10 + 15; barbel relatively elongate, thin; length of second anal spine, $\bar{x}$ 12% SL; body depth, $\bar{x}$ 29%; eye length, $\bar{x}$ 6%; upper jaw length, $\bar{x}$ 10%; pectoral fin length, $\bar{x}$ 18%.

Description Counts and measurements are given in Tables 1–6. Soft rays of second dorsal fin 26–30; soft anal rays 5–7; pectoral rays 16–20; gill rakers 16–21; snout length greater than eye length; pigment inside operculum occasionally appearing as muted, dark spot; barbel fully developed by 60 mm, bulbous between 30 and ~50 mm; lateral line scales 47–52, $\bar{x}$ 49.73, SE 0.08; faint brown stripes visible at 40–50 mm, occasionally evident to ~100 mm; ~9–10 dark, vertical bars frequently on specimens between ~30 and 95 mm; dorsal and caudal fins usually dusky, caudal occasionally lighter; pectoral, pelvic and anal fins unpigmented to lightly punctate.

Distribution Endemic to the Galapagos Is. (Fig. 4), found near beaches to 18 m.

Umbrina analis Günther
Figure 9

Synonymy
Umbrina analis Günther 1869(1866):426–427 (original description: holotype BMNH 1867.9.23.18, Panama).
Umbrina tumacoensis Wilson 1916:67 (original description: holotype, presumed lost (pers. commun.: M.E. Anderson, CAS, 2 March 1988; B. Chernoff, FMNH, 22 March 1988), paratypes CAS 62852, FMNH 56840).

Diagnosis A small species of *Umbrina* (max. length 231 mm) characterized by the following (based on nine specimens): peritoneum and inside gill cover pale to lightly punctate; soft dorsal fin rays 24–26; soft anal rays 6; pectoral rays usually 17; procurrent caudal rays 8–9 + 7–8; dorsal spines X + I; gill rakers usually 17–18;

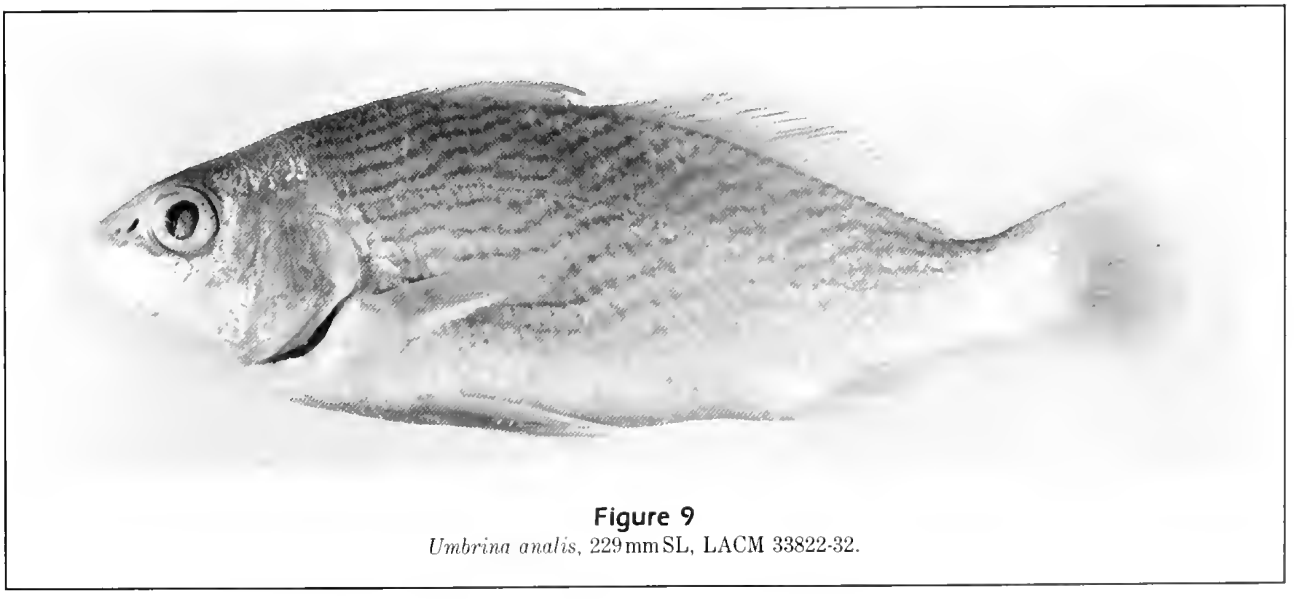

Figure 9
Umbrina analis, 229 mm SL, LACM 33822-32.

vertebrae 10 + 15; barbel relatively short, stout; length of second anal spine, $\bar{x}$ 19% SL; body depth, $\bar{x}$ 32%; eye length, $\bar{x}$ 8%; upper jaw length, $\bar{x}$ 11%; pectoral fin length, $\bar{x}$ 20%.

Description Counts and measurements are given in Tables 1–6. Soft dorsal and anal fin rays as in Diagnosis. Pectoral rays 16–18; gill rakers 16–21; barbel bulbous at 51 mm, more or less fully developed at 82 mm; no brown stripes on a 51 mm specimen, all stripes evident by 82 mm; second anal spine extremely long and thick; caudal peduncle deep; pectoral fins fairly long; lateral line scales 46–50, $\bar{x}$ 47.88, SE 0.44; dorsal and anal fins dusky or dark; caudal fin usually dusky; pectoral and pelvic fins with little or no pigment.

Distribution Known from five collections (one was split), ranging from Costa Rica to Colombia (Fig. 2). No depths recorded.

Umbrina wintersteeni n. sp.
Figure 10

Holotype SIO 60-366, 193 mm; Bahia Almejas, Baja California Sur, F.H. Berry and party, 25 August 1960.

Paratypes 146 specimens (49–298 mm) from 21 collections, all from Mexico: Baja California-west coast: SIO 60-366 (29); SIO 62–126 (10); SIO 64-84 (49); CAS 35536 (4); USNM 316655 (5); AMNH 5514a (1). Gulf of California: UCLA W50-27 (2); UCLA W52-48 (5); UCLA W52-49 (2); UCLA W52-50 (1); UCLA W53-84 (6); UCLA W53-95 (8); UCLA W57-34 (1); UCLA W57-36 (4); UCLA W57-42 (4); SIO 65–281 (3); SIO 76-275 (2); LACM 38104-26 (4); CAS-SU 375 (1); CAS-SU 2855 (3); CAS-SU 47933 (1); AMNH 5498 (1).

Diagnosis A relatively small species of *Umbrina* (max. size 298 mm) characterized by the following: inside gill cover pale to lightly punctate, little or no pigment in area of pseudobranch; peritoneum pale or lightly punctate; soft dorsal fin rays usually 25–27; soft anal rays usually 6; pectoral rays usually 16–18; procurrent caudal rays usually 7–8 + 6–7; dorsal spines X + I; gill rakers usually 17–20; vertebrae 10 + 15; barbel relatively short, stout; length of second anal spine, $\bar{x}$ 14% SL; body depth, $\bar{x}$ 29%; eye length, $\bar{x}$ 7%; upper jaw length, $\bar{x}$ 10%; pectoral fin length, $\bar{x}$ 17%.

Description Counts and measurements are given in Tables 1–6. Soft rays of second dorsal fin 23–28; soft anal rays 5–6; pectoral rays 15–18; gill rakers 14–23; snout length greater than eye length (adults); barbel bulbous at 49 mm, fully developed by ~100 mm; lateral line scales 48–51, $\bar{x}$ 49.14, SE 0.06; faint, brown stripes at 49 mm, nearly all present by 80–90 mm; ~8–11 dark, vertical bars on many juveniles, never on specimens >100 mm; dorsal, pelvic, and anal fins usually dusky to dark (Gulf of California specimens occasionally with light-to-dusky pelvic and anal fins); caudal fin dusky; pectoral fins lightly pigmented; background coloration tan to gold dorsally, grading to white or silver ventrally; dark-brown stripes: 15–20 oblique dorsolaterally, 8–10 more or less horizontal laterally in abdominal area, 4–5 horizontal on lateral caudal peduncle.

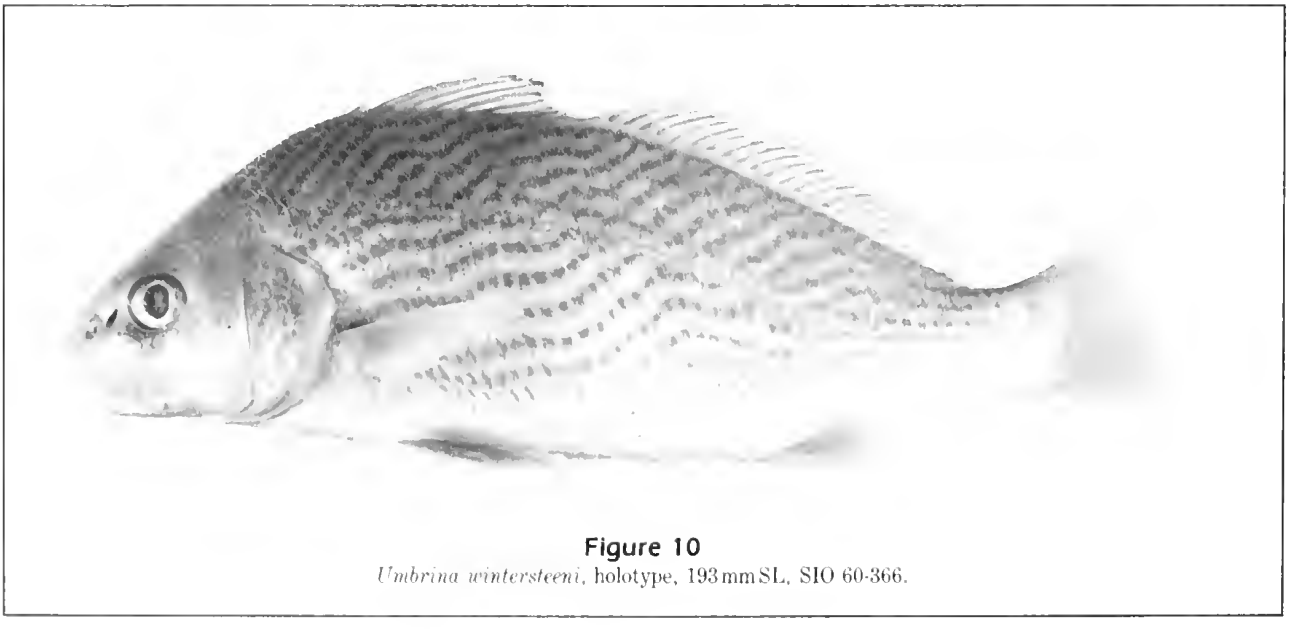

Figure 10
Umbrina wintersteeni, holotype, 193 mm SL, SIO 60-366.

Etymology Named for the late John Wintersteen, longtime researcher in the taxonomy of eastern Pacific sciaenids.

Distribution Just north of Bahia Magdalena (25°23′ N, 112°06′W), and the southern Gulf of California from ~27°N to Mazatlan (Fig. 1). Usually collected in bays; thus far, only recorded in depths to ~2m.

Relationships of New World *Umbrina* species

We did not attempt a phylogenetic analysis because we have not seen all *Umbrina* species. In addition, the status and limits of the only recognized sister genus, *Sciaena*, are uncertain. However, morphological similarity allows certain groups of the New World species to be distinguished. *Umbrina bussingi* and *U. milliae* (Atlantic) share several characters: compressed barbel, with anterior, slit-like opening; extremely long pectoral fins; very large eyes; caudal rays longest in middle of fin. They also lack stripes and differ slightly in relative body depth and length of second anal spine; we hypothesize that these are geminate species.

Umbrina analis, *U. broussonnettii* (Atlantic), *U. canosai* (Atlantic), *U. coroides* (Atlantic), *U. dorsalis*, and *U. reedi* share the following characters: relatively deep body; relatively long pectoral fins; dusky to dark anal fin. *Umbrina analis*, *U. canosai*, and *U. reedi* have fairly short, stout barbels and 6, 8, and 9 anal rays, respectively. *Umbrina analis* also has an extremely long, second anal spine. The other three species in this group have relatively slender, elongate barbels and 6 or 7 (*U. dorsalis*) anal rays. *Umbrina dorsalis* also has a relatively large eye and high number of dorsal rays; *U. broussonnettii* and *U. coroides* have low gill raker counts and differ slightly in certain scale and fin counts and pigmentation.

Umbrina galapagorum, *U. roncador*, *U. wintersteeni*, and *U. xanti* share the following characters: relatively elongate body; relatively short pectoral fins; little or no pigment on anal fin (exception: *U. wintersteeni*). Except for *U. wintersteeni*, these species have a somewhat elongate, slender barbel. The inside gill cover of *U. roncador* and *U. xanti* is dark to black and the anal ray counts are 7 and 6, respectively. *Umbrina galapagorum*, which usually lacks stripes (can be faint), and *U. wintersteeni*, which has a short, stout barbel, have 6 anal rays. Although we have no information for some species, juvenile characters (e.g., extreme differences in body depth, pectoral fin pigmentation, dorsolateral pigmentation; Fig. 11) corroborate the latter two major groups (six and four species), with *U. wintersteeni* possibly an intermediate form.

Distribution

As with the species of *Porichthys*, which also are associated with soft bottom (Walker and Rosenblatt 1988), the distributional limits of eastern Pacific species of *Umbrina* generally coincide with zoogeographic boundaries established for rocky shore fishes and other fauna (Springer 1958, Rosenblatt 1967, Briggs 1974, and others). In our area of concern, these boundaries are Point Conception, Bahia Magdalena area, La Paz for the western Gulf of California, and between Guaymas and Mazatlan for the eastern Gulf, Golfo de Tehuantepec area, and northern Peru. *Umbrina roncador* occurs in the northern Gulf of California (north of 27°N) and from Point Conception to the Bahia Magdalena area, which is also the northernmost Baja California (west coast) limit for *U. xanti*, *U. wintersteeni*, and *U. dorsalis*. Both *U. xanti* and *U. dorsalis* are wide-ranging, also occurring from the southern Gulf of California to northern Peru and Equador, respectively. *Umbrina wintersteeni* also is found in the southern Gulf as far south as Mazatlan. *Umbrina bussingi* and *U. analis* are each known from five collections. *Umbrina bussingi* occurs nearly throughout the eastern tropical Pacific (southern Gulf of California to Panama), while *U. analis* apparently is confined to the south (Costa Rica to southern Colombia).

Additional materials examined

Umbrina bussingi 140 specimens (56–257 mm) from 4 collections. **Mexico:** SIO 62-51 (130); SIO 70-160 (1); CAS 36615 (4). **Panama:** LACM 9099-28 (5).

Umbrina roncador 367 specimens (23–338 mm) from 88 collections. **California:** SIO H45-130 (17); SIO H45-162 (3); SIO H46-94 (6); SIO H47-160 (2); SIO H48-101 (1); SIO H51-235 (3); SIO H49-90 (5); SIO 86-63 (2); SIO 88-91 (17); CAS 18797 (8); CAS-SU 12666 (1); CAS-SU 19311 (2); CAS-SU 9913 (4); CAS 19515 (1); CAS 19672 (1); CAS 18532 (1); CAS 18527 (1); CAS 18347 (2); CAS 12934 (2); CAS 18272 (2); UCLA W57-208 (8); UMMZ 162170 (1); UMMZ 177364-5 (1); UMMZ 177457 (1); LACM W58-77 (2); LACM W50-126 (2); USNM 132385 (5); USNM 31316 (1); USNM 31317 (1); USNM 31270 (1); USNM 26872 (4); USNM 26758 (4); USNM 5299 (1); USNM 52978 (1); USNM 59496 (3); USNM 54332 (1); USNM 34781 (1); USNM 132394 (1); USNM 124991 (15); USNM 26849 (1). **Mexico, Baja-west coast:** SIO H46-215A (7); SIO H48-56 (1); SIO H48-55 (1); SIO H52-160 (8); SIO 62-729 (2); SIO H48-48 (12); SIO 62-113 (1); SIO H48-88 (1); SIO H52-137 (8); SIO H52-149 (8); SIO H52-135 (9); SIO 60-364 (5); SIO 60-364 (5); SIO 60-367 (1); SIO H48-91 (1); SIO 62-217 (3); UCLA W61-107 (2); UCLA W52-93 (3); UCLA W51-221 (1); UCLA W52-236 (3); LACM W52-248 (7); LACM W52-270 (3); LACM W51-234 (1); CAS-SU 58622 (8); CAS-SU 47932 (4); CAS W52-245 (8); CAS 11713 (2); CAS W52-183 (1); CAS W52-85 (2); CAS W52-93 (2); CAS W52-101 (2); USNM 54514 (1); USNM 132406 (1); USNM 46730 (2). **Mexico, Gulf of California:** UAZ 57 (1); UAZ 156 (71);

Figure 11
(upper) *Umbrina xanti*, 34 mm SL, SIO 61-232; (lower) *U. dorsalis*, 33 mm SL, SIO 61-232.

SIO 62-217 (3); SIO 63-532 (4); SIO 70-70 (1); CAS-SU 16585 (3); CAS-SU 6327 (1); CAS-SU 187 (1); UCLA W56-76 (3).

Umbrina xanti 397 specimens (20–296 mm) from 63 collections. **Mexico, Baja-west coast:** SIO 62-705 (10); SIO 62-706 (136); SIO 62-707 (2); SIO 62-708 (1). **Mexico, Gulf of California:** UCLA W51-22 (21); UCLA W51-24 (7); UCLA W51-56 (4); UCLA W51-57 (17); UCLA W56-118 (2); UCLA W59-248 (3); LACM W51-41 (1); LACM W51-49 (1); LACM W52-50; LACM W58-46 (1); CAS 2570 (1); CAS 2571 (1); CAS 4489 (1); CAS W51-53 (7); UBC BC 59-216 (1); UBC BC 59-236 (1); USNM 2996 (2); USNM 47443 (4); USNM 47463 (3); USNM 122659 (1); SIO 61-232 (4); SIO 65-349 (1). **Mexico, southern:** MCZ 485 (1); SIO 62-23 (31); SIO 62-28 (2); SIO 62-47 (1); LACM W58-12 (1); UBC BC 57-78 (2); UBC BC 57-85 (1); UBC BC 57-94 (1); UBC BC 57-98 (1);UBC BC 57-108 (1); UBC BC 57-129 (1); UBC BC 60-12 (1); UBC BC 60-13 (1). **Guatemala:** UCR 355-6 (2). **Nicaragua:** UCR 379-13 (1). **Costa Rica, incl. I. Cocos:** UCR 218-39 (1); UCR 259-3 (1); UCR 137-6 (3); LACM 35473-1 (40); SIO 77-89 (38). **Panama:** UCLA W53-283 (3); UCLA W53-285 (3); USNM 82233 (1). **Equador:** USNM 88744 (2). **Peru:** CAS-SU 29850 (2); CAS-SU 37491 (3); UCLA W60-34 (1); UBC BC 56-145 (1); UBC BC 56-149 (1); UBC BC 56-159 (1); UBC BC 56-162 (1); UBC BC 56-165 (1); UBC BC 56-234 (1); USNM 107150 (1); USNM 128009 (8); USNM 128010 (1). **Chile:** Univ. Antofagasta. uncat. (1).

Umbrina reedi 86 specimens (9–650 mm) from 9 collections. SIO 65-623 (1); SIO 65-625 (1); SIO 65-626 (2); SIO 65-655 (2); SIO 65-657 (34); UCLA W66-50 (2); UCLA W66-56 (29); USNM 176411 (7); USNM 88745 (8).

Umbrina dorsalis 93 specimens (28–327 mm) from 25 collections. **Mexico:** SIO 61-232 (12); SIO 61-236 (1); SIO 61-251 (7); SIO 62-23 (3); SIO 62-705 (1); UBC BC 57-100 (1); LACM W55-120 (1); LACM 9044-28 (34); LACM 9045-23 (2); LACM 9051-23 (2); UCLA W51-57 (1); UCLA W53-185 (1); UCLA W59-248 (1). **Costa Rica:** USNM 94000 (1); UCLA W54-168 (2); UCLA W54-172 (1). **Panama:** SIO 90-30 (1); UCLA W53-283 (1); UCLA W53-285 (1); UBC BC 60-117 (1); USNM 144680 (1); USNM 81213 (1); CAS-SU 8113 (2). **Colombia:** UMML Argosy 28, uncat. (1). **Equador:** UMML Argosy 44, uncat. (13).

Umbrina galapagorum 253 specimens (29–395 mm) from 27 collections. MCZ 8597, 8602 (38); MCZ 40448 (1); USNM 153626 (1); CAS 2311 (1); CAS 2313-2318 (6); CAS 2373 (1); CAS 2374-2379 (6); CAS 2384 (1); CAS 2385 (1); CAS 4486 (1); CAS 4657 (1); CAS 4952 (1); CAS 6326 (1); CAS 62979

(2); CAS-SU 24402 (2); CAS-SU 24413 (3); LACM W53-21 (5); LACM W53-28 (9); SIO 62-641 (151); SIO 79-51 (3); UBC BC 56-429 (2); UBC BC 56-437 (1); UCLA W50-219 (2); UCLA W53-144 (1); UCLA W55-314 (1); UCLA W56-325 (1).

Umbrina analis 8 specimens (51–229 mm) from 6 collections. **Colombia:** CAS 62852 (2); CAS 62853 (1); FMNH 56840 (2). **Panama:** USNM 81212 (1). **Costa Rica:** LACM 33822-32 (1); USNM 94612 (1).

Umbrina wintersteeni 9 specimens (56–276 mm) from 7 collections. **Mexico:** SIO 60-365 (3); UCLA W51-18 (1); CAS-SU 4827 (1); CAS W53-94 (1); USNM 29430 (1); USNM 46956 (1); USNM 47463 (1).

Acknowledgments

We are especially grateful to Carl L. Hubbs (deceased) for instigating this study and for providing data on many specimens. We wish to acknowledge the guidance, and data on holotypes, given by Labbish N. Chao. We thank the following individuals for loan material and/or correspondence relating to this study: M.E. Anderson, W. Baldwin, J.C. Briggs, W.A. Bussing, D. Buth, D. Catania, B. Chernoff, L.J. Dempster, A.W. Ebeling, W. Eschmeyer, R. Feeney, N. Feinberg, W.I. Follett, K. Fujita, K.E. Hartel, S. Jewett, L.W. Knapp, I. Kong U., R.J. Lavenberg, H.C. Loesch, J.D. McPhail, W.J. Rainboth, S. Raredon, C.R. Robins, L.P. Schultz, J.A. Siegel, P. Sonoda, M. Stehmann, C.C. Swift, D.A. Thomson, E. Trewavas, B. Walker, and W.J. Wilimovsky. We also appreciate the assistance of D. Gibson and C. Klepadlo at SIO. This paper is dedicated to S. Walker, T. Walker, J. Walker, and L. Walker for inspiration and support. Special thanks go to R.H. Rosenblatt and W. Watson for critically reviewing the manuscript.

Citations

Briggs, J.C.
1974 Marine zoogeography. McGraw Hill, NY, 475 p.

Chao, L.N.
1978 A basis for classifying western Atlantic Sciaenidae (Teleostei: Perciformes). NOAA Tech. Rep., Circ. 415, 64 p.
1986a A synopsis on zoogeography of the Sciaenidae. *In* Uyeno, T., et al. (eds.), Indo-Pacific fish biology: Proc., 2d Int. Conf. on Indo-Pacific fishes, p. 570–589. Ichthyol. Soc. Jpn., Tokyo.
1986b Sciaenidae. *In* Whitehead, P.J.P., et al. (eds.), Fishes of the northeastern Atlantic and the Mediterranean, vol. II, p. 865–874. UNESCO, Paris.

Chao, L.N., and R.V. Miller
1975 Two new species of sciaenid fishes (Tribe: Sciaenini) from the Caribbean Sea and adjacent waters. Bull. Mar. Sci. 25(2): 259–271.

Cuvier, G.
1816 Le regne animal, ed. 1, vol. 2. Paris.

Frey, H.W. (editor)
1971 California's living marine resouces and their utilization. Calif. Dep. Fish & Game, Mar. Resour. Agcy, Sacramento, 148 p.

Gilbert, C.R.
1966 Western Atlantic sciaenid fishes of the genus *Umbrina*. Bull. Mar. Sci. 16(2):230–258.

Gill, T.
1862 Catalogue of the fishes of lower California, in the Smithsonian Institution, collected by Mr. J. Xantus. Proc. Acad. Nat. Sci. Phila. 13:249–262.

Gistel, J.
1848 Naturgeschichte des Thierreichs. Für höhere Schulen. Scheitlin & Krais, Stuttgart, 216 p.

Günther, A.
1869 An account of the fishes of the states of Central America, based on collections made by Capt. J.M. Dow, F. Godman, Esq., and O. Salvin, Esq. Trans. Zool. Soc. Lond. 6:377–494.
1880 Report on the shore fishes. *In* Report on the scientific results of the voyage of H.M.S. *Challenger* during the years 1873–1876. Zool. Challenger Exped. Pt. 6, London, 82 p.

Hubbs, C.L.
1921 Description of a new sciaenid fish from Santa Catalina Island, California. Occas. Pap. Mus. Zool. Univ. Mich. 92, 3 p.

Hubbs, C.L., and K.F. Lagler
1958 Fishes of the Great Lakes region (rev. ed.). Cranbrook Inst. Sci. Bull. 26, 186 p.

Jordan, D.S., and C.H. Gilbert
1882 List of fishes collected by Lieut. Henry E. Nichols, U.S.N., in the Gulf of California and on the west coast of lower California, with descriptions of four new species. Proc. U.S. Natl. Mus. 4:273–279.

Leviton, A.E., R.H. Gibbs Jr., E. Heal, and C.E. Dawson
1985 Standards in herpetology and ichthyology: Part I. Standard symbolic codes for institutional resource collections in herpetology and ichthyology. Copeia 1985:802–832.

Linnaeus, C.
1758 Systema naturae. Regnum animale. Tome I, 10th ed., Holmiae, 824 p.

Lopez S., M.I.
1980 *Umbrina bussingi*, a new sciaenid fish from the tropical eastern Pacific Ocean. Rev. Biol. Trop. 28(1):203–208.

McPhail, J.D.
1958 Key to the croakers (Sciaenidae) of the eastern Pacific. Univ. Brit. Col., Inst. Fish., Mus. Contrib. 2, Vancouver, 17 p.

Miller, D.J., and R.N. Lea
1972 Guide to the coastal marine fishes of California. Calif. Dep. Fish & Game Bull. 157, 235 p.

Miller, R.V.
1971 A new sciaenid fish (Pisces: Umbrinini) with a single mental barbel, from the southern Caribbean. Copeia 1971: 300–306.

Ostroumoff, A.A.
1896 Zwei neue Relicten-Gattungen im Azow'schen Meere. Zool. Abz. v. 19(493):30.

Rosenblatt, R.H.
1967 The zoogeographic relationships of the marine shore fishes of tropical America. Stud. Trop. Oceanogr. 5:579–592.

Scofield, N.B.
1896 Family Sciaenidae. *In* Jordan, D.S., Notes on fishes, little known or new to science, p. 220–221. Proc. Calif. Acad. Sci., 2d ser., 6:201–244.

Springer, V.G.
1958 Systematics and zoogeography of the clinid fishes of the subtribe Labrisomini Hubbs. Publ. Inst. Mar. Sci., Univ. Tex. 5:417–492.

Steindachner, F.
1878 Uber zwei neue Fischarten von den Galapagos-Insulen. *In* Ichthyologische Beitrage (VII), p. 19–21. Akad. Wiss. Wien Sibzber. Abth. 1. 1878 (1879):1–24.

Trewavas, E.
1977 The sciaenid fishes (croakers or drums) of the Indo-West-Pacific. Trans. Zool. Soc. Lond. 33:253–541.

Walker, H.J. Jr., and R.H. Rosenblatt
1988 Pacific toadishes of the genus *Porichthys* (Batrachoididae) with descriptions of three new species. Copeia 1988:887–904.

Wilson, C.
1916 Some marine fishes from Colombia and Ecuador. Ann. Carnegie Mus. 10(1–2):57–76.

Table 1
Number of soft dorsal fin rays in eastern Pacific species of *Umbrina*. (Asterisks indicate count of primary type.)

	21	22	23	24	25	26	27	28	29	30	31	32	33	$\bar{x}$	SE
U. analis				6	1	2*								24.56	0.29
U. bussingi	5	19*	4											21.96	0.11
U. dorsalis								1	3	15	21	8	2*	30.76	0.14
U. galapagorum						9	59*	89	58	24				28.12	0.07
U. reedi	1	1	4	22*	21	1								24.28	0.12
U. roncador				4	11	72	110	105*	46	6	1			27.32	0.06
U. wintersteeni			1	3	25	37*	23	3						25.95	0.10
U. xanti						13	77	168*	114	30	4	1		28.03	0.04

Table 2
Number of soft anal fin rays in eastern Pacific species of *Umbrina*. (Asterisks indicate count of primary type.)

	5	6	7	8	9	10	$\bar{x}$	SE
U. analis		9*					6.00	—
U. bussingi			30*				7.00	—
U. dorsalis			45*	5			7.10	0.04
U. galapagorum	1	164*	73				6.30	0.03
U. reedi				2	46*	2	9.00	0.04
U. roncador		17	339*				6.95	0.01
U. wintersteeni	2	89*					5.98	0.02
U. xanti		402*	6				6.01	0.01

Table 3
Number of pectoral fin rays in eastern Pacific species of *Umbrina*. (Asterisks indicate count of primary type.)

	14	15	16	17	18	19	20	$\bar{x}$	SE
U. analis			2	14*	2			17.00	0.11
U. bussingi				3	30*	19		18.31	0.08
U. dorsalis		1	65*	33				16.32	0.05
U. galapagorum			1	57	323*	78*	4	18.06	0.03
U. reedi				12	69	19*		18.07	0.06
U. roncador		1	11	175*	422	48	1	17.77	0.02
U. wintersteeni		2	16	147*	17			16.98	0.04
U. xanti	1	1	20	532	192*	8		17.24	0.03

Table 4
Number of total gill rakers in eastern Pacific species of *Umbrina*.

	14	15	16	17	18	19	20	21	22	23	24	25	$\bar{x}$	SE
U. analis			1	5	3			1					17.60	0.43
U. bussingi				1	4	6	11	3	2				19.63	0.23
U. dorsalis					8	35	25	17	7	4	1	1	20.01	0.14
U. galapagorum			1	38	248	126	48	4					18.42	0.04
U. reedi					1	14	11	3	1				19.63	0.16
U. roncador		12	26	48	121	160	120	23	1				18.66	0.06
U. wintersteeni	2	5	12	21	46	43	17	5	4	2			18.32	0.13
U. xanti			10	91	475	90	21	1					18.03	0.03

Table 5

Selected morphometrics of eastern Pacific species of *Umbrina*. HL = head length; SN = snout length; INT = interorbital width; SUB = suborbital width; UJ = upper jaw length; PED = caudal peduncle depth; PEL = caudal peduncle length; PA = preanal length; PF = pectoral fin length; PRD = predorsal fin length; DEP = greatest depth; ASP = second anal spine length.

SL (mm)	Range (10^{-3}SL)												
	HL	EYE	SN	INT	SUB	UJ	PED	PEL	PA	PF	PRD	DEP	ASP
U. analis													
52–231	292–332	67–96	76–103	61–87	50–63	91–120	100–117	220–263	670–721	183–204	362–386	302–342	170–214
U. bussingi													
59–229	338–401	87–108	62–92	70–94	41–57	111–135	76–99	233–265	663–742	239–287	332–417	298–344	154–186
U. dorsalis													
49–327	282–364	57–116	81–103	80–125	37–59	115–173	92–117	235–278	607–652	185–265	344–369	315–378	117–181
U. galapagorum													
30–394	269–354	43–90	86–110	69–96	44–68	87–132	83–103	240–292	610–676	168–190	341–376	249–322	92–172
U. reedi													
85–650	310–360	40–88	83–113	74–101	41–62	110–147	98–122	209–263	634–685	216–247	378–409	306–396	82–159
U. roncador													
22–339	267–342	38–88	71–99	68–102	31–49	93–152	77–116	219–282	641–685	155–195	333–361	247–329	91–146
U. wintersteeni													
30–271	279–344	57–97	83–105	66–100	51–60	92–134	88–112	218–255	648–686	161–199	334–365	261–315	112–168
U. xanti													
20–287	267–316	49–105	69–107	66–99	31–36	85–152	80–113	239–316	605–642	150–172	328–358	235–330	97–157

Table 6

Number of procurrent caudal fin rays in eastern Pacific species of *Umbrina*.

	Dorsal							Ventral						
	6	7	8	9	10	$\bar{x}$	SE	6	7	8	9	10	$\bar{x}$	SE
U. analis			4	2		8.33	0.21		2	4			7.66	0.21
U. bussingi		6	12			7.67	0.11		12	5	1		7.39	0.14
U. dorsalis	1	17	16	4		7.61	0.12	10	22	1			6.73	0.09
U. galapagorum			2	40	12	9.19	0.03		4	33	13		8.18	0.08
U. reedi			1	19	9	9.28	0.05			15	10	2	8.52	0.12
U. roncador			5	29	15	9.20	0.05		1	27	13		8.29	0.08
U. wintersteeni		12	30	2		7.77	0.08	7	27	4			6.92	0.05
U. xanti			16	33	5	8.79	0.08		8	30	12		8.08	0.08

Behavioral reactions of humpback whales *Megaptera novaeangliae* to biopsy procedures

Mason T. Weinrich
Cetacean Research Unit, P.O. Box 159, Gloucester, Massachusetts 01930

Richard H. Lambertson
Department of Physiological Sciences, College of Veterinary Medicine
University of Florida, Box J-144, JHMHC, Gainesville, Florida 32610

Cynthia R. Belt
Mark R. Schilling
Heidi J. Iken
Cetacean Research Unit, P O Box 159, Gloucester, Massachusetts 01930

Stephen E. Syrjala
Resource Assessment and Conservation Engineering, Alaska Fisheries Science Center
National Marine Fisheries Service, NOAA
7600 Sand Point Way NE, Seattle, Washington 98115-0070

Abstract.—Accurate and precise descriptions of behavioral indicators of human activities which disturb cetaceans are required to better control adverse human impacts on these animals. We hypothesize that the application of a technique used to remove a small piece of innervated tissue, a biopsy darting procedure, is likely to result in the display of such behavioral indicators. In order to describe such displays, we recorded behavior of 22 humpback whales *Megaptera novaeangliae* before and after biopsy procedures in the southern Gulf of Maine. Reactions varied considerably among animals. Although respiratory responses were not consistent, biopsied whales generally decreased their ratio of surface to dive time and their net movement rate. Hard tail flicks occurred as an immediate reaction in approximately half the cases. Although 31 behaviors were tested for variation, only hard tail flicks significantly increased in either the number of animals that displayed them or the overall frequency of occurrence during postbiopsy reaction periods. While not statistically significant, some increase was noted in the frequency of trumpet blows and tail slashes, while slow swimming and apparent investigative behavior were noted to decrease. The strongest reactions, observed in two cases, occurred when the dart and retrieval line briefly snagged the whale's flukes. These findings complement and extend other studies on the response of baleen whales to human activity at sea.

The humpback whale *Megaptera novaeangliae* is an endangered species that has been protected from commercial catches since the mid-1960s. Protection from hunting in the North Atlantic portion of its range extends back to 1955. The most recent population estimates suggest close to 10,000 animals remain worldwide, with 5500 in the western North Atlantic (Johnson and Wolman 1985).

The endangered status of this species as well as its affinity for nearshore habits has brought increasing concern that the collective effects of industrial development, resource exploitation, and rapid increase in the whale watching industry could result in displacement, habitat degradation, and behavior modification. It thus has become important to determine whether human activity that is not directly lethal to individual whales could still have deleterious effects on the recovery of this species.

To assess potential deleterious effects of artificial stimuli on the normal behavior of a whale, definitions of disturbed behavior must be clarified. Disturbed behavior can be defined as behavior that results from a noxious stimulus that would not otherwise have occurred. Previous observations have been made under conditions of potential disturbance, such as the presence of boats or divers or the production of underwater noise (Baker and Herman 1982, Malme et al. 1983 and 1985, Bauer and Herman 1985, Richardson et al. 1985). However, a cause-and-effect relationship between the stimulus and a whale's response has been difficult or impossible to achieve, since baseline data on behavioral reactions to clearly noxious stimuli are almost entirely lacking.

Since 1979, humpback whales have been studied intensively in the southern Gulf of Maine to evaluate the demographics, behavior, and ecology of a group of annually-returning individuals (Mayo et al. 1985, Weinrich 1985 and 1986, Clapham and Mayo 1987). In 1983, the University of Florida began studies to determine the genetic characteristics and sex of known individuals in this group of

Manuscript accepted 1 June 1992.
Fishery Bulletin, U.S. 90:588–598 (1992).

whales. To obtain the tissue samples for this project, a projectile biopsy dart was used (Lambertsen 1987, Lambertsen and Duffield 1987, Lambertsen et al. 1988).

In an attempt to better understand the disturbance response of large whales, the present study was undertaken to assess the behavioral reaction of humpback whales to the biopsy procedures previously described (Lambertsen 1987). We reason that since the biopsy dart removes a small piece of innervated tissue, it is likely to be perceived by the whale as a noxious stimulus and should cause some observable response. Our results compare the behaviors of the whales before and after exposure to this relatively short-term, moderate-level stressful stimulus.

Materials and methods

Cruises to collect biopsy samples took place each year from 1983 to 1985 on Jeffrey's Ledge or Stellwagen Bank in the Gulf of Maine. In 1983 and 1984 various types of small power vessels (≤12.8m) were used, including an 11.6m sportfishing vessel equipped with one Detroit Diesel 671 engine, and a 12.8m pilot boat with two Detroit Diesel 671 engines. In 1985, a 6.1m runabout with a 175hp outboard engine and an 11m sailing sloop were used simultaneously. The use of two vessels allowed one (the 6.1m runabout) to be dedicated to collection of behavioral data in the methodology described below. The immediate response of whales to biopsy darting was recorded on two days in 1983, two in 1984, and six in 1985.

The biopsy apparatus used in this study consisted of a tethered retrievable biopsy dart, aimed at the flank below the dorsal fin, fired from a 68kg crossbow (Lambertsen 1987). A small biopsy punch fitted with internal prongs and attached to the tip of the dart shaft removed the tissue from the animal. A small tissue sample, including both epidermis and dermis, was thus obtained by a cutting action on penetration, and tearing on rebound. Upon penetration of the dart into the whale, a rebound was forced by a 2.5cm diameter flange set 2cm back from the tip of the biopsy punch.

In the first 2 years of the study, emphasis was placed on collecting as many biopsies as possible during brief periods at sea. Behavioral observations were collected opportunistically to provide qualitatively classified data on immediate reactions. For comparative purposes, these observations were ranked in a manner similar to that used by Mathews (1986), who studied the reactions of eight gray whales *Eschrichtius robustus* to a similar biopsy procedure. Categories used in this initial analysis included:

No reaction The whale continued its prebiopsy behavior with no detectable change.

Low-level reaction The animal modified its behavior, but displayed none of the overtly forceful behaviors listed as moderate or strong reactions (e.g., immediate dive).

Moderate reaction The animal modified its behavior in a more forceful manner (trumpet blows, hard tail flicks), but gave no prolonged evidence of behavioral disturbance.

Strong reaction The animal modified its behavior to a succession of forceful activities (continuous surges, tail slashes, numerous trumpet blows).

To test statistical differences in reaction levels among age-classes, non- and low-level reaction frequencies were combined, as were moderate and strong reactions. This was necessitated by the low expected values of the frequencies in a chi-square table based on the data in Table 1.

All data from 1983–85 were used to categorize immediate response levels; in 1985, a 30-min prebiopsy **control** period and a 30-min postbiopsy **response** period were defined to standardize a paired data set of respiratory and other surface behaviors. This approach used the vessel dedicated to behavioral data collection to institute a focal sampling technique (Altmann 1974) to allow quantitative comparison of the pre- and postbiopsy focal periods as "paired samples." Upon sighting a group of whales, each individual was distinguished through 7×50 binoculars using distinctive natural markings on the dorsal fin or the ventral surface of the tail flukes (Katona and Whitehead 1981). Because of the necessity of identifying individual respirations and behaviors within the group, dorsal fin shape was used whenever possible during focal samples; permanent identification came from fluke photographs taken during the approach for the biopsy strike. Once individuals were distinguished from one another, a 30-min "control" (i.e., pretreatment) focal sample was then initiated. During this period the engines of the observation vessel were shut down to eliminate engine noise. No approaches closer than 100m were made prior to the onset of, or during, the 30-min control period. If the whale moved farther than 1000m from the research vessel, making data collection difficult, the engine was started and approach was made slowly to within ~300m of the whale. At the conclusion of the 30-min "control" focal sample the whale was then approached at close range (3–40m) for the biopsy attempt. The same protocol was followed after the biopsy for a comparable "experimental" (i.e., post-treatment) data set, which started at the moment of impact by the dart.

During focal samples, data were collected on four respiratory variables: (1) number of respirations ("blows") during a given surface interval, (2) time between each respiration ("blow interval"), (3) time

the animal spent at the surface ("surface interval"), and (4) time spent below the surface during each dive ("dive time"), defined as the period of submergence following typical sounding behavior (i.e., a prominent, high arching of the back and tail, often followed by bringing the tail flukes above the water surface). The surface interval during which the biopsy strike took place was excluded from our analyses of both the pre- and postbiopsy respiratory variables. We determined (using chi-square goodness-of-fit tests) that the distribution of the observed data was not significantly different from a normal distribution, thus differences between the pre- and postbiopsy values were compared using two-tailed paired t-tests (Zar 1984). Surface-interval to dive-time ratios were calculated for each whale during pre-biopsy and postbiopsy focal samples, and compared using a Wilcoxon sign rank test (Zar 1984). The surface-interval/dive-time ratio integrates several respiratory values into a single measure of the respiratory "strategy" for each individual.

LORAN-C positions, which have an error of ~30 m in the study area (Day 1983), were used in estimating the net rate of movement of a whale as defined by its surfacings. LORAN positions were recorded at the start and end of each focal sample. With each LORAN-C reading, the bearing to the whale to the nearest 5 degrees and the visually-estimated distance from the vessel to the whale were also recorded. This information was used to correct the LORAN-C data if the whale was >30 m from the vessel, which was likely given the limitations of vessel movement during focal samples described above. To estimate the net movement rate, the distance between the first and last calculated whale positions within each focal sample period was divided by the elapsed time (30 minutes), yielding a net movement rate in knots. Actual swimming speed could not be determined due to uncertainty about the direction of a whale's movement underwater or the linearity of its track. Results between pre- and postbiopsy periods were compared using a Wilcoxon sign rank test (Zar 1984).

Photographs of the dorsal fin and tail flukes of individual whales were taken upon approach for biopsy. Each whale was identified using the catalog of Gulf of Maine humpback whales kept at the Cetacean Research Unit, where individuals are assigned a two-letter, one-number file code. If the animal could not be identified in the catalog, it was assigned a three-digit code. When possible, each animal was assigned to one of the following age groups: juvenile (1–3 yr), adolescent (4–6 yr), or adult (>6 yr). Age classifications were based on previous and/or subsequent repeated annual observations of the same individuals by the authors from calf year (used for juveniles and adolescents), sightings of the individual as an initially small and subsequently larger animal (juveniles and adolescents), or annually repeated sightings of an individual with no appreciable growth over several years (adults). If an animal was sighted only during the year in which it was biopsied, it was not classified by age-class.

During focal samples collected in 1985, a total of 30 behavior types were observed and analyzed. Behavior types were defined using an ethogram for humpback whales developed by the Cetacean Research Unit prior to this study (unpubl. data). The probability that any given behavior was displayed by more or fewer animals in the pre- vs. postbiopsy focal samples was tested using the binomial distribution (with the probability of each period containing an occurrence of the behavior assumed as 0.5), while the change in frequency of each behavior in individuals, given that the behavior was observed at all, was compared using Wilcoxon signed rank tests (Zar 1984). All 30 behaviors were tested for variation. Many of the behaviors did not show any variation between control and response periods, and therefore are not described in detail. These were belly-up rolls, breaches, bubble clouds (bubble clouds followed by obvious surface feeding), bubble cloud behaviors (bubble clouds not followed by obvious surface feeding), defecations, flipper flares, flipper flicks, flipper in air, flukes, half flukes, hangs, high flukes, high head-ups ("spyhops"), lobtails, logging, low flukes, quarter rolls, single bubbles, snakes (a twisting of the body), surges, tail breaches, and passing under a boat. Definitions of those behaviors which either varied significantly in frequency or showed some notable variation in the frequency of display following the biopsy procedure are the following:

Back rise Animal breaks surface while swimming, with no accompanying exhalation.

Belly-up lobtail Animal, ventral side up, elevates tail into the air, then slaps the water surface with the dorsal surface of its flukes.

Hard tail flick Animal rapidly and forcefully flexes tail up and down one time during otherwise normal swimming behavior; much spray can be thrown; flukes clear surface. The hard tail flick is faster and presents a less regular arching movement of the tail than a lob-tail.

Low head-up Animal lifts head into air at 30–45° angle to surface.

Sounding dive Animal arches its back in a typical diving posture but does not bring its tail flukes above the surface.

Tail rise Animal slowly straightens its caudal peduncle at the surface during normal swimming.

Tail slash Animal moves tail forcefully from side to side, flukes at or just below the surface; creates white water frothing.

Trumpet blow Loud, broad-band, wheeze-like sound made during exhalation at the surface.

In addition, the following behaviors showed a variation in frequency during the special case of SI4's reaction (discussed below):

Belly-up Animal rolls so that the whale has its ventral surface exposed above the surface (often for longer than a second).

Half fluke Animal rolls on its side exposing one fluke above and perpendicular to the surface.

Results

Immediate behavioral reactions, or the absence thereof, to the biopsy procedure were recorded for 71 biopsy strikes during the period 1983–85. Of these, 22 (recorded in 1985) are paired samples including a 30-min prebiopsy and 30-min postbiopsy focal sample. Two cases contained clearly unusual reactions, including one from the 1985 paired samples. These cases are discussed separately. This leaves 21 paired samples of behavioral data; however, in five cases some respirations could not be accurately assigned to a whale within the focal group, leaving 16 paired samples of complete respiratory data for analysis.

Immediate behavioral response

Of the 71 total biopsy attempts for which immediate behavioral reactions were recorded, 7.0% involved no behavioral reaction, 26.8% involved a low-level reaction, 60.6% involved a moderate reaction, and 5.6% involved a strong reaction (Table 1). All the strong reactions involved snagging of the flukes by the monofilament line attached to the biopsy dart.

Immediate dives were the most common response to the biopsy dart striking the animal, observed in 35 (49.2%) cases, hard tail flicks were present in 34 (47.8%), and trumpet blows were observed in 31 (43.6%) cases. Less than 20% of all reactions involved immediate surges or visually detectable increases in swimming speed.

Although an immediate dive was a frequently observed response, this may have been due to the time it took to approach the whale for the biopsy strike, i.e., the whale would have taken a dive at that point regardless of the biopsy attempt. However, the mean number of blows (4.89) during the surfacing interval in which the biopsy dart was fired was significantly lower than in the accompanying complete surfacings immediately prior to the biopsy attempt (7.17) (paired t-test: t −2.76, 15 df, p 0.015),suggesting those dives which occurred immediately after the strike of the biopsy dart were initiated as a response to the biopsy procedure.

Table 1
Qualitative ranking of intensity of behavioral responses in humpback whales *Megaptera novaeangliae* to biopsy procedures. NR = No reaction.

	NR	Low	Moderate	Strong	Total
Juveniles (1–3 yr)	2	3	10	3	18
Adolescents (4–6 yr)	0	4	6	0	10
Adults (>6 yr)	3	12	23	1	39
Unclassified	0	0	4	0	4
Total	5	19	43	4	71

Study animals could be categorized by age-class in 68 of the 71 trials. There was no significant difference in the intensity of reactions by age-class (χ^2 2.88, 3 df, p 0.41) (Table 1). However, 3 of the 4 reactions we ranked as strong were from juveniles. Also, strong reactions were always associated with a snagging of the retrieval line on the animals' flukes.

Respiratory and dive variables

There were no significant differences between pre- vs. postbiopsy focal samples for any of the four respiratory variables (paired t-tests (15 df): blow interval t 0.82, p 0.42; number of blows/surfacing interval t −0.93, p 0.36; surfacing interval t 1.65, p 0.11; dive time t 0.61, p 0.55). There was a significant decrease in the surface-interval/dive-time ratios during postbiopsy focal samples (Wilcoxon signed rank test, Z −2.11, p 0.03).

Substantial individual variation was found in respiratory variables. Seven animals (43.8%) showed a decrease in their mean blow interval following the biopsy procedure, and eight (50.0%) showed an increase (Table 2). Eleven individuals (68.8%) showed a decrease in the number of blows per surfacing, while in only four (25.0%) did it increase (Table 3). Similarly, eleven whales (69.0%) reduced their surface interval in the postbiopsy period, while in five (32.0%) this variable increased (Table 4). Finally, eight of the 16 individuals (50.0%) were found to decrease their dive times during the postbiopsy period, while in the other eight (50.0%) it increased (Table 5). The surface-interval/dive-time ratio also showed a decrease in 9 of the 16 animals (57.0%), while in 5 (32.0%) there was no change and in 2 (13.0%) there was an increase (Table 6). Based on binomial distribution, any case with 9 or more, or 2 or less, animals showing a change in a particular

direction would be significant at p 0.07 (based on 11 samples, ignoring the 5 that showed no change), indicating a significant decrease in the surface-interval/dive-time ratio in the sample.

To determine whether the immediate behavioral response to the biopsy dart affected subsequent

Table 2

Mean blow intervals (s) and standard deviations in humpback whales *Megaptera novaeangliae* during focal samples before and after biopsy procedures. Each individual whale is represented by a two-letter one-number code or a three-number code.

	Prebiopsy			Postbiopsy			
Animal	N	$\bar{x}$	SD	N	$\bar{x}$	SD	Difference
CO7	18	27.9	35.9	17	22.0	14.8	−5.9
SE6	11	49.2	43.2	15	46.3	45.9	−2.9
ZE1	19	36.4	23.7	23	26.8	23.4	−9.6
547	23	34.7	27.2	18	38.2	18.5	3.5
SW1	26	23.3	24.0	21	32.8	16.5	9.5
TH6	22	28.3	15.8	16	28.9	22.5	0.6
LA5	17	22.3	12.1	25	22.3	15.5	0.0
TR2	23	19.3	20.5	26	24.5	14.4	5.2
KE2	12	83.7	74.3	11	51.7	37.1	−32.0
ME1	22	14.5	2.6	19	16.0	2.0	1.5
CO9	22	16.3	5.3	21	15.9	4.0	−0.4
ST1	19	34.6	23.8	30	33.3	26.4	−1.3
OC1	38	30.4	20.4	36	32.6	27.1	2.2
SM1	32	27.8	22.8	21	33.7	27.1	5.9
CI1	23	14.3	5.1	17	18.3	13.3	4.0
RA6	12	31.8	20.3	10	19.3	7.1	−12.5
Sample		30.9	16.8		28.9	9.5	−2.0

Table 3

Mean number of blows per surface interval in humpback whales *Megaptera novaeangliae* during focal samples before and after the biopsy procedure. Each individual whale is represented by a two-letter one-number code or a three-number code.

	Prebiopsy			Postbiopsy			
Animal	N	$\bar{x}$	SD	N	$\bar{x}$	SD	Difference
CO7	4	4.4	1.1	4	8.6	4.2	4.2
SE6	2	8.3	6.0	5	3.7	1.9	−4.6
ZE1	3	10.0	6.0	5	5.0	3.7	−5.0
547	5	4.7	2.9	5	4.0	2.0	−0.7
SW1	3	5.8	1.0	4	5.8	1.7	0.0
TH6	5	6.5	2.4	6	6.0	2.9	−0.5
LA5	8	4.2	2.8	5	2.8	2.2	−1.4
TR2	3	8.7	3.1	4	7.3	3.0	−1.4
KE2	4	4.0	2.5	5	3.2	2.3	−0.8
ME1	7	4.1	1.9	2	8.0	2.8	3.9
CO9	5	5.4	2.5	11	2.9	1.6	−2.5
ST1	7	3.9	1.5	5	7.0	6.6	3.1
OC1	4	10.5	6.4	5	8.2	6.8	−2.3
SM1	6	6.3	4.3	5	5.2	4.8	−1.1
CI1	6	4.4	1.8	2	2.3	1.5	−2.1
RA6	4	2.3	1.7	4	3.5	1.3	1.2
Sample		5.8	2.4		5.2	2.1	−0.6

Table 4

Mean surface interval length (s) in humpback whales *Megaptera novaeangliae* during focal samples before and after the biopsy procedure. Each individual whale is represented by a two-letter one-number code or a three-number code.

	Prebiopsy			Postbiopsy			
Animal	N	$\bar{x}$	SD	N	$\bar{x}$	SD	Difference
CO7	4	117.7	135.2	4	196.4	123.2	78.7
SE6	2	399.0	291.9	5	140.8	156.1	−258.2
ZE1	3	369.3	251.4	5	110.3	119.0	−259.0
547	5	158.0	115.7	5	121.0	58.5	−37.0
SW1	3	115.5	49.3	4	199.5	87.0	84.0
TH6	5	206.6	96.2	6	135.8	94.8	−70.8
LA5	8	62.5	71.5	5	46.3	21.6	−16.2
TR2	3	154.0	104.5	4	168.0	106.6	14.0
KE2	4	256.8	177.2	5	135.4	106.5	−121.4
ME1	7	61.1	47.2	2	122.0	42.4	60.9
CO9	5	76.0	41.4	11	29.6	19.6	−46.4
ST1	7	113.9	104.6	5	222.4	244.1	108.5
OC1	4	390.3	292.3	5	264.4	282.4	−125.9
SM1	6	216.8	157.3	5	138.6	163.8	−78.2
CI1	6	57.5	35.8	2	36.1	49.9	−21.4
RA6	4	64.5	21.5	4	32.0	14.4	−32.5
Sample		176.2	120.1		131.1	70.0	−45.1

Table 5

Mean dive interval length (s) in humpback whales *Megaptera novaeangliae* during focal samples before and after the biopsy procedure. Each individual whale is represented by a two-letter one-number code or a three-number code.

	Prebiopsy			Postbiopsy			
Animal	N	$\bar{x}$	SD	N	$\bar{x}$	SD	Difference
CO7	4	92.2	84.6	4	194.8	112.7	102.6
SE6	2	171.3	94.7	5	177.2	79.8	5.9
ZE1	3	181.0	23.5	5	145.4	87.0	−35.6
547	5	146.7	113.6	5	314.0	76.7	167.3
SW1	3	394.7	149.8	4	145.8	121.8	−248.9
TH6	5	127.5	22.9	6	200.0	88.3	72.5
LA5	8	254.5	35.4	5	216.5	48.9	−38.0
TR2	3	412.5	9.2	4	391.3	253.4	−21.2
KE2	4	228.5	90.6	5	125.0	90.6	−103.5
ME1	7	250.5	125.5	2	565.5	38.9	315.0
CO9	5	161.0	129.9	11	120.3	62.9	−40.7
ST1	7	122.0	107.1	5	204.6	251.3	82.6
OC1	4	153.8	75.7	5	124.3	127.8	−29.5
SM1	6	96.7	57.7	5	199.0	109.2	102.3
CI1	6	170.3	35.0	2	113.6	76.9	−56.7
RA6	4	324.8	115.4	4	355.0	167.5	30.3
Sample		205.5	98.9		224.5	18.4	19.0

responses in respiratory variables, we examined separately those animals that reacted to the biopsy strike with an immediate hard tail flick (n 9), the most obviously forceful immediate response to the biopsy strike. This subset would therefore eliminate those animals who may have not been affected by the biopsy strike. However, variation among individuals during the postbiopsy period was not appreciably different from that portion of the sample where no hard tail flick was observed (binomial test). Hence, the occurrence of an immediate forceful response to the biopsy procedure does not appear to be associated with subsequent changes in respiratory variables.

Net movement rate

For 11 of the 21 animals, LORAN-C fixes allowed a calculation of the animal's net movement rate in pre- and postbiopsy focal samples. During the prebiopsy sample, only two animals showed values >1 kn. During the postbiopsy period, the average rate did not increase significantly (Wilcoxon signed rank test, Z −1.82, p 0.07). However, only three animals had rates <1 kn, and a generally increasing trend was recorded (Table 7).

Other behavioral responses

To consider changes in behavior elicited by the biopsy procedure, the possibilities of introducing new behaviors or altering display rates of regularly observed behaviors were both considered. The former was examined using the number of pre- and postbiopsy focal samples during which each behavior type was observed, while the latter was examined using the direction and magnitude of changes in observed behavior types within individual paired samples (Tables 8, 9). Only one of the 30 tested behavior types showed significant differences between the pre- and postbiopsy period.

Eleven of the 21 (52.3%) postbiopsy focal samples contained a hard tail flick, while the behavior was not observed in the prebiopsy focal samples (binomial distribution, $p<0.001$). Only once was a hard tail flick observed more than one time after a biopsy strike. This also was the only case in which the hard tail flick was not an immediate response to the biopsy dart. The percentage of biopsy strikes where the reaction included a hard tail flick among paired samples was not significantly different from that of the larger 1983–84 sample, where 34 of 50 animals displayed the hard tail flick (χ^2 1.54, 1 df, p 0.21).

As was the case in the number of 30-min samples in which a behavior was displayed, only hard tail flicks showed a significant increase in frequency during the postbiopsy period (binomial distribution, p 0.001). While results were not significant, one or more animals also showed notable increases in the numbers of trumpet blows, tail slashes, and belly-up lobtails following the biopsy procedure; similar nonsignificant but notable decreases were seen in back rises, tail rises, and low head-ups (Tables 8, 9). The latter three behaviors are associated with slow, unhurried travel, resting, or interest in nonessential environmental stimuli (e.g., boats, seaweed).

Table 6

Mean surface-interval/dive-time ratio in humpback whales *Megaptera novaeangliae* during focal samples before and after the biopsy procedure. Each individual whale is represented by a two-letter one-number code or a three-number code.

Animal	Prebiopsy	Postbiopsy	Difference
CO7	1.3	1.0	−0.3
SE6	2.3	0.8	−1.5
ZE1	2.0	0.8	−1.2
547	1.1	0.4	−0.7
SW1	0.3	1.4	1.1
TH6	1.6	0.7	−0.9
LA5	0.2	0.2	0.0
TR2	0.4	0.4	0.0
KE2	1.1	1.1	0.0
ME1	0.2	0.2	0.0
CO9	0.5	0.2	−0.3
ST1	0.9	1.1	0.2
OC1	2.5	2.1	−0.4
SM1	2.2	0.7	−1.5
CI1	0.3	0.3	0.0
RA6	0.2	0.1	−0.1
Sample	1.1	0.7	−0.4

Table 7

Net movement rate (kn) in humpback whales *Megaptera novaeangliae* during focal samples before and after the biopsy procedure. Each individual whale is represented by a two-letter one-number code or a three-number code.

Animal	Prebiopsy	Postbiopsy	Difference
CO7	0.5	1.7	1.2
SW1	0.7	1.5	0.8
TR2	0.8	2.0	1.2
ME1	0.8	4.5	3.7
ST1	0.5	0.6	0.1
OC1	0.9	0.6	−0.3
SM1	0.8	1.3	0.5
RA6	3.8	1.5	−2.3
BI1	1.5	3.8	2.3
PE4	0.5	1.1	0.6
SI4	0.5	0.7	−0.2
Sample	1.0 (SD 0.9)	1.7 (SD 1.3)	0.7

Table 8

Frequency of various behavior types in humpback whales *Megaptera novaeangliae* before the biopsy procedure ("control period"). Each individual whale is represented by a two-letter one-number code or a three-number code.

	CO7	SE6	ZE1	547	SW1	TH6	LA5	TR2	KE2	ME1	CO9	ST1	OC1	SM1	CI1	RA6	BI1	CR1	SI4	FL2	PE4	Total
Half fluke				2								1		1				1				5
Quarter roll						1																1
Bubble cloud																					2	2
Single bubble																						0
Breach									1					1								2
Back rise	9	3	11	2	1	1	2					1	7	3			1	1				42
Tail breach									2													2
Belly up												1										1
Belly-up lobtail																						0
Cloud behavior												2									8	10
Defecation																					1	1
Flipper flick																						0
Flipper in air												2										2
Flipper flare																						0
Fluke	3		2	2	2	1	3	2		4	4	3	2	1	4	3		3	4	5	7	55
Hang																						0
High fluke												1										1
High head-up	1											1										2
Hard tail flick																						0
Low fluke				1		1								1			1		1	3	1	9
Low head-up		3	4			1						1										9
Log (min)		9.3	9.5																			19
Lobtail														1				1	1			3
Snake																			1			1
Sounding dive	4	2		2	2			1	2	1	3	1	3	3	2		1	1			1	29
Surge					2											1	1					4
Tail rise		2		3		3	1		3	1		2	1	2	1		11	1	7		2	44
Trumpet blow				4	1	2				2	2	3	2	1		2	4	5	3	4		38
Tail slash				1		1				1										7		3
Under boat												1						1				2

Feeding behavior was observed with equal frequency in both the pre- and postbiopsy samples. Those animals engaged in feeding activity showed virtually no reaction to the biopsy attempt. A hard tail flick was never observed from an animal engaged in feeding activity, although it was observed during all other prebiopsy behavioral modes. Logging (resting) behavior was also displayed equally in both sample periods; however, whales logging when biopsied were observed to temporarily interrupt their logging period immediately following the biopsy.

Special cases

Two special cases of behavior modification were noted in conjunction with the biopsy procedure. Both involved the monofilament retrieval line becoming briefly snagged around one of the flukes of the whale. These represent the most vigorous and prolonged reactions to the biopsy procedure we observed.

In one case, for a period of time after the biopsy strike (~16 min) the line remained looped around the tip of one fluke of the tail and the animal behaved abnormally, swimming at elevated speeds (6–7 knots) in a roughly S-figured course. Although visually estimated, this speed appears higher when compared with values reported above. Another whale accompanied this animal in its vigorous swimming.

SI4 exhibited another unusual reaction after a biopsy (at a different time than the reaction reported for the same individual in Table 9). This whale had been associated with CR1 during the day of the biopsy effort; 40 min prior to the first strike of SI4, CR1 was sampled with little reaction. When SI4 was first struck by the biopsy dart its reaction was also minimal, but a tissue sample was not obtained. The next shot (29 min later) missed the whale, but involved a momentary snag of the line on the animal's tail stock. In response, the animal started to trumpet blow with increasing frequency but remained stationary and was easily approached. A third firing of the biopsy dart 11 min later was successful in obtaining a tissue sample.

Table 9

Frequency of various behavior types in humpback whales *Megaptera novaeangliae* following the biopsy procedure ("reaction period"). Each individual whale is represented by a two-letter one-number code or a three-number code.

	CO7	SE6	ZE1	547	SW1	TH6	LA5	TR2	KE2	ME1	CO9	ST1	OC1	SM1	C11	RA6	B11	CR1	S14	FL2	PE4	Total
Half fluke				3	1	2							1	1							1	9
Quarter roll			1			1															1	3
Bubble cloud																					2	2
Single bubble			2																			2
Breach																						0
Back rise	1	1	1	1	3	1	1		3			1	3	4								20
Tail breach									2													2
Belly up				1																		1
Belly-up lobtail									20													20
Cloud behavior																					7	7
Defecation																						0
Flipper flick														1								1
Flipper in air																						0
Flipper flare												1										1
Fluke	4	2	2	1	2	4	1	2	3	2	7	2	2	2	3	2		1	2	4	7	55
Hang												1										1
High fluke				1						1		1			1	1						5
High head-up																						0
Hard tail flick				1	1	1	1	1	1				1	2	1		1	1				12
Low fluke			1				1				1	1	1	1	2		1	2		1	2	14
Low head-up			1											1								2
Log (min)													3	3				13				19
Lobtail									4		1				1						1	7
Snake																						0
Sounding dive		4	6		2		3	1	5		2	2	1	4	5		1			3	5	44
Surge					1								1	1								3
Tail rise	3		2	2	3	2		1	1		1	1	1	4	3		2	2	2	1		31
Trumpet blow	1	1		3	2	8	1	1	1		1	1	4	9	5			4		5	10	57
Tail slash		1				2		1						1					1			11
Under boat																			1		1	2

Following the final biopsy attempt, SI4 started a series of stereotypic actions. Every 45–60 s, the animal would trumpet blow loudly, then tail slash or low-lobtail (a quick, low version of lob-tailing behavior), surge forward, and roll sideways with great force, often rolling ventral-side-up and spiraling underwater. Periods of submergence were <30 s in all cases. The swimming path was erratic, but the animal was never >100 m from the vessel. It passed immediately below the vessel twice, repeatedly surfacing on alternating sides of the boat. Swimming speed appeared greater than normal, although net movement in any one direction was minimal. During the same period CR1 appeared placid, although it did trumpet blow three times. After 14 min, the vigorous behavior of SI4 suddenly ended, and both animals started logging side by side. At this point, they were within 25 m of the vessel. Logging behavior continued for at least 15 min at which point the observation was terminated.

In order to compare the intensity of SI4's reaction with the sample analyzed above, we compared the rate at which it displayed various behavior types in the postbiopsy focal sample with the larger paired sample (n 21). To obtain a mean number of occurrences of each behavior type in the postbiopsy period, the total number of observations of each behavior type was divided by the number of paired samples (Table 10). From these data, it is clear that unusually high numbers of tail rises, trumpet blows, half flukes, belly-ups, lobtails, tail flicks, and tail slashes occurred in SI4's response.

Discussion

The results of this study indicate that behavioral reactions of individual whales to the biopsy procedure are detectable but do not appear to be severe. Immediate reactions (hard tail flicks) took place in >50% of 71 biopsy strikes, which is especially noteworthy given the rarity of this behavior in any other context. However, no significant difference was seen in most of the 30 observed behaviors in 30-min pre- and postbiopsy

Table 10

Frequency of various behavior types observed in a humpback whale *Megaptera novaeangliae* (animal SI4) subjected to repeated strikes of the biopsy dart compared with mean for the entire study population (not including SI4). Values given represent average over the 30-min postbiopsy focal sample. *N* of study population = 21.

Behavior	Study population	SI4
Half fluke	0.42	19
Quarter roll	0.14	2
Bubble cloud	0.09	0
Single bubble	0.09	1
Breach	0.00	0
Back rise	0.95	7
Tail breach	0.08	1
Belly up	0.04	12
Belly-up lobtail	0.95	0
Cloud behavior	0.33	0
Defecation	0.00	0
Flipper flick	0.04	1
Flipper in air	0.00	3
Flipper flare	0.04	2
Fluke	2.61	5
Hang	0.04	0
High fluke	0.23	0
High head-up	0.00	1
Low fluke	0.65	0
Low head-up	0.09	4
Log (min)	0.90	0
Lobtail	0.33	26
Snake	0.00	0
Sound	2.09	0
Surge	0.14	6
Tail flick	0.57	11
Tail rise	1.47	13
Trumpet blow	2.71	29
Tail slash	0.52	11
Under boat	0.09	2

behavioral focal samples. A significant decrease in the ratio of surface interval to dive time followed the biopsy procedure. Although not statistically significant, increases in trumpet blows and, to a lesser extent tail slashes and sounding dives, were noted following biopsy strikes, as were decreases in the amount of slow swimming and some nonessential behaviors.

Two of the behavior types that were noted to increase, trumpet blows and tail slashes, have been previously suggested to be agonistic (Baker and Herman 1984, Watkins and Wartzok 1985). A tail slash may be used by a humpback whale as a means of aggression against another whale in what has been interpreted as courtship battles (Baker and Herman 1984). Norris and Reeves (1977) identify "tail swishing" (our "tail slashing") as one of the more common behavioral responses to harassment.

The behaviors elicited by the biopsy procedure in most cases are not intrinsically different from those behaviors which occur naturally in this species. Thus we emphasize that it may be the change in frequency of behaviors that should be viewed as indicative of "affected" behavior, rather than the occurrence of such displays *per se*. The one notable exception is the hard tail flick, which rarely has been observed other than in response to the biopsy procedure.

The possibility exists that the hard tail flick reaction we observed is a reflex response. This reaction typically occurred at the instant of dart impact and thereafter was rarely repeated. Moreover, in some individuals a single hard tail flick at the time of the biopsy was followed by a period during which no other behavioral change was observed. A reflex response is consistent with our finding of no correlation of respiratory variation with the occurrence of this reaction.

While some of the hard tail flicks may have been purely reflexive, the same behavior was seen once in response to an extremely close vessel approach when no physical contact was made. Further, a similar reaction was reported by Watkins (1981), who labeled it a "startle response." Hence it is uncertain whether this behavior is reflexive or cognitive. It may have both components.

In other studies of whale disturbance in response to noxious stimuli, both Watkins (1981) and Mathews (1986) mention the approach of the vessel as contributing to the reaction of the animal. We made every effort to diminish vessel effects. Both previous studies were conducted from power-driven vessels approaching at moderate to rapid speeds. In over half of our paired samples, data were collected from the relatively silent approach of a sailboat. Those approaches made under power in paired samples were done at slow speed. Further, we limited movement of the research vessels near whales, except in the brief approach for the biopsy, to lessen effects of vessels. While the effect of the vessels was minimized, this approach is a necessary part of the biopsy procedure and need not be considered separately in an analysis of responses.

Our results are comparable with those found by Mathews (1986), who examined the response of eight gray whales to a similar biopsy procedure. Both studies established great variability in the reaction of whales to biopsy procedures. One clear difference is that the blow interval of gray whales showed a significant increase in the postbiopsy period, while that of the humpback whales we studied did not. Even so, four of the eight gray whales studied by Mathews (1986) showed a reduction in their surface-interval/dive-time ratios, as did 57.0% of the larger sample; only one gray whale showed an increased surface-interval/dive-time ratio.

There have been other studies of the response of humpback whales to human-induced stimuli. In Alaska, 17 humpback whales exhibiting "affected" behavior associated with the proximity of vessels increased their mean and maximum dive intervals, while their mean blow interval decreased (Baker and Herman 1982). In comparison, although the whales in our study did not consistently increase the length of their dives following the biopsy, blow intervals decreased slightly. In both studies, whales decreased surface-interval/dive-time ratios on average. The whales in our study and in that of Baker and Herman (1982) also responded with an increased rate of net movement.

Our results generally agree with other studies of the reactions of baleen whales to a variety of human-induced stimuli. Richardson et al. (1985) found that bowhead whales *Balaena mysticetus* respond to a variety of man-made stimuli (drillships, vessels, aircraft) by reducing their surface-interval/dive-time ratios. Swimming speeds increased in response to vessel traffic. Migrating gray whales, by comparison, have been reported to slow down as their migration route took them toward simulated offshore industrial activity (Malme et al. 1983, 1985). Bauer and Herman (1985) found that humpback whales on Hawaiian breeding grounds reduced their surface interval as vessels approached closely. The blow interval decreased as either the proximity or the number of vessels increased. Similarly, pod speed increased as vessels approached. Hence, the net effect in all these studies was the same as we have found; namely, that the animal avoids the source of the stimulus.

It is important to note that the reactions we describe in most cases were elicited by a noxious stimulus of brief duration and low-to-moderate amplitude. On this basis, our findings likely underestimate the effects of a more prolonged noxious stimulus, or one of greater force. For example, extreme responses, including escape, hard tail flicks, and immediate submergence, has been documented in harpooned right whales *Eubalaena glacialis* (Scammon 1874) and fin whales *Balaenoptera physalus* (Lambertsen and Moore 1983).

In the context of current management problems, the response of a whale to a prolonged sublethal noxious stimulus is a critical issue, as habitat intrusion may establish conditions of continuing, if not constant, exposure to diverse noxious stimuli. Recognizing this, Bauer and Herman (1985) considered the relationship of stimulus amplitude and duration (expressed as the number of whale-watching vessels and the length of time a whale group was in close proximity to whale-watching vessels) to elicited responses in their study of the effects of vessel traffic on humpback whales. In both cases, their data indicate a graded response in strenuous episodes of breaching, lobtailing, and flippering behavior and in movement away from the path of vessels.

Although our present study was not designed to evaluate the effects of increasing stimulus duration, including that approximated by stimulus repetition, the special case of SI4 is illuminating. Its progressively increasing reaction to repeated biopsy strikes was dramatic. After the first strike, the whale seemed unperturbed. After the second, it appeared, from its trumpet blowing and stationary position, to be annoyed but passive. After the third, it reacted with great intensity and subsequently appeared exhausted.

Based on these observations we conclude that adverse responses to rapidly repeated or prolonged noxious stimuli in whales may be incorrectly modeled as a linear function. Given the lack of any detectable response to the biopsy procedure in some animals, there seems to be a threshold for stressor amplitude below which no response will occur. Further, this threshold of tolerance may be dependent upon the specific activity in which the animal is engaged immediately prior to the time the stressor is applied; e.g., in our study animals engaged in feeding were unlikely to react to the strike of a biopsy dart. There likely are also individual differences in this threshold, as suggested by the wide variation in reactions observed.

Moreover, although one evidently can expect a graded response in the disturbance of the animal above its tolerance threshold, such gradation might be better modeled as an exponentially increasing stimulus-response function. As such, continuous or rapidly repeated moderate-level noxious stimulation could potentially lead to a general somatic alarm reaction, with endocrinologic consequences (Selye 1936, 1946). Thus, one of the important implications of this study for current management strategies to promote the recovery of endangered whale populations is that uncontrolled increases in the level or frequency of noxious intrusion into cetacean habitat may, suddenly and unexpectedly, have serious deleterious effects.

Acknowledgments

We are grateful to M. Gassel and P. Reid of the Cetacean Research Unit, and S. Frohock of the Atlantic Cetacean Research Center, who helped collect the data presented in this study. S. Sears, T. Leland, C. Gunson, S. Larkin, Dr. R. Schaper, and Dr. D. Senior provided great assistance at sea and in logistical arrangements. D. Beach, T. McKenzie, and two anonymous reviewers provided helpful comments on an early draft of the manuscript. Funding for the study was provided by the National Marine Fisheries Service (PO 40EANF-501-0396) and Contract 50EANF-00094,

with additional support to R.H.L. in the form of a fellowship from the Committee on the Challenges of Modern Society, Division of Science and Environment, North Atlantic Treaty Organization. The study by R.H. Lambertsen and M.J. Moore referred to in the discussion was undertaken with the cooperation of commercial whalers at the request of the Humane Killing Subcommittee and the Secretariat of the International Whaling Commission (IWC). Biopsy sampling was conducted under Marine Mammal Research Permit 393 issued by the National Marine Fisheries Service, National Oceanic and Atmospheric Administration, U.S. Department of Commerce.

Citations

Altmann, J.
1974 Observational study of behavior: Sampling methods. Behaviour 49(3,4):227–267.

Baker, C.S., and L.M. Herman
1982 The impact of vessel traffic on the behavior of humpback whales in southeast Alaska. Unpubl. rep. to NMFS Natl. Mar. Mammal Lab., Contract 81-ABC-00114, Seattle, 39 p.
1984 Aggressive behavior between humpback whales wintering in Hawaiian waters. Can. J. Zool. 62:1922–1937.

Bauer, G.B., and L.M. Herman
1985 Effects of vessel traffic on the behavior of humpback whales in Hawaii. Unpubl. rep. to NMFS Honolulu Lab., 163 p.

Clapham, P.J., and C.A. Mayo
1987 Reproduction and recruitment of individually identified humpback whales, *Megaptera novaeangliae*, observed in Massachusetts Bay, 1979–1985. Can. J. Zool. 65:2853–2863.

Day, B.
1983 Operator's guide for the SITEX-757 LORAN-C receiver. SITEX Co., Baltimore, 98 p.

Johnson, J.H., and A.A. Wolman
1985 The humpback whale. Mar. Fish. Rev. 46(4):30–37.

Katona, S.K., and H.P. Whitehead
1981 Identifying humpback whales using their natural markings. Polar Rec. 20:439–444.

Lambertsen, R.H.
1987 A biopsy system for large whales and its use for cytogenetics. J. Mammal 68:443–445.

Lambertsen, R.H., and D.A. Duffield
1987 Biopsy studies of the humpback whale, *Megaptera novaeangliae*. NTIS Rep., Springfield, VA, 151 p.

Lambertsen, R.H., and M.J. Moore
1983 Behavioral and post mortem observations on fin whales killed with explosive harpoons with preliminary conclusions concerning killing efficiency. Rep. IWC/TC/36/HK3 to Int. Whaling Comm. Dep. Physiol. Sci., Coll. Vet. Med., Univ. Florida, Gainesville, 23 p.

Lambertsen, R.H., C.S. Baker, D.A. Duffield, and J. Chamberlin-Lea
1988 Cytogenetic determination of sex among individually identified humpback whales. Can. J. Zool. 66:1243–1248.

Malme, C.I., P.R. Miles, C.W. Clark, P. Tyack, and J.E. Bird
1983 Investigations of the potential effects of underwater noise from petroleum industry activities on migrating gray whale behavior. Unpubl. rep. 5366 by Bolt, Beranek, & Newman, Inc., Cambridge, MA 02238, to Minerals Manage. Serv., 183 p.
1985 Investigations of the potential effects of underwater noise from petroleum industry activities on feeding humpback whale behavior. Unpubl. rep. 5851 by Bolt, Beranek, & Newman, Inc., Cambridge, MA 02238, to Minerals Manage. Serv., 128 p.

Mathews, E.A.
1986 Multiple uses of skin biopsies collected from free-ranging gray whales: Sex chromatin analysis, collection and processing for cell culture, microbiological analysis of associated organisms, behavioral responses of whales to biopsying, and future prospects for using biopsies in genetic and biochemical studies. M.S. thesis, Univ. Calif., Santa Cruz, 118 p.

Mayo, C., C. Carlson, P. Clapham, and D. Mattila
1985 Humpback whales of the Southern Gulf of Maine. Provincetown Cent. Coastal Stud., Provincetown, MA, 62 p.

Norris, K.S., and R.R. Reeves
1977 Report on a workshop related to humpback whales in Hawaii. NTIS Rep. PB-280 794, Springfield, VA, 90 p.

Richardson, W.J., M.A. Fraker, B. Wursig, and R.S. Wells
1985 Behavior of bowhead whales summering in the Beaufort Sea: Reactions to industrial activities. Biol. Conserv. 32: 195–230.

Scammon, C.A.
1874 The marine mammals of the northwest coast of North America. John H. Carmany, San Francisco, 319 p.

Selye, H.
1936 A syndrome induced by diverse nocuous agents. Nature (Lond.) 62:32–33.
1946 The general adaptation syndrome and the diseases of adaptation. J. Clin. Endocrinol. 6(2):117–240.

Watkins, W.A.
1981 Reaction of three species of baleen whales *Balaenoptera physalus*, *Megaptera novaeangliae*, and *Balaenoptera edeni* to implanted radio tags. Deep-Sea Res. 28(A):589–599.

Watkins, W.A., and D. Wartzok
1985 Sensory biophysics of marine mammals. Mar. Mammal Sci. 1:219–260.

Weinrich, M.T. (editor)
1985 Humpback whales of the Southern Gulf of Maine: Recent findings on habitat use, social behavior, and feeding patterns. Unpubl. spec. rep. 2, Cetacean Res. Unit, Gloucester, 42 p.

Weinrich, M.T.
1986 Observations: The humpback whales of Stellwagen Bank, 2d ed. Whale Res. Press, Gloucester, 162 p.

Zar, J.H.
1984 Biostatistical analysis. Prentice-Hall, Englewood Cliffs, 718 p.

Abstract.–Commercial landings data and research-vessel survey data collected by the Northeast Fisheries Science Center during 1982–86 were analyzed to identify spatial and temporal patterns as well as possible mechanisms associated with juvenile cod *Gadus morhua* distribution. Analysis of survey data indicated that cod ages 1–2, age 3, and age 4+ were distributed at different depths during the spring; however, during the autumn, age-3 fish co-occurred with age 1–2 fish.

Analysis of commercial landings data revealed the following patterns of distribution for age-2 cod: In quarter 1, concentrations appeared in the Nantucket Shoals region and the central portion of Georges Bank; in quarter 2, the concentration was northeast of Nantucket Shoals and also remained on Georges Bank; in quarter 3, both aggregations moved northeastward into deeper waters, along the 100 m contour of the Great South Channel and the Northern Edge, respectively; and in quarter 4, the Nantucket Shoals concentration had moved southwestward to shallower water, resuming locations identified in quarter 1, while the Georges Bank concentration remained as in quarter 3.

While intraseasonal spatial distributions did not appear to be defined by temperature, seasonal shifts in concentration of juvenile cod were most likely associated with temperature.

Manuscript accepted 20 May 1992.
Fishery Bulletin, U.S. 90:599–606 (1992).

Spatial and temporal distribution of juvenile Atlantic cod *Gadus morhua* in the Georges Bank-Southern New England region

Susan E. Wigley
Fredric M. Serchuk

Woods Hole Laboratory, Northeast Fisheries Science Center
National Marine Fisheries Service, NOAA
166 Water Street, Woods Hole, Massachusetts 02543-1097

The Atlantic cod *Gadus morhua* has accounted for more catch, by weight, than any other species in the U.S. Atlantic coast groundfish fishery during the past two decades (Serchuk and Wigley In press). Recent declines in annual landings of cod from the Georges Bank–Southern New England region (N. Atl. Fish. Org. Div. 5Z) have generated concern for the fishery. Total nominal catches (U.S. and Canadian commercial landings, plus U.S. recreational catch) from this area dropped from a high of 64,000 metric tons (t) live weight in 1982, to 27,900 t in 1986. Although catches increased to 33,700 t in 1987, 64% of the catch in numbers and 36% in weight consisted of age-2 fish from the strong 1985 year-class (NEFSC 1988). Of the various commercial market categories of cod, 'scrod' generally represents the smallest size grouping of cod landed. Scrod landings paralleled the general decline of Georges Bank cod landings, decreasing from 8100 t in 1982 to 3400 t in 1986. In addition, Northeast Fisheries Science Center (NEFSC) research-vessel survey abundance indices for spring and autumn 1987 were among the lowest observed for cod in the 25-year survey time-series (Serchuk and Wigley In press).

During the period December 1986–March 1987, anomalously high discard rates of juvenile cod below the legal minimum landed size of 19 inches (48.3 cm) TL were associated with commercial trawling operations using small mesh in the Nantucket Shoals area. This high discard level led to an emergency action extending large mesh regulation (5.5-inch mesh in codend) to this region during 23 February–31 March 1988 to "reduce fishing effort and mortality on juvenile Atlantic cod stocks found in high concentrations in this area at this time" (Federal Register, 50 CFR Part 651, 26 Feb. 1988). Large mesh regulation was permanently extended to the Nantucket Shoals area in January 1989 (Federal Register, 50 CFR Part 651, 31 Jan. 1989) (Fig. 1). In addition, the "Nantucket Shoals scrod slaughter" may have prompted the development and implementation of the Flexible Area Action System (FAAS) by the New England Fishery Management Council (NEFMC) and the National Marine Fisheries Service (NMFS). Under this plan, the Regional Director, NMFS Northeast Region, could close an area to fishing, impose mesh size restrictions, or establish catch limits for a period of 3 weeks to 6 months to minimize discards of juvenile fish. This represents a significant departure from the traditional uses of seasonal or areal closures, such as protection of adult haddock *Melanogrammus aeglefinus* during spawning (Halliday 1987).

For such a plan to be effective, knowledge of fish distribution pat-

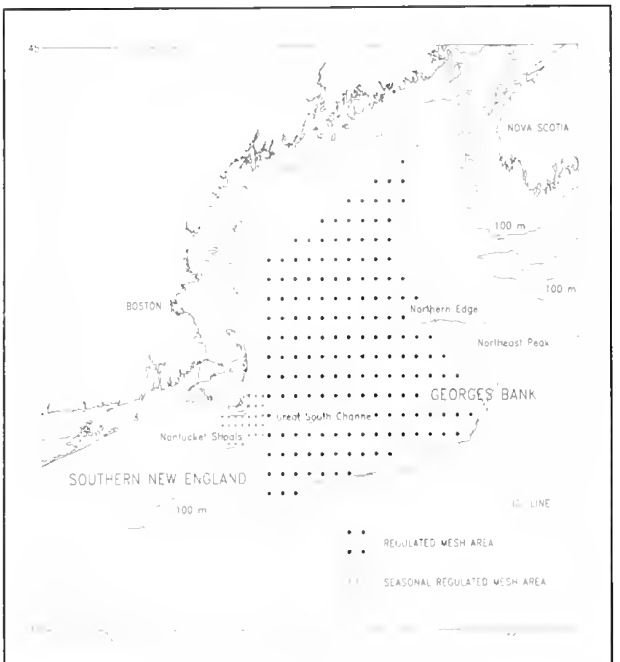

Figure 1
Georges Bank–Southern New England region of the Northwest Atlantic Ocean, showing geographic features and regulated mesh (5.5-inch) areas under the Northeast Multispecies Fishery Management Plan of the New England Fishery Management Council.

terns is necessary. In addition to documenting geographic, seasonal, and age-specific aspects of distribution, studies must examine mechanisms (such as temperature, depth, spawning, or feeding behavior) underlying these observed patterns. Numerous tagging studies have been conducted for Atlantic cod in the Northwest Atlantic: McKenzie (1934, 1956) and McCracken (1956) described cod movements in Canadian waters based on tagging experiments, and Smith (1902), Schroeder (1928, 1930), and Wise (1958, 1962) tagged cod from Woods Hole, Nantucket Shoals, and Nova Scotia to New Jersey, respectively. More recently, cod distributions delineated by bottom-trawl survey data from research vessels have been presented by Scott (1988) for Canadian waters and Grosslein and Azarovitz (1982) and Almeida et al. (1984) for U.S. waters. None of these studies considered fish size in the analyses. Overholtz (1984) found age-specific patterns of distribution for another gadoid species, haddock, in the Georges Bank region. Wigley and Gabriel (1991) and Bowman et al. (1987) examined distributions of several juvenile fishes, including cod, using NEFSC bottom-trawl survey data collected from Cape Hatteras, NC to Nova Scotia, Canada.

In our study, NEFSC commercial landings data and research-vessel survey data collected during 1982–86 were analyzed to identify spatial and temporal patterns as well as possible mechanisms associated with distributions of juvenile cod. The study period corresponds roughly to the duration of the NEFMC's Interim Fishery Management Plan for Atlantic Groundfish (31 March 1982 to 18 September 1986; NEFSC 1987). During this period, fishing practices were reasonably unchanged, although (1) an increase in minimum mesh size for the Georges Bank region from 5.125 inches (130 mm) to 5.5 inches (140 mm) was implemented on 1 April 1983, and (2) the International Court of Justice (ICJ) line dividing Georges Bank into U.S. and Canadian portions (Fig. 1) was established in October 1984. The study period also encompasses years of both strong and weak recruitment as well as a 50% reduction in spawning-stock biomass, events that allow evaluation of resulting distributions over varying year-class strengths and stock sizes.

Materials and methods

Distribution by temperature and depth

Temperature and depth analyses were based upon data collected for Atlantic cod during NEFSC spring and autumn bottom-trawl surveys during 1982–86 in the Georges Bank–Southern New England region in depths of 9–366 m. The stratified-random survey design and the standardization of survey gear and methodology are described in detail by Grosslein (1969) and Azarovitz (1981). Water-column temperature profiles, including bottom temperature (recorded to 0.1°C), were obtained on approximately half the survey stations via expendable bathythermographs; depths (m) were recorded using research-vessel electronic depth-sounding equipment. All cod were measured (FL to nearest cm) and a subset sampled for age, growth, and maturity information. Otoliths were processed and age determinations obtained according to procedures described by Penttila (1988); maturity staging was performed using classification criteria outlined by Burnett et al. (1989).

Estimates of mean temperature and depth (weighted by number of fish in each tow), and associated standard errors and ranges, were calculated by age for each season and tested for age-specific effects. Based upon results from analyses of individual age-groups, ages 1 and 2 were combined as well as fish age 4 or greater. These age-groups, as well as age-3 fish, were then retested for age-group specific effects. Assumptions of data normality were complicated by two factors. The first is the inherent nature of survey catch data as described by Pennington and Grosslein (1978), who found that the two most likely models for the distribution of fish (i.e., heterogeneous Poisson and randomly-

distributed clumps) both generated a negative binomial distribution. The second factor is that cod are not fully recruited to the survey sampling gear until age 3 or 4 (Serchuk and Wigley 1986). For these reasons, a distribution-free analysis of variance (Kruskal and Wallis 1952) was employed for statistical comparisons of temperature and depth distributions by age groups.

Spatial and temporal distribution

Commercial landings data (see Burns et al. [1983] for a detailed explanation of the commercial catch sampling program in the northeastern United States) for scrod cod collected by NEFSC during 1982–86 from the Georges Bank–Southern New England region (NEFSC Statistical Areas 521–526 and 537–539) were examined for spatial and temporal aspects of juvenile cod occurrences. Biases associated with the use of landings data were assumed to be negligible for this highly-directed fishery. Otter trawl catches account for 86–90% of the annual total cod landings (Serchuk and Wigley 1986); hence other gear types were excluded from subsequent analysis.

Table 1

Mean lengths-at-age, sample sizes, standard errors (SE), and range of observed values for age 0–10 cod *Gadus morhua* collected during NEFSC spring and autumn bottom-trawl surveys, 1982–86, in the Georges Bank–Southern New England region.

			Length (cm)		
Season	Age	N	$\bar{x}$	SE	Range
Spring	1	106	24.2	0.565	13.0–46.0
	2	458	43.8	0.253	26.0–58.0
	3	349	59.5	0.398	34.0–75.0
	4	212	69.0	0.570	46.0–89.0
	5	170	77.1	0.666	51.0–96.0
	6	69	84.7	1.013	64.0–108.0
	7	41	93.2	1.338	76.0–110.0
	8	24	102.5	2.235	79.0–124.0
	9	15	104.9	2.439	92.0–127.0
	10	5	102.8	5.678	87.0–119.0
Autumn	0	99	11.7	0.400	6.0–25.0
	1	279	36.9	0.308	23.0–51.0
	2	306	53.7	0.313	32.0–71.0
	3	145	68.0	0.557	42.0–83.0
	4	37	74.3	1.373	49.0–89.0
	5	16	85.4	2.432	60.0–99.0
	6	7	90.3	3.227	80.0–102.0
	7	6	98.8	2.613	94.0–110.0
	8	4	96.3	4.608	86.0–105.0
	9	3	105.0	5.196	96.0–114.0
	10	1	118.0	—	—

Fish in the scrod market category weigh 0.7–1.4 kg, measure 40–60 cm TL, and are 1–3 yr of age according to the growth function developed by Penttila and Gifford (1976).

Geographic resolution within Statistical Areas (SAR) was obtained by assigning the landings within each SAR to 10-min squares of latitude and longitude (~100 nm^2) based upon information from interviewed (i.e., dockside interviews of captains in which precise catch-location information was obtained) trips landing scrod cod. Scrod landings associated with interviewed trips were prorated upward for each 10-min square by the ratio, derived for each SAR, of total monthly landings to monthly interviewed landings. Prorated scrod landings were summarized quarterly for each year for each 10-min square.

Scrod cod landings were partitioned into age-groups 1, 2, 3 and 4+ by constructing a catch-at-age matrix using a technique described by Serchuk and Wigley (1986). In this method, quarterly mean weights for scrod cod were calculated by applying a length-weight equation to quarterly scrod length-frequency data; these means, in turn, were divided into scrod landings for the corresponding quarter to generate numbers landed. Age compositions for scrod landings were derived by applying quarterly age/length keys to numbers at length landed; resulting proportions at age were then applied to prorated scrod landings for each 10-min square to obtain estimates of landings by weight for each age-group.

Results

Temperature and depth distribution

Analyses of survey data were based upon 1455 and 904 cod collected during spring and autumn bottom-trawl surveys, respectively, during 1982–86. Mean lengths-at-age and associated statistics for cod ages 0–10 are presented in Table 1. Geographically, juvenile cod (defined as fish <37 cm, the minimum size at first maturity; Morse 1979) exhibited seasonal patterns of distribution. In spring, juveniles are dispersed throughout the Georges Bank–Southern New England region (Fig. 2A), while in autumn they are concentrated along the 100 m contour west of the Great South Channel and the Northern Edge and Northeast Peak of Georges Bank (Fig. 2B).

Differences in distribution with respect to both mean temperature and depth were noted for all age-groups of cod (Table 2). Mean temperatures were approximately 5.3°C in spring and 9.2°C in autumn for all age-groups, despite the fact that there was considerable overlap in the temperatures for the two seasons (Table 2). However, within seasons, differences in mean

temperature observed between age-groups were within 0.5°C, except for age-0 cod in the autumn (Table 2). In general, distribution patterns were delineated more by differences in depth than temperature.

No age-0 cod were captured during spring surveys due to their pelagic larval existence at this time (early April–early May). Age-1 and age-2 cod were found at significantly shallower mean depths than age-3 and age 4+ cod (57.0 and 58.0 m vs. 68.4 and 86.3 m, respectively; Table 2). The difference between mean depths of age-3 and age 4+ cod was also significant (Kruskal-Wallis ANOVA, $p<0.01$; Table 3). In the autumn surveys (corresponding to late September–late October), age-3 cod were observed at a mean depth similar to those for ages 1–2 (85.8 m vs. 86.8 and 85.2 m, respectively; Table 2) and significantly different (Kruskal-Wallis ANOVA, $p<0.01$; Table 3) from that for age 4+ cod (116.0 m; Table 2). Additionally, age-0 cod were captured in the autumn and observed to be distinct from all other age-groups with respect to both temperature and depth (Table 2).

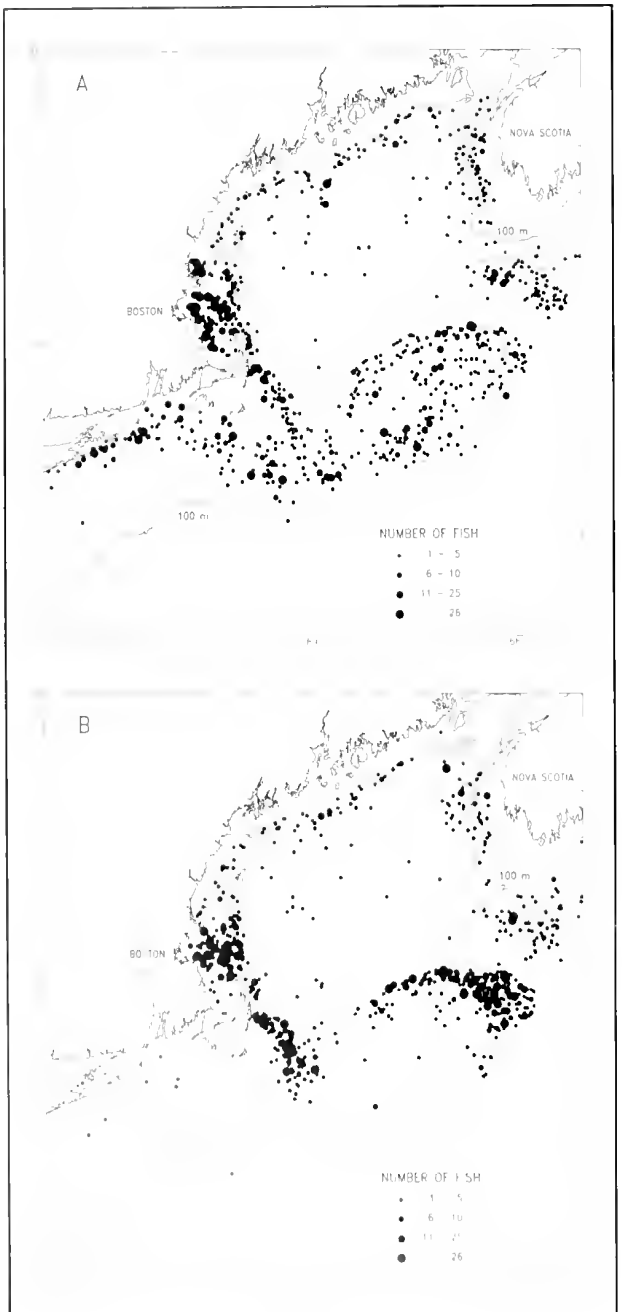

Figure 2
Geographic distribution (number/tow) of juvenile cod *Gadus morhua* <37 cm in length collected during NEFSC spring (A) and autumn (B) bottom-trawl surveys, 1968–86, in the Georges Bank–Southern New England region.

Spatial and temporal distribution

Statistical Area 521 accounted for 49% of total prorated scrod landings during the sampling period 1982–86, from a high of 57% in 1983 to a low of 29% in 1986, while SAR 523 and 522 contributed 14% and 13%, respectively; landings from Southern New England (SAR 537–539) accounted for only about 2% of total scrod landings (Table 4). Interviewed coverage was obtained for a high percentage of scrod landings

Table 2
Mean temperatures and depths, sample sizes, standard errors (SE), and range of observed values for age-groups 0, 1, 2, 3, and 4+ of cod *Gadus morhua* collected during NEFSC spring and autumn bottom-trawl surveys, 1982–86, in the Georges Bank–Southern New England region.

Season	Age	N	$\bar{x}$	SE	Range
			Temperature (°C)		
Spring	1	106	5.18	0.124	2.8–9.0
	2	458	5.03	0.050	3.3–12.1
	3	349	5.51	0.064	2.8–9.4
	4+	542	5.42	0.051	3.0–12.1
Autumn	0	99	10.02	0.233	5.8–14.3
	1	279	8.75	0.123	5.4–14.3
	2	306	9.02	0.108	5.4–14.3
	3	145	9.33	0.195	5.2–19.2
	4+	75	9.33	0.292	5.1–15.3
			Depth (m)		
Spring	1	106	56.98	2.001	25–122
	2	458	57.97	1.307	24–237
	3	349	68.36	1.966	24–210
	4+	542	86.34	2.346	25–307
Autumn	0	99	68.77	2.934	28–153
	1	279	86.80	2.185	28–230
	2	306	85.19	2.618	28–230
	3	145	85.80	3.945	31–205
	4+	75	116.00	7.793	26–328

Table 3

Results of Kruskal-Wallis analyses of variance of age-specific cod *Gadus morhua* distribution by temperature and depth by season, based on data for cod collected during NEFSC bottom-trawl surveys, 1982–86, in the Georges Bank–Southern New England region. NS = not significant, $p>0.05$; **highly significant, $p<0.01$.

Season	Age-group	Temp.	Depth
Spring	3 vs. 4+	NS	**
	1–2 vs. 3	**	**
	1–2 vs. 4+	**	**
Autumn	3 vs. 4+	NS	**
	1–2 vs. 3	NS	NS
	1–2 vs. 4+	NS	**

Table 4

Scrod cod *Gadus morhua* landings (t, live weight) by Statistical Area and year, 1982–86, in the Georges Bank–Southern New England region. Percentages of NEFSC commercial scrod landings for which interviewed coverage was obtained are given in parentheses. (Statistical Areas are shown in Figs. 3A–3D.)

Area	1982	1983	1984	1985	1986
521	4564(76)	4350(76)	1396(81)	3033(93)	1022(87)
522	1025(71)	978(73)	415(75)	855(93)	476(84)
523	1215(83)	958(95)	766(91)	939(87)	365(96)
524	554(68)	411(92)	517(92)	568(92)	757(84)
525	240(66)	109(80)	150(77)	204(91)	118(83)
526	466(92)	665(76)	413(90)	743(95)	579(84)
537	76(68)	135(73)	103(76)	60(74)	168(50)
538	4(30)	7(59)	3(61)	5(20)	5(60)
539	10(28)	3(22)	1(30)	<1(27)	<1(14)
Total	8154(76)	7616(79)	3764(84)	6407(92)	3490(84)

Table 5

Age composition by weight (t, live weight) of scrod cod *Gadus morhua* landings by quarter, 1982–86, in the Georges Bank–Southern New England region.

Year	Age-group	Quarter 1	2	3	4	Scrod total
1982	1	0	0	4	230	234
	2	417	1140	3141	1836	6534
	3	190	469	203	31	893
	4+	198	240	56	0	494
	Total	805	1849	3404	2097	8155
1983	1	0	0	16	61	77
	2	199	976	1554	1260	3989
	3	437	1170	965	502	3074
	4+	212	156	93	15	476
	Total	848	2302	2628	1838	7616
1984	1	0	0	1	78	79
	2	73	381	395	418	1266
	3	611	672	395	102	1780
	4+	236	182	185	33	636
	Total	920	1235	976	631	3762
1985	1	0	0	10	101	111
	2	304	1002	1813	1826	4945
	3	192	510	335	123	1160
	4+	96	46	43	6	191
	Total	592	1558	2201	2056	6407
1986	1	0	0	0	120	120
	2	162	467	193	249	1071
	3	948	850	289	52	2139
	4+	148	4	8	0	160
	Total	1258	1321	490	421	3490

(76–92% annually during the period; Table 4), suggesting that the proration procedure employed in this study accurately depicts the patterns of landings.

Age-2 cod dominated commercial landings of scrod in all years except 1984 and 1986, when age-3 fish comprised the majority (Table 5); this exception is due to weak 1982 and 1984 year-classes (Serchuk and Wigley In press). Age-1 fish are too small to be caught by the commercial gear until quarters 3 and 4; conversely, age 4+ fish grow out of the scrod market category and into the next market category after quarter 2 (Table 5). Based upon these observations, and the observation above from analysis of survey data that age-3 cod are seasonally segregated from ages 1–2, analysis of juvenile cod distribution from commercial data was confined to age-2 fish.

The following patterns of age-2 juvenile cod distribution emerged. In quarter 1, juvenile cod were concentrated in the Nantucket Shoals region (south of the stepped portion of the boundary between SAR 521 and 526) as well as being dispersed generally across the shallower central portions of Georges Bank, primarily in SAR 522 and 524 (Fig. 3A). By quarter 2, the area concentration was north of Nantucket Shoals (in SAR 521), while on Georges Bank there continued to be a dispersed distribution as in quarter 1 (Fig. 3B). In quarter 3, the Nantucket Shoals concentration had moved northeastward within SAR 521 to deeper water along the 100 m contour of the west slope of the Great South Channel; similarly, juveniles on Georges Bank had formed concentrations along the 100 m contour in SAR 522 (the east slope of the Great South Channel) and 523 (the Northern Edge and Northeast Peak areas; Fig. 3C). By quarter 4, the Nantucket Shoals concentration had

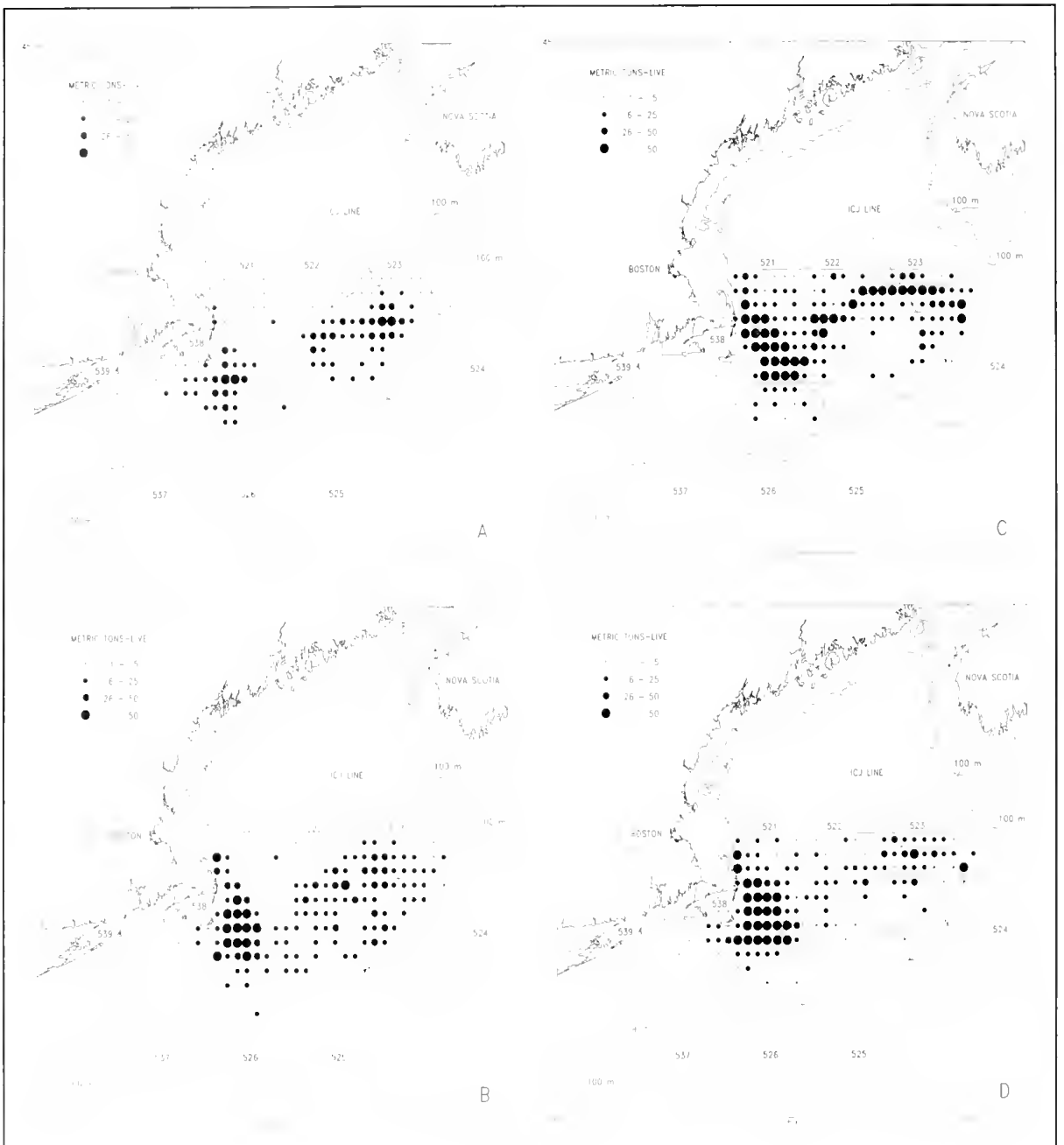

Figure 3

Distribution of age-2 cod *Gadus morhua* by 10-min squares of latitude and longitude from NEFSC serod landings data (t, live weight), 1982–86, for quarters 1 (A), 2 (B), 3 (C), and 4 (D) in the Georges Bank–Southern New England region.

shifted south and southwestward within SAR 521 to shallower water and into SAR 526, resuming locations identified in quarter 1; however, the concentration on Georges Bank in SAR 523 was still present (Fig. 3D).

Visual inspection of quarterly distribution plots for each year suggested that these patterns of juvenile cod concentrations persisted over varying year-class strengths and stock sizes; however, in the interest of space, only aggregate plots are presented (Figs. 3A–3D). Age-2 cod from strong 1980 and 1983 year-classes (Serchuk and Wigley In press) exhibited the same seasonal movements described above, as did age-2 fish from the relatively weak 1982 and 1984 year-classes. Similarly, no changes in observed annual patterns were evident from 1982 to 1986, during which time spawning-stock biomass diminished from over 80,000 t to about 33,000 t (Serchuk and Wigley In press).

Discussion

The observed seasonal variation in distribution of age-3 cod relative to age groups 1–2 and 4+ may be associated with a transitional period involving both maturation and feeding habits. Age 3 encompasses a period in which there is a mismatch in size-at-first-maturity and the attainment of the adult diet. Median size and age at sexual maturity for cod is about 50 cm and 2.5 yr, respectively (Livingstone and Dery 1976), and during spring some age-3 fish recruit to the spawning population. Autumnal co-occurrence of age-3 fish with ages 1–2 may be related to diet. Bowman and Michaels (1984) presented data which indicate that cod <66–70 cm have not assumed the adult diet dominated by fish; the mean length of age-3 cod in autumn is 68.0 cm (Table 1).

In a mathematical evaluation of spatial distributions of several North Sea species, Houghton (1987) suggested that cod distributions were more complex and less persistent than those observed for haddock or flatfish. In this study, however, the spatial and temporal patterns observed for juvenile Atlantic cod from landings data were remarkably uniform over the study period, and did not seem to vary according to stock size or year-class strength. The use of commercial data in this study is somewhat constrained by management regulations, fishing practices, and the distribution of fishing effort, yet results from analysis of survey data in this study seem to corroborate these conclusions.

The use of mean values in this study to define patterns of temperature and depth distribution may better reflect general tendencies rather than absolute preferences; in actuality, cod of all ages except age 0 were found at virtually all available temperatures and depths. Yet the patterns that emerged in this study are, for the most part, consistent with those identified in other studies. Both Schroeder (1930) and Wise (1962) noted the tendency for older cod to move into greater depths. Scott (1988) found that cod in colder Canadian waters were distributed at temperatures of 2–10°C, with largest catches occurring at 4–6°C. The apparent contradiction posed by the movement of cod to deeper, warmer water in winter–spring observed by Scott (1988), and the observations in this study of movement to shallower water on Nantucket Shoals and Georges Bank during this period, is an artifact of the different temperature regimes for the two regions; in each case, cod are changing depth locations to maintain preferred temperatures. Schroeder (1930) reported cod occurrences within an annual range of 0–17°C in the region from Nantucket Shoals to North Carolina, and attributed the triggering of the autumn migration of Nantucket Shoals adult cod westward to New Jersey for winter spawning to falling bottom temperatures in October. Similarly, movements of juvenile cod from Nantucket Shoals to deeper water off Chatham and the Great South Channel in summer–early autumn were thought to be in response to locally-available, cooler temperatures (Schroeder 1930). Wise (1958, 1962) determined from tagging studies that a resident population of cod inhabited the Nantucket Shoals–Great South Channel area year-round, but that Nantucket Shoals also represented the summer residence for the population of cod that wintered off the coast of New Jersey. Thus, the distribution patterns observed in this study within SAR 521 and 526 would most likely reflect seasonal movements of resident cod, although the migratory population may partially contribute to landings for quarters 2 and 3 in SAR 526.

Scott (1982) concluded from an analysis of fish distribution by bottom type that, although generally associated with sand-gravel sediments, cod occurred over all substrates and that observed patterns of distribution were more likely due to the bottom-type preferences of major prey items (e.g., *Cancer* crabs, sand lance, *Ammodytes* sp., etc). Although no quantitative analysis of distribution by bottom sediment was undertaken here, the seasonal shifts in concentration identified in this study do not suggest any major change in substrate preference of cod. However, the Great South Channel and the Northern Edge–Northeast Peak regions, where concentrations of scrod cod occur in quarters 3 and 4, are characterized by coarser sediment types than those generally found elsewhere on Georges Bank (Wigley 1961, Schlee 1973).

Based on the above analyses, there is evidence for well-defined seasonal and geographic shifts in concentration for juvenile Atlantic cod in the Georges Bank–Southern New England region. Moreover, these patterns of concentration appear to be associated primarily with temperature. The high level of spatial and temporal resolution possible, i.e., 10-min squares of latitude and longitude and quarters, suggest that this type of study may be useful in assisting fisheries managers with decisions regarding seasonal and areal closures under the Flexible Area Action System.

Acknowledgments

We express our thanks to S.L. Brunenmeister for her assistance in the initial stage of this work, J. Burnett and R.K. Mayo of the NEFSC and anonymous reviewers for their helpful comments and review of this manuscript, and N.G. Buxton of the NEFSC for graphic assistance.

Citations

Almeida, F.P., T.R. Azarovitz, L. O'Brien, and E.M. Pritchard
1984 The distribution of major finfish and shellfish species collected during NEFC bottom trawl surveys, 1965–1978. Ref Doc. 84-21, NMFS Woods Hole Lab.,101 p.

Azarovitz, T.R.
1981 A brief historical review of the Woods Hole laboratory trawl survey time series. *In* Doubleday, W.G., and D. Rivard (eds.), Bottom trawl surveys, p. 62–67. Can. Spec. Publ. Fish. Aquat. Sci. 58.

Bowman, R.E., and W.L. Michaels
1984 Food of seventeen species on northwest Atlantic fish. NOAA Tech. Memo. NMFS-F/NEC-28, Northeast Fish. Sci. Cent., Woods Hole, 183 p.

Bowman, R.E., T.R. Azarovitz, E.S. Howard, and B.P. Hayden
1987 Food and distribution of juveniles of seventeen northwest Atlantic fish species, 1973–1976. NOAA Tech. Memo. NMFS-F/NEC-45, Northeast Fish. Sci. Cent., Woods Hole, 57 p.

Burnett, J.M., L. O'Brien, R. Mayo, J. Darde, and M. Bohan
1989 The history of maturity sampling and classification schemes used during the NEFC bottom trawl survey program, 1963–1989. NOAA Tech. Memo. NMFS-F/NEC-76, Northeast Fish. Sci. Cent., Woods Hole, 33 p.

Burns, T.S., R. Schultz, and B.E. Brown
1983 The commercial catch sampling program in the northeastern United States. *In* Doubleday, W.G., and D. Rivard (eds.), Sampling commercial catches of marine fish and invertebrates, p. 82–95. Can. Spec. Publ. Fish. Aquat. Sci. 66.

Grosslein, M.D.
1969 Groundfish survey program of BCF Woods Hole. Commer. Fish. Rev. 31 (8–9):22–35.

Grosslein, M.D., and T.R. Azarovitz
1982 Fish distribution. MESA (Mar. Ecosyst. Anal.) N.Y. Bight Atlas Monogr. 15, 182 p.

Halliday, R.G.
1987 Haddock spawning area closures in the northwest Atlantic, 1970–87. NAFO (N. Atl. Fish. Org.) SCR Doc. 87/13, Ser. N1291, 22 p.

Houghton, R.G.
1987 The consistency of the spatial distribution of young gadoids with time. ICES CM 1987/D:15, 6 p.

Kruskal, W.H., and W.A. Wallis
1952 Use of ranks in one-criterion variance analysis. J. Am. Stat. Assoc. 47:583–621.

Livingstone, R. Jr., and L. Dery
1976 An observation on the age and length at maturity of cod on the Georges and Browns stock. ICNAF (Int. Comm. Northwest Atl. Fish.) Res. Doc. 76/VI/42, Ser. 3826, 2 p.

McCracken, F.P.
1956 Cod and Haddock tagging off Lockeport, Nova Scotia. Fish. Res. Board Can., Prog. Rep. Atl. coast stns 64: 10–15.

McKenzie, R.A.
1931 Cod movements on the Canadian Atlantic coast. Contrib. Can. Biol. Fish., new ser. 8 (31) [Ser. A, General (46)]: 434–458.
1956 Atlantic cod tagging off the southern Canadian mainland. Fish. Res. Board Can., Bull. 105, 93 p.

Morse, W.W.
1979 An analysis of maturity observations of 12 groundfish species collected from Cape Hatteras, North Carolina to Nova Scotia in 1977. Ref Doc. 79-32, NMFS Sandy Hook Lab., 20 p.

NEFSC
1987 Status of mixed species demersal finfish resources in New England and scientific basis for management. Ref. Doc. 87-08, NMFS Woods Hole Lab., 105 p.
1988 Status of the fishery resources off the northeastern United States for 1988. NOAA Tech. Memo. NMFS-F/NEC-50, Woods Hole, 132 p.

Overholtz, W.J.
1984 Seasonal and age specific distribution of the 1975 and 1978 year-classes of haddock on Georges Bank. NAFO (Northwest Atl. Fish. Organ.) Sci. Counc. Stud. 8:77–82.

Pennington, M.R., and M.D. Grosslein
1978 Accuracy of abundance indices based on stratified trawl surveys. ICNAF (Int. Comm. Northwest Atl. Fish.) Res. Doc. 77, Ser. 5264, 42 p.

Penttila, J.
1988 Atlantic cod *Gadus morhua*. *In* Penttila, J., and L.M. Dery (eds.), Age determination methods for Northwest Atlantic species, p. 31–36. NOAA Tech. Rep. NMFS 72.

Penttila, J.A., and V.M. Gifford
1976 Growth and mortality rates of cod from the Georges Bank and Gulf of Maine areas. ICNAF (Int. Comm. Northwest Atl. Fish.) Res. Bull. 12:29–36.

Schlee, J.S.
1973 Atlantic continental shelf and slope of the United States—sediment texture of the northeastern part. U.S. Geol. Surv. Prof. Pap. 529L, 64 p.

Schroeder, W.C.
1928 Cod studies. *In* Higgins, E. (ed), Progress in biological inquiries 1926, including the proceeding of the divisional conference, January 4–7, 1927. Rep. U.S. Comm. Fish., fiscal year 1927. Doc. 1029, app. 7, p. 601–605.
1930 Migrations and other phases in the life history of the cod off southern New England. Bull. U.S. Bur. Fish. 46, 136 p.

Scott, J.S.
1982 Selection of bottom type by groundfishes of the Scotian Shelf. Can. J. Fish. Aquat. Sci. 39:943–947.
1988 Seasonal spatial distributions of groundfish of the Scotian shelf and Bay of Fundy, 1974–79 and 1980–84. Can. Tech. Rep. Fish. Aquat. Sci. 1653, 75 p.

Serchuk, F.M., and S.E. Wigley
In press Assessment and management of the Georges Bank cod fishery: An historical review and evaluation. J. Northwest Atl. Fish. Sci.
1986 Assessment and status of the Georges Bank and Gulf of Maine Atlantic cod stocks—1986. Ref. Doc. 86-12, NMFS Woods Hole Lab., 84 p.

Smith, H.M.
1902 Notes of the tagging of 4,000 adult cod at Woods Hole, Mass. U.S. Comm. Fish Fish., Part 27, Rep. of the Comm., year ending June 30, 1901, p. 193–208.

Wigley, R.L.
1961 Bottom sediments of Georges Bank. J. Sediment Petrol. 31:165–188.

Wigley, S.E., and W.L. Gabriel
1991 Distribution of sexually immature components of ten Northwest Atlantic groundfish species, based on Northeast Fisheries Center Bottom Trawl Surveys, 1968–1986. NOAA Tech. Memo. NMFS-F/NEC-80, Northeast Fish. Sci. Cent., Woods Hole, 17 p.

Wise, J.P.
1958 The world's southernmost indigenous cod. J. Cons. Cons. Int. Explor. Mer 23:208–212.
1962 Cod groups in the New England. Fish Bull., U.S. 62:189–203.

Larval development of two sympatric flounders, *Paralichthys adspersus* (Steindachner, 1867) and *Paralichthys microps* (Gunther, 1881) from the Bay of Coquimbo, Chile

Humberto N. Zuñiga
Enzo S. Acuña

Departemento Biología Marina, Universidad Católica del Norte
Sede Coquimbo, Casilla 117, Coquimbo, Chile

Abstract.–Developmental series of two sympatric flounders of the genus *Paralichthys*, found in the Bay of Coquimbo, are illustrated and described. The series consist of yolksac to metamorphosed larvae of artificially-reared *Paralichthys adspersus* (1.7–13.0mm SL) and *P. microps* (1.5–11.0mm SL). Field-collected larvae correspond to the size ranges found in reared larvae. Degree of cephalic spination (in particular, sphenotic spines), pigmentation pattern, and number of elongated dorsal-fin rays are useful for identification of yolksac-to-postflexion larvae of both species.

During early metamorphosis the most valuable characteristics for identification are the number of elongated dorsal-fin rays, although after their reabsorption several morphometric relationships have to be used. *Paralichthys adspersus* preflexion larvae have two sphenotic spines and almost no pigmentation in the dorsal finfold, while *P. microps* larvae have only one sphenotic spine and a well-pigmented dorsal finfold. Beginning at notochordal flexion, the number of elongated dorsal-fin rays, six for *P. microps* and three for *P. adspersus*, can be used to identify the larvae. During late metamorphosis, morphometric relationships of SnL/HL, HL/SL, and BD/SL must be used to identify the larvae. Flexion is complete at 7.2mm SL and metamorphosis at ~11.0mm SL in *P. microps*, and at 8.6mm SL and 13.0 mm SL in *P. adspersus*, respectively.

Manuscript accepted 20 May 1992.
Fishery Bulletin, U.S. 90:607–620 (1992).

Paralichthys is one of the most important genera of flatfish on both coasts of North and South America (Ginsburg 1952), considering number of species, geographic distribution, and economic importance. Seven species of the genus have been reported in Chilean waters (Bahamonde and Pequeño 1975), *Paralichthys adspersus* (Steindachner 1867) and *P. microps* (Gunther 1881) being the most abundant and most widely distributed. The former is found from the coast of Paita (Peru) to Lota (Chile) and Juan Fernández Island; the latter from Huacho (Peru) to the austral tip of South America (Chirichigno 1974). Because these two morphologically-similar species co-occur over most of their distributional ranges, adult and larval identifications have been difficult. Muñoz et al. (1988) described larvae of *P. microps*, but recognized the possibility that specimens of both species were included in their sample. They indeed have one *P. adspersus* larva (3.2mm, Fig. 2b). Silva (1988) published photographs of the eggs and some larvae of *P. microps*.

In this paper, taxonomic characters which separate these two species during early-life-history stages, from yolksac larva to juvenile, are described.

Material and methods

Most of the material examined in the present study was obtained from several experiments, resulting from artificial fertilization of eggs and sperm from ripe specimens captured in the Bay of Coquimbo (29°59′S).

Larvae were cultured in 200L conical tanks, with a daily 25% water renewal. From hatching through flexion, larvae were fed the rotifer *Brachionus plicatilis* in concentrations of 5/mL, and from flexion through metamorphosis were fed *Artemia salina* nauplii in concentrations of 10/mL. Temperature range during the experiment was 13–17°C (Silva 1988). Larvae, sampled with a Bongo net (1m, 500μ mesh) and an epibenthic trawl (500μ mesh) at stations in Coquimbo Bay and adjacent coastal areas, were compared with cultured larvae.

A total of 49 larvae of *P. adspersus* and 46 of *P. microps* were used; of these, 39 larvae of both species were cleared and stained using Potthoff's (1984) method to determine the sequence of development of the axial skeleton. Pterygiophores and rays were counted when present, regardless of their state of development. Larvae were anesthesized with MS-222 before fixing in 5% formalin, and were later preserved in 3% buffered formalin.

Specimens were divided into developmental stages following the definitions of Ahlstrom et al. (1976).

Table 1

Morphometric relationships in *Paralichthys adspersus* and *P. microps* larvae. N = number of specimens; measurements in mm; length = NL for preflexion–flexion stages, SL for postflexion–juvenile.

	Preflexion			Flexion		
Measure	$\bar{x}$	SD	Range	$\bar{x}$	SD	Range
Paralichthys adspersus						
N		21			11	
Length	5.52	1.12	(3.6–7.0)	7.80	0.55	(6.9–8.6)
PAL/SL	41.40	1.32	(40.5–43.5)	39.60	3.08	(31.9–42.0)
BD/SL	13.90	3.80	(13.0–18.1) 17*	22.80	5.08	(17.4–31.4)
BD†/SL						
HL/SL	18.20	1.13	(16.7–20.0)	21.50	2.53	(18.6–26.7)
UJL/HL	37.30	4.52	(29.4–39.4) 17*	37.90	2.32	(33.3–41.7)
LJL/HL	46.30	3.08	(41.2–51.8) 19*	48.10	3.15	(44.7–54.7)
SnL/HL	22.10	2.22	(18.3–26.8)	21.10	1.02	(18.9–22.4) 10*
ED/HL	28.00	2.36	(24.8–33.3)	26.80	1.50	(24.7–28.9)
Paralichthys microps						
N		22			8	
SL	4.17	0.95	(2.95–6.0)	6.86	0.35	(6.2–7.2)
PAL/SL	41.15	1.83	(38–44)	40.90	3.27	(35–45)
BD/SL	13.30	2.16	(10–18)	25.60	6.40	(19–37)
BD†/SL						
HL/SL	18.10	1.48	(15–20)	21.60	3.70	(17–28)
UJL/HL	34.60	3.60	(29–37) 11*	44.50	4.20	(38–50)
LJL/HL	51.98	4.50	(43–59) 20*	57.10	3.86	(50–62)
SnL/HL	22.90	3.56	(16–31) 20*	23.90	2.88	(20–28)
ED/HL	30.10	4.10	(23–43) 21*	26.80	1.70	(24–29)

	Postflexion			Metamorphosis			Juvenile		
Measure	$\bar{x}$	SD	Range	$\bar{x}$	SD	Range	$\bar{x}$	SD	Range
Paralichthys adspersus									
N		7			6			4	
SL	8.90	0.35	(8.4–9.4)	10.00	0.53	(9.2–10.2)	13.60	1.04	(12.3–15.0)
PAL/SL	40.80	2.76	(37.6–45.2)	37.60	3.17	(33.9–43.5)	34.40	0.68	(33.3–35.0)
BD/SL	35.80	1.77	(33.7–38.2)	39.50	1.42	(36.6–41.3)	37.90	0.72	(37.2–39.0)
BD†/SL				41.90	2.90	(36.4–45.8)	35.30	0.83	(34.4–36.2)
HL/SL	30.60	2.35	(27.6–33.7) 6*	32.00	1.69	(29.7–34.7)	35.10	0.38	(34.7–35.7)
UJL/HL	34.10	1.71	(31.5–37.3)	34.50	1.49	(31.7–36.5)	34.40	0.94	(33.3–35.6)
LJL/HL	45.60	2.61	(41.7–50.5)	45.90	1.35	(42.9–48.4)	46.80	1.50	(44.4–48.1)
SnL/HL	20.70	2.55	(17.5–25.8)	18.30	1.66	(15.6–20.3) 5*	14.30	1.76	(11.5–16.3)
ED/HL	25.50	1.07	(24.1–26.8) 6*	25.00	2.57	(21.4–28.6)	28.70	2.09	(26.3–32.0)
Paralichthys microps									
N		4			8			4	
SL	6.90	0.77	(6–7.8)	9.30	0.67	(8.10–10.6)	15.20	1.95	(13.0–18.0)
PAL/SL	42.20	3.40	(37–46)	39.40	2.47	(36.2–43.5)	35.30	0.83	(34.4–36.2)
BD/SL	44.70	6.20	(35–46)	40.00	1.39	(37.7–42.0)	37.40	0.86	(36.2–38.5)
BD†/SL				46.50	1.03	(45.4–48.9)			
HL/SL	37.30	5.10	(32–46)	39.10	2.68	(35.8–43.0)	37.40	1.19	(36.3–39.4)
UJL/HL	38.90	2.10	(35–41)	37.80	2.09	(34.7–39.7) 6*	35.60	1.47	(34.3–38.0)
LJL/HL	50.70	4.30	(42–56)	47.90	2.70	(44.2–51.7) 6*	45.80	1.86	(43.1–46.9)
SnL/HL	23.20	1.90	(20–25)	23.30	1.73	(21.3–26.6) 6*	16.70	1.39	(15.5–19.0)
ED/HL	24.40	0.70	(23–25)	25.10	1.32	(23.0–26.6)	28.80	1.99	(25.4–30.2)

*N differs from number indicated above.

BD Body depth
BD† Body depth measured at anus
ED Eye diameter
HL Head length
LJL Lower jaw length
PAL Preanal length
SL Standard length
SnL Snout length
UJL Upper jaw length

Morphometric measurements follow the definitions of Gutherz (1970) and were made with an ocular micrometer (to 0.01 mm). Notochordal length (NL) was used for yolksac larvae through flexion: from then on, standard length (SL) was utilized. In preflexion and flexion larvae, body depth (BD) is defined as the vertical distance across the body at the anus including the dorsal-fin pterygiophores. After flexion, it is defined as the vertical distance across the body at the pelvic fin, from its base to the base of dorsal-fin rays. Head length (HL) is defined as the distance from the snout to the cleithrum, until and through flexion, and thereafter from snout to the opercle edge. The total number of myomeres and vertebrae does not include the urostyle. Drawings were made from a compound microscope equipped with a camera lucida.

Linear regression models were fitted to six morphometric relationships of the larvae, comparing the preflexion stages with flexion, postflexion, and metamorphosis, to separate larvae of both species. An F test (Neter and Wasserman 1974) was used to compare the morphometric relationships of these two groups of larvae within and between species.

Determination of *Paralichthys* adults was based on

Table 2

Osteological development sequence of fins in *Paralichthys adspersus* and *P. microps* larvae. Length = NL preflexion, SL postflexion.

	Paralichthys adspersus						*Paralichthys microps*					
	Rays + Pterygiophores		Rays + Radials		Rays		Rays + Pterygiophores		Rays + Radials		Rays	
SL	Dorsal	Anal	Pelvic	Pectoral	Caudal	Vertebrae	Dorsal	Anal	Pelvic	Pectoral	Caudal	Vertebrae
4.1							–	–	–	–	–	–
4.5							–	–	–	–	–	–
4.7	–	–	–	–	–	–						
4.8	–	–	–	–	–	–						
5.4	–	–	–	–	–	–						
5.5							0+1	–	–	–	–	–
5.9							0+2	–	–	–	–	–
6.1		–	–	–	–	–	2+2	–	–	–	–	–
6.2							3+3	–	–	–	–	–
6.2							3+3	–	–	–	–	–
6.5							3+4	–	–	–	–	3
6.5							4+5	0+20	–	–	–	27+–
6.7	2+3	–	–	–	–	–						
6.9	3+3	–	–	–	–	–						
7.0							9+60	24+49	–		6+7	29+–
7.1							64+62	53+51	3+0		8+7	30+–
7.2							69+68	?+53	5+0		1+9+8+1	34
7.7	3+3	–	–	–	–	9	71+69	57+55	5+0		1+10+8+1	34
7.7	3+4	–	–	–	–	26						
7.8							71+71	53+53	5+0		1+10+9+0	34
8.1	5+4	–	–	–	–	32	73+72	57+54	6+0		0+10+8+0	34
8.1	6+30	0+23	–	–	–	33						
8.1	10+60	0+48	–	–	–	33						
8.2	13+48	0+42	–	–	9+8	33						
8.5	45+64	38+51	3+0	–	9+9	33						
8.6	56+65	30+51	3+0	–	1+9+8+1	33	73+73	58+57	6+0	–	1+9+9+1	34
8.6	64+66	50+51	4+0	–	1+9+8+1	33						
8.6	69+67	55+53	5+0	–	1+9+8+1	33						
8.8	73+72	55+55	5+0	–	1+10+9+1	33						
9.2	71+71	57+57	5+0	–	1+9+9+1	32	75+75	60+59	6+0	0+2	1+10+8+1	34
9.7				–			75+75	64+61	6+0	3+0	1+10+8+1	35
10.1	74+72	59+57	6+0	–	1+9+9+1	34	72+71	58+56	6+2	6+3	1+10+9+1	33
10.2	70+70	54+53	6+0	0+3	1+9+9+1	33						
10.9	71+70	57+55	6+2	7+4	1+9+9+1	33						
11.3							70+68	59+57	6+3	14+4	1+9+9+1	34
12.3	68+66	55+54	6+3	14+4	1+10+9+1	33						
12.7							73+72	59+56	6+3	14+4	1+9+9+1	33
14.0	70+69	57+56	6+3	13+4	1+9+8+1	33						

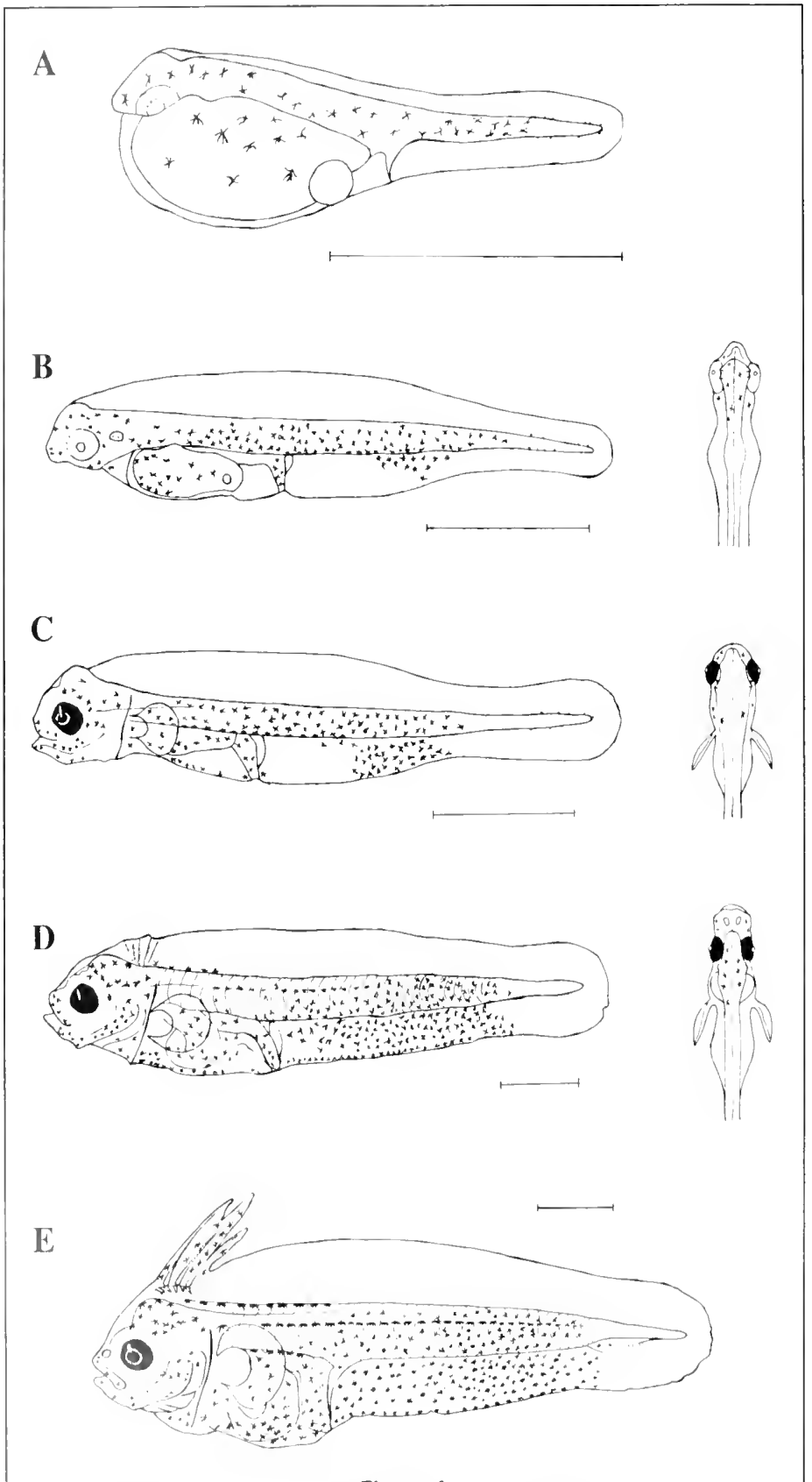

Figure 1

Parahchthys adspersus larvae. (A) Early yolksac, 1.7 mm NL; (B) late yolksac, 3.4 mm NL; (C) early preflexion, 3.9 mm NL; (D) late preflexion, 6.8 mm NL; (E) flexion, 7.7 mm NL. Drawings at right are dorsal head views.

the criteria of Ginsburg (1952), who observed that the origin of the dorsal fin in *P. microps* was over the center of the upper eye, while in *P. adspersus* it was over the eye's anterior margin. Furthermore, the number of gill rakers over the lower portion of the first arch is larger in *P. microps* (18–23) than in *P. adspersus* (15–19). An additional criterion found by Zuñiga (1988) referring to the size of the nostrils was also used.

Description

Paralichthys adspersus

Hatching occurs ~60 hours after fertilization. Larvae are ~1.7 mm NL; yolksac is more than half the body length; a small oil globule (0.13 mm) is present posterior to the yolksac (Fig. 1A).

Diagnosis The most important distinguishing features of preflexion *P. adspersus* larvae are the presence of two sphenotic spines (Fig. 2) and the lack of pigmentation in the dorsal finfold (Fig. 1). This last character may be useful through postflexion. Starting at notochord flexion, the presence of two groups of numerous opercular and preopercular spines, as well as 2–3 elongated dorsal-fin rays, is diagnostic. This last feature is useful until metamorphosis. Beyond metamorphosis, diagnosis should be based mostly on morphometric relationships.

Pigmentation Eyes of yolksac larvae are not pigmented. Few, relatively-large melanophores are found on the head, trunk, and yolksac except at the ventral margin (Fig. 1A). A series of small melanophores is present near the tip of the notochord. Pigment forms

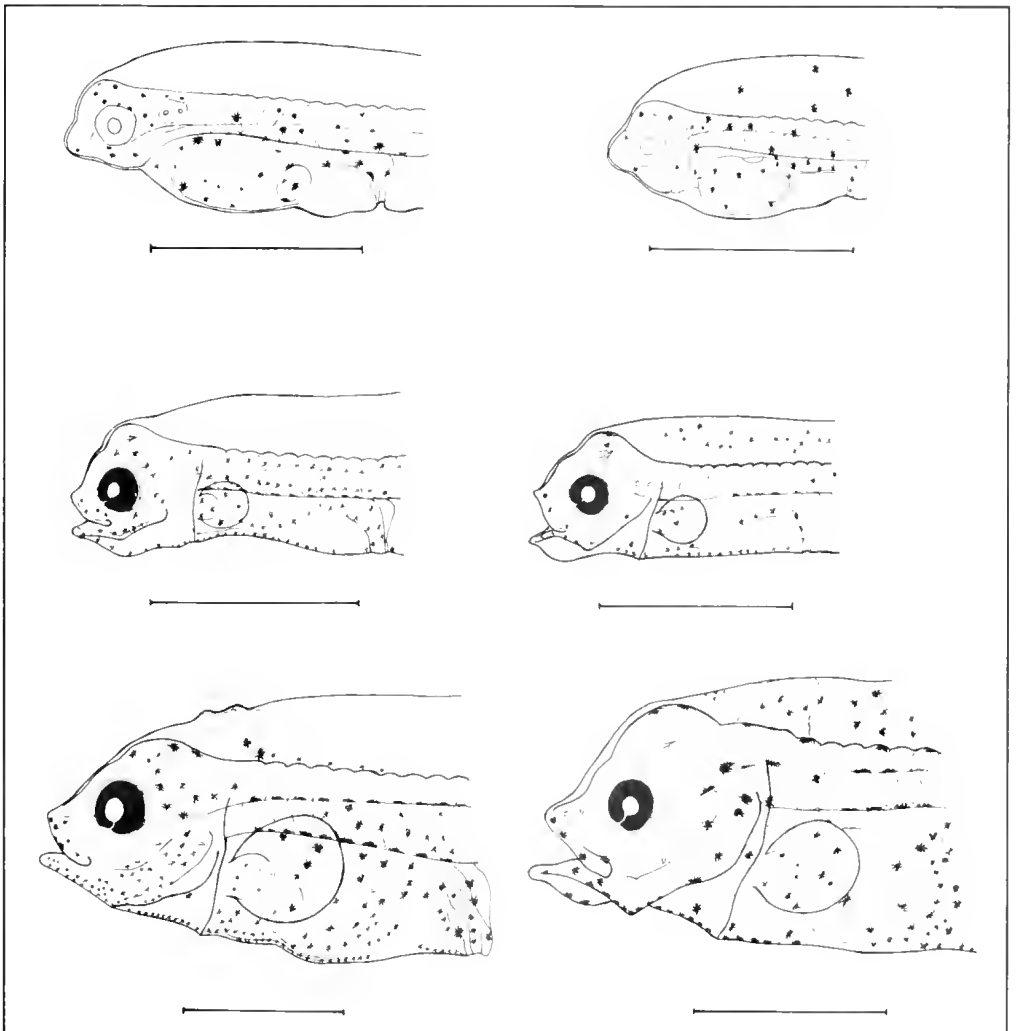

Figure 2

Heads of *Paralichthys adspersus* (left) and *P. microps* (right) larvae, showing number, size, and location of sphenotic, preopercular, and opercular head spines. Bars = 1.0 mm.

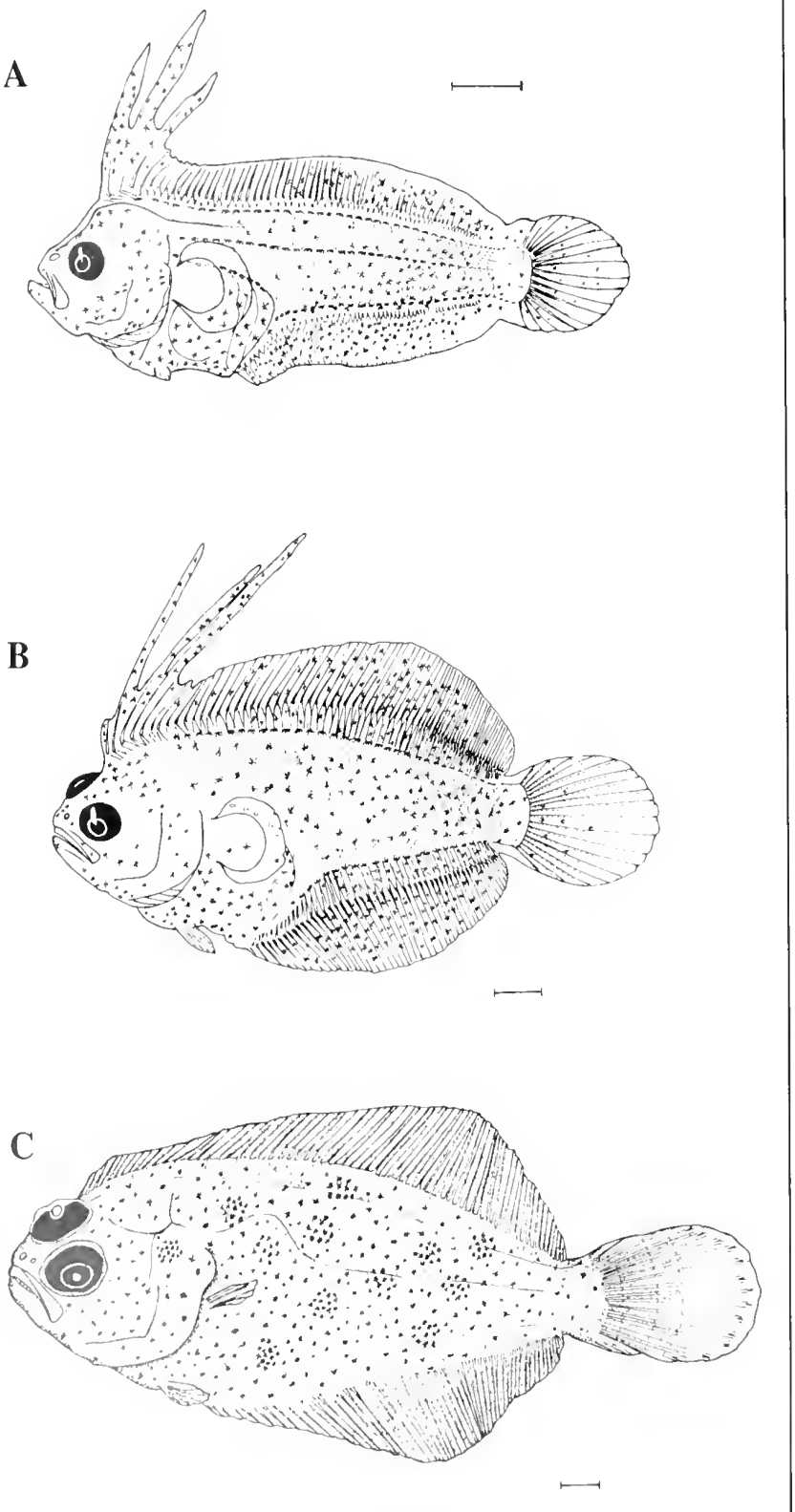

Figure 3

Paralichthys adspersus larvae. (A) Early postflexion, 8.8 mm SL; (B) early metamorphosis, 10.3 mm SL; (C) juvenile, 14.3 mm SL. Bars = 1.0 mm.

on the medial region of the pelvic fin. At the end of the stage (Fig. 1B), the eyes start to pigment.

During the preflexion stage (Fig. 1C, D), stellate melanophores are present on the head and over the anterior 2/3 of the body. Melanophores are absent on the dorsal finfold. At 3.5 mm NL, a series of melanophores forms on each side, slightly dorsal to the midline. At 4.0 mm NL, an embedded series of melanophores begins to develop dorsal to the notochord. A series of melanophores is present at the ventral margin of the body, from the gular region to the anus.

Head pigmentation consists of melanophores over both jaws, preopercle, opercle, and dorsal and lateral brain region. At about 5.0 mm NL, a melanophore is found internally above the palate, where it persists until metamorphosis.

At the beginning of the flexion stage (Fig. 3A), pigment intensifies in the tail region. The dorsal finfold generally remains unpigmented; however, a few melanophores appear in some specimens. A paired series of melanophores develops above the dorsum. Tail melanophores concentrate in the ventrolateral region, while the paired series dorsal to the notochord is less visible. The paired series dorsal to the gut becomes continuous with the gular–abdominal series. Head pigmentation increases. The interradial membrane of the elongated dorsal-fin rays becomes pigmented. Melanophores near the tip of the notochord persist but migrate as the caudal fin develops.

During postflexion (Fig. 3B), the melanistic pattern is similar to the previous stage except the paired dorsal series is more evident. The dorsal fin is pigmented, particularly in the posterior half, and the ventral region of the abdomen becomes pigmented.

During metamorphosis (Fig. 3C) pigmentation increases, especially on the left side of the body. Dorsal-fin pigmentation is concentrated in the posterior half of the fin. Groups of melanophores are present on the interradial membrane of the anal fin. The pelvic fin is almost completely pigmented.

Fin development Dorsal-fin pterygiophores and rays begin to form simultaneously at ~6.5 mm NL, reaching their full complements at 8.8 mm SL (Table 2). The anal-fin pterygiophores appear in advance of their corresponding fin rays, at 8.1–8.6 mm NL. In both fins, development proceeds posteriad. The pelvic fin appears at 8.5 mm NL, and all six rays are present at 10.1 mm SL. The hypural complex develops between 8.1 and 8.6 mm NL. There are 18 caudal-fin rays, plus 2 procurrent rays.

Morphology With absorption of the yolk, the yolksac larva becomes slender; the gut, jaws, and pectoral fins develop; and two sphenotic spines begin to develop on each side of the head. At 3.5 mm NL (4–5 days post-hatching), the yolk is exhausted, the mouth is functional, eyes are pigmented, and the pectoral fin is formed.

Two sphenotic spines appear at ~3.0 mm NL on each side of the head (Fig. 2); initially the upper one is the larger. Both spines are reabsorbed before development of elongated dorsal-fin rays, near the end of this stage. On some specimens, a third, smaller sphenotic spine can be found below the first two.

At about 4.5 mm NL, preopercular and opercular spines appear; the former are located along the posterior margin of the preoperculum and on the anterior preopercular ridge. Opercular spines are located at the upper portion of the bone and are more prominent than preopercular spines.

At ~6.5 mm NL, the elongated rays of the dorsal-fin crest begin to appear. Three rays (corresponding to the second, third, and fourth dorsal-fin rays of the adult) form the initial crest. At 6.2 mm NL the gut begins to coil. During preflexion, body depth is moderate (13.9% NL) and preanal distance is ~41.4% NL. These proportions remain relatively constant during later development (Table 1). There are 33 myomeres (11 preanal and 22 postanal) at the end of the stage.

The beginning of the flexion stage is characterized by an increase in body depth (22.8% NL) and development of the caudal fin. Preopercular spines are in two series in the upper and lower margins of the bone. Opercular spines are also in two groups: an upper group on the body of the operculum and a lower one along its margin. Elongated dorsal-fin rays remain, the middle one being the longest. At ~7.5 mm NL, the pelvic fins begin to form and, by the end of the stage, rays and pterygiophores of dorsal, anal and caudal fins are more evident.

Morphometric proportions are similar to those of the previous stage, except body depth which increases. A small increase in head length is also apparent (Table 1). There are 33 (9 preanal and 24 postanal) myomeres at the end of the stage.

During postflexion, body depth increases to 35.8% SL; head length reaches 30.6% SL (Table 1). Dorsal-crest fin rays increase in relative length; the second reaches 50% SL. The short dorsal-fin ray anterior to the crest begins to develop.

Preopercular and opercular spination increases in some specimens, but the spines begin to reabsorb at the end of the stage. The interocular region begins to change in preparation for eye migration. There are 33 (7–8 preanal and 25–26 postanal) myomeres at the end of the stage.

During metamorphosis, body depth continues to increase (39.0% SL), and snout length decreases (18.3% HL); however, other body proportions do not change substantially (Table 1). The second elongated dorsal-fin ray reaches its maximum length (~53.9% SL) before being reabsorbed. Migration of the right eye to the left side begins. Pectoral-fin rays form. Preopercular and opercular spines are lost, as are the elongated dorsal-fin rays. Eye migration is completed at ~13.0 mm. The smallest juvenile was 12.3 mm SL (Fig. 3C). There are 33 (4–6 preanal and 27–29 postanal) myomeres at the end of the stage.

Paralichthys microps

Hatching occurs 57–68 hours postfertilization; yolksac larvae are ~1.5 mm NL; one oil globule is present. Yolksac development is similar to *P. adspersus* yolksac larvae, except that melanophores form on the dorsal and anal finfold and a simple sphenotic spine begins to develop at yolk exhaustion (~3.2 mm NL, 4–5 days after hatching).

Diagnosis Distinguishing features of preflexion *P. microps* larvae are the presence of only one sphenotic spine (Fig. 2) and the dorsal finfold with pigmentation. After notochord flexion until metamorphosis, the most distinguishing feature is the presence of more than 3, and later 6, elongated dorsal-fin rays (Figs. 4E, 5). After reabsorption of these elongated rays, diagnosis is mostly based on morphometric relationships.

Pigmentation During the preflexion stage, the pigmentation pattern is similar to that of *P. adspersus*, but *P. microps* larvae have a different arrangement of body and finfold melanophores and less head pigment. Melanophores are relatively sparse over the trunk and

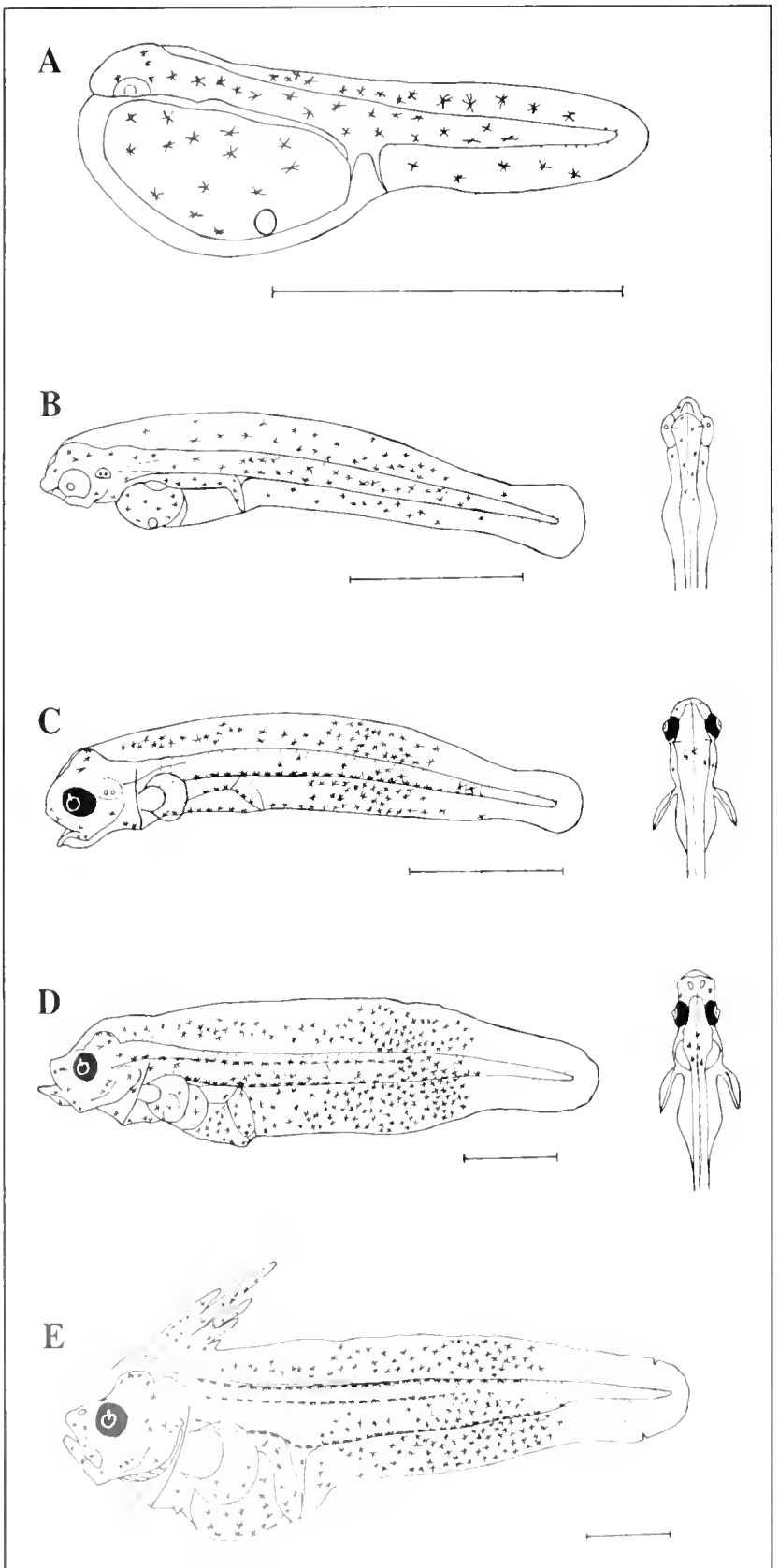

Figure 4

Paralichthys microps larvae: (A) Early yolksac, 1.5 mm NL; (B) late yolksac, 3.0 mm NL; (C) early preflexion, 3.4 mm NL; (D) middle preflexion, 5.3 mm NL; (E) late flexion, 7.0 mm NL. Drawings at right are dorsal head views. Bars = 1.0 mm.

anterior one-third of the tail. A dense zone of melanophores develops on the middle one-third of the tail and associated dorsal and ventral finfold regions (Fig. 4). Pigment is less dense on more anterior regions of the finfold and is absent on the posterior one-third of the tail and finfold. Head pigmentation is restricted to the jaws, dorsal brain, and opercle.

During the flexion stage, the melanistic zone on the tail and associated finfold region intensifies. The paired series along the dorsum and the epaxial region remains visible, while the embedded series dorsal to notochord is less visible due to the development of musculature. The number of ventral and ventrolateral abdominal melanophores increases. The ventral region of the gut has small melanophores, while those on the side of the gut are larger and stellate. The series above the gut and along its ventral midline are less apparent.

The pattern of melanophores on the head remains about the same, with brain melanophores the most conspicuous. Head pigmentation consists of small melanophores on the jaws, palate, preoperculum, operculum, and gular region, and larger and stellate melanophores in the brain region. The small melanophores located at the ventral margin near the tip of the notochord disappear with development of the caudal fin. Melanophores increase in number on the dorsal-fin crest and on the interradial membranes of the dorsal and anal fins during the postflexion stage (Fig. 5A).

Finally, during the metamorphosis stage (Fig. 5C) melanophores increase in numbers on the head and body, especially on the left side. Body melanophores are associated with myosepta. The paired dorsal series remains visible. Melanophores on the dorsal and anal fins are arranged in groups. The elongated dorsal-fin rays are covered with melanophores. The rear margins

of the hypural plates become pigmented, as do the bases of the caudal-fin rays.

Fin development Pterygiophores and fin rays of the dorsal fin appear at 5.5 mm NL; full complements are present at 7.7 mm SL (Table 2). Anal-fin pterygiophores and rays appear at 6.5 mm NL and have full complements at 7.7 mm SL. The pelvic-fin rays begin to develop at 7.0 mm NL and all are present at 8.1 mm SL; pterygiophores begin to develop at 10.1 mm SL and all are present at 11.3 mm SL. The first pectoral-fin rays appear at ~9.5 mm SL; full complements are present at 11.3 mm SL. The hypural complex develops between 6.2 and 7.2 mm NL. The number of caudal-fin rays is 18, plus 2 procurrent rays.

Morphology The sphenotic spine is more developed than in *P. adspersus* preflexion larvae (Fig. 2) (max. length is 24% eye diameter) and disappears with the appearance of the elongated dorsal-fin rays. At ~5 mm NL, up to 4 spines may be found at the preopercular margin; up to 3 spines are found in the upper region of opercle. At this size, the gut becomes coiled and the larva is moderately slender. Preanal distance is 41.2% NL; body depth (BD) is 13.3% NL, and upper jaw length (UJL) is 34.6% HL (Table 1).

At ~6 mm NL, three elongated rays appear on the dorsal fin crest. They correspond to the second, third, and fourth rays of the adult fin. The middle ray of the crest is the longest. There are 34 (11–12 preanal and 22–23 postanal) myomeres at the end of the stage.

The flexion stage is characterized by development of the hypural elements of the caudal fin. Body depth increases to 25.6%

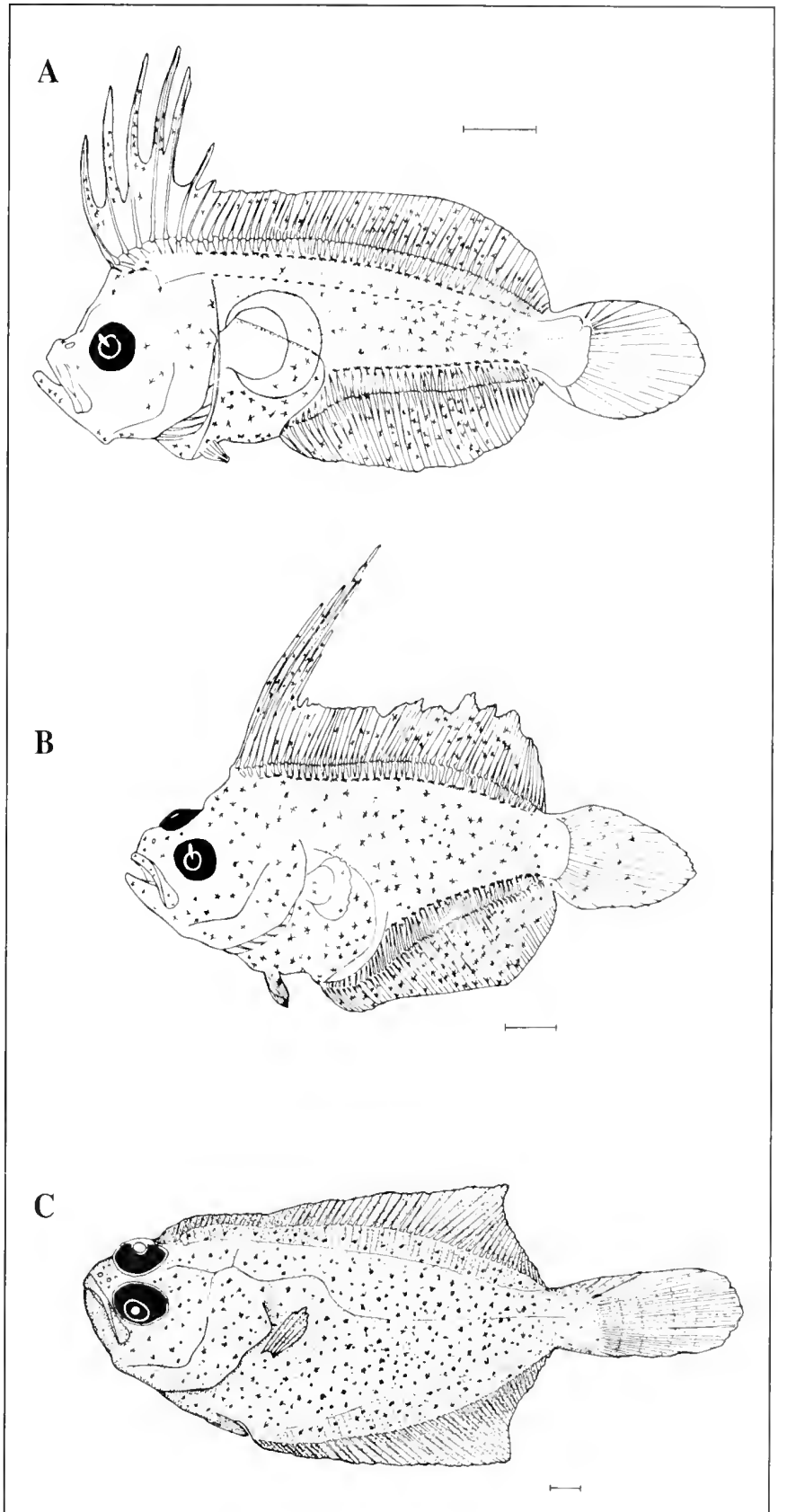

Figure 5
Paralichthys microps larvae. (A) early postflexion, 7.4 mm SL; (B) early to middle metamorphosis, 8.7 mm SL; (C) juvenile, 15.5 mm SL. Bars = 1.0 mm.

NL; upper and lower jaw lengths increase to 44.5% and 57.1% HL. Relative eye diameter decreases to 26.8% HL (Table 1).

The number and location of preopercular and opercular spines remain almost constant. The pelvic fin starts to develop at ~7.0 mm NL. Up to 6 elongated fin rays develop in the dorsal crest. There are 34 (9–11 preanal and 23–25 postanal) myomeres at the end of the stage.

The 6 (sometimes 7) fin rays of the dorsal crest continue to elongate during the postflexion stage. The fourth and fifth rays are more than half the body length; the first dorsal-fin ray is apparent but poorly developed. Rays and pterygiophores of median fins become more apparent.

By the end of this stage, preopercular and opercular spines start to disappear and the interocular region begins to deform in preparation for eye migration. Body depth increases (up to 44.7% SL) as does head length (up to 37% SL), with a corresponding decrease in relative jaw length and eye diameter (Table 1). There are 34 (7–9 preanal and 25–27 postanal) myomeres at the end of the stage.

Finally, during metamorphosis as the right eye migrates towards the left side of the body, the dorsal crest is lost, the mouth changes form, and pectoral-fin rays form (Fig. 5C).

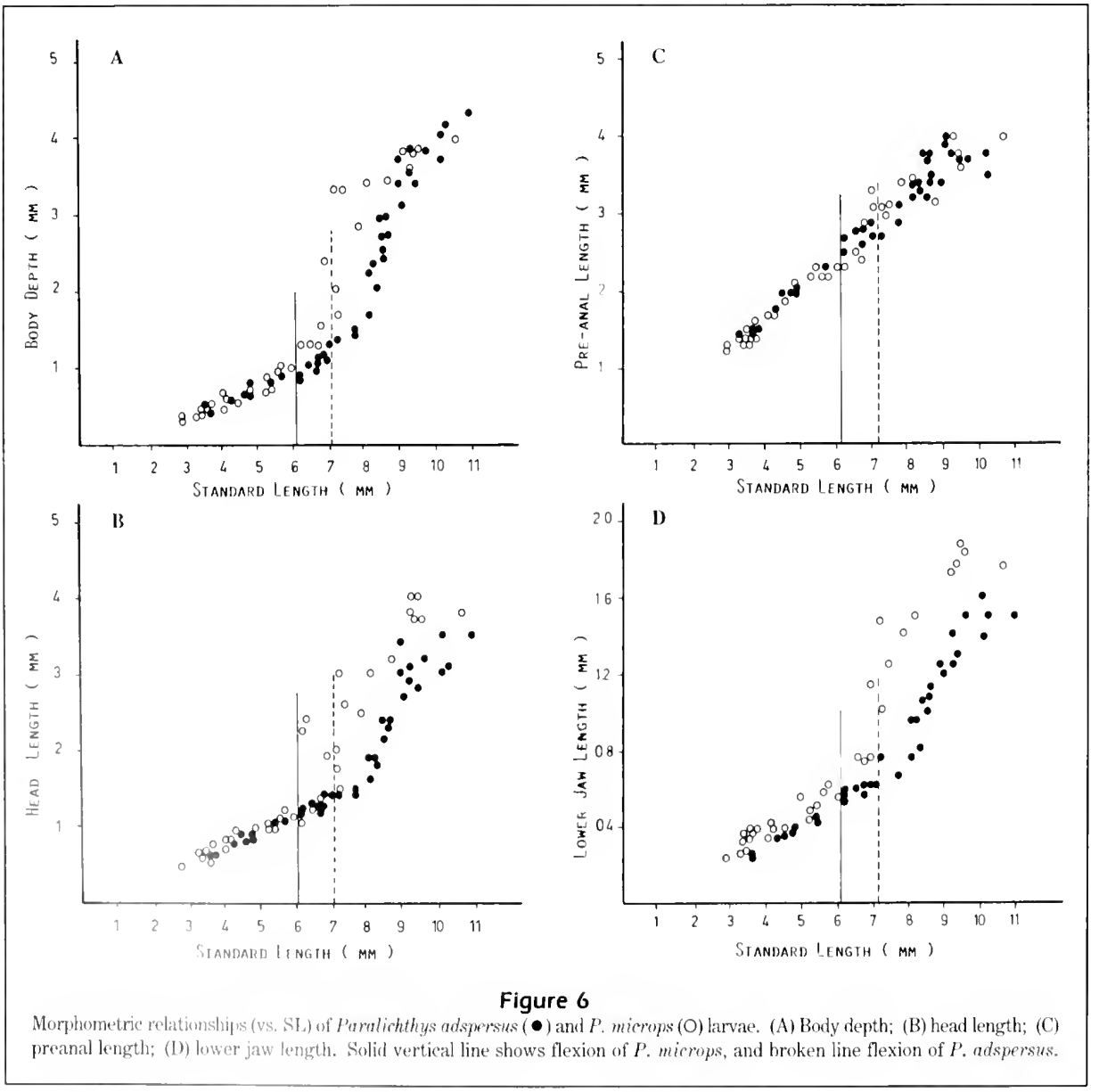

Figure 6

Morphometric relationships (vs. SL) of *Paralichthys adspersus* (●) and *P. microps* (○) larvae. (A) Body depth; (B) head length; (C) preanal length; (D) lower jaw length. Solid vertical line shows flexion of *P. microps*, and broken line flexion of *P. adspersus*.

Morphometrics

Six morphometric functional relationships are shown in Figures 6 and 7, and all linear regression models and their r^2 values are summarized in Table 3 (abbreviations as in Table 1). In general, all morphometric relationships were adequately described by the linear regression model, especially the preflexion *P. adspersus* larvae which always had higher r^2 values than those for other stages of the same species and all stages of *P. microps* (Table 3). The relationships are not so clear in *P. microps*, because the preflexion SnL/HL, PAL/SL, BD/SL, and HL/SL relationships had higher r^2 values than those of the other stages, while the relationships UJL/SL, LJL/SL, and ED/SL of other stages had higher values of r^2 than those from preflexion (Table 3).

F tests showed that models for all preflexion relationships and the PAL/SL of "other stages" could be considered statistically identical for both species, while all others were significantly different (Table 4). Regression models for all morphometric relationships (except SnL/HL and PAL/SL) between the two groups of developmental stages of *P. microps* were significantly different, while in *P. adspersus* all but SnL/HL, PAL/SL, and UJL/SL were significantly different (Table 5).

A summary of larval characters useful to identify larvae of both species during the different larval stages, including morphology, pigmentation, and morphometrics, is shown in Table 6.

Discussion

Characteristics of larval development of *P. adspersus* and *P. microps* are, in general, similar to those observed in other species of the genus (*P. dentatus* Smith and Fahay 1970; *P. olivaceus* Mito 1963, Okiyama 1967; *P. californicus*, Ahlstrom and Moser 1975). Important common characteristics are: presence of only one oil globule posteriad in the yolksac larvae; small size at hatching, notochordal flexion, and metamorphosis; presence of sphenotic spines; two groups of preopercular spines; elongated anterior dorsal-fin rays; a deep laterally-compressed body; and a large visceral mass. Opercular spines present in the two species described herein are uncommon in the family.

Length at hatching of Paralichthyid larvae varies between 1.5 and 3.7 mm NL with a mean of 2.2 mm, while the range described for the genus *Paralichthys* is 2.0–2.8 mm (Ahlstrom et al. 1984). Thus, hatching sizes (1.5–1.7 mm) of *P. adspersus* and *P. microps* larvae are smaller than any known congener. Lengths at flexion and metamorphosis of both species fall within

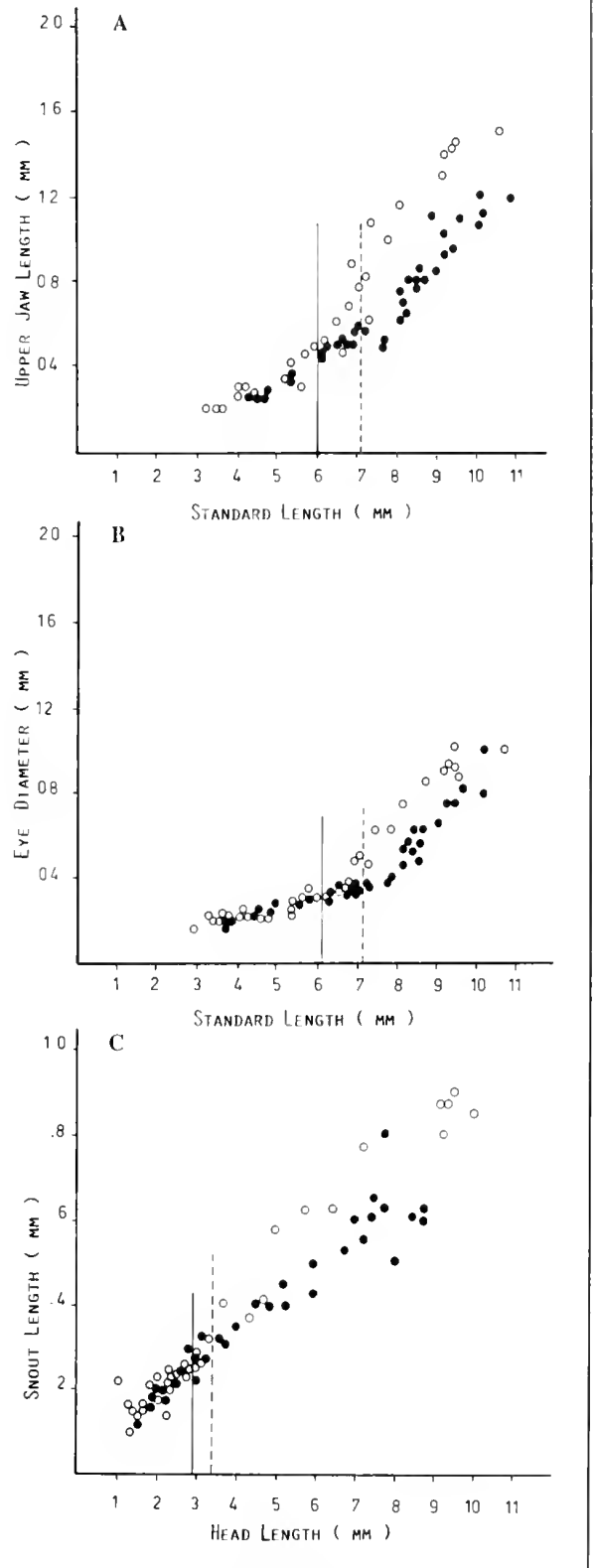

Figure 7
Morphometric relationships (vs. SL and HL) of *Paralichthys adspersus* (●) and *P. microps* (○) larvae. (A) Upper jaw length, (B) ocular diameter, (C) snout length. Symbols as in Fig. 6.

Table 3

Linear regression equations and r^2 values of selected morphometric relationships for preflexion and "other stages" larvae of *Paralichthys adspersus* and *P. microps*. Abbreviations as in Table 1.

	P. adspersus		*P. microps*	
Relationship	Preflexion	Other stages	Preflexion	Other stages
PAL/SL	0.091 + 0.397X r^2 0.975	0.652 + 0.328X r^2 0.557	0.088 + 0.388X r^2 0.957	0.534 + 0.338X r^2 0.772
BD/SL	−0.311 + 0.205X r^2 0.933	−5.446 + 0.944X r^2 0.873	0.328 + 0.214X r^2 0.901	−2.940 + 0.711X r^2 0.821
HL/SL	−0.189 + 0.218X r^2 0.971	−3.428 + 0.669X r^2 0.817	−0.149 + 0.217X r^2 0.937	−3.806 + 0.796X r^2 0.905
UJL/SL	−0.284 + 0.119X r^2 0.956	−1.012 + 0.215X r^2 0.701	−0.129 + 0.094X r^2 0.805	−1.060 + 0.258X r^2 0.889
LJL/SL	−0.137 + 0.110X r^2 0.974	−1.390 + 0.288X r^2 0.723	−0.034 + 0.104X r^2 0.815	−1.165 + 0.309X r^2 0.860
ED/SL	0.026 + 0.046X r^2 0.931	−1.114 + 0.199X r^2 0.911	0.047 + 0.042X r^2 0.785	−0.839 + 0.187X r^2 0.934
SnL/HL	−0.031 + 0.254X r^2 0.896	0.082 + 0.166X r^2 0.794	0.006 + 0.223X r^2 0.792	0.033 + 0.222X r^2 0.958

Table 4

Values of F for two regression models of morphometric relationships between preflexion and other developmental stages (flexion, postflexion, and metamorphosis) between *Paralichthys adspersus* and *P. microps*. Abbreviations as in Table 1.

	Preflexion			Other stages		
Relationship	F	df		F	df	
PAL/SL	1.18	(2, 41)	NS	0.05	(2, 38)	NS
BD/SL	0.66	(2, 38)	NS	11.24	(2, 38)	*
HL/SL	2.04	(2, 38)	NS	21.82	(2, 38)	*
UJL/SL	2.46	(2, 23)	NS	19.73	(2, 38)	*
LJL/SL	1.28	(2, 36)	NS	17.79	(2, 35)	*
ED/SL	0.67	(2, 38)	NS	34.97	(2, 33)	*
SnL/HL	1.25	(2, 38)	NS	14.81	(2, 35)	*

NS = Non-significant * Significant ($P<0.001$)

Table 5

F tests for two regression models of morphometric relationships between preflexion and other developmental stages (flexion, postflexion, and metamorphosis) within two species of *Paralichthys*. Abbreviations as in Table 1.

	P. adspersus			*P. microps*		
Relationship	F	df		F	df	
PAL/SL	0.79	(2, 43)	NS	1.48	(2, 36)	NS
BD/SL	50.90	(2, 41)	*	17.18	(2, 35)	*
HL/SL	22.90	(2, 41)	*	36.18	(2, 35)	*
UJL/SL	3.32	(2, 34)	NS	10.52	(2, 25)	*
LJL/SL	10.39	(2, 40)	*	18.03	(2, 35)	*
ED/SL	70.53	(2, 37)	*	51.96	(2, 34)	*
SnL/HL	2.11	(2, 40)	NS	0.83	(2, 33)	NS

NS = Non-significant * Significant ($P<0.001$)

the known range of the genus. *P. adspersus* is larger at metamorphosis than *P. microps* (9.6–13.0 mmSL vs. 8.0–11.0mmSL, respectively) and is comparable to the 10.2–14.2mmSL range for *P. olivaceus* (Okiyama 1967).

Early presence of elongated anterior dorsal-fin rays in *P. adspersus* and *P. microps*, at 6.5 and 6.0mmSL, respectively, is common in *Paralichthys* and related genera of paralichthyids (*sensu* Ahlstrom et al. 1984). The six elongated dorsal-fin rays observed in *P. microps* fall within the described range (4–8) for *Paralichthys*, while *P. adspersus* only has 3, as in the related genus *Citharichthys* (Ahlstrom et al. 1984). The shape and size of these dorsal-fin rays is characteristic of the genus *Paralichthys* and not *Citharichthys*.

The melanistic pattern of the larvae of both species is very similar to that described for the genera *Paralichthys* and *Pseudorhombus* (*sensu* Ahlstrom et al. 1984); however, the pigment series along the horizontal septum described for other species

Table 6

Summary of larval characters which distinguish larvae of *Paralichthys adspersus* and *P. microps* during different larval stages. Abbreviations as in Table 1.

Developmental stage	*P. adspersus*	*P. microps*
Preflexion	Two sphenotic spines present before development of dorsal-fin rays. Dorsal finfold unpigmented. LJL/HL = 46.3%	One sphenotic spine present before development of dorsal-fin rays. Dorsal finfold pigmented. LJL/HL = 52.0%
Flexion	Dorsal finfold unpigmented. LJL/HL = 48.1% 2–3 elongated dorsal-fin rays.	Dorsal finfold pigmented. LJL/HL = 57.1% 3–6 elongated dorsal-fin rays.
Postflexion	Dorsal fin poorly pigmented. HL/SL = 30.6%; BD/SL = 35.8% 3 elongated dorsal-fin rays. 33 myomeres.	Dorsal fin pigmented. HL/SL = 37.3%; BD/SL = 44.7% 6 elongated dorsal-fin rays. 34 myomeres.
Metamorphosis	3 elongated dorsal-fin rays (before reabsorption). SnL/HL = 18.3%; HL/SL = 32.0%; BD†/SL = 41.9% 33 myomeres.	6 elongated dorsal-fin rays (before reabsorption). SnL/HL = 23.3%; HL/SL = 39.1%; BD†/SL = 46.5% 34 myomeres.
Juvenile	33 vertebrae. Meristics (see Table 7).	34 vertebrae. Meristics (see Table 7).

BD† measured at the anus.

Table 7

Meristics of adult *Paralichthys adspersus* and *P. microps* of use in identifying juveniles.

Character Norman (1937)	*P. adspersus* Ginsburg (1952)	*P. microps*	
Origin of dorsal fin	Between anterior margin of eye and pupil (7–12 cm). Over anterior margin of eye or near it (20–39 cm).	Over or slightly anterior to center of eye.	
Gill rakers			
Upper	15–19	18–23	
Lower	7–8 ($\bar{x}$ 7)	9–10	Chirichigno (1974)
Total	22–27 ($\bar{x}$ 25–26)	27–33	
Fin rays			
Dorsal	68–76	68–80	
Anal	54–61	56–65	
Pectoral	11–13	11–12	

is not present in *P. adspersus* or *P. microps*. Reared and field-caught specimens of *P. adspersus* lack pigmentation in the dorsal finfold during the first half of their larval development, a unique feature among described paralichthyid larvae.

In flounders, the main change in body shape occurs during flexion, with an increase in body depth and head length. This stage is characterized by development of skeletal structures and by a change in swimming and feeding (Balart 1984). After flexion, the rate of growth of the head, snout, and jaws is comparatively greater in *P. microps*, while the rate of increase in body depth is greater in *P. adspersus*.

Preflexion larvae of *P. adspersus* and *P. microps* are statistically indistinguishable using morphometrics. After flexion and loss of the elongated dorsal-fin rays, separation is based mostly on morphometric characteristics, especially SnL/HL and HL/SL. After metamorphosis, during the juvenile stage when all fin rays are already developed, the adult range of meristic counts can be used (Table 7).

Acknowledgments

The authors are deeply indebted to Mr. Alfonso Silva for allowing them to use reared larvae which were part of a culturing experiment and to Mr. Alejandro Aron for providing field-collected larvae. Also, comments and editorial recommendations of two anonymous reviewers are greatly appreciated. This research was financed by D.G.I. Universidad Católica del Norte.

Citations

Ahlstrom, E.H., and H.G. Moser
1975 Distributional atlas of fish larvae in the California Current region: Flatfishes, 1955 through 1960. Calif. Coop. Oceanic Fish. Invest. Atlas 23, 207 p.

Ahlstrom, E.H., J.L. Butler, and B.Y. Sumida
1976 Pelagic stromateoid fishes (Pisces, Perciformes) of the eastern Pacific: Kinds, distributions, and early life histories and observations on five of these from the Northwest Atlantic. Bull. Mar. Sci. 26:285–402.

Ahlstrom, E.H., K. Amaoka, D.A. Hensley, H.G. Moser, and B.Y. Sumida
1984 Pleuronectiformes: Development. *In*Moser, H.G., et al. (eds.), Ontogeny and systematics of fishes, p. 640–670. Spec. Publ. 1, Am. Soc. Ichthyol. Herpetol. Allen Press, Lawrence, KS.

Bahamonde, N., and G. Pequeño
1975 Peces de Chile. Lista sistemática. Bol. Mus. Nac. Hist. Nat. (Chile), Publ. Occas. 22:3–20.

Balart, E.
1984 Osteological development in two teleost fishes *Engraulis japonicus* and *Paralichthys olivaceus*, and their relation to swimming and feeding function. M.Sc. thesis, Dep. Fish., Fac. Agric., Kyoto Univ., Japan, 149 p.

Chirichigno, N.
1974 Clave para identificar los peces marinos del Perú. Inf. Inst. Mar. Perú 44:1–387.

Ginsburg, I.
1952 Flounders of the genus *Paralichthys* and related genera in America waters. Fish. Bull., U.S. 52:267–351.

Gutherz, E.J.
1970 Characteristics of some larval Bothid flatfish, and development and distribution of larval spotfin flounder, *Cyclopsetta fimbriata* (Bothidae). Fish. Bull., U.S. 68:261–283.

Mito, S.
1963 Pelagic fish eggs from Japanese waters. III. Percina. VIII. Cottina. IX. Echeneida and Pleuronectida. Jpn. J. Ichthyol. 11:39–102.

Muñoz, H., G. Herrera, and H. Fuentes
1988 Desarrollo larval del lenguado de ojos chicos *Paralichthys microps*. Rev. Biol. Mar. Valparaíso, 24(1):35–53.

Netter, J., and W. Wasserman
1974 Applied linear statistical models. Richard D. Irwin, Homewood IL, 842 p.

Norman, J.R.
1937 Coast fishes. Part II. The Patagonian region. Discovery Rep. 16(2):1–150.

Okiyama, M.
1967 Study on the early life history of a flounder, *Paralichthys olivaceus* (Temminck et Schlegel). I. Descriptions of postlarvae. Bull. Jpn. Sea Reg. Fish. Res. Lab. 17:1–12.

Potthof, T.
1984 Clearing and staining techniques. *In* Moser, H.G., et al. (eds.), Ontogeny and systematics of fishes, p. 35–37. Spec. Publ. 1, Am. Soc. Ichthyol. Herpetol. Allen Press, Lawrence, KS.

Silva, A.
1988 Observaciones sobre el desarrollo del huevo y estadios larvarios del lenguado, *Paralichthys microps* (Gunther, 1881). Rev. Latinoam. Acui. Lima (Perú) 35:19–44.

Smith, W.G., and M.P. Fahay
1970 Description of eggs and larvae of the summer flounder, *Paralichthys dentatus*. U.S. Fish. Wildl. Serv. Res. Rep. 75, 21 p.

Zuñiga, H.
1988 Comparación morfológica y dietaria de *Paralichthys adspersus* (Steindachner, 1867) y *Paralichthys microps* (Günther, 1881) en Bahía de Coquimbo. Mar. biol. thesis, Univ. católica del Norte, Coquimbo, Chile, 144 p.

An estimate of the tag-reporting rate of commercial shrimpers in two Texas bays

R. Page Campbell
Terry J. Cody
Texas Parks and Wildlife Department
100 Navigation Circle, Rockport, Texas 78382

C.E. Bryan
Gary C. Matlock
Maury F. Osborn
Albert W. Green
Texas Parks and Wildlife Department
4200 Smith School Road, Austin, Texas 78744

Tag return rates are used to estimate exploitation rates for many animal species including penaeid shrimp. To avoid systematic underestimation of exploitation, the number of tagged animals recaptured but not reported must be reliably estimated (Paulik 1963, Youngs 1972, Seber 1973). Some investigators have offered rewards for tags to increase the tag return rate, but have incorrectly assumed that all or nearly all harvested tagged animals were reported (Kutkuhn 1966) or the rate of non-reporting remained the same throughout the experiment (Klima 1974, Kutkuhn 1966). Studies to measure the reporting rate of commercially-caught shrimp were conducted by Klima (1974) and Johnson (1981). The numbers of shrimp placed in both studies were small (n 71 and 20, respectively) and return rates differed markedly (82% and 10%, respectively). One drawback of these studies is that tagged shrimp were placed into the catch at shrimp houses or in the final processing stages, and not on the vessel during shrimping operations. Therefore, return rates during fishing operations were not measured.

Accurate reporting rates for recovered tags are essential for the determination of fishing mortality rates. The objective of the present study was to determine reporting rates of tagged shrimp captured during regular shrimping operations. To that end, tagged shrimp were surreptitiously placed in unculled catches. The reporting rates determined in this study are intended for use in correcting fishing-mortality estimates generated from a tagging program conducted during the same period.

Materials and methods

Texas Parks and Wildlife Department (TPWD) personnel placed tagged shrimp in the catch aboard Galveston and Aransas Bays' commercial bay and bait shrimp boats, May–November 1984. TPWD personnel and game wardens boarded shrimp vessels during bay shrimping operations. While a game warden distracted the crew by checking licenses, other TPWD personnel placed a single tagged shrimp in unculled catches (on deck) or in a live bait box. To conceal surreptitious placement of shrimp, 20 individuals of the target species *Penaeus aztecus* or *P. setiferus* were measured to the nearest mm total length (TL) on each vessel. A total of 219 shrimp (115 brown and 104 white) were surreptitiously placed aboard vessels in Aransas (n 125) and Galveston (n 94) Bay systems during the study period. No more than 12 shrimp were surreptitiously placed in each bay system in any one week.

Each tag was a uniquely-numbered black vinyl streamer (95mm long × 4mm wide) tapered at each end (Klima et al. 1987). Each tag was inserted between the second and third abdominal segments of the shrimp. Shrimp in Aransas Bay were measured (TL) prior to placement and after being returned by the fisherman. Since lengths were not required in the original study, measurements were not recorded in Galveston Bay. Lengths of shrimp placed in the catches and lengths of shrimp returned by fishermen were compared using student's t-test. Also, length frequencies of measured shrimp on commercial boats (n 2402) and of shrimp surreptitiously placed (n 105) aboard boats were compared visually using length-frequency histograms.

As part of a larger bay shrimp-tagging program conducted jointly by the TPWD and the National Marine Fisheries Service (NMFS), rewards were offered for tag returns. The program was promoted by distribution of posters to area shrimp dealers and through newspaper articles. No information was provided to the public concerning the surreptitious tagging activity.

Reporting rates (n reported/n placed, expressed as percent) were estimated for each species and bay system. Reporting rates and confidence intervals were estimated for the two bay systems combined. Reporting rates between species and between bay systems were compared using a Chi-square test (Sokal and Rohlf 1981).

Manuscript accepted 11 June 1992.
Fishery Bulletin, U.S. 90:621–624 (1992).

Results

Overall, 16% (95%CI, 11–21%) of 219 tagged shrimp were returned (Table 1). The return rate of 21% for brown shrimp was greater than the 11% for white shrimp (χ^2 4.415, 1df, $P \leq 0.05$). Reporting rates did not differ between bay systems for brown shrimp (χ^2 2.081, 1df, $P > 0.05$) or white shrimp (χ^2 1.059, 1df, $P > 0.05$). Reporting rates for the two species of shrimp were similar in Galveston Bay (χ^2 0.001, 1df, $P > 0.05$); in Aransas Bay, reporting rates were greater for brown shrimp (χ^2 6.890, 1df, $P \leq 0.05$). Sixty-eight percent of shrimp returned were reported found on the same day as placement.

Mean lengths of placed and returned brown shrimp from Aransas Bay were similar (t −0.48, $P > 0.05$) (Fig. 1), while the mean length of placed white shrimp was smaller than the mean length of those returned (t −4.01, $P \leq 0.05$). Placed brown shrimp were similar in length to those measured from the unculled catches on commercial shrimp boats (Fig. 2) whereas placed white shrimp were clearly smaller than those measured on commercial boats.

Discussion

Tag reporting rates for bay-caught shrimp have been reported by Klima (1974) and Johnson (1981). Tag reporting rates presented in this study are more precise because sample sizes were larger than in previous studies. Moreover, tag return rates in this study are more realistic because the tagged shrimp were placed in the catch before any processing occurred, rather than at dockside during the final processing stages.

The detection rate, and thus the reporting rate, of tagged shrimp in unculled catches may be influenced by size of tagged shrimp relative to size of other shrimp in the catch and by overall volume of catch being processed. In the fall shrimping season (15 August–15 December), there are no restrictions on the amount of shrimp that can be retained. During 15 August–31 October, when white shrimp dominate the catch, the minimum shrimp count size is 50 (heads-on) per pound in major Texas bays (State of Texas 1987–88). Thus, commercial fishermen selectively retain larger shrimp during this interval. Since the TPWD gear used to collect white shrimp for tagging was relatively nonselective, surreptitiously-placed shrimp in Aransas Bay were smaller than those in the catch in which they were placed. In contrast, brown shrimp dominated the catch in summer when there was no count size restriction, and thus placed shrimp were similar in size to those in the commercial catch. Because the placed white

Table 1

Number and percent of tagged *Penaeus* shrimp surreptitiously placed on shrimp boat decks which were found and returned to TPWD.

Species	Bay system	No. tagged	Returned	
			n	%
P. aztecus (brown shrimp)	Galveston	43	6	14
	Aransas	72	18	25
	Total	115	24	21
P. setiferus (white shrimp)	Galveston	51	7	14
	Aransas	53	4	8
	Total	104	11	11
Combined species	Galveston	94	13	14
	Aransas	125	22	18
	Total	219	35	16

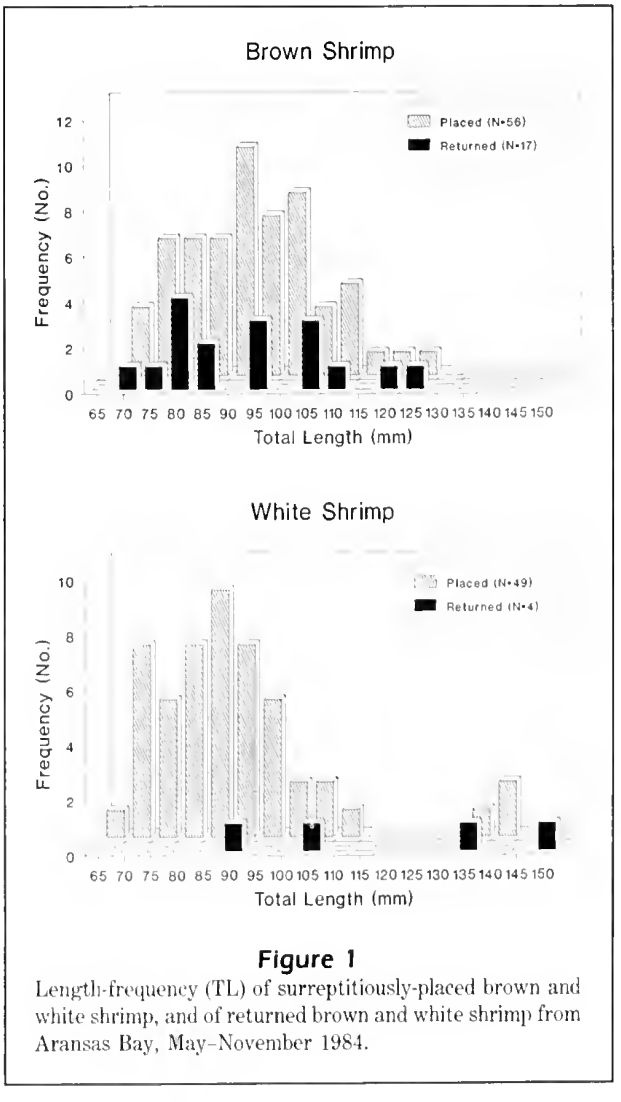

Figure 1

Length-frequency (TL) of surreptitiously-placed brown and white shrimp, and of returned brown and white shrimp from Aransas Bay, May–November 1984.

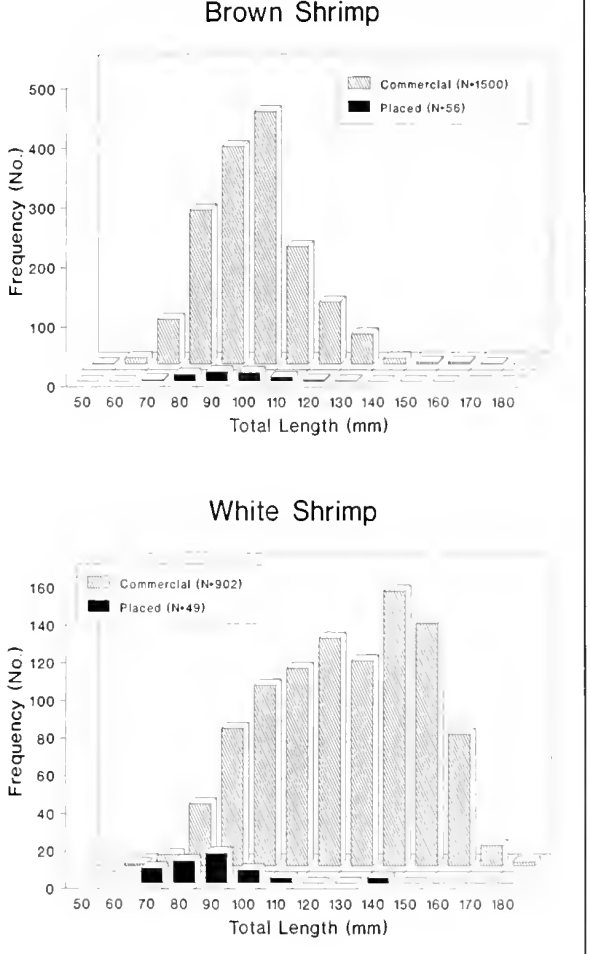

Figure 2

Length-frequency histograms of brown shrimp and white shrimp measured in commercial catches, and of tagged shrimp surreptitiously placed aboard boats in Aransas Bay, May–November 1984.

shrimp were smaller than those in the commercial catch, they may have been more difficult to detect and hence, were reported at a lower rate than if they had been similar in size to those in the commercial catch. The overall reporting rate with these white shrimp excluded was 19% (95%CI, 13–26%) which is similar to the reporting rate for brown shrimp (21%). Tagged and untagged brown shrimp sizes were similar.

Complete return of tags cannot be assumed even if rewards are offered. All tags used in the present study were potential reward tags ($50–500) inserted into the shrimp and placed into unculled shrimp catches; however, only 19% of these shrimp were reported. Past studies have relied on the use of monetary incentives to promote the return of tags. Rawstron (1971) determined that some reward tags in his fish-tagging study were not returned, but believed that this number was negligible. Likewise, Kutkuhn (1966) assumed low non-reporting rates for reward tags. Published estimates of tag-return rates for fish generally have ranged between 55 and 65%, with rewards. Green et al. (1983) reported much lower return rates by saltwater recreational anglers (29%) than had previously been estimated, and that rates differed among species and areas. Therefore, even with rewards, complete or high reporting rates cannot be assured.

Previous studies have relied on public-information dissemination plans to achieve high reporting rates of reward and non-reward tags. Matlock (1981) found that 83% (n 102) of the anglers not reporting tags in their catch knew about TPWD tagging programs, and that 78% of these anglers failed to find the tag. This suggests that public-information programs cannot assure high reporting rates. Even if fishermen are aware of tagging programs, they may not report recaptured tags if these programs have continued over a long period. The shrimp fishery in Texas had been subjected to frequent tagging experiments during the previous 10 years, and the shrimp fishermen's enthusiasm for reporting tags may have decreased. However, there are no data to examine this possibility.

Tag-return rates can be affected by many factors. Each tagging study that depends on volunteer tag returns would be enhanced by a concurrent estimate of non-reporting rates. This would improve estimates developed from returned tags. For example, during the tagging program conducted during the same period as this study, there were 2% of 25,870 released tagged shrimp returned (Peng Chai, TPWD, Austin, pers. commun.). If the reporting rate had been assumed to be 100% rather than the observed 19%, fishing mortality would be overestimated about five times.

Acknowledgments

We would like to thank each member of the TPWD Harvest and Resource Monitoring programs, without whose assistance this task could not have been accomplished. Thanks also go to the Texas Parks and Wildlife Department Law Enforcement officers who accompanied personnel into the bays and assisted in placement of tagged shrimp on the commercial boats, and also to the National Marine Fisheries Service for their support. This study was funded by the Texas Parks and Wildlife Department and by NMFS under P.L. 88-309 (Proj. 2-400-R).

Citations

Green, A., G.C. Matlock, and J.E. Weaver
1983 A method for directly estimating the tag-reporting rate of anglers. Trans. Am. Fish. Soc. 112:412–415.

Johnson, M.F.
1981 Shrimp mark-release investigations. Vol. II. *In* Jackson, W.B., and E.P. Wilkens (eds.), Shrimp and redfish studies; Bryan Mound brine disposal site off Freeport, Texas, 1979–1981. NOAA Tech. Memo. NMFS-SEFC-66, Southeast Fish. Sci. Cent., Miami, 110 p.

Klima, E.F.
1974 A white shrimp mark-recapture study. Trans. Am. Fish. Soc. 103:107–113.

Klima, E.F., Refugion Gmo. Castro Melandez, N. Baxter, F.J. Patella, T.J. Cody, and L.F. Sullivan
1987 "MEXUS-Gulf shrimp research, 1978–1984." *In* Richards, W.J., and R. Juhl (eds.), The Cooperative MEXUS-Gulf research program: Summary reports for 1977–85, p. 21–30. Mar. Fish. Rev. 49(1).

Kutkuhn, J.H.
1966 Dynamics of a penaeid shrimp population and management implications. Fish. Bull., U.S. 65:313–338.

Matlock, G.C.
1981 Nonreporting of recaptured tagged fish by saltwater recreational boat anglers in Texas. Trans. Am. Fish. Soc. 110:90–92.

Paulik, G.J.
1963 Detection of incomplete reporting of tags. Int. Comm. Northwest Atl. Fish. Spec. Publ. 4:238–247.

Rawstron, R.R.
1971 Nonreporting of tagged white catfish, largemouth bass, and bluegills by anglers at Folsom Lake, California. Calif. Fish Game 57:246–252.

Seber, G.A.F.
1973 The estimation of animal abundance and related parameters. Griffin, London, 654 p.

Sokal, R.R., and F.J. Rohlf
1981 Biometry. W.H. Freeman, San Franc., 859 p.

State of Texas
1987–88 Texas Parks and Wildlife Laws. West Publ. Co., St. Paul, MN, 455 p.

Youngs, W.D.
1972 Estimation of natural fishing mortality rates from tag recaptures. Trans. Am. Fish. Soc. 101:542–545.

Power to detect linear trends in dolphin abundance: Estimates from tuna-vessel observer data, 1975-89

Elizabeth F. Edwards
Peter C. Perkins
Southwest Fisheries Science Center, National Marine Fisheries Service, NOAA
P.O. Box 271, La Jolla, California 92038-0271

Trends in abundance of dolphin stocks affected by the tuna purse-seine fishery in the eastern tropical Pacific Ocean (ETP) are of intense interest to a number of organizations concerned about the stocks' continued survival (Hammond and Laake 1983, Gerrodette 1987, Holt et al. 1987, Buckland and Anganuzzi 1988, Anganuzzi and Buckland 1989, Anganuzzi et al. 1991). The most straightforward method for estimating such trends is linear-regression analysis of relative abundance indices across time (e.g., Anganuzzi and Buckland 1989). Such abundance indices can be derived from data collected by observers aboard the tuna vessels (Buckland and Anganuzzi 1988, Anganuzzi and Buckland 1989, Anganuzzi et al. 1991). Linear trends in abundance over successive 5-year periods have been reported by Buckland and Anganuzzi (1988), Anganuzzi and Buckland (1989), and Anganuzzi et al. (1991).

Power analysis provides a method to quantify the probability of not detecting low rates of change in abundance over a specified time-period. It also provides a method, in cases where no statistically-significant trends are apparent, for determining the steepness of change necessary for its statistical detection given observed variability in the data, i.e., detectable trend (Gerrodette 1987, Peterman 1990). We use power analysis here to assess the efficacy of weighted linear-regression analysis for estimating linear trends in abundance of eight stocks of ETP dolphins. While it is instructive to evaluate the power of conclusions about observed trends, it is perhaps even more important to determine the magnitude of change required for detection of a trend, given observed variability in the dolphin abundance estimates. Therefore, we also calculate detectable trends, in addition to power of observed trends.

We present here estimates of observed trend, power to detect trends, and detectable trends for eight stocks of ETP dolphins, over time-series of 5, 8, and 10-years, assuming a two-sided hypothesis with $\alpha = 0.10$, using the noncentral t-distribution for the alternative hypothesis. Detectable trends were estimated assuming Type I (α) and Type II (β) error levels equal 0.10. We estimated power and detectable trends for all three sets of time-series to determine how much improvement might be expected by increasing the number of years included in the trend estimate. We did not include longer time-series, as it is unlikely that even a population with reproductive and individual growth rates as relatively slow as ETP dolphins would follow a linear trend for more than a decade, if that long.

Methods

Relative abundance indices and their associated bootstrap standard errors for eight stocks of ETP dolphins during the years 1975–89 (Table 1, Fig. 1) formed the database for the regression analyses presented here. Indices and standard errors for 1975–87 were taken from Anganuzzi and Buckland (1989), and for 1988 and 1989, from Anganuzzi et al. (1991). The eight dolphin stocks included northern offshore and southern offshore stocks of the pantropical spotted dolphin *Stenella attenuata*, the eastern spinner dolphin *Stenella longirostris orientalis*, northern and southern stocks of whitebelly spinner dolphin (hybrid/intergrades between *Stenella l. orientalis* and *Stenella l. longirostris* [Perrin 1990]), and northern, central and southern stocks of the common dolphin *Delphinus delphis*.

Observed trends

We estimated linear trends in relative abundance for each of the eight stocks over sequential series of 5, 8, and 10 years, using standard weighted least-squares regression (Wilkinson 1989). The slope of the regression (b) estimates the trend in abundance. The estimated standard error of the estimated trend (s_b) indicates the variability associated with the trend estimate. Weights were the reciprocal of the square of the bootstrap standard errors (Buckland and Anganuzzi 1988). We eliminated the estimate for 1983 from all analyses, because the presence of a very strong El Niño that year caused biologically unreasonable estimates of abundance for many of the stocks, in particular for northern offshore spotted dolphins, the stock affected by the fishery in greatest numbers (Buckland and Anganuzzi 1988, Anganuzzi et al. 1991). In the absence of any objective criteria for choosing which stocks were (or were not) affected by the El Niño, we elected to treat

Manuscript accepted 1 June 1992.
Fishery Bulletin, U.S. 90:625–631 (1992).

Table 1

Estimated abundances (first row) and bootstrapped standard errors (second row) for eight stocks of dolphins affected by the tuna purse-seine fishery in the eastern tropical Pacific Ocean. Values are in thousands. Data for 1975–87 from Buckland and Anganuzzi 1988; data for 1988–89 from Anganuzzi and Buckland 1989. Dashes indicate no values reported for that year. Asterisks indicate values from 1983 omitted as anomalous. SOPS boundaries (Anganuzzi and Buckland 1989) used in estimating southern offshore spotted dolphins. See text for scientific names.

	Dolphin stocks							
	1	2	3	4	5	6	7	8
1975	3949	—	599	490	—	122	404	385
	996	—	197	181	—	51	138	227
1976	4253	574	535	1205	115	344	287	586
	908	212	190	293	62	130	80	223
1977	3828	924	514	588	203	637	466	229
	751	332	152	163	87	200	90	162
1978	3212	584	395	613	65	358	329	—
	543	302	124	150	47	126	105	—
1979	2950	1040	428	366	—	650	644	—
	559	394	202	183	—	248	287	—
1980	3335	260	447	342	124	512	251	230
	582	168	112	99	86	191	85	139
1981	2536	199	255	694	124	513	111	435
	443	83	165	287	80	330	35	142
1982	2550	591	202	416	100	—	232	103
	557	180	91	132	47	—	101	90
1983	*	*	*	*	*	*	*	*
	*	*	*	*	*	*	*	*
1984	2158	244	340	253	182	—	71	—
	362	115	85	72	71	—	91	—
1985	2884	238	586	648	247	—	265	249
	352	68	124	128	64	—	105	318
1986	3165	154	584	451	—	475	169	—
	302	60	108	95	—	237	50	—
1987	2953	—	384	650	—	304	60	—
	293	—	87	105	—	123	18	—
1988	2689	79	717	484	88	323	241	253
	326	30	110	92	33	93	50	100
1989	2910	560	389	515	190	243	125	179
	275	140	71	78	69	107	24	47

1 = northern offshore spotted dolphin
2 = southern offshore spotted dolphin
3 = eastern spinner dolphin
4 = northern whitebelly spinner dolphin
5 = southern whitebelly spinner dolphin
6 = northern common dolphin
7 = central common dolphin
8 = southern common dolphin

all eight stocks similarly by eliminating the 1983 estimate.

For each series, we calculated regressions using as many data points as existed for each species for that number of years. In some cases, this resulted in as few as three data points contributing to the regression. Because we omitted data from 1983, the 10-year series contained at most nine data points. Because some years were omitted or were missing abundance indices, not all year-series comprised strictly consecutive x-values (year values).

We reexpressed the slope estimate of trend (b) in terms of a change parameter r, where

$$r = b/A_1$$

and A_1 (estimated abundance in first year of series) is calculated from the estimated slope and intercept for each year-series. For these linear regressions, the parameter r expresses the annual rate of change as a fraction of the estimated initial abundance (Gerrodette 1987). Linear regressions were calculated only for series with at least three data points.

Power

We estimated power of statistical conclusions about the significance of each slope by assuming a two-sided alternative hypothesis and using the non-central t (nct) distribution. In all cases, we assumed error levels $\alpha = \beta = 0.10$. We used a two-sided hypothesis test to be consistent with earlier estimates of 5-year trends in abundance (Buckland and Anganuzzi 1988, Anganuzzi and Buckland 1989, Anganuzzi et al. 1991).

To calculate power using the nct distribution, we utilized a series of programs (available upon request) designed to return power estimates as a function of three input variables:

$t_{\alpha,\mathrm{df}}$ = normal t statistic given a level of α and degrees of freedom,

IDF = degrees of freedom, and

δ = b/s_b.

Degrees of freedom were $n-2$ where n is the number of years for which abundance estimates existed in a series. Values for b and s_b were calculated from the weighted linear regressions.

δ is the offset of the alternative distribution (the nct) standardized by the standard error of the offset. In all cases, we assumed as the alternative distribution the observed trend for a series. δ is thus the distance, expressed as standard deviation units, between the mean of the null distribution (taken here to be zero slope) and the mean of the alternative distribution (the slope estimated from regression of the data).

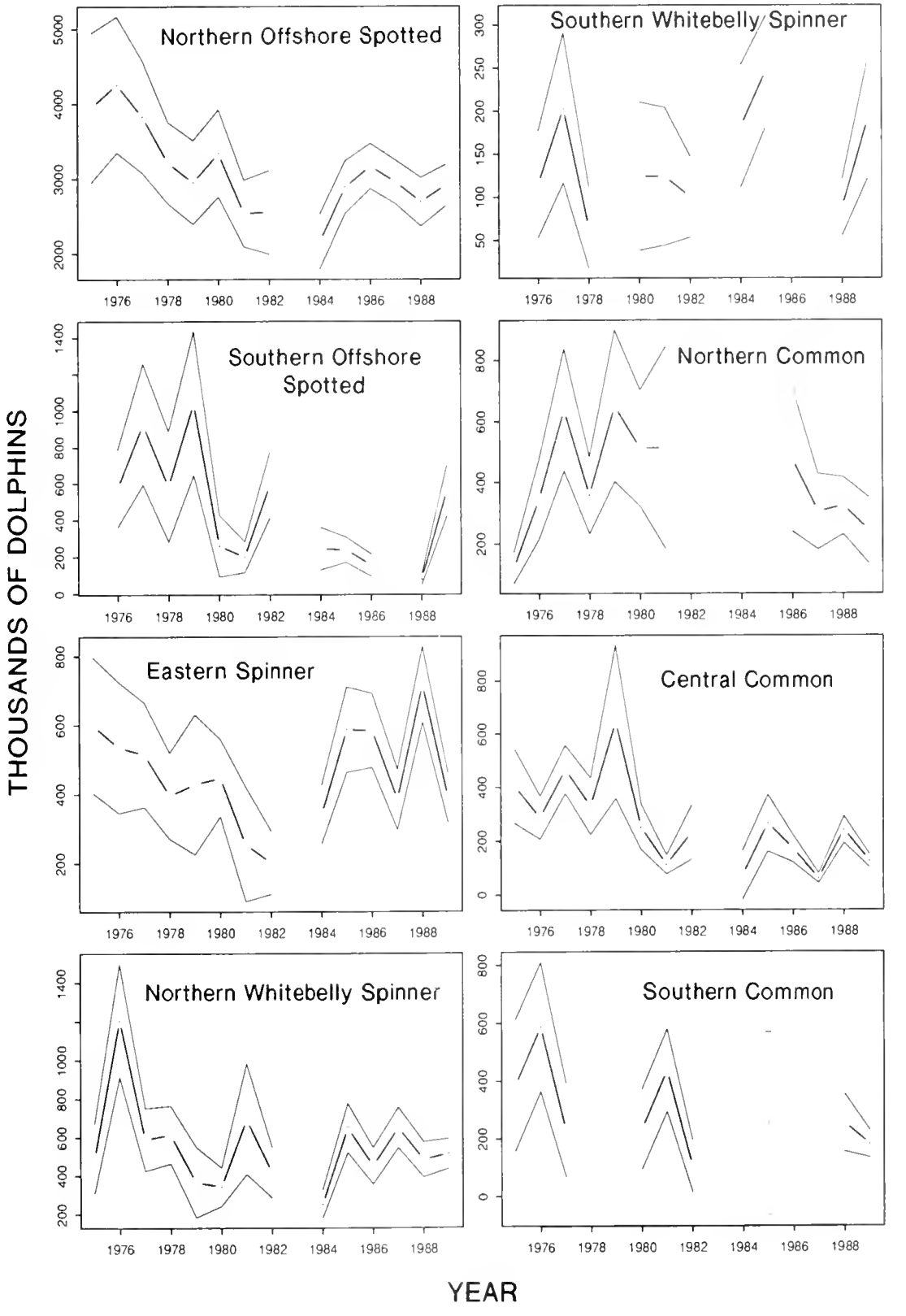

Figure 1

Estimated abundances (dashed line) of dolphins bounded by 1 bootstrap standard error (solid lines). Years for which no estimates were reported are omitted; estimates for 1983 are omitted as anomalous.

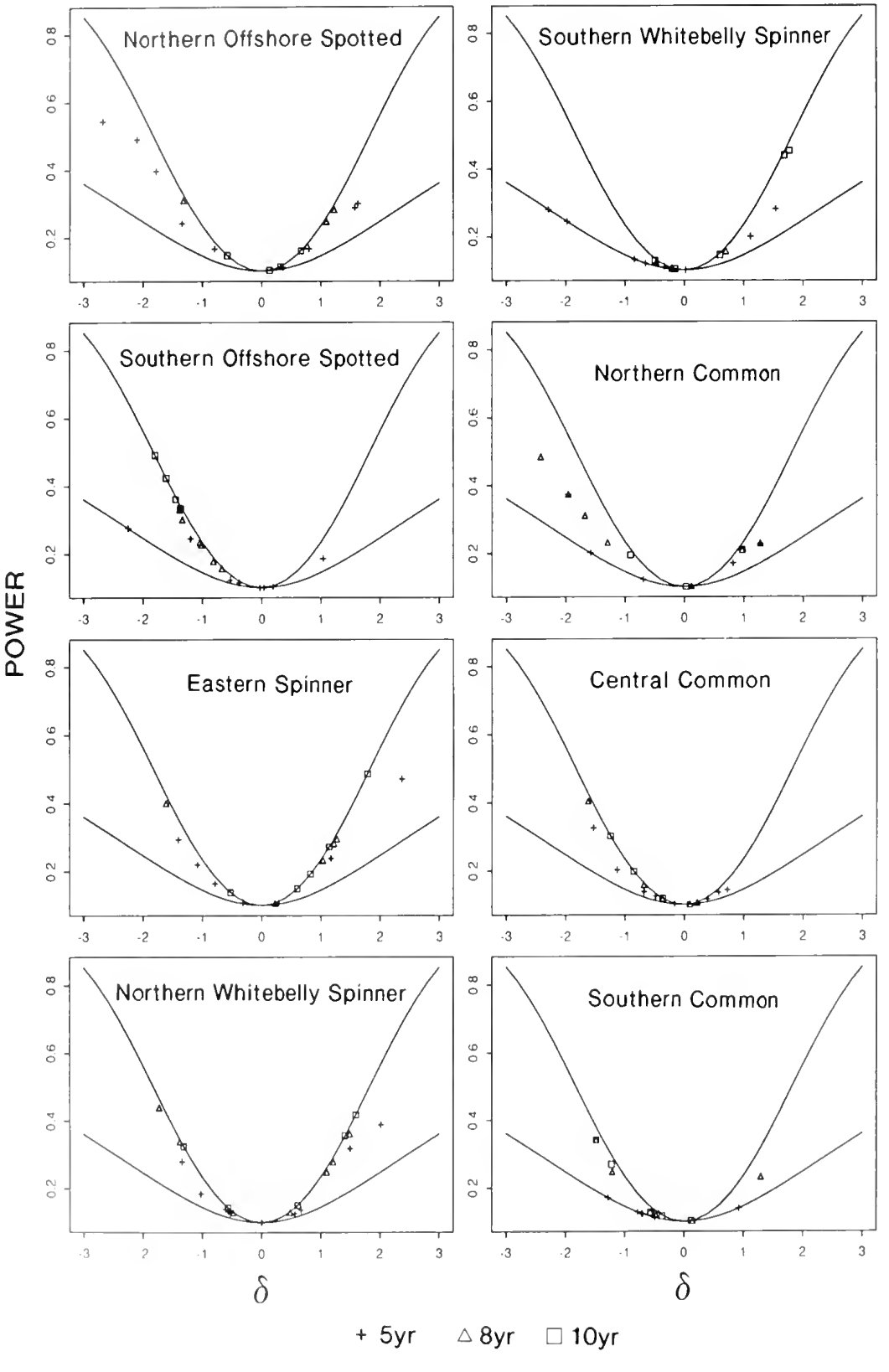

Figure 2

Power of conclusions about lack of statistical significance for estimated 5, 8, and 10-year trends in dolphin abundance. Power calculated for two-tailed noncentral t, assuming $\alpha = 0.10$. Solid lines indicate maximum (7 df) and minimum (1 df) power envelope. δ is the noncentral t parameter.

Detectable trends

We estimated detectable trends (r_d) for all data-series. All estimates of r_d assume error levels $\alpha = \beta = 0.10$. Detectable trends were estimated by determining the value of Delta ($\delta_{0.9}$) that returns a power value of 0.90 from the nct algorithm. As before, input value for IDF was $n-2$, and for s_b was the value estimated from the weighted regression. Then the value of b generating the desired power level (b_{nct}) is

$$b_{nct} = \delta_{0.9}/s_b$$

and the detectable initial trend per year is

$$r_d = b_{nct}/A_1.$$

Results

Observed trends

The majority (151/192; 79%) of the series showed no significant trend (specific data available from the authors). Of those that did, most showed decreases prior to the mid-1980s and no consistent trends since. Where population-abundance indices changed relatively regularly over time, successively longer time-series retained the same general patterns as found in shorter series. For example, observed trends were significantly negative for northern offshore spotted dolphin during the 5-year series 75/79 and 77/81, the 8-year series 75/83, 76/83, and 77/84, and the 10-year series 75/84 and 76/85. Similarly, 5-year negative trends were also reflected in 8- and 10-year series for southern offshore spotted dolphin, eastern spinner dolphin, northern whitebelly spinner dolphin, and central common dolphin.

Data were so sparse and variable for southern whitebelly spinner dolphin and southern common dolphin that little can be said about trends in these stocks. Northern common dolphin were the only species for which trends may have switched during the period of investigation (from negative during earlier years, to positive more recently); but it is obvious that here, as in the other series, the pattern in trend estimates is simply a function of the length of the series selected and its placement in time.

Power

Power to reject a false null hypothesis increases with increases in either or both of series length (as degrees of freedom increase) or δ (offset) (Fig. 2), but for TVOD the increases generally were not sufficient to be of practical use. Where no significant trends (slopes) were found, power to detect a false null hypothesis was low, averaging 20–30% in most cases and never exceeding 60%. Power for each test was small because the alternative hypothesis for these power calculations was taken to be the observed slope, which was usually fairly small, and also because scatter around the regression line tended to be large. Therefore the null and alternative distributions overlapped considerably. The low power of these tests simply means that if the true slope equaled the observed slope, the power to distinguish the true slope from a slope of zero (i.e., no change in abundance) would be quite small in most cases.

Detectable trends

The range of detectable trends decreased rapidly with increasing series-length in all cases (Fig. 3), as this increases the degrees of freedom (number of data points). The decrease is misleading in most cases, however. Although the improvement in ability to detect smaller trends with longer time-series appears dramatic, in most cases even the smallest detectable trends are still much too large to be of use.

Even with as many as 10 years of data in a series, linear trends less than about 10% per year could be detected consistently only for northern offshore spotted dolphin. For all other stocks, trends of at least 15–20% per year would be required to produce a significant result (Fig. 2). Series lengths would have to be such that populations more than doubled or decreased to zero in order for the change to be statistically detectable. This would require series lengths of at least 10 years.

In many cases, where significant trends were found, these trends were of lesser magnitude than the estimated detectable trend. This occurs because the estimated detectable trend is the expected value of the alternative distribution. Any trend value which falls below this expected value, but which also falls above the Type-I error limit for the null distribution, will be assumed significantly different from the null even though the trend could actually belong to either distribution. For example, if the Type-I error limit for the null distribution occurs at a trend value of 0.75 (i.e., if the cut-off point for values assumed to belong to the null distribution is 0.75), and the expected value (i.e., the mean) for the alternative distribution falls at 0.85, any trend value within the range 0.75–0.85 will be assigned to the alternative distribution even though it is smaller than the expected value of the alternative distribution. In practice for the ETP data, this effect is unimportant compared with the overall problem of high variability obscuring the possibility of detecting managerially-relevant trends in abundance (i.e., the

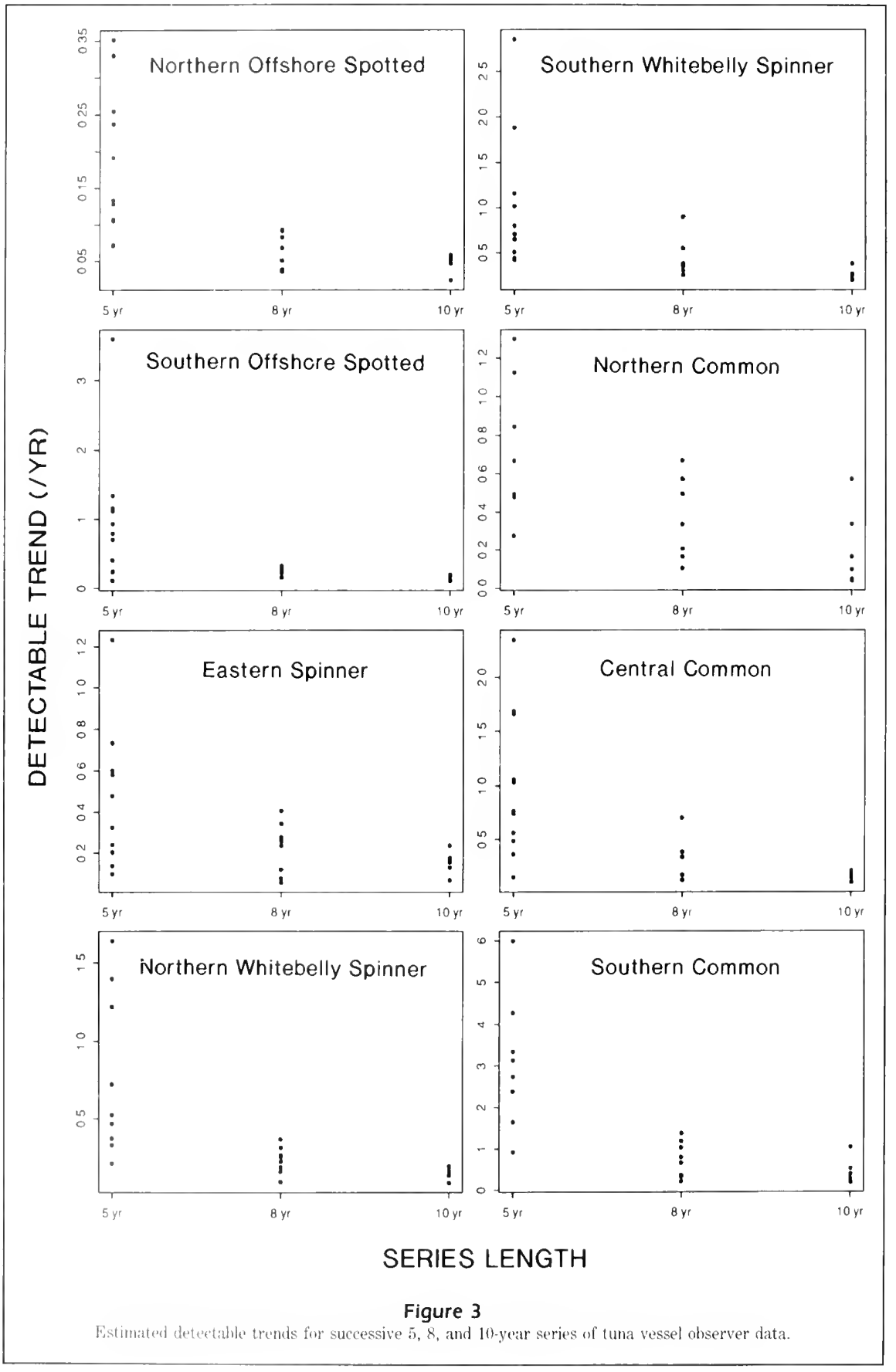

Figure 3

Estimated detectable trends for successive 5, 8, and 10-year series of tuna vessel observer data.

spread and subsequent overlap between null and alternative distributions is so great that differences between the cut-off point in the null and the mean of the alternative is effectively inconsequential).

Discussion

Given the observed variability in TVOD, it does not appear that linear trends in dolphin abundance estimated from these data with these techniques will be detectable at any levels practical for management purposes, except possibly for the stock of northern spotted dolphin. Even for this stock, survey series at least a decade in length are required.

Our estimates of 5-year trends agree with previously published estimates derived by the same methods, where 1983 has been omitted from the analyses (Anganuzzi and Buckland 1989). Our results imply that for time-periods as short as 5 years, considerably larger trends than those observed would be necessary to produce estimates of significant change with any reasonable power. Except for northern offshore spotted dolphin, this applies also to all other stocks, even for the maximum time-series tested (10 years in this study). It appears that other methods must be found to determine whether trends truly exist in dolphin abundance in the ETP. For management purposes, longer time-series must be monitored, for which linearity cannot be assumed. Other regression procedures making greater use of the precision estimates (standard errors) of the indices could have more power, but for linear analyses, at least, it is uncertain whether the increase in power could overcome the inherent variability and probable nonlinearities in the data.

A more effective approach to estimating trends in dolphin abundance is probably represented by the sophisticated smoothing method applied recently to these data by Buckland et al. (1992). The method reduces the relatively-scattered abundance estimates to smoothly-changing estimates of abundance, but with the advantage of producing confidence limits about the smoothed trend and generating a more biologically-reasonable result (abundance of natural populations rarely changes linearly). However, simulation experiments will be required to determine the circumstances under which the smoothed trends do, or do not, reflect accurately the true underlying dynamics of the stocks. Such simulations are currently underway, but results are as yet unavailable (Alejandro Anganuzzi, Inter-Am. Trop. Tuna Comm., La Jolla, pers. commun., July 1991).

Regardless of the results of the tests of various smoothing methods, it appears fruitless, based on the results presented here, to use linear-regression techniques to estimate trends in abundance of dolphin stocks in the ETP, even for periods as long as a decade. The power to detect ecologically (or managerially) relevant trends, given the observed variability in the data, is simply not sufficient.

Future efforts should, as suggested by Buckland et al. (1992), focus on developing or applying robust, curvilinear smoothing techniques that are reasonably responsive to the underlying processes or mechanisms controlling actual changes in dolphin abundance.

Acknowledgments

This study has benefited greatly from technical assistance by Cheryl Glick and extensive helpful discussions with Tim Gerrodette and Doug DeMaster.

Citations

Anganuzzi, A.A., and S.T. Buckland
1989 Reducing bias in estimated trends from dolphin abundance indices derived from tuna vessel data. Rep. Int. Whaling Comm. 39:323–334.

Anganuzzi, A.A., S.T. Buckland, and K.L. Cattanach
1991 Relative abundance of dolphins associated with tuna in the eastern tropical Pacific, estimated from tuna vessel sightings data for 1988 and 1989. Rep. Int. Whaling Comm. 41:497–506.

Buckland, S.T., and A.A. Anganuzzi
1988 Estimated trends in abundance of dolphins associated with tuna in the eastern tropical Pacific. Rep. Int. Whaling Comm. 38:411–437.

Buckland, S.T., K.L. Cattanach, and A.A. Anganuzzi
1991 Estimating trends in abundance of dolphins associated with tuna in the eastern tropical Pacific, using sighting data collected on commercial tuna vessels. Fish. Bull., U.S. 90: 1–12.

Gerrodette, T.
1987 A power analysis for detecting trends. Ecology 68: 1364–1372.

Hammond, P.S., and J.L. Laake
1983 Trends in abundance of dolphins involved in the purse-seine fishery for tuna in the eastern tropical Pacific Ocean, 1977–1981. Rep. Int. Whaling Comm. 33:565–588.

Holt, R.S., T. Gerrodette, and J.B. Cologne
1987 Research vessel survey design for monitoring dolphin abundance in the eastern tropical Pacific Ocean. Fish. Bull., U.S. 85:435–446.

Perrin, W.F.
1990 Subspecies of *Stenella longirostris* (Mammalia: Cetacea: Delphinidae). Proc. Biol. Soc. Wash. 103(2):453–463.

Peterman, R.M.
1990 The importance of reporting statistical power: The forest decline and acidic deposition example. Ecology 71:2024–2027.

Wilkinson, L.
1989 SYSTAT: The system for statistics. Systat, Inc., Evanston.

Superintendent of Documents **Subscriptions** Order Form

Order Processing Code:
* 5178

☐ **YES,** enter my subscription as follows:

Charge your order. It's Easy! MasterCard VISA

To fax your orders (202) 512–2233

____ subscriptions to **FISHERY BULLETIN (FB)** for $24.00 per year ($30.00 foreign).

The total cost of my order is $_____. Price includes regular domestic postage and handling and is subject to change.

(Company or Personal Name) (Please type or print)

(Additional address/attention line)

(Street address)

(City, State, ZIP Code)

(Daytime phone including area code)

(Purchase Order No.)

May we make your name/address available to other mailers? YES ☐ NO ☐

Please Choose Method of Payment:

☐ Check Payable to the Superintendent of Documents

☐ GPO Deposit Account ☐☐☐☐☐☐☐☐ – ☐

☐ VISA or MasterCard Account

☐☐☐☐☐☐☐☐☐☐☐☐☐☐☐☐

☐☐☐☐ (Credit card expiration date)

Thank you for your order!

(Authorizing Signature) 11/91

Mail To: New Orders, Superintendent of Documents
P.O. Box 371954, Pittsburgh, PA 15250–7954

Fishery Bulletin

Guidelines for Contributors

Form of manuscript

The document should be in the following sequence: Title Page, Abstract (not required for Note), Text, Acknowledgments, Citations, Text footnotes, Appendices, Tables, Figure legends, and Figures.

Title page should include authors' full names and mailing addresses and the senior author's telephone and FAX numbers.

Abstract Not to exceed one double-spaced typed page. Should include a sentence or two explaining to the general reader why the research was undertaken and why the results should be viewed as important. Abstract should convey the main point of the paper and outline the results or conclusions. No footnotes or references.

Text A brief introduction should portray the broad significance of the paper. The entire text should be intelligible to readers from different disciplines. All technical terms should be defined, as well as all abbreviations, acronyms, and symbols in text, equations, or formulae. Abbreviate units of measure only when used with numerals or in tables and figures to conserve space. Measurements should be expressed in metric units, with other equivalent units given in parentheses. Follow the *U.S. Government Printing Office Style Manual*, 1984 ed., and the *CBE Style Manual*, 5th ed. Fishery and invertebrate nomenclature should follow the *American Fisheries Society Special Publication 12* (for fishes), *16* (for mollusks), and *17* (for decapod crustaceans).

Text footnotes should be numbered in Arabic numerals and typed on a separate sheet from the text. Footnotes are not used for reference material or personal communications, but rather to explain or define terms in the text and for contribution numbers on the title page.

Informal sources Personal communications, unpublished data, and untitled manuscripts in preparation are noted parenthetically in the text (full name, affiliation, brief address including zip code, and month and year when appropriate).

Acknowledgments Gather all acknowledgments into a brief statement at the end of the text. Give credit only for exceptional contributions and not to those whose contributions are part of their normal duties.

Citations All titled sources should be listed in the Citations section, including unpublished and processed material. In text, cite as Smith and Jones (1977) or (Smith and Jones 1977); if more than one citation, list chronologically (Smith 1936, Jones 1975, Doe In press). All sources cited in the text should be listed alphabetically by the senior authors' surnames under the heading CITATIONS. Abbreviations of periodicals and serials should conform to *Serial Sources for the BIOSIS Data Base*™. Indicate whether sources are in a language other than English. For informal literature, include address of author or publisher. Authors are responsible for the accuracy of all citations.

Tables should supplement, not duplicate, the text. Each table should be numbered and cited consecutively, with headings short but amply descriptive so that the reader need not refer to the text. For values less than one, zeros should precede all decimal points. Indicate units of measure in column headings; do not deviate from the unit of measure within a column. Table footnotes should be noted consecutively in Roman letters across the page from left to right and then down. Since all tables are typeset, they need not be submitted camera-ready.

Figures Photographs and line drawings should be of professional quality—clear and concise—and reducible to 42 picas for full-page width or to 20 picas for a single-column width, and to a maximum 55 picas high. All graphic elements in illustrations must be proportioned to insure legibility when reduced to fit the page format. Line weight and lettering should be sharp and even. Lettering should be upper and lower case, and vertical lettering should be avoided whenever possible (except for vertical, y, axis). Zeros should precede all decimal points for values less than one. Reproductions of line artwork are accepted in the form of high-quality photographic prints from negatives or photomechanical transfer (PMT). Halftones should be sharply focused with good contrast. Micron rules should be inserted on electron micrographs, even when magnification is included in the figure legend. There should be clear distinction between identifying letters (press-on or overlay) and background of photograph. Label each figure in pencil on the back. Send only xerox copies of figures to the Scientific Editor; originals or photographic prints will be requested later when the manuscript is accepted for publication.

Copyright Government publications are in the public domain, i.e., they are not protected by copyright.

Submission of manuscript

Disks Authors are encouraged to retain manuscripts on word-processing storage media (diskettes, floppy disks) and submit a double-spaced hardcopy run from the storage media. Submit disks as MS-DOS "print" or "nondocument" files (often called "ASCII files"). If a disk cannot be converted to an ASCII file, the author should indicate on the disk the source computer and software language along with the file name. Either 5¼-inch or 3½-inch disks from IBM-compatible or Apple/MacIntosh systems (non-graphics only) can be submitted, double-sided/double-density or high-density, limiting each file to 300 kilobytes. All 8-inch word-processing disks (e.g., Wang or NBI) must be converted onto 5¼- or 3½-inch MS-DOS print disks.

Send original hardcopy and two duplicated copies to:

Dr. Ronald W. Hardy, Scientific Editor
Northwest Fisheries Science Center
National Marine Fisheries Service, NOAA
2725 Montlake Boulevard East
Seattle, WA 98112-2097

Copies of published articles and notes
The senior author and his/her organization each receive 50 separates free-of-charge. Additional copies may be purchased in lots of 100.

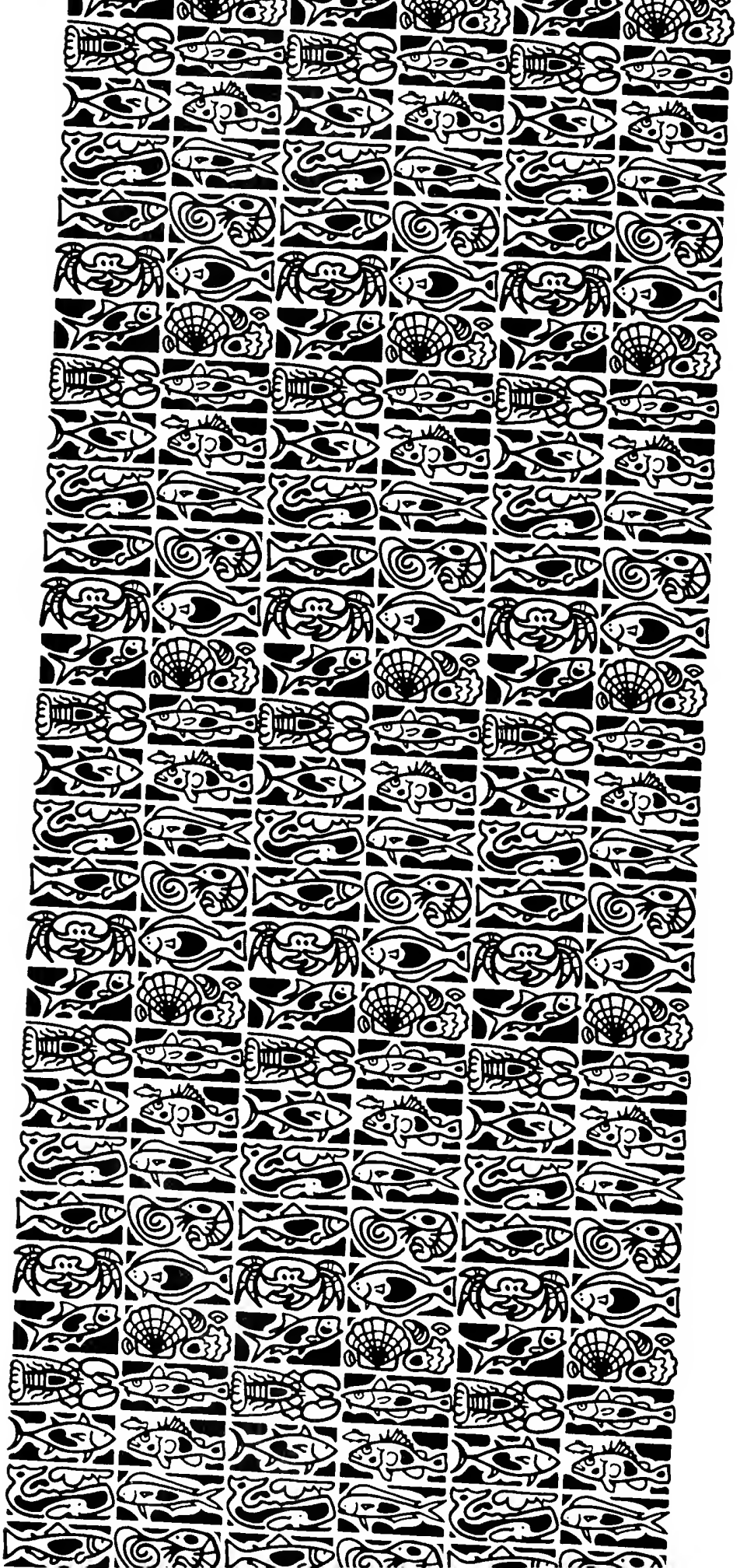

U.S. Department
of Commerce

Volume 90
Number 4
October 1992

Fishery Bulletin

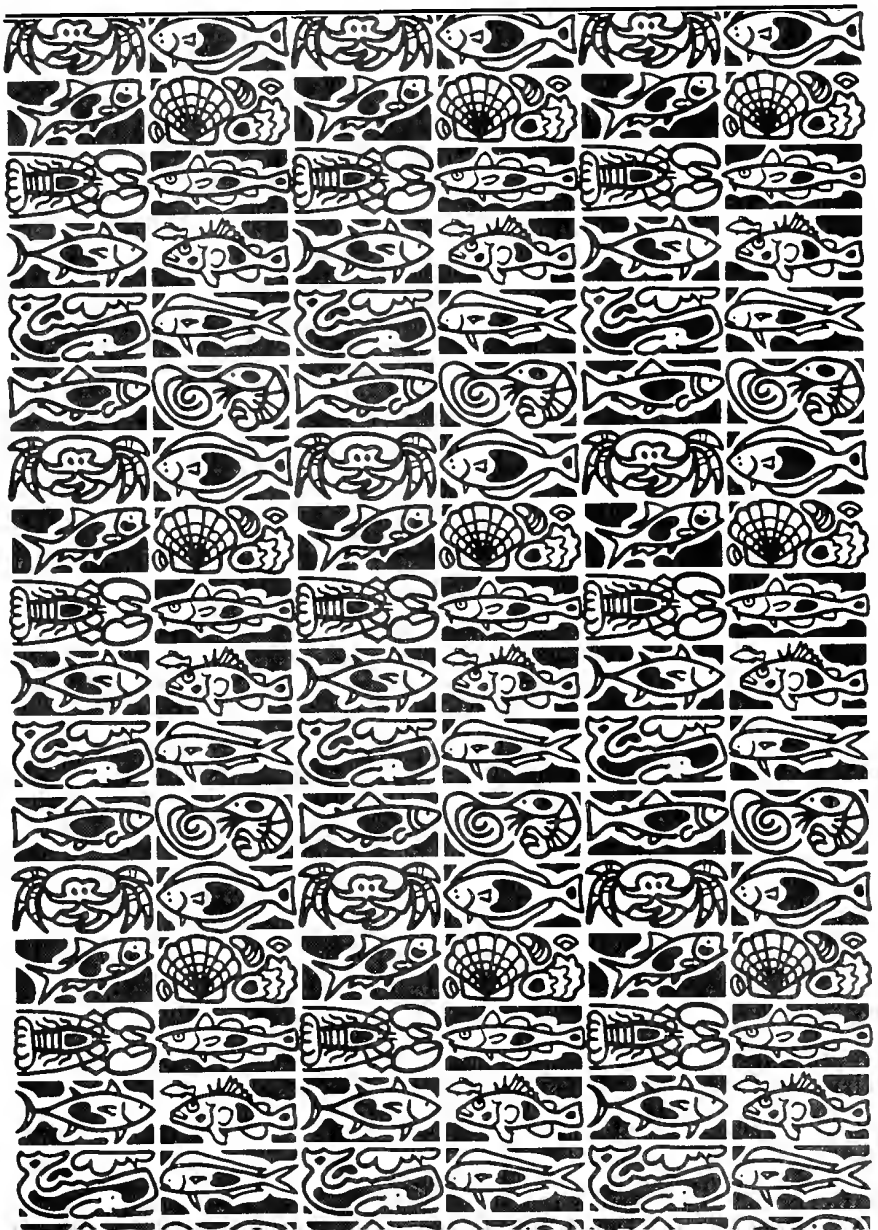

Fishery Bulletin

The *Fishery Bulletin* (ISSN 0090-0656) is published quarterly by the Scientific Publications Office, National Marine Fisheries Service, NOAA, 7600 Sand Point Way NE, BIN C15700, Seattle, WA 98115-0070. Second class postage is paid in Seattle, Wash., and additional offices. POSTMASTER send address changes for subscriptions to Fishery Bulletin, Superintendent of Documents, Attn: Chief, Mail List Branch, Mail Stop SSOM, Washington, DC 20402-9373.

The Secretary of Commerce has determined that the publication of this periodical is necessary in the transaction of the public business required by law of this Department. Use of funds for printing of this periodical has been approved by the Director of the Office of Management and Budget.

For sale by the Superintendent of Documents, U.S. Government Printing Office, Washington, DC 20402. Subscription price per year: $24.00 domestic and $30.00 foreign. Cost per single issue: $12.00 domestic and $15.00 foreign. **See back page for order form.**

The *Fishery Bulletin* carries original research reports and technical notes on investigations in fishery science, engineering, and economics. The Bulletin of the United States Fish Commission was begun in 1881; it became the Bulletin of the Bureau of Fisheries in 1904 and the Fishery Bulletin of the Fish and Wildlife Service in 1941. Separates were issued as documents through volume 46; the last document was No. 1103. Beginning with volume 47 in 1931 and continuing through volume 62 in 1963, each separate appeared as a numbered bulletin. A new system began in 1963 with volume 63 in which papers are bound together in a single issue of the bulletin. Beginning with volume 70, number 1, January 1972, the *Fishery Bulletin* became a periodical, issued quarterly. In this form, it is available by subscription from the Superintendent of Documents, U.S. Government Printing Office, Washington, DC 20402. It is also available free in limited numbers to libraries, research institutions, State and Federal agencies, and in exchange for other scientific publications.

U.S. Department
of Commerce
Seattle, Washington

Volume 90
Number 4
October 1992

Fishery Bulletin

Contents

Notes

Abstract. – Commercial and sport landings of white seabass have declined, particularly in southern California, and the populations now appear to be severely impacted. To provide information critical to the management of this species, settlement patterns of white seabass within the Southern California Bight were investigated for 1988–89. Data were obtained from 16 stations sampled along the southern California coastline during June–October 1988, and at 12 stations sampled along the coasts of the mainland and four Channel Islands May–August 1989. At each station, four 5-minute tows were taken with a 1.6 m beam trawl at each of two depths, 5 and 10 m.

Most young-of-the-year white seabass were <10 mm SL and had settled within 2–3 weeks of capture. Density estimates for white seabass off southern California were low, ranging from 0.3 to only 37.8 individuals per hectare. In 1988, catch-per-unit-effort (CPUE) peaked in July (1.10/tow) with differences being statistically significant among months. In 1989, CPUE peaked in June (0.45/tow) with differences being statistically significant among distance blocks from the mainland. CPUE was 15 times higher at the mainland stations compared with the island stations (0.59/tow vs. 0.04/tow). Abundance was significantly correlated with warm bottom-water temperatures in 1988, although not in 1989.

Multivariate analysis of the catches with selected environmental variables indicated that distance from the mainland and bottom temperature may have been important factors influencing settlement. However, in combination, these two variables accounted for only 5% of the total variance (R^2 0.05) in abundance. This finding implies that other factors, most notably the availability of premetamorphic larvae, probably have an influence on white seabass settlement and need to be considered in future studies.

Manuscript accepted 8 July 1992.
Fishery Bulletin, U.S. 90:633–641 (1992).

Abundance, distribution, and settlement of young-of-the-year white seabass *Atractoscion nobilis* in the Southern California Bight, 1988-89*

Larry G. Allen
Department of Biology, California State University, Northridge, California 91330

Michael P. Franklin
Department of Biology, California State University, Northridge, California 91330
Present address: Department of Biological Sciences
University of California, Santa Barbara, California 93106

The white seabass *Atractoscion nobilis* is the largest croaker (family Sciaenidae) occurring off southern California (Miller and Lea 1974), where it is important in both commercial and sport fisheries. Despite attempts to improve the fishery (e.g., imposing minimum size requirements and limits on sport and commercial catches; Frey 1971), landings continue to decline and the stocks appear to be severely impacted (Vojkovich and Reed 1983), particularly in southern California waters.

Despite their impacted status and economic importance, little was known about the early-life-history stages of white seabass until recently. Moser et al. (1983) described the larval development from hatchery-reared eggs. Field investigations of early-life-history stages were limited to reports of larval occurrence within California Cooperative Fisheries Investigations (CalCOFI) collections from 1950 to 1978. For example, Moser et al. (1983) found that only 15% of white seabass larvae were taken in southern California waters. Most were taken near Sebastian Viscano and San Juanico Bays, Baja California.

A few studies have provided limited information on the young-of-year (YOY) stages of white seabass. Allen and Franklin (1988) examined the abundance and distribution of juvenile white seabass in the vicinity of Long Beach harbor and developed a model for locating YOY white seabass in coastal waters. We observed that YOY white seabass were captured over sandy bottoms in shallow water near the breaker line, most often with submerged aquatic vegetation (drift algae: green, brown, and red), encrusting bryozoans, and terrestrial debris. This area seems to be the nursery grounds for white seabass. The drift material may be an important component of these nursery areas because these fish appear to be structure-oriented early in life (Allen and Franklin 1988, Margulies 1989, Donohoe 1990). Donohoe (1990), based on field collections, found that young seabass were associated with the drift, and also observed that the larvae and juveniles moved toward structures in laboratory experiments. A significant relationship was found between the mass of drift algae and the occurrence of YOY white seabass from Oceanside, California to the Mexican border, suggesting that the drift habitat may influence the distribution patterns

* Contribution 67 of the Ocean Studies Institute, California State University.

of these young fish (Donohoe 1990). Margulies (1989) concluded that the visual perception of YOY seabass improves with age, and that young fish begin to avoid predators by moving to the drift.

Our studies on white seabass settlement were undertaken in southern California where the main fishery for this species still exists. The specific objectives were to (1) examine the patterns of abundance, distribution, and settlement of YOY white seabass off the coast of southern California between Point Conception and San Mateo Point and along the coastlines of four of the larger Channel Islands, and (2) identify environmental factors that may influence these patterns.

Materials and methods

YOY white seabass were captured during the summers of 1988 and 1989 as part of the Ocean Resources Enhancement and Hatchery Program (OREHP) of the California Department of Fish and Game, which emphasized studies within the Southern California Bight. Trawls were made over flat bottoms just offshore of open sand beaches, using two 5.2 m whalers. At each station four 5-minute replicate tows were made in the shallow, potential nursery areas by two whalers simultaneously sampling along each of two isobaths (5 and 10 m) using a 1.6 m beam trawl. The trawl was comprised of 4 mm mesh in the wings and 2 mm knotless mesh in the codend. Calibration tows using a meter wheel indicated that a 5-minute tow covered an average of 183 m of bottom, yielding a mean coverage of 293 m^2. Bottom profiles were monitored using depth finders mounted in each whaler. Temperature, salinity, dissolved oxygen, and pH were monitored at the surface and bottom at each station at both isobaths, using a Hydrolab Surveyor II Water Quality Measurement System. Submerged aquatic vegetation (drift algae) captured in each tow was weighed (to nearest kg) at all stations. White seabass were measured to the nearest 0.1 mm standard length (SL).

Sixteen stations were established along the coast of southern California from Point Conception to San Mateo Point in 1988 (Fig. 1). These stations were approximately 10 nmi apart and were sampled from June through October. The sampling regime yielded 128 tow samples (4 tows at 2 depths at each of 16 stations) over 5 months, for a total of 640 tow samples in 1988.

In 1989, sampling was designed to examine the settlement patterns along the mainland and around the four largest offshore islands. Four mainland stations and eight island stations were sampled each month from May through August (Fig. 1). The mainland stations were those with the greatest consistency of catch of YOY white seabass in 1988: Stns. 6 (Ventura), 10 (Malibu), 13 (Belmont Shore), and 15 (Laguna Beach). Two new stations were established at each of four Channel Islands: Stns. 17 and 18 (Santa Cruz), 19 and 20 (Santa Rosa), 21 and 22 (Santa Catalina), and 23 and 24 (San Clemente). The twelve stations sampled in 1989 were divided subjectively into three groups of four stations based on relative distance from shore or distance blocks (DSTBLK). Stns. 6, 10, 13, and 15 were designated as being at the mainland (MAINLAND); Stns. 17, 18, 21, and 22 as near-island stations (NEAR ISL); and Stns. 19, 20, 23, and 24 as far-island stations (FAR ISL). The 1989 sampling regime yielded 96 tow samples (4 tows at 2 depths at each of 12 stations) for each month except May, when only 80 tows were made because poor weather conditions prevented sampling the Santa Rosa Island stations, for a total of 368 tows overall.

Analysis of variance, t-test, and correlation analyses were completed using the CSS:Statistica for desktop computers (Stat Soft, Inc., Tulsa). For 1988 data, a

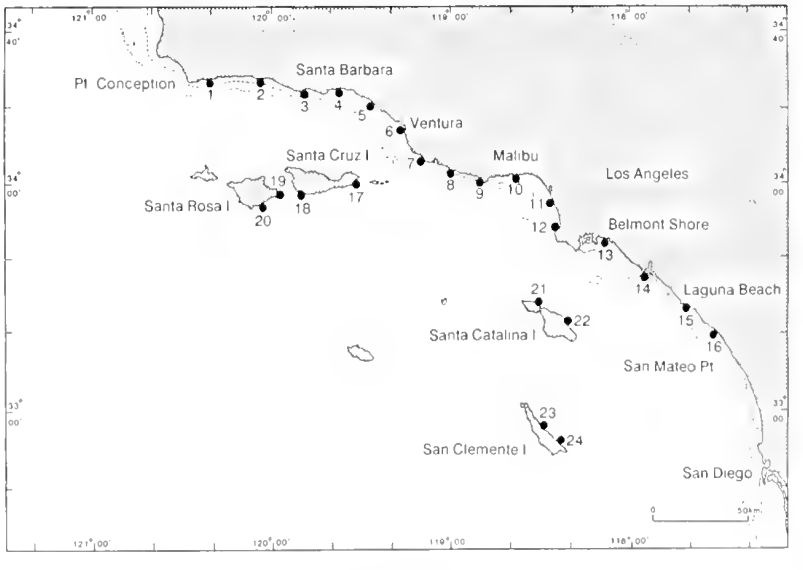

Figure 1

Map of locations of mainland and Channel Island stations sampled during the YOY white seabass *A. nobilis* survey, 1988–89.

balanced design, three-way ANOVA was used to test the effects on catch-per-unit-effort (CPUE) of combinations of independent variables (station, month, and depth). In 1989, a similar three-way ANOVA design was used to test the effects of distance block (distance from the mainland), month, and depth on CPUE. CPUE was used in all parametric analyses in order to minimize any negative impact that the large number of zero-catch tows would have on the analysis. Since replicates had to be combined, the three-way-interaction mean square was utilized as a conservative estimate of sampling error for the 1988 ANOVA test. In 1989, the ANOVA design was unbalanced due to two missing stations in May at Santa Rosa Island. In this case, cell means estimation was utilized to overcome the imbalance. Since the three-way-interaction term was originally found to be significant in the 1989 analysis, its mean square was pooled with the within-sample error in order to partition out the effect of the interaction on the main effects of distance block, month, and depth individually. Correlations and canonical correlation analysis were utilized to examine the possible association of various environmental factors with settlement of YOY white seabass.

Results

Length-frequencies

The YOY white seabass captured during the 1988 survey ranged from 4.2 to 78 mm SL ($\bar{x}$ 9.8 mm SL). In 1989, the range was 4.5–51.7 mm SL ($\bar{x}$ 12.1 mm SL). Most YOY, however, ranged from 5 to 20 mm SL (Fig. 2). Newly settled fish (<10 mm SL) were caught from June through September. Individuals >20 mm SL were more common from July through October.

Newly settled fish (<10 mm SL) made up 75% of all YOY seabass in 1988 and 1989. Fish <20 mm SL comprised 93% of the total catch. The paucity of larger YOY in the samples (Fig. 2) from July to September indicates that our beam-trawl catch may be biased toward smaller, less-mobile fish.

Studies utilizing the daily growth rings on white seabass otoliths (Franklin and Allen, unpubl. data) indicate that fish of 5–20 mm SL are ~37–104 days old. Since settlement occurred consistently at ~5 mm SL, white seabass in this range settled at 0–68 days before capture. The majority of those <10 mm SL had settled 14–21 days before capture.

Abundance and distribution

Summer 1988 Sampling along the mainland yielded 270 YOY white seabass. Most (58%) were captured at five of the 16 stations: Stn. 2 (Refugio Beach, *n* 38), Stn. 6 (Ventura, *n* 28), Stn. 10 (Malibu, *n* 30), Stn. 13 (Belmont Shore, *n* 31), and Stn 15 (Laguna Beach, *n* 31) (Fig. 3). Mean catches (CPUE) were highest at these five stations; furthermore, the variance of these five means was also very high. This was especially true at Stn. 2 (Refugio Beach) where 36 of the 38 YOY captured were taken during a single month (July).

The CPUE for all stations was low in June 1988 (0.15 individuals/tow), peaked in July (1.10/tow), and declined to 0.08/tow in October (Fig. 4). Catches in July accounted for 52% (141 individuals) of YOY white seabass taken in 1988. In June, catch was low (19 individuals) and white seabass were collected only from southern stations (12, 13, and 15) (Fig. 5). By July,

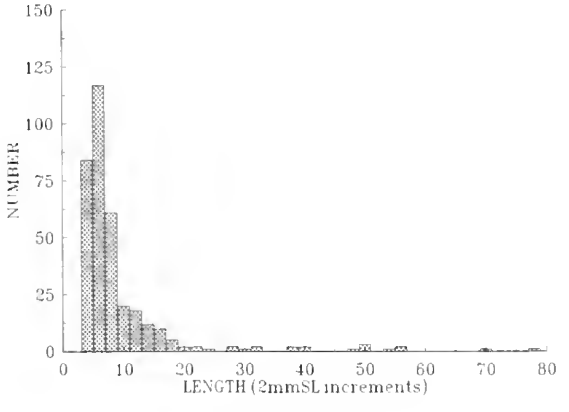

Figure 2
Length-frequencies of YOY white seabass *A. nobilis* from all samples combined, 1988–89. Length increments are 2 mm (*n* 354).

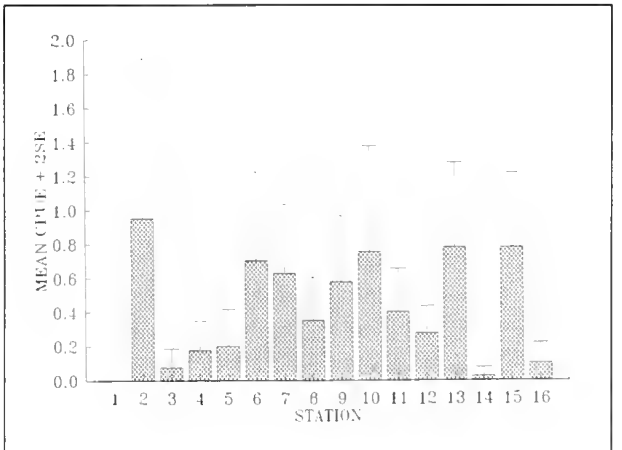

Figure 3
CPUE of YOY white seabass *A. nobilis* by station, summer 1988. Bars represent 2 SE of the mean.

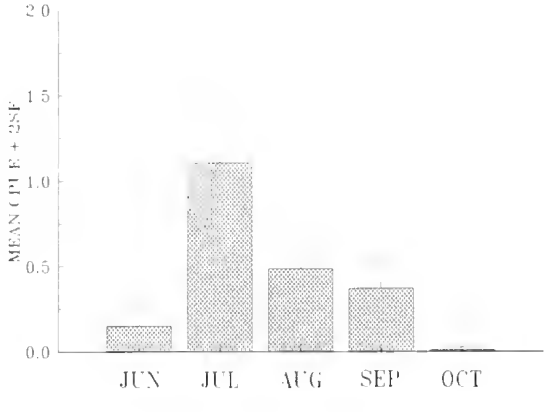

Figure 4
CPUE of YOY white seabass *A. nobilis* by month, summer 1988. Bars represent 2SE of the mean.

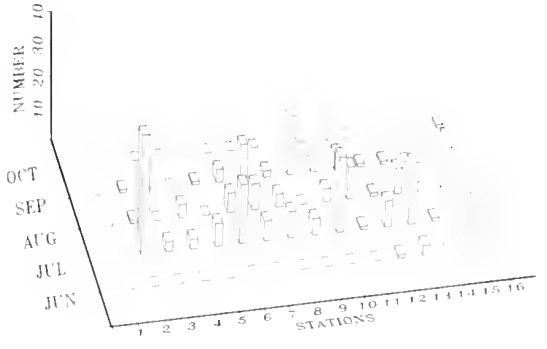

Figure 5
Abundance of YOY white seabass *A. nobilis* by station over the five months (June–October) of the 1988 survey.

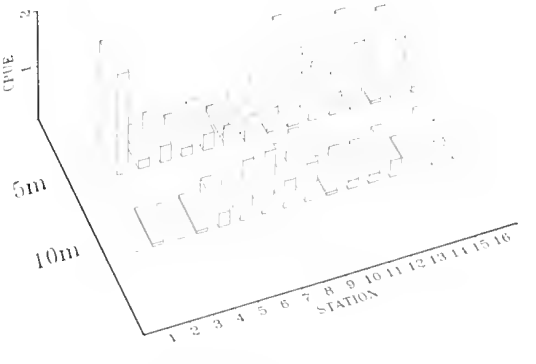

Figure 6
CPUE of YOY white seabass *A. nobilis* by station and depth for the 1988 survey.

relatively heavy settlement was observed throughout the coastal area, as far north as Stn. 2. The greatest numbers were taken off Stns. 2 (Refugio Beach), 6 (Ventura), 10 (Malibu), and 13 (Belmont Shore). None were taken at Stn. 15 (Laguna Beach) where they were most abundant a month earlier. In August, the number of recently-settled white seabass had declined from the July peak. Moderate numbers were captured at Stns. 7 (Hueneme), 11 (El Segundo), 13 (Belmont Shore), and 15 (Laguna Beach). In September, young seabass settled at the middle stations (stns. 6–11). By October, no new settlement was detected at any of the study sites (Fig. 5). The only YOY white seabass was an older fish (78mmSL) taken at Stn. 16 (San Mateo Pt.).

Sixty-three percent (170 individuals) of all YOY were taken at the 5m depth in 1988. YOY white seabass were most numerous at the 5m isobath at Stns. 2–4, 10–13, and 15, but were more abundant at 10m at Stns. 5–9 (Fig. 6).

Analysis of variance of CPUE values in 1988 indicated that only the observed monthly differences were statistically significant (Table 1). Differences in CPUE among stations and depths were not significant in 1988.

YOY white seabass densities ranged from a low of 0.3 individuals/ha in October 1988, to a high of 37.8 in July 1988. In 1988, population estimates varied greatly along the approximately 300km of coastline (excluding the offshore islands) covered in 1988. Overall density for the 5-month period yielded a population estimate of 130,000 individuals in the area of southern California covered by the sampling.

Summer 1989 Sampling from May to August 1989 along the coastlines of the mainland and the offshore islands produced 85 YOY. The catch rate at the mainland stations was 15 times higher than at island stations (CPUE 0.59/tow in 128 tows vs. 0.04/tow in 240 tows) (Fig. 7). Most (88%) of the YOY were captured at three of the mainland stations: Stns. 6 (Ventura, n 22), 10 (Malibu, n 14), and 15 (Laguna Beach, n 38). Five YOY were captured at Stns. 17 and 18 on Santa Cruz I., four were taken at Stn. 22 (White's Cove) on Santa Catalina I., and none were taken at Santa Rosa or San Clemente I.

The CPUE was low in May (0.14/tow), peaked in June (0.45/tow), and declined through July–August (0.14/tow) (Fig. 8). Settlement was restricted to the southern mainland stations (13 and 15) in May (Fig. 9). By June, settlement was observed as far north as Stn. 6 (Ventura) with the greatest numbers occurring off Stns. 10 (Malibu) and 15 (Laguna Beach). In July and August settlement was highly variable at the mainland stations. The five YOY white seabass taken at Santa Cruz I. (Stns. 17 and 18) were captured during June, July,

Table 1

Summary of three-way ANOVA results for catches of young-of-year white seabass *A. nobilis* during the 1988 and 1989 coastal surveys. Dependent variable in all cases was CPUE. DSTBLK = distance block; * $p<0.05$; ** $p<0.001$.

Test	Effect	df	MS	F	p
1988 Survey					
Station × Month × Depth	Station	15	0.9832	1.0086	0.4590
	Month	4	5.7207	5.8686	0.0005**
	Depth	1	1.9141	1.9635	0.1663
	S × M	60	1.0263	1.0529	0.4212
	S × D	15	1.3441	1.3788	0.1875
	M × D	4	0.9687	0.9938	0.4180
Error	S × M × D	60	0.9748	—	—
1989 Survey					
DSTBLK × Month × Depth	DSTBLK (DB)	2	2.9712	11.8180	0.0000**
	Month	3	0.6036	2.4008	0.0745
	Depth	1	0.5481	2.1801	0.1440
	DB × M	6	0.4784	1.9029	0.0915
	DB × D	2	0.3110	1.2371	0.2962
	M × D	3	0.7950	3.1623	0.0295*
Error	DB × M × D	74	0.2514	—	—

and August. Stn. 22 (White's Cove, Santa Catalina I.) was the only other Channel Island station where YOY seabass were taken (Fig. 9).

During 1989, 69% (n 59) of YOY white seabass were taken at 5m, while 31% (n 26) were captured at 10m. Most of the fish taken at the 10m isobath were captured at Stns. 6 (Ventura) and 15 (Laguna Beach). Two YOY white seabass were taken at 10m off Santa Cruz I. (Stns. 17 and 18).

In 1989, catches (CPUE) were then examined according to distance block, month, and depth of capture. Analysis of variance revealed the significant effect of distance block (Table 1; Fig. 10) which was highly significant ($p<0.0001$). Although month and depth were not significant main effects, a significant month-by-depth interaction was detected in the three-way ANOVA. The month-by-depth interaction indicated that depth distributions changed significantly over the period of May–August. Catches of YOY white seabass increased at the 10m depth stratum and decreased at 5m over the course of the summer (Fig. 11).

The population estimate for 1989 based on mean density along ~600km of mainland and offshore islands coastland was about 118,000 individuals over the 4-month sampling.

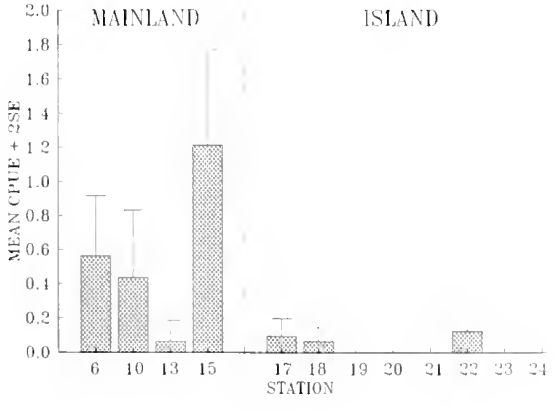

Figure 7

CPUE of YOY white seabass *A. nobilis* by station, summer 1989. Bars represent 2SE of the mean. Stations are grouped into mainland and island sites for comparison.

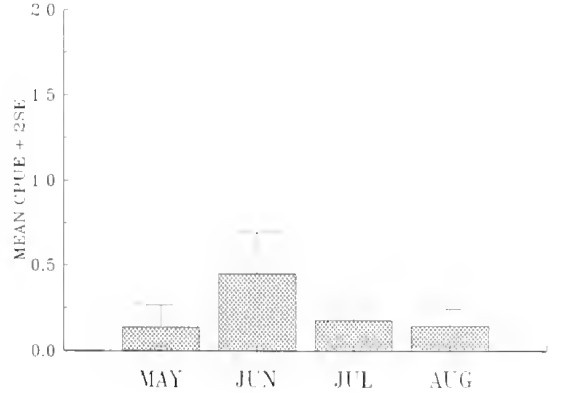

Figure 8

CPUE of YOY white seabass *A. nobilis* by month, summer 1989. Bars represent 2SE of the mean.

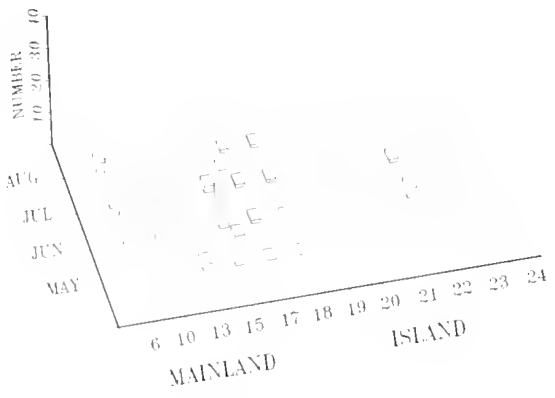

Figure 9

CPUE of YOY white seabass *A. nobilis* by station over the four months (June–October) of the 1989 survey. Stations are grouped into mainland and island sites for comparison. Stns. 19 and 20 (Santa Rosa I.) were not sampled in May due to severe weather conditions.

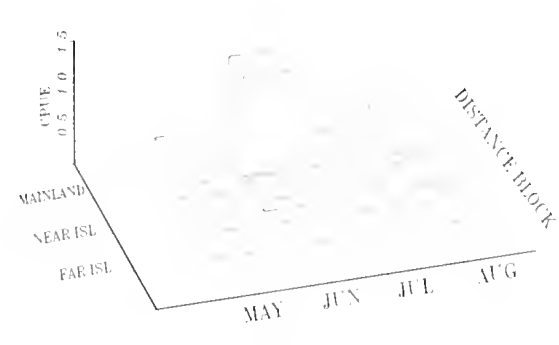

Figure 10

CPUE of YOY white seabass *A. nobilis* within stations grouped by distance block (MAINLAND = four mainland stations, NEAR ISL = four near-island stations, FAR ISL = four far-island stations) over the four months (May–August) of the 1989 survey.

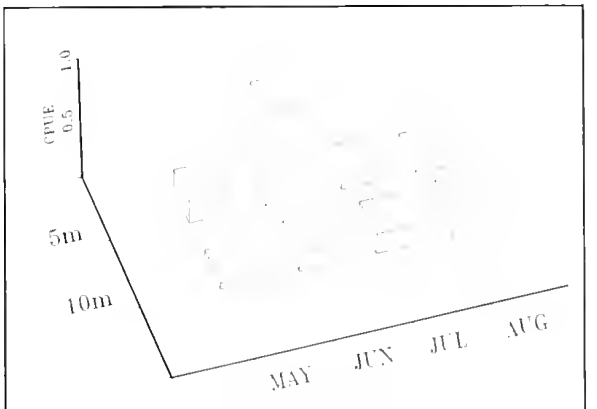

Figure 11

Abundance of YOY white seabass *A. nobilis* by depth over the four months (June–October) of the 1989 survey.

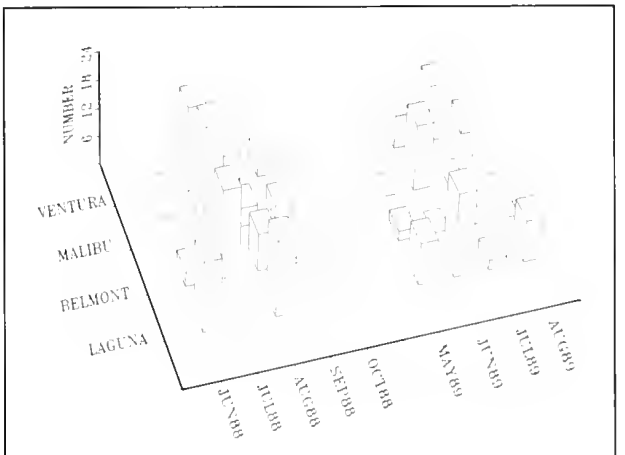

Figure 12

CPUE of YOY white seabass *A. nobilis* at each of four mainland stations by month over the summers of 1988 and 1989. (Stn. 6 = VENTURA, Stn. 10 = MALIBU, Stn. 13 = BELMONT, Stn. 15 = LAGUNA).

Comparison of 1988 and 1989 at four mainland stations

Settlement success in 1988 was compared with that in 1989 by examining the catch at the four mainland stations sampled during both years (Fig. 12). Abundance varied significantly among months over the two summers (one-way ANOVA; F 2.52; 8,27 df; $p<0.05$), but not among stations. Settlement among the four stations was consistent during 1988, but highly variable in 1989. Also, CPUE was higher in 1988 (0.75/tow) than in 1989 (0.59/tow) but the difference was not significant (t-test; t 1.23; 15 df; p 0.24). Catches differed most between years at Stn. 13 (Belmont Shore) where abundance dropped from 0.78/tow in 1988 to 0.06/tow in 1989, and at Stn. 15 (Laguna Beach) where abundance increased from 0.78/tow to 1.21/tow. The lack of significant differences in catches between 1988 and 1989 was probably due to the high variability and low numbers at individual stations within each year. The relatively high catch at Laguna Beach in 1989 was directly opposed to the lower catches at the other three stations.

Influence of environmental factors

Distance from the mainland Of the environmental variables examined, only the distance of the station from the mainland was significantly correlated with CPUE over both years (Table 2), and this correlation was negative. This corroborates the ANOVA results from 1989 where the effect of distance block was highly

Table 2

Correlation coefficients among catch-per-unit-effort (CPUE) of young-of-year white seabass *A. nobilis* and six environmental variables during the 1988 and 1989 coastal surveys (* $p<0.05$, 219 df).

	CPUE	DSTMN	BTMP	BSAL	BDO	BSLOP	BALGA
CPUE	–						
DSTMN	**−0.2030***	–					
BTMP	0.0993	−0.0115	–				
BSAL	0.0513	−0.0349	−0.0279	–			
BDO	−0.0084	−0.0425	0.0674	−0.0402	–		
BSLOP	0.0967	**−0.3761***	−0.0718	−0.0365	**0.1427***	–	
BALGA	0.0357	−0.0204	−0.0139	−0.0118	−0.0305	−0.1063	–

DSTMN Distance from mainland
BTMP Bottom temperature
BSAL Bottom salinity
BDO Bottom dissoved oxygen
BSLOP Bottom slope
BALGA Biomass algae

significant, further emphasizing the inshore-offshore distribution pattern of white seabass settlement.

Temperature Bottom temperature ranked second among environmental variables in its correlation to CPUE over both years, although the correlation of 0.10 was not statistically significant (Table 2). The lack of significance may be due to the fact that the relationship of catch to temperature differed noticeably in the 2 years and that overall catches were lower in 1989.

In 1988, the heaviest and most widespread settlement of YOY coincided with the striking rise in coastal temperature during July in the study area, resulting in a significant correlation between log-transformed [$\log_{10}$ (x + 1)] abundance of YOY and bottom temperature (r 0.25, $P<0.05$, 74 df). In 1989, however, the greatest and most widespread YOY abundance was encountered in June when temperatures were generally depressed. Thus the peak settlement in 1989 occurred 1 month earlier than in 1988 and was apparently not as closely related to a rise in sea temperature as it seemed to be in 1988.

Biomass of drift algae Samples of submerged drift algae ranged from trace amounts (<50 g) to >500 kg per tow for each depth and station. No significant correlation (r 0.036; Table 2) was found between the weight of drift algae and the abundance of young white seabass. However, only two fish (both >60 mm SL) were captured without drift algae in the nets. Thus, drift algae and YOY white seabass may be related on a presence/absence rather than a quantitative basis.

Correlations of catch with other physicochemical variables were too low to warrant consideration.

Multivariate model A combination of three environmental variables—distance from the mainland, bottom temperature, and biomass of drift algae—produced a significant canonical correlation with CPUE (Table 3). Though significant, the correlation accounted for only 5% (R^2 0.052) of the variation in CPUE. A significant canonical correlation with distance and bottom temperature alone accounted for slightly less variation in CPUE (R^2 0.051).

Discussion

Density estimates for white seabass off the coast of southern California were low. Population estimates based on these densities for the Southern California Bight were only 130,000 and 118,000 individuals in 1988 and 1989, respectively. The lower value in 1989 is not surprising since catches at the island stations were extremely low (a high of five YOY at Santa Cruz I., and none at Santa Rosa and San Clemente Is.). Even if these estimates are assumed to be within an order of magnitude of the real population levels, it is obvious that settlement of white seabass was poor in southern California waters. Our data showing relatively low numbers of YOY white seabass in southern California for both sampling years present a similar picture to that presented in Moser et al. (1983) for larval white seabass. The major settlement areas for this species undoubtedly occur to the south in Mexican waters.

Catches of YOY white seabass were highly variable in space and time. Only a small portion of this variability was explained by the environmental variables measured. Monthly differences in catch were marked

Table 3

Results of canonical correlation runs with catch-per-unit-effort (CPUE) of young-of-year white seabass *A. nobilis*, 1988–89, as the dependent variable and selected environmental (independent) variables (* $p<0.05$, ** $p<0.01$).

Successive canonical correlation runs

Run	Variables	Canonical R	Canonical R^2	χ^2	df	P
1	DSTMNLD BTMP BALGA	0.2274	0.0517	11.495	3	0.0093**
2	DSTMNLD BTMP	0.2250	0.0506	11.274	2	0.0036**

Canonical weights within runs

Variables	Run 1	Run 2
DSTMNLD	−0.8848	−0.8973
BTMP	0.4287	0.4312
BALGA	0.1450	

DSTMNLD Distance from mainland
BTMP Bottom temperature
BALGA Biomass algae

in both years, due to the peaks in abundance of YOY observed in both 1988 and 1989, although monthly differences were significant only in 1988. In 1989, a significant spatial pattern of catches was detected, related to distance from the mainland and depth of capture over months.

Both the distance block ANOVA from 1989 data and the overall correlation analyses strongly suggest that the abundance of YOY white seabass decreases rapidly with distance from the mainland. Other factors are less important. Nonetheless, the combination of distance, temperature, and biomass of drift algae produced a highly significant canonical correlation with distance and temperature contributing most heavily to the relationship.

The large amount of unexplained variation in the multivariate model suggests that important factors may be missing from the analysis. We believe that one such factor is the initial availability of presettlement larvae in the plankton. A dearth of premetamorphic larvae at a potential settlement site results in low settlement, no matter how favorable the environmental conditions. Population sizes off southern California might be limited largely by number of settling larvae rather than site-specific environmental factors or density-dependent survival of YOY. Only when larval input is constantly high, as we suspect is the case in Mexican waters, could the influence of environmental factors on settlement success be determined with any precision.

Factors affecting larval availability are not well known. Spawning of white seabass occurs in the summer and may be related to lunar periodicity (moon phase) (Franklin and Allen, unpubl. data) early in the reproductive period. Lunar periodicity of spawning activity coupled with adult stock size, larval transport mechanisms, and larval growth dynamics could all ultimately influence the availability of white seabass larvae.

Distance from the mainland, the strongest correlate with YOY abundance, probably reflects larval availability which may decrease with distance from coastal stocks occurring in both southern and Baja California. Island populations of adults were either not reproducing or their larvae were being carried away from settlement sites. Long-term settlement success of white seabass to islands may be sporadic and highly variable. For example, Cowen (1985) found that California sheephead (*Semicossyphus pulcher*) settled only sporadically to the offshore islands. The pattern of settlement success of sheephead over a 7–9 year period in areas without larval sources "upstream" of typical current direction was highly variable and dependent on episodic events, such as the El Niño climatic anomaly (Cowen 1985).

Warm water currents may be important to white seabass settlement for two reasons: (1) Large numbers of larvae carried northward from more southern waters by warm water currents may settle after metamorphosis and locate suitable habitat; and (2) the warm water itself may induce locally spawned larvae to settle. On a larger scale, major water movements such as the California Current, gyral circulation ("eddies"), and other mesoscale flows (e.g., internal waves) may

control white seabass settlement in the Southern California Bight. Parrish et al. (1981) demonstrated that seasonal effects of the California Current and upwelling in central California had a major effect on the distribution patterns of marine fish. The spawning activities of most fishes coincide with the onshore flow which is characteristic of the late winter and early spring months and transports eggs and larvae into shallow waters. The effects of major hydrographic events on the abundance and distribution of YOY white seabass remain largely unknown.

The main geographic source of white seabass larvae that settle successfully in southern California is also unknown. Southern California populations of adults may be reduced to the point that they may be only a minor source of larvae. Since larvae remain in the plankton as long as 4–5 weeks, population centers of adults off northern Baja California may constitute the major source of southern California YOY seabass. Thus, successful settlement to southern California waters may depend largely on the northward-flowing, warm-water currents best developed in the summer months. Satellite infrared-imagery data indicated that such a large, warm-water mass moved north along the southern California coastline in early July 1988 (Jan Svedkowsky, Ocean Imaging, San Diego, pers. commun.). The resulting dramatic rise in surface and bottom temperatures may have accounted for the marked increase in settlement of white seabass between June and July of that year if the water mass also contained a sufficient number of premetamorphic larvae. Studies of subpopulation structure utilizing restriction fragment length polymorphism (RFLP) analysis of nuclear DNA are currently underway in our laboratory in an attempt to identify the source of newly-settled white seabass in southern California coastal waters. If the main parental population of these fish is located in more southerly waters, joint U.S. and Mexican management efforts may be necessary to prevent the decline of these major breeding stocks in the south.

Acknowledgments

A study of this magnitude could not have been accomplished without the support of many people. We thank those who ably assisted with the demanding field work, especially Jan Cordes, Monica Lara, Julia Sears-Hartley, Phyllis Travers, and Lisa Wooninck. The crew of the RV *Yellowfin*, Jim Cvitanovich, Danny Warren, and Dennis Dunn, assisted greatly through their capable handling of vessels in shallow and often turbulent waters. Al Ebeling and three anonymous reviewers greatly improved this paper through careful readings and numerous, helpful comments. We also gratefully acknowledge the assistance provided by Steve Crooke and Paul Gregory of the California Department of Fish and Game. This research was supported through contracts with the Ocean Resource Enhancement and Hatchery Program (OREHP) and the Bay, Estuarine, and Nearshore Ecosystem Studies (BENES) program, administered by the California Fish and Game.

Citations

Allen, L.G., and M.P. Franklin
1988 Distribution and abundance of young-of-the-year white seabass (*Atractoscion nobilis*) in the vicinity of Long Beach harbor, California, 1984–1987. Calif. Fish Game 74:245–248.

Cowen, R.K.
1985 Large scale pattern of recruitment by the labrid, *Semicossyphus pulcher*: Causes and implications. J. Mar. Res. 43:719–742.

Donohoe, C.
1990 Distribution, abundance, food habits, age determination, and growth, of late larval and early juvenile white seabass, *Atractoscion nobilis*, off San Diego County, Calif. Unpubl. master's thesis, Calif. State Univ., San Diego, 95 p.

Frey, H.W. (editor)
1971 California's living marine resources and their utilization. Calif. Dep. Fish Game, Sacramento, 148 p.

Margulies, D.
1989 Size-specific vulnerability to predation and sensory system development of white seabass, *Atractoscion nobilis*, larvae. Fish. Bull., U.S. 87:537–552.

Miller, D.J., and R.N. Lea
1974 Guide to coastal marine fishes of California. Calif. Fish Game, Fish Bull. 157:1–249.

Moser, H.G., D.A. Ambrose, M.S. Busby, J.L. Butler, E.H. Sandknop, B.Y. Sumida, and E.G. Stevens
1983 Description of early stages of white seabass, *Atractoscion nobilis*, with notes on their distribution. Calif. Coop. Oceanic Fish. Invest. Rep. 24:182–193.

Parrish, R.H., C.S. Nelson, and A. Bakun
1981 Transport mechanisms and reproductive success of fishes in the California current. Biol. Oceanogr. 1:175–203.

Vojkovich, M., and R. Reed
1983 White seabass, *Atractoscion nobilis*, in California–Mexican water: Status of the fishery. Calif. Coop. Oceanic Fish. Invest. Rep. 24:79–83.

Abstract.—To resolve the uncertainty in estimating capture depths of fish on pelagic longline gear, electronic microchip hook timers were attached to branch lines to record when bites occurred, and time-depth recorders (TDRs) were attached to longline gear, off Hawaii in January 1989 and January–February 1990. Hook timers indicated that 32% of the striped marlin *Tetrapturus audax*, 21% of the spearfish *T. angustirostris*, and 12% of the bigeye tuna *Thunnus obesus* were caught on sinking or rising hooks, demonstrating that capture time data are needed to correctly estimate capture depth. Recorded and predicted longline depths differed greatly, indicating that TDRs are essential for describing depth distributions of fish from longline catches. Most (>60%) of the spearfish and striped marlin were caught on settled hooks (not sinking or rising) at depths of <120 m, whereas most bigeye tuna were caught at depths of >200 m. This suggests that eliminating shallow hooks could substantially reduce the bycatch of spearfish, striped marlin, and other recreationally important billfish without reducing fishing efficiency for bigeye tuna. Bigeye tuna and striped marlin survived up to 6–9 hours after capture, and over 50% of 12 frequently-caught taxa were alive when retrieved, suggesting that the release of live fish can be an effective management option.

Manuscript accepted 5 May 1992.
Fishery Bulletin, U.S. 90:642–658 (1992).

Depth, capture time, and hooked longevity of longline-caught pelagic fish: Timing bites of fish with chips

Christofer H. Boggs

Honolulu Laboratory, Southwest Fisheries Science Center
National Marine Fisheries Service, NOAA
2570 Dole Street, Honolulu, Hawaii 96822-2396

Targeting specific depths can improve longline catches of desired species, such as bigeye tuna *Thunnus obesus* (Saito 1975, Hanamoto 1976, Suzuki et al. 1977, Suzuki and Kume 1982), and reduce bycatch of other species, such as billfish (Suzuki 1989). However, considerable uncertainty exists in estimating the fishing depth of longline gear. Predicted longline depth based on catenary geometry, line length, and distance between floats (Yoshihara 1954) differs from true depth (Saito 1973, Hanamoto 1974, Nishi 1990) because of currents and other factors, yet depth is often inferred rather than measured (Suzuki et al. 1977, Suzuki and Kume 1982, Hanamoto 1987, Grudinin 1989). Furthermore, fish may be caught while the hooks are sinking, during deployment of the gear, or rising during its retrieval (Saito 1973), making capture depths impossible to estimate accurately without known capture times.

Accurate estimates of fishing depth can be made if time-depth recorders (TDRs) are attached to longline gear. Longline studies using TDRs (Saito et al. 1970, Saito 1973, Yamaguchi 1989, Nishi 1990) have also interpreted TDR depth fluctuations as records of times of capture, but few such measurements exist. Instead, capture has been assumed to occur when the gear is settled, so capture depth has been estimated as settled hook depth (Hanamoto 1976, Suzuki and Kume 1982). Hook timers, designed to indicate when each hook is struck (Somerton et al. 1988), provide a way to measure capture times and survival times of hooked fish. Capture times, together with TDR records, can be used to estimate capture depths accurately.

Billfish catch rates in recreational fisheries may be negatively affected by nearby longline fisheries (Squire and Au 1990), and interest in finding ways to reduce the longline take of billfish without reducing fishing efficiency for target species is increasing (Rockefeller 1989). Information on capture depth, capture time, and hooked longevity can be used to design fishing methods that reduce billfish mortality. Data on the selectivity and efficiency of longline gear at various depths are also critical for stock assessments (Suzuki 1989).

The present study improves methods for estimating capture depths of fish on longline gear using electronic timing devices, and describes the depth distributions and capture times of tunas, billfishes, sharks, and other pelagic fishes in Hawaiian waters in winter. Water temperature and dissolved oxygen (DO) were measured to describe the physical habitat in the study area, since these variables appear to cause geographic variation in depth distributions of fish (Hanamoto 1975, 1987). Relative fishing efficiency and the bycatch of billfish were predicted for several gear configurations.

Table 1

Summary of longline fishing operations conducted by the NOAA ship *Townsend Cromwell* off Hawaii, January 1989 and January–February 1990, giving averages for three set types (ranges in parentheses). Baskets were intervals of continuous main line between floats with snap-on branch lines, not spliced units of gear. Shortening rate was the ratio between ship speed and thrower speed. Depths do not include branch line length. Predicted depths were calculated from the shortening rate and the main line length per basket, assuming a catenary shape. TDR = time depth recorder.

Year	Set type	Sets (no.)	Time		Hooks per set (no.)	Line per basket (m)	Shortening rate (ratio)	Predicted depth (m)	Deep TDR depth (m)	Middle TDR depth (m)
			Begin set	End retrieval						
1989	Regular	6	8:09 (4:31–10:05)	15:24 (14:20–16:41)	199 (128–278)	795 (640–1103)	0.80 (0.69–0.98)	222 (88–304)	111[1] (43–180)	82[2] (32–133)
	Deep	6	8:55 (5:29–12:47)	16:36 (10:34–20:40)	257 (185–392)	1085 (990–1146)	0.59 (0.46–0.83)	415 (273–489)	260 (241–303)	191[2] (178–224)
	Very deep	4	8:23 (8:16–8:41)	19:10 (17:58–20:40)	405 (356–474)	1117 (1053–1146)	0.54 (0.45–0.71)	447 (349–496)	367 (329–400)	270[2] (243–295)
1990	Regular	5	6:50 (6:14–7:18)	19:08 (16:24–22:07)	456 (212–591)	809 (611–1068)	0.78 (0.67–0.90)	243 (150–355)	142 (78–183)	104 (71–140)
	Deep	13	7:18 (6:12–10:04)	19:38 (17:57–20:42)	474 (173–594)	1069 (798–1265)	0.60 (0.40–0.70)	409 (298–499)	249 (193–318)	180 (122–232)
	Very deep	4	5:29 (4:45–6:21)	19:03 (15:30–21:05)	404 (219–600)	1165 (937–1427)	0.62 (0.50–0.74)	436 (303–592)	416 (340–517)	291 (251–381)

[1] TDR data obtained for only three sets.
[2] Calculated from the ratio (0.73) between middle and deep TDR depths of sets in which middle-position data were available.

Materials and methods

Longline fishing was conducted on board the NOAA ship *Townsend Cromwell* in January 1989 and January–February 1990. Sets were made between lat. 14° and 20°N, long. 148° and 159°W, 20–500 nmi from the main Hawaiian Islands, and within an area typically fished by Hawaii's domestic longline fishery. Gear was usually deployed in the morning and retrieved in the afternoon or evening (Table 1), or occasionally at midday to permit a second set on the same day. No sets were made at night. Except for the hook timers and TDRs, the fishing gear and operations were similar to commercial longline fishing methods for tuna in Hawaii (Kawamoto et al. 1989) prior to the advent of night fishing for swordfish *Xiphias gladius*. Both this study and the contemporary commercial longline fishery used a wide variety of fishing depths. Commercial fishermen used more gear (~1000 hooks), let it stay in the water longer (~12 h), and retrieved it faster than in this study.

The fishing gear consisted of 3.5 mm-diameter nylon monofilament main line deployed with a line thrower (Kawamoto et al. 1989). The main line was supported at intervals by vertical, 18 m lines with floats at the ends. Snap-on branch lines made of 2.1 mm-diameter clear-blue nylon monofilament (20 m long in 1989 and 11 m long in 1990) were baited with thawed saury *Cololabis saira* on curved tuna hooks (one hook/branch line) and attached to the main line between float lines. Hooks were size 3.6 (Japanese size is 10.9 cm from eye to point). Each portion of the longline between floats and the attached branch lines constituted a "basket," a term taken from older gear in which the number of branch lines is fixed. However, this study used varying numbers of snap-on branch lines (12, 14, 16, or 20/basket), depending on the length of main line per basket.

Hook position was controlled by timing the attachment of branch lines as the main line was thrown overboard mechanically at a controlled speed. A computer program was used to signal and record attachment times. Deviations from the programmed instructions were noted, providing a record of set times for each hook. The total number of hooks in each set was 128–600, and the amount of main line deployed per set was 9–44 km (Table 1). The amount of gear increased with crew experience but also varied because of inclement weather and equipment failures.

Set depths

Fishing depth was altered by varying the slack in the main line and the length of line per basket (Table 1) and by exogenous factors such as wind and currents. Line slack was quantified as the shortening rate (Saito 1973), or sagging rate (Suzuki et al. 1977), equal to the horizontal distance between floats divided by the length of line per basket (a dimensionless ratio). At deploy-

ment, the shortening rate was the same as the ratio of ship speed through the water to line-thrower speed: 0.40 (maximum slack) to 0.98 (no slack). The length of main line per basket was 640–1427 m. The predicted maximum depth of the main line during each set was calculated from the shortening rate and the main line length per basket (Table 1), assuming a catenary shape (Yoshihara 1954).

The depth of each set was recorded with electronic TDRs (Wildlife Computers, models MKII and MKIII) programmed to sample depth once per minute. The TDRs were attached at the deep positions, defined as the attachment points for the branch line midway between floats (e.g., position 10 or 11 of 20 between floats). In 1990, TDRs were also attached at the middle positions between the deep positions and the float line (e.g., at position 5 or 15 of 20 between floats).

The time that the gear took to sink during deployment (0.5 h) and to rise during recovery (0.5 h) was quantified from TDR records. Set depth was described as the typical depth observed in records from the deep-positioned TDRs during the period after sinking and before rising. Recorded depth was examined after each set and compared with predicted depth. Shortening rate, the length of line per basket, or both were adjusted in the subsequent set to reach targeted depths.

Hook depths

The settled depth of each attachment point for the branch line was estimated by interpolating between (1) the TDR record for the deep and middle positions or (2) the latter point and the shallowest depth of the main line (assumed to equal the length of the float line). Settled hook depth was calculated by adding the branch line length to the interpolated depth of the branch line snap. Not enough TDRs were available (2 in 1989, 10 in 1990) to put 1 TDR on every basket. When fish were caught by baskets without TDRs, average TDR depths for that set were used to interpolate settled hook depths. For middle positions without TDRs in 1989, depth was estimated from the mean ratio of the middle position to deep-position TDR depths based on 1990 data.

Hook timers

Hook timers were made of a plastic resin cast around a battery-powered microchip clock controlled by a magnet (Somerton et al. 1988). They were attached to the branch lines near the snap, bridging a bend in the line (Fig. 1). A fish striking the hook pulled the magnet, thus triggering the timer. In 1989, a rubber band held the magnet in place against a test weight of about 1–2 kg. In 1990, thread with a breaking strength of

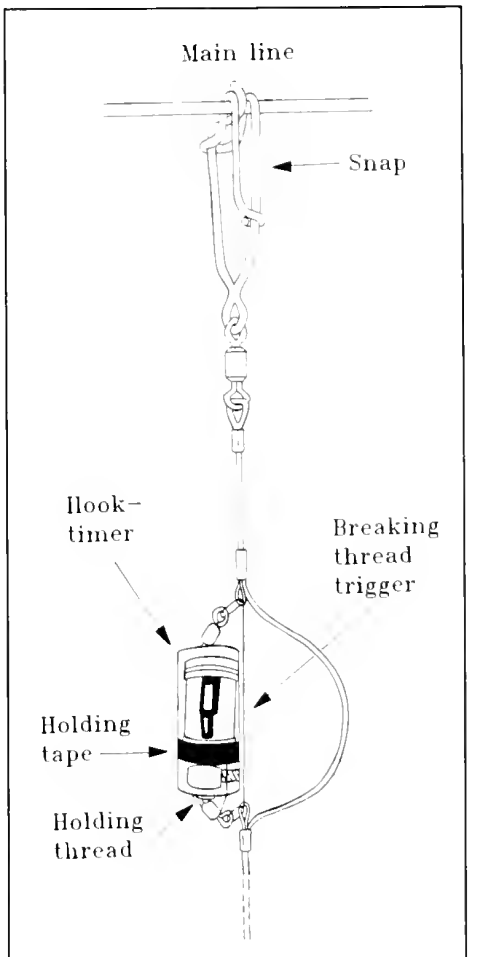

Figure 1
A hook timer and its trigger mechanism as arranged in 1990, when thread triggers were used. In 1989, rubber bands served as the trigger. The slack loop in the branch line was pulled taut when a fish struck the hook, breaking the trigger and pulling the magnet from its recess in the bottom of the hook timer.

4–5 kg bridged the bend in the line, and the magnet was held in place by a weaker thread until the bridging thread was broken (Fig. 1). Some branch lines were set without timers (14% in 1989, 35.5% in 1990) to preclude interruptions in fishing when timers were tangled or otherwise unavailable.

Hook timers indicated elapsed time in whole minutes (e.g., 0 min indicated 0–59 s). Timers were read as the branch lines were recovered, or soon after, with corrections made for delays. Timers were categorized as being triggered (1) at recovery (≤1 min before removing the branch line snap), (2) while rising (>1 min–0.5 h before recovery), (3) while settled (>0.5–<1.0 h, 1–<2, 2–<3 h, and so on before recovery), (4) while

sinking (<0.5 h after gear deployment), (5) at deployment (≤2 min after deployment), and (6) before deployment (timer triggered before setting commenced). Timers activated but without fish were categorized similarly except all settled categories (>0.5–9.0 h) were combined. Untriggered hook timers with fish also were tallied, and hooks with timers that were damaged, broken loose, or tangled too badly to be triggered were counted as hooks without timers.

The numbers of fish caught while the gear was sinking, settled, and rising were summarized. The unconfirmed depth of capture of each fish was defined as the settled depth of the hook. Capture depths were considered confirmed only if hook timers indicated the capture occurred within the period in which the gear was settled.

Catch and effort

Live fish that were not needed as specimens were tagged and released. Steel head "H" type dart tags (Squire 1987) were applied using a 3 m tagging pole while the fish remained in the water. Billfish were also injected with 5–20 mg oxytetracycline/kg of fish using pole-mounted syringes (Foreman 1987) to mark hard parts for validation of growth increments. Fish were released by cutting the branch lines close to the hooks with a tree-trimming pole. The condition (alive or dead) of the retained fish was noted, and it was weighed to the nearest 0.5 kg or measured to the nearest 0.1 cm. For the five most-frequently-caught species of commercial importance, catch, number of hooks, and number of hooks with timers were stratified into 40 m strata (40–<80 m, 80–<120 m, and so on) based on settled hook depths. The catch-per-unit-effort (CPUE) in each depth stratum was examined in two ways: (1) by confirmed capture depth ($CPUE_D$ in number of fish/1000 hooks with timers) representing the depth distribution of fish; and (2) by settled hook depth ($CPUE_H$ in number of fish/1000 hooks), representing the total effectiveness of hooks while sinking, settled, or rising.

The $CPUE_H$ for each depth was used to predict catch rates of "standardized" types of gear to illustrate the use of catch by hook position in estimating relative gear efficiency for different gear configurations. Total CPUE for each standardized gear configuration was estimated by calculating the weighted average $CPUE_H$, with weights corresponding to a given number of hooks per depth stratum for each configuration. Total CPUE was calculated from 1989 and 1990 data separately and averaged. Gear efficiency was calculated as the ratio of the predicted CPUE for each configuration to that of the regular configuration.

Standardized regular and deep longline gear configurations were assumed to have 6 and 13 hooks/basket, respectively. A shortening rate of 0.6 and the dimensions in Suzuki et al. (1977; without adjustment for currents) indicated hook depths of about 95, 140, and 170 m (for regular gear) and 100, 145, 190, 230, 265, 290, and 300 m (for deep gear). These depths correspond roughly to the midpoints of hook depth strata in the present study (100, 140, 180, 220, 260, and 300 m).

In addition to regular and deep gear, CPUE values for two hypothetical gear types were predicted: (1) shallow gear for which hooks are limited to the first three depth strata of this study; and (2) a proposed new gear for which no hooks would be deployed in the first three depth strata and the distribution of deeper hooks would match that of deep gear. The shallow gear configuration may be representative of that achieved by Hawaii's longline fishermen in 1989 and 1990 when they first began using monofilament longline and had difficulty achieving the depths formerly fished with traditional rope gear. With the rope gear, slack was obtained by manually throwing the baskets with the main line partially coiled. The [predicted] CPUE for the new gear type was estimated to indicate the reduction in bycatch of some species by the elimination of shallow hooks.

To show CPUE as it would appear in a study of gear configurations without hook position, capture depth, or capture time information, $CPUE_S$ values were calculated from catch and effort by set type. Sets were categorized on the basis of depth (TDR depth plus branch line length) into three groups: 60–<200 m (regular), 200–<330 m (deep), and 330–530 m (very deep). The first two groups contained depth ranges roughly comparable to those expected for regular and deep longline gear types, assuming a variety of shortening rates and variation due to ocean currents (Suzuki et al. 1977).

Oceanography

Vertical temperature structure in the area of each set was measured by expendable bathythermographs (XBTs; 400 m depth) and conductivity-temperature-depth casts (CTDs; 500–1000 m depth, usually 500 m) before or after each set. Water samples were taken with Niskin bottles to measure DO and to calibrate DO measurements made by CTDs.

Many of the TDRs were equipped with a second channel to record temperature. The TDRs were attached to the CTD probe to calibrate depth and temperature measurements. The TDR temperature data were used to estimate set depths exceeding 400 m (the lower limit for accurate range depth measurement from the TDRs).

Table 2

Catch data for 14 frequently-caught taxa in research longline sets off Hawaii, January 1989 and January–February 1990. Some weights were calculated from length measurements; some fish (i.e., those released) were not weighed.

Species	No. caught	No. weighed or measured	Weight (kg)		Alive (%)
			Average	Range	
Bigeye tuna *Thunnus obesus*	76	32	31.5	2.5–69.5	83
Yellowfin tuna *T. albacares*	16	11	39.5	7.5–62.5	63
Skipjack tuna *Katsuwonus pelamis*	5	5	9.0	7.0–11.0	20
Wahoo *Acanthocybium solandri*	4	3	17.5	7.5–25.0	0
Striped marlin *Tetrapturus audax*	67	20	18.0	9.5–37.0	71
Spearfish *T. angustirostris*	41	23	13.5	8.5–18.5	56
Mahimahi *Coryphaena hippurus*	90	60	6.5	2.5–16.0	88
Pomfrets (Bramidae)	17	15	5.5	2.0–10.0	86
Lancetfish *Alepisaurus ferox*	132	111	1.5	0.1–8.0	64
Ribbonfish *Trachipterus ishikawae*	4	2	8.0	7.0–8.0	75
Brown ray *Dasyatis violacea*	8	4	2.0	1.0–2.5	88
Whitetip shark *Carcharhinus longimanus*	26	—	—	—	85
Blue shark *Prionace glauca*	21	1	68.0	—	100
Thresher shark *Alopias* spp.	6	1	91.0	—	60

Results

A total of 16 longline sets caught 149 fish in 1989 and 22 sets caught 401 fish in 1990. Fishing effort totaled 14,410 hooks including 10,236 hooks with timers. There were 14 taxa for which more than 3 fish were caught (Table 2).

Achieving deep sets when intended was sometimes difficult. Backlash of the main line into the hydraulic line thrower created problems at high thrower speeds, and ship speed through the water was sometimes underestimated, reducing the shortening rate. Wind and currents reduced set depth by dragging floats and parts of the line in opposing directions. In particular, current shear between the surface and the waters below the thermocline, observed with an acoustic Doppler current profiler, seemed to prevent deep sets. Observed set depths were highly variable and usually less than the predicted depths (Table 1, Fig. 2). For example, at a predicted depth of about 490m, observed depths were 200–400m (Fig. 2). Sets averaged only 54% and 68% of the predicted depths in 1989 and 1990, respectively. For the first three sets in 1989, the TDRs failed, so depth was estimated as a percentage of the predicted depth based on the average percentage (49.3%) obtained from the next three sets with similar configurations.

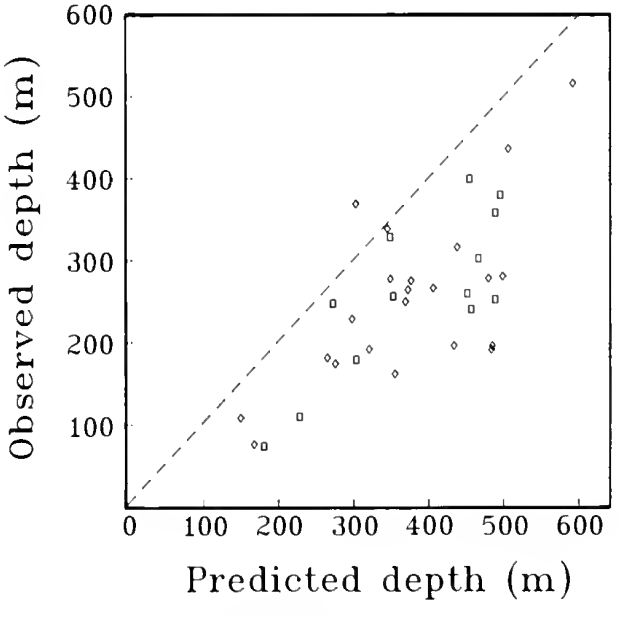

Figure 2

Relationship between predicted and observed set depths in 1989 (□) and 1990 (◊). Observed depths were measured with time-depth recorders, and predicted depths were calculated from the shortening rate and the main-line length per basket, assuming a catenary shape.

Capture depths

Capture depths were confirmed for those fish caught >0.5h after deployment and >0.5h before retrieval, because the TDR records showed that the main line usually took 0.5h to sink to within about 90% of its settled depth and about 0.5h to rise to the surface during retrieval (Fig. 3). Records of settled depth sometimes varied ≤100m for the deep sets (e.g., set 14;

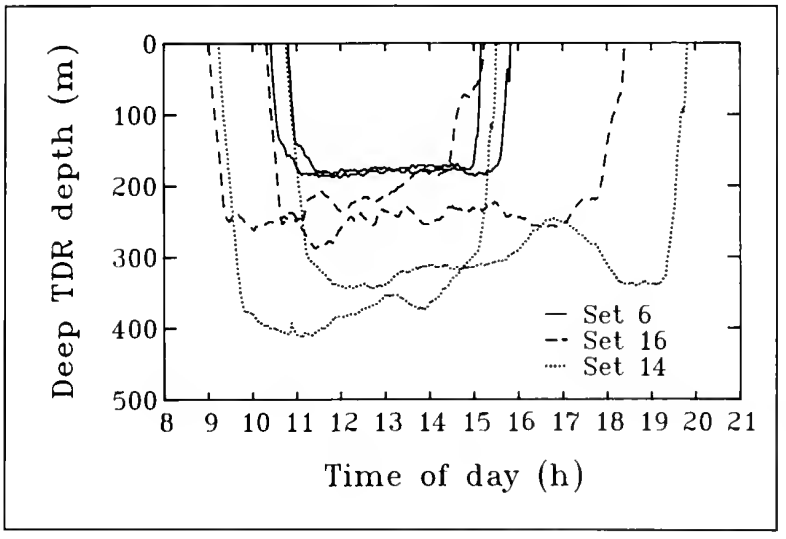

Figure 3 (left)
Sample records from time-depth recorders (TDRs) measuring the deep positions on three sets (each with two TDRs) in 1989, illustrating the typical sinking time (0.5 h), variation in settled depth, and typical rising time (0.5 h).

Figure 4 (below)
Hook depths for catches of 14 frequently-caught taxa in a study off Hawaii, winter 1989 and 1990 (combined). Settled hook depths are shown for all hooks that caught fish (unconfirmed) and for those hooks that caught fish while settled (i.e., not sinking or rising) as indicated by hook-timer data (confirmed).

Fig. 3) and ⩽40 m for the regular sets. Also, the gear sometimes took more than 0.5 h to rise (e.g., the first TDR on set 16; Fig. 3) or sink. Such deviations contributed to the variation in estimated capture depths. Capture depths of fish caught with hook timers on baskets with TDRs were based on the TDR depth at the time of capture; however, most catches were made by baskets without TDRs.

A comparison between the unconfirmed depths of all hooks that caught fish and those confirmed to have caught fish while settled (Fig. 4) showed that without hook-timer confirmation, many fish appeared to be caught at greater depths than they actually were. For example, mahimahi *Coryphaena hippurus* had unconfirmed capture depths of ⩽420 m and confirmed capture depths of <190 m. Most confirmed capture depths were <100 m for mahimahi and skipjack tuna *Katsuwonus pelamis*. Striped marlin *Tetrapturus audax*, whitetip shark *Carcharhinus longimanus*, blue shark *Prionace glauca*, and wahoo *Acanthocybium solandri* had unconfirmed depths of ⩽350–420 m and confirmed depths of <200–230 m. Species having a preponderance of confirmed capture depths of <150 m were yellowfin tuna *Thunnus albacares*, striped marlin, and spearfish *Tetrapturus angustirostris*. Most confirmed capture depths were >200 m for thresher

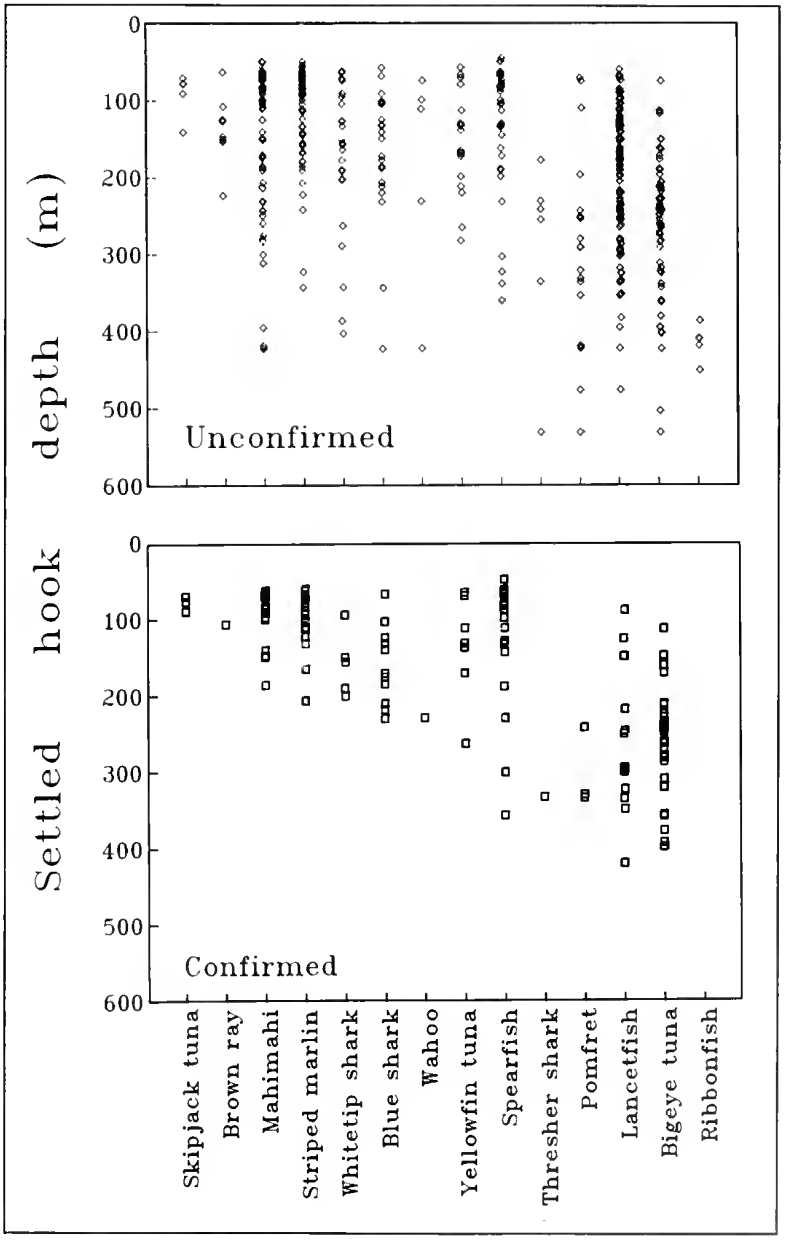

shark *Alopias* spp., pomfrets (Bramidae; species included *Taractichthys steindachneri, Taractes rubescens, and Eumegistus illustris*), lancetfish *Alepisaurus ferox*, and bigeye tuna (Fig. 4).

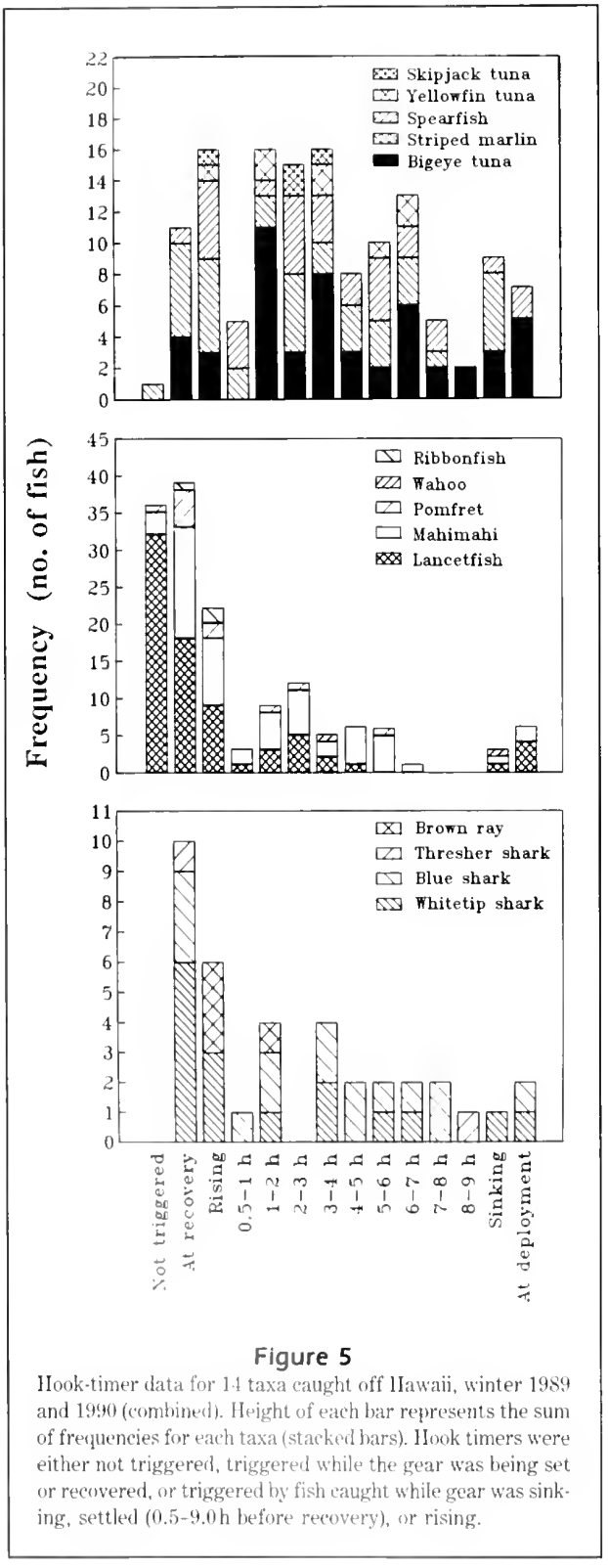

Figure 5

Hook-timer data for 14 taxa caught off Hawaii, winter 1989 and 1990 (combined). Height of each bar represents the sum of frequencies for each taxa (stacked bars). Hook timers were either not triggered, triggered while the gear was being set or recovered, or triggered by fish caught while gear was sinking, settled (0.5–9.0 h before recovery), or rising.

Capture times

Most of the fish (except ribbonfish *Trachipterus ishikawae* and brown ray *Dasyatis violacea*) were caught

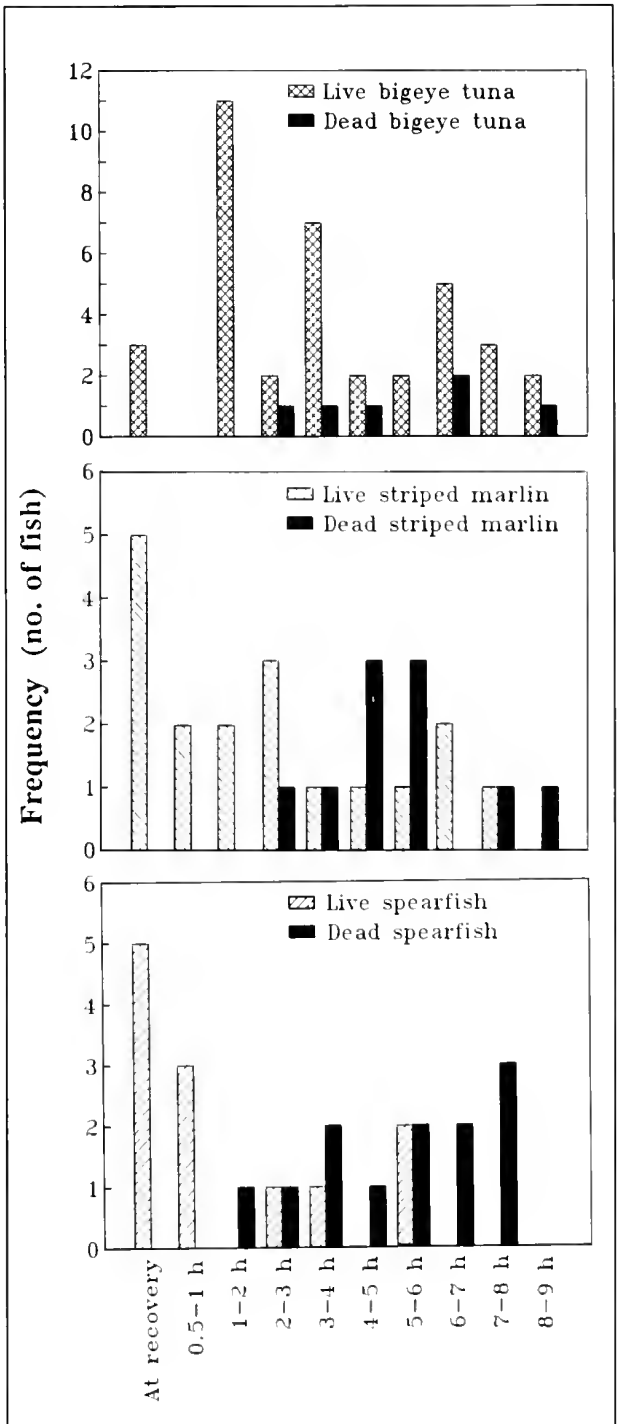

Figure 6

Condition (alive or dead) of three important species in relation to the elapsed time between capture and recovery as indicated by hook timers, during a study off Hawaii, winter 1989 and 1990 (combined).

while the gear was settled rather than while it was sinking or rising (Fig. 5), probably because the gear spent much more time in the settled position. However, substantial numbers of mahimahi, billfish, and other species were caught while the gear was rising (Fig. 5), which explains how fish were caught on deep-positioned hooks (unconfirmed depths) when their confirmed depth distribution was shallow (confirmed depths; Fig. 4).

For many species, catch-per-unit-time (CPUT) may have been highest while the gear was rising. The CPUT values at <3 and ≥3 h before recovery were not directly comparable because short sets resulted in lower effort (number of hooks with timers) ≥3 h before recovery. The catch in the 1–2 h and 2–3 h periods (Fig. 5) must be divided by 2 for comparison with the CPUT in the 0.5 h and 0.5–<1.0 h periods. For periods of 0.5–1.0, 1–2, and 2–3 h before recovery, CPUT values were less than during the rising period for ribbonfish, pomfrets, mahimahi, lancetfish, striped marlin, spearfish, brown ray, and whitetip shark (Fig. 5). In contrast, the values for yellowfin and skipjack tunas were not much different between settled and moving gear and were highest for bigeye tuna 1–2 h and 3–4 h before recovery. Blue shark CPUT values were highest 1–2 h before recovery.

Relatively large numbers of fish were categorized as caught at recovery (Fig. 5). However, estimates of the delay between recovery and reading each timer were not precise (± 1 minute). Thus some fish caught "at recovery" actually had timers triggered after recovery. Hook timers that did not catch fish were most often triggered "at recovery" (Table 3), suggesting that handling activated the timers. A similar lack of precision affected capture times "at deployment."

Hooks with timers triggered by small fish or without catching fish may have resulted in false capture times if larger fish were caught later on those hooks. Fortunately, small (<10 kg) fish, particularly lancetfish (Table 2), were most frequently caught without triggering the timers (Fig. 5). It was unusual for larger (~10–90 kg) fish, such as tunas, billfishes, or sharks (Table 2, Fig. 5), to be caught without triggering the timers. The increase in breaking strength of the triggers in 1990 (Fig. 1) decreased the relative number of small fish that triggered timers, and reduced the proportion of timers triggered without catching fish from 18.5% in 1989 to 9.7% in 1990 (Table 3).

Survival and release

Over 56% of the fish other than wahoo and skipjack tuna were alive when recovered, and for most species, survival was higher than 70% (Table 2). Based on fish with hook-timer data, over half of the bigeye tuna recovered up to 9 h after capture were alive. None of the 11 bigeye tuna recovered 1–2 h after capture were dead, and the shortest period between capture and recovery of dead bigeye tuna was 2–3 h (Fig. 6). Striped marlin were less hardy, with over half recovered dead ≥3 h after capture; nevertheless, many were recovered alive up to 6–8 h after capture (Fig. 6). Spearfish were the least hardy: The longest survival time was 5–6 h, and dead fish were recovered at <1–2 h after capture (Fig. 6).

Of the 29 bigeye tuna, 35 striped marlin, and 11 spearfish tagged during the study, 2 bigeye tuna and 1 striped marlin were recaptured 3–10 months later. These three fish were tagged after having been on branch lines for 3–6 h. The marlin had been injected

Table 3

Frequencies of activated hook timers on branch lines without fish (as percentage of total timers) categorized by elapsed time since the timers were triggered (range of values from individual sets in parentheses).

	Elapsed time							
	Before retrieval			After deployment				
Year	At retrieval (≤1 min)	Rising (>1–30 min)	Settled (≥30 min)	Sinking (≤30 min)	At deployment (≤2 min)	Activated before deployment	No. timers	Branch lines with timers (%)
1989	6.4 (—)*	1.2 (0–3.2)	3.9 (0.8–7.1)	1.0 (0–5.7)	4.8 (1.6–7.1)	1.0 (0–3.3)	3744 (126–356)	86.0 (61–100)
1990	3.8 (1.1–6.2)	1.5 (0–4.8)	2.6 (0.8–6.5)	0.4 (0–1.1)	1.0 (0–2.6)	0.4 (0–2.4)	6492 (167–418)	64.5 (34–99)
Combined	4.7*	1.4	3.1	0.6	2.4	0.6	10236	71.0

* Number recorded only during the first set in 1989. To calculate the combined frequency (4.7%), frequency was assumed to be 6.4% throughout 1989.

with 6 mg/kg oxytetracycline, but no flourescent mark was found in the otolith or vertebrae.

Abundance in relation to depth

For bigeye tuna, the depth distribution of $CPUE_D$ values (number of fish/1000 hooks with timers) was similar in 1989 and 1990, with $CPUE_D$ highest at 360–400 m and relatively high at 200–400 m (Fig. 7). Hooks with timers triggered before or at deployment could not be subsequently triggered; therefore, they were counted as hooks without timers when $CPUE_D$ was calculated (Table 4). The data from wider depth ranges in both years were pooled to obtain sample sizes (number of hooks with timers; Table 4) large enough to determine whether significant differences existed between depths (Fig. 8). For bigeye tuna, $CPUE_D$ values were significantly higher at depths of >200 m than at depths of <200 m ($P<0.05$, based on 95% CI for the difference between proportions). Few (12%) of

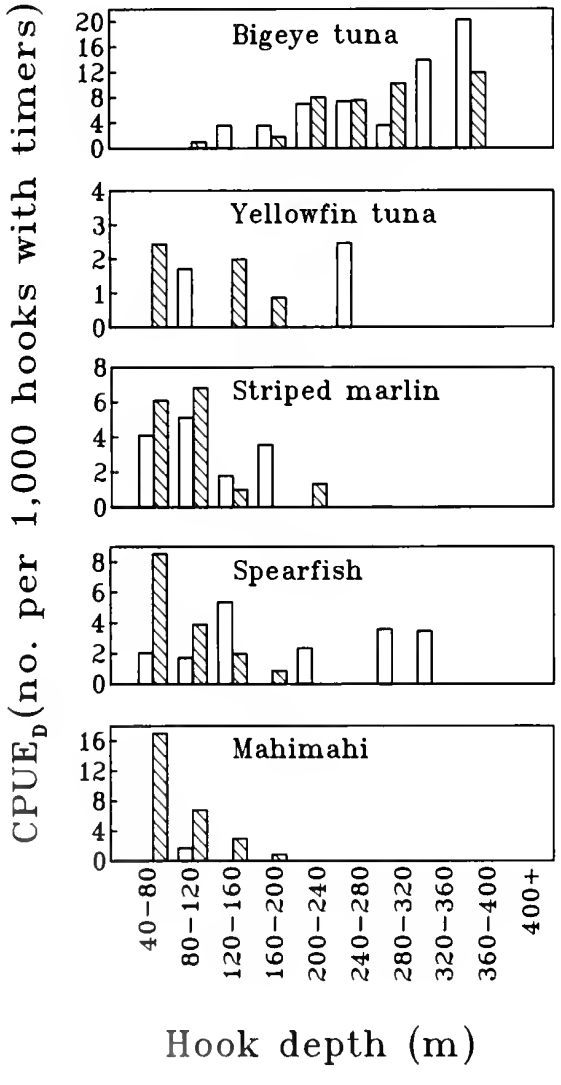

Figure 7

Indices of fish abundance vs. depth, calculated as the number of fish caught/1000 hooks with timers ($CPUE_D$) in ten depth strata. Indices for 1989 (open bars) and 1990 (crosshatched bars) are based on fish captured while the gear was settled (as confirmed by hook timers) (Table 4).

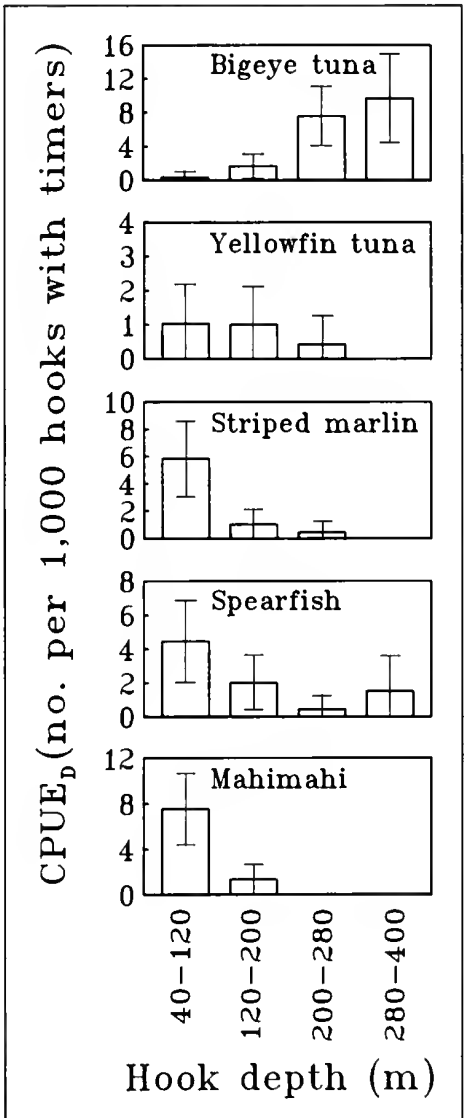

Figure 8

Indices of fish abundance vs. depth, calculated as the number of fish caught/1000 hooks with timers ($CPUE_D$) in four pooled hook-depth strata. Indices for 1989 and 1990 combined are based on fish captured while the gear was settled (as confirmed by hook timers) (Table 4). Error bars indicate 95% CI of the $CPUE_D$ values for each depth category.

the bigeye tuna with hook timers were caught while the hooks were moving (sinking or rising; Table 4). No clear relationship existed between depth and the proportion caught on moving hooks (Table 4).

Yellowfin tuna were not very abundant, which is typical for the winter months off Hawaii. The $CPUE_D$ for yellowfin tuna was not the same in both years (Fig. 7), but the number of fish caught with timers was very small, particularly in 1989 (Table 4). Pooled $CPUE_D$ was highest at 40–200 m (Fig. 8) although no significant difference in $CPUE_D$ by depth was found. The 40 m end of the depth range did not indicate the shallowest depths preferred by any species, since no hooks fished depths of <40 m.

Timer-confirmed catches by settled hooks indicated the highest catch rates for striped marlin were at 40–120 m in both years (Fig. 7), and pooled $CPUE_D$ was clearly the highest at this depth range (Fig. 8). The overall proportion of striped marlin caught on moving hooks was high (32%; Table 4) and increased with depth. At >120 m most striped marlin were caught by moving hooks, and at >200 m only one was caught by a settled hook (Table 4).

For spearfish, the pattern of $CPUE_D$ vs. depth differed between years. In 1989, the highest $CPUE_D$ was at 120–160 m although several fish were caught as deep as 280–360 m; however, in 1990 the highest $CPUE_D$ was at 40–80 m, and no confirmed capture depths were recorded at >200 m (Fig. 7). Pooled data suggested that spearfish were more abundant at <120 m, but the $CPUE_D$ at 40–120 m was not significantly different from that at 120–200 m (Fig. 8). In 1989, a large proportion (43%) of the spearfish were caught on moving hooks, but none were caught on moving hooks in 1990 (Table 4). Furthermore, for each of the major species, a higher proportion of fish were caught on moving hooks in 1989 than in 1990 (Table 4). An early report (Boggs 1990) on this research was based on 1990 data (Table 4) wherein only 12% of the tuna and billfish (combined) were caught on moving hooks.

Table 4

Catch of five commercially-important species in research longline sets off Hawaii, 1989 and 1990, giving fishing effort (number of hooks and timers) by depth strata, number caught (N) on known hook position, number confirmed by timers to be caught on moving (M; i.e., sinking or rising) and settled (S) hooks (in parentheses), and percentage of fish caught on moving hooks. Depth ranges include branch line length. Timers do not include those triggered at or before deployment. Catch totals are sometimes less than in Table 2 and Figure 5 because hook number and depth were not known for a few fish.

Hook depth (m)	Year	Hooks in stratum	Timers in stratum	Bigeye tuna		Yellowfin tuna		Striped marlin		Spearfish		Mahimahi	
				N (M,S)	Moving (%)	N (M,S)	Moving (%)	N (M,S)	Moving (%)	N (M,S)	Moving (%)	N (M,S)	Moving (%)
40–80	1989	546	489	1 (0,0)	–	0 (0,0)	–	5 (0,2)	0	4 (1,1)	50	3 (0,0)	–
	1990	1214	822	0 (0,0)	–	4 (0,2)	0	16 (1,5)	17	8 (0,7)	0	41 (5,14)	26
80–120	1989	684	586	0 (0,0)	–	1 (0,1)	0	9 (1,3)	25	4 (1,1)	50	2 (0,1)	0
	1990	1612	1026	2 (0,1)	0	0 (0,0)	–	15 (2,7)	22	5 (0,4)	0	14 (1,7)	12
120–160	1989	658	558	2 (0,2)	0	0 (0,0)	–	6 (2,1)	25	5 (1,3)	25	1 (0,0)	–
	1990	1611	1007	0 (0,0)	–	3 (0,2)	0	3 (1,1)	50	3 (0,2)	0	5 (1,3)	25
160–200	1989	350	281	1 (0,1)	0	0 (0,0)	–	2 (1,1)	50	1 (1,0)	100	0 (0,0)	–
	1990	1812	1151	6 (1,2)	33	4 (0,1)	0	5 (1,0)	100	5 (0,1)	0	6 (0,1)	0
200–240	1989	553	427	6 (1,3)	25	1 (1,0)	100	2 (0,0)	–	1 (0,1)	0	1 (1,0)	100
	1990	1160	748	11 (1,6)	14	1 (0,0)	–	1 (0,1)	0	0 (0,0)	–	4 (0,0)	–
240–280	1989	524	406	5 (0,3)	0	1 (0,1)	0	0 (0,0)	–	0 (0,0)	–	1 (0,0)	–
	1990	1321	795	11 (0,6)	0	1 (0,0)	–	0 (0,0)	–	0 (0,0)	–	6 (1,0)	100
280–320	1989	353	279	3 (0,1)	0	0 (0,0)	–	0 (0,0)	–	1 (0,1)	0	1 (0,0)	–
	1990	626	395	7 (0,4)	0	0 (0,0)	–	0 (0,0)	–	0 (0,0)	–	1 (0,0)	–
320–360	1989	384	288	7 (1,4)	20	0 (0,0)	–	2 (1,0)	100	4 (2,1)	67	0 (0,0)	–
	1990	198	152	0 (0,0)	–	0 (0,0)	–	0 (0,0)	–	0 (0,0)	–	0 (0,0)	–
360–400	1989	214	148	6 (1,3)	25	0 (0,0)	–	0 (0,0)	–	0 (0,0)	–	0 (0,0)	–
	1990	108	84	2 (0,1)	0	0 (0,0)	–	0 (0,0)	–	0 (0,0)	–	1 (0,0)	–
400+	1989	87	60	2 (0,0)	0	0 (0,0)	–	0 (0,0)	–	0 (0,0)	–	0 (0,0)	–
	1990	276	225	2 (0,0)	–	0 (0,0)	–	0 (0,0)	–	0 (0,0)	–	2 (1,0)	100
Total	1989	4352	3522	33 (3,17)	15	3 (1,2)	33	26 (5,7)	38	20 (6,8)	43	9 (1,1)	50
	1990	10,058	6402	41 (2,20)	9	13 (0,5)	0	40 (5,14)	26	21 (0,14)	0	80 (9,25)	26
Combined total		14,410	9924	74 (5,37)	12	16 (1,7)	12	66 (10,21)	32	41 (6,22)	21	89 (10,26)	28

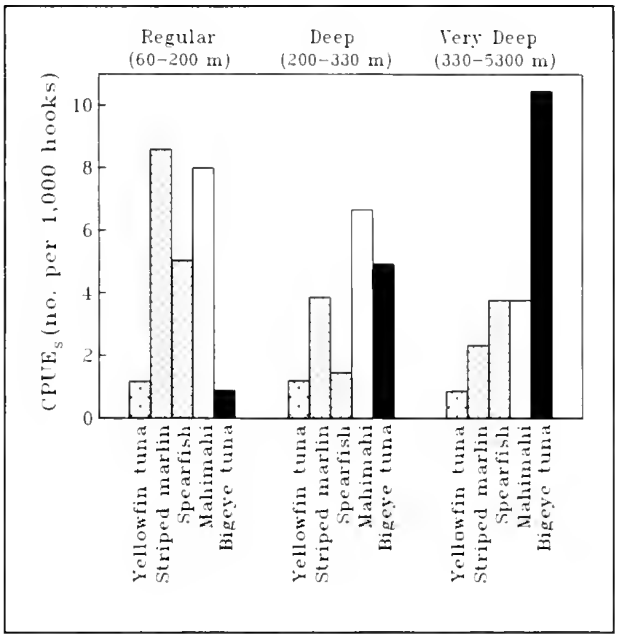

Figure 9

Comparison between indices of fish abundance from different types of longline sets, calculated as the number of fish caught/1000 hooks without regard to capture depth of individual fish ($CPUE_S$). Three types of longline sets were categorized on the basis of the deepest hooks, but every set contained some hooks as shallow as 40–80 m. Data are combined for 1989 and 1990.

Although relatively few mahimahi were captured with timer data, these data indicated maximum abundance was at 40–80 m in 1990 (only one fish was caught on a settled hook in 1989; Fig. 7, Table 4). Pooled data clearly indicated that $CPUE_D$ was highest at 40–120 m (Fig. 8). At >200 m, all mahimahi with timer data were caught on moving hooks.

Examining the $CPUE_S$ data as if the only available depth information were the set type (Fig. 9) made it difficult to correctly qualify the relative abundance of fish in relation to depth. For example, mahimahi appeared almost as abundant in deep sets as in shallow sets, and spearfish appeared more abundant in very deep than in deep sets, illustrating that it is impossible to correctly describe fish depth distributions without data on catch by hook position, hook depth, and capture time.

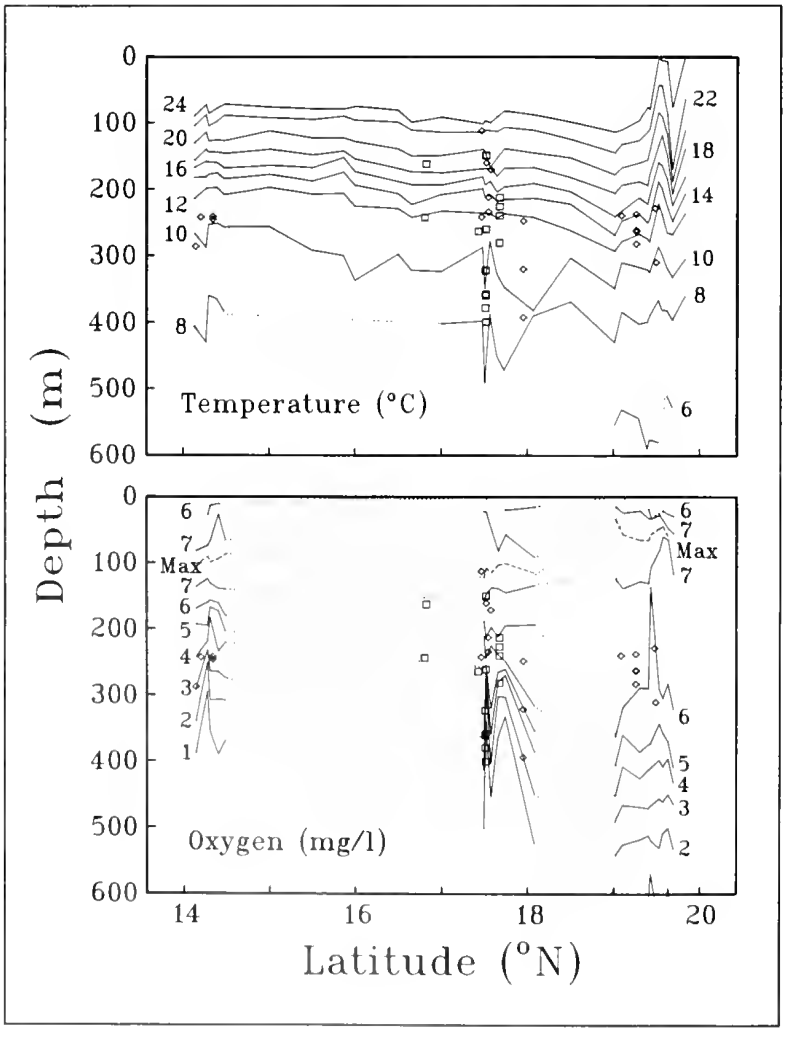

Figure 10

Temperature and dissolved oxygen profiles of the study area (lat. 14°–20°N, long. 148°–159°W) in 1990 (similar to 1989). Confirmed capture depths of bigeye tuna in 1989 (□) and 1990 (◊) are indicated.

Oceanographic habitat

The temperature profile in 1990 (Fig. 10) was representative of the study area in both years, except the bottom of the thermocline (i.e., the 12°C isotherm) was ~40 m deeper in 1989. In both years, the highest catch rate of bigeye tuna with confirmed capture depths occurred at lat. 17°–18°N at 360–400 m in temperatures of 8°–10°C (Fig. 10).

The oxycline in 1990 (Fig. 10) also was similar to that in the previous year (i.e., the 3.0 mg/L isopleth was only 10–20 m deeper in 1989). Most bigeye tuna were caught at DO concentrations of 2–6 mg/L. In both years, the highest catch rate was at 2–3 mg/L.

Table 5

Standardized distribution of hooks by depth stratum for four standardized gear types and predicted catch-per-unit-effort (CPUE) for each gear type based on the weighted average observed CPUE by hook depth for five commercially-important species in research longline sets off Hawaii, 1989 and 1990. For each species, relative gear efficiency is given as the ratio between the CPUE for each gear type and for regular gear (too few yellowfin tuna (N 3) were caught in 1989 to warrant calculating relative gear efficiency).

Model gear type	Hook number by depth (m)								Bigeye tuna		Yellowfin tuna		Striped marlin		Shortbill spearfish		Mahimahi	
	40-80	80-120	120-160	160-200	200-240	240-280	280-320	Year	CPUE	CPUE ratio	CPUE	CPUE ratio	CPUE	CPUE ratio	CPUE	CPUE ratio	CPUE	CPUE ratio
Regular	0	2	2	2	0	0	0	1989	1.93	1.00	0.47		9.30	1.00	5.37	1.00	1.43	1.00
								1990	1.52	1.00	1.36	1.00	4.83	1.00	2.57	1.00	5.03	1.00
								$\bar{x}$	1.73	1.00	0.91		7.07	1.00	3.97	1.00	3.23	1.00
Deep	0	2	2	2	2	2	3	1989	5.95	3.08	0.78		4.85	0.52	3.50	0.65	1.88	1.31
								1990	6.02	3.97	0.88	0.65	2.36	0.49	1.19	0.46	4.45	0.88
								$\bar{x}$	5.99	3.53	0.83		3.60	0.51	2.34	0.56	3.16	1.10
Shallow	2	2	2	0	0	0	0	1989	1.60	0.83	0.47		10.43	1.12	6.83	1.03	3.23	2.26
								1990	0.41	0.27	1.72	1.27	8.12	1.68	3.85	1.50	15.18	3.02
								$\bar{x}$	1.01	0.55	1.09		9.28	1.40	5.34	1.39	9.21	2.64
New	0	0	0	2	2	2	3	1989	7.93	4.10	0.82		2.04	0.22	2.09	0.39	1.76	1.22
								1990	8.42	5.55	0.85	0.63	0.93	0.19	0.61	0.24	3.81	0.76
								$\bar{x}$	8.18	4.82	0.84		1.49	0.20	1.35	0.32	2.78	0.99

The area (lat. 17°–18°N) of highest catch rates for bigeye tuna was on the south edge of a northward transition to a deeper thermocline and oxycline (Fig. 10). The north-south pattern is typical of the central Pacific Ocean at these latitudes, whereas the highly variable pattern in the thermocline between lat. 19.4° and 20°N was probably caused by the proximity to the lee side of the island of Hawaii.

With regard to the other species, the thermal structure of the habitat (Fig. 10) and the confirmed depth distribution of fish (Figs. 4, 7, and 8) suggested that yellowfin tuna were most abundant in the mixed layer (24°–25°C) and the steepest part of the thermocline down to about 15°C. Striped marlin appeared to be most abundant in the mixed layer and the top of the thermocline to ~20°C. Spearfish appeared to occupy a habitat between that of yellowfin tuna and striped marlin, and mahimahi occupied the mixed layer.

Standardized gear efficiency

For bigeye tuna in 1989–90, the CPUE ranges for standardized deep gear and proposed new gear were about 3.1–4.0 and 4.1–5.6 times, respectively, as great as those for regular gear (Table 5). Shallow gear on average was about half as efficient as regular gear in catching bigeye tuna, whereas it was about 40% more efficient than regular gear in catching spearfish and striped marlin. Deep gear was only about half as efficient as regular gear in catching striped marlin and spearfish, and the proposed new gear was only about 20% as efficient for striped marlin and about 30% as efficient for spearfish.

The numbers of yellowfin tuna and mahimahi caught in 1989 were much lower than in 1990, so the latter year provided better data for calculating gear efficiency for these species (Table 5). Shallow gear was about 3.0 times as efficient at catching mahimahi, and deep and new gear reduced efficiency to about 90% and 75% in comparison with regular gear. For yellowfin tuna, shallow gear was about 25% more efficient than regular gear, whereas the deep and new gear types were each about 65% as efficient.

Discussion

Habitat depth

Hook timers are useful in confirming whether fish are caught while longline hooks are sinking, settled, or rising. Combined with capture depths from TDRs, hook timers offer a new method for establishing the habitat depth of large pelagic fishes. Stock assessments (Suzuki 1989) depend on the estimation of effective effort, defined as fishing effort corrected for differences in efficiency due to gear and habitat depth (Suzuki et al. 1977). Improving the definition of tuna and billfish habitats and the estimation of effective effort in those habitats should lead to significant improvements in assessing true abundance.

Comparisons of CPUE by two gear types provide only qualitative information on habitat depth. For

example, since deep gear is more efficient than regular gear for bigeye tuna, this species must occupy a relatively deep habitat (Suzuki et al. 1977). More specific information on habitat depth is provided by catches and $CPUE_H$ by hook position (Hanamoto 1979 and 1987, Hanamoto et al. 1982, Suzuki and Kume 1982), especially when TDRs are used to record gear depth (Saito 1973 and 1975, Hanamoto 1974, Nishi 1990). Capture depth estimates without TDR records ignore major variations in actual gear depth (Fig. 2; Nishi 1990), and those without hook timers are biased by the inclusion of inappropriate hook depths.

A possible source of bias in the present study is the inclusion of some falsely confirmed depths due to fish being caught with timers already activated. The proportion of false estimates should be similar to the frequency of timers that were without fish and were triggered while settled, which was only 3.9% in 1989 and 2.6% in 1990 (Table 3). Thus it is unlikely that >4% of confirmed capture depths in this study are incorrect because of false timer readings.

Many pelagic longline studies (Saito 1975, Hanamoto 1976, Yang and Gong 1988) assume that fish are caught while hooks are at settled depths. Supporting this assumption, Saito (1973) has shown that albacore *Thunnus alalunga* are caught almost exclusively by settled hooks, based on capture times indicated by fluctuations in TDR records. Using hook timers, the present study adds new information: Almost 90% of bigeye and yellowfin tuna also are caught while hooks are at settled depths (Table 4). However, hook timers indicate this generalization does not extend to striped marlin, spearfish, mahimahi (Table 4), and most of the commercially unimportant species (Fig. 5). Although most of these fish are also caught on settled hooks, a substantial fraction are not, and this must be considered when quantifying their depth ranges (Fig. 4).

Besides the present study, little information exists on longline capture depths for mahimahi, spearfish, and striped marlin. In the study area, $CPUE_D$ values for these species (Fig. 7) indicate maximum abundance at depths in the mixed layer for mahimahi (<100 m, 24°–25°C; Fig. 10), extending into the top of the thermocline for striped marlin (120 m, 20°C) and into the middle of the thermocline for spearfish. Striped marlin are reported to be caught most frequently on longline hooks closest to the surface (60–90 m) in the eastern tropical Pacific and Indian Oceans, but they may be more abundant above this depth (Hanamoto 1979, Hanamoto et al. 1982). Mahimahi and spearfish may also be more abundant above the uppermost stratum (40–80 m) in the present study, since their catch rates appear to increase towards the surface (Fig. 7).

Striped marlin are also reported caught on deep longline hooks (~200 m; Hanamoto et al. 1982) and at the deep end of vertical longline gear (336 m; Saito 1973); but in the present study, their deepest confirmed capture depth is 210 m. Tracking data on striped marlin off California indicate a shallow (<60 m) depth distribution with most of the daytime spent within 10 m of the surface (Holts and Bedford 1989).

The depth distribution (200–400 m) of bigeye tuna in the present study is deeper than in many previous reports (Hanamoto 1974, 50–160 m; Saito 1975, 207–245 m; Suzuki and Kume 1982, 170–300 m; Yang and Gong 1988, 260–300 m; Nishi 1990, 140–180 m), although these studies have found bigeye tuna are most abundant on the deepest hooks fished. Hanamoto (1987) hypothesizes a habitat depth of 250–400 m for the central Pacific Ocean at latitude 25°N, based on the observed maximum longline CPUE at temperatures of 10°–15°C. The highest $CPUE_D$ values in the present study are at the cold, deep end of this range (Fig. 7), deeper than most hooks used in commercial fishing gear. However, the $CPUE_D$ value at 280–400 m is not significantly different from that at 200–400 m (Fig. 8). Although these results may be specific to January and February, perhaps commercial CPUE could be improved by increasing fishing depth, at least during winter months.

Seasonal and geographic variation in temperature and DO profiles may affect the depth preferences of pelagic fish. Hanamoto (1975, 1987) has hypothesized that the deep end of bigeye tuna habitat is limited by DO concentrations below 1 mL/L (1.4 mg/L) and by temperatures below 10°C. Results of the present study suggest that bigeye tuna are seldom caught in waters with a DO concentration of ~<2 mg/L (Fig. 10). Oxygen concentrations of ~2–3 mg/L cause significant reductions in bigeye tuna cardiac output (1.9–2.6 mg/L) and heart rate (2.7–3.5 mg/L), suggesting that bigeye tuna cannot maintain a full range of activity at lower DO concentrations (Bushnell et al. 1990).

Longline data to support the hypothesis of a 10°C temperature limit independent of the DO limit are sparse. Few hooks have been deployed in waters colder than 9°–10°C with DO concentrations of >1 mL/L (Hanamoto 1975, 1987). In the present study, the only area with DO values >2 mg/L and temperatures <8°C was at lat. 10°–20°N (Fig. 10). Currents prevented hooks from reaching cold (6°–8°C) water in this area.

Sonic tracking of bigeye tuna around Hawaii indicates a depth distribution slightly shallower than that in longline studies (Hanamoto 1987, 250–400 m; present study, 200–400 m). Holland et al. (1990) have reported that tracked bigeye tuna spend most of the daytime at 200–240 m in 14°–17°C water. This may be due to the association of the tracked bigeye tuna with fish aggregating devices or due to a size-related difference. The 72- to 74 cm bigeye tuna studied by Holland

et al. (1990) weighed ~10–12kg, whereas longline-caught bigeye tuna in the present study averaged >30kg.

Results of the present study apply predominantly to daytime habitat depths, but an important difference apparently exists between the daytime and nighttime depth distributions of bigeye tuna (Holland et al. 1990). At night, tracked bigeye tuna move upward to ~70–90m at temperatures of 23°–25°C. Confirmation of this nocturnal behavior comes from a new nighttime longline swordfish fishery that has recently developed in Hawaii using chemical light sticks. Although this fishery deploys very shallow (generally <90m) gear, the bycatch of bigeye tuna is surprisingly high (S. Pooley, NMFS Honolulu Lab., pers. commun., April 1991), indicating that bigeye tuna have a shallow nighttime depth distribution.

The small number of yellowfin tuna caught in this study makes estimated habitat depth (40–200m) less certain, but it does not differ much from the 90–230m depth found in Suzuki and Kume (1982) and Yang and Gong (1988). Tracking studies (Carey and Olson 1982, Holland et al. 1990) show yellowfin tuna spend most of their time at depths <100m. Depths of the highest longline $CPUE_D$ for yellowfin tuna in the present study (40–80m; Fig. 7) are similar to the depths (30–80m) at which tracked yellowfin tuna in Hawaii spend over 50% of their time during the day (Holland et al. 1990), tending to confirm that yellowfin tuna habitat is mostly in the mixed layer.

Methods for estimating habitat depths in the present study could be improved by increasing the number of TDRs deployed or by developing a model, calibrated with TDRs, to predict gear depth based on wind and current measurements, divergence or convergence of floats, and stops and starts in deployment and retrieval. Procedures to estimate the capture depths of fish caught while hooks are sinking or rising could also be developed, but would depend on very accurate timekeeping, since the gear rises rapidly during retrieval (Fig. 3).

Catch by moving hooks

The catch of shallow-swimming species on deep hooks moving through shallower depths could reduce the selectivity of gear designed to catch deep-swimming species. The results show that moving longline hooks are more effective (per unit time) than settled hooks at catching billfish, mahimahi, some sharks, and most other non-tuna species. However, the majority of these fish are caught on settled hooks, because of the longer time that hooks are settled (Fig. 5). The relative amount of time hooks are moving vs. settled is the only aspect of the commercial daytime tuna longline operations that differs much from the fishing method used in this study. The gear is left in the water longer and then retrieved more rapidly during commercial fishing, so hooks spend less time moving and more time settled. This may result in greater proportions of fish being caught on settled hooks by commercial fishermen than in the present study.

Eliminating shallow-settled hooks should greatly reduce the catch of shallow-swimming species. For non-tuna species, deploying and retrieving the gear less often (as in commercial operations) should decrease the CPUT (catch-per-unit-time), but would increase the CPUE because the latter increases with set duration. In contrast, bigeye tuna CPUT and CPUE should increase with less frequent deployment and retrieval, because CPUT is highest for settled hooks.

The mechanism for increased CPUT on moving hooks for non-tuna species is unclear. Moving bait may be more attractive than settled bait, but the low number caught on sinking hooks (Fig. 5) suggests that gear motion alone is not responsible for increased catch rate. Perhaps a gradual aggregation of fish around the gear (or the vessel) while the gear is settled contributes to the catch rate by rising hooks.

Although hook timer data provide a reliable way to confirm when fish are caught on settled hooks, such data may be less reliable as a measure of fish caught on moving hooks, because of the uncertainty regarding fish with timers triggered at recovery (Fig. 5). These fish are not included in the number captured on moving hooks (Table 4); their timer readings cannot be distinguished from ones triggered after being brought aboard. Therefore, the estimates of fish caught on moving hooks (Table 4) may be too low. Alternatively, if these readings indicate a tendency for some fish to not activate timers until they struggle during recovery, then the estimates of fish caught on moving hooks may be too high. In either case, only inferences regarding CPUT on moving and non-moving hooks, and the estimated proportions of fish caught on moving hooks, are affected by this uncertainty. The estimates of catches on non-moving hooks are conservative, and confirmed capture depths are not affected.

The higher proportion of fish caught on moving hooks in 1989 compared with 1990 (Table 4) could have been caused by moving hooks being less visible in 1990, since branch lines were more often recovered after dark (Table 1). Sets also lasted longer in 1990 (Table 1); this may have increased the relative proportion of catches on settled vs. moving hooks. The CPUT in relation to sinking, settled, and rising gear, and to the time of day, should be explored further using the techniques developed in the present study.

A TDR attached to vertical and regular rope longline gear sometimes records abrupt depth changes as a fish

is caught, making the TDR equivalent to a hook timer if it is close to a branch line that catches a fish (Saito et al. 1970, Saito 1973, Yamaguchi 1989). The records of TDRs at positions close to fish caught with hook timers in the present study were checked to see whether they indicated the time of capture, but the depth of the monofilament longline gear was much less stable (Fig. 3) than in the depth records of Saito et al. (1970), Saito (1973), and Yamaguchi (1989) using TDRs on rope gear. On monofilament longline gear, frequent depth changes resembling fish captures occur even when no fish are caught, making TDRs unreliable as substitutes for hook timers.

Viability of released fish

Before the present study, it was believed that fish would survive only a few hours after capture on longline gear (Grudinin 1989, Yamaguchi 1989) despite large pelagic species being known to survive capture and release from other types of gear (Foreman 1987, Squire 1987, Holts and Bedford 1989). Commercial longline fishermen in Hawaii speculated that much of their catch was made as hooks were sinking or rising, because most were alive or appeared long dead (F. Amtsberg, Der Fischen Co., Honolulu, HI 96822, pers. commun., March 1988). Based on TDR data from fish on regular longline gear (Yamaguchi 1989), vertical movements stop 1.0–1.5 h after capture for yellowfin tuna, 1.5–4.0 h for bigeye tuna, and ~0.5 h for spearfish and shark. This cessation of vertical movement has been interpreted as death (Yamaguchi 1989). Grudinin (1989) has reported on the diurnal periodicity of bigeye and yellowfin tuna catch rates based on the proportion recovered alive, assuming that tuna survive ≤2 h on longline gear. However, hook-timer results (Fig. 6) show that fish survive much longer than this, suggesting that vertical movement is not a reliable indicator of survival. Alternatively, the results of the present study could be specific to monofilament gear, which could have less resistance to moving through the water than does rope gear.

Clearly the high proportion of live fish (Table 2) is not primarily the result of capture during the 0.5 h rising period. The viability of longline-caught fish is indicated by their hooked longevity and the recovery of tagged fish. As a management option, non-retention of striped marlin and spearfish could reduce fishing mortality due to longline fishing. The importance of the reduction would depend on the length of the fishing operation; but in the present study, longline fishing mortality for striped marlin could have been reduced by 70% (Table 2) if all live fish had been released and had survived.

Gear efficiency and selectivity

Gear efficiency, defined as the dimensionless ratio of the CPUE of one gear type (i.e., deep gear) divided by the CPUE of the regular gear type, is the factor used to calculate effective effort by gear fishing at different depths (Suzuki et al. 1977). Total effective effort can then be used to calculate indices of relative abundance and to model stock production (Suzuki 1989). The most thorough approach thus far has been to calculate gear efficiency by area and season (Suzuki and Kume 1982). A better understanding of the variables that alter habitat depth would permit gear efficiency to be predicted as a function of environmental conditions, and help account for variation in abundance indices caused by environmental anomalies.

The relative efficiency of standardized deep gear (Table 5) follows the pattern observed in previous studies (Suzuki et al. 1977, Yang and Gong 1988) in which deep gear is more efficient at catching bigeye tuna and less efficient at catching yellowfin tuna and istiophorid billfish. However, the estimated efficiency of the standardized deep gear for bigeye tuna in the present study is greater (ratio 3.1–4.0 over the 2 years; Table 5) than that reported by Suzuki et al. (1977) for the central and western equatorial Pacific (1.8) or by Yang and Gong (1988) for the Atlantic (1.9). Suzuki and Kume (1982) have presented graphs of deep and regular CPUE for bigeye tuna on a quarterly basis by area throughout the Pacific, and these data indicate very little difference between gear types in the central Pacific north of lat. 15°N. The high efficiency estimated for deep gear in the present study may partly result from using measured depths rather than inferred depths to define deep and regular gear types. Also, a high relative efficiency for deep gear may be specific to the Hawaii area in the winter season.

The relative efficiency of deep gear for yellowfin tuna in the Atlantic (0.95, Yang and Gong 1988) is greater than in the central and western equatorial Pacific (0.73, Suzuki et al. 1977) and in the present study (0.65, Table 5). Relative efficiency of deep gear for striped marlin in the central and western equatorial Pacific (0.28, Suzuki et al. 1977) is much lower than in the central Pacific north of Hawaii (0.74, Suzuki 1989), nicely bracketing the estimate from the present study (0.51, Table 5).

The model estimates of gear efficiency (Table 5) are not meant to supplant earlier estimates based on much larger data sets (Suzuki et al. 1977, Suzuki and Kume 1982, Yang and Gong 1988, Suzuki 1989), but rather to show how catch by hook position can be used to estimate CPUE by different gear configurations, especially hypothetical configurations for which no real data exist. Efficiency estimates (Table 5) suggest that

shallow sets of the type hypothesized to represent early use of monofilament longline gear in Hawaii would be expected to catch about 40% more billfish and 160% more mahimahi than would regular longline gear. Large increases in longline catches of these fish in Hawaii have occurred in recent years (1989–90, Boggs 1991) as the expanding Hawaii fishery adopted a new type of gear. The proposed new gear configuration would be an effective way to reduce the catch of spearfish and striped marlin by ~70–80% below that of regular gear.

Hook timers and TDRs are useful in documenting the depth distribution and habitat of pelagic fish and in showing how different configurations of longline gear and the release of live fish can be effective means of reducing fishing mortality for some species. Better methods of identifying the habitats of pelagic fishes should make it easier to estimate real changes in fish abundance by accounting for changes in fishing methods and the environment.

Acknowledgments

Several of Hawaii's longline fishermen, especially F. Amtsberg, provided technical advice without which few fish would have been caught. Many of the staff at the Honolulu Laboratory participated in the cruises, and their creativity and hard work contributed substantially to this study, especially R.K.C. Chang, A.E. Chun, R. Ito, L.A. Koch, R.A. Skillman, D. Therry, J.H. Uchiyama, and S. Yano. L.A. Koch tabulated the data and produced the figures, and B.S. Kikkawa provided invaluable help in acquiring and manufacturing the hook timers. Volunteer assistance on the research cruises was given by H. Dewer, P. Fields, C. Hayashi, and A. Sesawa. The officers and crew of the NOAA ship *Townsend Cromwell* also were very helpful, especially LT R. Brainard, LTC B. Dearbaugh, H. Lariosa, and CDR R. Marriner.

Citations

Boggs, C.H.
1990 Longline research on tuna and marlin. *In* Relatorio, X Semana das Pescas dos Acores, March 12–16 1990, p. 249–252. Sec. Reg. Agric. Pescas, Dir. Reg. Pescas, Horta, Faial, Azores.
1991 A preliminary examination of catch rates in Hawaii's troll and handline fisheries over a period of domestic longline fishery expansion. Admin. Rep. H-91-05, NMFS Southwest Fish. Sci. Cent., Honolulu, 62 p.

Bushnell, P.G., R.W. Brill, and R.E. Bourke
1990 Cardiorespiratory responses of skipjack tuna (*Katsuwonus pelamis*), yellowfin tuna (*Thunnus albacares*), and bigeye tuna (*Thunnus obesus*) to acute reductions of ambient oxygen. Can. J. Zool. 68:1857–1865.

Carey, F.G., and R.J. Olson
1982 Sonic tracking experiments with tunas. Int. Comm. Conserv. Atl. Tunas Collect. Vol. Sci. Pap. 17:458–466.

Foreman, T.J.
1987 A method of simultaneously tagging large oceanic fish and injecting them with tetracycline. Fish. Bull., U.S. 85: 645–647.

Grudinin, V.B.
1989 On the ecology of yellowfin tuna (*Thunnus albacares*) and bigeye tuna (*Thunnus obesus*). J. Ichthyol. 26(6):22–29.

Hanamoto, E.
1974 Fishery oceanography of bigeye tuna—I. Depth of capture by tuna longline gear in the eastern tropical Pacific Ocean. La Mer (Bull. Soc. Franco-Japonaise Oceanogr.) 12(3):128–136.
1975 Fishery oceanography of bigeye tuna—II. Thermocline and dissolved oxygen content in relation to tuna longline fishing grounds in the eastern tropical Pacific Ocean. La Mer (Bull. Soc. Franco-Japonaise Oceanogr.) 13(2):58–71.
1976 The swimming layer of bigeye tuna. Bull. Jpn. Soc. Fish. Oceanogr. 29:41-44. [Engl. transl. no. 21 by Tamio Otsu, 1977, 7 p.; avail. NMFS Honolulu Lab., Honolulu 96822-2396.]
1979 Fishery oceanography of striped marlin—IV swimming layer in the tuna longline fishing grounds. Bull. Jpn. Soc. Sci. Fish. 45:687–690.
1987 Effect of oceanographic environment on bigeye tuna distribution. Bull. Jpn. Soc. Fish. Oceanogr. 51:203–216.

Hanamoto, E., T. Shibata, and H. Okui
1982 Some considerations on the vertical distribution particularly of the striped marlin in the Indian Ocean and on the fishing characteristics of the tuna longline gear. Kanagawa Prefect. Fish. Exp. Stn. Res. Rep. 4:17–21.

Holland, K.N., R.W. Brill, and R.K.C. Chang
1990 Horizontal and vertical movements of yellowfin and bigeye tuna associated with fish aggregating devices. Fish Bull., U.S. 88:493–507.

Holts, D., and D. Bedford
1989 Activity patterns of striped marlin in the Southern California Bight. *In* Stroud, R.H. (ed.), Planning the future of billfishes, research and management in the 90's and beyond. Part 2: Contributed papers. Mar. Rec. Fish. 13: 81–93. Natl. Coalition Mar. Conserv., Savannah, GA.

Kawamoto, K.E., R.Y. Ito, R.P. Clarke, and A.E. Chun
1989 Status of the tuna longline fishery in Hawaii, 1987–1988. Admin. Rep. H-89-10, NMFS Southwest Fish. Sci. Cent., Honolulu, 34 p.

Nishi, T.
1990 The hourly variations of the depth of hooks and the hooking depth of yellowfin tuna (*Thunnus albacares*), and bigeye tuna (*Thunnus obesus*), of tuna longline in the eastern region of the Indian ocean. Mem. Fac. Fish. Kagoshima Univ. 39: 81–98.

Rockefeller, W.
1989 Looking to the future of billfishes. *In* Stroud, R.H. (ed.), Planning the future of billfishes, research and management in the 90's and beyond. Part 1: Fishery and stock synopses, data needs and management. Mar. Rec. Fish. 13:11–14. Natl. Coalition Mar. Conserv., Savannah, GA.

Saito, S.
1973 Studies on fishing of albacore, *Thunnus alalunga* (Bonnaterre) by experimental deep-sea tuna long-line. Mem. Fac. Fish. Hokkaido Univ. 21:107–185.
1975 On the depth of capture of bigeye tuna by further improved vertical long-line in the tropical Pacific. Bull. Jpn. Soc. Sci. Fish. 41:831–841.

Saito, S., K. Ishii, and K. Yoneta
1970 Swimming depths of large sized albacore in the South Pacific Ocean — 1. Fishing of albacore by a newly designed vertical longline. Bull. Jpn. Soc. Sci. Fish. 36:578–584.

Somerton, D.A., B.S. Kikkawa, and C.D. Wilson
1988 Hook timers to measure the capture time of individual fish. Mar. Fish. Rev. 50(2):1–5.

Squire, J.L.
1987 Striped marlin, *Tetrapturus audax*, migration patterns and rates in the northeast Pacific Ocean as determined by a cooperative tagging program: Its relation to resource management. Mar. Fish. Rev. 49(2):26–43.

Squire, J.L., and D.W.K. Au
1990 Striped marlin in the northeast Pacific—a case for local depletion and core area management. *In* Stroud, R.H. (ed.), Planning the future of billfishes, research and management in the 90's and beyond. Part 2: Contributed papers. Mar. Rec. Fish. 13:199–214. Natl. Coalition Mar. Conserv., Savannah, GA.

Suzuki, Z.
1989 Catch and fishing effort relationships for striped marlin, blue marlin, and black marlin in the Pacific Ocean, 1952 to 1985. *In* Stroud, R.H. (ed.), Planning the future of billfishes, research and management in the 90's and beyond. Part 1: Fishery and stock synopses, data needs and management. Mar. Rec. Fish. 13:165–177. Natl Coalition Mar. Conserv., Savannah, GA.

Suzuki, Z., and S. Kume
1982 Fishing efficiency of deep longline for bigeye tuna in the Atlantic as inferred from the operation in the Pacific and Indian Oceans. Int. Comm. Conserv. Atl. Tunas Collect. Vol. Sci. Pap. 17:471–486.

Suzuki, Z., Y. Warashina, and M. Kishida
1977 The comparison of catches by regular and deep tuna longline gears in the western and central equatorial Pacific. Bull. Far Seas Fish. Res. Lab. 15:51–83.

Yamaguchi, Y.
1989 Tuna long-line fishing IV: Fish ecology in the context of tuna long-line fishing. Mar. Behav. Physiol. 15:45–73.

Yang, W.S., and Y. Gong
1988 The vertical distribution of tunas and billfishes, and fishing efficiency between Korean regular and deep longlines in the Atlantic Ocean. Bull. Natl. Fish. Res. Dev. Agency [Pusan, Korea] 42:39–42.

Yoshihara, T.
1954 Distribution of catch of tuna longline-IV. On the relation between k and φ° with a table and diagram. Bull. Jpn. Soc. Sci. Fish. 19:1012–1014.

Abstract. – In the summers of 1982, 1983, and 1985, almost 5000 commercial lobsters were transplanted from an area on the northeast coast of Newfoundland to St. Michael's Bay in southern Labrador, about 200 km beyond their reported northern limit of distribution, in an attempt to establish a self-sustaining population. Biological sampling of these lobsters was carried out each summer from 1986 to 1991. A continuous shift to larger sizes and a generally high incidence of new-shell animals indicated molting was a common occurrence in these lobsters. All nonovigerous females had ovaries developing for extrusion that summer, and their seminal receptacles were full. In contrast, percentages of ovigerous females were low and most of these had extruded recently. Many ripe females apparently failed to extrude, and many that did extrude lost the entire clutch before the following summer. Exposure to temperatures near or below 0°C from mid-November to mid-May, and to near-continuous darkness below a layer of ice during most of this period, may cause a high incidence of resorption of ripe ovaries. The incidence of ovigerous females with recently-extruded eggs increased substantially in the later years of the study, indicating a degree of physiological adjustment to the adverse environmental conditions. However, loss of the entire clutch of eggs continued to be prevalent. Prolonged low temperature certainly retarded embryonic development for the females that extruded and retained their eggs. Six of 17 ovigerous females with old, eyed eggs had less than half the yolk remaining. Only one brood would have hatched by early August, long enough in advance of autumn cooling for development to Stage IV and settlement in the area to be possible. Lobsters transplanted to St. Michael's Bay will not likely become a self-sustaining population. Any recruitment that might occur would certainly be too little and too irregular to support a fishery.

Manuscript accepted 15 July 1992.
Fishery Bulletin, U.S. 90:659–667 (1992).

Reproduction in American lobsters *Homarus americanus* transplanted northward to St. Michael's Bay, Labrador

Frank A. Boothroyd

Biology Department, Memorial University of Newfoundland
St. John's, Newfoundland A1B 3X9, Canada

Gerald P. Ennis*

Department of Fisheries and Oceans, P O. Box 5667
St. John's, Newfoundland A1C 5X1, Canada

The American lobster *Homarus americanus* occurs in the western Atlantic Ocean from the Strait of Belle Isle area of southern Labrador and the northern tip of the island of Newfoundland south to North Carolina (Cooper and Uzmann 1980). The species supports commercial fisheries of considerable economic importance throughout most of its range. Its high commercial value led to repeated attempts to establish lobster populations on the Pacific coast of North America, but none of the transplants was successful (Conan 1986). In recent years, the Provincial Government of Newfoundland and Labrador transplanted commercial (mostly adult) lobsters from an area on the northeast coast of the island of Newfoundland to a location ~200 km beyond the reported northern limit of distribution in St. Michael's Bay, Labrador (Fig. 1). The bay extends inland ~28 km from the open coast and contains numerous small islands, features promoting a circulation pattern that would aid retention and eventual settlement in the area of any larvae produced by the transplanted lobsters. This was an important consideration, since the aim of the transplant was to establish a self-sustaining population that would eventually support a fishery.

Lobsters were transplanted to St. Michael's Bay in the summers of 1982, 1983, and 1985. Biological sampling was conducted each summer from 1986 to 1991. Our purpose is to present observations related to various aspects of population biology, in particular, molting, mating, ovary development, spawning and embryonic development, and consider the possibility of this transplanted population being or becoming self-sustaining.

Methods and materials

Lobsters transplanted to St. Michael's Bay were caught during May–June by commercial fishermen near Comfort Cove, Notre Dame Bay, on the northeast coast of Newfoundland (Fig. 1). They were purchased from a local buyer by the Newfoundland and Labrador Department of Fisheries and transported directly to St. Michael's Bay by float plane. Transplants were made in 1982, 1983, and 1985 and totaled 2174 males, 81–114 mm carapace length (CL), and 2310 nonovigerous females, 81–112 mm CL. Lobsters were released once only at eight widely-separated sites around the bay where the shallow-water habitat appeared quite suitable for lobsters.

The authors conducted biological sampling annually in the summer-

* Reprint requests should be addressed to this author.

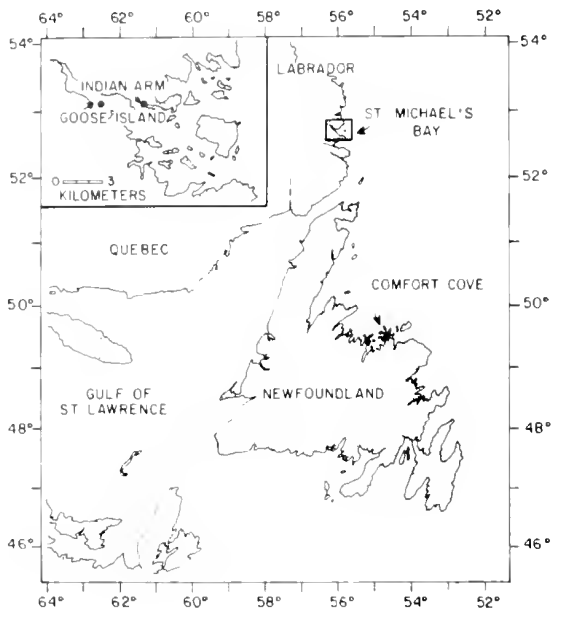

Figure 1

Locations of Comfort Cove, Newfoundland, and St. Michael's Bay, Labrador, the donor and recipient sites, respectively, for lobsters *Homarus americanus* transplanted to Labrador. Insert shows Goose I. and Indian Arm, the main sites in St. Michael's Bay where transplanted lobsters were sampled.

time from 1986 to 1990. In 1991, less detailed sampling was carried out by the Department of Fisheries of the Province of Newfoundland and Labrador. Sampling focused on lobsters in Indian Arm (transplanted in 1982) and at Goose Island (transplanted in 1985) (Fig. 1). These two sites were selected to include lobsters from the earliest and latest transplants. Also, in initial trap sampling in 1986, lobsters were caught more readily at these sites than at others. Lobsters were caught in baited traps in 1986, 1987, and 1991 and by scuba-diving from 1988 to 1990. Samples over the 6 years totaled 295 males and 392 females. Numbers included in sampling for various purposes described below are summarized by year and sampling site in Table 1. Carapace length of each lobster was measured to the nearest mm. Shell condition was determined by external macroscopic examination in 1986 and 1988–90. In over 90% of the lobsters examined for shell condition, those that molted the previous summer (new shell) could be readily distinguished from those that did not (old shell) by general brightness of coloration, sharpness of spines, and the degree of darkening due to abrasion on the leading edges and undersides of the claws. The others could be categorized with reasonable confidence. Each summer from 1987 to 1990, subsamples of nonovigerous females totaling 111 for the 4 years were sacrificed. For each of these, ovary color, ova diameter, contents of seminal receptacles,

Table 1

Summary of numbers included in sampling of lobsters *Homarus americanus* transplanted to St. Michael's Bay, Labrador (Indian Arm in 1982, Goose I. in 1985), 1986–91.

Year sampled	Number and carapace lengths		Shell condition		Setal development		Nonovigerous females			Ovigerous females			
	Male	Female	Male	Female	Male	Female	Ovaries	Seminal receptacles	Cement glands	New eggs	Old eggs	Egg counts	Yolk content of old eggs
Indian Arm													
1986	87	109	87	74	–	–	–	–	–	–	21*	–	–
1987	10	25	–	–	–	–	7	7	7	1	1	2	1
1988	32	48	32	42	–	–	27	27	27	5	2	7	2
1989	24	21	24	21	24	20	8	8	8	7	6	–	6
1990	17	22	17	22	17	21	8	8	8	11	3	–	3
1991	4	9	–	–	–	–	–	–	–	4	3	–	3
Goose Island													
1986	30	32	30	30	–	–	–	–	–	0	0	–	–
1987	7	33	–	–	–	–	23	23	23	0	0	–	–
1988	16	38	10	25	–	–	7	7	7	0	0	–	–
1989	29	20	29	20	29	20	15	15	16	2	2	–	2
1990	23	22	23	22	23	22	15	15	15	7	0	–	–
1991	15	13	–	–	–	–	–	–	–	10	0	–	–

*In 1986, old- and new-egg ovigerous females were not distinguished.

and the extent of pleopod cement gland development (Aiken and Waddy 1982) were determined. In 1989 and 1990, pleopod setal development (Aiken 1973) was determined for 47 nonovigerous females and 93 males. Eighty-four ovigerous females were included among the 392 females sampled over the 6 years. Egg numbers were determined for nine collected in Indian Arm in 1987 and 1988. Five of these were small egg masses that were counted directly, the other four were estimated by drying and weighing the entire mass, then weighing and counting a subsample representing about 10% of the total. Yolk content of eggs (to the nearest tenth, i.e., 0.1) was determined for 17 ovigerous females carrying old, eyed eggs collected from 1986 to 1991. Perkins Eye Indices (PEI), which provide a measure of embryonic development (Perkins 1972), were determined for four of the latter.

From July 1986 to September 1988, a continuously recording thermograph was maintained in St. Michael's Bay at 7m within the depth range occupied by the transplanted lobsters. Mean daily temperature was obtained from the tapes. These were averaged for the first and second half of each month, with data for the different years combined. Temperature during most of June each year was not obtained because the recording tape expired in 1987 and the instrument malfunctioned in 1988. The June portion of the annual temperature regime was approximated by extrapolating from temperatures which were rising in a near-linear fashion before and after.

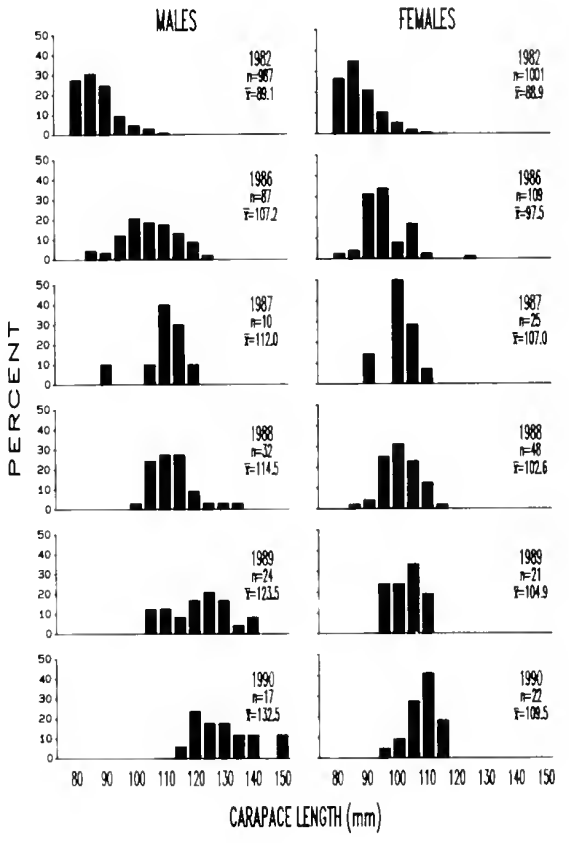

Figure 2

Size-frequencies for all male and female lobsters *Homarus americanus* transplanted to St. Michael's Bay, Labrador, in 1982, and when sampled at the Indian Arm release site, 1986–90.

Results

Changes in size composition

Indian Arm Mean CL of all the lobsters transplanted to St. Michael's Bay in the summer of 1982 was 89.1 mm (range 81–114mm, *N* 987) for males and 88.9mm (range 81–112mm, *N* 1001) for females (Fig. 2). We assume that these are also representative of the lobsters released at the Indian Arm site. When first sampled in the summer of 1986, mean CL of lobsters in Indian Arm had increased significantly (Tukey test; $P<0.001$) to 107.2mm for males (*N* 87) and 97.5mm for females (*N* 109). There were further shifts to larger sizes each year, especially among males, and in the summer of 1990, mean CL was significantly larger ($P<0.001$) than in all previous years at 132.5mm (range 116–153mm, *N* 17) for males and 109.6mm (range 98–116mm, *N* 22) for females.

Goose Island Mean CL of all the lobsters transplanted to St. Michael's Bay in the summer of 1985 was 84.1mm (range 81–95mm, *N* 687) for males and 84.4 mm (range 81–92mm, *N* 811) for females (Fig. 3), significantly smaller (*t*-test; $P<0.001$) than for those transplanted in 1982. We assume that these means are representative of the lobsters released at Goose I. At Goose I., annual shifts to larger sizes were small until 1988, when mean CL had increased significantly (Tukey test; $P<0.001$) to 96.4mm for males (*N* 16) and 92.6mm for females (*N* 38). By summer 1990, mean CL had increased significantly again ($P<0.001$) to 105.6mm (range 90–131mm, *N* 23) for males and to 95.9mm (range 89–105mm, *N* 22) for females.

Incidence of new-shell lobsters

The donor population at Comfort Cove is subjected to a very intensive fishery each spring which removes most of the commercial lobsters (nonovigerous and ≥81mm CL). Following the summer molting period, the vast majority of commercial-size animals in the population had molted and grown from smaller sizes

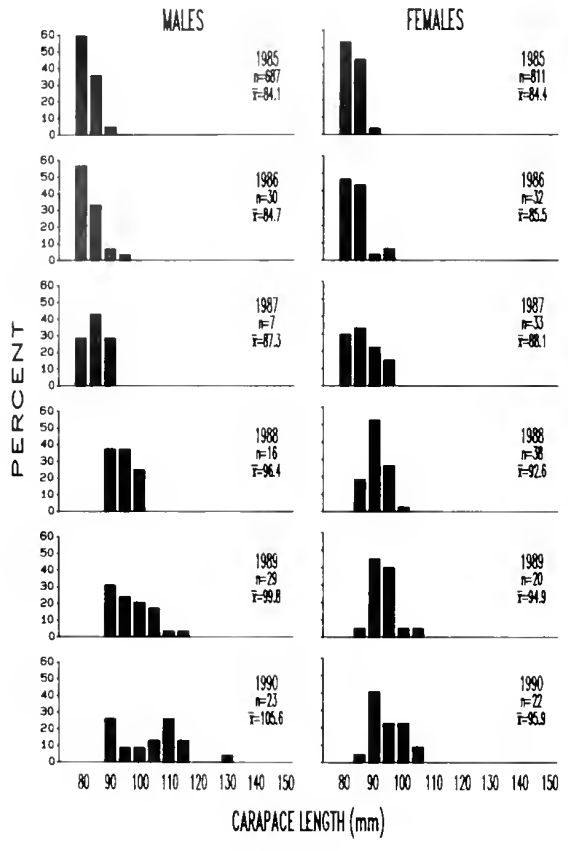

Figure 3
Size-frequencies for all male and female lobsters *Homarus americanus* transplanted to St. Michael's Bay, Labrador, in 1985, and when sampled at the Goose I. release site, 1986–90.

Table 2
Percentage with new shells (molted previous summer) among lobsters *Homarus americanus* transplanted to St. Michael's Bay, Labrador (Indian Arm in 1982, Goose I. in 1985) during sampling, 1986 and 1988–90. Number sampled in parentheses.

Year sampled	Indian Arm		Goose Island	
	Males	Females	Males	Females
1986	40.2 (87)	21.6 (74)	3.3 (30)	6.7 (30)
1988	53.1 (32)	42.9 (42)	80.0 (10)	92.0 (25)
1989	62.5 (24)	47.6 (21)	75.9 (29)	75.0 (20)
1990	52.9 (17)	31.8 (22)	52.2 (23)	63.6 (22)

Table 3
Pleopod setal development stages for male and nonovigerous female lobsters *Homarus americanus* transplanted to St. Michael's Bay, Labrador (Indian Arm in 1982, Goose I. in 1985) during sampling, 1989–90.

Year sampled	Setal development stages* (%)					
	Males			Females		
	N	0–2.0	2.5–5.0	*N*	0–2.0	2.5–5.0
Indian Arm						
1989	24	70.8	29.2	8	62.5	37.5
1990	17	47.1	52.9	8	0	100
Goose Island						
1989	29	69.0	31.0	16	81.2	18.8
1990	23	39.1	60.9	15	0	100

* From Aiken (1973). Stages 0–2.0 indicate molting is unlikely, and stages 2.5–5.0 that molting is probable in the current summer.

during the summer. As a consequence, the incidence of new shells among commercial sizes averaged 96% and 94% for male and female lobsters, respectively, in autumn samples from 1986 to 1990 (Ennis, unpubl. data). These are much higher percentages than could be expected for the transplanted lobsters in St. Michael's Bay. There has been no lobster fishing in St. Michael's Bay and, because of their larger sizes, lobsters there are less likely to molt. Old-shell lobsters are therefore likely to be much more prevalent.

Among Indian Arm lobsters, the incidence of new shells (indicating lobsters molted the previous summer) ranged from 40.2% in 1986 to 62.5% in 1989 for males and from 21.6% in 1986 to 47.6% in 1989 for females (Table 2). In 1986, the incidence of new shells was very low among Goose I. lobsters (3.3% for males and 6.7% for females) indicating few molted in summer 1985 when they were transplanted. However, in 1988 and 1989 the incidence of new shells was quite high (75.0–92.0%) for males and females (Table 2).

Pleopod setal development was determined in 1989 and 1990 only. Percentages with advanced stages (2.5 and higher), which indicated molting would occur later in the summer, varied between years and sexes at both sampling sites. Among males, advanced stages increased from 29.2% to 52.9% and from 31.0% to 60.9% in Indian Arm and Goose I. samples, respectively, between 1989 and 1990 (Table 3). Among females, it increased from 37.5% in the Indian Arm sample and 18.8% in the Goose I. sample in 1989, to 100% in both in 1990 (Table 3).

Reproductive condition of nonovigerous females

Ovaries of 110 nonovigerous females from Indian Arm and Goose Island combined were examined from 1987 to 1990 and all were found to be medium- to dark-green

Table 4

Ovary color and ova diameter among nonovigerous female lobsters *Homarus americanus* transplanted to St. Michael's Bay, Labrador (Indian Arm in 1982, Goose I. in 1985) during sampling, 1987–90.

Year sampled	*N*	Ovary color		Ova diameter (mm)	
		Med. green	Dark green	$\bar{x}$	Range
Indian Arm					
1987–88	34	11[a]	23	1.4	0.9–1.5
1989	8	0	8[b]	1.0	0.9–1.3
1990	8	1	7	1.0	0.8–1.2
Goose Island					
1987–88	30	21[a]	9	1.3	0.9–1.5
1989	15	1	14	1.0	0.8–1.3
1990	15	0	15	1.1	0.9–1.2

[a]The high proportion with medium-green ovaries in the 1987–88 sample is probably due to a different observer than in 1989–90.
[b]Includes one specimen with yellow specks throughout the ovary, indicating resorption underway.

Table 5

Pleopod cement gland stages for nonovigerous female lobsters *Homarus americanus* transplanted to St. Michael's Bay, Labrador (Indian Arm in 1982, Goose I. in 1985) during sampling, 1987–90.

Year	*N*	Cement gland stages*			
		1	2	3	4
Indian Arm					
1987	7	7	0	0	0
1988	27	27	0	0	0
1989	8	7	0	1	0
1990	8	8	0	0	0
Goose Island					
1987	23	23	0	0	0
1988	7	7	0	0	0
1989	16	15	0	1	0
1990	15	15	0	0	0

*From Aiken and Waddy (1982). Stages 3 and 4 indicate extrusion will occur in the current summer.

in color, with ova 0.8–1.5 mm in diameter (Table 4). All these ovaries were developing for extrusion in the summer they were sampled; one had yellow specks characteristic of an ovary being resorbed. However, of these nonovigerous females, only 2 of 24 sampled in 1989 (2 out of 111 overall) had sufficient pleopod cement gland development (Stage 3) to indicate egg extrusion would occur (Table 5). The seminal receptacles of all of the nonovigerous females examined from 1987 to 1990 were full, which means each had mated at the last molt and was capable of fertilizing a clutch of eggs. Pleopod setal development indicated 25% of 24 and 100% of 23 nonovigerous females sampled in 1989 and 1990, respectively, would molt (Table 3). While molting does not preclude egg extrusion in the same summer, this is unlikely to occur among lobsters in St. Michael's Bay. This phenomenon probably involves only animals extruding for the first time and <81 mm CL (Ennis 1984a).

Incidence of ovigerous females

The reproductive cycle in female lobsters normally covers 2 years. Molting and mating occur one summer, egg extrusion one year later, followed by hatching of eggs, molting, and mating again in the third summer (Aiken and Waddy 1980a). Departures from this 2-year cycle known to occur in the wild include molting, mating, and extrusion in the same summer (mentioned in the preceding section) and resorption of ripe ovaries just before extrusion (Aiken and Waddy 1976 and 1980ab, Ennis 1984b). While variability in the incidence of these phenomena may contribute somewhat, the intensity of the commercial fishery and its timing in relation to the spawning season exert by far the greatest impact on the incidence of ovigerous females in a lobster population.

At Comfort Cove, most of the nonovigerous commercial-size females in the population are removed by the spring fishery just before the summer spawning period. In autumn sampling from 1986 to 1990 an average 6% of commercial-size females were ovigerous, excluding those that molted and grew from subcommercial sizes and extruded as well during the summer (Ennis, unpubl. data). Not being fished and being more likely to spawn as well because of their larger size, the percentage of females ovigerous among St. Michael's Bay lobsters by comparison should be quite high.

In St. Michael's Bay, the percentages of females that were ovigerous with old eggs each summer (i.e., extruded previous summer) were very low, particularly in 1986–88 samples, considering all nonovigerous females examined the previous summer had ripe ovaries. In the 1986 Indian Arm sample, 19.3% of the females were ovigerous, including both new- and old-egged females which were not distinguished at the time. In subsequent years, the incidence of ovigerous females with old eggs increased from 4.0% in 1987 to 33.3% in 1991 (Table 6). No ovigerous females were included in Goose I. samples until 1989, when 10% of the females carried old eggs. In 1990 and 1991 samples, however, there were none with old eggs (Table 6).

Table 6

Percentage of females that were ovigerous among lobsters *Homarus americanus* transplanted to St. Michael's Bay, Labrador (Indian Arm in 1982, Goose I. in 1985) during sampling, 1986–91.

	Indian Arm				Goose Island			
Sampling dates	No. females	% new eggs	% old eggs	% ovigerous	No. females	% new eggs	% old eggs	% ovigerous
22 July–25 Aug. 1986	109	–	–	19.3*	32	0	0	0
18–25 July 26 Aug.–3 Sept. 1987	25	4.0	4.0	8.0	33	0	0	0
25 June–2 July 1988	48	10.4	4.2	14.6	38	0	0	0
19–25 July 1989	21	33.3	23.8	57.1	20	10.0	10.0	20.0
13–20 Aug. 1990	22	50.0	13.6	63.6	22	31.8	0	31.8
14–19 Aug. 1991	9	44.4	33.3	77.8	13	76.9	0	76.9

*In 1986, old- and new-egg ovigerous females were not distinguished.

The percentages of females that were ovigerous with new eggs (i.e., extruded within the preceding 2 or 3 weeks) ranged from 4% in 1987 to 50% in 1990 in the Indian Arm samples, and increased from 10% in 1989 to 32% in 1990 in the Goose I. samples (Table 6). Of 64 ovigerous females included in the combined 1987–91 samples, 73% had new eggs and, overall, there was a substantially higher incidence of ovigerous females among St. Michael's Bay lobsters in 1989–91 than previously.

The low incidence of ovigerous females in samples up to 1988 indicates most of the nonovigerous females, all of which had ripe ovaries in summer, failed to extrude eggs. In subsequent years, however, the proportion of nonovigerous females extruding increased substantially. There was no evidence of hatching of old eggs prior to our sampling each summer, which might have accounted for the scarcity of old-egged relative to new-egged females. This indicates that many females that extruded lost their entire clutch of eggs sometime prior to the following summer.

Fecundity and egg development

Egg numbers were determined for 9 ovigerous females included in the 1987 and 1988 samples from Indian Arm. Four of these egg counts were <0.1% of expected numbers as determined from a size-fecundity relationship for a population on the south coast of Newfoundland, one had 2%, and the others had 30–105% of the expected number of eggs (Table 7). The extremely low numbers in 5 of the 9 specimens cannot be attributed to high variability generally associated with such data, but rather indicate a high incidence of massive egg loss. Although egg numbers were not determined for any of 21 ovigerous females included in the 1989 and 1990 samples, cursory examination indicated that most had what appeared to be full clutches, although one had just a few hundred eggs.

Table 7

Egg numbers for nine ovigerous female lobsters *Homarus americanus* transplanted to St. Michael's Bay, Labrador, included in 1987 and 1988 samples from Indian Arm.

Carapace length (mm)	No. of eggs	% of expected number*
97	15	<0.1
97	7	<0.1
101	122	<0.1
102	186	<0.1
94	334	2.0
103	6588	30.0
104	10122	45.0
102	17878	84.0
95	17854	105.0

*Expected number of eggs was calculated from a CL–fecundity relationship ($\log_{10} F = 3.0984 \log_{10} CL - 1.8963$) for a population in Placentia Bay on the south coast of Newfoundland (Ennis 1981).

The extent of embryonic development for 17 ovigerous females with old, eyed eggs collected from 1986 to 1991 ranged from 0.8 to 0.3 yolk content (Table 8). Only 6 had less than half the yolk remaining when examined. Perkins Eye Indices (PEI) were determined for four specimens. One with 0.3 yolk content had a mean PEI of 470 on 29 June 1988. At an assumed constant developmental temperature of 10°C, it was estimated, using Perkin's (1972) formula, that hatching would have occurred by 4 August. Another with 0.4 yolk content had a mean PEI of 431 on 1 August 1986, for which hatching by 21 September was estimated.

Table 8

Yolk content of eggs for 17 ovigerous females with old, eyed eggs included in 1986–91 samples of lobsters *Homarus americanus* transplanted to St. Michael's Bay, Labrador. Yolk content to the nearest tenth.

Sampling date	Carapace length (mm)	Yolk content
1 Aug. 1986	94	0.4
19 July 1987	92	0.7
29 June 1988	95	0.3
30 June 1988	97	0.8
20 July 1989	88	0.4
21 July 1989	110	0.6
21 July 1989	108	0.6
21 July 1989	103	0.7
21 July 1989	109	0.6
21 July 1989	106	0.5
22 July 1989	92	0.7
16 Aug. 1990	116	0.3
16 Aug. 1990	111	0.4
16 Aug. 1990	104	0.5
19 Aug. 1991	101	0.5
19 Aug. 1991	114	0.5
19 Aug. 1991	107	0.4

The other two PEIs were 108 and 127 (0.8 and 0.7 yolk content, respectively). Even at 10°C, well above the temperature in St. Michael's Bay beyond September, it was estimated these broods would not be ready to hatch until late December–early January.

Temperature

Bottom temperature at 7 m in St. Michael's Bay drops below 0°C in late November, remains around −1°C throughout the winter, and rises above 0°C in early June (Fig. 4). Summer warming is rapid. Temperature reaches 9°C between mid- and late-July and peaks at just over 10°C in late August. By mid-September, autumn cooling is underway and temperature starts to drop rapidly around the end of September. At Comfort Cove, where the transplanted lobsters originated, sub-zero temperatures prevail for only about 2 months in late winter (Fig. 4). Summer warming begins in late April–early May and reaches a slightly higher peak at around 11°C in late August. Autumn cooling begins somewhat later and proceeds more slowly. In St. Michael's Bay, transplanted lobsters are exposed to a similar range in temperature as at Comfort Cove, but to a substantially lower mean temperature during most of the year.

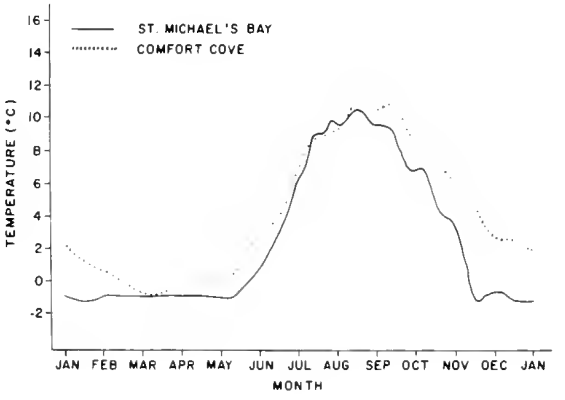

Figure 4

Annual temperature (°C) regimes from continuous-recording thermographs maintained on the bottom at 7 m in St. Michael's Bay, Labrador, summer 1986–autumn 1988, and at 9 m in Comfort Cove, Newfoundland, during the same period.

Discussion

The very low incidence of new-shell lobsters in the 1986 Goose I. sample indicates few molted in summer 1985 when they were transplanted. This was most likely due to molt inhibition caused by handling-induced stress, possibly including wide temperature fluctuations, during transplant. The high incidence of new-shell lobsters at Goose I. in 1988, and the substantial shift to larger sizes among the Indian Arm lobsters (transplanted in 1982) by 1986, indicate the transplanted lobsters acclimated over time and resumed molting despite the lower temperatures in St. Michael's Bay.

All nonovigerous females examined during the study had advanced ovaries developing for extrusion in the summer they were sampled. All of these had full seminal receptacles indicating they mated at the last molt. However, only 1.8% (2 out of 24 examined in 1989) had advanced pleopod cement gland development indicating extrusion was imminent. Some ovigerous specimens with recently-laid eggs were observed each year. This suggests most nonovigerous females that were going to extrude each summer had done so by the time our samples were collected. These amounted, however, to only 23% (N 104) of the females (excluding old-egg ovigerous) examined at Indian Arm from 1987 to 1990, and 22.5% (N 40) of those examined at Goose Island in 1989 and 1990. In 1991, this percentage increased to 66.7% (N 6) and 77% (N 13) in the Indian Arm and Goose I. samples, respectively. Advanced pleopod setal development among the ripe nonovigerous females that were examined in 1989 and 1990 indicated 62% would soon molt.

Based on the foregoing observations, it appears that up until 1990 at least most of the mature, nonovigerous females in St. Michael's Bay did not extrude. Rather, they resorbed the lipovitellin accumulated in the ripening oocytes, and many then proceeded to molt. Resorption of the ripe ovary has been associated with unfavorable holding conditions near the expected time of extrusion (Templeman 1940) but appears to be common in the wild as well (Ennis 1984b). Resorption occurs when the molting and reproductive cycles are out of phase, and molting is due to occur within 3 or 4 months after egg extrusion (Aiken and Waddy 1976, 1980ab). These cycles are normally synchronized by temperature and photoperiod regimes to ensure that when a female lobster extrudes eggs in one summer, it will not molt until after the eggs have hatched sometime the following summer.

In their experiments on the effects of winter temperature and photoperiod on spawning, Aiken and Waddy (1989) found a high incidence of resorption among mature females held at high temperature throughout the winter, particularly when a short-day photoperiod was maintained throughout the summer (55% resorbed). Onset of a long-day photoperiod in spring was necessary to trigger spawning among females held at high winter temperature. The incidence of spawning was high ($\geq$90%) among those held at low winter temperature, even without onset of a long-day photoperiod in spring, and only a few resorbed.

These results do not explain the high incidence of resorption among female lobsters in St. Michael's Bay where they are exposed to environmental conditions well outside the foregoing experimental treatments. From mid-November to mid-May, the bottom temperature is near or below 0°C and the bay is frozen over for most of this period. Visual acuity of lobsters at very low light intensity has not been described. It seems unlikely, however, that sufficient light would penetrate a layer of snow-covered sea ice underlaid by low-salinity water (from continuous river discharge and slow mixing under the ice) for lobsters to detect a light:dark cycle. This combination of very low temperature and near continuous darkness for 5–6 months from late autumn to spring is probably the main cause of the high incidence of ovary resorption that has prevailed among female lobsters in St. Michael's Bay.

Most of the ovigerous females collected in St. Michael's Bay had extruded quite recently. The remainder were old-egged females that spawned the previous summer. Apparently, many females that extruded lost the entire clutch of eggs before the following summer. Massive but incomplete loss of eggs was also observed. Of 9 ovigerous females collected in Indian Arm in 1987 and 1988, 5 had numbers of eggs ranging from 7 to 334. Only one of the 21 ovigerous females collected in 1989 and 1990 had just a few hundred eggs. The overall incidence of ovigerous females, particularly those with new eggs, increased substantially in 1989 and 1990 and especially in 1991. At Goose I., no ovigerous females at all were included in samples until 1989, 4 years after they were transplanted. This indicates a high degree of acclimation or physiological adjustment to environmental conditions in St. Michael's Bay on the part of females, resulting in much less resorption of ripe ovaries and much more extrusion in recent years. However, loss of the entire clutch of eggs appeared to be still quite prevalent. Ovigerous females sometimes lose their entire clutch of eggs by molting (Ennis 1984b). This may have been a more common occurrence in later years, which could explain the near absence of tiny clutches compared with the high incidence observed in 1987 and 1988, and would also be consistent with a high incidence of new shells and advanced setai development among females in 1989 and 1990. Despite some physiological adjustment resulting in more extrusion, for most females the molting and reproductive cycles continued to be out of phase.

Embryonic development in lobsters proceeds slowly at temperatures below 6°C, and hatching can be delayed by as long as 6 months if temperature remains at 2–3°C throughout spring, summer, and autumn, although it will eventually occur, even at that temperature (Aiken and Waddy 1986). Perkins (1972) found that advanced embryos will develop more slowly than less advanced ones when held at the same temperature. In one specimen with 29-week-old eggs on 10 January held at the Boothbay Harbor Laboratory under local water conditions, there was no measurable development for an 18-week period starting in early December. Over most of the period, temperature ranged from 0.1°C to 1.5°C.

In St. Michael's Bay, bottom temperature drops below 6°C by mid-October, below 3°C by mid-November, and below 0°C by late November. Of the old-egged ovigerous specimens from there, which are presumed to have extruded the previous summer, there was one with 0.8 yolk remaining when examined at the end of June, three with 0.7 remaining around 20 July, and three with 0.5 remaining in mid-August. Possibly some of these females carry their eggs through a second winter and may represent the ones observed in our samples with sufficiently advanced development for hatching to occur before the end of summer (i.e., hatching 2 years after extrusion rather than the usual 1).

Only 6 of the 17 old-egged ovigerous females collected in St. Michael's Bay from 1986 to 1991 had less than half the yolk remaining in the eggs when examined. Four of these would likely have been ready for

hatching by sometime in September, around the time autumn cooling begins. The other, which had 0.3 yolk remaining and a PEI of 470 at the end of June, would probably have hatched by early August. This was the only specimen for which hatching as much as 4 or 5 weeks in advance of autumn cooling was a possibility. However, extensive plankton sampling (130 15-min tows with a 1 m diameter net) conducted near the sites where lobsters were released in St. Michael's Bay, from 28 July to 22 August 1986, and from 18 July to 30 August 1987, failed to produce lobster larvae.

Bottom temperature at 7 m in St. Michael's Bay during August ranged from around 9°C to 10.5°C. Assuming temperature in the surface layer was around 15°C, at which lobster larvae will reach Stage IV in 25 days (Templeman 1936), it is possible that larvae hatching in early August would be in Stage IV at the end of August and ready to settle by mid-September. Larvae hatching in late August would be exposed to temperatures below 10°C well in advance of reaching Stage IV. At 10°C, it takes 2 months from hatching to Stage IV; and at 5°C, larvae generally die without reaching Stage IV (Templeman 1936). Caddy's (1979) consideration of the influence of seasonal temperature regime on survival of lobster larvae indicates poor chances of survival if larvae have not reached Stage IV by the end of August. Any larvae hatching in St. Michael's Bay in late August–early September appear to have little chance of reaching Stage IV and settling in the area. The 1988–90 diver-collected samples involved 12 dives totaling about 30 diver hours searching at the Indian Arm and Goose I. sites. Not a single small lobster was found, suggesting there had been very little if any recruitment since lobsters were transplanted in 1982.

The possibility that the lobsters transplanted to St. Michael's Bay will become a self-sustaining population is remote. While the portion of females with ripe ovaries that actually extrude has increased substantially during this study, many of these lose all or most of their clutch of eggs before the following summer. Of those females that carry their eggs for at least a year, very few have eggs ready for hatching sufficiently early in the summer that any larvae are likely to settle in the area. Any local recruitment that might occur would be too little and too irregular to support a fishery for lobsters in St. Michael's Bay.

Citations

Aiken, D.E.

1973 Proecdysis, setal development, and molt prediction in the American lobster (*Homarus americanus*). J. Fish. Res. Board Can. 30:1337–1344.

Aiken, D.E., and S.L. Waddy

1976 Controlling growth and reproduction inthe American lobster. *In* Avaulk, J.W. Jr. (ed.), Proc., 7th Annu. meet. world maricult. soc., p. 415–430. Louisiana St. Univ. Press, Baton Rouge.

1980a Reproductive biology. *In* Cobb, J.S., and B.F. Phillips (eds.), The biology and management of lobsters, vol. 1, Physiology and behavior, p. 215–276. Academic Press, NY.

1980b Maturity and reproduction in the American lobster. *In* Anthony, V.C., and J.F. Caddy (eds.), Proc., Canada–U.S. workshop on status of assessment science for N.W. Atlantic lobster (*Homarus americanus*) stocks, p. 59–71. Can. Tech. Rep. Fish. Aquat. Sci. 932.

1982 Cement gland development, ovary maturation, and reproductive cycles in the American lobster, *Homarus americanus*. J. Crustacean Biol. 2:315–327.

1986 Environmental influence on recruitment of the American lobster, *Homarus americanus*: A perspective. Can. J. Fish. Aquat. Sci. 43:2258–2270.

1989 Interaction of temperature and photoperiod in the regulation of spawning by American lobsters, *Homarus americanus*. Can. J. Fish. Aquat. Sci. 46:145–148.

Caddy, J.F.

1979 The influence of variations in the seasonal temperature regime on survival of larval stages of the American lobster (*Homarus americanus*) in the southern Gulf of St. Lawrence. Rapp. P.-V. Reun. Cons. Int. Explor. Mer 175: 204–216.

Conan, G.Y.

1986 Summary of session 5: Recruitment enhancement. Can. J. Fish. Aquat. Sci. 43:2384–2388.

Cooper, R.A., and J.R. Uzmann

1980 Ecology of juvenile and adult *Homarus*. *In* Cobb, J.S., and B.F. Phillips (eds.), The biology and management of lobsters, vol. II, p. 97–142. Academic Press, NY.

Ennis, G.P.

1981 Fecundity of the American lobster, *Homarus americanus*, in Newfoundland waters. Fish. Bull., U.S. 79:796–800.

1984a Incidence of molting and spawning in the same season in female lobsters, *Homarus americanus*. Fish. Bull., U.S. 82:529–530.

1984b Comparison of physiological and functional size-maturity relationships in two Newfoundland populations of lobsters *Homarus americanus*. Fish. Bull., U.S. 82:244–249.

Perkins, H.C.

1972 Development rates at various temperatures of embryos of the northern lobster (*Homarus americanus* Milne-Edwards). Fish. Bull., U.S. 70:95–99.

Templeman, W.

1936 The influence of temperature, salinity, light and food conditions on the survival and growth of the larvae of the lobster (*Homarus americanus*). J. Biol. Board Can. 2:485–497.

1940 The life history of the lobster. Newfoundland Dep. Nat. Resour., Serv. Bull. (Fish.) 15, 42 p.

Abstract. – Cobia is a highly prized recreational species of worldwide distribution in tropical and subtropical seas, but the development, distribution, and ecology of its early life stages are poorly known. Eggs are spherical, average 1.24 mm in diameter, and have a single oil globule (mean diameter 0.45 mm). The perivitelline space is narrow and the embryo heavily pigmented. Eggs hatch in about 24 h at 29°C based on the relationship between egg diameter and water temperature to predict development time in other marine fishes. Larvae hatch at about 2.5 mm SL. Cobia spawn in both estuarine and shelf waters during the day, and eggs and larvae are usually collected in the upper meter of the water column. Larvae are recognized by the large supraorbital ridge with a single spine, laterally swollen pterotics, heavy body pigmentation, minute epithelial spicules covering the body integument, and a pair of moderate-to-large, simple spines on either side of the angle of the posterior preoperculum. Only 70 larvae <20 mm SL were collected and identified from the Gulf of Mexico between 1967 and 1988; most occurred between June and September at surface temperatures ≥25°C, salinities >27‰, and within the 100 m depth contour. Similar patterns of head spination provide evidence of a sister-group relationship between cobia and dolphinfish rather than that previously hypothesized between cobia and remoras.

Larval development, distribution, and ecology of cobia *Rachycentron canadum* (Family: Rachycentridae) in the northern Gulf of Mexico*

James G. Ditty
Richard F. Shaw

Coastal Fisheries Institute, Wetland Resources Building
Louisiana State University, Baton Rouge, Louisiana 70803-7503

Cobia, in the monotypic family Rachycentridae, is distributed worldwide in tropical and subtropical seas (Briggs 1960), except the eastern Pacific, and is found seasonally in temperate waters (Hassler and Rainville 1975). A highly prized recreational species, most of the U.S. landings are from Gulf of Mexico (Gulf) waters; they are also caught incidentally in commercial fisheries (Shaffer and Nakamura 1989). Recreational landings are not well documented, but cobia are reportedly not abundant and recruitment is considered low (Gulf of Mexico & S. Atl. Fish. Manage. Counc. 1985). Cobia are migratory and usually absent from commercial and recreational catches of the northern Gulf during late fall and winter at which time they are caught off the Florida Keys. They migrate north and west along the Gulf coast during the spring (Shaffer and Nakamura 1989) and reappear in northern Gulf waters during March and April (Springer and Pirson 1958). Cobia are usually caught in shallow coastal waters (Shaffer and Nakamura 1989), although they are often taken offshore along the Louisiana and Texas coasts in association with oil and gas platforms and rafts of *Sargassum* (RFS, pers. observ.).

Despite the recreational value of cobia, its ecology, distribution, and morphological development during early life stages are poorly known. Only 23 specimens <20 mm SL are reported in the historical literature for the Gulf (Dawson 1971, Finucane et al. 1978ab, Houde et al. 1979). Richards (1967) reviewed cobia general life history, Shaffer and Nakamura (1989) compiled biological data, and Hassler and Rainville (1975) developed techniques for hatching and rearing cobia. In addition, Johnson (1984) discussed the utility of cobia early life stages for examining previous phylogenetic hypotheses and the evolutionary interrelationships of echeneoids (Rachycentridae–Coryphaenidae–Echeneididae). Aspects of early egg development have been described (Ryder 1887, Joseph et al. 1964, Hassler and Rainville 1975) but not development of early larvae <12.6 mm SL. Most larval illustrations and photographs are of poor quality (Ryder 1887, Dawson 1971, Hassler and Rainville 1975, Finucane et al. 1978a, Johnson 1984). The objectives of this study are to describe cobia egg and larval development, to provide data on the seasonal occurrence, distribution, and ecology (i.e., relationship of larvae to water temperature, salinity, and station depth at time of capture) of early life stages of cobia in the Gulf, and to further examine the interrelationships of the echeneoids.

Manuscript accepted 16 July 1992.
Fishery Bulletin, U.S. 90:668–677 (1992).

*Contribution LSU-CFI-91-6 of the Coastal Fisheries Institute, Louisiana State University.

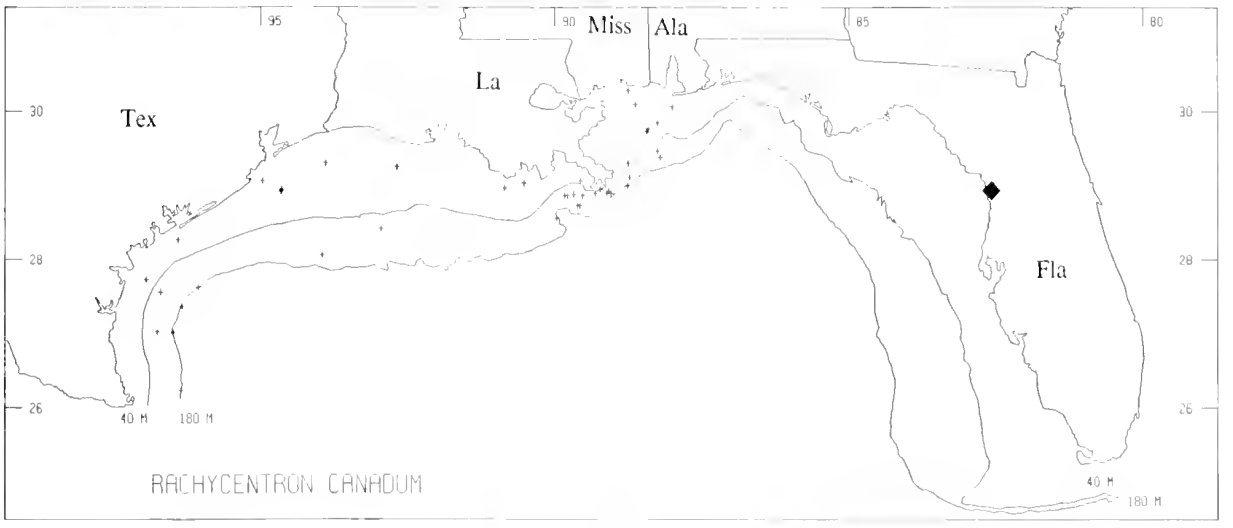

Figure 1

Distribution of larval cobia *Rachycentron canadum* in the northern Gulf of Mexico. Plus signs are positive catch stations; diamond is location of Crystal River estuary where cobia eggs and yolksac larvae were collected.

Methods

Eggs and larvae were obtained from museum collections along both the Gulf and Atlantic coasts. We examined 70 cobia eggs (all late-stage embryos) and 76 larvae 2.6–25 mm SL and determined their seasonal occurrence, distribution, and ecology. Hydrographic parameters were weighted by the total number of larvae caught at each station to derive mean and median values. All specimens were formalin-preserved except those from Southeast Area Monitoring and Assessment Program (SEAMAP) ichthyoplankton surveys of the Gulf which were in ethyl alcohol. We considered lat. 26°00′N as the southern boundary of our survey area (Fig. 1). Temperature and salinity data were from the surface only.

Body measurements were made to the nearest 0.1 mm with an ocular micrometer in a dissecting scope and follow Hubbs and Lagler (1958) and Richardson and Laroche (1979). All lengths refer to standard length (SL) unless otherwise noted. A compound scope was used to examine the origin and location of epithelial spicules. Representative specimens were illustrated with the aid of a camera lucida. Specimens were not cleared and stained because of the paucity of material. Fin rays were counted when their pterygiophores were visible; spines when they resembled formed structures (Richardson and Laroche 1979). Myomeres were difficult to count in fish >6 mm due to heavy larval pigmentation and opacity of the musculature, even under polarized light, but all specimens <6 mm had 24 myomeres. Cobia undergoing transition to the juvenile stage were those with a full complement of formed rays in all fins. Egg staging followed Moser and Ahlstrom (1985).

Egg and larval development

Cobia eggs were spherical and measured 1.15–1.3 mm ($\bar{x}$ 1.24, N 31), with a single oil globule 0.4–0.65 ($\bar{x}$ 0.45, N 13) in diameter. The oil globule was pigmented and lay near the vegetal pole opposite the developing embryo. The perivitelline space was narrow with the embryo occupying about 85% of egg volume (range 70–92%, N 13). The chorion was smooth and unornamented. Cobia eggs hatch in about 24 h at 29°C based on Pauly and Pullin's (1988) relationship between egg diameter and water temperature to predict development time in marine fishes.

The embryo of late-stage Gulf cobia eggs was heavily pigmented except for the caudal peduncle which was unpigmented. Late-stage embryos from north of Cape Hatteras, NC, had pigment lightly scattered over the peduncle. Early yolksac larvae (2.6–3.2 mm) were heavily pigmented externally and lacked a functional mouth, eye pigment, and all fins. A single oil globule with pigment was also present in the middle of the yolksac. External pigment occurred over the snout and in a band immediately behind the primordial eye. The eye remained unpigmented until larvae were 3.5–4.0 mm (Fig. 2). At higher magnification, tiny epithelial

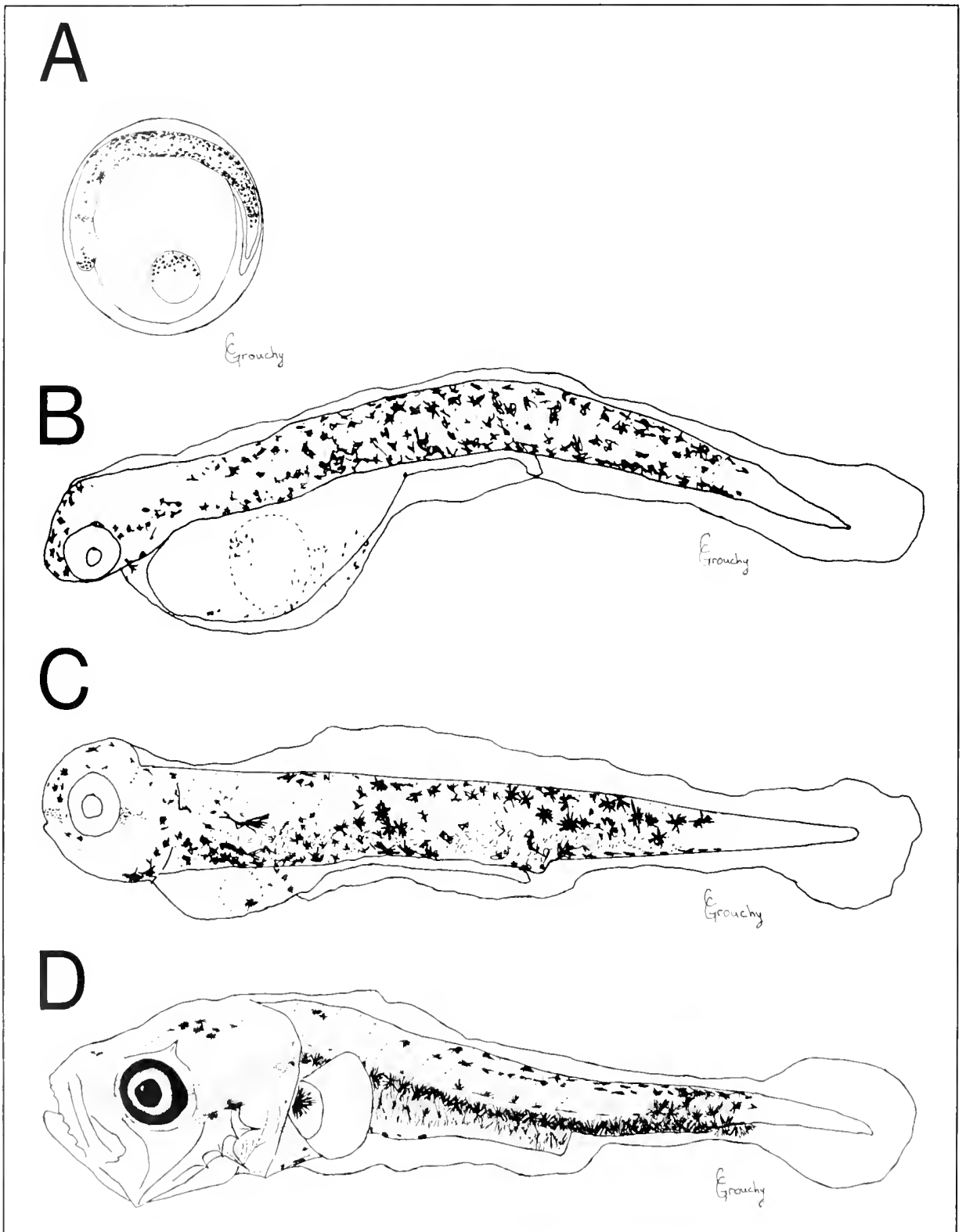

Figure 2

Eggs and larval development of cobia *Rachycentron canadum*. (A) Late-stage egg, diameter 1.24 mm; (B–C) yolksac larvae 2.6 and 3.0 mm SL; (D–H) larvae 4.5 mm, 6.8 mm, 10.0 mm, 14.1 mm, and 18.9 mm SL.

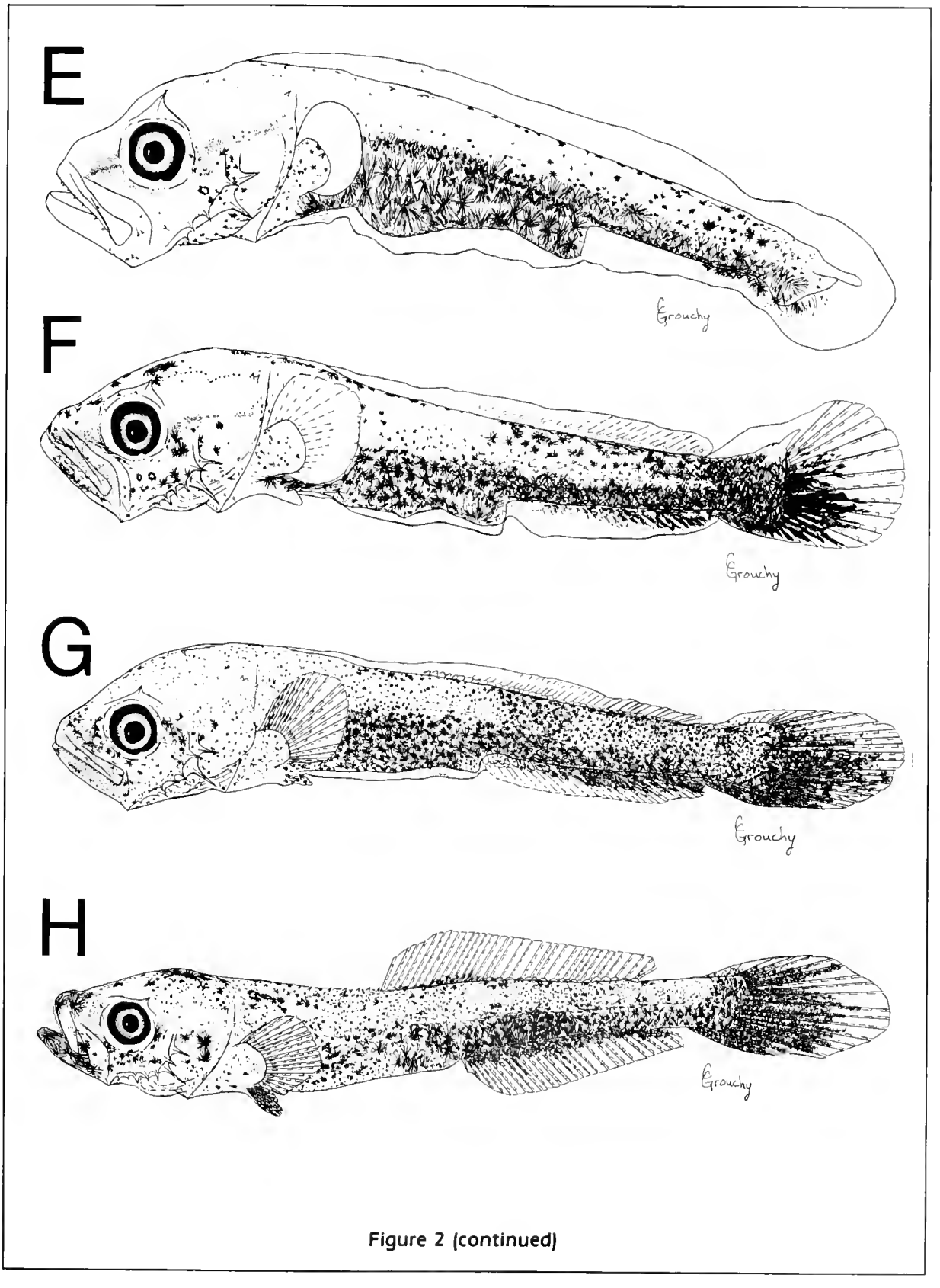

Figure 2 (continued)

Table 1

Body proportions of larval cobia *Rachycentron canadum* from the Gulf of Mexico, expressed as % standard length (SL).

SL	*N*	Preanal length	Head length	Snout length	Orbit diameter	Upper jaw length	Body depth cleithrum	Predorsal length	Prepelvic length	Peduncle length
2.6	1	61.5								
3.2	1	62.5								
4.0–4.9	2	64.4–65.0	27.8–31.2	6.7–7.5	10.0–11.2	10.0–13.8	18.9–21.2			
5.0–5.9	3	68.0–68.6	31.4–34.0	7.6–10.0	11.0–12.7	13.6	20.3–20.6		33.9	
6.0–6.9	3	63.2–67.2	27.9–31.7	7.3–8.3	8.8–10.8	10.3–12.7	19.8–23.3		30.9	
7.0–7.9	3	64.1–65.3	26.9–29.5	7.0–8.7	9.0–10.0	10.9–13.3	17.9–20.0	52.6	30.8–33.3	12.0–12.8
9.8	1	64.3	30.6	8.7	9.2	12.8	21.4	51.0	33.7	12.8
10.0–10.9	3	57.1–64.1	27.5–29.5	7.0–8.1	9.0–10.0	11.5–13.3	19.0–20.0	50.0–56.3	30.0–36.9	12.1–13.3
11.0–11.9	3	57.3–60.9	27.7–29.9	6.7–7.8	8.4–8.7	11.3–12.0	18.3–19.2	49.6–52.2	31.1–34.2	11.5–12.6
12.0–12.9	2	63.2–63.7	28.2–28.8	7.2–8.0	8.8–8.9	11.2–11.3	16.1–18.4	49.2–50.4	32.0–32.2	12.5–12.8
14.0–14.9	2	56.6–58.7	26.2–27.3	6.9–7.0	8.0–8.3	11.0–11.2	17.2–17.5	49.0–50.3	29.4–30.3	11.0–11.2
16.0–16.9	3	58.4–59.9	26.5–26.9	7.2–7.8	7.8–8.4	10.2–10.5	15.0–16.8	48.2–49.4	28.9–30.1	12.0–13.6
19.5	1	57.4	27.2	7.7	7.7	10.2	15.4	46.2	29.7	12.8
21.0	1	57.1	24.8	6.7	7.1	9.5	14.3	47.6	27.1	12.8
25.0	1	56.0	24.0	6.0	7.2	8.8	14.9	46.8	26.8	12.0

spicules were also visible over the entire body integument, except the pupil of the eye, by 4 mm.

Body measurements were made on 30 cobia larvae to examine developmental morphology (Table 1). Preanal length was 61.5–62.5% SL in yolksac larvae and increased slightly during preflexion, but decreased steadily thereafter. A single intestinal loop, visible through the body wall, gave the ventral visceral mass a bulbous appearance by 7 mm. Body depth was about 20% SL in larvae <10 mm but decreased to about 15% by 25 mm. Likewise, orbit diameter decreased from about 11–7% SL as larvae increased in length. Other body proportions were relatively stable until larvae were >10 mm. Thereafter, a slow but steady decline occurred in all proportions when compared with SL, except caudal peduncle length which remained constant (Table 1). The relationship between standard and total lengths (TL), as defined by regression analysis, was linear and highly correlated (SL = 0.73TL + 1.44; N 29, r^2 0.998) at all sizes.

The supraorbital ridge and two largest preopercular spines were visible by 4 mm, and the pterotics were laterally swollen. The two preopercular spines were located on either side of the angle of the posterior preopercle. Three smaller spines, the largest of which was inserted between the two posterior preopercular spines, were also present along the anterior preopercle. Spines were added along both the anterior and posterior preopercle until a total of 4 anterior and 4–5 posterior preopercular spines was reached by 14–15 mm. A single spine occurring along the supraorbital ridge of each frontal bone by 4.5 mm was directed posterolaterally by 6 mm. The supraorbital spine and swollen pterotics were best observed when viewed dorsally (see Hardy 1978 for illustration). A supracleithral spine also occurred about 10.5–11 mm, and two posttemporal spines (supratemporal of Dawson 1971) originating from a common base were visible by 12 mm. All head spination was simple and unserrated.

In early larvae, internal pigment on the roof of the mouth and ventral to the hindbrain and otic capsule formed a mediolateral stripe through the head. Externally, melanophores were scattered over the snout, fore- and midbrains, on the nape, and over the operculum. Pigment also occurred immediately anterior to the cleithral symphysis and along the isthmus. Both the tip of the quadrate bone and dentary remained unpigmented until 7–7.5 mm. Head pigmentation increased with length (Fig. 2). Minute epithelial spicules (Johnson 1984) covered the body by 4 mm, but were best observed on the head and larval finfold. Spicules were more easily observed on the integument as larvae increased in length.

Along the dorsal midline, a bilateral row of melanophores extended posteriorly from the nape to above the anus, behind which these rows coalesced to form a continuous band of postanal, dorsal pigment. By 4.5 mm, pigment occurred on the pectoral fin base, and larvae were sparsely pigmented dorsolaterally but heavily pigmented ventrolaterally. The caudal peduncle was unpigmented in early larvae, but pigment extended onto the peduncle by 5.5–6.5 mm and over the lower hypural bones by 7 mm. Pigment was also present on the posterior third of the anal finfold and proximally on the ventral caudal-fin rays by 7.5 mm. Body and anal- and caudal-fin ray pigment increased with length. Pigment occurred on the posterior dorsal-fin pteryio-

Table 2
Fin ray counts of larval cobia *Rachycentron canadum* from the Gulf of Mexico.

Size (mm SL)	*N*	Dorsal*	Anal	Pectoral	Pelvic
9.8	1	30	25	9	
10.0–10.9	3	27–30	22–25	12–13	
11.0–11.9	3	28–31	24–26	13–17	
12.0–12.9	2	30–33	24–26	14	
14.0–14.9	2	31	25	17	3
16.0–16.9	3	28–32	I,24–26	17–19	I,5
19.5	1	31	I,25	20	I,5
21.0	1	31	I,25	21	I,5
25.0	1	29	I,25	20	I,5

* Dorsal spines are virtually impossible to count on uncleared or unstained specimens.

phores by about 10.5mm. Fin pigmentation progressed anteriorly along the dorsal base and extended onto posterior dorsal rays by about 18–19mm. Pelvic rays were first pigmented at about 13mm, but pectoral fins remained unpigmented at all sizes examined (Fig. 2).

A 49mm juvenile had a jet black caudal fin except for the distal tips of the upper principal rays. Pelvic fins were completely black, but pigment was present basally on only the upper few rays of the pectoral fin. Pigment also covered all of the posterior rays of both the dorsal and anal fins. Fin pigment decreased anteriorly, however, such that only the basal portions of the anterior dorsal and anal rays were pigmented. All dorsal spines were visible and the integument was entirely jet black.

Fin development

A continuous median finfold extended posteriorly along the body from the nape to the cleithral symphysis of early larvae. About 5mm, a ventral thickening occurred near the tip of the unflexed notochord. Anlagen began to form obliquely downward in the caudal finfold during flexion (~6.5–8mm). As the hypural complex shifted to a terminal position, caudal ray development proceeded both dorsally and ventrally until the adult complement of 9+8 principal rays was present at 10.5–11mm. By 19.5mm, the caudal fin was distinctly spatulate and heavily pigmented. Dorsal- and anal-fin-base development coincided with notochord flexion. These fin bases began to differentiate centrally, and development proceeded both anteriorly and posteriorly with all pteryiophores countable by 10–11mm in both fins. Dorsal- and anal-ray anlagen, however, began to develop along the posterior fin base and proceeded anteriorly. Development of anal rays consistently preceeded that of dorsal rays. All anal fin elements were countable by 17mm. Dorsal spines were very difficult to count in specimens not cleared and stained because spines were short and often covered by integument. One partially cleared 16.7mm specimen had 7 poorly-formed, short dorsal spines, 11 precaudal and 14 caudal vertebrae (including urostyle), and 7 branchiostegal rays. Pelvic buds were visible by 6mm, with the full complement of elements (I,5) present by 16.5–17mm. Pectoral rays were first visible at about 10mm and the full complement (20–21 rays) was present by 19–20mm. A full complement of rays in all fins (around 20mm) marked the beginning of transition to the juvenile stage (Table 2).

Distribution and ecology

The only confirmed collection of both cobia eggs and yolksac larvae from the Gulf was from the Crystal River estuary, Florida, during July 1984. These specimens were collected from waters 28.1–29.7°C and 30.5–34.1‰, except for a single 3.2mm yolksac larva from a power plant discharge canal at 36.7°C and 25.2‰. All other eggs and early larvae were from stations along the outer perimeter of the study area at station depths of 3–6m. No eggs or larvae were collected at stations located over oyster reefs, in the salt marsh, or in tidal creeks. Gulfwide, larvae were first collected during late May, with most (98%) collected June–September. Cobia larvae also primarily (85%) occurred at 25–30°C ($\bar{x}$ 28.2°C, range 24.2–32.0°C), at >27‰ ($\bar{x}$ 30.8‰, range 18.9–37.7‰), and most (75%) at station depths <100m (median 50m, range 3.1–300m) (Fig. 3).

Discussion

Our data suggest that cobia eggs hatch in about 24h at 29°C. Ryder (1887) projected a 36h incubation time at an unspecified temperature. Based on Pauly and Pullin's (1988) predictive relationship to derive incubation time and a mean egg diameter of 1.24mm from this study, Ryder's cobia eggs were probably incubated at about 25°C. In cooler waters of the mid-Atlantic Bight and northward during the spring/early summer (i.e., ~20°C), projected incubation time increases to 56h. Cobia hatch at about 2.5mm based on collection of wild-caught early yolksac larvae (2.6–3.2mm) with unpigmented eyes and on the work of Hassler and Rainville (1975).

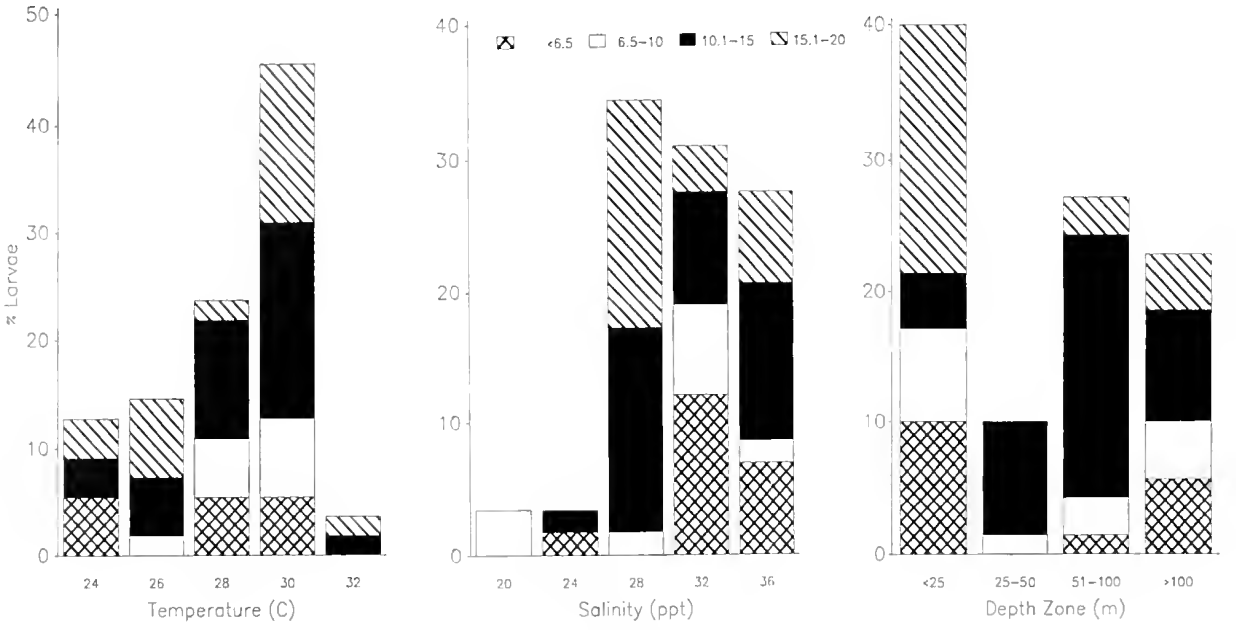

Figure 3

Distribution of cobia *Rachycentron canadum* larvae in the Gulf of Mexico with respect to hydrography. Larval stage/length class was assigned as follows: preflexion, <6.5 mm SL; flexion/early postflexion, 6.5–10.0 mm SL; late postflexion, 10.1–15.0 mm SL; and transition larvae, 15.1–20.0 mm SL.

Our data on egg and oil globule diameter agree with historical data (Ryder 1887, Joseph et al. 1964, Richards 1967, Hassler and Rainville 1975) except that our mean oil globule diameter (0.45 mm) is greater than that found for eggs from the Chesapeake Bay area (0.37 mm, Richards 1967; 0.38 mm, Joseph et al. 1964). Only two cobia eggs are previously illustrated, one in early- and the other in midstage development (Ryder 1887). The diameter of the early-stage egg, however, is considerably smaller than that of the midstage egg, and the specific identification of the early egg is unclear.

Cobia spawn during the day, since all embryos examined from the Gulf are at similar stages of development (i.e., late stage after Ahlstrom and Moser 1980) when collected during midmorning, except for one collection of late-stage eggs near midnight. Furthermore, daytime spawning cobia have been reported about 48 km southwest of Panama City, Florida (see Shaffer and Nakamura 1989 for details) in waters we estimate at 82–165 m deep. Our data also show that cobia larvae occur in both estuarine and shelf waters of the Gulf (Figs. 1,3), primarily during May–September. The only confirmed cobia eggs and yolksac larvae collected together in the Gulf are from the Crystal River estuary at station depths of 3–6 m. Early larvae (≤6.8 mm) are also collected at stations within the 65–134 m isobath range off Texas during September (Finucane et al. 1978b). The location of these collections suggests that some spawning also occurs on the shelf 50–90 km from the coast. Offshore waters beyond the edge of the continental shelf are relatively well sampled during May (SEAMAP 1983–87) when histological analyses indicated adult cobia are ripe (Thompson et al. 1991), but no cobia larvae were identified. Seven cobia larvae (all >9.5 mm) were identified from beyond the 180 m depth contour during this study and all were collected off the Mississippi River delta. Distribution of larvae centered around the Mississippi River delta, however, may reflect the intensity of neuston net sampling in this area rather than actual distribution of spawning adults. Only two larvae were collected off Florida during a comprehensive multiyear survey of eastern Gulf waters >10 m, both during August (Houde et al. 1979).

Seasonal occurrence and ecological data from along the Atlantic coast of the United States support our findings from the Gulf. Cobia eggs occur primarily between May and August at surface water temperatures >20°C (Joseph et al. 1964, Hassler and Rainville 1975, Eldridge et al. 1977; W.F. Hettler and L. Settle, NMFS Southeast Fish. Sci. Cent., Beaufort NC, pers. commun.; P. Berrien, NMFS Northeast Fish. Sci. Cent., Sandy Hook NJ, pers. commun.; D. Hammond, S.C. Dep. Wildl. Mar. Resour., Charleston SC, pers. commun.). Eggs are collected in lower Chesapeake Bay (Joseph et al. 1964), inlets to North Carolina estuaries

(W.F. Hettler and L. Settle, pers. commun.), in coastal waters 20–49 m deep (App. Table 1), and both near the edge of the Florida Current and in the Gulf Stream (Hassler and Rainville 1975, Eldridge et al. 1977). Off North Carolina, cobia eggs are usually collected on flood tides but few larvae are found in tidal inlets (W.F. Hettler and L. Settle, pers. commun.). Cobia eggs and larvae are usually collected in the upper meter of water with surface-towed nets (Joseph et al. 1964, Hassler and Rainville 1975 [implied], Eldridge et al. 1977; W.F. Hettler, pers. commun.). Neither cobia study off the Atlantic coast of the United States (Joseph et al. 1964, Hassler and Rainville 1975) provides environmental data, but eggs are successfully hatched at 19–35‰ (Hassler and Rainville 1975).

Similarities in larval morphology provide evidence of a sister-group relationship between cobia and dolphinfishes (Coryphaenidae) rather than that previously hypothesized between cobia and remoras (Echeneididae) (Johnson 1984). Larvae of both cobia and the dolphinfishes share similar patterns of head spination: laterally swollen pterotics; a single, simple spine on the supraorbital ridge of each frontal bone (except in pompano dolphin *C. equiselis*, which may have multiple spines along the ridge; JGD, pers. observ.); a small posttemporal spine; and several spines along the anterior and posterior preopercule, including an enlarged spine on either side of the angle. However, cobia have a small supracleithral spine (Dawson 1971, this study) that dolphinfishes lack. Remoras completely lack head spines. Both cobia and the dolphinfishes have epithelial spicules, a specialization unique to larvae of these species (Johnson 1984). We found spicules visible on the integument of both cobia and the dolphinfishes by 4 mm (JGD, pers. observ.) and they cover the entire body surface, except the pupil of the eye. Spicule composition and function, however, are unknown (Johnson 1984). Larval cobia are further separated from superficially similar remoras by the presence of large hook-like teeth on the dentary in remoras. Cobia lack these teeth. Larval cobia differ from the dolphinfishes by the lack of dorsal and anal spines and a higher vertebral count in the dolphinfishes (25 in cobia vs. 30–34 in dolphinfishes). Dolphinfishes also usually have 50+ soft dorsal rays, whereas cobia have 27–33.

Acknowledgments

This study was supported by the Marine Fisheries Initiative (MARFIN) Program (contract nos. NA90AA-H-MF111 and NA90AA-H-MF727). Thanks to those who loaned us specimens or provided data: Karen Burns, Mote Marine Lab, Sarasota FL; John Caruso, Tulane University Museum, New Orleans LA; L. Alan Collins and Churchill Grimes, NMFS Southeast Fisheries Science Center, Panama City FL; Wayne Forman and Leroy Kennair, Freeport-McMoRan, New Orleans LA; Bruce Comyns and Stuart Poss, Gulf Coast Research Lab, Ocean Springs MS; Peter Berrien, NMFS Northeast Fisheries Science Center, Sandy Hook NJ; Bill Hettler and Larry Settle, NMFS Southeast Fisheries Science Center, Beaufort NC; and Karsten Hartel, Museum of Comparative Zoology at Harvard. Thanks also to the Southeast Area Monitoring and Assessment Program (SEAMAP) and the Gulf States Marine Fisheries Commission for providing specimens and environmental data; to the Marine Resources, Monitoring, Assessment and Prediction (MARMAP) program for providing eggs collected during ichthyoplankton surveys; to Cathy Grouchy for illustrating the egg and larvae; and to Joe Cope for computer assistance.

Citations

Ahlstrom, E.H., and H.G. Moser
1980 Characters useful in identification of pelagic marine fish eggs. Calif. Coop. Oceanic Fish. Invest. Rep. 21:121–131.

Briggs, J.C.
1960 Fishes of worldwide (circumtropical) distribution. Copeia 1960(3):171–180.

Dawson, C.E.
1971 Occurrence and description of prejuvenile and early juvenile Gulf of Mexico cobia, *Rachycentron canadum*. Copeia 1971(1):65–71.

Eldridge, P.J., F.H. Berry, and M.C. Miller III
1977 Test results of the Boothbay neuston net related to net length, diurnal period, and other variables. S.C. Mar. Resour. Cent. Tech. Rep. 18, 22 p.

Finucane, J.H., L.A. Collins, and L.E. Barger
1978a Determine the effects of discharges on seasonal abundance, distribution, and composition of ichthyoplankton in the oil field. *In* Jackson, W.B. (ed.), Environmental assessment of an active oil field in the northwestern Gulf of Mexico, 1977–1978. NOAA Rep. to EPA (EPA-IGA-D5-E693-EO), NMFS Southeast Fish. Sci. Cent., Galveston, 299 p.

Finucane, J.H., L.A. Collins, L.E. Barger, and J.D. McEachran
1978b Ichthyoplankton/mackerel eggs and larvae. Environmental studies of the south Texas outer continental shelf, 1977. Final Rep. to Bur. Land Manage. by NMFS Southeast Fish. Sci. Cent., Galveston, 504 p.

Gulf of Mexico & South Atlantic Fishery Management Councils
1985 Final Amendment 1, fishery management plan and environmental impact statement for coastal pelagic resources (mackerels) in the Gulf of Mexico and south Atlantic region. Gulf Mex. Fish. Manage. Counc., Tampa, FL.

Hardy, J.D. Jr.
1978 Development of fishes of the mid-Atlantic Bight, an atlas of egg, larval, and juvenile stages. Vol. III. Aphredoderidae through Rachycentridae. U.S. Fish. Wildl. Serv., Biol. Serv. Prog. FWS/OBS-78/12, 394 p.

Hassler, W.W., and R.P. Rainville
1975 Techniques for hatching and rearing cobia, *Rachycentron canadum*, through larval and juvenile stages. Univ. N.C. Sea Grant Coll. Prog., UNC-SG-75-30, Raleigh, 26 p.

Houde, E.D., J.C. Leak, C.E. Dowd, S.A. Berkeley, and W.J. Richards
1979 Ichthyoplankton abundance and diversity in the eastern Gulf of Mexico. Univ. Miami Rep., BLM Contract AA550-CT7-28, Miami, 546 p.

Hubbs, C.L., and K.F. Lagler
1958 The fishes of the Great Lakes region. Univ. Mich. Press, Ann Arbor, 213 p.

Johnson, G.D.
1984 Percoidei: Development and relationships. *In* Moser, H.G., et al. (eds.), Ontogeny and systematics of fishes, p. 464-498. Spec. Publ. 1, Am. Soc. Ichthyol. Herpetol., Allen Press, Lawrence, KS.

Joseph, E.B., J.J. Norcross, and W.H. Massmann
1964 Spawning of the cobia, *Rachycentron canadum*, in the Chesapeake Bay area, with observations of juvenile specimens. Chesapeake Sci. 5:67-71.

Moser, H.G., and E.H. Ahlstrom
1985 Staging anchovy eggs. *In* Lasker, R. (ed.), An egg production method for estimating spawning biomass of pelagic fish: Application to the northern anchovy, *Engraulis mordax*, p. 37-41. NOAA Tech. Rep. NMFS 36.

Pauly, D., and R.S.V. Pullin
1988 Hatching time in spherical, pelagic, marine fish eggs in response to temperature and egg size. Environ. Biol. Fish. 22(4):261-271.

Richards, C.E.
1967 Age, growth, and fecundity of the cobia, *Rachycentron canadum*, from Chesapeake Bay and adjacent mid-Atlantic waters. Trans. Am. Fish. Soc. 96(3):343-350.

Richardson, S.L., and W.A. Laroche
1979 Development and occurrence of larvae and juveniles of the rockfishes *Sebastes crameri*, *Sebastes pinniger*, and *Sebastes helvomaculatus* (Family Scorpaenidae) off Oregon. Fish. Bull., U.S. 77:1-46.

Ryder, J.A.
1887 On the development of osseous fishes, including marine and freshwater forms. Rep. U.S. Fish. Comm., Pt. 13, 1885 (1887):489-604.

SEAMAP (Southeast Area Monitoring and Assessment Program)
1983-87 Plankton data for 1982-1986. Fisheries-independent survey data/National Marine Fisheries Service, Southeast Fisheries Center. Produced by Gulf States Mar. Fish. Comm., Ocean Springs, MS (ASCII file).

Shaffer, R.V., and E.L. Nakamura
1989 Synopsis of biological data on the cobia *Rachycentron canadum* (Pisces: Rachycentridae). NOAA Tech. Rep. NMFS 82 [FAO Fish. Synop. 153], 21 p.

Springer, V.G., and J. Pirson
1958 Fluctuations in the relative abundance of sport fishes as indicated by the catch at Port Aransas, Texas 1952-1956. Publ. Inst. Mar. Sci., Univ. Tex. 5:169-185.

Thompson, B.A., C.A. Wilson, J.H. Render, and M. Beasley
1991 Age, growth, and reproductive biology of greater amberjack and cobia from Louisiana waters. Year 1. Rep. to U.S. Dep. Commer., NOAA, NMFS, Coop. Agreement NA90AA-H-MF089, under Mar. Fish. Initiative (MARFIN) Prog., Coastal Fish. Inst., Louisiana St. Univ., Baton Rouge, 55 p.

Appendix Table 1

Station location, collection, and environmental data for cobia *Rachycentron canadum* eggs and larvae. All specimens from the Gulf of Mexico, except those loaned by the MCZ at Harvard and eggs from the NMFS Southeast Fisheries Science Center, Beaufort NC. Water temperature and salinity values were at the surface. NA = data not available.

Station	Date	Lat.	Long.	Stn. depth (m)	Temp. (°C)	Salinity ‰	Gear	*N*	Size (mm SL)	Eggs
4353[1]	6-05-67	30°13	88°47	11	25.9	28.9	7	2	16.6-18.2	
4357	6-05-67	30°02	88°40	18	26.4	29.4	7	1	17.0	
4355	6-10-68	29°24	88°17	55	32.0	36.6	7	2	12.6-15.3	
4356	6-12-67	29°19	88°14	73	30.3	27.8	7	3	13.6-14.2	
4354	6-18-68	29°42	88°27	37	29.4	37.7	7	1	12.9	
00807[1]	6-23-71	29°40	88°28	20	NA	NA	8	1	17.0	
01613	May/Jun 67	27°40	96°59	20	NA	NA	8	1	7.8	
01614	May/Jun 76	28°12	96°27	22	NA	NA	8	1	16.7	
01687	May/Jun 76	27°30	96°45	45	NA	NA	8	3	9.8-12.5	
EPA IV-A[2]	7-13-77	28°51	94°42	17	24.8	33.0	9	2	6.0-12.4	
EPA V-A	7-13-77	28°52	94°41	17	24.8	33.5	9	1	16.6	
EPA V-B	7-13-77	28°51	94°42	17	24.7	33.0	9	1	16.6	
EPA V-D	7-13-77	28°51	94°42	17	24.5	32.8	9	1	13.0	
EPA II-B	7-14-77	28°53	94°41	17	25.5	34.0	9	1	19.5	
BLM II-3[2]	7-06-77	27°18	96°23	131	>25	36.0	10	1	3.8	
BLM III	9-07-75	26°57	96°32	106	<25	36.0	11	1	5.9	
BLM IV-3	9-07-77	26°10	96°24	91	>25	36.0	10	1	12.4	
BLM III-2	9-08-77	26°58	96°48	65	>25	36.0	10	1	6.8	
BLM I-3	9-10-77	27°37	96°06	134	24.2	36.2	10	2	5.0-5.1	

Appendix Table 1 (continued)

Station	Date	Lat.	Long.	Stn. depth (m)	Temp. (°C)	Salinity ‰	Gear	*N*	Size (mm SL)	Eggs
9114 A-2[3]	7-18-84	28°56	82°35	4.6	29.6	31.5	12	1	6.8	14
9121 C-1	7-18-84	28°56	82°35	4.0	36.7	25.2	12	1	3.2	
9179 H-3	7-18-84	28°56	82°35	5.8	29.7	32.6	12	1	7.5	16
9008 H-4	7-18-84	28°56	82°35	6.1	29.7	32.6	12	1	3.1	
9266 I-1	7-18-84	28°56	82°35	6.0	29.4	31.3	12	1	2.6	6
9545 I-2	7-31-84	28°56	82°35	3.7	28.1	30.5	12	2	2.6-4.0	20
9086 I-2	7-18-84	28°56	82°35	4.1	29.6	34.1	12	—	—	4
9584 K-2	7-31-84	28°56	82°35	3.1	28.2	32.2	12	1	4.5	
3088[4]	6-14-84	28°58	90°33	13	28.0	18.9	13	2	6.7-7.8	
5370	6-18-86	28°54	90°53	7	29.7	27.9	10	1	10.5	
426	6-18-82	29°11	92°43	19	29.5	27.6	13	3	16.0-19.5	
432	6-23-82	29°14	93°56	15	NA	30.2	13	1	22.3	
573	6-16-82	28°30	90°00	100	29.4	33.3	10	1	5.0	
1644	6-07-83	30°00	88°02	26	25.0	NA	13	1	12.5	
1647	6-08-83	29°47	88°17	33	25.0	24.0	13	1	12.0	
3166	6-24-84	29°00	95°00	15	30.5	27.2	13	3	16.0-21.0	
3220	7-13-84	28°21	93°00	53	30.3	29.3	13	1	25.0	
4484	9-17-85	29°00	89°36	27	27.3	27.3	13	1	10.3	
94374[5]	6-01-85	34°54	75°40	33	NA	NA	NA	1	6.0	
94505	8-21-68	38°07	70°03	NA	NA	NA	NA	4	10.0-14.5	
AL8507-142[6]	7-28-85	36°50	75°27	21	25.0	31.9	14	—	—	2
AL8507-143	7-28-85	37°06	75°11	36	25.0	32.7	14	—	—	1
DL8604-83	6-21-86	38°38	74°48	20	20.2	31.9	14	—	—	1
DL8604-152	6-25-86	36°47	75°14	26	22.4	32.4	14	—	—	1
EK8006-1	7-16-80	35°41	74°58	49	25.2	36.0	14	—	—	1
EK8006-2	7-16-80	35°16	75°14	24	26.6	35.7	14	—	—	8
P-1[2]	9-12-86	28°48	89°52	82	29.8	27.0	13	1	10.1	
P-5	9-13-86	28°40	89°39	96	28.4	33.0	13	1	11.8	
P-17	9-25-86	28°53	89°16	63	28.6	33.0	13	1	11.0	
P-23	9-25-86	28°50	89°05	195	29.4	34.0	13	4	10.2-18.5	
P-31	9-26-86	28°56	88°48	300	28.6	34.0	13	2	10.7-12.3	
4[2]	5-27-88	29°14	88°47	63	25.1	31.7	13	1	9.5	
31	5-29-88	28°48	89°34	78	25.2	30.3	13	1	12.2	
12	8-26-88	28°40	89°37	101	29.0	NA	13	2	10.0-14.0	
24	8-26-88	28°49	89°43	70	28.8	26.8	13	2	14.0-19.0	
39	8-27-88	28°50	89°21	72	30.1	29.5	13	1	13.0	
44	8-27-88	28°52	89°07	111	29.6	28.0	13	3	10.0-24.5	
45	8-28-88	28°50	89°09	203	29.6	30.5	13	1	9.5	
60	8-27-88	29°03	88°46	157	29.5	29.5	13	1	15.0	

Stations:
[1]Gulf Coast Research Lab, Ocean Springs MS
[2]NMFS, Panama City Lab
[3]Mote Marine Lab, Sarasota FL
[4]SEAMAP 1982-1986
[5]Museum of Comparative Zoology, Harvard
[6]NMFS, Sandy Hook Lab, NJ

Gear:
[7]1 m, surface tow
[8]Neuston net (size unknown)
[9]0.5×1.0 m neuston net, 0.505 mm mesh
[10]60 cm bongo, 0.333 mm mesh, oblique tow
[11]1 m, 0.250 mm mesh, oblique tow
[12]1 m, stepped-oblique tow, 0.505 mm mesh
[13]1×2 m neuston net, 0.948 mm mesh
[14]60 cm bongo, 0.505 mm mesh, oblique tow

Abstract. – The basis for the curious association between yellowfin tuna *Thunnus albacares* and spotted dolphin *Stenella attenuata* in the eastern tropical Pacific Ocean has never been explained. Consideration of the bioenergetics of the associated tuna and dolphins suggests that the association may be based on the combined effects of a shallow thermocline, overlapping size (length) ranges of associated yellowfin and young dolphins, congruent diets, hydrodynamic constraints on swimming speeds of dolphin schools, and social (caregiving) behavior of dolphins. Insights developed during construction and exercise of comparative bioenergetics models for the tuna and dolphin suggest that tunas are more likely to follow dolphins than dolphins to follow tunas, and that the strength of the association in a given area may be related to oceanographic conditions affecting prey distribution and abundance.

Energetics of associated tunas and dolphins in the eastern tropical Pacific Ocean: A basis for the bond

Elizabeth F. Edwards

Southwest Fisheries Science Center, National Marine Fisheries Service, NOAA
P.O. Box 271, La Jolla, California 92038

In the eastern tropical Pacific Ocean, yellowfin tuna *Thunnus albacares* and spotted dolphin *Stenella attenuata* form an association strong enough that the fish can be captured by capturing the associated dolphins (e.g., Orbach 1977). The dolphins, easier to locate than the tuna, form the sighting cue for locating tuna schools. Despite chases lasting on average about half an hour (and occasionally as long as 2–3 hours) the fish tend to remain with the dolphins throughout. Eventually the dolphins tire and can be encircled, along with the associated tunas, with a purse-seine net.

Although the subject of substantial conjecture (e.g., Perrin 1969, Orbach 1977, Au and Pitman 1986, Au 1991), no definitive explanation exists for the association, perhaps in part because conjectures to date have been qualitative rather than explicitly quantitative. Quantifying the advantages or disadvantages of the association in terms of the energetics of its component groups holds promise for helping understand the bond, because such quantification can more readily expose conceptual errors, lead to unexpected insights, and form the basis for testable hypotheses. Expressing relationships in terms of energy flow (e.g., cost of finding food, cost of reproduction, feeding requirements, etc.) has often proved a useful format for developing understanding of biological phenomena. Following this precedent, I present here bioenergetics models for both tunas and dolphins in a "typical" association in the eastern tropical Pacific Ocean. I use these models to estimate feeding rates of tuna and dolphins, and discuss implications concerning the ecological advantage to tuna (or dolphins) when associated with dolphins (or tuna).

Estimates of forage requirements predict that tuna and dolphins should experience severe competition under some circumstances of prey distribution and abundance, but perhaps not under others. Observations of overlaps in sizes between associated tuna and dolphins and of morphological similarities between the animals have implications for the importance of swimming energetics to the association.

These estimated forage requirements and considerations about swimming energetics are discussed in terms of their implications for determining which component (tuna or dolphins) controls the association, how the competition might be mitigated, when the association might be more likely to occur, and how these factors might be used to locate large yellowfin tuna unassociated with dolphins. The last point is important in relation to current interest in eliminating the practice of "dolphin-fishing" in the eastern tropical Pacific Ocean. "Dolphin-fishing" involves location and capture of tuna schools by locating and capturing associated dolphin schools; as air-breathers, the dolphins are more easily sighted than the tuna due to the dolphin's surface activity. Other explanations for the bond, and poten-

Manuscript accepted 29 July 1992.
Fishery Bulletin, U.S. 90:678–690 (1992).

tial conflicting evidence, are discussed briefly as they relate to the energetics models and results presented here.

Methods: Model development and description

The tuna-dolphin association

The tuna-dolphin association occurs in the eastern tropical Pacific Ocean (ETP) in a triangular region roughly the size of the continental United States (~10 million km^2), extending along the western coast of the Americas from the tip of Baja California (~20°N) south to Peru (~20°S) and seaward to ~140°W (Fig. 1). Total productivity in this area tends to be low relative to all other oceans, but high relative to other tropical oceans. Ocean currents and winds generate a typical pelagic environment in which areas of high productivity are distributed in dynamic, nonrandom, complex patterns (Fiedler et al. 1990, Fiedler 1992).

The ETP is characterized by an exceptionally shallow surface mixed layer. In contrast to other areas of the equatorial Pacific where the thermocline is generally 150–200 m deep (Kessler 1990), the depth of the thermocline layer throughout much of the ETP extends only 50–100 m below the surface (Fig. 1). Water temperatures in this wind-mixed layer are quite warm (25–30°C) and oxygen concentrations are high (Wyrtki 1966 and 1967, Fiedler et al. 1990, Fiedler 1992). Below this layer, water temperatures fall relatively rapidly (from ~27 to ~15°C) through the thermocline (usually 5–25 m vertical extent), stabilizing again below the thermocline (Fiedler et al. 1990). Oxygen concentrations also decrease relatively rapidly through the thermocline, increasing again in cold water at greater depths.

Strong dependence on warm water and on high concentrations of oxygen apparently force both tuna and dolphins into this unusually shallow mixed layer. Tuna must swim more or less constantly both to provide an adequate flow of sufficiently-oxygenated water over their gills and to locate adequate food supplies (e.g., Magnuson 1978, Olson and Boggs 1986). Yellowfin tuna would likely have difficulty maintaining an adequate energy balance swimming in the colder waters below the mixed layer, nor can they afford being caught for long in the oxygen minima characteristic of the thermocline.

Dolphins are constrained to reside near the ocean surface in order to breathe. Only temporary excursions below the mixed layer are tolerable, both because of this requirement for gaseous oxygen and because the blubber layer of the tropical dolphins involved in the tuna-dolphin association is too thin to maintain thermoneutrality in waters much colder than that in the mixed layer (unpubl. estimates). This is not necessarily a disadvantage, as the major prey for associated tuna and dolphins (small fish and squid; Perrin et al. 1973) also tend to concentrate in this upper mixed layer, at least periodically throughout a 24-hour day.

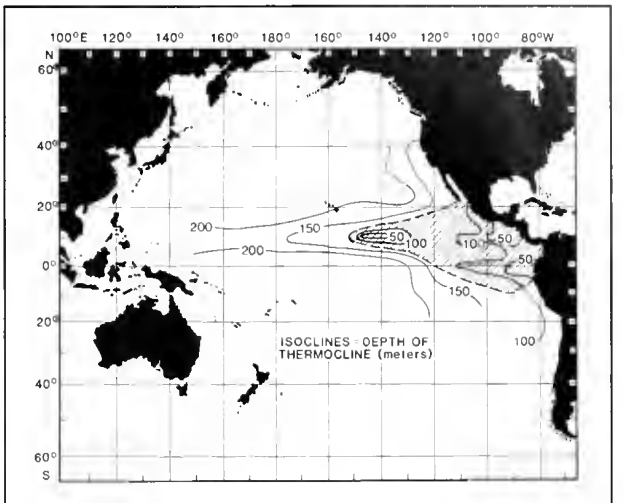

Figure 1

Depth of mixed layer in the area of the eastern tropical Pacific Ocean characterized by associations between yellowfin tuna *Thunnus albacares* and spotted dolphins *Stenella attenuata*. Tuna-dolphin fishery occurs roughly in area delimited by the 300 m isocline.

Although any individual tuna-dolphin association is doubtless dynamic in the details of its spatial configurations and component individuals, the association in general can be envisioned as a loose aggregation of animals characterized by dolphins swimming relatively near the ocean surface, separated vertically from the tuna swimming below by only a few meters (Fig. 2).

Although several species of dolphins and two species of tuna have been found to associate in the ETP, one species of dolphin (spotted dolphin *Stenella attenuata*) and one species of tuna (yellowfin *Thunnus albacares*) comprise the majority (>80%) of the associations (e.g., Orbach 1977, IATTC 1989). The remainder of this paper assumes the "tuna-dolphin association" includes only these two groups.

Energetics models

Both models followed the same format, using the standard bioenergetics approach of balancing food requirements against estimated energy costs for metabolism and energy savings as growth in biomass (University of Wisconsin Sea Grant 1989). The Wisconsin bioenergetics model derives estimates of consumption by

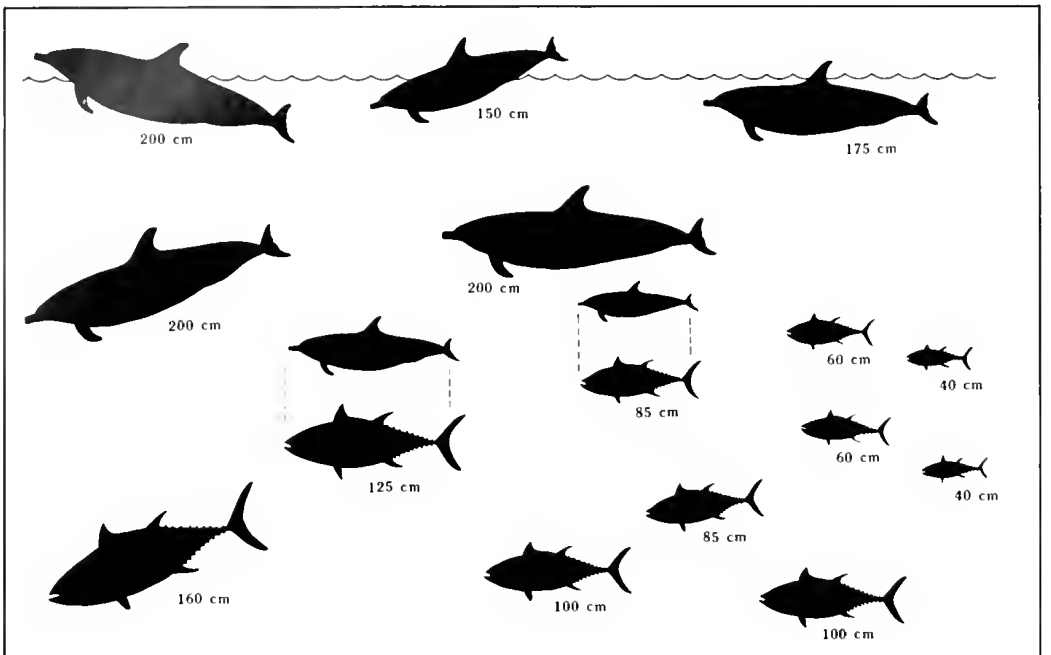

Figure 2
Idealized representation of a typical association of yellowfin tuna *Thunnus albacares* and spotted dolphins *Stenella attenuata*. Sizes and size-frequencies of tuna and dolphins are representative. Overlap in sizes between age-III yellowfin and neonate–1st yr dolphins (85–125 cm TL) is emphasized.

iteratively fitting an energetics equation for growth in body weight over time, to observed growth-rate curves derived from field samples of the organism in question. When the model growth curve simulates well the observed growth curve, the other fluxes estimated by the model are presumed to be reasonably accurate.

Specific rates (calories of flux · calories of animal^{-1} · day^{-1}) of energy flux were estimated based on data derived from various sources for individual tunas and dolphins as a function of size. Rates of energy flux for schools of dolphins and tuna were estimated as the sum of weight-specific estimates for individuals in each group.

Costs of reproduction were ignored for both yellowfin and spotted dolphins; in the yellowfin model because the model focuses on the sizes of yellowfin associated with dolphins, which tend to be relatively immature fish. Spawning activity in yellowfin does not occur in fish much smaller than 80 cm, and increases slowly to the maximum activity in fish larger than ~150 cm (Joseph 1963). Energy costs of reproduction for spotted dolphins were omitted because the fraction of pregnant, lactating, or pregnant and lactating females in a typical school at any time is relatively small (~25%; see School composition).

Some of the energetics parameters reported here for spotted dolphins are based on morphological measurements from 4 dolphin specimens from the ETP; 3 spotted dolphins measuring 81–189 cm total length (TL), plus 1 spinner dolphin *Stenella longirostris* 114 cm in length. The 81 cm individual was a very late-term fetus carried by the 189 cm animal. Although this sample is very small, all morphological measurements from these 4 animals fall well within the bounds of size-related regressions of morphological characteristics derived subsequently for a sample of 34 spotted dolphins measuring 74–215 cm TL (tip of rostrum to fluke notch) (unpubl. data).

School composition The yellowfin model addresses only those sizes of yellowfin found associated with dolphins (relatively large age-II and age-III fish, 55–125 cm TL; Fig. 3). Based on catch records from the fishery, an "average" association was assumed to include 500 yellowfin with an age composition of 65% age-II and 35% age-III fish per school (Ashley Mullin, IATTC, c/o Scripps Inst. Oceanogr., La Jolla; unpubl. data from commercial fishery).

Dolphin school composition was assumed to reflect the apparent age distribution of the spotted dolphin population, which in turn was assumed to appear as the length (age) distribution of dolphins collected during purse-seining operations in the ETP (Smith 1979, Barlow and Hohn 1984; A. Hohn, NMFS Southwest

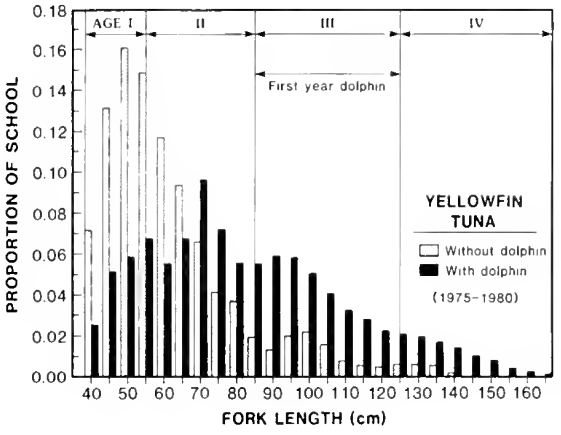

Figure 3

Sizes and ages of yellowfin tuna *Thunnus albacares* caught with and without dolphins in the eastern tropical Pacific Ocean, and length-interval during the first year of life by spotted dolphins *Stenella attenuata*. Data include all years 1975–84, all areas fished, all fleets (U.S. plus non-U.S.). (Unpubl. data from Ashley Mullin, IATTC, La Jolla).

Fish. Sci. Cent., La Jolla, unpubl. data). Proportions of nursing calves (ages 0–2 yr), adolescents (ages 3–14 yr), sexually adult males (ages 15 and up), and sexually adult females (ages 11 and up) in an average school were 0.05, 0.40, 0.25, and 0.30, respectively. Proportions of adult females not pregnant or lactating, lactating, pregnant, and pregnant and lactating animals were 0.05, 0.15, 0.08, and 0.02, respectively.

Weight-length conversions The tuna model used, as the calibration growth curve, the Gompertz fit derived by Wild (1986) for yellowfin tuna from the ETP. When necessary, body fork lengths in centimeters (cm FL) were converted to wet weights in grams (WW_g) using the length-weight relationship (Alex Wild, IATTC, La Jolla, unpubl. data for yellowfin tuna from the ETP)

$$FL = e^{((\ln(WW_g/1000)+11.184)/3.08612)},$$

The calibration growth curve for expected size-at-age in spotted dolphins was derived from equations and figures in Hohn and Hammond (1985) and unpublished data (A. Hohn, Southwest Fish. Sci. Cent., La Jolla). Weight-length conversions assumed the relationship

$$WW_{kg} = 1.4 * 10^{-5} * TL^{2.95},$$

where WW_{kg} is wet weight in kilograms, and TL is total length (tip of rostrum to fluke notch) in centimeters, based on weight-length measurements from a sample of 50 spotted dolphins ranging in size from 82 to 210 cm TL.

Equations Each model included equations for specific rates of consumption (C_{sp}), respiration (R_{sp}; including both swimming activity ACT_{sp}, and standard metabolism STD_{sp}), heat of digestion (specific dynamic action, SDA_{sp}), and waste losses (excretion plus egestion; WL_{sp}). Specific rate of growth is estimated simply as the difference between consumption and the sum of energy expenditures.

The form of the equation for each specific rate was the same for both models, with the exception of R_{sp}, which was estimated for yellowfin using Boggs' (1984) experimental results. R_{sp} was estimated for dolphins following Magnuson's (1978) procedure for estimating cost of swimming by carangiforms.

No effect of water temperature on consumption or respiration rates appears in either model. Ambient water temperature was assumed to be constant at 27°C, as most of the tuna-dolphin habitat occurs in waters of this temperature.

Consumption Specific rate of consumption (C_{sp}; calories food consumed · calories of animal^{-1} · day^{-1}) was estimated as

$$C_{sp} = CONS_{cal}/CAL_{an}$$

CAL_{an} is total caloric content of an individual yellowfin or spotted dolphin, estimated as a function of wet weight in grams,

$$CAL_{an} = CD * WW_g,$$

where CD is caloric density (cal/g wet wt) of yellowfin tuna[1] or spotted dolphins[2].

$CONS_{cal}$ is total calories consumed per individual per day, estimated as

$$CONS_{cal} = CONS_{ind} * CD_f,$$

where CD_f is caloric density of food (cal/g wet wt) for

[1] 1440 cal/g wet wt (Boggs 1984).

[2] CD_d = 1860 cal/g wet wt; average caloric density of four dolphins measuring 81–189 cm TL. Caloric density of each animal was determined as the sum of calories contained in blubber, muscle, viscera, and bone divided by total animal wet weight in grams. Average caloric density of individual dolphins ranged from 1985 cal/g wet wt in the 81 cm animal, to 1760 cal/g wet wt in the large adult female (189 cm TL). Assuming constant energy density for spotted dolphins is acceptable, as spotted dolphins do not appear to exhibit any significant seasonal, and little age-related, changes in thickness of their blubber layer.

yellowfin tuna[3] or spotted dolphins[4], and $CONS_{ind}$ is wet weight in grams of food consumed, estimated as

$$CONS_{ind} = C_{max} * P_{val} * WW_g,$$

where C_{max} is maximum possible consumption (expressed as a fraction of wet weight) for the largest yellowfin or dolphin, estimated as

$$C_{max} = C_a * WW_g^{Cb},$$

where [5]$C_a = 1.2$ and [6]$C_b = -0.22$ for yellowfin, or [7]$C_a = 3.98$ and [8]$C_b = -0.29$ for spotted dolphins.

P_{val} is an iteratively fitted unitless value in the range 0–1 that, when "correct," results in the simulated growth curve matching the observed growth curve (University of Wisconsin Sea Grant 1989), and WW_g is body wet weight in grams.

Respiration (yellowfin tuna) Specific rate of respiration (R_{sp}; calories respired · calories of animal^{-1} · day^{-1}) for yellowfin tuna was estimated as

$$R_{sp} = (STD_w + ACT_w) * (20650/CD),$$

with energy costs of standard (STD_w) and active (ACT_w) metabolism expressed in watts. The factor 20650 converts watts to cal/day. Dividing by caloric density of the animal (CD) produces the specific rate.

Weight-specific energy cost of standard metabolism for yellowfin was assumed constant for all sizes of yellowfin (Boggs 1984) as

$$STD_w = 0.464 \text{ watts/g wet weight.}$$

Energy cost of active metabolism (watts/g wet wt) was estimated using Boggs' (1984) equations and data for energy costs of activity in yellowfin,

$$ACT_w = F * VL^G * FL^H,$$

where VL is velocity in cm/sec and $F(=1.59\ E^{-4})$, $G(=1.64)$, and $H(=-1.28)$ are fitted parameters derived from Boggs' (1984) laboratory studies on yellowfin energetics.

Yellowfin were assumed to swim at length-specific optimum-sustained cruising speeds, with velocity scaling to fish length as

$$VL = VL_a * FL^{VLb},$$

where [9]$VL_a = 20.6$, and [10]$VL_b = 0.4$.

Respiration (spotted dolphins) Specific rate of respiration (R_{sp}; calories respired · calories of animal^{-1} · day^{-1}) for spotted dolphins was estimated as

$$R_{sp} = (ACT_{sp} + STD_{sp} + HL_{rsp}),$$

where ACT_{sp} is specific rate of swimming activity, STD_{sp} is specific rate of standard (basal) metabolism, and HL_{rsp} is specific rate of residual heat loss.

Specific rates of swimming activity and standard metabolism are estimated as

$$ACT_{sp} = ACT_{cal}/CAL_{an}$$

and

$$STD_{sp} = STD_{cal}/CAL_{an}.$$

Caloric cost of **standard metabolism** was estimated as

$$STD_{cal} = S_a * WW_g^{Sb},$$

[3] Energy density of yellowfin food was based on an assumed diet of 70% fish, 20% squid, and 10% invertebrates (Olson and Boggs 1986), with undigestible fractions of 0.124, 0.066, and 0.025, and caloric densities of 1440, 1260, and 1000 cal/g wet wt, respectively. Average ingested energy density (including the undigestible fraction) is 1380 cal/g wet wt.

[4] Energy density of spotted dolphin food changes with age (size). Spotted dolphins nurse throughout their first year (Perrin et al. 1976). They do not begin to ingest solid food until their second year, and they do not stop nursing entirely until their third year when they are ~145 cm in length. In this simulation, dolphins up to 1 yr of age were assumed to consume only milk (2855 cal/g wet wt) (Pilson and Walker 1970). Diet during the second year was assumed to be the same as that for yellowfin tunas, with an ingested energy density (CD_f) of 1380 cal/g wet wt.

[5] Based on the assumption that maximum specific feeding rate for very large yellowfin tunas (95000 g wet wt) would not exceed 10%/day, then solving for the intercept C_a (i.e., $C_a = 0.10/(95000^{-0.22})$) yields $C_a = 1.2$. In practice, the exact value chosen for C_{max} is flexible, as higher values simply reduce the fitted value of P_{val}, and vice versa.

[6] By analogy to walleye *Stizostedion vitreum* (Kitchell et al. 1977).

[7] Assuming maximum possible ration for adult spotted dolphins (~75 kg) would not exceed 15% of body weight/day (Sergeant 1969), and with $C_{max} = 0.15$, $WW_g = 85000$ g, and $C_b = -0.29$, then $C_a = 3.98$.

[8] As a compromise between the unresolved arguments of Kleiber (1961; $C_b = -0.25$) and Heusner (1982; $C_b = -0.33$) for scaling of metabolic rate with size in mammals. This compromise was chosen because consumption is not strictly a metabolic rate. While Huesner's argument for metabolic rate is supported by data for metabolic rate changes with size (see formulation for dolphin respiration), no such data exist for consumption rates.

[9] Intercept estimate based on 100 cm FL yellowfin swimming on average 130 cm/sec *in situ* (Holland et al. 1990).

[10] Slope estimate based on theoretical and empirical studies by Weihs (1973, 1981).

where $^{11}S_a = 1380$, and $^{12}S_b = 0.67$.

Caloric cost of activity[13] was estimated as

$$ACT_{cal} = PWR * 20650,$$

where 20650 converts watts to calories/day. Power required to swim (PWR) was estimated as

$$PWR = MP/(ME * PE),$$

where MP is mechanical power required to overcome drag, ME is mechanical efficiency,[14] and PE is "propeller efficiency" (efficiency of propulsion by flukes)[15]. MP (in watts) was estimated as a function of total drag (D_t; in dynes) and velocity (VL; in c/sec) as

$$MP = (D_t * L)/10^7,$$

where the factor 10^7 converts the product $D_t * L$ to watts.

Total drag was estimated as a function of drag due to body, fins, and movements by flukes as

$$D_t = (0.5 * N * VL^2 * S_w * C_t)/(1.0 - FID),$$

where N is density of seawater (1.025g/cm^3), S_w is wetted surface area of the body, C_t is coefficient of total drag, and FID is (fin + induced) drag. FID[16] is expressed here as the fractional increase in estimated total drag due to adding the effects of fins and moving flukes.

S_w is wetted surface area of the body, excluding flippers, dorsal fin, and flukes, estimated as[17]

$$S_w = 0.1636 * TL^{2.14}.$$

Surface areas of fins are excluded from this calculation because fin drag is incorporated into the equation for total drag as an increase of 21% over drag estimated from body dimensions alone.

C_t was estimated from the formula for drag of submerged streamlined bodies moving with constant velocity

$$C_t = C_f * [1 + (1.5 * (D_a/TL)^{3/2}) + (7 * (D_a/TL)^3)]$$

(Hoerner 1965, Webb 1975). C_f is the coefficient of friction drag, and D_a is the maximum body diameter (cm; derived from girth at axilla (G_a)) where

$$G_a = G_{aa} * WW_{kg}^{Gab},$$

with $G_{aa} = 25$ and $G_{ab} = 0.28$, based on measurements of 50 spotted dolphins measuring 82–210cmTL.

C_f was estimated from the equation for streamlined bodies moving submerged at constant velocity in turbulent flow as

$$C_f = 0.072\ R_L^{-1/5},$$

where R_L is Reynolds number, estimated here as

$$R_L = (TL * VL)/v,$$

where v is kinematic viscosity (= 0.01 Stokes) assuming turbulent flow at the boundary layer (Webb 1975), and VL is velocity (cm/sec), estimated as

$$VL = VL_a * TL^{VLb},$$

[11] Sa was assumed constant for all sizes of spotted dolphins. Given an observed rate of 0.45mg $O_2 \cdot g$ wet $wt^{-1} \cdot hr^{-1}$ for a spinner dolphin *Stenella longirostris* weighing 68000 WW_g (Hampton and Whittow 1976) and assuming 3.25 cal/mg O_2 (Elliot and Davidson 1975), then 2,386,800 (0.45*3.25*68000) calories are expended daily in standard metabolism, and $S_a = 1380$ (2,386,800/68,000$^{0.67}$). The observed resting rate of oxygen consumption is consistent with the range of resting rates (0.3–0.6mg $O_2 \cdot g$ wet wt^{-1}) reported for bottlenose dolphins under various conditions (Hampton et al. 1971, Karandeeva et al. 1973, Hampton and Whittow 1976).

[12] Heusner (1982) presents convincing statistical arguments that intraspecific relationships between basal (standard) metabolism and body weight in adult mammals are better described by the 2/3 power than the 3/4 power proposed by Kleiber (1961). Heusner's argument is based on observed differences between adults of similar species (e.g., breeds of dog); but Huesner's curve is also more realistic because it predicts a relatively higher weight-specific rate in smaller (younger) animals of a given species. This is more consistent with Kleiber's (1961) observation that younger animals tend to have elevated weight-specific metabolic rates compared not only with adults of the same species, but with small adults of similar species. In young marine mammals, weight-specific standard metabolic rate is often at least twice the standard rate of adults (Ashwell-Erickson and Elsner 1981, Lavigne et al. 1982). The parameterization above results in weight-specific estimates of S that are 2.3–1.3 times higher in dolphins measuring 80–140cmTL than in adult dolphins (~190cmTL). This differs by 0–11% (increasing with increasing size) from basal metabolic rates of juvenile through adult seals of similar weight (Ashwell-Erickson and Elsner 1981).

[13] Dolphins were assumed to swim steadily far enough below the surface to eliminate the effects of surface drag (e.g., Hertel 1969). This formulation ignores the costs of surfacing to breathe, and the attendant increase in total distance swum to follow a sinusoidal rather than a straight path through the water. Preliminary estimates of these additional costs for individual dolphins of several sizes, for reasonably realistic depths of dive and distance between surfacings, ranged from 10 to 25% of steady swimming costs. As this cost is relatively low, the dolphin model was not reformulated to include these added costs of surfacing.

[14] ME = 0.20, by analogy to observed muscle efficiencies of terrestrial mammals.

[15] PE = 0.85 by analogy to tunas (Magnuson 1978).

[16] FID was assumed = 0.21, based on the fraction of estimated total (body + fin + induced) drag accounted for by (fin + induced) drag in the 4-dolphin sample.

[17] Based on measurements of wetted surface area in the 34-dolphin sample.

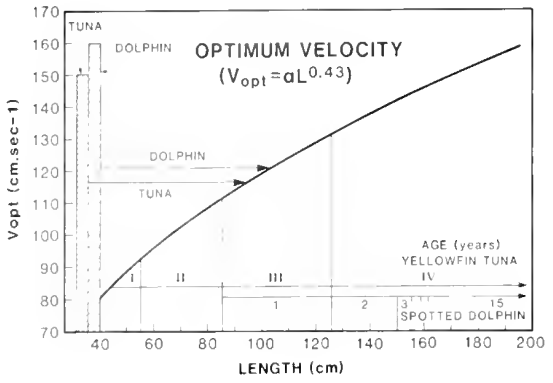

Figure 4

Estimated optimum sustained swimming speed (curved line) of yellowfin tuna *Thunnus albacares* and spotted dolphins *Stenella attenuata* from the eastern tropical Pacific Ocean. Lengths: fork length for tuna; rostrum to fluke notch ("total length") for dolphins. Vertical bars indicate range of optimum speeds predicted for sizes of tuna and dolphins occurring in mixed associations. Arrows indicate observed average swimming speeds of a radio-tagged 96 cm yellowfin tuna and of tagged individual spotted dolphins swimming *in situ*. Size-ranges for yellowfin tuna ages I–IV, and for spotted dolphins from birth, are indicated above abscissa.

where $VL_a = 20.6$ and $VL_b = 0.43$, assuming swimming velocity scales with length in the same manner for both spotted dolphins and yellowfin tuna (Fig. 4). Using the same formula and parameters to predict velocity as a function of length in both the tuna and dolphin models maintains comparability between results from the two models. As geometrically similar swimmers, hydrodynamic constraints should be approximately the same for both tuna and dolphins.

Specific rate of residual heat loss (HL_{rsp}; calories heat lost in excess of that generated by active and standard metabolism, and specific dynamic action · calories of animal^{-1} · day^{-1})[18] was estimated as

$$HL_{rsp} = HL_{usp} - (ACT_{sp} * (1.0 - ME) + STD_{sp} + SDA_{sp}),$$

where $HL_{rsp} > 0$, otherwise $HL_{rsp} = 0$.

[18] Because spotted dolphins are warm-blooded relative to their environment and because their blubber layer is not a perfect insulator, they will constantly lose heat to surrounding water. If the sum of estimated heat production generated by muscle activity, standard metabolism, and specific heat of digestion equals or exceeds this unavoidable passive loss, the term has no effect. Otherwise, the additional heat loss was added to the animal's energy cost. In practice, the influence of the term was negligible, as differences between H_a and the sum of STD, ACT, and SDA were < 10%.

The term (1.0 – ME) in conjunction with ACT_{sp} expresses the fraction of total active metabolism that is dissipated as heat, rather than converted to mechanical energy. The term H_{rsp} was taken to be zero when the estimate of H_{rsp} yielded a negative result. In this case, all passive losses were more than offset by heat generated by metabolism.

Specific rate of unavoidable passive heat loss (HL_{usp}; calories lost passively as heat · calories of animal^{-1} · day^{-1}) was estimated following Brodie's (1975) procedure for passive losses in large whales,

$$HL_{usp} = \frac{((21.18/BD_a) * (37.0 - T_a) * S_m/10000.0) * 24}{WW_g * (CD_d/1000.0)},$$

where [19]BD_a is average blubber depth, CD_d is caloric density of spotted dolphins, 37.0 (°C) is the assumed core temperature for spotted dolphins (Hampton and Whittow 1976), T_a is ambient temperature (assumed constant at 27°C), 21.18 is the conductivity factor for whale blubber (Brodie 1975), and [20]S_m is metabolic surface area, estimated as

$$S_m = 0.84 * S_w.$$

Unavoidable heat loss from fins and head is assumed negligible, as blood flow to these areas can be adjusted to minimize or maximize heat loss, as needed.

Specific dynamic action Specific rate of specific dynamic action (SDA_{sp}; calories lost as heat of digestion · calories of animal^{-1} · day^{-1}) was estimated as

$$SDA_{sp} = SDA * C_{sp},$$

where SDA (the fraction of consumption converted to heat energy during digestion) = 0.15 for both yellowfin tuna[21] and spotted dolphins[22].

Waste losses Specific rate of waste losses (WL_{sp}; calories lost as feces or urine · calories of animal^{-1} · day^{-1}) were estimated as the sum of fractional losses to egestion (F_a) and excretion (U_a)

[19] BD_a = 0.65 cm, based on measurements of blubber depth at maximum girth for a sample of 72 spotted dolphins measuring 80–190 cm TL.

[20] S_m is the surface area of the body beneath the blubber layer. S_m averaged 84% of S_w in the 4-dolphin sample.

[21] Reflecting the relative high-protein low-carbohydrate diet ingested by yellowfin tunas (Olson and Boggs 1986).

[22] SDA is primarily a function of the protein content of ingested food, and is ~15% for a variety of carnivores, including sea otters eating clams and squid (10–13%, Costa and Kooyman 1984), harp seals eating fish (17%, Gallivan and Ronald 1981), and various terrestrial mammals fed a mixed diet (Kleiber 1961).

$$WL_{sp} = (F_a + U_a) * C_{sp},$$

where $^{23}F_a = 0.20$ and $^{24}U_a = 0.07$ for yellowfin tuna; $F_a = 0.125$ and $U_a = 0.07$ for spotted dolphins[25].

Growth Specific rate of growth (calories available for growth · calories of animal^{-1} · day^{-1}) was estimated as

$$G_{sp} = C_{sp} - (R_{sp} + SDA_{sp} + WL_{sp}).$$

Total calories available for growth (G_{cal}) is

$$G_{cal} = G_{sp} * CAL_{an}.$$

Total grams wet-weight biomass available for growth (G_{wwg}) is then

$$G_{wwg} = G_{cal}/CD.$$

The formulas and parameter values presented above produce reasonable model estimates of the various energy fluxes for both yellowfin tuna and spotted dolphins (Edwards 1992).

Results: Estimated consumption

Despite the apparent similarity between yellowfin tuna and spotted dolphins in food **composition** (prey type and size[26]), estimated food **requirements** for tuna and dolphins differ considerably. Estimated food requirements for individual tuna and dolphins imply that each dolphin requires 5–10 times more food per day than each yellowfin tuna, depending on the sizes of the tuna and dolphin being compared (Fig. 5). In a "typical" association of 200 dolphins and 500 tuna, total dolphin requirements are still 2–5 times higher than total tuna requirements per time-period (Fig. 6), despite the greater number of tuna than dolphins.

[23] Based on the relative assumed nondigestible portions of tuna diet items by analogy to similar items (Cummins and Wuycheck 1971).
[24] Based on measurement of non-fecal excretion by carnivorous fish (Brett and Groves 1979).
[25] Together these processes probably account for 15–20% of ingested food energy in spotted dolphins, as found for other small marine mammals eating fish (Shapunov 1973, Ronald et al. 1984, Ashwell-Erickson and Elsner 1981, Lavigne et al. 1982, and references therein.)
[26] Diet is undoubtedly an important factor in the tuna-dolphin association, as associated yellowfin tuna and spotted dolphins apparently have nearly identical feeding preferences (Perrin et al. 1973). Stomach contents of co-occurring tuna and spotted dolphins consisted primarily of small pelagic schooling fish (e.g., mackerel *Auxis thazard*) and squid of similar types and sizes.

Discussion: Model implications

The strict "result" of exercising the models is estimation of food consumption by yellowfin tuna and spotted dolphins of various sizes. This information alone is not particularly helpful in furthering our understanding of the tuna-dolphin bond. However, the process of model

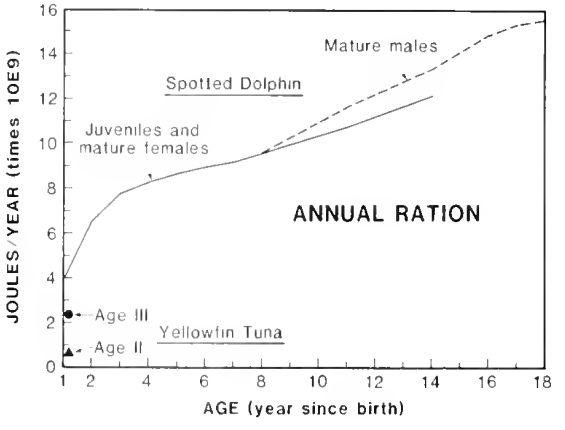

Figure 5
Estimated annual ration for individual spotted dolphins *Stenella attenuata* ages birth–18 yr, and yellowfin tuna *Thunnus albacares* ages II–III, occurring in mixed associations in the eastern tropical Pacific Ocean.

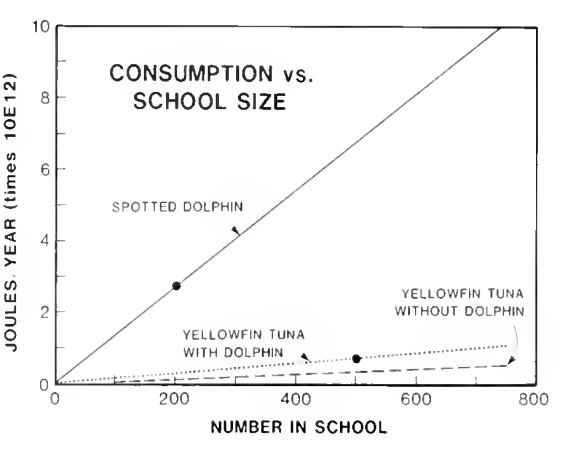

Figure 6
Estimated annual ration for schools of yellowfin tuna *Thunnus albacares* and spotted dolphins *Stenella attenuata* occurring in mixed associations in the eastern tropical Pacific Ocean (ETP). Solid circles indicate number of individual dolphins and individual tuna in a typical mixed association. Ration estimates for schools were based on average observed size-frequency distributions of tuna and dolphin in the ETP.

development and comparisons of similar energy fluxes in the completed models generated several interesting observations with potentially significant implications.

Hydrodynamics and body length

Length frequencies of the tuna and dolphins in a typical association show a surprisingly strong overlap between age-III yellowfin and neonate–1st yr dolphins. Both animals begin their respective years at ~85 cm TL, and complete the year at ~125 cm TL (Fig. 4). This is significant for two reasons. First, this size range comprises the majority of the yellowfin tuna found associated with dolphins (Fig. 3)[27]. Second, both animals have relatively stiff torpedo-shaped bodies with stiff fins and carangiform swimming behavior. Because theory predicts that optimum swimming speeds (the speed at which the least energy is consumed for a given distance covered) of geometrically-similar swimmers will be comparable (Weihs 1973, Webb 1975), the similar body forms and swimming behaviors of the tuna and the dolphins imply that optimum swimming speeds will also be similar for either animal of a given length.

Swimming speeds of sonic-tagged yellowfin tuna measured *in situ* show that individual undisturbed yellowfin, of the size most often found associated with dolphins, choose in their natural environment to swim on average at their predicted optimum cruising speed (e.g., yellowfin 90–100 cm FL swim at 100–130 cm/sec; Holland et al. 1990). Because yellowfin tuna tend to associate in schools of like-sized individuals, the expected speed of the tuna group is similar to the expected speed of the individuals involved.

In contrast, tracking studies (Perrin et al. 1979) of spotted dolphins in the ETP indicate that dolphin schools swim on average not the speed most efficient for the majority of the individuals in the school (i.e., ~160–170 cm/sec for large adults) but the speed most efficient for the neonate–1st yr animals (~120 cm/sec; Fig. 4).

These observations imply that yellowfin associating with dolphin schools may do so at little or no added hydrodynamic cost. The associated fish, unlike larger or smaller sizes of yellowfin, need swim neither faster nor slower than their apparently preferred optimum in order to maintain an association with dolphins.

The observation that associating with dolphins may cost tuna little does not explain **why** the tuna participate. The similarity in feeding preferences and probable similarity in feeding behaviors provides one explanation and suggests that tuna are more likely to follow dolphins than the reverse.

Who follows whom

The higher forage requirements of dolphins both individually and as an association imply that dolphins following tuna, particularly single dolphin schools following single tuna schools, would fall far short of meeting their daily energy requirements. Dolphin schools might avoid this energy deficit by switching from one tuna school to another, but they would have to switch consistently from recently-successful to soon-to-be-successful schools of foraging tuna. This frequent switching could be difficult because it would likely involve periods of searching at speeds greater than sustainable by the young dolphins, in order to find new tuna schools (and new patches of forage) faster than the patches could be found by the current tuna school.

Measurements of muscle mass and estimates of power-time curves for various sizes of spotted dolphins imply that the relatively small muscle mass of neonate–1st yr dolphins probably cannot sustain speeds much faster than their predicted optimum for any extended length of time (unpubl. data). If searching for new schools of tuna requires sustained accelerated swimming, the young dolphins could have trouble keeping up with the rest of the school. Because it is unlikely that dolphins, as nursing mammals and highly social animals, would simply leave their young behind, switching frequently from one tuna school to another may not be a practical option.

The disparity in feeding requirements implies that, while dolphins would probably be disadvantaged by having to rely upon tuna to locate sufficient prey, the tuna could recognize an advantage by following dolphins. The fish would then be associating with another predator that is searching for the same prey, but which must encounter that prey either more often or in considerably larger patches than required by the tuna, per time period.

However, the greater need of the dolphins for food implies concomitantly that competition for resources, if those resources are limited, could be fierce. The schooling characteristics of the predators and prey, coupled with feeding behaviors and differing sizes of the predators, provide one possible explanation for the ability of the smaller yellowfin tuna under some circumstances to persist in this potentially competitive association despite the dolphin's greater size, and need for food.

[27] Figure 3 includes fish from all areas of the fishery, not just the offshore areas where most dolphin fishing occurred during the years these data were collected, causing dolphin-fish distribution to be skewed to left.

WHEN SHOULD TUNA ASSOCIATE WITH DOLPHIN?

PREY ABUNDANCE:	LOW		HIGH	
PATCH TYPE:	RARE LARGE	FREQUENT SMALL	RARE LARGE	FREQUENT SMALL
ABILITY TO LOCATE PREY:				
D>T	YES	NO	YES	NO
D=T	NO	NO	NO	NO
D<T	NO	NO	NO	NO

Figure 7

Decision table predicting conditions under which yellowfin tuna *Thunnus albacares* and spotted dolphins *Stenella attenuata* should (or should not) associate.

Avoiding competition for food

As is characteristic of pelagic ocean systems, both predators and prey in the ETP occur in clumped distributions. Individuals occur in schools or aggregations separated by (often vast) distances devoid of other individuals. The prey, like the yellowfin tuna, will tend to occur in schools of like-sized individuals with similar swimming speeds. Aggregations of tuna and dolphins will typically consist of dolphins of assorted sizes accompanied by tuna of approximately one size. The feeding strategy of the predators will involve searching for a clump of prey, simultaneous (or nearly so) arrival at the prey patch by both tuna and dolphins, and repeated incursions by individuals of both predator groups into the clump of prey wherein prey are seized and swallowed whole individually.

Associated yellowfin tuna may be able to mitigate this direct competition with dolphins for food on the basis of the difference in size between the fish and the feeding adult dolphins (~100cm vs. 200cmTL). Because the tuna are smaller, they have smaller maximum stomach capacity (~400g wet wt for age-2 yellowfin, ~1100g wet wt for age-3 yellowfin; Olson and Boggs 1986) compared with spotted dolphins (~2000g wet wt in adults; Bernard and Hohn 1989). Even if the smaller, presumably more-agile tuna could seize individual prey only as fast as the dolphins and no faster, they would satiate more quickly than the dolphins.

As both groups would begin feeding at the same time, when the prey concentration was maximum, the tuna at any time would be relatively closer than the dolphins to satiation, given the observed (average) relative proportions of tunas and dolphins in a typical association. The tuna would be filling their stomachs while the prey were still relatively dense. Depending on the size of the prey patch, dolphins might never succeed in satiating, even though the tuna had their fill. Even if the prey patch was sufficiently limited that neither group achieved satiation, the tuna would always be relatively more full at any given time. Thus, although the dolphins require more prey overall, the tuna could succeed competitively by satiating sooner (being relatively more successful) during any given prey encounter.

However, it may not always be to the tuna's advantage to associate with dolphins, even given this scenario. The benefit (or not) can be assessed by evaluating the relative advantages of associating or not, given the range of possibilities for prey spatial distribution and abundance.

When should the association occur?

The possibilities can be summarized in a simple decision table (Figure 7). At the extremes, prey abundance may be either low or high and any given abundance may be either homogeneously distributed (frequent) or clumped (rare). The possibilities for locating prey are that (1) dolphins are more adept than tuna, (2) both are equally adept, or (3) dolphins are less adept than tuna. The advantages for tuna to associate with dolphins can be assessed for each cell in the table.

Consideration of each cell in the table suggests that tuna may benefit from associating with dolphins only when (1) prey are distributed in rare patches and (2) dolphins are more adept than the tuna in finding these patches. This would be true regardless of prey concentration within the patches, because whenever tuna and dolphin associate they will compete for food. If tuna are more adept than dolphins at finding food, then there will be no foraging-related advantage for the tuna to associate with their competitors. The tuna would be able to find food more easily on their own than by following dolphins, and would not have to risk sharing these resources once located. If the tuna and dolphins are equally adept, there is still no advantage, for the same reason.

If the prey are distributed in relatively small but numerous patches, there is still no advantage for tuna to associate with dolphins, again because the spatial frequency of schools would produce a relatively high probability of tuna encountering the food on their own without risk of sharing with their competitor. In addition, when patches are small, the tuna would be especially disadvantaged by having to compete with dolphins because the presence of dolphins could prevent the tuna from satiating, despite the fact that the tuna would still be relatively more full than the dolphins when the patch had been exhausted.

But when the prey are distributed in rare patches **and** the dolphins are more adept than the tuna at locating these patches, then tuna could benefit from associating with dolphins because the fish could encounter food more often than if they were not associated. This will be true regardless of the density of the prey patch.

It is never the case that dolphins benefit energetically from depending entirely on tuna for finding prey, because dolphin forage requirements are so much higher than tuna requirements.

These conclusions lead to the hypothesis that tuna-dolphin associations should be more prevalent in areas where oceanic conditions encourage strong clumping of prey, and less prevalent when conditions encourage a more homogeneous distribution of prey. I am currently exploring, with a simulation model of tuna, the movements of dolphin and prey in response to environmental characteristics of the ETP (work in progress). Further studies correlating oceanic environmental characteristics with catches of various size-classes of tuna are planned but not yet underway. If the suggestions described above are borne out, it may be possible to identify areas of the ETP where large yellowfin tuna could be captured without having to rely on dolphin-associated fishing.

Caveats

This study assumes that average size of dolphin schools remains constant at about 200 animals. This is the average school size for spotted dolphins observed during dolphin survey research cruises in the ETP. In fact, neither school size nor school composition are constant. Observers on both research and commercial vessels report school sizes ranging from a few animals to many hundreds. Scott (1991) reports diel changes in sizes of schools sighted by tuna fishermen in the ETP.

However, these inconsistencies may not significantly affect the implications of the energetics estimates presented here. Average sizes of dolphin schools captured with tuna in the ETP are considerably larger (400–600 animals) than the average school size observed during research surveys because the fishermen preferentially search and capture large schools of dolphins, which tend to carry more tuna. Estimates concerning the relative importance of tuna and dolphins to energetics of the association are probably reasonably similar for both large and small associations, because in both cases the proportions of tuna and dolphins tend to be similar (i.e., as the number of dolphins increases, in general the number of associated tuna increases). The study of diel differences (Scott 1991) shows that school sizes of dolphins sighted in association with tuna vary from a morning low to a late-afternoon high, but the change is relatively small, from ~450 to ~600 animals on average.

Other explanations for the bond

Other hypotheses have been proposed to explain the tuna-dolphin association. The two most-often suggested are the possibility that tuna perceive dolphin schools as FADs (fish aggregating devices) or as protection from sharks. Both of these factors may well contribute to the strength of the bond; neither precludes the energetics results discussed above.

The propensity for fish to collect around floating objects is well known, although the reasons are not yet understood. Presumably, floating objects provide a reference point for the aggregating tuna and in some way increase foraging success, perhaps by concentrating prey items or by tracking convergence areas where prey densities may be higher than elsewhere.

The FAD hypothesis has merit for the sizes of tuna actually found with dolphins in the ETP, for two reasons in particular. First, associating with dolphins may increase foraging success for the associated tuna because both tuna and dolphins are apparently seeking the same prey and dolphins may be more adept at finding it. Thus, tuna are associating with a FAD that does not simply attract appropriate prey passively, but actively searches and finds it. Second, tuna are required to swim constantly in order to ventilate their gills. It appears convenient that the average observed speed of dolphin schools is also the optimum speed of the sizes of tuna usually found associated with these schools. Rather than circling a stationary FAD, tuna associated with dolphin schools will cover a much larger area while moving at their most efficient cruising speed, and will cover that area in the presence of a sentient foraging FAD.

The shark protection hypothesis derives from a common perception that dolphins actively protect their young by driving sharks from their vicinity. If this is so, tuna associating with dolphins may be associating with the best of all possible FADs; a floating object that moves at the tuna's optimal speed, moves in search of the same prey the tuna would like to find, is probably at least as adept as the tuna at finding that preferred prey, and which provides protection against, rather than increased risk of, predation (FADs of course concentrate not only fish, but also their predators).

Both the FAD and shark hypotheses assume that tuna follow dolphins. Not all hypotheses assume that tuna are the followers. Au and Pitman (1986) and Au (1991) suggest, for example, that dolphins follow tuna in order to take advantage of tuna foraging in conjunction with bird flocks. This would be an advantage for dolphins during the actual feeding event. However, it

does not solve the problem that dolphins apparently must locate not only the same type of prey as large yellowfin tuna, but quite a bit more of it during any given time-period. Following tuna does not appear adequate to fulfill dolphin schools' energy requirements.

This fundamental difference in food energy requirements may be the single most important **biological** factor underlying the association. Oceanographic conditions (the shallow mixed layer) set the stage; energetics requirements (hydrodynamics and foraging patterns) appear to constrain the roles. Although the definitive answer has yet to be demonstrated quantitatively, the energetics-based hypotheses presented here are at least consistent with currently available data. The tuna-dolphin association may be a consequence of a combination of oceanography, hydrodynamics, foraging energetics, and life-history characteristics, i.e, a consequence of the ecology of the association's components.

Acknowledgments

This study could not have been completed without generous sharing of data, time, and constructive advice by helpful individuals from, but not limited to, the National Marine Fisheries Service, Southwest Fisheries Science Center, and the Inter-American Tropical Tuna Commission. This work was completed while the author was a National Research Council PostDoctoral Research Associate at the Southwest Fisheries Science Center, La Jolla, CA.

Citations

Ashwell-Erickson, S., and R. Elsner
1981 The energy cost of free existence for Bering Sea harbor and spotted seals. *In* Hood, D.W., and J.A. Calder (eds.), The eastern Bering Shelf: Oceanography and resources, vol. 2, p. 869–899. Univ. Wash. Press, Seattle.

Au, D.W.
1991 Polyspecific nature of tuna schools: Shark, dolphin, and seabird associates. Fish. Bull., U.S. 89:343–354.

Au, D.W.K., and R.L Pitman
1986 Seabird interactions with dolphins and tuna in the eastern tropical Pacific. Condor 88(3):304–317.

Barlow, J., and A. Hohn
1984 Interpreting spotted dolphin age distribution. NOAA-TM-NMFS-SWFC-48, Southwest Fish. Sci. Cent., La Jolla, 21 p.

Bernard, H.J., and A.A. Hohn
1989 Difference in feeding habits between pregnant and lactating spotted dolphins (*Stenella attenuata*). J. Mammal. 70(1):211–215.

Boggs, C.H.
1984 Tuna bioenergetics and hydrodynamics. Diss. Abstr. Int. 45/02-B:482.

Brett, J.R., and D.D. Groves
1979 Physiological energetics. *In* Hoar, W.S., et al. (eds.), Fish physiology, vol. 8, p. 280–354. Academic Press, NY.

Brodie, P.F.
1975 Cetacean energetics, an overview of intraspecific size variations. Ecology 56:152–161.

Costa, D.P., and G.L. Kooyman
1984 Contribution of specific dynamic action to heat balance and thermoregulation in the sea otter, *Enhydra lutris*. Physiol. Zool. 57(2):199–203.

Cummins, K.W., and J.W. Wuycheck
1971 Caloric equivalents for investigations of ecological energetics. Int. Assoc. Theor. Appl. Limnol. Proc. 18:1–158.

Edwards, E.F.
1992 Evaluation of energetics models for yellowfin tuna (*Thunnus albacares*) and spotted dolphin (*Stenella attenuata*) in the eastern tropical Pacific Ocean. Admin. Rep. LJ-92-01, NMFS Southwest Fish. Sci. Cent., La Jolla, 43 p.

Elliot, J.M., and W. Davidson
1975 Energy equivalents of oxygen consumption in animal energetics. Oecologia (Heidelb.) 19:195–120.

Fiedler, P.C.
1990 Seasonal climatologies and variability of eastern tropical Pacific surface waters. NOAA Tech. Rep. NMFS 109, 65 p.

Fiedler, P.C., L.J. Lierheimer, S.B. Reilly, S.N. Sexton, R.S. Holt, and D.P. DeMaster
1990 Atlas of eastern tropical Pacific oceanographic variability and cetacean sightings, 1986–1989. NOAA-TM-NMFS-SWFSC-144, Southwest Fish. Sci. Cent., La Jolla, 142 p.

Gallivan G.J., and K. Ronald
1981 Apparent specific dynamic action in the harp seal (*Phoca groenlandica*). Comp. Biochem. Physiol. 69A:579–581.

Hampton, I.F.G., and G.C. Whittow
1976 Body temperature and heat exchange in the Hawaiian spinner dolphin *Stenella longirostris*. Comp. Biochem. Physiol. 55A:195–197.

Hampton, I.F.G., G.C. Whittow, J. Szekerczes, and S. Rutherford
1971 Heat transfer and body temperature in the Atlantic bottlenose dolphin, *Tursiops truncatus*. Int. J. Biometrics 15(2–4):247–253.

Hertel, H.
1969 Hydrodynamics of swimming and wave-riding dolphins. *In* Anderson, H.T. (ed.), Biology of marine mammals, p. 31–63. Academic Press, NY.

Heusner, A.A.
1982 Energy metabolism and body size. Part 1. Is the 0.75 mass exponent of Kleiber's equation a statistical artifact? Respir. Physiol. 48:1–12.

Hoerner, S.F.
1965 Fluid dynamic drag: Practical information on aerodynamic drag and hydrodynamic resistance. Published by author, Midland Park, NJ, 468 p.

Hohn, A.A., and P.S. Hammond
1985 Early postnatal growth of the spotted dolphin in the offshore eastern tropical Pacific. Fish. Bull., U.S. 83:533–556.

Holland, K.M., R.W. Brill, and R.K.C. Chang
1990 Horizontal and vertical movements of yellowfin and bigeye tuna associated with fish aggregating devices. Fish. Bull., U.S. 88:493–507.

IATTC (Inter-American Tropical Tuna Commission)
1989 Annual report, 1988. Inter-Am. Trop. Tuna Comm., Scripps Inst. Oceanogr., La Jolla, 288 p.

Joseph, J.
1963 Fecundity of yellowfin tuna (*Thunnus albacares*) and skipjack (*Katsuwonus pelamis*) from the eastern Pacific Ocean. Int.-Am. Trop. Tuna Comm. 7(4):257–292.

Karandeeva, O.G., S.K. Matisheva, and V.M. Shapunov
1973 Features of external respiration in the Delphinidae. *In* Chapskii, K.K., and V.E. Salokov (eds.), Morphology and ecology of marine mammals, p. 196–206. John Wiley, NY.

Kessler, W.S.
1990 Observations of Long Rossby Waves in the northern tropical Pacific. J. Geophys. Res. 95(C4):5183–5217.

Kitchell, J.F., D.J. Stewart, and D. Weininger
1977 Application of a bioenergetics model to yellow perch (*Perca flavescens*) and walleye (*Stizostedion vitreum vitreum*). J. Fish. Res. Board. Can. 34:1922–1935.

Kleiber, M.
1961 The fire of life. John Wiley, NY, 453 p.

Lavigne, D.M., W. Barcyard, S. Innes, and N.A. Oritsland
1982 Pinniped bioenergetics. *In* Mammals in the sea, vol. 4, p. 192–235. FAO Fish. Ser. 5.

Magnuson, J.J.
1978 Locomotion by scombrid fishes: Hydrodynamics, morphology and behavior. *In* Hoar, W.S., et al. (eds.), Fish physiology, vol. 7, p. 239–313. Academic Press, NY.

Olson, R.J., and C.H. Boggs
1986 Apex predation by yellowfin tuna (*Thunnus albacares*): Independent estimates from gastric evacuation and stomach contents, bioenergetics, and cesium concentrations. Can. J. Fish. Aquat. Sci. 43(9):1760–1775.

Orbach, M.
1977 Hunters, seamen and entrepreneurs. The tuna seinermen of San Diego. Univ. Calif. Press, Berkeley, 304 p.

Perrin, W.F.
1969 Using porpoises to catch tuna. World Fishing 18(6), 4 p.

Perrin, W.F., R.W. Warner, C.L. Fiscus, and D.B. Holts
1973 Stomach contents of porpoise, *Stenella* spp., and yellowfin tuna, *Thunnus albacares*, in mixed-species aggregations. Fish. Bull., U.S. 71:1077–1092.

Perrin, W.F., J.M. Coe, and J.R. Zweifel
1976 Growth and reproduction of the spotted porpoise, *Stenella attenuata*, in the offshore eastern tropical Pacific. Fish. Bull., U.S. 74:229–269.

Perrin, W.F., W.E. Evans, and D.B. Holts
1979 Movement of pelagic dolphins (*Stenella* spp.) in the eastern tropical Pacific as indicated by results of tagging, with summary of tagging operations, 1969–1976. NOAA Tech. Rep. NMFS-SSRF-737, 14 p.

Pilson, M.E.Q., and D.W. Walker
1970 Composition of milk from spotted and spinner dolphins. J. Mammal. 51(1):74–79.

Ronald, K., K.M. Keiver, F.W.H. Beamish, and R. Frank
1984 Energy requirements for maintenance and faecal and urinary losses of the grey seal (*Halichoerus grypus*). Can. J. Zool. 62:1101–1105.

Scott, M.
1991 The size and structure of pelagic dolphin herds. Ph.D. thesis, Univ. Calif, Los Angeles, 165 p.

Sergeant, D.E.
1969 Feeding rates in cetacea. Fiskeridir. Skr. Ser. Havunders. 15:246–258.

Shapunov, V.M.
1973 Food requirements and energy balance in the black sea bottlenose dolphin (*Tursiops truncatus ponticus barabasch*). *In* Chapskii, K.K., and V.E. Solokov (eds.), Morphology and ecology of marine mammals, p. 207–212. John Wiley, NY.

Smith, T.D. (editor)
1979 Report of the status of porpoise stocks workshop, Aug. 27–31, La Jolla, CA. Admin. Rep. LJ-79-41, NMFS Southwest Fish. Sci. Cent., La Jolla, 138 p.

University of Wisconsin Sea Grant
1989 A generalized bioenergetics model of fish growth for microcomputers. WIS-SG-87-245, Univ. Wisc., Madison, 47 p.

Webb, P.W.
1975 Hydrodynamics and energetics of fish propulsion. Fish. Res. Board Can. Bull. 190, 159 p.

Weihs, D.
1973 Optimal fish cruising speed. Nature (Lond.) 245:48–50.
1981 Voluntary swimming of speeds of two species of large carcharhinid sharks. Copeia 1:219–222.

Wild, A.
1986 Growth of yellowfin tuna, *Thunnus albacares*, in the eastern Pacific Ocean based on otolith increments. Int.-Am. Trop. Tuna Comm. Bull. 18(6), 56 p.

Wyrtki, K.
1966 Oceanography of the eastern equatorial Pacific Ocean. Oceanogr. Mar. Biol. Annu. Rev. 4:33–68.
1967 Circulation and water masses in the eastern equatorial Pacific Ocean. Int. J. Oceanol. Limnol. 1(2):117–147.

Abstract.– A principal mechanism underlying a production hypothesis that artifical reefs increase environmental carrying capacity and eventually the biomass of reef-associated organisms is that these structures reduce predation on reef residents. We tested this predation mechanism with a series of field experiments at two sites (inner-bay sand-seagrass flat, and outer-bay seagrass bed adjacent to coral reefs) in Bahia de la Ascension, Mexico. We examined survival of two size-classes of juvenile Caribbean spiny lobster *Panulirus argus* tethered in seagrass beds with and without access to artificial lobster shelters, and at different distances from the shelters. The artificial shelters were concrete structures (casitas) that simulate lobster dens. Large juvenile lobsters (56–65 mm CL) attained a relative size refuge when tethered 60 m away from casitas compared with smaller (46–55 mm CL) lobsters. Conversely, the small lobsters survived better beneath casitas than did large lobsters. Small juveniles also survived better at casitas or 30 m away from casitas than at 15 m or 70 m away. Observations indicated that the daytime predator guild, composed primarily of snappers (family Lutjanidae), seldom foraged more than 60 m from casitas and were typically within 15 m of casitas. There was also a significant positive correlation between predation-induced lobster mortality and numbers of snapper associated with casitas at the inner-bay site. Thus, tethering lobsters 70 m away from casitas appeared adequate to examine survival of lobsters in an environment uninfluenced by daytime predators aggregating to casitas. These results indicate that (1) the relative importance of a lobster-size refuge from predators varies according to shelter availability, and (2) that there is a nonlinear relationship between predation risk and distance from an artifical shelter. Our results demonstrate that casitas increase survival of small juvenile lobsters but reduce survival of larger juveniles. Small casitas scaled according to body size may enhance survival of large juvenile lobsters in nursery habitats where large conspecifics are removed from large casitas.

Manuscript accepted 13 July 1992.
Fishery Bulletin, U.S. 90:691–702 (1992).

Artificial shelters and survival of juvenile Caribbean spiny lobster *Panulirus argus*: Spatial, habitat, and lobster size effects*

David B. Eggleston

The College of William and Mary, Virginia Institute of Marine Science
Gloucester Point, Virginia 23062
Caribbean Marine Research Center, Lee Stocking Island, Exuma Cays, Bahamas
Present address: College of Ocean and Fishery Sciences WH-10
University of Washington, Seattle, Washington 98195

Romuald N. Lipcius

The College of William and Mary, Virginia Institute of Marine Science
Gloucester Point, Virginia 23062
Caribbean Marine Research Center, Lee Stocking Island, Exuma Cays, Bahamas

David L. Miller

Department of Geography, State University of New York, Cortland, New York 13045

Artificial reefs are in use worldwide as a means of increasing local abundance of finfish and invertebrates (see reviews by Bohnsack and Sutherland 1985, Grove and Sonu 1985, Mottet 1985, Bohnsack 1989). The use of artificial reefs to increase fisheries production remains controversial because it is unknown whether these structures (1) provide critical resources that increase the environmental carrying capacity and eventually the biomass of reef-associated organisms (production hypothesis), or (2) merely attract and aggregate organisms from surrounding areas without increasing total biomass (attraction hypothesis) (Bohnsack 1989). The attraction hypothesis is an important consideration for artificial-reef-based fisheries that may be vulnerable to overexploitation. Thus, there is a need for ecological investigations capable of assessing the impact of artificial reefs upon species distribution, abundance, and survival patterns, and the processes underlying these patterns.

Artificial reef technology has traditionally been based on the assumption that obligate reef dwellers (e.g., reef fishes and lobsters) are limited locally or regionally by the availability of shelter (Bohnsack 1989, Hixon and Beets 1989, Eggleston et al. 1990 and references therein). Conversely, artificial reefs also concentrate numerous potential predators (Hixon and Beets 1989, Eggleston et al. 1990); increased predation pressure at or near these structures could outweigh the benefits from increases in production. For instance, fishes and lobsters normally dispersed over a wide area could be concentrated and consumed by predators more rapidly in a smaller area. Thus, artificial shelters may either enhance or reduce the survival of their inhabitants, depending upon predator responses. In this paper, we present the results of a series of field experiments comparing survival rates of two size-classes of juvenile Caribbean spiny lobster *Panulirus argus*

* Contribution 1725 of the Virginia Institute of Marine Science.

Latreille, with and without access to artificial shelters at different spatial scales in seagrass beds. We then discuss these mortality patterns in terms of the relative importance of lobster size, shelter availability, and distance of lobsters from the artifical shelter. Moreover, we use daytime abundance and foraging ranges of shelter-associated predators to speculate on the mechanisms underlying these mortality patterns.

Juvenile *P. argus* inhabit shallow bays throughout the tropical and subtropical western Atlantic where they frequently aggregate during the day in crevices of coral and rocky reefs (Berrill 1975, Herrnkind et al. 1975). Gregarious behavior within dens probably enhances individual survivorship because spiny lobsters collectively use their spinose antennae to fend off diurnally active predators (Berrill 1975, Cobb 1981, Zimmer-Faust and Spanier 1987, Eggleston and Lipcius 1992). However, intra- and interspecific competition for suitable dens can force smaller juvenile *P. argus* out of these dens (Berrill 1975). Predation represents a major source of mortality for juvenile spiny lobsters (Munro 1974, Herrnkind and Butler 1986, Howard 1988, Smith and Herrnkind 1992), and when individuals are displaced or forced to shelter in an inadequate den they may be subject to increased predation rates (Herrnkind and Butler 1986, Eggleston et al. 1990).

Large juvenile and adult spiny lobsters are the focus of intense commercial and recreational fisheries in south Florida and the Caribbean, with the possibility of regional overexploitation of spiny lobster fisheries (U.S. Agency for International Development 1987). Several Caribbean nations have met increased market demand with the large-scale use of artificial shelters to concentrate lobsters and facilitate harvest (e.g., Mexico—Miller 1989, Lozano-Alvarez et al. 1991; Cuba—Cruz and Brito 1986; Bahamas—R.W. Thompson, Dep. Fish., Nassau, Bahamas, pers. commun., May 1991). These artificial shelters, commonly referred to as "casitas Cubanas" (see Fig. 1), attract and concentrate a broad size-spectrum of juvenile *P. argus*, particularly in nursery areas (Eggleston et al. 1990, Lozano-Alvarez et al. 1991).

Predation intensity in and around artificial shelters is affected by numerous factors including the sizes of predator, prey, and shelter (Hixon and Beets 1989, Eggleston et al. 1990), and distance from the reef (Shulman 1985). Moreover, since most crustaceans have indeterminate growth (Hartnoll 1982), they must continually search for larger shelters as they grow, a process that involves predation risk that is inversely related to body size (e.g., Scully 1983, Reaka 1987, Vermeij 1987). Hence, we hypothesized that (1) the relative importance of a lobster size refuge would vary according to shelter availability, and (2) that the impact of artificial shelters upon predation-induced mortality of juvenile lobsters would vary according to the distance of unprotected lobsters from these shelters. We tested these hypotheses experimentally in the field by quantifying the survival of tethered spiny lobster juveniles in seagrass beds of Bahia de la Ascension, Mexico. This bay is a productive nursery for juvenile *Panulirus argus* and supports a commercial fishery for large juveniles and adults (Miller 1989, Lozano-Alvarez et al. 1991). Experimental factors included (1) presence or absence of artificial shelter, i.e., casitas Cubanas, (2) lobster size, (3) site, and (4) distance between tethered, unprotected lobsters and artificial shelters.

Methods and materials

Study site

Tethering experiments were conducted in Bahia de la Ascension, a large bay (~740 km^2) within the Sian Ka'an Biosphere Reserve, Mexico (19°45′N, 87°29′W) (Fig. 2). Two experimental sites with contrasting

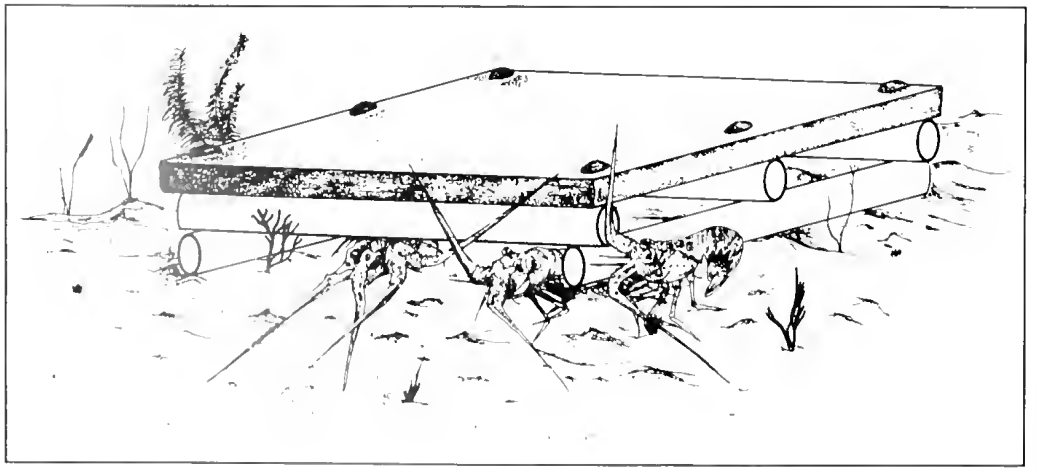

Figure 1
A large "casita Cubana" constructed with a frame of PVC-pipe and roof of cement (177 cm length × 118 cm width × 6 cm height of opening).

habitats were chosen to compare relative rates of predation: an inner-bay sand-seagrass (*Thalassia testudinum*) flat located at the northwestern portion of the bay, and an outer-bay seagrass meadow adjacent to a coral reef (Fig. 2). Seagrass and algal habitats likely provide the only natural daytime refuge for juvenile *P. argus* in this system because of an apparent lack of crevices (formed by rocky outcrops, patch coral reefs, sponges, solution holes, or undercut seagrass banks). Anecdotal information from lobster fishermen present in Bahia de la Ascension prior to the introduction of casitas (around 1974) indicated that juvenile lobsters commonly resided solitarily under dense stands of *Thalassia* or complex red algae (e.g., *Laurencia*), or aggregated around existing structures such as sponges or cobble. Moreover, previous tethering experiments with juvenile *P. argus* in this system demonstrated that seagrass and algae provide some protection for spiny lobster juveniles from predators (R.N. Lipcius et al., unpubl. data).

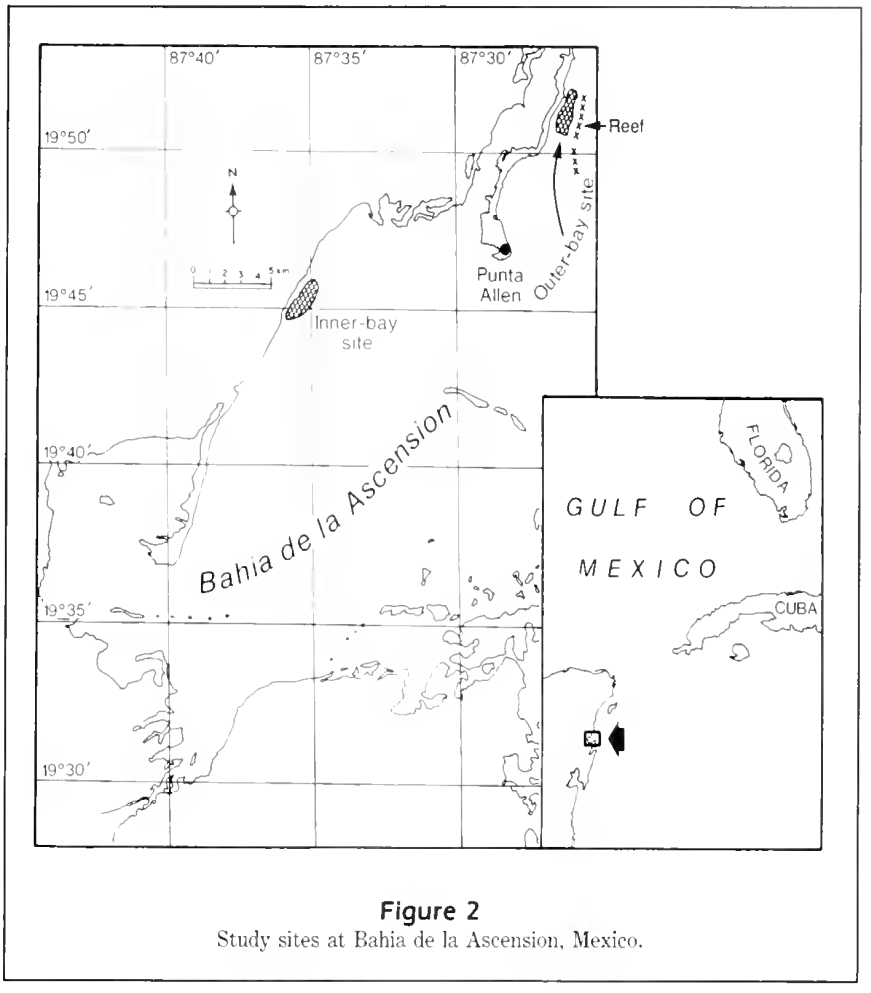

Figure 2
Study sites at Bahia de la Ascension, Mexico.

Differences in seagrass density between and within sites were determined prior to experiments by measuring dry-weight biomass (g) of *Thalassia* removed from 0.25 m^2 plots. The inner-bay site was composed of sparse seagrass patches ($\bar{x}$ *Thalassia* biomass 62.4 g/m^2, N 6, SD 10.7) interspersed among coarse calcareous sand and coral rubble. The coral rubble was covered mostly by green and red algae (*Dasycladus* spp. and *Laurencia* spp., respectively), but also supported larger sponges. The outer-bay site was located shoreward of a fringing coral reef and composed of sand patches and patch corals interspersed among moderate to dense seagrass beds ($\bar{x}$ *Thalassia* biomass 111.6 g/m^2, N 6, SD 13.4, and 210.0 g/m^2, N 6, SD 12.6, respectively). Further details of the study site are described in Eggleston et al. (1990).

Artificial shelters

Our design of artificial lobster shelters was based on "casitas Cubanas"—sunken wood and concrete structures that simulate lobster dens (Miller 1989) (Fig. 1). The large casitas used in this study (177x118x6 cm) were constructed with a reinforced concrete roof bolted to a supporting PVC-pipe frame. Several physical properties of the casita appear to make it an optimal lobster den: (1) shaded cover provided by the wide concrete roof, (2) a low ceiling that excludes large piscine predators, and (3) multiple den openings which are smaller than the inner roof height of the casita (Fig. 1) (Eggleston et al. 1990). Hence, the use of casitas permitted us to standardize den size and availability in different habitats.

Tethering experiments and predator observations

Spiny lobsters were collected from existing casitas and held in traps for 1–2 days prior to initiation of each experiment. Only intermolt lobsters exhibiting strong "tail flipping" responses were used in tethering experiments. Tethers were constructed by locking a plastic cable-tie around the cephalothorax of a lobster, between the second and third walking legs, and securing the cable-tie with cyanoacrylate cement. The cyano-

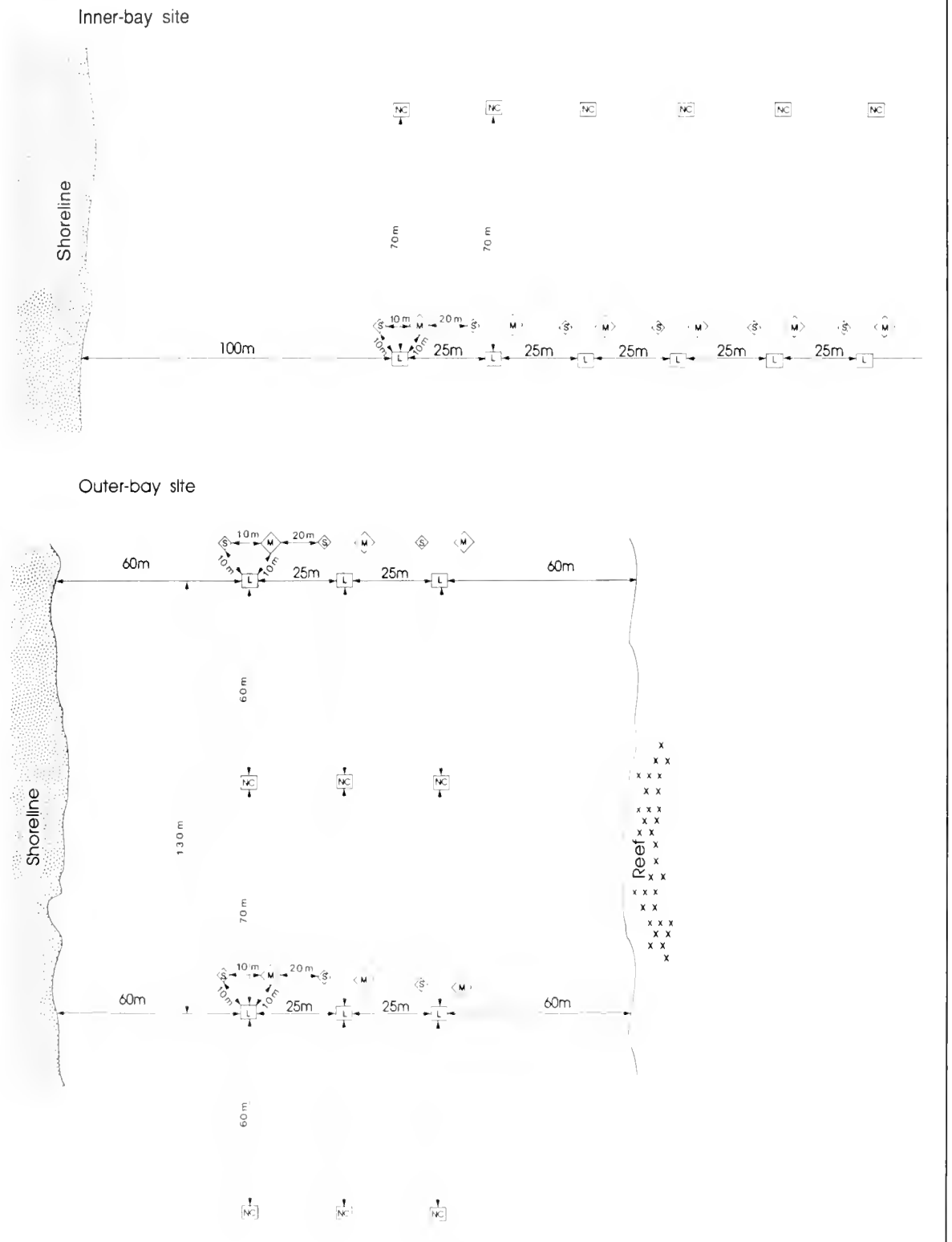

Figure 3

Schematic of casita layout at the (upper) inner-bay and (lower) outer-bay sites for the January 1989 experiment. S = small casita, M = medium casita, L = large casita, and NC = no-casita station.

acrylate cement ensured that a piece of carapace remained on the line as evidence of predator-induced mortality. An empty cable tie without a piece of carapace attached to it was scored as an escape. Each cable-tie was connected with 30lb test monofilament line either to another cable-tie and attached to a shelter, or attached to a square wire-metal frame that was positioned outside of the triangular casita station (Fig. 3) on the seagrass bed with lead weights. The wire-metal frame had the same length-width dimensions as the large casita but did not provide shelter. The metal frame was chosen over stainless-steel stakes because stakes could not penetrate the underlying carbonate platform at the inner-bay site. The metal frames were visually inconspicuous because they were covered by a thin layer of sediment. Tether lengths of 0.7m provided a foraging area of about 1.5m^2 and prevented tangling between adjacent lobsters. Although tethering does not necessarily measure absolute rates of predation, it does measure relative rates of predation (Heck and Thoman 1981), which can serve to compare mortality rates as a function of different experimental treatments.

We used a stationary visual census technique (Bohnsack and Bannerot 1986) to quantify the community structure of potential predators associated with casita and no-casita stations during the experimental period (January and August 1989). Visual censuses were performed between 10:00 and 14:00 hours with three replicate samples taken during the experimental period. By performing the visual censuses during midday, we maximized the visibility available for species identification. Nighttime observations were not performed because our previous study (Eggleston et al. 1990) indicated that the predator guild normally associated with the casitas dispersed widely over the seagrass bed at night. However, predator movements were observed during one dawn and dusk crepuscular period.

We examined the daytime foraging ranges of casita-associated predators by swimming along a transect perpendicular to each casita. When potential predators were observed, a float was set to mark the location, whereupon a scuba diver then followed the predators to assure that they were associated with the casita. Our initial observations indicated that piscine predators associated with casitas seldom moved more than 30–40m away from a casita.

Experimental design

Before initiating the tethering experiments in 1989, we deployed casitas at the inner-bay and outer-bay sites during 1988. During July 1988 at the inner-bay site, we positioned a row of six large casitas 25m apart from one another (Fig. 3). Each large casita had one medium and one small casita placed 10m away, yielding six stations with one small, medium, and large casita arranged in a triangle (Fig. 3). At the outer-bay site during August 1988, we positioned six small, medium and large casitas equidistant between the shore and reef line and arranged these in two rows, each containing three triangular stations (Fig. 3b). See Eggleston et al. (1990) and Eggleston and Lipcius (1992) for a complete description of the small and medium casitas and their use in other field experiments. Two separate tethering experiments were then performed during January and August 1989.

The first experiment was performed during January 1989. In this study we examined the survival of two sizes of juvenile lobsters with and without access to shelter at both the inner-bay and outer-bay sites. Six metal-frame, no-casita stations were placed 60–70m away and perpendicular to the casitas in sparse-to-moderate-density *Thalassia* at both sites (Fig. 3). Juvenile lobsters were divided into two size-classes: small, 46–55mm carapace length (CL) as measured dorsally from the base of the supraorbital spines to the posterior border of the cephalothorax; and large, 56–65mm CL. Lobsters were tethered for 7 days. Each casita and no-casita station at both sites had six tethered lobsters from either of two size-classes for a total of 144 tethered lobsters (2 sites × 6 lobsters × 2 sizes × 2 treatments (casita vs. no-casita) × 3 replicate stations).

Based on our initial observations of predator foraging ranges (see above), we assumed that our choice of 60–70m for the no-casita station was well beyond the foraging range of diurnally active predators, thereby providing unbiased estimates of lobster survival in the absence of artificial shelters (i.e., mortality estimates were not biased towards finding significantly higher predation rates on lobsters tethered within the foraging range of casita-associated predators). However, our observations during the January 1989 experiment indicated that some predators moved nearly 60m from the casitas (see Results). Thus, although the 70m distance from the large casitas was probably beyond the foraging range of casita-associated predators, the 60m distance from the small and medium casitas was probably not.

Before initiating the second tethering experiment, we positioned a row of three large casitas equidistant between the shore and reef line in July 1989 at the outer-bay site (Fig. 4). In August 1989 we examined how lobster survival varied with distance from the casitas. Three metal-frame no-casita stations were placed 15, 30, and 70m away and perpendicular to the large casitas (Fig. 4). Based on the foraging ranges of predators during the January experiment (see above), we assumed that 70m was an adequate distance to

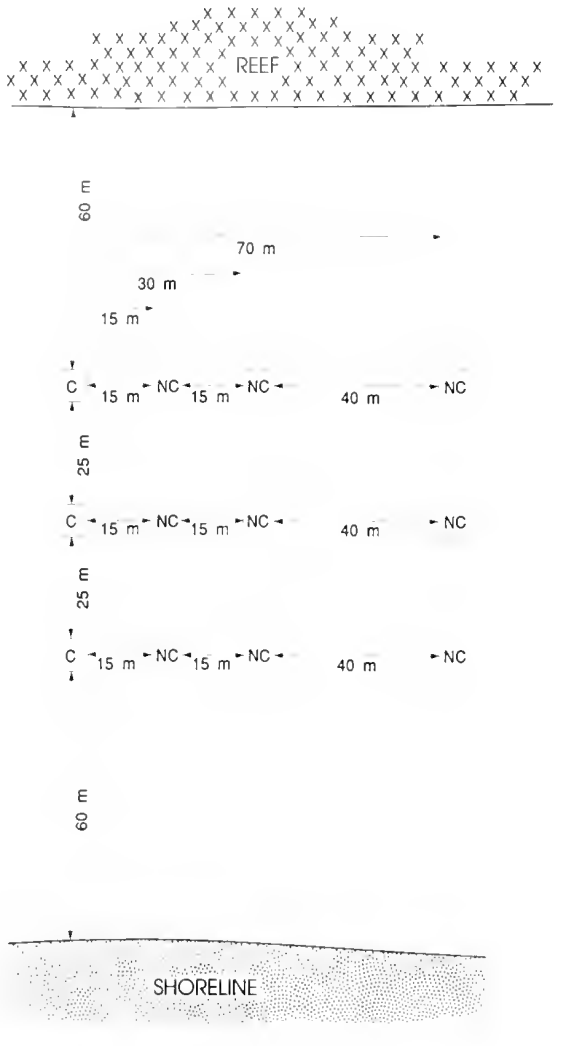

Figure 4

Schematic of casita layout at the outer-bay site for the August 1989 experiment. S = small casita, M = medium casita, L = large casita, and NC = no-casita station.

Table 1

(a) Three-way ANOVA table (model I) describing the effects of site (inner-bay sand-seagrass flat, and outer-bay seagrass bed adjacent to coral reefs), lobster *Panulirus argus* size (small 46–55 mm CL; large 56–65 mm CL) and shelter availability (casita vs. no-casita station 60 m away) on proportional mortality rates (arc-sine square-root transformed) of tethered lobsters during January 1989. $^{*}P<0.05$, $^{**}P<0.01$, ns $P>0.05$.

Source of variation	SS	df	MS	F
Site	0.002	1	0.002	0.402 ns
Lobster size	0.040	1	0.040	7.174**
Shelter availability	0.001	1	0.001	0.006 ns
Site × lobster size	0.001	1	0.001	0.112 ns
Site × shelter availability	0.001	1	0.001	0.235 ns
Lobster size × shelter availability	0.023	1	0.023	4.179*
Site × lobster size × shelter availability	0.001	1	0.001	0.187 ns
Error	0.089	16	0.006	

(b) Ryan's Q tests of mean proportional mortality rates (arc-sine square-root transformed) of tethered lobsters for the interaction effect of lobster size × shelter availability. Treatment levels not significantly different at the 0.05 level share an underline. Treatment levels are arranged in increasing order of proportional mortality.

Interaction

Shelter availability	Lobster size	
Casita	large	small
No Casita	large	small

Lobster size	Shelter availability	
Small	Casita	No Casita
Large	No Casita	Casita

assess predation in an environment uninfluenced by the casitas. This assumption held true for the diurnal predator guild during August 1989 (see Results). Only juvenile lobsters approximating the small size-class ($\bar{x}$ 53.2 mm CL, range 45.2–59.0 mm CL, N 72, SD 4.1) were tethered for 7 days. We chose only small lobsters in the second experiment because logistical considerations limited us to one size-class, and we wanted to verify that survival of small lobsters was enhanced when residing beneath casitas (See Results for first experiment below). Each casita and no-casita (i.e., metal frame) station contained 6 tethered lobsters for a total of 72 tethered lobsters (6 lobsters × 4 distances (0, 15, 30, and 70 m) × 3 replicate stations).

Lobsters were checked and predation losses scored every 1–2 days during experiments. Fewer than 4% of tethered lobsters escaped, and these were not used in subsequent statistical analyses. Lobsters that were eaten or missing were not replaced. Cumulative losses were converted to proportional mortality/day/casita (or station). Proportions were analyzed as a function of shelter availability (casita vs. no casita), distance from the casita (0, 15, 30, and 70 m), lobster size (small vs. large), and site (inner-bay vs. outer-bay) with two- and three-way, fixed-factor analyses of variance (ANOVA) models (after procedures in Underwood 1981). Proportional mortality was arc-sine square-root transformed to meet assumptions of normality and homogeneity of variance (Underwood 1981). In all cases, the variances were homogeneous as determined by Cochran's C-test. Differences among means were revealed by use of

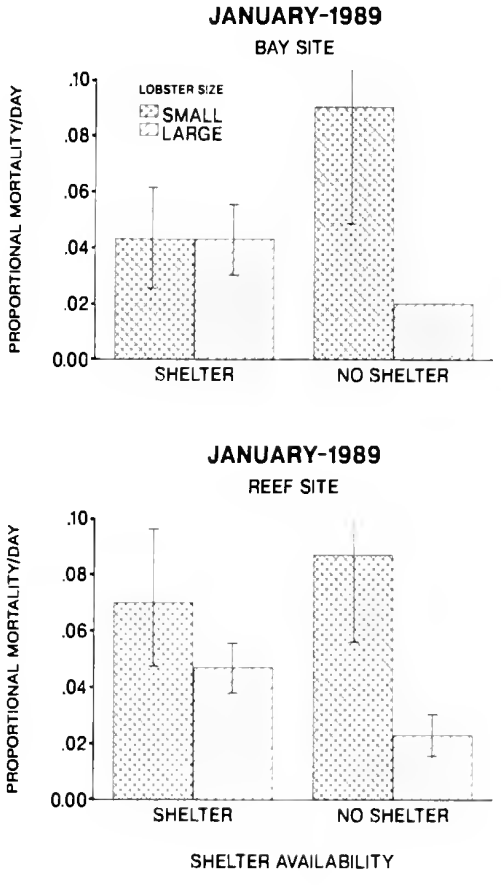

Figure 5
Results of field tethering of *Panulirus argus* at the inner-bay and outer-bay sites during January 1989, describing mortality as a function of lobster size (small 46–55 mm CL; large 56–65 mm CL) and shelter availability (casita vs. no casita). Values are mean proportional mortality · casita^{-1} · d^{-1} resulting from a total of 18 lobsters tested. Vertical bars are 1 SE.

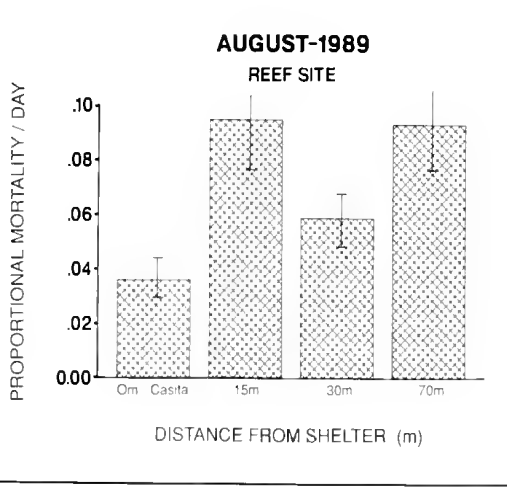

Ryan's Q multiple comparison test (Einot and Gabriel 1975) as recommended by Day and Quinn (1989).

Results

Tethering experiments

During January 1989, mortality of juvenile lobsters varied significantly as a function of lobster size but not according to site or shelter availability (i.e., tethered to casitas or 60–70 m away in seagrass) (Table 1a, Fig. 5). However, the interaction effect of lobster size by shelter availability was significant; this interaction effect was due to the significantly higher mortality of small vs. large lobsters tethered in seagrass, and by the significantly higher mortality of large lobsters in casitas compared with those tethered in seagrass (Table 1b).

At the outer-bay site in August 1989, mortality rates of small juvenile lobsters varied significantly according to distance from the casita (i.e., 0, 15, 30, and 70 m away from the casita) (Fig. 6; one-way ANOVA; F 5.89, df 3, $P<0.02$). Lobsters suffered significantly higher mortality rates when tethered 15 and 70 m away from casitas than when tethered to casitas or 30 m away from casitas (Fig. 6; Q Ryan's test, experiment-wise error rate 0.05).

Predator observations

The visual census of potential lobster predators at the inner-bay site during January 1989 indicated two predatory crab species (stone crab *Menippe mercenaria*, and a portunid *Portunus spinimanus*) and two piscine predators (gray snapper *Lutjanus griseus*, and schoolmaster snapper *L. apodus*) associated with the casitas (Table 2). No potential predators were observed in the vicinity of the no-casita stations. Mixed schools of gray snapper and schoolmaster snapper were typically found within 10 m of large casitas. Schools associated with small and medium casitas were usually located within 5 m of the casitas. Observed movements of snappers were seldom more than 15–20 m from the shelters. Similarly, two snapper species predominated at the outer-bay site during January 1989: mutton snapper *L. analis* and yellowtail snapper *Ocyurus chrysurus* (Table 2). Casitas at the outer-bay site also attracted octopus (*Octopus* spp.), green moray eel *Gymnothorax funebris*, the stone crab

Figure 6
Results of field tethering of *Panulirus argus* at the outer-bay site during August 1989, describing mortality of small juvenile lobsters (46–55 mm CL) as a function of distance from the casita (i.e., 0, 15, 30, and 70 m away from the casita). Values are mean proportional mortality · casita^{-1} · d^{-1} resulting from a total of 18 lobsters tested. Vertical bars are 1 SE.

Table 2

Summary of results from visual census of potential lobster *Panulirus argus* predators associated with 18 casitas of three sizes (small, medium, large) at two sites (inner-bay, outer-bay) during 10–16 January 1989 at Bahia de la Ascension, Mexico. Results below are pooled from censusing 18 casitas on three different sampling dates. Fish size is fork length (cm) and crab size is carapace width (cm).

Species	Total abundance	Mean individuals/ sample/casita	Frequency/ casita size (N 18)	Percent frequency	Size (cm)		
					Mean	Min.	Max.
Inner-bay site							
Large Casita							
Lutjanus griseus (gray snapper)	213	11.8	18	100.0	23.4	9	37
Lutjanus apodus (schoolmaster snapper)	27	1.50	6	33.3	10.0	8	11
Menippe mercenaria (stone crab)	3	0.17	3	16.7	11.0	11	11
Medium Casita							
Lutjanus griseus	12	0.66	12	66.7	7.5	6	10
Menippe mercenaria	2	0.13	2	11.1	7.0	4	10
Portunis spinimanus (portunid crab)	2	0.11	2	11.1	8.0	8	8
Small Casita							
Lutjanus griseus	30	1.67	12	66.7	7.5	6	10
Lutjanus apodus	2	0.11	1	5.6	9.0	9	9
Menippe mercenaria	1	0.06	1	5.6	4.0	—	—
Portunis spinimanus	4	0.22	2	0.1	8.5	7	12
Outer-bay site							
Large Casita							
Lutjanus analis (mutton snapper)	15	0.83	6	33.3	25.3	20	40
Ocyurus chrysurus (yellowtail snapper)	24	1.30	6	33.3	22.0	19	25
Menippe mercenaria	3	0.17	3	16.7	10.0	10	10
Octopus	3	0.16	3	16.7	—	—	—
Medium Casita							
Lutjanus analis	4	0.22	4	22.2	12.8	10	15
Portunis spinimanus	2	0.11	2	11.1	9.5	6	13
Small Casita							
Lutjanus analis	3	0.16	2	11.1	8.0	8	8
Gymnothorax funebris (green moray eel)	3	0.16	3	16.7	50.0	50	50
Portunis spinimanus	3	0.16	3	16.7	7.5	6	11

M. mercenaria, and the portunid crab *P. spinimanus* (Table 2). As above, no potential predators were observed in the vicinity of the no-casita stations, and mixed schools of snapper seldom strayed more than 15–20 m from casitas. However, several large snapper of both species (*L. griseus* at the inner-bay site and *L. analis* at the outer-bay site) were observed ~60 m from the casitas. We also witnessed a stone crab feeding on a lobster tethered beneath a casita, and on two separate occasions observed octopus feeding on tethered lobsters beneath a casita.

During January 1989 at the inner-bay site, there was a significant positive correlation between mean lobster proportional mortality per day at a particular casita station and the mean number of potential predators occupying the same casita station (r 0.92, n 6, $P<0.01$; Fig. 7). Conversely, there was no significant correlation between lobster proportional mortality and numbers of predators inhabiting casitas at the outer-bay site (r 0.11, n 6, NS), nor between proportional mortality and the sizes of piscine predators (mm total length; TL) at both sites (inner-bay: r 0.64, n 6, NS; outer-bay: r 0.59, n 6, NS).

Predator observations at the outer-bay site in August demonstrated a more diverse predator guild than that observed during January (compare Tables 2 and 3). Although mutton snapper and yellowtail snapper were abundant at large casitas, they were joined by larger predators, including Nassau grouper *Epinephelus striatus* and a great barracuda *Sphyraena barracuda*. One barracuda was identified by particular scars near the mouth and a broken tooth. This barracuda roamed the entire experimental area. We also observed one Nassau grouper that moved between the 70 m no-casita stations and the reef (see Fig. 4 for geography). Another slightly smaller grouper moved back and forth between the casitas, the 15 m no-casita stations, and the reef.

Table 3

Summary of results from visual census of potential lobster *Panulirus argus* predators associated with three large casitas at the outer-bay site during 3–10 August 1989 at Bahia de la Ascension, Mexico. Results below are pooled from censusing three casitas on three different sampling dates. Fish size is fork length (cm).

Species	Total abundance	Mean individuals/ sample/casita	Frequency/ casita size (N 18)	Percent frequency	Size (cm)		
					Mean	Min.	Max.
Lutjanus analis (mutton snapper)	12	1.33	9	100.0	20.3	15	30
Ocyurus chrysurus (yellowtail snapper)	15	1.67	9	100.0	22.0	19	25
Sphyraena barracuda (great barracuda)	2	0.22	2	22.2	100.0	100	100
Epinephelus striatus (Nassau grouper)	2	0.22	2	22.2	45.0	40	50
Dasyatis americana (southern stingray)	1	0.11	1	11.1	60.0*	—	—

* Measured from wingtip to wingtip (cm).

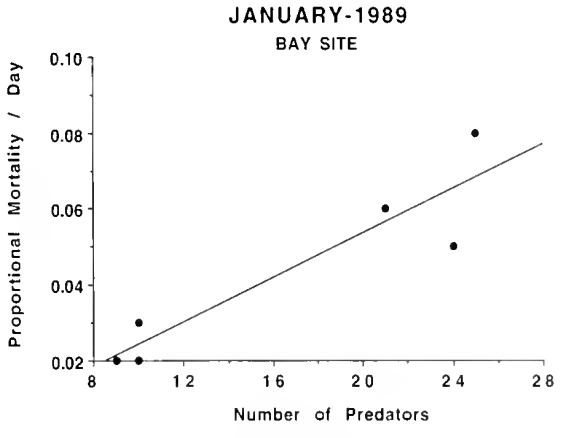

Figure 7

Mean proportional mortality of juvenile lobsters *Panulirus argus* · large casita^{-1} · d^{-1} compared against the mean number of potential predators · casita station^{-1} · d^{-1} at the inner-bay site during January 1989 ($y = -0.0051 + 0.0029x$; r^2 0.85, n 6, $P<0.009$).

Discussion

The impact of artificial shelters upon juvenile spiny lobster survival varied both by lobster size and the distance of unprotected lobsters from shelter. During our January 1989 experiment, which emphasized the effects of lobster size and shelter availability, large lobsters (56–65 mm CL) survived better than small lobsters (46–55 mm CL) in sparse-to-moderate-density seagrass (*Thalassia*) 60 m from casitas. Conversely, small lobsters survived better than large lobsters when tethered beneath casitas. During our August 1989 experiment, small lobsters survived better at casitas or 30 m away from casitas than 15 m or 70 m away. We interpret these patterns in terms of the relative importance of shelter availability and body size upon lobster survival, and then speculate on the influence of artificial-shelter-associated predators and seagrass density relative to these patterns in lobster survival.

We reemphasize that predation estimates based on tethering are likely biased by the technique and may not reflect natural predation rates. For example, lobster dens which are normally abandoned at night may become "traps" for tethered lobsters because they cannot effectively flee and conspecifics are not available to help detect and repel predators. However, predation rates on early juvenile *Panulirus argus* tethered in open sand, seagrass, and algal habitats in Florida Bay were similar both day and night (Herrnkind and Butler 1986, Smith and Herrnkind 1992). Moreover, most casita-associated predators are widely dispersed among the seagrass flats at night in Bahia de la Ascension, Mexico (Eggleston et al. 1990). Thus, we feel that the tethering technique is not only useful for comparing relative rates of predation between different size-classes of juvenile spiny lobster, but also for comparing predation rates between representative benthic habitats (e.g., crevices, algal clumps, seagrass).

Results from our January 1989 experiment support the hypothesis that large juvenile lobsters (56–65 mm CL) attain a relative-size refuge from predation compared with small juvenile lobsters (45–55 mm CL), and that the relative importance of this size refuge varies according to shelter availability. Increased predation

on small juvenile lobsters tethered in seagrass suggests that sparse-to-moderate-density *Thalassia* does not provide adequate protection from predators, and that the addition of shelter greatly enhances survival for these smaller juvenile lobsters. Thus, the use of artificial lobster shelters in sparse-to-moderate-density *Thalassia* beds may effectively reduce predation-induced mortality rates of small juvenile lobsters and thereby enhance production of this size-class. However, given the general relationship of increasing survival with habitat complexity for many decapod crustaceans (Heck and Thoman 1981, Wilson et al. 1987, Heck and Crowder 1991 and references therein), the relative importance of shelter availability upon survival of small juvenile lobsters may be reduced in habitats with dense *Thalassia*. Thus, further studies are required to understand the relationship between shelter availability and increasing habitat complexity upon survival of small juvenile lobsters.

The reduced survival of large juvenile lobsters near casitas compared with seagrass 60–70 m away during the January 1989 experiment is consistent with our previous results for this lobster size-class. For example, survival of small lobsters (46–55 mm CL) in large casitas was significantly higher than survival of large lobsters (56–65 mm CL) (Eggleston et al. 1990). Moreover, large lobsters survived better in medium than in large casitas (Eggleston et al. 1990). Eggleston et al. (1990) suggested that medium casitas excluded predators that were able to prey on large lobsters, and postulated that larger predators associated with large casitas may selectively prey upon larger lobsters, due to better visual perception with increasing predator and prey size (Kao et al. 1985, Ryer 1988). The significant positive correlation between the numbers of predators (primarily gray snapper *L. griseus*) occupying specific casita stations and predation rates at these same stations suggests that gray snapper may be the principle predator of juvenile lobsters inhabiting casitas at the inner-bay nursery site. Gray snapper (15 cm TL) have successfully attacked small early-juvenile lobsters tethered in Florida Bay (Herrnkind and Butler 1986).

The combined results from this study and previous work in Bahia de la Ascension, Mexico (Eggleston et al. 1990), suggest that juvenile lobsters would survive better by leaving large shelters to take up residence in smaller shelters or nearby seagrass habitats when they reach a body size of ~56–65 mm CL. This idea of enhancing survival through size-specific emigration from large shelters was partially supported during our recent observations of habitat-specific and size-specific patterns of shelter use by juvenile *P. argus* in Bahia de la Ascension, Mexico. Our recent field observations (Eggleston and Lipcius 1992) indicated that shelter-seeking behavior of *P. argus* is highly flexible to local social conditions (i.e., presence of conspecifics) and shelter scaling. For example, in a habitat containing very few conspecifics (e.g., outer-bay site), large juvenile lobsters chose smaller, safer medium casitas over large casitas as predicted by our tethering results (this study; Eggleston et al. 1990). However, in a habitat containing large numbers of conspecifics (e.g., inner-bay site), large juvenile lobsters occupied large casitas with large conspecifics (Eggleston and Lipcius 1992). The tethering technique in this study did not address the potential benefits of gregarious residency to lobster survival. Gregarious occupancy by more than the six tethered lobsters appeared to be inhibited because of the tethering technique, i.e., lobsters did not colonize casitas containing tethered individuals (pers. observ.). Since gregarious sheltering has been implicated as a mechanism for reducing predator-induced mortality (Berrill 1975, Herrnkind et al. 1975, Eggleston and Lipcius 1992), final conclusions regarding the impact of casitas upon predation-induced mortality rates of large juvenile lobsters must not only consider the size-specific relationship between shelter-associated predators and lobsters, but also the potential benefits of gregarious sheltering.

Results from our August 1989 experiment support the hypothesis that the impact of artificial shelters upon predation-induced mortality of juvenile lobsters varies according to the distance of unprotected lobsters from these shelters. During the August experiment at the outer-bay site, small lobsters survived equally well whether they were tethered beneath casitas or 30 m away. These tethering results, combined with observations on predator movements, suggest that 30 m is beyond the daytime foraging range of most casita-associated predators. However, the lack of a significant correlation between the numbers of potential predators at a specific casita station and predation rates on lobsters at these same stations at the outer-bay site during the January 1989 experiment suggests that transient predators such as jacks (*Caranx* spp.), groupers (*Epinephelus* spp.), sharks (*Ginglymostoma cirratum* and *Sphyrna* spp.), and stingrays (*Dasyatis* spp.) may be moving from the nearby barrier reef (see Figs. 3 and 4 for geography) and preying on tethered lobsters. Gut contents of stingrays (*Dasyatis* spp.) and bonnethead sharks *Sphyrna tiburo*, captured at night in nearshore Florida Bay waters, contained a high proportion of early-juvenile spiny lobsters (Smith and Herrnkind 1992). Nurse sharks *Ginglymostoma cirratum* are also known predators of juvenile *P. argus* (Cruz and Brito 1986). Thus, our observations on the daytime abundance and movements of casita-associated predators (i.e., primarily mutton and yellowtail snapper, *Lutjanus analis* and *O. chrysurus*) at the outer-

bay site may not reflect potential predation intensity as previously suggested for the inner-bay site.

Predation risk on artifical reefs usually decreases with distance from a natural, larger reef. For example, mortality of tethered juvenile grunts (family Pomadasyidae) in St. Croix, U.S. Virgin Islands, was 40% higher at the reef edge than 20 m away (Shulman 1985). Our results are somewhat consistent with those of Shulman (1985) in that predation of lobsters decreased from 15 to 30 m from the casitas. However, increased predation rates from 0 to 15 m and from 30 to 70 m indicate that predation risk does not simply decrease linearly with increasing distance from the artificial reef (casita). We hypothesize that the predator guild originating from the nearby barrier reef at the outer-bay site (see Figs. 3 and 4 for geography) forages within the adjacent seagrass habitat and is attracted to the casitas, thereby leaving a relative "gap" in predator abundance between 15 and 60 m from the casitas. Thus, predator encounter rates with lobsters tethered only 15 m from casitas were probably high relative to lobsters tethered 30 m away. The patterns of survival of small *P. argus* within close proximity to casitas (i.e., 15 m) in this study are consistent with our previous work in seagrass habitats of Bahia de la Ascension, Mexico. For example, survival of small lobsters (46–55 mm CL) was significantly higher at medium and large casitas than in seagrass 15 m away (Eggleston et al. 1990). Predation rates also increased from 30 to 70 m, and predators not associated with the casitas, such as Nassau grouper *E. striatus*, were observed moving from nearby natural reefs to the 70 m no-casita stations rather than from the casitas.

Resident piscivores set the upper limit of the number and sizes of prey species that can occupy a given reef (Hixon and Beets 1989, Eggleston et al. 1990). For example, Hixon and Beets (1989) found an inverse relationship between the number of piscivorous fishes on a reef and the maximum number of co-occurring potential prey fishes. The results from our study indicate that large casitas are more effective at reducing mortality on small juvenile lobsters than seagrass habitats, even though seagrass and algal beds provide some refuge for juvenile spiny lobsters (Herrnkind and Butler 1986; R.N. Lipcius et al., unpubl. data). Hence, for small lobsters, our results from both the January and August experiments strongly suggest that artificial lobster shelters such as casitas increase lobster production by enhancing survival in nursery areas. However, our results for the outer-bay site during January indicated that survival of large juvenile lobsters was significantly lower when tethered beneath large casitas compared with nearby seagrass habitats. These results are consistent with the notion of building artificial lobster shelters that are scaled according to body size to enhance survival of larger juveniles in nursery habitats, particularly in areas where large conspecifics are removed from large casitas by the fishery (Eggleston et al. 1990, Eggleston and Lipcius 1992). However, further research on the impact of casitas upon lobster survival, growth rates, local and regional population structure, and benthic community structure will be required to assess the efficacy of this technology as a fisheries enhancement tool.

Acknowledgments

We thank L. Coba-Cetina, T. Camarena-Luhrs, and E. Sosa-Cordero with the Centro de Investigaciones de Quintana Roo, and J. Cohen, J. Eggleston, K. Kennedy, and numerous Earthwatch volunteers for their able field assistance. Special thanks to Armando Lopez and Sonja Lillvick for the fine accommodations and logistical support, and R. Wicklund and G. Wenz of the Caribbean Marine Research Center for their administrative guidance. We thank J. Bohnsack, L. Jones, M. Luckenbach, J. van Montfrans, and two anonymous referees for critical comments. This work was funded by Sigma-Xi, Earthwatch–The Center for Field Research, the National Undersea Research Program of the National Oceanic and Atmospheric Administration, the Caribbean Marine Research Center, the Commonwealth of Virginia, L.L. Glucksman, and the National Science Foundation (INT-8617945 to D.M. and R.L. and OCE 87-00414 to R.L. and A. Hines).

Citations

Berrill, M.
1975 Gregarious behavior of juveniles of the spiny lobster, *Panulirus argus* (Crustacea: Decapoda). Bull. Mar. Sci. 25: 515–522.

Bohnsack, J.A.
1989 Are high densities of fishes at artificial reefs the result of habitat limitation or behavioral preference? Bull. Mar. Sci. 44:631–645.

Bohnsack, J.A., and S.P. Bannerot
1986 A stationary visual census technique for quantitatively assessing community structure of coral reef fishes. NOAA Tech. Rep. NMFS 41, 15 p.

Bohnsack, J.A., and D.L. Sutherland
1985 Artificial reef research: A review with recommendations for future priorities. Bull. Mar. Sci. 37:11–39.

Cobb, J.S.
1981 Behaviour of the Western Australian spiny lobster, *Panulirus cygnus* George, in the field and laboratory. Aust. J. Mar. Freshwater Res. 31:399–409.

Cruz, R., and R. Brito
1986 Ecologia de la langosta (*Panulirus argus*) al SE de Isla de la Juventud. I. Colonizacion de arrecifes artificiales. Rev. Invest. Mar. 7:3–17.

Day, R.W., and G.P. Quinn
1989 Comparisons of treatments after an analysis of variance in ecology. Ecol. Monogr. 59:433–463.

Eggleston, D.B., and R.N. Lipcius
1992 Shelter selection by spiny lobster under variable predation risk, social conditions and shelter size. Ecology 73: 992–1011.

Eggleston, D.B., R.N. Lipcius, D.L. Miller, and L. Coba-Cetina
1990 Shelter scaling regulates survival of juvenile Caribbean spiny lobster *Panulirus argus*. Mar. Ecol. Prog. Ser. 62: 70–88.

Einot, I., and K.R. Gabriel
1975 A study of the powers of several methods of multiple comparisons. J. Am. Stat. Assoc. 70:574–583.

Grove, R.S., and C.J. Sonu
1985 Fishing reef planning in Japan. *In* D'Itri, F. (ed.), Artificial reefs: Marine and freshwater applications, p. 187–251. Lewis Publ., Chelsea, MI.

Hartnoll, R.G.
1982 Growth. *In* Abele, L.G. (ed.) The biology of crustacea, vol. 2, p. 111–196. Academic Press, NY.

Heck, K.L. Jr., and L.B. Crowder
1991 Habitat structure and predator-prey interactions in vegetated aquatic systems. *In* Bell, S.S., E.D. McCoy, and H.R. Mushinsky (eds.), Habitat structure: The physical arrangement of objects in space, p. 281–299. Chapman & Hall, NY.

Heck, K.L. Jr., and T.A. Thoman
1981 Experiments on predator-prey interactions in vegetated aquatic habitats. J. Exp. Mar. Biol. Ecol. 53:125–134.

Herrnkind, W.F., and M.J. Butler
1986 Factors regulating postlarval settlement and juvenile microhabitat use by spiny lobsters *Panulirus argus*. Mar. Ecol. Prog. Ser. 34:23–30.

Herrnkind, W.F., J. Vanderwalker, and L. Barr
1975 Population dynamics, ecology and behavior of spiny lobsters, *Panulirus argus*, of St. John, U.S. Virgin Islands: Habitation and pattern of movements. Sci. Bull., Nat. Hist. Mus., Los Angel. Cty. 20:31–34.

Hixon, M.A., and J.P. Beets
1989 Shelter characteristics and Caribbean fish assemblages: Experiments with artificial reefs. Bull. Mar. Sci. 44:666–680.

Howard, R.K.
1988 Fish predators of the western rock lobster (*Panulirus cygnus* George) in a nearshore nursery habitat. Aust. J. Mar. Freshwater Res. 39:307–316.

Kao, T., T.K. Wetterer, and N.G. Hairston Jr.
1985 Fish size, visual resolution and prey selectivity. Ecology 66:1729–1735.

Lozano-Alvarez, E., P. Briones-Fourzan, and B.F. Phillips
1991 Fishery characteristics, growth, and movements of the spiny lobster *Panulirus argus* in Bahia de la Ascension, Mexico. Fish. Bull., U.S. 89:79–89.

Miller, D.L.
1989 Technology, territoriality and ecology: The evolution of Mexico's Caribbean spiny lobster fishery. *In* Barkes, F. (ed.), Common property resources: Ecology and community-based sustainable development, p. 185–198. Valhaven Press, London.

Mottet, M.G.
1985 Enhancement of the marine environment for fisheries and aquaculture in Japan. *In* D'Itri, F. (ed.), Artificial reefs: Marine and freshwater applications, p. 13–112. Lewis Publ., Chelsea, MI.

Munro, T.
1974 The biology, ecology, and bionomics of Caribbean reef fishes. Part VI. Crustaceans (spiny lobsters and crabs). Univ. West Indies Zool. Dep., Res. Rep. 3:1–57.

Reaka, M.L.
1987 Adult-juvenile interactions in benthic reef crustaceans. Bull. Mar. Sci. 41:108–134.

Ryer, C.H.
1988 Pipefish foraging: effects of fish size, prey size and altered habitat complexity. J. Exp. Mar. Biol. Ecol. 48:37–45.

Scully, E.P.
1983 The behavioral ecology of competition and resource utilization among hermit crabs. *In* Rebach, S., and D.W. Dunham (eds.), Studies in adaptation: The behavior of higher Crustacea, p. 23–56. John Wiley, NY.

Shulman, M.J.
1985 Recruitment and coral reef fishes: Effects of distribution of predators and shelter. Ecology 66:1056–1066.

Smith, K.N., and W.F. Herrnkind
1992 Predation on early juvenile spiny lobsters *Panulirus argus* (Latreille): Influence of size and shelter. J. Exp. Mar. Biol. Ecol. 157:3–18.

Underwood, A.
1981 Techniques of analysis of variance in experimental marine biology and ecology. Oceanogr. Mar. Biol. Annu. Rev. 19: 513–605.

U.S. Agency for International Development
1987 Caribbean marine resources: Oppurtunities for economic development and management. U.S. Agy. Int. Develop., Wash. DC, 53 p.

Vermeij, G.
1987 Evolution and escalation: An ecological history of life. Princeton Univ. Press, Princeton, 527 p.

Wilson, K.A., K.L. Heck Jr., and K.W. Able
1987 Juvenile blue crab, *Callinectes sapidus*, survival: An evaluation of eelgrass, *Zostera marina*, as refuge. Fish. Bull., U.S. 85:53–58.

Zimmer-Faust, R.K., and E. Spanier
1987 Gregariousness and sociality in spiny lobsters: Implications for den habitation. J. Exp. Mar. Biol. Ecol. 105:57–71.

Stock structure of the bluefish *Pomatomus saltatrix* along the mid-Atlantic coast*

John E. Graves
Jan R. McDowell
Ana M. Beardsley
Daniel R. Scoles

Virginia Institute of Marine Science, School of Marine Science
College of William and Mary, Gloucester Point, Virginia 23062

Abstract.–Restriction-fragment length polymorphism analysis of mitochondrial DNA (mtDNA) was used to investigate the genetic basis of stock structure of the bluefish *Pomatomus saltatrix* along the U.S. mid-Atlantic coast, and to determine the degree of genetic differentiation between mid-Atlantic bluefish and Australian conspecifics. A total of 472 young-of-the-year (YOY) and yearling bluefish collected in New Jersey, Virginia, and North Carolina over a period of 3 years, and 19 YOY bluefish collected in New South Wales, Australia were analyzed with 9 informative restriction endonucleases. Despite considerable mtDNA variation within samples of U.S. mid-Atlantic bluefish, no significant genetic differentiation was detected among spring-spawned and summer-spawned (YOY) bluefish, YOY and yearling bluefish from different geographic locations along the mid-Atlantic coast, or yearling bluefish collected at the same location in different years. Mid-Atlantic bluefish differed from their Australian conspecifics by three or more restriction site differences, or a mean nucleotide sequence divergence of 1.96%. In addition, Australian bluefish demonstrated greatly reduced levels of mtDNA variation relative to the mid-Atlantic samples. The results of this study suggest that bluefish along the mid-Atlantic coast comprise a single genetic stock and that significant differentiation occurs among geographically disjunct populations of this widely distributed marine fish.

The bluefish *Pomatomus saltatrix* is broadly distributed in temperate and warm-temperate coastal waters of the world's oceans (Briggs 1960), although it is absent from the eastern Pacific (Smith 1949). In the United States, bluefish occur along the Atlantic and Gulf coasts, supporting large recreational and commercial fisheries.

The movements and biology of the bluefish, like many fishes along the Atlantic coast, are closely tied to large seasonal fluctuations in water temperature (reviewed in Wilk 1977). Spawning appears to be concentrated in two spatially and temporally distinct events: a spring spawn at the inside edge of the Gulf Stream in the south Atlantic bight, and a summer spawn in the shelf waters of the mid-Atlantic bight (Kendall and Walford 1979). However, the presence of eggs and larvae indicates that some spawning occurs throughout the year, especially in the southern portion of the south Atlantic bight (Kendall and Walford 1979, Collins and Stender 1988). Presumably, eggs and larvae are transported by cross-shelf currents to estuaries along the Atlantic coast which serve as nursery grounds for the young bluefish.

The discrete temporal nature of the two spawning events is evidenced by a bimodal size distribution of juvenile bluefish within the estuaries during the middle and late summer (Nyman and Conover 1988, McBride 1989), a difference that is still evident in yearling fish and may persist until fish reach 4 years of age (Lassiter 1962). The extent to which each of the major spawning events contributes juveniles to specific areas appears to vary annually (Chiarella and Conover 1990).

A general mixing of bluefish from different coastal areas may occur at the end of the first summer. Tagging studies indicate that as water temperatures cool, young bluefish move out of the estuaries in a southerly direction and probably overwinter in the south Atlantic bight (Lund and Maltezos 1970, Wilk 1977), while adults move further offshore (Wilk 1977). As temperatures along the mid-Atlantic coast warm in the spring, there is a general movement of bluefish up the Atlantic coast, with larger bluefish making more extensive migrations into northern waters (Wilk 1977).

Although the seasonal movements of bluefish may be conducive to a mixing of fish from different coastal areas, mark and recapture studies suggest that a large fraction of bluefish are recaptured in the same general area in which they were tagged (Lund and Maltezos 1970, Wilk 1977). The degree to which this fidelity affects stock structure is not known.

Manuscript accepted 29 July 1992.
Fishery Bulletin, U.S. 90:703–710 (1992).

* Contribution 1750 of the Virginia Institute of Marine Science.

Table 1

Sample size, date, location, and age of bluefish *Pomatomus saltatrix* collected and analyzed in this study. YRL = yearling; YOY = young-of-the-year.

Sample	*n*	Date	Location	Age
VA88	100	7/88	York River VA	YRL
VA89	102	7/89	York River VA	YRL
VA90	39	7/90	York River VA	YRL
NC88	83	7/88	Hatteras NC	YRL
NC89	57	7/89	Hatteras NC	YRL
NC90	40	7/90	Hatteras NC	YOY
NJ90-Sp	26	8/90	southern NJ	YOY
NJ90-Su	25	8/90	southern NJ	YOY
AU91	19	2/91	Port Stephens, N.S.W., Australia	YOY

The genetic basis of population structure of the bluefish is poorly understood. Based on studies of morphological and scale characteristics, Wilk (1977) suggested that two populations exist along the mid-Atlantic coast. These populations correspond to the fish which spawn off North Carolina in the spring, and those that spawn in the northern mid-Atlantic during the summer. Lund and Maltezos (1970) also concluded on the basis of mark and recapture analysis that several populations are present along the mid-Atlantic coast. Chiarella and Conover (1990) used scales from summer-spawning fish in the New York Bight to back-calculate length at age-1 and found that most summer-spawning fish had lengths corresponding to a spring birthdate, a result not consistent with spring- and summer-spawning stocks. They concluded that the morphological and life-history differences found between spring- and summer-spawned bluefish are probably ecophenotypic in nature, and suggested that a direct genetic analysis of stock structure was warranted.

In this paper, we present the results of a restriction-fragment length polymorphism (RFLP) analysis of bluefish mitochondrial DNA (mtDNA) among bluefish collected along the mid-Atlantic coast over a period of 3 years. We employed RFLP analysis of mtDNA to evaluate genetic differentiation between spring- and summer-spawned bluefish collected at a single location at the same time, among similarly-sized bluefish collected at the same location over several years, and among bluefish collected during the same year from the north and south mid-Atlantic coast, as well as from a disjunct population in Australia.

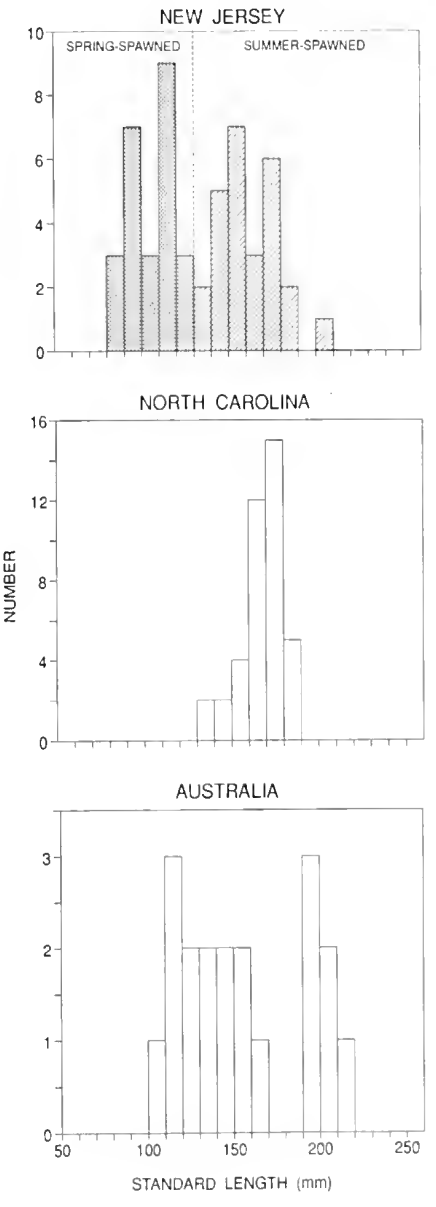

Figure 1

Frequency distribution of standard lengths among YOY bluefish *Pomatomus saltatrix* collected in New Jersey, North Carolina, and Port Stephens, N.S.W., Australia. The New Jersey fish were separated into spring- and summer-spawned groups based upon their standard length on the date of capture relative to a standard length of 125 mm (Nyman and Conover 1988, McBride 1989).

Materials and methods

Experimental design and collections

Bluefish were collected along the mid-Atlantic coast during 1988–90, and in Australia during 1991 (Table 1). To test the hypothesis that spring- and summer-spawned bluefish represent genetically distinct stocks, young-of-the-year bluefish were collected by trawl on New Jersey state survey cruises during August 1990 (NJ90-Sp, NJ90-Su, Table 1). Fish were classified as spring- or summer-spawned based on the date of capture using a standard length of 125 mm used as the cut-off between the two groups in August (Nyman and Conover 1988, McBride 1989). The distribution of lengths is presented in Figure 1.

To obtain an estimate of the degree of temporal genetic variation between bluefish year-classes at a single collection location, 1-year-old (yearling) bluefish were purchased from commercial fishermen on the York River, Virginia during July 1988 (VA88), 1989 (VA89), and 1990 (VA90), and in Hatteras, North Carolina during 1988 (NC88) and 1989 (NC89). The distribution of lengths of the Virginia and North Carolina samples is presented in Figure 2.

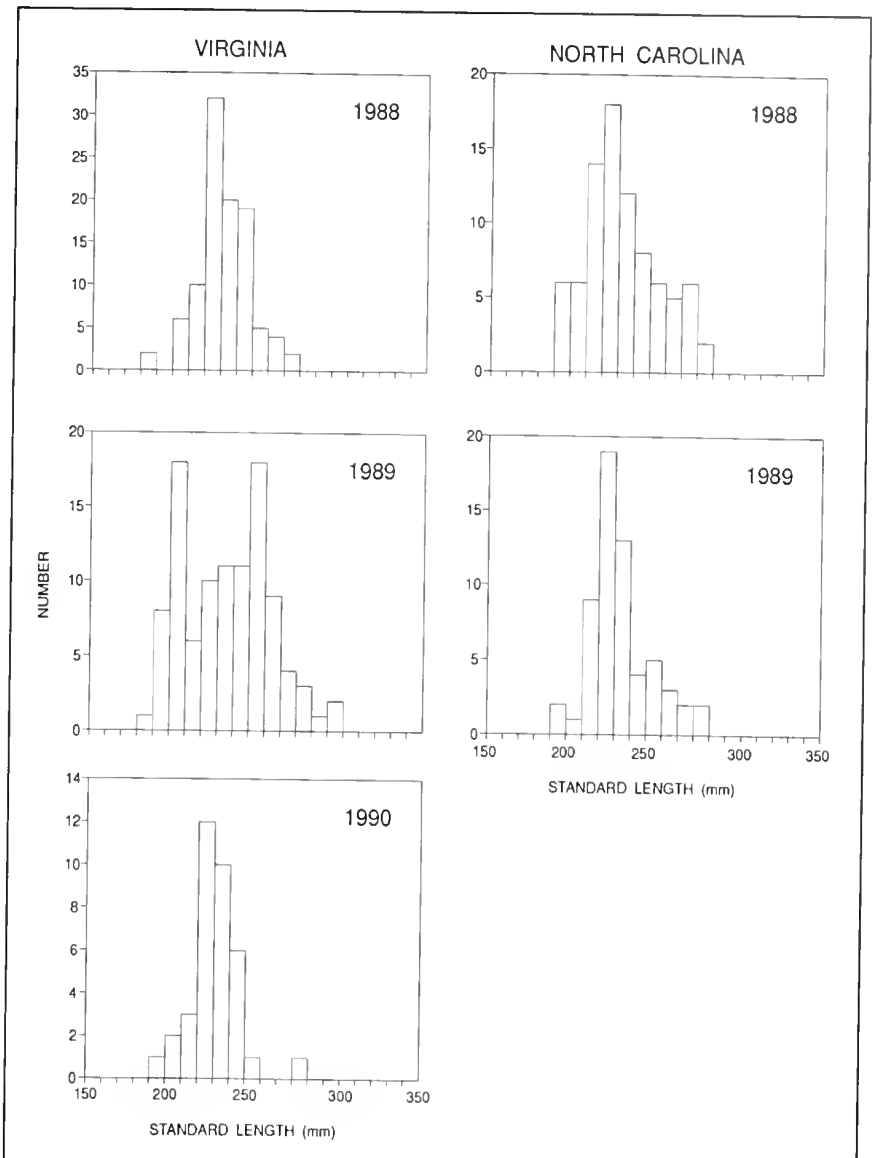

Figure 2

Frequency distribution of standard lengths among yearling bluefish *Pomatomus saltatrix* collected in (left) the York River, VA during summer 1988, 1989, and 1990, and (right) Hatteras, NC during summer 1988 and 1989.

An analysis of geographic population structure of highly vagile fishes, like the bluefish, is problematic. The presence of an adult bluefish in one geographic location is not very meaningful, as the fish could easily travel to another location several hundred kilometers away within a few weeks. If discrete geographic stocks of bluefish exist, such stocks might be expected to separate at the time of spawning. However, collection of adults at this critical time is difficult since bluefish spawn at the edge of the continental shelf during the spring and in the middle of the shelf during the summer (Kendall and Walford 1979). Thus we decided to focus our study on their products, YOY bluefish. Although some mixing probably occurs during cross-shelf transport, the genetic composition of YOY bluefish should reflect the composition of the offshore spawning population.

To determine genetic differentiation among bluefish along the mid-Atlantic coast, samples of YOY individuals were collected during summer 1990 in New Jersey (described above) and purchased from commercial fishermen in Hatteras, North Carolina (NC90). In addition, to obtain an estimate of the degree of mtDNA differentiation between isolated bluefish populations, a sample of 19 YOY bluefish was collected by hook-and-line in Port Stephens, N.S.W., Australia during February 1991 (AU91). The size composition of all YOY collections is presented in Figure 1.

mtDNA analysis

Depending on size and quality of the bluefish, three different procedures were used to analyze bluefish mtDNA. The rapid isolation procedure of Chapman and Powers (1984) was used to obtain mtDNA from samples of lateral red muscle from the yearling bluefish collected in 1988 and 1989. After digestion, restriction fragments were separated electrophoretically on 0.8–1.5% agarose gels run at 2 volts/cm overnight and visualized directly with ethidium bromide staining. For those samples in which there was not sufficient mtDNA

for direct visualization, restriction digestions were endlabeled before electrophoresis with a mixture of all four ^{35}S nucleotide triphosphates using the Klenow fragment (Maniatis et al. 1982). After electrophoresis, gels were treated with a scintillation enhancer, dried, and autoradiographs exposed at −70°C for 5 days.

Mitochondrial DNA was purified from YOY and yearling bluefish collected in 1990 and 1991 following the protocols of Lansman et al. (1981) and ^{35}S-end-labeled restriction fragments were visualized autoradiographically after electrophoresis. Due to the thermal history of many of these specimens, yields of supercoiled mtDNA were low. In those instances, the nuclear band containing both nuclear DNA and relaxed mtDNA was collected and dialyzed as described for mtDNA bands in Lansman et al. (1981), or mtDNA was reisolated following the Chapman and Powers (1984) protocol. For these samples, the Southern transfer and

Table 2

Distribution of mtDNA genotypes among bluefish *Pomatomus saltatrix* samples. Each letter represents the fragment pattern for a particular restriction endonuclease: from left to right, *Ava*I, *Hin*dIII, *Pvu*II, *Dra*I, *Eco*RV, *Sst*I, *Pst*I, *Sst*II, and *Nci*I. A description of all fragment patterns and sizes is available from the authors upon request.

Composite genotype	VA88	VA89	VA90	NC88	NC89	NC90	NJ90-Sp	NJ90-Su	AU91	Total
AAAAAAAAA	44	45	24	50	33	17	20	18	0	250
AAAAAAAAB	0	0	0	1	1	1	0	0	0	3
AAAAAAAAC	1	2	0	1	1	0	0	2	0	7
AAAAAAAAD	6	1	0	0	0	0	0	0	0	7
AAAAAAAAG	0	1	1	0	1	0	0	0	0	3
AAAAAAAAH	0	0	1	0	0	0	0	0	0	1
AAAAABAAA	0	0	1	0	0	0	0	1	0	2
AAAABAAAA	11	11	1	5	3	5	1	1	0	38
AAAABAAAB	0	0	0	0	1	0	0	0	0	1
AAAABAABA	0	1	0	1	0	0	0	1	0	3
AAAACAAAA	6	6	3	2	3	2	2	0	0	24
AAAACAAAC	0	0	0	0	0	1	0	0	0	1
AAAACAABA	0	0	0	0	0	1	0	0	0	1
AAAADAAAA	7	13	3	4	2	4	1	1	0	35
AAABAAAAA	0	0	1	0	1	0	0	0	0	2
AAACAAAAA	1	1	0	1	0	0	0	0	0	3
AAAEEAAAD	0	0	0	0	0	0	0	0	18	18
AAAEFAAAD	0	0	0	0	0	0	0	0	1	1
AABAAAAAA	0	2	0	1	1	0	0	0	0	4
AABABAAAA	3	4	0	2	1	3	1	0	0	14
AABABAAAB	1	0	0	0	0	0	0	0	0	1
AABABAAAC	0	0	0	0	1	0	0	0	0	1
AABABAAAE	0	2	0	2	0	1	0	0	0	5
AACAAAAAA	1	0	0	2	1	0	0	0	0	4
AACACAAAA	2	2	0	0	0	0	0	0	0	4
BAAAAAAAA	6	2	0	4	3	2	0	1	0	18
BAAAAAAAC	0	1	0	0	0	0	0	0	0	1
BAAACAAAA	5	1	0	2	0	0	0	0	0	8
BAAACAAAD	1	0	0	0	0	0	0	0	0	1
BAAACBAAA	0	1	0	0	0	0	0	0	0	1
BAAADAAAA	0	0	0	1	1	0	0	0	0	2
BADAAAAAA	1	0	0	0	0	0	0	0	0	1
BADACAAAA	0	0	0	1	0	0	0	0	0	1
CAAAAAAAA	1	1	0	0	1	0	0	0	0	3
CAAAAAAAC	3	1	1	0	0	2	0	0	0	8
CAAABAAAC	0	1	0	0	0	0	0	0	0	1
DAAAAAAAA	0	2	0	1	1	1	0	0	0	5
DAAACAAAA	0	1	0	0	0	0	0	0	0	1
DACAAAAAA	0	0	0	0	1	0	0	0	0	1
EAAAAAAAF	0	0	0	1	0	0	0	0	0	1
FAAAAAAAA	0	1	0	1	0	0	0	0	0	2
Totals	100	102	36	83	57	40	26	25	19	469

hybridization protocols of Maniatis et al. (1982) were followed after digestion and electrophoresis. Highly purified bluefish mtDNA, nick translated with biotin-7-dATP, was used as a probe for mtDNA fragments. Hybridization filters were visualized after strigency washes using the BRL BlueGene Nonradioadtive Nucleic Acid Detection System.

All mtDNA samples were digested with the following nine restriction endonucleases used according to the manufacturers' instructions: *Ava*I, *Dra*I, *Eco*RV, *Hin*dIII, *Nci*I, *Pst*I, *Pvu*II, *Sst*I, and *Sst*II. The different restriction-fragment patterns produced by each restriction endonuclease were assigned a letter, and a composite mtDNA genotype, consisting of nine letters representing the fragment patterns generated by each of the restriction endonucleases, was constructed for each individual. The nucleon diversity (Nei 1987) was calculated for each sample and for the pooled samples. The nucleotide sequence divergence among mtDNA genotypes was estimated by the site approach of Nei and Li (1979). The mean nucleotide sequence diversity within samples and mean nucleotide sequence divergence between samples were calculated following the method of Nei (1987), with the latter value being corrected for within-group diversity (Nei 1987). The distribution of genotypes was evaluated for homogeneity among collections using the G-test (Sokal and Rohlf 1981); however, as several of the genotypes were represented by one individual, we employed the Roff and Bentzen (1989) Monte Carlo approach to estimate the significance of heterogeneity χ^2 values determined from the raw data.

Results

The analysis of 472 mid-Atlantic bluefish with 9 restriction endonucleases revealed 40 mtDNA genotypes, and 2 mtDNA genotypes were encountered among 19 Australian bluefish. A total of 77 restriction fragments was visualized, and the average individual was scored for 34 fragments, accounting for approximately 1.4% of the mtDNA genome. The restriction endonucleases, *Hin*dIII and *Pst*I, revealed no variant fragment patterns, while the remaining seven enzymes revealed from two (*Sst*I and *Sst*II) to eight (*Nci*I) different fragment patterns. Restriction-site gains or losses were inferred from completely additive changes in fragment patterns.

Considerable RFLP variation was detected within Atlantic bluefish samples (Table 2). The most common mtDNA genotype, AAAAAAAAA, ranged in frequency from 0.43 (NC 1990 YOY) to 0.75 (NJ 1990 YOY). The large number of variant genotypes resulted in nucleon diversities ranging from 0.416 to 0.798 (Table 3). Because many of the variant genotypes differed from the common genotype by several site changes, the within-sample mean nucleotide sequence diversities were also relatively high, varying from 0.63% to 1.49%. In contrast to the mid-Atlantic bluefish, the Australian sample was quite depauperate of variation. Of the 19 fish in the sample, 18 shared a common mtDNA genotype (AAAEEAAAD), and one fish had a genotype differing from the common type by a single site change (Table 2). The lack of variation in the Australian sample was reflected in a low nucleon diversity (0.105) and a within-sample mean nucleotide sequence diversity of 0.07%.

Significant genetic differentiation was not found between the samples of spring- and summer-spawned YOY bluefish collected in New Jersey during the summer of 1990. The corrected mean nucleotide sequence divergence between the two samples was extremely small (0.02%), indicating that average sequence divergence between two individuals randomly drawn from either the spring- or summer-spawned sample was the same as the divergence between two individuals randomly drawn from each group.

Table 3

Genetic variation within bluefish *Pomatomus saltatrix* samples expressed as nucleon diversity and mean nucleotide sequence diversity. The spring- and summer-spawned NJ YOY bluefish collections were pooled (NJ90 combined) for comparison with the NC90 YOY sample, and all NJ, VA, and NC bluefish collections were pooled (mid-Atlantic combined) for comparison with the AU91 YOY sample. YRL = yearling; YOY = young-of-the-year.

Sample	Age	n	Nucleon diversity	Mean nucleotide sequence diversity
VA88	YRL	100	0.781	1.34%
VA89	YRL	102	0.777	1.41%
VA90	YRL	36	0.565	0.89%
NC88	YRL	83	0.632	1.15%
NC89	YRL	57	0.663	1.20%
NJ90-Sp	YOY	26	0.416	0.72%
NJ90-Su	YOY	25	0.467	0.63%
NJ90 combined	YOY	51	0.438	0.67%
NC90	YOY	40	0.798	1.49%
mid-Atlantic combined		372	0.696	1.23%
AU91	YOY	19	0.105	0.07%

Considerable genetic differentiation was not detected among samples of yearling bluefish collected at the same site in different years. The mean nucleotide sequence divergences (Table 4) among the VA88, VA89, and VA90 collections, and between the NC88 and NC90 samples, were of the same magnitude as the within-sample mean nucleotide sequence diversities (Table 3). Consequently, when adjusted for within-sample diversity (Nei 1987), the corrected mean nucleotide sequence divergences among samples were nearly zero (Table 4).

Table 4

Mean nucleotide sequence divergences (%) among selected bluefish *Pomatomus saltatrix* collections. Values are presented with and without correction for within-sample variation.

Collections	Uncorrected	Corrected
Among collections at a single location over 2 or more years		
VA88 vs. VA89	1.39	0.11
VA88 vs. VA90	1.20	0.18
VA89 vs. VA90	1.20	0.05
NC88 vs. NC89	1.18	0.01
Between spring- and summer-spawned bluefish		
NJ90-Sp vs. NJ90-Su	0.69	0.02
Between mid-Atlantic YOY fish		
NJ90-combined vs. NC90	1.19	0.11
Between mid-Atlantic and Australian bluefish		
mid-Atlantic combined vs. AU91	2.60	1.96

Analysis of YOY bluefish from the northern and southern mid-Atlantic bight revealed little mtDNA genetic differentiation. The corrected mean nucleotide sequence divergence between the combined NJ90 YOY sample and the NC90 YOY collection was 0.11%, suggesting little population structuring along the mid-Atlantic coast. This inference was further supported by an analysis of heterogeneity which demonstrated no significant differences in the distribution of six major mtDNA genotypes (those occurring in 10 or more of the 472 fish) and the pooled rare genotypes among the seven mid-Atlantic collections ($G_H = 39.5$, $0.25 < P < 0.50$). Heterogeneity χ^2 analysis of the distribution of all genotypes, including those represented by a single individual, was performed using the Monte Carlo simulation of Roff and Bentzen (1989). A total of 320 of the 1000 randomizations produced χ^2 values greater than the original data set, indicating no significant heterogeneity.

The low levels of mtDNA differentiation among mid-Atlantic bluefish collections contrasted with the substantial difference encountered between the combined mid-Atlantic bluefish and the Australian sample. The average mid-Atlantic bluefish could be distinguished from its Australian conspecific by three or more restriction-site changes. Two of the site changes were unique to the Australian sample, and the third (*Nci*I pattern D) occurred at a low frequency (0.01) in the combined mid-Atlantic sample. The corrected mean nucleotide sequence divergence between the Australian sample and the combined mid-Atlantic bluefish samples was 1.95%. Significant heterogeneity was noted among the pooled samples when the Australian sample was included with the mid-Atlantic bluefish ($G_H = 177$, $p < 0.001$).

A sample of 10 yearling bluefish was analyzed from the northeast Gulf of Mexico (Panama City, FL). Unlike the Australian bluefish, all of the mtDNA genotypes found in the Gulf of Mexico mtDNA individuals were also present in the mid-Atlantic samples, and 7 of the 10 Gulf of Mexico bluefish had the common mid-Atlantic mtDNA genotype. Because of the small size of the Gulf of Mexico sample, it was not appropriate to test for frequency differences between bluefish from the mid-Atlantic coast and the Gulf of Mexico.

Discussion

Mid-Atlantic bluefish demonstrated considerable mtDNA genotypic variation. It is difficult to directly compare the nucleon diversities calculated in this study with those from other studies because the value is sensitive to the number of restriction sites surveyed, and analyses employing larger numbers of restriction endonucleases typically have higher nucleon diversities. The value of 0.696 for the pooled mid-Atlantic bluefish samples is higher than those reported for many marine fishes surveyed with a larger number of enzymes (Avise et al. 1989, Gold and Richardson 1991), and indicates a relatively high degree of genetic variation within the bluefish. This trend becomes more apparent when mean nucleotide sequence diversities, a measure of intrasample diversity that is much less sensitive to the number of restriction sites surveyed, are compared. The value calculated in this study for the pooled mid-Atlantic samples, 1.23%, is higher than values reported for many other marine fishes (Ovenden 1990).

The Australian bluefish demonstrated much less variation than their mid-Atlantic conspecifics. The sample of 19 Australian bluefish had a nucleon diversity five times lower than the combined Atlantic samples, and a mean nucleotide sequence diversity that was an order of magnitude lower (Table 3). A similar difference in the level of mtDNA variation between

conspecific populations has been noted between Atlantic and Pacific blue marlin (Graves and McDowell, unpubl. data). The striking lack of variation within the Australian sample could be the result of a smaller effective population size of females resulting from population bottlenecks, or may simply reflect a period of isolation sufficient for the sorting of gene trees (Nei 1987, Avise et al. 1988, Chapman 1990, Bowen and Avise 1990).

We found little evidence to support the hypothesis that genetically distinct stocks of bluefish exist along the mid-Atlantic coast. Although appreciable mean nucleotide sequence divergences were found between sampling locations (Table 4), when corrected for within-group variation the values became extremely small, indicating that most of the observed differentiation could be accounted for by variation within the samples. The lack of population structuring was also supported by the homogeneous distribution of all genotypes and the fact that the level of genetic divergence among sampling locations was not appreciably greater than the level of divergence among samples taken at any one location in different years.

The extent of gene flow among populations can also be inferred from the frequency distribution of rare alleles (Slatkin 1989). An inspection of Table 2 indicates that almost all mtDNA genotypes that occurred more than once were found in different collections, suggesting significant gene flow among sampling locations. For example, the genotype AAAABAABA, which was present in three individuals, occurred in the VA89, NC88, and NJ90-Su collections. An exception to this pattern was presented by the genotype AAAAAAAAD, which occurred seven times: in six individuals of the VA88 sample and one individual of the VA89 sample. However, an examination of bluefish mtDNA genotypes not included in this analysis—because the individuals were greater than one year old, or because they came from a sample that was too small for inclusion in this analysis—suggests that the observed distribution of the AAAAAAAAD genotype may be an artifact of sampling error. The genotype was present in two bluefish collected in 1988 (one in New York and one in Connecticut) and in six bluefish collected in 1989 (two in New York, two in Virginia, and two in North Carolina).

In contrast to the genetic similarity among mid-Atlantic samples, a large, consistent genotypic difference was noted between the mid-Atlantic bluefish and a conspecific population in Australia. The corrected mean nucleotide sequence divergence of almost 2% is more than an order of magnitude larger than the values detected among mid-Atlantic samples, and is similar to values reported between northwest Atlantic and Barents Sea capelin populations (Dodson et al. 1991) or among populations of freshwater fishes of different river systems (Bermingham and Avise 1986).

While significant genetic differentiation was found between mid-Atlantic and Australian bluefish, no major differences were detected between mid-Atlantic bluefish and a small sample from the Gulf of Mexico. Consistent restriction-site differences have been reported between Gulf of Mexico and mid-Atlantic populations of a number of marine organisms, including horshoe crabs *Limulus polyphemus* (Saunders et al. 1986), oysters *Crassostrea virginica* (Reeb and Avise 1990), and black sea bass *Centropristis striata* (Bowen and Avise 1990). These preliminary results suggest that bluefish from the Gulf of Mexico and the mid-Atlantic are not as genetically isolated as many other coastal marine species, although much larger samples will have to be surveyed to determine if significant mtDNA genotypic frequency differences exist between the two areas. Considering the high vagility of bluefish and their continuous distribution around Florida, this result is not unexpected.

The lack of significant genetic differentiation between spring- and summer-spawned bluefish is consistent with the results of Chiarella and Conover (1990), who found no correlation between the season in which an adult bluefish spawned and the hatch-date of an individual. These data suggest that the bimodal distribution of YOY bluefish in mid-Atlantic estuaries results from two major spawning events of the same population of bluefish, rather than the participation of different stocks. The morphological differences found between spring- and summer-spawned bluefish are probably ecophenotypic, resulting from early-life-history development in appreciably different environments. Similar morphological plasticity has been demonstrated in many other marine fishes (Barlow 1961).

The high degree of genetic homogeneity detected within mid-Atlantic bluefish is also consistent with the results of tag and recapture studies. While many bluefish return to the same site for several years (Lund and Maltezos 1970), migratory habits appear to change with age (Wilk 1977). Thus, the potential exists for considerable interchange, and it is important to note that even small levels of exchange can prevent the accumulation of genetic differentiation (Hartl 1988).

The results of this study cannot disprove the null hypothesis that bluefish along the mid-Atlantic coast share a common gene pool. There appears to be sufficient gene flow to prevent the accumulation of even slight genetic differences. Determining the magnitude of exchange between geographic regions would require an extensive tag and recapture program. Until such data are available, the resource should be managed as assumed in the Fishery Management Plan for the Bluefish—as a single, genetically homogeneous stock.

Acknowledgments

Bluefish were kindly provided by Hunt Howell, Alice Webber, Raoul Castaneda, Bill Andrews, Katy West, Debbie Fabel, Steve Battaglane, and R. Bill Talbot. This project resulted from a study initiated by Herb Austin and Brian Meehan of the Virginia Institue of Marine Science. Robert Chapman provided helpful advice with the statistical analysis. Critical reviews of the manuscript were provided by John Olney and John Musick. Funding for this research was provided by the U.S. Fish and Wildlife Service (F-60-R) and the Commonwealth of Virginia.

Citations

Avise, J.C., R.M. Ball, and J. Arnold
1988 Current versus historical population sizes in vertebrate species with high gene flow: A comparison based on mitochondrial DNA lineages and inbreeding theory for neutral mutations. Mol. Biol. Evol. 5:331–344.

Avise, J.C., B.W. Bowen, and T. Lamb
1989 DNA fingerprints from hypervariable mitochondrial genotypes. Mol. Biol. Evol. 6:258–269.

Barlow, G.W.
1961 Causes and significance of morphological variation in fishes. Syst. Zool. 10:105–117.

Bermingham, E., and J.C. Avise
1986 Molecular zoogeography of freshwater fishes in the southeastern United States. Genetics 113:939–965.

Bowen, B.W., and J.C. Avise
1990 Genetic structure of Atlantic and Gulf of Mexico populations of sea bass, menhaden, and sturgeon: Influence of zoogeographic factors and life-history patterns. Mar. Biol. (Berl.) 107:371–381.

Briggs, J.C.
1960 Fishes of world-wide (circumtropical) distribution. Copeia 1960:171–180.

Chapman, R.W.
1990 Mitochondrial DNA analysis of striped bass populations in Chesapeake Bay. Copeia 1990:355–366.

Chapman, R.W., and D.A. Powers
1984 A method for the rapid isolation of mitochondrial DNA from fishes. Tech. Rep. UM-SG-TS-84-01, Md. Sea Grant Prog., Univ. Md., College Park, 11 p.

Chiarela, L.A., and D.O. Conover
1990 Spawning season and first-year growth of adult bluefish from the New York bight. Trans. Am. Fish. Soc. 119:455–462.

Collins, M.R., and B.W. Stender
1988 Larval king mackerel (*Scomberomorus cavalla*), Spanish mackerel (*S. maculatus*), and bluefish (*Pomatomus saltatrix*) off the southeast coast of the United States, 1973–1980. Bull. Mar. Sci. 41:822–834.

Dodson, J.J., J.E. Carscadden, L. Bernatchez, and F. Colombani
1991 Relationship between spawning mode and phylogeographic structure in mitochondrial DNA of north Atlantic capelin *Mallotus villosus*. Mar. Ecol. Prog. Ser. 76:1103–113.

Gold, J.R., and L.R. Richardson
1991 Genetic studies in marine fishes. IV. An analysis of population structure in the red drum (*Sciaenops ocellatus*) using mitochondrial DNA. Fish. Res. 12:213–241.

Hartl, D.L.
1988 A primer of population genetics. Sinauer Assoc., Sunderland, MA, 305 p.

Kendall, A.W. Jr., and L.A. Walford
1979 Sources and distribution of bluefish, *Pomatomus saltatrix*, larvae and juveniles off the east coast of the United States. Fish. Bull., U.S. 77:213–227.

Lansman, R.A., R.O. Shade, C.F. Shapira, and J.C. Avise
1981 The use of restriction endonucleases to measure mitochondrial DNA sequence relatedness in natural populations. III. Techniques and potential applications. J. Mol. Evol. 17:214–226.

Lassiter, R.R.
1962 Life history aspects of the bluefish fish, *Pomatomus saltatrix* Linnaeus, from the coast of North Carolina. Master's thesis, N.C. State College, Raleigh, 103 p.

Lund, W.A. Jr., and G.C. Maltezos
1970 Movements and migrations of the bluefish, *Pomatomus saltatrix*, tagged in waters of New York and southern New England. Trans. Am. Fish. Soc. 99:719–725.

Maniatis, T., I.F. Fritsch, and J. Sambrook
1982 Molecular cloning: A laboratory manual. Cold Spring Harbor Lab., Cold Spring Harbor, NY, 545 p.

McBride, R.S.
1989 Comparative growth and abundance of spring versus summer-spawned juvenile bluefish, *Pomatomus saltatrix*, recruiting to New Youk bight. Master's thesis, State Univ. New York, Stony Brook, 61 p.

Nei, M.
1987 Molecular evolutionary genetics. Columbia Univ. Press, NY, 512 p.

Nei, M., and W-H. Li
1979 Mathematical model for studying genetic variation in terms of restriction endonucleases. Proc. Natl. Acad. Sci. 76:5269–5273.

Nyman, R.M., and D.O. Conover
1988 The relation between spawning season and the recruitment of young-of-the-year bluefish, *Pomatomus saltatrix*, to New York. Fish. Bull., U.S. 86:237–250.

Ovenden, J.R.
1990 Mitochondrial DNA and marine stock assessment: A review. Aust. J. Mar. Freshwater Res. 41:835–53.

Reeb, C.A., and J.C. Avise
1990 A genetic discontinuity in a continuously distributed species: Mitochondrial DNA in the American oyster, *Crassostrea virginica*. Genetics 124:397–406.

Roff, D.A., and P. Bentzen
1989 The statistical analysis of mitochondrial DNA polymorphisms: χ^2 and the problem of small samples. Mol. Biol. Evol. 6:539–545.

Saunders, N.C., L.G. Kessler, and J.C. Avise
1986 Genetic variation and geographic differentiation in mitochondrial DNA of the horshoe crab, *Limulus polyphemus*. Genetics 112:613–627.

Slatkin, M.
1989 Gene flow and the geographic structure of natural populations. Science (Wash. DC) 236:787–792.

Smith, J.L.B.
1949 The sea fishes of southern Africa. Central News Agency, Cape Town, 550 p.

Sokal, R.R., and F.J. Rohlf
1981 Biometry. W.H. Freeman, NY.

Wilk, S.J.
1977 Biological and fisheries data on bluefish, *Pomatomus saltatrix* (Linnaeus). Tech. Ser. Rep. 11, Sandy Hook Lab., NMFS Northeast Fish. Sci. Cent., Highlands, NJ, 56 p.

Abstract. – Age, growth, and mortality of larval Atlantic bumper *Chloroscombrus chrysurus* were compared between cruise samples collected during August–September 1986 and September 1987 off the Louisiana–Mississippi barrier islands. Calcein-marked Atlantic bumper otoliths (sagitta) were used for age validation. The first growth increment formed on the sagitta approximately 2 days after spawning, and daily increments formed thereafter. Length at hatching was estimated at 0.7–0.9 mm SL. Growth rates were determined from sagitta and length-frequency data. Highest growth rates occurred in August 1986 (0.40 mm/day) and were associated with highest mean temperature and zooplankton standing stock estimates. The length exponent for Atlantic bumpers' dry weight-length relationship was 3.25. Instantaneous daily mortalities (M) ranged from 0.62 in August 1986 to 0.17 in late September 1987.

Age validation, growth, and mortality of larval Atlantic bumper (Carangidae: *Chloroscombrus chrysurus*) in the northern Gulf of Mexico

Deborah L. Leffler

Florida Marine Research Institute, Florida Department of Natural Resources
3 Jackson Street, Fort Walton Beach, Florida 32548

Richard F. Shaw

Coastal Fisheries Institute, Center for Wetland Resources
Louisiana State University, Baton Rouge, Louisiana 70803-7503

Manuscript accepted 1 July 1992.
Fishery Bulletin, U.S. 90:711–719 (1992).

Atlantic bumper *Chloroscombrus chrysurus*, a carangid, is an abundant coastal pelagic fish that is widely distributed in the western Atlantic and Gulf of Mexico (Leak 1977). Exploratory fishing surveys indicate that Atlantic bumper may be abundant enough in the northern Gulf of Mexico to harvest commercially (Juhl 1966, Bullis and Carpenter 1968, Bullis and Thompson 1970, Klima 1971). Presently, Atlantic bumper is mainly a commercial bycatch, marketed primarily for petfood, with little potential as a food fish in the United States (Klima 1971, Leak 1977). It, however, may be an important food source for many predatory fish (Reintjes 1979).

Atlantic bumper spawn primarily in nearshore coastal waters, especially off Louisiana and Mississippi (Boschung 1957, Perret et al. 1971, Christmas and Waller 1973, Ditty 1986, Shaw and Drullinger 1990), and the larvae of this species were most abundant during surveys off the Louisiana–Mississippi (LA–MS) barrier islands (Stuck and Perry 1982, Leffler 1989). Larvae have been collected from June to October, with abundance peaks usually occurring in July or August (Sabins 1973, Stuck and Perry 1982, Williams 1983, Ditty 1986).

Very little early-life-history work has been conducted on Atlantic bumper (Shaw and Drullinger 1990). Early-life-history information is a critical component in estimating future year-class strength (Cushing 1975, Leak and Houde 1987). For example, slow larval growth rates influence mortality by extending the duration of vulnerable larval stages (Bannister et al. 1974, Houde 1987), while a fast growth rate can possibly increase interaction with predators (Pepin 1991), thereby influencing recruitment. Early-life-history data are needed for Atlantic bumper to determine their ecological role and to assist in the prudent development of any directed fishery.

The abundance of Atlantic bumper over a wide geographic range, their perceived potential as a commercial resource, and their probable ecological importance as a forage fish, provided the impetus for conducting this larval age-and-growth study. The goals of this ichthyoplankton study were to (1) validate the periodicity of growth increments on larval and juvenile Atlantic bumper otoliths, (2) estimate Atlantic bumper length at hatching, (3) estimate the age structure of the sample population, (4) describe larval growth and mortality rates, and (5) relate larval growth

and mortality rates to environmental parameters and food availability.

Materials and methods

Sampling procedure

Atlantic bumper larvae were collected during five cruises off the Louisiana–Mississippi barrier islands in the Gulf of Mexico (Chandeleur Is., Ship I., and Horn I.; 29°50′–30°15′N and 88°40′–89°00′W; Fig. 1). Three cruises were completed in 1986 (5–7 Aug., 8–9 Sept., and 22–24 Sept.) and two in 1987 (8–10 and 24–26 Sept.). Adverse weather conditions canceled the scheduled August 1987 cruise.

The sampling design consisted of a 4×4 grid of stations (N 16) randomly sampled on two consecutive nights, and a 3×3 grid of stations (N 9) randomly sampled during daylight, starting 12 hours after the initiation of the first nocturnal sampling. The sampling grid had a fixed compass orientation with respect to three windowshade, subsurface current drogues (five drogues were used in 1987) which were released at the beginning of each cruise (Shaw et al. 1988). The change to five drogues in 1987 allowed for a more defined sampling grid. Surface-water temperature and salinity, as well as water depth, were recorded for each ichthyoplankton tow.

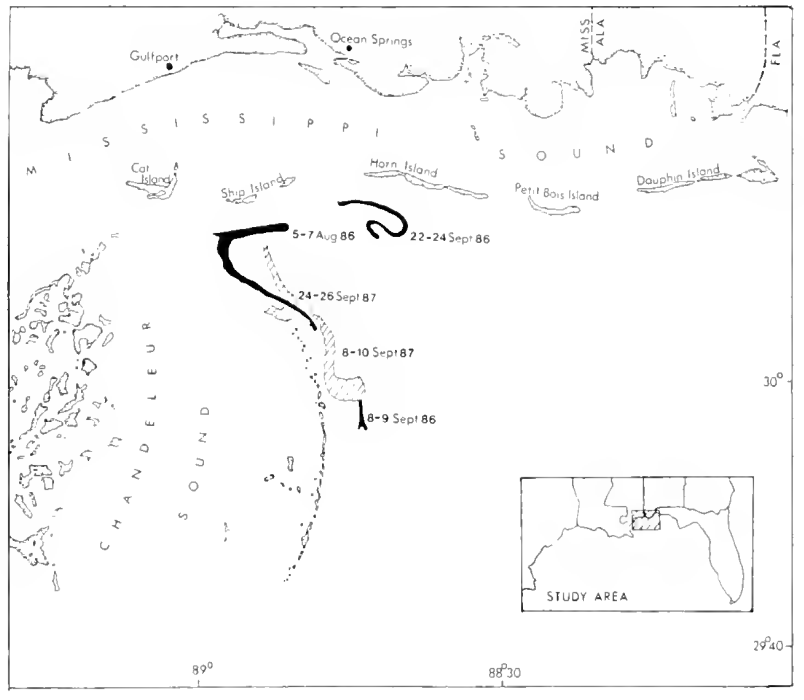

Figure 1

Location and dates of ichthyoplankton cruises during 1986–87 in which Atlantic bumper *Chloroscombrus chrysurus* were collected for age determination. Shaded areas represent trajectory of the water mass followed by current drogues during 1986 cruises, and diagonally-lined areas represent 1987 cruises.

Three-minute surface tows were taken at ~1.0 m/s using a 60 cm "bongo-type" plankton sampler fitted with a flowmeter (General Oceanics model 2030). In 1986, samples were collected using a 202 μm mesh net, while in 1987 a 333 μm mesh net was used. During the two cruises in September 1987, the bongo sampler was fitted with one 202 μm mesh net and one 333 μm mesh net for comparisons of daytime collections. Atlantic bumper collected using the two mesh sizes were placed into 1 mm size-classes and tested for differences using a Median test (α 0.05; SAS Inst. 1985). Ichthyoplankton samples used for age determination were preserved with 95% ethanol, stored in ice water, and later transferred to 70% ethanol in the lab.

Live larval and juvenile Atlantic bumper were collected for an age-validation experiment and length-weight measurement analysis by dipnetting the jellyfish *Aurelia aurita* with which the fish are often associated (Reid 1954, Franks 1970). Fish were then transferred to a cooler containing 100 ppm calcein (2,4-bis-[N,N′-di(carbomethyl)aminomethyl]fluorescein) in 13 L of aerated ambient seawater to create a fluorescent mark in their otoliths using the method described by Wilson et al. (1987). Fish were held between 6 and 12 h in the seawater-calcein solution and then transferred into a 127 L aquaria. Fish were held under a 12h/12h photoperiod in 23°C and 25 ppt water and fed *ad libidium* on brine shrimp. Fish were sacrificed 2, 7, and 10 days after marking.

Lab analysis

Ichthyoplankton samples from the bongo net collections were split once with a Folsom plankton splitter (Van Guelpin et al. 1982). *Chloroscombrus chrysurus* larvae were sorted, counted, and measured to the nearest 0.1 mm standard length (SL). Preflexion larvae were measured to the end of their notochord, otherwise larvae were measured to the posterior tip of the hypural plate. When more than 52 fish were present,

a random subsample of 50 fish were measured, as well as the shortest and longest. Ethanol-related shrinkage was assumed to be uniform for each fish collected and preserved (3-min tow, alcohol preservation; see Radtke 1989).

Validation, age, and growth

Sagittal otoliths were removed from each Atlantic bumper larvae using a dissection microscope equipped with polarized light. The sagitta from nine postlarval and juvenile Atlantic bumper (8.3–25.0 mm SL) that were immersed in the calcein-seawater solution were prepared and viewed using the method described by Wilson et al. (1987). Growth increments, following the fluorescent mark, were counted at 400× and verified at 1000×. The number of growth increments counted from the calcein mark to the otolith edge were compared with the number of days fish were held in captivity after marking.

Age estimation of larval Atlantic bumper was performed using sagitta that were air-dried and mounted in S/P Accu-mount 60 on a glass microscope slide. Most larval otoliths were thin enough that only viewing under a compound microscope was necessary to make total increment counts and otolith radius measurements. A few larger otoliths were ground with 600 WetorDry grit sandpaper and polished using 0.3μ Alumina 2 Alpha Micropolish until growth rings were countable. The counting and measurement procedure was enhanced by using a digital imaging system which produced images on a video monitor at 400× or 1000×. Independent increment counts were made twice by the same person without knowledge of fish length or previous otolith count. Only otoliths for which replicate counts were identical were used in the analysis. Eleven of the 170 otoliths prepared were discarded.

Separate linear growth equations of standard length on increment number were developed for fishes collected on the five cruises. These five equations were compared using analysis of covariance (ANCOVA, α 0.05; SAS Inst. 1985). Exponential and other nonlinear models (e.g., Laird-Gompertz) used to describe larval growth were also tested (Campana and Neilson 1985). A General Linear Model ANOVA, followed by a multiple comparisons test (Duncan, α 0.05; SAS Inst. 1985), were used to detect differences in surface-water temperature between years, months, and cruises.

Zooplankton biomass

Zooplankton displacement volumes (mL/m^3) were determined (Yentsch and Hebard 1957) for each net tow. A mean zooplankton standing stock value was then calculated for each cruise and net mesh type. A simple regression of zooplankton standing-stock values (202 vs. 333μm mesh nets) was developed for both September 1987 cruises. ANCOVA (α 0.05) was used to test for differences between the two cruises. The data from the two cruises were combined into one zooplankton standing-stock regression to standardize the values from the two mesh sizes.

Dry weight-length relationship

Larval and juvenile Atlantic bumper (N 120, 8.0–32.0 mm SL) collected by dipnetting for jellyfish, were measured to the nearest 0.1 mm SL, oven dried for 6h at 62°C, and then weighed to the nearest 1.0 mg. A log-log dry weight-length relationship was established and described by the equation $W = aL^b$, where $W = \log_{10}$ dry weight (mg), and $L = \log_{10}$ standard length (mm). A 95% confidence interval placed around the estimated slope (b) was used to test for differences in the estimated length power term (b) and the classical b estimate of 3.0 for adult fish (LeCren 1951) and 4.0 for larval fish (Power 1989).

Mortality

Atlantic bumper densities for each 1 mm SL category were converted into mortality estimates following the length-frequency method described by Essig and Cole (1986). Sampling with respect to the windowshade drogues allowed us to monitor larval densities from the same mass of water for an entire collecting period. Only nighttime collected larvae >2.0 mm or <5.0 mm were utilized in our mortality estimates to minimize biases from net avoidance by larger larvae or extrusion through the mesh openings by the smallest larvae. The descending limb of each age-frequency distribution corresponding to a length range of 2.0–5.0 mm SL was described by the equation $Dt = Do\exp^{(-Mt)}$, where M = the instantaneous daily mortality coefficient, Dt = larval fish density at time t, Do = larval fish density in the first fully recruited group (i.e., time = 0), and t = time in days (Peebles and Tolley 1988). Mortality estimates were tested for statistical differences between cruises and years using ANCOVA (α 0.05).

Results

Validation, age, and growth

Daily increment formation on Atlantic bumper sagitta was validated using calcein. Each otolith from the nine fish treated had distinct growth increments between the green fluorescent calcein mark and the edge of the otolith (Fig. 2). On each sagitta examined, the number of increments counted after the calcein mark was

Figure 2

Photomicrograph (400×) of the transverse-sectioned sagittal otolith of a 23.5 mm SL juvenile Atlantic bumper *Chloroscombrus chrysurus* observed under ultraviolet light. The lower light band displays the uptake of calcein during the immersion process.

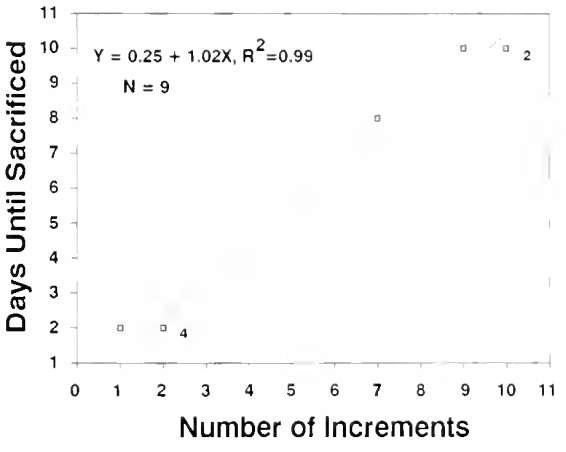

Figure 3

Regression of the number of otolith growth increments subsequent to the fluorescent calcein mark on the number of days each fish was held in captivity before sacrificing. Numbers associated with points represent overlapping values.

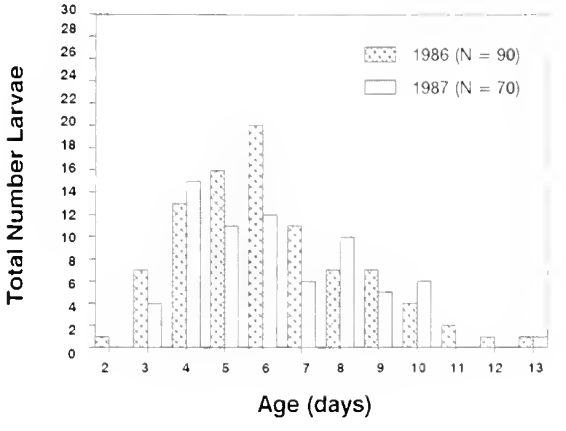

Figure 4

Age distribution of Atlantic bumper *Chloroscombrus chrysurus* larvae captured off the Louisiana–Mississippi barrier islands, 1986–87.

equivalent to the number of days the fish was held in captivity. The slope (1.02) of a least-squares linear regression (Fig. 3) was not significantly different from 1.0 (t-test, $p>0.05$), confirming daily increment formation in otoliths of larval and juvenile Atlantic bumper.

Larval Atlantic bumper have circular sagitta, with a central core. Yolksac larvae (0.8 mm SL, preserved length) lacked increments. However, all other aged fish between 1.0 and 5.0 mm (preserved length; N 158) had countable increments (i.e., 1–11 increments or 3–13 days old; Fig. 4). Growth models were based only on 2–13 day-old fish.

Larval Atlantic bumper growth rates during the first two weeks of life were best described using a linear model. A separate growth curve was estimated for the 5–7 August 1986 data (Table 1). Growth curve comparisons for the two cruises in September 1986 (days 8–9 and 22–24) showed no significant differences within month (intercept, p 0.44; slope, p 0.48). Similarly, no significant difference was found between the two September cruises in 1987 (days 8–10 and 24–26; intercept, p 0.07; slope, p 0.42). Therefore, the paired September data sets were combined into a single regression for each year (1986 and 1987; Table 1). Atlantic bumper length-frequencies displayed no significant differences (p 0.93) between the two different mesh sizes (202 vs. 333 μm) during the 1987 daytime

Table 1

Estimates of three linear growth equations used to describe the growth rate (mm/day) of larval *Chloroscombrus chrysurus* (0.8–4.8 mm) collected off the Louisiana–Mississippi barrier islands during 1986 and 1987, and the associated mean surface-water temperatures (°C) including ranges. R^2 is the coefficient of determination for the respective models; L = standard length (mm); X = age (days).

Sampling date	Number fish aged	Size (range)	Equations	R^2	Growth rate (mm/day)	Mean surface-temperature (°C) (range)
5–7 August 1986	9	0.8–3.7	L = 0.40X − 0.13	0.94	0.40	29.6 (29.0–30.8)
8–9, 22–24 Sept. 1986	81	1.2–4.8	L = 0.26X + 0.70	0.61	0.26	28.4 (28.0–29.0)
8–10, 24–26 Sept. 1987	69	1.3–4.5	L = 0.31X + 0.71	0.72	0.31	27.8 (26.5–30.0)

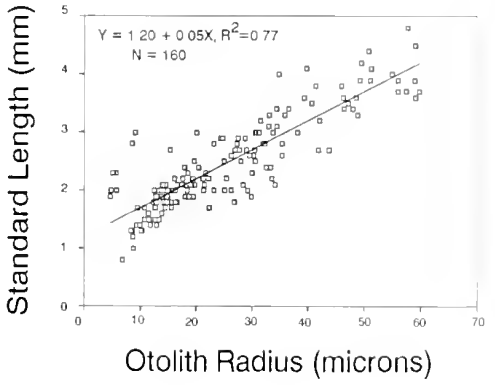

Figure 5

Regression of larval standard length (mm) on sagittal otolith radius (μ) for Atlantic bumper *Chloroscombrus chrysurus* larvae collected off the Louisiana–Mississippi barrier islands, 1986–87.

Table 2

Zooplankton standing-stock estimates (mL/m³ ± SE) with 1987 values converted to equivalent 202 μm mesh net values, based on the conversion study done during both September cruises in 1987. The number of samples taken during each cruise is indicated in parentheses. The following equation was used in the conversion: Y = 0.785X − 0.054 (R^2 0.86).

	1986	1987	
Month	(202 μm)	Converted	(333 μm)
August	0.83 ± 0.17 (34)	–	–
early Sept.	0.61 ± 0.13 (25)	0.57 ± 0.04 (40)	0.39 ± 0.04 (40)
late Sept.	0.32 ± 0.05 (41)	0.39 ± 0.03 (40)	0.25 ± 0.03 (40)

collections. Comparisons of the growth curves for September 1986 and 1987 and August 1986 indicated a significant difference in both the August intercept ($p<0.04$) and slope ($p<0.03$) of the regressions. Even though the sample size (N 9) was small, the observed growth rate for August (0.40 mm/day) was significantly higher than for September (0.26 mm/day in 1986 and 0.31 mm/day in 1987). The higher August growth rate occurred at a higher mean surface-water temperature, 29.6°C (Table 1). In September of 1987, the water temperature range (26.5–30.0°C) was wider than the other sampling periods due to a cold front passing through before the late-September cruise. There was, however, no significant difference (p 0.11) in temperature between months because of the low number of cruises.

Atlantic bumper standard lengths were regressed on the otolith radius (measured in microns; Fig. 5). The coefficient of determination (r^2) for the relationship was 0.77 and the equation is L = 120 + 0.05R, where L = standard larval length (mm) at the otolith radius, R (Fig. 5). The relationship between the age and otolith radius explained less variability (r^2 0.68) and fit the following equation A = 2.96 + 0.13R, where A = age in days at the otolith radius, R. Otolith radius was observed to increase with both larval length and age.

Zooplankton biomass

Zooplankton mean biomass values for 1986 were similar to the converted 1987 values. The 202 vs. 333 μm mesh regression equation Y = −0.054 + 0.785X (r^2 0.86), where Y = the 333 μm zooplankton standing-stock value, and X = the 202 μm zooplankton value, was used to establish a correction factor to convert the 1987 zooplankton values into estimates comparable to the 1986 values. The highest mean zooplankton biomass estimate (0.83 mL/m³) was found in August 1986 (Table 2). The mean standing-stock estimates declined throughout the September cruises within each year (Table 2).

Dry weight-length relationship

The dry weight-length relationship for postlarval and juvenile Atlantic bumper (Fig. 6) is described by the exponential model Weight = 0.0016 Length$^{3.25}$ (r^2 0.94), where weight = dry weight of the fish (mg) and length = standard length (mm). The dry weight-length power term for larval and juvenile Atlantic bumper, 3.25, is significantly different from the classical standard length-weight power term of 3.0 for adult fish (LeCren 1951) and 4.0 for larval fish (Power 1989) at the 95% confidence level ($p>0.05$).

Mortality

Instantaneous daily mortality (M) for larval Atlantic bumper was significantly higher during August 1986 (F 13.8, p 0.03) than in either September 1986 or 1987, with September values decreasing during successive cruises each year (Table 3). As a whole, however, the M values for all cruises in 1986 and 1987 were similar (F 0.74, p 0.45).

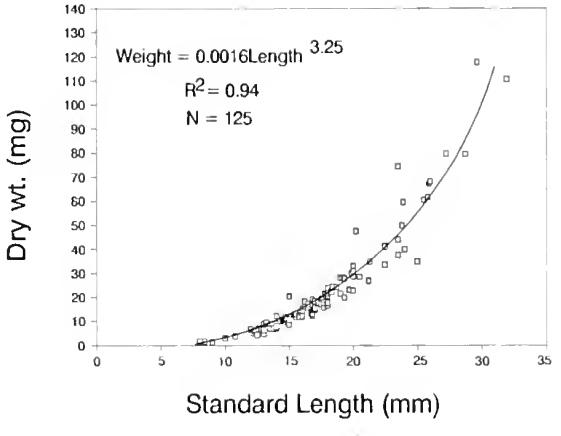

Figure 6
Relationship between dry weight and standard length of Atlantic bumper *Chloroscombrus chrysurus* collected off the Louisiana-Mississippi barrier islands, 1986-87.

Discussion

The age of larval and juvenile Atlantic bumper was estimated from counts of growth increments on sagittal otoliths. One growth increment formed daily on each sagitta of Atlantic bumper between 8 and 25 mm SL. We, like others (Pritcher 1988, Fowler 1989, Parsons and Peters 1989), assumed that this relationship held true for smaller larvae (1-8 mm). We validated the periodicity of otolith growth increments and established an otolith age-and-growth analysis for larval Atlantic bumper in the northern Gulf of Mexico.

Growth increments were not visible in the otoliths of yolksac Atlantic bumper larvae (0.8 mm NL), but at least one increment was visible in 1.0 mm SL larvae. The length at hatching appears to be between 0.7 and 0.9 mm SL (after preservation) based on the larval length measurements. Atlantic bumper larvae, therefore, appear to begin otolith increment deposition after yolksac absorption, approximately 2 days after spawning (allowing 1 day each for egg incubation and yolksac absorption). Pelagic species, such as Atlantic bumper, often begin growth increment formation on their sagitta at the time of yolksac absorption (Radtke 1984).

An isometric or linear relationship between the size of otolith radius and standard length was revealed for Atlantic bumper larvae. The variation observed in our otolith radius-fish size relationship could be influenced by growth- and age-related factors. For example, under unfavorable environmental conditions the fish may not continue to experience an increase in otolith radius or fish size, while daily increment formation may continue (Lyczkowski-Shultz et al. 1988, Secor and Dean 1989).

Table 3
Estimates of instantaneous daily mortality of larval *Chloroscombrus chrysurus* (2.0-5.0 mm SL) off the Louisiana-Mississippi barrier islands were calculated using the length-frequency method. Total larval Atlantic bumper densities and total larval fish densities were included for each cruise in 1986 and 1987. R^2 is the coefficient of determination for the respective models.

Sampling dates	Number of fish	Instantaneous daily mortality estimates (M)	R^2	Atlantic bumper total densities (# fish/100 m^3)	Total larval fish density (# fish/100 m^3)
5-7 August 1986	1912	0.62	0.82	608.9	1838.1
8-9 Sept. 1986	576	0.35	0.98	121.7	799.8
22-24 Sept. 1986	291	0.18	0.86	227.9	599.9
8-10 Sept. 1987	573	0.30	0.90	62.2	262.4
24-26 Sept. 1987	122	0.17	0.92	42.4	298.2

Temperature (Laurence 1978, Laurence et al. 1981, Houde 1989) and food availability (Methot and Kramer 1979, Laurence et al. 1981, Lyczkowski-Shultz et al. 1988, Warlen 1988) play important roles in larval growth and survival. Atlantic bumper growth rates were highest in August 1986, when mean surface-water temperatures and zooplankton biomass estimates were greatest.

The Atlantic bumper growth rate calculated over the two cruises in September 1987 may have been higher than the September 1986 growth rate because of the increase in zooplankton availability (Tables 1 and 2). Zooplankton displacement volume values calculated from the samples taken in 1986 declined from August to September. Relative zooplankton biomass values have peaked, however, as late as October off the Chandeleur Is. within Chandeleur Sound (102,000 animals/100 m^3; Gillespie 1971; Fig. 1). Our zooplankton standing-stock estimates were high compared with values obtained from Mississippi River plume fronts during July 1987 (0.04–0.43 mL/m^3; R.F. Shaw, unpubl. data).

Atlantic bumper larvae had a dry weight-length exponent value of 3.25 which is similar to that of 3.32 determined for larval northern anchovy *Engraulis mordax* (Lasker et al. 1970). This power term, however, is lower than values determined for seven laboratory-reared, cold-water marine larval species (3.76–4.77; Laurence 1979), or the hypothesized standard value for developing larval fish (4.0; Power 1989).

The highest Atlantic bumper instantaneous daily mortality estimate (M 0.62), observed during August, was similar to that reported for estuarine larval spotted seatrout *Cynoscion nebulosus* (0.64; Peebles and Tolley 1988) and, to some extent, another carangid, jack mackerel *Trachurus symmetricus* (0.80; Hewitt et al. 1985). Mortality estimates, which declined throughout September 1986 (0.35–0.18) and 1987 (0.30–0.17), were similar and were within the reported range for several larval marine species (Essig and Cole 1986, Houde 1987 and 1989, Pepin 1991). The highest daily mortality rate was associated with highest temperatures, highest macrozooplankton displacement volumes, and highest larval Atlantic bumper densities (Tables 1–3). In late September 1986, however, there was a low mortality rate during a time of relatively high Atlantic bumper densities, lower zooplankton biomass estimates, and lower temperatures. Two factors—larval size and lower water temperatures—may have influenced this lower mortality rate (Weinstein and Walters 1981). Mean larval Atlantic bumper standard lengths (1.2 mm) were similar for all the cruises. Lower surface-water temperatures, therefore, may have enhanced survival, reducing the Atlantic bumper mortality estimate. Larval growth (i.e., daily development) and mortality rates have been reported to increase with temperature (Houde 1989, Pepin 1991). The high growth-rate and mortality estimate observed in August 1986 is consistent with these findings.

The high natural mortality observed in August is probably related to predation, based on two existing theories. Larval Atlantic bumper are usually aggregated in patches (Leffler 1989) and, therefore, may offer exceptional feeding opportunities to any predator that encounters them (McGurk 1987). Pepin (1991) suggested that increased mortality rates were associated with increasing growth rates, resulting from increased encounters with predators. These higher growth rates require a higher intake of food, causing increased activity which leads to increased predator encounters.

Another possible cause for the high August mortalities may be associated with competition for limited food resources, i.e., density-dependent mortality (Cushing 1974). Food availability as indexed by the zooplankton biomass estimate was highest during August, but the high total larval fish density may have rapidly depleted the food source, causing elevated mortalities. Larval Atlantic bumper density was high during the August cruise (608.9 larvae/100 m^3) as was the total larval fish density (1838.1 larvae/100 m^3; Leffler 1989).

This study provides preliminary information on the early life history of larval Atlantic bumper. Further studies need to be conducted on larval Atlantic bumper to determine the relationship between these early-life-history parameters and fluctuating temperatures and food availability.

Acknowledgments

The authors would like to thank J. Ditty, D. Drullinger, R. Raynie, and K. Edds for assistance in the field and laboratory. Also we would like to acknowledge L. Rouse, E. Turner, C. Wilson, R. McMichael, and two anonymous reviewers for critical reviews of the manuscript, and M. Mitchell and B. McLaughlin for their assistance in preparing the graphics. Special thanks to the captains and staff at Gulf Coast Research Laboratory, Ocean Springs, MS, for use of their boats and aquarium facilities.

Financial support was provided through the Louisiana Sea Grant College Program, a part of National Sea Grant College Program maintained by NOAA U.S. Department of Commerce.

Citations

Bannister, C.A., D. Harding, and S.J. Lockwood
1974 Larval mortality and subsequent year-class strength in the plaice (*Pleuronectes platessa* L.). *In* Blaxter, J.H.S. (ed.), The early life history of fish, p. 21–37. Springer-Verlag, NY.

Boschung, H.T.
1957 The fishes of Mobile Bay and the Gulf Coast of Alabama. Ph.D. diss., Univ. Alabama, Tuscaloosa, 626 p.

Bullis, H.R. Jr., and J.S. Carpenter
1968 Latent fisheries resources of the central West Atlantic region. *In* de Witt, G. (ed.), The future of the fishing industry of the United States, p. 61–64. Univ. Wash. Publ. Fish., New Ser. 4, Seattle.

Bullis, H.R. Jr., and J.R. Thompson
1970 Bureau of commercial fisheries exploratory fishing gear research base, Pascagoula, Mississippi—July 1, 1967 to June 30, 1969. U.S. Fish Wildl. Serv., Circ. 351, 29 p.

Campana, S.E., and J.D. Neilson
1985 Microstructure of fish otoliths. Can. J. Fish. Aquat. Sci. 42:1014–1032.

Christmas, J.Y., and R.S. Waller
1973 Estuarine vertebrates, Mississippi. *In* Christmas, J.Y. (ed.), Cooperative Gulf of Mexico estuarine inventory and study–Mississippi, p. 320–439. Gulf Coast Res. Lab., Ocean Springs.

Cushing, D.H.
1974 The possible density-dependence of larval mortality and adult mortality in fishes. *In* Blaxter, J.H. (ed.), The early life history of fish, p. 103–112. Springer-Verlag, NY.
1975 Marine ecology and fisheries. Cambridge Univ. Press, Cambridge, 278 p.

Ditty, J.G.
1986 Ichthyoplankton in nertic waters of the northern Gulf of Mexico off Louisiana: Composition, relative abundance and seasonality. Fish. Bull., U.S. 84:935–946.

Essig, R.J., and C.F. Cole
1986 Methods of estimating larval fish mortality from daily increments in otoliths. Trans. Am. Fish. Soc. 115:34–40.

Fowler, A.J.
1989 Description, interpretation and use of the microstructure of otoliths from juvenile butterfly fish (family Chaetodontidae). Mar. Biol. (Berl.) 102:167–181.

Franks, J.S.
1970 An investigation of the fish population within the inland waters of Horn Island, Mississippi, a barrier island in the northern Gulf of Mexico. Gulf Res. Rep. 3:3–104.

Gillespie, M.C.
1971 Analysis and treatment of zooplankton of estuarine waters of Louisiana. *In* Cooperative Gulf of Mexico estuarine inventory and study, Louisiana Phase IV, Biology, p. 108–175. La. Wildl. Fish. Comm., New Orleans.

Hewitt, R.P., G.H. Theilacker, and N.C.H. Lo
1985 Causes of mortality in young jack mackerel. Mar. Ecol. Prog. Ser. 26:1–10.

Houde, E.D.
1987 Fish early life dynamics and recruitment variability. *In* Hoyt, R.D. (ed.), 10th annual larval fish conference, p. 17–29. Am. Fish. Soc. Symp. 2, Bethesda.
1989 Comparative growth, mortality, and energetics of marine fish larvae: Temperature and implied latitudinal effects. Fish. Bull., U.S. 87:471–495.

Juhl, R.
1966 Experimental trawling survey along the Florida west coast. Commer. Fish. Rev. 28(6):1–5.

Klima, E.F.
1971 Distribution of some coastal pelagic fishes in the Western Atlantic. Commer. Fish. Rev. 33(6):21–34.

Lasker, R., H.M. Feder, G.H. Theilacker, and R.C. May
1970 Feeding, growth, and survival of *Engraulis mordax* larvae reared in the laboratory. Mar. Biol. (Berl.) 5:345–353.

Laurence, G.C.
1978 Comparative growth, respiration, and delayed feeding abilities of larval cod (*Gadus morhua*) and haddock (*Melanogrammus aeglefinus*) as influenced by temperature during laboratory studies. Mar. Biol. (Berl.) 50:1–7.
1979 Larval length-weight relations for seven species of Northwest Atlantic fishes reared in the laboratory. Fish. Bull., U.S. 76:890–895.

Laurence, G.C., A.S. Smigielski, T.A. Halavik, and B.R. Burns
1981 Implications of direct competition between larval cod (*Gadus morhua*) and haddock (*Melanogrammus aeglefinus*) in laboratory growth and survival studies at different food densities. Rapp. P.-V. Reun. Cons. Int. Explor. Mer 178:304–311.

Leak, J.C.
1977 Distribution and abundance of carangidae (Pisces, perciformes) larvae in the eastern Gulf of Mexico, 1971–1974. M.S. thesis, Univ. Miami, Coral Gables, 83 p.

Leak, J.C., and E.D. Houde
1987 Cohort growth and survival of bay anchovy, *Anchoa mitchilli*, larvae in Biscayne Bay, Florida. Mar. Ecol. Prog. Ser. 37:109–122.

LeCren, E.D.
1951 The length-weight relationship and seasonal cycle in gonad weight and condition in the perch (*Perca flavescens*). J. Anim. Ecol. 20(2):201–219.

Leffler, D.L.
1989 Composition, abundance, and small-scale distribution of ichthyoplankton off the Louisiana–Mississippi barrier islands, with special emphasis on the age, growth, and mortality of *Chloroscombrus chrysurus*. M.S. thesis, Louisiana State Univ., Baton Rouge, 151 p.

Lyczkowski-Shultz, J., J.P. Steen Jr., and B.H. Comyns
1988 Early life history of red drum (*Sciaenops ocellatus*) in the north central Gulf of Mexico. MASGP-88-013, Gulf Coast Res. Lab., Ocean Springs, MS, 147 p.

McGurk, M.D.
1987 Natural mortality and spatial patchiness: Reply to Gulland. Mar. Ecol. Prog. Ser. 39:201–206.

Methot, R.D. Jr., and D. Kramer
1979 Growth of northern anchovy, *Engraulis mordax*, larvae in the sea. Fish Bull., U.S. 77:413–423.

Parsons, G.R., and K.M. Peters
1989 Age determination in larval and juvenile sheepshead, *Archosargus probatocephalus*. Fish. Bull., U.S. 87:985–988.

Peebles, E.B., and S.G. Tolley
1988 Distribution, growth, and mortality of larval spotted seatrout, *Cynoscion nebulosus*: A comparison between two adjacent estuarine areas of southwest Florida. Bull. Mar. Sci. 42(3):397–410.

Pepin, P.
1991 Effect of temperature and size on development, mortality, and survival rates of the pelagic early life history stages of marine fish. Can. J. Fish. Aquat. Sci. 48:503–518.

Perret, W.S., W.R. Latapie, J.F. Polland, W.R. Mock, G.B. Adkins, W.J. Gaidry, and C.J. White
1971 Fishes and invertebrates collected in trawl and seine samples in Louisiana estuaries, Section I. *In* Cooperative Gulf of Mexico estuarine inventory and study, Louisiana, Phase IV, Biology, p. 39–105. La. Wildl. Fish. Comm., New Orleans.

Power, J.H.
1989 Sink or swim: Growth dynamics and zooplankton hydromechanics. Am. Nat. 133(5):706–721.

Pritcher, C.R.
1988 Validation of a technique for reconstructing daily patterns in the recruitment of coral reef damselfish. Coral Reefs 7:105–111.

Radtke, R.L.
1984 Formation and structural composition of larval striped mullet otoliths. Trans. Am. Fish. Soc. 113:186–191.
1989 Larval fish age, growth, and body shrinkage: Information available from otoliths. Can. J. Fish. Aquat. Sci. 46: 1884–1894.

Reid, G.K.
1954 An ecological study of the Gulf of Mexico fishes in the vicinity of Cedar Key, Florida. Bull. Mar. Sci. Gulf Caribb. 4:1–94.

Reintjes, J.W.
1979 Coastal herrings and associated species: A profile of species or groups of species, their biology, ecology, and current exploitation with economic and social information. Prepared for Gulf of Mexico Fish. Manage. Counc. by NMFS Southeast Fish. Sci. Cent., Beaufort NC, 170 p.

Sabins, D.S.
1973 Diel studies of larval and juvenile fishes of the Caminada Pass area, Louisiana. M.S. thesis, Louisiana State Univ., Baton Rouge, 163 p.

SAS Institute Inc.
1985 SAS User's Guide: Statistics, 1982 Edition. SAS Inst. Inc., Cary NC, 584 p.

Secor, D.H., and J.M. Dean
1989 Somatic growth effects on the otolith–fish size relationship in young pond-reared striped bass, *Morone saxatilis*. Can. J. Fish. Aquat. Sci. 46:113–121.

Shaw, R.F., and D.L. Drullinger
1990 Early-life-history profiles, seasonal abundance, and distribution of four species of carangid larvae off Louisiana during 1982 and 1983. NOAA Tech. Rep. NMFS 89, 37 p.

Shaw, R.F., D.L. Drullinger, K.A. Edds, and D.L. Leffler
1988 Fine-scale spatial distribution of red drum, *Sciaenops ocellatus*, larvae. Contrib. Mar. Sci. 30(suppl.):109–116.

Stuck, K.C., and H.M. Perry
1982 Ichthyoplankton community structure in Mississippi coastal waters. *In* Fishery monitoring and assessment completion report, 1 Jan. 1977 to 31 Dec. 1981, p. VI-I-1 thru VI-I-53. Proj. 2-296-R, Gulf Coast Res. Lab., Ocean Springs, MS.

Van Guelpin, L., D.F. Markle, and D.J. Duggan
1982 An evaluation of accuracy, precision, and speed of several zooplankton sampling techniques. J. Cons. Perm. Int. Explor. Mer 40:226–236.

Warlen, S.M.
1988 Age and growth of larval gulf menhaden, *Brevoortia patronus*, in the northern Gulf of Mexico. Fish. Bull., U.S. 86:77–90.

Weinstein, M.P., and M.P. Walters
1981 Growth, survival and production in young-of-year populations of *Leiostomus xanthurus* Lacepede residing in tidal creeks. Estuaries 4(3):185–197.

Williams, L.W.
1983 Larval fish assemblages of lower Mobile Bay. M.S. thesis, Univ. South. Alabama, Mobile, 55 p.

Wilson, C.A., D.W. Beckman, and J.M. Dean
1987 Calcein as a fluorescent marker of otoliths of larval and juvenile fish. Trans. Am. Fish. Soc. 116:668–670.

Yentsch, C.S., and J.F. Hebard
1957 A gauge for determining plankton volume by the mercury immersion method. J. Cons. Cons. Int. Explor. Mer 22(2):184–190.

Evaluation of ghost fishing in the Hawaiian lobster fishery

Frank A. Parrish
Thomas K. Kazama

Honolulu Laboratory, Southwest Fisheries Science Center
National Marine Fisheries Service, NOAA
2570 Dole Street, Honolulu Hawaii 96822-2396

Abstract.– Mortality due to retention of lobsters in derelict traps was evaluated over a 2-year period using two approaches. First, a string of eight empty, single-chamber, plastic traps was deployed at 40 m depth off Oahu, Hawaii, and monitored periodically by scuba during a 6-month period in 1990. The traps were stable and remained intact despite adverse oceanic conditions. Numerous entries and exits of lobsters were recorded. For the second test, the ability of lobsters to exit traps was tested in a series of field and laboratory trials of trap strings stocked with Hawaiian spiny lobster *Panulirus marginatus* and slipper lobster *Scyllarides squammosus*. The number of lobsters that died in stocked traps was less than 4% of the test population and differed significantly from zero only in the laboratory evaluation (χ^2 5.42, P 0.02). The two species exited similarly; however, the pattern of exits in laboratory and field tests differed significantly (χ^2 23.889, P 0.03). All lobsters exited within 56 days in a pattern generally approximating an exponential decline. Our evidence suggests that little direct mortality of lobsters is due to the inability to exit traps, and consequently ghost fishing by these traps is not considered a problem for spiny and slipper lobsters.

Manuscript accepted 14 August 1992.
Fishery Bulletin, U.S. 90:720–725 (1992).

Continued fishing by lost traps has become the focus of increasing concern by both fishery managers and scientists. The recent trend for trap fisheries to replace their degradable traps with designs made from more persistent synthetic materials has heightened the seriousness of possible ghost fishing by such unrecovered traps. Ghost fishing has been defined as the continued fishing of irretrievable gear (Smolowitz 1978). Such a definition fails to distinguish between permanent entrapment and temporary occupation of a trap (e.g., for feeding or shelter). Mortality occurring in abandoned traps should be measured to assess the impact of ghost fishing on a particular fishery.

The phenomenon of ghost fishing has been observed in a wide range of trap fisheries with diverse trap designs (e.g., High 1976, Pecci et al. 1978, Smolowitz 1978, Paul 1983). Despite this attention, few studies have effectively assessed the ghost fishing problem for any species. The more rigorous evaluations rely on continued underwater field observations of simulated lost traps (Breen 1990). With this method, mortalities have been clearly demonstrated in temperate fisheries in which animals were unable to exit traps fitted with nonreturn entrance devices. Features such as spring-loaded doors and slick plastic entrance chutes effectively reduce the ability of some animals to exit actual and simulated lost traps, resulting in reported mortalities of 26–55% (High 1976, Miller 1977, Breen 1987). Conventional wooden, two-chamber or "parlor-type" traps designed for the American lobster *Homarus americanus* have produced mortalities of 12–25% (Sheldon and Dow 1975, Pecci et al. 1978, Smolowitz 1978).

Ghost fishing poses a potential risk to at least some trap fisheries, and such a risk requires assessment for each species and trap configuration. Tropical lobsters have been largely neglected in the controlled evaluation of mortality by ghost traps. Isolated anecdotal reports of tropical lobsters found in lost traps (Sutherland et al. 1983) and tank studies made to date (Paul 1983) do little to predict realistic, long-term effects of lobsters interacting with modern traps in the field.

Hawaii's lobster fishery targets two species, Hawaiian spiny lobster *Panulirus marginatus* and slipper lobster *Scyllarides squammosus*. A laboratory study by Paul (1983) used California parlor-type traps made of wire to determine the effectiveness of escape vents in releasing undersized Hawaiian spiny lobster. Paul (1983) suggested that ghost fishing might occur in these traps and recommended that the Hawaiian fishery consider incorporating degradable escape panels to facilitate the escape of adult lobsters. By 1985 the fishery had adopted a more cost-effective molded-plastic trap design as the standard gear. Degradable panels have not been included.

In 1989 the Hawaiian lobster industry reported that more than 1 million traps were set in the Northwestern

Hawaiian Islands (NWHI); an estimated 2000 of these traps were unrecovered (Landgraf et al. 1989). The annual accumulation of lost plastic traps on the banks where commercial trapping occurs must be considered a potential hazard to the lobster stocks. No field studies have been done on the interactions between lost traps and the adults of the two target lobster species. The objectives of this study were to (1) evaluate the persistence of lost commercial traps under field conditions, (2) estimate retention of target species in plastic traps with bait depleted, and (3) assess mortality of lobsters unable to exit traps.

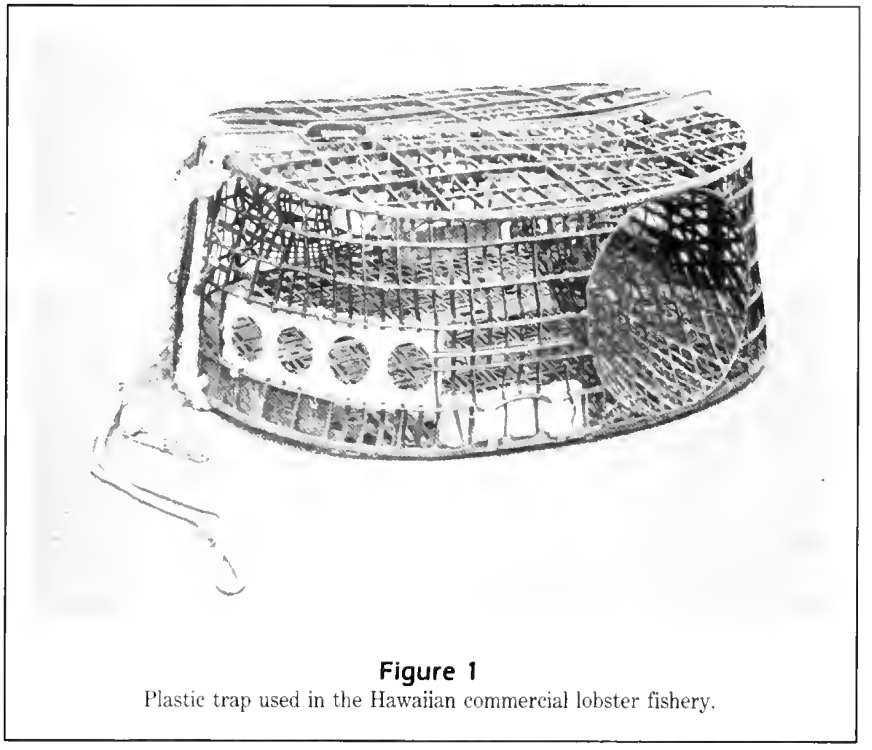

Figure 1
Plastic trap used in the Hawaiian commercial lobster fishery.

Methods

Study sites

The prohibitive cost of prolonged, ship-supported diving operations in the NWHI dictated that all field experiments be conducted at Oahu. Sites close to the windward shore of Oahu provided appropriate depths (30–40 m) and habitat consistent with the NWHI commercial banks. The area is known to harbor exploitable numbers of the lobster fishery's target species. Its heavy seas, strong bottom surge, and swift currents (Bathen 1978) might mimic NWHI conditions and thus could test the stability of lost traps. Traps placed in such rough conditions, without surface markers, were unlikely to be disturbed by fishermen and other recreational users.

Trap stability and faunal interactions

A string of eight empty traps was deployed in a linear orientation from February to July 1990. The selected area afforded two types of adjacent habitat—high-relief rugose bottom, and hard relatively-flat bottom—allowing comparisons of trap stability and use by lobsters in the different environments. Individual traps were set 10 m apart, four on high-relief bottom and four on adjacent even bottom. The molded-plastic traps (Fig. 1) used in the study were a standard commercial model employed throughout the commercial fishery in Hawaii (Fathoms Plus Marine Implementation, P.O. Box 6307, San Diego, CA 92106). Each trap consisted of a single chamber with two side entrances and was weighted with about 10 kg of lead, as is conventional in the fishery. Traps remained in place over a 6-month period. They were observed monthly by scuba divers during three dives conducted at 48-hour intervals. Physical condition, movement, and contents of the traps were noted on each dive, along with general observations of the surrounding area. The monthly censuses recorded the initial presence of lobsters from the surrounding study site and any exits or entries over the following 4 days. The area in and under the traps was examined for exoskeleton remnants that might indicate molting or mortality. One additional trap with its hinge pins removed was deployed on flat bottom near the trap string to mimic a trap with corrodible hinge pins that had deteriorated.

Trap stocking experiment

In the summers of 1990 and 1991, traps of the same type (Fig. 1) were deployed in the field and laboratory, and stocked with spiny and slipper lobsters from the NWHI to evaluate their ability to exit and the extent of mortality. Prior to the traps being stocked, lobsters had spent 3–8 days in transit in continuously-flushing shaded bait wells where they were fed daily. Mean carapace lengths were 87.6 mm (N 96, range 67.4–121.7 mm) for spiny lobster, and 83.3 mm (N 96, range 50.1–99.7 mm) for slipper lobster. Antennae were tagged with color-coded, plastic, self-locking, electrical ties to permit visual identification of individuals without their being handled during the experiment. Molt stage

of lobsters prior to their deployment in traps was determined using Lyle's (1982) adaptation of Drach's (1939) staging technique.

In the field test, 128 tagged lobsters were placed by divers in 4 strings of 8 unbaited traps each (2 spiny and 2 slipper lobsters per trap). Two strings were placed on and around high-relief substrate, one in summer 1990 and the other in summer 1991; two strings were placed on relatively-flat hardbottom, at least 300m from any relief that could provide lobsters shelter, in summer 1991. The contents of the traps were checked every 48 hours until all tagged lobsters had exited or died.

In the laboratory trials, 64 additional tagged lobsters were placed in 16 traps (2 spiny and 2 slipper lobsters per trap) in a large, shaded, outdoor concrete tank. Throughout the tank, food and other suitable shelter were provided outside the traps to encourage exiting. Contents of the traps were monitored daily, and any lobsters found outside the trap in which they were originally stocked were removed from the tank. Lobster death totals in the laboratory (where predation could not occur) and in the field were compared in an attempt to separate losses by predation from other mortality (e.g., starvation, conspecific aggression) in the field.

This study employed a modified experimental cohort design to examine the effects of multiple categories (replicate, habitat type, species) on exiting by lobsters. The design permits cross-classified categorical analysis to be applied (Fienberg 1987). Using chi-square tests, comparisons were made between replicates, habitat types, and species in a systematic order. Categories were collapsed or pooled when justified by the lack of significant differences (Siegel and Castellan 1988).

Results

Trap stability and faunal interactions

Estimated seas of 4–6 ft and currents of 1–2 knots were common at the study site. They produced no observable effect on the physical integrity of the plastic traps. Movement of traps across the substrate was not detected, despite frequent observations of the interconnecting groundline actively moving in the bottom surge. The two halves of the trap without hinge pins shifted 2cm apart. Over the 6-month period, the traps became encrusted with sessile organisms, including bryozoans, corals, and fish eggs. Occasionally adult fish larger than the opening of the escape vent were found in the traps; however, most of these departed through the trap entrance as a diver approached.

Adults of both spiny and slipper lobsters local to the surrounding study site entered the traps. Of the 12 such occurrences of lobsters recorded during the 6-month survey, 7 lobsters left before the last inspection of the monthly observation period, indicating that they did not occupy the traps for more than 30 consecutive days. Three lobsters were observed entering and exiting within the same 48-hour observation period. Nine of the 12 lobsters were found in traps on even bottom.

One dead spiny lobster comprised the only mortality observed within the 6-month field evaluation. Postmortem examination and the presence of lobster debris in the area around the trap suggested death by predation. Sightings of known predators such as octopus, eels, jacks, and sharks were routine. Large eels often occupied the traps, occasionally with lobsters.

Trap stocking experiment

Molt-stage evaluation indicated that 27% of the spiny lobsters and 1% of the slipper lobsters were in the premolt stage at deployment. Mortality was limited to seven spiny lobsters, five in the laboratory and two in the field. All of these lobsters were in premolt stage at deployment and died during or shortly after molting. Despite the limited mortality, the number of deaths in the laboratory trials differed significantly from zero

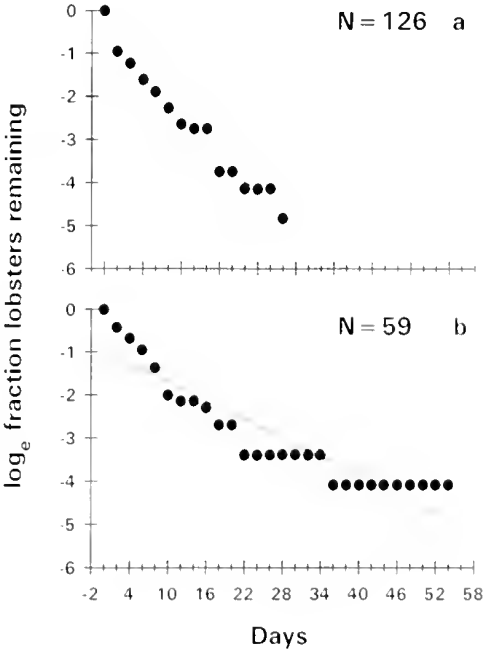

Figure 2
Persistence of occupancy of plastic traps stocked with spiny *Panulirus marginatus*, and slipper *Syllarides squamosus*, lobsters (combined) in the (a) field and (b) laboratory.

(χ^2 5.42, P 0.02). This was not true for the field trials (χ^2 2.06, P 0.15), and mortalities in the laboratory and field were significantly different (χ^2 4.74, P 0.03). Consequently, the two test situations were evaluated separately, with all animals that died excluded from the trap-occupation analysis.

Contingency tables were used to test for differences in the exit distributions for various groups of the data (Fienberg 1987). Within each species, the distributions of exits were first compared between replicate trap strings within the same habitat type and were found not to be significantly different (spiny lobster—high relief, χ^2 3.22, P 0.50; even substrate, χ^2 10.00, P 0.19; slipper lobster—high relief, χ^2 3.33, P 0.50; even substrate χ^2 9.52, P 0.22). Therefore, the distributions of exits for the two replicates were pooled within each habitat type. Within each species, exits were then compared for the effect of the two habitat types and were found not significantly different (spiny lobster—χ^2 10.81, P 0.21; slipper lobster—χ^2 4.53, P 0.72). The distributions of two habitat types were then pooled within each species, and exits of the two species were not significantly different (χ^2 16.93, P 0.08). Consequently, the distributions of the two species in all field trials were combined (N 126 lobsters after 2 early mortalities) for further comparisons.

Within each species, exits observed in the tank were compared with the field data pooled by replicate and habitat type and were not significantly different (spiny lobster—χ^2 14.42, P 0.21; slipper lobster—χ^2 13.63, P 0.09). Exits of spiny and slipper lobsters in the tank were not significantly different (χ^2 11.55, P 0.32), and the data were subsequently pooled (N 59 lobsters after 5 early mortalities). A comparison of exits of all lobsters in the tank (pooled) and all lobsters in the field (pooled) showed a significant difference (χ^2 23.889, P 0.03).

Half of the 126 spiny and slipper lobsters stocked in the field and 33% of the lobsters stocked in the laboratory exited within 48 hours after being placed in the traps. Ninety percent or more of the exits in both tank and field trials occurred within the first 16 days. All field animals had left by day 30, and all laboratory animals by day 56. The overall exit pattern of the lobsters suggested an exponential model. The data were fitted to the log-transformed exponential function

$$\ln_e (N_t/N_0) = bt,$$

where N_t is the number of lobsters remaining after time t from N_0 lobsters initially stocked. The parameter b was estimated with a log-linear regression procedure for the field traps ($b = -0.16$/day; r^2 0.992, SE 0.284, $P<0.001$) and for the laboratory traps ($b = -0.094$/day, r^2 0.961, SE 0.632, $P<0.001$; Fig. 2).

Stocked spiny and slipper lobsters exited and reentered field traps in at least 13 instances; 6 lobsters returned to the same trap. One spiny lobster was observed exiting three traps within 6 days.

Discussion

Trap stability

The lack of structural damage and appreciable movement of the plastic traps in the field contrasts with the popular opinion of experienced fishermen that lost traps break up and roll off the banks into waters beyond the depth range of lobsters. Fishermen routinely report movement of trap strings as a result of powerful swells moving across the commercial banks. Despite the frequently observed movement of the groundline by swells at the Oahu study site, it is likely that the study site does not fully duplicate the power of the long-term swells common in the NWHI. Lost traps may not shift on the bottom as much as actively fished traps. Buoys and interconnecting polypropylene line provide additional lift and resistance to water motion; therefore, fully rigged strings of traps are more likely to move than isolated traps severed from the groundline. A 1990 systematic diving survey of 33 sites around 2 of the prominent NWHI commercial lobster fishing banks revealed only 2 mangled derelict traps (F. Parrish, unpubl. data). The failure to locate large amounts of lost gear may be partly explained by this survey being incidental to other work. Total gear losses in 1989 averaged about 1 trap/nm^2 over the total estimated area of the lobster fishing grounds (Landgraf et al. 1989). Lost gear could be heavily concentrated in a few of the more intensively fished areas that the survey may have missed.

A trap manufacturer (Fathoms Plus Marine Implementation) has made available a corrodible pin which is intended to allow the halves of plastic traps to eventually fall apart once the pin deteriorates. The fact that our pinless trap remained relatively intact for 6 months in the field suggests that the synthetic plastic clips on the trap roof will continue to hold the trap together, especially for fisheries conducted in calmer seas.

Mortality and movement of lobsters

Seven deaths among the 192 spiny and slipper lobsters within the 56-day study represent low mortality when compared with the natural mortality estimates from the fishery population modeling by Haight and Polovina (1992). Extrapolation of the experiment's percentage of mortality from 2 months to 1 year (22%) is close to half the fishery's annual estimated natural mortality (40%). The fact that only animals that began the trials

in premolt condition died suggests that lobsters at this stage are less fit. The probability that this mortality would occur only with premolt individuals by chance alone is <0.001 (Agresti 1990). Increased vulnerability to a poor physical environment, conspecific aggression, or predation have been associated with molting (Conan 1985). It seems likely that the higher percentage of spiny lobster in premolt stage accounts for some of the difference in mortality between spiny and slipper lobsters.

The significantly higher mortality observed in the laboratory compared with the field does not support the idea that undetected predation substantially affected the field results. The relatively low absolute level of total mortality suggests that such predation is probably minimal at the field site. However, with mortality being higher in the laboratory than in the field, no estimate of predation is possible.

More than twice as many deaths were observed in the laboratory as in the field, even though the field trials involved twice as many lobsters and three times as many were in the premolt stage. This suggests a less healthy or fit laboratory population, which is consistent with the significantly slower exit of pooled species from traps in the laboratory versus in the field. Aspects of the laboratory environment (e.g., water quality, lighting, diet) may have degraded the physical condition of the lobsters or affected their behavior, inhibiting their exit, or providing less inducement to leave the traps than that encountered in the field. It seems likely that our field assessment provides a better estimate of natural exit patterns.

With a study design similar to ours, Munro (1974) examined the rate of fish exiting unbaited traps. His theoretical model suggests that the number exiting per day may be a fixed fraction of the current trap occupancy, and that catch eventually reaches an asymptote when trap entrances are balanced by exits. Our number of stocked lobsters declined approximately exponentially, approaching zero asymptotically. However, the total occupancy of traps declined daily until it reached a low and varying level at which exits were roughly matched by entrances of lobsters. This final, low level of trap occupancy at the end of the stocking experiment seems consistent with native occupancy observed during the monthly field monitoring.

In our stocking tests, some individuals likely left a trap and reentered it undetected between censuses, particularly in the field test where the observation interval was 48 hours. Based on independent probabilities of exit and entry estimated from our field data, the theoretical joint probability of such reentry was as high as 0.06, and probably about 12 individuals left and reentered the same trap undetected during the full 26-day field stocking experiment.

Conclusion

Our results indicate that spiny and slipper lobsters are not restrained by lost molded-plastic traps for periods long enough to cause serious harm. There is no evidence that such lost traps result in increased mortality. The absence of any apparent trap-induced mortality and the low incidence of identifiable in-trap mortality due to predation suggest that ghost fishing by these traps contributes little to the total mortality of the population. Such traps, when unbaited and intact, may best be considered short-term artificial shelters that lobsters enter and exit occasionally, more or less at will.

Acknowledgments

Thanks are due to Steve Kaiser for advice on selection of study sites and to Bill and Joanne Goebert for providing ready access to those sites. Ray Boland, Karl Bromwell, Theresa Martinelli, and Leslie Timme assisted in the rigorous program of field monitoring. Greatly appreciated are the statistical and substantive comments of Deborah Goebert, Robert Moffitt, James Parrish, and Jeffrey Polovina.

Citations

Agresti, A.
1990 Categorical data analysis. John Wiley, NY, 558 p.

Bathen, K.H.
1978 Circulation atlas for Oahu, Hawaii. Misc. Rep. UNIHI-SEAGRANT-MR-78-05, Univ. Hawaii Sea Grant Coll. Prog., Honolulu, 22 p.

Breen, P.A.
1987 Mortality of Dungeness crabs caused by lost traps in the Fraser River estuary, British Columbia. N. Am. J. Fish. Manage. 7:429–435.
1990 A review of ghostfishing by trap and gill nets. *In* Shomura, R.S., and M.L. Godfrey (eds.), Proceedings, Second international conference on marine debris, 2–7 April 1989, Honolulu, p. 571–599. NOAA Tech. Memo. NMFS-SWFSC-154, NMFS Southwest Fish. Sci. Cent., Honolulu.

Conan, G.Y.
1985 The periodicity and phasing of molting. *In* Wenner, A.M. (ed.), Crustacean issues, factors in adult growth, vol. 3, p. 73–99. A.A. Balkema, Boston.

Drach, P.
1939 Mue et d'intermue chez les Crustaces Decapodes. Ann. Inst. Oceanogr. 19:103–392.

Fienberg S.E.
1987 The analysis of cross-classified categorical data, 2d ed. MIT Press, Boston, 198 p.

Haight W.R., and J.J. Polovina
1992 Status of lobster stocks in the Northwestern Hawaiian Islands, 1991. Admin. Rep. H-92-02, NMFS Southwest Fish. Sci. Cent., Honolulu, 19 p.

High, W.L.
1976 Escape of Dungeness crabs from pots. Mar. Fish. Rev. 38(4):19–23.

Landgraf, K.C., S.G. Pooley, and R.P. Clarke
1989 Annual report of the 1989 western Pacific lobster fishery. Admin. Rep. H-90-06, NMFS Southwest Fish. Sci. Cent., 30 p.

Lyle, W.G.
1982 Molt stage determination in the Hawaiian spiny lobster *Panulirus marginatus*. M.S. thesis, Univ. Hawaii, Honolulu, 29 p.

Miller, R.J.
1977 Resource underutilization in a spider crab industry. Fisheries (Bethesda) 2(3):9–13.

Munro, J.L.
1974 The mode of operation of Antillean fish traps and the relationships between ingress, escapement, catch and soak. J. Cons. Cons. Int. Explor. Mer 35:337–350.

Paul, L.M.B.
1983 Investigations into escape vent effectiveness and ghost fishing in captive populations of the spiny lobster *Panulirus marginatus*. *In* Grigg, R.W., and K.Y. Tanoue (eds.), Proceedings, Second symposium on resource investigations in the Northwestern Hawaiian Islands, vol. 2, p. 283–295. Misc. Rep. UNIHI-SEAGRANT-MR-84-01, Univ. Hawaii Sea Grant Coll. Prog., Honolulu.

Pecci, K.J., R.A. Cooper, C.D. Newell, R.A. Clifford, and R.J. Smolowitz
1978 Ghost fishing of vented and unvented lobster, *Homarus americanus*, traps. Mar. Fish. Rev. 40(5-6):9–24.

Sheldon, W.W., and R.L. Dow
1975 Trap contributions to losses in the American lobster fishery. Fish. Bull., U.S. 73:449–451.

Siegel, S., and N.J. Castellan
1988 Nonparametric statistics, 2d ed. McGraw-Hill, NY, 399 p.

Smolowitz, R.J.
1978 Trap design and ghost fishing: An overview. Mar. Fish. Rev. 40(5–6):2–8.

Sutherland, D.L., G.L. Beardsley, and R.S. Jones
1983 Results of a survey of the south Florida fish-trap fishing grounds using a manned submersible. Northeast Gulf Sci. 6(2):279–183.

Abstract. – Movements of 25 yellowtail rockfish *Sebastes flavidus* on Heceta Bank, off Oregon, were studied by acoustical tagging and tracking during the summers of 1988–90. Some fish were tracked discontinuously up to 1 month after transmitters were inserted into their stomachs. In each year, some fish remained at the capture site after release or returned after displacement to a different release site. In 1990, the year of most intensive tagging, 11 of 12 fish were detected near the capture location 13 days after release in August 1990, including 3 of 4 fish displaced 0.5 nmi (0.9 km), all 4 fish displaced 2.0 nmi (3.7 km), and all 4 of the fish released at the capture site. One fish homed overnight from the release site 0.5 nmi away. In September 1990, 1 month after release, eight of these fish had dispersed up to 0.1–0.7 nmi (0.2–1.3 km) to the south of their capture location, suggesting a change in site fidelity. Pressure-sensitive transmitters showed that tagged yellowtail rockfish usually remained at midwater depths of 25–35 m, well above the sea floor depth of ~75 m. Rapid descents to nearbottom depths were common, but no obvious diel vertical or horizontal migrations were detected.

Movements of acoustically-tagged yellowtail rockfish *Sebastes flavidus* on Heceta Bank, Oregon

William G. Pearcy

College of Oceanography, Oregon State University, Corvallis, Oregon 97331-5503

The yellowtail rockfish *Sebastes flavidus* is a common rockfish along the west coast of North America. It is caught by both commercial and recreational fishermen and was one of the most abundant rockfish species in commercial groundfish landings from the U.S. west coast from 1982 to 1990 (Pacific Fisheries Management Council 1991).

Schools of yellowtail rockfish may persist at the same location for many years. Carlson (1986) reported that a school of adult yellowtail rockfish in southeastern Alaska consisted of individuals from one or two year-classes and had negligible recruitment over an 11-year period. Because their aggregrations may be site-specific with limited interchange of adults, and because rockfish are long-lived, late-maturing, and of low fecundity (Gunderson et al 1980, Love et al. 1990, Eldridge et al. 1991), overfishing or disturbances, such as habitat modifications from offshore mining or petroleum development, may have long-lasting effects in a local area. On the other hand, a rockfish species whose individuals move freely from reef to reef may be less vulnerable to localized disturbances (Love 1979). The stability and areal range of rockfish aggregations have important implications for assessment, availability, and management of rockfish species.

The yellowtail rockfish is the most abundant, large-sized schooling fish seen from submersibles over the shallow, rocky areas on the top of Heceta Bank, a deep reef located ~55 km off the central Oregon coast (Pearcy et al. 1989; Figs. 1 and 2). Large pelagic schools, sometimes of a thousand or more individuals, were observed over shallow portions of the bank (<150 m) during the summer. Based on both observations from submersible dives and the occurrence of large echo-groups recorded by the ships' echosounders, these schools were often associated with pinnacles or high-relief topography (Pearcy et al. 1989).

During one dive, a school of yellowtail rockfish followed the submersible along the bottom for over an hour before abruptly turning and swimming back toward the location where the school was initially encountered (Pearcy et al. 1989). This observation and those of Carlson and Haight (1972), who found that individual rockfish returned to a home site in southeast Alaska after being displaced as far as 22.5 km, suggest that schools of yellowtail rockfish may have home ranges centered around a specific site on the bank.

Pelagic rockfishes, such as the yellowtail rockfish, may range over wider areas than benthic rockfishes. However, little is known about the vertical distribution or diel vertical migrations of yellowtail rockfish, or the relationships between vertical and horizontal movements.

This study used acoustical tracking to determine the horizontal and vertical movements and site-specificity of yellowtail rockfish on Heceta Bank. In this paper, I define site-specificity as the tendency of fish to inhabit a specific localized area as opposed to free-ranging or vagrant

Manuscript accepted 13 July 1992.
Fishery Bulletin, U.S. 90:726–735 (1992).

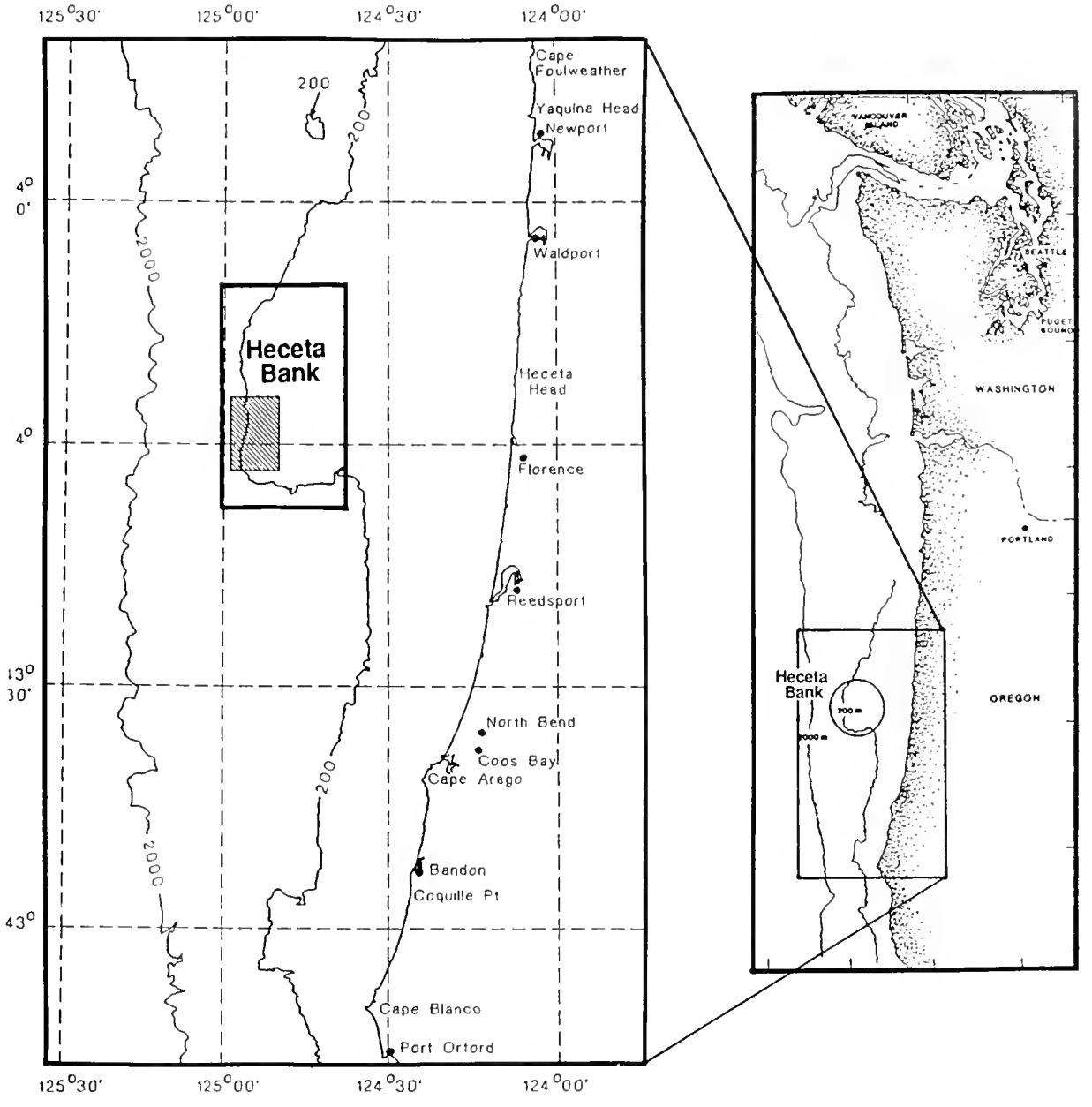

Figure 1

Location of Heceta Bank off Oregon. Hatched area of the bank encompasses the area of this study as shown in Figure 2 (depth contours in meters).

behavior. Homing is defined as returning to a site formerly occupied instead of to equally probable locations. Homing does not imply a direct, straight-line course back to the home site.

Yellowtail rockfish are ideal for acoustical tracking because they are common, large in size, and do not suffer from the lethal embolisms of other rockfishes when brought to the surface, but instead expel swimbladder gases during decompression*.

* Bubbles of gas were observed emanating from the region of the opercle as yellowtail rockfish were reeled from about 2–3 m depth to the surface. By immersing fish in tanks aboard ship, these bubbles were seen forming and being expelled from under the thin skin between the last gill and the cleithrum anterior to the base of the pectoral fin. Samples of the gas were collected in syringes and analyzed with a microgasometer using the methods of Scholander et al. (1955). The gas was comprised of about 75% oxygen, indicating that gases from the swimbladder were released without causing lethal embolisms when yellowtail rockfish were rapidly decompressed.

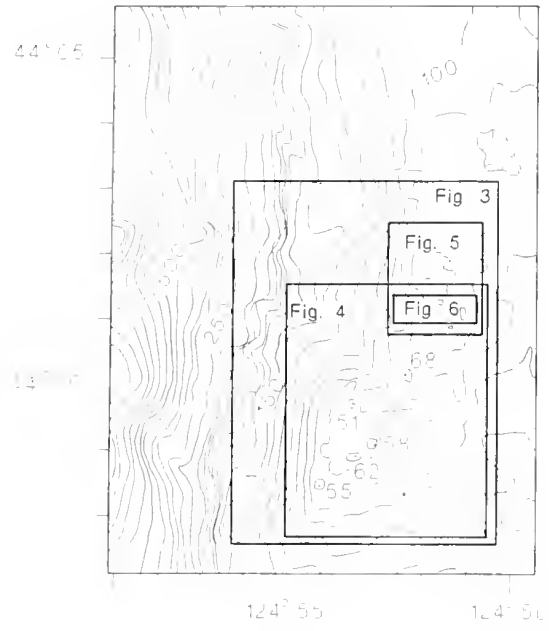

Figure 2
Topography of the southern portion of Heceta Bank and the areas encompassed in Figures 3–6. Depths are in meters.

Table 1
Information on tag retention in 5 yellowtail *Sebastes flavidus*, and 5 black *S. melanops*, rockfishes aboard ship (S) and in the laboratory ashore (L). ARM = tags with hooks (anti-regurgitation mechanisms).

Date	S/L	Tag	Days to regurgitate (or die)
S. flavidus			
Sep 1988	S	External	(3)
	S	Stomach	1,2,(6)
Aug 1990	L	Stomach-ARM	11
S. melanops			
Apr 1990	L	Stomach	1
	L	Stomach-ARM	9
Jul 1990	L	Stomach	0.5
	L	Stomach-ARM	2,89

Methods

Yellowtail rockfish were captured with hook-and-line during the daytime and placed in deck tanks with circulating seawater. Acoustical transmitters were inserted into the stomachs of large (42–54 cm fork length), active, uninjured, unanesthetized fish with a 1 cm diameter rod. Most fish were males. Fish were released within 15 min at the capture site or within 30 min at displaced locations. Displaced fish were released over bottom topography and depths known to be inhabited by yellowtail rockfish (except in 1988), and within 2 nmi of the capture location to facilitate survey of several release sites during a cruise. They were tracked using a directional hydrophone and acoustical receiver. Four fish tracked during 1989 were also tagged with external Floy tags.

Preliminary tagging

Before this study began, a few tests were conducted in circulating seawater tanks aboard ship or in the laboratory to evaluate methods of tagging pelagic rockfishes on five yellowtail and five black rockfishes (Table 1). Dummy tags of the same dimensions and weight as those used in the study were inserted into the stomach or attached externally to the side of fish under the dorsal fin. The external tag attachment, similar to the one used by Matthews et al. (1990) for benthic rockfish, caused one fish to list to one side and interfered with its swimming. It died after 3 days in the ship's tank. Three fish with tags inserted in their stomachs had normal orientation in deck tanks and were more active. One of these fish died after 6 days.

Stomach insertion of tags was used in this study. This method is quick and minimizes handling and trauma to the fish (Stasko and Pinock 1977). The major disadvantage was possible regurgitation of tags (Table 1 and Results), although Stasko and Pincock (1977) reported that transmitters inserted into the stomachs of many other species of fishes were not disgorged. During the last year, to increase the retention of tags in the stomachs, one or two small (no. 18 steel dry fly) hooks were attached to the ends of tags with epoxy as anti-regurgitation mechanisms (ARM's). Hooks protruded 2 mm from the tag. In experiments in large aquaria or tanks in the laboratory, tags with ARM's stayed inside either black rockfish *S. melanops* or yellowtail rockfish a total of 2, 9, 11, and 89 days compared with 0.5, 1, 1, and 2 days (and one that died after 6 days) for controls without ARM's (Table 1).

Equipment

Acoustical tracking equipment (VEMCO Ltd.) was used in this study, including a VR-60 receiver with preset channel frequencies, a telemetry decoder and display unit, directional hydrophone, and transmitters or tags with five different crystal-controlled frequencies. Transmitters were 16 mm in diameter, 48–65 mm in length, with batteries of 4.5, 9, 21, and 60 days rated life-span. In 1990, transmitters with the same frequencies had different pulse widths and pulse periods which

were decoded and displayed by the receiver. The transmitters had a rated range of 500–1500 m.

Pressure-telemetering transmitters with battery durations of 4.5 days were used in 1989 and 1990. The pulse rates of these transmitters were linearly proportional to pressure, and individual calibrations were incorporated into the receiver program. The manufacturer claimed accuracy was 5% of the full range, or 5 psi (~3 m depth), similar to my test of two tags lowered vertically on a metered line at sea. Data on depths of fish and time of day from these transmitters were printed at regular intervals aboard ship and stored in the receiver. During 1989, depths and times were recorded manually every 5 min or less. During 1990, data on time and depth were stored automatically by the receiver every 0.5 sec. Median depths were calculated for every 25-sec period and plotted by computer.

Field procedures

Research was conducted using either the RV *William A. McGaw*, a 32 m ship used to support submersible research, or the FV *Corsair*, an 18 m trawler. Echosounders were used to scout concentrations of fish over the shallow (60–90 m) portions of Heceta Bank. When dense midwater schools of fish were detected, weighted fishing lines with jigs were lowered to catch fish. Only yellowtail rockfish were caught from these midwater schools, which were usually at depths of 20–40 m. Often the schools were so compact that our fishing weights bounced off fish at these depths. If yellowtail rockfish were readily caught, our position was recorded and an anchored surface float was released from the *Corsair* to provide a fixed reference to prevent drifting off-station and assist tracking of fish.

Transmitter signals were detected with a directional hydrophone attached to the end of a 4 m rotatable pole mounted to the side of the vessels. The hydrophone pole was rotated through 360° until the signal strength of a transmitter was maximal. Then the vessel headed directly toward the transmitter. Signal strength increased as the range closed. When signal strength was equally high in all directions or when the direction of the signal decreased rapidly, we assumed that the fish was in the vessel's immediate vicinity and our location was then determined by LORAN C. Repeated positions for stationary transmitters on the bottom were within 0.1 nmi (~180 m) from one another. Repeatable accuracy of Loran C for one vessel is about 100 m (Dugan and Panshin 1979).

Results

Horizontal movements

1988 (Fig. 3) Four yellowtail rockfish were caught near the bottom, tagged, and released during September 1988. Three fish were released where they were caught, and the fourth was displaced about 1 nmi seaward of its catch location. Fish 1 was caught and released over a shallow (71 m), high-relief rocky area of Heceta Bank on 15 September (Fig. 3). Three locations were determined

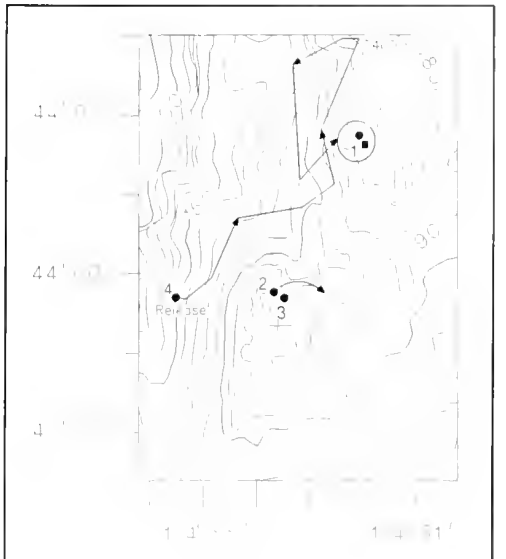

Figure 3
Locations and tracks of yellowtail rockfish *Sebastes flavidus* tagged and released in 1988. Fish 1, released 15 September at 1919 h (●), was located 24 h later (■), and was found within the open circle (○) during seven intervening fixes. Fishes 2, 3, and 4 were released 13 September (●) and followed indicated paths. Fish 3 moved less than 200 m.

immediately after release, three after 12 h, and two after ~24 h. All locations were within 0.5 nmi of one another, and the last was 0.1 nmi from the capture site. Fish 2 and 3 were caught, released, and detected once over the southernmost shallow portion of Heceta Bank at a depth of 80 m on 13 September. One of these fish was located ~0.75 nmi (1400 m) east of its capture location after 7 h. The other fish was found within 200 m of the release site 17 h after release.

To determine if a stationary transmitter location was the result of a regurgitated tag, the submersible *Delta*, with a separate hydrophone and receiver, dove on Fish 3, which remained close to the release site. The ship maintained position over this transmitter as the submersible was launched. Although a strong signal was recorded from the transmitter, its bearing changed frequently, indicating that the tag was moving and had not been regurgitated. This was confirmed when the bearing of the transmitter changed 180° as a school of several hundred fish swam under the submersible. The fish transmitting the signal had two external Floy tags but was not seen.

The fourth fish was captured at the southern high spot of Heceta Bank (80m depth, same date and capture site as Fishes 2 and 3) and released 27min after capture 1.3nmi offshore in a habitat where yellowtail rockfish were rarely seen—where the bottom was 150m, flat, and comprised of fine sediments. Between 1727h on 7 September and 0730h the next day, this fish was tracked continuously (Fig. 3). It moved to the northeast until 0400h, turned south, but then resumed its northeasterly course, ending up near the 75m depth contour just west of a shallow region of the bank, about 2nmi from its capture location.

1989 (Fig. 4) Two experiments were conducted in 1989 to further investigate horizontal movements: one involved three fish caught and released with pressure-telemetering transmitters at a station on 21 August (1 fish) and 24 August 24 (2 fish). The other experiment included six fish, three of which were released at the capture site and three displaced 1.1 miles away, on 25 August. All fish were caught in midwater at ~79m.

Fish 2 in the first experiment was released at site A and was tracked continuously for 11h after release. During this time it stayed within ~0.2nmi of the release site, which was marked by a surface buoy. We returned to this location 36h later and found this fish 0.5nmi to the east. After 1.5h it returned to the release site and was located several times in this vicinity during the next 56h (Fig. 4).

Two other fish were caught, tagged, and released 3 days later, at site B, and tracked for about 24h. Acoustical signals of these two fish stayed within 0.2nmi of the release location during this period.

In the second experiment, six fish were caught at site B on 25 August. Three fish (10, 11, 12) were released at the capture location and three (7, 8, 9) were displaced 1.1nmi to the northeast of site C and released in 77m of water. When we returned to these locations 9 days later, two (7 and 9) of the three tags from fish displaced to site C were detected and remained there over the next 36h. Distinctive double pings from these two tags were heard on the receiver, indicating that the tags had been regurgitated and were on the bottom.

Fish 10 and 11, which were released at capture site B, were detected ~0.1nmi south of site B 9 days after capture. Signals from the third fish (12) were not detected. The transmitter from displaced Fish 8 was detected ~0.4nmi to the east of the capture site. Within the next 36h, this fish moved to within 0.2nmi of the capture location, and its last position was 0.3nmi from the capture site.

The submersible *Delta* was used to dive on one of the tags that was stationary at the displacment location (site C). This transmitter was found lying on top of a large rock.

1990 (Figs. 5 and 6) During 1990, transmitters with ARM's were inserted into 12 yellowtail rockfish. All fish were caught during early evening (1900h) on 15 August in mid-

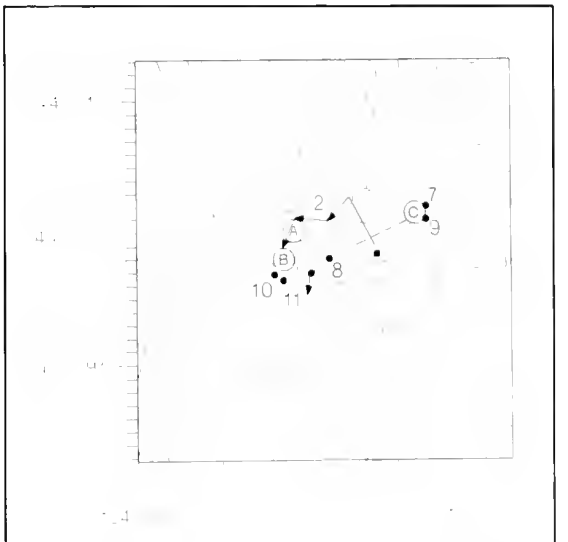

Figure 4
Locations and tracks of yellowtail rockfish *Sebastes flavidus* released in 1989. See text for details. Dashed line is the assumed path of Fish 8.

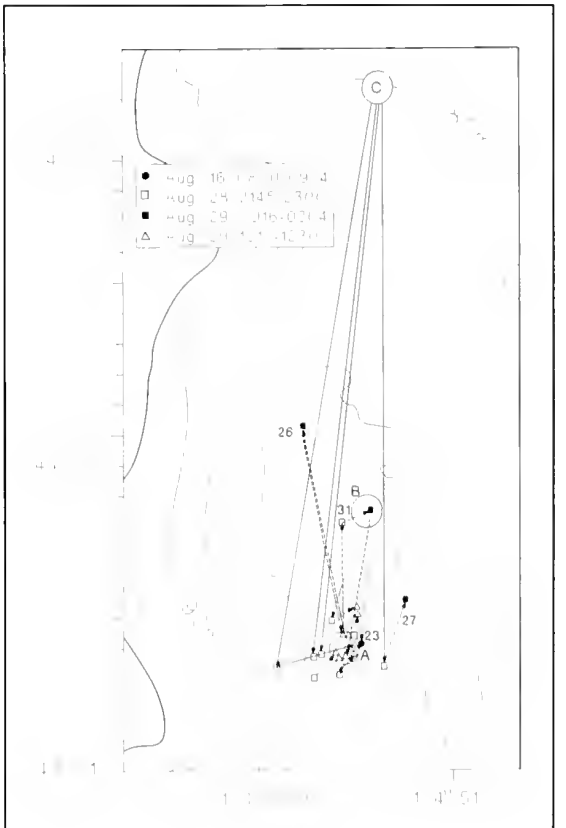

Figure 5
Tracks of 11 yellowtail rockfish *Sebastes flavidus* captured at site A and released at sites A (dashed lines), B (dotted lines), and C (solid lines) on 15 August 1990. Symbols designate dates and times that positions were obtained (see legend).

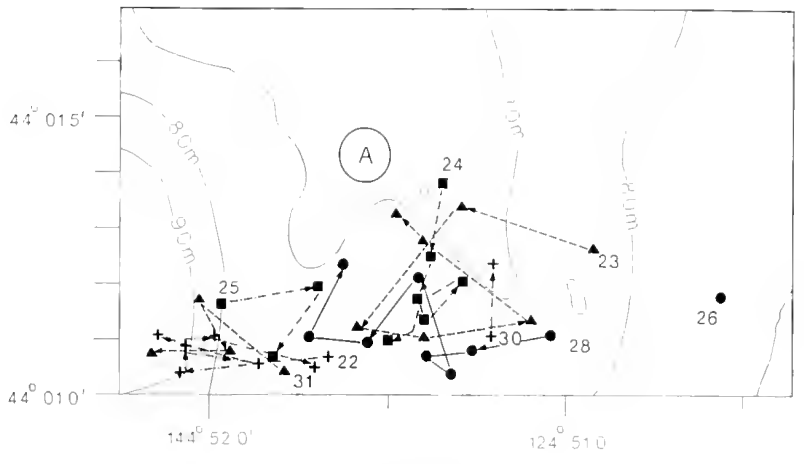

Figure 6

Tracks of eight of the yellowtail rockfish *Sebastes flavidus* released on 15 August, one month later during the period 16–18 September 1990. Symbols designate positions of each fish.

water above a 68m rocky bottom. Four of these fish were released at capture site A, four at 0.5 nmi to the north (site B, bottom depth 70m), and four at 2.0nmi to the north (site C, bottom depth 87m) (Fig. 5). The two release sites to the north of the capture site had high-relief bottom topography, similar to the capture site. In addition, schools of rockfish, similar in appearance acoustically to those comprised of yellowtail rockfish, were observed in the vicinity of the two displacement sites. Since yellowtail rockfish are numerous over shallow (<100m) rocky ridge, boulder, and cobble habitats of Heceta Bank, and schools of yellowtail rockfish were seen from submersibles near release sites B and C (Pearcy et al. 1989, Hixon et al. 1991), I assumed that the transplant release sites were habitable by yellowtail rockfish.

The morning after the releases, all four of the transmitters in fish released at capture site A were detected within 0.1nmi of site A. One of the fish (23) released 0.5nmi to the north returned to the capture site overnight, after 17h. No transmitters were detected at the other two release sites on the following day when the ship passed over these locations and departed the bank.

Eleven of the twelve fish were located 13 days after release when we returned to Heceta Bank, including all four released at site C (2.0nmi to the north) (Fig. 5). The missing transmitter was from site B. All 11 fish were found at least once within 0.15nmi of the capture site (Fig. 5). These results are evidence for a strong homing tendency.

Two fish that were caught and released at the original capture location (site A) showed the most extensive short-term movements (Fig. 5). Fish 26 was located 0.8nmi and Fish 31 was found 0.5nmi north of site A during the night and early morning of 28–29 August, 14 days after release. Both returned to site A about 11h later. Fish 27, displaced to site C, was found 0.15 nmi east of capture site A and then moved 0.24nmi to the north during a 2-hour period on the evening of 29 August.

One month after releases, we returned to the capture location to study longer-term movements. No transmitters were detected in the immediate vicinity of the original capture location. Using an expanding rectangular search pattern, 8 of the 12 transmitters were discovered, all south and a distance of ~0.1–0.7nmi from the capture location. Locations of these fish were determined over the next 2.5 days during three periods between submersible operations. The fish were scattered along a 1.1nmi east-west axis (Fig. 6). Most fish demonstrated short-term movements of over 0.1 nmi (our nominal error of navigation) during these 2.5 days. Two fish (23 and 28) moved ~0.5nmi. Only one fish (22) ended up near the location where it was initially found on this cruise. None of these eight fish was found closer than 0.1nmi to the original capture site, and most were 0.4nmi away. There was no evidence that these fish stayed in a common school or within a small home range, as found earlier in the summer.

Vertical movements

Pressure-telemetering (depth sensor) transmitters were used during 1989 and 1990, but due to problems with the receiver, limited data were obtained. Figure 7 shows the maximum and minimum depths for 10-min intervals for three fish monitored almost continuously during 21–22 and 24–25 August 1989. Fish were usually in midwater, inhabiting depths of 25–50m where the bottom was ~75m. Short-duration vertical movements were seen for all fish, usually rapid descent/ascent ("bounce") dives to or close to the bottom, followed by rapid vertical ascents back to depths of 25–35m. Fish 2 made nine of these "bounce dives" to the bottom during the early morning of 24 August over about a 4h period. Other than this series of dives, there was little evidence for any diel patterns in the frequency of vertical migrations of fish that were tagged. Fish 3 either regurgitated its transmitter or rested on the bottom after 0700h on 25 August (Fig. 7).

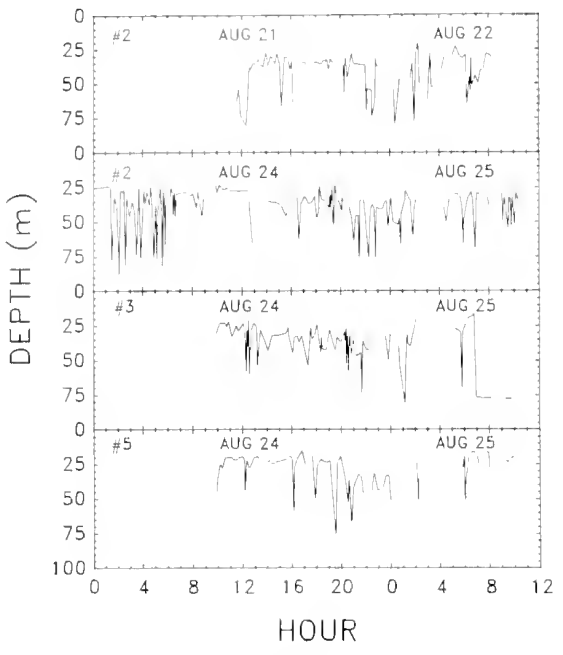

Figure 7
Depths of yellowtail rockfish *Sebastes flavidus* nos. 2, 3, and 5 measured with pressure-telemetering transmitters during 21–25 August 1989. Bottom depths 75–99 m during this period.

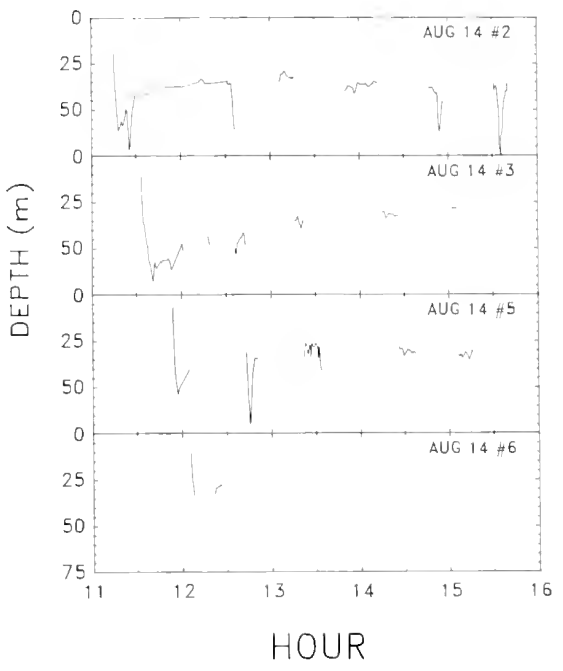

Figure 8
Depths of yellowtail rockfish *Sebastes flavidus* nos. 2, 3, 5, and 6 measured with pressure-telemetering transmitters during 14 August 1990. Bottom depths 75–80 m.

Vertical excursions of fish during late morning and afternoon of August 1990 showed a similar pattern, with fish occupying midwater depths and occasionally diving to deep water (Fig. 8). The records for Fishes 2 and 3 show that these fish descended toward the bottom immediately after release and then rose to progressively shallower depths during the next several hours. Synchronous vertical movements of several fish were not common (Figs. 7, 8) but some did occur among the three fish tracked during 25 August 1990 (Fig. 8). Sometimes fish dove as the vessel approached, perhaps a response to ship noise (Ona and Godoe 1990), but at other times fish descended when the vessel was not underway.

Maximum rates of descent for fish shown in Figure 8 were 0.16–0.40 m/sec; maximum ascents were 0.15–0.31 m/sec. Figure 9 shows the dive of Fish 5 after release, with the most rapid descent during the first minute, and slower rates in the next 3 minutes. Rapid vertical movements were also observed during 1989, with maximum rates of descent of 0.15–0.45 m/sec, and rates of ascent of 0.15 m/sec.

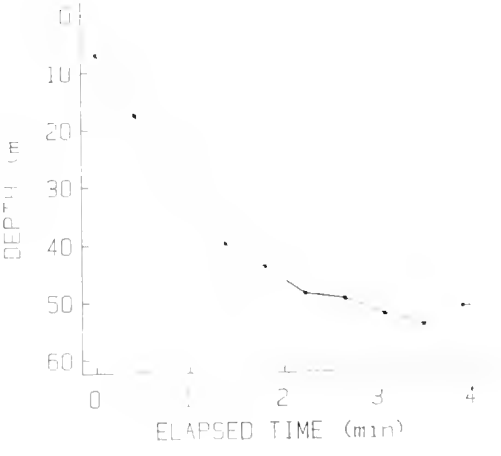

Figure 9
Initial descent of yellowtail rockfish *Sebastes flavidus* no. 5, starting at 1154 h, 14 August 1990, after release at the surface (see Fig. 8).

Discussion

Homing and horizontal movements

During all three years of the study, yellowtail rockfish on Heceta Bank demonstrated site fidelity and homing. Displaced fish returned from as far as 2 nmi from their capture site, and those released over rocky habitat and at similar depths returned to the location of capture in 1990. Eleven of twelve fish tagged in 1990 returned to or remained close to the original capture site 13 days after release. One fish that was displaced 0.5 nm returned overnight to the location where it was captured.

Carlson and Haight (1972) also found that adult yellowtail rockfish returned to their home site, some from as far as 22.5km, some after displacement to other yellowtail schools, and some after 3 months in captivity. In both studies, yellowtail rockfish homed even if released at sites where the habitat was similar to that at the capture site and near other schools of yellowtail rockfish. This demonstrates fidelity to a home site.

Not all yellowtail rockfish demonstrate site fidelity, however. Eight of ten recoveries of 153 yellowtail rockfish tagged in Puget Sound were from the open Washington coast, 58–2214 days after release, indicating an offshore migration probably related to the onset of maturation of these fish (Mathews and Barker 1983). In another study, Stanley (1988) tagged 4622 yellowtail rockfish in Queen Charlotte Sound, British Columbia during 1980 and 1981. As of 1987, the five that were recovered moved from <10km to >300km. Of 9417 yellowtail rockfish tagged southwest of Vancouver Island, 24 were recovered. Twelve moved <10km while others were recovered 23 to >500km from the tagging location (Stanley 1988).

The degree of site fidelity and movement of yellowtail rockfish may be related to the bottom topography of the tagging location. This appears to be the case for black rockfish, another offshore pelagic species. Culver (1987; B.N. Culver, Wash. Dep. Fish., Montesano, pers. commun.) found that black rockfish tagged over a 5-year period from rocky habitats of northern Washington exhibited "no significant movement," whereas fish tagged in areas that had sandy sediments or small pinnacles off the central Washington and northern Oregon coast displayed appreciable movements. Perhaps yellowtail rockfish on Heceta Bank, and other rocky banks, are less mobile than those inhabiting areas with level seafloors.

Carlson and Haight (1972) found that fish displaced to sites across open water with depths >100m returned to the site of capture with much less frequency than did fish released along the adjacent coast in shallower depths. One fish in my study, released in relatively deep water off Heceta Bank and tracked continuously for 14 hours (Fish 4, Fig. 3), was not oriented toward its home site. These observations suggest that homing is most effective over relatively shallow water (<100m), even though yellowtail rockfish are basically midwater fish. Homing may also be influenced by topography. Matthews et al. (1987) reported that displaced copper and quillback rockfishes *S. caurinus* and *S. maliger* returned to high-relief, but not to low-relief, reefs.

The sensory mechanisms and environmental cues used for homing and home-site recognition by yellowtail rockfish are not known. Possibly the fish on Heceta Bank recognized familiar topography and prominent "landmarks." Movements of up to 0.75nmi by yellowtail rockfish (Figs. 5 and 6) indicate that they do not always have as small a home range and may range over a large portion of the bank. Perhaps they learn visual "landmarks" over much of the bank in this way.

One fish returned to its home site from 925m after only 11 hours, mainly during the night when recognition of visual landmarks would have been more difficult. This fish returned home more rapidly than substrate-associated copper and quillback rockfishes that took 8–25 days to return home after displacement of only 500m (see Matthews 1990 for this and summary of homing by other rockfishes). This suggests oriented or directed movement.

Eight of the twelve fish tagged in August 1990 were relocated 1 month after release but were all south of the capture location and scattered in an east-west direction. None was found within 0.1nmi of the capture site. This dispersal from the capture site suggests reduced site fidelity and perhaps seasonal dissociation of individuals from the large schools observed earlier during the summer. This dispersal may be associated with seasonal changes, perhaps related to mating behavior and the fact that most of the fish tagged were large males. Carlson and Barr (1977) reported that the spatial distribution and activity of yellowtail and dusky (*S. ciliatus*) rockfishes differed markedly between May–October, when they were seen in the water column and apparently actively feeding, and November–April, when they withdrew into crevices between boulders. Although no distinct seasonal changes are known in the bathymetric distribution of yellowtail rockfish (J. Tagart, Wash. Dep. Fish., Olympia, pers. commun., Aug. 1991), the spatial distributions of other species of rockfishes are known to change seasonally (Miller and Geibel 1973, Patten 1973, Matthews et al. 1987). Several species of juvenile rockfishes are known to move to deeper reefs with the onset of fall and winter storms (Love et al. 1991). It would be interesting to learn if the yellowtail rockfish of Heceta Bank disperse and become more benthic during the late fall and winter, and then if they eventually regroup at the original capture location next spring after spawning, or instead acquire new home sites on the bank. Studies are obviously needed on seasonal and long-term movements of yellowtail rockfish.

Diel vertical movements

Most yellowtail rockfish were seen swimming above the bottom during submersible dives on Heceta Bank. However, a few were observed resting on the sea floor. More fish were observed inactive on the bottom during night than day dives. The tagged yellowtail rockfish of Heceta Bank were pelagic, swimming far above the

bottom most of the time. Data from pressure-telemetering tags show that fish dove toward the bottom but remained there only briefly. Only one fish with a pressure transmitter either rested on the bottom for an extended period or disgorged its transmitter (Fig. 7).

Little is known about the diel vertical distribution of rockfishes. Schools of *S. entomelas* and *S. proriger* are known to rise off the bottom during the night and become more diffuse than dense schools on the bottom during the day (Leaman et al. 1990). Rockfish may intercept vertically-migrating pelagic organisms that constitute their primary prey, feeding closer to the surface at night or during crepuscular periods and descending with their prey during the day. Sometimes vertically migrating prey, such as euphausiids, are advected onto banks and seamounts and trapped near the bottom during the day where they are devoured by rockfishes (Isaacs and Schwartzlose 1965, Chess et al. 1988, Genin et al. 1988, Hobson 1989). Euphausiids are often the primary prey of adult yellowtail rockfish (Lorz et al. 1983). About 50% of the diet by weight of yellowtail rockfish from Heceta Bank was comprised of euphausiids (Brodeur and Pearcy 1984). However, vertically-migrating mesopelagic fishes and shrimp were the primary food items of yellowtail rockfish collected in deeper water (137 m bottom depth) along the southern edge of Astoria Canyon (Pereyra et al. 1969).

Yellowtail rockfish from Heceta Bank did not demonstrate obvious diel changes in their behavior by either rising closer to the surface at night or swimming over deeper water to intercept more oceanic organisms. Such behavior has been observed for other species of rockfishes (Chess et al. 1988, Leaman et al. 1990), and predatory shore fishes are known to migrate offshore at night to feed in midwater (Hobson 1968). One yellowtail rockfish on Heceta Bank with a pressure-telemetering transmitter made more dives to the bottom during night than day.

The reasons for dives to the bottom are unclear. One possible explanation is that these dives assist the fish in localizing their position on the bank and preventing drift of the school away from their home station. Surface currents often set the ship away from tagged fish that appeared to be geostationary. Yellowtail rockfish must be able to orient to a specific site and swim against prevailing currents to maintain their position.

Tagging-tracking techniques

Sonic tags inserted into the stomachs of yellowtail rockfish without retention hooks were useful for tracking fish for several days. Most fish showed detectable movements up to 2 days after release. Horizontal movements greater than the accuracy of fixes were found in one fish 10 days later, but this was an exception. Depth sensor tags provided reliable information on the retention of tags since fish were almost always in midwater. Fish with depth transmitters remained in midwater up to 5 days, the rated duration of the batteries. One pressure-sensitive tag (Fish 3, Fig. 7) was apparently regurgitated after 22 h and fell to the bottom. If ARM's were employed on tags, fish movements were measurable for 1 month after release. One ARM tag dropped to the bottom immediately after the fish was released, demonstrating that restraining hooks are not a guarantee that tags will stay in the stomach. Eight of the twelve fish with non-pressure telemetering ARM tags that were relocated moved significant distances 30 days after the release of fish, indicating long-term retention of transmitters.

Effects of the transmitter on behavior of the fish are not known. However, one fish apparently schooled soon after release. Although fish dove toward the bottom immediately after release, they rose to typical midwater depths after less than an hour. These observations suggest that the trauma of being caught, tagged, and released, and the added weight of the transmitter, did not have prolonged effects and tagged fish behaved normally.

Acknowledgments

This research was supported by the Department of Interior's U.S. Minerals Management Service (Cooperative Agreement 14-12-0001-30445). NOAA's National Undersea Research Program provided supplemental shiptime and submersible support. I thank J.P. Fisher, B.N. Tissot, R. Albright, and the Captain of the FV *Corsair*, W. Dixon, and his crew for conducting this research at sea, J.P. Fisher for his help with analyses of the data, and J.P. Fisher, A. Schoener, M.A. Hixon, and two anonymous reviewers for helpful comments on the manuscript. A. Ebeling and M.A. Hixon provided the microgasometer and advice to determine the composition of gas escaping from decompressed yellowtail rockfish.

Citations

Brodeur, R.D., and W.G. Pearcy
1984 Food habits and dietary overlap of some shelf rockfishes (genus *Sebastes*) from the northeastern Pacific Ocean. Fish. Bull., U.S. 82:269–293.

Carlson, H.R.
1986 Restricted year-class structure and recruitment lag within a discrete school of yellowtail rockfish. Trans. Am. Fish. Soc. 115:490–492.

Carlson, H.R., and L. Barr
1977 Seasonal changes in spatial distribution and activity of two species of Pacific rockfishes, *Sebastes flavidus* and *S. ciliatus*, in Lynn Canal, southeastern Alaska. Mar. Fish. Rev. 39(3):23–24.

Carlson, H.R., and R.E. Haight
1972 Evidence for a home site and homing of adult yellowtail rockfish, *Sebastes flavidus*. J. Fish. Res. Board Can. 29: 1011–1014.

Chess, J.R. , S.E. Smith, and P.C. Fischer
1988 Trophic relationships of the shortbelly rockfish, *Sebastes jordani*, off central California. Calif. Coop. Oceanic Fish. Invest. Rep. 29:129–136.

Culver, B.N.
1987 Results from tagging black rockfish (*Sebastes melanops*) off the Washington and northern Oregon coast. *In* Proc., Int. rockfish symp., p. 231–239. Univ. Alaska Sea Grant Rep. 87-2, Fairbanks.

Dugan, R.F., and D.A. Dashin
1979 How to get the most out of LORAN-C. Oregon State Univ. Ext. Mar. Advis. Prog. SG-54, Corvallis, 12 p.

Eldridge, M.B., J.A. Whipple, M.J. Bowers, B.M. Jarvis and J. Gold
1991 Reproductive performance of yellowtail rockfish, *Sebastes flavidus*. Environ. Biol. Fish. 30:91–102.

Genin, A., L. Haury, and P. Greenblatt
1988 Interactions of migrating zooplankton with shallow topography: Predation by rockfishes and intensification of patchiness. Deep-Sea Res. 35:151–175.

Gunderson, D.R., P. Callahan, and B. Goiney
1980 Maturation and fecundity of four species of *Sebastes*. Mar. Fish. Rev. 42(3):74–79.

Hixon, M.A., B.N. Tissot, and W.G. Pearcy
1991 Fish assemblages of rocky banks of the Pacific Northwest. Final Rep. to U.S. Dep. Int., Minerals Manage. Serv., MMS 91-0052, Oregon State Univ., Corvallis, 409 p.

Hobson, E.S.
1968 Predatory behavior of some shore fishes in the Gulf of California. U.S. Fish. Wildl. Serv. Res. Rep. 73, 92 p.
1989 Predation on ocean krill. Science (Wash. DC) 243:237.

Isaacs, J.D., and R.A. Schwartzlose
1965 Migrant sound scatterers: Interaction with sea floor. Science (Wash. DC) 150:1810–1813.

Leaman, B.M., R. Kieser, P. Withler and R.D. Stanley
1990 *W.E. Ricker* hydroacoustic cruise to study rockfish behavior off northern Vancouver Island, March 14–23, 1990. Can. Manuscr. Rep. Fish. Aquat. Sci. 2091, 63 p.

Lorz, H.V., W.G. Pearcy, and M. Fraidenburg
1983 Notes on the feeding habits of the yellowtail rockfish, *Sebastes flavidus*, off Washington and in Queen Charlotte Sound. Calif. Fish Game 69:33–38.

Love, M.S.
1979 Isolation of olive rockfish, *Sebastes serranoides*, populations off southern California. Fish. Bull., U.S. 77:975–983.

Love, M.S., P. Morris, M. McCrae, and R. Collins
1990 Life history aspects of 19 rockfish species (Scorpaenidae: *Sebastes*) from the southern California Bight. NOAA Tech. Rep. NMFS 87, 38 p.

Love, S.M., M.H. Carr, and L.J. Haldorson
1991 The ecology of substrate-associated juveniles of the genus *Sebastes*. Environ. Biol. Fish. 30:225–243.

Mathews, S.B., and M.W. Barker
1983 Movements of rockfish (*Sebastes*) tagged in northern Puget Sound, Washington. Fish. Bull., U.S. 82:916–922.

Matthews, K.R.
1990 A telemetric study of the home ranges and homing routes of copper and quillback rockfishes on shallow rocky reefs. Can. J. Zool. 68:2243–2250.

Matthews, K.R., B.S. Miller, and T.P. Quinn
1986 Movement studies of nearshore demersal rockfishes in Puget Sound, Washington. *In* Proc., Int. rockfish symp., p. 63–72. Univ. Alaska Sea Grant Rep. 87-2, Fairbanks.

Matthews, K.R., T.P. Quinn, and B.S. Miller
1990 Use of ultrasonic transmitters to track demersal rockfish movements on shallow rocky reefs in Puget Sound, Washington. *In* Parker, N., et al. (eds.), Fish marking techniques, p. 375–379. Am. Fish Soc. Symp. 7, Bethesda.

Miller, D.J., and J.J. Geibel
1973 Summary of blue rockfish and lingcod life histories; a reef ecology study; and giant kelp, *Macrocystis pyrifera*, experiments in Monterey Bay, California. Calif. Fish Game Fish Bull. 158, 137 p.

Ona, E., and O.R. Godoe
1990 Fish reaction to trawling noise: The significance to trawl sampling. *In* Karp, W.A. (ed.) Developments in fisheries acoustics: A symposium held in Seattle, 22–26 June 1987. Rapp. P.-V. Reun. Cons Int. Explor. Mer 189:159–166.

Pacific Fisheries Management Council
1991 Status of the Pacific coast groundfish fishery through 1991 and recommended acceptable biological catches for 1992. Pac. Fish. Manage. Counc., Portland, 69 p.

Patten, B.G.
1973 Biological information on copper rockfish in Puget Sound, Washington. Trans. Am. Fish. Soc. 102:412–416.

Pearcy, W.G., D.L. Stein, M.A. Hixon, E.K. Pikitch, W.H. Barss, and R.M. Starr
1989 Submersible observations of deep-reef fishes of Heceta Bank, Oregon. Fish. Bull., U.S. 87:955–965.

Pereyra, W.T. , W.G. Pearcy, and F.E. Carvey
1969 *Sebastes flavidus*, a shelf rockfish feeding on mesopelagic fauna, with consideration of ecological implications. J. Fish. Res. Board Can. 26:2211–2215.

Scholander, P.F., L. Van Dam, C.L. Claff, and J.K. Kanwisher
1955 Micro gasometric determination of dissolved oxygen and nitrogen. Biol. Bull. (Woods Hole) 109:328–334.

Stanley, R.D.
1988 Shelf rockfish (silvergray, yellowtail, and canary rockfish. *In* Fargo, J., et al. (eds.), Groundfish stock assessments for the west coat of Canada in 1987 and recommended yield options for 1988, p. 227–272. Can. Tech. Rep Fish. Aquat. Sci. 1617.

Stasko, A.B., and D.G. Pincock
1977 Review of underwater biotelemetry, with emphasis on ultrasonic techniques. J. Fish. Res. Board Can. 34:1261–1285.

A simple simulation approach to risk and cost analysis, with applications to swordfish and cod fisheries

Victor R. Restrepo
University of Miami, Rosenstiel School of Marine and Atmospheric Science
4600 Rickenbacker Causeway, Miami, Florida 33149

John M. Hoenig
Department of Fisheries and Oceans, Science Branch
P O Box 5667, St. John's, Newfoundland A1C 5X1, Canada

Joseph E. Powers
Southeast Fisheries Science Center, National Marine Fisheries Service, NOAA
75 Virginia Beach Drive, Miami, Florida 33149

James W. Baird
Department of Fisheries and Oceans, Science Branch
P O. Box 5667, St. John's, Newfoundland A1C 5X1, Canada

Stephen C. Turner
Southeast Fisheries Science Center, National Marine Fisheries Service, NOAA
75 Virginia Beach Drive, Miami, Florida 33149

Abstract.– Monte Carlo simulation is used to quantify the uncertainty in the results of sequential population analysis and related statistics. Probability density functions describe the measured or perceived uncertainty in the inputs to the assessment model. Monte Carlo simulation is then used to examine the variability in the resulting parameter estimates (stock sizes and fishing mortalities), derived statistics (e.g., $F_{0.1}$), and in the management regulations necessary to achieve various management objectives. We show how relative frequency histograms of the simulation results can be used to describe the risk of not meeting a given management goal as a function of the catch quota selected. We also show how to compute the expected cost, in terms of potential yield foregone, associated with picking a conservative quota. This enables one to balance risks and costs or to allow risk to vary within proscribed limits while keeping the catch quota stable. We illustrate the use of the Monte Carlo approach with examples from two fisheries: North Atlantic swordfish and northern cod.

Manuscript accepted 29 July 1992.
Fishery Bulletin, U.S. 90:736–748 (1992).

Fishery managers recognize the dangers of accepting parameter estimates without consideration of the variability inherent in the estimates of fish stock status and related parameters. Early strategies for dealing with this were quite simple, such as replacing the estimate of the fishing mortality giving the maximum yield (F_{max}) by a more conservative value. Sensitivity analyses, in which the effects of various perturbations of the inputs are observed, have commonly been employed to obtain impressions of the probable bounds on the errors (e.g., Pope 1972, Pope and Garrod 1975). Recently, various authors have used the delta method (see Kendall and Stuart 1977: 246–248) to obtain analytical expressions or numerical solutions for the variances and covariances of outputs from simple sequential population analyses (SPAs) (Saila et al. 1985, Sampson 1987, Prager and MacCall 1988, Kimura 1989). These solutions tend to be complex, only asymptotically valid, and highly model-specific. They have only been worked out for the simplest SPA models and some simple quota-setting procedures (e.g., Pope 1983).

It is possible to measure how well the population estimates correspond to trends in indices of abundance when calibration procedures are applied to sequential population analyses. The variance-covariance matrix of the stock sizes estimated directly in the optimization procedure is calculated from the inverse Hessian or its approximation (Seber and Wild 1989); the variance of any function of these parameters is then approximated by the delta method. But estimates of standard errors of population sizes obtained in this way do not reflect all the variability in the inputs and the uncertainty in the model, because they are conditioned on a number of assumptions such as natural mortality being exactly

known. For example, similar trends in population abundance may be obtained when two very different values of natural mortality rate are assumed as inputs; despite the similar trends (and hence correlation with the abundance indices), there may be large differences in the absolute estimates of abundance.

In this paper we use the term "uncertainty" to describe any variability or error that arises during the stock assessment process. Uncertainty can enter into an assessment in various ways. There may be uncertainties in the values of the inputs, e.g., the total catch may be estimated with error. Also, the formulation of the assessment model may be subject to uncertainty, and the analyst may make data-dependent decisions during the analysis which are subject to error. The degree to which these sources of error are incorporated into the analyses will determine the perceived uncertainty in the overall assessment results. If all sources of error are not appropriately accounted for, then estimates of the uncertainty in the assessment results may be too small.

Monte Carlo simulation is a convenient tool for studying a model's outputs given different types and levels of error in the model's inputs (e.g., Restrepo and Fox 1988). In a sensitivity analysis framework, Pope and Gray (1983) and Rivard (1983) used a Monte Carlo approach to study the relative contribution of various inputs to the overall uncertainty in total allowable catch (TAC) estimates obtained from calibrated SPAs. Francis (1991) used Monte Carlo simulation analysis to construct risk curves describing the chances of not meeting management objectives as a function of the catch quota. In this paper, we present a general method, also based on Monte Carlo simulation, to account for uncertainty in assessment results, including the parameters directly estimated from the SPAs as well as derived statistics used to set management targets and allowable catches. We also show how the simulation results can be used to quantify the risk (of not meeting a management goal) associated with the selection of a given TAC, and we describe a measure of the cost of picking a conservative catch quota.

We apply the simulation method to swordfish *Xiphias gladius* in the North Atlantic Ocean and cod *Gadus morhua* off eastern Newfoundland and southeastern Labrador. These fisheries are quite different in nature. Swordfish are highly migratory, managed internationally with fishing mortality controls, and the data set allows for the estimation of only a few parameters in models with many constraints. Northern cod, on the other hand, are demersal, managed by quota, and the availability of age-specific survey indices allows for the estimation of many parameters with a minimum number of assumptions.

Quantifying uncertainty by simulation

Suppose the only uncertainty in the inputs to an assessment model concerns the value of the instantaneous natural mortality rate, M, and that M could be anywhere in the interval 0.15–0.25/yr with equal likelihood. One could compute the assessment model results for a large number of uniformly spaced values of M in this interval (e.g., 100) and make histograms of the results. This would represent the perceived information about the relative likelihood of the estimated output taking on various values. If not all values of M were believed to be equally likely, one could weight the 100 outputs by the probability associated with the corresponding inputs.

The above procedure becomes awkward when there are a number of inputs subject to uncertainty, because the number of combinations of input parameter values becomes very large. An alternative is to use a Monte Carlo approach in which values of the inputs are drawn randomly from probability distributions. A sufficiently large number of plausible input data sets are thus generated and used to compute the assessment model results such that the distributions of the estimated outputs are clearly defined. This may involve hundreds or thousands of runs, depending on the types of data and models used (in our work we found that 500–1000 data sets were necessary to obtain stable results).

A typical assessment of a fish stock using SPA involves three levels of analysis. First, data are prepared for the SPA. This usually involves estimating and ageing the annual catch, and computing indices of abundance for calibration. Second, the SPA itself is carried out (it is also frequently termed "VPA," for Virtual Population Analysis). In many cases, several SPAs are carried out to examine the goodness-of-fits of the input data to alternative model formulations or simply to examine the sensitivity of the results to the alternative formulations. Third, derived statistics are computed. These are commonly biological reference points (F_{max}, $F_{0.1}$; Gulland and Boerema 1973), and forward projections of stock status and catches under alternative management actions.

It is easy to see how the Monte Carlo approach can be used to characterize the uncertainty in the entire analysis process, starting with the raw data collected for the first step in the above procedure. For instance, the total annual catches and their proportions at age can be obtained by resampling the original data that led to the catch estimates, through a non-parametric bootstrap (Efron 1982). These bootstrapped catches would then be used in the SPAs, whose results, in turn, would affect the values of projected future catches.

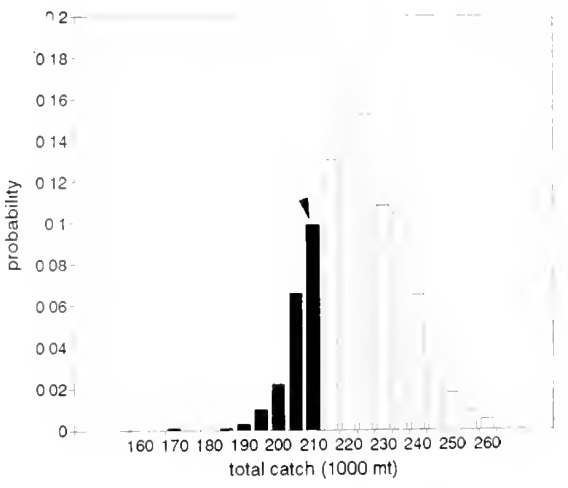

Figure 1

Probability mass distribution (relative frequency) for estimates of total catch of cod *Gadus morhua* necessary to have 1991 fishing mortality equal to that of 1990. Estimates were obtained from 1000 simulated data sets analyzed by the ADAPT approach. If a total catch of 210,000 mt is selected (arrow), the probability that fishing mortality will exceed the status quo is estimated by the sum of histogram bar heights to the left of 210,000 (i.e., the shaded portion).

In practice, however, the time and computer resources required to carry out such a large-scale simulation make it more practical to derive the input uncertainty distributions from parametric statistical analyses of data. This would involve assuming a distribution type for the inputs and estimating their mean and variance. For example, by virtue of the central limit theorem, an estimated mean has an approximately normal distribution if the sample size is sufficiently large.

Often, the distributions determined for some of the inputs will not be based on a rigorous statistical treatment of the data, but rather will represent educated guesses about the likelihood of the inputs taking on particular values (this is probably most true for the natural mortality rate, M, which is usually assumed and not estimated). The outputs would then represent the analyst's personal uncertainty in the assessment results.

The above approach can be generalized to allow for uncertainty in the formulation of the SPA model as well. Suppose one believes that there is a 70% chance that the fishing mortality rate in the last year does not decline with age after a fully recruited age (this is often known as a "flat-topped" partial recruitment curve), and a 30% chance that it does decline ("dome-shaped" partial recruitment). Then one could conduct 70% of the simulations with an SPA that assumes the flat-topped curve and 30% with the dome-shaped curve. The resulting combination of outputs would reflect the intuitive estimate of uncertainty about the SPA model formulation. Similarly, the approach can also account for uncertainty concerning data-dependent decision making. For example, if several abundance indices are available, one might subject each index to a preliminary test to decide whether the index is acceptable for calibrating the SPA, e.g., via analysis of residuals. One can repeat this decision-making process for each of the simulated data sets and thus account for the uncertainty associated with screening indices.

In summary, the Monte Carlo approach to quantifying uncertainty consists of generating a large number of pseudo-data sets, drawn at random from specified distributions, and carrying out *the entire assessment* procedure for each data set. The distributions of the assessment outputs and derived statistics are then summarized, e.g., as histograms. The simulation is thus viewed as a means for translating input and model uncertainties (measured and/or perceived) into output uncertainties.

Analyzing the consequences of management options

Estimating risks

The simulation results can also be used to quantify the uncertainty associated with a future management action. An example is the determination of uncertainty in the catch of the current year that would maintain the fishing mortality at the level of the previous year ($F_{\text{status quo}}$). A point estimate might be computed as follows. An SPA of some sort is used to estimate the population size at the end of the previous year and the fishing mortality during that year. Assuming that recruitment in the current year is equal to the long-term average, the estimated population size in the current year can be computed. Finally, the harvest which causes the population to experience the same fishing mortality rate as that estimated for the previous year can be computed. To quantify the uncertainty in this result, the whole procedure can be repeated 1000 times, each time perturbing each input to the SPA by a random amount (as per the specified uncertainty distributions). This results in 1000 sets of estimates of population size, fishing mortality, and natural mortality rate which, together with a set of randomly-drawn values for recruitment, can be used to generate 1000 estimates of the total allowable catch which will cause the fishing mortality to remain unchanged. These values can be organized into a relative-frequency histogram such as in Figure 1.

From the histogram, it appears that the most likely (modal) value for achieving the management goal

($F_{status\ quo}$) is a quota of 220,000 mt, but the actual value might be anywhere from ~170,000 to 260,000 mt. If the TAC is set at 220,000 mt, then these results suggest there is roughly a 50% chance of the fishing mortality increasing and a 50% chance of it decreasing. Suppose one is risk averse and chooses a TAC of 210,000 mt instead. What would be the perceived risk, or probability of exceeding the target fishing mortality, under this quota?

The risk of exceeding the target fishing mortality ($F_{status\ quo}$) is given by the proportion of the area under the histogram to the left of the TAC chosen (Fig. 1). Thus,

$$\text{Prob}(F_{achieved} > F_{target}) = \sum_{i=1}^{I} p(i)$$

where p(i) is the probability mass (relative frequency of outcomes) associated with the ith bar of the histogram, and I is the number of bars to the left of the chosen TAC. This probability can be computed for any value of the TAC. In practice, the risk would be computed by sorting in ascending order the 1000 catch values obtained from the simulation, and then plotting the cumulative count of outcomes less than any value of the TAC versus that value of the TAC (Fig. 2). One can also derive a family of risk curves. For example, separate curves could be generated for the risk of exceeding $F_{status\ quo}$ by each of several amounts (in absolute or relative numbers). For each of the 1000 simulation runs, one computes the value of $F_{status\ quo}$ and the catch that causes current F to exceed the status quo by the specified amount. The resulting histogram of catches is summed to obtain the risk curve.

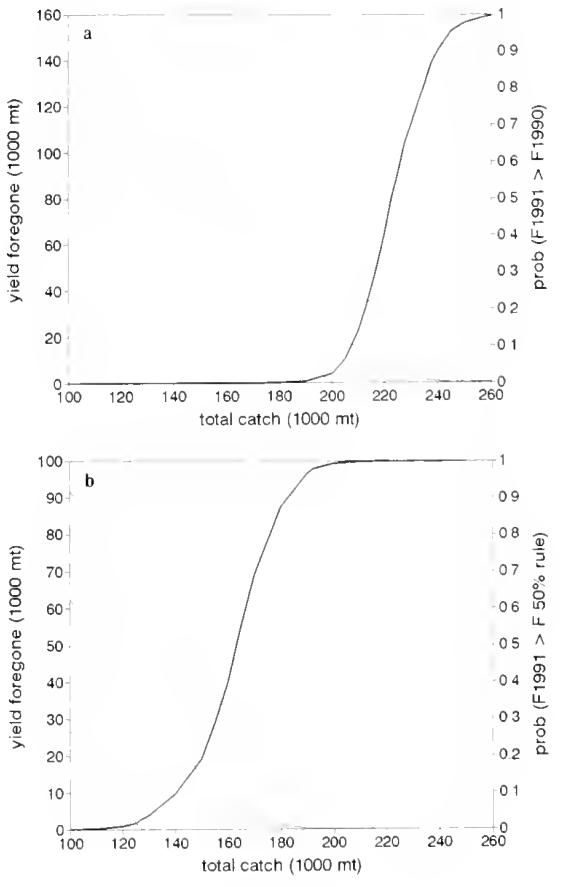

Figure 2

(a) Probability of exceeding the current (1990) cod *Gadus morhua* fishing mortality and expected value of the potential yield foregone (with 95% confidence band determined as the 2.5th and 97.5th percentiles of the distribution resulting from 1000 simulations) as functions of total catch selected for 1991. (b) Probability of the 1991 fishing mortality exceeding the 50% rule fishing mortality, and expected value of the yield foregone (with 95% confidence band), as functions of the total catch selected for 1991.

Estimating cost as yield foregone

If we choose a conservative value for the TAC in order to ensure that risk of exceeding the target fishing mortality will be small, then we are probably passing up some of the yield we could have had in the short term while still meeting our objective (e.g., see Bergh and Butterworth 1987). It is possible to describe this cost in economic or biological terms. Here, we express the cost as the expected value of the potential yield foregone, which we define as follows. For any TAC, x, let

$$\delta(i) = \begin{cases} 0, \text{ yield associated with ith interval of histogram} \leq x \\ 1, \text{ yield associated with ith interval of histogram} > x. \end{cases}$$

Then,

$$E(\text{potential yield foregone}) = \sum_{i=1}^{\infty} p(i)\,\delta(i)\,(y(i) - x)$$

where E(||) denotes the expectation operator, the summation is over all intervals of the histogram (Fig. 1), and

y(i) is the yield associated with the ith interval of the histogram. The expected potential yield foregone can be plotted against the corresponding TAC (Fig. 2). Here, y(i) − x is a possible value of the yield foregone provided it is non-negative; negative values are eliminated by the indicator function δ(i); p(i) is the probability that the yield foregone is equal to δ(i) (y(i) − x). In practice, the expected yield foregone would be computed by setting all simulated catches which are less than the TAC equal to zero and then computing the mean of the 1000 values minus the TAC. The results can then be plotted versus the TAC for various choices of TAC (Fig. 2).

It should be noted that this cost relates to the upcoming year only. One can also calculate the fate of the biomass left in the water at the end of the upcoming year. That is, one can ask whether this biomass left in the water will increase or decrease over the year. In general, for a quantity of biomass left in the water, the relative change in its biomass over the year is given by

relative change in unfished biomass =

$$e^{-M}\frac{\sum_a P_a W_{a+1}}{\sum_a P_a W_a} - 1.$$

Here, P_a is the proportion of the stock that is age a; W_a, the average weight of animals at age a; M, the (constant) instantaneous natural mortality rate; and the summations are over all age groups of interest.

Trade-offs in decision making

The manager can now choose how to trade off potential yield and risk. For example, consider the option of a TAC of 210,000 mt as a means of maintaining the fishing mortality at a constant level. From Figure 2a, the perceived risk of the fishing mortality exceeding the target mortality is ~14%. The expected value of the potential yield foregone for this TAC is ~14,000 mt. If, instead, a TAC of 215,000 mt is selected, the risk of exceeding the target fishing mortality becomes 26% and the expected value of the potential yield foregone becomes 10,000 mt. Thus, an increase in the TAC of 5,000 mt would almost double the risk of exceeding $F_{status\ quo}$ while reducing the expected potential yield foregone by 30%.

Another way to present the results of the SPA simulations is to plot percentiles of output distributions versus the TAC selected. For example, for each SPA run on simulated data, one can take the estimated population size and iteratively seek the fishing mortalities that will result in each of several TACs. Then, for any value of TAC one can compute the median and 2.5th and 97.5th percentiles of the distribution of fishing mortalities. Since instantaneous fishing mortality may not be meaningful to some interested parties (such as fishing industry groups), one may wish to look at the distribution of changes in population biomass associated with particular choices of the TAC (Fig. 3).

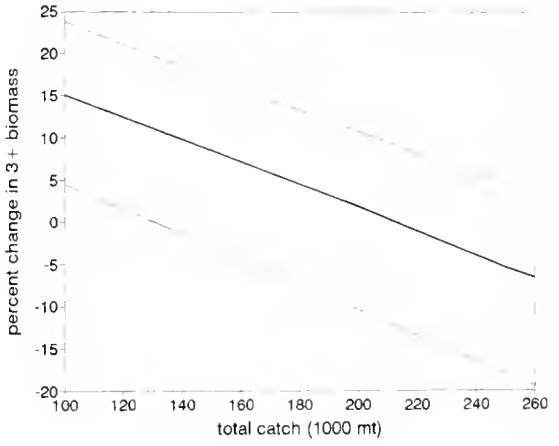

Figure 3

Percentiles of the distribution of relative change (%) in biomass of cod *Gadus morhua* age 3 and above, as a function of the total catch selected for 1991. Dotted lines: (top) 97.5th percentile; (middle) 50th percentile; (bottom) 2.5th percentile.

Thus, we have two approaches which we can summarize as follows. The first approach is to select a goal or objective (such as $F_{status\ quo}$ or $F_{0.1}$) and then quantify the chances of achieving that goal as a function of the TAC or effort restriction selected. The second is to quantify the consequences of choosing different quotas or effort restrictions. Both approaches are useful to managers. A manager might first ask how a specific management objective like $F_{0.1}$ can be met. A graph similar to Figure 2a makes it clear that the trade-off between risks and costs must be balanced. The manager might also want to know the consequences of picking particular quotas or effort restrictions. For example, for economic or political reasons, it may be difficult to stick with a management policy if a large quota reduction is called for. In this case, the consequences to the stock of maintaining the status quo or reducing the quota by various intermediate amounts may be of interest. A graph similar to Figure 3 may be helpful for this.

Managers and industry have a strong interest in maintaining stability in a fishery. Conflicts can easily arise when annual assessments provide only point estimates of the quota required to achieve a specified goal. This is because random error in the estimates

implies that annual adjustments in the quota will be proscribed even when no changes are in fact necessary. Instead of letting the quota "float" from year to year, one can stabilize the quota and let the risks float from year to year. Thus, as long as the risks remain within certain limits, there is no need to adjust the quota. (Here, the risks can include potential stock collapse as well as foregone potential yield.)

The sequential population analysis model: ADAPT

The examples presented below use data from two very different fisheries that are assessed with the same SPA approach, known as ADAPT (Gavaris 1988). ADAPT is widely used in the eastern United States and Canada. Here we describe the basic method briefly and direct the interested reader to more details in Parrack (1986), Gavaris (1988), Conser and Powers (1990), and Powers and Restrepo (1992).

The objective in ADAPT is to minimize deviations between observed (age-specific) indices of abundance and those predicted by what is commonly referred to as virtual population analysis (VPA). Let the subscripts t, a, and i denote time, age, and abundance-index sequence number, respectively. The basic equations governing the model are

$$N_{at} = N_{a+1,\,t+1}\, e^{Z_{at}}, \tag{1}$$

$$C_{at} = F_{at}\, N_{a+1,\,t+1}\, (e^{Z_{at}} - 1)/Z_{at}, \text{ and} \tag{2}$$

$$I_{it} = q_i\, N_{at}\, (1 - e^{-Z_{at}})/Z_{at}, \tag{3}$$

where N = stock size in numbers of fish, C = catch in numbers, I = index of relative stock abundance (each index is associated with one or more ages which must be specified), F = instantaneous fishing mortality rate, Z = total instantaneous mortality rate (Z = F + M), and q = coefficient of proportionality between relative abundance and absolute abundance. Inputs to the model are the catch, natural mortality, and relative abundance indices. Given that there are T years of data, A ages, and Y indices, a search algorithm, e.g., Marquardt-Levenberg (Seber and Wild 1989), is used to estimate the parameters q_i (i = 1 . . . Y) and $N_{a,\,T+1}$ (a = 2 . . . A) that minimize the weighted residual sum of squares:

$$RSS = \min \sum_i \sum_t \lambda_i\, (I_{it} - \widehat{I_{it}})^2, \tag{4}$$

where the weights, λ_i, may be input or estimated via iteratively-reweighted least squares.

ADAPT, like other VPA calibration procedures, requires model constraints in order to reduce the number of parameters. Hence, the stock sizes for the last age each year are not normally estimated but are instead derived from a specified relationship between F_{At} and $F_{A-1,\,t}$. Additional constraints may be required when the amount of relative-abundance data does not support the estimation of a large number of parameters. Often, as in the swordfish example below, this involves estimating the relative selectivities of the various age-groups in year T in some fashion external to the calibration process. This leads us to add to our explanation the notion that ADAPT is generally thought of as a framework rather than a rigid model. Thus the reader is likely to encounter applications that deviate from the model in equations (1) through (3). For example, for swordfish, A is a "plus" group consisting of ages A and older. For cod in Atlantic Canada, the objective function (4) is modified to allow for lognormal errors. A detailed presentation of some of the most commonly used options in ADAPT can be found in Powers and Restrepo (1992).

Assessment uncertainty: Application to North Atlantic swordfish

Swordfish in the North Atlantic Ocean are assessed by the International Commission for the Conservation of Atlantic Tunas (ICCAT). Interest is centered on the level of fishing mortality relative to reference values (e.g., F_{max}), and on trends in mortality and stock abundance. Potential management options involve restrictions aimed at controlling fishing mortality. The assessment procedure is continually changing as experience is gained. The procedure below was used for the 1989 assessment (ICCAT 1990).

Assessment procedure

Nine age-groups were recognized in the commercial catch, ages 1 to 9+. There were 11 years of catch-at-age data from 1978 to 1988. Fleets from the United States, Japan, and Spain accounted for most of the catch. Eleven abundance indices were available based on fleet-specific catch rates from the longline fisheries (ICCAT 1990).

Details of this assessment of the stock are presented in ICCAT (1990). Briefly, the procedure used was as follows. (1) A separable virtual population analysis, SVPA (Pope and Shepherd 1982), was computed in order to obtain estimates of the age-effects or partial recruitment in the last year for which data were available. Data from 1983 to 1988 were used for this under

the assumption that the selectivity pattern remained stable during that period. For that analysis the terminal fishing mortality was set to 0.2/yr and selectivity for the oldest age group was 3.0. (2) The ADAPT approach to sequential population analysis was then used for calibration, with each abundance index used separately. A weighting factor for each index was obtained by setting the weight for the ith index equal to the reciprocal of the mean squared error after calibrating with the index. In performing the calibrations, ages 5 and above were assumed to be fully recruited ($S_a = 1.0$ for $a = 5, 6, \ldots, 9+$) and the partial recruitment for the other ages was as determined from the SVPA (i.e., from step 1). (3) The set of weights computed for the abundance indices were then rescaled so that they summed to unity. (4) The weights were then used in recalibrating the ADAPT SPA using all of the abundance indices at once. In doing so, the following constraints were used: S_1 was taken from the separable virtual population analysis, S_2 through S_5 were directly estimated through calibration, and S_6 through S_{9+} were set equal to the estimated S_5. The objective function used in the calibration was to minimize the weighted sum of the squared deviations from the predicted abundance indices as in equation (4).

After the fishing mortalities and population sizes were computed by the sequential population analysis, the values of F_{max} and $F_{0.1}$ were calculated from yield-per-recruit computations. Data from the terminal year (i.e., the most recent year available) were used to project the catch in the current year and then project the catch for the next year. For this, recruitment in the current year and the following year were assumed by ICCAT to be equal to the long-term mean recruitment obtained in the sequential population analysis. The projections were made for a variety of fishing mortalities, specifically $F_{0.1}$, F_{max}, and $F_{status\ quo}$.

Specification of uncertainty in the inputs

One thousand simulated data sets were analyzed using a version of ADAPT written in FORTRAN 77 (available from the authors). The formulation of the problem was made to mimic the 1989 ICCAT assessment for North Atlantic swordfish. However, we emphasize that the uncertainties in the inputs specified below are our *ad hoc* choices and, although realistic, are intended mainly for illustrative purposes.

Natural mortality Uncertainty in the natural mortality rate (M) was specified as a uniformly-distributed random variable in the interval 0.1–0.3/yr. The value of 0.2 used by ICCAT (1990) is at the center of this range, and the choice of a uniform distribution places equal confidence in all values in the interval.

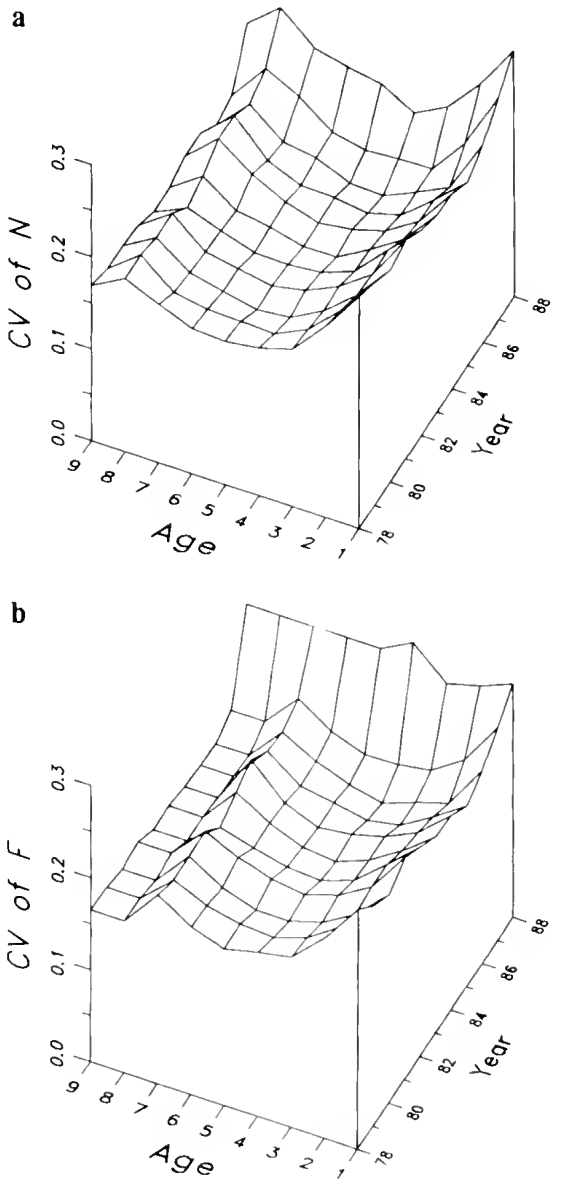

Figure 4
Coefficients of variation of outputs from the sequential population analyses of simulated swordfish *Xiphias gladius* data sets. (a) Age- and year-specific estimates of population numbers; (b) age- and year-specific estimates of instantaneous fishing mortality.

Catch-at-age Total annual catches were represented by lognormally-distributed random variables with coefficients of variation of 10% and expected values equal to those in the assessment. A coefficient of variation of 10% indicates that the catches are known with high precision. The proportions of the total catch in any year that make up each age component were assumed to follow a multinomial distribution with expected values

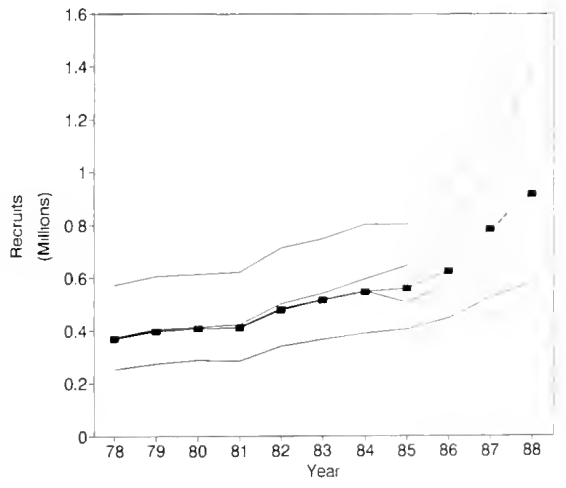

Figure 5

Distribution of swordfish *Xiphias gladius* recruitment estimates, by year, from the sequential population analyses. Outer lines are from the Monte Carlo simulations and show 95% confidence bands (determined as the 2.5th and 97.5th percentiles of the distribution resulting from 1000 simulations). Inner pair of lines shows confidence bands obtained from the information matrix after a single run of the ADAPT program using actual data. Line with symbols gives median estimate for each year from the simulations.

equal to the observed proportions and sample size equal to 1% of the annual catch. This model for the uncertainty was purely heuristic rather than based on measured variances.

Abundance (CPUE) indices The 11 available indices from the longline fisheries were also assumed to be lognormally distributed with a coefficient of variation of 10%. We chose a value of 10% as a rough approximation for all indices in all years. However, there is no reason why each index could not have a different coefficient of variation for each year depending on the amount of data available.

Results of swordfish simulations

The simulations gave rise to 1000 sets of age- and year-specific fishing mortality rates and population sizes. We computed the coefficient of variation of these sets of estimates for each age-year combination (Figs. 4a, b). As expected, the coefficients of variation were highest in the most recent year, 1988. Also, the age groups which form the bulk of the catch (ages 3–5) were the best determined. It is interesting to note that the coefficients of variation of fishing mortality rates for ages 8 and 9 were consistently lower than those for preceding ages. This is due to the manner in which the estimates for ages 8 and 9 were determined: it was assumed that $F_{8t} = F_{9t}$ (subscripts refer to age and year, respectively), and these were computed as a weighted average of fishing mortalities for ages 5–7. Thus, the uncertainty in the estimates of fishing mortality for the last two age-groups is solely a function of the uncertainties in the estimates for ages 5–7. This underscores the fact that the simulation results are conditional not only on the input-uncertainty distributions but on the formulation of the model being fitted as well.

The median recruitment (age 1) from the simulations increased over time (Fig. 5). However, the 95% confidence bands, defined by the 2.5th and 97.5th percentiles of the 1000 estimates, are quite wide. The confidence bands provided by the delta method for a single run with the actual data are much narrower than the ones obtained by the Monte Carlo approach. The former confidence bands indicate there is no uncertainty in the results for the converged part of the SPA in contrast to the simulation results. This is because the delta method results, based on the information matrix of a single run, are conditional on the natural mortality rate, catch at age, etc., being known exactly whereas the simulation accounts for uncertainty in these inputs. For this reason, we believe the simulation results are more reasonable.

Note that there appears to be very little interannual recruitment variability in the time-series (Fig. 5). This is probably due to the fact that fish ages were estimated from lengths deterministically by inverting the Gompertz growth equation, and this tends to blur the age-groups.

The population of fish age 5 and above appears to have declined rather steadily over time while the weighted fishing mortality rate appears to have increased (medians, Figs. 6a, b). Here, weighted fishing mortality is defined as the mean of the fishing mortality estimates for ages 5 through 9+, computed with weights proportional to the estimated population size at age. Again, the confidence bands are very wide.

It should be noted that for each run the estimates of fishing mortality, F_{at}, and population size, N_{at}, are highly correlated not only with each other but also with the value of natural mortality, M, used in the simulation run. For this reason, it is appropriate to examine trends in an estimated quantity one run at a time. We computed the ratio of the weighted fishing mortality in a given year t to the weighted F in the base year (taken to be 1978 in this example) for each simulation run (Fig. 7). The distribution of the fishing mortality ratio in 1979 was centered around 1.0; the ratio in 1986, 1987, and 1988 was >1.0 in 100% of the runs, thus clearly indicating that fishing mortality has increased. This result is not obvious from examination of Figure

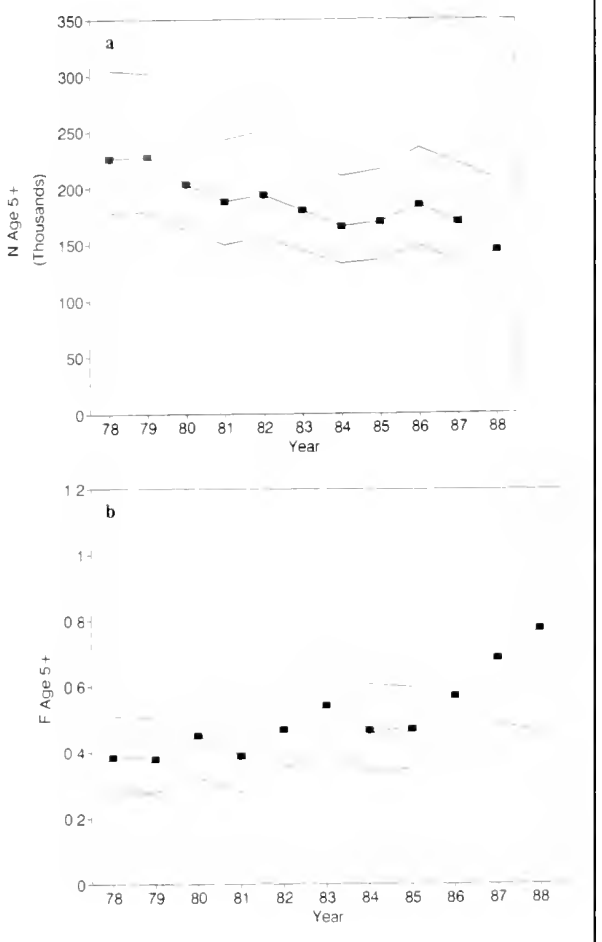

Figure 6

Medians, 2.5th percentiles, and 97.5th percentiles of the output distributions from the Monte Carlo simulations. (a) Distribution of estimates of the population size of swordfish *Xiphias gladius* aged 5 and above; (b) distribution of estimates of fishing mortality for swordfish aged 5 and above.

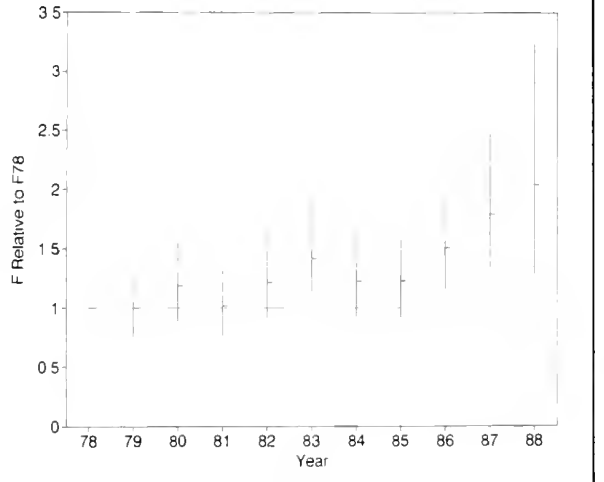

Figure 7

Distribution of the ratio of swordfish *Xiphias gladius* fishing mortality in year y to that in 1978 as a function of the year. Vertical bars indicate 95% confidence intervals based on percentiles; horizontal bars represent the median ratio.

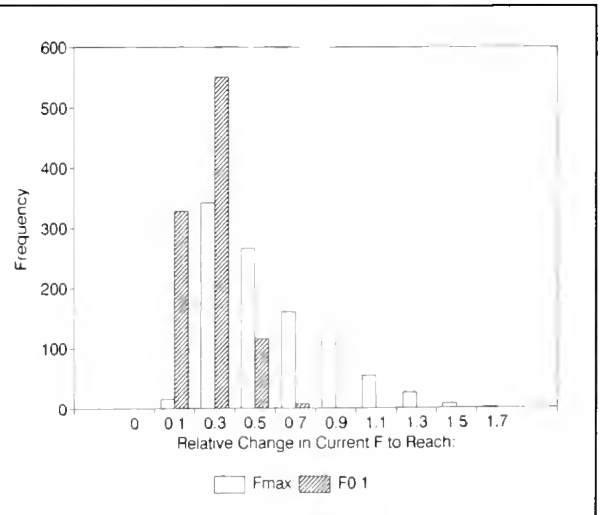

Figure 8

Multipliers necessary to bring the vector of age-specific fishing mortalities in the terminal year to the $F_{0.1}$ and F_{max} levels, for 1000 simulated data sets for swordfish *Xiphias gladius*.

6b and illustrates how very easily the Monte Carlo approach lends itself to hypothesis testing.

Of course, the goals of an assessment are not restricted to estimating population sizes and mortality rates. Interest is often centered on catch projections and quotas, effort regulations, and risk analyses. For swordfish assessments, it is useful to contrast the estimated current level of fishing mortality against reference points such as $F_{0.1}$ and F_{max}. The uncertainty in such comparisons (e.g., the ratio of current F to $F_{0.1}$) can easily be quantified using the Monte Carlo procedure. For each simulation run, we computed the multiplier that would be necessary to bring the estimated vector of age-specific fishing mortalities in the terminal year to the $F_{0.1}$ and F_{max} levels (Fig. 8). For the computations, we used the run-specific natural mortality rate and the weight-at-age relationships used by ICCAT in the 1989 assessment. No uncertainty was specified for weight relationships although this could easily be added if appropriate information were available. From Figure 8 it is evident that, to achieve the $F_{0.1}$ goal, fishing mortality must be cut to ~25% of its current value. With respect to F_{max}, it appears that fishing mortality must be cut by ~50% (Fig. 8). Note, however, that this conclusion is considerably less

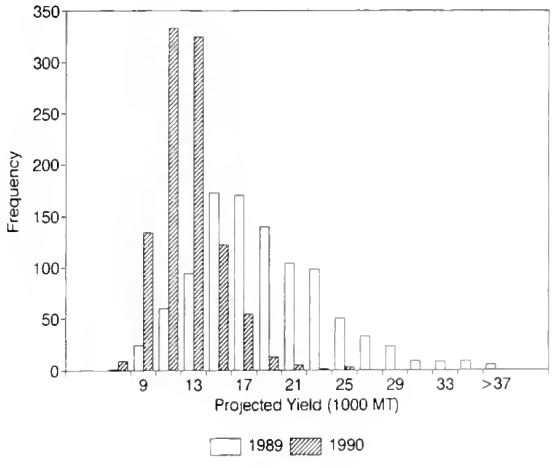

Figure 9

Distribution of 1989 estimated swordfish *Xiphias gladius* catches when fishing mortality is kept the same as in 1988 (open bars), and distribution of 1990 estimated catches when fishing mortality is equal to the midpoint between the 1988 fishing mortality and $F_{0.1}$, assuming 1989 fishing mortality was the same as in 1988 (cross-hatched bars).

certain than that for $F_{0.1}$ as evidenced by the fact that the distribution of multipliers is broader for F_{max} than for $F_{0.1}$. But, as an anonymous reviewer pointed out, it is interesting to note that the mode of both distributions is about one-third of the status quo F.

We also computed 1000 projected catches in weight for 1989 with fishing mortality equal to that in 1988. We then projected the catch for 1990 with fishing mortality set at the midpoint between the fishing mortality in 1988 and $F_{0.1}$ (Fig. 9). This method gradually reduces fishing mortality to minimize the short-term impact of decreased landings on fishermen (see Pelletier and Laurec 1990, for a discussion). Recruitments for 1989 and 1990 were drawn randomly from the empirical distribution of recruitments estimated from 1978–87 on each iteration. If the fishing mortality does not change in 1989 from the level in 1988, catches are likely to be somewhere around the 1988 yield of ~18,000 mt. The 1990 yields are likely to be ~11,000–13,000 mt.

Using the Monte Carlo results, it is equally simple to obtain distributions of catches for fishing at other exploitation levels or to obtain distributions of fishing mortalities for fixed catch quotas. Similarly, the distribution of other projected variables, such as the spawning-potential ratio that results from various catch and fishing mortality options, can be computed. In doing so, it is important to have the values of the inputs used in calibrating the SPAs (e.g., natural mortality) stored in each iteration, so that the projection computations use the same values.

Risks and costs: Application to northern cod

We studied the cod fishery in NAFO Divisions 2J + 3KL and based our simulations on the data and methods described in Baird et al. (1990). Additional data, described below, were obtained from the files at the Northwest Atlantic Fisheries Centre, St. John's, Newfoundland. The simulations reflect our own perceptions and experience about the sources and nature of the uncertainties in the assessment. As with the swordfish example, the selection of management objectives for simulation was made for illustrative purposes.

This cod fishery is managed by quota. The assessment uses trawl-survey data and commercial catch-rate data to calibrate the SPA.

Assessment and simulation procedures

Only a brief description of the assessment procedure is given here since the details are not important for understanding the use of the simulation method. The catch-at-age data for ages 3–13 for each year from 1978 to 1989 were taken from Table 7 of Baird et al. (1990). Coefficients of variation of these catch estimates were computed using the method of Gavaris and Gavaris (1983); these coefficients were available in the files. The coefficients of variation ranged from 2 to 17%. Age- and year-specific catch rates from research-vessel surveys for the period 1978–89 and associated coefficients of variation (Baird et al. 1990, table 23) were used to tune the sequential population analysis. The coefficients of variation were ≤30% in 87% of the cases. Age- and year-specific catch rates from the offshore commercial trawl fishery for ages 5–8 for the period 1983–89 were standardized by the method of Gavaris (1980) for use as an index of abundance for tuning the SPA (Baird et al. 1990, table 39). We developed estimates of the coefficients of variation for the commercial catch-rate indices. In all cases, these were close to 10%. Natural mortality for this stock is believed to be around 0.2/yr.

In the simulations, the point estimates of the inputs were replaced by random variables with the same expected values and coefficients of variation as specified above. Catch at age values were generated as normal random variables, while the research-vessel and the commercial catch rates were generated as lognormal random variables. The value of the natural mortality rate was generated as a uniform random number between 0.15 and 0.25/yr.

The specific formulation of the ADAPT model was as follows. The research-vessel indices were obtained in the fall and were assumed to represent population size at the end of November. The commercial catch-rate indices were assumed to represent population size at the beginning of the year. The fishing mortality F for the oldest age-group (13) was calculated as 50% of the mean F for ages 7–9 weighted by population number at age. The objective function to be minimized differed from equation (4) in that lognormal errors were assumed and the weights, λ_i, were fixed to be 1.0.

Projections for 1990 and 1991 were made using the same procedures used in the most recent annual assessment (Baird et al. 1990). Population and fishing mortality projections for 1990 were made by randomly selecting a value for recruitment from the historical set of estimated recruitments and assuming that (1) the total catch in 1990 is 225,000 mt (the fixed Canadian quota in place when the assessment was done in 1990, plus an additional 25,000 mt in expected foreign catch), and (2) the partial recruitment (selectivity) vector for 1990 is equal to that estimated for 1989 in each simulated SPA.

Catch projections for 1991 were made in two ways. In one, we set the fishing mortality for 1991 equal to that for 1990 and solved for the catch. In the other, we set the fishing mortality for 1991 equal to

$$\min \{(\hat{F}_{0.1} + \hat{F}_{1990})/2,\ 2\ \hat{F}_{0.1}\}.$$

This is the 50% rule formulated by the Canadian Atlantic Fisheries Scientific Advisory Committee (Canada Department of Fisheries and Oceans 1991) for a gradual movement towards $F_{0.1}$. We also computed the fate of yield foregone and the distribution of population changes for various choices of the total catch.

Results of cod simulations

We generated risk curves for two fishing mortality objectives for 1991 (Figs. 2a,b). These curves can be put in perspective by noting that the Canadian total allowable catch for 1990 was 199,262 mt while the total catch (Canadian plus international) may have been as high as 235,000 mt. To have a 50% risk of increasing the fishing mortality in 1991 over the 1990 level, one would set the total catch at 225,500 mt; to have a 50% chance of exceeding the fishing mortality associated with the 50% rule would entail setting the total catch at 163,000 mt. It appears that a cut in the TAC would be necessary to have a reasonable chance of preventing the fishing mortality from exceeding the 1990 value. Substantial cuts in the harvest would be required to ensure a high probability of meeting the 50% rule.

For values of the TAC for which the risk is less than 25%, the expected value of the yield foregone is approximately a linear function of the TAC (Figs. 2a,b). That is, for every change in the TAC of 1000 mt, the expected yield foregone changes by ~1000 mt. The fate of biomass left in the water is to increase by ~13% in a year (mean of 1000 simulations = median = 12.9%; 95% confidence band based on 2.5th and 97.5th percentiles is 7.2% and18.4%). The relative change in biomass of fish aged 3 and above is also a linear function of the TAC (Fig. 3). Note, however, that the relative change in biomass cannot be determined very precisely as evidenced by the wide confidence bands.

We presented results of catch projections for two scenarios. Often, one might like to examine a larger number of options. For example, if current fishing mortality exceeds F_{max}, then one could explore various ways to reduce fishing mortality in gradual steps as well as exploring the consequences of various types of "status quo" options. The simulation approach is versatile enough to handle fixed catch, fishing mortality, and biomass objectives, as well as objectives involving relative change. Thus, one could have any of the following objectives for fishing mortality: achieve F = 0.40/yr, achieve $F = F_{0.1}$, reduce F by 40%, or adjust F so that biomass changes a given fixed or relative amount.

In some fisheries, catch and population projections may be highly dependent on the assumptions made about recruitment. When this is the case, it may be helpful to quantify the uncertainty separately for various segments of the population. For example, we computed the distribution of relative change in age 3+ biomass of cod (from 1989 to 1991) for various choices of the TAC. The wide confidence bands (Fig. 3) reflect the large uncertainty in future recruitment. We could have quantified the relative change in the biomass of age 5+ fish. From the ADAPT run based on 1989 data, we already have an estimate of age-3 biomass in 1989. This biomass can be projected forward to age 5 in 1991; hence, we do not need to generate a random value for recruitment. The uncertainty in the biomass of age 5+ fish should thus be smaller than the uncertainty in age 3+ biomass. Unfortunately, the latter quantity may be of greater interest.

Conclusions

Monte Carlo simulation has long been regarded as a very useful quantitative tool, especially for sensitivity analysis (e.g., Pope and Gray 1983, Rivard 1983). It is also quite useful for studying the properties of specific assessment procedures (e.g., Mohn 1983, Kimura 1989). Here, we follow Francis (1991) and use it to quantify the risks of not meeting the objectives

for the fishery as a function of the management measures imposed. The simulation approach we present can be used with assessment models other than ADAPT. For example, one could use Monte Carlo simulation to quantify the effects of uncertainty in input data, assumptions, and model formulation on the outputs from the CAGEAN (Deriso et al. 1985) or stock synthesis (Methot 1990) methods. We believe that this simulation framework is not only a versatile and intuitive method to estimate uncertainty, risks, and costs, but in many cases it may also be the only practical way to incorporate some types of input uncertainty which are not estimated statistically. Because the estimated uncertainties in the model outputs are conditional on what is known and what is assumed about the inputs, failure to acknowledge possible sources of uncertainty in a realistic manner may lead to overly optimistic views of the uncertainties in the model outputs. The Monte Carlo approach forces one to examine the nature and magnitudes of the uncertainties in the inputs and in the model formulation, and it allows one to study how uncertainties are propagated through the assessment and into the projections ultimately used for management recommendations.

It appears feasible to quantify risks and costs for a wide variety of management options when the assessments are accomplished by any of a variety of analytical models. It remains to determine what risks (and costs) should be quantified, how much risk is acceptable, and for how long. For example, we do not know how to quantify the risk of stock collapse due to recruitment failure, but we might wish to quantify the risk of the spawning biomass falling below 20% of the virgin level in three years out of five. If we assume that this represents a dangerous situation (see Beddington and Cooke 1983, Brown 1990, and Goodyear 1990, for thoughtful discussions), then the risk should be kept low. On the other hand, if we consider the risk of exceeding the economically-optimal fishing mortality (however defined), then we might like the risk to be close to 50%, i.e., as likely to be above the optimum as below it. (Of course, we should consider the relative costs of over- and undershooting the target mortality). If F is not close to the economic optimum fishing mortality, then one must also devise a way to determine what is the best trajectory to take for arriving at the long-term goal. It is beyond the scope of this paper to address what are appropriate goals, biological reference points, and trajectories.

Finally, for any stock assessment, the results of a Monte Carlo simulation study are necessarily conditional on what is assumed about the sources of uncertainty, including the model chosen for the assessment. Since decisions about some of the sources of uncertainty are subjective, the results are personal views of uncertainty, risk, cost, etc. If three scientists assess a given stock, they can generate three separate sets of simulation outputs. The combination of their simulations provides a picture of their collective uncertainty about the assessment results. Alternatively, they can agree that a minimal estimate of the uncertainty is provided by the one set of results that are the least uncertain.

A more detailed study of the relative sensitivities of the assessment outputs and risk curves to the choice of input distributions can be carried out via sensitivity analysis (Miller 1974). In this Monte Carlo framework, sensitivity analysis would consist of introducing planned perturbations to the input-uncertainty distributions and then measuring the overall effect on the model's outputs. This should aid in the identification of key inputs so that more effort could be placed on improving their estimates. This is more difficult than it may seem. A given input that is perturbed during the sensitivity analysis (say, catch at age) will cause different degrees of change in the various output distributions: stock sizes, fishing mortalities, $F_{0.1}$, projected catches, etc. Furthermore, this impact may change over time. For instance, assumptions about recruitment become very dominant as the projections are made further ahead in time. Nonetheless, sensitivity analysis can be very useful in identifying trade-offs between the benefits of precision and the cost of obtaining that precision.

Acknowledgments

Partial support for this study was provided through the Cooperative Institute for Marine and Atmospheric Studies by National Oceanic and Atmospheric Administration (NOAA) Cooperative Agreement NA90-RAH-0075 and by the Canadian Government's Atlantic Fisheries Adjustment Program (Northern Cod Science Program). We thank Nicholas Payton for programming assistance and Peter Shelton, Al Pinhorn, Donald Parsons, and two anonymous reviewers for helpful comments.

Citations

Baird, J.W., C.A. Bishop, and W.B. Brodie
1990 The assessment of the cod stock in NAFO Divisions 2J, 3K and 3L. CAFSAC (Can. Atl. Fish. Sci. Adv. Comm.) Res. Doc. 90/18.

Beddington, J.R., and J.G. Cooke
1983 The potential yield of fish stocks. FAO Fish. Tech. Pap. 242, 50 p.

Bergh, M.O., and D.S. Butterworth
1987 Towards rational harvesting of the South African anchovy considering survey imprecision and recruitment variability. S. Afr. J. Mar. Sci. 5:937–951.

Brown, B.
1990 Use of spawning stock size considerations in providing fishery management advice in the North Atlantic—a brief review. ICCAT (Int. Comm. Conserv. Atl. Tunas) Collect. Vol. Sci. Pap. 32(2):498–506.

Canada Department of Fisheries and Oceans
1991 1991 Atlantic groundfish management plan 1990. Ottawa, 114 p.

Conser, R.J., and J.E. Powers
1990 Extensions of the ADAPT tuning method designed to facilitate assessment work on tuna and swordfish stocks. ICCAT Collect. Vol. Sci. Pap. 32: 461–467.

Deriso, R.B., T.J. Quinn II, and P.R. Neal
1985 Catch-age analysis with auxiliary information. Can. J. Fish. Aquat. Sci. 42:815–824.

Efron, B.
1982 The jackknife, the bootstrap and other resampling plans. Soc. Ind. Appl. Math, Philadelphia.

Francis, R.I.C.C.
1991 Risk analysis in fishery management. Northwest Atl. Fish. Organ. Sci. Counc. Stud. 16:143–148.

Gavaris, S.
1980 Use of a multiplicative model to estimate catch rate and effort from commercial data. Can. J. Fish. Aquat. Sci. 37: 2272–2275.
1988 An adaptive framework for the estimation of population size. CAFSAC (Can. Atl. Fish. Sci. Adv. Comm.) Res. Doc. 88/29.

Gavaris, S., and C.A. Gavaris
1983 Estimation of catch at age and its variance for groundfish stocks in the Newfoundland region. Can. Spec. Publ. Fish. Aquat. Sci. 66:178–182.

Goodyear, C.P.
1990 Spawning stock biomass per recruit: The biological basis for a fisheries management tool. ICCAT Collect. Vol. Sci. Pap. 32:487–497.

Gulland, J.A., and L.K. Boerema
1973 Scientific advice on catch levels. Fish. Bull., U.S. 71: 325–335.

ICCAT (International Commission for the Conservation of Atlantic Tunas)
1990 Appendix 10 to Annex 8. *In* Report for biennial period, 1988–89, Part II (1989). Madrid, Spain [Engl. version].

Kendall, M., and A. Stuart
1977 The advanced theory of statistics, vol. 1, 4th ed. Macmillan, NY.

Kimura, D.K.
1989 Variability, tuning, and simulation for the Doubleday-Deriso catch-at-age model. Can. J. Fish. Aquat. Sci. 46: 941–949.

Methot, R.D.
1990 Synthesis model: An adaptable framework for analysis of diverse stock assessment data. Int. N. Pac. Fish. Comm. Bull. 50:259–277.

Miller, D.R.
1974 Sensitivity analysis and validation of simulation models. J. Theor. Biol. 48:345–360.

Mohn, R.K.
1983 Effects of error in catch and effort data on tuning cohort analysis, with a postscript on logistic production models. Can. Spec. Publ. Fish. Aquat. Sci. 66:141–150.

Parrack, M.L.
1986 A method of analyzing catches and abundance indices from a fishery. ICCAT (Int. Comm. Conserv. Atl. Tunas) Collect. Vol. Sci. Pap. 24:209–221.

Pelletier, D., and A. Laurec
1990 Toward more efficient adaptive TAC policies with error-prone data. Northwest Atl. Fish. Organ. SCR Doc. 90/100 (ser. N1835).

Pope, J.G.
1972 An investigation of the accuracy of virtual population analysis using cohort analysis. Int. Comm. Northwest Atl. Fish. Res. Bull. 9:65–74.
1983 Analogies to the status quo TACs: Their nature and variance. Can. Spec. Publ. Fish. Aquat. Sci. 66:99–113.

Pope, J.G., and D.J. Garrod
1975 Sources of error in catch and effort quota regulations with particular reference to variations in the catchability coefficient. Int. Comm. Northwest Atl. Fish. Res. Bull. 11:17–30.

Pope, J.G. and D. Gray
1983 An investigation of the relationship between the precision of assessment data and the precision of total allowable catches. Can. Spec. Publ. Fish. Aquat. Sci. 66:151–157.

Pope, J.G., and J.G. Shepherd
1982 A simple method for the consistent interpretation of catch-at-age data. J. Cons. Cons. Int. Explor. Mer 40:176–184.

Powers, J.E., and V.R. Restrepo
1992 Additional options for age-sequenced analysis. ICCAT (Int. Comm. Conserv. Atl. Tunas) Collect. Vol. Sci. Pap. 39: 540–553.

Prager, M.H., and A. MacCall
1988 Sensitivities and variances of virtual population analysis as applied to the mackerel, *Scomber japonicus*. Can. J. Fish. Aquat. Sci. 45:539–547.

Restrepo, V.R., and W.W. Fox Jr.
1988 Parameter uncertainty and simple yield-per-recruit analysis. Trans. Am. Fish. Soc. 117:282–289.

Rivard, D.
1983 Effects of systematic, analytical, and sampling errors on catch estimates: A sensitivity analysis. Can. Spec. Publ. Fish. Aquat. Sci. 66:114–129.

Saila, S.B., E. Lorda, and H.A. Walker
1985 The analysis of parameter error propagation in simple fishery models. Mar. Res. Econ. 1(3):235–246.

Sampson, D.B.
1987 Variance estimators for virtual population analysis. J. Cons. Cons. Int. Explor. Mer 43:149–158.

Seber, G.A.F., and C.J. Wild
1989 Nonlinear regression. John Wiley, NY.

Behavior of individually-identified sei whales *Balaenoptera borealis* during an episodic influx into the southern Gulf of Maine in 1986

Mark R. Schilling
Cetacean Research Unit, P.O. Box 159, Gloucester, Massachusetts 01930

Irene Seipt
Cetacean Research Program, Center for Coastal Studies
Provincetown, Massachusetts 02657

Mason T. Weinrich*
Cetacean Research Unit, P.O. Box 159, Gloucester, Massachusetts 01930

Steven E. Frohock
Atlantic Cetacean Research Center, P.O. Box 1413, Gloucester, Massachusetts 01930

Anne E. Kuhlberg
Cetacean Research Unit, P.O. Box 159, Gloucester, Massachusetts 01930

Phillip J. Clapham
Cetacean Research Program, Center for Coastal Studies
Provincetown, Massachusetts 02657
Department of Zoology, University of Aberdeen, Aberdeen AB9 2TN, Scotland

Abstract.–Sei whales *Balaenoptera borealis* are noted for major fluctuations in distribution, often in response to local availability of prey. An influx of sei whales occurred in the southern Gulf of Maine during summer 1986. Forty-seven individuals (including four mothers with calves) were photographically identified using natural markings, including dorsal-fin notches, placement of small circular scars on the animal's flank, and natural variation in dorsal-fin shape and pigment swaths along the dorsal surface behind the blowholes. Seventeen of these whales (36.1%) were photographed on more than one day, and the period between first and last sighting of individuals ranged from one to 66 days. Only six animals were sighted in more than one region in the southern Gulf of Maine. Observed behavior included traveling, nearsurface skim feeding, lunge feeding, and (rarely) "milling" or breaching. Group sizes were small and variable. Two individuals were matched to photographs taken in other regions in or near offshore Gulf of Maine waters. We hypothesize that the southern Gulf of Maine represents a short-term feeding site. The occurrence of individuals without sufficient marks for individual recognition suggests that photoidentification is of limited value in the study of this species.

Most species of baleen whales undertake seasonal migrations between high-latitude feeding grounds and warmer breeding areas (Kellogg 1929, Slijper 1962, Mackintosh 1965). Populations often show annual variations in local spatial distribution within these areas (Wursig et al. 1985). While the factors causing these variations are not well defined for breeding grounds, it has been suggested that they are explained on feeding grounds by differences in prey distribution (Whitehead and Carscadden 1988, Payne et al. 1990). Because of the energetic demands upon large whales (Lockyer 1981) and the unpredictable distribution of their prey, such areal variation would be expected if the animals were seeking to maximize their feeding efficiency.

Sei whales *Balaenoptera borealis* have been reported to have greater variation in distribution on their feeding grounds than most baleen whale species (Horwood 1987). Sei whales have been reported in considerable numbers for brief periods outside of their regular range in Norway (1885, 1898, and 1919), Finland (1885), and Scotland (1906) (Tomilin 1957, Jonsgard and Darling 1977). Ingebrigtsen (1929) reported large annual changes in distribution off the Faroe Islands. These changes are hypothesized to be related to local increases in planktonic productivity (International Whaling Commission 1977, Horwood 1987).

Sei whales off the northeastern United States and southeastern Canada have been little studied. Mitchell and Chapman (1977) hypothesized

Manuscript accepted 5 July 1992.
Fishery Bulletin, U.S. 90:749–755 (1992).

* Author to whom reprint requests should be sent.

the existence of a "stock" of sei whales centered around Nova Scotia. During the spring these animals are thought to occur on the southern edge of George's Bank (Mitchell and Chapman 1977, CETAP 1982). During June and July, they move north to the southern Scotian Shelf, then onto Brown's, Bacarro, and Roseway Bank from August to October (Sutcliffe and Brodie 1977). The lack of sightings in these areas, plus late-winter/early-spring strandings in South Carolina, Louisiana, and Mississippi suggest a southward movement after October (Mead 1977). The inshore waters of the southern Gulf of Maine are rarely used by sei whales (CETAP 1982, Payne et al. 1990).

In this paper, we report on the photoidentification, occupancy patterns, surface behavior, and social behavior of individual sei whales found in the Gulf of Maine during an unexpected summer influx of this species in 1986, documented through daily shipboard surveys. We also report results of photographic identification of individual sei whales, and evaluate the feasibility of such techniques for investigations of this species.

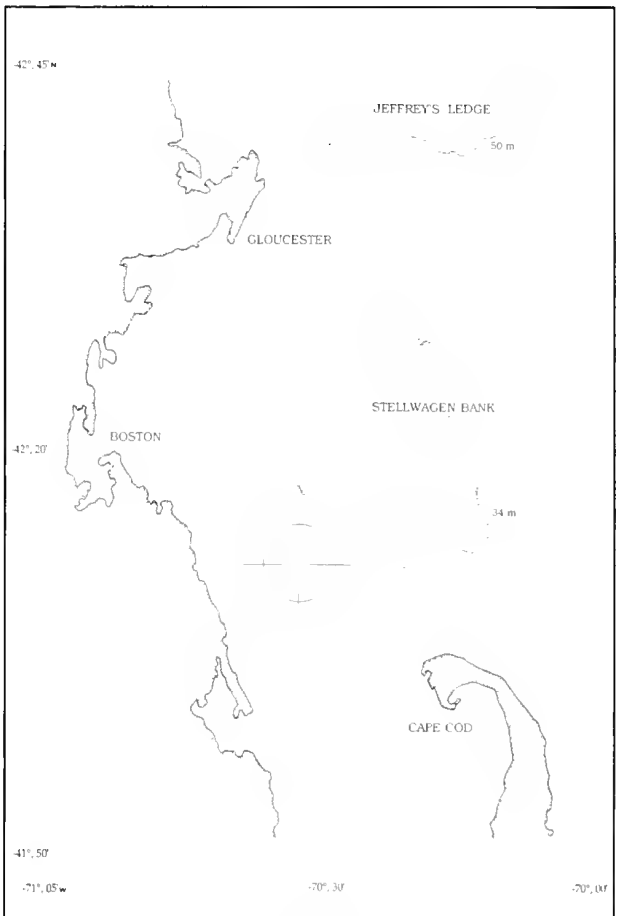

Figure 1
Study area in the Gulf of Maine.

Methods

Non-systematic surveys of the southern Gulf of Maine were conducted daily (weather permitting) from mid-April through October on commercial whale-watching and research vessels operating out of Provincetown and Gloucester, Massachusetts during 1980–91. In 1986, the only year of sei whale abundance, the number of vessels collecting data varied. There were usually six to nine 4-hr cruises daily from each port. Vessels were 18–30 m long diesel-powered whale-watching vessels and 6.7–14 m long research vessels powered by sail, diesel, or outboard engines. Whale-watch cruises were typically 4–5 hr in duration, while research-vessel cruises often lasted from dawn until dusk.

Search effort by whale-watching vessels was concentrated on the southern and northern edges of Stellwagen Bank and the southern edge of Jeffrey's Ledge because of the concentrations of whales there (Fig. 1). Stellwagen Bank is a shallow glacial deposit with a sand substrate, at 20–40 m. Southern Jeffrey's Ledge has a mean depth of 48 m, and is a mixture of sand, gravel, and rocks. Depths surrounding both areas extend to 182 m. In both areas there is upwelling, caused by steep topography which enriches the biological productivity of the area, providing food for whales (Kenney and Winn 1986).

For each sighting data included location, direction and speed of animal movement (based on LORAN-C readings taken every 5–10 min), environmental conditions, behavioral information including respiration intervals (to the nearest second) of individuals recognizable by natural marks, notable non-respiratory surface behavior, and associations among whales. Two or more whales were considered associated if they were in close proximity and consistently coordinated in the timing and direction of their surfacings.

Cow/calf pairs were treated as single animals for an analysis of occupancy periods (the time between first and last sighting), assuming that the calf's movements are determined by those of its mother. Calves were designated based on the animal being considerably smaller than any other animals, and on the continuous association between two individuals for at least 30 min or on more than one day. Personnel were experienced in observing mother-calf pairs of humpback *Megaptera novaeangliae* and fin *Balaenoptera physalus* whales. To determine mean associated group size, mother and calf pairs were counted as two individuals.

Fecal samples were scooped from the surface in a 5-gallon bucket on two days in August 1986 near northern Stellwagen Bank. The material was frozen until

examination. Prey remains were identified to species by staff of Allied Whale at the College of the Atlantic, Bar Harbor, Maine.

High-speed (ISO 400) black-and-white film was used in 35 mm single-lens reflex cameras equipped with telephoto lenses (range 200–400 mm) to photograph whales. When possible, three regions were photographed on each side of a whale: between the tip of the snout and the blowhole, the flank between the blowhole and dorsal fin, and the dorsal fin.

Photos were classified as matchable or unmatchable based on the same criteria defined by Seipt et al. (1990) for fin whale photoidentification. Unmatchable photos had poor focus, were not perpendicular to the whale, or were too far from the whale to distinguish marks clearly (generally photos taken at distances >100 m from the whale). For photos judged matchable, a whale was classified as a unique individual based on the presence of one or more of the following characters: recognizable scars, a distinctive dorsal-fin shape (including dorsal-fin notches), or detectable pigmentation on the flank between the blowhole and dorsal fin. If at least one of these features was not present in a photograph, it was discounted.

Matches of individual whales were made within independent photographic collections of the Atlantic Cetacean Research Center (Gloucester MA), the Center for Coastal Studies (Provincetown MA), and the Cetacean Research Unit (Gloucester MA) by personnel experienced in photo-identifying individual humpback or fin whales. The independent catalogs of identified whales from each organization were compared, with matches being confirmed by both other groups, resulting in a single collective catalog of identified whales. Only matches agreed upon by all parties were accepted.

In order to examine long-range movements of sei whales, photographs were solicited from researchers working in the Gulf of Maine for comparison with the unified catalog described above. Each set of photographs obtained in different geographic areas or years were treated separately.

Data for this study were stored on PC-based microcomputers and statistical analyses were performed using SPSS (1989) statistical software package for PC's, including calculation of mean values and standard deviations. A two-tailed t-test was used to compare mean values for associated group sizes between different parts of the study area, and a χ^2 test was used to test potential differences in group sizes when a mother-calf pair was present in the group (Zar 1984).

Results

Photoidentification

A total of 240 sei whale sightings took place between 29 June and 20 September 1986. Photographs were taken on 182 sightings (75.8%). In 51 photographed sightings (28.0% of all photographed sightings) the animal could not be reliably identified because of poor photographic quality.

Photoidentification of some individual sei whales was possible using variation in dorsal-fin shape, placement of small circular scars on either flank, and light pigment swaths behind the dorsal fin (Fig. 2). A total of 47 identifiable non-calf sei whales and 4 calves were photographed; of these, 19 were identifiable based on notches in their dorsal fin alone, 4 based on the locations of small circular scars on the flanks, and 10 based on both distinctive dorsal fins and circular scars. No attempt was made to photoidentify calves. Twelve whales were identified based on dorsal-fin shape and pigment swaths behind the blowhole. One sei whale was missing its dorsal fin, and one had a large white scar visible on the lower portion of its right caudal peduncle. In 12 cases, animals did not have distinctive marks by which they could be identified reliably.

Occurrence and occupancy

The 47 individual sei whales were sighted on as few as 1 and as many as 15 separate days ($\bar{x}$ 2.4, SD 3.0) (Fig. 3). Seventeen individuals (36.2%) were observed on more than one day; the mean period for resighted animals between first and last sighting was 26.8 days (SD 24.1, median 20.0). No individual sighting record spanned more than 66 days from first to last sighting.

Twenty-six individuals (55.3%) were initially photographed on southern Stellwagen Bank, 15 (31.9%) on northern Stellwagen Bank, 4 (8.5%) on Jeffrey's Ledge, 1 (2.1%) in Massachusetts Bay (west of Stellwagen Bank), and 1 (2.1%) in the Great South Channel. Only 6 animals out of the 17 resighted were photographed in more than one of these areas. Of these, four were first seen on southern Stellwagen and subsequently moved north on the Bank; one animal showed the reverse pattern. The remaining one was first photographed on southern Jeffrey's Ledge and later resighted on northern Stellwagen Bank. One of these whales moved between northern and southern Stellwagen Bank at least five times; this individual also had the greatest number of sightings (15) and the longest period between first and last sighting.

Behavior and movement patterns

A total of 752 respiration intervals were recorded during 53 sei whale sightings (from at least 15 different individuals). Inter-respiration intervals showed a range of 2–928 sec, with a mean of 60.8 sec (SD 78.0 sec). The most common respiratory pattern was a single breath followed by a short dive of 45–90 sec. On only four sightings did the whales submerge for prolonged dives of 6–11 min, and they did so repeatedly within the observation.

The regular breath intervals and lack of prolonged dives often appeared associated with near-surface feeding. In the most common feeding behavior, sei whales would take a breath and then roll 45–90° around their longitudinal axis while ~3 m below the surface. The mouth was often slightly open as the animal swam forward. There were four observations of lunge feeding, when the whale rapidly surfaced with its mouth opened. During lunges, no rolling was observed. On one of four occasions of lunging, the same individual alternated lunges with the more common nearsurface feeding behavior.

During feeding and swimming, the whales often remained in an area of ~0.5 km^2 for over an hour. Whales would either change swimming direction with each breath, or travel in a straight line for 10 min or less before reversing, resulting in minimal net movement at the surface.

Figure 2

Photographic match of sei whale *Balaenoptera borealis* #22, utilizing both circular scars and dorsal-fin notches as aids in identification. Note the pattern of circular scars below the dorsal fin, particularly the large circular scar below and immediately posterior to the dorsal fin, and the slightly blunted tip of the fin itself. Top photograph was taken 10 August 1986, bottom photograph on 22 August 1986.

Defecations were observed nine times. Feces were bright red and contained chunks of particulate matter. Only mandibles from the copepod *Calanus finmarchicus* were subsequently identified in fecal material.

While feeding and traveling comprised most of the behavioral events (both time and number), milling (at least three socializing with one another while moving in apparently random directions, rolling, and remaining on the surface continually for over 10 min) was seen four times. This was always associated with one whale leaving the group either during or immediately after the milling period. Breaching was seen once, when a single animal breached twice in rapid succession.

Social behavior

Sei whales were seen in groups of 1–6 individuals. Mean group size was 1.8, and was the same on both

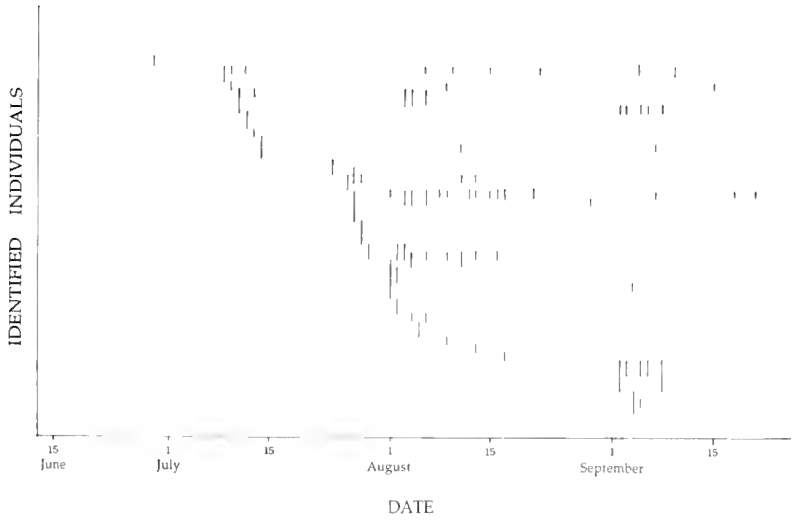

Figure 3

Occurrence of individual sei whales *Balaenoptera borealis* in the southern Gulf of Maine during 1986. Individual whales are ordered (top to bottom) by date of first sighting; each row of marks represents the dates on which one individual was seen during the year. Vertical marks represent single whales.

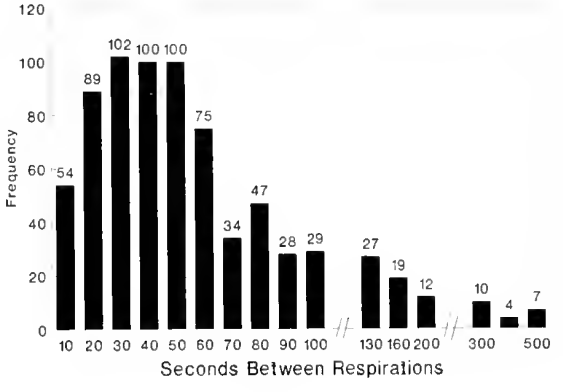

Figure 4

Histogram showing the distribution of breath intervals (sec) from sei whales *Balaenoptera borealis* recorded during 52 sightings in the 1986 season on northern Stellwagen Bank. Note the scale change for the longer breath intervals due to their infrequent occurrence.

northern and southern Stellwagen Banks, where most observations took place (two-tailed t-test, p 0.93, 1 df). Resightings of individual animals on successive days were recorded 14 times. In cases where all members of an associated group were photoidentified, only one pair of animals was seen together on two days; one whale from this pair was later sighted with a different associate two days later. These data indicate that individual associations were transient, generally lasting less than 24 hr.

Of 13 cow/calf pairs, 3 (23.0%) were associated with 1 or more other whales, while 48 (51.6%) of the 93 non-calf groups involved 2 or more whales. Frequency of association with another whale was not statistically significant between groups with and without mother-calf pairs (χ^2 3.7, p 0.06, 1 df). Cow/calf pairs were never seen with more than one associate.

Comparisons with other data sets

Sei whales identified in the southern Gulf of Maine in 1986 were compared with one 1984 photograph from Georges Bank (Atlantic Cetacean Research Center), one from Stellwagen Bank in 1987 (Plymouth Marine Mammal Center), one from Jeffrey's Ledge in 1988 (Cetacean Research Unit), three from the Scotian Shelf in 1988 (Atlantic Cetacean Research Center and Nancy Miller), and four from the Scotian Shelf in 1989 (New England Aquarium). There were two matches. Sei whale 33 was photographed on 11 June 1984 between Wilker's and Oceanographer's Canyon on the southern edge of Georges Bank (40°05′N, 68°19′W), 176 nmi from the 1986 sighting; sei whale 19 was photographed on 28 August 1989 on the Nova Scotian Shelf (42°57′N, 65°09′W), 211 nmi from its 1986 sighting.

Discussion

Photoidentification of individual animals has been accomplished for numerous baleen and toothed whales (Katona et al. 1980, Dorsey 1983, Agler et al. 1990, Seipt et al. 1990). Our results indicate that some sei whales can be identified using variations in natural markings. Dorsal-fin shape, natural pigment patterns, and scarring were all useful features. The presence of circular scars along the flank—hypothesized to be caused by small sharks (Shevchenko 1977), lampreys, or pathogenic microorganisms (Tomilin 1957, Rice 1977)—and dorsal-fin notches (unknown origin) both facilitated identification of the individuals. While these techniques work within a single season, the possibility of acquiring new dorsal-fin notches, new scars, or

having scars change with age (Shevchenko 1977) might make identification over a prolonged period difficult.

The lack of distinctive markings on some individuals indicates that while photoidentification is useful in studies of sei whales, it is not likely to allow identification of all members of the population. Because we were unable to determine the sex and/or age of the animals involved, it is impossible to indicate whether distinctive markings were related to age or sex.

The photographic matches of sei whales in the southern Gulf of Maine to both Georges Bank and the Scotian Shelf lend some support to the idea that whales in the 1986 influx were from the closest-known geographic stock. However, given the dearth of knowledge concerning the biogeography of this species, and Brown's (1977) record of a sei whale moving 4000km in 10 days, many or all of the animals reported here may come from other locations in the North Atlantic. During the year of the southern Gulf of Maine influx, abnormally high levels of *Calanus finmarchicus* were present on Stellwagen Bank (Payne et al. 1990). Our findings therefore lend support to the hypothesis that sei whales show annual areal fluctuations to take maximal advantage of changes in local productivity throughout their range. Whether each individual independently found the increased copepod productivity, or whether social factors were involved in the influx, remains an open question which our data do not address.

Most of the sei whales in 1986 were seen during late July and early August, with a secondary peak in early September (Fig. 3). This suggests that the local productivity provided a brief stop-over point during the summer feeding season. Repeated resightings of a few individuals during the study suggest that a small number of animals found prey levels adequate to allow a prolonged occupancy period.

Observed behavior of sei whales was similar to that previously described (Tomilin 1957, International Whaling Commission 1977, Horwood 1987). The relatively small variation around the mean breath interval shows a departure from the standard balaenopterid pattern of hyperventilation, e.g., several breaths taken in rapid succession followed by a longer diving period (Gunther 1949, Leatherwood et al. 1976). The rolling we observed during apparent feeding behavior differs from that described by Tomilin (1957) who did not observe this species roll during feeding.

Social groups observed in this study are similar to those reported by studies of other balaenopterids, with individuals being sighted either alone or in small groups (Nemoto 1964, Dorsey 1983, Whitehead and Carlson 1988). Lockyer (1977) reported a mean associated group size of 2.4, slightly higher than the 1.8 reported here. Since she did not define an associated group, however, direct comparisons are difficult. Further, if there is a correlation between the associated group-size and prey patch-size (such as that described for humpback whales by Whitehead 1983), it is possible that the larger group size observed could be explained by the more productive Antarctic waters. Our limited data also suggest that, as in other baleen whales, cow/calf pairs were more solitary than other animals, both in frequency of association with other individuals and in overall group size. This has previously been documented in humpback whales (Clapham and Mayo 1987), gray whales *Eschrichtius robustus* (Swartz 1986), and right whales *Eubalaena australis* (Payne 1986).

Acknowledgments

Many people helped gather field data including Cindy Belt, Carole Carlson, Peggy Christian, Lisa Frohock, David Mattila, Sharon Pittman, and many interns. Polly Hamlin (CCS), Maribel Marcy (CRU), and Lisa Frohock (ACRC) helped considerably in compiling raw data. Scott Kraus (New England Aquarium), Nancy Miller, Fred Wenzel, and Dave Wiley all provided photographs of sei whales for comparison with our 1986 sightings. Dr. Steven Katona and his colleagues at the College of the Atlantic generously took their time to examine the fecal material. We thank the owners and crews of the Dolphin Fleet, Cape Ann Whale Watch, Cap't Bill and Sons Whale Watch, and Gloucester Whale Watch for their logistical help and support. Funding for this study came from the National Marine Fisheries Service, the American Cetacean Society/Los Angeles Chapter, the Essex County Ecology Center, and Gloucester Whale Watch: we are indebted to them all.

Citations

Agler, B.A., J.A. Beard, R.S. Bowman, H.D. Corbett, S.E. Frohock, M.P. Hawvermale, S.E. Katona, S.S. Sadove, and I.E. Seipt
1990 Finback whale, *Balaenoptera physalus*, photographic identification: Methodology and preliminary results from the western North Atlantic. Rep. Int. Whaling Comm. (Spec. Issue 12):349-356.

Brown, S.G.
1977 Some results of sei whale marking in the Southern Hemisphere. Rep. Int. Whaling Comm. (Spec. Issue 1):39-43.

CETAP (Cetacean and Turtle Assessment Program)
1982 A characterization of marine mammals and turtles in the mid- and north Atlantic areas of the U.S. outer continental shelf. Final Report of the Cetacean and Turtle Assessment Program, University of Rhode Island, to the Bureau of Land Management, Washington D.C. Kingston, 450 p.

Clapham, P.J., and C.A. Mayo
1987 Reproduction and recruitment of individually identified humpback whales, *Megaptera novaeangliae*, observed in Massachusetts Bay, 1979–1985. Can. J. Zool. 65:2853–2863.

Dorsey, E.M.
1983 Exclusive adjoining ranges in individually identified minke whales in Washington state. Can. J. Zool. 61:174–181.

Gunther, E.R.
1949 Habits of the fin whale. Discovery Rep. 25:113–142.

Hammond, P.S., S.A. Mizroch, and G.P. Donovan (editors)
1990 Individual recognition of cetaceans: Use of photo-identification and other techniques to estimate population parameters. Rep. Int. Whaling Comm. (Spec. Issue 12), 440 p.

Horwood, J.W.
1987 The sei whale: Population biology, ecology, and management. Croom Helm Ltd., Kent, England, 375 p.

Ingebrigtsen, A.
1929 Whales caught in the North Atlantic and other seas. Int. Counc. Explor. Sea, Rapp. P.V. Reun. 56:1–26.

International Whaling Commission
1977 Report of the special meeting of the scientific committee on sei and Bryde's whales. Rep. Int. Whaling Comm. (Spec. Issue 1):1–9.

Jonsgard, A., and K. Darling
1977 On the biology of the eastern North Atlantic sei whale. Rep. Int. Whaling Comm. (Spec. Issue 1):124–129.

Katona, S.K., P. Harcourt, J.S. Perkins, and S.D. Kraus
1980 Humpback whales: A catalog of individuals identified by fluke photographs. College of the Atlantic, Bar Harbor, ME, 169 p.

Kellogg, R.
1929 What is known of the migration of some of the whalebone whales. Smithson. Inst. Annu. Rep., 1928, Publ. 2981, p. 467–494.

Kenny, R.D., and H.E. Winn
1986 Cetacean high-use habitats of the northeast United States continental shelf. Fish. Bull., U.S. 84:345–357.

Leatherwood, S., D.C. Caldwell, and H.E. Winn
1976 Whales, dolphins and porpoises of the western North Atlantic: A guide to their identification. NOAA Tech. Rep. NMFS CIRC-396, 176 p.

Lockyer, C.
1977 Some possible factors affecting age distribution of the catch of sei whales in the Antarctic. Rep. Int. Whaling Comm. (Spec. Issue 1):63–70.
1981 Growth and energy budgets of large baleen whales from the southern hemisphere. *In* FAO Advisory Committee on Marine Resources Research, Working Party on Marine Mammals (ed.), Mammals in the seas: Vol. 3. Large cetaceans, p. 379–487. FAO, Rome, 504 p.

Mackintosh, N.A.
1965 The stocks of whales. Fishing News (Books), Ltd., London, 232 p.

Mead, J.
1977 Records of sei and Bryde's whales from the Atlantic coast of the United States, the Gulf of Mexico, and the Caribbean. Rep. Int. Whaling Comm. (Spec. Issue 1):113–116.

Mitchell, E.A., and D.G. Chapman
1977 Preliminary assessment of stocks of the Northwest Atlantic sei whales. Rep. Int. Whaling Comm. (Spec. Issue 1): 117–120.

Nemoto, T.
1964 Schools of baleen whales in the feeding areas. Sci. Rep. Whales Res. Inst. 18:89–110.

Payne, P.N., D. Wiley, S. Young, S. Pittman, P.J. Clapham, and J. Jossi
1990 Recent fluctuations in the abundance of baleen whales in the southern Gulf of Maine in relation to changes in prey abundance. Fish. Bull., U.S. 88:687–696.

Payne, R.
1986 Long term behavioral studies of the southern right whale (*Eubalaena australis*). Rep. Int. Whaling Comm. (Spec. Issue 10):161–167.

Rice, D.W.
1977 Synopsis of biological data on the sei whale and Bryde's whale in the Eastern North Pacific. Rep. Int. Whaling Comm. (Spec. Issue 1):92–97.

Seipt, I.E., P.J. Clapham, C.A. Mayo, and M.P. Hawvermale
1990 Population characteristics of individually identified fin whales *Balaenoptera physalus* in Massachusetts Bay. Fish. Bull., U.S. 88:271–277.

Shevchenko, V.I.
1977 Application of white scars to the study of the location and migrations of sei whale populations in Area III of the Antarctic. Rep. Int. Whaling Comm. (Spec. Issue 1):130–134.

Slijper, E.J.
1962 Whales. Basic Books, NY, 475 p.

SPSS
1989 Statistical package for the social sciences (PC+3.1). SPSS, Inc., Chicago.

Sutcliffe, W.H. Jr., and P.F. Brodie
1977 Whale distribution in Nova Scotia waters. Fish. Mar. Serv. Tech. Rep. 22, Fisheries and Environment Canada, 22 p.

Swartz, S.L.
1986 Gray whale migratory, social, and breeding behavior. Rep. Int. Whaling Comm. (Spec. Issue 8):207–229.

Tomilin, A.G.
1957 Mammals of the U.S.S.R. and adjacent countries. Vol. 9, Cetacea. Akad. Nauk SSSR, Moscow, 756 p. [in Russ.]. (Trans. by the Israel Prog. Sci. Transl., Jerusalem, 1967, 717 p.; avail. NTIS, Springfield VA, as TT-65-50086.)

Whitehead, H.
1983 Structure and stability of humpback whale groups off Newfoundland. Can. J. Zool. 61:1391–1397.

Whitehead, H., and C. Carlson
1988 Social behavior of feeding finback whales off Newfoundland: Comparisons with the sympatric humpback whale. Can. J. Zool. 66:217–221.

Whitehead, H., and J.E. Carscadden
1985 Predicting inshore whale abundance—Whales and capelin off the Newfoundland coast. Can. J. Fish. Aquat. Sci. 42: 976–981.

Wursig, B., E.M. Dorsey, M.A. Fraker, R.S. Payne, and W.J. Richardson
1985 Behavior of bowhead whales *Balaena mysticetus* summering in the Beaufort Sea: A description. Fish. Bull., U.S. 83: 357–377.

Zar, J.H.
1984 Biostatistical analysis. Prentice-Hall Inc., Englewood Cliffs, 718 p.

Population dynamics of pelagic armorhead *Pseudopentaceros wheeleri* on Southeast Hancock Seamount

David A. Somerton

Honolulu Laboratory, Southwest Fisheries Science Center
National Marine Fisheries Service, NOAA
2570 Dole Street, Honolulu, Hawaii 96822-2396
Present address: Alaska Fisheries Science Center, National Marine Fisheries Service, NOAA
7600 Sand Point Way NE, Seattle, Washington 98115-0070

Bert S. Kikkawa

Honolulu Laboratory, Southwest Fisheries Science Center
National Marine Fisheries Service, NOAA
2570 Dole Street, Honolulu, Hawaii 96822-2396

Abstract.–Pelagic armorhead *Pseudopentaceros wheeleri* are the target of a directed trawl fishery on many of the southern Emperor–northern Hawaiian Ridge seamounts. The population dynamics of armorhead for the period 1970–90 were reconstructed for Southeast Hancock seamount, the southernmost of the seamounts commercially fished, by using commercial catch-and-effort statistics, various biological measurements, and research stock-survey data. The population declined almost continuously from a 1972 high of 5500 metric tons (t) to a 1989 low of 25 t. In addition to the intense fishery, this decline was due partly to the sporadic pattern of armorhead recruitment. Natural mortality rate was estimated as 0.54/year; however, females had a higher mortality rate than males.

Manuscript accepted 5 July 1992.
Fishery Bulletin, U.S. 90:756–769 (1992).

Pelagic armorhead *Pseudopentaceros wheeleri* have an unusual life history that includes two distinct postlarval phases: a pelagic juvenile phase, and a demersal adult phase. During the first 1.5–2.5 years of their lives (Uchiyama and Sampaga 1990), juvenile armorhead inhabit the epipelagic zone over a broad area of the northeast Pacific, where they acquire large fat reserves before migrating westward to the southern Emperor–northern Hawaiian Ridge (SE–NHR) seamounts (Boehlert and Sasaki 1988, Humphreys et al. 1989). After arriving at the seamounts, armorhead mature and assume demersal habits. Because of the rigors of spawning or the inability to obtain sufficient prey (Seki and Somerton, In prep.), adult armorhead subsequently lose weight to such an extent that they eventually become emaciated and moribund (Humphreys et al. 1989).

Armorhead form dense nighttime aggregations over the relatively flat summits of the SE–NHR seamounts. Soon after these aggregations were discovered in 1967, they were subjected to intense fishing effort first by Soviet trawlers (Komrakov 1970) and 2 years later by Japanese trawlers (Sasaki 1986). The combined annual catch of armorhead rapidly increased and reached a high of 164,000 metric tons (t) in 1973 (Borets 1975, Takahashi and Sasaki 1977) before plummeting to 875 t in 1978. This decline in catch was evidently due to a decline in armorhead abundance, because the Japanese catch-per-unit-effort (CPUE) showed a corresponding drop from a high of 54.0 t/hr in 1972 to 0.4 t/hr in 1978 (Sasaki 1986).

Although never a participant in this fishery, the United States became involved in 1976 when implementation of the Magnuson Fishery Conservation and Management Act extended its exclusive economic zone (EEZ) to include the Hancock Seamounts, the southernmost of the SE–NHR seamounts supporting the armorhead fishery. Although Soviet trawlers ceased operations on the Hancock seamounts after the jurisdictional change, Japanese trawlers continued to fish but were subject to an annual harvest quota and were required to carry U.S. observers who monitored the catch. Regardless of these management efforts, catch rates continued to decline and the Japanese discontinued fishing on the Hancock Seamounts in 1984. In response to the apparent stressed condition of the armorhead population, the National Marine Fisheries Service (NMFS) in 1985 initiated a stock

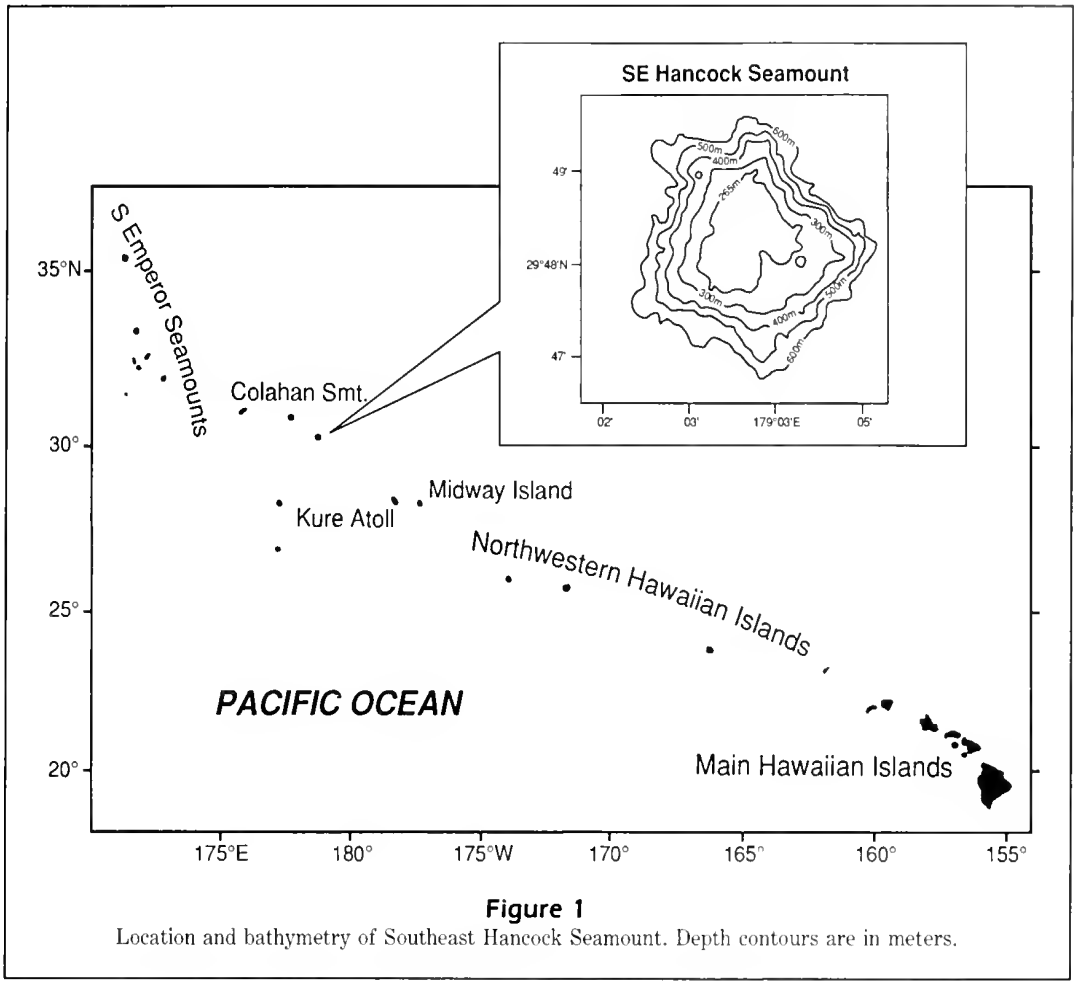

Figure 1
Location and bathymetry of Southeast Hancock Seamount. Depth contours are in meters.

assessment program to monitor armorhead abundance, and in 1986 enacted a 6-yr moratorium prohibiting trawl fishing on the Hancock Seamounts.

The population dynamics of pelagic armorhead have been previously examined (Borets 1975, Wetherall and Yong 1986); however, the results of these studies are questionable because they were based on either Soviet or Japanese catch-and-effort statistics but not both. The present paper attempts to rectify the problem of incomplete data by focusing solely on the stock of armorhead inhabiting the Southeast (SE) Hancock Seamount, where catch-and-effort statistics were supplemented with various biological and vessel performance data after the initiation of the U.S. observer program in 1977 and were completely replaced by research stock-survey data when the commercial fishery ended. With these additional data, it is possible to obtain absolute estimates of armorhead abundance, rather than relative estimates, and to extend the time-series of such estimates beyond the termination of the commercial fishery. In addition to developing a continuous record of armorhead abundance since the initiation of the fishery, this paper also includes estimates of the natural mortality rate and annual recruitment of pelagic juveniles to the seamounts.

Materials and methods

SE Hancock Seamount

The Hancock seamounts consist of two peaks, Northwest (NW) and SE Hancock Seamount, separated by 61 km and situated on the NHR ~293 km northwest of Kure Atoll, the northernmost of the Hawaiian Islands, and ~287 km southeast of Colahan Seamount, the closest seamount supporting an armorhead fishery (Fig. 1). The SE Hancock Seamount is shaped somewhat like a truncated cone with a relatively flat, smooth summit and steep, rugged flanks (Fig. 1). This topography, combined with the tendency of armorhead to nocturnally migrate from the flanks to the summit (Humphreys and Tagami 1986), constrained the commercial trawl fishery to operate primarily on the summit (<300 m) at night (Sasaki 1986).

Types of data and preliminary analysis

Since the types of data available for describing the population dynamics of armorhead have changed with time, it is convenient to separate the entire 1970–90 interval into three periods: (1) 1985–90, when NMFS stock surveys were conducted but no commercial fishing occurred; (2) 1978–84, when regulated Japanese fishing occurred with U.S. observers aboard the vessels; and (3) 1970–77, when unregulated Japanese and Soviet fishing occurred.

Period 1 In the period 1985–90, NMFS conducted 10 armorhead stock-survey cruises to SE Hancock Seamount. Although bottom trawls were occasionally used, the primary sampling gear was a bottom longline. Unlike trawls, longlines could be used on the steep flanks of the seamount and allow sampling of the entire population. Longlines consisted of 30 rigid poles (droppers), each with 5 equally-spaced hooks on short leaders, attached at 18m intervals along a 600m groundline (Shiota 1987). On all cruises, longlines were set perpendicular to the depth contours to maximize the depth range sampled and were fished with the same bait (squid), hook size (no. 20 circle), soak time (1 hr), and fishing period (0800–1830 hr) to maintain constant catchability. Starting in 1986, however, catchability changed slightly when hook timers (small timing devices that are activated when a fish strikes the hook; Somerton et al. 1989) were installed on the leaders. To estimate the effect of timers on armorhead catchability, a comparison experiment was conducted in 1990 in which droppers were alternated with and without timers along the longline. A correction coefficient accounting for the effect of timers on catchability was then estimated as the ratio of the armorhead catches for droppers with timers to those without timers (this ratio was 0.77).

Since preliminary information indicated that armorhead density varied with depth on the seamount, stock surveys were based on a depth-stratified sampling design. Fishing depths were estimated by recording a depth profile of the bottom as the longline was set, then partitioning the measured distance between the terminal anchors into 30 equal intervals (the number of droppers). To help correct for possible differences between fathometer depths and actual fishing depths due to horizontal drift while the longline sank, maximum depth recorders were placed on both anchors and at the midpoint of all longline sets. Recorded maximum depths were used instead of fathometer depths to determine where the anchors and midpoint lay along each depth profile.

When longlines were retrieved, the species identity of each captured fish was recorded along with the number of the hook on which it was caught. All fish from each 5-dropper segment of the longline were then placed together into a basket for later collection of the following biological attributes: sex, fork length (FL, mm), and body depth (BD, mm) which is the shortest distance between the bases of the first anal spine and the dorsal fin. In 1985, body weight (W, g) was also measured on some specimens in addition to body depth. Equations predicting BD from W and FL, and predicting W from BD and FL, were calculated from these data by using multiple regression. These equations are:

Females (n 436)

BD	86.69 − 0.19FL + 0.10W	(R^2 0.91)
W	−936.25 + 9.06BD + 2.49FL	(R^2 0.90)

Males (n 476)

BD	75.55 − 0.18FL + 0.10W	(R^2 0.85)
W	−934.02 + 7.52BD + 2.82FL	(R^2 0.87)

Although the depth distribution of armorhead on the longline could be determined unambiguously with the sampling procedure used, this was not true for the depth distribution of any of the measured or derived biological attributes, because the catch from each 5-dropper segment was aggregated before the attributes were measured. As a means of approximating such depth distributions, the biological attributes of individual fish within each segment group were randomly assigned to the capture depths within the segment.

The relative abundance of armorhead during each stock-assessment cruise was expressed as the mean catch in numbers per hook ($\bar{U}$) estimated as a weighted average over four depth strata (<265, 265–300, 301–400, 401–500m). Algebraically, ($\bar{U}$) is

$$\bar{U} = \frac{\sum_{i=1}^{4} U_i A_i}{\sum_{i=1}^{4} A_i}, \quad (1)$$

where U_i is the catch per hook, and A_i is the bottom area in depth stratum i. Values of U_i were corrected for the influence of hook timers, and values of A_i were estimated as planar areas between the strata depth boundaries measured on a bathymetric map of the SE Hancock Seamount (Fig. 1).

Since armorhead begin to lose weight after arriving at the seamounts, we examined an index of relative fatness (FI), defined as body depth divided by fork length, as an index of post-recruitment age. Frequency distributions of FI were calculated as weighted averages, where the weighting factors were proportional to the estimated abundance of armorhead in each depth stratum. Algebraically, this is expressed as

$$\bar{N}_{\cdot j} = \frac{\sum_{i=1}^{4} N_{ij} A_i U_i}{\sum_{i=1}^{4} A_i U_i}, \quad (2)$$

where N_{ij} is the number of fish in FI category j and depth stratum i.

The frequency distributions of FI usually display two or three distinct modes which are similar in appearance to the modes often present in length-frequency distributions of temperate fishes. Since armorhead recruitment to the seamounts is seasonal (Boehlert and Sasaki 1988), these modes were assumed to represent annual cohorts of fish. To estimate the proportion of the population contributed by each cohort (P_k) and the mean and variance of its FI distribution, the FI distributions were separated into their component distributions by fitting a distribution mixture model using a procedure developed for length-frequency data (Macdonald and Pitcher 1979).

Several of the year-class modes in the FI distributions were so distinct that they could be followed through the time-series in an orderly progression from when they were fat (high FI) to when they were lean (low FI). This feature of the FI distributions was used in two ways. First, the rate at which armorhead decrease in fatness was estimated by following the particularly strong year-class recruiting to the seamount in 1986. Mean FI of this cohort (μ_k) on each cruise was regressed against the time (in months), and the time squared, since the cohort was considered fully recruited to the seamount. Linearity of the relationship was determined by the significance of the coefficient of the squared term.

Second, the instantaneous natural mortality rate (M) of armorhead was estimated by following two cohorts, one composed of armorhead recruiting to the seamount in 1986 and the other composed of all armorhead present on the seamount during the first cruise in 1985. Relative abundance of each cohort at each time (t) was first estimated as the product of the catch-per-hook and the proportion of the population within the appropriate cohort on each cruise; that is, $P_{k,t}\,\bar{U}_t$. Instantaneous natural mortality rate was then estimated by regressing the natural logarithm of relative abundance against the time (in months) since the cohort was considered fully recruited. Analysis of covariance (ANCOVA) was used to test whether the slopes of the regression lines (i.e., the estimated values of M) differed between cohorts. A best estimate of M was computed as the average of the estimates for the two cohorts weighted by the inverses of their variances. Additionally, M was estimated for each sex separately, considering only the 1986 cohort. ANCOVA was again used to test whether the estimated values of M differed between sexes. These and all subsequent applications of ANCOVA herein will first test a model with one slope and two intercepts against a model with two slopes and two intercepts. If such a test is not significant, then a model with one slope and one intercept is tested against a model with one slope and two intercepts.

Period 2 In the period 1978–84, Japanese trawlers conducted 10 fishing trips to SE Hancock Seamount. For all trips, U.S. observers recorded the weight of armorhead caught and the duration of each trawl-haul. In addition, fork length and body weight were recorded for a random sample of armorhead drawn from each haul.

The biomass of armorhead at the start of each fishing trip was estimated by using the Leslie method (Leslie and Davis 1939) in which the change in CPUE over time is related to the cumulative catch removed. Algebraically, this is expressed as

$$U_d = B_0\, q - q\, K_d, \quad (3)$$

where U_d is the daily average catch (in kg) of armorhead per hour of fishing on day d, K_d is the cumulative catch of armorhead up to the beginning of day d, q is the catchability coefficient, and B_0 is the initial biomass. Two parameters (q, B_0) were estimated by regressing U_d on K_d; variance of B_0 was estimated using the equation from Polovina (1986). Mean catchability, $\bar{q}_j$, and its variance were calculated from the per-trip estimates.

Frequency distributions of FI were computed the same as for Period 1, except that body depths were not measured but were estimated from body weights and fork lengths using the regression equation previously described. Since the distributions showed apparent cohort modes similar to those observed during Period 1, the mean and variance of the FI distribution for each cohort and the proportional contribution of the cohort to the population were again estimated with a distribution mixture model. The rate at which FI decreased with time was estimated by regressing the mean FI of the cohort recruiting in 1980 against the time (in months), since the cohort was considered fully recruited.

Period 3 In the period 1970–77, Japanese trawlers fished Hancock Seamounts for at least 1 month in every year; however, data from NW and SE Hancock Seamounts could not be separated. Soviet trawlers also likely fished the Hancock Seamounts over this period, but the available Soviet data (Borets 1975) were aggregated over all seamounts and were not useful for determining the stock dynamics on the Hancock Seamounts.

Relative abundance of armorhead was therefore based solely on Japanese data and was calculated as the reported monthly catch divided by the fishing effort (in hr). Annual mean catch-per-hour ($\bar{U}_t$) and its variance were calculated from the unweighted monthly means. FI could not be calculated during this period due to insufficient data.

Biomass estimation

Armorhead abundance could be estimated in absolute terms as biomass only in Period 2. In the other periods, abundance was estimable in relative terms as CPUE. To allow estimation of biomass from CPUE in Periods 1 and 3 and to allow the merging of all three periods into one continuous time-series, several parameters were required that could be estimated only with data from Period 2. For this reason, we will start by describing the biomass estimation procedures for Period 2.

Period 2 The initial biomass estimates obtained for Period 2 (i.e., Leslie estimates of initial biomass in each year, $B_{0,t}$) may not include the total biomass of armorhead on the SE Hancock Seamount. Instead, the initial estimates may include only the biomass of the fishable stock or that portion of the stock occurring on the summit at night and therefore vulnerable to trawls. The question of whether $B_{0,t}$ includes the total population was addressed by testing the equality of two different estimators of annual recruitment to the seamount. The first (R_1) was calculated as the difference between the estimated biomass in 1 year minus the expected biomass surviving from the previous year. Assuming that the catch was taken in a brief interval at the start of the year, this relationship can be expressed as

$$R_{1,t+1} = B_{0,t+1} - (B_{0,t} - C_t)\, e^{-M}, \tag{4}$$

where $B_{0,t}$ and $B_{0,t+1}$ are the biomass estimates in years t and t+1, C_t is the catch in year t, and e^{-M} is the annual survival rate. The second (R_2), is calculated as the proportion of the biomass composed of recently recruited fish:

$$R_{2,t+1} = B_{0,t+1}\, P_{r,t+1}, \tag{5}$$

where $P_{r,t+1}$ is the proportion of the population composed of the cohort recruiting in year t+1. If $B_{0,t}$ estimates include the total biomass, then they will be appropriately scaled to C_t, and R_1 will equal R_2. But if the $B_{0,t}$ estimates are less than the total biomass, then R_1 will be greater than R_2. Equality was tested using the statistic

$$Z = \frac{R_1 - R_2}{\sqrt{\mathrm{Var}\,(R_1 - R_2)}}, \tag{6}$$

where Z was assumed to be distributed as a normal random variable. Estimates of $\mathrm{Var}(R_1 - R_2)$ were computed as described in the Appendix.

The fishable proportion of the stock (P_f) was estimated in two stages. First, total biomass of the 1980 cohort was estimated for each year in 1980–84, when the 1980 cohort represented more than 90% of the total population, by using an age-structured analysis (Megrey 1989) applied to a single cohort. Starting with a known or assumed value of biomass at the beginning of 1985, this analysis sequentially predicts biomass in each preceding year by accounting for catch and natural mortality. If the catch occurs over a short period at the start of the year, total biomass of this cohort in each year (B^*_t) can be expressed as

$$\begin{aligned} B^*_{t0-1} &= B^*_{t0}\, e^{M} + C_{t0-1} \\ B^*_{t0-2} &= B^*_{t0-1}\, e^{M} + C_{t0-2} \\ &= B^*_{t0}\, e^{M} + C_{t0-1}\, e^{M} + C_{t0-2} \\ &\;\;\vdots \\ B^*_{t0-n} &= B^*_{t0}\, e^{nM} + \sum_{i=1}^{n} C_{t0-1}\, e^{(n-i)M}, \end{aligned} \tag{7}$$

where B^*_{t0} is an estimate of total biomass at the start of the last year (t_0) in the time-series (terminal biomass), and C_{t0-i} is the catch in year t_{0-i}. Second, the proportion fished in each year ($P_{f,t}$) was then estimated as $B_{0,t}/B^*_t$, and mean P_f was then estimated as the average of the five annual estimates. This estimate of P_f, however, was not unique because it depended on B^*_{t0}, and B^*_{t0} was chosen arbitrarily because no independent estimate was available. Therefore, the terminal biomass B^*_{85} (the terminal fishing year was defined as 1985 as a later convenience) was estimated along with P_f. Assuming P_f is a constant, the two parameters were estimated by minimizing the weighted sum of squares of the $P_{f,t}$ with weights equal to the inverse of the variance of each $P_{f,t}$.

Once the estimate of mean P_f had been obtained, corrected estimates of the initial biomass in each year (i.e., corrected Leslie estimates) were estimated as

$$B^*_{0,t} = \frac{B_{0,t}}{P_f}, \tag{8}$$

and the mean annual biomasses were then estimated as

$$B^*_t = \frac{U_t}{q_t P_f}, \quad (9)$$

where U_t and q_t are the mean annual CPUE and catchability. Variance of B^*_t was estimated with methods described in the Appendix.

Period 3 Biomass during Period 3 was estimated from the mean catch-per-hour of Japanese trawlers (U_t) as

$$B^*_t = \frac{U_t}{q_j P_f}, \quad (10)$$

where q_j is the mean catchability of Japanese trawlers estimated for Period 2. Variance of B^*_t was estimated with methods described in the Appendix.

Period 1 Biomass during Period 1 was estimated from longline catch-per-hook (U_t) as

$$B^*_t = \frac{U_t W_t}{q_l}, \quad (11)$$

where W_t is the mean individual weight of armorhead caught during sampling Period t, and q_l is the catchability of the longlines. Estimation of q_l required an independent estimate of B^*_t for at least one of the sampling periods, and the estimate chosen was the terminal biomass of the 1980 year-class in 1985. Catchability was thus estimated as

$$q_l = \frac{U_{85} P_{80} W_{85}}{B^*_{80,85}}, \quad (12)$$

where U_{85} is the catch-per-hook, W_{85} is the mean body weight in 1985, $B^*_{80,85}$ is the terminal biomass of the survivors of the 1980 year-class at the start of 1985, and P_{80} is the proportion of the 1985 population composed of the 1980 year-class survivors. Variances of B^*_t and q_l were estimated with the methods described in the Appendix.

Spawning and recruitment biomasses

Spawning and recruitment biomasses were estimated for Periods 1 and 2 in which FI information was available. Spawning biomass in each year (S_t) was estimated as:

$$S_{t+1} = \left(B^*_t - \frac{C_t}{2}\right) e^{-\frac{M}{2}} (1 - P_{r,t}), \quad (13)$$

where $P_{r,t}$ is the proportion of B^*_t comprised of newly-recruited fish, and all other terms are as previously defined. This formulation assumes that B^*_t was always estimated on 1 July, the midpoint of both the fishing season and the stock-assessment cruise. Natural mortality between 1 July and 31 December, the assumed peak of spawning (Bilim et al. 1978), was accounted for by the term $e^{-M/2}$, where M is the annual instantaneous natural mortality rate. $P_{r,t}$ was estimated as the proportion of the population (P_k) within the modal group with the largest mean FI, or as zero if no model group had a mean FI>0.25. $P_{r,t}$ was included in the estimate of spawning biomass because, based on samples collected on the August 1988 stock-assessment cruise (R. Humphreys, NMFS Honolulu Lab., unpubl. data), female armorhead appear to be nonreproductive during the first spawning season after they recruit to the seamounts. Recruitment biomass was estimated as

$$R_t = \left(B^*_t + \frac{C_t}{2}\right) P_{r,t}. \quad (14)$$

This formulation assumes that recruitment occurs from March to May (Boehlert and Sasaki 1988) and is complete by the time B^*_t is estimated. Since young armorhead recruit to the seamounts at approximately 24–30 months of age (Uchiyama and Sampaga 1990), recruitment follows spawning by 3 calendar years. Spawner-recruit relationships were therefore examined using a 3-year lag between spawning and recruitment.

Results and discussion

The armorhead population on SE Hancock Seamount fluctuated tremendously between 1970 and 1990 (Fig. 2) and declined steadily after the population high in 1972, except for small increases occurring in 1980 and 1986. Before the forces producing these changes (i.e., natural mortality, fishing mortality, and recruitment) are examined, the potential biases and the precision of the biomass time-series will be considered.

Biomass estimates

Construction of the time-series of biomass estimates required (1) merging two time-series of CPUE data that were non-overlapping in time and were from distinctly different gear types, and (2) the conversion of a relative measure of abundance (CPUE) into the absolute measure of biomass. Since Japanese trawls and research longlines were never used simultaneously, the time-series could not be merged by simply standardizing the catchability of one gear relative to the other. Fortunately, however, the armorhead popula-

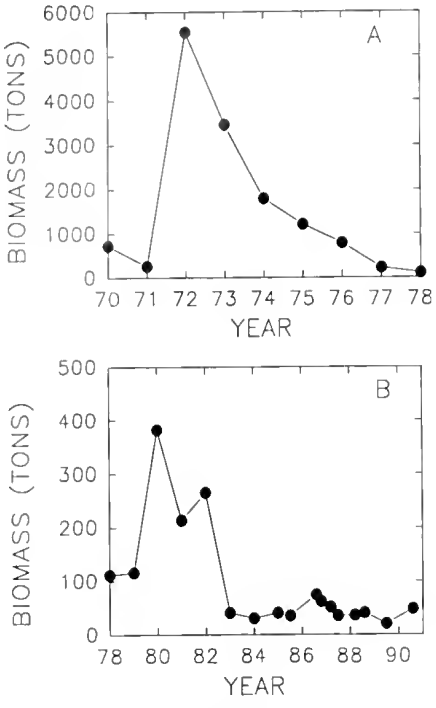

Figure 2

Pelagic armorhead *Pseudopentaceros wheeleri* biomass on Southeast Hancock Seamount during periods of (A) high abundance (1970–78) and (B) low abundance (1979–90). Prior to 1985, when routine stock-assessment surveys were initiated, the biomass estimates are annual means and are shown at the beginning of the year. Starting in 1985, the biomass estimates are for each stock-assessment survey and are shown for the appropriate month.

Table 1

Leslie estimates of initial biomass (B_0) and catchability (q) of pelagic armorhead *Pseudopentaceros wheeleri* for each of the Japanese fishing trips during Period 2 (1978–84) on SE Hancock Seamount.

Year	Month	Vessel ID no.	Days fished	Catch (t)	B_0 (t)	q	$P(q=0)$
1978	May	1	11	204	198	0.00197	<0.001
1979	Jun	2	18	68	80	0.00059	<0.005
1980	Aug	3	29	453	551	0.00047	<0.001
1981	Jun	2	5	161	297	0.00101	>0.10
	Aug	3	20	44	55	0.00067	>0.10
1982	May	4	10	180	269	0.00064	0.10
	Jul	2	12	8	17	0.00071	>0.10
1983	Jul	3	19	39	38	0.00066	<0.001

tion on SE Hancock seamount was sufficiently small and the fishing effort was sufficiently large to allow use of the Leslie method to estimate both the mean catchability of the trawlers (q_j) and the biomass at the initiation of each fishing season ($B_{0,1}$) during the period just prior to replacement of commercial trawling by research longlining. The time-series was merged by using the estimate of q_j and P_f to compute biomass from Japanese trawl CPUE and by using the estimates of $B_{0,t}$ to estimate q_l and thereby compute biomass from longline CPUE. Thus, the Leslie method provided the means to merge the two time-series and to express the resulting time-series in terms of biomass.

Because success of this procedure rests on the successful application of the Leslie method, any biases in the biomass estimates are likely the result of violations of the underlying assumptions. One of the most important assumptions of the Leslie method is that the change in size of the population is solely due to removals by the fishery. In practice, this requires that the population is closed to immigration and the fishery is sufficiently short and intense so that the effect of natural mortality is negligible. In nearly all cases examined, these requirements were met; that is, fishing usually occurred well after the spring peak in recruitment of pelagic juveniles (Table 1; Boehlert and Sasaki 1988) and the catch was usually obtained in 1 or 2 months and represented a large fraction of the estimated biomass (Table 1). One further indicator of the successful application of the Leslie method is the significance of the slope of the regression, or q. Although the estimates of q obtained using the Leslie method were not always significantly greater than zero, they were remarkably similar among years for each vessel that had fished repeatedly (Table 1). Such similarity was used as justification for using the non-significant estimates in later calculations.

Bias could also result from violation of another assumption of the Leslie method, that the entire population is equally vulnerable to the sampling gear. Such bias was considered likely when initial biomass estimates from Period 2 seemed too small to be consistent with the observed catches. This apparent inconsistency was examined statistically by testing the equality of two estimators of recruitment, one that included catch (R_1; Eq. 4), and one that did not (R_2; Eq. 5). The bias was confirmed since in 4 of the 5 years examined, R_1 was significantly ($P<0.05$) greater than R_2, a condition that could occur only if the biomass estimates were too small.

The most likely explanation for the underestimation of armorhead biomass is that the $B_{0,t}$ estimates do not include the entire population and instead include only the fishable population or the part actually exposed to trawls. This result was surprising because we believed that the population would be sufficiently mixed by the nocturnal vertical migration so that all armorhead would be equally vulnerable even though the trawls were topographically restricted to only a part of the armorhead depth range. Our

finding, however, indicates either that mixing is minimal or that the rate of mixing is relatively low compared with the 2- to 4-week duration of a typical Japanese fishing trip.

Although the bias in $B_{0,t}$ was corrected by estimating the proportion of the stock vulnerable to trawling (P_f= 0.27), adequacy of this correction rests on the assumption that P_f does not vary with time. However, P_f may vary with time because the depth distribution of armorhead may vary. For example, the proportion of the population occurring in the shallowest depth stratum (<250m) averaged 15% over the 10 research cruises, but ranged from 0 to 40%. It is unclear if such variation in the daytime distribution is reflected in the nighttime distribution, because armorhead do not feed at night and therefore cannot be sampled effectively with longlines (M.P. Seki and D.A. Somerton, NMFS Honolulu Lab., unpubl. data). Bias in the biomass estimates could additionally occur if P_f depends on the degree of mixing of deep and shallow fish, because P_f would likely be larger when fishing periods were longer and less intense. Since fishing periods tended to be longer during Period 3 than in Period 2, this would lead to an overestimate of biomass during Period 3.

Precision in the estimates of biomass, which is expressed as the coefficient of variation (CV) to compensate for the large range in biomass, was smallest in Period 1 (Fig. 3), because longline CPUE estimates were more precise than trawl CPUE estimates. Expressed differently, based on the mean CV over the period 1970–84 (excluding 1971 when data were not sufficient to estimate the variance of U_t), the 95% confidence intervals for B^*_T was $\pm 1.70\ B^*_T$, which in all years includes zero. Over the period 1985–90, however, the 95% confidence interval was $\pm 0.29\ B^*_T$, and never included zero.

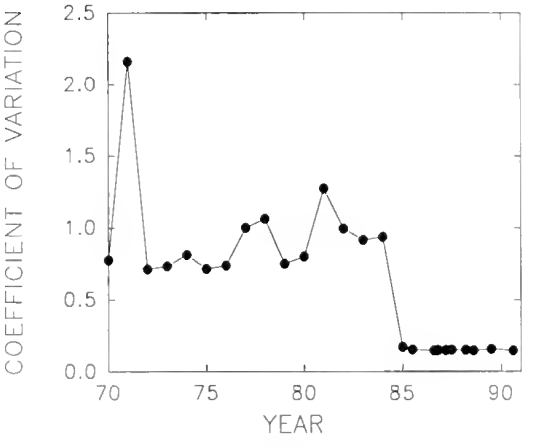

Figure 3
Coefficient of variation of the biomass estimates of pelagic armorhead *Pseudopentaceros wheeleri* as a function of time.

Post-recruitment ageing

The estimates of natural mortality rate and annual recruitment required estimates of the age distribution. Although the ages of armorhead can be determined using either daily or annual growth increments on their otoliths (Uchiyama and Sampaga 1990), they are easily obtainable only for individuals in the pelagic phase of their life history, because somatic growth ceases once armorhead recruit to the seamount (Humphreys et al. 1989) and growth increments become so closely spaced that they are exceedingly difficult to count (R. Humphreys, NMFS Honolulu Lab., pers. commun.). Thus, we expressed age on a scale relative to the presumed time of recruitment. Such post-recruitment ages were based on the decrease in FI over time.

Frequency histograms of FI display modes which can be tracked sequentially from one histogram to the next over time as they move from the right (high FI or fat) to the left (low FI or lean). Two examples of this are the large mode that appeared in 1980 and could be followed until 1984 (Fig. 4A) and the large mode that appeared in 1986 and could be followed until 1990 (Fig. 4B). Since the first appearance of these modes was always associated with an increase in CPUE (Fig. 2B), they were interpreted to represent cohorts of fish that had recruited to the seamount.

To further substantiate our interpretation of the modes, the rate of decrease in FI was examined for consistency both over time and between the two presumed year-classes. Plots of FI versus time appeared to have slight curvature (Fig. 5), but for both the 1980 and 1986 year-classes the curvature was not significant ($P>0.05$). Changes in FI, therefore, are proportional to changes in post-recruitment age. The rates of decrease in FI of the 1986 (0.00169/mo) and the 1980 (0.00157/mo) year-classes did not differ significantly (ANCOVA, $P>0.05$). In addition, sexual equality in the rate of decrease in FI was tested for the 1986 year-class alone, and the male rate was not significantly different (ANCOVA, $P>0.05$) from the female rate. Taken together, these findings indicate that all armorhead decrease in FI at approximately the same rate and that once established by the recruitment of a strong year-class, the coherency of an FI mode should be preserved over time.

Natural mortality

Natural mortality was estimated from the change in the relative abundance of two cohorts over time during a period when no commercial fishing occurred. The first of these cohorts, which consisted

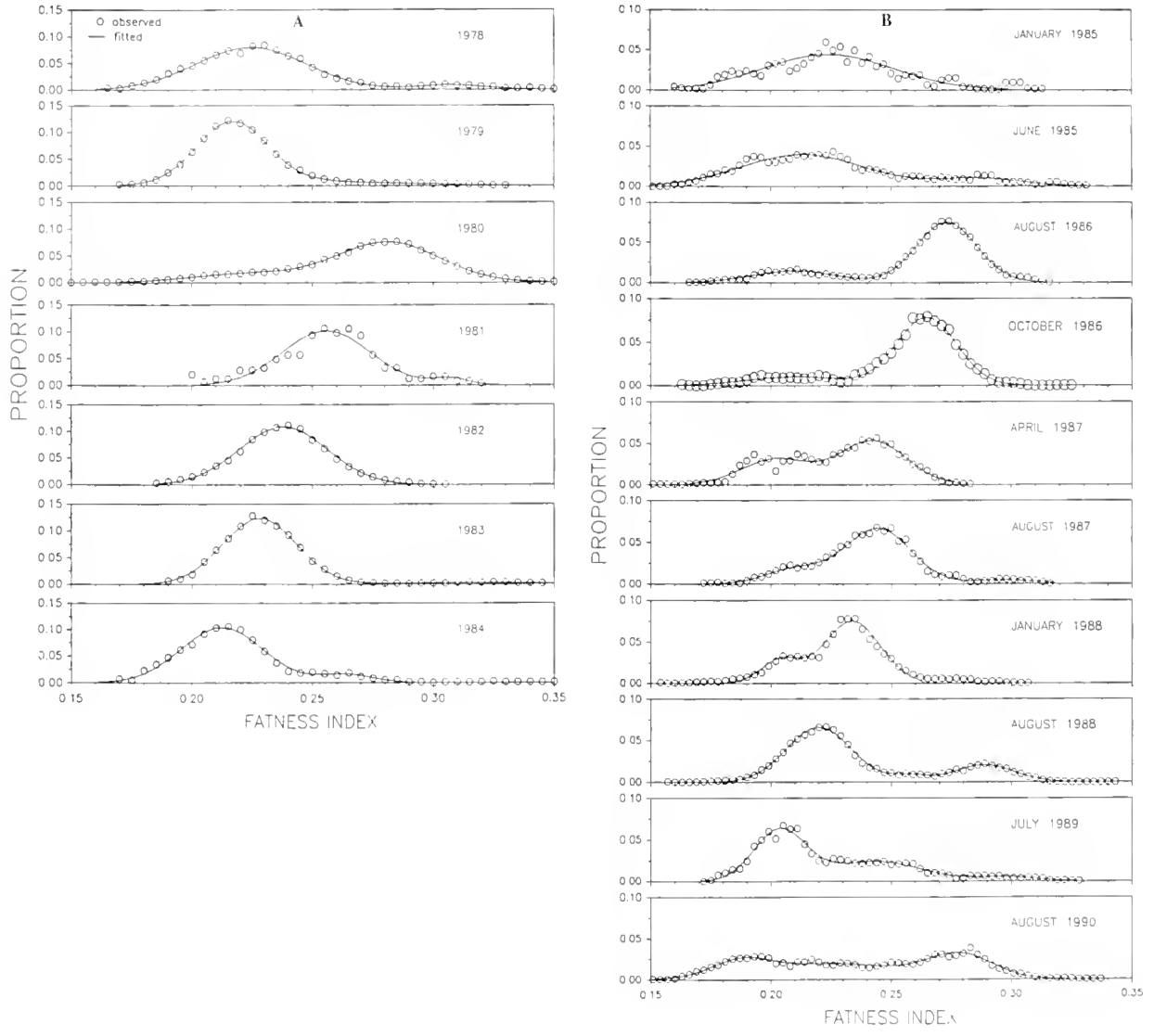

Figure 4

Frequency histograms of fatness index are shown for Japanese commercial catch of pelagic armorhead *Pseudopentaceros wheeleri* in (A) each year during 1978–84 and (B) for each of the research cruises during 1985–90.

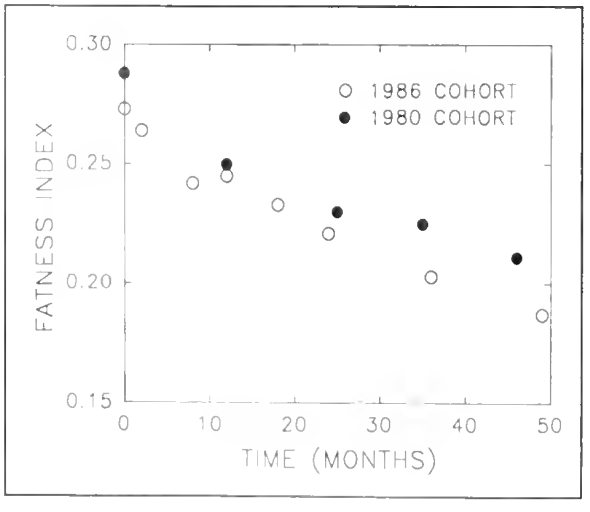

of the extant armorhead population in January 1985, was identifiable for seven consecutive samplings and had an instantaneous natural mortality (M) of 0.054/mo. The second, which consisted of the year-class recruiting in 1986, was identifiable for eight consecutive samplings and had an M of 0.044/mo (Fig. 6). Although the two estimates were significantly different (ANCOVA, $P<0.05$), the weighted average (0.045/mo or 0.54/yr) was chosen as

Figure 5

Decrease in fatness index of pelagic armorhead *Pseudopentaceros wheeleri* with time for the 1980 and 1986 year-classes on Southeast Hancock Seamount.

the most representative value. For both cohorts, log-relative abundance was clearly a linear function of time, and M is therefore invariant with age (Fig. 6A).

When M was estimated separately for each sex, considering the 1986 cohort alone, the value for males (0.037/mo) was significantly different (ANCOVA, $P<0.001$) from the value for females (0.045/mo). Furthermore, the intercept of the regression, i.e., the log-relative abundance at the time of recruitment) appeared to be smaller for males (4.27) than for females (4.94), but the difference could not be tested because of the strong difference in slopes (Fig. 6B). Taken together, these results indicate that, at least for the 1986 cohort, females recruited to the seamounts in greater abundance than males but subsequently died at a greater rate. It is also possible that the higher mortality rate of females was primarily restricted to the first year of residence on the seamount (Fig. 6B).

Since a sexual difference in mortality seemed inexplicable to us, we examined the possibility that longlines preferentially selected fat females. This was done by examining whether the ratio of females to males, expressed as proportion female, changed with FI similarly for trawls as for longlines. Since the FI values of females and males decrease identically with time, any change in female proportion with FI would indicate either selective sampling or differential mortality, depending on whether one or both gear types showed the change. To test for such changes, female proportion was regressed on FI for various samples. When these regressions were performed on the longline samples, all 10 had a significant ($P<0.05$) positive slope. When the regressions were performed on the research trawl samples, four of five had a significant positive slope. Thus a sampling bias is unlikely, unless both gears produced a similar bias.

The estimate of natural mortality rate (0.54/yr) is more than twice that reported in Borets (0.25/yr; 1975). His estimate, however, was based on age data that were likely biased for two reasons. First, the age range [i.e., 7 yr, ages 5–12], reported in Borets (1975) appears to be excessive when compared with the range estimated from modal progression through the research FI histograms (4–5 yr). Second, the mean age of the catch between 1968 and 1974 reported in Borets (1975) did not decrease as would be expected in a developing fishery. On the other hand, our estimate of natural mortality rate was less than the rate implied in the studies of Uchida and Tagami (1984), Humphreys et. al. (1989), and Uchiyama and Sampaga (1990), which all suggested that armorhead were semelparous and, like Pacific salmon *Oncorhynchus* spp., died soon after spawning.

Fishing mortality

Fishing mortality rate (F) can be estimated only between 1978 and 1983 when the total catch and effort on SE Hancock Seamount are known with reasonable certainty, based on the U.S. observer program. Over this period, F, which was calculated as the estimated value of $q_j \times$ total annual effort, averaged 1.03/yr or roughly twice the natural mortality rate. The mean exploitation rate (which was approximated as $(F/Z)(1-e^{-Z})$ where $Z=F+M$), was ~0.50. Therefore, provided that no recruitment occurred and that fishing effort was continuous throughout the year, then an average of roughly 50% of the population at SE Hancock Seamount was removed annually by the fishery over this period.

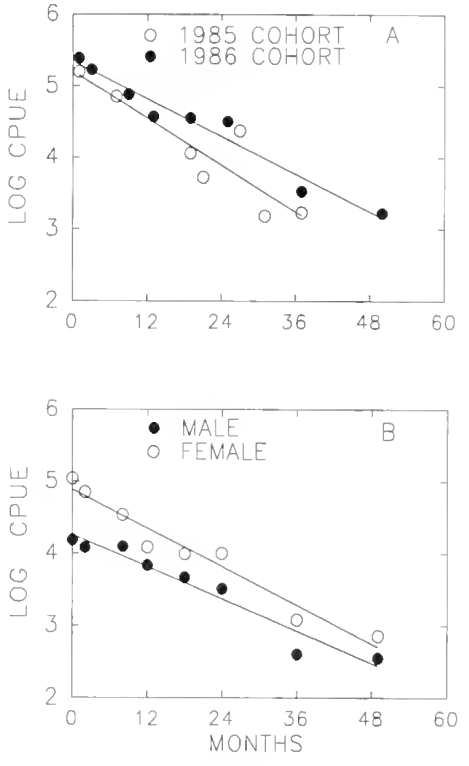

Figure 6

Change in log CPUE of pelagic armorhead *Pseudopentaceros wheeleri* versus time for the (A) cohort composed of the extant population in 1985 and the cohort recruiting in 1986, and (B) for males and females of the 1986 recruiting cohort.

Recruitment

Annual recruitment to SE Hancock Seamount was extremely intermittent between 1978 and 1990. When expressed in metric tons, the 1980 recruitment clearly dominated the entire record (Fig. 7A). However, the total biomass changed considerably over this period, and, when expressed as a percentage of the total biomass, the 1986 recruitment and—to a lesser extent—the 1988 and 1990 recruitments were also relatively important (Fig. 7B). For some

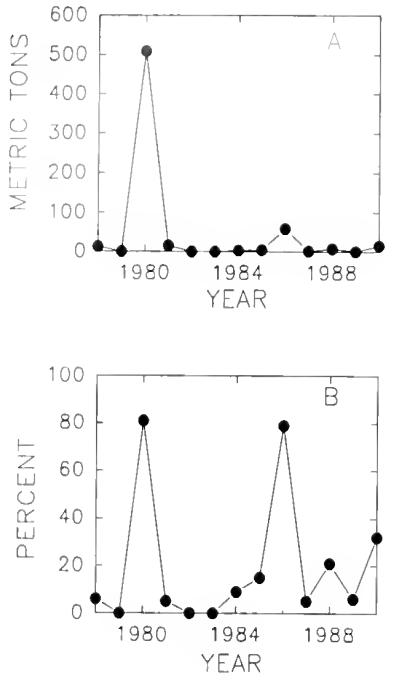

Figure 7

Annual recruitment to Southeast Hancock Seamount expressed in (A) metric tons and (B) percent of the population biomass of pelagic armorhead *Pseudopentaceros wheeleri*.

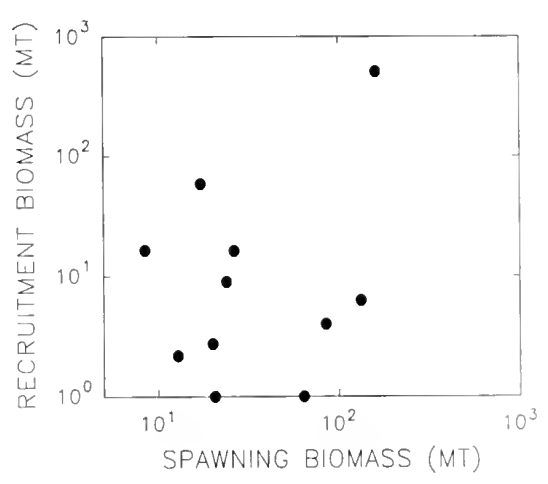

Figure 8

Annual recruitment versus spawning biomass of pelagic armorhead *Pseudopentaceros wheeleri* 2 years earlier.

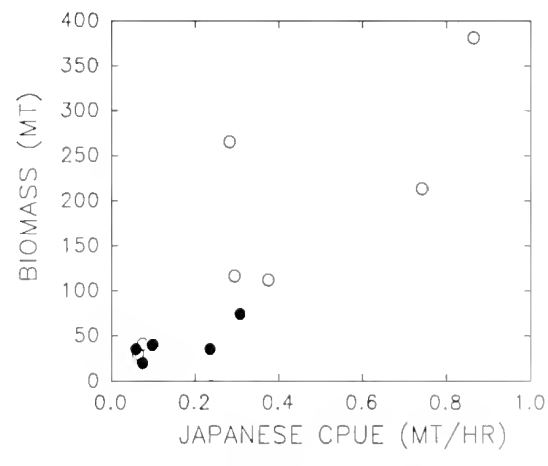

Figure 9

Biomass of pelagic armorhead *Pseudopentaceros wheeleri* on Southeast Hancock Seamount and Japanese trawl catch/hr on all other southern Emperor–northern Hawaiian Ridge seamounts during (●) Period 1 (1985–90) and (○) Period 2 (1978–84) when the Southeast Hancock Seamount population experienced fishing.

unknown reason, recruitment in the even years tended to be larger than it was in the odd years (Mann-Whitney test, $P = 0.06$).

Prior to 1978, it is difficult to estimate annual recruitment because the data required to calculate FI were not routinely collected. However, an examination of the large increase in abundance in 1972 (Fig. 2A) cannot be avoided. Interpretation of the 1972 increase is troublesome because the evidence for an unusually large recruitment is equivocal. A large recruitment, for example, should have resulted in a large increase in the proportion of the population comprised of fat armorhead as it did in 1980 and 1986 (Fig. 4A, B), yet the proportion of the population categorized as fat during the period of maximum recruitment was smaller in 1972 than it was in 1973 when recruitment did not appear to be exceptionally large (Boehlert and Sasaki 1988). Armorhead measured in 1972, however, were markedly smaller than in any other year (Takahashi and Sasaki 1977, Borets 1975). One proposed explanation for the small size is that the tremendous abundance of armorhead in 1972 resulted in a density-dependent suppression of growth in the pelagic phase (Borets 1977). This might also have reduced the FI of recruits and thereby masked the FI signature of a large recruitment.

An alternate explanation for the 1972 increase in abundance is that it is an illusion due to a rapid increase in trawl catchability as the newly-developed fishery progressed from an exploratory phase to a production phase (Takahashi and Sasaki 1977, Uchida and Tagami 1984). If, however, the 1972 increase was due simply

to changing catchability, then such an increase should not be evident in the Soviet catch-and-effort data, because the Soviet fishery had developed earlier and was likely beyond its "fishing-up" phase. Soviet data do display an increase from 1971 to 1972 (73–104 million fish/vessel day; Borets 1975), but this is considerably less than that experienced by the Japanese fishery. Thus, it is not entirely clear whether the apparent increase in 1972 was real and due to recruitment or an artifact due to changing catchability.

The dependance of recruitment on spawning biomass was examined by Wetherall and Yong (1986) and found to be essentially nonexistent, at least at the high levels of spawning biomass extant during 1969–77. Recruitment, however, must ultimately be limited by spawning biomass at low population levels; therefore, we reexamined the relationship over the period 1980–90, when the spawning biomass was considerably lower. This was done by plotting, on a log-log scale, the estimated spawning biomass on SE Hancock Seamount against the estimated recruitment 2 years later (Fig. 8). Since a clear relationship is not evident, it is possible that recruitment and spawning biomass are only weakly related even at the low population levels examined. There are, however, at least two other possible reasons why no relationship was found. First, since no apparent genetic difference exists among the armorhead collected at the various seamounts (Borets 1979), recruits to SE Hancock Seamount are likely the progeny of the entire North Pacific population. If the SE Hancock Seamount population does not vary concordantly with the entire North Pacific population, any relationship between recruitment and spawning biomass would be obscured. However, plots of the estimated biomass on SE Hancock Seamount against Japanese CPUE on all SE-NHR seamounts show a strong concordance (Fig. 9). Second, if spawning biomass does exert an influence on recruitment, it may do so only by limiting the maximum level attained. Thus, at higher levels of spawning biomass, higher levels of recruitment are possible—but not assured—because of environmental variability. One interpretation of Figure 8 could therefore be that recruitment did increase with spawning biomass, but at the higher levels of biomass there were several environmentally-poor recruitment years.

Management implications

Since armorhead do not grow after they recruit to the fishery and therefore cannot be growth-overfished, management strategies could be designed solely to achieve some optimum level of spawning stock biomass (SSB). One approach is to define this optimum SSB by using a spawner-recruit relationship as is done for some species of Pacific salmon (Ricker 1975). Another approach is to define it in terms of a fixed percentage of the equilibrium biomass in the absence of a fishery (Beddington and Cooke 1983). But in either case, the spawning population must include the entire SE-NHR population rather than the small component examined here. In addition, some form of international agreement controlling the armorhead catch will be required before any management measures are effective.

Acknowledgments

We thank George Boehlert, Bob Humphreys, Bill Lenarz, and Jeff Polovina for reviewing the manuscript and offering helpful suggestions.

Citations

Beddington, J.R., and J.G. Cooke
1983 The potential yield of fish stocks. FAO Fish. Tech. Pap. 242, 47 p.

Bilim, L.A., L.A. Borets, and M.K. Platoshina
1978 Characteristics of ovogenesis and spawning of the boarfish on the region of the Hawaiian Islands. *In* Fisheries oceanography, hydrobiology, biology of fishes and other denizens of the Pacific Ocean. Izv. Tikhookean. Nauchno-Issled. Inst. Rybn. Khoz. Okeanogr. (TINRO) 102:51–57 [in Russ.]. (Engl. transl. 106 by W.G. Van Campen, 1986, 9 p.; avail. NMFS Honolulu Lab.)

Boehlert, G.W., and T. Sasaki
1988 Pelagic biogeography of the armorhead, *Pseudopentaceros wheeleri*, and recruitment to isolated seamounts in the north Pacific Ocean. Fish. Bull., U.S. 86:453–466.

Borets, L.A.
1975 Some results of studies on the biology of the boarfish (*Pentaceros richardsoni*). Invest. of the biology of fishes and fishery oceanography. Izv. Tikhookean. Nauchno-Issled. Inst. Rybn. Khoz. Okeanogr. (TINRO, Vladivostok) 6:82–90. (Engl. transl. 97 by W.G. Van Campen, 1984, 9 p.; avail. NMFS Honolulu Lab.)
1977 Dynamics of size-age composition of the boerfish (*Pentaceros richardsoni*). Invest. of the biology of fishes and fishery oceanography. Izv. Tikhookean. Nauchno-Issled. Inst. Rybn. Khoz. Okeanogr. (TINRO, Vladivostok) 8:65–69 [in Russ.] (Engl. transl. 115 by W.B. Van Campen, 1987, 6 p; avail. NMFS Honolulu Lab.)
1979 The population structure of the boarfish, *Pentaceros richardsoni*, from the Emperor Seamounts and the Hawaiian Ridge. J. Ichthyol. 19:15–20.

Efron, B., and G. Gong
1983 A leisurely look at the bootstrap, the jackknife and cross-validation. Am. Stat. 37:36–48.

Humphreys, R.L. Jr., and D.T. Tagami
1986 Review and current status of research on the biology and ecology of the genus *Pseudopentaceros*. *In* Uchida, R.N., et al. (eds.), Environment and resources of seamounts in the North Pacific, p. 55–62. NOAA Tech. Rep. NMFS 43.

Humphreys, R.L. Jr., G.A. Winans, and D.T. Tagami
1989 Synonymy and life history of the North Pacific pelagic armorhead, *Pseudopentaceros wheeleri* Hardy. Copeia 1989: 142–153.

Komrakov, O.E.
1970 Distribution and fishery of the boarfish (*Pentaceros richardsoni*) in the Hawaiian region. Avail. as Transl. 117 from NMFS Honolulu Lab.

Leslie, P.H., and D.H.S. Davis
1939 An attempt to determine the absolute number of rats on a given area. J. Anim. Ecol. 8:94–113.

Macdonald, P.D.M., and T.J. Pitcher
1979 Age groups from size-frequency data: A versatile and efficient method of analyzing distributions mixtures. J. Fish. Res. Board Can. 36:987–1001.

Megrey, B.A.
1989 Review and comparison of age-structured stock assessment models from theoretical and applied points of view. *In* Edwards, E.F., and B.A. Megrey (eds.), Mathematical analysis of fish stock dynamics, p. 8–48. Am. Fish. Soc. Symp. 6., Bethesda.

Polovina, J.J.
1986 A variable catchability version of the Leslie model with application to an intensive fishery experiment on a multispecies stock. Fish. Bull., U.S. 84:423–428.

Ricker, W.E.
1975 Computation and interpretation of biological statistics of fish populations. Bull. Fish. Res. Board Can. 191, 382 p.

Sasaki, T.
1986 Development and present status of Japanese trawl fisheries in the vicinity of seamounts. *In* Uchida, R.N., et al. (eds.), Environment and resources of seamounts in the North Pacific, p. 21–30. NOAA Tech. Rep. NMFS 43.

Seber, G.A.F.
1973 The estimation of animal abundance. Hafner Press, NY, 506 p.

Seki, M.P., and D.A. Somerton
In prep. Feeding ecology and daily ration of the pelagic armorhead, *Pseudopentaceros wheeleri*, at Southeast Hancock Seamount. NMFS Honolulu Lab., 30 p.

Shiota, P.M.
1987 A comparison of bottom longline and deep-sea handline for sampling bottom fishes in the Hawaiian Archipelago. Admin. Rep. H-87-5, NMFS Honolulu Lab., 18 p.

Somerton, D.A., B.S. Kikkawa, and C.D. Wilson
1989 Hook timers to measure the capture time of individual fish. Mar. Fish. Rev. 50(2):1–5.

Takahashi, Y., and T. Sasaki
1977 Trawl fishery in the central North Pacific seamounts [Kita Taiheiyo chubu kaizan ni okeru tororu gyogryo. Hokuyo sokouo gyogyo—Shiryo (3)] Northern waters groundfish fishery—Data (3). Div. North. Waters Groundfish Resour., Far Seas Fish. Res. Lab., 45 p. [In Jpn.; Engl. transl. 22 by T. Otsu, 1977, 49 p.; avail.NMFS Honolulu Lab.]

Uchida, R.N., and D. Tagami
1984 Groundfish fisheries and research in the vicinity of seamounts in the North Pacific Ocean. Mar. Fish. Rev. 46(2):1–17.

Uchiyama, J., and J. Sampaga
1990 Age and growth of the pelagic armorhead *Pseudopentaceros wheeleri* from the Hancock Seamounts. Fish. Bull., U.S. 88:217–222.

Wetherall, J.A., and M.Y. Yong
1986 Problems in assessing the pelagic armorhead stock on the central North Pacific seamounts. *In* Uchida, R.N. et al. (eds.), Environment and resources of the seamounts in the North Pacific, p. 73–86. NOAA Tech. Rep. NMFS 43.

Appendix

Variances of several of the estimators described in Materials and Methods were approximated by using the Delta method (Seber 1973) and assuming all covariance terms were negligible. Variance of $(R_1 - R_2)$ was estimated as

$$\mathrm{Var}(R_1 - R_2) = (P_{r,t+1} - 1)^2\,\mathrm{Var}(B_{0,t+1}) + (B_{0,t+1})^2\,\mathrm{Var}(P_{r,t+1}) + e^{-2M}\,[\mathrm{Var}(B_0, t) + \mathrm{Var}(C_t) + (B_{0,t} - C_t)^2\,\mathrm{Var}(M)], \tag{15}$$

where all variables are defined in text Equations 5 and 6. Variances of $B_{0,t}$ and $B_{0,t+1}$ were computed by using the method in Polovina (1986). Variance of C_t was assumed to be negligible because catch was measured by U.S. observers. Variance of M was estimated as the variance of the slope of the regression of log-relative abundance on postrecruitment age (in years). Variance of $P_{r,t+1}$ was estimated with a bootstrap method (Efron and Gong 1983). Bootstrap estimates were obtained from trawl samples of armorhead biological data by iteratively repeating the following steps: (1) A subsample of n fish from each sample was randomly chosen with replacement, where n is equal to the size of the original sample; (2) an FI frequency distribution was constructed from the subsample; (3) $P_{r,t+1}$ was estimated by fitting the distribution mixture model to the FI frequency distributions. In all cases, variance of $P_{r,t+1}$ was calculated as the variance among 100 bootstrap estimates.

Variance of B^*_t during Period 2 was as

$$\mathrm{Var}(B^*_t) = \left[\frac{1}{q_t P_f}\right]^2 \mathrm{Var}(U_t) + \left[\frac{U_t P_f}{(q_t P_f)^2}\right]^2 \mathrm{Var}(q_t) + \left[\frac{U_t q_t}{(q_t P_f)^2}\right]^2 \mathrm{Var}(P_f) \tag{16}$$

where all variables are defined in Equation (9). Variance of U_t was estimated as the variance among the daily U within each year. Variance of q_t was estimated as the variance of the slope of the Leslie model. When more than one vessel fished in each year, however, variance of q_t was the average of the individual variance estimates weighted by catch.

Variance of P_f was estimated by using a Monte Carlo model. Each iteration of the model consisted of generating a random value of $B_{0,t}$ for each year and a value of M, assuming all were normally distributed with means and variances equal to the original estimated values. With these generated values, B^*_t was estimated for each year with Equation (9) and $P_{f,t}$ was estimated as $B_{0,t}/B^*_t$. Mean estimates of P_f and $B^*_{80,85}$ (B^*_{t0} in Eq. 7), were obtained by using the iterative procedure to minimize the weighted sum of squares of the $P_{f,t}$ estimates. In all cases variances of P_f and $B^*_{80,85}$ were estimated from 100 iterations of the Monte Carlo model.

Variance of B^*_t during Period 3 was estimated using Equation (16) but with q_t replaced by q_j. Variance of U_t was estimated as the variance among the monthly means. Variance of q_j was estimated as the variance among the q estimates in Table 1. Variance of P_f is the same as for Period 2.

Variance of B^*_t during Period 1 was estimated as

$$\mathrm{Var}(B^*_t) = \left[\frac{W_t}{q_l}\right]^2 \mathrm{Var}(U_t) + \left[\frac{U_t}{q_l}\right]^2 \mathrm{Var}(W_t) + \left[\frac{U_t W_t}{q_l^2}\right]^2 \mathrm{Var}(q_l), \tag{17}$$

where all variables are defined in Equation (11). Variance of W_t was estimated from the biological samples from each research cruise. Variance of U_t was estimated as the variance of U among the four depth strata.

Variance of q_l was estimated as

$$\mathrm{Var}(q_l) = \left[\frac{U_{85} W_{85}}{B^*_{80,85}}\right]^2 \mathrm{Var}(P_{80}) + \left[\frac{U_{85} P_{80}}{B^*_{80,85}}\right]^2 \mathrm{Var}(W_{85}) + \left[\frac{P_{80} W_{85}}{B^*_{80,85}}\right]^2 \mathrm{Var}(U_{85}) + \left[\frac{U_{85} P_{80} W_{85}}{B^*_{80,85}}\right]^2 \mathrm{Var}(B^*_{80,85}), \tag{18}$$

where all variables are defined in Equation (12). Variances of W_{85} and U_{85} were estimated as described above for W_t and U_t. Variance of P_{80} was estimated as described for $P_{r,t+1}$. Variance of $B^*_{80,85}$ was estimated with the previously described Monte Carlo model.

Genetic isolation of previously indistinguishable chinook salmon populations of the Snake and Klamath Rivers: Limitations of negative data

Fred M. Utter
Robin S. Waples
David J. Teel

Coastal Zone and Estuarine Studies Division
Northwest Fisheries Science Center, National Marine Fisheries Service, NOAA
2725 Montlake Boulevard East, Seattle, Washington 98112

Abstract.–An anomalous inability to distinguish certain geographically-separated chinook salmon *Oncorhynchus tshawytscha* populations of the Snake River and the Klamath River from a survey of 18 polymorphic loci led to a prediction that distinction would ultimately be found through sampling of additional polymorphic loci. Recently published studies involving pertinent groups within each of these rivers included data from an additional 15 polymorphic loci, and therefore allow a reexamination of the relationships between these groups. Comparison of results for the new studies shows the formerly indistinguishable groups from two areas to be as distinct from one another as from other major groupings of the species with a mean genetic distance between populations of each river (0.014) that is double that of the maximum within-group genetic distance. Two newly-resolved gene loci (*mMDH-2** and *sMEP-1**) are particularly good at distinguishing populations from the two rivers. In addition to resolving the anomalous similarity between populations inhabiting geographically separated areas, the new results illustrate the care that must be used in drawing inferences from negative data.

A variety of characteristics can be useful in distinguishing particular groups of organisms from other related groups. In humans, for instance, major ancestral groups can be identified by heritable morphological traits, as well as by characteristic frequencies of alleles detected by molecular or immunological procedures. Conversely, although two groups lacking any distinguishing characteristics may, in fact, be closely related, the possibility of undetected differences often prevents a conclusive determination of the degree of relatedness. For example, two cryptic species of bonefishes in Hawaii were considered members of a common gene pool until biochemical genetic analysis revealed that the two forms diverged perhaps 20 million years ago (Shaklee and Tamaru 1981). Other examples of genetic distinctions between and within species of fishes previously considered to be homogeneous are listed in Allendorf et al. (1987).

The motivation behind our present study was a puzzling instance of apparent genetic similarity between two geographically separated groups of chinook salmon *Oncorhynchus tshawytscha*. Indigenous chinook salmon from the Klamath River and spring- and summer-run chinook salmon from the Snake River are well differentiated from nearby populations at several protein-coding gene loci (Utter et al. 1989, Bartley and Gall 1990, Waples et al. 1991, Bartley et al. 1992). However, a comparison of the two river groups by Utter et al. (1989) failed to distinguish them despite their substantial geographic separation. The mouths of the Snake and Klamath Rivers are separated by a distance of almost 600 river-ocean miles, and a number of ancestrally distinct groups of populations (Utter et al. 1989) are found in intervening areas.

This apparent genetic similarity was even more puzzling because of substantial life-history differences between chinook salmon from the two rivers. The populations that were not well differentiated in the Utter et al. (1989) study included four spring-run and two summer-run populations from the Snake River and two fall- and one spring-run population from the Klamath River. Utter et al. (1989) also sampled fall-run fish from the Snake River, but this population is genetically quite different both from Snake River spring- and summer-run fish and chinook salmon from the Klamath River. Whereas the fall-run fish migrate to sea as subyearlings, the other populations produce juveniles that spend an additional winter in freshwater and outmigrate as yearlings.

Manuscript accepted 5 July 1992.
Fishery Bulletin, U.S. 90:770–777 (1992).

Utter et al. (1989) speculated that the anomalously high degree of genetic similarity between Klamath and Snake River populations was due to coincidentally high frequencies of the same common alleles (possibly a reflection of restricted gene flow among populations and reduced population sizes over an extended time interval) rather than to a recent common ancestral origin. Of the 25 polymorphic loci examined, only 18 were variable in either the Snake or Klamath River groups, and populations from these two areas had the lowest average heterozygosities (0.027–0.045; Utter et al. 1989, App. A) of any populations included in the study. Utter et al. (1989) predicted that additional genetic surveys would ultimately reveal divergent frequencies of alleles in the two areas. If such differences were not found in more extensive studies, alternate explanations for this apparent similarity would be required.

This paper retests and rejects the null hypothesis of no genetic difference between these two groups based on two recently published studies, which sample several new populations and an additional 15 polymorphic loci. Comparison of results for the new studies shows the formerly-indistinguishable chinook salmon populations of the Klamath and Snake River to be quite distinct, with a mean genetic distance between populations of each river (0.014) that is double that of the maximum within-group genetic distance. In addition to resolving the anomalous apparent similarity between these chinook salmon populations of these geographically separated areas, the new results illustrate the care that must be used in drawing inferences from negative data.

Table 1

Collection data for samples of chinook salmon *Oncorhynchus tshawytscha* from the Klamath (K1–K10; Bartley et al. 1992) and Snake (S1–S11; Waples et al. 1991) Rivers. Samples from hatchery stocks are marked by a dagger (†); other samples were from naturally spawning populations. Locations included in the study of Utter et al. (1989) are indicated by an asterisk (*). Run timing indicates the season of entry of adults into freshwater.

Map code	Location	Run timing	Sample size
Klamath River			
K1	Omagar Creek	Fall	100
K2	Blue Creek	Fall	100
K3	Camp Creek	Fall	106
K4	Horse Linto Creek	Fall	100
K5	S. Fork Trinity River	Fall	100
*K6	Trinity River†	Fall	120
K7	Upper Salmon River	Fall	98
K8	Shasta River	Fall	100
K9	Bogus Creek	Fall	128
K10	Iron Gate Hatchery†	Fall	99
Snake River			
*S1	Valley Creek	Spring	99
*S2	Sawtooth Hatchery†	Spring	100
S3	Salmon River	Spring	99
S4	Marsh Creek	Spring	100
*S5	Johnson Creek	Summer	97
*S6	McCall Hatchery†	Summer	100
S7	Secesh River	Summer	92
*S8	Rapid River Hatchery†	Spring	100
S9	Imnaha River	Summer	100
S10	Imnaha Hatchery†	Summer	100
S11	Lostine River	Spring	100

Materials and methods

Our analyses used the data from Bartley et al. (1992) for Klamath River populations and Waples et al. (1991) for Snake River populations; comparisons also were made with earlier data from Utter et al. (1989). Sampling locations included 10 areas from the Klamath River and 11 from the Snake River drainages (Table 1, Fig. 1). Samples of juvenile fish from hatcheries and naturally-spawning populations were collected between 1986 and 1989 for the Klamath River, and 1989 and 1990 for the Snake River. Starch gel electrophoresis for all three studies followed procedures described by Aebersold et al. (1987). The data used in these analyses were part of a larger baseline dataset used by management agencies to help determine natal origins of chinook salmon harvested in mixed-stock fisheries (Shaklee and Phelps 1990).

Genetic nomenclature and abbreviations followed a system suggested by Shaklee et al. (1989). Data were collected from 21 enzyme systems and 30 presumptive gene loci that were polymorphic in at least one of the populations (Tables 2,3). The observed polymorphisms were attributed to 26 disomic loci and 2 isolocus pairs (*sAAT-1,2** and *sMDH-B1,2**; see Allendorf and Thorgaard 1984). A single, average allele frequency was computed for each isolocus pair for purposes of comparing populations.

Genetic data were analyzed using the BIOSYS program of Swofford and Selander (1981). Analyses included calculation of unbiased pairwise genetic distances between populations (Nei 1978), unweighted pair group method (UPGM) projection of a matrix of these distances (Sneath and Sokal 1973), average heterozygosities, and the number of alleles per locus.

Results and discussion

Our analyses focused on a comparison of genetic characteristics between chinook salmon from the Klamath and Snake Rivers. Discussion of population structure within these two areas appears elsewhere, as do more

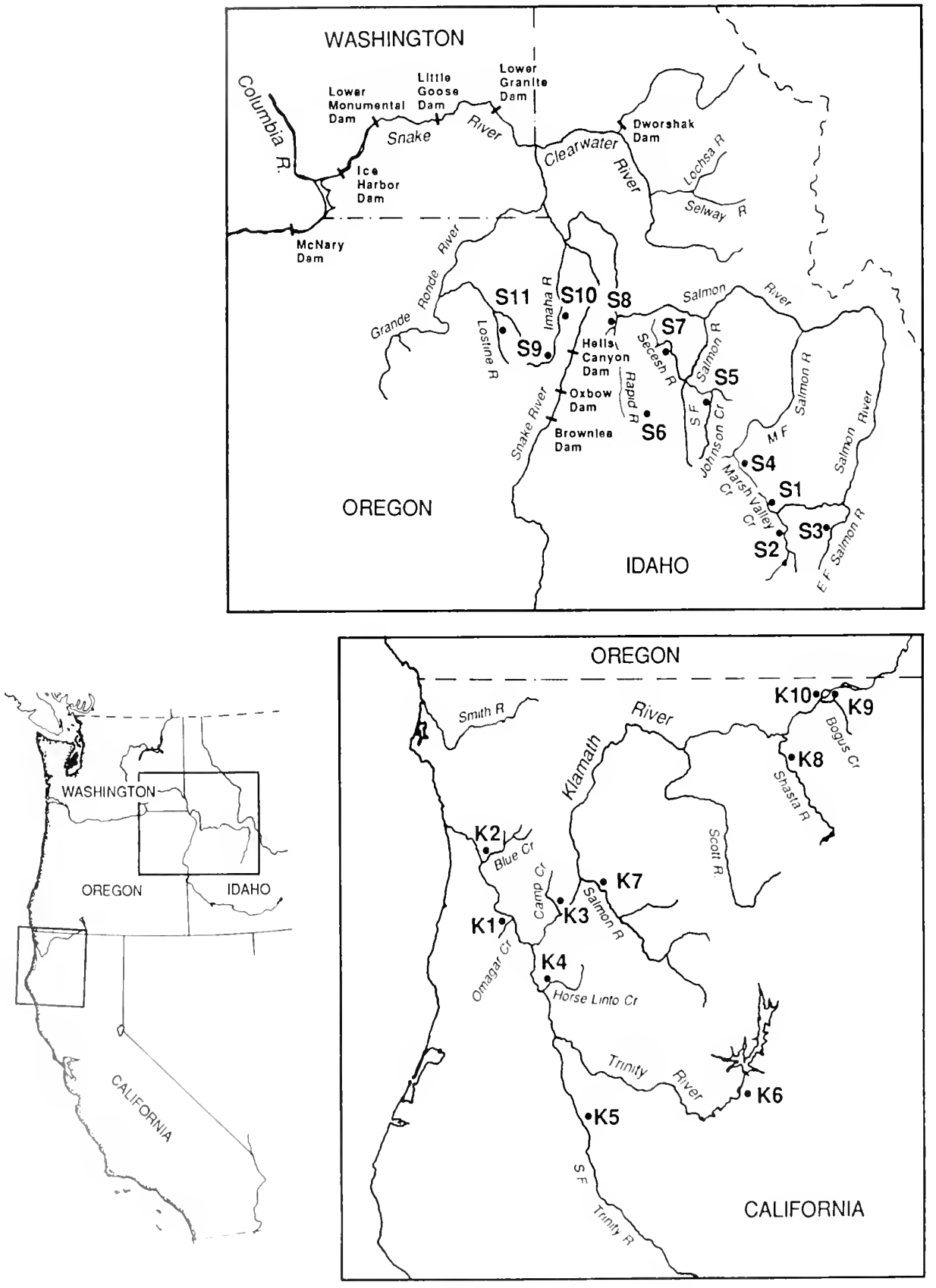

Figure 1

Sampling locations of chinook salmon *Oncorhynchus tshawytscha* in the Klamath and Snake River drainages. See Table 1 for names of locations.

Table 2

Enzymes and loci examined (enzyme nos. in parentheses) of chinook salmon *Oncorhynchus tshawytscha*.

Enzyme	Locus	Enzyme	Locus
Aspartate aminotransferase (2.6.1.1)	*sAAT-1,2**	Tripeptide aminopeptidase (3.4.11.4)	*PEPB-1**
	*sAAT-3**	Leucine-tyrosine dipeptidase (3.4.–.–)	*PEP-LT**
	*sAAT-4**	Malate dehydrogenase (1.1.1.37)	*sMDH-B1,2**
Adenosine deaminase (3.5.4.4)	*ADA-1**		*mMDH-1**
Alcohol dehydrogenase (1.1.1.1)	*ADH*4*		*mMDH-2**
Aconitate hydratase (4.2.1.3)	*sAH-1**	Malic enzyme (1.1.1.40)	*sMEP-1**
	*mAH-4**	Mannose-6-phosphate isomerase (5.3.1.8)	*MPI**
Glyceraldehyde-3-phosphate dehydrogenase (1.2.1.12)	*GAPDH-3**	Phosphogluconate dehydrogenase (1.1.1.44)	*PGDH**
Dipeptidase (3.4.13.11)	*PEPA**	Phosphoglycerate kinase (2.7.2.3)	*PGK-2**
Glutathione reductase (16.4.2)	*GR**	Phosphoglucomutase (2.7.5.1)	*PGM-2**
Hydroxyacylglutathione hydrolase (3.1.2.6)	*HAGH**	L-Iditol dehydrogenase (1.1.1.14)	*IDDH-1**
Isocitrate dehydrogenase (1.1.1.42)	*sIDHP-1**	Superoxide dismutase (1.15.1.1)	*sSOD-1**
	*sIDHP-2**	Triose-phosphate isomerase (5.3.1.1)	*TPI-4**
Lactate dehydrogenase (1.1.1.27)	*LDH-B2**		
	*LDH-C**		

Table 3

Range of common allele frequencies in samples of chinook salmon *Oncorhynchus tshawytscha* from the Snake and Klamath Rivers reported in three investigations. Parenthetical entries summarize data from studies (2) and (3), respectively, for those populations studied in (1). Subset (A) are loci common to all studies; subset (B) are isolocus pairs unique to study (1); subset (C) are loci newly resolved in studies (2) and (3).

		(1) Utter et al. 1989		(2) Waples et al. 1991	(3) Bartley et al. 1992	
	Locus	Snake	Klamath	Snake	Klamath	
(A)	*sAAT-1,2**	0.981–1.000	0.995–1.000	0.957–1.000 (0.957–1.000)	1.000	(1.000)
	*sAAT-3**	0.994–1.000	0.995–1.000	0.965–1.000 (0.980–1.000)	0.985–1.000	(0.985–1.000)
	*ADA-1**	0.953–0.969	1.000	0.846–1.000 (0.894–1.000)	0.995–1.000	(1.000)
	*sAH-1**	0.994–1.000	0.995–1.000	0.985–1.000 (0.990–1.000)	0.940–1.000	(0.940–1.000)
	*PEPA**	0.994–1.000	0.990–1.000	0.995–1.000 (0.995–1.000)	0.770–1.000	(0.930–1.000)
	*GR**	1.000	0.995–1.000	0.995–1.000 (0.985–1.000)	0.995–1.000	(1.000)
	*LDH-B2**	0.972–1.000	1.000	0.970–1.000 (0.970–0.995)	1.000	(1.000)
	*LDH-C**	0.976–1.000	1.000	0.920–1.000 (0.920–1.000)	0.890–1.000	(0.980–1.000)
	*PEPB-1**	0.944–0.976	0.949–0.990	0.904–0.985 (0.904–0.985)	0.860–1.000	(0.980–1.000)
	*sMDHB-1,2**	0.995–0.998	0.997–1.000	0.942–0.997 (0.944–0.990)	0.993–1.000	(0.997–1.000)
	*MPI**	0.910–0.953	0.975–0.990	0.770–0.990 (0.884–0.990)	0.860–1.000	(0.970–0.992)
	*PGK-2**	0.062–0.139	0.146–0.350	0.065–0.187 (0.065–0.187)	0.148–0.400	(0.148–0.320)
	*sSOD-1**	0.944–0.976	0.895–0.990	0.885–0.980 (0.939–0.980)	0.755–0.992	(0.845–0.992)
(B)	*sIDHP-1,2**	0.913–0.937	1.000	—	—	
	*PGM-1,2**	1.000	0.942–0.990	—	—	
(C)	*TPI-4**	—	—	0.825–0.955	0.995–1.000	
	*sAAT-4**	—	—	0.919–1.000	0.985–1.000	
	*ADH**	—	—	0.985–1.000	1.000	
	*mAH-4**	—	—	0.985–1.000	0.775–1.000	
	*GAPDH-3**	—	—	1.000	0.871–1.000†	
	*HAGH**	—	—	0.902–1.000	1.000	
	*sIDHP-1**	—	—	0.783–0.950	0.992–1.000	
	*sIDHP-2**	—	—	0.945–1.000	0.900–1.000	
	*PEP-LT**	—	—	0.870–0.985	0.985–1.000	
	*mMDH-1**	—	—	0.995–1.000	0.795–1.000	
	*mMDH-2**	—	—	0.490–0.800	0.905–1.000	
	*sMEP-1**	—	—	0.010–0.079	0.150–0.465	
	*PGDH**	—	—	1.000	0.910–1.000	
	*PGM-2**	—	—	1.000	0.860–1.000	
	*IDDH-1**	—	—	0.897–1.000	0.990–1.000	

† Data from Gall et al. 1989

complete details of the individual studies. (Bartley et al. 1992, Waples et al. 1991).

Variability within populations

The levels of genetic variation within populations were evaluated using only the loci found to be polymorphic. Because this restriction does not represent a random sample of gene loci, values reported here are applicable only for comparisons among populations included in this study or with other studies using the same set of loci. Indices of genetic variability were consistently slightly higher in the Snake River samples; the average number of alleles per locus was 1.63 vs. 1.51 for the Klamath River, and the average heterozygosity was 0.079 vs. 0.065 ($0.05>p>0.01$ in both instances, based on Mann-Whitney tests). Heterozygosities ranged from 0.058 to 0.090 in the Snake River populations and were less uniform in the Klamath River groups, where both the lowest (0.039 in Shasta River) and the highest (0.126 in Omagar Creek) values were found. Neither of these latter two populations were represented in the initial study of the Klamath River by Utter et al. (1989). The actual heterozygosity values reported here are higher than those reported by Utter et al. (1989), primarily because a number of new, very polymorphic systems are included in the more recent analyses. Nevertheless, Utter et al. (1989) also found a slightly higher average heterozygosity in Snake River spring-run and summer-run chinook salmon (0.035–0.045) than in those from the Klamath River (0.027–0.032). Based on the new data, Waples et al. (1991) concluded that, in comparison with other Columbia River populations, Snake River spring-run and summer-run chinook salmon have somewhat reduced levels of genetic variability, but that the difference is apparently not as large as suggested by earlier studies (Utter et al. 1989, Winans 1989).

Variability between regions

Allele frequency distributions differed substantially between the two regions at a number of gene loci. Although three or more alleles were found at some of these loci, most of the important differences were reflected in differing frequencies of the common allele (Table 3). Particularly large differences were found at *mMDH-2** and *sMEP-1** (Fig. 2); for these loci, the range of allele frequencies was nonoverlapping between regions, with substantially higher frequencies of the common (i.e., *100**) allele found in the Klamath River samples at both loci.

Genetic differences between the two regions based on data for all 30 loci are summarized in a phenogram resulting from clustering of pairwise genetic distances

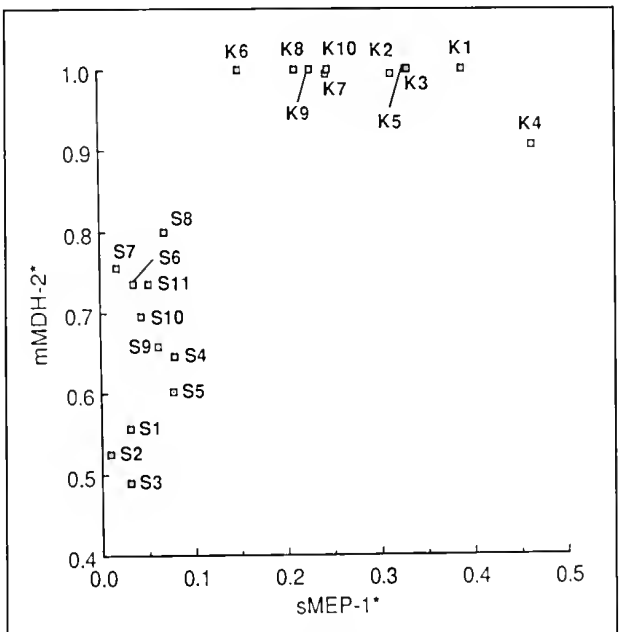

Figure 2

Plot of frequencies of common alleles of Klamath (K) and Snake (S) River populations of chinook salmon *Oncorhynchus tshawytscha* at the *mMDH-2** and *sMEP-1** loci.

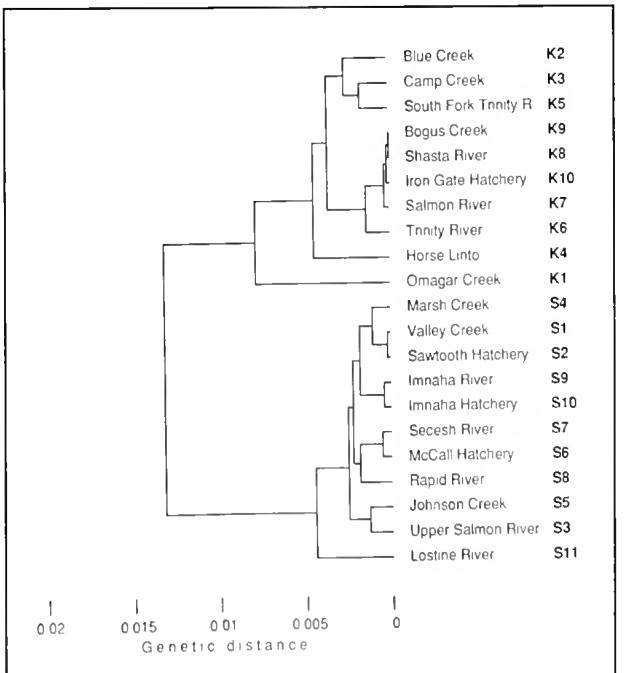

Figure 3

UPGM projection of Nei's genetic distances between Klamath and Snake River populations of chinook salmon *Oncorhynchus tshawytscha*.

(Fig. 3). The Snake and Klamath River populations are separated by a mean genetic distance of 0.014, whereas the within-river separations average 0.004 and 0.007,

respectively. The present data, then, clearly identify two genetically-distinct groups on the basis of the 30 polymorphic loci that were examined.

This genetic distinction clearly rejects a hypothesis of a recent common ancestry for populations of these regions. The topography of the clustering within Klamath and Snake River groups and the relative genetic distance between them are very similar to those distinguishing Klamath River populations from other genetically-distinct population groups of California and the Oregon Coast based on a similar set of polymorphic loci (Bartley et al. 1992).

Comparison with previous information

Because the clear separation of Snake and Klamath River populations reported here contrasts sharply with the minimal differences detected between these groups by Utter et al. (1989), an examination of results from that earlier study is warranted. A direct comparison of the original study with the two more recent studies is complicated by (1) the addition of a number of new gene loci in the more recent studies, (2) the greater discriminatory capabilities for some loci used in the newer studies, and (3) the more extensive sampling of populations in the newer studies. A comparison of the 15 loci common to both the original and more recent studies was made for the five Snake River sampling sites (S1, S2, S5, S6, S8) and two Klamath River sites (K6, K10) that were sampled in both investigations. In general, very similar allele frequencies were found at most loci in the two sets of samples (Table 3). None of the allele frequency differences between the original and the more recent studies exceeded 0.06 (at *PEPA** in the Klamath River comparisons). Thus, the more recent samples confirm the minimal differences between the two regions reported by Utter et al. (1989) based on the loci and populations originally examined.

The improved resolution in the more recent studies, therefore, can be attributed to an increase in the number and type of usable genetic characters. Particularly important was the addition of 15 gene loci not included in the earlier study (Table 3). Although regional differences are strongest at *mMDH-2** and *sMEP-1**, clear contrasts between the regions are also seen at five other loci (*mAH-4**, *GAPDH-3**, *HAGH**, *PEP-LT**, and *TPI-4**). In addition, the more recent studies resolve individual loci that had previously been considered isolocus pairs, which further enhanced the discriminating power of two genetic systems. This effect was most apparent for the enzyme IDH. Utter et al. (1989), as have other previous studies (e.g., Utter et al. 1987), reported variation for the isolocus pair *sIDHP-1,2**; subsequently, Shaklee et al. (1990) showed that it is possible to resolve the two loci individually. Whereas the most extreme frequency difference between the two regions at *sIDHP-1,2** was 0.087 (1.0–0.913; Table 3) in the original study, the maximum difference at *sIDHP-1** in the newer studies was 0.217 (1.0–0.783). Similarly, the protocol of Gall et al. (1989) for partitioning variation at the *PGM-1,2** isolocus increased the discriminatory power of this genetic system.

General implications of the results

During the 1960s, the newly found capability to resolve numerous genetic systems exhibiting Mendelian inheritance led to a flood of studies that continues to this day (see Lewontin 1991). Protein electrophoresis has been used extensively in fishery research and management (Utter 1991); such data have proven particularly useful in modifying previously held assumptions about the genetic structure of fish species (Allendorf et al. 1987). The results discussed here are instructive with regard to both the power and the limitations of such information.

The power of Mendelian data lies in the identification of genetic differences among individuals, populations and species. The regional differences among populations of North American chinook salmon originally described by Utter et al. (1989) have also been apparent in subsequent studies (Bartley and Gall 1990, Waples et al. 1991, Bartley et al. 1992). These differences have generally been interpreted to reflect more recent ancestries of populations within a particular genetically-defined region than between populations of different regions.

However, in spite of the power of electrophoretic data to detect genetic differences when present, there are limits to the conclusions that one can draw from the failure to detect such differences. That is, although a finding of a statistically-significant allele frequency difference may provide evidence that gene flow is restricted (or that some other evolutionary force is operating), the inability to identify such differences does not prove that genetic differences do not exist. The present example, in which genetically divergent groups were not well distinguished in a previous study, emphasizes the potential significance of this limitation. Although Utter et al. (1989) hypothesized that the apparent similarity between Klamath and Snake River chinook salmon was a coincidence that did not reflect a common ancestral origin, the distinctness of the two groups could not be demonstrated until new data became available. The situation is analogous to a classical genetic comparison between populations of *Drosophila pseudoobscura* from Berkeley, California and Bogata, Colombia, in which an initial apparent genetic similarity was puzzling in view of the exten-

sive geographic separation of the two regions (Lewontin and Hubby 1966). A subsequent study that found previously-unknown genetic variants (Singh et al. 1976) demonstrated clear genetic differences between populations of each region.

The important message here is to beware of the danger of drawing positive conclusions from negative data. It should also be emphasized that problems of this nature are not confined to genetic data; rather, the limitations of nondiscriminatory information (i.e., the power to reject the null hypothesis) should be considered in evaluating any kind of comparative data for two or more samples.

Similar allele frequencies among samples, then, support but do not confirm hypotheses that the samples are drawn from a common breeding group. This well-established principle requires restatement from time to time (e.g., Utter 1981, Waples 1991). Such awareness serves to safeguard against a premature conclusion of identity for groups that are distinct and thus may be subject to different management criteria.

In these instances it is important to recognize the power of Mendelian data involving multiple polymorphic loci to detect differences between populations when they do exist. For example, assuming that most allozyme variation is neutral, it will take populations that are divided into large units a considerable amount of time before significant divergence will occur. Thus, Atlantic herring *Clupea harengus* populations of the eastern and western Atlantic Ocean that have likely been isolated for thousands of years could not be distinguished because of similar allele frequencies at a number of polymorphic loci (Grant 1984). The observed value for Wright's (1943) fixation index (F_{st}) of 0.0042 approximates an F_{st} value of 0.003 expected for neutral markers among populations of effective size of 1 million individuals separated over 3000 generations (Nei and Chakravarti 1977). Such dynamics preclude genetic distinction of these herring populations through neutral genetic markers (and thus rejection of the null hypothesis) even with very large samples of loci and individuals. Under such circumstances, other criteria (e.g., tagging data) are needed to determine whether one or more populations is being sampled.

Finally, we note the complementary nature of relationships among populations indicated by many phenotypic traits on one hand and by most molecular genetic markers on the other hand. A strong selective component appears to be involved in the maintenance of phenotypic traits such as timings of spawning and migration (e.g., Ricker 1972, Helle 1981); consequently, relationships inferred from such traits tend to reflect relative similarities in adaptations among populations. Conversely, the apparent absence of strong selection at most electrophoretically detectable loci permits the estimation of relative degrees of gene flow within and among regions (e.g., Chakraborty et al. 1978, Allendorf and Phelps 1981), and such estimations provide useful insights about ancestral relationships. In view of the complementary nature of these different categories of genetic information, adequate sets of both molecular markers (for clarifying ancestral relationships) and phenotypic traits (for identifying adaptive differences within lineages) should be included in genetic surveys of a particular species whenever possible. Such adaptive differences have been noted within a number of apparent ancestral groupings of chinook salmon, including both spring- and fall-spawning migrations within the Klamath River populations of the species (Utter et al. 1989).

Acknowledgments

Research funded in part through contract DE-AI79-89BP0091 with Bonneville Power Administration.

Citations

Aebersold, P., G. Winans, D. Teel, G. Milner, and F. Utter
1987 Manual for starch gel electrophoresis: A method for the detection of genetic variation. NOAA Tech. Rep. NMFS 61, 19 p.

Allendorf, F., and S. Phelps
1981 Use of allelic frequencies to describe population structure. Can. J. Fish. Aquat. Sci. 38:1507–1514.

Allendorf, F., and G. Thorgaard
1984 Tetraploidy and the evolution of salmonid fishes. *In* Turner, B (ed.), Evolutionary genetics of fishes, p. 1–53. Plenum Press, NY.

Allendorf, F., N. Ryman, and F. Utter
1987 Genetics and fishery management: Past, present, and future. *In* Ryman, N., and F. Utter (eds.), Population genetics and fishery management, p. 1–20. Wash. Sea Grant Prog., Univ. Wash. Press, Seattle.

Bartley, D., and G. Gall
1990 Genetic structure and gene flow in chinook salmon populations of California. Trans. Am. Fish. Soc. 119:55–71.

Bartley, D., B. Bentley, J. Brodziak, R. Gomulkiewicz, M. Mangel, and G.A.E. Gall
1992 Geographic variation in population genetic structure of chinook salmon from California and Oregon. Fish. Bull., U.S. 90:77–100 (authorship amended per errata, Fish. Bull. 90(3):iii).

Chakraborty, R., P. Fuerst, and M. Nei
1978 Statistical studies on protein polymorphism in natural populations: II. Gene differentiation between populations. Genetics 88:367–390.

Gall, G.A.E., B. Bentley, C. Panattoni, E. Childs, C. Qi, S. Fox, M. Mangel, J. Brodziak, and R. Gomulkiewicz
1989 Chinook mixed fishery project 1986–1989. Report of the Department of Animal Science and the Department of Applied Mathematics, Univ. Calif., Davis, under Interagency Agreement C-1335 with Calif. Dep. Fish & Game, 192 p.

Grant, W.
1984 Biochemical population genetics of Atlantic herring. Copeia 1984:357–364.

Helle, J.
1981 Significance of the stock concept in artificial propagation of salmonids in Alaska. Can. J. Fish. Aquat. Sci. 38: 1665–1671.

Lewontin, R.
1991 Electrophoresis in the development of evolutionary genetics: Milestone or millstone? Genetics 128:657–662.

Lewontin, R., and J. Hubby
1966 A molecular approach to the study of genetic heterozygosity in natural populations. II. Amount of variation and degree of heterozygosity in natural populations of *Drosophila pseudoobscura*. Genetics 54:595–609.

Nei, M.
1978 Estimation of average heterozygosity and genetic distance from a small number of individuals. Genetics 89: 583–590.

Nei, M., and A. Chakravarti
1977 Drift variances of F_{st} and G_{st} statistics obtained from a finite number of isolated populations. Theor. Popul. Biol. 11:307–25.

Ricker, W.
1972 Hereditary and environmental factors affecting certain salmonid populations. *In* Simon, R., and P. Larkin (eds.), The stock problem in Pacific salmon, p. 19–161. H.R. MacMillan Lectures in Fisheries, Univ. Brit. Col., Vancouver.

Shaklee, J., and S. Phelps
1990 Operation of a large-scale, multiagency program for genetic stock identificiation. *In* Parker, N.C., et al. (eds.), Fish marking techniques, p. 817–830. Am. Fish. Soc. Symp. 7, Bethesda.

Shaklee, J., and C. Tamaru
1981 Biochemical and morphological evolution of Hawaiian bonefishes (*Albula*). Syst. Zool. 30:125–146.

Shaklee, J., F. Allendorf, D. Morizot, and G. Whitt
1989 Genetic nomenclature for protein-coding loci in fish: Proposed guidelines. Trans. Am. Fish. Soc. 118:218–227.

Shaklee, J., C. Busack, A. Marshall, M. Miller, and S. Phelps
1990 The electrophoretic analysis of mixed-stock fisheries of Pacific salmon. *In* Ogita, Z.I., and C.L. Markert (eds.), Isozymes: Structure, function, and use in biology and medicine, p. 235–265. Wiley-Liss, NY.

Singh, R., R. Lewontin, and A. Felton
1976 Genetic heterogeneity within electromorphic alleles of xanthine dehydrogenase in *Drosophila pseudoobscura*. Genetics 84:609–629.

Sneath, P., and R. Sokal
1973 Numerical taxonomy. W.H. Freeman, San Francisco, 573 p.

Swofford, D., and R. Selander
1981 BIOSYS-1--A FORTRAN program for the comprehensive analysis of electrophoretic data in population genetics and systematics. J. Hered. 72:281–283.

Utter, F.
1981 Biological criteria for definition of species and distinct intraspecific populations of salmonids under the U.S. Endangered Species Act of 1973. Can. J. Fish. Aquat. Sci. 38: 1626–1635.
1991 Biochemical genetics and fishery management: An historical perspective. J. Fish. Biol. 39(Suppl. A):1–18.

Utter, F., D. Teel, G. Milner, and D. McIsaac
1987 Genetic estimates of stock compositions of 1983 chinook salmon, *Oncorhynchus tshawytscha*, harvest off the Washington coast and the Columbia River. Fish. Bull., U.S. 85:13–23.

Utter, F., G. Milner, G. Ståhl, and D. Teel
1989 Genetic population structure of chinook salmon in the Pacific Northwest. Fish. Bull., U.S. 87:238–264.

Waples, R.
1991 Pacific salmon and the definition of "species" under the Endangered Species Act. Mar. Fish. Rev. 53(3):11–22.

Waples, R., D. Teel, and P. Aebersold
1991 A genetic monitoring and evaluation program for supplemented populations of salmon and steelhead in the Snake River Basin. Annu. Rep. Res., Contract DE-A179-89BP00911, U.S. Dep. Energy, 50 p. (Avail. Bonneville Power Admin., P.O. Box 3621, Portland OR 97208.)

Winans, G.
1989 Genetic variability in chinook salmon stocks from the Columbia River Basin. N. Am. J. Fish. Manage. 9:47–52.

Wright, S.
1943 Isolation by distance. Genetics 28:114–138.

Differentiating *Paralithodes* larvae using telson spines: A tail of two species*

Gregory C. Jensen
Helle B. Andersen
David A. Armstrong
School of Fisheries WH-10, University of Washington, Seattle, Washington 98195

Identification of larvae belonging to closely related species of decapod Crustacea is frequently dependent upon few (often single) morphological characters. Since larvae used in descriptions are often the offspring from a single captive, very little is known about how intraspecific variability may affect the ability to differentiate species. Two congeneric decapods whose zoeae are separated on the basis of a single morphological character are the red king crab (RKC) *Paralithodes camtschaticus*, and blue king crab (BKC) *P. platypus*. Larvae of these commercially-important species are distinguished from each other by the number of spines or processes on the telson, RKC having 7 pairs of spines and BKC 8 pairs, excluding a minute seta (Sato 1958, Haynes 1984). However, when viewed together there are other apparent differences: BKC zoeae have proportionately shorter rostrums and carapace spines, larger bodies at each stage, and larger eyes.

During the course of extensive plankton sampling for king crab larvae in Herendeen Bay within Port Moller, Alaska, considerable variability in telson morphology was noted. A large proportion of zoeae resembling BKC were captured having an asymmetrical pattern of 8+7 telson spines, while others, also appearing to be BKC in other respects, had only 7 pairs; such interspecific character overlap had not been noted with these two species near the Pribilof Islands, Alaska (Armstrong et al. 1985). To confirm the identity of these zoeae and provide additional characters to separate the two species, several measurements were taken on specimens from Herendeen Bay and the Pribilof Islands to establish a stronger, more quantitative basis to distinguish these larvae.

* Contribution 867 of the School of Fisheries, University of Washington.

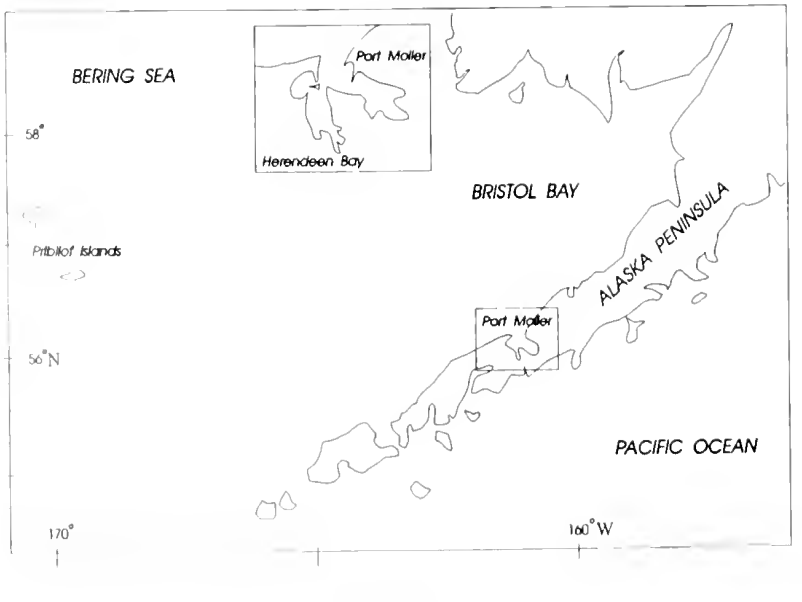

Figure 1
Locations of *Paralithodes* spp. zoeae collections.

Materials and methods

Paralithodes zoeae were collected near the Pribilof Islands, Alaska, in May 1983 and April 1984, and from Herendeen Bay, Alaska (Fig. 1) in May and June of 1990, using either a 505 μm mesh Tucker trawl or a 60 cm bongo net with a mesh of 333 or 505 μm. Samples were preserved in 5% buffered formalin in seawater and later sorted for target species, which were transferred to a solution of 70% ethanol and 5% glycerol. The number of telson spines (excluding a minute seta) was recorded for each specimen, and three measurements were taken: tip of rostrum to the anteriormost edge of the eye ("rostrum length"), anterior edge of eye to the tip of the posteriolateral carapace spines ("carapace length"), and the longest dimension of the eye ("eye length," Fig. 2). Damaged or distorted specimens were not used for measurements, but spine counts were recorded. A total of 608 larvae were measured; 371 from Herendeen Bay and the remainder from around the Pribilof Islands. The ratios of rostrum length to carapace length were plotted against carapace length for "normal" (i.e., 7+7 telson spine RKC and 8+8 BKC)

Manuscript accepted 1 July 1992.
Fishery Bulletin, U.S. 90:778–783 (1992).

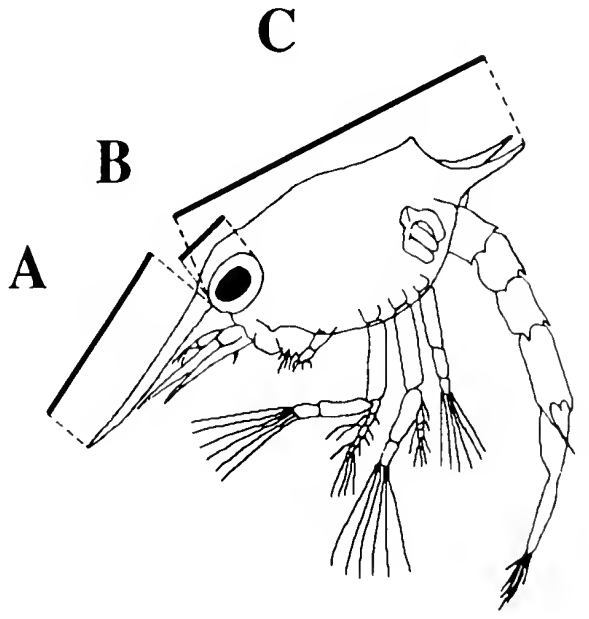

Figure 2
Measurements taken from *Paralithodes* spp. zoeae. (A) rostrum length, (B) eye length, (C) carapace length.

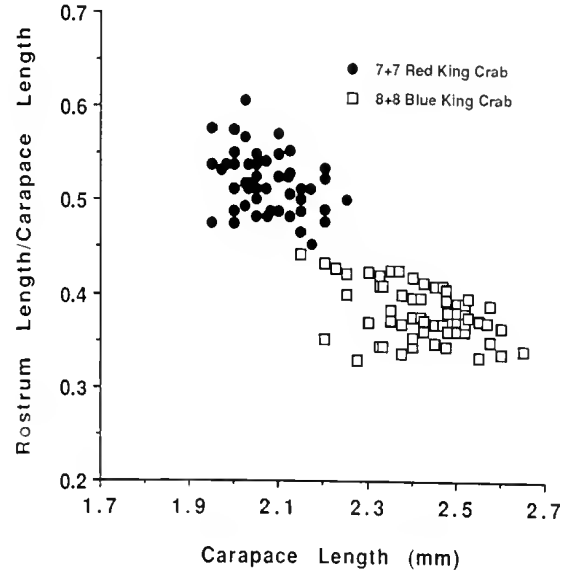

Figure 3
Ratios of rostrum length/carapace length for first-stage *Paralithodes* spp. collected near the Pribilof Islands, Alaska.

zoeae of both species in the two areas. Those with an anomalous number of spines (8+7 and "BKC" with 7+7) were then similarly plotted for comparison.

Unless otherwise indicated, data are presented as mean ±1 standard deviation. ANOVAs were used to test for significant differences ($\alpha \leq 0.05$) between the means of different groups, and the means compared using Tukey's T method. A two-way ANOVA was used to examine intraspecific variation in zoeae I between the two areas.

Results

Plotted ratios of rostrum length/carapace length for Pribilof Island specimens fell into two distinct clouds representing those thought to be RKC (longer rostrum) and BKC (Fig. 3). These were not so clearly separated in the samples from Herendeen Bay; nevertheless, all those with an asymmetric telson spine pattern or a short rostrum, large body, and spine count of 7+7 fell within the cloud of 8+8 BKC larvae (Fig. 4). These larvae were designated as BKC and divided into groups based on number of telson spines. The ratios for all of these groups were significantly different ($p<0.05$) at each zoeal stage from the means for RKC zoeae; Figure 5 shows combined results for both species at the two locations. Both the carapace and eyes of BKC larvae were significantly longer than those of RKC at all

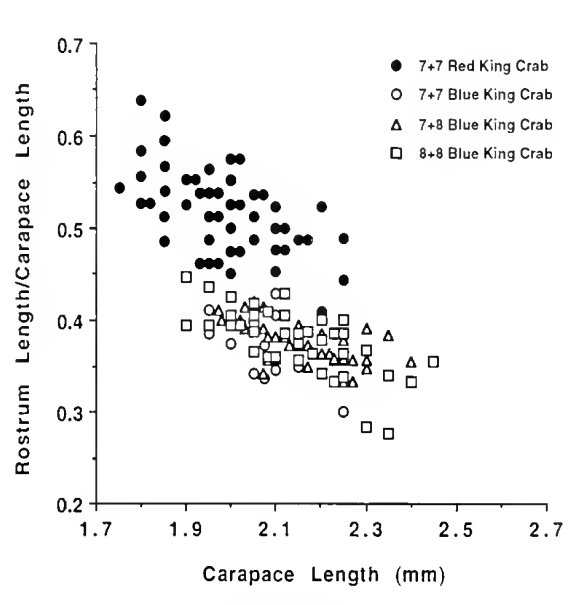

Figure 4
Ratios of rostrum length/carapace length for first-stage *Paralithodes* spp. zoeae collected from Herendeen Bay, Alaska.

stages, but these differed considerably between the two areas. Two-way ANOVA revealed no significant difference in rostrum/carapace length ratio for zoeae-I BKC from the two areas, but significantly smaller

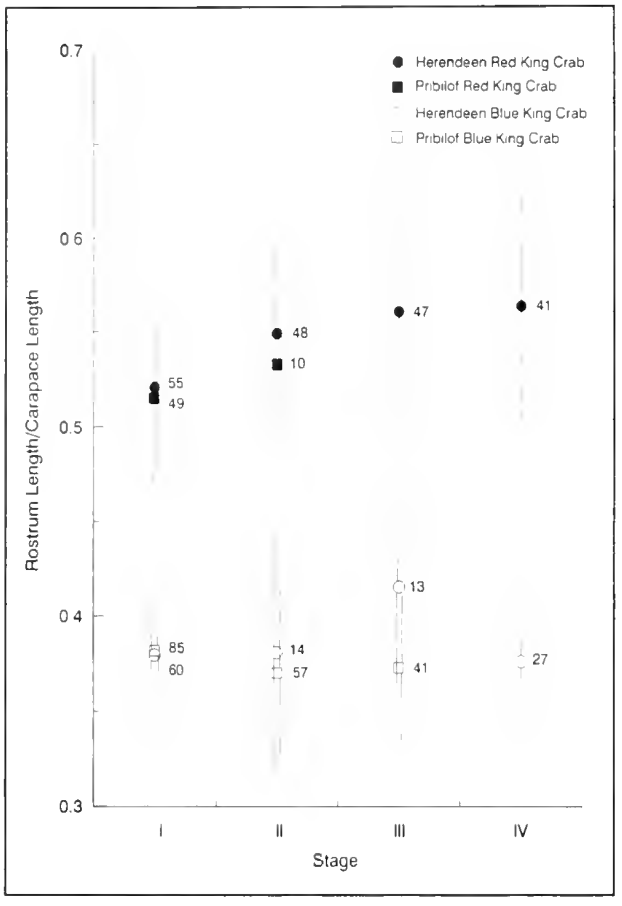

Figure 5

Paralithodes spp. rostrum length/carapace length by stage. Values are mean ratios (± 1 SD); numbers are the number of zoeae measured for each value.

eyes for Herendeen Bay BKC, suggesting that eye length is not reliable for distinguishing the two species. No intraspecific differences between areas were detected for either rostrum/carapace length or eye length for RKC.

The mean eye length of RKC larvae was significantly less ($p<0.05$) at each stage than the means of all groupings of BKC. In addition, the mean of the 7+7 zoeae-I BKC was significantly less than those with 8+8 (Fig. 6). BKC larvae from Herendeen Bay showed great variation in number of telson spines. Only 45.9% of all BKC larvae had a spine count of 8+8, the majority having some other combination of 7, 8, or 9 spines on each side of the telson. In contrast, the majority of BKC zoeae from the Pribilof Islands (84%) had a spine count of 8+8 (Fig. 7). RKC larvae showed little variation in telson spines, with only 0.9% of the zoeae from Herendeen Bay and 3.2% from the Pribilof Islands deviating from the count of 7+7.

Discussion

BKC zoeae are generally distinguished from RKC zoeae by the presence of an additional pair of inner spines on the telson (Fig. 8A,B), and for king crab zoeae collected near the Pribilof Islands this was a reliable character for separating the two species. Only 3.2% of the RKC zoeae collected from this area deviated from the 7+7 pattern. Even though 16% of the BKC zoeae differed from 8+8, this difference was almost invariably in the form of an extra 1 or 2 inner spines, making confusion with RKC unlikely. BKC zoeae were visibly much larger as confirmed by their greater carapace length, and had shorter rostrums and larger eyes.

A substantially different pattern was apparent in samples from Herendeen Bay, where 42% of zoeae-I BKC were missing one spine from the telson (Fig. 8C) and an additional 18% missing two spines (Fig. 8D). Because the missing spines are the innermost of the two pairs, those remaining tend to be considerably longer than the single pair in RKC; yet as Figure 8D

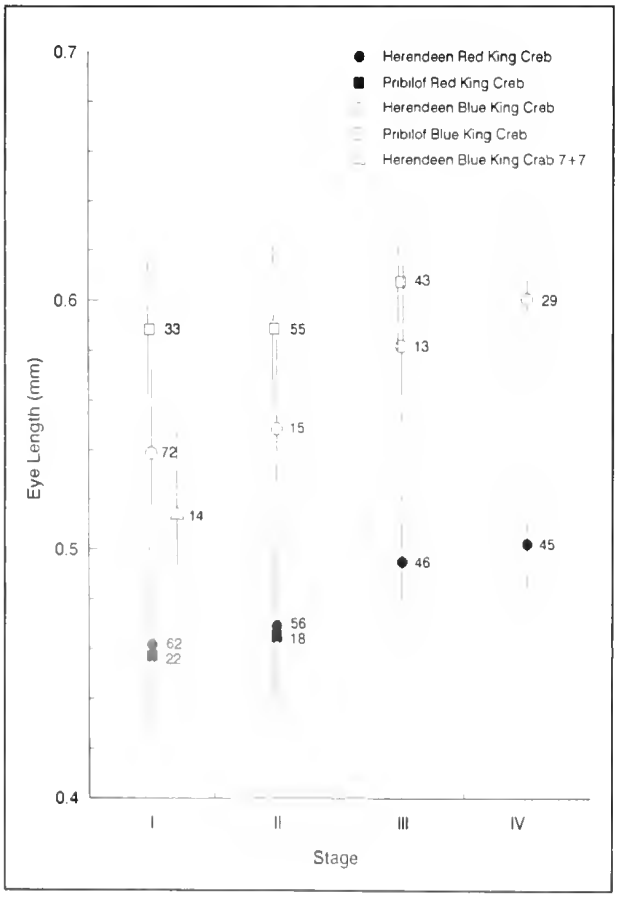

Figure 6

Mean eye length (± 1 SD), and number of *Paralithodes* spp. zoeae measured.

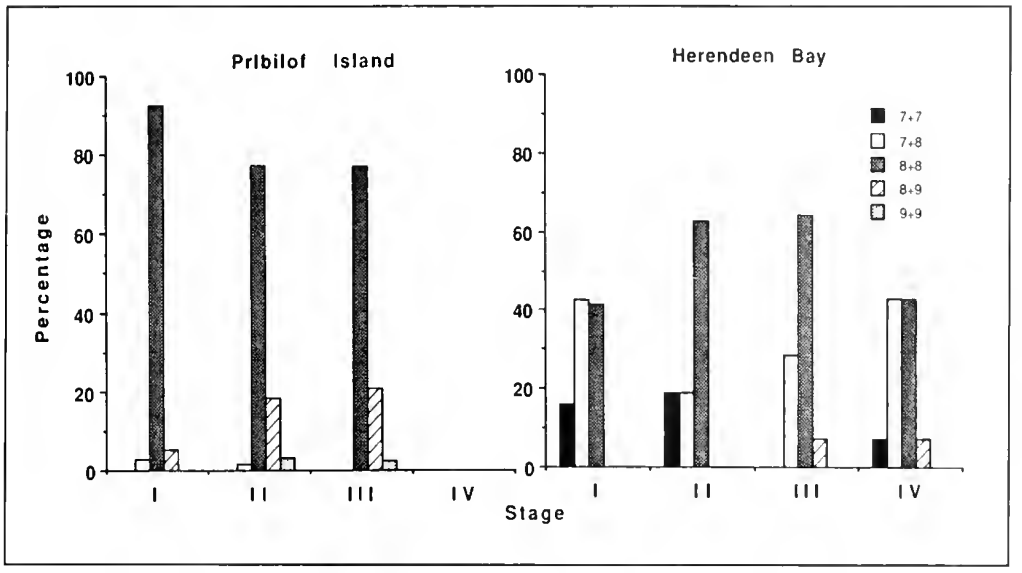

Figure 7
Number of telson spines of *Paralithodes platypus* zoeae collected from the Pribilof Islands and Herendeen Bay.

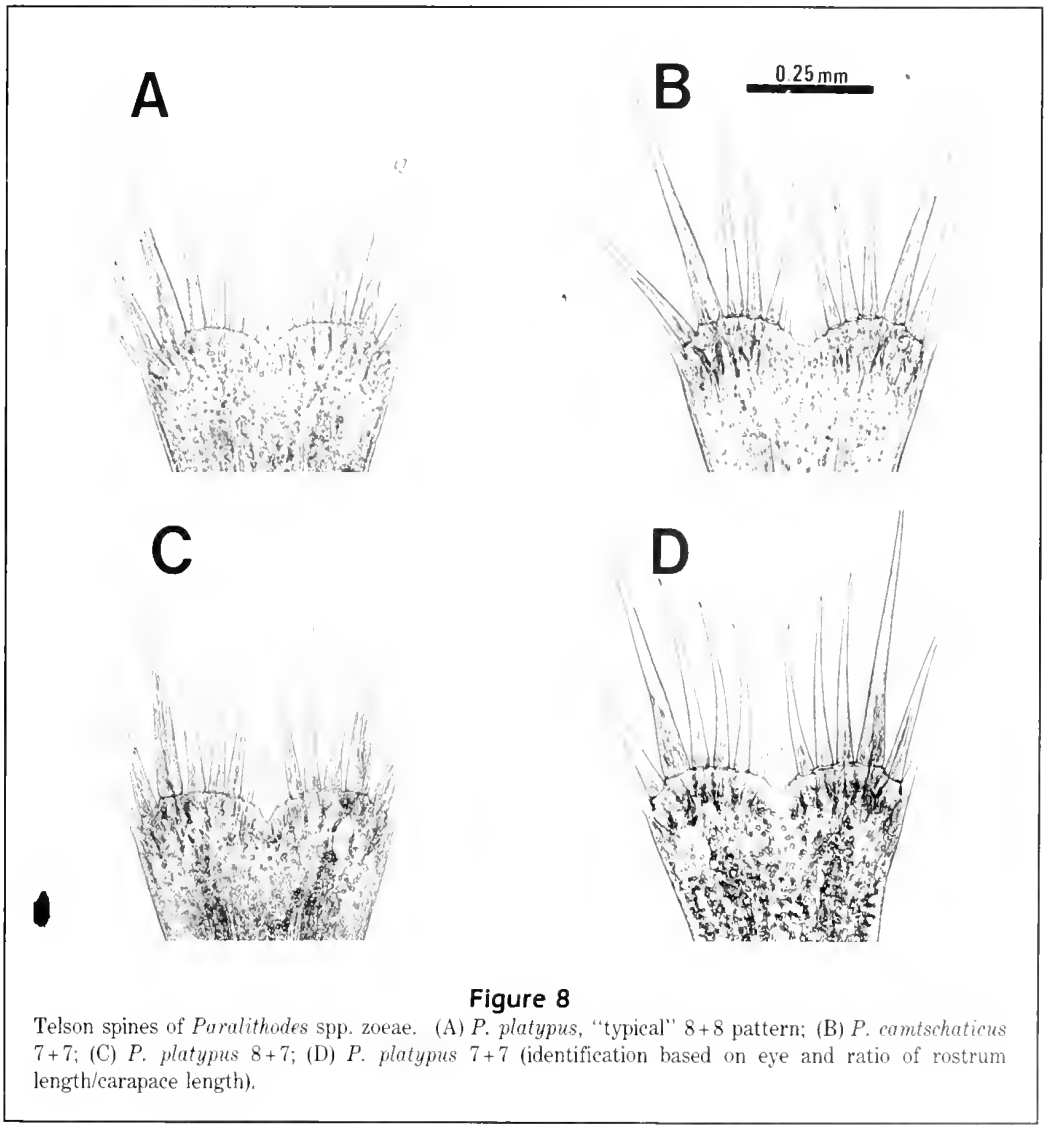

Figure 8
Telson spines of *Paralithodes* spp. zoeae. (A) *P. platypus*, "typical" 8+8 pattern; (B) *P. camtschaticus* 7+7; (C) *P. platypus* 8+7; (D) *P. platypus* 7+7 (identification based on eye and ratio of rostrum length/carapace length).

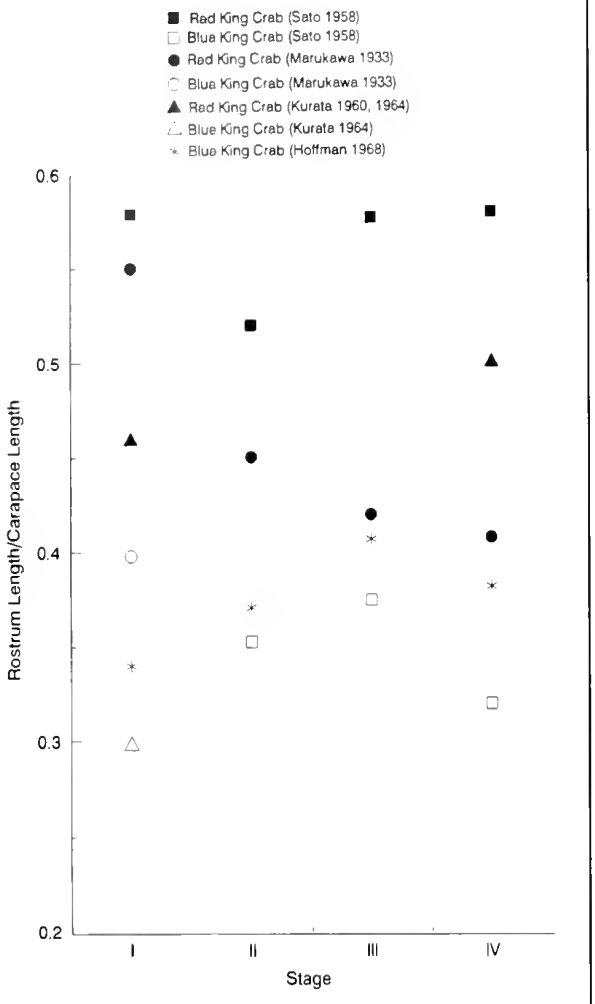

Figure 9
Rostrum/carapace length ratios of *Paralithodes* spp. zoeae taken from published illustrations.

shows, this difference is sometimes negligible. However, BKC were readily distinguished from RKC by their proportionately shorter rostrums, larger eyes, and larger bodies, but the differences were not as great as those seen in the Pribilof Islands. Zoeae in both locations appeared to gain additional telson spines with larval stage, a pattern noted previously for other lithodid larvae by Kurata (1964). While rostrum length alone was not reliable for separating the two species (due to intraspecific variation between the two areas), the proportion of rostrum length to carapace length remained constant and appears to be a useful method of differentiating the two. Whether this is reliable in other areas is not known, but it is consistent with illustrations in published descriptions of the two species (Fig. 9).

Of particular interest is the intraspecific variability exhibited both between the two areas and within the population in Herendeen Bay. While there were no significant differences between populations of RKC, all linear measurements of BKC zoeae from Herendeen Bay averaged 10–12% smaller than those of conspecifics from the Pribilof Islands. The cause of this variation is not known, but environmental factors such as temperature can affect both the number of decapod larval stages (Knowlton 1974) and their morphology (Shirley et al. 1987). Temperatures differed considerably between the two areas at the time of larval collection. At the Pribilof Islands in May 1983 the water was 2–4°C, and −1–1.5°C in April 1984 (Armstrong et al. 1985). In Herendeen Bay larvae stayed above a 40m thermocline in water 2.5–8.5°C, and developmental times were exceptionally fast (Wainwright et al. 1991).

BKC have an extremely disjunct distribution (Somerton 1985), and it is also possible that size differences could be related to their reproductive isolation. But although local environmental features or isolation may explain differences between the two populations, they are unlikely to account for the variation seen within the relatively small scale of Herendeen Bay. The eyes of BKC zoeae having a 7+7 spine pattern were intermediate in length between the 8+8 or 8+7 BKC larvae and RKC from Herendeen Bay (Fig. 7). The cause of such differences cannot be known without appropriate experiments and genetic studies, but the recent report of an adult RKC-BKC hybrid from the Sea of Okhotsk (Nizyayev 1991) raises the possibility that some interbreeding may occur within the confines of Herendeen Bay.

Because all larvae were collected from the plankton rather than hatched in captivity, we cannot state unequivocally that these differences in spine count are due to intraspecific variation of BKC rather than a mixture of other lithodid species. However, megalopae, juveniles, and adults of RKC and BKC were collected within Herendeen Bay during the course of this study; despite extensive trawling, pot fishing, dredging, and intertidal surveys, the only other lithodid found was *Hapalogaster grebnitzkii*. Larvae matching the description for *H. grebnitzkii* were also the only other lithodid zoeae occurring in the plankton samples. The large size, shape, and position of the posterolateral carapace spines, coupled with a lack of carapace sculpturing, readily distinguish RKC and BKC zoeae from other described species of Bering Sea lithodids. We believe it is extremely unlikely that the variation is due to a fourth, undescribed species.

No single character for reliably separating BKC and RKC zoeae was observed, but since the number of telson spines is useful for differentiating the two species in some areas (e.g., Pribilof Islands), we suggest using this count along with the rostrum/carapace

length ratio until the extent of character overlap is known. A ratio of >0.45 (RKC) or <0.45 (BKC) usually distinguished the species in our samples from both areas. Eye measurements, like spine counts, vary with area but can be useful when the rostrum or carapace is damaged or distorted. In our samples the overlap in telson spine counts was greatest in zoeae I, but fortunately this was the stage when the two species could be most reliably distinguished by the proportion of rostrum to carapace length.

Acknowledgments

We thank Mike McGurk and Dave Warburton of Triton, Ltd., for their help in the field, and Trent McDonald, Pam Wardrup, and Tom Wainwright for suggestions and advice. This study was funded by Minerals Management Service of the Department of the Interior, through an interagency agreement with the National Oceanic and Atmospheric Administration, Department of Commerce, as part of the Alaska Outer Continental Shelf Environmental Assessment Program (OCSEAP).

Citations

Armstrong, D.A., J.L. Armstrong, R. Palacios, G. Williams, G.C. Jensen, and W. Pearson
1985 Early life history of juvenile blue king crab, *Paralithodes platypus*, around the Pribilof Islands. *In* Melteff, B.R. (ed.), Proceedings of the international king crab symposium, p. 211–229. Rep. 85-12, Univ. Alaska Sea Grant Prog., Fairbanks.

Haynes, E.B.
1984 Early zoeal stages of *Placetron wosnessenskii* and *Rhinolithodes wosnessenskii* (Decapoda, Anomura, Lithodidae) and review of lithodid larvae of the northern North Pacific Ocean. Fish. Bull., U.S. 82:315–324.

Hoffman, E.G.
1968 Description of laboratory-reared larvae of *Paralithodes platypus* (Decapoda, Anomura, Lithodidae). J. Fish. Res. Board Can. 25:439–455.

Knowlton, R.E.
1974 Larval developmental processes and controlling factors in decapod Crustacea, with emphasis on Caridea. Thalassia Jugosl. 10:138–158.

Kurata, H.
1960 Last stage zoea of *Paralithodes* with intermediate form between normal last stage zoea and glaucothoe. Bull. Hokkaido Reg. Fish. Res. Lab. 22:49–56 [in Jpn., Engl. synop.].
1964 Larvae of decapod Crustacea of Hokkaido. 6. Lithodidae (Anomura). Bull. Hokkaido Reg. Fish. Res. Lab. 29:49–65 [in Jpn., Engl. summ.].

Marukawa, H.
1933 Biological and fishery research on Japanese king-crab *Paralithodes camtschatica* (Tilesius). J. Imp. Fish. Exp. Stn. 4, 152 p. [in Jpn., Engl. abstr.].

Nizyayev, S.A.
1991 Finding of a hybrid crab specimen with the characters of *Paralithodes camtschatica* and *P. platypus* in the Sea of Okhotsk. Zool. Zh. 9:128–131 [in Russ., Engl. summ.].

Sato, S.
1958 Studies on larval development and fishery biology of king crab, *Paralithodes camtschatica* (Tilesius). Bull. Hokkaido Reg. Fish. Res. Lab. 17:1–102 + plates [in Jpn., Engl. summ.].

Shirley, S.M., T.C. Shirley, and S.D. Rice
1987 Latitudinal variation in the Dungeness crab, *Cancer magister*: Zoeal morphology explained by incubation temperature. Mar. Biol. (Berl.) 95:371–376.

Somerton, D.A.
1985 The disjunct distribution of blue king crab, *Paralithodes platypus*, in Alaska: Some hypotheses. *In* Melteff, B.R. (ed.), Proceedings of the international king crab symposium, p. 13–21. Rep. 85-12, Univ. Alaska Sea Grant Prog., Fairbanks.

Wainwright, T.C., D.A. Armstrong, H.B. Andersen, P.A. Dinnel, D.W. Herren, G.C. Jensen, J.M. Orensanz, and J.A. Shaffer
1991 Port Moller king crab studies: Annual report. Fish. Res. Inst. Rep. FRI-UW-9203, Univ. Wash., Seattle, 38 p.

A telemetric study of the home ranges and homing routes of lingcod *Ophiodon elongatus* on shallow rocky reefs off Vancouver Island, British Columbia

Kathleen R. Matthews

Pacific Southwest Research Station, U.S. Forest Service
Box 245, Berkeley, California 94701

Lingcod *Ophiodon elongatus* are an important commercial and recreational fish in the northeast Pacific (Miller and Geibel 1973, Cass et al. 1990). In some areas lingcod show serious population declines. In Washington, after signs of depletion, the fishery was closed in central Puget Sound for 5 years (1978–83) to allow rebuilding (Buckley et al. 1984). Currently in central Puget Sound, the now tightly-restricted fishery allows only recreational use, a 6-week opening, and a daily limit of 1 fish. Similarly in British Columbia, landings and average size of the catch have declined and tighter regulations imposed (Richards and Hand 1991). Because of lingcod declines, it is crucial to understand their life-history characteristics in order to determine possible causes of decline and to help recovery efforts. One area of uncertainty regarding lingcod life history is their movement behavior.

Despite a number of studies of lingcod movements (Miller and Geibel 1973, Mathews and La Riviere 1987, Jagielo 1990, Smith et al. 1990), many questions remain about their movement patterns. Most studies describe lingcod as sedentary (Miller and Geibel 1973, Mathews and La Riviere 1987, Smith et al. 1990); yet lingcod do make migrations, and movement up to 385km has been documented (Mathews and La Riviere 1987, Jagielo 1990). Although not verified through tagging, it is thought that most lingcod movements, including possible homing behavior, are related to spawning. Female lingcod may seasonally leave deeper reefs and move inshore to lay demersal eggs that the shallower living males guard. There is indirect evidence for the inshore movement of females; an increase of larger gravid females in the inshore catch occurs during fall months just prior to spawning (Miller and Geibel 1973).

Furthermore, some studies have indicated the homing behavior of lingcod, similar to many rocky reef fishes (Hart 1943, Williams 1957, Carlson and Haight 1972, Matthews 1990); i.e., when fish move away for any reason (including spawning, experimental displacement, etc.) they will return to areas previously occupied (Gerking 1959). In an early study in Canada, 4 of 14 displaced lingcod returned 9.7km to original capture sites (Hart 1943). Additional evidence of lingcod homing behavior came from an attempt to enhance overfished areas by transplanting lingcod (Buckley et al. 1984). None of the transplanted lingcod were resighted at the release area (i.e., the enhancement was unsuccessful), whereas nine of the transplanted lingcod were caught close to the original capture site (190km from release site).

Lingcod movement behavior has implications for enhancement efforts and habitat management. Attempts to rebuild populations in overfished areas by transplanting lingcod from areas of higher abundance would be unsuccessful if lingcod simply returned to their original home sites. Furthermore, movement information is valuable because if lingcod preferentially home to certain reefs, then those reefs could be designated as management reserves. Thus, any new knowledge of lingcod homing will lead to a better understanding of their movement behavior and the effect of rehabilitation efforts. The objectives of this pilot study were to use ultrasonic tagging to (1) describe home ranges and movements of lingcod on rocky reefs, and (2) determine the homing routes of displaced lingcod.

Methods

Study sites

The study was conducted during April 1990 off eastern Gabriola Island on the eastern side of Vancouver Island, British Columbia (Fig. 1). The area is characterized by extensive shallow rocky reefs and pinnacles. Depths encountered during ultrasonic tracking were in the range 3–35m. Two reef areas were chosen for the tracking work: Gabriola reefs and Valdes reefs (each is actually a series of small, separate reefs) (Fig. 1). Both reefs are approximately 15–30m deep, although shallower areas were sometimes encountered. Although bullkelp *Nereocystis leutkeana* is present on these reefs during the summer and fall, no surface kelp was present during this April study.

Ultrasonic tagging

The transmitters (48×15mm, 18g in air, 8.3g in seawater) were ex-

Manuscript accepted 29 July 1992.
Fishery Bulletin, U.S. 90:784–790 (1992).

ternally attached using methods used for tuna (Holland et al. 1985). The nylon loop on the transmitter anchored one inelastic pull tie, with another tie wrapped around the tag's opposite end. The two pull ties were inserted through the dorsal musculature and cinched down to prevent the transmitter from dangling.

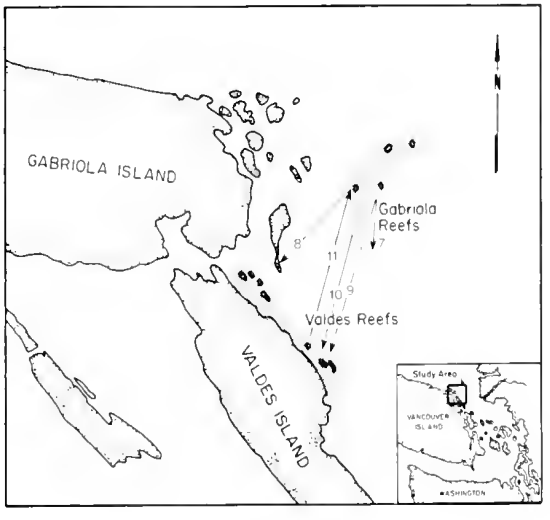

Figure 1
Map of study area and general displacement directions for *Ophiodon elongatus* fish nos. 7–11. Fish were captured and displaced in the direction shown by arrow.

Lingcod were captured on hook-and-line, placed in a seawater-filled cooler, and anesthetized (methomidate hydrochloride). After tags were attached, lingcod were allowed to recover in fresh (without anesthetic) seawater prior to release. Fish appeared completely recovered from the anesthetic and tagging procedure ~5–10 min after tagging.

Eleven transmitters with replaceable batteries (Vemco V3-1H-R pingers, Vemco Ltd., Nova Scotia, Canada B3L 4J4) were operated at five crystal-controlled frequencies: 50.0 (2 tags), 60.0 (2 tags), 65.54 (3 tags), 69.0 (2 tags), and 76.8 (2 tags) kHz, corresponding to pre-set channels on the Vemco VR-60 receiver. Tags assigned to the same channel were easily differentiated by their unique pulse period, which was automatically decoded and displayed by the receiver. To locate the transmitters, a Vemco V-10 directional hydrophone was employed from a small boat. Once a tag was located, the boat's position was determined, using LORAN-C readings, depth, and visual compass bearings of four charted features (buoys, lights, etc.), in the study area on an almost daily basis (one of 21 tracking days was missed due to boat breakdown) for the life of the transmitter (21 d battery life). One reason this study area was chosen was the presence of several flashing lights and buoys which made navigation and location determination easier, especially at night.

During 5–27 April 1990, 11 lingcod (57.0–80.6 cm total length, TL) were tagged and monitored (Table 1).

Table 1
Summary of total lengths and duration of tracking of lingcod *Ophiodon elongatus* equipped with ultrasonic transmitters in the Strait of Georgia, British Columbia, and monitored 5–27 April 1990 to measure home ranges and homing routes. Nocturnal movement occurred 24:00–06:00.

Tag no.	Sex	Length (TL cm)	Date tracking began	Duration (d)	Nondisplaced lingcod home ranges			
Controls								
1	Female	67.5	4/5/90	20	Captured and released at Valdes reefs			
2	Male	62.1	4/5/90	16	Captured and released at Valdes reefs			
3	Male	59.5	4/9/90	19	Captured and released at Valdes reefs			
4	Male	69.8	4/8/90	15	Captured and released at Gabriola reefs			
5	Female	80.6	4/9/90	12	Captured and released at Gabriola reefs			
6	Female	68.4	4/9/90	15	Captured and released at Gabriola reefs			
					Displaced lingcod homing routes			
					Distance moved (km)	Total time to return (h)	Movement rate (m/h)	Nocturnal movement rate (m/h)
Experimentals								
7	Male	66.2	4/12/90	14	1.0	40	25	83.3
8	Male	57.0	4/16/90	12	2.2	Did not return		
9	Male	64.0	4/19/90	9	2.8	60	48	233.3
10	Male	64.5	4/23/90	5	2.8	35	80	233.3
11	Male	69.5	4/25/90	3	2.8	33	85	233.3

Up to seven tagged fish were deployed within the study area at one time. One procedure was conducted on two rocky reefs to determine the home ranges of lingcod during the day, night, and periods of strong current which were predicted up to 14.8km/h (8.0kn) (Canadian tide and current tables, Canadian Hydrographic Service 1990). Six lingcod were captured, tagged, released, and monitored at the original point of capture, either Gabriola reefs area or Valdes reefs. Their geographic locations were determined on an almost daily basis (the only exception being 18 April) for the duration of the tag battery life.

To determine the homing routes of displaced lingcod, five males were captured, tagged, and displaced up to 2.8km in two opposite directions (Fig. 1). Four of the five displaced fish were moved south, while one fish was moved north. Because there was no information on the time required for lingcod to home, the first fish was moved a short distance (1km) to allow enough time to track its homeward movement. Of the remaining four lingcod, one was displaced 2.2km, and three were displaced 2.8km. The movements were then monitored almost continuously, with occasional rest breaks, until the transmitter batteries expired. Displaced fish were individually tracked because they required continuous monitoring. When the displaced fish were first released, an attempt was made to stay with the fish for several hours to detect any homeward movement.

The field schedule started with two teams each working 12h on the boat for a full 24h coverage. After the first few days of field work, we changed the schedule to devote our efforts to covering nighttime lingcod movement (16:00–08:00). The entire study covered 21 tracking days during 5–27 April (only 18 April was canceled due to boat problems) for a total of 336 tracking hours. When the nondisplaced fish were first released, an entire day was spent tracking those fish. Subsequently, each fish was periodically (about 15–20 times/tracking day) checked for its position, which allowed several tagged fish to be concurrently monitored. The five displaced fish were followed one at a time to ensure that their homing route could be detected.

On two separate dates, I conducted scuba observations to search for tagged lingcod and to collect information not available through telemetry. When a signal cannot be located, it was impossible to determine whether the tag battery has died or the fish has left the area; hence, I searched underwater for two tagged fish in their last recorded location after the signal could no longer be detected. Also, to determine the accuracy of telemetric locations, I used scuba observations to compare underwater positions of tagged fish with those provided by telemetry. Once the directional hydrophone positioned the boat directly over the tag's signal I then anchored the boat, descended, and searched for the tagged fish.

Results

Nondisplaced fish (controls)

The six lingcod (three females and three males) tagged and released at Gabriola and Valdes reefs were generally found close to release sites during the day, night, and periods of swift current. When relocated, the six lingcod were essentially in the same position (latitude–longitude differences were within 0.01–0.02 nmi, which is the normal resolution of the LORAN unit). Thus, there was no detectable difference in their home range size. Fish were monitored for 12–20d ($\bar{x}$ 16.2+2.9d) until the tag batteries expired.

These telemetry findings were verified by visual (scuba) resightings of two tagged lingcod. After determining the position of an ultrasonic tag, I later (within a few minutes) observed the tagged fish sitting on the bottom. These visual sightings also verified that the tags were still attached to the fish. Furthermore, after the signal had apparently died on two tagged fish, I searched underwater and saw the two tagged lingcod in their last recorded telemetry position.

The six individual lingcod were also monitored on six separate nights when the current ranged from slack to 10.4km/h (5.6kn) for a total of 50h of nighttime observation. Home ranges were similar to those observed in the day. However, signals were louder suggesting that the fish were out in the open, i.e., not under a rock (Matthews et al. 1990).

Displaced fish (experimentals)

The five displaced lingcod remained close to release sites and did not move for several hours following release (Figs. 2–6). These first few hours (both during the day and night) following release may be a recovery period in response to capture, handling, and tagging. Subsequently, four of the five displaced fish moved back to the capture site. Each fish had returned to the capture site by the end of the second night following release. Return trips were confined to the immediate vicinity of the Gabriola and Valdes Islands study area.

The four homing lingcod (nos. 7, 9–11) remained near the release site for 4–6h and returned to home sites in 33–60h (Figs. 2–5). These four fish started their homeward movements at night (20:30–06:00), and movement terminated once it became light at ~06:00.

No clear pattern was detected in the homeward movement, as lingcod did not appear to follow obvious features such as depth contours or currents. Homing lingcod traversed depths of 5–35m. Occasionally the

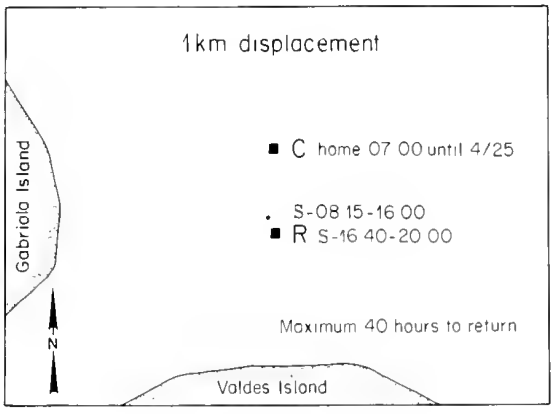

Figure 2
Positions of *Ophiodon elongatus* fish no. 7 (66.2 cm male) captured from site C, moved 1 km south to release site R, and monitored 12–25 April. S = stationary.

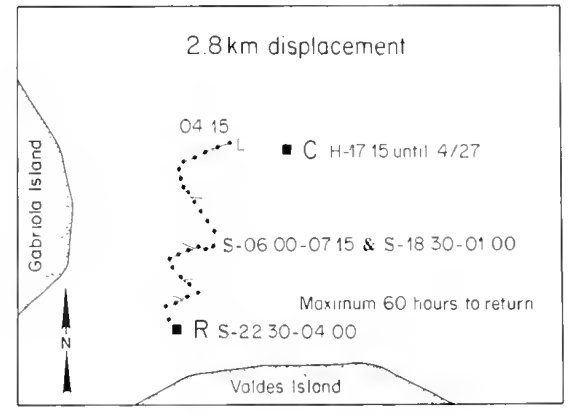

Figure 3
Positions of *Ophiodon elongatus* fish no. 9 (64.0 cm male) captured from site C, moved 2.8 km south to release site R, and monitored 19–27 April. S = stationary, L = temporarily lost.

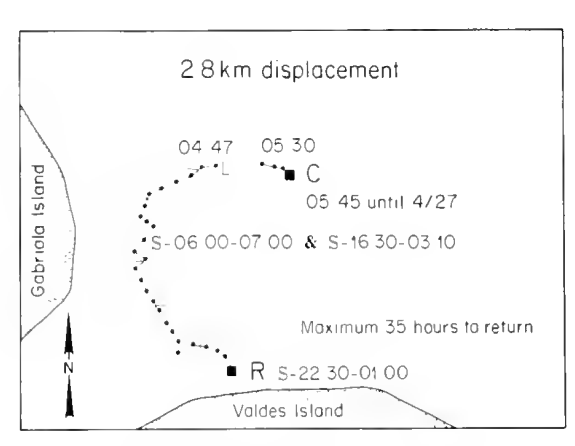

Figure 4
Positions of *Ophiodon elongatus* fish no. 10 (64.5 cm male) captured from site C, moved 2.8 km south to release site R, and monitored 23–27 April. S = stationary, L = temporarily lost (04:47–05:30).

signals became quite strong, suggesting homing lingcod were traversing areas without much rock relief. Lingcod encountered the deepest water (35 m) when crossing open areas. The four lingcod returned to their original capture sites where they remained until the transmitter batteries died or the tracking project was completed.

The first displaced fish (no. 7, a 66.2 cm male) was caught on 12 April in 10 m of water, moved 1 km south, and released in 18 m of water (Fig. 2). Because this was the first release and I did not know what movement to expect, I stayed directly over the fish from release time (16:40) until 20:30. However, no movement was detected. When I returned the following morning (07:30), the fish had moved about halfway (500 m, Fig. 2) back to the capture site. I stayed with the fish from 07:30 to 16:30, but no additional movement was detected. When tracking resumed the following morning (07:00), the fish was back at the original capture site where it remained for 12 d (until 25 April) when the battery apparently died. This fish moved at least 1 km, the displacement distance, in ~40 h. Because all homeward movement of the fish apparently occurred at night, the remaining displaced fish were tracked at night.

Fish no. 9 (64.0 cm male) was captured on 19 April in 12 m of water, tagged and moved 2.8 km south, and released into water 18 m deep (Fig. 3). It was stationary from release at 22:30 until 04:00 when it moved in a northerly direction for 2 h and stopped. Tracking was terminated at 07:15; when it reconvened at 18:30, the fish was in the same location. At 01:00 it moved to the northwest and the northeast until 04:30 when its signal was lost. Tracking was terminated at 08:30, and when it resumed at 17:15 the fish was back at the capture site. I assumed that the fish homed between 04:30 (when the signal was lost) and daybreak because all other lingcod movement occurred at night. It remained at the capture site for 7 days until tracking ended on 27 April. The 2.8 km return trip was completed in less than 60 h.

Fish no. 10 (64.5 cm male) was captured in 10 m of water, tagged and displaced 2.8 km south, and released in water 18 m deep (Fig. 4). The fish was stationary for 2.5 h after release (22:30–01:00) and moved sporadically from 01:00 to 06:00. The fish was stationary from 06:00 to 07:00 when tracking ended. When tracking

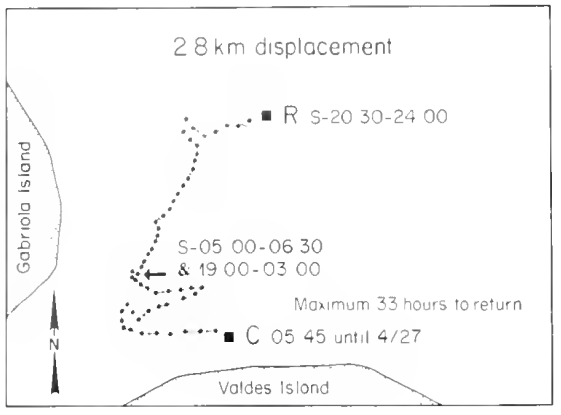

Figure 5
Positions of *Ophiodon elongatus* fish no. 11 (69.5 cm male) captured from site C, moved 2.8 km north to release site R, and monitored 25–27 April. S = stationary.

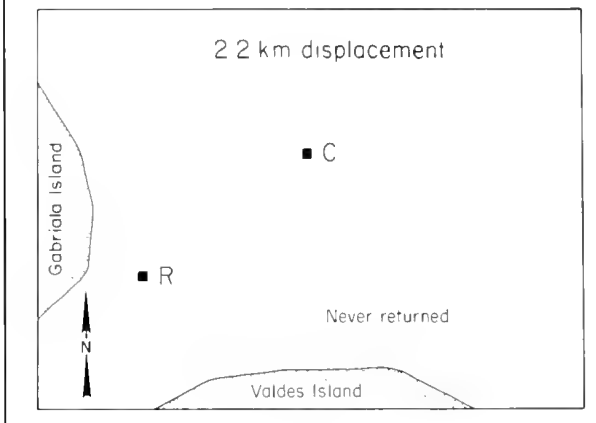

Figure 6
Positions of *Ophiodon elongatus* fish no. 8 (57.0 cm male) captured from site C, moved 2.2 km south to release site R, and monitored 16–27 April.

reconvened at 16:30, the fish was in the same position where it remained until 03:15. It then moved from 03:15 to 04:47 when the signal was temporarily lost. When relocated at 05:30, it was followed back to the capture site (05:30–05:45). It was at this site 4 days later that tracking stopped. The 2.8 km return trip took about 35 h.

Fish no. 11, a 69.5 cm male, was captured in 15 m of water, tagged and displaced 2.8 km to the north, and released in 12 m of water (Fig. 5). The fish remained stationary from release (20:30) until 24:00, when it moved to the west and south until 05:00. It remained at this position until tracking ended at 06:30. Later that day, the fish was relocated in the same location where it remained until 03:00. At this time the fish moved southeast and southwest and reached its original capture site at 05:45. It remained there until 27 April when tracking ended. The 2.8 km return trip took ~33 h.

One fish did not return from displacement. Fish no. 8, a 57.0 cm male was caught, tagged, and transplanted 2.2 km (Fig. 6) to the release site. Tracking continued for 12 d, during which time the fish apparently remained at the release site and no movement was detected. Because I was unable to make scuba observations at this site, it is possible that the tag was shed, which would also result in a stationary signal.

Lingcod took 33–60 h to return from their 1.0–2.8 km displacements for an average homing speed of 59.5 m/h (Table 1). Actually, their movement rate was faster since they moved only at night. If averaged over the total period when movement was documented (6 h, 24:00–06:00) for two consecutive nights (total of 12 h) then the rates are 83.3–233 m/h ($\bar{x}$ 195.8 m/h or 1175.0 m/d).

Discussion

Similar to intertidal fishes (Williams 1957) and several species of rockfishes (Carlson and Haight 1972, Matthews 1990), lingcod are another rocky reef fish capable of homing. Ultrasonic tracking is limited by low sample sizes due to tag cost and labor-intensive tracking. This study represents the first attempt to use ultrasonic telemetry to research lingcod movement behavior, but this was limited to displaced males soon after their nesting season. Additional work is necessary to determine whether males behave differently (e.g., do not home) at other times of the year. Telemetry would also be valuable to determine whether females make inshore-offshore movements to relocate previously used areas.

Lingcod movement occurred at night (24:00–06:00, Figs. 3–5) sometimes under dark, moonless skies. Little work has been done on fish vision in cold-temperate water systems (see review in Loew and McFarland 1990). Nevertheless, water at night is darker and has lower visibility than during the day, and as Ebeling and Bray (1976) point out, "...the relatively turbid, temperate waters are often a dark and gloomy place at night." Moreover, during our April tracking study, most nights were overcast and rainy, further reducing the water's visibility. The low visibility at night presumably precludes lingcod from using visual landmarks which usually requires precise recognition of specific features such as coral heads or rocks (Hasler 1966, Reese 1989). Still, an important question remains: Why should lingcod move at night when visibility is better during the day? Perhaps their nocturnal movement is to avoid predation since lingcod some-

times crossed flat, open areas that had no hiding places. Locally, harbor seals feed on lingcod, and recently their numbers have dramatically increased (Olesiuk et al. 1990). On the other hand, perhaps lingcod are simply more active at night, as my nighttime home-range observations indicated, which would explain their nighttime movement.

Lingcod homing was fairly directional and confined to the immediate area of Gabriola Island. In contrast, when displaced shorter distances (500 m), copper and quillback rockfishes, which co-occur with lingcod, moved along a bimodal northwest–southeast axis and sometimes retraced that path before finally moving in a westerly direction that led to their home site (Matthews 1990). After displacement, initial movement of lingcod was in the homeward direction only, i.e., no back-and-forth movement between the release site and home site was observed. The more direct and nocturnal homing in lingcod suggests they are navigating rather than orienting along one compass course or relying on olfactory cues. Orientation can be ruled out (Baker 1978, Able 1980) because lingcod successfully homed from north and south displacements. It is currently unknown whether rocky-reef fish, including lingcod, recognize olfactory cues.

Lingcod homing was fast in comparison with copper and quillback rockfishes, which took 8–25 d to return from 500 m displacements (Matthews 1990). From an analysis of a large-scale tagging program during 1982–87, Smith et al. (1990) estimated that mean dispersal rates for male and female lingcod were 500 m/d and 1040 m/d, respectively, similar to those observed in the present study (1173.7 m/24 h). Presumably, lingcod movement rates vary depending upon seasonal requirements (e.g., feeding, spawning, etc.).

Several hypotheses could explain why the smallest male (no. 8) did not return from displacement. Perhaps lingcod do not develop a resident or homing response until they are older and larger. The length-maturity relationship is determined by their geographic area (Richards et al. 1990), and the 50% maturity level for male lingcod at a similar latitude off the west coast of Vancouver Island is 57.1 cm. Thus, if fish no. 8 (57.0 cm) was not sexually mature, it may have lacked the ability to home. Buckley et al. (1984) also noted a lack of homing in small male lingcod. In that study, after 4.5 yr, the smallest transplanted lingcod (a 57 cm male) remained close to the release site after most transplanted lingcod had apparently homed. Alternatively, the lack of homeward movement could be due to tag shedding, which would also produce a stationary signal.

This study revealed new information on lingcod homing behavior. After displacement up to 2.8 km, lingcod moved at night back to home sites within 60 h and followed a fairly direct route. Because this was a pilot study and I displaced only male lingcod, more tracking studies are needed to increase sample sizes, include females, and attempt longer-distance transplants. Whether they home and reuse spawning areas will be important to document, as this information is crucial if lingcod preserves are established. It does appear that transplant attempts to rebuild lingcod stocks may be ineffective with larger, older males but may be successful if the lingcod are moved before they reach a certain size or age.

Acknowledgments

Claudia Hand, John Candy, and Bronwyn Lewis ably caught the lingcod and assisted in all phases of the field work including the tortuous all-night trips. This research was conducted while I held a Natural Sciences and Engineering Research Council Visiting Scientist Fellowship at the Canadian Department of Fisheries and Oceans Pacific Biological Station under the sponsorship of Dr. Laura Richards. The Institute of Ocean Sciences in Sidney kindly loaned us the use of the research vessel *Orca*. Dr. Richards and two anonymous reviewers provided helpful comments which greatly improved the manuscript.

Citations

Able, K.P.
1980 Mechanisms of orientation, navigation, and homing. *In* Gauthreaux, S.A. Jr. (ed.), Animal migration, orientation, and navigation, p. 283–373. Academic Press, NY.

Baker, R.R.
1978 Evolutionary ecology of animal migration. Holmes and Meier Publ., Inc., NY, 1012 p.

Buckley, R., G. Hueckel, B. Benson, S. Quinnel, and M. Canfield
1984 Enhancement research on lingcod (*Ophiodon elongatus*) in Puget Sound. Wash. Dep. Fish. Prog. Rep. 216, 93 p.

Canadian Hydrographic Service
1990 Canadian tide and current tables. Pacific Coast, vol. 5.

Carlson, H.R., and R.E. Haight
1972 Evidence for a home site and homing of adult yellowtail rockfish, *Sebastes flavidus*. J. Fish. Res. Board Can. 29: 1011–1014.

Cass, A.J., R.J. Beamish, and G.A. McFarlane
1990 Lingcod (*Ophiodon elongatus*). Can. Spec. Publ. Fish. Aquat. Sci. 109, 40 p.

Ebeling, A.W., and R.N. Bray
1976 Day versus night activity of reef fishes in a kelp forest off Santa Barbara, California. Fish. Bull., U.S. 74:703–717.

Gerking, S.D.
1959 The restricted movement of fish populations. Biol. Rev. Camb. Philos. Soc. 34:221–242.

Hart, J.L.
1943 Migration of lingcod. Fish. Res. Board Can., Prog. Rep. Pac. Coast Stn. 57:3–7.

Hasler, A.D.
1966 Underwater guideposts. Univ. Wisc. Press, Madison, 155 p.

Holland, K., R. Brill, S. Ferguson, R. Chang, and R. Yost
1985 A small vessel technique for tracking pelagic fish. Mar. Fish. Rev. 47(4):26–32.

Jagielo, T.H.
1990 Movement of tagged lingcod *Ophiodon elongatus* at Neah Bay, Washington. Fish. Bull., U.S. 88:815–820.

Loew, E.R., and W.N. McFarland
1990 The underwater visual environment. *In* Douglas, R., and M. Djamgoz (eds.), The visual system of fish, p. 1–43. Chapman and Hall, London.

Mathews, S.B., and M. LaRiviere
1987 Movement of tagged lingcod, *Ophiodon elongatus*, in the Pacific Northwest. Fish. Bull., U.S. 85:153–159.

Matthews, K.R.
1990 An experimental study of movement patterns and habitat preferences of copper, quillback, and brown rockfishes on three habitat types. Environ. Biol. Fishes 29:161–178.

Matthews, K.R., T.P. Quinn, and B.S. Miller
1990 Use of ultrasonic transmitters to track demersal rockfish movements on shallow rocky reefs. *In* Parker, N.C., et al. (eds.), Fish marking techniques, p. 375–379. Am. Fish. Soc. Symp. 7, Bethesda.

Miller, D.J., and J.J. Geibel
1973 Summary of blue rockfish and lingcod life history histories; a reef ecology study; and giant kelp *Macrocystis pyrifera*, experiments in Monterey Bay, California. Calif. Dep. Fish Game, Fish. Bull. 158:1–137.

Olesiuk, P.F., M.A. Bigg, G.M. Ellis, S.J. Crockford, and R.J. Wigen
1990 An assessment of the feeding habits of harbour seal (*Phoca vitulina*) in the Strait of Georgia, British Columbia, based on scat analysis. Can. Tech. Rep. Fish. Aquat. Sci. 1730, 135 p.

Reese, E.S.
1989 Orientation behavior of butterflyfishes (family Chaetodontidae) on coral reefs: Spatial learning of route specific landmarks and cognitive maps. Environ. Biol. Fishes 25:79–86.

Richards, L.J., and C.M. Hand
1991 Lingcod. *In* Fargo, J., and B.M. Leaman (eds.), Groundfish stock assessments for the west coast of Canada in 1990 and recommended yield options for 1991, p. 19–42. Can. Tech. Rep. Fish. Aquat. Sci. 1778.

Richards, L.J., J.T. Schnute, and C.M. Hand
1990 A multivariate maturity model with comparative analysis of three lingcod (*Ophiodon elongatus*) stocks. Can. J. Fish. Aquat. Sci. 47:948–959.

Smith, B.D., G.A. McFarlane, and A.J. Cass
1990 Movements and mortality of tagged male and female lingcod in the Strait of Georgia, British Columbia. Trans. Am. Fish. Soc. 119:813–824.

Williams, G.
1957 Homing behavior of California rocky shore fishes. Univ. Calif. Publ. Zool. 59:249–284.

An investigation of bottlenose dolphin *Tursiops truncatus* deaths in East Matagorda Bay, Texas, January 1990

W. George Miller

Naval Ocean Systems Center, Code 514, San Diego, California 92152

There are reports of massive mortalities of bottlenose dolphins *Tursiops truncatus* over periods of months in areas as large as the U.S. Atlantic coast and the Persian Gulf. From early June 1987 until March 1988, over 740 bottlenose dolphins (estimated at about 50% of the coastal migratory stock) stranded along the U.S. Atlantic coast from New Jersey to Florida (Scott et al. 1988, Geraci 1989). Geraci concluded the dolphins were poisoned by brevetoxin, a neurotoxin produced by the red tide organism *Ptychodiscus brevis*.

During 23 August to 30 October 1986, 527 dead dolphins were found on the eastern and western shores of the Persian Gulf. Several dead turtles, dugongs, and one 6.1 m unidentified whale were also found, along with many fish that washed ashore. Of the 78% of mammal carcasses identified to species, 64% were bottlenose dolphins, 34% were humpback dolphins *Sousa chinensis*, 1.7% were common dolphins *Delphinus delphis*, and 0.3% were finless porpoises *Neophocoena phocoenoides*. The dead dolphins included adults, neonates, calves, and juveniles. Cause(s) of the deaths could not be determined, since only four animals were necropsied (Anonymous 1986).

The subject of this study is an unusual stranding of 26 *T. truncatus* that occurred in January 1990 around East Matagorda Bay (EMB), Texas. There are no previous reports of this number of strandings in a relatively small area in a single day. On 20 January 1989, a helicopter pilot reported the stranded dolphins to the U.S. Coast Guard, who notified the Texas Marine Mammal Stranding Network at Texas A&M University and Texas Parks & Wildlife Department (TPW). These organizations collected 26 carcasses, 23 from within the Bay and 3 from the Gulf side of East Matagorda Peninsula. I performed necropsies on the dolphins on 24–25 January to determine cause of death.

Methods

Examination of dolphins

Each *T. truncatus* dolphin was assigned an identification number and its stranding location noted (Fig. 1). State of decomposition was noted: freshly dead with no bloating (1 animal), detectable bloating, or severe decomposition. Animals were sexed and weighed, and length was measured via a straight-line from the notch in the tail flukes to the most rostral aspect of the mandible. Measurements of blubber thickness were taken at six locations along the animal's left side using the standard protocol of the Naval Ocean Systems Center (NOSC) (Fig. 2). Skin condition and abnormal marks or deteriorated areas were recorded. Condition and position of thoracic and abdominal organs were noted before removal and collection of tissue samples.

Site inspection and background information

On 26 January 1990, I conducted an aerial survey of the stranding site, comparing the actual configuration of East Matagorda Bay with an existing map (NOAA nautical chart #11319) to determine exit routes for dolphins from the Bay to the deeper waters of the outer coast. The main exit is a narrow cut connecting the Bay and the Gulf (Fig. 1).

The Texas Parks and Wildlife Department monitored water-temperature changes in the Bay almost daily during 15–29 December 1989 (Fig. 3). The Bay was completely frozen over for 2.5 days with partial ice remaining for 4 days. On 22 December, a helicopter pilot flew close to the Bay to observe about 12 dolphins swimming and breaking ice (~5 cm thick) in a 4–7 km area in the east-central region of the Bay.

Rapidly-moving weather systems from the north with strong northerly winds can significantly lower tidal levels in the Bay (Steve Marwitz, Texas Parks & Wildlife, Rockport, TX 78382, pers. commun.). Within the period 15–22 December 1989, when two cold-weather systems moved through the area, an estimated range for the mean low tide level was 30–60 cm below normal (Mark Mazot, Tex. Parks Wildl. Dep., pers. commun., Feb. 1990); however, there were no official measurements. Thus it is possible that lowered water depths around the periphery of the Bay could have impeded dolphin movement between the Bay and the Gulf of Mexico via the Caney Creek Gulf Cut or the intercoastal canal.

Results

Of the 26 *Tursiops truncatus* examined, 23 dolphins were from within East Matagorda Bay and consisted of 6 mature males (MM), 5 immature males (IM), 7 mature

Manuscript accepted 9 September 1992.
Fishery Bulletin, U.S. 90:791–797 (1992).

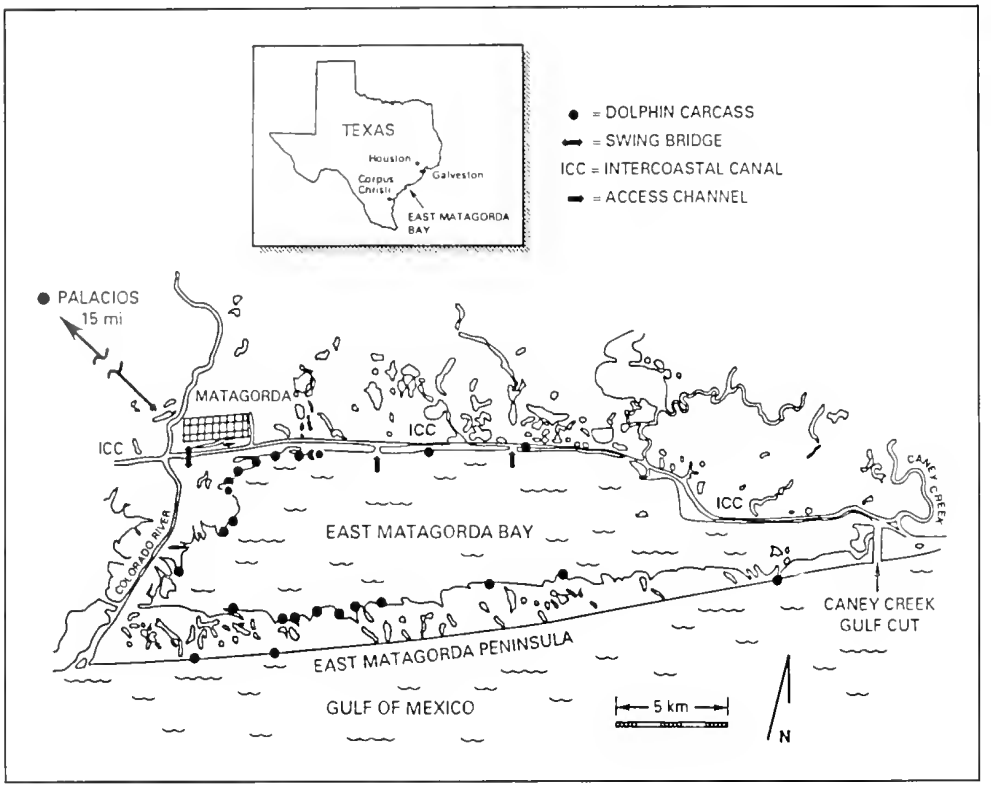

Figure 1
Map of East Matagorda Bay, Texas, showing location of recovered bottlenose dolphin carcasses.

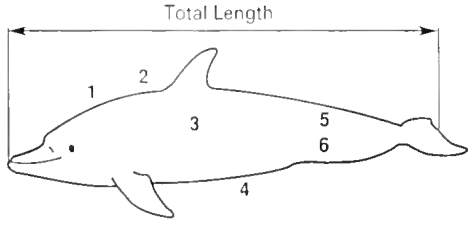

Site 1) Dorsal midline 10cm to 15cm caudal to the blow hole.
Site 2) Dorsal midline 10cm to 15 cm cranial to the insertion of the dorsal fin.
Site 3) Lateral midline at the midpoint of the dorsal fin.
Site 4) Ventral midline 10cm cranial to umbilicus.
Site 5) Dorsolateral aspect of tail stock at level of the anus.
Site 6) Lateral midline at level of the anus.

Figure 2
Blubber measurement sites on bottlenose dolphins collected in East Matagorda Bay, based on Naval Ocean System Center collection procedures.

females (MF) (4 with fetus), and 5 immature females (IF); 2 females and 1 male were from outside the Bay on East Matagorda Peninsula. I could not make an accurate determination of time of death because decomposition varies markedly depending on environmental conditions. The condition of the carcasses at necropsy suggested that death occurred ~5–10 days prior to siting, with the exception of one freshly dead animal collected outside the Bay on East Matagorda Peninsula.

Table 1 shows blubber thickness measured at NOSC (site 2), length, sex, and weight data from 24 East Matagorda Bay dolphins for which there were complete data, and from a comparison group of 16 Texas coast dolphins which stranded over the period 1981–89. Average blubber thickness for 21 stranded dolphins recovered in the Bay was 12.7 mm, while the average thickness for the comparison group of 16 dolphins recovered on the Texas coast during the winter months of November–March 1981–89 was 18.6 mm at the same measurement site. This difference was significant (Student's t test, $P<0.001$). In addition, the subcutaneous fat layer that is prominent between the blubber and skeletal muscles in healthy robust dolphins (Ridgway and Fenner 1982) was greatly reduced or absent in all of the dolphins taken from inside the Bay.

A linear regression was used to (1) show the relationship of blubber thickness (mm) to weight (kg) for the comparison group of dolphins stranded along the Texas coast during winter months and (2) test the similarity of slopes between the Texas-coast and East Matagorda Bay groups (Fig. 4). In Texas coast strandings, there was a significant positive correlation between blubber thickness and body weight (r 0.9); while in the Bay group, blubber thickness decreased with increased weight (r −0.38).

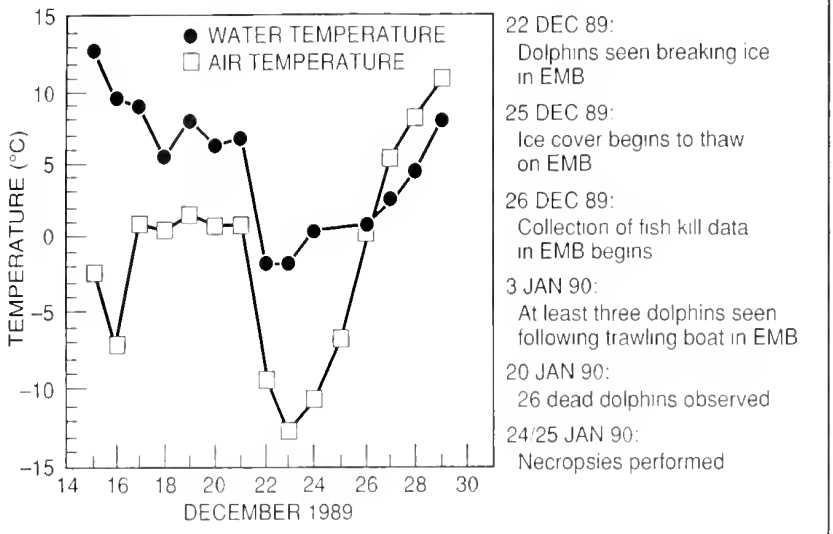

Figure 3

Water and air temperatures at East Matagorda Bay (EMB) during December 1989, and chronology of significant events related to January 1990 strandings of bottlenose dolphins. Air temperatures recorded at Palacios, Texas (the closest recording weather station, 15 mi away), (from Naval Oceanogr. Command Detachment, Asheville, NC). Water-temperature data from Texas Parks & Wildl. Dep., Fish. Div., Coastal Branch, Palacios, TX. Water temperatures in East Matagorda Bay for the dates 1, 15, and 29 January 1992 were 13.5, 16, and 14.5°C, respectively.

Two mature females (MF) and a mature male (MM) had thickened hepatic capsules. One MF had marked lobulation and increased fibrous tissue throughout the liver. Five mature animals (2 MM, 3 MF) had an unusual and unidentified thin, smooth creamy-white layer on the endothelial surface of the hepatic portal vessels.

Three animals had abnormalities associated with the gastrointestinal (GI) system. An immature female (IF) had a section of small

Table 1

Summary data from 24 bottlenose dolphins *Tursiops truncatus* taken in East Matagorda Bay and Peninsula, January 1990, and from Texas coast bottlenose dolphins recovered in November–March 1981–89 (data from Texas Marine Mammal Stranding Network).

East Matagorda				Texas coast			
Blubber thickness (mm)	Length (cm)	Sex	Weight (kg)	Blubber thickness (mm)	Length (cm)	Sex	Weight (kg)
Peninsula				12	100	F	14
9	198	M	68	12	115	M	17
15	240	F	123	15	205	F	91
28	235	F	NA	16	212	M	104
Bay				17	219	M	109
4	216	M	114	18	177	F	59
5	269	M	182	18	206	F	107
5	282	F	170	18	221	F	102
7	262	F	139	18	235	F	139
8	288	M	189	18	240	F	141
9	262	M	159	18	235	F	143
10	275	M	180	20	227	M	136
11	176	F	43	20	179	M	120
11	216	F	91	24	280	M	150
11	270	M	170	25	237	M	193
13	191	M	55	28	260	M	216
13	258	M	141				
14	207	F	82				
15	245	F	114				
15	261	F	136				
15	255	F	150				
15	256	F	166				
16	256	M	150				
22	220	F	82				
22	254	F	145				
26	218	M	77				

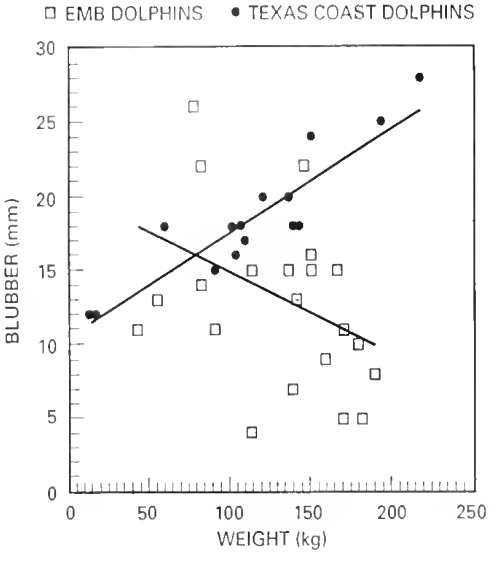

Figure 4

Linear regression of blubber thickness and weight for bottlenose dolphins recovered from East Matagorda Bay, in January 1990, and for comparison group of bottlenose dolphins from the Texas coast during November–March 1981–89.

intestine ~1.5 m long containing extremely-hard dehydrated feces, and its stomach contained partially-digested fish and bones. Two IF had peritoneal adhesions throughout the GI tract. One of these had a serofibrinous exudate on the serosal surfaces of the entire small intestine, and the gastric compartments were empty. Four animals (2 MF, 2 IM) had nematodes in the forestomach and fundic chamber. Clear, crystallized deposits adhered to the parietal and visceral surfaces of the thoracic and abdominal cavities of all animals. These deposits were ≤1 mm in size, felt "gritty," and imparted a "sandpaper-like" texture to the surface, a condition not uncommon in decomposed dolphins in the region (Raymond J. Tarpley, Texas A&M Univ., College Station, pers. commun., March 1990).

Every mature animal in the Bay group had hard, white, spherical deposits in the pancreatic interstitial tissue. These deposits were ≤2 mm in size and were scattered throughout the central pancreas. When crushed with a knife, the deposits were the same white color and consistency throughout.

Stomach contents were noted in 19 of the 23 Bay animals. Stomachs of 6 animals (3 MM, 2 IF, 1 MF) were void of food. Ten animals had unidentified fish, bones, and scales in the stomach. Three animals (2 MF, 1 IM) had undigested and partially-digested fish in the forestomach; in two of these animals, there was a 30 cm undigested fish in the esophagus.

No other gross abnormalities were noted in the respiratory, cardiovascular, renal, musculoskeletal, or reproductive systems of the Bay dolphins. Eyes were too decomposed for examination. Data concerning infectious agents (viral, bacteriological, fungal, etc.) could not be obtained because of advanced decomposition of the carcasses.

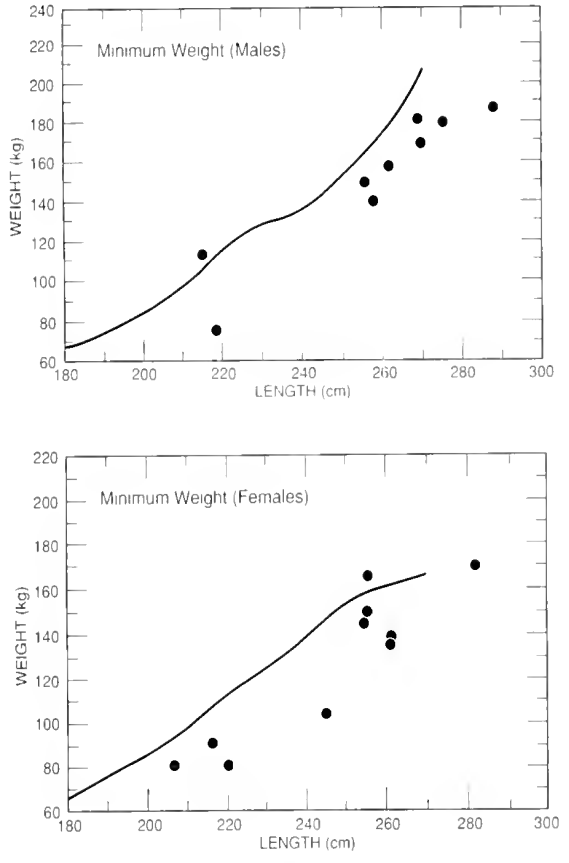

Figure 5
Weight-length data for male and female bottlenose dolphins from East Matagorda Bay, plotted on Ridgway and Fenner's (1982) minimum weight-length graph.

Discussion

Several factors might have contributed to the East Matagorda Bay dolphin mortality. First, an abnormally rapid drop in water temperature which resulted in the Bay freezing over; second, abnormally low tidal levels, possibly preventing exit from the Bay; and third, striped mullet, an important food source for the dolphins, may have been significantly depleted by the freeze. The poor condition of Bay dolphins was indicated by the ~89% of males and 80% of females in states of emaciation or near-emaciation, based on minimum weight-length guidelines established by Ridgway and Fenner (1982) (Fig. 5). In addition, average blubber thickness of the Bay dolphins was a third less than that of the Texas-coast dolphins during winter, based on records over the previous 9-year period.

Gunter (1941) and Gunter and Hildebrand (1951) reported on the death of fishes and other organisms during severe cold periods along the Texas coast. In 1940, water temperature fell from 18.3°C to −3.9°C in 4 hours (Gunter and Hildebrand 1951). Concerning dolphins, Gunter (1941) write, "It is probably worth recording that two porpoises, T. truncatus, were stranded in St. Charles Bay by the low tide and were forced to remain there, only partially submerged, during the coldest days of the freeze. They did not die and it was reported that they escaped when the tide rose." There are other reports of bottlenose dolphins in frozen seas; for example, Manton (1986) reports that *T. truncatus* have been seen breaking ice in the northern part of the Adriatic Sea. There are no records of dolphin deaths associated with other recent freezes in East Matagorda Bay, i.e., in 1983–84 or February 1989; however, local fishermen stated that the only previous sightings of dead dolphins (reported as 4 or 5) in the Bay followed the 1983–84 storm. No data on water

temperatures or duration of ice on the Bay was available for the 1983–84 freeze.

There may have been no possible escape route for the dolphins because of the very low water level and the ice formation on the surface of the Bay. Smith et al. (1983) state that ice may impede the movement of dolphins in an area, and Shane (1980) studied the distribution of bottlenose dolphins in southern Texas and found that some animals had a home range that was limited to shallow bays. In our study, local fishermen stated that they repeatedly saw the same animals, which they could recognize by marks on the dorsal fin and flukes, and that the approximate number of dolphins in the Bay usually was "in the 20's." If the dolphins in East Matagorda Bay were resident, then many of the older animals stranded in January 1990 likely had experienced and survived the severe weather conditions in 1983 when the Bay froze over.

There are no precise data available to accurately determine the food biomass available to the EMB dolphins during and after the December 1989 freeze, but it is possible that an essential food source was not available. Fish mortality is greatest during a rapid decrease in water temperature (Springer and Woodburn 1960). Data from Dailey et al. (1991a) show that the relative abundance (gillnet entrapment technique, n/hour) of subadult and adult striped mullet *Mugil cephalus* along the Texas coast in spring 1989 was double that of previous years, while the relative abundance (bag-seine entrapment technique, n/ha) of juveniles in 1989 was only 60% of the value for the two previous years. Following the December 1989 freeze, the relative abundance of subadult and adult striped mullet in the spring of 1990 was far below that of spring 1989, while the relative abundance of juveniles (for recruitment to the population) was 380% higher in 1990 than it was in 1989. The large increase in relative abundance of young for spring recruitment to the population following the December 1989 freeze has been attributed to a lack of adult predator fish (Lawrence McEachron, Texas Parks Wildl., Rockport, TX 78382, pers. commun., Oct. 1991).

Table 2 shows estimated freeze kills for a variety of marine fish species in East Matagorda Bay for periods in 1983–84, February 1989, and December 1989 (McEachron et al. 1991). Although freezes are common on the Texas coast, fish kills of the magnitude of the December 1989 freeze in the Bay had never before been recorded, with *Mugil cephalus* mortality estimated to be over 2.5 million fish.

And thus, a compounding problem for the dolphins in the December 1989 freeze is the unprecedented kill of striped mullet. It is probable that a food source essential to the Bay dolphins was severely depleted at a critical time when the dolphins needed calories. Barros (1992), Barros and Odell (1990), and Cockcroft and Ross (1990) show that bottlenose dolphins utilize a variety of food resources, composed primarily of fish (4 to 6 major prey species common to their respective areas) and cephalopods (primarily 1 species common to their respective areas), and occasionally crustaceans. Pryor et al. (1990) suggest that mullet has been a staple dolphin food for centuries. Gunter (1942) reported on prey in freshly-killed, presumably-healthy *T. truncatus*: 1 from deeper waters and 33 from the shallows of Aransas and St. Charles Bays, Aransas County, Texas.

Table 2

Estimated marine fish-freeze kill in East Matagorda Bay for the periods 1983–84, February 1989, and December 1989 (McEachron et al. 1991). ND = no data.

Species	1983–84	February 1989	December 1989
Micropogonias undulatus			
Atlantic croaker	700	100	<100
Pogonias cromis			
Black drum	3300	89,900	5600
Brevoortia patronus			
Gulf menhaden	7100	100	2400
Arius felis			
Hardhead catfish	ND	200	ND
Lagodon rhomboides			
Pinfish	300	200	100
Sciaenops ocellatus			
Red drum	500	23,500	400
Cynoscion arenarius			
Sand seatrout	ND	ND	ND
Archosargus probatocephalus			
Sheepshead	4300	11,600	200
Leiostomus xanthurus			
Spot	ND	ND	ND
Paralichthys lethostigma			
Southern flounder	ND	ND	ND
Cynoscion nebulosus			
Spotted seatrout	900	170,400	600
Mugil cephalus			
Striped mullet	**178,400**	**21,200**	**2,684,100**
Other fish	19,400	67,400	6,400
Total fish	214,900	384,600	2,699,800

Although Gunter found 12 species of fish and 1 shrimp, 83% of fish consumed were *Mugil cephalus*.

A significant difference between stranded (presumably ill) and net-caught/capture-killed (presumably healthy) dolphins is that stranded dolphins (Barros 1992, Barros and Odell 1990) have a high percentage of empty stomachs (empty or <1g, 32–54%) while net-caught or captured dolphins (Cockcroft and Ross 1990, Gunter 1942) have a very low percentage of empty stomachs (<3%). The reason for this discrepancy is not documented, but ill dolphins often have a decreased appetite or may not be able to catch food. Another reason for a high percentage of empty stomachs in the Bay dolphins may be lack of food availability. Of 19 Bay dolphins examined, 32% had empty stomachs and 37% had only unidentifiable bones and scales (no flesh). Gunter (1942) observed 34 killed specimens of *T. truncatus*; none of the stomachs were void of food. In addition, Gunter (1942) showed that the average number of recognizable fish/stomach was 18, whereas the 15% of EMB dolphins that had eaten recently had no more than 2 recognizable fish/stomach. These data, along with the Texas Parks & Wildlife fish freeze-kill and biomass data, indicate that food was in short supply for the Bay dolphins. I suspect that many of them might have survived if they had sufficient nutrition.

Ridgway and Fenner (1982) state that the blubber may thin as weight loss progresses to emaciation, and reduced blubber thickness at necropsy is one sign of emaciation. Studies on healthy, well-fed dolphins at the Naval Ocean Systems Center in San Diego show that *T. truncatus* have thicker blubber as body weight increases, and that *T. truncatus* may respond within 2 weeks to water-temperature changes by increasing or decreasing blubber thickness for cooler or warmer temperatures, respectively (William A. Friedl, NOSC, Kaneohe, HI, pers. commun., Nov. 1990). Level of starvation may not be the only reason for differences in blubber thickness between EMB and Texas coast dolphins: the EMB dolphins might originally have had thinner-than-normal blubber resulting from living in a shallow bay with higher-than-average water temperatures (29, 25, and 19°C monthly average water temperatures in EMB for September, October, and November 1989, respectively); or the normal prey field in EMB might be limited compared with other areas. Further work on blubber constituents and factors affecting blubber thickness is needed to determine if blubber thickness is an indicator of starvation as a cause of death.

The December 1989 EMB freeze, in which temperatures stayed near freezing for about 4 days, resulted in devastation of the dolphins' most-likely major food source, the striped mullet. The dolphins' emaciated condition, the substantial reduction in their blubber thickness, lack of food in their stomachs, the assessment that dolphins lived for 2 weeks following the freeze, and the EMB fish freeze-kill and biomass data suggest, in addition to any direct effects to the dolphins of the extreme cold, that decimation of the food resource contributed to this acute dolphin mortality event.

Acknowledgments

I thank the following organizations and individuals for their contributions that made this report possible: Texas Marine Mammal Stranding Network (Dr. Raymond Tarpley, founder of the TMMSN; Gina Barron, for her untiring efforts and organizational skills; Elsa Haubold and all the other members of the network who have graciously devoted their time); Texas Parks and Wildlife Department (Steve Marwitz and Lawrence McEachron, Rockport, Texas); U.S. Coast Guard; Houston Helicopter (Mike Boyaki and Dave Beard); Dr. James Calvin, Department of Statistics, Texas A&M University, College Station; and Naval Oceanographic Command Detachment, Asheville, North Carolina. Special thanks to Dr. Sam H. Ridgway (Naval Ocean Systems Center) for his critique and support for this work, and to F.G. Wood for his suggestions. Dr. Raymond J. Tarpley (TMMSN and Texas A&M University), provided NOSC with information on blubber measurements taken from dolphins stranded on the Texas coast from 1981 to June 1989.

Citations

Anonymous
1986 Regional organization for the protection of the marine environment, Report of the first meeting of experts on mortality of marine animals, Kuwait, Nov. 22–23, 1986.

Barros, N.B.
1992 Food habits. *In* Hansen, L.J. (coordinator), Report on investigation of 1990 Gulf of Mexico bottlenose dolphin strandings, p. 41–46. Contrib. MIA-9293, NMFS Southeast Fish. Sci. Cent., Miami.

Barros, N.B., and D.K. Odell
1990 Food habits of bottlenose dolphins in the southeastern United States. *In* Leatherwood, S., and R.R. Reeves (eds.), The bottlenose dolphin, p. 309–328. Academic Press, San Diego.

Cockcroft, V.B., and G.J.B. Ross
1990 Food and feeding of the Indian Ocean bottlenose dolphin off southern Natal, South Africa. *In* Leatherwood, S., and R.R. Reeves (eds.), The bottlenose dolphin, p. 295–308. Academic Press, San Diego.

Dailey, J.A., J.C. Kana, and L.W. McEachron
1991 Trends in relative abundance in size of selected finfish and shellfish along the Texas coast: November 1975–December 1989. Manage. Data Ser. 53, Texas Parks Wildl. Dep., Fish. Wildl. Div., Coastal Fish. Br., Austin, 241 p.

Geraci, J.R.
1989 Clinical investigation of the 1987–1988 mass mortality of bottlenose dolphins along the U.S. central and south Atlantic coast. Report to the National Marine Fisheries Service, U.S. Navy, Office of Naval Research, and the Marine Mammal Commission, April 1989.

Gunter, G.
1941 Death of fishes due to cold on the Texas coast, January, 1940. Ecology 22:203–208.
1942 Contributions to the natural history of the bottlenose dolphin, *Tursiops truncatus* (Montague), on the Texas coast, with particular reference to food habits. J. Mammal. 23: 267–276.

Gunter, G., and H.H. Hildebrand
1951 Destruction of fishes and other organisms on the south Texas coast by the cold wave of January 28–February 3, 1951. Ecology 32:731–736.

Manton, V.J.A.
1986 Water management. *In* Bryden, M.M., and R. Harrison (eds.), Research on dolphins, p. 189–208. Clarendon Press, Oxford.

McEachron, L.W., G.C. Matlock, C.E. Bryan, P. Unger, T.J. Cody, and J.H. Martin
1991 Winter mass mortality of animals in Texas bays. Texas Parks Wildl. Dep., Fish. Wildl. Div., Coastal Fish. Br., Austin, 47 p.

Pryor, K., J. Lindbergh, S. Lindbergh, and R. Milano
1990 A dolphin-human fishing cooperative in Brazil. Mar. Mammal Sci. 6(1):77–82.

Ridgway, S.H., and C.A. Fenner
1982 Weight-length relationships of wild-caught and captive Atlantic bottlenose dolphins. J. Am. Vet. Med. Assoc. 181(11):1310–1315.

Scott, G.P., D.M. Burn, and L.J. Hansen
1988 The dolphin die-off: Long-term effects and recovery of the population. Proc., Oceans '88, p. 819–823. IEEE, NY.

Shane, S.H.
1980 Occurrence, movements, and distribution of bottlenose dolphins, *T. truncatus*, in Southern Texas. Fish. Bull., U.S. 78:593–601.

Smith, T.G., J.R. Geraci, and D.J. St. Aubin
1983 Reaction of bottlenose dolphins, *Tursiops truncatus*, to a controlled oil spill. Can. J. Fish. Aquat. Sci. 40:1522–1525.

Springer, V.G., and K.D. Woodburn
1960 An ecological study of the fishes of the Tampa Bay area. Fla. State Board Conserv. Prof. Pap. Ser. 1:1–104.

Application of otolith microchemistry analysis to investigate anadromy in Chesapeake Bay striped bass *Morone saxatilis**

David H. Secor

The University of Maryland System, Center for Environmental and Estuarine Studies
Chesapeake Biological Laboratory, Solomons, Maryland 20688-0038

Management of Chesapeake Bay and coastal striped bass *Morone saxatilis* fisheries is affected by migration of large Chesapeake adults into coastal waters. Tagging studies during the 1930s and 1950s indicated that a small percentage of Chesapeake striped bass contribute to the coastal fishery (Vladykov and Wallace 1952, Mansueti 1961, Massman and Pacheco 1961). However, work on age- and sex-specific migration patterns (Chapoton and Sykes 1961, Kohlenstein 1981) suggested that about half of the females aged 3+ migrate out of the Bay. The current consensus appears to be that young striped bass remain in or near the tributary in which they were spawned for 2 or 3 years; thereafter most males remain in the Bay, while a substantial number of females migrate out of the Bay and remain in coastal waters until sexually mature (Chapman 1987, Setzler-Hamilton and Hall 1991). Although facultative anadromy is suggested by tagging studies, age- and sex-specific rates of anadromy remain largely unknown (ASMFC 1990).

Wave-length dispersive electron microprobe analysis of strontium/calcium ratio (Sr/Ca) in otoliths has recently been employed as a method for distinguishing between freshwater and marine life-history phases of individual fishes (Casselman 1982, Radtke et al. 1988, Kalish 1990). Sr is substituted for Ca into the lattice of aragonitic calcium carbonate (Kinsman and Holland 1969), and in otoliths the rate of substitution is in proportion to its abundance in the endolymph (Kalish 1989). Sr concentration in seawater is more than one order of magnitude greater than in freshwater (Bagenal et al. 1973, Radtke et al. 1988, Kalish 1990, Ingram and Sloan 1992). Therefore, Sr levels in otoliths of fish exposed to seawater should be substantially higher than those exposed to freshwater.

Sr/Ca ratio in otoliths of anadromous striped bass was analyzed to determine its usefulness in charting individual migratory histories. In a prospectus, Coutant (1990) suggested a similar application to investigate patterns of estuarine use by Chesapeake Bay and Roanoke River striped bass. Here, I looked for a seasonal pattern in otolith Sr/Ca ratios that was consistent with anadromous behavior. An annual cycle of low Sr/Ca ratios during spring (exposure to Sr-poor freshwater) and high ratios during fall and winter (exposure to Sr-rich saltwater) was expected in large adults. If such a pattern existed, then further research and application would be justified. Analysis of Sr/Ca composition could be applied to problems of migratory behavior, spawning, hatchery contribution to coastal stocks, definition of life-history traits, environmental degradation (Coutant 1990), and consequences of anadromy to recruitment (e.g., Kalish 1990).

In this investigation, I related Sr/Ca ratios to annuli which are assumed to form in spring (see Discussion). I used a less traditional definition for annulus, "...a ridge or a groove in or on the [hard] structure..." (Wilson et al. 1987), because opaque and translucent zones did not adequately describe the microstructure observed under scanning electron microscopy or light microscopy.

Methods

Sr/Ca ratios were examined for five large adults from the Chesapeake Bay and South Carolina (Table 1). Adults from the Chesapeake were presumed to be anadromous based on their size (Setzler-Hamilton and Hall 1991); the South Carolina population is a freshwater population, resident to the Santee-Cooper watershed (Secor et al. 1992). Chesapeake Bay fish (n 3) were collected by charterboat fisherman from Solomons, Maryland during the May 1991 "Maryland Trophy Season", presumably caught in upper Bay waters. South Carolina fish were collected at a 1989 fishing tournament. Otoliths were removed, cleaned in 10% sodium hypochlorite solution (bleach), and rinsed with deionized water. They were embedded in Spurr epoxy, sectioned in a transverse plane with a Buehler Isomet saw, and mounted on a glass slide. Otoliths were polished (see Secor et al. 1991) until all annuli were visible with transmitted light on a compound microscope. Otolith sections were further polished with 3μm alumina to limit any surface structure that could cause artifacts

* Contribution 2368, Center for Environmental and Estuarine Studies, The University of Maryland System.

Manuscript accepted 13 July 1992.
Fishery Bulletin, U.S. 90:798–806 (1992).

Table 1

Striped bass *Morone saxatilis* from Chesapeake Bay (MD and Juv) and Santee-Cooper (SC) populations used in electron microprobe analyses.

ID	Population	Sex	Age	TL (cm)	Weight (kg)
MD-1	Chesapeake	Female	21	119	15.5
MD-2	Chesapeake	?	8	94	7.3
MD-3	Chesapeake	?	9	93	8.1
SC-1	Santee-Cooper	Female	6	80	4.8
SC-2	Santee-Cooper	Female	5	81	5.4
Juv-1	Patuxent River	Juvenile	0	–	–

in microprobe analysis (Kalish 1991). Otolith sections were carbon-coated in a high-vacuum evaporator.

A sagitta from a juvenile striped bass sampled from the Patuxent River (Chesapeake Bay tributary) was similarly prepared and polished so that the core and all increments were sectioned (Secor et al. 1991). The juvenile's parentage, a 20kg female that was assumed to be migratory based on its size (Kohlenstein 1981), was known because the juvenile was a marked hatchery fish released as a 9-day-old larva.

X-ray intensities for Sr and Ca elements were quantified using a JXA-840A JEOL wave-length dispersive electron microprobe (Central Facility for Microanalysis, Univ. Maryland, College Park MD 20742), with Calcite ($CaCO_3$) and Strontianite ($SrCO_3$) as standards. Striped bass otoliths were resilient to high-beam power densities compared with previous work on salmonid otoliths (Kalish 1990) and showed no diffusion of elements over a 32-sec counting period (Table 2). This permitted analysis of small sample points ($5 \times 5\mu m$) at high accelerating voltage (25kV) and probe current (20nA). Background and peak counting times were each 20 sec for Sr, and 5 sec for Ca. Background counting times were equally divided below and above the peak position. The detection limit for Sr was 580ppm. Precision was calculated at <1% for Ca counts and 8.2% for Sr counts (at Sr/Ca = 0.003) (1.96σ; Goldstein et al. 1981). The electron beam caused a physical disruption (a pit) at the section's surface which limited the proximity of adjacent points that could be accurately sampled. Initial analyses of Chesapeake sample otoliths at "step" distances of $8\mu m$ resulted in no Sr X-ray counts. This was probably due to physical disruptions among adjacent points because surface structure can cause artifacts in microprobe analysis (Kalish 1991). Analysis was therefore conducted at 13 and $20\mu m$ step sizes where positive counts occurred (Table 3). Transects (700–2600μm in length) across annuli in the otolith sections were selected. The electron microprobe sampled 60–130 points along these transects. Each point required ~70sec of microprobe time. X-ray intensities were calculated using the ZAF procedure (Reed 1975), normalized to standards, and converted to elemental (atomic weight) ratios.

Due to their close proximity, individual points were not always visible in probed otolith sections. To relate Sr/Ca ratios to the

Table 2

Effect of counting time on strontium and calcium counts. Accelerating voltage = 25kV, probe current = 20nA, sample size = $5\mu m^2$. Note that Sr and Ca show no decline with counting time which would indicate sample destruction.

Seconds counted	Counts/sec	
	Sr	Ca
0	585	16763
4	586	16678
8	576	16725
12	589	16869
16	586	16748
20	578	16847
24	570	16828
28	592	16850
32	603	16813

Table 3

Summary statistics for Sr/Ca ratios of Chesapeake Bay and Santee-Cooper samples. All ratio statistics have been multiplied by 1000 for presentation purposes. Age is given in parentheses below each sample. Step = distance between sampled points along transect.

Sample	Transect	Step (μm)	N	$\bar{x}$	SE	Mode	Median
MD-1	1	20	99	2.753	0.094	3.4	2.8
(21)	2	20	99	2.645	0.095	2.3	2.6
	3 (age ≥7)	13	60	3.713	0.124	4.7	4.0
MD-2 (8)	–	13	99	2.974	0.155	0	3.0
MD-3	1	20	100	2.385	0.097	2.8	2.4
(9)	2	13	70	2.323	0.086	1.7	2.3
SC-1 (6)	–	20	130	0.937	0.061	0	0.9
SC-2 (5)	–	13	99	0.241	0.054	0	0

opaque zones of annuli checks, probed sections were viewed under a compound microscope and transect distances between annuli measured with an ocular scale. Because the distance between each microprobe measurement was known, distances between measurements can be converted to distances between annuli. Distances between annuli (annular increments) became narrow with increasing age (<50 μm) (Fig. 1), and points did not always sample directly on annuli. Therefore, it was necessary to assign an annulus to the closest sampled point. Points between annuli were assumed to sample age in linear proportion. For instance, if 10 points were sampled between annuli 5 and 6, then points would be assigned ages 5.0, 5.1, 5.2,...6.0. A replicate scan was performed on two of the otolith samples. In the juvenile's otolith, not all daily increments were visible along the transect with scanning electron microscopy or light microscopy. Therefore, Sr/Ca ratios were related to standard length using an otolith/fish-length relation documented for the Potomac River population (Houde and Rutherford 1992).

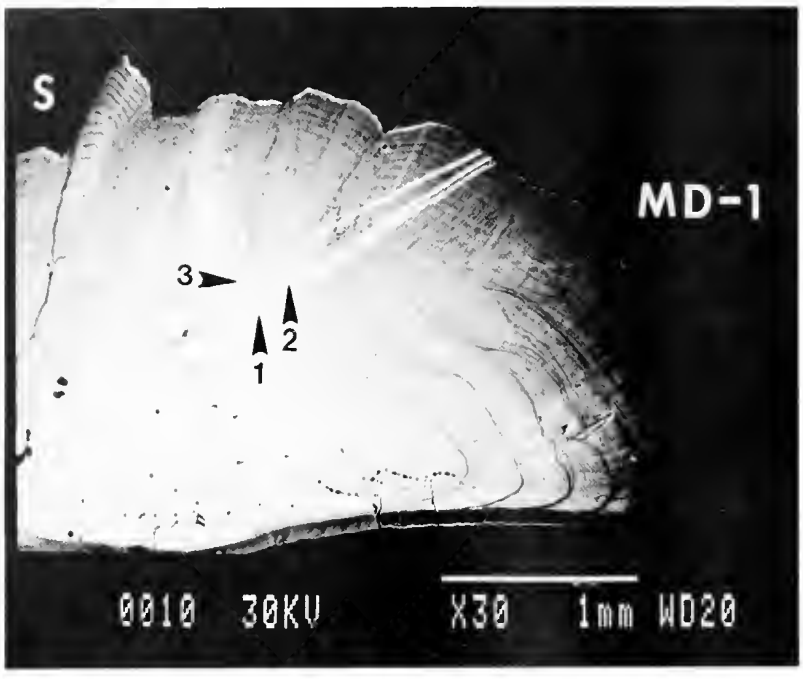

Figure 1

Back-scatter electron micrograph of otolith from striped bass *Morone saxatilis* Sample MD-1. Twenty-one annuli are clearly visible along the sulcus (s) and sulcal ridge. Transects 1 and 2 were performed at 20μm step size; Transect 3 began at the 7th annular check and 13μm step size. The probed transect previous to Transect 3 was performed at 8μm step size and resulted in no positive Sr counts. Note that individual probed points are visible in a series of physical disruptions (pits) for Transects 1 and 2.

Results

Mean Sr/Ca ratios in Chesapeake striped bass were three to four times greater than Santee-Cooper striped bass (Table 3; Figs. 2,3). This trend is consistent with a salinity influence on the ratio, because Santee-Cooper striped bass are confined to freshwater and both Santee-Cooper females were sexually mature. Although substantial variation occurred in Sr/Ca between South Carolina samples, both samples were near the electron microprobe's detection limit of Sr/Ca (Sr/Ca =0.0008). Instrumental precision decreases markedly as the detection limit is approached, which may produce spurious variation. Peaks and nadirs in the Sr/Ca ratios were apparent in Chesapeake striped bass, and in fish >age-4, these patterns generally showed an annual cycle (Fig. 2). This is most apparent for sample MD-1. Because low Sr/Ca ratios can be associated with freshwater excursions, results indicate yearly migration for this large female.

Lack of agreement among replicate transects (Fig. 2) probably was due to the manner in which ages were assigned, spatial resolution, and within-sample variability. Probed points of replicate transects could not be directly "lined up" with respect to annuli. This offset occasionally resulted in the interpretation that an annuli was associated with a peak in one transect and a nadir in the other transect (e.g., annuli 15, 18, and 19 in Transect 1 vs. these annuli in Transect 2 for MD-1; Fig. 2). Transects 1 and 2 for Sample MD-1 (20μm step size) sampled few points between successive annuli at older ages, and the accuracy with which points could be assigned to annuli was less (Fig. 4). Transect 3 for MD-1 (13μm step size) clearly shows increased resolution of the ratio across annular increments. Similarly, Transect 2 (13μm) for MD-3 revealed several more peaks and nadirs after the 5th annulus than did Transect 1 (20μm). The overall Sr/Ca ratio was significantly different between Transects 1 and 2 for MD-3 (Table 4, t 3.06, $p<$ 0.01). Replicate transects in MD-1, where step size

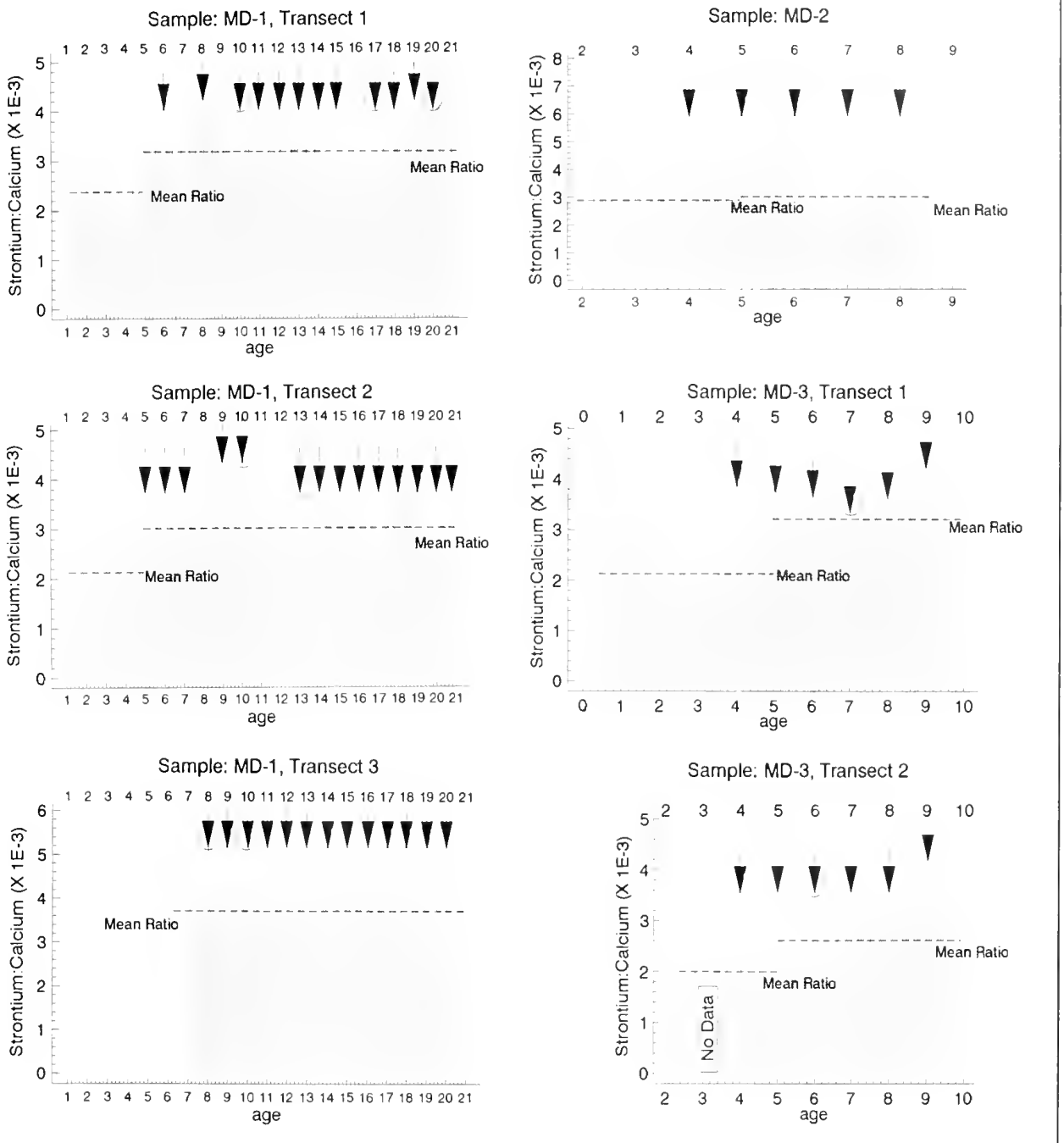

Figure 2

Transects of Sr/Ca ratios across annuli increments of Maryland striped bass *Morone saxatilis*. Mean ratios are plotted for ages <5 and ages ≥5 for each sample. See Table 3 for step sizes. Arrows indicate presumed freshwater excursions. Circled arrows indicate nadirs in ratios which were consistent with an annual cycle but did not coincide with annuli.

was 20 μm for both transects, did not significantly differ.

Despite the differences among transects, the overall trend in Chesapeake fish was a nadir in Sr/Ca ratio at or shortly after annuli that coincided with spring spawning runs (Merriman 1941, Robinson 1960). This trend occurred only in fish >4 years old. There was a significant increase in the overall Sr/Ca ratio in fish >5 years for two of three Chesapeake fish (Table 4).

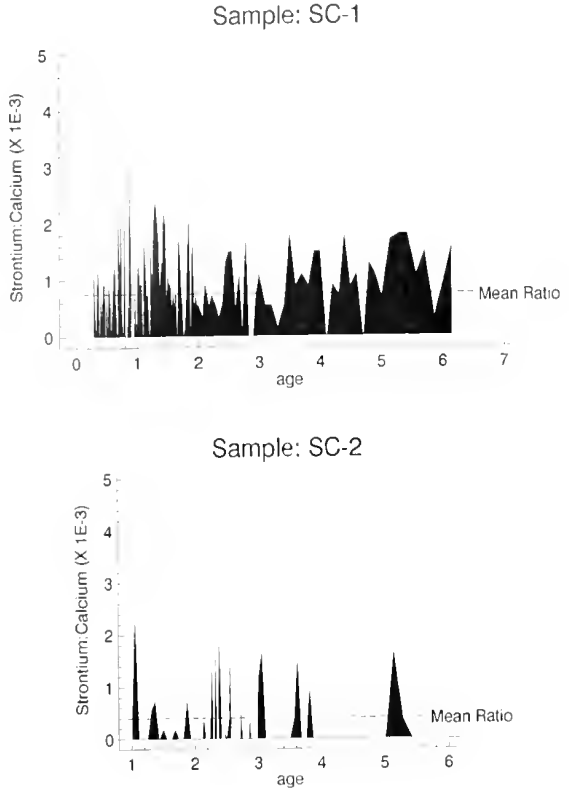

Figure 3

Transects of Sr/Ca ratios across annuli of adult female Santee-Cooper (SC) striped bass *Morone saxatilis*. Mean ratios are plotted across all ages.

Strontium was not detected in the Patuxent River juvenile striped bass otolith until it reached ~8 mm SL (Fig. 5). Because larvae less than this size tend to utilize freshwater nurseries (Houde and Rutherford 1992), this further verified that freshwater residence results in low levels of otolith Sr.

Discussion

Annulus formation

Rate and season of annulus formation in striped bass otoliths are critical to interpretation of the results on annual and seasonal changes in otolith microchemistry. Heidinger and Clodfelter (1987) validated the hypothesis of yearly annulus formation for young (<5 years old) striped bass. However, no directed research has documented the time of annulus formation in striped bass otoliths or scales despite their widespread use in fisheries (e.g., Beamish and McFarlane 1983). Several investigators have made the observation that annuli are not observed until spawning season in scales (Merriman 1941, Robinson 1960) and otoliths (M. White, S.C. Wildl. Mar. Resour., Bonneau SC 29431, pers. commun.). Based on these limited observations and the general trend of spring annulus formation in other North American temperate fishes, it was assumed that annular check formation occurred during or just prior to the spawning season (February–April).

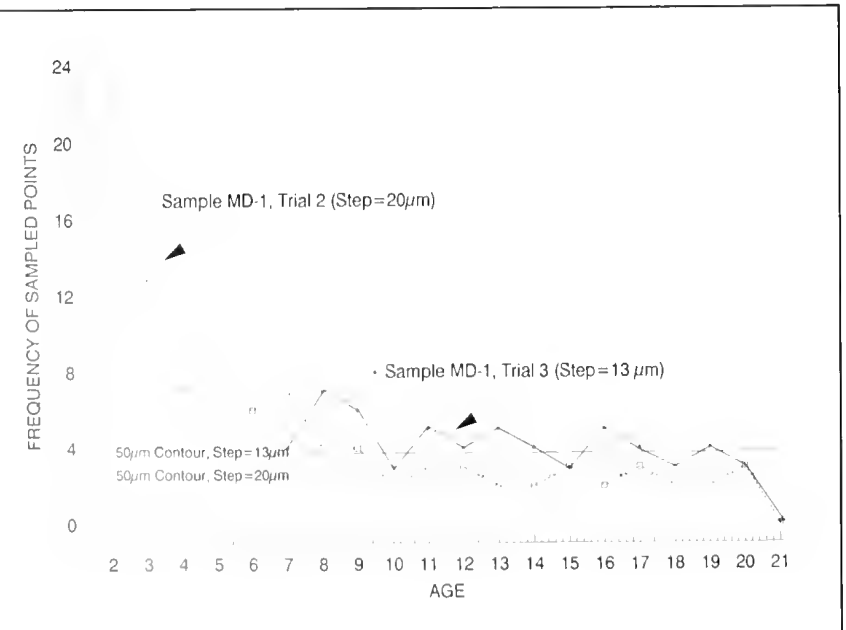

Figure 4

Number of sampled points between annuli checks at two step sizes. Contours for a hypothetical 50 μm annular increment are plotted at 13 and 20 μm step sizes.

Salinity effect on otolith microchemistry

Because Chesapeake samples had substantially higher Sr/Ca ratios than South Carolina samples, there appears to be a salinity effect on the ratio. This conclusion is further substantiated by the juvenile otolith that was examined and showed nondetectable Sr/Ca ratio during the early-larval period, a time when Chesapeake tributary larvae generally occur above the salt-wedge (Uphoff 1989, Houde and Rutherford 1992). Patterns in otolith Sr/Ca in adults were consistent with expected seasonal changes in ambient salinity. The range of ratios found for Chesapeake striped bass was similar to those found by Kalish (1989) for 12 marine species (Sr/Ca 0.0018

Table 4

Comparison of ratios between probed points <5 or ≥5 years. Significant differences ($p<0.001$) are shown by an asterisk.

		Age <5			Age ≥5			
Sample	Transect	$\bar{}$	SD	N	$\bar{}$	SD	N	t
MD-1	1	2.17	0.89	44	3.22	0.68	55	6.62*
	2	2.16	0.89	44	3.03	0.64	55	5.09*
MD-2	—	2.96	1.50	65	3.01	1.66	34	0.15
MD-3	1	2.15	0.93	78	3.20	0.67	22	4.95*
	2	2.01	0.62	35	2.61	0.70	35	3.78*

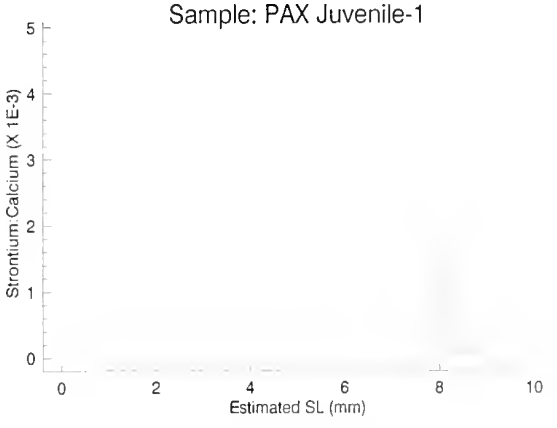

Figure 5

Transect of Sr/Ca ratios for the early-larval period from a juvenile striped bass *Morone saxatilis* sampled from the Patuxent River, 1991. Transect distance was converted to standard length using regression of standard length on otolith length for Potomac River striped bass larvae (Houde et al. 1992). Transect points were converted to larval lengths assuming a linear growth rate and constant otolith length:fish length relationship.

-0.0062) and 1 freshwater species (Sr/Ca 0.0005-0.0010).

Radtke (1984) and others (Townsend et al. 1989, Radtke et al. 1990) have shown an inverse relationship between temperature and otolith Sr/Ca ratio. If there were such an inverse relationship in adult striped bass otoliths, then ratios would increase during fall and winter and decrease during spring and summer, a pattern which would to some degree parallel the pattern seen for anadromous striped bass.

Kalish (1989, 1991) in recent directed research found no temperature relationship for otolith Sr/Ca ratio, and suggested that seasonal changes in fish physiology can cause incidental correlation between temperature and Sr/Ca ratios. Based on evidence for seasonal, growth, and age effects on Sr/Ca ratios, he postulated that during certain periods of active metabolism, Ca-binding proteins are more abundant in the serum which results in a higher relative fraction of free Sr available for deposition onto the otolith. If Sr/Ca ratios in the otolith are controlled by physiological processes alone, then a different pattern of Sr/Ca ratios would be expected compared with those observed for striped bass, i.e., Sr/Ca ratios would tend to rise in late-winter and early-spring during vitellogenesis but might also be high during periods of active growth. However, physiological effects such as sexual maturation and stress could explain both the increase in Sr/Ca ratio after the 5th annulus in Samples MD-1 and MD-3, and seasonal (subannular) patterns which varied among samples (e.g., the major peak which proceeded the 6th annulus in Sample MD-2; Fig. 2).

Although results exist for few species, the magnitude of the salinity effect found in this and other studies (Casselman 1982, Kalish 1989 and 1990) may be greater than differences expected due to physiological condition (Kalish 1989, 1991) and temperature alone (Radtke 1984, Townsend et al. 1989, Radtke et al. 1990). Similar to my findings, Kalish (1989, 1991) reported a three- to four-fold difference in Sr/Ca ratio between groups of young rainbow trout exposed to either freshwater or saltwater. Casselman (1982) reported a three-fold difference in Sr/Ca ratio between the marine and freshwater life-history phases of American eel. In laboratory-rearing studies on larval herring *Clupea harengus*, temperature effects resulted in no more than a two-fold difference in Sr/Ca ratios (Townsend et al. 1989, Radtke et al. 1990), although a complementary field study conducted by Townsend et al. (1989) showed that temperatures of 1-12°C had a four-fold effect on Sr/Ca ratio. Physiological condition has been associated with an approximate two-fold effect on Sr/Ca ratio in juvenile Australian salmon *Arripis trutta* (Kalish 1989).

A three-fold difference in Sr/Ca ratio in otoliths is consistent with the probable influence of ambient concentrations of Sr and Ca, since the Sr/Ca ratio is at least four times greater in saltwater than in freshwater (Casselman 1982, Radtke et al. 1988, Kalish 1989 and 1990). Further, Berg (1968) has shown substantially less physiological discrimination against Sr than Ca in scale formation, and Kalish (1989) shows excellent correspondence between otolith microchemistry and the chemical composition of endolymph that bathes the otolith. Therefore, ambient levels of Sr could be reflected in the otolith's microchemistry (Mugiya and Takahashi 1985, Kalish 1989) dependent upon the degree of physiological discrimination against Sr.

Otolith microchemistry and migratory history

The otolith microchemistry method offers great potential to address questions related to time of maturation and frequency of spawning. A distinct positive shift in Sr/Ca ratio at 5 years in samples MD-1 and MD-3 could be indicative of maturation or onset of coastal migration. Current estimates of age-at-maturation for Chesapeake population females indicate that <30% of females are mature by age 5 years (Maryland DNR 1991). Kohlenstein (1981) showed through a tagging study that the majority of female striped bass migrate by 5 years. Lack of a shift in MD-2 might indicate that this individual was a male or had a different migration history.

All Maryland striped bass samples showed annual peaks and valleys in Sr/Ca ratios. Based on a salinity effect, it can be inferred that valleys represent excursions into strontium-poor freshwater habitats. Assuming that large, mature adults venture into freshwater or low-salinity habitats to spawn, then spawning frequency can be estimated.

Precision error and spatial resolution of the electron microprobe analysis is critical in the proposed application of charting individual migratory histories. Precision errors were indicated by differences in Sr/Ca patterns and overall level between transects of the same sample (e.g., MD-3). Changing spatial resolution between measurements of 20 and 13 μm permitted greater resolution of seasonal (subannular) patterns. A more complete series of measures along a transect is taken at lower step sizes because gaps between measured points become narrower. This effect could explain variation in mean Sr/Ca levels among transects for the same sample. Alternatively, lack of agreement between transects could indicate machine precision limits in detecting Sr/Ca levels.

A decline in otolith growth rate with age also caused a decrease in spatial resolution (Fig. 4). At a 13 μm step size, four or five measurements were taken per annular increment in fish >7 years. Therefore, each measurement can correspond to several months of the fish's life. This would explain why nadirs in Sr/Ca ratio rarely approached zero after the 5th annulus. Tagging studies indicate that adult striped bass can migrate between freshwater and coastal habitats within a month (Mansueti 1961, Chapoton and Sykes 1961, Waldman et al. 1990). Peaks and nadirs observed in otolith Sr/Ca ratio may therefore represent temporally-averaged values. Laboratory verification studies are planned to gauge the spatial sensitivity of otolith microchemistry to resolve changes in ambient salinity.

Other life-history applications

An ingenious application of the Sr/Ca method to early-life-history consequences of anadromy was made by Kalish (1990). He was able to detect Sr in the core of salmonid otoliths (the earliest deposited material). Under the rationale that maternally-derived protein influenced offspring otolith microchemistry, it was possible to segregate offspring on the basis of whether they originated from eggs spawned by anadromous (high Sr/Ca) or nonanadromous (low Sr/Ca) females. In my study, a single striped bass juvenile of known anadromous parentage had no detectable Sr in the otolith core. In contrast to salmonid embryos and larvae, striped bass obtain relatively small amounts of maternal protein and lipids, and the period of endogenous feeding is considerably shorter. Also, the chorion of striped bass eggs is highly permeable; therefore, ambient concentrations of Sr could have a greater influence on otolith microchemistry.

Substantial variation in Sr/Ca ratio occurred for young adult (≤5 years old) Chesapeake fish. In all samples, values ranged below detection limits. Presumably these values represent excursions unrelated to spawning by young fish into freshwater systems. Freshwater and slightly saline environments in the upper reaches of Chesapeake Bay tributaries may serve as foraging grounds. Future research could analyze the duration and seasonality of freshwater habitation by fishes that reside in the Chesapeake Bay.

Further verification studies are needed to establish whether estuarine and marine phases can be distinguished using Sr/Ca ratios. Ratios tended to continuously increase following nadirs, and this pattern could indicate exposure to waters of increasing salinity. A verification study could be carried out by probing the last deposited otolith material (the edge) for Sr/Ca and relating that ratio to the salinity in which the striped bass was sampled in the field or through laboratory rearing studies (Kalish 1989, Townsend et al. 1989, Radtke et al. 1990). A key comparison will be that between samples from estuarine habitats (salinity 5–20 ppt) and marine habitats (≥32 ppt). Should differences be detectable between these groups, then it will be possible to infer detailed patterns of anadromy and related life-history traits.

Acknowledgments

Dr. Philip Picoli at the Central Facility for Microanalysis, University of Maryland, generously provided expertise and assistance with the electron microprobe. Drs. Ed Houde, John Kalish, and David Townsend gave useful criticisms on earlier versions of this manuscript.

Dr. John Dean made available samples of otoliths from South Carolina striped bass. Bunky's Charter Boat Service provided Chesapeake Bay samples. This research was supported by the U.S. Fish and Wildlife Service Emergency Striped Bass Study.

Citations

ASMFC (Atlantic States Marine Fisheries Commission)
1990 Amendment 4 to the Atlantic States Marine Fisheries Commission Interstate Striped Bass Management Report. Fish. Manage. Rep. 16, Versar Inc., Columbia, MD, 200 p.

Bagenal, T.B., F.J.H. Mackereth, and J. Heron
1973 The distinction between brown trout and sea trout by the strontium content of their scales. J. Fish Biol. 5:555–557.

Beamish, R.J., and G.A. McFarlane
1983 The forgotten requirement for age validation in fisheries biology. Trans. Am. Fish. Soc. 112:735–743.

Berg, A.
1968 Studies on the metabolism of calcium and strontium in freshwater fish. I. Relative contribution of direct and intestinal absorption. Mem. Ist. Ital. Idrobiol. 23:161–196.

Casselman, J.M.
1982 Chemical analysis of the optically different zones in eel otoliths. *In* Loftus, K.H. (ed.), Proc., 1980 North American eel conference, p. 74–82. Ont. Fish. Tech. Rep. Ser. 4, Ont. Minist. Nat. Resour.

Chapman, R.W.
1987 Changes in the population structure of male striped bass, *Morone saxatilis*, spawning in three areas of the Chesapeake Bay from 1984 to 1986. Fish. Bull., U.S. 85:167–170.

Chapoton, R.B., and J.E. Sykes
1961 Atlantic coast migration of large striped bass as evidence by fisheries and tagging. Trans. Am. Fish. Soc. 90:13–20.

Contant, C.C.
1990 Microchemical analysis of fish hard parts for reconstructing habitat use: Practice and promise. *In* Parker, N.C., et al. (eds.), Fish marking techniques, p. 574–580. Am. Fish. Soc. Symp. 7, Bethesda.

Goldstein, J.I., D.E. Newberry, P. Echlin, D.C. Joy, C. Fiori, and E. Lifshin
1981 Scanning electron microscopy and x-ray microanalysis. Plenum Press, NY, 675 p.

Heidinger, R.C., and K. Clodfelter
1987 Validity of the otolith for determining age and growth of walleye, striped bass, and smallmouth bass in power cooling ponds. *In* Summerfelt, R.C. (ed.), Age and growth of fish, p. 241–251. Iowa State Univ. Press, Ames.

Houde E.D., and E.S. Rutherford
1992 Egg production, spawning biomass and factors influencing recruitment of striped bass in the Potomac River and Upper Chesapeake Bay. Final Rep. to Maryland Dep. Nat. Resour., Contract CB89-001-003. Univ. Maryland, Cent. Environ. Estuarine Stud., Ref. [UMCEES]-CBL 92-017, 313 p.

Ingram, B.L., and D. Sloan
1992 Strontium isotopic composition of estuarine sediments as paleosalinity-paleoclimate indicator. Science (Wash. DC) 255:68–72.

Kalish, J.M.
1989 Otolith microchemistry: Validation of the effects of physiology, age and environment on otolith composition. J. Exp. Mar. Biol. Ecol. 132:151–178.
1990 Use of otolith microchemistry to distinguish the progeny of sympatric anadromous and non-anadromous salmonids. Fish. Bull., U.S. 88:657–666.
1991 Determination of otolith microchemistry: Seasonal variation in the composition of blood plasma, endolymph and otoliths of bearded rockcod *Pseudophycis barbatus*. Mar. Ecol. Prog. Ser. 74:137–159.

Kinsman, D.J.J., and H.D. Holland
1969 The co-precipitation of cations with $CaCO_3$—IV. The co-precipitation of Sr^{2+} with aragonite between 16° and 96°C. Geochim. Cosmo. Acta. 33:1–17.

Kohlenstein, L.C.
1981 On the proportion of the Chesapeake Bay stock of striped bass that migrates into the coastal fishery. Trans. Am. Fish. Soc. 110:168–179.

Mansueti, R.J.
1961 Age, growth and movements of the striped bass, *Roccus saxatilis*, taken in size selective fishing gear in Maryland. Chesapeake Sci. 2:9–36.

Maryland DNR
1991 Investigation of striped bass in Chesapeake Bay. USFWS Federal Aid Project F-42-R-3, 1989–1990. Md. Dep. Nat. Resour., Tidewater Admin., 193 p.

Massman, W.H., and A.L. Pacheco
1961 Movements of striped bass in Virginia waters of the Chesapeake Bay. Chesapeake Sci. 2:37–44.

Merriman, D.
1941 Studies on the striped bass, *Roccus saxatilis*, of the Atlantic Coast. U.S. Fish Wildl. Serv. Fish. Bull. 50:1–77.

Mugiya, Y., and K. Takahashi
1985 Chemical properties of the saccular endolymph in the rainbow trout, *Salmo gairdneri*. Bull. Fac. Fish. Hokkaido Univ. 36:57–63.

Radtke, R.L.
1984 Formation and structural composition of larval striped mullet otoliths. Trans. Am. Fish. Soc. 113:186–191.

Radtke, R.L., R.A. Kinzie III, and S.D. Folsom
1988 Age at recruitment of Hawaiian freshwater gobies. Environ. Biol. Fishes 23:205–213.

Radtke, R.L., D.W. Townsend, S.D. Folsom, and M.A. Morrison
1990 Strontium: Calcium ratios in larval herring otoliths as indicators of environmental histories. Environ. Biol. Fishes 27:51–61.

Reed, S.J.B.
1975 Electron microprobe analysis. Cambridge Univ. Press, Cambridge, 400 p.

Robinson, J.B.
1960 The age and growth of striped bass (*Roccus saxatilis*) in California. Calif. Fish Game 46:279–290.

Secor, D.H., J.M. Dean, and E.H. Laban
1991 Manual for otolith removal and preparation for microstructure examination. Baruch Press, Univ. South Carolina, Columbia, 85 p.

Secor, D.H., J.M. Dean, T.A. Curtis, and F.W. Sessions
1992 Effect of female size and propagation methods on larval production at a South Carolina striped bass (*Morone saxatilis*) hatchery. Can. J. Fish Aquat. Sci. 49:1778–1787.

Setzler-Hamilton, E.M., and L.W. Hall Jr.
1991 Striped bass *Morone saxatilis*. *In* Funderburk, S.L., et al. (eds.), Habitat requirements for Chesapeake Bay living resources, 2d ed., p. 13-1–13-31, plus maps. Living Resources Subcommittee, Chesapeake Bay Program, Annapolis.

Townsend, D.W., R.L. Radtke, M.A. Morrison, and S.D. Folsom
1989 Recruitment implications of larval herring overwintering distributions in the Gulf of Maine, inferred using a new otolith technique. Mar. Ecol. Prog. Ser. 55:1–13.

Uphoff, J.H.
1989 Environmental effects on survival of eggs, larvae and juveniles in the Choptank River, Maryland. Trans. Am. Fish. Soc. 118:251–263.

Vladykov, V.D., and D.H. Wallace
1952 Studies of striped bass *Roccus saxatilis* (Walbaum) with special reference to the Chesapeake Bay region during 1936–1938. Bull. Bingham Oceanogr. Collect., Yale Univ. 14(1):132–177.

Waldman, J.R., D.J. Dunning, Q.E. Ross, and M.T. Mattson
1990 Range dynamics of Hudson River striped bass along the Atlantic coast. Trans. Am. Fish. Soc. 119:910–919.

Wilson, C.A. et al.
1987 Glossary. *In* Summerfelt, R.C., and G.E. Hall (eds.), Age and growth of fish, p. 527–530. Iowa State Univ. Press, Ames.

Leatherback turtle captured by ingestion of squid bait on swordfish longline

Robert A. Skillman
George H. Balazs

Honolulu Laboratory, Southwest Fisheries Science Center
National Marine Fisheries Service, NOAA
2570 Dole Street, Honolulu, Hawaii 96822-2396

The leatherback turtle *Dermochelys coriacea* is the only species of the family Dermochyidae. The other six extant marine turtles are hard-shelled members of the family Cheloniidae. The leatherback inhabits the pelagic marine environment, apparently only leaving to breed in coastal waters. With recorded dives to 475m, it is among the world's deepest-diving vertebrates (Eckert et al. 1986). With weights up to 916 kg, it is the world's largest turtle (Eckert and Luginbuhl 1988). The leatherback is listed as endangered under the U.S. Endangered Species Act, the International Union for Conservation of Nature, and the Convention on International Trade in Endangered Species. Consequently, fishery interactions involving the leatherback are of concern. This paper reports an interaction with longline gear while fishing for swordfish.

Leatherbacks ingest and become entangled in marine debris (Balazs 1985), and they are taken by operative fishing gear (Nishemura and Nakahigashi 1990). Entanglement has been reported with lobster pot lines (Lazell 1976), drift nets (Balazs 1982, Wetherall et al. In Press); pelagic longline (Witzell 1984, Tobias 1991); gillnets (Margaritoulis 1986); and swordfish *Xiphias gladius* tangle nets (Frazier and Brito Montero 1990). Interactions with tuna and swordfish longline fishing have involved entanglement and foul-hooking, particularly with the leatherback's long flippers (Honolulu Star-Bulletin 1935, Witzell 1984, Dollar 1991, Tobias 1991, USFWS 1969). In the Hawaii swordfish fishery, sightings of leatherbacks and reported interactions are not rare, particularly in the area of the seamounts above the Northwestern Hawaiian Islands (Robert Dollar, NMFS Honolulu Lab., pers. commun.). It is not uncommon for leatherbacks to become entangled in driftnets set north of Hawaii between 30° and 45°N. However, virtually nothing is known about their overall distribution, abundance, and life history including stock structure (Wetherall et al., In press). The nearest colonies of nesting leatherbacks occur in the eastern Pacific along the coast of Mexico and Costa Rica and in the western Pacific in peninsular Malaysia. To our knowledge, ingestion of baited hooks has not been reported in the literature.

Leatherbacks are known to feed on gelatinous, pelagic animals. These include the medusa of sychozoan coelenterates (true jellyfish) (Bleakney 1965, Brongersma 1969) and hydrozoan coelenterates (Portuguese man-of-war *Physalia arethusa*) (Bacon 1970). Davenport (1988) and Davenport and Balazs (1991) have suggested the potential importance of bioluminescence in the predation of free-swimming colonial tunicates (pyrosomas) by leatherbacks during the night or on deep dives. Neither fish (tuna bait) nor squid (swordfish bait) have been cited in the literature as prey of leatherbacks. Accordingly, Witzell (1984) stated that leatherbacks are not likely to be taken on a baited hook.

The present paper presents documentation of a leatherback captured after ingesting squid bait on swordfish longline gear. The chemical light sticks used to attract swordfish may have attracted the leatherback to the gear.

On 24–25 January 1991, while experimental longline fishing operations were being conducted for swordfish from the NOAA research ship *Townsend Cromwell*, a leatherback turtle was hooked and released alive at lat. 26°58.3′N, long. 168° 53.5′W. The turtle swam vigorously while being hauled next to the research vessel and after being released. The hook line could be seen coming from the turtle's mouth, but the exact location of the hook was not apparent. No blood or external injuries were apparent. A tree branch lopper on the end of an extendable fiberglass pole was used to cut the hook line a few centimeters from the turtle's mouth. The estimated carapace length of the turtle was 170cm. The turtle was too large to haul on board, and the prevalence of sharks, including blue shark *Prionace glauca*, made it impossible to enter the water for accurate measurement or tagging. Other site specifics included the following: 2400m bottom depth, 21.4°C sea surface-water temperature, 18.9°C air temperature, 150–180cm sea swells, northeasterly trade winds at 15kn, and approximate depth of the upper mixed layer at 85m.

Details of the set and gear are as follows. The longline gear consisted of ~16km of 4.0 or 3.2mm monofilament main line suspended with floats every 3 hook lines. The gear, with 206 hooks, was set on 24

Manuscript accepted 6 August 1992.
Fishery Bulletin, U.S. 90:807–808 (1992).

January 1991 starting at lat. 27°01.720′N, long. 168°56.153′W, in the vicinity of an unnamed seamount some 940km east of Midway Is. and 150km north-northeast of Raita Bank, Northwestern Hawaiian Is. The gear was hauled on 25 January beginning at lat. 26°59.094′N, long. 168°57.810′W. The turtle was taken on the first hook of a 3-hook basket located about mid-set. This hook was set at 1818h and hauled at 0907h the next day, for a soak time of 14h 49 min. Because the hook timer (a 7.5×3cm cylinder of clear plastic resin with an embedded clock chip; Somerton et al. 1988) on that line was lost, an estimate of the time of hooking is not available. The hook timer on the second hook-line, with full bait remaining, was set off at 0511h; the hook timer on the first hook of the previous basket, with the bait missing, was set off at 0159h. The float lines, made of polypropylene rope, were 9m long. The hook droppers, made of 2.1mm monofilament, were 13m long with a 60g weighted swivel 4m from the hook. Thus, the depth of hook 1 was nominally ~22m, unless altered by currents, since the first hook-line of each basket was attached within 3m of the float. Green, 12h chemical light sticks were placed ~2m above each of the 206 hooks (the light sticks still glowed weakly at the time of hauling). Each hook was baited with a whole, previously-frozen Argentinean squid (*Illex* sp.), weighing ~0.34kg.

While entanglement of leatherbacks in pelagic longline and other gears has been described, ours is apparently the first report of a hook and bait being eaten. Chemical light sticks used on swordfish longline may impose an added hazard for leatherbacks by simulating natural prey. The magnitude of the take, the level of mortality or serious injury, and the impact on the leatherback stock are unknown. Additional data on the take by pelagic fisheries as well as information on leatherback feeding habits, stock structure, and population dynamics would be needed to evaluate the impact of the take.

Citations

Bacon, P.R.
1970 Studies on the leatherback turtle *Dermochelys coriacea* (L.), in Trinidad, West Indies. Biol. Conserv. 2:213–217.

Balazs, G.H.
1982 Driftnets catch leatherback turtles. Oryx 16:428–430.
1985 Impact of ocean debris on marine turtles: Entanglement and ingestion. *In* Shomura, R.S., and H.O. Yoshida (eds.), Proceedings, Workshop on the fate and impact of marine debris, 27–29 November 1984, Honolulu, p. 387–429. NOAA Tech. Memo. NMFS-SWFC-54, NMFS Honolulu Lab.

Bleakney, J.S.
1965 Reports of marine turtles from New England and eastern Canada. Can. Field-Nat. 19:120–128.

Brongersma, L.D.
1969 Miscellaneous notes on turtles, IIB. Proceedings, K. Ned. Akad. Wet. Ser. C, Biol. Med. Sci. 72:90–102.

Davenport, J.
1988 Do diving leatherbacks pursue glowing jelly? Br. Herpetol. Soc. Bull. 24:20–21.

Davenport, J., and G.H. Balazs
1991 'Fiery bodies'—Are pyrosomas an important component of the diet of leatherback turtles? Br. Herpetol. Soc. Bull. 37:33–38.

Dollar, Robert A.
1991 Summary of swordfish longline observations in Hawaii, July 1990–March 1991. Admin. Rep. H-91-09, NMFS Honolulu Lab., 13 p.

Eckert, K.L., and C. Luginbuhl
1988 Death of a giant. Mar. Turtle Newsl. 43:2–3.

Eckert, S.A., D.W. Nellis, K.L. Eckert, and G.L. Kooyman
1986 Diving patterns of two leatherback sea turtles (*Dermochelys coriacea*) during internesting intervals at Sandy Point, St. Croix, U.S. Virgin Islands. Herpetologica 42(3):381–388.

Frazier, J.G., and J.L. Brito Montero
1990 Incidental capture of marine turtles by the swordfish fishery at San Antonio, Chile. Mar. Turtle Newsl. 49:8–13.

Honolulu Star-Bulletin
1935 [Photograph with a caption indicating a 200kg leatherback turtle was found entangled in the line and hooks of a sampan, a Japanese-style fishing boat probably using longline gear.] Honolulu Star-Bulletin, 8 April 1935, p. 3.

Lazell, J.D. Jr.
1976 This broken archipelago. Cape Cod and the islands, amphibians and reptiles. Demeter Press Book, Gräfelfing, Germany, p. 191.

Margaritoulis, D.N.
1986 Captures and strandings of the leatherback sea turtle, *Dermochelys coriacea*, in Greece (1982–1984). J. Herpetol. 20(3):471–474.

Nishemura, W., and S. Nakahigashi
1990 Incidental capture of sea turtles by Japanese research and training vessels: Results of a questionnaire. Mar. Turtle Newsl. 51:1–4.

Somerton, D.A., B.S. Kikkawa, and C.D. Wilson
1988 Hook timers to measure the capture of individual fish. Mar. Fish. Rev. 50(2):1–5.

Tobias, W.
1991 Incidental catch a continuing problem in the Mediterranean. Mar. Turtle Newsl. 51:10–12.

USFWS (U.S. Fish & Wildlife Service)
1969 Cruise report, USFWS ship *Townsend Cromwell*, cruise 44. USFWS Hawaii Area Biol. Lab., 4 p. [Avail. NMFS Honolulu Lab.]

Wetherall, J.A., G.H. Balazs, R.A. Tokunaga, and M.Y.Y. Yong
In press Bycatch of marine turtles in North Pacific high-seas driftnet fisheries and impacts on the stocks. *In* Proc., Int. North Pac. Fish. Comm., Nov. 4–6, 1991, Tokyo.

Witzell, W.N.
1984 The incidental capture of sea turtles in the Atlantic U.S. Fishery Conservation Zone by the Japanese tuna longline fleet, 1978–81. Mar. Fish. Rev. 46(3):56–58.

Reproductive biology of the swordfish *Xiphias gladius* in the Straits of Florida and adjacent waters

Ronald G. Taylor
Michael D. Murphy

Florida Marine Research Institute, Department of Natural Resources
100 Eighth Avenue SE, St. Petersburg, Florida 33701-5095

The swordfish *Xiphias gladius* Linnaeus inhabits all tropical, subtropical, and temperate oceans of the world, including the Mediterranean Sea and the Gulf of Mexico. In the western Atlantic, it is found from Newfoundland to Argentina (Palko et al. 1981, Nakamura 1985). Swordfish occur in the Florida Straits at all times of the year. Prior to 1970, swordfish were pursued primarily by recreational fishermen. During the 1970s, the fishery in Florida attracted displaced Cuban-Americans and New England longline fishermen, and by 1980 commercial landings from the east coast of Florida had reached nearly 1500 mt (Berkeley and Irby 1982).

Little is known about the reproductive biology of swordfish in the western Atlantic. Ovchinnikov (1970) and Berkeley and Houde (1980) reported contradictory findings on male and female sizes-at-maturity. Wilson (1984) reported that males mature at younger ages than do females in the U.S. south Atlantic. Descriptions of swordfish spawning season and spawning grounds have been based on the temporal and areal distribution of infrequently-collected larvae and juveniles (Arata 1954, Tibbo and Lauzier 1969, Markle 1974, Grall et al. 1983). Our research objectives were to determine the size- and age-at-maturity, spawning season, and approximate spawning grounds of swordfish in the Straits of Florida and adjacent waters. Data were collected as part of a joint Florida Marine Research Institute and University of Miami investigation of the fishery and biology of the swordfish. Samples gathered during this research have been used to develop a method to determine the ages of swordfish and to describe their growth (Berkeley and Houde 1984).

Methods and materials

Swordfish were sampled from recreational and commercial catches made off southeast Florida (Fig. 1) from June 1977 through November 1980. Each year most of the collections were made April through September. Samples were taken at least once each month over the 2.5 yr sampling period, except in December when no samples were taken either year. Because of the varied conditions of landed swordfish, a variety of length measurements (to the nearest cm) were taken: total length (TL), distance from the tip of the bill to the midpoint of the line connecting the distal edges of the caudal-fin lobes; fork length (FL), from the tip of the bill to the distal end of the central ray of the caudal fin; lower jaw to fork length (LJFL), from the tip of the lower jaw to the distal end of the central ray of the caudal fin; eye to fork length (EFL), from the posterior margin of the eye's bony orbit to the distal end of the central ray of the caudal fin; and trunk length (TRNKL), from the posterior margin of the gill cavity to the point of least circumference of the caudal peduncle. Lower jaw to fork length is used throughout this paper unless otherwise noted. For fish measured only for TL, FL, EFL, or TRNKL, LJFL was estimated using the appropriate regression equation (Table 1). Whole weight (W) was determined to the nearest pound and converted to kilograms for our analyses. Portions of ovaries and testes were collected and preserved in Davidson's fixative (Humason 1972). Whole gonads, macroscopically judged ripe or mature based on the presence of transparent eggs, were preserved and then weighed to the nearest gram.

Swordfish maturity was described using histological features to define gonadal development. Subsamples of preserved gonads were embedded in paraffin, sectioned at 6 μm, stained with Mayer's haematoxylin and eosin, and mounted for microscopic examination. Swordfish were assigned to one of eight developmental classes following Murphy and Taylor (1990) and based on the appearance of histological features described by Grier (1981) for males and Wallace and Selman (1981) for females. These developmental classes and the mean observed oocyte diameters are (1) Immature, $<20\,\mu$m; (2) Developing, 71 μm; (3) Maturing, 160 μm; (4) Mature, 434 μm; (5) Gravid, 723 μm; (6) Spawning/Partially Spent, 823 μm; and (7) Spent, 181 μm. The relationship between swordfish maturity and length was described for each sex using maturity data for fish grouped into 10 cm size-classes. A logistic distribution function was fit to the percentages of mature fish ($\geq$ Class 4) and the midpoints of their size-classes (Saila et al. 1988) in order to predict a maturity schedule. A similar distribution function was generated for maturity against age.

Manuscript accepted 2 July 1992.
Fishery Bulletin, U.S. 90:809-816 (1992).

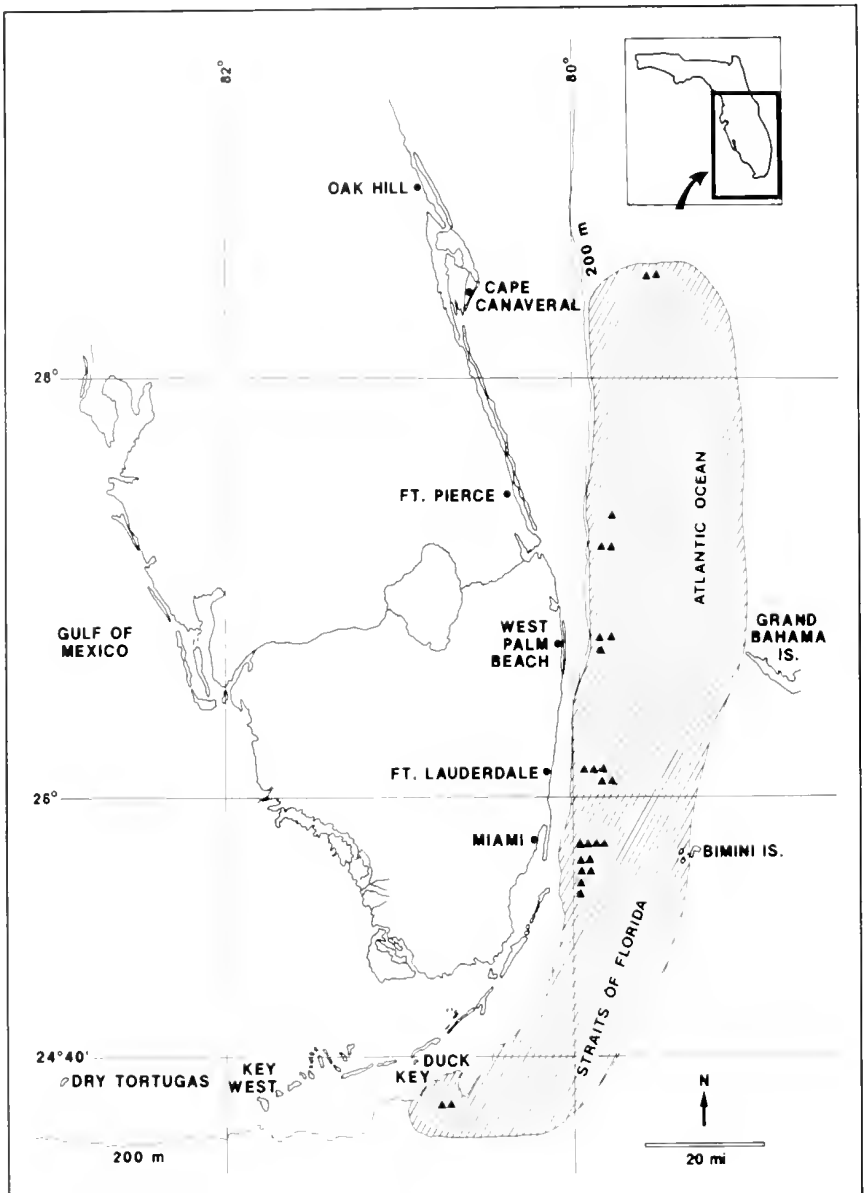

Figure 1

Areal extent of sampling locations (shaded area) off southeast Florida during June 1977–November 1980. Triangles indicate where female swordfish *Xiphias gladius* were found with histological evidence for recent (postovulatory follicles) or imminent (hydrated oocytes) spawning (see "Methods and materials").

Table 1

Linear regressions of lower jaw to fork length (LJFL) on total length (TL), fork length (FL), eye to fork length (EFL), or trunk length (TRNKL); and nonlinear regressions of whole weight (W) on lower jaw to fork length and LJFL on W, for swordfish *Xiphias gladius* off southeast Florida (regression analysis, SAS 1982).

Equation	N	Range	r^2
LJFL = −6.03 + 0.662(TL)	401	32–432 cm TL	0.982
LJFL = −5.51 + 0.714(FL)	100	30–396 cm FL	0.983
LJFL = 8.89 + 1.076(EFL)	316	68–249 cm EFL	0.995
LJFL = 15.71 + 1.402(TRNKL)	324	18–189 cm TRNKL	0.987
$W = 1.050 \times 10^{-5}\,LJFL^{3.035}$	127	27–281 cm LJFL	0.973
$LJFL = 48.58W^{0.305}$	127	0.090–168.0 kg W	0.980

Ages for the swordfish that comprise this data set were determined by Berkeley and Houde (1984), who counted unvalidated age marks found on thin-sections of the second anal-fin spine.

Temporal differences in mean oocyte diameters were used to define spawning season. To determine mean oocyte diameter for each individual, 100 oocytes in a common lamella were measured with an ocular micrometer. Mean oocyte diameters were calculated for all collections in a given month and plotted to examine monthly changes. The distribution of oocyte diameters was also examined within individuals to determine whether swordfish undergo multiple spawns or a single spawn each year.

We used the distribution of swordfish captured in near-term spawning condition to delimit their spawning grounds off southeast Florida. Histological features indicative of recent or imminent spawning included postovulatory follicles and hydrated oocytes (DeMartini and Fountain 1981, Hunter and Macewicz 1985). For a variety of fishes, it has been found that oocytes hydrate during the late-afternoon or evening just prior to spawning (*Serrifus politus*, DeMartini and Fountain 1981; *Engraulis mordax*, Hunter and Macewicz 1985; *Cynoscion nebulosus*, Brown-Peterson et al. 1988; *Sciaenops ocellatus*, Fitzhugh et al. 1988). Postovulatory follicles are identifiable only for a short time. Following spawning, they are rapidly absorbed (within 6 h for *Callionymus enneactis*, Takita et al. 1983) and quickly become indistinguishable from other atretic structures (within 2 d in *Engraulis mordax*, Hunter and Macewicz 1985).

Batch fecundity was estimated gravimetrically from counts of ova >750 μm diameter in a 2–3 g portion from the midsection of each preserved ovary (n 7).

Results

Sex and length data were collected from 554 swordfish: 211 females 72–281 cm, and 343 males 82–235 cm. Gonads were available for histological processing from 295 fish (133 males and 162 females), of which 149 were ascribed ages.

Table 2

Observed and predicted percentages of mature (≥Class 4, see "Methods and materials") swordfish *Xiphias gladius* in 10 cm LJFL length intervals. Predicted percentages were calculated from logistic distribution functions fit to observed maturity data (see "Results"). Numbers in parentheses are numbers of fish examined.

Lower jaw to fork length interval midpoint (cm)	Male		Female	
	Observed %(*N*)	Predicted %	Observed %(*N*)	Predicted %
80			0(1)	0
90	0(3)	11	0(2)	0
100	33(3)	24	0(7)	0
110	46(11)	45	0(17)	0
120	64(11)	69	0(19)	1
130	90(10)	85	0(14)	3
140	96(24)	94	0(8)	5
150	93(14)	98	0(2)	10
160	100(11)	99	0(3)	18
170	100(14)	100	50(4)	30
180	100(11)	100	60(10)	47
190	100(8)	100	56(16)	64
200	100(6)	100	71(14)	78
210	100(5)	100	75(16)	87
220	100(1)	100	100(10)	93
230	100(1)	100	100(6)	97
240			100(3)	98
250			100(5)	99
260			100(2)	100
270				
280			100(3)	100

Table 3

Observed and predicted percentages of mature (≥Class 4, see "Methods and materials") swordfish *Xiphias gladius* by assigned age group (ages from Berkeley and Houde 1984). Predicted percentages were calculated from logistic distribution functions fit to observed maturity data (see "Results"). Numbers in parentheses are numbers of fish examined.

Age (years)	Male		Female	
	Observed %(*N*)	Predicted %	Observed %(*N*)	Predicted %
0	0(1)	4		
1	30(10)	29	0(13)	0
2	80(10)	79	0(18)	1
3	93(14)	97	0(6)	5
4	92(12)	100	18(11)	14
5	100(12)	100	38(8)	37
6	100(8)	100	60(10)	66
7			100(3)	87
8	100(2)	100	83(6)	96
9			100(4)	99
10			100(1)	100

Male swordfish mature at a smaller size and younger age than do females. Males begin to mature at ~100 cm at age 1 (Tables 2, 3). The proportion of mature males in our samples increased rapidly thereafter, and all males were mature by 160 cm or age 5. In contrast, the smallest mature females were ~170 cm or age 4, and all females were mature by 220 cm or age 9. The predicted length at 50% maturity, based on the fit of logistic distribution functions to the percentage mature within size-classes, was significantly less (approximate t-test, Sokal and Rohlf 1981; t' 36.5, df 33, $P<0.001$) for males (112 cm) than for females (182 cm). Likewise, age at 50% maturity was significantly younger for males (1.4 yr) than for females (5.5 yr; t' 17.7, df 16, $P<0.001$). The logistic distribution functions for maturity by size-class and age fit observed data well (Tables 2, 3) and are as follows:

Males:

$$\%\ \text{Mature} = 1/(1+e^{(-0.0976(\text{LJFL}-112))}) \quad (n\ 15,\ r^2\ 0.980)$$

$$\%\ \text{Mature} = 1/(1+e^{(-2.223(\text{AGE}-1.40))}) \quad (n\ 8,\ r^2\ 0.990)$$

Females:

$$\%\ \text{Mature} = 1/(1+e^{(-0.0690(\text{LJFL}-182))}) \quad (n\ 20,\ r^2\ 0.966)$$

$$\%\ \text{Mature} = 1/(1+e^{(-1.234(\text{AGE}-5.45))}) \quad (n\ 10,\ r^2\ 0.976).$$

Swordfish from southeast Florida waters demonstrate group-synchronous oocyte maturation (*sensu* Wallace and Selman 1981). This pattern of oocyte development is characterized by the presence of at least two distinct groups of dissimilar-sized oocytes during the spawning season. Ovaries from all swordfish in our samples contained a dominant group of oocytes <200 μm diameter (Fig. 2). All oocytes within Maturing ovaries (Class 3) were <200 μm, although lipid deposition suggests preparation for active vitellogenesis. Mature ovaries (Class 4) contained an additional distinct group of vitellogenic oocytes at 200–600 μm. A third group of oocytes, 600–1100 μm, were present only in Gravid and Spawning/Partially Spent fish (Classes 5 and 6). This largest

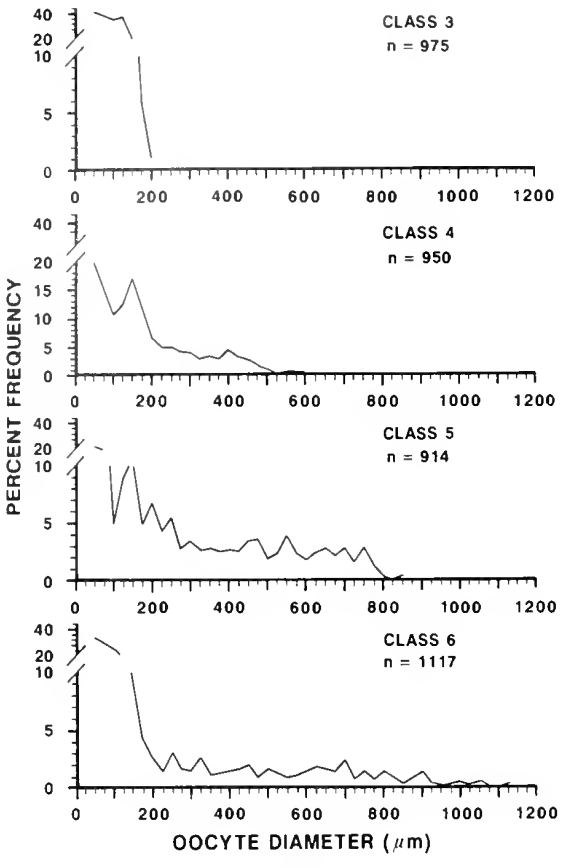

Figure 2

Percent frequency of oocyte diameters for swordfish *Xiphias gladius* collected during the spawning season off southeast Florida with ovaries in Classes: (3) Maturing, (4) Mature, (5) Gravid, and (6) Spawning/Partially Spent (see "Methods and materials").

group of oocytes proceeds through final maturation and represents the clutch (Wallace and Selman 1981) to be shed during the next spawning event.

The reproductive season for swordfish is protracted. Mature or actively spawning females were found during each month sampled, except January. Gravid or actively spawning males were found during all months sampled (Fig. 3). The greater numbers of spawning fish taken from late-spring to midsummer suggests increased spawning activity then. In addition, mature swordfish show a sharp increase in their maximum oocyte diameters to >800 μm beginning in April and extending through July, indicating peak spawning activity then (Fig. 4).

Histological features (postovulatory follicles and hydrated oocytes) provide evidence for active swordfish spawning off the Atlantic coast of Florida from about 24°40′N in the Straits of Florida southwest of Duck Key to about 28°25′N just west of Cape Canaveral (Fig. 1). The easternmost location where fish in spawning condition were collected was 16 km east of Grand Bahama Island at 480 m depth. About 25% of the fish collected at the westward extent of our sampling area (about the 200 m contour) exhibited evidence of recent or imminent spawning.

There was a preponderance of smaller males in our spring and summer samples. Overall, males significantly dominated the catch (345 M:216 F; χ^2 29.7, df 1, $P<0.001$); although at sizes >200 cm, females significantly outnumbered males (22 M:67 F; χ^2 22.8, df 1, $P<0.001$). There was no histological indication of hermaphroditism throughout the 72–281 cm length range. During spring and summer, males were dominant (266 M:152 F; χ^2 31.1, df 1, $P<0.001$); but during the fall and winter there was no significant difference in abundances of sexes (79 M:64 F; χ^2 1.6, df 1, $P>0.05$).

The batch fecundity of the seven swordfish sampled was 1.4–4.2 million eggs for swordfish 177–281 cm and 69–268 kg (Table 4). There was no obvious relationship between our estimates of batch fecundity and length or weight. The correlation coefficients between batch fecundity and length (r 0.21) and between batch fecundity and weight (r 0.64) were not significantly different from zero (table of critical values for correlation coefficients, df 5, $P>0.05$, Rohlf and Sokal 1981).

Discussion

Sizes-at-maturity have been reported for swordfish in the Atlantic and Pacific Oceans and Mediterranean Sea (Ovchinnikov 1970, Berkeley and Houde 1984, DeMetrio et al. 1989). However, in these reports maturity was determined by visual inspection of gonads, and no explanations were given as to whether the sizes reported were for first maturity or for 50% maturity. Berkeley and Houde (1984) reported that western Atlantic male and female swordfish mature at ~21 kg and 74 kg, respectively. This corresponds closely to the lengths-at-50%-maturity we present for swordfish off southeast Florida. Using equations in Table 1, we determined 50% maturity of males at 18 kg (112 cm LJFL converted to whole weight) and 50% maturity of females at 77 kg (182 cm). Ovchinnikov (1970) reported that male swordfish "reach maturity" in the Atlantic at about 100 cm (type of measure unknown). However, he reported a smaller size-at-maturity for females (70 cm). DeMetrio et al. (1989) reported that male swordfish in the eastern Mediterranean Sea first begin to mature at 82–105 cm LJFL and that nearly all are mature when >135 cm. Females

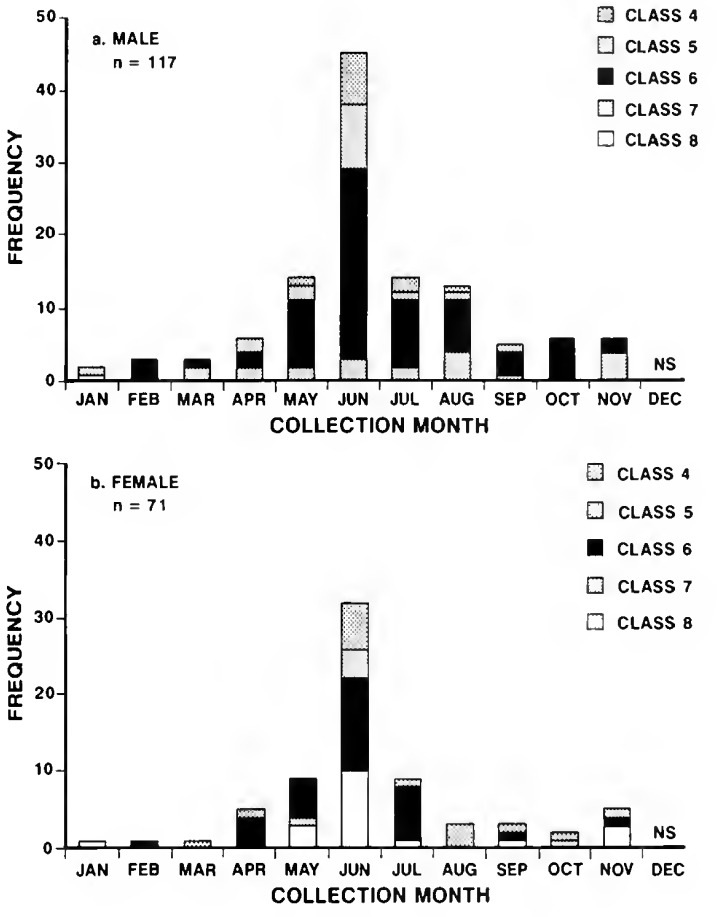

Figure 3

Monthly frequencies of gonad development classes for mature (≥Class 4, see "Methods and materials") swordfish *Xiphias gladius* collected off southeast Florida during the period June 1977–November 1980. NS indicates no samples taken.

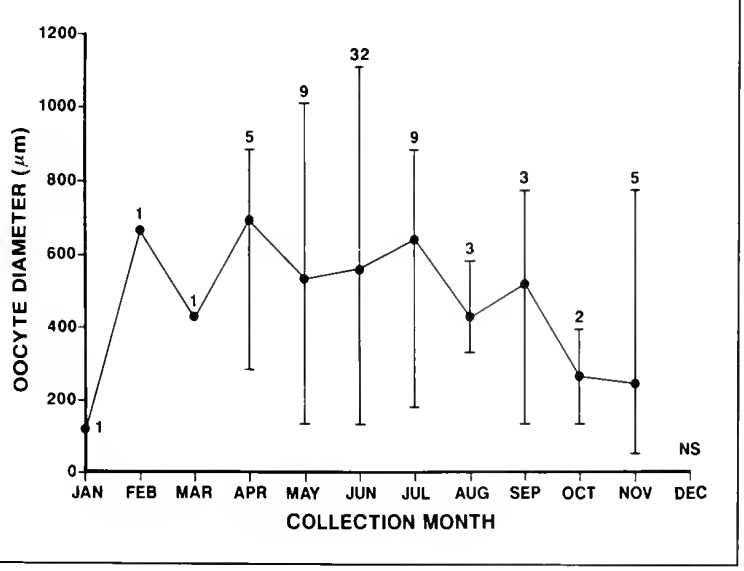

Figure 4

Monthly mean and range (vertical bars) of individual mean oocyte diameters for all mature (Class ≥4) swordfish *Xiphias gladius* collected off southeast Florida during the period June 1977–November 1980. Numbers indicate sample size; NS indicates no samples taken.

in the Mediterranean first reach maturity at 106–135 cm LJFL, and about 50% of the females >135 cm are mature. This is in contrast to our findings that the smallest mature females off Florida were ~170 cm LJFL and that 50% of females reached maturity when ~180 cm.

Female swordfish from the Pacific Ocean mature at sizes comparable to or somewhat smaller than those in the western Atlantic. From 1949 to 1958, Yabe et al. (1959) examined 372 female swordfish taken by a Japanese longline fleet in the North Pacific. They found only five mature females and suggested that females in the North Pacific begin to mature at 150–170 cm EFL (170–192 LJFL). Kume and Joseph (1969) concluded that female swordfish off California begin to mature at slightly smaller sizes, 139 cm EFL (158 cm LJFL), and are regularly found in ripe condition at >170 cm (192 cm LJFL).

The ages-at-maturity we estimated for male (1.4 yr) and female (5.5 yr) swordfish off southeast Florida are somewhat younger and older, respectively, than those determined for male and female swordfish collected farther north in the U.S. South Atlantic. From a relatively small sample collected off North Carolina and South Carolina, Wilson (1984) determined that males mature between ages 2 and 3 (15 mature males of 24 examined). Females mature between ages 4 and 5 (2 mature females of 18 examined). Although Wilson (1984) relied on a different technique (thin-sectioned otoliths) than did our study (thin-sectioned spines) to determine swordfish ages, he compared the two aging techniques and found they provided similar swordfish ages through at least age 5.

Female swordfish mature at a younger age in the eastern Mediterranean Sea than in the western Atlantic or Pacific Oceans. In the eastern Mediterranean,

Table 4

Estimates of batch fecundity for seven swordfish *Xiphias gladius* sampled off southeast Florida, including lower jaw to fork length, age (Berkeley and Houde 1984), whole weight, gonad development class, and oocyte diameters.

Batch fecundity (millions)	Lower jaw to fork length (mm)	Age (yr)	Whole weight (kg)	Gonad class	Hydrated oocyte size		
					N	$\bar{x}$	range
1.398	256	6	107	6	1754	0.98	0.83–1.16
2.814	252	9	223	6	1288	1.04	0.75–1.14
2.836	207	8	116	6	1656	1.56	1.30–1.77
3.071	177	–	69	6	2036	1.55	1.33–1.73
3.125	233	–	170	6	2121	1.35	1.17–1.57
4.220	281	–	268	6	2912	1.54	1.34–1.68
4.220	256	9	210	6	1232	1.11	0.96–1.23

DeMetrio et al. (1989) found mature female swordfish as young as age 2, with most mature by age 3. However, Yabe et al. (1959) suggested that female swordfish in the North Pacific mature at age 5 or 6. This is in agreement with our age-at-50%-maturity for females (5.5 years). Although we found no information on maturation of male swordfish from the Pacific, most male swordfish in the eastern Mediterranean reach maturity by age 2 (DeMetrio et al. 1989), again similar to our findings off southeast Florida.

The observed protracted spawning of swordfish off southeast Florida, with peak activity during April through July, agrees with reported spawning seasons determined from temporal changes in the abundance of larvae and juveniles. Taning (1955) reported that spawning off Florida and elsewhere in the North Atlantic occurs throughout the year, with peak larval abundances during February through April. The temporal distribution of larval abundance in the western North Atlantic suggests that swordfish spawn during December through September, with a peak in April (Arata 1954, Markle 1974, Grall et al. 1983). Off the coast of southern California, gonads of female swordfish are inactive from late-August through mid-November (Weber and Goldberg 1986). This period of inactivity coincides with low mean oocyte diameters of swordfish in the western Atlantic (Fig. 4), suggesting that swordfish in the eastern Pacific and western Atlantic may have similar annual spawning seasons.

Two histological features present in ovarian tissue—hydrated oocytes and postovulatory follicles—provided evidence that female swordfish spawn off the coast of southeast Florida between the Florida Keys and Cape Canaveral. The presence of hydrated oocytes indicates an imminent spawn, certainly within 12 h. Young postovulatory follicles found in many female swordfish provide evidence that spawning occurred within 24 h of capture. Further, short-term studies of the movement of swordfish, using acoustic tags, have shown that fish that were likely mature (70–140 kg) remained in the same general area (<90 km from tagging) for up to 5 d during the peak of the spawning season (April) off Baja California (Carey and Robison 1981). More extensive movement occurred for a 70 kg swordfish tracked for 2.5 d in November in the vicinity of Cape Hatteras, North Carolina. This fish traveled 240 km in 67 h, heading from cold continental shelf waters off Cape Hatteras to warmer Sargasso Sea waters. The combination of this information on net random movement of swordfish with our observed histological evidence for recent or imminent spawning suggests that spawning occurs in our sampling area. Additionally, Grall et al. (1983) found major concentrations of swordfish larvae and juveniles in the western Atlantic in the waters near the Lesser Antilles, in the Yucatan Straits, and in the Florida Straits, implying the presence of a large spawning population in these areas.

Changes in sex ratios as swordfish increase in size apparently result from differences in growth between the sexes and possibly from seasonal differences in their distribution. Swordfish larger than ~230 cm are female because males have shorter life spans and slower growth rates (Berkeley and Houde 1984, Wilson 1984). The dominance of males in our summer collections may be explained by seasonal differences in the distribution of the sexes. Guitart-Manday (1964) found a similar preponderance of males (72%) in samples from the mainly summertime commercial fishery off Cuba. Beckett (1974) reported that few males were taken in the northern swordfish fisheries in waters <18°C, whereas in more tropical latitudes, males account for 67–100% of the catch. Off southeast Florida, surface-water temperatures remain >18°C throughout the year, ranging from ~22°C in February to 29°C in August (Atkinson et al. 1983). Our observed seasonal changes in sex ratios of swordfish collected off southeast Florida imply that whereas some males and females are year-round inhabitants of these waters, more females than males move north during the summer, which results in a dichotomous distribution that becomes more acute the farther north the fish migrate. At the northern extent of the range in the western North Atlantic, off New England and the Canadian maritimes, most, if not all, fish captured are females (Lee 1942, Tibbo et al. 1961).

Our estimates of batch fecundity (1.4–4.2 million ova) are comparable to the estimate of Yabe et al. (1959) and to estimates for smaller swordfish by Uchiyama and Shomura (1974). Our estimates are somewhat less than those made for larger fish collected by the latter authors. Yabe et al. (1959) estimated the fecundity of a swordfish 186 cm TRNKL (276 cm LJFL from Table 1) to be 3–4 million ova (1.2–1.6 mm in diameter). Uchiyama and Shomura (1974) estimated the fecundity of an 80 kg swordfish (185 cm LJFL from Table 1) to be 3.0 million ova, which closely agrees with our determinations. However, they estimated that a 200 kg swordfish (244 cm LJFL from Table 1) would have a fecundity of ~6 million ova, which is more than our estimates for swordfish over 200 kg.

Our estimates of fecundity and maturity schedules can be used in analyzing the effect of fishing on the spawning-stock biomass or spawning potential of swordfish in the U.S. South Atlantic (e.g., spawning-stock biomass per recruit analysis, Gabriel et al. 1989). Recent assessments of the status of swordfish in the Atlantic have utilized several techniques, including dynamic pool models ("yield per recruit"), to determine the effects that fishing and age at entry to the fishery have on yield (ICCAT 1991). Our quantitative estimates of the female maturation process and fecundity can be used in further analyzing the effect of fishing on the abundance of mature swordfish (and by implication the production of new recruits).

Acknowledgments

Credit for collecting the samples and data for this research is given to E. Houde, S. Berkeley, E. Irby, J. Jolley, and D. Nickerson. Data collected for this study were funded in part by a grant/cooperative agreement from the National Oceanic and Atmospheric Administration through the National Sea Grant College, Grant NA80AA-D-00038. The views expressed herein are those of the authors and do not necessarily reflect the views of NOAA or any of its subagencies. We thank L. French, J. Leiby, M. Myers, and anonymous reviewers for their editorial assistance.

Citations

Arata, G.F. Jr.
1954 A contribution to the life history of the swordfish, *Xiphias gladius* Linnaeus, from the South Atlantic coast of the United States and the Gulf of Mexico. Bull. Mar. Sci. Gulf Caribb. 4:183–243.

Atkinson, L.P., T.N. Lee, J.O. Blanton, and W.S. Chandler
1983 Climatology of the southeastern United States Continental Shelf waters. J. Geophys. Res. 88:4705–4718.

Beckett, J.S.
1974 Biology of swordfish, *Xiphias gladius* L., in the Northwest Atlantic Ocean. *In* Shomura, R.S., and F. Williams (eds.), Proc., Int. billfish symp.; Part 2, Review and contributed papers, p. 105–106. NOAA Tech. Rep. NMFS SSRF 675.

Berkeley, S.A., and E.D. Houde
1980 Swordfish dynamics in the Straits of Florida. Int. Counc. Explor. Sea CM 1980/H:59 Pelagic Fish Committee, 11 p.
1984 Age determination of broadbill swordfish, *Xiphios gladius*, from the Straits of Florida, using anal fin spine sections. *In* Prince, E.D., and L.M. Pulos (eds.), Proc., International workshop on age determination of oceanic pelagic fishes: Tunas, billfishes, and sharks, p. 137–143. NOAA Tech Rep. NMFS 8.

Berkeley, S.A., and E.W. Irby
1982 Analysis of catch, effort and landing data in the swordfish longline fishery of the Florida Straits. Int. Counc. Explor. Sea CM 1982/H:53, 12 p.

Brown-Peterson, N., P. Thomas, and C.R. Arnold
1988 Reproductive biology of the spotted seatrout, *Cynoscion nebulosus*, in South Texas. Fish. Bull., U.S. 86:373–388.

Carey, F.G., and B.H. Robison
1981 Daily patterns in the activities of swordfish, *Xiphias gladius*, observed by acoustic telemetry. Fish. Bull., U.S. 79:277–292.

DeMartini, E.E., and R.K. Fountain
1981 Ovarian cycling frequency and batch fecundity in the queenfish, *Seriphus politus*: Attributes representative of serial spawning fishes. Fish. Bull., U.S. 79:547–555.

DeMetrio, G., P. Megalofonou, S. Tselas, and N. Tsimedides
1989 Fishery and biology of the swordfish *Xiphias gladius* L., 1758 in Greek waters. *In* Savini, M., and J.F. Caddy (eds.), Report of the second technical consultation on stock assessment in the eastern Mediterranean, p. 135–145. FAO Fish. Rep. 412.

Fitzhugh, G.R., T.G. Snider III, and B.A. Thompson
1988 Measurement of ovarian development in red drum (*Sciaenops ocellatus*) from offshore stocks. Contrib. Mar. Sci. (Suppl.) 30:79–83.

Gabriel, W.L., M.P. Sizenmore, and W.J. Overholtz
1989 Analysis of spawning stock biomass per recruit: An example for Georges Bank haddock. N. Am. J. Fish. Manage. 9:383–391.

Grall, C., D.P. DeSylva, and E.D. Houde
1983 Distribution, relative abundance, and seasonality of swordfish larvae. Trans. Am. Fish. Soc. 112:235–246.

Grier, H.J.
1981 Cellular organization of the testis and spermatogenesis in fishes. Am. Zool. 21:345–357.

Guitart-Manday, D.
1964 Biología pesquera del emperador o pez de espada, *Xiphias gladius* Linnaeus (Teleostomi: Xiphiidae) en las aguas de Cuba. Poeyana Inst. Biol. (Habana), Ser. B. 1, 37 p. [transl. by Foreign Language Div., Canada].

Humason, G.L.
1972 Animal tissue techniques. W.H. Freeman, San Francisco, 641 p.

Hunter, J.R., and B.J. Macewicz
1985 Measurement of spawning frequency in multiple spawning fishes. *In* Lasker, R. (ed.), An egg production method for estimating spawning biomass of pelagic fish: Application to the northern anchovy, p. 79–94. NOAA Tech. Rep. NMFS 36.

ICCAT (International Commission for the Conservation of Atlantic Tunas)
1991 Reference paper on 1991 swordfish stock assessments by SCRS swordfish assessment group. SCRS/91/16, Int. Comm. Conserv. Atl. Tuna, Madrid, 19 p.

Kume, S., and J. Joseph
1969 Size composition and sexual maturity of billfish caught by the Japanese longline fishery in the Pacific Ocean east of 130°W. Bull. Far Seas Fish. Res. Lab. (Shimizu) 2:115-162 [in Engl., Japanese summ.].

Lee, R.E.
1942 The occurrence of female swordfish in southern New England waters, with a description of their reproductive condition. Copeia 2:117-119.

Markle, G.E.
1974 Distribution of larval swordfish in the Northwest Atlantic Ocean. *In* Shomura, R.S., and F. Williams (eds.), Proc., Int. billfish symp.; Part 2, Review and contributed papers, p. 252-260. NOAA Tech. Rep. NMFS SSRF 675.

Murphy, M.D., and R.G. Taylor
1990 Reproduction, growth, and mortality of red drum *Sciaenops ocellatus* in Florida waters. Fish. Bull., U.S. 88:531-542.

Nakamura, I.
1985 Billfishes of the world. FAO Fish. Synop. 125(5), 58 p.

Ovchinnikov, V.V.
1970 Mech-ryba i parusnikovye (Atlanticheskii okean. Ekologia i funktsional naya morfologiya). (Swordfish and billfishes of the Atlantic Ocean. Ecology and functional morphology.) Nauch-Issled. Inst. Ryb. Knoz. Okeanogr., Kaliningrad, 106 p. [Transl. by Israel Prog. Sci. Transl., 77 p.; avail. NTIS, Springfield, VA, TT71-50011.]

Palko, B.J., G.L. Beardsley, and W.J. Richards
1981 Synopsis of the biology of the swordfish, *Xiphias gladius* Linnaeus. NOAA Tech. Rep. NMFS Circ. 441, 21 p.

Rohlf, F.J., and R.R. Sokal
1981 Statistical tables, 2d ed. W.H. Freeman, NY, 219 p.

Saila, S.B., C.W. Reckseik, and M.H. Prager
1988 Basic fishery science programs, a compendium of microcomputer programs and manual of operation. Elsevier, NY, 230 p.

SAS
1982 SAS user's guide: Basics, 1982 ed. SAS Inst., Inc., Cary NC, 923 p.

Sokal, R.R., and F.J. Rohlf
1981 Biometry, 2d ed. W.H. Freeman, NY, 859 p.

Takita, T., T. Iwamoto, S. Kai, and I. Sogabe
1983 Maturation and spawning of the dragonet, *Callionymus enneactis*, in an aquarium. Jpn. J. Ichthyol. 30(3):221-226.

Taning, A.V.
1955 On the breeding areas of the swordfish (*Xiphias*). Pap. Mar. Biol. Oceanogr. Deep Sea Res. Suppl. to Vol. 3:3248-3251.

Tibbo, S.N., L.R. Day, and W.F. Doucet
1961 The swordfish (*Xiphias gladius* L.), its life-history and economic importance in the northwest Atlantic. Fish. Res. Board Can. Bull. 130:1-47.

Tibbo, S.N., and L.M. Lauzier
1969 Larval swordfish (*Xiphias gladius*) from three localities in the western Atlantic. J. Fish. Res. Board Can. 26: 3248-3251.

Uchiyama, J.H., and R.S. Shomura
1974 Maturation and fecundity of swordfish from Hawaiian waters. *In* Shomura, R.S., and F. Williams (eds.), Proc., Int. billfish symp.; Part 2, Review and contributed papers, p. 142-148. NOAA Tech. Rep. NMFS SSRF 675.

Wallace, R.A., and K. Selman
1981 Cellular and dynamic aspects of oocyte growth in teleosts. Am. Zool. 21:325-343.

Weber, E.C., and S.R. Goldberg
1986 The sex ratio and gonad indices of swordfish, *Xiphias gladius*, caught off the coast of southern California in 1978. Fish. Bull., U.S. 84:185-186.

Wilson, C.A. III
1984 Age and growth aspects of the life history of billfishes. Ph.D. diss., Univ. South Carolina, Columbia, 180 p.

Yabe, H.S., S. Ueyanagi, S. Kikawa, and H. Watanabe
1959 Studies of the life history of the swordfish, *Xiphias gladius* Linnaeus. Rep. Nankai Reg. Fish. Res. Lab. 10: 107-150 [in Jpn., Engl. summ.; transl. by CEP Multilingual Serv. Div., Dep. Sec. of State, Canada].

Fishery Bulletin Index

Volume 90 (1-4), 1992

List of Titles

90(3)

90(4)

Fishery Bulletin Index

Volume 90 (1-4), 1992

List of Authors

Fishery Bulletin Index

Volume 90 (1-4), 1992

List of Subjects

Statement of Ownership, Management and Circulation

(Required by 39 U.S.C. 3685)

1A Title of Publication	1B PUBLICATION NO	2 Date of Filing
Fishery Bulletin	3 6 6 - 3 7 0	9-16-92
3 Frequency of Issue: Quarterly	3A No. of Issues Published Annually: 4	3B Annual Subscription Price: 24.00 domestic 30.00 foreign

4 Complete Mailing Address of Known Office of Publication *(Street, City, County, State and ZIP+4 Code) (Not printer)*

NMFS Scientific Publicatione Office
7600 Sand Point Way NE, Seattle, WA 98115-0070

5 Complete Mailing Address of the Headquarters of General Business Offices of the Publisher *(Not printer)*

National Marine Fisheries Service, NOAA/DOC
1335 East-West Highway, Silver Spring, MD 20910

6 Full Names and Complete Mailing Address of Publisher, Editor, and Managing Editor *(This item MUST NOT be blank)*

Publisher *(Name and Complete Mailing Address)*
Willis Hobart, Scientific Publications Office
7600 Sand Point Way NE, Seattle, WA 98115-0070

Editor *(Name and Complete Mailing Address)*
Nancy Peacock, Scientific Publications Office
7600 Sand Point Way NE, Seattle, WA 98115-0070

Managing Editor *(Name and Complete Mailing Address)*
Same as above

7 Owner *(If owned by a corporation, its name and address must be stated and also immediately thereunder the names and addresses of stockholders owning or holding 1 percent or more of total amount of stock. If not owned by a corporation, the names and addresses of the individual owners must be given. If owned by a partnership or other unincorporated firm, its name and address, as well as that of each individual must be given. If the publication is published by a nonprofit organization, its name and address must be stated.) (Item must be completed.)*

Full Name	Complete Mailing Address
U. S. Dept. of Commerce	14th St., NW, Washington, DC 20230

8 Known Bondholders, Mortgagees, and Other Security Holders Owning or Holding 1 Percent or More of Total Amount of Bonds, Mortgages or Other Securities *(If there are none, so state)*

Full Name	Complete Mailing Address
NONE	

9 For Completion by Nonprofit Organizations Authorized To Mail at Special Rates *(DMM Section 424.12 only)*
The purpose, function, and nonprofit status of this organization and the exempt status for Federal income tax purposes *(Check one)*

(1) [X] Has Not Changed During Preceding 12 Months
(2) [ ] Has Changed During Preceding 12 Months

(If changed, publisher must submit explanation of change with this statement.)

10 Extent and Nature of Circulation *(See instructions on reverse side)*	Average No. Copies Each Issue During Preceding 12 Months	Actual No. Copies of Single Issue Published Nearest to Filing Date
A Total No. Copies *(Net Press Run)*	2074	2080
B Paid and/or Requested Circulation handled by U.S. Supt. of Documents, Washington, DC 20240 1 Sales through dealers and carriers, street vendors and counter sales	"	"
2 Mail Subscription *(Paid and/or requested)*	600	600
C Total Paid and/or Requested Circulation *(Sum of 10B1 and 10B2)*	600	600
D Free Distribution by Mail, Carrier or Other Means Samples, Complimentary, and Other Free Copies	1455	1457
E Total Distribution *(Sum of C and D)*	2055	2057
F Copies Not Distributed 1 Office use, left over, unaccounted, spoiled after printing	19	23
2 Return from News Agents	--	--
G TOTAL *(Sum of E, F1 and 2—should equal net press run shown in A)*	2074	2080

11 I certify that the statements made by me above are correct and complete

Signature and Title of Editor, Publisher, Business Manager, or Owner

PS Form 3526, January 1991 *(See instructions on reverse)*

Superintendent of Documents **Subscriptions** Order Form

Order Processing Code:
* 5178

☐ **YES,** enter my subscription as follows:

Charge your order. It's Easy! MasterCard VISA

To fax your orders (202) 512–2233

____ subscriptions to **FISHERY BULLETIN (FB)** for $24.00 per year ($30.00 foreign).

The total cost of my order is $_____. Price includes regular domestic postage and handling and is subject to change.

(Company or Personal Name) (Please type or print)

(Additional address/attention line)

(Street address)

(City, State, ZIP Code)

(Daytime phone including area code)

(Purchase Order No.)

May we make your name/address available to other mailers? YES ☐ NO ☐

Please Choose Method of Payment:

☐ Check Payable to the Superintendent of Documents

☐ GPO Deposit Account ☐☐☐☐☐☐☐–☐

☐ VISA or MasterCard Account

☐☐☐☐☐☐☐☐☐☐☐☐☐☐☐☐☐☐☐☐

☐☐☐☐ (Credit card expiration date)

Thank you for your order!

(Authorizing Signature) 11/91

Mail To: New Orders, Superintendent of Documents
P.O. Box 371954, Pittsburgh, PA 15250–7954

Fishery Bulletin

Guidelines for Contributors

Form of manuscript

The document should be in the following sequence: Title Page, Abstract (not required for Note), Text, Acknowledgments, Citations, Text footnotes, Appendices, Tables, Figure legends, and Figures.

Title page should include authors' full names and mailing addresses and the senior author's telephone and FAX numbers.

Abstract Not to exceed one double-spaced typed page. Should include a sentence or two explaining to the general reader why the research was undertaken and why the results should be viewed as important. Abstract should convey the main point of the paper and outline the results or conclusions. No footnotes or references.

Text A brief introduction should portray the broad significance of the paper. The entire text should be intelligible to readers from different disciplines. All technical terms should be defined, as well as all abbreviations, acronyms, and symbols in text, equations, or formulae. Abbreviate units of measure only when used with numerals or in tables and figures to conserve space. Measurements should be expressed in metric units, with other equivalent units given in parentheses. Follow the *U.S. Government Printing Office Style Manual*, 1984 ed., and the *CBE Style Manual*, 5th ed. Fishery and invertebrate nomenclature should follow the *American Fisheries Society Special Publication 12* (for fishes), *16* (for mollusks), and *17* (for decapod crustaceans).

Text footnotes should be numbered in Arabic numerals and typed on a separate sheet from the text. Footnotes are not used for reference material or personal communications, but rather to explain or define terms in the text and for contribution numbers on the title page.

Informal sources Personal communications, unpublished data, and untitled manuscripts in preparation are noted parenthetically in the text (full name, affiliation, brief address including zip code, and month and year when appropriate).

Acknowledgments Gather all acknowledgments into a brief statement at the end of the text. Give credit only for exceptional contributions and not to those whose contributions are part of their normal duties.

Citations All titled sources should be listed in the Citations section, including unpublished and processed material. In text, cite as Smith and Jones (1977) or (Smith and Jones 1977); if more than one citation, list chronologically (Smith 1936, Jones 1975, Doe In press). All sources cited in the text should be listed alphabetically by the senior authors' surnames under the heading CITATIONS. Abbreviations of periodicals and serials should conform to *Serial Sources for the BIOSIS Data Base*™. Indicate whether sources are in a language other than English. For informal literature, include address of author or publisher. Authors are responsible for the accuracy of all citations.

Tables should supplement, not duplicate, the text. Each table should be numbered and cited consecutively, with headings short but amply descriptive so that the reader need not refer to the text. For values less than one, zeros should precede all decimal points. Indicate units of measure in column headings; do not deviate from the unit of measure within a column. Table footnotes should be noted consecutively in Roman letters across the page from left to right and then down. Since all tables are typeset, they need not be submitted camera-ready.

Figures Photographs and line drawings should be of professional quality—clear and concise—and reducible to 42 picas for full-page width or to 20 picas for a single-column width, and to a maximum 55 picas high. All graphic elements in illustrations must be proportioned to insure legibility when reduced to fit the page format. Line weight and lettering should be sharp and even. Lettering should be upper and lower case, and vertical lettering should be avoided whenever possible (except for vertical, y, axis). Zeros should precede all decimal points for values less than one. Reproductions of line artwork are accepted in the form of high-quality photographic prints from negatives or photomechanical transfer (PMT). Halftones should be sharply focused with good contrast. Micron rules should be inserted on electron micrographs, even when magnification is included in the figure legend. There should be clear distinction between identifying letters (press-on or overlay) and background of photograph. Label each figure in pencil on the back. Send only xerox copies of figures to the Scientific Editor; originals or photographic prints will be requested later when the manuscript is accepted for publication.

Copyright Government publications are in the public domain, i.e., they are not protected by copyright.

Submission of manuscript

Disks Authors are encouraged to retain manuscripts on word-processing storage media (diskettes, floppy disks) and submit a double-spaced hardcopy run from the storage media. Submit disks as MS-DOS "print" or "nondocument" files (often called "ASCII files"). If a disk cannot be converted to an ASCII file, the author should indicate on the disk the source computer and software language along with the file name. Either 5¼-inch or 3½-inch disks from IBM-compatible or Apple/MacIntosh systems (non-graphics only) can be submitted, double-sided/double-density or high-density, limiting each file to 300 kilobytes. All 8-inch word-processing disks (e.g., Wang or NBI) must be converted onto 5¼- or 3½-inch MS-DOS print disks.

Send original hardcopy and two duplicated copies to:

Dr. Ronald W. Hardy, Scientific Editor
Northwest Fisheries Science Center
National Marine Fisheries Service, NOAA
2725 Montlake Boulevard East
Seattle, WA 98112-2097

Copies of published articles and notes
The senior author and his/her organization each receive 50 separates free-of-charge. Additional copies may be purchased in lots of 100.